Surface Chemistry of Synthetic Protein Analogues. VII. Polytyrosine and its Related Polypeptides

By Toshizo ISEMURA and Takuya YAMASHITA

(Received July 22, 1958)

We have previously studied[1-6] the monolayers of synthetic polypeptides with non-electrolytic side chains as well as those with electrolytic side chains at air/water interface. It is well known that tyrosine residue is very specific among other amino acid residues in protein because of the potency of its hydrogen bonding. In the present experiment, poly-L-tyrosine and poly-DL-tyrosine were studied at air/water and oil/water interfaces, in order to investigate the effect of hydrogen bond on the nature of polypeptide monolayer. The monolayer of poly-DL-phenylalanine which lacks only a phenolic OH group per residue was also studied in comparison with polytyrosine. The effect of the phenolic OH group was also investigated by its esterification with benzyl group.

Experimental

Among the samples used in the present investigation, poly-DL-phenylalanine, poly-DL-tyrosine and poly-*o*-benzyl-DL-tyrosine were synthesized by Dr. H. Tani and Dr. H. Yuki of our University, and poly-L-tyrosine by Dr. E. Katchalski and Dr. M. Sela of the Weizmann Institute of Science. The solvents used for the speading solution for each polypeptide are listed in Table I.

Surface pressure and surface potential were measured simultaneously. Surface pressure was measured by Wilhelmy's hanging plate method and surface potential by vibrating air electrode method. The pH of the substrate was adjusted by adding hydrochloric acid or potassium carbonate to any desired pH without buffering. The pH was measured with Beckman's glass electrode or with Toyo pH test paper. Interfacial pressure and interfacial potential were measured by the procedure which was reported previously by Hotta[7-9] of our laboratory, excepting the use of hanging plate instead of detaching ring. At oil/water interface, the interfacial concentration was changed by successive injection method using micrometer syringe. Measurement was carried out five minutes later after every injection. Petroleum ether of boiling point of 90~120°C was used as an oil phase. All the experiments were carried out at room temperature without any temperature regulation. The temperature change never exceeded more than one degree in the course of experiment.

Results and Discussion

Poly-DL-phenylalanine.—We studied at first the film of poly-DL-phenylalanine at air/water and oil/water interfaces as an example of the polypeptide film containing the side chain of benzyl group. In Fig. 1, surface (or interfacial) pressure and surface (or interfacial) moment were plotted per phenylalanyl residue. The surface (or interfacial) moment was calculated from

TABLE I
SOLVENTS USED FOR EACH POLYPEPTIDE

Polypeptide	Solvent	Interface
Poly-DL-phenylalanine	Benzene (9) + Dichloroacetic acid (1)	A/W
	Chloroform	A/W
	Benzene (25) + Dichloroacetic acid (1)	O/W
Poly-L-tyrosine (D. P. 45)	Pyridine (1) + Isopropyl alcohol (1)	A/W, O/W
	Benzene (3) + Dichloroacetic acid (7)	A/W
Poly-DL-tyrosine	Pyridine (1) + Isopropyl alcohol (1)	A/W, O/W
Poly-*o*-benzyl-DL-tyrosine	Benzene (3) + Dichloroacetic acid (2)	A/W, O/W

1) T. Isemura and K. Hamaguchi, This Bulletin, **25**, 40 (1952).
2) T. Isemura and K. Hamaguchi, ibid., **26**, 425 (1953).
3) T. Isemura and K. Hamaguchi, ibid., **27**, 125 (1954).
4) T. Isemura and K. Hamaguchi, ibid., **27**, 339 (1954).
5) K. Hamaguchi and T. Isemura, ibid., **28**, 9 (1955).
6) T. Isemura, K. Hamaguchi and H. Kawasato, ibid., **28**, 185 (1955).
7) T. Isemura, H. Hotta and T. Miwa, ibid., **26**, 380 (1953).
8) H. Hotta, ibid., **26**, 386 (1953).
9) H. Hotta, ibid., **27**, 412 (1954).

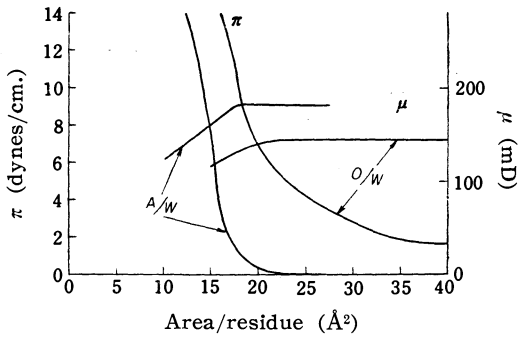


Fig. 1. Surface (or interfacial) pressure (π)-area and surface (or interfacial) moment (μ)-area curves of poly-DL-phenylalanine on distilled water. (A/W interface, 10°C and O/W interface, 13°C).

the observed surface (or interfacial) potential using Helmholtz's formula. $\Delta V = 4\pi n\mu$. The force-area curves of this polypeptide film spread from chloroform solution* and from benzene solution containing a small amount of dichloroacetic acid were exactly identical. A limiting area per residue was found from compressibility-area relation to be 15.8 Å². This area is somewhat larger than that of the typical polypeptide with non-electrolytic paraffine side chains, namely 14.7 Å². Mishuck and Eirich[10] reported that this polypeptide has a small limiting area and attributed this fact to the multilayer formation. On the other hand, Cumper and Alexander[11] found 14.4 Å as the limiting area per residue of this polypeptide from the surface viscosity-area relation. The area found per residue from the force-area relation by them is in rather good agreement with our present result. The surface moment at the area where the film begins to form multilayer is designated by μ_c. μ_c of this polypeptide is 182 mD and is in the same order of magnitude with that of most polypeptide films of non-electrolytic side chains which are spread in β-configuration, whereas Davies[12] reported the surface moment of this polypeptide to be about 100 mD at 30 Å²/residue. At oil/water interface the film is considerably expanded as shown in Fig. 1, because of release of van der Waals force between large side chains such as benzyl groups by oil phase. μ_c was found to be 144 mD and markedly higher than that found by Davies (about 80 mD at 30 Å²).

Poly-L-tyrosine and poly-DL-tyrosine.— The force-area relations of poly-L-tyrosine and poly-DL-tyrosine spread from solutions of respective polypeptide in a mixture of pyridine and isopropyl alcohol (1 : 1) was investigated as a function of pH of the substrate water. The surface pressure-area curves for poly-L-tyrosine and poly-DL-tyrosine are shown in Fig. 2 and Fig. 3, respectively. As shown in these figures on the substrate at pH's less than 9.4 the film considerably condensed. The small area of these polypeptides can not be attributed to partial dissolution of the film as shown in Fig. 4; the presence of salt such as potassium chloride in the substrate water at the concentration of 1.0 mol. per liter scarcely affects the expansion of film. On the other hand, the film is considerably expanded on a substrate at pH's more

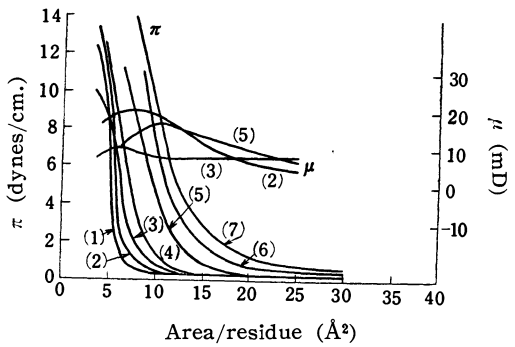


Fig. 2. Surface pressure (π)-area and surface moment (μ)-area curves of poly-L-tyrosine (spread from pyridine-isopropyl alcohol solution). (1) pH 2.0, (2) pH 5.6, (3) pH 7.2, (4) pH 9.4, (5) pH 11.0, (6) pH 11.3 and (7) pH 12.5. (26°C).

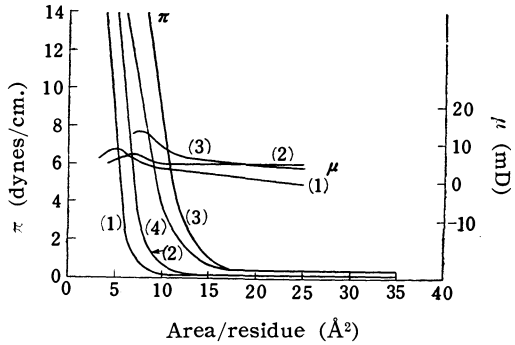


Fig. 3. Surface pressure (π)-area and surface moment (μ)-area curves of poly-DL-tyrosine. (1) pH 5.6, (2) pH 9.2, (3) pH 11.0 and (4) pH 12.5. (24°C).

* Unpublished experiment by Dr. K. Hamaguchi in our laboratory.

10) E. Mishuck and F. R. Eirich, *J. Polymer Sci.*, **16**, 397 (1955).

11) C. W. N. Cumper and A. E. Alexander, *Trans. Faraday Soc.*, **46**, 235 (1950).

12) J. T. Davies, *Biochim. Biophys. Acta*, **11**, 165 (1953).

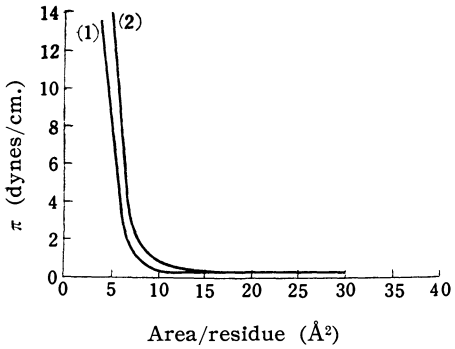


Fig. 4. Effect of the salt on poly-L-tyrosine (spread from pyridine-isopropyl alcohol solution) at pH 5.6. (1) no salt and (2) 1 mol. KCl. (26°C).

than 11.0. However, when the pH of the substrate becomes more than 13, it dissolves rather than expands. In Figs. 2 and 3, the surface moment-area relations of poly-L-tyrosine and poly-DL-tyrosine are also shown, respectively. Surface moment is very small in comparison with that of poly-DL-phenylalanine. The trend of the curve is very different from that of other polymer films. These facts may be caused by the cancellation of dipole by intramolecular hydrogen bond. Several years ago, Masuda and Eda[13] reported the small area per tyrosine residue for poly-DL-tyrosine film. They found a smaller area on acid substrate than on alkaline substrate. This may be caused by partial dissolution of polypeptide because of the smaller degree of polymerization of the polypeptide which they used.

Polytyrosine films spread at air/water interface occupy much less area than the films of other polypeptides such as polyphenylalanine and show much smaller surface moment as mentioned above. These anomalous properties of polytyrosine might come from the hydrogen bonding of phenolic OH group in tyrosine residue. Without this hydroxyl group, polytyrosine may assume exactly a structure of polyphenylalanine. Accordingly, the film would have a limiting area of about 15 Å² per residue. Nevertheless, the limiting area per residue for poly-L-tyrosine was found to be 5.7 Å² and that for poly-DL-tyrosine to be 5.8 Å² both at pH 5.6. These small areas per residue may be attributed to the spreading of these polypeptides in a coiled state, owing to the strong hydrogen bonding of phenolic OH groups. The extremely low value of surface moment supports also this inference. Even on alkaline substrate, the spreading of the film is not complete, although the film expands considerably at pH region between 8.0 and 11.5. As shown in Fig. 5, this finding corresponds to the partial breaking of hydrogen bonds and to the partial dissociation of phenolic OH groups, and to the result of spectrophotometric titration by Katchalski and Sela[14,15]. On the other hand, we obtain the film which seems to assume β-keratin configuration irrespective of the pH of the substrate if we spread it from a solution in dichloroacetic acid which is a strong hydrogen-bond breaking agent. The surface moment of the film thus obtained is about 120~130 mD, as shown in Fig. 6, suggesting the intramolecular cancellation of OH contributions to surface moment

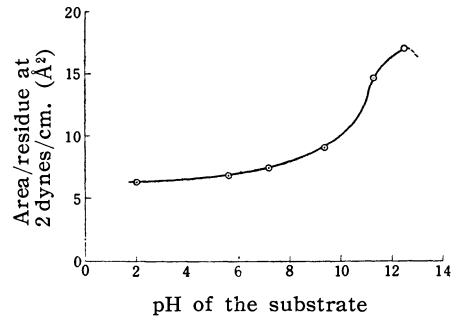


Fig. 5. Effect of pH of the substrate water on the area at 2 dynes/cm. of poly-L-tyrosine (spread from pyridine-isopropyl alcohol solution) at air/water interface.

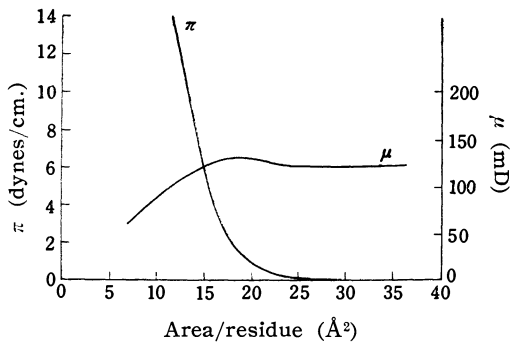


Fig. 6. Surface pressure (π)-area and surface moment (μ)-area curves of poly-L-tyrosine (spread from dichloroacetic acid and benzene solution) on distilled water. (16°C).

13) Y. Masuda and K. Eda, *Science [Japan] (Kagaku)*, **21**, 470 (1951).

14) E. Katchalski and M. Sela, *Bull. Research Council of Israel*, **2**, 315 (1952).

15) E. Katchalski and M. Sela, *J. Am. Chem. Soc.*, **75**, 5284 (1953).

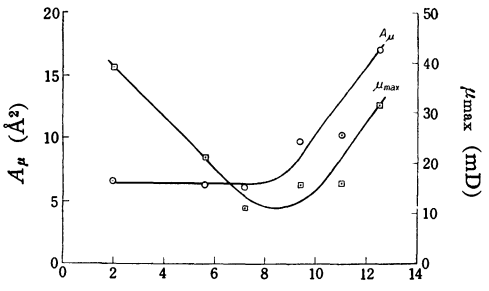


Fig. 7. Monolayers of poly-L-tyrosine (spread from pyridine-isopropyl alcohol solution). Area at maximum surface moment (A_μ)-pH and maximum surface moment (μ_{max})-pH curves.

and tending to the value of surface moment of ordinary polypeptide films. In Fig. 7, the surface moment of polytyrosine increases as the film is compressed and passes a maximum and then decreases, whereas most usual well-spread linear polymer shows a constant surface moment, μ_c until the polymer film is closely packed as the film is compressed and further compression causes the decrease of surface moment. The maximum surface moment, μ_{max} and the area where the maximum moment was found, A_μ, are plotted against pH. μ_{max} increases considerably above pH 8.5. This might be caused by the unfolding and reorientation of polypeptide owing to the breaking of some hydrogen bonds. The reason why μ_{max} increases at the extreme acid substrate is not clear but is presumably due to the formation of oxonium ions[16].

In Figs. 8 and 9, the results obtained at petroleum ether/water interface are shown. The film is considerably expanded.

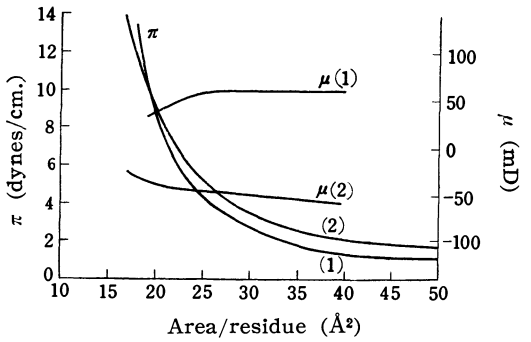


Fig. 8. Interfacial pressure (π)-area and interfacial moment (μ)-area curves of poly-L-tyrosine. (1) pH 2.0, 13°C and (2) 11.0, 15°C.

16) I. Sawai, *Trans. Faraday Soc.*, **31**, 765 (1938).

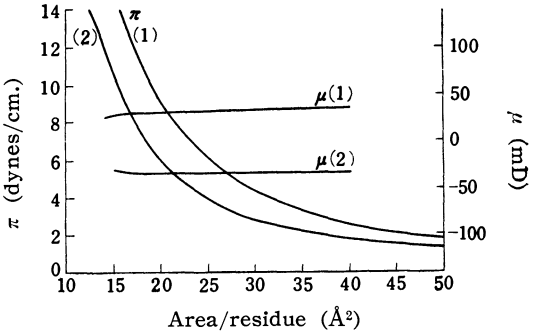


Fig. 9. Interfacial pressure (π)-area and interfacial moment (μ)-area curves of poly-DL-tyrosine. (1) pH 2.0 and (2) pH 11.0. (22°C).

Poly-L-tyrosine film is more expanded at pH 11.0 than at 2.0, whereas poly-DL-tyrosine is more expanded at pH 2.0 than at pH 11.0. The force-area curves are like those of the monolayers of polypeptide with nonpolar side chains such as poly-DL-phenylalanine. At pH 2 all the side chains of *p*-hydroxybenzyl group might be dissolved in the oil phase. Interfacial potential was found to be 60 mD (μ_c) for poly-L-tyrosine and 32 mD at 25 Å²/residue for poly-DL-tyrosine. These values are markedly less than that for poly-DL-phenylalanine (144 mD (μ_c)). This difference might be caused by the contribution of phenolic OH group of tyrosine. Poly-DL-tyrosine is more expanded than poly-L-tyrosine corresponding to the general tendency of expansion of poly-DL-amino acid more than poly-L-amino acid as previously reported[3]. On the other hand, the fact that at air/water interface the film of poly-DL-tyrosine occupies less area than poly-L-tyrosine does at pH 12.5 is due to the general tendency of higher solubility of poly-DL-amino acid than poly-L-amino acid. If the aqueous phase is alkaline, the phenolic OH dissociates and dissolves in the aqueous phase at both air/water and oil/water interfaces. In this case the contribution of dipole is inverse. The negative surface moment was found at oil/water interface, namely −44 mD at 25 Å²/residue for poly-L-tyrosine and −34 mD (μ_c) for poly-DL-tyrosine.

From these results we can conclude that both poly-L-tyrosine and poly-DL-tyrosine spread incompletely at air/water interface and the film is in a partially coiled state because of the hydrogen bonding of phenolic OH group if it is not ionized. However, at oil/water interface by the release of van der Waals force between

side chains due to the intervening of oil, hydrogen bonds are readily broken, and the monolayer which seems to be in β-configuration is obtained. Even at air/water interface, similar monolayer is obtained when we spread the film from a solution in hydrogen bond breaking agent. The obtained force-area curve is very similar to that of poly-DL-phenylalanine. With this monolayer, surface moment of 132 mD (μ_{max}) is found.

Poly-*o*-benzyl-DL-tyrosine. — Force-area and surface (interfacial) moment-area curves of poly-*o*-benzyl-DL-tyrosine at air/water and oil/water interfaces are shown in Fig. 10. Because of lacking of hydrogen bonding agency by esterification of phenolic OH groups, the film is well spread at air/water interface. The area per residue at minimum compressibility is somewhat less than that of poly-DL-phenylalanine and polytyrosine which was spread from the solution containing dichloroacetic acid. The large van der Waals force between side chains seems to cause the condensation of the film. The maximum value of surface moment reached 123 mD. Surface moment increased as the film was compressed, especially when the force-area curve begins to stand steeply at about 20 Å^2 residue. This change is based on the reorientation of large polar side chains. At oil/water interface, poly-*o*-benzyl-DL-tyrosine expanded considerably more than any other polypeptides mentioned above. All large side chains may be in the oil phase, and there is no interaction between the side chain because of the release of van der Waals force between them by intervening of oil. The size and difficulty of packing such large chains may be the cause of the expansion of the film. Interfacial moment was found to be 150 mD

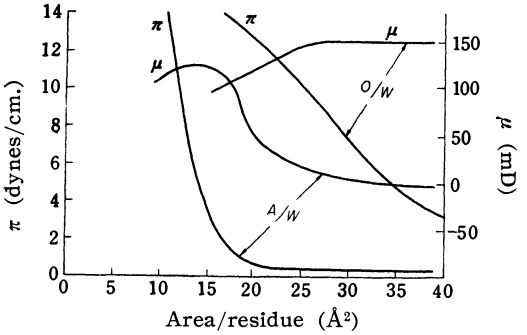


Fig. 10. Surface (or interfacial) pressure (π)-area and surface (or interfacial) moment (μ)-area curves of poly-*o*-benzyl-DL-tyrosine on distilled water. (24°C).

TABLE II

AREAS AND SURFACE AND INTERFACIAL MOMENTS FOR EACH POLYPEPTIDE

	Interface	Aqueous phase	pH	Temp. (°C)	A_π (Å^2/residue)	$A_{\pi=5}$ (Å^2/residue)	μ (mD)	A_μ (Å^2/residue)
Poly-DL-phenyl-alanine	A/W	d.w	5.4	10	15.8	15.6	182(C)	17.8
	O/W	d.w	5.4	13		22.8	144(C)	23.0
Poly-L-tyrosine (Pyridine-Isopropyl alcohol)	A/W	d.w	5.6	26	5.7	5.7	21(M)	6.2
		0.01 N K_2CO_3	11.0	26	10.4	10.0	10(M)	16.0
	O/W	0.01 N HCl	2.0	13		23.7	60(C)	25.0
		0.01 N K_2CO_3	11.0	15		25.0	−44 (at 25 Å^2)	
Poly-L-tyrosine (Dichloroacetic acid-Benzene)	A/W	d.w	3.0	16	15.4	15.6	132(M)	18.8
Poly-DL-tyrosine	A/W	d.w	5.6	24	5.8	5.6	9(M)	4.8
		0.01 N K_2CO_3	11.0	24	11.0	11.0	8(M)	14.0
	O/W	0.01 N HCl	2.0	22		28.0	32 (at 25 Å^2)	15.2
		0.01 N K_2CO_3	11.0	22		22.5	−34(C)	16.0
Poly-*o*-benzyl-DL-tyrosine	A/W	d.w	4.0	24	13.8	13.9	123(M)	14.2
	O/W	d.w	4.2	24		33.7	150(C)	29.2

A_π: Area at minimum compressibility (limiting area), $A_{\pi=5}$: Area at 5 dynes/cm., μ: Surface (or interfacial) moment, (C): Constant value, (M): Maximum value, A_μ: Area at which μ begins suddenly decrease, or area at the maximum value of μ, d.w: Distilled water.

(μ_c) which corresponds namely to the value of poly-DL-phenylalanine.

All the results are summarized in Table II.

Summary

The monolayer properties of synthetic polypeptides which have phenolic OH groups in the side chains such as poly-L-tyrosine and poly-DL-tyrosine were studied to investigate the effect of hydrogen bonding by tyrosyl OH groups. Poly-*o*-benzyl-DL-tyrosine and poly-DL-phenylalanine were also studied for comparison.

At air/water interface, poly-L-tyrosine and poly-DL-tyrosine occupy much smaller area per residue than any other polypeptide films, and have very small surface moment, if they were spread from the solution in pyridine and isopropyl alcohol mixture. These polypeptides might be spread in a strict sense not in an extended monolayer but in a coiled state, suggesting the hydrogen bond between phenolic OH and —CO— or —NH— groups in the main chain. On the alkaline substrate the film expands considerably because of the breaking of hydrogen bonds by the ionization of phenolic OH. At petroleum ether/water interface, the film is also expanded by releasing of van der Waals force. Interfacial moment changes its sign due to whether the aqueous phase is acid or alkaline. It suggests that *p*-hydroxybenzyl groups are in the oil phase at oil/acid solution, whereas they are in the aqueous phase at oil/alkaline solution. Poly-L-tyrosine assumes the configuration very similar to that of poly-DL-phenylalanine, if poly-L-tyrosine is spread from a solution in dichloroacetic acid which is a strong hydrogen bond breaking agent.

Poly-*o*-benzyl-DL-tyrosine gives a monolayer which is somewhat more condensed than poly-DL-phenylalanine at air/water interface, whereas it occupies a larger area per residue than poly-L-tyrosine, poly-DL-tyrosine and poly-DL-phenylalanine at oil/water interface. All these findings are caused by the existence of very large side chains in poly-*o*-benzyl-DL-tyrosine.

The authors express their hearty thanks to Dr. H. Tani and Dr. H. Yuki of the Faculty of Science of Osaka University and Professor E. Katchalski and Dr. M. Sela of the Weizmann Institute of Science in Israel who gave them the valuable samples of synthetic polypeptides. The expense for the experiment was partly defrayed from the grant given by the Ministry of Education, to which the authors' thanks are due.

The Institute of Scientific and Industrial Research, Osaka University, Sakai, Osaka
and
The Institute for Protein Research Osaka University, Tosabori Nishi-ku, Osaka

Catalytic Hydrogenation in Vapor Phase with Urushibara Nickel Catalyst

By Kazuo HATA, Ken-ichi WATANABE and Hamao WATANABE

(Received July 31, 1958)

It has been reported[1] that catalytic hydrogenation in vapor phase with Urushibara nickel catalyst (U-Ni in abbreviation) was carried out for the first time and the experimental results were fairly good. In consequence, it has been proved that U-Ni as a catalyst for hydrogenation is able to be used effectively in vapor phase as well as in liquid phase[2]. It is not as troublesome to use U-Ni as to use other catalysts such as Sabatier's reduced nickel catalyst.

From the previous investigations, we got a suggestion of preparing U-Ni from

1) K. Hata, K. Watanabe and S. Sato, This Bulletin, **30**, 431 (1957).

2) Y. Urushibara and S. Nishimura, ibid., **27**, 480 (1954); Y. Urushibara, S. Nishimura and H. Uehara, ibid., **28**, 446 (1955); K. Hata et al., *J. Chem. Soc. Japan, Pure Chem. Sec.* (*Nippon Kagaku Zasshi*), **77**, 1405 (1956).

nickel chloride solution and aluminum metal in place of zinc dust. In this paper, we introduce a new study using U-Ni which is made from nickel chloride and aluminum metal. It was found that U-Ni thus made was a more excellent hydrogenation catalyst in vapor phase than any other one because of its activity and convenience in practical use.

At first aluminum powder was used for the precipitating agent, and the precipitated nickel was treated with alkali. The catalyst thus obtained was found to be useful for the reduction of some organic substances. However, aluminum powder did not seem to be entirely suitable for the preparation of the catalyst, although the preparation could be carried out more easily by the addition of some detergent. Then grained aluminum (45 meshes) was chosen instead of aluminum powder. Nickel was precipitated from nickel chloride solution on the surface of aluminum grains, and the precipitated nickel was treated with acetic acid containing inorganic salt such as sodium chloride, whereby the precipitated nickel did not separate from the aluminum grains*. U-Ni catalyst thus prepared, which is called U-Ni-AA** in abbreviation, was proved to be a very convenient catalyst for vapor phase hydrogenation because the grains of aluminum remained undissolved after they were treated with acetic acid, and served as carrier.

A similar catalyst prepared by digesting the precipitated nickel with alkali is called U-Ni-BA**, which is also useful for hydrogenation. U-Ni-BA for the liquid phase hydrogenation must be prepared with grained aluminum[3], but for the vapor phase hydrogenation, it was proved that U-Ni-BA prepared from nickel chloride and commercially available aluminum powder was effective enough. The conditions of preparation of these U-Ni catalysts are shown in Table I.

The results of hydrogenation with these catalysts are summarized in Table II. Nitrobenzene was reduced to aniline, phenol to cyclohexanol. Both styrene and acetophenone were hydrogenated with U-Ni-BA to ethylbenzene (Exp. No. 3 and 4); when U-Ni-AA was used, they were reduced further to ethylcyclohexane (Exp. No. 9 and 10). It is very remarkable that benzene was reduced to cyclohexane[4] with U-Ni-AA, but not with U-Ni-BA (prepared with aluminum powder). Benzonitrile was largely reduced to toluene and ammonia[5], and the result of this cleavage reaction was different from that of previous experiments[1] using U-Ni-A (prepared from nickel chloride and zinc dust).

From these results, it is evident that the aromatic ring is able to be reduced by the use of this new type catalyst U-Ni-AA, while not by U-Ni-A*** or U-Ni-B***. In addition, it is interesting to note that U-Ni-AA can also be used in the hydrogenation in liquid phase under the condition of room temperature and ordinary pressure of hydrogen. For example, nitrobenzene was reduced to aniline in 70% yield in ethanol. Thus U-Ni-AA is shown to be effective for hydrogenation both in vapor and liquid phase as well as reduced nickel catalyst. It may be expected that U-Ni prepared from aluminum will be widely applied in the field of catalytic chemistry.

Experimental

U-Ni-AA.—To 60 g. of grained aluminum (45 meshes), a small amount of water is added. In another vessel, 80 cc. of nickel solution containing 32 g. of $NiCl_2 \cdot 6H_2O$ is heated to 50~60°C, and added to the aluminum with stirring. An exchange reaction occurs and nickel deposits on the surface of the aluminum. The reaction is controlled by cooling with cold water or by heating with hot water. The precipitated nickel is washed with cold water. Then 40% acetic acid solution (385 cc., 70°C) containing 89 g. of sodium chloride is added to the nickel. After 3~7 minutes, the acid solution is decanted, and the residue washed with ca. 2 l. of warm water (50~60°C) and then with methanol. The catalyst thus obtained contains 8 g. of nickel.

U-Ni-BA (for vapor phase hydrogenation).—Ten g. of aluminum powder (200 meshes) is suspended in a small amount of water, and heated on a boiling water bath. Then 10 cc. of warm nickel chloride solution containing 4 g. of $NiCl_2 \cdot 6H_2O$ (ca. 90°C) is added to the aluminum. After a violent exchange reaction ceases, all

* The procedure of preparing the catalyst and of the hydrogenation was quite different unless the salt was used, and the catalyst thus prepared was not suitable for hydrogenation.

** In abbreviation, the last A means aluminum as precipitating agent, and the first A and B mean acid and base as the digesting solution for the precipitated nickel.

3) K. Hata, S. Taira and I. Motoyama, This Bulletin, **31**, 776 (1958).

4) P. Sabatier and J. B. Senderens, *Compt. rend.*, **132**, 210 (1901).

5) P. Sabatier and J. B. Senderens, ibid., **140**, 482 (1905); K. Hata, *Sci. Papers Inst. Phys. Chem. Research (Tokyo)*, **23**, 224 (1944); M. Tanaka, K. Watanabe and K. Hata, *J. Chem. Soc. Japan, Pure Chem. Sec. (Nippon Kagaku Zasshi)*, **76**, 1392 (1955).

*** Only phenol was reduced to cyclohexanol in 20~30% yield with U-Ni-A or U-Ni-B (unpublished).

TABLE I
PREPARATION OF CATALYSTS

Catalyst	$NiCl_2 \cdot 6H_2O$ (g.)	Al (g.)	Al (mesh)	Digesting solution	NaCl (g.)	Carrier
U-Ni-AA	32	60	45	40% CH_3CO_2H (385 cc.)	89*	—
U-Ni-BA	4	10	200	20% NaOH (200 cc.)	—	Pumice stone
U-Ni-BA	12	15	45	20% NaOH (350 cc.)	—	"Hyflosupercel"

* The quantity to saturate the acid solution.

TABLE II
VAPOR PHASE CATALYTIC HYDROGENATION WITH U-Ni CATALYSTS

Exp. No.	Catalyst	Compounds	Weight of sample (g.)	Nickel (g.)	Temp. (°C)	Time (hr.)	Flow velocity of sample (g./min.)	Products and Yields (%)	
1	U-Ni-BA	Nitrobenzene	8	1	240[1]	5	0.038	Aniline[2]	(58)
2	U-Ni-BA	Phenol	10	4	185[1]	6	0.034	Cyclohexanol	(79)
3	U-Ni-BA	Styrene	4.3	1	195[1]	4	0.029	Ethylbenzene	(91)
4	U-Ni-BA[3]	Acetophenone	5	3	200	$1^3/_4$	0.114	Ethylbenzene	(52)
5	U-Ni-AA	Nitrobenzene	5	8	230	2	0.094	Aniline[2]	(65)
6	U-Ni-AA	Phenol	5	8	180	$3^1/_2$	0.111	Cyclohexanol	(66)
7	U-Ni-AA	Benzonitrile	5	8	250	2	0.075	Toluene	(76)
8	U-Ni-AA	Benzene	5	8	176	$2^1/_3$	0.046	Cyclohexane[4]	(83)
9	U-Ni-AA	Styrene	5	8	150	2	0.073	Ethylcyclohexane[5]	(94)
10	U-Ni-AA	Acetophenone	5	8	190	2	0.069	Ethylcyclohexane[6]	(71)

1) The temperature of the oil bath.
2) Besides aniline, high molecular amines were obtained as by-products.
3) Grained aluminum (45 meshes) was used, and "Hyflosupercel" was used as carrier.
4) B.p. 80~81.2°C, $n_D^{20}=1.4270$ (lit. 1.4266).
5) B.p. 127~128°C, $n_D^{20}=1.4347$ (lit. 1.4324).
6) B.p. 128~131.8°C, $n_D^{20}=1.4332$ (lit. 1.4324).

the contents are heated to dryness, and 200 cc. of 20% sodium hydroxide solution is added gradually. Since a vigorous exothermic reaction takes place, the contents are stirred well and cooled with running water, and the aluminum is completely dissolved in a short time. Treatment of the nickel precipitate is accomplished by heating for about five minutes. The supernatant solution is decanted, and the residue washed with warm water (50~60°C) until the washing becomes neutral to litmus, and then with methanol thoroughly. The catalyst thus obtained contains about 1 g. of nickel.

Method of hydrogenation.—In the earlier period of these experiments, a special U-tube apparatus was used for hydrogenation reactions, and the reaction tube was heated in an oil bath, as previously reported[1]. In Table II, the experiments, Nos. 1—3, were carried out by the above method.

The U-tube method being somewhat troublesome, the usual hydrogenation method, e.g. with Sabatier's hydrogenation apparatus, has been adopted for convenience. Further experiments, Nos. 4—10, were carried out by such a method in a hard glass reaction tube, 1.8 cm. in diameter and 90 cm. in length, heated in an electric furnace. In experiment No. 4, "Hyflosupercel" (purified kieselguhr) was used as a carrier.

The catalyst was put into the reaction tube, and heated up to an appropriate reaction temperature, while methanol, which was used for washing the catalyst, was expelled by heating. The vaporized sample, together with a large excess of hydrogen, was introduced into the reaction tube. The reaction products flowing out of the tube were collected into the receiver through a condenser, and were isolated by means of fractional distillation. Then each product was identified by preparing an appropriate derivative respectively, except in the case of cyclohexane and ethylcyclohexane.

Summary

Catalytic hydrogenation in vapor phase with new types of Urushibara nickel catalyst was carried out.

1) New types of U-Ni were prepared from nickel chloride and aluminum. U-Ni-BA and U-Ni-AA were respectively obtained by treating the precipitated nickel with alkali or acetic acid.

2) These catalysts are quite easy to prepare and were proved to be useful for hydrogenation. Above all, U-Ni-AA is the most convenient for vapor phase hydrogenation, since it was found to be highly active and the aluminum served as carrier. It was also used in hydrogenation in liquid phase.

The authors express their gratitude to the Ministry of Education for the financial support of this research.

Department of Chemistry
Faculty of Science
Tokyo Metropolitan University
Setagaya-ku, Tokyo

Reactions of Active Methylene Compounds. IV. Synthesis of 2-Hydroxyphenyl Benzyl Ketones and 4-Hydroxy-3-phenylcoumarins (Continued)

By Yoshiyuki KAWASE

(Received August 4, 1958)

In the previous paper[1], 2-hydroxyphenyl benzyl ketones (III) and 4-hydroxy-3-phenylcoumarins (V) were prepared from 2-methoxybenzoyl-phenylacetonitriles (I) and ethyl 2-methoxybenzoyl-phenylacetates (II). Afterwards, it was known that Chatterjea and Roy[2] had reported a preparation of III (R, R′=H) and V (R, R′=H) from I (R, R′=H) by the action of hydrobromic acid in acetic acid.

The present paper describes a preparation of an analogous series of compounds (Ia, IIa, IIIa, IVa, b, b′ and Va, a′, b) by the same procedure described in the previous paper.

By the action of anhydrous aluminum chloride (2 moles) in nitrobenzene, 4-hydroxy-3-phenylcoumarin-2-imides (IVa, b) were obtained from nitriles Ia, b, methoxy groups of which all, except one in the *o*-position of the carbonyl group, were unaffected. 4-Hydroxy-3-phenylcoumarins (Va, b) were obtained from the imides IVa, b by acid hydrolysis, and Va was also obtained from IIa by means of aluminum chloride in nitrobenzene. By the use of an increased amount (4.5 moles) of aluminum chloride, small amounts of IVb′ and Va′ were obtained from Ib and IIa respectively, 4′-methoxy groups of which were demethylated. Attempted preparations of imide IVa′ from Ia, of coumarins Vb, b′ from IIb, and of IVa by ester condensation of methyl salicylate with *p*-methoxyphenylacetonitrile were unsuccessful.

1) Y. Kawase, This Bulletin, **31**, 390, 440 (1958).
2) J. N. Chatterjea and S. K. Roy, *J. Indian Chem. Soc.*, **34**, 155 (1957) [*Chem. Abst.*, **52**, 1987 (1958)]; cf. J. N. Chatterjea and S. K. Roy, *J. Indian Chem. Soc.*, **34**, 98 (1957) [*Chem. Abst.*, **51**, 16445 (1957)].

Experimental[3]

2-Methoxybenzoyl-4-methoxyphenylacetonitrile (Ia).—To a solution of methyl 2-methoxybenzoate (5.5 g.) and 4-methoxyphenylacetonitrile (4.5 g.) in anhydrous benzene (100 cc.), sodium hydride (1.5 g., 2 moles) was added and the mixture was heated for 4 hr. on an oil-bath (95~100°), most of the benzene being distilled off in the meantime. The well-cooled mixture was treated with water and extracted with ether. The alkaline aqueous solution was acidified and the solid product separated was collected, washed with aqueous sodium bicarbonate, and recrystallized from ethanol in colorless prisms, m.p. 109~110.5°; yield 6 g. or 70%.

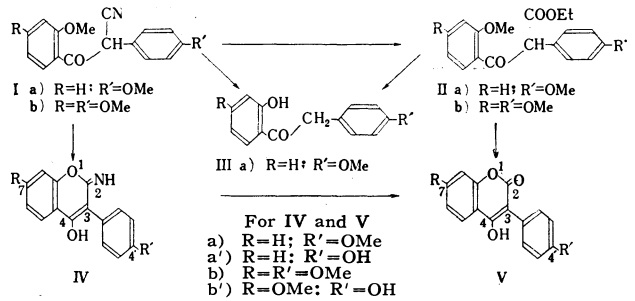
Anal. Found: C, 72.37; H, 5.27; N, 5.05. Calcd. for $C_{17}H_{15}O_3N$: C, 72.58; H, 5.37; N, 4.98%.

Ethyl 2-Methoxybenzoyl-4-methoxyphenylacetate (IIa).—A solution of nitrile Ia (2.2 g.) in anhydrous ethanol (50 cc.) containing one mole of water (0.14 cc.) was saturated with hydrogen chloride with cooling. After three days at room temperature, water was added and ethanol was removed in vacuo. The gummy product separated was taken up in ether, washed with aqueous sodium hydroxide, and distilled to give colorless viscous oil, b. p. 180~200°/0.004mm. (bath-temperature); yield 1.6 g. or 62%.

Anal. Found: C, 69.23; H, 5.90. Calcd. for $C_{19}H_{20}O_5$: C, 69.50; H, 6.14%.

2-Hydroxyphenyl 4-Methoxybenzyl Ketone (IIIa).—(*a*) *From nitrile Ia.*—A solution of Ia (0.5 g.) in acetic acid (10 cc.) containing concentrated hydrochloric acid (5 cc.) was heated on a

3) Melting and boiling points are uncorrected.



steam-bath for 15 hr. The cooled solution was made alkaline with aqueous sodium hydroxide and extracted with ether. The residue obtained from the ether solution was distilled to give colorless oil, b. p. 160~180°/0.003 mm. (bath-temperature); yield 0.2g. 2,4-Dinitrophenylhydrazone, m. p. 198~199° (from ethanol).

Anal. of 2, 4-dinitrophenylhydrazone. Found: C, 59.66; H, 4.11; N, 13.28. Calcd. for $C_{21}H_{18}O_6N_4$: C, 59.71: H, 4.30; N, 13.27%.

(*b*) *From ester IIa.*—By the same procedure described for (a), 0.2 g. of IIIa was obtained from 0.5 g. of IIa; b. p. 160~180°/0.003 mm. (bath-temperature). 2, 4-Dinitrophenylhydrazone, m. p. 197~198°, was identical with the sample from (a).

4-Hydroxy-4'-methoxy-3-phenylcoumarin-2-imide (IVa).—A mixture of Ia (0.5 g.) and anhydrous aluminum chloride (0.5 g., 2.1 moles) in nitrobenzene (5 cc.) was heated on a steam-bath for 1 hr. The cooled solution was treated with water, and nitrobenzene was removed by steam-distillation. The semi-solid product separated from the residue was taken up in ethyl acetate, and extracted with dilute hydrochloric acid. The acid aqueous solution was made alkaline with aqueous sodium bicarbonate, and the precipitates obtained were crystallized from ethanol in colorless microcrystals, m. p. 214.5~215.5°; yield 0.1 g.

Anal. Found: C, 71.75; H, 5.34; N, 5.16. Calcd. for $C_{16}H_{13}O_3N$: C, 71.90; H, 4.90; N, 5.24%.

4-Hydroxy-4'-methoxy-3-phenylcoumarin (Va).—(*a*) *From imide IVa.*—A solution of IVa (ca. 0.05 g.) in 2 cc. of dilute hydrochloric acid (1 : 1) was heated on a steam-bath for 2 hr. The separated crystals were collected and recrystallized from dilute ethanol in colorless microcrystals, m.p. 228~229°; identical with the sample from (b).

(*b*) *From ester IIa.*—A mixture of IIa (0.5 g.) and aluminum chloride (0.5 g., 2.4 moles) in nitrobenzene (5 cc.) was heated for 1 hr. The cooled solution was treated with dilute hydrochloric acid, and nitrobenzene was removed by steam-distillation. The semi-solid product separated from the residue was taken up in ethyl acetate and extracted with aqueous sodium carbonate. The product obtained by acidifying the alkaline solution was recrystallized from dilute ethanol; m. p. 230~231°, yield 0.1 g.

Anal. Found: C, 71.63; H, 4.54. Calcd. for $C_{16}H_{12}O_4$: C, 71.63; H, 4.15%.

4, 4'-Dihydroxy-3-phenylcoumarin (Va').—A mixture of IIa (0.5 g.) and aluminum chloride (0.8 g., 4 moles) in nitrobenzene was worked up as before, and nitrobenzene was removed by steam-distillation. The residual aqueous mixture was filtered while hot, and the crystalline product formed from the filtrate on cooling was recrystallized from dilute ethanol; m. p. 254~255°, yield ca. 0.05 g. It was identical with the sample which will be described in the next paper.

The semi-solid precipitates obtained in the above mentioned filtration were dissolved in ethyl acetate, and treated as before to give Va (ca. 0.05 g.), m. p. 226~227° (from ethyl acetate); identical with the sample described before.

4-Hydroxy-4', 7-dimethoxy-3-phenylcoumarin-2-imide (IVb).—By the same procedure as described before, 0.1 g. of the compound was obtained from 0.5 g. of Ib and 0.5 g. (2.5 moles) of aluminum chloride; m. p. 214~215° (from ethanol).

Anal. Found: C, 68.59; H, 5.33; N, 5.55. Calcd. for $C_{17}H_{15}O_4N$: C, 68.67; H, 5.08; N, 4.71%.

4-Hydroxy-4', 7-dimethoxy-3-phenylcoumarin (Vb).—By hydrolysis of imide IVb with hydrochloric acid, Vb was obtained in colorless needles, m. p. 213~214° (from dilute ethanol). Reported m. p. is 219~220°[4].

Anal. Found: C, 68.10; H, 5.24. Calcd. for $C_{17}H_{14}O_5$: C, 68.45; H, 4.73%.

4, 4'-Dihydroxy-7-methoxy-3-phenylcoumarin-2-imide (IVb').—By the same procedure as described before, a small amount of the compound was obtained from 0.8 g. of Ib and 1.5 g. (4.5 moles) of aluminum chloride; m. p. 287~288° (from ethanol), soluble in acid and in cold aqueous sodium hydroxide.

Anal. Found: C, 67.33; H, 4.66; N, 4.79. Calcd. for $C_{16}H_{13}O_4N$: C, 67.83; H, 4.59; N, 4.94%.

From the ethanolic mother liquor of recrystallization, 0.1 g. of IVb was obtained.

The author wishes to express his hearty thanks to Professor K. Fukui for his helpful advice and encouragement, and to the members of the Agricultural Department of Kyoto University for microanalyses.

Faculty of Literature and Science
Toyama University, Toyama

4) J. Boyd and A. Robertson, *J. Chem. Soc.*, **1948**, 174.

*Reactions of Active Methylene Compounds. V. New Synthesis of Hydroxy Substituted 2-Hydroxyphenyl Benzyl Ketones and 4-Hydroxy-3-phenylcoumarins, and Structures of the Latter and Related 2-Imides**

By Yoshiyuki KAWASE

(Received August 4, 1958)

The present paper describes the action of anhydrous pyridine hydrochloride on methoxy substituted ethyl 2-methoxybenzoyl-phenylacetates (II) and 2-methoxybenzoyl-phenylacetonitriles (I) to give hydroxy substituted 2-hydroxyphenyl benzyl ketones (III) and 4-hydroxy-3-phenylcoumarins (V) respectively, and the structures of the latter and the intermediate, 2-imides IV of V are discussed through their infrared spectra.

Anhydrous pyridine hydrochloride is often used for demethylation of methyl ether of phenols[1]; for instances, similar to the present work, 2-methoxybenzal-phenylacetonitriles were transformed into 3-phenylcoumarins[2] and 4-hydroxy-2′-methoxy-3-phenylcoumarins into coumarino (3′, 4′: 3, 2) coumarones[3].

The action of this reagent on nitriles Ia~d[4] under reflux caused demethylation of all the methoxy groups and subsequent cyclization to give the intermediate imides IV, which were readily converted into hydroxy substituted 4-hydroxy-3-phenylcoumarins (Va~d) by acid hydrolysis. Methoxy substituted IV and V had been obtained[5] by the action of aluminum chloride on I and II respectively, methoxy groups of which in the *p*-position of carbonyl group were unaffected. On the other hand, the action of pyridine hydrochloride on esters IIa~d[4] caused at first cleavage of ester group, decarboxylation, and then demethylation of all the methoxy groups to give hydroxy substituted 2-hydroxyphenyl benzyl ketones (IIIa~d). Methoxy substituted III had been obtained[4] by the action of hydrochloric acid on I and II, methoxy groups of which expect one in the *o*-position of the carbonyl group were unaffected.

It is reported that absorptions by carbonyl groups of 4-hydroxycoumarins[6,7] are in a shorter region, and that of chromones[7,8] are in a longer region, than 6 μ.

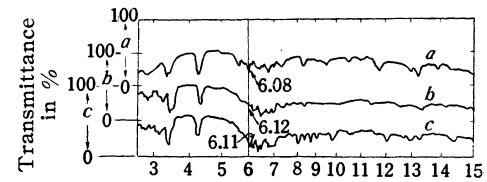


Fig. 1. Infrared spectra of VIII (a), VIa (b) and VIe (c).

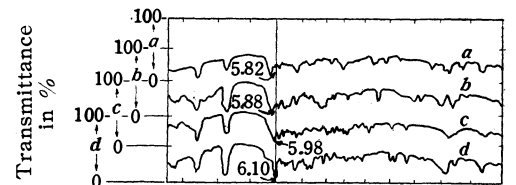


Fig. 2. Infrared spectra of IX (a), X (b), VIIa (c) and XIa(d).

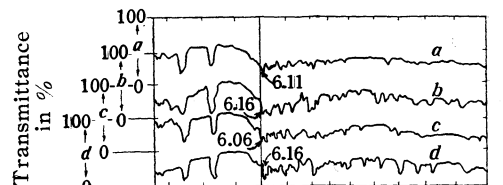


Fig. 3. Infrared spectra of VIIb (a), XIb (b), VIIe (c) and XIc (d).

* Preliminary report: Y. Kawase, *Experientia*, **14**, Nov. (1958).

1) V. Prey, *Ber.*, **74B**, 1219 (1941); **75B**, 350 (1942).

2) Ng. Ph. Bun-Hoï et al., *J. Chem. Soc.*, **1951**, 2307; *J. Org. Chem.*, **21**, 1022 (1956).

3) T. R. Govindachari et al., *J. Chem. Soc.*, **1957**, 548.

4) Y. Kawase, This Bulletin, **31**, 390 (1958); **32**, 9 (1959).

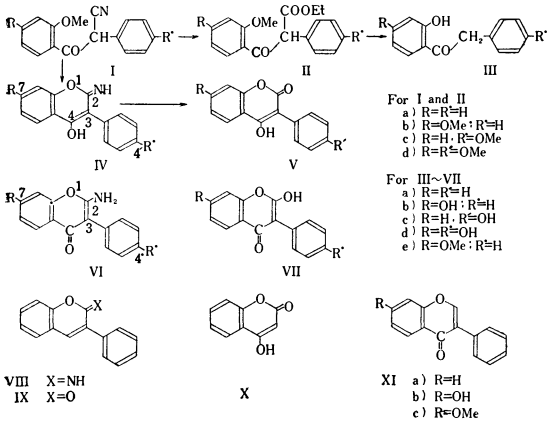
5) Y. Kawase, ibid., **31**, 440 (1958); **32**, 9 (1959).

6) T. R. Govindachari et al., *J. Chem. Soc.*, **1956**, 629; F. M. Dean et al., ibid., **1957**, 3497.

7) a) C. H. Stammer et al., *J. Am. Chem. Soc.*, **80**, 137, 140 (1958); b) A. Fujino and M. Yamaguchi, *J. Japan. Chem.* (*Kagaku no Ryôiki*), *Extra Voll.* **28**, 124, 126 (1958).

8) H. L. Hergert and E. F. Kurth, *J. Am. Chem. Soc.*, **75**, 1622 (1953); B. L. Shaw and T. H. Simpson, *J. Chem. Soc.*, **1955**, 655; G. E. Inglett, *J. Org. Chem.*, **23**, 93 (1958).

The infrared spectra of IVa, e and Va, b, e were measured in Nujol and compared* with those of related 3-phenylcoumarin-2-imide (VIII), 3-phenylcoumarin (IX), 4-hydroxycoumarin (X) and isoflavones (XIa~c). (see Figs. 1—3). (Preparation of IVa, e and Va, e was reported in the previous paper[5]). It seems that 4-hydroxycoumarin structures of IV and V will rather be replaced by chromone structures, namely 2-amino- (VI) and 2-hydroxy-isoflavones (isoflavonols) (VII) respectively, from the whole shapes of their infrared spectra, and from the absorptions by their carbonyl groups in a longer region than 6 μ.



Experimental[9]

2-Hydroxyphenyl Benzyl Ketone (IIIa).—A mixture of ester IIa (0.3 g.) and anhydrous pyridine hydrochloride (1.5 g.) was refluxed for 20 min. on an oil-bath (ca. 220°). The cooled mixture was treated with dilute hydrochloric acid and heated for several minutes on a steam-bath. After being cooled, the solid product separated was collected and recrystallized from ethanol; m. p. 57~58°, identical with the authentic sample[4]; yield 0.1 g. The three following ketones were prepared in the same way.

2, 4-Dihydroxyphenyl Benzyl Ketone (IIIb).—From 0.3 g. of IIb, 0.1 g. of IIIb was obtained, m. p. 110~113° (from water), identical with the authentic sample[10].

2-Hydroxyphenyl 4-Hydroxybenzyl Ketone (IIIc).—From 0.3 g. of IIc, 0.1 g. of IIIc was obtained, m. p. 106~107° (from oqueous ethanol, and dried at 80°).

Anal. Found: C, 73.58; H, 5.30. Calcd. for $C_{14}H_{12}O_3$: C, 73.67; H, 5.30%.

2, 4-Dihydroxyphenyl 4-Hydroxybenzyl Ketone (IIId).—From 0.3 g. of IId, 0.1 g. of IIId was obtained, m. p. 183~184° (from dilute ethanol, and dried at 120°). Reported m. p. is 191~192°[11].

Anal. Found: C, 68.78; H, 5.20. Calcd. for $C_{14}H_{12}O_4$: C, 68.84; H, 4.95%.

2-Hydroxyisoflavone (Isoflavonol) (VIIa).—A mixture of nitrile Ia (0.3 g.) and anhydrous pyridine hydrochloride (1.5 g.) was refluxed for 20 min. on an oil-bath. The cooled mixture was treated with dilute hydrochloric acid and heated on a steam-bath for 1 hr. After being cooled, the deposits were collected and crystallized from ethanol; m. p. 228~229°, yield 0.15 g.; identical with the authentic sample[5]. The following compounds were prepared in the same way.

2, 7-Dihydroxyisoflavone (VIIb).—From 0.3 g. of Ib, 0.15 g. of VIIb was obtained; m. p. 277~278° (from ethanol). Reported m. p. is 284~285°[12] or 285°[13].

Anal. Found: C, 70.68; H, 4.06. Calcd. for $C_{15}H_{10}O_4$: C, 70.86; H, 3.96%.

2-Amino-4'-hydroxyisoflavone (VIc) and 2, 4'-Dihydroxyisoflavone (VIIc) —In the case of Ic, intermediate imide VIc was isolated together with VIIc by the same procedure as described before. Ic (0.3 g.) was treated with pyridine hydrochloride and with dilute hydrochloric acid, and the precipitates thus formed were crystallized from ethanol to give VIc in colorless microcrystals, m. p. ca. 330° (decomp.); yield 0.1 g.

Anal. Found: C, 71.15; H, 4.50; N, 5.42. Calcd. for $C_{15}H_{11}O_3N$: C, 71.14; H, 4.37; N. 5.53%.

From the ethanolic mother liquor of crystallization, VIIc (0.1 g.) was obtained; m. p. 255~256° (from dilute ethanol, and dried at 150°).

Anal. Found: C, 70.64; H, 3.98. Calcd. for $C_{15}H_{10}O_4$: C, 70.86; H, 3.96%.

VIIc was also obtained from imide VIc by hydrolysis with dilute hydrochloric acid for a longer time; m. p. 252~254°.

2, 4', 7-Trihydroxyisoflavone (VIId).—From Id (0.5 g.) and pyridine hydrochloride (2.5 g.), 0.2 g. of VIId was obtained; m. p. ca. 340° (decomp.) (from methanol, and dried at 150°).

Anal. Found: C, 66.63; H, 3.84. Calcd. for $C_{15}H_{10}O_5$: C, 66.67; H, 3.73%.

The author wishes to express his hearty thanks to Professor K. Fukui for his helpful advice and encouragement, to Professor K. Matsui of Kanazawa University for the sample of 4-hydroxycoumarin, to Mr. M. Yamaguchi of Osaka City University for infrared spectroscopy, and to the members of the Agricultural Department of Kyoto University for microanalyses.

Faculty of Literature and Science
Toyama University, Toyama

* λ_{max} (C=O) of coumarin and umbelliferone are 5.80 and 5.95 μ respectively (A. Fujino and M. Yamaguchi, loc. cit.), and that of 2,7-dihydroxychromone is 6.0 μ (C. H. Stammer et al., loc. cit.).

9) Melting points are uncorrected.

10) E. Chapman and H. Stephen, *J. Chem. Soc.*, **123**, 404 (1923).

11) E. Walz, *Ann.*, **489**, 118 (1931).

12) J. Boyd and A. Robertson, *J. Chem. Soc.*, **1948**, 174.

13) C. Menzter and P. Vercier, *Monatsh.*, **88**, 264 (1957) [*Chem. Abst.*, **51**, 14705 (1957)].

Studies on Dehydroalanine Derivatives. I. Synthesis of N-Carboxy-dehydroalanine Anhydride

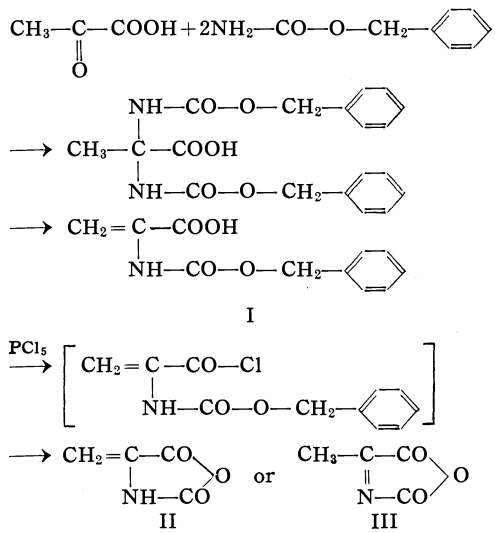
By Shumpei SAKAKIBARA

(Received August 5, 1958)

It is supposed that thermal or alkaline decomposition of serine, cysteine and peptides containing those amino acids proceed via dehydroalanine[1], and that dehydroalanine must play an important role as a transient intermediate in the course of enzymatic transformations of those substances[2]. If the synthesis of dehydroalanine were possible, this substance would be hydrolysed immediately into pyruvic acid and ammonia because of the presence of very unstable enamine structure in the molecule[3]. On the other hand, *N*-acyl derivatives of dehydroalanine are comparatively stable toward water, and actually some derivatives have been synthesized previously[4-6]. *N*-acetyl[4], *N*-carboethoxy, *N*-carbobenzoxy and *N*-formyl dehydroalanine[5] have been reported to be polymerized into *N*-acyl derivatives of poly-α-amino acrylic acid through a vinyl type polymerization. However, all efforts to prepare the poly-α-amino acrylic acid from these polymer derivatives remain unsuccessful because of the difficulty of the acid or alkaline hydrolysis of these polymers.

Each of the double bonds of suitable dehydroalanine derivatives is supposed to be reactive toward some reagents such as active hydrogen, hydrogen cyanide, hydrogen sulfide, indole and so on, and poly-dehydroalanine[7], if its synthesis is possible, may be converted into poly-alanine, poly-asparagine, poly-cysteine and poly-tryptophane theoretically by the action of such reagents as described above. In this series of papers, the synthetic studies on poly-dehydroalanine and on poly-α-amino acrylic acid will be described chiefly and the reactivities of the obtained polymers will be discussed.

For the starting material of poly-dehydroalanine and of poly-α-amino acrylic acid, *N*-carboxy dehydroalanine anhydride (II) was prepared from *N*-carbobenzoxy dehydroalanine (I) and phosphorous pentachloride in dry ether. The substance I was first synthesized by Frankel and Reichmann[5] through the procedure resembling that for *N*-acetyl dehydroalanine by Bergmann and Grafe[4].



The reagent, phosphorous pentachloride, and its reacted residuals scarcely affected the double bond of the substance II (or III) in the course of the reaction, but the reaction product crystallized very easily. After recrystallization from ethyl acetate and petroleum ether, colorless prisms with melting point of 111~113° (decomp.) were obtained. This substance sublimed at 80° or higher temperature (0.1 mmHg) accompanied by partial polymerization.

If the structure III is more stable than

1) M. Bergmann and A. Miekeley, *Ann.*, **458**, 40 (1927); M. Bergmann and D. Delis, ibid., **458**, 76 (1927); B. H. Nicolet, *J. Biol. Chem.*, **95**, 389 (1932); B. H. Nicolet and L. A. Shinn, ibid., **140**, 685 (1941).

2) C. V. Smythe, ibid., **142**, 387 (1942); E. Chargaff and D. B. Sprinson, ibid., **148**, 249 (1943); C. Fromageot, *Bull. soc. chim.*, **13**, 202 (1946).

3) H. Scheibler and U. Scheibler, *Ber.*, **87**, 379 (1954).

4) R. Adams, J. L. Johnson and B. Englund, *J. Am. Chem. Soc.*, **72**, 5080 (1950).

5) M. Frankel and M. E. Reichmann. *J. Chem. Soc.*, **1952**, 289.

6) T. Wieland, G. Ohnacker and W. Ziegler, *Ber.*, **90**, 194 (1957).

7) This name represents the polypeptide of dehydroalanine in distinction from the vinyl-type polymer of dehydroalanine which is named as poly-α-amino acrylic acid in this series of papers.

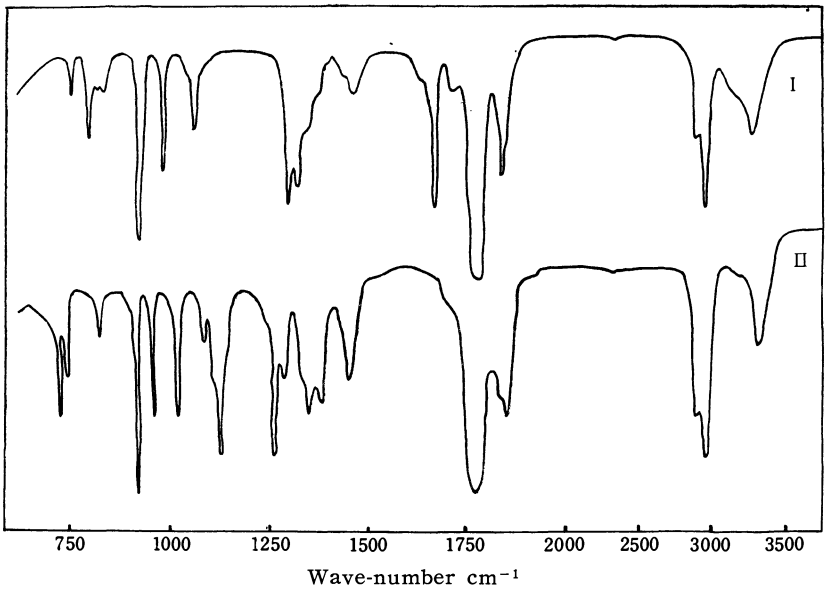
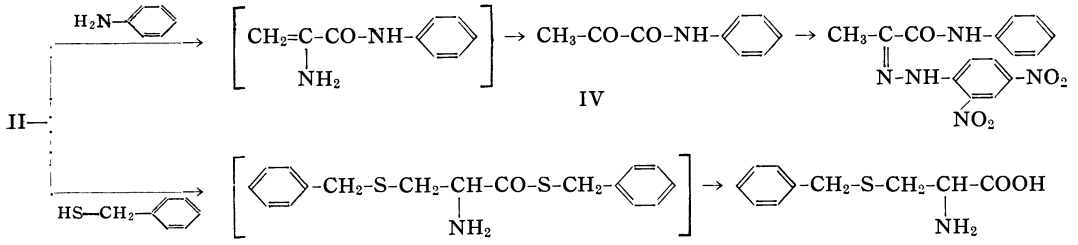


Fig. 1. Infrared spectra recorded on an Adam-Hilger H-80 infrared spectrophotometer: I, *N*-carboxy dehydroalanine anhydride; II, *N*-carboxy DL-alanine anhydride. Nujol suspension.

II, the position of the double bond in the molecule may shift from C=C to C=N in the course of the reaction. The infrared spectrum (Fig. 1) of the product, however, showed absorption bands which were all identical with those supposed for the structure II; that is, the absorption bands at 3050~3300 cm^{-1} indicated the presence of —NH— groups in the molecule, and the absorption bands at 1750~1900 cm^{-1} corresponding to carbonyl groups in a five-membered ring were identified completely as those of *N*-carboxy DL-alanine anhydride. The sharp band at 1675 cm^{-1}, which was not observed in the same region of the spectrum of *N*-carboxy DL-alanine anhydride, may be due to the presence of a double bond directly attached to the five-membered ring in the structure II. The absence of δN-H(amide II) band in both the spectra must be explained by the fact that both NH groups exist in five-membered rings of the respective *N*-carboxy anhydride.

In addition, the structure II was confirmed by the reactions with aniline and with benzylmercaptane. In the case of the former, pyruvic acid anilide IV was obtained in a yield of about 60%, and the structure IV was confirmed by the formation of the 2,4-dinitrophenyl hydrazone. In the case of the latter, *S*-benzyl cysteine formed was identified with an authentic sample by paper-chromatography. These results all supported the structure II for the product.

One of the characteristics of the substance II was its relative stability toward water and amines in comparison with ordinary *N*-carboxy anhydrides. For example, the substance II, which had been prepared about half a year ago and stored in a usual desiccator over phosphorous pentoxide without any precautions, indicated almost the same melting point as that of the original one in spite of the fact that almost all of drying agents have already become tarry. Moreover, the



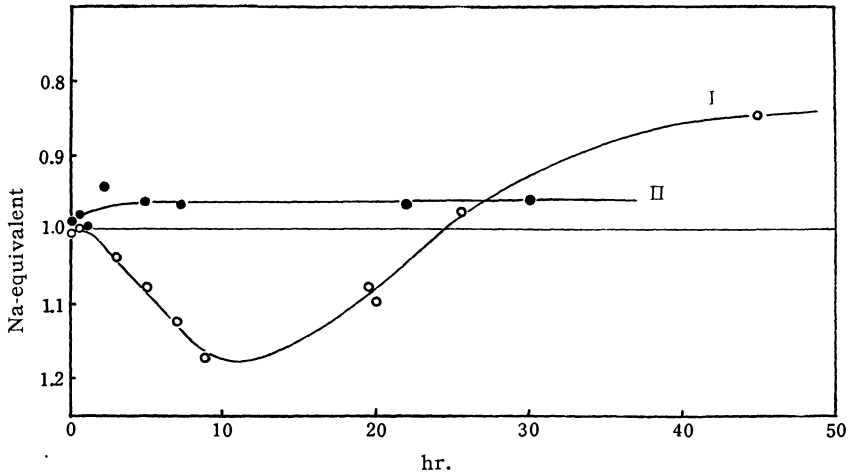
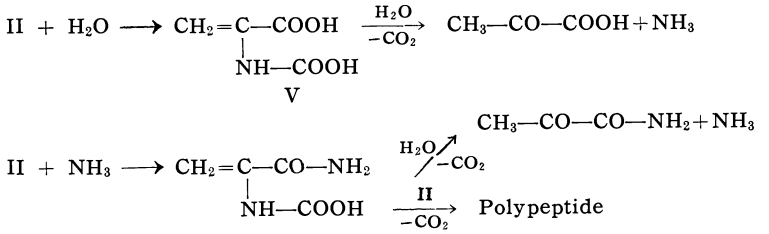
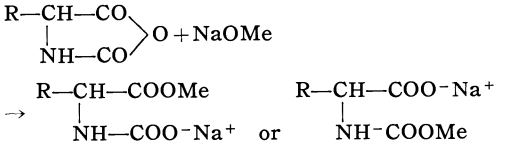


Fig. 2. Time—Na-equivalent curves of *N*-carboxy anhydrides at 30°±0.1° in dioxane containing an equal mole of water: I, *N*-carboxy dehydroalanine anhydride: II, *N*-carboxy DL-alanine anhydride.



substance II immersed in water seemed to be rather stable below 30° and decomposed gradually under evolution of carbon dioxide at 35° or higher temperature.

For clarifying the hydrolytic reaction of the *N*-carboxy anhydride II, it was dissolved in dioxane containing an equal mole of water (against II) and the solution was allowed to react in a bath at 30° ±0.1°. Then, the solution was titrated with sodium methoxide at times according to the procedure of Berger et al.[8] and equivalent values obtained



(the residual amount of the *N*-carboxy anhydride plus acidic material formed, such as pyruvic acid) were plotted against time (curve I on Fig. 2). This curve I was compared with that of *N*-carboxy-DL-alanine anhydride (curve II) under the same condition. In this comparison, it was very interesting to find that the curve I fell down at first, then, recovered gradually and began to rise only after 30 hours, notwithstanding the fact that no practical change of titration values was observed within 30 hours in the case of the *N*-carboxy-DL-alanine anhydride. The reason for the increase in the titration values for the substance II beyond the original line should be explained by the formation of carbamic acid V by hydrolysis. Furthermore, this carbamic acid V would possibly be more stable than those from other ordinary *N*-carboxy amino acid anhydrides at room temperature, since the carbamic acid contains the conjugated double bond in the molecule. If the assumption is reasonable, the considerable stability of the *N*-carboxy anhydride II above mentioned should be explained by the retardation of the chain reactions for polypeptide-forming polymerization. On the other hand, *N*-carboxy-DL-alanine anhydride may be hydrolyzed gradually into carbamic acid of DL-alanine, which is decarboxylated immediately into DL-alanine; then, it will be possible to consider that the titration values

8) A. Berger, M. Sela and E. Katchalski, *Anal. Chem.*, **25**, 1554 (1953).

of the solution should not change practically, since alanine formed is titrated by sodium methoxide in the same manner as *N*-carboxy anhydride under this condition. The upward tendency of the latter part of the titration curve I may also be explained by the gradual formation of the pyruvic acid amide or by the gradual polymerization which was initiated by the formed ammonia.

This material II will be expected to undergo the poly-peptide-forming polymerization and the vinyl type polymerization independently. The details of both cases will be published in later communications.

Experimental

N-Carbobenzoxy dehydroalanine (I). — It was prepared from α,α-dicarbobenzoxyamido propionic acid[9] (m.p. 138.5°) according to the procedure of Frankel and Reichmann[5]. The yield of the low product with m.p. 107° was about 76~83%. After successive recrystallizations from toluene containing a small amount of hydroquinone, colorless plates with m.p. 112~113° (decomp. at 160°) were obtained. Frankel[5] reported m. p. 105° (decomp.) and Wieland[6] m. p. 119° (decomp.).

Anal. Found: C, 59.65; H, 4.50; N, 6.33; No. of double bond, 0.982[10]. Calcd. for $C_{11}H_{11}O_4N$: C, 59.72; H, 5.01; N, 6.33; No. of double bond, 1.00.

N-Carboxy dehydroalanine anhydride (II). —A solution of 10 g. of I in 50 ml. of dry ether was cooled to 0° in an ice water bath and 10.5 g. of powdered phosphorous pentachloride was added in one portion. Then, the suspension was shaken vigorously with intermittent cooling in the bath for about 50 min. The supernatant was decanted quickly into a distillation flask and was concentrated to syrup under reduced pressure at 25~30°. During the course of the treatment, the residual syrup crystallized gradually. After about 30 min., 50 ml. of petroleum ether was added to the residual crystalline mass and the mixture was cooled in an ice water bath for about one hr. Then, the crystalline mass was filtered off and washed with some petroleum ether. The crude crystals were recrystallized from ethyl acetate-petroleum ether after treatment with some active charcoal. The yield of the light yellow prisms with m.p. 105~108° (decomp.) was 3.5 g. (70%). After recrystallization from the same solvents, the colorless prisms of 3.1 g. with m.p. 111° (decomp.) were obtained. After sublimation at 80~90° (0.1 mmHg), this substance melted and decomposed at 111~113°.

Anal. Found: C, 42.56; H, 2.60; N, 12.13. Calcd. for $C_4H_3O_3N$: C, 42.49; H, 2.67; N, 12.39%.

Reaction of II with aniline.—*Formation of pyruvic acid anilide (IV).*—A solution of 1.13 g. of II in 20 ml. of ethyl acetate was cooled to −10° and 5 g. of aniline was added into the solution, then the mixture was allowed to react overnight in a refrigerator at 0~4°. A small amount of yellow precipitate formed was filtered off and the mother liquor was washed successively with 0.5 N hydrochloric acid, water, 0.5% sodium bicarbonate solution and water, dried over anhydrous sodium sulfate and concentrated to dryness under reduced pressure. The residual syrup was transferred into a sublimation vessel with some ethyl acetate. The main product IV was then separated by sublimation at 100° (0.1 mmHg) from yellow by-products. The colorless needles with m.p. 103~105° were obtained in the yield of 1.0 g. (60%); Nef[11] reported m.p. 104°.

Anal. Found: N, 8.65. Calcd. for $C_9H_9O_2N$: N, 8.60%.

2, 4-Dinitrophenyl hydrazone of IV.—To a solution of 50 mg. of IV in 5 ml. of ethanol was added a solution of 100 mg. of 2, 4-dinitrophenyl hydrazine in 5 ml. of 2 N hydrochloric acid, and the mixture was heated for a short time in a boiling water bath and cooled. The voluminous yellow crystals which formed were filtered off, washed with dil. hydrochloric acid and water, and dried. The yield of the yellow crystals was about quantitative and they melted at 245~247° after recrystallizasion from glacial acetic acid.

Anal. Found: C, 52.48; H, 3.82; N, 21.2. Calcd. for $C_{15}H_{13}O_5N_5$: C, 52.49; H, 3.82; N, 20.4%.

Reaction of II with benzyl mercaptane.— A solution of 100 mg. of II and 500 mg. of benzyl mercaptane in 5 ml. of dry acetone was allowed to react overnight at room temperature. The mixture was concentrated to dryness and the residuals were hydrolyzed for one hr. with 6 N hydrochloric acid. The hydrolysate was extracted with ether and the aqueous layer was concentrated to dryness. The residuals were extracted with absolute ethanol and the extract was concentrated. From the residuals, *S*-benzyl cysteine was detected by paper-chromatography, which was identified by comparison with an authentic sample.

Reaction of II with water.—The substance II (350 mg.) was dissolved in 15.00 ml. of freshly distilled dry dioxane containing 56 mg. of water. The solution was divided into 14 test tubes so that each tube contains 1.00 ml. of the solution, and the tubes were sealed. Then, they were allowed to react in a bath at 30°±0.1° simultaneously. Each of the portions was opened successively at times and dry nitrogen was introduced for about one min. into the solution, which was then titrated with a methanol-benzene solution (ca. 0.3 N) of sodium methoxide using thymol blue as an indicator according to the procedure of Berger, et al.[8]. The sodium methoxide solution was standardized every 5 hr.

9) E. Martell and R. M. Herbst, *J. Org. Chem.*, **6**, 878 (1941).

10) This value was determined by back-titration of the bromine using sodium thiosulfate after a sufficient amount of bromine in glacial acetic acid was added to the sample.

11) J. U. Nef, *Ann.*, **270**, 299 (1892).

with purified benzoic acid. After about 8 hr. the reacting solution began to become turbid, and after about 20 hr. yellow precipitates began to form. (Curve I on Fig. 2)

Reaction of *N*-carboxy-DL-alanine anhydride with water.—*N*-Carboxy -DL-alanine anhydride[12] (m.p. 45°) (356 mg.) was subjected to the reaction under the same condition described above. After about 30 hr. the reacting solution remained clear (Curve II on Fig. 2). A suspension of 18.3 mg. of DL-alanine in 1 ml. of dimethyl formamide was titrated with a methanol-benzene solution (0.306 N) of sodium methoxide with an indicator of thymol blue, and 0655 ml. (0.975 equivalent for DL-alanine) of the solution was required for neutralization.

Summary

N-Carboxy dehydroalanine anhydride was first synthesized from carbobenzoxy dehydroalanine. The structure of the *N*-carboxy anhydride was confirmed by the analysis of its infrared spectrum and by the investigation of its chemical behavior. The hydrolytic reaction of the *N*-carboxy anhydride was compared with that of *N*-carboxy DL-alanine anhydride, and it was supposed that dehydroalanine carbamic acid might exist stably in dioxane at ordinary temperature.

The author wishes to express his thanks to Professor Shiro Akabori and Professor Shunsuke Murahashi for their guidance and encouragement throughout the course of this study, and to Mr. Yukio Okuda for his kind assistance in a part of the experiment.

Department of Chemistry
Faculty of Science
Osaka University, Kita-ku, Osaka
and
Institute for Protein Research
Osaka University
Nishi-ku, Osaka

12) J. L. Bailey, *J. Chem. Soc.*, **1950**, 3461.

Thermal Effects of Some Kaolin Minerals. II. Halloysite

By Hiroshi TAKAHASHI

(Received March 18, 1958)

In the preceding part of this series, studies were made on the structural changes of kaolinite and kaolin mineral of fireclay type with heat-treatment in the relatively low temperature region with respect to the degree of the crystallinity[1].

In the early stage of heat-treatment, the progress of the crystallinity is remarkable. It is mainly due to the loss of the adsorbed water. In the next stage, there occurs the lowering of crystallinity due to the break of the kaolin structure resulting from the loss of the lattice water. In the following stage, the rearrangement of ions for the mullite nucleation becomes remarkable, though the X-ray diagram indicates that this state is an amorphous structure.

Halloysite is composed of the same structural units as those of kaolinite, but the stacking of almino-silicate layers is in almost entirely disorder and generally contains the inter-layer water between unit layers. The crystallinity of halloysite, except a certain type of halloysite[2,5], is lower than that of kaolinite. And, it was also found by Brindley and Robinson that the theory of the reflection for a random layer lattice is applicable to the structure of halloysite[3]. The change in the structure of halloysite owing to the loss of the inter-layer water, was studied in details by Brindley and Goodyear[4].

In this paper, the structural changes of halloysite with heat-treatment in the relatively low temperature region, are presented, through X-ray diffraction method, differential thermal analysis and the density measurement from the point of view of the degree of crystallinity of kaolin minerals and are compared with those of kaolinite.

1) H. Takahashi, This Bulletin, **31**, 1031 (1958).

2) G. Honjo and K. Mihama, *Acta Cryst.*, **5**, 511 (1954).

3) G. W. Brindley and K. Robinson, *Min. Mag.*, **28**, 393 (1948).

4) G. W. Brindley and J. Goodyear, ibid., **28**, 407 (1948).

5) H. Takahashi, This Bulletin, **31**, 275 (1958).

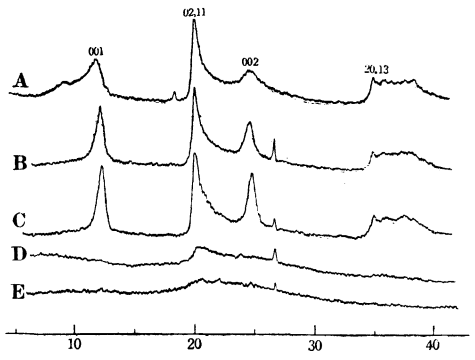
Experimental

Twelve samples of halloysite with the various degrees of crystallinity were used in this study. From the point of view of the degree of crystallinity in halloysite, the following four samples are generally representative for the structural changes through heat-treatment. Four samples mentioned above are as follows; Halloysite from Spruce Pine, N. C., U. S. A.; Halloysite from Bedford, Ind., U. S. A.; Halloysite from Tintic, Utah, U. S. A. and Shichinoe-clay from Shichinoe, Aomori, Japan.

These samples, except for Shichinoe-clay, are the API Standard Clay Minerals. Of all kinds of halloysite used in this study, Shichinoe-clay has the lowest degree of crystallinity. The structural characteristics of these samples have been discussed in the previous paper[5], and those of Shichinoe-clay was also discussed by Sudo[6]. The method of preparation of the experimental specimens and the experimental conditions of all measurements are the same as those in kaolinite and Kibushi-clay.

Results and Discussion

X-ray Diffraction Studies.—Fig. 1 shows the X-ray diffractometer traces of heat-treated specimens of Tintic halloysite. As shown in these traces, the reflections which correspond to hydrated halloysite disappear owing to the loss of the inter-layer water when heat-treated, and it changes into a dehydrated halloysite. With the rise of the treated temperature, the intensity of all reflections increases and (001) reflection becomes sharp to 400°C. In the 545°C heat-treated specimen, the reflections which are apparent in the original sample are not observable, but only a wedge-like background. In the 700°C heat-treated specimen, only a very diffuse and indistinct band is observable. In Tintic halloysite, it is considered that the crystallinity progresses up to 400°C. This is because the residual inter-layer water which exists sporadically between the kaolin layers is lost with the rise of treated temperature, which causes the arrangement of kaolin unit layers to be ordered. Past 400°C, the structure of halloysite begins to disintegrate due to the gradual disappearance of the lattice water. Then the lattice water completely vanishes. Therefore, its crystallinity drops. The X-ray diagram shows also that the rate of change in the heat-treated specimens of other halloysites is similar to that of Tintic halloysite. The only difference is that the loss of lattice water occurs at a lower temperature according to the order of crystallinity of the original sample. The temperature which eliminates the lattice water is the highest in Spruce Pine halloysite and lowest in Shichinoe-clay. This is quite natural in the light of the thermal data.



Degrees 2θ Cu K_α

Fig. 1. X-ray diffractometer traces of heat-treated specimens of Tintic halloysite.
A, original halloysite
B, treated at 200°C
C, treated at 400°C
D, treated at 545°C
E, treated at 700°C

It is known by Brindley that halloysite has a pseudo-hexagonal form in symmetry and has a two-dimensional like structure[3]. To the two-dimensional structure, Warren's theory is applicable[7]. This theory has been applied to various kinds of substance[8], particularly to amorphous carbon in the process of graphitization[9]. The structure of halloysite is more complex than that of amorphous carbon in in the chemical composition and the crystal structure. So, it is very dangerous to apply this theory entirely to halloysite. However, the values obtained by the application of this theory should have some relation with the real values to some extent. For this reason, the crystallite dimensions were obtained from the broadening of (001) and (02, 11) reflection lines. There are two elements determining the broadening of the reflection line. One is the crystallite size, and the other is the lattice distortion. Accordingly, to obtain the real crystallite size from the line broadening, the factor of the lattice distortion must be eliminated[10]. However, the

6) T. Sudo, *Clay Min. Bull.*, **2**, 96 (1954).

7) B. E. Warren, *Phys. Rev.*, **59**, 693 (1941).
8) E. Aruja, *Nature*, **154**, 53 (1944).
9) J. Biscoe and B. E. Warren, *J. App. Phys.*, **13**, 364 (1942). H. Akamatu et al., This Bulltin, **29**, 574 (1956).
10) C. R. Houska and B. E. Warren, *J. App. Phys.*, **25**, 1503 (1954).

increase of the line breadth correlates the fact that the lattice distortion becomes remarkable and that the crystallite size becomes reduced. These two facts mean a lowering in the crystallinity. Therefore, the crystallite sizes thus obtained indicate the relative degree of crystallinity rather than the real crystallite sizes. Consequently, the crystallite sizes are not the real crystallite sizes, but the values are proportional to the real crystallite sizes. However, the real crystallite sizes of halloysite are not much different from the values thus obtained, which are probably, approximate values. This fact was also described in the separate paper[11]. The crystallite dimension along the direction of the *c*-axis (L_c) was measured by the Bragg's equation[12] and the crystallite dimension parallel to the layer plane (L_a) was measured by Warren's equation[7].

$$L_c = \frac{0.9\,\lambda}{\beta_c \cos\theta} \quad \text{(Bragg's equation)}$$

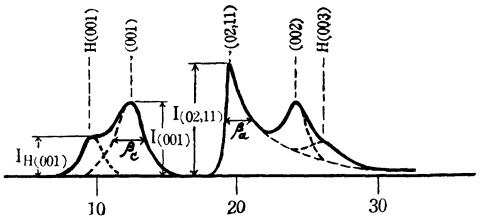
$$L_a = \frac{1.84\,\lambda}{\beta_a \cos\theta} \quad \text{(Warren's equation)}$$

λ: wave length (Cu K_α: 1.5418 Å)
θ: diffraction angle (degree)
β: half value of breadth (radian)

In these measurements, quartz was used for a correction substance for the instrumental broadening of the reflection line.

Kaolin minerals generally change in their shapes and physico-chemical properties according to the structural characteristics. Kaolin minerals have two kinds of crystallinity; that is, one is the internal crystallinity and the other is the crystallinity in the stacking of layers[5]. Therefore, these two kinds of crystallinity must be considered. So, the ratio of the intensity of (001) reflection to that of (02,11) band is measured. This term seems to indicate somewhat the order of the crystallinity of halloysite samples. The original samples of halloysite, except for Spruce Pine halloysite, are partially hydrated halloysite. In Fig. 2 is shown the schematic drawing of the X-ray diagram of the partially hydrated halloysite. In Fig. 2, the intensity ratio was obtained by the following equation[4].

$$\text{Intensity ratio} = \frac{I_{(001)} + \frac{I_{H(001)}}{4}}{I_{(02,11)}}$$



Degrees 2θ Cu K_α

Fig. 2. Schematic drawing of the X-ray diagram of the partially hydrated halloysite.

Fig. 3 shows the change of the spacings of (001) and (02, 11) reflections, the crystallite dimensions and the intensity ratios with heat-treatment. Figs. 3-A, -B, -C and -D show the data for four samples of halloysite.

On the crystallite dimensions, L_c-dimension increases with the rise of the treated temperature; when the regularity along the direction of *c*-axis disappears, L_c-dimension sharply decreases. L_a-dimension, in the partially hydrated halloysite, reaches a maximum value, it then decreases slowly, and then sharply decreases, In Spruce Pine halloysite, L_a-dimension curve has no maximum point perhaps owing to the original sample being dehydrated halloysite. The increase of L_c-dimension with heat-treatment, is caused by the progress of regularity along the direction of *c*-axis because of the loss of the inter-layer water, while the decrease in L_a-dimension is due to the fracturing of kaolin layers.

As for the change of the intensity ratio, the value increases and reaches a maximum point with the rise of treated temperature, and then sharply decreases. The value of the intensity ratio is larger as the crystallinity is higher. This means that the higher the crystallinity of halloysite is, the higher is the regularity along the direction of *c*-axis. From the value of the intensity ratio, it is understood that Spruce Pine halloysite has very high crystallinity. The maximum value in the change of the intensity ratio is considered to indicate the degree of crystallinity of halloysite. In the hydrated halloysite with very low crystallinity, found in Japan, the results are reverse to those so far described, as far as the intensity ratio is concerned. This is for the reason that there is a remarkable disorderliness in the kaolin layers[6].

As for the changes in spacing, the spacing of (001) reflection slowly reduces

11) H. Takahashi, "Proc. Sixth Natl. Coference on Clay and Clay Minerals", Natl. Acad. Sci.-Natl. Res. Council, U.S.A. (in Press).
12) W. L. Bragg, "The Crystalline State", Vol. I, p. 189 (1933).

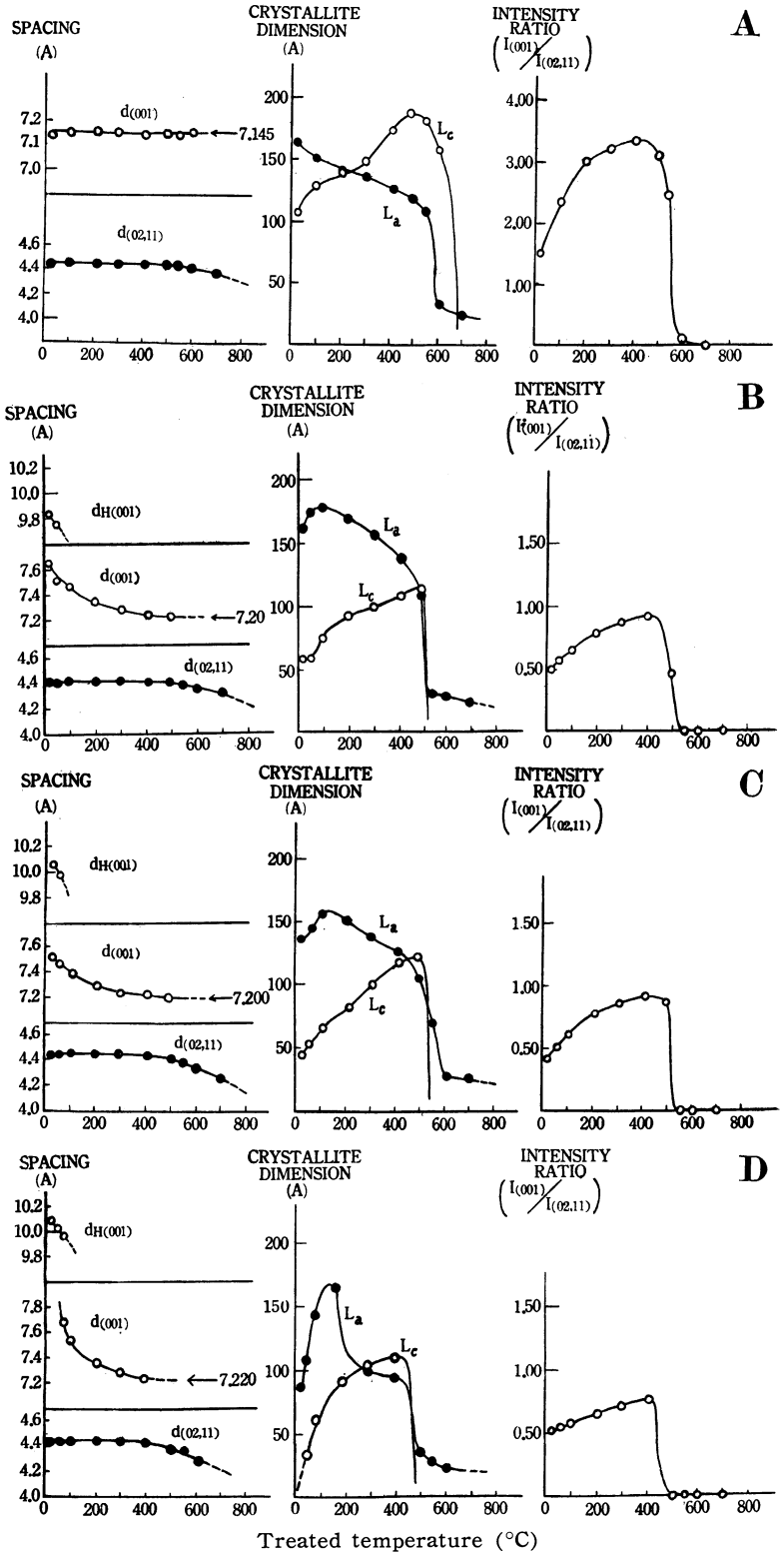


Fig. 3. Curves showing the changes of the spacing of (001) and (02, 11) reflections, the crystallite dimensions and the intensity ratios with the heat-treated temperature..

A, Spruce Pine halloysite
B, Bedford halloysite
C, Tintic halloysite
D, Shichinoe halloysite

with the loss of the inter-layer water until it reaches a nearly constant value. This maintained value seems to indicate the order of the crystallinity in halloysite. The spacing of (02,11) band decreases sharply with the loss of lattice water. This corresponds to the disintegration of the kaolin structure.

Differential Thermal Analysis.—The differential thermal analysis curves of some specimens with heat-treatment are shown in Fig. 4, and Table I shows the thermal data obtained from these curves.

In the heat-treated specimens of halloysite except for Spruce Pine halloysite, the endothermic reaction (E_{n1}) associated with the loss of the inter-layer or adsorbed water is observable even in the 400°C heat-treated specimen of halloysite. This might be due to the fact that after the heat-treatment it adsorbs water vapor so rapidly from the atmospheric air. This phenomenon corresponds to the crystallinity of the original sample in the low stage.

In the endothermic reaction (E_{n2}) caused by the loss of the lattice water in Spruce Pine halloysite, the peak height and area of this reaction reduce in the 545°C heat-treated specimen. And in the 700°C heat-treated specimen, this reaction is unobservable. In the 545°C heat-treated specimen of Shichinoe-clay, this reaction disappears. This means that the structure

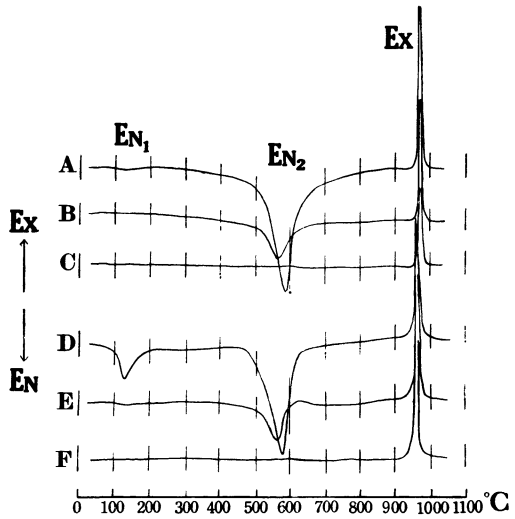


Fig. 4. Differential thermal analysis curves of heat-treated specimens of Spruce Pine and Tintic halloysite.
A, original Spruce Pine halloysite
B, treated at 545°C
C, treated at 700°C
D, original Tintic halloysite
E, treated at 545°C
F, treated at 700°C

TABLE I
THERMAL DATA OF HEAT-TREATED SPECIMENS OF HALLOYSITE
(ALL TEMPERATURES ARE DEGREES CENTIGRADE)

Specimen	Treated-temp.	E_{n1}		E_{n2}		E_x		
		Temp. at peak	Height of peak	Temp. at peak	Height of peak	Temp. at peak	Height of peak	Breadth of peak
Halloysite	original	125°	1	583°	17	973°	45	4.0°
(Spruce Pine, N. C.)	200°	—	—	581	17	971	46	3.4
	400	—	—	573	15	969	48	2.2
	545	—	—	555	5	968	51	3.4
	700	—	—	—	—	967	52	3.6
Halloysite	original	125	2	574	16	970	34	4.5
(Bedford, Ind.)	200	120	1	574	16	969	32	4.2
	400	120	1	574	14	967	32	4.7
	545	—	—	563	6	966	30	4.8
	700	—	—	—	—	964	38	5.1
Halloysite	original	130	4	571	12	969	16	9.4
(Tintic, Utah)	200	115	2	570	15	963	24	4.3
	400	115	1	565	13	965	34	4.2
	545	—	—	558	4	964	30	4.9
	700	—	—	—	—	959	46	5.2
Halloysite	original	129	6	550	12	885	7	23.4
(Shichinoe, Aomori)	200	115	2	546	13	885	8	23.4
	400	125	1	543	9	886	9	25.6
	545	—	—	—	—	883	12	26.6
	700	—	—	—	—	881	12	27.0

of Shichinoe-clay disintegrates at a lower temperature as compared with that of Spruce Pine halloysite. This fact corresponds to the fact that the original sample of Shichinoe-clay has the lowest degree of crystallinity of all the halloysite samples used in this study.

In the exothermic reaction (E_x) associated with the mullite nucleation, the features of this reaction are the same as those of kaolinite. That is, the peak temperature tends to lower, though very slightly, and the peak height gradually increases with the rise of treated temperature.

In the 700°C heat-treated specimen, the peak height is large as compared with that of the original sample. This fact seems to indicate that in the metakaolin state, the rearrangement of ions takes place for the mullite nucleation though this state is amorphous from the X-ray diagram. Therefore, the heat-treatment accelerates the rearrangement of ions for the mullite nucleation. As a result, the peak height of the exothermic reaction increases. The peak breadth of this reaction reduces with the rise of the heat-treatment, and attains a minimum value, and then slightly increases again.

Density.—In Fig. 5 are shown the changes of the density of halloysite specimens with heat-treatment. Measurements were made on dried specimens.

The rate of change in the density are very similar to those of kaolinite and Kibushi-clay described in the preceding part of this study. The density increases at first with the rise of treated temperature, and reaches a maximum point; then it falls suddenly and maintains the minimum value. Past the minimum point in the density curve which corresponds to the disappearance of the lattice water, the density increases sharply and straight. The curve is steeper as the crystallinity of the original sample is higher. The same phenomena were also observable in kaolinite and Kibushi-clay.

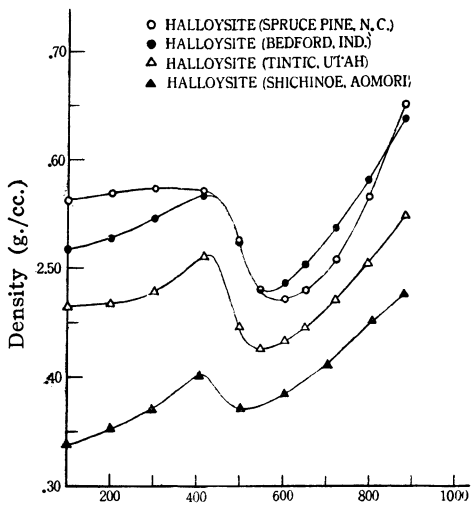


Fig. 5. Curves showing the changes of the density of the halloysite specimens with heat-treated temperature.

When the inclinations in the density curves of kaolinite and ordinary halloysite are compared, that of kaolinite is larger than that of the other.

Therefore, past the minimum point on the density curve, it is considered that the inclination of the density curve of kaolin mineral is corrected to the degree of crystallinity of the kaolin mineral, particularly to the internal degree of crystallinity. This indicates that the rearrangement of ions occurs in the metakaolin state, despite of the fact that the structure is amorphous by the X-ray diagram, and that the stronger the structure of the original sample is, the faster and more perfect is the rearrangement of ions. The mullite nucleation is more remarkable as the crystallinity of the original kaolin mineral is higher.

Mechanism of Structural Change of Halloysite with Heat-treatment.—In the heat-treatment process of halloysite, there are three steps of the structural change with respect to the degree of crystallinity. In the first process, crystallites in one neighborhood aggregate as the inter-layer water vanishes gradually, and so the apparent crystallite size and the value of the density increase and its crystallinity therefore progresses. This tendency is remarkable particularly along the direction of c-axis. In the second process, the hydroxyl ions oriented with the metal ions are cut out and dehydrated, and then kaolin changes into metakaolin. The density decreases suddenly in this stage. As the result, the crystallinity owing to the disintegration of the structure of halloysite. Past this stage, the structure of halloysite becomes amorphous. However, the value of the density of all kinds of halloysite sharply increases with the rise of treated temperature similar to that in kaolinite. The higher the crystallinity is, the larger is the proportion of the increase of the density in all kaolin minerals. This fact shows that even in this amorphous state,

the rearrangement of ions for the mullite nucleation occurs. The higher the original crystallinity is, the more perfect is the rearrangement.

Summery

The structural change of halloysite with heat-treatment in the relatively low temperature region has been studied, and was compared with those of kaolinite and Kibushi-clay. There are three processes, same as in the case of kaolinite. The first process is accompanied by the loss of the inter-layer and adsorbed water, and thə second process by the loss of the lattice water. In the third process, which is an amorphous state corresponding to the metakaolin state, the rearrangement of ions takes place for the mullite nucleation. The rate of the structural change depends on the degree of crystallinity of the original kaolin mineral.

The author wishes to express his hearty thanks to Professor H. Akamatu for his continuous advice and encouragement.

Department of Chemistry
Faculty of Science, the
University of Tokyo
Hongo, Tokyo

Polarographic Studies of Metallic Complexes. III.[1] *Pentammine Series of Cobalt(III) Complexes*[2]

By Nobufumi MAKI, Yoichi SHIMURA and Ryutaro TSUCHIDA

(Received June 9, 1958)

The relation between the structure of metallic complexes and their half-wave potentials has been studied to some extent[3-12]. For instance, Hall et al.[9] studied several kinds of platinum(IV) complex and found the following facts. Platinum (IV) complexes of halogenopentammine type were reduced irreversibly to platinum (II) complexes in one step and the half-wave potentials were at more positive values for halogenopentammineplatinum (IV) complexes than for hexammineplatinum(IV) ion, $[Pt(NH_3)_6]^{4+}$. The shift, however, was to a more negative value for hydroxypentammineplatinum(IV) complex. Namely the polarographic stability of the pentammineplatinum(IV) complexes, $[Pt(NH_3)_5X]$, increases in the following order of ligand X;

$$Br^- < Cl^- < NH_3 < OH^-$$

They also found that tris(ethylenediamine)-platinum(IV) complex ion was reduced irreversibly to $[Pt\,en_3]^{2+}$, through $[Pt\,en_3]^{3+}$, in two steps at a little more negative potential than the corresponding reduction of hexammineplatinum(IV) ion.

Brigando[11] reported that, on the basis of polarographic measurements and absorption spectra, the following complexes were ranked in order of increasing stability;

$[Co(NH_3)_4(NH_2CH_3)_2]Cl_3$

$[Co(NH_3)_6]Cl_3$, $[Co\,en_3]Cl_3$

$[Co(NH_2CH_2CH_2NHCH_2CH_2NH_2)_2]Cl_3$

The half-wave potentials for these complexes at the dropping mercury electrode in 0.6 F sodium perchlorate were respectively as follows; −0.215 V., −0.297 V., −0.392 V., and −0.420 V. (vs. S. C. E.).

For the same purpose, the present paper deals with the polarography of pentam minecobalt(III) complex ions, $[Co(NH_3)_5X]^{(3-n)+}$.

1) Part II of this series: N. Maki, Y. Shimura and R. Tsuchida, This Bulletin, **31**, 413 (1958).
2) Partly presented at the Eleventh Annual Meeting of the Chemical Society of Japan, Tokyo, April 6, 1958.
3) T. Uemura, K. Morinaga, H. Takesawa and H. Kobayashi, presented at the Symposium on Co-ordination Compounds, Tokyo, Nov. 13, 1951.
4) J. B. Willis, J. A. Friend and D. P. Mellor, *J. Am. Chem. Soc.*, **67**, 1680 (1945).
5) H. F. Holtzclaw, Jr., ibid., **73**, 1821 (1951).
6) H. F. Holtzclaw, Jr. and D. P. Sheetz, ibid.. **75**, 3053 (1953).
7) J. Brigando, *Compt. rend.*, **236**, 708 (1953).
8) H. F. Holtzclaw, Jr., *J. Phys. Chem.*, **59**, 300 (1955).
9) J. R. Hall and R. A. Plowman, *Australian J. Chem.*, **8**, 158 (1955).
10) J. R. Hall and R. A. Plowman, ibid., **9**, 143 (1956).
11) J. Brigando, *Bull. soc. chim. France*, **1957**, 221.
12) N. Maki, Y. Shimura and R. Tsuchida, This Bulletin, **30**, 909 (1957).

TABLE I

HALF-WAVE POTENTIALS OF PENTAMMINE SERIES OF COBALT(III) COMPLEXES

Complex compound	Supporting electrolyte; 0.1 F KCl		Supporting electrolyte; 0.5 F K_2SO_4	
	$E_{1/2}$ of 1st wave [Co(III)→Co(II)]	$E_{1/2}$ of 2nd wave [Co(II)→Co(0)]	$E_{1/2}$ of 1st wave [Co(III)→Co(II)]	$E_{1/2}$ of 2nd wave [Co(II)→Co(0)]
$[Co(NH_3)_5I]Cl_2$[13]	+	-1.24_5	+	—
$[Co(NH_3)_5Br]Br_2$[14]	+	-1.24_5	+	—
$[Co(NH_3)_5Cl]Cl_2$[15]	+	−1.24	+	—
$[Co(NH_3)_5NO_3](NO_3)_2$[16]	+	-1.25_5	-0.05_5	−1.28
$[Co(NH_3)_5N_3]Cl_2$[17]	+	−1.23	-0.12_5	-1.28_5**
$[Co(NH_3)_5SO_4]ClO_4$[18]	-0.10_5	-1.23_5	-0.24_5	-1.27_5
$[Co(NH_3)_5NO_2](ClO_4)_2$[19]	−0·12	*	−0.26	-1.28_5
$[Co(NH_3)_5S_2O_3]Cl$[20]	−0.13	-0.96_5	about −0.12	*
$[Co(NH_3)_5C_2O_4]Br\cdot 1.5\,H_2O$[21]	−0.21	-1.23_5	−0.33	−1.29
$[Co(NH_3)_5OCOCH_3](ClO_4)_2$[22]	-0.22_5	−1.24	−0.37	−1.27
$[Co(NH_3)_6](NO_3)_3$	-0.23_5	-1.25_5	−0.43	−1.28
$[Co(NH_3)_5CO_3]NO_3$[23]	-0.38_2	−1.25	−0.50	*
$[Co(NH_3)_5HCO_3](NO_3)_2$[24]	—	—	-0.50_2	−1.28
$[Co(NH_3)_5OH_2]_2(SO_4)_3\cdot 3H_2O$[25]	−0.38	-1.24_5	−0.47	-1.27_5
$[Co(NH_3)_5OH]SO_4\cdot 1.5\,H_2O$[26]	−0.39	-1.25_5	-0.47_5	-1.27_5
$[Co(NH_3)_5CrO_4]Cl$[27]	+	*	+	*
$[Co(NH_3)_5NCS]SO_4\cdot 2\,H_2O$[28]	+	*	+	*

* Maximum wave.

** The data obtained in the presence of 0.0016% Tween-80.

1) The concentration of the complex; 0.001 gram complex ion per liter.

2) Potential unit; V. vs. S. C. E.

3) Temperature, 25°C.

Experimental

The experimental setup and technique are the same as in the previous work and have been described in the earlier communications[1,12]. The capillary had an m-value of 1.356 mg./sec. and a drop time of 5.82~6.23 sec./drop in 0.1 F potassium chloride or 0.5 F potassium sulfate at a potential of 0.0 V. against the saturated calomel electrode with the mercury head of 96 cm. All the measurements were made at 25±0.1°C, the temperature being maintained by a water thermostat. The reversibilities of the electrode reaction were examined by determining the slope of $\log i/(i_d-i)$ vs. potential. Slopes of the log plots indicated irreversible reaction throughout.

The complex compounds studied were prepared by the method described in previous literature[13-27]. (The references are given in Table I.) Each solution for the electrolysis was made freshly from the dry crystalline cobalt(III) complexes before use and polarographic measurements were made as soon as possible after the removal of oxygen dissolved in solution. No maximum suppressor was used except in the case of azidopentamminecobalt(III) ion. Regarding the complexes of pentammine type, the presence of the maximum suppressor causes the lowering of the diffusion current and the shift of the half-wave potential to negative direction. The supporting electrolytes used were 0.5 F potassium sulfate and 0.1 F potassium chloride.

Results and Discussion

In Table I are shown the half-wave potentials of the cobalt(III) complexes of pentammine series. All the compounds are irreversibly reduced in two steps at the dropping mercury electrode with two exceptions. One of the exceptions is the complexes which contain the ligand reducible by itself, such as chromate ion. The other is the complexes which aquate easily in solution.

From Table I it is seen that the first wave exhibits various half-wave potential

13) R. G. Yalman, *J. Am. Chem. Soc.*, **77**, 3219 (1955).
14) H. H. Willard and D. Hall, ibid., **44**, 2220 (1922).
15) W. A. Hynes, L. K. Yanowsky and M. Schiller, ibid., **60**, 3253 (1938).
16) A. Benrath and A. Miens, *Z. anorg. allgem. Chem.*, **177**, 289 (1929).
17) M. Linhard and H. Flygare, *Z. anorg. Chem.*, **262**, 340 (1950).
18) F. Ephraim and W. Flügel, *Helv. Chim. Acta*, **7**, 738 (1924).
19) M. Linhard, H. Siebert and M. Weigel, *Z. anorg. allgem. Chem.*, **278**, 287 (1955).
20) P. R. Rây, *Quart. J. Indian Chem. Soc.*, **4**, 71 (1927).
21) J. C. Duff, *J. Chem. Soc.*, **1923**, 566, 573: S. M. Jörgensen, *Z. anorg. Chem.*, **11**, 425 (1896).
22) M. Linhard and B. Rau, *Z. anorg. allgem. Chem.* **271**, 121 (1953).
23) A. B. Lamb and K. J. Mysels, *J. Am. Chem. Soc.*, **67**, 468 (1945).
24) A. Werner, *Ber.*, **40**, 4098 (1907).
25) S. M. Jörgensen, *Z. anorg. Chem.*, **17**, 461 (1898).
26) A. Werner, *Ber.*, **40**, 4104 (1907).
27) S. H. C. Briggs. *J. Chem. Soc.*, **1919**, 70.
28) A. Werner and A. Müller, *Z. anorg. Chem.*, **22**, 102 (1900).

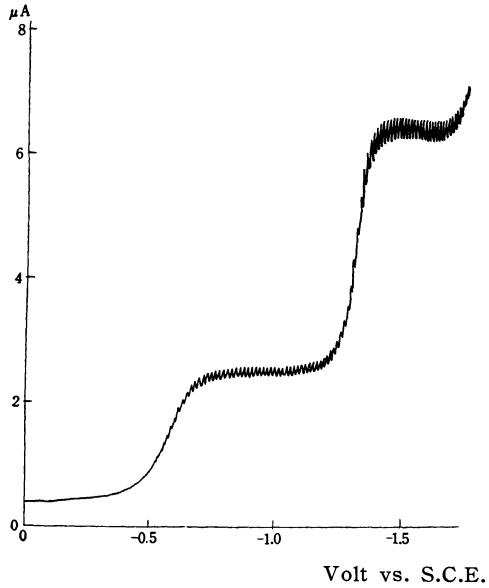


Fig. 1. The polarogram of $[Co(NH_3)_5CO_3]^+$ at the concentration of 0.001 F in the solution of 0.5 F K_2SO_4.
The first wave: $E_{1/2}=-0.50$ V., $i_d=1.52$ μA.
The second wave: $E_{1/2}=-1.28$ V., $i_d=3.04$ μA.

values from compound to compound, while the potentials of the second reduction are always in close proximity to that of hexaquocobalt(III) ion. (−1.428 V. vs. S. C. E. in 0.5 F potassium sulfate solution[4]). Fig. 1 shows the typical polarogram of the pentamminecobalt(III) complexes.

The height of the second wave was very close to twice that of the first wave. The heights of either waves were linearly related with the concentration of the complex ion in the range of $1\times10^{-2}\sim5\times10^{-4}$ F. Accordingly the first wave, corresponding to a one-electron transfer, represents the reduction of cobalt(III) to cobalt(II), and the second, corresponding to a two-electron, represents the reduction of cobalt(II) to metallic state.

As regards the process of the reduction of pentamminecobalt(III) complexes in dilute solution, Willis et al.[4] proposed the following mechanism;

$$[Co(NH_3)_5X]^{n+} + e^- \longrightarrow [Co(NH_3)_5X]^{(n-1)+}$$

$$[Co(NH_3)_5X]^{(n-1)+} + 6\,H_2O \xrightarrow{\text{rapidly}} [Co(OH_2)_6]^{2+} + 5\,NH_3 + X^{-n+3}$$

$$[Co(OH_2)_6]^{2+} + 2e^- \longrightarrow Co + 6\,H_2O$$

From the reduction scheme, it may be seen that the first step in the polarographic reduction of the pentamminecobalt(III) complexes corresponds to the disruption of the complexes, so its half-wave potential of the first wave may be regarded as a measure of the stability against the polarographic reduction.

The polarographic stability of the pentammine series of cobalt(III) complexes increases in the following order of the ligands;

$$I^-, Br^-, Cl^-, CrO_4^{2-}, NCS^- < NO_3^- < SO_4^{2-} < NO_2^- < S_2O_3^{2-} < C_2O_4^{2-} < CH_3COO^- < NH_3 < CO_3^{2-} < OH_2 < OH^-$$

(Supporting electrolyte; 0.1 F potassium chloride).

This order of the stability varied scarcely by the kind of the supporting electrolyte. The reverse of the order is seen between carbonate and water molecule when 0.5 F potassium sulfate was used as a supporting electrolyte.

$$I^-, Br^-, Cl^-, CrO_4^{2-}, NCS^- < NO_3^- < N_3^- < SO_4^{2-} < NO_2^- < C_2O_4^{2-} < CH_3COO^- < NH_3 < OH_2 < OH^- < CO_3^{2-}, HCO_3^-$$

(Supporting electrolyte; 0.5 F potassium sulfate).

No relation between the above order of the polarographic stability and that of the spectrochemical series[29] could be found.

Polarographic Behavior of Individual Complexes.—Some cobalt(III) complexes of pentammine series gave a "prewave" which precedes the actual second

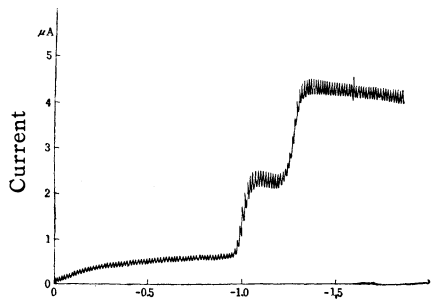


Fig. 2. The polarogram of $[Co(NH_3)_5Br]^{2+}$ at the concentration of 0.001 F in the solution of 0.1 F KCl.
The diffusion current of the second wave: 3.62 μA.
A prewave occurs at around −1.0 V.

29) Y. Shimura and R. Tsuchida, This Bulletin, **29**, 311 (1956).

wave. Brdička[30] explained the prewave as being due to the pentaquomonohydroxocobalt(II) ion formed by hydrolysis, the ion being in slow equilibrium with the hexaquocobalt(II) ion. Fig. 2 shows Brdička's prewave obtained in the reduction of bromopentamminecobalt(III) ion. Similar prewaves were found in the following ions;

$[Co(NH_3)_5I]^{2+}$, $[Co(NH_3)_5Br]^{2+}$

$[Co(NH_3)_5Cl]^{2+}$, $[Co(NH_3)_5SO_4]^{+}$

$[Co(NH_3)_5NO_2]^{2+}$, $[Co(NH_3)_5OH]^{2+}$

$[Co(NH_3)_5OH_2]^{3+}$, $[Co(NH_3)_5OCOCH_3]^{2+}$

On the other hand in the following ions the prewave was completely absent;

$[Co(NH_3)_5S_2O_3]^{+}$, $[Co(NH_3)_5SO_3]^{+}$

$[Co(NH_3)_5HCO_3]^{2+}$, $[Co(NH_3)_5CO_3]^{+}$

$[Co(NH_3)_5C_2O_4]^{+}$

The ion, $[Co(NH_3)_5NO_3]^{2+}$ shows a prewave in 0.1 F potassium chloride, but does not in 0.5 F potassium sulfate.

Thiosulfato- or sulfono-pentamminecobalt(III) ion[31] gave the first wave which had too small a slope at the reduction potential to determine its half-wave potential exactly. This is considered to be due to the aquation of the ion. In 1 F sodium sulfite a well-defined wave of the ion, $[Co(NH_3)_5SO_3]^{+}$ was obtained, because the presence of an overwhelming amount of sulfite ions causes an interruption of the aquation of the complex to some extent (Fig. 3).

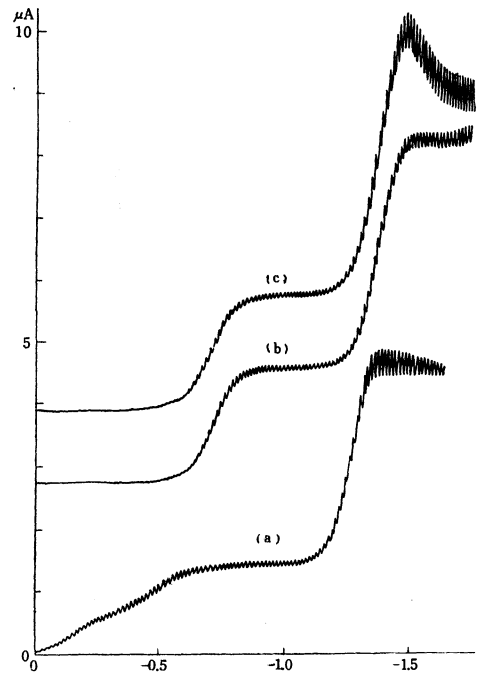


Fig. 3. The polarograms of $[Co(NH_3)_5SO_3]^{+}$ obtained at the concentration of 0.001 F in the solution of 0.5 F K_2SO_4 and of 1 F Na_2SO_3.
a) Supporting electrolyte: 0.5 F K_2SO_4
b) Supporting electrolyte: 1 F Na_2SO_3, in the presence of 0.0016% Tween-80.
c) Supporting electrolyte: 1 F Na_2SO_3, in the absence of the maximum suppressor.

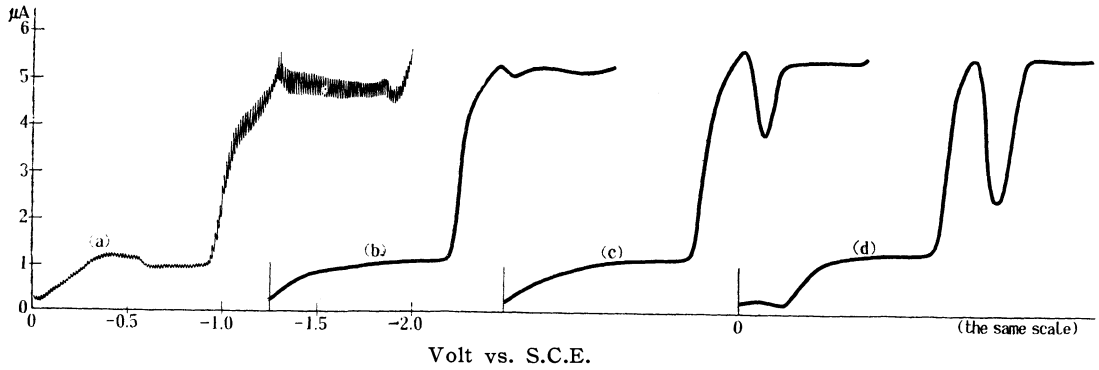


Fig. 4. The effects of maximum suppressor on the current-voltage curves of $[Co(NH_3)_5NCS]^{2+}$ at the concentration of 0.001 F in the solution of 0.5 F K_2SO_4.
a) The polarogram obtained in the absence of maximum suppressor.
b) Current-voltage curve taken in the presence of 0.0032% Tween-80.
c) In the presence of 0.0065% Tween-80.
d) In the presence of 0.0097% Tween-80.

30) R. Brdička, *Collection Czechoslov. Chem. Communs.*, **5**, 113 (1933).

31) The "sulfono group" is SO_3^{2-} radical bound to the central metal ion by the sulfur atom.

The reduction potential of the second step of thiosulfato-pentamminecobalt(III) ion, $[Co(NH_3)_5S_2O_3]^+$, is -0.965 V. vs. S. C. E. in 0.1 F potassium chloride. This value is quite different from that of the other pentamminecobalt(III) complexes. This fact means that through the reduction of the thiosulfatopentamminecobalt (III) ion, a cobalt(II) complex ion was formed, which was reducible more easily than hexaquocobalt(II) ion. The cobalt (II) complex is probably thiosulfatopentaquocobalt(II) ion or a similar one.

The first wave of isothiocyanatocobalt (III) ion has a small maximum wave which can easily be suppressed in the presence of 0.0032% Tween-80.* The effect of the maximum suppressor on the wave form of the ion, $[Co(NH_3)_5NCS]^{2+}$, are shown in Fig. 4. Chromatopentamminecobalt(III) ion shows many complicated waves. This may be an overlap of the waves of the cobalt(III) complexes and of chromate ion (Fig. 5).

In a neutral solution the first wave of aquopentamminecobalt(III) complex ion has always a smaller slope at the half-wave potential than the other pentamminecobalt(III) complexes (Fig. 6). On the other hand, in 1 F perchloric acid, a well-defined wave which had a sharp slope was obtained. One of the reasons for this is considered to be the shift of the equilibrium between the aquopentamminecobalt (III) ion and the hydroxopentamminecobalt(III) ion.

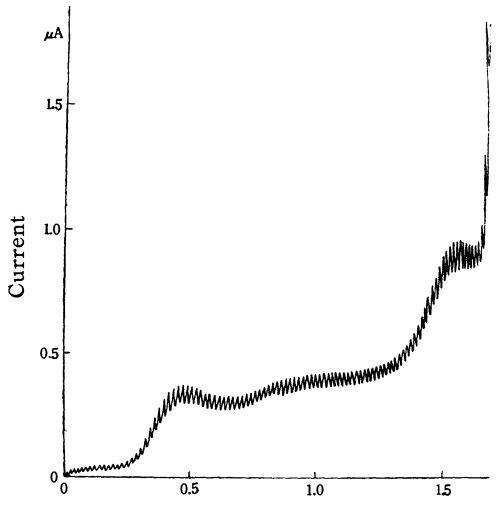


Fig. 5. The polarogram of $[Co(NH_3)_5CrO_4]^+$ obtained at the concentration of 0.001 F in the solution of 0.5 F K_2SO_4.

* Polyoxyethylene sorbitan mono-oleate.

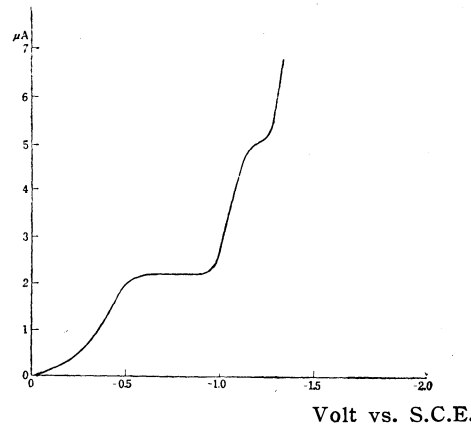


Fig. 6. Current-voltage curve of $[Co(NH_3)_5OH_2]^{3+}$ at the concentration of 0.001 F in the solution of 0.1 F KCl.

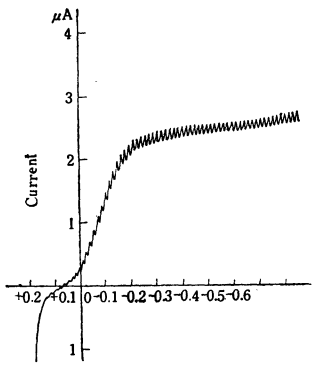


Fig. 7. The polarogram of $[Co(NH_3)_5OH_2]^{3+}$ obtained at 0.001 F in 1 F $HClO_4$. $E_{1/2}$ and i_d, respectively, -0.045 V. and 2.25 μA.

$$[Co(NH_3)_5OH_2]^{3+} \rightleftarrows [Co(NH_3)_5OH]^{2+} + H^+$$

In perchloric acid the above equilibrium is markedly shifted to the left hand. Consequently the well-defined wave of the aquopentamminecobalt(III) ion could be obtained (Fig. 7).

Summary

1. Most of the cobalt(III) complex ions of pentammine series, $[Co(NH_3)_5X]^{(3-n)+}$, are reduced irreversibly in two steps at the dropping mercury electrode. The first diffusion current corresponds to the reduction, cobalt(III) → cobalt(II) and the second to the reduction, cobalt(II) → cobalt (0). The diffusion current and concentration were linearly related.

2. The polarographic stability of cobalt (III) complexes of the pentammine series increases in the following order of the ligands;

I^-, Br^-, Cl^-, CrO_4^{2-}, $NCS^- < NO_3^-$
$< N_3^- < SO_4^{2-} < NO_2^- < C_2O_4^{2-}$
$< CH_3COO^- < NH_3 < OH_2 < OH^-$
$< CO_3^{2-}$, HCO_3^-

(Supporting electrolyte; 0.5 F potassium sulfate).

The reverse of the order was found between carbonate and water molecule when 0.1 F potassium chloride was used as a supporting electrolyte. This order did not agree with that of the spectrochemical series of the pentamminecobalt(III) complexes.

3. In dilute perchloric acid the well-defined wave was obtained for aquopentamminecobalt(III) ion, $[Co(NH_3)_5OH_2]^{3+}$, while the ion gave a modified wave in the first reduction step in neutral supporting electrolyte, potassium chloride or potassium sulfate.

The authors wish to thank Dr. J. Fujita for his kindness in giving them some of the complex compounds used in this study.

Department of Chemistry
Faculty of Science
Osaka University
Kita-ku, Osaka

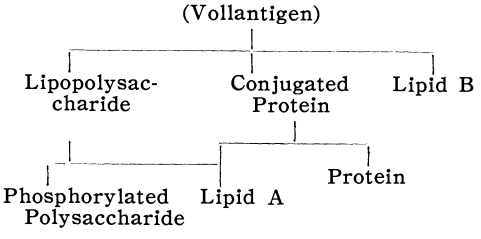
Studies on the Cephalin of Escherichia Coli

By Masaharu KUROKAWA, Kyoko HOTTA, Tomoko YOSHIMURA, Mitsuo MAKITA and Ichiro HARA*

(Received June 16, 1958)

To investigate the lipids of gramnegative bacilli two procedures are available. One of these is concerned with the lipids extracted directly from bacilli[1] and the other is carried out on the lipids of lipopolysaccharide protein complxes isolated from bacteria. The lipopolysaccharide-protein complexes of gramnegative bacilli are designated as O-antigen[2]. According to Westphal and Lüderitz[3], lipopolysaccharide-protein complexes are divided into several components as represented in Fig. 1.

Fig. 1
Lipopolysaccharide-lipid-protein complex (Vollantigen)



There were two kinds of lipid in the complex; one of these, designated as lipid B, was separated readily in contrast to the other lipid A, which could be extracted only by treatment with chloroform-ethanol mixture containing hydrochloric acid. The latter was also designated as the bound lipids by Čmelik. Lipid B was regarded as cephalin and like phospholipid, nonantigenic.

This report accounts for the chemical nature of the lipid B(possibly containing some lipid A), which was isolated to investigate the antigenic properties, especially of hapten or testantigen to anti-E. coli rabbit sera. Serological and biological properties of this lipid fraction will be reported later.

Experimental

Preparation of crude toxic substance.—A culture of *E. coli* 0—23 was autolyzed at 37°C for 48 hr. by addition of chloroform. Zinc complex of crude toxic substance was precipitated from the culture by adding 50% solution of zinc chloride in proportion of 20 ml./l. of the culture. The zinc complex was separated by centrifuge, treated with 40% disodium phosphate solution, and centrifuged to remove zinc phosphate. The supernatant was dialyzed against distilled water. The dialyzate was treated with its twothirds

* Present Address, Department of Chemistry, Faculty of Liberal Arts, Chiba University, Konakadai-cho, chiba.

1) S. Čmelik, *Z. physiol. Chem.*, **293**, 222 (1953); ibid., **296**, 67 (1954); ibid., **302**, 20 (1955).
2) H. Zinsser and J. T. Parker, *J. Exper. Med.*, **37**, 275 (1923).
3) O. Westphal and O. Lüderitz, *Angew. Chem.*, **66**, 407 (1954).

volume of saturated ammonium sulfate solution to precipitate crude toxic substance. The precipitate of crude toxic substance was dialyzed toxic and then lyophilized. Total yield of crude substance was 1 g. per 10 l. culture.

In the paperelectrophoretic pattern (Fig. 2), three peaks were shown by protein staining[4] and two peaks by lipid staining[5], but no further purification was carried out.

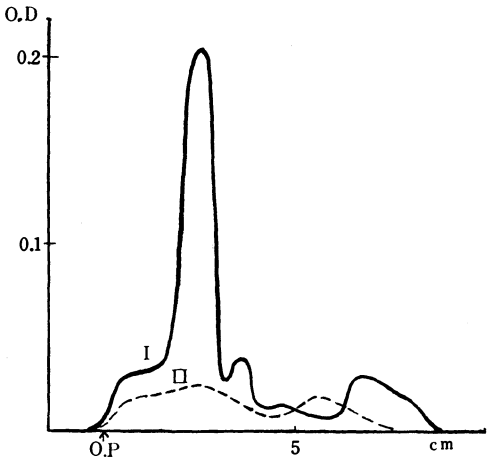


Fig. 2. The paperelectrophoretic pattern. I—Protein, II—Lipid, 0.2 mA/cm; 17 hr's electrophoresis. Veronal buffer pH 8.6, μ 0.05. Filterpaper Tōyō-roshi No. 51

Chemical analysis.—Phosphorus was assayed by King's method[6]. One to two mg. of lipids was digested with 1.2 ml. of perchloric acid, and then colorimetrically determined with 1.0 ml. of 5% ammonium molybdate solution and 0.5 ml. of 1-amino-2-naphthol-4-sulfonic acid solution (0.25 g. of 1-amino-2-naphthol-4-sulfonic acid in 125 ml. of water containing 15 g. of sodium bisulfite and 3 g. of sodium sulfite). Total nitrogen was assayed by the micro Kjeldahl procedure. After hydrolyzing the lipids according to the procedure described in the next section, the main chemical constituents were analyzed respectively. Cholin was assayed by Entenman's method[7]. To the hydrolyzate containing 100 mg. of cholin was added the ammonium reineckate solution (2 g. of ammonium reineckate in 100 ml. of 1.2 N hydrochloric acid). The precipitated cholin reineckate was dissolved in acetone and colorimetrically determined at 500~570 mμ. Serine and ethanolamine were assayed by Axelrod-Reichenthal's method[8]. To the hydrolyzate containing 100 μg of serine and 50 μg ethanolamine was added 0.1 ml. of dinitrofluorobenzene (DNFB) reagent (0.1 ml. of DNFB in 2ml. of absolute ethanol). The dinitrophenyl ethanolamine (DNP-EA) was extracted with chloroform, dinitrophenyl serine (DNP-S) remaining in aqueous solution. DNP-EA and DNP-S were colorimetrically determined at 420 mμ. Total glycerophosphoric acid was determined by Burmaster's method[9]. To the hydrolyzate containing 10~50 μg. of phosphorus were added 1 ml. of 4% sodium sulfite solution, 1 ml. of 10 N sulfuric acid, 1 ml. of 7% sodium molybdate solution and 1 ml. of stannous chloride solution (40 g. of stannous chloride was dissolved in 100 ml. hydrochloric acid and 1 ml. of this solution was diluted with 200 ml. of distilled water). According to this procedure, the inorganic-phosphate phosphorus (Inorg.-P) was colorimetrically determined at 540 mμ. To the hydrolyzate containing 10~50 μg of phosphorus were added 1 ml. of 10 N sulfuric acid and 1 ml. of 0.05 M periodic acid. This solution was immersed in boiling water for 1 hr. and to this were added 1 ml. of 4% sodium bisulfite solution, 0.5 ml. of 10 N sulfuric acid, 1 ml. of 7% sodium molybdate solution and 1 ml. of the diluted stannous chloride solution after cooling. By this procedure the glycerophosphoric acid phosphorus (GPA-P) plus the inorganic phosphate phosphorus were determined. (GPA-P+Inorg-P) $-$ Inorg-P = GPA-P. Sugar was determined with anthrone reagent[10]. Neutralization values of fatty acids were also determined.

Intact lipids and their constituents in the hydrolyzates were qualitatively determined by paper chromatography on Toyo-roshi No. 51 paper with a mixture of *n*-butanol, ethylene glycol and water (4:1:3); phosphorus was identified by spraying Hanes-Isherwood's reagent[11] and amino compounds were by spraying 0.2% ninhydrin in *n*-butanol. In paper chromatography, the ascending method was used at 35°C, for 6 hr.

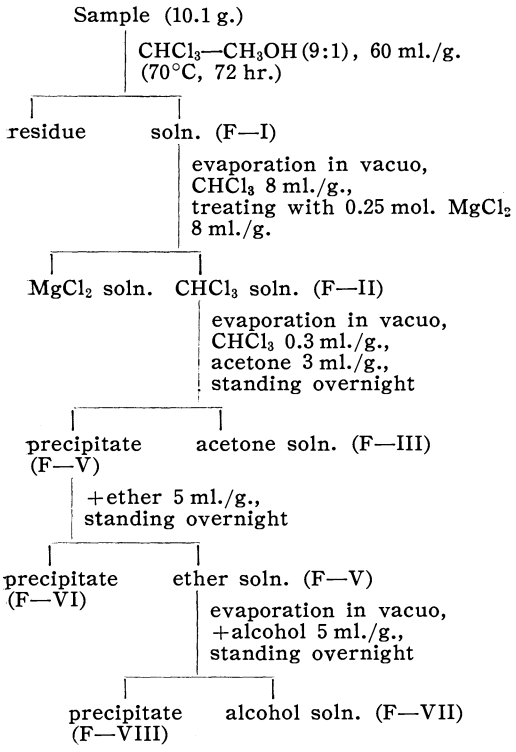
Fractionation and Hydrolysis.—From lyophilized crude toxic substance (10.1 g.), lipids were extracted with a mixture of chloroform and methanol (9:1 v/v) in a hot-water bath for 72 hr. Extractions were repeated 3 times with new solvents in the same way. Extracted lipids were fractionated according to the following scheme (Fig. 3).

Nitrogen-containing impurities removed from F—I with 0.25 M magnesium chloride solution by McKibbin's method[12]. Six fractions were obtained from F—II (Table I).

F—VII and F—VIII were hydrolyzed as follows, respectively: 50 mg. of lipids was refluxed with 30 ml. of saturated barium hydroxide solution for 5 hr., and then 3.25 ml. of concentrated hydrochloric acid was added. Hydrolysis was continued for 75 min. After cooling, the extraction of fatty acids was carried out thrice with each 15 ml. of chloroform. To the aqueous layer was added 18 ml. of 2 N sulfuric acid to precipitate

4) E. L. Durrum, *J. Am. Chem. Soc.*, **72**, 2943 (1950).
5) B. Swahn, *Scand. J. Clin. Lab. Invest.*, **4**, 98 (1952).
6) E. J. King, *Biochem. J.* **26**, 292 (1932).
7) C. Entenman et al., *J. Biol. Chem*, **155**, 13 (1944).
8) J. Axelrod and J. Reichenthal, ibid., **204**, 903 (1953).
9) C. F. Burmaster, ibid., **164**, 233 (1946).
10) F. A. Loewus, *Anal. Chem.*, **24**, 219 (1952).
11) C. S. Hanes and F. A. Isherwood, *Nature*, **164**, 1107 (1949).
12) J. M. McKibbin and W. E. Taylor, *J. Biol. Chem.*, **178**, 17 (1949).

Fig. 3



barium sulfate. To remove the residual hydrochloric acid, vacuum distillations were repeated. Both aqueous solutions free from hydrochloric acid, were analyzed according to the procedures described above (Table II).

There was no choline in F—VII, F—VIII, and F—I hydrolyzates. It could not be seen that lecithin and sphingomyelin were contained in these fractions. The results agreed with those of many researches on the bacterial lipids. From Table II it was concluded that F-VII and F—VIII were so-called cephalin fractions. The principal nitrogen-containing constituents of F—VII and F—VIII were ethanolamine and serine respectively. Glycerophosphoric-acid contents in these fractions were 17.7% and 14.6% respectively, but these amounts were less than the calculated amounts (24% for F—VII and 22% for F—VIII), if F—VII and F—VIII consisted of only phosphatidyl ethanolamine and phosphatidyl serine respectively. There was also some inorganic phosphorus in these hydrolyzates, but its origin was obscure. Neutralization values of fatty acids of F—VII and F—VIII were 194 and 239 respectively, but detailed researches on the natures of fatty acids were not satisfactorily completed.

R_f values of paper chromatography of intact lipids and their hydrolyzates indicated similarly that F—VII consisted mainly of phosphatidyl ethanolamine and that F—VIII was a mixture of phosphatidyl ethanolamine and phosphatidyl serine. There were neither free amino acids nor related compounds in F—VII and F—VIII according to the spots of paper chromatography.

TABLE I

ANALYTICAL DATA AND YIELDS OF THE FRACTIONS

	Yield*		N(%)	P(%)	N/P
F—I	100	7.3	1.01	2.28	0.98
F—II	81.3	6.0	0.84	2.20	0.85
F—III	44.2	3.2	0.02	0.09	0.45
F—IV	32.0	2.4	1.54	2.85	1.20
F—V	27.9	2.0	1.45	3.11	1.03
F—VI	4.2	0.3	1.29	0.00	—
F—VII	12.5	0.9	1.52	3.50	0.96
F—VIII	14.6	1.1	1.12	3.46	0.72

* For F—I for crude toxin.

TABLE II

ANALYTICAL DATA OF THE HYDROLYZATES

	F—VII (33040 μg)		F—VIII (36800 μg)		Note
	μg	%	μg	%	
Intact Lipid N	664	1.52	412	1.12	
Intact Lipid P	1170	3.54	1275	3.46	
$CHCl_3$ solution	19100	57.9	23000	62.5	
$CHCl_3$ N and P	none	—	none	—	
Aqueous solution	13900	42.1	13800	37.5	
N	630	95.0	372	90.3	% to total N
Choline-N	none	—	none	—	
Serine-N	72	10.8	224	54.4	% to total N
Serine	480	1.5	1680	4.6	% to total lipid
Ethanolamine-N	522	78.6	164	39.8	% to total N
Ethanolamine	2310	7.0		2.0	% to total lipid
P	1140	97.5	1240	97.3	% to total P
Inorganic P	66	5.6	168	13.5	% to water sol. P
G.P.A.—P	1053	92.6	964	77.7	% to water sol. P
G.P.A.	5850	17.7	5360	14.6	% to total lipid
Sugar	2265	6.9	1008	2.7	% to total lipid
Neutralization Value	194		239		Fatty acids

TABLE III

R_f VALUES OF FRACTIONS AND THEIR HYDROLYZATE

	Intact Lipid				Hydrolyzates			
	P-Staining		Ninhydrin		P-Staining	Ninhydrin		
F—IV	0.60	0.82	0.59	0.81				
F—VII		0.80		0.79	0.03	0.13	0.39	
F—VIII	0.60	0.80	0.60	0.80	0.03	0.02	0.14,	0.38
Cephalin	0.60	0.80	0.60	0.79				
Ethanolamine							0.38	
Serine						0.15		
G.P.A.*					0.03			

*Glycerophosphoric acid

Discussion

It could be supposed from the value N/P (0.96) that F—VII contained only monoaminophosphoglyceride. The calculated amounts of phosphatidyl ethanolamine and phosphatidyl serine, based upon Table II, were 88% and 12% respectively. Glycerophosphoric acid amounts calculated from the above estimation were 23.7%, being 6% more than the observed values.

From the value N/P (0.76) it was considered that F-III might contain not only monoaminophosphoglyceride, but also phosphatidic acids. The calculated amounts of phosphatidyl ethanolamine and phosphatidyl serine were 28% and 33% respectivly. The calculated glycerophosphoric acid amount was 18.0%, being 4% more than the observed. The discrepancies of phosphor values in both cases were compensated for by inorganic phosphorus amounts, but the origins of the latter were not ascertained.

Sugars were also contained 6.9% in F—VII and 2.7% in F—VIII. There was no cerebroside because the chloroform-soluble portions of these two hydrolyzates contained no sphingosine-nitrogen. But it was considered that these are probably some sugar containing lipids, such as phosphatidylinosito-dimannoside in *Mycobacterium tuberculosis* reported by Lederer[13].

Summary

The lipids were extracted from the crude toxic substances, isolated from *Escherichia coli* by Hosoya's method[14]. These lipids which were 7.2% of the crude toxic substances by weight, were fractionated by solvents. One of these fractions, that was soluble in diethyl ether and ethanol, contained 7.0% ethanolamine and 1.5% serine, and the other that was soluble in diethyl ether, but insoluble in ethanol contained 2.0% ethanolamine and 4.6% serine. There was no choline in any fraction. Average neutralization values of fatty acids in these two fractions were 194 and 239 respectively.

The authors wish to express their deepest appreciation to Professor Susumu Mitsuhashi, M. D., Gumma University Medical School, for much useful guidance and helpful discussion.

The Kitasato Institute for Infectious Diseases, Minato-ku, Tokyo

13) E. Vilkas and E. Lederer, *Bull. soc. chim. biol.*, **38**, 111 (1956).

14) S. Hosoya and S. Miyata, *C. R. Soc. Biol.*, **99**, 773 (1928); S. Hosoya, et al., *Jikken Igaku*, **28**, 420 (1944).

Silica in Water. V. Salt Effect on the Colorimetric Determination of Silica in Concentrated Salt Solution*

By Iwaji IWASAKI and Toshikazu TARUTANI

(Received June 13, 1958)

In a concentrated salt solution, the amount of silica obtained by colorimetric methods (silicomolybdate and molybdenum blue method) is lower than that obtained in the absence of salt**. This phenomenon is called the salt effect or the salt error, and the ratio of the true silica content to the value obtained in the presence of salt is called the salt factor, since it gives a measure of the salt effect. Some salt factors were reported for the colorimetric determination of silica in sea water[1-5], and the salt effect was also investigated for the colorimetric determination of small amounts of silica in alkali[6]. The properties of silicomolybdic acid in a concentrated salt solution have not been studied systematically. The following experiments were carried out to make clear the properties of salt effect and to find the method for correcting the salt effect.

Silicomolybdate Method

Reagents and apparatus. — *Silica solution.*— Portions 0.500 g. of anhydrous silica were fused with 4 g. of sodium carbonate, the melt was dissolved in distilled water, and diluted to 1000 cc. Solutions of a suitable concentration of silica were prepared by diluting this stock solution.

Ammonium molybdate solution.—10%.

Sulfuric acid.—Various normalities.

Salts.—All chemicals were of analytical reagent grade or C. P. purity.

Apparatus.—Hitachi EPU-2 spectrophotometer, 10 mm. cell.

Variations of absorption spectrum of molybdate with acidity and salts.—In the measurement of absorbance of silicomolybdic acid by using a spectrophotometer or a photoelectric colorimeter, distilled water or a solution prepared by adding acid and ammonium molybdate solution to distilled water (or salt solution) is used as the reference. When the latter is used, it must be considered that the absorption spectrum of molybdate in the solution varies with acidity. The absorption spectra of molybdate in the solutions prepared by adding 2 cc. of sulfuric acid of various normalities and 2 cc. of 10% ammonium molybdate solution to 50 cc. of distilled water were measured against distilled water. The results are shown in Fig. 1. The absorption spectra of

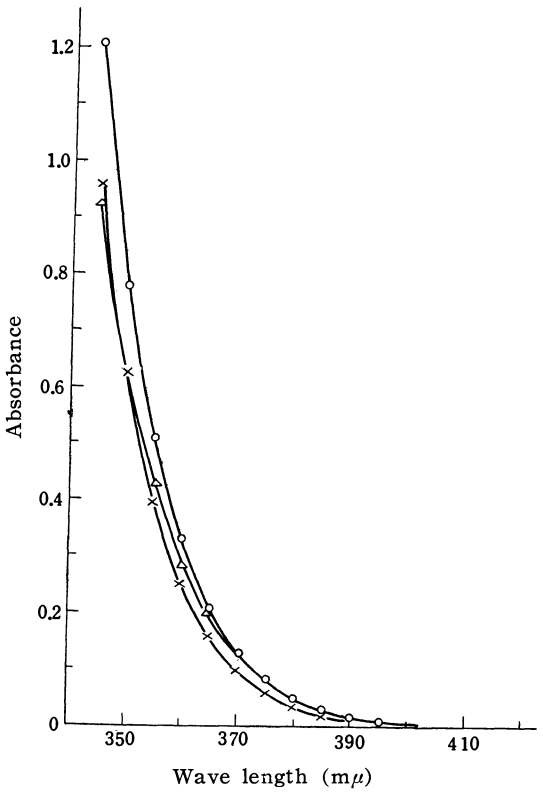


Fig. 1. Variation of absorption spectrum of molybdate with acid concentration.
× 0.037 N
○ 0.11 N (0.074 N, 0.15 N)
△ 0.22 N

* For previous paper in this series see T. Tarutani, *J. Chem. Soc. Japan, Pure Chem. Sec.* (*Nippon Kagaku Zasshi*), **77**, 1815 (1956).

** The latter gives the true content of silica.

1) D. T. W. Chow and R. J. Robinson, *Anal. Chem.*, **25**, 646 (1953).
2) R. J. Robinson and H. J. Poor, *Ind. Eng. Chem., Anal. Ed.*, **8**, 455 (1936).
3) A. Saeki, *J. Oceanog. Soc. Japan*, **6**, 39 (1950).
4) I. Iwasaki, T. Tarutani, T. Katsura and H. Shimojima, *Japan Analyst* (*Bunseki Kagaku*), **2**, 210 (1953).
5) J. B. Mullin and J. Riley, *Anal. Chim. Acta*, **12**, 162 (1955).
6) O. A. Kenyon and H. A. Bewick, *Anal. Chem.*, **25**, 145 (1953).

molybdate in 0.074 N or 0.15 N sulfuric acid is almost the same as that in 0.11 N. However, in 0.037, 0.11, and 0.22 N sulfuric acid, the spectra are different from one another.

In the concentrated salt solution, the absorption spectrum of molybdate varies with the kind of salt and the concentration of salts, even when quantities of reagents added to the solution are constant. The absorption spectra of molybdate in distilled water, 1 M sodium chloride solution, and 0.5 M sodium sulfate solution, were measured against distilled water (Fig. 2). These solutions contained the same quantity of ammonium molybdate, and the concentration of sulfuric acid was 0.11 N. It can be seen that the absorption spectrum of molybdate varies with the concentration of salts and the kind of salt.

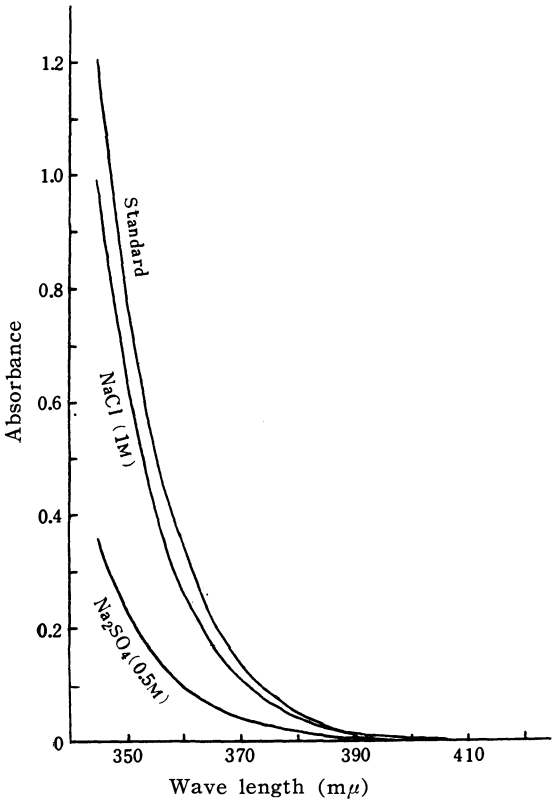


Fig. 2. Variation of absorption spectrum of molybdate with salts.

From the results shown in Figs. 1 and 2, the following conclusions may be drawn. When the solution prepared by adding definite quantities of reagents to distilled water is used for zero standard and the absorbance of silicomolybdic acid in the sample solution containing very small amounts of salt is determined, ultraviolet light can be used.

In the colorimetric determination of silica in the concentrated salt solution, when a wave length above 400 mμ is used, the solution prepared by adding definite quantities of reagents to distilled water can be used as zero standard, but when ultraviolet light is used, the solution of the same concentration of salt as the sample solution has to be used after addition of definite quantities of reagents, because the absorption spectrum of molybdate varies with the concentration of salts.

Time required for the maximum color development of silicomolybdic acid and the stability of color.—The time required for the maximum color development of silicomolybdic acid and the stability of color varies with acidity, temperature, kind of salt, concentration of salts, and quantity of molybdate. The effect of acidity, temperature, and quantity of molybdate on the time required for the maximum color development of silicomolybdic acid were already reported[7]. In a concentrated salt solution, the stability of color is smaller than that in the solution of a negligibly small salt concentration. An example is shown in Fig. 3. These experiments were carried out at 15°C. In Fig. 3, the time necessary for maximum

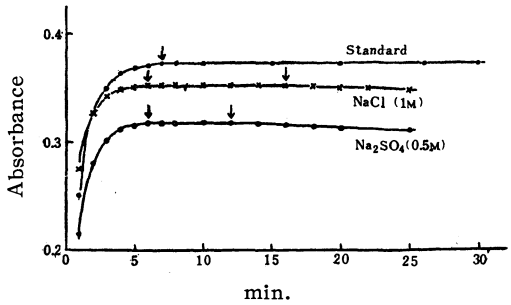


Fig. 3. Stability of color.

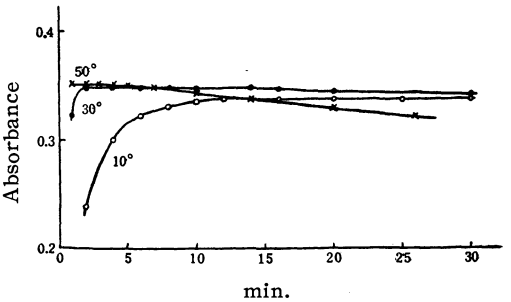


Fig. 4. Color change of silicomolybdic acid with temperature.

7) T. Tarutani, *J. Chem. Soc. Japan, Pure Chem. Sec.* (*Nippon Kagaku Zasshi*), **77**, 743 (1956).

color development are shown by the left arrow, and the time when the color intensity begins to decrease is shown by the right arrow. The color change of silicomolybdic acid with temperature are shown in Fig. 4. These experiments were carried out by the following procedure. Fifty cc. of the sample solution containing 10 p.p.m. of silica was taken, and 2 cc. of 3 N sulfuric acid and 2 cc. of 10% ammonium molybdate solution were added, and the absorbance of silicomolybdic acid was measured against distilled water at 400 mμ. From the results shown in Figs. 3 and 4, in the determination of absorbance of silicomolybdic acid, the time required for the maximum color development must be measured to obtain an accurate result.

Salt effect.—In this section, the experiments were carried out by the following procedure. The absorbance of silicomolybdic acid in the solution prepared by adding 2 cc. of 3 N sulfuric acid and 2 cc. of 10% ammonium molybdate solution to 50 cc. of the salt solution was measured against a blank containing the same amounts of salt, molybdate and acid.

Table I summarizes the previous data on the salt factor of sea water. The value reported by Iwasaki and Tarutani is differs from others. These data are supposed to suggest that the salt effect may vary with the wave length used.

TABLE I
SALT FACTOR OF SEA WATER

Author	Apparatus used	Wave length used	Salt factor
Robinson, Chow[1]	Spectro-photometer	430 mμ	1.23
Robinson, Poor[2]	Pulfrich photometer	430 mμ (filter)	1.16
Saeki[3]	Ukena tube	—	1.25
Iwasaki, Tarutani[4]	Duboscq colorimeter	—	1.09
Mullin, Riley[5]	Spectro-photometer	812 mμ (Mo-blue)	1.1

Therefore, the salt effects were measured at various wave lengths (Fig. 5). The concentration of silica in the salt solution was 10 p. p. m. The ordinate in Fig. 5 is the ratio of the absorbance of salt solution to the absorbance of standard silica solution. As will be seen in Fig. 5, the salt effect varies with wave length used and the salt effect at a longer wave length is greater than that at shorter wave length. And also the salt effect varies with the kind of salt, for example, the effect of sulfate is greater than that of chloride. In the salt solution having large salt effect e. g. ammonium sulfate solution, the variation of salt effect with wave length is large, but in the salt solution having smaller salt effect, e. g., sodium chloride solution, this variation is small.

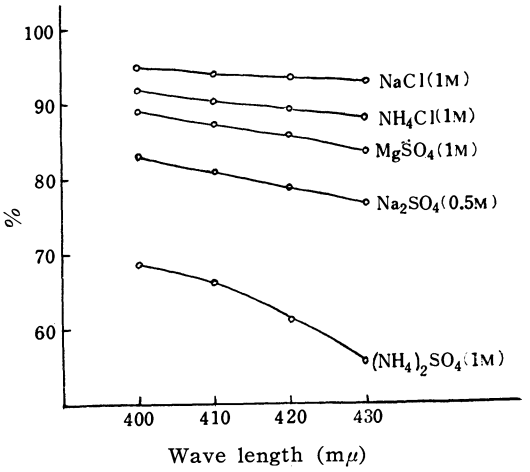


Fig. 5. Salt effect.

The absorbance was measured for a number of concentrations of sodium sulfate solution containing 10 p. p. m. of silica (Fig. 6). The straight line was obtained and it is shown that the salt effect is proportional to the salt concentration.

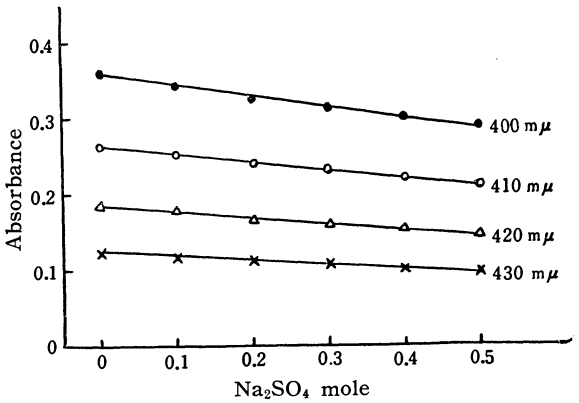
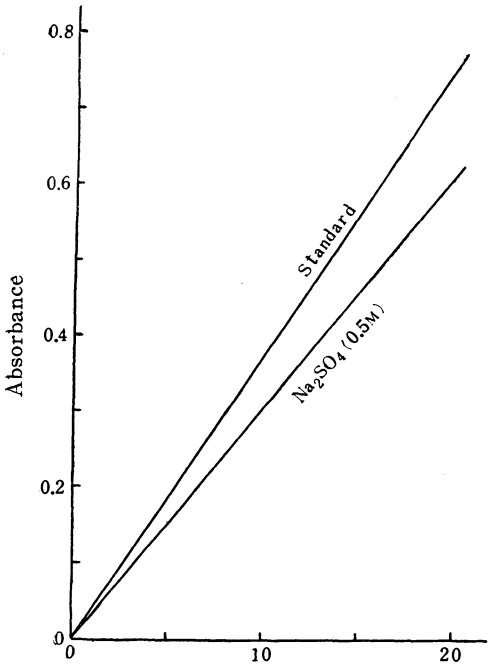


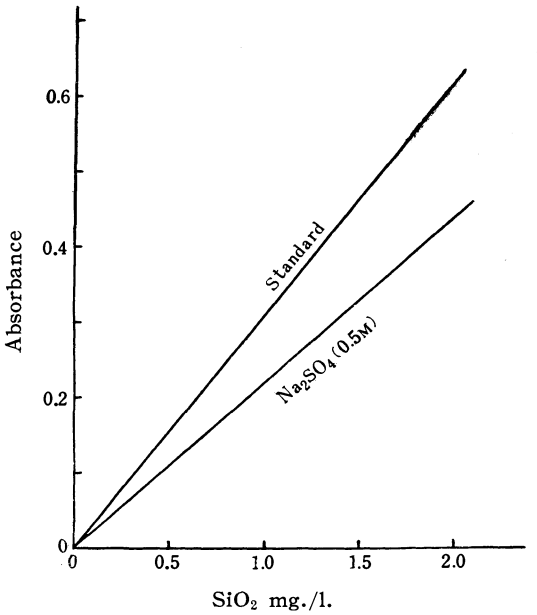
Fig. 6. Relation between absorbance and Na_2SO_4 concentration.

The absorbance was measured for different concentrations of silica in distilled water and in 0.5 M sodium sulfate solution (Fig. 7). Wave length of 400 mμ was used. A straight line was obtained. The absorbance of silicomolybdic acid in the salt solution obeys Beer's law. The ratio of the slopes of the two straight lines obtained for distilled water and salt solution gives the value of salt factor.



SiO_2 mg./l.

Fig. 7. Calibration curve.



SiO_2 mg./l.

Fig. 8. Calibration curve.

Molybdenum Blue Method

Reagents.—*Sulfuric acid.*—3 N.

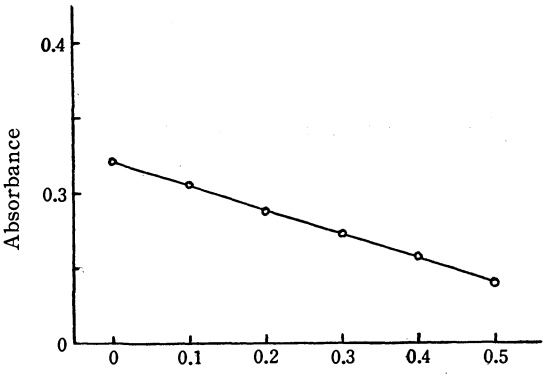
Ammonium molybdate solution.—10%.

Reducing agent. — Twenty grams of sodium bisulfite, 2 g. of anhydrous sodium sulfite, and 0.5 g. of 1-amino-2-naphthol-4-sulfonic acid were dissolved in 200 cc. of distilled water, and stored in an amber-colored glass bottle.

Experiments.—Fifty cc. of a sample solution was taken, and 2 cc. of 3 N sulfuric acid and 2 cc. of 10% ammonium molybdate solution were added. After the color of yellow silicomolybdic acid reaches maximum, 5 cc. of reducing agent was added. After the color of molybdenum blue reaches maximum, the absorbance was measured against a blank containing the same amount of reagents at 820 mμ. Fine crystals sometimes separated out from the solution, when the concentration of salts were very high and temperature was low.

The absorbance was measured for different concentrations of silica in distilled water and in 0.5 M sodium sulfate solution, and the results obtained are shown in Fig. 8. Straight lines were obtained—i. e. the absorbance of molybdenum blue complex in the salt solution obeys Beer's law as in silicomolybdate method, and the ratio of the slopes of two straight lines gives the salt factor.

The variation of salt effect with wave length was not measured, but in this method, the salt effect will vary with wave length as in the silicomolybdate method. The absorbance was measured for a number of concentrations of solution containing 1 p.p.m. of silica (Fig. 9). A straight line was obtained. The salt effect is proportional to the salt concentration.



Na_2SO_4 mole

Fig. 9. Relation between absorbance and Na_2SO_4 concentration.

Conclusion

1) Wave length, kind of salt, and concentration of salts are important factors which affect the salt effect in both silicomolybdate method and molybdenum blue method.

2) In the silicomolybdate method, the salt effect is great at a longer wave length. Also, it varies with the kind of salt. The effect of sulfate is greater than that of chloride.

3) The absorbance of both silicomolybdic acid and molybdenum blue complex

in a salt solution obeys Beer's law, when the concentration of salt and reagents are maintained constant, and a definite wave length is used.

4) In the salt solutions containing definite quantities of silica, the absorbance decreases linearly with salt concentration under the conditions described above.

5) From the properties of salt effect mentioned above, it is possible to explain the reasons that several different salt factors were reported for sea water by different authors.

6) In order to obtain the true silica content in the concentrated salt solutions by the colorimetric method, one of the following procedures may be used.

(a) A sample solution is diluted with distilled water to the extent that the salt effect can be neglected, and then absorbance is measured.

(b) The calibration curve is made by using the same concentration of salt as that of the sample solution.

(c) The calibration curve is made by using the standard silica solution, and it is used for the determination of silica in a concentrated salt solution. The concentration (A) of silica in the sample solution is determined and the concentration (B) of silica in the sample solution diluted twice with distilled water is measured. The true silica content (S) can be obtained by the following formula.

$$S = A + 2(2B - A)$$

The cost of this research was defrayed from the Scientific Research Encouragement Grant from the Ministry of Education, to which the authors wish to express their thanks.

Laboratory of Analytical Chemistry and Geochemistry
Tokyo Institute of Technology
Meguro-ku, Tokyo

Antioxygenic Activity of Lecithin and its Hydrolysis Products. II. α- and β-Glycerophosphoric Acids*

By Chieko URAKAMI, Haru KAMEYAMA and Mitsuko OKADA

(Received May 30, 1958)

Since the last paper on the subject[1] was published, we have observed considerable variations in the activities of α- and β-glycerophosphoric acid with different batches of crude oleic acid obtained from beef tallow. Thus it became necessary to find some means of overcoming this difficulty. In the method of purification by low temperature crystallization, it was found difficult to remove acetone completely and we suspected that some impurities soluble in acetone might have been carried over to the final product to give these varied results. This difficulty was overcome, however, by crystallizing oleic acid as urea complex. The samples of the substrate purified in this way gave rather consistent results.

Further evidences were obtained as to the formation of oil-soluble products from both α- and β-glycerophosphoric acid during autoxidation, as suggested in the previous paper, by applying chromatographic techniques and measuring the ultraviolet absorption of the fractions obtained.

Experimental

Materials.—*Oleic acid.*—Crude oleic acid from beef tallow was supplied by the laboratory of Nihon Yushi Co., Ltd. Olive oil was treated according to the procedure described by Knight, et al.[2] to obtain crude oleic acid. These crude products were purified by the following two methods: *Method A*; The samples were purified by low temperature crystallization from acetone, as described in the previous paper. *Method B*;

* The preceding paper (This Bulletin **29**, 921 (1956).) will be designated as Part I of the series under this new title.

1) Chieko Urakami, Y. Kakutani and H. Okura, This Bulletin, **29**, 921 (1956).

2) H. B. Knight, E. F. Jordan, Jr., E. T. Roe and D. Swern, "Biochemical Preparation," Vol. 2, John Wiley & Sons, Inc., New York (1952). pp. 100.

The samples of oleic acid obtained in the above manner were treated with urea according to the procedure described by Swern and Parker[3]. The constants of these samples are summarized in Table I.

TABLE I
CONSTANTS OF SAMPLES OF OLEIC ACID

Source	Code No.	b. p.	n_D^{20}	Iodine No.	Acid No.
Beef tallow					
Method A	O-1	200~201/2	1.4596	90.2	197.9
〃	O-2	189~192/2	1.4589	91.8	198.3
Olive oil					
Method B	O-3	214/5	1.4600	90.0	198.2
Lit. or calcd. values		210/5	1.4585 1.4599	89.9	198.6

Methyl oleate.—Esterification of oleic acid was carried out by following the procedure described by Knight et al.[2] The samples of the ester prepared from the oleic acid which was purified by Method A and those prepared from the oleic acid which was purified by Method B are classed in the respective group in Table II.

TABLE II
CONSTANTS OF SAMPLES OF METHYL OLEATE

Source	Code No.	b. p.	n_D^{20}	Iodine No.	Acid No.
Beef tallow					
Method A	M-1	173~174/2	1.4520	84.5	194.2
〃	M-2	205/12	1.4352	88.6	196.1
Method B	M-3	160~164/3	1.4515	81.8	195.2
Olive oil					
Method B	M-4	166~169/1.8	1.4526	86.1	188.3
Lit. or calcd. values		172~173/2	1.4526 1.4522	85.7	189.2

α-Glycerophosphoric acid.—An ethanolic solution of the free acid was prepared from the sodium salt (procured from Daito Seiyaku Co., Ltd.) in the same manner as described in the previous paper[1]. This sample was found to contain about 21% β-glycerophosphoric acid and was used in the experiments with oleic acid. A sample containing 14% β-isomer was prepared by isomerization in an acid medium[4] and used in the runs with methyl oleate.

β-Glycerophosphoric acid.—An ethanolic solution was prepared from its sodium salt (obtained from Yashima Yakuhin Co., Ltd.) as described above. The sample was found to be 100% pure. The concentrations of the ethanolic solutions were determined by Burmaster's method[5].

Autoxidation.—The procedure employed was essentially the same as that described previously, except that the bath temperature was maintained at 45°C for the runs with methyl ester, instead of 50°C used for runs with the acid. The concentration of the glycerophosphoric acids in the substrate was 0.1%.

Peroxide determinations. — The method described in the previous paper was followed, except that the use of nitrogen gas was omitted. As shown in Table III, the values obtained by titration under nitrogen did not significantly differ from those obtained without bubbling nitrogen through the sample solution, as long as one to two drops of a 0.05% solution of hydroquinone in isopropanol had been added to each aliquot taken.

TABLE III
PEROXIDE VALUES OBTAINED BY TITRATION UNDER NITROGEN AND IN AIR

	Sample wt. g.	P. V. mM/100 g.
Under nitrogen	0.1824	2.54
	0.2107	2.53
In air	0.2180	2.52
	0.1926	2.58

Recovery test.—The recovery of the water-soluble glycerophosphoric acids from the substrates during autoxidation was examined in the same manner as described previously. The results are shown in Figs. 1 and 2 and Table IV.

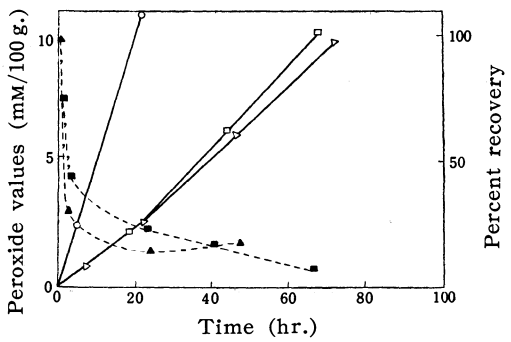


Fig. 1. Peroxide values and percent recovery against time.
○ Oleic acid, O-1, alone. △ Peroxide values for the same sample of oleic acid containing 0.1% α-glycerophosphoric acid (79% purity). □ Peroxide values for the same sample of oleic acid containing 0.1% β-glycerophosphoric acid. ▲ Percent recovery of the α-glycerophosphoric acid. ■ Percent recovery of the β-glycerophosphoric acid.

Chromatography. — Since the method described by Huennekens and his associates[6] affords separation of oleid acid from phosphorus containing substances of biological interest, we utilized the method in removing the substrate from the substance which seemed to be formed from the glycerophosphoric acids added initially. The

3) D. Swern and W. B. Parker, *J. Am. Oil Chemists' Soc.*, **29**, 614 (1955).
4) E. Chargaff, *J. Biol. Chem.*, **144**, 455 (1942).
5) C. F. Burmaster, ibid., **164**, 233 (1946).
6) F. M. Huennekens, D. J. Hanahan and M. Uziel, ibid., **206**, 443 (1954).

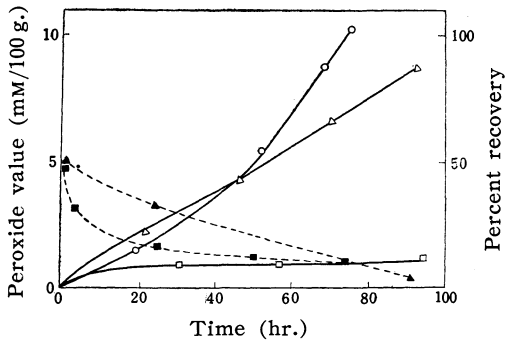


Fig. 2. Peroxide values and percent recovery against time
○ Methyl oleate, M-1, alone. △ Peroxide values for the same sample of methyl oleate containing 0.1% α-glycerophosphoric acid (86% purity). □ Peroxide values for the same sample of methyl oleate containing 0.1% β-glycerophosphoric acid. ▲ Percent recovery of the α-glycerophosphoric acid. ■ Percent recovery of the β-glycerophosphoric acid.

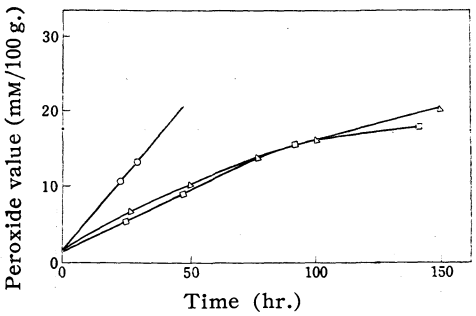


Fig. 3. Peroxide values against time
○ Oleic acid, O-2, alone. △ The same sample of oleic acid containing 0.1% α-glycerophosphoric acid (79% purity). □ The same sample of oleic acid containing 0.1% β-glycerophosphoric acid.

TABLE IV
RECOVERY OF GLYCEROPHOSPHORIC ACIDS FROM SUBSTRATES

Time hr.	P. V. mM/100g.	Sample wt. g.	Recovery in water, mg. α	β	Total
0	0	0.1345[a]	10.03	4.11	14.15 (36.1)
87.5	1.18	0.1487[a]	0.104	0.045	0.149 (0.38)
39	15.07	1.3200[b]	0.0036 (1.5)		
82	23.85	1.7680[c]		0.0064 (2.0)	

a) Methyl oleate obtained from beef tallow containing 7% α-isomer. The ratio of the recovered α:β before and after oxidation remained the same, 70:30. b) Methyl oleate obtained from olive oil containing 0.1% α-isomer. c) Oleic acid from olive oil containing 0.1% β-isomer. The figures in the parentheses represent percent recovery.

last two samples shown in Table IV were subjected to chromatography, after removing any unreacted glycerophosphoric acids by repeated washing with water.

By a trial run with paper, using about 200 mg. each of the samples and a mixture of 1-propanol and water (8:1) as a developing solvent (at 21°C for 15.5 hr.), it was found that a significantly large amount of phosphorus was present in the upper half (toward the solvent front) of the chromatogram. This was somewhat more concentrated in the section 3/4 from the original point of application. Therefore, the upper half of the chromatogram was extracted successively three times with a 50 cc. portion of diethyl ether, twice with 25 cc. of ethanol and finally with 10cc. of a 0.1 N solution of sodium hydroxide. Each extract was tested for the presence of phosphorus and it was found to be present only in the alkaline extract. Therfore, the same sample was subjected to column chromatography in the same manner, using cellulose powder (Toyo-Roshi No. 50), except that a larger amount of diethyl ether was used in place of extracting with ethanol. A blank run was made in exactly the same way. The ultraviolet absorption curves obtained with the ether extract are shown in Fig. 9 and those of the alkaline extracts in Fig. 10 (corrected for the absorption of the blank).

Measurements of ultraviolet absorption.— A Beckman DU-spectrophotometer was used. For the purpose of comparison of the sample obtained from the incorporation of the α- and that from the incorporation of the β-isomer, the extinction coefficients were calculated on the basis of mg. %* of phosphorus since their molecular weights are unknown.

Results

In the present study with oleic acid obtained from two different batches of beef tallow and purified by Method A, both glycerophosphoric acids were found to be active in a comparable strength (see Figs. 1 and 3) but marked differences in activity were observed in the methyl ester prepared from the corresponding sample of oleic acid. In one sample the β-isomer was found to be strongly active, while the α-isomer almost inactive in the early stages of autoxidation as shown in Fig. 2. The activity shown in the later stages is considered to be due to the presence of some 14% β-isomer since the curve obtained by another run with the α-isomer containing 21% β-isomer runs closely parallel to the one shown here, except with an increased activity in the later stages. In

* This expression is used for a matter of convenience instead of the conventional expression, for the products have neither been isolated in pure form nor characterized. However, the estimated values for their molecular extinctions at certain characteristic wave lengths are given in the discussion section.

another sample of the substrate, on the other hand, both acids were found to be active in comparable strength as shown in Fig. 3, although some difference was observed in the later stages. These results are not only in disagreement with our previous finding but also are peculiar in that the activity of the same substance differs in oleic acid and in the methyl ester prepared from the corresponding sample of oleic acid. (Fig. 1 and 2).

The results of the recovery of the glycerophosphoric acids in the aqueous phase during the autoxidation (see Fig. 1 and 2) show, however, that a marked decrease in recovery occurs in the first several hours regardless of whether or not the activity is observed, although a somewhat gradual decrease is shown with the α-isomer during the period in which its activity is depressed. Therefore, it is considered that some minor impurities which could not be removed by low-temperature crystallization from acetone may have interfered so as to give the varied results observed, rather than the difference in the configurations of the glycerophosphoric acids as we suggested in the previous paper.

In the methyl oleate prepared from beef tallow and purified by Method B, both acids were found to be active in an equal strength, (Fig. 4). Comparable results were obtained in oleic acid and its methyl ester prepared from olive oil and purified by the same method, (Figs. 5 and 6). In the latter case, the α-isomer was found to be consistently somewhat more active than the β-isomer. When samples of the substrate obtained from olive oil purified by Method A were used (not presented here), on the other hand, a marked difference in activity was observed, the α-isomer being more strongly active than the β-isomer. It should be pointed out, however, that the β-isomer in methyl oleate did not show activity up to a peroxide value of 10 mM/100 g. but a strong activity in the later stages, Fig. 6. This might have been the case with the β-isomer in the previous report where the experiment was carried out up to this level of peroxide value.

From these results, it is probably certain that α- and β-glycerophosphoric acid are active antioxidants of a comparable strength at a concentration of 0.1%. It is also evident from these results that the purification by low-temperature crystallization from acetone is unsuitable for the study of this nature. Accordingly, those results obtained by using substrates which have been purified by merely repeating distillation of saponified products of fats should be subjected to re-examination.

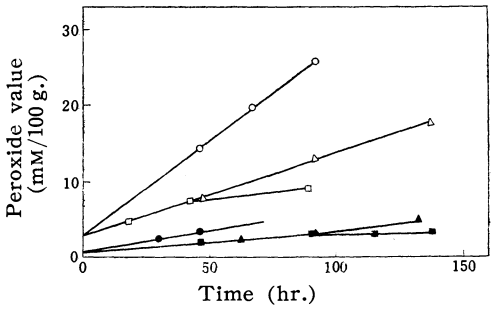


Fig. 4. Peroxide values against time. ○ Methyl oleate, M-2, alone. △ Methyl oleate, M-2, containing 0.1% α-glycerophosphoric acid (86% purity). □ Methyl oleate, M-2, containing 0.1% β-glycerophosphoric acid. ● Methyl oleate, M-3, alone. ▲ Methyl oleate, M-3, and 0.1% α-glycerophosphoric acid (86% purity). ■ Methyl oleate, M-3, containing (0,1%) β-glycerophosphoric acid.

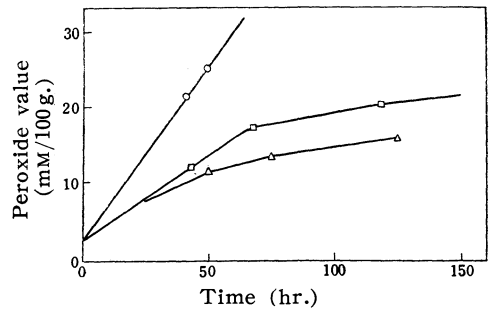


Fig. 5. Peroxide values against time. ○ Oleic acid, O-3, alone. △ The same sample of oleic acid containing 0.1% α-glycerophosphoric acid (79% purity). □ The same sample of oleic acid containing 0.1% β-glycerophosphoric acid.

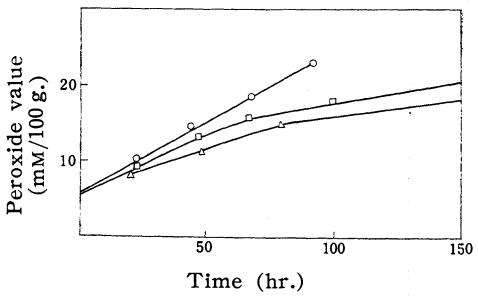


Fig. 6. Peroxide values against time. ○ Methyl oleate, M-4, alone. △ The same sample of methyl oleate containing 0.1% α-glycerophosphoric acid (86% purity). □ The same sample of methyl oleate containing 0.1% β-glycerophosphoric acid.

The absorption spectra observed in the region longer than 300 mμ in Fig. 7 are due to the presence of the α-isomer at a concentration of 7% since the E values calculated for the sample of glycerophosphoric acid employed (see Fig. 8) are much greater than those of the substrate before and after autoxidation (see Fig. 9). Therefore, the absorption spectrum observed after 87.5 hours' autoxidation indicates the presence of a substance other than the glycerophosphoric acid itself, probably a substance formed from it during the autoxidation.

With a low concentration of either α- or β-glycerophosphoric acid as actually used (0.1%) for testing their antioxygenic activities, it would be in possible to observe such an absorption in the ultraviolet region before autoxidation but it should be possible after autoxidation, only, however with the sample to which the α-isomer has been incorporated. This is shown in Fig. 9 A where the curve indicated by the solid line represents the absorption due to the presence of an intensely absorbing substance since the substrate isolated from it by the chromatographic means shows a lower intensity of absorption (dotted line). This sort of observation would not be possible with the

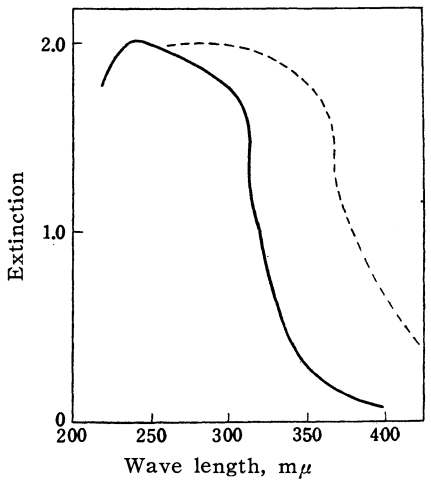


Fig. 7. Absorption curves of 1% ether solutions of methyl oleate containing 7% α-glycerophosphoric acid.
—— At zero time (in ether). ------ At the end of 87.5 hours of autoxidation (in ether).

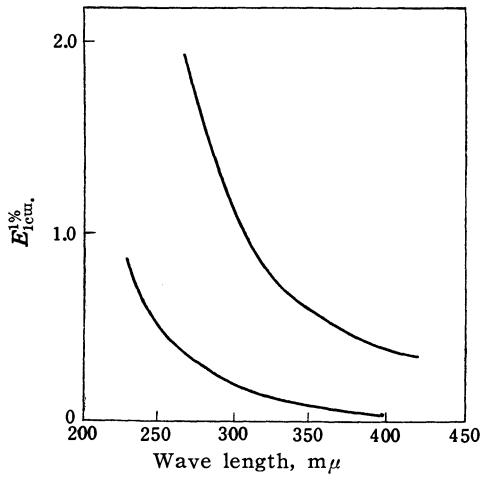


Fig. 8. Absorption curves of the glycerophosphoric acids (ethanol).
The upper curve, α-glycerophosphoric acid.
The lower curve, β-glycerophosphoric acid.

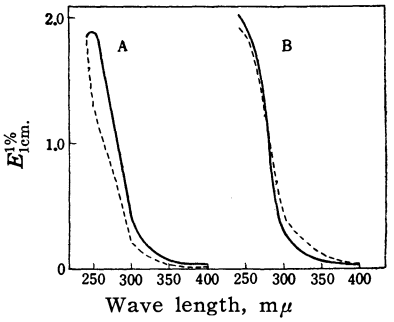


Fig. 9. Absorption curves of the ether solutions of: A, solid line, methyl oleate containing 0.1% α-glycerophosphoric acid (sample b, Table IV); dotted line, the ester isolated by the column chromatography. B, solid line, oleic acid containing 0.1% β-glycerophosphoric acid (sample c, Table IV); dotted line, oleic acid isolated by the column chromatography.

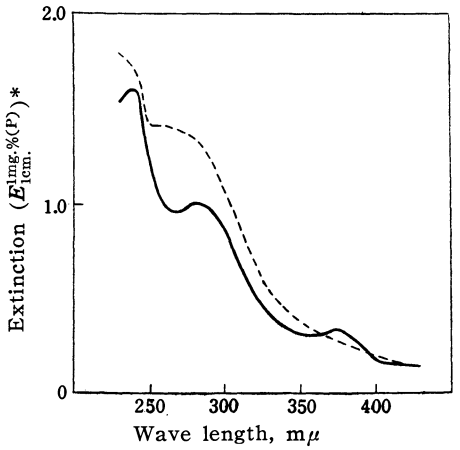


Fig. 10. Absorption curves of 0.1 N sodium hydroxide solutions of the phosphorus containing substances isolated by the column chromatography: dotted line, from the α-glycerophosphoric acid added sample (sample b, Table IV); solid line, from the β-glycerophosphoric acid added sample (sample c, Table IV).

β-isomer since the absorption of its ethanolic solution is much less intense than that of the α-isomer (see Fig. 8), and this found to be the case as shown in Fig. 9B where the absorption curve of the isolated substrate coincides with that of the substrate to which the β-isomer has been added.

Fig. 10 shows the absorption spectra of the phosphorus-containing substances found to be present in the alkaline extracts of the column chromatograms. They differ from those of the glycerophosphoric acids (see Fig. 8). The unknown substance which appears to be formed from β-glycerophosphoric acid shows $E_{1cm}^{1mg\%(P)}$ 1.6 at 240 mμ and 1.0 at 380 mμ and 0.96 at 270 mμ, an inflection. The substance believed to be formed from the α-isomer does not show a sharp maximum but an inflection at 250 mμ with $E_{1cm}^{1mg\%(P)}$ 1.42. This substance is probably a mixture of at least two compounds, one formed from the α- and the other from the β-isomer since the sample incorporated contained some 14% β-isomer and no isomerization is apparent as indicated in Table IV.

Discussion

Although varied reactivities of α- and β-glycerophosphoric acid were observed in different samples of the substrate, both must be active antioxidants since the consistent results could be obtained when highly purified oleic acid and methyl oleate were used. This may reasonably be supported by the isolation of the unknown substances with high intensity of absorption in the ultraviolet region from the substrates to which both α- and β-glycerophosphoric acid have been incorporated.

The antioxygenic activity of the glycerophosphoric acids may, however, be secondary in nature; that is, the unknown substances formed during autoxidation may be responsible for the activity observed, rather than the glycerophosphoric acids themselves. It is unlikely that the involvement of the glycerophosphoric acid molecule is analogous to that of hydroquinone where the molecule itself is ultimately oxidized to quinone after terminating free radical chain reactions by reacting with peroxy radicals[7]. Strong indications for this are that recovery of the glycerophosphoric acids drops sharply in the early stages of autoxidation and that the unknown substances with high intensity of absorption in the ultraviolet region can be isolated from samples which are still exhibiting antioxygenic activity, Table IV and Figs. 7 and 10.

Assuming the molecular weight of the unknown substances to be about 436, (which is the sum of the molecular weight of oleic acid and that of the glycerophosphoric acid minus a mole of water and is considered to be the lowest limit of those oxidized products retaining the original carbon chain length) their molecular extinctions are calculated to be about 42,000 at 270 mμ, at the inflection of the solid line (Fig. 10), and 70,000 at 240 mμ (the maximum). These values are probably higher than those calculated from absorption measured in non-polar solvents but they, nevertheless, indicate that the K-bands are involved. The absorption curve with λ_{max} at 240 and 380 and $\lambda_{infl.}$ at 270 resembles, in its general trend, those reported for oxidized products of ethyl oleate[8] and for the olefinic keto-acids[9]. Therefore, it appears that the glycerophosphoric acids have reacted with some highly conjugated form of compounds produced from the substrate molecule by a free-radical attack during autoxidation.

These results do not reveal, however, whether the phosphoryl group of the glycerophosphoric acid molecule is involved in such a reaction. Because compounds with the same absorption characteristics can possibly be formed, too, if a coordination takes place between a radical of a highly conjugated form (produced from the substrate molecule) and a radical of the glycerophosphoric acid involving the glycerol moiety, or between the former and inorganic phosphoric acid released from the glycerophosphoric acid, as a result of a free radical attack on the glycerol moiety, has been observed to take place in aqueous solutions by irradiation of ionizing radiations[10]. The latter case is least feasible, however, in the system under consideration. Some evidence for this can be provided by the results obtained here. If it had occurred, the absorption band indicated by the solid line in Fig. 9 A or the absorption spectrum observed after 87.5 hours of autoxidation (see Fig. 7) would not have been detected since the *E* value

7) J. L. Bolland and P. Ten Haave, *Trans. Faraday Soc.*, **43**, 2011 (1947).

8) R. T. Holman, W. O. Lundberg, W. M. Lauer and G. O. Burr, *J. Am. Chem. Soc.*, **67**, 1285 (1945).

9) G. King, *J. Chem. Soc.*, **1951**, 1980.

10) G. Scholes, W. Taylor and J. Weiss, Ibid., **1957**, 235.

of orthophosphoric acid in ethanol at λ_{max} 250 mμ is 0.024(measured in our laboratory) and its extinction even at a concentration of 7% is less than 0.167, which is smaller than the E value of β-glycerophosphoric acid, 0.18 at 265 mμ. The β-isomer does not show absorption of the product in the presence of the substrate, (Fig. 9B). The question as to the former case will be treated in a later paper. A highly probable case is, however, participation of the phosphoryl group since phosphoric acid or its alkaline acid salts are known to add readily to ethylene oxide[11] or react with hydroperoxides obtained from lard[12].

Confirmation of the structures of the unknown substances containing phosphorus and exhibiting the high intensity of absorption in the ultraviolet region is of great importance in providing information as to requirements of molecular structures of phosphorus containing compounds of this nature for antioxygenic activity. It also appears to be important from the standpoint of elucidating free radical chain reaction mechanism which is yet obscure and of current interest to a number of workers[8,9,13-15]. The method employed in the present work for the isolation of the unknown substances may find its usefulness in the study of structures of products formed in early stages, if not primary products of a free-radical attack, of autoxidation of ethylenic compounds.

11) F. R. Atherton, H. T. Openshaw and A. R. Todd, ibid **1945**, 382.
12) F. Q. Quackenbush and O. S. Privett, *J. Am. Oil Chemists' Soc.*, **31**, 225 (1954).
13) R. W. Brauer and L. T. Steadman, *J. Am. Chem. Soc.*, **66**, 563 (1944).

Summary

It has been demonstrated that the method of purification of the substrate by low temperature crystallization is not suitable for the study of antioxidant activity of the glycerophosphoric acids and that further purification by crystallization as the urea complex gives consistent results. In such a highly purified substrate, both acids have been found to be active in a comparable strength.

The study of ultraviolet absorption of the phosphorus-containing substances isolated by the column chromatography has shown that the glycerophosphoric acid molecule acquires a highly conjugated system during autoxidation. Discussions have been presented as to possibilities incurred in the formation of such highly conjugated compounds.

Faculty of the Science of Living
Osaka City University
Nishi-ku, Osaka

14) L. Bateman and J. L. Bolland, *The British Rubber Producers' Association Publication*, No. 126 (1950); L. Bateman and A. L. Morris, ibid., No. 173 (1952); L. Bateman, G. Gee, A. L. Morris and W. F. Watson, ibid., No. 155 (1951).
15) D. Swern, H. B. Knight and J. E. Coleman, *J. Am. Oil Chemists' Soc.*, **28**, 498 (1951); **32**, 79, 221 (1955).

*Rapid Analysis of Gamma-Emitters Using Gamma-Ray Scintillation Spectrometer. II. Determination of ^{137}Cs in Fission Products**

By Fumio AOKI, Seishi YAJIMA** and Toshio KUROSAWA

(Received June 20, 1958)

The rapid and accurate determination of ^{137}Cs in fission products is very important for instance, in the determination of the "fine structure" of the fission yield curve, or in the treatment of the fuel elements and radioactive wastes.

Beta-ray assay, which has been generally used, involves many tedious procedures and requires skill[1], because the object must be isolated prior to the activity measurement. The chemical yield through the procedures is not always highly reliable.

A gamma-ray scintillation spectrometer has been favorably used owing to the speediness of its procedure and

* Read at 11th Annual Meeting of the Chemical Society of Japan.

** Present, address, Japan Atomic Energy Research Institute, Tokai, Ibaragi-Prefecture.

1) F. Brown, *J. Inorg. Nuclear Chem.*, **1**, 248 (1955).

eliability. But when the sample contains nany gamma-emitters, it is, in general, lifficult or impossible to determine the ndividual activity accurately without separation, because of the possible superposition of the spectra of the gamma-rays.

Peirson[2] analysed the fission products from uranium 235 without chemical separations using a two-crystal gamma-ray scintillation spectrometer, which does not give rise to the Compton continua but shows only the photopeaks in the recorded spectrum. Even if such an excellent instrument is available, chemical separations will still be necessary in such cases as:

i) When the gamma-energy of a nuclide in question can not be resolved from superposing spectra of other nuclides.

ii) When the gamma-intensity of the nuclide is weak and overwhelmed by those of others.

Woodhead et al.[3] determined the activity of ^{137}Cs in fission products. They separated ^{137}Cs solely by anion exchange resin using carriers, and measured its gamma-intensity with a gamma-ray scintillation spectrometer. If it were not necessary to separate ^{137}Cs solely, the procedures would become more simple.

The authors have worked out a method for the rapid determination of ^{137}Cs in fission products combining the partial separation of nuclides with anion exchange resin followed by gamma-ray spectrometry.

Method. — *Extraction of Uranium.* — The bulk of the uranium is extracted from the solution of the irradiated fuel elements with a mixture of tributyl phosphate (T. B. P.) and diethyl ether. (1 : 1), together with most of neptunium formed. The residual neptunium is removed by the resin treatment shown below (Table I). In this process the loss of ^{137}Cs is in the order of 10^{-5}, which is negligible in its determination.

Anion Exchange.—In treating the fission product solution, free from uranium, by a mixed bed of carbonate- and oxalate-form anion exchange resin (see section III), alkali metals go completely through the column together with some of alkali earths, while almost all of the other ions are retained in the column[4].

The leakage of alkali earths is reduced by the addition of strontium ions. Tables

TABLE I
RETENTION OF MAIN ELEMENTS (%)

pH of the soln.	Retention of				
	I	Ru	Rare earths. Y	Transition metals	Np
6	93	96	100	100	100
8	96	96	100	100	100
10	98	98	100	100	100

TABLE II
LEAKAGE OF Ba AND Sr (%)

Addition of Sr^{2+} mg/20 ml	Leakage of	
	Ba	Sr
0	89	80
5	53	65
10	46	10
20	36	0
30	30	0
40	42	0
60	42	0

I and II show the retention and leakage of some elements.

Measurement.—The fission product solution after the resin treatment will contain ^{140}Ba-^{140}La and ^{137}Cs-^{137m}Ba, when it is short-aged, and ^{137}Cs-^{137m}Ba only, when it is long-aged. (^{133m}Cs and ^{135m}Cs are also formed in fission, but their lives are extremely short. ^{135}Cs, the daughter of ^{135m}Cs, emits no gamma-ray and its life is very long. They are all left out of consideration.)

The activity of ^{137}Cs is represented by the peak height of 0.661 MeV gamma of ^{137m}Ba in equilibrium with ^{137}Cs, the parent. Some of ^{137m}Ba is retained in the resin column, but the parent and daughter soon (about 30 min. after the resin treatment) reach a state of equilibrium. Because of the short half life of ^{137m}Ba (2.6 min.) compared with that of ^{137}Cs (30 y.), the difference between the activities of ^{137m}Ba in equilibrium before and after the resin treatment is negligible.

^{140}La, originally present in the sample, is also removed by the resin treatment, but it grows form ^{140}Ba in the effluent and reaches a state of equilibrium within a week.

When the effluent is measured by a scintillation spectrometer for long-aged samples, the 0.661 MeV peak height gives the activity of ^{137}Cs without correction, because no other nuclides are present. But when the sample is short-aged, the peak is superposed by the Compton pulses of ^{140}Ba-^{140}La gammas, which must be subtracted from the observed peak

2) D. H. Peirson, *Brit. J. Appl. Phys.*, **6**., 444 (1955).
3) J. L. Woodhead et al., *Analyst*, **81**, 570 (1956).
4) S. Yajima et al., not yet published.

height[5]. The correction factor depends on the crystal dimensions and geometry. In our case pure ^{140}Ba-^{140}La source (in equilibrium) gives Compton pulses of 59% of the 0.82 MeV peak height at the photo-peak of ^{137m}Ba gamma.

Experimental

Chemical Procedures.—Two kinds of sample were prepared, one for the long-aged and the other for the short-aged, which are:

a) F. P. (about 0.4 μC) + uranyl nitrate (several mg.) + pure ^{137}Cs solution (x ml).

b) Sample a) (F. P. and pure ^{137}Cs activities suffered a little change) + ^{140}Ba-^{140}La (about 0.2μC)*.

The cooling time of the fission products, which had been supplied by United State Atomic Energy Commitee, was about 3 years. The quantity of the ^{137}Cs (x) was taken as 0, 0.1, 0.3, 0.5, 0.75, 1.0, 1.25, 1.5, 1.75 and 2.0. One ml. of the pure ^{137}Cs solution corresponded to about 0.01 μC and 0.05 μC in sample a and b, respectively. Other elements of fission products than ^{140}Ba-^{140}La are almost completely retained in the resin column; hence they were left out of consideration. After the samples were dissolved in 50 ml of 5 N nitric acid, uranium was extracted with a mixture of T. B. P. and diethyl ether (1 : 1).

The same quantities of two forms of anion exchange resin (Dowex 1—X7.5, 50—100 mesh, treated by 5% oxalic acid solution and by 10% ammonium carbonate solution) were mixed in a beaker. After carbon dioxide gas was thoroughly removed, a column of about 6 mm. in diameter and 100 mm. in length was set up out of the mixture.

Each fission product sample in nitric acid solution free from uranium was taken in a beaker. After evaporating off most of the nitric acid, the residue was dissolved in 20 ml. of 3 N hydrochloric acid solution and again evaporated to dryness. This process was taken so that the resin column could retain almost all ^{106}Ru, which had been proved empirically. Each of the short-aged samples was dissolved in 20 ml. of 0.5% ammonium chloride solution which contains 30 mg. of strontium ion. The pH value was adjusted to 9 with aqueous ammonia solution. The solution was allowed to run through the resin column followed by a passage of 30 ml. of 1% aqueous ammonia solution. Each effluent was concentrated to 2 ml. and transferred to a polyethylene tube in order to measure the gamma-intensity in the same condition.

Measurements.—The same scintillation spectrometer as that used in the previous study[6] was used. One week after the resin treatment, the samples in polyethylene tubes were placed in the well of the sodium iodide (activated with thallous ions) crystal and the activity was measured. Typical gamma-ray spectra of the samples are shown in Figs. 1 and 2.

The effluents of the long-aged samples contained no other radioactive nuclides than ^{137}Cs-^{137m}Ba,

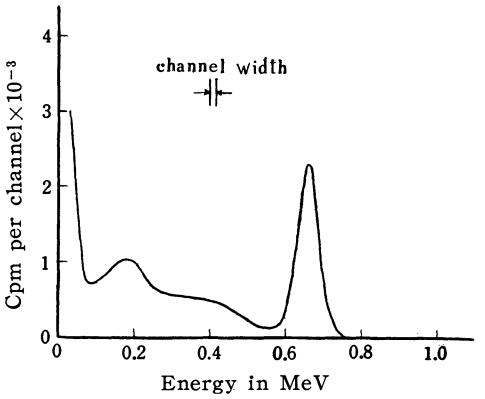


Fig. 1. Gamma-ray spectrum of the long-aged sample treated by the resin column.

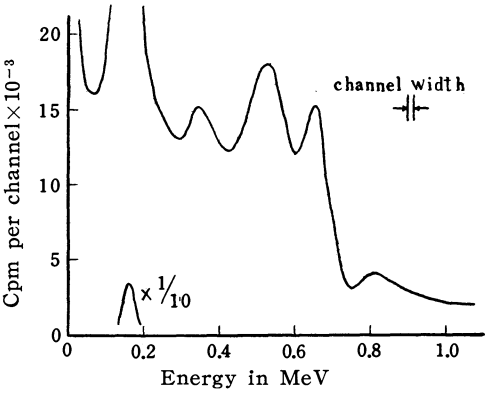


Fig. 2. Gamma-ray spectrum of the short-aged sample treated by the resin column.

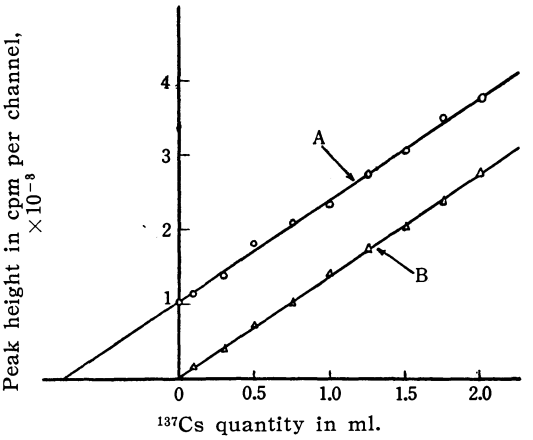


Fig. 3. 0.66 MeV peak heights vs. added ^{137}Cs quantities of the long-aged samples.

5) R. E. Connally M. Leboeuf, *Anal. Chem.*, **25**, 1075 (1953).

* In practice this case was first investigated, but because of the unexpected results, as shown in Fig. 4, the sample a) was next studied. The changes of the activities were due to the shortage of the F. P. and pure ^{137}Cs solution.

6) F. Aoki et al., This Bulletin, **30**, 583 (1957).

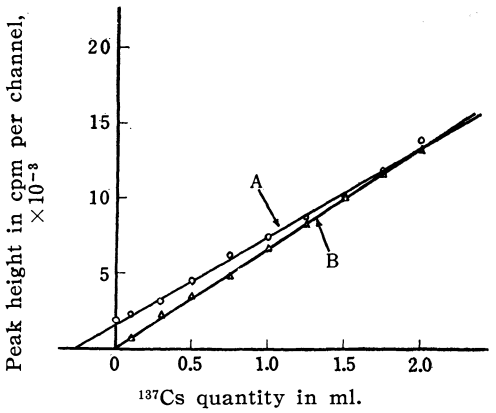


Fig. 4. 0.66 MeV peak heights vs. added ^{137}Cs quantities of the short-aged samples.

but those of the short-aged contained ^{137}Cs-^{137m}Ba and ^{140}Ba-^{140}La, which were identified by the gamma-energies.

The real peak heights of the 0.66 MeV gamma were plotted against the quantities of the added ^{137}Cs solutions (Figs. 3 and 4).

The straight lines, 'A' and 'B' show the 0.66 MeV peak height of the samples and that of pure ^{137}Cs solution added to the fission products, respectively; both have good linearities. In Fig. 3, both lines are parallel, but in Fig. 4 the slope of the straight line 'B' is a little greater than that of 'A'. This fact shows that the peak height, in spite of the correction for the Compton pulses of ^{140}Ba-^{140}La gammas, does not represent the ^{137}Cs quantity, but always gives too low a value. This phenomenon has not yet been sufficiently investigated, but one possible explanation is that some of the 0.66 MeV gamma pulses are summed up with photoelectric or Compton pulses of ^{140}Ba-^{140}La gammas to form higer pulses. However, the length between the origin of the coordinate and the intersection of the straight line 'A' and the abscissa gives the quantity of ^{137}Cs originally present in the fission products, which does not depend on the presence of ^{140}Ba-^{140}La. When the straight line 'A' is determined by the method of least squares, the most probable value of the quantity in question is obtained.

The results are shown in Table III, where N is the 0.66 MeV peak height in counts per minute per channel and x the volume of ^{137}Cs solution in milli litres. The analysed ^{137}Cs quantity corresponds to the absolute value of x at $N=0$, and is given in the same unit as that of the added ^{137}Cs solution whose activity is temporarily shown in milli litres.

TABLE III
ANALYSIS OF ^{137}Cs IN THE FISSION PRODUCTS

Sample	Straight line	^{137}Cs quantity (ml)
Long-aged	$N=1037.44-1370.83x$	0.757
Short-aged	$N=1553.51-5963.95x$	0.260

In this experiment the quantities of ^{137}Cs originally present in the fission products were unkown, so the errors of the measured quantities can not be shown. The maximum deviations of the peak heights from the straight lines determined by the method of least squere are 6% and 10% in the case of the long-aged and the short-aged, respectively.

Summary

A method for the rapid determination of ^{137}Cs in fission products has been studied. Simple and reliable analysis is possible by combining oxalate- and carbonate-form anion exchange resin and a gamma-ray scintillation spectrometer as follows.

Take several samples of equal quantity from a given fission products solution. Add various known quantities of pure ^{137}Cs to them respectively. Extract the bulk of uranium with T. B. P. in diethyl ether. Treat them through a mixed bed of carbonate- and oxalate-form anion exchange resin. Measure each aliquot using a gamma-ray scintillation spectrometer. Plot the real peak height of the 0.66 MeV gamma vs. the added ^{137}Cs quantity, and determine the straight line by the method of least square. Find the intersection of the straight line and the abscissa.

The quantity in question is given by the length of the abscissa between the intersection and the origin.

The authors wish to thank Dr. S. Uchida and Mr. K. Hashimoto for encouraging the prosecution of this work.

Government Chemical Industrial Research Institute
Shibuya-ku, Tokyo

Normal Vibrations and Calculated Thermodynamic Properties of Methyltrichlorosilane

By Kazuhiro SHIMIZU and Hiromu MURATA

(Received June 27, 1958)

Methylchlorosilane is the simplest of those methylchlorosilanes which are both industrially important and theoretically interesting. The infrared and the Raman spectrum of this compound have been reported by several investigators[1-5]. But the normal vibrational frequencies have been calculated and assigned only by a method in which a methyl group is regarded as one particle. Therefore, the vibrational frequencies accompanied by the motion of hydrogen atoms have been excluded from the calculations, and the coupling between the skeletal vibrations and the characteristic modes of the methyl group has been ignored. To make all the normal modes clear, it is necessary that the vibrations of hydrogen atoms are taken into account. In this paper, the fundamental frequencies are calculated and assigned, their normal modes are determined, and the thermodynamic properties are calculated.

Normal Coordinate Treatment. — In methyltrichlorosilane, there are two symmetrical groups, CH_3 and $SiCl_3$. Because of the interaction between the CH_3 and the $SiCl_3$ group, the internal rotation is restricted, and it is more correct in the present consideration to treat the relative movement of CH_3 and $SiCl_3$ as torsional oscillation rather than as free internal rotation. This molecule belongs to the point group C_{3v} whether the groups have staggered or eclipsed forms. According to the group theory, it is clearly shown that this molecule has twelve fundamental frequencies of which five belong to species a_1, one to species a_2, and six to species e. All vibrations except the a_2 torsional mode are both infrared and Raman active. If this molecule has the torsional angle about the Si—C axis, it belongs to the point group C_3. The species a_1 and a_2 of the point group C_{3v} correspond to the species a of the point group C_3. Previous work by Collins and Nielsen[6] shows a normal coordinate treatment of the staggered configuration of methyltrifluorosilane having a structure similar to methyltrichlorosilane. But, in this investigation, at first, we undertake to make an attempt to carry out a normal coordinate treatment with an arbitrary torsional angle, and, next, to calculate the normal vibrational frequencies of the point group C_{3v} molecule for which the torsional angle θ is 0° in the eclipsed from, and 180° in the staggered form. We do not calculate the a_2 mode which is both infrared and Raman inactive. A normal coordinate treatment was carried out using the Wilson *FG* matrix method[7]. The *F* matrix elements were formed from the force constants in a Urey-Bradley force field[8].

The various bond distances, the interbond angles, and the distances between nonbonded atoms used to determine the internal coordinates are shown in Fig. 1. From the internal coordinates the following orthonormal symmetry coordinates were found; for the a vibrations,

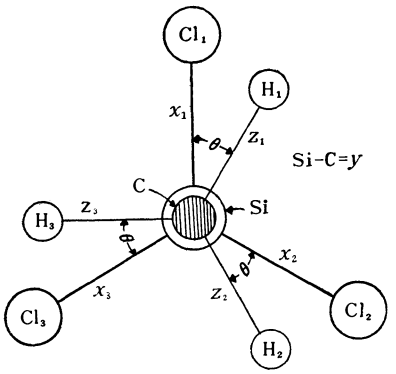


Fig. 1. Internal coordinates of methyltrichlorosilane.

1) J. Goubeau, H. Siebert and M. Winterwerb, *Z. anorg. Chem.*, **259**, 239 (1949).
2) T. Shimanouchi, I. Tsuchiya and Y. Mikawa, *J. Chem. Phys.*, **18**, 1306 (1950).
3) L. Burnelle and J. Duchesene, ibid., **20**, 1324 (1952).
4) H. Murata, *J. Chem. Soc. Japan, Pure Chem. Sec.*, (*Nippon Kagaku Zasshi*), **73**, 465 (1952).
5) A. L, Smith, *J. Chem. Phys.*, **23**, 1997 (1953).
6) R. L. Collins and J. R. Nielsen, Ibid., **23**, 351 (1955).
7) E. B. Wilson, Jr., ibid., **7**, 1047 (1939); **9**, 76 (1941).
8) T. Shimanouchi, Ibid., **17**, 245, 734, 848 (1949).

$$R_1=\Delta(z_1+z_2+z_3)/\sqrt{3}$$
$$R_2=\Delta(z_1y+z_2y+z_3y-z_1z_2-z_1z_3-z_2z_3)/\sqrt{6}$$
$$R_3=\Delta y$$
$$R_4=\Delta(x_1+x_2+x_3)/\sqrt{3}$$
$$R_5=\Delta(x_1y+x_2y+x_3y - x_1x_2-x_1x_3-x_2x_3)/\sqrt{6}$$

and for the e vibrations

$$R_{6a}=\Delta(2z_1-z_2-z_3)/\sqrt{6}$$
$$R_{7a}=\Delta(2z_2z_3-z_1z_3-z_1z_2)/\sqrt{6}$$
$$R_{8a}=\Delta(2z_1y-z_2y-z_3y)/\sqrt{6}$$
$$R_{9a}=\Delta(2x_1-x_2-x_3)/\sqrt{6}$$
$$R_{10a}=\Delta(2x_1y-x_2y-x_3y)/\sqrt{6}$$
$$R_{11a}=\Delta(2x_2x_3-x_1x_3-x_1x_2)/\sqrt{6}$$

The numbering of these coordinates corresponds to the numbering of the fundamentals in Table II.

From the coefficients of the symmetry coordinates and the potential constants of a Urey-Bradley force field, one gets the following F matix elements:
for the a vibrations,

$$F_{11}=K_z+4s^2_{zz}F_{zz}+s^2_{zy}F_{yz}+t^2_{zy}F'_{yz}$$
$$F_{12}=[(t_{yz}s_{zy}F_{yz}+t_{zy}s_{yz}F'_{yz})y - 2t_{zz}s_{zz}(F_{zz}+F'_{zz})z]/\sqrt{2}$$
$$F_{13}=\sqrt{3}\,(s_{yz}s_{zy}F_{yz}-t_{yz}t_{zy}F'_{yz})$$
$$F_{22}=(H_{yz}+t_{yz}t_{zy}F_{yz}-s_{yz}s_{zy}F'_{yz})yz/2 + (H_{zz}+t^2_{zz}F_{zz}-s^2_{zz}F'_{zz})z^2/2+3\sqrt{2}\kappa'/4$$
$$F_{23}=\sqrt{6}\,(t_{zy}s_{yz}F_{yz}+t_{yz}s_{zy}F'_{yz})z/2$$
$$F_{33}=K_y+3(s^2_{yx}F_{xy}+t^2_{yx}F'_{xy}) +3(s^2_{yz}F_{yz}+t^2_{yz}F'_{yz})$$
$$F_{34}=\sqrt{3}\,(s_{xy}s_{yx}F_{xy}-t_{xy}t_{yx}F'_{xy})$$
$$F_{35}=\sqrt{6}\,(t_{xy}s_{yx}F_{xy}+t_{yx}s_{xy}F'_{xy})x/2$$
$$F_{44}=K_x+4s^2_{xx}F_{xx}+s^2_{xy}F_{xy}+t^2_{xy}F'_{xy}$$
$$F_{45}=[(t_{yx}s_{xy}F_{xy}+t_{xy}s_{yx}F'_{xy})y - 2t_{xx}s_{xx}(F_{xx}+F'_{xx})x]/\sqrt{2}$$
$$F_{55}=(H_{xx}+t^2_{xx}F_{xx}-s_{xx}F'_{xx})x^2/2 + (H_{xy}+t_{xy}t_{yx}F_{xy}-s_{xy}s_{yx}F'_{xy})xy/2 +3\sqrt{2}\kappa/4$$
$$F_{14}=F_{15}=F_{24}=F_{25}=0$$

for the e vibrations

$$F_{66}=K_z+s^2_{zz}F_{zz}+3t^2_{zz}F'_{zz}+s^2_{zy}F_{yz}+t^2_{zy}F'_{yz}$$
$$F_{67}=-t_{zz}s_{zz}(F_{zz}+F'_{zz})z$$
$$F_{68}=(t_{yz}s_{zy}F_{yz}+t_{zy}s_{yz}F'_{yz})y$$
$$F_{77}=(H_{zz}+t^2_{zz}F_{zz}-s^2_{zz}F'_{zz})z^2+\sqrt{2}\kappa'/4$$
$$F_{78}=-\kappa'/\sqrt{2}$$
$$F_{88}=(H_{yz}+t_{yz}t_{zy}F_{yz}-s_{yz}s_{zy}F'_{yz})yz+\sqrt{2}\kappa'/4$$
$$F_{99}=K_x+s^2_{xx}F_{xx}+3t^2_{xx}F'_{xx}+s^2_{xy}F_{xy}+t^2_{xy}F'_{xy}$$
$$F_{910}=(t_{yx}s_{xy}F_{xy}+t_{xy}s_{yx}F'_{xy})y$$
$$F_{911}=-t_{xx}s_{xx}(F_{xx}+F'_{xx})x$$
$$F_{1010}=(H_{xy}+t_{yx}t_{xy}F_{xy}-s_{xy}s_{yx}F'_{xy})xy+\sqrt{2}\kappa/4$$
$$F_{1011}=-\kappa/\sqrt{2}$$
$$F_{1111}=(H_{xx}+t^2_{xx}F_{xx}-s^2_{xx}F'_{xx})x^2+\sqrt{2}\kappa/4$$

and

$$F_{69}=F_{610}=F_{611}=F_{79}=F_{710}=F_{711}=F_{89}=F_{810}=F_{811}=0$$

where the following abbreviations are adopted:

$$s_{zz}=4z/3q_{zz} \qquad t_{zz}=2\sqrt{2}\,z/3q_{zz}$$
$$s_{zy}=(3z+y)/3q_{yz} \qquad t_{zy}=2\sqrt{2}\,y/3q_{yz}$$
$$s_{yz}=(3y+z)/3q_{yz} \qquad t_{yz}=2\sqrt{2}\,z/3q_{yz}$$
$$s_{yx}=(3y+x)/3q_{xy} \qquad t_{yx}=2\sqrt{2}\,x/3q_{xy}$$
$$s_{xy}=(3x+y)/3q_{xy} \qquad t_{xy}=2\sqrt{2}\,y/3q_{xy}$$
$$s_{xx}=4x/3q_{xx} \qquad t_{xx}=2\sqrt{2}\,x/3q_{xx}$$

and the symbols used for the equilibrium values of the interatomic distances are x=Si—Cl, y=Si—C, z=C—H, q_{xx}=Cl···Cl, q_{xy}=C···Cl, q_{yz}=Si···H and q_{zz}=H···H.

The G matrix elements are obtained by use of the table of Decius[9]. In terms of the abbreviations ρ_x, ρ_y and ρ_z for the reciprocals of the Si—Cl, Si—C and C—H bond lengths, respectively, and μ_x, μ_y, μ_c and μ_h for the reciprocals of the atomic masses of the Cl, Si, C and H, the following G matrix elements are found, assuming all angles to be tetrahedral:
for the a vibrations,

$$G_{11}=\mu_h+\mu_c/3$$
$$G_{12}=4\rho_z\mu_c/3$$
$$G_{13}=-\mu_c/\sqrt{3}$$
$$G_{22}=2(\mu_h+8\mu_c/3)\rho^2_z$$
$$G_{23}=-4\rho_z\mu_c/\sqrt{3}$$
$$G_{33}=\mu_y+\mu_c$$
$$G_{34}=-\mu_y/\sqrt{3}$$
$$G_{35}=-4\rho_x\mu_y/\sqrt{3}$$
$$G_{44}=\mu_x+\mu_y/3$$
$$G_{45}=4\rho_x\mu_y/3$$
$$G_{55}=2(\mu_x+8\mu_y/3)\rho^2_x$$
$$G_{14}=G_{15}=G_{24}=G_{25}=0,$$

for the e vibrations,

$$G_{66}=\mu_h+4\mu_c/3$$

9) J. C. Decius, ibid., **16**, 1025 (1948).

$$G_{67}=4\sqrt{2}\,\rho_z\mu_c/3$$
$$G_{68}=-\sqrt{2}\,(3\rho_y+\rho_z)\,\mu_c/3$$
$$G_{610}=\sqrt{2}\,\rho_y\mu_c\cos\theta$$
$$G_{77}=(8\mu_c/3+5\mu_h/2)\,\rho^2{}_z$$
$$G_{78}=-2(3\rho_y+\rho_z)\,\rho_z\mu_c/3+\rho^2{}_z\mu_h/2$$
$$G_{710}=2\rho_y\rho_z\mu_c\cos\theta$$
$$G_{88}=3\rho^2{}_y\mu_y/2+(3\rho_y+\rho_z)^2\mu_c/6+\rho^2{}_z\mu_h$$
$$G_{89}=\sqrt{2}\,\rho_y\mu_y\cos\theta$$
$$G_{810}=-[(3\rho_y+\rho_x)\,\mu_y+(3\rho_y+\rho_z)\,\mu_c]\,\rho_y\cos\theta/2$$
$$G_{811}=2\rho_x\rho_y\mu_y\cos\theta$$
$$G_{99}=\mu_x+4\mu_y/3$$
$$G_{910}=-\sqrt{2}\,(3\rho_y+\rho_x)\,\mu_y/3$$
$$G_{911}=4\sqrt{2}\,\rho_x\mu_y/3$$
$$G_{1010}=\rho^2{}_x\mu_x+(3\rho_y+\rho_x)^3\mu_y/6+3\rho^3{}_y\mu_c/2$$
$$G_{1011}=\rho^2{}_x\mu_x/2-2(3\rho_y+\rho_x)\,\rho_x\mu_y/3$$
$$G_{1111}=(5\mu_x/2+8\mu_y/3)\,\rho^2{}_x$$
$$G_{69}=G_{611}=G_{79}=G_{711}=0$$

Since the repulsive force constants between non-bonded atoms are ignored, the F matrix elements of an eclipsed configuration are equal to those of a staggered one. Also, as shown in the G matrix elements, the different point between an eclipsed and a staggered configuration is only the change of the signs of G_{610}, G_{710}, G_{89}, G_{810} and G_{811} elements. However, the calculated values of GF for both the configurations are equivalent.

The C—H stretching vibrations were split off by the method of Wilson. The molecular constants and the potential constants used are listed in Table I. As an aid in determining some of the potential constants, K_x, K_y, K_z, H_{xx}, H_{xy}, H_{zz}, F_{xx}, F_{xy}, F_{zz} and κ, the results from previous investigations of methane[8] and the skeletal vibrations of this molecule[2] were used. But for K_y, a slightly lower value was adopted. We gave -0.05 md/A to the value of κ', taking into consideration the corresponding constants found for methane, monochloromethane, monofluoromethane and methyl alchohol. The values of H_{yz} and F_{yz} were selected so as to give the good agreement with the observed fundamentals. The values of F' are assumed to be $-0.1\,F$.

TABLE I
MOLECULAR AND POTENTIAL CONSTANTS OF METHYLTRICHLOROSILANE

Bond distance and angle	Potential constants (md/A) Type	
x=Si—Cl	K_x(Si—Cl)	2.59
=2.021 A	K_y(Si—C)	2.72
y=Si—C	K_z(C—H)	4.63
=1.876 A	H_{xx}(Cl—Si—Cl)	0.059
z=C—H	H_{xy}(Cl—Si—C)	0.035
=1.093 A	H_{yz}(Si—C—H)	0.20
all angles	H_{zz}(H—C—H)	0.40
=tetrahedral	F_{xx}(Cl···Cl)	0.29
	F_{xy}(Cl···C)	0.162
	F_{yz}(Si···H)	0.13
	F_{zz}(H···H)	0.10
	κ($CSiCl_3$)	0.17 A^2
	κ'($SiCH_3$)	-0.05 A^2

Normal Frequencies.—A normal coordinate treatment of the skeletal vibrations which assumed the methyl group to be one particle was carried out by Goubeau et al.[1] and Shimanouchi et al.[2]. The calculated frequencies of all the normal vibrations are in good agreement with the observed, if the assignment of these frequencies is made adequately as shown in Table II. In it, the results of previous investigations are listed together for comparison.

The L matrices, whose components give the modes of vibrations and the potential energy distribution for each normal vibration were calculated. They are shown in Tables III and IV. Since the ν_1 and ν_6 are considered to have almost pure C—H streching frequencies, their L mairices and potential energy distributions are omitted.

Judging from the values of the contribution of each symmetry coordinate to the normal coordinates Q_{10} and Q_{11} in Table III and the distribution of potential energy in the symmetry coordinates for the normal frequencies ν_{10} and ν_{11} in Table IV, it is reasonable to designate the frequencies 229 cm^{-1} and 164 cm^{-1} respectively as "$SiCl_3$ rocking" and "$SiCl_3$ non-symmetric deformation". Thus, the classification given in Table II is reasonable.

As shown in Tables III and IV, the skeletal vibrations and the vibrations accompanied by the motion of hydrogen atoms are separated to a considerable extent. Therefore, the calculated values of the skeletal vibrations are expected to be in good agreement with their corresponding observed values.

Internal Rotation.—The torsional vibration belongs to the species a_2 and is both infrared and Raman inactive. The frequency can be calculated if the height of the potential barrier hindering the internal rotation is known. However, the

TABLE II

RAMAN AND INFRARED DATA, PROBABLE VALUES OF THE OBSERVED FUNDAMENTALS, CALCULATED WAVE NUMBERS, AND ASSIGNMENTS FOR METHYLTRICHLOROSILANE

Type	Mode of vibration	G.S.W.[a]	S.T.M.[b]	B.D.[c]	M.[d]	S.[e]	calc.	obs.
a_1	$\nu_1(CH_3$ sym. str.)	—	—	2915	—	2923	2928	2923
	$\nu_2(CH_3$ sym. def.)	—	—	1271	—	1271	1274	1271
	ν_3(Si—C str.)	758	761	764	760	764	760	764
	ν_4(Si—Cl sym. str.)	450	450	457	450	458	449	458
	$\nu_5(SiCl_3$ sym. def.)	228	229	—	230	229	228	229
e	$\nu_6(CH_3$ nonsym. str.)	—	—	2977	—	2990	2980	2990
	$\nu_7(CH_3$ nonsym. def.)	—	—	1416	—	1417	1431	1417
	$\nu_8(CH_3$ rocking)	—	—	807	—	804	843	804
	ν_9(Si—Cl nonsym. str.)	569	576	578	575	577	597	577
	$\nu_{10}(SiCl_3$ rocking)	351	229	—	230	164	227	229
	$\nu_{11}(SiCl_3$ nonsym. def.)	162	164	—	165	229	165	164

a Goubeau, Siebert and Winterwerb, reference 1;
b Shimanouchi, Tsuchiya and Mikawa, reference 2;
c Burnelle and Duchesene, reference 3;
d Murata, reference 4;
e Smith, reference 5.

TABLE III

L MATRICES OF THE NORMAL VIBRATIONS OF METHYLTRICHLOROSILANE

a_1 vibrations,

	Q_2	Q_3	Q_4	Q_5
$R_2(CH_3$ sym. def.)	1.41	0.17	0.03	0.01
R_3(Si—C str.)	−0.16	0.30	0.04	0.01
R_4(Si—Cl sym. str.)	0.01	−0.09	0.18	−0.01
$R_5(SiCl_3$ sym. def.)	0.01	−0.14	0.07	0.19

e vibrations,

	Q_7	Q_8	Q_9	Q_{10}	Q_{11}
$R_7(CH_3$ nonsym. def.)	1.47	−0.27	−0.03	0.01	0.00
$R_8(CH_3$ rocking)	0.36	0.88	0.12	−0.02	−0.01
R_9(Si—Cl nonsym. str.)	−0.01	−0.06	0.27	0.02	0.00
$R_{10}(SiCl_3$ rocking)	−0.03	0.11	−0.12	0.16	0.10
$R_{11}(SiCl_3$ nonsym. def.)	0.00	−0.04	0.12	−0.09	0.13

TABLE IV

POTENTIAL ENERGY DISTRIBUTION $F_{ii}L_{ia}^2/\lambda_a$ FOR THE NORMAL VIBRATIONS OF METHYLTRICHLOROSILANE

a_1 vibrations,

	ν_2	ν_3	ν_4	ν_4
$R_2(CH_3$ sym. def.)	0.96	0.03	0.00	0.00
R_3(Si—C str.)	0.08	0.89	0.04	0.01
R_4(Si—Cl sym. str.)	0.00	0.07	0.94	0.01
$R_5(SiCl_3$ sym. def.)	0.00	0.04	0.03	0.96

e vibrations,

	ν_7	ν_8	ν_9	ν_{10}	ν_{11}
$R_7(CH_3$ nonsym. def.)	0.92	0.08	0.00	0.01	0.00
$R_8(CH_3$ rocking)	0.06	0.90	0.03	0.01	0.00
R_9(Si—Cl nonsym. str.)	0.00	0.02	0.98	0.04	0.00
$R_{10}(SiCl_3$ rocking)	0.00	0.01	0.04	0.55	0.40
$R_{11}(SiCl_3$ nonsym. def.)	0.00	0.00	0.05	0.23	0.79

question as to the potential hill has not been definitely settled. Here, the potential barrier of monomethylsilane, methyltrichlorosilane and methyltrifluorosilane are compared with the values of ethane, 1,1,1-trichloroethane and 1,1,1-trifluoroethane, respectively. The heights of ethane[10], 1,1,1-trichloroethane[11] and 1,1,1-trifluoroethane[12] are respectively 2.875±0.125 kcal/mole, 2.97 kcal/mole and 3.25±0.40 kcal/mole. That is to say, the value of 1,1,1-trichloroethane is found between the value of ethane and of 1,1,1-trifluoroethane. On the other hand, the value of monomethylsilane[13] and of methyltrifluorosilane[14] are respectively 1.314±0.229 kcal/mole and 1.20 ±0.16 kcal/mole. Thus it seems that the height of the potential barrier of methyltrichlorosilane is 1.30±0.25 kcal/mole.

TABLE V
HEAT CAPACITY, ENTROPY, FREE ENERGY, AND HEAT CONTENT OF METHYLTRICHLOROSILANE FOR THE IDEAL GASEOUS STATE AT 1 ATOMS PRESSURE (cal. deg.$^{-1}$ mol.$^{-1}$)

T°K		$\frac{(H^0-E^0_0)}{T}$	$-\frac{(F^0-E^0_0)}{T}$	S^0	C^0_p
	torsional:	0.58	0.26	0.84	1.39
100	other:	9.71	51.47	61.18	13.28
	total:	10.29	51.73	62.02	14.67
		1.32	1.23	2.55	1.89
273.15		15.03	63.61	78.64	22.27
		16.35	64.84	81.19	24.16
		1.36	1.35	2.71	1.90
298.15		15.66	64.96	80.62	22.98
		17.02	66.31	83.33	24.88
		1.37	1.35	2.72	1.90
300		15.70	65.05	80.75	23.15
		17.07	66.40	83.47	25.05
		1.51	1.77	3.28	1.94
400		17.94	69.89	87.83	26.11
		19.45	71.66	91.11	28.05
		1.60	2.12	3.72	1.96
500		19.82	74.10	93.92	28.41
		21.42	76.22	97.64	30.37
		1.66	2.42	4.08	1.97
600		21.40	77.85	99.25	30.19
		23.06	80.27	103.33	32.16
		1.70	2.67	4.37	1.97
700		22.76	81.32	104.08	31.66
		24.46	83.99	108.45	33.63
		1.74	2.90	4.64	1.97
800		23.95	84.37	108.32	32.85
		25.69	87.27	112.96	34.82
		1.76	3.11	4.87	1.98
900		25.00	87.25	112.25	33.88
		26.76	90.36	117.12	35.86
		1.78	3.29	5.07	1.98
1000		25.93	89.93	115.86	34.76
		27.71	93.22	120.93	36.74

In the present investigation, the usual $V=V_0\ (1-\cos 3\theta)/2$ is adopted as the form of the potential barrier. In this formula, V_0 is the height of the potential barrier and θ is the torsional angle. The torsional frequency can now be obtained from V_0. The calculated value $147\pm15\ \mathrm{cm}^{-1}$ is believed to be not far from the real torsional frequency.

Thermodynamic Properties.—The probable values of the wave numbers of the normal frequencies given in Table II were used to calculate values of the heat content, free energy, entropy and heat capacity for the ideal gaseous state at 1 atoms pressure (rigid rotator, harmonic oscillator approximation). The bond distances and the interbond angles given in Table I were used to calculate the product of the principal moments of inertia, using the Hirschfelder formula[15]. The value obtained was $I_aI_bI_b=1.48102\times10^{-112}\ \mathrm{gm}^3\ \mathrm{cm}^6$. The molecular weight used was 149.496 and the symmetry number was 3. In Table V, the contributions of the torsional frequency and the others (translational, rotational and vibrational except torsinal) are listed separately to facilitate revision of the table, if and when a better way is found to calculate the contribution for the former.

The authors wish to thank Professor Y. Morino and Dr. T. Shimanouchi of the University of Tokyo and Dr. H. Shingu of Kyoto University for making many valuable discussions.

Osaka Municipal Technical Research Institute, Kita-ku, Osaka

10) K. S. Pitzer, *Disc. Faraday Soc.*, **10**, 66 (1951).
11) K. S. Pitzer and J. L. Hollenberg, *J. Am. Chem. Soc.*, **75**, 2219 (1953).
12) H. W Thompson and R. B. Temple, *J. Chem. Soc.* **1948**, 1428.
13) D. R. Lide and D. K. Coles, *Phys. Rev.*, **80**, 911 (1950).
14) J. Sheridand and W. Gordy, *J. Chem. Phys.*, **19**, 965 (1951).
15) J. O. Hirschfelder, ibid., **8**, 431 (1940).

*Phase Transition of Lithium Ferrospinel-Lithium Aluminospinel Solid Solution**

By Eizo KATO**

(Received July 8, 1958)

The phase transition of lithium ferrospinel was studied by means of thermal, electric[1] and X-ray measurements[2]. Lithium aluminospinel is a compound in which ferric ion in LFS changes into aluminum ion. Kordes[3], Verwey[4], Braun[5] and Yamaguchi[6] found that the crystal structure of LAS is the same as that of LFS, but its physico-chemical properties are not evident. No information pertaining to a phase transition of LFS-LAS solid solution has ever been presented in the literature. In the present paper, some physico-chemical changes attributed to exchange ferric ion for aluminum ion in LFS-LAS solid solution are systematically investigated by means of X-ray diffraction and differential thermal analysis, besides, formation of LFS-LAS solid solution is discussed.

Experimental

Specimens***.—Hydroxides coprecipitated from mixed aqueous solutions of ferric and aluminum nitrate were mixed with lithium oxalate in acetone, then dried, pressed and calcined in an electric furnace at 1200°C for three days. Specimens in a low temperature form (an ordered phase) were obtained by annealing in the same furnace from ca. 1200°C to the room temperature for a day, while specimens in a high temperature form (a disordered phase) were quenched by immersion into water from ca. 1300°C in 1~2 seconds.

Apparatus and Procedures. — Thermal analyses were carried out up to 1000°C at a heating rate of 10°/min. by the apparatus reported already[7]. The measurements above 1000°C were performed at a rate of 3°/min. by an apparatus with a sample holder of sillimanite. X-ray powder photographs were taken with Co $K\alpha$ radiation by a back-reflection technique, and lattice constants

TABLE I

CHEMICAL COMPOSITIONS, LATTICE CONSTANTS AND ENDOTHERMIC TEMPERATURES OF SOLID SOLUTIONS

Specimen	Composition, Fe/Al	Lattice constant (Å)			Endothermic temperature (°C)
		Ordered phase	Disordered phase	Δ (%)	
A	0/5	7.909	7.911	0.03	ca. 1200
B	1/4	7.999	8.010	0.14	ca. 1130
C	1.5/3.5	8.005 8.206	8.053_6	—	ca. 1090 ca. 880
P	2/3	8.004 8.206	8.095_8	—	875~880
R	2.5/2.5	8.004 8.206	8.143	—	880
Q	3/2	8.177_3	8.183_8	0.08	916
D	3.5/1.5	8.00 8.210	8.212	0.03	887
E	4/1	8.257	8.263	0.08	826
F*	5/0	8.329_6	8.332_6	0.04	765

* given from the previous report[1]

* Lithium ferrospinel and lithium aluminospinel are abbreviated to LFS and LAS, respectively, in the following.

** Present adress, Idemitsu Kōsan Co. Ltd., Chuō-ku, Tokyo.

1) E. Kato, This Bulletin, **31**, 113 (1958).
2) E. Kato, ibid., in press.
3) E. Kordes, *Z. Krist.*, **91**, 193 (1935).
4) E. J. W. Verwey and E. L. Heilmann, *J. Chem. Phys.*, **15**, 174 (1947).
5) P. B. Braun, *Nature*, **170**, 1123 (1952).
6) G. Yamaguchi, This Bulletin, **26**, 206 (1953).

*** By Kordes[3] lithium fluoride was used as a mineralizer in order to prepare homogeneous specimens. It was proved by X-rays that fluoride was scarcely reacted with ferric oxide, so that this synthesis was not employed.

7) E. Kato, This Bulletin, **31**, 108 (1958).

were accurately determined by an extrapolation method against $1/2(\cos^2\theta/\sin\theta+\cos^2\theta/\theta)$

Results and Discussion

Order-Disorder Transition of Solid Solution.—From spacings and reflection intensities measured by X-ray diffraction, the crystal structures of the low temperature and the high temperature form of LFS–LAS solid solution were found to be an ordered lattice, O^6—$P4_33$, and a disordered lattice, O_h^7—$Fd3m$, respectively. Both lattices are identified by arrangements of cations at octahedral interstices, and have the same structures with those in LFS or LAS alone. The values of the lattice constant as a function of the chemical composition for the ordered and the disordered phase of the solid solution are shown in Table I and Fig. 1. The relation of the lattice constants vs. the composition for disordered phases was calculated by a method of least squares.

$$y=7.912_5+0.4907x-0.0699x^2$$

where x is the mole fraction of LFS in the solid solution, and y thelattice constant of disordered phase.

On the other hand, experimental results for the ordered phase were too few to find an equation similar to the above one. Lattice expansions (Δ) at the transition from the ordered phase to the disordered one is small as is listed in Table I, and these values are in 0.03~0.14% regardless of the composition. If the magnitude of the expansion is estimated at 0.05%, the observed values of lattice constant of the ordered phase will agree with those calculated by the above equation.

Physico-chemical changes of the solid solution in occurrence of the transition were observed by differential thermal analysis. The endothermic reaction due to the transition was already seen in the measurement of LFS, and thermal changes similar to LFS or LAS were found in all specimens of ordered phase of the solid solution*. Though the transition temperature of LFS or LAS** is known, no paper was reported for those of the solid solutions. The exact value of the transition temperature had better be measured by a dilatometry with a considerable slower heating rate. The dilatometry was, however, not carried out, because of difficulty to prepare aluminum-rich specimens by sintering. In place of the relation of the transition temperature vs. the chemical composition, that of the endothermic temperature vs. the composition in a series of specimens was measured and is shown

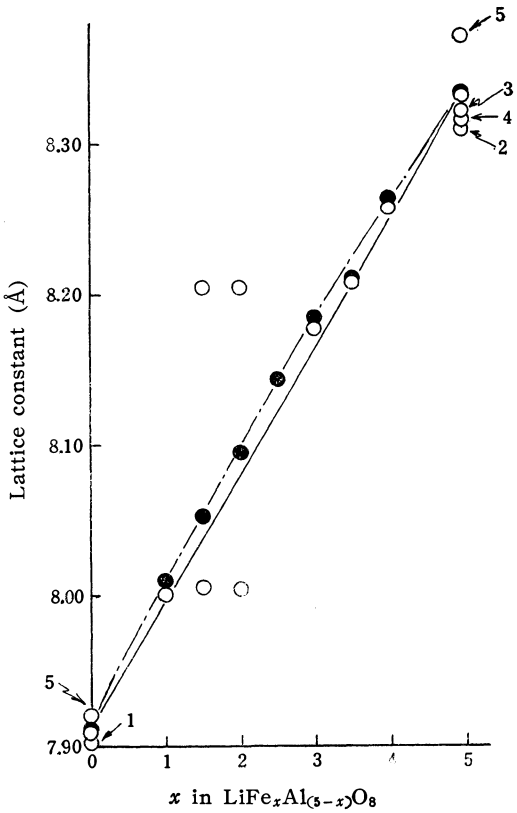


Fig. 1. Relation between the lattice constant and the chemical composition in the solid solutions.
○: ordered phase, present author
●: disordered phase, present author
1: disordered phase, E. Kordes[3]
2: disordered phase, A. Hoffman[9]
3: disordered phase, F. Barblan et al.[10]
4: disordered phase, R. Collongues and G. Chaudron[11]
5: disordered phase, E. Kordes and E. Röttig[12]

* Thermal analysis of LAS was studied by the present author for the first time. The endothermic reaction due to a ferromagnetism, which was found in LFS, was not observed in the case of the solid solution.

** By Braun[5] the transtion takes place at the temperature below 1350°C.

8) H. Forestier and M. Vetter, *Compt. rend.*, **209**, 164 (1939).
9) A. Hoffmann, *Naturwiss.*, **26**, 431 (1938).
10) F. Barblan, E. Brandenberger and P. Niggli, *Helv. Chim. Acta*, **27**, 88 (1944).
11) R. Collongues and G. Chaudron, *Compt. rend.*, **231**, 143 (1950).
12) E. Kordes and E. Rötting, *Z. anorg. allgem. Chem.*, **264**, 34 (1951).

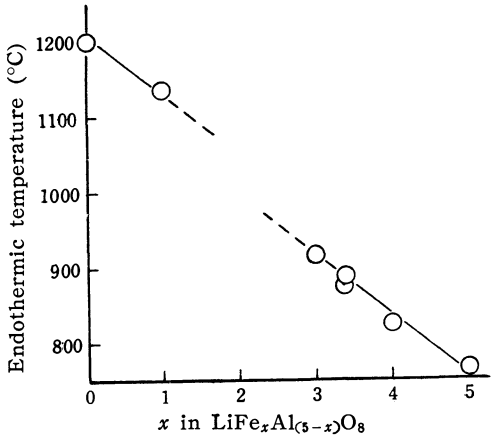


Fig. 2. Relation between the endothermic temperature and the chemical composition in the solid solutions.

in Table I and Fig. 2. The endothermic temperature of LFS is lower than that of any composition of the solid solution, and the more the aluminum content, the higher this temperature. An analogous relation is seen in that of ferromagnetic Curie point vs. chemical composition in nickel-magnesium, cupric-nickel and zinc-nickel ferrospinel solid solution[8]. It is very remarkable that no continuous change of the endothermic temperature against the composition is found in any kinds of specimens of the solid solution but in those of the compositions rich in ferric ion or aluminum ion. This is supposed to be caused by some differences in crystal structure between iron-rich and aluminum-rich compositions. The true transition temperatures, which are provided to be lower than the endothermic temperatures by 10~30° from the result of LFS, will also be given in the similar manner as above-mentioned.

It is concluded that the transition of LFS-LAS solid solution is the order-disorder transition of the same type as that of LFS or LAS from the results on the crystal structure and the endothermic reaction.

Formation of Homogeneous Solid Solution. —In the disordered phase, homogeneous solid solutions were formed at any compositions. In the ordered phase, however, the solid solutions were homogenized in the specimens of iron-rich composition (D and E in Table I) or of aluminum-rich (B). There might be two phases separated in the specimens of intermediate compositions (C, P and R). The compositions of the separated phases were estimated by the measurements of lattice constants and the use of the above equation, and it was determined that in one of these two phases it is of 20 mole per cent LFS, and in the other 68 mole per cent. In thermal analysis, the only endothermic temperature was measured in the case of specimens B, D and E, while two endothermic temperatures corresponded to two phases were revealed in the case of C, P and R. X-ray diffraction results were in conformity with thermal analysis'. The formation of a homogeneous solid solution in the ordered phase of Q, though it was annealed on the same condition as others, is assumed due to a difference in a disordering velocity* from that of the others. Whether the homogeneous solid solution can be formed in the ordered phase at a higher temperature or in the disordered phase quenched at a lower temperature, no knowledge is offered from the present work.

Homogeneous solid solutions were not formed in the region of 20~68 mole per cent LFS, where the discrepancy in the relation of the transition temperature vs. the chemical composition was also observed. The conditions necessary to form a homogeneous solid solution are usually those mentioned below[13]; (1) both phases have the same crystal structure, (2) the values of lattice constants resemble each other, (3) the chemical properties are also similar, (4) the ionic radii of constructing ions are the similar size. Typical examples are revealed in the ferrospinel mentioned above, lead phosphate-lead arsenate and lead phosphate-lead vanadate solid solution[14]. Systematic studies on relations of solid solutions of solid solution with order-disorder transition have hitherto been reported very rarely. The ordered phase of LFS and that of LAS have the same crystal structure and the difference between their lattice constants is small. It is also the case in the disordered phase. These is a considerable agreement between an ionic radius of ferric ion (0.67 Å) and that of aluminum ion (0.55 Å). Though having the conditions necessary to be homogenized, LFS-LAS solid solutions cannot

* From the condition of annealing, the transition velocity of each composition was found to be very rapid as that of LFS.

13) R. Kiriyama and S. Seki, "Crystal Chemistry (Kesshō no Kagaku)", Part II, Sōgensha, Osaka, 1950, p. 135.

14) M. Amadori, *Gazz. chim. Ital.*, **49**, 38 (1919).

be formed over all ratios. Such phenomena might be caused by an averaged structure, i. e., a cation arrangement at the octahedral or the tetrahedral interstices in the crystal. Detailed experiments along this line will be discussed in the following paper.

The author wishes to express his sincere thanks to Mr. Kazuo Sasaki of Osaka City University for his discussion.

Institute of Polytechnics
Osaka City University
Kita-ku, Osaka

*Experiments on Synthetic Mica Crystal Growing. Crystal Growing with Carbon Granule Resistance Furnace**

By Tokiti NODA and Yoshihiro SUMIYOSHI

(Received July 2, 1958)

In experiments on the growing of synthetic fluor-phlogopite, it is necessary first to melt the mixture of raw materials of fluor-phlogopite composition to a clear liquid by heating it at about 1450°C and then to maintain the resultant melt for many hours at temperatures within a range of several tens of degrees around its crystallizing temperature of about 1350°C. For the growing of large crystals, the melt should be cooled very slowly.

The rate of cooling necessary for the growing of large crystals may be acquired in two ways.

1) For small melts, by precise control of the temperature of the melt; 2) by using a large enough quantity of melt to obtain the necessary rate through natural cooling or by less precise control of temperature. A large mass of melt will provide sufficient space for growing large crystals.

The first way may be carried out by applying the technique originally designed by Stöber[1], Bridgman[2] and Kyropoulos[3] for growing large single crystals, techniques which have been used in the manufacture of optical crystals. The results of experiments done along this line will be reported later; experiments on growing synthetic mica crystals in large melts are described in the present paper.

* Summary of papers published in *J. Chem. Soc. Japan, Ind. Chem. Sec.*, (*Kogyo Kagaku Zasshi*), **59**, 352, 1323 (1956); and *J. Ceram. Assoc. Japan.* (*Yogyo Kyokai Shi*), **64**, 95 (1956).

1) F. Stöber, *Z. Krist.*, **61**, 299 (1925).

2) P. W. Bridgman, *Proc. Am. Acad. Arts. Sciences*, **60**, 303 (1925).

3) S. Kyropoulos, *Z. anorg. Chem.*, **154**, 308 (1926); *Z. Phys.*, **63**, 849 (1930).

Experimental

Apparatus.—Among various types, platinum resistance, silicon carbide resistance, carbon resistance and gas-fired furnaces may meet the requirements for the temperature range for synthetic mica crystal growing. In small-scale experiments, the first two types of furnace were used. In large-scale experiments, however, carbon granule resistance furnaces, designed especially for this purpose, were used. Because, the platinum resistance furnace being excluded for its prohibitive expense, a silicon carbide resistance furnace was unexpectedly found to serve only a short time, as heating resistors were attacked by fluorine-containing vapor evolved from the melt.

The first requisite was to design and construct a carbon granule resistance furnace having all the characteristics needed to meet the requirements of temperature control necessary for synthetic mica crystal growing, because this type of furnace is usually considered inadequate for precise temperature control and the furnace is apt to have a reducing atmosphere.

As a preliminary step in designing the furnace, characteristic data, such as electric power input per unit surface area of heating zone, specific resistance of carbon granule heating element, and power input per unit volume of carbon granule heating element, were investigated by a critical examination of several commercial furnaces of the carbon granule resistance type.

A furnace of 2 kg. melting capacity of this type was constructed, employing these characteristic data as a design basis, and used for medium scale experiments on synthetic mica crystal growing. Then based on a close examination of both calculated and observed characteristic data of this furnace, a furnace of carbon granule resistance type having a 30 kg. melting capacity was constructed for large-scale experiments on synthetic mica crystal growing. The furnace

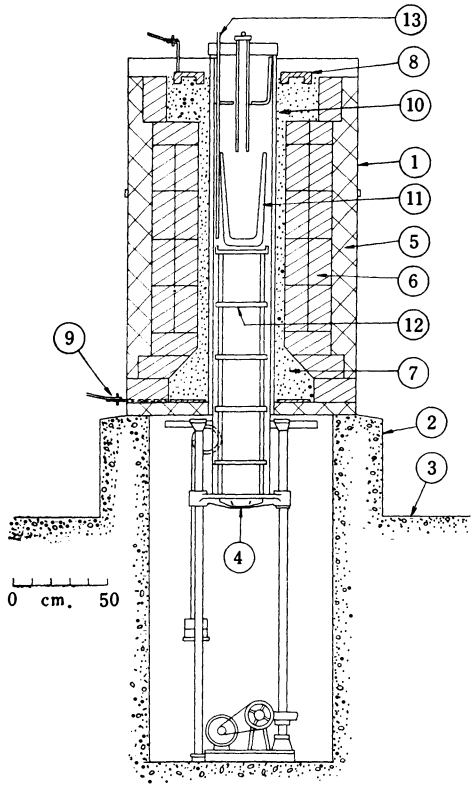


Fig. 1. Carbon granule resistance furnace.

1: Steel case 2: Concrete foundation 3: Floor 4: Motor-driven lift 5: Heat insulator 6: Refractories 7: Carbon granule resistance 8: Upper electrode 9: Lower electrode 10: Core tube 11: Clay crucible 12: Buffer plate 13: Thermocouple protection tube
Inner dia. of core tube 30 cm., Outer dia. of core tube 34 cm., Width of heating element 6 cm., Height of heating element L 110 cm., Sectional area of heating element A 154 cm^2, L/A 0.15_9 cm^{-1}, Volume of heating element V 82.9 l,
Specific resistance of carbon granule resistor
ρ 1.44 Ω cm. (room temp.)
0.50_6 Ω cm. (at 1675 °C),
Total resistance of heat element R
0.21_6 Ω (room temp.) 0.07_8 Ω (at 1675 °C),
Surface area of heating zone A_i 104 dm^2,
Power input per unit surface area of heating zone EI/A_i
0.09_6 kW./dm^2 (room temp.)
0.38_4 kW./dm^2 (1675 °C),
Total input EI
10 kW. (room temp.) 40 kW. (1675 °C),
Power input per unit volume of heating element EI/V
0.12_0 kW/l (room temp.) 0.46_2 (1675 °C),
Current I 215 amp. (room temp.)
720 amp. (1675 °C),
Terminal voltage E 46.5 V. (room temp.)
55.8 V. (1675 °C),

was remodeled several times in the process of the research and a sectional sketch of the furnace in its final form is given in Fig. 1, with its characteristic data.

The power input(P) for heating the furnace up to a certain temperature and the power input (P') for keeping the furnace at that temperature are related to temperature(θ), the effective surface area of heating zone(a), and the time(t) required for heating the furnace up to the temperature by the following equations[4]:

$$P = ca^{0.9}\theta^{1.55}t^{-0.5} \quad (1)$$

$$P' = c'a^{0.9}\theta^{1.55} \quad (2)$$

For this furnace, the values of c and c' were found to be 76 and 7.5 respectively. The power input for keeping the furnace at 1350°C was about 20 kW, the heat loss at the furnace side wall being about 65% of total input, and at the top and the bottom of the furnace, about 35%.

The furnace was harnessed with two voltage regulators in sequence, i.e. a motor-driven induction regulator, controlled by an electronic controller, was used with a saturable reactor combined with a magnetic amplifier and a D.C. voltage stabilizer. With this device, the temperature of the furnace could be controlled within ±2~3°C in the temperature range of 1300° and 1400°C by regulating the terminal voltage within ±0.05%.

A motor-driven lift was attached under the furnace, so that a crucible placed on the lift could be raised to a predetermined height in the furnace.

Raw Materials.—Raw materials, such as quartzite, alumina, magnesia, talc and potassium silicofluoride, were of commercial grade except the poassium carbonate which was of chemical grade. These materials were analysed and were found to have sufficient purity for the present purpose. All gradients of these raw materials were taken into account in calculating the mixing ratio of the raw materials for the preparation of batch mixtures.

Because the loss of fluorine due to decomposition of fluoride in the batch during heating is accelerated by the presence of water vapor[5], the mixture of calculated amounts of silica, magnesia, talc, alumina and potassium carbonate was first calcined at about 1000°C to expel water and carbon dioxide contained in the mixture and then the calculated amout of potassium silicofluroride was added.

Batches of POM 2 composition were used in most of the experiments of the present series because it was found, from results of experiments on the determination of crystallizing

4) T. Hayashi, *J. Electrochem. Soc. Japan*, (*Denki Kagaku*), **15**, 55 (1947).
5) a. V. Middel, PB 32546 (1947); b. R. A. Hatch and R. A. Humphrey, *Office of Naval Research* (1950), The Synthetic Mica Program 2; c. A. Van Valkenburg and R. G. Pike, *J. Res. Natl. Bur. Stand.*, **48**, 360 (1952); d. W. Eitel, R. A. Hatch and M. V. Denny, *J. Amer. Ceram. Soc.*, **36**, 341 (1953).

temperature of fluor-phlogopite[6] and also from results of a large number of crystal growing experiments[7], that this composition was one of the most favorable compositions for crystal growing. Two examples of batch mixtures are given in Table I.

TABLE I

	POM 2 composition %		Batch mixture I %	Batch mixture II %
SiO_2	40.58	Alumina	11.72	11.30
Al_2O_3	11.60	Talc	60.29	48.07
MgO	27.32	Magnesia	5.88	10.51
K_2O	10.79	Potassium silicofluoride	18.38	18.77
F	9.71	Potassium carbonate	3.73	2.35
		Quartzite		7.61

Experimental Procedure.—The evaporation of fluorine in the batch is highest in the course of reaction during heating above 1000°C and is comparably low in the molten state. Therefore, it was planned to melt the batch as quickly as possible to minimize the evaporation of fluorine.

At first it was our plan to follow the melting procedure in this way, viz: the crucible containing the batch is placed in a low position within the furnace (c.f. Fig. 1), heated up to about 1000°C, and then moved to a higher temperature region which had already been heated to 1400°C. After completion of the melting, the crucible is raised or lowered to ensure the required temperature difference between the top and the bottom of the crucible and then cooled slowly by controlling the power input of the furnace. The heating and cooling curve of the experiment carried out in this way is shown in Fig. 2.

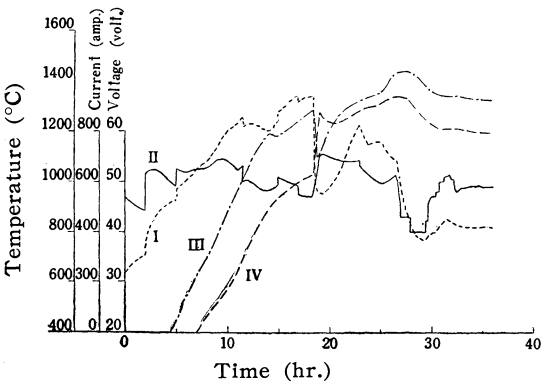


Fig. 2. Heating and cooling curve of experiment No. 1.
I: electric current
II: terminal voltage
III: temperature at the top of the crucible
IV: temperature at the bottom of the crucible

This procedure was abandoned because of operational difficulties, such as failure to get the crucible, buffer plates, thermocouple protecting tube and other furnace furnitures on the lift to raise smoothly, and the increase of undesired updraft of cold air during and after the raising operation. Most of the experiments were carried out in the following way. An unfilled crucible is first placed in the furnace; then the furnace is heated by passing electric current through the resistance element. After the temperature has reached about 1400°C, the crucible is charged several times with the batch until it is filled with the melt. Upon completing the charge, the crucible is covered with a lid, the temperature of the crucible is maintained above 1400°C for 5~6 hours to obtain the clear melt, and then cooled slowly by controlling the power input of the furnace.

Because well-sintered high-aluminous clay crucibles used in the earlier stages of this series of experiments were found to be less resistant to thermal shock, calcined but unsintered high-aluminous clay crucibles were used in later stages of the series. They were first heated in the furnace up to 1650°C to sinter. After the sintering, the temperature of the furnace was lowered to about 1400°C, the crucible was charged with the batch material and after completion of the melting, the melt was cooled slowly, as described above. The heating and cooling curve of a typical experiment of this series is given Fig. 3.

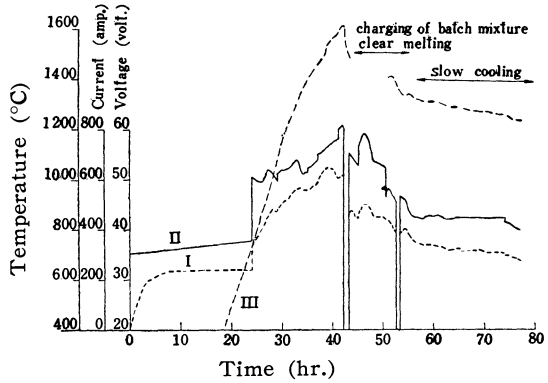


Fig. 3. Heating and cooling curve of experiment No. 13.
I: electric current
II: terminal voltage
III: temperature at the bottom of the crucible

Crucible Material. — Graphite and high-aluminous clay crucibles were used in the experiments because graphite was known not to be wetted and corroded by the melt, and a well-sintered alumina or high-aluminous clay body

6) T. Noda and S. Sugiyama, *J. Chem. Soc. Japan, Ind. Chem. Sec.*, (*Kogyo Kagaku Zasshi*), **46**, 1082 (1943); cf. T. Noda, *J. Amer. Ceram. Soc.*, **38**, 147 (1955).

7) T. Noda, *Industrial Physical Chemistry* (*Kogyo Butsuri Kagaku*), No. 1, 108 (1948); cf. T. Noda, This Bulletin, **23**, 40 (1950).

was found to resist the corrosion[8].

Graphite crucibles used were cylindrical in shape, 25 cm. in outer diameter, 50 cm. in height and 46 cm. in depth. The crucible was placed in a sagger made of fire clay, with grog powder packed in the intersticial space between the crucible and the sagger, thus preventing the oxidation of graphite. Buffer plates and cylinders made of fire clay were placed on and under the sagger in the furnace in order to decrease unfavorable convection current in the furnace.

Mica aggregates which crystallized in graphite crucibles were gray, minute carbon particles deposited in interstitial glass between mica crystals discoloring them. Crystals grown in graphite crucibles were generally small, and even when they grew large, they were mostly of mosaic nature.

It seems that one of the causes of small crystal formation is that the wall of graphite crucible is not wetted with the melt and consequently the wall does not initiate the nucleation of mica, so that the melt tends to become supercooled and forms a large number of nuclei when it starts to crystallize at a supercooled temperature.

In one experiment with graphite crucible, the molten state was maintained down to a temperature of about 150°C below the crystallizing temperature and small mica crystals rapidly formed around a steel wire when it was quickly dipped into the melt, while glass adhered to a wire quickly dipped into a melt in a high-aluminous clay crucible.

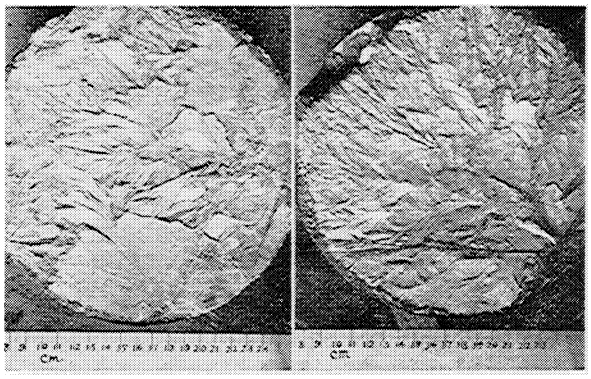
These observations suggest that the melt in graphite crucible was in a supercooled state or was in a state of easy crystallization with slight stimulus. Another suspected cause for small crystal formation was that a change in chemical composition of the melt was accelerated by the reducing atmosphere, but the change was not verified by chemical analysis. Also, the presence of minute carbon particles might stimulate the nucleation, although no positive assertion can be made.

High-aluminous clay crucibles used in the experiments were of alumina and silica, about 50% each. Crucibles sintered at about 1600°C or below were heavily corroded by the melt, so that the thickness of crucible wall decreased to about one-half of its original thickness, changing the chemical composition of the melt markedly and often leaking the melt completely.

Crucibles sintered at about 1650°C were found to withstand corrosion of the melt. The wall of clay crucibles initiated the nucleation of mica crystals, so that in the earlier stage of crystallization, large numbers of small crystals were formed in the vicinity of the wall. However, in the course of slow cooling, some of these crystals or crystal nuclei which were spontaneously formed in the melt grew to large single crystals of good quality. Mica aggregates crystallized in clay crucibles were slightly colored brown owing to iron contamination coming from crucible material. These aggregates contained a slightly larger amount of glass than those crystallized in the graphite crucible, but contained no carbon.

Result

Temperature Gradient in Melt and Oriented Growing of Crystals.—The formation of large crystals grown horizontally in the surface layer of melt was often observed when the temperature difference between the top and the bottom of the crucible was small during the crystallization period. Crystals grown in this way are shown in Fig. 4a. The crystal in the lower part of the figure measured 7 cm. by 12 cm. and was slightly curved. The evaporation of potassium and fluorine from the surface of the melt must have caused the crystallizing temperature of the surface layer of the melt to become higher and the early-formed crystals in this layer may have been in contact with the melt and may have had a longer time to grow than crystals formed later in the bulk of the melt. This may be the reason for small crystals growing at random in the bulk of the melt in spite of the formation of large crystals in the surface layer. Crystals grew upwards from the bottom of the crucible when the bottom temperature was sufficiently lower than the top temperature to cause the crystal nuclei to form originally at the bottom of the crucible. Edges of basal planes of vertically grown crystals can be seen on the surface of the crystalline mass shown in Fig. 4b. Rapid cooling causes new crystal nuclei to form in a slightly displaced direction from the orientation of



(a) (b)

Fig. 4. Top view of crystallized mass

8) T. Noda and M. Konno, *J. Ceram. Assoc. Japan*, (*Yogyo Kyokai Shi*), **57**, 25 (1949); T. Noda and K. Mori, ibid., **57**, 104 (1949); T. Noda and T. Ikenoue, Ibid., **57**, 163 (1949).

TABLE II
TEMPERATURE GRADIENT AND ORIENTED CRYSTAL GROWING

Experiment	Height of melt cm.	Temperature difference °C	Temperature gradient °C/cm.	Oriented growing
5	30	10	0.3	none
6	30	40～150	1.3～5	slight
8	30	115	3.8	slight
9	30	150	5	noticeable

the original crystals. This type of formation results in curved crystals of mosaic nature and under the most unfavorable conditions in dendritic crystals which are manifested by the branched edges of basal plane, as seen in Fig. 4b.

For the purpose of obtaining the relationship between the temperature gradient in the melt and the oriented growing of crystals, the temperature difference between the top and the bottom of the crucible and the qualitative degree of oriented crystal growing are given in Table II.

Although temperature readings with thermocouples placed at the top and bottom level of the crucible may not always indicate true temperatures of the melt at the same levels, the temperature gradient calculated by dividing the temperature difference by the depth of melt may, for practical purposes, be used for deduction of the experimental result. It can be seen from data of Table II that no oriented growth of crystals was observed when the temperature gradient was 1～2°C /cm. and that the temperature gradient of 4～5°C/cm. may be needed for oriented growth.

Rate of Growth and Quality of Crystal. —In one experiment in which the temperature at the bottom was higher than that at the top, a steel wire was frequently dipped into the charge contained in a graphite crucible to see the start of crystallization. When the temperature was 1230°C at the top and 1375°C at the bottom, the charge was in the molten state; when the temperature was 1205°C at the top and 1335°C at the bottom, a part of the charge began to solidify, the main part being a viscous melt; the crystallization was completed when the temperature was 1185°C at the top and 1325°C at the bottom. Because of the inverted temperature gradient, the convection may have occurred in the melt to equalize the temperature difference, so the real temperature of the upper layer of the melt may have been higher than the measured value. However, a considerable temperature gradient may still have been held, because crystals grew vertically downward from the upper layer. The crystallizing temperature of the melt was estimated to be about 1350°C, while in the above case the actual crystallization began between 1325°C and 1205°C.

This means that a great supercooling took place. It seems that a rapid rate of cooling may favor the occurrence of supercooling. Therefore the melt does not always begin to crystallize when the temperature of the melt is cooled to that corresponding to its crystallizing temperature, and the rate of cooling of the melt, calculated by dividing temperature-drop in the slow cooling period by the duration of slow cooling, does not necessarily correspond to the true rate of cooling during the crystallization. However, in the course of slow cooling, a slow-down of the cooling rate due to the generation of the heat of crystallization* was generally observed, and it can be assumed that the period of the slow-down of the cooling rate corresponds to the duration of crystallization. Therefore the rate of crystal growth of basal plane can be calculated by dividing the size of the largest crystal found in the solidified mass by the duration of crystallization, assuming that the crystal had grown throughout the duration of crystallization, although the solidified mass in the crucible was usually composed of a large number of crystals of various sizes. The rate of crystal growth thus calculated and the quality of crystals produced are given in Table III.

In experiment No. 13, using a well-sintered high-aluminous clay crucible, several clear single crystals measuring about 5 cm. by 5 cm. could be split from the solidified mass, although the yield of crystals of this size was very small. Two of these crystals are shown in Fig. 5. In this experiment, the rate of cooling was 2～5°C/hr.. The quality of these crystals is designated in Table III as "excellent". Crystals which are not perfect

* 74±3 cal./g., N. Daimon, T. Horibe, K. Mukumoto and T. Noda, *J. Chem. Soc. Japan, Ind. Chem. Sec.*, (*Kogyo Kagaku Zasshi*), **55**, 762 (1952).

TABLE III
RATE OF CRYSTAL GROWTH AND QUALITY OF CRYSTAL

Exp. No.	Crucible used	Crystallization time hr.	Cooling rate °C/hr.	Largest crystal cm.	Crystal growth rate mm./min.	Quality of crystal
5	Graphite	21	2～ 5	10	0.08	good
6	〃	17	3～20	13	0.13	poor
8	〃	2	rapid cooling	5	0.42	very poor
9	〃	2	15～20	3	0.25	poor
13	High aluminous clay	13	2～ 5	5	0.06	excellent

TABLE IV
CHEMICAL COMPOSITION OF BATCHES AND PRODUCTS

Exp. No.		MgO %	SiO_2 %	SiO_2 %mod*	SiO_2 Δ%**	Al_2O_3 %	Al_2O_3 %mod*	Al_2O_3 Δ%**	K_2O %	K_2O %mod*	K_2O Δ%**	F %	F %mod*	F Δ%**
11	batch	27.64	42.92			12.16			11.43			9.93		
	product	27.03	43.74	44.74	+1.84	13.61	13.92	+1.76	10.42	10.65	−0.78	9.33	9.54	−0.39
12	batch	26.84	41.07			12.58			11.26			9.46		
	product	26.75	43.79	43.92	+2.85	14.98	15.02	+2.50	9.71	9.74	−1.52	8.09	8.11	−1.35
13	batch	27.35	39.19			15.43			11.07			9.50		
	product	24.14	43.02	48.74	+9.55	17.21	19.57	+4.41	10.65	11.96	+0.90	8.11	9.19	−0.31

* %mod = (% in product) × (MgO % in batch) / (MgO % in product)
** Δ% = (%mod) − (% in batch)

single ones, but are of mosaic nature are designated as "poor" in quality. When they were split from the solidified mass, these crystals separated into many small ones. Crystals grown at a rate higher than 0.1 mm./min. were always imperfect mosaic crystals. It can be deduced then that in order to grow good single crystals which can be split from the solidified mass, the rate of growth should be less than one-tenth of a millimeter per minute.

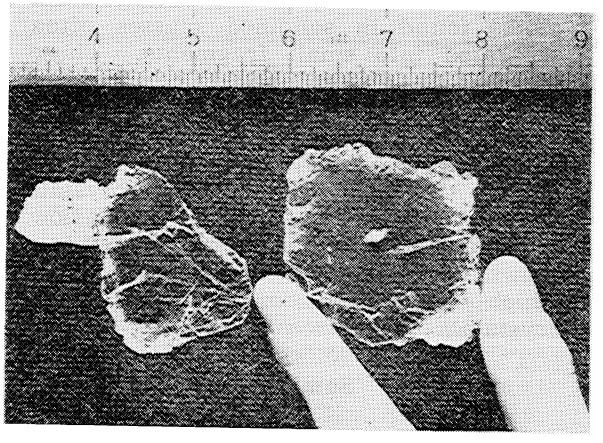


Fig. 5. Single crystals of fluor-phlogopite.

Change in Chemical Composition of Charge during Process.—Chemical compositions of batch mixtures and solidified products of three experiments are given in Table IV.

We used in experiment No. 11, a slightly-sintered high-aluminous clay crucible for melting for a relatively short period, in experiment No. 12, a slightly-sintered high-aluminous clay crucible for a long period and, in experiment No. 13, a well-sintered high aluminous clay crucible for a long period. Changes in individual components of the charge during the melting were calculated on the assumption that the content of magnesia was kept constant because no magnesia came from the crucible and the evaporation of magnesium fluoride was negligible.

In experiment No. 11 where the short period melting and the rapid cooling were used, small crystals resulted without remarkable change in the chemical composition of the melt. In experiment No. 12, the clay crucible was heavily corroded. This resulted in a considerable increase in content of alumina and silica. The loss of fluorine and potassium due to the evaporation was also remarkable. The great shift of the chemical composition and especially a remarkable deficit of fluorine in the melt, may be to blame for the formation of small crystals. The well-sintered clay crucible used in experiment No. 13 strongly resisted the corrosion of melt. The slow-cooling procedure was carried out as planned and the solidified mass contained many large crystals, as described above. The chemical composition

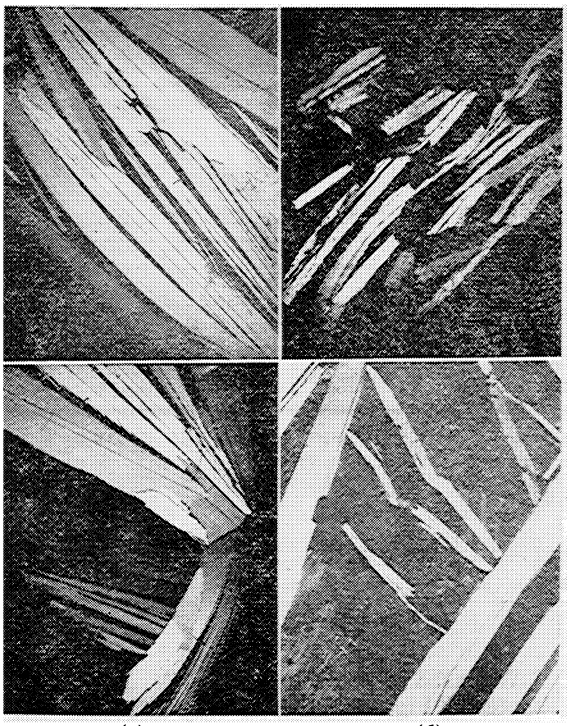


Fig. 6. Microphotograph of fluor-phlogopite (1).

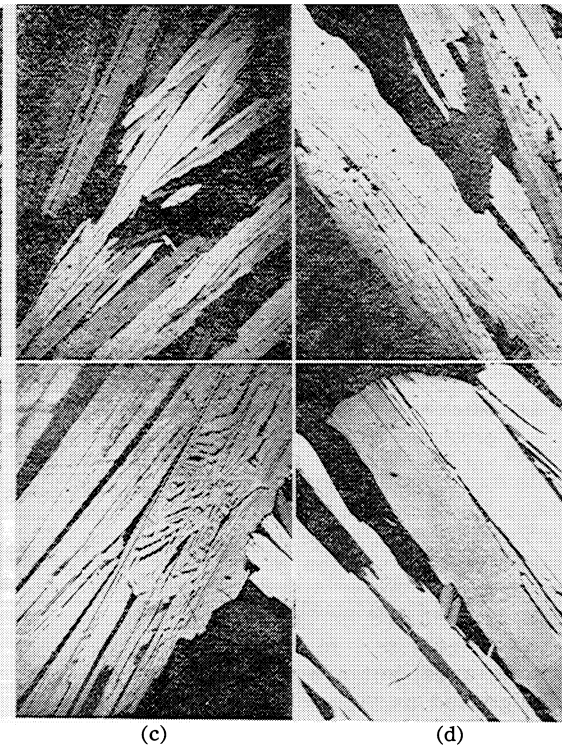


Fig. 7. Microphotograph of fluor-phlogopite (2).

of the product of experiment No. 13, given in Table IV, shows a remarkable increase of silica and alumina content, a slight increase of potassium and a slight decrease of fluorine. Because the excessive potassium of the batch usually concentrates in the glassy part of solidified mass, the analysed sample may have contained a slightly larger amount of glass than average. However, it seems to be essential that in order to obtain good large crystals, the fluorine and potassium content of the melt must not be deficient.

Microscopic Observation.—Curved crystals were often found in solidified masses. Some crystals bent 90° or more. A slightly curved crystal is shown in Fig. 6a. The curved crystals may have been bent by crystals growing from other directions. The curved crystals retain their form after they have been split from the mass. Sometimes the growing pressure of the other crystals was so great that the bent crystal was deformed to become a mosaic crystal, as shown in Fig. 6c. In Fig. 6b there is another example of imperfect curved crystals. Small crystals grown in interstices between large crystals perpendicular to the basal plane of large crystals were bent and ruptured by the pressure of contraction action on the basal planes of large crystals while the temperature was cooling (Fig. 6d).

As was previously described, large basal plates found in solidified masses often separated into small fragments. These plates were almost entirely composed of small crystals grown in the same direction or slightly inclined toward each other or were imperfect skeleton crystals, as shown in Fig. 7a, b, and c. All these crystals were formed by rapid cooling. With slow cooling, we obtained perfect crystals grown parallel to each other (Fig. 7d), which when split made clear single crystals.

Summary

Synthetic mica crystal growing experiments were carried out with a graphite crucible and a well-sintered high-aluminous clay crucible in a carbon granule resistance furnace of 30 kg. melting capacity, specially designed for this purpose. In experiments with a graphite crucible, the

melt often became supercooled and crystallized rapidly, to result in small crystals once crystallization started at the supercooled temperature. With a clay crucible, several experiments failed because of cracks in the crucible or because of corrosion of the crucible by the melt. Only with a well-sintered high-aluminous clay crucible and under the condition of small loss of fluorine and potassium in the melt were perfect large single crystals measuring about 5 cm. by 5 cm. formed even at a mean cooling rate of 2~5°C/hr. in the range of 1360°C to 1300°C. The yield of large single crystals was very small, doubtless because only the few crystals which had formed earlier had enough time and space to be in contact with the melt and thus to grow to large size. If the growing crystals come into contact or collide with other growing crystals, the crystals are either prevented from growing further or become strained or bent. Consequently, for crystals to grow to a large size, they must be in contact with the melt for a long time without being disturbed by other crystals. This can be done when crystals grow in the same direction. It was found that the temperature gradient of 4~5°C/cm. was necessary for crystals to grow in one direction.

Among many factors affecting the growth of crystals, the rate of cooling should be controlled to secure the rate of crystal growth at less than 0.06 mm./min. in order to grow perfect and flawless single crystals of mica.

Needless to say, a sufficient volume of melt is necessary to grow large crystals, i. e. a large quantity of melt gives more opportunity for large crystals to grow. Crystals measuring 5 cm. by 5 cm. were never obtained before the 30 kg. melting experiments were carried out.

This research was carried out during the period from 1946 to 1954 by the cooperation of Messrs. K. Tamura, S. Kanatsu, I. Tate, M. Horiguchi, K. Inagaki, E. Kato, D. Ishii and K. Hata with the aid of the Scientific Research and Development Fund of the Ministry of Education, the Asahi Science Promotion Fund and a special aid by the Electocommunication Laboratory, the Japan Telegram and Telephone Corporation.

Department of Applied Chemistry
Faculty of Engineering
Nagoya University
Chikusa-ku, Nagoya

Raney Nickel and Platinized Rany Nickel with Higher Catalytic Activities

By Shigeo NISHIMURA

(Received July 8, 1958)

Preparation of Raney Nickel Catalysts. —In a previous paper[1], it was reported that a Raney nickel catalyst with a higher activity can be obtained by adding aqueous sodium hydroxide in portions to the suspension of a Raney alloy in water. To obtain a catalyst of high activity the usual methods of developing the Raney alloy, e. g. the method of Adkins and Billica[2], seemed unfavorable for the following reasons.

a) The reaction of the Raney alloy with sodium hydroxide in an aqueous solution is strongly exothermic and it is very difficult to put the alloy into the solution within a short time. Therefore, a catalyst developed uniformly can not be obtained, because the portion of the alloy added at the beginning is treated with the most concentrated sodium hydroxide for the longest time and that added last with the most dilute sodium hydroxide for the shortest time.

The lack of uniformity can not be neglected in such a catalyst as W-7 of Adkins and Billica[2], which is prepared with a

1) S. Nishimura and Y. Urushibara, This Bulletin, **30**, 199 (1957).
2) H. Adkins and H. R. Billica, *J. Am. Chem. Soc.*, **70**, 695 (1948).

comparatively small quantity of sodium hydroxide and contains a considerable amount of aluminum, or in a catalyst prepared from an alloy containing less nickel.

b) In the preparation of Urushibara nickel catalysts[3,4], which are obtained by treating finely divided nickel, precipitated from a nickel chloride solution by zinc dust, with aqueous caustic alkali or with acetic or propionic acid, it proved harmful to the activity of the catalysts to use a concentrated solution of the developing reagent and mild conditions are favorable so far as the time for the preparation is tolerable. It suggests that use of a strong alkali may be unfavorable also in the preparation of the Raney nickel catalyst.

From this point of view, the author attempted with success to prepare Raney nickel catalyst with a higher activity by adding a sodium hydroxide solution in portions to the suspension of a Raney alloy in water. In the course of this study, it was found that the Raney alloy, after being partly leached with a very dilute sodium hydroxide solution, reacts with, and is developed by, water, forming a large quantity of white aluminum hydroxide, which was confirmed to be bayerite by the X-ray diffraction analysis[5]. After the reaction with water has subsided and the alloy has been covered with grey films of bayerite, the product reacts only very mildly with a concentrated sodium hydroxide solution, which can be added at one time without arousing a violent reaction. Then the digestion is continued to remove the bayerite and to complete the development.

The Raney nickel catalyst prepared in this way (denoted as T-4 when prepared from an alloy containing 40% of nickel) is more active than the W-7 catalyst of Adkins and Billica. The catalyst prepared under the same conditions as W-7 except that a larger quantity of the sodium hydroxide solution of the same concentration was used (denoted as W-7′) was less active than W-7.

It suggests that the W-7′ catalyst was overdeveloped or partly deactivated with the strong alkali in the course of the development. Table I shows the activities of these three catalysts in the hydrogenation of various organic compounds under the ordinary pressure and at 25°C.

TABLE I

TIME (min.) FOR THE HYDROGENATION OF ORGANIC COMPOUNDS WITH RANEY NICKEL CATALYSTS UNDER THE ORDINARY PRESSURE AND AT 25°C

Compound	Amount (g.)	Hydrogen absorbed (mole/mole)	Catalyst T-4	W-7	W-7′
Cyclohexanone	3.93	1	17	21	24
Acetophenone	4.81	1	34	40	50
Cyclohexene	3.29	1	7	9	9
Quinoline	2.58	2	83	84	
Benzonitrile	2.06	2	49	76	80
Cyclohexanone oxime	2.26	2	92	126	

a) The catalyst was prepared from 2 g. of a Raney alloy containing 40% of nickel each time just before the hydrogenation.
b) 20 cc. of 95% ethanol was used as the solvent.

From some apparently similar methods in the literature[6-9] the present method differs in the fact that the Raney alloy is developed mostly with water, but not with an alkali, forming a large quantity of bayerite, which prevents the catalyst from direct contact with a strong alkali and facilitates the later addition of the main portion of the sodium hydroxide solution. The procedure to prepare the T-4 catalyst is given in details in the experimental part.

Preparation of the Platinized Raney Nickel Catalysts. — In many hydrogenations it has been shown that the Raney nickel catalyst is greatly promoted by treatment with chloroplatinic acid. Delépine and Horeau[10,11] showed that a Raney nickel platinized with chloroplatinic acid was effective for the hydrogenation of carbonyl compounds with addition of a little aqueous sodium hydroxide. Lieber, Smith and their co-workers[12-17] showed

3) Y. Urushibara and S. Nishimura, This Bulletin, **27**, 480 (1954).
4) Y. Urushibara, S. Nishimura and H. Uehara, ibid., **28**, 466 (1955).
5) A small amount of bayerite is also formed in the preparation of the W-7 Raney nickel catalyst. cf. G. W. Watt and S. G. Parker, *J. Am. Chem. Soc.*, **74**, 1103 (1952).
6) F. Fischer and K. Meyer, *Ber.*, **67**, 253 (1934).
7) E. B. Maxted and R. A. Titt, *J. Soc. Chem. Ind.*, **57**, 197 (1938).
8) J. Yasumura, *Science and Ind.*, (*Kagaku to Kogyo*), **22**, 21 (1948).
9) R. Cornubert and J. Phélisse, *Bull. soc. chim. France*, [5], **19**, 399 (1952).
10) M. Delépine and A. Horeau, *Compt. rend.*, **201**, 1301 (1935); **202**, 995 (1936).
11) M. Delépine and A. Horeau, *Bull. soc. chim.* France, [5], **4**, 31 (1937).
12) E. Lieber and G. B. L. Smith, *J. Am. Chem. Soc.*, **58**, 1417 (1936).
13) J. R. Reasenberg, E. Lieber and G. B. L. Smith, ibid., **61**, 384 (1939).

that treatment with chloroplatinic acid or with chloroplatinic acid and triethylamine was also effective for many hydrogenations. These methods agree in the fact that the Raney nickel is treated with chloroplatinic acid, and may supposedly have the following disadvantages:

a) The activity of nickel itself may be partly lost on treatment with chloroplatinic acid and the nickel ion then formed may be a catalytic poison[12].

b) The chloride ion and/or the hydrogen ion may be also catalytic poisons[18] and it is not certain if they can be completely removed by mere addition of sodium hydroxide[19] or triethylamine.

Recently Blance and Gibson[20] prepared a platinized Raney nickel from a nickel-aluminum alloy containing 2% of platinum but such an alloy has to be made specially and may not always be readily available.

The present author improved the preparation of the platinized Raney nickel by platinizing and simultaneously leaching the Raney alloy: A chloroplatinic acid solution made alkaline with a little sodium hydroxide is added to the suspension of a Raney alloy in water. The partly leached and platinized Raney alloy reacts with water, forming a large quantity of bayerite, and then can be treated in the same way as in the preparation of the T-4 catalyst. The details of the procedure for the preparation are given in the experimental part.

The platinized T-4 catalyst prepared in this way is more active than the T-4 catalyst platinized by the method of Delépine and Horeau. Table II shows the activities of these two catalysts in the hydrogenation of some organic compounds, T-4-Pt denoting T-4 platinized by the present method and T-4-Pt (D. H.) T-4 platinized by the method of Delépine and Horeau.

TABLE II

TIME (min.) FOR THE HYDROGENATION OF ORGANIC COMPOUNDS WITH THE PLATINIZED RANEY NICKEL CATALYSTS UNDER THE ORDINARY PRESSURE AND AT 25°C

Compound	Amount (g.)	Hydrogen absorbed (mole/mole)	Catalyst	
			T-4-Pt	T-4-Pt (D.H.)
Cyclohexanone	3.93	1	10	13
Acetophenone	4.81	1	13	17
Quinoline	2.58	2	27	38
Benzonitrile	2.06	2	11	14
Cyclohexanone oxime	2.26	2	17	19

a) The catalyst was prepared from 2 g. of a Raney alloy containing 40% of nickel and 50 mg. of chloroplatinic acid, $H_2PtCl_6 \cdot 6H_2O$.

b) 20 cc. of 95% ethanol was used as the solvent.

Experimental

Preparation of T-4 Catalyst.—To a mixture of 2 g. of a Raney nickel-aluminum alloy containing 40% of nickel[21] and 10 cc. of water, contained in a 30 cc. Erlenmeyer flask with a stirrer and heated in a water bath of 50°C, 0.4 cc. of 20% aqueous sodium hydroxide is added with vigorous stirring, care being taken not to let the reaction become violent, and the mixture is stirred. In about one hour, the partly leached Raney alloy begins to react with water and turns grey in color, and the reaction almost subsides in one hour and a half. Then 6 cc. of 40% aqueous sodium hydroxide is added at one time with continued stirring.

The digestion is continued for one additional hour at 50°C with good stirring, until the upper layer becomes snow-white. The catalyst is washed by stirring and decanting four times with 15 cc. of water of 50°C and then three times with the same volume of ethanol. A specimen of the T-4 catalyst thus prepared contained 13.3% of aluminum and a little aluminum hydroxide.

Preparation of W-7 and W-7′ Catalysts.—W-7 catalyst was prepared from 2 g. of the alloy and 12 cc. of a 20 per cent sodium hydroxide solution exactly as described by Adkins and Billica[2] except that the catalyst was washed as described above for the T-4 catalyst. W-7′ catalyst was prepared from 2 g. of the alloy and 24 cc. of 20 per cent aqueous sodium hydroxide. The W-7 and W-7′ catalysts thus prepared contained 13.3 per cent and 12.5 per cent of aluminum, respectively.

Preparation of Platinized T-4 Catalyst.—To a suspension of 2 g. of the Raney alloy in 10 cc. of water, 50 mg. of chloroplatinic acid, $H_2PtCl_6 \cdot 6H_2O$, dissolved in 2 cc. of water made alkaline with 0.4 cc. of 20 per cent aqueous sodium hydroxide, was added with vigorous stirring in a water bath of 50°C.

The procedure hereafter is exactly the same as described above for the T-4 catalyst. Incomplete digestion, which is indicated by the grey

14) S. S. Scholnik, J. R.Reasenberg, E. Lieber and G. B. L. Smith, ibid., **63**, 1192 (1941).
15) D. R. Levering and E. Lieber, ibid., **71**, 1515 (1949).
16) D. R. Levering, F. L. Morritz and E. Lieber, ibid., **72**, 1190 (1950).
17) G. S. Samuelsen, V. L. Garik and G. B. L. Smith, ibid., **72**, 3872 (1950).
18) J. N. Pattison and Ed. F. Degering, *J. Am. Chem. Soc.*, **73**, 611 (1951).
19) S. Watanabe, *Science and Ind.* (*Kagaku to Kogyo*), **31**, 195 (1957).
20) R. B. Blance and D. T. Gibson, *J. Chem. Soc.*, **1954**, 2487.
21) A 50-50% alloy can be used with a somewhat lower activity of the resulting catalyst.

color of the upper layer, does not develop the activating effect by platinum.

Platinization of the T-4 Catalyst by the Method of Delépine and Horeau.—To a suspension of the T-4 catalyst, prepared from 2 g. of the Raney alloy, in 10 cc. of water, 50 mg. of chloroplatinic acid, dissolved in 2 cc. of water, is added with vigorous stirring in a water bath of 50°C. In a few minutes, when the reaction is complete, a little sodium hydroxide solution is added with stirring, and then the catalyst is washed.

Hydrogenation. — After the catalyst, suspended in 15 cc. of ethanol, was saturated with hydrogen at 25°C, the substance dissolved in 5 cc. of ethanol was added and the mixture was shaken with hydrogen at 400—500 oscillations per minute.

Identification of Bayerite.—The snow-white precipitate in the upper layer formed during the digestion with alkali was collected by centrifuging and analyzed by means of the X-ray diffraction.

The diffraction pattern shown in Fig. 1 shows that the precipitate is bayerite, one form of aluminum trihydroxide. But the bayerite is different from that formed in the reaction of the alloy with water as shown in Fig. 2. According to Fricke[22], the former is bayerite a and the latter bayerite b.

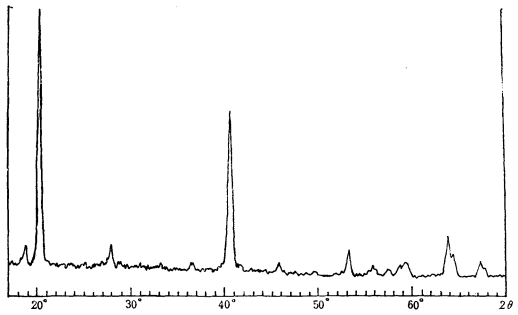


Fig. 1. Diffraction pattern of the precipitate formed during the digestion with alkali.

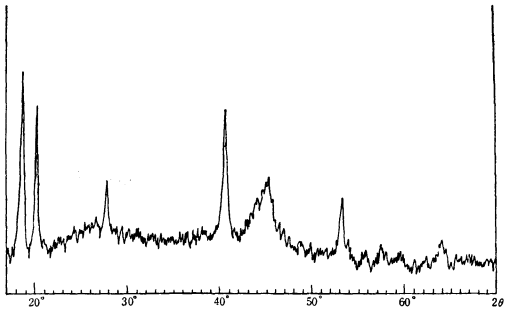


Fig. 2. Diffraction pattern of Raney alloy after the reaction with water.

The patterns were obtained by an X-ray diffractometer with Ni-filtered Cu-K_α radiation.

The author wishes to express his hearty thanks to Professor Yoshiyuki Urushibara for his kind guidance and valuable suggestion given throughout this work. The author is also indebted to Dr. Hiroshi Takahashi and Mr. Haruo Kuroda for their kind help in the measurement of the X-ray diffraction. This study has been supported by the Scientific Research Grant of the Ministry of Education.

Department of Chemistry
Faculty of Science
The University of Tokyo
Hongo, Tokyo

22) R. Fricke, *Z. anorg. allg. Chem.*, **175**, 249 (1928)

The Density of the Polycyclic Aromatic Compounds

By Hiroo INOKUCHI and Masayuki NAKAGAKI

(Received July 16, 1958)

It is already generally known that the physico-chemical properties of the polycyclic aromatic compounds are correlated closely to the number of carbon atoms comprised in the molecule. For instance, it has been found that the inner heat of sublimation of these hydrocarbons possesses a linear function of the number of carbon atoms with an average value of 1.5 kcal./mol. per carbon atom[1] and also that the increment of the number of benzene rings in the molecule of this series shows the increase of the electrical conductivity of these compounds[2].

These compounds belong to typical molecular crystal, in which molecules interact with each other by the van der Waals force. Lattice energies of crystals built up of homopolar molecules such as nitrogen or carbondioxide were first calculated by London[3]. The main object of this paper is to apply similar calculations of computing the density of the polycyclic aromatic compounds in comparison with the number of carbon atoms.

Experimental Procedures

The measurements of density for the polycyclic aromatic compounds were carried out at room temperature by means of the pycnometer as shown in Fig. 1. The total volume of this vessel, made of glass tubing of 15 mm. in diameter, was approximately 5 cc. The addition of the ground-on caps to cover the entrances of the vessel was helpful to prevent the evaporation of the pycnometer liquid.

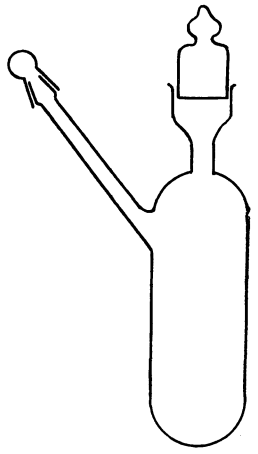


Fig. 1. The pycnometer

Since the solubility of violanthrene and *iso*-violanthrene in organic solvents is negligiblly small at room temperature, ethanol can be used as the pycnometer liquid. The solubilities of anthanthrene and naphthacene were, however, fairly high in the alcohol. Therefore, distilled water mixed with a very small amount of a surface-active agent was employed as the pycnometer liquid for these compounds.

Through a preliminary experiment, it was recognized that the adherence of bubbles of air on a surface of an organic compound was a serious reason for the fluctuation of the observed density values. In order to remove as much of the air as possible, the vessel containing the specimen and liquid had to be attached to a water-pump and to be kept under a reduced pressure.

The polycyclic aromatic compounds used in this experiment were purified thoroughly by the methods already described in previous reports[2].

Results and Discussion

The potential energy of a molecule as

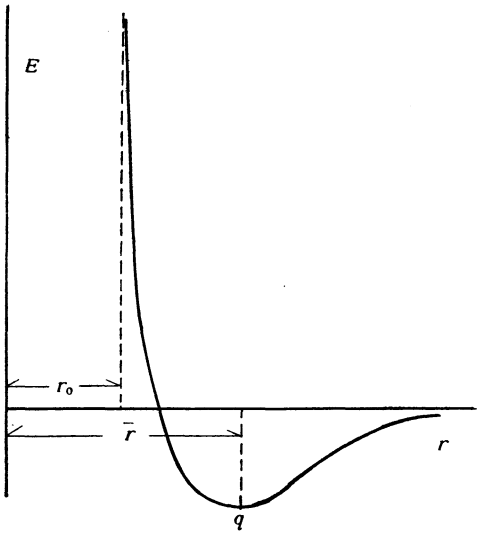


Fig. 2. The potential energy curve for intermolecular force.

1) H. Inokuchi, S. Shiba, T. Handa and H. Akamatu, This Bulletin, **25**, 299 (1952).
2) H. Akamatu and H. Inokuchi, *J. Chem. Phys.*, **18**, 810 (1950); **20**, 1481 (1952). H. Inokuchi, This Bulletin, **24**, 222 (1951); **25**, 28 (1952)
3) F. London, *Z. physik. Chem.*, **B11-12**, 222 (1930-1).

a function of an intermolecular distance, r, is generally expressed by a curve as shown in Fig. 2. This curve is made up of the sum of the dispersion and the repulsive force, the latter arising when the clouds of valence electrons of two molecules interpenetrate each other. These two forces are equal at the minimum point, q, of the potential energy curve. In addition, a strong repulsion due to the interpenetration of inner electron shells is assumed when the intermolecular distance is smaller than r_0. When the molecular weight of the hydrocarbon is very large, that is to say, the interaction between these molecules is very strong, it is reasonable to assume that the equilibrium distance between two molecules, $\bar{r}$, is nearly equal to r_0.

The molecule of the aromatic compound, a member of the series from benzene to graphite, has a plate-like shape, and is packed to make the molecules parallel to one another. Therefore, we can introduce the theory that r_0 corresponds to the interlayer spacing of graphite, 3.35Å, assuming that graphite is a kind of polycyclic aromatic compound having infinitely large molecular weight.

In calculating the sum of the dispersion forces and repulsive forces of atoms in the molecule, the contribution of hydrogen atoms may be neglected. Hence, the interation energy per one molecule $E(r)$ is expressed as,

$$E(r)=\frac{-AN^2}{(r-r_0)^6}+\frac{BN}{(r-r_0)^n} \tag{1}$$

in which N is the number of carbon atoms included in that molecule and A and B are constants.

At the equilibrium condition,

$$\left(\frac{\partial E(r)}{\partial r}\right)_{r=\bar{r}}=0=\frac{6AN^2}{(\bar{r}-r_0)^7}-\frac{nBN}{(\bar{r}-r_0)^{n+1}} \tag{2}$$

Therefore, $(\bar{r}-r_0)$ is represented as

$$(\bar{r}-r_0)^{n-6}=\frac{nB}{6A}\times\frac{1}{N} \tag{3}$$

The density of the aromatic compounds ρ is related to $\bar{r}$ by the equation

$$M/\rho=N_A S\bar{r} \tag{4}$$

in which M and S are the molecular weight and the area of one molecule of the aromatic hydrocarbon respectively, and N_A is Avogadro's number.

Since M and S may be proportional approximately to N, the number of carbon atoms in that molecule, Equation 4 can be rewritten in the form

$$\bar{r}=C/\rho \qquad C=M/N_A S=\text{constant} \tag{5}$$

and also

$$r_0=C/\rho_\infty \tag{6}$$

Equation 3, therefore, becomes

$$\left(\frac{1}{\rho}-\frac{1}{\rho_\infty}\right)^{n-6}=\left(\frac{nB}{6AC^{n-6}}\right)\frac{1}{N} \tag{7}$$

This equation may be reduced to

$$\log\left(\frac{1}{\rho}-\frac{1}{\rho_\infty}\right)=-\frac{1}{n-6}\log N+\log Q \tag{8}$$

Here,

$$Q=nB/6AC^{n-6} \tag{9}$$

When we use the following numerical values

$\rho_\infty=2.26$ (density of graphite)

n=8

$B/AC^2=0.99$

in the above equation,

TABLE I
THE DENSITY OF POLYCYCLIC AROMATIC HYDROCARBONS

Compound	N	Density		Reference
		Observed	Calculated	
Benzene	6	1.04	1.02	
Naphthalene	10	1.15_2	1.16	4)
Anthracene	14	1.25	1.26	5)
Pyrene	16	1.27	1.29_5	6)
Naphthacene	18	1.33	1.33	
Tri-phenylene	18	1.3	1.33	7)
Perylene	20	1.35	1.36	
Benzperylene	22	1.35	1.38	8)
Anthanthrene	22	1.39	1.38	
Coronene	24	1.37_7	1.41	9)
Mesonaphtho-dianthrene	28	1.46	1.45	
Pyranthrene	30	1.47_5	1.46	
Ovalene	32	1.47_7	1.48	10)
Violanthrene	34	1.49	1.50	
Iso-violanthrene	34	1.50_5	1.50	
Circuman-thracene	40	1.52	1.54	I1)
Graphite	∞	2.26	(2.26)	

4) J. M. Robertson, *Proc. Roy. Soc.*, **A142**, 674 (1933).
5) J. M. Robertson, ibid., **A140**, 79 (1932).
6) J. M. Robertson and J. G. White, *J. Chem. Soc.*, **1947**, 358.
7) A. Klug, *Acta Cryst.*, **3**, 165 (1950).
8) J. G. White, *J. Chem. Soc.*, **1948**, 1398.
9) J. W. Robertson et al., *Proc. Roy. Soc.*, **A220**, 311 (1953).
10) D. M. Donaldson and J. M. Robertson, ibid., **A207**, 101 (1951).
11) E. Clar, W. Kelly, J. M. Robertson and M. G. Rossman, *J. Chem. Soc.*, **1956**, 3878.

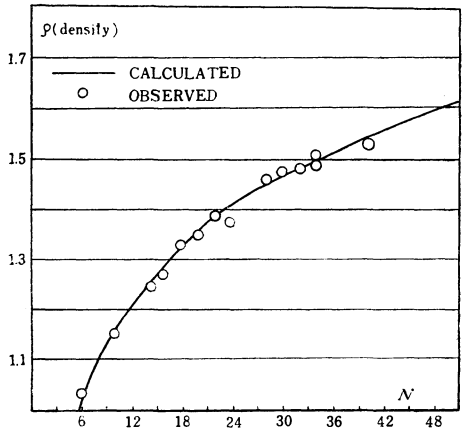


Fig. 3. The density of the polycyclic aromatic compounds.

$$\log\left(\frac{1}{\rho}-\frac{1}{2.26}\right)=-\frac{1}{2}\log N+0.120 \quad (10)$$

can be obtained.

The computed and also observed values of ρ are given in Table I and Fig. 3 for several polycyclic aromatic compounds. The agreement of these values in the table is satisfactory.

Table II
THE DENSITY OF CARBON BLACKS.

Specimen	L_a (Å)[12]	N	Density	
			observed	calculated
Royal Spectra	13.1	66	1.68	1.66
Philblack E	12.0	55	1.76	1.63
Peerless II-A	14.2	77	1.82	1.69
Tokyo Gas Carbon	13.4	69	1.68	1.67
Statex B	16.9	111	1.81	1.76
Philblack O	13.3	67	1.81	1.67

Applying Equation 10 to calculate the density of carbon blacks, we have the result in Table II. By means of the X-ray diffraction analysis, the dimension of a condensed polycyclic aromatic layer of the carbon, L_a, was calculated from the breadth of (10) reflection at half of the maximum intensity, applying Warren's formula for the random layer lattice. The area occupied by a carbon atom in the layer, may be assumed an equilateral triangle, for which b has the value of $a \sin 60°$, as illustrated in Fig. 4. Here, a possesses the distance of C−C bonding, 1.41Å. Thus, the number of carbon atoms in the layer is expressed

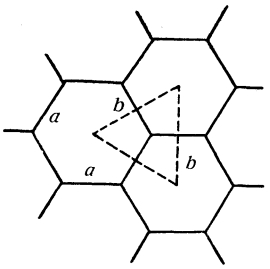


Fig. 4. The area occupied by a carbon atom in graphite layer.

$$N=4L_a^2/3\sqrt{3}\,a^2 \quad (11)$$

On the basis of this table the authors are inclined to think that they have derived a relation between the density and the molecular weight of carbon blacks.

Summary

The density (ρ) of the polycyclic aromatic hydrocarbons, from benzene (C_6H_6) to circumanthracene ($C_{40}H_{16}$), are correlated closely to the number of carbon atoms (N) included in the molecule. We may be expressed the relation as $\log(1/\rho-1/\rho_\infty) = -(1/2)\log N+0.120$, in which ρ_∞ is the density of graphite, 2.26. The agreement of the computed values with the observed results is satisfactory. A trial to apply the equation to calculate the density of carbons is made with some success.

The authors express hearty thanks to Professor H. Akamatu for his kind direction in this work. The cost of this research has been defrayed from the Scientific Research Encouragement Grant from the Ministry of Education to which the authors' thanks are due.

Department of Chemistry
Faculty of Science
The University of Tokyo
Hongo, Tokyo

12) H. Kuroda, *J. Colloid Sci.*, **12**, 496 (1957).

Formation and Aging of Precipitates. X. An Electron Micro-Diffraction Study on Crystal Habit of Barium Sulfate Precipitates*

By Kazuyoshi TAKIYAMA

(Received July 19, 1958)

The shapes of precipitated particles of sparingly soluble salts are usually classified into groups of perfect crystals having simple forms and dendrites having irregular forms. The author has previously reported the relationship between the condition of precipitation and the shape and size of precipitated particles of barium sulfate, by the direct mixing of reagents[1]. The rectangular perfect crystals were prepared from a solution below about 0.0005 M of initial concentration of barium sulfate, and the spindle-shaped dendrites having rugged edges were prepared in a range of initial concentration from about 0.001 to 0.2 M. Above 0.5 M, the precipitate was jelly-like at the beginning, but it changed gradually to the crystalline precipitate. Fischer[2] also studied the morphology of barium sulfate precipitates by electron microscopy and reported that the crystals formed as elevated temperature were somewhat more perfect than those formed at room temperature, and that the fairly perfect crystals were formed when very dilute solutions of reagents were mixed slowly by ionic diffusion through a thin membrane.

An attempt has been made in the present investigation to employ the electron micro-diffraction method for clarifying the crystal habit of barium sulfate.

Sample.—Solutions of 0.001 and 0.1 M barium chloride were placed in small beakers, which were kept at room temperature and at 80°C. Small thin films of Formvar were then floated on the surface of the solutions, and a drop of 0.001 M sulfuric acid was placed on each film. A few minutes were allowed for the reactant ions to diffuse slowly through the thin film and form the precipitates. Then the films with the drops were removed with the aid of a glass slide and refloated on the surface of water in another beaker. About ten minutes were allowed for diffusion of ions from the drop of mother liquid into the water below. Then the films with drops were scooped with specimen grids. After drying the specimen, the precipitates were observed with an electron microscope.

Rectangular perfect crystals were formed from 0.001 M solution independently of the reaction temperature. Dendrites were formed from 0.1 M solution. The growth direction of dendrite was dependent on the reaction temperature as mentioned later. The crystals formed by the diffusion mixing method are generally thin laminae, so they are suitable to study by the electron diffraction method. Crystals precipitated by the direct mixing of reagents have the same morphological characteristics as those precipitated by the diffusion mixing of ions, when the concentration and the reaction temperature are kept at the same condition.

Results

Morphology of Barium Sulfate Precipitates by Electron Microscopy.—A perfect crystal of barium sulfate is a rectangular platelet as shown in Fig. 1a. In a particular case of precipitation in dilute aqueous alcohol, octagonal or hexagonal platelet is formed as shown in Fig. 3a.

The dendrite prepared at room temperature is made of two main stems crossed perpendicularly to each other, which grow from the center of the crystal. Many primary and secondary branches are seen which grow from the main stems parallel to the stems (Fig. 4a). The dendrites prepared at elevated temperature are shown in Figs. 7a and 8a. The primary branches grow obliquely to the main stems crossed perpendicularly with each other (Fig. 7a). The main stems of the crystals shown in Fig. 8a has defects, and the large protuberances of these crystals correspond to the primary branches of the crystals shown in Fig. 7a. The secondary branchings are parallel to the primary branches, that is, they are oblique to the main stems (Figs. 7a and 8a). The relation of the main stems and the branches are shown in Figs. 9a and b.

* The nineth paper of this series, This Bulletin, **31**, 950 (1958).

1) E. Suito and K. Takiyama, ibid., **27**, 121, 123 (1954); **28**, 305 (1955).

2) R. B. Fischer, *Anal. Chem.*, **23**, 1667 (1951); R. B. Fischer and T. B. Rhinehammer, ibid., **25**, 1544 (1953).

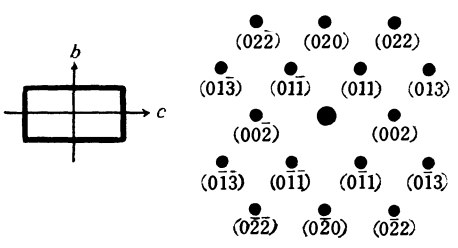
The dendrite grows generally in two-dimension as shown by a replica of crystal in Fig. 10. The dendrite shown in Fig. 11 is sometimes observed. Here the platelet particle is set perpendicular to the supporting film. The crystal seems to be a twin, and twin planes estimated to be (110) were observed.

Analysis of N-Pattern Obtained by Electron Micro-Diffraction Method. — All electron diffraction patterns obtained from the crystals in the present study are N-patterns. The arrangement for orientation between the electron microscopic image and the electron diffraction pattern as well as the fixing of the index of each reflection spot were made as follows. The image of electron microscope is rotated at a certain angle with respect to the electron diffraction pattern owing to the difference of lens current. The method for an arrangement of these two images is described below, in Fig. 1 as an example. The electron diffraction pattern obtained from a selected crystal in Fig. 1a is shown in Fig. 1c. When the current of the intermediate lens is increased a little more than the value which gives the diffraction pattern, a pattern shown in Fig. 1b is obtained. In Fig. 1b the small bright field image appears at the center of the pattern and many small dark field images appear at the similar positions to the electron diffraction spots. The orientations of the bright and dark field images are the same, so the relative orientation of the electron microscopic image to the electron diffraction pattern can be known. All crystals are, of course, barium sulfate and belong to V_h^{16}. The reciprocal lattice of barium sulfate crystal and the intersection with Ewald sphere are obtained. Then N-pattern constructed is compared with that obtained by experiment (Fig. 1c), and the Miller's indices of reflection spots are fixed as shown in Fig. 2b.

Crystal Habit of Barium Sulfate Precipitates by Electron Micro-Diffraction Method. — All electron micrographs and diffraction patterns shown in this paper are arranged to the same orientation. Electron diffraction patterns obtained from most crystals are N-patterns same as that shown in Fig. 2b. From this, it has been revealed that the platelet crystals have grown along (100) plane. The laminae that give the N-pattern shown in Fig. 2b are perpendicular to the electron beam.

The short- and the long-axes of rectangular crystal shown in Fig. 1a are *b*- and *c*-axes respectively as shown in Fig. 2a. The normal to the platelet is *a*-axis. The normal to the octagonal lamina shown in Fig. 3a is also *a*-axis, and the side planes of that crystal are {010}, {011} and {001} groups.

The main stems of dendrite shown in Fig. 4a have grown to the direction along



(a) (b)

Fig. 2. The direction of axes and the indices of electron diffraction pattern of perfect crystal of barium sulfate shown in Fig. 1.

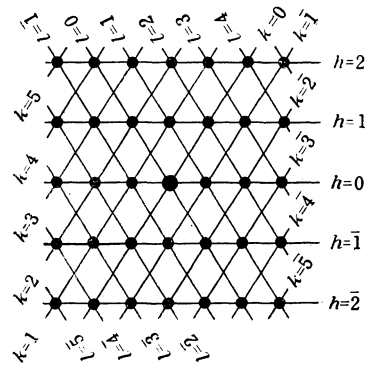
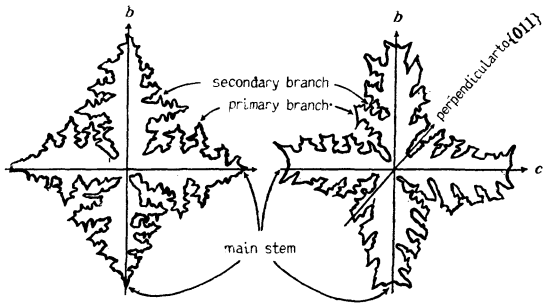


Fig. 6. The indices of electron diffraction pattern of dendrite of barium sulfate shown in Fig. 5.



a b

Fig. 9. Schematic diagrams of two typical dendrites of barium sulfate crystals.
a: room temperature
b: 80°C

b- and *c*-axes. Small branchings also grow in parallel to these axes (Fig. 9a). The platelet of dendrite shown in Fig. 5a was placed inclined to the electron beam, and the angle between *a*-axis (normal to platelet) and the electron beam was proved 64° from the analysis of N-pattern as shown in Fig. 6. The main stems of the dendrite shown in Fig. 7a have grown along *b*- and *c*-axes, but the branches have grown to the direction perpendicular to the plane of {011} group (Fig. 9b). The dendrites shown in Fig. 8a have grown markedly to the direction perpendicular to the plane of {011} group.

Consideration

Generally speaking, when a crystal grows from a dilute reagent, the growth rate is so small that the perfect crystal is formed. The perfect crystal of barium sulfate is generally a rectangular platelet and the octagonal or hexagonal crystal is formed in a rare case.

Dendrite of barium sulfate crystal is formed in a range of initial concentration from about 0.001 M to 0.2 M. At the concentration above this range, the rate of nucleation is very rapid, so numerous nuclei appear but their growth immediately after mixing of reagents does not proceed. At the concentration below that range, the rate of nucleation is very slow and a small number of nuclei grows slowly to the perfect crystals. In the range of initial concentration mentioned above (0.001 to 0.2 M), both rates of nucleation and growth are a little more rapid than that in the case just mentioned above, and the edge or the corner of a crystal grows preferentially to form the dendrite.

Watson and Freemann[3] believed that the dendrite formed in an iron sol is composed of aggregated small cubic particles. However, the electron diffraction pattern of the dendrite of barium sulfate is N-pattern, which indicates a single crystal and that the crystal has grown from a single nucleus to the dendrite.

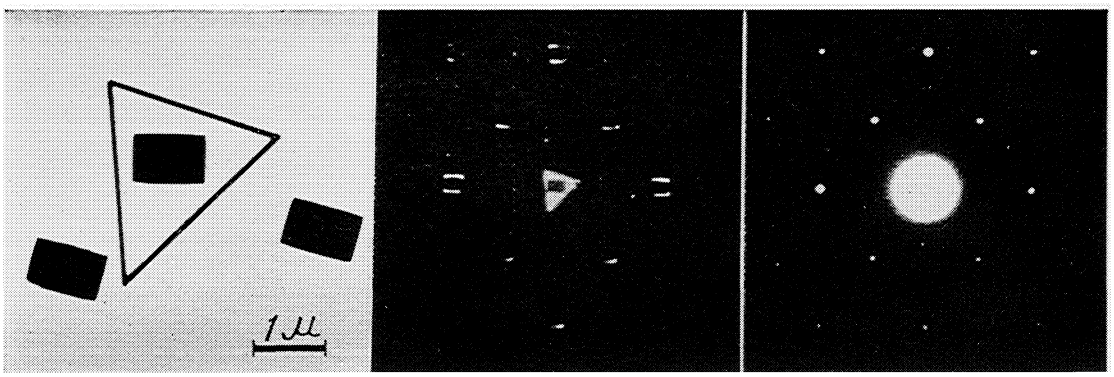
Summary

Barium sulfate precipitates in a form of rectangular perfect crystal from a solution of low initial concentration, and in a form of dendrite from a solution of higher initial concentration. They are platelets grown along (100) plane. The short- and long-axes of rectangular crystal are *b*- and *c*-axes respectively. The dendrite grows along *b*- and *c*-axes, or along the direction perpendicular to the plane of {011} group.

The author acknowledges his thanks to Professor Eiji Suito of Kyoto University for his guidance and discussion. He also wishes to express his hearty thanks particularly to Professor Masayoshi Ishibashi of Kyoto University for his continual advice and encouragement.

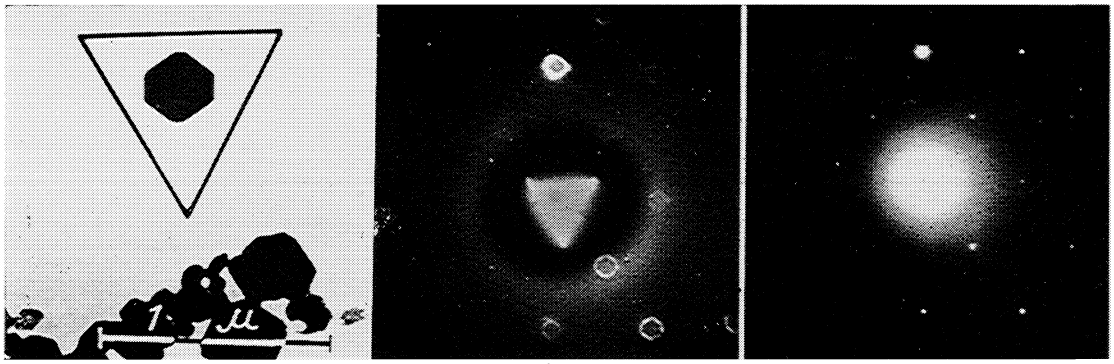
Institute for Chemical Research
Kyoto University
Takatsuki, Osaka

3) J. H. L. Watson and M. W. Freemann, *Kolloid-Z.*, **148**, 127 (1956).



a (×10,000) b c

Fig. 1. Perfect crystal of barium sulfate prepared by diffusion mixing of 0.001 M H_2SO_4 and 0.001 M $BaCl_2$ at room temperature.



a (×30,000) b c

Fig. 3. Perfect crystal of barium sulfate prepared by direct mixing of H_2SO_4 and $Ba(OH)_2$ at the initial concentration of 0.05 M in 2.5% aqueous alcohol medium at room temperature.

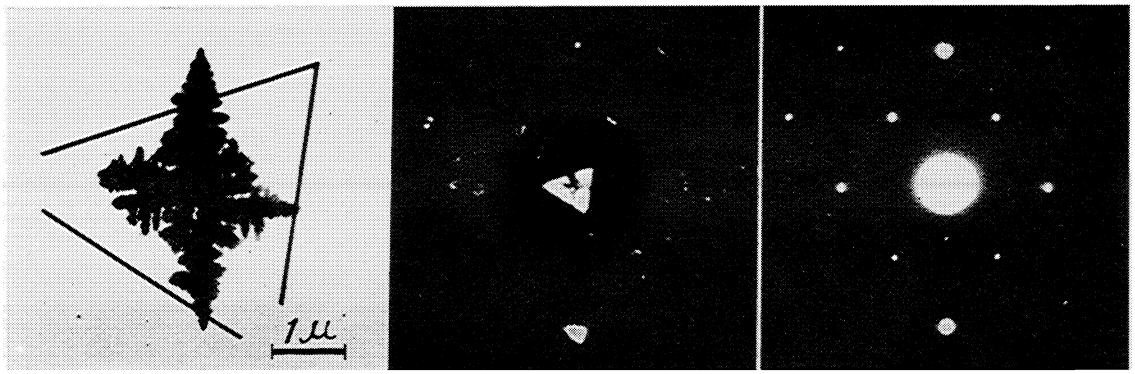
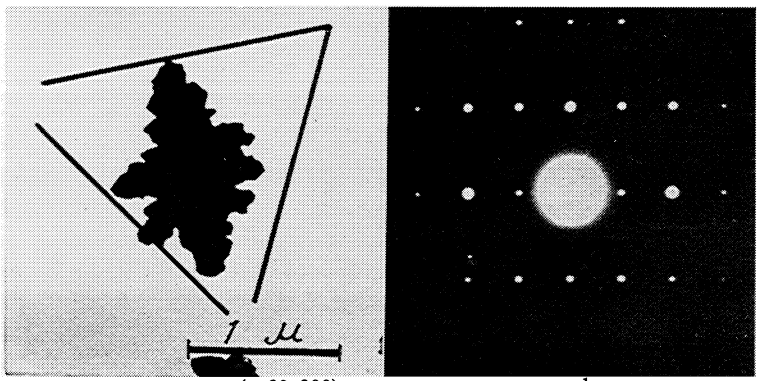
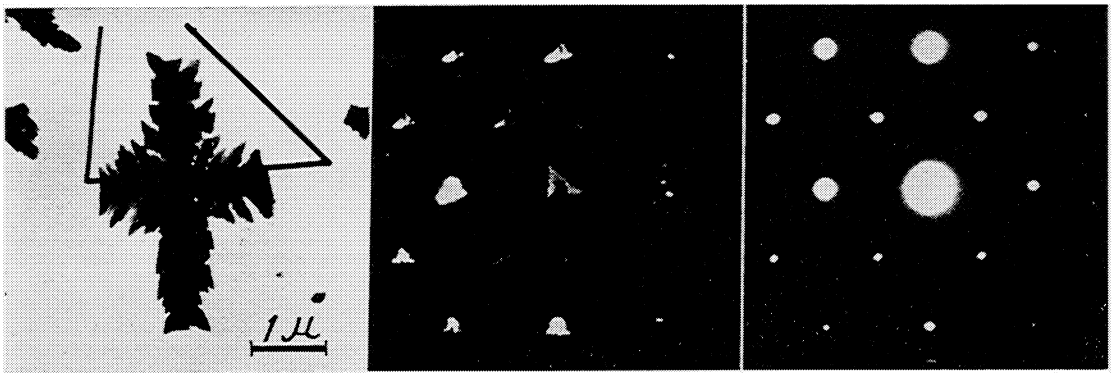


Fig. 4. Dendrite of barium sulfate prepared by diffusion mixing of 0.001 M H_2SO_4 and 0.1 M $BaCl_2$ at room temperature.



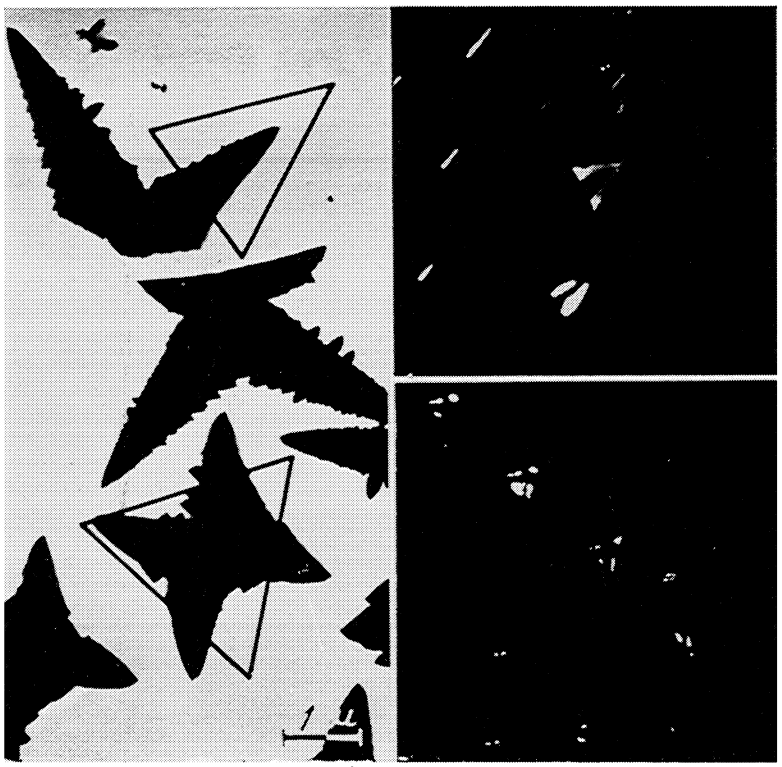
a (×20,000) b

Fig. 5. Dendrite of barium sulfate prepared by direct mixing of H_2SO_4 and $Ba(OH)_2$ at the initial concentration of 0.02 M at room temperature.



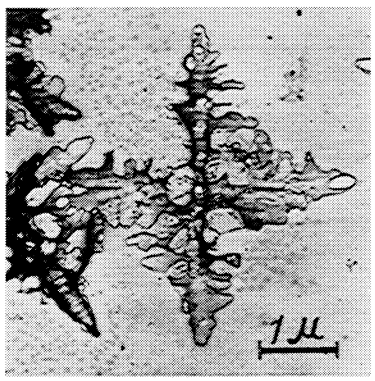
a (×10, 000) b c

Fig. 7. Dendrite of barium sulfate prepared by diffusion mixing of 0.001 M H_2SO_4 and 0.1 M $BaCl_2$ at 80°C.



a (×10, 000) b

Fig. 8. Dendrite of barium sulfate prepared by diffusion mixing of 0.001 M H_2SO_4 and 0.1 M $BaCl_2$ at 80°C.



(×10, 000)

Fig. 10. Replica of dendrite of barium sulfate prepared by direct mixing of 0.001 M H_2SO_4 and 0.1 M $BaCl_2$ at room temperature.



(×10, 000)

Fig. 11. Twin of dendrite of barium sulfate prepared by direct mixing of H_2SO_4 and $Ba(OH)_2$ at the initial concentration of 0.01M at room temperature.

Untersuchungen über die Bildung der Proteinase aus einem Aspergillus awamori-Stamm. II. Charakterisierung des Proteinasebildungsvermögens des Mycels im Kultursverlauf durch seinen Stickstoffwechsel

Von Jiro HOSHINO

(Eingegagen am 23. Juli, 1958)

Aus dem ausgewaschenen ruhenden Mycel des Schimmelpilzes, ebenso wie Bakterie sind reichliche Mengen von Enzyme im reinen Zustand leicht zugänglich. Die Enzymbildung wird aber bei diesem experimentalen System durch verschiedene äussere Faktoren stark beeinflusst. Es ist bekannt, wie auch der Verfasser in der vorigen Mitteilung[1] über die Proteinasebildung bestätigt hat, dass sich das Vermögen der Zelle zur Enzymbildung, die eine der Mikroorganismus eigenen biochemischen Aktivitäten darstellt, mit der Züchtungsdauer ändert.

Nach der Angabe von O. Tanabe[2] wurde das Amylasebildungsvermögen des *Asp. oryzae*-Stammes in den früheren Stufen der Züchtung grösser erwiesen. Derselbe Tatbestand wurde von C. P. Hegarty bei der *„adaptiven"* Bildung von Enzyme aus *Streptococcus lactis* festgestellt[3]. Die Bakterien betreffend wurden noch von mehreren Forschern darüber mit den mannigfachen Ergebnisse verfolgt[4-8].

Es liegt nahe anzunehmen, dass verschiedene Stoffe innerhalb des Mycels für die Änderung dieser physiologischen oder biochemischen Aktivitäten verantwortlich sind, von denen die Nucleinsäuren als Spezifität-Donator und die Aminosäuren als Bausteine des Enzymproteins eine entschiedene Rolle spielen sollen.

Da die Ergebnisse über die Änderung des Proteinasebildungsvermögens mit der Züchtungsdauer, die der Verfasser in der vorigen Mitteilung kurz dargelegt hatte, eine sehr Wichtige zu bedeuten scheint, hat der Verfasser nun diese vorige Aufgabe wieder sich aufgestellt, um damit tiefere Übersicht auf die Beziehung des Proteinasebildungsvermögens mit dem Sammelbecken von Aminosäuren des Mycels und seinem Stickstoffwechsel gewinnen zu können.

1) J. Hoshino, Dieses Bulletin, **31**, 883 (1958).
2) O. Tanabe und K. Tonomura, *J. Agr. Chem. Soc., Japan* (*Nippon Nōgei-Kagaku Kaishi*), **30**, 596 (1956).
3) C. P. Hegarty, *J. Bact.*, **37**, 145 (1939).
4) E. F. Gale, "Chem. Act. of Bacteria" p. 51, Academic Press, Inc., New York, (1948).
5) D. Billen, *J. Bact.*, **61**, 515 (1951).
6) M. J. Pinsky, ebenda, **64**, 337 (1952).
7) M. Suda, *Symp. Enz. Chem.* (*Kōso Kagaku Symposium*), **4**, 18 (1950).
8) J. Fukumoto und T. Yamamoto, *J. Agr. Chem. Soc. Japan* (*Nippon Nōgei-Kagaku Kaishi*), **31**, 421 (1957).

Arbeitsmethode

Bestimmung des Proteinasebildungsvermögens des Mycels. — Zur Ermittelung des Proteinasebildungsvermögens des Mycels wurde die Aktivität der in die Kulturflüssigkeit sezernierten Proteinase nach dem zwanzigstündigen Schütteln des ausgewaschenen Schüttelmycels (1.0 g feuchtes: ungefähr 0.2 g trocknes), welches aus den verschiedenen Phasen einer Entwicklungskultur abgeerntet worden war, in der 1.0 prozentige Glucose haltigen M/5-Phosphatpufferlösung (pH=6.1) nach der Folinschen Methode bestimmt und mit derselben pro g trocknes Mycels angegeben. Diese Aktivität wird vom Verfasser provisorisch als *„potentiale Aktivität des Proteinasebildungssystems"* (PAPS) bezeichnet.

Züchtung des Pilzes und Gewinnung des ausgewaschenen Schüttelmycels wurden in der vorigen Mitteilung ausführlich dargelgt.

Bestimmung des organischen Stickstoffs des Mycels.—Zur Bestimmung des organischen Stickstoffs des Mycels wurde die semi-mikro Kjeldahlsche Methode nach A. O. A. C. verwendet. Den organischen Gesamtstickstoffgehalt hat der Verfasser experimentell in zwei Gruppen, d. h. Proteine- und non-Proteine-N, eingeteilt, wobei der erstere denjenigen Gesamtstickstoff bedeutet, der sich in der 5.0 prozentigen Trichloressigsäure löslichen Fraktion befindet. Den letztere kann man rechnerisch leicht erreichen. Bestimmung dessen ist wie folgt: Das üblicherweise gut ausgewaschene und abgepresste Mycel (ungefähr 0.2 g trocknes) wurde mit 40 ccm 5 prozentiger Trichloressigsäurelösung 20 Minuten am Rückfluss gekocht. Das Extrahieren wurde in analoger Weise noch zweimal wiederholt. Sodann wurde das rückstehende Mycel getrocknet und zur Ermittelung des Stickstoffs herangezogen.

Ergebnisse

Abhängigkeiten der PAPS und N-Konstitution des Mycels von seinen Entwicklungsphasen. — Das Proteinasebildungsvermögen (PAPS) des Mycels und seine Gehalte am Gesamt-(N_t), Proteine-(N_p) und non-Proteine-N(N_{np}) wurden in den verschiedenen Entwicklungsphasen ermittelt, um damit auf die Frage zu beantworten, welche Bestandteile an die Biosynthese von Proteinase teilnehmen. Die Resultate sind in der Abb. 1 illustriert.

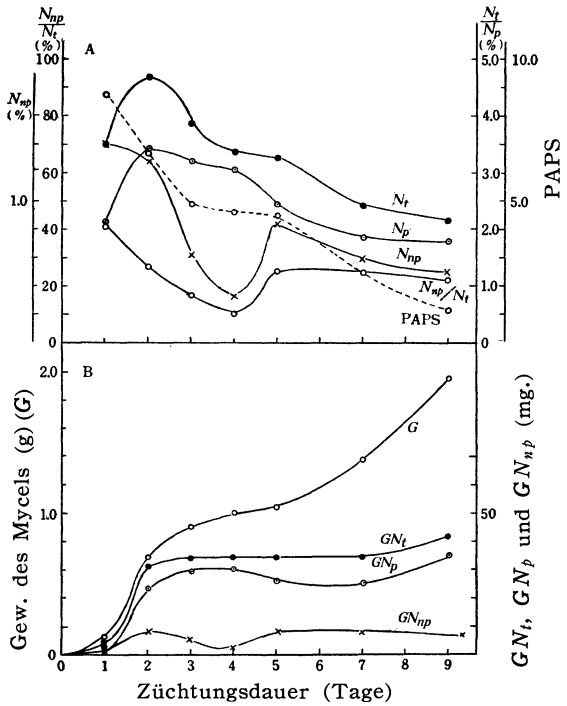


Abb. 1. Abhängigkeiten der PAPS und N-Konstitution des Mycels von seiner Züchtungsdauer.
N_t: totaler Stickstoffgehalt des Mycels
N_p: Proteinstickstoffgehalt des Mycels
N_{np}: non-Proteinstickstoffgehalt des Mycels

Die Sporen wurden in der vorliegenden Arbeit nicht behandelt, weil die Dauer kurz nach dem Impfen dieselbe der Keimung darstellt und der Stoffwechsel dabei von der Mycelentwicklung recht verschieden sein soll[9].

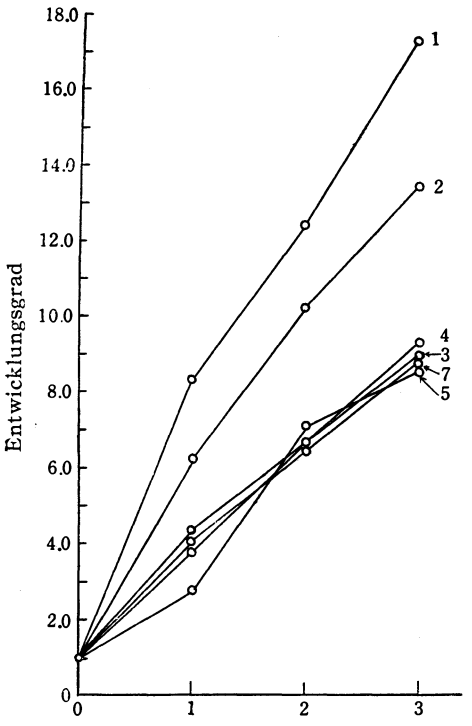
Vom ersten bis zum zweiten Tagen nach dem Impfen hat sich das Mycel sehr stark entwickelt, und solche Phase wurde 4~5 Tage danach wieder beobachtet. Dass das Mycel in dieser Entwicklungsphase allmählich reicher an N_t und N_p, und im Gegenteil armer an N_{np} geworden ist, ist es nun bedeutungsvoll. Daraus geht es klar hervor, dass in dieser Entwicklungsphase die Myceleiweisskörpern aus den Aminosäuren kräfting synthetisiert werden, wobei also der anabolische Stoffwechsel den Eiweissstoff betreffend eine dominierends Rolle spielt. Vom 4 Tage nach dem Impfen fängt der Amino-N Gehalt des Mycels plötzlich an zuzunehmen und dementsprechend fängt der N_p Gehalt an abzunehmen. In Anbetracht, dass der Gesamt-N inzwischen unveränderlich bleibt, (Abb. 1, B) müssen die Aminosäuren innerhalb des Mycels unter dem Verbrauch von Myceleiweisskörpern anhäufen. In dieser Phase scheint daher der catabolische Stoffwechsel den Eiweisskörper betreffend in analogem Sinne eine dominierende Rolle zu spielen.

Die in der Figur gegebenen Versuche zeigen weiter, dass sich das Proteinasebildungsvermögen (PAPS) in der anabolischen Phase allmählich erschwächt und es gerade mit dem Aminosäuregehalt des Mycels gleichläuft. Daraus folgt es, dass die Proteinasebildung von der Menge der inneren Aminosäuren beschränkt wird, und sich vermindert, wenn die Aminosäuren zur Myceleiweissstoffbildung verbraucht worden sind.

Den Züchtungsverlauf in der Figur kann man in zwei „Lebenskreise" einteilen, von denen das Erste einen typischen Entwicklungs- oder Stoffwechselsprozess bietet: die catabolische Phase entspricht der „*lag*" Phase und die anabolische Phase der „*log*" d.h. kräftig entwickelnden Phase. Das Mycel, das sich zwischen diesen beiden Phasen befindet und also die Aminosäuren am meisten enthält, hat das grösste Proteinasebildungsvermögen in jedem Kreis.

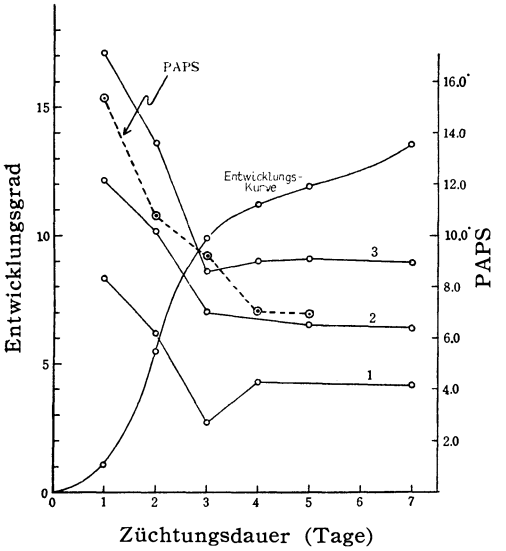
Beziehung der Änderung des Vermögens zur Mycelentwicklung mit der Proteinasebildung. — Da das Mycel, das ein erhebliches Vermögen zur Proteinasebildung besitzt, nicht dasjenige, das ein sich kräftig entwickelendes Mycel, sondern dasjenige ist, das sich in der Vorstufe der „*log*" Phase befindet und damit, wie aus der Abb. 1 ersichtlich ist, uns seine kommende kräftige Entwicklung erwarten liess, hat der Verfasser das potentiale Entwicklungsvermögen des Mycels in den jeden Phase in folgender Weise ermittelt: 1.0 g wie üblich dargestelltes Schüttelmycel wurde in die frische Nährlösung unter sterilen Bedingungen übergetragen und weiter bei

9) T. Yanagita, *Arch. für Mikrobiol.*, **26**, 329 (1957).



Schüttelungsdauer bei der Entwicklungsprüfung (Tage)

Abb. 2. Entwicklungsverläufe der in verschiedenen Entwicklungsphasen abgeernteten Mycel. Die Ziffern in der Figur zeigen die Züchtungsdauer an.



Züchtungsdauer (Tage)

Abb. 3. Abhängigkeiten der PAPS und Entwicklungsvermögens des Mycels von seiner Züchtungsdauer. Die Ziffern in der Figur zeigen die Schüttelungsdauer bei der Entwicklungsprüfung an.

30°C fortgeschüttelt. Je nach 1, 2 und 3 Tagen wurde je ein Kolben abgebrochen und die sich entwickelte Mycel abgeerntet, ausgewaschen, sodann zur Wägung getrocknet.

Als Entwicklungsgrad wurde das Gewichtsverhältnis dieses Mycels zum unterworfenen Mycel ermittelt. In der Abb. 2 werden die Entwicklungsgrade der Mycel verschiedener Züchtungsphasen in Kurvenform gegeben. Dabei ergab es sich, dass das jüngere Mycel ein grösseres Entwicklungsvermögen besitzt, ohne „*lag*" Phase zu zeigen. Die Mycel in den Züchtungsphasen von 3, 4, 5 und 7 Tagen zeigten aber beinahe gleichartige Entwicklungsverläufe. Diese Umstände sind auf der Abb. 3 leicht begreiflich. Hierbei wurde es gezeigt, dass ein deutlicher Parallelismus zwischen dem Proteinasebildungs- und dem Entwicklungsvermögen des Mycels auch in diesem Falle besteht.

Der „*lag*" Phase des zweiten "Lebenskreises" entpricht also die Phase, wovon die Fläche der Kurven des Entwicklungsvermögens beginnt. Während der Prüfung über das Entwicklungsvermögen wurde keine massgebende Bildung der Proteinase beobachtet.

Unter Berücksichtigung dieser Tatsachen wurde es festgestellt, dass das erhebliche Proteinasebildungsvermögen einem Mycel gehört, welches ein kräftiges Entwicklungsvermögen besitzt und reichliche Mengen von Aminosäuren enthält. Diese Erscheinungen stellen daher vermutlich zwei Seiten eines Attributes dar, und sie antagonieren einander gegen ein Sammelbecken von Aminosäuren. Dieser Befund steht in voller Übereinstimmung mit den Untersuchungen von M. Nomura[10], in denen er eine antagonistische Biosynthese von Amylase durch *Bacillus subtilis* gegen dieselbe der Zelleiweissstoffen beobachtet und die Amylasebildung als „*abnorme*" Biosynthese bezeichnet hat.

Beziehung des Proteinasebildungsvermögens der in verschiedenen Bedingungen entwickelten Mycel mit seinem Amino-N Gehalt. — Aus den hierher geschilderten Ergebnisse schien der Aminosäuregehalt des Mycels bei der Proteinasebildung eine dominierende Rolle zu spielen. In Anbetracht dessen wurden die N-Bestandteile desjenigen Mycels in Bezug auf seine Proteinasebildungs- und Entwicklungsvermögen untersucht, das sich unter der

10) M. Nomura, J. Hosoda, B. Maruo und S. Akabori, *J. Biochem.*, **43**, 841 (1956).

TABELLE I

PAPS UND N-KONSTITUTION DES SICH UNTER VERSCHIEDENEN BEDINGUNGEN ENTWICKELTEN MYCELS

N-Quelle % C-Quelle %	Gew. des Mycels in mg	N_t (%)	N_p (%)	N_{np} (%)	N_{np}/N_t (%)	PGA*	PAPS**
NH_4NO_3 4 % Rohrzucker 4 %	312	5.7	3.5	2.2	38.3	4.6	5.1
NH_4NO_3 1.5% Rohrzucker 10 %	345	5.2	3.6	1.6	29.8	4.4	5.5
NH_4NO_3 0.2% Rohrzucker 20 %	427	4.0	3.2	0.8	20.8	4.7	6.2

* Entwicklungsvermögen: dies wurde mit dem Entwicklungsgrad der 24-stündigen Prüfung angegeben.

** Proteinasebildungsvermögen: dies steht im Text geschrieben.

variierenden N-Konzentration entwickelt hatte. Die Ergebnisse sind in der Tabelle I zusammengestellt.

Dabei hat es sich ergeben, dass kein wesentlicher Parallelismus zwischen dem Aminosäuregehalt und den beiden Vermögen des Mycels besteht, während es dem Verfasser gelungen ist, auf obige Weise den Aminosäuregehalt des Mycels zu verändern. Daraus darf festgestellt werden, dass der Gehalt des Mycels an Aminosäuren nicht immer für die Proteinasebildung ein entschiedener Faktor ist. Doch ist es so zu deuten, dass das Mycel, das erhebliche Proteinasebildungs- und Entwicklungsvermögen besitzt, stets reichliche Aminosäuren darin enthält.

Die Aufgabe, was für ein Substanz auf die Proteinasebildung in diesem experimentalen System eine dominierende Rolle spielt, bleibt auf Grund der oben dargelegten Resultaten noch unlöslich und bedarf noch weitere Untersuchungen.

In der vorliegenden Arbeit wurde am Schlusse das Proteinasebildungsvermögen des Mycels im Kultursverlauf in Bezug auf das Mycelentwicklung durch seinen Stickstoffwechsel charakterisiert.

Schlusswort

Die Proteinasebildungsvermögen des Pilzmycels wurde in Anbetracht seines Stickstoffwechsels verfolgt. Gleichungen wurden durch die Verfolgungen der Änderung der Stickstoffskonstitution und des Entwicklungsvermögens des Mycels im Kultursverlauf abgeleitet, um damit auf die Frage zu beantworten, ob ein Sammelbecken von Aminosäuren bei der Biosynthese von Proteinase eine dominierende Rolle spielt.

Es wurde gezeigt, dass ein „Lebenskreis" des Mycels in einige metabolische Phasen, d. h. catabolische und anabolische usw. eingeteilt wird und dass Mycel, das sich zwischen diesen beiden Phasen befindet, wo der Vorstufe der gebräuchlichen „*log*" Phase entspricht und Aminosäuren am meisten enthalten sind, das grösste Proteinasebildungsvermögen zeigt.

Das erhebliche Proteinasebildungsvermögen gehört zu einem Mycel, welches neben dem grossen Sammelbecken von Aminosäuren ein kräftiges Entwicklungsvermögen besitzt.

Aus dem Versuch mit dem Mycel, das sich unter der variierenden N-Konzentration entwickelt hatte, wurde es aber festgestellt, dass der Aminosäuregehalt des Mycels nicht immer für die Proteinasebildung ein dominanter Faktor ist.

In der vorliegenden Arbeit konnte der Verfasser zusammenfassend das Proteinasebildungsvermögen des Mycels im Kultursverlauf in Bezug auf das Mycelentwicklung durch seinen Stickstoffwechsel charakterisieren.

Zum Schlusse ist es mir eine angenehme Pflicht, Herrn Professor Dr. N. Taketomi, und Herrn ausserordentlichen Professor H. Suzuki für ihre vielfache Anregungen und Revisionen bei der Anfertigung dieser Arbeit meinen besten Dank auszusprechen.

Laboratorium der Gärungs- und Biochemie
Abteilung für Angewandte Chemie
Naturwissenschaftlich-Technische Fakultät
Universität Waseda, Shinjuku-ku, Tokyo

Dichroism of Dyes in the Stretched PVA Sheet. II[1]. *The Relation between the Optical Density Ratio and the Stretch Ratio, and an Attempt to Analyse Relative Directions of Absorption Bands**

By Yoshié TANIZAKI

(Received July 26, 1958)

Hitherto, dichroic properties have been mainly utilized to investigate dyeing mechanism[2] or the percentage orientation of fibres[3]. A conclusion derived from a number of experimental results shows that almost all dye molecules in dyed state should lie lengthwise along the cellulose chains[4]. In the previous paper[1], this conclusion was applied to presume the relative direction of transition moments of absorption bands of certain direct dyes in the stretched polyvinyl alcohol sheet from their dichroic properties. A similar attempt may not be applied to short molecules which show poor dichroism, and it is still more difficult, as it is not sure that such molecules are adsorbed on a fibre so as to orient parallel to the fibre axis. However, the fact that an observed optical density ratio (to be defined later) depends upon the stretch ratio of the sheet may give a key to analyse the direction of transition moment of the absorption band of the dye molecule. The purpose of this paper is to derive an expression for the density ratio as a function of the stretch ratio, to apply it to absorption bands of certain basic dyes, and to analyse their relative direction.

Experimental

Materials.—Polyvinyl alcohol (abbreviated to PVA) with the polymerization degree of about 1500 was used for preparing sheets by the method described in the previous paper[1].

Dyes used were crystal violet and auramine yellow which were recrystallized twice from ethanol, starting from the pure ones produced in the Laboratory of Hodogaya Kagaku Co., Ltd. The paper chromatography detected no colored impurities in these dyes.

PVA sheets, swollen fully in distilled water, were soaked in the aqueous dye solution at room temperature.

Measurements.—Measurements were carried out with a Shimadzu QB-50 spectrophotometer, in filter hole of which a sheet-polarizer of PVA-iodine[5] was set. To determine the correlation between the electric vector of polarized incident light and the stretching direction of the sample sheet, an apparatus shown in Fig. 1 was used. A colored and an uncolored PVA sheet were respectively pasted on a metal ring to be fixed in R_1 and R_2. The disk D graduated 0° to 360° on its circumference can be rotated at will in concentric with the toothed wheel G_1, and at the same time the rotation is transmitted through G_2, being used as a change gear, to R_1 and R_2. Gear ratios are all the same. This apparatus is set in the cell box of the spectrophotometer in place of

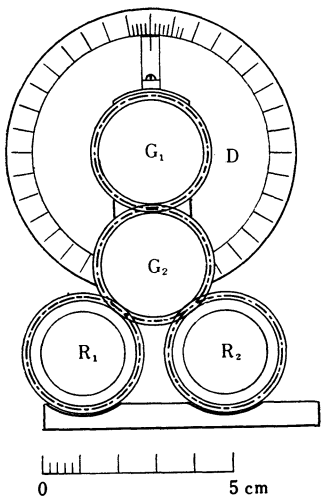


Fig. 1. Apparatus for rotating sample sheets.

1) Part I of this series, Y. Tanizaki and N. Ando, *J. Chem. Soc. Japan, Pure Chem. Sec.* (*Nippon Kagaku Zasshi*), **78**, 542 (1957).

* Presented at 11th Annual Meeting of the Chemical Society of Japan, April 1958.

2) T. H. Morton, *J. Soc. Dyers Col.*, **62**, 272 (1946); H. H. Summer, T. Vickerstaff and E. Waters, ibid., **69**, 181 (1953).

3) J. M. Preston, ibid., **47**, 312 (1931); D. R. Morey, *Tex. Research*, **4**, 491 (1934); **5**, 105 (1935); J. M. Preston and P. C. Tsien, *J. Soc. Dyers Col.*, **62**, 368 (1946); **66**, 361 (1950); J. M. Preston and Y. F. Su, ibid., **66**, 357 (1950); D. R. Morey and E. V. Martin, *Tex. Research J.*, **21**, 607 (1951).

4) T. Vickerstaff, "The Physical Chemistry of Dyeing", Second Edition, Oliver and Boyd, London (1954), p. 183.

5) Y. Tanizaki, This Bulletin, **30**, 935 (1957).

the cell holder. Thus the correlation mentioned above was determined by means of the Malus' law.

Notations.—A circle drawn on the sheet before stretching is deformed into an ellipse after stretching. The ratio of the long axis of the ellipse to the short one is defined as the *stretch ratio* R_s[6]. $D_{\parallel}$ and $D_{\perp}$ are optical densities for completely and linerly polarized lights whose electric vectors are respectively parallel and perpendicular to the stretching direction. An *optical density ratio* R_d is then defined as $D_{\parallel}/D_{\perp}$.

Theoretical

Let us suppose that an imaginary sphere in substrate of PVA sheet is deformed, being kept at a constant volume by stretching into a spheroid. If the optical property around the stretching direction were isotropic and any unit vector with an angle θ_0 against the stretching direction in the sphere were transformed into a unit vector with θ in the spheroid, the distribution of vectors after stretching, $f(\theta)$, would be determined in the following way,

$$f(\theta)=\int_0^{\pi/2} G(\theta,\theta_0)F(\theta_0)\,\mathrm{d}\theta_0 \qquad (1)$$

where $F(\theta_0)$ means a function of distribution before stretching, and $G(\theta,\theta_0)$ is a function of transformation which makes θ_0 transform to θ by stretching. Since it is natural to consider that the distribution of vectors before stretching is quite at random, then $F(\theta_0)$ may be expressed as follows,

$$F(\theta_0)=\sin\theta_0$$

or

$$=\frac{\tan\theta_0}{\sqrt{1+\tan^2\theta_0}} \qquad (2)$$

On the basis of the assumption that the deformation takes place under a constant volume, the relation between θ_0 and θ is expressed as follows,

$$\tan\theta_0=R_s\tan\theta$$

where R_s is the axial ratio of the ellipsoid and is equal to the stretch ratio mentioned above. Then the transformation function may be written as follows

$$G(\theta,\theta_0)=\delta(\tan^{-1}(R_s\tan\theta)-\theta_0)\rho(\theta_0) \qquad (3)$$

where δ is a delta-function and ρ is a surface element, namely

$$\rho(\theta_0)=R_s\frac{\sin\theta_0\cos^2\theta_0}{\sin\theta\cos^2\theta} \qquad (4)$$

By the combination of Eqs. 1, 2, 3 and 4,

$$f(\theta)=\int_0^{\pi/2}\delta(\tan^{-1}(R_s\tan\theta)-\theta_0)\times\frac{R_s}{\sin\theta\cos^2\theta}\frac{\tan^2\theta_0\,\mathrm{d}\theta_0}{(1+\tan^2\theta_0)^2}$$

The interval of this integration involves zero. So that, according to the nature of δ-function[7], this integration becomes equal to the integrand excluding δ-function, in which θ_0 is replaced by $\tan^{-1}(R_s\tan\theta)$, that is,

$$f(\theta)=\frac{R_s^3\tan^2\theta}{\sin\theta\cos^2\theta(1+R_s^2\tan^2\theta)^2}$$

or

$$f(\theta)=\frac{R_s^3\sin\theta}{\{1+(R_s^2-1)\sin^2\theta\}^2} \qquad (5)$$

where $R_s\geq 1$ and $0\leq\theta\leq\pi/2$. Determining $N(R_s)$ so as to make the integration with respect to θ unity, namely,

$$\int_0^{\pi/2}N(R_s)f(\theta)\,\mathrm{d}\theta=1$$

$N(R_s)f(\theta)$ for several values of R_s provides the curves shown in Fig. 2. This figure indicates that for large R_s values, that is, when the PVA sheet is stretched to a high degree, the greater part of vectors becomes able to meet the stretching direction. This

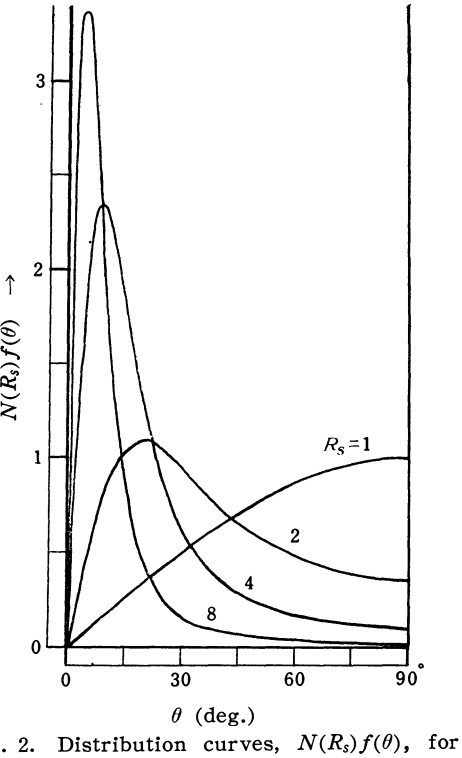


Fig. 2. Distribution curves, $N(R_s)f(\theta)$, for several values of the stretch ratio, R_s.

6) E. H. Land, *J. Opt. Soc. Am.*, **41**, 957 (1951).

7) P. A. M. Dirac, "Quantum Mechanics", Third Edition, Oxford (1947), p. 58.

will correspond to a distribution of a characteristic direction, which is regarded as a vector and is called hereafter an *orientation axis*, of the molecular species. So that, when the direction of the transition moment corresponding to an absorption band is on the orientation axis, the problem is rather easy to be dealt with. For the present purpose, however, it is necessary to consider a general case where transition-directions of dye molecules do not always coincide with orientation axes. Therefore, it will be convenient to introduce here an imaginary plane made of an orientation axis and a direction of transition moment. This plane does not necessarily coincide with the usual molecular plane, and is temporarily called a *light absorption-plane*. The transition moment μ of an absorption band can be decomposed into two components within the light absorption-plane, one of which is normal and the other parallel to the orientation axis, namely μ_b and μ_a respectively. Consequently, if the value of $|\mu_a/\mu_b| = r$ can be obtained, $\cot^{-1} r$ will give the angle of a direction of transition against the orientation axis of a molecule.

Now, if we imagine rectangular coordinates in the PVA substrate, so as to run the Z axis parallel with the stretching direction (see Fig. 3), and if the angle between Z and μ_a is θ, then three components of μ_a can be written as follows,

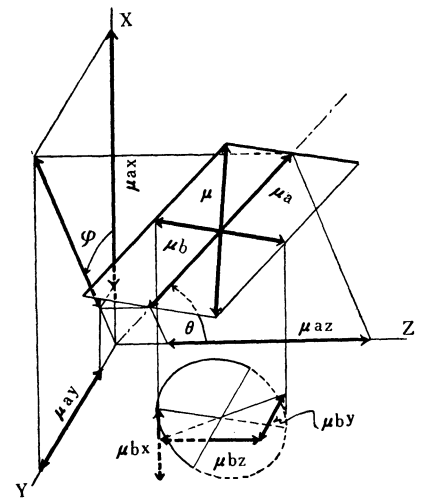


Fig. 3. Rectangular coordinates in the PVA substrate, of which the Z axis is taken parallel to the stretch direction of the PVA sheet. A transition moment μ of a dye molecule is decomposed to a parallel component μ_a and a normal μ_b to the orientation axis in the light absorption-plane.

$$\begin{cases} \mu_{aX} = \mu_a \sin\theta \cos\varphi \\ \mu_{aY} = \mu_a \sin\theta \sin\varphi \\ \mu_{aZ} = \mu_a \cos\theta \end{cases} \tag{6}$$

where φ is the angle between X and the projection of μ_a on the XY-plane. Similarly, corresponding ones for μ_b can be represented by

$$\begin{cases} \mu_{bX} = \mu_b(\cos^2\theta + \sin^2\theta \sin^2\varphi)^{1/2} \cos\phi \\ \mu_{bY} = \mu_b\left(\dfrac{\sin^4\theta \sin^2\varphi \cos^2\varphi \cos^2\phi + \cos^2\theta \sin^2\phi}{\cos^2\theta + \sin^2\theta \sin^2\varphi}\right)^{1/2} \\ \mu_{bZ} = \\ \mu_b\left(\dfrac{\sin^2\theta \cos^2\theta \cos^2\varphi \cos^2\phi + \sin^2\theta \sin^2\varphi \sin^2\phi}{\cos^2\theta + \sin^2\theta \sin^2\varphi}\right)^{1/2} \end{cases} \tag{7}$$

where φ is the angle between the X axis-orientation axis-plane and the light absorption-plane. The angle θ takes values of zero to $\pi/2$, and φ and ϕ values of zero to 2π. Integration with respect to φ and ϕ must be averaged for the region. Thus the components of μ for the X, Y and Z directions should be of the form

$$\begin{cases} \mu_X^2 = \displaystyle\int_{\theta=0}^{\pi/2} \frac{1}{2\pi} \int_{\varphi=0}^{2\pi} \frac{1}{2\pi} \int_{\phi=0}^{2\pi} \\ \qquad \times (\mu_{aX}^2 + \mu_{bX}^2) N(R_s) f(\theta) \mathrm{d}\phi \mathrm{d}\varphi \mathrm{d}\theta \\ \text{etc.} \end{cases} \tag{8}$$

Substitution of Eqs. 6 and 7 for Eq. 8, and integrations with respect to φ and ϕ, give

$$\begin{cases} \mu_X^2 = \mu_Y^2 = \dfrac{1}{4} \displaystyle\int_0^{\pi/2} \{2\mu_a^2 \sin^2\theta \\ \qquad + \mu_b^2(1+\cos^2\theta)\} N(R_s) f(\theta) \mathrm{d}\theta \\ \mu_Z^2 = \dfrac{1}{2} \displaystyle\int_0^{\pi/2} (2\mu_a^2 \cos^2\theta \\ \qquad + \mu_b^2 \sin^2\theta) N(R_s) f(\theta) \mathrm{d}\theta \end{cases} \tag{9}$$

Since the optical density D is proportional to μ^2, it may be possible to write

$$R_d \equiv \frac{D_\parallel}{D_\perp} = \frac{\mu_Z^2}{\frac{1}{2}(\mu_X^2 + \mu_Y^2)} = \frac{\mu_Z^2}{\mu_X^2} \tag{10}$$

For non-stretched state, i. e. $R_s = 1$, integration of Eq. 9 gives $\mu_X^2 = \mu_Y^2 = \mu_Z^2 = \mu^2/3$. Hence the following relation can be obtained by the aid of Eq. 10,

$$R_d = 1 \quad (R_s = 1)$$

For $R_s > 1$, combination of Eqs. 9 and 10, and integration with respect to θ give

$$R_d = \frac{2 + 2(2r^2 - 1) T(R_s)}{(2r^2 + 1) - (2r^2 - 1) T(R_s)} \tag{11}$$

where

$$T(R_s)=\frac{R_s^2}{R_s^2-1}\left\{1-\frac{N(R_s)}{\sqrt{R_s^2-1}}\log(R_s+\sqrt{R_s^2+1})\right\}$$

$$N(R_s)=2\left\{\frac{1}{\sqrt{R_s^2-1}}\log(R_s+\sqrt{R_s^2-1})+R_s\right\}^{-1}$$

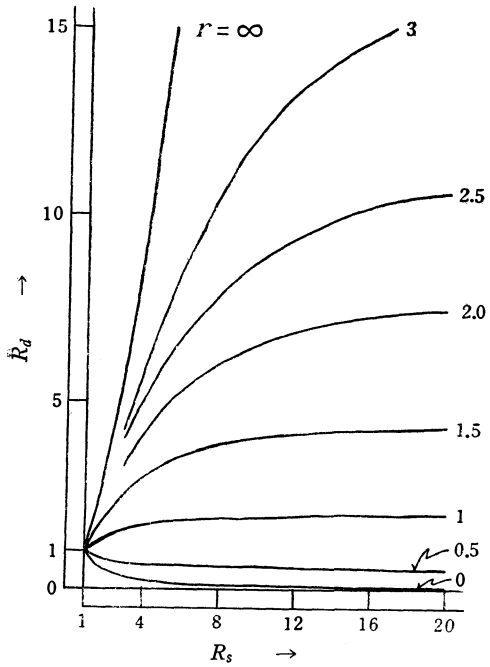


Fig. 4. Relation between R_d and R_s for various values of r.

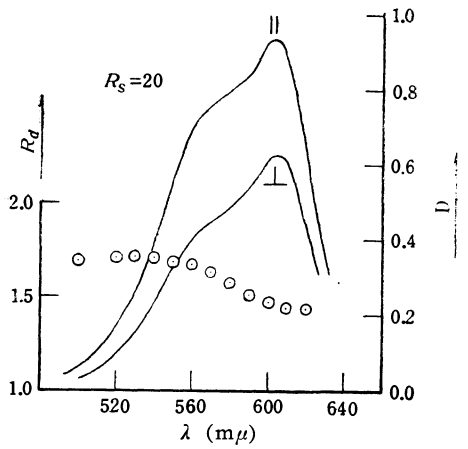


Fig. 5. Absorption spectra by polarized light of the crystal violet ion in the stretched PVA sheet. ∥ means the absorption curve when the electric vector of incident light is parallel and ⊥ means when the vector is normal to the stretch direction. Circles indicate the optical density ratio, R_d.

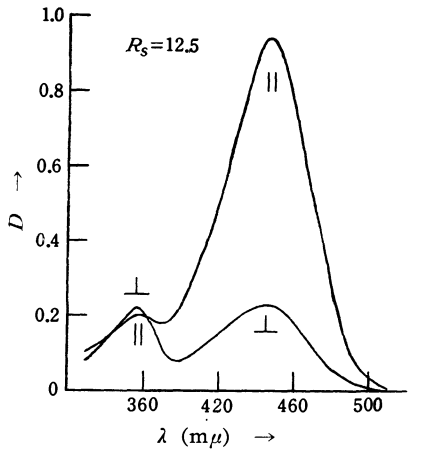


Fig. 6. Absorption spectra by polarized light of the auramine yellow ion in the stretched PVA sheet. The meaning of ∥ and ⊥ is the same as in Fig. 5.

and $R_s>1$.

This is the final expression. Plotting R_d against R_s for various values of a parameter r curves representing Eq. 11 are obtained as shown in Fig. 4.

Results

Absorption spectra by polarized light of the crystal violet and the auramine yellow ion in stretched PVA sheets are shown in Figs. 5 and 6, respectively. Fig. 5 shows that the crystal violet ion has an absorption maximum at about 605 mμ and a shoulder at about 560 mμ, and that R_d values near the shoulder are larger than that at the absorption maximum. Fig. 6 shows that the auramine yellow ion has the first (445 mμ) and the second (~375 mμ) band whose dichroic properties are different from each other. This means that transition moments corresponding to these absorption bands have different directions.

Observed and calculated relations between R_d and R_s of each absorption band are shown in Figs. 7 and 8. Fig. 7 shows the case of the crystal violet ion; the observed values at 605 mμ are represented by the white circles and those of 560 mμ by the half solid circles, and the full lines are the curves obtained from Eq. 11 putting $r=0.86$ for the 605 mμ band and $r=0.90$ and 0.92 for the 560 mμ band. Similarly, Fig. 8 shows the result of the auramine yellow ion; the observed values for the first band are indicated by the white circles and for the second band (375 mμ)

by the half solid circles, and the corresponding full lines are calculated by Eq. 11 putting $r=1.55$ and 1.60 for the first band and $r=0.60$, 0.65 and 0.70 for the second band, respectively. In Fig. 8 it is noticed that, in the small region of R_s, the observed value of R_d are smaller for the first band and larger for the second band than the calculated ones represented by the full lines. This fact may be simply interpreted as the effect due to the overlap of both bands. That is to say, on account of the mutual superposition of the bands the first band with large R_d may apparently increase the small R_d value of the second band and the converse would hold good. For the large R_s value, however, the observed R_d values roughly run along the respective calculated lines. In the case of crystal violet (Fig. 7), the observed R_d values for small R_s values are smaller than the calculated ones, and these differences are larger at 560 mμ than at 605mμ.

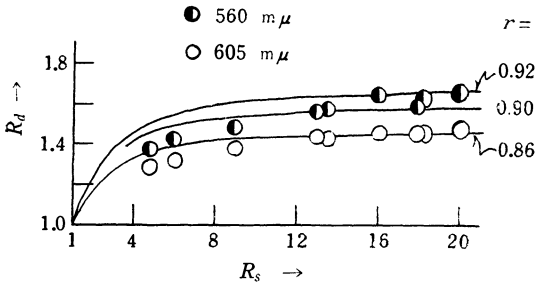


Fig. 7. Observed and calculated relations between R_d and R_s of the crystal violet ion in the stretched PVA sheet.

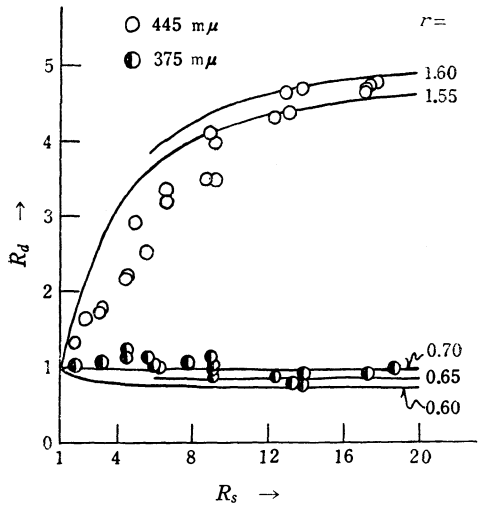


Fig. 8. Observed and calculated relationships between R_d and R_s of the auramine yellow ion in the stretched PVA sheet.

Thus, it can be said that Eq. 11 explains the experimental relation between R_d and R_s except for the smaller region of R_s and accordingly that Eq. 5 represents approximately well the nature of the distribution of such short molecules as the crystal violet ion in the stretched PVA substrate.

Discussion

The crystal violet ion. — Lewis and his coworkers[8] considered that the absorption band in the visible region of the crystal violet ion consists of those of isomers A and B. According to their consideration, the isomer A has a structure like a propeller with three blades (i. e. three benzene rings) and the isomer B has a similar form in which one blade is turned in the opposite direction from the others. As regards the absorption band here discussed, the main band belongs to the A isomer and the shoulder indicates the superposition of two bands A and B. In radially symmetrical molecules such as crystal violet, so-called x and y bands, which are both in the molecular plane[9], coincide with each other. In such a case, the transition moment is equal in all directions of the plane. This should be indeed the case of the A isomer. Furthermore, if we assume that the orientation axis is in the molecular plane, we should expect the value of r to be unity; that is, the angle of the direction of the transition moment against the orientation axis is expected to be 45°. According to our result, however, r equals to 0.86 and the corresponding orientation angle is $\cot^{-1} r=$ 49°. On the other hand, though the B isomer has not the same symmetry as the A isomer, the apparent moment would be regarded to be still equal in all directions of the molecular plane of the B isomer in the statistical sense, because the spacial extent, which may be one principal factor to govern the orientation of the molecule, seems to be passably symmetrical considering its solid thickness. So that, also in the case of the B isomer the angle mentioned above would be expected again to be 45°. But the present result indicates that r equals 0.92~0.90, hence $\cot^{-1} r$ equals to 47.5°~48°.

Fig. 5 indicates that the R_d values near the absorption maximum are always

8) G. N. Lewis, T. T. Magel and D. Lipkin, *J. Am. Chem. Soc.*, **64**, 1774 (1942).
9) G. N. Lewis and J. Bigeleisen, ibid., **65**, 2102 (1943).

smaller than that of the shoulder. According to resolution of the observed band into those of isomers made by Lewis and his coworkers[8], the maximum corresponding to the isomer A is scarcely overlapped by the band of the isomer B, while the slope of the former almost covers the latter. This implies that the observed R_d value at the maximum wavelength gives the true R_d value for the A isomer, but the observed one at the shoulder, gives the smaller than the true value for the B isomer. Accordingly, it is considered that the absorption corresponding to the B isomer has the possibility of taking the r value of unity (i. e. the corresponding angle is 45°). From this fact we should be led to the conclusion that the orientation axis of the molecule deviates from its plane in the A isomer rather than in the B isomer. This seems indeed to be improbable from the point of view of their geometrical shapes. Therefore it seems wise to discard the abovementioned explanation and to adopt the alternative[10] that both bands originate from only one species. That is to say, the light absorption bands originate from two kinds of transition in one molecular species, one of which lies on the molecular plane and the other of which has two components parallel and normal to the plane. The former may correspond to the 560 mμ band and the latter to 605 mμ. Thus we can explain the experimental facts that the 560 mμ band has always the greater R_d value than that at 605 mμ, and the R_d value of the former has the possibility to take the r value of unity.

The auramine yellow ion.—For the first band of the auramine yellow ion, the corresponding r value is 1.55~1.60 (see Fig. 8). Accordingly the angle of the transition-direction against the orientation axis is 32.5°~32°. Similarly, since the most probable value of r for the second band is 0.65, the corresponding angle is obtained as 57°. Since the mutual correlation of the absorption planes of both bands is unfortunately unknown, the angle between two directions of the corresponding transition moments can not be decided directly. Nevertheless, when it is supposed that the absorption planes coincide with each other, namely when both transitions are on the same molecular plane, the angle just mentioned would be 57°+32°=89° or 57°−32°=25°. Here the former value approximates to a right angle. This fact is of interest, because, in such a molecule as the auramine yellow ion, there may exist the x and y bands which are on the molecular plane and at right angles to each other[9].

10) Y. Mori, Presented at the Symposium of Electronic State, Nagoya, Oct. 1956.

Summary

1) An expression for the optical density ratio was derived as a function of the stretch ratio.

2) Dichroism of the crystal violet and auramine yellow ion in stretched PVA sheets was observed, and the relation of the optical density ratio to the stretch ratio was plotted. It was shown that the theoretical expression derived here could explain rather well the experimental relation between these two quantities.

3) The analytical results were as follows. The main absorption band and the shoulder of the crystal violet ion did not orginate from the two isomers but were perhaps due to one species. For the auramine yellow ion the angle between the transition directions corresponding to the first and the second band might be approximately a right angle provided that the *absorption-planes* were in a same plane.

The author is indebted to Professor Noboru Ando and Dr. Ikuzo Tanaka for their encouragement to carry out this work and also to Dr. Hideo Yamazaki for his helpful suggestions on the theoretical part. Many thanks are due to Mr. Junzo Ito of Nippon Gosei Kagaku Co., Ltd. who gave polyvinyl alcohol, to Mr. Norio Ikari of Hodogaya Kagaku Co., Ltd. who gave the dye samples, and also to Mr. Toshiro Iijima who helped the author in chromatographical tests.

Laboratory of Physical Chemistry
Tokyo Institute of Technology
Meguro-ku, Tokyo

Studies on Antibiotics and Related Substances. VII. The Structure of Kanamycin

By Sumio UMEZAWA, Yukio ITŌ and Shunzō FUKATSU

(Received August 5, 1958)

Kanamycin has been described by H. Umezawa and coworkers[1] as an antibiotic produced by a strain of *Streptomyces kanamyceticus*. It is low toxic and very active against a variety of Gram-positive and Gram-negative bacteria including streptomycin-resistant strain. Kanamycin was isolated in a pure state as a crystalline monosulfate which was converted into a crystalline free base[2,3]. Analysis and electrometric titrations of the salt and the free base indicated that the antibiotic is a tetra-acidic base of the composition $C_{18}H_{36}O_{11}N_4$. Acetylation of kanamycin with acetic anhydride in methanol gave tetra-*N*-acetyl kanamycin[3,4]. On the other hand, when kanamycin was acetylated with acetic anhydride and pyridine, undeca-acetylkanamycin was obtained[4].

Information about the degradation products of kanamycin was obtained by studying the products formed by acid hydrolysis[3,4]. From the hydrolyzate of kanamycin by 6 N hydrochloric acid, Maeda, et al.[4], isolated two kinds of reducing aminohexoses and diamino-trihydroxycyclohexane which was identical with deoxystreptamine (I) isolated from the vigorous hydrolysis of neomycin[5]. Moreover, Ogawa and Itō[6] obtained deoxystreptamine and two kinds of methylaminohexosides by methanolysis of kanamycin. Recently, we received an information from Hooper and others[7] that they identified the two aminohexose-moieties of kanamycin to be D-6-amino-6-deoxyglucose (pyranose form) (II) and 3-amino-3-deoxyaldohexose (pyranose form) (III).

Therefore, the hydrolytic cleavage of kanamycin could be represented by the following equation:

$$C_{18}H_{36}O_{11}N_4 + 2H_2O \rightarrow C_6H_{14}O_3N_2 + 2C_6H_{13}O_5N$$
(I) (II) and (III)

The present authors[8] recently reported in a short communication that the acid-hydrolysis of exhaustively methylated *N*-acetylkanamycin resulted in the isolation of mono-*O*-methyldeoxystreptamine which presents evidence to show that both of the two aminohexose moieties are directly joined to deoxystreptamine. The situation is different from streptomycin in which streptidine is linked with streptobiosamine, or from neomycin in which deoxystreptamine is linked with neobiosamine.

The present paper deals with the sites of glucosidic linkages occurring between the above-mentioned three moieties in detail.

The tetra-*N*-acetylkanamycin prepared by the method of Cron and others[3] was methylated with dimethyl sulfate and sodium hydroxide by the method of West and Holden[9] to yield a crude methylated product, which was chromatographed through a cellulose powder column to yield a colorless gum. The acetyl determination showed that the methylated product is partially de-*N*-acetylated. When the methylated product was acetylated again to make sure, the tetra-*N*-acetyl-hepta-*O*-methylkanamycin was obtained. It was further ascertained by infrared spectrum that no free hydroxyl group is contained in the methylated product.

The methylated product was hydrolyzed with 6 N hydrochloric acid. Paper chromatography studies of the hydrolyzate showed three ninhydrin positive spots of

1) H. Umezawa, M. Ueda, K. Maeda, K. Yagishita, S. Kondo, Y. Okami, R. Utahara, Y. Osato, K. Nitta and T. Takeuchi, *J. Antibiotics, Series A*, **10**, (5), 181 (1957).
2) K. Maeda, M. Ueda, K. Yagishita, S. Kawaji, S. Kondo, M. Murase, T. Takeuchi, Y. Okami and H. Umezawa, ibid., 228 (1957).
3) M. J. Cron, D. L. Johnson, F. M. Palermiti, Y. Perron, H. D. Taylor, D. F. Whitehead and I. R. Hooper, *J. Am. Chem. Soc.*, **80**, 752 (1958).
4) K. Maeda, M. Murase, H. Mawatari and H. Umezawa, *J. Antibiotics, Series A*, **11**, (2), 73 (1958).
5) F. A. Kuehl, M. N. Bishop, K. Folkers, L. H. Sommer, N. S. Marans, G. M. Goldberg, J. Rockett and P. P. Pioch, *J. Am. Chem. Soc.*, **73**, 881 (1951).
6) H. Ogawa and T. Itō, *J. Antibiotics, Series A*, **10**, (6), 267 (1957); ibid., **11**, (2), 70, 72 (1958).
7) M. J. Cron, O. B. Farding, D. L. Johnson, H. Schmitz, D. F. Whitehead, I. R. Hooper and R. V. Lemieux, *J. Am. Chem. Soc.*, **80**, 2342, 4741 (1958).
8) S. Umezawa, Y. Itō and S. Fukatsu, *J. Antibiotics, Series A*, **11** (5), 120 (1958).
9) E. S. West and R. F. Holden, *J. Am. Chem. Soc.*, **56**, 930 (1934).

R_f 0.08, 0.32 and 0.41 with a *n*-butanol-ethanol-water mixture. The hydrolyzate was evaporated to dryness, taken up in methanol and treated with ether to yield an amorphous precipitate, which consisted of the product of R_f 0.08, containing a small amount of the product of R_f 0.32. The precipitate was chromatographed through a cellulose powder column to yield the colorless, crystalline hydrochloride of mono-*O*-methyldeoxystreptamine (IV), which was optically inactive and, upon oxidation with periodate, consumed two moles of periodate without the formation of formic acid.

The hydrochloride was acetylated with acetic anhydride in pyridine to yield the colorless prisms of the diacetate (V) of mono-*O*-methyl-di-*N*-acetyldeoxystreptamine.

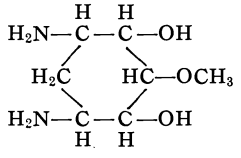
Finally, the diacetate was subjected to de-*O*-acetylation with ammonia in absolute methanol solution at 0°C to yield the colorless prisms of mono-*O*-methyl-di-*N*-acetyldeoxystreptamine (VI). This consumed no periodate and was also optically inactive.

The compounds (IV, VI) with the *O*-methyl group in the 5-position should be optically inactive while the compounds with the *O*-methyl group in the 4- or 6-position should be optically active. The di-*N*-acetyl compound (VI) with the *O*-methyl group in the 5-position should consume no periodate while the corresponding compound with the *O*-methyl group in the 4- or 6-position should consume one mole of periodate. The compound IV with the *O*-methyl group in the 5-position should be oxidized with two moles of periodate without the formation of formic acid while the corresponding compound with the *O*-methyl group in the 4- or 6- position should consume two moles of periodate with the formation of one mole of formic acid.

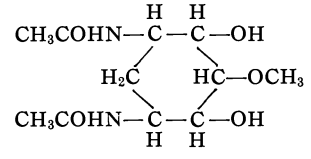
Therefore, the experimental evidences presented above have led the authors to conclude that the mono-*O*-methyl-deoxystreptamine (IV) is 1, 3-diamino-4, 6-dihydroxy-5-methoxycyclohexane and, considered with the previous findings, permit the assignment of structure VII to kanamycin.

Experimental

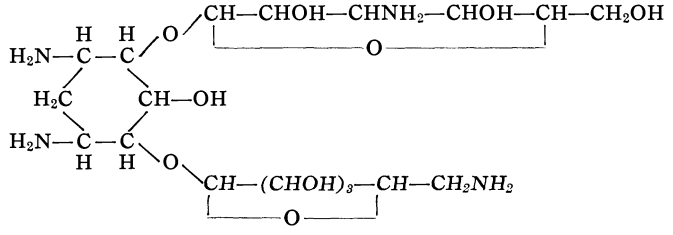
Methylation of *N*-Acetylkanamycin.—To a vigorously stirred solution of tetra-*N*-acetylkanamycin (4.0 g.) in water (8 cc.) was added a solution of dimethyl sulfate (52 g.) in carbon tetrachloride (40 cc.). During this and the subsequent addition of alkali the temperature of the reaction was kept at 50~55°C. A solution of sodium hydroxide (108 g.) in water (100 cc.) was then added dropwise over a one-hour period, with vigorous stirring. The temperature was then raised slowly to 70~75°C and dimethyl sulfate (103 g.) was added dropwise over a 30-minute period. Again, a solution of sodium hydroxide (36 g.) in water (30 cc.) was added and then dimethyl sulfate (52 g.) was added gradually in a 15-minute period. After this addition the water-bath was heated to boiling and kept at this temperature for 30 min. The temperature was then lowered to about 50°C and the mixture was stirred vigorously with chloroform (150 cc.) for 15 min. The mixture was filtered and the sodium sulfate precipitate was washed with chloroform. The aqueous portion of the filtrate was re-extracted with chloroform as described above. The chloroform extracts were combined and dried with sodium sulfate. Evaporation of the solvent in vacuo left an amber



(IV)



(VI)



(VII)
Kanamycin

gum (3.22 g.) soluble in methanol, ethanol, chloroform and water. A sample was dried in vacuo at 60~70°C. The determination of methoxyl content gave 27.44% OCH_3.

The crude product (11.17 g.) was dissolved in a solution (30 cc.) of *n*-butanol-ligroin-water (38 : 60 : 2) and chromatographed on a column (2.5×40 cm.) of cellulose powder washed with the same solvent. Sixteen fractions of eluate with the same solvent were limited to 40 cc. each, evaporated in vacuo to dryness and weighed. Fractions 7-14 were combined to yield 7.0 g. of exhaustively methylated *N*-acetyl-kanamycin, m. p. 80°C (sintered at about 65°C). The determinations of methoxyl and acetyl content gave 28.35% OCH_3 and 12.25% $COCH_3$.

It was ascertained by infrared spectrum that no free hydroxyl group is contained in the methylated product.

A portion (2.5 g.) of the methylated product of tetra-*N*-acetylkanamycin was dissolved in absolute methanol (22.5 cc.) and to the solution acetic anhydride (4.3 cc.) was added. After being allowed to stand overnight, the acetylation mixture was filtered and evaporated to dryness. The residue was dissolved in water (20 cc.) and extracted thrice with chloroform (20 cc.). The chloroform extracts were combined and dried with sodium sulfate. Evaporation of the solvent left a colorless gum which resisted attempts to crystallize it (1.17 g.).

Anal. Found: OCH_3, 27.5; $COCH_3$, 21.6. Calcd. for $C_{18}H_{21}O_4(OCH_3)_7(NHCOCH_3)_4$: OCH_3, 28.9; $COCH_3$, 22.9. Calcd. for $C_{18}H_{22}O_5(OCH_3)_6(NHCOCH_3)_4$: OCH_3, 25.3; $COCH_3$, 23.4%.

Isolation of Mono-*O*-methyldeoxystreptamine Hydrochloride (IV) from Hydrolyzed Methylated *N*-acetylkanamycin.—Exhaustively methylated *N*-acetyl-kanamycin (7.0 g.) was refluxed with 6 N hydrochloric acid (100 cc.) for 1.5 hr. The reaction mixture was evaporated to dryness at 60°C in vacuo. The residue was dissolved in water (100 cc.) and evaporated again to dryness. The evaporation to remove hydrogen chloride was repeated thrice. The residue was dissolved in water (100 cc.) and the solution was decolorized with active charcoal (1.0 g.).

Paper chromatography of the hydrolyzate using the top-layer of *n*-butanol-ethanol-water (4 : 1 : 5) gave 3 zones with ninhydrin. The R_f values were 0.08 (brown), 0.32 (orange) and 0.41 (violet), respectively.

The decolorized solution was evaporated at 60°C in vacuo to dryness and dried in a desiccator overnight. The amber residue was dissolved in methanol (20 cc.) and the solution was diluted with ether (50 cc.) to yield a precipitate (1.90 g.). Paper chromatography of the precipitate using the above-mentioned solvent showed the main spot with R_f 0.08 (brown) and a trace with R_f 0.32 (orange).

The precipitate (1.90 g.) was dissolved in the top-layer (10 cc.) of *n*-butanol-ethanol-water (4 : 1 : 5) and chromatographed on a column (1.5×50 cm.) of cellulose powder (18 g.) washed with the same solvent. Twenty fractions of eluate with the same solvent were limited to 20 cc. each, evaporated to dryness in vacuo and weighed. Fractions 6—9 were combined to yield the crude hydrochloride of mono-*O*-methyldeoxystreptamine (1.65 g.).

Three recrystallizations from methanol-ethanol gave colorless needles (350 mg.) of the hydrochloride of 1, 3-diamino-4, 6-dihydroxy-5-methoxycyclohexane (IV), m. p. 207~209°C (decomp.), which was optically inactive.

Anal. Found: C, 34.03; H, 7.17; N, 10.94; OCH_3, 11.65. Calcd. for $C_6H_7(OH)_2(NH_2)_2(OCH_3)\cdot 2HCl$: C, 33.73; H, 7.23; N, 11.24; OCH_3, 12.45%.

Periodate Oxidation. — The accurately weighed sample (20.1 mg.) of 1, 3-diamino-4, 6-dihydroxy-5-methoxycyclohexane hydrochloride was dissolved in 0.023 N sodium periodate solution (20 cc.) and 2 cc. aliquots were titrated with 0.1 N sodium arsenite at the intervals listed in Table I, according to the procedure of Fleury and Lange[10]. Two moles of periodate was consumed without the formation of formic acid.

TABLE I
PERIODATE OXIDATION*

	Time (hr.)					
	0.5	1	2	3	4	6
1, 3-Diamino-4, 6-dihydroxy 5-methoxy-cyclohexane·2HCl	1.91	1.88	—	1.98	—	1.95
1, 3-Diacetamido-4, 6-dihydroxy-5-methoxy-cyclohexane	0.18	0.25	0.14	—	0.23	—

* Expressed in terms of moles of periodate consumed per mole of substance.

1, 3-Diacetamido-4, 6-diacetoxy-5-methoxycyclohexane (V). — The crude hydrochloride (1.2 g.) of 1, 3-diamino-4, 6-dihydroxy-5-methoxycyclohexane was acetylated with acetic anhydride-pyridine (18 cc. : 36 cc.) at 27°C for 24 hr. The acetylation mixture was concentrated to dryness at 40°C in vacuo; the residue was dissolved in water (20 cc.) and decolorized with active charcoal (0.5 g.). The filtrate was again evaporated to dryness in vacuo and dried in a desiccator overnight. The residue was washed with ether (30 cc.), and taken up in chloroform (20 cc.); a small quantity of insoluble part was filtered off and the filtrate was dried with sodium sulfate. Evaporation of the solvent was followed by extraction with hot ethyl acetate. Crystallization from the extract yielded colorless prisms (215 mg.), m. p. 220°C (decomp. sintered at about 170°C).

Anal. Found: C, 52.35; H, 6.65; N, 8.18; OCH_3, 9.22. Calcd. for $C_6H_7(OCH_3)(OCOCH_3)_2\cdot(NHCOCH_3)_2$: C, 52.32; H, 6.98; N, 8.14; OCH_3, 9.01%.

10) P. F. Fleury and J. Lange, *J. pharm. chim.*, [8] **17**, 107, 196 (1933).

The mother liquor was concentrated and allowed to stand at room temperature to yield the second crop of crystals (350 mg.).

1,3-Diacetamido-4,6-dihydroxy-5-methoxycyclohexane (VI). — A solution of 1,3-diacetamido-4,6-diacetoxy-5-methoxycyclohexane (460 mg.) in absolute methanol (130 cc.) was treated with a stream of dry ammonia gas for 1 hr. After being allowed to stand 3 hr. at room temperature, the mixture was evaporated at about 50°C in vacuo to dryness. The residue was dissolved in absolute methanol (50 cc.) and evaporated again to dryness in vacuo. The residue was taken up in absolute ethanol (30 cc.) and the solution was filtered to remove a small quantity of insoluble part. When the filtrate was concentrated and cooled, colorless needles crystallized out. Recrystallization from absolute ethanol yielded 130 mg. of 1,3-diacetamido-4,6-dihydroxy-5-methoxycyclohexane. The product was optically inactive.

Anal. Found: C, 50.94; H, 7.47; N, 10.64; OCH_3, 11.32; *N*-acetyl, 32.99, 33.87. Calcd. for $C_6H_7(OH)_2(OCH_3)(NHCOCH_3)_2$: C, 50.77; H, 7.69; N, 10.77; OCH_3, 11.9. *N*-acetyl, 33.08%.

Periodate Oxidation. — An accurately weighed sample (25.3 mg.) of 1,3-diacetamido-4,6-dihydroxy-5-methoxycyclohexane was dissolved in 0.0287 N sodium periodate (20 cc.) and 2 cc. aliquots were titrated with 0.1 N sodium arsenite at the intervals listed in Table I.

Summary

Evidence is presented to show that both the two aminohexose moieties in kanamycin are directly joined to deoxystreptamine through hydroxyl groups by glucosidic linkages. Proof for the sites of attachment of the two aminohexose moieties rests on the periodate oxidation of the optically inactive 1,3-diamino-4,6-dihydroxy-5-methoxycyclohexane and its *N*-acetyl derivative which were obtained by the degradation of exhaustively methylated *N*-acetylkanamycin by acid hydrolysis followed by acetylation. Kanamycin is therefore represented by formula VII.

The authors wish to express their appreciation to Professor H. Umezawa of National Institute of Health, Dr. I. R. Hooper of Bristol Laboratories and Dr. H. Ogawa of Research Laboratories of Meiji Seika Co. for helpful advice and to Meiji Seika Co. for the generous gift of kanamycin samples.

Department of Applied Chemistry
Engineering Faculty of Keio University
Koganei, Tokyo

Vapor Pressure of Molecular Crystals. XIII. Vapor Pressure of α-Glycine Crystal. The Energy of Proton Transfer

By Sadao TAKAGI*, Hideaki CHIHARA and Syûzô SEKI

(Received August 7, 1958)

Glycine is the simplest amino acid, having the zwitterion configuration within the crystal lattice[1]. Three modifications have been reported[2] and the α-form is probably the most stable one at room temperature. The molecular structure of glycine in the vapor phase is not known probably owing to low vapor pressure of the crystal. If glycine sublimes with the molecular configuration (and not the zwitterion configuration), a proton must be transferred from an NH_3^+ group of a zwitterion to a COO^- group of the neighboring zwitterion in the crystalline state. Or, in an alternative way, the proton transfer must occur in the vapor state after the zwitterion has sublimed, and this transfer undoubtedly accompanies greater energy change than it would in the crystalline state[3]. On the other hand, if the sublimation does not accompany the proton transfer, the heat of sublimation would be as great as that of an ionic crystal. The present study aims at the energetics of sublimation, with a hope of obtaining some information about such

* Present address, The Institute of Polytechnics, Osaka City University, Kita-ku, Osaka.

1) G. Albrecht and R. Corey, *J. Am. Chem. Soc.*, **61**, 1087 (1939); H. Baba, et al., *J. Chem. Soc. Japan, Pure Chem. Sec.* (*Nippon Kagaku Zasshi*), **70**, 333 (1949); K. Kuratani, ibid., **70**, 453 (1949).

2) Y. Iitaka, *Proc. Japan Acad.*, **30**, 109 (1954); J. Bernal, *Z. Krist.*, **78**, 363 (1931).

3) R. W. Gurney, "Ionic Processes in Solution", McGraw-Hill, N. Y., 1953.

proton transfer. The determination of the relative stability of the modifications of glycine crystals by measurements of vapor pressures presents another interesting problem but will not be considered here.

Experimental

Material.—Glycine (Organic Synthetic Chemicals Co., special grade) was recrystallized from aqueous solution repeatedly and dried over phosphorus pentoxide. The more satisfactory method of drying crystals by vacuum sublimation was not applied because it was found that sublimation gave a mixture of α and γ form of glycine. The modifications were identified by use of the X-ray powder diffraction patterns. Occlusion of water within the crystal lattice may cause a serious error in the measurement of vapor pressure[4] and it is highly probable particularly when we deal with crystals of polar molecules. Pieces of glycine crystals, of the same batch as that used for the pressure measurements, were heated in vacuo to see if the occluded water was present, with the result that no water evolution was detected up to the decomposition temperature, ca. 230°C. The constancy of the vapor pressure at a fixed temperature during a fixed length of time, a few hours, was considered to provide another assurance.

Measurements of Vapor Pressures.—The sublimation pressure was measured between 138 and 153°C with an apparatus, the same as the one reported elsewhere[5], based on the Knudsen effusion method.

Results.—The vapor pressures are listed in Table I. These data well fit the vapor pressure equation

$$\log P(\text{mmHg}) = 13.666 - (6816.8/T)$$

obtained by the method of least squares. The heat, entropy and free energy of sublimation derived from the equation are given in Table II.

Table I

Vapor pressure of α-glycine

t°C	P(mmHg) $\times 10^3$	t°C	P(mmHg) $\times 10^3$
138.9_8	1.344	145.9_7	2.459
140.6_6	1.557	147.3_3	2.877
142.0_9	1.789	149.2_6	3.289
143.4_9	1.978	150.6_6	3.899
144.7_9	2.360	152.6_8	4.362

Table II

Heat, entropy and free energy of sublimation

Heat	Entropy	Free Energy at 298.16°K
31.18±0.49 kcal./mole	49.33±1.17 cal./deg.mole	16.47±0.60 kcal./mole

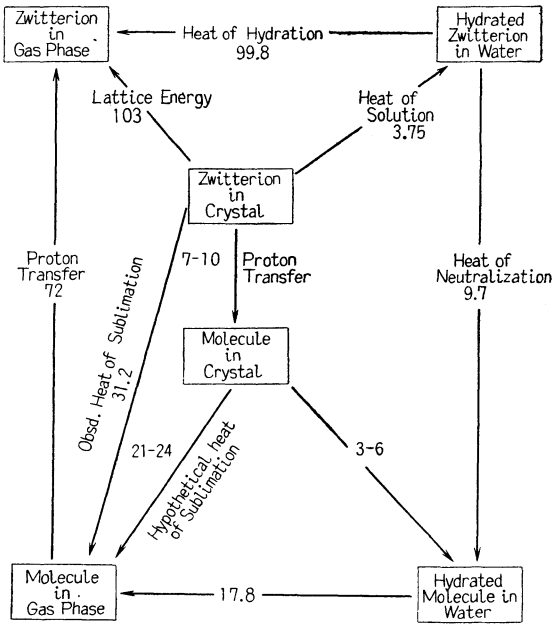


Fig. 1. Energy cycle of glycine (in kcal./mole). Arrows indicate the direction of endothermic changes.

Discussion of the Results

Fig. 1 illustrates an energy-cycle for glycine constructed by use of available thermochemical values. Arrows in Fig. 1 indicate the directions of endothermic changes. This is the final set-up of the energy diagram and we examined other possibilities also, because it was not a priori apparent that the measured heat of sublimation 31.2 kcal./mole corresponds to the change from 'zwitterion in crystal' to 'molecule in gas phase'.

It was first assumed that the observed 31.2 kcal. is the change in heat content in going from the crystal to zwitterions in vapor; in other words this value represents the lattice energy of the crystal if allowance is made for the average kinetic energy of dipolar-ions in vapor. An independent estimate of the lattice energy of glycine has been reported by Shimura from the measured partial molal volume of glycine in aqueous solution by help of Kirkwood's theory on the free energy of hydration[6]. This estimate gives the lattice energy a value as great as 103 kcal./mole. The dipole moment of glycine determined by Buckingham[7] (13.3D) shows

4) S. Seki, H. Chihara and K. Suzuki, "Hydrogen Bond", Iwanami Co. (1956), p. 40.
5) I. Nitta, S. Seki, M. Momotani and K. Sato, *J. Chem. Soc. Japan, Pure Chem. Sec.* (*Nippon Kagaku Zasshi*), **71**, 378 (1950).
6) K. Shimura, *J. Agr. Chem. Soc. Japan* (*Nippon Nōgei-Kagaku Kaishi*), **24**, 412 (1951).
7) A. D. Buckingham, *Australian J. Chem.*, **6**, 323 (1953).

that it is reasonable to assume that unit point charges rest on N and O atoms in a zwitterion so that the electrostatic interaction energy alone in the crystal would amount to about 60 kcal./mole. The total lattice energy including the van der Waals and the hydrogen bond energy will be at least 80 kcal./mole. Therefore our first assumption was wrong and the observed heat of sublimation must correspond not to the lattice energy but to the change in heat content in going from the crystal to molecules in vapor state.

Estimation of the heat of sublimation of a hypothetical crystal composed of glycine molecules, NH_2CH_2COOH.*—The van der Waals energy will contribute about 7.7 kcal. to this hypothetical lattice energy, which is the heat of sublimation[8] of 2-methyl-1-butene, a molecule which is isoelectronic with glycine. The following energy values are assigned to the three hydrogen bonds: 5~6 kcal. for the NH···O 2.76Å long (in diformylhydrazine[9] 2.80Å), 2.5~3.5 kcal. for the bifurcated bonds 2.93 and 3.05Å long (in urea[9] 2.99 and 3.04Å) and 3~4 kcal. for the bond of intermediate length 2.88Å. The sum of all these energy values 20.7~24.7 kcal./mole will be taken as the hypothetical heat of sublimation of molecular crystal of glycine**.

The energies of proton transfer.—By combining the hypothetical heat of sublimation with the observed heat of sublimation 31.2 kcal./mole, we see that the zwitterion crystal is more stable than the molecular crystal by about 7~10 kcal./mole, or in other words a proton transfer in the crystal (a change from $N^+H\cdots O^-$ to $OH\cdots N$) would accompany a heat absorption of 7~10 kcal./mole. If the proton transfer occurred in vapor state, the change

$$NH_2CH_2COOH \rightarrow NH_3^+CH_2COO^-$$

would accompany as much energy absorption as 72 kcal./mole and the "molecular" configuration would be extremely stable in vapor phase in contrast to the situation in the crystalline state. The result that the energy of proton transfer in vapor is about ten times as great as that in a crystal shows that the proton transfer can occur non-adiabatically in the crystal lattice: i.e. as a proton moves along the N···O bond by absorbing the necessary energy, the potential energy curve changes its shape as illustrated schematically in Fig. 2. The strong crystal field may be participating in such a change in the potential

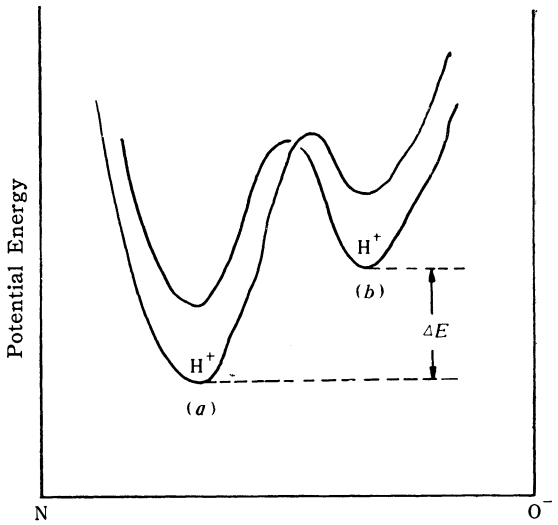


Fig. 2. Change of the potential energy curve in the course of proton transfer. ΔE is the energy of proton transfer (from *a* to *b*) in crystal.

energy diagram. Thus the energy of proton transfer in crystal here obtained does not represent the energy for a single proton to move within a fixed "double minimum" potential field, but the energy required for the overall rearrangement of electronic charges in the entire volume of a crystal is included.

This is a piece of information which we consider to be important in connection with energetics of hydrogen bonding. Participation of hydrogen bonding has often been assumed in various chemical reactions such as in simple hydrogen-deuterium exchange reactions and keto-enol isomerization reactions. Nuclear resonance studies in solution has come to attention of many investigators[10] in relation to the acid-base interaction and they will be one of significant methods of attack against proton transfer in solution.

Glycine is the simplest amino acid constituting complex protein molecules. In

* By hypothetical it is meant that the crystal structure is the same as that of the zwitterion-crystal except for the position of a hydrogen atom; actually the OH···O bonds would be formed if the molecular crystal were more stable.

8) S. S. Todd, G. D. Oilver and P. M. Huffman, *J. Am. Chem. Soc.*, **69**, 1519 (1947); D. W. Scott, G. Waddington, J. C. Smith and H. M. Huffman, ibid., **71**, 2767 (1949).

9) K. Suzuki, S. Onishi, T. Koide and S. Seki, This Bulletin, **29**, 127 (1956).

** The range of uncertainty was taken wide enough in order to cover the limit of validity of discussions.

10) J. N. Shoolery and B. J. Alder, *J. Chem. Phys.*, **23**, 805 (1955); E. Grunwald, A. Loenstein and S. Meiboom, ibid., **27**, 630, 641 (1957).

view of relatively small amount of energy required for a proton jump in a strong crystalline field, it may be reasonably supposed that such proton jumps can frequently occur in many protein systems with or without bound water molecules. Thus a diminishingly small degree of stimulation, given one end of a fibrous nerve protein coiled in a helical arrangement through NH···O hydrogen bonds, may easily be conveyed to the other end of that nerve protein by synchronous proton transfer. Such a mechanism, in fact, has been proposed by several authors[11] and we believe that we could here present some grounds for such speculative discussions.

The energy of proton transfer in vapor state may be very roughly evaluated by the sequence of changes:

$$NH_2CH_2COOH \underset{D}{\rightarrow} NH_2CH_2COO + H \underset{A}{\rightarrow}$$

$$NH_2CH_2COO^- + H \underset{I}{\rightarrow} NH_2CH_2COO^- + H^+$$

$$\underset{P}{\rightarrow} NH_3^+CH_2COO^-$$

D, A, I and P may be replaced by the bond dissociation energy of an O—H bond (110.2 kcal./mole), the electron affinity of an O atom (−87.7 kcal./mole), the ionization energy of a hydrogen atom (312.1 kcal./mole) and the proton affinity of an NH_3 molecule (−219 kcal./mole[12]), respectively. The overall change in energy will be 116 kcal./mole in comparison with 72 kcal./mole given in Fig. 1.

Estimation of the heat of self-neutralization in solution and other heats derived therefrom.—The process of self-neutralization in solution may be divided into two steps;

$$H_3N^+CH_2COO^- + H^+ = H_3N^+CH_2COOH - \Delta H_a$$

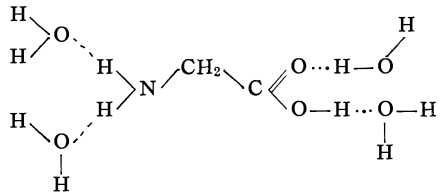
and

$$H_3N^+CH_2COOH = H_2NCH_2COOH + H^+ + \Delta H_b.$$

ΔH_a can be evaluated from the temperature variation of pK_a, giving 1.16 kcal./mole[13]. ΔH_b may be approximated by the heat (10.8 kcal./mole) associated with the change

$$H_3N^+CH_2COO^- = H_2NCH_2COO^- + H^+.$$

It is believed that this approximation will not cause a significant error since the reaction takes place in aqueous solution having the static dielectric constant larger than 80. The heat of self-neutralization will then be 9.7 kcal./mole (Fig. 1). This value was used to obtain the heat of solution of hypothetical crystals of molecular glycine 3∼6 kcal./mole and the heat of solution of glycine vapor (heat of hydration) 17.8 kcal./mole, both giving a hypothetical solution of molecular glycine*. This is reasonable for a heat of hydration if we assume the hydrogen bond formation scheme like the following one:



The difference 82 kcal./mole between the heat of hydration of zwitterion in vapor and the heat of hydration of molecules in vapor (giving ionic and molecular solutions, respectively) is a rough indication of the effect of ionic charge on N and O atoms when placed in aqueous solution.

Concluding remarks. — The molecular-dipolar ion (zwitterion) relationship now demonstrated for glycine is by no means an exceptional case but may be found in other more familiar systems such as ammonium chloride decomposing into ammonia and hydrogen chloride in the vapor state. Here are apparently the proton jumps occurring in sublimation process, to which a formal analogy of the present treatment may be applicable. It will be interesting to examine the movement of protons or the rôle of hydrogen bonding in more complex amino acids or polypeptides by more-or-less direct means.

Summary

Sublimation pressures of crystalline α-glycine were measured between 138 and 153°C by the effusion method. The pressure equation

$$\log P(\text{mmHg}) = 13.666 - (6816.8/T)$$

11) I. Oshida, Y. Oshika and R. Miyasaka, *J. Phys. Soc. Japan*, **10**, 849 (1955); M. L. Huggins, *Am. Scientist*, **31**, 338 (1943); N. Riel, *Naturwissenshaften*, **43**, 145 (1956).

12) H. Tsubomura, private communication.

13) E. J. Cohn and J. T. Edsall, "Proteins, Amino Acids and Peptides as Ions and Dipolar Ions", Reinhold, New York (1943), p. 80.

* This heat of hydration may be compared with the heat of hydration (7.8 kcal.) of propionic acid corrected for the difference in the interaction energy of a methyl group (3.4 kcal.) and that of an amino group (5.6 kcal.) with water, where it has been assumed that three water molecules accommodate to each of methyl and amino groups (cf. J. A. V. Butler, *General Discussion of the Faraday Soc. on the Structure and Molecular Forces in Pure Liquid and Solution*, 229 (1936));
7.8+(3×5.6)−(3×3.4)=14.4 kcal./mole.

fits well the experimental data. The heat, entropy and free energy (at 25°C) of sublimation were 31.18±0.49 kcal./mole, 49.33 ± 1.17 cal./deg. mole and 16.47 ± 0.60 kcal./mole, respectively. An energy cycle was constructed which correlates zwitterion and molecule in crystal and vapor states, and hydrated zwitterion and molecule in solutions. The observed heat of sublimation corresponds to the change in heat content in going from the zwitterion-crystal to gaseous molecules. The molecular configuration is more stable in vapor state. By using the experimental values of the heat of sublimation, the heat of solution of crystals into water and the temperature dependence of pK_a in solution, with the help of the theoretical values of the lattice energy of the crystal, the following heat values were determined; the heat of proton jump in vapor, $NH_3^+CH_2COO^- \rightarrow NH_2CH_2COOH$, −72 kcal./mole, the heat of proton jump in the crystal 7∼10 kcal./mole, hypothetical heat of sublimation of crystals composed of molecules 21∼24 kcal./mole, the heats of hydration of a zwitterion and a molecule −99.8 and −17.8 kcal./mole, respectively, the heat of solution of the hypothetical crystal to give a solution of molecular glycine 3∼6 kcal./mole, and the heat of self-neutralization in aqueous solution 9.7 kcal./mole. The negative quantities show that the processes are exothermic. It was shown that the proton transfer in a medium of large dielectric constant or in a strong crystalline field requires only a small amount of energy and its significance in chemical reactions and biochemical activities was suggested. Each of the derived heat values was examined by independent checks from different sources, except for the energies of proton transfer.

The authors wish to express their sincere gratitude to Professor I. Nitta for his interest in this research. They are also indebted to the Ministry of Education for the financial support.

Department of Chemistry
Faculty of Science
Osaka University
Kita-ku, Osaka

*Photometric Study on the Change of Basic Rhodochromium Ion to Basic Erythrochromium Ion in Aqueous Solution**

By Masayasu MORI, Shigeru UESHIBA and Hideo YAMATERA**

(Received August 7, 1958)

The so-called rhodochromium salt has attracted the attention of some investigators in coordination chemistry because of the peculiar reaction of its aqueous solution toward aqueous alkalis. This reaction may be represented by the scheme in Table I.

When Jörgensen discovered these salts, he thought that I and IV were isomers, while II was isomeric to III. Wilmarth, Graff and Gustin[1] investigated this problem using various methods. By careful analyses they denied this isomerism and found the correct formulae of the basic erythro salt and the erythro salt to be as given in Table I.

The reaction II → III may, therefore, be considered as a kind of replacement reaction of the coordinated ammonia molecule. Wilmarth and others called attention to the ease with which this reaction occurs and attributed it to the peculiar structure of the basic rhodo salt with a possible π-bonding as demonstrated by their magnetic measurements. They also found by visual observation that the reaction velocity is not affected by the hydroxide ion concentration ranging from 10^{-4} to 6.0 N in alkali.

It seemed to the present authors that the quantitative study of the kinetics of this reaction II → III would be of value in knowing the energy relation and the

* Presented at the Symposium on Coordination Chemistry, held in Nagoya on Nov. 16~17, 1957.

** Present Address: Faculty of Science, Rikkyo University, Toshima-ku, Tokyo,

1) W. K. Wilmarth, H. Graff and S. T. Gustin, *J. Am. Chem. Soc.*, **78**, 2683 (1956).

TABLE I

THE RELATION BETWEEN THE RHODOCHROMIUM SALT AND ITS DERIVATIVES

Rhodochromium Salt		Erythrochromium Salt
$[Cr(NH_3)_5OHCr(NH_3)_5]X_5$		$[Cr(NH_3)_5OHCr(NH_3)_4OH_2]X_5$
(I)		(IV)
red		red
Alkali ⇄ Acid		Alkali ⇄ Acid
Basic Rhodochromium Salt		Basic Erythrochromium Salt
$[Cr(NH_3)_5OCr(NH_3)_5]X_4$	$\xrightarrow[\text{Time}]{}$	$[Cr(NH_3)_5OHCr(NH_3)_4OH]X_4$
(II)		(III)
blue		red

TABLE II

THE RESULT OF ANALYSIS OF DECAMMINE-μ-OL-DICHROMIUM(III) CHLORIDE PERCHLORATE

$[Cr(NH_3)_5OHCr(NH_3)_5]_2Cl_3(ClO_4)_7 \cdot xH_2O$

	Cr	N	Cl	Cl in ClO_4	H_2O
Calcd. $x=0$	15.02	20.22	7.68	17.91	0
Calcd. $x=2$	14.64	19.71	7.49	17.46	2.54
Found in Sample I	15.10	19.56	7.40	16.45	1.74
Found in Sample II	15.22	18.78	7.18	16.78	2.8, 3.4
Found in Sample III	15.07	19.60	6.90	17.15	2.58
Found in Sample IV	15.27	19.82	7.53	17.02	1.57

The poor agreement of the analytical data with the calculated values in some samples is possibly due to the incomplete removal of perchloric acid owing to the fineness of crystals. Special attention has been paid in sample IV to avoid this. It seemed difficult to determine the content of water molecules on account of the slow decomposition of the complex at 100°C.

structure of the related compounds. These salts have characteristic absorption spectra in the visible and ultraviolet region and, therefore, the reaction velocities can be readily pursued by the aid of a spectrophotometer.

Experimental

Materials.—Decammine-μ-ol-dichromium(III) chloride perchlorate, $[Cr(NH_3)_5OHCr(NH_3)_5]_2Cl_3(ClO_4)_7 \cdot xH_2O$ has been used in most of the present research. The chloride prepared as described by Jörgensen was converted into this salt by dissolution in water and addition of perchloric acid. Even recrystallization with perchloric acid did not alter the composition. The preparation of the perchlorate was the first aim, but it was found fairly difficult owing to the high solubility and ready decomposition of the salt. The results of analyses of some chloride perchlorate preparations are given in Table II.

Absorption Measurements.—The absorption mearsurement was carried out with a Beckman DU spectrophotometer. In the kinetic study a solution of rhodo salt (about 0.004 g. ion/l. in 0.1 N perchloric acid) and an equal volume of aqueous ammonia (about 4 N) were first mixed. At the moment of mixing ($t=0$) the whole complex salt should be of the form of basic rhodo salt (II), which will be changed to basic erythro salt (III) as the reaction proceeds. Then at proper intervals the absorbance (A_t) at 392 mμ and the time (t) of the measurement were recorded. Finally the absorbance was measured after the lapse of sufficient time, when the reaction was virtually complete. This absorbance A_∞ should correspond to that of the basic erythro salt (III). It is readily seen that $A_t - A_\infty$ is proportional to the amount of the rhodo salt remaining at time t.

Results and Discussion

When $\log(A_t - A_\infty)$ is plotted against time, the resulting curves are nearly straight lines as shown in Figs. 1a~1d. The slight bending of the curve at the end of each experiment is possibly due to further decomposition of the basic erythro salt produced. A very slow change of absorbance is actually observed in a solution of purified basic erythro salt. However, its velosity is quite low compared with that of the main reaction and its effect seems negligible in the present discussion.

The reaction is, therefore, of the first order and represented by the equation:

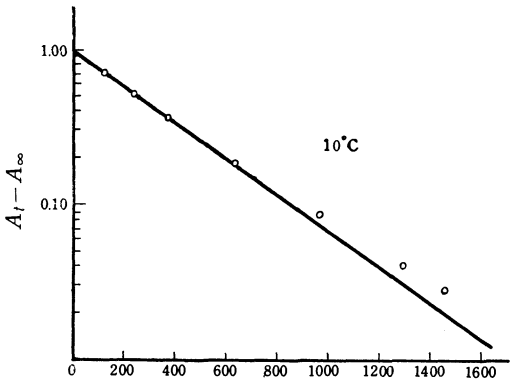


Fig. 1a.

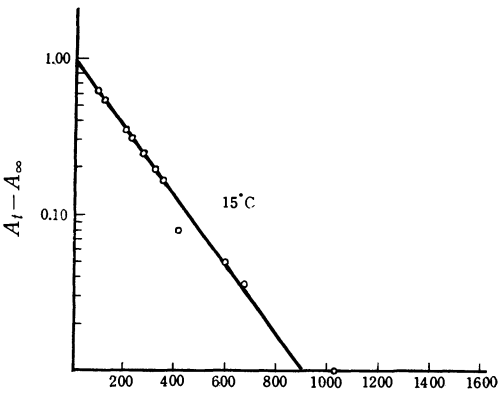


Fig. 1b.

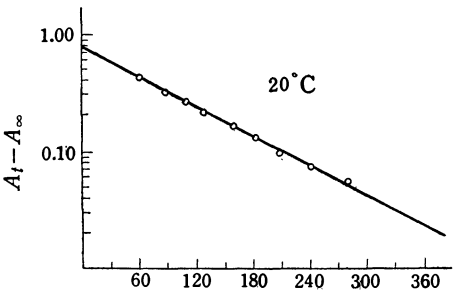


Fig. 1c.

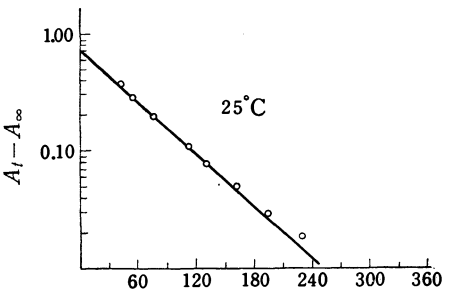


Fig. 1d.

Fig. 1. Change of A_t-A_∞ with time (in a semilog scale).

$$kt=\ln(A_0-A_\infty)-\ln(A_t-A_\infty)$$

where k is the velocity constant and A_0 is absorbance at $t=0$ and corresponds to the absorbance of the basic rhodo salt initially present. These values are readily estimated from the plot in Fig. 1. In Table III are given the velocity constant k and the half-value period $\tau=0.693/k$ obtained in this way.

TABLE III
THE VELOCITY CONSTANT AND HALF-VALUE PERIOD OF THE REACTION

T°C	10	15	20	25
$k\times10^3$	2.64	5.08	9.66	17.3
τ	258	136	72	40

The k values at different temperatures give us the energy of activation E, the frequency factor A and the entropy of activation ΔS^* according to the relations:

$$\ln k = \ln A - E/RT$$

$$\ln A = \ln(kT/h) + \Delta S^*/R - 1$$

The numerical data thus obtained are as follows: $E=21$ kcal/mole, $A=4.5\times10^{13}$ l./mole sec., $\Delta S^*=2$ kcal/deg. mole.

The effect of the hydroxide ion concentration on the reaction velocity was examined by the use of different species and concentration of alkalis. The result, given in Table IV, shows that the increase in

TABLE IV
THE EFFECT OF THE HYDROXIDE ION CONCENTRATION ON THE VELOCITY CONSTANT AT 10°C

Concentration of the complex (In the reacting system)	Concentration of the alkali (In the reacting system)	k
0.00215 g. ion/l.	2.25 N in NH_3	0.00264
0.00107 〃	〃 3.37 N in NH_3	0.00259
0.00107 〃	〃 0.0735 N in NaOH	0.00237
0.00215 〃	〃 0.490 N in NaOH	0.00223
0.00107 〃	〃 0.735 N in NaOH	0.00214

the hydroxide ion concentration caused the decrease in the observed velocity constant. This decrease in the reaction velocity may be due to the increase in the viscosity of the solution; but there is also a possibility that some side reactions or slow deposition of hydrous chromium oxide increased the apparent absorption, and consequently decreased the calculated velocity constant. However, the fact that the reaction is not accelerated by the hydroxide ion excludes the possibility of the S_{N2} mechanism involving a direct attack of the complex by the hydroxide ion.

The addition of sodium perchlorate to the reacting system at 20°C showed that the ionic strength over 0.08 to 1.32 has little effect on the velocity constant. When the concentration of sodium perchlorate exceeded 2.5F, the reaction velocity seemed to decrease, but the fluctuation of the data was significant. This fluctuation may be due to the formation of a fine precipitate of basic rhodo perchlorate even though not visually perceptible.

As seen from the preceeding argument, the aqueous solution of basic rhodo salt is unstable, so that it is difficult to obtain its absorption spectrum directly. When the kinetic data are available, however, the absorbance of the basic rhodo salt (A_0) can be derived from A_t and A_∞ by calculation or on the graph. The curve of the absorption spectrum drawn in this way is shown in Fig. 2. The very characteristic feature of the absorption spectrum probably demonstrates the different electronic structures of the basic rhodo salt from those of other chromium ammines, but the assignment of any electronic transition to each observed absorption band possibly requires a further investigation.

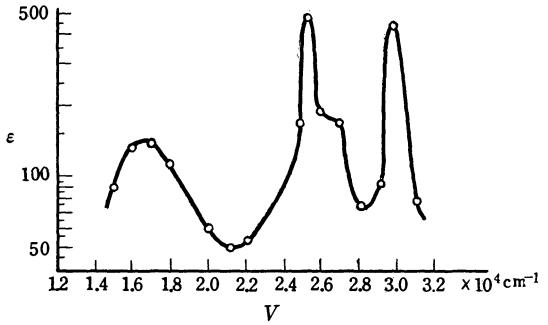


Fig. 2. Absorption spectrum of basic rhodo salt obtained from kinetic data.

Summary

The conversion reaction of the basic rhodo ion to the basic erythro ion in an alkaline solution was found to be of the first order. The velocity constants at 10°, 15°, 20° and 25°C were measured, and the energy of activation, the frequency factor and the entropy of activation calculated. The reaction velocity appeared to be somewhat diminished by higher concentration of sodium hydroxide. The absorption spectrum of unstable basic rhodo salt was derived from the kinetic data.

The authors wish to express their debt of gratitude to Assistant Professor Yukio Kondo of the Rikkyo University for sending them a reprint of his paper concerning the absorption spectra of binuclear ammine complexes.

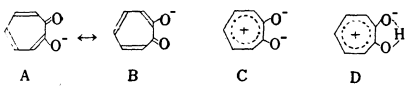
Institute of Polytechnics
Osaka City University
Kita-ku, Osaka

The Dissociation Constants of Carboxytropone and Carboxytropolones

By Nobuyuki TANAKA, I. T. OIWA*, Toshiko KUROSAWA** and Tetsuo NOZOE

(Received August 4, 1958)

Although tropolones possess the properties characteristic of enols and phenols, they may be regarded, in respect of acidity, as vinylogs of carboxylic acids. Their dissociation constants are closer to the latter than to those of phenols[1-4]. This is attributed to the resonance of the ions A and B. However, the acidity is not so enhanced as would be expected



from the stabilization of the ion species A and B. This fact has been explained by considering the "aromatic" resonance of the species C and D, the former being less favored than the latter[2].

In this study, the dissociation constants of 2-carboxytropone, 3-carboxytropolone and its derivatives have been determined by potentiometric titrations with a glass electrode. From the results obtained, the chelation between the substituted carboxyl group and the hydroxyl group of tropolones is discussed.

Experimental

Materials.—Eight compounds that were investigated in the present study were prepared in this laboratory and had the properties given in Table I. Ten milligrams of each compound was weighed accurately and dissolved in redistilled water ($\kappa < 10^{-6}$ mho/cm.) to prepare a solution of approximately 10^{-3} mole/l. in concentration (Table I). A 0.01 M carbonate-free sodium hydroxide solution was prepared by the usual method[16], and its concentration was standardized against recrystallized oxalic acid. The solution was kept in a bottle with a buret which had an arrangement for protection against carbon dioxide.

Three buffer solutions recommended by the National Bureau of Standards (U. S. A.)[17] were employed for the standard for the pH measurement. They are 0.05 M potassium hydrogen phthalate of pH 4.008 at 25°C, 0.025 M potassium

TABLE I

CARBOXYTROPONE AND CARBOXYTROPOLONES INVESTIGATED

No.	Compound	Molecular weight	M. p., °C	Conc. of soln., mM	Reference
1	2-Carboxytropone	150.13	148 (decomp.)	0.574	5
2	3-Carboxytropolone	166.13	218 (decomp.)	1.004	6, 7
3	4-Carboxytropolone	166.13	218	1.194	8, 9, 10
4	5-Carboxytropolone	166.13	290 (decomp.)	0.461	9, 11
5	3-Carboxy-4-methyltropolone	180.15	196 (decomp.)	1.001	12, 13
6	3-Carboxymethyltropolone	180.15	174 (decomp.)	1.001	14
7	Anhydride of 3,4-dicarboxytropolone[a]	192.12	254	0.825	12, 15
8	3-Carboxy-4-carboxymethyltropolone	244.16	183 (decomp.)	1.018	10, 12

a) This substance gives 3,4-dicarboxytropolone when dissolved in water.

* Present address, Research Laboratories, Shin-etsu Chemical Industry, Iriarai, Ohta-ku, Tokyo.
** Present address, 2217, 5-Chome, Matsumoto-cho, Mito.

1) W. von E. Doering and L. H. Knox, *J. Am. Chem. Soc.*, **73**, 828 (1951).
2) P. L. Pauson, *Chem. Revs.*, **55**, 9 (1955).
3) N. Yui and T. Nozoe, *Sci. Repts. Tôhoku Univ. First Ser.*, **35**, 83 (1951).
4) N. Yui, ibid., **40**, 102, 114 (1956).
5) T. Nozoe, K. Takase, et al., to be published.
6) T. Nozoe, Y. Kitahara and S. Masamune, *Proc. Japan Acad.*, **29**, 17 (1953).
7) J. W. Cook, L. D. Loudon and D. K. V. Steel, *J. Chem. Soc.*, **1954**, 530.
8) T. Nozoe and Y. Kitahara, *Proc. Japan Acad.*, **30**, 204 (1954).
9) Y. Kitahara, *Sci. Repts. Tôhoku Univ. First Ser.*, **40**, 74 (1956).
10) R. D. Haworth and J. D. Hobson, *J. Chem. Soc.*, **1951**, 561.
11) J. W. Cook, R. A. Raphael and A. I. Scott, ibid., **1952**, 4416.
12) T. Nozoe, Y. Kitahara, K. Doi, S. Masamune, M. Endo, M. Ishii and Je-Gyun, *Sci. Repts. Tôhoku Univ. First Ser.*, **38**, 257 (1954),
13) R. D. Haworth, B. P. Moore and P. L. Pauson, *J. Chem. Soc.*, **1948**, 1045.
14) T. Nozoe, Y. Kitahara, et al., to be published.
15) D. W. Crow, R. D. Haworth and P. R. Jefferies, *J. Chem. Soc.*, **1952**, 3705.
16) I. M. Kolthoff and E. B. Sandell, "Textbook of Quantitative Inorganic Analysis," MacMillan Co., New York, p. 526 (1952).
17) R. G. Bates, "Electrometric pH meaurements," John Wiley & Sons, Inc., New York, p. 118 (1954).

dihydrogen phosphate and 0.025 M disodium hydrogen phosphate of pH 6.857 at 25°C and 0.05 M borax of pH 9.180 at 25°C.

Apparatus and Procedure.—The cell

Ag-AgCl	0.1 M HCl (inner)	glass membrane		
	sample solution +NaOH (outer)	saturated KCl	Hg_2Cl_2-Hg	

was constructed for the pH measurement. The glass electrode which was designed by one of the authors (I. T. O.) had the shape of a small flask of approximately 30 ml. capacity. A standardized 0.1 M hydrochloric acid was placed inside. A titration cell used is shown in Fig. 1.

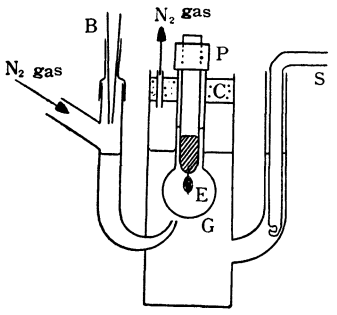


Fig. 1. Schematic diagram of the titration cell: G, glass membrane; E, silver-silver chloride electrode: P, polyethylene seal; C, cork; S, salt bridge; B, buret.

The pH of the solution was determined by the measurement of the electromotive force (e. m. f.) of the above cell. The measurement of e. m. f. was made by means of an instrument which consisted of a potentiometer and the combination of a UX-54 type vacuum tube (corresponding to the FP-54 type vacuum tube in the United States) and a galvanometer[18].

In order to remove the dissolved carbon dioxide and to stir the solution, purified nitrogen gas was passed through the solution before the titration and also after every addition of sodium hydroxide solution during the titration. The e. m. f. was measured with an accuracy of 0.0001 volt; therefore the pH was determined with an accuracy of 0.005 pH-unit. All measurements were carried out in a thermostat of 25.00±0.01°C.

Results

Titration Curves. — Typical titration curves obtained are reproduced in Fig. 2.

Calculation of Dissociation Constants.— (a) *Monobasic acid (HA).*—The dissociation constant of a monobasic acid, K_1, was calculated with the equation

$$K_1=\frac{a_{H^+}\times a_{A^-}}{a_{HA}}=\frac{a_{H^+}\left(b+\frac{a_{H^+}}{f_{H^+}}\right)f_{A^-}}{c-\left(b+\frac{a_{H^+}}{f_{H^+}}\right)} \qquad (1)$$

where c means the total concentration of an acid titrated, b the concentration of sodium hydroxide added, a_{H^+}, a_{HA} and a_{A^-} mean the activities of the hydrogen ion, the undissociated acid and the dissociated acid anion, respectively, and f_{H^+} and f_{A^-} the activity coefficients of the hydrogen ion and the dissociated acid anion, respectively. The activity coefficient of the undissociated acid HA was assumed to be unity, while those of the dissociated acid anion A^- and the hydrogen ion were calculated with the equation

$$\log f_i=-\frac{0.358Z_i^2\sqrt{I}}{1+0.2325a_i\times10^8\sqrt{I}} \qquad (2)$$

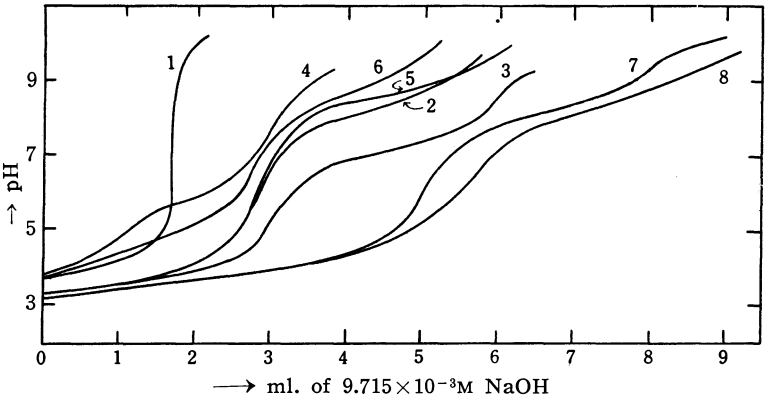


Fig. 2. Titration curves of carboxytropone and carboxytropolones. The curves are given the same number as in Table I.

18) N. Tanaka, I. T. Oiwa and M. Kodama, *Anal. Chem.*, **28**, 1555 (1956).

where Z_i represents the ionic charge, Γ the total ionic concentration, and a_i the ion-size parameter[19]. Because 2-carboxytropone was considered to have a molecular volume similar to that of benzoic acid, its ion-size parameter was assumed to be 6 Å according to Kielland's[19] tables.

(b) *Dibasic acids* (H_2A).—When $K_1/K_2 \geq 10^3$, the first dissociation constant, K_1, was calculated with eq. 1 in which f_{A^-} was replaced by f_{HA^-}, the effect of the second dissociation being neglected. In this calculation, the part of the titration curve before the equivalence point for the first dissociation was used. The second dissociation constant, K_2, was calculated with the equation

$$K_2 = \frac{a_{H^+} \times a_{A^{2-}}}{a_{HA^-}} = \frac{a_{H^+}\left(b + \frac{a_{H^+}}{f_{H^+}} - [OH^-]\right) f_{A^{2-}}}{\left(2c + [OH^-] - \frac{a_{H^+}}{f_{H^+}} - b\right) f_{HA^-}} \quad (3)$$

from the observed values which were obtained between the equivalence points for the first and the second dissociations on the titration curve.

(c) *Tribasic acids* (H_3A).—From the titration curves given in Fig. 2 it was seen that K_1/K_2 is not greater than 10^3, so that K_1 and K_2 were not able to be calculated by the procedure given in (b). In this case they were calculated with the equations

$$K_1K_2 = \frac{a_{H^+}^2 \times a_{HA^{2-}}}{a_{H_3A}} = a_{H^+}^2 \left(\frac{b + \frac{a_{H^+}}{f_{H^+}} - [OH^-]}{2c - b - \frac{a_{H^+}}{f_{H^+}} + [OH^-]} \right) \times \left\{ 1 + \frac{K_1 f_{H^+}}{a_{H^+}} \left(\frac{b - c + \frac{a_{H^+}}{f_{H^+}} - [OH^-]}{b + \frac{a_{H^+}}{f_{H^+}} - [OH^-]} \right) \right\} f_{HA^{2-}} \quad (4)$$

$$K_1 = a_{H^+} \left(\frac{b + \frac{a_{H^+}}{f_{H^+}} - [OH^-]}{c - b - \frac{a_{H^+}}{f_{H^+}} - [OH^-]} \right) \times \left\{ 1 - K_1K_2 \left(\frac{f_{H^+}}{a_{H^+}} \right)^2 \left(\frac{2c - b - \frac{a_{H^+}}{f_{H^+}} + [OH^-]}{b + \frac{a_{H^+}}{f_{H^+}} - [OH^-]} \right) \right\} f_{H_2A^-} \quad (5)$$

from the values obtained before the equivalence point for the second dissociation on the titration curve.

The third dissociation constant, K_3, was calculated with the equation,

$$K_3 = \frac{a_{H^+} \times a_{A^{3-}}}{a_{HA^{2-}}} = \frac{a_{H^+}\left(b + \frac{a_{H^+}}{f_{H^+}} - [OH^-]\right) f_{A^{3-}}}{\left(3c - b - \frac{a_{H^+}}{f_{H^+}} + [OH^-]\right) f_{HA^{2-}}} \quad (6)$$

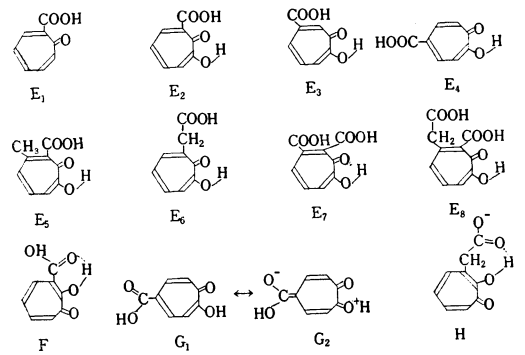
from the values obtained between the equivalence points for the second and third dissociations on the titration curve.

In Table II are given the typical examples of calculation for the mono- and di-basic acid, and in Table III, the dissociation constants obtained for the compounds investigated. For comparison, the dissociation constants of several substances which have structures similar to the compounds investigated in this study are also given in Table III.

Discussion

2-Carboxytropone (E_1).— This acid is stronger than benzoic acid. This is attributed to the fact that the inductive (electron withdrawal) effect of a tropone ring is stronger than that of a benzene ring.

3-Carboxytropolone (E_2) and 3-carboxy-4-methyltropolone (E_5).— The values of pK_1 are smaller than those of benzoic acid and 2-carboxytropone. This shows the stronger inductive effect of the tropolone ring as well as the existence of chelation



19) J. Kielland, *J. Am. Chem. Soc.*, **59**, 1675 (1937).

TABLE II

RESULTS OF TITRATION

2-Carboxytropone with 9.715×10^{-3}M NaOH

NaOH, ml.	pH	$a_{H^+}\times10^4$	f_{H^+}	$b\times10^4$	$[A^-]\times10^4$	f_{A^-}	$K_1\times10^4$
0.14	3.66	2.18_3	0.982	0.448	2.592	0.982	1.88
0.31	3.73	1.86_2	.981	0.993	2.890	.981	1.89
0.57	3.85	1.39_0	.980	1.811	3.229	.980	1.82
0.75	3.95	1.12_2	.979	2.369	3.515	.979	1.85
0.91	4.04	0.91_2	.978	2.860	3.791	.978	1.89
1.10	4.18	0.65_4	.977	3.436	4.105	.977	1.82
						mean	1.86
						$pK_1=3.73\pm0.01$	

3-Carboxytropolone with 9.715×10^{-3}M NaOH

NaOH, ml.	pH	$a_{H^+}\times10^4$	f_{H^+}	$b\times10^4$	$[HA^-]\times10^4$	f_{HA^-}	$K_1\times10^4$
0.15	3.30	5.01_2	0.973	0.483	5.623	0.973	6.28
0.42	3.35	4.41_6	.973	1.341	5.877	.973	6.26
0.61	3.39	3.99_9	.973	1.951	6.060	.973	6.22
0.88	3.46	3.46_8	.973	2.768	6.326	.973	6.23
1.12	3.52	3.02_0	.972	3.496	6.601	.972	6.28
						mean	6.25
						$pK_1=3.20\pm0.01$	

NaOH, ml.	pH	$a_{H^+}\times10^9$	f_{H^+}	$b\times10^4$	$[HA^-]\times10^4$	f_{HA^-}	$[A^{2-}]\times10^4$	$f_{A^{2-}}$	$[OH^-]\times10^6$	$K_2\times10^8$
4.46	8.29	5.12	0.944	12.57	4.939	0.941	12.55	0.787	1.79_7	1.08
4.64	8.38	4.16	.943	13.01	4.417	.941	12.98	.785	2.66_7	1.02
4.93	8.65	2.23	.942	13.71	3.591	.940	13.66	.782	4.22_1	1.02
									mean	1.04
									$pK_2=7.98\pm0.01$	

TABLE III

DISSOCIATION CONSTANTS OF CARBOXYTROPONE, CARBOXYTROPOLONES AND THE RELATED COMPOUNDS

Compound	pK_1	pK_2	pK_3
2-Carboxytropone	3.73 ± 0.01		
3-Carboxytropolone	3.20 ± 0.01	7.98 ± 0.01	
4-Carboxytropolone	3.42 ± 0.005	7.03 ± 0.01	
5-Carboxytropolone	4.05 ± 0.01	6.41 ± 0.02	
3-Carboxy-4-methyltropolone	3.15 ± 0.01	8.29 ± 0.01	
3-Carboxymethyltropolone	4.52 ± 0.02	8.77 ± 0.05	
3, 4-Dicarboxytropolone	3.24 ± 0.03	6.26 ± 0.03	8.57 ± 0.01
3-Carboxy-4-carboxymethyltropolone	3.75 ± 0.03	5.90 ± 0.05	8.08 ± 0.02
Acetic acid	4.756[20]		
Benzoic acid	4.201[20]		
Tropolone	6.92[3]		
4-Methyltropolone	7.26[3]		

such as given in structure F. The larger values of pK_2 also show the existence of stable chelation.

4-Carboxytropolone (E_3) and 5-carboxytropolone (E_4). — In these substances the carboxyl group will not be able to form the chelation of type F, which 3-carboxytropolone forms. The magnitudes of pK_1 of these acids, therefore, are expected to be larger than those of 3-carboxytropolone and 3-carboxy-4-methyltropolone, and the magnitudes of pK_2 of the former, smaller than those of the latter. The experimental results agree with this expectation; The pK_1 of 5-carboxytropolone is much greater than that of 4-carboxytropolone, this may be attributed to the contribution of structure G_2. It is also interesting to notice that the difference between pK_1

20) R. A. Robinson and R. H. Stokes, "Electrolytic Solutions," Butterworths Scientific Publications, London, p. 436 (1955).

and pK_2 of 5-carboxytropolone is much smaller than the differences of other monocarboxytropolones (See Table III).

3-Carboxymethyltropolone (E_6). — The methylene group shields the inductive effect of a tropolone ring upon the carboxyl group, and, consequently, the pK_1 value is close to that of acetic acid. The large pK_2 value indicates the existence of the stable chelation (structure H).

3, 4-Dicarboxytropolone (E_7) **and 3-carboxy-4-carboxymethyltropolone** (E_8).— 3, 4-Dicarboxytropolone gives a pK_1 value which is nealy equal to that of 3-carboxytropolone (E_2), while 3-carboxy-4-carboxymethyltropolone gives a somewhat larger pK_1. This seems to be due to the greater steric interference of a carboxymethyl group in the 4-position.

Summary

The thermodynamic dissociation constants of 2-carboxytropone, 3-carboxytropolone, 4-carboxytropolone, 5-carboxytropolone, 3-carboxy-4-methyltropolone, 3-carboxymethyltropolone, 3, 4-dicarboxytropolone and 3-carboxy-4-carboxymethyltropolone have been determined by means of the pH titration with a glass electrode.

The relationships between the magnitudes of the dissociation constants and the structures of these compounds have been discussed.

The authors thank the Ministry of Education for the financial support granted for this research.

Department of Chemintry,
Faculty of Science,
Tohoku University
Katahira-cho, Sendai

SHORT COMMUNICATIONS

Absolute Estimation of the Ionic Entropies of Transfer

By Toshio IKEDA

(Received September 9, 1958)

The earlier attempts[1,2] of estimating the absolute ionic entropies of transfer are all based on an artificial assumption. Recently, the first absolute estimation has been carried out successfully by Agar and Breck[3]. The present report would give the second way of estimating these values exclusively from the observed data concerning the "Soret effect" and thermocells without making any assumption except the additivity of the ionic entropies of transfer, which was originally proposed by Eastman[1] and lately has been confirmed by Alexander[4] at low concentrations. For a thermocell of the system, $Ag|AgCl_s$, MCl_{aq}, $AgCl_s|Ag$, we can write, when the Soret effect is hindered, as follows:

$$\boldsymbol{F}\frac{d\varphi}{dT} = -t_+S_+^* + t_-S_-^* - S_{el}^* + S_{Ag} - S_{AgCl} + t_+S_{MCl} \qquad (1)$$

where $\boldsymbol{F}$ is Faraday's constant, $d\varphi$ is the thermopotential difference due to the temperature gradient dT, t_+ and t_- are the transference numbers of positive and negative ions of the salt MCl (here uni-univalent) respectively, S_+^*, S_-^* and S_{el}^* are the entropies of transfer of hydrated positive and negative ions in solution phase and that of electron in metallic phase respectively, S_{Ag} and S_{AgCl} are the molar entropies of metallic silver and solid silver chloride respectively, and S_{MCl} is the molar

1) E. D. Eastman, *J. Am. Chem. Soc.*, **50**, 283, 292 (1928).
2) J. C. Goodrich, F. M. Goyan, E. E. Morse, R. G. Preston and M. B. Young, ibid., **72**, 4411 (1950).
3) J. N. Agar, and W. G. Breck, *Trans. Faraday Soc.*, **53**, 167, 179 (1957).
4) K. F. Alexander, *Z. physik. Chem.*, **203**, 213 (1954).
5) H. B. Callen, *Phys. Rev.*, **73**, 1349 (1948); S. R. de Groot, "Thermodynamics of Irreversible processes", North Holland Publ. Co., Amsterdam and Intersc. Publ., New York., (1951).

TABLE I

IONIC ENTROPIES OF TRANSFER (cal./deg./mole) IN AQUEOUS m-MOLAL SOLUTION OF MCl AT 25°C. σ(deg.$^{-1}$), dφ/dT(μV/deg.), S_{Ag}=10.1, S_{AgCl}=23.0, S_{Hg}=18.3, S_{HgCl}=23.4 cal./deg./mole.

System MCl	Ag/AgCl, MCl(m=0.05)					Ag/AgCl, MCl(m=1.0)					Hg/HgCl,MCl(m=1.0)		
	t_+[g]	$\sigma\times10^3$	dφ/dT[b]	S_+*	S_-*	t_+[g]	$\sigma\times10^3$	dφ/dT[b]	S_+*	S_-*	dφ/dT[e]	S_+*	S_-*
HCl	0.829	−1.76[c]	145	10.4	18.4[f]	0.845	−7.3[a]	− 83	4.1	18.2	330	3.5	19.9
LiCl	0.321	+0.31[a]	511	6.5	24.5	0.26	0. [d]	289	0.2	19.6	630	0.2	19.6
NaCl	0.388	−1.91[a]	482	18.1	24.9	0.363	−1.56[d]	228	13.1	18.8	560	13.2	18.7
KCl	0.490	−1.20[a]	493	27.4	24.9	0.485	−0.93[d]	261	22.6	19.4	610	22.3	19.7
NH_4Cl	0.491	0.0 [c]	498	29.0	24.4	—	—	—	—	—	—	—	—

a, K. F. Alexander, *Z. physik. Chem.*, **203**, 213 (1954); b, H. A. Bernhardt and H. D. Crockford, *J. Phys. Chem.*, **46**, 473 (1942); c, J. Chipman, *J. Am. Chem. Soc.*, **48**, 2577 (1926); d, C. C. Tanner, *Trans. Faraday Soc.*, **23**, 75 (1927); e, Th. W. Richards, *Z. physik. Chem.*, **24**, 39 (1897); f, This anomalous value might be due to the fact that Chipman's value of σ here used is incorrect, probably too low; g, I. C. T; B. E. Conway "Electrochemical Data", Elsevier Publ. Co., Amsterdam, (1952).

entropy of MCl in solution phase. Here $S_{MCl}=S_+ + S_-$, S_+ and S_- being the partial molar entropies of hydrated positive and negative ions produced from one molecule of the salt MCl in solution phase.

Coupling the relations[5], $S_+^*=Q_+^*/T+S_+$ and $S_-^*=Q_-^*/T+S_-$, with the approximation formula[6] $\sigma=-(Q_+^*+Q_-^*)/2\boldsymbol{R}T^2$ for the Soret coefficient σ, one may yield the molecular entropy of transfer of the salt MCl as

$$S_+^*+S_-^*=-2\boldsymbol{R}T\sigma+S_{MCl} \qquad (2)$$

where Q_+^* and Q_-^* are the heat of transfer of hydrated positive and negative lons of MCl in solution phase, and $\boldsymbol{R}$ is the gas constant.

Upon solving Eqs. 1 and 2 with respect to S_+^* and S_-^* by the aid of the relation of $t_+ + t_- = 1$, one may yield

$$\left.\begin{aligned} S_-^* &= \boldsymbol{F}\mathrm{d}\varphi/\mathrm{d}T - S_{Ag} + S_{AgCl} \\ &\quad -2t_+\boldsymbol{R}T\sigma + S_{el}^* \\ S_+^* &= -\boldsymbol{F}\mathrm{d}\varphi/\mathrm{d}T + S_{Ag} - S_{AgCl} \\ &\quad -2t_-\boldsymbol{R}T\sigma - S_{el}^* + S_{MCl} \end{aligned}\right\} \qquad (3)$$

Since S_{el}^* is very small as compared with the other terms in Eq. 3, sufficiently correct values of the ionic entropies of transfer may be obtained even by omitting term of S_{el}^* from Eq. 3. Some of the values of S_+^* and S_-^* thus estimated for the 0.05 and 1 molal aqueous solutions of some electrolytes at 25°C are tabulated in Table I. There can be seen some remarkable facts: (1) the values of S_+^* and S_-^* persist their proper values, independent of what system they are originated from; (2) the value of S_-^* is consistently the same, entirely independent of the nature of its conjugate cations present in the chloride solutions; (3) S_i^* is a function of the concentration.

Finally it is very interesting to have a possibility of determing the heats of transfer for positive and negative ions separately, if only the individual ionic activity coefficients are known.

Department of Chemistry, Faculty of Liberal Arts and Science, Shizuoka University, Oiwa-cho, Shizuoka

6) S. R. de Groot, *J. Phys. Radium*, **8**, 129, 193 (1947).

*Studies of the Structure of Bergenin**

By Shin-ichiro FUJISE, Morio SUZUKI, Yasuhiko WATANABE and Sumu MATSUEDA

(Received October 21, 1958)

Two reports on the structure of bergenin were published recently by J. Evelyn Hay et al.[1] and by Posternak et al.[2]. We also wish to report here our results on the structure of bergenin (I) from the bark of *Corylopsis Spicata*[3].

The periodate oxidation of di-*O*-methylbergenin (II) gave 5, 6, 7-trimethoxyisocoumarin-3-aldehyde (III). By careful catalytic hydrogenation of III, 3-hydroxymethyl-5, 6, 7-trimethoxyisocoumarin (IV)

* The paper was read at Annual Meeting of Chemical Society of Japan, April 5, 1958.

1) J. E. Evelyn Hay et al., *J. Chem. Soc.*, **1958**, 2231.

2) Posternak et al., *Helv. Chim. Acta*, **41**, 1159 (1958).

3) Hattori, *Acta Phytochim.*, (*Japan*), **4**, 327 (1929).

(its 3-acetoxymethyl derivative (V)), 3-methyl-5, 6, 7-trimethoxyisocoumarin (VI) and 3-methyl-5, 6, 7-trimethoxy-3, 4-dihydroisocoumarin (VII) were isolated through three steps.

The alkaline treatment of III gave 5, 6, 7-trimethoxy-3, 4-dihydroisocoumarin-3-carboxylic acid (VIII), i. e., an intermolecular Cannizzaro reaction was observed. The values of U. V. spectrum of these compound are given in Tables I and II.

TABLE I

U. V. ABSORPTION OF BERGENIN AND ITS DERIVATIVES

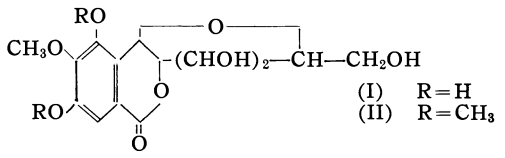
(λ_{max} in mμ)

Group 1			Group 2		
Compound	λ_{max}	log ε	Compound	λ_{max}	log ε
I	275	3.903	III	335	3.856
	220	4.426		245	4.600
II	268	3.914	IV	338	3.726
	220	4.482		247	4.680
VII	305	3.485	V	335	3.705
	265	3.962		247	4.684
	220	4.415			
VIII	303	3.397	VI	340	3.658
	265	3.874		245	4.655
	220	4.388			

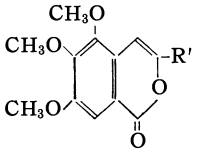
TABLE II

CARBONYL STRETCHING FREQUENCIES IN I. R. SPECTRA OF BERGENIN AND ITS DERIVATIVES

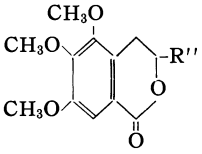
Compound	ν(cm^{-1})
I	1703
II	1721, 1711
Penta-*O*-acetylbergenin	1775, 1733



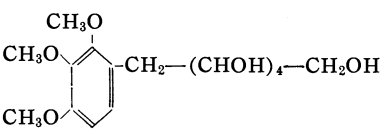
(I) R=H
(II) R=CH_3



(III) R'=CHO
(IV) R'=CH_2OH
(V) R'=CH_2OCOCH_3
(VI) R'=CH_3



(VII) R''=CH_3
(VIII) R''=COOH



(IX)

From the results shown in Table I, we conclude that bergenin and di-*O*-methylbergenin have dihydroisocoumarin-ring, but not isocoumarin-ring (the absence of 330 mμ absorption). The results also agreed with those in Table II, i. e., I. R. spectrum of 3-methyl-3, 4-dihydroisocoumarin (1716 cm^{-1}) indicated the identical structure with that of bergenin and of di-*O*-methylbergenin.

The catalytic reduction of II, by using Raney catalyst (at 200°, 100 atm.) resulted in obtaining 6-(2, 3, 4-trimethoxyphenyl)-1, 2, 3, 4, 5-heptahydroxyhexane IX, being accompanied by both decarboxylation and hydrogenation. The products was stable to Fehling's solution. The constitution of IX was also confirmed by the oxidation with sodium metaperiodate. In the case that 4 moles of this reagent were consumed, oxidation product was isolated to be prove as 2, 3, 4-trimethoxy phenylacetaldehyde 2, 4-dinitrophenyl hydrazone.

The alkaline hydrogen peroxide oxidation of I gave arabinose (as 2, 4-dinitrophenylhydrazone). II was found to be also stable to Fehling's solution. Deducing from the above-mentioned experimental results, bergenin is concluded to be represented by the formula I.

TABLE III

ANALYSES

No.	Formula, m. p.	Found. C%	Found. H%	Calcd. C%	Calcd. H%
III	$C_{13}H_{12}O_6$ m. p. 160~161°	58.85	4.53	59.09	4.58
IV	$C_{13}H_{14}O_6$ m. p. 141~142°	58.88	5.51	58.64	5.30
V	$C_{15}H_{16}O_7$ m. p. 93~94°	58.42	5.06	58.44	5.23
VI	$C_{13}H_{14}O_5$ m. p. 84~86°	62.57	5.71	62.39	5.64
VII	$C_{13}H_{16}O_5$ m. p. 67~69°	61.60	6.10	61.89	6.39
VIII	$C_{13}H_{14}O_7$ m. p. 157~158°	55.33	5.08	55.32	5.00
IX	$C_{15}H_{24}O_8$ m. p. 182~183°	54.87	6.51	54.21	7.28

Department of Chemistry, Faculty of Science, Tohoku University
Katahira-cho, Sendai

4) J. Blair et al., *J. Chem. Soc.*, **1955**, 2871.

*Paramagnetic Resonance Absorption in Solution of the Sodium Adducts of Styrene and 1, 1-Diphenylethylene**

By Kozo Hirota, Keiji Kuwata and Kazuo Morigaki

(Received November 21, 1958)

As reported already[1], paramagnetic resonance absorption with hyperfine structure could be observed on the red adduct of styrene with sodium in tetrahydrofuran (THF) solution. Such absorption has been observed by Weissman and his collaborators[2] in caces of polynuclear condensed aromatic hydrocarbons, e. g., naphthalene, anthracene, and naphthacene. Moreover, it is interesting that the adduct of styrene polymerizes easily, turning into a so-called "living polymer". The research, therefore, was continued with an apparatus of higher sensitivity, thus obtaining more interesting and confirmative results. It is the object of the present communication to report them and also a similar research on 1,1-diphenylethylene (DPE), which also forms a living polymer[3].

As shown in Figs. 1a and 1b, two kinds of spectrum were observed in the adduct of styrene, and it was found that they could be observed in the solutions when the adduct of high degree of polymerization was depolymerized with metallic sodium, and after repeated experiment it

1) K. Hirota, K. Kuwata and K. Morigaki, This Bulletin, **31**, 538 (1958).

2) D. Lipkin, D. E. Paul, J. Townsend and S. I. Weissman, *Science*, **117**, 534 (1953); T. L. Chu, G. E. Pake, D. E. Paul, J. Townsend and S. I. Weissman, *J. Phys. Chem.*, **57**, 504 (1953); S. I. Weissman, J. Townsend, D. E. Paul and G. E. Pake, *J. Chem. Phys.* **21**, 2227 (1953); T. R. Tattle, Jr. and S. I. Weissman, ibid., **25**, 189 (1956).

* Part of this communication was already spoken at the meetings of the Phys. Soc. of Japan (March 1958, Tokyo), and of the Chem. Soc. of Japan (April 1958, Tokyo).

3) K. Kuwata, S. Ishida and K. Hirota, *J. Chem. Soc. Japan, Pure Chem. Sec.* (*Nippon Kagaku Zasshi*), to be published.

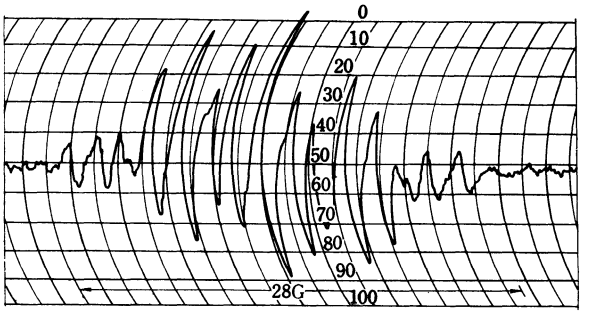


Fig. 1a. Resonance spectrum of styrene radical.

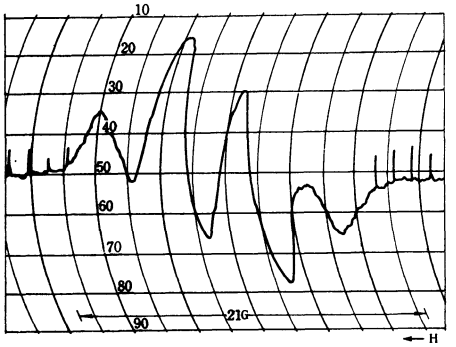


Fig. 1b. Resonance spectrum of styrene radical.

was confirmed that, according as the depolymerization is performed to much extent or not, the spectra observed were composed of about 23 lines or of four lines, as shown in Figs. 1a and 1b, but the reproducibility of the former was not confirmed. It is noteworthy that the spectrum of four lines did not separate into more lines when the measurment was done at such low temperature as about −100°C and when dioxane was used as the solvent, or potassium was substituted for sodium to prepare the adduct.

Similar situation was found on the adduct of DPE whose spectra are shown in Figs. 2a and 2b. The spectrum composed of 32~33 lines (Fig. 2a) could be obtained on the adduct freshly prepared from DPE monomer and sodium in THF. The spectrum, changed into the one composed of nine lines (Fig. 2b), when the sample was kept at 110°C for two days. Now it is clear that solutions of the sodium adducts of styrene and DPE contain some free radicals. Taking such fact into consideration, some discussions on the nature of these adducts were attempted.

These radicals in the adduct of styrene are considered to have the following

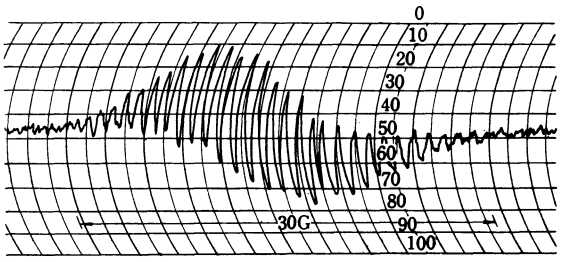


Fig. 2a. Resonance spectrum of DPE radical.

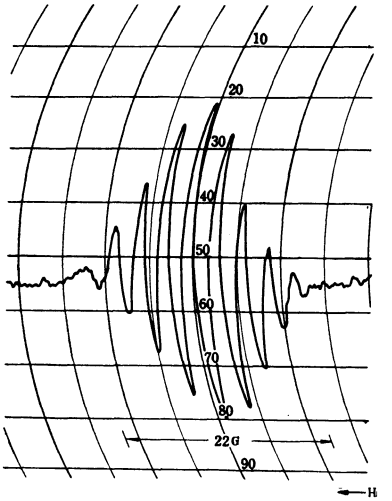
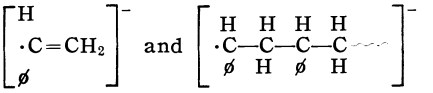
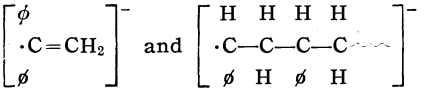


Fig. 2b. Resonance spectrum of DPE radical.

structures on the view of the polymerization reaction, it is believed that these two radicals are the origin of such two resonance spectra*:



In case of DPE the situation is similar, but is more confirmative by the analysis of the spectra. The structures of the radicals corresponding to the spectra shown by Fig. 2a and Fig. 2b are as follows, respectively:



The detailed result and discussion will be published in near future.

* By these formulae all resonace formulae are represented for both adducts.

The writers express sincere thanks to Professor Junkichi Itoh of Osaka University who made the measurement of the paramagnetic resonance absorption possible.

Faculty of Science, Osaka University
Kita-ku, Osaka

2ξ, 3-(3'-Oxocyclohex-4'-eno)-cholest-4-ene and 2ξ, 3-(3'-Oxocyclohex-4'-eno)-5α-cholestane (Preliminary Note)

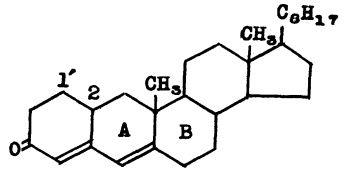
By Yoshiyuki URUSHIBARA and Jihei INOMATA

(Received December 10, 1958)

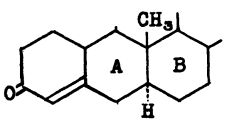
Chololest-4-en-3-one (I) was condensed with ethyl formate by the action of sodium methoxide to give 2-hydroxymethylene-cholest-4-en-3-one (II), m. p. 110°C[1]. The substance II was then condensed with freshly distilled methyl vinyl ketone in ethyl acetate in the presence of trimethylamine[2], and chromatography of the product on alumina and recrystallization from ethanol-methanol yielded 2ξ-(3'-oxobutyl)-cholest-4-en-3-one (III), m. p. 86~88°, λ_{max} 242 mμ(ethanol) (ε=14500), infrared absorptions 5.813, 5.970, and 6.160 μ (Found: C, 82.11; H, 11.19. Calc. for $C_{31}H_{50}O_2$: C,81.88; H, 11.08%). The diketone (III) gave a dioxime melting at 84°C (Found: N, 5.83. Calcd. for $C_{31}H_{52}O_2N_2$: N, 5.78%).

Treatment of the diketone (III) with alcoholic potash in the stream of nitrogen, chromatography of the product on alumina and recrystallization from ethanol, gave 2ξ,3-(3'-oxocyclohex-4'-eno)-cholest-4-ene (IV), m. p. 149—150° (Found: C, 85.08; H, 11.17. Calcd. for $C_{31}H_{48}O$: C, 85.26; H, 11.08%). The substance IV dissolved in ethanol showed an absorption maximum at 296 mμ (ε=30000) and in Nujol gave infrared absorptions at 6.000, 6.143 and 6.301 μ, which are proofs of the dienone structure IV.

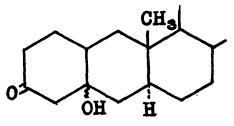
Reaction of 2-hydroxymethylene-cholest-4-en-3-one (II), methanolic sodium methoxide and freshly prepared 4-(diethylamino)-2-butanone methiodide[3], followed by chromatography of the product on alumina and recrystallization from ethanol, gave directly the same dienone (IV), m. p. 141°C, which could be purified with difficulty.



(IV)



(IX)



(VIII)

5α-Cholestan-3-one (V) was transformed into a monohydroxymethylene derivative, m. p. 180~185°C, in the same way as mentioned above(Found: C, 81.14; H, 11.31. Calcd. for $C_{28}H_{46}O_2$: C, 81.13; H, 11.11%). The structure of the product was proved to be 2-hydroxymethylene-5α-cholestan-3-one (VI)[4] by the formation of 2,3-seco-5α-cholestane-2,3-dioic acid, m. p. 193~194°C, on oxidizing the substance with hydrogen peroxide and caustic soda[5]. The dicarboxylic acid was identified with the specimen prepared from 5α-cholestan-3β-ol by the method of Windaus et al.[6]

Reaction of 2-hydroxymethylene-5α-cholestan-3-one (VI), 4-(diethylamino)-2-butanone methiodide and ethanolic potash, followed by chromatography of the product on alumina and recrystallization, gave 2ξ-(3'-oxobutyl)-5α-cholestan-3-one (VII), m. p. 113~114°C, infrared absorption 5.808~5.840μ (Found: C, 81.63; H, 11.52. Calc. for $C_{31}H_{52}O_2$: C, 81.52; H, 11.48%), and 2ξ,3-(3'-oxocyclohexano)-5α-cholestan-3ξ-ol (VIII), m. p. 230~231°C, infrared absorptions 2.826 and 5.790 μ (Found: C, 81.80; H, 11.70. Calcd. for $C_{31}H_{52}O_2$: C, 81.52; H, 11.48%).

1) J. G. Burr, Jr., W. F. Holton and C. N. Webb., *J. Am. Chem. Soc.*, **72**, 4903 (1950); R. B. Woodward., A. A. Patchett, D. H. R. Barton, D. A. J. Ives and R. B. Kelly, *J. Chem. Soc.*, **1957**, 1131.

2) G. I. Poos, G. E. Arth, R. E. Beyler and L. H. Sarett, *J. Am. Chem. Soc.*, **75**, 422 (1953).

3) Cf. E. C. Du Feu, F. J. McQuillin and R. Robinson, *J. Chem. Soc.*, **1937**, 53.

4) Cf. L. Ruzicka, U. S. Patent, 2,281,622; *Chem. Abstr.*, **36**, 5958 (1942).

5) Cf. D. Arigoni, H. Bosshard, H. Bruderer, G. Büchi, O. Jeger and L. J. Krebbaum, *Helv. Chim. Acta*, **40**, 1733 (1957); D. H. R. Barton et al., *J. Chem. Soc.*, **1954**, 4660.

6) A. Windaus and Cl. Uibrig, *Ber.*, **47**, 2384 (1914).

Compounds VII and VIII yielded the same 2ξ, 3-(3′-oxocyclohex-4′-eno)-5α-cholestane (IX), m. p. 153°C, on treatment with sodium hydroxide in the stream of nitrogen, followed by chromatography of the product on alumina and recrystallization from ethyl acetate (Found: C, 84.75; H, 11.57. Calcd. for $C_{31}H_{50}O$: C, 84.86; H, 11.49%). The substance IX dissolved in ethanol showed an absorption maximum at 243 mμ(ε=15000) and in Nujol infrared absorptions at 5.970 and 6.160μ, which prove the structure IX.

2-Hydroxymethylene-5α-cholestan-3-one (VI) reacted with methyl vinyl ketone on addition of a few drops of 10% ethanolic potash in the heat, and treatment of the product, m. p. 134~135°C, probably the 2-formyl intermediate, with ethanolic potash in the stream of nitrogen gave the same 2ξ-(3′-oxobutyl)-5α-cholestan-3-one (VII).

The 2ξ, 3-(3′-oxocyclohexano)-5α-cholestan-3ξ-ol (VIII), m. p. 231~232°C, and its 3-stereoisomeride, m. p. 217~219°C (Found: C, 81.16; H, 11.42. Calcd. for $C_{31}H_{52}O_2$: C, 81.52; H, 11.48%), were obtained by the action of *N*-ethylanilinomagnesium bromide on 2ξ-(3′-oxobutyl)-5α-cholestan-3-one (VII) followed by hydrolysis of the intermediate product with dilute hydrochloric acid[7].

No experimental evidence has yet been obtained concerning the configuration around the carbon atom 2 in compounds III, IV, VII, VIII and IX[8], but it seems almost certain for these deformylated compounds that carbon atom 1′ is situated at the more stable α-configuration and consequently the hydrogen in position 2 is attached there with the β-bond, axial to both ring A and the added ring.

Details will follow.

Department of Chemistry
Faculty of Science
The University of Tokyo
Hongo, Tokyo

7) Cf. J. Colonge, *Bull. soc. chim. France*, (5), **1**, 1101 (1934).

8) Cf. S. A. Szpilfogel, W. J. van Der Burg, C. M. Siegmann and D. A. van Dorp, *Rec. trav. chim.*, **75**, 1043 (1956) and A. Wettstein, K. Heusler, H. Ueberwasser and P. Wieland, *Helv. Chim. Acta*, **40**, 323 (1957).

High Resolution Proton Magnetic Resonance in Fluorobenzene

By Shizuo Fujiwara, Mikio Katayama and Hiroshi Shimizu

(Received November 11, 1958)

Gutowsky et al. resolved the proton nuclear magnetic resonance spectrum of fluorobenzene into a doublet and interpreted that it would refer to the case where the fluorine was equally coupled through electrons with the ortho-, meta-and paraprotons[1]. Baker also presented the same conclusion[2]. But this conclusion is a quite perplexing one to the chemists, and we continued the efforts to resolve the spectrum further and observed that the components of the doublet were different in the intensity from each other, consistent with the observation by Gutowsky et al.[1], each having the structure as shown in Fig. 1.

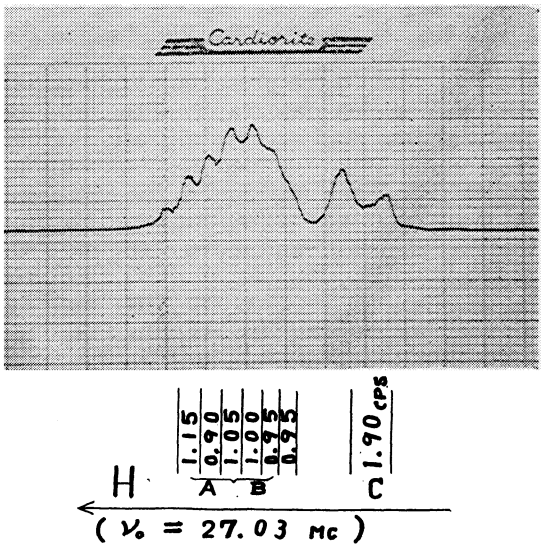


Fig. 1. Proton resonance in fluorobenzene.

The separation between each component of the multiplets is shown in Figure 1. In spite of the argument given by Baker[2] for the fluorine spectrum of this compound, we assume that the proton resonance spectrum of Fig. 1 would refer to the case where the effect of the non-equivalent distribution of electrons participates in

1) H. S. Gutowsky, L. H. Meyer and D. W. McCall, *J. Chem. Phys.*, **23**, 982 (1955).
2) E. B. Baker, ibid., **13**, 984 (1955).

the resonance phenomena. A possible assignment of the line components may be done with the help of the molecular theory[3] by taking the peaks of A, B and C (A is the highest in the resonant field) as referring to meta-, para- and ortho-protons, respectively.

During this experiment, we could know that Bak, Shoolery and Williams[4] reached the same conclusion as ours of unequal H-F couplings, but, in their article, the spectrum of the proton resonance is not shown. Further efforts to make the assignments of each component line and to make measurements at higher field are now being on.

Our thanks are due to Dr. G. A. Williams of Stanford University who sent us the preprint. Thanks are also due to Professor O. Simamura of the University of Tokyo who supplied us the sample.

University of Electro-Communications
Chôfu, Tokyo

3) For example C. A. Coulson: "Valence," Oxford University Press, (1953).
4) B. Bak, J. N. Shoolery and G. A. Williams, III, to be published in *J. Molecular Spectroscopy*.

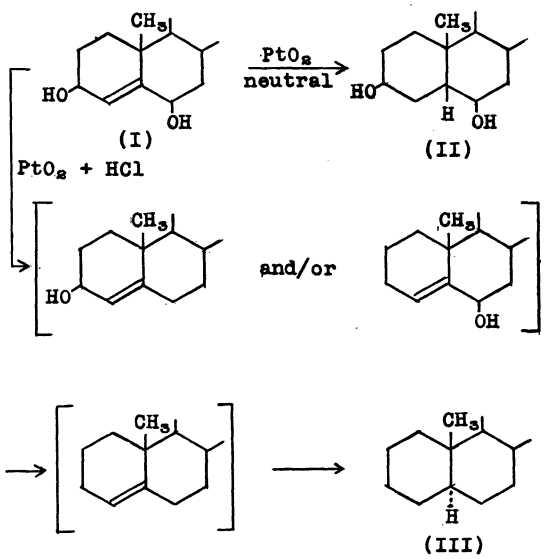
Hydrogenolysis and Hydrogenation of Some 2, 3-Unsaturated Alcohols with Platinum Oxide and with Platinized Raney Nickel

By Shigeo NISHIMURA and Kazuko MORI

(Received December 10, 1958)

The hydrogenation of cholest-4-ene-3β, 6β-diol (I) in neutral ethanolic solution with platinum oxide as a catalyst gives 5β-cholestane-3β,6β-diol (II)[1]. The present authors carried out the same reaction in the presence of a trace of hydrochloric acid, when a little less than three moles of hydrogen were absorbed and 5α-cholestane (III) was obtained as the main product[2] (Table I). Shoppee et al.[3] obtained similar results in the hydrogenation of cholest-4-en-3-ols and related compounds, but they gave no account on the course of the hydrogenation.

Since it has been found that neither 5α-cholestane-3β, 6β-diol nor 5β-cholestane-3β, 6β-diol can be hydrogenolyzed with platinum oxide and hydrochloric acid, it can be assumed that the cholestenediol (I) underwent for the most part the hydrogenolysis before the saturation of the double bond, giving 5α-cholestane as the main product as illustrated below:



The above assumption is further supported by the fact that the product obtained by an incomplete hydrogenation of the cholestenediol (I) gave coloration with tetranitromethane in chloroform, while the cholestenediol (I) is entirely indifferent to the reagent.

The formation of 5β-cholestane from 3α-acetoxycholest-4-ene[3] can not be explained in a similar way, because, if cholest-4-ene were an intermediate product, then 5α-cholestane should be the main product as in the hydrogenation of the cholestenediol (I).

Similar results have been obtained in the hydrogenation of other 2,3-unsaturated alcohols and phenol, as summarized in Table I.

In the presence of platinum oxide and hydrochloric acid the substances absorbed more hydrogen than is necessary to transform them into the corresponding saturated alcohols. Since none of 3-phenyl-1-propanol, tetrahydrofurfuryl alcohol and

1) V. Prelog and E. Tagmann, *Helv. Chim. Acta*, **27**, 1880 (1944).

2) In ether-acetic acid solution, two moles of hydrogen are absorbed by the diacetate of the diol, and 5α-cholestane-3β,6β-diol, 5α-cholestan-3β-ol and 5α-cholestane are obtained: O. Rosenheim and W. W. Starling, *J. Chem. Soc.*, **1937**, 383.

3) C. W. Shoppee, B. D. Agashe and G. H. R. Summers, ibid., **1957**, 3107.

TABLE I
MOLES OF HYDROGEN ABSORBED IN 95% ETHANOL AT THE ORDINARY TEMPERATURE AND PRESSURE

Compound	Catalyst		
	PtO_2	PtO_2 +HCl	Platinized Raney Ni[5]
Cholest-4-ene-3β,6β-diol	1.0	2.7	1.1
Cinnamyl alcohol	1.0	1.5	0.98
Furfuryl alcohol[4]		3.1	2.1
Phenol		3.4	3.0

cyclohexanol could be hydrogenolyzed under the same conditions, it is concluded that the hydrogenolysis took place prior to the saturation of the double bond. On the other hand, in neutral ethanolic solution cinnamyl alcohol absorbed only 1 mole of hydrogen in the presence of either platinum oxide or platinized Raney nickel prepared in alkaline solution[5], while furfuryl alcohol gave a quantitative yield of tetrahydrofurfuryl alcohol with the latter catalyst.

It has been reported that cinnamyl alcohol gives about equal moles of 3-phenyl-1-propanol and propylbenzene with palladium-charcoal and hydrogen[6]. It is very probable that the catalyst contained a trace of hydrochloric acid.

The authors wish to express their hearty thanks to Professor Yoshiyuki Urushibara for his kind guidance.

Department of Chemistry, Faculty of Science, The University of Tokyo
Hongo, Tokyo

4) Furfuryl alcohol absorbs about 2.5 moles of hydrogen in the hydrogenation with platinum oxide either in the presence or in the absence of ferrous chloride or sulfate giving tetrahydrofurfuryl alcohol along with other products: W. E. Kaufmann and R. Adams, *J. Am. Chem. Soc.*, **45**, 3029 (1923); J. S. Pierce and C. Parks, ibid., **51**, 3384 (1929).

5) S. Nishimura, This Bulletin **32**, 61, (1959).

6) R. Baltzly and J. S. Buck, *J. Am. Chem. Soc.*, **65**, 1984 (1943). Cf. W. H. Hartung and R. Simonoff, "Org. Reactions", Vol. VII, p. 267, John Wiley & Sons (1953).

Phase Relationship in the System $3CaO \cdot P_2O_5$—$CaO \cdot MgO \cdot 2SiO_2$—$SiO_2$

By Toshiyuki Sata

(Received August 4, 1958)

According to the present writer's published studies[1,2], slowly cooled specimens of fused phosphatic fertilizer and of bone-ash magnesia porcelain are composed of β-tricalcium phosphate, apatite, diopsidic pyroxene, and silica minerals. The equilibrium study of the system composed of these minerals, therefore, must be of great importance for the industrial manufacture of these products. Henceforth the author constructed the phase diagrams of the ternary system $3CaO \cdot P_2O_5$—$CaO \cdot MgO \cdot 2SiO_2$—$SiO_2$, on which no paper has ever been presented. This investigation is continued from his preceding report on the system $3CaO \cdot P_2O_5$—$MgO \cdot SiO_2$—SiO_2[3].

Experimental

Of the three-component system concerned, data of the two partial systems, $3CaO \cdot P_2O_5$—SiO_2 and $CaO \cdot MgO \cdot 2SiO_2$—$SiO_2$, were given by other authors, the former by Pierre[4] and Wojciechowska[5], and the latter by Bowen[6]. Another partial system $3CaO \cdot P_2O_5$—$CaO \cdot MgO \cdot 2SiO_2$ and the three-component system were investigated by usual quenching method in this study.

Powdered batches of selected compositions, prepared by quenching into glass after being kept at above their melting points, were again held at constant temperatures in a silicon carbide resistor furnace and then quenched in water. Thenceforth the equilibrium phases found therein were determined by the optical and the X-ray examination. For measuring the temperature a thermocouple of platinum-platinum rhodium(10%) was used. Details of experimental

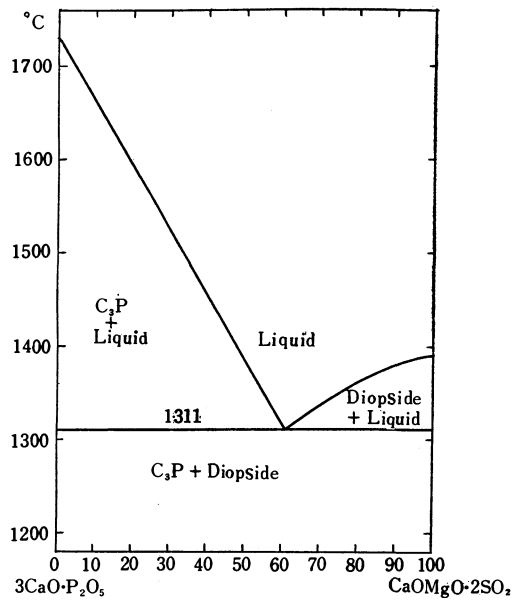


Fig. 1. The system $3CaO \cdot P_2O_5$—$CaO \cdot MgO \cdot 2SiO_2$

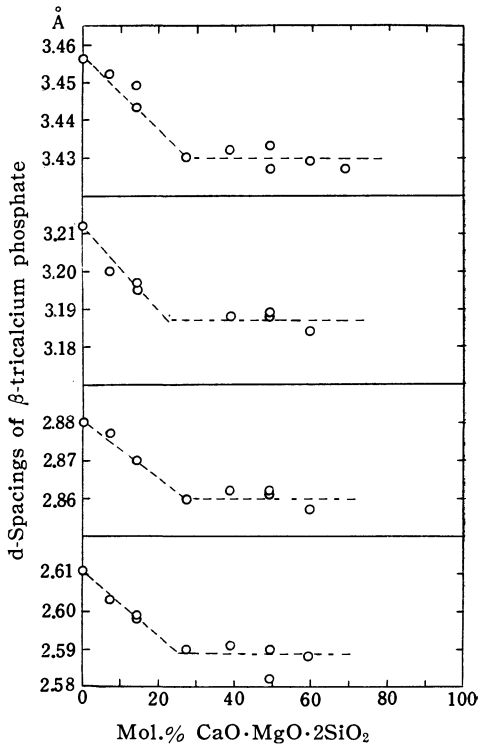


Fig. 2. The change in spacings of β-tricalicium phosphate at 1250~1300°C (pure tricalicium phosphate at 1100°C)

1) T. Sata and R. Kiyoura, *J. Chem. Soc. Japan, Ind. Chem. Sec.* (*Kogyo Kagaku Zasshi*), **62**, 63 (1959).
2) T. Sata and R. Kiyoura, *J. Cer. Assoc., Japan* (*Yogyo Kyokai Shi*), **66**, 294 (1958).
3) T. Sata, This Bulletin, **31**, No. 4 408 (1958).
4) D. D. S. St Pierre, *J. Am. Cer. Soc.*, **37**, (6) 243 (1954), **39**, (4) 147 (1956).
5) J. Wojciechowska et al., *Roczniki Chem.*, **30**, 743 (1956).
6) N. L. Bowen, *Am. J. Sci.*, (4) **38**, 207 (1914), *Z. anorg. allgem. Chem.*, **90**, 1 (1914).

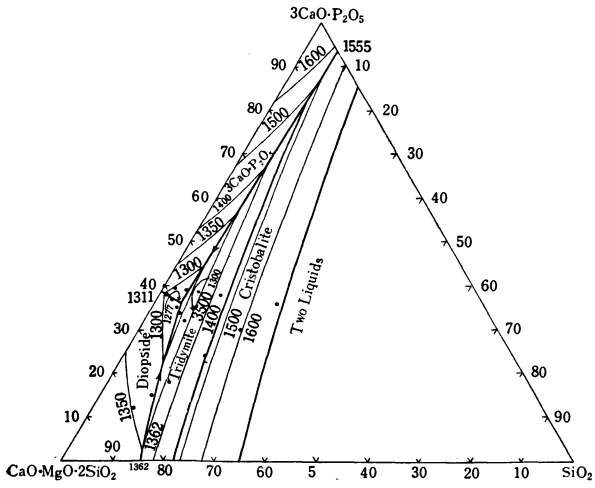


Fig. 3. The system $3CaO \cdot P_2O_5$—$CaO \cdot MgO \cdot 2SiO_2$—$2SiO_2$

procedures are similar to those already described in the author's preceding report[3].

Results

The system $3CaO \cdot P_2O_5$—$CaO \cdot MgO \cdot 2SiO_2$.—Data on the quenching runs for this two-component system are listed in Table I, from which the equilibrium diagram was constructed as shown in Fig. 1. It is found that this system seems to be perfectly described as a binary one, whose eutectic is located at 39% of $3CaO \cdot P_2O_5$ and 61% of $CaO \cdot MgO \cdot 2SiO_2$, melting point at 1311±4°C. In the region rich in $3CaO \cdot P_2O_5$ (over 80%), the following facts were observed. (1) The crystallization of diopside did not take place when samples were kept for about 1 hr. even under the eutectic temperature. (2) The transition temperature of tricalcium phosphate from

TABLE I

QUENCHING DATA IN THE SYSTEM $3CaO \cdot P_2O_5$—$CaO \cdot MgO \cdot 2SiO_2$

No.	Composition wt.% C_3P	Composition wt.% CMS_2*	Holding temp. °C	Holding time min.	Phases present
248	95	5	1500	45	α-C_3P, glass
			1400	120	α-C_3P, β-C_3P, glass
			1292	60	β-C_3P
113	90	10	1500	30	α-C_3P, glass
			1450	60	α-C_3P, small β-C_3P, glass
			1400	60	β-C_3P, glass
			1292	300	β-C_3P, diopside
100	80	20	1600	20	small α-C_3P, glass
			1520	30	α-C_3P, β-C_3P, glass
			1450	60	β-C_3P, glass
			1307	30	β-C_3P
			1272	70	β-C_3P, small diopside
112	70	30	1314	30	β-C_3P, glass
			1302	30	β-C_3P, trace diopside
			1292	50	β-C_3P, diopside
99	60	40	1455	30	glass
			1422	30	very small β-C_3P, glass
			1314	40	small β-C_3P, glass
			1307	40	β-C_3P, diopside, glass
111	50	50	1382	30	very small β-C_3P, glass
			1357	30	small β-C_3P, glass
98	40	60	1324	40	glass
			1314	60	small β-C_3P, glass
			1307	40	β-C_3P, diopside, glass
			1282	40	all crystal
119	35	65	1314	40	small diopside, glass
118	30	70	1340	20	glass
			1324	30	trace diopside, glass
			1314	30	diopside
97	20	80	1364	30	glass
			1358	40	diopside, glass

* Abbreviations: $C_3P = 3CaO \cdot P_2O_5$, $CMS_2 = CaO \cdot MgO \cdot 2SiO_2$

TABLE II

QUENCHING DATA IN THE SYSTEM $3CaO \cdot P_2O_5$—$CaO \cdot MgO \cdot 2SiO_2$—$SiO_2$

No.	Composition wt.%		C_3P	CMS_2 wt.%	S*	Holding Temp. °C	Time min.	Phases present
	CMS_2	No. 23						
195	80	20	12	80	8	1340	30	glass
						1334	30	diopside, glass
						1304	30	almost crystal
200	75	25	15	75	10	1330	60	glass
						1323	40	very small diopside, glass
196	70	30	18	70	12	1354	30	cristbl.,* glass
						1314	60	cristbl., glass
						1304	30	cristbl., diopside, glass
						1237	120	β-C_3P, diopside, cristbl.
197	60	40	24	60	16	1354	30	cristbl., glass
						1294	60	cristbl., glass
						1284	60	cristbl., diopside, glass
						1279	60	cristbl., diopside, small glass
						1274	60	all crystal
198	50	50	30	50	20	1354	30	cristbl., glass
						1284	60	cristbl., glass
						1279	60	all crystal
199	40	60	36	40	24	1292	40	β-C_3P, cristbl., glass
						1277	60	all crystal
						1237	120	β-C_3P, diopside, cristbl., tridymite
	No. 197	No. 98						
203	50	50	32	60	8	1299	40	small cristbl., glass
						1282	50	cristbl., glass
						1273	50	all crystal
204	40	60	33.6	60	6.4	1290	50	diopside, cristbl., glass
						1282	50	almost crystal
205	30	70	35.2	60	4.8	1290	50	glass
						1281	60	diopside, glass
206	19.4	80.6	36.9	60	3.1	1290	50	glass
						1281	60	diopside, glass
	No. 199	No. 98						
202	50	50	38	50	12	1315	40	cristbl., glass
201	30	70	38.8	54	7.2	1315	40	very small cristal., glass
						1299	40	cristbl., glass
						1282	50	cristbl., β-C_3P, glass
						1277	50	all crystal
207	20	80	39.2	56	4.8	1290	50	very small C_3P, glass
						1282	50	diopside, almost crystal
208	10	90	39.6	58	2.4	1290	50	small β-C_3P, glass
						1282	50	diopside, almost crystal

* Abbreviations; S=silica, cristbl.=cristobalite

β to α increased with diopside content, 1350 ~1400°C with 5%, 1450~1450°C with 10%, and 1450~1520°C with 20% of diopside (the transition temperature of pure tricalcium phosphate is 1180°C). (3) The spacings for diffraction lines in β-tricalcium phosphate decreased with diopside contents as indicated in Fig. 2, showing apparent formation of solid solution with some diopside (25±2 mol.% or 19±2 wt.%). These facts occurring in the region rich in tricalcium phosphate will be discussed with more data in the near future.

The system $3CaO \cdot P_2O_5$—$CaO \cdot MgO \cdot 2SiO_2$—$SiO_2$.—This three-component system is a perfect ternary one, and its eutectic was decided from the quenching data of the 14 samples shown in Table II, whose compositions lie along the tie lines connecting No. 23 (C_3P60—SiO_240) with $CaO \cdot MgO \cdot 2SiO_2$ corner and No. 98 (C_3P40—$CaO \cdot MgO \cdot 2SiO_260$) with No. 197 or No. 199, as

plotted in Fig. 3. The ternary eutectic is located at 36±1% C_3P, 59±1% $CaO \cdot MgO \cdot 2SiO_2$, and 5±1% SiO_2, and at 1277±3°C, which is close to the $3CaO \cdot P_2O_5$—$CaO \cdot MgO \cdot 2SiO_2$ join. Accordingly the silica field covers over a very wide area. The isotherms on the liquidus surface were approximately represented in the ternary system.

Summary

The phase relationship in the system $3CaO \cdot P_2O_5$—$CaO \cdot MgO \cdot 2SiO_2$—$SiO_2$ was investigated by the usual quenching method. The two partial systems $3CaO \cdot P_2O_5$—SiO_2 and $CaO \cdot MgO \cdot 2SiO_2$—$SiO_2$ have already been reported by previous investigators. Another partial system $3CaO \cdot P_2O_5$—$CaO \cdot MgO \cdot 2SiO_2$ seems to be approximately binary, whose eutectic is located at 39% of $3CaO \cdot P_2O_5$ and 61% of $CaO \cdot MgO \cdot 2SiO_2$, and at 1311±4°C. In the region rich in $3CaO \cdot P_2O_5$, it was observed that the crystallization velocity of diopside is rather slow under the solidus temperature, that the transition temperature of tricalcium phosphate is considerably increased with diopside content, and that β-tricalicium phosphate apparently makes solid solution with diopside (19 wt.%).

The system $3CaO \cdot P_2O_5$—$CaO \cdot MgO \cdot 2SiO_2$—$SiO_2$ is of a perfect ternary one, whose eutectic is at 36% of $3CaO \cdot P_2O_5$, 59% of $CaO \cdot MgO \cdot 2SiO_2$ and 5% of SiO_2, and at 1277±3°C. Its isotherms of the liquidus surface were approximately represented.

The author acknowledges the constant help and encouragement given by Professor R. Kiyoura, Tokyo Institute of Technology, and also much helpful advice supplied by Professor H. Yamada and Assistant Professor S. Kawakubo, Tokyo Institute of Technology. This work was conducted as a part of a program to investigate the corrosion problems of various refractory bricks in the manufacture of fused phosphatic fertilizer.

Research Laboratory for Ceramics
Tokyo Institute of Technology
Meguro-ku, Tokyo

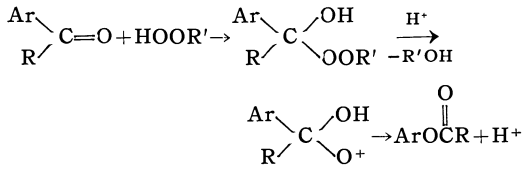
Kinetics of the Acid-Catalyzed Peroxide Oxidation of 4-Hydroxybenzaldehyde in Acetic Acid

By Yoshiro OGATA and Iwao TABUSHI

(Received July 5, 1958)

It is well known that aromatic ketones and aldehydes give on oxidation with peroxides (e. g., hydrogen peroxides or organic peracids) aryl esters or their hydrolysis products, i. e., phenols and carboxylic acids[1-3].

In general, the reaction is acid-catalyzed. It is of interest to note that *o*- or *p*-hydroxyl, amino or mercapto group facilitates the reaction to such an extent that it takes place at a high pH even in aqueous alkaline media[4], where a mechanism involving an initial attack of hydrogen peroxide to the active hydrogen of these groups was postulated[5]. In contrast, the reaction in acidic media occurs without these activating groups[6,7]. In this case, the mechanism has been suggested to be an addition of peroxide to the carbonyl group followed by a rearrangement[2,3].



R: alkyl or H[8] Ar: aryl.

1) D. Swern, *Chem. Revs.*, **45**, 1 (1949).
2) J. E. Leffler, ibid., **45**, 385 (1949).
3) C. H. Hasall, *Organic Reactions*, **9**, 73 (1957).
4) a) H. D. Dakin, *Proc. Chem. Soc.*, **25**, 194 (1909).
b) H. D. Dakin, *Am. Chem. J.*, **42**, 477 (1909).
5) a) E. Bamberger, *Ber.*, **36**, 2042 (1903).
b) E. Bamberger and H. O. Eppinger, ibid., **73**, 644 (1940).
6) W. Dilthy, M. Inckel and H. Stephan, *J. prakt. Chem.*, **154**, 219 (1940).
7) W. Dilthy and F. Quint, ibid., **131**, 1 (1931).
8) A. Wacek and A. Bezard, *Ber.*, **74**, 845 (1941).

However, few detailed mechanistic studies from the kinetic standpoint have been reported on the hydrogen peroxide oxidation in acidic media. The present study was undertaken to elucidate the mechanism as well as the true oxidizing agent of the acid-catalyzed hydrogen peroxide oxidation of hydroxybenzaldehyde in aqueous acetic acid by estimating the effects of acidity on the rate.

Experimental

Materials.—*p*-Hydroxybenzaldehyde was purified by recrystallization from water, m. p. 116°.

Kinetic Procedures.—*Procedure A. Simultaneous Addition of the Reactants.*—Hydroxybenzaldehyde, acetic acid, sulfuric acid and water were mixed in a flask in the above order, thermostated at 15° or 20°; then hydrogen peroxide was added to the mixture. To avoid the temperature increase during the addition of hydrogen peroxide, a lower concentration of sulfuric acid and relatively high water content should be used. In the procedure, however, the apparent rate constant usually increases during the reaction except at high acidity.

Procedure B. Addition of Aldehyde to an Equilibrium Mixture of Peroxides.—Hydrogen peroxide was added to a cooled mixture of aqueous acetic acid and sulfuric acid in a brown flask, and the mixtue thermostated at 15±0.1 or 20±0.1° until the equilibrium state between hydrogen peroxide and peracetic acid was attained. Then hydroxybenzaldehyde was added to a known amount of the peroxide solution, the oxidation being started here. The reaction temperature was 15±0.1 or 20±0.1°.

In order to ascertain the establishment of the equilibrium and also to estimate hydrogen peroxide and peracetic acid contents in the preliminary equilibrium mixture, permanganate titration for hydrogen peroxide and iodometry for the peracetic acid were employed. Aliquots were taken out at appropriate intervals from the preliminary mixture before the addition of the aldehyde, run into a cooled mixture of ice and sulfuric acid and titrated rapidly at ca. −5° with potassium permanganate to determine the hydrogen peroxide content. An aqueous solution of potassium iodide was then added to the mixture, warmed and titrated with thiosulfate to estimate the peracid content. In general, the aliquot consumes a slight excess of permanganate because of the obscurity of the end point; it was corrected by a separate determination of total peroxides.

When the ratio a/b (where the equivalent amount of hydrogen peroxide present is a, that of peracetic acid b) becomes constant within experimental error, the equilibrium constant K_1 and the forward and the reverse rate constant of peracetic acid formation (k_1 and k_{-1}, respectively) may be calculated by means of equations:

$$K_1 = k_1/k_{-1}, \qquad k+k_{-1} = \frac{2.303}{t}\log\left(\frac{a_0-a_e}{a-a_e}\right)$$

where a_0 is the initial concentration and a_e is the equilibrium concentration of hydrogen peroxide.

In kinetic runs after the addition of hydroxybenzaldehyde, aliquots were withdrawn and their total peroxide content was determined iodometrically. The rate constants were then calculated by means of the usual second-order rate equation. The spontaneous decomposition of the peroxides in the absence of hydroxybenzaldehydes under these conditions is so small that it may be assumed that the amount of consumed peroxides minus the known amount of the spontaneous decomposition is the amount of peroxides reacted.

Reaction Products Criterion.—The reaction mixture gave, on long standing, a product containing hydroquinone or catechol. As mentioned previously, the formates of these phenols are probably produced at an initial stage, since the conversion percentage is not in accord with those of peroxide, when calculated spectrophotometrically on the assumption that hydroquinone is produced directly. These esters could not be isolated in appreciable quantities presumably because of the rapid hydrolysis during isolation procedures, as the hydrolysis was accelerated in the presence of considerable amounts of water and sulfuric acid.

Results and Discussion

The Equilibrium between Hydrogen Peroxide and Peracetic Acid.—When the rate measurements were carried out by adding hydrogen peroxide to an equilibrium mixture of aqueous acetic acid, sulfuric acid and hydroxybenzaldehyde (Procedure A), an induction period was observed at the initial stage and the apparent second-order rate constants increased rapidly at

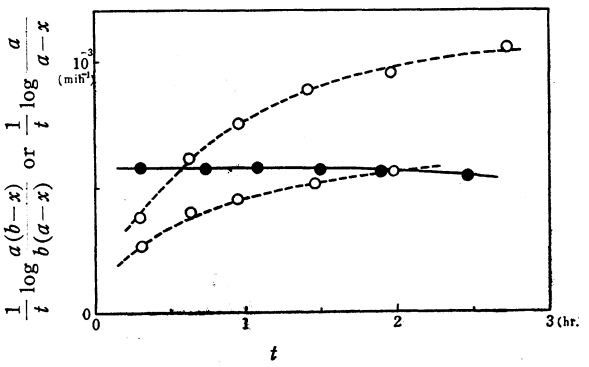


Fig. 1. Comparison of the results with Procedure A and B in the reaction of hydroxybenzaldehyde with peroxide.
dotted line: $\frac{1}{t}\log\left(\frac{a}{a-x}\right)$ vs. t at the early stages of the reaction with Procedure A. (Initial concentration of the aldehyde is considerably higher than that of hydrogen peroxide). solid line: $\frac{1}{t}\log\frac{a(b-x)}{b(a-x)}$ vs. t with Procedure B.

TABLE I

THE APPARENT SECOND-ORDER RATE CONSTANTS OF *p*-HYDROXYBENZALDEHYDE WITH PROCEDURE B

p-HOC_6H_4CHO 10^{-2}M	Total peroxide[a] 10^{-2}M	H_2SO_4 M	H_2O M	$k\times10^3$ [b] l. $mole^{-1}sec^{-1}$	Temp. °C
1.64	2.4	0.392	5.55	4.06±0.02	15
0.984	2.4	0.392	5.55	4.08±0.05	15
1.64	4.8	0.392	5.55	4.07±0.06	15
1.64	2.4	0.392	5.55	5.10±0.05	20
1.64	2.4	0.196	5.55	2.62±0.02	15
1.64	2.4	0.784	5.55	8.70±0.06	15
1.64	2.4	0.784	5.55	10.3 ±0.1	20
1.64	2.4	1.18	5.55	13.9 ±0.1	15
1.64	2.4	0.078	5.55	1.52±0.03	15
1.64	2.4	0.392	3.33	7.44±0.06	20
1.64	2.4	0.392	11.1	2.64±0.05	15
1.64	2.4	0.392	16.7	1.91±0.02	15
1.64	2.4	0.392	16.7	2.27±0.05	20

a) The average value of different initial concentrations of peroxide.
b) Figures following ± show probable errors.

TABLE II

THE APPARENT PSEUDO-FIRST-ORDER RATE CONSTANTS AND APPARENT EQUILIBRIUM CONSTANTS OF THE PERACETIC ACID FORMATION FROM HYDROGEN PEROXIDE AND ACETIC ACID

H_2O M	H_2SO_4 M	H_2O_2 10^{-2} M	K_1	$k_1\times10^{-4}$ sec^{-1}	$k_{-1}\times10^{-4}$ sec^{-1}
5.55	0.392	1.2	3.01	—	—
5.55	0.392	2.4	3.03	1.74	0.58
5.55	0.392	4.8	3.05	1.82	0.60
5.55	0.078	2.4	2.44	0.206	0.084
5.55	0.196	2.4	2.50	0.711	0.284
5.55	0.784	2.4	3.64	4.42	1.20
5.55	1.18	2.4	5.15	—	—
11.1	0.392	2.4	2.75	0.668	0.242
16.7	0.392	2.4	2.33	—	—

first, and then slowly. This trend was remarkable especially with low concentrations of sulfuric acid and with a relatively high initial concentration of hydroxybenzaldehyde compared with that of hydrogen peroxide. Typical examples are shown in Fig. 1.

On the other hand, when hydrogen peroxide is allowed to reach equilibrium with aqueous acetic and sulfric acid before hydroxybenzaldehyde is added to start the reaction (Procedure B), no such initial suppression of apparent rate constant is observed. The rate constant holds a satisfactory constancy during the reaction except near the end of the reaction where a slight decrease of the constant is appreciable. The constant does not, of course, vary with changing initial concentrations of the reactants. Table I shows the apparent second-order constants with Procedure B.

The facts cited above suggest that an active intermediate is formed by the acid-catalyzed interaction of hydrogen peroxide and acetic acid, the rate of its formation being comparable to that of the main reaction of hydroxybenzaldehyde with the intermediate. The facts that the initial suppression of the rate becomes remarkable by reducing the rate of formation of the intermediate and that the apparent rate constant estimated by Procedure A is much lower at an early stage than that by procedure B, agree well with the assumption of such an active intermediate. For example, a "rate constant" with Procedure A at 10% conversion is ca. 1/12.6 of that with Procedure B in the following condition. $[H_2O]=5.55$ M and $[H_2SO_4]=0.0736$ M at 20°.

It is most probable that the intermediate is peracetic acid, the equilibrium constant of its sulfuric acid-catalyzed formation having been estimated by D'Ans[9].

9) J. D'Ans and W. Frey, O; *Z. anog. Chem.* **84**, 145 *Chem. Abstr.*, **8**, 923 (1914).

$$H_2O_2+CH_3COOH \underset{k_{-1}}{\overset{k_1}{\rightleftarrows}} CH_3CO_3H+H_2O \quad (1)$$

$$CH_3CO_3H+\text{hydroxybenzaldehyde} \xrightarrow{k_2} \text{product} \quad (2)$$

In addition to peracetic acid, the formation of Caro's acid may be expected. It seems rational, however, that peracetic acid is the main oxidizing agent, since the acidities used are not very high and the rate of formation of Caro's acid is very low under these conditions, although it may become appreciable at higher acidities[10]. The possibility that the active attacking agent is OH^+ (or $H_3O_2^+$) may be eliminated, since the protonation of hydrogen peroxide should be very rapid.

Approximate rate constants and equilibrium constants of the formation of peracetic acid determined under the same conditions as those of the kinetic experiments are shown in Table II. Both constants increase with increasing acidity in accord with the previous observation in such an equilibrium as hydrogen peroxide-performic acid or hydrogen peroxide-monoperoxysulfuric acid[10].

Since the magnitude of k_1 was moderate in these experiments, conditions where v_1 and v_2 (v's are rates of the subscripted steps) are comparable may easily be attained[11].

Our qualitative observation on the initial suppression of the rate agrees with the above discussion and provides another evidence for the justification of eqs. 1 and 2. Furthermore, the oxidation rate measurements in pure aqueous media of the same acidity show that the rate is too slow to measure, thus indicating that no intermediate is produced by the interaction of hydrogen peroxide and sulfuric acid alone.

Effects of Acidity and Water Content.— A study of the effects of sulfuric acid concentration and water content on the apparent second-order rate constant according to Procedure B (k) shows that the results can not be expressed in a simple form, unless corrections for peracetic acid concentration and acidity are made. (see Figs. 2 and 3).

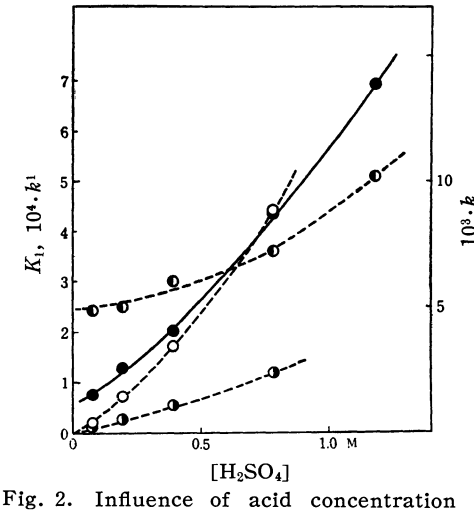


Fig. 2. Influence of acid concentration on the rate and the equilibrium constant for the reaction of peracetic acid formation at 15° and for the oxidation of hydroxybenzaldehyde. $[H_2O]=5.55$ M.
Dotted lines correspond to the peracetic acid formation:
◐, equilibrium constant K_1
○, forward rate constant $k_1 \cdot 10^4$
◑, reverse rate constant $k_{-1} \cdot 10^4$
Solid line correspond to the rate constant of oxidation: $k \cdot 10^3$.

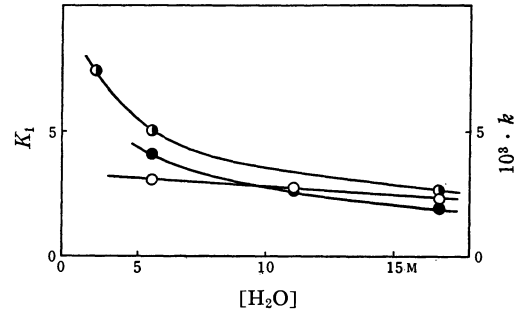


Fig. 3. Influence of water concentration on the rate and the equilibrium constant for peracetic acid formation of 15° and oxidation of p-hydroxybenzaldehyde at 15° and 20°.
○, equilibrium constant of peracetic acid formation K_1
◑, for rate constant of the oxidation at 20°
●, at 10°
$[H_2SO_4]=0.392$ M.

10) J. M. Monger and O. Redlich, *J. Phys. Chem.*, **60**, 797 (1956).

11) Under these conditions the observed initial suppression of the rate in Procedure A becomes remarkable. In the following equations (total peroxide is nearly equal to $[H_2O_2]$ in the early stages of the reaction)

$v_1=k_1[H_2O_2][AcOH]$

$v_2=k_2[CH_3CO_3H][\text{hydroxybenzaldehyde}]$

$=k_2'[\text{total peroxide}][\text{hydroxybenzaldehyde}]$

The observed rate constants with p-hydroxybenzaldehyde at $[H_2O]=5.55$ M, $[AcOH]=15$ M and $[H_2SO_4]=0.392$ M were found to be

$k_1=1.78\times10^{-4}$ l. mole^{-1}sec.$^{-1}$

$k_2'=4.07\times10^{-3}$ l. mole^{-1}sec^{-1}.

Here, k_2' is the apparent rate contant and k is the rate constant of the subscripted step. Therefore,

$v_2/v_1=4.07\times10^{-3}\times[\text{hydroxybenzaldehyde}]/(1.78\times10^{-4}\times15)$

Namely, if the initial concentration of hydroxybenzaldehyde exceeds 10^{-2} M, v_2 appoaches to v_1. This approach should become remarkable as the acidity decreases, since k_1 appreaches to zero with decreasing acidity, while k_2' approaehes to a definite value (see Fig. 2).

The concentration of peracetic acid is obtainable from the concentration of total peroxide [T] as follows.

$$K_1=\frac{[H_3O]\,[CH_3CO_3H]}{[H_3O_3]\,[CH_3CO_2H]} \quad (3)$$

Here, both $[CH_3CO_2H]$ and $[H_3O]$ may be regarded as constant. Since

$$[T] = [H_2O_2] + [CH_3CO_3H] \quad (4)$$

$$[CH_3CO_3H] = \frac{[CH_3CO_2H]\,K_1}{[CH_3CO_3H]\,K_1 + [H_2O]} \cdot [T] \quad (5)$$

$$[H_2O_2] = \frac{[H_2O]}{[CH_3CO_2H]\,K_1 + H_2O} \cdot [T]$$

$$v = k\,[Hy]\,[T] = k_p\,[Hy]\,[CH_3CO_3H] + k_h\,[Hy]\,[H_2O_2] \quad (6)$$

are obtained, where Hy means hydroxybenzaldehyde, k_p and k_h are rate constants for reactions of peracetic acid and hydrogen peroxide, respectively. Therefore,

$$k = k_p\frac{[CH_3CO_2H]\,K_1}{[CH_3CO_2H]\,K_1 + [H_2O]} + k_h\frac{[H_2O]}{[CH_3CO_2H]\,K_1 + [H_2O]} \quad (7)$$

From the above discussion, it may be concluded that the second term of the right hand side of equation 7 expressing hydrogen peroxide oxidation is far less important than the first term. Hence,

$$k = k_p\frac{[CH_3CO_2H]\,K_1}{[CH_3CO_2H]\,K_1 + [H_2O]} \quad (8)$$

The value of k_p calculated by means of equation 8 holds sufficient constancy as noted later; therefore it is confirmed that the second term participation has little effect on the kinetics. This is supported numerically, comparing k in Procedures A and B at the initial stage of reaction, and the ratio of peracid to hydrogen peroxide in the equilibrium state.

For the expression of the acidity of the solutions, the Hammett's acidity function H_0 was used, the indicators being *o*- and *p*-nitranilines and 4-chloro-2-nitraniline. Plots of H_0 vs. log k_p gave no straight line, but a curve whose slope approaches -1 with increasing acidity, while it approaches zero with decreasing acidity. This fact seems to mean that the rate constant k_p may further be separable into the acid-independent (k_n) terms:

$$k_p = k_n + k_a k_0 \quad (9)$$

where h_0 relates to H_0 in expression $\log h_0 = -H_0$.

Plot of k_p vs. h_0 gives a satisfactory straight line as shown in Fig. 4. A slight decrease of k_a at very high acidity or its change in varying water-sulfuric acid ratio at the same acidity is probably due to the unequality of h_0 and proton activity[12].

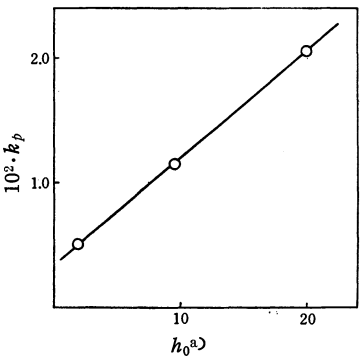


Fig. 4. The plot of k_p vs. h_0 for the reaction of *p*-hydroxybenzaldehyde in moderate acidities at 20°.

Reaction Mechanism.—The above results imply that there is a preliminary, relatively rapid and reversible peracetic acid formation, then acid-catalyzed or uncatalyzed attack of the peracetic acid on the carbonyl group takes place to form an addition complex followed by a rearrangement of the complex to the product. The rearrangement would not perhaps be a rate-determining step, since no stable complex has been isolated, and furthermore, in our preliminary experiments no appreciable difference was observed between the ultraviolet spectrum of the original aldehyde solution and that of the aldehyde solution immediately after mixing it with peracetic acid solution.

On the basis of the observed kinetics, there are two possible mechanisms, i. e., mechanism A involving steps 10, 11, 13, 14 and 16 and mechanism B involving steps 10, 12, 14, 15 and 16.

$$CH_3CO_2H + H_2O_2 + H^+ \rightleftarrows CH_3CO_3H + H_2O + H^+ \quad (10)$$

$$CH_3CO_3H + H^+ \rightleftarrows CH_3CO_3H_2^+ \quad (11)$$

$$ArCHO + H^+ \rightleftarrows ArC^+HOH \quad (12)$$

12) For the ionization and dissociation of sulfuric acid in aqueous acetic acid, see S. Bruckenstein and I. M. Kolthoff, *J. Am. Chem. Soc.*, **78**, 10 (1956).

a) The values of h_0 were calculated from the observed H_0's under these experimental conditions. The values of H_0 were calculated by Hammett's equation $H_0 = pK_a + \log(c_B/c^+_{BH})$ to be -0.28, -0.99 and -1.30 with $[H_2SO_4] = 0.392$ M, 0.784 M and 1.18 M, respectively, where $[H_2O] = 5.55$ M is constant.

$$CH_3CO_3H_2^+ + ArCHO \rightarrow$$
$$ArCHO \cdot CH_3CO_3H_2^+ \text{(complex, } I \cdot H^+) \quad (13)$$
$$CH_3CO_3H + ArCHO \rightarrow$$
$$ArCHO \cdot CH_3CO_3H \text{ (complex, I)} \quad (14)$$
$$CH_3CO_3H + ArC^+HOH \rightarrow I \cdot H^+ \quad (15)$$
$$I \text{ (or } I \cdot H^+) \rightarrow$$
$$ArOCHO + CH_3CO_2H \text{ (or } +H^+) \quad (16)$$

Since the mobile equilibria 11 and 12 probably tend to shift to the left side, step 12 in mechanism A and 11 in B may be neglected except at high acidity. The apparent rate constants k_A and k_B, corresponding to mechanism A and B, respectively, are easily expressed in terms of the equilibrium and rate constants of equations 11—15, where K and k denote equilibrium and rate constants of the subscripted steps, respectively.

$$k_A = k_{13} \cdot \frac{1}{1+K_{12}[H^+]} \cdot \frac{K_{11}[H^+]}{1+K_{11}[H^+]} + k_{14} \cdot \frac{1}{1+K_{11}[H^+]} \cdot \frac{1}{1+K_{12}[H^+]} \quad (17a)$$

$$k_B = k_{15} \cdot \frac{1}{1+K_{11}[H^+]} \cdot \frac{K_{12}[H^+]}{1+K_{12}[H^+]} + k_{14} \cdot \frac{1}{1+K_{11}[H^+]} \cdot \frac{1}{1+K_{12}[H^+]} \quad (17b)$$

Here, k_{13}, k_{14} and k_{15} are acidity-independent constants. At lower acidity, equations 17a and 17b may be simplified in the following way, since both $K_{11}[H^+]$ and $K_{12}[H^+]$ are far smaller than unity.

$$k_A = k_{13}K_{11}[H^+] + k_{14} \quad (18a)$$
$$k_B = k_{15}K_{12}[H^+] + k_{14} \quad (18b)$$

Since both equations 18a and 18b agree with the observed expression 9 and also with the rate-acidity relationship, it seems impossible, on the basis of the kinetics alone, to determine which mechanism is favored in so far as the values of K_{11} and K_{12} are unavailable. However, step 13 is more favorable than step 15, since it involves an attack of a more electrophilic agent $CH_3CO_3H_2^+$.

Summary

The sulfuric acid-catalyzed oxidations of 4-hydroxybenzaldehyde with hydrogen peroxide in aqueous acetic acid were kinetically investigated at 15° and 20° by iodometric estimation of the peroxides. The rates of peroxide consumption were found to be proportional to the product of the concentrations of hydroxybenzaldehyde and peroxide, when the aldehyde was added after the equilibrium between hydrogen peroxide and peracetic acid was attained. The rate constant is a linear function of Hammett acidity function h_0.

Hydrogen peroxide itself reacts slowly with the aldehyde, but it reacts more easily through the formation of peracetic acid. A mechanism involving a ratedetermining attack of protonated and free peracetic acid was postulated and discussed.

Department of Industrial Chemistry
Faculty of Engineering
Kyoto University
Sakyo-ku, Kyoto

Studies on the Interaction of Surface Films with Solute in Solution. IV. Effect of Congo Red Dissolved in Aqueous Substrate upon the Monolayers of Octadecylamine, Cetyl Alcohol, Ethyl n-Hexadecyl Ether, Ethyl Stearate and Cholesterol

By Mitsuo MURAMATSU

(Received August 8, 1958)

In the Part II[1] of this series, the interaction between various dyes in aqueous solutions and stearic acid in the built-up film has been studied. There it was suggested that pH dependence of the amount of dye taken up by the film may be explained by the interaction between dye and stearic acid, involving ionic, dipolar and van der Waals' force. This was generally in agreement with the effect of aqueous dye solution on the monolayer of stearic acid spread on it[2] and has further been supported by the experimental results of a profound effect of aqueous dye on the monolayer of octadecylamine[3]. As has been pointed out in Part II[1], however, there still remained some uncertainty in establishing the mechanism of the interaction between amphoteric dye and the surface film.

Of many amphoteric dyes, Congo red is most familiar to us and the surface-chemical properties of its solution have widely been studied by the measurement of ultrasonic velocity[4], diffusion coefficient[5], viscoelasticity of the adsorbed film[6], and foaming power[7]. Hence Congo red was also adopted in the present work as a representative for the amphoteric dyes and its effect upon the monolayers of several amphipathic compounds has been studied. It may be expected that such a study would also contribute to the understanding of the mechanism of dyeing processes of fibers by so-called direct dyes to which many of the amphoteric dyes belong.

Experimental

Apparatus and procedure were the same as used in the preceding work[3]. The same samples of Congo red[1] and octadecylamine[3] as those which appeared in the preceding reports were used also in of the present experiments. Cetyl alcohol was first grade of Katayama Pure Chemical Co. Ethyl *n*-hexadecyl ether and ethyl stearate were synthesized by the reaction of sodium ethylate with purified hexadecyl bromide and stearyl chloride, respectively. All these amphipathic compounds were purified repeatedly by fractional distillation in vacuo and successive recrystallization from suitable solvents. The highly purified sample of cholesterol was kindly supplied by Dr. E. Kimoto of Kurume Medical College.

Results

Octadecylamine. — It has been suggested[3,8] that the surface pressure, F, of

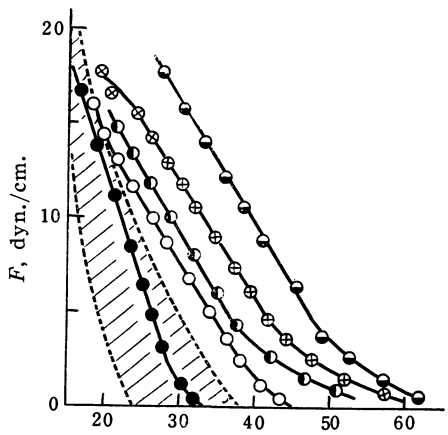


Fig. 1. $F\sim A$ curves for the monolayers of octadecylamine spread on the solutions of Congo red.
Substrate pH; ◑, 1.0; ⊕, 3.6; ◒, 5.5; ○, 7.3; ●, 9.3: $F\sim A$ curve for monolayer spread on water lie always in a range of hatched zone.

1) M. Muramatsu, This Bulletin, **31**, 871 (1958).
2) R. Matuura, ibid., **24**, 282 (1951).
3) M. Muramatsu, ibid., **31**, 878 (1958).
4) T. Sasaki and T. Yasunaga, to be published.
5) M. Nakagaki, This Bulletin, **23**, 104 (1950).
6) K. S. G. Doss, *Kolloid-Z.*, **84**, 138 (1938); **86**, 205 (1939); **87**, 272 (1939), etc.; H. Kimizuka, This Bulletin, **26**, 33 (1953).
7) M. Nakagaki, ibid., **23**, 47 (1950); T. Sasaki and H. Kimizuka, ibid., **24**, 230 (1951).
8) T. Sasaki and M. Muramatsu, ibid., **26**, 96 (1953).

this film fluctuated considerably for a given molecular area, A. This came from the effects of ageing of the film, carbon dioxide in the substrate, velocity of compression, etc. This tendency disappeared when Congo red was added to the substrate phase. The effect of dye upon $F\sim A$ curve of the monolayer of octadecylamine is shown in Fig. 1 in which the hatched zone is quoted from the preceding report[3]. It can be seen in this figure that the addition of dye results in a remarkable expansion of the monolayer when pH of the substrate is around 5.5. In Fig. 2 curve

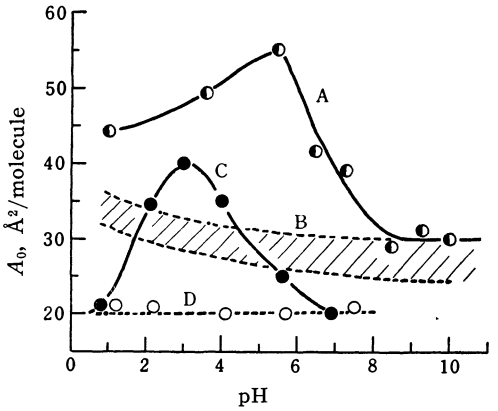


Fig. 2. Effect of Congo red upon A_0 for the monolayer of octadecylamine and cetyl alcohol.
A and B, amine on the substrate with or without dye, respectively; C and D, alcohol on the substrate with or without dye, respectively.

A shows the effect of substrate pH on the area, A_0, of octadecylamine molecule in the monolayer which spread on the solution of dye and is compressed to $F=2$ dyn./cm. In the same figure the hatched zone B expresses the limit of fluctuation of A_0 for a given pH value of the substrate without dye. Maximum expansion of the monolayer was observed at pH 5.5.

Cetyl Alcohol. — No effect of substrate pH was observed upon A_0 for the monolayer spread on the surface of water. When the dye was dissolved in the substrate of pH 2~4, the film expanded considerably. Such an effect of dye is shown in Fig. 2, in which the curve C and D express the pH dependence of A_0 for the monolayer spread on aqueous substrate containing or lacking the dye, respectively. Maximum expansion of the monolayer occurred at pH 3 in this case.

Ethyl *n*-Hexadecyl Ether. — Characteristic kinds of behavior in $F\sim A$ relationship were observed for this film. When the monolayer on the surface of water was compressed, we usually observed an instantaneous rise and subsequent lowering of the surface pressure. A typical example is shown in Fig. 3 (a). The behavior could be reproduced fairly well, though F was determined by means of the vertical plate method which proves to be unsuitable when we measure the decreasing surface pressure. A similar curve was obtained for the film spread on the surface of water of any acidity. The pH dependence of the area, A_0, at $F=2$ dyn./cm. is expressed as curve B in Fig. 4.

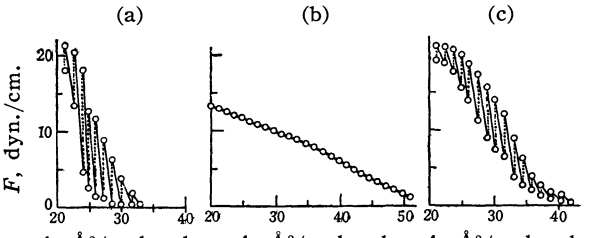


Fig. 3. $F\sim A$ curves for the monolayers of ethyl *n*-hexadecyl ether spread on (a) water of pH 4.0, (b) dye solution of pH 3.8, and (c) dye solution of pH 1.9.

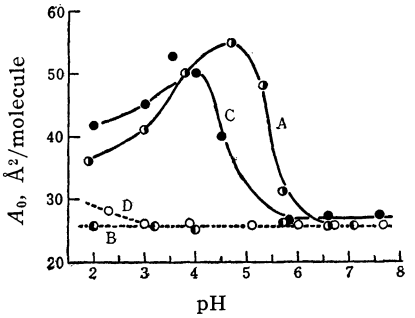


Fig. 4. Effect of Congo red upon A_0 for the monolayer of ethyl *n*-hexadecyl ether and ethyl stearate.
A and B, the ether on the substrate with or without dye, respectively; C and D, the ester on the substrate with or without dye, respectively.

The addition of the dye to the substrate generally resulted in an expansion of the monolayer, as shown in curve A of Fig. 4. The maximum expansion seemed to appear when pH of the dye solution was around 4.4. Precisely speaking, however, there is a difference between the form of $F\sim A$ curve for the region of pH 3.5~5.5 and that for the rest of pH region. In the former region, as illustrated in Fig. 3 (b) for example, dye not only expanded the

monolayer remarkably but also prevented the subsequent lowering of the initial surface pressure. In contrast to this, the effect of surface pressure lowering was evident in the latter region as illustrated in Fig. 3 (c).

Ethyl Stearate.—Effect of substrate pH upon A_0 for the monolayer spread on water is shown by curve D in Fig. 4. Apparently no change in the $F\sim A$ curve was observed throughout pH 3~8. When the monolayer was spread on a substrate water of pH 2.3 and compressed to $F>$ 15 dyn./cm., we usually observed an instantaneous rise and subsequent fall of surface pressure which reached finally an equilibrium value. Such a tendency was most remarkable when the film was compressed fifteen minutes after initial spreading. Any time of elapse longer or shorter than this proved to result in less exaggeration. These phenomena may be due to the hydrolysis of the ester, which was reported for the same film spread on an alkaline substrate[9], and to the change in surface pressure effected by ethanol thereby formed at and ejected from the surface phase. Actually, standing of the monolayer for sixty minutes caused an $F\sim A$ relationship identical with that for stearic acid.

The effect of added dye upon A_0 of the monolayer is shown by curve C in Fig. 4 in which, however, A_0 at pH 1.9 accompanies an inevitable error due to the hydrolysis mentioned above. Even if we took account of this ambiguity, it would be clear that the maximum expansion was observed at pH 3.0.

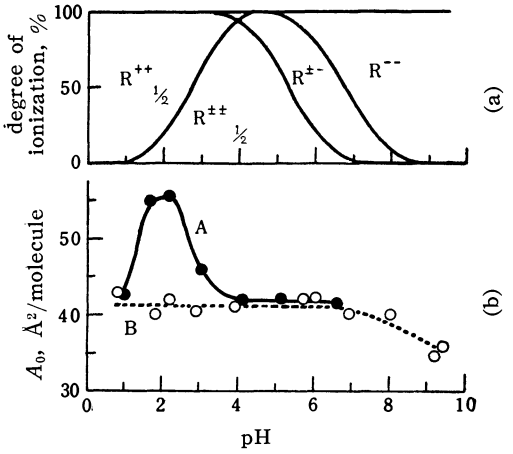


Fig. 5. (a) Effect of pH on the degree of ionization of Congo red. (b) Effect of pH on A_0 for the monolayer of cholesterol spread on the substrate, (A) containing Congo red and (B) lacking it.

Cholesterol.—Curve B in Fig. 5 (b) shows pH dependence of A_0 for the monolayer of cholesterol spread on the surface of water. In conforminity with the results appearing in the other reports[10], the monolayer proved to be of low compressibility and of large area when it was spread on distilled water pH of which was less than 7. In more alkaline region, however, A_0 decreased slighty with increasing pH, while the compressibility was scarcely affected at all by the change of the acidity throughout all pH region investigated. This might be ascribed to the dissolution of cholesterol, as predicted by the experimental results on surface evaporation[11].

For the aqueous substrate containing dye, pH dependence of A_0 is shown by the curve A in Fig. 5 (b). Maximum expansion was observed at pH 2 where A_0 was larger by ca. 15 Å²/molecule than that for the control experiment.

Discussion

In Fig. 5 (a) are shown the ionization curves for each ionizable groups in the molecule of Congo red. They are obtained from respective values of the ionization constants which have been reported in Part I[12] of this series. It should be emphasized that the calculations for the dissociation constants were based on the treatment of the dye as a high-polymer electrolyte. When we compare these curves with $A_0\sim$pH curves shown in Figs. 2 and 4, it can be seen that the interaction of Congo red with various amphipathic compounds is favored in the isoelectric region, irrespective of the types of their polar heads. In Part II[1] of this series, it has been presumed that the conditions for mutual cohesion of dye molecules among themselves would play simultaneously an important rôle in its interation with film materials. Actually the film materials seem to interact with the colloidal aggregates of dye formed in the solution. Remarkable changes both in the ultrasonic velocity in bulk[4] and in the rheological property of the surface[6] of the solution

9) A. E. Alexander and J. H. Schulman, *Proc. Roy. Soc.*, **A161**, 115 (1937).

10) e. g., J. H. Schulman and E. K. Rideal, *Proc. Roy. Soc.*, **B122**, 29 (1937), etc.

11) E. Sebba and H. V. A. Briscoe, *J. Chem. Soc.*, **1940**, 114.

12) M. Muramatsu, This Bulletin, **31**, 864 (1958).

13) A. Inaba, unpublished.

TABLE I

EFFECT OF CONGO RED UPON A_0 OF VARIOUS MONOLAYERS

Film substance		$pH_{max.}$	Area, Å²/molecule			Surface polarity	
Name	Mol. wt.		$(A_0)_{H_2O}$	$(A_0)_{dye}$	ΔA_0	ΔV, mV	$(A_0)_{H_2O}\cdot\Delta V$ Å²·mV/molecule
Cholesterol	386	2.0	41	56	15	ca. 400[10]	16.1×10^3
Cetyl alcohol	242	3.0	20	40	20	400[14]	$8.0\times$ 〃
Ethyl stearate	312	4.0	25	50	25	370[9]	$9.3\times$ 〃
Ethyl *n*-hexadecyl ether	270	4.4	25	55	30	——	——
Octadecylamine	269	5.5	28	55	27	710[15]	$19.9\times$ 〃

of Congo red being in the same pH range have also been attributed to the formation of colloidal aggregates of dye. Therefore the present results had better be discussed along this line. Additional support for this suggestion was obtained by Matuura[2] who has reported an expanded film of stearic acid spread on a solution of Congo red, pH of which was ca. 3. Inaba[13] has observed that a surface of paraffin was wetted thoroughly by the same solution. All these phenomena emphasize the importance of the rôle of van der Waals' attraction in the interaction. For the other region of pH, ionic repulsion due to the same sign of the charge of dye molecules would suppress the tendency of forming colloidal aggregates in which the molecules of dye interlink each other by the molecular forces other than ionic.

In Table I is summarized the effect of added Congo red on A_0 for various monolayers spread on the substrates, pH values of which are optimum corresponding to the largest expansion. In this table $(A_0)_{H_2O}$ and $(A_0)_{dye}$ represent values of A_0 on pure water and dye solution respectively. Further, the data on surface potential, ΔV, of the monolayer on water are quoted from other literatures. As is seen in the table the amount of increase, ΔA_0, in the area due to the addition of dye seems to depend on the quantity, $(A_0)_{H_2O}\cdot\Delta V$, which may be expressed as the surface polarity, rather than the molecular weight of the monolayer substance. Noticeable deviation from this is observed only for cholesterol which differs in its molecular structure from the other substances. This suggests the distinct contribution to $A\Delta_0$ of the dipolar attraction, in addition to van der Waals' force. It was pointed out[16] that dipolar attraction acting between each other of dye molecules of zwitterion type enhanced the possibility of forming colloidal aggregates of the dye in aqueous medium. A similar explanation was also made for the mechanism of dyeing of fibers[17].

Let us draw attention to the conspicuous nature of the monolayer of ethyl *n*-hexadecyl ether spread on distilled water. As far as the author is aware, the nature of this film has not been studied before. In the case of the monolayer of octadecyl methyl ether, some investigators[18] reported an intramolar rotation of —O—CH_3 bond when the film was compressed to some extent. There the methyl group was considered to orientate itself toward the bulk of substrate, so that the process resulted in a decrease of resultant dipole. It seems to be probable, however, that such a distortion is accompanied by a strong resistance when the end group is ethyl radical as was the case in the present experiment. In Fig. 3 (a) the instantaneous rise and subsequent lowering in surface pressure due to the compression would be an evidence for this effect. In connection with this, it is of interest to note that such an effect disappears whenever Congo red is added to the substrate of pH 3.5~5.5 where the largest expansion of the film is observed. Intramolecular rotation is evidently hindered by Congo red with which the film substance interacts. It should be further noticed that the molecules of dye are almost in the form of $R^{\pm\pm}{}_{1/2}$, as seen in Fig. 5 (a). This increases the possibility of the dipolar attraction between dye and ethyl *n*-hexadecyl ether, if we take account of the hindrance toward reorientation of ethyl group accompanying the change of resultant dipole moment. Presumably both van der Waals' and dipolar force are

14) J. Marsden and J. H. Schulman, *Trans. Faraday Soc.*, **34**, 748 (1938).
15) J. Glazer and M. Z. Dogan, ibid., **49**, 448 (1953).
16) W. Pauli and F. Lang, *Monatsh.* **67**, 159 (1936).
17) e. g., E. L. Valko, "Colloid Chemistry", edited by J. Alexander, Vol. 6, Reinhold Publ. Corp., New York, 1946, p. 594.
18) J. H Schulman and A. H. Hughes, *Proc. Roy. Soc.*, **A138**, 430 (1932); A. E. Alexander, *Trans. Faraday Soc.*, **37**, 426 (1941).

chiefly responsible for the expansion of the monolayer.

Similar kinds of attractive force can also be mentioned to explain the mechanism of the interaction of dye with cetyl alcohol or ethyl stearate. Optimum pH values for the maximum expansion of these films lie in a range of 3~4 where dye molecules are also in the form of zwitterion. On the other hand it is of interest that ΔA_0 for cetyl alcohol is less than that for ethyl *n*-hexadecyl ether. This comes from a decreasing van der Waals' force corresponding to ethyl group. Presumably such a force overwhelms the attraction due to hydrogen bond through the hydroxyl radical of alcohol even if it would be possible. Thus the present result suggests the importance of the rôle of van der Waals' force rather than hydrogen bond in the dyeing process of fibers by the direct dye[17].

Differing from such non-ionic compounds as mentioned above, we may suggest a possibility of ionic interaction in addition to hydrogen bonding, dipole-dipole and van der Waals' force to explain the mechanism of the interaction between Congo red and octadecylamine. The largest expansion of this film is observed when it is spread on the solution of dye of pH 5.5, where a considerable amount of dye molecules are partly ionized, while the molecules of octadecylamine in the film are considered to be perfectly ionized[15]. Therefore we should take account of the additional contribution of ion-ion attraction between dye and octadecylamine to explain the expansion of the monolayer. This is similar to the fact which the present author has pointed out in the case of interaction of basic dye with stearic acid[1] and acid dye with octadecylamine[3]. In connection with this it may be of some values to discuss the effect of dissolved Congo red upon mono- and multilayers of stearic acid and barium stearate. Matuura[2] reported an expansion of the monolayer of stearic acid spread on the dye solution of pH 3. The present author has reported a remarkable increase in thickness of the built-up film of stearic acid and decrease in thickness in the case of barium stearate, when each of them soaks into the dye solution of pH 3.6[1]. In this case both increase have been attributed to the strong interaction. The dye molecules in such a solution are considered to be charged somewhat positively, as shown in Fig. 5 (a). However, no negative charge seems to exist in the molecules of stearic acid in the monolayer spread on pH <6[15,19]. It is probable that the same arguments can also be applied to the case of the multilayers of the same substance. Therefore it would be reasonable to ignore the ion-ion attraction between stearic acid and dye. On the other hand we can not ignore the ion-dipole attraction arising from the positive charge of dye, when dye molecules are allowed to orientate and bind themselves to stearic acid.

Various kinds of behavior of interaction of cholesterol with dye are somewhat erratic. Apparently they are similar to the case of stearic acid rather than cetyl alcohol. This may come from the molecular structure of sterol back-bone being hydrophobic. We can only say at present that the explanation is similar to the case of stearic acid. The detailed discussion may be a future problem.

Summary

Effect of dissolved Congo red upon the monolayers of octadecylamine, cetyl alcohol, ethyl *n*-hexadecyl ether, ethyl stearate and cholesterol spread on the substrate containing the dye has been studied, under varying pH of the solution. It has been observed generally that all monolayers expanded when they were spread on aqueous solution, the pH of which was in such a region that the molecules of dye were almost in zwitterion form. Dipolar and van der Waals' attraction were tentatively postulated to explain the nature of the cohesive force by which the molecules of dye were bond together so that the colloidal aggregates were formed in the solution. The expansion of the monolayer can be accounted for by the binding of the aggregate to film materials. This explanation could successfully be applied to the films of such nonionic substance as cetyl alcohol, ethyl *n*-hexadecyl ether and ethyl stearate.

The largest expansion of the monolayer of octadecylamine was observed when the substrate containing dye showed acidity so that the molecules of dye were partly of negative charge while those of octadecylamine were of positive charge. In this case we had better take account of the possibility of ion-ion attraction between octadecylamine and dye, in addition to the

19) E. Havinga and M. der Hertog-Polak, *Rec. trav. chim.*, **71**, 64 (1952); E. Havinga, ibid., **71**, 72 (1952).

forces which appeared in the cases of nonionic substances.

The author wishes to express his hearty thanks to Professor T. Sasaki for his kind guidance and encouragement in this work. He is also indebted to Professor R. Matuura of Kyūshū University for his helpful discussion, to Professor H. Saikachi of the same university for the elemental analysis of the samples, and to Mr. H. Ōshima of Fukuoka Gakugei University for his assistance on the synthesis and purification of amphipathic compounds. The cost of this research has been defrayed from the Scientific Research Expenditure of the Ministry of Education.

Department of Chemistry, Faculty of Science, Tokyo Metropolitan University
Setagaya-ku, Tokyo

Absorption Spectra of Dyes. II[1]. *On Non-additivity of Absorption Spectra of Binary Mixtures of a Direct Dye and Some Acid Dyes in Aqueous Solution**

By Yoshié TANIZAKI, Teruaki KOBAYASHI and Noboru ANDO

(Received July 7, 1958)

It has been known that absorption spectra of binary mixtures of dyes in aqueous solution are not always additive[2,3] probably owing to the formation of complexes between dyes in solution, and it is also well known that in dyeing from solutions of mixtures of two dyes, the amounts of dyes adsorbed are frequently non-additive (i. e. a reduction in adsorption)[3]. Moreover in such cases, it seems that there exist some relations between non-additive properties in the amounts of dyes adsorbed and those in absorption spectra. In practical dyeing, mixtures are more frequently used than a single dye in order to produce any desired shade, so that the scientific study on dye mixtures is not only interesting from the physicochemical point of view, but also important practically. For this reason, in our laboratory, the investigation about dye mixtures has been started and the attention is first focused on non-additivity in spectrum.

Hitherto, only a few studies on non-additivity in absorption spectrum of dye mixtures have been carried out[2,3]. Neale and Stringfellow[3] showed that the mixture of Chlorazol Sky Blue FF and an acid dye (*o*-anisidine → H acid) shows non-additive property in absorption spectra, while the mixture of Chlorazol Sky Blue FF and Orange II has an additive spectrum. In this paper, selecting several monoazo acid dyes, the formula of which can be expressed *p*-X-aniline → γ acid with different substituents X, the authors investigated the spectra of pairs of Chlorazol Sky Blue FF and these acid dyes, ranging over the visible and near ultraviolet regions, and found that all of them were more or less different from the sum of the corresponding spectra of their components.

In this paper, a qualitative explanation of non-additivity in spectrum of such mixtures will be given by means of the conventional quantum chemical concept.

Experimental

Materials.—Direct Sky Blue 6B of Mitsubishi-Kasei Co., Ltd. was used as the sample of Chlorazol Sky Blue FF and it was purified by the usual method of Robinson and Mills[4], and the acid dyes made by coupling diazotized *p*-X-aniline with γ acid in acid or alkali solution, were purified by the same method.

Preparation of Samples.—Conductivity water of about 3.5×10^{-7} mho at room temperature was used for the preparation of dye solutions. The

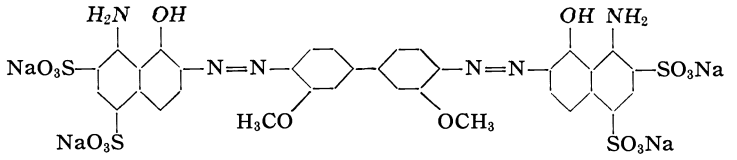
1) Part I of this series, Y. Tanizaki and N. Ando, *J. Chem. Soc. Japan, Pure Chem. Sec.* (*Nippon Kagaku Zasshi*), **78**, 343 (1957).

* Presented at the 11th Annual Meeting of the Chemical Society of Japan, April 1958.

2) D. R. Lemin and T. Vickersraff, *Trans. Faraday Soc.* **43**, 491 (1947); A. N. Derbyshire and R. H. Peters, *J. Soc. Dyers Col.*, **72**, 268 (1956).

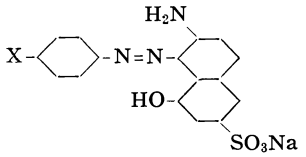
3) S. M. Neale and W. A. Stringfellow, ibid., **59**, 241 (1943).

4) C. Robinson and H. A. T. Mills, *Proc. Roy. Soc.* (London), **A131**, 576 (1931).

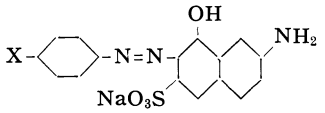


concentrations were 3.59×10^{-6} moles/liter and $1.78\sim1.81\times10^{-5}$ moles/liter for Direct Sky Blue 6B and acid dyes, respectively; these concentrations were determined by the fact that the change in spectrum was the largest when the ratio was about 1 : 5[5].

Dye samples will be conveniently abbreviated in this paper as follows: Direct Sky Blue 6B will be referred to briefly as "Sky Blue". And monoazo acid dyes (p-X-aniline $\rightarrow\gamma$ acid)



(I) (X-α)



(II) (X-β)

will be represented by substituents X, which means here H, CH_3, OCH_3, Cl and NO_2, of diazotized components and their coupling positions α or β; namely dyes of I will be briefly called X-α, or H-α, CH_3-α, etc. according to their substituents, and similarly those of II will be called X-β or H-β, CH_3-β, etc.

Measurements of Absorption Spectra.—For measurements of absorption spectra of dye solutions, the Shimadzu QB-50 and QR-50 spectrophotometers were used at room temperature (14° to 16°C). Absorption cells were 1 cm. and 2 cm. thick, and optical densities are always reduced to values corresponding to 1 cm. thick.

Results

The most marked non-additivity in absorption spectrum was found for the pair, Sky Blue and the acid dye with substituent NO_2, and in the case of Sky Blue and the acid dye with H for X the least non-additivity was found. As examples, spectra of the combinations of Sky Blue with NO_2-α and NO_2-β, whose non-additivity is the most remarkable, are shown in Figs. 1 and 2, respectively, with those of the components. In each figure curves I and II show the observed absorption curves of Sky Blue and the acid dye, respectively, curve III the sum of them,

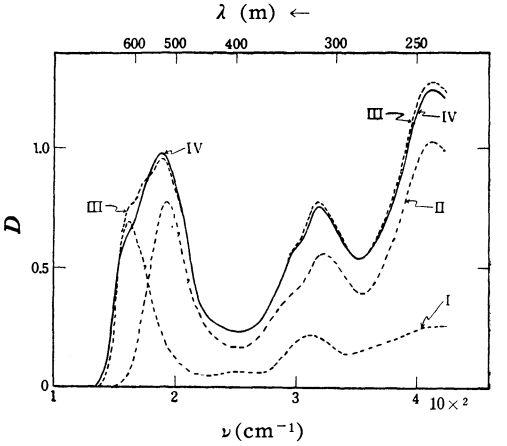


Fig. 1. Absorption spectra of a mixture of Sky Blue and NO_2-α, and its components. Curves I and II show the absorption spectra of Sky Blue and NO_2-α, respectively, curve III shows the resultant of curves I and II, and curve IV observed of the mixture.

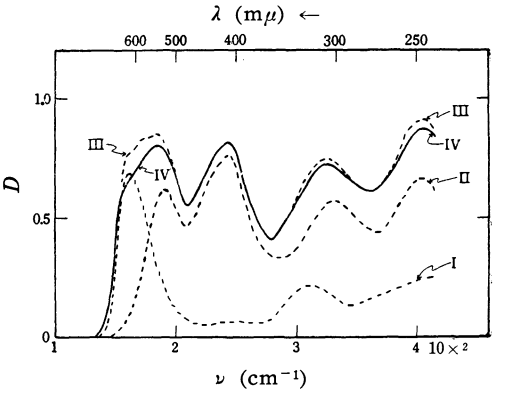


Fig. 2. Absorption spectra of a mixture of Sky Blue and NO_2-β, and its components. Curves show just the same case as in Fig. 1.

and curve IV the observed curve of the mixture. The difference, ΔD, between the sum of optical densities of its components and the observed one of a mixture is the largest in the neighborhood of a wave length of the principal band of Sky Blue ($\sim$620 mμ). And here, it is of interest that the bands corresponding to those of NO_2-β in the range of 400$\sim$460 mμ ($25\sim22\times10^3$ cm^{-1}) are additive, and that

5) T. Kobayashi, Y. Tanizaki and N. Ando, This Bulletin, to be published.

at the position corresponding to the first band of NO_2-α (~530 mμ) the observed absorption is more intense than the resultant one.

Now, observed wave numbers of absorption maxima of each component are shown in Fig. 3, in which values of difference ΔD between maximum densities of the resultant curve and those of the observed one of a mixture are also shown in round brackets at corresponding positions of absorption bands of acid dyes. Values of ΔD at the principal band of Sky Blue (161×10^2 cm^{-1}), however, are shown in the lowest line corresponding to each acid dye component. Fig. 3 shows distinctive facts to be summarized as follows.

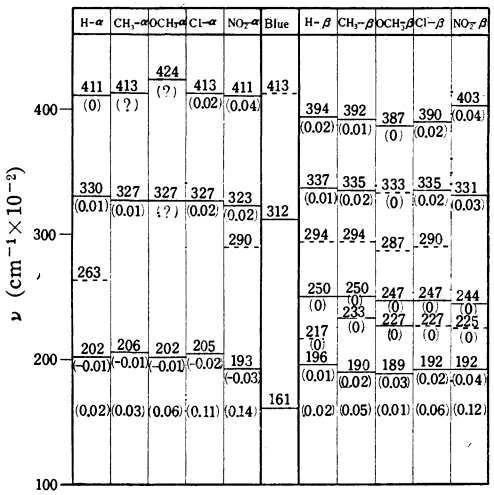


Fig. 3. Observed wave numbers of absorption bands of component dyes. Full and dotted lines mean the maximum positions and shoulders, respectively. Numbers in brackets show the difference between maximum optical densities of the sum of component spectra and observed ones of mixtures.

(1) It can be seen that non-additivity of absorption spectra appears in such positions that the absorption maxima of each component of a mixture are close to each other and there appears such a tendency as that the smaller the difference in wave number between them the larger the difference ΔD.

(2) The observed density near the position corresponding to a wavelength of the first band of each acid dye is smaller than the resultant in the case of Sky Blue and X-β, while it is larger when the acid dye component is X-α, that is to say, ΔD has the negative sign in the latter case.

(3) Absorption bands of the combination with X-β show the additive property in the region of $22\sim25\times10^3$ cm^{-1} (460~400 mμ).

(4) Every mixture shows the largest ΔD at the position corresponding to the wavelength of the principal band of Sky Blue.

Discussion

It may be supposed that such non-additivity in a spectrum comes from the formation of so loose complexes in a solution of dye mixture that the intermolecular charge-transfer does not occur, but some interaction between energy levels of components probably appears provided that their energies are close by. In such a case, for instance, when the excited levels A and B responsible for the absorptions of component dye molecules of a complex interact slightly with each other, it would be assumed that the absorption bands due to the individual transitions change only in wave number, not changing approximately in shape and intensity. Thus, if the spatial configuration of two molecular species were settled, the magnitude of the perturbation would naturally depend upon the difference between energies of A and B, the relative orientation of them in complex or the respective oscillator strength. But if it could be regarded that the effects of the latter two factors were not large and were the same in any complex considered here, the difference between the energies of excited states would become the main factor; namely, the nearer the energies, the larger the perturbation. According to the above consideration, the change in the spectrum of the complex may be approximately discussed by only the difference

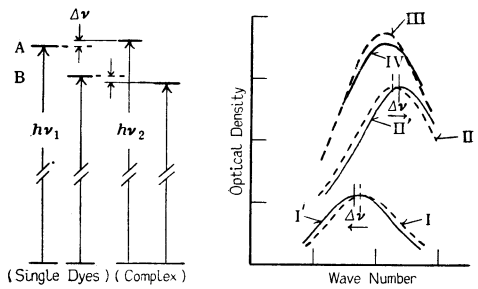


Fig. 4. A schematic illustration of the spectral change in a loose complex. Absorption curves are drawn with a shift of 200 cm^{-1} of each band of the component to the opposite side.

in wave numbers of the corresponding absorption bands of the components. In Fig. 4 the relation between the absorption band of a mixture and those of its components are shown schematically*. In this figure, curves I and II are the absorption bands of the components before interacting, curves I′ and II′ are those after interacting, and curves III and IV are the sums of curves I and II and of curves I′ and II′, respectively. The figure indicates that the intensity of the absorption band composed of those of components after interacting is always smaller than that composed of those before. From studies of dichroism for such dyes as used here, it could be regarded that an apparent single band in the ultraviolet region is the superposition of two, of which the directions of oscillation are orthogonal to each other, originated from the aromatic nucleus of the complicated coupling component[6]. And for this case an explanatory figure also might be given. For example, instead of A mentioned above, $A_{\parallel}$ and $A_{\perp}$ which are orthogonal and close in energy to each other might be considered and the following cases should occur. According to whether $A_{\parallel}$ is directed parallel, normal or inclined to $B_{\parallel}$, the resulting curves will become somewhat different in shape. But practically, the main features of drawn curves for respective cases showed a similar tendency as shown in Fig. 4, indicating a decrease in intensity of the curve after interacting. Anyway, a qualitative and reasonable illustration thus can be obtained for ΔD described in (1) in the foregoing section.

Quite similarly the above consideration will be applied to explain the difference ΔD between the sum of densities of Sky Blue and X-β and the observed one of the mixture at the position corresponding to the first band of X-β. This band is perhaps due to a single absorption and could interact with the first band of Sky Blue in complexes. On the other hand, when a component is X-α the corresponding ΔD has the negative sign. This can be explained, however, if it may be assumed that the first band of X-α consists of two absorption bands, of which one has the same property as the first band of X-β and the other has the different. This assumption is based on the evidence from the dichroic measurement of such dyes in stretched polyvinyl alcohol-sheet[7]. Dichroic properties of some of the dyes used are shown in Fig. 5, in which the curves show absorption spectra when the

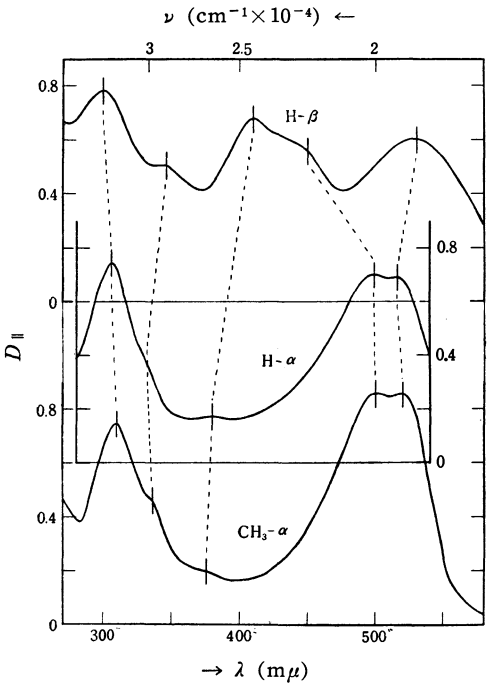


Fig. 5. Absorption spectra for plane polarized light of H-α, CH_3-α and H-β in stretched polyvinyl alcohol sheets when the stretch direction is parallel to the electric vector of incident polarized light.

direction of the electric vector of incident polarized light coincided with the stretch direction. These suggest that respective bands in each curve connected by dotted lines would correspond to each other[7]. It is now possible to assume that the band of the longer wavelength side of two subsidiary bands composing the main band of X-α corresponds to the first band of X-β and is able to interact with the first band of Sky Blue, while the other band of the shorter side has less or no interaction with that of Sky Blue. On the other hand, in Fig. 1 or 2, in which the shoulder of the first band of component Sky Blue ($\sim$580 mμ) becomes more distinctive in the

* The polarizability of such a molecule used here may be more responsible for its excited states than the ground state. Therefore, in a complex the interaction between the excited states of the components may be larger than that between the ground states. In Fig. 4, in order to discuss the relative change in levels, all the ground states are indicated on the same line.

6) Y. Tanizaki and N. Ando, *J. Chem. Soc. Japan, Pure Chem. Sec.* (*Nippon Kagaku Zasshi*), **78**, 542 (1957).

7) Y. Tanizaki, presented at the 9th Annual Meeting of the Chemical Society of Japan, April 1956.

resultant curve, it may be presumed that the main absorption band of Sky Blue also consists of such two bands as those just mentioned for X-α. Further the subsidiary band of the longer wavelength side of Sky Blue seems to be more sensitive to the change in external condition than that of the shorter side[8]. Consequently, the correlation shown in Fig. 4 may be able to be diverted by the following method to illustrate the facts described in 2 and 4 in the last section, that is, values of ΔD, near the wavelengths of the first bands of the acid dyes, have the positive sign for pairs of Sky Blue and X-β but the negative sign for those of Sky Blue and X-α, and the largest value is found at the wavelength of the principal band of Sky Blue. If it is supposed schematically that the first absorption band of an X-α consists of two bands shown by curves I′ and II′ in Fig. 4 and is expressed by curve IV, it will be changed to curve III, after being perturbed, with the relative shift of the just-mentioned two bands composing it, while for Sky Blue the reverse is the case; that is, curve III means the principal band of Sky Blue before being perturbed and curve IV that after being perturbed.

Now, supposing that the bands of the shorter wavelength side shown by curves I_b and II_b in Fig. 6, which are constituents of the first bands of Sky Blue (I) and NO_2-α (II), respectively, would remain unchanged, and only the bands of the longer side, curves I_a and II_a, interact with each other, there can be obtained curve IV which, corresponding to the observed absorption, is the resultant of the new component bands coming from the shift just mentioned ($I_a \rightarrow I_a'$, $II_a \rightarrow II_a'$). And curve III shows the sum of curves I and II. The case of the mixture of Sky Blue and NO_2-β is shown in Fig. 7, in which the band of NO_2-β indicated by curve II is assumed to be a single band. In these figures the resolution of the main band into subsidiary bands has been properly made. The curve IV in each figure shows the coincidence in character with those observed (see Figs. 1 and 2). In Fig. 7 it is seen that curve IV is also stronger in intensity near a wave number of 20×10^3 cm^{-1} than curve III; in fact observed results showed, though not very clearly, such a tendency.

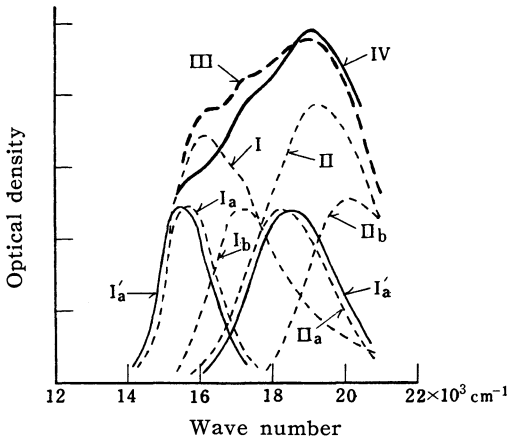


Fig. 6. Absorption curves of a mixture of Sky Blue and NO_2-α, before and after interacting, of the first bands. It is assumed that the interaction occurs only between the bands in the low wave number side, each of which shows a shift of 200 cm^{-1}.

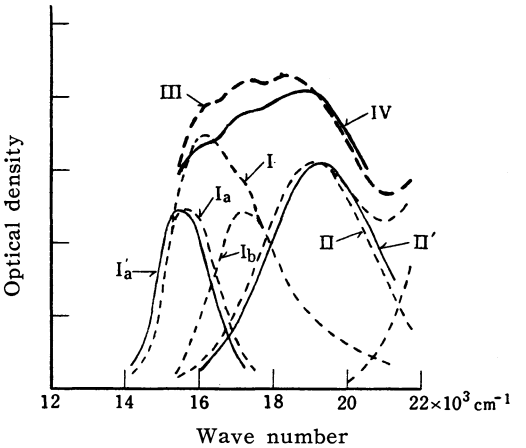


Fig. 7. Absorption curves of a mixture of Sky Blue and NO_2-β, before and after interacting, of the first bands. It is assumed that the interaction occurs between the first band of NO_2-β, which is a single band, and the band of the low wave number side of Sky Blue, each of which shows a shift of 200 cm^{-1}.

It was assumed above that the band of the shorter wavelength side of two constituents of the first band of X-α has less or no interaction with the main band of Sky Blue, corresponding to the second band of X-β (see Fig. 5). If it is true, the second band of X-β should show the

8) Y. Horiki, unpublished. For example, the maximum wavelengths of the first band of Sky Blue in water and in water-pyridine (20% for pyridine) solution were 618 mμ and 630 mμ, respectively, indicating the shift $\Delta\nu$= 310 cm^{-1}. On the other hand, though the determination for the convex parts was not so accurate, it seemed that $\Delta\nu$ was smaller than 290 cm^{-1}, and the shoulder was more distinctive in pyridine solution than in water.

additive spectrum in the combination with Sky Blue. The results observed are indeed in agreement with this expectation. At the same time, the third band also shows the additive property as shown in Figs. 2 and 3. Consequently, it might be considered another reason for the fact described in 3 in the last section that even the band of Sky Blue nearest to the X-β band under consideration lies too far apart for them to interact with each other.

It is well known that the first absorption band of such a dye as used here is quite generally ascribed to the electronic oscillation along the longest conjugated system which includes, as terminal groups, auxochromes characterized by lone-paired electrons in them. That is, the excited state is produced by the migration of an electron on such a terminal group to the inner π-electron system. On the other hand, such frontier electrons may be less protected from the change in the external condition, and are therefore affected easily. It may be, therefore, considered that the first band is more sensitive to the external change than the other bands. Thus, this may be followed by the fact described in (4) in the foregoing section that every mixture shows the largest ΔD at the position corresponding to the principal band of Sky Blue.

Finally, it is interesting to note that ΔD is the largest when X is NO_2 and the smallest when X is H (see Fig. 3). This might be related to the difference in nature of substituents X, but at present there could be found no interpretation for it from these qualitative investigations. As an empirical fact, it can be said that in order to investigate complexes formed in binary mixtures of Sky Blue and the acid dyes used here, NO_2-α or -β will be the most suitable to be selected.

Summary

1. Absorption spectra of mixtures of Direct Sky Blue 6B with p-X-aniline→γ acid, in which the substituent X means H, CH_3, OCH_3, Cl or NO_2, and the components in aqueous solution were observed in the visible and near ultraviolet regions.

2. All the absorption bands showed non-additive property, excepting the bands in the region of 400~460 mμ of the mixtures of Sky Blue and X-β shown in Figs. 2 and 3. And optical densities of observed bands of a mixture were generally smaller than sums of the values of each component, but when the acid dyes made by α coupling were used as other components, increases were seen at the positions corresponding to wave lengths of the first bands of them.

3. An explanation for these non-additive properties was given by means of the interaction between the corresponding bands of components.

4. At the same time, in this connection, it is pointed out that the apparent single band of the first of p-X-aniline→γ acid in α coupling consists of two bands and similarly the first band of Direct Sky Blue 6B may also consist of two bands.

The authors are indebted to Dr. Ikuzo Tanaka for his useful advice, and they also wish to express their sincere thanks to Mr. Toshiro Iijima for his generous offer of purified acid dyes and to Mitsubishi Kasei Co., Ltd. for the kind contribution of a sample of Direct Sky Blue 6B.

Laboratory of Physical Chemistry
Tokyo Institute of Technology
Meguro-ku, Tokyo

Photochemical Reactions between Methylene Blue and Tri-, Di- and Monomethylamine. III. The Behavior of Methylene Blue in the Presence of Oxygen

By Hiroshi OBATA, Kenichi KOGASAKA and Masao KOIZUMI

(Received August 11, 1958)

In the preceding papers[1], the photochemical reactions between methylene blue and three kinds of amine in vacuo were investigated, and the following scheme was proposed.

$$MB^+ + OH^- + Am \underset{k_2}{\overset{k_1}{\rightleftharpoons}} \text{Intermediate} \xrightarrow{k_3} MBH + AmO \quad (1)$$

Thus, methylene blue when irradiated, reacts with hydroxyl ions and amine and produces a certain type of intermediate with a life time of a few minutes, a part of the intermediate then transforming into leucodye and amine oxide. Now according to a recent paper of Oster[2], methylene blue is photobleached by various kinds of secondary and tertiary amine including ethylenediaminetetraacetic acid, and the reaction which is somewhat similar to ours, was interpreted to take place via the triplet state of dye ion on the ground that the fluorescence of methylene blue is not affected by the added amines. His conclusion will certainly apply to our case, since we have afterwards ascertained that the fluorescence of methylene blue in aqueous solution is practically the same as that of the solution used for the photochemical reaction, both in intensity and in structure.

The objective of the present paper is to elucidate the following three kinetic features which are considered to be important in relation to the above reaction.

(1) *The decision of a species which reacts with oxygen, when the aerobic solution of methylene blue containing amine is irradiated.*—In the studies of photosensitization by methylene blue, Weil[3] observed that amine is oxidized but methylene blue does not practically bleach, and we have also ascertained this fact under our experimental conditions. As to the regeneration of methylene blue in such cases, it seems generally considered especially by biochemists, that the attack of oxygen on leucodye reproduces the original dye. But on the basis of our scheme 1, the possibility of oxygen attack on the intermediate can not be excluded a priori, especially in view of our result that cupric ions react with the intermediate very effectively. The problem must therefore be decided experimentally and for this purpose, a quantitative comparison of the rate of photobleaching in vacuo and that of oxygen absorption by the same solution was undertaken.

(2) *The reactivity of oxygen with a triplet state (T state) of methylene blue.*—Generally, triplet states of dye ions are easily attacked by oxygen[4] as exemplified by the case of eosine studied by Imamura and Koizumi[5]. In the photobleaching of the aqueous solution of eosine under aerobic condition, the reaction takes place chiefly via T state, but most part of the intermediate in the T state is deactivated by oxygen and only a very small fraction of it interacts with oxygen in such an effective way as to lead a bleaching reaction. On this view, the question is raised whether the T state of methylene blue, in the presence of amine, is not attacked altogether by oxygen or alternatively, although attacked by oxygen it is only deprived of its excitation energy, no genuine chemical reaction occurring. This problem is intimately connected with the first one. As a help for the elucidation of this problem, the photobleaching reaction of methylene blue in the aqueous

1) H. Obata and M. Koizumi, This Bulletin, **30**, 136, 142 (1957).
2) G. Oster and N. Wotherspoon, *J. Am. Chem. Soc.*, **79**, 4836 (1957).
3) L. Weil and J. Maher, *Arch. Biochem.*, **29**, 241 (1950).
4) e. g. G. O. Schenck, *Z. Elektrochem.*, **55**, 505 (1951); **56**, 855 (1952); **57**, 675 (1953); *Naturwiss.*, **40**, 205, 229 (1953).
5) M. Imamura and M. Koizumi, This Bulletin, **28**, 117 (1955); **29**, 913 (1956).

solution involving no amine was investigated. It turned out that the rate is somewhat slower than that of eosine under similar conditions, and in relation to the above mentioned question, further investigations were undertaken to make clear of the effect of pH and oxygen pressure on the photobleaching rate.

3) *The behavior of T state of methylene blue in the presence of amine and oxygen.*— A quantitative comparison was made between the rate of photobleaching of methylene blue in vacuo by virtue of trimethylamine and that of oxygen absorption by the same system when irradiated, taking into account of the rate with which the aqueous solution of methylene blue is photobleached by oxygen. A conclusion is that T state of methylene blue is very efficiently deactivated by oxygen in the absence of amine, but such a process is practically suppressed by the presence of amine, oxygen only reacting with leucodye.

Experimental and Results

I. Measurement of the rate of oxygen absorption.—*a*) *Apparatus and Procedure.*—For our purpose, the rate of oxygen absorption must be compared with that of photobleaching under as much the same condition as possible. This requirement imposes some severe conditions on the apparatus, and as a result of examination of various methods from this viewpoint, it was decided to adopt Tödt's electrochemical method[6].

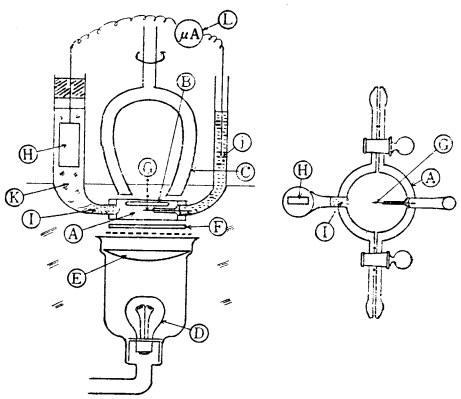


Fig. 1. Apparatus for the measurement of oxygen absorption
A reaction vessel
B magnetic stirrer
C magnet
D light source (automobile head-light lamp 35 w/35 w)
E condensor lens to prepare parallel light
F filter to cut off below 600 mμ
G cathode (platinum wire)
H anode (iron)
I KCl-agar bridge
J mercury
K 0.1 N KCl
L microammeter or galvanometer

The apparatus constructed is shown in Fig. 1. In this figure, A is a reaction vessel with an internal diameter of 28 mm. and a depth of 10 mm., B is a magnetic stirrer, a magnet C being rotated by a phonomotor 80 r.p.m. The cell is irradiated by an automobile head-light lamp 35 w/35 w (D) placed below the cell, E is a condensor lens to prepare parallel light and F is a filter which cuts off below 600 mμ. The intensity of illuminating light is approximately the same as that of the preceding papers[1]. A cathode G., which is polarizable, is a platinum wire 0.3 mm. diameter and 4 mm. length and an anode H, which is unpolarizable, is a piece of iron 30 mm.×10 mm.×4 mm. Tödt's anode contains 2% carbon and 0.6% copper and according to him, the iron rich in carbon and copper generally gives a better stability. Our anode contains 0.18% carbon and 0.98% copper, the specimen being supplied from Osaka Special Steel Ltd. The anode is dipped in 0.1 N potassium (K) solution and is connected to a cell via a potassium chloride-agar bridge I. As shown by Tödt, the amount of current supplied by this cell is determined by the diffusion of oxygen in the neighborhood of platinum electrode, and is given by the following relation after the establishment of a steady state.

$$i = nFDqc/\delta$$

(n=4, F: Faraday, D: diffusion constant, q: area of the cathode surface, c: oxygen concentration in the bulk solution, δ: thickness of diffusion layer).

In our experiment the speed of rotation of the magnet is slower than that in Tödt's experiment, hence the diffusion current is very dependent on the rotating speed and particular caution must be paid to keep constant the speed of rotation. Another thing to be added is that a platinum electrode needs to be dipped in hydrochloric acid to make its surface clean before use. Perhaps a platinum electrode, when exposed in the air, would have its surface covered with a thin film of oxide or the like, which would reduce the current.

b) *Calibration.*—Calibration between the diffusion current and the concentration of dissolved oxygen was made using the same solution for the absorption experiment, the composition being 2.0×10^{-5} M methylene blue, 0.1 N potassium chloride and pH 9.2 controlled by borate buffer. Firstly, the air mixed with a certain amount of nitrogen gas was passed through the solution immersed in a thermostat at 40°C, and the cell was filled quickly with this solution without any gaseous phase left behind. The current was measured in 30°C thermostat by a microammeter

6) F. Tödt, *Z. Elektrochem.*, **54**, 485 (1950); F. Tödt et al., *Biochem. Z.*, **323**, 192 (1952); **325**, 210 (1954); F. Tödt, D. Burk and O. Warburg, *Biochim. et Biophys. Acta*, **12**, 347 (1953).

in higher oxygen concentration or a galvanometer in lower oxygen concentration, while the concentration of oxygen was analyzed by Winkler's method[7] using the remaining solution. Winkler's method, however, when applied directly to the above solution did not give correct results owing to some difficulty in iodometry. Hence the dissolved oxygen was excluded by a flow of nitrogen gas and then redissolved in the mixed solution of manganese chloride and sodium hydroxide which was analyzed by the same method. Between the current and the concentration of oxygen, a good linear relationship holds, as shown in Fig. 2.

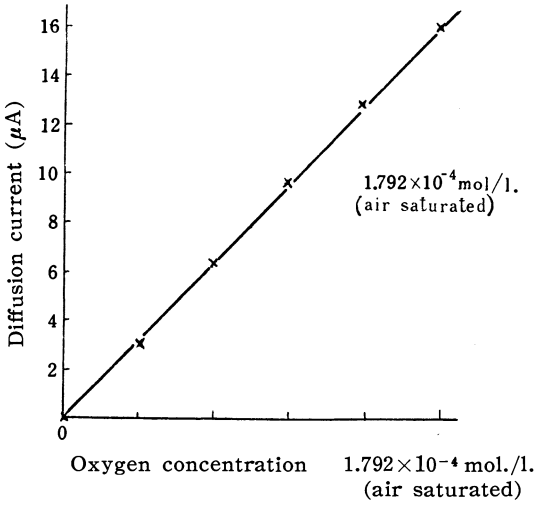


Fig. 2. Calibration curve between the diffusion current and the concentration of oxygen.

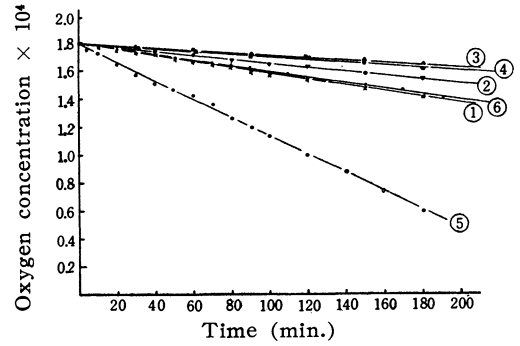


Fig. 3. Oxygen absorption by methylene blue solution containing amines.

①	trimethylamine	2×10^{-3} M
②	〃	1.5×10^{-3} M
③	〃	1.0 〃
④	〃	0.6 〃
⑤	dimethylamine	4×10^{-2} M
⑥	monomethylamine	〃

7) L. W. Winkler, *Ber.*, **21**, 2843 (1888); F.P. Treadwell and W. T. Hall, "Analytical Chemistry", vol 2. John Wiley of Sons, New York (1942) p. 704.

c) *Results.* — The composition of the solutions employed were usually 2×10^{-5}M methylene blue, 0.1 N potassium chloride pH 9.2 controlled by borate buffer, the amount of trimethylamine being varied from 0.6×10^{-3}M to 2.0×10^{-3}M. In cases of dimethylamine and monomethylamine, the concentration was raised to 4.0×10^{-2}M. A few results obtained for the relation between the concentration of oxygen and time are shown in Fig. 3. As seen from the figure, a linearity holds in all cases. But for a later stage (below about 3×10^{-5}M of oxygen), not shown in the figure, an abnormally rapid decrease of oxygen is observed in cases of trimethyl and monomethylamine, but not in dimethylamine. The origin of the above phenomena is not known at the present stage. It may perhaps be related to the electrode process and different kinds of behavior may partly be due to the mechanism of each reaction in this region. For our present purpose, however, only those regions of the normal behavior were employed and the rate of oxygen absorption was evaluated from its inclination.

The results are summarized in Table I. In this table two kinds of calculated value were obtained as follows.

Calculation A. If one assumes that leucodye, when formed, reacts very rapidly with oxygen according to the following stoichiometric relation

$$MBH+\frac{1}{2}O_2 \longrightarrow MB^+ + OH^-*$$

then, the rate of oxygen consumption will be given by

$$-\frac{d[O_2]}{dt}=\frac{1}{2}\frac{k_1k_3}{k_1+k_2+k_3}[MB]_0$$

where $[MB]_0$ is the analytical concentration of methylene blue.

Figures given under the heading Cal. A are the values by the above formula.

Calculation B. If one assumes that as soon as the intermediate is produced, it is attacked by oxygen immediately according to the following stoichiometric relation,

$$(MB\cdots HO\cdots Am)+\frac{1}{2}O_2 \longrightarrow MB^+ + OH^- + AmO$$

then the rate of oxygen absorption will be given by

* In view of Weil's results that hydrogen peroxide was not detected by an ordinary method though perceptible by pyruvic acid method, the overall reaction in the main would be such as written above.

TABLE I

Methylene blue (MB) 2.0×10^{-5}M
pH=9.2, Temp. 30°C

[TA]	[TA]/[MB]	k_1	k_2	k_3	$-\frac{d[O_2]}{dt}$ Cal. A	Cal. B	obs.
2.0×10^{-3} M	100	0.109	0.055	0.039	2.07×10^{-7}	1.09×10^{-6}	1.98×10^{-7}
1.5 〃	75	0.057	0.028	0.026	1.373 〃	5.7×10^{-7}	1.42 〃
1.0 〃	50	0.052	0.044	0.027	1.122 〃	5.2 〃	0.9 〃
0.6 〃	30	0.039	0.025	0.024	1.018 〃	3.9 〃	0.96 〃
*1.5 〃	75	0.325	0.216	0.170	7.75 〃	3.25×10^{-6}	5.69 〃
**2.0 〃	100	0.202	0.127	0.071	3.06 〃	1.72 〃	2.73 〃

* pH=10.0
** pH=9.2, temp. 40°C and MB=1.7×10^{-5}

[DA]	[DA]/[MB]	k_1	k_2	k_3	Cal. A	Cal. B	obsd.
4.0×10^{-2}	2000	0.052	0.060	0.041	1.392×10^{-7}	5.2×10^{-7}	5.73×10^{-7}

[MA]	[MA]/[MB]	k_1	k_2	k_3	Cal. A	Cal. B
4.0×10^{-2}	2000	0.052	0.049	0.035	1.334×10^{-7}	5.2×10^{-7}	2.0×10^{-7}

$$-\frac{d[O_2]}{dt}=\frac{1}{2}k_1[MB]_0$$

Figures given under the heading Cal. B are the values obtained by this formula. k_1, k_2 and k_3 are the constants evaluated from the analysis of the bleaching of the dye ion in vacuo in the same solution used for the oxygen absorption experiment.

II. The photobleaching of the aqueous solution of methylene blue by dint of dissolved oxygen.—*a) Apparatus and procedure.*— The experiment was done in a similar way to that described in Imamura and Koizumi's paper[5]. The concentration of dye was usually 1.6×10^{-5}M. The rate of photobleaching was calculated from the fall of the maximum absorbance. In certain cases the position of maximum absorption showed a slight shift toward a shorter wave length giving rise to some ambiguity to the analysis, although the initial rate generally adopted is quite reliable. The data can be analyzed by Imamura and Koizumi's method and the relation

$$\{\ln(1-e^{-\alpha c_0 d})+\alpha c_0 d)\}-\{\ln(1-e^{-\alpha cd})+\alpha cd\}=k't \quad (2)$$

can express the experimental results satisfactorily. Thus in almost all cases the plot of $\{\ln(1-e^{-D})+D\}$ (D, optical density) against t gives a straight line and from its inclination the value of k' is evaluated, k' is related with the quantum yield k by the following equation

$$k'=\alpha d I_0 k \quad (3)$$

in which α is not a genuine extinction coefficient but is to be considered rather a kind of experimental parameter. By an experiment employing a thermopile, k was determined for a certain solution and the proportionality constant between k and k' thus obtained was utilized for calculating k from k' for all the other solutions.

b) Effect of oxygen pressure on the bleaching rate of the aqueous methylene blue solution.—The aqueous solution of methylene blue was found to bleach gradually when irradiated, but if evacuated there occurs no bleaching perceptible. Thereupon, in order to examine the effect of oxygen concentration on the rate, the experiments were done with the solutions which had been previously brought to equilibrium with the air of various pressures. The concentration of the dissolved oxygen was calculated by use of Ostwald's absorption coefficient of oxygen in water neglecting the effect of a small quantity of dye. The results obtained are summarized in Table II and a plot of $1/k$ against the reciprocal of the oxygen concentration is given in Fig. 4, which shows a good straight line.

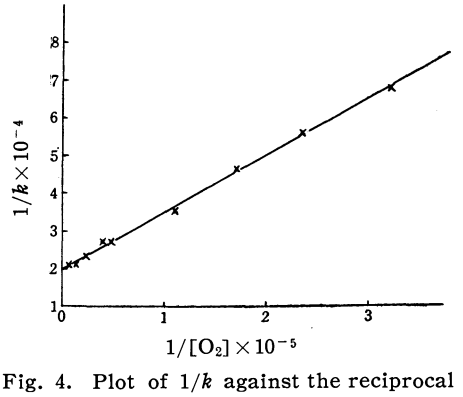


Fig. 4. Plot of $1/k$ against the reciprocal of the oxygen concentration.

TABLE II

Concentration of oxygen mole/l.	k'	k
2.5×10^{-4}	0.0240	4.63×10^{-5}
1.07×10^{-4}	0.0247	4.75×10^{-5}
4.95×10^{-5}	0.0239	4.61×10^{-5}
4.85×10^{-5}	0.0225	4.34×10^{-5}
2.38×10^{-5}	0.0174	3.36×10^{-5}
2.15×10^{-5}	0.0180	3.48×10^{-5}
9.1×10^{-6}	0.0143	2.76×10^{-5}
5.76×10^{-6}	0.0117	2.26×10^{-5}
4.25×10^{-6}	0.00912	1.76×10^{-5}
3.13×10^{-6}	0.00766	1.48×10^{-5}
1.16×10^{-6}	0.00288	5.55×10^{-6}

As the reaction goes via T state, k is to be related with the constants of various steps by the same formula already applied to the case of eosine.

$$k=\varphi_{S\to T}\frac{k^{I}_{D_2}[O_2]}{k^{IS}_{O_2}[O_2]+k^{I}_{H_2O}[H_2O]}\times\frac{k^{II}_{H_2O}}{k^{IIS}_{H_2O}}$$

or $$\frac{1}{k}=\frac{1}{\varphi_{S\to T}}\frac{k^{IS}_{O_2}}{k^{I}_{O_2}}\frac{k^{IIS}_{H_2O}}{k^{II}_{H_2O}}+\frac{1}{\varphi_{S\to T}}\frac{k^{I}_{H_2O}[H_2O]}{k^{I}_{O_2}[O_2]}\frac{k^{IIS}_{H_2O}}{k^{II}_{H_2O}}$$

where $\varphi_{S\to T}$ means transition probability for the suffixes I, II refer respectively to the first and second step and the suffix S means the sum of all the reactions of the related species. Other symbols are evident. From the inclination and the intercept of the plot in Fig. 4,

$$\frac{1}{\varphi_{S\to T}}\times(k^{I}_{H_2O}[H_2O]/k^{I}_{O_2})(k^{IIS}_{H_2O}/k^{II}_{H_2O})=1.55\times10^{-1} \quad (4)$$

$$\frac{1}{\varphi_{S\to T}}\times(k^{IS}_{O_2}/k^{I}_{O_2})(k^{IIS}_{H_2O}/k^{II}_{H_2O})=2.0\times10^{4}$$

or $$\varphi_{S\to T}(k^{I}_{O_2}/k^{IS}_{O_2})(k^{II}_{H_2O}/k^{IIS}_{H_2O})=5\times10^{-5} \quad (5)$$

From 4 and 5

$$k^{I}_{H_2O}[H_2O]/k^{IS}_{O_2}=7.75\times10^{-6} \quad (6)$$

and putting $[H_2O]=55.5$ M

$$k^{I}_{H_2O}/k^{IS}_{O_2}=1.4\times10^{-7}$$

For eosine the above quantities have already been evaluated as follows[8]

$$\varphi_{S\to T}(k^{I}_{O_2}/k^{IS}_{O_2})(k^{II}_{H_2O}/k^{IIS}_{H_2O})=2.8\times10^{-4}$$

$$k^{I}_{H_2O}/k^{IS}_{O_2}=1.3\times10^{-8}$$

Comparing the two sets of values, it may be said that the reactivity (deactivation+genuine reaction) of T state of methylene blue against oxygen is about 1/10 of that of eosine.

c) The effect of pH on the bleaching rate. —The pH effect on the photobleaching was examined only for the solution saturated with air. It is to be noted that absorption spectra of methylene blue change above and below a certain pH value and especially in the strong alkaline region, the dye seems to be quite unstable even in the dark. Hence the effect was examined only in the region where absorption spectra are not affected or affected little. In most experiments the pH values were controlled by the veronal-sodium acetate-hydrochloric acid buffer. All the data could be analyzed by 2, a linearity between $\{\ln(1-e^{-D})+D\}$ and t holding exactly except for a single case of pH 8.59 (the most alkaline solution).

The results are summarized in Table III and are shown in Fig. 5.

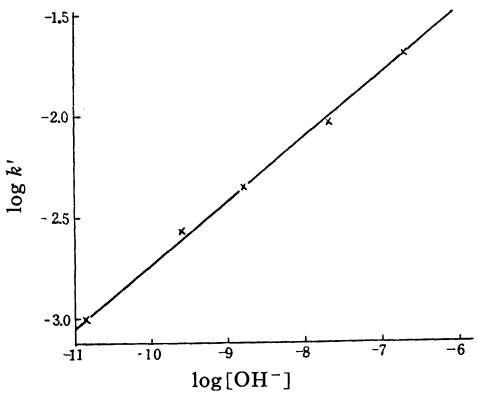


Fig. 5. Relation between $\log k'$ and $\log[OH^-]$.

TABLE III

buffered solution		non-buffered solution	
pH	k'		k'
3.35	0.001	10^{-3}N HCl	0.0019
4.40	0.0027	*pure water	0.024
5.20	0.0043	10^{-3}N NaOH	0.062
6.34	0.0086		
7.30	0.0196		
8.59	0.023		

* pH of the aqueous solution MB 1.6×10^{-5} M was measured by pH meter to be ca. 6.8.

From this figure, it can be said that k is approximately proportional to $[OH^-]^{1/3}$ for the buffered solution and the results for the non-buffered solution are somewhat higher at pH<7.0.

8) M. Imamura, This Bulletin, **30**, 249 (1957).

Discussion

Firstly, the discussion will be given about a species which is attacked by oxygen in the amine added solution of methylene blue. The solution of methylene blue containing trimethylamine does not practically bleach in spite of the presence of oxygen and this fact conforms well with the result that the quantum yield of amine induced photobleaching (reversible photoreduction) in vacuo ($10^{-3}\sim10^{-2}$) is quite larger than that of the oxygen induced photobleaching (irreversible photoöxidation) of the aqueous methylene blue solution ($\sim4.6\times10^{-5}$)***. From the above results the possibility that oxygen attacks T state decomposing methylene blue molecules can be excluded in the amine added solution. And whether oxygen attacks intermediate or leucodye, the rate must be so fast that as soon as the intermediate (or the leucodye) is formed, the consumption of oxygen must immediately take place, because the rate of oxygen absorption is the zeroth order in oxygen concentration. However, there is one thing to be taken into consideration. That is the possibility of deactivation of T state by oxygen. From the results of the irreversible photoöxidation of the aqueous solution, although the value of quantum yield is quite small

$$\varphi_{S\to T}(k^{I}_{O_2}/k^{IS}_{O_2})(k^{II}_{H_2O}/k^{IIS}_{H_2O})=k=5\times10^{-5}$$

the rate constant $k^{IS}_{O_2}$ (for the whole process consisting of deactivation and genuine reaction) is quite larger than $k^{I}_{H_2O}[H_2O]$ ($k^{IS}_{O_2}/k^{I}_{H_2O}[H_2O]=1.3\times10^{5}$). Therefore, there is no reason to deny a priori the posibility of such a deactivation in the solution of methylene blue containing amine. But if this should occur in about the same order as in the aqueous methylene blue solution, the rate of oxygen consumption ought to be exceedingly smaller than the calculated value in Table II. The agreement between the calculated and the observed value in the order of magnitude definitely denies such a possibility, and for the case of trimethylamine, the close agreement between the observed and the calculated value (Cal. A) strongly supports the view that oxygen attacks only on leucodye and not on intermediate. Thus it may be concluded that the behavior of T state toward oxygen is essentially different in two solutions with and without amine. For the solution containing amine, such a view as that competitive reactions of T state with oxygen on the one hand and with amine and OH^- on the other take place, the latter greatly predominating over the former, can not be adopted. Rather, the interpretation that oxygen in the solution containing amine loses the power of deactivating T state or alternatively loses a chance of effective encounter with T state, seems to fit experimental results. This interpretation is further supported from the following argument about the different features of the kinetics already established in the reversible photoreduction and the irreversible photoöxidation. On the basis of a broad outline of the reaction scheme proposed in the previous paper[1], let us asume tentatively a more detailed mechanism which of course must await further studies to confirm it. One plausible scheme would be such as the following

$$\begin{array}{l} MB^+ + h\nu \longrightarrow MB^{+*} \longrightarrow MB^{+t} \\ \qquad\qquad \overrightarrow{k}^{I}_{q} \\ \qquad MB^{+t} \longrightarrow MB^+ \\ \overrightarrow{k}^{I}[OH^-] \Big\downarrow\Big\uparrow \overleftarrow{k}^{II} \qquad \overrightarrow{k}^{II}[Am] \\ \qquad MB\cdots OH \longrightarrow MB\cdots HO\cdots Am \\ \qquad\qquad\qquad\qquad\qquad\quad \downarrow k_2 \\ \qquad\quad k_3 \\ \qquad\longrightarrow \text{Product} \end{array}$$

Applying the stationary state condition to T state and MB $\cdots$OH, k_1 in 1 can be expressed as follows in the above scheme

$$k_1\sim\frac{I_{ab}\varphi_{S\to T}\overrightarrow{k}^{I}\overrightarrow{k}^{II}[OH^-][Am]}{\overrightarrow{k}^{I}_{q}\overleftarrow{k}^{II}+\overrightarrow{k}^{I}[OH^-]\overrightarrow{k}^{II}[Am]+\overrightarrow{k}^{I}_{q}\overrightarrow{k}^{II}[Am]}$$

Although somewhat different relations may result from different mechanisms, the essential point would not be affected. It is that the relation experimentally found, $k_1\propto[OH^-][Am]$ requires a far larger magnitude of $\overrightarrow{k}^{I}_{q}\overleftarrow{k}^{II}$ term or the like compared with other terms involved in the denominator. Thus it is a natural expectation that the reaction of T state with OH^- and amine leading to an intermediate is slower than the deactivation or quenching process of T state by water molecules or itself.

The above situations are in sharp contrast with those of the solution without amine, in which T state is deactivated by

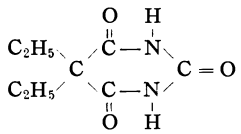
*** To avoid confusion let us designate the two reactions as reversible photoreduction and irreversible photooxidation hereafter.

O_2 far more rapidly than water. Thus the different kinds of behavior in two cases are comprehensive only from the viewpoint mentioned above.

Lastly it is to be added that for the case of monomethylamine, the observed rate of oxygen absorption coincides approximately with the values calculated by A method while it lies near to the values calculated by B method for the case of dimethylamine. But in view of few data and their accuracy being not very good, further studies will be necessary for a decisive conclusion except the case of trimethylamine for which the statement that oxygen attacks leucodye may be beyond doubt.

Next the retarding effect of veronal upon the irreversible photoöxidation may be taken up.

A structural formula of veronal



contains two secondary amino nitrogens, and in view of the results reported by Oster[2], it is a natural expectation that another reaction competing with the irreversible photoöxidation takes place between T state of methylene blue and veronal molecule. To ascertain this conjecture, it was examined whether the evacuated buffered solution displays the photobleaching or not. The result as shown in Fig. 6, is that the photobleaching does really take place and moreover the introduction of oxygen into the bleached solution recovers a greater part of the lost color. Such a bleaching process does not occur in the evacuated dye solution containing 10^{-3}M sodium hydroxide.

Thus, there is no doubt that a reversible photoreduction such as the formation of leucodye is taking place in this case. The retardation of the irreversible photoöxidation caused by the addition of veronal, can be attributed to this competitive reductive reaction, the produced leucodye being recovered by the existent oxygen. Veronal can be said to have amino-like action although to a far lesser extent. It may be worthy of adding here that an enough caution must be paid when the buffer solution is used for such experiments as the present one, since the buffer solutions usually employed often involve such a N-containing compound

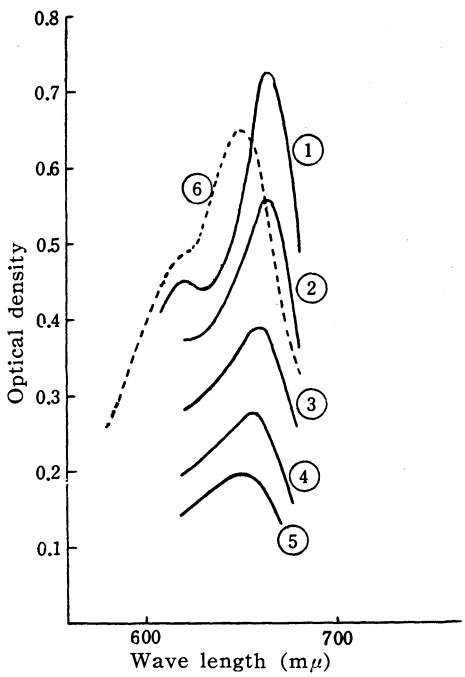


Fig. 6. Photobleaching of the methylene blue solution containing veronal in vacuo.
1 initial
2 after 10 minutes
3 after 20 minutes
4 after 40 minutes
5 after 60 minutes
6 after exposed to the air

like veronal.

Studies on the pH dependence of the rate certainly be essential for the elucidation of a detailed mechanism of the irreversible photoöxidation. But the results obtained in this paper are difficult to interpret because of the complexity introduced by the above circumstances and of the lack of experiments for examining the effect of oxygen concentration upon the rate in various pH solutions. A further more careful and extensive study will be necessary in order to make clear a detailed mechanism of the present reaction.

Summary

In connection with the reversible photoreduction of methylene blue in vacuo published already, the rate of the consumption of oxygen in the irradiated solution of methylene blue containing three kinds of amine was measured. In addition, the irreversible photoöxidation of the aqueous methylene blue solution was

studied, particular attention being paid to the effect of oxygen pressure and pH on the rate. The following conclusions were drawn from the above two series of experiments.

1) In the irradiated aqueous solution of methylene blue containing trimethylamine, oxygen does not affect the T state of dye and attacks only the leuco form, reproducing the dye molecule. Oxygen reacts almost instantaneously with the leucodye as soon as the former is produced.

2) In the aqueous solution of methylene blue (with no amine added) the reactivity of T state against oxygen is about one order less than that of eosine in the analogous condition. The deactivation of T state by oxygen in case of methylene blue is about 10^{-7} times greater than that by water.

3) Comparison of the above results 1 and 2 (taking into account of the result that in the evacuated state the reactivity of T state against OH^- and amine is much less than the deactivation by water) leads to the conclusion that the deactivation of T state by oxygen is almost completely suppressed by the addition of amine.

4) The rate of irreversible photoöxidation increases with the alkalinity of the solution. But in the buffer solution containing N-compound like veronal, a competitive reaction somewhat like that between methylene blue and amine occurs. It is pointed out that enough caution must be taken for such a possibility when the buffer solutions are employed.

A part of this research was done in the Institute of Polytechnics of Osaka City University. The cost of this research has been partially defrayed from the Scientific Research Grant from the Ministry of Education.

Department of Chemistry, Faculty of Science, Tohoku University
Katahira-cho, Sendai

Photometric Determination of Indicator End Points in Complexometric Titrations

By Sôichirô MUSHA, Makoto MUNEMORI and Kin'ya OGAWA

(Received August 13, 1958)

In photometric titrations with an indicator, the color does not develop linearly with the titrant added. This characteristic has been elucidated by a mathematical treatment of complexometric titration with specific indicator for a certain metal[1].

In a previous communication[2], the present authors proposed a graphical method for determining indicator end point in the complexometric titration by a photometric technique and applied it with success to the titration of magnesium with disodium salt of ethylenediaminetetraacetic acid (Complexon III) using Eriochrome Black T (EBT) as indicator. This method is, however, an approximate one and therefore its utility and limitation will be discussed in the present paper.

1) J. M. H. Fortuin, P. Karsten and H. L. Kies, *Anal. Chim. Acta*, **10**, 365 (1954).
2) S. Musha, M. Munemori and K. Ogawa, This Bulletin, **30**, 675 (1957).

Theoretical

List of Principal Symbols.—

m_t, total concentration of metal in titration system
i_t, total concentration of indicator in titration system
c_t, total concentration of titrant in titration system
$\mu = c_t/m_t$, relative concentration of titrant
$\alpha = [I^*]/i_t$, ratio of $[I^*]/([MI] + [I^*])$
$[I^*] = [I] + [HI] + [H_2I] + \cdots\cdots$, sum of the concentrations of metal-free indicator components
$[Y^*] = [Y] + [HY] + [H_2Y] + \cdots\cdots$, sum of the concentrations of metal-free titrant
$K_Y^* = [MY]/[M][Y^*]$, apparent stability constant
$K_I^* = [MI]/[M][I^*]$, apparent indicator constant
A_s, absorbancy during the course of titration

A_{sI}, absorbancy of metal-free indicator
A_{sMI}, absorbancy of metal-indicator complex
V, volume of titrant solution added, in ml.
V_{eq}, volume of titrant solution equivalent to the total concentration of metal, in ml.
V_0, volume of metal ion solution to be titrated, in ml.
C, molarity of titrant

General Expression and Approximate Expression. — In titrating the metal ion with such a reagent as Complexon-III in an aqueous system, there are the following equilibria:

$$M+Y^*=MY \quad \text{and} \quad M+I^*=MI \tag{1}$$

From K_Y^* and K_I^* it follows that:

$$[MY]=K_Y^*[M][Y^*] \tag{2}$$

$$[MI]=K_I^*[M][I^*] \tag{3}$$

On the other hand, m_t, c_t and i_t are expressed by the following equations:

$$m_t=[M]+[MY]+[MI] \tag{4}$$

$$c_t=[MY]+[Y^*] \tag{5}$$

$$i_t=[MI]+[I^*] \tag{6}$$

From Eqs. 2, 3, 4, 5 and 6, the following relationship is derived.

$$c_t=m_t-[MI]\left(1+\frac{1}{K_I^*[I^*]}\right)+[I^*]\frac{K_I^*}{K_Y^*}\left\{\frac{m_t}{[MI]}-\left(1+\frac{1}{K_I^*[I^*]}\right)\right\} \tag{7}$$

By replacing Eq. 7 by the relative values μ and α, comes the following equation:

$$\mu=1-\frac{1}{m_t}(1-\alpha)\left(i_t+\frac{1}{\alpha K_I^*}\right)+\alpha\frac{K_I^*}{K_Y^*}\left\{\frac{1}{1-\alpha}-\frac{1}{m_t}\left(i_t+\frac{1}{\alpha K_I^*}\right)\right\} \tag{8}$$

Eq. 8 is the general expression for the spectrophotometric titration curve and will be called *general equation.*

Now, if $[Y^*]$ and i_t are so small that they can be neglected in the course of titration, Eqs. 4 and 5 are converted into the followings:

$$m_t=[M]+[MY] \tag{9}$$

$$c_t=[MY] \tag{10}$$

From Eqs. 2, 3, 9 and 10 it follows that:

$$c_t=m_t-\frac{1}{K_I^*}\frac{[MI]}{[I^*]} \tag{11}$$

If the dilution of solution by titrant is neglected, Eq. 12 will be obtained by substituting Eq. 11 with V and V_{eq}:

$$V=V_{eq}-\frac{V_0}{C}\frac{1}{K_I^*}\frac{[MI]}{[I^*]} \tag{12}$$

Values of $[MI]/[I^*]$ can be computed from the absorbancy readings by means of the following equation:

$$[MI]/[I^*]=(A_{sI}-A_s)/(A_s-A_{sMI}) \tag{13}$$

If $(A_{sI}-A_s)/(A_s-A_{sMI})$ is plotted against V will result a straight line whose intercept on the V-axis is equal to V_{eq}[2]. By replacing Eq. 11 by μ and α, comes Eq. 14:

$$\mu=1-\frac{1}{m_t}\frac{1}{K_I^*}\frac{1-\alpha}{\alpha} \tag{14}$$

Eq. 14 is the approximate expression for the spectrophotometric titration curve and will be called *approximate equation.*

Discussion

On the basis of general equation, Fortuin et al.[1] discussed the condition to be fulfilled for the accurate determination of indicator end point in complexometric titration by a photometric method. In the present paper, however, we shall discuss the conditions under which the approximate equation is established within experimental errors.

When Eq. 14 is compared with Eq. 8, i_t and K_Y^* are omitted in Eq. 14, and therefore the effects of these variables on the deviation of the approximate equation from the general equation will be mainly examined.

If the magnitudes of m_t, i_t, K_Y^* and K_I^* are assigned in Eq. 8, α and hence $(1-\alpha)/\alpha$ can be evaluated as a function of μ. The curves in Figs. 2 and 4 illustrate the manner in which α changes with μ for the systems defined by Tables I and II, respectively. Corresponding curves in Figs. 1 and 3 illustrate the variation of $(1-\alpha)/\alpha$ with μ. Line A_0 in Fig. 1 and line B_0 in Fig. 3 show the plots obtained by Eq. 14.

1) Effect of i_t.—The effect of the magnitude of i_t was examined when K_I^* is much smaller than K_Y^*. From Fig. 1 it is seen that the deviation of the approximate equation from the general equation becomes greater at higher indicator concentration. Therefore, it may be concluded that in order to estimate μ with precision of 1%, the molarity of the indicator must be ten times smaller than $1/K_I^*$ in numero. Fig. 2, which represents actual behavior of photometric titration curve, shows ambiguous end point at higher indicator concentration.

2) Effect of K_Y^*. — The effect of the magnitude of K_Y^* was examined when the

TABLE I

Curve	$m_t\times10^2$	$i_t\times10^5$	$K_I^*\times10^{-4}$	$K_Y^*\times10^{-12}$
A_1	1/3	3	1/8	4
A_2	1/3	30	1/8	4
A_3	1/3	300	1/8	4

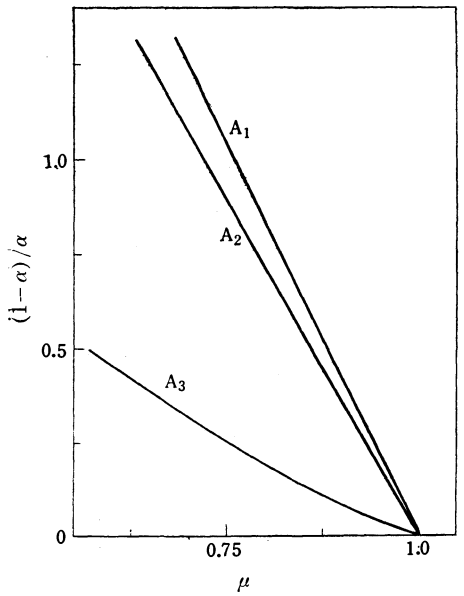


Fig. 1. Variation of $(1-\alpha)/\alpha$ with μ for the systems defined by Table I.

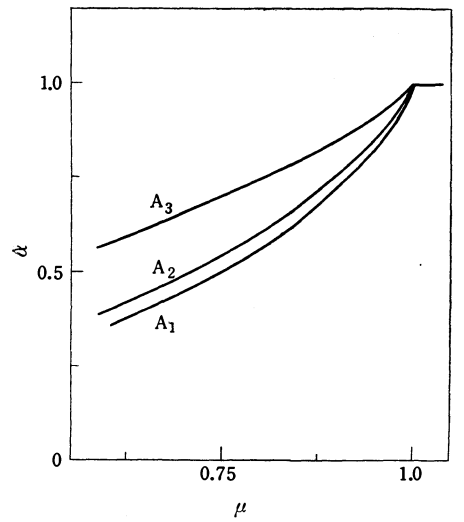


Fig. 2. Variation of α with μ for the systems defined by Table I.

TABLE II

Curve	$m_t\times10^2$	$i_t\times10^5$	$K_I^*\times10^{-4}$	$K_Y^*\times10^{-5}$	$\log\left(\frac{K_Y^*}{K_I^*}\right)$
B_1	1/3	3	1/8	1/8	1
B_2	1/3	3	1/8	10/8	2
B_3	1/3	3	1/8	100/8	3

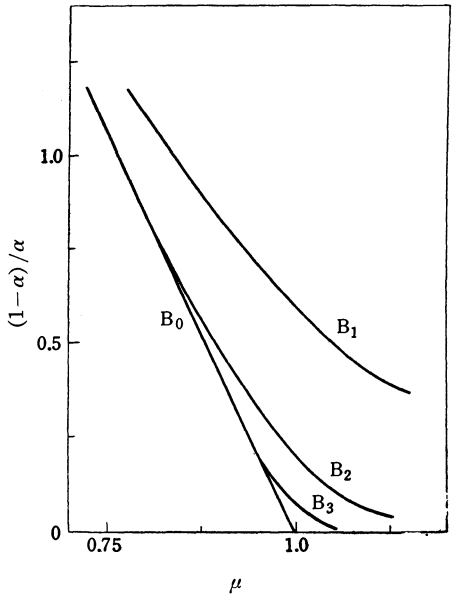


Fig. 3. Variation of $(1-\alpha)/\alpha$ with μ for the systems defined by Table II.

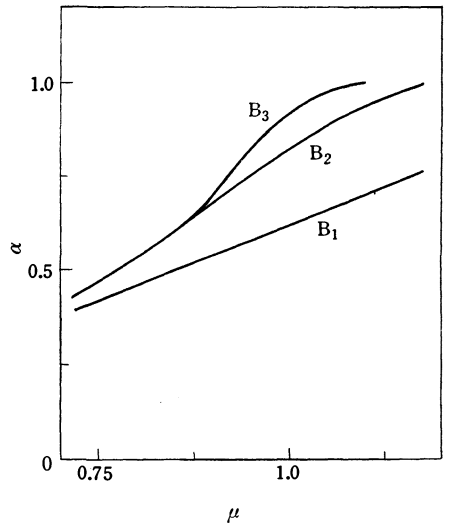


Fig. 4. Variation of α with μ for the systems defined by Table II.

molarity of the indicator was ten times smaller than $1/K_I^*$ in numero. From Fig. 3 it is seen that the deviation of the approximate equation from the general equation becomes larger as the value of $\log(K_Y^*/K_I^*)$ decreases.

In a usual plot of the titration curve (Fig. 4), the end point can be accurately determined only when $\log(K_Y^*/K_I^*)$ is larger than 4. However, if $(1-\alpha)/\alpha$ is plotted against μ (Fig. 3), the end point can be determined through extrapolation even when $\log(K_Y^*/K_I^*)$ is equal to 2 (curve B_2).

3) Slope of the line expressed by the approximate equation.—It is seen from Eq. 14 that the slope of the line expressed by the approximate equation is proportional to the product of m_t and K_I^*. Accordingly, in case of titration where Eq. 12 is well established, the apparent indicator constant can be estimated from the slope of the line expressed by this equation.

Experimental

In order to test the applicability of the linear plot described above, the following titrations were investigated:

1) Micro-titration of calcium at pH 12 using Murexide indicator, as an example of lower concentration of metal ion.

2) Titration of calcium at pH 10 using EBT indicator, as an example of lower value of K_I^*.

3) Titration of magnesium at pH 10 using EBT indicator, as an example of the case where value of log (K_Y^*/K_I^*) is smaller than 3.

Apparatus.—Yanagimoto Photometric Titrator Model PT-1 and Yanagimoto pH meter were used.

Reagents.—All chemicals used were the reagent grade. Standard solution of calcium was prepared by dissolving calcium carbonate (dried at 110°C), in dilute hydrochloric acid and diluting it with distilled water. Standard solution of magnesium was prepared by dissolving magnesium sulfate heptahydrate in distilled water and its concentration was gravimetrically determined with oxine[3]. Standard solution of Complexon-III was prepared by dissolving disodium ethylenediaminetetraacetate dihydrate in distilled water to produce approximately 0.01 M solution. Murexide indicator solution was prepared by shaking 40 mg. of the dye with 10 ml. of distilled water and 2 ml. of its supernatant was used. This solution was prepared daily. EBT indicator solution was prepared by dissolving 0.5 g. of Eriochrome Black T and 4.5 g. of hydroxylamine hydrochloride in 100 ml. of ethanol and its 0.5 ml. was used. This solution was stable for at least 5 months. For the adjustment of pH of the solution to 10 and 12, 1 N ammonium chloride-ammonia buffer solution and 1 N sodium hydroxide solution were used, respectively.

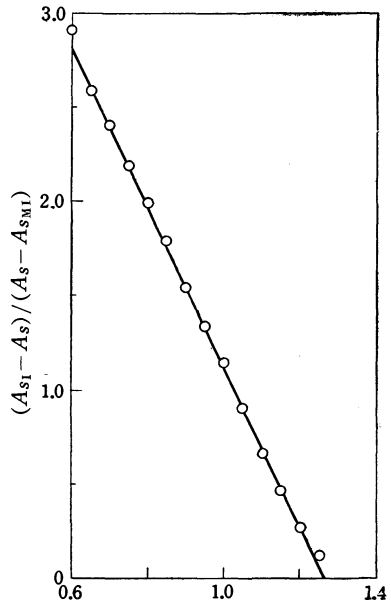
Procedure.—An aliquot of sample solution and a few ml. of buffer solution were placed in the titration cell and diluted to 50 ml. with distilled water. Appropriate wave-length was set and the absorbancy scale was adjusted to zero with slit. The indicator solution was pipetted into the titration cell and then titration was carried out. Absorbancies were recorded at the beginning of titration and at every 0.05 ml. of the titrant added during the titration, until the constant value of absorbancy was obtained.

Results and Discussion. — *Titration of calcium at pH 12 using Murexide indicator.* —Absorbancy measurement was made at 580 mμ. In this titration system, the values of log K_Y^* and log K_I^* are 10.5 and 5.0, respectively[4]. Although the value of log (K_Y^*/K_I^*) is sufficiently large, the photometric titration curve (Fig. 6) is somewhat round near the equivalence point, owing to the lower concentration of the calcium ion in the titration system. The plot of $(As_1-A_s)/(A_s-As_{MI})$ against the volume of the titrant added (Fig. 5) gives a straight line, the intercept of which corresponds to the equivalence point. The

TABLE III

RESULTS OF PHOTOMETRIC TITRATION OF CALCIUM AT pH 12 WITH 0.01 M COMPLEXON-III USING MUREXIDE INDICATOR

Calcium taken, mg.	Titrimetric end point, ml.	Calcium found, mg.	Error %
0.50_7	1.26_6	0.50_7	0
0.50_7	1.26_6	0.50_7	0
1.01_8	2.54_0	1.01_8	0
1.01_8	2.54_0	1.01_8	0
1.28_7	3.16_0	1.26_7	−1.6
1.28_7	3.18_5	1.27_6	−0.7

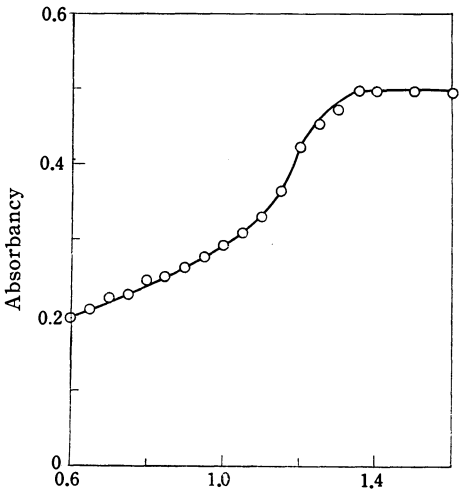


0.01 M Complexon-III, ml.

Fig. 5. Plot for titration of 0.50_7 mg. of calcium at pH 12 with Complexon-III using Murexide indicator.

3) F. P. Treadwell and W. T. Hall, "Analytical Chemistry", Vol. II, (9th ed.), John Wiley and Sons, New York, (1942) p. 259.

4) G. Schwarzenbach, "Die komplexometrische Titration", Ferdinand Enke Verlag, Stuttgart, (1956) pp. 7, 31 and 36.



0.01 M Complexon-III, ml.

Fig. 6. Titration curve of the same titration as in Fig. 5.

results given in Table III show that the titration can be carried out with high precision.

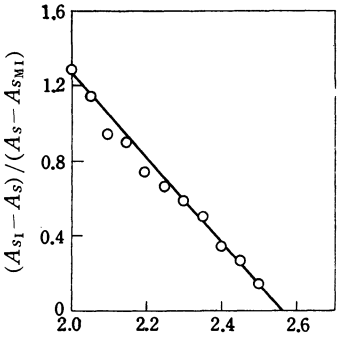
Titration of calcium at pH 10 using EBT indicator. — In this titration system, the values of $\log K_Y^*$ and $\log K_I^*$ are 10.2 and 4.03, respectively[4]. Visual titration of this system fails owing to the ambiguous color change at the end point. Even by a photometric technique, the titration curve at 545 mμ (Fig. 8) does not give a sharp end point since the value of $\log K_I^*$ is too small. However, the plot of $(A_{sI}-A_s)/(A_s-A_{sMI})$ against the volume of the titrant added (Fig. 7) gives a straight line, the intercept on the V-axis representing the equivalence point. The results given in Table IV show that precisions of the order of a few tenths of one per cent were obtained in most instances.

Titration of magnesium at pH 10 using EBT indicator. — In this titration system, the values of $\log K_Y^*$ and $\log K_I^*$ are 8.5 and 5.44, respectively[4]. The value of $\log (K_Y^*/K_I^*)$ is about 3, so that the photometric titration curve at 545 mμ (Fig. 2 in the previous communication[2]) shows some rounding near the equivalence point. However, the plot of $(A_{sI}-A_s)/(A_s-A_{sMI})$ against the volume of the titrant added gives a straight line, the intercept on the V-axis representing the equivalence point (Fig. 1 in the previous communication[2]). The results (Table I in the previous communication[2]) show that the titration was carried out with precision of about 1%.

TABLE IV

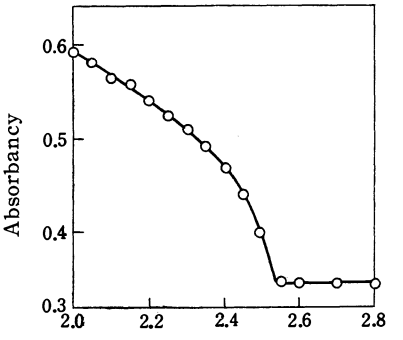
RESULTS OF PHOTOMETRIC TITRATION OF CALCIUM AT pH 10 WITH 0.01 M COMPLEXON-III USING EBT INDICATOR

Calcium taken, mg.	Titrimetric end point, ml.	Calcium found, mg.	Error %
1.01_8	2.55_2	1.02_3	+0.5
1.01_8	2.53_0	1.01_4	−0.4
1.01_8	2.55_2	1.02_3	+0.5
1.01_8	2.55_0	1.02_2	+0.4



0.01 M Complexon-III, ml.

Fig. 7. Plot for titration of 1.01_8 mg. of calcium at pH 10 with Complexon-III using EBT indicator.



0.01 M Complexon-III, ml.

Fig. 8. Titration curve of the same titration as in Fig. 7.

Apparent indicator constant.—It was previously pointed out that the apparent indicator constant would be estimated from the slope of the linear plot of $(A_{sI}-A_s)/(A_s-A_{sMI})$ against the volume of titrant added. The values of $\log K_I^*$ obtained in the above titrations are given in Table V and compared with those described by Schwarzenbach[4] (given in the fifth column in Table V). It is seen that there are considerable discrepancies between them. These discrepancies may be due to the differences in ionic strength and temperature and also to some unknown factor such as the influence of buffer components in the equilibria.

TABLE V
VALUES OF LOGARITHM OF APPARENT INDICATOR CONSTANT FOR CALCIUM AND MAGNESIUM

Metal ion	pH	Indicator	$\log K_I^*$	
			Values obtained	Values reported
Calcium(II)	12	Murexide	4.3_9	5.0
Calcium(II)	10	EBT	4.0_3	3.84
Magnesium(II)	10	EBT	5.2_8	5.44

Determination of calcium and magnesium in their mixture.—Total amount of calcium and magnesium in their mixture was titrated at pH 10 with standard Complexon-III solution using EBT indicator. Absorbancy measurements were made at 545 mμ. with another aliquot of the sample solution, magnesium was masked by sodium hydroxide and calcium was titrated at pH 12 using Murexide indicator. Absorbancy measurements were made at 580 mμ. The amount of magnesium was calculated by their differences. The linear plots obtained in the titrations of total calcium and magnesium and of calcium give the same pictures as obtained in 3 and 1, respectively. The results are tabulated in Table VI.

TABLE VI
RESULTS OF TITRATION OF CALCIUM AND MAGNESIUM IN THEIR MIXTURE WITH 0.01 M COMPLEXON-III

Calcium, γ			Magnesium, γ		
taken	found[a)]	deviation	taken	found[b)]	deviation
513	507	−2	254	256	+2
203	203	0	254	249	−5
203	203	0	508	507	−1

a) Each value is the average of three separate determinations.

b) Each value was calculated from the difference between the average of the volume of titrant for total and that for calcium in three separate titrations.

Department of Applied Chemistry
College of Engineering
University of Osaka Prefecture
Sakai, Osaka

Vapor Pressures of Molecular Crystals. XIV[1]. *Sulfamide and Diacetylhydrazine*

By Sadao TAKAGI*, Ryuichi SHINTANI, Hideaki CHIHARA and Syûzô SEKI

(Received August 7, 1958)

The energy of the hydrogen bond can be determined by various methods in vapor, liquid, solution, and crystalline solid. All but one method, that have been reported by the authors and other investigators in cases of liquids and crystals, estimate the energy from the temperature variation of the equilibrium constant for the association-dissociation equilibrium due to hydrogen bonding in vapor or in solution state. Those determinations, however, can not be correlated with the so-called hydrogen bond distances with only one exception for the case of gaseous carboxylic acid dimers, the structure of which could be determined by means of the electron diffraction technique. On the other hand when we deal with crystalline solids, it is possible to determine the hydrogen bond distance by the X-ray investigation although we can not obtain the state, in which only the hydrogen bond ceases to act, other forces such as the dispersion forces and the dipolar forces being unchanged. Usually the compromise has been adopted that the contributions other than the hydrogen bond to be subtracted from the total lattice energy may be estimated by one of the following

1) The Report XIII may be found in This Bulletin, **32**, 84 (1959).

* Present address: The Institute of Polytechnics, Osaka City University, Minami-Ogimachi, Osaka.

2) I. Nitta, S. Seki and K. Suzuki, This Bulletin, **24**, 63 (1951).

two methods: (1) the dispersion energy is calculated by using the interatomic distances and the atomic polarizabilities, and the electrostatic energy by assuming the electron density on each atom; (2) the dispersion and the electrostatic energies of the hydrogen-bonded crystal are substituted by the heat of sublimation of the crystal that is isoelectronic with the crystal in question but that possesses no hydrogen bond between molecules[2].

We have here chosen sulfamide and diacetylhydrazine as compounds having NH···O hydrogen bonds in crystals, whose structures were determined[3,4], and we have applied the former method of obtaining the energies of hydrogen bonds.

Experimental

Materials.—Sulfamide $(NH_2)_2SO_2$ was prepared by Goehring's method from liquid ammonia and sulfuryl chloride[5], and purified by fractional sublimation in high vacuum, m. p. 91.9°C (*Anal.* found S 32.84% and N 28.45%.) Diacetylhydrazine $CH_3COHN\text{-}NHCOCH_3$ was supplied by Miss A. Yamaguchi of the University of Tokyo*. This was recrystallized from aqueous solution and dehydrated** and sublimed in high vacuum; m. p. 123°C. The crystal modifications of both substances were checked against the reported crystal structures by X-ray diffractometer.

Apparatus.—The vapor pressures were measured with the apparatus already reported elsewhere[1] except for minor alterations. In the experiments with diacetylhydrazine, it was found that effused vapor condensed on the quartz helical balance which was kept at room temperature, causing a considerable error in the determination of the weight changes. In order to remove this difficulty the balance container was heated with a ribbon heater from outside the glass tubing to maintain the temperature of the balance at about 70°C. The treatment of the quartz balance with dimethyldichlorosilane vapor was also useful in preventing condensation of diacetylhydrazine.

Results and Discussion

The vapor pressures are listed in Table I for both sulfamide and diacetylhydrazine. The experimental values are well reproduced by the equations,

$$\log P = 11.047 - (5300.4/T) \quad \text{(sulfamide)}$$

and

$$\log P = 12.1947 - (5384.4/T) \quad \text{(diacetylhydrazine)}$$

The heat, entropy and free energy changes of sublimation computed by these equations are given in Table II.

TABLE I

VAPOR PRESSURES OF SULFAMIDE CRYSTAL

T°K	P(mmHg) $\times 10^5$	T°K	P(mmHg) $\times 10^5$
347.8_9	6.370	352.7_5	10.43
348.7_0	7.017	354.7_8	12.81
349.7_4	7.960	357.7_9	17.04
350.7_8	8.671		

VAPOR PRESSURES OF DIACETYLHYDRAZINE CRYSTAL (ANHYDROUS)

T°K	P(mmHg) $\times 10^4$	T°K	P(mmHg) $\times 10^4$
342.3_9	2.876	349.6_2	6.100
343.4_8	3.269	350.6_8	6.913
344.9_4	3.946	352.2_5	8.046
347.3_6			

TABLE II

HEATS, ENTROPIES AND FREE ENERGIES OF SUBLIMATION

	ΔH (kcal./mole)	ΔS (cal./deg. mole)	ΔG at 298.16°K (kcal./mole)
Sulfamide	24.25±0.24	37.26±0.68	13.11±0.31
Diacetylhydrazine	24.63±0.39	42.60±1.13	11.93±0.51

The heat of sublimation here obtained may be safely regarded as the lattice energy of the crystal*.

Calculation of the energies of the NH···O hydrogen bonds.—*a) Sulfamide.*—The calculation of the dispersion energy was made by the same procedure as was reported earlier[2]. The summation of r^{-6} (r: interatomic distance) for nonbonded pairs of atoms or atomic groups within 10 Å from a 'central atom' is shown in Table III, which was obtained on the basis of the atomic

TABLE III

SUMMATION FOR SULFAMIDE

Non-bonded pairs	$\sum(1/r^6) \times 10^6$ in Å^{-6}
S～S	906.63
NH_2～NH_2	7367.64
O～O	5962.20
S～NH_2	6006.26
S～O	5002.95
NH_2～O	14792.97*

* The hydrogen-bonded pairs were excluded.

3) K. N. Trueblood and S. W. Mayer, *Acta Cryst.*, **9**, 628 (1956) (sulfamide).

4) R. Shintani and I. Nitta, read before the 4th International Congress of Crystallography, July 1957 (Montreal, Canada); A full paper will be published in *Acta Cryst.* or elsewhere (diacetylhydrazine).

5) M. Goehring, J. Heinke, H. Malz and G. Ross, *Z. anorg. u. allgem. Chem.*, **273**, 200 (1953).

* The authors are indebted to her for her kindness.

** The monohydrate of diacetylhydrazine is more stable than the anhydrous form at room temperature and humidity.

* Association in vapor can be ignored as the vapor pressure is very low.

parameters determined by Trueblood and Mayer[3]. The atomic polarizabilities were calculated from the molecular refractions R_D for O (in a carbonyl), NH_2 (in a primary amine) and SO_2 (in dialkyl sulfate) compiled by Vogel[6]. The static polarizabilities given in Table IV have been corrected for the dispersion effect by subtracting 3% from the values for the NaD light[7]. The dispersion energy was then computed by using the Slater-Kirkwood formula[8] by summation within the 10 Å sphere and by integration outside that sphere. The summation part contributed 13.71 kcal and the integration part contributed 0.014 kcal. to the dispersion energy. The number of terms included in the summation was 1128. The dipolar interaction energy in sulfamide was obtained by summing up the contribution from each pair of molecules in the crystal by using the value of the dipole moment 3.9 D[9]. The dipolar energy contribution within the 10 Å sphere amounted only to 2.87 kcal. and this was taken as the total electrostatic energy as the integration diverges. The hydrogen bond energy was set equal to the difference between the observed lattice energy and the sum of the dispersion and electrostatic energies; $24.25-(12.08+2.9)=9.30$ kcal./mole. There are two NH···O hydrogen bonds per molecule of sulfamide and therefore the energy of a hydrogen bond is 4.6_5 kcal./mole. Omission of the repulsive potential energy in the calculation may be partly justified by the fact that in many molecular crystals the Margenau potential of r^{-8} factor nearly cancels out the repulsive contribution[10].

TABLE IV
STATIC POLARIZABILITIES

	No. of outer shell electrons	Static polarizability
S	6	1.382×10^{-24} cc.
O	6	0.8162 〃
NH_2	7	1.707 〃

b) Diacetylhydrazine. — The summation of r^{-6} and the static polarizabilities are given in Tables V and VI. The dispersion energy is 19.30 kcal./mole for summation within the 10 Å sphere (1064 terms) from "central atoms" and 0.39 kcal./mole for integration outside the sphere. The electrostatic contribtion to the total lattice energy was calculated by point charge model with unbalanced charges on C and O atoms, $\pm2.002\times10^{-10}$ c. g. s. e. s. u., estimated from the bond moment of C=O 2.50 D and the bond length 1.249 Å. The resultant energy was 1.15 kcal./mole, being repulsive. The total hydrogen bond energy is then about 6.06 kcal./mole or 3.03 kcal./mole for each bond.

TABLE V
SUMMATION FOR DIACETYLHYDRAZINE

Non-bonded pairs	$\Sigma(1/r^6)\times10^6$ in Å^{-6}
NH∼NH	4286.9
C∼C	3674.0
O∼O	5361.7
CH_3∼CH_3	4126.3
C∼O	11359.2
CH_3∼O	8470.5
NH∼O	9038.3*
C∼CH_3	5110.5
C∼NH	6778.2
CH_3∼NH	3455.5

* H-bond pairs were excluded.

TABLE VI
STATIC POLARIZABILITIES

	No. of outer shell electrons	Polarizability
O	6	$0.816_2\times10^{-24}$ cc.
C	4	1.60 〃
CH_3	7	1.89 〃
NH	6	1.61 〃

Comparison of the energy of NH···O hydrogen bond.—In Table VII are summarized the energies of NH···O hydrogen bonds in crystals hitherto reported. In general the NH···O energies fall in a range of values between 3 and 6 kcal. and are in comparable magnitude with the energies of OH···O bands. However, from the point of view that the energy should decrease with increasing length of the bond, it seems hopeless to correlate the energies with the bond lengths in Table VII. This is partly due to the difference of the method of evaluation of the energy and partly due to relatively small contribution of hydrogen bonding forces to the total lattice forces. The situation is in a sense analogous to the evaluation of the resonance energy of conjugated molecules from the experimental heat of formation and the energy of a Kekulé structure.

6) A. I. Vogel, *J. Chem. Soc.*, **1948**, 1833; see also J. R. Partington, "An Advanced Treatise of Physical Chemistry", Vol. IV, Longmans, London (1953), p. 50.
7) S. Seki and H. Chihara, *Sci. Papers Osaka University*, No. 1 (1949).
8) J. C. Slater and J. G. Kirkwood, *Phys. Rev.*, **87**, 684 (1931).
9) G. Devoto and R. D. Nola, *Gazz. chim. ital.*, **63**, 495 (1953); The gaseous dipole moment of $SO_2(CH_3)_2$ is 4.41D and thus it was assumed that the effect of association of sulfamide in dioxane solution would be small.
10) I. Nitta and S. Seki, *J. Chem. Soc. Japan, Pure Chem. Sec.* (*Nippon Kagaku Zasshi*), **64**, 475 (1943).

TABLE VII
ENERGY OF HYDROGEN BONDS

Crystal	N···O length	Energy in kcal./bond	Method	Reference
Diketopiperazine	2.88	5.3	**a**	i
Diformylhydrazine	2.788	6.1	**a**	ii
δ-Valerolactam	—	(7.2)*	**a**	ii
ε-Caprolactam	—	(7.0)*	**a**	ii
Oxamide	—	(4.2)*	**a**	ii
Acetamide	2.89, 2.99	3.0	**a**	ii
Urea	2.99, 3.04	3.5	**a**	ii
Sulfamide	3.02	4.7	**b**	iii
Diacetylhydrazine	2.875	3.0	**c**	iii

i: S. Seki, K. Suzuki and T. Koide, *J. Chem. Soc. Japan, Pure Chem. Sec.* (*Nippon Kagaku Zasshi*), **77**, 346 (1956).
ii: K. Suzuki, S. Onishi, T. Koide and S. Seki, This Bulletin, **29**, 127 (1956).
iii: Present study.
a: Subtraction of the heat of sublimation of the isoelectronic compound possessing no dipole moment.
b: Calculation of the dispersion and the electrostatic energies by use of theoretical formulae (point dipole model).
c: Calculation of the dispersion and electrostatic energies by use of theoretical formulae (point charge model).
* It is uncertain how many bonds there are per molecule.

The method **a** gives the hydrogen bond energy in which the energy required for the rearrangement of molecules from the structure of the isoelectronic crystal to the hydrogen-bonded structure is included. This rearrangement energy is quite analogous to the compression energy[11] and should differ from compound to compound. Thus this type of hydrogen bond energy does not represent the energy localized in the hydrogen bond but includes all the contributions to the change in the lattice energy that would be needed if the hydrogen-bonded structure were transformed into a non-bonded structure, i. e. the energy localized at the hydrogen bonds, the energy of electronic rearrangement within a molecule to make it non-polar within the crystal lattice and the energy for the change of crystal structure[12]. In other words, such "hydrogen bond energy" is a measure of how much gain in stability would result in a crystal as a whole by forming the hydrogen bonds compared with a hypothetical non-bonded structure.

The methods **b** and **c** are less unambiguous than the method **a** in that the former give the energy values in the approximation, the origin of which is less obscure. The estimation of the electrostatic energy is always a hard thing to do correctly; the point dipole model would be a very rough approximation in short-range interaction as in crystals and the charge distribution in crystal is rarely known except in cases of fully refined analysis of the crystal structures. Although the resultant contribution of the electrostatic energy to the total lattice energy is usually small, it is still so large as to affect the hydrogen bond energy value significantly.

The precision with which the dispersion energy is estimated by use of the Slater-Kirkwood formula depends primarily on the choice of the values for the static polarizability of atoms or atomic groups. We have some ground for believing that the calculated dispersion energy is a good measure to the actual interaction energy because we obtained relatively good agreement with the experimental heats of sublimation of nonpolar compounds as is shown in Table VIII. The difference between the calculated and the observed energies still amounts to a few kcal./mole which can not be ignored in comparison with the energy of a hydrogen bond. It may be concluded that the method of evaluating the energy of hydrogen bonds by subtracting contributions of other sources than the hydrogen bonds from the total lattice energy may be applied only to those crystals in which the hydrogen bonding plays an overwhelmingly important role in determining the crystal structure such as ice.

11) C. A. Coulson, "Valence", Clarendon Press, Oxford (1953), p. 236.
12) H. Chihara, *J. Japanese Chem.* (*Kagaku no Ryoiki*), **10**, 31 (1956).

TABLE VIII
CALCULATED AND OBSERVED LATTICE ENERGIES OF NONPOLAR COMPOUNDS (kcal./mole)

	Calculated	Observed	Reference
Tin tetraiodide SnI_4	20.6	18.1	(10)
Titanium tetraiodide TiI_4	16.4	14.9	(10)
Iodine, I_2	15.5	14.8	(10)
Benzene, C_6H_6	10.7	9.2	(13)
Naphthalene, $C_{10}H_8$	18.2	15.9	(10)
Anthracene, $C_{14}H_{10}$	27.2	22.8	(10)
Hexamethylbenzene $C_6(CH_3)_6$	19.4	19.3	(7)

The lattice forces in relation to the crystal structure.—Only one of two hydrogen atoms in each NH_2 group participates in hydrogen bonding in sulfamide crystal. The closest approach between molecules is through the hydrogen bonds but their distance is longer than in diformlyhydrazine. Diformylhydrazine is probably the crystal possessing the shortest NH···O hydrogen bonds (2.788Å) ever known* and its closest approach in the crystal is through hydrogen bonds and not at the contact CH ···O between neighboring molecules (the non-bonded closest distance CH···O is 3.69 Å, which is longer than the sum of the van der Waals radii 3.4 Å). Therefore the equilibrium distance in the system NH···O would be 2.788 Å**. In sulfamide also, there is nothing hindering the neighboring molecules from approaching nearer and nevertheless its hydrogen bond is longer than in diformlyhydrazine. This may be explained by the difference in electronic configuration in these two compounds. In fact the infrared absorption spectrum of sulfamide, recorded with Hilgar Model H800 spectrometer, showed NH stretching absorptions at 3338 and 3248 cm^{-1} by the Daifloil mull method in comparison with about 3100 cm^{-1} in diformylhydrazine[14].

Sulfamide is a polar crystal with parallel orientation of molecular dipoles in the direction of the *c* axis. This may plausibly give rise to the spontaneous polarization of the crystal unless twinning masks the effect. An estimation of the spontaneous polarization gives about 44226 e. s. u. by using the dipole moment 3.9 D. This is surprisingly large polarization being in comparable magnitude with the case of ferroelectric barium titanate $BaTiO_3$ (the saturation polarization 48000 e. s. u.). The measurement of the polarization should give the value of the dipole moment of a molecule in the crystal, and a study along this line is now going on.

The heat of sublimation of diacetylhydrazine is by about one kcal./mole smaller than would be predicted by the additivity of lattice energies; the heat of sublimation of diformylhydrazine is 24.1 kcal./mole and an increment of about one kcal./mole may be predicted for the addition of a CH_2 unit*. The melting point 132°C and the density 1.35 are lower than 158°C and 1.59 of diformylhydrazine. Diacetylhydrazine is very hygroscopic and changes to the monohydrate in air under ordinary condition within an hour. Such properties are reflected on relatively weak hydrogen bonds in diacetylhydrazine. The fact that the electrostatic interaction is acting as repulsive** is somewhat surprising result

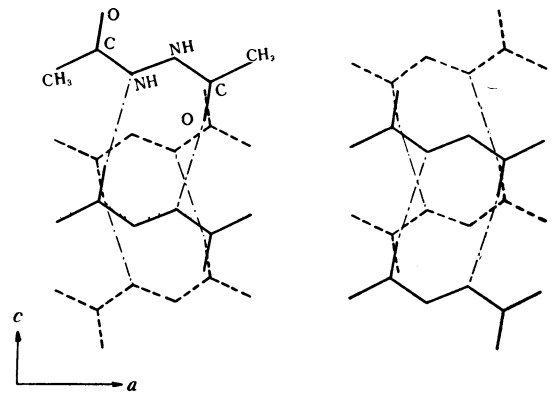


Fig. 1. The arrangement of diacetylhydrazine molecules projected along the *b* axis. Full line shows the molecules lying on *c* plane and dotted line shows molecules displaced halfway in *b*-direction. Hydrogen bonds are represented by chain lines.

13) J. H. de Boer, *Trans. Faraday Soc.*, **32**, 10 (1936).

* 2.75Å for NH···O bond was reported for amino acids or peptides (cf. H. L. Yakel and E. W. Hughes, *Acta Cryst.*, **7**, 291 (1954); R. A. Pasternak, L. Katz and R. B. Corey, Ibid,, **7**, 225 (1954)) but these are the bonds, $N^+H\cdots O^-$, between zwitterions.

** In ice and in solid and gaseous hydrogen fluoride there is nothing that hinders the molecules from getting nearer exceptthe inherent potential energy along the hydrogen bonds, so that the actual distances found 2.76Å and 2.55Å would correspond to the shortest approach in linear OH···O and FH···F systems, respectively, if other effects like conjugation do not greatly modify the electronic structure of the molecules. In other words the single minimum OH···O bond will not exist unless the hydrogen bond is very strongly conjugated with the molecular network.

14) T. Miyazawa, *J. Chem. Soc. Japan, Pure Chem. Sec.*, (*Nippon Kagaku Zasshi*), **76**, 341 (1955).

* Mr. Hiroshi Suga of our laboratory has found a lambda-type phase transition of diacetylhydrazine at about 50°C with the heat of transition of probably less than one kcal./mole. In comparing the heats of sublimation of these two compounds the heat of transition must be considered and then the discrepancy would be much smaller. This transition, however, does not affect much the discussion on the hydrogen bond energy.

** Solid carbon dioxide is another example of repulsive electrostatic energy.

in view that the molecules are packed in layers so that C=O bonds are directing antiparallel, one over another (see Fig. 1). This is only a deceptive appearance in the arrangement and actually the lattice is mainly constructed by the dispersion forces.

Summary

The vapor pressures of crystalline sulfamide and diacetylhydrazine were measured between 347°K and 358°K and between 342°K and 353°K, with the results, $\log P = 11.047 - (5300/T)$ and $\log P = 12.195 - (5384/T)$, respectively. The heats of sublimation were found to be 24.25±0.24 kcal./mole and 24.63±0.39 kcal./mole, respectively. The hydrogen bond (NH···O) energies were evaluated by subtracting from the observed heat of sublimation the contribution of the dispersion energy (by Slater-Kirkwood formula) and the contribution of the electrostatic interaction energy. The latter contribution was obtained by adopting the point dipole model with the dipole moment 3.9 D (for sulfamide) and by adopting the point charge model with the charges ±2.002 e.s.u. at C and O atoms diacetylhydrazine). The NH···O energies were 4.7 kcal. and 3.0 kcal., respectively. The electrostatic interaction in diacetylhydrazine is repulsive. Critical discussions are given on the significance of the hydrogen bond energy values obtained by various methods. The inter-relation between the lattice forces and the packing of molecules in the crystals is discussed on the basis of the calculation of separated contributions to the lattice energy and it is shown that the principal forces, acting between diacetylhydrazine molecules are the dispersion forces and the antiparallel arrangement of C=O dipoles in crystal is only a deceptive appearance. It is suggested that the nearest approaches in the linear systems OH···O and FH···F are 2.76 Å and 2.55 Å, respectively, unless very strong conjugation with the molecular network occurs. The NH stretching modes of vibration in sulfamide absorb at 3338 and 3248 cm^{-1}.

The authors wish to express their sincere thanks to Professor I. Nitta for his interest and encouragement during the present series of works. The cost of the research was partly defrayed by the financial support of the Ministry of Education to which their thanks are also due.

Department of Chemistry
Faculty of Science
Osaka University
Kita-ku, Osaka

Studies on the Graphitization II. Sub-structure and Crystallite Growth of Carbon Black

By Haruo KURODA and Hideo AKAMATU

(Received August 29, 1958)

The Graphitization is a process of crystallite growth and continuous improvement of the crystal structure of carbon to graphite with heat-treatment. The most powerful method of investigation is the X-ray diffraction by which not only the crystallite growth but also the ordering of crystal structure can be well defined[1].

In the previous paper[2], we have examined the graphitization of several kinds of carbon and found that petroleum-coke as well as coal-tar-coke are well graphitized, but carbon blacks are less graphitized with heat-treatment even in the same conditions. With heat-treatment up to 3000°C, the crystallites grow up to 444Å (L_a) for petroleum-coke and their lattice layers are stacked in graphitic orientation, while for Kosmos Carbon Black, for example, the crystallites grow to only

1) R. E. Franklin, *Acta Cryst.*, **3**, 107 (1950); **4**, 253 (1951); *Proc. Roy. Soc.*, **A209**, 196 (1951).
C. R. Houska and B. E. Warren, *J. Appl. Phys.*, **25**, 1503 (1954).
B. E. Warren, "Proceeding of lst. and 2nd. Conference on Carbon", University of Buffalo, p. 49 (1956).

2) H. Akamatu, H. Inokuchi, H. Takahashi and Y. Matsunaga, This Bulletin, **29**, 574 (1956).

129Å and about 89 per cent of their layers still remains in disordered stacking. The strongest characteristic for carbon blacks is the fact that the crystallite growth does stop. L_a as well as L_c attain to a limited size respectively at about 2500°C, and these values depend on the original particle size of raw carbon blacks. It is widely known that the maximum value of layer diameter, L_a, is about one-third of the original particle size.

The results with both these cases of soft-cokes and carbon blacks, with violanthrone-coke and polyvinyl chloride-coke, show that there is a wide variety in graphitizability, and this should be attributed to the difference in micro-structures or sub-structures of these original cokes or carbons. In this paper, the sub-structures of carbon blacks and their change with heat-treatment will be discussed, from the results of investigation by means of X-ray small-angle scattering and electron microscopy. The sub-structures of soft-cokes will be discussed in the following paper.

Materials and Heat-Treatment.—Three kinds of commercial carbon black were used in the present investigation; Kosmos-15A (LFT, United Carbon Co.), Tokyo Gas Carbon (Tokyo Gas Co.) and Thermax (MT. Thermatomic Co.). The average particle size of Kosmos-15A is 400Å, that of Tokyo Gas Carbon 350Å, and that of Thermax 3000Å. The heat-treatment has been made in vacuo at several temperatures from 1000 to 3000°C. The data for crystallite size, by X-ray diffraction method, are summerized in Table I.

TABLE I
GROWTH OF CRYSTALLITE DIMENSION WITH HEAT-TREATMENT

	Temperature of H.T. (°C)	L_a(Å)	L_c(Å)
Kosmos-15A	original	33.6	15.9
	1570	50.4	19.1
	1750	56.3	27.8
	1960	68.8	34.0
	2500	124	44.6
	3000	129	44.7
Tokyo Gas	original	30.6	13.3
	1350	38.0	15.9
	1750	51.3	24.0
	2040	77.5	32.3
	2500	113	36.6
	3000	118	39.4
Thermax	original	38.5	17.0
	1500	47.5	20.2
	1900	78	73
	2500	326	152
	3000	320	177

The crystallite sizes are similar to one another in these original carbon blacks. This is the case even after being heat-treated below 2000°C. However, after being heated over 2000°C, where generally crystallite growth proceeds rapidly, the crystallite size of Thermax becomes much greater than that of the other blacks. The diffractometer records show that, for Kosmos and Tokyo Gas Carbon, (10) and (11)-diffraction still maintain the wedge-like profiles characteristic of the random orientation of layers even after heated to 3000°C, while for Thermax a remarkable modulation of the diffraction profile can be observed after being heated to 3000°C, and the ordering parameter shows that 50 per cent of layers are in the graphitic orientation.

X-Ray Small-Angle Scattering.—*Experimental.*—A X-ray small-angle scattering camera is designed[3] which consists of collimation system, specimen holder and camera body. The collimation system is made of metal tube with two apertures separated by 500 mm.. Several sizes of aperture are prepared; the smallest one is 0.09 mm. in width and 0.1 mm. in length. Each aperture is fixed on a holder which can be fitted to the collimator tube and is easily exchangeable with others without a rearrangement of setting. Thus we can use a selected pair of apertures. The specimen is packed into a circular cavity of 10 mm. diameter in a flat metal plate of 0.5 mm. thickness, and placed immediately behind the second aperture. The camera body is made of a metal tube with a film cassette at one end. The distance from specimen to film is 549 mm.. A beam stopper is placed in front of the film, the thickness of which is controlled so that the image of the direct beam can be registered faintly on the film. The apparatus is evacuated except for the specimen. Cu-K_α radiation filtered with a nickel foil is used.

About twenty diagrams are usually registered for each specimen, with various exposure times from 5 minutes to 20 hours and with different aperture sizes. Of a microphotometer trace, only a restricted range of the photographic density is used for an intensity curve, so that a linear relation can be assumed between the incident energy of X-rays and the corresponding photographic density. A series of intensity curves for each specimen are combined by graphical matching to a complete scattering angle.

Results. — The results for the heat-treated samples of Kosmos and Tokyo Gas Carbon are shown in Fig. 1 and Fig. 2, where the scattering intensity in logarithmic scale is plotted against the scattering angle.

The geometrical condition of our camera, using filtered X-rays, is not applicable to the correct investigation of a very small angle part. We omitted Thermax, since its particle size is too large and the

3) H. Kuroda, *J. Chem. Soc. Japan Pure Chem. Sec.* (*Nippon Kagaku Zasshi*), **77**, 1298 (1956).

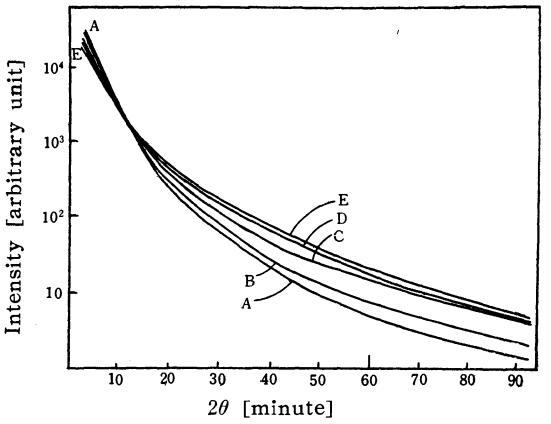


Fig. 1. Intensity curves of small-angle scattering by heat-treated Kosmos-15A Carbon Black.
(A) original, (B) 1325°C, (C) 1570°C, (D) 1950°C, (E) 2500°C.

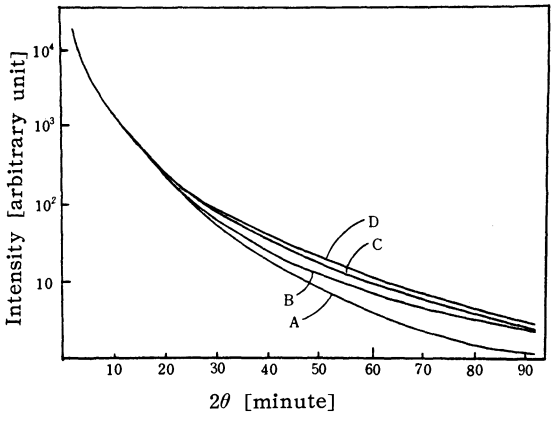


Fig. 2. Intensity curves of small-angle scattering by heat-treated Tokyo Gas Carbon Black.
(A) original, (B) 1350°C, (C) 2100°C, (D) 3000°C.

important part of scattering is presumed to be in such a very small angle part.

It can be seen in Fig. 1 and Fig. 2 that the intensity increases in higher angle part as the heat treatment temperature is higher, while in the lower angle part no remarkable change or slight decrease in intensity is observed. It can be assumed qualitatively that the scattering at a higher angle is due to smaller particles or heterogeneity of smaller dimension, and at lower angle due to larger particles or heterogeneity of larger dimension.

The X-ray small-angle scattering by raw carbon blacks has been discussed in a previous paper[4], where it has been reasonablly interpreted by Porod's theory[5]. According to this theory, a parameter called the distance of heterogeneity, l_c, can be known from the observed intensity curve by means of the following integration,

$$l_c = \pi \int_0^\infty h \cdot I(h) \cdot \mathrm{d}h \Big/ \int_0^\infty h^2 \cdot I(h) \cdot \mathrm{d}h$$

where $h = 4\pi \sin\theta/\lambda$ at scattering angle of 2θ, with X-ray wave length λ, and $I(h)$ is the intensity at h. There is the following relation between the distance of heterogeneity and the average diameter of particle,

$$D = \frac{4}{3} l_c$$

when the system consists of spherical particles and the inter-particle interference is absent.

It has been revealed that in the case of raw carbon blacks, the average diameter of particles estimated from the above relation is in good agreement with the particle size observed by electron microscope. This is the case also for untreated samples of Kosmos and Tokyo Gas Carbon. Therefore, in raw carbon blacks, the structural unit which is responsible for the greater part of the observed scattering is an individual carbon black particle which is observed directly by electron microscope. In consequence, one can assume that each particle is made of homogeneous material density. This is true, however, in the first approximation. According to the theory, the scattering intensity is expected to be proportional to h^{-4} in the higher angle region, when a system consists of particles of homogeneous density. In the case of raw carbon blacks, the region in which $h^4 I(h)$ is nearly constant is observed as seen on curve a in Fig. 3. However, this is realized only in a limited region below a certain scattering angle, and beyond this angle the intensity deviates from the prediction of the theory. This deviation in the higher angle region is presumablly due to the heterogeneity of electron density in a particle.

The change in the parameter l_c with heat-treated temperature is illustrated in Table II. The value of this parameter decreases as heat treated temperature increases. However, the geometrical significance of this parameter is not so simply

4) H. Kuroda, *J. Colloid Sci.*, **12**, 496 (1957).

5) G. Porod, *Kolloid-Z.*, **124**, 83 (1951); **125**, 51 (1952).

TABLE II
CHANGE IN DISTANCE OF HETEROGENEITY WITH HEAT-TREATMENT.

	Temperature of H.T. (°C)	l_c (Å)
Kosmos-15A	original	289
	1325	281
	1570	243
	1950	230
	2500	215
Tokyo Gas	original	261
	1350	232
	2100	216
	3000	208

interpreted as in the case of raw carbon blacks. The decrease in the size parameter can not be attributed to the shrinkage of carbon black particles, since their shape and size do not change appreciably, by electron microscope, below 2000°C, and so also the density even after being heated up to 3000°C.

In Fig. 3 the plot of $h^4I(h)$ versus h is shown. Although a horizontal part is realized for the untreated sample, the deviation from the constancy of $h^4I(h)$ becomes more and more serious as heat treated temperature is higher. This is presumablly due to the advancement of heterogeneity in a particle. Thus, after being heated, the structure unit responsible for the observed scattering is not the individual particle, but the sub-structures which developed in the particle; the substructure made of crystallites which grow in the particle.

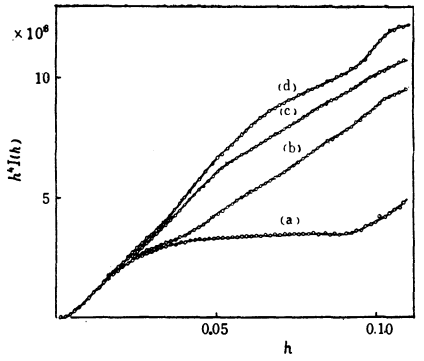


Fig. 3. Plot of $h^4I(h)$ versus h. Tokyo Gas Carbon Black.
(a) original, (b) 1325°C, (c) 2100°C, (d) 3000°C.

The distance of heterogeneity decreases as heat trated temperature is higher, while the crystallite size increases. Thus, at an extreme both these dimensions might approach each other. Neverthless, in reality they do not coincide with each other, since strong interference is likely to be present between crystallites.

In Fig. 4, $\log I(h)$ is plotted against $\log h$. On this curve, the inclination of the curve is illustrated, the value of which is around 2 or 3. This value indicates that the intensity of scattering by heated sample to above 2500°C is nearly proportional to the inverse of the second power of the scattering angle. It can be expected, when a system consists of plate-like particles, that the intensity will be proportional to the inverse of the second power of the scattering angle in a wide

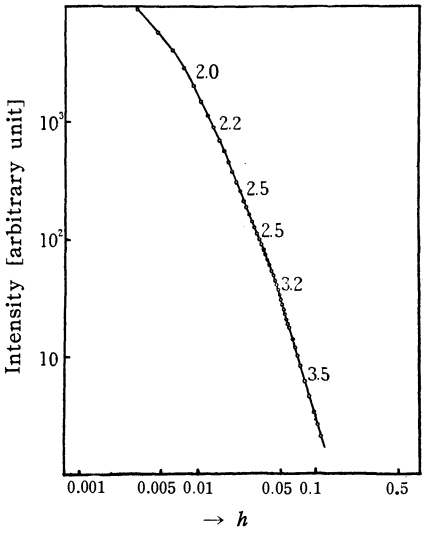


Fig. 4. $\log I(h)$ vs. $\log h$. Kosmos-15A heat-treated to 2500°C.

range[6]. One can conclude that the most part of the observed scattering for a heated sample above 2500°C is caused by crystallites which have a plate-like shape.

The results from X-ray small-angle scattering leads to the following conclusion. A particle of raw carbon black is made of nearly homogeneous density. With heat-treatment, sub-structures develop to plate-like crystallites; at an extreme, however, the carbon black particle does not grow to a large crystalline unit but splits into smaller crystalline units. These small crystallites are quite independent of each other, as each of them can be the center of scattering, but they are still in aggregation so tightly that interference between them is sure to be strong.

6) A. Guinier and G. Fournet, "Small-Angle Scattering of X-Rays" John Wiley, Chapt. 2, New York (1955).

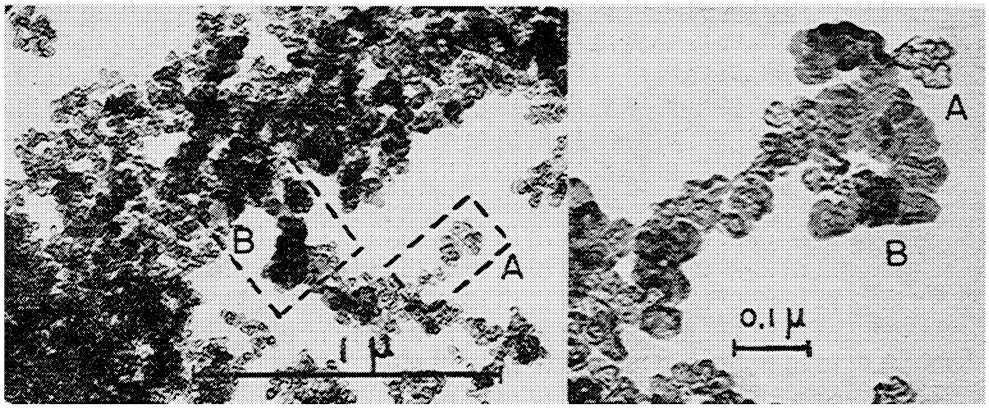


Fig. 5. Electron Micrograph of Tokyo Gas Carbon Black, heated to 3000°C. (Unshadowed).

Electron Microscopic Observation.— *Experimental.* — Electron micrographs were made with Hitachi Electron Microscope, Model-10-A. Special precautions are required to observe the details of structure, with high resolution as well as contrast, of such a minute particle as carbon black. Recently, Sakata[7] in our laboratory has developed a technique of making a collodion grid, whose pore size is one micron or less. This is called micro-grid. One can spread over a micro-grid a very thin collodion film, less than 50A in thickness. The specimen is mounted on this thin film. Thus, the undesirable effects from mounting the film is avoidable to a great extent. Experimental procedures were conducted so as to reduce the effects of contamination[8] to the minimum.

Results.—The electron micrographs show that the appearance of particles does not change appreciably when the heat treated temperature is lower than 2000°C ; particles keep their spherical shape, the average size being similar to those of untreated carbon black. Only a slight change of contrast is seen in the inner part of images of particles. However, after being heated up to 2500°C, the particles suddenly show a completely different appearance. This will be seen in Fig. 5. In these figures, one can see two modes of particle shape. Some particles have very irregular contours and are transparent to an electron beam. These are shown in the region lettered A. Other particles have rather round outlines and are less transparent to an electron beam. These can be seen in the region lettered B. The particles of mode-A have plate-like shape with sharp edges. The particle size is nearly 100 A, which is comparable to the crystallite size determined from X-ray diffraction pattern. Each of these minute particles might be a crystallite. The particles of mode-B show a heterogeneity of density ; the inner part is more transparent than the peripheral part, which suggests a hollow structure of particle. They consist of minute grains whose size is also comparable to the crystallite size. These facts indicate that a particle of mode-B is a shell-like cluster of crystallites, with a loose packing in the inner part. Such a structure is presumably not different from the structure of heat-treated Thermax. It can be easily presumed that particles of mode-A are produced by disintegration from particles of mode-B.

Thermax is most advantageous for electron microscopic observation, for the particle size is very large. The electron micrographs of heat-treated Thermax have been presented by Ragoss, Hoffman and Holst[9], and by Kmetko[10]. Kmetko has given a polyhedron model of graphitized carbon black particles, based on electron microscopic observation by replica technique. In the present investigation, we used a high accelerating potential, 10 kV, in operating the electron microscope. This gives a clear internal structure of particles. Some typical micrographs are illustrated in Fig. 6, 7 and 8.

Below 1500°C of heat treated temperature, no appreciable change can be seen. However, at this temperature, fine contrast is seen in the images. This fine contrast develops to dark radiated strips along the periphery of particle as heat treated temperature is higher. Finally, above 2500°C, the dark strips grow up to trigonal or trapezoidal dark patterns. The

7) S. Sakata, *J. Electronmicroscopy*, **6**, 75 (1958).
8) J. H. L. Watson, *J. Appl. Phys.*, **18**, 153 (1947).
9) A. Ragoss, U. Hoffman and R. Holst, *Kollod-Z.*, **105**, 118 (1943).
10) E. A. Kmetko, "Proceeding of lst. and 2nd. Conference on Carbon," University of Buffalo, 21 (1956).

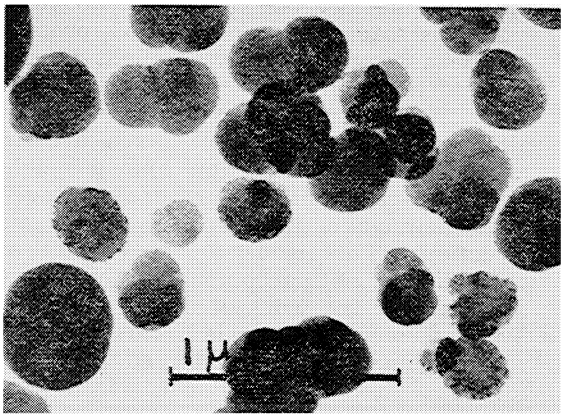


Fig. 6. Thermax heated at 1540°C.

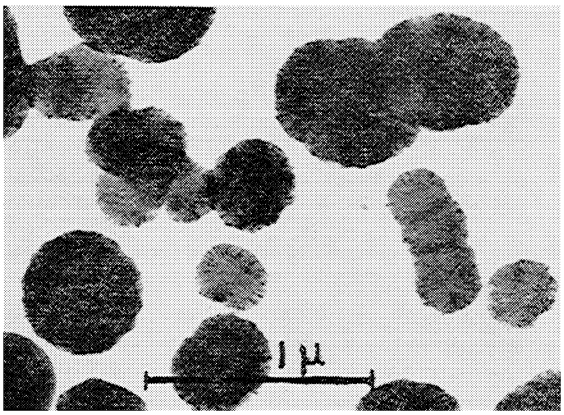
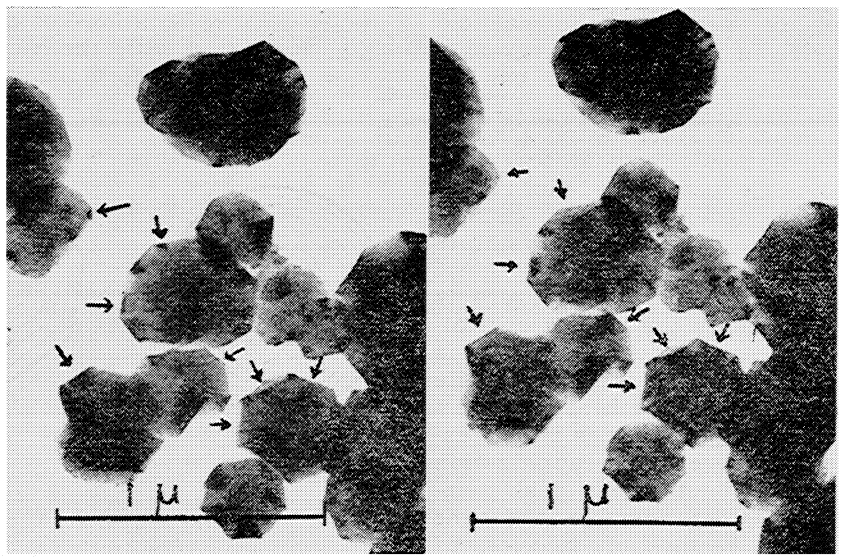


Fig. 7. Thermax heated at 1900°C.

bases of trigons or trapezoids coincide with the edges of the polygonal outlines of the particles. These dark patterns are not due to the difference in thickness of material, but are produced by the diffraction effect. This is illustrated in two micrographs (a) and (b) of Fig. 8. Both the micrographs were made from the same field, but made with different inclination to incident beam by 12°. The dark patterns in each particle change the shape, or disappear, depending sensitively on the direction of incident beam. This is indicated by arrows. It can be easily presumed that these dark patterns are due to (002)-diffractions by the graphite-like crystals. This leads to the conclusion that crystallites are orientated with their c-axes being in the direction normal to the particle surface. The length of edges of the polygonal outlines is in the order of 1000Å, which is only a few times that of L_a-dimension determined by X-ray diffraction. Therefore, the area corresponding to each dark pattern might be a single crystal or a cluster made of a few crystallites with a common direction of their c-axes.

Discussion

Carbon black is deposited from a gas phase in the process of incomplete combustion or thermal decomposition of hydrocarbon gas or vapor. The resulting solid



(a) (b)

Fig. 8. Thermax heated at 3000°C.
(a) and (b) were made from the same field with different directon to incident beam by 12°. The dark patterns in each images are slightly different in (a) and (b).

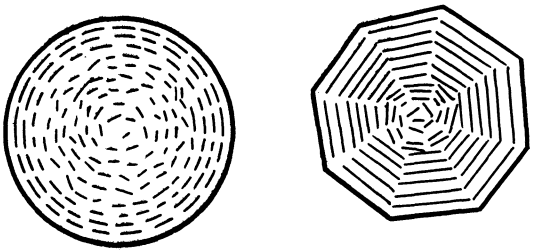
particles consist mainly of turbostratic carbon crystallites. However, the spheroidal shape suggests that the particles are in a fluid-state when they are produced at a higher temperature. The X-ray small-angle scattering by raw carbon black indicates that the material density is nearly homogeneous in the particle. The minute turbostratic crystallites may be imbedded among heavy hydrocarbon molecules or cross-linkages of disorganized carbon atoms. However, alignment of minute crystallites would not be at random, but may be in a preferential orientation. As this is due to the effective action of surface tension, which is responsible for the spheroidal shape, the preferential orientation should be most effectively conducted along the surface of the particle, with the basal planes of crystallites being tangent to the surface. Hall[11] found indications of such a preferential orientation at the surface of a raw carbon black. The schematic diagram of such a model is illustrated in Fig. 9, A.

In the process of heat-treatment, minute crystallites grow by the condensation process at the expense of the disorganized carbon atoms with liberating hydrogen. Meanwhile, the alignment of crystallites will be further improved. The crystallite growth proceeds mainly in such a way in an early stage of heat-treatment, presumablly below 1500°C. The rate of growth is not different between smaller particles and larger ones. No appreciable change can be seen in the particle shape nor size in electron micrographs, excepting a fine structure which can be seen in images of large particles of Thermax, which indicate rather clearly the preferential orientation of crystallites. The X-ray small-angle scattering can reveal the continuous development of heterogeneity which results from the crystallite growth.

When the heat treated temperature is over 2000°C, suddenly the rate of crystallite growth is greatly advanced. This is so, when the particle size is greater, while in small particles the growth attains very rapidly to a limited size. It is widely experienced that the degree of graphitization is primarily dependent on the peak temperature, but less dependent on the time of soaking. The remarkably accelerated rate of crystallite growth at the higher temperature demands an explanation other than the mechangism mentioned above.

At this stage, the condensation process has been completed, leaving slight defects or distortions between neighboring crystallites. As the crystallites are in such an alignment in that their c-axes are in nearly the same direction among neighbors, they can easily be further rearranged with their c-axes in completely the same direction. This leads to the growth of crystallites, not accompanied by mass transfer nor the work of breaking bonds. The intermediate state is a cluster. The rearrangement would be forced thermally to relax the stresses caused from the distortions.

At a temperature higher than 2000°C, a plastic deformation or creep is known for carbons, therefore, the thermal relaxation would be advanced only at a higher temperature. Mrozowski[12] proposed a driving force of the crystallite growth, which is the anisotropic expansion of crystallites along c-axes. This leads to the creation of local stresses which lead to and become relieved by the growth and rearrangement of crystallites. This process, however, would be practically effective if the crystallites are in alignment in such a manner as mentioned above. The crystallite growth would be accelerated along the surface of the particle in preference to the inner part, as the alignment would be found primarily along the surface. This is what we observed. Thus, the polyhedral particle will result from the preferential orientation of crystallites, which developed with their c-axes being in the direction of normal to the surface. The schematic diagram is given in Fig. 9, B.



A B

Fig. 9. Schematic diagram of alignment of crystallites in a carbon black particle. (A) before heat-treatment, (B) after heat-treatment.

11) C. E. Hall, *J. Appl. Phys.*, **19**, 271 (1948).

12) S. Mrozowski, "Proceeding of 1st. and 2nd. Conferences on Carbon", University of Buffalo, 31 (1956).

As the crystallite growth proceeds in this way, however, the mutual relation between the neighbors becomes different from the alignment mentioned above. This is easily seen when one compares the diagram (A) with (B). Moreover, great stresses would be stored up between crystallites, especially when the anisotropic expansion of crystallites are made at a higher temperature. We observed, for Tokyo Gas Carbon heated to 3000°C, a remarkably asymmetrical profile of (002)-diffraction, which suggests the presence of a large distorsion in lattice.

In this stage, the scheme proposed by Mrozowski must be modified, but becomes rather more important. When the stresses become too great, they are not likely to be relieved practically and the rearrangements of crystallites are not likely to be realized. There is no place for the energy dissipation within the particle, and this is the characteristic for carbon blacks which differ from soft-cokes. This would be so, as the size or the mass of a particle is smaller. Thus, the limited size of crystallite growth would be proportional to the original particle size. The result which would be expected from the further heattreatment is disintegration or rather bursting into individual crystallites, as this is the only way to relieve the stored stresses. This is the case we observed in the case of the small particles of Kosmos-15A and Tokyo Gas Carbon Black.

As the crystallites grow by the mechanism discussed, the turbostratic structures still remain unimproved. It is believed that the crystallite growth proceeds in advance of ordering of crystal structure. The crystal structure will be improved by the rearrangement of layers as pairs of the nearest neighboring layers take on graphitic orientation. The mechanism would not be far from that discussed above. However, this process begins when the layer diameter, L_a reaches a value of about 150Å. For small particies, the growth of crystallites stops for the reason discussed above, even when less than 150Å. In consequence, the crystal structure can not be improved. This is the reason why one can not make graphitization of carbon blacks with small particle size. A similar argument can be extended to hard carbons. The graphitization is primarily dependent on the sub-structures of raw materials.

Summary

The sub-structures of carbon black and its change with heat-treatment have been investigated by means of X-ray small-angle scattering and electron microscopy.

With heat-treatment, the X-ray small-angle scattering intensity increases in the higher angle region, indicating the development of heterogeneous sub-structures to minute crystallites. Above 2000°C, the crystallite growth is rapidly accelerated, and at an extreme, a carbon black particle disintegrated to smaller crystalline units. Electron microscopic observations, especially for Thermax which has a large particle size, revealed that the crystallites are in alignment with their c-axes being in the direction of normal to the particle surface. This alignment leads to the polyhedral shape of the heat-treated particles. From these observations, the sub-structures and the mechanism of crystallite growth in carbon black particles have been discussed.

This investigation is a part of the research project for carbons, which is supported by Committee 117 in Nippon Gakujutsu Shinkokai, and the expense has been defrayed in part from a grant given by the Ministry of Education, for which the authors' thanks are due.

Department of Chemistry
Faculty of Science
University of Tokyo
Hongo, Tokyo

Polarographic Studies of Metallic Complexes. IV.[1] *Bisethylenediamine Series of Cobalt(III) Complexes*[2]

By Nobufumi MAKI, Yoichi SHIMURA and Ryutaro TSUCHIDA

(Received August 13, 1958)

There have been reported, heretofore, some polarographic studies on the ethylenediaminecobalt(III) complexes[3-10]. Holtzclaw et al.[3-5] studied several kinds of *cis*- and *trans*-bisethylenediaminecobalt (III) complex and found that the *trans*-isomer having two negative ligands in its coordination sphere exhibits a little more negative half-wave potential than the corresponding *cis*-isomer. This fact was explained as being due to the stabilization of the complex compound by the trans effect of the two negative ligands. On the other hand the *trans*-isomer containing one or two neutral ligands in its coordination sphere showed almost the same half-wave potential as the corresponding *cis*-isomer.

As regards the reduction wave of tris-ethylenediaminecobalt(III) ion, Kivalo[8] and Laitinen et al.[7] obtained the following results. The ion, $[Co\ en_3]^{3+}$, is reduced reversibly to $[Co\ en_3]^{2+}$ ion in the presence of an excess of 0.1~0.5 F ethylenediamine. ($E_{1/2} = -0.456$ V. vs. S.C.E) However, in the absence of an excess of ethylenediamine the irreversible wave of $[Co\ en_3]^{3+}$ was given. This fact was considered to be due to the following reason. The apparent irreversibility of the reduction is due to the aquation of the reduction product, or to the decrease in the coordination number of cobalt(II) complex ion, though the electron transfer reaction for $[Co\ en_3]^{3+} + e^- \rightarrow [Co\ en_3]^{2+}$ is fast enough to be reversible. While the reversible electrode reaction in the presence of excessive ethylenediamine was explained as being due to the existence of the stable ion, $[Co\ en_3]^{2+}$, which is in equilibrium with an excess of ethylenediamine, being different from the reduction product of hexamminecobalt(III) ion. The latter ion gave an irreversible wave, even if an excess of ammonia was present in solution.

However, Doležal[9] obtained a somewhat different result recently. Namely, his polarographic and oscillopolarographic studies showed that the redox system, $[Co\ en_3]^{3+}/[Co\ en_3]^{2+}$, is not perfectly reversible. It was found that the difference of the half-wave potentials between the anodic and the cathodic wave was 30 mV. under equal conditions. The dependence of the cathodic wave on the pH value of the solution and on the concentration of ethylenediamine and of gelatin was also different from that of the anodic wave. The anodic wave approaches reversibility more perfectly than the cathodic wave.

In the previous work of this series[1] the present authors determined the order of the polarographic stability for the cobalt (III) complexes of pentammine series, $[Co(NH_3)_5X]$. For the same purpose, a comparison of the half-wave potentials of the first waves has been carried out for the cobalt(III) complexes of bis-ethylenediamine series, $[Co\ en_2X_2]$ or $[Co\ en_2Y]$. The polarographic behavior of these complexes has also been dealt with in the present paper.

Experimental

Apparatus.—A Yanagimoto model 104 polarograph with the sensitivity of galvanometer of $2\times10^{-9}\mu$A/mm./m. was used. For the accurate evaluation of curves and half-wave potentials the method described previously was used[10]. As an electrolysis cell an H-type vessel with a saturated calomel electrode was employed. The capillary used had a rate of flow of mercury, 0.615 mg./sec. and a drop time of 7.42~6.98 sec./drop in the solution of 0.5 F potassium sulfate and of 0.1 F potassium chloride at an open circuit with a mercury head of 65.5 cm.. The capillary was

1) Part III of this series; N. Maki, Y. Shimura and R. Tsuchida, This Bulletin, **32**, 23 (1959).
2) Presented in part at the Eleventh Annual Meeting of the Chemical Society of Japan, Tokyo, April 6, 1958.
3) H. F. Holtzclaw, Jr., *J. Am. Chem. Soc.*, **73**, 1821 (1951).
4) H. F. Holtzclaw, Jr. and D. P. Sheetz, ibid., **75**, 3053 (1953).
5) H. F. Holtzclaw, Jr., *J. Phys. Chem.*, **59**, 300 (1955).
6) J. B. Willis, J. A. Friend and D. P. Mellor, *J. Am. Chem. Soc.*, **67**, 1680 (1945).
7) H. A. Laitinen and M. W. Grieb, ibid., **77**, 5201 (1955).
8) P. Kivalo, ibid., **77**, 2678 (1955).
9) J. Doležal, *Coll. Czech. Chem. Communs.*, **21**, 113 (1956).
10) N. Maki, Y. Shimura and R. Tsuchida, This Bulletin, **30**, 909 (1957).

connected to the mercury reservoir by a tube of polyvinylchloride. All the measurements were made at 25±0.1°C, the temperature being maintained by a water thermostat. The reversibility of the electrode reaction was examined by determining the slope of $\log i/(i_d-i)$ vs. potential. Slopes of the log plots indicated irreversible reaction throughout.

Material.—The complex compounds studied were prepared by the method described in literature[11-27,30]. (The references are given in Tables I, II and III.) Each solution for the electrolysis was made freshly from the dry crystalline cobalt(III) complexes before use and the polarographic measurements were made as soon as possible after the removal of oxygen. The concentration of the solution was 0.001 gram complex ion per liter.

In order to remove the dissolved oxygen, a vigorous stream of nitrogen which was purified from oxygen by means of an alkaline solution of pyrogallol, was passed through the cell solution for an hour prior to each electrolysis, preventing the evaporation.

In order to compare the half-wave potentials with each other, no maximum suppressor was used, because its presence at the concentration which is enough to suppress the maxima of the second waves of bisethylenediaminecobalt(III) complxes, causes lowering of the diffusion current, shift of the half-wave potential of the first wave towards negative direction, and sometimes deformation of the wave. The supporting electrolytes used are 0.5 F potassium sulfate and 0.1 F potassium chloride.

Results and Discussion

In Tables I and II are shown the half-wave potentials of the cobalt(III) complexes of bisethylenediamine series.

All the compounds are reduced irreversibly in two steps at the dropping mercury electrode in the solution of 0.1 F potassium chloride or 0.5 F potassium sulfate except the case of the complexes which aquate easily in solution. The complex ions such as $[Co\ en_2S_2O_3]^+$, $[Co\ en_2gly]^{2+}$*, $[Co\ en_2leuc]^{2+}$* show two waves in 0.5 F potassium sulfate at the potential corresponding to the reduction of cobalt(III) → cobalt(II). The height of the second wave was very close to twice that of the first wave in the presence of Tween-80**, a maximum suppressor. The height of the first wave was proportional to the concentration of the complex ion in the range of the concentration $1\times10^{-2}\sim5\times10^{-4}$ F. In the case of the mixed solution of a complex ion and its aquated species, the total height of the waves of the original ion and of the aquated species was roughly proportional to the original concentration of the cobalt(III) complex. Hence, the first wave, corresponding to a gain of one electron, represents the reduction of cobalt(III) to cobalt(II) and the second, corresponding to two electrons, represents the reduction of cobalt(II) to metallic state.

In the solution of a non-complexing supporting electrolyte such as potassium chloride or potassium sulfate, the reduction processes of bisethylenediaminecobalt(III) complexes are considered to be in the following:

$$[Co\ en_2X_2]^{(3-2n)+}+e^-\rightarrow[Co\ en_2X_2]^{(2-2n)+}$$

$$[Co\ en_2X_2]^{(2-2n)+}+mH_2O\rightarrow\begin{cases}[Co\ en_2(OH_2)_2]^{2+}+2X^{n-}\\ [Co\ en_2(OH_2)X]^{(2-n)+}+X^{n-}\\ [Co\ en(OH_2)_4]^{2+}+2X^{n-}+en\\ \text{etc., etc.}\end{cases}$$

$$[Co\ en_2(OH_2)_2]^{2+}+2e^-\rightarrow Co+2H_2O+2en$$

$$[Co\ en_2(OH_2)X]^{(2-n)+}+2e^-\rightarrow Co+H_2O+X^{n-}+2en$$

$$[Co\ en(OH_2)_4]^{2+}+2e^-\rightarrow Co+4H_2O+en\ \text{etc.}$$

From the scheme of the reduction processes, it may be seen that the first step in the polarographic reduction of these cobalt(III) complexes corresponds to the disruption of the cobalt(III) complexes, resulting in the formation of aquo-ethylenediaminecobalt(II) ions such as $[Co\ en_2(OH_2)_2]^{2+}$, $[Co\ en_2(OH_2)X]^{(2-n)+}$ and $[Co\ en(OH_2)_4]^{2+}$, so its half-wave potential may be regarded as a measure of the stability toward polarographic reduction.

* The following abbreviations are used; gly, $NH_2CH_2COO^-$; leuc, $NH_2CH(COO^-)CH_2CH(CH_3)_2$; ox, $(COO^-)_2$.

** Polyoxyethylene sorbitan mono-oleate (Atlas Powder Co. in U. S. A.).

11) P. Rây and B. Sarma, *J. Indian Chem. Soc.*, **28**, 59 (1951).
12) A. Werner and K. R. Lange, *Ann.*, **386**, 88 (1912).
13) A. Werner, ibid., **386**, 1 (1912).
14) Y. Shimura and R. Tsuchida, This Bulletin, **29**, 311 (1956).
15) A. Werner and E. Humphrey, *Ber.*, **34**, 1728 (1901).
16) A. Werner, ibid., **44**, 2453 (1911).
17) A. Werner, H. Müller, R. Klien and F. Bräunlich, *Z. anorg. Chem.*, **22**, 91 (1900).
18) W. C. Fernelius et al., "*Inorganic Synthesis*", vol 2, McGraw-Hill Co., New York (1946) p. 222.
19) S. M. Jörgensen, *J. prakt. Chem.*, **39**, 1 (1889).
20) A. Werner, *Ann.*, **386**, 1 (1912).
21) M. Linhard, *Z. Elektrochem.*, **50**, 224 (1944).
22) P. Pfeiffer and O. Angern, *Ber.*, **60**, 305 (1927).
23) A. Werner and M. Pokrowska, *Ann.*, **386**, 1 (1912).
24) J. C. Duff, *J. Chem. Soc.*, **1922**, 450.
25) J. Meisenheimer, L. Angerman and H. Holsten, *Ann.*, **438**, 261 (1924).
26) A. Werner and A. Vilmos, *Z. anorg. Chem.*, **21**, 145 (1899).
27) Y. Shimura, This Bulletin, **31**, 315 (1958).

TABLE I

HALF-WAVE POTENTIALS OF COBALT(III) COMPLEXES OF [Co en_2X_2] TYPE

Compound	Supporting electrolyte; 0.5 F K_2SO_4		Supporting electrolyte; 0.1 F KCl	
	$E_{1/2}$ of 1st wave [Co(III)→Co(II)]	$E_{1/2}$ of wave of aquated complexes [Co(III)→Co(II)]	$E_{1/2}$ of 1st wave [Co(III)→Co(II)]	$E_{1/2}$ of wave of aquated complexes [Co(III)→Co(II)]
[Co $en_2(CN)_2$]Cl[11]	−0.85	—	−0.80	−0.61
cis-[Co $en_2(OH_2)_2$] $(NO_3)_3$[12]	−0.50	—	−0.42	—
trans-[Co $en_2(NH_3)_2$] $Cl_3 \cdot H_2O$[13]	−0.45	—	−0.31	—
cis-[Co $en_2(NH_3)_2$] $(ClO_4)_3$[14]	−0.45	—	−0.31	—
trans-[Co $en_2(NO_2)_2$]Cl[15]	−0.26	−0.5	−0.27***	−0.40***
cis-[Co $en_2(NO_2)_2$] ClO_4[16]	−0.25	−0.5	−0.24***	−0.41***
trans-[Co $en_2(NCS)_2$]Cl·H_2O[17]	+	−0.51**	+	*
cis-[Co $en_2(NCS)_2$]Cl·H_2O[17]	+	−0.51**	+	*
trans-[Co en_2Cl_2]Cl[18]	+	*	+	*
cis-[Co en_2Cl_2]Cl[19]	+	*	+	*
trans-[Co en_2Br_2]Br[20]	+	*	+	*
cis-[Co en_2Br_2]Br[20]	+	*	+	*

1) The concentration of the complex ion; 0.001 F.
2) The characteristics of capillary used; m=0.615 mg./sec., t=7.42～6.98 sec./drop.
3) Potential unit; V. vs. S. C. E.
4) Temp., 25°C.
* Maximum wave.
** The data obtained in the presence of 0.0016% Tween-80.
*** The data adopted from H. F. Holtzclaw, Jr. and D. P. Sheetz, *J. Am. Chem. Soc.*, **75**, 3053 (1953).

TABLE II

HALF-WAVE POTENTIALS OF COBALT(III) COMPLEXES OF [Co en_2Y] TYPE

Compound	Supporting electrolyte; 0.5 F K_2SO_4		0.1 F KCl	
	$E_{1/2}$ of 1st wave Co(III)→Co(II)	$E_{1/2}$ of wave of aquated complexes Co(III)→Co(II)	$E_{1/2}$ of 1st wave Co(III)→Co(II)	$E_{1/2}$ of wave of aquated complexes Co(III)→Co(II)
[Co en_3] $(ClO_4)_3$[21]	−0.51	—	−0.41	—
[Co en_2CO_3]Cl·H_2O[22]	-0.45_5	—	−0.40	—
[Co en_2SO_3]Cl·$3H_2O$[23]	−0.43	*	*	*
[Co $en_2S_2O_3$]Br·$3H_2O$[24]	—	-0.49_5	—	**
[Co en_2gly] $Cl_2 \cdot H_2O$[25]	−0.41	−0.5	−0.36	—
[Co en_2ox]Cl[26]	−0.31	−0.5	−0.32****	—
[Co en_2leuc] $(ClO_4)_2$[27]	-0.30_5	−0.5	-0.33_5***	—

1) The experimental conditions are the same as mentioned in Table I.
2) Potential unit; V. vs. S. C. E.
* The waves of the original complex ion and of the aquated species are so near located that both the waves cannot be discriminated one another. However, it was noticed that the half-wave potential shifted towards negative direction with the decreasing concentration due to the aquation of the complex ion.
** Maximum wave.
*** The data obtained in the presence of 0.0016% Tween-80.
**** The data obtained in the solution of 1 F $(NH_4)_2C_2O_4$.

The polarographic stability of the cobalt (III) complexes of [Co en_2X_2] type increases in the following order of the ligand X;

$Br^-, Cl^- < NCS^- < NO_2^- < NH_3 < OH_2 < CN^-$

(Supporting electrolyte; 0.5 F K_2SO_4)

The same order was also obtained in 0.1 F potassium chloride. For the complexes of [Co en_2X_2] type the difference of the half-wave potentials between *cis*- and *trans*-isomer is far smaller than that among the other kinds of the complex of this series, hence the difference between *cis*- and *trans*-isomer need not be taken

into consideration in this case.

The order of stability of [Co en_2Y] type complexes was in the following order of the ligands;

$leuc^- < ox^{2-} < gly^- < SO_3^{2-} < CO_3^{2-} < en$

(0.5 F K_2SO_4 or 0.1 F KCl as supporting electrolyte)

No relation between the above orders of the polarographic stability and that of the spectrochemical series[28] could be found in accordance with the result obtained in the previous paper[1].

Polarographic Behavior of Individual Complexes.—The second waves of all the bisethylenediaminecobalt(III) complexes indicated the maxima which could be suppressed by the maximum suppressor, Tween-80, except the case of dicyanobis-

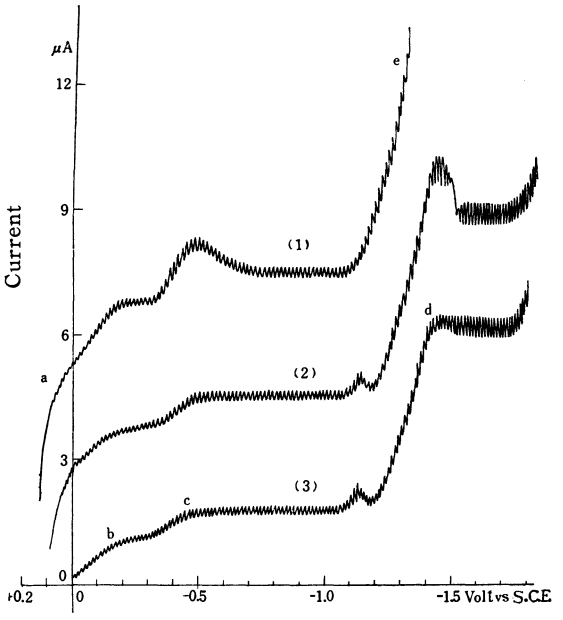


Fig. 1. The polarograms of *trans*-[Co $en_2(NCS)_2]Cl \cdot H_2O$ obtained at the concentration of 0.001 F in the solution of 0.1 F KCl.
1) In the absence of maximum suppressor
2) In the presence of 0.0016% Tween-80
3) In the presence of 0.0032% Tween-80
a Anodic wave
b The first wave of *trans*-$[Co\ en_2(NCS)_2]^+$
c The reduction wave of the aquated complexes
d The second wave of *trans*-$[Co\ en_2(NCS)_2]^+$
e Maximum wave
Sensitivity; 0.06 μA/mm., Damping; 200

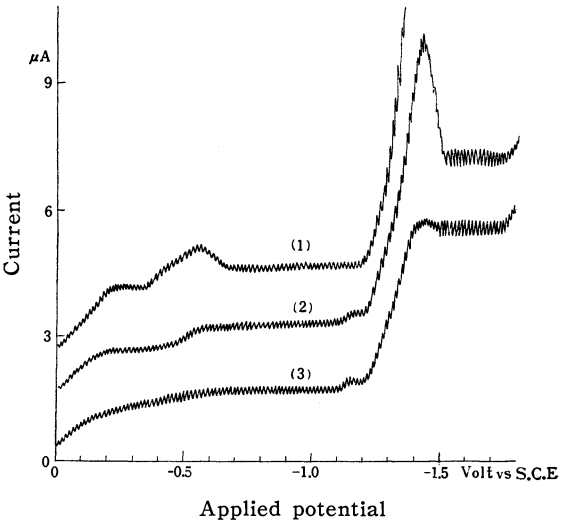


Fig. 2. The polarograms of *cis*-[Co $en_2(NCS)_2]Cl \cdot H_2O$ obtained at the concentration of 0.001 F in the solution of 0.5 F K_2SO_4.
1) In the absence of maximum suppressor
2) In the presence of 0.0016% Tween-80
3) In the presence of 0.0032% Tween-80
Sensitivity; 0.06 μA/mm., Damping; 200

ethylenediaminecobalt(III) ion, [Co $en_2(CN)_2]^+$. Trisethylenediaminecobalt(III) and monoethylenediamine-tetramminecobalt(III) ions have also the maxima in the second step of the reduction, which was reported briefly in an earlier communication[10]. Therefore, it can be said that all the cobalt(III) complexes containing one or more ethylenediamine in their coordination sphere show the maxima at the second wave corresponding to the reduction for Co(II)→Co(0).

Figs. 1 and 2 show the polarograms of *cis*- and *trans*-diisothiocyanato-bisethylenediaminecobalt(III) ions, $[Co\ en_2(NCS)_2]^+$, respectively. It is expected that these ions aquate to some extent in solution. In fact, for *trans*-$[Co\ en_2(NCS)_2]^+$ ion, the small maximum wave was given at around −0.4 V. (vs. S. C. E.), which could be suppressed in the presence of 0.0016% Tween-80. The half-wave potential of this small wave is near to that of diaquobisethylenediamine-cobalt(III) ion, $[Co\ en_2(OH_2)_2]^{3+}$. ($E_{1/2} = -0.44$ V. vs. S. C. E. in 0.1 F KCl) Therefore, this small wave is considered to correspond to the reduction wave of the aquated species such as $[Co\ en_2(NCS)OH_2]^{2+}$ and $[Co\ en_2(OH_2)_2]^{3+}$. Similarly, for *cis*-$[Co\ en_2(NCS)_2]^+$ ion, the small wave of the aquated cobalt(III) ions was given at around −0.51 V. (vs. S. C. E.)

28) Y. Shimura and R. Tsuchida, ibid., **29**, 311 (1956).

in a solution of 0.5 F potassium sulfate. The half-wave potential of $[Co\ en_2(OH_2)_2]^{3+}$ ion is −0.50 V. in 0.5 F potassium sulfate.

In a dilute supporting electrolyte, a similar wave of the aquated cobalt(III) complex ions was found for the following ions;

$[Co\ en_2Cl_2]^+$, $[Co\ en_2Br_2]^+$
$[Co\ en_2(NCS)_2]^+$, $[Co\ en_2ox]^+$
$[Co\ en_2gly]^{2+}$, $[Co\ en_2S_2O_3]^+$
$[Co\ en_2(CN)_2]^+$

Among these ions it was noticed that the height of the wave of the aquated species increases gradually with time for some complex ions, but does not for the others. This is considered to be due to the variety of the rate of the aquation. Namely, the aquation of some ions is comparatively slow, compared with the time of the polarographic measurement, while for the others, the aquation is so rapid that the usual polarographic method can not detect and trace the change of the height of the wave. The ions, $[Co\ en_2(CN)_2]^+$, $[Co\ en_2SO_3]^+$ belong to the former and the ions, $[Co\ en_2Cl_2]^+$, $[Co\ en_2Br_2]^+$ to the latter.

In a solution of 0.1 F potassium chloride dicyano-bisethylenediaminecobalt(III) ion,

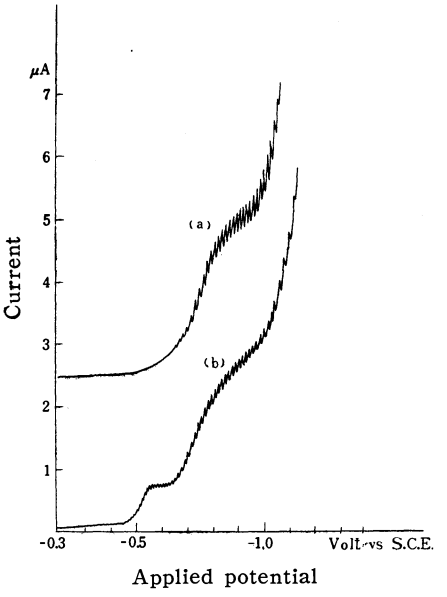


Fig. 3. The polarograms of $[Co\ en_2(CN)_2]Cl$ obtained at the concentration of 0.001 F.
a) In the solution of 0.5 F K_2SO_4
b) In the solution of 0.1 F KCl
Sensitivity; 0.04 μA/mm., Damping; 100

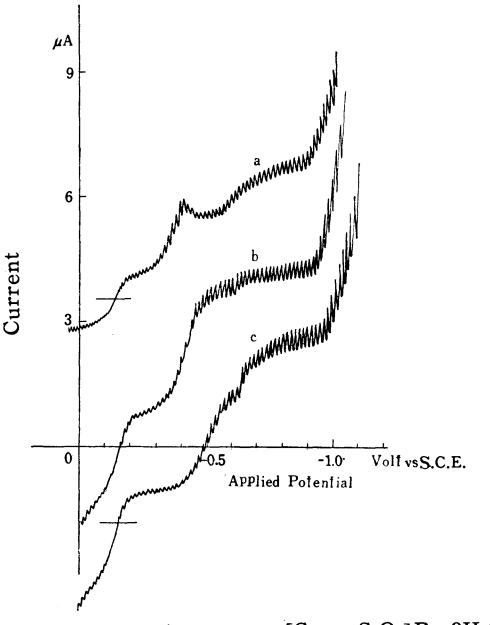


Fig. 4. The polarograms $[Co\ en_2S_2O_3]Br \cdot 3H_2O$.
a) obtained at the concentration of 0.001 F complex ion in the solution of 0.1 F KCl
b) obtained at the concentration of 0.005 F complex ion in the solution of 0.1 F KCl
c) obtained at the concentration of 0.005 F complex ion in the solution of 0.5 F K_2SO_4
Sensitivity; 0.06 μA/mm., Damping; 200

$[Co\ en_2(CN)_2]^+$ showed the wave of the aquated complexes at around −0.80 V., but did not show anything in 0.5 F potassium sulfate. It seemed that the wave of the aquated species was probably covered by the wave of the original ion in the solution of potassium sulfate, because the waves of the original and the aquated ions were located very near to each other. The reduction potential of the aquated ions of $[Co\ en_2(CN)_2]^+$ did not coincide with that of $[Co\ en_2(OH_2)_2]^{3+}$ ion, so it is considered that the main species of the aquated ions is a partly aquated complex ion, $[Co\ en_2(CN)OH_2]^{2+}$. (Fig. 3)

In 0.1 F potassium chloride, thiosulfato-bisethylenediaminecobalt(III) ion, $[Co\ en_2S_2O_3]^+$ has the small maximum wave which could be suppressed in the presence of 0.0016% Tween-80. (Fig. 4) The half-wave potential of the first wave of this ion could not be determined owing to the interference of the anodic wave of the thiosulfate ion liberated from the original complex by the aquation.

Fig. 5 shows the polarogram of the first wave of *cis*-diaquo-bisethylenediaminecobalt(III) ion, $[Co\ en_2(OH_2)_2]^{3+}$ in 0.5 F potassium sulfate. The wave has always

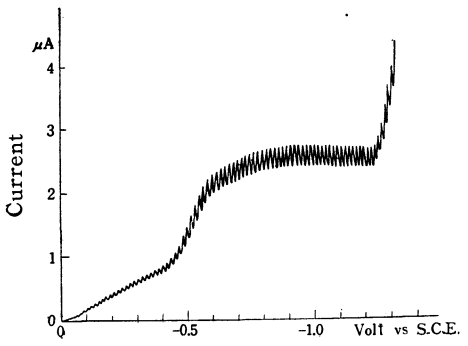


Fig. 5. The polarogram of *cis*-[Co $en_2(OH_2)_2]^{3+}$ obtained in the solution of 0.5 F K_2SO_4 at the concentration of 0.001 F complex ion.
Sensitivity; 0.04 μA/mm., Damping; 200

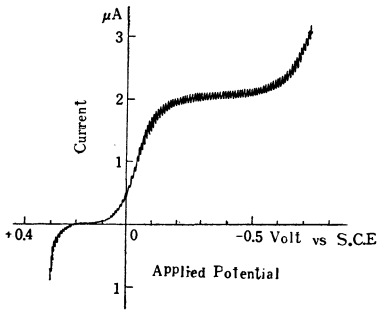


Fig. 6. The polarogram of *cis*-[Co $en_2(OH_2)_2]^{3+}$ obtained in 1 F $HClO_4$ at the concentration of 0.001 F complex ion.
Sensitivity; 0.04 μA/mm., Damping; 200
$E_{1/2}=-0.01$ V. (vs. S. C. E.)
$i_d=2.09$ μA.

a slower slope at the half-wave potential than that of the other complex ions of bisethylenediamine series. A gradually rising current near the zero potential was observed. However, it can not necessarily be said that this current is a residual current, since the diffussion current reaches a plateau parallel to the axis of the potential. (Usually, the diffusion current, runs parallel to the residual current, not to the axis of the potential.) Moreover in 1 F perchloric acid, a well-defined wave is obtained, which has a steep slope at the half-wave potential. (Fig. 6) One of the reasons for this is the presence of an equilibrium between the aquo-bisethylenediaminecobalt(III) ion and hydroxo-bisethylenediaminecobalt(III) ion.

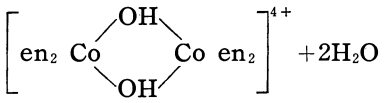
$$[Co\ en_2(OH_2)_2]^{3+} \rightleftarrows [Co\ en_2(OH_2)OH]^{2+} + H^+$$

$$[Co\ en_2(OH_2)OH]^{2+} \rightleftarrows [Co\ en_2(OH)_2]^{+} + H^+$$

In perchloric acid the above equilibrium is markedly shifted to the left hand. Consequently, the steep wave of diaquo-bisethylenediaminecobalt(III) ion could be obtained.

Another reason for this is the polymerization of diaquo-bisethylenediaminecobalt (III) ion in neutral solution. Namely, as verified by the spectrochemical studies of Rasmussen et al.[29], various kinds of polynuclear cobalt(III) complex are formed in solution. For instance,

2 *cis*-$[Co\ en_2(OH_2)OH]^{2+} \rightarrow$



It is also considered that in perchloric acid, the polymerization is inhibited due to the presence of an overwhelming

TABLE III
HALF-WAVE POTENTIALS OF AQUO-AMMINE AND DIAQUO-BISETHYLENEDIAMINE COBALT(III) COMPLEXES

Complex	Supporting electrolyte; 0.5 F K_2SO_4 $E_{1/2}$ of 1st wave [Co(III)→Co(II)]	1 F $HClO_4$ $E_{1/2}$ of 1st wave [Co(III)→Co(II)]
$[Co(NH_3)_6](ClO_4)_3$	-0.43_8	—
$[Co(NH_3)_5OH_2]_2(SO_4)_3\cdot 2H_2O$[30]	-0.47_5	−0.06
cis-$[Co(NH_3)_4(OH_2)_2]_2(SO_4)_3\cdot 3H_2O$[30]	-0.48_5	+0.14
$[Co(NH_3)_3(OH_2)_3]^{3+}$	-0.24_9*	—
cis-$[Co\ en_2(OH_2)_2](NO_3)_3\cdot H_2O$[12]	−0.50	−0.01

1) The concentration of the complex ion; 0.001 gram complex ion per liter.
2) Potential unit; V. vs. S. C. E.
3) Temp., 25°C.
* The data adopted from J. B. Willis, J. A. Friend and D. P. Mellor, *J. Am. Chem. Soc.*, **67**, 1680 (1945).

29) S. E. Rasmussen and J. Bjerrum, *Acta Chem. Scand.*, **9**, 735 (1955).

30) S. M. Jörgensen, *Z. anorg. Chem.*, **17**, 461 (1898).

hydrogen ion. Consequently, only the original ion is present in solution. Therefore, the steep well-defined wave of this ion was obtained in perchloric acid.

A similar behavior was observed for the aquo-ammine cobalt(III) complexes, which were shown in Table III.

Summary

1. Most of the cobalt(III) complex ions of bisethylenediamine series, $[Co\ en_2X_2]^{(3-2n)+}$ or $[Co\ en_2Y]^{(3-m)+}$ are reduced irreversibly in two steps at the dropping mercury electrode. The first diffusion current corresponds to the reduction, Co(III)→Co(II) and the second to the reduction, Co(II)→Co(0). The second step always exhibits the maximum wave.

2. The polarographic stability of $[Co\ en_2X_2]$ type complexes increases in the following order of the ligands;

Br^-, $Cl^- < NCS^- < NO_2^- < NH_3 < OH_2 < CN^-$

(Supporting electrolyte; 0.5 F K_2SO_4)

Similarly, the order of the stability of $[Co\ en_2Y]$ type complexes is as follows;

$leuc^- < ox^{2-} < gly^- < SO_3^{2-} < CO_3^{2-} <$ en

(Supporting electrolyte; 0.5 F K_2SO_4)

These orders are independent of the kind of supporting electrolyte such as potassium chloride or potassium sulfate. The orders of the polarographic stability did not agree with that of the spectrochemical series.

3. In perchloric acid the well-defined wave of steep slope was obtained for diaquo-bisethylenediaminecobalt(III) ion, $[Co\ en_2(OH_2)_2]^{3+}$, while the ion gave a modified wave in the neutral solution of 0.1 F potassium chloride and of 0.5 F potassium sulfate. This phenomena was explained as being due to the inhibition of the dissociation and polymerization of the complex in the presence of an overwhelming hydrogen ion. A similar behavior was observed in the aquo-ammine cobalt (III) complexes.

Department of Chemistry
Faculty of Science
Osaka University
Kita-ku, Osaka

*A Note on the Proton Magnetic Resonance Spectra of Some Thiophene Derivatives**

By Kensuke TAKAHASHI, Yasuo MATSUKI, Tatsuo MASHIKO and Genjiro HAZATO

(Received August 19, 1958)

High resolution magnetic resonance spectra of the aromatic ring protons for a large number of substituted benzenes have at times been studied by several authors[1], but no available data were obtained for substituted thiophenes except for 2-bromo-5-chlorothiophene[2]. Here we present the experimental results and preliminary discussions on the proton magnetic resonance spectra of several thiophene derivatives. With respect to the number of the ring protons, they are less by two than the corresponding benzene derivatives, and so the spectra of mono-, di- and tri-substituted thiophenes are generally expected to show the structure of three quartets, two doublets and one singlet respectively. The analyses are simple for the ring protons of di- and tri-substituted thiophenes but more complicated for mono-substituted ones, and they will be discussed here qualitatively.

Experimental

The basic theory and experimental details of n-m-r measurements have been described by several authors in excellent articles, so they will not be given here.

* Presented partly at the 11th Annual Meeting of the Chemical Society of Japan, held on April 4, 1958, at Tokyo.

1) P. L. Corio and B. P. Dailey, *J. Am. Chem. Soc.*, **78**, 3043 (1956); H. S. Gutowsky, D. W. McCall, B. R. McGarvey and H. L. Meyer, ibid., **74**, 4809 (1952); H. S. Gutowsky, C. H. Holm, A. Saika and G. A. Williams, ibid., **79**, 4596 (1957).

2) W. A. Anderson, *Phys. Rev.*, **102**, 151 (1956).

TABLE I

Substituent	b. p. (°C)	Measured condition (Weight per cent)		
		Sample	CCl_4	C_6H_{12}
——		70.5		29.5
2-CH_3	107～112	95.9		4.1
3-CH_3	114～115	95		5
2, 3-$(CH_3)_2$	139～140	96.2		3.8
2, 4-$(CH_3)_2$	139～142	94.8		5.2
2-Cl		77.8		22.2
2-Br	148～151	81.0		19.0
2-I	72～74/15	82.5		17.5
2, 5-Cl_2		80.9		19.1
2, 5-Br_2		80.2		19.8
2, 5-I_2		26.5	67.2	6.3
2-Br, 3-CH_3	34.5～35.0/4.8	80.1		19.9
2-$COCH_3$	88/8	74.3		25.7
2-NO_2	m. p. 45～46	97		3
2-CHO	76/12	81.1		18.9
2-SO_2Cl	m. p. 32～33	93.2		6.8
2, 4-$(SO_2Cl)_2$	m. p. 76～77	8.3	89.9	1.8
2, 5-$(SO_2Cl)_2$	m. p. 44～45	28.8	68.3	2.9
2, 5-$(NO_2)_2$				
2-SO_2Cl, 3-CH_3	98～100/3	98.9		1.1
2-SO_2Cl, 5-CH_3		78.4		21.6
2, 4-$(SO_2Cl)_2$, 3-CH_3	m. p. 96	36.7	62.0	1.3
2, 5-$(SO_2Cl)_2$, 3-CH_3				

Materials.—All thiophene derivatives used in the present observations were synthesized by Y. M. and T. M., the details of the procedure will soon be published in the Journal of the Chemical Society of Japan, Ind. Chem. Sec..

Procedure and Apparatus. — The apparatus used in this research is a Bloch-type high resolution n-m-r spectrometer (Model V-4300B), purchased from Varian Associates, Palo Alto, California. Proton resonances were observed at a fixed frequency of 40 mc./sec. and the corresponding magnetic fields in the neighborhood of 9400 gauss.

The chemical shifts were read from the signals recorded with a Sanborn Model 127 Recorder, comparing with the shift of 227 cps for benzene-cyclohexane mixture, 1 : 1 by volume, as a reference, and the values given here are the averages, usually from about three recordings, and the small values were calibrated by running acetaldehyde, with its known splitting of 2.85 cps.

The values of chemical shift will not be sensitive to the presence of small amounts of impurities, especially in the case of C-H bonds, so that the samples were used after several times distillations or recrystallizations without any other special procedures of purification.

Samples which are solid at room temperature were measured in the super-cooled conditions after being heated above their melting points or dissolved in carbon tetrachloride. In such a case, it should be kept in mind that the occurrence of the additional shift due to the concentration effect or the molecular interaction is possible, so that the measured conditions are given in Table I.

Additional errors do not result from neglecting the bulk diamagnetic susceptibility corrections by using cyclohexane as a internal reference. Another error results from the difference of the reference concentration, but it is assumed that this error is small[3]. In some compounds, especially in 2-bromothiophene and in thiophene itself, it was observed that the line shapes were slightly changed with the variation of the concentration of the reference compound.

The results were reproducible within the deviation of about 4 cps.

Results and Discussion

Table of Chemical Shifts.—The chemical shifts of the ring protons obtained from the twenty-two compounds are given in Table II, in cps, indicating the separations from the cyclohexane signal, the larger value showing the lower field side. In the case where the signal is split by the indirect spin-spin interaction, the shift given here is that for the center of the resonance pattern. As for 2-methyl-, 3-methyl- and 2-bromothiophene, the assignments of their spectra are not given in Table II and they will be discussed in the latter paragraph of monosubstituted thiophenes.

3) P. L. Corio and B. P. Dailey, *J. Am. Chem. Soc.*, **78**, 3043 (1956); *J. Chem. Phys.*, **25**, 1291 (1956).

TABLE II

THE MAGNETIC RESONANCE DATA FOR THE RING PROTONS IN SUBSTITUTED THIOPHENES, REFERRED TO CYCLOHEXANE IN CPS, AT 40 mc./sec.

Substituent	Assignment				Mean shift	Mean shift from thiophene
	2-H	3-H	4-H	5-H		
——					220	0
2-CH_3	—				210	−10
3-CH_3		—			211	− 9
2,3-$(CH_3)_2$	—	—	203	211	207	−13
2,4-$(CH_3)_2$	—	197	—	197	197	−23
2-Cl	—	209	209	209	209	−11
2-Br	—				214	− 6
2-I	—	224	204	224	218	− 2
2,5-Cl_2	—	204	204	—	204	−16
2,5-Br_2	—	207	207	—	207	−13
2,5-I_2	—	214	214	—	214	− 6
2-Br, 3-CH_3	—	—	204	219	211	− 9
2-$COCH_3$	—	248	223	248	239	19
2-NO_2	—	252	227	252	244	24
2-CHO	—	255	229	255	246	26
2-SO_2Cl	—	257	230	257	248	28
2,4-$(SO_2Cl)_2$	—	266	—	281	273	53
2,5-$(SO_2Cl)_2$	—	258	258	—	258	38
2,5-$(NO_2)_2$	—	277	277	—	277	57
2-SO_2Cl, 3-CH_3	—	—	224	252	238	18
2-SO_2Cl, 5-CH_3	—	246	215	—	230	10
2,4-$(SO_2Cl)_2$, 3-CH_3	—	—	—	288	288	68
2,5-$(SO_2Cl)_2$, 3-CH_3	—	—	257	—	257	37

Indirect Spin-Spin Coupling Constants.—The indirect spin-spin coupling constants (J) for disubstituted thiophenes are given in Table III in cps, obtained by reading the scales of their spectra. In monosubstituted thiophenes, however, there are three independent coupling constants, the reasonable values of which can not be determined without theoretical calculations referring to the multiplet structure.

TABLE III

THE COUPLING CONSTANT (J) AND THE CHEMICAL SHIFT (δ) OF TWO RING PROTONS IN DISUBSTITUTED THIOPHENES IN CPS AT 40 mc./sec.

Substituent	J	δ
2,3-$(CH_3)_2$	5.2	5.9
2-Br, 3-CH_3	5.6	14
2-SO_2Cl, 3-CH_3	5.5	27
2-SO_2Cl, 5-CH_3	4.1	31
2-Br, 5-Cl*	3.9	6.2
2,4-$(SO_2Cl)_2$		15
2,4-$(CH_3)_2$		$\simeq 0$
2,5-Cl_2		0
2,5-Br_2		0
2,5-I_2		0
2,5-$(NO_2)_2$		0
2,5-$(SO_2Cl)_2$		0

* from Anderson's value[2].

The mean value (5.4 cps) of the indirect coupling constants between the 4- and 5-positioned protons (J_{45}) for three compounds, i.e. 2,3-dimethyl-, 2-bromo-3-methylthiophene and 3-methylthiophene-2-sulfonylchloride, is greater than the mean value of J_{34} (4.0 cps) for two compounds, 5-methylthiophene-2-sulfonylchloride and 2-bromo-5-chlorothiophene. The values of J_{35} can not be determined from the spectra of 2,4-dimethylthiophene and 2,4-thiophenedisulfonylchloride, for the signals of 3- and 5-positioned protons of these compounds are broad; perhaps they will have the unresolved multiplet structures.

With our results and the help of the values analyzed in detail for selenophene and furan[4], it can be assumed that $J_{45} \simeq J_{23} > J_{34} > J_{25} > J_{24} \simeq J_{35}$ in thiophene derivatives.

And also the methyl resonances for methylthiophenes have the fine structure due to spin-spin coupling with adjacent ring protons, having the approximate coupling constants of 1.0 cps, the signals of which are shown in b and d in Fig. 1.

Monosubstituted Thiophenes.—Nine compounds were measured and the spectra of

4) T. Isobe, Presented at the Symposium on the Structural Chemistry, held on Nov. 21, 1957, at Fukuoka.

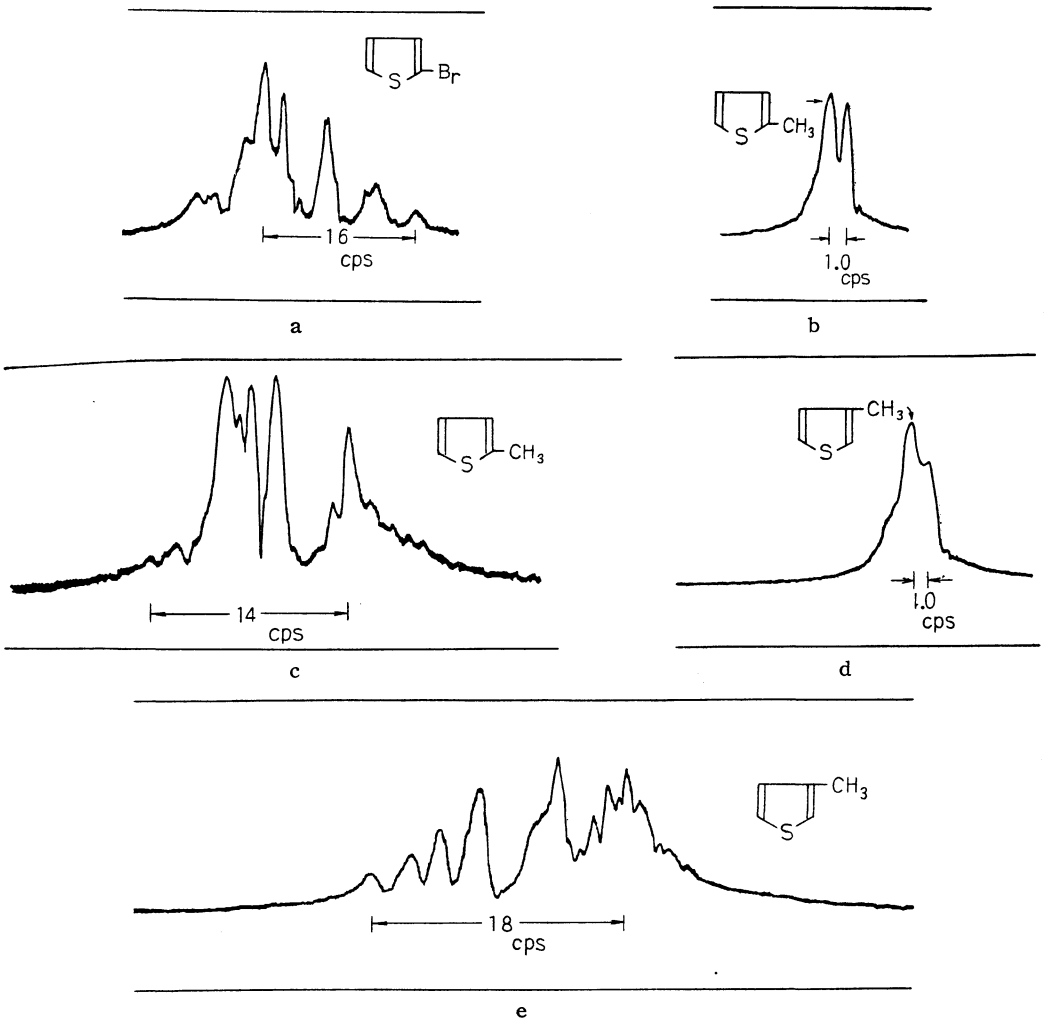


Fig. 1. The proton magnetic resonance spectra showing (a), 2-bromothiophene; (b), methyl group in 2-methylthiophene; (c), ring protons in 2-methylthiophene; (d), methyl group in 3-methylthiophene; (e) ring protons in 3-methylthiophene. Applied magnetic field increasing from left to right.

their ring protons can be classified into three types. The spectrum of 2-chlorothiophene is in the first type; it has a broad single line, so that the three protons in the ring are almost magnetically equivalent. The spectra of 2-bromo-, 2-methyl- and 3-methylthiophene are in the second type and they have the most complicated spectra as shown in a, c and e in Fig. 1, but their analyses are difficult for the present, so that they are not given in Table II. As for the others, 2-acetyl-, 2-iodo-, 2-nitrothiophene, 2-thiophenesulfonylchloride and 2-thiophenealdehyde, the spectra are in the third type and they are shown in a, b, c, d and e in Fig. 2. Their signals consist of two main parts separated approximately 20 cps or more. The intensity ratio of the high-field part to the low-field one is 1 : 2, corresponding to one proton and to two protons respectively. At the high-field side of the signal, there are three or four sub-lines. Therefore these sub-lines can be considered as the lines coming from the 4-positioned proton. At the low field side of their signal, there are two sub-lines and they can be assumed to be the lines coming from the 3- and 5-positioned protons, and that both protons have almost the same chemical shifts.

In the spectra of the ring protons in the third group, we can assume that J_{34} and J_{45} have approximately the same value of

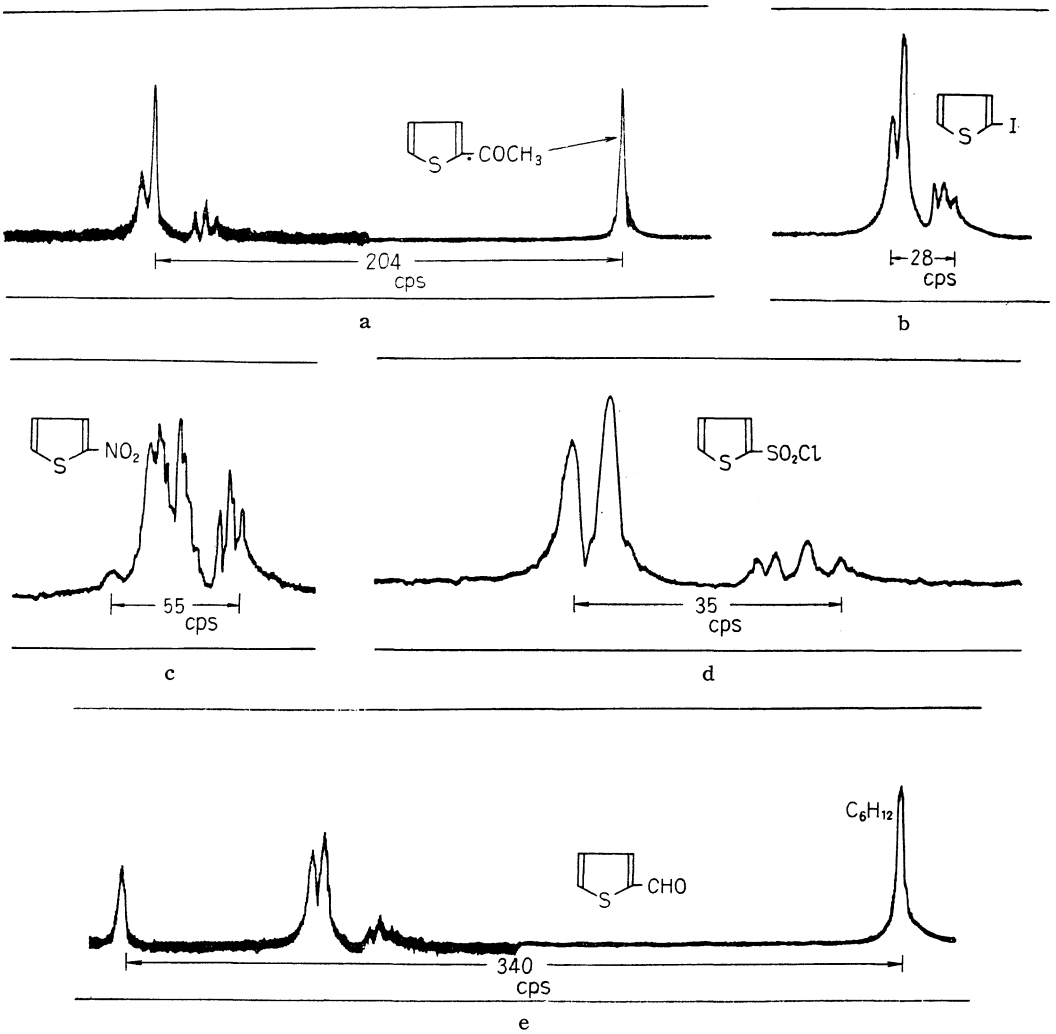
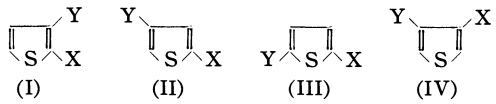


Fig. 2. The proton magnetic resonance spectra showing (a), 2-acetylthiophene; (b), 2-iodothiophene; (c), 2-nitrothiophene; (d), 2-thiophenesulfonylchloride; and (e), 2-thiophenealdehyde. Applied magnetic field increasing from left to right in all figures.

5 cps, closely consistent with the values shown in the preceding paragraph. The spectra of 2-nitrothiophene are more complicated than the others (Fig. 2 c), and in this figure, a signal which appeared at the lowest field side is assumed as coming from 2,5-dinitrothiophene by which the sample is contaminated.

In general, the multiplet structure of the n-m-r spectrum depends upon the ratio of the coupling constant to the chemical shift (J to δ). In monosubstituted thiophenes, it can be supposed that the chemical shifts are small as compared with the coupling constants in the first type, approximately the same in the second type and large in the third type.

Disubstituted Thiophenes. — The disubstituted thiophenes are the typical model of the two-proton system and there are four isomers as follows:



Their spectra consist of two doublets, but if X and Y are the same, the spectra for III and IV should have the single line.

The chemical shifts and coupling constants between the two ring protons are given in Table III; the samples in type IV were not measured. In the near future, we hope to obtain the measurements of this type for the determination of J_{25}, the coupling constant between the two protons

by way of the sulfur atom.

Trisubstituted Thiophenes. — Two compounds were measured and they have a single line.

Substituent Effects to Thiophene Ring. —The nitro, sulfonylchloro, aldehyde and acetyl groups have the strong electron withdrawing power. The introductions of these substituents to the thiophene nuclei should have lessened the electron density of the ring protons, we can see these aspects in the experimental results shown in the seventh column of Table II. In the case of 2-nitrothiophene, the magnitudes of the shifts are large in 3- and 5-H but small in 4-H toward lower field. On the contrary, the shift of the ring proton to the lower frequency in the spectra of methylthiophenes is consistent with the effect of higher electron density in the ring due to methyl substitution.

Also in the halogeno-substituted thiophenes, the similar shifts toward the higher field were observed as shown in Table II. The I-effect of the halogen-substituent withdraws charge from the ring, while the E-effect donated charge to the ring. Therefore, the situation here shows probably a predominance of the E-effect over the I-effect.

It is hoped that the present results will be usefull in determining the structure of unknown thiophene derivatives and in analyzing the spectrum for thiophene in detail.

Summary

1) The chemical shifts of the ring protons for twenty-two kinds of thiophene derivative were measured, and the qualitative discussions on the substituent effects were also given.

2) The coupling constants between the ring protons for thiophene derivatives can be generally assumed to be $J_{45} \simeq J_{23} > J_{34} > J_{25} > J_{24} \simeq J_{35}$.

The Chemical Research Institute of Non-aqueous Solutions
Tohoku University
Katahira-cho, Sendai

*The Fundamental Conditions for Countercurrent Distribution Studies of Clupeine**

By Fumio SAWADA

(Received September 5, 1958)

The heterogeneity of some protamines, protein moieties in sperm nuclei of fishes, namely clupeine[1-9] from herring, salmine[3,4] from salmon, iridine[3,4,10] from rainbow-trout, and mugiline[11,12] from mullet, has been reported from German[1-7] and Japanese[8-12] laboratories. Nevertheless, it is still uncertain how the heterogeneity of protamines originates and what the biological activities of different molecules are. Thus, as the first step to resolve the problem, clupeine has been examined

* Presented at the 8th Annual Meeting of the Chemical Society of Japan held on April 1, 1955, in Tokyo.

1) A. Kossel and E. G. Schenk, *Z. physiol. Chem.*, **173**, 278 (1928).

2) K. Felix and K. Dirr, ibid., **184**, 111 (1927); K. Felix and A. Mager, ibid., **249**, 111 (1937); H. M. Rauen, W. Stamm and K. Felix, ibid., **291**, 275 (1952).

3) H. M. Rauen, W. Stamm and K. Felix, ibid., **292**, 101 (1953).

4) K. Felix, "The Chemical Structure of Proteins", a Ciba Foundation Symp., J. & A. Churchil Ltd., London (1953) p. 151.

5) K. Felix, *American Scientist*, **43**, 431 (1955); K. Felix, A. Krekels and W. Rick, *Trans. Faraday Soc.*, **53**, 252 (1957).

6) E. Waldschmidt-Leitz, F, Ziegler, A. Schaeffner and L. Weil, *Z. physiol. Chem.*, **197**, 219 (1931); E. Waldschmidt-Leitz and L. Pflanz, ibib., **292**, 150 (1953); E. Waldschmidt-Leitz and K. Gauss, ibid., **293**, 10 (1953); E. Waldshmidt-Leitz and R. Voh, ibid., **298**, 257 (1954).

7) K. E. Rasmussen, ibid., **224**, 97 (1934).

8) T. Ando, E. Abukumagawa, Y. Nagai and M. Yamasaki, *J. Biochem. (Japan)*, **44**, 191 (1957); T. Ando, M. Yamasaki, E. Abukumagawa, S. Ishii and Y. Nagai, ibid., **45**, 429 (1958).

9) T. Ando, S. Ishii, M. Yamasaki, K. Iwai, C. Hashimoto and F. Sawada, ibid., **44**, 275 (1957).

10) F. Sawada and T. Ando, The 31th Annual Meeting of the Japanese Biochem. Soc., Sapporo, July 14, 1958.

11) T. Ikoma, *J. Japanese Biochem. Soc. (Seikagaku)*, **26**, 460 (1954).

12) S. Morisawa, Symp. on the Structure of Proteins, Fukuoka, Oct. 29, 1956.

for heterogeneity by means of Craig's countercurrent distribution (C. C. D.) method[13-15].

The usefulness of C.C.D., using a solvent system consisting of lauric acid in butanol and aqueous sodium acetate, for the fractionation of the methyl ester hydrochlorides of clupeine[3-5] and mugiline-β[11,12] has already been described. This solvent system, however, proved to be unsuitable for these protamine sulfates[3,11]. The sulfate is considered to represent more intact protein without any treatment of methyl esterification and to be suitable for the elucidation of the origin of the heterogeneity of clupeine. Thus, a course of study aiming to obtain desirable conditions for the fractionation of clupeine sulfate by means of C.C.D. is described in this paper.

Experimental

Preparation of Clupeine Sulfate[9]. — Dry powder** (50 g.) of the matured milts of herring (*Clupea pallasii*) obtained in 1951 (at Yoichi facing the Japan Sea, Hokkaido, Japan) was stirred with 0.2 N hydrochloric acid (600 ml.) under ice-cooling for 50 minutes, and clupeine was precipitated as picrate (yield 12.3 g.) by the addition of 0.125 M sodium picrate to the first extract. The clupeine picrate (5.29 g.) was then dissolved into 67% (wt./wt.) aqueous acetone, and converted in to the sulfate by adding sulfuric acid (to pH 2) and ethanol under cooling. The aqueous solution of clupeine sulfate reprecipitated once was passed through the Dowex-2 column (sulfate form) to remove the contaminating picric acid. Thus white glittering powder (yield 2.29 g.) of clupeine sulfate was obtained from the eluate after two reprecipitations.

Preparation of Clupeine *p*-Toluenesulfonate.—An aqueous acetone solution of clupeine picrate (253 mg. in 2.5 ml.) and an aqueous solution (6.8 ml.) of 4% *p*-toluenesulfonic acid (see below) were mixed. The liberated picric acid was removed by means of ether extraction (five times with 10 ml. each) and by means of treatment with Amberlite IRA-410 (*p*-toluenesulfonate form). The resultant solution (pH 2) was neutralized with Amberlite IR-4B (OH-form). White amorphous powder of clupeine *p*-toluenesulfonate was obtained by lyophilization (yield 99 mg.)***.

Solvents for the C.C.D.—*n*-Butanol, commercial grade; acetic, dichloroacetic, trichloroacetic and picric acid, commercial grade.

p-Toluenesulfonic acid—The commercial reagent was treated with charcoal and recrystallized from a hot solution in concentrated (1 : 1, by volume) hydrochloric acid, or by saturation of the aqueous solution with gaseous hydrogen chloride. The melting point was 104~105°C (cor.).

Principles of Method. — To the C.C.D. of proteins, only a few types of solvent systems, especially the so-called "butanol systems"[16] are applicable. The author tested, therefore, various systems consisting of *n*-butanol and aqueous solution containing some reagents such as hydrochloric, acetic, dichloroacetic, trichloroacetic, *p*-toluenesulfonic**** or picric acid, sodium *p*-toluenesulfonate and sodium chloride. In every case, the partition coefficients of clupeine in these systems were measured, and the system satisfying the conditions necessary for C. C. D.[14] —no irreversible effects on the solute and a linear partition isotherm***** with a partition coefficient not much shifted from unity—was searched for.

Determination of Partition Coefficient.—A mixture of 1 ml. of *n*-butanol and 1 ml. of an aqueous solution containing the known concentrations of a clupeine sample and a reagent or reagents (see above) were put into a test-tube (1×12 cm.) with a glass stopper, and left to stand at a constant temperature in an incubator for 30 minutes. Then the test-tube was vigorously shaken for about 30 seconds at room temperature, and allowed to stand again in an incubator for 10 minutes. After the phases separated, the amounts of clupeine in both of the phases were measured by the retention analysis using an acidic dye, ponceau 6RF[9]. The average value from three to six measurements was used. The ratio $K=C_1/C_2$, where C_1 and C_2 are the equilibrium concentration of the sample in the upper and the lower phases respectively, was defined as a partition coefficient.

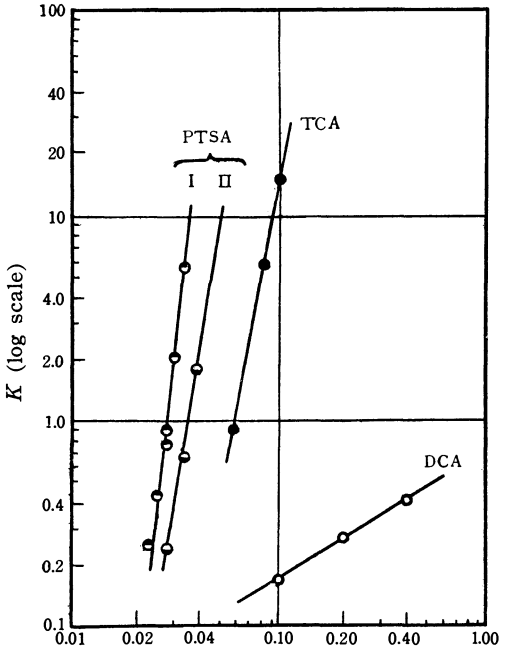
Results and Discussion

Dependence of the Partition Coefficient upon Concentration of the Reagents in the System.—In the systems consisting of *n*-butanol and aqueous solutions of various concentrations of hydrochloric, acetic or picric acid, the *K*-values of clupeine sulfate were found to be almost zero. Therefore these systems were discarded.

In the case of the systems containing

13) L. C. Craig, *J. Biol. Chem.*, **155**, 519 (1944).
14) L. C. Craig, C. Golumbic, H. Mighton and E. Titus, ibid., **161**, 321 (1945).
15) J. R. Weisiger, "Organic Analysis", Vol. 2, Interscience Publisher, New York (1954).
** The preparation of the dry powder of the milts was performed by Dr. M. Yamasaki according to the Rasmussen's method[7].
*** An atempt to obtain clupeine *p*-toluenesulfonate by elution of clupeine adsorbed on Amberlite XE-64 (IRC-50) with aqueous *p*-toluenesulfonic acid was unsuccessful.
**** Dichloroacetic, trichloroacetic and *p*-toluenesulfonic acids are known to be good complexing agents for peptides or proteins[16,17].
16) F. Sawada, *Protein-Nucleic Acid-Enzyme, (Tampakushitsu-Kakusan-Koso)*, **2**, 167 (1957).
17) L. C. Craig, *Anal., Chem.*, **28**, 723 (1956).
***** A plot of the concentration of solute in one phase in equilibrium with the concentration in the second one is called a partition isotherm. When a partion isotherm remains constant over a wide range of concentration, the isotherm is said to be linear (Ref. 15, p. 277).

dichloroacetic, trichloroacetic or *p*-toluenesulfonic acid, the *K*-values of clupeine sulfate at a definite concentration increased as the concentration of these acids increased (Fig. 1). Because of the low *K*-value for dichloroacetic acid and of the difficult solubility of the sample in trichloroacetic acid, only the system containing *p*-toluenesulfonic acid was found to be favorable for the distribution of clupeine.

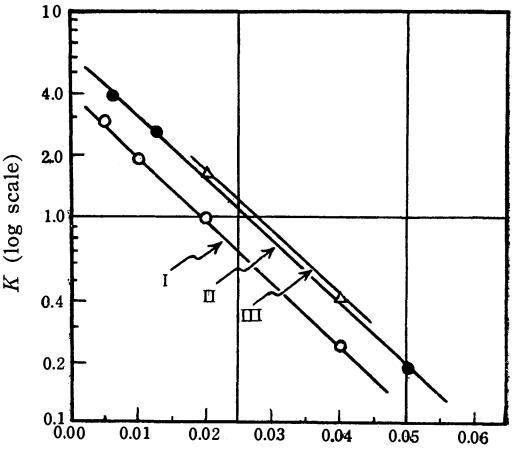


Concn. of acids (M in log scale)

Fig. 1. Dependence of *K*-value of clupeine sulfate upon the concn. of acid in the system of *n*-butanol vs. aq. acid (18~23°C).

Symbol	Acid	Concn. of clupeine sulfate (%)
○—○	dichloroacetic	0.025
●—●	trichloroacetic	0.025
I ◒—◒	*p*-toluenesulfonic	0.02
II ◒—◒	*p*-toluenesulfonic	0.04

Dependence of the Partition Coefficient upon the Concentration of the Sample.— In the solvent system consisting of *n*-butanol and an aqueous *p*-toluenesulfonic acid at a definite concentration, the partition isotherm was not linear; in other words the *K*-value of clupeine sulfate decreased as its concentration increased (curve I in Fig. 2). The same relation was observed when either clupeine *p*-toluenesulfonate was taken for its sulfate (curve II in Fig. 2) or *p*-toluenesulfonic acid was replaced with its sodium salt (curve III in Fig. 2); only in the last case *n*-butanol in the system was replaced by *n*-butanol-*n*-propanol mixture (3 : 1, v./v.) from the viewpoint of miscibility.



Concn. of clupeine (%)

Fig. 2. Dependence of *K*-value of clupeine salt upon its concn. in the system of *n*-butanol* vs. *p*-toluenesulfonic acid or its Na salt.

Symbol	Concn. of the acid or the salt	Clupeine	Temp. (°C)
I ○—○	0.029 M acid	sulfate	20
II ●—●	0.020 M acid	*p*-toluene-sulfonate	27
III △—△	0.021 M salt	sulfate	30

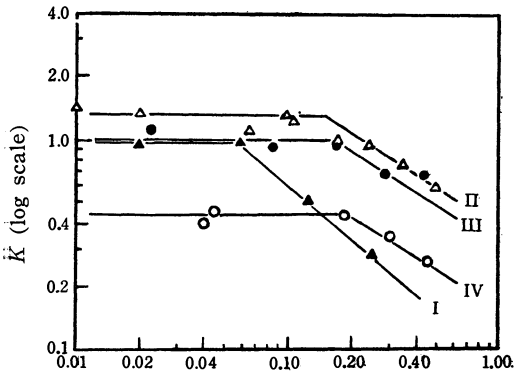
* In the case of III, *n*-butanol-*n*-propanol (3 : 1).

The non-linearity of an isotherm is generally observed in the partition of inorganic cations, and the favorable partition can be performed by the use of a solvent system containing a large excess of a complexing agent at a constant pH[18]. The same situation is expected in the case of clupeine which is a strongly basic protein.

Thus, the higher concentration of *p*-toluenesulfonic acid may bring a linear isotherm but with an undesirably large *K*-value and a very low pH. However, its salts, for example sodium *p*-toluenesulfonate, would have the same effect at neutral pH as the acid has, and the addition of sodium chloride in the system would make the *K*-value decrease because of its "salting-in" effect. Therefore, in the solvent system consisting of *n*-butanol and an aqueous solution containing a high and suitable concentration of both sodium *p*-toluenesulfonate and sodium chloride, a

18) E. Hecker, "Verteilungsverfahren im Laboratorium", Verlag Chemie, GMBH, Weinheim/Bergstr. (1955), pp. 18, 107.

linear isotherm with a suitable K-value would be obtained at a neutral pH range. In fact, these considerations were proved to be the case as shown in Fig. 3.



Concn. of clupeine sulfate (% in log scale)

Fig. 3. Dependence of K-value of clupeine sulfate upon its concn. in the system of n-butanol vs. aq. salts.

Symbol	Concn. of Na p-toluene-sulfonate	Concn. of NaCl	Temp. (°C)
I ▲—▲	ca. 0.07 M	0.20 M	23~24
II △—△	ca. 0.12 M	0.40 M	ca. 17
III ●—●	0.12 M	0.40 M	22~23
IV ○—○	0.12 M	0.48 M	22~23

The range of the clupeine concentration where the K-value remains constant becomes broader as the concentration of sodium p-toluenesulfonate increases (curves I and II, III or IV in Fig. 3). It seems that the constant K-value ranges depend only upon the concentration of sodium p-toluenesulfonate; temperature (curves II and III in Fig. 3) and concentration of sodium chloride (curves III and IV in Fig. 3) seem not to affect the constant ranges and the gradients of the curves.

Thus, the solvent system consisting of n-butanol and an equal volume of aqueous solution of 0.12 M sodium p-toluenesulfonate and 0.40 or 0.48 M sodium chloride (curve III or IV in Fig. 3) was found to possess at common temperature the linear isotherms with adequate K-values for clupeine sulfate, so far as its concentration was less than 0.2 per cent in the total volume of both phases. In ranges of the higher concentration of clupeine, the K-values suddenly decreased (see also Fig. 3).

Dependency of the Partition Coefficient upon Temperature. — The K-values of clupeine sulfate in the solvent system consisting of n-butanol and aqueous p-toluenesulfonic acid at 0°C and 40°C were equal (Table I). On the other hand, they decreased obviously in the system of n-butanol and an equeous solution containing sodium p-toluenesulfonate and sodium chloride as temperature increased (Table II). Therefore, we must do a C.C.D. procedure with the latter system at a constant temperature.

TABLE I

DEPENDENCE of K-VALUE OF CLUPEINE SULFATE (0.02%) UPON TEMP. IN THE SYSTEM OF n-BUTANOL VS. AQ. 0.029 M p-TOLUENESULFONIC ACID

Temp. (°C)	K-value
0	0.7_5
40	0.7_9

TABLE II

DEPENDENCE OF K-VALUE OF CLUPEINE SULFATE (0.022%) UPON TEMP. IN THE SYSTEM OF n-BUTANOL VS. AQ. 0.14 M Na p-TOLUENESULFONATE—0.40 M NaCl

Temp. (°C)	K-value
1	3.9_2
11~12	2.8_3
19~20	1.5_7
34~35	1.0_3

The solvent system described in the above, well satisfies the conditions necessary for C.C.D. procedure (see principles of the method). In such a system of neutral condition, a danger of secondary transformation of protamines would be minimized. In this system the K-value can be easily controlled by changing the concentration of the components. Moreover, the presence of sodium chloride increases the capacity of the system to dissolve the sample and reduces the time necessary for the separation of phases.

The usefulness of the present system was practically proved by a preliminary experiment of C.C.D., in which the heterogeneity of clupeine sulfate was evidently demonstrated[9], contrary to Rauen's result******[3]. Recently, Scanes and Tozer[19] reported the fractionation of clupeine sulfate by C.C.D. technique, using a unique solvent system, n-propanol-3 M sodium acetate (3 : 2, by volume). The fractionation efficiency of their system seems to be nearly the same as ours.

In connection with the unique effect of p-toluenesulfonate anion in the solvent system, a strange phenomenon was pointed

****** In the Rauen's system, undesirably small K-values were obtained for the sulfates of clupine[3] and mugiline-β[11].

19) F. S. Scanes and B. T. Tozer, *Biochem. J.*, **63**, 565 (1956).

out by Pierce[20] in the case of C.C.D. of an ox pituitary growth hormone. In spite of the fact that the distribution pattern of the hormone protein agreed with the theoretical curve in the solvent system consisting of *sec*-butanol and 0.0044 M aqueous *p*-toluenesulfonic acid, some disagreement was found between the experimental and theoretical curves, when the acid concentration was 0.0022 M. This phenomenon might be explained by such non-linearity of the partition isotherm of the hormone as is shown above in clupeine, though Pierce denied its possibility in his paper.

Summary

The conditions and solvent system suitable for C.C.D. of clupeine sulfate, were systematically studied and the following results were obtained.

1. In the solvent system consisting of *n*-butanol and aqueous hydrochloric, acetic or picric acid, the partition coefficient (K) of clupeine sulfate was almost zero.

2. In the system consisting of *n*-butanol and aqueous dichloroacetic, trichloroacetic or *p*-toluenesulfonic acid, the K-value increased with the increase of the acid concentration at a constant solute concentration. In the last system, at a constant acid concentration, the K-value decreased with the increase of the solute concentration.

3. The system consisting of *n*-butanol and an equal volume of aqueous solution containing 0.12 M sodium *p*-toluenesulfonate and 0.40 or 0.48 M sodium chloride was found to satisfy all the conditions necessary for the C.C.D. of clupeine sulfate.

The author wishes to express his hearty thanks to Professor T. Ando for his guidance and encouragement throughout this work, as well as to Dr. I. Ishii for his helpful discussions and also to Dr. C. Hashimoto for her cooperation in the preparation of clupeine. The present work was supported in part by the Scientific Research Grant from the Ministry of Education given to Professor T. Ando.

Department of Biophysics and Biochemistry, Faculty of Science the University of Tokyo Hongo, Tokyo

20) J. G. Pierce, ibid., **57**, 16 (1954).

Crystal and Molecular Structure of 1-Oxa-azulan-2-one. I. X-ray Determination of Crystal Structure

By Yoshio SASADA

(Received August 18, 1958)

We investigated previously the crystal and molecular structures of sodium salt[1] and hydrochloride of tropolone[2,3] as a part of the serial structural studies of the compounds containing planar seven-membered carbon rings. We have extended our study to the related compounds of azulene. Azulene, a fused five- and seven-membered ring system, is a well-known representative of non-benzenic aromatic compounds. Since Hückel[4] explained the large dipole moment of this compound by molecular orbital treatment, many theoretical and experimental researches especially measurements of dipole moment and absorption spectra, on azulene and its derivatives have been made. These studies were reviewed by several authors[5]. However, there have appeared only a few investigations using diffraction methods which can determine the molecular structures in detail. Even for the mother substance, azulene, it was in 1956 that its structure was reported by Takeuchi and Pepinsky[6] and Robertson and Shearer[7] independently, but no accurate molecular dimension sufficient to discuss in comparison with the theoretical results has

1) Y. Sasada and I. Nitta, *Acta Cryst.*, **9**, 205 (1956).
2) Y. Sasada, K. Osaki and I. Nitta, ibid., **7**, 113 (1954).
3) Y. Sasada and I. Nitta, This Bulletin, **30**, 62 (1957).
4) E. Hückel, *Z. Physik.*, **70**, 204 (1931).
5) e. g., M. Gordon, *Chem. Rev.*, **50**, 127 (1952).
6) Y. Takeuchi and R. Pepinsky, *Science*, **124**, 126 (1956).
7) J. M. Robertson and H. M. M. Shearer, *Nature*, **172**, 885 (1956).

yet been reported. The other few papers on structures of azulene derivatives[8] deal only with crystal data or approximate structures.

Thus the accurate determination of these compounds by means of X-ray analyses will be desirable to the structural chemistry of non-benzenic aromatic compounds. Moreover, the accumulation of knowledge on the molecular orientation in the crystals so determined may contribute to the crystal chemistry of organic compounds, because, for example, azulene is isomer to naphthalene but the electron density distributions in the molecules are more or less different from each other.

Nozoe and his collaborators[9] have obtained, since several years ago, many related compounds of azulene from corresponding derivatives of tropolone, and they kindly supplied us with their valuable products. We have determined the crystallographic data of these compounds[10], some of which were further analysed[11,12]. The present account deals with the structure determination of 1-oxa-azulan-2-one, together with some remarks on the method of X-ray analysis.

Experimental

Crystals are obtained as very fine yellow needles elongated in the c axis direction.

Crystallographic and physical data obtained are as follows:

1-Oxa-azulan-2-one, $C_9H_6O_2$, m. p. 69~70°C; Orthorhombic; $a=21.45\pm0.08$, $b=8.28\pm0.04$, $c=3.96\pm0.02$ Å; Absent spectra, ($h00$), ($0k0$) and ($00l$) when h, k and l are odd respectively; Space group, $P2_12_12_1-D_2^4$; Four molecules per unit cell; Volume of unit cell, 703 Å^3; Density (by floatation); 1.36 g. cm^{-3}; Density (calc.), 1.38 g. cm^{-3}; Linear absorption coefficient for Cu K_α radiation, $\mu=9.45$ cm^{-1}; Total number of electrons per unit cell, $F(000)=304$.

For the structure analysis, a complete set of relative intensities for ($hk0$), ($hk1$) and ($hk2$) was obtained by the integrated Weissenberg procedure. The specimen used has the following maximum and minimum dimensions at right angles to the axis of rotation: 0.01×0.02 cm.

Intensities were estimated by visual comparison with a calibrated scale. The multiple-film technique was used to correlate strong and weak reflexions, ranging in relative intensities from 22000 to 1. Reflexions from only 128 planes were observed out of 232 possible ($hk0$)'s. The corrections for polarization and Lorentz factors were made in the usual way, and that for absorption was neglected.

Results and Discussion

Structure Determination. — Patterson functions[13] have been customarily used in order to obtain some clues to the structure determination problems. However, the two-dimensional Patterson method is generally powerless in the case of the crystals containing no heavy atoms.

For several years, proposals of the so-called direct methods of crystal analysis[14,15] have been made and some of them were applied with success to the actual structure determinations. However, these successful applications are only for the fortunate cases. Some empirical remarks on this point were made by Watase and Nitta[16]. The cause of the inapplicability is due to the fact that the limiting conditions for deriving these analytical forms, such as the non-negativity principle of electron density, are scarcely severe enough. As the actual situations are more complicated, analytical processes based on such rather simple conditions are not enough to solve the crystal structures containing more than, e. g. five independent atoms in the cell.

Therefore the applications of the systematic methods mentioned above may not be effective for the present case. Otherwise information given by individual intensity of each reflexion had to be used carefully as it is.

The very short period of the c axis suggests that the approximate crystal structure can be obtained by the use of the ($hk0$) reflexions alone. The starting-point was very favorable; that is, the shape of the molecule was already known from the preceding studies of the related compounds. Moreover, the shortest axis of the unit cell strongly limited the inclination of the molecular plane to the (001) plane.

As the plane group of this projection is pgg, the structure factors are represented as follows:

For the reflexions with $h+k=2n$

$$F(hk0)=\sum_j f_j \cos 2\pi hx_j \cos 2\pi ky_j$$

and for the reflexions with $h+k=2n+1$

8) e. g., K. H. Jost, *Naturwiss.*, **43**, 224 (1956).
9) T. Nozoe, Festschrift Arthur Stoll (Birkhauser A.G.) Basel, p 746 (1957).
10) Y. Sasada, to be published.
11) C. Tamura, Y. Sasada and I. Nitta, to be published.
12) Y. Takaki, Y. Sasada and I. Nitta, to be published.
13) A. L. Patterson, *Z. Krist.*, **90**, 517 (1935).
14) D. Harker and J. S. Kasper, *Acta Cryst.*, **1**, 70 (1948).
15) J. Karle and H. Hauptmann, ibid., **3**, 181 (1950).
16) H. Watase and I. Nitta, This Bulletin, **31**, 714 (1958).

$$F(hk0) = -\sum_j f_j \sin 2\pi hx_j \sin 2\pi ky_j$$

The structure factor maps, graphical representations of the above formulae, were made for all reflexions in the region within $2\sin\theta = 1.2$, the maps being drawn in the scale of 4 cm. = 1 Å.

The planes with very strong or weak intensities in the region with small $2\sin\theta$ severely limit the allowable approximate regions of molecular position and orientation together with symmetry considerations. For example, the value of the unitary structure factor of (400) is 0.36 and that of (200) is very small. As shown in Fig. 1, these facts require that the molecule should be in the regions A or B

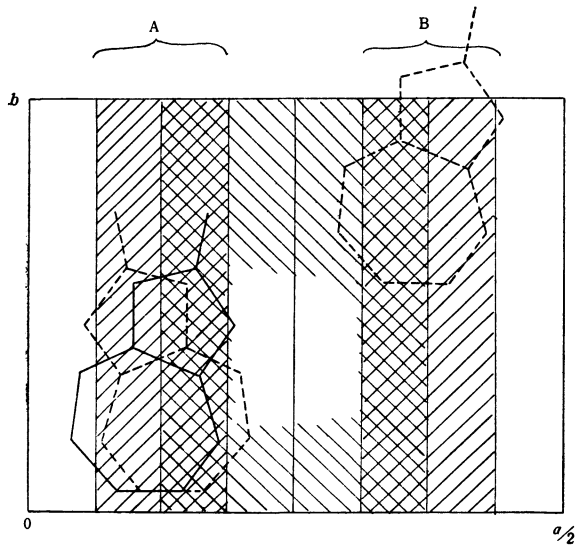


Fig. 1. Example of the determination of the allowable approximate regions using the structure factor maps. The areas shaded with lines obliqued right and left represent the negative regions in the structure factor maps of (400) and (200) respectively.

and the direction of the long axis of the molecule is nearly parallel to the *b* axis. From symmetry considerations, the molecule shown by the dotted line in the region B is equivalent crystallographically to that shown by the dotted line in the region A. Therefore, it was sufficient to apply the trial only to the region A.

The number of possible sets of atomic coordinates in this region which explains the intensities of lower order reflexions was reduced by elimination because of the requirements of the intensities of the higher order reflexions using the structure factor maps. After these successive procedures the structure has been obtained for which the agreement between the observed and the calculated structure factors is fairly good. (After the completion of this structure determination, it was found that the coordinates so obtained deviated from the final positions only by 0.2 Å or less.) Then ordinary Fourier and $(F_o - F_c)$ syntheses followed.

It is noted that the distinction of two structures shown by solid and dotted lines occurs only for the structure factors (*hk*0) with odd *h*. In fact, the structure shown by the dotted line, which was concluded to be false from the detailed trial for (*hk*0) with odd *h*, can also give a Fourier map pretty well to some extent. The detail on this point will be discussed elsewhere.

In the structure-factor calculation, the atomic scattering factors were taken from McWeeny[17], using for oxygen $\overline{f_o} = \frac{1}{3}(f^{\parallel} + 2f^{\perp})$ and for carbon the values for 'valence states'. The corrections were made only for isotropic *B* factors of individual atoms, though it was observed from the $(\rho_o - \rho_c)$ map that thermal motions of some atoms were anisotropic. The best *B* factors were: 6.0 for O_1, C_3, C_4, C_8, C_9 and C_{10}; 7.5 for O_2, C_2, C_5, C_6 and C_7.

The *R* index decreased to 0.134 including the contributions from hydrogen atoms placed radially at a distance of 1.0 Å from the carbon atoms.

TABLE I

ATOMIC COORDINATES (AT ROOM TEMPERATURE)

Atom	*x/a*	*y/b*	*z/c*
O_1	0.100	0.552	0.218
O_2	0.169	0.721	0.470
C_2	0.158	0.588	0.344
C_3	0.194	0.448	0.319
C_4	0.180	0.173	0.110
C_5	0.145	0.051	−0.034
C_6	0.084	0.052	−0.160
C_7	0.042	0.179	−0·168
C_8	0.050	0.335	−0.043
C_9	0.101	0.399	0.115
C_{10}	0.161	0.331	0.168

In Table I are listed the final atomic coordinates. Fig. 2 shows the comparison between observed and calculated structure factors and Fig. 3 the final Fourier projection of the electron density on the (001) plane.

Determination of *z* Coordinates.—As this crystal is a very fine needle in shape, the Weissenberg photographs about the *a* and *b* axes could not be taken. However, the

17) R. McWeeny, *Acta Cryst.*, **4**, 513 (1951).

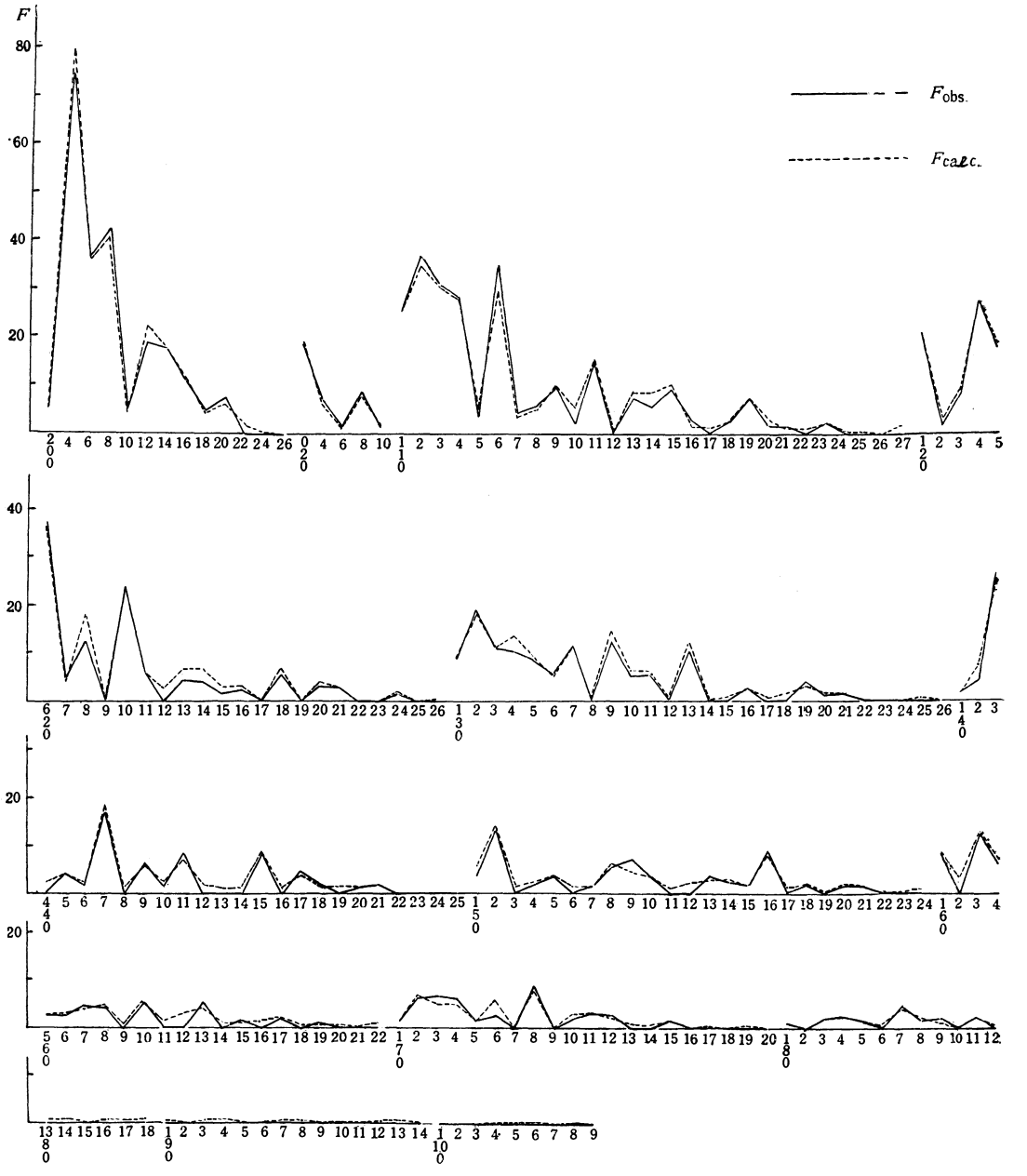


Fig. 2. Observed and calculated structure factors, $F(hk0)$.

very short period of the c axis does not require the full zonal reflexions about the a and b axes in order to estimate z coordinates. The data for $(0kl)$ and $(h0l)$ reflexions were taken from the equi-inclination Weissenberg photographs for the $(hk1)$ and $(hk2)$.

The process of the trial was very simple because the x and y parameters were already known. The coordinates so obtained were refined by the least squares method with suitable weights. For convenience, at the early two cycles, the four parameters, that is, z coordinate of the mass centre of the molecules, angles of the long and short axes of the molecule with the (001) plane and z coordinate of O_2, were corrected assuming the planarity of the fused system of five- and seven-membered rings. In the succeeding two cycles, the z coordinates of eleven atoms were shifted independently.

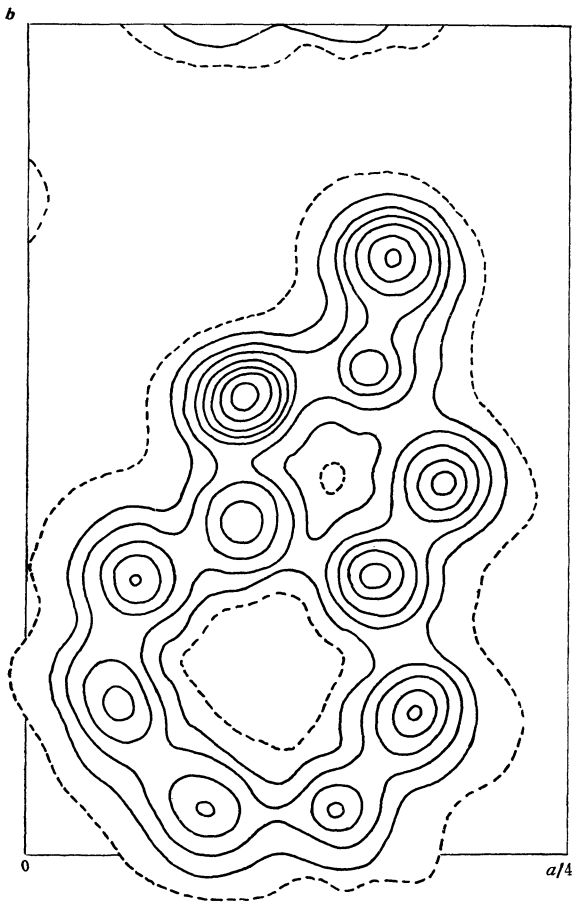


Fig. 3. The final Fourier projection of the electron density on (001). Contours at intervals of 1 e. Å^{-2}. Contour at 1 e. Å^{-2} is broken.

The final z coordinates are listed in Table I and the comparison between observed and calculated structure factors in Fig. 4.

Description of the Structure.—Fig. 5 shows the crystal structure projected on the (001) plane together with intra- and intermolecular distances.

The detailed discussions on the molecular structure are not significant, because the estimated standard deviations of bond lengths reach the values of about 0.04 Å owing to large thermal motions of atoms in the crystal.

There are no intermolecular distances deviating greatly from the sums of normal van der Waals radii.

As seen from Fig. 5, the molecular arrangement is somewhat characteristic. The seven-membered carbon ring, which is supposed to be the electrically positive part of the molecule, has as the first neighbors six five-membered rings, the negative parts, if we include the one within its own molecule. The five-membered ring is also surrounded by six seven-membered rings. Such characteristics of the molecular orientations are in contrast with those of azulene[6,7] and 2-amino azulene[12]. Mutual molecular orientations in these crystals are similar to those in naphthalene[18]. As the basic principles of the packing of molecules in organic crystals are yet to be explored, we shall only point out the parallel relation between molecular orientation and magnitudes of dipole moments of these substances. (According to Kurita and Kubo[19], the values of dipole moments are 5.64, 2.09 and 1.0 D for the present molecule, 2-amino azulene and azulene itself respectively.)

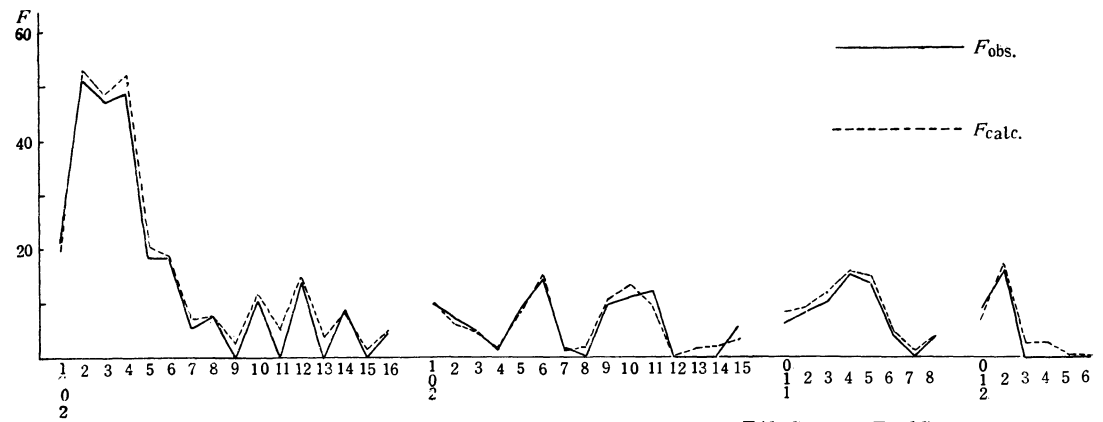


Fig. 4. Observed and calculated structure factors, $F(h0l)$ and $F(0kl)$.

18) S. C. Abrahams, J. M. Robertson and J. G. White, ibid., **2**, 238 (1949).

19) Y. Kurita and M. Kubo, to be published.

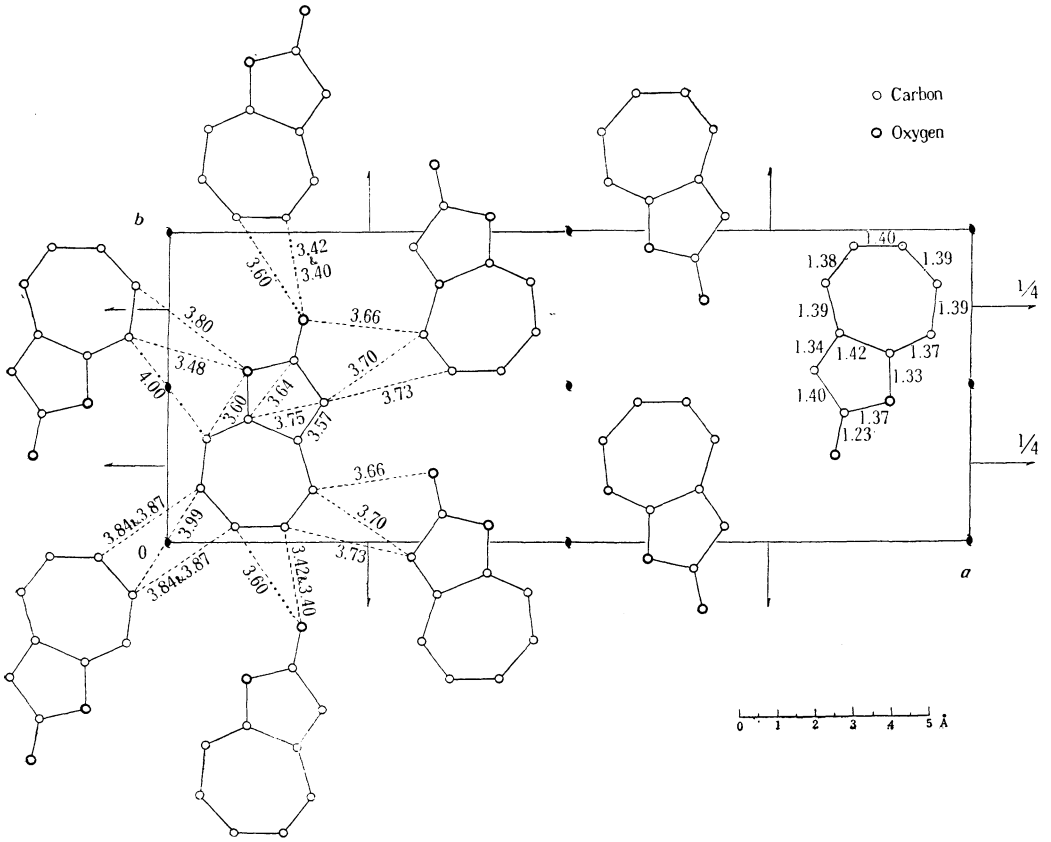


Fig. 5. Crystal structure projected on (001), together with intra- and intermolecular distances (Å).

Finally it was noticed that the B factor of each atom increases with increasing distance of an atom from the mass center of the molecule. This may correspond to the oscillational vibration of the molecule about its mass center.

Further discussion on these points will be given in the following paper which describes the refinement of the structure of this substance by low temperature technique.

The present author wishes to express his sincere thanks to Professor I. Nitta for his guidance and encouragement throughout this work. He is also indebted to Professor T. Nozoe for supplying the sample and also for continued interest.

Department of Chemistry
Faculty of Science
Osaka University
Kita-ku, Osaka

Crystal and Molecular Structure of 1-Oxa-azulan-2-one. II. A Refinement of the Structure by Low Temperature Technique

By Yoshio SASADA

(Received August 18, 1958)

As a part of the serial investigations of the compounds containing planar seven-membered carbon rings[1-5], the crystal structure of 1-oxa-azulan-2-one was reported in a preceding paper[6]. In that case the great thermal agitation at room temperature did not permit us to give the detailed determination of its crystal structure. The last Fourier projection indicated, moreover, considerably large anisotropic thermal vibrations of some atoms in the molecule. Therefore, it was highly desirable to carry out intensity measurement at low temperature in order to obtain the molecular dimensions with enough accuracy to discuss the molecular structure quantitatively.

Recently Cruickshank has published several papers[7,8] on the method dealing with molecular motions in crystals, which he applied to the cases of naphthalene[9,10] and anthracene[10-12] and compared the molecular vibrations obtained using X-ray data with those from infrared studies. Thus it will also be interesting to examine the thermal vibration of this polar molecule in order to make comparison with naphthalene and anthracene.

For these two main objects, the study of the crystal structure at low temperature was attempted and the present account deals with the analysis of this compound at $-110°C$.

Apparatus.—For several years, low temperature single crystal diffraction techniques have been adopted by several authors[13]. There are two main distinct procedures: one is the cold gas flow and the other the conduction method. The latter method has the advantage that good constancy of temperature is attained. However, for the present purpose, the former procedure is sufficient because fluctuation of temperature less than 5°C is allowable throughout the experiment.

The apparatus used for this work is shown in Fig. 1. This is a modification of the device described by J. H. Robertson. A large Dewar-vessel, 4 liters in volume, is fitted with a wooden cap in which there are holes for a large tube for filling, a level indicator, a vacuum jacketed nozzle and a pair of wires containing the heating element. Careful regulation of the current in this heating element allows sufficiently constant temperature to be maintained. The leakage of cold nitrogen gas, which make precise temperature control impossible, is avoided by the use of rubber packing.

The cold nitrogen stream is directed at the crystal on the goniometer head of a Weissenberg camera. A thermocouple fixed at the tip of the slit was placed between the tip of the nozzle and the crystal, the distance from the crystal being 3 mm. Difference between temperatures at this position and at the crystal was found to be less than 5°C at $-110°C$.

Special care was taken to prevent the frost from condensing on the crystal itself. For this purpose the cold nitrogen stream is surrounded by a supplementary stream of dry nitrogen gas of about 5°C. The velocity of the latter is controlled so as to reduce the frosting. When kept at $-110°C$, 0.7 litre of liquid nitrogen is necessary for one hour.

Experimental

Preliminary tests were made at 0°C, $-45°C$ and $-110°C$. The cell dimensions at these three temperatures show no sign of discontinuous change of considerable magnitude, the values being as follows: $a=21.4_5$, $b=8.28$, at 0°C; $a=21.3_7$, $b=8.28_5$, at $-45°C$; $a=21.2_6$, $b=8.28_5$Å, at $-110°C$. These values were obtained from the reflexions of (20, 0, 0) and (0, 8, 0) recorded on the same film respectively.

The intensity of each reflexion increases continuously with lowering temperature and the change of intensity is more significant with increasing angles. This corresponds to reduction of thermal motion without any phase transitions.

From these preliminary tests, it was expected that a satisfactory result for the present purpose could be obtained from an experiment at $-110°C$.

The final cell dimensions at $-110°C$ and space

1) Y. Sasada and I. Nitta, *Acta Cryst.*, **9**, 205 (1956).
2) Y. Sasada and I. Nitta, This Bulletin, **30**, 62 (1957).
3) K. Furukawa, Y. Sasada and T. Watanabé, to be published.
4) C. Tamura, Y. Sasada and I. Nitta, to be published.
5) Y. Takaki, Y. Sasada and I. Nitta, to be published.
6) Y. Sasada, This Bulletin, **32**, 165 (1959).
7) D. W. J. Cruickshank, *Acta Cryst.*, **9**, 754 (1956).
8) D. W. J. Cruickshank, ibid., **9**, 747 (1956).
9) D. W. J. Cruickshank, ibid., **10**, 504 (1957).
10) D. W. J. Cruickshank, ibid., **9**, 1005 (1956).
11) D. W. J. Cruickshank, ibid., **9**, 915 (1956).
12) D. W. J. Cruickshank, ibid., **10**, 470 (1957).
13) W. N. Lipscomb, *Norelco Rep.*, **4**, 54 (1957).

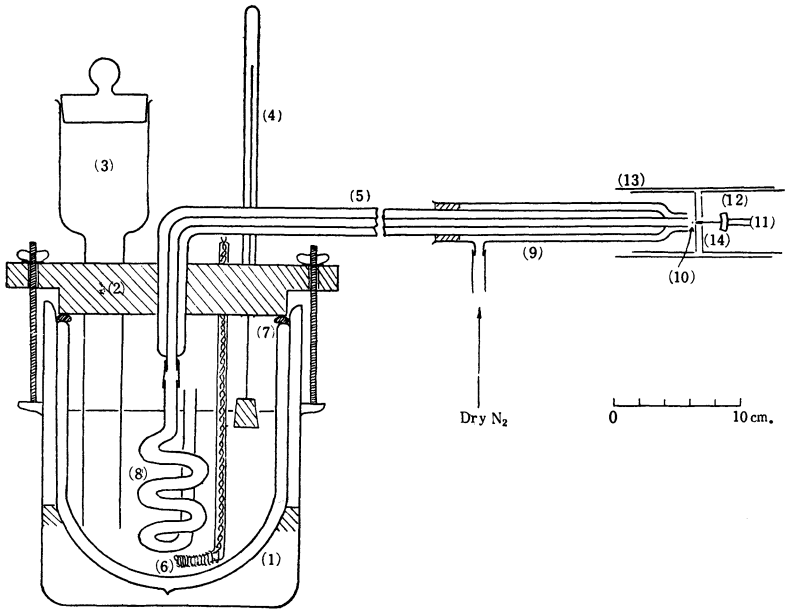


Fig. 1. Cooling apparatus.
(1) Dewar bottle. (2) Wooden cap. (3) Tube for filling. (4) Level indicator. (5) Vacuum jacketed nozzle. (6) Heating coil. (7) Rubber packing. (8) Copper tube. (9) Supplementary nozzle for dry nitrogen. (10) Thermocouple junction. (11) Goniometer head. (12) Screen. (13) Film pack. (14) Crystal.

group are: $a=21.26\pm0.06$, $b=8.28_5\pm0.04$, $c=3.91\pm0.03$Å and $P2_12_12_1$-D_2^4.

Using Cu K_α radiation, three complete sets of relative intensities for ($hk0$) were obtained by the Weissenberg procedure. Throughout the experiment temperature was kept within the range of ±5°C. The specimens used have the following maximum and minimum dimensions at right angle to the axis of rotation: crystal 1, 0.005×0.023; crystal 2, 0.004×0.018; crystal 3, 0.005×0.020 cm.

Intensities were estimated by visual comparison with a scale, which was prepared by counting the number of times of the repeating reflexion of the crystal 3. The multiple-film technique was used to correlate strong and weak reflexions, ranging in relative intensities from 25000 to 1. The corrections for polarization and Lorentz factors were made in the usual way. The effect due to the shape of the specimen was also allowed for.

The values of structure factors used in the following analysis are the weighted means of the values in the above mentioned three sets. Reflexions from 188 planes were observed out of 229 possible ($hk0$)'s.

Results

Refinement of the (001) Projection and Location of the Hydrogen Atoms. — The structure factors observed at -110°C almost agreed with those observed at room temperature, if the mean temperature factor of 4.0×10^{-16}cm^2 was applied to the former. This implies that the structure at low temperature remains essentially the same as that of room temperature so that the refinement can be made starting from the coordinates reported in the preceding paper[6].

Two successive Fourier and an (F_o-F_c) syntheses on the (001) plane were applied to correct the atomic coordinates. The corrections were estimated from the equation

$$\Delta r=(\mathrm{d}(\rho_o-\rho_c)/\mathrm{d}r)_{r=0}/2p\rho(0)$$

where $\rho(0)$ is the electron density at an atomic centre and p is a constant, whose value was deduced from the second Fourier map assuming the electron density near an atomic centre to be represented by the equation

$$\rho(r)=\rho(0)\ \exp(-pr^2)$$

In the structure-factor calculation, the atomic scattering factors were taken from McWeeny[14], using for oxygen $\bar{f}_o=\frac{1}{3}\times(f^{\parallel}+2f^{\perp})$, and for carbon the values for 'valence states'.

It was observed from the $(\rho_o-\rho_c)$ map that the magnitudes of thermal motions of individual atoms are different from each other and some of them are considerably anisotropic. These thermal

14) R. McWeeny, *Acta Cryst.*, **4**, 513 (1951).

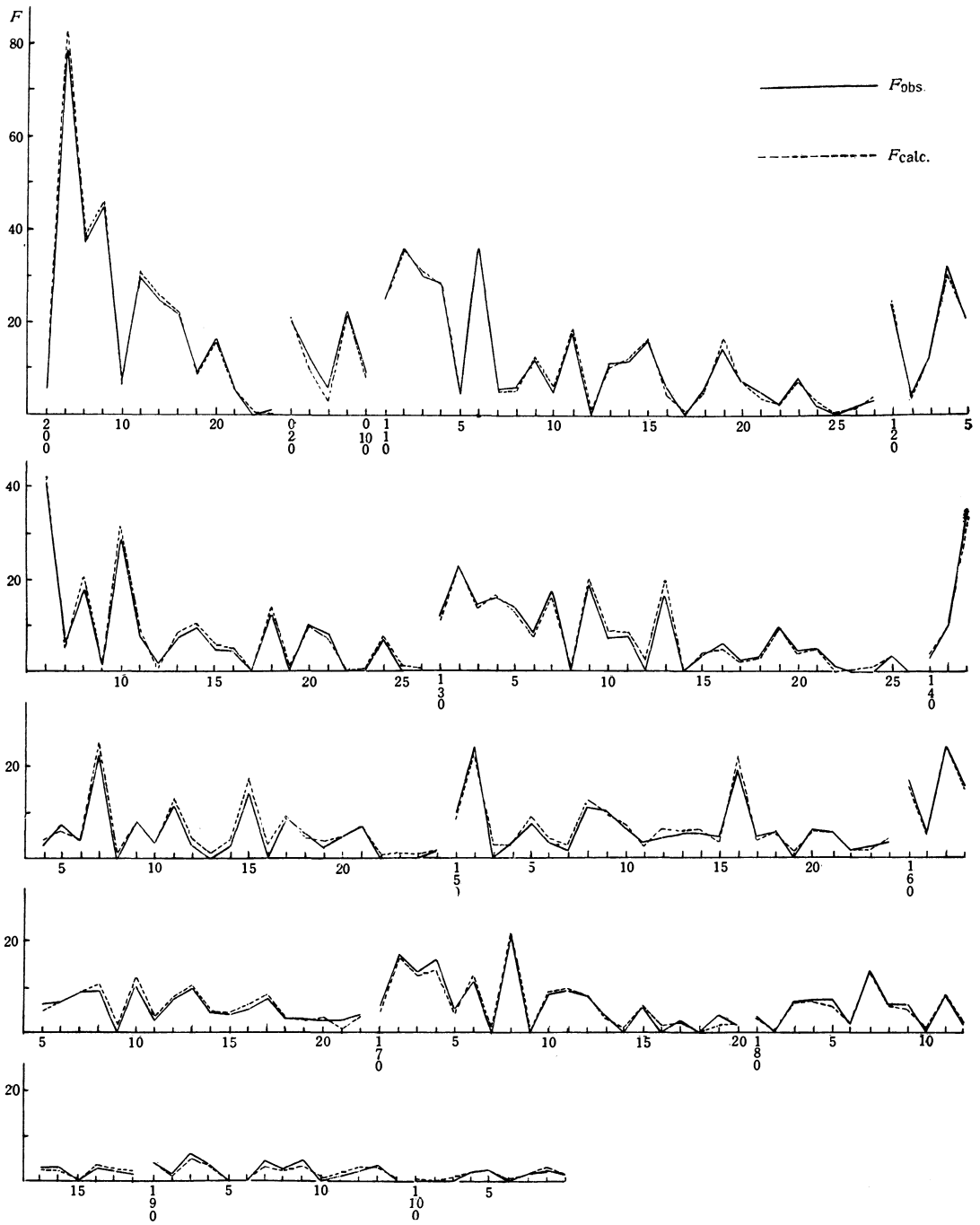


Fig. 2. Observed and calculated structure factors, $F(hk0)$.

factors for individual atoms and their anisotropy were obtained from the successive three (F_o-F_c) syntheses in the following way. The corrections for thermal factors were estimated from the equation[15]

$$\Delta B=\pi^2(\mathrm{d}^2(\rho_o-\rho_c)/\mathrm{d}r^2)_{r=0}/p^2\rho(0)$$

For the atoms vibrating anisotropically, the scattering factors of the form

$$f=f_0\exp[-\{\alpha+\beta\sin^2(\phi-\psi_b)\}(\sin\theta/\lambda)^2]$$

were employed[16,17], where α and β are

15) Y. Sasada, to be published.

16) E. W. Hughes, *J. Am. Chem. Soc.*, **63**, 1737 (1941).
17) W. Cochran, *Acta Cryst.*, **4**, 81 (1951).

constants, ψ_b is the angle between the direction of maximum vibration and the b axis, and $(2\sin\theta, \phi)$ are the polar coordinates of a point in the $(hk0)$ section of the reciprocal lattice, measured from the a^* axis. In the projection it should be noted that only two molecules are equivalent in dealing with the anisotropic vibrations.

Throughout these refinements F_c included the contributions from hydrogen atoms placed radially at a distance of 1.0 Å from the carbon atoms. In Table I are listed the final atomic coordinates and the final thermal parameters. The comparison between observed and calculated structure factors is shown in Fig. 2, where the R index becomes 0.097.

TABLE I
ATOMIC COORDINATES AND THERMAL FACTORS (AT −110°C)

Atom	x/a	y/b	z/c	α	β	ψ_b
O_1	0.099_5	0.554	0.218	2.3	0.5	97°
O_2	0.168	0.722	0.470	2.6	1.3	87
C_2	0.157	0.589	0.344	2.8	0.5	90
C_3	0.194	0.451	0.319	2.8	0.5	85
C_4	0.180	0.169	0.110	2.3	0.5	95
C_5	0.145_5	0.050	−0.034	2.3	1.7	92
C_6	0.084_5	0.052	−0.160	2.6	1.4	83
C_7	0.042	0.175	−0.168	3.3	0	—
C_8	0.049	0.336	−0.043	2.8	0	—
C_9	0.100_5	0.398	0.115	2.2	0	—
C_{10}	0.162	0.329	0.168	2.2	0	—

Figs. 3 and 4 show the final Fourier projection on the (001) plane and the fifth $(\rho_o-\rho_c)$ map respectively. In the calculation of the latter, F_c's do not include the contributions from the hydrogen atoms. The significant peaks on this map are evidently due to the hydrogen atoms.

Coordinates and Molecular Dimensions. —The x and y coordinates obtained by the low temperature refinement hardly differ at all from those at room temperature. The z coordinates, the changes of which have scarcely any influence on the intra- and intermolecular distances due to the short c period, were expected to show no significant differences with those at room temperature. In fact, the change of the c period is of the same order as that of the a axis and a few oscillation photographs at low temperature did not show essential differences. Therefore the same z coordinates as those at room temperature are used in the following discussions. The final coordinates of the carbon and oxygen atoms are shown in Table I.

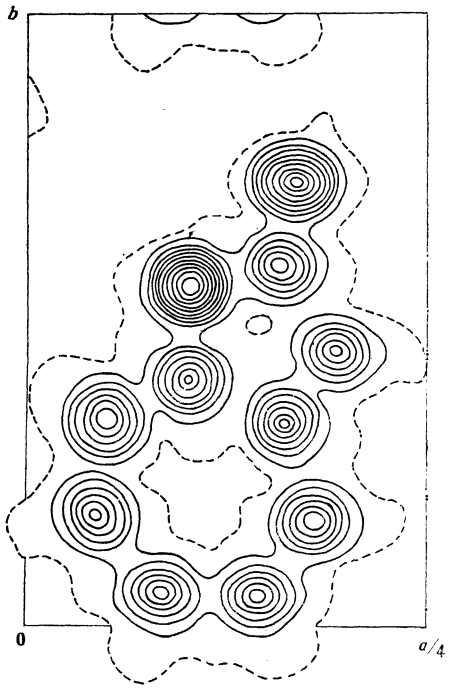


Fig. 3. The final Fourier projection of the electron density on (001). Contours at intervals of 1 e. Å^{-2}. Contour at 1 e. A^{-2} is broken.

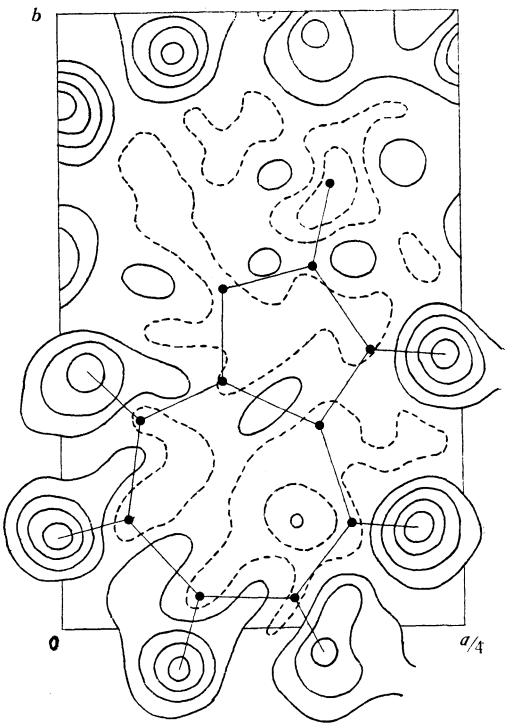


Fig. 4. The final $(\rho_o-\rho_c)$ projection on (001). Contours at intervals of 0.2 e. Å^{-2}. The zero and negative contours are broken.

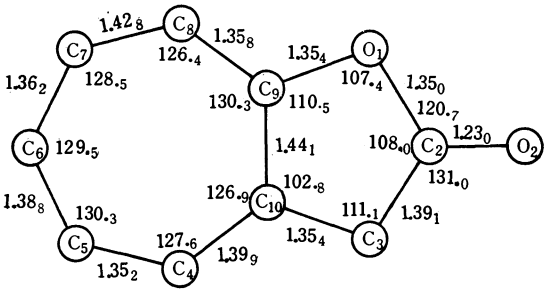
By the use of least squares method the best plane through all carbon and oxygen atoms in the fused ring was determined to be

$$z=0.3634x+0.3192y-1.4186$$

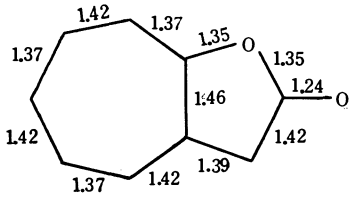
The perpendicular displacements of individual atoms from this mean plane are shown in Table II. The average displacement is 0.02$_4$ Å. The bond lengths and valency angles in the molecule are shown in Fig. 5 (a).

TABLE II
THE PERPENDICULAR DISPLACEMENT OF THE ATOMS FROM THE MEAN PLANE

Atom	Displacement (Å)
O_1	+0.033
O_2	+0.044
C_2	−0.007
C_3	−0.023
C_4	+0.010
C_5	+0.027
C_6	+0.002
C_7	−0.023
C_8	−0.015
C_9	+0.036
C_{10}	−0.042



(a)



(b)

Fig. 5. (a) Observed bond lengths (Å) and bond angles (°). (b) Bond lengths calculated by Pauling's relation.

The estimated positions of hydrogen atoms from the fifth ($\rho_o-\rho_c$) map are given in Table III, the z coordinates being obtained by substituting the estimated x and y values in the equation of the mean plane of the molecule, although the assumed positions were used in the calculations of the ($hk0$) structure factors.

TABLE III
HYDROGEN COORDINATES AND BOND LENGTHS OF C—H

Atom	x(Å)	y(Å)	z(Å)
H_3	5.14	3.62	1.61
H_4	4.72	1.33	0.72
H_5	3.40	−0.31	−0.28
H_6	1.53	−0.58	−1.05
H_7	0.04	1.22	−1.02
H_8	0.36	3.46	−0.18

C_3—H_3=1.09, C_4—H_4=0.94, C_5—H_5=0.80, C_6—H_6=1.13, C_7—H_7=0.95, C_8—H_8=0.91 Å

Estimation of Accuracy.—The standard deviations of the atomic coordinates, $\sigma(x)$ and $\sigma(y)$ were estimated by the method of Cruickshank[18-20] as follows: $\sigma(x)$= 0.010−0.012; $\sigma(y)$=0.007−0.009 Å for carbon; $\sigma(x)$=0.007−0.008; $\sigma(y)$=0.005 Å for oxygen.

If the small error introduced by the uncertainty of the molecular orientation is ignored, the standard deviation of a bond length can be shown, in this case, to be

$$\sigma(b)=\sigma(d)\times b/d$$

where b is the length of the bond and d is its length in the projection on (001). From this equation the standard deviation of a C—C bond comes out to be about 0.018Å, and that of a C—O bond about 0.012 Å. The average standard deviation of bond angles was found to be 0.7°, and the standard deviation of electron density was 0.18 e. Å^{-2} for the (001) projection.

Discussion

Molecular Structure. — It is recognized clearly from Fig. 5 (a) that a larger and a

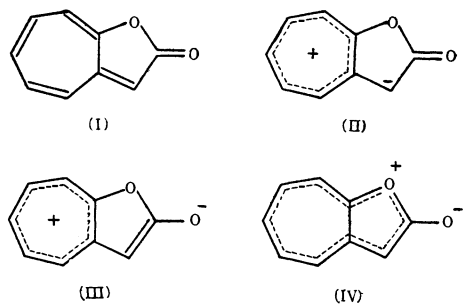


Fig. 6. Canonical formulae.

18) D. W. J. Cruickshank, ibid., **2**, 65 (1949).
19) D. W. J. Cruickshank, ibid., **7**, 519 (1954).
20) F. R. Ahmed and D. W. J. Cruickshank, ibid., **6**, 385 (1953).

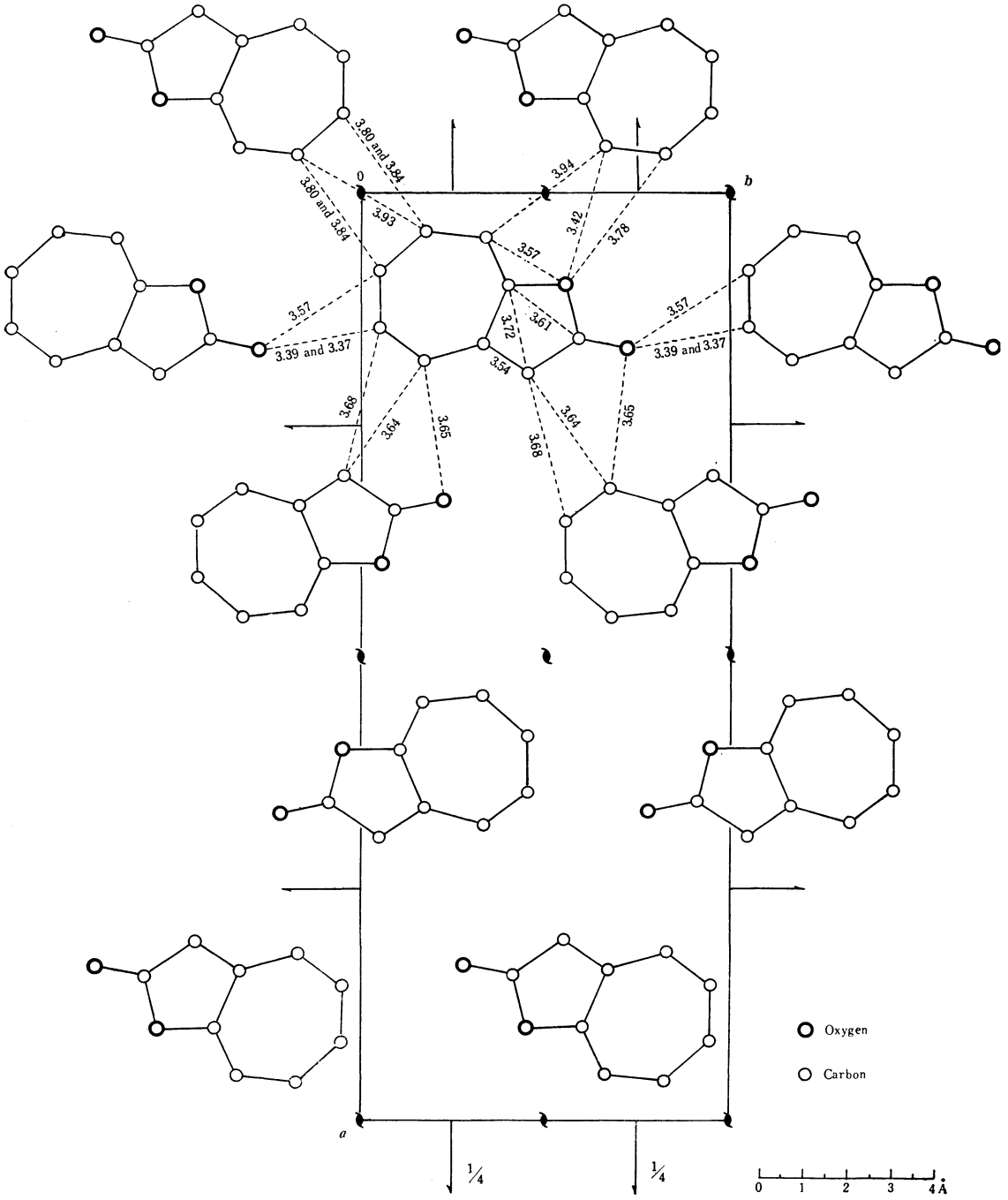


Fig. 7. Arrangement of molecules in the (001) projection with intermolecular distances (Å).

shorter C—C bonds are disposed alternately. The mean values for the larger and shorter C—C bonds are 1.40_9 and 1.35_7Å with estimated standard deviations of 0.01_0 Å respectively. The difference between these two values is highly significant, and this fact favors the conventional chemical formula I shown in Fig. 6.

However, the mean value of the larger C—C bonds and that of two C—O bonds in the five-membered ring (with standard deviation of 0.01_0 Å) are significantly different from their pure single bond lengths respectively. Thus, in order to interpret the bond distances more quantitatively, it becomes necessary to take into account the many resonance structures shown in Fig. 6.

In other words this molecule is not a simple γ-lactone but has the contributions from the structures similar to those in azulene and tropolone. As in the case of tropolone, the carbonyl oxygen is responsible for the drawing out of the ring electron and the lone pair electrons of the oxygen atom in 1-position supply the electron to carbonyl oxygen. The best agreement between measured and calculated bond lengths was obtained taking the following contributions: I, 34%; II (seven structures), each 3%; III (seven structures), each 3%; IV (two structures), each 12%, the relation[21]

$$R=R_1-(R_1-R_2)3x/(2x+1)$$

being used with $R_1=1.54$(C—C), $R_2=1.34$ Å (C=C), $R_1=1.42$ (C—O) and $R_2=1.20$ Å (C=O), (Fig. 5 (b)).

Considering the resonance structures given above, it seems that the seven-membered ring itself is somewhat positively charged. This is justified by the large dipole moment of this molecule[22] and by some chemical evidences[23], and also compatible with characteristic molecular arrangement in the crystal described in Part I of this series[6].

Molecular Arrangement. — The crystal structures projected on the (001) and (010)

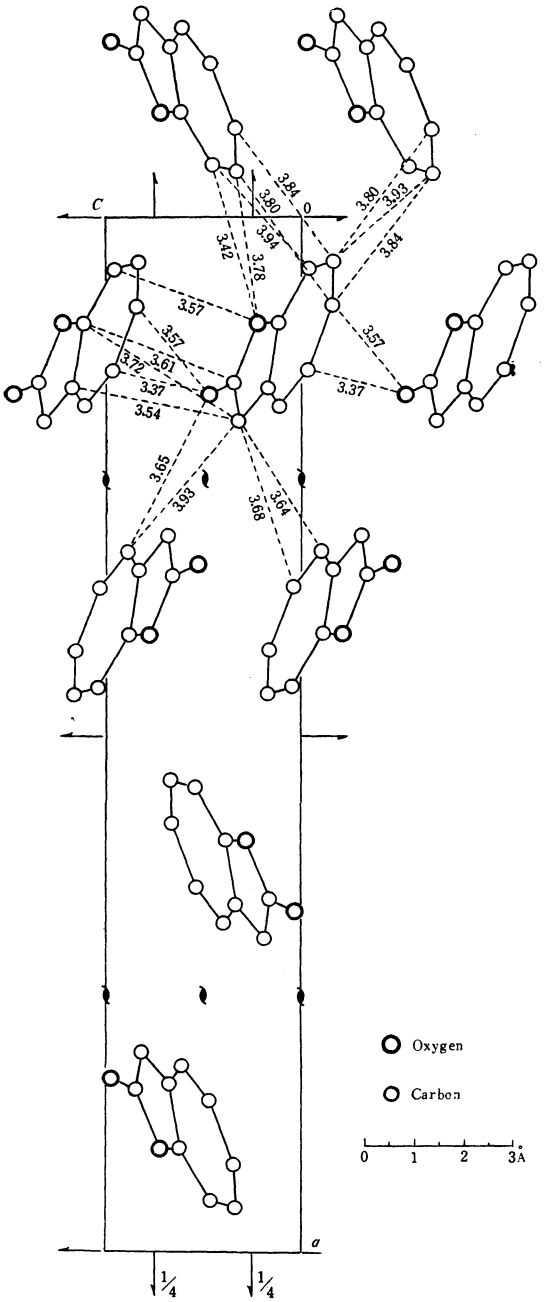


Fig. 8. Arrangement of molecules in the (010) projection with intermolecular distances (Å).

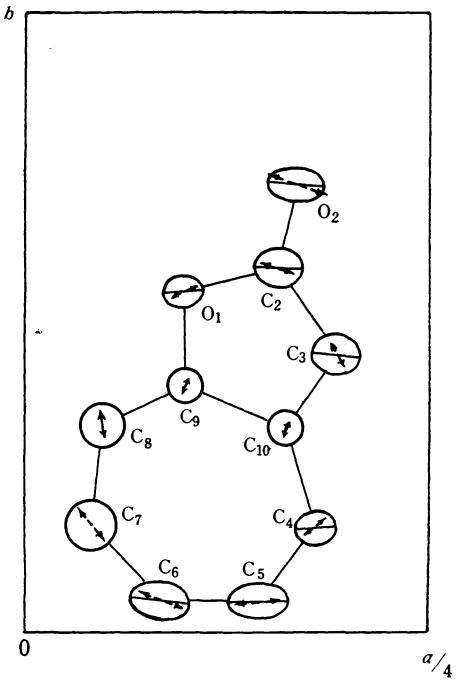


Fig. 9. Anisotropic thermal motions of individual atoms. Dimensions of solid circles and ellipses are proportional to the r. m. s. amplitudes estimated from B factors. The dotted arrows show the direction and relative magnitudes of the vibration of individual atoms due to the rigid-body angular oscillation of the molecule about its mass centre.

21) L. Pauling, "The Nature of the Chemical Bond", Ithaca, Cornell University Press, (1948).
22) Y. Kurita and M. Kubo, to be published.
23) S. Seto, *Sci. Rep. Tahoku Univ., Ser. I*, **37**, 367 (1953).

planes are shown in Figs. 7 and 8 respectively, together with the intermolecular distances. Intermolecular distances at a low temperature are shorter by about 0.03 Å than those at room temperature. Anisotropy of the change of the intermolecular distances, however, can not be detected owing to the greater standard deviations for them at room temperature.

Although an outline of the crystal structure is the same as that mentioned in Part I, the molecular arrangement can also be described as an assembly of the rods in which the molecules are joined together in a file by the interaction of dipoles in the same directions. The interaction between rods is less than that in the rod.

The thermal expansion coefficient along the *b* axis, which agrees approximately with the direction of the rod, is of negative sign, and those along the *a* and *c* axes are positive and of the same order as those in ordinary organic crystals[24]. This fact can be interpreted well from the point of view mentioned above, and will be further discussed in the following paragraph in connection with the anisotropic thermal vibrations.

Anisotropic Thermal Motion. — Fig. 9 shows the anisotropic thermal vibrations schematically. Dimensions of solid circles and ellipses are proportional to the r.m.s. amplitudes estimated from the *B* factors. These can be understood as the coupling of rigid-body libration of the molecule about its mass centre and the translational vibration whose amplitude along the *a* axis is greatest. The r. m. s. amplitudes of angular oscillation are about 3° and those of the translational vibration along the *a* and *b* axes 0.17 and 0.15 Å respectively. Contrary to the cases of naphthalene[9] and anthracene[11,12], the translational amplitude along the long axis of the molecule is smaller than that along the short axis. This is compatible with the characteristic arrangement of the polar molecules mentioned above.

The present author wishes to express his sincere thanks to Professor I. Nitta for his guidance and encouragement throughout this work. He is also indebted to Professor T. Nozoe for supplying the sample and for his continued interest and to Professor T. Watanabé for his kind advice particularly on the low temperature techniques.

Department of Chemistry, Faculty of Science, Osaka University
Kita-ku, Osaka

24) I. Woodward, *Acta Cryst.*, **11**, 441 (1958).

*The Roles of Prolyl Residue in Polypeptide Monolayers. I. On the Chain Configurations Deduced from Surface Pressure and Potential Measurements**

By Toshizo ISEMURA and Shoichi IKEDA

(Received August 25, 1958)

During the last decade, investigations on synthetic polypeptides as model substances of protein have made great progress. Their monolayer properties have also been studied and clarified by the present authors[1] and many other workers[2,3]. In these studies synthetic polypeptides with non-electrolytic or unionized electrolytic side chains are found to spread as condensed monolayers at the air-water interface. Many globular proteins also give condensed monolayers at the same interface. Generally, monolayers of high polymeric substances are of condensed type under the strong interaction between

* Surface Chemistry of Synthetic Protein Analogus VIII.

1) T. Isemura and K. Hamaguchi, This Bulletin, **26**, 425 (1953); **27**, 125. 339 (1954).
K. Hamaguchi and T. Isemura, ibid., **28**, 9 (1955).
T. Isemura, K. Hamaguchi and S. Ikeda, *J. Polymer Sci.*, **23**, 651 (1957).

2) D. F. Cheesman and J. T. Davies, *Adv. Protein Chem.*, **9**, 439 (1954).

3) C. H. Bamford, A. Elliott and W. E. Hanby, "Synthetic PolyPeptides", Academic Press, New York (1956), p. 355-360.

constituent monomer units and of expanded type under the weak interaction.

Among amino acid residues constituting polypeptide chains in protein, prolyl residue is specific in respect to several properties: (1) it can not be incorporated into the β-configuration of a polypeptide chain because it has a pyrrolidine ring which makes a part of the main chain; (2) it reduces the degree of stertic rigidity because it is inhibited from rotating around some bonds involved; and (3) it can form no hydrogen bond with other carbonyl group because the nitrogen atom of keto-imido bond has no hydrogen atom to participate in the hydrogen bonding.

Synthetic polypeptides, the monolayers of which have so far been studied, contain no prolyl residue. It is of great importance to investigate how these properties of prolyl residue affect the behavior of monolayers of polypeptides and to correlate it with the chain configuration, the chain flexibility and the hydrogen bonding. These studies appear to be useful to interpret monolayer properties of gelatin and collagen.

In this connection, we have investigated the monolayers of synthetic polypetides composed of various proportions and arrangements of prolyl residues, that is, poly-DL-alanine, poly-L-prolyl-L-leucylglycine, copoly-1 : 1 : 1-(L-proline, L-leucine, DL-alanine) and poly-L-proline. Poly-L-hydroxyproline was also examined for comparison with poly-L-proline. In this paper, we will describe the results and some inferences derived from the measurements of surface pressure and potential.

Experimental

Materials.—Poly-DL-alanine is a sample prepared by Dr. Tani[4], the degree of polymerization of which was found to be about 300 by surface pressure measurement. It was spread from the solution in a mixed solvent, dichloroacetic acid-benzene (1 : 9 v/v). Poly-L-prolyl-L-leucylglycine is a sample synthesized by Dr. Sakakibara[5]. Its degree of polymerization was found to be 13 by end-group analysis and surface chemical method. Copoly-1 : 1 : 1-(L-proline, L-leucine, DL-alanine), poly-L-proline II[6] and poly-L-hydroxy-proline are gifts of Dr. Kurtz through Professor Noguchi. The degree of polymerization of copoly-1 : 1 : 1-(L-proline, L-leucine, DL-alanine) was found to be 129 by surface pressure measurement. Poly-L-prolyl-L-leucylglycine and copoly-1 : 1 : 1-(L-proline, L-leucine, DL-alanine) were spread from the solution in a mixed solvent, dichloroaceticacid-benzene (1:4 v/v). The spreading solvent for poly-L-proline II (D. P. 50) and poly-L-hydroxyproline (D. P. unknown) was 50% (v/v) isopropyl alcohol. Because of their hygroscopic nature, poly-L-prolyl-L-leucylglycine, poly-L-proline II and poly-L-hydroxyproline were dried for several hours at the boiling point of toluene in an Abderhalden's pistol, before weighing for preparing the spreading solutions. Poly-L-prolyl-L-leucylglycine contains one molecule of water of crystallization per periodic unit after such drying.

Distilled water was used as aqueous subphases, unless otherwise stated. The pH of subphases was adjusted by 0.01 N hydrochloric acid or by 0.01 M potassium carbonate, if necessary. To certify the minimum solubility of the sample into the aqueous phase, potassium chloride was often added, which was recrystallized from water after removing surface active impurities by using active charcoal as adsorbent and then baked.

Methods.—Surface pressure was measured by a surface balance of float type with a mica float and a double torque system. Its sensitivity was better than 0.01 dyne per cm. Surface potential was measured by the vibrating electrode method. The electrode was made of gold of 2 cm. in diameter. The signal picked up by the electrode was amplified by a three stage A. C. amplifier and detected by an oscilloscope. The potential was determined by the compensation method with a potentiometer. The trough was made of polymethyl methacrylate, the rim of which was coated by a thin paraffin layer to ensure a high contact angle.

All the measurements were carried out at room temperature, but the fluctuation of temperature never exceeded 1° during the experiments. The solution was spread by means of a micrometer syringe. Fifteen minutes after spreading, the compression of film was started. The films of all polypeptides other than poly-L-proline and poly-L-hydroxyproline showed no time effect.

Results

Surface pressure-area (Π-A) and surface potential-area ($\Delta V - A$) curves of poly-DL-alanine, poly-L-prolyl-L-leucylglycine and copoly-1 : 1 : 1-(L-proline, L-leucine, DL-alanine) are shown in Figs. 1, 2, and 3, respectively. For comparison with poly-L-prolyl-L-leucylglycine, area of copoly-1 : 1 : 1-(L-proline, L-leucine, DL-alanine) in Fig. 3 was denoted in the unit of A^2 per three amino acid residues. In Fig. 4 the Π-A and ΔV-A curves of poly-L-proline together with the Π-A curve of poly-L-hydroxyproline both on 1 M potassium chloride are shown. The Π-A and ΔV-A curves of all these polypeptides other than the last

4) H. Tani and C. Ooizumi, Symposium on Synthetic Polypeptids, Osaka, Oct. 28, 1957.
5) H. Kitaoka, S. Sakakibara and H. Tani, This Bulletin, **31**, 802 (1958).
6) A. Berger, J. Kurtz and E. Katchalski, *J. Chem. Soc.*, **76**, 5552 (1954).

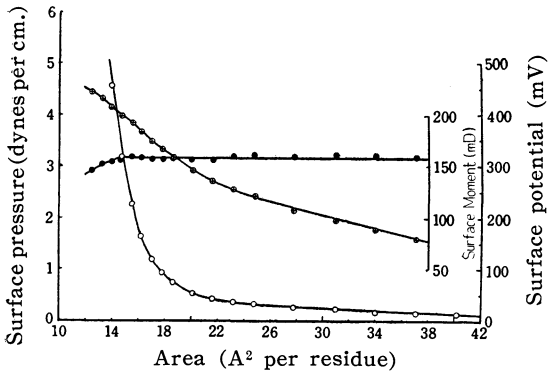


Fig. 1. Surface pressure (○), potential (⊕) and moment (●) *vs.* area curves of poly-DL-alanine at 18°C.

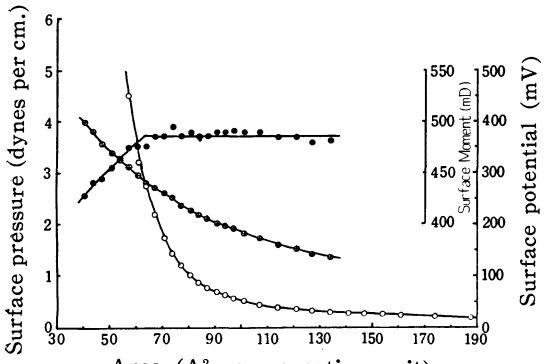


Fig. 2. Surface pressure (○), potential (⊕) and moment (●) *vs.* area curves of poly-L-prolyl-L-leucyglycine at 27°C.

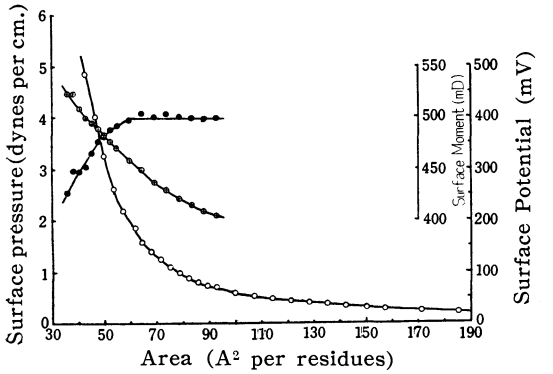


Fig. 3. Surface pressure (○), potential (⊕) and moment (●) *vs.* area curves of copoly-1 : 1 : 1-(L-proline, L-leucine, DL-alanine) at 16°C.

two were not affected by the addition of potassium chloride in the concentration of 0.1 M into the aqueous subphase. Therefore, they are considered to be spread completely as monomolecular films. The surface moment-area (μ-A) curves are also shown in these figures, which were calculated by the Helmholtz equation,

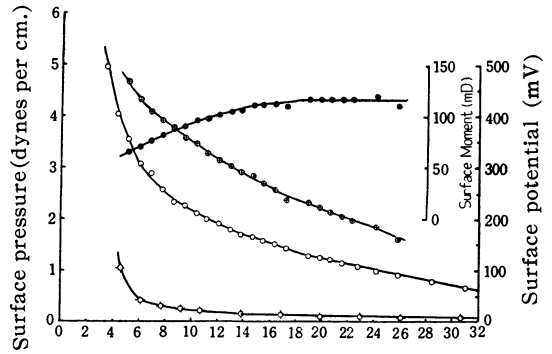


Fig. 4. Surface pressure (○), potential (⊕) and moment (●) *vs.* area curves of poly-L-proline and surface pressure-(◇) area curve of poly-L-hydroxyproline on 1 M potassium chloride at 29°C.

$$\Delta V = \frac{4\pi\mu}{A}$$

In the Π-A curve there appears an area, A_Π, where the surface compressibility

$$\delta = -\frac{1}{A}\frac{\partial A}{\partial \Pi}$$

is a minimum. This area corresponds to that occupied by a repeating unit in the close-packed monolayer. The surface moment is constant, namely, μ_c, over certain regions of area. When the monolayer is compressed, the surface moment begins to decrease at a certain definite area, A_μ. This area is that where the electric dipole of repeating unit begins to change its orientation. Since the dipole is considered to be contributed mainly by the carbonyl groups of peptide bonds in the polypeptides studied (except for poly-L-hydroxyproline), the values of surface moment are concerned with the orientation of carbonyl groups in the monolayer. All these characteristics are summarized in Table I.

TABLE I
MONOLAYER CHARACTERISTICS OF POLYPEPTIDES

Polypeptides	A_Π A² per repeating unit	A_μ A² per repeating unit	μ_c mD
Poly-DL-alanine	14.9	14.8	158
Poly-L-prolyl-L-leucyl-glycine	57	63	162×3
Copoly-1 : 1 : 1-(L-proline, L-leucine, DL-alanine)	46*	60*	166×3

* A² per three amino acid residues.

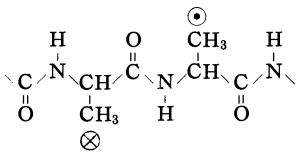
In spite of the marked difference in surface pressure among three polypeptides completely spread as monolayer, that is,

poly-DL-alanine, poly-L-prolyl-L-leucylglycine and copoly-1 : 1 : 1-(L-proline, L-leucine, DL-alanine), the values of surface moment were found to be nearly equal to one another, μ_c being about 160 mD per amino acid residue, as seen in Table I. This means that the orientation of the carbonyl groups of all these polypeptides are almost the same. Taking the electric moment of carbonyl group to be 360 mD, following Davies[7], it may be directed to 30° downwards to the aqueous surface.

Discussion

Chain Configuration in Polypeptide Films. — *a) Poly-DL-alanine.* — Poly-DL-alanine gives a monolayer of condensed type. Its Π-A and ΔV-A curves have already been reported by Glazer and Dogan[8], and its μ-A curve has been measured by Davies[7]. The Π-A curve in Fig. 1 shifts somewhat to larger area than that of Glazer and Dogan's, but the ΔV-A curve is in good agreement. The A_μ value found from the μ-A curve is much less than Davies'. The monolayer of poly-DL-alanine is much more condensed than some vinyl polymers with side-chains of the same order of length, such as polyvinyl acetate[9-12] and polyethyl acrylate[9]. This is attributed to the fact that the polypeptide chain is held together rigidly by the intrachain hydrogen bonds and is less flexible by the partial double bond nature of peptide bonds. The minor dependence of surface pressure on temperature also supports this view.

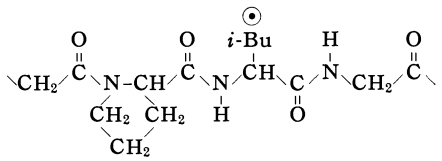
From the data in Table I, it appears probable that the β-configuration with the alternation of side-chains, methyl groups, up and down to the surface,



⊙ above the interface
⊗ below the interface

makes most parts of the chain, as Cumper and Alexander[13] and Davies[7,14] suggested from the surface viscosity and surface potential measurements, respectively.

b) Poly-L-prolyl-L-leucylglycine.—Recently, Leung and Marsh[15] determined the crystal structure of the tripeptide, L-leucyl-L-prolylglycine, which is similar to the repeating unit of poly-L-prolyl-L-leucylglycine. They found that all the peptide bonds are planar-*trans* and the tripeptide is in a highly extended configuration. Such a configuration appears to be probable also in this polypeptide. On the basis of these requirements and data in Table I, a possible configuration at the interface may be suggested as follows:



⊙ above the interface

in which the main chain assumes a β-configuration except for the glycyl-L-prolyl bond, and the side-chain of L-leucyl residue stands up out of the aqueous surface. While at the area larger than A_μ all pyrrolidine rings of L-prolyl residues lie flat on the aqueous surface, at the area less than A_μ some of them rise on the surface and at the area equal to A_Π all of them rise and are closely packed.

c) Copoly-1 : 1 : 1-(L-proline, L-leucine, DL-alanine). — Although copoly-1 : 1 : 1-(L-proline, L-leucine, DL-alanine) has the same proline content as poly-L-prolyl-L-leucylglycine, the arrangements of prolyl and the other residues in the amino acid sequences might be different from each other. As seen in Table I, whereas the values of A_μ are equal for these two polypeptides, A_Π for the former is much less than that of the latter. The former monolayer is more expanded. At the area larger than A_μ, their chain configurations appear to be similar to each other, and they should, however, be different at the area less than A_μ. The amino acid sequence in the former polypeptide cannot, therefore, be entirely periodic as in the latter. On the other hand, if it would contain any successive prolyl residues in some parts of the chain, no prolyl residues could always

7) J. T. Davies, *Biochim. Biophys. Acta*, **111**, 165 (1953).
8) J. Glazer and M. Z. Dogan, *Trans. Faraday Soc.*, **49**, 448 (1953).
9) D. J. Grisp, *J. Colloid Sci.*, **1**, 49 (1946).
10) G. C. Benson and R. L. McIntosh, ibid., **3**, 223 (1948).
11) T. Isemura, H. Hotta and T. Miwa, This Bulltetin, **26**, 380 (1953).
12) M. J. Shick, *J. Polymer Sci.*, **25**, 465 (1957).
13) C. W. N. Cumper and A. E. Alexander, *Trans. Faraday Soc.*, **46**, 235 (1950).
14) J. T. Davies, ibid., **49**, 949 (1953).
15) Y. C. Leung and R. F. Marsh, *Acta Cryst.*, **10**, 815. (1957); **11**, 17 (1958).

exist at the interface in an equivalent manner, orientating the pyrrolidine rings and carbonyl groups irregularly. Then the $A_{//}$ and μ_c values would be less than those observed. Thus the copolypeptide should contain the considerable amounts of L-prolyl-R-L-prolyl sequences, where R is either L-leucyl or DL-alanyl residue. Such parts of the chain will be folded by the steric hindrance and rigidity, submerging a part of the main chain into the aqueous subphase, instead of raising the pyrrolidine rings out of the surface, when the monolayer is compressed to the area less than A_{μ}. The other parts of the chain will remain the same as in poly-L-prolyl-L-leucylglycine. Hence, $A_{//}$ is much less than A_{μ}. It may, therefore, be considered that copoly-1:1:1-(L-proline, L-leucine, DL-alanine) is composed of a polypeptide with no successive but irregular arrangements of prolyl residues.

d) Poly-L-proline. — Poly-L-proline exists in two forms[16]. Poly-L-proline I is prepared by polymerization of N-carboxy-L-proline anhydride in pyridine and precipitated by adding ether to the reaction mixture. It is partly soluble in water and dextro-rotatory, $[\alpha]_D^{25}=+40°$. When it is dissolved in formic acid and precipitated by ether, it is transformed into poly-L-proline II, which is soluble in water and highly levo-rotatory, $[\alpha]_D^{25}=-540°$. But poly-L-proline I is regenerated when poly-L-proline II is dissolved into higher alcohols[17].

The poly-L-proline sample given to us was poly-L-proline II. However, at least, its most part is probably transformed into poly-L-proline I in the present spreading solution, that is, in 50% (v/v) isopropyl alcohol solution. The *Π-A* curves of poly-L-proline on various aqueous subphases are shown in Fig. 5. It is unstable on salt-free subphases, and the higher the pH of the aqueous subphase, the more stable and the more expanded the film. The addition of potassium chloride into the water phase also aids the spreading of film. In any cases examined, films are of expanded type and pressure-soluble.

According to the study of X-ray diffraction by Cowan and McGavin[18], poly-L-proline II in the crystalline state exists in a left-handed helix with 3 residues per

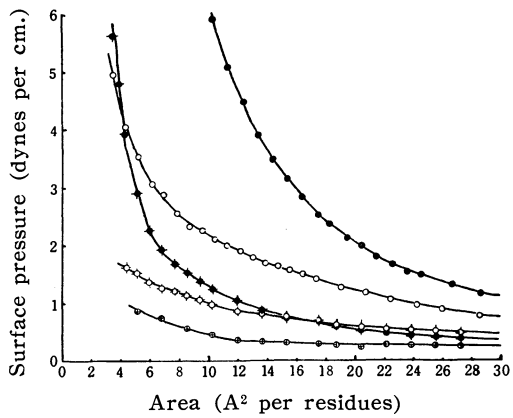


Fig. 5. Surface pressure-area curves of poly-L-proline on various aqueous subphases at 29°C: ⊕, 0.01 N HCl; ◇, H_2O; ○, 1 M KCl; ◆, 0.01 M K_2CO_3; ●, 0.01 M K_2CO_3; 1 M KCl.

turn, the keto-imido bonds being planar-*trans*. On the other hand, though no data on the structure of poly-L-proline I is available, Katchalski[17] inferred it to be a right-handed helix with *cis* bonds, and actually Crick and Rich[19] have deduced it to have approximately $3^1/_8$ residues per turn. Both structures have a high degree of steric rigidities, only permissible to the *cis-trans* transformation. Harrington and Sela[20] have demonstrated this for aqueous solutions. It will be found that no proline residues of poly-L-proline can always exist in an equivalent manner, when it is spread at the interface. Then no carbonyl groups can always orientate to the same direction, and the surface moment is, therefore, relatively low, owing to the intrachain cancellation of dipole moments. In fact, the values of μ_c did not exceed 120 mD in the cases of various subphases examined. The results obtained in the present investigation suggest that the *trans* peptide bonds in poly-L-proline dissolve into the aqueous subphase and the *cis* bonds remain on the surface, after being subjected to the *cis-trans* transformation, as soon as poly-L-proline I is spread. The lower the pH of subphase, the more feasible the transformation will be. The dependence of film behavior on the pH appears to have some correlation with the mutarotation of poly-L-proline I in formic acid, acetic acid or water. The addition of potassium chloride will support the *trans-cis* transformation, reducing the water

16) J. Kurtz, A. Berger and E. Katchalski, *Nature*, **178**, 1066 (1956).
17) E. Katchalski, Symposium on Synthetic Polypeptides, Osaka, Oct. 28, 1957.
18) P. M. Cowan and S. McGavin, *Nature*, **176**, 501 (1955).
19) F. H. C. Crick and A. Rich, cited in ref. (20).
20) W. F. Harrington and M. Sela, *Biochim. Biophys. Acta*, **27**, 24 (1958).

activity. The expanded nature of poly-L-proline films may be attributed to their being devoid of hydrogen bond, as shown later.

General Behavior of Polypeptide Monolayers.—From the Π-A curves in Figs. 1, 2, 3 and 4, it can be noticed that the polypeptide films change from the condensed type to the expanded type in the following order:

poly-DL-alanine;

poly-L-prolyl-L-leucylglycine;

copoly-1 : 1 : 1-(L-proline, L-leucine, DL-alanine);

poly-L-proline.

This order suggests that the higher the prolyl content, the more expanded the film, although the extent of the expansion of film depends also on the arrangement of prolyl residues in the polypeptide sequence. Even poly-DL-alanine, which has the shortest side-chain among polypeptides to be spread as monolayer, gives a very condensed film. The film of poly-L-proline is one of the most expanded.

To distinguish which factor of prolyl residue mentioned earlier is the most responsible for the expansion of film, the film of poly-L-hydroxyproline was studied which differs from poly-L-proline only in the presence of hydroxyl groups on pyrrolidine rings capable of hydrogen bonding. Its Π-A curve on 1 M potassium chloride solution is shown in Fig. 4. The film was unstable and spread incompletely even on such a concentrated salt solution. It is, however, of condensed type. Therefore, the expanded nature of poly-L-proline film may be attributed to the absence of hydrogen bond. The order of expansion of polypeptide films will mainly come from the fact that the prolyl residues involved reduce the number of hydrogen bonds in the film state. The hydrogen bonds in film hold the polypeptide chain together and make it rigid, and, conversely, their decrease in number will make the chain extended and flexible. Accordingly, it is believed that the chain flexibility caused by the reduced number of intrachain hydrogen bonds is generally more effective than the steric rigidity in the monolayer of polypeptide containing prolyl residues.

It is found from Table I that while the condensed poly-DL-alanine monolayer has equal values of A_{Π} and A_{μ}, the expanded monolayer of the other two polypeptides has A_{Π} values less than A_{μ} values. Such a difference between monolayers of condensed and expanded type is extensively observed in other polymers so far reported. Since the condensation and expansion of monolayers of polymers are related to the intrachain interaction, this property depends on the chain configuration in monolayer. The condensed monolayer will collapse if it is compressed beyond the close-packed area, because the molecular chain is held together rigidly. In the expanded monolayer, however, the molecular chain can readily reorientate or fold itself on compression, as it is flexible. The difference in chain configuration or intrachain interaction is considered to be manifested in the monolayer property mentioned above.

Summary

To elucidate the roles of prolyl residue in polypeptide monolayers, the surface films of poly-DL-alanine, poly-L-prolyl-L-leucylglycine, copoly-1 : 1 : 1-(L-proline, L-leucine, DL-alanine), poly-L-proline and poly-L-hydroxyproline were studied by the surface pressure and potential measurements.

The area of minimum surface compressibility and the smallest area of constant surface moment were assigned to each of the first three polypeptides which were found to form monomolecular films. In the region of large area their surface moments were equal to one another and, therefore, the orientations of carbonyl groups might be the same. From these data their chain configurations at the interface were deduced. Poly-DL-alanine exists in the β-configuration and the other two have the similar configuration except for the bonds attached to prolyl residues. Based on the departure in surface pressure behavior of copoly-1 : 1 : 1-(L-proline, L-leucine, DL-alanine) from that of poly-L-prolyl-L-leucylglycine, the arrangement of prolyl residues in the sequence of the former polypeptides was discussed. In the poly-L-proline film it is likely that the parts of *cis* peptide bond form the film and the parts of *trans* bond dissolve into the aqueous subphase.

The polypeptide films were found to be more expanded as the prolyl content was higher, although the arrangement of prolyl residues also affected the expansion of film. From the comparison of poly-L-proline film with poly-L-hydroxyproline,

the evidence was obtained that the expansion of film comes from the decrease in number of hydrogen bonds because of the presence of prolyl residues. The condensation or expansion and its related properties of the film were interpreted in terms of the chain rigidity or flexibility and the intrachain interaction.

The authors are indebted to Dr. H. Tani and Dr. S. Sakakibara of the Faculty of Science, Osaka University, to Dr. J. Kurtz of the Weizmann Institute of Science in Israel and to Professor J. Noguchi of Kanazawa University for supplying the valuable samples. This work was partly supported by a grant given by the Ministry of Education, to which the authors' thanks are also due.

Institute of Scientific and Industrial Research, and Institute for Protein Research Osaka University, Osaka

The Electrolytic Reduction of Ketones at a Mercury Cathode.—Preparation of Organomercuric Compounds

By Toshio ARAI

(Received September 1, 1958)

Tafel[1] reported that on an electrolytic reduction, acetone might be reduced to isopropyl alcohol at a mercury cathode, and later he reported[2] that methyl ethyl ketone was reduced to diisobutyl mercury at a mercury cathode, and acetone to diisopropyl lead at a lead cathode. Haggerty[3] investigated the possibility of preparing diisobutyl mercury from acetone in a sulfuric acid solution at a mercury cathode. Dimenthyl mercury[4] was also obtained from menthone in a strong sulfuric acid electrolyte at a mercury cathode at a higher temperature.

It has been thought that on electrolytic reduction of ketones in a sulfuric acid solution at a mercury cathode, organomercury compounds are produced according to the following formula:

$$2\begin{matrix}R\\R\end{matrix}\!\!>\!C{=}O + 6H^+ + 6F + Hg \rightarrow \begin{matrix}R\\R'\end{matrix}\!\!>\!CH{-}Hg{-}CH\!<\!\begin{matrix}R\\R'\end{matrix} \quad (1)$$

and when the organomercury compounds obtained are treated with mercuric halide in an alcoholic solution, organomercuric halides are prepared as follows:

$$R{-}CH_2{-}Hg{-}CH_2{-}R + HgX_2 \rightarrow 2R{-}CH_2{-}HgX \quad (2)$$

It has been also recognized that when they are treated with hydrogen chloride gas in an alcoholic solution, organomercuric chloride and hydrocarbon are obtained:

$$R{-}CH_2{-}Hg{-}CH_2{-}R + HCl \rightarrow R{-}CH_2HgCl + R{-}CH_3 \quad (3)$$

The author has investigated electrolytic reduction of aryl alkyl ketones and cyclic ketones and prepared organomercury compounds from several ketones by using a diluted sulfuric acid solution at a mercury cathode at a higher temperature. Phenylacetone, acetylbenzoyl[5], cyclopentanone, cyclohexanone, and methylcyclohexanone were reduced to organomercury compounds, and their halides were prepared. These organomercury compounds were shown in Table II. The preparation of other ketones, namely, acetophenone, propiophenone, *p*-methylacetophenone, *p*-bromoacetophenone, benzoin, benzil, 1-acetonaphthone, and dibenzyl ketone were tried in this experiment in the same way, but mercury compounds were not obtained, and corresponding pinacol and alcohol were produced.

In general, it is thought that ketones which have carbonyl radical adjacent to phenyl radical are not reduced to mercury compounds.

1) J. Tafel, *Z. Elektrochem.*, **8**, 288 (1902).
2) J. Tafel, *Ber.*, **39**, 3626 (1906).
3) C. J. Haggerty, *Trans. Am. Electrochem. Soc.*, **56**, 421 (1929).
4) C. Schall and W. Kirst, *Z. Electrochem.*, **29**, 537 (1923).
5) T. Arai, unpublished.

Organomercury compounds were synthesized by many kinds of methods, and dicyclohexyl mercury and its halides were already obtained purely chemically[6,7], but other compounds obtained in this experiment, were not prepared by pure chemical methods. In this experiment the yield of organomercury compounds was not very good; this method, however, seems to be an easy and effective method of syntheses.

Experiment and Discussion

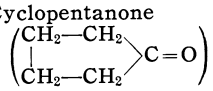
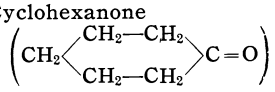
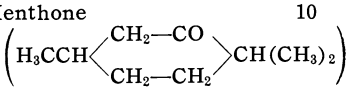
In most cases the cathodic solution consisting of 120 ml. of 5% sulfuric acid in which a ketone was suspended and alcohol was not used as electrolyte. A 5% solution of sulfuric acid served as an anodic solution and cylindrical lead was employed as anode. The anode was separated from the catholyte by means of porous pot. An electrical connection was made with the mercury at the bottom of a cathode by means of platinum wire sealed into a glass narrow tubing. Mercury was purified by washing with nitric acid. The electrolyte was first heated to 50° and during the electrolysis the catholyte was maintained at 50~55° by the reaction heat. The electrolytic chamber was kept upright and the cathodic solution was stirred vigorously. After the current was passed for a short time, a black turbidity appeared in the catholyte. It has been thought[8] that this turbidity seemed to be due to finely divided mercury.

As the electrolysis continued, the cathodic solution gradually cleared up. The amount of electric current passed was about one and a half of the theoretical one. After the electrolysis, a heavy viscous oil floated on the surface of the mercury. The catholyte was placed in a separate funnel, the oil was removed, the residue was extracted with ether, the ether extracts were evaporated under reduced pressure and a solid residue or a viscous oil was obtained. It was mercury compound and the yield of crude product was about 25~30% of the theoretical amount. As the compounds was unstable,

TABLE I

ELECTROLYTIC CONDITIONS

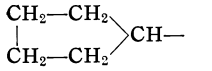
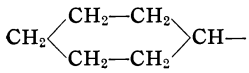
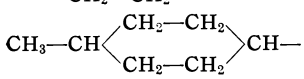
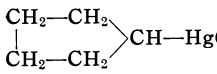
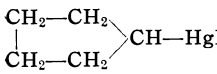
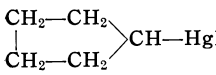
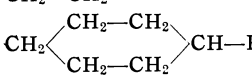
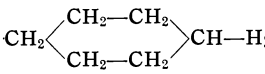
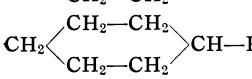
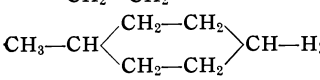
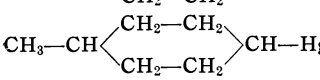
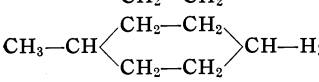
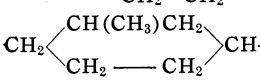
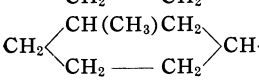
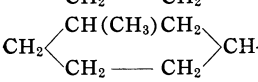
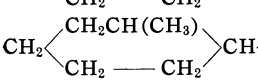
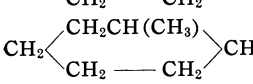
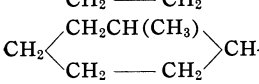
Cathode: Hg 15.2 cm^2; anode: Pb, cylindrical; anolyte: 5% H_2SO_4

Ketones	wt. (g.)	Elect. current amp.	Elect. current hours	Temp. °C	Catholyte	Products
Phenylacetone ($C_6H_5CH_2COCH_3$)	7	2	6	18°	5% H_2SO_4 120 ml.	Recovered
〃	10	2	6	20°	30% H_2SO_4 120 ml.	Hg Compd.
〃	10	3	4	55°	5% H_2SO_4 120 ml.	〃
〃	10	2	6	18°	6 N HCl 60 ml. + glac. HAc 60 ml.	〃
Cyclopentanone 	12	2	8.5	16°	5% H_2SO_4 120 ml.	〃
〃	15	3	5	50°	5% H_2SO_4 120 ml.	〃
〃	10	3	5	20°	6 N HCl 60 ml. + 50% H_2SO_4 60 ml.	〃
〃	10	3	5	21°	6 N HCl 60 ml. + glac. HAc 60 ml.	〃
Cyclohexanone 	20	4	6	55°	5% H_2SO_4 120 ml.	〃
〃	50	4	15	55°	5% H_2SO_4 90 ml.	Pinacol and Hg Compd.
〃	12	3.5	5	16°	30% H_2SO_4 120 ml.	Hg Compd.
2-Methylcyclohexanone	10	3	4	55°	5% H_2SO_4 120 ml.	〃
3-Methylcyclohexanone	10	3	4	55°	5% H_2SO_4 120 ml.	〃
4-Methylcyclohexanone	10	3	4	55°	5% H_2SO_4 120 ml.	〃
Menthone 	10	3	4	60°	50% H_2SO_4 120 ml.	Recovered
Cyclohexanol	10	6	8	60°	50% H_2SO_4 120 ml.	〃
Dibenzylketone ($C_6H_5CH_2COCH_2C_6H_5$)	8	6	6	60°	50% H_2SO_4 120 ml.	〃

6) G. Gruttner, *Ber.*, **47**, 1651 (1914).

7) O. Tiffeneau and O. Gannage, *Chem. Zentr.*, **1**, 766 (1921).

TABLE II
PROPERTIES OF ORGANOMERCURY COMPOUNDS

R—	m.p. °C	Appearance	Solvent	Hg % Calcd.	Hg % Found	References
R—Hg—R (Group I)						
$C_6H_5CH_2CH(CH_3)$—	69～71°	needles	Et-OH	48.25	48.45	
	106～108°	needles	50% Et-OH	59.20	59.51	
	149～151°	needles	50% Et-OH	54.68	54.45	6,7
	172～174°	needles	Et-OH	50.80	50.41	7
R—Hg—X (Group II)						
$C_6H_5CH_2CH(CH_3)$—HgCl	80～81°	needles	Et-OH	56.47	56.49	
$C_6H_5CH_2CH(CH_3)$—HgBr	88°	needles	Et-OH	50.19	50.05	
$C_6H_5CH_2CH(CH_3)$—HgI	90°	needles→ pale yellow	Et-OH	44.91	44.71	
	106～107°	needles	Et-OH	65.73	65.58	10
	108～109°	leaflets	Et-OH	57.37	56.37	
	117～118°	needles→ pale yellow	Et-OH	50.57	50.40	
	158°	needles	50% Me_2CO	62.84	61.90	7,9
	141～142°	leaflets	50% Me_2CO	55.16	54.79	6,9
	142～144°	needles→ pale yellow	Et-OH	48.85	48.75	7
	161～162°	plates	Et-OH	60.56	60.62	7
	157°	leaflets	80% Et-OH	53.39	53.17	7
	144°	plates	80% Et-OH	47.26	46.86	
	86～87°	needles	50% Et-OH	60.56	60.51	
	87～89°	plates	50% Et-OH	53.39	53.02	
	85～86°	plates	Et-OH	47.26	46.28	
	66～67°	needles	Et-OH	60.56	60.35	
	64～65°	leaflets	50% Et-OH	53.39	53.10	
	68～69°	plates	50% Et-OH	47.26	46.95	

crude product was dissolved in alcohol and the solution was used to prepare organomercuric halides. The product was crystallized from dilute alcohol, but some mercury compounds were difficult to crystallize.

The compound in the product was heated with alcoholic solutions of mercuric chloride, mercuric bromide, or mercuric iodide and white precipitates were formed as shown by Eq. 2. These substances were organomercuric halides; they were recrystallized from alcohol or acetone, and fine crystals were obtained. A quantitative yield was obtained.

The crude products were dissolved in alcohol and hydrogen chloride was passed into the solution and the hot reddish solution was cooled in an ice bath. Precipitates were produced as seen in Eq. 3; they were filtered and recrystallized from dilute alcohol containing charcoal. Fine crystals were obtained. It was organomercuric chloride and was identical with the compound obtained by treating the crude organomercury compound with mercuric chloride.

The analysis of mercury was carried out according to the convenient thiocyanate method recommended by Kharasch and Flenner (cited by Hillebrand and Lundell[8]) and good results were obtained.

The influence of various electrolytic conditions on the reduction of several ketones are shown in Table I. Phenyl acetone was not reduced to mercury compound in 5% sulfuric acid solution at a low temperature; it was recovered almost intact, and was not reduced to secondary alcohol or pinacol. It was mercurised in 30% sulfuric acid or in a mixture of glacial acetic acid and 18% hydrochloric acid solution at a low temperature; however, it was mercurised even in 5% sulfuric acid solution at a high temperature. Cyclohexanone behaves similarly to phenylacetone. Cyclopentanone was easily mercurised at a low temperature in various cathodic solution. By the use of 50 g. of cyclohexanone, in catholyte, pinacol[11] (dihydroxy-dicyclohexyl) was produced by about half the amount.

The ketones mentioned above were reduced to mercury compound even in a mild condition; however, in the case of menthone, it was reported[4] that menthone was reduced to dimenthyl mercury only in a strong sulfuric acid at 77~80° with a high current density and to methone or menthol in a weak sulfuric acid electrolyte at a mercury cathode.

Dibenzyl ketone, which was expected to be reduced to organomercury compound and tried in this experiment, was not reduced to mercury compound.

The formation of these mercury compounds is not a continuation of a secondary-alcohol formation because secondary alcohol was not reduced by electrolytic methods under various conditions; namely, cyclohexanol was reduced under the same conditions as above mentioned, but it was recovered almost as it was.

Dialkyl mercuries are volatile liquids and miscible with organic solvents, practically insoluble in water, decompose on standing at room temperature and are sensitive to light. Diaryl mercuries are solid and stable. The mercury compounds obtained in this experiment were also solid and soluble in ether and hot alcohol, but less soluble in cold alcohol and insoluble in water. Dicyclohexyl mercury was unstable and changed its color from white to gray slowly in several hours after recrystallization. It was reported[6] that dicyclohexyl mercury was unstable and decomposed to black oil after 25 hours in a vacuum desiccator over phosphrous pentoxide. Dicyclopentyl mercury was stable as compared with the former, but both compounds turned from gray to black in a few days and at last they decomposed to yellow liquid and black residue. These compounds, above mentioned, were very unstable in the pure and dried state, but comparatively stable in sulfuric acid, ether, and alcohol. Dicycloalkyl mercury has a strong specific odor like camphor and diisopropylmercury like aromatic hydrocarbon.

It was reported[7] that di-4-methylcyclohexyl mercury was a liquid, but this compound is a crystal and di-3-methyl, and di-2-methylcyclohexyl mercury might be solid; however, they were not obtained crystalline in this experiment and it seems that they have a lower melting point compared with the melting point of its halides, and di-4-methylcyclohexyl mercury and its halide have a high melting point owing to its symmetric structure.

Organomercuric halides are exceedingly stable, and are fine crystals with sharp melting points without odor; they are soluble in pyridine, hot alcohol, and acetone, less soluble in alcohol and insoluble in water. Iodides are white crystals, but their color changes to yellow on standing very slowly.

8) W. F. Hillebrand and G. E. F. Lundell, "Applied Inorganic Analysis," John Wiley & Sons, New York, (1953).
9) E. L. Hill, *J. Am. Chem. Soc.*, **50**, 167 (1928).
10) N. Turkiewitz and St. Pilat, *Ber.*, **71**, 284 (1938).
11) 1,1-dihydroxydicyclohexyl, m. p. 129~130°, plates.

The author expresses his sincere thanks to Professor Buhei Sakurai for his kind guidance and encouragement throughout this experiment.

Department of Chemistry, Faculty of Liberal Arts and Science
Shinshu University
Matsumoto

Syntheses of Pyrimidine Derivatives. XVII. On the Reaction Mechanism of Some Pyrimidine Syntheses

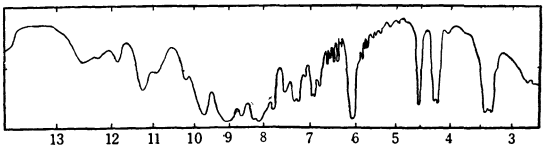
By Akira TAKAMIZAWA, Kanji TOKUYAMA and Kazuo TORI

(Received September 3, 1958)

Some interesting reactions have been presented in the previous papers[1-4] dealing with the syntheses of pyrimidine derivatives from 3-alkoxypropionitriles and acetamidine. These reactions can be divided into two types according to their reaction behavior, which are represented by A and B. In the case of reaction A, 2-methyl-4-amino-5-ethoxymethylpyrimidine (II) can be obtained directly by the reaction of 2-methoxymethylene-3-ethoxypropionitrile (I) with acetamidine.

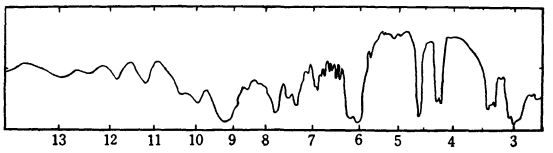
On the other hand, in the case of the reaction of 2-methoxyethoxymethyl-3-ethoxypropionitrile (III) (derived from I) with acetamidine in alcohol, an intermediate IV′ can be detected spectrophotometrically in the reaction mixture (λ_{max} = 275 mμ), without being successfully isolated. Being heated with another one mole of acetamidine, the intermediate IV′ is converted into 2,7-dimethyl-5,6-dihydropyrimido(4,5-d)pyrimidine (V), hydrolysis of which produces 2-methyl-4-amino-5-acetaminomethylpyrimidine (VI), but treatment of IV′ with hydrogen chloride results in II (Reaction B). In view of these facts, the structure of IV′ has reasonably been supposed as 2-acetamidinomethylene-3-ethoxypropionitrile (IV). Besides the above-mentioned facts, it has been shown[5,6] that 2-methyl-4-hydroxy-5-ethoxymethylpyrimidine (VII) could be obtained by the reaction of ethyl 2-methoxymethylene-3-ethoxypropionate (VIII) or ethyl 2-methoxyethoxymethyl-3-ethoxypropionate (IX) with acetamidine in ethanol. One of the important purposes of the present investigations is to identify IV′ with IV, and to present the most reasonable mechanism of these reactions. Another purpose is to check and see if the mechanism of analogous reactions can be explained in a similar manner.

Identification of the Intermediate IV′.— In order to compare the structure of the intermediate IV′ with that of IV, the



Wave length (μ)

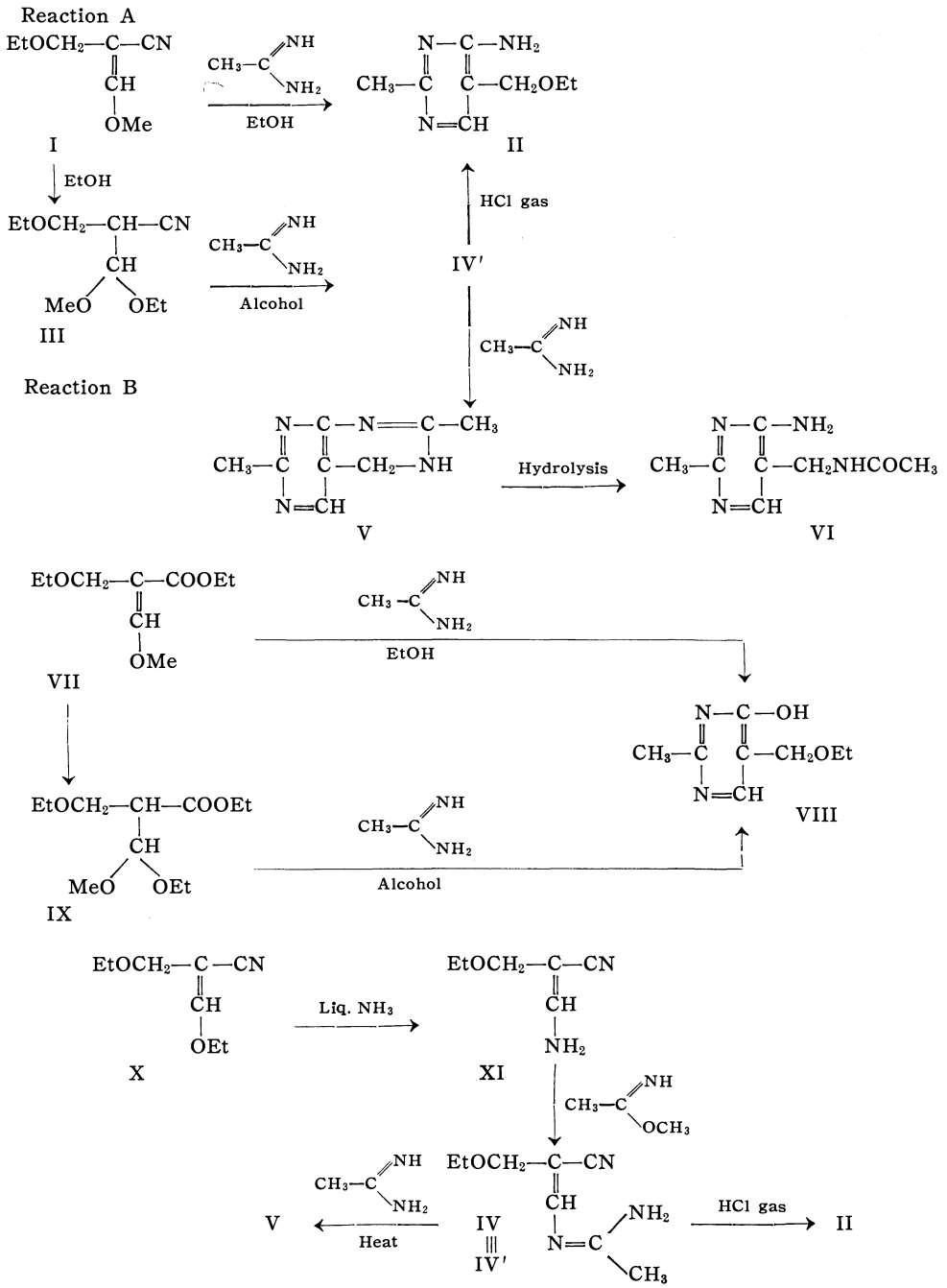
Fig. 1. Infrared absorption spectrum of 2-ethoxymethylene-3-ethoxypropionitrile (X) in nujol. 4.51 μ (conj. C≡N), 6.08 μ (—C=C—), 8.17 μ (=C—O—C). (Perkin-Elmer Model 12C IR spectrometer).



Wave length (μ)

Fig. 2. Infrared absorption spectrum of 2-aminomethylene-3-ethoxypropionitrile (XI) in nujol. 2.85 μ, 2.95 μ (NH_2), 4.56 μ (conj. C≡N), 6.05 μ (—C=C—), 6.19 μ (δ NH_2). (Perkin-Elmer Model 12C IR spectrometer).

1) M. Tomita, S. Uyeo, A. Takamizawa and R. Maeda, *J. Pharm. Soc. Japan*, (*Yakugaku Zasshi*), **74**, 742 (1954); A. Takamizawa and R. Maeda, ibid., **74**, 746 (1954); A. Takamizawa, ibid., 748, 759 (1954).
2) A. Takamizawa, K. Ikawa and M. Narisada, ibid., **78**, 832, 637, 643 (1958).
3) A. Takamizawa, K. Ikawa and K. Tori, ibid., **78**, 649 (1958).
4) A. Takamizawa, S. Hayashi and K. Tori, ibid., **78**, 1166 (1958).
5) A. Takamizawa, ibid., **74**, 752, 756 (1954).
6) A. Takamizawa, K. Tokuyama and H. Satoh, ibid., **79**, (1959), in press.



synthesis of the latter from 2-aminomethylene-3-ethoxypropionitrile (XI) and acetiminomethyl ester was undertaken. 2-Ethoxymethylene-3-ethoxypropionitrile (X) was dissolved in liquid ammonia, and after this solution was kept for a long time at room temperature, XI was obtained as a dark brown viscous liquid. The infrared spectra of this product and X were measured. From the results given in Figs. 1 and 2, it is clear that the absorption band due to —C=C—O— group of initial substance X disappears and that of an amino group newly appears. XI thus obtained being unstable, it easily liberated ammonia on heating. Furthermore, its picrate, hydrochloride, etc. could not be derived because of its weak basicity, and the expected derivatives could not be formed by the reactions of XI with acetic

anhydride, methyl iodide and 2,4-dinitrobromobenzene, but acetamide, ammonium iodide and 2,4-dinitroaniline were obtained, respectively.

It is quite natural to expect that IV can be prepared by the reaction of XI with acetiminomethyl ester. The reaction process was traced spectrophotometrically. The result given in Fig. 3 shows that the product has an absorption band (λ_{max}= 275 mμ) identical with that of the intermediate IV′ in the reaction B. The reaction mixture was converted into II by adding hydrochloric acid under cooling and into V by treating with acetamidine under heating. From the above facts, it seems conclusive that the intermediate IV′ is identical with IV.

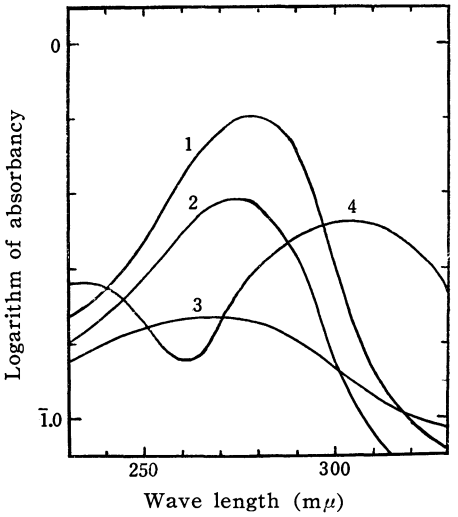
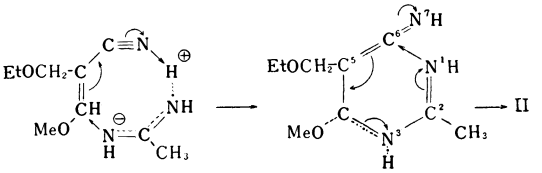


Fig. 3. Changes of ultraviolet absorption spectra of the reaction mixture, XI and acetiminomethyl ester. Curve (1), XI: (2), after 12 hr. at room temperature (IV was formed): (3) after treating IV (curve (2)) with hydrochloric acid gas: (4) after treating IV (curve (2)) with acetamidine. (Beckman DU spectrophotometer).

Reaction Mechanism of Pyrimidine Syntheses.—Thus it is easily inferred that there are two reaction processes for pyrimidine syntheses: namely, the first (reaction B) is the reaction of III with acetamidine whose characteristic is to produce the intermediate IV which is converted into V by heating with acetamidine, and the second (reaction A) is that of I with acetamidine in which II is formed directly without passing through any detectable intermediate.

On the basis of all the present data, the mechanisms of these two reactions may be surmised as below. In the first step of reaction A, the Michael type addition of acetamidine to I may conceivably occur. Then, the resulting intermediate XII may be immediately converted into II, since C^6 in $C^5=C^6=N^7H$ group in XII is positively charged to some extent owing to the polarity of C=N bond and N^1 in the acetamidino group has of course some amount of negative charge and therefore C^6 and N^1 can easily be bonded[7].



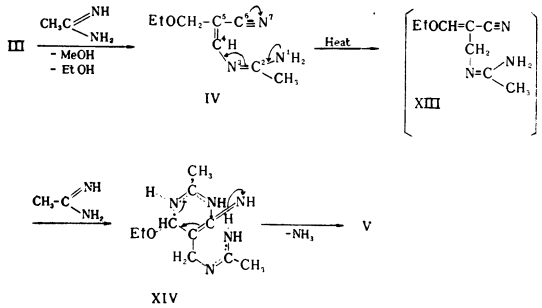
In the case of reaction B, however, the intermediate IV is derived from III by the replacement reaction. The N^1 atom in IV has probably a somewhat positive charge since the electron attracting effect of the $C^2=N^3$ bond and of the nitrile group is considerably large[8]. Moreover, the great dipole moment of $C^6\equiv N^7$ bond (3.5 D) suggests that the C^6 atom is charged positively to a large extent. Therefore, the bond formation between C^6 and N^1 may be very difficult. In addition to this, the intermediate IV can be stabilized by the resonance of the ordinary structure with polar structures where non-bonding electrons in the NH_2 group migrate to C=N and C≡N groups. These are the reasons why IV is fairly stable in the solution and can be detected spectrophotometrically. By heating the solution, the prototropy may occur continually to form the structure XIII, because of the strong electron attracting effect of the nitrile group. Then, another acetamidine molecule may be added to XIII, resulting in XIV which is finally converted into V eliminating an ammonia molecule[9].

However, by treating IV with a reagent such as hydrochloric acid, the nitrile group

7) In the structure XII, C^6 and N^7 have respectively about 16% positive and negative charges because of the difference in the electronegativity values between C^6 and N^7 of C=NH group. The above value can be evaluated by the aid of the bond moment of C=N. (0.9 D; C. P. Smyth, "Dielectric Behavior and Structure", McGraw Hill, New York, (1955), p. 245).

8) N^1 has a positive charge because of the strong electron attracting power of $C^2=N^3$ bond and of nitrile group affecting through the conjugated system of IV, although N^1 seems to charge negeatively due to the difference of electronegativity between C^2 and N^1 of C^2-N^1H_2 group, the moment of which is only 0.22 D.

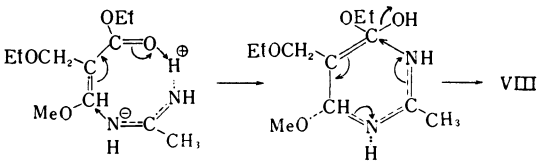
9) Further investigation seems to be required for the final conclusion on these reaction mechanisms.



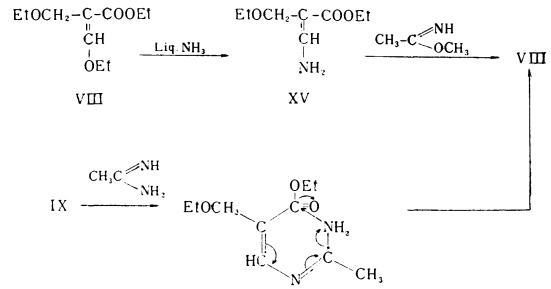
in it may be broken. Thereby the strong electron attracting effect of this group probably decreases and IV is conceivably converted into II[10] through a course similar to that of reaction A mentioned above.

In short, the important difference between these two reactions is that intermediate IV in reaction B has a nitrile group with strong electron attracting power and an amino group with electron donating property at both ends of its conjugated system and between these two groups resonance is possible, whereas the intermediate XII in the reaction A has no longer such a resonating system, since its nitrile group is converted into imino type.

It is quite natural from the above consideration that ethyl 2-methoxymethylene-3-ethoxypropionate (VII) gives 2-methyl-4-hydroxy-5-ethoxymethylpyrimidine (VIII) by the reaction with acetamidine[5,6] in the same manner as in the reaction A.



The situation is the same for the reaction of ethyl 2-aminomethylene-3-ethoxypropionate (XV) and acetiminomethyl ester. In this case, VIII was also obtained directly[11]. Now let us consider the reaction of ethyl 2-methoxyethoxymethyl-3-ethoxypropionate (IX) with acetamidine. In the course of this reaction, the intermediate like IV could not be observed spectrophotometrically but the reaction product VIII was obtained directly[5,6]. At the first glance, this fact looks strange because in the intermediate of this reaction, the stabilization due to resonance between the electron attracting (COOEt) and donating (NH_2) groups may be expected. However, this fact may probably be explained by taking account of the small electron attracting power of the carbethoxyl group compared with that of the nitrile group[12]. Further mention on this point will be made below.



According to these two reaction mechanisms for pyrimidine syntheses, it is possible to explain consistently some analogous reactions indicated in the literatures, which have been re-investigated in our laboratory.

The reactions of ethoxymethylenemalondinitrile (XVI) (reaction C) and ethyl ethoxymethylenecyanoacetate (XVII) (reaction D) with acetamidine give 2-methyl-4-amino-5-cyanopyrimidine (XVIII) (reaction C) and 2-methyl-4-hydroxy-5-cyanopyrimidine (XIX) with 2-methyl-4-amino-5-carbethoxypyrimidine (XX) (reaction D), respectively. On the other hand, aminomethylenemalondinitrile (XXI) (reaction E) and ethyl aminomethylenecyanoacetate (XXII) (reaction F) are converted by the reaction with acetiminomethyl ester into acetamidinomethylenemalondinitrile (XXIII) and ethyl acetamidinomethylenecyanoacetate (XXIV), respectively[13-15], yielding the corresponding pyrimidines only by treating with alkali. It is probably that in the cases of the reaction C and D, the intermediates, XXV and XXVI, are led to the corresponding pyrimidines directly in a way similar to that of reaction A, since their nitrile groups disappear, whereas in the cases of the reactions E and F the

10) 2-Methyl-5-carbethoxy-3,4-dihydropyrimidine is also obtained. In this case, it must be considered that the nitrile group is converted into an iminoester group.

11) A. Takamizawa and K. Tokuyama, *J. Pharm. Soc. Japan*, (*Yakugaku Zasshi*), **79**, (1959), in pretss.

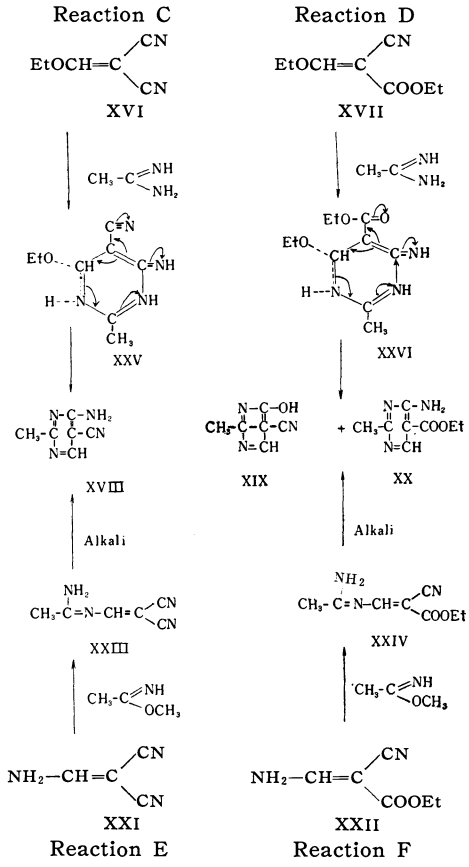
12) This is inferred from the fact that the σ vlaue (Hammett's substituent constant) for the nitrile group is apparently larger than that for the carboxyl group.

13) A. R. Todd and F. Bergel, *J. Chem. Soc.*, **1937**, 364.

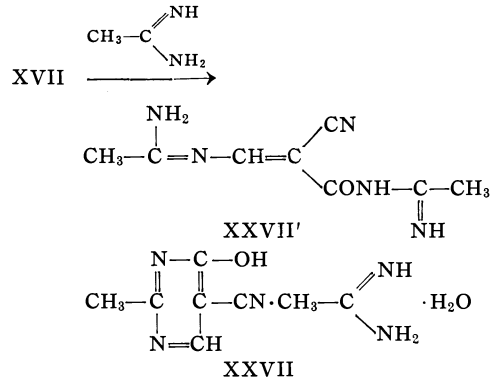
14) T. Matsukawa, *J. Pharm. Soc. Japan* (*Yakugaku Zasshi*), **62**, 417 (1942).

15) Y. Sawa and T. Tsuji, This work was read at the Kinki Congress of Pharmaceutical Society of Japan, Osaka, 1955.

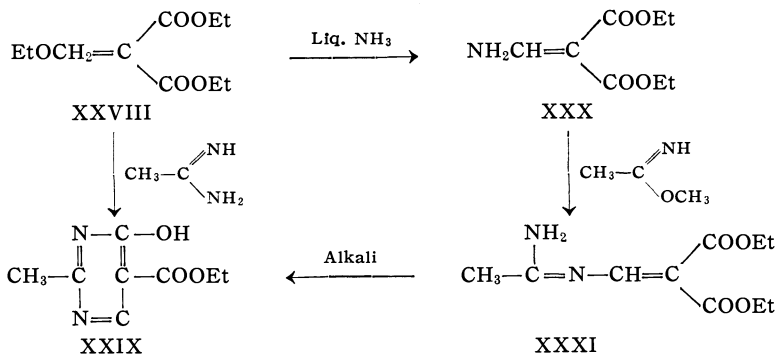
intermediates, XXVII and XXVIII, have still their nitrile groups and therefore do not react further without treating with alkali. That is to say, this mechanism is similar to that of reaction B.



According to Todd[13], the intermediate XXVI was obtainable in the course of the reaction D, but this assertion has been refuted by Sawa and Tsuji[15], who reported that XXVI could not be obtained under the experimental conditions they employed. This result seems to be consistent with the above consideration that the intermediate like XXVI is too unstable to be detected. Moreover, Sykes et al.[16] have reported that XXVII′ was obtained by the reaction of XVII with two moles of acetamidine, but their result is not convincing. It contradicts the present authors' opinion. Inspecting more completely their data on the melting point and elemental analysis, we are led to the conclusion that the compound obtained by Sykes et al. is acetamidinate XXVII[15] of XIX.



As mentioned above, the electron attracting effect of one carbethoxy group is weaker than that of a nitrile group, but the following fact indicates that two carbethoxy groups roughly correspond to one nitrile group in their electron attracting power. While 2-methyl-4-hydroxy-5-carbethoxypyrimidine (XXIX) was obtained at once by the reaction of diethyl ethoxymethylenemalonate(XXVIII) with acetamidine, diethyl aminomethylenemalonate (XXX) was converted with acetiminomethyl ester into diethyl acetamidinomethylenemalonate (XXXI), which gave XXIX on treatment with alkali.



16) P. Nesbitt and P. Sykes, *J. Chem. Soc.*, **1954**, 3057.

Experimental

2-Aminomethylene-3-ethoxypropionitrile (XI).—A solution of 2-ethoxymethylene-3-ethoxypropionitrile (X) (5.0 g.) dissolved completely in liquid ammonia (20 cc.) was left at room temperature for 45 days. After removal of the liquid ammonia and the alcohol produced under reduced pressure, a dark brown liquid (3.8 g.) was obtained. $n_D^{20.5}$, 1.4759.

Anal. Found: C, 56.62; H, 7.64; N, 22.21; $-OC_2H_5$, 34.66. Calcd. for $C_6H_{10}N_2O$: C, 57.11; H, 7.99; N, 22.21; $-OC_2H_5$, 35.71%.

Reaction of 2-aminomethylene-3-ethoxypropionitrile (XI) with acetiminomethyl ester.—To an ice-cold solution of sodium (0.3 g.) in absolute methanol (50 cc.), was added acetiminomethyl ester hydrochloride (1.5 g.); the mixture was shaken for few minutes and quickly filtered from precipitated sodium chloride. To the cooled filtrate was added 2-aminomethylene-3-ethoxypropionitrile (XI) (1.3 g.) in portions with shaking. After being allowed to stand overnight at room temperature, (i) dry hydrochloric acid was vigorously passed into the solution during three hours at 10~15°C, and the solution was again allowed to stand overnight. After removal of methanol in a vacuum, the residue was neutralized with sodium carbonate, washed with ethyl acetate, made strongly alkaline with sodium hydroxide and extracted with benzene. The benzene layer was dried over sodium sulfate and purified by passing through an alumina column. After evaporation of the solvent, 2-methyl-4-amino-5-ethoxymethylpyrimidine (II) was given; it was crystallized from ethanol in colorless rods, m. p. 89~90°C. Yield, 10 mg., (5.86%). Picrate, m. p. 189~190°C.

Anal. Found: C, 42.44; H, 4.18; N, 21.57. Calcd. for $C_{14}H_{16}N_6O_8$ (as picrate): C, 42.42; H, 4.44; N, 21.21%.

(ii) A mixture of absolute methanol (20 cc.), sodium (0.3 g.) and acetamidine hydrochloride (1.4 g.) was added. After being boiled for three hours, the precipitated sodium chloride was filtered off and the solvent was removed. To the residue was added 10% aqueous solution of sodium hydroxide; the mixture was heated on a water-bath for one hour. After cooling, colorless crystals separated on salting out with 50% aqueous solution of sodium hydroxide. Recrystallization from water gave 2-methyl-4-amino-5-acetaminomethylpyrimidine (VI) of colorless prisms (1.0 g.), m. p. 204~206°C. Picrate was yellow needles, m. p. 200°C.

Anal. Found: N, 23.98. Calcd. for $C_{14}H_{15}N_7O_8$ (as picrate): N, 23.96%.

Reaction of diethyl aminomethylenemalonate (XXX) with acetiminomethyl ester.—To an ice-cold solution of sodium (0.6 g.) in absolute ethanol (50 cc.), was added acetiminomethyl ester hydrochloride (3.2 g.); the mixture was shaken for a few minutes and quickly filtered from precipitated sodium chloride. To the cooled filtrate was added diethyl aminomethylenemalonate (XXX) (3.7 g.) in portions with shaking. After being allowed to stand overnight at room temperature, the solvent was removed in a vacuum. The residue, m. p. ca. 190°C, decomposed by recrystallization. This may be diethyl acetamidinomethylenemalonate (XXXI).

The above product was heated on a water-bath for 15 minutes with an ethanolic sodium ethoxide (0.2 g.; 50 cc.). The yellow solution was cooled, acidified with acetic acid, and concentrated in vacuo to about half the original volume. On standing, 2-methyl-4-hydroxy-5-carbethoxypyrimidine (XXIX) separated; it crystallized from acetone in colorless needles, m. p. 190°C. Yield, 0.1 g.

Anal. Found: N, 15.11. Calcd. for $C_8H_{10}N_3O$: N, 15.38%.

Summary

The mechanism of the reactions of 2-alkoxymethylene-3-alkoxypropionitrile and 2-dialkoxymethyl-3-alkoxypropionitrile with acetamidine was studied. The results show that these two nitriles react with acetamidine in completely different manners. In the case of the reaction of 2-alkoxymethylene-3-alkoxypropionitrile with acetamidine, the final product (2-methyl-4-amino-5-alkoxymethylpyrimidine) can be obtained directly, while in the case of the reaction of the other nitrile with acetamidine, the intermediate with the absorption maximum at 275 mμ can be detected spectrophotometrically. This intermediate could be identified with 2-acetamidinomethylene-3-alkoxypropionitrile. The difference in the mechanism between these two reactions might be explained by taking into consideration the fact that the intermediate in the latter case can be stabilized by the resonance among the usual structure and the polar structures in which non-bonding electrons on the nitrogen atom of the amino group migrate into C≡N or C=N group.

We wish to acknowledge our indebtedness to Professors M. Tomita, University of Kyoto, and S. Uyeo, University of Osaka, and Dr. K. Takeda, Director of our laboratory, for their kind guidance and encouragement and we are also indebted to Assistant Professor S. Nagakura, the University of Tokyo, for his helpful discussion. We are grateful to Messrs. K. Kubota, M. Narisada and H. Miyazaki for the measurements of infrared and ultraviolet spectra and to Messrs. T. Iyeki and K. Miyahara and Misses H. Nakai and K. Numoto for the elemental analyses.

Shionogi Research Laboratory
Shionogi & Co., Ltd.
Imafuku, Amagasaki

Electron Diffraction Investigation on the Molecular Structure of 1,1,2-Trifluoro-1,2,2-trichloroethane

By Machio IWASAKI

(Received August 5, 1958)

In previous publications[1-3] it has been reported that the energy difference between *trans* and *gauche* isomer for 1,2-difluoro-1,1,2,2-tetrachloroethane is 0~500 cal./mol., and that for 1,1,2,2-tetrafluoro-1,2-dichloroethane is 440±110 cal./mol. In order to compare these results with the data for the well-known series of chlorinated ethanes[4] (CH_2Cl-CH_2Cl, $CHCl_2$-CH_2Cl and $CHCl_2CHCl_2$), it is desirable to elucidate the molecular structure of 1,1,2-trifluoro-1,2,2-trichloroethane. However, the problem of rotational isomerism in this molecule has not yet been studied except when an earlier study was made by Glockler and Sage[5]. Based solely on the number of observed Raman lines, they concluded that two isomers were present, but no attempt was made at the determination of the energy difference between the two isomers.

This report presents the results of studies on the molecular structure of CF_2Cl-$CFCl_2$ carried out by the sector-microphotometer method of electron diffraction mainly to find the effect of fluorine substitution on the energy difference between the two isomers. An attempt was also made at the determination of the equilibrium angle of the stable configuration.

Experimental

The sample was prepared by S. Nagase in this laboratory from hexachloroethane, which was fluorinated with antimony trifluoride under superatmospheric pressures in the presence of antimony pentachloride as a catalyst[6]. The product distilled at 47.8°C. The purity of this sample was tested with an infrared absorption spectrum and there were no absorptions due to impurities.

The diffraction patterns were taken at a room temperature of about 20°C using an apparatus[7] having an r^3-sector, which was rapidly rotated during photographic exposure. The apparatus and the experimental procedures were the same as described in the previous paper[3]. Two nozzle-to-plate distances of 125 mm. and 285 mm. were used: the former was used for large angle scattering and the latter for small angle scattering, which was sensitive to the internal rotation. The wavelength of the electron beam was about 0.055Å. The extraneous scatterings were removed by a beam trap and the spreading of the sample was prevented by a trap cooled with liquid air.

The molecular intensity curve qI_m shown by the top curve in Fig. 5 was obtained by the method similar to that employed by Karle and his coworker[8], the index of resolution being about 1.0.

Analysis

Radial Distribution Curve.—The radial distribution (RD) curve was calculated by the following equation:

$$f(r) = \sum_{q=0}^{q_{\max}} qI_m \exp(-aq^2) \sin(\pi qr/10) \qquad (1)$$

where I_m is the molecular scattering intensity. The artificial damping factor a was chosen so as $\exp(-aq^2)=0.1$ at $q=100$. $q=(40/\lambda)\sin(\theta/2)$, where θ is the angle of scattering and λ is the wavelength of the electron beam.

In the calculation of the RD curve, a theoretical intensity curve which was computed with constant coefficients for the assumed model was substituted in place of the observed intensity below $q=6$. Furthermore, a correction for the effect of non-nuclear scatterings[9] was made. The RD curve shown in Fig. 2 was obtained after several steps of successive

1) M. Iwasaki, S. Nagase and R. Kojima, *J. Chem. Phys.*, **22**, 959 (1954).
2) M. Iwasaki, S. Nagase and R. Kojima, This Bulletin, **30**, 230 (1957).
3) M. Iwasaki, This Bulletin, **31**, 1071 (1958).
4) S. Mizushima, "Structure of Molecules and Internal Rotation", Academic Press, Inc., New York, N. Y., 1954.
5) G. Glockler and C. Sage, *J. Chem. Phys.*, **9**, 387 (1941).
6) R. Kojima, M. Iwasaki, S. Nagase and H. Baba, *Repts. Govt. Ind. Research Inst., Nagoya, (Nagoya Kogyo Gijutsu Shikenjo Hokoku)*, **5**, 225 (1956).
7) Y. Morino, M. Kimura and M. Iwasaki, The Sixth Annual Meeting of the Chemical Society of Japan, April 1953.
8) J. Karle and I. L. Karle, *J. Chem. Phys.*, **18**, 957 (1950).
9) L. S. Bartell, L. O. Brockway and R. H. Schwedeman, ibid., **23**, 1854 (1955).

approximations based on Karle's criteria[8].

The RD curve has maxima at 1.34_5, 1.75_5, 2.0~3.7, 3.89_0, and 4.31_3Å. The first two peaks at 1.34_5 and 1.75_5Å are assigned to C—F and C—Cl bond distances, respectively. The unresolved peak at 2.0~3.7Å is due to the superposition of various non-bonded distances, that at 3.89_0Å to the *trans* F···Cl distance, and that at 4.31_3Å to the *trans* Cl···Cl distance.

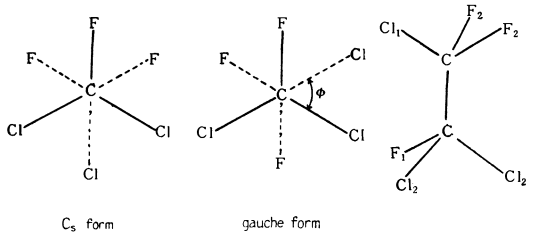


Fig. 1. Rotational isomers of CF_2Cl-$CFCl_2$.

Two configurations are conceivable for this molecule. One of them is a form having the C_s symmetry as shown in Fig. 1. This form will be called the C_s form. The other form having no symmetry is called the *gauche* form. Because the *trans* Cl···Cl distance is characteristic of the *gauche* form, the peak at 4.31_3Å evidently shows the existence of the *gauche* form. On the other hand, the *trans* F···Cl distance appears in both forms, but the number of this distance is three for the C_s form whereas it is one for the *gauche* form. Therefore, the ratio of the areas under these two peaks is expected to depend on whether there exists only the *gauche* form or whether two isomers exist. Because the area under the RD peak is approximately proportional to Z_iZ_j/r_{ij}, the ratio of the two forms, N_{C_s}/N_g, can be calculated from the areas of the two peaks mentioned above by means of the following formula:

$$\frac{N_{C_s}}{N_g} = \frac{Z_{Cl}r_{F\cdots Cl}A_{F\cdots Cl}}{3Z_Fr_{Cl\cdots Cl}A_{Cl\cdots Cl}} - \frac{1}{3} \qquad (2)$$

where Z_F and Z_{Cl} are, respectively, the atomic numbers of fluorine and chlorine, $A_{Cl\cdots Cl}$ and $A_{F\cdots Cl}$ are the areas of the peaks, and $r_{Cl\cdots Cl}$ and $r_{F\cdots Cl}$ are the *trans* Cl···Cl and the *trans* F···Cl distances. The ratio of the areas was hardly affected at all by the assumed value of the abundance ratio of the two isomers, because the correction for non-nuclear scatterings made it possible to use the observed values to such a small q value as 7. In this way, the amount of the *gauche* form was estimated as 80 per cent from the RD curve in applying Eq. 1. This value was further tested by the consideration of theoretical intensity curves described in the next section.

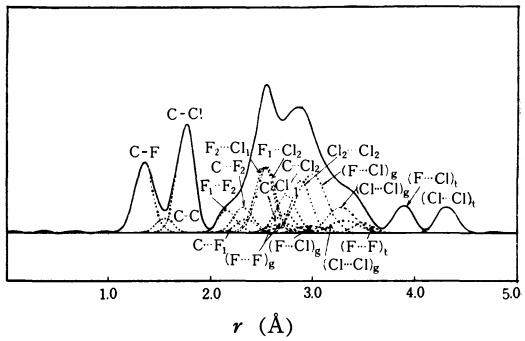


Fig. 2. Radial distribution curve for CF_2Cl-$CFCl_2$.

When the contributions from the C—F and C—Cl distances were subtracted from the composite peak ranging from 1.0 to 2.0Å, the remaining area forms a smooth curve having a maximum at 1.54_5Å which is attributable to the C—C bond distance. These three components of the first composite peak of the RD curve are illustrated in Fig. 2, and the areas under these peaks are in good agreement with the theoretical values shown in Table I.

According to the results of the previous reports[1-3] and many other papers about fluorochloromethane[10], the C—F and the C—Cl bond distances decrease with the number of fluorine atoms bonded with one and the same carbon atom. Therefore, the C—F and the C—Cl bond distances may probably be different for two halves of this molecule. In fact, the values of 1.38Å (C—F) and 1.76Å (C—Cl) in $CFCl_2$-$CFCl_2$, and those of 1.33_0Å (C—F) and 1.74_5Å (C—Cl) in CF_2Cl-CF_2Cl being assumed for the two halves of this molecule, the weighted mean values of the C—F and the C—Cl distances were 1.34_7 and 1.75_5Å, respectively; those values are in good agreement with the observed values of 1.34_5 and 1.75_5Å.

In analyzing the part of the RD curve from 2.0 to 3.7Å, an assumption was made that the bonded distances and the bond angles in two halves of the molecule were equal to those of $CFCl_2$-$CFCl_2$ and CF_2Cl-CF_2Cl, respectively. Furthermore, the

10) The C-F and the C-Cl distances in many organic fluorine compounds have been tabulated in the previous paper, ref. 2.

TABLE I
THE RESULT OF ANALYSIS OF THE RD CURVE
(THE DISTANCES ARE GIVEN IN Å UNITS)

		C—F	C—C	C—Cl	(F···Cl)$_t$	(Cl···Cl)$_t$
Distance		1.34_4	1.54_5	1.75_5	3.89_0	4.31_3
Mean amplitude.	obs.	0.055_5	0.041_7	0.054_0	0.063_8	0.069_5
	calc.	0.045	0.050	0.054	0.070	0.074
c_{ij}	obs.	0.259	0.055	0.514	0.307	0.335
	calc.	0.255	0.057	0.481	0.337	0.364

assumed values listed in Table II were used for the mean amplitudes. When contributions from distances that do not change with internal rotation were subtracted from the experimental RD curve, the remaining curve shown in Fig. 3 was

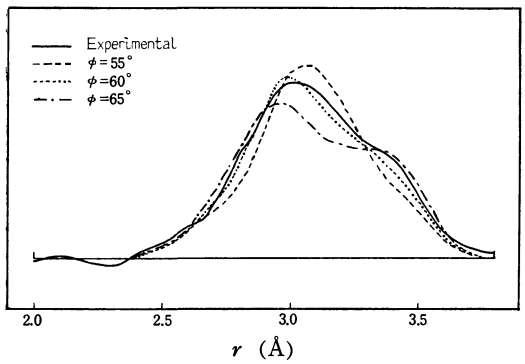


Fig. 3. Comparison between the experimental and the calculated RD curves which are attributable to the contributions from the distances that vary with the internal rotation.

TABLE II
MEAN AMPLITUDES USED IN THIS ANALYSIS
(IN Å)

Distance	Mean amplitude	Distance	Mean amplitude
C—F	0.045	(F···F)	0.114
C—C	0.050	(F···Cl)$_g$	0.120
C—Cl	0.054	(Cl···Cl)$_g$	0.125
F···F	0.056	(F···F)$_t$	0.061
C···F	0.059	(F···Cl)$_t$	0.070
F···Cl	0.065	(Cl···Cl)$_t$	0.074
C···Cl	0.073		
Cl···Cl	0.070		

obtained, the part from 2.4 to 3.7Å of this curve corresponding to the contribution from the *gauche* F···F, the *gauche* F···Cl, the *gauche* Cl···Cl, and the *trans* F···F distances, which change with the azimuthal angle of the *gauche* form and the relative amount of rotational isomers. The fact that the part of the remaining curve from 2.0 to 2.4Å which is attributable to the contribution from the distances that are independent of the internal rotation, is almost equal to zero reflects the correctness of the assumption about the bonded distances and bond angles. When the remaining curve thus obtained was compared with the theoretical one calculated for various azimuthal angles[11], ϕ, of the *gauche* form, the curve for $\phi=60°$ was found to be in good agreement with the observed one as shown in Fig. 3.

The mean amplitudes listed in Table I were obtained by fitting the RD peaks with Gaussian functions, no corrections being made for second order effects, such as a sample spread, multiple scatterings and the failure of Born approximation[12]. The observed mean amplitudes are in good agreement with those calculated by Morino et al.[13] from spectroscopic data.

Theoretical Intensity Curves. — The theoretical intensity curves were calculated using the following equation:

$$qI_m(q)=\sum_{i\neq j}\sum(c_{ij}/r_{ij}) \times\exp(-b_{ij}q^2)\sin(\pi qr_{ij}/10) \qquad (3)$$

where r_{ij} denotes the interatomic distance between i-th and j-th atoms, b_{ij} is the temperature factor, and

$$c_{ij}=Z_iZ_j/\sum_i(Z_i^2+Z_i) \qquad (4)$$

In the region of small q-values the effect of non-nuclear scattering was corrected for the experimental intensity and then the constant coefficient was used over the whole q region in calculating theoretical intensity curves. The summations of Eq. 3 were performed by use of punched cards and a Remington Rand Type-285 Model-2 Tabulating machine[14,15].

In determining the range of uncertainty of 13 structural parameters and 14 mean

11) The azimuthal angle of the *gauche* form is that for the two C-Cl bonds in the molecule.
12) R. Glauber and V. Schomaker, *Phys. Rev.*, **89**, 667 (1953); L. S. Bartell and L. O. Brockway, *Nature*, **171**, 978 (1953); J. A. Ibers and J. A. Hoerni, *Acta Cryst.*, **7**, 405 (1954).
13) Y. Morino, K. Kuchitsu, A. Takahashi and K. Maeda, *J. Chem. Phys.*, **21**, 1927 (1953).
14) Y. Morino and K. Kuchitsu, *X-Ray*, (*X-sen*), **8**, 37 (1954).
15) The calculation by use of punched cards was carried out by K. Kuchitsu of the University of Tokyo.

amplitudes, it was not feasible to exhaust the possible variations in all parameters. Therefore, all the parameters except the ratios, $\rho_{Cl}=C-Cl_2/C-Cl_1$ and $\rho_F=C-F_1/C-F_2$ the azimuthal angle of the *gauche* form, ϕ, and the fraction of the *gauche* form, N_g, were kept constant throughout the analysis. The mean amplitudes used were the same as those in the previous papers[2,3]. The majority of these values listed in Table II were taken from those calculated by Morino et al.[13] from spectroscopic data or obtained by Karle et al.[16,17] from electron diffraction experiments. The C—C distance and all the bond angles were assumed to be equal to those in $CFCl_2$–$CFCl_2$ and CF_2Cl–CF_2Cl, that is, C—C=1.54Å, $\angle CCCl_1=\angle CCCl_2=112°$, $\angle CCF_1=107°05'$, $\angle CCF_2=108°$, $\angle F_1CCl_2=107°30'$, $\angle F_2CCl_1=110°$, $\angle F_1CFl_2=108°44'$ and $\angle Cl_1CCl_2=110°30'$. It was already shown in the RD analysis that this assumption was quite adequate.

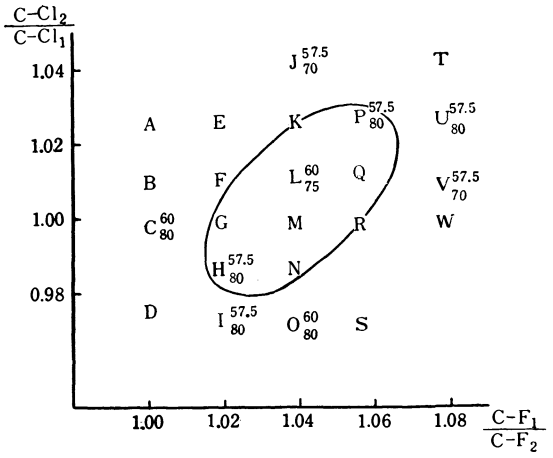


Fig. 4. Parameter chart. The positions of letters indicate the parameters of models for which intensity curves were computed. The values of the superscripts and the subscripts indicate the azimuthal angles and the amounts of the *gauche* form both of which were used in calculating the intensity curves reproduced in Fig. 5.

For each model indicated in a $\rho_{Cl}-\rho_F$ parameter chart (Fig. 4), parameters, ϕ and N_g, were further varied. The projection of the $\rho_{Cl}-\rho_F$ parameter chart on a $\phi-N_g$ plane is shown in Fig. 6. Some of the computed curves are reproduced in Fig. 5. The relative depth of the 5th and the 6th minimum, the position of the 3rd maximum and the 4th minimum and the feature of a shelf on the inner portion of the 4th maximum are very sensitive to small changes in the parameters. The models A–F, J and T in the parameter chart can be ruled out because the relative depth of the 5th and the 6th minimum contradicts with experiments, while the models, O, S, V and W, are unacceptable because the 6th minimum is too deep as compared with experiments. The model I can also be rejected because of the prominence of a shelf on the inner portion of the 4th maximum. The model U is unsatisfactory because the 7th and the 8th maximum are too faint. The models, G, H, L, M, N, P and Q, are regarded as acceptable fits, while the models, K and R, can be accepted as borderline fits. In Table III is given the comparison between the observed and the calculated intensity curve for the best model L. In Table IV

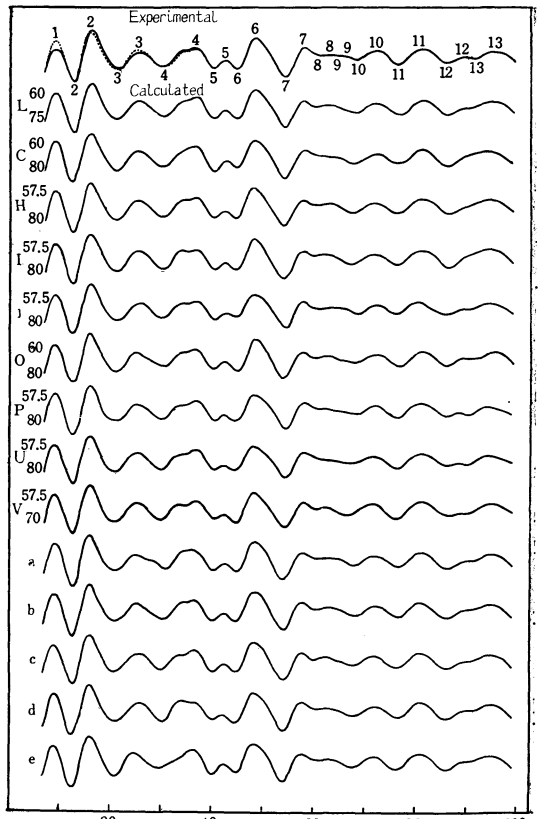


Fig. 5. Experimental and calculated intensity curves. In the experimental curve the dotted line indicates the correction for non-nuclear scatterings.

16) D. A. Swick, I. L. Karle and J. Karle, *J. Chem. Phys.*, **22**, 1242 (1954).
17) D. A. Swick and I. L. Karle, ibid., **23**, 1499 (1955).

TABLE III
COMPARISON BETWEEN EXPERIMENTAL AND THEORETICAL INTENSITY CURVES

Max.	Min.	Peak position			Peak height		
		q_o	q_c	q_c/q_o	I_o	I_c	I_o/I_c
1		9.0	9.0	1.000	+1.30	+1.24	1.048
	2	12.5	12.5	1.000	−1.90	−1.98	0.960
2		16.0	16.0	1.000	+2.05	+2.00	1.025
	3	21.0	21.0	1.000	−0.98	−0.90	1.089
3		25.2	25.2	1.000	+0.61	+0.58	1.052
	4	30.2	30.2	1.000	−0.73	−0.71	1.028
4		36.6	36.7	1.003	+0.80	+0.82	0.976
	5	40.2	40.2	1.000	−0.85	−0.86	0.988
5		42.5	42.5	1.000	−0.18	−0.20	0.900
	6	44.8	44.8	1.000	−1.00	−0.93	1.075
6		48.3	48.4	1.002	+1.62	+1.51	1.073
	7	54.3	54.2	0.998	−1.52	−1.57	0.968
7		58.0	57.8	0.997	+0.78	+0.67	1.164
	8	61.4	60.6	(0.987)	+0.15	+0.05	(3.000)
8		63.4	62.4	(0.984)	+0.24	+0.26	(0.923)
9		66.2	65.5	(0.989)	+0.07	−0.05	(——)
	10	68.5	68.2	0.996	−0.26	−0.42	0.619
10		72.1	72.2	1.001	+0.52	+0.37	1.405
	11	76.5	76.7	1.003	−0.52	−0.55	0.982
11		81.1	81.2	1.001	+0.60	+0.65	0.923
	12	86.2	86.2	1.000	−0.54	−0.65	0.831
12		89.5	89.5	1.000	−0.03	0.00	(——)
13		95.4	95.0	0.996	+0.45	+0.50	0.900
Average				1.000			1.005
Average deviation				0.001			0.096

TABLE IV
DISTANCES OBTAINED FROM q_c/q_o VALUES
(THE DISTANCES ARE GIVEN IN Å UNITS)

Acceptable models	Average q_c/q_o	Average deviation	C—F_1	C—F_2	C—Cl_1	C—Cl_2	C—C
L_{75}^{60}	1.000	0.001	1.38_0	1.33_0	1.74_5	1.76_0	1.54_0
N_{70}^{60}	0.999	0.003	1.37_9	1.32_9	1.76_8	1.74_3	1.53_8
$K_{80}^{57.5}$	1.001	0.003	1.38_1	1.33_1	1.72_6	1.77_1	1.54_1
$G_{80}^{57.5}$	0.999	0.002	1.36_3	1.33_8	1.75_4	1.75_4	1.53_9
$H_{80}^{57.5}$	0.999	0.003	1.36_2	1.33_7	1.76_8	1.74_6	1.53_8
$P_{80}^{57.5}$	1.000	0.003	1.39_5	1.32_0	1.72_5	1.77_0	1.54_0
Q_{75}^{60}	0.999	0.003	1.39_4	1.31_9	1.74_3	1.75_8	1.53_9
Most probable value			1.37_9	1.32_9	1.74_7	1.75_8	1.53_9

are listed the mean values of the q_c/q_o ratio for these acceptable models as well as the molecular parameters calculated therefrom. The accepted values of these parameters and the limits of errors are as follows:

C—F_1=1.37_9±0.02_1Å C—F_2=1.32_9±0.01_4Å

C—Cl_1=1.74_7±0.02_7Å C—Cl_2=1.75_8±0.02_0Å

With respect to the parameter N_g the models for N_g=100 per cent were all unsatisfactory because the positions of the 3rd maximum and the 4th minimum did not agree with experiments. This discrepancy could not be removed without taking into account the coexistence of the C_s form. Therefore, the existence of the C_s form is definitly concluded from the diffraction data. From the acceptable domains estimated for acceptable models

in the $\rho_F - \rho_{Cl}$ parameter chart, the limits of errors for the N_g and ϕ parameters were determined as follows:

$$N_g = 76 \pm 7 \text{ per cent } \phi = 59.5 \pm 3.5^\circ$$

These values coincide with the results from the analysis of the RD curve.

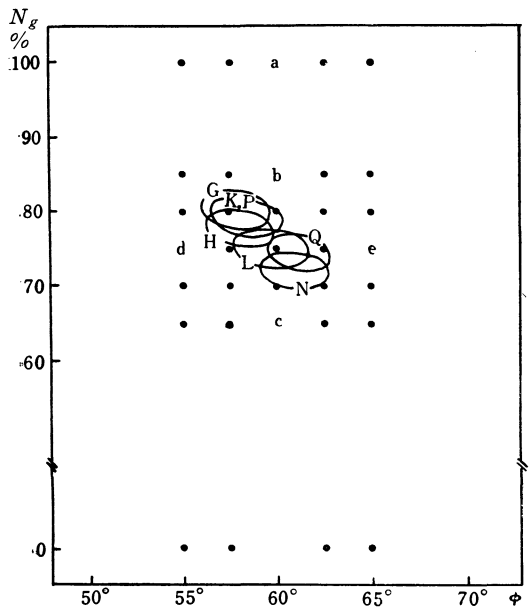


Fig. 6. Parameter chart for N_g and ϕ. The positions of the small letters and dots indicate the parameters of the models for which intensity curves were computed. The areas enclosed in the curved lines roughly indicate the acceptable regions for the models represented by the capital letters, which correspond to the positions in the $\rho_{Cl} - \rho_F$ parameter chart. The theoretical intensity curves corresponding to the positions indicated by the small letters are reproduced in Fig. 5.

Discussion of the Results

The shortening of the C—F bond distance found in $CF_2Cl—CF_2Cl$[3] is also revealed in this molecule. It is concluded that the C—F bond distance in a $-CF_2Cl$ group is different from that in a $-CFCl_2$ group. Moreover, the values of these distances are almost the same as those found in CF_2Cl-CF_2Cl and $CFCl_2-CFCl_2$. It implies that the structure of one half of the molecule scarcely affects the other half of the molecule. With respect to the C—Cl bond distances it appears that the similar difference in two halves of the molecule also exists, although great uncertainties of the data do not permit to draw a definite conclusion. From the analysis described in the preceding section, it was definitly concluded that there exist two rotational isomers, C_s and *gauche* forms for $CF_2Cl-CFCl_2$ molecules in the vapor state, the amount of the *gauche* form being 76 ± 7 per cent. If the ratio of the vibrational and rotational partition functions for the C_s and the *gauche* form is assumed to be equal to unity, the energy difference, ΔE, between the isomers is calculated as 270 ± 250 cal./mol. (the *gauche* form is more stable than the C_s form.) from diffraction data, in remarkable contrast to the value of 2900 cal./mol.[18,19] for $CH_2Cl-CHCl_2$. It appears that this lowering of energy difference arises mainly from the decrease in the difference of electrostatic interactions between the C_s and the *gauche* form due to the fluorine substitution, because the C—Cl bond moment is nearly equal to the C—F bond moment. The decrease in the difference of steric repulsion between the C_s and the *gauche* form, of course, should not be neglected, because the van der Waals' radius of a fluorine atom is larger than that of a hydrogen atom. However, the effect of the change in the steric interaction is less important for this lowering because it was reported[20] that the methyl substitution does not appreciably affect the energy differences in chlorinated ethanes.

In the case of 2-methylbutane, $CH_2(CH_3)-CH(CH_3)_2$, which has a similar skeletal structure to that of $CH_2Cl-CHCl_2$ but has a large difference in electrostatic interaction, the energy difference is reported by Sheppard and Szasz[21] to be almost zero. In this connection, it is interesting to mention that a large energy difference was not observed in a $CF_2Cl-CFCl_2$ molecule, in which the difference of electrostatic interactions decreases.

The azimuthal angle of the *gauche* form was determined to be 59.5° in contrast to the value of 70° in $CH_2Cl-CHCl_2$[22]. This change in the equilibrium position of the *gauche* form seems to have some relation to the lowering of the energy difference.

18) J. R. Thomas and W. D. Gwinn, *J. Am. Chem. Soc.*, **71**, 2785 (1949).
19) K. Kuratani and S. Mizushima, *J. Chem. Phys.* **22**, 1403 (1954).
20) I. Miyagawa, *J. Chem. Soc. Japan, Pure Chem. Sec.*, (*Nippon Kagaku Zassi*), **75**, 1162 (1954).
21) N. Sheppard and G. J. Szasz, *J. Chem. Phys.*, **18**, 145 (1950).
22) A. Turkevich and J. Y. Beach, *J. Am. Chem. Soc.*, **61**, 3127 (1939).

The result in this investigation is consistent with the conclusion reached by Mizushima, Morino and Shimanouchi[23] that the most important force in dtermining stable configurations of rotational isomers is the steric repulsion and that the electrostatic force plays an important role in determining the energy difference between the rotational isomers because the steric repulsion may become of the same order of magnitude as the electrostatic force in the stable configurations.

Summary

The molecular structure of 1,1,2-trifluoro-1,2,2-trichloroethane was investigated by means of the sector-microphotometer method of electron diffraction. The existence of the two isomeric forms, C_s and *gauche* was ascertained and the amount of the *gauche* form was found to be 76±7 per cent at 20°C. This corresponds to the energy difference of 270±250 cal./mol., the *gauche* form being more stable than the C_s form. The interatomic distances were determined as follows: $C-F_1=1.37_9\pm0.02_1$Å, $C-F_2=1.32_9\pm0.01_4$Å, $C-Cl_1=1.74_7\pm0.02_7$Å, $C-Cl_2=1.75_8\pm0.02_0$Å and the equilibrium angle of the *gauche* form is 59.5±3.5°, where the C—C bond distance and the bond angles were assumed to be equal to the value of CF_2Cl-CF_2Cl and $CFCl_2$-$CFCl_2$ molecules, which have already been investigated by the present author.

The diffraction patterns and the microphotometer traces were taken by using apparatuses in Nagoya University. The author wishes to express his sincere gratitude to Professor M. Kubo, Professor R. Uyeda and Dr. Kimura for giving him facility to use the apparatuses and for their valuable advice. Thanks are also due to Dr. S. Shibata, Mr. H. Morimoto and Mr. K. Kimura of Nagoya University for their friendly assistance, and to Mr. K. Kuchitsu of the University of Tokyo for his help in calculating theoretical intensities by means of a punched card machine. Further, the author is much indebted to Professor Y. Morino of the University of Tokyo for his helpful criticism on this investigation.

Government Industrial Research Institute, Nagoya, Kita-ku, Nagoya

23) S. Mizushima, Y. Morino and T. Shimanouchi, *J. Phys. Chem.*, **56**, 324 (1952).

SHORT COMMUNICATIONS

Nuclear Magnetic Resonance Spectra of Dibromothiophene

By Shizuo Fujiwara, Mikio Katayama, Shôichi Hayashi, Hiroshi Shimizu and Shôji Nishimura*

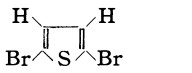
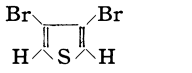
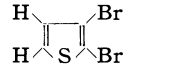
(Received November 17, 1958)

An extensive investigation of nuclear magnetic resonance of substituted thiophenes was carried out recently by Hazato et al.[1], and the results of the measurements of the chemical shifts and of the indirect spin-spin coupling constants J for these molecules were reported. The observed values of the chemical shifts were found in good accord with the values expected from the electronic structures of the substituents, but the chemical shifts due to the difference in the substituent positions were not fully elucidated, since their measurements were not made of 2,3- or 3,4-disubstituted thiophene. We, thus, report here the results of the measurements of these compounds.

The apparatus used is the one constructed in this laboratory of the type of high resolution slow-sweep setup which is composed of oscillator, null-T bridge, pre-amplifier, Collins 51J4 receiver, Sanborn recorder, oscillograph, magnet and saw-tooth generator. The magnet has the same structure as the one previously described by Gutowsky[2]. The field strength of the magnet is about 6200 gauss in 4.8 cm. gap with 12.5 cm. pole face diameter.

The resonance was observed at 27.030 Mc. The disubstituted thiophene and cyclohexane were mixed equally in volume, and sealed in a capillary of about 1 mm. diameter. The shifts were measured as the separations between the spectra of the sample and of cyclohexane. The results are shown in Table I. As the two protons of 2,3-dibromothiophene are not chemically equivalent, multiple resonance lines should be observed. It was, however, unsuccessfull probably owing to the lack of the intensity.

TABLE 1
CHEMICAL SHIFTS OF DIBROMOTHIOPHENE

substance	shift from cyclohexane
 2,5-dibromothiophene	140 cps
 3,4-dibromothiophene	150
 2,3-dibromothiophene	145

We see in Table I that the diamagnetic shieldings for the 3,4-protons in 2,5-dibromothiophene are larger than those for the 2,5-protons in 3,4-dibromothiophene. The shift of 2,3-dibromothiophene falls in the middle of the former two molecules. Our results presented here may be taken as the supplementary data for those of Hazato et al., and all the results will be used for the interpretations of the electronic nature of substituted thiophene.

Our thanks are due to Dr. Yonezô Morino of the University of Tokyo for his suggestion to make measurements on these compound.

University of Electro-Communications
Chofu, Tokyo

* Department of Chemical Engineering, University of Osaka Prefecture, Sakai, Osaka.

1) K. Takahashi, Y. Matsuki, T. Mashiko and G. Hazato. Lectured at the Annual Meeting of Chemical Society of Japan, Tokyo, April. 1958.

2) H. S. Gutowsky, L. H. Meyer and R. E. McClure: *Rev. Sci. Inst.*, **24**, 644 (1953).

Crystal Structure of Pyrazinamide

By Yoshito TAKAKI, Yoshio SASADA and Tokunosuké WATANABÉ

(Received December 9, 1958)

The crystal structure of pyrazinamide*, $C_5H_5N_3O$, (a new potential medicine for tuberculosis[1]) has been examined by X-ray analysis. The crystal data obtained were:

$a=23.07$, $b=6.72$, $c=3.72$Å, $\beta=100.8°$,

space group $P2_1/a$, four molecules per unit cell.

The analysis was carried on by two-dimensional procedures. By considering the molecular packings, all the atoms were roughly located in the projections onto (001) and (010). The atomic coordinates were refined by using structure factor maps and further by successive Fourier projections. At the present stage the discrepancy indices ($R=\sum||F_o|-|F_c||/\sum|F_o|$) are 0.17 for ($hk0$) and 0.20 for ($h0l$).

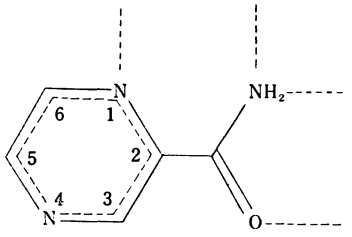


Fig. 1.

The molecule as shown in Fig. 1 is found to be approximately planar. Moreover the bond lengths C—C and C—N in the pyrazine ring show intermediate values between their single and double bonds. These suggest that there is a considerable amount of conjugation between the ring and the amide group.

Two amide groups are linked by a pair of NH—O hydrogen bonds forming a dimer molecule. These dimers are arranged in the direction (011), combining each other by NH—N'_1 hydrogen bonds. This structure explains the cleavage plane parallel to (100).

Further refinement is now going on by $(\rho_o-\rho_c)$ and least squares methods. The details of this work will be shortly published.

Faculty of Science
Osaka University
Kita-ku, Osaka

* The sample used was supplied from Sankyo Co., Ltd.

1) S. Kushner et al., *J. Am. Chem. Soc.*, **74**, 3617 (1952).

The Reaction of Glycine Cobalt Complex with Acetaldehyde

By Yoshikazu IKUTANI, Tôru OKUDA, Mikio SATO and Shiro AKABORI

(Received January 8, 1959)

Considerable progress in the chemical synthesis of threonine has recently been made by Sato, Okawa and Akabori by means of a Knoevenagel-type condensation of acetaldehyde with the active methylene groups of glycine copper complex[1]. As a continuation of their study we have investigated a similar type of reaction using acetaldehyde and glycine cobalt complex. The triglycino-cobalt was reported to occur in two isomeric forms, namely α- and β-form[2]. These two isomers can be obtained separately owing to the difference of their specific gravities.

A 0.02 g. portion of glycine cobalt complex was allowed to react with 0.1 cc. of acetaldehyde in the presence of 0.1 cc. of 6% aq. sodium carbonate as a condensing catalyst in a sealed tube. After suitable periods of time the total yields of products (threonine+allothreonine) and the ratios of threo- to allo-form in the products were determined by the dinitrofluorobenzene method[3] and a simplified ninhydrin method, respectively.

In general, the yields, especially when the β-form complex was used, were poor, while the threo/allo ratios obtained were much higher than those observed in the case of the copper complexes (threo/allo =1.8). The highest ratio was obtained when the condensation was carried out at 70°C for 2 hr. using the α-isomer. Under this condition the total yield (allo+threo) was 32%, (see Table I).

The poor yield may be due to remarkable stability of glycine cobalt complex, and the changes in the threo/allo ratios with reaction temperature and/or time (see Tebles I and II) suggest that the stabilities of cobalt threonine and cobalt

TABLE I

INFLUENCE OF REACTION TEMPERATURE ON THE THREO/ALLO RATIO AT A REACTION TIME OF 2hr.

Reaction Temp.	α-form			β-form		
	threo, %	allo, %	threo/allo	threo, %	allo, %	threo/allo
50°C	77	23	3.4	78	22	3.5
70°C	88	12	7.6	81	19	4.2
90°C	76	24	3.1	70	30	2.3

TABLE II

INFLUENCE OF REACTION TIME ON THE THREO/ALLO RATIO AT 70°C

Reaction Time	α-form			β-form		
	threo, %	allo, %	threo/allo	threo, %	allo, %	threo/allo
1/2 hr.	78	22	3.5	74	26	2.9
1 hr.	82	18	4.5	75	25	3.0
2 hr.	88	12	7.6	81	19	4.2
4 hr.	85	15	5.6	78	22	3.5

1) M. Sato, K. Okawa and S. Akabori, This Bulletin, **30**, 937 (1957).

2) H. Ley and H. Winkler, *Ber.*, **42**, 3894 (1909).

3) J. C. Perrone, *Nature*, **167**, 513 (1951).

allothreonine complexes are different. Moreover, as can be seen in Tables I and II, the ratios obtained with the α-form appear to be slightly higher than those obtained with the β-form.

The effect of catalysts other than sodium carbonate was also examined and only potassium carbonate was effective. Disodiumhydrogenphosphate and sodium acetate were completely inactive. The detailed results on this reaction will be reported elsewhere.

Division of Organic Chemistry
Institute for Protein Research
Osaka University, Osaka

Molecular Structure and Rotational Isomerism of Some Fluorochloroethanes

By Machio IWASAKI

(Received August 15, 1958)

The problem of rotational isomerism in chlorinated ethanes has been well elucidated by a number of investigators from various points of view. In the series of CH_2Cl-CH_2Cl, $CHCl_2$-CH_2Cl and $CHCl_2$-$CHCl_2$, the energy differences between the *trans* (or C_s) and the *gauche* forms are expected to be almost equal, from simple considerations on the interaction between non-bonded atoms. Contrary to this expectation, the experimental evidence shows that there are remarkable variations in the energy differences in these three compounds: the energy difference for CH_2Cl-CH_2Cl is reported to be 1.0~1.3 kcal./mol. by many investigators[1-4], that for $CHCl_2$-CH_2Cl is 2.9kcal./mol.[5,6] and that for $CHCl_2$-$CHCl_2$ is nearly 0 kcal./mol.[5,7], these data being evaluated in the vapor state.

Miyagawa[8] suggested that this variation of the energy difference for these three compounds arises from the induction effect and the difference in bond angles. Kreevoy and Mason gave in their recent paper[9] the same explanation for this experimental result. Miyagawa[10] also reported that the substitution of a hydrogen atom in chloroethanes with a methyl group having a van der Waals' radius almost equal to that of chlorine atom gave no appreciable decrease of the energy difference between the isomers. This fact stimulates the investigation of the effect of fluorine substitution which introduces the C—F bond moment that is almost equal to the C—Cl bond moment in contrast to the methyl substitution which introduces inappreciable change in electrostatic interaction.

Furthermore, the general applicability and the merits of various potential functions[8,9] that have recently been proposed can not be criticized until comprehensive data on the molecular parameters are available. Therefore, it is desirable to carry out a study on the molecular structure and the rotational isomerism of some fluorochloroethanes by electron diffraction which will give the data for the energy difference and the azimuthal angle of the *gauche* form in addition to other molecular parameters.

The present writer has undertaken studies on the molecular structure of CF_2Cl-CF_2Cl, $CFCl_2$-CF_2Cl and $CFCl_2$-$CFCl_2$ in order to find the effect of fluorine substitution on the energy difference between the isomers and on the bond distances.

Apparatus. — In earler investigations, the molecular scattering term required for the analysis of molecular structures was estimated visually from the total scattering which was the supperposition of small oscillation corresponding to the molecular term and the steeply falling background corresponding to atomic and incoherrent scatterings, because the background fell off very rapidly with an increasing scattering angle so that it was difficult to record and measure the pattern accurately. Therefore, the visual method may essentially be free from a large error in the estimation of intensities. As a matter of fact, there is a limit in the accuracy of the molecular parameters determined by the visual method; moreover this method is not sufficiently reliable to provide solutions for such a complicated problem as that of rotational isomerism.

This difficulty has been overcome by the use of a rotating sector to compensate for the sharp drop in intensity by screening electrons appropriately before they reach the photographic emulsion used to record the pattern, and by the measurement of the resulting diffraction patterns with a recording microphotometer. The sector-microphotometer method has been proposed independently by C. Finbak[11] and by P. Debye[12] and has been developed by the

1) I. Watanabe, S. Mizushima and Y. Morino, *Sci. Papers Inst. Phys. Chem. Research (Tokyo)*, **39**, 401 (1942).
2) T. Shimanouchi, H. Tsuruta and S. Mizushima, ibid., **42**, 51 (1944).
3) H. J. Bernstein, *J. Chem. Phys.*, **17**, 258 (1949).
4) W. D. Gwinn and K. S. Pitzer, ibid., **16**, 303 (1948).
5) J. R. Thomas and W. D. Gwinn, *J. Am. Chem. Soc.*, **71**, 2785 (1949).
6) K. Kuratani and S. Mizushima, *J. Chem. Phys.*, **22**, 1403 (1954).
7) K. Naito, *Repts. Osaka Ind. Research Inst.*, (*Osaka Kogyogijutsu Shikenjo Kiho*), 8, 1 (1957).
8) I. Miyagawa, *J. Chem. Soc. Japan, Pure Chem. Sec.* (*Nippon Kagaku Zasshi*), **75**, 1169, 1173, 1177 (1954).
9) M. M. Kreevoy and E. A. Mason, *J. Am. Chem. Soc.*, **79**, 4581 (1957).
10) I. Miyagawa, *J. Chem. Soc. Japan, Pure Chem. Sec.* (*Nippon Kagaku Zasshi*), **75**, 1162 (1954).
11) C. Finbak, *Avhandl. Norske Videnskaps-Akad. Oslo I. Mat.-Naturv. Kl.* **13**, (1937).
12) P. P. Debye, *Physik. Z.*, **40**, 404 (1939).

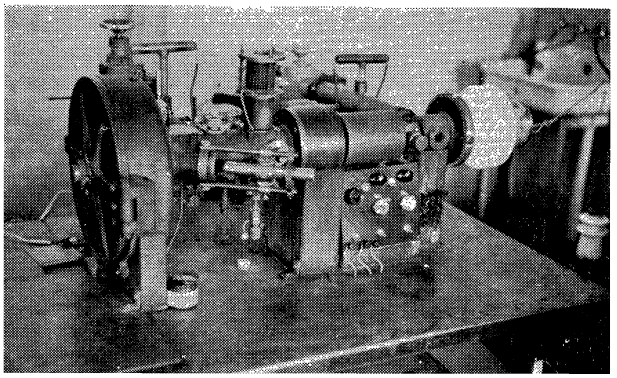


Fig. 1. External appearance of an electron diffraction unit.

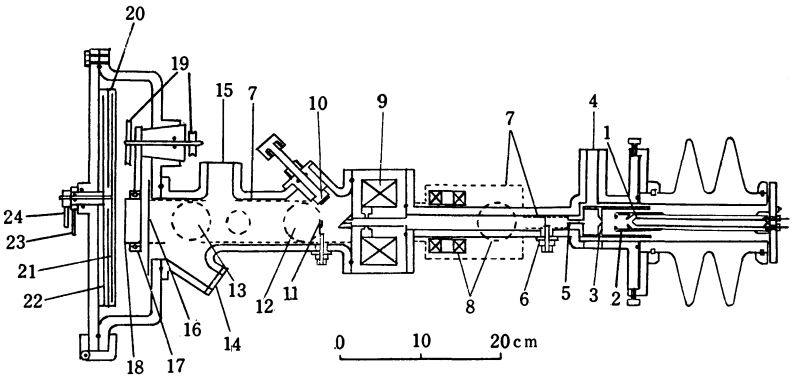


Fig. 2. Sectional drawing of an electron diffraction unit.
1. filament, 2. Trichter, 3. anode, 4. to pump, 5. diaphragm, 6. slit, 7. shield case made of permalloy, 8. Helmholz coil, 9. magnetic lens, 10. stop valve, 11. slit, 12, 13. port for specimen injection, 14. window, 15. to pump, 16. fluorescent screen, 17. ball bearing, 18. sector, 19. pulley for rotating the sector, 20. cassette, 21. fluorescent screen, 22. photographic plate, 23. handle for rotating photographic plates, 24. handle for rotating fluorescent screen.

Norwegian school[13]. Several laboratories[13-18] now use this method in electron diffraction investigation on molecular structures. In our country, the first apparatus having a rotating sector was constructed by Ino[19] and applied to thin amorphous films of a high polymer. The apparatus[20] used in this study was designed and constructed after the example of Ino's apparatus and some device was made for the treatment of gaseous samples.

Figs. 1 and 2 show the external appearance and the sectional drawing of the electron diffraction unit, respectively. It consists of four parts: an electron gun, a collimating system, a specimen chamber and a diffraction chamber. Cylinders made of permalloy were used for shielding electron beams from the external magnetic field. The electron gun was of a hot cathode type, consisting of a filament, a Trichter[21] biasing cup and an anode. The divergent beam from the gun was focused on the plane of photographic plates by a single magnetic lens. The direction of the beam was precisely controlled and adjusted to the center of the sector by means of two pairs of Helmholtz coils which are set at a right angle to each other. Two ports are provided for introducing specimens into the electron beam, one at 125 mm. and the other at 285 mm. from the photographic plate. The shorter distance is suitable for studies on moderate and wide-angle scatterings, $20 < q < 105$, and the longer distance

13) C. Finbak, O. Hassel and B. Ottar, *Arch. Math. Naturvidenskap.*, **44**, No. 13 (1941); O. Hassel and H. Viervoll, *Acta Chem. Scand.*, **1**, 149 (1947); O. Bastiansen, *Det 8. Nordiske Kjemikermfte. Beretning og Foredrag.*, **1954**, 139; O. Bastiansen, O. Hassel and E. Risberg, *Acta Chem. Scand.*, **9**, 232 (1955).
14) I. L. Karle and J. Karle, *J. Chem. Phys.*, **17**, 1052 (1949); J. Karle and I. L. Karle, ibid., **18**, 957 (1950); I. L. Karle and J. Karle, ibid., **18**, 963 (1950).
15) H. J. Yearian and W. M. Barss, *J. Appl. Phys.*, **19**, 700 (1948).
16) L. O. Brockway and L. S. Bartell, *Rev. Sci. Instr.*, **25**, 569 (1954).
17) F. A. Keidel and S. H. Bauer, *J. Chem. Phys.*, **25**, 1218 (1956); R. B. Harvey, F. A. Keidel and S. H. Bauer, *J. Appl. Phys.*, **21**, 860 (1950).
18) C. Romers and J. E. G. Creutzbergs, *Recucil trav. chim.*, **75**, 331 (1956).
19) T. Ino, *J. Phys. Soc. Japan*, **8**, 92 (1953).
20) Y. Morino, M. Kimura and M. Iwasaki, The Sixth Annual Meeting of the Chemical Society of Japan (1953).
21) K. H. Steigerwald, *Optik*, **5**, 459 (1949).

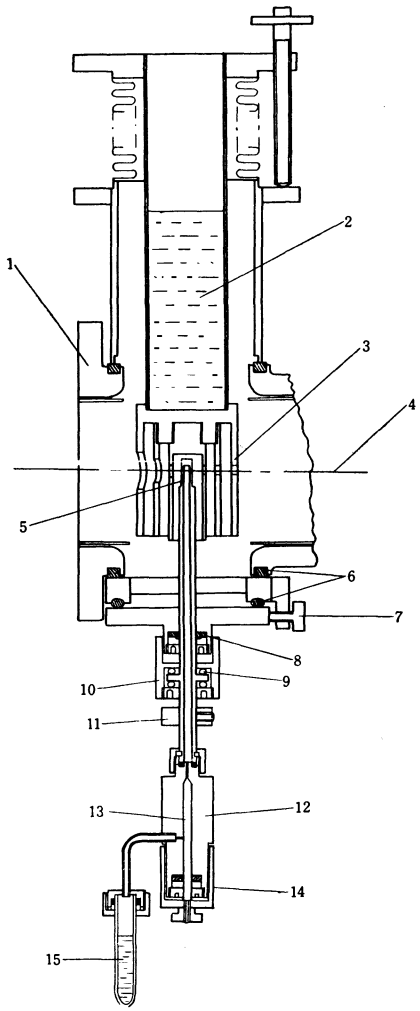


Fig. 3. Sectional drawing of a specimen injection system.
1. body of a diffraction unit, 2. liquid air, 3. cold trap, 4. electron beam, 5. nozzle, 6. rubber packing, 7. cross leader, 8. Wilson seal, 9. ball, 10. screw for adjusting the position of the nozzle, 11. nob, 12. needle valve, 13. needle, 14. screw for adjusting the inlet pressure, 15. sample.

is useful for examination of small angle scattering, $7 < q < 45$. The system of specimen injection is shown in Fig. 3 and the nozzle of a drum type is used. At first sight, it seems likely that in the nozzle of this type the spreading of samples is rather large and so the multiple and extraneous scatterings are serious. However, in practical use, a nozzle of this type makes it possible to take very clean diffraction patterns in lower inlet pressure of gas than that in the case of a nozzle of the ordinary type. Even if the inlet pressure of gas is sufficiently low and the cold trap is used, the diffraction patterns obtained have an index of resolution of 0.95~1.00; that is, the ratio of the amplitude of the molecular scattering terms to the magnitude of the smooth background upon which the molecular terms are superposed is 0.95~1.00 times that given by theory for a perfect pattern. The inlet gas pressure can precisely be controlled by a needle valve having a mildly tapered needle. The spreading gas is caught by using the cold trap which consists of three-fold concentric cylinders. The stop valve which is set behind the magnetic lens permits the electron gun to be isolated from the other parts of the apparatus and to keep it evacuated in placing photographic plates as well as in altering the nozzle-to-plate distance. The wavelength of the electron beam is determined by means of a gold foil attached to the nozzle. The sector which has a spiral form with an angular opening increasing as the square of the radius[22] is provided because this form is somewhat more profitable than the heart form with respect to the accuracy of figuring and finish. The sector is mounted on the inner race of a ball bearing of phosphor bronze, which is rotated by a power supply introduced into the vacuum space through a Wilson seal and transmitted by a pulley and a phosphor bronze wire. The fluorescent screen placed in front of the sector assembly makes it possible to observe the diffraction patterns in their innate state without replacing the sector. Moreover, it serves as a shutter of the electron beam.

The experimental procedure and the method for deriving the molecular scattering intensity from diffraction data has been already described in previous papers[23-25].

Results

The detailed description of the analysis has already been reported in this Bulletin[23-25]. Only the results are briefly described in this paper.

The experimental and the theoretical intensity curves are reproduced in Fig. 4, and the radial distribution curves derived from the experimental intensities are shown in Fig. 5. The molecular parameters obtained by the radial and the correlation method are listed in Tables I and II. In all cases, the analyses were made on the assumption that the structural frame of molecules does not change with rotation about the C—C bond. In the case of a CF_2Cl—$CFCl_2$ molecule, the C—C distance and the bond angles for the two halves of the molecule were assumed to be equal to those of CF_2Cl–CF_2Cl and $CFCl_2$–$CFCl_2$, respectively.

22) At present, an r^3-sector constructed by S. Shibata is available as well as an r^2-sector. S. Shibata, Symposium on the X-ray and electron diffraction held in Osaka City University, Nov. 1956.
23) M. Iwasaki, S. Nagase and R. Kojima, This Bulletin, **30**, 230 (1957).
24) M. Iwasaki, ibid. **31**, 1071 (1958).
25) M. Iwasaki, ibid. **32**, 194 (1959).

TABLE I

THE MOLECULAR PARAMETERS FOR CF_2Cl-CF_2Cl, $CFCl_2$-CF_2Cl AND $CFCl_2$-$CFCl_2$

	CF_2Cl-CF_2Cl	$CFCl_2$-CF_2Cl	$CFCl_2$-$CFCl_2$
C—F(Å)	$1.33_0 \pm 0.01_5$	$1.32_9 \pm 0.01_4$ $1.37_9 \pm 0.02_4$	1.38 ±0.02
C—Cl(Å)	$1.74_5 \pm 0.01_5$	$1.74_7 \pm 0.02_7$ $1.75_8 \pm 0.02_0$	1.76 ±0.01
C—C(Å)	1.54 ±0.04	1.53_9(*)	1.54 ±0.06
∠CCCl	112 ±1.5°	112°(*) 112°(*)	112 ±2°
∠CCF	108 ±1.5°	108°(*) 107°05′(*)	107°05′
∠FCCl	110 ±1°	110°(*) 107.5°(*)	107.5±1.5°
∠FCF	108°44′	108°44′(*)	
∠ClCCl		110.5°(*)	110.5±1°

(*): Assumed

TABLE II

OBSERVED MEAN AMPLITUDES FOR CF_2Cl-CF_2Cl, $CFCl_2$-CF_2Cl AND $CFCl_2$-$CFCl_2$

	CF_2Cl-CF_2Cl	$CFCl_2$-CF_2Cl	$CFCl_2$-$CFCl_2$
C—F	0.052Å	0.055_5Å	0.064Å
C—Cl	0.061	0.054_0	0.062
C—C	0.045	0.041_7	——
$(F\cdots Cl)_t$	0.062	0.063_8	0.070
$(Cl\cdots Cl)_t$	0.088	0.069_5	0.081

The mean amplitudes were not determined except the values listed in Table II and the values estimated from the spectroscopic data and other electron diffraction data were used throughout these analyses.

The energy difference between the rotational isomers and the azimuthal angles of the *gauche* form in these three molecules are listed in Table III and the stable configurations are shown in Fig. 6. In the case of the CF_2Cl-$CFCl_2$ molecule, the configuration having the C_s symmetry is called the C_s form and that having no symmetry the *gauche* form as shown in Fig. 6. In all cases, the *trans* (or C_s) form was assumed to possess the C_{2h} (or C_s) symmetry but the azimuthal angle of

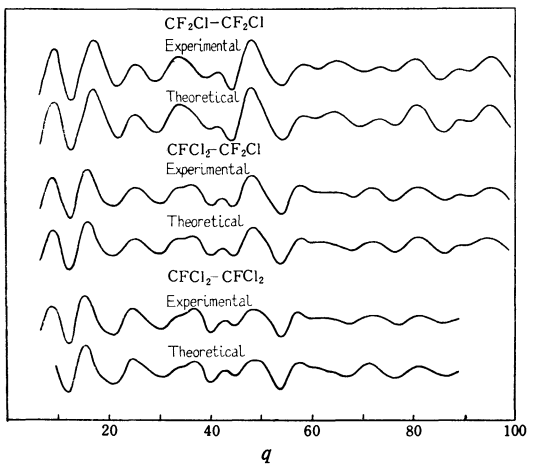


Fig. 4. Experimental and theoretical intensity curves.

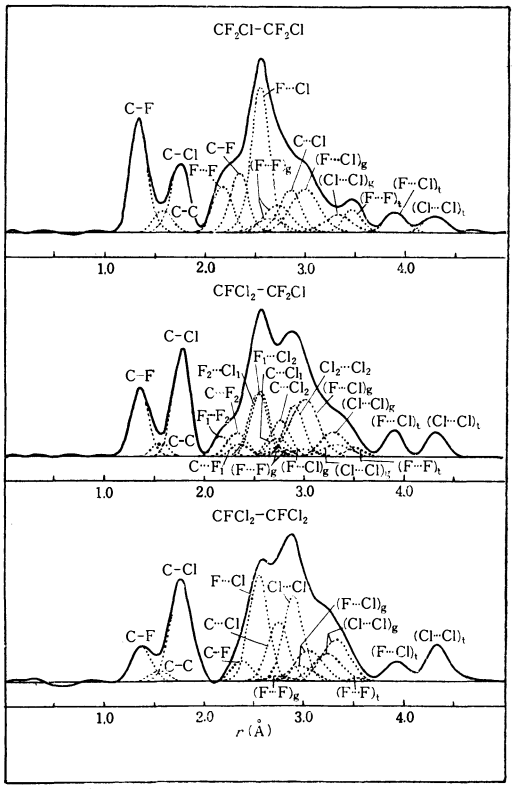


Fig. 5. Radial distribution curves.

TABLE III

THE ENERGY DIFFERENCE BETWEEN THE ROTATIONAL ISOMERS AND THE AZIMUTHAL ANGLE OF THE *GAUCHE* FORM FOR CF_2Cl-CF_2Cl, $CFCl_2$-CF_2Cl AND $CFCl_2$-$CFCl_2$

Molecules	Stable form	N_g(%)	ΔE (cal./mol.)	Azimuthal angle of the *gauche* form
CF_2Cl-CF_2Cl	*trans* (C_{2h})	48± 5 (10°C)	440±110	62.5±3° (Cl-C-C-Cl)
$CFCl_2$-CF_2Cl	*gauche* (C_1)	76± 7 (20°C)	−270±250	59.5±3.5° (Cl-C-C-Cl)
$CFCl_2$-$CFCl_2$	*trans* (C_{2h})	55±10 (15°C)	280±240	59 ±4° (F-C-C-F)

N_g: Amount of the *gauche* form.

ΔE: Energy difference between the isomers. $\Delta E = E_g - E_t$ (or E_{C_s})

the *gauche* form was taken as an unknown parameter. The amounts of the rotational isomers were obtained from the area under the radial distribution peaks by using the successive approximation and further confirmation was made by analyzing the small angle scattering ($20 < q < 40$) that was precisely measured by use of the long camera length. The azimuthal angle of the *gauche* form was also determined by the analysis of the radial distribution curve and the small angle scattering ($20 < q < 40$).

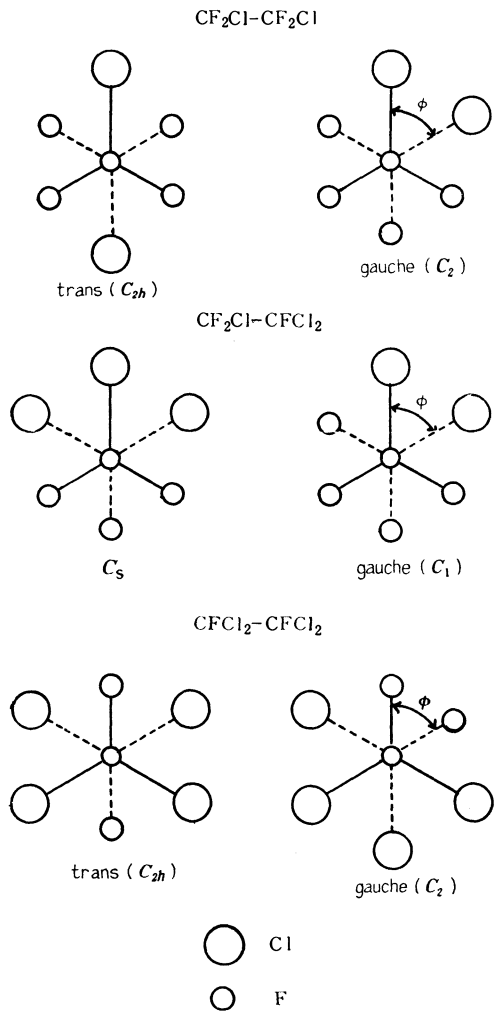


Fig. 6. Stable configurations.

Discussion

Bond Distances and Bond Angles.—The shortening of the C—X bond (X=halogen or carbon atom) by the substitution of hydrogen atoms in H_3C—X compounds with fluorine atoms was a historical problem which has been stimulating many investigators working in the field of electron diffraction and microwave spectroscopy. Brockway and Livingston[26] have first reported this shortening for many fluorinated hydrocarbons from the results of visual electron diffraction. On the other hand, Bauer[27] doubted whether or not this shortening was real, because of the great ambiguity inherent to visual electron diffraction. Thereafter, the development of microwave spectroscopy and the sector-microphotometer method of electron diffraction revealed that this shortening was real in the case of carbon-halogen bonds, although the magnitude of this shortening was somewhat smaller than that reported by Brockway and Livingston.

In the series in question, it was shown that the C—F bond distance decreased with the number of fluorine atoms attached to one and the same carbon atom, i.e., in a —$CFCl_2$ group the C—F bond distance is 1.38Å and in a —CF_2Cl group it is 1.33Å. These results coincide with the results of other organic fluorine compounds as shown in Table IV. The value of 1.38Å for $CFCl_2$-$CFCl_2$ coincides with those of the groups having a single fluorine atom attached to one and the same carbon atom. The value of 1.33$_0$Å for CF_2Cl-CF_2Cl seems to be slightly shorter than that for the group having two fluorine atoms attached to one and the same carbon atom,

26) L. O. Brockway and R. Livingston, *U. S. Naval Research Lab. Project M-510, Report No. 547.1. XA C-R-1080, A-3786.*

27) S. H. Bauer, *U. S. Atomic Energy Com. Report, MDDC* 1494 (1947).

TABLE IV

THE MOLECULAR STRUCTURES OF SOME FLUORINATED HYDROCARBONS

Compounds	C—F(Å)	C—Cl(Å)	Other structure parameters	Method	Ref.
CH_3F	1.385		$\angle HCF=110°0'$	MW	a
CH_2ClF	1.378±0.006	1.759±0.003	$\angle FCCl=110°01'\pm2'$	MW	b
$CHCl_2F$	1.41 ±0.03	1.73 ±0.04	$\angle ClCCl=112°\pm2°$, $\angle FCCl=10.9°\pm2°$	V	c
CCl_3F	1.40 ±0.04	1.76 ±0.02	$\angle ClCCl=111.5°\pm1°$, $\angle FCCl=107.5°\pm1°$	V	c
$C(CH_3)_3F$	1.38 ±0.02		$\angle CCF=108°\pm1.5°$	S	d
CH_3CH_2F	1.375		$\angle CCF=109°28'$ (assumed)	MW	e
CH_2F_2	1.358±0.001		$\angle FCF=108°17'\pm6'$	MW	f
$CHClF_2$	1.36 ±0.03	1.73 ±0.03	$\angle FCF=110.5°\pm1°$, $\angle FCCl=110.5°\pm1°$	V	c
CCl_2F_2	1.35 ±0.03	1.74 ±0.03	$\angle FCF=109°\pm2°$, $\angle ClCCl=113°\pm2°$	V	c
	1.33_5 ±0.02	1.77_5 ±0.02	$\angle FCF=109.5°\pm3°$, $\angle ClCCl=108.5°\pm2°$	V	g
CHF_3	1.332±0.008		$\angle FCF=108°48'\pm45'$	MW	h
$CClF_3$	1.328±0.002	1.751±0.004	$\angle FCF=108.6°\pm0.4°$	S	i
	1.328±0.002	1.748±0.009	$\angle FCF=108.6°\pm0.4°$ (assumed)	MW	i
CH_3CF_3	1.335±0.005		C—C=1.530±0.005, $\angle CCF=111°2'\pm17'$	MW	j
CF_3CF_3	1.32 ±0.01		$\angle CCF=109.5°\pm1.5°$	S	k
CF_4	1.323±0.005			S	l

MW: microwave, V: visual, S: sector

a) O. R. Gillam, H. D. Edwards and W. Gordy, *Phys. Rev.*, **75**, 1014 (1949).
b) N. Muller, *J. Am. Chem. Soc.*, **75**, 860 (1954).
c) L. O. Brockway, *J. Phys. Chem.*, **40**, 747 (1936).
d) F. Andersen, J. R. Andersen, B. Bak, O. Bastiansen, E. Risberg and L. Smedvik, *J. Chem. Phys.*, **21**, 373 (1953).
e) J. Kraitchman and B. P. Dailey, ibid., **23**, 184 (1955).
f) D. R. Lide, *J. Am. Chem, Soc.*, **74**, 3548 (1952).
g) R. L. Livingston and R. H. Lyon, *J. Chem. Phys.*, **24**, 1283 (1956).
h) S. N. Ghosh, R. Trambarulo and W. Gordy, ibid., **20**, 605 (1952).
i) L. S. Bartell and L. O. Brockway, ibid., **23**, 1860 (1955).
j) W. F. Edgell, ibid., **16**, 1002 (1948).
k) D. A. Swick and I. L. Karle, ibid., **23**, 1499 (1955).
l) L. O. Brockway, C. G. Thornton and L. S. Bartell, Am. Chem. Soc. Meeting, Los Angeles, California, March 1953.

but the difference is inappreciable in view of errors involved in experiments.

On the other hand, although the inaccuracies of the data do not permit us to draw a definite conclusion, it appears to be likely that the C—Cl distance also decreases with the number of fluorine atoms. Recently, Livingston and Lyon[28] reported a slightly greater value 1.77_5Å for the C—Cl distance in CF_2Cl_2 in disagreement with the present value, although the difference is within experimental errors. Their result seems to be related to the fact that the ClCCl bond angle 108.5°, obtained by them, is slightly shorter than the tetrahedral value, 109.5°. In this connection, it is desirable to determine the C—Cl distance in CF_2Cl_2 by the sector-microphotometer method or the microwave spectroscopy. The value of the C—Cl distance determined for the extreme case of a $CClF_3$ molecule in which three atoms except one chlorine atom were replaced by fluorine atoms was reported to be 1.748Å[29,30] from the microwave spectroscopy and 1.751Å[30] from the sector-microphotometer method of electron diffraction. In the case of a CF_2Cl-CF_2Cl molecule having two fluorine atoms attached to one and the same carbon atom, the C—Cl bond distance was found to be slightly shorter than the extreme value, the difference being also within experimental errors.

With regard to the C—C bond distance, although a definite conclusion could not be drawn because of the greater ambiguity of the data, experimental results could be explained by the normal distance of the C—C bond. It is not likely that such a

28) R. L. Livingston and D. H. Lyon, *J. Chem. Phys.*, **24**, 1283 (1956).

29) D. K. Coles and R.H. Hughes, *Phys. Rev.*, **76**, 858(1949).
30) L. S. Bartell and L. O. Brockway, *J. Chem. Phys.*, **23**, 1860 (1955).

large shortening as reported in earlier investigations was realized in the present molecules.

With respect to bond angles, it is to be noted that the FCF angle is less than the tetrahedral value, in agreement with recent determinations on other fluorinated hydrocarbons. This is interesting together with the fact that the decrease in the FSiF angle from the tetrahedral value was also reported in the case of organosilicon compounds. For example, the FSiF angle is $108°17' \pm 30'$ for $SiHF_3$[31] and $107°56' \pm 6'$ for SiH_2F_2[32]. Other bond angles are also consistent with the values found in other related molecules.

Such a shortening of the carbon-halogen bond was originally explained by Pauling[33] by the assumption of resonance structures of the type

$$X-\overset{\overset{F^-}{|}}{\underset{|}{C}}=X^+ \quad (X=F \text{ or } Cl)$$
$$\quad\quad\; X$$

The fact that the C—F shortening is more marked than the C—Cl shortening is attributed to the great tendency of a fluorine atom to form double bonds. It is conceivable that the structures of this type can also contribute to the slight closing of the FCF angle because of the Coulomb attraction between F^- and F^+.

Rotational Isomerism.—From the present studies, it was definitly confirmed that there exist two isomers, the *trans* (or C_s) and the *gauche* forms, in the vapor state for the series of the molecules in question. As shown in Table III the energy differences were almost of the same magnitude and considerably small compared with the remarkable variation and large values (except $CHCl_2$—$CHCl_2$) observed in the series of chloroethane: CH_2Cl-CH_2Cl (1.2 kcal./mol.), $CHCl_2$-CH_2Cl (2.9 kcal./mol.) and $CHCl_2$-$CHCl_2$ (0 kcal./mol.). It is said that the internal rotation is subject mainly to the steric and electrostatic interactions. According to the replacement of a hydrogen atom with a fluorine atom, the nature of three atoms contained in two groups rotating against each other is more close together in both "steric" and "electrostatic" senses as compared with the case of chloroethanes. As a concequence of this circumstance, it is likely that the potential energy of the *trans* (or C_s) form becomes nearly equal to that of the *gauche* form. It was reported by Miyagawa[10] that the replacement of a hydrogen atom with a methyl group in chloroethanes gave no serious decrease of the energy difference between the isomers and did not affect the tendency of the change in the energy differences with the number of chlorine atoms substituted in the molecules, although a methyl group having almost the same van der Waals' radius as a chlorine atom was introduced. Moreover, a fluorine atom may be closer to a hydrogen atom in the magnitude of the steric interaction than a chlorine atom, because the potential barrier of CF_3-CF_3, 3.92 kcal./mol.[34] is close to that of CH_3-CH_3, 2.875 kcal./mol.[35] as compared with the value in CCl_3-CCl_3, 10.8 kcal./mol.[36]. Accordingly, the main factor contributing to this lowering of energy difference in fluorochloroethane is presumably due to the decrement of the electrostatic interaction rather than the steric interaction. In fact, it is well known that the bond moment of C—F is approximately equal to that of C—Cl.

From a simple assumption of the additivity of interaction energy and the constancy of the bond distances as well as bond angles, it is expected that the energy differences are all the same in the series of 1,2-di-, 1,1,2-tri- and 1,1,2,2-tetrasubstituted ethanes. However, the observed energy differences in chloroethanes were not the same and indicated a remarkable variation which was explained by the induction effect and the opening of the ClCCl bond angle[8] as described in foregoing section. In the series of chlorofluoroethanes, the changes of the energy difference caused by the effect of induction are very small and the ClCCl bond angles are close to the tetrahedral angle. As a result of this circumstance, it appears to be likely that the energy differences in the present series represent almost the same value.

From the theoretical side, many attempts have been made to predict the hindering potential for the internal rotation about single bonds, based on a simple model for interactions between non-bonded atoms or groups. Among a number of attempts, the treatments recently made with tolerable success by Miyagawa[8] and Mason

31) G. A. Heath, L. F. Thomas and J. Sheridan, *Trans. Faraday Soc.*, **50**, 779 (1954).
32) V. W. Laurie, *J. Chem. Phys.*, **26**, 1359 (1957).
33) L. Pauling, "*The Nature of the Chemical Bond*", Cornell University Press, Ithaca, N. Y., 1945, p. 235.
34) D. E. Mann and E. K. Plyler, *J. Chem. Phys.*, 21, 1116 (1953).
35) K. S. Pitzer, *Disc. Faraday Soc.*, **10**, 66 (1951).
36) Y. Morino and E. Hirota, *J. Chem. Phys.*, 28, 185 (1958).

TABLE V
OBSERVED AND CALCULATED ENERGY DIFFERENCES (kcal./mol.)

Molecule	ΔE_{obs}	ΔE_e	Lennard-Jones		Buckingham	
			ΔE_s	ΔE_{total}	ΔE_s	ΔE_{total}
CF_2Cl-CF_2Cl	0.44	0.15	−0.10 (0.00)	0.05 (0.15)	0.30	0.45
$CFCl_2$-CF_2Cl	−0.27	−0.17	0.15 (0.05)	−0.02 (−0.12)	−0.20	−0.37
$CFCl_2$-$CFCl_2$	0.28	0.15	−0.25 (−0.13)	−0.10 (0.02)	−0.05	0.10

$\Delta E = E_g - E_t$ (or E_{Cs})

TABLE VI
OBSERVED AND CALCULATED AZIMUTHAL ANGLE OF THE *GAUCHE* FORM

Molecule	ϕ_{obs}	ϕ_{calc}(I)	ϕ_{calc}(II)
CF_2Cl-CF_2Cl	117.5°	118° (119°)	116°
$CFCl_2$-CF_2Cl	122	123 (122)	124
$CFCl_2$-$CFCl_2$	121	120 (120)	118

ϕ_{calc}(I): Lennard-Jones
ϕ_{calc}(II): Buckingham

and Kreevoy[9] seem to be most promising. The former author used a Lennard-Jones type potential while the latter a modified Buckingham type potential for interatomic interactions.

In order to estimate quantitatively the energy differences, a similar treatment was applied to the present case. The Lennard-Jones type potential for fluorine-fluorine interaction was approximated by the following formula for neon-neon interaction[37],

$$V(\mathrm{F-F}) = 7.148\times10^4/r^{12} - 143.58\times r^6 \text{ kcal./mol.} \quad (1)$$

The application of this formula leads to the value of 2.4 kcal./mol. for the potential barrier in CF_3-CF_3, minor terms due to dipole interaction being added. Though this value is somewhat smaller than the observed value 3.92 kcal./mol.[34], the two values seem to coincide roughly with each other for such approximate calculation. The formula applied by Miyagawa[8] to chlorinated ethanes with a fair success,

$$V(\mathrm{Cl-Cl}) = 2.332\times10^6/r^{12} - 2.180\times10^3/r^6 \text{ kcal./mol.} \quad (2)$$

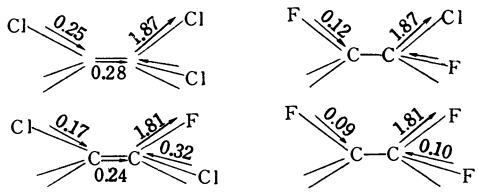
was adopted for chlorine-chlorine interaction. The expression for fluorine-chlorine interaction was derived through the method of averages proposed by Miyagawa[8] as follows:

$$V(\mathrm{F-Cl}) = 4.185\times10^5/r^{12} - 5.663\times10^2/r^6 \text{ kcal./mol.} \quad (3)$$

As a result of the application of these formulas, the values listed in the 4th column of Table V were obtained for the energy differences due to steric interaction.

For the sake of comparison, the modified Buckingham type potential given by Mason and Kreevoy[9] was also applied to this problem. The results are listed in the 8th column of Table V.

With respect to the electrostatic interaction, dipole interactions were calculated taking into account of induction effects. For the sake of this computation, the following induced moment were estimated from the observed dipole moments in many chlorofluoroalkanes, assuming a vanishing C—H bond moment and the tetrahedral angle.



The thick and slender arrows indicate original dipoles and induced dipoles, respectively. The dipole moments calculated on the assumption of the additivity of these induced moments were in good agreement with the observed values as shown in Table VII.

The energy differences contributed from the electrostatic interactions were estimated using these dipoles and induced dipoles as shown in the 3rd column of Table V. In this calculation, the center of the dipole moment is located at seven-eighth of the bonded distance from the carbon atom. Total energy differences listed in the 6th and the 9th column of Table V approximately coincide with the observed

37) J. Corner, *Trans. Faraday Soc.*, **44**, 914 (1948).

TABLE VII

CALCULATED AND OBSERVED DIPOLE MOMENTS IN CHLOROFLUOROALKANES (VAPOR STATE)

Molecule	μ(calc.)	μ(obs.)	Ref.	Molecule	μ(calc.)	μ(obs.)	Ref.
CH_3F	1.81	1.81	a	CH_3CF_2Cl	2.16	2.14	n
CH_3Cl	1.87	1.87	b, c, d	CH_3CF_3	2.33	2.32	d
CH_2F_2	1.97	1.96	e	$(CH_3)_3CF$	2.05	2.05	o
CHF_3	1.61	1.62	f	CF_3CHF_2	1.53	1.54	f
		(1.64_5)	(g)	CF_3CF_2Cl	0.51	0.52	f
CH_2Cl_2	1.63	1.62	h	CH_3CH_2Cl	1.96	2.03	p
$CHCl_3$	0.97	0.95	i	CH_3CHCl_2	2.01	2.07	j
		(1.02)	(j)	CH_3CCl_3	1.81	1.79	j
$CFCl_3$	0.44	0.45	k	$(CH_3)_3CCl_3$	2.15	2.13	q
CF_2Cl_2	0.52	0.51	k	CH_2ClCCl_3	1.39	1.39	r
		(0.55)	(l)	$CHCl_2CCl_3$	0.89	0.92	r
CF_3Cl	0.46	0.46	f	$(CH_2ClCH_2F)_g$	2.64 ($\phi=68°37'$)	2.64	n
$CHFCl_2$	1.20	1.29	k				
CHF_2Cl	1.41	1.39_6	k	$(CHCl_2CHF_2)_g$	2.10 ($\phi=60°$)	2.10	n
CH_3CH_2F	1.90	1.92	a				
CH_3CHF_2	2.28	2.24	m				

a) C. P. Smyth and K. B. McAlpine, *J. Chem. Phys.*, **2**, 499 (1934).
b) O. Fuchs, *Z. Physik*, **63**, 824 (1930).
c) R. Karplus and A. H. Sharbaugh, *Phys. Rev.*, **75**, 1449 (1949).
d) R. G. Shulman, B. P. Dailey and C. H. Towes, ibid., **78**, 145 (1950).
e) D. R. Lide, ibid., **87**, 227 (1952).
f) A. D. Giacomo and C. P. Smyth, *J. Am. Chem. Soc.*, **77**, 774 (1955).
g) J. N. Shovlery and A. H. Sharbaugh, *Phys. Rev.*, **82**, 95 (1951).
h) R. J. Myers and W. D. Gwinn, *J. Chem. Phys.*, **20**, 1420 (1952).
i) R. Sänger, *Physik. Z.*, **27**, 556 (1926).
j) A. A. Maryott, M. E. Hobbs and P. M. Gross, *J. Am. Chem. Soc.*, **63**, 659 (1941).
k) C. P. Smyth and K. B. McAlpine, *J. Chem. Phys.*, **1**, 190 (1933).
l) G. W. Epprecht, *Z. angew. Math. Physik.*, **1**, 138 (1950).
m) J. H. Gibbs and C. P. Smyth, *J. Am. Chem. Soc.*, **73**, 5115 (1951).
n) A. D. Giacomo and C. P. Smyth, ibid., **77**, 1361 (1955).
o) F. Andersen, J. R. Andersen, B. Bak, O. Bastiansen, E. Risberg and L. Smedvik, *J. Chem. Phys.*, **21**, 373 (1953).
p) R. Sänger, O. Steiger and K. Gachter, *Helv. Phys, Acta*, **5**, 200 (1932).
q) R. H. Wiswall, Jr. and C. P. Smyth, *J. Chem. Phys.*, **9**, 356 (1941).
r) J. R. Thomas and W. D. Gwinn, *J. Am. Chem. Soc.*, **71**, 2785 (1949).

values. The modified Buckingham type potential seems to give somewhat better results. However, if two constants in Lennard-Jones type potential are adjusted so as to give observed potential barrier in CF_3-CF_3, the agreement between the calculated and observed energy differences becomes better as shown in the 7th column of Table V. The modified potential functions used in this calculation are as follows:

$$V(\mathrm{F—F}) = 12.729\times10^4/r^{12} - 2.5569\times10^2/r^6 \text{ kcal./mol.} \quad (4)$$

$$V(\mathrm{F—Cl}) = 5.5839\times10^5/r^{12} - 7.5565\times10^2/r^6 \text{ kcal./mol.} \quad (5)$$

It is to be noted that the azimuthal angles of the *gauche* forms calculated from these potential functions are in excellent agreement with observed values as shown in Table VI. In this calculation, the angle was measured from the *trans* (or C_s) position. This agreement may indicate that the potential functions used were fairly adequate.

In the above calculation, the effects of resonance arising from the substitution with fluorine atoms were not included explicitly. However, the changes of the geometry caused by resonance were considered to be implicitly taken into account by using the molecular parameters obtained from the electron diffraction. Furthermore, the changes of the charge distribution were also considered to be implicitly contained in the estimation of the induced moment as a result of ascribing the lowering of the dipole moment caused by resonance to that by induction.

From the foregoing consideration, it is concluded that the substitution of hydrogen atoms in chlorinated ethanes with fluorine atoms decreases the difference of the electrostatic interaction between the *trans* (or C_s) and the *gauche* form, and that as a consequence the energy differences in fluorochloroethanes decrease and become almost equal to one another irrespective of the number of chlorine atoms substituted in the molecules. This fact is consistent with the conclusion reached by Mizushima, Morino and Shimanouchi[38] that the most important force in determining stable configurations of rotational isomers is the steric repulsion, but the electrostatic force plays an important role in determining the energy difference between the rotational isomers, because in the stable configurations the steric repulsive force may become of the same order of magnitude as the electrostatic force.

TABLE VIII
THE ENERGY DIFFERENCES FOR RELATED COMPOUNDS (cal./mol.)

Molecule	X=H	X=F	Difference
CX_2Cl-CX_2Cl	1140	440	700
CX_2Cl-CX_2Br	1460	600	860
CX_2Br-CX_2Br	1700	945	755

As an example of the lowering of the energy difference caused by the fluorine substitution, one can point out the case of bromofluoroethanes studied by Kagarise et al.; that is, the energy difference in CF_2Br-CF_2Br is 945±50 cal./mol.[39] and that in CF_2Cl-CF_2Br is 600±200 cal./mol.[40] as compared with the value of 1700±40 cal./mol. for CH_2Br-CH_2Br[41] and 1460±30 cal./mol. for CH_2Br-CH_2Cl[41]. It is interesting to note that the lowering of energy difference caused by the fluorine substitution shows almost the same value as shown in Table VIII. In other words, this fact indicates that the electrostatic part of the energy difference in these molecules is of almost the same magnitude as 0.7~0.8 kcal./mol. This is caused by the fact that the C—F, C—Cl and C—Br bond moments are of almost the same magnitude. Moreover, the order of the energy differences in the series of CH_2Cl-CH_2Cl, CH_2Cl-CH_2Br and CH_2Br-CH_2Br does not change with the fluorine substitution and a considerable amount of the energy difference exists after the fluorine substitution. This fact indicates that the steric part cannot be neglected and its contribution becomes larger with the number of bromine substitutions.

38) S. Mizushima, Y. Morino and T. Shimanouchi, *J. Phys. Chem.*, **56**, 324 (1952).
39) R. E. Kagarise and L. W. Daasch, *J. Chem. Phys.*, **23**, 130 (1955).
40) R. E. Kagarise, ibid., **26**, 380 (1957).
41) K. Kuratani, T. Miyazawa and S. Mizushima, ibid., **21**, 1411 (1953).

Summary

In order to investigate the molecular structure and rotational isomerism, the electron diffraction camera having a rotating sector was designed and constructed and its application to some fluorochloroethanes was made successfully. The shortening of the C—F and the C—Cl bond by the substitution of atoms attached to one and the same carbon atom with other fluorine atoms was also revealed in fluorochloroethanes as well as fluorochloromethanes, although in the case of the C—Cl bond distance the inaccuracy of the data does not permit a definite conclusion to be drawn. It was definitly confirmed that there exist two rotational isomers, the *trans* (or C_s) and the *gauche* forms, in the vapor state for the molecules in question. The energy differences between the isomers and the azimuthal angles of the *gauche* form were determined and further discussed from the standpoint of intramolecular potential.

It was found that three fluorochloroethanes in question have almost equal and small energy differences in contrast to the remarkable variation in the case of chloroethanes. This is caused by the fluorine substitution which produces the decrease of the electrostatic part in the energy difference between the isomers.

The author wishes to express his sincere gratitude to Professor M. Kubo, Professor R. Uyeda and Dr. M. Kimura of Nagoya University for their valuable advice and encouragement throughout the course of this work, and to Professor Y. Morino of the University of Tokyo for his helpful criticism on this investigation. The author is also indebted to Dr. I. Miyagawa of the University of Tokyo for his helpful discussion.

Government Industrial Research Institute, Nagoya, Kita-ku Nagoya

Kinetics of the Selenium Dioxide-Catalyzed Hydrogen Peroxide Oxidation of Dimethylaniline in Aqueous Methanol

By Yoshiro OGATA and Iwao TABUSHI

(Received August 23, 1958)

It has been reported that the oxidation of organic compounds with hydrogen peroxide was accelerated by selenium dioxide catalyst[1-3], but the mechanism of these reactions has not yet been clarified satisfactorily.

In general, there seem to be two main types of catalysts in organic oxidations with hydrogen peroxide; i. e., (i) the oxidation-reduction interaction between hydrogen peroxide and catalysts produces OH free radical, (e. g., in Haber-Weiss scheme[4] using Fenton's reagent) which can rapidly oxidize organic substances, and (ii) the combination of hydrogen peroxide with a catalyst gives peroxide as a relatively stable intermediate which is a more active oxidizing agent than hydrogen peroxide itself.

As the latter example, there are many organic and inorganic peroxides which oxidize organic substances without generating free radicals; for example, in the acid-catalyzed hydrogen peroxide oxidation of salicylaldehyde in acetic acid, intermediary peracetic acid reacted faster than hydrogen peroxide itself[5], and also Caro's acid, obtained from the reaction of hydrogen peroxide and sulfuric acid[6], was found to be a far more effective oxidant for tertiary amines than hydrogen peroxide itself[7,8].

As to the selenium dioxide-catalyzed reaction, there seems to be no direct evidence to decide which of these mechanistic types is operating. However, it has been reported that acrolein is oxidized to acrylic acid with neither hydroxylation nor polymerization, suggesting a non-radical mechanism for the reaction. But these peroxide intermediates may react by generating free radicals. For example, it has been considered that osmium, vanadium[9] and tungsten oxide[10] produced intermediary peroxides which could generate an OH radical during their reactions.

The present paper describes the rate data and a probable mechanism of the selenium dioxide-catalyzed hydrogen peroxide oxidation of dimethylaniline (DMA) in aqueous methanol in the presence of perchloric acid.

Experimental

Materials.—DMA and methanol were purified by duplicate fractional distillations.

Kinetic Procedures. — The reaction was carried out in brown flasks with ground-glass stoppers at 40, 50 and 60° (reflux condensers were used for runs at 60°). The solvent used was 50~90 volume % aqueous methanol.

An aqueous methanol solution of DMA was mixed with an aqueous solution of hydrogen peroxide, selenium dioxide and perchloric acid after being thermostated at the reaction temperatures, thus the reaction was started. Aliquots were withdrawn at appropriate intervals of time to estimate the sum of the amount of selenium dioxide and hydrogen peroxide iodimetrically, using ammonium pyrophosphate as accelerator. Since no selenium was precipitated in the course of the reaction and the rate of selenic-acid formation was slow and also equilibrium amounts of intermediate complex were low as stated later, the amount of hydrogen peroxide was obtained as the difference of total oxidizing agents and the selenium dioxide initially present.

The hydrogen-peroxide content in a mixture of hydrogen peroxide and selenium dioxide was determined by introducing it into an aqueous solution of ceric sulfate and then titrating the excessive ceric ion potentiometrically with ferrous sulfate[11,12]. But this method could not be applied

1) C. W. Smith and R. T. Holm, *J. Org. Chem.*, **22**, 746 (1957).
2) G. B. Payne and C. W. Smith, ibid., **22**, 1680 (1957).
3) P. Seguin, *Compt. rend.*, **216**, 667 (1943).
4) C. Walling, "Free Radicals in Solution", John Willey & Sons, Inc., New York, 1957, p. 566.
5) Y. Ogata and I. Tabushi, *This Journal.*
6) J. M. Monger and O. Redlich, *J. Phys. Chem.*, **60**, 797 (1956).
7) E. Bamberger and L. Rudolf, *Ber.*, **35**, 1082 (1902).
8) The rate constant in the neutral aqueous solution for Caro's acid oxidation of DMA is 10^7 times larger than that of hydrogen peroxide of triethylamine (S. D. Ross, *J. Am. Chem. Soc.*, **68**, 1484 (1946)).
9) N. A. Milas, ibid., **59**, 2342 (1937).
10) G. A. Bogdonov and T. I. Berkengeim, *Chem. Abstr.*, **49**, 2842 (1955); Zhur. Fiz. Khim., **26**, 1659 (1952).
11) F. J. Hughes and D. S. Martin Jr., *J. Phys. Chem.*, **59**, 410 (1955).
12) H. H. Willard and P. Young, *J. Am. Chem. Soc.*, **52**, 553 (1930).

in the presence of DMA, because a rapid oxidation of DMA took place.

Selenate and selenic acid were determined gravimetrically by precipitating lead selenate by the addition of aqueous lead nitrate[13a] or acetate[13b] in aqueous ethanol solution.

Reaction Products.—To examine the reaction products, nearly equimolar amounts of hydrogen peroxide and DMA were used. A mixture of 50 cc. of 1 M methanol solution of DMA, 10 cc. of 0.2 M aqueous solution of selenium dioxide, 6 cc. of 30% aqueous hydrogen peroxide and 2 cc. of concentrated perchloric acid (ca. 10 N) were introduced into a flask with a reflux condenser and heated to 50° for 20 hr. and then at 60° for 5 hr.

After methanol was distilled on a water bath, the residual aqueous solution was treated with potassium hydroxide until it became weakly basic. The solution was cooled and, after filtration of potassium perchlorate, freed from remaining DMA (ca. 1 g.) by extraction with ether.

The residual aqueous layer was neutralized and condensed under a reduced pressure, then poured into a boiling aqueous solution of picric acid (10 g. of picric acid in 200 cc. of water) to precipitate the picrate of DMA oxide[14]. The precipitate consisted of yellow crystals (10.7 g.) and brown amorphous material (2.5 g.); the former, after several recrystalization from ethanol showed no depression of m. p. on admixture with the authentic sample[14]. The brown material was also found to yield the same crystals but with difficulty. The total yield of the oxide amounted to 73% on the basis of the hydrochloride, obtained on the addition of hydrochloric acid into the picrate of DMA oxide.

Vinyl Polymerization. — DMA and peroxide (hydrogen peroxide or benzoyl peroxide) and/or selenium dioxide were added in acrylonitrile, thermostated at 50° in flasks with ground-glass stoppers, to start the reaction. After appropriate time, cold methanol was poured into the reaction mixture to stop the reaction and to precipitate the polymer produced. The precipitates obtained were filtered, dried and weighed. The results are summarized in Table VII.

TABLE I

THE EFFECT OF CONCENTRATION OF SELENIUM DIOXIDE ON k_0: [DMA] = 5/30 M, [$HClO_4$] = 2/30 M and [H_2O_2] = ca. 0.017 M

[SeO_2], M	k_0, min^{-1}	k_0/[SeO_2] 1. mole min^{-1}
1/250	2.68×10^{-3}	0.670
2/750	1.76×10^{-3}	0.660
1/750	9.02×10^{-4}	0.676
1/1500	$4,37\times10^{-4}$	0.651

TABLE II

THE EFFECT OF CONCENTRATION OF DMA ON k_0 AT 40, 50 AND 60°

[DMA] M	[$HClO_4$] M	[SeO_2] M	k_0, $min^{-1}\times10^4$	k_0/[SeO_2] 1. mole min^{-1}
Temp. 40°				
5/30	2/30	1/750	4.74	0.356
7.5/45	2/45	1/1125	3.39	0.382
6/45	2.4/45	1/1125	2.74	0.308
5/45	2.0/45	1/1125	2.10	0.236
4/45	1.6/45	1/1125	1.97	0.222
4/45	1.6/45	2/1125	4.25	0.238
2/45	0.8/45	2/1125	2.59	0.143
Temp. 50°				
5/30	2/30	1/750	9.02	0.676
7/45	2.8/45	1/1125	5.40	0.607
6/45	2.4/45	1/1125	5.04	0.567
5/45	2.0/45	1/1125	4.30	0.484
4/45	1.6/45	1/1125	3.40	0.382
3/45	1.2/45	1/1125	3.06	0.344
2/45	0.8/45	1/1125	2.16	0.243
1/45	0.4/45	1/1125	1.60	0.180
Temp. 60°				
8/45	3.2/45	1/1125	12.4	1.396
6/45	2.4/45	1/1125	10.8	1.220
5/45	2.0/45	1/1125	9.82	1.105
4/45	1.6/45	1/1125	8.92	1.002
3/45	1.2/45	1/1125	7.55	0.850
2/45	0.8/45	1/1125	6.30	0.709
1/45	0.4/45	1/1125	5.11	0.576

Results and Discussion

Rate Equations. — The rate of the selenium dioxide-catalyzed hydrogen peroxide

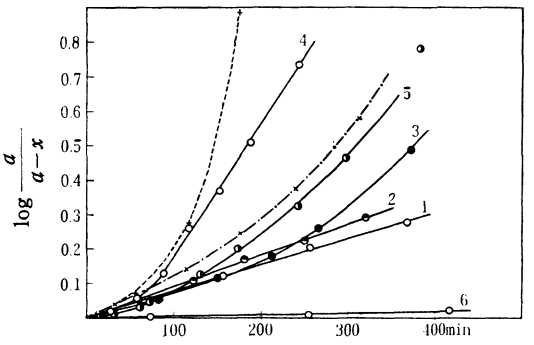


Fig. 1. The effects of acidity and substituent on the rate; solid lines correspond to DMA, where [DMA] = 5/30 M, [SeO_2] = 1/750 M and [$HClO_4$]: 1. 1/30 M, 2. 2/30 M, 3. 4/30 M, 4. 5/30 M, 6. 4/3 M; dotted line corresponds to *p*-methoxydimethylaniline where [amine] = 2.25/30 M, [SeO_2] = 1/750 M, [$HClO_4$] = 1.6/30 M; broken line corresponds to *p*-methyldimethylaniline where [amine] = 5/30 M, [SeO_2] = 1/750 M, [$HClO_4$] = 2/30 M.

13) a) R. Ripan-Tilici, *Z. Anal. Chem.*, **102**, 28 (1935). b) P. Spaw, *Bull. Soc. Chim. France*, [5], **3**, 159 (1936).
14) E. Bamberger and F. Tschirner, *Ber.*, **32**, 342 (1899).

oxidation of DMA was much faster than the uncatalyzed reaction with selenium dioxide or hydrogen peroxide alone. The rate of consumption of hydrogen peroxide was of first-order with hydrogen peroxide (equation 1) as shown in Fig. 1.

$$-\frac{d[H_2O_2]}{dt} = k_0[H_2O_2] \quad (1)$$

The pseudo first-order rate constant k_0 was found to be proportional to the concentration of selenium dioxide, when the concentrations of DMA and perchloric acid were both kept constant (Fig. 2), while it was linearly related to the concentration of DMA in the range of 5/30~1/45 M, when the concentration of selenium dioxide was constant and the apparent acidity of the solution estimated by pH meter was kept constant by changing the concentration of perchloric acid, where the ionic strength

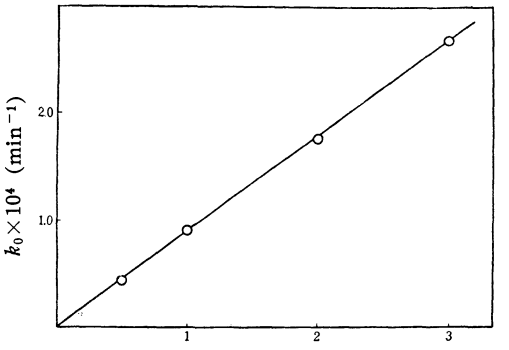


Fig. 2. The effect of concentration of selenium dioxide on the rate; where [DMA] = 5/30 M and [$HClO_4$] = 2/30 M at 50°.

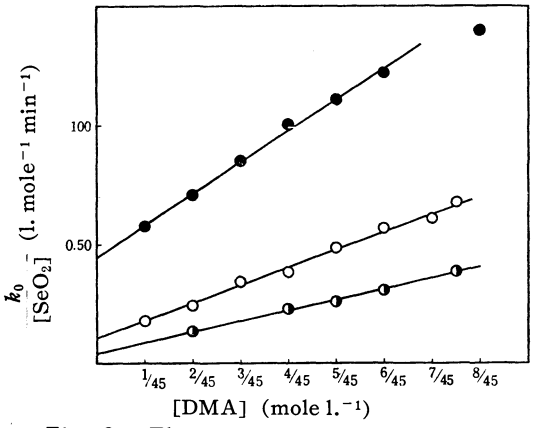


Fig. 3. The effect of concentration of DMA on the rate at various temperature.

was controlled by the addition of neutral salt (sodium perchlorate) (see Fig. 3).

Hence, rate equation 1 can be modified to

$$-\frac{d[H_2O_2]}{dt} = k[H_2O_2][SeO_2][DMA] + k'[H_2O_2][SeO_2] \quad (2)$$

The first term of equation 2 may correspond to the rate-determining attack of an intermediate comples between selenium dioxide and hydrogen peroxide on DMA molecule[15].

The reaction is different from the peracetic acid oxidation[4] in that the main route of complex formation can not be a slow step, since no induction period was observed and the difference between the rates with variation of the time of allowing the mixture of hydrogen peroxide and selenium dioxide to stand before a solution of DMA was added.

The rate of the peroxide consumption in aqueous methanol in the absence of DMA was found to be considerably less than the second term of equation 2 (see Table VIII), thus the second term of equation 2 should mainly express a reaction involving the participation of DMA and only partly a reaction independent of DMA. The former reaction may be a slow reaction between hydrogen peroxide and selenium dioxide to produce an intermediate complex II, which reacts with DMA rapidly.

Hence two complexes I and II may be possible, which respectively react with DMA slowly and rapidly.

$$H_2O_2 + SeO_2 \underset{\text{mobile equilibrium}}{\rightleftarrows} \text{complex(I)} \xrightarrow[+DMA]{\text{slow } k_3} \text{DMAO (amino oxide)}$$

$$H_2O_2 + SeO_2 \underset{k_2}{\overset{k_1}{\rightleftarrows}} \text{complex(II)} \xrightarrow{k_4} \text{DMAO (amino oxide)}$$

where $k_4 \gg k_2 \gg k_1$, so that the formation of the complex II is the rate determining step in the lower reaction.

Active Oxidizing Species.—Hughes[11] assumed the formation of intermediate perselenious acid in the kinetic study of the selenic acid formation, while Smith[1] suggested that the catalytic action of selenium dioxide in hydrogen peroxide oxidation

15) Although the possibilities of the complex formation between H_2O_2 and DMA, or SeO_2 and DMA, followed by the oxidation by the other oxidizing agent may be conceivable, these mechanisms are less probable, since the accelerating effect of selenium dioxide on the H_2O_2 oxidation is not limited to amines but was observed also in aldehydes[1], ketones[2] and olefins[3].

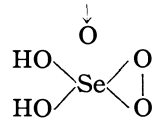
might be due to the formation of selenic acid or its higher peroxides.

To clarify this point, we examined the participation of selenate in the reaction. The reaction with sodium selenate instead of hydrogen peroxide and selenium dioxide or that using sodium selenate and hydrogen peroxide instead of hydrogen peroxide and selenium dioxide was fairly slow (Table III, V), hence selenic acid or a complex of selenic acid and peroxide can not be an active species, I or II. This conclusion is in accord with our observation that the rate of selenic-acid formation estimated cerimetrically was slower than the main reaction, and also with Hughes' data[11].

When besides hydrogen peroxide and selenium dioxide a large amount of sodium selenate was added, a small increase in the rate was observed and the increment was proportional to the concentration of sodium selenate added (Table V). But no salt effect was observed with the addition of sodium perchlorate (Table V). This fact suggests that the increment may be due to the selenium dioxide existing in a selenate solution.

The rate of hydrogen peroxide consumption in the absence of DMA was followed cerimetrically as well as iodimetrically, but no remarkable change in concentration of hydrogen peroxide was observed. This fact suggests that concentrations of I and II are both very small in their equilibrium states.

It may well be assumed that I and II are a kind of peroxide such as HO—Se(=O)—O—O—H (perselenious acid) or



, but no information of I and II could be obtained by us by means of ultraviolet absorption spectroscopy.

Effects of Acidity and Substituents.— Rates of the reaction satisfied equation 2 only at a relatively low concentration of perchloric acid (less than 0.1 M where DMA 5/30 M). In this range, the k_0 values was found to increase with increasing concentration of the acid. But at higher a concentration of the acid (more than 4/30 M where DMA 5/30 M), a tendency of induced reaction was observed in the early stage (before reaching the pseudo-first order kinetics), and it became remarkable as the acidity increased. Typical examples are shown in Fig. 1. This behavior made the quantitative investigation of the effect of acidity difficult, but qualitatively, the rate began to decrease markedly through maximum ($[HClO_4] \fallingdotseq 5/30\ M = [DMA]$) as the acidity increased. This decrease of rate may be ascribed to a decrease in the concentration of DMA by the protonation. The first small increase of the rate, inexplicable by the change of the concentration of DMA, may be due to the suppression of the dissociation of acids I and/or II (equation 4) just as discussed in the case of Caro's acid[16] if I and II have

TABLE III

THE RATE OF DISAPPEARANCE OF SELENATE IN THE OXIDATION OF DMA WITH SELENATE ALONE, ESTIMATED BY GRAVIMETRY OF LEAD SELENATE: $[DMA] = 1/5$ M, $[Na_2SeO_4] = 735$ mg. in 50 cc. and $[HClO_4] = 4/50$ M at 50°

Time, min.	0	88	262	394
$PbSeO_4$, mg.	117.0	116.2	117.3	115.8

TABLE IV

THE RATE OF DISAPPEARANCE OF HYDROGEN PEROXIDE IN A MIXTURE OF HYDROGEN PEROXIDE AND SELENIUM DIOXIDE BY MEANS OF BACK TITRATION OF EXCESS CERIC ION WITH AN AQUEOUS FERROUS SULFATE SOLUTION: 1 m. mole of H_2O_2, 5 m. mole of SeO_2 and 4 m. mole of $HClO_4$ were mixed with 15 cc. of water and 28 cc. of methanol

Time, min.	0	110	191	∞
$FeSO_4$ required	1.37	1.91	2.53	27.90[a]

a) The theoretical vol. of $FeSO_4$ necessary for the complete disappearance of hydrogen peroxide.

TABLE V

THE EFFECTS OF ADDED MATERIALS ON THE RATE: $[SeO_2] = 1/750$ M, $[DMA] = 5/30$ M and $[HClO_4] = 2/30$ M at 50°

Added material		$k_0 \times 10^3$, min^{-1}
Na_2SeO_4	100 mg. in 30 cc. of solution	1.13
Na_2SeO_4	46 mg. in 30 cc. of solution	1.02
Na_2SeO_4	25 mg. in 30 cc. of solution	0.951
Na_2SeO_4	0 mg.	0.902[b]
$NaClO_4$	1/30 M	0.895
Hydroquinone	2.5 mg. in 30 cc. of solution	0.896
None	time of standing was 0 min.[a]	0.893
None	time of standing was 60 min.	0.898

a) In the other runs, time of standing was 15~30 min.

b) In the absence of selenium dioxide, the rate was considerably low.

16) Y. Ogata and I. Tabushi, This Bulletin, 31, 969 (1958).

their pK_a values near the acidity of maximum rate.

$$DMA + H^+ \overset{\text{mobile}}{\rightleftarrows} DMAH^+ \quad (3)$$

$$HO_2SeOOH \overset{\text{mobile}}{\rightleftarrows} HSeO_4^- + H^+ \quad (4)$$

$$DMA + HO_2SeO_2H \overset{\text{slow}}{\longrightarrow} \text{prod.} \quad (5)$$

The rate of the oxidation of *p*-methyl- and *p*-methoxydimethyl-anilines showed a tendency toward induced reaction even at the low acidity, so that their kinetics could not be followed, but, qualitatively these substituents increased the rate, which supports the above electrophilic substitution mechanism.

Other Factors Influenceing the Rate.—Rate measurements carried out at 40, 50 and 60° gave linear relations of k_0 vs. DMA (Fig. 3) and thus gave the values of k and k' at these temperatures. From these values activation energies and log PZ were calculated, but as to k', Arhenius plot did not give a straight line, probably because the second term of equation 2 contained more than one reaction (for example, selenic acid formation, spontaneous decomposition of hydrogen peroxide and oxidation of methanol). Activation energies and other data were summarized in Table VIII.

TABLE VI

THE EFFECT OF SOLVENT COMPOSITION ON THE RATE. TEMP. 50° $[SeO_2] = 1/750$ M

vol. % of methanol	[DMA], M	k_0, $\text{min}^{-1} \times 10^4$
50	3/30	4.13
66.7	3/30	6.40
66.7	5/30	9.02
80	5/30	14.8
90	5/30	24.2
95	5/30	28.4

TABLE VII

POLYMERIZATION OF ACRYLONITRILE ADDED WITH VARIOUS REAGENTS

ACRYLONITRILE; 5 cc.

BPO mg.	DMA mg.	30% H_2O_2	SeO_2 mg.	Time min.	Polymer obtained mg.
20	60	0	0	2.2	0
20	60	0	0	4.0	24.9
20	60	0	0	11.0	598.5
20	60	0	2	300.0	0[c]
20	60	0	0	4.5	86.8
0	60	2 drops	0	2 days	0
0	60	2 drops	2	2 days	0
20	60	0[a]	0	4.0	46.0
0	60	2 drops[b]	0	2 days	0
0	0	2 drops	2	2 days	0
0	0	0	0	Several days	0

a) 0.1 cc. of water was added.
b) 2 drops of conc. $HClO_4$ were added.
c) The solution was slightly turbid.

TABLE VIII

TEMPERATURE COEFFICIENTS, ACTIVATION ENERGY AND ACTIVATION ENTROPY OF k AND k'

$k_{60}/k_{50} = 5.95\,(1.^2\ \text{mole}^{-2}\ \text{min}^{-1})/3.36\,(1.^2\ \text{mole}^{-2}\ \text{min}^{-1}) = 1.74$

$k_{50}/k_{40} = 3.36/1.93 = 1.77$

$\Delta H^{\ddagger}$ (40 and 50°) = 11.50 kcal./mole

$\Delta H^{\ddagger}$ (50 and 60°) = 11.86 kcal./mole

av. $\Delta H^{\ddagger} = 11.68$ kcal./mole

$\Delta S^{\ddagger}(50°) = 11.8$ E. U.

$k'_{60}/k'_{50} = 4.02$ (0.446/0.110)[a]

$k'_{50}/k'_{40} = 2.45$ (0.110/0.045)[a]

a) The unit of the constants is l. mole^{-1} min^{-1}.

The addition of water to methanol markedly decreases the rate (Table VI). This marked solvent effect may partly be attributed to the participation of water in the formation of the intermediate (perselenious acid), since it was reported[11] from the oxygen isotope exchange study that the formation of perselenious acid from selenious acid was attained through dehydration of selenious acid as shown in equations 6 and 7,

$$H_2SeO_3 \rightleftarrows H_2O + SeO_2 \quad (6)$$

$$SeO_2 + H_2O_2 \rightleftarrows HO_2SeOOH \quad (7)$$

and partly to the suppression of the dissociation of the attacking acids I and/or II.

Possibility of Free Radical Mechanism.—The observation that sulfur dioxide and hydroperoxide initiated vinyl polymerization[17]

$$ROOH + SO_2 \rightarrow RO\cdot + \cdot[SO_3H] \quad (8)$$

may suggest the possibility of a free radical mechanism of the reaction of selenium dioxide with hydrogen peroxide. But the addition of a small amount of hydroquinone has no appreciable effect on the rate at lower acidity of the solution where no induced reaction has been observed[18].

Furthermore, the tests of the polymerization of acrylonitrile was carried out, indicating that the free radical mechanism was not operating. The polymerization of acrylonitrile was tested in the presence

17) E. I. Thinyakova, B. A. Dolgoplosk and V. N. Reich, *Izvestia A. N. SSSR*, 1957, 851.
18) At higher acidities, hydroquinone markedly consumed hydrogen peroxide under these reaction conditions.

of BPO+DMA, (hydrogen peroxide+DMA), (hydrogen peroxide+selenium dioxide+DMA), (hydrogen peroxide+selenium dioxide), (hydrogen peroxide+selenium dioxide+DMA+perchloric acid) or (BPO+DMA+selenium dioxide), where BPO means benzoyl peroxide. In most of these experiments, no polymerization was observed. But two exception were observed; i. e., the reagent (BPO+DMA) could easily initiate the polymerization in accord with previous investigators[19], and the reagent (BPO+DMA+selenium dioxide) initiated it only with great difficulty.

These observations indicate that (i) the interaction of hydrogen peroxide and DMA can not produce any effective free radical; (ii) selenium dioxide has an effective inhibitory action for the radical polymerization; (iii) I or II can not participate in the radical chain.

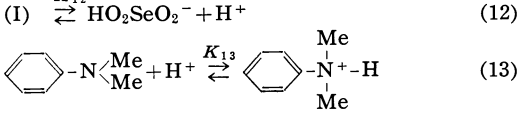
The Over-all Reaction Mechanism.—The results obtained above suggest a set of steps for the over-all reaction.

$$H_2SeO_3 \overset{K_9}{\rightleftarrows} SeO_2+H_2O \tag{9}$$

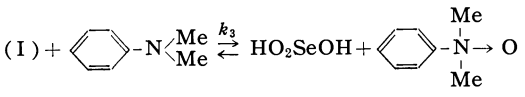
$$SeO_2+H_2O_2 \overset{K_{10}}{\rightleftarrows} HO_2SeOOH\ (I) \tag{10}$$

$$H_2SeO_3+H_2O_2 \underset{k_2}{\overset{k_1}{\rightleftarrows}} \text{complex (II)} \tag{11}$$

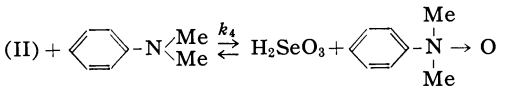
$$(I) \overset{K_{12}}{\rightleftarrows} HO_2SeO_2^- + H^+ \tag{12}$$



(13)



(14)



(15)

19) e. g., L. Horner and E. Schwenk, *Ann.*, **566**, 69 (1949); L. Horner, *Angew. Chem.*, **62**, 359 (1950), *J. Polymer Sci.*, **18**, 438 (1955); M. Imoto, T. Otsu and K. Kimura, ibid., **15**, 495 (1955).

K's denote mobile equilibrium constants and k's denote rate constants, of which k_1 and k_3 correspond to those of rate-determining steps via complex II and I, respectively.

Summary

The selenium dioxide-catalyzed oxidation of dimethylaniline with hydrogen peroxide was investigated kinetically at 40~60° in 50~95 volume % aqueous methanol. The rate of the consumption of hydrogen peroxide at constant acidity of the reaction mixture was expressed as

$$v=k[H_2O_2][SeO_2][\text{Dimethylaniline}]+k'[H_2O_2][SeO_2]$$

The first term of this equation seems to correspond to the rate of a reaction between dimethylaniline and a complex (I) produced rapidly from selenium dioxide and hydrogen peroxide, while the second term corresponds mainly to a slow reaction between selenium dioxide and hydrogen peroxide to yield the complex (II) followed by a rapid reaction with dimethylaniline. The energy of activation was 11.7 kcal.

When perchloric acid was added to the reaction mixture, the pseudo-first-order rate constant with respect to hydrogen peroxide first increased and then decreased via a maximum, which was explicable by the assumptions of the dissociation of the intermediate and the protonation of dimethylaniline. Electron-releasing groups tended to increase the rate. An increase of the water content in the solvent methanol decreased the rate. There was no evidence for the radical mechanism under these experimental conditions.

Department of Industrial Chemistry
Faculty of Engineering
Kyoto University
Sakyo-ku, Kyoto

Separation and Determination of Microgram Quantities of Molybdenum in Natural Waters

By Ken SUGAWARA, Motoharu TANAKA and Shiro OKABE*

(Received September 4, 1958)

Despite the importance of the role of molybdenum in the biochemical cycle of nitrogen and especially in plant growth, the only accessible datum of the content of this element in an inland water is that of Ter Meulen[1] who reported 0.9 μg. Mo/l. for a canal water in the Netherlands. As for sea water, more data have been reported. However, these data are often discordant, apparently because of defects in some of the methods employed. Thus, while Ishibashi et al.[2] found 10.6 μg./l. for the North Pacific water, Ernst and Hoermann[3] reported 0.3~0.7 μg./l. for the Atlantic.

Considering these facts, the present writers have elaborated a new method of determination, applicable to both sea and fresh waters, by which they plan to conduct an extensive study of the distribution of molybdenum in various kinds of natural water.

The method consists of two steps: 1) the element is co-precipitated together with either hydrated manganese oxide or ferric hydroxide and 2) the molybdenum is then extracted by a solvent consisting of *n*-butanol and chloroform in the form of thiocyanate to be subjected to spectrophotometry. Special care is taken in adjusting the pH of the solution to 3.8 where quantitative co-precipitation of molybdenum is ensured, resulting in a nearly 100% recovery of molybdenum[4].

Of these two different kinds of coprecipitant, manganese oxide is preferred because with this element, a precipitate is obtained which is quickly and easily filtered. This precipitate is more easily soluble in dilute hydrochloric acid containing a small amount of hydrogen peroxide, and the optimal range of pH is wider where a perfect co-precipitation of molybdenum is ensured[4].

Experimental

Reagents. — *Ferrous ammonium sulfate solution.* — Dissolve 0.70 g. of the salt in 100 ml. of 0.2 N sulfuric acid. The solution thus prepared contains 1.0 mg. of ferrous iron per ml. and is good for only one week after being prepared.

Sodium hypochlorite solution. — Neutralize 7.1 ml. of alkaline hypochlorite solution having 7% available chlorine with glacial acetic acid, using *p*-nitrophenol as indicator. Then add 0.6 ml. excess of the same acid and water bringing the solution to 50 ml. The solution is 1% for chlorine and is buffered at pH 3.7.

Potassium permanganate solution. — Dissolve 0.86 g. of potassium permanganate in 100 ml. water. The solution contains about 3 mg. Mn/ml.

Manganous sulfate solution.—Dissolve 1.0 g. of hydrated manganous sulfate in 100 ml. water. The solution contains 2 mg. Mn/ml.

Bromocresol purple. — Ethanolic solution, 0.1% wt./vol.

Potassium iodide solution.—10%, reagent quality.

Sodium sulfite solution.—10%, reagent quality.

Potassium thiocyanate solution. — 10%, reagent quality.

Hydrogen peroxide solution.—1%, 30% reagent is diluted.

Stannous chloride solution.—Ten g. of hydrated salt is dissolved in 100 ml. of 1 N hydrochloric acid. It is recommended that the preparation be made each week.

Solvent mixture of n-butanol and chloroform.—One part of *n*-butanol and four parts of chloroform are mixed. The components must be previously subjected to distillation and those fractions which distil 118°C and 61~63°C respectively are separated.

Standard molybdenum solution. — An amount (0.750 g.) of reagent quality molybdenum trioxide is dissolved in 10 ml. of 0.1 N sodium hydroxide solution and diluted to about 50 ml. After being slightly acidified with hydrochloric acid, the solution is made up to 500 ml. In practice, a dilute solution is prepared each week and used as the standard. The primary standard solution containing 1.0 mg. Mo per ml. is properly diluted

* Present address: Fukuoka College of Liberal Arts, Kurume, Fukuoka-ken.

1) G. Evelyn Hutchinson, "A Treatise on Limnology vol. 1- Geography, Physics, Chemistry", John Wily & Sons, Inc., New York, (1957), p. 824.

2) M. Ishibashi, T. Shigematsu and Y. Nakagawa, *Memoir of Chemical Research Laboratory, Kyoto University*, 32, 199 (1954).

3) T. Ernst and H. Hoermann, *Nach. Ges. Wiss. Göttingen Math. -Phys.* Kl., Fach. IV, N. F. **1**, 205 (1936).

4) M. Tanaka, *Mikrochimica Acta*, 1958, 204.

with 0.1 N hydrochloric acid so that one ml. of the dilute solution contains one μg. Mo per ml.

Procedure. — Depending upon the probable content of molybdenum, a sample of 1~5 liters is taken. After being warmed to 70~80°C, the sample is acidified with hydrochloric acid. The solution is neutralized with 4 N sodium hydroxide solution by using bromocresol purple as indicator and is buffered to approximately pH 3.8 by adding 12 ml. of glacial acetic acid and 5 ml. of 4 M sodium acetate solution per liter. Then 2 ml. of the manganous sulfate solution and 2 ml. of the potassium permanganate solution are successively added, while stirring vigorously. The solution is heated to 80°C whereby coagulation of the formed hydrated oxide of manganese is hastened. After cooling, the coagulum is filtered and then dissolved in a small amount of 2 N hydrochloric acid containing 1 ml. of 1% hydrogen peroxide. The solution is transferred into a 100 ml. beaker and boiled gently about 30 minutes until the excess of hydrogen peroxide is expelled. After cooling, 1 ml. of sodium sulfite solution is added whereby the remaining hydrogen peroxide is decomposed and ferric ions are reduced. Further addition of the potassium iodide solution ensures elimination of traces of hydrogen peroxide and the ferric iron. The liberated iodine is driven out by heating the solution for 10 minutes on a water bath. The final volume of the solution is 10~15 ml. Two ml. of concentrated hydrochloric acid, 2 ml. of ferrous ammonium sulfate solution and 3 ml. of potassium thiocyanate solution are successively added. Then the whole is transferred into a 100 ml. separatory funnel. After thoroughly mixing, 3 ml. of the stannous chloride solution is added and then shaken[5].

The next step is the extraction of formed molybdenum thiocyanate by the *n*-butanol—chloroform mixture[6]. After the addition of 7 ml. of the mixture, the contents of the funnel are vigorously shaken for two minutes. When the layers separate, the bottom oil layer is drawn out into a 10 ml. measuring flask and the remaining aqueous fraction is treated with 2 ml. of the solvent mixture. The joint extracts in the flask are made to just 10 ml. Then a few mg. of solid stannous chloride is added to protect the ferrous iron against oxidation. Otherwise, a red coloration by ferric thiocyanate may interfere with the measurement of the coloration. The absorbance measurement is made at 475 mμ. The molybdenum determination is made in reference to the standard curve previously prepared.

Checking the method and application of the method to natural waters.—1) Recovery of molybdenum by the co-precipitation procedure was checked as follows: an amount of molybdenum ranging 5~15 μg. in one liter of water was co-precipitated together with hydrated manganese oxide or ferric oxide, each equivalents to 10 mg. and 100 mg. of Mn and Fe respectively. As shown in Table I, the molybdenum recovery is from 98 to 100% by the use of either manganese or iron.

2) The interferences by ordinary elements and tungsten with the final colorimetry were examined. The results proved that these elements cause no interference at concentrations as are usually found in ordinary natural waters.

3) Examples of the results of the application of the present methods to various natural waters are given in Table II.

TABLE I

CO-PRECIPITATION OF MOLYBDENUM WITH HYDRATED MANGANESE OXIDE AND FERRIC HYDROXIDE

Mn used (mg.)	Mo added (μg.)	Mo found (μg.)
10	5.0	5.1
10	10.0	10.0
10	15.1	15.0
100	10.0	10.1
Fe used (mg.)	**Mo added (μg.)**	**Mo found (μg.)**
10	5.0	5.2
10	10.0	10.0
10	15.1	15.2
100	10.0	10.2

TABLE II

EXAMPLES OF APPLICATION

Description	Sample taken (l.)	Mo added (μg.)	Mo found (μg.)
Ground water from a well on the campus of Nagoya University.	5		3.0
	5	5.0	8.2
River water from Nagaragawa, Gifu Prefecture.	5		2.5
	5	5.0	7.4
Sea water from the Antarctic Ocean.			
68°52.5'S	1		9.8
25°33.5'E	1	5.0	14.6
Pacific Ocean.			
04°14.0'N	1		10.0
128°55.0'E	1	10.0	19.8
Indian Ocean.			
12°48.0'S	1		12.2
78°03.8'E			

Chemical Institute, Faculty of Science
Nagoya University, Chikusa-ku
Nagoya

5) E. B. Sandell, "Colorimetric Determination of Traces of Metals.", Interscience Publishers, Inc., New York, (1950), p. 455.

6) S. Kanamori, private communication.

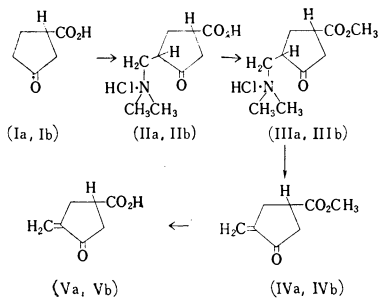
Studies on Antibiotics and Related Substances. VIII. Syntheses of the Two Enantiomorphs of 5-Methylenecyclopentanone-3-carboxylic Acid

By Mitsuhiro KINOSHITA and Sumio UMEZAWA

(Received September 5, 1958)

The present authors[1] previously reported the synthesis of 5-methylenecyclopentanone-3-carboxylic acid, an antitumor isomer of sarkomycin[2]. The structure of sarkomycin had been established by Hooper et al.[3] to be 2-methylenecyclopentanone-3-carboxylic acid, the hydrogenated product being (+)-2-methylcyclopentanone-3-carboxylic acid. More recently, Toki[4] reported the synthesis and the resolution of *dl*-sarkomycin.

The present paper describes the syntheses of optically active 5-methylenecyclopentanone-3-carboxylic acids and their antitumor activities. The synthetic routes are analogous to the synthesis of *dl*-5-methylenecyclopentanone-3-carboxylic acid previously described[1].



dl-Cyclopentanone-3-carboxylic acid prepared by the Kay and Perkin's method[5] was resolved into its optically active components (Ia and Ib) by fractionally crystallizing its brucine salt. Both (+)- and (−)-cyclopentanone-3-carboxylic acids were condensed with dimethylamine hydrochloride and paraformaldehyde by means of the Mannich reaction to yield (+)- and (−)-5-(dimethylaminomethyl)-cyclopentanone-3-carboxylic acid hydrochlorides (IIa and IIb), respectively, which were esterified with methanol by the Fischer-Speier method to yield methyl (+)- and methyl (−)-5-(dimethylaminomethyl)cyclopentanone-3-carboxylate hydrochlorides (IIIa and IIIb), respectively.

Though each of the two products consists of a pair of diastereoisomers differing in the configuration respecting C_5, the separation of components is not required for the preparation of 5-methylenecyclopentanone-3-carboxylic acid. Therefore, each of the two diastereoisomeric mixtures of methyl 5-(dimethylaminomethyl)cyclopentanone-3-carboxylate hydrochloride was directly degraded by vacuum distillation to yield methyl (+)- or methyl (−)-5-methylenecyclopentanone-3-carboxylate (IVa and IVb).

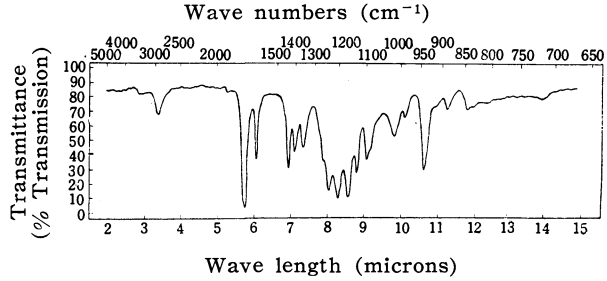


Fig. 1. Infrared absorption spectrum of methyl (+)-5-methylenecyclopentanone-3-carboxylate in carbon tetrachloride.

Mild hydrolysis of IVa and IVb with dilute sulfuric acid, followed by extraction with ethyl acetate and by evaporation of the solvent in vacuo gave (+)- and (−)-5-methylenecyclopentanone-3-carboxylic acid (Va and Vb), respectively.

The ultraviolet absorptions of IVa and IVb in methanol solution showed maxima at 231 and 335~336 mμ, suggesting the presence of an α,β-unsaturated ketone group in each as shown in Fig. 2. The infrared absorption of IVa in carbon tetrachloride showed maxima as follows: 5.74 μ (conjugated carbonyl group), and 6.05 μ

1) S. Umezawa and M. Kinoshita, This Bulletin, **30**, 267 (1957).
2) H. Umezawa, T. Yamamoto, T. Takeuchi, T. Osato, Y. Okami. S. Yamaoka, T. Okuda, K. Nitta, K. Yagishita, B. Utahara and S. Umezawa, *Antibiotics and Chemotherapy*, **4**, 514 (1954).
3) I. R. Hooper, L. C. Cheney, M. J. Cron, O. B. Fardig, D. L. Johnson, F. M. Palermiti, H. Schmitz and W. B. Wheatley, ibid., **5**, 585 (1955).
4) K. Toki, This Bulletin, **30**, 450 (1957); ibid., **31**, 333 (1958).
5) F. W. Kay and W. H. Parkin, Jr., *J. Chem. Soc.*, **1906**, 1646.

(carbon-carbon double bond) as shown in Fig. 1. The ultraviolet absorptions of Va and Vb in methanol solution showed maxima at 232 and 333 mμ suggesting the presence of an α, β-unsaturated ketone group in each.

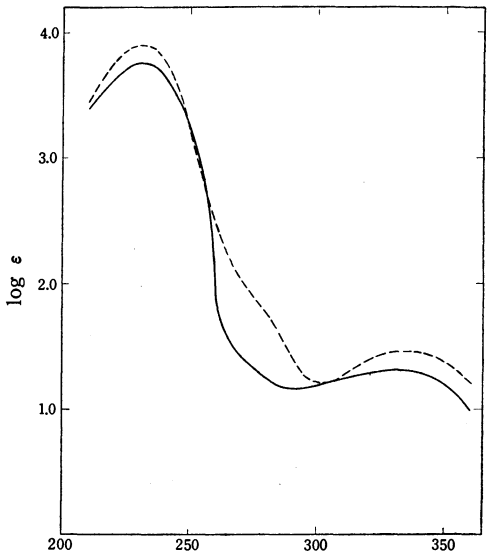


Fig. 2a. Ultraviolet absorption spectra of (+)-5-methylenecyclopentanone-3-carboxylic acid (——) and methyl (+)-5-methylenecyclopentanone-3-carboxylate (------) in methanol.

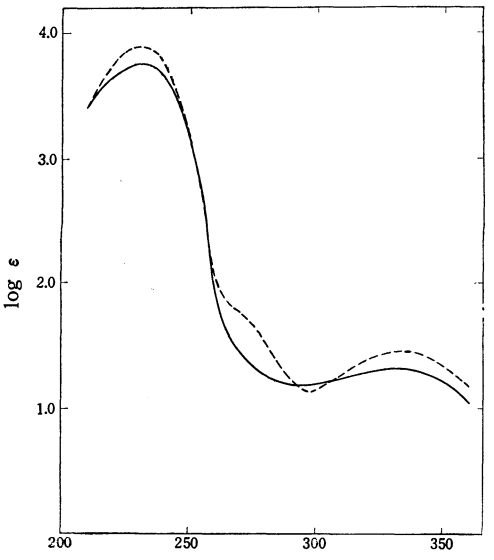


Fig. 2b. Ultraviolet absorption spectra of (−)-5-methylenecyclopentanone-3-carboxylic acid (——) and methyl (−)-5-methylenecyclopentanone-3-carboxylate (------) in methanol.

Moreover, ozonolysis of (−)-5-methylenecyclopentanone-3-carboxylic acid (Vb) gave formaldehyde (isolated as the methone derivative) as one of the products. This established the presence of an exomethylene group in Vb.

Methyl (+)- and methyl (−)-5-methylenecyclopentanone-3-carboxylates (IVa and IVb) possessed significant activities against *Staph. aureus* 209-P. The both enantiomorphs (Va and Vb) of 5-methylenecyclopentanone-3-carboxylic acid possessed strong antitumor activities of the same extent.

Experimental

Resolution of *dl*-Cyclopentanone-3-carboxylic Acid. — (+)-*Cyclopentanone-3-carboxylic Acid* (Ia). — A mixture of *dl*-cyclopentanone-3-carboxylic acid (48 g.), brucine tetrahydrate (178.5 g.) and 90% methanol (380 cc.) was heated until solution was effected. After cooling and storing at 11~12°C for 2 hr., the first crystalline crop was separated, and washed with a small quantity of 90% methanol. The weight of the dried product 103 g. On decomposing a small portion of the crop in the same way as described below, the free acid of $[\alpha]_D^{10}+12.0°$ (c 4, methanol) was obtained. Recrystallization of the crude salt from 90% methanol (120 cc.) gave 80 g. of the purified salt, which, on decomposition, gave the free acid of $[\alpha]_D^{9}+18.5°$ (c 4, methanol).

A second crop (41 g.) was obtained by evaporation of the mother liquor and recrystallized three times from 90% methanol to give 16.7 g. of the salt [free acid: $[\alpha]_D^{10}+19.0$ (c 4, methanol)]. The crops were collected and recrystallized from 90% methanol (1.2 cc./g.) to give 82.5 g. of the nearly pure salt [free acid: $[\alpha]_D^{9}+23.0°$ (c 4, methanol)]. The product was further recrystallized twice from the same solvent and subjected to decomposition.

To a solution of the recrystallized brucine salt (66 g.) of (+)-acid in boiling water (160 cc.) was added dropwise 14% sodium carbonate solution (142 cc.) with stirring. After being cooled in a refrigerator overnight, the brucine was filtered off. The filtrate was acidified with hydrochloric acid to pH 2.4, saturated with ammonium sulfate and extracted with ether repeatedly. After drying the extract, evaporation of ether gave 10.3 g. (43% from *dl*-acid) of (+)-cyclopentanone-3-carboxylic acid (Ia), $[\alpha]_D^{7.5}+27.2°$ (c 2.0, methanol)*. Recrystallization from ether gave colorless plates, m. p. 66~67°C.

Anal. Found: C, 56.49; H, 6.28. Calcd. for $C_6H_8O_3$: C, 56.24; H, 6.29%.

(−)-*Cyclopentanone-3-carboxylic Acid* (Ib). — By concentration of the mother liquor of the above-mentioned second crop, 54.6 g. of the third crop was obtained. The corresponding free acid

* Rotation reported by Toki[4] is $[\alpha]_D^{21}+22.1°$ (c 1.9, methanol).

obtained by decomposition showed $[\alpha]_D^8 -17.5°$ (c 4, methanol). Recrystallization from 85% ethanol (55 cc.) gave 34.5 g. of crystals. The corresponding free acid showed $[\alpha]_D^{9.5} -15.7°$ (c 3.94, methanol). The recrystallized salt was mixed with the crystalline residue obtained by evaporation of the recrystallization mother liquors of the first and the second crops described above and dissolved in hot 85% ethanol. The solution was left at 14°C for 1.5 hr. and the less soluble salt there separated was filtered off. Evaporation of the mother liquor gave 8 g. (crystal A) of the more soluble salt. Evaporation of the mother liquor separated from the third crop and the recrystallization mother liquor of the third crop gave 14 g. (crystal B) and 13 g. (crystal C) of crystalline residues, respectively. Crystals A, B and C correspond to the brucine salt of (−)-cyclopentanone-3-carboxylic acid which is more soluble than the salt of the (+)-acid described above.

For decomposition 14% sodium carbonate solution (76 cc.) was added dropwise to a hot solution of the brucine salt of (−)-acid (35 g., collected crystals A, B and C) and the resulting mixture was processed, in the same manner as described in the preceding paragraph, to yield the crystals of (−)-cyclopentanone-3-carboxylic acid; yield 4.6 g. (19.2% from *dl*-acid), $[\alpha]_D^{10} -23.4°$ (c 2.0, methanol)**. A sample for analysis was prepared by recrystallization from ether, m. p. 65~67°C.

Anal. Found: C, 56.63; H, 6.20. Calcd. for $C_6H_8O_5$: C, 56.24; H, 6.29%.

(+)-*5-(Dimethylaminomethyl)cyclopentanone-3-carboxylic Acid Hydrochloride* (IIa).—A mixture of (+)-cyclopentanone-3-carboxylic acid (9.5 g.) and dimethylamine hydrochloride (6.03 g.) was heated on a water bath. To the resulting melt was added paraformaldehyde (2.22 g.) and the mixture was stirred at 85°C for 1 hr. and then evaporated under reduced pressure to remove moisture. The resulting syrup was dissolved in absolute methanol (13 cc.) and a small amount of insoluble solid was removed by filtration. After addition of acetone (35 cc.) the solution was allowed to stand overnight in a refrigerator to afford the crystalline hydrochloride of (+)-5-(dimethylaminomethyl)cyclopentanone-3-carboxylic acid; yield 3.95 g. (24%), m. p. 136~139°C (dec.). Recrystallization from absolute methanol raised the melting point to 141~142°C (dec.); $[\alpha]_D^{11.5}$ +51.3° (c 1.385, methanol).

Anal. Found: C, 48.81; H, 6.99; N, 6.27. Calcd. for $C_9H_{16}O_3NCl$: C, 48.80; H, 7.28; N, 6.32%.

(−)-*5-(Dimethylaminomethyl)cyclopentanone-3-carboxylic Acid Hydrochloride* (IIb).—A mixture of (−)-cyclopentanone-3-carboxylic acid (4.5 g.) and dimethylamine hydrochloride (2.76 g.) was heated on a water bath. To the resulting melt was added 1.05 g. of paraformaldehyde and the mixture was stirred at 85°C for 1 hr. and then evaporated under reduced pressure. The residue was processed by the same procedure as employed for the preparation of IIa to afford the crystalline hydrochloride of (−)-5-(dimethylaminomethyl)-cyclopentanone-3-carboxylic acid hydrochloride; yield 1.8 g. (23%). The hydrochloride was recrystallized from absolute methanol; m. p. 140~141°C (dec.), $[\alpha]_D^{18} -62.3°$ (c 0.566, methanol).

Anal. Found: C, 48.60; H, 7.16; N, 6.29. Calcd. for $C_9H_{16}O_3NCl$: C, 48.80; H, 7.28; N, 6.32%.

Methyl (+)-5-(Dimethylaminomethyl)cyclopentanone-3-carboxylate Hydrochloride (IIIa).—A mixture of (+)-5-(dimethylaminomethyl)cyclopentanone-3-carboxylic acid hydrochloride (3.3 g.) and absolute methanol (38 cc.) was saturated with dry hydrogen chloride and allowed to stand overnight. The solvent was removed by distillation under reduced pressure. The resulting crystals were dissolved in a small quantity of absolute methanol and the solution was diluted with absolute ether, whereupon there separated colorless, minute plates of methyl(+)-5-(dimethylaminomethyl)cyclopentanone-3-carboxylate hydrochloride; yield 3 g. (86%). The hydrochloride was recrystallized from absolute methanol, m. p. 144~145.5°C (dec.); $[\alpha]_D^{11} +73.2°$ (c 0.95, methanol).

Anal. Found: C, 50.86; H, 7.42; N, 5.86. Calcd. for $C_{10}H_{18}O_3NCl$: C, 50.95; H, 7.64; N, 5.94%.

Methyl (−)-5-(Dimethylaminomethyl)cyclopentanone-3-carboxylate Hydrochloride (IIIb).—A mixture of (−)-5-(dimethylaminomethyl)cyclopentanone-3-carboxylic acid hydrochloride (1.5 g.) and absolute methanol (22 cc.) was saturated with dry hydrogen chloride and processed in the same manner as described in the preceding paragraph. Yield 1.4 g. (88%). Recrystallization from absolute methanol, m. p. 144~146°C (dec.); $[\alpha]_D^{13} -65.0°$, (c 0.65, methanol).

Anal. Found: C, 50.75; H, 7.46; N, 5.78. Calcd. for $C_{10}H_{18}O_3NCl$: C, 50.95; H, 7.64; N, 5.94%.

Methyl (+)-5-methylenecyclopentanone-3-carboxylate (IVa).—A sample (0.7 g.) of methyl (+)-5-(dimethylaminomethyl)cyclopentanone-3-carboxylate hydrochloride was placed in a small round-bottom flask and heated at 160~163°C in an oil bath under highly reduced pressure (0.0035mmHg). Colorless crystals of methyl (+)-5-methylenecyclopentanone-3-carboxylate were obtained in a receiver cooled in a dry ice-acetone bath; m. p. 46~48.5°C, $[\alpha]_D^9 +43.3°$ (c 0.82, methanol), yield 0.38 g. (83%). The ultraviolet absorption of the product showed maxima at 231 mμ (ε 7,800) and 335 mμ (ε 29.4) in methanol. The infrared spectrum showed maxima at 5.74, 6.05 and 10.61 μ in carbon tetrachloride as shown in Fig. 1.

Anal. Found: C, 62.42; H, 6.32. Calcd. for $C_8H_{10}O_3$: C, 62.32; H, 6.54%.

Methyl (−)-5-Methylenecyclopentanone-3-carboxylate (IVb).—The ester was prepared from 0.7 g. of methyl (−)-5-(dimethylaminomethyl)cyclopentanone-3-carboxylate hydrochloride by the same procedure as described above; yield 0.36 g. (79%), m. p. 46~48°C, $[\alpha]_D^{12} -36.5°$ (c 0.65, methanol). The ultraviolet absorption spectrum

** Rotation reported by Toki[4] is $[\alpha]_D^{21} -22.2°$ (c 2.0, methanol).

of the product showed maxima at 231 mμ (ε 7.780) and 336 mμ (ε 28.6) in methanol (Fig. 2).

Anal. Found: C, 62.40; H, 6.40. Calcd. for $C_8H_{10}O_3$: C, 62.32; H, 6.54%.

(+)-*5-Methylenecyclopentanone-3-carboxylic Acid* (Va).—A mixture of freshly prepared methyl (+)-5-methylenecyclopentanone-3-carboxylate (1.44 g.) and 1.5 N sulfuric acid (30 cc.) was stirred at 27~28°C for 2 hr. to give a clear solution, which was kept cold in an ice-bath, adjusted to pH 7.8 with a saturated solution of sodium bicarbonate, and shaken with three 30 cc. portions of ethyl acetate to remove any unchanged ester. The water-layer was adjusted to pH 2.0 with 1.5 N sulfuric acid and extracted with four 25 cc. portions of ethyl acetate. After the extract was dried over sodium sulfate, the ethyl acetate was removed by distillation under reduced pressure at 14°C to yield a crude product of (+)-5-methylenecyclopentanone-3-carboxylic acid, a colorless, viscous oil which rapidly crystallized; yield 0.48 g. (37%), m. p. 46~60°C, $[\alpha]_D^{10}$+34.9° (c 1.0, methanol). The freshly prepared sample was soluble in methanol and in water. However, on standing at room temperature in the absence of polymerization inhibitor, the product gradually polymerized and became much less soluble in methanol or water. It resisted attempts to recrystallize it. The ultraviolet absorption spectrum of the product showed maxima at 232 mμ (ε 5.670) and 333 mμ (ε 20.7) in methanol, showing the presence of α, β-unsaturated ketone group.

(−)-*5-Methylenecyclopentanone-3-carboxylic Acid* (Vb).—This acid was prepared from methyl (−)-5-methylenecyclopentanone-3-carboxylate (0.65 g.) by the same procedure as described above; yield 0.2 g. (34%), m. p. 48~57°C $[\alpha]_D^{12}$−29.3° (c 0.517, methanol). The product polymerized gradually and resisted attempts to recrystallize it. The ultraviolet absorption spectrum of the product showed maxima at 232 mμ (ε 5.650) and 333 mμ (ε 20.5) in methanol, showing the presence of α, β-unsaturated ketone group.

Ozonolysis of Vb.—A solution of 200 mg. of freshly prepared (−)-5-methylenecyclopentanone-3-carboxylic acid (Vb) in ethyl acetate (10 cc.) was treated with an approximately 2% (by weight) ozone-oxygen mixture at 0°C at a rate of 500 cc./min. for 19 min. The resulting solution was mixed with water (10 cc.) and zinc dust (300 mg.) and the mixture was refluxed for 30 min. The reaction mixture was filtered while hot into a solution of methone (300 mg.) in 10 cc. of ethanol. Dilution with 20 cc. of water afforded the needles of formaldehyde methone, m. p. 183~186°C; yield 128 mg. (31%). Recrystallization from 80% ethanol gave pure crystals of m. p. 187~189°C. Admixing with an authentic specimen of formaldehyde methone showed no change of melting point.

Bioassays.—Preliminary results have indicated that methyl (+)-5-methylenecyclopentanone-3-carboxylate (IVa) and the other isomer (IVb) possess potencies of 5.2 and 6.5 unit/mg. (in terms of sarkomycin potency) in 10% ethanol against *Staph. aureus* 209-P respectively. The minimum necessary concentrations of (+)-5-methylenecyclopentanone-3-carboxylic acid (Va) and the other isomer (Vb) for the anti-HeLa-cell effect were 62.5 and 62.5 mcg./cc. respectively. The daily intraperitoneal injections of 0.15 mg. of Va and 0.25 mg. of Vb inhibited the ascites increase and prolonged the survival period of mice bearing ascites type of Ehrlich cartinoma by intraperitoneal route.

A detailed report on the biological activities of IVa, IVb, Va and Vb will be published elswhere.

Summary

1) The two diastereoisomeric mixtures (IIa and IIb) of 5-(dimethylaminomethyl)-cyclopentanone-3-carboxylic acid hydrochloride were synthesized from the two enantiomorphs of cyclopentanone-3-carboxylic acid by means of the Mannich reaction.

2) The two diastereoisomeric mixtures (IIIa and IIIb) of methyl 5-(dimethylaminomethyl)cyclopentanone-3-carboxylate hydrochloride were degraded to give methyl (+)- and methyl (−)-5-methylenecyclopentanone-3-carboxylates (IVa and IVb), which were hydrolyzed into (+)- and (−)-5-methylenecyclopentanone-3-carboxylic acid (Va and Vb), respectively.

3) It was found that IVa and IVb possess high potency against *Staph. aureus* and both Va and Vb show significant antitumor activities of the same extent.

The authors are indebted to Professor H. Umezawa, National Institute of Health, Tokyo, for antitumor assays, and to Mr. S. Nakada of this Laboratory for the microanalytical data.

Applied Chemistry Department
Engineering Faculty
Keio University
Koganei, Tokyo

Selective Oxidation of Allylic Alcohols with Active N-Halogen Compounds. II[1]

By Ken-ichi MORITA*

(Received September 9, 1958)

It was shown in the previous paper[1] that active *N*-halogen compounds are effective reagents for the selective oxidation of allylic alcohols[2]. This article presents examples of selective oxidation of dihydroxylic compounds, each carrying an allylic and a primary or equatorial hydroxyl group, to α,β-unsaturated ketones with the unaffected primary or equatorial hydroxyl group, which may be difficult when manganese dioxide is employed[4,5], and of an allylic alcohol with an isolated ethylenic linkage to an α,β-unsaturated ketone without affecting the isolated double bond.

Reduction of methyl 3-keto-23,24-dinorchol-4-en-22-oate[6] (I) with lithium aluminum hydride gave a product which is presumed a mixture consisting essentially of 23,24-dinorchol-4-en-3β,22-diol and its 3α-epimeride. Oxidation of the mixture III by means of *N*-bromoacetamide in benzene-pyridine gave 23,24-dinorchol-4-en-22-ol-3-one (IVa)[7] in an overall yield of 78% from keto ester I. Similarly, reduction[8] of 3-keto-23,24-dinorchol-4-en-22-al[9] (II) with sodium borohydride to diol mixture III followed by oxidation with *N*-bromoacetamide or with isocyanur bromide[10] yielded 23,24-dinorchol-4-en-22-ol-3-one (IVa)[11].

The lithium aluminum hydride reduction of methyl 3-keto-20-*iso*-23,24-dinorchol-4-en-22-oate (V)[6] to diol mixture VII and the succeeding oxidation with *N*-bromoacetamide furnished 20-*iso*-23,24-dinorchol-4-en-22-ol-3-one (VIIIa) in an overall yield of 72%. The same compound VIIIa was also obtained from 3-keto-20-*iso*-23,24-dinorchol-4-en-22-al[6] (VI) by sodium borohydride reduction followed by the selective oxidation with *N*-bromoacetamide.

Treatment of methyl 3-keto-23,24-dinorchol-4-en-22-oate (I) with ethylene glycol in benzene solution in the presence of *p*-toluenesulfonic acid furnished methyl 3-ethylenedioxy-23,24-dinorchol-5-en-22-oate (IX), m.p. 188~189°C, α_D −46°. The rotatory dispersion curve[14] of this compound (negative plain) is consistent with a 5-ene-ketal. Djerassi et al.[15] have shown that 5-ene-steroids give negative plain dispersion curves. Acid hydrolysis of ketal ester IX regenerated methyl 3-keto-23,24-dinorchol-4-en-22-oate (I). Reduction of ketal ester IX with lithium aluminum hydride gave 3-ethylenedioxy-23,24-dinorchol-5-en-22-ol (Xa), m.p. 181~182°C, α_D −33°. Hydrolysis of ketal alcohol Xa gave 23,24-dinorchol-4-en-22-ol-3-one (IVa), which was identical with the sample derived from compound I or II through diols III.

Addition of hypobromous acid to 3-ethylenedioxy-cholest-5-ene (XI) by means of *N*-bromoacetamide in dioxane containing

* Present address: Ben May Laboratory for Cancer Research, University of Chicago 37, Ill. U. S. A.

1) Part I. K. Morita, This Bulletin, **31**, 450 (1958). (Steroids Part XXIV; Part XXIII, Idem., ibid., **31**, 379 (1958)).

2) Though Romero[3] recently reported that the reaction of cholest-4-ene-3β,6β-diol with *N*-bromosuccinimide in aqueous dioxane furnished cholest-4-en-6β-ol-3-one only in a low yield, it should be noted that the presence of water markedly decreases the yield of the reaction[1].

3) M. A. Romero, *J. Org. Chem.*, **22**, 1267 (1957).

4) H. Bruderer, D. Arigoni and O. Jeger, *Helv. Chim. Acta*, **39**, 858 (1956).

5) C. Amendolla, G. Rosenkranz and F. Somdheimer, *J. Chem. Soc.*, **1954**, 1226.

6) M. E. Herr and F. W. Heyl, *J. Am. Chem. Soc.*, **74**, 3627 (1952).

7) C. Meystre and K. Miescher, *Helv. Chim. Acta*, **31**, 211 (1949). Identity was established by a direct comparison with the sample kindly provided by Dr. C. Meystre of CIBA Ltd. The author wishes to express his hearty thanks to him.

8) Partial reduction of keto aldehyde II to corresponding keto alcohol IVa may be probable. cf. E. H. Jensen and W. A. Struck, *Anal. Chem.*, **27**, 271 (1955).

9) G. Slomp, Jr. and L. J. Johnson, *J. Am. Chem. Soc.*, **80**, 915 (1958); cf. D. A. Shepherd et al., ibid., **77**, 1212 (1955).

10) K. Morita, This Bulletin, **31**, 347 (1958).

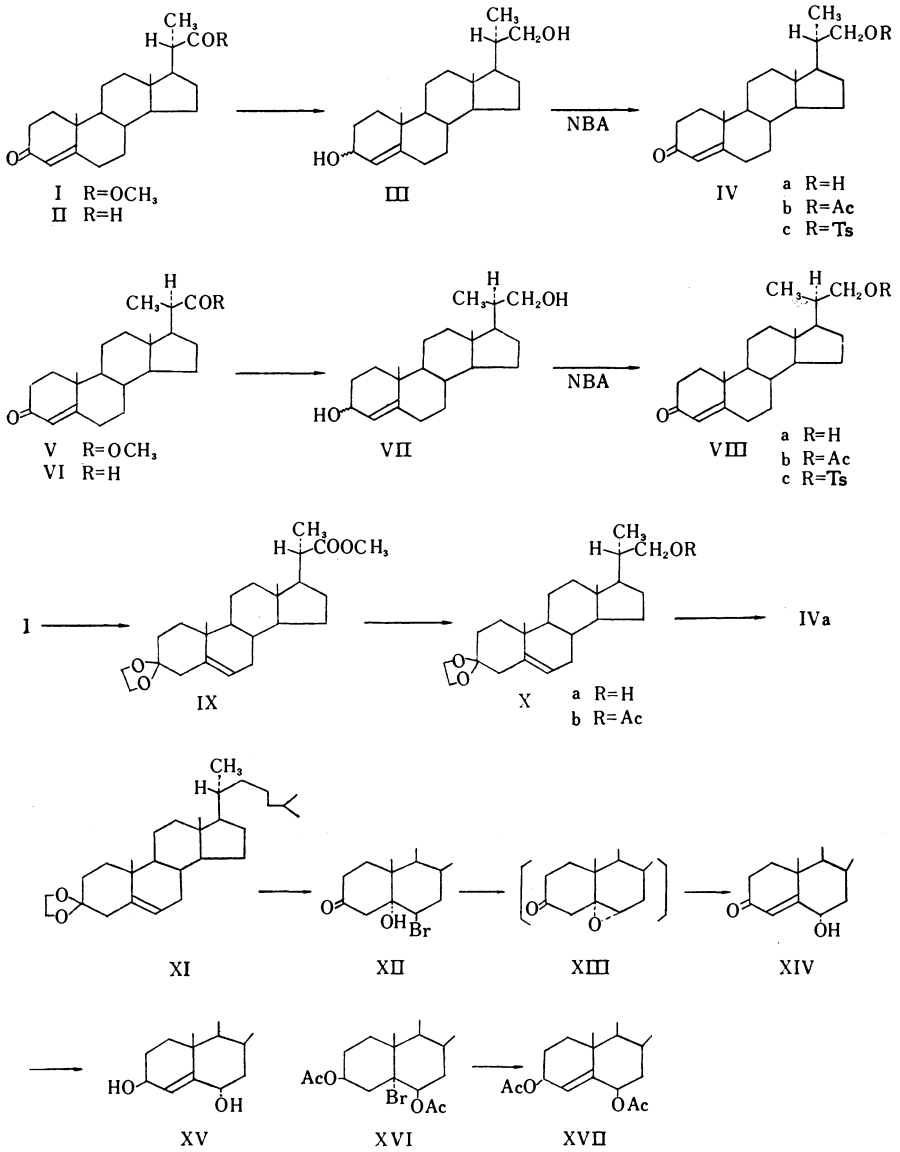
11) In this case the yield was lower than that of the reduction by means of lithium aluminum hydride, probably owing to the formation of a small amount of by-products (saturated compound[12], etc.[13]) during the reduction with sodium borohydride.

12) F. Sondheimer et al., *Chem. & Ind.*, **1954**, 1482; J. K. Normberski and G. F. Woods, *J. Chem. Soc.*, **1955**, 3426; C. Djerassi et al., *J. Am. Chem. Soc.*, **79**, 3528 (1957).

13) W. W. Zorbach, ibid., **75**, 6344 (1953).

14) Determination of the rotatory dispersion curve was kindly carried out by Professor Carl Djerassi of Wayne State University. The author wishes to express his hearty thanks to him.

15) C. Djerassi, W. Closson and A. E. Lippman, *J. Am. Chem. Soc.*, **78**, 3163 (1956).



dilute perchloric acid yielded 6β-bromocholestan-5α-ol-3-one (XII) in 50% yield[16]. Treatment of compound XII with sodium hydroxide in methylenechloride-methanol at room temperature gave 6α-hydroxycholest-4-en-3-one (XIV), which was converted into cholest-4-ene-3β,6α-diol (XV)[17] by lithium aluminum hydride reduction. Dehydrobromination of 5α-bromocholestane-3β,6β-diol diacetate (XVI)[18] with boiling pyridine gave cholest-4-ene-3β,6β-diol diacetate (XVII).

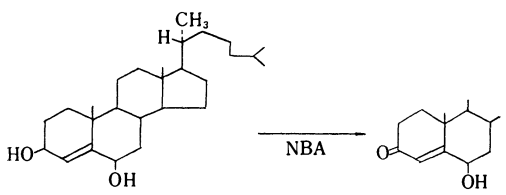
Oxidation of cholest-4-ene-3β,6β-diol (XVIII) and cholest-4-ene-3β,6α-diol (XV) by means of about one equivalent of *N*-bromoacetamide gave cholest-4-en-6β-ol-3-one (XIX) and cholest-4-en-6α-ol-3-one (XIV) in good yields, respectively. Proofs for these structures were obtained from their conversion into acetates and into 5α-cholestane-3,6-dione by a reaction with hydrochloric acid[19]. The method may be applica-

16) Cf. S. Mori, K. Morita and F. Mukawa, *Proc. Japan Acad.*, **32**, 585 (1956).

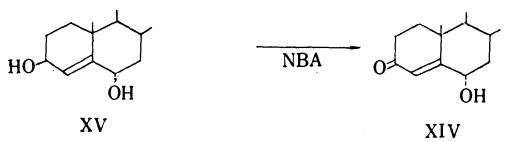
17) Y. Urushibara and K. Mori, *Abstract of the 10th Annual Meeting of the Chemical Society of Japan*, p. 204 (1957).
Detail of the experimental for preparation of cholest-4-ene-3β, 6α-diol (XV) from cholest-4-ene-3β-ol-6-one by hydride reduction was informed by Miss K. Mori to whom author's thanks are due.

18) Y. Ueno, *J. Pharm. Soc. Japan* (*Yakugaku Zasshi*), **71**, 1626 (1952).

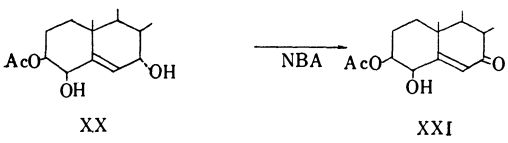
19) B. E. Ellis and V. A. Petrow, *J. Chem. Soc.*, **1939**, 1078.



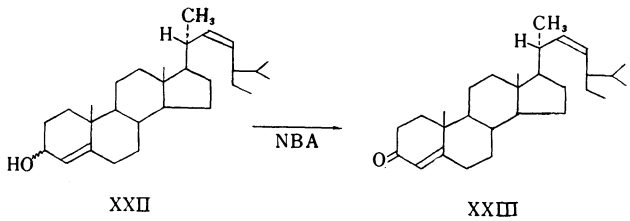
XVIII XIX



XV XIV



XX XXI



XXII XXIII

ble to a general synthesis of 6β-hydroxy-3-keto-4-ene-steroids[20,21] and of 6α-hydroxy-3-keto-4-ene-steroids[20,22]. Amendolla et al.[5], reported that manganese dioxide oxidation of cholest-4-ene-3β,6β-diol (XVIII) gave cholest-4-en-6β-ol-3-one (XIX) in a good yield while the oxidation of cholest-4-ene-3β,6α-diol (XV), in which $C_{(6)}$-hydroxyl group is equatorial, gave cholest-4-ene-3,6-dione even under mild conditions.

It is noteworthy that on the *N*-bromoacetamide oxidation of compound XVIII 3β-hydroxy group (quassi equatorial) was selectively oxidized whereas 6β-hydroxy group (axial) remained unaffected. This fact is contrary to the general rule for the oxidation by means of *N*-bromoacetamide to the effect that axial hydroxyl groups are more readily oxidized than equatorial ones. Lieberman and Fukushima[23] reported the selective oxidation of cholest-5-ene-3β,4β,7α-triol 3-monoacetate (XX) to cholest-5-ene-3β,4β-diol-7-one 3-monoacetate (XXI), in which quassi axial hydroxyl group 7α was selectively oxidized and axial hydroxyl group 4β remained unaffected. It might be expected that *N*-bromoacetamide oxidation of allylic hydroxyl groups to give s-trans α,β-unsaturated ketones is easier than that of allylic hydroxyl groups to give s-*cis* α,β-unsaturated ketones.

Reduction of stigmasta-4,22-dien-3-one (XXIII)[24] with lithium aluminum hydride gave a mixture of stigmasta-4,22-dien-3β-ol and the corresponding 3α-ol. Oxidation of the mixture XXII by means of about one equivalent of *N*-bromoacetamide gave stigmasta-4,22-dien-3-one (XXIII) in 80% yield. *N*-Halogen compounds may also be effective for the selective oxidation of allylic alcohols containing isolated ethylenic double bonds to α,β-unsaturated ketones without affecting the isolated double bonds.

Experimental[25]

23,24-Dinorchol-4-en-22-ol-3-one (IVa).—*a) From Methyl 3-Keto-23,24-dinorchol-4-en-22-oate (I).*—A mixture of 165 mg. of ketoester I[6] and 100 mg. of lithium aluminum hydride in 15 ml. of anhydrous tetrahydrofuran was heated under reflux for 5 hours. After careful decomposition of excessive lithium aluminum hydride with a small amount of water, tetrahydrofuran was evaporated under a reduced pressure. The solid was collected, dried, and washed well with dioxane. Evaporation of the solvent under a reduced pressure yielded a solid, m.p. 187~204°C, in a quantitative yield.

A solution of the above solid (162.3 mg.) in 2 ml. of benzene and 4 ml. of pyridine was treated with 82 mg. of *N*-bromoacetamide at room temperature (17~18°C) for two and a half hours in the dark. The solution was diluted with benzene and washed successively with 10% aqueous sodium bisulfite, with 10% aqueous sodium hydroxide, with water, with dilute sulfuric acid, and again with water, and dried over anhydrous sodium sulfate. The solvent was evaporated under a reduced pressure, and 165 mg. of a crystalline solid was obtained. The solid was dissolved in 10 ml. of benzene and adsorbed on a column of alumina (5 g.). Elution with ether gave 129 mg. (78% from I) of IVa with m.p. 135~136°C. Recrystallization from aqueous acetone yielded pure IVa, m.p. 137~138°C, $[\alpha]_D^{18}$ +94 (C, 1.125), λ_{max} 241 mμ, log ε, 4.20, ν_{max}^{Nujol} 2.90 (OH), 6.09 (C=O), 6.18 μ (C=C). The melting point was not depressed on admixture with an authentic sample (m.p. 137.5~138°C) kindly provided by Dr. C. Meystre[7].

20) M. Ehrenstein et al., *J. Org. Chem.*, **16**, 1051 (1951); **17**, 1587 (1952); **19**, 1331 (1954). L. F. Fieser, *J. Am. Chem. Soc.*, **75**, 4377 (1953).
21) F. Sondheimer et al., *J. Chem. Soc.*, **1954**, 1226; *J. Am. Chem. Soc.*, **76**, 5020 (1954).
22) K. Morita, *Proc. Japan Academy.*, **32**, 588 (1956).
23) S. Lieberman and D. K. Fukushima, *J. Am. Chem. Soc.*, **72**, 5211 (1950).
24) G. Slomp, Jr., et al., ibid., **77**, 1216 (1955). Cf. D. A. Shepherd et al., ibid., **77**, 1212 (1955).
25) All melting points are uncorrected. Rotations are all measured in chloroform solution.

Anal. Found: C, 79.51; H, 10.42. Calcd. for $C_{22}H_{34}O_2$: C, 79.95; H, 10.37%.

b) From 3-Keto-23, 24-dinorchol-4-en-22-al (II) by use of N-Bromoacetamide.—To a suspension of 1.5 g. of keto aldehyde II[9] in 90 ml. of methanol, a solution of 0.3 g. of sodium borohydride in 0.7 ml. of water and 15 ml. of methanol was added with stirring at room temperature. After standing for 2 hours at room temperature excessive sodium borohydride was decomposed by careful addition of a small amount of dilute acetic acid. Then the solution was poured into an excess of water. The solid was collected and well washed with water. The solid melted at 175~190°C. Yield, 1.4 g.

The mixture, dissolved in 15 ml. of benzene and 30 ml. of pyridine, was treated with 700 mg. of *N*-bromoacetamide as described above, and 870 mg. of compound IVa with m.p. 135~138°C was obtained. Identity was established by a mixed melting point determination.

c) From 3-Keto-23, 24-dinorchol-4-en-22-al (II) by use of Isocyanur Bromide[10].—To a solution of 5 g. of keto aldehyde II in 100 ml. of tetrahydrofuran, 2 g. of sodium borohydride in 10 ml. of water was added at room temperature. After allowed to stand overnight at room temperature the solution was poured into an excess of water. The solid was collected by filtration. The solid melted at 196~205°C. Yield, 4.8 g.

A mixture of 404 mg. of the above solid, 25 ml. of *tert*-butyl alcohol, 1 ml. of pyridine and 205 mg. of 83% isocyanur bromide[10] was treated as usual, and 260 mg. of compound IVa with m.p. 134~138°C was obtained.

d) From 3-Ethylenedioxy-23, 24-dinorchol-5-en-22-ol (Xa).—To a suspension of 128 mg. of ketal alcohol Xa in 13 ml. of methanol, 1.3 ml. of 8% (by volume) sulfuric acid was added, and the mixture was refluxed for one hour. A few drops of water were added and the precipitated needles were collected by filtration and recrystallized from aqueous acetone to give 72 mg. of IVa in needles, m.p. 137~138°C. The melting point was not depressed on admixture with the above samples.

23, 24-Dinorchol-4-en-22-ol-3-one acetate (IVb).—The substance was obtained in a usual way, and recrystallized from *n*-hexane, m.p. 131~132°C, $[\alpha]_D^{22}$ +95 (c, 1.248).

Anal. Found: C, 76.89, H, 9.91. Calcd. for $C_{24}H_{36}O_3$: C, 77.37, H, 9.74%.

When a mixture of 21 mg. of the acetate IVb, 3 ml. of methanol and 0.3 ml. of 0.8% (by volume) sulfuric acid was heated under reflux for 45 minutes, compound IVa was obtained.

23, 24-Dinorchol-4-en-22-ol-3-one tosylate (IVc).—To 249 mg. of compound IVa in 2 ml. of pyridine, 0.19 g. of *p*-toluenesulfonyl chloride was added and the mixture was allowed to stand overnight at room temperature. The mixture was poured into an excess of water. The solid was collected, washed with dilute hydrochloric acid and with water, dried, and recrystallized from acetone to give IVc in plates, m.p. 175~177°C (dec.), ν_{max}^{Nujol} 5.99 (C=O), 6.17, 6.24 (C=C), 7.30, 8.51 μ (—O—SO_2—).

Anal. Found: C, 72.66, H, 7.05. Calcd. for $C_{29}H_{36}SO_4$: C, 72.46, H, 7.55%.

Methyl 3-Keto-23,24-dinorchol-4-en-22-oate (I).—To a suspension of 50 mg. of ketal ester IX in 4 ml. of methanol, 0.4 ml. of 8% (by volume) sulfuric acid was added and the mixture was refluxed for 40 minutes. The solid soon disappeared and in about 10 minutes a new crystalline substance began to separate out. The suspension was diluted with water and the solid (m.p. 170~172°C; 45 mg.) was collected and recrystallized from acetone to give I in crystals with m.p. 178~180°C. The identity was established by a mixed[6] melting point determination.

Methyl 3-Keto-20-*iso*-23, 24-dinorchol-4-en-22-oate (V).—3-Keto-20-*iso*-23, 24-dinorchol-4-en-22-al (II)[6] (391 mg.) (m.p. 142~143°C from methylene chloride-isopropyl alcohol; reported m.p. 140~142°C[6], 137.5~139°C[26]), dissolved in 8 ml. of benzene and 8 ml. of glacial acetic acid, was oxidized with 118 mg. of chromic acid in 0.25 ml. of water and 8 ml. of acetic acid according to Herr and Heyl[6].

The ethereal extract was washed twice with 10% sodium carbonate. The sodium salt was collected centrifugally, and washed with ether. Treatment of the salt with 20% sulfuric acid gave 135 mg. of 3-keto-23, 24-dinorchol-4-en-22-oic acid with m.p. 233~243°C, which gave a pure sample, m.p. 265~268°C, on recrystallization from methylene chloride-methanol.

The alkaline solution was neutralized with 20% sulfuric acid and 262 mg. of crude 3-keto-20-*iso*-23, 24- dinorchol-4-en-22-oic acid with m.p. 201~204°C was obtained. Methylation of the crude acid with diazomethane yielded 123 mg. of V with m.p. 118~121°C. Reported m.p. 119~121°C[6].

20-*Iso*-23, 24-dinorchol-4-en-22-ol-3-one (VIIIa).—*a) From Methyl 3-Keto-20-iso-23, 24-dinorchol-4-en-22-oate (V).*—A mixture of 73.7 mg. of keto ester V and 52 mg. of lithium aluminum hydride in 2 ml. of tetrahydrofuran was treated in the same way as described above (reflux for 5 hours) to give 73.4 mg. of a mixture (VII) with m.p. 188~205°C.

The above solid was dissolved in a mixture of 1 ml. of benzene and 3 ml. of pyridine and the solution was treated with 37 mg. of *N*-bromoacetamide (standing for 3 hours at room temperature). After being treated as usual, the crystalline residue (73.6 mg.; m.p. 120~138°C) was dissolved in 10 ml. of benzene and adsorbed on a column of alumina (3 g.). Elution with ether and recrystallization from aqueous acetone gave 53 mg. of VIIIa, m.p. 147~148°C, $[\alpha]_D^{21.5}$ +96 (c, 0.532), λ_{max} 241 mμ, log ε, 4.24, ν_{max}^{Nujol} 2.89 (OH), 6.03 (C=O) 6.20 μ (C=C).

Anal. Found: C, 79.90, H, 10.48. Calcd. for $C_{22}H_{34}O_2$: C, 79.95, H. 10.37%.

b) From 3-Keto-20-iso-23, 24-dinorchol-4-en-22-al (VI).—To a mixture of 1 g. of compound VI[6] in 60 ml. of methanol, a solution of 0.2 g. of sodium borohydride in 1 ml. of water and 5 ml. of methanol was added with stirring at the room

26) K. Tsuda. R. Hayatsu, Y. Kishida and S. Akagi, *J. Am. Chem. Soc.*, **80**, 921 (1958).

temperature. After one hour the reaction mixture was diluted with water and the solid (m. p. 175～195°C) was collected by filtration. Yield, 1 g.

A mixture of 203.7 mg. of the above solid, 2 ml. of benzene, 5 ml. of pyridine and 108.2 mg. of *N*-bromoacetamide was treated in the same way as described above to give 135 mg. of compound VIIIa with m. p. 145～147°C. The melting point was not depressed on admixture with the sample obtained above.

20-*Iso*-23,24-dinorchol-4-en-22-ol-3-one acetate (VIIIb). — The substance was prepared in the usual way from 34 mg. of compound VIIIa. The crude substance showed m. p. 85～91°C, $[\alpha]_D^{22}$ +94 (c, 0.726). No attempt was made to purify it further, because only a few mg. of this substance which is crystallized with difficulty was available.

20-*Iso*-23,24-dinorchol-4-en-22-ol-3-one tosylate (VIIIc).—To 138 mg. of compound VIIIa in 3 ml. of pyridine, 87 mg. of *p*-toluenesulfonyl chloride was added and the mixture was left to stand overnight. Treatment in the usual way gave VIIIc in plates with m. p. 176～178°C (dec.), ν_{max}^{Nujol} 5.99 (C=O), 6.20, 6.26 (C=C), 7.31, 8.51 μ (—O—SO_2—).

Anal. Found: C, 72.35, H, 7.08. Calcd. for $C_{25}H_{36}SO_4$: C, 72.46, H, 7.55%.

Methyl 3-Ethylenedioxy-23,24-dinorchol-5-en-22-oate (IX).—A mixture of 2 g. of compound I[6], 140 ml. of dry benzene, 10 ml. of ethylene glycol and 0.2 g. of *p*-toluenesulfonic acid monohydrate was distilled until 30 ml. of the distillate was azeotropically removed in about 1 hour, and the mixture was refluxed for further 8 hours[27]. After cooling, the mixture was extracted with benzene, and the extract was washed with 10% aqueous potassium carbonate and with water, and dried over anhydrous sodium sulfate. The solvent was evaporated under a reduced pressure, and the crystalline residue was recrystallized from acetone to give 1.4 g. of IX in needles, m. p. 188～189°C, $[\alpha]_D^{20}$ −46 (c, 1.410), ν_{max}^{Nujol} 5.80 (C=O). 7.95 (O=C—O—C), 9.25 μ (ketal)[28].

Anal. Found: C, 74.64, H, 9.86. Calcd for $C_{25}H_{38}O_4$: C, 74.58, H, 9.51%.

3-Ethylenedioxy-23,24-dinorchol-5-en-22-ol (Xa).—A mixture of 748 mg. of ketal ester IX, 170 mg. of lithium aluminum hydride and 20 ml. of anhydrous tetrahydrofuran was treated in the same way as described above (reflux for 4 hours), and recrystallization of the product from methanol gave 610 mg. of Xa in fine needles, m. p. 181～182°C, $[\alpha]_D^{16.5}$ −33 (c, 1.28).

Anal. Found: C, 77.07, H, 9.93. Calcd for $C_{24}H_{38}O_3$: C, 76.96, H, 10.23%.

3-Ethylenedioxy-23,24-dinorchol-5-en-22-ol acetate (Xb). — The substance was prepared in the usual way. Recrystallization from aqueous ethanol gave Xb in long needles, m. p. 122～123°C, $[\alpha]_D^{21.5}$ −32 (c, 1.75).

Anal. Found: C, 74.89, H, 10.00. Calcd. for $C_{26}H_{40}O_4$: C, 74.96, H, 9.68%.

A mixture of 9 mg. of acetate XIb, 3 ml. of methanol and 0.3 ml. of 0.8% (by volume) sulfuric acid was treated in the same way as described above (reflux for 50 min.) to give IVa, m. p. and mixed m. p. 137～138°C.

6β-Bromocholestan-5α-ol-3-one (XII). — A suspension of 1 g. of 3-ethylenedioxy-cholest-5-ene (XI) in 50 ml. of dioxane and 3 ml. of water was mixed with 1 ml. of 60% perchloric acid and 350 mg. of *N*-bromoacetamide, and the mixture was shaken occasionally at room temperature. The whole solid soon went into solution and in a few hours a new solid appeared. After being kept overnight the suspension was diluted with 10 ml. of water and left to stand in a refrigerator for two hours, and the solid was collected, dried, and triturated with hot acetone to give 520 mg. of XII melting at 176～178°C. Recrystallization from acetone raised the melting point to 181～182°C (dec.), which was not depressed on admixture with an authentic sample of XII[29].

Cholest-4-en-6α-ol-3-one (XIV).—To a solution of 59 mg. of bromohydrin XII in 5 ml. of methylene chloride and 10 ml. of methanol, 17 mg. of potassium hydroxide in 8.5 ml. of methanol was added. After being kept at room temperature overnight, the solution was neutralized with acetic acid and concentrated to half the volume under a reduced pressure. Water was added and crystals were collected by filtration to obtain 51 mg. of XIV, m. p. 152～156°C. The melting point was raised to 160～161°C on recrystallization from aqueous ethanol. Identity was established by a mixed[22] melting point determination.

It was shown in a previous paper[22] that sodium bicarbonate hydrolysis of 6β-chlorocholestan-5α-ol-3-one furnished compound XIV in a good yield while sodium bicarbonate hydrolysis of bromohydrin XII in the same manner as described previously furnished compound XIV only in a low yield. When a mixture of bromohydrin XII (0.4 g.) in ethanol (30 ml.) and potassium bicarbonate (0.2 g.) in water (3 ml.) was heated under reflux for 5 hours, 0.35 g. of 5α-cholestane-3,6-dione was obtained, m. p. 169～170°C, $[\alpha]_D^{25}$ +5 (c, 2.50).

Cholest-4-en-3β,6α-diol (XV).—A mixture of 108 mg. of XIV and 50 mg. of lithium aluminum hydride in 3 ml. of tetrahydrofuran was treated in the same manner as described above (reflux for 1 hour). The residue (107 mg.) exhibited m. p. 126～148°C, $[\alpha]_D^{24}$ +47 (c, 1.07). Two recrystallizations from methanol gave 48 mg. of XV in needles, m. p. 178～179°C, $[\alpha]_D^{25}$ +31 (c, 0.388). Reported m. p. 175～178°C, $[\alpha]_D$ +29[30], 176～177°C[17], 178～179°C[31]. Identity was established

27) cf R. Antonucci, S. Bernstein, R. Littel, K. J. Sac and J. H. Williams, *J. Org. Chem.*, **17**, 1341 (1952).
28) S. Bernstein, R. H. Lenhard and T. B. Williams, ibid., **19**, 41 (1954).
29) S. Mori and F. Mukawa, *Proc. Japan Acad.*, **31**, 31 (1955). cf. D. H. R. Barton and E. Miller, *J. Am. Chem. Soc.*, **72**, 1066 (1950).
30) V. Prelog and E. Tagmann, *Helv. Chim. Acta*, **27**, 1867 (1944).
31) Y. Urushibara, This Bulletin, **16**, 184 (1941).

by a mixed[17] melting point determination.

Cholest-4-ene-3β,6β-diol (XVIII).—5α-Bromocholestan-3β, 6β-diol diacetate[18] (2 g.) in dry pyridine (15 ml.) was heated under reflux for 8 hours. The mixture was diluted with ice-cold water and extracted with ether. The extract was washed with diluted hydrochloric acid and with water, dried over anhydrous sodium sulfate, and evaporated. Recrystallizations (twice) from methanol gave 1.2 g. of cholest-4-ene-3β, 6β-diol diacetate, m. p. 132~135°C.

Hydrolysis of the diacetate (1 g.) in methanol (20 ml.) with potassium hydroxide (0.3 g.) in methanol (3 ml.) at room temperature gave 0.7 g. of diol XVIII, m. p. 255~258°C. Identity was established by a mixed[32] melting point determination.

Cholest-4-en-6β-ol-3-one (XIX).—A solution of 200 mg. of 3β, 6β-diol XVIII in 3 ml. of benzene and 4 ml. of pyridine was treated with 72 mg. (1.05 equiv.) of *N*-bromoacetamide at room temperature for 18 hours. After being treated as usual, the crystalline residue was recrystallized from acetone—*n*-hexane to give 155mg. of XIX in needles, m. p. 185~189°C. The melting point was raised to 190~191°C by recrystallizations (twice) from acetone—*n*-hexane and was not depressed when mixed with an authentic sample of XIX[22].

The identity was further established by conversion into the acetate, m. p. and mixed m. p. 101~102°C, and into 5α-cholestan-3, 6-dione, m. p. and mixed m. p. 170~171°C, on treating with hydrochloric acid in ethanol.

Cholest-4-en-6α-ol-3-one (XIV).—A solution of 157 mg. of 3β, 6α-diol XV in 3 ml. of benzene and 4 ml. of pyridine was treated with 57 mg. of *N*-bromoacetamide at room temperature overnight. After being treated as usual, the crystalline residue was recrystallized from acetone-*n*-hexane to give 121 mg. of XIV in needles, m. p. 150~155°C. The melting point was raised to 160~161°C when recrystallized from aqueous ethanol. Identity was established by a mixed[22] melting point determination.

The identity was further established by conversion into the acetate, m. p. and mixed[33] m. p. 103~104°C, and into 5α-cholestane-3, 6-dione, m. p. and mixed m. p. 170~171°C, on treating with hydrochloric acid in ethanol.

Stigmasta-4, 22-dien-3-ol (XXII).—A mixture of 0.5 g. of stigmasta-4, 22-dien-3-one (XXIII)[24], m. p. 123~125°C, and 0.2 g. of lithium aluminum hydride in 15 ml. of anhydrous tetrahydrofuran was treated in the same manner as described above (reflux for 1.5 hours) to give a mixture, m. p. 134~163°C, $[\alpha]_D^{24}$ +32 (c, 1.57). It is presumed that the mixture consists essentially of stigmasta-4, 22-dien-3β-ol and the corresponding 3α-ol.

Stigmasta-4, 22-dien-3-one (XXIII).—A solution of 200 mg. of the above mixture (XXII) in 3 ml. of benzene and 4 ml. of pyridine was treated with 70 mg. (1.05 equiv.) of *N*-bromoacetamide at room temperature for 2 hours. After being treated as usual, the crystalline residue was recrystallized from acetone to give 162 mg. of XXIII in needles, m. p. 118~122°C. The melting point was raised to 126~127°C by three recrystallizations from acetone and was not depressed when admixed with an authentic sample of XXIII[24].

Ultraviolet and Infrared Absorption Spectra. — They were measured by use of Hitachi Photoelectric Spectrophotometer Model EPU-2 and ŌYŌ-KŌKEN instrument, respectively. Samples for ultraviolet spectra were dissolved in 95% ethanol. Infrared spectra were kindly measured at Institute of Physical and Chemical Research.

The author is indebted to Professor S. Mori, Tokyo Metropolitan University, Dr. M. Nakamura, Director of this Institute, and Mr. R. Mamine, this Institute, for their encouragement.

Sugiyama Chemical Research Institute
Mure, Mitaka, Tokyo

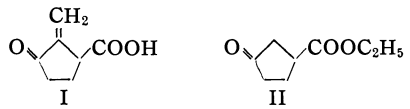
32) V. A. Petrow, O. Rosenheim and W. W. Straling, *J. Chem. Soc.*, **1938**, 677.
33) L. F. Fieser, *J. Am. Chem. Soc.* **75**, 4377 (1953).

Synthesis of Sarkomycin. II.[1] *A New Synthesis of the Alkyl Cyclopentanone-3-carboxylate*

By Katsuyuki TOKI

(Received September 11, 1958)

In the previous report[1], the present author described the synthesis of *dl*-sarkomycin (2-methylenecyclopentanone-3-carboxylic acid) (I) starting from ethyl cyclopentane-3-carboxylate[2] (II).



Though the alkyl cyclopentanone-3-carboxylate (II) is a key substance for the preparation of *dl*-sarkomycin, the hitherto published methods are so complicated for the commercial preparation of alkyl cyclopentanone-3-carboxylate (II) that the present author has studied the synthesis of this intermediate by means of a new convenient route.

It was found that the cyclopentanone-3-carboxylate (II) can be readily obtained by the thermal decomposition of monoester of 1,2,4-butanetricarboxylic acid (3-alkoxycarbonyladipic acid) (VI) which was prepared from butadiene (III) and alkyl acrylate (IV) according to the following new scheme. (See Fig. 1).

Cyclohexene-4-carboxylate[3] (V) was prepared in a good yield (71.4%) by heating butadiene (III) with alkyl acrylate (IV) in an autoclave at 170~180° in the presence of polymerization inhibitors such as hydroquinone.

Monoester of 1,2,4-butanetricarboxylic acid (VI) was obtained by the oxidation[4] of V with potassium permanganate in a 67.2% yield. While cyclopentanone-3-carboxylic acid (X) could be prepared from the triester VII according to Kay's precedure[2], the cyclopentanone-3-carboxylate (II) was formed directly when monoester VI was heated at 200~300° at atmospheric pressure and then distilled under a reduced pressure. The cyclopentanone-3-carboxylate (II), thus obtained, was identical with the specimen prepared by Kay's method[2].

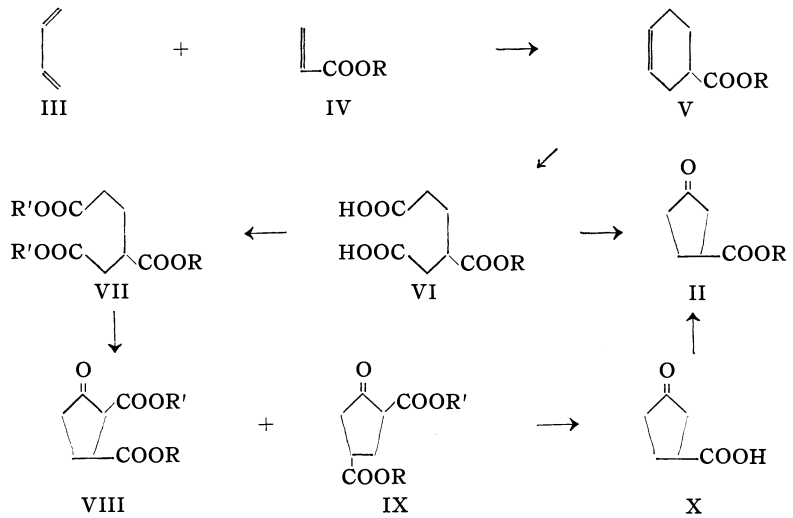


Fig. 1. The new route for the synthesis of alkyl cyclopentanone-3-carboxylate.

1) I. Synthesis. of *dl*-sarkomycin (2-methylenecyclopentane-3-carboxylic acid). K. Toki, This Bulletin, **30**, 450 (1957).

2) F. W. Kay et al., *J. Chem. Soc.*, **89**, 1640 (1906).

3) Ger., Pat., 857, 637, Dec. 1, (1952).

4) Brit. Pat., 688, 344, Mar. 4, (1953).

Experimental

Methyl cyclohexene-4-carboxylate (V, R=CH_3).—A mixture of 86 g. (1 mole) of methyl acrylate (IV, R=CH_3), 108 g. (2 moles) of butadiene[5] (III) and 1 g. of hydroquinone was heated in an autoclave at 170° for twenty hours. The reaction mixture was distilled in vacuo to remove the polymeric materials and the distillate was fractionated through a Widmer-column. The fraction boiling at 182~185° (99~107°/100 mm.), n_D^{31} 1.4574, was collected. The yield was 90 g. (64.3%).

Anal. Found: C, 68.56; H, 8.58. Calcd. for $C_8H_{12}O_2$: C, 68.57; H, 8.57%.

Ethyl cyclohexene-4-carboxylate (V, R=C_2H_5).—A mixture of 100 g. (1 mole) of ethyl acrylate (IV, R=C_2H_5), 108 g. (2 moles) of butadiene and 1 g. of hydroquinone was treated in the same manner as above. The yield of V (R=C_2H_5), b.p. 105~110°/100 mm., was 110g. (71.4%).

Anal. Found: C, 70.03; H, 8.88. Calcd. for $C_9H_{14}O_2$: C, 70.13, H, 9.09%.

Monoester of 1,2,4-butanetricarboxylic acid (3-Alkoxycarbonyladipic acid (VI)).—*a*) *Methylester.*—Finely powdered potassium permanganate (461 g.) was added in small portions to a mixture of 140 g. (1 mole) of V and 2000 ml. of water with vigorous stirring over a period of five hours at temperatures below 50°. Manganese dioxide was filtered off and the filtrate was acidified with diluted hydrochloric acid and extracted with ether in a large continuous extracter for five days. The ether layer was dried over anhydrous sodium sulfate, the ether was removed and the residue was then distilled in vacuo. The yield of VI, (R=CH_3) b.p. 209~213°/0.4 mm., was 137.1 g. (67.2%). It was recrystallized from a mixture of ethyl acetate and petroleum ether, m.p. 95~97°.

Anal. Found: C, 47.05; H, 5.79. Calcd. for $C_8H_{12}O_6$: C, 47.06; H, 5.88%.

b) *Ethylester.*—A suspension of 154 g. (1.0 mole) of V (R=C_2H_5) in 2000 ml. of water was oxidized with 461 g. of potassium permanganate in the same manner as described above. The yield of VI (R=C_2H_5), b.p. 217~220°/0.5 mm., was 140 g. (64.2%).

Anal. Found: C, 49.48; H, 6.37. Calcd. for $C_9H_{14}O_6$: C, 49.54; H, 6.42%.

Diethyl methyl 1,2,4-butanetricarboxylate (VII, R=CH_3, R'=C_2H_5).—A mixture of 102 g. (0.5 mole) of VI (R=CH_3), 1000 ml. of absolute ethanol and 10 g. of concentrated sulfuric acid was refluxed on a water bath for eight hours. After concentration of the reaction mixture, the residue was poured into ice and water. The oily layer was extracted with ether, washed with 5% aqueous sodium bicarbonate solution and dried over anhydrous sodium sulfate. The ether was removed and the residue was distilled under a reduced pressure. The yield of VII, b.p. 185~190°/28 mm., n_D^{24} 1.4412, was 80 g. (61.5%).

Anal. Found: C, 55.34; H, 7.53. Calcd. for $C_{12}H_{20}O_6$: C, 55.38; H, 7.69%.

5) Butadiene was prepared by the procedure described in "Organic Syntheses", Coll. Vol. II, John Wiley and Sons, Inc., New York (1943), p. 102.

Triethyl 1,2,4-butanetricarboxylate (VII, R=R'=C_2H_5).—A mixture of 109 g. (0.5 mole) of VI (R=C_2H_5), 1000 ml. of absolute ethanol and 10 g. of concentrated sulfuric acid was refluxed on a water bath for eight hours. The reaction mixture was warked up in the same manner as above. The final product, b.p. 190~202°/24 mm., weighed 73 g. (53.3%).

Anal. Found: C, 57.00; H, 8.00. Calcd. for $C_{13}H_{22}O_6$: C, 56.93; H, 8.03%.

Methyl cyclopentanone-3-carboxylate (II, R=CH_3).—After heating 51 g. (0.25 mole) of VI (R=CH_3) with 1 g. of barium oxide at 250~300° for 10~30 minutes, the mixture was distilled under a reduced pressure. The product came over at 122~125°/18 mm. and weighed 10.2 g. (28.7%).

Anal. Found: C, 59.18; H, 7.00. Calcd. for $C_7H_{10}O_3$: C, 59.15; H, 7.04%.

The 2,4-dinitrophenylhydrazone melted at 182~184° (recrystallized from a mixture of ethyl acetate and petroleum ether).

Ethyl cyclopentanone-3-carboxylate (II, R=C_2H_5) from VII (R=R'=C_2H_5).—To a suspension of 13 g. of sodium-sand in 300 ml. of benzene was added 137 g. (0.5 mole) of triethyl 1,2,4-butanetricarboxylate (VII, R=R'=C_2H_5). When the vigorous reaction subsided, the reaction mixture was heated for two hours with stirring and acidified with diluted hydrochloric acid.

The whole mixture was extracted with ether and the ether layer was washed with 5% aqueous solution of sodium bicarbonate and then with water. The ether solution was dried over anhydrous calcium chloride, the ether was removed and the residue was distilled. The yield of diethyl cyclopentanone-2,3- and -2,4-carboxylates, b.p. 131~137°/0.6 mm., was 96 g. (84%).

A solution of 96 g. (0.42 mole) of diethyl cyclopentanone-2,3- and -2,4-carboxylates in 1. of 8% sulfuric acid was boiled for three hours. Cyclopentanone-3-carboxylic acid (X) was extracted from the reaction mixture with ether, the ether layer was dried over anhydrous calcium chloride and the ether was distilled off. The residue was distilled at 138~145°/0.3 mm., m.p. 64~65°, and weighed 45 g. (83%).

A mixture of 45 g. (0.35 mole) of X, 180 ml. of benzene, 75 ml. of 99% alcohol and 4 g. of *p*-phenolsulfonic acid was refluxed for two days, a water separator being used. The ethyl ester (II) was obtained in a yield of 51 g. (93%): b.p. 127~128°/20 mm.

Anal. Found: C, 61.48 H, 7.63. Calcd. for $C_8H_{12}O_3$: C, 61.54; H, 7.69%.

The 2,4-dinitrophenylhydrazone melted at 153~154°.

Anal. Found: C, 49.77; H, 4.65; N, 16.93. Calcd. for $C_{14}H_{16}O_6N_4$: C, 50.00; H, 4.76; N, 16.67%.

Summary

Cyclopentanone-3-carboxylate which is the starting material for the synthesis of *dl*-sarkomycin (2-methylenecyclopentanone-3-carboxylic acid) was obtained by a new

route from butadiene and alkyl acrylate through alkyl cyclohexene-4-carbonylate and thence 3-alkoxycarbonyl adipic acid.

The author wishes to express his deep appreciation to Professor Shiro Akabori, Professor Hamao Umezawa and Professor Masanao Matsui, for their continuous interest in this work. The author is also indebted to Mr. Noboru Nishimura for carrying out micro-analyses and Messrs. Hiroo Wada and Yoshio Suzuki for their kind collaboration.

Osaka Works, Sumitomo Chemical Co., Ltd.
Konohana-ku, Osaka

Effects of Dry Grinding on Kaolin Minerals. I. Kaolinite

By Hiroshi TAKAHASHI

(Received September 10, 1958)

Considerable work has been done on the effects of dry grinding on clay minerals and related minerals, particularly kaolinite[1]. The resolution of the grinding effects on kaolin minerals has proved helpful in the study of the structure of kaolin minerals. It is considered that understanding of the grinding process is useful for the study of weathering processes, soil fertility and the active solid.

It is well known that the grinding of kaolinite increases the base exchange capacity, but there is no consistent explanation of this increase. In the result of study concerning the dry grinding effect of kaolinite, there are two lines of thought, at least. One asserts that the dry grinding of kaolinite brings about only a reduction in particle size of kaolinite owing to cleavage and fracturing of the kaolinite crystal. The cleavage and fracturing of kaolinite crystal increases the specific surface and the broken bond. These facts lead to an increase in the base exchange capacity. The other insists that the dry grinding of kaolinite causes the formation of a zeolitic substance having a structure similar to that of the original kaolinite; that is, it distorts the lattice, and or decomposes kaolinite to alumina and silica gel. It is considered that wet grinding of kaolinite is effective in causing a change on the surface property but not in the structural change.

Studies heretofore of the grinding on kaolin minerals have been made mostly by ball-milling. Incidentally, it was found by Mackenzie and Milne that mechanical mortar is very effective in causing a change in structure of mica[2]. From this point of view, effects of several-hundred-hours mechanical-mortar dry grinding of kaolinite were studied by X-ray diffraction, thermal, electron microscopic and other methods in this study.

The purposes of this study are to obtain the fundamental information of the structure of kaolinite and the correct explanation of the grinding process of kaolinite, and to present the variation of the grinding effects of kaolin minerals with respect to the crystallinity.

Experimental

The following kaolinites were investigated: Kaolinite from Mesa Alta, N. M., U. S. A.; Kaolinite from Drybranch, Geor., U. S. A.. Both clays are the API Standard Clay Minerals. The structural characteristics of these original clays were discussed in the previous paper[3], and from

1) W. P. Kelly, W. H. Dore and S. M. Brown, *Soil Sci.*, **31**, 25 (1931).
W. P. Kelly and H. Jenny, ibid., **41**, 367 (1936).
C. E. Marshall, *J. Phys. Chem.*, **41**, 935 (1937).
M. L. Jackson and E. Truog, *Soil Sci. Soc. Am., Proc.*, **4**, 136 (1939).
B. T. Shaw, *J. Phys. Chem.*, **46**, 1032 (1942).
W. D. Laws and J. B. Page, *Soil Sci.*, **62**, 319 (1946).
C. W. Parkert, A. T. Perkins and R. D. Dragsdorf, *Trans. Kansas Acad. Sci.*, **51**, 386 (1950).
R. D. Dragsdorf, H. E. Kissinger and A. T. Perkins, *Soil Sci.*, **71**, 439 (1951).
S. J. Gregg, T. W. Parker and M. J. Stephens, *Clay Min. Bull.*, **2**, 34 (1953).
S. J. Gregg, K. J. Hill and T. W. Parker, *J. App. Chem.*, **4**, 631 (1954).
S. J. Gregg, T. W. Parker and M. J. Stephens, ibid., **4**, 666 (1954).

2) R. C. Mackenzie and A. A. Milne, *Clay Min. Bull.*, **2**, 57 (1953).
R. C. Mackenzie and A. A. Milne, *Min. Mag.*, **32**, 178 (1953).
3) H. Takahashi, This Bulletin, **31**, 275 (1958).

these results, it is found that Mesa Alta kaolinite is a triclinic in symmetry and so it has the highest degree of crystallinity of all kaolin minerals. The crystallinity of Drybranch kaolinite is somewhat lower than that of Mesa Alta kaolinite.

A 30 g. portion of the original kaolinite was charged and ground by a mechanical mortar (15.2 cm. in diameter and 8.4 cm. in depth). Specimens were taken out at intervals of 24 hour and examined by X-ray, thermal and electron microscopic method. In conjunction with the above measurements, base exchange capacity and density were measured.

X-ray diagrams were recorded by an X-ray diffractometer (Geigerflex). Experimental conditions are as follows: filtered Cu radiation (Cu$K\alpha$: 1.5418 Å) at 35 kV and 15 mA is used; scanning speed is 1° or 1/2° 2θ per minute; time constant is 4 seconds; receiving slit is 0.2 mm. or 0.1 mm.; angular aperture is 1° or 1/2°. The differential thermal analysis curves were obtained by the apparatus described by Sudo et al.[4]. Care was taken to pack a specimen into the sample block in a homogeneous manner and also keep the weight of the specimen constant. The mean heating rate is 12.5°C per minute. The density was measured by pycnometer in carbon tetrachloride. The base exchange capacity was measured by the following procedures. The specimen was treated with hydrochloric acid, thus convert it into "hydrogen-clay", and after being washed with water was titrated with sodium hydroxide solution. The base exchange capacity was expressed as the number of milli-equivalents of cation, per 100 g. of specimen, required to bring the pH to 7. Measurements of the density and the base exchange capacity were made after it had been dried at 110°C to avoid the influence of the adsorbed water. Electron micrographs were obtained by a Hitachi HU-10A type Electron Microscope.

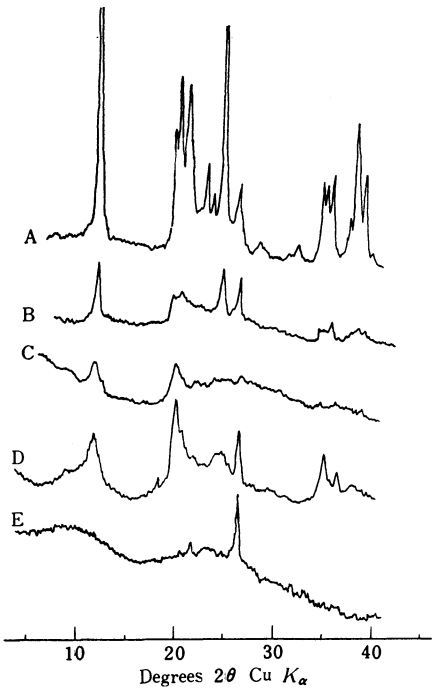


Fig. 1-a. X-ray diffractometer traces of ground kaolinite (Mesa Alta, N. M.).
A, original kaolinite
B, ground 168 hours
C, 168-hour-ground kaolinite treated with 0.1N NaOH
D, 168-hour-ground kaolinite treated with 0.1N HCl after 0.1N NaOH
E, ground 312 hours

4) T. Sudo, K. Nagasawa, M. Amafuji, M. Kimura, S. Honda and M. Tanemura, *J. Geol. Soc. Japan* (*Chishitsu-Gaku Zasshi*), **58**, 679 (1952).

Results and Discussion

X-Ray Diffraction Studies. — X-ray diffractometer traces are shown in Figs. 1 and 2. Figs. 1-a and -b show the X-ray diffractometer traces at various stages of grinding of Mesa Alta kaolinite, and Figs. 2-a and -b show that of Drybranch kaolinite. The data obtained from the X-ray diagrams are shown in Tables I and II.

The following major differences, noted in the X-ray diagrams, were used as criteria to determine the structural characteristics:

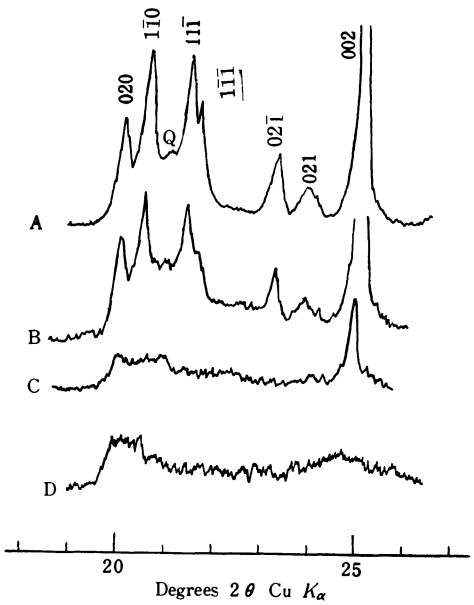


Fig. 1-b. Detailed X-ray diffractometer traces of ground kaolinite (Mesa Alta, N. M.).
A, original kaolinite
B, ground 48 hours
C, ground 96 hours
B, ground 168 hours

TABLE I

POWDER DATA OF GROUND KAOLINITE (MESA ALTA, N. M.) IN ANGSTROM UNITS

Brindley and Robinson			Original Kaolinite		Ground 48 hr.		Ground 96 hr.		Ground 168 hr.		Ground 168 hr. treated with 0.1N NaOH		Ground 168 hr. treated with 0.1N HCl after 0.1N NaOH		Ground 312 hr.	
d	*I*	*hkl*	*d*	*I*	*d*	*I*	*d*	*I*	*d*	*I*	*d*	*I*	*d*	*I*	*d*	*I*
											10.0	Wbr	9.6	Wbr		
7.15	10+	001	7.14	VS	7.14	S	7.16	M	7.15	M	7.37	Mbr	7.5	Mbr	8.0	Mvbr
4.45	4	020	4.46	M	4.47	M	4.46	M	4.44	Mbr	4.44	Mbr	4.43	S		
4.35	6	$1\bar{1}0$	4.35	S	4.35	M	4.32	W								
4.17	6	$11\bar{1}$	4.18	S	4.18	M										
4.12	3	$1\bar{1}\bar{1}$	4.13	W	4.14	VW										
3.837	4	$02\bar{1}$	3.84	M	3.85	M										
3.734	2	021	3.73	W	3.75	W										
3.566	10+	002	3.57	VS	3.58	S	3.58	M	3.58	Wbr	3.2	Wvbr	3.62	Mbr	4.0	Mvbr
3.365	4	111	3.37	M	3.38	W										
3.138	2	$11\bar{2}$	3.14	W												
3.091	2	$1\bar{1}\bar{2}$	3.09	W												
2.748	2	022	2.75	W	2.75	W	2.75	VWbr								
2.553	8	$20\bar{1}, 1\bar{3}0, 130$	2.55	S	2.56	M	2.56	Wbr	2.57	VWbr	2.58	VWbr	2.55	M		
2.521	4	$13\bar{1}, 1\bar{1}2$	2.53	M	2.53	W	2.53	Wbr								
2.486	9	$1\bar{3}\bar{1}, 200, 112$	2.49	S	2.49	M	2.50	Wbr	2.50	VWbr	2.47	VWbr	2.46	M		
2.374	7	003	2.37	M	2.38	W	2.39	Wbr								
2.331	10	$20\bar{2}, 1\bar{3}1, 11\bar{3}$	2.33	VS	2.34	M	2.34	Wbr	2.34	VWbr			2.35	Wbr		
2.284	9	$1\bar{1}\bar{3}, 131$	2.29	S	2.29	M	2.29	Wbr	2.29	VWbr	2.30	VWbr				
2.243	1	$13\bar{2}, 040$	2.24	W												
2.182	3	$1\bar{3}\bar{2}, 220$	2.18	W	2.19	W	2.19	VWbr								
2.127	2	$02\bar{3}, 041$	2.13	W	2.13	VW										
2.057	1	$2\bar{2}\bar{2}$	2.06	W												

Key to Abbreviation: VS: very strong, S: strong, M: medium, W: weak, VW: very weak, br: broad, vbr: very broad.

TABLE II

POWDER DATA OF GROUND KAOLINITE (DRYBRANCH, GEOR.) IN ANGSTROM UNITS

Original Kaolinite		Ground 48 hr.		Ground 96 hr.		Ground 144 hr.		Ground 144 hr. treated 0.1N HCl after 0.1N NaOH		Ground 264 hr.		Ground 264 hr. treated with 0.1N NaOH		Ground 264 hr. treated with 0.1N HCl after 0.1N NaOH		Ground 384 hr.	
d	*I*	*d*	*I*	*d*	*I*	*d*	*I*	*d*	*I*	*d*	*I*	*d*	*I*	*d*	*I*	*d*	*I*
										8.5	Mbr	9.2	VWvbr			8.5	VWvbr
7.15	VS	7.15	VS	7.16	S	7.20	M	7.22	VS	7.2	W						
4.45	S	4.45	M	4.45	W	4.44	Mbr	4.45	S	4.35	Wbr						
4.36	M	4.36	M	4.35	W	4.30	Wbr	4.20	W								
4.17	M	4.16	W														
3.86	W																
3.74	VW													3.8	Mbr	3.7	Wvbr
3.58	VS	3.57	VS	3.58	S	3.60	M	3.58	S	3.6	W	3.4	Mvbr	3.54	W	3.54	W
3.37	VW																
2.74	VW																
2.56	S	2.56	M	2.56	W	2.57	VWbr	2.57	M								
2.53	W	2.53	W	2.53	VW												
2.49	S	2.49	M	2.50	W	2.50	VWbr	2.50	W								
2.38	M	2.38	M	2.38	W	2.39	VWbr	2.38	M								
2.34	S	2.34	S	2.34	M	2.35	VWbr	2.34	W								
2.29	M	2.29	M	2.30	W												
2.24	VW																
2.18	W																

Key to Abbreviation: VS: very strong, S: strong, M: medium, W: weak, VW: very weak, br: broad, vbr: very broad.

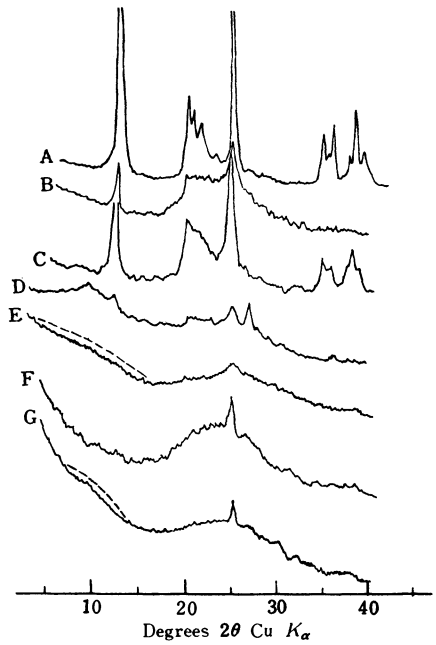


Fig. 2-a. X-ray diffractometer traces of ground kaolinite (Drybranch, Geor.).
A, original kaolinite
B, ground 144 hours
C, 144-hour-ground kaolinite treated with 0.1N HCl after 0.1N NaOH
D, ground 264 hours
E, 264-hour-ground kaolinite treated with 0.1N NaOH
F, 264-hour-ground kaolinite treated with 0.1N HCl after 0.1N NaOH
G, ground 384 hours

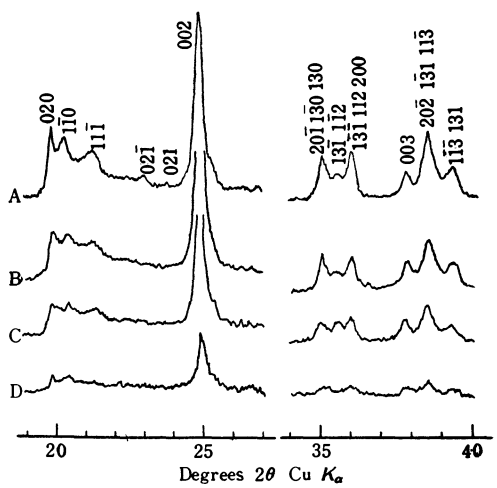


Fig. 2-b. Detailed X-ray diffractometer traces of ground kaolinite (Drybranch, Geor.).
A, original kaolinite
B, ground 48 hours
C, ground 96 hours
D, ground 144 hours

(1) Intensity and sharpness of the reflections.
(2) Number of reflections.
(3) Change in the basal spacing.
(4) Resolution between closely spaced reflections.
(5) Absence of certain reflections.
(6) Intensity of the background.

As shown in Fig. 1 and Table 1, the original sample of Mesa Alta kaolinite has the structural characteristics with the highest degree of crystallinity, since the $11\bar{1}$ and $1\bar{1}\bar{1}$ reflections are resolved each other and the $11\bar{2}$, $1\bar{1}\bar{2}$ and 022 reflections are present[5].

Important features of the initial stage of grinding are a decrease in the intensity of 00*l* reflections; however, the breadth of 00*l* reflections are considerably sharper than that of original kaolinite. In the 48-hour-ground specimen, it is found that the intensity of $02\bar{1}$ and 021 reflections decrease and $11\bar{2}$, $1\bar{1}\bar{2}$ and 022 reflections disappear, and that $11\bar{1}$ and $1\bar{1}\bar{1}$ reflections are nearly consistent. These facts show that the grinding causes some displacement of layers parallel with the *b*-axis in the structure of kaolinite. In the 96-hour-ground specimen, all reflections broaden, and the reflections of $1\bar{1}0$, $11\bar{1}$, $02\bar{1}$ and 021 disappear. These facts suggest that the crystalline part of the specimen has a pseudemonoclinic in symmetry similar to that of kaolin mineral of fireclay type, which indicates the displacement of layers by $nb_0/3$ along the *b*-axis[6]. After grinding for 168 hours, the structure of this specimen has the lowest degree of crystallinity among the kaolin minerals with the exception of halloysite which has a two-dimensional structure. That is, the assymmetric 02, 11 band and the broad band similar to that of 20, 13 band on the X-ray diagram of halloysite are observable. These facts mean that the structure of this specimen has a displacement of layers along the *a*-axis in addition to the displacement along the *b*-axis. In other words, it suggests that the two-dimensional kaolinite is formed by dry grinding. As shown in Fig. 1, after 312 hours, only two very broad bands are apparent.

With the grinding progresses, the background increases as the intensity of the reflections weaken. These facts lead to a non-crystalline substance is produced by

5) G. W. Brindley and K. Robinson, *Trans. Faraday Soc.*, **42B**, 198 (1946).
6) G. W. Brindley and K. Robinson, *Trans. Brit. Ceram. Soc.*, **46**, 49 (1947).

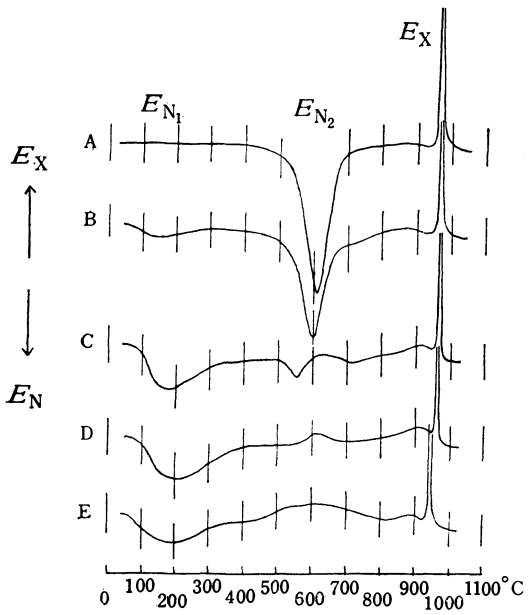


Fig. 3. Differential thermal analysis curves of ground kaolinite (Mesa Alta, N. M.).
A, original kaolinite
B, ground 48 hours
C, ground 96 hours
D, ground 168 hours
E, ground 312 hours

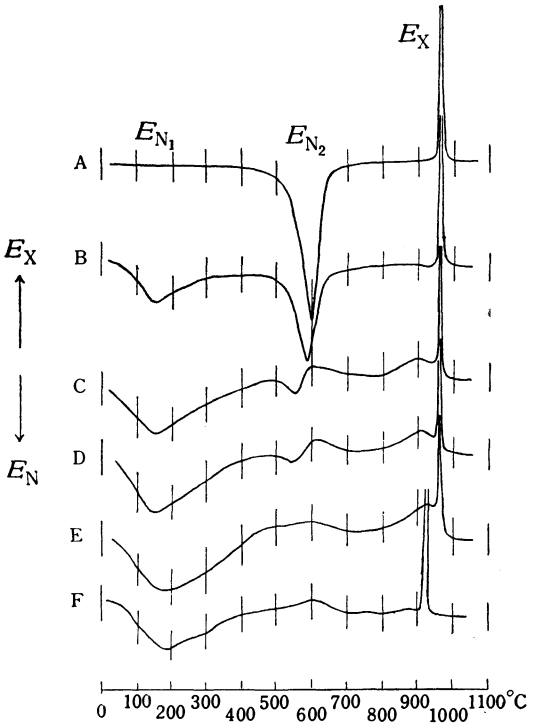


Fig. 4. Differential thermal analysis curves of ground kaolinite (Drybranch, Geor.).
A, original kaolinite
B, ground 48 hours
C, ground 96 hours
D, ground 144 hours
E, ground 264 hours
F, ground 384 hours

TABLE III
THERMAL DATA OF GROUND KAOLINITE (MESA ALTA, N. M.).
(ALL TEMPERATURES ARE DEGREES CENTIGRADE)

Grinding time (hr.)	E_{n1} Temp. at peak	E_{n1} Height of peak	E_{n1} Area of peak	E_{n2} Temp. at peak	E_{n2} Height of peak	E_{n2} Area of peak	E_x Temp. at peak	E_x Height of peak	E_x Area of peak	E_x Breadth (half value of breadth)
0	—	—	—	604°C	16	1080	966°C	39	220	5.1°
48	—155°C—	1	90	597	13	960	962	43	240	4.3
96	—170—	5	470	554	5	220	961	60	220	2.8
168	—175—	7	890	543	3	35	960	67	240	2.5
312	—180—	7	1110	—	—	—	937	58	260	3.5

TABLE IV THERMAL DATA OF GROUND KAOLINITE (DRYBRANCH, GEOR.).
(ALL TEMPERATURES ARE DEGREES CENTIGRADE)

Grinding time (hr.)	E_{n1} Temp. at peak	E_{n1} Height of peak	E_{n1} Area of peak	E_{n2} Temp. at peak	E_{n2} Height of peak	E_{n2} Area of peak	E_x Temp. at peak	E_x Height of peak	E_x Area of peak	E_x Breadth (half value of breadth)
0	—	—	—	592°C	20	1280	964°C	41	250	4.8°
48	—155°C—	6	670	582	15	750	963	45	270	4.0
46	—155—	10	1570	554	3	140	958	48	240	3.2
144	—160—	10	1960	548	2	70	957	56	250	3.1
264	—170—	10	1740	—	—	—	956	58	260	2.2
384	—190—	6	910	—	—	—	919	48	260	4.2

dry grinding. To ascertain this fact, the following treatment was made. That is, the 168-hour-ground specimen of Mesa Alta kaolinite was treated with a weak alkali solution. It forms a permutite-like substance. When it is immersed in a weak hydrochloric acid solution to dissolve the gel-like substance, the crystalline portion of the specimen is left. Fig. 1-D shows the X-ray diffractometer trace of the remaining crystalline portion; this diagram closely resembles that of halloysite. X-ray data and the following electron micrograph (Fig. 8-F) reveal that the structure of the kaolinite has changed into a two-dimensional structure.

In Drybranch kaolinite, as shown in Fig. 2 and Table II, it follows just the same process as Mesa Alta kaolinite in dry grinding. The difference is only that the structure of the original sample has a slightly lower degree of crystallinity than that of Mesa Alta kaolinite, so, the time it takes to become amorphous is somewhat shorter than that of Mesa Alta kaolinite.

Differential Thermal Analysis. — Differential thermal analysis curves and data of the grinding process of kaolinite are shown in Figs. 3 and 4 and Tables III and IV.

Measurements which were used are as follows:

(1) The peak temperature, height and area of the first endothermic reaction (E_{n1}) associated with the loss of the adsorbed water. The peak area was measured by planimeter from the base line of the thermal curve.

(2) The peak temperature, height and area of the second endothermic reaction (E_{n2}) associated with the loss of the lattice water.

(3) The peak temperature, height, area and breadth of the final exothermic reaction (E_x) corresponding to the mullite nucleation.

The endothermic reaction (E_{n1}) associated with the loss of adsorbed water, which is not present in the original sample, appears and its height and area increase; These phenomena mean that the substance produced by the dry grinding adsorbs more and more water vapor as grinding progresses. The peak temperature of this reaction gradually rises a little. This fact indicates that the water adsorbed by the ground substance is combined strongly as the grinding progresses.

In the second endothermic reaction (E_{n2}) associated with the loss of the lattice water, are observable a lowering in peak temperature, and a reduction in height and area. Finally this reaction disappears thoroughly. This corresponds with the gradual and complete disintegration of the kaolinite structure due to grinding. In the 96-hour-ground specimen of kaolinite, the X-ray diagram is similar to that of Kibushi-clay, but the height of this reaction is very small as compared with that of Kibushi-clay which is a kaolin mineral of fireclay type. This fact corresponds to the increase of the background of this specimen in its X-ray diagram, that is, a considerable amount of non-crystalline substance is produced by dry grinding.

In the exothermic reaction (E_x), there are some interesting phenomena. The peak temperature falls very slightly. But after 312 hour grinding the peak temperature lowers remarkably although the peak area is relatively unchanged. Except for the 312-hour-ground specimen on which grinding had progressed to an extreme degree, the peak height increases while the breadth decreases. As shown in the X-ray results, the perfectly ordered structure of kaolinite changes to a disordered structure as the grinding progresses. It is well known that the temperature range of the exothermic reaction (E_x) of kaolin with a higher degree of crystallinity is narrower than that of kaolin with a lower degree of crystallinity[7].

It is, therefore, difficult to draw a conclusion on the basis of the most important character of the exothermic reaction. Incidentally, it is known that the exothermic reaction corresponds to the transformation of kaolinite into mullite[8]. This transformation includes two elements of reaction, that is, nucleation of mullite and growth of mullite nuclei. Consequently, it is clear that kaolinite becomes liable to grow into mullite crystal from mullite nuclei produced by dry grinding.

To ascertain the character of the exothermic reaction of the ground specimen, the X-ray diffractometer traces of ground specimens obtained just after the exothermic reaction on the differential thermal analysis curves are recorded, which are given in Fig. 5.

As the grinding progresses, the presence of the reflection line of mullite becomes clear. That is to say, development of the

7) H. H. Murray, *Am. Mineral.*, **39**, 97 (1954).
8) W. D. Jones, *Min. Mag.*, **30**, 186 (1953). G. W. Brindley and K. Hunter, ibid., **30**, 574 (1955).

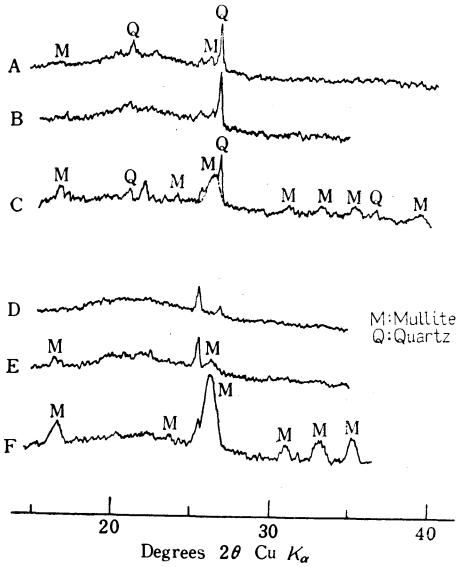


Fig. 5. X-ray diffractometer traces of ground kaolinite obtained just after the final exothermic reaction (E_x) on the differential thermal analysis curve.
A, original kaolinite (Mesa Alta, N. M.)
B, ground 168 hours
C, ground 312 hours
D, original kaolinite (Drybranch, Geor.)
E, ground 144 hours
F, ground 384 hours

mullite reflection corresponds to the increasing height of the exothermic peak as grinding progresses.

The features of the exothermic reaction of kaolinite are different from that of halloysite with a lower degree of crystallinity. Results of halloysite are reported in the following part III. From the comparison with the result of the grinding effects of halloysite, it is concluded that a non-crystalline substance produced by dry grinding of kaolinite, even in the 312-hour-ground specimen of Mesa Alta kaolinite or the 384-hour-ground specimen of Drybranch kaolinite, is an allophanic substance rather than the perfectly amorphous substance similar to the silica-alumina mixed gel.

Base Exchange Capacity and Density.— In Fig. 6 are shown the changes in the base exchange capacity at various periods of grinding.

As grinding progresses, the base exchange capacity at first increases. After reaching a maximum value, it gradually decreases until it attains a constant value. These features on the base exchange capacity curve show that the broken bonds of kaolinite increase at first owing to the

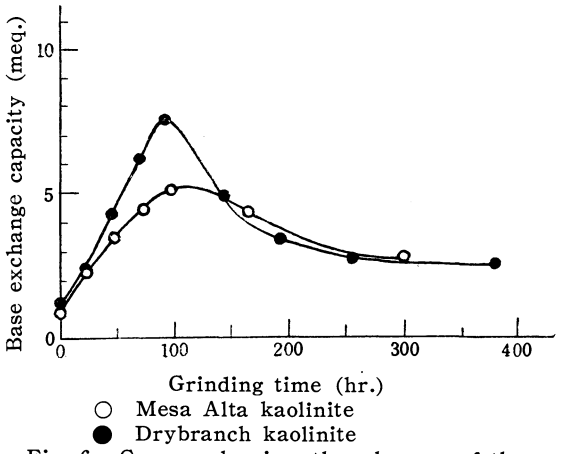


Fig. 6. Curves showing the changes of the base exchange capacity with the time of grinding.

cleavage and fracturing by dry grinding and that a non-crystalline substance gradually increases through dry grinding. These results support the thoughts of Laws and Page in the explanation of the increase on the base exchange capacity through dry grinding of kaolinite[1].

In Fig. 7 are shown the changes in the density at the various stages of grinding. As the grinding progresses, the density sharply decreases, but after reaching a certain point, it is maintained at a constant value. This constant value is nearly equal to the values of a silica-alumina-mixed gel or allophane which is a non-crystalline clay mineral. These facts show also that kaolinite changes to a non-crystalline or an amorphous substance by dry grinding.

The point of bend in the density curve and the maximum point in the base

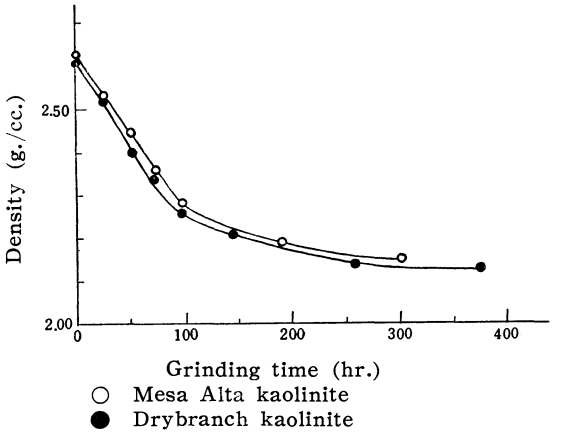


Fig. 7. Curves showing the changes of the density with the time of grinding.

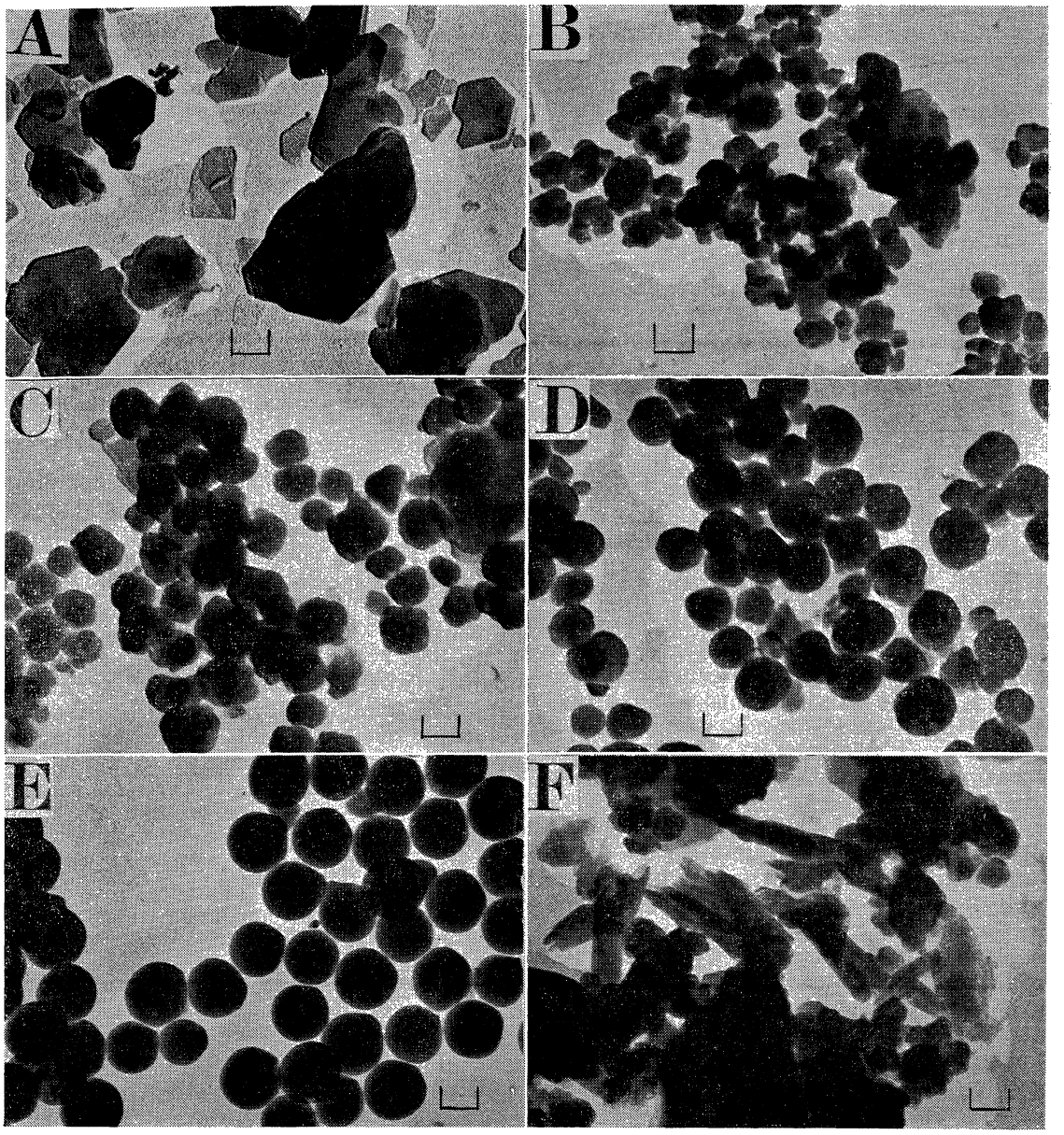


Fig. 8 Electron micrographs of ground kaolinite (Mesa Alta, N. M.).
The linear dimension on the micrograph represents 0.1 μ.

A, original kaolinite
B, ground 48 hours
C, ground 96 hours
D, ground 168 hours
E, ground 312 hours
F, 168-hour-ground kaolinite treated with 0.1N HCl after 0.1N NaOH

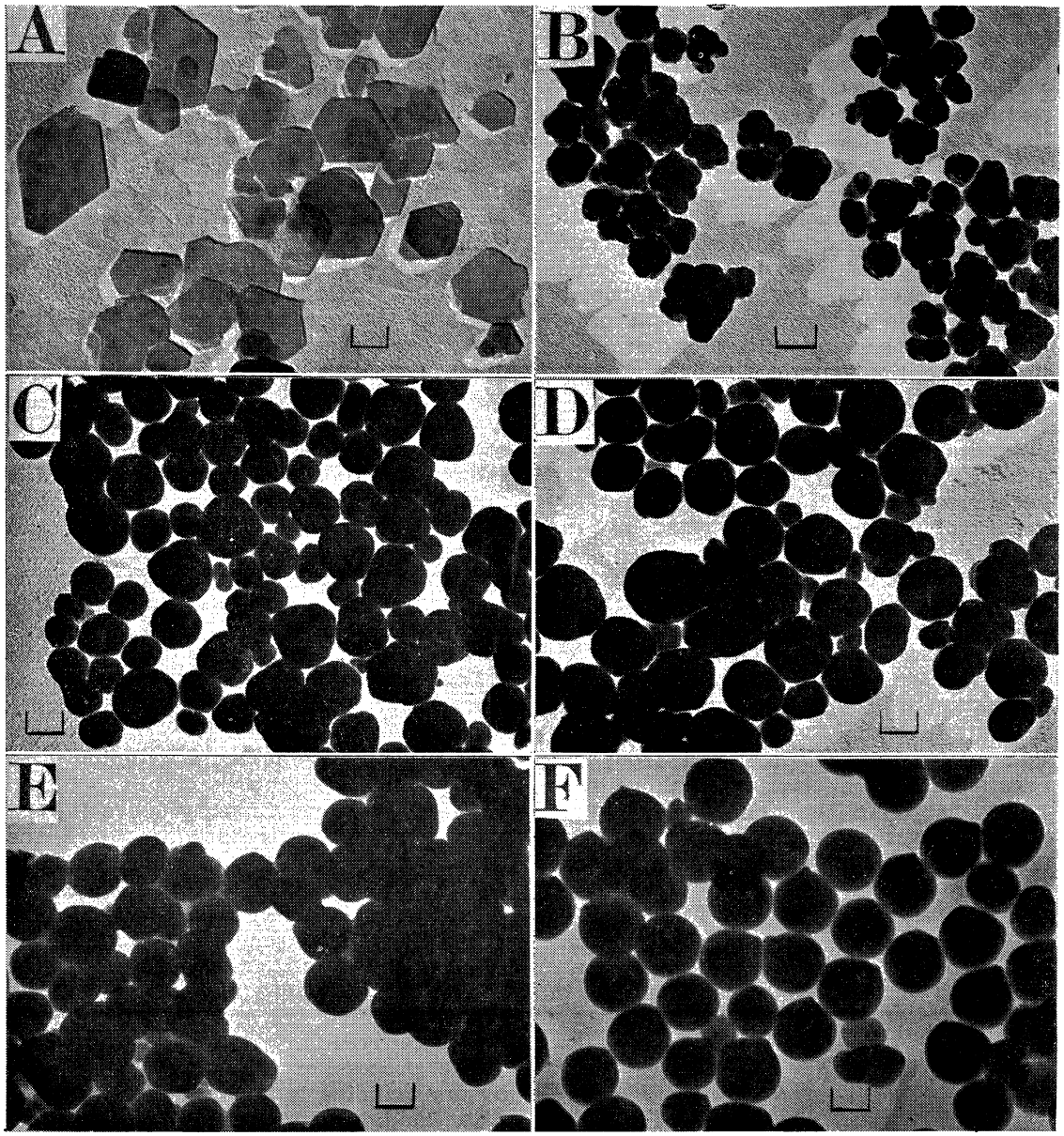


Fig. 9 Electron micrographs of ground kaolinite (Drybranch, Geor.). The linear dimension on the micrograph represents 0.1 μ.

A, original kaolinite
B, ground 48 hours
C, ground 96 hours
D, ground 144 hours
E, ground 264 hours
F, ground 384 hours

exchange capacity curve are at nearly identical positions. In the light of the X-ray data, this stage seems to correspond to the point at which kaolinite changes into a zeolitic substance by dry grinding.

Electron Microscopic Studies. — Figs. 8 and 9 show electron micrographs of kaolinite after various periods of grinding. It is observable that, in the early stage of grinding, fine crystallites are produced by cleavage and fracturing of the kaolinite crystal. The fine crystallites reaggregate, and reaggregated particles become radial and the particle size increases, slowly changing into uniformly spherical particles. The specimen with a radial shape has a zeolitic structure and is made of both crystalline and non-crystalline portions. That is, in this specimen, the non-crystalline substance produced by dry grinding falls between the crystalline substance. The crystalline portion in the zeolitic substance is separated by the alkali and acid treatment from the original ground speimen. Fig. 8-F shows the electron micrograph of this crystalline portion. As is clear from these electron micrographs and X-ray data, the crystalline portion which makes a zeolitic substance has a considerably lower degree of crystallinity than that of the original kaolinite. As was presumed from the results of Kibushi-clay and halloysite to be described in the following parts, it seems that these radial particles grow irregularly as the grinding further progresses.

If the mean sizes of the fine particles which are produced through dry grinding and those of the particles which are produced through the reaggregation of such fine particles are plotted against the grinding time, the results are as shown in Fig. 10.

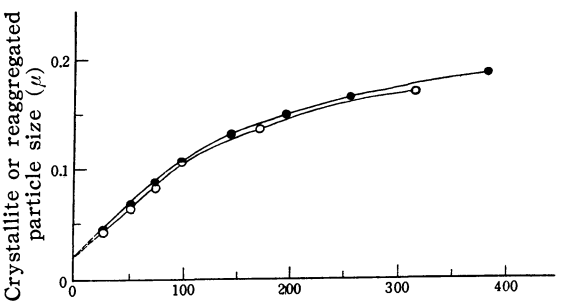


Fig. 10. Crystallite or reaggregated particle size of ground kaolinite plotted against the time of grinding.

The curve, if extrapolated to zero time, indicates almost the same value of about 200 Å for both kaolinites. Judging from this, it seems that the crystallites which separate from the original crystal during the early stage of grinding are about 200 Å in size. This value is consistent with the value in the "most dispersed state" of kaolinite in ball-milling obtained by Gregg et al., through the B. E. T. method[1].

Mechanism of Change in Kaolinite Structure with Dry Grinding. — When kaolinite is ground, kaolinite crystals cleave and fracture and then split into fine crystals that are considered unit crystallites. Such fine crystallites promptly reaggregate in groups of several. The assemblages of the original kaolinite crystallites produced through dry grinding disintegrate partially into allophane or gel-like substances. These substances and crystalline particles promptly reaggregate.

With grinding, the structure of the crystalline part of the reaggregated particle slowly becomes disordered kaolin and as an increase in the amorphous part, the reaggregated particles of the disordered kaolin and the amorphous substance become radial.

At a certain point in the grinding time corresponding to the maximum point on the base exchange capacity curve and the inflection point on the density curve, the particle becomes almost uniformly spherical. The structure of this spherical particle is considered to be zeolitic. This structure, with continued grinding, changes finally into a structure similar to the perfectly amorphous structure as silica-alumina mixed gel and its particle size increases irregularly.

The process of the structural change by dry grinding is the same in both Mesa Alta kaolinite and Drybranch kaolinite, except that the structural change of Drybranch kaolinite occurs slightly faster than that of Mesa Alta kaolinite. This means that the grinding effect on kaolinite is related to the structural perfectness of the original kaolinite. This fact has been ascertained by the study of the dry grinding effect of all kaolin minerals.

Summary

The effects of several-hundred-hour mechanical-mortar dry grinding of kaolinite were studied by X-ray, thermal,

electron microscopic and other methods. It has been found that there are two sorts of structural change in the process of dry grinding of kaolinite. One is the production of a non-crystalline substance attended by the disordering of the crystalline part, and the other is the reaggregation process. The process of the reduction in the particle size and the process of the production of the non-crystalline substance are connected to the process of the reaggregation. In a certain stage of the dry grinding, the reaggregates are spherical particles which have a zeolitic structure. As the grinding further progresses, the structure of the crystalline part in this radial particle becomes disordered due to the mechanical stress, and it changes into an amorphous substance at last. Consequently, the effect of dry grinding of kaolin mineral depends on the structural perfectness of aluminosilicate layers of the kaolin mineral, that is, the internal crystallinity of the kaolin mineral.

Department of Chemistry
Faculty of Science
The University of Tokyo
Hongo, Tokyo

Effects of Dry Grinding on Kaolin Minerals. II. Kibushi-clay

By Hiroshi TAKAHASHI

(Received September 29, 1958)

In the preceding part of this series, the effect of dry grinding of kaolinite was discussed.[1] From these results, it was ascertained that the dry grinding by a mechanical-mortar is more effective than that by ball-milling in its structural change, and the mechanism of the process of dry grinding of kaolinite was found. There are two sorts of change in structure. That is, one is the production of a non-crystalline substance resulting from the disordering of a crystalline part. The other is the process of reaggregation. In a certain stage of grinding, a zeolitic structure is formed and it changes finally into an amorphous structure.

A considerable amount of work was done on the grinding effect of kaolinite, but the grinding effects of kaolin minerals with the exception of kaolinite were not studied much. The disordering of kaolinite in the process of dry grinding follows each of the structural variations as reported by Brindley and Robinson[2]. From these facts, the effects of dry grinding of fireclay type kaolin mineral were studied with respect to the degree of crystallinity of the original structure.

Experimental

The sample used in this study is Kibushi-clay from Shidare, Gifu, Japan. This clay is a kaolin mineral of fireclay type and contains a little organic substance[2,3]. The structural characteristics of this clay were discussed in the previous paper[4]. The grinding conditions were the same as those of kaolinite described in the preceding part. The experimental specimens were examined by X-ray diffraction, differential thermal, electron microscopic and other methods. All experimental conditions were the same as those of kaolinite.

Results and Discussion

X-Ray Diffraction Studies.—X-ray diffractometer traces in the process of dry grinding of Kibushi-clay are shown in Fig. 1, and X-ray powder data observed from the X-ray traces are given in Table I. As shown in the X-ray diagram of the original sample, the structure of Kibushi-clay is similar to that of fireclay. That is, in the X-ray diagram, 020 and $1\bar{1}0$ reflections are not resolved to each other and become a wedge-like band, 001 reflection is considerably broad and weak, $13\bar{1}, 1\bar{1}2$ reflections are weak and $20\bar{1}, 130$ reflections are broad.

1) H. Takahashi, This Bulletin, **32**, 235 (1959).
2) G. W. Brindley and K. Robinson, *Trans. Faraday Soc.*, **42B**, 198 (1946).
3) G. W. Brindley and K. Robinson, *Trans. Brit. Ceram. Soc.*, **46**, 49 (1947).
4) H. Takahashi, This Bulletin, **31**, 275 (1958).

TABLE I

POWDER DATA OF GROUND KIBUSHI-CLAY IN ANGSTROM UNITS

Fireclay from Brindley and Robinson			Original clay	Ground 48 hr.	Ground 96 hr.	Ground 144 hr.	Ground 144 hr. treated with 0.1 N HCl after 0.1 N NaOH	Ground 192 hr.	Ground 384 hr.
d	*I*	*hkl*	*d* *I*	*d* *I*	*d* *I*	*d* *I*	*d* *I*	*d* *I*	*d* *I*
7.15	10	001	7.20 S	7.20 S	7.3 M br	7.7 M br		8.0 W vbr	
4.45	8	02,11	4.45 S	4.45 S	4.44 M br				
4.36	2	110	4.33 VW						
4.14	2	11$\bar{1}$							
3.57	10	002	3.58 S	3.58 S	3.57 M br	3.6 M br	3.7 M vbr	3.5 M vbr	3.6 W vbr
2.55	7	20$\bar{1}$,130	2.56 M	2.57 M	2.57 W br				
			2.53 W	2.55 VW					
2.50	7	13$\bar{1}$,200	2.50 M	2.50 M					
2.375	7	003	2.38 W	2.38 VW					
2.325	8b	20$\bar{2}$,131	2.34 M	2.34 M	2.35 W br				

Key to Abbreviation: S: strong, M: medium, W: weak, VW: very weak, br: broad, vbr: very broad.

When Kibushi-clay is ground, its structure gradually becomes more and more disordered. That is, the background increases as the intensity of the reflection weakens. In the X-ray diagrams of the ground specimens during the early stage of grinding, a lowering in the intensity of 001 reflections is remarkable, and the 131, 112, 200 reflections are very indistinct in the ground specimen after 72 hours.

In the X-ray diagrams of the ground specimens after 96 hours, only 02, 11 and 20, 13 bands are observable. When the 144-hour-ground specimen which has an amorphous structure is treated with a weak alkaline solution, it changes into a permutite-like substance. In the next place, it is treated with a weak acid solution to dissolve the amorphous substance produced by dry grinding. The X-ray diagram of the residual part produced by the above treatments is shown in Fig. 1-b-B

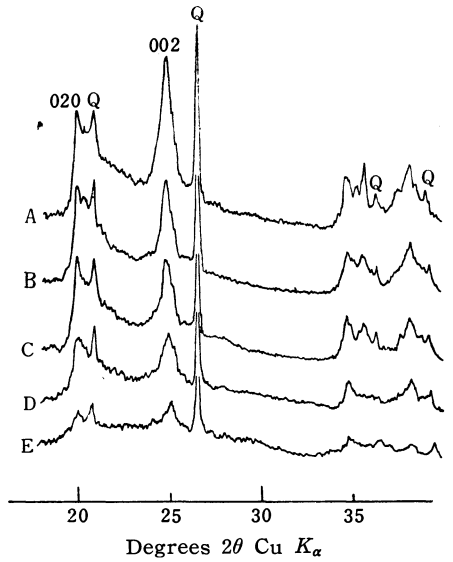


Fig. 1-a. X-ray diffractometer traces of Kibushi-clay. (I)
A, original Kibushi-clay
B, ground 24 hours
C, ground 48 hours
D, ground 72 hours
E, ground 96 hours

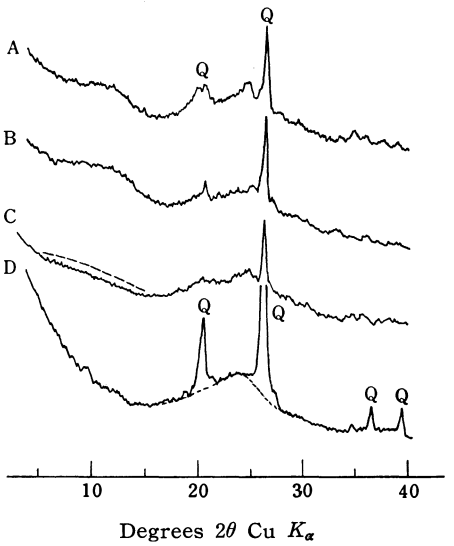


Fig. 1-b. X-ray diffractometer traces of ground Kibushi-clay. (II)
A, ground 144 hours
B, 144-hour-ground Kibushi-clay treated with 0.1 N HCl after 0.1 N NaOH.
C, ground 192 hours
D, 192-hour-ground Kibushi-clay treated with 0.1 N HCl after 0.1 N NaOH.

and its electron micrograph is shown in Fig. 6-F. The above-mentioned alkali-acid treatment was done for the 192-hour-ground specimen, too. The X-ray diagram of the residual part is shown in Fig. 1-b-D. As shown in this trace, the X-ray diagram is closely similar to that of the silica gel. This fact indicates that the crystalline part is absent in this specimen and it has changed into a gel-like substance. The specimen of Kibushi-clay ground after this stage gives a perfectly amorphous pattern in its X-ray diagram. The above-mentioned alkali-acid treatment of this specimen leaves only the impurities such as quartz.

When the result of X-ray study in Kibushi-clay is compared with that of kaolinite, it is clear that Kibushi-clay takes to become amorphous in far shorter than grinding time the case of kaolinite. On the basis of the X-ray data in the various stages of grinding of Kibushi-clay, it can be concluded that the effects of dry grinding of kaolinite and Kibushi-clay depend on the perfectness of kaolin unit layer, that is, the internal degree of crystallinity.

Differential Thermal Analysis.—Differential thermal analysis curves and data of ground specimens of Kibushi-clay are shown in Fig. 2 and Table II.

The tendency observed from the differential thermal analysis curves are similar to those in the kaolin specimens, but the only difference observable is that all of them have a broad exothermic reaction at about 600°C caused by the presence of some organic substances.

The first endothermic reaction (E_{n1}) associated with the loss of adsorbed or inter-layer water, which is not so remarkable in the original sample, becomes apparent and its height and area grow as the grinding progresses. These phenomena mean that the substance produced by the grinding adsorbs water vapor and its quantity increases with grinding. The peak temperature of this reaction rises slightly. This fact suggests that the substance produced by the grinding adsorbs more and more strongly the water vapor as the grinding progresses.

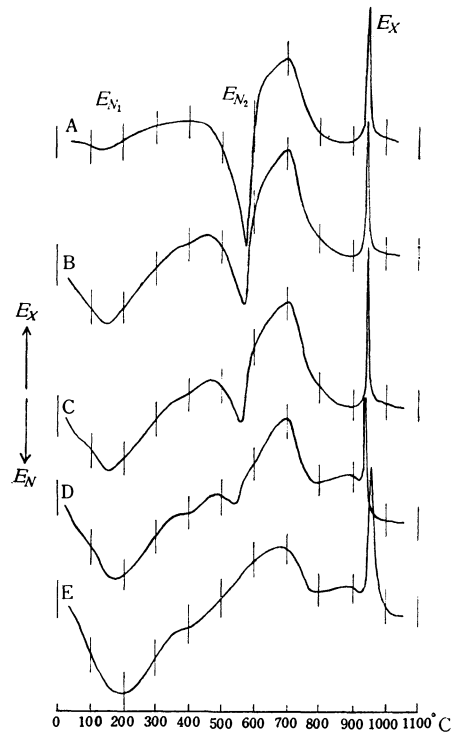


Fig. 2. Differential thermal analysis curves of ground Kibushi-clay.
A, original Kibushi-clay
B, ground 48 hours
C, ground 96 hours
D, ground 192 hours
E, ground 384 hours

In the second endothermic reaction (E_{n2}) associated with the loss of lattice water, a lowering in its peak temperature, and a reduction in the peak height and area

TABLE II
THERMAL DATA OF GROUND KIBUSHI-CLAY
(ALL TEMPERATURES ARE DEGREES CENTIGRADE)

Grinding time (hr.)	E_{n1}			E_{n2}			E_x			
	Temp. at peak	Height of peak	Area of peak	Temp. at peak	Height of peak	Area of peak	Temp. at peak	Height of peak	Area of peak	Breadth (half value of breadth)
0	130°	1	140	574°C	14	740	945°C	13	140	10.5°C
48	—140—	12	1320	563	12	480	941	28	160	6.4
96	—145—	10	1410	551	7	260	941	36	180	4.6
192	—160—	10	1830	534	1	30	940	53	220	3.9
384	—180—	10	1780	—	—	—	960	15	200	14.0

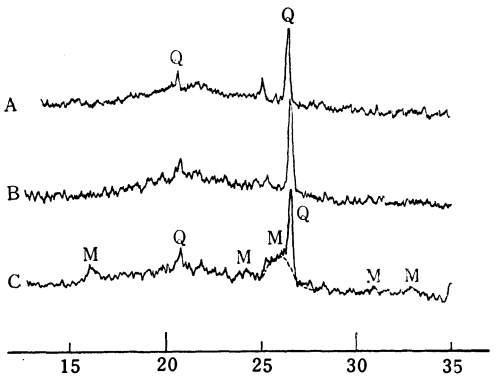
are observable. Finally, this reaction disappears completely. This leads to the disintegration of kaolin structure while it is being ground for long periods.

The final exothermic reaction (E_x) which corresponds to the mullite nucleation, is somewhat different from that of kaolinite. The peak temperature tends to fall, though very slightly, up to 192 hours of grinding. Except for the 384-hour-ground specimen, the peak height and area of the other specimens increase and the peak breadth is reduced. For the 240-hour-ground specimen, the peak temperature is almost the same as that of the 192-hour-ground specimen but the breadth is broader. In the 384-hour-ground specimen, the peak temperature rises above that of all other ground specimens, and the height and the area are smaller than those of the 192-hour-ground or the 240-hour-ground specimens. These facts mean that the structure of a non-crystalline substance produced by dry grinding changes into a more disordered structure as the grinding progresses. In the early stage of grinding, the strcture of a non-crystalline substance becomes to some extent a regular structure which is related to the original kaolin structure, but the structure of the 384-hour-ground specimen is not regular, it is an entirely disordered gel-like substance. From these facts, it might be seen that the temperature for the transformation of kaolin into mullite is high.

As shown in Figs. 2-D and -E, the slight endothermic reaction is observable just before the exothermic reaction. It has been known that the presence of this slight endothermic reaction is observable on the thermal curve of kaolin mineral with the highest degree of crystallinity[6]. The 192-hour-ground specimen of Kibushi-clay has a non-crystalline structure according to the X-ray and other data. Why does this slight exothermic reaction exist in this specimen? It is difficult to draw a conclusion as yet. But it is supposed that this fact is related to the considerable sharpness of the peak of the exothermic reaction and its remarkable height. There are two interpretations of this fact. One is that the way of transformation of kaolin into mullite is different from that of the original sample, and the other is that the tranformation of kaolin into mullite becomes more liable to grow than in the case of the original sample.

5) H. H. Murray, *Am. Mineal.*, **39**, 27 (1954).

To ascertain the character of the final exothermic reaction, X-ray diagrams were taken of some specimens after the exothermic reaction on the differential thermal analysis curve. Their traces are shown in Fig. 3.



Degrees 2θ Cu K_α
M: Mullite, Q: Quartz

Fig. 3. X-ray diffractometer traces of ground Kibushi-clay obtained just after the final exothermic reaction (E_x) on the differential thermal analysis curve.
A, original Kibushi-clay
B, ground 96 hours
C, ground 192 hours

In this case, too, it is indicated that as the grinding progresses, the reflection line of mullite crystal becomes clear. The final exothermic reaction has two elements, that is, the nucleation of mullite from the original kaolin mineral and the growth of mullite crystal from the mullite nuclei.

This is true because the presence of this weak endothermic reaction in the kaolin mineral with the highest degree of crystallinity corresponds to the nucleation of mullite. In the case of this ground specimen, it is clear that the nucleation of mullite from the kaolin mineral is easy, but the crystal growth of mullite nuclei is hard. But in the case of the ground specimen such as the 192-hour-ground Kibushi-clay, the presence of its endothermic reaction corresponds to the crystal growth of mullite nuclei. That is in the 192-hour-ground specimen or the 384-hour-ground specimen of Kibushi-clay, though the nucleation of mullite from the kaolin mineral is hard, the crystal growth of mullite nuclei is easy. Consequently, in the specimen of Kibushi-clay which is ground for a long period, the temperature of the transformation into mullite rises, because the nucleation of mullite is hard.

But, as the crystal growth of mullite nuclei is easy and rapid, the reflection of mullite is distinctly detected in its X-ray diagram, and so the height of the exothermic peak increases.

Base Exchange Capacity and Density.— In Fig. 4 are shown the changes of the base exchange capacity with the grinding time. Measurements were made on the dried specimens.

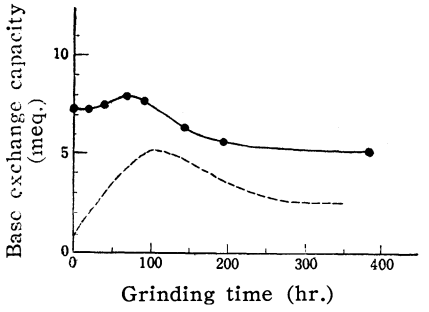


Fig. 4. Curve showing the change of base exchange capacity with the time of grinding.
------: The change in the grinding process of Mesa Alta kaolinite.

In this figure, the change in the grinding process of Mesa Alta kaolinite is drawn for reference.

The features obtained from the curve of base exchange capacity are slightly different from those of kaolinite. The maximum point is observable on the base exchange capacity curve of the grinding process of kaolinite, but it is not distinct on this curve. As shown in the micrograph of the original clay to be noted in the following section, the particle size of the original Kibushi-clay is very fine as compared with that of other kaolin minerals. Therefore, the fracturing into crystallites from the original crystal during the early stage of grinding is not so remarkable as that of kaolinite. In this clay, an increase in the broken bond which results in an increase of the capacity is not remarkable. As the result, it seems that the maximum point on the base exchange capacity curve is unobservable. In this case, the change of the base exchange capacity depends mainly on the production of a non-crystalline substance by dry grinding. This tendency also supports the thought shown by Laws and Page in the explanation for the change of the base exchange capacity due to dry grinding[6].

6) W. D. Laws and J. B. Page, *Soil Sci.*, **62**, 319 (1946).

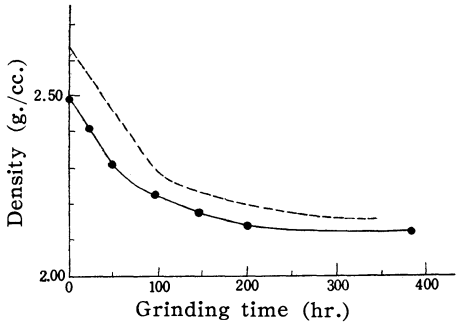


Fig. 5. Curve showing the change of density with the time of grinding.
------: The change in the grinding process of Mesa Alta kaolinite.

In Fig. 5 are shown the changes of the density with the grinding time. Measurements were made on the dried specimens.

In this figure, the change of density in the process of grinding of Mesa Alta kaolinite is drawn for reference. As the original sample of Kibushi-clay contains only a little organic substance, its density value is small.

As the grinding progresses, the density sharply decreases, but after reaching a certain point, it is maintained at a constant value. This constant value is nearly equal to the value of a silica-alumina mixed gel or allophane. These facts mean that Kibushi-clay changes into a non-crystalline substance by dry grinding.

Electron Microscopic Studies. — Fig. 6 shows the electron micrographs in the various periods of grinding of Kibushi-clay. The original clay is very fine and hexagonal platty, and the particle has a considerably sharp edge. In the early stage of grinding, fine crystallites separated from the original crystal are observable. These fine crystallites are nearly hexagonal and platty. As the grinding progresses, the fine crystallites promptly reaggregate, and reaggregated particles become spherical and the particle size increases gradually. As the grinding further progresses, the irregular growth of particles is observable. On the basis of the results obtained through the X-ray and other methods, it is understood that this irregular growth of reaggregated particles indicates that an amorphous substance is produced by dry grinding. The same thing is also found in halloysite as shown latter.

If the mean sizes of the fine particles which are produced through dry grinding and the particles which are produced by

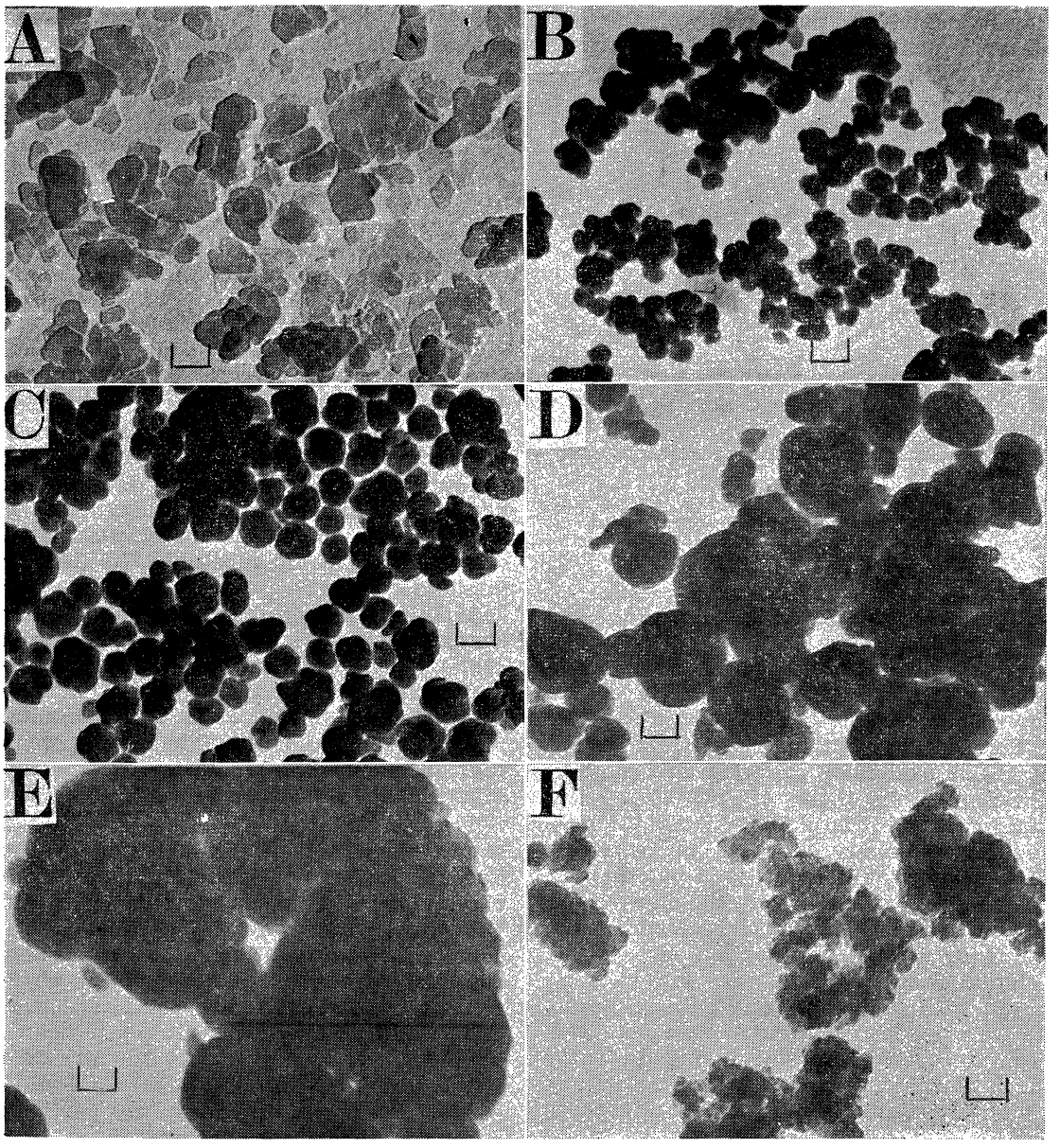


Fig. 6. Electron micrographs of ground Kibushi-clay. The linear dimension on the micrographs represents 0.1 μ.

A, original Kibushi-clay
B, ground 48 hours
C, ground 96 hours
D, ground 192 hours
E, ground 384 hours
F, 144-hour-ground Kibushi-clay treated with 0.1 N HCl after 0.1 N NaOH.

the reaggregation of such particles are plotted against the grinding time, the results are as shown in Fig. 7.

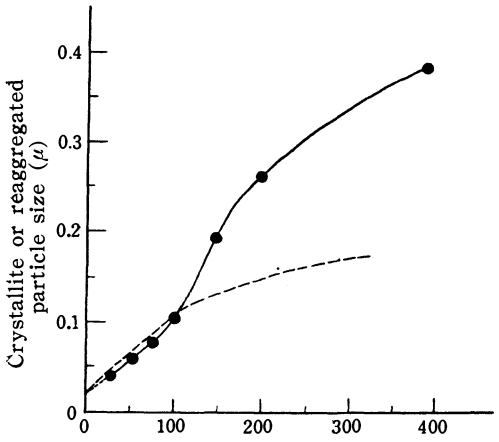


Fig. 7. Crystallite or reaggregated particle size of ground Kibushi-clay plotted against the time of grinding.
------: The change in the grinding process of Mesa Alta kaolinite.

In this figure, the curve showing the change of the crystallite or reaggregated particle with the grinding time in Alta kaolinite is drawn for reference. The curve, if extrapolated to zero time, indicates the value of about 200 Å. This value is the same as that in the case of kaolinite. As in kaolinite, in Kibushi-clay, too, the crystallites produced in the early stage of grinding seem to have about 200 Å in size. It is supposed that the time when the irregular growth begins is related to the degree of crystallinity of the original sample. This tendency is found also in halloysite. That is, the lower the crystallinity, the faster the irregular growth.

Summary

The effects of several-hundred-hour mechanical-mortar dry grinding of Kibushi-clay which is a kaolin mineral of fireclay type were studied by X-ray diffraction, thermal, electron microscopic and other methods and compared with those of kaolinite. It has been found that the process of a production of a non-crystalline substance attended with a disordering of a crystalline part and the process of a reaggregation are present in the dry grinding of Kibushi-clay as in kaolinite. Finally, Kibushi-clay changes into an amorphous substance as the result of dry grinding. In a certain stage of grinding, a zeolitic structure is formed. As the grinding progresses, the particle size increases owing to reaggregation. When an amorphous substance like silica-alumina mixed gel is produced, the particle size grows irregularly. In Kibushi-clay, the time it takes to become amorphous by dry grinding is shorter than in the case of kaolinite. Consequently, the effects of dry grinding of kaolinite and kaolin mineral of fireclay type depend on the structural perfection of unit layers of the original kaolin minerals.

Department of Chemistry
Faculty of Science
The University of Tokyo
Hongo, Tokyo

Effects of Dry Grinding on Kaolin Minerals. III. Halloysite

By Hiroshi TAKAHASHI

(Received September 29, 1958)

In the preceding parts of this series, the effects of dry grinding of kaolinite and Kibushi-clay have been studied[1]. From the results, a common mechanism in the structural change of kaolinite and Kibushi-clay by dry grinding was presented. That is, in the process of dry grinding, the separation into unit crystallites from the original crystal, the reaggregation of crystallites, the production of a non-crystalline material, the disordering of the crystallites, the reaggregation of crystallites and a non-crystalline material, the formation of a zeolitic structure in a certain period of grinding and the change into an amorphous substance such as silica-alumina mixed gel are observable. The effects of grinding of halloysite have been little studied so far. In this paper, the effects of dry grinding of halloysite are studied with respect to the degree of crystallinity of kaolin minerals with various degrees of crystallinity.

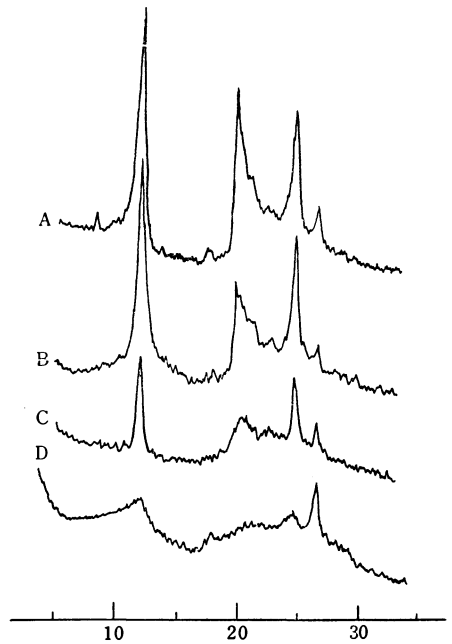
Experimental

The following samples were used in this study: Halloyste from Spruce Pine, N. C., U. S. A.; Halloysite from Bedford, Ind., U. S. A.; Halloysite from Tintic, Utah, U. S. A. These samples are the API Standard Clay Minerals and their structural characteristics are discussed in the previous paper[2]. As shown in the paper, it is considered that the structural differences among varieties halloysite chiefly depend on the internal variations rather than their stacking variation. Of halloysite, Spruce Pine halloysite has the highest degree of crystallinity. This was ascertained by the electron diffraction method[3]. Bedford halloysite has a lower degree of crystallinity than Spruce Pine halloysite. Tintic hallosite has the lowest degree of crystallinity of all the kinds of halloysite used in this study. Both Bedford and Tintic halloysite are partially hydrated halloysites.

The grinding conditions were the same as for kaolinite described in part I of this series. Experimental specimens were examined by X-ray diffraction, thermal, electron microscopic and other methods. The experimental conditions were the same as for kaolinite. The base exchange capacity and the density in various stages of dry grinding were measured after the specimens had been dried at 110°C in order to avoid the effect of the inter-layer or adsorbed water.

Results and Discussion

X-Ray Diffraction Studies.—X-ray diffractometer traces in the processes of grinding of halloysite are shown in Fig. 1. Figs. 1-a, -b and -c show the X-ray diffractometer traces of Spruce Pine halloysite, Bedford halloysite and Tintic halloysite, respectively. In Tables I-a, -b and -c, the interplanar spacing and the relative intensity measured from their X-ray diagrams are given.



Degrees 2θ Cu K_α

Fig. 1-a X-ray diffractometer traces of ground halloysite (Spruce Pine, N. C.).
A, original halloysite
B, ground 48 hours
C, ground 96 hours
D, ground 192 hours

1) H. Tahakashi, This Bulletin, **32**, 235, 245 (1959).
2) H. Takahashi, ibid. **31**, 275 (1958).
3) G. Honjo and K. Mihama, *Acta Cryst.*, **7**, 511 (1954).

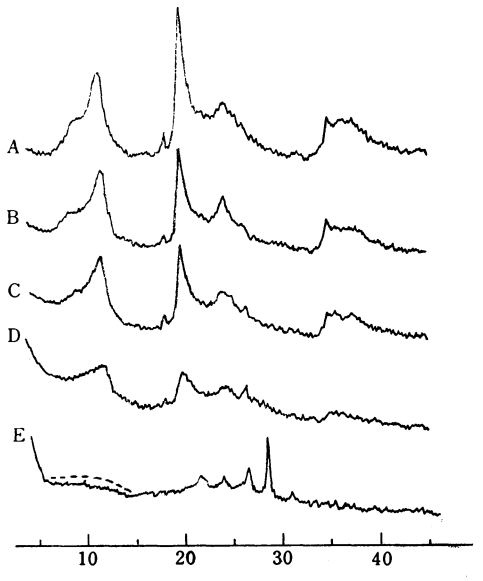


Fig. 1-b. X-ray diffractometer traces of ground halloysite (Bedford, Ind.).

A, original halloysite
B, ground 48 hours
C, ground 96 hours
D, ground 144 hours
E, ground 312 hours

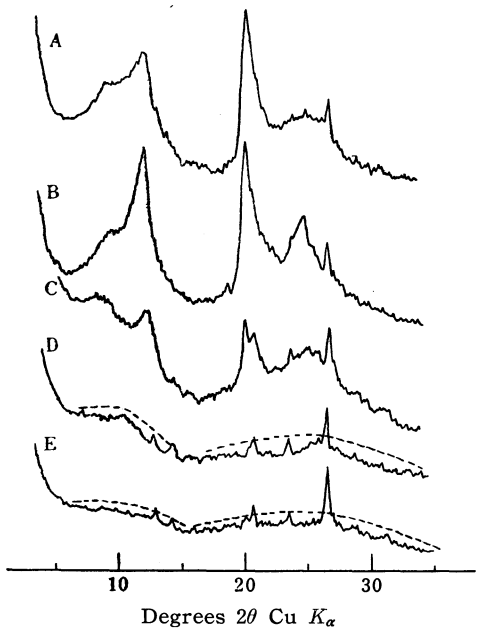


Fig. 1-c. X-ray diffractometer traces of ground halloysite (Tintic, Utah).

A, original halloysite
B, ground 48 hours
B, ground 96 hours
D, ground 144 hours
E, ground 240 hours

When halloysite is ground, it gradually assumes a more and more disordered structure; that is, the background increases as the intensity of the reflection weakens. In the X-ray diagrams of the original samples of Bedford and Tintic halloysite which are partially hydrated halloysites, the reflection of about 10 Å spacing is present in both original samples. It is known that this reflection indicates the presence of a hydrated halloysite in these samples. This reflection is observable even in the 96-hour-ground specimen of Tintic halloysite and the 144-hour-ground specimen of Bedford halloysite. This fact indicates that the loss of the inter-layer water due to the heat caused by dry grinding does not occur in these specimens. This leads to the theory that the dry grinding does not produce so much local heat. The intensity of all the reflections apparent in the X-ray diagrams decreases as the grinding progresses. The manner of the disappearance of the reflections depends on the degree of crystallinity of original halloysite samples. In the X-ray diagram of the 144-hour-ground specimen of Tintic halloysite which has the lowest degree of crystallinity in the original state, 02,11 bands are not distinct and very diffuse. Whereas, in the X-ray diagram of the 144-hour-ground specimen of Bedford halloysite, the reflection is considerably distinct though its intensity lowers. As the grinding progresses further, the X-ray diagram of this specimen comes to correspond to the amorphous pattern. In Spruce Pine halloysite, which has the highest degree of crystallinity of all the kinds of halloysite, all reflections in the X-ray diagram are considerably distinct even with a 192-hour-ground specimen.

In the early stage of grinding of all halloysite, the lines of basal reflections become sharp as compared with those of the original samples. This tendency is observable also in the case of kaolinite. The structure of halloysite is pseudo-hexagonal in symmetry, and is nearly two-dimensional[4]. The structure of halloysite is not precisely two-dimensional; however, if it is supposed that the theory of the reflection of the two-dimensional lattice is applicable to the structure of halloysite, the crystallite dimension in the process of grinding can be calculated from the breadths of reflection lines[5]. It is

4) G. W. Brindley and K. Robinson, *Min. Mag.*, **28**, 393 (1948).
5) B. E. Warren, *Phys. Rev.*, **59**, 693 (1941).

TABLE I-a
POWDER DATA OF GROUND HALLOYSITE (SPRUCE PINE, N. C.) IN ANGSTROM UNITS

Brindley and Robinson			Original Halloysite		Ground 48 hr.		Ground 96 hr.		Ground 192 hr.	
d	*I*	00*l* or *hk*	*d*	*I*	*d*	*I*	*d*	*I*	*d*	*I*
7.2~7.5	8	001	7.15	VS	7.15	VS	7.20	S	7.3	M
4.422	10+	02, 11	4.44	S	4.44	S	4.43	M br	4.3	M vbr
3.578	8	002	3.57	S	3.58	S	3.59	M	3.5	W br
2.559	7	13, 20	2.56	M	2.57	M	2.57	W br	2.57	W vbr
			2.53	W						
(2.48)			2.49	M	2.49	W	2.49	VW		
2.403	2	003	2.38	W	2.39	W	2.36	VW		
(2.33)	2		2.33	M	2.33	W	2.30	VW		
2.218	1	04, 22	2.29	W						
			1.997	MW	1.994	W				
1.800	1	004								
1.678	5	31, 15, 24	1.670	MW	1.67	W br	1.68	VW br		
1.481	8	06, 33	1.488	M	1.49	MW br	1.49	VW br		

Key to Abbreviation: VS: very strong, S: strong, M: medium, MW: medium weak, W: weak, VW: very weak, br: broad, vbr: very broad.

TABLE I-b
POWDER DATA OF GROUND HALLOYSITE (BEDFORD, IND.) IN ANGSTROM UNITS

Original halloysite		Ground 48 hr.		Ground 96 hr.		Ground 144 hr.		Ground 312 hr.	
d	*I*	*d*	*I*	*d*	*I*	*d*	*I*	*d*	*I*
9.6	W br	9.8	W br	9.8	VW br			8.5	VW vbr
7.3	S	7.5	S	7.5	S br	7.5	M vbr		
4.45	VS	4.45	S	4.45	S	4.44	M		
3.63	M br	3.67	M	3.69	M	3.65	W br	4.0	W vbr
2.57	M br	2.57	M br	2.57	M br	2.56	W vbr		
1.80	W								
1.68	M br	1.68	W br						
1.48	M br	1.48	W br	1.48	W br				

Key to Abbreviation: VS: very strong, S: strong, M: medium, W: weak, VW: very weak, br: broad, vbr: very broad.

TABLE I-c
POWDER DATA OF GROUND HALLOYSITE (TINTIC, UTAH) IN ANGSTROM UNITS

Original halloysite		Ground 48 hr.		Ground 96 hr.		Ground 144 hr.		Ground 240 hr.	
d	*I*	*d*	*I*	*d*	*I*	*d*	*I*	*d*	*I*
10.1	M	10.0	M	10.0	M br	8.2	M vbr	8.1	W vbr
7.37	S	7.36	S	7.3	M br				
4.44	VS	4.44	VS	4.44	M				
3.66	M br	3.61	M	3.54	M br	3.6	M vbr	3.5	M vbr
2.56	M br	2.56	M br	2.56	W br				
1.68	M br	1.68	W br						
1.48	M br	1.48	M br	1.48	W br				

Key to Abbreviation: VS: very strong, S: strong, M: medium, W: weak, br: broad, vbr: very broad.

known that the breadth of a reflection line is determined by two factors, that is, the particle size and the distortion of lattice. These factors must be separated for the precise measurement of crystallite dimension[6]. However, the broadening of the line breadth is due to a reduction in crystallite size or a remarkable distortion of lattice. These two elements which correspond to the broadening in the line breadth are related to a lowering in the degree of crystallinity. Therefore, the crystallite dimensions obtained from the line breadth seem to be terms which re-

6) C. R. Houska and B. E. Warren, *J. Appl. Phys.*, **25**, 1503 (1954).

present the relative degree of crystallinity of the specimens rather than the real crystallite sizes. To calculate the crystallite dimension from the line breadth, Bragg's equation was used for the dimension along the c-axis (L_c) from 001 reflection[7], and Warren's equation was used for the dimension of the broadening, parallel to the layer plane of crystallite (L_a) from 02,11 band[5]. Fig. 2 shows the changes of the crystallite dimensions with the grinding time.

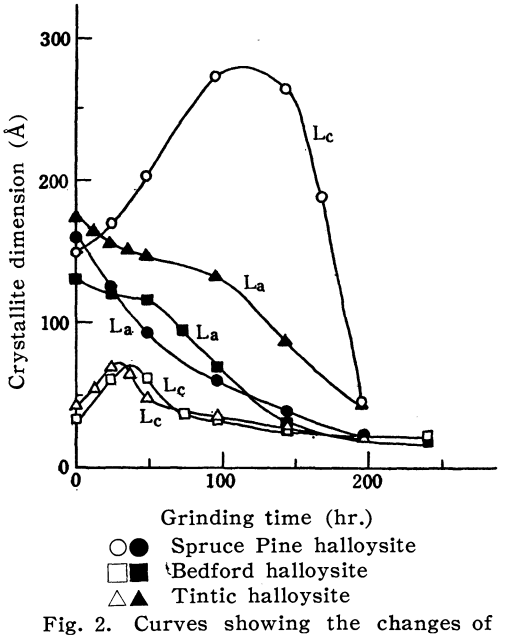


Fig. 2. Curves showing the changes of crystallite dimensions with the time of grinding.

From the curve shown in this figure, it is observable that the breadth of the basal reflection becomes sharper in the early stage of grinding. Of these curves, some features are observable; that is, the maximum point on L_c-dimension curve of Spruce Pine halloysite with the highest degree of crystallinity is apparent when ground for a considerably long time. For the crystallite dimension of Spruce Pine halloysite along a-axis (L_a), it decreases quickly with the grinding, whereas, it does not change in Bedford halloysite and Tintic halloysite up to some extent of grinding. When the grinding passes this stage, the L_a-dimensions of Bedford halloysite and Tintic halloysite decrease as that of Spruce Pine halloysite does. This fact means that Bedford halloysite and Tintic halloysite are more resistant to dry grinding than Spruce Pine halloysite, presumably because of the lubricating action of the water layers between the kaolin layers. This resistant action of the interlayer water is also found in vermiculite[8]. The quick decrease in the L_a-dimension is correlated to the fracturing of the kaolin layer.

The increase of the background in the X-ray diagram of halloysite is similar to those of kaolinite or Kibushi-clay, and is correlated to the production of a non-crystalline material. It is considered that the structure of non-crystalline materials produced by dry grinding of halloysite with lower crystallinity is considerably disordered and is similar to a gel-like structure.

For some ground specimens, the alkali-acid treatment noted in the case of kaolinite was made to ascertain the disordering of the crystallite. Throughout all these specimens, the same tendency is observable as that of kaolinite. The 240-

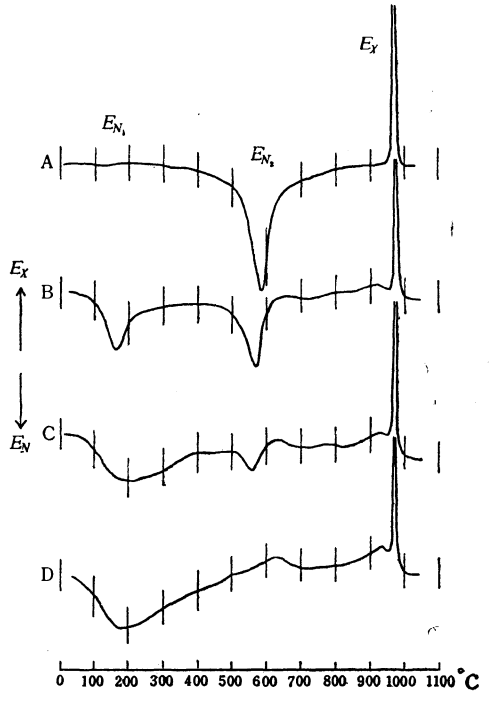


Fig. 3-a. Differential thermal analysis curves of ground halloysite (Spruce Pine, N. C.).
A, original halloysite
B, ground 48 hours
C, ground 96 hours
D, ground 192 hours

7) W. L. Bragg, "The Crystalline State", Vol. I, 189 (1933).

8) R. C. Mackenzie and A. A. Milne, *Clay Min. Bull.*, 2, 57 (1953).

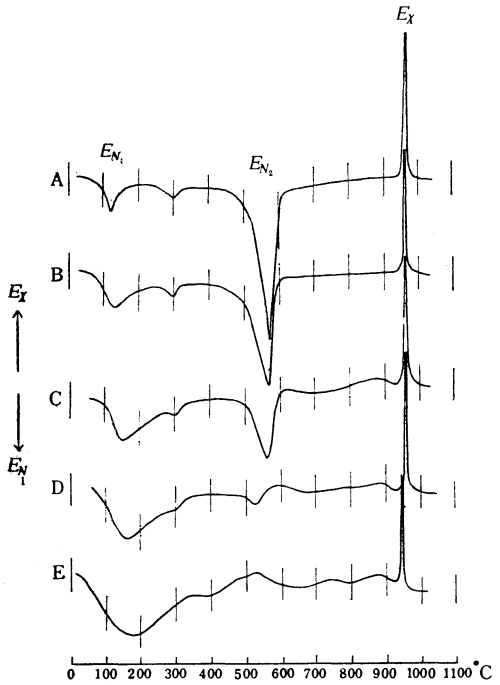


Fig. 3-b. Differential thermal analysis curves of ground halloysite (Bedford, Ind.).
A, original halloysite
B, ground 48 hours
C, ground 96 hours
D, ground 144 hours
E, ground 312 hours

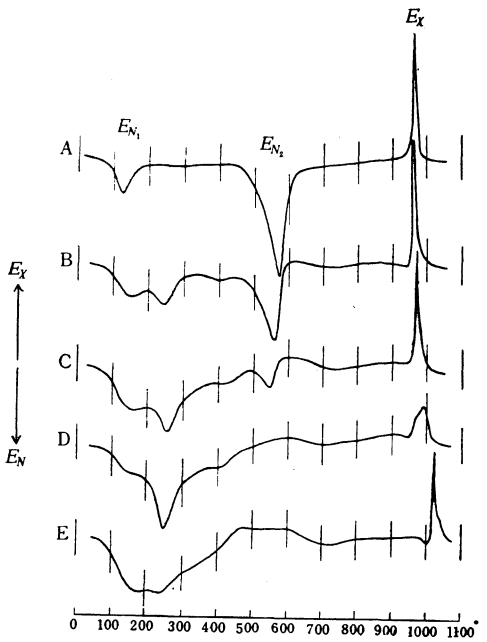


Fig. 3-c. Differential thermal analysis curves of ground halloysite (Tintic, Utah).
A, original halloysite
B, ground 48 hours
C, ground 96 hours
D, ground 144 hours
E, ground 240 hours

TABLE II-a
THERMAL DATA OF GROUND HALLOYSITE (SPRUCE PINE, N. C.).
(ALL TEMPERATURES ARE DEGREES CENTIGRADE)

Grinding time (hr.)	E_{n1} Temp. at peak	E_{n1} Height of peak	E_{n1} Area of peak	E_{n2} Temp. at peak	E_{n2} Height of peak	E_{n2} Area of peak	E_x Temp. at peak	E_x Height of peak	E_x Area of peak	E_x Breadth (half value of breadth)
0	125°C	1	70	583°C	17	1380	973°C	45	220	4.0°
48	—130—	5	640	568	10	560	972	43	220	3.8
96	—160—	6	820	563	5	480	971	48	220	3.7
144	—190—	8	960	555	2	310	971	53	230	3.7
192	—190—	9	1940	—	—	—	970	58	230	3.1

TABLE II-b
THERMAL DATA OF GROUND HALLOYSITE (BEDFORD, IND.).
(ALL TEMPERATURES ARE DEGREES CFNTIGRADE)

Grinding time (hr.)	E_{n1} Temp. at peak	E_{n1} Height of peak	E_{n1} Area of peak	E_{n2} Temp. at peak	E_{n2} Height of peak	E_{n2} Area of peak	E_x Temp. at peak	E_x Height of peak	E_x Area of peak	E_x Breadth (half value of breadth)
0	125°C	2	110	574°C	16	720	970°C	34	170	4.5°
48	—128—	4	410	569	15	590	968	34	180	4.5
96	—150—	6	630	566	9	450	968	43	200	3.3
144	—160—	6	790	535	2	60	967	50	200	2.7
312	—190—	6	1090	—	—	—	951	68	200	3.0

TABLE II-c
THERMAL DATA OF GROUND HALLOYSITE (TINTIC, UTAH).
(ALL TEMPERATURES ARE DEGREES CENTIGRADE)

Grinding time (hr.)	E_{n1}			E_{n2}			E_x			
	Temp. at peak	Height of peak	Area of peak	Temp. at peak	Height of peak	Area of peak	Temp. at peak	Height of peak	Area of peak	Breadth (half value of breadth)
0	130°C	4	170	571°C	12	680	969°C	16	170	9.4°
48	—155— —240—	5 6	350	562	10	480	966	30	200	3.6
96	—165— —260—	5 9	790	548	3	100	967	19	150	7.5
144	—250—	11	1120	—	—	—	994	5	140	39.2
240	—170— —260—	8	1340	—	—	—	1023	15	130	7.3

hour-ground specimen of Tintic halloysite which has an amorphous pattern in its X-ray diagram dissolved completely through the alkali-acid treatment and leaves only the impurities such as quartz, felspars and others. When the X-ray diagram of the ground specimen of halloysite is compared with those of kaolinite and Kibushi-clay, it is clear that the dry grinding is not so effective on kaolinite and Spruce Pine halloysite in the structural change, but is most effective on Kibushi-clay and Tintic halloysite. From the X-ray data, it is concluded that the effects of dry grinding of kaolin minerals in the structural change depend on the perfectness of kaolin unit layers, that is, the internal degree of crystallinity.

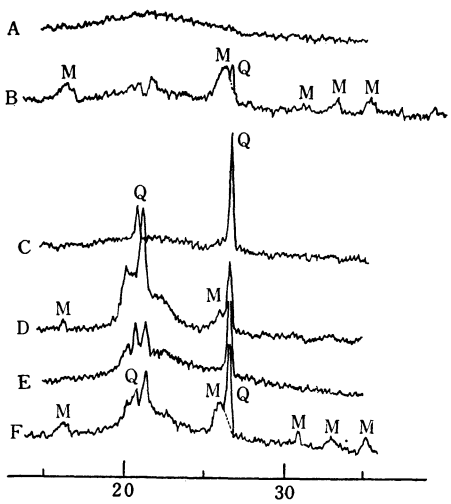
Differential Thermal Analysis. — Differential thermal analysis curves and data of the grinding process of halloysite are shown in Fig. 3 and Table II.

The first endothermic reaction (E_{n1}) associated with the loss of the inter-layer or adsorbed water, is not present in the original sample of Spruce Pine halloysite, but is present in the original samples of Bedford and Tintic halloysite. It is natural that this reaction is apparent in the original sample of Bedford and Tintic halloysite, because they are partially hydrated halloysite. As the grinding progresses, this reaction appears and its height and area increase. These facts mean that the substance produced by dry grinding adsorbs water vapor and its quantity increases as the grinding progresses. The peak temperature of this reaction gradually rises. This leads to the water adsorbed by the ground substance being combined more strongly as the grinding progresses. In the original sample of Bedford halloysite, a weak endothermic reaction is apparent at about 300°C, probably due to the presence of gibbsite as impurity. This reaction is wholy apparent in the process of grinding. The rates of change in the first endothermic reaction are the same as those in the cases of Spruce Pine and Bedford halloysite. But, in the grinding process of Tintic halloysite, this reaction is slightly different from those of Bedford and Spruce Pine halloysite. On the differential thermal analysis curves of the ground specimens of Tintic halloysite after 48 hours of grinding, the second maximum is apparent in this reaction, and the height and area increase, and the peak temperature gradually rises. In the 240-hour-ground specimen of Tintic halloysite, this reaction increases more, and the second maximum becomes indistinct.

In the second endothermic reaction (E_{n2}) associated with the loss of the lattice water, it is observable that the features of this reaction are similar to those of kaolinite. That is, a lowering in the peak temperature, and a reduction in the peak height and area are observable. When the grinding progresses for a long time, in such specimens as the 144-hour-ground specimen of Tintic halloysite, the 162-hour-ground specimen of Bedford halloysite and the 192-hour-ground specimen of Spruce Pine halloysite, this reaction is unobservable. This fact indicates that the kaolin structure finally disintegrates due to dry grinding. The grinding time in which this reaction disappears is shorter as the crystallinity of the original sample is lower.

In the exothermic reaction (E_n) are found some interesting phenomena. The exothermic reactions of ground specimens of Bedford halloysite and Spruce Pine halloysite are similar to that of kaolinite. The peak temperatures tend to fall very slightly, and in the specimens ground for a long period, the peak temperature falls

remarkably. Except for the 312-hour-ground specimen of Bedford halloysite, the peak height and area of the exothermic reaction increase and the breadth of peak decreases. The exothermic reaction behaves the same as in the case of kaolinite. But, the exothermic reaction of Tintic halloysite behaves very differently from that of kaolinite and the other halloysite. At first the peak temperature tends to be somewhat low, but as the grinding progresses, the temperature rises rapidly. The peak height increases at first, but soon reduces remarkably. The peak height, as the temperature becomes higher, increases again. The peak breadth also becomes narrower at first, but soon increases and then decreases again. To determine whether there is a difference between their exothermic reactions, X-ray diagrams were taken of several specimens just before and after the exothermic reactions on the differential thermal analysis curve. These traces are shown in Fig. 4. It is indicated that as the grinding progresses, the growth of mullite crystal becomes remarkable, but the presence of mullite is unobservable just before the exothermic reaction.



Degrees 2θ Cu K_α

M: Mullite Q: Quartz

Fig. 4. X-ray diffractometer traces of ground halloysite obtained just before or after the final exothermic reaction (E_x) on the differential thermal analysis curve.

A, original Bedford halloysite just after E_x

B, 312-hour-ground Bedford halloysite just after E_x

C, original Tintic halloysite just after E_x

D, 144-hour-ground Tintic halloysite just after E_x

E, 240-hour-ground Tintic halloysite just before E_x

F, 240-hour-ground Tintic halloysite just after E_x

This tendency was also found in the process of grinding of kaolinite. From this fact, it is certain that the exothermic reaction is attributed to the mullite nucleation in halloysite[9]. It is difficult to draw a conclusion from the character of the exothermic reaction as to the grinding effects of halloysite used in the experiment, but it may be interpreted as follows. When the crystallinity of the halloysite is at a considerably low stage, the non-crystalline material produced by dry grinding has a completely amorphous structure, whereas, when the halloysite with a higher degree of crystallinity is ground, the non-crystalline substance produced by grinding has a structure which is somewhat related to that of the original halloysite; that is, it is not a perfectly amorphous substance. This substance is hard to change into a perfectly amorphous substance. The tranformation of kaolin mineral into mullite is closely related to the original structure. In the case of Tintic halloysite, however, the original structure completely disintegrates by dry grinding. The transformation to mullite from kaolin mineral requires much more energy than that of kaolinite, Spruce Pine halloysite and Bedford halloysite. It is considered that the reaction produces a higher temperature. In kaolinite, Spruce Pine and Bedford halloysite, the non-crystalline substance produced by dry grinding may be an allophanic substance rather than gel-like. In all ground specimens of halloysite, the weak endothermic reaction immediately before the exothermic reaction becomes distinct as the grinding progresses. This fact was also found in kaolinite and Kibushi-clay as discussed above. In the transformation of kaolin into mullite, there are two steps of the structural change. The first step is the nucleation of mullite, and the second step is the crystal growth of mullite nuclei. The dry grinding accelerates the reaction of the second step, that is, the crystal growth of mullite nuclei.

Base Exchange Capacity and Density.— In Fig. 5 are shown the changes of the

9) R. C. Mackenzie, "Differential Thermal Investigation of Clays", Mineralogical Society (London), (1957), p. 108.

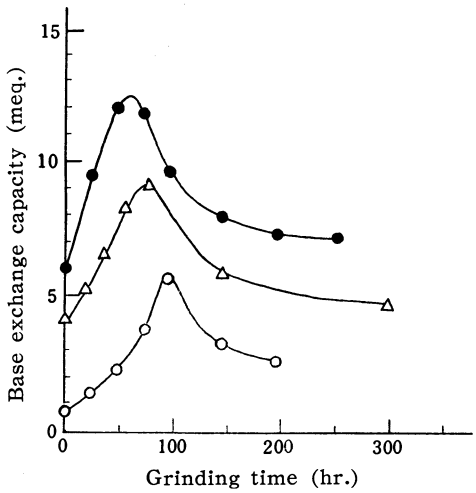


Fig. 5. Curves showing the changes of base exchange capacity with the time of grinding.

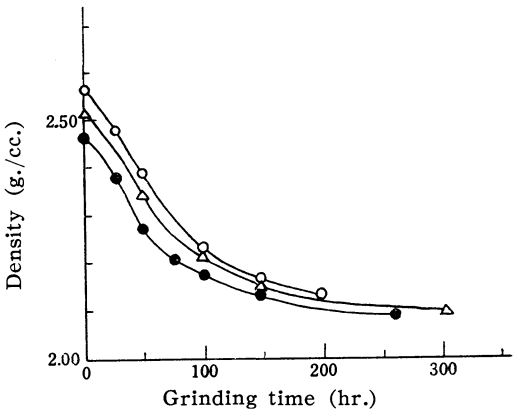


Fig. 6. Curves showing the changes of density with the time of grinding.

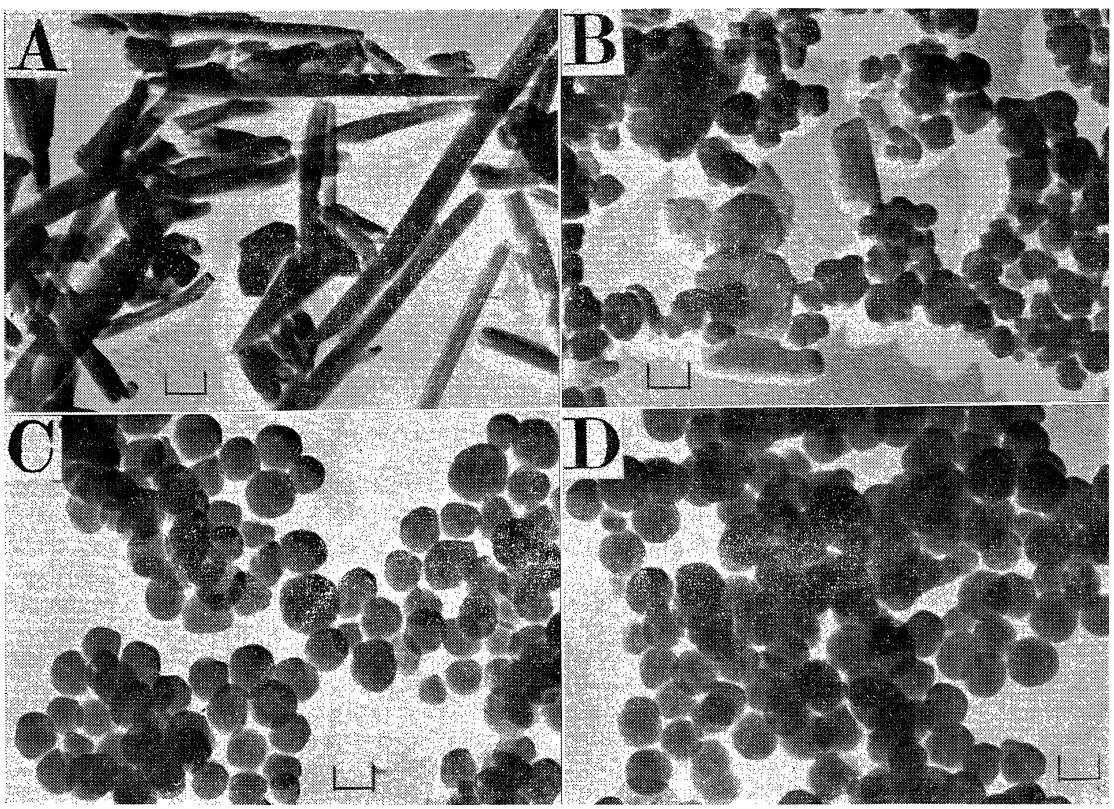


Fig. 7-a. Electron micrographs of ground halloysite (Spruce Pine, N. C.). The linear dimension on the micrographs represents 0.1 μ.

A, original halloysite
B, ground 48 hours
C, ground 96 hours
D, ground 192 hours

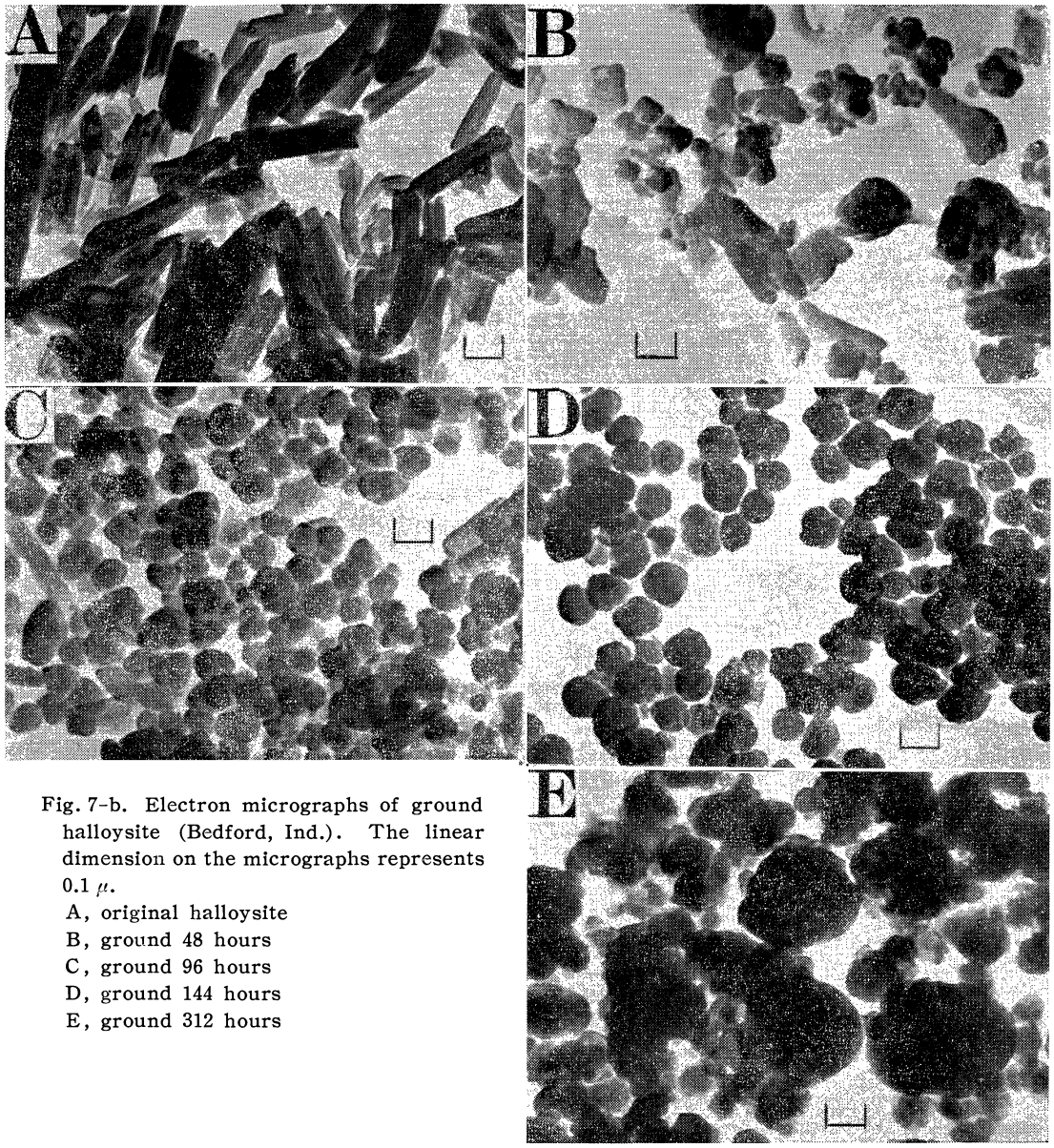


Fig. 7-b. Electron micrographs of ground halloysite (Bedford, Ind.). The linear dimension on the micrographs represents 0.1 μ.
A, original halloysite
B, ground 48 hours
C, ground 96 hours
D, ground 144 hours
E, ground 312 hours

base exchange capacity with the grinding time.

As the grinding progresses, the base exchange capacity at first increases. After reaching a maximum value, it gradually decreases until it attains the constant value. The maximum value and the constant value vary according to the order of the original sample. The lower the crystallinity of the original sample, the shorter the time in which the base exchange capacity attains its maximum point. The rates of change of base exchange capacity against the grinding time are similar to those of kaolinite. As in kaolinite, these results also support the thought of Laws and Page for the explanation of the change on the base exchange capacity through dry grinding[10].

In Fig. 6 are shown the changes of the density with the grinding time.

As the grinding progresses, the density sharply decreases, but after reaching a certain point, it slowly attains a constant value. This constant value is nearly equal to the value of a silica-alumina mixed gel or allophane. These facts mean that halloysite changes into a non-crystalline substance by dry grinding.

10) W. D. Laws and J. B. Page, *Soil Sci.*, 62, 319 (1946).

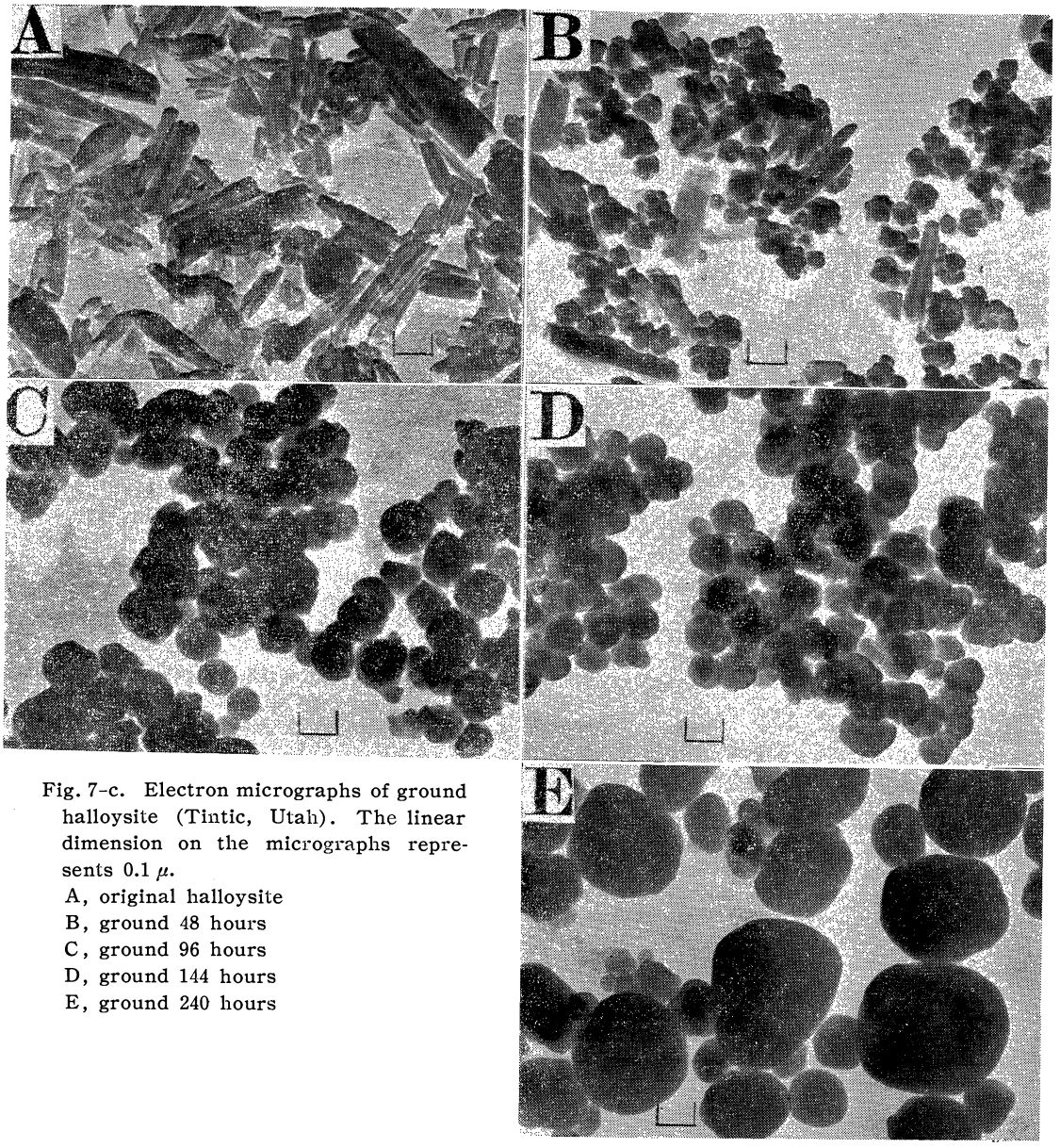


Fig. 7-c. Electron micrographs of ground halloysite (Tintic, Utah). The linear dimension on the micrographs represents 0.1 μ.
A, original halloysite
B, ground 48 hours
C, ground 96 hours
D, ground 144 hours
E, ground 240 hours

The point of the bend in the density curve and the maximum point in the base exchange curve are at nearly identical positions. This phenomenon was also seen in kaolinite. This stage seems to correspond to the point at which the kaolin structure changes to zeolitic.

Electron Microscopic Studies.—Electron micrographs of halloysite in the process of dry grinding are shown in Fig. 7. Figs. 7-a, -b and -c show those of Spruce Pine halloysite, Bedford halloysite and Tintic halloysite, respectively.

The particles of the original halloysite samples have a tubular shape. It is observable that in the early stage of dry grinding, fine crystallite is produced from the original crystal. The shapes of these crystallites are platty with a considerably sharp edge though the shape of the original halloysite is tabular. As the grinding progresses, the fine crystallites reaggregate, and raggregated particles become spherical and the particle size increases, and then the reaggregated particles slowly change into uniformly spherical particles. As the grinding progresses further, for example in the 240-hour-ground specimen of Tintic halloysite or in the 312-hour-ground specimen of Bedford halloysite,

the remarkable and irregular growth of particles is observable. In the light of X-ray and thermal data, the irregular growth of reaggregated particles corresponds to the fact that an amorphous substance is produced by dry grinding.

If the mean size of the fine particles which are produced through dry grinding and the particles which are produced by the reaggregation of such fine particles are plotted against the grinding time, the results are as shown in Fig. 8.

The curve, if extrapolated to time zero, indicates the value of about 200 Å in all kinds of halloysite, and this value is the same as that in the case of kaolinite. It seems that the crystallites which separate from the original crystal during the early stage of grinding are about 200 Å in size. As shown on these curves, the time in which the reaggregated particles begin to grow irregularly corresponds to the degree of crystallinity of the original samples. The irregular growth of the reaggregated particles is found also in Kibushi-clay. It is considered that the

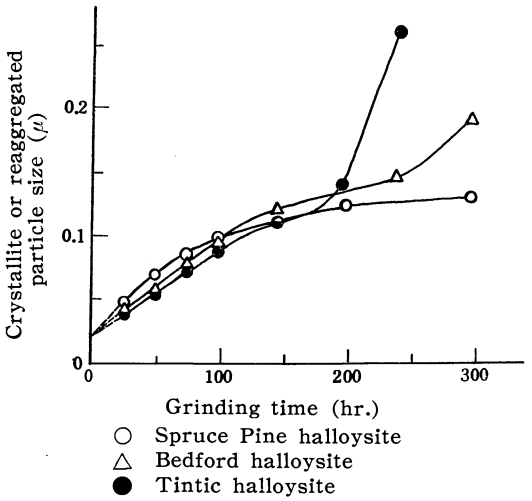


Fig. 8. Crystallite or reaggregated particle size of ground halloysite plotted against the time of grinding.

irregular growth of such particles indicates the change into a perfectly amorphous substance from a non-crystalline substance produced by dry grinding.

Mechanism of Change in Halloysite Structure due to Dry Grinding. — When halloysite is ground, halloysite crystals cleave and fracture and then split into fine crystals which are considered unit crystallites. These crystallites are very similar to those in case of kaolinite in shape and size. Groups of several such fine crystallites promptly reaggregate. The reaggregated crystallites change partially or thoroughly into a non-crystalline material. These non-crystalline substances reaggregate with the crystallites. As the grinding progresses, the crystalline part of the reaggregated particle decreases and the size of the reaggregated particle increases gradually. In a certain stage of grinding, a zeolitic structure is formed. The reaggregated particles which have a zeolitic structure become uniformly spherical. This period in grinding corresponds to the maximum point on the base exchange capacity curve and the inflection point on the density curve. The structure, with the progress of grinding, changes finally to the perfectly amorphous structure as silica-alumina mixed gel and the particle size grows irregularly.

The process of the structural change by dry grinding is the same as in the cases of all kinds of halloysite. The only difference is that Spruce Pine halloysite is less easily subject to the effect of the structural change than Tintic halloysite. This means that the effect of dry grinding of halloysite depends on the structural perfectness of the original halloysite. Generally, the effects of dry grinding on kaolin minerals are related to the internal degree of crystallinity of the original kaolin minerals.

Summary

The effects of several-hundred-hour mechanical-mortar dry grinding of halloysite were studied by X-ray diffraction, differential thermal, electron microscopic and other methods and they were compared with those of kaolinite and Kibushi-clay. It has been found that there are two sorts of structural change caused by dry gringing in halloysite as in the case of kaolinite. One is the production of a non-crystalline material attended with disordering of crystallites, and the other is the process of reaggregation. In a certain stage of grinding, the reaggregates come to have a zeolitic structure. This stage of grinding corresponds to the maximum point on the base exchange capacity curve and the inflection point on the density curve. The particle which has a zeolitic structure is uniformly spherical. As the grinding progresses further, halloysite changes into an amorphous substance, and the particle size increases irregularly. In consequence, it

was found that the effects of dry grinding on kaolin minerals depend strikingly on the structural perfectness of unit layers of the original kaolin minerals, that is, the internal degree of crystallinity.

The author wishes to express his hearty thanks to Professor H. Akamatu for his continuous advice and encouragement. Thanks are due to Professor T. Sudo of the Tokyo University of Education and Professor R. E. Grim of the University of Illinois for their valuable suggestions and discussions.

Department of Chemistry
Faculty of Science
The University of Tokyo
Hongo, Tokyo

The Crystal Structure of trans-Dibromo-bisethylenediamine-cobalt(III) Bromide Hydrobromide Dihydrate

By Shun'ichiro Ooi, Yoshimichi Komiyama, Yoshihiko Saito and Hisao Kuroya

(Received September 13, 1958)

The crystal structure of the ethylenediamine-"praseo"-chloride, *trans*-$[Co\ en_2Cl_2]Cl\cdot HCl\cdot 2H_2O$, was determined before by Nakahara and two of us[1]. An attempt has been made now to investigate the crystal structure of the bromine-analogue, namely, the *trans*-dibromo-bisethylenediamine cobalt(III) bromide hydrobromide dihydrate, *trans*-$[Co\ en_2Br_2]Br\cdot HBr\cdot 2H_2O$. This compound has almost the same properties, physical and chemical, as the corresponding chlorine-complex, and, therefore, may be expected to be isotype with the latter. However, the analysis was carried out with caution in consideration of the fact that the configuration of the chloro-dinitro-triammine-cobalt(III), $[Co(NH_3)_3(NO_2)_2Cl]$, is quite different from that of the apparently analogous bromo-compound, $[Co(NH_3)_3(NO_2)_2Br]$[2),3)].

Experimental

The crystals are well-formed dark green tablets, showing predominant (100) faces. This habit is the same as that of $[Co\ en_2Cl_2]Cl\cdot HCl\cdot 2H_2O$. They are monoclinic and belong to the monoclinic holohedral class. Crystals show marked dichroism; in polarized light they appear blue when the electric vector is normal to the *b*-axis and yellowish green when this vector is parallel to the *b*-axis. From oscillation and Weissenberg photographs with Fe $K\alpha$ radiation ($\lambda=1.937$ Å) the unit cell dimension is found to be: $a=10.98$, $b=8.18$, $c=9.46$Å, $\beta=113.2°$. The space group determined from extinctions, is $P2_1/c-C_{2h}^5$.

The cell contains two formula units of $[Co\ en_2Br_2]Br\cdot HBr\cdot 2H_2O$ (density calculated 2.28 g.cm^{-3}; found 2.21 g.cm^{-3}) and cobalt atoms must therefore occur on centers of symmetry.

The intensities of reflections ($h0l$), ($hk0$) were estimated by comparison with a standard scale. The exposures were taken with Fe $K\alpha$ radiation, using multiple film technique. After correction for Lorentz and polarization factors, relative F values were obtained. No correction for absorption was made.

Determination of the Structure

The structure determination is based on the analysis of the ($hk0$) and ($h0l$) reflections, which could be carried out in a rather straightforward fashion. Because of the occurrence of the cobalt atoms at symmetry centers, the Patterson functions were simple and comparison of these results with those obtained for $[Co\ en_2Cl_2]Cl\cdot HCl\cdot 2H_2O$ revealed that both structures were isotype. Therefore, the Patterson function could be solved without difficulty, yielding an approximate position not only for bromine atoms but for most of the lighter atoms as well. The signs of all but weak reflections could be derived on the basis of the sets of parameters thus

1) A. Nakahara, Y. Saito and H. Kuroya, This Bulletin, **25**, 331 (1952).
2) Y. Tanito, Y. Saito and H. Kuroya, ibid., **26**, 420 (1953).
3) Y. Komiyama, ibid., **31**, 26 (1958).



Fig. 1. Electron density projected along the *b*-axis. Contours are drawn at 4 e. Å^{-2} intervals and 20 e. A^{-2} for heavy lines of Co and Br peaks. Broken lines show zero electron level.

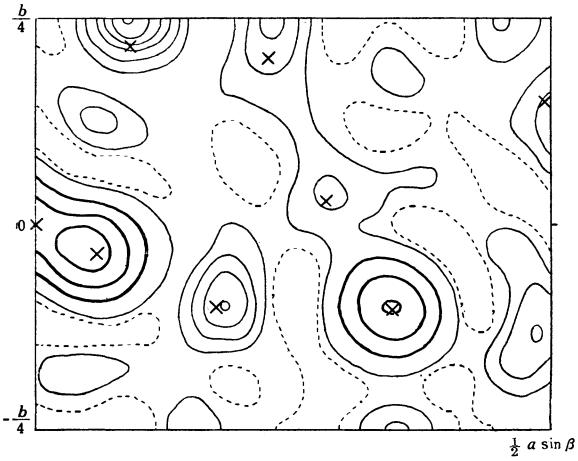


Fig. 2. Electron density projected along the *c*-axis. Contours are drawn in the same manner as Fig. 1.

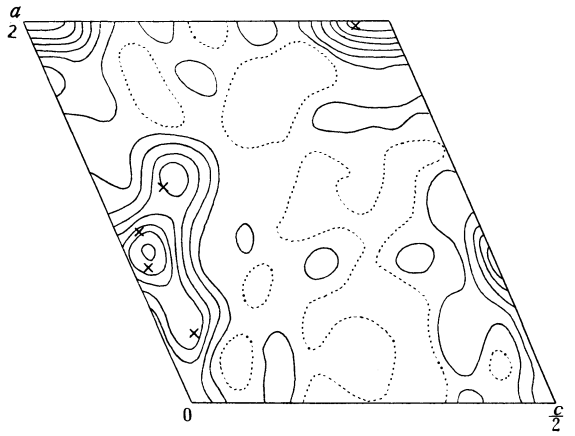


Fig. 3. Residual electron density projected along the *b*-axis, showing the positions of light atoms. Contours are drawn at 2 e. Å^{-2} intervals.

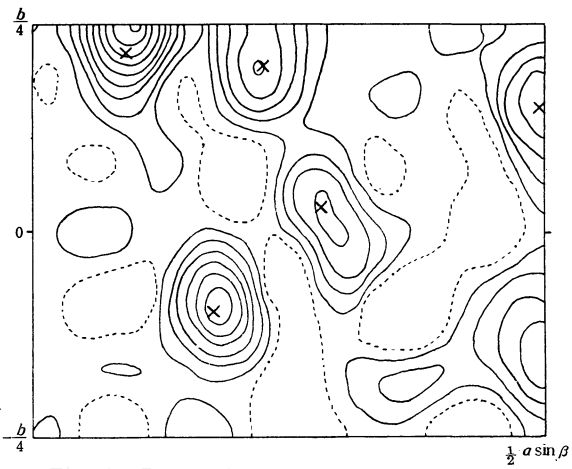


Fig. 4. Residual electron density projected along the *c*-axis, showing the positions of light atoms. Contour lines as in Fig. 3.

deduced. Then the Fourier syntheses of the electron density projected along [001] and [010] were evaluated. In the *c*-axis projection almost every atom was resolved. But it was not the case in the *b*-axis projection. The outlines of the ethylenediamine ligands did not come out clearly, probably due to the diffraction effect of heavy bromine atoms. In order to improve the situation, the contribution of the cobalt and bromine atoms was subtracted from the observed structure factors and trial of computing the residual electron density projections along the *b*-axis was made. (The result is given in Fig. 3).

Fourier refinements were repeated as usual. Final projections shown in Fig. 1—Fig. 4 lead to the structure illustrated in Fig. 5 and Fig. 6. Parameter values are listed in Table I. The parameter of the oxygen atom is less reliable because of poor resolution of the projection. The parameters listed in Table I gave the reliability index $R=\sum||F_o|-|F_c||/\sum|F_c|$ of 0.133 and 0.130 for $(h0l)$ and $(hk0)$ respectively. Calculated and observed structure amplitudes are given in Table II. In the calculation of structure factors,

TABLE I

FINAL ATOMIC COORDINATES

	x/a	*y/b*	*z/c*
Co	0	0	0
Br(1)	0.060	−0.037	0.275
Br(2)	0.344	−0.397	0.269
N(1)	0.092	0.216	0.045
N(2)	0.175	−0.099	0.024
C(1)	0.225	0.201	0.032
C(2)	0.281	0.029	0.091
O	0.494	0.150	0.452

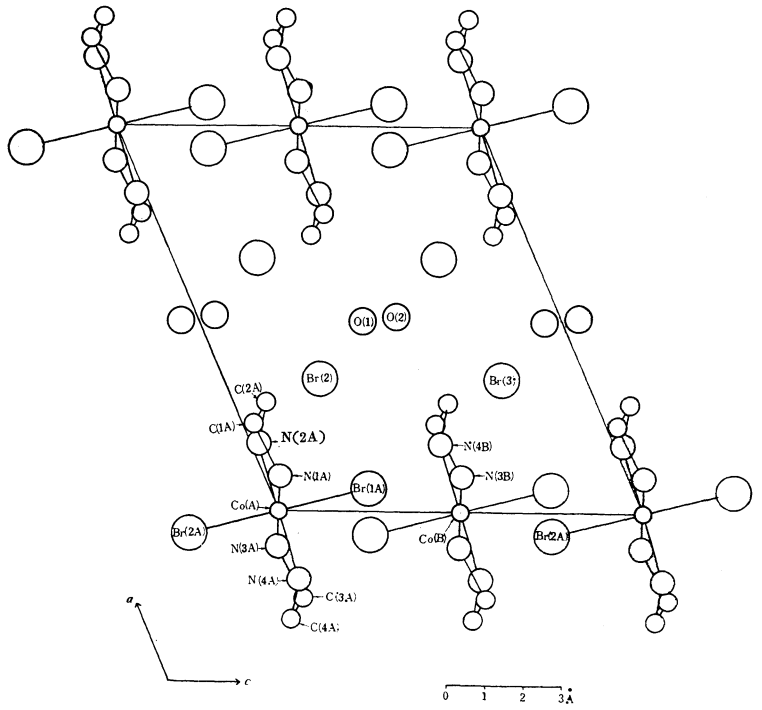


Fig. 5. Projection of the structure upon a plane normal to the *b*-axis.

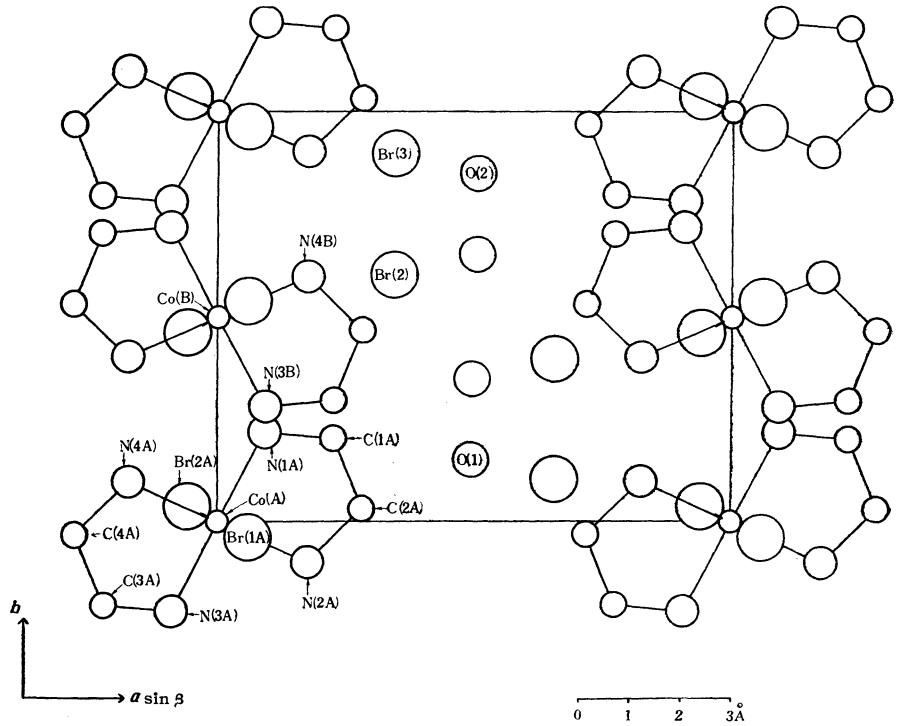


Fig. 6. Projection of the structure upon a plane normal to the *c*-axis.

Table II
Observed and calculated structure amplitudes

hkl	F_o	F_c	*hkl*	F_o	F_c	*hkl*	F_o	F_c	*hkl*	F_o	F_c
100	101	106	410	40	53	002	82	−104	502	66	59
200	82	82	420	32	24	004	236	226	50$\bar{2}$	86	67
300	233	158	430	88	104	006	75	−74	504	<16	−9
400	<12	−6	440	70	74	008	81	63	50$\bar{4}$	10	16
500	35	−34	450	53	51				506	54	55
600	75	60	460	60	73	102	<9	13	50$\bar{6}$	50	58
700	127	−115	470	28	22	10$\bar{2}$	12	5	50$\bar{8}$	23	26
800	41	−36				104	<14	−18			
900	<14	6	510	65	−54	10$\bar{4}$	153	158	602	47	38
1000	55	−60	520	<12	11	106	54	68	60$\bar{2}$	24	−18
			530	16	−30	10$\bar{6}$	32	−23	604	<14	7
020	163	169	540	14	22	108	26	−44	60$\bar{4}$	112	119
040	16	6	550	53	63	10$\bar{8}$	116	96	60$\bar{6}$	41	−46
060	<14	−9	560	23	17				60$\bar{8}$	120	118
080	25	28	570	99	103	202	<11	−9			
						20$\bar{2}$	12	15	702	145	142
110	51	54	610	33	38	204	58	40	70$\bar{2}$	134	114
120	122	115	620	22	13	20$\bar{4}$	89	83	704	96	−96
130	135	129	630	63	71	206	<17	−6	70$\bar{4}$	50	−67
140	150	146	640	64	−78	20$\bar{6}$	32	39	70$\bar{6}$	38	43
150	13	13	650	48	47	20$\bar{8}$	42	23	70$\bar{8}$	43	38
160	54	51	660	27	−24						
170	28	13				302	97	−93	802	83	69
180	<8	−11	710	70	49	30$\bar{2}$	206	−203	80$\bar{2}$	132	112
			720	17	−25	304	56	59	80$\bar{4}$	70	−60
210	65	−60	730	74	56	30$\bar{4}$	167	187	80$\bar{6}$	99	83
220	84	86	740	35	42	306	<15	7	80$\bar{8}$	63	−54
230	10	−14	750	40	29	30$\bar{6}$	106	−122			
240	88	88				30$\bar{8}$	168	140	902	33	30
250	57	53	810	17	−20				90$\bar{2}$	21	14
260	56	61	820	44	−39	402	134	135	90$\bar{4}$	20	19
270	91	95	830	62	−60	40$\bar{2}$	70	82	90$\bar{6}$	<14	3
280	<7	4	840	13	−15	404	72	−85	90$\bar{8}$	20	37
			850	10	10	40$\bar{4}$	65	71			
310	34	30				406	145	123	100$\bar{2}$	151	131
320	124	122	910	17	18	40$\bar{6}$	48	−43	100$\bar{4}$	82	−75
330	80	81	920	35	−29	40$\bar{8}$	102	79	100$\bar{6}$	104	97
340	13	4	930	<9	13						
350	49	63							110$\bar{4}$	41	−48
360	<14	−19	1010	<7	1						
370	56	51									

atomic scattering factors listed in the International Table were employed. Temperature correction of the form $\exp -B(\sin\theta/\lambda)^2$, where $B=0.9$ Å^2, was applied in the final calculation of the structure factors.

Discussion

The structure is isotype with [Co en$_2$ Cl$_2$] Cl·HCl·2H$_2$O. The principal points of stereochemical interest which emerge from this X-ray analysis are as follows.

(1) The structure is essentially ionic and consists of [Co en$_2$Br$_2$]$^+$, [H$_2$O···H···H$_2$O]$^+$ and Br$^-$. Since the structure is isotype with chloro-analogue, a similar consideration of the arrangement of bromine ions leads us to locate a proton midway between the two water molecules. The O···O distance is found to be 2.60 Å. The existence of the group [H$_2$O···H···H$_2$O]$^+$ was suggested by Huggins and this was indeed verified by our investigation on the structures of *trans*-dihalogeno-*iso*-ethylenediamine complexes[4].

4) M. L. Huggins, *J. Phys. Chem.*, **40**, 723 (1936).

(2) The interatomic distances are given in Table III. Co-Br distance is found to be 2.44 Å. This is 0.14 Å larger than the corresponding Co-Cl distance and the difference agrees with that in covalent bond radius of chlorine and bromine atom. Other distances agree well with those found in [Co en_2 Cl_2] Cl·HCl·$2H_2O$.

TABLE III
INTERATOMIC DISTANCES AND BOND ANGLES

Co—Br(1)	2.44 Å
Co—N(1)	2.00
Co—N(2)	2.01
N(1)—C(1)	1.52
N(2)—C(2)	1.51
C(1)—C(2)	1.55
Br(1A)···N(3B)	3.58
Br(2A)···N(3B)	3.46
Br(2)···N(4B)	3.58
Br(3)···N(4B)	3.37
Br(2)···O(2)	3.24
Br(3)···O(2)	3.26
O(1)···O(2)	2.60
N(1)—Co—N(2)	86.5°
Co—N(1)—C(1)	109.2°
Co—N(2)—C(2)	108.3°
N(1)—C(1)—C(2)	107.6°
N(2)—C(2)—C(1)	110.3°

(3) The dichroism of the crystal has been measured by Yamada et al. and their investigation revealed that the general features of the absorption curve are essentially the same as those obtained for [Co en_2 Cl_2] Cl·HCl·$2H_2O$[5]. This is quite feasible since both structures are isotype. The marked dichroism is reasonable since all the Br-Co-Br bonds are nearly parallel to the *c*-crystal axis.

5) S. Yamada et al., This Bulletin, 28, 222 (1955).

Summary

The structure of *trans*-dibromo-bisethylenediamine cobalt(III) bromide hydrobromide dihydrate has been determined by X-ray analysis.

[Co en_2Br_2] Br·HBr·$2H_2O$ is monoclinic, $a=10.98$, $b=8.18$, $c=9.46$ Å, and $\beta=113.2°$, space group $P2_1/c$, two formula units in the cell. The structure consists of [Co en_2Br_2]$^+$, [H_2O···H···H_2O]$^+$ and Br^-, and is isotype with [Co en_2Cl_2] Cl·HCl·$2H_2O$. The complex ion has a center of symmetry. Two enantiomorphous ethylenediamine molecules, taking "*gauche*" configration, are coordinated to a cobalt atom. A cobalt atom is surrounded in a square coplanar configuration by four nitrogen atoms at distances 2.0 Å, and on a line approximately perpendicular to the plane of nitrogen atoms are two bromine atoms at distances 2.44 Å. The marked dichroism of the crystal is explainable in terms of the characteristic features in the arrangement of the complex ions in the crystal.

Part of the cost of this investigation was defrayed from the Fund for Scientific Research Expenditure of the Ministry of Education to which the authors' thanks are due.

Institute of Polytechnics
Osaka City University
Kita-ku, Osaka

*The Interaction between Dyes and Surfactants. I**

By Tamotsu KONDO and Kenjiro MEGURO

(Received July 7, 1958)

In previous works[1,2], we found the fact that the dye in aqueous solution is flocculated by adding a small amount of ionic surfactant, when the charge of surfactant is opposite to that of the dye.

We also found this flocculate** is dispersed again with further addition of surfactant. We call these phenomena "flocculation and deflocculation of dye by surfactant". To clarify the mechanism of these phenomena, we studied the interaction between anionic surfactants with

* Presented before the 11th Annual Meeting of the Chemical Society of Japan held in Tokyo, April, 1958.

** This flocculate is considered to be a stoichiometric complex salt formed between dye and surfactant. Details of its properties will be described in a later paper.

1) K. Meguro *J. Chem. Soc. Japan, Pure Chem. Sec.* (*Nippon Kagakn Zasshi*), **77**, 72 (1956).

2) T. Kondo et al., ibid., **77**, 1240 (1956).

alkyl chains of different lengths and a cationic dye, and also between cationic surfactants having gegenions of different degrees of hydration and an anionic dye.

Experimental

Materials.—Rhodamine 6G and Eosine were used as cationic and anionic dyes respectively. Both were commercial samples and were purified by the method described previously[3].

The anionic surfactants employed were sodium decyl (Na. De. S.), dodecyl (Na. D. S.) and tetradecyl sulfates (Na. T. S.). These alkyl sulfates were prepared from the corresponding alcohols by sulfation. The details of the preparation and the purification of these compounds were described already[4].

Dodecylpyridonium chloride (D. Py. Cl.), bromide (D. Py. Br.) and iodide (D. Py. I.) were used as cationic surfactants. These dodecylpyridonium halides were prepared by refluxing the dodecyl halides with pyridine for several hours. The salts were purified by recrystallization from acetone and by extraction with petroleum ether.

Procedure.—As described above, when the surfactant ion has a charge opposite to that of the dye ion, the ionic dye in solution is flocculated by adding surfactant solutions of low concentration. It was also mentioned that the flocculate disperses again in a more concentrated solution of surfactant. In order to treat these phenomena quantitatively, the flocculation value and the deflocculation value were defined as the minimum concentration of surfactants required to cause the complete flocculation and deflocculation of dye in 24 hours at constant temperature after mixing dye and surfactant.

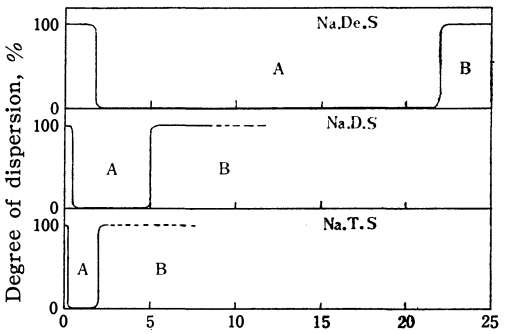
In practice, 2 ml. of dye solution of a constant concentration and equal volume of surfactant solutions of various concentrations were mixed in small test tubes, and these test tubes were permitted to stand at 30°C for 24 hours. At the end of 24 hours, the degree of flocculation was observed visually or spectrophotometrically, if necessary, after centrifuging. The flocculation and deflocculation values correspond to the minimum number of millimoles of surfactant per liter of mixed solution required to cause the complete flocculation and deflocculation. By repeating the same procedure for the dye solutions of various concentrations, the dependence of flocculation and deflocculation values upon the dye concentration was also investigated.

In order to study the properties of the complex formed between dye and surfactant, the transfer of flocculate to nonpolar solvent, such as benzene, was observed by the same procedure described already[5]. That is, 2 ml. of dye-surfactant mixture were shaken with equal volume of benzene in test tubes. After a few hours the degree of coloring of benzene phase was measured photometrically.

Results

The flocculation and deflocculation values varied with the difference in alkyl chain length and gegenion of surfactant, and furthermore with the addition of salt or organic solvent.

Effect of alkyl chain length of surfactant.—Results obtained with the alkyl sulfate—Rhodamine 6G systems in which the dye concentration was kept to be 0.5 mM/l. are shown in Fig. 1.



Concn. of alkyl sulfate, mM/l.
A: flocculation zone, B: deflocculation zone
Fig. 1. Flocculation pattern of Rhodamine 6G by sodium alkyl sulfates.

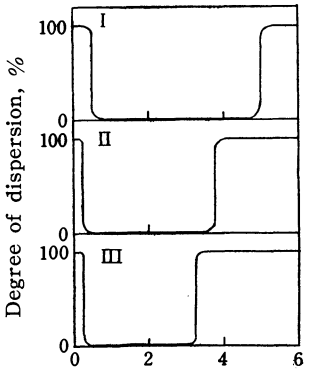
This figure shows that the minimum amounts of sulfate required to cause the complete flocculation and deflocculation markedly decrease with the increase in alkyl chain length of sulfate. In other words, the width of flocculation zone, i.e., the value obtained by subtracting the flocculation value from the deflocculation value, which is the net amount of surfactant necessary for the complete deflocculation of flocculate, decreases with increasing alkyl chain length.

As the dye concentration decreased, the flocculation and deflocculation values became smaller. Results for Rhodamine-dodecyl sulfate system are shown in Fig. 2. Similar results were obtained with decyl and tetradecyl sulfates.

The plots of the width of flocculation zone against the dye concentration gave a straight line. Results are shown in Fig. 3. It can be seen that the slope of the straight line rises with decreasing alkyl chain length of sulfate.

Effect of gegenion of surfactant.—Fig. 4 shows the flocculation and deflocculation

3) T. Kondo, ibid., 77, 1281 (1956).
4) O. Yoda, K. Meguro, T. Kondo and T. Ino, ibid., 75, 1272 (1954).
5) K. Meguro, *Memoirs of the Musashi University, Supplement*, 5, 33 (1957).



Concn. of Na. D. S., mM/l.
Rhodamine 6G concn.: I 0.50 mM/l., II 0.25 mM/l., III 0.125 mM/l.

Fig. 2. Effect of Rhodamine 6G concentration on its flocculation by Na. D. S.

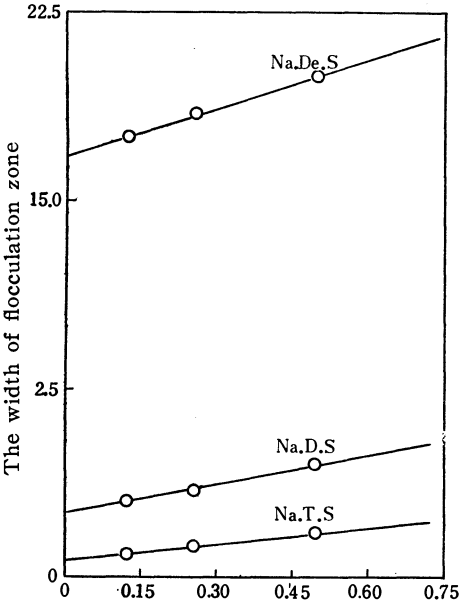
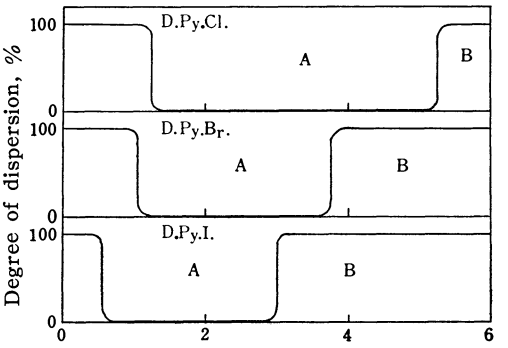


Fig. 3. The value of width of flocculation plotted against the dye concentration Rhodamine 6G. Sodium Alkyl Sulfate systems.

of Eosine, the concentration of which is 0.5 mM/l., by dodecylpyridonium halides.

In this figure, the chloride gives the largest flocculation and deflocculation values while the iodide gives the smallest ones. That is, the larger the hydration of gegenion of surfactant, the greater the width of flocculation zone.

The linear relation between the width of flocculation zone and the dye concentration for Eosine-dodecyl pyridonium halide systems is as shown in Fig. 5.



Concn. of dodecyl pyridonium halide, mM/l.
A: flocculation zone, B: deflocculation zone

Fig. 4. Flocculation pattern of Eosine by dodecyl pyridonium halides.

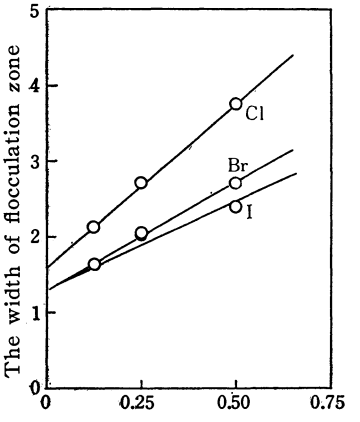
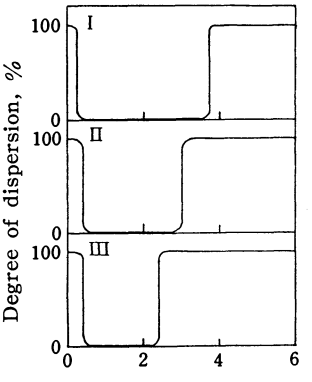
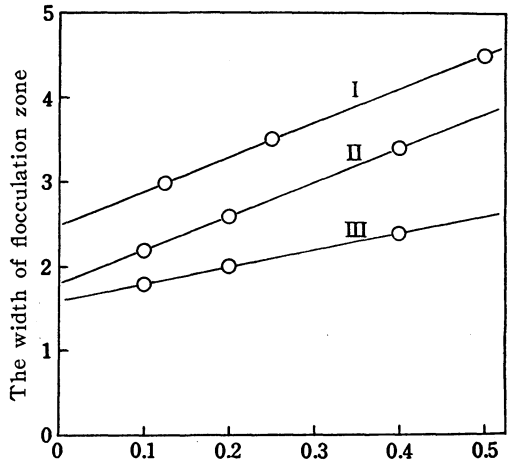


Fig. 5. The value of the width of flocculation zone plotted against the dye concentration for Eosine-D. Py. Halide systems.



Concn. of Na. D. S., mM/l.
I: no salt, Rhodamine 6G 0.25 mM/l.
II: NaCl 8 mM/l., Rhodamine 6G 0.20 mM/l.
III: NaCl 16 mM/l., Rhodamine 6G 0.20 mM/l.

Fig. 6. Effect of NaCl on the flocculation of Rhodamine 6G by Na. D. S.

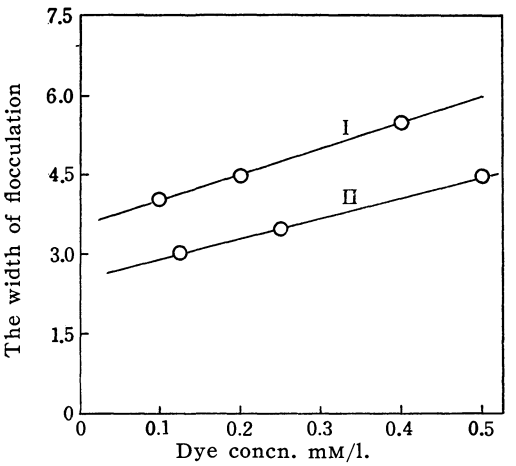


I: no salt, II: NaCl 8 mM/l.
III: NaCl 16 mM/l.

Fig. 7. Effect of NaCl on the relation between the width of flocculation zone and the dye concentration in Rhodamine 6G—Na. D. S. system.

Effect of added salt.—Added salt depressed the flocculation to a certain extent but promoted the dispersion of flocculates. A typical result obtained with Rhodamine 6G—Na. D. S.—sodium chloride system is shown in Fig. 6. and 7.

Effect of added alcohol.—The addition of ethanol to Rhodamine 6G – Na. D. S. system did not alter the flocculation value of dodecyl sulfate but exerted a slight influence on its deflocculation value. The width of flocculation zone, therefore, varies slightly as shown in Fig. 8.



I: ethanol 8.1 wt. %, II: no alcohol.

Fig. 8. Relation between the width of flocculation zone and dye concentration for Rhodamine 6G—Na. D. S. system in water-ethanol mixture.

Transfer of dye-surfactant complex into organic solvent.—Results for the transfer of Rhodamine 6G—D. S. complex into benzene are shown in the following table.

TABLE I
TRANSFER OF RHODAMINE 6G—D. S. COMPLEX INTO BENZENE

Dye concn. mM/l.	Na. D. S. concn. mM/l.						
	0.10	0.25	0.50	1.00	2.50	3.75	5.00
0.125	++	+++	++	+	+	−	−
0.25	++	+++	++	++	+	−	−
0.50	+	++	+++	++	++	+	−

In this table, the number of + signs denotes the degree of coloring of benzene phase, and the − sign shows the non-coloring.

It is noticed that the complex has a strong oilphilic property when the concentration of Na. D. S. is equivalent to that of dye. Furthermore, it is remarkable that this oilphilic property decreases again in more concentrated Na. D. S. solutions.

Discussion

The slope of straight lines shown in Figs. 3, 5, 7 and 8 will represent the minimum number of surfactant ions required to cause the complete deflocculation of a dye ion or a dye surfactant complex.

This number is termed "the deflocculation number of surfactant" and denoted by N_d in this series of papers. N_d values for surfactants employed in this work are collected in Table II.

TABLE II
VALUES OF N_d

Dye	Surfactant	N_d
Rhodamine 6G	Na. De. S.	6.7
	Na. D. S.	4.0
	Na. T. S.	2.2
Eosine	D. Py. Cl.	4.2
	D. Py. Br.	2.8
	D. Py. I.	1.9

The plots of $\log N_d$ against the number of carbon atoms of sulfate give a straight line as shown in Fig. 9, which is similar to that found between the C.M.C. and the number of carbon atoms in alkyl chain of surfactant.

On the other hand, with dodecylpyridonium halides, a linear relation between N_d value and lyotropic number of gegen-

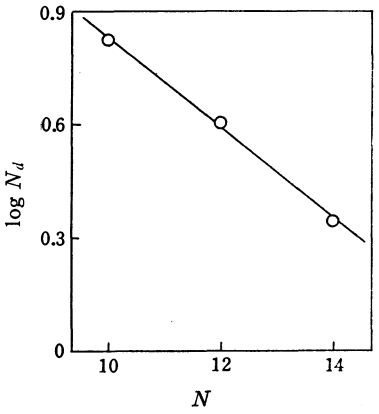


Fig. 9. Relation between log N_d and the number of carbon atoms in alkyl chain of sulfate.

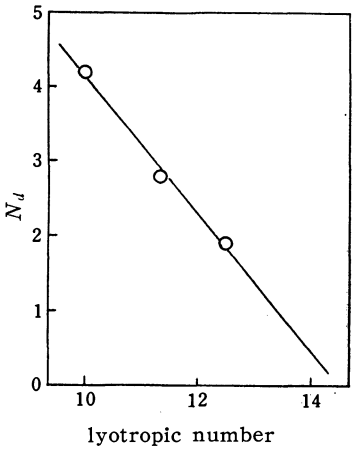


Fig. 10. Relation between N_d values and lyotropic number of gegenions of dodecylpyridonium halides.

ions is obtained as shown in Fig. 10. A similar relation is held between C.M.C. values of these cationic surfactants and lyotropic numbers of their gegenions[6].

It may be suggested that the deflocculation phenomenon of dye is closely related to the association properties of surfactant from the above-mentioned facts. As the magnitude of C.M.C. value measures the ability of micelle formation of surfactant, the N_d value seems to have a close relation with micelle forming ability of surfactant. The facts that the flocculation takes place at the equivalence between dye and surfactant, and that the deflocculation occurs in more concentrated surfactant solutions, and the facts that the flocculate has the oilphilic property, and that the deflocculate loses this oilphilic property, suggest the existence of dye surfactant aggregate composed of a dye surfactant complex, as the nucleus, and few surfactant ions. This dye-surfactant aggregate suggested by the present authors is pictured in Fig. 11.

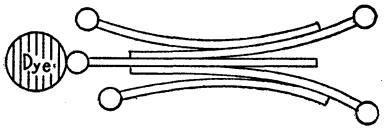


Fig. 11. Schematic representation of a dye-surfactant aggregate.

In connection with these considerations, it will be mentioned that the deflocculation of dye-surfactant complex occurs in surfactant solutions of the concentration below the C.M.C.

If we accept the above argument that a few surfactant ions can combine with a dye—surfactant complex in the deflocculation, we should expect that the surfactant ions themselves can form an aggregate owing to the interaction between their long alkyl chains below the critical concentration for micelle formation[7].

Nezu Chemical Laboratory
Musashi University
Nerima, Tokyo

6) K. Meguro, T. Kondo et al., Presented at the Symposium on Colloid and Surface Chemistry held in Tokyo, November 1956.

7) K. Meguro et al., This Bulletin 31, 472 (1958).

*Reaction of 2-Chloro-3-phenyltropone and 2-Chloro-7-phenyltropone with Ammonia and Amines**

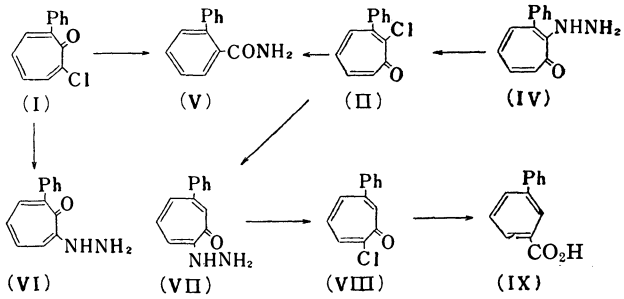
By Toshio MUKAI

(Received September 19, 1958)

The present writer has been examining the reactivity of 2-phenyltropone[1,2] and taking a great interest in comparing its chemical and physical properties with those of 3- and 4-phenyltropones. As a preliminary step, the synthesis of 3-phenyltropone from 2-phenyltropone was attempted. The objective would be realized if the expected abnormal substitution** could occur in the reaction of ammonia and 2-chloro-3-phenyltropone, easily obtainable from 2-phenyltropone through 3-phenyltropolone. However, such an abnormal substitution of 3- or 7-substituted 2-chlorotropone has not been carried out, although the reaction has been tried often with 4(or 6)- and 5-substituted 2-chlorotropones[3,4]. In the first step of this experiment, therefore, the reaction of not only 2-chloro-3-phenytropone but also 2-chloro-7-phenyltropone with ammonia and amines was examined.

The starting material, the 2-chloro derivatives, were prepared by the reaction of 3-phenyltropolone and thionyl chloride. This afforded a mixture of 2-chloro-7-phenyltropone (I) and 2-chloro-3-phenyltropone(II) in a good yield, in which the quantity of I was 4~5 times as large as that of II. In some cases, a small amount of colorless crystals III, m. p. 86.5°C, was obtained during this reaction. In 1951, Cook and others[5] reported the formation of a *o*-chlorobenzaldehyde, besides 2-chlorotropone, by the reaction of tropolone and thionyl chloride. The analytical values of III also agree with those of the corresponding chlorophenylbenzaldehyde but its infrared spectrum[6] does not exhibit the absorption in the carbonyl region. The ultraviolet absorption spectrum of III, shown in Fig. 1, does not exhibit the absorption in the longer wave length, characteristic of the tropone nucleus[7], so that III must be a compound formed by aromatization, but its structure is still under examination.

The structure of I is proved by the fact that its alkaline hydrolysis affords a biphenyl-2-carboxylic acid and that its hydrogenolysis forms 2-phenyltropone. The structure of II was established by its identity with a compound, obtained by the



decomposition of 2-hydrazino-3-phenyltropone (IV) with copper sulfate in hydrochloric acid solution[8]. IV is derived from the structurally known 2-methoxy-3-phenyltropone[9].

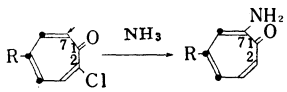
Reaction of 2-chloro-3-phenyltropone (II) by standing in ethanolic solution saturated with ammonia at a room temperature

*) Paper presented before the 8th Scientific Meeting of the Chemical Research Institute of Non-aqueous Solution, Tohoku University, October 22, 1956.

1) T. Mukai, *Sci. Repts. Tohoku Univ., First Ser.*, **38**, 280 (1954).

2) T. Nozoe, T. Mukai, J. Minegishi and T. Fujisawa, ibid., **37**, 388 (1953).

**) 2-Halotropones react with ammonia to give 2-aminotropones, but it has been found by T. Sato that the replacement of halogen by ammonia does not occur directly, and an abnormal substitution at C_7 rather than at C_2 occurs in the majority of cases (see ref. 3 and 4).



3) The dissertation of T. Sato, to be published.

4) T. Nozoe, S. Seto and T. Sato, *Proc. Japan Acad.*, **30**, 473 (1954).

5) B. J. Abadir, J. W. Cook, J. D. Loudon and D. K. V. Steel, *J. Chem. Soc.*, **1952**, 2350.

6) Infrared spectra were measured with Perkin-Elmer Model 21 double beam Spectrophotometer by Mr. Yusaku Ikegami of the Chemical Research Institute of Non-aqueous Solution, Tohoku University, to whom the author is deeply indebted.

7) M. Tsuboi, This Bulletin, **25**, 369 (1952).

8) S. Seto, *Sci. Repts. Tohoku Univ., First Ser.*, **37**, 275 (1953).

9) T. Muroi, *J. Chem. Soc. Japan, Pure Chem. Sec.* (*Nippon Kagaku Zasshi*), **77**, 1084 (1956).

resulted in its rearrangement to biphenyl-2-carboxamide (V) in a good yield, instead of undergoing the expected abnormal substitution. The reaction of 2-chloro-7-phenyltropone (I) and ethanolic ammonia also ended in the same rearrangement.

On heating a mixture of 2-chloro-7-phenyltropone (I) and hydrazine in ethanol, the structurally known 2-hydrazino-7-phenyltropone[2] (VI) was obtained in a good yield. On the other hand, the reaction of 2-chloro-3-phenyltropone (II) and hydrazine afforded yellow crystals VII, m. p. 137°C without the rearrangement. The melting points of IV and VII were very close but their admixture showed them to be different substances. The ultraviolet spectrum of VII, shown in Fig. 2, indicated the absorption of a 2-aminotropone type[10] and its analytical values also agreed with those for a hydrazino compound. The ultraviolet spectra of other hydrazinotropones, IV and VI, are also given in Fig. 2, from which it is seen that the absorption in the longest wavelength region has disappeared in IV alone owing to the steric hindrance of the hydrazino group.

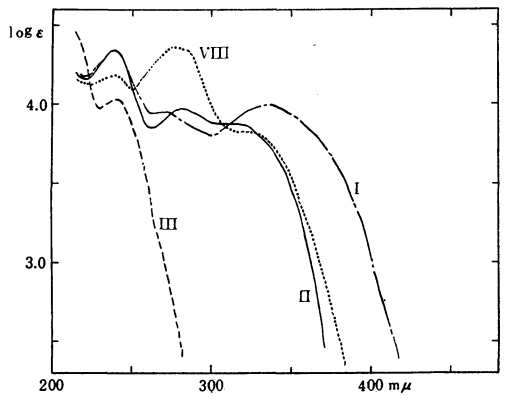


Fig. 1. U. V. Spectra of 2-Chloro-7-phenyltropone (I), 2-Chloro-3-phenyltropone (II), III of m. p. 86.5°C, and 2-Chloro-6-phenyltropone (VIII) in methanol.

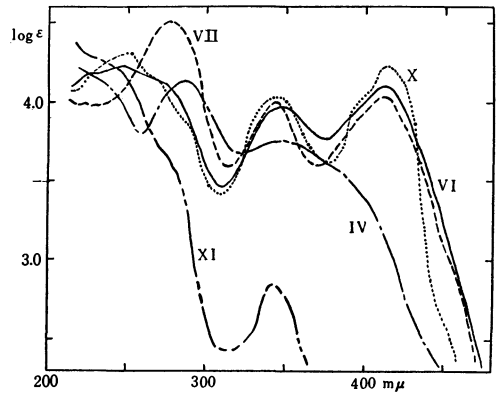
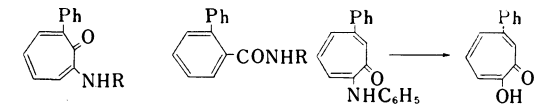


Fig. 2. U. V. Spectra of 2-hydrazino-3-phenyltropone (IV), 2-hydrazino-7-phenyltropone (VI), 2-hydrazino-6-phenyltropone (VII), 2-methylamino-7-phenyltropone (X), and biphenyl-2-carboxymethylamide (XI) in methanol.

Decomposition of VII with copper sulfate in hydrochloric acid medium affords the corresponding chlorotropone VIII which easily undergoes rearrangement on being heated with ethanolic alkali to form biphenyl-3-carboxylic acid (IX)[11]. It follows that VII and VIII are respectively 2-hydrazino- and 2-chloro-6-phenyltropone. The occurrence of an abnormal substitution with hydrazine was observed for the first time in this compound. It is interesting to note that the reaction with hydrazine is so vastly different from that with ammonia. The ultraviolet spectrum of VIII is given in Fig. 1. It is noted that II and VIII are the chlorine derivatives of 3-phenyltropone, their absorption curve shifts to a shorter wave length region than that of 2-phenyltropone derivatives and they have a maximum near 280 mμ.

The reaction of I and II with alkyl- and arylamines was next examined. When I or II was heated with methylamine in ethanol solution, I afforded yellow crystals X, m. p. 159°C and II gave pale yellow crystals XI, m. p. 165°C. The ultraviolet spectra of X and XI are indicated in Fig. 2. The spectrum of X exhibits two peaks of high intensity at above 340 mμ, indicating a typical 2-aminotropone type, while that of XI lacks the corresponding absorption, indicating the possibility of an aromatization. Since the analytical values of X agree with those of 2-methylaminotropones and the hydrolysis of X by heating with alkali in ethanolic solution affords 3-phenyltropolone, X must be 2-methylamino-7-phenyltropone. The structure of



(X): R=CH3 (XI): R=CH3 (XIII) (XIV)

(XV): R=C6H5 (XII): R=C6H5

10) The absorption in the longer region of ultraviolet spectra of 2-amino- and 2-hydrazinotropones splits into two maxima when measured in methanol (cf. Ref. 2).

11) H. Hey, *J. Chem. Soc.*, 1934, 1966.

XI was established by admixture of the methylamide, m. p. 166°C, of biphenyl-2-carboxylic acid, prepared by an unequivocal process.

The reaction with aniline was found to be somewhat more complicated. On heating 2-chloro-3-phenyltropone (II) and aniline in ethanol solution, orange plates XII, m. p. 110°C, were obtained from an easily soluble portion, and yellow crystals XIII, m. p. 173°C, from a sparingly soluble portion. The ultraviolet spectra of XII and XIII are shown in Fig. 3. XII shows absorption of a different type from that of the troponoids while that of XIII is similar to the absorption curve of 2-aminotropones[10]. XII is a neutral substance, is stable to acids and alkalis, and from its analytical values, it is assumed to be the rearrangement anilide of product, biphenyl-2-carboxylic acid. In fact, XII showed no depression of the melting point on admixture with the same anilide, m. p. 110°C, prepared by unequivocal process. Hydrolysis of XIII by heating with alkali in ethanolic solution afforded colorless crystals XIV, m. p. 97°C, an acid substance which gave the coloration with ferric chloride characteristic to tropolones. The ultraviolet spectrum of XIV is also characteristic of that of tropolones[7] as shown in Fig. 3. Previously, Doering and Knox[12] prepared 4-phenyltropolone and gave its melting point at 97°C, and measured its ultraviolet spectrum (in cyclohexane). From the comparison of elemental analytical values and ultraviolet spectra, XIV is undoubtedly 4-phenyltropolone and XIII would then

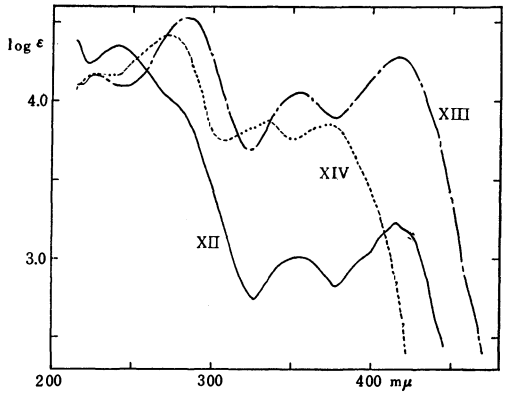


Fig. 3. U. V. Spectra of biphenyl-2-carboxyanilide (XII), 2-anilino-6-phenyltropone (XIII), and 4-phenyltropolone (XIV) in methanol.

12) W. von E. Doering and L. H. Knox, *J. Am. Chem. Soc.*, 75, 297 (1953).

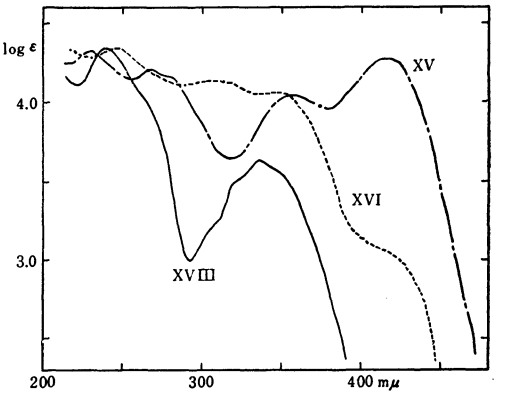
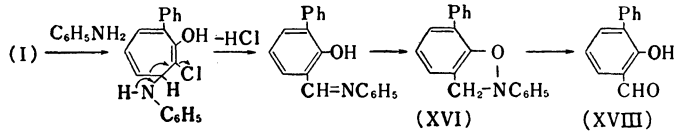


Fig. 4. U. V. Spectra of 2-anilino-7-phenyltropone (XV), the Schiff's Base (XVI), and 2-hydroxy-3-phenylbenzaldehyde (XVIII) in methanol.

be 2-anilino-6-phenyltropone. This fact indicates clearly that an abnormal substitution occurred in the reaction of II and aniline. This is the first example of an abnormal substitution occuring with an arylamine.

In the reaction of 2-chloro-7-phenyltropone (I) and aniline, yellow crystals XV, m. p. 124°C, and colorless crystals XVI, m. p. 103.5°C, are obtained with XVI predominating in yield. The ultraviolet spectra of XV and XVI are indicated in Fig. 4 and from the absorption curve and analytical date, XV was assumed to be 2-anilino-7-phenyltropone. This structure was actually established by the conversion of XV into 3-phenyltropolone (XVII) by alkaline hydrolysis. XVI is a neutral substance and undergoes facile decomposition on being heated in dilute acid or alkali, affording colorless crystals XVIII, m. p. 45.5°C. Although XVIII is an acid substance, it does not dissolve in sodium hydrogen carbonate and exhibits a dark violet coloration with ferric chloride in ethanol, like that of salicylaldehyde. The infrared spectrum of XVIII, exhibits absorptions due to hydroxyl group at 3200 cm^{-1} and that of carbonyl group at 1666 cm^{-1}, which are both displaced to a smaller frequency range. It would be rational to accept this shift by assuming an intramolecular hydrogen bonding between the carbonyl and hydroxyl groups. There is also a C-H stretching vibration of aldehyde group at 2820 and 2730 cm^{-1}. From these facts, the analytical data and ultraviolet absorption in Fig. 4, XVIII is assumed to be 2-hydroxy-3-phenylbenzaldehyde and XVI would then be a Schiff's



Base of XVIII and aniline. This assumption was proved to be correct from the facile formation of XVI by heating XVIII and aniline. However, the infrared spectrum of XVI does not exhibit the O-H stretching vibration and the C=N vibration is not distinct, although there is the aromatic C=C vibration at 1616 cm^{-1} (common with XVIII). Considering the fact that XVI is a neutral substance, it is more likely to have an oxazoline structure than that of Schiff's Base.

The formation of a salicylaldehyde derivative by the nucleophilic attack on tropones has already been observed in the reaction of 2,7-dihalotropone with alkali[13] or ammonia[3]. These reactions all belong to the same type and are assumed to have been instigated by the attack of aniline at 3-position of the tropone ring as suggested by Kitahara[14].

The afore-mentioned reactions are examples of ammonia and amines acting as nucleophilic reagents on 2-halo-3-(or 7)-phenyltropone, and the normal and abnormal substitutions and rearrangement reactions have been observed. These reactions are thought to be brought about in different directions by whether the amines attack the 1-position (C=O) of the tropone ring, or the 2-position (C-Cl) or 3- or the 7-position (C-H). Which of these reactions actually occurs depends on the structure of the reacting tropones to be reacted, the basicity and the size of the reagent used. For example, the reaction of ammonia with 2-chloro-7-phenyltropone (I) is principally directed towards its attack on the 1-position (C=O), resulting in aromatization to form V. With methylamine, which has a larger volume than ammonia, the attack occurs at the 2-position (C-Cl), perhaps due to the steric hindrance of the phenyl group at the 7-position a substitution reaction results, forming X. With further increase in the volume of the reagent to aniline, the attack occurs not only at the 2-position (C-Cl) but also at the 3-position (C-H) and results in the formation of XVI. In 2-chloro-3-phenyltropone (II), the steric hindrance of the phenyl and carbonyl groups toward the 2-position becomes so large that the normal substitution at the 2-position does not occur. In the reaction of II and amines, the attacks on the 1-position (C=O) and the 7-position (C-H) invariably occur competitively so that the attack of ammonia and methylamine, due to their volume and basicity, becomes effective on the 1-position (C=O) and rearrangement reaction is likely to occur in the majority. On the contrary, aniline and hydrazine are more liable to attack the 7-position rather than the 1-position and the result is likely to be an abnormal substitution reaction.

The foregoing experimental evidence (especially formation of VII) offers the possibility of deriving 3-phenyltropone from 2-phenyltropone and the writer expects to carry out the preparation of 3-phenyltropone along line.

Experimental[15]

Reaction of 3-Phenyltropolone and Thionyl Chloride. — To a solution of 1.0 g. of 3-phenyltropolone dissolved in 25 cc. of dehydrated benzene, 0.73 g. (1.2 mol. equiv.) of thionyl chloride was added and the mixture was refluxed for 3 hours on a water bath. Benzene was then distilled off, thionyl chloride was removed under reduced pressure, and the dark brown oily residue was dissolved in a mixture of 5 cc. each of chloroform and carbon tetrachloride. This solution was passed through an alumina column (1 $cm^2 \times 20$ cm.), which was eluted with chloroform, and the effluent was divided into seven fractions. Evaporation of the solvent from each fraction afforded pale yellow to yellow crystals with melting points listed below: (1) m. p. 65~70°C, (2) 72~74°C, and (3) 70~73°C, with a combined yield of 630 mg. (4) 90 mg. of m. p. 55~65°C. (5) Crystalline but its melting point cannot be determined. (6) 50 mg. of m. p. 80~87°C. (7) 110 mg. of m. p. 92~99°C. Fractions 1 to 3 were recrystallized from ethanol to yellow prisms I, m. p. 75°C.

Anal. Found: C, 72.34; H, 4.38. Calcd. for $C_{13}H_9OCl$: C, 72.06; H, 4.14%.

Fractions 6 and 7 were combined and recrystallized from ethanol and afforded pale yellow

13) S. Seto, *Sci. Repts. Tohoku Univ., First Ser.*, **37**, 378 (1954).

14) Y. Kitahara, ibid., **39**, 250 (1956).

15) All m. p. are uncorrected. The microanalyses were carried out by Miss Ayako Iwanaga and Mr. Shinichi Ohyama of this laboratory to whom the author is indebted.

prisms II, m. p. 103~104°C.

Anal. Found: C, 71.88; H, 4.46. Calcd. for $C_{13}H_9OCl$: C, 72.06; H, 4.14%.

The alumina column was finally eluted with ethanol and evaporation of ethanol from the effluent afforded pale yellow crystals. Low-pressure (3 mmHg) sublimation yielded 20 mg. of colorless crystals, m. p. 73~80°C, which recrystallized from cyclohexane to colorless plates III, m. p. 85.5~86.5°C. $\tilde{\nu}$ (in KBr): 3340, 3300~80, 3040, 2915, 2865, 1467, 1412, 1356, 1313, 1240, 1179, 1113, 1085, 1055, 1038, 845, 788, 757, 701 cm^{-1}.

Anal. Found: C, 71.44; H, 4.77. Calcd. for $C_{13}H_9OCl$: C, 72.06; H, 4.14%.

Hydrolysis of 2-Chloro-7-phenyltropone (I) with Alkali. — A solution of 150 mg. of I dissolved in a mixture of 4 cc. each of ethanol and 4 N potassium hydroxide was refluxed for 4 hours on a water bath. Ethanol was then distilled off, the residue was diluted with water, and extracted with benzene to remove a neutral portion. The aqueous layer was neutralized to weak acid and extracted three times with chloroform. The chloroform extract was washed with water and the solvent evaporated, leaving 120 mg. of yellowish brown oil. The residual oil was distilled under reduced pressure (2 mmHg) at a bath temperature of 140°C and the colorless oily distillate crystallized immediately to 90 mg. of crystals melting at 75~85°C. Recrystallization from petroleum ether—benzene mixture afforded colorless crystals, m. p. 107~109°C, undepressed on admixture with biphenyl-2-carboxylic acid, m. p. 109~110°C.

Catalytic Reduction of 2-Chloro-7-phenyltropone (I).—To a solution of 50 mg. of I dissolved in 5 cc. of methanol, 50 mg. of sodium acetate and 20 mg. of 5% palladium-carbon were added and the mixture was hydrogenated at ordinary temperature and pressure. The absorption of hydrogen was quite slow and only 8.1 cc. (1.5 mol. equiv.) was absorbed in 5 hours. The catalyst was filtered off, the residue was diluted with water, and the solution was extracted with benzene. Evaporation of the benzene gave 40 mg. of a pale yellow oil which crystallized on inoculation of 2-phenyltropone crystal. The crystalline mixture was allowed to stand with a small quantity of methanol and afforded needles, m. p. 81~83°C. The mixed m. p. 82~84°C on admixture with 2-phenyltropone, m. p. 84°C. Similar catalytic reduction of 2-chloro-3-phenyltropone (II) ended in the recovery of II and no product was obtained that would form a hydrochloride or a picrate.

Formation of 2-Hydrazino-3-phenyltropone (IV).—To a solution of 120 mg. of 2-methoxy-3-phenyltropone[9], m. p. 77~78°C, dissolved in a mixture of 4 cc. of ether and 1 cc. of methanol, 0.1 cc. of 80% aqueous solution of hydrazine hydrate was added and the mixture was allowed to stand overnight in a refrigerator. This solution was treated with water and the separated ether layer was evaporated at room temperature from which 120 mg. of orange yellow crystals were obtained. Recrystallization from ethanol afforded 70 mg. of deep yellow prisms IV, m. p. 140°C.

Anal. Found: N, 12.97. Calcd. for $C_{13}H_{12}NO_2$: N, 13.20%.

Formation of 2-Chloro-3-phenyltropone (II) from 2-Hydrazino-3-phenyltropone (IV). —A solution of 300 mg. of IV dissolved in 4 cc. of concentrated hydrochloric acid was added in a few minutes into a heated solution of 3 g. of copper sulfate dissolved in 3 cc. of water. Some evolution of nitrogen was observed but a fair amount of tarry substance separated out. After boiling for 5 minutes, the solution was cooled and extracted with chloroform. The chloroform extract was washed with water, passed through an alumina column, and the column was eluted with chloroform. The pale yellow crystals, m.p. 93~95°C, obtained on evaporation of chloroform, were recrystallized from ethanol to pale yellow plates, m. p. 104~105°C, undepressed on admixture with 2-chloro-3-phenyltropone (II), m. p. 104°C, as described above.

Reaction of 2-Chloro-3-phenyltropone (II) and Ammonia.—A solution of 100 mg. of II dissolved in 3 cc. of ethanol saturated with ammonia at room temperature was placed in a vessel, sealed tightly, and left to stand at room temperature for 50 hours. The color of the solution changed from yellow through brown to pale yellow. Ethanol was evaporated under reduced pressure at room temperature and 60 mg. of pale yellow crystals, m. p. 173~174°C, so obtained were recrystallized from benzene to colorless needles V, m. p. 174~174.5°C, undepressed on admixture with an authentic sample of biphenyl-2-carboxamide, m. p. 174°C.

Reaction of 2-Chloro-7-phenyltropone (I) and Ammonia. — A mixture of 120 mg. of I in 3.7 cc. of ethanol saturated with ammonia was allowed to stand in a sealed vessel for 50 hours. Ethanol was evaporated under a reduced pressure at room temperature and 80 mg. of brown crystals, m. p. 148~160°C (sint. 120°C), were recrystallized from benzene to 50 mg. of colorless needles V, m. p. 174~174.5°C, undepressed on admixture with biphenyl-2-carboxamide.

Reaction of 2-Chloro-7-phenyltropone (I) and Hydrazine. — To a solution of 50 mg. of I dissolved in 1.5 cc. of ethanol, 0.06 cc. of 80% hydrazine hydrate solution was added and the mixture was refluxed for 30 minutes on a water bath. The ethanolic solution was concentrated to about one-half and cooled. From this 45 mg. of golden yellow needles, m. p. 195~197°C, separated out. The crystals were recrystallized from ethanol to VI, m. p. 199~200°C[16], which showed no depression on admixture with the structurally known 2-hydrazino-7-phenyltropone, m. p. 192°C (decomp.)[16]. Benzylidene compound[2] of VI: m. p. 150°C.

λ_{max}^{MeOH} mμ (log ε): 240(4.38), 273(4.20), 280(4.14), 442(4.56).

16) VI was reported as melting at 192°C (cf. Ref. 2), but it is corrected to m. p. 200°C.

Reaction of 2-Chloro-3-phenyltropone (II) and Hydrazine.—To a solution of 100 mg. of II dissolved in 3 cc. of ethanol, 0.10 cc. of 80% hydrazine hydrate solution was added and the mixture was refluxed for 30 minutes on a water bath. Evaporation of ethanol and cooling of the residue separated 80 mg. of golden yellow crystals, m. p. 100~130°C, which were recrystallized from cyclohexane to 60 mg. of orange scales VII, m.p. 136~137°C.

Anal. Found: N, 13.28. Calcd. for $C_{13}H_{12}ON_2$: N, 13.20%.

Benzylidene compound of VII: Yellow needles, m. p. 203°C.

Anal. Found: N, 9.52. Calcd. for $C_{20}H_{16}ON_2$: N, 9.33%.

λ_{max}^{MeOH} mμ (log ε): 238(4.25), 285(4.42), 377(4.26), 438(4.59).

Formation of 2-Chloro-6-phenyltropone (VIII) from 2-Hydrazino-6-phenyltropone (VII) and its Aromatization. — A suspension of 80 mg. of VII and 1.5 cc. of concentrated hydrochloric acid was added to a heated solution of 1.5 g. of copper sulfate dissolved in 1.5 cc. of water. After boiling 30 minutes, the solution was diluted with water and extracted with benzene. The benzene extract was washed with water and passed through an alumina column. Evaporation of benzene eluate afforded 45 mg. of a yellowish crystals m. p. 110~112°C, which were recrystallized from ethanol to pale yellow needles VIII, m. p. 113~114°C.

Anal. Found: C, 71.72; H, 4.39. Calcd. for $C_{13}H_9OCl$: 72.06; H, 4.14%.

A solution of 40 mg. of VIII in 2 cc. of 10% ethanolic potassium hydroxide solution was refluxed for 30 minutes, ethanol was distilled off, 2 cc. of water was added to the residue, and the mixture was heated for a further 10 minutes. A small amount of brown precipitate that separated out was filtered off, the filtrate was acidified with 6 N sulfuric acid, and the white precipitate so formed was collected by filtration, yielding 20 mg. of colorless crystals, m. p. 145~153°C. The crystals were recrystallized from benzene-petroleum ether to colorless plates IX, m. p. 162~163°C. The reported melting point for biphenyl-3-carboxylic acid is 162~164°C[11].

Reaction of 2-Chloro-7-phenyltropone (I) and Methylamine.—To a solution of 100 mg. of potassium hydroxide dissolved in 2.5 cc. of ethanol, 180 mg. of methylamine hydrochloride was added and potassium chloride that separated out was removed by filtration. To this filtrate, 100 mg. of I was added and the mixture was refluxed for 3 hours on a water bath. The residue obtained on evaporation of ethanol was recrystallized from ethanol to 45 mg. of yellow plates X, m. p. 159°C.

Anal. Found: N, 6.97. Calcd. for $C_{14}H_{13}ON$: N, 6.63%.

Ethanol was evaporated from the recrystallization mother liquor, the residue was dissolved in benzene, and the solution was passed through an alumina column. From the benzene eluate, 30 mg. of yellow crystals, m. p. 75°C, was obtained and this was identified to be I by mixed fusion.

Hydrolysis of 2-Methylamino-7-phenyltropone (X) with Alkali.—A solution of 25 mg. of X dissolved in a mixture of 1.5 cc. of ethanol and 4 N potassium hydroxide was refluxed for 6 hours on a water bath, ethanol was evaporated, and the residue was diluted with water. This was extracted with benzene and 20 mg. of pale brown crystals, m. p. 105~110°C, obtained on evaporation of benzene were recrystallized from ethanol to crystals of m. p. 113°C, undepressed on admixture with an authentic sample of 3-phenyltropone, m. p. 118°C[2].

Reaction of 2-Chloro-3-phenyltropone (II) and Methylamine.—A solution of 100 mg. of II dissolved in a solution of 130 mg. of methylamine hydrochloride and 100 mg. of potassium hydroxide dissolved in 2.5 cc. of ethanol was sealed in a glass tube and heated for 3 hours at 100°C. The ethanol was evaporated from the mixture, the residue was extracted with benzene and the solid residue obtained on evaporation of benzene was recrystallized from ethanol to pale yellow needles XI, m. p. 162~164°C.

The oily acid chloride obtained on refluxing biphenyl-2-carboxylic acid with thionyl chloride in benzene was added to ethanolic solution of methylamine and the mixture was warmed on a water bath, from which biphenyl-2-carboxymethylamide was obtained as colorless crystals, m. p. 165~167°C. This showed no depression of the melting point on admixture with XI.

Reaction of 2-Chloro-3-phenyltropone (II) and Aniline. — A solution of 180 mg. of II and 400 mg. of aniline dissolved in 5 cc. of ethanol was refluxed for 3 hours on a water bath. Ethanol was then evaporated, the residue cooled, and 40 mg. of yellow crystals, m. p. 165~167°C, obtained from it were recrystallized from benzene to XIII, m. p. 172~173°C.

Anal. Found: C, 83.79; H, 5.42; N, 5.53. Calcd. for $C_{19}H_{15}ON$: C, 83.49; H, 5.53; N, 5.13%.

The ethanolic solution left after separation of the crystals was extracted with benzene, the benzene extract was shaken with 1 N hydrochloric acid solution to remove remaining aniline, and washed with water. The benzene solution was then passed through an alumina column and the column was eluted with benzene. The effluent was divided into two fractions and evaporation of benzene from the initial fraction left 100 mg. of pale orange oil. The latter fraction afforded 40 mg. of similar oil. Both oils crystallized immediately and respectively afforded crystals of m. p. 97~101°C and 102~105°C. These were combined and recrystallized from cyclohexane to 90 mg. of colorless prisms XII, m. p. 109~110°C.

Anal. Found: C, 83.14; H, 5.46; N, 5.38. Calcd. for $C_{19}H_{15}ON$: C, 83.49; H, 5.53; N, 5.13%.

The alumina column was further eluted with ethanol and 10 mg. of yellow crystals, m. p. 165~167°C, were obtained, which showed no depression of the melting point on admixture with XIII.

Biphenyl-2-carboxylic acid chloride was refluxed with aniline in benzene and colorless crystals

(from ethanol), m. p. 110°C, thereby obtained showed no depression of the melting point on admixture with XII.

Hydrolysis of 2-Anilino-6-phenyltropone (XIII).—To a solution of 30 mg. of XIII dissolved in 2.5 cc. of ethanol, 2.5 cc. of 3 N potassium hydroxide solution was added and the mixture was refluxed for 8 hours on a water bath. Ethanol was evaporated from the mixture, water was added to the residue, and this was extracted with benzene.

Alkaline aqueous solution was neutralized with dilute hydrochloric acid and the turbid solution that resulted was extracted three times with chloroform. The extract was washed with water and the solvent was evaporated, leaving 20 mg. of brown oil which crystallized immediately. Its recrystallization from ethanol afforded colorless needles XIV, m. p. 97°C.

Anal. Found: C, 78.23; H, 5.38. Calcd. for $C_{13}H_{10}O_2$: C, 78.77: H, 5.09%.

This substance colors red with aqueous solution of ferric chloride and the color transits to the chloroform layer. The reported melting point of 4-phenyltropolone is 97°C[12].

Reaction of 2-Chloro-7-phenyltropone (I) with Aniline. — A solution of 600 mg. of I and 1.8 g. of aniline dissolved in 6 cc. of ethanol was refluxed for 6 hours on a water bath. Evaporation of the solvent left 250 mg. of yellow crystals, m. p. 97~98°C. Ethanol was added to the filtrate, which was further refluxed for 3 hours, and 100 mg. of yellow crystals, m. p. 97~98°C, was obtained. The mother liquor left here will be designated as A. The two crops of the above crystals were combined, dissolved in carbon tetrachloride and passed through a short alumina column. Evaporation of carbon tetrachloride from the effluent afforded 250 mg. of orange plates, m. p. 101~102°C, and its recrystallization from ethanol gave XVI, m. p. 103~103.5°C. $\tilde{\nu}$ (in KBr): 3030, 1616, 1583, 1488, 1455, 1427, 1372, 1293, 1280, 1202, 1173, 1100, 1075, 1023, 1000, 980, 940, 906, 849, 830, 757, 692, 650 cm^{-1}.

Anal. Found: N, 5.29. Calcd. for $C_{19}H_{15}ON$: N, 5.13%.

XVI is insoluble in either dilute acid or alkali. The mother liquor (A) was dissolved in benzene, shaken with 1 N hydrochloric acid to remove excessive aniline, the benzene layer was washed thoroughly with water, and the benzene evaporated, leaving 190 mg. of yellow crystals, m. p. 89~106°C. The crystals were dissolved in a mixture of 5 cc. each of ethanol and 2 N hydrochloric acid and the mixture was refluxed for 30 minutes on a water bath. Ethanol was evaporated, residual solution was extracted with benzene after addition of water, and the benzene extract was shaken with dilute sodium hydroxide solution to remove an acid portion. The alkaline extract will be designated as B. The benzene extract was washed with water and the solvent evaporated, giving 150 mg. of yellow crystals, m. p. 110~113°C. Recrystallization from ethanol afforded 90 mg. of yellow prisms XV, m. p. 122~124°C.

Anal. Found: N, 5.22. Calcd. for $C_{19}H_{15}ON$: N, 5.13%.

The extract B was neutralized, acidified and extracted with chloroform. The extract was washed thoroughly with water; and evaporation of the solvent left 20 mg. of pale brown oil which soon solidified to colorless crystals, m. p. 38~40°C. This substance is probably identical with XVIII described below.

Hydrolysis of 2-Anilino-7-phenyltropone (XV) with Alkali.—A solution of 50 mg. of XV dissolved in a mixture of 4 cc. of ethanol and 2 cc. of 6 N potassium hydroxide was refluxed for 6 hours on a water bath. Ethanol was evaporated from this mixture, water was added to the residual solution, and extracted with benzene to remove a neutral portion. The aqueous alkali solution was acidified with dilute hydrochloric acid and extracted with chloroform. The extract was washed with water; evaporation of hlorcoform afforded 30 mg. of pale yellow crystals, m. p. 97~100°C. Its recrystallization from ethanol gave yellowish prisms, m. p. 114~116.5°C, which showed no depression with authentic 3-phenyltropolone, m. p. 118°C[2].

Hydrolysis of Schiff's Base (XVI).—A solution of 110 mg. of XVI dissolved in a mixture of 4 cc. of ethanol and 2 cc. of 6 N potassium hydroxide was refluxed for 1 hour. Ethanol was evaporated from this solution, water was added and then extracted with benzene to remove a neutral portion. The aqueous alkali solution was acidified and extracted with chloroform. The extract was washed with water, the chloroform evaporated, and 80 mg. of pale brown oily residue crystallized immediately, showing m. p. 40~42°C. Recrystallization from ethanol afforded colorless plates XVIII, m. p. 45.5~46°C. $\tilde{\nu}$ (in KBr) 3200, 3040, 2820, 2730, 1666, 1611, 1495, 1472, 1453, 1433, 1384, 1303, 1264, 1214, 1167, 1097, 1065, 1026, 911, 829, 794, 761, 720, 693 cm^{-1}.

Anal. Found: C, 78.33; H. 5.11. Calcd. for $C_{13}H_{10}O_2$: C, 77.98; H, 5.09%.

The halogen test is negative with XVIII and it does not transit to an alkali layer on shaking its benzene solution with saturated solution of sodium hydrogen carbonate. Ethanolic solution of XVIII becomes dark violet with ferric chloride.

Hydrolysis of 80 mg. of XVI by heating in a mixture of 2 cc. of each of ethanol and 2 N hydrochloric acid for 30 minutes also affords 50 mg. of XVIII, m. p. 45°C.

Reaction of 2-Hydroxy-3-phenylbenzaldehyde (XVIII) and Aniline. — A mixture of 80 mg. of XVIII and 200 mg. of aniline was heated on a water bath for 20 minutes and the resulting dark red oil separated crystals on being cooled. The addition of a small amount of ethanol afforded 90 mg. of almost colorless scales, m. p. 103°C, undepressed on admixture with XVI, m.p. 103.5°C.

The author takes this opportunity to express his sincere gratitude to Professor Tetsuo Nozoe for his kind guidance throughout the course of this work, to Professor Shuichi Seto and Assistant

Professor Yoshio Kitahara for much helpful advice, and to Mr. Mutsuo Ishii for his cooperation in carrying out the experiments.

Department of Chemistry
Faculty of Science
Tohoku University
Katahira-cho, Sendai

Spectrophotometric Determination of Uranium with Neo-thorone

By Shozo SHIBATA and Teiichi MATSUMAE

(Received July 7, 1958)

In an earlier communication[1] a photometric method for the determination of uranium with Neo-thorone (*o*-arsonophenylazo-chromotropic acid) was briefly described. The purpose of this paper is to treat the same subject in detail. Several colorimetric methods recently reported for the determination of uranium were based on the complex formation with such a reagent as dibenzoylmethane[2], 2-acetoacetylmethane[3], diethyldithiocarbamate[4], potassium ferrocyanide[5], potassium thiocyanate[6], or on the formation of peroxide with hydrogen peroxide[7].

Hydrogen peroxide is the common reagent used for the colorimetric determination of uranium, but it is not very sensitive. Kuznetsov[8] has reported a qualitative test; a very sensitive color reaction of uranium with *o*-arsonophenylazo-chromotropic acid. Neo-thorone in a solution of pH 1 or 2 has been used as a chromogenic reagent to determine thorium[9] and fluoride[10].

Experimental

Apparatus.—A Hitachi Model EPV-2 Spectrophotometer with 1 cm. cells was used for all absorbance measurements.

Reagents.—Neo-thorone (0.1%): dissolve 0.1 g. of reagent grade chemical (Hayashi Chemical Works, Osaka) in water and dilute to 100 ml.

Standard uranium nitrate solution: Dissolve 1.20 g. of reagent grade uranyl nitrate in water and dilute to 1 liter to prepare a stock solution. It was standardized gravimetrically by the oxine method. An aliquot of this solution was diluted to give a solution containing 5 μg. of uranium per ml.

Sodium ethylenediaminetetra-acetate (2%): Dissolve 20 g. of disodiumdihydrogen ethylenediaminetetra-acetate dihydrate in water and dilute to 1 liter.

Sodium acetate-acetic acid buffer: Dissolve 12 g. of sodium acetate in water and dilute to 1 liter. A 0.1 N acetic acid solution was used to make a buffer solution.

Other reagents were analytical grade chemicals.

General Procedure.—The following procedure was used to determine uranium in aqueous solution. The sample solution was adjusted to contain from 2 to 10 μg. of uranium per ml. One ml. aliquot was pipetted into 25 ml. glass stoppered volumetric flask. One ml. of 0.1% solution of Neo-thorone and 5 ml. of buffer solution of pH 6.0 were added, and then the solution was made up to 25 ml. with water. The solution was allowed to stand for five minutes, and then the absorbance was measured at 600 mμ, against a reference solution. The amount of uranium was determined by comparison with a previously prepared absorbance-uranium concentration curve.

Results and Discussion

Spectral Properties. — The absorption spectrum of an aqueous solution of Neothorone was obtained with water as the reference. The absorption peak of Neothorone in a buffered solution of pH 1.0~6.0 was found at 510 mμ. (Fig. 1). The absorption spectra of the aqueous solution of uranium—Neo-thorone complex at pH 2.0, 3.0 and 6.0 are shown in Fig. 2. Correction was applied for the reagent blank.

1) S. Shibata and T. Matsumae, This Bulletin, **31**, 377 (1958).
2) J. H. Yoe, F. Will III, and R. A. Black, *Anal. Chem.*, **25**, 1200 (1953).
3) T. Hara, *J. Chem. Soc. Japan, Pure Chem. Sec.* (*Nippon Kagaku Zasshi*), **78**, 331 (1957).
4) E. B. Sandell, "Colorimeteric Determination of Traces of Metals", 2nd Ed. Interscience Publishers, New York, 1950, p. 602.
5) ibid., p. 603.
6) J. E. Currah and F. E. Beamish, *Anal. Chem.*, **19**, 609 (1947).
7) O. Hackl, *Z. anal. Chem.*, **119**, 321 (1940).
8) V. I. Kuzenetsov, *Compt. Rend. Acad. Sci. URSS* **31**, 898 (1941).
9) M. Ishibashi and S. Higashi, *Japan Analyst* (*Bunseki Kagaku*), **4**, 14 (1955); **5**, 135 (1956).
10) K. Emi and J. Hayami, *J. Chem. Soc. Japan, Pure Chem. Sec.* (*Nippon Kagaku Zasshi*), **76**, 1291 (1955).

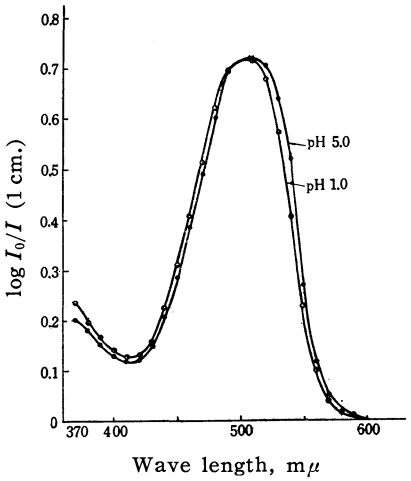


Fig. 1. Absorption spectra of Neo-thorone.

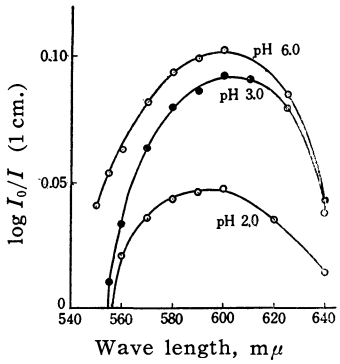


Fig. 2. Absorption spectra of uranium—Neo-thorone complex.

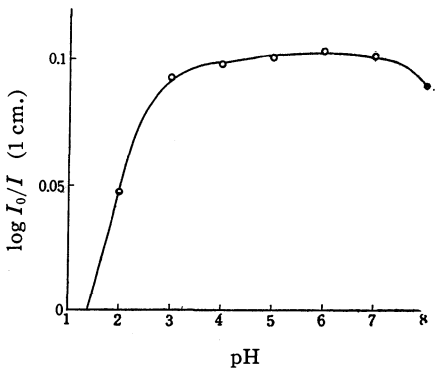


Fig. 3. Effect of pH on the color intensity.

Effect of pH. — Solutions of pH range 1.0~8.0 were prepared as previously described. The complex provides maximum intensity over a pH range of 5.0 to 7.0 (Fig. 3), the absorbance being constant over this range. With increasing pH values above 7.0, the color intensity decreased. All absorbance measurements were performed at 600 mμ.

Effect of Reagent Concentration. — The optimum amount of Neo-thorone was sought by adding various amounts of 0.1% solution of Neo-thorone to a solution containing 20 μg. of uranium, and the result is shown in Fig. 4. Corrections were made for reagent blank. In all cases the pH values were maintained constant. When more than 0.5 ml. of 0.1% Neo-thorone solution per 25 ml. was added, the absorbance become practically constant. The reagent blank increased slightly with increasing Neo-thorone concentration. Therefore, 1 ml. of 0.1% Neo-thorone solution was taken each time in the present work.

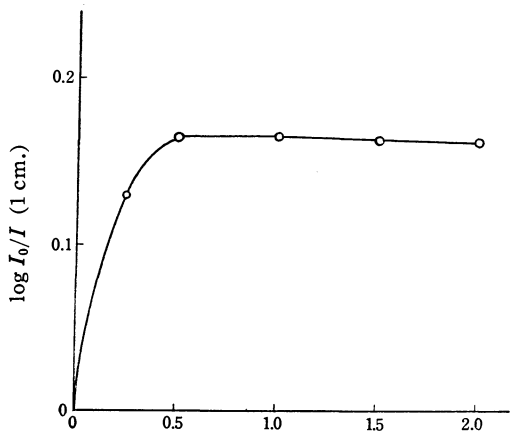


Fig. 4. Effect of Neo-thorone concentration. (20 μg. U taken, pH 6.0)

Temperature Effect. — Throughout the present investigation the experiments were carried out at room temperature which ranged from 10 to 25°C. In this range the temperature had no remarkable influence on the absorbance of uranium-Neo-thorone complex.

Stability of Color. — The color of the uranium—Neo-thorone complex in aqueous medium seemed to develop fully after a few minutes, and its intensity did not change for at least 4 hours, as shown in Table I.

TABLE I
STABILITY OF COLOR

Time after color developed.	Absorbancy (at 600 mμ)	
min.	20 μg.U/25 ml.	120 μg.U/25 ml.
5	0.081	0.429
15	0.080	0.429
60	0.081	0.429
120	0.082	0.428
240	0.081	0.429

Calibration Curve. — The calibration curve is shown in Fig. 5. It was found that the system conformed to Beer's law in the concentration range from 0 to 40 μg. of uranium per 25 ml.

Composition of Complex.—The composition of uranium—Neo-thorone complex was determined by the continuous variation method. The results obtained are shown in Fig. 6. From these results, the ratio of uranium to Neo-thorone would be 1 : 1*.

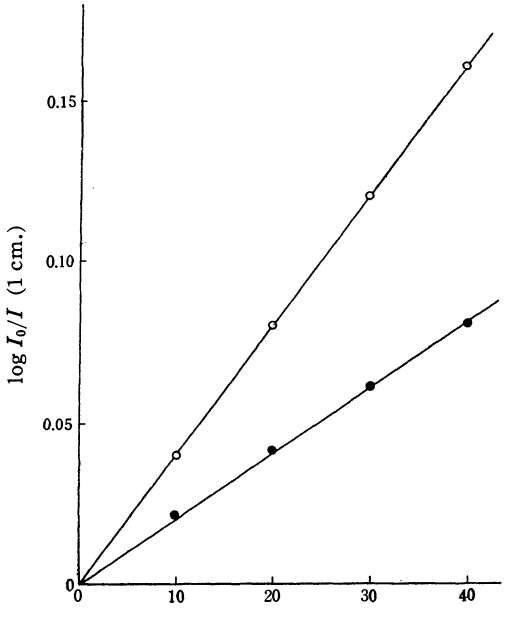


Fig. 5. Calibration curve, ○ pH 6.5, ● 1.0 ml. 1% sodium ethylenediaminetetra-acetate present.

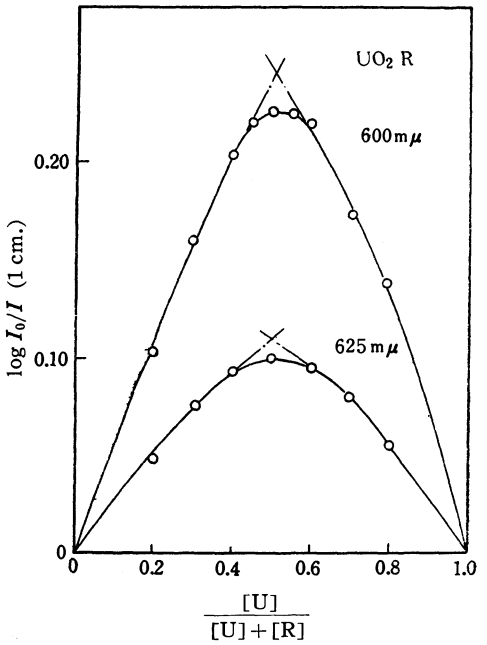


Fig. 6. Continuous variation method.

Effects of Foreign Ions.—A study was made on the effects of several anions and cations. Oxalate, fluoride, and phosphate interfered. A few grams of sodium, potassium, and ammonium which were present in the solution as acetate, sulfate, chloride, and nitrate did not interfere. Many of the cations, for example, aluminum, copper, iron(III), indium, titanium, zinc, thorium, cerium, and zirconium interfered because they formed respective complexes with Neo-thorone. But a proper amount of such metals as aluminum, iron(III), zinc, zirconium, thorium and lead can be masked by the use of sodium ethylenediaminetetra-acetate. For example absorbance measurements when using the ethylenediaminetetra-acetate as masking agents, were made for solutions containing aluminum, iron(III), zinc and thorium. The results are presented in Table II.

TABLE II
DETERMINATION OF URANIUM IN THE PRESENCE OF Al, Fe, Zn AND Th

U taken	Metals added (mg.)				U found	Error
(μg.)	Al	Fe	Zn	Tn	(μg.)	(μg.)
0.0	0.4				0.3	+0.3
10.0	0.4				10.2	+0.2
20.0	0.4				20.0	±0.0
0.0		1.0			0.1	+0.1
10.0		1.0			10.3	+0.3
20.0		1.0			20.2	+0.2
0.0			0.2		0.2	+0.2
10.0			0.2		10.1	+0.1
20.0			0.2		20.5	+0.5
0.0				0.2	0.1	+0.1
10.0				0.2	10.1	+0.1
20.0				0.2	20.0	±0.0
10.0	0·2	0.5	0.1		9.8	−0.2
20.0	0.2	0.5	0.1		20.4	+0.4

As shown Table II; aluminum, zinc, iron(III) and thorium do not interfere.

Summary

The spectrophotometric method for the determination of microquantities of uranium with Neo-thorone was established. By this method 5 to 40 μg. of uranium in

* In preparing this paper, H. Matsuyama, T. Hara and K. Koyama, *J. Chem. Soc. Japan, Pure Chem. Sec.* (*Nippon Kagaku Zasshi*), **79**, 958 (1958). have reported independently a similar method for the determination of uranium by Neo-thorone. However they have stated that the complex was composed of 2 moles of uranium to 3 moles of Neo-thorone.

25 ml. solution can be determined easily and accurately. Interference by a small amount of aluminum, zinc, lead, thorium and iron could be avoided by using sodium ethylenediaminetetra-acetate. Therefore, complete separation of iron, thorium, and aluminum is not necessary.

The authors wish to express their heartfelt thanks to Professor Dr. Masayoshi Ishibashi for his encouragement and numerous suggestions throughout the investigation. Also the authors express hearty thanks to Mr. S. Higashi who kindly supplied Neo-thorone to them.

Government Industrial Research Institute, Nagoya
Kita-ku, Nagoya

Studies on Meso-ionic Compounds. IX[1]*. *Sydnone-4-carboxylic acid via Lithium Compound*

By Hiroshi KATO and Masaki OHTA

(Received September 24, 1958)

Although a large number of sydnone derivatives have been obtained, attempts to prepare sydnone-4-carboxylic acid (III) have not yet been successful. 3-Phenyl-4-bromosydnone (I) did not react with potassium cyanide[2], nor did the Grignard reagent derived from the bromo-compound I react with carbon dioxide[3]. On the other hand, many attempts to prepare III by oxidizing the methyl group of 3-phenyl-4-methylsydnone have not been promising[4]. After many trials, the authors have finally succeeded in preparing III via lithium compound.

Among many methods proposed for the preparation of organolithium compounds, the authors have tried halogen-metal interconversion method, because it has been known that the ease of interconversion depends on the degree of positive polarization of the halogen atom[5], and it has been reported that the bromine atom of 4-bromosydnone (I) has the tendency to be removed as positive ion[2]. In accordance with the above consideration, 3-phenyl-4-bromosydnone (I) reacted smoothly with *n*-butyl-lithium to give the corresponding lithium compound (II), which in turn,

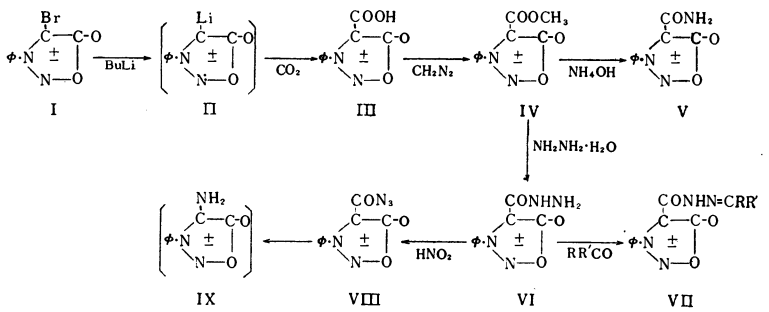


Fig. 1. Sydnone-4-carboxylic acid and its derivatives.

* Presented in part at the 11th Annual Meeting of the Chemical Society of Japan held in Tokyo, April, 1958.

1) Part VIII. M. Hashimoto and M. Ohta, This Bulletin, **31**, 1048 (1958).

2) H. Kato and M. Ohta, ibid, **30**, 210 (1957).

3) M. Ohta and H. Kato, *J. Chem. Soc. Japan, Pure Chem. Sec.* (*Nippon Kagaku Zasshi*), **78**, 1653 (1957).

4) Unpublished results of the experiment carried out by M. Hashimoto.

5) R. G. Jones and H. Gilman, *Organic Reactions*, **6**, 339 (1951).

reacted with carbon dioxide to give the expected 3-phenylsydnone-4-carboxylic acid (III). The acid gave the ester IV by reaction with diazomethane, and the ester gave the corresponding amide (V) or hydrazide (VI) by the action of ammonia or hydrazine hydrate, respectively. The hydrazide is rather unstable and is converted, by warming, into an unidentified compound. This compound is negative to Liebermann's nitroso test, but turns positive to it after being warmed with 5% sodium hydroxide solution, which suggests the maintenance of sydnone nucleus in that compound[6].

The hydrazide VI is characterized by its ready formation of hydrazones VII by reaction with ketones (see Table 1). When the hydrazide was treated with sodium nitrite in acetic acid, the corresponding azide VIII was obtained, but the authors succeeded in preparing neither aminosydnone IX nor its derivatives by Curtius or its modified reactions. As a considerable number of attempts to prepare aminosydnone IX by reduction of 4-nitrosydnone have been unsuccessful[4,7], the stability of this supposed compound might be called in question.

Experimental

3-Phenyl-4-bromosydnone (I).—The method of preparation of this compound is a little different from those reported earlier[8]. Into a solution of 50 g. of 3-phenylsydnone and 50 g. of fused sodium acetate in 400 cc. of glacial acetic acid was added dropwise 50 g. of bromine under cooling and stirring. After a few minutes, the solution was diluted with a large quantity of water and the precipitate which separated out was filtered off. Recrystallization from ethanol gave 57 g. of white needles, m.p. 141°C.

3-Phenylsydnone-4-carboxylic acid (III).—A solution of *n*-butyl-lithium in 100 cc. of ether prepared from 3.1 g. of lithium metal and 35 g. of *n*-butyl bromide[9] was added dropwise to a suspension of 35 g. of 3-phenyl-4-bromosydnone in 70 cc. of anhydrous ether under a stream of nitrogen and under stirring and cooling to −50°C. After thirty minutes, the reaction mixture was poured over 50 g. of powdered dry ice. When all the dry ice had been evaporated, the mixture was decomposed with water and the aqueous layer was washed three times with benzene and acidified with hydrochloric acid. The precipitate which separated out was collected and recrystallized from ethanol giving 25 g. of white needles, m.p. 193°C (decomp.).

Anal. Found: C, 52.16; H, 3.19; N, 13.68. Calcd. for $C_9H_6O_4N_2$ (III): C, 52.43; H, 2.93; N, 13.59%.

Methyl 3-phenylsydnone-4-carboxylate (IV).—Diazomethane prepared from 2 g. of *N*-nitroso-*N*-methyl-*p*-toluenesulfonamide was absorbed into a suspension of 0.5 g. of III in 20 cc. of ether. After a few minutes, the solution was concentrated and the crystals which separated out were collected and recrystallized from methanol giving 0.47 g. of colorless leaflets, m.p. 142°C (decomp.)

Anal. Found: N, 12.44. Calcd. for $C_{10}H_8O_4N_2$ (IV): N, 12.72%.

3-Phenylsydnone-4-carboxamide (V).—In 5 cc. of concentrated aqueous ammonia was suspended 0.2 g. of III. After being kept standing for three days under room temperature, the precipitate was collected and recrystallized from ethanol giving 0.13 g. of colorless needles, m.p. 227°C (decomp.).

Anal. Found: N, 20.50. Calcd. for $C_9H_7O_3N_3$ (V): N, 20.48%.

3-Phenylsydnone-4-carboxylic acid hydrazide (VI).—Into a solution of 10 cc. of hydrazine hydrate and 4 cc. of methanol was added 10 g. of IV. After three hours, the crystals which separated out were collected, dissolved in chloroform, and reprecipitated by addition of ligroin, giving 9 g. of yellow needles. This compound was turned into a dark red substance by warming; the latter decomposed at 303°C.

Anal. Found: C, 49.05; H, 3.99; N, 25.07. Calcd. for $C_9H_8O_3N_4$ (VI): C, 49.09; H, 3.66; N, 25.45%.

When VI was warmed in methanol or in xylene, a dark red substance of m.p. 303°C (decomp.) separated out, which is insoluble in most solvents.

Anal. Found: C, 45.92; H, 3.12; N, 25.36%.

This compound was negative to Liebermann's nitroso test, but turned positive to it after warming two hours with 5% sodium hydroxide solution.

When VI was treated with carbonyl compounds at room temperature, the corresponding hydrazones VII were obtained. Some of the derivatives of this type are listed in Table I.

Example: To 0.1 g. of VI was added a few drops of acetone. After a few minutes, petroleum ether was added and the crystals which separated out were collected, dissolved in acetone and reprecipitated by addition of petroleum ether giving 0.08 g. of white fine needles, m.p. 144~146°C (decomp.).

3-Phenylsydnone-4-carboxylic acid azide (VIII).—Into a solution of 0.6 g. of VI in 10 cc. of 50% aqueous acid, was added 0.2 g. of sodium nitrite under cooling. After thirty minutes, water was added and the crystals which separated out were collected, dissolved in acetic acid and reprecipitated by addition of water affording 0.52 g. of white needles, m.p. 102°C (decomp.).

Anal. Found: C, 46.78; H, 2.54; N, 30.37. Calcd. for $C_9H_5O_3N_5$ (VIII): C, 46.75; H, 2.18; N, 30.30%.

When VIII was heated in ethanol, water or a

6) J. C. Earl and A. W. Mackney, *J. Chem. Soc.*, **1935**, 899.
7) W. Baker, W. D. Oillis and V. D. Poole, ibid., **1950**, 1542.
8) H. Kato and M. Ohta, *J. Chem. Soc. Japan, Pure Chem. Sec.* (*Nippon Kagaku Zasshi*), **77**, 1304 (1956).
9) R. G. Jones and H. Gilman, *Organic Reactions*, **6**, 352 (1951).

TABLE I
HYDRAZONES (VII) DERIVED FROM 3-PHENYLSYDNONE-4-CARBOHYDRAZIDE (VI) AND CARBONYL COMPOUNDS

carbonyl compd.	m.p. (°C)*	characteristics	formula	N found	N calcd.
acetone	144~146	white needle[a)]	$C_{12}H_{12}O_3N_4$	21.59	21.53
methyl ethyl ketone	147	white needle[b)]	$C_{13}H_{14}O_3N_4$	20.50	20.43
benzaldehyde	219	pale yellow amorph.[c)]	$C_{16}H_{12}O_3N_4$	18.13	18.18
cyclohexanone	130	white amorph.[b)]	$C_{15}H_{16}O_3N_4$	17.93	18.66
acetophenone	224	pale yellow amorph.[c)]	$C_{17}H_{14}O_3N_4$	17.22	17.38

* All melting points are with decomposition.
Recrystallized from: a) acetone—petroleum ether; b) benzene—ligroin; c) benzene.

solution of phthalic anhydride in pyridine, no identifiable substance could be isolated. When VIII was heated in acetic anhydride for fifteen minutes on a water bath, the solvent was removed under reduced pressure, and the residue treated with water, a solid substance was obtained, which soon underwent decomposition with evolution of gas giving an unidentified oily substance.

The authors are indebted to Mr. Asaji Kondo for carrying out the microanalyses.

Laboratory of Organic Chemistry
Tokyo Institute of Technology
Meguro-ku, Tokyo

Study on Zinc Oxide-Chromium Oxide Catalyst. III. Promoting Effect of Chromium Oxide on Catalytic Activities for Methanol Synthesis and Decomposition

By Yoshisada OGINO, Masaaki OBA and Hiroshi UCHIDA

(Received September 19, 1958)

Several papers have appeared dealing with the promoting effect of chromium oxide in zinc oxide-chromium oxide catalysts on the catalytic activities for the methanol synthesis and decomposition. However only Natta's paper has been able to discuss the subject from the kinetic view point, since there had not been any rate equation of the methanol synthesis before the one given by Natta[1,2]. Recently the authors of this paper have proposed a rate equation that gives the rate constant of the synthesis from a relatively small number of measurements[3]. By the aid of this rate equation a quantitative expression of the activity becomes available more easily. This leads us to a further understanding of the promoting effect of chromium oxide.

Our previous paper[4] described the activity for the methanol decomposition in connection with the catalyst composition along with its structural dependence, but the catalyst used in the study proved to have such a poor activity that an accurate determination on the synthesis was somewhat difficult. In the present study the catalyst has been prepared by a procedure different from the previous one, and necessary attention has been paid to obtain homogeneous structure of the catalyst.

Experimental Procedure

Catalyst Preparation.—The catalysts were made by treating a commercial zinc oxide powder (grade, pure) with an appropriate chromic acid solution. The mixture was kneaded into a paste, which was divided into two portions. One of them was allowed to dry immediately at room temperature, while the other was washed with acetone before drying. According to the

1) G. Natta, P. Pino et al., *La Chimica e L' Industria*, **35**, 705 (1953).
2) G. Natta, "Catalysis III," 345 (1955) (Edited by P. H. Emmett, Rheinhold Publishing Corp., New York).
3) H. Uchida and Y. Ogino, This Bulletin, **31**, 45 (1958).
4) H. Uchida and Y. Ogino, ibid., **29**, 587 (1956).

paper by Feitknecht et al.,[5] the washing furnished a means for separating a solid product from a liquid product in the paste without decomposition. The dried cakes were powdered and pressed into tablets, which were crushed and screened to 2 to 3 mm. particles. The catalyst produced directly from the paste is denoted catalyst A, while the one from the separated solid is denoted catalyst B.

Further, another catalyst, denoted catalyst S, was prepared. A preparation of the catalyst B-9 whose chromic acid content was equivalent to Cr/Zn ratio of 0.5 was reduced in hydrogen at 350°C, and was leached with nitric acid at room temperature till any dissolution of uncombined oxide of zinc or chromium was hardly detectable. The remainder, according to the statement by T. Sato[6], was to give the crystal structure of zinc chromite spinel with no sign of either zinc oxide or chromium oxide. It was then treated in the same way as described above. The Cr/Zn ratio in the catalyst S was determined 1.6 by chemical analysis.

Catalytic Activities for Synthesis and Decomposition of Methanol. — A reactor as described in our previous paper[3] was used for the determination of catalytic activity for the methanol synthesis. The syntheses were conducted at several different temperatures from 300 to 360°C at a constant pressure (150 kg./cm^2 of $2H_2+1CO$ gas) and space velocity (about $1\cdot10^4$). Methanol concentration in the exit gas from the reactor gave a measure of the activity. On the other hand, activity for the methanol decomposition was given by a rate of carbon monoxide evolution, or percent of methanol decomposition, during a constant feed through a catalyst bed. The measurements were made at several different temperatures from 300 to 400°C. By-products in the synthesis as well as in the decomposition were determined by analytical methods as usually employed*1.

Specific Surface Area.—The specific surface area was determined from nitrogen adsorption data plotted according to the BET theory.

Results

Chemical Composition of Catalysts B.— In order to determine the time of kneading necessary for completion of the reaction between zinc oxide and chromic acid solution, change in chemical composition of the solid in the paste with kneading times was pursued. It appeared that after only one hour of the kneading both Cr/Zn ratio and the crystallisation-water in the solid attained respective values which were held approximately constant during the prolonged kneading extending twenty hours. The results clearly show that to the utmost two hours of the kneading are sufficient for completion of the reaction considered, and for producing a solid of homogeneous structure.

In Fig. 1, the Cr/Zn ratio in the catalysts B is plotted against the ratio in the original pastes after kneading for two hours. The full line in Fig. 1 illustrates the fact that the quantity of chromic acid which is removable from the paste by

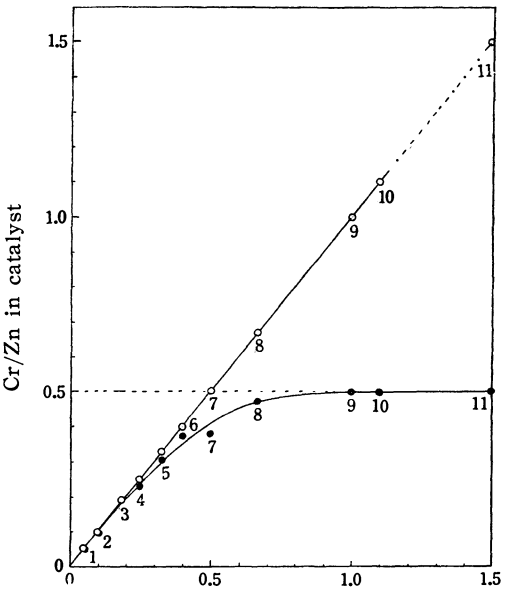


Fig. 1. Catalyst composition.

○ catalysts A; ● catalysts B

washing with acetone becomes larger according to the increasing ratio of Cr/Zn in the paste. The catalyst B, or the solid in the paste, can thus contain no more chromic acid than that equivalent to the Cr/Zn ratio of 0.5. The results also show that the solid is in equilibrium with the liquid of a higher chromic acid concentration, the amount of which becomes larger according to the increase in chromic acid content in the paste*2.

A plot corresponding to the series of

5) W. Feitknecht and L. Hugi-Carmes, *Helv. Chim. Acta.*, 37, 2107 (1954).

6) T. Sato, Lecture at the Fourth Symposium on Catalysis, 1956.

*1 Refer to our previous paper[3,4], and also the paper by Brown et al. (*Ind. Eng. Chem.*, **21**, 310 (1929)) for analysis of dimethylether.

*2 Chromic acid concentration of the liquids actually existing in equilibrium with the solids was determined, which follows:

Cr/Zn in paste	1/3	1/2	1/1.5	1	1.5	2.0
Cr/Zn in solid	0.31	0.38	0.47	0.50	0.50	0.50
Cr/Zn in liquid	0.82	1.17	1.78	1.85	1.89	1.95

The results are essentially in agreement with those by Groeger[7].

7) M. Groeger, *Z. anorg. Chem.*, **70**, 135 (1911).

catalysts A gives the straight line in the figure.

Catalytic Activity for Methanol Synthesis and Decomposition.—Part of the results is shown in Fig. 2 presenting the methanol concentration as a function of the reaction temperature. From the data available, rate constants, k, have been calculated by the aid of the following rate equation proposed by us[3],

$$r = k(p_{CO}p^2_{H_2})^{0.7} - p_{CH_3OH}\cdot(p_{CO}p^2_{H_2})^{-0.3}/K$$

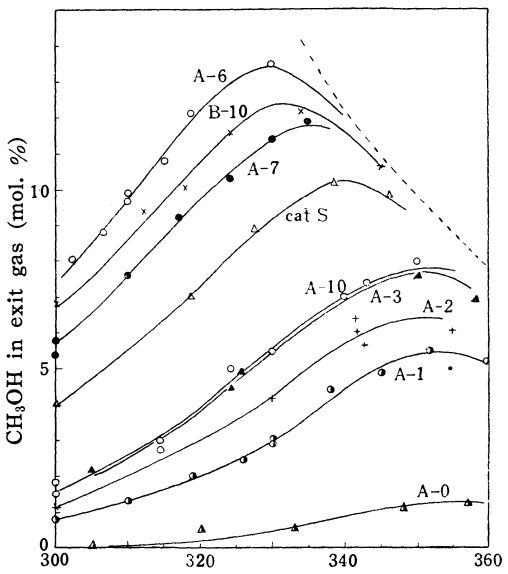


Fig. 2. Methanol concentration as a function of reaction temperature at 150 kg./cm² and S. V. of 0.95—1.05·10⁴.

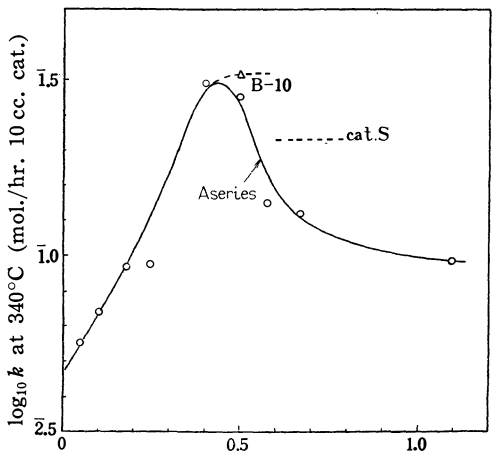


Fig. 3. Relation of Cr/Zn ratio to catalytic activity for synthesis.
k's were evaluated from the data in Fig. 2 after the corrected values at S. V. of 1·10⁴ had been estimated.

where K is the equilibrium constant of the synthesis, and are given in Fig. 3 as a function of Cr/Zn ratio in the catalysts. The figure reveals that the series of catalysts A exhibits maximum activity at the Cr/Zn ratio which is a little less than 0.5, whereas catalyst B-10 of Cr/Zn ratio of 0.5 gives activity higher than the catalyst A-7 of the same Cr/Zn ratio.

Molstad et al.,[8] and Frolich et al.[9] have done comprehensive work on the activity correlated to the Cr/Zn ratio in a wider range. The present results give a maximum activity at the same Cr/Zn ratio as pointed out by the former, but differ from the work of the latter in giving the maximum activity at a somewhat higher Cr/Zn ratio. The difference may mainly be due to our mode of catalyst preparation which is different from theirs.

Catalyst S is of intermediate activity between catalyst B-10 and catalyst A-10. Catalytic activity for the methanol decomposition is shown in Fig. 4 as a function

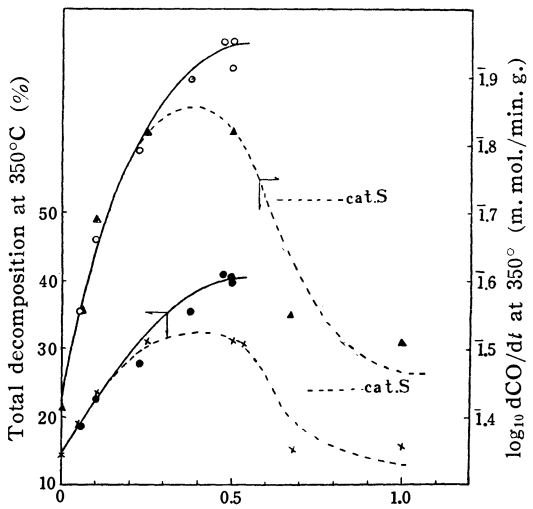


Fig. 4. Relation of Cr/Zn ratio to catalytic activity for decomposition.
dotted lines, A series; full lines, B series.

of Cr/Zn ratio in the catalyst. Tendencies similar to those found in the synthesis are found in the decomposition. Furthermore an asymptotic rise of the activities of catalysts B with the increasing Cr/Zn ratios up to 0.5 can be seen more clearly. The similarity between the changes in activity for the synthesis and for the

8) M. C. Molstad and B. F. Dodge, *Ind. Eng. Chem.*, 27, 134 (1935).
9) P. K. Frolich and D. S. Cryder, ibid., 21, 867 (1929).

TABLE I
SPECIFIC SURFACE AREAS OF CATALYSTS

Catalyst	A-0	A-0	A-1	A-2	A-3	A-6	A-7
Specific surface area[a], m^2/g.	5.8[b]	6.3	40	29	35	96	44
Catalyst	A-10	B-1	B-2	B-4	B-9	S	
Specific surface area[c], m^2/g.	20	40	31	68	90	43	

a), numerals listed, except b), show the specific surface areas determined on the catalysts after having been used in the synthesis: b) is the area determined on the catalyst A-O before the synthesis. c), the specific surface areas of catalysts B were determined on the specimens reduced in hydrogen at 320~350°C.

decomposition with the Cr/Zn ratios was once reported by Frolich et al..*3

Selectivity in Synthesis and Decomposition.—In the synthesis, gaseous products such as carbon dioxide and methane were produced in extremely small amounts: increase in carbon dioxide concentration in the gas after the synthesis did not exceed one percent, and hardly any methane was detectable. Among the liquid products both formaldehyde and methylformate were usually found to be very small in amount (0.1% and 0.5% respectively), and because of the too small quantity of dimethylether produced, no accurate determination was probable by the method employed in this work. On the other hand, the zinc oxide catalyst gave the highest yield of water, which diminished rapidly with the increasing Cr/Zn ratios in the catalysts (refer to Fig. 5). Anyhow, hardly any kind of effect of chromic acid addition undesirable to the selectivity of the synthesis has been found.

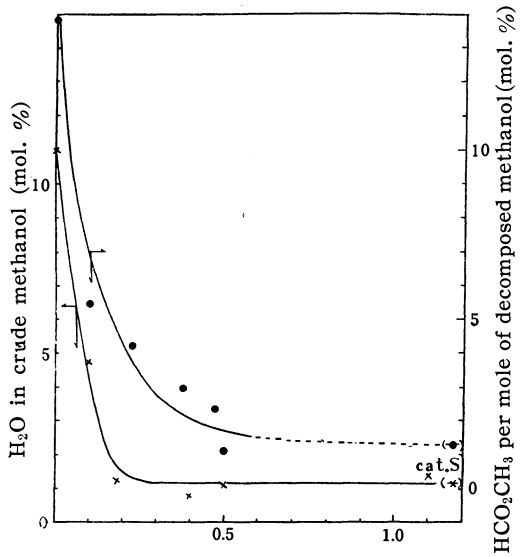


Fig. 5. Cr/Zn ratio in catalyst and selectivity in reactions.

*3 In this respect any similarity was hardly found by Storch (*J. Phys. Chem.*, 32, 1743 (1928)).

In the methanol decomposition, small quantities of carbon dioxide and formaldehyde were produced, independent of the Cr/Zn ratios in the catalysts, whereas the production of methylformate seemed closely correlated to the ratio (refer to Fig. 5). The correlation appeared remarkable on the series B of the catalysts: the yield was the greatest on the zinc oxide catalyst, and tended to decline regularly with the increasing Cr/Zn ratios. As for the series of the catalysts, a slight minimum of the yield appeared at a relatively small Cr/Zn ratio.

Specific Surface Area. — The specific surface areas which were determined on the catalysts after the synthesis are listed in Table I. With respect to the series A the area passes through a maximum at the Cr/Zn ratio of 0.4. The individual catalysts of the B series show a larger specific surface area than the corresponding ones of the series A.

Discussion

Catalyst Composition and Catalytic Activity.—In the course of our manufacturing the catalysts A, the liquid which contained chromic acid more abundantly than the solid in the paste left after drying the surface layer of higher chromic acid content at the back of the original solid particle, and the particle surface became more enriched with chromic acid than the particle interior. Therefore the chemical composition of the catalysts A can not indicate the real surface concentration of chromic acid. On the other hand, the chemical composition of the catalysts B can directly predict the concentration considered, since the catalyst was produced from the solid, free of the liquid. Only the B series of the catalysts thus gives a correct relation of the catalytic activity to the chemical composition.

For the reason mentioned above, a maximum of the activity appearing at the Cr/Zn ratio shortly before 0.5, which was usual in the previous work, is not the necessary relation between the activity and the chemical composition. An excessive addition of chromic acid may certainly cause decrease in the activity, since chromic acid alone is no more an active catalyst than zinc oxide alone, but an exact representation of the activity change in the intermediate range of the Cr/Zn ratio has not been established as yet*4.

Catalyst Composition and Specific Catalytic Activity per Unit Surface Area.—By dividing the activity per gram of the catalyst by the specific surface area, the specific catalytic activity per unit surface area is obtained, and is plotted against the Cr/Zn ratio of the catalyst in Fig. 6. Over a wide range of the relatively high ratios, the specific activities for both the synthesis and the decomposition vary a little, gradually approaching either one of catalyst S. However, in the range of the low Cr/Zn ratio the specific activity for the synthesis rises with the increasing Cr/Zn ratios, whereas the one for the decomposition indicates the opposite.

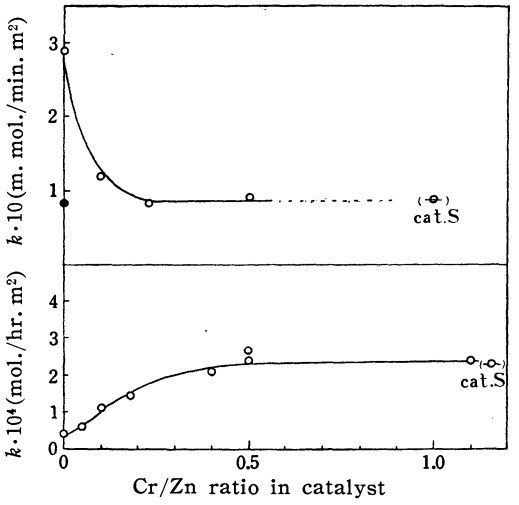


Fig. 6. Relation between Cr/Zn ratio in catalyst and specific activity per unit surface area.
above, decomposition; below, synthesis.
● shows the specific activity determined on catalyst A-0 after having been used in the synthesis.

*4 In this respect a catalyst prepared by coprecipitation of hydroxides of zinc and chromium from a mixed solution of the nitrates was at first expected to give information, however it has proved difficult to obtain a catalyst of homogeneous structure as well as one of moderate activity by this procedure of preparation.

It was at first sight apparently difficult to explain the results thus seemingly inconsistent with each other, but soon the following fact could shed some light upon the subject: the catalysts without and with a little chromic acid content turned gray after having been used in the synthesis for a few days, and came to give far lower activity for the decomposition than the original one having the clean surface, while regarding the catalyst of the higher chromic acid content neither darkening of the catalyst nor decrease in the activity for the decomposition occurred. This shows easier contamination of the surface of the former catalyst with carbon from carbon monoxide decomposition during the synthesis. If the catalyst surface remained clean, the series of catalysts with none and with a little chromic acid content should show the downward tendency of the activity for the synthesis with the increasing chromic acid contents.

At any rate change in the activity based on unit surface area is far smaller than that in the activity based on unit mass (volume) of the catalyst. This suggests an apparent proportionality of the catalytic activity to the extent of the specific surface area, and furthermore, when combined with the relation of the specific surface area to the Cr/Zn ratio, an intercrystalline promoting effect of chromic acid.

Relation of Catalyst Composition to Activation Energy and Frequency Factor in Methanol Synthesis and Decomposition.—From Arrhenius' plots of the rate constants of the synthesis and the decomposition, the constants being based on unit specific surface area, the activation energy and frequency factor have been evaluated*5. Fig. 7 shows the plots of the energy and factor vs. the Cr/Zn ratio in the catalyst. Both of the plots similarly fall with the increasing Cr/Zn ratio rapidly at first, and then asymptotically approach respective minimum values of catalyst S*6.

The addition of chromic acid thus causes decreases in both the frequency factor and the activation energy. The decrease in the former necessarily results in the fall

*5 In our previous paper the plots on the rate of decomposition were given on the catalysts of a different procedure of preparation, and were found intersecting with each other at a definite $1/T$. In the present results the plots certainly show different slopes, but no intersection appears in the temperature range which is far lower than that in the previous paper.

*6 Although the syntheses were not always conducted on the clean catalyst surface, the present tendency may be considered still inherent to the clean one.

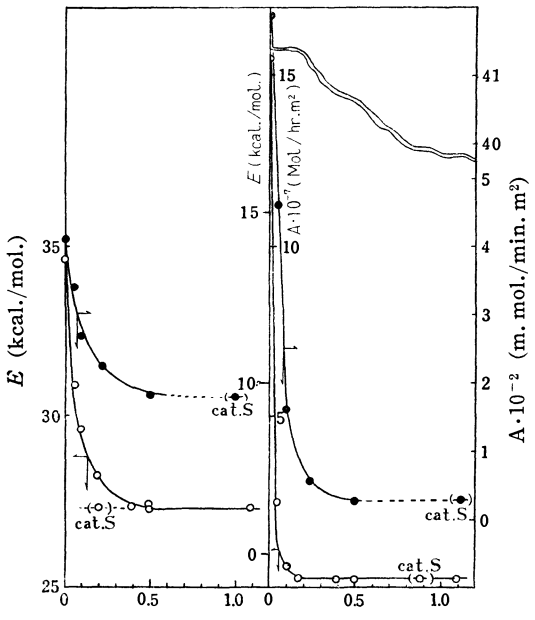


Fig. 7. Relation of Cr/Zn ratio in catalyst to activation energies and frequency factors of reactions.
○, synthesis: ●, decomposition.

of the specific activity per unit surface area, which is simultaneously compensated with decrease in the latter. Consequently the specific activity per unit specific surface area can be maintained at the level of catalyst S, presumably a zinc chromite spinel, of moderate activity.

At first sight one may be apt to consider chromic acid simply an intercrystalline promoter, namely a structural promoter responsible for production of high-area structure, but closer investigation as mentioned above leads us to the conclusion that chromic acid behaves not only as an intercrystalline but also as an intracrystalline promoter, namely a promoter modifying the structure of the catalyst advantageously for preservation of the specific activity*7. Moreover, we should like to emphasize the effect of chromic acid addition upon the improvement of the selectivity and prevention of carbon monoxide decomposition on the catalyst surface, which are suggestive rather of a intracrystalline than an intercrystalline promoting effect.

*7 Natta stated that chromium oxide was an intercrystalline promoter because of there being little change in the activation energy of the synthesis by the addition.

Summary

The catalysts have been prepared from pastes of zinc oxide powder kneaded with chromic acid solutions of different concentrations. From the pastes two series of the catalysts have been produced, namely the one directly from the paste and the other from the solid, free of the liquid, in the paste. Only the results on the latter series can give the correct relation of the catalyst composition to the catalytic activity, which indicates the activity rising with the higher chromic acid contents to an asymptotic maximum at the Cr/Zn ratio of 0.5.

The catalytic activity on the catalysts of different Cr/Zn ratios almost parallels the specific surface area of the catalysts, while the specific activity based on unit specific surface area of the catalysts changes in a far less degree than the change in activity per unit gram of the catalyst. These suggest an intercrystalline promoting effect of chromic acid. Moreover the closer investigation on the activity reveals that both the activation energy and the frequency factor of the reactions which are based on unit surface area show a downward tendency with the increasing Cr/Zn ratios asymptotically to their respective minimums of presumable zinc chromite spinel. This shows besides an intracrystalline promoting effect of chromic acid.

Within the range of the present study, hardly any effect of chromic acid addition undesirable to the selectivity in the synthesis has been found.

Government Chemical Industrial Research Institute, Tokyo
Shibuya-ku, Tokyo

Non-exchange of Sulfur Atoms between Sulfate and Sulfonate Ions

By Mitsuo MURAMATSU

(Received October 3, 1958)

Many works have been undertaken to determine whether the sulfur atoms in an organic molecule can exchange themselves with those in a molecule of another compound[1]. According to the reports published up to the present, a measurable rate was observed in the exchange reactions between alkyl disulfides and trisulfides[2], elementary sulfur and organic substances containing S-S or C=S bond[3], sulfite and alkylthiosulfates[4], and alkylpolysulfides and alkylmercaptides[5]. These facts may be explained by the easiness of opening and subsequent closing of sulfur bond in organic compounds. However, no exchange seemed to be reported between other sulfur-containing compounds[1].

In order to obtain further information regarding the lability of sulfur bond and to study the possibility of introducing radioactive sulfur atoms into the molecules of organic compounds, the present author has attempted to study the exchangeability of sulfur atom in sulfate with that in sulfanilate, naphthionate, β-naphthalenesulfonate, *o*-nitrophenolsulfonate, *o*-carboxybenzenesulfonate, *m*-nitrobenzenesulfonate and taurine.

Experimental

Sodium salts of taurine, sulfanilic acid and naphthionic acid were of reagent grade. Ammonium *o*-carboxybenzenesulfonate, sodium *m*-nitrobenzenesulfonate, *o*-nitrophenolsulfonate and β-naphthalenesulfonate were synthesized. All these sulfonates were recrystallized repeatedly and were dissolved to make a stock solution of 0.25 M. The solution of radioactive sulfate having specific activity of 10 mC/mol. was prepared by dissolving purified sodium sulfate into a solution of carrier-free $^{35}SO_4^{2-}$, to make a solution of 0.25 M.

Four cc. portions of sulfonate and sulfate solutions were transferred into a measuring flask and made up exactly to 10 cc. and to a desired acidity with distilled water and dilute hydrochloric acid or aqueous ammonia. The reaction mixture was then transferred into a reaction flask to which a reflux condenser was attached and was kept at desired temperature.

After the supposed exchange reaction, inorganic sulfate was separated as barium salt and the specific activity of the precipitate and the remaining sulfonate in the filtrate was determined separately after purification. In the case of naphthionate, another method of separation was also adopted; hydrochloric acid was added to the reaction mixture and the specific activity of naphthionic acid formed was determined.

TABLE I

FRACTION EXCHANGE, *F*, IN THE REACTION OF SODIUM SULFATE AND SODIUM NAPHTHIONATE: CONCENTRATION OF SODIUM SULFATE AND NAPHTHIONATE ARE BOTH 1/10 mol./1. pH=7

Time	Room temperature		91±2°C	
	F, %	Method of separation	*F*, %	Method of separation
1 hr.	0.1±0.1	$BaSO_4$		
2 〃			3.8±0·8	$BaSO_4$
4 〃	0.2±0.1	$BaSO_4$		
9 〃			−2.9±2.0	$BaSO_4$
12 〃			0.5±1.1	$BaSO_4$
21 〃	0.0±0.1	naphthionic acid		
28 〃	0.0±0.1	naphthionic acid	0.1±0.2	naphthionic acid
22 days	0.0±0.2	$BaSO_4$		
150 〃	0.1±0.8	naphthionic acid		
161 〃	0.6±0.6	$BaSO_4$		

1) G. Hevesy, "Radioactive Indicators" (1948), Interscience Publ., Inc., New York, p. 85; A. C. Wahl and N. A. Bonner, "Radioactivity Applied to Chemistry", (1951). John Wiley and Sons, Inc., New York, p. 346.

2) E. N. Gur'yanova and V. N. Vasil'eva, *Zhur. Fiz. Khim.*, 28, 60 (1954).

3) E. N. Gur'yanova, ibid., 28, 60 (1954).

4) A. Fava and G. Pajaro, *J. Am. Chem. Soc.*, 78, 5203 (1956).

5) A. Fava and A. Illiceto, *Ricerca Sci.*, 23, 839 (1954); S. Ikeda, *J. Chem. Soc. Japan, Pure Chem. Sec.* (*Nippon Kagaku Zasshi*), 79, 103 (1958).

Radioactivity of each sample was measured by means of an end-window type GM counter. The quantity of the sample to be counted was little enough to ignore the self absorption of soft β-ray of sulfur-35.

Results and Discussion

It was observed that no measurable exchange of sulfur took place between sulfate and any organic sulfonates during a few decades of hours at temperature up to 91±2°C or during six months at room temperature. This was indeed the case at any pH from 2 to 10. Separation-induced exchange did not take place for any compounds studied, irrespective of the method of separation. Typical examples are shown in Table I.

Such a difficulty of exchange may be ascribed to the firm C–S bond in the sulfonate ion, rather than the S=O bond in the sulfate. Actually, a slow rate of exchange of the oxygen atom in the reaction of sulfate ion with $H_2{}^{18}O$[6] is not sufficient to explain the present results. Such a conclusion is in accord with what is familiar in organic chemistry.

The author wishes to thank Professor T. Sasaki for his criticism and many helpful suggestions. The cost of this research was defrayed from the Scientific Research Expenditure of the Ministry of Education.

Department of Chemistry
Faculty of Science
Tokyo Metropolitan University
Setagaya-ku, Tokyo

6) T. C. Hoering and J. W. Kennedy, *J. Am. Chem. Soc.*, **79**, 56 (1957); T. Titani and K. Goto, This Bulletin, **14**, 77 (1939), etc.

Ion-Exchange Separation of Cerium and Thorium with Lead-EDTA Complex as Eluting Agent

By Tomitsugu TAKETATSU

(Received October 11, 1958)

Vickery[1] reported that when EDTA was used as eluant, separation of two metal ions by ion-exchange resin became more effective by introducing a third metal ion having a peak position of elution between those of the two ions, than the separation without the third metal ion. The method, using a third metal-EDTA complex solution as eluant was studied in this paper, instead of adding the third metal ion to the sample solution. Schwarzenbach et al.[2] determined the formation constants of cerium(III)-, lead(II)- and thorium(IV)-EDTA complexes and gave values $10^{16.0}$, $10^{18.0}$ and $10^{23.2}$, respectively. The separation of cerium and thorium ions was tried here by cation exchange resin with lead-EDTA.

Experimental

Reagents and apparatus.—Solution of lead-EDTA complex in various concentrations was prepared by adding a measured volume of a 0.1 mole solution of disodium salt of ethylenediaminetetraacetic acid to a 0.1 mole lead nitrate solution of the same volume, the pH controlled with aqueous ammonia and nitric acid and filled up to 1000 ml. with distilled water. Thorium or cerium standard solutions were prepared by dissolving their nitrate in distilled water and the concentrations were determined gravimetrically as their oxides. The results were 5.38 mg./ml. (ThO_2) and 12.00 mg./ml. (CeO_2).

The cation exchange resin Dowex 50 of ammonium form and of 50×100 mesh was used in a column of 5 cm.×0.6 cm^2.

General procedure.—The following procedure was recommended. A slightly acidic mixed solution of cerium and thorium ions was poured over the top of the column and the ions were adsorbed on the resin bed. After the resin bed was washed with 100 ml. of water, 250 ml. of a 0.015 M solution of lead-EDTA complex (pH 3.0) was passed through the column at a flow rate of 1.0~1.5 ml./min. in order to elute thorium ions. It was again washed with 100 ml. of water and cerium ions were eluted with 3 N hydrochloric acid. Lead ions remaining in the column were

1) R. C. Vickery, *J. Chem. Soc.*, **1952**, 4357.
2) G. Schwarzenbach, R. Gut and G. Anderegg, *Helv. Chim. Acta*, **37**, 937 (1954).

precipitated as lead chloride but gradually redissolved in hydrochloric acid and eluted from the resin bed.

Analytical method.—The first effluent containing thorium and lead ions was dried up, and treated with concentrated sulfuric and nitric acid to decompose EDTA[3]. Lead ions were thus removed as lead sulfate. The second effluent containing cerium and lead ions was similarly treated. Cerium and thorium ions were precipitated with aqueous ammonia and their concentrations determined gravimetrically as oxides.

Results and Discussion

The quantities of thorium and cerium used were 26.9 mg. (ThO_2) and 44.1 mg. (CeO_2), respectively. The effects of various conditions of the eluant on the rate of separation were examined, i.e., the concentration of lead-EDTA complex solution, the pH and the flow rate.

Effect of the concentration.—Lead-EDTA complex solution with concentrations varying from 0.010 to 0.020 mole was used as eluants. The pH value was fixed at 3.0 and the flow rate at 1.5 ml./min. Each 100 ml. of the effluents was collected and the concentration of thorium or cerium ions was determined. The data obtained are given in Fig. 1.

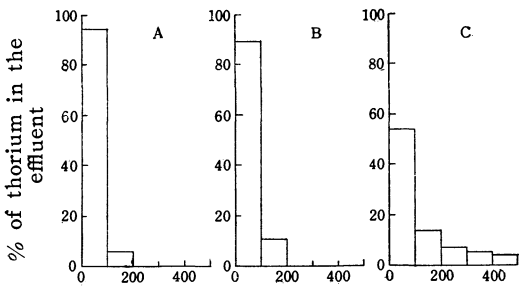


Fig. 1. Elution of thorium ion at different concentrations of eluants.
A: 0.020 mol. lead-EDTA complex solution.
B: 0.015 mol. lead-EDTA complex solution.
C: 0.010 mol. lead-EDTA complex solution.

It can be seen that thorium ions were completely eluted with 200 ml. of 0.020 and 0.015 mole eluants but incompletely with 500 ml. of 0.010 mole eluants. On the other hand, cerium ions were not eluted with the eluants under the same conditions.

Effect of pH.—In order to determine the optimum pH, 0.015 mole eluants of pH 2.4, 3.0 and 4.7 were used. The elution graphs for thorium ions are shown in Fig. 2.

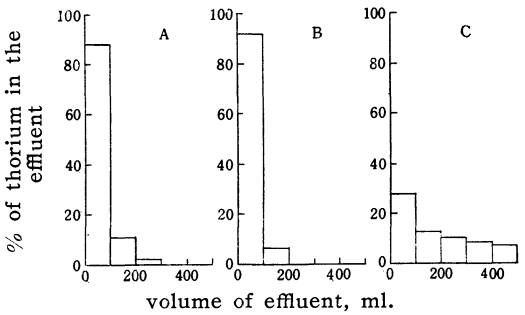


Fig. 2. Elution of thorium ion at different pH values of eluants.
A: pH 2.4 B: pH 3.0 C: pH 4.7

The data indicate that thorium ions were most effectively eluted at pH 3.0, whereas cerium ions were not eluted in the range of pH between 2.4 and 4.7.

Effect of flow rate.—The flow rate studied was 0.6, 1.2 and 2.0 ml./min. Each 50 ml. of the effluent was collected and the concentration of thorium ions was determined. The results are shown in Fig. 3.

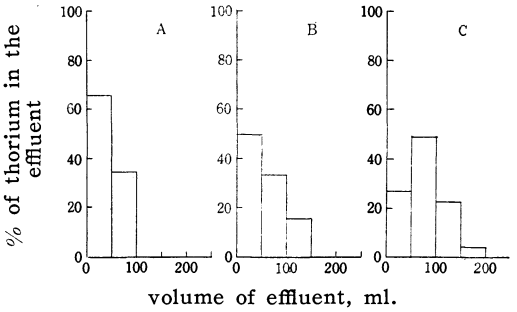


Fig. 3. Elution of thorium ion at different flow rates.
A: 0.6 ml./min. B: 1.5 ml./min.
C: 2.0 ml./min.

From the elution graphs it can be seen that the amount of thorium ions in the effluent increases with decrease of the flow rate. However, a flow rate of 1.0~1.5 ml./min. was employed to make the time taken for an experiment reasonable. Cerium ions were not eluted at any flow rate of the eluant.

The optimum conditions for the separation were as follows: the concentration of the lead-EDTA complex solution was 0.015 mole, pH 3.0 and the flow rate 1.0~1.5 ml./min. Fig. 4 shows that cerium ions

3) W. F. Hillebrand and G. E. F. Lundell, "Applied Inorganic Analysis" (1929), John Wiley & Sons, Inc., New York, p. 61.

were not eluted even with 1000 ml. of the lead-EDTA solution at the optimum conditions.

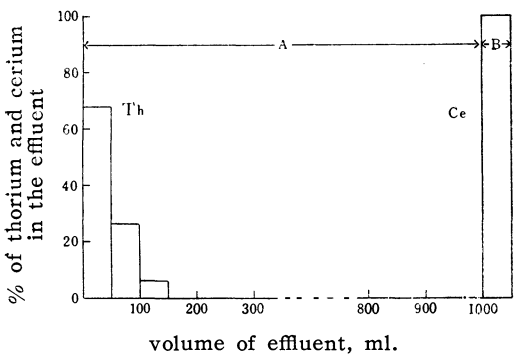


Fig. 4. Elution graph of thorium and cerium.
eluant { A: 0.015 ml. lead-EDTA complex solution.
B: 3 N HCl solution.

On the other hand, when only an EDTA solution of the concentration of 0.015 mole was used as eluant at pH 3.0 and at a flow rate 1.0~1.5 ml./min. instead of the lead-EDTA complex solution, cerium ions began to flow out even in the first fraction of the volume of 50 ml. This shows that lead ions as the third element in the lead-EDTA complex gave a remarkable effect on the efficiency of the separation.

The results of analyses for various quantities of the two ions by this procedure are shown in Table 1.

TABLE I
SEPARATION OF CERIUM AND THORIUM IONS

Taken. (mg.)		Found. (mg.)			
ThO_2	CeO_2	ThO_2	Error	CeO_2	Error
39.5	19.6	39.7	+0.2	19.6	±0.0
26.9	12.0	26.9	±0.0	11.7	−0.3
53.8	12.0	53.6	−0.2	11.9	−0.1

A qualitative detection by the fluorescent X-ray spectrometer "Norelco" showed that there was neither cerium in the thorium oxide fraction nor thorium in the cerium fraction. Thus, it was concluded that the separation of cerium and thorium ions was quantitatively carried out.

At the optimum conditions of the separation of cerium and thorium ions, the behavior of other rare earth ions was examined. Rare earth ions, i.e., lanthanum, cerium, praseodymium, neodymium, dysprosium and yttrium and a trace of thorium were extracted from allanite and adsorbed on the resin bed. The total weight of their oxides was about 123.2 mg. After 250 ml. of the 0.015 mole lead-EDTA solution (pH 3.0) was passed through the resin bed, the rare earth and thorium ions in the effluent and in the resin bed were separately determined gravimetrically as oxides. Each rare earth oxide was qualitatively detected by the fluorescent X-ray spectrometer. Heavy lanthanons, gadolinium, dysprosium and yttrium and thorium (total oxides 11.1 mg.) were detected in the effluent; on the other hand, light lanthanons, lanthanum, cerium, praseodymium, neodymium, samarium and gadolinium (total oxides 112.0 mg.) were found to remain in the resin bed.

Further studies are under way on the separation of the rare earths with the lead- and other-EDTA complex solutions as eluants.

Summary

The separation of cerium and thorium ions was studied with a lead-EDTA complex solution as eluant. The optimum conditions were determined as the following: the concentration of the lead-EDTA solution was 0.015 mole, pH 3.0 and the flow rate 1.0~1.5 ml./min. Thorium ions were completely eluted with 200 ml. of the eluant at the optimum conditions, while no cerium ions were detected in the effluent with 1000 ml. of the eluant. Thus the use of a lead-EDTA complex solution as eluant was concluded to be effective for separation of cerium and thorium ions.

The author wishes to express his gratitude to Professor S. Misumi for his valuable discussion and encouragement.

Department of Chemistry
Faculty of Science
Kyushu University
Hakozaki, Fukuoka

Phenothiazine Derivatives. III[1]. *Mechanism of the Reaction of Diphenylamine with Thionyl Chloride*

By Manabu FUJIMOTO

(Received September 24, 1958)

In the preceding paper[1] of this series, it was reported that diphenylamine (I) reacts violently with thionyl chloride, thionyl bromide and sulfuryl chloride, and that thionyl chloride transforms diphenylamine (I) into 1,3,7,9-tetrachlorophenothiazine (II), while thionyl bromide and sulfuryl chloride transforms it merely into 2,4,6,2′,4′,6′-hexabromodiphenylamine and the corresponding hexachlorodiphenylamine (III), respectively, as shown schematically in Chart I, where arrows with crosses indicate that the expected changes do not take place by the action of thionyl chloride.

Thionyl bromide is less stable than thionyl chloride, decomposing slowly even at room temperature as follows:

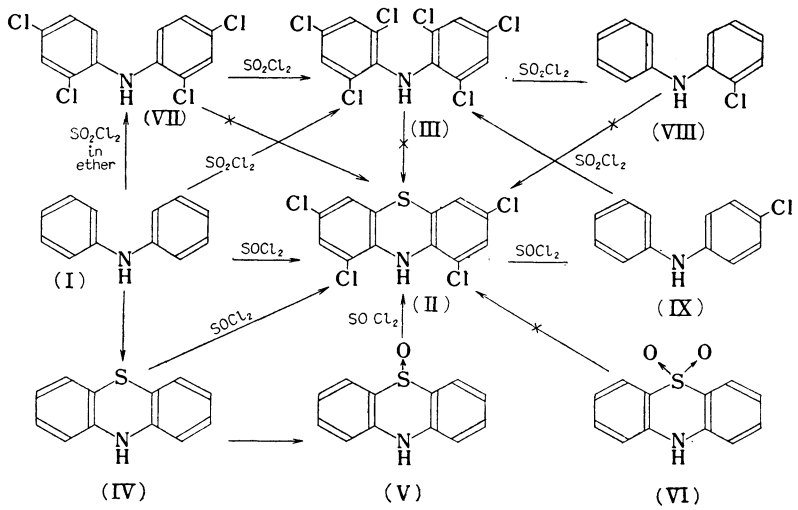
$$4SOBr_2 \rightarrow S_2Br_2 + 3Br_2 + 2SO_2$$

Therefore, in its reaction with diphenylamine (I) it gives an extensively brominated product, hexabromodiphenylamine. On the other hand, the sulfonyl group in sulfuryl chloride is so stable that the reagent can react with diphenylamine (I) only as a chlorinating agent (Chart I).

The present paper deals with the characteristic reaction of thionyl chloride with diphenylamine which has been further studied closely. The reaction involves at least two processes, namely, phenothiazine ring formation and chlorination of the benzene nuclei, but the sequence of the two processes is to be determined.

As already reported[1], phenothiazine (IV) and its 5-oxide (V) react with thionyl chloride to form the same tetrachlorophenothiazine (II). Nevertheless, it has now been found that the hexachlorodiphenylamine (III), 2,4,2′,4′-tetrachlorodiphenylamine (VII)[2], 2-chlorodiphenylamine (VIII) and phenothiazine 5,5-dioxide (VI) do not react with thionyl chloride. On the other hand, the tetrachlorophenothiazine (II) was obtained from the reaction of 4-chlorodiphenylamine (IX) and thionyl chloride. Therefore, it may be concluded that the first process of the reaction giving the chlorinated phenothiazine is the sulfur-bridge formation to

CHART I



1) Part II; H. Kanô and M. Fujimoto, *Pharm. Bull.*, 5, 393 (1957).

2) F. Krollpfeiffer et al., *Ber.*, 67, 914 (1934).

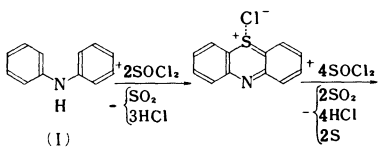
TABLE I

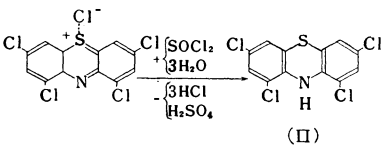
Solvent	Thionyl chloride (g.)	Volume of solvent (ml.)	Time of reflux	Recovered diphenylamine (%)	Diphenylamine hydrochloride (%)	Tetrachlorophenothiazine (%)
Benzene	0.7	30	1 hr.	71	26	2
	4.2	〃	〃	78	—	10
Carbon tetrachloride	0.7	20	〃	80	13	—
	4.2	〃	30 min.	58	33	—
	〃	〃	8 hr.	57	—	28

give the phenothiazine ring system, followed by the chlorination to yield the final product II.

It was expected that dilution with an inert solvent, such as benzene or carbon tetrachloride, might moderate the reaction and make it possible to catch an intermediate of the phenothiazine type, such as phenothiazine (IV), its 5-oxide (V), phenazathionium chloride or hydroxide. But moderation of the reaction gave mainly diphenylamine hydrochloride along with a small amount of the final product II (Table I). This result can be interpreted by assuming that the dilution with an inert solvent retards greatly the first process of phenothiazine formation, but the chlorination of the phenothiazine once formed is relatively rapid.

In the reaction of diphenylamine to give the tetrachlorophenothiazine (II), color development of brown to dark green and the presence of sulfur monochloride or dichloride in the thionyl chloride in reflux are always observed, which facts suggest intermediate formation of phenazathionium chloride, because it is known that penazathionium chloride and hydroxide form dark brown needles[3]. Thus the reaction mechanism may be represented as follows:





As phenothiazine 5,5-dioxide is a sulfone, so it would not be transformed into a phenazathionium compound, and thus it can reasonably be expected that it will resist the attack by thionyl chloride.

Experimental

Treatment with Thionyl Chloride. — The general procedure for the treatment with thionyl chloride was as follows. To a diphenylamine or a phenothiazine derivative (1 g.), 10 ml. of thionyl chloride was added dropwise, and the mixture was heated gently under reflux for 5 min. Hydrogen chloride and sulfur dioxide were evolved when a reaction took place. The cooled solution was poured onto crushed ice. 1,3,7,9-Tetrachlorophenothiazine (II) was obtained yellow crystals from diphenylamine (I), phenothiazine (IV), the 5-oxide (V) and 4-chlorodiphenylamine (IX). Recrystallized from benzene, it showed m.p. 235 ~236°C. The yield was nearly quantitative. 2,4,6,2',4',6'-Hexachlorodiphenylamine (III), 2,4,2',4'-tetrachlorodiphenylamine (VII), 2-chlorodiphenylamine (VIII) and phenothiazine 5,5-dioxide (VI) were recovered intact.

Treatment of Diphenylamine with Thionyl Chloride in Solution. — Diphenylamine (1 g.) was dissolved in a solvent, and thionyl chloride dissolved in the same solvent was added drop by drop. The mixture was refluxed, cooled, and poured on ice. After filtration, the organic layer was separated, dehydrated over sodium sulfate, and passed through a column of alumina. Elution first with the same solvent and then with a mixture of the solvent and acetone gave the results listed in Table I.

Diphenylamine Hydrochloride. — Recrystallized from methanol-ethyl acetate. Colorless needles, m.p. 195~196°C (decomp.).

Anal. Found: C, 69.80; H, 5.96; N, 6.75. Calcd. for $C_{12}H_{12}NCl$: C, 70.04; H, 5.88; N, 6.81 %.

Treatment with Sulfuryl Chloride. — One gram of each of diphenylamine (I), and chlorinated diphenylamines, VII, VIII and IX, was treated with 10 ml. of sulfuryl chloride. When the initial violent reaction ceased, the solution was refluxed for 30 min., and poured onto crushed ice. The precipitate was collected, dried, and recrystallized from ethanol. The product was always 2,4,6,2',4',6'-hexachlorodiphenylamine (III) which was obtained in colorless needles, m.p. 138~139°C. The yield was quantitative. 2,4,2',4'-Tetrachlorodiphenylamine (VII) was prepared from diphenylamine by the action of sulfuryl chloride in ethyl ether[2]. Colorless needles, m.p. 141~142°C (from acetic acid). Yield, 74%.

3) E. de B. Barnett and S. Smiles, *J. Am. Chem. Soc.*, **95**, 1235 (1909).

The author expresses his thanks to Professor Y. Urushibara, the University of Tokyo, for his helpful guidance throughout this work, to Dr. K. Takeda, Director of the Laboratory, for his permission to undertake this research, and also to the members of the Center of Microanalytical Services, Shionogi & Co., Ltd., for the elementary analyses.

Research Laboratory
Shionogi & Co., Ltd.
Imafuku, Amagasaki

Phenothiazine Derivatives. IV[1]*. Reactions of Thionyl Chloride with Some Substituted Diphenylamines and with Naphthylphenylamines*

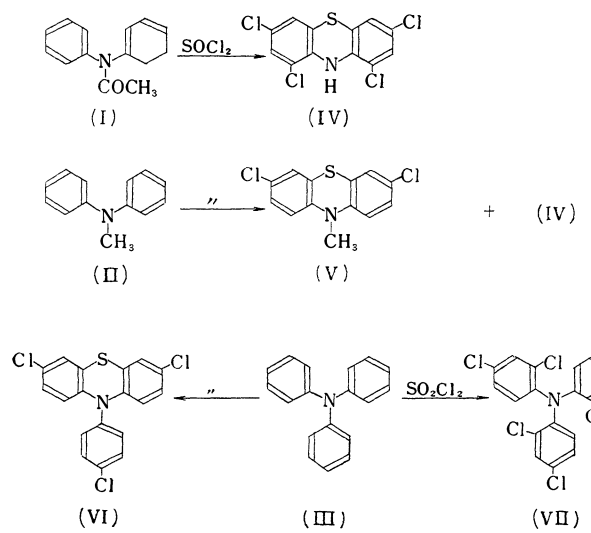
By Manabu FUJIMOTO

(Received September 24, 1958)

In part III[1] of this series, the reaction of thionyl chloride with diphenylamine was investigated in detail. The present paper describes similar reactions of thionyl chloride with some substituted diphenylamines and with naphthylphenylamines.

***N*-Substituted Diphenylamines.** — *N*-Acetyldiphenylamine (I), methyldiphenylamine (II), and triphenylamine (III) were treated with thionyl chloride with results represented schematically in Chart I. While *N*-acetyldiphenylamine (I) was completely transformed into 1,3,7,9-tetrachlorophenothiazine (IV), methyldiphenylamine (II) gave 7% of 3,7-dichloro-10-methylphenothiazine (V)[2] besides 89% of the same tetrachlorophenothiazine (IV). It appears that the substituents on the nitrogen atom exerted some steric hindrance on the *ortho* positions to the nitrogen atom, and they were either removed to give way to chlorine atoms entering these positions or retained to hinder chlorination in these positions. With thionyl chloride, triphenylamine (III) gave a nearly quantitative yield of a product $C_{18}H_{10}NCl_3S$, which is probably 3,7-dichloro-10-(4′-chlorophenyl)phenothiazine (VI) considered on the basis of the orienting and the steric effects, but with sulfuryl chloride it gave a hexachlorotriphenylamine in a high yield, which is supposed to be 2,4,2′,4′,2″,4″-hexachlorotriphenylamine (VII) from a similar consideration.

CHART I

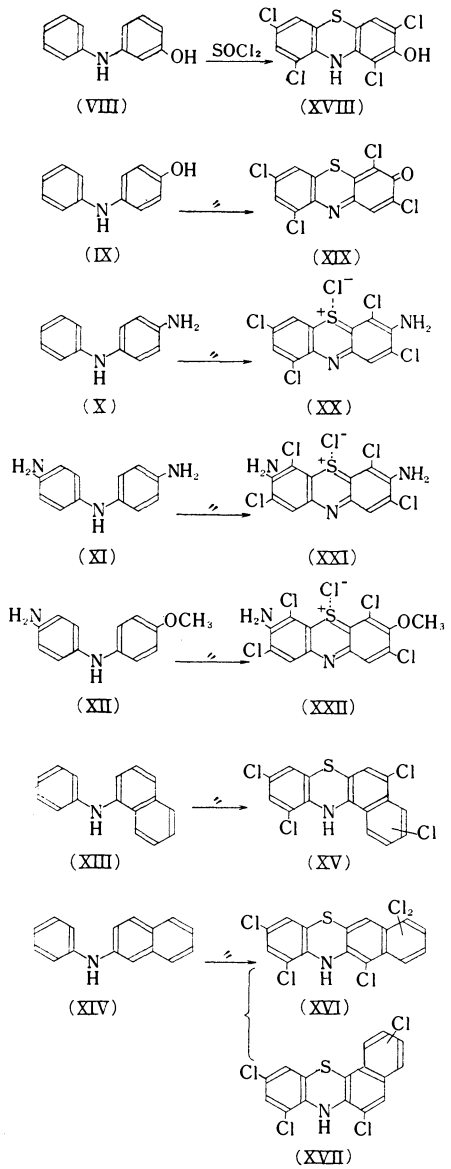


1) Part III: This Bulletin, **32**, 294 (1959).

2) A. C. Schmalz and Burger, *J. Am. Chem. Soc.*, **76**, 5458 (1954).

Diphenylamines Substituted in the Benzene Nuclei.—2-, 3- and 4-nitrodiphenylamines were found inert to thionyl chloride, and likewise, phenyl-(2-, 3-, and 4-)tolylamines did not give the corresponding phenothiazines. On the other hand, 3-hydroxy- (VIII), 4-hydroxy- (IX), 4-amino- (X), 4,4'-diamino- (XI) and 4-amino-4'-methoxy- (XII) diphenylamines reacted normally, as shown in Chart II. Assign-

CHART II



ment of the structures to the products is discussed below.

As observed previously[1], the reaction of unsubstituted diphenylamine with thionyl chloride proceeds through the formation of the intermediate phenazationium chloride and subsequent chlorination to give 1,3,7,9-tetrachlorophenothiazine, which shows that positions 1,3,7 and 9 of the intermediate phenazathionium chloride are rendered reactive in the chlorination by the effect of the nitrogen atom (position 10). 3-Hydroxydiphenylamine (VIII) is expected to produce 2-hydroxyphenazathionium chloride as the intermediate, in which the hydroxyl group will favor chlorination in positions 1 and 3. Thus, the product $C_{12}H_5ONCl_4S$ from 3-hydroxydiphenylamine (VIII) and thionyl chloride is assumed to be 1,3,7,9-tetrachloro-2-hydroxyphenothiazine (XVIII). Nevertheless, in the redundant 3-substituted phenazathionium intermediates from 4-hydroxy- (IX) and 4-amino- (X) diphenylamines, the hydroxyl group and the amino group in position 3 will orient chlorination to positions 2 and 4. As the hydroxyl group and the amino group have stronger orienting effects than the imino group, it is expected that positions 2, 4, 7 and 9 of the 3-substituted phenazathionium intermediates are reactive toward chlorination. Thus, the phenothiazone $C_{12}H_3ONCl_4S$ obtained from 4-hydroxydiphenylamine (IX) is assumed to be 2,4,7,9-tetrachloro-3-phenothiazone (XIX), and the phenazathionium chloride $C_{12}H_5N_2Cl_5S$ obtained from 4-aminodiphenylamine (X) to be 3-amino-2,4,7,9-tetrachlorophenazathionium chloride (XX). For similar reasons, the product $C_{12}H_6N_3Cl_5S$ from 4,4'-diaminodiphenylamine (XI) and thionyl chloride is supposed to be 3,7-diamino-2,4,6,8-tetrachlorophenazathionium chloride (XXI), and the product $C_{13}H_7ON_2Cl_5S$ from 4-amino-4'-methoxydiphenylamine (XII) and thionyl chloride to be 3-amino-2,4,6,8-tetrachloro-7-methoxyphenazathionium chloride (XXII). 2-Hydroxydiphenylamine gave exceptionally only an unpurifiable black tarry mass.

Naphthylphenylamines. — α-Naphthylamine (XIII) reacted normally with thionyl chloride to form a single product $C_{16}H_7NCl_4S$, probably x,5,9,11-tetrachlorobenzo[a]phenothiazine[3] (XV). There are two possibilities for the positions of cyclization in β-naphthylphenylamine (XIV), and in fact two products with formulae $C_{16}H_6NCl_5S$ and $C_{16}H_7NCl_4S$, respectively, were separated chromatographically from the reaction mixture of β-naphthylphenylamine (XIV) and thionyl chloride (Chart II). The product $C_{16}H_6NCl_5S$ obtained in a larger amount is supposed to be the

linearly cyclized compound, 1,3,x,x',11-pentachlorobenzo[b]phenothiazine[3] (XVI). It melts at 147~149°C, and gives dark blue coloration with sulfuric acid. Then the minor product $C_{16}H_7NCl_4S$ may be x,6,8,10-tetrachlorobenzo[c]phenothiazine[3] (XVII). It melts at 217~219°C (decomp.) and produces dark green color with sulfuric acid. These two benzophenothiazines could not be distinguished from each other in the ultraviolet and infrared absorption spectra.

Experimental

Thionyl chloride (10 ml.) was added dropwise to 1.0 g. of the compound to be treated with the reagent, and the mixture was gently heated under reflux for 30 min., when hydrogen chloride and sulfur dioxide were evolved. The cooled mixture was poured onto ice, and the product was collected and dried. The following substances were obtained, depending upon the starting materials.

1,3,7,9-Tetrachlorophenothiazine (IV) and 3,7-Dichloro-10-methylphenothiazine (V).—The mixed product, obtained from methyldiphenylamine (II) as the starting material, was recrystallized from a mixture of ethanol and benzene. 1,3,7,9-Tetrachlorophenothiazine (IV), m.p. 235~236°C, crystallized out in yellow needles in a yield of 89%. The mother liquor was evaporated, and the residue was recrystallized from 50% aqueous ethanol. 3,7-Dichloro-10-methylphenothiazine (V), m.p. 129~130°C, was obtained in yellowish-green needles in a yield of 7%. The two substances were identified with authentic samples[1,2], respectively. The former IV was also obtained quantitatively from *N*-acetyldiphenylamine (I).

3,7-Dichloro-10-(4'-chlorophenyl)phenothiazine (VI).—Obtained from triphenylamine (III). Yellow fine crystals from benzene, m.p. 131~132°C. Yield, 91%. The substance shows indigo-blue coloration with sulfuric acid.

Anal. Found: C, 57.54; H, 2.89; N, 4.16. Calcd. for $C_{18}H_{10}NCl_3S$: C, 57.09; H, 2.66; N, 3.70%.

1,3,7,9-Tetrachloro-2-hydroxyphenothiazine (XVIII).—Obtained from pure 3-hydroxydiphenylamine (VIII), and recrystallized from chloroform-ethanol. Fine powder with chocolate color, m.p. 202~203°C (decomp.). Yield, 92%. The substance is soluble in 10% aqueous caustic soda, and produces blue-violet color with sulfuric acid.

Anal. Found: C, 40.49; H, 1.54; N, 4.03. Calcd. for $C_{12}H_5ONCl_4S$: C, 40.82; H, 1.43; N, 3.97%.

2,4,7,9-Tetrachloro-3-phenothiazone (XIX).—Derived from freshly distilled 4-hydroxydiphenylamine (IX). White crystals with pinkish tinge from ethanol-benzene, m.p. 145~146°C. Yield, nearly quantitative. It gives cobalt-blue coloration with sulfuric acid.

Anal. Found: C, 41.11; H, 1.01; N, 4.00. Calcd. for $C_{12}H_3ONCl_4S$: C, 41.06; H, 0.86; N, 3.99%.

3-Amino-2,4,7,9-tetrachlorophenazathionium Chloride (XX).—Obtained from freshly rectified 4-aminodiphenylamine (X). Reddish-violet fine powder from chloroform, m.p. 185~186°C. Yield, 86%. It gives reddish-violet coloration with sulfuric acid.

Anal. Found: C, 37.40; H, 1.10; N, 7.30. Calcd. for $C_{12}H_5N_2Cl_5S$: C, 37.28; H, 1.30; N, 7.25%.

3,7-Diamino-2,4,6,8-tetrachlorophenazathionium Chloride (Tetrachlorothionine) (XXI).—From pure 4,4'-diaminodiphenylamine. Bluish-purple fine powder from methanol, m.p. over 360°C. Yield, 94%. It gives dark green coloration with sulfuric acid.

Anal. Found: C, 36.13; H, 1.78; N, 10.46. Calcd. for $C_{12}H_6N_3Cl_5S$: C, 35.90; H, 1.51; N, 10.47%.

3-Amino-2,4,6,8-tetrachloro-7-methoxyphenazathionium Chloride (XXII).—Obtained from 4-amino-4'-methoxydiphenylamine (XII). Bluish-violet fine powder from methanol, m.p. 281~284°C (decomp.). Yield, 82%. Its color in sulfuric acid is bluish violet.

Anal. Found: C, 37.22; H, 1.41; N, 6.97. Calcd. for $C_{13}H_7ON_2Cl_5S$: C, 37.47; H, 1.69; N, 6.73%.

x,5,9,11-Tetrachlorobenzo[a]phenothiazine (XV).—One gram of α-naphthylphenylamine (XIII) gave 1.7 g. (96%) of this compound (XV) in reddish-violet fine crystals, which was purified chromatographically, and then recrystallized from benzene, m.p. 266~268°C. Its coloration with sulfuric acid is bluish violet.

Anal. Found: C, 49.43; H, 2.19; N, 3.15. Calcd. for $C_{16}H_7NCl_4S$: C, 49.65; H, 1.82; N, 3.62%.

1,3,x,x',11-Pentachlorobenzo[b]phenothiazine (XVI) and x,6,8,10-Tetrachlorobenzo[c]phenothiazine (XVII).—One gram of β-naphthylphenylamine (XIV) gave 1.8 g. of a crude crystalline mixture. The mixture was dissolved in 20 ml. of benzene, and passed through a column of alumina. The chromatogram was eluted first with the same solvent and then developed with a mixture of chloroform and ethanol. The first fraction gave a substance in yellow fine crystals, which was assumed to be 1,3,x,x',11-pentachlorobenzo[b]phenothiazine (XVI). Recrystallized from chloroform-ethanol, it melts at 147~149°C and gives dark blue coloration with sulfuric acid, Yield, 1.2 g. (62%).

Anal. Found: C, 45.32; H, 1.88; N, 3.07. Calcd. for $C_{16}H_6NCl_5S$: C, 45.57; H, 1.43; N, 3.32%.

The second fraction, which was strongly fluorescent in solution, gave another substance in fine yellow crystals, which was assumed to be the other possible product, x,6,8,10-tetrachlorobenzo[c]phenothiazine (XVII). Recrystallized from chloroform-ethanol, it melts at 217~219°C (decomp.). Yield, 0.5 g. (28%). It gives dark green coloration with sulfuric acid.

Anal. Found: C, 49.70; H, 2.04; N, 3.57. Calcd. for $C_{16}H_7NCl_4S$: C, 49.65; H, 1.82; N, 3.62%.

Reaction of Triphenylamine (III) with Sulfuryl Chloride.—Sulfuryl chloride (10 ml.) was added to 1.0 g. of triphenylamine (III), and the mixture was gently refluxed for 30 min., and

3) The nomenclature of these benzophenothiazines conforms to the "Ring Index" (1940).

poured onto crushed ice. The precipitate was collected, dried, and recrystallized from ethanol. 2,4,2',4',2'',4''-Hexachlorotriphenylamine (VII) was obtained in colorless crystals, m.p. 78~79°C. Yield, 92% of the theory. It remains colorless with sulfuric acid.

Anal. Found: C, 47.66; H, 2.44; N, 3.17. Calcd. for $C_{18}H_9NCl_6$: C, 47.83; H, 2.01; N, 3.10%.

Summary

Reactions of thionyl chloride with some substituted diphenylamines and with naphthylphenylamines were studied. *N*-Acetyldiphenylamine gave the known 1,3,7,9-tetrachlorophenothiazine. Methyldiphenylamine gave a small yield of the known 3,7-dichloro-10-methylphenothiazine besides the same tetrachlorophenothiazine as the main product. The following new compounds were obtained from respective starting materials and their structures were deduced: 3,7-dichloro-10-(4'-chlorophenyl)-phenothiazine from triphenylamine, 1,3,7,9-tetrachloro-2-hydroxyphenothiazine from 3-hydroxydiphenylamine, 2,4,7,9-tetrachloro-3-phenothiazone from 4-hydroxydiphenylamine, 3-amino-2,4,7,9-tetrachlorophenazathionium chloride from 4-aminodiphenylamine, 3,7-diamino-2,4,6,8-tetrachlorophenazathionium chloride from 4,4'-diaminodiphenylamine, 3-amino-2,4,6,8-tetrachloro-7-methoxyphenazathionium chloride from 4-amino-4'-methoxydiphenylamine, x,5,9,11-tetrachlorobenzo[a]phenothiazine from α-naphthylphenylamine, and 1,3,x,x',11-pentachlorobenzo[b]phenothiazine and x,6,8,10-tetrachlorobenzo[c]phenothiazine from β-naphthylphenylamine.

The author expresses his thanks to Professor Y. Urushibara, the University of Tokyo, for his helpful guidance throughout this work, to Dr. K. Takeda, Director of the Laboratory, for his permission to undertake this research, and also to the members of the Center of Microanalytical Services, Shionogi & Co., Ltd., for the elementary analyses.

Research Laboratory
Shionogi & Co., Ltd.
Imafuku, Amagasaki

Studies on Organic Reagents for Inorganic Analysis. V. m-Nitrophenylfluorone for the Spectrophotometric Determination of Zirconium

By Hirotoshi SANO

(Received September 17, 1958)

For the determination of zirconium, the phenylfluorone (abbreviation for 2,3,7-trihydroxy-9-phenylfluorone) method was recommended previously by the present author and Kimura[1]. The reactions between phenylfluorone and several metals were also studied[2,3]. The method, which is about forty times more sensitive than the alizarin red S method[4], is the most sensitive method for the colorimetric determination of zirconium, but the absorbance of the chelate decreases with increasing acidity in the solution. On the other hand, several derivatives of phenylfluorone were synthesized by the author, and the effect of the substituent on the utility of the derivative as a spectrophotometric reagent was studied[5,6]. The results suggested that *m*-nitrophenylfluorone (abbreviation for 2,3,7-trihydroxy-9-(3′-nitrophenyl)fluorone) was one of the most excellent reagents in view of the sensitivity, stability, and other characteristics. In this paper, detailed procedure for the spectrophotometric determination of zirconium using this reagent is described.

1) K. Kimura and H. Sano, This Bulletin, **30**, 80 (1957).
2) H. Sano, ibid., **30**, 790 (1957).
3) H. Sano, *Japan Analyst* (*Bunseki Kagaku*), **7**, 235 (1958).
4) E. B. Sandell, "Colorimetric Determination of Traces of Metals", 2nd Ed., (1950), Interscience Publishers Inc., New York.
5) H. Sano, This Bulletin, **30**, 672 (1958).
6) H. Sano, ibid., **30**, 974 (1958).

Experimental and Results

Apparatus and Reagents Used. — The absorbance measurements were made with a UVISPEK spectrophotometer using a 10 mm. glass cell. The reference cell contained distilled water for all the measurements, except for the measurement of the absorption spectrum of the chelate, in which the blank solution was used as a reference solution.

Ethanolic solution of m-nitrophenylfluorone was made up in the following way: *m*-nitrophenylfluorone was synthesized from hydroxyhydroquinone triacetate and *m*-nitrobenzaldehyde according to the prescription reported previously[2,3], and 0.120 g. of this reagent was dissolved in 150 ml. of ethanol and 1 ml. of 5 N hydrochloric acid by warming. After being cooled, the solution was diluted to 200 ml. with ethanol.

Ethanolic solution of phenylfluorone was prepared dy dissolving 120 mg. of phenylfluorone in 150 ml. and 1 ml. of 5 N hydrochloric acid, and diluting to 200 ml. with ethanol.

Zirconyl chloride stock solution was prepared by dissolving analytical grade zirconyl chloride octahydrate in 1 N hydrochloric acid, and standardized gravimetrically using distilled aducous ammona. This solution contains 2.07 mg. of zirconium per ml. A working solution was prepared from the stock solution by dilution with dilute hydrochloric acid, every time an experiment was made,

Cyclohexanol.—Reagent grade cyclohexanol was used without further purification.

Ethanol: Reagent grade 99% ethanol was used.

Fundamental Reaction.—The treatment of slightly acidic solution of zirconyl ions with an excess of a standard *m*-nitrophenylfluorone solution results in a color change from yellow to red; an orange-red colored precipitate appears, aftar it is allowed to stand. Various organic solvents, such as acetic acid anhydride, acetone, benzene, carbon disulfide, carbon tetrachloride, chloroform, cyclohexane, cyclohexanol, dioxane, ethanol, ethyl acetate, diethyl ether, ethyl *iso*propyl ketone, *iso*butanol, *iso*propanol, di*iso*propyl ether, methanol, *n*-pentanol, *n*-butanol and petroleum ether were tried to dissolve the precipitate of zirconium *m*-nitrophenylfluoronate, with little success. Then an attempt was made to keep the complex in the supersaturated or colloidal solution with the addition of a suitable stabilizer. A cyclohexanol-ethanol mixed solution was found to be the most favorable stabilizer. In the experiments described below, all the solutions were made to a total volume of 25 ml. The order of the addition of the reagents was always the same. The zirconium solution was added first; and acid, ethanol, cyclohexanol, and ethanolic solution of *m*-nitrophenylfluorone were added in this order.

Spectral absorbance data for the reagent blank and 20.7 μg. of zirconium (following the standard procedure mentioned later) are given in Fig. 1. The absorption maximum of the dye and the chelate was found at 475 mμ and 550 mμ, respectively. The optimum wavelength was taken as 550 mμ because at this point the absorption caused by the blank solution is small and that by zirconium *m*-nitrophenylfluoronate is the greatest.

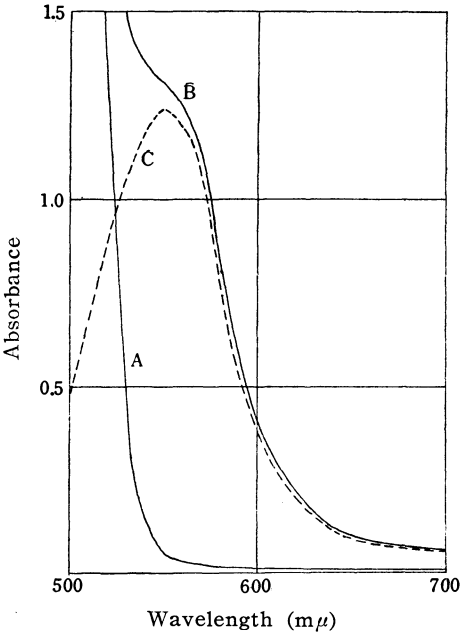


Fig. 1. Absorption spectra.

Curve A: Reagent blank (Reference solution: water)
Curve B: 20.7 μg. Zirconium (Reference solution: water)
Curve C: 20.7 μg. Zirconium (Reference solution: reagent blank solution)

Effect of Cyclohexanol and Ethanol Concentration.—A precipitate of zirconium *m*-nitrophenylfluoronate is obtained after a while from a solution containing no cyclohexanol and less than 5 ml. of ethanol. The colored solution becomes stable as an increasing amount of cyclohexanol is added, but cyclohexanol layer separates from ethanolic water layer when the amount of cyclohexanol becomes relatively great in comparison with that of ethanol. The solution shows no difference in the position of absorption maximum when the amount of cyclohexanol or ethanol added is changed, although there was a slight difference in the detailed shape of the absorption curve. From these results, 2.5 ml. of cyclohexanol, 5 ml. ethanol, and 5 ml. ethanolic solution of *m*-nitrophenylfluorone were taken as the optimum. In this condition, the solution gives no visible precipitate of *m*-nitrophenylfluoronate in zirconium concentration below 3 μg. per 25ml. by being allowed to stand for a day or more.

Effect of Acidity.—The effect of acid concentration upon the absorbance given by 20.7 μg. of zirconium and 3 mg. of *m*-nitrophenylfluorone is illustrated in Fig. 2, together with the case given by 20.7 μg. of zirconium and 3 mg. of

phenylfluorone* for the purpose of comparison. The absorbances shown in Fig. 2, are the values observed thirty minutes after the preparation of the solution. In the acidity range higher than 1.5 N hydrochloric acid concentration, the absorbances increase slowly with increasing digestion time, so the plateau range of the curve extends a little. In the case of *m*-nitrophenylfluoronate the absorbance is almost independent of hydrochloric acid concentration in the region below 0.1 N, whereas no plateau range is found above 0.05 N acid concentration in the case of phenylfluoronate.

Effect of Digestion Time. — The effect of digestion time on the absorbance given by 5.0 μg. of zirconium and 3 mg. *m*-nitrophenylfluorone in 0.1 N hydrochloric acid solution is shown in Fig. 3. In a solution containing zirconium above 4 μg., a precipitate of zirconium *m*-nitrophenylfluoronate is obtained after the solution is allowed to stand for a day, but the stable suspension can regenerate with a short shaking by hand. The absorbance remains nearly constant for forty minutes after the preparation.

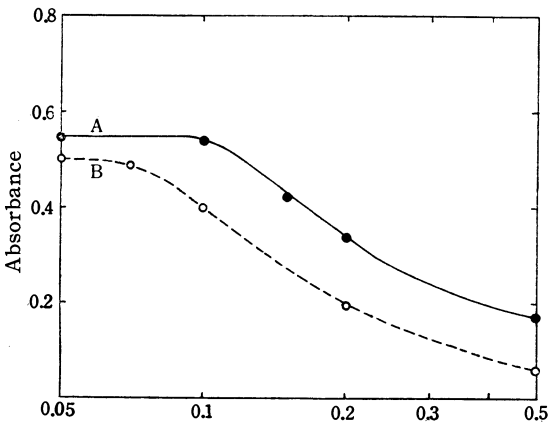


Fig. 2. Effect of acidity.
Curve A: Zirconium *m*-nitrophenylfluoronate (Reference solution: water)
Curve B: Zirconium phenylfluoronate (Reference solution: water)

Standard Procedure.—From the results above mentioned, the following was recommended as the optimum procedure.

Transfer the sample solution (less than 10 ml.) to a 25 ml. volumetric flask. When the sample contains more than 20 to 25 μg. zirconium, an aliquot portion of the sample solution containing the desired amount of zirconium in final volume is pipetted into a 25 ml. volumetric flask. Additional acid will then be required to bring the acidity up to 0.10 N hydrochloric acid used in the determination of zirconium with *m*-nitrophenylfluorone. Adjust the volume to about 10 to 12 ml. with distilled water. Add 5 ml. of ethanol, 2.5 ml. of cyclohexanol, and 5 ml. of ethanolic solution containing 3 mg. of *m*-nitrophenylfluorone in this order. Make up the solution to the mark with distilled water, mix with shaking by hand, allow to stand for an hour, and obtain the absorbance of the solution in the spectrophotometer at 550 mμ using a 10 mm. glass cell and distilled water as a control solution. Determine the amount of zirconium by reference to the standard working curve prepared previously.

Working Curve.—Data for the working curve are given in Fig. 4. These data were obtained following the standard procedure. A straight-line relationship between the absorbance and the amount of zirconium is shown up to 0.6 p. p. m. Solutions containing from 0.6 to 1.0 p. p. m.

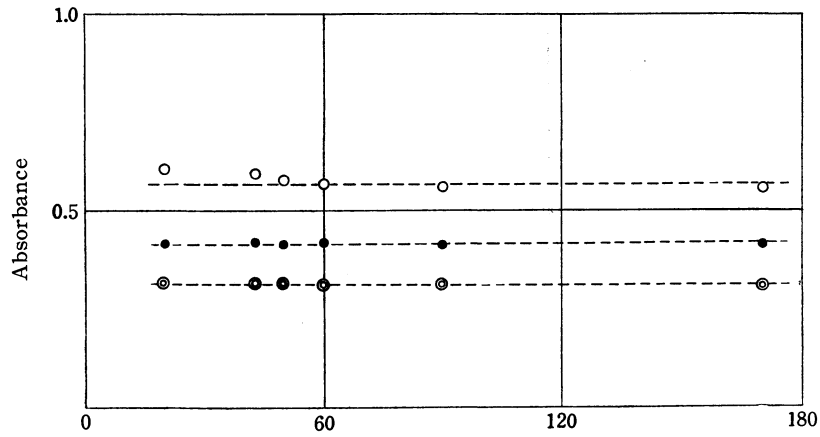


Fig. 3. Effect of digestion time.
-○- 540 mμ (Reference solution: water)
-●- 550 mμ (〃)
-◎- 560 mμ (〃)

* The absorbance measurements were made by a procedure similar to that of *m*-nitrophenylfluoronate.

deviate slightly from Beer's law but their absorbances are reproducible. The region from 0 to 0.10 p. p. m. of zirconium was examined in detail for any deviation from the straight-line relationship, but none was found. In Fig. 4, the working curves used in the Alizarin Red S method[4] and in the Phenylfluorone mothod[1] are shown for the comparison of the sensitivities of the methods.

Effect of Diverse Ions.—The effect of various ions was studied using 0.3 p. p. m. of zirconium. The standard procedure was employed, with the exception that the desired amount of the diverse ion was added into a volumetric flask prior to the addition of the zirconium solution. The concentrations of zirconium and diverse ion are expressed on the basis of the final volume 25 ml. The change in absorbance was then measured at 550 mμ. Errors of less than 3% of the zirconium present were considered to be negligible. A negligible error was obtained with the following maximum about;

2000 p. p. m. of: sodium, potassium, ammonium and magnesium ions.

1000 p. p. m. of: calcium, barium, strontium and mercuric ions.

500 p. p. m. of: lanthanum, neodymium, cerrous, cadmium and zinc ions.

100 p. p. m. of: aluminum and thorium ions.

Chloride, bromide, nitrate (2000 p. p. m.) and sulfate (1000 p. p. m.) ion do not interfere with the reaction. Some elements give interference by increasing the color intensity. Some elements quench the color due to zirconium *m*-nitrophenylfluoronate. Table I lists the interfering ions and their effect. Serious interference is given by the following ions: titanium, germanium, tin, iron (III), antimony, oxalate, phosphate and fluoride.

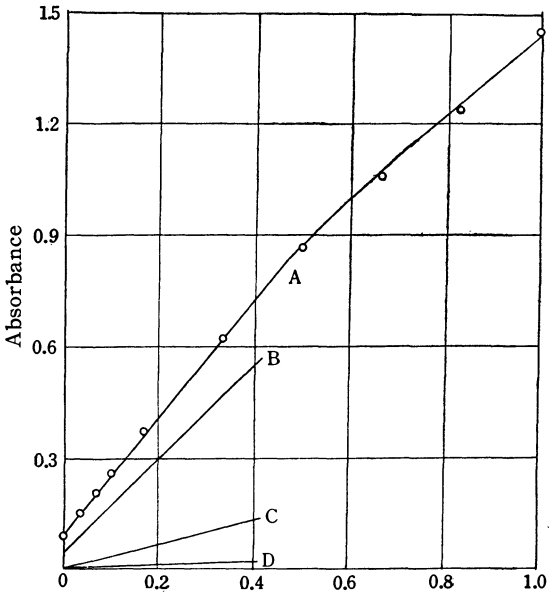


Fig. 4. Working curve.
Curve A: This method.
Curve B: Phenylfluorone method.
Curve C: Quercetin method.
Curve D: Alizarin S method.

TABLE I
INTERFERING DIVERSE IONS

Ion	Amount added p. p. m.	Error %	Permissible amount p. p. m.
Fe(II)	2.0	2	3
Fe(III)	2.0	10	0.6
Ti(IV)	0.2	40	0.01
Ge(IV)	0.4	20	0.06
Sn(IV)	0.4	10	0.1
As(III)	10	2	15
As(V)	10	10	3
Sb(III)	2	10	0.6
Sb(V)	2	10	0.6
F^-	2	25	0.2
$C_2O_4^{2-}$	5	20	0.7
HPO_4^{2-}	5	20	0.7

Discussion

The color change arising from the reaction of *m*-nitrophenylfluorone with zirconium closely resembles the case of phenylfluorone, namely the shift of the absorption maximum caused by chelate formation is 75 mμ in *m*-nitrophenylfluorone, and 72 mμ in phenylfluorone[2], whereas the differences of the absorption maximum between the phenylfluorone or its zirconium chelate and *m*-nitrophenylfluorone or its zirconium chelate are 7 and 10 mμ, respetively. The trend in the effect of the acidity of the solution on the absorbance is, however, considerably different. In the *m*-nitrophenylfluorone method recommended here the constancy of the absorbance is obtained at the region of the acidity below 0.10 N hydrochloric acid concentration, whereas there is no such constancy in the phenylfluorone method. This will be caused by the effect of the *m*-nitro group attracting the electron of the —OH group at 3 position and increasing the electronegativity of the oxygen atom. Furthermore, it was fortunately found that the absorbance of *m*-nitrophenylfluoronate was greater than that of the corresponding phenylfluoronate. The comparison of the sensitivities by several methods is shown in Fig. 4. The sensitivity of this method, given by the inclination of the working curve, is nearly fifty times as great as that the alizarin red S method[4], about five times that of the quercetin method[7], and about 1.2 times for the phenylfluorone method[1]. In

7) F. S. Grimaldi and C. E. White, *Anal. Chem.*, 25, 1886 (1953).

the region from zero to 0.15 p. p. m. of zirconium, the solution remains without any visible precipitation for three days or more, so the stability of the absorbance seems to be greater than that in the phenylfluorone method. These facts show the method is excellent for the determination of a micro amount of zirconium.

Summary

The spectrophotometric determination of a micro amount zirconium, using *m*-nitrophenylfluorone, has been described. The method recommended here, which is carried out in 0.1 N hydrochloric acid solution, shows nearly fifty times the sensitivity of the alizarin red S method, about five times that of the quercetin method, and about 1.2 times that of the phenylfluorone method reported previously as the most sensitive reagent by the author and K. Kimura. The solution becomes stable enough to carry on the spectrophotometric determination by adding some cyclohexanol and ethanol, and no precipitation is found for the small amount of zirconium. Furthermore, the stability for increasing acidity in the solution is greater than that of the phenylfluorone method. The method is found to be suitable for the determination of 0 to 0.5 p. p. m. of zirconium. Transfer the sample solution (less than 10 ml.) to a 25 ml. volumetric flask. Then add additional acid to bring the acidity up to 1.0 N hydrochloric acid and 7.5 ml. cyclohexanol-ethanol (1 : 2) mixed solution, and 5 ml. ethanolic solution containing 3 mg. *m*-nitrophenylfluorone in that order. Adjust the volume to 25 ml., shake the solution, allow to stand for one hour, and read the absorbance of the solution with a spectrophotometer at 550 mμ with 1-cm. glass cells and distilled water as a control solution. Oxalate, fluoride, phosphate, titanium, germanium, iron(III) and antimony cause serious interference.

The author is indebted to Professor Emeritus Kenjiro Kimura and Professor Nobufusa Saito for their encouragement in carrying out this study. The author is also grateful for a grant from the Ministry of Education.

Department of Chemistry
Faculty of Science
The University of Tokyo
Hongo, Tokyo

SHORT COMMUNICATIONS

*Synthesis of Trimethylboron from Boric Anhydride or Borate**

By Jun IYODA and Isao SHIIHARA

(Received November 26, 1958)

Many organoboron compounds have been prepared by the action of Grignard reagents[1] on boron trihalides or esters of boric acid. But so far as is known, there is no report** on the synthesis of organoboron compounds from naturally occuring materials such as boric anhydride or sodium borate directly. Related reactions are concerned only with sodium hydride[2] at a temperature as high as 330°C in an autoclave. Recently, with progress in the study of organoaluminum compounds, many attempts have been made to utilize organoaluminum compounds in related reactions in place of Grignard reagents[3,4]. Previously we[5] found that the silicon-oxygen bond in polymeric form was cleaved and alkylated simultaneously with organoaluminum compounds. In the present communication, this reaction was applied to boron-oxygen compounds and it was found that organoboron compound was obtained directly from inorganic boric anhydride or its salts in a good yield.

The reaction was carried out as follows. Methylaluminum sesquichloride[6] $(CH_3)_3Al_2Cl_3$ was added to a boron compound in an inert atmosphere and the reactant was refluxed at 150 to 170°C for several hours, and trimethylboron (b. p. −21.8°C) generated was caught by a dry-ice acetone trap.

The results obtained are shown in Table I. In the case of boric anhydride the yield of trimethylboron is especially good and almost quantitative but it is somewhat low in the case of borate. It is interesting to note that when the reaction was carried out in isoamyl ether solution, no trimethylboron was produced. Also, by the use of methylmagnesium chloride in the same ethereal solution, no methyl-boron

TABLE I

REACTION OF METHYLALUMINUM SESQUICHLORIDE WITH BORON COMPOUNDS

B compd.	$Me_3Al_2Cl_3$ (g.)	$Me_3Al_2Cl_3$ (m. mole)	(g.)	(m. mol.)	Reacn. temp. (°C)	Reacn. time (hr.)	BMe_3 (g.)	Yield (%)
$B(OBu)_3$	40	(172)	25.5	(124)	room temp.	over night	6.5	93.6
B_2O_3	10.5	(151)	54	(251)	100～170	6	14	68.8
$Na_2B_4O_7$	12	(60)	50	(244)	140～160	4	5.5	
					170*	3	4.0	71.2
B_2O_3	6	(87)	MeMgCl**/400 cc. i-Am_2O		150～160	6	—	
B_2O_3	6	(87)	42/50 g. i-Am_2O		150	5	—	

* after eight days.

** from 12 g. (0.5 mole) of Mg.

* Presnted before the Symposium of Organosilicon and Organometallic Compounds at Osaka, October 18, 1958.

1) M. S. Kharasch and O. Reinmth, "Grignard Reactions of Nonmetallic Substances", Prentice-Hall Inc., New York (1954). pp. 1335; M. F. Lappert, *Chew. Rev.*, **56**, 959 (1956).

** Recently, R. Köster reported briefly that trialkylborons were synthesized by the reaction of trialkylaluminum with trialkylboroxole $[RBO]_3$, but not obtained from boric anhydride directly because of the decomposition of the trialkylaluminum compounds. See ref. 4.

2) H. I. Schlesinger and H. C. Brown, U. S. Patent. 2534533 (1950); H. I. Schlesinger, H. C. Brown and A. E. Finholt, *J. Am. Chem. Soc.*, **75**, 208 (1953).

3) For examples, Kali-Chemie A. -G., Brit. P., 768, 765 (1957).
R. Köster and K. Ziegler, *Angew. Chem.*, **69**, 94 (1957).
Chem. and Ind. News, **36**, No. 17, 66 (1958).

4) R. Köster, *Angew. Chem.*, **70**, 371 (1958).

5) I. Shiihara, H. Takahashi and J. Iyoda, the 11th Annual Meetings of Chemical Society of Japan in Tokyo, April 1958.

6) J. Iyoda and I. Shiihara, the Symposium of Organosilicon and Organometallic Compounds at Osaka, October 15, 1957.

compounds were obtained. These results are explained as follows: both organometallic compounds are stabilized by the etherate formation with ether, and consequently their affinity toward the oxygen of the boron-oxygen bond are lowered.

Osaka Industrial Research Institute
Daini, Oyodo-ku, Osaka

Coexistence of Two Different Molecular Forms within a Single Crystal of L-Valine

By Masamichi Tsuboi, Tadao Takenishi* and Yoichi Iitaka

(Received December 25, 1958)

In the course of our work on the infrared absorption spectra of amino acids, we found that a crystal of L-valine gives a spectrum quite different from that of a crystal of DL-valine (Fig. 1). The number of the bands observed for the DL-valine crystal is that expected from one valine molecule[1], and almost every band has been assigned to one of the vibrational modes expected for the molecule[2]. While, the L-valine crystal shows much more bands than the DL-valine crystal does. For example, instead of the band at 680 cm^{-1} of the DL-crystal, which is assigned to the COO^- scissoring mode, the L-crystal shows two bands at 715 and 663 cm^{-1}. These are situated too far apart to be considered as arising from one molecular vibration due to the splitting in the crystalline force field. A pair of bands is also observed in the spectrum of the L-crystal, instead of each of the bands of the DL-crystal at 774, 818, 890, 925, 948, 1035, 1105, 1181, 1320, 1355, 1406, 1593 and 1629 cm^{-1}. These observations may lead us to a view that the L-valine crystal belongs to an unusual type of crystal composed of molecules of one species of two different forms.

This view is supported by an X-ray examination. From the oscillation- and Weissenberg-photographs of the L-valine crystal the following data were obtained: monoclinic, $a=9.71$ Å, $b=5.32$ Å, $c=12.08$ Å, $\beta=90.8°$. Its density was reported by Cohn et al.[3] to be 1.230 g. cm^{-3}, which shows that there are four molecules per one unit cell, its density calculated being 1.247 g. cm^{-3}. Systematic extinctions on the photographs indicate the space group to be either C_2^2–$P2_1$ or C_{2h}^2–$P2_1/m$. The piezoelectricity is detected of this crystal; accordingly, the possibility of C_{2h}^2–$P2_1/m$ is eliminated, and the space group is determined to be C_2^2–$P2_1$. This space group requires only two crystallographically similar units (related by the twofold screw axis) within one unit cell. This requirement is fulfilled by supposing that the four molecules in one unit cell are in two sets of two molecules of different forms[1].

The question may now be raised, what is the difference between these two forms. Considered on the basis of what are at present known on the internal rotation around the C–C single bond[4], three rotational isomers are possible for the valine molecule, i. e., *trans*, *gauche I*, and *gauche II* isomers (Fig. 2; A, B, and C). The energy differences among these three isomers may be very small as are the energy differences between the *trans* and *gauche* isomers of symmetric tetrachloroethane[5] and between those of symmetric tetrabromoethane[6,7] (Fig. 2; D and E). The two molecules of different forms, composing the L-valine crystal, are probably two of these three isomers.

Similar rotational isomers with the small energy differences are also possible for the isoleucine molecule, in which one of the two methyl groups of the valine molecule is substituted by the ethyl group. Then, the existence of isoleucine crystals composed of two rotational isomers may

* Central Research Laboratory, Ajinomoto Co., Inc. Kawasaki, Kanagawa.

1) That the DL-valine crystal is composed of molecules of one form is evident from the space group (C_i^1–P_1), the unit cell dimensions ($a=5.25$Å, $b=5.43$Å, $c=11.05$Å, $\alpha=91°$, $\beta=92.4°$, $\gamma=109.4°$), and the the density (1.315 g. $cm.^{-3}$) of this crystal; this space group requiring two crystallographically similar units within one unit cell, and the unit cell dimensions and the density requiring two molecules (D and L) in each unit cell. Details will be shown elsewhere (M. Tsuboi, T. Takenishi and Y. Iitaka, to be published).

2) M. Tsuboi and T. Takenishi, to be published.

3) E. J. Cohn, T. L. McMeekin, J. T. Edsall and J. H. Weare, *J. Am. Chem. Soc.*, **56**, 2270 (1934).

4) S. Mizushima, "Structure of Molecules and Internal Rotation" Academic Press, New York, 1954; M. Hayashi, T. Shimanouchi and S. Mizushima, This Bulletin, **29**, 802 (1956).

5) K. Naito, I. Nakagawa, K. Kuratani, I. Ichishima and S. Mizushima, *J. Chem. Phys.*, **23**, 1907 (1955).

6) R. E. Kagarise and K. H. Rank, *Trans. Faraday Soc.*, **48**, 394 (1952); R. E. Kagarise, *J. Chem. Phys.*, **23**, 207 (1955); **24**, 300 (1956).

7) M. Hashimoto, T. Shimanouchi and S. Mizushima, ibid., **24**, 172 (1956).

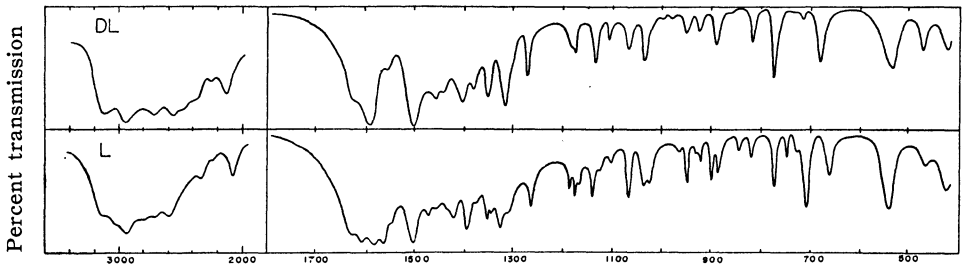


Fig. 1. Infrared absorption spectra of DL-valine and L-valine crystals.

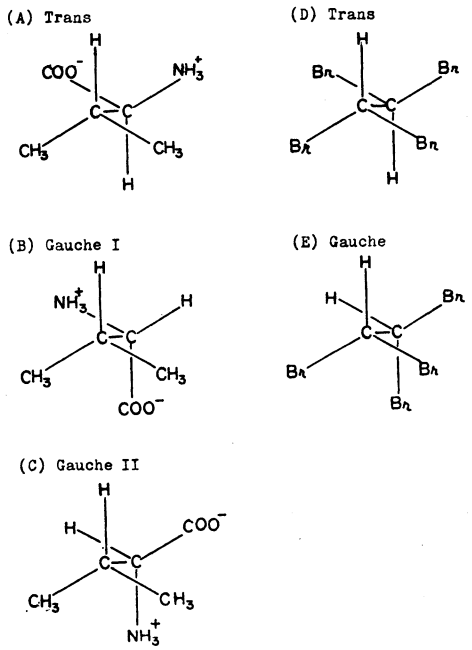


Fig. 2. Rotational isomers of L-valine and symmetric tetrabromoethane.

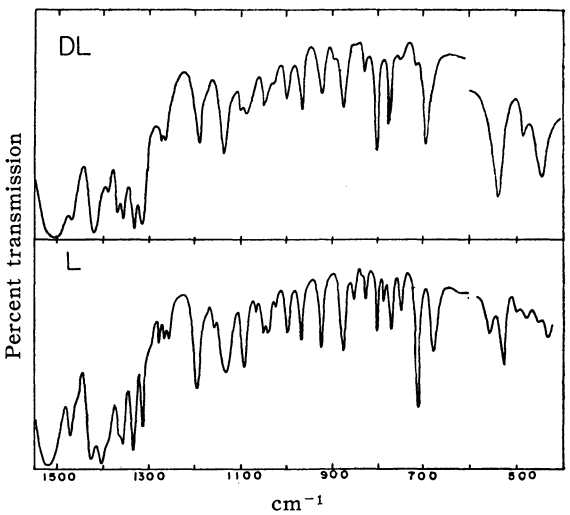


Fig. 3. Infrared absorption spectra of DL-isoleucine and L-isoleucine crystals.

be conjectured. As a matter of fact, there is an L-isoleucine crystal which shows much more bands than a DL-isoleucine crystal (Fig. 3). This may correspond to one of what have been above conjectured.

We wish to express our sincere thanks to Professor San-ichiro Mizushima and Dr. Takehiko Shimanouchi in the University of Tokyo, and to Professor Isamu Nitta and Mr. Hiroyuki Tadokoro in Osaka University for their kind helps and valuable suggestions. Our thanks are also due to Drs. Haruomi Oeda and Tetsuo Ogawa in Ajinomoto Co., Inc., for their encouragement throughout this work.

Faculty of Science
The University of Tokyo
Hongo, Tokyo

ν_{O-H} *Absorption of Cholesterol and Epicholesterol*[1]*

By Michinori Ōki and Hiizu Iwamura

(Received January 6, 1959)

The authors observed two ν_{O-H} absorptions with 3-buten-1-ol[2], and attributed

* Added in proof: While this paper was in press, P. von R. Schleyer, D. S. Trifan and R. Bacskai (*J. Am. Chem. Soc.*, **80**, 6691 (1958)) reported the same phenomenon for these compounds without noticing the unsymmetry of the O-H stretching band of cholesterol.

1) Part III of intramolecular interaction between hydroxyl group and π-electrons.

2) M. Ōki and H. Iwamura, This Bulletin, in press.

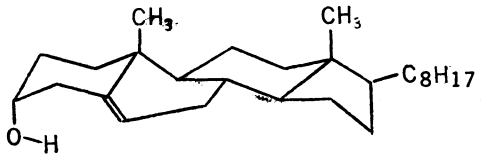
TABLE I

ν_{O-H} ABSORPTION OF CHOLESTEROL AND EPICHOLESTEROL

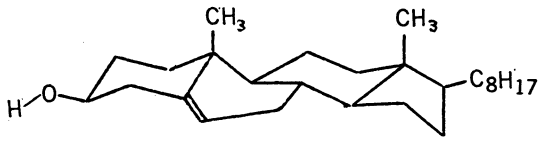
Compound	ν_{O-H} band	ν_{max} (cm^{-1})	$\Delta\nu_{1/2}$ (cm^{-1})	$A\times10^{-3}$ ($mole^{-1}\cdot liter\cdot cm^{-2}$)	$\Delta\nu_{max}$ (cm^{-1})
cholesterol	I	(3613.0)	(18.4)	(1.05)	10
	II	3623.0	16.4	3.47	
epicholesterol	I	3589.6	32.0	2.67	34.1
	II	3623.7	16.8	0.85	

one at the lower wave number (3596.1 cm^{-1}) to the intramolecular interaction between hydroxyl group and π-electrons of the double bond. Then it was naturally expected that the concept would be applicable to more complex molecules, such as steroids.

The molecular scale models indicate that the steric requirement is fulfilled for such a kind of interaction to take place in epicholesterol[3] (I), but not in cholesterol[3] (II).



I



II

Measurements of the O-H stretching absorption in the fundamental region showed that it is really the case. As shown in Fig. 1, epicholesterol gave two distinct maxima, while cholesterol a normal band for secondary alcohols, although the band can be divided into two as in the cases of other secondary alcohols[4] (Table I). The measurements and the calculation were carried out similarly as reported previously[2,5].

Comparison of the integrated intensities of band I (interacted form) and of band II (free) of epicholesterol with the corresponding values of 3-buten-1-ol shows that the number of molecules with internal interaction between hydroxyl group and the π-electrons of the double bond is much

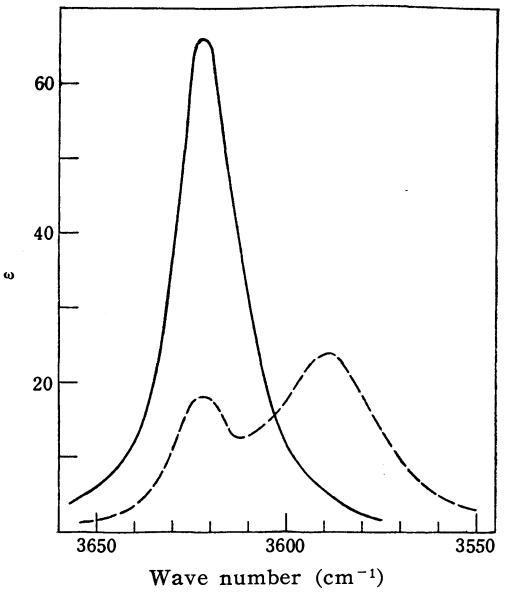
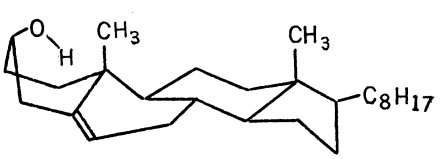


Fig. 1. ν_{O-H} absorption of cholesterol (——) and of epicholesterol (----).

greater in epicholesterol than in 3-buten-1-ol, since the integrated intensity of band I of epicholesterol is greater than that of 3-buten-1-ol (1.93×10^3 $mole^{-1}\cdot liter\cdot cm^{-2}$) and the A_I/A_{II} value is 3.1 for epicholesterol and 0.6 for 3-buten-1-ol. The reverse in the intensities of the two bands in these compounds can be attributed to the more favorable conformation of epicholesterol than that of 3-buten-1-ol. Namely, when the interaction takes place, the conformation of C–C–C–O must be a *gauche* form which will cause greater unstability in term of energy and unfavorable entropy change in 3-buten-1-ol, while the conformation favorable for the interaction is fixed in epicholesterol.



III

3) Pure samples of these substances were kindly donated by Miss K. Mori of this laboratory, to whom the authors' thanks are due.

4) M. Ōki and H. Iwamura, This Bulletin, in press.

5) M. Ōki, H. Iwamura and Y. Urushibara, ibid., **30**, 769 (1958).

The possibility for A ring of cholesterol to take a boat form (III) to some extent is denied, as far as the present data concern, because no absorption band was observed that would have been expected if cholesterol had possessed structure III favorable for the interaction.

This finding may be utilized for the analysis of epicholesterol in a mixture and similar phenomena will be observed in many other compounds of the same type. Examination of the scale models reveals that only the axial hydroxyl group is capable of forming this kind of interaction in steroids. Possibility for use in the diagnosis of the hydroxyl group is under investigation.

Department of Chemistry
Faculty of Science
The University of Tokyo
Hongo, Tokyo

Asymmetric Synthesis of Threonine by Optically Active Complex Ions of Cobalt

By Masuo MURAKAMI and Kozo TAKAHASHI*

(Received January 8, 1959)

The structure of an octahedral complex containing two or three molecules of an optically active bidentate coordinating agent is defined by the configuration of these bidentate molecules, and the number of stable isomers of these complexes is limited by asymmetric effect of these bidentate molecules[1]. For example, the reaction of dextro-1,2-*trans*-diaminocyclopentane with dichloro-bis(levo-cyclopentadiamine)cobalt(III) chloride gives only D[Co(*l*-cptdin)$_3$]Cl$_3$ and L[Co(*d*-cptdin)$_3$]·Cl$_3$[2].

On the basis of these results, Bailar et al. attempted to resolve some of racemic coordinating substances by the aid of an optically active complex. They failed to obtain optically active alanine, leucine, phenylalanine and propylenediamine[3], but succeeded in the case of tartaric, α-chloropropionic acid and lactic acids by this method[4]. These facts suggest possibility that an effective asymmetric synthesis may be brought about by a reaction whereby a new asymmetric carbon atom is formed through the coordinating molecule of an optically active octahedral complex.

Recently, Akabori et al. reported an excellent method for the synthesis of threonine by means of a Knoevenagel type condensation of acetaldehyde with the active methylene group of glycine copper complex[5]. We have attempted to synthesize optically active threonine by means of the reaction mentioned above from optically active complexes of the type [Co B$_2$ glycine].

One gram of levo-glycino-bis(ethylenediamine)cobalt(III) iodide, which was prepared according to the direction of Meisenheimer[6], was allowed to react at room temperature with 0.34 cc. of acetaldehyde in 5 cc. of 4% sodium carbonate aqueous solution. After 90 hr., 0.5 g. of sodium sulfide nonahydrate was added and cobalt(II) sulfide was removed and then the filtrate was flowed through a cation exchange resin column (H form Amberlite IR-120). The amino acids adsorbed on the resin were eluted with 2 N aqueous ammonia. The crude crystalline product (190 mg., 80% yield) obtained from the above eluate showed dextro rotation, $[\alpha]_D^{13}$ +3.84 (c 2.345, in water), m. p. 223~224°C. The paper chromatogram, obtained by developing with *n*-butanol-methylethylketone-concentrated aqueous ammonia-water (5 : 3 : 1 : 1), indicated that the crude product consisted of threonine, allothreonine and glycine with the relative ratio of the spot area of 7 : 2 : 1. The crude 2,4-dinitrophenylthreonine obtained from the reaction product showed levo rotation, $[\alpha]_D^{11}$ −8.22 (c 2.34, in 4% aq. sodium hydrogen carbonate), (asymmetric yield ca. 8%), m. p. 125~132°C[7].

Glycino-bis(levo-propylenediamine)-cobalt(III) chloride[8], which is considered to

* Present Address: Hasune Factory, Yamanouchi Pharmaceutical Co., Ltd., Itabashi-ku, Tokyo.

1) J. C. Bailar, Jr., "The Chemistry of the Coodination Compounds", Reinhold Publishing, Corporation, New York (1956), p. 313.

2) F. H. Jaeger and H. B. Blumendal, *Z. anorg. allgem. Chem.*, 175, 161 (1928).

3) J. C. Bailar, Jr., C. A. Stiegman, J. H. Balthis and E. H. Huffman, *J. Am. Chem. Soc.*, 61, 2402 (1939).

4) A. D. Gott and J. C. Bailar, Jr., ibid., 74, 4820 (1952).

5) M. Sato, K. Okawa and S. Akabori, This Bulletin, 30, 937 (1957).

6) J. Meisenheimer, L. Angerman, H. Holsten and E. Kiderlen, *Ann.*, 483, 217 (1924).

7) The specific rotation and m. p. of dinitrophenyl-L-threonine are described to be +107 and 145°C, respectively, by K. R. Rao and H. A. Sober, *J. Am. Chem. Soc.*, 76, 1328 (1954).

8) *Anal.* Found: C, 27.51; H, 6.75; N, 19.28. Calcd. for $C_8H_{24}O_2N_5Cl_2Co$: C, 27.21; H, 6.86; N. 19.88%.

be preferable to L[Co en_2 glycine] I_2, was prepared and treated with acetaldehyde in a similar manner described above. The threonine thus obtained was a syrup and probably contaminated with levo propylenediamine. The paper chromatogram showed that this crude threonine consisted of threonine, allothreonine and glycine with the approximate ratio of 6.5 : 3 : 0.5. This crude threonine was converted into dinitrophenyl derivative (75% yield), which showed a slight levo rotation, $[\alpha]_D^{11}$ −1.2 (c 5.822 in 4% aq. sodium hydrogen curbonate), (asymmetric yield ca. 1%).

These varied yields for the asymmetric product may depend largely on the stability of the complex ions.

Institute of Scientific and Industrial Research
Osaka University
Kitahanada-cho, Sakai

*The Crystal Structure of Phenylarsonic Acid**

By Akira SHIMADA

(Received December 28, 1958)

In the attempt to determine the molecular configuration of an organoarsenic compound and at the same time to compare the structure of this acid with that of other organic acids, this study was undertaken. Small needle crystals of phenylarsonic acid, $C_6H_5AsO(OH)_2$, were easily obtained by the slow evaporation of a water-ethanol solution. Oscillation and Weissenberg photographs prepared with Cu K_α radiation gave the following unit-cell dimensions:

$$a=10.42, \quad b=14.92, \quad c=4.70\ \text{Å}$$

Schröder et al.[1] already showed that this crystal was orthorhombic with the axial ratios 0.7048 : 1 : 0.203, and also that perfect cleavages were found along the (110) plane, and imperfect ones along the (100) plane. The axial ratios given by these authors can be compared with the values derived by the X-ray measurement, 0.698 : 1 : 0.315 = 0.698 : 1 : 0.210×3/2. With assumption of four chemical units in the unit cell with the dimension given above, one can calculate the density to be 1.84 g./cc., which agrees satisfactorily with the observed value, 1.804 g./cc., reported by Schröder[2]. The systematic absence of (h00) reflections for h=odd, (0k0) ones for k=odd, (00l) ones for l=odd, and nothing else lead to the space group D^4_{42}–$P2_12_12_1$. Intensities were estimated visually with a calibrated scale, by making use of the multiple-film technique. The corrections for polarization and Lorentz factors were made in the usual way and that for absorption was neglected.

Since the c axis is shorter and each projection has the center of symmetry with plane group P_{gg}, the Patterson projection onto the (001) plane was first synthesized, which revealed clearly interatomic vectors between arsenic atoms owing to their greater scattering powers. The first electron-density projection was then synthesized, the Fourier coefficients being the observed structure amplitudes $|F_{hk0}|$'s with the signs determined by the arsenic atoms alone, and the successive refinement of the electron-density projection made clearer all of the atomic positions except hydrogen atoms. The electro-density projection is shown in Fig. 1. The reliability index for (hk0) spectra is, at the present stage of refinement, 20% with a temperature factor $B=4.2\ \text{Å}^{-2}$ for all. Preliminary studies of electron-density projections along other axes with the same method of analyses were sufficient to give an approximate z coordinate of each atom, from which the outline of the molecular configuration as well as their orientation were derived.

Although the result given above is preliminary and not very accurate, some interesting features of crystal structure were revealed. The interatomic distances within a molecule as well as between nearest molecules were found to be plausible. Three As–O bonds, with a mean length of 1.6_9 Å, and an As–C_1 bond, with a length of 1.9_1 Å, are arranged in a distorted tetrahedron. Long chains are formed along the two-fold screw axis perpendicular to the (001) plane by two sets of non-equivalent hydrogen bonds $-OH_1\cdots O_3\cdots HO_2-$. One set of hydrogen bonds with

* The major part of this paper was read at the Autumnal Joint Meeting of Chemical Societies of Japan, Tokyo, 1958.

1) P. Groth, "Chemische Krystallographie", Bd. IV, 354, Engelmann Leipzig, (1917).

2) Schröder, *Ber.*, 12, 562 (1879).

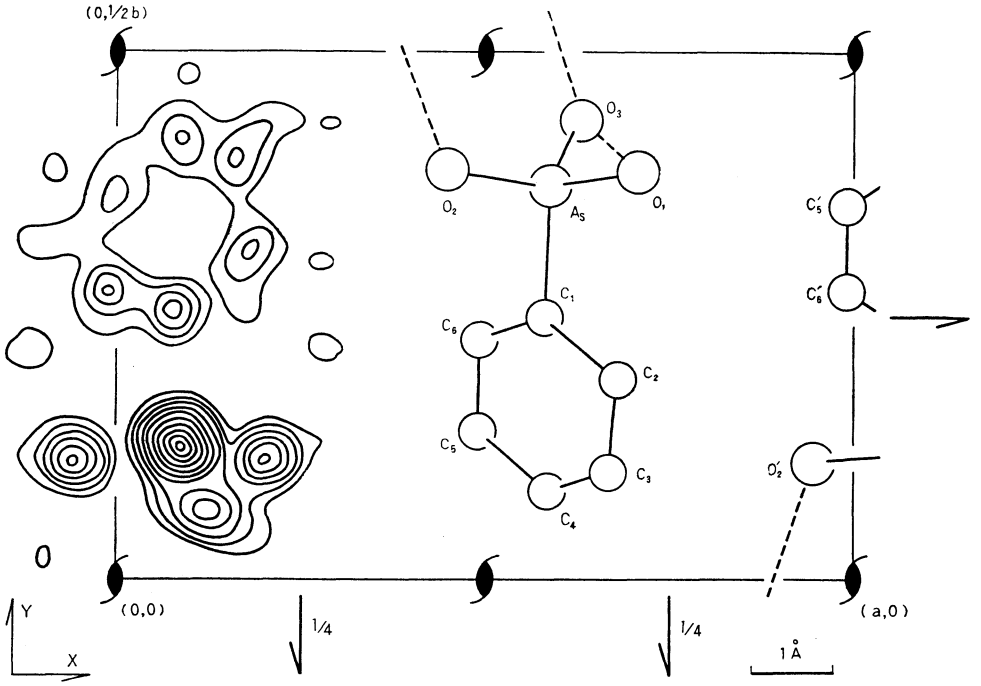


Fig. 1. Projection of the structure on (001). Contours are drawn at arbitrary intervals. Dashed line indicates the hydrogen bond between the molecules.

a distance 2.7_3 Å unites the oxygens, O_2 and O_3, of adjacent molecules around the screw axis, while the other set with a distance 2.5_6 Å unites the oxygens, O_3 and O_1, of adjacent molecules both along the *c* axis. The benzene rings are connected through the arsenic atoms to these chains and, hence, there might be no intermolecular forces other than those of the van der Waals type between these chains. This mode of packing of the molecules would explain the cleavages along the planes parallel to the (110) and (100) planes. Further refinement of the structure is now in progress.

The author wishes to express his sincere thanks to Professor I. Nitta and Professor T. Watanabé of Osaka University for their helpful advice, to Professor H. Nakata of Konan University for supplying the specimen, and to the other members of this University for their encouragement.

Department of Chemistry
Faculty of Science
Konan University
Higashinada, Kobe

Effect of Antioxidants on Polyethylene

By Shigeharu Okamoto and
Keisaku Takeuchi*

(Received January 9, 1959)

It is well known that oxidized polyethylene contains some amount of oxygen. Infrared spectrophotometric studies[1] have shown that during oxidation carbonyl groups are formed. The presence of these polar groups should be readily detected by measurements of the dielectric losses which imply the existence of the rotation of the polar groups under the influence of an externally applied alternating electric field. The oxidation resistance of polyethylene can be improved by the use of certain inhibitors and it is to be expected that increased knowledge of the effect of antioxidants on polyethylene will contribute toward this improvement.

* Present Address, Kijima Communication Wire Co., 6-1252, Kamimeguro, Meguro-ku, Tokyo.

1) F. M. Rugg, J. J. Smith and R. C. Bacon, *J. Polymer Sci.*, 13, 535 (1954).

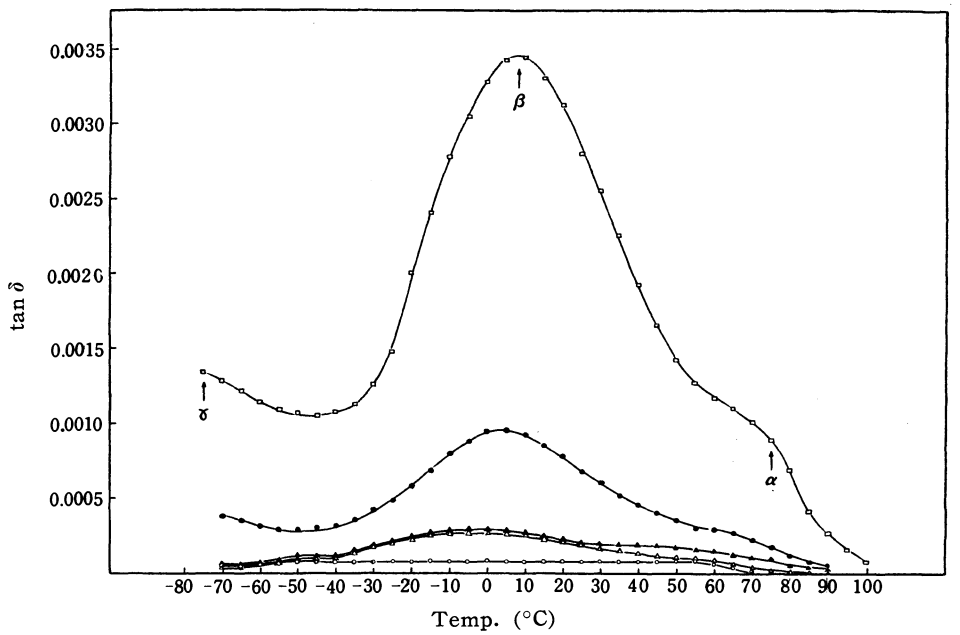


Fig. 1. The dissipation factor as a function of temperature for polyethylene exposed to ultraviolet radiation. Frequency 10 kc./sec. ○ before exposure; △ (20 hr.) and ▲ (40 hr.) exposure, with an antioxidant; ● (20 hr.) and □ (40 hr.) exposure, without antioxidant.

In this view we have studied the effect of an antioxidant on the change of the dielectric losses of polyethylene during aging. The polyethylene examined was Alathon 10-NC10-Natural and the antioxidant chosen was α-naphthylamine. A small amount of the antioxidant (1% by weight) was added on an open mill into the polyethylene sample. The photo-oxidation of polyethylene specimens has been carried out by exposure to the ultraviolet radiation from a mercury quartz lamp during 20 and 40 hr. Dielectric measurements were made over a temperature range of -75 to $+100$°C at a frequency of 10 kilocycles per sec. The results are given in Fig. 1.

As shown by the graph, for polyethylene samples containing no antioxidant, there exist three loss peaks and the maximum heights of the peaks increase as the time of exposure is increased. It is customary to label these peaks as α, β and γ descending from higher temperatures. On the other hand, far polyethylene samples containing a small amount of antioxidant, the α and β loss peaks which are attributed to the carbonyl activity in the crystalline regions and to that in the amorphous regions respectively, are markedly small and remain almost unchanged in intensity, independent of increasing exposure time. Furthermore, the γ peaks are missing as does that of original polyethylene sample before exposure.

It is concluded from the results that dielectric measurement is a sensitive method to estimate the degree of polarity of oxidation products and α-naphthylamine can be established to be an effective oxidation inhibitor for polyethylene by the use of dielectric method too.

Department of Applied Physics
Waseda University
Shinjuku-ku, Tokyo

On the Photochemical Decomposition of 2,4-Dinitrophenyl Peptides

By Shiro Akabori, Shumpei Sakakibara and Keiko Sakakibara*

(Received February 5, 1959)

In recent years, Blackburn[1], Mills[2] and others have pointed out the fact that

* Present address, Kobe Yamate Women's Junior College, Ikuta-ku, Kobe.

1) S. Blackburn, *Biochem. J.*, **45**, 579 (1949).
2) G. L. Mills, ibid., **50**, 707 (1952).

DNP-amino acids are unstable toward light, and Akabori et al.[3] have previously reported a semiquantitative investigation on the photochemical decompsition of the DNP-amino acids.

In the present investigation, photochemical decomposition of DNP-dipeptides, DNP-L-leucyl-glycine and DNP-glycyl-L-leucine, was examined. It was thus confirmed that the *N*-terminal amino acid residues of these peptides, together with the attached DNP-group, were completely decomposed under suitable conditions, resulting in the liberation of the *C*-terminal residues, glycine and leucine, in the form of free amino acids. The starting materials, DNP-L-leucyl-glycine and DNP-glycyl-L-leucine, were prepared from L-leucyl-glycine[4] and glycyl-L-leucine[5] according to Sanger's method[6] and their purity was confirmed by nitrogen analysis and two-dimensional paper chromatography under improved Levy's condition[7].

Anal. Found: N, 15.68**; N, 15.78***. Calcd. for $C_{14}H_{18}O_7N_4$: N, 15.81%. Found: N, 15.40****. Calcd. for $C_{14}H_{18}O_7N_4 \cdot 1/2\,H_2O$: N, 15.42%. Two milligrams of DNP-L-leucyl-glycine (m.p. 154~157°) on a glass dish (9 cm. in diameter) were dissolved in a small amount of ethanol or ether and then diluted with 20 ml. of suitable solvent such as distilled water, 1 N-hydrochloric acid, ether, benzene, chloroform and carbon tetrachloride. The solution was covered with cellophane sheet (0.02 mm. thick) and exposed to a 15 W. Mazda UV-sterilizing lamp for about 20 hr. at a distance of 20 cm., the principal line of the lamp being 2537 Å. The exposed solution was evaporated to dryness in a vacuum desiccator at room temperature and the residue was extracted as completely as possible with 1 ml. of water. One tenth milliliter of the extract was subjected to paper chromatography using a mixture of butanol, acetic acid and water (4:1:1) as solvent in order to detect the ninhydrin-positive products. The water-insoluble part of the photodecomposed residue was extracted with ethyl acetate and the extract was similarly analyzed by two-dimensional paper chromatography under improved Levy's condition (Fig. 1, Table I). When water or 1 N-hydrochloric acid was used as the solvent during irradiation, rather complicated results were obtained; dinitroaniline, dinitrophenol, glycine and other ninhydrin-positive materials, though small in amount, being detected as the products. In the case of benzene as the solvent,

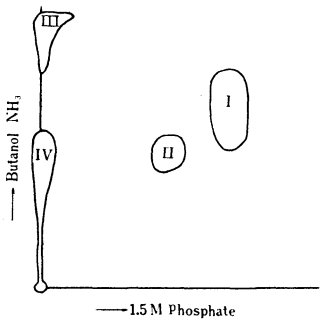


Fig. 1. An example of two-dimensional paper chromatograms of ethyl-acetate soluble parts of the photodecomposed products, the details of which are listed in Table I.

Spot I (yellow) corresponds to the DNP-leucyl-glycine and to the DNP-glycyl-leucine, spot II (yellow) to dinitrophenol, spot III (deep yellow) to dinitroaniline and sport IV (brown) probably to basic materials derived from dinitroaniline.

TABLE I

Starting material	DNP-leucyl-glycine						DNP-glycyl-leucine		
Reaction solvent	—[a]	Ether[b]	Benzene	Benzene[b]	Chloroform[b]	Carbon tetrachloride[b]	—[a]	Chloroform[b]	Carbon tetrachloride[b]
Spot I	###	###	###	##	+	−	###	+	±
Spot II	±	±	±	±	±	±	±	±	±
Spot III	−	+	+	##	##	−	−	##	##
Spot IV	−	−	−	−	−	##	−	−	+

a Starting material before irradiation.

b Solvent which was saturated with 1N-hydrochloric acid.

3) S. Akabori, T. Ikenaka, Y. Okada and K. Kohno, *Proc. Japan Acad.*, **29**, 509 (1953).

4) M. Bergmann, L. Zervas and J. S. Fruton, *J. Biol. Chem.*, 111, 238 (1935).

5) E. Fischer and J. Steingroever, *Ann.*, **365**, 167 (1909).

6) F. Sanger, *Biochem. J.*, **39**. 507 (1945); ibid., **45**, 563 (1949).

7) A. L. Levy, *Nature*, **174**, 126 (1964); G. Koch and W. Weidel, *Z. physiol. Chem.*, **303**, 213 (1956).

** DNP-L-leucyl-glycine (dried in vacuo at room temperature)

*** DNP-glycyl-L-leucine (dried in vacuo at 80° for 3hr.)

**** DNP-glycyl-L-leucine (dried in vacuo at room temperature)

especially when saturated with 1N-hydrochloric acid, only one faint but clear spot corresponding to glycine was obtained as ninhydrin-positive substance, but greater part of the starting material remained unchanged. More promising results were obtained in the case of chloroform and of carbon tetrachloride saturated with 1 N-hydrochloric acid. In both cases only one deep spot due to glycine (almost in the same density) was obtained, but a distinct difference was observed in the ethyl acetate soluble by-products.

Two milligrams of DNP-glycyl-L-leucine (sintered at 75~78°, resolidified and then decomposed at 110~115°) were dissolved in a small amount of ether and diluted with 20 ml. of chloroform or carbon tetrachloride, and treated exactly as in the case of DNP-leucyl-glycine. As expected, a clear single leucine spot was obtained in both solvents.

Application of these results to DNP-tri or higher peptides would be more interesting and the method may be utilizable as a new route for step-wise degradation of peptides from their *N*-terminal amino acid residues. Studies along this line are being pursued in this laboratory.

Institute for Protein Research
Osaka University, Nishi-ku, Osaka

Infrared Absorption Bands Possibly Associated with the Helical Structure of Polystyrene, Poly-p-methylstyrene and Poly-m-methylstyrene Prepared with Ziegler Catalyst

By Hiroyuki TADOKORO, Shun'ichi NOZAKURA, Tohru KITAZAWA*, Yutaka YASUHARA and Shunsuke MURAHASHI

(Received February 5, 1959)

In a previous paper[1] we have briefly suggested the possibility that the several bands of the spectrum of isotactic polystyrene might be associated with the threefold screw-axis of this polymer. On carrying out further studies in relation to this problem, we have found some experimental facts which supports this possibility as well as the inference that poly-*p*-methylstyrene and poly-*m*-methylstyrene prepared with Ziegler catalyst might have the isotactic structure, although they did not show distinct crystallinity.

Fig. 1 partly reproduces the spectra of of the films of crystallized and quenched

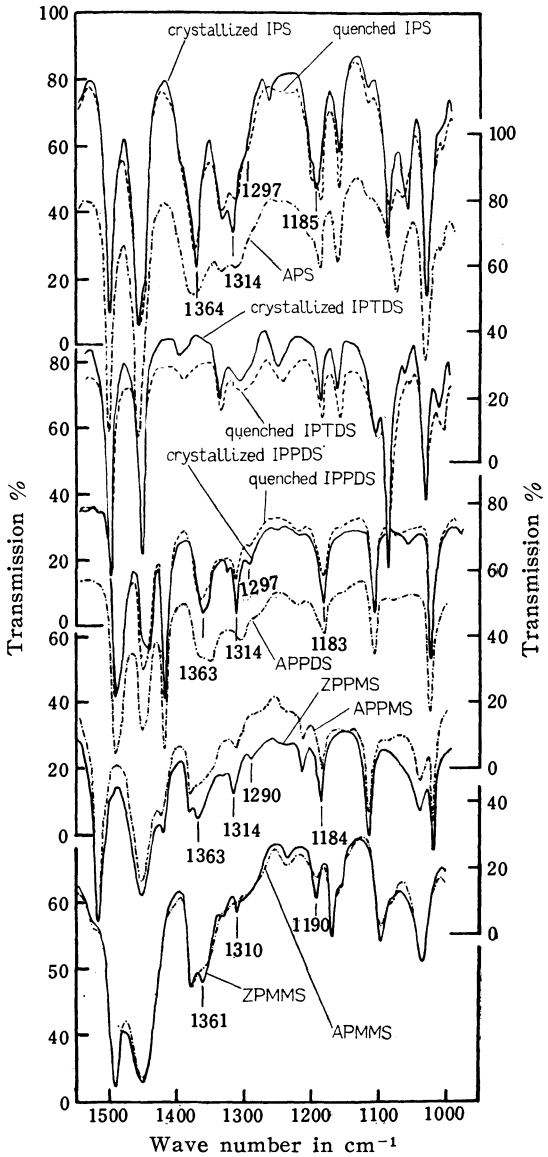


Fig. 1. Infrared spectra of crystallized and quenched IPS, APS, crystallized and quenched IPTDS, crystallized and quenched IPPDS, APPDS, ZPPMS, APPMS, ZPMMS and APMMS.

* Present address, Research Laboratories, Kanegafuchi Spinning Co. Ltd., Tomobuchi-chô, Miyakojima-ku, Osaka.

1) H. Tadokoro, N. Nishiyama, S. Nozakura and S. Murahashi, *J. Polymer Sci.*, to be published.

isotactic polystyrene (IPS)[2,3] atactic polystyrene (APS), crystallized' and quenched isotactic poly-α, β, β-trideuterostyrene (IPTDS)[1], $-(-CD_2-\underset{\underset{C_6H_5}{|}}{CD}-)_p-$, crystallized and quenched isotactic poly-*p*-deuterostyrene (IPPDS), $-(-CH_2-\underset{\underset{D}{|}}{CH}-)_p-$, atactic poly-*p*-deuterostyrene (APPDS), poly-*p*-methylstyrene prepared with Ziegler catalyst (ZPPMS), atactic poly-*p*-methylstyrene (APPMS), poly-*m*-methylstyrene prepared with Ziegler catalyst (ZPMMS) and atactic poly-*m*-methylstyrene (APMMS). Fig. 2 shows the polarized spectra of the oriented-and-crystallized IPS, IPTDS and IPPDS samples. The spectra of IPS and IPPDS exhibit several bands showing the same dichroism and the similar behavior on crystallization at nearly the same wave numbers; 1364 (⊥), 1314 (⊥), 1297 (∥) and 1185 cm^{-1} (∥). These four bands appear in weak intensity even in the spectra of quenched samples of IPS and IPPDS which give amorphous X-ray patterns, while they do not appear in the spectra of APS and APPDS. As these four bands are absent in the spectrum of IPTDS, these bands are considered to be not directly associated with the vibrations of the phenyl group, but with that of main chain. The first three bands at 1364, 1314 and 1297 cm^{-1} may be in the region assignable to CH_2 and CH wagging and CH_2 twisting, and the fourth at 1185 cm^{-1} in the region of CH_2 twisting and C–C stretching[4]. Hence the bands in these regions may be expected to be easily affected by the changes of the skeletal configurations. We could therefore consider that those bands are closely associated with the intramolecular interactions in the helical chain having the three-fold screw-axis (alternate sequence of *gauche* and *trans* conformation)[2,5]. The occurrence of these bands in the spectra of the quenched samples of IPS and IPPDS may be interpreted as indicating the existence of the locally remained helical structure in the amorphous region.

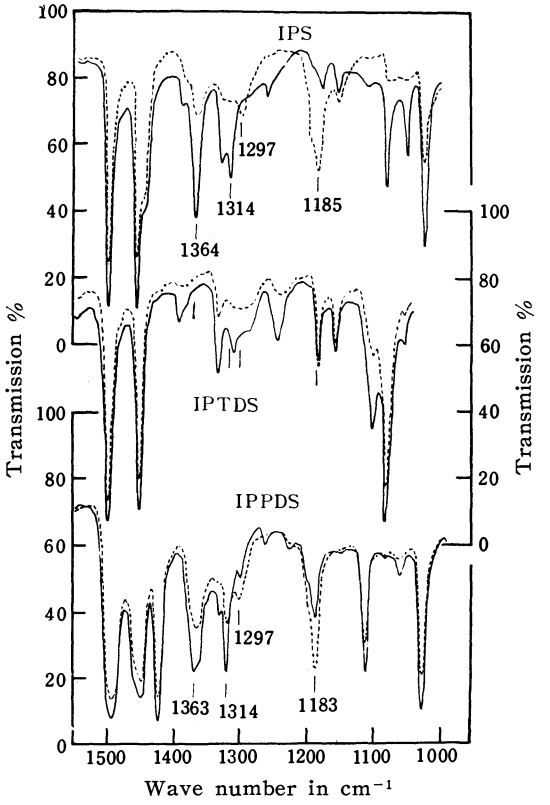


Fig. 2. Polarized infrared spectra of IPS, IPTDS and IPPDS.
—— electric vector perpendicular to elongation
------ electric vector parallel to elongation

It is interesting to note that the difference between the spectra of ZPPMS and APPMS as well as that between those of ZPMMS and APMMS are closely analogous to that between the spectra of quenched IPS and APS. Similar bands appear also at nearly the same positions in the spectra of ZPPMS (1363, 1314 and 1290 cm^{-1}) and ZPMMS (1361, 1310 and 1190 cm^{-1}) prepared with Ziegler catalyst, although these polymers are not appreciably crystalline. On the other hand, these bands are absent in the spectra of ordinary APPMS and APMMS. In view of the similarity pointed above, it can be inferred that ZPPMS and ZPMMS may have also isotactic and local helical structure just as quenched IPS has. Now the tentative explanation for the reason why these polymers are difficult to be crystallized in spite of their possible isotactic structure, would be that the packing of the neighboring molecular

2) G. Natta and P. Corradini, *Makromol. Chem.*, **16**, 77 (1955).
3) S. Murahashi, S. Nozakura, M. Sumi and K. Hatada, This Bulletin, to be published.
4) For example, Fig. 4 of the paper by Nielsen et al. J. R. Nielsen and A. H. Woollett, *J. Chem. Phys.*, **26**, 1391 (1957).
5) C. W. Bunn and E. R. Howells, *J. Polymer Sci.*, **18**, 307 (1955).

chains in hypothetical crystalline lattices of these polymers may be considered to be not so close on account of the existence of the *p*- or the *m*-substituent methyl groups.

The inference of the existence of local helical structure is strongly supported by the experimental results that the densities of several samples of ZPPMS ($1.015_2 \pm 0.0008$ g./cc.) were always higher than those of APPMS ($1.011_0 \pm 0.0008$ g./cc.). These density values were measured by the flotation method using aqueous sodium chloride solution at 25°C.

Thus, it may be considered that ZPPMS and ZPMMS might be crystallized if some adequate conditions of orientation and thermal treatments were found. In this standpoint of view, we are now going to study the crystallization of these polymers by use of X-ray-, infrared- and density measurements.

Department of Chemistry
Faculty of Science
Osaka University
Kita-ku, Osaka

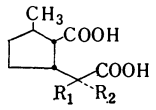
On the Structure of Actinidine and Matatabilactone, the Effective Components of Actinidia polygama

By Takeo SAKAN, Akira FUJINO, Fujio MURAI, Yasuo BUTSUGAN and Akio SUZUI

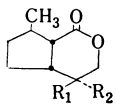
(Received February 10, 1959)

Deep interest has been held in Japan in *Actinidia polygama* Miq., a plant especially liked by the Felidae animals. The authors isolated two substances that excite cats from the leaves and gall of this plant. One is a base, named actinidine, $C_{10}H_{13}N$, b.p. 100~103°C/9 mm., $[\alpha]_D^{11}$ −7.2° (c 17.54, chloroform) (picrate: m.p. 143°C; *Anal.* Found: C, 51.45; H, 4.09; N, 14.97. Calcd. for $C_{16}H_{16}O_7N_4$: C, 51.06; H, 4.29; N, 14.89%), and the other, a neutral substance, named matatabilactone, $C_{10}H_{16}O_2$, b.p. 106~109°C/2 mm., $[\alpha]_D^{28}$ +31.9° (c 1.82, chloroform) (3,5-dinitrobenzoate of the methyl ester of the corresponding hydroxy acid: m.p. 78~79°C; *Anal.* Found: C, 54.88; H, 5.77; N, 7.09. Calcd. for $C_{18}H_{22}O_8N_2$: C, 54.82; H, 5.62; N, 7.10%).

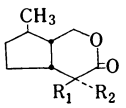
Permanganate oxidation of the hydroxy acid, obtained by alkali hydrolysis of matatabilactone, afforded two isomeric dicarboxylic acids, $C_{10}H_{16}O_4$, of m.p. 84~85°C, $[\alpha]_D^{13}$ +32.5° (c 0.63. chloroform), (*Anal.* Found: C, 60.32; H, 8.08. Calcd.: C, 59.98; H, 8.05%), and of m.p. 117~118°C, $[\alpha]_D^{12}$ +15.6° (c 0.93, chloroform), (*Anal.* Found: C, 60.32; H, 8.08.), which were found, through the good offices of Dr. McElvain, to be respectively identical with nepetalinic acids[1,2] of m.p. 85°C (Ia*) and of m.p. 117°C (Ib), obtained from nepetalactone by him.**



Ia $R_1=CH_3, R_2=H$
Ib $R_1=H, R_2=CH_3$



IIa $R_1=CH_3, R_2=H$
IIb $R_1=H, R_2=CH_3$



IIIa $R_1=CH_3, R_2=H$
IIIb $R_1=H, R_2=CH_3$

It follows, therefore, that the structure of matatabilactone may be represented by either II or III. In the inrared spectrum of matatabilactone, the value of $\nu_{C=O}$ (5.76 μ in carbon tetrachloride) differs from that[3] of isoiridomyrmecin[4] (iridolactone)[3,5,6](IIIa) and of iridomyrmecin[3,5-9] (IIIb), but is very similar to that of the dihydro derivative of nepetalactone*. Thus, matatabilactone is II, i.e. dihydronepetalactone[10]. Examination are now

* Heavy dots represent that the substituents are situated above the plane of the cyclopentane ring.

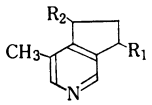
** Through mixed fusion test and comparison of infrared absorption spectra.

1) S. M. McElvain, R. D. Bright and P. R. Johnson, *J.Am. Chem. Soc.*, **63**, 1558 (1941).
2) S. M. McElvain and E. J. Eisenbraun, ibid., **77**, 1599 (1955).
*) A private communication from Dr. S. M. McElvain.
3) G. W. K. Cavill, D. L. Ford and H. D. Locksley, *Autralian J. Chem.*, **9**, 288 (1956).
4) S. M. McElvain and E. J. Eisenbraun, *J. Org. Chem.*, **22**, 976 (1957).
5) G. W. K. Cavill, D. L. Ford and H. D. Locksley, *Chem. & Ind.* (London), **1956**, 465.
6) G. W. K. Cavill and H. D. Locksley, *Australian J. Chem.*, **10**, 352 (1957).
7) M. Pavan, *Ricerca Sci.*, **19**, 1011 (1959) (*Chem. Abstr.*, **45**, 7309 (1951)); ibid **20**, 1853 (1950) (*Chem. Abstr.*, **45**, 5869 (1951)).
8) M. Pavan, *Chimica e industria* (Milan), **37**, 625, 714 (1955) (*Chem. Abstr.*, **49**. 16333, (1955); **50**, 13311 (1956)).
9) R. Fusco, R. Trave and A. Vercellone, ibid., **37**, 251, 958 (1955) (*Chem. Abstr.*, **50**, 6737 (1956)).
10) J. Meinwald, *J. Am. Chem. Soc.*, **76**, 4571 (1954).

being made to see whether this lactone is a mixture of IIa and IIb or not.

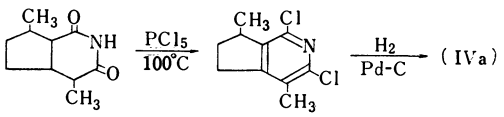
Actinidine was assumed to be a pyridine base from its color reaction (violet to 2,4-dinitrochlorobenzene and alkali) and from ultraviolet and infrared absorption spectra, λ_{max} 262 mμ (ethanol) (ε=2,400) and $\nu_{C=N}$ 6.30 μ (liquid). Several pyridine derivatives were actually isolated as the permanganate-oxidation products. One melting at 255°C with decomposition (*Anal.* Found: C, 53.19; H, 4.24; N, 8.00. Calcd. for $C_8H_7O_4N$: C, 53.04; H, 3.90; N, 7.73%), was found to be identical with 5-methylpyridine-3,4-dicarboxylic acid obtained by similar oxidation of 4-methylisoquinoline. Consideration of the natures of other oxidation products, a hydroxy compound, m.p. 132~133°C (*Anal.* Found: C, 73.11; H, 8.23; N, 8.48. Calcd. for $C_{10}H_{13}ON$: C, 73.59; H, 8.03; N, 8.58%) and a lactone, m.p. 92.5~93°C (*Anal.* Found: C, 66.33; H, 5.61; N, 8.28. Calcd. for $C_9H_9O_2N$: C, 66.24; H, 5.56; N, 8.58%), suggests formula IVa for actinidine.

The alternative formula IVb is excluded by the fact that a ketone, m.p. 47~49°C, $\nu_{C=O}$ 5.85 μ (liquid), (*Anal.* Found: C, 74.42; H, 6.92; N, 8.49. Calcd. for $C_{10}H_{11}ON$: C, 74.51; H, 6.88; N, 8.69%), was derived from actinidine-*N*-oxide, m.p. 123.5~124.5°C (*Anal.* Found: C, 73.94; H, 8.04; N, 8.45. Calcd. for $C_{10}H_{13}ON$: C, 73.59; H, 8.03; N, 8.58%) through rearrangement, hydrolysis and oxidation.



IVa $R_1=CH_3, R_2=H$
IVb $R_1=H, R_2=CH_3$

The structure IVa is closely related to that of II. Actually, actinidine was synthesized from nepetalinic acid imide as shown below.



It is very interesting to note that a monoterpene and an alkaloid having the same carbon skeleton following the isoprene rule have been found in one and the same plant.

The authors wish to express their sincere gratitude to Dr. S. M. McElvain for the identification of their samples with his nepetalinic acids.

Institute of Polytechnics
Osaka City University
Kita-ku, Osaka

Rapid Gas Chromatographic Analysis of a Mixture of Oxygen, Nitrogen, Methane, Carbon Monoxide, and Carbon Dioxide

By Yûichi Murakami

(Received February 10, 1959)

Gas chromatography has been widely used as method for separation or analysis of many complex mixtures of gases or liquids. However, a mixture of oxygen, nitrogen, methane, carbon monoxide, and carbon dioxide has not been separated successfully. "Molecular Sieves 5-A" is effective in separating hydrogen, carbon monoxide, oxygen, nitrogen, and methane but it adsorbs irreversibly carbon dioxide[1].

Activated charcoal can separate hydrogen, carbon monoxide, oxygen, methane, and other hydrocarbons, but for practical use carbon dioxide shows too long a retention time as well as too widely a diffuse band and nitrogen can not be separated from oxygen[2,3]. Silica gel is very poor in separating hydrogen, oxygen, and methane[2] but for some rather complex procedure[4], and gives longer retention time for carbon dioxide than that for the above gases. Alumina is also very poor in separating the above gases[2] and adsorbs irreversibly carbon dioxide.

The present author will propose a new method of gas chromatography, with which the above mixture can be completely analyzed within a few minutes. The principle and the procedure of the method are rather simple as follows.

1) G. Kyryacos, and C. E. Boord, *Anal. Chem.*, **29**, 787 (1957).
2) H. W. Patton, J. S. Lewis, and W. I. Kaye, ibid., **27**, 170 (1955).
3) N. H. Ray, *J. Appl. Chem.*, **4**, 82 (1954).
4) D. H. Szulczewski, and T. Higuchi, *Anal Chem.*, **29**, 1541 (1957).

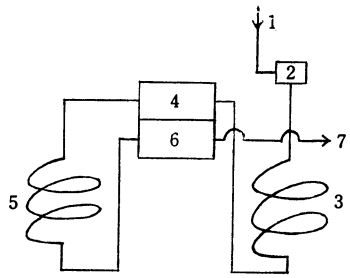


Fig. 1. Flow diagram of the present method.

1. Carrier gas inlet
2. Sample inlet
3. Column I
4. Cell I
5. Column II
6. Cell II
7. Outlet

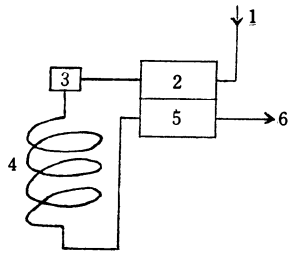


Fig. 2. Flow diagram of the usual method.

1. Carrier gas inlet
2. Reference cell
3. Sample inlet
4. Column
5. Sensitivity cell
6. Outlet

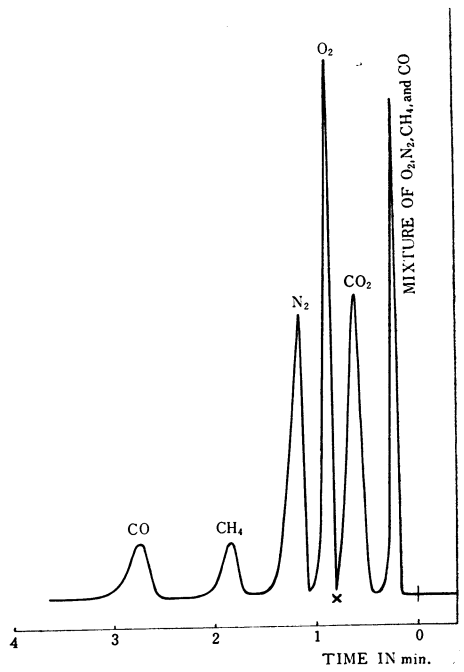


Fig. 3. Gas chromatogram.
× Switching the poles of recorder.

Apparatus.—The flow diagrams of the present new method and the usual one are illustrated in Figs. 1 and 2 respectively. In the usual method the carrier gas passes through successively a thermal-conductivity cell, a sample inlet, a column, and the other cell. The former cell works as a reference cell while the latter as a sensitivity cell. On the other hand, in the present method the carrier gas passes through successively a sample inlet, column I, thermal-conductivity cell I, column II, and cell II. The two cells are the same in construction. The electrical circuit comprises a Wheatstone bridge, the two arms of which are the platinium wires of the thermal-conductivity cells. In order to measure both positive and negative deflections, it is necessary either to adjust the base line to the middle of the chart or to be able to switch the poles of the recorder.

Columns.—*Column I*: A spiral copper column used was 40 cm. long and 4 mm. in inner diameter. Silica gel supplied by Chiyoda & Co. was used as the adsorbent. It was comminuted into 50~80 mesh and heated for one hour at 350°C. *Column II*: A spiral copper column used was 200 cm. long and 4 mm. in inner diameter, and "Molecular Sieves 5-A", comminuted into 50~80 mesh and heated for one hour at 400°C was used.

Procedure and Principle of the present method.—The test gas is separated firstly into carbon dioxide and a mixture of remaining gases by means of column I: they pass through thermal-conductivity cell I. During this period, in cell II the carrier gas alone is flowing, and then cell I is working as a sensitivity cell while cell II as a reference cell. Successively the mixture of remaining gases is separated further into oxygen, nitrogen, methane and carbon monoxide through column II and they pass through cell II. The situation in the second period is entirely changed, so that the role of each cell is interchanged and the direction of deflection is reversed.

The columns were operated at 80°C. The inlet pressure was 0.63 kg./cm^2 gage, the outlet atmospheric. The flow rate of hydrogen as carrier gas was 70 cc./min. Fig. 3. is an example of the gas chromatogram thus obtained and it shows that a mixture of oxygen, nitrogen, methane, carbon monoxide, and carbon dioxide has been completely separated. The time required for analysis is not more than four minutes.

The author wishes to express his sincere thanks to Dr. T. Keii and Mr. S. Terasawa for their kind encouragement.

Tokyo Institute of Technology
Meguro-ku, Tokyo

Changes of Dynamic Properties of Some Kaolin Minerals by Heat-treatment

By Shigeru MOCHIDA, Isao KAWASAKI and Yoichi NISHIMURA

(Received July 18, 1958)

In general, ceramic products are made by heating clay mineral at a high temperature in order to utilize its strength and hardness. In some cases, however, moderate abrasion as well as strength and hardness are required where clay mineral is used at the meta-stable state in the process of its structural changes, different from the general conception of ceramic products. It is therefore, important to study changes of dynamic properties of clay mineral when it is heated at a relatively low temperature region, and this study aims at clarifying the characteristics of the results of heat-treatment in air-tight and carbon dioxide atmosphere.

Mutual relationship between changes of dynamic properties, densities and structures of some kaolin minerals was investigated when they were heated in a closed vessel. On the dynamic properties, the Young's modulus and bending strength, and on the physical properties, bulk density and density were measured.

At the same time, the relationship between changes of dynamic properties and structures was partly tested by X-ray diffraction method. The results of Kibushi-clay heated in a closed vessel were compared with the results when it was heated in the open air.

Samples.—The following kaolin minerals were used in this study: Shidare-Kibushi clay from Shidare, Gifu, Japan; Yagusa-Kibushi clay from Yagusa, Aichi, Japan; Naegi-Kaolin from Naegi, Gifu, Japan; and Hongkong-Kaolin from Hongkong.

By the X-ray diffraction method, any of them excepting Hongkong-Kaolin is a kaolin mineral of fireclay type[1] and contains a small quantity of quartz in spite of being elutriated. Shidare-Kibushi clay contains a small quantity of organic matter as an impurity. Hongkong-Kaolin is halloysite with a high crystallinity[2]. The results of chemical analysis of the four samples which have been elutriated are shown in Table I.

In differential thermal analysis curves of all samples, the endothermic peak was reached due to the loss of inter-layer water between 100 and 200°C and to the loss of structural water between 400 and 500°C. The exothermic peak was reached at about 950°C corresponding to the structural change to mullite.

TABLE I
CHEMICAL ANALYSIS OF SOME KAOLIN MINERALS

Component	Shidare-Kibushi	Yagusa-Kibushi	Naegi-Kaolin	Hongkong-Kaolin
SiO_2	48.76	50.29	47.48	46.78
TiO_2	0.77	0.23	0.01	tr.
Al_2O_3	34.53	33.13	37.59	35.62
Fe_2O_3	1.50	2.10	0.40	0.46
MnO	0.00	tr.	0.00	tr.
CaO	0.27	0.24	0.11	0.81
MgO	0.20	0.64	0.02	0.63
K_2O	0.34	1.51	1.61	1.16
Na_2O	0.19	0.58	0.16	1.11
Ig·Loss	13.43	11.40	12.45	13.27
Total	99.99	99.82	99.83	99.84

All samples were elutriated, roll-milled with a proper amount of water and extruded into rods of about 3.5 mm. in diameter by a press. Each sample prepared as mentioned above was dried at 100°C in a drying oven for 24 hours. The samples were heated in an air-tight graphite crucible, the temperature of which is raised by 5°C per minute in an electric furnace with siliconit heaters, and then they were cooled down naturally in the crucible taken out of the furnace after having constantly been heated therein at a given temperature for an hour. In the case of heat-treatment in the open air, samples were heated in a porcelain crucible with many holes under the same conditions as in the case of the air-tight crucible. The temperatures of heat-treatment in both cases were 500, 800, 900, 1000, 1050, 1100, 1150, 1200 and 1250°C.

Experimental

Young's Modulus. — Young's modulus was measured in a cramp-free state by loading at a non-fixed end. It was calculated by the following equation[3]:

$$\text{Young's modulus} = (4l^3/\pi a^4 e)P/3$$

where l, distance between the fixed point and the loaded point = 10 cm.; P, load = 980 dynes; a, radius of sample (cm.); and e, length of strain (cm.).

1) G. W. Brindley and K. Robinson, *Trans. Faraday Soc.*, **42B**, 198 (1946).
2) G. Honjo and K. Mihama, *Acta Cryst.*, **7**, 511 (1954), and H. Takahashi, This Bulletin, **31**, 275 (1958).
3) Y. Tani, "Experimental Elasticity", (Iwanami Koza) V. F. 30 (1939).

TABLE II
BULK DENSITY OF SOME KAOLIN MINERALS

Temp. °C	Shidare-Kibushi		Yagusa-Kibushi	Naegi-Kaolin	Hongkong-Kaolin
100	1.72	open	1.92	1.86	1.68
500	1.64	1.58	1.88	1.78	1.63
800	1.64	1.61	1.80	1.72	1.55
900	1.72	1.76	1.95	1.88	1.63
1000	1.74	1.82	2.04	1.92	1.65
1050	1.86	2.03	2.37	2.14	1.74
1100	2.02	2.49	2.43	2.31	1.88
1150	2.34	2.46	2.43	2.44	2.13
1200	2.37	2.45	2.08	2.50	2.15
1250	2.44	2.39	—	—	—

TABLE III
DENSITY OF SOME KAOLIN MINERALS

Temp. °C	Shidare-Kibushi		Yagusa-Kibushi	Naegi-Kaolin	Hongkong-Kaolin
100	2.629	open	2.629	2.61	2.58
500	2.537	2.505	2.598	2.59	2.57
800	2.572	2.574	2.577	2.56	2.58
900	2.591	2.687	2.685	2.66	2.61
1000	2.672	2.695	2.716	2.68	2.66
1050	2.670	2.699	2.671	2.70	2.67
1100	2.675	2.688	2.647	2.66	2.68
1150	2.651	2.654	2.684	2.64	2.69
1200	2.662	2.669	2.613	2.66	2.69
1250	2.637	2.653	—	—	—

TABLE IV
YOUNG'S MODULUS ($\times 10^{11}$ dyne/cm^2)

Temp. °C	Shidare-Kibushi		Yagusa-Kibushi	Naegi-Kaolin	Hongkong-Kaolin
100	0.525	open	—	—	—
500	1.66	1.78	1.88	1.75	1.02
800	1.63	2.01	2.34	2.00	1.10
900	2.19	2.98	3.25	2.65	1.47
1000	2.52	3.58	4.40	2.83	1.56
1050	3.68	4.82	5.00	3.44	2.01
1100	4.85	5.91	5.92	5.08	2.85
1150	5.75	6.80	6.20	5.78	4.50
1200	6.05	7.18	5.92	6.53	4.27
1250	6.62	6.00	—	—	—

TABLE V
BENDING STRENGTH (g./mm^2)

Temp. °C	Shidare-Kibushi		Yagusa-Kibushi	Naegi-Kaolin	Hongkong-Kaolin
100	1300	open	1620	1490	470
500	2320	5140	2660	3260	1050
800	5100	6490	6950	5990	2570
900	5950	7970	8210	8110	3840
1000	7030	7720	8960	7720	4240
1050	8360	8130	12600	9040	6000
1100	10770	12900	17690	11130	6860
1150	12030	12920	17670	14600	9770
1200	13800	13350	11390	17500	9300
1250	14600	12600	—	—	—

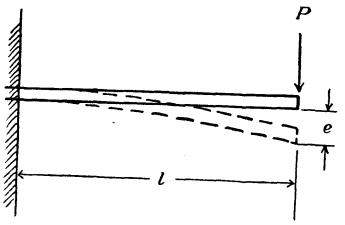


Fig. 1. Measuring procedure of Young's modulus.

Bending Strength. — Although a bending strength does, in an exact sense, not always mean a physical value, it is practically used as a breaking strength in industries. By supporting a sample on two knife edges, continuously loading on the middle of the sample and reading the weight of the load just breaking the sample the bending strength was calculated by the following equation[4]:

$$\text{bending strength} = 8Pl/\pi d^3$$

where P, weight of load just breaking the sample (g.); l, distance between two supporters 60 mm. and d, diameter of sample (mm.).

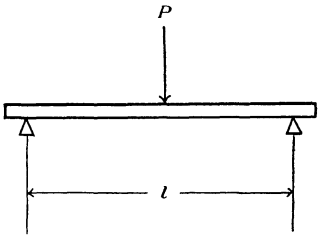


Fig. 2. Measuring procedure of bending strength.

Density. — The sample was ground into a powder finer than 200-mesh and its density was measured by a picnometer in mono-chlorbenzene at 25°C.

Results

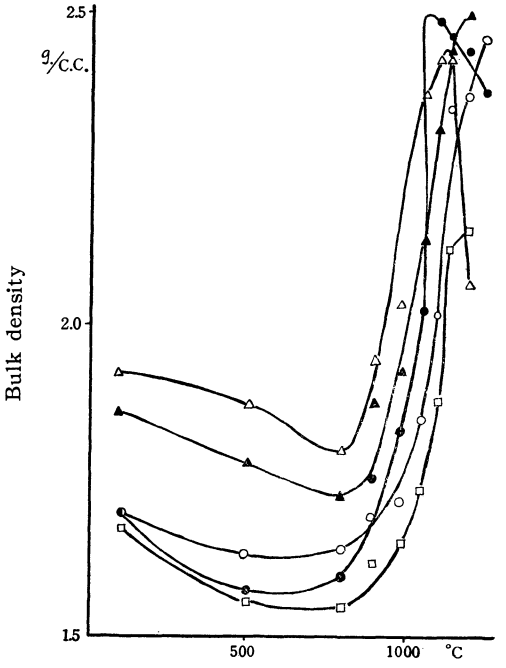
Bulk Density.—The value of bulk density is shown in Table II and Fig. 3, and there is the minimum point at about 800°C in each curve, except that the temperature corresponding to the minimum point of bulk density of Shidare-Kibushi clay heated in the open air moves down to about 500°C and its maximum point appears at about 1150°C.

Density.—As shown in Table III and Fig. 4, there is a minimum point between 500 and 800°C and a maximum point at about 1000°C in each curve of the density. Beyond 1000°C the density decreases gradually.

Young's Modulus.—As shown in Table IV and Fig. 5, the Young's modulus increases rapidly beyond 800°C and a maximum value is shown between 1100 and 1200°C.

Bending Strength.—As shown in Table V and Fig. 6, beyond 800°C the bending strength increases gradually and beyond 1000°C, it increases

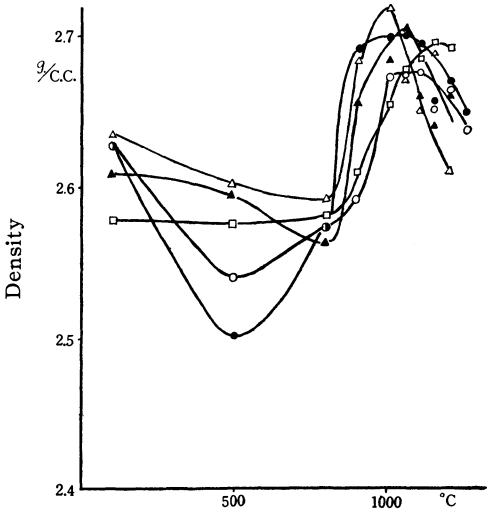
4) Japanese Industrial Standard (JIS), S·6005, 4 (1955).



Treated temperature

Fig. 3. Curves showing the changes of bulk density in the various stages of heat-treatment.

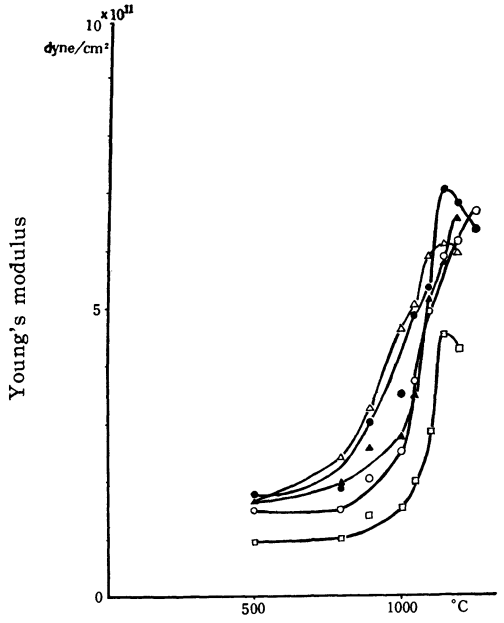
○ Shidare-Kibushi
● Shidare-Kibushi (open)
△ Yagusa-Kibushi
▲ Naegi-Kaolin
□ Hongkong-Kaolin



Treated temperature

Fig. 4. Curves showing the changes of density in the various stages of heat-treatment.

○ Shidare-Kibushi
● Shidare-Kibushi (open)
△ Yagusa-Kibushi
▲ Naegi-Kaolin
□ Hongkong-Kaolin



Treated temperature

Fig. 5. Curves showing the changes of Young's modulus in the various stages of heat-treatment.
- ○ Shidare-Kibushi
- ● Shidare-Kibushi (open)
- △ Yagusa-Kibushi
- ▲ Naegi-Kaolin
- □ Hongkong-Kaolin

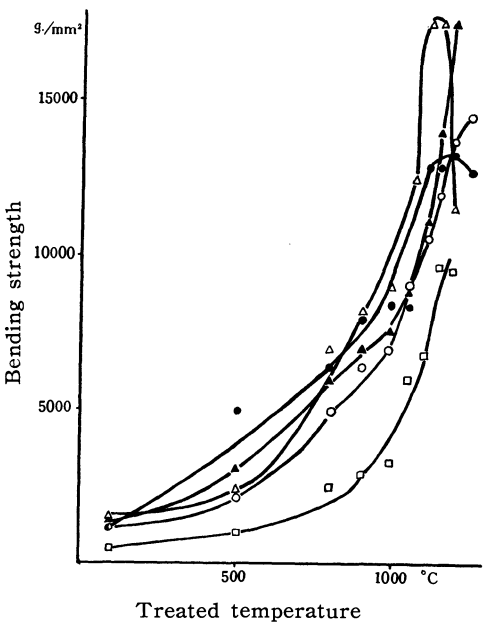
rapidly. In both cases, there are maximum values and, after reaching the maximum values, it decreases rapidly.

Discussion

Even clay minerals, which belong to the same "kaolin" group, differ from one another according to their kinds in regard to the bending strength and Young's modulus. There are many factors, for example, particle sizes, structural characteristics, impurities, etc., which influence the dynamic properties of kaolin minerals.

As only four samples were experimented with in regard to their dynamic properties, it is difficult to discuss and to relate the results of their dynamic properties with the results of chemical analysis. The effects of the impurity contained in kaolin mineral on the dynamic properties are studied now and their results will be reported in future.

In this paper, some relationships between the dynamic properties and the structural characteristics are discussed. The changes of the dynamic properties by heat-treatment beyond a certain temperature are not continuative but are abrupt.



Treated temperature

Fig. 6. Curves showing the changes of bending strength in the various stages of heat-treatment.
- ○ Shidare-Kibushi
- ● Shidare-Kibushi (open)
- △ Yagusa-Kibushi
- ▲ Naegi-Kaolin
- □ Hongkong-Kaolin

In the heat-treated specimens of Yagusa-Kibushi clay, for example, the bending strength increases to only 2000 g./mm² between 800 and 1000°C and as much as 8000 g./mm² between 1000 and 1100°C, but decreases rapidly between 1100 and 1200°C. Also, the Young's modulus and even density take a similar tendency. These phenomena seem to be attributed to the changes of crystal structures in clay minerals. Therefore, those causes which affect the changes of dynamic properties may be due to the following:

1. Change of plasticity of kaolin mineral by heating at an early stage.
2. Change of crystal structure of kaolin mineral and transformation of its macrostructure caused by the change of crystal structure by heating at a later stage.
3. Sintering.

Now, the value expressed by percentage which is obtained by dividing a bulk density by a density is called "filling ratio". The dynamic properties and the filling ratio will be discussed. As shown in Table VI and Fig. 7, the minimum value of filling ratio appears, generally speaking at the temperatures between 500 and 800°C. The changes of the filling ratio

TABLE VI
FILLING RATIO (PERCENTAGE)

Temp. °C	Shidare-Kibushi		Yagusa-Kibushi	Naegi-Kaolin	Hongkong-Kaolin
100	65.3	open	73.9	72.0	65.2
500	64.4	63.2	71.8	68.2	63.3
800	64.0	62.6	70.0	67.2	60.2
900	66.2	65.8	72.5	70.7	63.9
1000	65.2	67.7	74.9	71.7	62.1
1050	70.0	75.2	88.8	79.3	65.0
1100	75.5	92.5	91.7	86.8	72.5
1150	88.0	92.5	90.5	91.6	79.2
1200	89.0	91.8	82.7	93.8	80.6
1250	92.6	90.2	—	—	—

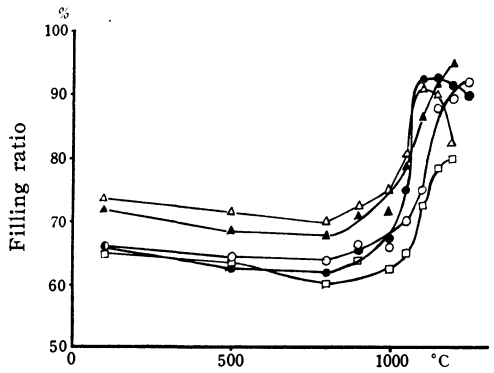


Fig. 7. Curves showing the changes of filling ratio in the various stages of heat-treatment.
○ Shidare-Kibushi
● Shidare-Kibushi (open)
△ Yagusa-Kibushi
▲ Naegi-Kaolin
□ Hongkong-Kaolin

may be due to the following. In the early stage of heating, the sample loses interlayer water. At the temperatures between 500 and 800°C, it has the minimum filling ratio, because it becomes porous owing to the loss of structural water while the shrinkage caused by sintering does not keep pace with it. Beyond 800°C, it is in the state of "meta-kaolin" and its filling ratio is recovered gradually between 800 and 1000°C, because the shrinkage by sintering is larger than the loss of structural water.

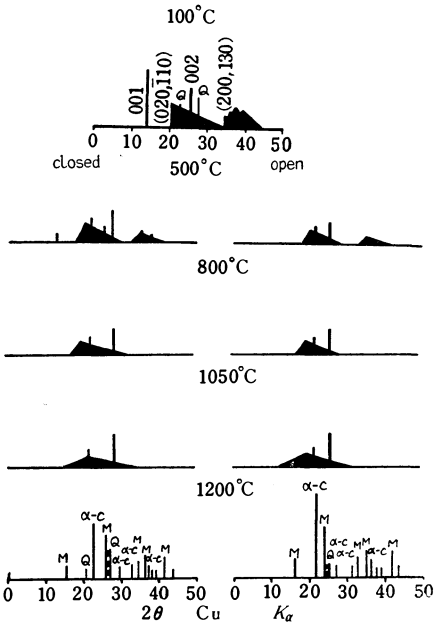
The Young's modulus changes a little until it reaches 800°C, but as soon as the temperature exceeds 800°C, the Young's modulus begins to increase in company with filling ratio. This indicates that the Young's modulus increase is accompanied by the sintering. The filling ratio increases rapidly beyond 1000°C which may be due not only to the sintering but also to the commencement of the structural changes of the kaolin minerals[5]. This rapid increase of the filling ratio has influence on the bending strength and the Young's modulus.

The temperature at which crystallization begins varies a little according to the kinds of kaolin mineral. That is to say, in the case of Yagusa-Kibushi clay, the Young's modulus begins to increase just beyond 1000°C, but in the case of Shidare-Kibushi clay and Naegi-Kaolin, it does at higher temperature. In the case of Hongkong-Kaolin, it begins to increase rapidly beyond 1050°C. However, when the temperature of heat-treatment rises up to a certain point along with the development of crystallization, the filling ratio does not increase but begins to decrease and, at the same time, the bending strength and the Young's modulus also are inclined to decrease. This may be explained as follows.

In the case of Shidare-Kibushi clay, the filling ratio continues to increase until 1250°C together with the bending strength and Young's modulus, which may be caused, to a great extent, by the sintering and the commencement of crystallization. Crystals of mullite and α-cristobalite do not yet grow at 1050°C, but they appear at 1200°C. In the case of Yagusa-Kibushi clay, the Young's modulus increases rapidly beyond 1000°C, and reaches the maximum value between 1100 and 1200°C. However, at 1200°C the Young's modulus apparently starts to decrease according to the decrease of the filling ratio. Moreover, the characteristics of the sample heated at 1200°C shows a distinguished expansion in diameter.

X-ray diffraction data will be discussed below. As shown in Fig. 8, in the case of Shidare-Kibushi clay, mullite begins to

5) W. F. Bradley and R. E. Grim, *Am. Mineral*, **36**, 182 (1951).



M: mullite, α-c: α-cristobalite, Q: quartz

Fig. 8. Schematic drawings of the X-ray diffractometer traces of heat-treated specimens of Shidare-Kibushi clay.

grow at about 1050°C. At about 1200°C, the crystallization to mullite is distinguishable and the quartz of impurity changes to α-cristobalite. Therefore, it is considered that when this clay begins to crystallize and its filling ratio increases rapidly owing to sintering, both the bending strength and the Young's modulus increase together. However, when the crysrallizations to mullite and α-cristobalite are remarkable, cracks grow along the crystals, and therefore, the filling ratio and bending strength together with the Young's modulus are reduced.

The difference between the heat-treatment in a closed vessel and in the open air will be discussed. In general, Kibushi clay changes at the lower temperature when heated in the open air. This may be clearly seen from the X-ray diffraction diagrams of the heat-treated specimens of Shidare-Kibushi clay shown in Fig. 8. That is, in the heat-treatment in a closed vessel, two reflections, (001) and (002), are clearly left at 500°C although their intensities are weaker, while in the heat-treatment in the open air, the reflections are thoroughly extinguished at the same temperature. The X-ray diffraction diagram of the 1100°C heat-treated specimen in the open air is almost exactly similar to that of the specimen heated at 1200°C in a closed vessel.

Summary

When kaolin mineral is heat-treated at a relatively low temperature region, its density has the minimum value between 500 and 800°C and the maximum at about 1000°C.

The value of dynamic properties of kaolin mineral increases slightly until about 800°C but increases rapidly beyond 1000°C to reach the maximum value. Then, the value is inclined to decrease rapidly beyond the temperatures, at which the maximum value is yielded. Similarly, the filling ratio also has the minimum value at about 800°C and increases rapidly beyond 1000°C to reach the maximum value. This indicates that when kaolin mineral is heat-treated at a relatively low temperature region, its dynamic properties have a close relation with its filling ratio. It is considered that these phenomena are due not only to the sintering of clay mineral by heat-treatment but also to the structural changes as shown in X-ray diffraction data.

The changes of dynamic and physical properties and of the structures of kaolin mineral heated in a closed vessel take place later than those heated in the open air. It may be due to the fact that the oxidation of the organic matters contained in kaolin mineral is oppressed in a closed vessel.

The writers wish to express their sincere thanks to Dr. Hiroshi Takahashi of the University of Tokyo for his valuable advice and assistance throughout this work.

Tombow Pencil Mfg. Co., Ltd.
Toshima, Kita-ku, Tokyo

*Crystal Structure and Lattice Energy of i-Erythritol. I. Crystal Structure of i-Erythritol**

By Akira SHIMADA

(Received August 13, 1958)

i-Erythritol ($CH_2OH \cdot C^*HOH \cdot C^*HOH \cdot CH_2OH$) is one of the polyalcohols, which has a close relationship with carbohydrates. Hence a knowledge of its stereochemical configuration would be of great interest and importance to the chemistry of carbohydrates. The molecule of this compound is built up of two and, in a sense, identical groups, each of which has an asymmetric carbon atom, C*, as indicated in the above chemical formula. It has already been reported that in the crystal of this substance these two identical groups are related to each other by a center of symmetry[1,2]. However, the detailed spatial configuration of this molecule still remains unexplored.

Interesting roles of the hydrogen bond have been elucidated for pentaerythritol in connection with its thermal and electrical properties[3-8]. Therefore, it seems highly promising to make an attempt to find out what types of hydrogen bond are linking molecules together in the crystal of *i*-erythritol, in order to understand some physical properties of this crystal.

Experimental

i-Erythritol crystallizes in the tetragonal bipyramidal class. Crystals were prepared by the slow evaporation of the solution in a mixture of ethyl alcohol and water. They were ground to cylindrical rods, elongated parallel to the [001] or [010] axis; their diameters are less than 0.4 mm. All photographs were taken with Cu K_α radiation. The crystal has been shown by the previous workers[1,2] to possess the space group symmetry $C_{4h}^6-I4_1/a$, with eight molecules in the unit cell. This assignment of the space group was verified by oscillation and Weissenberg photographs in the present experiment, and a redetermination of the unit cell dimensions gave the following values.

$$a=12.81\pm0.03\ \text{Å} \qquad c=6.81\pm0.02\ \text{Å}$$

The axial ratio $c/a=0.532\pm0.003$ as deduced from these lattice constants will give $c/\sqrt{2}\ a=0.376\pm0.002$ if we refer to the old choice of the crystallographic axes*, which is in excellent agreement with the goniometric value 0.3762[9]. Assuming eight molecules in the unit cell with the dimensions given above, the density is calculated to be 1.45 ± 0.01 g./cc., which is in good harmony with the value, 1.450 g./cc., reported by Schröder[10].

The ($hk0$) and ($h0l$) intensity data were estimated visually from multiple-film Weissenberg photographs. They were corrected for the Lorentz and polarization factors, using Cochran's chart[11]. Correction was applied to the absorption in the usual way, although this was found to be very small (absorption coefficient $\mu=12.7$ cm^{-1}). The observed structure ampliudes were first set on to an absolute scale using Wilson's method[12] which were further improved during the later stages of refinement.

Structure Determination

The unit cell contains only eight molecules, that is, sixteen C, sixteen C*, sixteen O_1 and sixteen O_2 atoms, suggesting that the center of gravity of each molecule must occupy a special position in the unit cell. In accord with the conclusion[1,2] already derived from a preliminary consideration of intensities of certain principal planes, it was confirmed that each molecule was situated at a center of symmetry. Hence each atom occupies the general positions given by,

* The major part of this paper was read at the 7th Annual Meeting of the Chemical Society of Japan, April, 1954. A short communication is now in press in Acta Crystallographica, and the present account describes the structure analysis in detail.

1) W. G. Burgers, *Phil. Mag.*, (7) 1, 289 (1926).
2) N. Schönfeldt, K. Hermann und O. Hassel, *Z. physik. Chem.* (A) **124**, 305 (1926).
3) I. Nitta and T. Watanabé, *Nature*, **140**, 365 (1937); *Sci. Papers Inst. Phys. Chem. Research*, **34**, 1669 (1938).
4) F. J. Llewllyn, E. G. Cox and T. H. Goodwin, *J. Chem. Soc.*, **1937**, 883.
5) I. Nitta, S. Seki and M. Momotani, *Proc. Japan Acad.*, **26**, (9) 25 (1950).
6) I. Nitta, S. Seki, M. Momotani, K. Suzuki and S. Nakagawa, ibid., **26**, (10) 11 (1950).
7) I. Nitta, T. Watanabé, S. Seki and M. Momotani, ibid., **26**, (10) 19 (1950).
8) R. Kiriyama, S. Yabumoto and I. Nitta, This Bulletin, **27**, 115 (1954).
9) P. Groth, "Chemische Krystallographie", Engelmann, Leipzig (1906), part III, p. 240.
* The old axes are such that the z axis is unchanged and the x axis is the diagonal of the basal plane of the new unit cell.
10) Schröder, *Ber.*, **12**, 562 (1879).
11) W. Cochran, *J. Sci. Instr.*, **25**, 253 (1948).
12) A. J. C. Wilson, *Nature*, **150**, 152 (1942).

$$(0,0,0;\ 1/2,1/2,1/2)+$$
$$x,y,z;\ \bar{x},1/2-y,z;\ 3/4-y,1/4+x,1/4+z;$$
$$1/4+y,1/4-x,1/4+z;$$
$$\bar{x},\bar{y},\bar{z};\ x,1/2+y,\bar{z};\ 1/4+y,3/4-x,3/4-z;$$
$$3/4-y,3/4+x,3/4-z$$

Because of the short c axis, it was expected that an approximate structure might appear in an electron density projection on the (001) plane, without complication due to overlappings of atoms. Since a molecule contains only lighter atoms, a Patterson projection $P(uv)$ on the (100) plane, shown in Fig. 1, did not give any useful information about the location of each atom. Hence, an attempt was made to solve the structure with a minimum function[13] derived from this Patterson projection. In order to get a minimum function, a location of rotation peaks must be determined and various minimum functions were tried, regarding acceptable peaks in the Patterson function as the possible image-seeking vectors. The location of rotation peaks, marked by a cross in the Patterson function, gave the most promising minimum function $M_4(xy)$ as shown in Fig. 2. Another approarch to the clue to an approximate structure was obtained by the inequality method[14] using Sakurai's chart[15], and the signs of five out of fifty-two observed reflections could be determined. The first Fourier map prepared with these terms, given in Fig. 3, shows a good resemblance to the minimum function $M_4(xy)$.

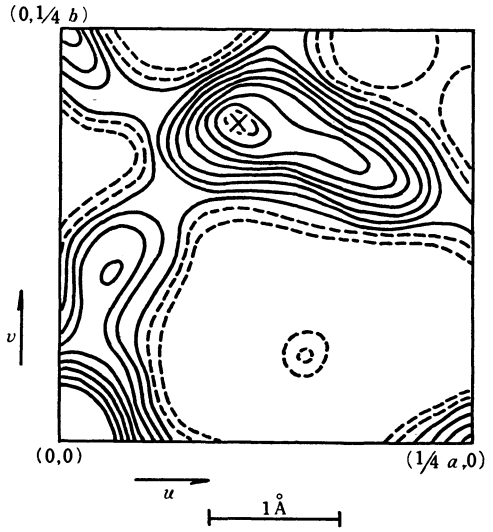


Fig. 1. Patterson projection $P(uv)$ onto (001) with contours at arbitrary intervals.

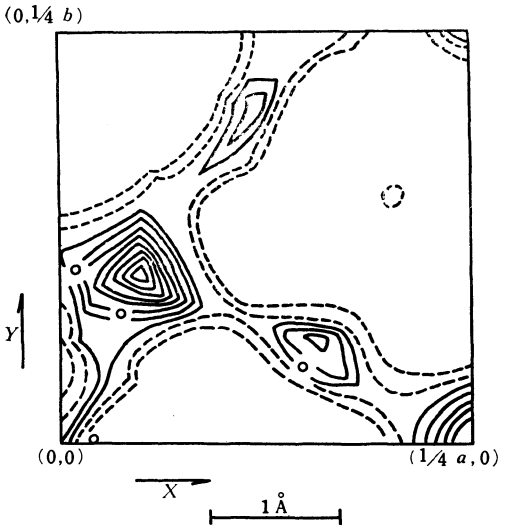


Fig. 2. Minimum function $M_4(xy)$ with contours at arbitrary intervals. Circles indicate the location of atoms corresponding to Fig. 4.

Based on these two promising figures, an effort was made to locate each atom at each peak by trial and error method. Starting from the approximate structure projected on the (001) plane, the structure was refined by successive Fourier syntheses with the aid of difference syntheses at later stages. The final Fourier

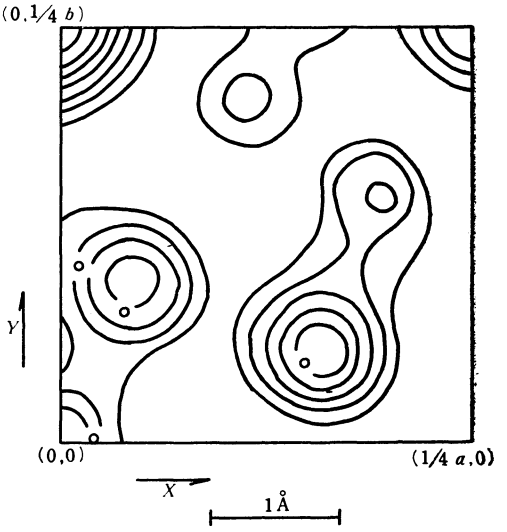


Fig. 3. First Fourier projection onto (001) prepared by inequality method with contours at arbitrary intervals. Circles indicate the location of atoms corresponding to Fig. 4.

13) M. J. Burger, *Acta Cryst.*, **4**, 531 (1951).
14) D. Harker and J. S. Kasper, ibid., **1**, 70 (1948),
15) K. Sakurai, ibid., **5**, 546 (1952).

projection on the (001) plane is shown in Fig. 4. The reliability index $R=(\sum||F_o|-|F_c||)/\sum|F_o|$ for $(hk0)$ spectra is reduced to 16.5%, the contributions from hydrogen atoms being excluded. Several plausible configurations of the molecule were derived from the Fourier projection on the (001) plane with the aid of the Patterson projection $P(uw)$ on the (010) plane, which is shown in Fig. 5. They were put to the test by the comparison of observed and calculated structure factors for $(h0l)$ spectra. One of these configurations led to an approximately good agreement between the observed and the calculated structure factors, so as to give an approximate value of z for each atom. Since the symmetry of the crystal is high, there are considerable overlappings of atoms in the (010) projection which make it difficult to refine x,y and z values by successive Fourier syntheses alone. We were able to overcome this difficulty by preparing difference syntheses with the coefficients F_o-F_c', where F_c' stands for the structure factor calculated by means of the coordinates of the atoms, the peaks of which were well resolved but equivalent peaks were overlapped by other atoms by the symmetry operations. The usual difference syntheses were also tried at later stages to refine the structure. The electron density projection on the (010) plane is shown in Fig. 6. The reliability index R for $(h0l)$ spectra is found to be 13.3%*, the contributions from

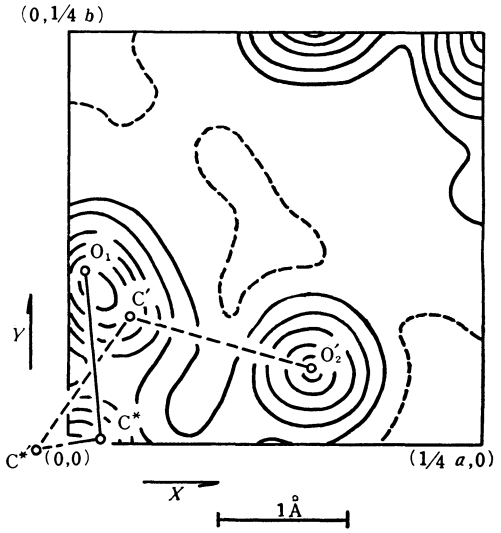


Fig. 4. Final electron density projection onto (001). Contours at intervals of 2 e.Å^{-2} with the lowest solid contour at 3 e.Å^{-2}.

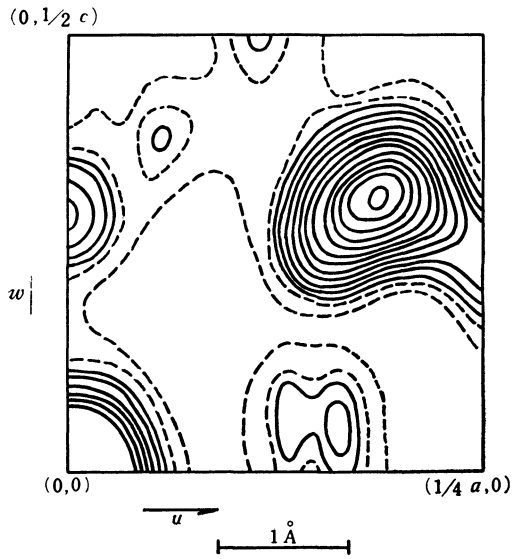


Fig. 5. Patterson projection onto (010) with contours at arbitrary intervals.

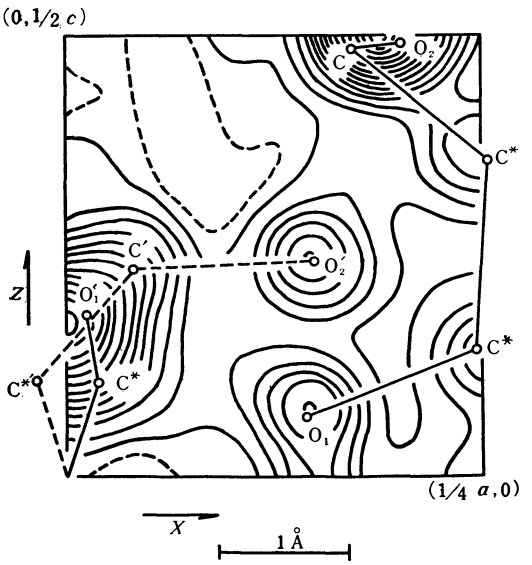


Fig. 6. Final electron density projection onto (010). Contours at intervals of 2 e.Å^{-2} with the lowest solid contour at 3 e.Å^{-2}.

TABLE I
ATOMIC COORDINATES

	x/a	y/b	z/c
C*	0.019	0.001	0.108
C	−0.039	−0.080	0.236
O_1	0.011	0.108	0.185
O_2	−0.148	−0.049	0.243

* The reliability indices for $(hk0)$ and $(h0l)$ spectra were reduced mainly because of the more careful measurement of intensity after the short communication was sent to Acta Crystallographica. The author hopes at some more favorable time to refine the structure by the use of I. B. M. computor which will be provided at his university in the near future.

TABLE II
VALUES OF CALCULATED AND OBSERVED STRUCTURE FACTORS

(*hk*0)

h	*k*	1/8(F_o)	1/8(F_c)	*h*	*k*	1/8(F_o)	1/8(F_c)	*h*	*k*	1/8(F_o)	1/8(F_c)	*h*	*k*	1/8(F_o)	1/8(F_c)
2	0	1.0	−0.8	2	4	11.8	−14.8	2	8	5.7	−4.5	2	12	2.5	2.1
4	0	6.8	5.6	4	4	8.2	−7.5	4	8	10.0	10.5	4	12	1.4	0.6
6	0	12.8	14.2	6	4	2.1	2.1	6	8	1.8	2.3	6	12	0.9	0.3
8	0	4.6	5.3	8	4	3.5	−3.1	8	8	2.1	2.7	8	12	0	−0.7
10	0	2.7	−2.6	10	4	6.3	−6.3	10	8	2.4	2.8	10	12	0.5	−0.5
12	0	1.2	0.7	12	4	2.3	2.9	12	8	1.9	1.6				
14	0	0	0.7	14	4	1.5	−1.9	14	8	0.8	1.0	2	14	2.3	2.3
16	0	0.4	−0.3									4	14	0.7	−1.0
				2	6	3.2	2.2	2	10	5.2	5.0	6	14	1.3	−1.6
2	2	15.4	13.9	4	6	0.8	2.0	4	10	4.4	4.9	8	14	0	−0.4
4	2	4.3	−4.4	6	6	2.6	−2.1	6	10	2.6	2.1				
6	2	5.1	5.2	8	6	1.2	0.3	8	10	0	−0.3	2	16	1.2	1.1
8	2	5.8	−6.8	10	6	1.5	1.5	10	10	4.1	3.6				
10	2	0.9	0.1	12	6	1.4	1.7	12	10	0	−0.5				
12	2	1.4	−1.7	14	6	0	0.8								
14	2	0.7	−0.8												
16	2	1.6	−1.3												

(*h*0*l*)

h	*l*	1/8(F_o)	1/8(F_c)	*h*	*l*	1/8(F_0)	1/8(F_c)	*h*	*l*	1/8(F_o)	1/8(F_c)	*h*	*l*	1/8(F_o)	1/8(F_c)
2	2	13.1	−12.2	2	6	2.4	−2.1	1	1	7.1	7.3	1	5	1.3	−0.4
4	2	3.3	−3.6	4	6	3.0	3.2	3	1	9.7	9.9	3	5	4.6	4.8
6	2	0.4	0.0	6	6	0	−0.6	5	1	4.9	−4.1	5	5	1.5	−1.6
8	2	4.2	−4.2	8	6	1.2	−1.1	7	1	8.0	8.3	7	5	0.8	1.1
10	2	2.9	2.6	10	6	2.2	3.3	9	1	0.9	1.4	9	5	0.8	0.6
12	2	0	−0.6	12	6	1.0	1.2	11	1	2.7	−2.2	11	5	0	−0.3
14	2	0	0.1					13	1	2.2	1.7	13	5	0.8	0.5
				0	8	2.0	2.0	15	1	0.5	0.3				
0	4	5.3	6.8	2	8	1.0	−1.4					1	7	2.1	−2.5
2	4	3.3	−3.2	4	8	0.4	0.5	1	3	10.8	−9.0	3	7	2.3	2.3
4	4	4.2	−4.6	6	8	0	0.0	3	3	0.9	−0.5	5	7	1.5	−1.5
6	4	4.3	4.1					5	3	8.2	−9.3	7	7	0.4	−0.8
8	4	4.4	−3.8					7	3	0	−0.3	9	7	0.6	0.6
10	4	0	−0.4					9	3	1.4	−1.2				
12	4	1.4	−1.6					11	3	2.4	−2.1				
14	4	0.6	0.6					13	3	0.9	0.2				
								15	3	0	−0.1				

hydrogen atoms being excluded. The atomic coordinates detemined in this way are listed in Table I. The observed and the calculated structure factors for (*hk*0) and (*h*0*l*) spectra are given in Table II. In the above calculation of structure factors, McWeeny's[16] scattering curves of "valence states" for carbon atom and of $f=1/3(f^{\parallel}+2f^{\perp})$ for oxygen atom were used with the isotropic temperature factor $B=2.17$ Å^2.

Discussion of the Structure

Since the molecule lies at the center of symmetry, two identical $CH_2OH\cdot C^*HOH$ groups constituting each half of the molecule are in the *trans*-position to each other, and the zig-zag chain of the four carbon atoms lies exactly in a plane, one of the C* atoms being of the nature *d* and the other *l*. All the valency angles for the carbon atoms are found to be approximately tetrahedral. Hence the configuration of the molecule as a whole can be described, only if we refer to the relative orientation of the outer C–O_2 bond with regard to the outer C*–C bond in each half of the molecule. The configuration of the molecule can be easily understood from Fig. 7, which shows the perspective view of a molecule in the C*–C bond direction. Intramolecular bond distances and bond angles are also listed in Table III. The plane of the C*–C–O_2

16) R. McWeeny, ibid., 4, 513 (1951).

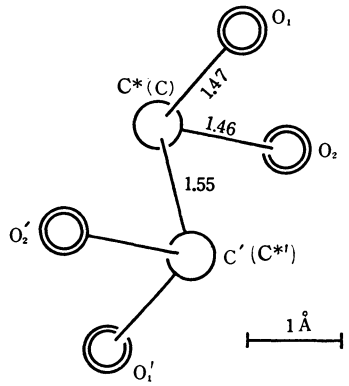


Fig. 7. *i*-Erythritol molecule projected on a plane at right angles to the C*-C bond. Intramolecular bond distances are given in Ångstrom units.

TABLE III
INTRAMOLECULAR BOND DISTANCES AND BOND ANGLES

C*-C	1.54 Å	∠C*'-C*-C	110°
C*-C*'	1.55 Å	∠C*'-C*-O_1	110°
C*-O_1	1.47 Å	∠C-C*-O_1	113°
C-O_2	1.46 Å	∠C*-C-O_2	108°

group forms a dihedral angle of 59° with the plane of the C-C*-O_1 group and an angle of 65° with that of the zig-zag chain of carbon atoms. In other words, the directions of the outer C-O_2 bond and the C*-C*' bond make the *gauche*-configuration with respect to the C*-C bond, and the two hydroxyl oxygen atoms in each half of the molecule are also in the *gauche*-positions around the C*-C bond. It is interesting to note that this relative configuration of the two hydroxyl groups with respect to the C*-C bond agrees with that found in tartaric acid and tartrate ion[17-21]. This mode of linkage is known to exist in carbohydrates. It must also be added that this configuration should be compared with the molecular configurations reported on ethylene glycol and glycerol on the basis of an electron diffraction study[22].

Fig. 8 gives the view of the crystal

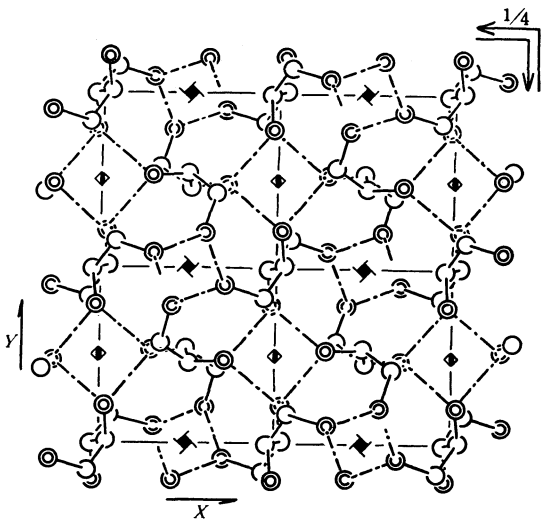


Fig. 8. A projection of the structure along the *c* axis of the crystal.

structure along the *c* axis. In this structure, important roles of two types of hydrogen bonds in the cohesion of the crystal can not be overlooked. The outer hydroxyl oxygen atom is linked to two oxygen atoms of the outer hydroxyl groups of the neighboring molecules, above and below, with a distance 2.66 Å forming a spiral chain arrangement of hydrogen bonds along the *c* axis. The inner hydroxyl oxygen atom, on the other hand, is linked to two oxygen atoms of the inner hydroxyl groups of the neighboring molecules. They form a distorted square of the side length 2.77 Å around the position given by the symmetry $\bar{4}$. They are making a lateral linkage, in a way, but at the same time they are uniting molecules within the same chain mentioned above. Thus, the crystal structure is held together by a three-dimensional net work of these hydrogen bonds, in which all the available hydrogen atoms and all the oxygen atoms also are joining, in agreement with the fact that this crystal has no cleavage.

The author is indebted to Professor I. Nitta, and Professor T. Watanabé for their helpful advice.

Department of Chemistry
Faculty of Science
Konan University
Higashinada-ku, Kobe

17) C. A. Beevers and W. Hughes, *Nature*, **146**, 96 (1940); *Proc. Roy. Soc.* A177, 251 (1941).
18) F. Stern and C. A. Beevers, *Acta Cryst.*, **3**, 341 (1950).
19) R. Sadanaga, ibid., **3**, 416 (1950).
20) G. S. Parry, ibid., **4**, 131 (1951).
21) A. J. van Bommel and J. M. Bijvoet, ibid., **11**, 61 (1958).
22) O. Bastiansen, *Acta chem. scand.*, **3**. 415 (1949).

Crystal Structure and Lattice Energy of i-Erythritol. II. Lattice and Hydrogen Bond Energies for i-Erythritol

By Akira SHIMADA

(Received August 13, 1958)

There have been already reported many studies on the lattice energy of crystalline substances, but most of them are dealing with crystals which are composed of ions. Viewed from the standpoint of the fact that the most powerful force capable of holding ions together is the electrostatic one, this situation seems to be very natural. On the other hand, there have been reported few studies on the lattice energy of crystals composed of more or less complicated molecules. Among these studies, a detailed calculation of the lattice energy has been already carried out for pentaerythritol[1], which gave a satisfactory result in comparison with the observed heat of sublimation. Of *i*-erythritol ($CH_2OH \cdot C^*HOH \cdot C^*HOH \cdot CH_2OH$), which is also a member of tetrahydric alcohols, various physical properties have been already reported and related to those of pentaerythritol[2,3]. Now that the crystal structure of *i*-erythritol has recently been determined by X-ray analysis[4], it was attempted to calculate the lattice energy and compare it with the observed heat of sublimation[2].

Calculation of the Lattice Energy.—The crystal of *i*-erythritol was found to belong to the tetragonal system with $a=12.81$ Å, $c=6.81$ Å and the space group $C_{4h}^6-I4_1/a$[5]. There are eight centro-symmetrical molecules in the unit cell. The structure projected on the (001) plane is shown in Fig. 1, in which the Roman numerals are given for the sake of convenience in the following calculations. The interesting feature of this structure is that two different types of hydrogen bonds, as shown in Fig. 1, link all the molecules firmly in a three-dimensional way*. One of these two types of the hydrogen bond, with a distance 2.77 Å, connects two CHOH groups of adjoining molecules while the other, with a distance 2.66 Å, connects two CH_2OH groups of adjoining molecules. The coordinates of atoms determined by X-ray analysis[4] were used in the following calculations.

The calculations of the lattice energy was carried out in the same way as in the case of pentaerythritol. This energy was supposed to be composed mainly of the van der Waals and electrostatic energies. Slater-Kirkwood's formula was applied to get the former energy, splitting the molecule into three kinds of force center; they are the CH, the CH_2 and the OH group. The polarizability α of each atomic group used in Slater-Kirkwood's formula is shown in Table I. They were

TABLE I
MOLECULAR REFRACTION AND POLARIZABILITY

Group	M_∞	$\alpha \times 10^{24}$ cc.
OH	2.48	0.981
CH	3.41	1.350
CH_2	4.32	1.709

esimated from the molecular refractions M_∞ at infinite wave length[1]. As for the molecules the centers of which lie within about 10 Å from the molecule 0 at the origin, the minus sixth power of distance between force centers was computed one by one and summed up. As for the molecules lying apart beyond 10 Å from the molecule 0, the summation was replaced by integration, assuming the uniform distribution of the force centers. The result of calculation is given in Table II, showing that the contribution of the integral part is found to be very small. The obtained value 20.42 kcal./mol. is somewhat greater than that of pentaerythritol (17.62 kcal./mol.) and this is possibly related to the

1) I. Nitta, S. Seki and K. Suzuki, This Bulletin, **24**, 63 (1951).
2) I. Nitta, S. Seki, M. Momotani, K. Suzuki and S. Nakagawa, *Proc. Japan Acad.*, **26**, (10) 11 (1950).
3) S. Seki and K. Suzuki, This Bulletin, **26**, 63 (1953).
4) A. Shimada, This Bulletin, **32**, 325 (1959).
5) For a detailed explanation of the crystallographic data, see "International Tables for X-ray Crystallography", Kynoch Press, Birmingham, England (1952).

* A preliminary infrared study on *i*-erythritol crystal shows that there is no marked band at the frequency of the unbonded OH stretching mode (3700 cm^{-1}), but at 3210cm^{-1} is observed a broad band which can be ascribed to the stretching modes of the hydrogen-bonded OH. Further study is now in progress.

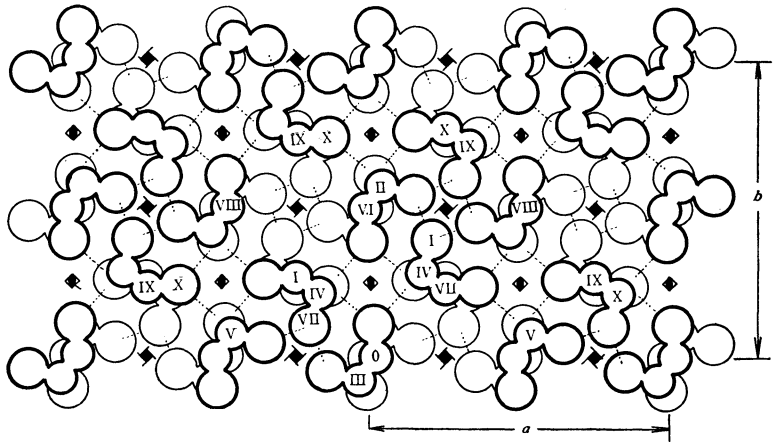


Fig. 1. View of molecular arrangement projected on (001) plane. The upper half of the centro-symmetrical molecule is shown by the broad outline, the large circle standing for OH group and the small one for CH and CH_2 groups. Dashed line indicates the hydrogen bond between the molecules.

TABLE II

VAN DER WAALS ATTRACTION ENERGY BETWEEN DIFFERENT ATOMIC GROUPS

Sort of molecule	van der Waals energy (cal./mol.)						
	CH∼CH	CH_2∼CH	CH_2∼CH_2	OH∼CH	OH∼CH_2	OH∼OH	Total
I	409.0	732.2	406.0	2393.7	3090.4	6168.9	13200.2
II	33.9	113.5	153.5	84.4	133.5	114.2	633.0
III	41.5	182.5	188.5	205.5	534.3	219.0	1371.3
IV	62.7	427.0	821.5	514.9	990.6	356.9	3173.6
V	35.5	102.4	59.4	273.7	264.2	376.4	1011.6
VI	7.6	27.5	22.6	23.8	45.6	36.7	163.8
VII	6.9	16.3	10.3	31.3	37.1	38.1	140.0
VIII	10.1	25.5	22.2	36.5	58.1	54.3	206.7
IX	1.4	14.3	11.1	25.2	35.5	27.7	115.2
Part of sum	608.6	1641.2	1695.1	3589.0	5189.3	7292.2	20015.4
Part of integral	38.1	48.1	59.6	64.4	81.3	112.0	403.5
			Total van der Waals energy:				20418.9

TABLE III

ELECTROSTATIC ENERGY BETWEEN DIFFERENT MOLECULES, USING DIFFERENT NET CHARGES

Sort of molecule	Distance from molecule 0 (Å)	Number of molecules	Electrostatic energy (kcal./mol.)		
			A	B	C
I	4.74	4	−16.687	−19.199	−21.711
II	6.41	2	− 1.260	− 1.809	− 2.344
III	6.81	2	0.166	0.192	0.226
IV	6.83	4	− 3.174	− 3.655	− 4.033
V	7.25	4	1.654	1.781	2.045
VI	9.35	4	− 0.412	− 0.769	− 1.065
VII	9.64	4	0.165	0.231	0.403
VIII	9.68	8	7.894	8.803	9.966
IX	9.94	8	− 0.522	− 0.531	− 0.545
X	11.05	8	0.364	0.435	0.508
		Total:	−11.812	−14.521	−16.550

difference of the packing in the two compounds (molecular volume: *i*-erythritol 84.2 cc./mol. and pentaerythritol 97.5 cc./mol. at room temperature).

In the calculation of electrostatic energy for this crystal, the point charge model was adopted, putting a net charge ε on the nuclear positions of the carbon atoms in CH and CH_2 groups, ε' on the hydrogen atoms in OH groups and $-(\varepsilon+\varepsilon')$ on the oxygen atoms. The positions of hydrogen atoms in OH groups were assumed to lie approximately on the line connecting two oxygen atoms at a distance 0.96 Å from the oxygen atom. A value 0.551×10^{-10} e. s. u. was assigned to the charge ε, and values 1.726 (Case A), 1.870 (Case B) and 2.015 (Case C) $\times10^{-10}$ e. s. u. were given for the charge ε', as in the case of pentaerythritol. These three cases correspond respectively to the three degrees of ionic characters 36, 39 and 42% of the OH bonds. The result of calculation is shown in Table III. In this calculation, the summation is taken over a sphere with its origin at the center of the molecule 0 and a radius of about 11 Å. The contribution of the outer part is neglected, in consideration of a possibility that it will decrease at least with the third power of distance. In fact, it can be shown by the Taylor's theorem that the electrostatic energy between each pair of molecules with no resultant permanent dipole moment will decrease at least with the fifth power of distance, and the number of pairs of molecules will increase with the second power of distance. Summing up the van der Waals and the electrostatic energies, the following three values are obtained, 32.23, 34.94 and 36.97 kcal./mol., corresponding respectively to the case A, B and C. The first value is in good agreement with the experimental value: 32.3± 0.2 kcal./mol[2]. It will be seen that for *i*-erythritol a good agreement is obtained for the case A, whereas the case B or C stands good for the case of pentaerythritol.

Estimation of the Hydrogen Bond Energy.—A part of the lattice energy may be attributed to the four hydrogen bonds, which are formed between a molecule of *i*-erythritol and its nearest neighbors. However, it is not easy to define and calculate that part of energy in this case, because in this complicated structure are appreciable the contributions of distant neighbors especially to the electrostatic energy and, furthermore, there is a rather even distribution of the hydrogen bonds, in contrast to the case of pentaerythritol where the hydrogen bonds connect the molecules to construct a typical layer lattice. Hence, in this case, the hydrogen bond energy is tentatively defined as the interaction energy between two OH groups directly linked together by the hydrogen bond. The van der Waals energies for the hydrogen bonds between two CHOH and two CH_2OH groups come out to be 1.35 and 1.65 kcal./mol. respectively. The corresponding electrostatic energies are computed, for the case A, to be 2.90 and 4.73 kcal./mol. Summing up these values, the hydrogen bond energies are to be 4.3 and 6.4 kcal./mol. The average value of these energies (5.4 kcal./mol.) seems to be somewhat larger than that of pentaerythritol (4.68 kcal./mol. for the case B or 5.16 kcal./mol. for the case C), although the definition of the hydrogen bond is somewhat different between these two compounds[1]. However, it is noteworthy to point out that a reasonable correlation of hydrogen bond energies (4.3 and 6.4 kcal./mol.) with hydrogen bond distances (2.77 and 2.66 Å) has been found in this calculation on the ground of rather simple model, while the model suggested by Lippincott[6] gives the values of hydrogen bond energies, 4.2 and 6.7 kcal./mol., corresponding to these two hydrogen bond distances.

Suzuki et al.[7] suggested another way for estimating hydrogen bond energy. This is to compare the heat of sublimation of the hydrogen-bonded substance with that of a reference substance, which is composed of isoelectronic molecules having similar configuration but no ability of hydrogen-bonding. This method was also applied to the cases of *i*-erythritol and pentaerythritol. The suitable reference substance chosen were 3, 4-dimethylhexane and 3, 3-diethylpentane each for these two compounds. The heat of sublimation of the reference substance was obtained by adding the heat of fusion[8] and that of vaporization. Since the heat of fusion of 3, 4-dimethylhexane is not yet known, it was estimated by adding the difference between the heat of fusion of 2, 3-dimethylbutane (0.194 kcal./mol.) and that of

6) E. R. Lippincott and R. Schroeder, *J. Chem. Phys.*, **23**, 1099 (1955).

7) K. Suzuki, S. Ōnishi, T. Koide and S. Seki, This Bulletin, **29**, 127 (1956).

8) F. D. Rossini, K. S. Pitzer, R. L. Arnett, R. M. Braun and G. C. Pimental, "Selected Values of Physical and Thermodynamical Properties of Hydrocarbons and Related Compounds", Carnegie Press, Pittsburgh, U. S. A. (1953).

n-butane (1.114 kcal./mol.) to that of *n*-hexane (3.114 kcal./mol.). The heat of vaporization was calculated from the temperature variation of vapor pressure[8] near the melting point. Table IV gives the latent heats associated with the phase

TABLE IV
HEAT OF PHASE CHANGE FOR THE REFERENCE SUBSTANCE (kcal./mol.)

	Reference substance	
	3,4-Dimethyl-hexane	3,3-Diethyl-pentane
Heat of fusion	2.19	2.35
Heat of vaporization	9.53	10.50
Heat of sublimation	11.7	12.9

changes for the reference substances. From these values, the hydrogen bond energies of 5.2 and 4.6 kcal./mol. have been estimated for *i*-erythritol and pentaerythritol respctively. These values are found to be in good agreement with the average values mentioned in the preceding paragraph.

At any rate, it seems likely that the average hydrogen bond energy for *i*-erythritol is larger than that for pentaerythritol, since the two methods of calculation gave parallel results. The values obtained above can be compared with those obtained on other alcohols[9]. Although in the calculation of the lattice energy mentioned above certain assumptions are involved, and the repulsive and other higher terms are ignored[10], it is noteworthy that the reasonable values for the lattice and hydrogen bond energies are obtained, based on the crystal structure.

The author wish to thank Professor I. Nitta, Professor T. Watanabé and Dr. S. Seki for their continued encouragement and Dr. K. Suzuki for his helpful discussion on the calculation of the lattice energy.

Department of Chemistry
Faculty of Science
Konan University
Higashinada-ku, Kobe

9) I. Nitta and S. Seki, *J. Chem. Soc. Japan, Pure Chem. Sec.* (*Nippon Kagaku Zasshi*), **69**, 143 (1948).

10) In the case of iodine crystal, these two terms were found to cancel out with each other. The agreement of the observed heat of sublimation with the lattice energy calculated by the use of Slater-Kirkwood's formula in many examples seems to indicate that these two terms cancel out with each other. See, I. Nitta and S. Seki, ibid., **64**, 475 (1943).

Electrical Conductance of Concentrated Aqueous Solutions of Copper Sulfate

By C. V. Suryanarayana and S. Alamelu

(Received September 19, 1958)

Numerous attempts have been made to extend the Debye-Hückel theory to electrolyte solutions of higher concentrations than 0.1 N. The attempts of Falkenhagen and Leist[1], Robinson and Stokes[2], Wishaw and Stokes[3], and Leist[4], are the most notable contributions in recent times in this direction.

Suryanarayana and Venkatesan[5,6] recently formulated the equation,

$$\Lambda_c = \Lambda_s + A\frac{(1-c_p)}{\eta_p} \qquad (1)$$

where

$$\Lambda_c = \frac{\text{specific conductance } (K_c)\times 1000}{c_p}$$

Λ_s = specific conductance at saturation $(K_s)\times 1000$

$$c_p = \frac{\text{mole fraction at a given concn.}}{\text{mole fraction at saturation at the same temp.}}$$

of course, at saturation $c_p = 1$

$$\eta_p = \frac{\text{viscosity at a given concn.}}{\text{viscosity at saturation}}$$

1) H. Falkenhagen and M. Leist, *Naturwiss.*, **41**, 570 (1954).
2) R. A. Robinson and R. H. Stokes, *J. Am. Chem. Soc.*, **76**, 1991 (1954).
3) B. F. Wishaw and R. H. Stokes, ibid., **76**, 2065 (1954).
4) M. Leist, *Z.phys.Chem.*, **205**, 16 (1955).
5) C. V. Suryanarayana and V. K. Venkatesan, *Nature*, **178**, 1461 (1956).
6) C. V. Suryanarayana and V. K. Venkatesan, *Acta. Chim. Hung.*, **17**, 327 (1958).

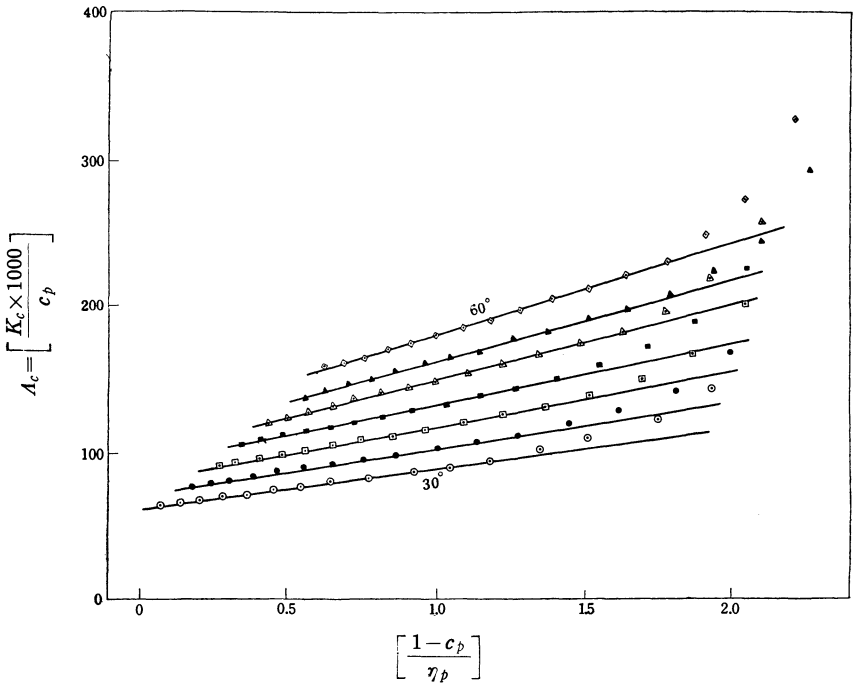


Fig. 1.

TABLE I

TEMPERATURE 30°C

Molality	Specific conductance $K_c \times 10^2$	Density	Relative viscosity	c_p	η_p	Λ_c	$\left[\frac{1-c_p}{\eta_p}\right]$
0.0992	0.9661	1.011	1.042	0.0673	0.4818	143.5	1.936
0.1965	1.638	1.027	1.070	1.1332	0.4946	122.9	1.752
0.2921	2.179	1.042	1.131	0.1977	0.5231	110.2	1.508
0.3862	2.673	1.057	1.182	0.2609	0.5468	102.4	1.352
0.4785	3.042	1.071	1.246	0.3228	0.5762	94.26	1.175
0.5693	3.413	1.085	1.288	0.3833	0.5958	89.04	1.035
0.6586	3.842	1.098	1.326	0.4428	0.6132	86.76	0.9088
0.7463	4.075	1.110	1.403	0.5009	0.6488	81.34	0.7693
0.8326	4.482	1.124	1.485	0.5581	0.6869	80.32	0.6433
0.9175	4.719	1.136	1.539	0.6141	0.7117	76.85	0.5423
1.0010	5.003	1.149	1.602	0.6688	0.7408	74.82	0.4471
1.0830	5.253	1.161	1.675	0.7231	0.7747	72.64	0.3575
1.1640	5.502	1.172	1.738	0.7759	0.8037	70.92	0.2788
1.2440	5.650	1.184	1.827	0.8273	0.8448	68.28	0.2044
1.3210	5.825	1.195	1.908	0.8780	0.8824	66.34	0.1382
1.3980	5.977	1.205	2.009	0.9281	0.9290	64.40	0.0774
1.5100 (Satd.)	—	1.223	2.162	1.0000	1.0000	—	—

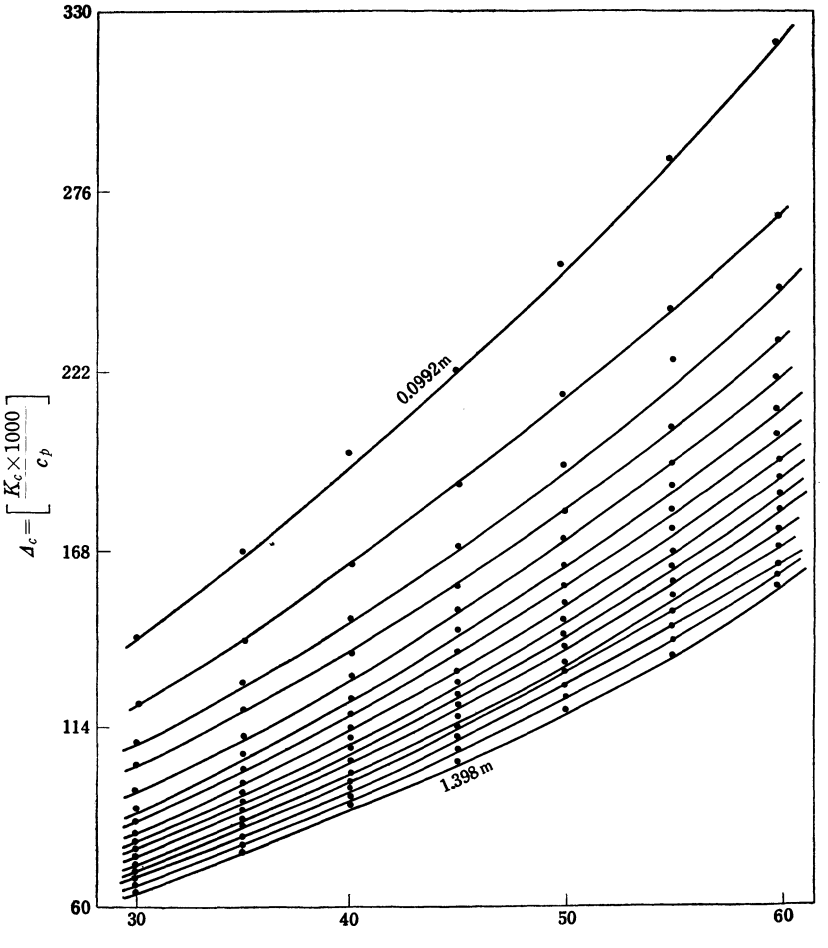


Fig. 2.

TABLE II
TEMPERATURE 35°C

Molality	Specific conductance $K_c \times 10^2$	Density	Relative viscosity	c_p	η_p	Λ_c	$\left[\frac{1-c_p}{\eta_p}\right]$
0.0992	1.041	1.009	1.047	0.0618	0.4722	168.6	1.9870
0.1965	1.738	1.025	1.078	0.1222	0.4863	142.2	1.8050
0.2921	2.343	1.040	1.124	0.1813	0.5069	129.2	1.6150
0.3862	2.874	1.054	1.172	0.2393	0.5286	120.0	1.4390
0.4785	3.321	1.068	1.225	0.2961	0.5525	112.1	1.2750
0.5693	3.778	1.082	1.273	0.3517	0.5741	107.4	1.1290
0.6586	4.151	1.095	1.318	0.4061	0.5944	102.2	0.9993
0.7463	4.482	1.109	1.385	0.4595	0.6247	97.54	0.8652
0.8326	4.872	1.121	1.442	0.5119	0.6504	95.17	0.7504
0.9175	5.172	1.133	1.502	0.5632	0.6775	91.83	0.6443
1.0010	5.508	1.146	1.555	0.6135	0.7013	89.78	0.5512
1.0830	5.821	1.158	1.619	0.6633	0.7318	87.76	0.4601
1.1640	6.009	1.170	1.687	0.7117	0.7608	84.43	0.3789
1.2440	6.169	1.181	1.760	0.7590	0.7938	81.28	0.3036
1.3210	6.341	1.192	1.830	0.8054	0.8254	78.74	0.2357
1.3980	6.528	1.203	1.914	0.8513	0.8632	76.67	0.1723
1.6500 (Satd.)	—	1.249	2.217	1.0000	1.0000	—	—

TABLE III
TEMPERATURE 40°C

Molality	Specific conductance $K_c \times 10^2$	Density	Relative viscosity	c_p	η_p	Λ_c	$\left[\frac{1-c_p}{\eta_p}\right]$
0.0922	1.143	1.007	1.047	0.0568	0.4619	201.3	2.042
0.1965	1.867	1.023	1.084	0.1123	0.4784	166.3	1.856
0.2921	2.504	1.038	1.119	0.1667	0.4937	150.2	1.689
0.3862	3.063	1.052	1.163	0.2200	0.5133	139.2	1.520
0.4785	3.576	1.066	1.207	0.2721	0.5325	131.4	1.367
0.5693	4.062	1.080	1.259	0.3232	0.5555	125.7	1.218
0.6586	4.482	1.093	1.305	0.3734	0.5757	120.0	1.088
0.7463	4.872	1.106	1.362	0.4224	0.6009	115.3	0.961
0.8326	5.253	1.119	1.417	0.4706	0.6252	111.6	0.847
0.9175	5.650	1.131	1.467	0.5177	0.6474	109.1	0.745
1.0010	5.942	1.143	1.520	0.5639	0.6707	105.4	0.650
1.0830	6.169	1.155	1.580	0.6096	0.6972	101.2	0.560
1.1640	6.441	1.167	1.640	0.6542	0.7236	98.47	0.478
1.2440	6.691	1.179	1.708	0.6976	0.7536	95.92	0.401
1.3210	6.901	1.190	1.771	0.7403	0.7814	93.22	0.332
1.3980	7.078	1.200	1.850	0.7807	0.8164	90.65	0.269
1.8000 (Satd.)	—	1.251	2.266	1.0000	1.0000	—	—

TABLE IV
TEMPERATURE 45°C

Molality	Specific conductance $K_c \times 10^2$	Density	Relative viscosity	c_p	η_p	Λ_c	$\left[\frac{1-c_p}{\eta_p}\right]$
0.0992	1.191	1.005	1.039	0.0525	0.4625	226.7	2.0480
0.1965	1.977	1.021	1.080	0.1040	0.4808	190.2	1.8630
0.2921	2.668	1.035	1.110	0.1543	0.4942	172.9	1.7120
0.3862	3.248	1.050	1.152	0.2036	0.5130	159.5	1.5520
0.4785	3.820	1.064	1.195	0.2519	0.5321	151.7	1.4060
0.5693	4.338	1.077	1.242	0.2991	0.5530	145.0	1.2680
0.6586	4.803	1.091	1.289	0.3455	0.5740	139.0	1.1400
0.7463	5.172	1.104	1.339	0.3909	0.5962	132.3	1.0220
0.8326	5.650	1.116	1.389	0.4355	0.6186	129.7	0.9126
0.9175	6.032	1.129	1.436	0.4792	0.6393	125.9	0.8147
1.0010	6.339	1.141	1.490	0.5219	0.6634	121.4	0.7206
1.0830	6.658	1.153	1.542	0.5643	0.6866	118.0	0.6346
1.1640	6.947	1.165	1.592	0.6054	0.7089	114.8	0.5567
1.2440	7.269	1.176	1.656	0.6457	0.7374	112.6	0.4805
1.3210	7.458	1.188	1.717	0.6852	0.7643	108.8	0.4118
1.3980	7.598	1.198	1.786	0.7243	0.7952	104.9	0.3466
1.9500 (Satd.)	—	1.268	2.246	1.0000	1.0000	—	—

A = a constant whose value is a function of temperature and dielectric constant of the medium.

The basis of the formulation of the concepts c_p and η_p has already been given[7].

In the present investigations the data collected for copper sulfate solutions are sought to be fitted into equation 1. We hoped to verify the equation of Wishaw and Stokes (loc. cit.) with the same data. Unfortunately, copper sulfate being an "intermediate electrolyte" and a bi-bivalent salt with complications regarding ionic hydration in solution, and owing to uncertainty regarding the actual value of the mean distance of closest approach '$\mathring{a}$', we could not test Wishaw and Stokes' equation or even that of Falkenhagen and Leist (loc. cit.). Equation 1 involves no such uncertain parameters since the very

7) C. V. Suryanarayana and V. K. Venkatesan, This Bulletin 31, 442 (1958).

TABLE V
TEMPERATURE 50°C

Molality	Specific conductance $K_c \times 10^2$	Density	Relative viscosity	c_p	η_p	Λ_c	$\left[\frac{1-c_p}{\eta_p}\right]$
0.0992	1.254	1.003	1.042	0.0485	0.4535	258.7	2.0980
0.1965	2.094	1.019	1.082	0.0959	0.4710	218.4	1.9200
0.2921	2.802	1.033	1.113	0.1423	0.4844	196.9	1.7710
0.3862	3.448	1.047	1.149	0.1878	0.5001	183.6	1.6240
0.4785	4.051	1.061	1.191	0.2324	0.5184	174.4	1.4800
0.5693	4.605	1.075	1.239	0.2759	0.5393	166.9	1.3430
0·6586	5.093	1.088	1.282	0.3187	0.5581	159.8	1.2210
0.7463	5.556	1.101	1.330	0.3606	0.5790	154.1	1.1040
0.8326	6.003	1.114	1.382	0.4017	0.6016	149.5	0.9945
0.9175	6.343	1.127	1.418	0.4420	0.6172	143.5	0.9040
1.0010	6.733	1.139	1.468	0.4814	0.6392	139.8	0.8114
1.0830	7.191	1.150	1.519	0.5205	0.6612	138.1	0.7252
1.1640	7.401	1.162	1.565	0.5585	0.6813	132.5	0.6480
1.2440	7.640	1.173	1.628	0.5955	0.7086	128.3	0.5709
1.3210	7.854	1.185	1.690	0.6320	0.7357	124.3	0.5001
1.3980	8.004	1.195	1.753	0.6680	0.7630	119.8	0.4351
2.1200 (Satd.)	—	1.285	2.296	1.0000	1.0000	—	—

TABLE VI
TEMPERATURE 55°C

Molality	Specific conductance $K_c \times 10^2$	Density	Relative viscosity	c_p	η_p	Λ_c	$\left[\frac{1-c_p}{\eta_p}\right]$
0.0992	1.311	1.001	1.039	0.0448	0.4401	292.5	2.1700
0.1965	2.172	1.016	1.076	0.0886	0.4560	245.0	1.9980
0.2921	2.936	1.030	1.108	0.1316	0.4693	223.1	1.8500
0.3862	3.634	1.045	1.140	0.1737	0.4831	209.2	1.7110
0.4785	4.241	1.059	1.180	0.2148	0.5000	197.4	1.5700
0.5693	4.838	1.073	1.223	0.2552	0.5182	189.5	1.4370
0.6586	5.379	1.086	1.266	0.2947	0.5365	182.5	1.3140
0.7463	5.898	1.098	1.311	0.3334	0.5555	176.9	1.2000
0.8326	6.284	1.111	1.355	0.3715	0.5741	169.2	1.0950
0.9175	6.723	1.124	1.398	0.4087	0.5926	164.5	0.9979
1.0010	7.145	1.136	1.437	0.4451	0.6088	160.5	0.9104
1.0830	7.471	1.148	1.486	0.4812	0.6298	155.2	0.8237
1.1640	7.782	1.160	1.530	0.5164	0.6483	150.7	0.7457
1.2440	8.082	1.170	1.582	0.5507	0.6705	146.8	0.6701
1.3210	8.289	1.182	1.641	0.5843	0.6953	141.9	0.5977
1.3980	8.405	1.192	1.702	0.6177	0.7206	136.1	0.5306
2.3000 (Satd.)	—	1.302	2.360	1.0000	1.0000	—	—

approach in its derivation was from a new angle (loc. cit.). Hence, equation 1 is now tested with the data of copper sulfate.

Experimental

All solutions were made by weight using "Analar" (British Drag House) variety of copper sulfate ($CuSO_4 \cdot 5H_2O$). A Jones and Bollinger type cell[8] of cell constant 0.6723 was used for conductivity determinations for all concentrations at different temperatures. The measurement of conductance was made by a Philip's GM 4249/01 bridge at a frequency of 1000 cycles/sec. Owing to the high concentration range in which measurements were made, the correction for conductance of pure solvent was quite negligible owing to high specific conductance in all the solutions and the correction was ignored. All connecting wires were heavily insulated, rigid, and well separated so that errors of poor insulation and induction effect were avoided. In the

8) G. Jones and G. M. Bollinger, *J. Am. Chem. Soc.*, 53, 411 (1931).

TABLE VII
TEMPERATURE 60°C

Molality	Specific conductance $K_c \times 10^2$	Density	Relative viscosity	c_p	η_p	Λ_c	$\left[\frac{1-c_p}{\eta_p}\right]$
0.0992	1.367	0.9988	1.034	0.0415	0.4319	329.3	2.219
0.1965	2.256	1.014	1.076	0.0822	0.4495	274.7	2.042
0.2921	3.063	1.028	1.099	0.1220	0.4592	251.1	1.912
0.3862	3.757	1.042	1.131	0.1609	0.4725	233.4	1.776
0.4785	4.438	1.056	1.169	0.1991	0.4884	222.9	1.640
0.5693	5.036	1.070	1.210	0.2364	0.5055	213.0	1.510
0.6586	5.603	1.083	1.251	0.2731	0.5225	205.1	1.391
0.7463	6.112	1.095	1.293	0.3089	0.5401	197.8	1.279
0.8326	6.560	1.109	1.331	0.3442	0.5560	190.5	1.180
0.9175	7.078	1.121	1.368	0.3787	0.5715	186.9	1.087
1.0010	7.521	1.133	1.411	0.4125	0.5893	182.4	0.997
1.0830	7.818	1.144	1.457	0.4460	0.6087	175.3	0.910
1.1640	8.175	1.157	1.502	0.4785	0.6275	170.8	0.831
1.2440	8.405	1.168	1.552	0.5102	0.6483	164.7	0.755
1.3210	8.735	1.180	1.600	0.5416	0.6683	161.3	0.686
1.3980	9.086	1.190	1.654	0.5724	0.6910	158.8	0.619
2.4900 (Satd.)	—	1.319	2.394	1.0000	1.0000	—	—

range of measurement of resistance the instrumental error was ±2.00%. The conductivity cell was immersed in a Gallenkamp b-12210 thermostat giving an accuracy of ±0.05°C.

The viscosities were determined using an Ostwald viscometer immersed in the same thermostat. After attainment of equilibrium the saturated solution was sucked through a tube plugged with cotton wool into a pipette which was kept at the same temperature as the thermostat to avoid crystallization of the saturated solution and transferred into the viscometer. The densities of all the solutions were also measured. Solubility data were obtained from Seidell[9].

Results obtained are given in the tables.

Discussion

A test of equation 1 consists in obtaining a linear plot when Λ_c is plotted against $(1-c_p)/\eta_p$. Fig. 1 shows that such a plot is a straight line at all the temperatures betweem 30° and 60°C, with a few points (right hand side)toward low concentrations going off the straight line at each temperature. This indicates that equation 1 is valid in the range of concentrations from 0.3862 M to saturation (1.5 to 2.5 M). Since the actual resistance measured at saturation at different temperatures happened to be small, attempt is not made here to compare the extrapolated value of Λ_s with that found experimentally owing to the limitations of the instrument used. This aspect is postponed to a future date.

Pearce and Pumplin[10] found out the partial molal volumes of copper sulfate in aqueous solutions upto saturation at 25°C. They observed that the data on copper sulfate solutions are especially interesting because of the negative values of the partial molal volumes in dilute aqueous solutions, quite similar to the phenomenon observed for lithium hydroxide, sodium hydroxide and magnesium sulfate solutions. The very low values in general for copper sulfate indicate a very large amount of electrostriction of the solvent produced by the cupric ion, the water dipoles being compressed around the cupric ion by the intense electrostatic field produced by the high charge density of the ion. Absence of any discontinuity in the curve and a constancy of the law of variation throughout the curve upto saturation indicate that no sudden changes occur either in the total number of water molecules surrounding the ion or the type of bonding between the ion and the water molecules. Stewart[11] observed that the variation of the partial molal volume of ions with concentration is closely linked with the change in structure of water in the same solutions, as revealed by X-ray studies.

9) Seidell "Solubilities of Organic and Inorganic Compounds," Van Nostrand Co., New York (1940), Vol. I.

10) J. N. Pearce and G. G. Pumplin, *J. Am. Chem. Soc.*, 59, 1221 (1937).

11). G. W. Stewart, *J. Chem. Phys.*, 7, 869 (1939).

Fig. 2 shows the temperature variation of Λ_c for all the sixteen concentrations of copper sulfate solutions investigated upon. The curves are not perfect straight lines but are slightly bent convex toward the X-axis. Usually the two factors that determine the form of the temperature conductance curve are: (1) the increase in the viscosity of the solution, and the corresponding decrease in the mobility of the ions, with decreasing temperature; and (2) the effect of temperature on association of ions. With complications of ionic hydration and uncertainties regarding the predominance of one or the other of the above two factors, it is difficult to explain the non-linear variation of Λ_c against temperature.

Equation 1 was originially derived for fully dissociated strong electrolytes based on the principle that the difference in the mobilities of an ion at two different concentrations is a function of the difference in the respective internal pressures at the two concentrations. Copper sulfate is known to be an intermediate electrolyte[12] and the above mentioned observations show that equation 1 holds well even with a bibivalent electrolyte like copper sulfate.

Summary

The electrical conductance of aqueous solutions of copper sulfate has been measured over a wide range of concentrations up to saturation. The equation connecting conductance and concentration in the range of high concentrations recently formulated by Suryanarayana and Venkatesan has been tested with the data obtained for copper sulfate solutions. The equation is found to be valid over a wide range of concentration from 0.3862 M to saturation at temperatures ranging from 30° to 60°C. Slight deviations have been observed at lower concentrations.

Physico-Chemical Laboratory
Annamalai University
Annamalainagar, South India

12) S. Glasstone, "The Electrochemistry of Solutions", Methuen and Co., London (1945), p. 67.

Substituent Effects on the Ultraviolet Absorption Spectrum of 1,3,5-Trinitrobenzene in Some Solvents

By Takehiro ABE

(Received August 22, 1958)

The near ultraviolet absorption spectrum of 1,3,5-trinitrobenzene shows an intense band at 223 mμ and two shoulders at about 300 and 340 mμ in ethanol[1,2]. The maximum absorption band has a shorter wavelength of 223 mμ and a greater molar absorbancy than that of nitrobenzene[2], which has been interpreted by Nagakura and Tanaka[3], in terms of the intramolecular charge transfer.

In the present paper, an attempt has been made to investigate the effects of four substituents on the spectra of 1,3,5-trinitrobenzene in some solvents. The ultraviolet absorption spectra of 1,3,5-trinitrobenzene (TNB), 2,4,6-trinitrotoluene (TNT), picryl chloride (PC), 2,4,6-trinitrophenylmethylnitramine (Tetryl) and picric acid (PA) have been compared in solvents like water, water-sodium hydroxide, ethanol, benzene and acetone, together with the solvent effects upon the spectra of PC, Tetryl and PA. The spectra of TNB and TNT, measured in the previous work[2], have been used here.

Experimental

Materials.—Trinitrobenzenes of commercial extra pure grade were purified by recrystallizing several times. PC: m. p. 82.5°C, Tetryl: m. p. 129.9°C, PA: m. p. 122.6°C. Commercial guaranteed solvents were fractionally distillated after usual treatments.

1) E. F. Caldin and G. Long, *Proc. Roy. Soc.*, **A228**, 263 (1955).
2) T. Abe, This Bulletin, **31**, 904 (1958).
3) S. Nagakura and J. Tanaka, *J. Chem. Phys.*, **22**, 236 (1954).

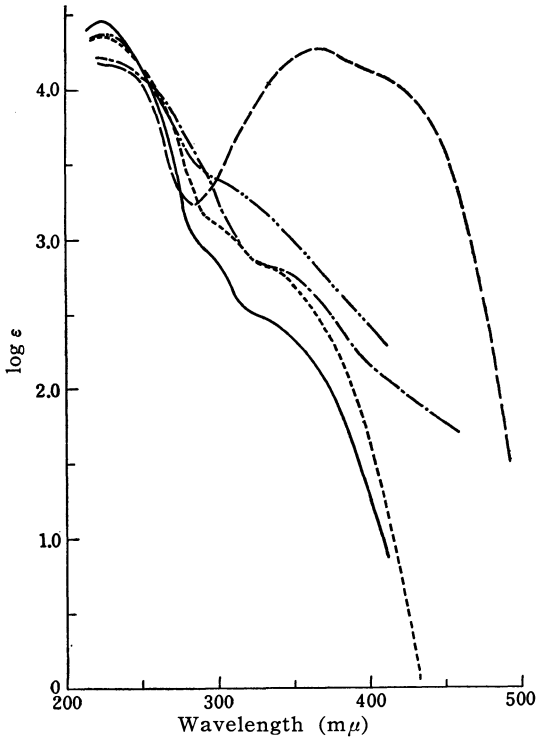


Fig. 1. Absorption spectra of TNB (——), TNT (------), PC (—·—), Tetryl (—··—) and PA (— —), all in ethanol.

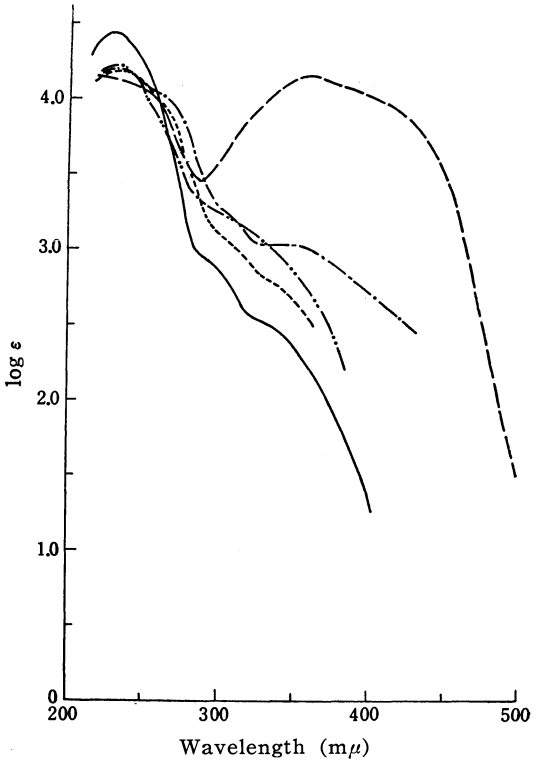


Fig. 2. Absorption spectra of TNB (——), TNT (------), PC (—·—), Tetryl (—··—) and PA (— —), all in water.

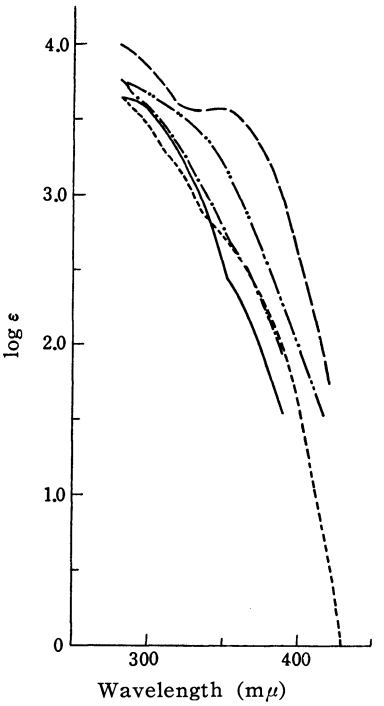


Fig. 3. Absorption spectra of TNB (——), TNT (------), PC (—·—), Tetryl (—··—) and PA (— —), all in benzene.

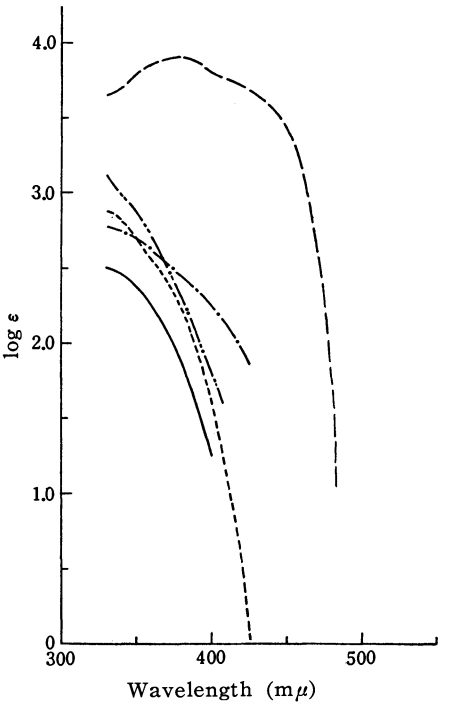


Fig. 4. Absorption spectra of TNB (——), TNT (------), PC (—·—), Tetryl (—··—) and PA (— —), all in acetone.

Spectra.—The spectra of the solution were measured with a Hitachi Model EPU-2 spectrophotometer at room temperature. Path length of absorption cells was 1 cm.

Results and Discussion

Spectra of Trinitrobenzenes in Some Solvents.—*In ethanol* (Fig. 1).—By substituting a group like $-CH_3$, $-Cl$, $-N(CH_3)NO_2$ or $-OH$, the 223 mμ band of TNB shifts to the red and its molar absorbancy decreases in the following order: TNB> Tetryl> TNT> PC> PA. Molar extinction coefficients of 300 and 340 mμ bands of the substituted trinitrobenzenes are greater than those of TNB, except those of PA that gives intense absorption bands at 350~450 mμ.

In the previous paper[2], it has been described that a benzene nucleus of polynitro-substituted benzene possesses some positive charge owing to the strong electron-attracting nature of nitro groups, and that the greater this positive charge, the greater becomes the blue shift of the maximum absorption band of the nitro compound. A benzene nucleus of each derivative of TNB possesses a less positive charge than that of TNB, because the electron of the $-CH_3$, $-Cl$, $-N(CH_3)NO_2$ or $-OH$ substituent can migrate to some extent toward the benzene nucleus in the direction opposite to the electron migration of the nitro groups, as indicated in Fig. 5. It is, therefore, known that the maximum absorption bands of the substituted trinitrobenzenes, benzene nuclei of which possess less positive charges than that of TNB, shift to the red with decreasing molar absorbancies, compared with the band of TNB.

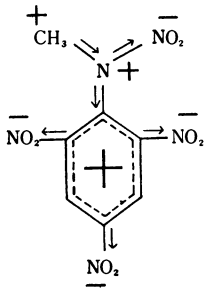


Fig. 5. Charge distribution of Tetryl.

In water (Fig. 2).—The substituted trinitrobenzenes show similar spectra as in ethanol, but give their maximum absorption bands at longer wavelengths and the smaller molar absorbancies in water than in ethanol. Both in ethanol and in water the molar absorbancies of their maximum absorptions are in the following order: TNB> Tetryl> TNT> PC> PA.

In benzene (Fig. 3).—The molar absorbancy of the 350 mμ shoulder of each substituted TNB is greater than that of TNB. Especially PA shows intense bands in this region.

In acetone (Fig. 4).—The molar absorbancies of the 340 mμ shoulders of the substituted trinitrobenzenes are greater than that of TNB. In addition to this shoulder, PA shows intense bands at 370~440 mμ. In all solvents the molar absorbancies of the 340 mμ bands of the trinitrobenzenes increase in the order of TNB, TNT, PC, Tetryl and PA, except the absorbancies of PC in water and in acetone.

It has been found that the visible absorption bands of TNB in acetone, indicated in the previous paper[2], are owing to the action of visible light on the trinitrobenzene used, because TNB that gives no visible absorption bands in acetone as shown in Fig. 4, shows such visible absorption spectra as indicated in the previous paper, after being irradiated by an usual incandescent lamp for a long time.

Solvent Effects on the Spectra of PC, Tetryl and PA (Figs. 1~4).—PC, Tetryl and PA give greater molar absorbancies of absorption bands near 300 mμ in benzene than in ethanol or in water. These great absorbancies in benzene seem probably to be due to formations of molecular complexes between the trinitrobenzenes and benzene, as TNB and TNT form complexes with benzene[2,4].

The absorption curves of PC and Tetryl in ethanol are not so closely resemble those in water as the curves of TNB and TNT. Only the 350 mμ band of PC exceptionally gives a greater molar absorbancy in water than in ethanol.

PA shows similar absorption curves in all three solvents like ethanol, water and acetone. This similarity seems to show that PA dissociates in negative ion not only in water, but also in ethanol and in acetone, losing a proton, because PA is known to be strongly acidic in water.

Spectra of Trinitrobenzenes in Aqueous Sodium Hydroxide Solution (Figs. 6~8).—In Fig. 6, visible absorption spectra of

4) G. Briegleb and J. Czekalla, *Z. Elektrochem.*, **59**, 184 (1955).

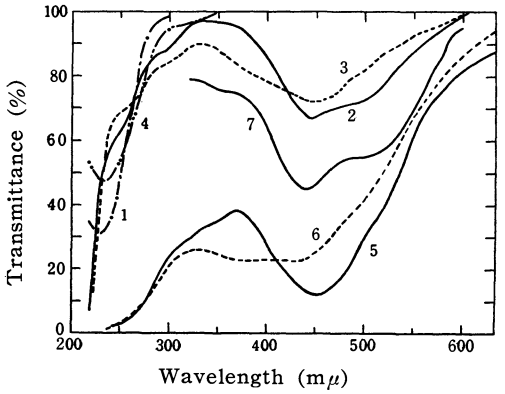


Fig. 6. Absorption curves of:
1. An aqueous solution of TNB;
2. A solution measured immediately after a few drops of 2 N sodium hydroxide solution were added into the solution (1);
3. A solution obtained by boiling the solution (2);
4. An aqueous solution of TNT;
5. A solution measured immediately after a few drops of 2 N sodium hydroxide solution were added into the solution (4);
6. A solution obtained by boiling the solution (5);
7. An aqueous solution of Tetryl, in which a few drops of 2 N sodium hydroxide solution were added.

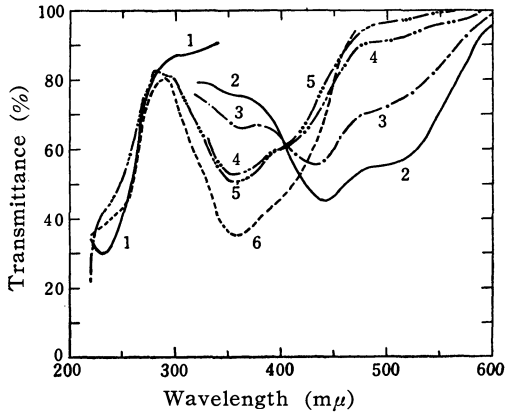


Fig. 7. Absorption curves of:
1. An aqueous solution of Tetryl;
2. A solution measured immediately after a few drops of 2 N sodium hydroxide solution were added into the solution (1);
3. A solution obtained by standing the solution (1) for about half an hour;
4. The solution (2) after an hour and forty minutes;
5. The solution (2) after two hours and a half;
6. An aqueous solution of PA.

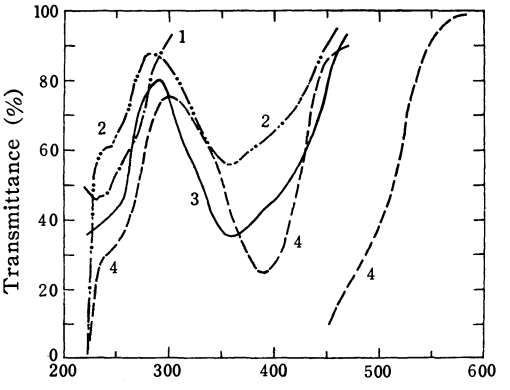


Fig. 8. Absorption curves of:
1. An aqueous solution of PC;
2. A solution in which a red color produced by adding a little of dilute sodium hydroxide solution into the solution (1), already discolored;
3. An aqueous solution of PA;
4. A solution obtained by adding a concentrated sodium hydroxide solution into the solution (3).

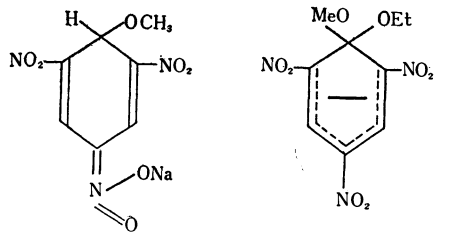
sodium hydroxide solutions of TNB, TNT and Tetryl are compared one another, and the absorption curves of the rather stable alkaline solutions of TNB and TNT, boiled to accelerate the rates of reactions between the trinitrobenzenes and alkali, are also indicated. The spectrum of TNB (curve 2) in sodium hydroxide solution closely resembles to that of Tetryl (curve 7). The spectrum of TNT (curve 5) in this solution also resembles them. These red colors are reversively decolorized by addition of weak acids.

On standing for two hours, the red color of the sodium hydroxide solution of Tetryl changes slowly to yellow, as described in Fig. 7. A spectrum of the yellow solution (curve 5) that yields no red color again by adding alkali, closely resembles that of PA (curve 6).

On treating an aqueous solution of PC with sodium hydroxide solution, a red color is produced and fades in a few minutes. By adding a concentrated solution of sodium hydroxide, a solution of PA at once gives a brownish orange color, which disappears in a moment. Absorption curves of yellow solutions to which these alkaline solutions of PC and PA change finally through red solutions, are given in Fig. 8. In a concentrated solution of sodium hydroxide, PA shifts a position of its maximum absorption band to the red by about 30 mμ, and shows a weak shoulder at about 500 mμ (curve 4).

From the above results, the red colors of the aqueous sodium hydroxide solutions of the substituted trinitrobenzenes are stable at room temperature in the following order: TNB and TNT> Tetryl> PC> PA. It is noticed that the substituted trinitrobenzenes that form the labile colors with sodium hydroxide, contain electron-donating substituents like $-N(CH_3)NO_2$, -Cl and -OH.

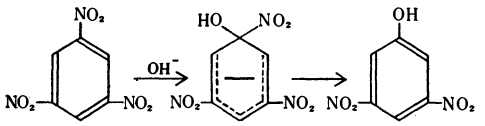
On boiling with dilute sodium hydroxide solution, TNB yields 3,3′,5,5′-tetranitroazoxybenzene and 3,5-dinitrophenol[5]. On standing in the cold with methanolic sodium methylate, TNB yields 3,5-dinitroanisol[6] and on boiling with alcoholic soda solution, it undergoes a partial reduction to form 3,3′,5,5′-tetranitroazoxybenzene[7]. The first product of the reaction of methanolic caustic alkali on TNB is a red crystalline addition product having the experimental composition, $TNB \cdot CH_3ONa \cdot 1/2H_2O$, isolated by Bruyn and Leent[8]. From these experimental results, the red product between TNB and sodium hydroxide seems probably to be an intermediate in the reaction of TNB to 3,5-dinitrophenol. The red products of TNT and Tetryl with sodium hydroxide may be also intermediates in their reactions. The transient colors of the sodium hydroxide solutions of PC and PA, absorption spectra of which have not been determined owing to their rapid discolorations, seem to be due to the same complexes as those of TNB, TNT and Tetryl. Actually, it has been reported that a methanol solution of TNT, treated with potassium methylate, yields a red product of an empirical composition, $TNT \cdot CH_3OK \cdot H_2O$[9]. A methanol solution of picryl chloride, treated with an excess of sodium methylate or of strong sodium hydroxide solution, also turns dark red and deposits red crystals of the empirical composition, $trinitroanisol \cdot NaOCH_3$[10]. The color reaction of sodium ethoxide with TNT and TNB in ethanol has been interpreted by Caldin and his co-workers[1,11] in terms of a proton-transfer reaction for TNT and in terms of an addition reaction for TNB.



(a) (b)

Fig. 9. Meisenheimer's structure for $TNB \cdot CH_3ONa$(a) and $TNA \cdot OEt^-$(b).

A structure of the red product of $TNB \cdot CH_3ONa$ was presented by Meisenheimer[12], as indicated in Fig. 9 (a). His structure seems to be doubtful in the following point. If the red product between TNB and sodium hydroxide has such a structure as given in Fig. 9 (a), PA may be produced from it at the end of the reaction, while 3,5-dinitrophenol is experimentally obtained as mentioned above. The absorption band of PA is not found also in the spectrum (curve 3) of the boiled alkaline solution of TNB in Fig. 6. It has been, by Nagakura[13], suggested to the present author that TNB should react with sodium hydroxide as follows:



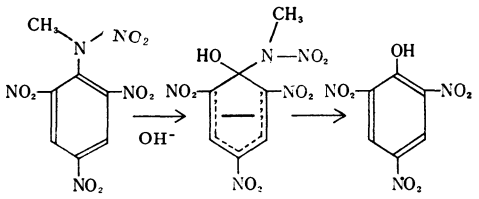
Pale yellow Red Yellow

It was suggested also by Meisenheimer[14] that a red product between 2,4,6-trinitroanisol (TNA) and sodium ethoxide had the probable constitution indicated in Fig. 9(b). In this case, he isolated as solids the products of the reaction of TNA with potassium ethoxide and of 2,4,6-trinitrophenetole with potassium methoxide, obtained a mixture containing trinitrophenetole on decomposing each of these solids with dilute sulfuric acid, and concluded that both red products consisted of the potassium salt of the anion (Fig. 9(b)). The structure presented by Meisenheimer for the complex between TNA and ethoxide ion, has been recently supported by Hamick and Foster[15,16], and by Nagakura and Tsubomura[13,17], who

5) L. de Bruyn and van Leent, *Rec. trav. Chim.*, **13**, 151 (1894).
6) L. de Bruyn, ibid., **9**, 208 (1890).
7) L. de Bruyn and van Leent, ibid., **13**, 148 (1894).
8) L. de Bruyn and van Leent, ibid., **14**, 150 (1895).
9) A. Hantzsch and H. Kissel, *Ber.*, **32**, 3140 (1899).
10) Jackson, *Am. Chem. J.*, **20**, 448 (1898); **23**, 294 (1901).
11) J. B. Ainscough and E. F. Caldin, *J. Chem. Soc.*, **1956**, 2528, 2540, 2546.
12) J. Meisenheimer, *Ann.*, **323**, 214, 241 (1902).
13) S. Nagakura, Private communication.
14) J. Meisenheimer, *Ann.*, **323**, 205 (1902).
15) D. L. Hamick and R. Foster, *J. Chem. Soc.*, **1954**, 2153.
16) R. Foster, *Nature*, **175**, 746 (1955).
17) H. Tsubomura, Private communication.

have succeeded in measuring an energy of activation for a decomposition reaction of a red complex of 2,4-dinitroanisol and hydroxyl ion to dinitrophenol.

In the reaction of Tetryl with sodium hydroxide PA seems to be finally produced through an intermediate, as indicated below, because the final absorption curve (5) of the reaction closely resembles that of PA (6) in Fig. 7. Although the red



products of TNB and Tetryl with alkali finally yield the different substances, that is, 3,5-dinitrophenol and PA, respectively, the resemblance between their spectra (curves 2 and 7 in Fig. 6) suggests that the structure of the red product of TNB may be similar to that of the red product of Tetryl. This is, thus, considered to support Meisenheimer's structure, since the resemblance of their spectra can be interpreted by assuming his structures in Fig. 9 (a), although the question pointed out above remains still.

Summary

(1) In ethanol and in water the maximum absorption bands of the substituted trinitrobenzenes are observed at longer wavelengths and possess smaller molar absorbancies than 1,3,5-trinitrobenzene, a benzene nucleus of which possesses some greater positive charge than those of the derivatives.

(2) Picric acid shows similar absorption curves in solvents like ethanol, water and acetone. This similarity seems to show that picric acid dissociates in all solvents.

(3) On treating the trinitrobenzenes with aqueous sodium hydroxide solution, the red colors are produced. The colors given by the trinitrobenzenes having substituents like $-N(CH_3)NO_2$, -Cl and -OH, are labile, while those produced from trinitrobenzene and 2,4,6-trinitrotoluene are rather stable. The spectrum of the red color of trinitrobenzene closely resembles that of Tetryl.

The author is particularly indebted to Professor Y. Nomura for his suggestion and encouragement of the present work. Thanks are also due to Associate Professor S. Maeda for use of the spectrophotometer.

Department of Chemistry
Defense Academy
Yokosuka, Kanagawa

*Penetration of Liquids into Filter Paper Used in Paper Chromatography**

By Masayuki NAKAGAKI and Kyoko OSAGAWA

(Received August 21, 1958)

The velocity of liquids ascending in filter paper, which is hung in a closed vessel and whose lower end is dipped in a liquid, is interesting from two viewpoints. The one is as the basis of the paper chromatography, in which the knowledge on the mechanism of the ascending of the developer liquid in a filter paper and on the properties of the filter paper seems to be fundamental to understand the physico-chemical details in the process of paper chromatography. The other standpoint is as a part of the studies of the penetration of liquids into porous materials. The latter, for example, the penetration of detergent solutions into clothes, is important when we consider the treatment of textiles in water.

The phenomenon can be treated by assuming that the penetration of liquids is due to the capillary force under the

* Presented before the Himeji Meeting held by the Chemical Society of Japan on May 31, 1958.

resistance by the viscosity and the hydrostatic pressure. Many theoretical and experimental investigations have already been made from this standpoint. Brittin[1] and Ikeda and Soeya[2] studied the ascending of liquids in capillary tubes. Lucas[3], Peek and McLean[4] and Fujita[5] studied the penetration into filter paper. Wolkowa[6] studied the penetration of liquids into a tube packed with powdered material. Carman[7] also studied the layer of powders on the basis of Kozeny's theory.

According to these investigations, the velocity of ascending, dh/dt, is given by[3,4]

$$dh/dt = (1/8\eta h)(2r\gamma \cos\theta - r^2 h\rho g) \quad (1)$$

and the equation for the initial stage of penetration is[3,4,6]

$$h^2 = kt \quad (2)$$

with $$k = r\gamma \cos\theta/2\eta \quad (2a)$$

In the present paper, a model of laminar capillary gaps will be used besides the model of tubular gaps already used by investigators cited above. Moreover, parameters will be used to take into account the winding of the gaps and the adsorption of liquids by the fibre. Finally, the penetration of liquids into the filter paper actually used in the paper chromatography will be studied.

Experimental

Organic Liquids.—Ethanol was boiled for 4 hours on a water bath with calcium oxide and distilled. The fraction distilled out at 78°C was dehydrated with sodium metal and distilled to collect the fraction at 78°C. Finally, it was again distilled on calcium oxide and the fraction of 78°C was used.

Benzene of the guaranteed reagent grade was distilled and the fraction at 80°C was used.

Acetone of the extra pure reagent grade was distilled and the fraction at 56.3°C was used.

Carbon tetrachloride of the extra pure reagent grade was treated with potassium hydroxide solution in an alcohol water mixture (KOH: H_2O:Alcohol=1:1:2) and shaken on a water bath for 30 min. at 50~60°C. Then it was washed with water, dehydrated with sodium metal and distilled to collect the fraction at 76.7°C.

Method of the Measurement. — Toyo filter paper No. 50 (for chromatography) was cut in pieces of 1 cm. in width and 25 cm. in length, and marked every 1 cm. with a pencil to show the distance from one end. A piece of the filter paper was hung in a measuring cylinder of 200 cc. closed with a cork stopper. In the cylinder, 10 cc. of liquid for study was placed in advance. The filter paper was hung so that its lower end was just 1 cm. below the surface of the liquid. The time when the front of the liquid passed every pencil mark was measured by a stop watch. All measurements were made in a thermostat held at 20°, 30° or 40°±0.02°C.

Theoretical Consideration of the Penetration

It may be natural to assume that liquid goes up in a piece of filter paper owing to the capillary force, under the resistance by the viscosity and the hydrostatic pressure. The shape of the capillary gap may be assumed to be one dimensional (tube like) or two dimensional (laminar).

In the case of the one dimensional gap, the amount of the liquid which penetrates into the gap per unit time, Q (cc./sec.), is given by Poiseuille's law,

$$Q = (\pi r^4/8\eta l)p \quad (3)$$

where η is the viscosity of the liquid, r the radius of the gap, p the pressure difference and l the length of the capillary filled with the liquid. The value of l may be different from the height of the liquid penetrated, because the capillary may be curved or wound. Therefore, the factor f is introduced here to indicate the degree of winding of the capillary by the equation,

$$f = l/h \quad (4)$$

where h is the height to which the liquid has gone up.

Now, the pressure difference p is the difference of the pressure by the surface tension and the hydrostatic pressure by the gravity,

$$p = (2\gamma \cos\theta)/r - h\rho g \quad (5)$$

where γ is the surface tension of the liquid, θ is the advancing contact angle and ρ is the density of the liquid and g is the constant of the gravity. At the equilibrium, $h=h_\infty$ and $p=0$, so that

$$h_\infty = 2\gamma \cos\theta/r\rho g \quad (6)$$

Then, another factor must be introduced here. If it is assumed that a fraction of the liquid which penetrates into the filter paper, α, is absorbed in fiber and $(1-\alpha)$ remains in the capillary gap, then,

$$(1-\alpha)Q = \pi r^2(dl/dt) = \pi r^2 f(dh/dt) \quad (7)$$

1) W. E. Brittin, *J. Appl. Phys.*, **17**, 37 (1946).
2) Y. Ikeda and T. Soeya, *J. Phys. Soc. Japan*, **4**, 306 (1949).
3) R. Lucas, *Kolloid-Z.*, **21**, 105 (1917); **23**, 15 (1918).
4) R. L. Peek and D. A. McLean, *Ind. Eng. Chem., Anal. Ed.*, **6**, 85 (1934).
5) H. Fujita, *J. Phys. Chem.*, **56**, 625 (1952).
6) Z. W. Wolkowa, *Kolloid-Z.*, **67**, 280 (1934).
7) P. C. Carman, *J. Soc. Chem. Ind.*, **57**, 225 (1938); **58**, 1 (1939).

Integrating this equation with Eqs. 2 and 4,

$$t/\tau = -h/h_\infty - \ln(1-h/h_\infty) \quad (8)$$

is obtained, where

$$\tau = 8\eta f^2 h_\infty/(1-\alpha)r^2\rho g \quad (9)$$

On the other hand, if the gap is two dimensional and its width is w and the half distance of the gap is a, $(w \gg a)$, then Eqs. 3, 5, 6, 7 and 9 should be replaced by

$$Q = (2wa^3/3\eta l)p \quad (3a)$$

$$p = \gamma\cos\theta/a - h\rho g \quad (5a)$$

$$h_\infty = \gamma\cos\theta/a\rho g \quad (6a)$$

$$(1-\alpha)Q = 2awf\mathrm{d}h/\mathrm{d}t \quad (7a)$$

and

$$\tau = 3\eta f^2 h_\infty/(1-\alpha)a^2\rho g \quad (9a)$$

respectively. However, the final equation 8 holds also in this case, although the interpretation of the constants h_∞ and τ is different from the former case. The assumption of two-dimensional gaps seems to be more reasonable than the one-dimensional gaps in the case of the filter paper.

On the basis of Eq. 8, it is easily seen that h^2 is proportional to the time, t, at the initial stage of the penetration,

$$h^2/t = 2h_\infty{}^2/\tau \quad (h/h_\infty \ll 1) \quad (9)$$

which agrees with Eq. 2 if $2h_\infty{}^2/\tau$ is equal to k.

According to the experimental data, the h^2-t curve is, however, straight only in the very initial range. The curve is not straight in the later stage. It is, therefore, desirable to expand Eq. 8 in a power series. It can be done in two ways:

$$h^2/t = (2h_\infty{}^2/\tau)\{1-(2/3)(h/h_\infty) - (1/18)(h/h_\infty)^2 - \cdots\cdots\} \quad (11a)$$

and

$$t/h^2 = (\tau/2h_\infty{}^2)\{1+(2/3)(h/h_\infty) + (1/2)(h/h_\infty)^2 + \cdots\cdots\} \quad (11b)$$

These equations show that the plot of h^2/t or t/h^2 against h should be almost linear if h is sufficiently small compared to h_∞. These equations also show that the deviation from the linearity should be smaller in h^2/t than in t/h_2, because the coefficient of the term of $(h/h_\infty)^2$ is smaller in Eq. 11a than in Eq. 11b. This is shown in Fig. 1, where curve I shows Eq. 11a and curve II shows Eq. 11b. The straight lines I′ and II′ are the initial slope of these curves. The symbols a and b show the deviation of curves I or II from the linearity by 1% and 5%, respectively.

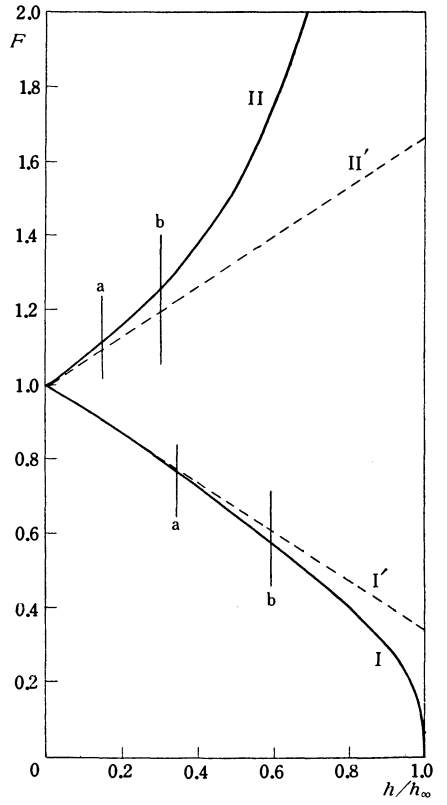


Fig. 1. Theoretical curves and their deviation from the linearity.

I: $F = (\tau/2h_\infty{}^2)(h^2/t)$
I′: $F = 1-(2/3)(h/h_\infty)$
II: $F = (2h_\infty{}^2/\tau)(t/h^2)$
II′: $F = 1+(2/3)(h/h_\infty)$
a: 1% deviation
b: 5% deviation

On the basis of the fact that curve I can be approximated by a straight line I′ in a fairly wide range of (h/h_∞), it is proposed to plote experimental values of (h^2/t) against h. The initial slope of this plot will give the values of A and B in the equation

$$h^2/t = A - Bh \quad (12)$$

and A and B are related to h_∞ and τ by the relations:

$$h_\infty = 2A/3B \quad (13)$$

and

$$\tau = 8A/9B^2 \quad (14)$$

as easily derived from Eq. 11a.

Results and Discussion

The height of the ascent of water and ethanol against time is shown in Fig. 2. The curves in this figure are the theoretical curves by Eq. 8, using the values of h_∞ and τ obtained by (h^2/t) vs. h plots on the basis of Eqs. 12, 13 and 14. These values are shown in Table I together with the

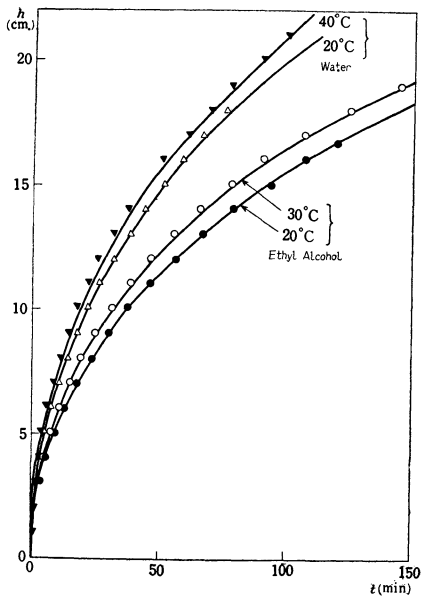


Fig. 2. The $h-t$ plot for water and ethanol.

TABLE I
CONSTANTS FOR THE PENETRATION OF WATER AND ETHANOL

	Water		Ethanol	
	20°C	40°C	20°C	30°C
A (cm²/min.)	5.45	6.10	3.10	3.87
B (cm./min.)	0.070	0.075	0.044	0.069
h_∞ (cm.)	51.9	54.2	47.5	37.4
τ (min.)	990	965	1460	722
x (μ)	14.3	13.1	6.09	7.50
y (μ)	1.65	1.37	1.59	1.84

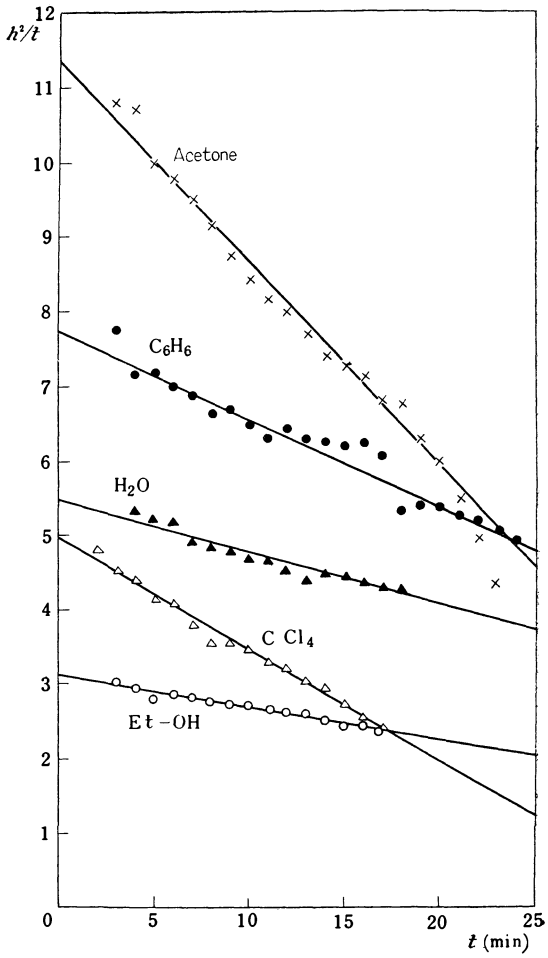


Fig. 3. The $h^2/t-h$ plot for acetone, benzene, water, carbon tetrachloride and ethanol.

TABLE II
CONSTANTS FOR THE PENETRATION OF SEVERAL LIQUIDS AT 20°C

	Acetone	Benzene	Water	CCl_4	Ethanol
A (cm²/min.)	11.37	7.71	5.45	4.95	3.10
B (cm./min.)	0.271	0.117	0.070	0.150	0.0435
η (c. p.)	0.323	0.647	1.009	0.970	1.200
γ (dyne/cm.)	23.70	28.88	72.75	26.77	22.27
ρ	0.7901	0.8788	0.9982	1.594	0.7893
x (μ)	10.9	7.65	14.3	7.78	6.09
y (μ)	2.06	1.82	1.65	1.88	1.59
$\cos\theta$	0.559	0.797	0.426	0.783	(1.00)
θ	55.0°	37.2°	64.8°	38.5°	(0°)
Two dimensional gap ($a=6.09\ \mu$)					
f ($\alpha=0.16$)	2.71	3.06	3.38	2.95	3.50
f ($\alpha=0$)	2.96	3.34	3.69	3.22	3.83
One dimensional gap ($r=12.2\ \mu$)					
f ($\alpha=0.16$)	3.33	3.75	4.15	3.63	4.30
f ($\alpha=0$)	3.64	4.10	4.54	3.96	4.70

values of A and B of Eq. 12.

In order to eliminate the factors depending on the properties of the liquid penetrating and in order to obtain the parameters depending mostly on the properties of the filter paper, two quantities, x and y, are introduced, both of which are proportional to the half distance, a, in the case of two-dimensional gap and are proportional to the radius, r, of the gap in the case of the one-dimensional gap. That is,

$$x=\gamma/\rho gh_\infty=a/\cos\theta \text{ or } r/2\cos\theta \qquad (15)$$

and

$$y=(3/2)(\eta B/\rho g)^{1/2}=(1-\alpha)^{1/2}a/f \text{ or } (3/8)^{1/2}(1-\alpha)^{1/2}r/f \qquad (16)$$

The values of x and y are cited in Table I. The values of x for water and ethanol are different from each other, while the values of y are approximately the same for both water and ethanol.

The relationship between (h^2/t) and h are shown in Fig. 3 for acetone, benzene, water, carbon tetrachloride and ethanol at 20°C. The linearity expected from Eq. 12 is satisfied. The values of A and B obtained from this linearity are listed in Table II. Using the values of the viscosity, surface tension and density of these liquids listed also in Table II, the values of x and y are calculated and shown in the same table. It is seen that the value x varies widely depending on the nature of the liquid, while the value of y is roughly the same.

According to Eq. 15, the difference of the value of x should be due to the difference of the contact angle. If the contact angle is assumed to be zero in the case of the smallest value of x, that is the case of ethanol (this corresponds to the assumption that $a=6.09\,\mu$ or $r=12.2\,\mu$), then, the largest possible values of $\cos\theta$ and the smallest possible values of the advancing contact angle, θ, are calculated as shown in Table II. For fat-free filter paper, it is said that the value of θ was zero for many liquids[4], but it is not so for the filter paper used in the actual paper chromatography.

In order to make further estimation, the value of α is assumed to be as follows. In the case of water, the amount of water contained in 1 cm^2 of the filter paper was 0.0165 g./cm^2, and the weight of the dried filter paper was 0.0133 g./cm^2. Therefore, the amount of water contained in 1 g. of the filter paper was 1.24 g. On the other hand, the amount of water adsorbed by 1 g. of the fiber of the filter paper may be about 0.2 g., referring to the data by Marshall and Peters[8]. Therefore, the value of α is assumed to be 0.16. If a liquid other than water is adsorbed less in the fiber, the value of α should be smaller than this. The values of f calculated under this assumption were listed in Table II. Assuming the value of $a=6.09\,\mu$ in the case of two-dimensional gap model, the mean value of f is 3.12 if $\alpha=0.16$ and 3.41 if $\alpha=0$. In the case of one-dimensional gap model of $r=12.2\,\mu$, the mean value of f is 3.85 if $\alpha=0.16$ and 4.21 if $\alpha=0$. Therefore, the length of the gap is three to four times larger than the length of the filter paper.

The value of $6.09\,\mu$ for the half distance of the gap seems to be reasonable, because the diameter of fibers of the filter paper measured under a microscope was about $15\,\mu$. In this connection, it may be good to point out the generally accepted fact that the dimension of the gap obtained by the measurement of the permeability of liquid is usually five to fifteen times greater than the value obtained by the measurement of the permeability of particles.

Summary

The penetration of liquid into a piece of filter paper hung vertically above a liquid is studied theoretically and experimentally. The height of the ascent of the liquid is proportional to the square root of the time at the initial stage of the penetration, but the proportionality does not hold in a wide range of time. The equation which describes this relationship between the height and time has been derived. The values of the parameters in the equation have been determined for acetone, benzene, water, carbon tetrachloride and ethanol. It is concluded that the capillary gap in the filter paper is about $6\,\mu$ in the half distance and the length of the gap is about 3 times larger than the length of the filter paper, if the gap is assumed to be two dimensional.

Faculty of the Science of Living
Osaka City University
Nishi-ku, Osaka

8) W. J. Marshall and R. H. Peters, *J. Soc. Dyers and Colourist*, 63, 446 (1947).

The Aconite Alkaloids. XXIV. Oxidation of Miyaconitine and Miyaconitinone*

By Shichiro KAKIMOTO

(Received September 4, 1958)

Miyaconitine (I) $C_{23}H_{29}O_6N$ and miyaconitinone (II) $C_{23}H_{27}O_6N$ were isolated from *Aconitum miyabei*, Nakai, and the following extended formulae were given to them, respectively, in Part XVI[1].

$C_{16}H_{20}$ { $OCOCH_3$, OH, $(CO)_3$, $N\text{-}C_2H_5$ } I

$C_{15}H_{19}$ { $OCOCH_3$, $(CO)_4$, $N\text{-}C_2H_5$ } II

Since these alkaloids were relatively unstable to oxidation with either potassium permanganate or nitric acid, no crystalline oxidation product could be isolated even by the best method[2] found for the aconite alkaloids by H. Suginome. But, when miyaconitinone was oxidized with potassium permanganate under milder conditions, oxomiyaconitinone (III) $C_{20}H_{20}O_6$ ($-CO-N-C_2H_5$) was obtained only in a small yield.

In Part XVI[1] it was shown that an α-diketone group exists in these two alkaloids, and it seemed that oxidation with hydrogen peroxide would be successful. But all attemps of oxidative ring opening under the vigorous conditions described, for instance, by Holleman[3] and by Boeseken[4], to open the ring of *o*-camphorquinone, were unsuccessful. The present author has established a milder method to oxidize *o*-camphorquinone almost quantitatively to camphoric acid and these alkaloids have been oxidized successfully to dibasic acids by this method.

Namely, oxidation of miyaconitine with dilute alkaline hydrogen peroxide gave a basic substance, oxymiyaconitine (IV) $C_{23}H_{29}O_7N$, and an acid, miyaconinic acid (V) $C_{21}H_{29}O_7N$. It was determined that miyaconinic acid retains the original ethylimino group but not the acetyl group. It was titrated as a monobasic acid and gave a monomethyl ester (VI) $C_{22}H_{31}O_7N$ by esterification with diazomethane, while the dimethyl ester (VII) $C_{23}H_{33}O_7N$ could be derived with dimethyl sulfate in a concentrated potassium hydroxide solution. Acetylation of the dimethyl ester afforded a diacetyl compound (VIII) $C_{27}H_{37}O_9N$. Miyaconinic acid as well as these derivatives could not be hydrogenated by the method[1] described as a method for comparison of miyaconitine with miyaconitinone. These experiments showed that miyaconitine was hydrolyzed and then oxidized at the α-diketone group to give a dibasic acid V and its transformations into the above-mentioned derivatives are represented by the following schema:

I → $C_{16}H_{20}$ { $(OH)_2$, CO, $(COOH)_2$, $N\text{-}C_2H_5$ } V → $C_{16}H_{20}$ { $(OH)_2$, CO, COOH, $COOCH_3$, $N\text{-}C_2H_5$ } VI →

$C_{16}H_{20}$ { $(OH)_2$, CO, $(COOCH_3)_2$, $N\text{-}C_2H_5$ } VII → $C_{16}H_{20}$ { $(OCOCH_3)_2$, CO, $(COOCH_3)_2$, $N\text{-}C_2H_5$ } VIII

Oxidation of miyaconitinone by the same method gave miyaconinic acid and miyaconitinonic acid (IX) $C_{23}H_{29}O_8N$. The formation of miyaconinic acid from miyaconitinone is analogous to the alkaline hydrolysis of miyaconitine and miyaconitinone to miyaconine. Miyaconitinonic acid had an acetyl group and absorbed 1 mole of hydrogen, so that its relation to miyaconinic acid may be similar to the relation of miyaconitinone to miyaconine. Accordingly, formula IX is given to miyaconitinonic acid.

$C_{15}H_{19}$ { $OCOCH_3$, $(CO)_2$, $(COOH)_2$, $N\text{-}C_2H_5$ } IX

* This constitutes a part of a series entitled "The Aconite Alkaloids" by H. Suginome. The report, "On Lucaconine" presented in *Proc. Japan Acad.*, **22**, 122(1946) will be called Part XXIII. Part XXII is H. Suginome and S. Umezawa, *J. Fac. Sci. Hokkaido Univ., Ser. III Chem.*, **4**, 44 (1950).

1) H. Suginome, S. Furusawa, Y. Chiba and S. Kakimoto, ibid., **4**, 1 (1950).

2) H. Suginome, ibid., **2**, 95 (1937); *Ann.*, **533**, 172 (1931).

3) M. A. F. Holleman, *Rec. trav. chim.*, **23**, 169 (1904).

4) M. J. Boeseken, ibid., **30**, 142 (1911).

Miyaconinone that had been obtained by acid hydrolysis of miyaconitinone was oxidized to miyaconinic acid. This relation also had the same resemblance as observed previously. Miyaconine was oxidized to isomiyaconinic acid (X) differing from miyaconinic acid in melting point, optical rotation and crystalline form, but possessing the same formula $C_{21}H_{29}O_7N$ and the same chemical properties.

When miyaconitinonic acid was treated with acetic anhydride or heated under a reduced pressure, carbon dioxide and water were split off, producing a weak base, anhydrodecarboxymiyaconitinonic acid (XI) $C_{22}H_{27}O_5N$. It absorbed 1 mole of hydrogen, and had still an acetyl group. It could be distilled in high vacuum and it corresponded to a base resulting from original miyaconitinone by loss of one carbonyl group. It would be the most useful substance for succeeding degradation to clarify the constitution of the original alkaloid. The same treatment of miyaconinic acid with acetic anhydride afforded a weak base, diacetyldecarboxymiyaconinic acid (XII) $C_{24}H_{33}O_7N$. From isomiyaconinic acid, diacetyldecarboxyisomiyaconinic acid (XIII) $C_{24}H_{33}O_7N$ was obtained.

These acids and derivatives were produced by opening of one ring containing the α-diketone group just as expected. Further, anhydrodecarboxy compound XI was derived by closing the ring and splitting off carbon dioxide and water.

As the acids were titrated as monobasic, the ring opening might have occurred in the neighborhood of the ethylimino group. Accordingly, it was expected that the ethylimino group would be changed in its chemical properties and attacked in the ordinary degradation process. But, methiodides of their esters returned readily with alkali to the original substances such as miyaconitine and miyaconitinone.

Experimental

Oxomiyaconitinone (III).—Two g. of miyaconitinone was added to a solution of 0.15 g. of potassium permanganate and 5 cc. of glacial acetic acid in 30 cc. of acetone and the solution was allowed to stand for 24 hr. After filtration to remove manganese dioxide, the solution was evaporated to dryness and the residue was dissolved in water. The crude oxomiyaconitinone was extracted from the aqueous solution with chloroform and recrystallized from ethanol. Yield, 0.2 g. White needles, m. p. 210°.

Anal. Found: C, 64.86; H, 6.10; (N)-C_2H_5, 7.49. Calcd. for $C_{21}H_{20}O_7N$-C_2H_5: C, 64.62; H, 5.90; (N)-C_2H_5, 6.80%.

A Modified Method for Preparation of Camphoric Acid.—To a mixture of 2.5 cc. of 3 percent hydrogen peroxide, 2.5 cc. of N potassium hydroxide solution and 5 cc. of water, 0.2 g. of *o*-camphorquinone was added and the mixture was shaken for 24 hr. The reaction mixture was acidified and concentrated to give 0.2 g. of camphoric acid. m. p. 186~187°. $[\alpha]_D^{10}$ +57.3° (acetone).

Anal. Found: C, 59.90; H, 7.99. Calcd. for $C_{10}H_{16}O_4$: C, 59.98; H, 8.06%.

Oxidation of Miyaconitine with Hydrogen Peroxide.—*a) Oxymiyaconitine (IV).*—A suspension of 1.7 g. of powdered miyaconitine in a mixture of 8 cc. of 3 percent hydrogen peroxide, 10 cc. of N potassium hydroxide solution and 20 cc. of water, was shaken for 24 hr. The mixture of unchanged miyaconitine and oxymiyaconitine was collected and fractionally recrystallized from ethanol; 0.25 g. of oxymiyaconitine was obtained. m. p. 244~245° (decomp.). $[\alpha]_D^{9.5}$ +44.6° (N acetic acid).

Anal. Found: C, 64.33; H, 6.69. Calcd. for $C_{23}H_{29}O_7N$: C, 64.02; H, 6.78%.

b) Miyaconinic acid (V).—The basic filtrate from miyaconitine and oxymiyaconitine, was acidified with dilute hydrochloric acid and dried up under a reduced pressure. The residue was extracted with ethanol, the extract was evaporated to dryness and the residue was treated with dilute acetic acid. The crude acid thus obtained was dissolved in dilute ammonia water and reprecipitated with dilute acetic acid. Yield, 0.17 g. Needles, m. p. 295° (decomp.). $[\alpha]_D^{18}$ +17.7° (N ammonia). It contained 1 mole of water of crystallization.

Anal. Found: H_2O, 4.18. Calcd. for $C_{21}H_{29}O_7N$-H_2O: H_2O, 4.25. Found: C, 61.79; H, 6.96; N, 3.65; COOH*, 12.41. Calcd. for $C_{21}H_{29}O_7N$: C, 61.90; H, 7.18; H, 3.44; COOH, 11.08%.

c) Monomethyl ester of miyaconinic acid (VI).—To a suspension of 0.1 g. of miyaconinic acid in 25 cc. of ether, 0.1 g. of diazomethane was added and the mixture was allowed to stand for 24 hr. The precipitate was dissolved in dilute acetic acid and reprecipitated with dilute ammonia water. The precipitate was recrystallized from methanol. Yield, 0.1 g., m. p. 285° (decomp.). It contained 2 moles of water of crystallization.

Anal. Found: H_2O, 7.52. Calcd. for $C_{22}H_{31}O_7N \cdot 2H_2O$: H_2O, 7.88. Found: C, 62.73; H, 7.41; OCH_3, 7.76. Calcd. for $C_{22}H_{31}O_7N$: C, 62.69; H, 7.41; OCH_3 7.36%.

Its perchlorate melted at 210° with decomposition.

Anal. Found: Cl, 6.49. Calcd. for $C_{22}H_{31}O_7N \cdot HClO_4$: Cl, 6.80%.

Its methiodide melted at 271~272° with decomposition.

Anal. Found: C, 48.50; H, 5.51; I, 23.87. Calcd. for $C_{22}H_{31}O_7N \cdot CH_3I$: C, 48.90; H, 6.03; I, 23.53%.

d) Dimethyl ester (VII).—To a solution of 0.2 g. of miyaconinic acid in 1.3 cc. of 15 percent

* Titrated with 0.01 N potassium hydroxide (Indicator: Phenolphthalein).

potassium hydroxide solution, 1 cc. of dimethyl sulfate was added and the mixture was warmed at 60°. The reaction mixture was acidified with dilute sulfuric acid and filtered. The solution was alkalized with dilute ammonia water, producing 0.19 g. of the dimethyl ester. It melted at 296~297° with decomposition and formed a perchlorate and a methiodide.

Anal. Found: C, 63.58; H, 7.10; OCH_3, 14.08; (N)-C_2H_5, 7.18. Calcd. for $C_{23}H_{33}O_7N$: C, 63.41; H, 7.41; OCH_3, 14.24; (N)-C_2H_5, 6.67%. Found: Cl, 6.47. Calcd. for $C_{23}H_{33}O_7N\ HClO_4$; Cl, 6.62%.

e) Diacetyl dimethyl ester (VIII).—To a solution of 0.2 g. of dimethyl ester in 2 cc. of glacial acetic acid, 2 cc. of acetic anhydride and 2 cc. of pyridine were added. After 24 hr., the solvent was distilled off under a reduced pressure. The residue was dissolved in water, and dilute ammonia water was added to give 0.2 g. of diacetyl dimethyl ester. It was recrystallized from methanol. m. p. 167~168°.

Anal. Found: C, 62.65; H, 7.34; OCH_3, 11.12; (N)-C_2H_5, 5.43; $COCH_3$, 16.39. Calcd. for $C_{27}H_{37}O_9N$: C, 62.41; H, 7.18; OCH_3, 11.94; (N)-C_2H_5, 5.59; $COCH_3$, 16.57%.

Oxidation of Miyaconitinone. — Three g. of miyaconitinone was oxidized by the above-described method. After the separation of 0.32 g. of crude miyaconinic acid from the reaction mixture, chloroform was added to the filtrate and the mixture was stirred for several minutes. The semicrystalline product, presumably containing chloroform, was separated and warmed in water to remove the contained chloroform. From the concentrated solution, 0.17 g. of crude miyaconitinonic acid crystallized out in white needles. It was recrystallized from ethanol, m. p. 259° (decomp.). $[\alpha]_D^{10}$ −84.7° (N ammonia water).

Aanl. Found: C, 61.28; H, 6.57; COOH, 10.16; $COCH_3$, 9.83. Calcd. for $C_{23}H_{29}O_8N$: C, 61.73; H, 6.54; COOH, 10.05; $COCH_3$, 9.62%. 8.120 Mg. of sample absorbed 0.442 cc. of hydrogen (1.04 mol.).

Oxidation of Miyaconine. — Oxidation of 0.7 g. of miyaconine afforded 0.2 g. of isomiyaconinic acid. It melted at 268° with decomposition. White plates, $[\alpha]_D^{9.3}$ +27.3° (N ammonia water).

Anal. Found: H_2O, 4.55; C, 59.53; H, 7.06; COOH, 10.53. Calcd. for $C_{21}H_{29}O_7N\cdot H_2O$: H_2O, 4.25; C, 59.28; H, 7.35; COOH, 10.53%.

Oxidation of Miyaconinone. — From 0.45 g. of miyaconinone, 0.05 g. of miyaconinic acid was obtained, m. p. 295°.

Anal. Found: C, 62.69; H, 6.88. Calcd. for $C_{21}H_{29}O_7N$: C, 61.90; H, 7.18%.

Anhydrodecarboxymiyaconitinonic Acid (XI).—Miyaconitinonic acid (0.2 g.) was heated at 259° in a high vacuum for a few minutes. After cooling, the residue was recrystallized from ethanol to give anhydrodecarboxymiyaconitinonic acid. Yield, 0.13 g., m. p. 164~165°, $[\alpha]_D^{10}$ −117.0° (chloroform). XI was soluble in dilute hydrochloric acid, but almost insoluble in dilute acetic acid, and it was precipitated with ammonia water from the acidic solution. XI was also obtained from 0.1 g. of the original acid by heating with a mixture of 0.5 cc. of glacial acetic acid and 3 cc. of acetic anhydride for 1 hr., evaporating the solvent and adding water. XI was recrystallized from ethanol. Yield, 0.04 g.

Anal. Found: C, 67.43; H, 6.77; N, 3.74; $COCH_3$, 11.54. Calcd. for $C_{22}H_{27}O_6N$: C, 68.55; H, 7.06; N, 3.63; $COCH_3$, 11.09%. 8.533 Mg. of sample absorbed 0.442 cc. of hydrogen (1.15 mol.).

When this base was heated with 45 per cent ethanol for 2 hr., it was converted into a weak base, m. p. 194~195°, $[\alpha]_D^{10}$ −142.4° (chloroform). The latter base corresponded to decarboxymiyaconitinonic acid.

Anal. Found: C, 65.63; H, 6.94; $COCH_3$; 10.63. Calcd. for $C_{22}H_{29}O_6N$: C, 65.50; H, 7.25; $COCH_3$, 10.67%. 8.637 Mg. of sample absorbed 0.446 cc. of hydrogen (0.93 mol.).

Diacetyldecarboxymiyaconinic Acid (XII).—When 0.22 g. of miyaconinic acid was treated with acetic anhydride as mentioned above, 0.11 g. of diacetyldecarboxymiyaconinic acid was obtained in white prisms, m. p. 215~216°.

Anal. Found: C. 63.57; H, 6.39; $COCH_3$, 18.98. Calcd. for $C_{24}H_{33}O_7N$: C, 64.41; H, 7.43; $COCH_3$, 19.68%.

Diacetyldecarboxyisomiyaconinic Acid (XIII).—From 0.1 g. of isomiyaconinic acid, 0.01 g. of diacetyldecarboxyisomiyaconinic acid was obtained in white needles, m. p. 200~202°.

Anal. Found: C, 63.73; H, 6.50; $COCH_3$, 19.80. Calcd. for $C_{24}H_{33}O_7N$: C, 64.41; H, 7.43; $COCH_3$, 19.68%.

The author wishes to express his thanks to Professor Harusada Suginome, President of Hokkaido University, for his exceedingly kind direction throughout this work.

Department of Chemistry
Faculty of Science
Hokkaido University
Sapporo

The Aconite Alkaloids. XXV. Selenium Dehydrogenation of Miyaconitinone and Lucidusculine*

By Harusada SUGINOME and Shichiro KAKIMOTO

(Received September 4, 1958)

Miyaconitinone[1], $C_{23}H_{27}O_6N$, which has been isolated from *Aconitum miyabei*, Nakai, belongs to the aconine group that may be derived from the fundamental base, $C_{19}H_{29}N$; while lucidusculine[2], $C_{24}H_{35}O_4N$, which has been isolated from *Aconitum lucidusculum*, Nakai, may be derived from the fundamental base, $C_{20}H_{31}N$, similar to atisine. These two aconite alkaloids, belonging to different fundamental bases, were subjected to dehydrogenation by selenium, producing the following results:

Miyaconitinone → $C_{21}H_{38}$ (unsure), phenanthrene, anthracene

Lucidusculine → phenanthrene, 3-methylphenanthrene, pimanthrene (unsure)

Hetisine, atisine, napelline and staphisine all yielded neutral fractions consisting of complex mixtures of phenanthrene hydrocarbons, some of which were identified to be phenathrene, 1-methyl-, 1,7-dimethyl-, 1-methyl-6-ethylphenanthrene, 3-methylretene, and $C_{17}H_{16}$ or $C_{18}H_{18}$[3].

The conditions, employed at first, to dehydrogenate miyaconitinone were rather more vigorous than Lowson's procedure, but a good result was not obtained. Only an oily mixture of unsaturated hydrocarbons and a saturated hydrocarbon, which melted at 60° and seemed not to be pure but near to $C_{21}H_{38}$, were obtained.

When miyaconitinone was dehydrogenated under more drastic conditions, e. g., heated in a sealed tube at 300~320° for 24 hr. and then at 370~380° for 24 hr., an oily mixture of unsaturated hydrocarbons was yielded. High vacuum distillation of the mixture afforded crystalline hydrocarbons from which pure phenanthrene and anthracene were separated by means of recrystallization. Each of them was determined by observation of ultraviolet absorption spectrum and preparation of quinone and picrate.

Under the same condition, giving phenanthrene and anthracene from miyaconitinone, lucidusculine was dehydrogenated. The main part of mixture of crystalline hydrocarbons was phenanthrene, and two other hydrocarbons were obtained in small quantities. One of them was determined to be a methylphenanthrene by elementary analysis. It melted at 62° and was converted into the picrate, bright yellow needles, m. p. 130°, and into the quinone, orange plates, m. p. 204°. Therefore, it was decided to be a 3-methylphenanthrene[4]. The other hydrocarbon melted at 80° and was converted into the picrate, yellow needles, m. p. 125°, and into the quinone, reddish needles, m. p. 182°. It seemed to be 1,7-dimethylphenanthrene (pimanthrene)[5]. From lucidusculine no anthracene derivative was yielded, but only the derivatives of phenanthrene.

It has not yet been reported that anthracene is obtained from other aconite alkaloids. The authors have been able to obtain anthracene from miyaconitinone. But it may be too early to conclude that the aconite alkaloid, having the fundamental base, $C_{20}H_{31}N$, has a constitution with a skeleton that yields both phenanthrene and anthracene, because miyaconitinone has so many oxygen atoms that it is very unstable to oxidation (cf. Part XXIV) and because it requires a drastic condition for dehydrogenation. It is of interest that some cholestanediols can be converted readily into anthracene ring system[6].

* Part XXIV, S. Kakimoto, This Bulletin, **32**, 349(1959).

1) H. Suginome, S. Furusawa, Y. Chiba and S. Kakimoto, *J. Fac. Sci. Hokkaido Univ., Ser. III Chem.*, **4**, 1 (1950).

2) H. Suginome, S. Kakimoto and J. Sonoda, ibid., **4**, 25 (1950); R. Majima and S. Morio, *Ber.*, **65**, 599 (1936).

3) A. Lowson and J. E. C. Toops, *J. Chem. Soc.*, **1937**, 1640; W. A. Jacobs and L. C. Craig, *J. Biol. Chem.*, **143**, 589 (1942); L. C. Craig and W. A. Jacobs, ibid., **152**, 645, 651 (1944); W. A. Jacobs and C. F. Huebner, ibid., **170**, 189 (1947); C. F. Huebner and W. A. Jacobs, ibid., **169**, 211 (1946); **170**, 203 (1947).

4) R. D. Haworth, *J. Chem. Soc.*, **1932**, 1125.

5) L. Ruzicka and Fr. Balas, *Helv. Chim. Acta.*, **6**, 689 (1923).

6) K. Tsuda and R. Hayatsu, *J. Am. Chem. Soc.*, **77**, 3089 (1955).

Experimental

Dehydrogenation of Miyaconitinone. — A mixture of 3 g. of miyaconitinone and 15 g. of selenium was divided into four portions. Each of them was sealed in a hard glass tube and heated at 320° for 35 hr. The reaction mixtures were combined and extracted with ether, and from the extract, basic substances from which no crystalline substance could be isolated, were removed by extraction with dilute hydrochloric acid. After ether was distilled off, the residue was fractionated by high vacuum distillation (over 10^{-3} mm.). Three hundred mg. of first fraction, distilled at 80~130°, was treated with glacial acetic acid. The insoluble part was recrystallized three times from methanol to give 13 mg. of white leaflets, m. p. 60°. The material has no color reaction with tetranitromethane and may be $C_{21}H_{38}$ or hydrocarbon near $C_{21}H_{38}$.

Anal. Found: C, 85.36; H, 14.38. Mol. Wt. 294 (Rast's method). Calcd. for $C_{21}H_{38}$: C, 86.79; H, 13.21%. Mol. Wt. 290.

When water was added to the solution of unsaturated hydrocarbon in glacial acetic acid, oil was separated. It was distilled to give 230 mg. of oil which was colored by tetranitromethane. It seemed to be a mixture of unsaturated hydrocarbons.

Anal. Found: C, 89.64; H, 7.98%.

Since it was not possible to isolate the pure substance in the above described experiment, more drastic conditions were employed as the following.

A mixture of 20 g. of miyaconitinone and 80 g. of selenium was divided into ten portions. Each of them was heated at 300~320° for 24 hr., and then at 370~380° for the same period in a sealed tube. The reaction mixtures were combined and extracted with ether. Ethereal extract was washed with dilute hydrochloric acid, next with dilute sodium bicarbonate solution and then with water. After removal of the ether, the residue was distilled under a high vacuum to give one part of oil and 460 mg. of crystalline part. The latter was fractionally recrystallized from methanol into three parts, i) melted at 90~100°, ii) melted at 190~200°, iii) melted at 120~150°. Recrystallization through picrate and chromatographic separation of crude substance was not effective to obtain pure compounds. The part i thus separated was able to be purified through the picrate which was recrystallized from ethanol, and then the derived free hydrocarbon was recrystallized from methanol again to yield 25 mg. of phenanthrene, m. p. 99~100°. The substance was characterized by the observation of ultraviolet absorption spectrum and by preparing the picrate, m. p. 144° and phenanthrenequinone, m. p. 205°, which was derived by oxidation with chromic trioxide in glacial acetic acid. These derivatives gave no depression of the melting points on admixture with the corresponding derivatives of pure phenanthrene.

Anal. Found: C, 94.33; H, 5.24. Calcd. for $C_{14}H_{10}$: C, 94.34; H, 5.66. Found: C, 80.70; H, 3.66. Calcd. for $C_{14}H_8O_2$: C, 80.69; H, 3.87%. Found: C, 59.37; H, 2.71. Calcd. for $C_{14}H_{10}$. $C_6H_3O_7N$: C, 58.97; H, 2.80%.

The part ii, mentioned above, was recrystallized from methanol to yield 20 mg. of an anthracene, m. p. 215°. The derived anthraquinone melted at 283°.

Anal. Found: C, 94.35; H, 5.65. Calcd. for $C_{14}H_{10}$: C, 94.34; H, 5.66. Found: C, 80.41; H, 3.62. Calcd. for $C_{14}H_8O_2$: C, 80.69; H, 3.87%.

The part iii was found to be a mixture of i and ii. Recrystallization through picrate and chromatographic separation afforded no good result. Therefore, the mixture was oxidized with chromic trioxide in glacial acetic acid. The oxidized substance was dissolved in alcohol and the product was adsorbed on neutral alummina and eluted with benzene; 20 mg. of pure phenanthrenequinone and 15 mg. of anthraquinone could be separated.

Dehydrogenation of Lucidusculine. — The conditions of dehydrogenation were the same as those used for miyaconitinone to obtain phenanthrene and anthracene. Neutral oil in an amount of 1.731 g. was obtained from 20 g. of lucidusculine. From the oil, 426 mg. of crystalline hydrocarbon mixture was separated by high vacuum distillation. The mixture was repeatedly recrystallized from methanol, but only 45 mg. of phenanthrene, m. p. 98°, (its picrate, m. p. 142°, the quinone, m. p. 204°) was isolated and no anthracene could be obtained. Other parts of hydrocarbon mixture were converted into picrate. The recrystallization was repeated again to give phenanthrene picrate and two other picrates. One of them was in the form of bright yellow needles, m. p. 130° and the other of yellow needles, m. p. 125°. From the former, 38 mg. of 3-methylphenanthrene, m. p. 62° was obtained and it was oxidized to the quinone, m. p. 204°. Orange plates.

Anal. Found: C, 93.58; H, 6.06. Calcd. for $C_{15}H_{12}$: C, 93.71; H, 6.26%. Found: C, 80.92; H, 4.79. Calcd. for $C_{15}H_{10}O_2$: C, 81.10; H, 4.54%.

From the latter, 9 mg. of hydrocarbon, m. p. 80° was obtained. Five mg. of this substance was oxidized to quinone which was recrystallized from methanol and melted at 182°. Reddish needles. But its yield was too small to be recrystallized repeatedly for analysis. It seemed to be pimanthrene (1,7-dimethylphenanthrene).

Department of Chemistry
Faculty of Science
Hokkaido University
Sapporo

The Aconite Alkaloids. XXVI. On Lucaconine and Monoacetyllucaconine*

By Harusada SUGINOME and Sijô FURUSAWA**

(Received September 4, 1958)

In Part XXIII[1] of this series, it was reported that a new alkaloid, lucaconine, $C_{21}H_{33}O_6N$, was isolated from the roots of *Aconitum luciduscul*um, Nakai and it was suggested that it had two methoxyl, four hydroxyl, and a secondary amino group. One of the present authors with Amiya[2] found that diacetyllucaconine had two active hydrogens. Therefore, *N*-alkyl and other functional groups had to be determined more precisely. As the results of repeated examinations, it was found that the base had an *N*-ethyl and three methoxyl groups, and, therefore, the older molecular formula of lucaconine, $C_{21}H_{33}O_6N$, should be revised to $C_{24}H_{39}O_7N$***.

On the other hand, a new alkaloid was isolated from the roots of the above mentioned *Aconitum* species, viz., on the basis of the difference of solubility in benzene from the crude bases containing lucaconine. The content of the base was about one-tenth of that of lucaconine and was about 0.012 per cent that of dried roots. The new alkaloid was purified through a perchlorate, from which the free base was liberated and recrystallized from ethanol. The purified base had m.p. 187°, $[\alpha]_D^{18}+42.7°$, and molecular formula $C_{26}H_{41}O_8N$. On hydrolysis with alcoholic potassium hydroxide it split off one mole of acetic acid and produced the alkamine, lucaconine.

$$C_{26}H_{41}O_8N+H_2O\rightarrow CH_3COOH+C_{24}H_{39}O_7N$$

Therefore, this new base was named monoacetyllucaconine.

Acetylation of lucaconine I and monoacetyllucaconine II with acetic anhydride gave the same diacetyl compound, diacetyllucaconine III, $C_{28}H_{43}O_9N$, m. p. 124°, $[\alpha]_D^{16}+15.3°$, which afforded lucaconine on hydrolysis with alcoholic potassium hydroxide.

From these results the formulae of lucaconine I and monoacetyllucaconine II may be extended as follows:

$C_{19}H_{21}$ { $(OCH_3)_3$, $(OH)_4$, $N\text{-}C_2H_5$ } Lucaconine (I)

$C_{19}H_{21}$ { $(OCH_3)_3$, $OCOCH_3$, $(OH)_3$, $N\text{-}C_2H_5$ } Monoacetyllucaconine (II)

Lucaconine and monoacetyllucaconine are assumed to have hexacyclic structure based on the skeletal formula, $C_{19}H_{29}N$[3].

Experimental

Isolation of Lucaconine.—As described in the previous reports[1,4], 293.6 kg. of dried roots of *Aconitum luciduscul*um, Nakai was treated. The percolate thus obtained was divided into three fractions, which were named fraction I, fraction II, and fraction III as previously described[4]. The yield of fraction III was 1,062 g. (0.36% of dried roots). Treatment of fraction II with acetone gave 357 g. of crystalline material, which was recrystallized from ethanol to give 210 g. of crude lucaconine, melting at 197°.

From 5.5 g. of this crude lucaconine, 6.8 g. of crystalline perchlorate was prepared, which was recrystallized from ethanol to give 5.1 g. of pure perchlorate, m. p. 210° (decomp.). From this salt, 3.9 g. of a free base melting at 198° was liberated; on three recrystallizations from ethanol, the base melted at 200°, and showed no depression of the melting point on admixture with an authentic sample of lucaconine[1]. $[\alpha]_D^{14}+57.1°$ (chloroform).

Anal. Found: C, 63.48; H, 8.39; N, 3.55; OCH_3, 20.86; (N)-C_2H_5, 6.59. Calcd. for $C_{24}H_{39}O_7N$: C, 63.55; H, 8.45; N, 3.09; 3-OCH_3, 20.53; (N)-C_2H_5, 6.19%.

Determination of N-ethyl group[5].—Lucaconine was treated in the usual manner for Willstätter's *N*-alkyl determination. Trimethyl ethyl ammonium iodide thus obtained was analyzed.

* Part XXV, H. Suginome and S. Kakimoto, This Bulletin, **32**, 352 (1959).

** Present address, Faculty of Technology, Chû-ô University, Tokyo, Japan.

1) H. Suginome, S. Kakimoto, J. Sonoda and S. Noguchi, *Proc. Japan Acad.*, **22**, 122 (1946).

2) H. Suginome and T. Amiya, unpublished work.

*** The compositions calculated for these two formulae are nearly identical as follows: Calcd. for $C_{21}H_{33}O_6N$: C, 63.77; H, 8.41; N, 3.57%. Calcd. $C_{24}H_{39}O_7N$: C, 63.55; H, 8.45; N, 3.09%.

3) H. Suginome and K. Ohno, *J. Fac. Sci., Hokkaido Univ., Ser. III. Chem.*, **4**, 36 (1950).

4) H. Suginome, S. Furusawa, Y. Chiba and S. Kakimoto, ibid., **4**, 1 (1950).

5) R. Willstätter and M. Utzinger, *Ann.*, **382**, 148(1911); R. Majima and K. Tamura, ibid., **526**, 116 (1936).

Anal. Found: I, 60.38. Calcd. for $(CH_3)_3(C_2H_5)NI$: I, 59.02%.

The pure lucaconine was also obtained by treatment of the crude base melting at 197° with ethanolic potassium hydroxide, followed by recrystallization from ethanol.

Perchlorate.—m. p. 210° (decomp.).

Anal. Found: C, 51.68; H, 7.08; Cl, 6.39. Calcd. for $C_{24}H_{39}O_7N \cdot HClO_4$: C, 52.01; H, 7.75; Cl, 6.36%.

Hydrochloride.—m. p. 216~217° (decomp.) (from abs. ethanol).

Anal. Found: C, 58.81; H, 8.31; Cl, 7.32. Calcd. for $C_{24}H_{39}O_7N \cdot HCl$: C, 58.80; H, 8.22; Cl, 7.24%.

Hydrobromide.—m. p. 223° (decomp.) (from abs. ethanol).

Anal. Found: C, 54.30; H, 7.54; Br, 14.81. Calcd. for $C_{24}H_{39}O_7N \cdot HBr$: C, 53.91; H, 7.54; Br, 14.93%.

Methiodide.—m. p. 174° (from water).

Anal. Found: C, 49.23; H, 7.29; OCH_3, 16.36; I, 19.51. Calcd. for $C_{24}H_{39}O_7N \cdot CH_3I$: C, 50.40; H, 7.11; 3-$OCH_3$, 15.91; I, 21.32%.

The methiodide readily returned to the original base by means of alkali.

Isolation of Monoacetyllucaconine. — On being left to stand in a refrigerator, the mother liquor, obtained by removal of the lucaconine-rich base, gave 90 g. of crystalline substance melting at 168~172°. This substance was recrystallized from benzene and then from ethanol to give a crystalline base melting at 186°. Yield 12.8 g. From this base perchlorate was obtained, which after three recrystallizations from ethanol showed m. p. 202~202.5° (decomp.). Yield, 9.0 g. Free base, obtained from this perchlorate, showed m. p. 187°, $[\alpha]_D^{18}$+42.7° (ethanol) after recrystallization from ethanol. Yield, 3.75 g.

Anal. Found: C, 63.11; H, 8.22; N, 2.85; OCH_3, 18.90; (N)-C_2H_5, 5.05; $COCH_3$, 10.80. Calcd. for $C_{26}H_{41}O_8N$: C, 63.07; H, 8.34; N, 2.83; 3-OCH_3, 18.79; (N)-C_2H_5, 5.86; $COCH_3$, 8.68%.

This base, monoacetyllucaconine, was easily soluble in methanol and in ethanol and moderately so in benzene but sparingly so in water and in petroleum ether.

Perchlorate.—m. p. 202~202.5° (decomp.).

Anal. Found: Cl, 5.85. Calcd. for $C_{26}H_{41}O_8N \cdot HClO_4$: Cl, 5.95%.

Hydrobromide.—m. p. 190~191° (decomp.).

Anal. Found: H_2O, 2.42. Calcd. for $C_{26}H_{41}O_8N \cdot HBr \cdot 3/4H_2O$: H_2O: 2.29%.

Anal. (anhydrous) Found: Br, 13.21. Calcd. for $C_{26}H_{41}O_8N \cdot HBr$: Br, 13.85%.

Hydrolysis of Monoacetyllucaconine.— After monoacetyllucaconine was hydrolyzed with 0.5 N ethanolic potassium hydroxide, a crystalline substance was obtained. After recrystallization from ethanol, it was identified as lucaconine by the mixed melting point test.

Anal. Found: C, 63.34; H, 8.77. Calcd. for $C_{24}H_{39}O_7N$: C, 63.55; H, 8.45%.

Acetic acid produced on hydrolysis of monoacetyllucaconine was identified as silver salt.

Anal. Found: Ag, 64.67. Calcd. for CH_3CO_2Ag: Ag, 64.64%.

Diacetyllucaconine (III). — *a) From Lucaconine (I).*—Lucaconine was heated in acetic anhydride for 30 min., and the reaction mixture was treated in the usual manner. After recrystallization from dilute ethanol, diacetyllucaconine was obtained in colorless needles, m. p. 124°, $[\alpha]_D^{16}$+15.3° (94% ethanol).

Anal. Found: C, 62.40; H, 8.01; N, 2.69; $COCH_3$, 15.93. Calcd. for $C_{28}H_{43}O_9N$: C, 62.55; H, 8.05; N, 2.61; 2-$COCH_3$, 15.9%.

b) From Monoacetyllucaconine (II).—Upon the same treatment as in the case of lucaconine described above, monoacetyllucaconine afforded the same diacetyllucaconine, m. p. and mixed m. p. 124°.

After being heated at 145° for 10 min. under reduced pressure (1×10^{-5} mmHg), diacetyllucaconine was recovered unchanged.

Hydrolysis of Diacetyllucaconine (III).— Diacetyllucaconine was hydrolyzed by heating with 0.5 N ethanolic potassium hydroxide. After removal of most of the ethanol, the reaction mixture was extracted with chloroform and then the chloroform extract was evaporated to give lucaconine, which melted at 198° after recrystallization.

Anal. Found: C, 63.58; H, 8.67; N, 3.44. Calcd. for $C_{24}H_{39}O_7N$: C, 63.55; H, 8.45; N, 3.09%.

Department of Chemistry
Faculty of Science
Hokkaido University
Sapporo

The Molecular Cross-sectional Areas for the Determination of Specific Surface Areas of Solids. I. Carbon Black

By Kumasaburo KODERA and Yoshito ONISHI

(Received September 11, 1958)

Various methods have been developed to estimate the specific surface areas of solids from the theory of physical adsorption. Among them, most widely used is the Brunauer-Emmett-Teller, or B. E. T. method[1]. In this method, the number of adsorbed molecules necessary to cover the surface of 1 g. of a solid completely with a monomolecular layer is evaluated by so-called B. E. T. equation, i. e.,

$$\frac{P}{V(P_s-P)} = \frac{1}{V_mC} + \frac{(C-1)}{V_mC}\cdot\frac{P}{P_s} \qquad (1)$$

where P is the equilibrium pressure, P_s the saturation pressure of the adsorbate gas, V the volume of the gas adsorbed at S. T. P., V_m that necessary to cover the surface with a monomolecular layer, and C a constant.

Specific surface area is then obtained by multiplying V_m with the molecular cross-sectional area, σ, which is given by the following equation:

$$\sigma = 1.091(M/N\rho)^{2/3} \qquad (2)$$

where M is the molecular weight, ρ the density in the liquid (or solid) state of the adsorbate, and N Avogadro number. If the number of molecules in a monomolecular layer and the cross-section obtained above were correct, the calculation would give an absolute surface area, and the values obtained by different adsorbates should agree. But it is well known, generally, that this is not the case. For instance, Jacobs and Tompkins[2] stated that most adsorbates yield surface areas that require multiplication by a factor of between 1.2 and 1.5, and in extreme cases 2 or 3, to give areas agreeing with those calculated from the nitrogen isotherms. This disagreement may arise from either of two reasons: (1) the B. E. T. equation cannot be applied satisfactorily for the isotherms; and (2) equation 2 for σ fails to give a correct cross-section of an adsorbate molecule on the surface. Existence of chemisorption, active spots, and pores or cracks on the surface mainly affects the type of isotherm while packing of adsorbate molecules on the surface affects σ because the factor 1.091 in equation 2 is calculated from the assumption that the adsorbate molecules on the surface is spherical closest packing, i. e., three dimensionally 12 co-ordination and two dimensionally 6 co-ordination. Therefore, it is very difficult to know the absolute value of the surface area by this method. Thus, to compare surface areas using different gases, relative values of cross-sections should be determined beforehand.

On the other hand, Harkins and Jura[3] have developed the absolute calorimetric method to measure the absolute surface area without the knowledge of the cross-section of the adsorbate molecule. But this method has not been employed generally, because it can not be applied to solids which have pores and cracks and the method of measurement is so difficult that its applicability is rather limited.

Livingston[4] examined published data about the measurements of the specific surface areas of oxides by the B. E. T. method and assigned the cross-sections of adsorbate molecules which might give the consistent areas for oxides. He took the case of adsorption of nitrogen at $-195°$ as a standard process and assigned the value 15.4 Å^2 for the cross-section of a nitrogen molecule instead of widely used value, 16.2 Å^2, obtained from equation 2 using liquid density of nitrogen. Cross-sections of the other gas molecules were, then, determined so as to give equal surface area with nitrogen. These values are shown in Table V, column 5. These values, however, can not necessarily give consistent surface areas for other solids than oxides. In the experiments described below, adsorption of several gases on carbon black samples was measured by the same

1) S. Brunauer, P. H. Emmett and E. Teller, *J. Am. Chem. Soc.*, **60**, 301 (1938).

2) P. W. M. Jacobs and F. C. Tompkins, "Chemistry of the Solid State", edited by W. E. Garner, Butterworth Scientific Publications, London (1955), p. 91.

3) W. D. Harkins and G. Jura, *J. Am. Chem. Soc.*, **66**, 1362 (1944).

4) H. K. Livingston, *J. Colloid Sci.*, **4**, 447 (1949).

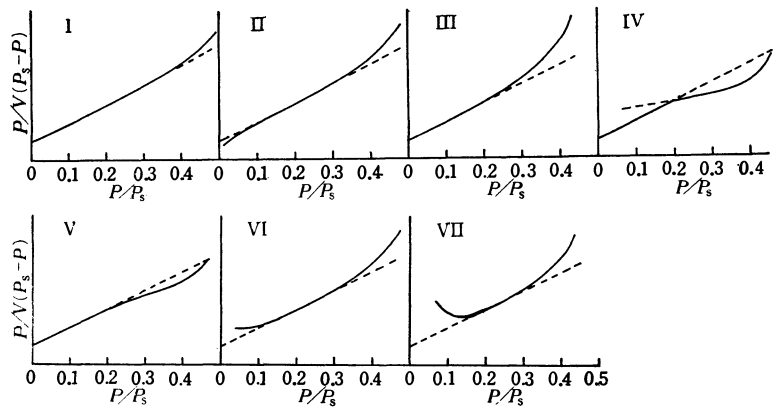


Fig. 1. Types of B.E.T. curves.

apparatus under similar experimental conditions. The specific surface areas of the adsorbents were then calculated and by comparing them with each other and with the values obtained from the electron microscopy, and taking into consideration of the two dimensional van der Waals' constant of argon, the molecular cross-section for each adsorbate gas which would give consistent surface area was determined. Gases were also examined to discover whether they were suitable for this purpose or not.

Experimental Method and Results

A series of 8 commercial carbon blacks listed in column 2, Table I, were used in this experiment. Nitrogen, argon, oxygen, carbon dioxide and *n*-butane were chosen as adsorbate gases.

The apparatus for the adsorption measurement was an ordinary volumetrical type. Temperatures of the adsorbents were measured by a vapor-pressure thermometer with suitable vapors. Samples of carbon black were heated at 200°C in the apparatus and evacuated until pressure in the apparatus reached 1×10^{-5} mmHg every time before the adsorption was measured. In most cases adsorption isotherms were taken between the relative pressures of 0.02 to 0.35, and in some cases up to 0.90. Measured values of $P/V(P_s-P)$ were plotted as a function of P/P_s, according to equation 1. Curves obtained were classified in 7 types as shown in Fig. 1.

Curves I and III have similar forms, but the former has a longer linear portion which extends over 0.35 of P/P_s. Curve II is the most general form which has the linear part from 0.05 to 0.2 or more, and below 0.5 deflects downwards. Curves IV to VII are of special types which appear in a few cases.

In Table I, types of curves obtained are listed together with the appearance of the hysteresis in the measured pressure range.

V_m was calculated from the linear parts of these curves and shown in Table II. From these values of V_m, specific surface areas of the adsorbent were calculated using molecular cross-sections in column 4, Table V, which were calculated by equation 2 using the liquid density of each gas at measured temperatures[5]. The values are shown in Table III. The ratio S_{N_2}/S is that between surface area measured by nitrogen and that of the other gas. Surface areas measured by the absolute method by Okuda and Tanaka[6] and from electron microscopy by Suito and Arakawa[7] are shown for comparison. It should be remembered that the latter values were calculated from average particle diameter $d_1=\sum nd/\sum n$, assuming the density of carbon black to be 1.8, whereas values from the adsorption correspond to $S=K(\sum nd^2/\sum nd^3)$, where K is a shape factor.

Discussion

As are shown in Table III, the ratios of surface area by nitrogen adsorption to that by argon adsorption (S_{N_2}/S), for both adsorption temperatures are 1.14 and their standard deviations are small. For oxygen and *n*-butane, the standard deviations in area ratios are greater and for carbon dioxide the greatest, even with the exclusion of No. 6.

Applicability of the B.E.T. isotherm can be judged from the range of the linear part on the curve. From Fig. 1 and Table I, it is seen that argon (−183°C) and oxygen show largest range of linear part and then follow nitrogen and argon (−196°C). Of

5) P. H. Emmett and S. Brunauer, *J. Am. Chem. Soc.*, **59**, 1153 (1937).

6) S. Okuda and N. Tanaka. The report to be published soon in *J. Ceramic Association, Japan.* (*Yogyo Kyokai Shi*).

7) E. Suito and M. Arakawa, "Collaborative Research Reports of the Ministry of Education." (Chemistry), p. 120 (1956). Data given by the authors were average particle diameter d_1, from which the surface areas shown in the table were calculated.

TABLE I
TYPES OF B. E. T. CURVES

No.	Black	$N_2(-196°C)$		Ar(−196°C)		Ar(−183°C)		$O_2(-183°C)$		$CO_2(-78°C)$		n-C_4H_{10}(0°C)	
		Type	Hyst.	Type	Hyst.	Type	Hyst.	Type	Hyst.	Type	Hyst.	Type	Hyst
1	Peerless II A	III	−	III	−	III	−	III	−	III	−	III	+
2	Philblack-E	I	−	I	−	I	−	I	−	II	+	I	−
3	Tokai S. 285	III	−	III	−	II	−	I	−	II	+	I	+
4	Denka 2000	III	−	III	−	I	−	I	−	II	−	I	−
5	Mi-ike 20	II	−	I	−	I	−	II	−	II	−	IV	+
6	P-33	III	−	I	−	I	−	II	−	II	−	II	+
7	Denka granular	IV	−	V	−	II	−	II	−	VII	−	II	+
8	Witoco	III	−	III	−	I	−	II	−	II	−	II	+

TABLE II
VALUES OF V_m

No.	N_2 cc./g.	Ar(−196°C) cc./g.	Ar(−183°C) cc./g.	O_2 cc./g.	CO_2 cc./g.	n-C_4H_{10} cc./g.
1	80.7	85.4	80.3	89.6	58.5	27.5
2	30.6	30.6	29.5	32.4	19.6	11.3
3	21.1	22.0	21.2	23.8	14.5	7.58
4	9.93	10.1	9.76	10.0	6.21	3.83
5	3.97	4.15	3.88	3.88	2.69	1.51
6	3.67	3.66	3.62	3.53	1.12	1.38
7	14.6	16.0	14.7	15.2	10.3	5.98
8	27.1	27.1	26.2	33.1	20.8	9.23

TABLE III
SPECIFIC SURFACE AREAS MEASURED BY VARIOUS GASES

No.	$N_2(-196°C)$	Ar(−196°C)		Ar(−183°C)		$O_2(-183°C)$		$CO_2(-78°C)$		n-C_4H_{10}(0°C)		Electron micro-scope	Absolute method
	S_{N_2} $m^2/g.$	S $m^2/g.$	S_{N_2}/S	S $m^2/g.$	S_{N_2}/S	S $m^2/g.$	S_{N_2}/S	S $m^2/g.$	S_{N_2}/S	S $m^2/g.$	S_{N_2}/S		
1	351.5	317.3	1.11	311.0	1.13	340.0	1.03	267.7	1.31	237.0	1.48	99.0	
2	133.0	113.4	1.17	114.2	1.16	123.0	1.08	89.7	1.47	97.2	1.38	112.2	
3	91.9	81.6	1.13	81.9	1.12	90.3	1.02	66.4	1.38	65.4	1.41	60.6	46.4
4	43.2	37.6	1.15	37.8	1.14	37.9	1.14	28.4	1.52	33.0	1.31	81.3	
5	17.4	15.4	1.13	15.0	1.16	14.7	1.18	12.3	1.41	13.0	1.34	17.9	
6	16.0	13.6	1.18	14.0	1.14	13.4	1.19	5.1	(3.14)	11.9	1.35	22.8	
7	63.6	59.2	1.08	57.0	1.12	57.6	1.10	47.0	1.35	51.6	1.23	49.2	
8	118.0	100.5	1.17	101.4	1.16	125.5	0.94	95.3	1.34	79.6	1.48	91.6	109
Avarage			1.14		1.14		1.09		1.38		1.37		
Standard deviation			0.03		0.02		0.08		0.09		0.08		

The value in parentheses is excluded from the average.

TABLE IV
COMPARISON OF SURFACE AREA FROM B. E. T. METHOD AND ELECTRON MICROSCOPY

No.	N_2	Ar(−196°C)	Ar(−183°C)	O_2	CO_2	n-C_4H_{10}
1	(3.54)	(3.20)	(3.14)	(3.44)	(2.10)	(2.40)
2	1.18	1.01	1.02	1.10	0.80	0.87
3	1.52	1.35	1.35	1.49	1.10	1.08
4	(0.53)	(0.46)	(0.46)	(0.47)	0.35	(0.41)
5	0.97	0.86	0.84	0.82	0.69	0.73
6	0.70	0.60	0.61	0.59	(0.22)	0.52
7	1.29	1.20	1.16	1.17	0.96	1.05
8	1.29	1.10	1.11	1.37	1.04	0.87
Average	1.16	1.02	1.02	1.09	0.823	0.853
Mol. cross-section	14.0	13.5	14.2	12.9	20.7	37.6 Å^2

these two, argon (−196°C) has longer linear portions though not listed in the table. By *n*-butane, linear parts are also large but in most cases isotherms show hysteresis. Carbon dioxide is inferior to the other gases. Among the adsorbents used, No. 7 exhibits anomalous isotherms for all gases.

From the above facts, nitrogen and argon turned out to be the most suitable adsorbates for the surface area measurement of carbon black, while oxygen and *n*-butane are seen to be somewhat inferior to the former two. Carbon dioxide is not suitable for this purpose. From the surface ratio values in Table III, except for No. 6 by carbon dioxide, it is possible to eliminate the differences in surface areas measured by different gases by assigning a proper molecular cross-section for each gas. In doing this, a gas which might be considered to give the specific surface area nearest to the absolute surface should be chosen as a standard gas; then, the cross-section of other gases could be determined to give the equal surface area as the standard gas. Generally, nitrogen is used for the B. E. T. method with the cross-section of 16.2 Å^2, but it generally gives a larger surface area when compared with that by the other gases and also with the value obtained by electron microscopy or the absolute method. To compare surface area values by the B. E. T. method with those by electron microscopy, ratio of the values by the two methods was calculated for each carbon black with various gases and listed in Table IV*. It is seen from the table that the agreement of values between the two methods is best for argon, whereas nitrogen adsorption gives somewhat greater values. The molecular cross-section of each gas used for the evaluation of the surface area was divided by the respective average ratio and shown in the bottom of the table. These are cross-sections which will give surface areas in agreement with those from electron microscopy. For carbon black, Anderson and Emmett[8] concluded that 16.2 Å^2 is better than 13.8 Å^2 calculated from the solid density. On the other hand, Arnell and Henneberry[9] compared the surface areas of carbon blacks measured by permeability, electron microscopy, and the B. E. T. method using nitrogen cross-section of 16.2Å^2. The results revealed that the surface areas measured by the B. E. T. method was 30% larger in average than those by the other methods (except for samples which had pores and cracks as mentioned by Arnell et al.).

From the above considerations, the value 16.2 Å^2 for nitrogen cross-section would be too large. The concept of two dimensional gas of adsorbed molecules suggests that the molecular cross-section should be nearly equal to the two-dimensional van der Waals' constant[10]. For nitrogen this value is 15.4 Å^2; Livingston used this value as a standard and estimated the cross-section of other gases from this value. In the above experiment both nitrogen and argon proved to be suitable for this method, but from Table IV, it is seen that argon gives surface areas more consistent with those by electron microscopy than nitrogen does. In addition, the following facts point to the superiority of argon to nitrogen, i. e., in the plot of equation 1, generally, the former has longer linear part than the latter. Moreover, argon shows no chemisorption and exhibits more ideal packing state on the surface as it consists of monoatomic molecules and has no quadruple moment which nitrogen has to some extent[11]. The fact that the agreement between the two dimensional van der Waals' constant and the value from the equation 2 is better in argon than in nitrogen, seems to show that the former exhibits more ideal packing state on the surface than the latter does. Therefore, argon was taken as a standard. For the molecular cross-section of argon, three values were obtained, i. e., 13.5 Å^2 from comparison with electron microscopy, 13.8 Å^2 from equation 2 using liquid density at −195°C, and 13.6 Å^2 from the van der Waals' constant. Among these three values, 13.8 Å^2 from equation 2 was employed as a standard, because the differences among these values are rather small and there is no serious reason to change the generally employed value from equation 2. The molecular cross-section thus determined, those given by Livingston,

* Values in parentheses are the largest and the smallest ratios for each gas and are excluded from the average, because corresponding samples might have some undesirable surface states or particle size distributions for this comparison.

8) R. B. Anderson and P. H. Emmett, *J. Applied Phys.*, **19**, 367 (1948).

9) J. C. Arnell and G. O. Henneberry, *Canadian J. Res.*, **A, 26**, 29 (1948).

10) J. H. de Boer, "Dynamical Character of Adsorption", Oxford (1953), p. 172.

11) W. V. Smith and R. Howard, *Phys. Rev.*, **77**, 132 (1950).

TABLE V
MOLECULAR CROSS-SECTIONAL AREAS

Gas	Temp.	van der Waals' const.	Eq. 2 Liq. state.	Livingston's	Present Authors'
N_2	−196°C	15.4 Å²	16.2 Å²	15.4 Å²	14.2 Å²
Ar	−196	13.6	13.8	14.6	13.8
Ar	−183	13.6	14.4	15.5	14.4
O_2	−183	13.5	14.1	14.6	13.5
CO_2	− 78	16.5	17.0	19.5	20.8
n-C_4H_{10}	0	33.0	32.1	44.6	38.6

TABLE VI
SPECIFIC SURFACE AREAS

No.	N_2 S m²/g.	Ar(−196°C) S m²/g.	Ar(−183°C) S m²/g.	O_2 S m²/g.	CO_2 S m²/g.	n-C_4H_{10} S m²/g.	Elec. micro.	Abs. method
1	304.0	317.3	311.0	325.0	327.0	285.0	99.0	
2	116.7	113.4	114.2	117.7	109.6	116.7	112.2	
3	80.5	81.6	81.9	86.3	81.1	78.8	60.6	46.4
4	37.9	37.6	37.8	36.3	34.7	39.7	81.3	
5	15.3	15.4	15.0	14.1	15.0	15.6	17.9	
6	14.0	13.6	14.0	12.8	6.2	14.3	22.8	
7	55.8	59.2	57.0	55.1	57.5	62.1	49.2	
8	103.5	100.5	101.4	120.0	116.6	95.8	91.6	109

ordinary values from equation 2 and the two dimensional van der Waals' constants are shown in Table V. It is seen that the values agree surprisingly well with those in Table IV except oxygen. The value for oxygen agrees with that of van der Waals' constant. The value for nitrogen becomes smaller than that from equation 2 and of Livingston. Livingston said that according to the results of Arnell and Henneberry for 9 carbon blacks, nitrogen adsorption surfaces are about 12% higher than the values by permeability and electron microscopy. It is not clear how Livingston estimated the value of 12%, but if nitrogen cross-section 16.2 Å² used by Arnell and Henneberry is reduced by 12%, it gives 14.5 Å² which nearly agrees with the present value.

The specific surface areas calculated by these cross-sections are listed in Table VI. Comparison with the values by the absolute method shows good agreement in case of No. 8, while in No. 3, the absolute method gives a far smaller value. The electron microscopy also gives a smaller value for the latter sample. If there were small pores and cracks on the surface of the latter, unobservable by the electron microscope, these would be covered by the adsorbate in the case of the absolute method, so that both methods might give lower values than the B. E. T. method does. Other small values by electron microscopy are also explainable by the existence of pores and cracks. Thus, Nos. 1, 3 and 8 show somewhat lower values also by n-butane adsorption which suggest the existence of small pores, into which rather large n-butane molecules can not penetrate.

In electron microscopy, as is described above, the surface areas were calculated from $d_1=\sum nd/\sum n$, assuming all the particles to be spherical. Calculation from d_1 gives correct surface area only when all the particles have the same size. Generally, this is not the case, and owing to the particle size distribution, this calculation gives too large a surface area. Moreover, as was pointed out by Arnell and Henneberry, if a small number of large particles were overlooked in measuring particle size by the electron microscope, surface area estimated from the results would give also higher value. Therefore, larger values than those by the B. E. T. method are not unexplainable.

No. 6 shows a remarkably small surface for carbon dioxide. The surface area of this sample for carbon dioxide increased as the temperature of heating before the adsorption rose above 200°C, although it remained constant for nitrogen and argon. This effect of heating temperature was seen only in this sample. This might be explained as the heat treatment above 200°C changed surface state of this sample, and also changed the state of adsorption of carbon dioxide molecules, but the

adsorption of nitrogen and argon, which should be purely physical, would not be affected.

Conclusions

For the measurement of the specific surface areas of solid adsorbents, argon and nitrogen are most suitable for adsorbate gases. Oxygen and *n*-butane are also applicable but carbon dioxide may give unreliable results in some cases. The cross-sectional areas of adsorbed molecules listed in Table V, column 6, were determined to give consistent surface areas for different gases. The anomaly for carbon dioxide may be explained by the surface state of the carbon black.

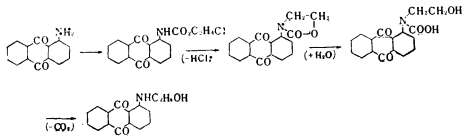
Department of Chemistry, Faculty of Industrial Arts, Kyoto Technical University, Sakyo-ku, Kyoto

*Studies on 3-(Anthraquinon-1-yl)oxazolidin-2-ones. I. 3-(Methylanthraquinon-1-yl)oxazolidin-2-ones and Their Related Compounds**

By Kō NAIKI

(Received September 18, 1958)

In a previous paper[1], it was reported that 1-aminoanthraquinone reacted with 2-chloroethyl chloroformate and formed 2-chloroethyl anthraquinon-1-yl carbamate. The chloroethyl anthraquinonyl carbamate was converted into 1-*N*-2-hydroxyethylaminoanthraquinone by the action of potassium hydroxide, and 3-(anthraquinon-1-yl)oxazolidin-2-one could not be separated from reaction mixture by fractional recrystallization. The reactions are explained as follows (Scheme I).



Sheme 1

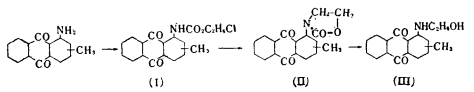
In another paper[2], it was found that 2-chloroethyl anthraquinon-1-yl carbamates which contain 2-substituent in anthraquinone nucleus were converted into 2′-substituted 3-(anthraquinon-1-yl)oxazolidin-2-ones by the action of potassium hydroxide.

The result of these investigations suggests the existence of a steric hindrance of 2′-substituent in the anthraquinonyl-oxazolidinones which plays an important part in the stability of the anthraquinonyl-oxazolidinones in aqueous solution of potassium hydroxide. Similarly, an electronic effect of substituent should be considered to be important and this is being investigated in the author's laboratory.

In the present study, 3-(methylanthraquinon-1-yl)-oxazolidin-2-ones, 1-*N*-2-hydroxyethylaminomethylanthraquinones and 2-chloroethyl methylanthraquinon-1-yl carbamates were synthesized and the effect of the methyl group by its position on the stability of the anthraquinonyloxazolidinones was investigated. None of them has yet been prepared, so far as is known.

Preparation and Results

The syntheses of the compounds were carried out according to the following processes (Scheme II).



Scheme II

2-Chloroethyl 2-methylanthraquinon-1-yl carbamate(Ia), 3-methylanthraquinon-1-yl carbamate(Ib) and 4-methylanthraquinon-1-yl carbamate(Ic) were obtained from the corresponding 1-aminomethylanthraquinones by the action of 2-chloroethyl

* Presented at the 11th Annual Meeting of the Chemical Society of Japan, April, 1958.

1) K. Naiki, *J. Soc. Org. Syn. Chem. Japan*, (*Yūki Gōsei Kagaku Kyokaishi*), **12**, 364 (1954).

2) K. Naiki, Ibid., **14**, 84 (1956).

chloroformate in the presence of sodium carbonate in boiling xylene. 1-*N*-2-Hydroxyethylamino-2-methylanthraquinone(IIIa), 1-*N*-2-hydroxyethylamino-3-methylanthraquinone(IIIb) and 1-*N*-2-hydroxyethylamino-4-methylanthraquinone(IIIc) were obtained from the corresponding 2-chloroethyl methylanthraquinonyl carbamates by the action of 20% aqueous solution of potassium hydroxide at 105~107°. Mixtures of the hydroxyethylaminomethylanthraquinones, the 3-(methylanthraquinon-1-yl)-oxazolidin-2-ones(II) (IIa, 2′-methyl; IIb, 3′-methyl; IIc, 4′-methyl) and the unchanged 2-chloroethyl methylanthraquinonyl carbamates were obtained from the corresponding 2-chloroethyl methylanthraquinon-1-yl carbamates by the action of 20% aqueous solution of potassium hydroxide at 98~99° for 1 hour.

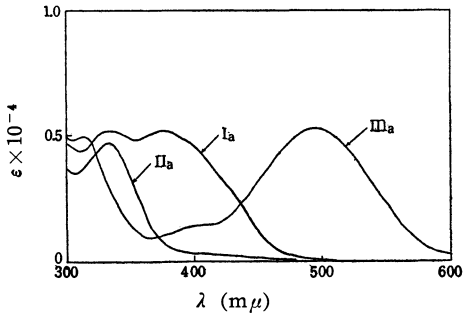


Fig. 1. Absorption spectra of the derivatives of 1-amino-2-methylanthraquinone (in toluene)
Ia: 2-Chloroethyl 2-methylanthraquinon-1-yl carbamate
IIa: 3-(2-Methylanthraquinon-1-yl) oxazolidin-2-one
IIIa: 1-*N*-2-Hydroxyethylamino-2-methylanthraquinone

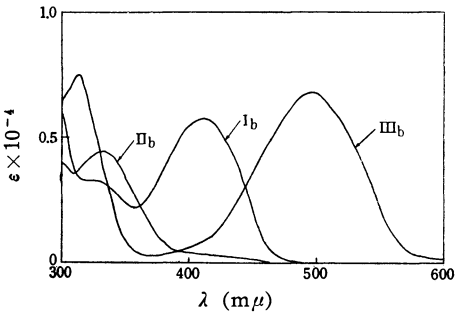


Fig. 2. Absorption spectra of the derivatives of 1-amino-3-methylanthraquinone (in toluene)
Ib: 2-Chloroethyl 3-methylanthraquinon-1-yl carbamate
IIb: 3-(3-Methylanthraquinon-1-yl) oxazolidin-2-one
IIIb: 1-*N*-2-Hydroxyethylamino-3-methylanthraquinone

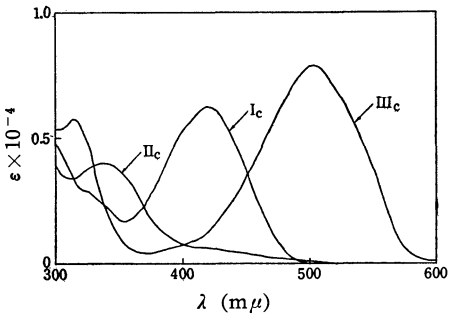


Fig. 3. Absorption spectra of the derivatives of 1-amino-4-methylanthraquinone (in toluene)
Ic: 2-Chloroethyl 4-methylanthraquinon-1-yl carbamate
IIc: 3-(4-Methylanthraquinon-1-yl) oxazolidin-2-one
IIIc: 1-*N*-2-Hydroxyethylamino-4-methylanthraquinone

The proportion of the constituents of the reaction mixtures was determined by spectrophotometry. These results are shown in Table I. Each of the constituents was separated from the reaction mixtures by column chromatography from benzene on alumina.

Absorption spectra of the compounds obtained above are shown in Figs. 1, 2 and 3, respectively. Absorption maxima and extinction coefficients are given in Table III.

Discussion

Effects of the Methyl Group According to its Position on the Stability of the Methylanthraquinonyloxazolidinones.— On account of aqueous dispersion of solid materials, various difficulties may be introduced in the discussion when their stabilities are compared with one another. Nevertheless, it may probably be considered that there exists some close relation between the stability and the factors such as electronic and steric effects of groups. Table I shows clearly that the 2′-methyl group increases the stability of

TABLE I
THE PROPORTION OF THE CONSTITUENTS OF THE REACTION PRODUCT FROM THE 2-CHLOROETHYL METHYLANTHRAQUINON-1-YL CARBAMATES AND 20% AQUEOUS SOLUTION OF POTASSIUM HYDROXIDE*

Position of CH_3	I %	II %	III %
2	7	77	16
3	13	23	64
4	14	51	35

* Determined by the spectrophotometry.

the anthraquinonyloxazolidinone in aqueous solution of potassium hydroxide. In other words, it shows the existence of steric hindrance of the methyl group in the hydrolysis process (cf. Scheme I).

The reaction mixture obtained from the chloroethyl methylanthraquinonyl carbamates and potassium hydroxide can be separated into the constituents by the column chromatography from benzene on alumina. It is observed, however, that the unreacted 2-chloroethyl methylanthraquinonyl carbamates are gradually converted into the corresponding methylanthraquinonyloxazolidinones on alumina in the column. For this reason, the use of the column chromatography to determine exactly the proportion of the constituents is not desirable in a strict sense. Thus, the determination of the proportion of the constituents was attempted by the spectrophotometry. Since the principal absorption bands of the constituents are apart from one another as shown in Figs. 1, 2 and 3, the determination of the proportion of the constituents was carried out exactly.

The Effect of the 2-Methyl Group on Absorption Spectra.—A marked difference in intensity of light absorption between mono- and dimethylated 1-aminoanthraquinones was explained by the steric hindrance of the *N*-methyl group with the adjacent carbonyl group[3]. Accordingly, it may be expected that another substituent at 2-position provides a further steric effect. This expectation agrees with the experimental result of the 1-amino-2-methoxyanthraquinones shown in Table II[4].

TABLE II
ABSORPTION SPECTRA OF 1-AMINO-2-METHOXYANTHRAQUINONES

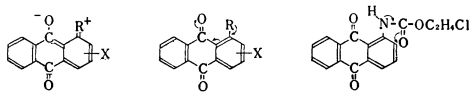
Compound	Principal absorption band (in ethanol)
1-Amino-2-methoxyanthraquinone	478 mμ
1-Methylamino-2-methoxyanthraquinone	520 mμ
1-Dimethylamino-2-methoxyanthraquinone	506 mμ

It is now apparent that the steric hindrance of the methyl group of the compounds discussed here plays an important part. It has been known that the first absorption band of the 1-substituted anthraquinones can be attributed to resonance hybrid of the normal and the extreme ionic form (IV). The explanation of the formation of the ionic form is given by the well-known mechanism (V) which shows a mesomeric shift of the electrons from the 1-substituted group to the carbonyl oxygen atom. Thus, the contribution of the ionic form will be further increased by the 1-substituent with the greater electron-donating ability, resulting in the stronger the donating power, the longer the wave length of absorption maxima. This is illustrated in the case of the hydroxyethylaminoanthraquinones (Table III). However, in the 2-chloroethyl anthraquinonyl carbamates, another electron shift may be introduced in the opposite sense(VI). This alternative effect will counter the shift of the electrons to the anthraquinone ring and lower the wave length of absorption.

TABLE III
ABSORPTION SPECTRA OF 1-AMINOMETHYLANTHRAQUINONES*

Compound	$\lambda_{max.}$ (mμ)		$\varepsilon_{max.} \times 10^{-4}$	
Ia	336	378	0.518	0.520
Ib	320	414	0.335	0.580
Ic	~325	421	(0.271)	0.618
IIa	332	~400	0.469	(0.021)**
IIb	333	~405	0.443	(0.040)**
IIc	337	~420	0.388	(0.052)**
IIIa	312	492	0.501	0.518
IIIb	313	497	0.768	0.687
IIIc	315	504	0.580	0.792

Bracketed values are absorption bands of low intensity.
~ denotes point of inflexion.
* Measured by a Shimadzu QB-50 Electrophotometer. Solvent: toluene; concn. 1×10^{-4} mol./l.
** Concn. 1×10^{-3} mol./l.



The further effect will come into play if such a group as methyl is introduced in the 2-position, for the steric hindrance from both the carbonyl and the methyl group forces atoms attached to the substituting group out of the plane of the anthraquinone nucleus. Consequently, in the case of the spectrum of 2-chloroethyl 2-methylanthraquinon-1-yl carbamate, the intensity of the corresponding absorption band (336 mμ) to that of anthraqinone becomes stronger and the primary band (378 mμ)

3) R. H. Peters et al., *J. Chem. Soc.*, **1953**, 2101.
4) K. Naiki, *J. Org. Syn. Chem. Japan* (*Yūki Gōsei Kagagu Kyokaishi*), 11, 113 (1953).

becomes weaker than the other methylanthraquinonyl carbamates. If a more bulky group such as the oxazolidinonyl group is at the 1-position of the anthraquinone nucleus, the steric effect inhibits the shift of the electrons from the nitrogen atom to the anthraquinone nucleus, and spectra of the anthraquinonyloxazolidinones are very similar to that of anthraquinone itself.

In the case of the methylanthraquinonyloxazolidinones, it seems that the 2-methyl group in the anthraquinone nucleus increases the steric inhibition and the absorption intensity at about 400 mμ becomes weaker than the other methylanthraquinonyloxazolidinones.

Experimental

2-Chloroethyl 2-Methylanthraquinon-1-yl carbamate (Ia).—The synthesis of the compound was reported in the previous paper[2]. The product was recrystallized from ethanol, giving yellow needles, m. p. 173~174°.

2-Chloroethyl 3-Methlanthraquinon-1-yl carbamate (Ib). — A mixture of 1.08 g. of 1-amino-3-methylanthraquinone (m. p. 185~189°), 0.76 g. of 2-chloroethyl chloroformate, 0.54 g. of sodium carbonate and 70 ml. of xylene was refluxed with stirring for 2 hours. Insoluble substance was removed by hot filtration and the filtrate was evaporated to a volume of about 20 ml. for crystallization. Yield, 1.27 g. (83% of the theory) of yellow needles, m. p. 198~200°. The product was recrytallized from ethanol, giving yellow needles, m. p. 201~202°. *Anal.* Found: N, 4.34. Calcd. for $C_{18}H_{14}O_4NCl$: N, 4.07%.

2-Chloroethyl 4-Methylanthraquinon-1-yl carbamate (Ic). — A mixture of 1.88 g. of 1-amino-4-methylanthraquinone (m. p. 180~182°), 1.24 g. of 2-chloroethyl chloroformate, 0.95 g. of sodium carbonate and 18 ml. of xylene was refluxed with stirring for 6 hours. The insoluble substance was removed by hot filtration and the filtrate was cooled. The crystal formed was collected and dried. Yield, 2.45 g. (90% of the theory) of yellow needles, m. p. 187~188°. It was recrystallized from ethanol, giving yellow needles, m. p. 190~191°. *Anal.* Found: N, 4.25. Calcd. for $C_{18}H_{14}O_4NCl$: N, 4.07%.

Behavior of 2-Chloroethylmethylanthraquinon-1-yl carbamates on Alumina.—2-Chloroethyl 3-methylanthraquinon-1-yl carbamate (0.40g., m. p. 198~199°) was dissolved in benzene, then adsorbed on alumina, stood overnight and eluted by the use of ethanol. The substance (0.30 g., m. p. 213~215°), consisting of 3-(3-methylanthraquinon-1-yl) oxazolidin-2-one and unchanged 2-chloroethyl 3-methylanthraquinon-1-yl carbamate, was obtained. It was separated into the constituents by means of chromatography on alumina from benzene. 2-Chloroethyl 3-methylanthraquinon-1-yl carbamate passed through the column; 3-(3-methylanthraquinon-1-yl) oxazolidin-2-one was eluted by the use of ethanol. Pure 3-(3-methylanthraquinon-1-yl) oxazolidin-2-one was obtained.

Similar treatment of 2-chloroethyl 2-methylanthraquinon-1-yl carbamate and 4-methylanthraquinon-1-yl carbamate gave 3-(2-methylanthraquinon-1-yl) oxazolidin-2-one and 3-(4-methylanthraquinon-1-yl) oxazolidin-2-one, respectively.

3-(2-Methylanthraquinon-1-yl)oxazolidin-2-one (IIa).—The synthesis was reported in the previous paper[2]. Pale yellow needles, m. p. 226~227°.

3-(3-Methylanthraquinon-1-yl) oxazolidin-2-one (IIb).—A mixture of 1.00 g. of finely powdered 2-chloroethyl 3-methylanthraquinon-1-yl carbamate (m. p. 198~199°) and 30 g. of 20% aqueous solution of potassium hydroxide was heated in a boiling water bath with vigorous stirring for 1 hour. After being diluted with water, the precipitate was collected, washed with water and dried. Yield, 0.82 g. of reddish powder. The product, consisting of unchanged 2-chloroethyl 3-methylanthraquinon-1-yl carbamate, 3-(3-methylanthraquinon-1-yl) oxazolidin-2-one and 1-*N*-2-hydroxyethylamino-3-methylanthraquinone, was dissolved in benzene and chromatographed on alumina. 1-*N*-2-Hydroxyethylamino-3-methylanthraquinone is most strongly adsorbed and 3-(3-methylanthraquinon-1-yl) oxazolidin-2-one is more strongly adsorbed than 2-chloroethyl 3-methylanthraquinon-1-yl carbamate. The red band, containing 1-*N*-2-hydroxyethylamino-3-methylanthraquinone, was eluted by the use of ethanol. Yield, 0.38 g. of red needles, m. p. 234~235°. The pale orange band, containing 3-(3-methylanthraquinon-1-yl) oxazolidin-2-one, was eluted by the use of ethanol. Yield, 0.18 g. of pale orange needles, m. p. 235~236°. It was recrystallized from ethanol, giving pale orange needles, m. p. 235~236°. *Anal.* Found: N, 4.50. Calcd. for $C_{18}H_{13}O_4N$: N, 4.56%. The yellow eluate, containing 2-chloroethyl 3-methylanthraquinon-1-yl carbamate, was evaporated for crystallization. Yield, 0.14 g. of yellow needles, m. p. 198~199°

3-(4-Methylanthraquinon-1-yl) oxazolidin-2-one (IIc).—A mixture of 0.50 g. of finely powdered 2-chloroethyl 4-methylanthraquinon-1-yl carbamate (m. p. 187~188°) and 15 g. of 20% aqueous solution of potassium hydroxide was heated with vigorous stirring in a boiling water bath for 1 hour. After being diluted with water, the precipitate was collected, washed with water and dried. Yield, 0.33 g. of reddish brown powder. It was fractionally recrystallized from ethanol, giving pale brown needles, m. p. 201~202°. *Anal.* Found: N, 4.58. Calcd. for $C_{18}H_{13}O_4N$: N, 4.56%.

The chromatographic separation of the reaction product obtained above, consisting of 1-*N*-2-hydroxyethylamino-4-methylanthraquinone, 3-(4-methylanthraquinon-1-yl) oxazolidin-2-one and unchanged 2-chloroethyl 4-methylanthraquinon-1-yl carbamate, was carried out in the same with the 3-methyl derivative. Yield, 0.100 g. of 1-*N*-2-hydroxyethylamino-4-methylanthraquinone, m. p. 153~154°, 0.130 g. of 3-(4-methylanthraquinon-1-yl) oxazolidin-2-one, m. p. 201~202°, and 0.060 g. of

2-chloroethyl 4-methylanthraquinon-1-yl carbamate, m. p. 189~190°.

Determination of the Proportion of the Constituents of the Reaction Product Obtained from the 2-Chloroethyl Methylanthraquinon-1-yl Carbamates and 20% Aqueous Solution of Potassium Hydroxide.—A mixture of 0.20 g. of finely powdered 2-chloroethyl methylanthraquinon-1-yl carbamate and 6.00 g. of 20% aqueous solution of potassium hydroxide was heated with vigorous stirring in a boiling water bath for 1 hour. After being diluted with water, the precipitate was collected, washed with water and dried. Yield, 0.16 g. of pale red powder, m. p. 192~201°, from 2-chloroethyl 2-methylanthraquinon-1-yl carbamate; 0.15 g. of brownish red powder, m. p. 139~149°, from 2-chloroethyl 3-methylanthraquinon-1-yl carbamate; 0.16 g. of reddish brown powder, m. p. 148~167°, from 2-chloroethyl 4-methylanthraquinon-1-yl carbamate.

The proportion of the constituents of the products obtained above were determined by the use of a Shimadzu QB-50 Electrophotometer. Optical densities (D) of the benzene solutions of the products are shown in Tables IV, V and VI. It was found by simple caluculation that the reaction product obtained from 2-chloroethyl 2-methylanthraquinon-1-yl carbamate contains 21 mg. of 1-*N*-2-hydroxyethylamino-2-methylanthraquinone, 124 mg. of 3-(2-methylanthraquinon-1-yl) oxazolidin-2-one and 12 mg. of 2-chloroethyl 2-methylanthraquinon-1-yl carbamate; the product obtained from 2-chloroethyl 3-methylanthraquinon-1-yl carbamate contains 91 mg. of 1-*N*-2-hydroxyethylamino-3-methylanthraquinone, 33 mg. of

Table IV

Optical densities of the product obtained from 2-chloroethyl 2-methylanthraquinon-1-yl carbamate* and extinction coefficients of the constituents

λ (mμ)	D	$\varepsilon\times10^{-4}$		
		Ia	IIa	IIIa
330	0.670	0.511	0.469	0.346
380	0.086	0.511	0.037	0.109
490	0.128	0.004	0.003	0.518

* Solvent: toluene; conc. 47 mg./l.

Table V

Optical densities of thf product obtained from 2-chloroethyl 3-methylanthraquinon-1-yl carbamate*and extinction coefficients of the constituents

λ (mμ)	D	$\varepsilon\times10^{-4}$		
		Ib	IIb	IIIb
340	0.475	0.318	0.401	0.685
420	0.147	0.538	0.036	0.124
500	0.357	0.005	0.007	0.672

* Solvent: toluene; concn. 48 mg./l.

Table VI

Optical densities of the product obtained from 2-chloroethyl 4-methylanthraquinon-1-yl carbamate* and extinction coefficients of the constituents

λ (mμ)	D	$\varepsilon\times10^{-4}$		
		Ic	IIc	IIIc
340	0.472	0.206	0.378	0.197
420	0.254	0.618	0.051	0.119
500	0.438	0.002	0.015	0.778

* Solvent: toluene; concn. 48 mg./l.

3-(3-methylanthraquinon-1-yl)oxazolidin-2-one and 26 mg. of 2-chloroethyl 3-methylanthraquinon-1-yl carbamate; the product obtained from 2-chloroethyl 4-methylanthraquinon-1-yl carbamate contains 51 mg. of 1-*N*-2-hydroxyethylamino-4-methylanthraquinone, 82mg. of 3-(4-methylanthraquinon-1-yl)oxazolidin-2-one and 27 mg. of 2-chloroethyl 4-methylanthraquinon-1-yl carbamate.

1-*N*-2-Hydroxyethylamino-2-methylnathraquinone (IIIa).—The synthesis was reported in the previous paper[2]. It was purified by means of chromatography from benzene on alumina and recrystallized from toluene, giving red needles, m. p. 141~142°.

1-*N*-2-Hydroxyethylamino-3-methylanthraquinone (IIIb).—A mixture of 1.00 g. of finely powdered 2-chloroethyl 3-methylanthraquinon-1-yl carbamate (m. p. 198~199°) and 30 g. of 20% aqueous solution of potassium hydroxide was refluxed with stirring in an oil bath for 1 hour. After being diluted with water, the precipitate was collected, washed with water, dried and recrystallized from toluene. Yield, 0.67 g. (83% of the theory) of red needles, m. p. 180~181°. It was recrystallized from toluene, giving red needles, m. p. 180.5~181.0°. *Anal.* Found: N, 5.21. Calcd. for $C_{17}H_{15}O_3N$: N, 5.02%.

1-*N*-2-Hydroxyethylamino-4-methylanthraquinone (IIIc).—A mixture of 0.50 g. of finely powdered 2-chloroethyl 4-methylanthraquinon-1-yl carbamate (m. p. 187~188°) and 15 g. of 20% aqueous solution of potassium hydroxide was refluxed with stirring in an oil bath for 1 hour. After being diluted with water, the precipitate was collected, washed with water, dried and recrysatllized from toluene. Yield, 0.30 g. (73% of the theory) of brownish red needles, m. p. 163~164°. It was recrystallized from toluene, giving brownish red needles, m. p. 164~165°. *Anal.* Found: N, 5.04. Calcd. for $C_{17}H_{15}O_3N$: N, 5.02%.

The writer is indebted to Mr. Yoshié Tanizaki for his advice.

The Laboratory of Dyestuff Chemistry
Tokyo Institute of Technology
Meguro-ku, Tokyo

Polyterpenes. II[1]. *Oxidation of Thujopsene with Lead Tetra-acetate**

By Shizuo NAGAHAMA, Hiroshi KOBAYASHI and Saburo AKIYOSHI

(Received September 19, 1958)

It has been reported by Kawamura[2] and recently by Nozoe et al.[3], that thujopsene, the main constituent of Hiba (*Thujopsis dolabrata Sieb. et Zucc.*) wood oil, affords a glycol, m. p. 91°, by the oxidation with permanganate in acetone containing water. On the other hand, the authors obtained a ketonic acid, m. p. 165° as a main product and no glycol was found when the oxidation was carried out in acetone solution without addition of water[1].

To obtain the glycol by an alternate route, oxidation of this sesquiterpene with lead tetra-acetate was attempted. However, contrary to the expectation, a ketone and its enol acetate were found to be the main products.

It is well known that the olefines, when oxidized with lead tetra-acetate, usually give a mixture of acetates produced partly by the addition of acetoxyl group to the double bond and partly by the substitution to the alpha position of the double bond or simultaneous occurrence of these cases[4]. As a single example of ketone formation, there are some reports concerning the formation of R-homocamphenylone from camphene[5,6], which accompanied by ring-enlargement**. In the present case, however, the oxidation was considered to be accompanied by ring-contraction, a novel reaction which seems not to have appeared in literature. The reaction was carried out in two ways. (1) To the benzene solution of the terpene was added solid lead tetra-acetate in portions. (2) The minium was added to the mixture of the terpene and acetic acid. The reaction product was fractionated by distillation under reduced pressure, and the main fraction was found to be the same in both cases. As an example, one of the results obtained by method 1 is shown in Table I.

TABLE I

Frn.	b. p.	mm.	Yield g.	n_D^{25}	d_4^{25}	E. V.*
1	92~102°	8	3.25	1.4984	0.9296	—
2	~105°	7.5	2.90	1.5025	0.9232	—
3	~106°	7.5	3.31	1.5045	0.9355	—
4	~119°	7	1.15	1.5050	0.9517	16.5
5	~127°	7	13.25	1.4870	0.9802	68.5
6	~137°	6	2.97	1.4909	0.9897	97.7
7	~144°	6	3.81	1.4934	1.0026	174
8	~155°	6	2.45	1.4970	1.023	204

* Ester value. Calcd. for $C_{17}H_{26}O_2$: 214

The infrared spectra were examined concerning all fractions, and no appreciable band was found in 3400 cm^{-1} region. Fraction 5 had an infrared band at 1708 cm^{-1} (cf. Fig. 1) and its greater part proved to be a ketone I which gave a semicarbazone m. p. 214° (decomp.) and a 2, 4-dinitrophenylhydrazone m. p. 170°. The highest boiling fraction showed a band at 1745 cm^{-1} suggesting that it was probably a mixture of normal ester (1735~1740 cm^{-1}) and enol ester (1755 cm^{-1}). This was confirmed by the fact that the saponification product of this fraction showed bands at 3450 and 1708 cm^{-1} and gave a 2, 4-dinitrophenylhydrazone, m. p. 168°, which was identified with that of ketone I by mixed melting-point test and infrared spectrum. In the spectra of fractions 6 and 7, rather weak bands were observed at 1825 and 1666 cm^{-1}.

Since ketone I, $C_{15}H_{24}O$ gave an acid $C_{14}H_{22}O_2$, m. p. 102° (II) by hypohalite oxidation, it was presumed to be a methyl ketone. Alkaline permanganate oxidation

* Partly presented before the Kyushu Local Meeting of the Chemical Society of Japan held at Kumamoto, October 29, 1957, and before the Symposium on Perfumery, Terpene and Essential Oil Chemistry held at Fuse City November 30, 1957.

1) Part I, This Bulletin, **30**, 886 (1957).

2) J. Kawamura, *Bull. Govt. Forest Expt. Station*, **30**, 59 (1930).

3) T. Ozeki, S. Seto and T. Nozoe, 10th Annual Meeting of the Chemical Society of Japan, April, 1957.

4) R. Criegee, *Ann.*, **481**, 263 (1930).

5) M. Ishidate, N. Inoue, and H. Fukushima, This Bulletin, **17**, 491 (1942): *J. Pharm. Japan* (*Yakugaku Zasshi*), **63**, 104 (1943).

6) Y. Matubara, *J. Chem. Soc. Japan, Pure Chem. Sec.* (*Nippon Kagaku Zasshi*), **76**, 1088, 1092 (1955), ibid., **78**, 726, 730 (1957).

** Added in proof: Another example of this type of reaction had been reported by P. Naffa and G. Ourisson (*Bull. soc. chim. France* **1954**, 1115., *C. A.*, **49**, 12386^h (1955)), where longihomocamphenylone was obtained from longifolene by this reagent.

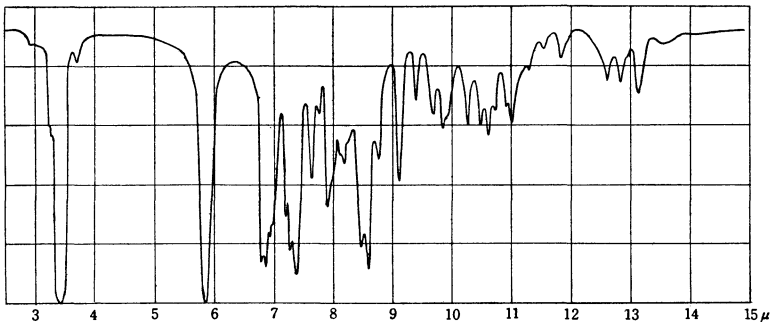


Fig. 1. Ketone I (regenerated from semicarbazone. Spectrum of Fraction 5 was essentially identical with this.)

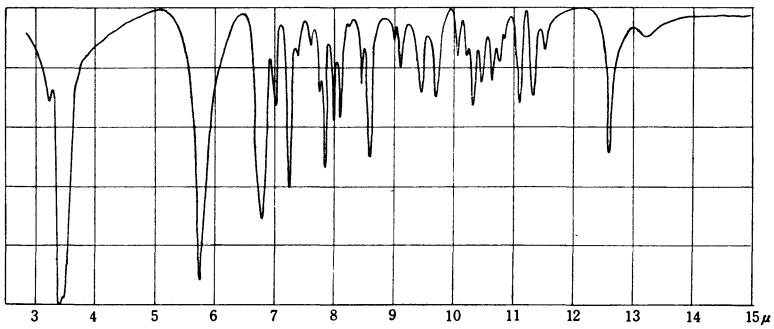


Fig. 2. Ketone VII (Nujol).

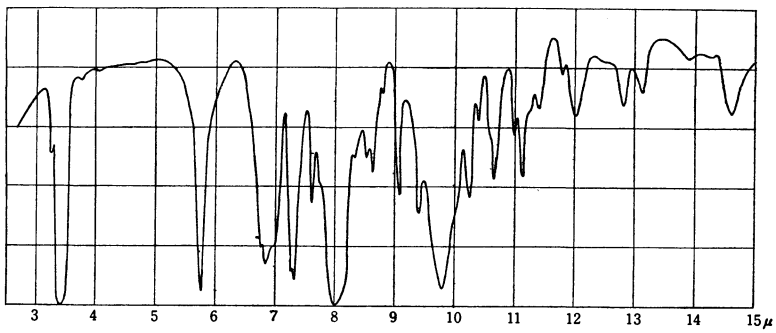


Fig. 3. Ester V.

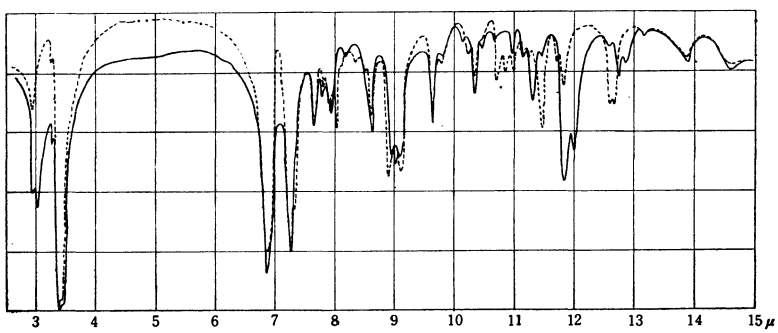
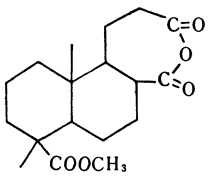


Fig. 4. —— Peroxide X, ------ Peroxide XI (Nujol).

of I gave mainly a dicarboxylic acid $C_{13}H_{20}O_4$ (III) accompanied by a small amount of acid II. Acid III was readily converted into an anhydride, m. p. 211~212° (IV) by heating or treating with acetic anhydride. Since this anhydride shows infrared absorption at 1799 and 1754 cm^{-1} (in carbon tetrachloride) and is stable toward heating, it may be considered to be of glutaric anhydride type.

Peracetic acid oxidation of ketone I followed by saponification and alumina chromatography gave an alcohol $C_{13}H_{22}O$, m.p. 78° (VI), and a ketone $C_{13}H_{20}O$, m.p. 118.5~121° (VII) (Fig. 2). When chromatographic separation was performed prior to the saponification, an ester V (Fig. 3) was obtained. Saponification of ester V gave alcohol VI, which in turn gave ketone VII by the chromic acid oxidation***. It is noticeable that ketone VII shows infrared absorption at 1727 cm^{-1} (in carbon tetrachloride) which is intermediate value of cyclopentanone (1745 cm^{-1}) and cyclohexanone (1715 cm^{-1}). Alcohol VI was oxidized with permanganate under a condition similar to the oxidation of ketone I, giving the same dicarboxylic acid III.

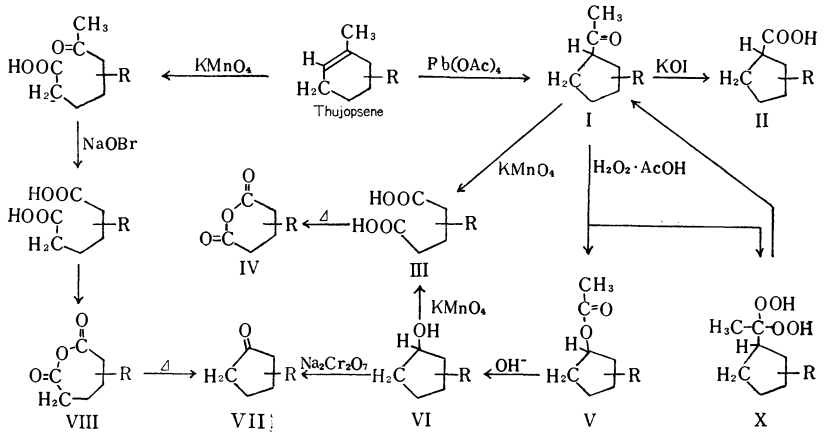
It has been reported[1] that the dicarboxylic acid obtained from thujopsene by permanganate oxidation followed by hypobromite treatment, gave an anhydride VIII, m. p. 110°, to which a glutaric anhydride was suggested from the infrared spectrum. However, an adipic anhydride IX from methyl vouacapenate showed anhydride bands at 1808 and 1764 cm^{-1} (in chloroform)[7]. Furthermore, Ozeki, Seto and Nozoe[3] obtained the "pyroketone" m. p. 121° by treating the dicarboxylic acid with acetic anhydride, followed by heating to 310°. On reexamining the experiment, it was confirmed that the pyroketone was identical with the above-mentioned ketone VII. Therefore, it must be considered that the anhydride VIII is of an adipic anhydride type, and the ring containing double bond in thujopsene is of a six-member type.



IX

The result mentioned above is formulated as Scheme I, assuming the cyclopentyl methyl ketone structure I for ketone I. Infrared absorption at 1708 cm^{-1} supports the validity of this inference.

In the case of the peracetic acid oxidation of ketone I, two kinds of crystalline ketone peroxide were separated. One of them $C_{15}H_{26}O_4$ (X) was obtained in 47% yield when the reaction was carried out below 20°. By means of iodometric titration, it was proved that two -OOH groups are present in X. When the acetic acid solution of X was warmed, the peroxide was decomposed and the original ketone I was regenerated. When the oxidation



Scheme I. R=C_8H_{18}

*** The same ketone VII was separated from the neutral parts of permanganate oxidation products of thujopsene.

7) M. Arakawa, Private communication.

was conducted at about 25°, another peroxide XI was obtained in a poor yield. It decomposed at 135~138°, but it was not studied further owing to lack of material. The infrared spectra of X and XI are shown in Fig. 4.

Further investigations on the structure of thujopsene are being carried on.

Experimental

Thujopsene was obtained by the fractionation of Hiba wood oil as previously described[1].

Reaction of Thujopsene with Lead Tetra-acetate.—(a) Thujopsene (35 g.) was dissolved in 165 cc. of dry benzene, and lead tetra-acetate (prepared from 305 g. of acetic acid, 105 g. of minium, and recrystallized from acetic acid) was added portionwise with stirring for half an hour. The flask was immersed now and then in the water bath to keep the temperature below 40°. Stirring was continued for an additional one and a half hours. The reaction mixture was filtered, sodium bicarbonate solution was added to the filtrate and the organic layer was separated. This was washed twice with water, again with diluted sodium bicarbonate solution and finally with water and dried over sodium sulfate. Solvent was removed and the residue was fractionated. The result of a typical run is shown in Table I. Fraction 5 which boiled mainly at 125~127°/7 mm., gave a yellow 2,4-dinitrophenylhydrazone m. p. 170~170.5°, and a semicarbazone, m. p. 213~214°C (decomp.).

Anal. Found: C, 69.53; H, 9.83; N, 15.41. Calcd. for $C_{16}H_{27}ON_3$: C, 69.27; H, 9.81; N, 15.15%.

Regenerated ketone from the semicarbazone showed the following constants. B. p. 132~133°/9 mm. n_D^{20} 1.4920, d_4^{20} 0.979, M. R. 65.1. Calcd. for $C_{15}H_{24}O$, 64.91. Infrared spectrum, Fig. 1. The ketone separated in another run on the second distillations gave the following constants. B. p. 125°/5 mm. n_D^{26} 1.4897, d_4^{26} 0.9762, $[\alpha]_D^{30}$ +1.23°.

(b) To a mixture of 35 g. of thujopsene, 305 g. of acetic acid and 105 g. of acetic anhydride, was added 160 g. of minium in portions for 1.5 hours, the temperature being kept below 60°. Stirring was continued for one additional hour. Water was added, and the solution was neutralized with sodium carbonate, filtered and extracted with benzene. Fractionation gave 13.3 g. of ketone I, b. p. 125~127°/7 mm.

Hypohalite Oxidation of Ketone I.—The ketone (1 g.) was dissolved in 10 cc. of dioxane and oxidized with the hypobromite solution prepared from 4.8 g. of sodium hydroxide, 75 cc. of water and 2.1 cc. of bromine. When the mixture was warmed gradually, the reaction set in at about 80°. The crude acid II was precipitated by acidification of the alkaline solution, yield 850 mg. Repeated crystallization from methanol-water and final sublimation under reduced pressure gave a sample of m. p. 101~102°. The same acid was obtained by potassium hypoiodite oxidation according to the procedure of Heer and Miescher[8].

Anal. Found: C, 75.72; H, 10.10. Calcd. for $C_{14}H_{22}O_2$: C, 75.63; H, 9.97%.

Permanganate Oxidation of I.—The ketone (1 g.) was suspended in 40 cc. of 5% sodium hydroxide solution and 100 cc. of 4% potassium permanganate solution was added portionwise with stirring at 50~60°. Permanganate was consumed in 7 hours. On dissolving manganese dioxide with sodium bisulfite and hydrochloric acid, an acid mixture was precipitated, which was collected and dissolved in benzene. The benzene solution was extracted with sodium bicarbonate and sodium hydroxide solution successively. Acid III (122 mg.) was obtained from the former extract and recrystallized from methanol-water.

Anal. Found: C, 65.37; H, 8.05. Calcd. for $C_{13}H_{20}O_4$: C, 64.98; H, 8.39%.

The sodium hydroxide extract gave 4 mg. of crude acid II m. p. 98~99°.

Anhydride IV.—Acid III (192 mg.) was heated with 5 cc. of acetic anhydride for 3 hours and acetic anhydride was removed under reduced pressure. The residue was crystallized by rubbing and recrystallized from acetic anhydride, m. p. 211~212°, yield 80 mg. When acid III was heated in a small tube, dehydration occurred at about 190° and melted at 211°. After being cooled, the contents solidified, and this solid also melted at 211°. The infrared spectrum coincided with that of the anhydride obtained by acetic anhydride treatment. Mixed melting point of III and IV showed no appreciable depression. Though the anhydride was heated to 450°, evolution of carbon dioxide was not observed practically and the anhydride could be recovered.

Peracetic Acid Oxidation of Ketone I.—(a) Ketone I (3.0 g.) was dissolved in 30 cc. of acetic acid (treated with chromium trioxide) and 24 cc. of hydrogen peroxide (30%) was added with swirling. After being kept at room temperature (about 25°) for 38 hours, the mixture was diluted with water and extracted with ether, and the ether extract was washed three times with sodium bicarbonate solution and then twice with water. On evaporation of ether, 1.95 g. of reaction product was obtained. This was dissolved in 5 cc. of methanol, and sodium hydroxide solution (1 g. in 5 cc. of water) was added to it and the mixture was allowed to stand overnight; then it was poured into water, and extracted with ether. Ether was removed and the residue was dissolved in petroleum ether and chromatographed with alumina column of 1.8×10 cm. The petroleum ether eluate was an oil (0.5 g. n_D^{20} 1.4965) and the infrared spectrum suggested the presence of unchanged I. The benzene and ethyl acetate eluates gave a crystalline alcohol, 0.42 g., m. p. 74~76°. An analytical sample was prepared by purification with the aid of sublimation under reduced pressure, m. p. 78°.

8) J. Heer and K. Miescher, *Helv. Chim. Acta*, 28, 156 (1945).

Anal. Found: C, 80.10; 11.64. Calcd. for $C_{13}H_{22}O$: C, 80.35; H, 11.41%.

In another run where the reaction mixture was allowed to stand for 3 days, the product was distilled under reduced pressure, saponified and chromatographed; the petroleum ether eluate gave crystalline ketone, m. p. 113~114° (100 mg. from 2.9 g. of I) and its infrared spectrum was identical with that of ketone VII obtained by chromic acid oxidation of alcohol VI.

(b) The ketone (5.4 g.) was oxidized for 5 days as before and a solid substance XI (195 mg.) was separated from the reaction mixture. This was filtered and recrystallized from benzene-petroleum ether mixture, which decomposed at 135~138°. The infrared spectrum is shown in Fig. 4. The attempted elementary analysis failed because of an explosion. The filtrate was treated as before (without distillation and saponification) and the product was chromatographed. Petroleum ether eluate (0.4 g. n_D^{26} 1.4863, d_4^{22} 0.9957) and benzene eluate (1.3 g. n_D^{20} 1.4858, d_4^{22} 1.044, infrared spectrum Fig. 3) were combined and saponified with methanolic sodium hydroxide solution, and alcohol VI was obtained in quantitative yield. Although ethyl acetate eluate (0.5 g. n_D^{22} 1.5000) did not crystallize, its infrared spectrum was essentially identical with that of VI.

(c) The ketone (3.67 g.) was dissolved in 45 cc. of acetic acid, to which 30 cc. of hydrogen peroxide (30%) was added. When the reaction mixture being kept below 20° overnight, a large quantity of crystalline substance X separated out. This was collected on a glass filter, recrystallized from benzene, yield 2.11 g. (47%), decomposed at about 120°.

Anal. Found: C, 66.78; H, 9.69. Calcd. for $C_{15}H_{26}O_4$: C, 66.63; H, 9.69%.

A 13.2 mg. and a 15.0 mg. portion of the sample required 1.98 cc. and 2.19 cc. of 0.1 N sodium thiosulfate solution (f=1.008). Calcd. for $C_{15}H_{24}\cdot 2OOH$: 1.93 and 2.19 cc.

Acetic acid solution of X was warmed and water was added. On cooling there separated out an oil, from which a semicarbazone of m. p. 214° (decomp.) was obtained. The infrared spectrum of this semicarbazone was identical with that of semicarbazone of I.

Chromic Acid Oxidation of VI.—Sodium dichromate (100 mg.) was dissolved in 0.5 cc. of acetic acid and alcohol VI (194 mg.) in 0.5 cc. of acetic acid was added. The mixture was warmed for a few minutes and allowed to stand for one day. Water was added and the oil which separated was extracted with ether. Ether was evaporated and residue was crystallized by rubbing. Yield 148 mg. Recrystallization from methanol-water and sublimation under reduced pressure gave a sample of m. p. 118.5~121°C.

Anal. Found: C, 81.46; H, 10.37. Calcd. for $C_{13}H_{20}O$: C, 81.20; H, 10.48%.

2, 4-Dinitrophenylhydrazone orange m. p. 215~216°.

Permanganate Oxidation of VI. — Alcohol VI (1.0 g.) was suspended in 40 cc. of 5% sodium hydroxide solution and 50 cc. of 4% permanganate solution was added to it dropwise with vigorous stirring. The temperature was kept below 55° by cooling with a water bath. After being stirred for 4 hours, the reaction mixture was acidified with hydrochloric acid and sodium bisulfite was added to it. The precipitate which separated was dissolved in sodium bicarbonate solution, filtered and reprecipitated with hydrochloric acid; yield 647 mg. The infrared spectrum of it was identical with that of III obtained from ketone I. It gave the anhydride of m. p. 211~212°.

The authors wish to express their gratitude to Professor M. Hamana and Professor H. Saikachi of the Pharmaceutical Department of this University for elementary analysis and measurement of rotation. They are also indebted to Mr. M. Shido for elementary analysis.

Department of Synthetic Chemistry
Faculty of Engineering
Kyushu University
Hakozaki, Fukuoka

Phenothiazine Derivatives. V[1]*. Synthesis of Hydroxyphenothiazines*

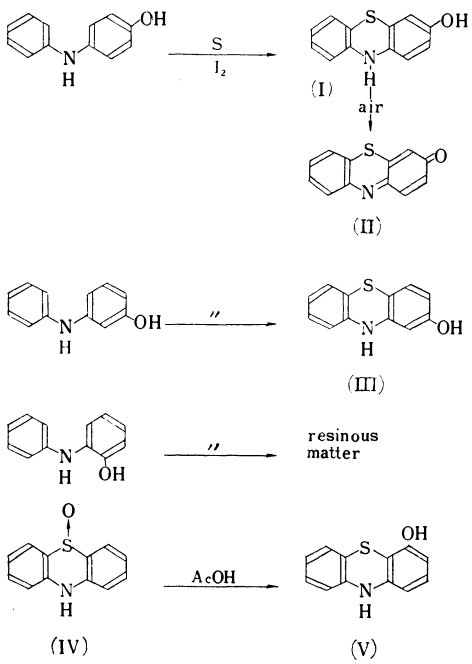
By Manabu FUJIMOTO

(Received September 24, 1958)

Of the theoretically possible four hydroxyphenothiazines, the 3-hydroxy compound I only has been reported[2,3]. By treating 4-hydroxydiphenylamine with sulfur and iodine, Houston et al.[2] prepared the compound as a dark greenish brown solid with m. p. 170~175°C and with a tendency to be easily oxidized in air to 3-phenothiazone (II) (Chart I).

Before Houston et al., Hilditch and Smiles already prepared the supposed 3-hydroxyphenothiazine[3] by an intramolecular rearrangement of phenothiazine 5-oxide in acetic acid. It was a purple crystalline mass that defied purification. They submitted it to reduction with zinc and hot acetic acid and obtained a colorless soft crystalline substance which rapidly recovered purple color in the presence of air.

Chart I



The present author repeated the experiment of Hilditch and Smiles and obtained a reddish-violet substance in fine powder melting at 141~143°C. It showed a distinct depression of the melting point on admixture either with 3-hydroxyphenothiazine (I) or with 3-phenothiazone (II), prepared according to the method of Houston et al[2]. Although the rearranged product was chromatographically pure and phenolic in nature, it was evidently different from the substances of Houston et al.

The investigation described below presents a contribution to the solution of the problem concerned. In the first place, an attempt was made to synthesize all of the unknown hydroxyphenothiazines.

It was reported by Charpentier et al.[4] that the reaction of a *meta* substituted diphenylamine with sulfur and a small amount of iodine as a catalyst gives a mixture of a 2-substituted phenothiazine and its 4-isomer, although the 2-substituted product is formed in a greater yield, and that 3-methoxydiphenylamine gives only 2-methoxyphenothiazine.

The present author obtained one hydroxyphenothiazine by thionation of 3-hydroxydiphenylamine, but could not isolate the expected isomeric product. Therefore, the hydroxyphenothiazine is supposed to be 2-hydroxyphenothiazine (III). As a very unstable compound, 2-hydroxydiphenylamine gave only a black resinous matter by a similar treatment. If 1-hydroxyphenothiazine, were obtained by the reaction of 2-hydroxydiphenylamine it would have a tendency to form 1-phenothiazone similarly to the 3-hydroxy isomer I.

As an alkaline solution of the substance, obtained by the intramolecular rearrangement of phenothiazine 5-oxide IV with acetic acid according to Hilditch and Smiles resists aeration, it is considered to be a phenol with the hydroxyl group in a *meta* position to the nitrogen atom. Two such hydroxyphenothiazine are possible,

1) Part IV: This Bulletin, **32**, 296 (1959).
2) D. F. Houston et al., *J. Am. Chem. Soc.*, **71**, 3818 (1949).
3) T. P. Hilditch and S. Smiles, *J. Chem. Soc.*, **101**, 2295 (1912).
4) P. Charpentier et al.: *Compt. rend.*, **235**, 59 (1952).

namely, 2-hydroxy- and 4-hydroxy-phenothiazines. As the substance from the rearrangement of the 5-oxide (IV) differs conspicuously from 2-hydroxyphenothiazine (III) described above, it must be 4-hydroxyphenothiazine (V). The position 4 is quite a reasonable place where the sulfoxide oxygen atom may migrate.

Experimental

3-Hydroxyphenothiazine (I) and 3-Phenothiazone (II). — Essentially the method of Houston et al.[2] was followed.

2-Hydroxyphenothiazine (III). — A mixture of 3.7 g. of 3-hydroxydiphenylamine and 1.4 g. of sulfur was ground in a mortar and placed in a 100 ml. flask. Then 0.04 g. of iodine was added, and the flask was stoppered and placed in a metal bath preheated to 190°C. The bath temperature was kept at 190~200°C during 30 min., while hydrogen sulfide was evolved, and then for additional 10 min. The reaction mass was poured into a porcelain dish and allowed to cool. It solidified to a greenish-yellow cake. Yield, 4.2 g. Fractional recrystallization from benzene gave 3.2 g. of the pure substance III in dark yellow powder, m. p. 270~272°C. It gives cobalt-blue coloration with sulfuric acid.

Anal. Found: C, 67.11; H, 4.09; N, 6.40. Calcd. for $C_{12}H_9ONS$: C, 66.85; H, 4.21; N, 6.50%.

4-Hydroxyphenothiazine (V). — Acetic acid (20 ml.) was added to phenothiazine 5-oxide (IV) (1.0 g.), and the reddish-violet solution was refluxed for 3 hr. Acetic acid was evaporated in vacuo, and the residue was recrystallized from absolute ethanol. The yield was quantitative. It forms reddish-violet fine powder, m. p. 141~143°C, and gives sepia-brown coloration with sulfuric acid. It is soluble in 10% aqueous caustic soda. The benzene solution showed a single adsorption band in the chromatogram on alumina.

Anal. Found: C, 67.01; H, 4.08; N, 6.45. Calcd. for $C_{12}H_9ONS$: C, 66.85; H, 4.21; N, 6.50%.

Summary

The phenolic compound resulting from the rearrangement of phenothiazine 5-oxide in acetic acid was found to be 4-hydroxyphenothiazine, and to be different from 2- and 3-hydroxyphenothiazines which were derived from 3- and 4-hydroxydiphenylamines, respectively, by fusion with sulfur and iodine.

The author expresses his thanks to Professor Y. Urushibara, Tokyo University, for his helpful guidance throughout this work, to Dr. K. Takeda, Director of the Laboratory, for his permission to complete this research, and also to the members of the Center of Microanalytical Services, Shionogi and Co., Ltd., for the elementary analyses.

Research Laboratory
Shionogi & Co., Ltd.
Imafuku, Amagasaki

*Heat of Solution of Methanolized Cellulose**

By Yoshizo TSUDA

(Received September 19, 1958)

In our previous papers[1,2], the lateral order distribution of cellulose was determined and discussed. In our laboratory the lateral order distribution has been determined from the solubility data of methanolized cellulose in aqueous sodium hydroxide solution of various concentrations.

Recently it has been shown that the solubility of methanolized cellulose depends on the degree of polymerization of the methanolized cellulose and that distribution obtained by such a method gives rather a longitudinal order distribution of crystallites. On the other hand, it has been shown that the effect of the degree of polymerization of hydrolyzed cellulose on its solubility is smaller than that of the lateral order[3].

The present investigation of heat of solution of methanolized cellulose was undertaken to obtain some informations

* This paper was presented at the 11th Annual Meeting of the Chemical Society of Japan, April, 1958.

1) Y. Tsuda and S. Mukoyama, This Bulletin, **29**, 748 (1956).

2) Y. Tsuda and S. Mukoyama, *Textile Research J.*, **27**, 945 (1957).

3) H. Sobue, S. Fukuhara and M. Moriya, *J. Chem. Soc. Japan, Ind. Chem. Sec.* (*Kogyo Kagaku Zasshi*), **61**, 1015 (1958).

about the dependency of the solubility of methanolized cellulose on the cohesive energy of crystallites.

Experimental

Cellulose Samples. — Cuprammonium rayon, Shin-toramomen, BX-yarn[4], viscose rayon, tire-cord rayon A (conventional) and tire-cord rayon B (all-skin type) were used.

Methanolysis. — Methanolysis of the samples was performed at 40° for 24 hours with 1 N hydrogen chloride in absolute methyl alcohol. After methanolysis, the residue was filtered, washed with methanol until it became chloride-free and then dried.

Measurement of Heat of Solution. — The apparatus was a simple non-adiabatic calorimeter composed of a 100 ml. pyrex vacuum bottle, a Beckmann thermometer (in 0.01° division), a stirring rod and a sample inlet tube, as shown in Fig. 1.

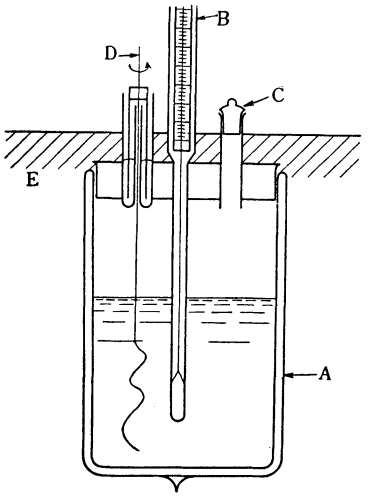


Fig. 1. Calorimeter.
A, 100 ml. pyrex vacuum bottle
B, Beckmann thermometer
C, Sample inlet tube
D, Stirrer
E, Thermostat

The apparatus was immersed in a thermostat kept at 20°. Methanolized sample (50 mg.) was bone-dried and kept at 20°. The solvent was 50 ml. of 11% aqueous sodium hydroxide solution, which was kept at 20° in the calorimeter. The stirring was done at a constant speed because constancy of the mechanical generation of heat was necessary for the measurement of small heat change. Under these experimental conditions observed temperature rise was about 0.05°, which was estimated to 0.001°. The dissolution of methanolized cellulose in the alkaline solution was a relatively rapid reaction. The heat capacity of calorimeter was determined experimentally under working conditions by measuring the heat of solution of potassium chloride in water.

Degree of polymerization was measured using cuprammonium solvent. Lateral order distribution was obtained by the same method as described in a previous paper[2].

Results

In Table I are shown the values of the heat of solution together with the statistical quantities which indicate their reliability. Degree of polymerization of methanolized cellulose is also shown in Table I. It is evident from Table I that the heats of solution of samples I, II and III are smaller than the others and those of samples V and VI are larger than the rest. The lateral order distribution of these samples is shown in Fig. 2.

TABLE I
HEAT OF SOLUTION

	Methanolized	Heat of solution cal./g.	95% Confidence limit	Degree of polymerization
I	Cuprammonium Rayon	27.6	±1.3	50
II	Shin-toramomen	27.8	±1.2	45
III	BX-yarn	29.2	±1.3	40
IV	Viscose Rayon	31.4	±1.2	33
V	Tire-cord Rayon A	33.4	±1.3	28
VI	Tire-cord Rayon B	34.3	±1.1	25

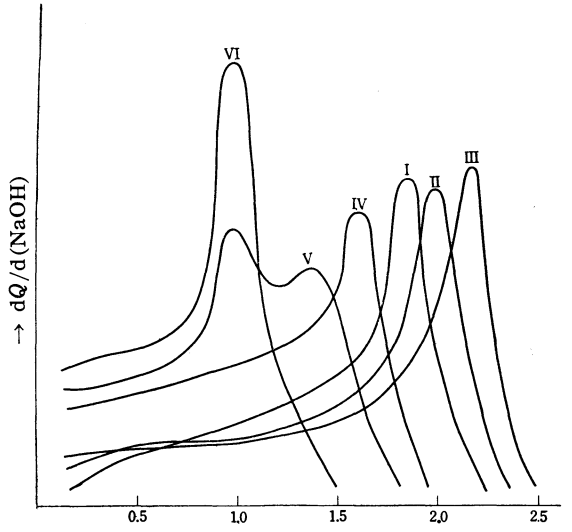


Fig. 2. Lateral order distribution (types identified in Table I).

Discussion

The heat of solution of the cellulose sample, H_s, can be separated in two parts as follows;

4) N. Drisch and L. Soep, *Textile Research J.*, 23, 513 (1953).

$$H_s = H_a - E_c$$

where H_a is the heat of solution of amorphous cellulose in the alkaline solvent and E_c is the cohesive energy of the cellulose sample. H_a is a constant value with respect to all cellulose samples under a given experimental condition. Therefore the difference in the heat of solution of two samples can be regarded as the difference in their cohesive energies; that is, the larger the heat of solution, the smaller the cohesive energy. It will be seen from the results in Table I that the methanolysis residue of Shin-toramomen, Bx-yarn and cuprammonium rayon have large cohesive energy values and tire-cord rayons have rather low values. On the other hand, as shown in Fig. 2, the former shows high lateral order distributions and the latter shows low lateral order distributions. These relationships indicate that the distribution obtained from the fractional dissolution of methanolized cellulose corresponds to the distribution of cohesive energy. Although the degree of polymerization can be regarded as another factor of the fractional dissolution, its effect would be relatively small in comparison with the effect of cohesive energy.

It may be accepted from these relationships that the length of crystallite depends on the lateral order of crystallite and a portion of high lateral order can form a long crystallite, and therefore the dependency of lateral order distribution on the degree of polymerization has been observed.

If it is assumed that methanolysis destroys only the aggregated portion of very low cohesive energy, the cohesive energy of the methanolysis residue would be almost identical with that of the original cellulose.

Summary

The heat of solution of methanolysis residue of cellulose fibers was measured and then the difference in the cohesive energy of different samples was estimated. It was elucidated that the cohesive energy of methanolized cellulose corresponds to the experimentally evaluated lateral order.

Research Center, Toyo Rayon Co. Ltd., Otsu, Shiga

Effects of Dry Grinding on Talc

By Hiroshi TAKAHASHI

(Received October 2, 1958)

In the previous papers, the effects of dry grinding on kaolin minerals were studied, and the mechanism of the structural change caused by dry grinding was presented[1]. That is, there are two ways of change in structure. One is the production of a non-crystalline material attended with disordering of a crystalline portion, and the other is the reaggregation process. Finally, the kaolin mineral changes into a completely amorphous substance through a formation of a zeolitic substance. The mechanism of the dry grinding on kaolin minerals must be common somewhat to any substances with layered structure. In the ball-milling of graphite, too, a remarkable disordering in structure was observed by Bacon[2]. However, the effects of grinding for substances with the layered structure have not been studied very much heretofore, with the exceptions of kaolinite and mica[3]. The mechanism of dry grinding on kaolin minerals is somewhat common to that of other clay and related minerals, for example, such as montmorillonite, mica, attapulgite, pyrophyllite, serpentine and chrysotile. The results of the grinding

1) H. Takahashi, "Proc. Sixth Natl. Conference on Clay and Clay Minerals", Natl. Res. Council-Natl. Acad. Sci., (in press); H. Takahashi, This Bulletin, **32**, 235, 245, 252 (1959).

2) G. E. Bacon, *Acta Cryst.*, **5**, 392 (1952).

3) M. L. Jackson and E. Truog, *Soil Sci. Soc. Am., Proc.*, **4**, 136 (1939); R. C. Mackenzie and A. A. Milne, *Min. Mag.*, **32**, 178 (1953); R. C. Mackenzie and A. A. Milne, *Clay Min. Bull.*, **2**, 57 (1953).

effects on these clay and related minerals are reported in the following papers. Talc is an end-member of clay mineral with three-layered structure. In this study, the effects of a mechanical-mortar dry grinding on talc are discussed in the structural change, and compared with those of kaolin minerals.

Experimental

The sample used in this study is talc from Kanjun, China. The dry grinding was done in the same manner as for kaolin minerals. That is, 30 g. of original sample was charged and ground by a mechanical-mortar (15.2 cm. in dia. and 8.4 cm. in depth). Experimental specimens were taken out at intervals of 48 hours and examined by X-ray diffraction, differential thermal and electron microscopic methods. The density was also measured.

X-ray powder diagrams were recorded by an X-ray diffractometer (Geigerflex). Experimental conditions are as follows. Filtered Cu radiation (Cu $K\alpha$: 1.5418Å), at 35 kV and 15 mA is used, scanning speed is 1° or 1/4° 2θ per minute, time constant is 4 seconds, receiving slit is 0.2 mm. or 0.1 mm., angular aperture is 1° or 1/2° were used. The differential thermal analysis curves were recorded by the apparatus described by Sudo et al.[4]. Care was taken to pack a specimen into the sample block in the homogeneous manner and also to keep the weight of specimen constant. The mean heating rate is 12.5°C per minute. The density was measured by pycnometer in carbon tetrachloride. It was done after it had been dried at 110°C in order to avoid the effect of the adsorbed water. Electron micrographs were obtained by the Hitachi HU-10A type Electron Microscope.

Results and Discussion

X-Ray Diffraction Studies.—X-ray diffractometer traces and data are given in Fig. 1 and Table I. In this table, the interplaner spacing and the relative intensity measured from the X-ray trace are shown and the values described in ASTM Card are given for reference.

Generally, as the grinding progresses, even though the X-ray diagram is similar to that of the original sample, a decrease in the intensity of reflections except for some reflections and an increase in the background are observable. The intensity of reflections belonging to the basal reflections come to decrease sharply as compared with that of the original sample during the early stage of grinding. Another distinct feature observable in the X-ray

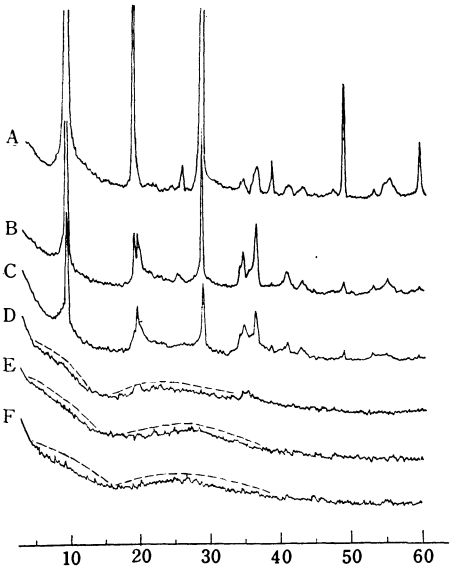


Fig. 1. X-ray diffractometer traces of ground specimens of talc.
A, original talc
B, ground 96 hours
C, ground 192 hours
D, ground 240 hours
E, ground 384 hours
F, ground 528 hours

diagram is that the reflection of 4.60Å spacing comes to be remarkably distinctive as the reflection of 4.69Å spacing weakens due to the progress of grinding. The profile of this reflection becomes an assymmetric broad band which is similar to the (02,11) band found in the X-ray diagram of halloysite. It seems that this reflection is related to the structure of talc and has (020) index rather than a spurious line[5]. The above-mentioned two characteristics with respect to the intensities of reflection line and background observed in the early stage of grinding become more and more distinct as the grinding progresses up to 192 hours. After 192 hours in grinding, the change of the interplaner spacing is not so remarkable. When the grinding progresses further, the X-ray diagram changes remarkably in contrast with that observed thus far. In the 240-hour-ground specimen, the X-ray diagram scarcely has any distinct reflection, but only two very diffuse bands. It is clear that a non-crystalline substance is produced by dry grinding. In the process of the grinding of talc, a remarkable change

4) T. Sudo et al., *J. Geol. Soc. Japan*, (*Chishitsu-Gaku-Zasshi*), 58, 679 (1952).

5) D. M. C. MacEwan, "X-Ray Identification and Crystal Structures of Clay Minerals", Mineralogical Society (London), Edited by G. W. Brindley, p. 311 (1951).

TABLE I
POWDER DATA OF GROUND TALC

A.S.T.M. Index (No. II-1238)		Original Talc		Ground 96 hr.		Ground 192 hr.		Ground 240 hr.		Ground 384 hr.		Ground 528 hr.	
$d(kX)$	I	d(Å)	I	d	I	d	I	d	I	d	I	d	I
9.4	8	9.4	VS	9.3	VS	9.3	MS	9.8	W vbr	9.8	VW vbr	9.8	VW vbr
4.69	4	4.69	S	4.70	M	4.69	W						
		4.60	VW	4.59	M	4.58	M br	4.55	VW				
3.88	1b												
3.37	3	3.45	MW	3.50	W			3.8	W vbr	3.3	W vbr	3.4	W vbr
3.11	10	3.12	VS	3.11	MS	3.12	M						
2.70	1	2.63	W	2.63	MW	2.64	VW						
2.59	2	2.60	W	2.60	MW	2.60	MW	2.60	VW				
2.47	5	2.48	MW	2.49	MS	2.49	M br						
2.32	1	2.34	MW	2.34	VW	2.34	VW						
2.20	3	2.21	W br	2.21	W br	2.22	W br						
2.09	2	2.11	W br	2.11	W br	2.12	W br						
1.92	0.5	1.927	W										
1.86	3	1.870	MS	1.870	W	1.873	W						
1.725	2	1.731	W	1.73	W	1.73	VW br						
1.67	4	1.665	MW br	1.67	MW br	1.68	VW br						
1.652	1—2												
1.632	1b												
1.55	3	1.560	M	1.56	W br	1.56	VW br						

Key to abbreviatin: VS: very strong, S: strong, MS: medium strong, MW: medium weak, W: weak, VW: very weak, br: broad, vbr: very broad.

occurs in the structure at the period between 192 hours and 240 hours under the experimental condition of this experiment. In the 384-hour-ground specimen, the X-ray diagram is nearly similar to that of the 240-hour-ground specimen. As the grinding progresses, the maximum points of diffuse bands in the X-ray diagram gradually become more and more indistinct, and the intensity of the background at the small angle part of a scattering angle increases progressively.

That a zeolitic substance is formed in the dry grinding of kaolin minerals can be supported on the basis of the X-ray diagram of the ground specimen treated with a weak alkali- and acid-solution as described in the previous papers[1]. These procedures were used for some ground specimens of talc. A part of these X-ray traces are shown in Fig. 2.

From a comparison of these X-ray traces with those of the original ground specimen, the following conclusions are drawn. In the alkali-treated specimen of 192-hour-ground talc, only a slight increase in the intensity of background is observable in the X-ray diagram, as compared with that of the original ground specimen. The X-ray pattern of the acid-treated specimen after being treated with the above weak alkaline solution is almost similar to that of

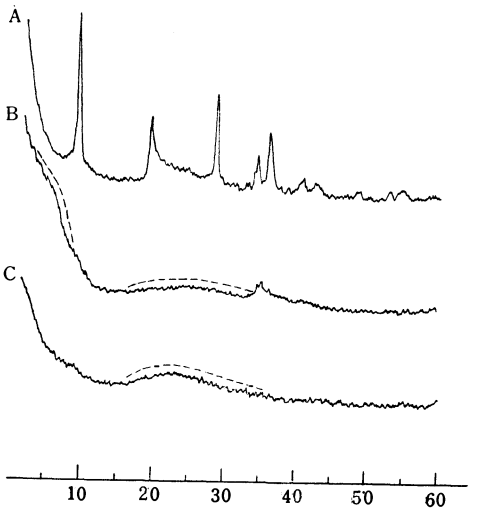


Fig. 2. X-ray diffractometer traces of alkali- and acid-treated specimens of ground talc.
A, 192-hour-ground talc treated with 0.1 N HCl after treated with 0.1 N NaOH
B, 240-hour-ground talc treated with 0.1 N NaOH
C, 240-hour-ground talc treated with 0.1 N HCl after treated with 0.1 N NaOH

TABLE II
THERMAL DATA OF GROUND TALC
(ALL TEMPERATURES ARE DEGREES CENTIGRADE)

Grinding time (hr.)	E_{n1}		E_x		E_{n2}	
	Temp. at peak (°C)	Height of peak	Temp. at peak (°C)	Height of peak	Temp. at peak (°C)	Height of peak
0	—	—	—	—	990	13
48	—138—	6	807	9	980	8
96	—135—	9	805	20	970	6
192	—140—	14	807	50<	968	4
240	—150—	13	807	8	945	2
528	—140—	15	825	1	—	—

the original ground specimen, however, the pattern becomes somewhat distinct owing to a dissolution of an amorphous substance produced by dry grinding. In the X-ray diagram of the weak alkali-treated 240-hour-ground specimen, two very diffuse bands are noticeable as is clear by comparison of Fig. 1-D and Fig. 2-B. The positions of the maximum points of these bands are about 14.7Å and 3.5Å in the interplaner spacings. In addition to these diffuse bands, a very remarkable scattering is also observable in the region of a scattering angle as low as six degrees. To dissolve the amorphous substance produced by dry grinding, acid treatement was given. The X-ray diagram of the residual part has a broad band with a maximum of 3.86Å in spacing. The background decreases below that before acid treatment. This fact indicates that in the 192-hour-ground specimen, the disordering in the talc structure is observable but the production of an amorphous substance is yet remarkable. In this stage, a zeolitic substance is not to be formed. In the 240-hour-ground specimen, the crystalline substance is not present. This fact is ascertained by the X-ray diagram of a residual substance treated with alkali and acid. Therefore, it is considered that the structure of this specimen is not perfectly amorphous, but it is related somewhat to the original structure though the original talc structure disintegrates due to dry grinding. In the light of the X-ray data, the structure of the 384-hour-ground specimen is considerably similar to that of the 240-hour-ground specimen. In the 528-hour-ground specimen, the amorphous substance dissoluble by the alkali-acid treatment considerably increases. This means an increase of the amorphous substance by dry grinding.

Consequently, it is concluded that in the dry grinding of talc, the disordering of structure is remarkable up to a certain stage of grinding, and past this stage, the specimen changes wholly into a non-crystalline substance and then gradually changes into a completely amorphous substance. Therefore, the formation of a zeolitic substance is not remarkable as compared with that of kaolin mineral.

Differential Thermal Analysis. — Differential thermal analysis curves of the specimens in the various periods of grinding are shown in Fig. 3, and thermal data measured from these curves are given in Table II.

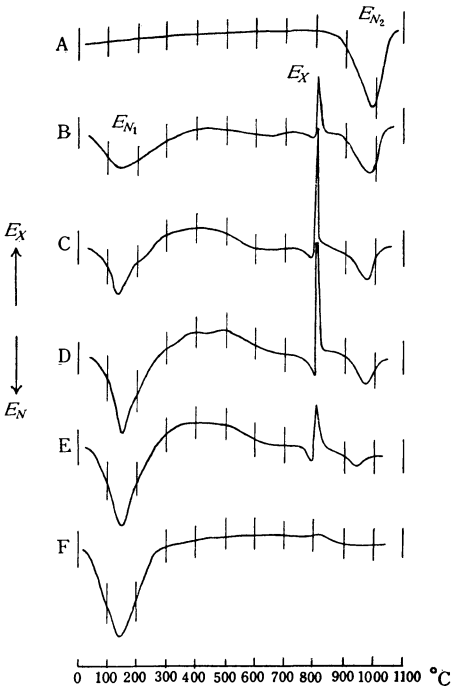


Fig. 3. Differential thermal analysis curves of ground talc.
A, original talc
B, ground 48 hours
C, ground 96 hours
D, ground 192 hours
E, ground 240 hours
F, ground 528 hours

The original sample has only an endothermic reaction (E_{n2}) associated with the loss of lattice water. The peak temperature of the endothermic reaction is 990°C, which is nearly equal to the value given in literature[6]. In the 96-hour-ground specimen, the first endothermic reaction (E_{n1}) associated with the loss of adsorbed water is apparent. This fact means that a non-crystalline substance is produced by dry grinding. As that of a kaolin mineral, a lowering in the peak temperature and a decrease in the height are observable in the second endothermic reaction (E_{n2}). It seems that these characteristics are related to the partial disintegration of the original structure. In the differential thermal analysis curve of this specimen, another important characteristic is observable. That is, a sharp exothermic reaction (E_X) is apparent at about 800°C, and there is the presence of a slight but distinct endothermic reaction immediately before this reaction. In the 192-hour-ground specimen, all features observed in the differential thermal analysis curves of the 48- and 96-hour-ground specimens become all the more distinct. An increase in the height of the first endothermic reaction, a remarkable increase in the intensity of the exothermic reaction, a lowering in the peak temperature and a decrease in the height of the second endothermic reaction are observable. Moreover the endothermic reaction just before the exothermic reaction becomes more distinct. The first endothermic reaction of ground specimens up to 192 hours is considered to be caused by a non-crystalline substance produced by grinding rather than by the water which gets into the inter-layers of talc as an inter-layer water, because the basal spacing of these specimens does not change much. In the 240-hour-ground specimen, the height of the exothermic reaction sharply decreases and the height of the second endothermic reaction decreases remarkably as compared with those of the 192-hour-ground specimen. In a many-hour-ground specimen, for example, the 528-hour-ground specimen, the reaction which is present in the original specimen is absent. Only the first endothermic reaction associated with the loss of the adsorbed water, and the weak and broad exothermic reaction at 825°C are observable. Then the endothermic reaction just before the exothermic reaction has already disappeared.

On the differential thermal analysis curves of the ground specimens, an important and interesting phenomenon is observable. That is, a new phase different from the original structure is apparent in the course of dry grinding. To ascertain this new phase, the X-ray traces of the 192-hour-ground specimen taken out just before and after the exothermic reaction on the differential thermal analysis curve are compared. A difference is observable in that only a reflection of 2.885Å spacing is apparent. From the facts that all reflections of the original 192-hour-ground specimen remain in the X-ray diagram of the specimen taken out just after the exothermic reaction and that a new reflection appears, it is supposed that the exothermic reaction on the differential thermal analysis curve is not based on the structural change of original talc. And from the fact that this exothermic reaction disappears again in many-hour-ground specimens, it is supposed that this exothermic reaction is not also based on the structural change of a perfectly amorphous substance produced by dry grinding. Therefore, it is clear that this exothermic reaction is based on crystallization from the new phase formed by dry grinding which is not the talc structure and is not a perfectly amorphous structure. This sort of structural change is not found at all in the case of kaolin minerals. The appearance of a new phase

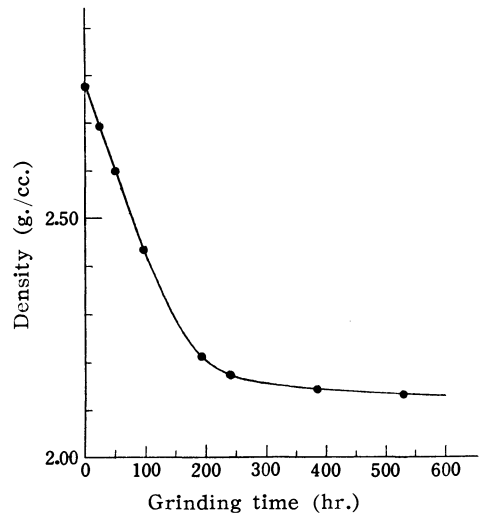


Fig. 4. Curve showing the change of the density with the time of grinding.

6) M. M. Taboadela and V. A. Ferrandis, "Differential Thermal Investigation of Clays", Mineralogical Society (London), Edited by R. C. Mackenzie (1957). p. 176.

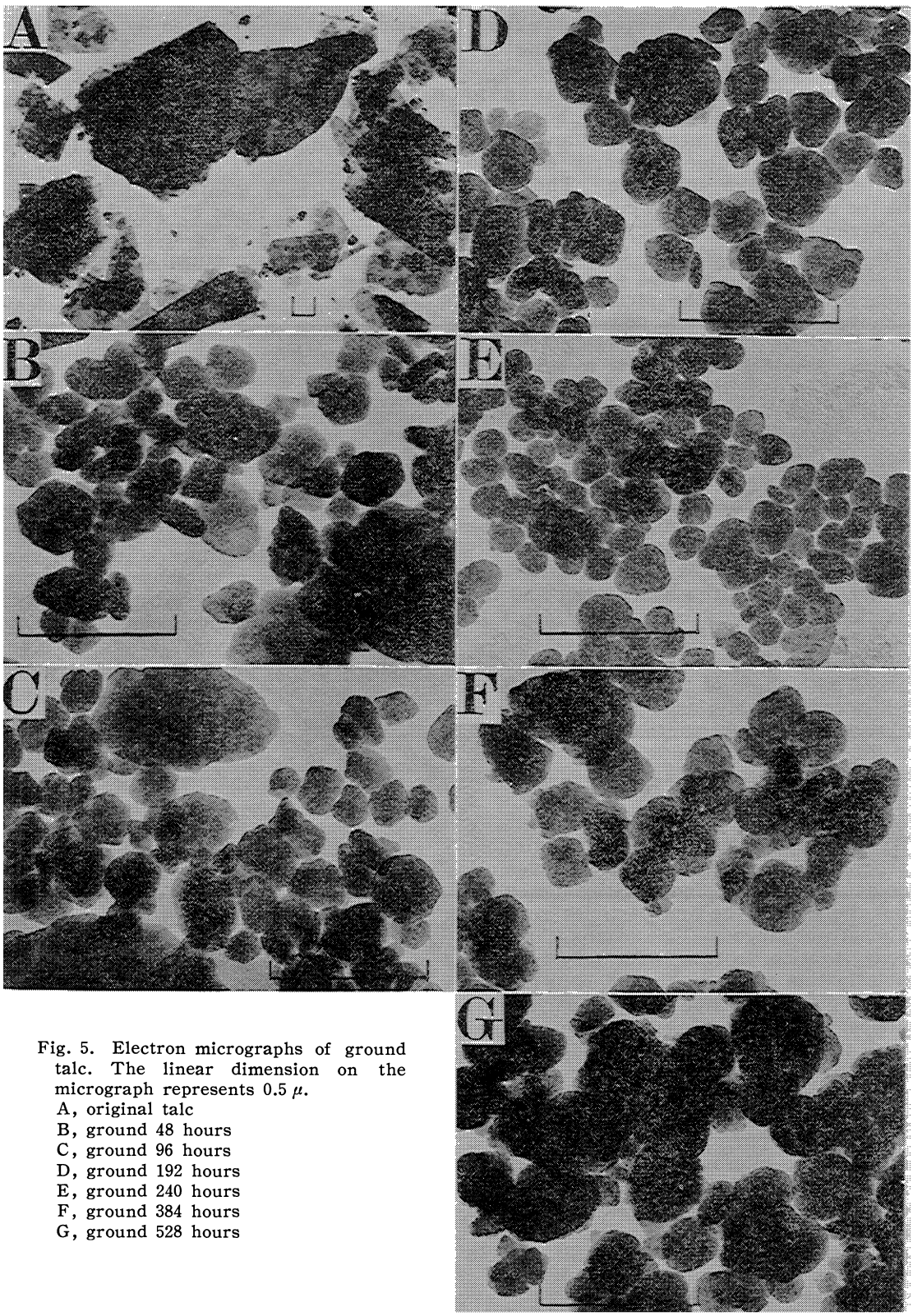


Fig. 5. Electron micrographs of ground talc. The linear dimension on the micrograph represents 0.5 μ.
A, original talc
B, ground 48 hours
C, ground 96 hours
D, ground 192 hours
E, ground 240 hours
F, ground 384 hours
G, ground 528 hours

by dry grinding is an important characteristic of talc.

Density.—A curve showing the change of the density in the process of the dry grinding on talc is shown in Fig. 4.

The density sharply decreases up to about 200 hours in the grinding, but thereafter it reaches a nearly constant value. This constant value is nearly equal to that of a gel-like substance. The point of the bend in the density curve is existent between the points of 192 hours and 240 hours. In the light of the X-ray and thermal data, this point corresponds to the point where the structure of talc changes wholly into a new structure by dry grinding. In talc, grinding takes a longer time for the density to reach the constant value than that of kaolin minerals. This means that talc suffers the effects of dry grinding less than kaolin minerals do, for the structure of talc is stronger than that of kaolin minerals.

Electron Microscopic Studies. — Fig. 5 shows the electron micrographs in the process of grinding on talc.

The original sample is an irregular and platty particle with a sharp edge, and the particle has several microns in size. In the 48-hour-ground specimen, it is observed that the particles are fine as compared with those of the original particle, while considerably large particles are also observable. It seems that the fine particles do not aggregate unlike the fine particles in the grinding process of kaolin minerals, and the edge of this particle is not sharp. The shape of the considerably large particle is spherical. As the grinding progresses, number of large particles decreases and that of fine particles increases, but the size of the fine particles remains almost unchanged. This means that the reaggregation process is not very remarkable in this case. In the 240-hour-ground specimen, the shape of the particle is almost uniformly spherical as compared with that of the 192-hour-ground specimen but it is not so spherical as the shape of particles found in the process of dry grinding of kaolin minerals. The mean value of the particle size of this specimen is about 0.1 micron. Past this stage in grinding, the particle size increases as compared with that of the 240-hour-ground specimen. As the grinding further progresses, an irregular growth of the particle is observable. This corresponds to the fact that the completely amorphous substance has been produced by grinding.

Summary

The several-hundred-hour mechanical-mortar dry grinding on talc was examined by X-ray diffraction method, differential thermal analysis, electron microscopy and density measurements, and they were compared with those of kaolin minerals. In the dry grinding on talc, some characteristics in the structural changes by dry grinding were found. As the grinding progresses, the original crystals cleave and fracture and then split into fine crystals. Disordering in structure of these fine crystals is observable before the talc structure disintegrates completely. In talc, a new substance is produced by dry grinding, which is somewhat related to but different from the original talc structure. The appearance of this new phase is most remarkable in the stage of grinding where the crystalline pattern of talc entirely disappears in the X-ray diagram. This new phase has a non-crystalline structure, but the strurcture is not completely amorphous. It crystallizes into a new crystal at about 800°C. As the grinding progresses, the structure of this new phase gradually disintegrates to a completely amorphous structure similar to that of a silica-magnesia mixed gel. The formation of a zeolitic structure is not so remarkable; also, even if this structure is formed, the period of its stage is very short. It is an important characteristic that talc wholly changes into a new non-crystalline substance by dry grinding. It is generally supposed that talc does not easily suffer the effects of dry grinding because the structure is stronger than that of kaolin minerals.

The author wishes to express his hearty thanks to Professor H. Akamatu for his continuous advice and encouragement. Thanks are due to Professor T. Sudo of the Tokyo University of Education and Professor R. E. Grim of the University of Illinois for their valuable suggestions and discussions.

Department of Chemistry
Faculty of Science
the University of Tokyo
Hongo, Tokyo

Wet Grinding on Kaolin Minerals

By Hiroshi TAKAHASHI

(Received October 2, 1958)

In the previous studies, the effects of dry grinding on the structural change of kaolin minerals have been presented[1]. It was concluded that the effect of dry grinding depends on the internal degree of crystallinity of the original kaolin mineral, and there are two processes in the structural change. One is the production of a non-crystalline material attended by disordering of the crystalline portion, and the other is the reaggregation process. At a certain period in the grinding, a zeolitic structure is formed; then finally, kaolin mineral changes into a completely amorphous substance like a silica-alumina mixed gel.

Considerable work has been done on the dry grinding of kaolinite, but comparatively little is known on the wet grinding. It was found by Shaw that the wet grinding of kaolinite causes a shearing along the cleavage plane[2]. This will lead to weakening the stacking force between kaolin unit layers. The wet grinding of kaolinite has been made heretofore using ball-mill with water or organic liquid such as benzene. Judging from the fact that wet grinding causes a shearing stress, it is obvious that a higher viscous liquid is more effective in the grinding process than the lower one. Therefore, glycerol was used in the present experiment, combined with a mechanical-mortar as it is very effective in causing a change in structure as discussed in the previous papers[1].

The purpose of this study is to know the correlation between the effect of the wet grinding and that of the dry grinding from the point of view of the degree of the crystallinity of kaolin minerals. It is hoped that this will lead to the fundamental information concerning kaolin minerals.

1) H. Takahashi, "Proc Sixth Natl. Conference on Clay and Clay Minerals", Natl. Res. Council-Natl. Acad. Sci., (in press). H. Takahashi, This Bulletin, **32**, 235, 245, 252 (1959).

2) B. T. Shaw, *J. Phys. Chem.*, **46**, 1032 (1942).

Experimental

The following kaolin minerals were investigated: Kaolinite from Mesa Alta, N. M., U. S. A.; Halloysite from Spruce Pine, N. C., U. S. A.; Halloysite from Tintic, Utah, U. S. A.. These specimens are API Standard Clay Minerals. The structural characteristics of these specimens were discussed in the previous paper[3]. Of all kaolin minerals, Mesa Alta kaolinite has the highest degree of crystallinity, of all halloysites, Spruce Pine halloysite has the highest degree of crystallinity, and Tintic halloysite has a lower degree of crystallinity than Spruce Pine halloysite.

30 g. of each original kaolin mineral was charged, mixed with 100 cc. glycerol. The mixture was wet-ground by a mechanical-mortar (15.2 cm. dia. and 8.4 cm. in depth). The specimen was taken out at intervals of 48 hours and washed with water throughly and then air-dried. The experimental specimen thus prepared was examined by X-ray, thermal and electron microscopic methods. In parallel with these examinations, its density was measured.

X-ray powder diagrams were recorded by an X-ray diffractometer (Geigerflex). Experimental conditions are as follows. Filtered Cu radiation (Cu K_α: 1.5418 Å) at 35 kV and 15 mA is used, scanning speed is 1° or 1/4° 2θ per minute, time constant is 4 seconds, receiving slit is 0.2 mm. or 0.1 mm., angular aperture 1° or 1/2° were used. The differential thermal analysis curves were recorded by the apparatus described by Sudo et al.[4]. Care was taken to pack the specimen into the sample block in a homogeneous manner and also to keep the weight of the specimen constant. The mean heating rate is 12.5°C per minute. The density was measured by pycnometer in carbon tetrachloride. The electron micrographs were obtained by the Hitachi HU-10A type Electron Microscope.

Results and Discussion

X-Ray Diffraction Studies. — X-ray diffractometer traces in the wet grinding process of kaolin minerals are given in Fig. 1. Fig. 1-a and Table I show the X-ray traces and the data of Mesa Alta kaolinite in their various stages of the wet grinding.

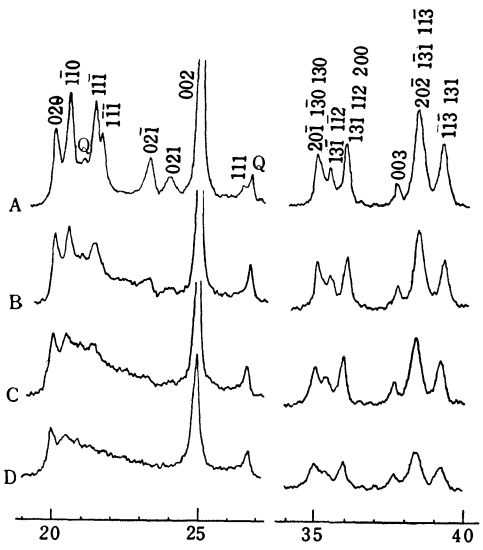
3) H. Takahashi, This Bulletin, **31**, 275 (1958).

4) T. Sudo et al., *J. Geol. Soc. Japan*(*Chishitu-Gaku-Zasshi*), **58**, 679 (1952).

TABLE I
POWDER DATA OF WET-GROUND KAOLINITE (MESA ALTA, N. M.)

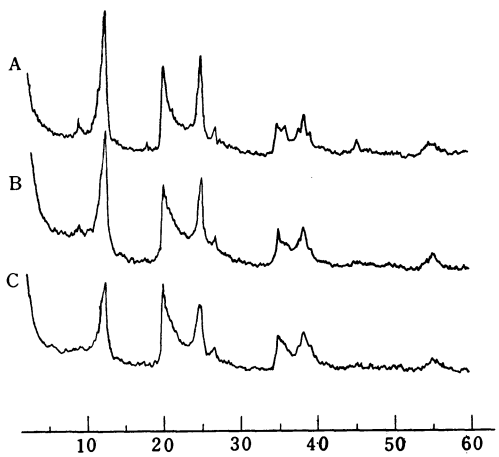
Brindley and Robinson			Original Kaolinite		Ground 96 hr.		Ground 192 hr.		Ground 384 hr.	
d	*I*	*hkl*	*d*	*I*	*d*	*I*	*d*	*I*	*d*	*I*
7.15	10+	001	7.14	VS	7.15	VS	7.16	VS	7.165	S
4.45	4	020	4.46	M	4.46	M	4.46	M	4.46	W
4.35	6	$1\bar{1}0$	4.35	S	4.35	M	4.36	W	4.36	W
4.17	6	$11\bar{1}$	4.18	S	4.18	M	4.18	W		
4.12	3	$1\bar{1}\bar{1}$	4.13	M						
3.837	4	$02\bar{1}$	3.84	M	3.84	W				
3.734	2	021	3.73	W	3.73	VW				
3.566	10+	002	3.57	VS	3.57	VS	3.58	VS	3.58	S
3.365	4	111	3.37	M						
3.138	2	$11\bar{2}$	3.14	W						
3.091	2	$1\bar{1}\bar{2}$	3.09	W						
2.748	2	022	2.75	W						
2.553	8	$20\bar{1}, 1\bar{3}0, 130$	2.55	S	2.56	M	2.56	M	2.56	W
2.521	4	$13\bar{1}, 1\bar{1}2$	2.53	M	2.53	W	2.53	W	2.53	VW
2.486	9	$1\bar{3}\bar{1}, 200, 112$	2.49	S	2.49	M	2.49	M	2.49	M
2.374	7	003	2.37	M	2.38	W	2.38	W	2.39	W
2.331	10	$20\bar{2}, 1\bar{3}1, 11\bar{3}$	2.33	S	2.33	S	2.34	S	2.34	M
2.284	9	$1\bar{1}\bar{3}, 131$	2.29	S	2.29	M	2.29	M	2.29	M
2.243	1	$13\bar{2}, 040$	2.24	W						
2.182	3	$1\bar{3}\bar{2}, 220$	2.18	W						
2.127	2	$02\bar{3}, 041$	2.13	W						
3.057	1	$2\bar{2}\bar{2}$	2.06	W						

Key to abbreviation: VS: very strong, S: strong, M: medium, W: weak, VW: very weak, br: broad, vbr: very broad.



Degrees 2θ Cu K_α

Fig. 1-a. X-ray diffractometer traces of wet-ground specimens of Mesa Alta kaolinite.
A, original kaolinite
B, ground 96 hours
C, ground 192 hours
D, ground 384 hours



Degrees 2θ Cu K_α

Fig. 1-b. X-ray diffractometer traces of wet-ground specimens of Spruce Pine halloysite.
A, original halloysite
B, ground 192 hours
C, ground 384 hours

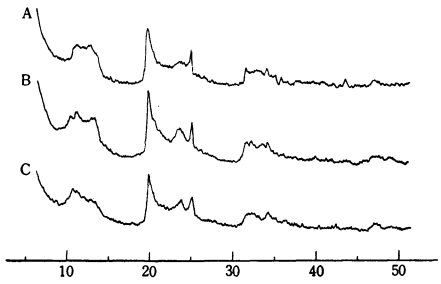


Fig. 1-c. X-ray diffractometer traces of wet-ground specimens of Tintic halloysite.

A, original halloysite
B, ground 192 hours
C, ground 528 hours

As the grinding progresses, the intensities of all reflections decrease and those of the background increase slowly. The X-ray diffraction diagram of the 48-hour-ground kaolinite is not much different from that of the original kaolinite. However, all the reflection lines become broad, $(1\bar{1}\bar{1})$ reflection becomes weak and the resolution of $(20\bar{1}, 130, 1\bar{3}0)$ reflection and $(13\bar{1}, 1\bar{1}2)$ reflection slightly fall. In the 96-hour-ground specimen, $(11\bar{1})$ and $(1\bar{1}\bar{1})$ reflections become broad, and they are hardly resolved at all with each other. The intensities of $(02\bar{1})$ and (021) reflections decrease and $(11\bar{2})$, $(1\bar{1}\bar{2})$ and (022) reflections disappear. These facts mean that the unit layers are displaced slightly in parallel to *b*-axis. In the 192-hour-ground specimen, a decrease in the intensity and a broadening of (020) and $(1\bar{1}0)$ reflections are observable, but $(02\bar{1})$ reflection can scarcely be detected. From these phenomena, it can be seen that a displacement occurs in this specimen, which is more random than the displacement by $b_0/3$ in parallel to *b*-axis. In the X-ray diagram of the 288-hour-ground specimen, the lowering in the resolution of (020) and (110) reflections is observable, but the broad $(1\bar{1}\bar{1})$ line can not be seen. In the X-ray diagram of the 384-hour-ground specimen, a wedge-like (02, 11) band is observable, but (003), $(20\bar{2}, 1\bar{3}1, 11\bar{3})$ and $(1\bar{1}3, 131)$ reflections resolve distinctly with one another. The structure of the 384-hour-ground specimen becomes similar to that of fireclay[5]; however, it has still more regular displacement comparing with that of fireclay. As shown in Table I, in the process of wet grinding, the value of the basal spacing grows gradually, though slightly, as the grinding progresses. This means that the local water gets into the space between the kaolin unit layers as the inter-layer water, or that the stacking of the unit layers becomes looser owing to the shearing stress. From the above results, it is clear that the structural change of kaolinite caused by wet grinding results from cleavages in the kaolin crystal.

In the case of halloysite, however, the features observed in kaolinite are not so remarkable. Figs. 1-b and -c show the X-ray traces in various stages of wet grinding of Spruce Pine halloysite and Tintic halloysite, respectively. As seen in these figures, the X-ray traces for various stages of wet grinding are only slightly different from one another. In the wet-ground specimen of Spruce Pine halloysite, all reflections become slightly broad; only the intensity of (00*l*) reflection decreases and the background increases, as the grinding progresses. In Tintic halloysite, the changes in X-ray traces due to wet grinding are similar to that of Spruce Pine halloysite. In the 528-hour-ground specimen, it is observable that the halloysite-glycerol complex is formed.

The reflection lines generally become slightly broad by wet grinding. To ascertain the broadening of the reflections, crystallite dimensions in the wet grinding process of Tintic halloysite are measured from (001) reflection and (02, 11) band[6], as reported in the previous papers[1,7]. Their values are shown in Table II.

The crysatllite dimensions thus obtained

TABLE II
CRYSTALLITE DIMENSIONS IN THE VARIOUS STAGES OF WET GRINDING OF TINTIC HALLOYSITE

Grinding time (hr.)	Crystallite dimension (Å)	
	L_c (from 001 reflection)	L_a (from 02, 11 band)
0	80	155
192	76	141
288	70	118
384	66	110
528	58	105

5) G. W. Brindley and K. Robinson, *Trans. Farad. Soc.* **42B**, 198 (1946).
6) W. L. Bragg, "The Crystalline State", I, 189 (1933); B. E. Warren, *Phys. Rev.*, **59**, 693 (1941); C. W. Brindley and K. Robinson, *Min. Mag.*, **28**, 393 (1948); C. R. Houska and B. E. Warren, *J. Appl. Phys.*, **25**, 1503 (1054).
7) H. Takahashi, This Bulletin, **32**, 17 (1959).

are, of course, not accurately real crystallite sizes but relative values. The change of the basal spacing in the process of wet grinding of halloysite is not so remarkable as that of kaolinite. This indicates that the cleavage caused by wet grinding is not very remarkable in halloysite compared with that of kaolinite. The dry grinding is in general more effective than the wet grinding in causing the structural change. However, it is observable that there is a great difference in the wet grinding effects between kaolinite and halloysite. As clearly shown in X-ray data, kaolinite is subjected to its effects more than halloysite though its degree of crystallinity is originally higher. In kaolinite, the shearing stress acts in parallel to the layer planes, as kaolinite is made of stacking of parallel unit layers. On the other hand, in halloysite, its crystal has a tubular shape, resulting from the rolling up of the unit layers[8]. So, it is hard to make cleavage by shearing stress through wet grinding. Furthermore, as halloysite has originally a two-dimensional structure; even if a small displacement takes place along the unit layers, it does not affect its X-ray diagram.

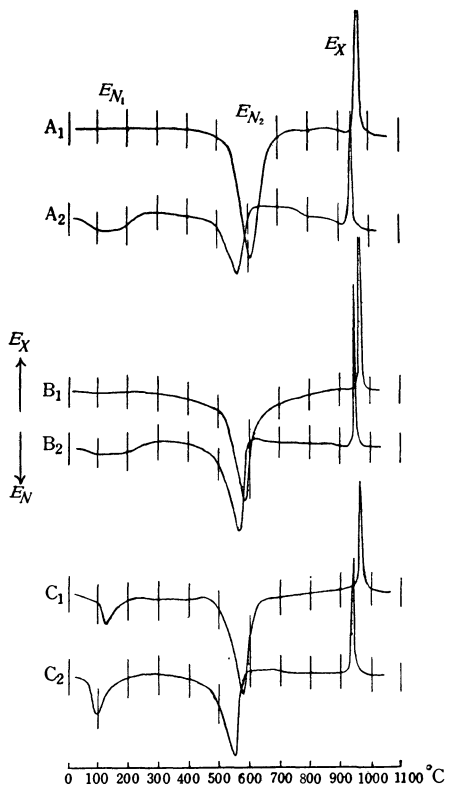


Fig. 2. Differential thermal analysis curves of wet-ground specimens of kaolin minerals.
A_1, original Mesa Alta kaolinite
A_2, ground 384 hours
B_1, original Spruce Pine halloysite
B_2, ground 384 hours
C_1, original Tintic halloysite
C_2, ground 528 hours

Differential Thermal Analysis.—Differential thermal analysis curves and data in the process of wet grinding of kaolin minerals are shown in Fig. 2 and Table III.

In ground specimens of kaolinite, the the first endothermic reaction (E_{n1}) associated with the loss of the inter-layer or adsorbed water becomes apparent and its height increases as the grinding progresses. This means that the water gets locally into the increased spaces between kaolin layers because of cleavages through wet grinding, and it becomes the inter-layer water, and/or that the non-crystalline material which adsorbs some amounts of water is produced by wet grinding. For the second endothermic reaction (E_{n2}) associated with the loss of the lattice water, as the grinding progresses, the lowering in its peak temperature and the decrease in its peak height and area are observable. In the final exothermic reaction (E_x) due to the mullite nucleation, as the grinding progresses, the lowering in the peak temperature, the increase in the peak breadth and the decrease in the peak height and area are observable. However, in halloysite, these features observed in this reaction are not so remarkable compared with that of kaolinite. This fact corresponds to the fact that kaolinite is more liable to suffer the effects of wet grinding than halloysite as shown in X-ray data. That is, in halloysite, although a lowering in the peak temperature is observable, the peak breadth decreases and the peak height is either invariable or increases. These phenomena indicate that the effect of wet grinding of halloysite is nearly the same as the effect at the early stage of dry grinding[1].

Density.—In Fig. 3 is shown the density at various periods of grinding. Measurements were made after the specimens had been dried at 110°C in order to avoid the effect of the adsorbed water.

In halloysite, the density gradually decreases at first; after reaching a certain point of grinding, it rapidly decreases. On

8) T. F. Bates, F. A. Hildebrand and A. Swineford, *Am. Mineral.*, **35**, 463 (1950).

TABLE III
THERMAL DATA OF WET-GROUND KAOLIN MINERALS
(ALL TEMPERATURES ARE DEGREES CENTIGRADE)

Specimen	E_{n1}			E_{n2}			E_x			
	Temp. (°C)	Height	Area	Temp. (°C)	Height	Area	Temp. (°C)	Height	Area	Breadth (°C)
Kaolinite (Mesa Alta, N.M.)										
Original	—	—	—	604	16	1080	966	39	220	5.1
Wet-Ground 384 hr.	120—170	2	230	566	13	660	947	31	190	8.4
Halloysite (Spruce Pine, N.C.)										
Original	125	1	70	583	17	1380	973	45	220	4.0
Wet-Ground 384 hr.	100—200	1	200	564	15	900	971	53	190	3.5
Halloysite (Tintic, Utah)										
Original	130	4	170	571	12	680	969	16	170	9.4
Wet-Ground 432 hr.	-110-	5	240	555	10	560	952	16	130	7.3

the other hand, in kaolinite, the decrease in the density is remarkable in the early stage of grinding, then the density slowly decreases, and finally it attains a nearly constant value. The rate of change in the density corresponds to the fact that kaolinite is more liable to suffer the effect of wet grinding than halloysite, at least in the early stage of grinding as indicated in previous sections.

The structure of kaolinite changes into a disordered structure due to cleavage caused by the wet grinding, while halloysite scarcely suffers the effect in the early stage of grinding. In a considerably long time of grinding, the structure of halloysite gradually decomposes due to fracturing and cleavage caused by grinding. This corresponds to the somewhat rapid decrease in the density.

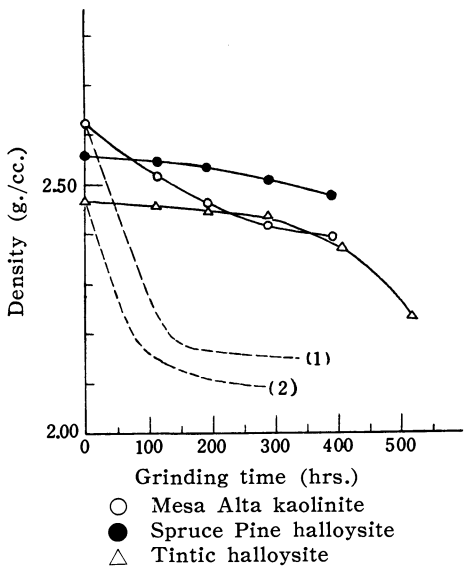


Fig. 3. Curves showing the changes of the density of wet-ground specimens of kaolin minerals with the time of grinding. (1), (2): Curves showing the changes in the process of dry grinding of Mesa Alta kaolinite and Tintic halloysite, respectively.

Electron Microscopic Studies.—The electron micrographs of some ground specimens are shown in Fig. 4.

In the early stage of grinding of kaolinite, it is seen that the edge of a kaolin crystal tends to curl. This tendency is interpreted in the light of the characteristic of the shape of kaolin unit layer by Bates et al.[8]. That is, kaolin mineral with a random displacement has generally the tubular shape like halloysite. The relation between the degree of crystallinity of a kaolin mineral and the shape of the crystal was presented in the previous paper[3]. As the grinding progresses, the shape of the kaolin crystal gradually change into a circular but platty shape. The particle size does not change remarkably. Finally, it changes into spherical aggregates of fine platty particles.

In halloysite, various shapes such as split tubular, platty, lath-shaped, cabbage-like and other variations are observable in the wet grinding process. From these phenomena, it seems that the force of wet grinding causes fracturing rather than shearing.

Mechanism of Structural Change of Kaolin Mineral due to Wet Grinding.—When kaolinite is wet-ground, the crystal

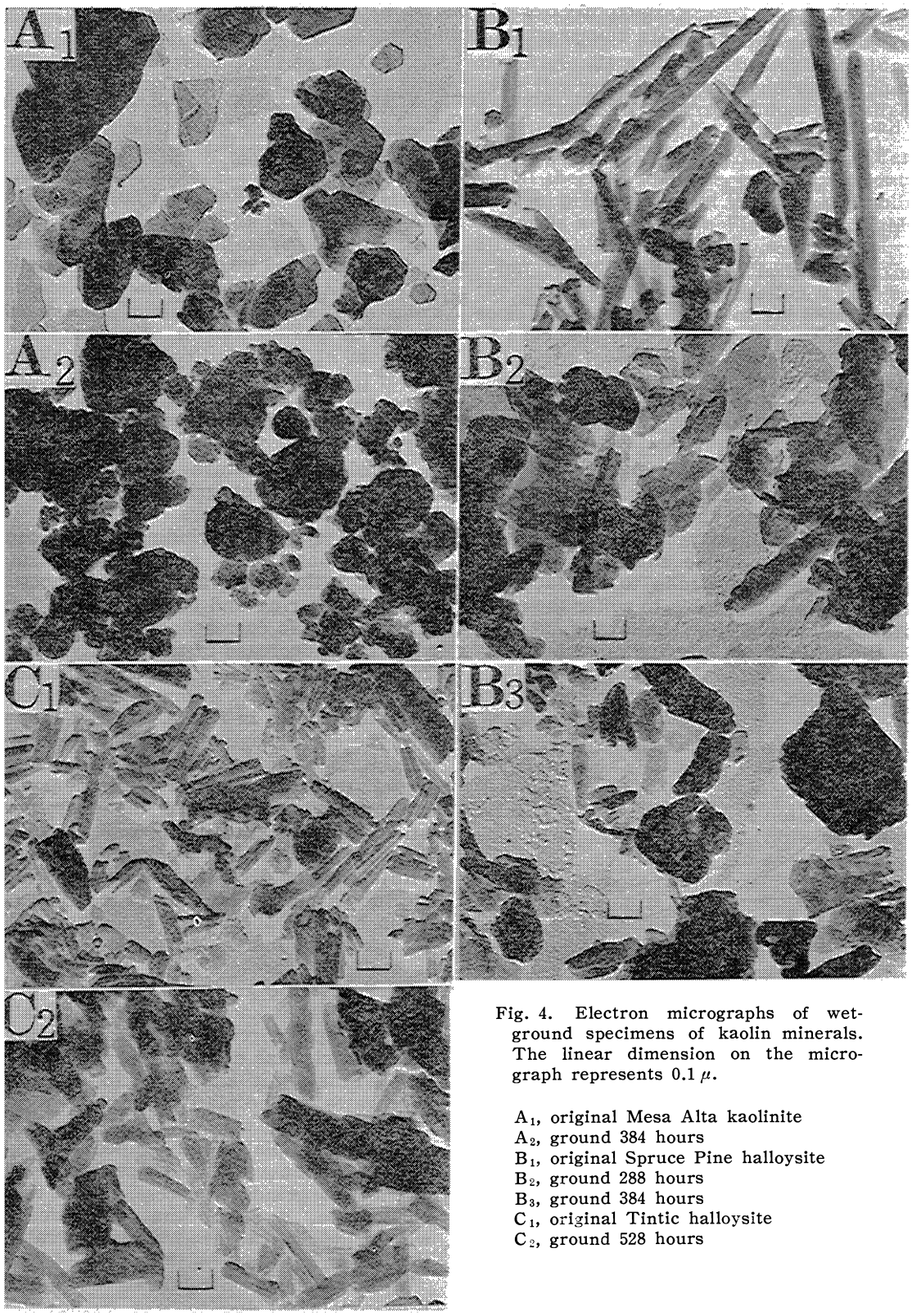


Fig. 4. Electron micrographs of wet-ground specimens of kaolin minerals. The linear dimension on the micrograph represents 0.1 μ.

A_1, original Mesa Alta kaolinite
A_2, ground 384 hours
B_1, original Spruce Pine halloysite
B_2, ground 288 hours
B_3, ground 384 hours
C_1, original Tintic halloysite
C_2, ground 528 hours

cleaves along the layer plane owing to shearing stress. In consequence, displacement of layers takes place in parallel to *b*-axis. As the grinding progresses for a long time, the structure of the original kaolinite with a triclinic in symmetry change into the more disordered structure. These displacements are remarkable in the early stage of grinding. The change of the particle shape due to wet grinding is observable as the gradual formation of fine and radial platty particles though it is not so remarkable in the early stage. When the grinding further progresses, kaolinite with a higher degree of crystallinity gradually changes into kaolin with a random displacement similar to that of halloysite.

In the early stage of grinding of halloysite, the original crystal splits and fractures owing to the fracturing force. Therefore, the change on the X-ray diagram is not so remarkable and the thermal data also indicate the same tendency. From the electron micrographs, too, it can be concluded that the force of wet grinding acts as a fracturing force, which results in splitting tubular crystal. The process of the structural change through wet grinding for the platty particle of halloysite produced by splitting is similar to that of kaolinite.

Summary

The effects of wet grinding on kaolin minerals were examined by X-ray diffraction method, differential thermal analysis, electron microscopy and density measurement. The effects of wet grinding of kaolin minerals are different from those of dry grinding, particularly at the early stage of grinding. It has been considered that the force of dry grinding acts as fracturing and cleaving forces, while the force of wet grinding acts as a weak cleaving force for kaolinite and as a weak fracturing force for halloysite in the early stage of grinding. It has been revealed that the effects of wet grinding depend on the shape of crystal in the original kaolin mineral in the early stage of grinding, and beyond a certain stage of grinding, they depend on the structural perfectness of the kaolin layer, that is, the internal degree of crystallinity of the original kaolin mineral.

The author wishes to express his hearty thanks to Professor H. Akamatu for his continuous advice and encouragement. Thanks are due to Professor T. Sudo of the Tokyo University of Education for his valuable suggestions and discussions.

Department of Chemistry
Faculty of Science
the University of Tokyo
Hongo, Tokyo

Formation and Aging of Precipitates. XI. An Electron Micro-Diffraction Study on Nucleation of Barium Sulfate Precipitate from Homogeneous Solution*

By Kazuyoshi TAKIYAMA

(Received October 6, 1958)

In the course of precipitate formation, the nucleation process is the idea generally accepted. The nucleation involves a process of formation of embryo, which is an unstable intermediate, and a process of the nucleus formation. When the precipitate is formed with direct mixing of ions, the growth of the nuclei formed in small numbers plays a predominant part in the region of the lower concentration, and the nucleation plays a predominant part in the higher concentration region[1,2]. When the precipitate is formed from a homogeneous solution, the nucleation occurs when a certain degree of supersaturation is attained[3]. During the

* The tenth paper of this series, This Bulletin, 32, 68 (1959).

1) K. Takiyama, ibid., 31, 950 (1958).
2) K. Takiyama, ibid., 32, 68 (1959).
3) V. K. LaMer and R. H. Dinegar, *J. Am. Chem. Soc.*, 73, 380 (1951).

precipitation process the crystal property of particles seems to appear after nucleation.

An attempt has been made in the present investigation to employ the electron micro-diffraction method with a view to observe the nucleation process during the formation of barium sulfate precipitate according to LaMer and Dinegar's method[3].

Experimental

Procedure.—Fifty ml. of 0.02 M ammonium persulfate solution was added to a 200 ml. beaker containing 50 ml. of 0.02 M barium nitrate solution. Barium sulfate formed from the sulfate in persulfate was filtered with a glass filter. Ten ml. of 0.1 M sodium thiosulfate solution was then added to the clear filtrate and the reaction solution thoroughly mixed was kept in a thermostat at 25°C. The precipitate, when examined with a beam of white light, exhibited Tyndal beam 7 minutes after the addition of thiosulfate.

The reaction mixture was poured into a spray bottle which was kept in the thermostat, and was sprayed on tiny Formvar films floating on the surface of distilled water 5, 6, 7, 8, 9 and 10 minutes after the addition of thiosulfate. A few minutes were allowed for diffusion of soluble salts from the drop of reaction mixture into the water below. The films were scooped with specimen grids for observation with an electron microscope.

Calculation of Size of Crystalline Nucleus.—From the Thomson's equation[4] on nucleation in the supersaturated vapor, the size of nucleus formed in the supersaturated sparingly soluble salt solution is expressed by the following equation,

$$r=\frac{2M\sigma}{iRT\rho \ln S/S_\infty} \qquad (1)$$

where r is the radius of spherical nucleus, M the molecular weight, σ and ρ are the surface tension and the density of the crystal, R is the gas constant, T the absolute temperature, S the supersaturation concentration, S_∞ the solubility of the salt and i the van't Hoff factor. According to LaMer and Dinegar[3], the value of the supersaturation ratio, $\sqrt{K^\circ_{SS}/K^\circ_{SP}}$ (K°_{SS} and K°_{SP} are the activity products of both supersaturated and saturated solutions), is a constant and is 22 on an average at 25°C. The value of r is calculated in the present case, as 100 Å from the equation 1, when this limiting value, 22, is substituted for S/S_∞. On the other hand, the condition of concentration of reacting ions at the time that the precipitate begins to appear in the case of homogeneous solution method, seems to correspond to the limiting supersaturation concentration at which the precipitate appears without an induction period in the case of direct mixing method. This limiting supersaturation concentration is about 0.002 M[1]. The size of nucleus, r, is calculated as 60 Å according to the equation 1, when this value of 0.002 is substituted for S. It seems that the size of crystalline nucleus formed under the experimental condition mentioned above is in the range of 100 to 200 Å in diameter.

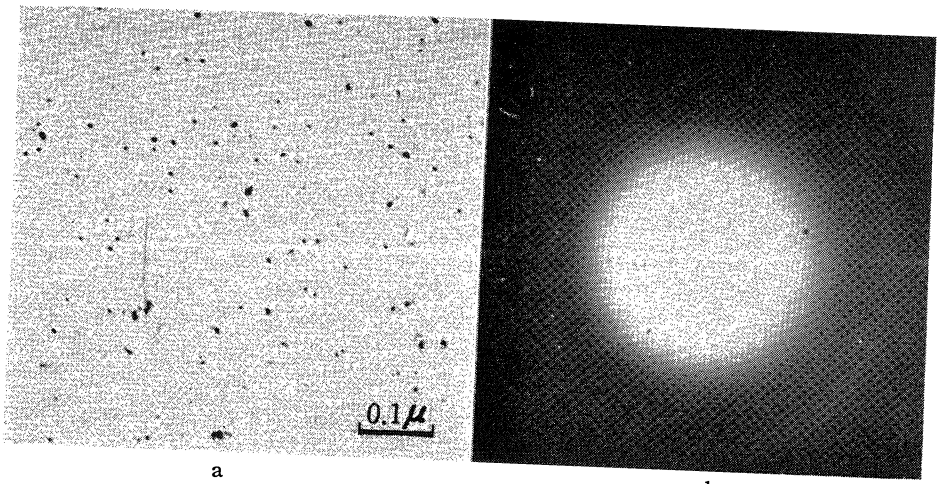
Results

The image of particles began to be observed with the electron microscope after 6 minutes and the particles grew gradually as the time passed. An electron micrograph and an electron diffraction pattern obtained from the six minutes' specimen are shown in Figs. 1 a and b. The diameter of particles shown in Fig. 1 a measures 30 to 80 Å and the particles looked like unstable embryos formed by aggregation of monomers. As the crystal structure of these particles is not perfect, the diffraction pattern is composed of a few broad rings. The particles in the seven minutes' specimen are nearly spherical and measure 100 to 200 Å in diameter as shown in Fig. 2 a. The size of these particles coincides with that obtained by the calculation from equation 1. The electron diffraction pattern obtained from these particles is composed of indistinct coarse rings as shown in Fig. 2 b. But the rings indicate that the crystal structure of particles is more perfect than that of particles shown in Fig. 1 a. The size of particles in the eight minutes' specimen is 300 to 400 Å in diameter as shown in Fig. 3 a. The electron diffraction pattern is composed of distinct coarse Debye-Scherrer rings as shown in Fig. 3 b. The crystal structure of particles seems to have been completed in this stage. The particles in the ten minutes' specimen are spindle-shaped and the length of the long axis is about 1000 Å as shown in Fig. 4 a. The electron diffraction pattern obtained from one of the particles arrow is N-pattern as shown in Fig. 4 b. Each particle is obviously a single crystal, and the long axis proves to be b-axis from the analysis of the pattern shown in Fig. 4 b. The shape of the particle grown completely is oval. The oval particle of barium sulfate seems to be formed through dendritic growth in every direction from a crystal nucleus and the particle has a single crystal structure. The growth along b-axis seems to be more or less marked.

The particles of barium sulfate began

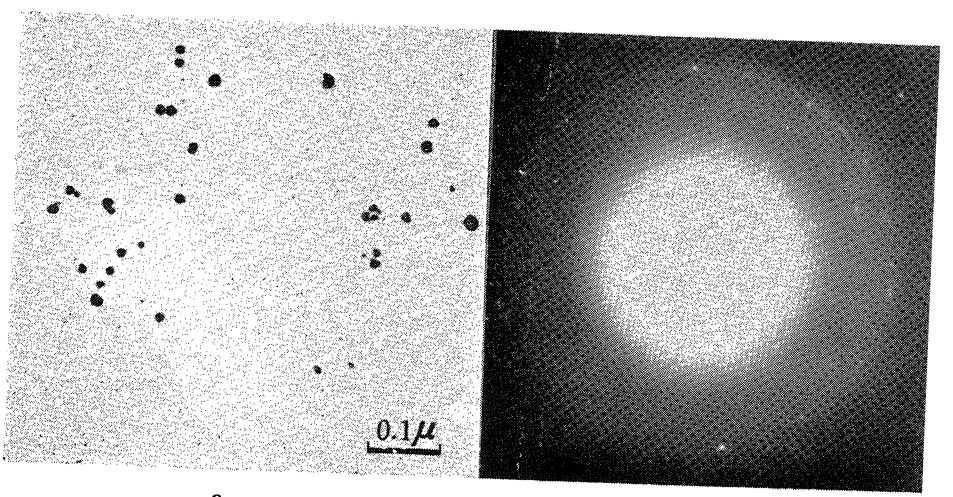
4) W. Thomson, *Phil. Mag.*, **42**, 448 (1871).

Electron micrographs and diffraction patterns of barium sulfate presipitates.



a (×100, 000) b

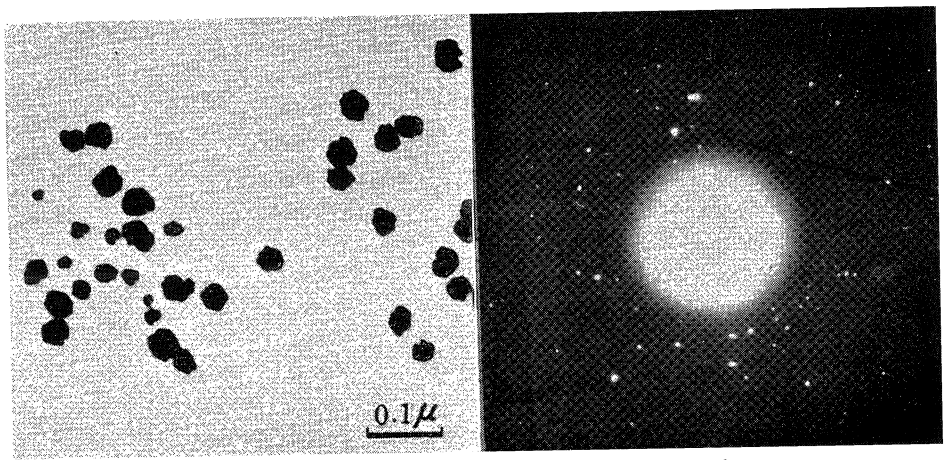
Fig. 1. Embryos of barium sulfate precipitate sampled after 6 minutes.



a (×100, 000) b

Fig. 2. Crystal nuclei of barium sulfate precipitate sampled after 7 minutes.

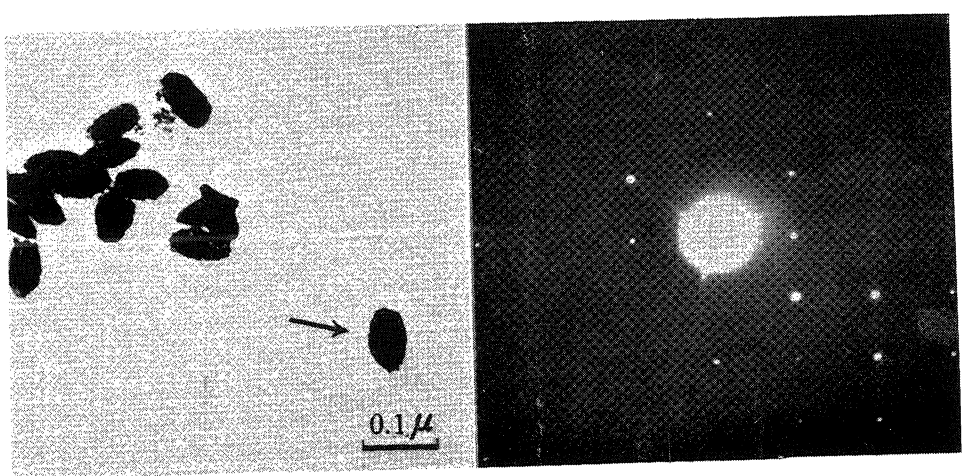
Electron micrographs and diffraction patterns of barium sulfate presipitates.



a b

(×100, 000)

Fig. 3. Crystals of barium sulfate precipitate sampled after 8 minutes.



a b

(×100, 000)

Fig. 4 Single crystals of barium sulfate precipitate sampled after 10 minutes.

to appear after 6 minutes and grew up continuously into large crystals. During the precipitation process, the existence of the nucleus with a certain size can be logically proved from the standpoint of thermodynamics[3,4], but in fact only the continuous growth of a particle is observed by electron microscopy and the particle appears to form a distinct crystal structure when it has attained the size as large as that of the nucleus calculated thermodynamically.

Summary

The nucleation process of the precipitation of barium sulfate from the homogeneous solution of persulfate-thiosulfate system was observed by the electron micro-diffraction method. The particles grew continuously, but the distinct crystal structure began to appear in the particles having the length of 100 to 200 Å in diameter, corresponding to the nucleus calculated thermodynamically.

The author gratefully acknowledges the guidance of Professor Eiji Suito of Kyoto University. He also wishes to express his hearty thanks particularly to Professor Masayoshi Ishibashi of Kyoto University for his continuous advice and encouragement.

Institute for Chemical Research
Kyoto University
Takatsuki, Osaka

Studies on the Interaction of Surface Films with Solute in Solution. V Deposition of Monolayers of Several Amphipathic Compounds from Surfaces of Aqueous Solutions of Congo Red and Crystal Violet

By Mitsuo MURAMATSU

(Received September 18, 1958)

It has been shown by several investigators that useful knowledge could frequently be obtained for the surface interaction of the insoluble monolayer formed at air-water interface with the other additives, by investigating the nature of the built-up film obtained from the surface of aqueous substrate. Thus, the nature of the mixed monolayer of stearic acid and normal paraffin[1] or cetyl alcohol[2] has been studied by means of this method. In the latter case, formation of a stoichiometric complex of 1:1 ratio was suggested by the measurement of the surface potential, which was in agreement with the experimental result on the mixed monolayer of the same materials spread on the surface of water[3]. Such a method could sometimes be applied to study the interaction between the insoluble monolayer and the aqueous solute in the solution underlying the film. The present author[4] obtained the built-up film of stearic acid of low refractive index by transferring the monolayer from the surface of aqueous solutions containing copper, aluminum and thorium ions and discussed the structure of metal soap formed at the solution-air interface. A similar method could successfully be applied to the case of interaction between dicarboxyacids in aqueous phase and octadecylamine in the monolayer spread on it[5].

In the preceding reports[6,7] it has been shown that the addition of dye to aqueous substrate resulted in a remarkable expansion of the monolayer of amphipathic compound spread on it, when pH of the substrate was in a proper range where the binding of dye to the film material as well as the aggregation of the former

1) H. Sobotka and S. Rosenberg, *J. Colloid Sci.*. 5, 581 (1950).
2) T. Isemura and R. Nakagawa, *Memoirs Inst. Sci. Ind. Research, Osaka Univ.*, 8, 140 (1951).
3) J. Marsden and J. H. Schulman, *Trans. Faraday Soc.*, **34**, 748 (1938).
4) M. Muramatsu and T. Sasaki, This Bulletin, **25**, 21, 25 (1952).
5) T. Sasaki and M. Muramatsu, ibid., **26**, 96 (1953).
6) M. Muramatsu, ibid., **31**, 878 (1958).
7) M. Muramatsu, ibid., **32**, 114 (1959).

was remarkable. This could be ascribed to the interaction between the dye and the amphipathic compound, involving ionic, dipolar and van der Waals' forces. A similar conclusion was obtained by Matuura[8] in the case of the monolayer of stearic acid. To obtain further confirmations for such an interaction, the present author has intended to study the nature of the built-up films of several amphipathic compounds transferred from the surfaces of aqueous solutions of Congo red and Crystal violet.

Experimental

Materials. — Amphipathic compounds and dyes were purified thoroughly by the methods similar to those used in the former experiments[6,7]. Oleic acid and castor oil as piston oils were pure grade commercial products of Kahlbaum and Takeda, respectively, which were used without any further purification. Tri-*p*-cresyl phosphate was synthesized by the reaction of *p*-cresol and phosphorus pentachloride[9] and was distilled three times in vacuo.

Method.—Monolayers were spread from the benzene solutions of amphipathic compounds onto the aqueous substrates, containing or lacking the dyes. They were built up onto the base echelon of successive Y-multilayers of barium stearate deposited on a highly polished slide of stainless steel, by means of Langmuir-Blodgett technique[10] under the spreading pressure, F, of either of tri-*p*-cresyl phosphate ($F=10$ dyn./cm.), castor oil (15 dyn./cm.) or oleic acid (30 dyn./cm.), unless otherwise mentioned. The spacing of the built-up film was determined by means of the simplified optical method[11], assuming the same refractive index of 1.462 for the film as that of the base echelon, spacing of which was reported to be 24.4Å[10].

Concentration of the dye solution was kept to 10^{-4}mol./l. The acidity of the substrate was adjusted simply by twice-distilled hydrochloric acid and ammonia using the Beckman glass electrode. In the case of dye solution, experiments were conducted under the pH of largest expansion of each monolayer[7,8].

Results

Ease of Building-up of the Films.— Successive Y-multilayer of stearic acid could easily be obtained in pH range of 4～7 by transferring the monolayer under the spreading pressure of oleic acid or castor oil from the surface of water containing no dye. When pH of water was less than 4, however, the monolayer adherred neither to the bare surface of the slide nor to the base echelon of barium stearate. These facts are in agreement with what was reported[10]. In contrast with this, the successive Y-multilayer was obtained from the surface of the aqueous solution of Congo red the pH of which was 3.2. Deposition of the monolayer was clearly favored by the addition of the dye at least in the region of low pH, presumably owing to an increased stability of the film. From the surface of the solution of Crystal violet, we could obtain the Y-multilayer only when the monolayer was compressed by oleic acid and the slide was dried thoroughly after each transfer of the film.

Attempts were made to build the multilayers of cholesterol from the substrates of water and solution of Congo red. In the former case the substrate water of pH 5.8 proved to be favorable for obtaining the successive Y-layer for any piston oil used, while deposition of the monolayer was unsuccessful on the substrate of pH 2.0. Here, the addition of Congo red to the substrate resulted in promoting the easiness of building-up of the film even at pH 2.0. In this case the use of oleic acid and castor oil as piston oil effected Y-layer and occasionally X-layer.

The monolayers of cetyl alcohol, ethyl *n*-hexadecyl ether and ethyl stearate adhered neither to the bare surface of the slide nor to the base echelon, irrespective of the addition of Congo red to the substrate. This was indeed the fact under the spreading pressure of any piston oil used. Further efforts were also made to build up the multilayers under the spreading pressure of benzene solutions of film material placed near the slide covered with the base echelon. This method proved to be suitable for the deposition of such monolayers as copper, aluminum and thorium stearate, to which the ordinary technique of Langmuir-Blodgett method failed to apply[4]. However, it was unsuccessful in the present case even with this method.

The monolayer of octadecylamine could be deposited onto the base echelon only when the fiilm was compressed by tri-*p*-cresyl phosphate, under the substrate pH of 5～9. This was in agreement with the results reported in a former paper[5]. When Crystal violet was added to the aqueous substrate, no monolayer could be deposited in many cases onto the solid surface. Even when it could be built up,

8) R. Matuura, This Bulletin, **24**, 282 (1951).
9) W. Autenrieth and A. Geyer, *Ber.*, **41**, 146 (1908).
10) K. B. Blodgett and I. Langmuir, *Phys. Rev.*, **51**, 964 (1937), etc.
11) T. Tachibana, *J. Japanese Biochem. Soc.* (*Seikagaku*), **20**, 8 (1948).

TABLE I

BUILT-UP FILMS OF STEARIC ACID, CHOLESTEROL AND OCTADECYLAMINE TRANSFERRED FROM THE SURFACES OF AQUEOUS SUBSTRATES CONTAINING OR LACKING DYE

Film material	Conditions of building-up: Substrate sol.		Conditions of building-up: Piston oil*	Nature of the built-up film: Type of the film	Nature of the built-up film: Apparent spacing, Å	Nature of the built-up film: Wetting toward	
	Dissolved dye	pH				water	benzene
Stearic acid	none	4~7	C or O	Y	23.1±0.2	hydrophobic	oleophobic
〃	Congo red	3.2	C or O	Y	22.1±0.4	〃	oleophilic
〃	Crystal violet	7.2	O	Y	29.2±2.9	〃	〃
Cholesterol	none	5.8	T, C or O	Y	18.4±0.2	〃	〃
〃	Congo red	2.0	C or O	Y or X	25.8±0.3	〃	〃
Octadecylamine	none	5~9	T	Y	24.4±0.5	〃	oleophobic
〃	Congo red	5.5	T	Y	22.4±0.4	〃	oleophilic

* C, castor oil; O, oleic acid; T, tri-*p*-cresyl phosphate

we merely obtained optically heterogeneous films, irrespective of the nature of the piston oil and of the substrate pH. In contrast with this, homogeneous Y-multilayer was obtained successively from the surface of the solution of Congo red of pH 5.5, when the monolayer was compressed by tri-*p*-cresyl phosphate and the built-up film was dried after each transfer of the film.

The conditions for the successful deposition of the film were summarized in the columns of Table I from the first to the fourth columns. In this table the fifth column expresses the types of the multilayers thus obtained.

Spacing of the Built-up Films. — In Table I, the sixth column shows the spacing of the built-up films of stearic acid, cholesterol and octadecylamine, transferred from the surfaces of aqueous substrates containing or lacking dye. They are expressed in average values of 5—12 independent experiments. When the monolayer was deposited from the surface of water, the spacing depended only a little on the acidity of substrate throughout the whole region of pH investigated and on the choice of piston oil. The latter condition was valid also in the case of the solution of dye as substrate. This might come from the low compressibility of these films[7].

Wettability of the Films. — As is cited in the seventh column of Table I, all built-up films were of hydrophobic character when they were once dried. Of these films, the film of stearic acid was reported to be wetted profoundly by aqueous solutions of copper, aluminum and thorium ions[4,12]. Such an effect of metal ions was observed in the present experiments for the built-up films of stearic acid transferred from the surfaces of water, solution of Congo red and of Crystal violet. However, there were some differences between the three films in their behaviors towards the subsequent procedure. For the first film, the solid surface remained in its hydrophilic condition for at least two minutes after final rinsing with water. For the second and the third films, the procedure under the same condition resulted in peeling-back of rinsing water. After the films were once dried, the subsequent conditioning by aqueous metal ions gave rise to no wetting of the first film, while it rendered the remaining two films wettable.

The last column of Table I represents the wettability of these films toward a drop of benzene placed on them. Though the test was merely qualitative, the result was sufficient to classify the film into two groups with respect to their wetting characters. Benzene showed a large contact angle toward the films of stearic acid and of octadecylamine both transferred from the surface of water. When the slide was tilted, the drop slid on the film on which less color change was observed at the track. On the contrary, the contact angle was very small for the rest of the films and the sliding of the drop resulted in a remarkable change in color, showing the profound dissolution of film materials into the benzene drop.

Discussion

As mentioned in the preceding section, the monolayers of cetyl alcohol, ethyl *n*-hexadecyl ether and ethyl stearate spread on the surfaces of water adhered neither to the metal surface nor to the base echelon of barium stearate. Isemura

12) I. Langmuir, *Science*, **87**, 493 (1938); A. Inaba, This Bulletin, **26**, 43 (1953).

and Nakagawa[2] have obtained a similar result for the case of cetyl alcohol. In the case of ethyl stearate it was reported[13] that the monolayer could be deposited successively only under the delicate control of substrate pH, speed of down- and up-trip of the slide. The built-up film thus obtained however seems to consist of large crystals transferred heterogeneously on the slide, as was pointed out by the microscopic observation[14]. All these phenomena, as well as the present results, seem to show the difficulty of building up a non-ionic monolayer spread on water. A similar result was obtained for the monolayers of these compounds spread on aqueous solutions of Congo red. Under the present conditions of pH of substrate, the majority of dye molecules were considered to be in a zwitterion form as pointed out in a preceding report[7]. Therefore, there is no net charge in the molecules either of film materials or of dye.

On the other hand, building-up was successful in the cases of the monolayers of stearic acid, cholesterol and octadecylamine spread on the solutions of Congo red, and of stearic acid on the solution of Crystal violet. Of these films, it is noticeable that the building-up of the monolayers of stearic acid and cholesterol is facilitated by an addition of Congo red to the substrate. Here, because of Congo red being in the region more acidic than the isoelectric point, the molecules of the dye have a positive charge while the monolayers are not in a charged state[7]. In the remaining two cases, dye and film materials are charged oppositely to each other, as pointed out in the preceding reports[7,15]. These facts lead us to a presumption that a suitable attachment of charged dye to the film material does not decrease the easiness of obtaining a built-up film of its own.

As seen in Table I, the apparent spacing of the built-up film of stearic acid or octadecylamine is decreased by an addition of Congo red to the substrate of the monolayer. It has been reported that the monolayers of stearic acid[8] and octadecylamine[7] expanded remarkably when they were spread on aqueous solution of Congo red and were compressed to a surface pressure of piston oil used in the present experiment. This could be explained by an attachment of colloidal aggregates of dye to the monolayer. Therefore the attachment of Congo red to the film may cause an increase in film thickness, while it may result in a decrease in surface density of *n*-hydrocarbon chain of the amphipathic compound and consequently a decrease of refractive index of the film. These two effects contribute oppositely to each other to the apparent spacing which we actually measured assuming the same refractive index of the upper layer as that of the base echelon. In the present case, the effect of the former seems to be overwhelmed by that of the latter. A similar effect of solute was observed in the case of the built-up film of stearic acid obtained from the surface of aqueous solutions of copper, aluminum and thorium ions[4]. In contrast with this, an overwhelming contribution of the former is observed for the film of cholesterol spread on the solution of Congo red and for the film of stearic acid on the solution of Congo red and for the film of stearic acid on the solution of Crystal violet.

It is of interest to show that, though all the films studied exhibit hydrophobic property, they are wettable toward benzene, except for the films of stearic acid and octadecylamine transferred from the surface of water which proved to be oleophobic. Zisman et al.[16] obtained the oleophobic monolayers of methyl-rich surface being non-wettable toward methylene liquid such as *n*-hexadecane, benzene, etc. They explained the phenomenon by a difference between methyl-methyl and methylene-methylene attractions[17]. As was pointed out by several investigators[18], the oleophobic character toward methylene liquid seems to suggest the existence of the methyl-rich surface, in which the molecules are closely packed and orientate towards the contacting phase. In Table I the built-up films of stearic acid and octadecylamine show an oleophobic property while the cholesterol film proves to be oleophilic, when they are transferred from the surface of water. This can be explained by the greater difficulty of packing of methyl head for the case of cholesterol, as would be expected from the special structure of

13) E. Stenhagen, *Trans. Faraday Soc.*, **34**, 1328 (1938).
14) G. Knott, J. H. Schulman and A. F. Wells, *Proc. Roy. Soc.*, **A176**, 534 (1940).
15) M. Muramatsu, This Bulletin, **31**, 871 (1958).
16) W. A. Zisman et al., *J. Colloid Sci.*, **1**, 513 (1946); **2**, 563 (1947).
17) W. A. Zisman et al., ibid., **7**, 109, 166, 428, 465 (1952).
18) See, *Discussions Faraday Soc.*, **3**, 250 (1948).

cholesterol. Similarly, the oleophilic nature of the films taking up the dye can reasonably be explained by the structure of built-up film consisting of widely spaced *n*-hydrocarbon chain. We can find that this is also in a conformity with the effect of added dyes upon the limiting area of the monolayers of stearic acid, cholesterol and octadecylamine[7,8].

Summary

Attempts were made to obtain the built-up films of stearic acid, cholesterol, cetyl alcohol, ethyl *n*-hexadecyl ether, ethyl stearate and octadecylamine, by transferring each monolayer from the surfaces of water and aqueous solutions of Congo red and Crystal violet. Deposition of the monolayers of cetyl alcohol, ethyl *n*-hexadecyl ether and ethyl stearate was unsuccessful, irrespective of whether the substrate contained dye or not. On the other hand, the monolayers of the remaining compounds could easily be deposited onto the solid phase from the surfaces of water and dye solution.

The effect of added dye upon the apparent spacing of the film thus obtained seems to show an attachment of dye to the film substance, though the spacing varied from one case to another. This variation could be explained taking account of the balance of two contributing factors mutually opposite to the apparent spacing: one, increase of the film thickness due to the attachment of dye, and the other, decrease of the refractive index of the film due to the wide separation of *n*-hydrocarbon chain. Such a consideration was supported by the data on the wettability toward benzene. All these phenomena are in agreement with the data on the effect of dissolved dye upon the limiting area of the monolayer spread on it.

In conclusion the author expresses his hearty thanks to Professor T. Sasaki for his kind guidance in the course of this study. The cost of this research has been defrayed from the grant of the Ministry of Education given to the Professor.

Department of Chemistry
Faculty of Science
Tokyo Metropolitan University
Setagaya-ku, Tokyo

Remarks on the Molecular Calculation of Naphthalene and Anthracene

By Noboru MATAGA, Kichisuke NISHIMOTO and Shizuyo MATAGA

(Received September 22, 1958)

The calculations made by Pariser and Parr[1,2] and also by Pople[3] in terms of semi-empirical molecular orbital (MO) method, have made a remarkable progress in the interpretation of the spectra of π-eletron systems. However, the agreement between the experimental and the theoretical results on the spectra of naphthalene which should come to our attention naturally next to benzene, does not seem to be satisfactory as yet. Although the results of Pople's SCF calculation[3] and Pariser's ASMOCI calculation[2] seem to be fairly well founded experimentally, the results of SCF and ASMOCI calculations of Moser and Lefebvre[4] in various degrees of approximations are in rather an unfortunate disagreement with experimental observations. Such an undesired circumstance is not restricted only to the case of electronic spectra, but, for example, the calculated bond orders of naphthalene and anthracene seem to agree hardly at all with observed values. The bond orders of naphthalene calculated with naive MO's are in a serious discrepancy with experimental values, but those of anthracene calculated in the same way are in good cor-

1) R. Pariser and R. G. Parr, *J. Chem. Phys.*, **21**, 466, 767 (1953); ibid., **23**, 711 (1955).
2) R. Pariser, ibid., **24**, 250 (1956).
3) J. A. Pople, *Proc. Phys. Soc.*, **A68**, 81 (1955).
4) R. Lefebvre and C. Moser, *J. Chem. Soc.*, **1956**, 1557, 2734.

TABLE I
CALCULATED AND OBSERVED SPECTRA OF NAPHTHALENE

State	Calcd. (i)		(ii)		(iii)		Pople		Pariser		Obs.	
	$h\nu$(e.V.)	f	$h\nu$(e.V.)	f	$h\nu$(e.V.)	f	$h\nu$(e.V.)	f	$h\nu$(e.V.)	f	$h\nu$(e.V.)	f
$^1B_{3u}$	4.253	0.00	4.256	0.00	4.245	0.00	4.40	—	4.018	0.000	3.99	0
$^1B_{2u}$	4.503	0.33	4.465	0.25	4.680	0.29	4.65	—	4.493	0.256	4.30	0.18
$^1B_{3u}$	5.803	2.03	5.813	2.09	5.860	2.18	6.13	—	5.939	2.115	5.50	2.0
$^1B_{2u}$	6.337	0.46	6.415	0.83	6.490	0.89	6.20	—	6.309	0.699	7.30	0.6
$^3B_{2u}$	2.584	0.00	2.627	0.00	2.725	0.00	3.09	—	2.180	0.000	2.6	—
$^3B_{3u}$	3.758	0.00	3.762	0.00	3.740	0.00	4.09	—	3.639	0.000	3.7(?)	—
$^3B_{3u}$	4.253	0.00	4.256	0.00	4.245	0.00	4.40	—	4.018	0.000	—	—
$^3B_{2u}$	4.334	0.00	4.269	0.00	4.380	0.00	4.83	—	4.220	0.000	—	—

TABLE II
CALCULATED AND OBSERVED SPECTRA OF ANTHRACENE

State	Calcd. (i)		(iii)		Pople		Pariser		Obs.	
	$h\nu$(e.V.)	f	$h\nu$(e.V.)	f	$h\nu$(e.V.)	f	$h\nu$(e.V.)	f	$h\nu$(e.V.)	f
$^1B_{2u}$	3.279	0.26	3.481	0.39	3.72	—	3.648	0.386	3.30	0.1
$^1B_{3u}$	3.898	0.00	3.908	0.00	4.15	—	3.715	0.000	3.50	0
$^1B_{3u}$	5.098	2.74	5.185	3.00	5.64	—	5.499	3.229	4.80	2.20
$^1B_{2u}$	6.648	1.03	6.441	0.81	6.44	—	6.586	0.644	5.64	0.65
$^3B_{2u}$	1.713	0.00	1.691	0.00	2.23	—	1.660	0.000	1.8	—
$^3B_{3u}$	3.595	0.00	3.585	0.00	3.96	—	3.503	0.000	—	—
$^3B_{3u}$	3.898	0.00	3.908	0.00	4.15	—	3.715	0.000	—	—
$^3B_{2u}$	4.793	0.00	4.824	0.00	5.39	—	5.230	0.000	—	—

respondence with experiment. The application of the semiempirical SCFMO method of Pople to these molecules leads to a nice agreement with experiment in the case of naphthalene[5] but at the same time to a wrong prediction in the case of anthracene[6]. However, employing the values of molecular integrals which we have been using for studying the electronic structures of nitrogen heterocycles[7], the electronic spectra and other properties of naphthalene and anthracene seem to be satisfactorily interpreted. In the present report, the results of our calculation on the aromatic hydrocarbons will be described with some critical discussions comparing our results with those of other authors.

I. Electronic Spectra.—As indicated in Tables I and II, the calculated spectra of naphthalene and anthracene employing our parameters[7] are in a satisfactory agreement with experimental values. In these tables the results obtained by Pople and Pariser, respectively, are also given for the purpose of comparison. In both of these tables, "i" is the result of the ordinary Hartree-Fock SCF calculation with the approximation of zero differential overlap, and "ii" is obtained by an approximate SCF calculation in which $F_{\mu\nu}$'s for the neighbors more distant than the nearest are neglected, and in "iii" the naive MO's are used for the calculation of excitation energies and oscillator strengths. The calculated results in "iii" are close to those "i" or "ii", and the agreement with the observed values is satisfactory. This fact is in accordance with the circumstance that, as pointed out by Dewar and Longuet-Higgins[8], owing to the uniform charge distribution in aromatic hydrocarbons, their naive MO's themselves are fairly close to SCFMO's.

Now, the results obtained by Lefebvre and Moser are collected in Table III. In this table, A is the result of the calculation which involves the penetration integrals to hydrogen atoms, in addition to other parameters which are the same as used by Pariser and Parr. Accordingly, the pairing property between the bonding and the antibonding orbitals is lost in this

5) J. A. Pople, *Trans. Faraday Soc.*, **49**, 1375 (1953).
6) H. O. Pritchard and F. H. Sumner, *Proc. Roy. Soc.*, **A226**, 128 (1954).
7) N. Mataga and K. Nishimoto, *Z. physik. Chem. N. F.* **13**, 140 (1957); N. Mataga, This Bulletin, **31**, 453, 459, 463 (1958).
8) M. J. S. Dewar and H. C. Longuet-Higgins, *Proc. Phys. Soc.*, **A67**, 795 (1954).

case. In B, $F_{\mu\mu}$, the diagonal element of Fock's Hamiltonian in terms of AO, has been assumed to be constant regardless of the position of carbon atoms, resulting in the pairing property, and all the off-diagonal elements, $F_{\mu\nu}$'s for nearest neighbors have been assumed to be equal to each other. For more distant neighbors, $F_{\mu\nu}$ is calculated by $F_{\mu\nu}=H_{\mu\nu}-1/2\ P_{\mu\nu}\gamma_{\mu\nu}$, where $H_{\mu\nu}$ is the off-diagonal element of core Hamiltonian, $P_{\mu\nu}$ is the bond order and $\gamma_{\mu\nu}$ is the electronic Coulomb repulsion integral. In C, it has been assumed that all values of $H_{\mu\nu}$ for nearest neighbors are equal.

TABLE III
SPECTRA OF NAPHTHALENE CALCULATED BY LEFEBVRE AND MOSER (SINGLET STATES)

(A)

MO's state	$h\nu$(e.V.)			f		
	Hückel	Cyclic	SCF	Hückel	Cyclic	SCF
B_{3u}	4.668	3.819	4.696	0.02	0.02	0.13
B_{2u}	4.984	4.180	4.995	0.05	0.00	0.00
B_{3u}	6.655	6.799	6.333	2.47	3.43	1.51
B_{2u}	6.542	5.939	6.538	1.28	1.01	1.15

(B)

MO's state	$h\nu$(e.V.)		f	
	Hückel	Cyclic	Hückel	Cyclic
B_{3u}	4.722	4.586	0.00	0.00
B_{2u}	4.161	4.086	0.30	0.35
B_{3u}	7.563	7.466	2.54	3.80
B_{2u}	6.762	6.993	1.11	0.59

(C)

MO's state	$h\nu$(e.V.)		f	
	Hückel	Cyclic	Hückel	Cyclic
B_{3u}	4.403	4.120	0.00	0.00
B_{2u}	4.289	4.314	0.20	0.20
B_{3u}	6.343	7.000	2.36	3.56
B_{2u}	6.597	5.834	1.05	0.71

The most important difference of our calculation from Lefebvre's and Moser's is in the choice of parameters, especially of $\gamma_{\mu\nu}$ values. In this respect, some discussions will be given in the latter part of this paper.

II. Bond Orders.—As mentioned in the introductory part of the present paper, Pople's self-consistent treatment as applied to the calculation of bond orders gave good agreement with the experiment for naphthalene, but not for anthracene, whereas with the simple treatment without the inclusion of electronic interaction, the situation was reversed. In view of this circumstance, Pritchard and Sumner[9] tried to hit the experimental values calculating the bond orders of naphthalene and anthracene by various approximations. This was, however, a rather hard task. Among various approximations (six approximations), only one (their approximation 5) gave results for both molecules free from significant error. In this approximation, Pople's self-consistent MO method was used with variation of α, the diagonal element of core Hamiltonian in terms of μth AO; the correction used was $\Delta\alpha=\beta$ in the sense that atoms labelled 3 in Fig. 1 are more electronegative than other atoms in the system.

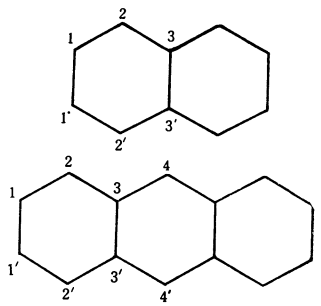


Fig. 1. Numbering of atoms in naphthalene and anthracene.

Now, as indicated in Table IV, the bond lengths calculated by the self-consistent field MO method using our parameters, are in good correspondence with experiment, where the results of Pritchard and Sumner by approximation 5 (abbreviated as P.S.) are also indicated for the purpose of comparison. In this table, the calculated

TABLE IV
CALCULATED AND EXPERIMENTAL BOND LENGTHS OF NAPHTHALENE AND ANTHRACENE (IN A)

Naphthalene

bond	Calcd. (i)*	(ii)*	P.S.	Expt.
1—2	1.374	1.369	1.369	1.365±0.006
2—3	1.414	1.417	1.420	1.425±0.005
3—3'	1.412	1.406	1.409	1.393±0.010
1—1'	1.405	1.412	1.413	1.404±0.009

Anthracene

bond	Calcd. (i)*	P.S.	Expt.
1—2	1.370	1.365	1.371±0.006
2—3	1.423	1.430	1.424±0.005
3—4	1.396	1.403	1.396±0.004
3—3'	1.436	1.432	1.436±0.007
1—1'	1.408	1.422	1.408±0.010

* The meaning of i and ii is the same as those in Tables I and II.

9) H. O. Pritchard and F. H. Sumner, *Trans. Faraday Soc.*, 51, 457 (1955).

bond lengths were obtained from the bond orders using the equation

$$R_{\mu\nu}=S-\frac{S-D}{1+\kappa\left(\frac{1-P_{\mu\nu}}{P_{\mu\nu}}\right)}$$

where S is taken to be 1.54 Å, D=1.33 Å and κ=0.765.

None of the calculated values using our parameters differs from the experimental mean by more than two and a quater times the "estimated standard deviation," and may be regarded as correct.

III. Ionization Potentials and Electron Affinities.—The ionization potentials and electron affinities are important quantities for studying the molecular sturctures. We have examined whether our calculation can predict correctly the ionization potentials and electron affinities of naphthalene and anthracene. The calculated values have been standardized to the observed values of benzene, i.e., after adding $\Delta I=I^{\text{obs.}}_{\text{benz.}}-I^{\text{calc.}}_{\text{benz.}}$ or $\Delta A=A^{\text{obs.}}_{\text{benz.}}-A^{\text{calc.}}_{\text{benz.}}$ to the calculated ionization potentials or electron affinities, respectively; the theoretical values have been compared with experiment. As shown in Table V, the calculated values agree satisfactorily with observed values.

TABLE V
CALCULATED AND OBSERVED IONIZATION POTENTIALS OF NAPHTHALENE AND ANTHRACENE (IN e.V.)

Molecule	Ionization Potential Calcd. (i)*	(ii)*	(iii)*	Obsd.
Benzene	(9.24)			9.24
Naphthalene	8.116	8.125	8.068	8.12 (a)
Anthracene	7.414	—	7.400	—
Molecule	**Electron Affinity Calcd. (i)***	**(ii)***	**(iii)***	**Obsd.**
Benzene	(−0.54)			−0.54 (b)
Naphthalene	0.595	0.585	0.643	0.65 (b)
Anthracene	1.297	—	1.310	1.19 (b)

* The meaning of i, ii and iii is the same as in other tables.

(a) K. Watanabe and J. R. Mottl, *J. Chem. Phys.*, **26**, 1773 (1957).

(b) Blackedge and Hush, quoted in, N. S. Hush and J. A. Pople, *Trans. Faraday Soc.*, **51**, 600 (1955).

Discussion

As has been described so far, the electronic spectra, bond lengths, ionization potentials and electron affinities calculated with our parameters are in an excellent agreement with experimental values, and the main difference of our calculation from that of other authors' is in the choice of $\gamma_{\mu\nu}$ values. Our values are somewhat smaller than those used by Pariser and Parr and by Pople. The procedure employed by Pariser and Parr for evaluating $\gamma_{\mu\mu}$ is analogous to the Moffitt's method of "atoms in molecules"[10] which takes into account accurately the energy difference between the separated pairs of ions and neutral atoms. In other words, it may also be regarded as an appropriate consideration of the effect of electronic correlation for the one-center interaction integral $\gamma_{\mu\mu}$, by the use of the experimental values of atomic valence state ionization potential and electron affinity[11]. In Moffitt's method, $\gamma_{\mu\nu}$'s where $\mu\neq\nu$, are calculated theoretically using, for example, Slater type AO's. In the procedure used by Pariser and Parr, $\gamma_{\mu\nu}$'s for neighbors more distant than the nearest are calculated in terms of Slater type AO's or by uniform charge sphere approximation. $\gamma_{\mu\nu}$'s for nearest neighbors are evaluated by interpolation formula of the type: ar^2+br+c, where r is the interatomic distance and $c=\gamma_{\mu\mu}$. When atoms are combined to form a molecule, however, the effective charges for σ-electrons may be rather increased compared with the case of isolated atoms and the electron clouds associated with σ-bonds may somewhat contract.

In contrast to this, the effective changes for π-electrons may by decreased. Owing to this circumstance, one should use a little smaller values of $\gamma_{\mu\nu}$'s than those used by Pariser and Parr and by Pople, which may be a cause of the excellent agreement of our calculated results with experiment. In addition, our procedure for evaluating $\gamma_{\mu\nu}$'s is very simple and straightforward. One can easily obtain them if one can only know the values of valence state ionization potentials and electron affinities of the atoms involved. Another reason for the use of our $\gamma_{\mu\nu}$ values may be as follows, although it might be essentially the same as described above. When applied to some simple molecules such as hydrogen[12,13] and lithium molecules[14], the method of Moffitt gives

10) W. Moffitt, *Proc. Roy. Soc.*, **A210**, 245 (1951); *Report Progr. Phsics*, **17**, 173 (1954).
11) W. Kotos, *Acta Phys. Polon.*, **16**, 299 (1957).
12) C. W. Scherr, *J. Chem. Phys.*, **22**, 149 (1954).
13) A. C. Hurley, *Proc. Phys. Soc.*, **A68**, 149 (1955).
14) A. Rahman, *Physica*, **20**, 623 (1954).

rather unsatisfactory results. For example, it leads to the conclusion that the ground state of the hydrogen molecule is almost completely ionic[13]. A similar conclusion is also reached in the case of the diamond[15]. In the latter case, however, if one calculate non-empirically the energies and wave functions employing Slater AO's, one can obtain the result that the ground state is homopolar even if the agreement between the calculated and the observed cohesive energy is very unsatisfactory.

Then, one may be able to improve the results in the following way. For example, if $\gamma_{\mu\mu}$ calculated with Slater AO's is κ times the $\gamma_{\mu\mu}$ evaluated by Moffitt's method, one divides by κ all $\gamma_{\mu\nu}$'s calculated with Slater AO's and one uses $\gamma_{\mu\nu}=(1/\kappa)\gamma_{\mu\nu}$ (Slater) in the calculation of molecular energy and wave function. Actually, in the case of the diamond, a satisfactory improvement has been brought about in this way[15]. Although the real theoretical ground for doing it in this way is not very clear, the physically unsatisfactory results at which Moffitt's method arrives originate from the inconsistent use of, for example, $\gamma_{\mu\mu}$ values which are obtained empirically on the one hand and $\gamma_{\mu\nu}$ $(\mu\neq\nu)$ values which are calculated with ordinary orbital functions on the other hand. Thus, even if the interatomic part of energy is very small compared with its intra-atomic part, the former still affects the calculated results to such an extent as described above.

When studing the π-electronic structures, such a circumstance may not be very serious as in the case of σ-electronic structures. Nevertheless, our calculation in the present paper seems to indicate that such a circumstance still exists in the case of π-electronic structures. Actually, the ratio $\gamma_{\mu\nu}$ (Slater)$/\gamma_{\mu\nu}$, where $\gamma_{\mu\nu}$ is the value we have used, is approximately constant and close to κ when μ-th and ν-th atoms are one or two bond distances apart from each other and approaches gradually to unity as they become more distant.

15) T. Yamaguchi, Private communication.

Summary

Electronic structures of naphthalene and anthracene have been studied by the self-consistent field MO method employing our semiempirical parameters. The calculated electronic spectra, bond lengths, ionization potentials and electron affinities are in a good agreement with expriment. Some discussions have been given in connection with the method of "atoms in molecules" and others.

We are grateful to Professor R. Fujishiro for his encouragement. One of the authors (N.M.) expresses with pleasure his cordial thanks to Mr. T. Yamaguchi of Osaka University for his helpful discussions.

Institute of Polytechnics
Osaka City University
Kita-ku, Osaka

The Aconite Alkaloids. XXVII. On Lucaconine*

By Sijô FURUSAWA**

(Received September 4, 1958)

In the previous paper[1] the extended formulae of lucaconine (I), $C_{24}H_{39}O_7N$, and monoacetyllucaconine (II), $C_{26}H_{41}O_8N$, were given as follows:

$C_{19}H_{21}\begin{cases}(OCH_3)_3\\(OH)_4\\N\text{-}C_2H_5\end{cases}$ $C_{19}H_{21}\begin{cases}(OCH_3)_3\\OCOCH_3\\(OH)_3\\N\text{-}C_2H_5\end{cases}$

Lucaconine (I) Monoacetyllucaconine (II)

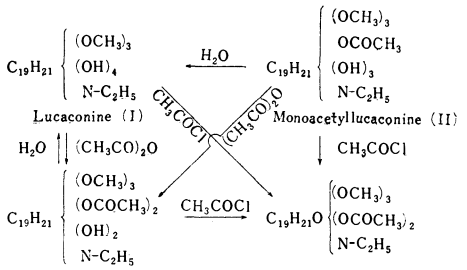
The present paper describes further experiments, undertaken with the object of characterizing the hydroxyl groups of lucaconine. Acetylation of lucaconine (I)

* This constitutes a part of a series entitled "The Aconite Alkaloids" by H. Suginome. Part XXVI, cf. foot note 1).

** Present address, Faculty of Technology, Chû-ô University, Tokyo, Japan.

1) H. Suginome and S. Furusawa, This Bulletin, **32**, 354.

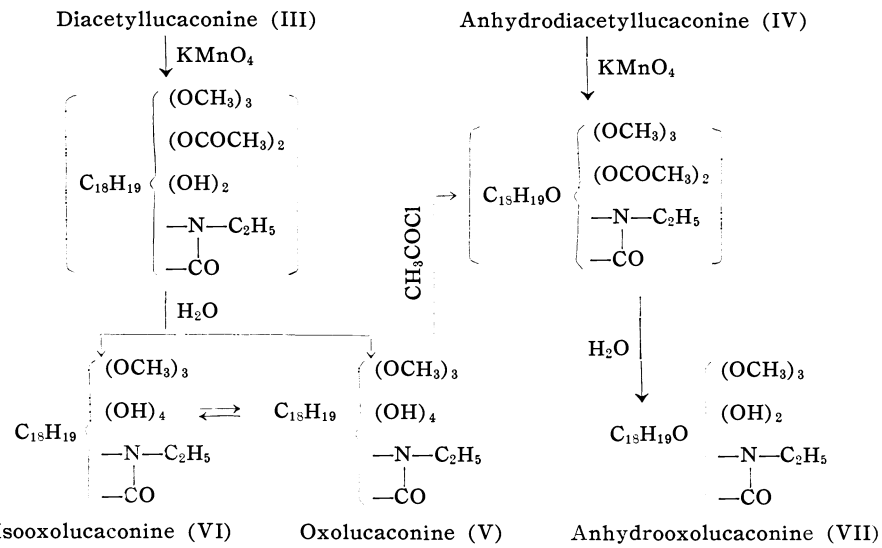
with acetic anhydride gave diacetyllucaconine(III), $C_{28}H_{43}O_9N$[1], while, on treatment with acetyl chloride, lucaconine (I) yielded anhydrodiacetyllucaconine(IV), $C_{28}H_{41}O_8N$, m. p. 156°, $[\alpha]_D^{27}+20.0°$. This anhydrodiacetyl-compound IV was obtained also from monoacetyllucaconine (II) and diacetyllucaconine (III) by the similar treatment. Anhydrodiacetyllucaconine (IV) decolorized bromine in acetic acid and absorbed one mole of hydrogen over platinum catalyst, showing the presence of a double bond. A small quantity of isodiacetyllucaconine, $C_{28}H_{43}O_9N$, m. p. 188° (decomp.), $[\alpha]_D$ 0°, was isolated as a by-product when lucaconine (I) was treated with a large quantity of acetyl chloride.



Oxidation of diacetyllucaconine (III) with potassium permanganate in acetone, followed by hydrolysis, gave two neutral products, oxolucaconine (V), $C_{24}H_{37}O_8N\cdot 1\,3/4\ H_2O$, m. p. 132°, $[\alpha]_D^{16.2}+24.2°$, as a main product and isooxolucaconine (VI), $C_{24}H_{37}O_8N$, m. p. 242°, $[\alpha]_D^{22.6}+44.8°$, as a by-product. The latter compound VI was also obtained by heating V at about 150° for 10 minutes under reduced pressure (1×10^{-5} mmHg) and VI was partly converted reversely into V on action of methanolic hydrogen chloride or alcoholic sodium hydroxide in a sealed tube. Treatment of oxolucaconine V with acetyl chloride, followed by hydrolysis, gave anhydrooxolucaconine (VII), m. p. 256°, $[\alpha]_D^{27}-25.0°$. This compound VII was also obtained directly from anhydrodiacetyllucaconine(IV)by oxidation with potassium permanganate, followed by hydrolysis.

Acetylation of isooxolucaconine(VI) and of anhydrooxolucaconine (VII) by acetic anhydride gave no crystalline product, but the determination of acetyl groups of these amorphous products showed the production of diacetyl-compounds by these reactions.

On treatment with chromic acid in glacial acetic acid lucaconine (I) was converted into lucaconinone-I (VIII), $C_{24}H_{37}O_7N$, m. p. 210°, $[\alpha]_D^{27}+15.0°$, which showed bands in the infrared spectrum at 2.99 and 5.72 μ, corresponding to hydroxyl and five-membered ring ketone group[2], and formed a monoxime melting at 223~224° (decomp.). Oxolucaconine(V)was converted by the same procedure into a diketo-compound, oxolucaconinedione(IX), $C_{24}H_{33}O_8N$, m. p. 209°, $[\alpha]_D^{26.7}+139°$, which showed bands in the infrared spectrum at 2.90, 5.72, 5.83 and 6.08 μ, characteristic of hydroxyl, five-membered ring ketone, six-membered ring ketone and lactam carbonyl group, respectively[2], and further furnished

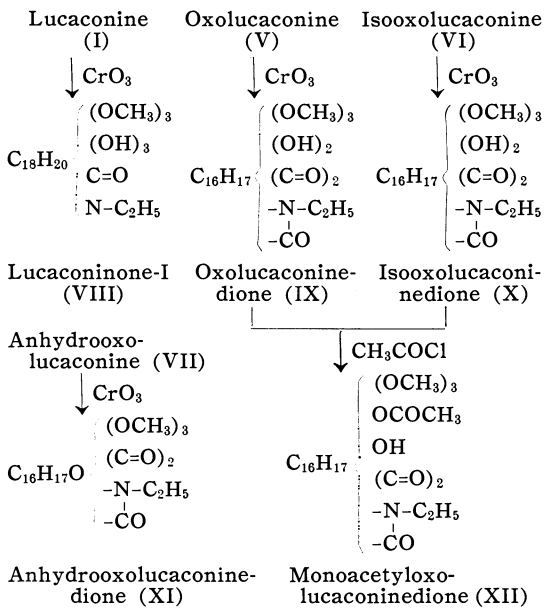


2) H. Suginome, T. Amiya and T. Shima, unpublished work.

a monoxime melting at 246~248° (decomp.). In this case, a by-product, isooxolucaconinedione (X), $C_{24}H_{33}O_8N \cdot H_2O$, m. p. 136° (decomp.), $[\alpha]_D^{26}$ +33.7°, which formed the same monoxime (m. p. 246~248°) as described above, was obtained***. Isooxolucaconine (VI) gave only isooxolucaconinedione (X) by similar procedure. Anhydrooxolucaconine (VII) was similarly oxidized into a diketo-compound, anhydrooxolucaconinedione (XI), $C_{24}H_{31}O_7N$, m. p. 272°, $[\alpha]_D^{26.5}$ −84.2°, which showed bands in the infrared spectrum at 5.72 and 5.83 μ [2], and gave a monoxime melting at 268° under decomposition.

Upon treatment with acetyl chloride, both oxolucaconinedione (IX) and isooxolucaconinedione (X) gave the same monoacetyloxolucaconinedione (XII), $C_{26}H_{35}O_9N$, m. p. 269° (decomp.), $[\alpha]_D^{26.7}$ +113°. On hydrolysis with methanolic sodium hydroxide, this compound XII afforded nearly an equal amounts of IX and X.

Selenium was liberated on heating lucaconinone-I (VIII) and oxolucaconinedione (IX) with selenium dioxide in glacial acetic acid. On the contrary, lucaconine (I) and oxolucaconine (V) did not give selenium under similar conditions. That may probably be due to the presence of a methylene group adjacent to a keto group in VIII and IX.



On the basis of these facts, it may be reasonably concluded that, of four hydroxyl groups of lucaconine, two can be acetylated or oxidized to oxo groups, one being attached to a five-membered ring and the other to a six-membered ring, but the remaining two hydroxyl groups can be neither acetylated nor oxidized under usual conditions. Furthermore, it is to be noted that the latter two hydroxyl groups split off one mole of water on treatment with acetyl chloride. These observations will be discussed in a later paper.

In conclusion mention will be made of the action of nitric acid on lucaconine. Upon treatment with concentrated nitric acid, lucaconine (I) was converted into nitronitrosolucaconinic acid (XIII), $C_{16}H_{19}O_9N_3$, m. p. 214° (decomp.), $[\alpha]_D^{27}$ −117°. This compound contained two methoxyl groups but no *N*-ethyl group and was soluble in alkali with a pale yellowish green color.

Experimental

Anhydrodiacetyllucaconine (IV).—*a) From Lucaconine.*—A mixture of 2.0 g. of lucaconine and 10 cc. of acetyl chloride was allowed to stand in a sealed tube for ten days. After removal of the excess of acetyl chloride, the residue was treated with ice-water and made alkaline with aqueous ammonia to give a white precipitate. This material was recrystallized from ethanol to obtain anhydrodiacetyllucaconine in colorless plates, m. p. 156°, $[\alpha]_D^{27}$ +20.0° (94% ethanol). Yield 1.5 g.

Anal. Found: C, 64.63; H, 7.83; N, 2.90; OCH_3, 19.73; $COCH_3$, 18.14. Calcd. for $C_{28}H_{41}O_8N$: C, 64.72; H, 7.95; N, 2.70; OCH_3, 17.90; 2-$COCH_3$, 16.56%. 6.459 mg. of the substance absorbed 2.84 cc. of hydrogen (1.04 mol.).

When a mixture of 1.0 g. of lucaconine and 10 cc. of acetyl chloride was refluxed for 40 min., and treated in the usual manner, it yielded 0.4 g. of anhydrodiacetyllucaconine and a small quantity (ca. 0.01 g.) of a crystalline substance, isodiacetyllucaconine, m. p. 188° (decomp.), $[\alpha]_D$ 0°.

Anal. Found: C, 62.69; H, 8.37; N, 2.80; OCH_3, 16.84; $COCH_3$, 16.81. Calcd. for $C_{28}H_{43}O_9N$: C, 62.55; H, 8.05; N, 2.61; 3-OCH_3, 17.31; 2-$COCH_3$, 16.02%.

b) From Monoacetyllucaconine (II).—A mixture of 0.5 g. of monoacetyllucaconine and 4.5 cc. of acetyl chloride was refluxed for 40 min. The reaction mixture was treated in the usual manner to give 0.38 g. of anhydrodiacetyllucaconine.

c) From Diacetyllucaconine (III).—A mixture of 0.25 g. of diacetyllucaconine and 5 cc. of acetyl chloride was allowed to stand at room temperature for a week. After treatment as described above, 0.2 g. of anhydrodiacetyllucaconine was obtained.

Oxolucaconine (V).—To a solution of 3.2 g. of diacetyllucaconine in 100 cc. of acetone, 3.5 g. of powdered potassium permanganat was gradually added under stirring and chilling. Manganese

*** There is a possibility that isooxolucaconinedione (X) is a hydrate of oxolucaconinedione (IX), but it is preferable to call it an "iso-" compound because of difference in optical activities.

dioxide was filtered off and the filtrate was evaporated to dryness. The residue was treated with boiling ethanolic potassium hydroxide for 30 min. After cooling, the solution was made slightly acidic with hydrochloric acid and was evaporated up. The residue was then extracted with absolute ethanol and the ethanolic extract was evaporated to give ca. 1.8 g. of colorless crystals which were recrystallized from ethanol. Oxolucaconine was obtained in colorless crystals, m. p. 132°, $[\alpha]_D^{16.2}$+24.2° (94% ethanol). This material was insoluble in water, diluted hydrochloric acid and diluted aqueous ammonia, and it seemed to be neutral.

Anal. Found: C, 57.54; H, 7.96; N, 2.72; H_2O, 6.06; (N)-C_2H_5, 4.32. Calcd. for $C_{24}H_{37}O_8N$. 1¾ H_2O: C, 57.75; H, 8.18; N, 2.81; H_2O, 6.32; (N)-C_2H_5, 5.82%.

From the mother liquor of the above recrystallization, a small quantity of a crystalline substance, m. p. 242°, identical with isooxolucaconine mentioned next, was obtained.

Isooxolucaconine (VI). — When 0.2 g. of oxolucaconine was heated at 150° for 5 min. under reduced pressure (1×10^{-5} mmHg), it decomposed under foaming, became glassy and crystallized on cooling. On recrystallization from ethanol, isooxolucaconine was obtained in colorless needles, melting at 242°, $[\alpha]_D^{22.6}$+44.8° (94% ethanol).

Anal. Found: C, 61.17; H, 8.16; OCH_3, 20.73. Calcd. for $C_{24}H_{37}O_8N$: C, 61.65; H, 7.98; 3-OCH_3, 19.93%.

Upon heating with methyl iodide in a sealed tube, isooxolucaconine could not be methylated but yielded oxolucaconine. The same substance was also produced when isooxolucaconine was heated in a sealed tube with ethanolic potassium hydroxide or with methanolic hydrogen chloride.

Acetylation of Isooxolucaconine (VI).—A solution of isooxolucaconine in a mixture of pyridine and acetic anhydride (1:1) was allowed to stand at room temperature overnight. After removal of the solvents, an amorphous product was treated with aqueous ammonia and extracted with ether. An amorphous residue, obtained on evaporating the ethereal extracts, was purified by repeated precipitation from dilute ethanol.

Anal. Found: $COCH_3$, 16.85. Calcd. for $C_{24}H_{35}O_8N(COCH_3)_2$: 2-$COCH_3$, 15.60%.

Anhydrooxolucaconine (VII). — *a) From Anhydrodiacetyllucaconine (IV).*—To a solution of 0.6 g. of anhydrodiacetyllucaconine in 20 cc. of acetone, 0.4 g. of powdered potassium permanganate was added. After being kept for 24 hr. manganese dioxide was filtered off and the filtrate was evaporated to give 0.5 g. of an amorphous residue. This product was treated with ethanolic potassium hydroxide and then crystallized from ethanol. On repeated recrystallization from ethanol, anhydrooxolucaconine, m. p. 256°, $[\alpha]_D^{27}$−25.0° (94% ethanol) was obtained. It was soluble in methanol and slightly so in acetone, ether and water.

Anal. Found: C, 64.32; H, 7.91; N, 3.27; OCH_3, 20.69; (N)-C_2H_5, 4.72. Calcd. for $C_{24}H_{35}O_7N$: C, 64.17; H, 7.85; N, 3.12; 3-OCH_3, 20.72; (N)-C_2H_5, 6.46%.

b) From Oxolucaconine (V).—A mixture of 2.0 g. of oxolucaconine and 20 cc. of acetyl chloride was refluxed for 30 min. After removal of the excess of acetyl chloride, the residue was treated with alkali to give 1.0 g. of a crystalline substance. On recrystallization from ethanol, anhydrooxolucaconine, m. p. 257°, was obtained.

Acetylation of Anhydrooxolucaconine (VII).—A mixture of 0.05 g. of anhydrooxolucaconine, 0.5 cc. of pyridine and 0.2 cc. of acetyl chloride was allowed to stand at room temperature overnight. After removal of the solvent, the residue was treated with aqueous ammonia to give a white precipitate. This precipitate was dissolved in ethanol and was reprecipitated by addition of water. After repetition of this treatment, the precipitate was dried and analyzed.

Anal. Found: $COCH_3$, 17.64. Calcd. for $C_{24}H_{33}O_7N(COCH_3)_2$: 2-$COCH_3$, 16.15%.

Lucaconinone-I (VIII).—To a solution of 2.0 g. of lucaconine in 25 cc. of glacial acetic acid, a solution of 0.7 g. (2 mol.) of chromic trioxide in 15 cc. of acetic acid was dropped in under stirring and coolling. After standing overnight and after the removal of the solvent, a glassy substance was obtained. This material was dissolved in water; the solution was made alkaline and was extracted with chloroform. On evaporation of the chloroform solution, 0.64 g. of a crystalline residue was yielded, which was recrystallized from 99% ethanol to give crystals melting at 200~201°. Yield 0.4 g. This substance was converted into perchlorate, melting at 236° after being recrystallized from ethanol. It was transformed into the free base by the usual method. The base, lucaconinone-I, thus obtained melted at 210°, $[\alpha]_D^{27}$+15.0° (94% ethanol).

Anal. Found: C, 63.82; H, 8.31; N, 3.18. Calcd. for $C_{24}H_{37}O_7N$: C, 63.83; H, 8.26; N, 3.11%.

Perchlorate. — m. p. 236° (decomp.) (from ethanol).

Anal. Found: Cl, 6.92. Calcd. for $C_{24}H_{37}O_7N\cdot HClO_4$: Cl, 6.79%.

Oxime. — m. p. 223~224° (decomp.) (from ethanol).

Anal. Found: N, 6.12. Calcd. for $C_{24}H_{38}O_7N_2$: N, 6.01%.

Oxolucaconinedione (IX).—To a solution of 0.8 g. of oxolucaconine in 10 cc. of glacial acetic acid, a solution of 0.28 g. (2.2 mol.) of chromic anhydride in 10 cc. of the same solvent was added slowly under stirring and cooling. After the mixture was set aside overnight, it was treated in the usual manner to give 0.3 g. of a crystalline product which was recrystallized from ethanol. Oxolucaconinedione was obtained as colorless needles melting at 209°, $[\alpha]_D^{26.7}$+139° (94% ethanol).

Anal. Found: C, 62.10; H, 7.40; N, 3.11. Calcd. for $C_{24}H_{33}O_8N$: C, 62.13; H, 7.18; N, 3.02%.

Oxime. — m. p. 246~248° (decomp.) (from ethanol).

Anal. Found: N, 5.91. Calcd. for $C_{24}H_{34}O_8N_2$: N, 5.86%.

The mother liquor from which the above mentioned crystals were separated was extracted with chloroform and the chloroform extracts were evaporated to dryness. The residue was crystallized from ethanol to give 0.1 g. of a colorless crystalline substance, m. p. 136~137° (decomp.), which was identified with isooxolucaconinedione mentioned below.

Isooxolucaconinedione (X).—Isooxolucaconine was oxidized with chromic anhydride in glacial acetic acid by the method described above to give isooxolucaconinedione, colorless crystals melting at 136~137° (decomp.), $[\alpha]_D^{26}+33.7°$ (94% ethanol).

Anal. Found: C, 59.77; H, 7.43; N, 3.17; H_2O, 3.62. Calcd. for $C_{24}H_{33}O_8N\cdot H_2O$: C, 59.82; H, 7.34; N, 2.91; H_2O, 3.75%.

The oxime prepared from isooxolucaconinedione melted at 246~248° (decomp.) and showed no depression of the melting point on admixture with the above-mentioned oxolucaconinedione oxime.

When isooxolucaconinedione was heated in an oil bath at 160~170° for 10 min. under reduced pressure (1×10^{-5} mmHg), it melted under foaming and crystallized on cooling. Recrystallization from ethanol gave a crystalline substance, m. p. 136° (decomp.), which showed no depression of the melting point on admixture with the starting material.

Anhydrooxolucaconinedione (XI).—With 0.08 g. of chromic anhydride in acetic acid, 0.25 g. of anhydrooxolucaconine was oxidized as described above to give 0.2 g. of anhydrooxolucaconinedione, which was recrystallized from ethanol, m. p. 272°, $[\alpha]_D^{26.5}-84.2°$. It was sluble in methanol, ethanol and acetone and sparingly soluble in ether and benzene.

Anal. Found: C, 64.30; H, 7.50; N, 3.27. Calcd. for $C_{24}H_{31}O_7N$: C, 64.70; H, 7.01; N, 3.14%.

Oxime.—m. p. 268° (decomp.).

Anal. Found: N, 6.52. Calcd. for $C_{24}H_{32}O_7N_2$: N, 6.08%.

Monoacetyloxolucaconinedione (XII).—A mixture of 0.26 g. of oxolucaconinedione and 3 cc. of acetyl chloride was heated under reflux for 30 min. After removal of the solvent, the residue was treated with aqueous ammonia to give white precipitate which was crystallized from ethanol. Monoacetyloxolucaconinedione melted at 269° (decomp.), $[\alpha]_D^{26.7}+113°$ (ethanol). It was soluble in methanol and ethanol and sparingly soluble in acetone, benzene and water.

Anal. Found: C, 62.62; H, 7.56; $COCH_3$, 8.79. Calcd. for $C_{24}H_{32}O_8N(COCH_3)$: C, 61.80; H, 6.98; $COCH_3$, 8.51%.

This substance was also obtained from isooxolucaconinedione by the same procedure as described above.

Hydrolysis of Monoacetyloxolucaconinedione (XII).—A solution of 0.1 g. of monoacetyloxolucaconinedione in 2 cc. of N-methanolic sodium hydroxide was heated for 20 min. After removal of the solvent, the residue was treated with water and the precipitate was fractionally recrystallized from ethanol. Isooxolucaconinedione melting at 132° (decomp.) and oxolucaconinedione melting at 207° were yielded in nearly equal amounts.

Nitronitrosolucaconinic Acid (XIII).—A mixture of 3.0 g. of lucaconine and 20 cc. of nitric acid (*d*: 1.43) was heated on a water bath at 80° for 1 hr. with stirring. After cooling, 30 cc. of water was added and yellow precipitate was collected, which was repeatedly precipitated from diluted ethanol and finally crystallized from diluted acetone. Nitronitrosolucaconinic acid was obtained in pale yellow plates, melting at 214°, $[\alpha]_D^{27}-117°$. It was easily soluble in acetone and sparingly so in water, methanol, ethanol, ether and chloroform.

Anal. Found: C, 48.60; H, 4.81; N, 10.83; OCH_3, 15.32; COO-, 24.64; (N)-C_2H_5, neg. Calcd. for $C_{12}H_{13}O_3N_3(OCH_3)-(COO)_2$: C, 48.47; H, 4.78; N, 10.57; 2-OCH_3, 15.62; 2-COO-, 22.66%.

The author wishes to express his sincere thanks to Professor Harusada Suginome, President of Hokkaido University, for his kind guidance throughout this work.

Department of Chemistry
Faculty of Science
Hokkaido University
Sapporo

The Study of Adsorption of Detergents at a Solution-Air Interface by Radiotracer Method. II. The Kinetics of Adsorption of Sodium Alkyl Sulfates

By Ryohei MATUURA, Hideo KIMIZUKA, Shigeru MIYAMOTO, Ryosuke SHIMOZAWA and Katsumasa YATSUNAMI

(Received September 24, 1958)

It is usual in the case of the solution of detergents that a considerable time is required to attain true equilibrium of adsorption at the solution-air interface. The process has been studied chiefly from the measurement of the change in surface tension with time. The suggestion that the diffusion of solute to the surface is a cause of the alteration of surface tension with time was first made by Milner[1], and equations to describe the phenomena in terms of diffusion have been deduced by Bond and Puls[2], Ross[3], Ward and Tordai[4], Bartholomé and Schäfer[5], Lange[6] and Fordham[7]. However, it has been proved that there are many cases in which the process can not be explained in terms of simple diffusion alone, and the factors governing the adsorption rate other than diffusion have been proposed. For example, the concept of energy barrier has been introduced by Doss[8], Blair[9] and Addison[10].

In the preceding paper[11] the Gibbs adsorption equation has been checked in the case of sodium dodecyl sulfate, tetradecyl sulfate and hexadecyl sulfate at the solution-air interface. It is perfectly clear that the Gibbs equation refers only to the adsorption equilibrium. It has nothing to do with the process of reaching the equilibrium, and so to calculate the surface excess at the stage of non-equilibrium from surface tension by using the Gibbs equation is incorrect. In order to study the kinetics of adsorption, therefore, it is preferable to measure the change in the adsorbed amount with time directly. By using radioisotopes this can easily be done. The method is simple and accurate, and is most suitable since the adsorption can be measured at a liquid surface without any mechanical disturbances. It is the purpose of the present experiment to measure the rate of adsorption of sodium alkyl sulfates at the solution-air interface by radiotracer method and to make discussions as to the theories of the adsorption rate presented by earlier authors.

Experimental

Surface active substances used in the present experiment were the same as those in the preceding paper[11], i.e., sodium dodecyl sulfate (SDS), sodium tetradecyl sulfate (STS), and sodium hexadecyl sulfate (SHS). Labelling these compounds with S-35 was described earlier[11].

The counting apparatus was also the same as that used in the preceding paper[11]. After the formation of a fresh plane surface of a detergent

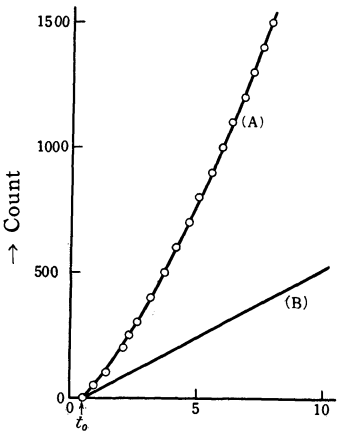


Fig. 1. Count vs. time curves for the solution of SHS (A) and sulfuric acid (B). Concentration, 4.24×10^{-6} mole/l.

1) S. R. Milner, *Phil. Mag.*, (6), **13**, 96 (1907).
2) W. N. Bond and H. O. Puls, ibid., (7), **24**, 864 (1937).
3) S. Ross, *J. Am. Chem. Soc.*, **67**, 990 (1945); *J. Phys. Chem.*, **49**, 377 (1945).
4) A. F. H. Ward and L. Tordai, ibid., **14**, 453 (1946).
5) E. Bartholomé and K. Schäfer, *Melliand Textilber.*, **31**, 487 (1950).
6) H. Lange, *Kolloid-Z.*, **121**, 130 (1951); **136**, 136 (1954).
7) S. Fordham, *Trans. Faraday Soc.*, **50**, 593 (1954).
8) K. S. G. Doss, *Kolloid-Z.*, **86**, 205 (1939); **87**, 272 (1939).
9) C. M. Blair, Jr., *J. Chem. Phys.*, **16**, 113 (1948).
10) C. C. Addison and S. K. Hutchinson, *J. Chem. Soc.*, **1949**, 3387.
11) R. Matuura, H. Kimizuka, S. Miyamoto and R. Shimozawa, This Bulletin, **31**, 532 (1958).

solution, the measuring arrangement was quickly set in and the count from the solution was measured with time. An example is shown in Fig. 1 (curve A). The curve B in the same figure shows a change in the counting with time of a sulfuric acid solution with the same concentration and specific activity as the detergent solution. The two series of measurements should be done under exactly the same conditions. t_0 in Fig. 1 is the starting time of counting. The tangent of the curve at any time t is clearly the intensity of radiation from the bulk of the solution, I_i, plus that from the adsorbed layer at that time, $I_{s(t)}$. The intensity of radiation from sulfuric acid solution does not show any change with time and it can be regarded as equal to I_i since no surface adsorption will take place with sulfuric acid solution of so low a concentration as in the present experiment. Then,

$$I_{s(t)} = (I_i + I_{s(t)}) - I_i \quad (1)$$

i.e., the counting rate at time t of the surface layer can be obtained from the difference between the counting rate of the detergent solution at that time and that of sulfuric acid solution. The surface excess at time t, Γ_t, is calculated from $I_{s(t)}$ by using the following relation;

$$\Gamma_t = I_{s(t)}/SA \quad (2)$$

where S is the specific activity of the radioactive substance and A is the surface area of the solution. S can be determined as in the preceding paper[11].

Results

The change in adsorption with time of SDS, STS and SHS at the solution-air interface is plotted in Figs. 2, 3 and 4, respectively. The abscissa is represented as the square root of time for the convenience of discussions.

Discussions

It is seen from Figs. 2, 3 and 4 that at the initial stage of adsorption the surface excess of the detergents is proportional to the square root of time, i.e., the adsorption at constant temperature can be expressed by the relation,

$$\Gamma_t = Kt^{1/2} \quad (3)$$

were, t is the time of aging and K is a constant independent of time but dependent on the concentration of the detergent solution. When K is plotted against concentration, C, approximately linear relation can be found as shown in Fig. 5, i.e.,

$$K = K_0C \quad (4)$$

where K_0 is a constant characteristic of each detergent. From Eqs. 3 and 4 the

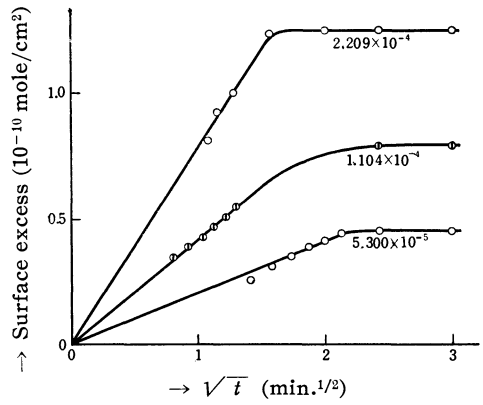


Fig. 2. Surface excess vs. time curves of SDS, at 28±1°C. Numericals of each curve represent the concentration of the detergent solution in mole/l.

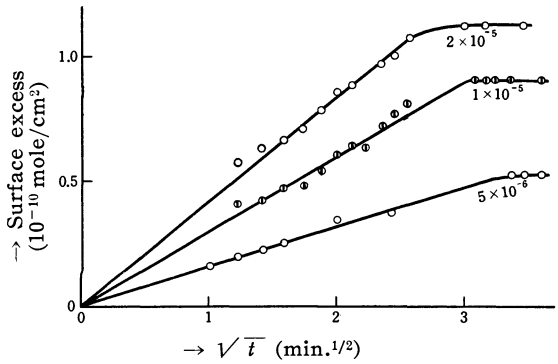


Fig. 3. Surface excess vs. time curves of STS, at 28±1°C. Numericals of each curve represent the concentration of the detergent solution in mole/l.

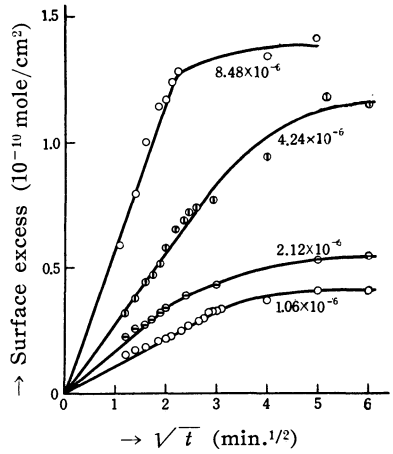


Fig. 4. Surface excess vs. time curves of SHS, at 28±1°C. Numericals of each curve represent the concentration of the detergent solution in mole/l.

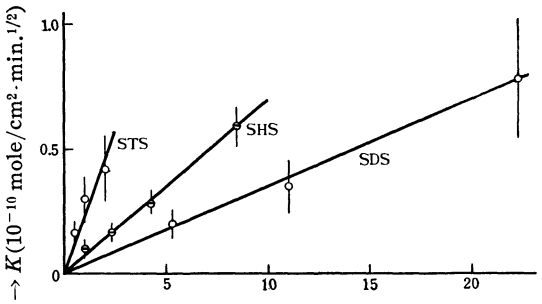


Fig. 5. K vs. concentration of detergents at 28±1°C.

following relation is obtained;

$$\Gamma_t = K_0 C t^{1/2} \tag{5}$$

Now the simple diffusion theory[4] tells us that the surface excess at time t, Γ_t, is given by the relation,

$$\Gamma_t = 2C(Dt/\pi)^{1/2} \tag{6}$$

where D is the diffusion coefficient of the solute molecules. At first sight it is seen that Eq. 6 is similar in form to Eq. 5, and this similarity of the two equations may seem to lead to the conclusion that the rate of adsorption is determined solely by the diffusion of solute molecules from the bulk phase to the surface layer. But further insight makes it clear that discrepancy is involved in the simple diffusion theory. If the simple diffusion theory could be applied to the present case, K_0 in Eq. 5 should be equal to $2(D/\pi)^{1/2}$ in Eq. 6. Then we should be able to calculate the diffusion coefficient from the experimental values of K_0. The calculated values of diffusion coefficient of three alkyl sulfates used are shown in Table I as D_{calc}. In order to check the diffusion theory it is necessary to compare these values of D_{calc} with the observed values of diffusion coefficient. We could not find in any literature the experimental values of diffusion coefficient of sodium alkyl sulfates in aqueous solutions, but we can estimate the values from conductivity data of Lottermoser and Püschel[12] by using the Nernst's equation,

$$D = \Lambda_0 RT/|Z|F^2 \tag{7}$$

where Λ_0 is the conductivity at infinite dilution of surface active ion with the valency Z and F, R and T are Faraday constant, gas constant and absolute temperature, respectively. The estimated values of diffusion coefficient for three alkyl sulfate ions used are shown in Table I as D_{est}. These values are, of course, diffusion coefficients at infinite dilution, but the concentrations so small as in the present experiment would not alter the values appreciably.

TABLE I
COMPARISON OF DIFFUSION COEFFICIENTS

Detergents	SDS	STS	SHS
Temp. (°C)	28±1	28±1	28±1
D_{calc}(cm^2/sec.)	1.60×10^{-9}	7.69×10^{-6}	6.32×10^{-7}
D_{est}(cm^2/sec.)	6.80×10^{-6}	4.54×10^{-6}	4.01×10^{-6}

As seen from Table I the calculated values of the diffusion coefficient are in general much smaller than the estimated ones. Moreover, the most embarrassing point is that the diffusion coefficient calculated by the simple diffusion theory decreases considerably with decrease in the chain length of the detergent molecule. This is quite unreasonable. Therefore, we can conclude that the simple diffusion theory can not explain the rate of adsorption of sodium alkyl sulfates at the solution-air interface under the conditions of the present experiment.

Salley et al.[13] measured the rate of adsorption of Aerosol OTN at the solution-air interface by radiotracer method and obtained the rate equation,

$$\Gamma_t = kt^n \tag{8}$$

where k and n are constants. They found that n is nearly 1/2. They calculated the diffusion coefficient of sulfosuccinate ion from the experimental values of k by making use of the simple diffusion equation. The calculated diffusion coefficient was $0.7\sim2.2\times10^{-4}$ cm^2/min., which was, according to them, comparable to the observed value, $3\sim4\times10^{-4}$ cm^2/min. However, we suppose that the agreement is not so good as to confirm the validity of the simple diffusion theory, and various surface active compounds, especially with varying chain length, should be examined in order to check the diffusion theory.

In the case of the adsorption of surface active electrolytes, such as those used in the present experiment, it is reasonable to take the energy barrier idea into consideration. Let λ be the energy barrier to the adsorption, then the rate equation[9] may be given by

$$\Gamma_t = 2C(Dt/\pi)^{1/2} \exp(-\lambda/RT) \tag{9}$$

12) A. Lottermoser and F. Püschel, *Kolloid-Z.*, **63**, 175 (1933).

13) D. J. Salley, A. J. Weith, Jr., A. A. Argyle and J. K. Dixon, *Proc. Roy. Soc.*, **A203**, 42 (1950).

in which the simple diffusion equation is combined with the idea of energy barrier. Tentatively we applied Eq. 9 to the present case and calculated the energy barrier to the adsorption of three alkyl sulfates used in the present experiment. That is, from Eqs. 5 and 9

$$K_0 = 2(D/\pi)^{1/2} \exp(-\lambda/RT) \qquad (10)$$

Using the value of D, estimated from the conductivity data of Lottermoser and Püschel, and K_0, obtained in the present experiment, the values of energy barrier were calculated*. They are shown in Table II.

TABLE II

ENERGY BARRIER, λ, TO THE ADSORPTION

Detergents	SDS	STS	SHS
Temp. (°C)	28±1	28±1	28±1
Energy barrier, λ, (kcal./mole)	2.5	1.2	0.6

We could not compare the calculated energy barrier with the observed one, and therefore the validity of the energy barrier theory has not been established. This point will be discussed by further study of the adsorption rate, especially in the presence of inorganic electrolytes.

* Strictly speaking, we should calculate λ from the slope of $\ln K_0/2(D/\pi)^{1/2}$ vs. $1/T$ plot.

Summary

The rate of adsorption of sodium dodecyl sulfate, sodium tetradecyl sulfate and sodium hexadecyl sulfate at the solution-air interface has been measured by radiotracer method. It has been found that the surface excess of a detergent is proportional to the concentration of the solution and the square root of time of aging at the initial stage of adsorption. The simple diffusion theory has been checked and it has been found that the results of the present experiment can not be explained by the simple diffusion theory. The idea of energy barrier has tentatively been applied and the values of energy barrier have been calculated.

The authors wish to express their thanks to Professor Tunetaka Sasaki of Tokyo Metropolitan University for his kind advice and encouragement throughout this study. The expenses of this research were defrayed from the Scientific Research Grant of the Ministry of Education, to which the authors' thanks are also due.

Department of Chemistry
Faculty of Science
Kyushu University
Hakozaki, Fukuoka

The Different Distribution of Rubidium and Cesium in Natural Plants

By Noboru YAMAGATA, Toshiko YAMAGATA and Shunji MATSUDA

(Received October 9, 1958)

The uptake of rubidium and cesium by plants in relation to potassium absorption was studied by several investigators. Collander[1] found that the differences between the plant species, the eleven phanerogams studied, were only moderate for potassium, rubidium and cesium contents; all plants absorbed rubidium and cesium with almost the same rapidity as for potassium. The data of Collander and the experiments of other investigators[2-4] suggested the possible use of radioactive rubidium-86 as a tracer for potassium in plant growth experiments, since an isotope of potassium having a suitable half-life was not readily available. On the other hand, cesium-137 is one of the principal long-lived products of nuclear fission and its absorption by cultured plants is a matter of keen interest.

If cesium is hardly differentiated in uptake by plants as in the case of rubidium, and its translocation up to the aerial part is similar to that of rubidium, the distribution of these elements in the leaves of natural plants must be of the same nature. The present paper points

1) R. Collander, *Plant Physiol.*, **16**, 691 (1941).
2) E. Epstein, *Proc. Fourth Ann. Oak Ridge Summer Symp.*, **TID-5115**, 418 (1952).
3) F. J. Richards, *Ann. Bot.*, 8, 323 (1945).
4) J. C. Martin et al., *Soil Sci. Soc. Amer. Proc.*, **10**, 94 (1946).

TABLE I
RUBIDIUM AND CESIUM CONTENT OF NATURAL PLANT
(Dry basis)

Name	Location	K %	Rb p.p.m.	Cs p.p.m.
Usnea longissima	Ozegahara, forest	0.249	0.8	0.01
〃	〃 , 〃	0.256	0.7	0.004
Thelypteris oligophlebia	Ōmine-mine	2.92	50	0.05
Lepisorus Thumbergianus	Ozegahara, forest	1.07	4	0.1
Dicranopteris glauca	Mt. Ōdaigahara	0.631	20	0.01
Osmunda cinnamomea	Ozegahara, bog	1.61	5	0.1
〃	〃 , forest	1.83	6	0.3
Equisetum arvense	Ōmine-mine	5.02	30	0.01
〃	〃	2.27	20	0.05
Abies Mariesii	Mt. Zaō	0.287	3	0.05
Tsuga Sieboldii	Ozegahara, forest	0.601	2	0.03
Pinus densiflora	Tsubaki, sea-shore	0.378	2	0.01
P. pumira	Mt. Zaō	0.346	3	0.05
P. parvifolia	Mt. Shibutsu	0.347	1	0.01
Myrica gale var. tomentosa	Ozegahara, bog	0.354	2	0.08
Ostrya Japonica	Mt. Zaō	0.802	10	0.02
Fagus japonica	〃	0.514	10	0.05
Quercus crispula	Mt. Ōdaigahara	0.816	5	0.02
〃	Ozegahara, forest	0.707	2	0.4
〃	Mt. Shibutsu	0.531	2	0.01
Reynoutria japonica	Mt. Shibutsu	0.837	3	0.6
Dianthus superbus var.	Mt. Shibutsu	0.964	4	0.3
Nuphar pumilum var. ozeense	Ozegahara, bog	0.887	10	0.05
Nymphaea tetragona	〃 , 〃	0.743	10	0.05
Ranunculus nipponicus var.	〃 , 〃	1.91	5	0.3
Magnolia obovata	Mt. Zaō	0.866	10	0.02
〃	Ōmine-mine	2.01	20	0.004
Hydrangea hirta	〃	1.22	10	0.3
Saxifraga Fortunei	Mt. Shibutsu	0.801	1	0.01
Sorbus commixta	〃	0.987	4	0.002
Sanguisorba sitchensis	〃	1.15	4	0.03
Sieversia pentapetala	〃	0.310	2	0.05
Skimmia japonica	Mt. Ōdaigahara	0.726	6	0.2
Empetrum nigrum var. japonicum	Mt. Shibutsu	0.233	1	0.05
Acer Tschonoskii	Mt. Zaō	0.677	6	0.05
A. Mono	Ozegahara, forest	1.39	4	0.05
Aesculus turbinata	〃 , 〃	1.20	3	0.02
Tilia japonica	〃 , 〃	1.71	5	0.03
Kalopanax pictus	〃 , 〃	1.90	6	0.07
Phyllodoce aleutica	Mt. Zaō	0.338	3	0.02
Rhododendron sp.	〃	0.677	6	0.05
R. Tchonoskii	Mt. Shibutsu	0.324	0.8	0.05
R. Fauriae	〃	0.300	1	0.05
Andromeda Polifolia var. grandiflora	Ozegahara, bog	0.456	1	0.05
Arcterica nana	Mt. Shibutsu	0.173	0.6	0.1
Menyanthes trifoliata	Ozegahara, bog	1.81	6	0.4
Adenophora nikoensis	Mt. Shibutsu	2.64	8	1
〃	〃	2.10	3	0.1
Cirsium spicatum	Mt. Zaō	1.25	30	0.3
〃	Ōmine-mine	1.90	20	0.04
Sasa paniculata	Mt. Ōdaigahara	0.490	4	0.01
S. oseana	Ozegahara, bog	1.34	8	0.1

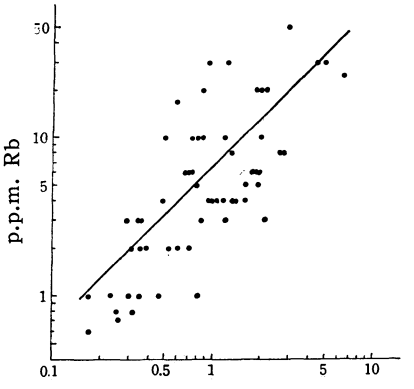
Name	Location	K %	Rb p.p.m.	Cs p.p.m.
Miscanthus sinensis	Gunma-mine	0.171	1	0.1
〃	Mt. Zaō	0.934	30	0.2
〃	Ozegahara, bog	0.869	20	1
Phragmites communis	〃 , 〃	1.37	4	0.5
Lisichiton camtschatcense	〃 , 〃	6.45	25	0.5
Veratrum stamineum	〃 , 〃	4.35	30	0.01
〃	Mt. Shibutsu	2.71	8	0.05
Narthecium asiaticum	Ozegahara, bog	1.98	10	0.1
Iris laevigata	〃 , 〃	1.63	4	0.05

out the different distribution of rubidium and cesium in natural plants and deals with the discussion of the different nature of these elements in the biological cycle from soil to plant.

Distribution of Rubidium and Cesium in Natural Plants.—The distribution studies on the rare alkali elements in soil, plants, and waters have been carried out and reported by one of the authors[5]. Sixty-one samples of natural plants consisting of fifty different species were collected from various districts in Japan and analyzed for leaves by a spectrographic method by use of cathode-layer arc excitation. The plant species consist of two mosses, seven ferns, five gymnosperms, and eleven monocotyledons, the rest being dicotyledons. The analytical data are summarized in Table I. Rubidium varied from 0.6 to 50 p.p.m. and cesium from 0.002 to 1 p.p.m. on the dried material.

The determination of rubidium and cesium in plants has been reported by G. Bertrand and D. Bertrand[6]. The values for land plants examined by them ranged from 2.1 to 81 (average, 20.3) p.p.m. of rubidium and from 3 to 88.5 (average, 22) p.p.m. of cesium for phanerogams on the dried material. The values for rubidium are in good agreement with those given by the authors; however, the values for cesium given by Bertrand et al. are an order similar to the values for rubidium, showing surprisingly high values. Recently, Smales and Salmon analysed seaweed and the ratios of $0.55\sim1.4\times10^{-2}$ (average, 1.0×10^{-2}) were given for the ratio Cs/Rb[7]. Rubidium is more abundant than cesium by factors of approximately 100 in rocks, soils, seaweeds, and other natural materials; the land plants could not be the only exception. The result of the authors' determination indicates the variation of the Cs/Rb ratio from 2×10^{-4} to 2×10^{-1} and the average 3×10^{-2}.

Relationships between the potassium content and the rubidium or the cesium content of natural plants were examined;



$Rb=5.3\times K^{0.94}$, $r=0.72$

Fig. 1. Relation between potassium and rubidium contents of natural plant.

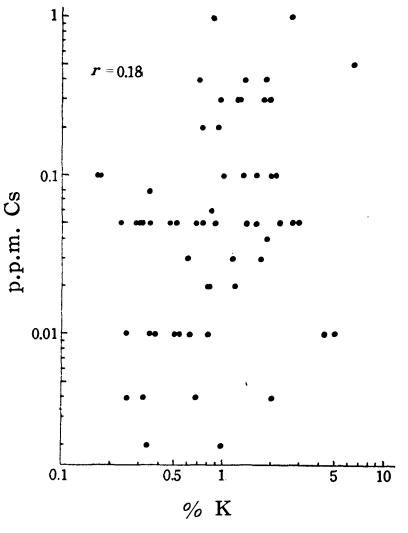


Fig. 2. Relation between potassium and cesium contents of natural plant.

5) N. Yamagata, *J. Chem. Soc. Japan, Pure Chem. Sec.* (*Nippon Kagaku Zasshi*), 71, 288, 567 (1950); 72, 154, 157, 247, 299, 530, 610, 753 (1951); N. Yamagata and T. Kurobe, ibid., 72, 944 (1951).

6) G. Bertrand and D. Bertrand, *Compt. rend.*, 219, 325 (1944); 229, 453 (1949).

7) A. A. Smales and L. Salmon, *Analyst*, 80, 37 (1955).

TABLE II
RUBIDIUM AND CESIUM CONTENTS OF SOIL IN JAPAN
(Dry basis, hot conc. HCl soluble)

Soil Type	Location	K %	Rb p.p.m.	Cs p.p.m.
Kwantō loam	Meguro, Tokyo	0.04	0.8	0.02~0.2
〃 , uppon layer	Nishigahara, Tokyo	0.05	0.8	0.1 ~1
〃 , lower layer	〃 〃	0.04	0.6	0.01~0.1
Volcanic ashy soil	Hokkaido	0.02	0.3	0.06~0.6
Bog soil, upper layer	Aomori Pref.	0.13	20	0.5
Meadow soil, upper layer	Akita Pref.	0.08	8	0.1 ~1
〃 , middle layer	〃	0.07	40	0.4
〃 , lower layer	〃	0.05	10	0.2
Volcanic ashy soil	Ibaragi Pref.	0.01	2	0.03
Tertiary diluvium, upper layer	Aichi Pref.	0.04	3	0.03~0.3
〃 lower layer	〃	0.06	10	0.2
Alluvial paddy soil	Shiga Pref.	0.11	80	0.3 ~3
Granitic alluvium	Shiga Pref.	0.07	20	0.2 ~2
Sandy alluvium (I)	Kagawa Pref.	0.07	10	0.03
〃 (II)	〃	0.07	2	0.04~0.4
Average		0.06	14	(0.3)

the Rb/K ratio varied from 1.2×10^{-4} to 3.2×10^{-3} and the average was 7.3×10^{-4} for sixty-one samples. The variation of Cs/K ratio was greater than that of Rb/K and covered from 2×10^{-6} to 1×10^{-3}. Fig. 1 is a plot in logarithmic scale of the potassium content in percent versus the rubidium content in p.p.m. The existence of a linear relationship between rubidium and potassium contents can easily be seen; the coefficient of correlation (r) is 0.72. Fig. 2 is a plot in logarithmic scale of the potassium versus the cesium content. In this case, the existence of a linear relationship is doubtful ($r=0.18$). The coefficient of correlation between rubidium and cesium contents was also calculated and the value of 0.0073 appears to indicate no relation between the contents of these elements in the examined plants.

The variation of the Cs/K ratio greater than the Rb/K ratio and the doubtful existence of correlation between cesium and potassium contents may be accounted for by one or several reasons as under described.

(1) The variation of total cesium content of the soils on which the plants were growing is greater than that of rubidium.

(2) The uptake of cesium into the aerial portions of the plants is irregular as compared with that of rubidium; for example, the uptake tends to increase at the higher concentrations of cesium in soil solution.

(3) The ion-exchange or adsorption mechanism between soil and solution that makes the release of cesium and rubidium for soil colloids and minerals is different.

Distribution of Rubidium and Cesium in Soil.—Soils usually contain 20~500[8] or 5~100 (average, 60[9] or 100[10]) p.p.m. of total rubidium and only less than 1 to 25.7 (max.) p.p.m.[8] of total cesium in contrast with 1.36% of total potassium on the average[9]. Although the data for cesium are too incomplete to guess the average content, Vinogradov gave a value of approximately 5 p.p.m.[9,10]. The average ratio of Rb/K is $4\sim7\times10^{-3}$ and the average Cs/K is approximately 4×10^{-4}. Those data appear to be reasonable in accordance with Horstman's recent work[11]. He gave 240~460 for the average ratios K/Rb of various rocks ($Rb/K=2.2\sim4.2\times10^{-3}$) and 6700 for K/Cs of granitic rocks ($Cs/K=1.5\times10^{-4}$). On the weathering of rocks, absolute loss of the three elements occurs with the fastest leaching and the least adsorption of potassium, as the result, the ratios of Rb/K and Cs/K increase. However, the above-mentioned data indicate that soils differ not so much from fresh rocks in the averaged ratios of Rb/K and Cs/K.

No biological activities can ever extend to the complete decomposition of soil forming silicate minerals, although the total elements existing in soil are reserved

8) D. J. Swaine, "Trace-Element Content of Soils". Commonwealth Bureau of Soil Sci. Tech. Comm., No 48 (1955) p. 34, 88.

9) V. I. Vernadsky, "Selected Papers" (in Russian), ed. by A. P. Vinogradov, Acad. Sci. U. S. S. R. Moscow (1954) Vol. I, p. 365.

10) A. P. Vinogradov, "Geochemistry of Rare and Disperse Chemical Elements in Soil" (in Russian), Acad. Sci. U. S. S. R. Moscow (1957) p. 86-94, 216.

11) E. L. Horstman, *Geochim. et. Cosmochim. Acta*, 12, 1-28 (1957).

for living matter to be utilized in far future. In this respect, we often consider the amount of elements extractable with mineral acid as a measure for the availability by plants in the near future.

Fifteen representative Japanese soils were extracted with hot hydrochloric acid (31%) and analyzed; the result[12] has been recalculated and summarized in Table II. The variation of rubidium and cesium covered from 0.3 to 80 and from 0.01 to 3 p.p.m. respectively when potassium varied from 0.01 to 0.13%. The Rb/K ratio varied from 1.5×10^{-3} to 7×10^{-2} and the Cs/K ratio varied from 4×10^{-5} to 1×10^{-3}. These values indicate that the variations of levels of rubidium and cesium in soil are of the same order and it appears to us that the first reason (1) for the different distribution of these elements in natural plants fails to elucidate the fact.

Culture Experiment.—Many investigators carried out the culture experiments with solutions of various concentrations of rubidium and cesium; an example is shown in Table III. When the uptake by natural or cultivated plants growing in soil comes into question, we must consider the natural levels of rubidium and cesium concentrations in soil. Indeed, the culture experiment with higher concentrations may serve for certain physiological purposes, however, for the present purpose, it will be desirable to make the levels of these elements in culture solution as close as possible to those in natural soil conditions.

TABLE III
RUBIDIUM, CESIUM AND POTASSIUM LEVELS IN CULTURE SOLUTION USED BY SEVERAL INVESTIGATORS

	Rb meq./l.	Cs meq./l.	K meq./l.
Collander[1]	0.1 2	0.1	2
Menzel and Heald[13]	0.054 0.0054	0.054 0.0054	0.54
Murphy et al.[14]	Rb/K (weight) 1/1, 1/2, 1/5, 1/10		

It is not the total or acid soluble but only a fraction of the elements that the root of a plant can readily absorb. It is well known that rubidium and cesium are more firmly held by the clay fraction of soil than potassium, probably on account of their greater ionic polarizability. We can therefore assume that the Rb/K and the Cs/K ratios in the neutral ammonium acetate extract of soil or in the actual soil solution are probably smaller respectively than the ratios of the total or strong acid soluble elements in soil.

As the concentrations of available or active rubidium and cesium in soil had not been estimated when the present cultue experiment was undertaken, the standard ratios of Rb/K and Cs/K were temporarily fixed to approximately 10^{-2} and 2×10^{-4} respectively except where varied as an experimental condition.

Experimental

The experiment was conducted in a greenhouse and cucumber, rice-plant, and soy-bean were chosen for the experiment plants. The seedlings were grown in nutrient solutions in 3 liter porcelain pots from 3rd July to 11th July when tracer isotopes were added. After that, a long period experiment was carried on for thirty days with occasional renewal of nutrient solution and radio isotopes.

The culture solution was prepared with extra pure chemicals and distilled water; the elementary composition was as follows[15]: (p.p.m. in solution)

NO_3-N: 130, NH_4-N: 23, K: 200, Ca: 200, Na: 20, Mg: 40, Si: 20, P: 50, Cl: 20, S: 50, Fe: 2, Mn: 0.4, B: 0.4, Zn: 0.4, Cu: 0.04, Mo: 0.002.

Two isotopes ^{137}Cs and ^{86}Rb were added together in a concentration of about 10 μc/l. each of nutrient solution. Another experiment to determine the uptake velocity of these elements by plants in a short period was conducted with higher concentrations of isotopes.

The harvested plant leaves were incinerated and counted for the total activity of ^{137}Cs and ^{86}Rb. After thirty-nine days the sample was recounted for the activity. As the difference was to be ascribed to the decay of a short-lived isotope ^{86}Rb (half-life: 19.5 days), each of the activities of these isotopes could be calculated. After the activity determination, the plant ash was analyzed for potassium by a chemical method. The ratio of counts from ^{137}Cs (or ^{86}Rb) and concentration of potassium in the plant were compared with the same ratio in the culture solution. The distribution factors between plant and solution were calculated by dividing the two ratios: (^{86}Rb/K in plant)/(^{86}Rb/K in solution) for rubidium, and (^{137}Cs/K in plant)/(^{137}Cs/K in solution) for cesium.

12) N. Yamagata, *J. Chem. Soc. Japan, Pure Chem. Sec.* (*Nippon Kagaku Zasshi*), **71**, 567 (1950).
13) R. G. Menzel and W. R. Heald, *Soil Sci.*, **80**, 287 (1955).
14) W. S. Murphy, A. H. Hunter and P. F. Pratt, *Soil Sci. Soc. Amer. Proc.*, **19**, 433 (1955).
15) N. Yamagata and T. Yamagata, Culture experiment with a universal solution. Presented at the Annual Meeting of the Society of the Science of Soil and Manure, Tokyo, Apr., 1958.

Results

A short period experiment was performed to examine whether there were any differences between rubidium and cesium of the transport velocity into the aerial part. The result of the experiment is shown for rice-plant (Fig. 3). The transport velocity is represented by plotting the increase of distribution factors against time, consequently, it does represent an increase of rubidium or cesium in the plant not absolutely but relatively to potassium. Rapid absorption is observed in several early hours and steeper slope for rubidium appears to indicate faster transport in the plant or rubidium than of cesium at the early stage of absorption, although the difference between these elements will have no connection with the absorption during the prolonged period.

A long period experiment was conducted with the three crop plants over a range of concentrations of rubidium and cesium from 0.02 to 20 and about 0.0001 to 4 p.p.m. respectively. The results are shown in Table IV. The effect of concentration was not clear except for rubidium in the case of soy-bean. The relatively small variation of distribution factors with concentration in nutrient solution indicates that the effect of concentration on rubidium and cesium uptake relative to potassium is small, by a factor of two or three at most. The results also indicate that a difference exists between plant species. It can be seen that the distribution factor for cesium is greater in leaves than roots only in the case of soy-bean. The rice-plant accumulates less cesium relative to potassium than the other plants. These results are in good agreement with Rediske and Selders' experiement with several other crop plants[16].

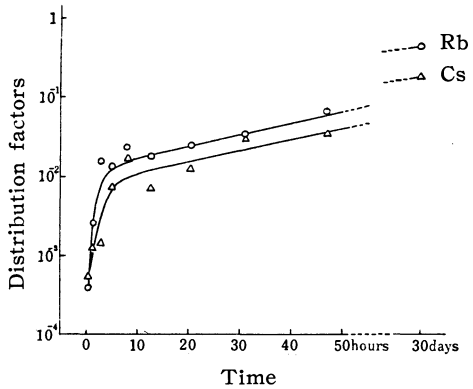


Fig. 3. Uptake velocity of cesium and rubidium by rice-plant as represented by distribution factor between solution and plant leaf.

Distribution of Rubidium and Cesium in Tobacco Leaf.—The analytical data for the distribution of the alkali elements in cultivated tobacco leaves were previously presented by one of the authors[17]. The recorded value for rubidium varied from 5 to 90 p.p.m. on the dried material and the average was 30 p.p.m. The Rb/K ratio varied from 5×10^{-4} to 3×10^{-3} and the average was 1×10^{-3}; these values are in good agreement with those of the natural plants.

On the other hand, the concentration of cesium in tobacco leaves was very low and for this reason it was only successfully determined quantitatively for one sample among seventeen (No. 10a in the original paper). This sample contained 0.17 p.p.m. cesium in ash or 0.02 p.p.m. in the dried material, and the Cs/K ratio for the whole leaf was 1.2×10^{-6}. The Cs/K ratios for the rest of the sample are considered to be less than this value. It can thus be concluded that the Cs/K ratios for cultivated tobacco leaves are surprisingly low as compared with those for the natural plants ($2\times10^{-6}\sim1\times10^{-3}$).

According to the experiment conducted by Menzel[18], the uptake of rubidium and cesium by plants was inversely proportional to the available potassium in the soil, and the uptake of cesium was more affected than that of rubidium by the increase in available potassium. Thus, the remarkable discrimination in the cultivated tobacco plant of cesium from potassium will be accounted for by the possible existence of a greater quantity of available potassium in the soil as compared with the case of natural plants.

Another interesting phenomenon should be pointed out, that of the different distribution with in the tobacco leaf of cesium from rubidium and potassium. The tobacco leaf was divided into two portions, the principal vein and the remaining part, and separately analyzed. Qualitative examination indicated in every sample of tobacco leaves the considerable enrichment of potassium and rubidium in the vein and the inverse trend for cesium. Quantitative determinaion was made with the tobacco leaf No. 10a and the result is

16) J. H. Rediske and A. A. Selders, *U. S. Atomic Energy Comm.*, HW-35174 (1953).
17) N. Yamagata, *J. Chem. Soc. Japan, Pure Chem. Sec.* (*Nippon Kagaku Zasshi*), **71**, 288 (1950).
18) R. G. Menzel, *Soil Sci.*, **77**, 419 (1954).

TABLE IV

DISTRIBUTION FACTORS FOR Rb-K AND FOR Cs-K IN LEAF AND ROOT OF PLANTS OF SEVERAL CROP SPECIES

(K: 200 p.p.m. in nutrient solution)

Pot No.	Ratios in Nutrient soln. (in weight)		Part	Distribution Factors					
				Cucumber		Rice-plant		Soy-bean	
	Rb/K	Cs/K		Rb/K	Cs/K	Rb/K	Cs/K	Rb/K	Cs/K
1	10^{-4}	5×10^{-7}	L	0.30	0.66	0.35	0.31	0.17	0.40
			R	*0.14*	*0.62*	*0.26*	*0.33*	*0.72*	*0.28*
2	10^{-3}	2×10^{-5}	L	0.56	0.91	0.57	0.23	0.24	0.82
			R	*0.13*	*1.75*	*0.50*	*0.49*	*0.65*	*0.40*
3 (standard)	10^{-2}	2×10^{-4}	L	0.32	0.40	0.45	0.18	0.39	0.54
			R	*0.18*	*0.81*	*0.45*	*0.46*	*0.65*	*0.33*
4	10^{-1}	2×10^{-3}	L	0.50	0.52	0.88	0.57	0.48	0.57
			R	*0.30*	*1.25*	*0.32*	*0.25*	*0.42*	*0.30*
5	10^{-2}	2×10^{-2}	L	0.72	0.57	0.17	0.15	0.72	0.72
			R	*0.35*	*0.76*	*0.22*	*0.58*	*0.24*	*0.33*
Average			L	0.48	0.61	0.48	0.29	0.40	0.61
			R	*0.22*	*1.04*	*0.35*	*0.42*	*0.54*	*0.33*

TABLE V

THE DIFFERENT DISTRIBUTION IN TOBACCO LEAF OF CESIUM FROM RUBIDIUM AND POTASSIUM

(Sample No. 10a, recalculated from the previous report[17])

	K %	Rb p.p.m.	Cs p.p.m.	Rb/K	Cs/K
Whole leaf	1.77	40	0.02	2×10^{-3}	1.2×10^{-6}
Principal vein	3.70	90	0.006	2.5×10^{-3}	1.5×10^{-7}
The remaining part	1.35	20	0.02	1.5×10^{-3}	1.5×10^{-6}

shown in Table V. The Rb/K ratio is similar in the principal vein and in the rest. On the other hand, the Cs/K ratio in the former is approximately one tenth of the ratio in the latter, that is to say, the cesium is relatively enriched in the latter as compared with potassium and rubidium. These results appear to be inconsistent with the conclusions by Glueckauf[19] who considered the possible enrichment of cesium and strontium occurring in flowers, leaf veins and root substrate.

Conclusion

1. The greater variation of cesium in natural plants than that of rubidium could not be attributed to the variations of total or acid soluble elements in the soil.

2. The relative uptake by plants of rubidium and cesium to potassium was only slightly affected by the concentrations of these elements in nutrient solution. It appears that a difference does exist between plant species in their ability to accumulate cesium and rubidium relative to potassium.

3. The greater variation of the Cs/K ratio and the doubtful existence of correlation between cesium and potassium contents of natural plants may be principally attributed to the complicated mechanisms of ion-exchange or adsorption between soil and solution.

Fixation by soils and uptake by plants of cesium have been investigated by several authors[20-22] in connection with the problems of radioactive contamination from nuclear fission explosions and also with a view to the ultimate disposal of fission products. The fate of cesium-137 in the biogeochemical cycle from soil to plant has usually been considered likely to follow that of potassium. This appears not to be true after both the results ascertained by us and other investigators. When consideration is taken of the difference of the ionic radii between rubidium (1.49Å) and cesium (1.63Å), we can not expect that cesium can replace potassium (1.33Å) as freely as rubidium does. In this regard, the concept of the "Cesium Unit" temporarily adopted by U.N. authorities to evaluate the concentration of cesium-137 in natural

19) E. Glueckauf, *Atomic Energy Research Establishment*, Harwell, SPAR/7 (1956).

20) C. B. Amphlett, *Research*, 8, 335 (1955).

21) C. B. Amphlett and L. A. McDonald, *J. Inorg. & Nuclear Chem.*, 2, 403 (1956).

22) H. Nishita et al., *Soil Sci.*, 81, 317 (1956).

materials relatively to potassium has little meaning. We believe that the future burden of mankind with radioactive cesium-137 will properly be estimated on the basis of the concept of isotopic dilution.

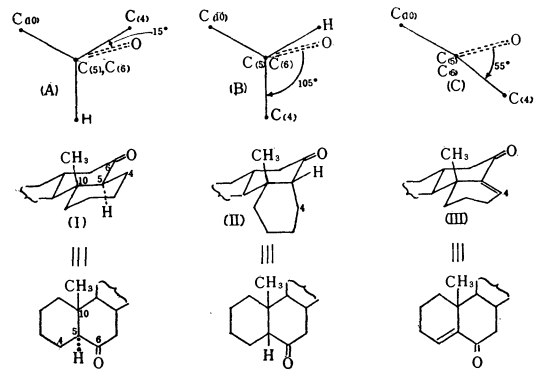
Kiriu College of Technology
Gunma University, Kiriu

Stereochemistry of Some Steroidal Ketones

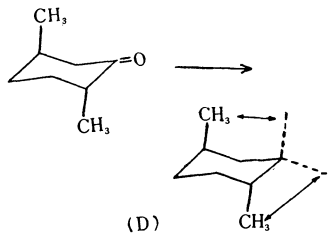
By Ken-ichi MORITA

(Received November 12, 1958)

According to Barton's rule[1a] for calculating the relative degrees of steric hindrance of carbonyl groups, the degree of steric hindrance of a $C_{(6)}$-carbonyl group must be the same whether it is in a 5α-steroid or in a 5β-steroid[2]. However, the fact that reduction of a $C_{(6)}$-carbonyl group in a 5α-steroid (I) with lithium aluminum hydride gives exclusively an axial isomer[3] whereas reduction of a $C_{(6)}$-carbonyl group in a 5β-steroid (II) with the same reagent gives a considerable amount of an equatorial isomer[4] suggests[1b,5] that the degrees of steric hindrance of the two carbonyl groups may be different. In the two compounds, the geometrical circumstances around the carbonyl groups are equal except the $C_{(4)}$-methylene groups (see I and II). The expressions A and B show the views[6] looking down the $C_{(5)}$-$C_{(6)}$-axes of a 5α-6-ketone (I) and a 5β-6-ketone (II), respectively. The angle between the $C_{(6)}$-oxo-group and the $C_{(4)}$-methylene group is much greater in II than in I. The interaction between the oxo-group and the $C_{(4)}$-methylene group may be smaller in II than in I. Thus the oxo-group in II must be less hindered[7]. This postulation is well in line with the results of the hydride reduction, if we accept the generalization[1b,5] that the more hindered ketone gives the more axial hydroxyl group by lithium aluminum hydride reduction.



This view may be extended to carbonyl groups in other positions. As far as the steroid nucleus of 5α-series is concerned, the angular methyl groups at positions $C_{(10)}$ and $C_{(13)}$ are axial with respect to A and C ring, respectively. Therefore the degrees of steric hindrance of the carbonyl groups at positions $C_{(1)}$ and $C_{(12)}$ may be less[8] than Barton's degree[1a]. If we



1) D. H. R. Barton, *J. Chem. Soc.*, **1953**, 1027, (a) p. 1034, (b) p. 1029 footnote 23.

2) Barton has stated that systems having cis-fused rings may prove more complex.

3) C. W. Shoppee and G. H. R. Summers, *J. Chem. Soc.*, **1952**, 3361.

4) Y. Urushibara and K. Mori, This Bulletin, in press.

5) Cf. W. G. Dauben, E. J. Blanz, Jr., J. Tin and R. A. Micheli, *J. Am. Chem. Soc.*, **78**, 3752 (1956).

6) W. Klyne, *Experientia*, **12**, 119 (1956).

7) It may be noted that the conformation of 5α-6-ketone system (I) is still favored from a viewpoint of relative stability[6].

8) An axial methyl group attached at α-carbon atom may have less hindering effect than an axial methyl group attached at β-carbon atom, and steric effect by these axial methyl groups seems to be important in the intermediates. The expression D shows the necessary intermediates for the reactions with reagents like lithium aluminum hydride[9], semicarbazide, phenylhydrazines[10], and so on.

9) L. W. Trevoy and W. G. Brown, *J. Am. Chem. Soc.*, **71**, 1675 (1949).

10) See, e. g., Hammett, "Physical Organic Chemistry", McGraw-Hill Book Co., p. 333 (1940).

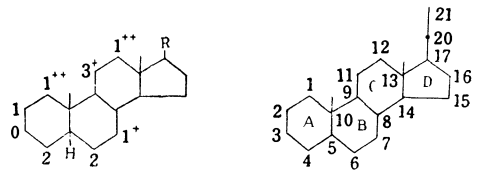
TABLE I

REDUCTION OF STEROIDAL KETONES WITH LITHIUM ALUMINUM HYDRIDE

Compounds	Position of carbonyl groups*	Relative degrees of steric hindrance		Products	Composition of products		Ref.
		Barton's degree	Modified degree		Equatorial (%)	Axial (%)	
cholestan-1-one	1	2^+	1^{++}	cholestan-1-ol	35	65	11
cholestan-2-one	2	1	1	cholestan-2-ol	37	52	5
cholestan-3-one	3	0	0	cholestan-3-ol	90	10	12, 13, 14
coprostan-3-one	3(5β)	0	0	coprostan-3-ol	94	4	12
cholest-5-en-3-one	3(5-ene)	0	0	cholest-5-en-3-ol	90	5	12
cholestan-4-one	4	2	2	cholestan-4-ol	7	86	15
cholest-5-en-4-one	4(5-ene)	—	less than 2	cholest-5-en-4-ol	main	—	16, 15
cholestan-6-one	6	2	2	cholestan-6-ol	6	93	3
coprostan-3, 6-dione	6(5β)	2	1^+	coprostan-3, 6-diol	considerable amount of 6α(equatorial)-compd.		4
cholest-4-en-6-one	6(4-ene)	—	less than 2	cholest-4-en-6-ol	main	—	16, 15
cholest-4-en-3β-ol-6-one acetate	6(4-ene)	—	less than 2	cholest-4-en-3β, 6-diol	75(crude)	—	17
cholestan-3β-ol-7-one acetate	7	1^+	1^+	cholestan-3β, 7-diol	45	55	5
4-chloro-17α-hydroxy-3,20-bisethylenedioxy-pregnan-11-one	11	3^+	3^+	4-chloro-11, 17α-dihydroxypregnane-3, 20-dione bisethylene-ketal	trace	90	18
25D, 5α-spirostan-3β-ol-12-one acetate	12	2^+	1^{++}	25D, 5α-spirostane-3β, 12-diol	50	50	19

* In 5α-steroids unless otherwise stated

arbitrarily indicate the degree of the steric effect by an axial substituent attached at α-carbon atom by the + sign, indicating a positive magnitude less than one unit, Barton's degrees may be modified as shown in IV (see also Table I). The results of reduction of steroidal ketones with lithium aluminum hydride (Cf. Table I) suggest[20] that the sum (indicated by the + + sign)



IV

of the steric effect by the γ-carbon atom which is bent round so as to hinder the carbonyl group and the steric effect by the axial substituent attached at α-carbon atom may be smaller than one unit in magnitude. If it is true, the order of relative degrees of steric hindrance of the $C_{(1)}$- or $C_{(12)}$-carbonyl group and of those of the $C_{(4)}$- or $C_{(6)}$-carbonyl group reverses in the two estimations.

Becker et al.[1,6] and Jones et al.[15] recorded that reduction of cholest-4-en-6-one with lithium aluminum hydride gave mainly cholest-4-en-6α-ol. Urushibara and Mori[17] reported that reduction of cholest-4-en-3β-ol-6-one acetate with lithium aluminum hydride gave mainly cholest-4-en-3β, 6α-diol. These facts are of interest in connection with the foregoing discussion.

11) H. B. Henbest and R. C. L. Wilson, *J. Chem. Soc.*, **1956**, 3289.
12) C. W. Shoppee and G. H. R. Summers, ibid., **1950**, 687.
13) H. R. Nace and G. L. O'Connor, *J. Am. Chem. Soc.*, **73**, 5824 (1951).
14) W. G. Dauben, R. A. Micheli and J. F. Eastham, ibid., **74**, 3852 (1952).
15) D. N. Jones, J. R. Lewis, C. W. Shoppee and G. H. R. Summers, *J. Chem. Soc.*, **1955**, 2876.
16) E. J. Becker and E. S. Wallis, *J. Org. Chem.*, **20**, 353 (1955).
17) Y. Urushibara and K. Mori, This Bulletin, in press.
18) R. H. Levin et al., *J. Am. Chem. Soc.*, **76**, 546 (1954). Cf. L. H. Sarett et al., ibid., **73**, 1777 (1951).
19) R. Hirshmann, C. S. Snoddy, Jr., C. F. Hiskey and N. L. Wendler, ibid., **76**, 4013 (1954).
20) It may be necessary to study the relative degrees of steric hindrance of these carbonyl groups by using carbonyl reagents such as ethyleneglycol, ethanedithiol, semicarbazide and the phenylhydrazines, etc., since the degrees of steric hindrance of the carbonyl groups may not exactly be reflected redution with lithium aluminum hydride[21].
21) Cf. K. D. Hardy and R. J. Wicker, ibid., **80**, 640 (1958).

Cholest-4-en-6-one and cholest-4-en-3β-ol-6-one acetate exhibit the maximum absorption bands at 243 mμ (ε=6,360)[22] and 236 mμ (ε=6,300)[23] in the ultraviolet region, respectively. A method of calculating the principal absorption band of α,β-unsaturated ketones was devised by Woodward[24] and was extended by Fieser and Fieser[25]. The calculated value of the absorption maximum for the 4-ene-6-ketone system is 242mμ, which is in agreement with the observed wavelengths within 6 mμ. In Woodward-Fieser-Fieser's method of calculation no steric factor is considered. We may thus assume[26] that the steric hindrance involved in the system does not cause an abnormal change in wavelength but causes a decrease in absorption intensity and is associated with the transition between the non-planar ground state and the near-planar excited state[27]. Hence, the interplanar angle θ between the $C_{(6)}$-carbonyl double bond and the 4,5-ethylenic bond in the ground state may be calculated[30] from Braude-Sondheimer's equation[26] as roughly 55°[31], if the value of intensity for the unhindered system is arbitrarily taken as 18,000[33]. The expression C shows the view looking down the $C_{(5)}$-$C_{(6)}$-axis of the 4-ene-6-ketone (III). The interaction between the carbonyl group and the $C_{(4)}$-methylene group may be smaller in III than in I; it means that the carbonyl group in III is less hindered, and then may be reduced to the stable form in a more proportion. The result of the hydride reduction corroborates the assumption. Jones et al.[15] reported that reduction of cholest-5-en-4-one, λ_{max} 242 mμ (calculated value; 242 mμ), ε=5,900, with lithium aluminum hydride gave mainly the 4α (equatorial)-hydroxy compound. This phenomenon may also be explained in a similar way ($\theta \simeq 55°$). Another example was recorded by Shapiro et al.[34] who reduced 5,16-pregnadien-3β-ol-20-one acetate with lithium aluminum hydride, obtaining the 20α-hydroxy compound (stable form). 16,17-Saturated $C_{(20)}$-ketones are exclusively reduced to 20β-isomers[35].

The author is indebted to Professor S. Mori, Tokyo Metropolitan University, Dr. M. Nakamura, Director of the Institute, and Mr. R. Mamine, the Institute, for their interest in the present study.

Sugiyama Chemical Research Institute
Mure, Mitaka, Tokyo

22) H. Reich, F. W. Walker and R. W. Collins, *J. Org. Chem.*, **16**, 1753 (1951).
23) E. R. H. Jones et al., *J. Chem. Soc.*, **1937**, 801; ibid., **1940**, 659.
24) R. B. Woodward, *J. Am. Chem. Soc.*, **63**, 1123 (1941); **64**, 76 (1942).
25) L. F. Fieser and M. Fieser, "Natural Products related to Rhenanthorene", 3rd. ed., Reinhold Publishing Corp., (1949) p. 190.
26) E. A. Braude and F. Sodheimer, *J. Chem. Soc.*, **1955**, 3754.
27) It should be noted that the wavelengths of the absorption maxima of the semicarbazone (253 mμ; ε, 7,050) and of the 2, 4-dinitrophenylhydrazone (375 mμ; ε, 24,900) of cholest-4-en-6-one are abnormally low[22,28,29] with low intensity. Steric hindrance involved in the systems seems to be strong, because of bulkiness of =NNHCONH$_2$ and =NNHC$_6$H$_3$(NO$_2$)-2,4 moieties, and to be associated with transitions between non-planar ground states and non-planar excited states.
28) L. Dorfman, *Chem. Revs.*, **53**, 86 (1953).
29) K. Hirayama, "Zikken Kagaku Koza", 1, I, Maruzen, Tokyo, (1957), p. 91, 97.
30) The rough interplanar angles for other α,β-unsaturated ketosteroids may also be calculated.
31) Turner and Voitle[32] ascribed the fact that compounds having the s-cis configuration exhibit diminished absorption intensity to the decrease in the distance separating the ends of the conjugated system.
32) R. B. Turner and D. M. Voitle, *J. Am. Chem. Soc.*, **73**, 1403 (1951).
33) Cf. K. Morita, This Bulletin, **31**, 379 (1958); see also Idem., *J. Chem. Soc. Japan, Pure Chem. Sec.* (*Nippon Kagaku Zasshi*), **78**, 1581 (1957).
34) E. L. Shapiro, D. Gould and E. B. Hershberg, *J. Am. Chem. Soc.*, **77**, 2912 (1955).
35) *Inter al.*, W. Klyne and E. Miller, *J. Chem. Soc.*, **1950**, 1972; H. Hirschmann et al., *J. Biol. Chem.*, **192**, 115 (1951); R. B. Turner and D. M. Voitle, *J. Am. Chem. Soc.*, **73**, 2283 (1951).

SHORT COMMUNICATIONS

Crystal Structures of Silicon Nitride

By Kiichi NARITA and Kenji MORI

(Received September 28, 1958)

Leslie, Carrol and Fisher[1] separated silicon nitride from nitrided silicon steel and, by studying the X-ray and the electron diffractions of the nitride, proposed an orthorhombic cell for Si_3N_4. More recently Turkdogan and Ignatowiez[2] reported that non-metallic inclusions extracted from the nitrided Iron-Silicon alloys are identical with one of the two silicon nitrides synthesized.

It has been established[2-5] that when silicon is nitrided at high temperatures varying from 1200 to 1400°C, a mixture of two phases (α and β) of nitrides is formed. Vassiliou and Wilde[3] mentioned that these two phases were regarded as orthorhombic (α) and hexagonal (β), respectively. But Popper and Ruddlesden[4] reported that one of them (β) can be indexed as rhombohedral, while both of the two phases were claimed to be hexagonal by Hardie and Jack[6]. More recently Forgeng and Decker[5] have come to the same view as Hardie and Jack's. The spacings, however, calculated by the various investigators are in good agreement with one another, notwithstanding that they differ in opinions on these two phases. Thus, it may not yet be concluded that the behavior of silicon nitride in steel is unequivocally solved.

The present authors prepared silicon nitrides in the following way and made a study on their X-ray and electron diffractions, using an electron microscope also at the same time. As it was difficult to obtain the appropriately large single crystal of silicon nitride for X-ray diffraction, the N-pattern obtained with a selected area electron diffraction was used for a study of the crystal structure of this material, in the place of the precession diagram in the X-ray diffraction study. This paper is to present a brief report of the results obtained.

The samples of silicon nitrides were prepared by heating the powdered elementary silicon in a current of ammonia* in the temperature range 1200° to 1500°C. Caution, however, was paid: at every several hours' interval the reaction product was taken out, ground into particles of about 150 mesh in size, and then submitted to the repeated reactions.

The final product is composed of the two specimens; the major part is grayish white powder, and the other of less quantity white mould growing on the former. When the mould-form product is ground, it changes into grayish white powder similar to that of the major part. It is to be noted that there is no distinguishable difference between these two specimens, as far as the X-ray diffraction spectra obtained with a diffractometer are concerned. This leads the present authors to a suggestion that both of these two specimens can be regarded as a mixture of α and β silicon nitride and others, as described below.

Table I shows the results from our studies of the X-ray diffraction (on both two specimens) and the selected area electron diffraction (on the material shown in Fig. 1). The spacings are in good agreement with those given by other investigators. One of the substances, which is more frequently found in the mould-form portion, is in the form of the flat needle as shown in Fig. 1. Its pattern of the selected area electron diffraction in the form of rectangle-shaped N-pattern is illustrated in Fig. 2. It is regarded that this pattern corresponds to the reciprocal lattice of $(11\bar{2}0)$ plane of hexagonal α-silicon nitride

1) W. C. Leslie, K. G. Carroll and R. M. Fisher, *Trans. Am. Inst. Mining Met. Engrs.*, **194**, 204 (1952).
2) E. T. Turkdogan and S. Ignatowiez, *J. Iron and Steel Inst.*, **185**, 200 (1957).
3) B. Vassiliou and F. G. Wilde, *Nature*, **179**, 435 (1957).
4) P. Popper and S. N. Ruddlesden, ibid., **179**, 1129 (1957).
5) W. D. Forgeng and B. F. Debker, *Trans. Am. Inst. Mining Met. Engrs.*, **212**, 343 (1958).
6) D. Hardie and K. H. Jack, *Nature*, **180**, 332 (1957).

* Purification of ammonia was made following the method of A. Farkas and H. W. Melville: "Experimental methods in Gas Reactions", Macmillan, London (1939), p. 162. Flow rate was regulated as 250 cc./min./3.14 cm^2.

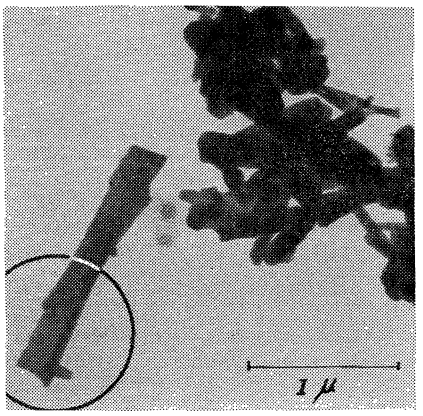


Fig. 1. Electron Micrograph of α-silicon nitride.

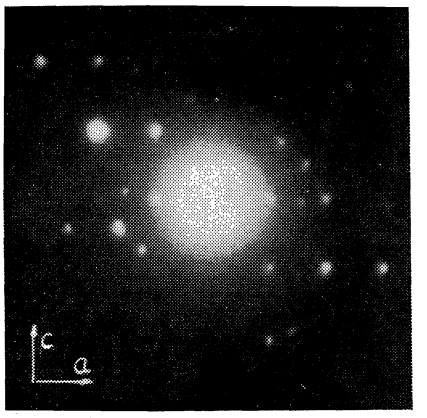


Fig. 2. Electron diffraction pattern of nitride, pertinent to the portion as enclosed by the circle in Fig. 1.

TABLE I

X-RAY DATA FOR THE SILICON NITRIDE

Electron diffraction	Diffractometer		α-Si_3N_4		β-Si_3N_4		Forgeng, Decker[5] Si_2ON	
d Obsd.	*d* Obsd.	Int.	*hkl*	*d* Calcd.	*hkl*	*d* Calcd.	*hkl*	*d*
6.68 Å	6.67 Å	13	100	6.74 Å				
	6.63	9			100	6.58 Å		
5.76			001	5.64				
	5.15	9						
	4.64	9					110	4.69 Å
	4.46	13					020	4.44
4.29	4.32	100	101	4.33				
	3.89	36	110	3.88				
	3.82	13			110	3.80		
	3.47	13						
3.34	3.37	36	200	3.37			111	3.38
	3.30	27			200	3.29		
2.84	2.89	82	201	2.89				
2.78	2.82	9	002	2.82				
	2.67	32			101	2.73	200	2.75_3
2.58	2.60	77	102	2.60				
	2.54	73	210	2.54				
	2.49	23			210	2.49		
	2.43	9					002	2.42_9
	2.39	13					201	2.39_4
	2.32	45	211	2.32	111	2.31	131	2.30_1
	2.28	9	112	2.28				
2.21	2.24	4	300	2.25			040	2.22_5
	2.18	9			201	2.19		
2.12	2.16	27	202	2.16			112	2.15_1
	2.13	5					022	2.12_9
2.05	2.08	32	301	2.08			221	2.10_7
			220	1.94				
					220	1.90		
	1.88_7	10	212	1.88_8	211	1.89_3		
1.87			003	1.88_0				
	1.86_7	13	310	1.86_5				
	1.80_8	9	103	1.81_3			202	1.81_9
	1.76_8	9	311	1.77_0			310	1.79_7
1.72	1.75_4	9	302	1.75_4	301	1.75_3	132	1.77_9

mentioned by the other investigators[5,6]. And it can not be indexed according to Leslie's[1] orthorhombic lattice.

In view of the above, the crystal structure of α-silicon nitride is regarded more likely as hexagonal. The selected area electron diffraction could not be applied to β-silicon nitride; however, considering the structure of β silicon nitride as hexagonal, as mentioned by the other investigators[5,6], the X-ray diffraction data shown in Table I can be explained as resulting from the mixture of α and β nitrides.

The parameters of these hexagonal cells of α and β silicon nitrides which are yielded from the X-ray diffraction data are as follows:

α-silicon nitride $a_0=7.76\pm0.05$ Å

$c_0=5.64\pm0.006$ Å $\quad c/a=0.727$

β-silicon nitride $a_0=7.59\pm0.06$ Å

$c_0=2.92\pm0.008$ Å $\quad c/a=0.385$

There are some discrepancies between the observed values for spacings obtained with the diffractometer and the calculated values. One of such discrepancies is also found in Leslie's data[1]. These discrepant spacings coincide with those of silicon oxynitride determined by Forgeng and Decker[5] as shown in Table I.

Research Department
Kobe, Steel Works, Ltd.
Fukiai-ku, Kobe

Chemical Shifts of Proton Resonance and Mesomeric Effects in Substituted Benzene

By Hiroshi SHIMIZU, Mikio KATAYAMA and Shizuo FUJIWARA

(Received December, 8, 1958)

In regard to the chemical shift phenomena of nuclear magnetic resonance, efforts have been made to correlate the observed values with the bond characters of the compounds including the resonating nuclei, and successful results have been obtained with the fluorine resonances in binary systems[1]. Further study for the dependence of the chemical shifts on the substituents in polyatomic molecules were made by Gutowsky et al. and showed that *mata* and *para* substituents in substituted fluorobenzenes produced fluorine shifts proportional, respectively, to the inductive and the resonance effects of the substituents as is inferred from chemical reactivities. They showed also that the substituent effects in polysubstituted fluorobenzenes are reasonably additive[2]. Since these results offer most valuable informations for the investigations of the reactions of simple organic molecules, further study of the problem has been made by Corio and Dailey for the proton shifts in monosubstituted benzenes[3], but the results are rather complicated and have been interpreted in terms of the polarization effects in aromatic substitution reactions.

As the last results are complicated by the electron coupling of the proton spins, we have planned here to make measurements of proton resonance in substituted benzenes at a moderate resolution, where the ring protons will give a sharp line, and to investigate the proton shifts in relation with the characters of the substituent groups. The apparatus used is the one constructed in this laboratory, being operated at 27.030 Mc and using a permanent magnet.

In the actual experiments of the measurements, each sample was mixed with cyclohexane at the ratio of 1 : 1 by volume and the shift was measured as the average of the separations between the sample and cyclohexane in several records. Then, as shown in Table I, the shift values were

TABLE I

CHEMICAL SHIFT OF PROTON MAGNETIC RESONANCE IN SUBSTITUTED BENZENES

Substance	Chemical shifts (ref. benzene)
C_6H_5-NO_2	+14.5±0.5 cps
-COCl	+14.5 〃
-CH_3	− 2.5 〃
-F	− 8.0 〃
-Cl	− 4.0 〃
-Br	− 3.5 〃
-I	− 0.5 〃
-OH	− 9.5 〃
-NH_2	−19.5 〃

resonance frequency: 27.030 Mc.

1) H. S. Gutowsky and C. J. Hoffman, *J. Chem. Phys.*, **19**, 1259 (1951).

2) H. S. Gutowsky, D. W. McCall, B. R. McGarvey and L. H. Meyer, *J. Am. Chem. Soc.*, **74**, 4809 (1952).

3) P. L. Corio and B. P. Dailey, ibid., **78**, 3043 (1956).

4) C. K. Ingold, "Strurcture and Mechanism in Organic Chemistry", G. Bell & Sons Ltd. (1953).

calculated taking benzene as the reference.

It is noted in Table I that there are observed very small but definite shifts for both bromo and chlorobenzene from benzene and, furthermore, our results in the table show a fine proportionality with the ability of each group to cause mesomeric effect[4].

Authors are very grateful to Professor Osamu Simamura of the University of Tokyo for valuable discussions. Our thanks are also due to Miss M. Nakahara who has made the purification of some of the samples.

University of Electrocommunications
Chofu, Tokyo

The Poisoning Effect of Lead Acetate and Quinoline

By Tosao FUKUDA

(Received February 23, 1959)

As previously reported[1], when palladium-calcium carbonate catalyst was poisoned by lead acetate, the activity for the hydrogenation of 1,4-butenediol decreased with increasing amount of lead acetate. It seems likely that, when it is poisoned by a large amount of lead acetate, the activity for the hydrogenation of 1,4-butynediol as well as 1,4-butenediol disappears completely. On the other hand, when palladium-calcium carbonate catalyst was poisoned by quinoline, the activity for the hydrogenation of 1,4-butenediol disappeared almost completely, while that for the hydrogenation of 1,4-butynediol decreased to about a half. Accordingly, it was suggested that the partial hydrogenation of 1,4-butynediol can be achieved by using quinoline as a poison, but not by using lead acetate.

It is a well known fact that the catalyst properties may be changed complicatedly by the adsorption of the poisons[2]. It seems that the properties of palladium-calcium carbonate catalyst are also affected by the adsorption of lead acetate or quinoline. The effect of quinoline might be different from that of lead acetate. Accordingly, the partial hydrogenation of 1,4-butynediol takes place as observed.

However, it seems that the difference in the poisoning effect of lead acetate and quinoline originated also in the difference of the adsorbability between lead acetate and quinoline.

The experiments were carried out by using the aqueous solution of 1,4-butynediol and 1,4-butenediol, at 25°C. The concentration of 1,4-butynediol and 1,4-butene-

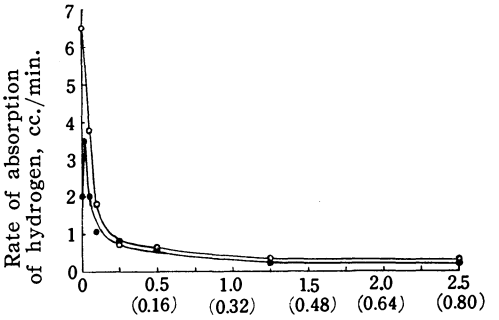


Fig. 1. The poisoning effect of acetate on the hydrogenation of 1,4-butynediol and 1,4-butenediol.
Pd-$CaCO_3$(5%) 300 mg.
Concentration of 1,4-butynediol (or 1,4-butenediol) 175 μmol./cc.
Oscilaltion 250 turns/min.
● 1,4-butynediol
○ 1,4-butenediol

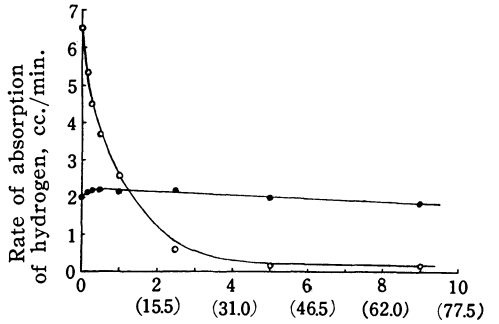


Fig. 2. The poisoning effect of quinoline on the hydrogenation of 1,4-butynediol and 1,4-butenediol.
Pd-$CaCO_3$(5%) 300 mg.
Concentration of 1,4-butynediol (or 1,4-butenediol) 175 μl./cc.
Oscillation 250 turns/min.
● 1,4-butynediol
○ 1,4-butenediol

1) T. Fukuda and T. Kusama, This Bulletin, 31, 339 (1958).
2) R. Suhrman and K. Schultz, *Z. Phys. Chem. N. F.*, 1, 69 (1954); W. H. Sachtler, *J. Chem. Phys.*, 25, 751 (1956); L. E. Moore and P. W. Selwood, *J. Am. Chem. Soc.*, 78, 697 (1956).

diol was 175 μ mol./cc. The results are shown in Fig. 1 and Fig. 2.

When lead acetate was added to the reactant, the activity of palladium-calcium carbonate catalyst disappeared almost completely with 0.4 μ mol./cc. of lead acetate. When quinoline was used with 0.4 μ mol./cc., the activity for the hydrogenation remained almost unchanged. When it was used 40 μ mol./cc. the activity for the hydrogenation of 1,4-butynediol decreased only a little, but that for the hydrogenation of 1,4-butenediol disappeared almost completely. It is interesting to note that, when the catalyst was poisoned by a small amount of quinoline, the activity for the hydrogenation of 1,4-butynediol increased at first and then decreased with increasing amount of quinoline.

When palladium-calcium carbonate catalyst was poisoned by the larger amount of lead acetate, the activity for the hydrogenation of 1,4-butynediol as well as 1,4-butenediol disappered completely. But, when it was poisoned by quinoline, the activity for the hydrogenation of 1,4-butenediol disappeared completely, while that for the hydrogenation of 1,4-butynediol decreased only a little. These results may explain clearly that lead acetate is adsorbed much more strongly than 1,4-butynediol, but quinoline is not. The catalyst properties are affected by quinoline. Quinoline might be adsorbed competitively with 1,4-butynediol and 1,4-butenediol. As a result, the hydrogenation of 1,4-butenediol is stopped by quinoline, while that of 1,4-butynediol is only retarded.

It may be concluded that the difference in the poisoning effect of lead acetate and quinoline originates also in the difference of the adsorbability between lead acetate and quinoline.

The author is grateful to Professor T. Kusama, Yokohama National University, for his unfailing kindness in encouraging this work.

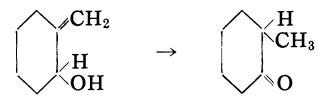
Faculty of Engineering
Yokohama National University
Minami-ku, Yokohama

*Isomerization of Luciculine**

By Takashi Amiya

(Received February 25, 1959)

Lucidusculine (I) ($C_{24}H_{35}O_4N$) is one of the aconite alkaloids; upon hydrolysis it gives a trihydric amino alcohol, luciculine (II) ($C_{22}H_{33}O_3N \cdot H_2O$)[1]. In contact with palladium-carbon in the presence of hydrogen and methanol, compound II was found to isomerize to a ketone base, isoluciculine (III), m. p. 131~136C°, λ_{max} in MeOH 302 mμ, logε1.4 (*Anal.* Found: C, 71.22; H, 9.33; N, 332; H_2O, 2.33. Calcd. for $C_{22}H_{33}O_3N \cdot {}^1/_2H_2O$: C, 71.71; H, 9.30; N, 3.80; H_2O, 2.44%). Compound III showed a band at 5.82 μ in the infared spectrum, and was considered therefore to be a cyclic six-membered ketone. Since it was shown previously that a terminal methylene group exists in compound II[1], this isomerization seems to proceed similarly to that of Shimoburo base I[2], hypognavine[3] or napellonine[4,**] as follows:



(II) (III)

On the basis of these observations, the presence of an allyl alcohol moiety in the structure of compound II may be claimed.

The author is grateful to Professor Harusada Suginome, President of Hokkaido University, for his unfailing kindness in encouraging this work.

Department of Chemistry
Faculty of Science
Hokkaido University
Sapporo

---

* This paper constitutes a part of a series entitled "The Aconite Alkaloids" by H. Suginome.

1) H. Suginome, T. Amiya and T. Shima, in preparation.

2) T. Sugasawa, *Pharm. Bull. Japan*, **4**, 6 (1956).

3) S. Sakai, ibid., **5**, 1 (1957).

4) K. Wiesner, Z. Valenta, J. F. King, R. K. Maudgal, L. G. Hamber and Shô Itô, *Chem. and Ind.*, **1957**, 173.

** It has been shown that napellonine is identical with Shimoburo base I[5].

5) K. Wiesner, Shô Itô and Z. Valenta, *Exper.*, **14**, 167 (1958).

Preparation of Chromium-51 of a High Specific Activity by the Szilard-Chalmers Process

By Nagao SHIBATA and Kenji YOSHIHARA

(Received January 16, 1959)

High specific activity ^{51}Cr has been prepared by neutron irradiation of electromagnetically enriched ^{50}Cr in a pile[1]; but this method offered only a small enrichment factor (about 23). The Szilard-Chalmers process of chromate or dichromate was investigated by Green and Maddock[2], and by Kahn, Freedman and Bryant[3], and it was found that about 30% and 8% tervalent chromium were formed from chromate, and dichromate, respectively (crystalline in both cases). This effect is applicable to the enrichment of ^{51}Cr but the yield is not very high.

In this paper, the authors studied the preparation of high specific activity ^{51}Cr by the Szilard-Chalmers process of neutron-irradiated, highly stable dye, Palatine Fast Blue GGN (Fig. 1), and succeeded in preparing highly enriched ^{51}Cr with a high yield.

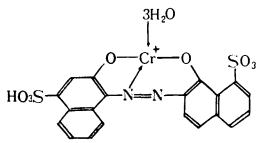


Fig. 1. Palative Fast Blue GGN.

This dye is water-soluble and slightly acid. It has an affinity to an anion- but not to a cation- exchange resin, whilst tervalent chromium is caught by the latter. The present separation is based on this difference.

The dye which was irradiated in the reactor, JRR-1 (neutron flux: 4×10^{11} n/cm^2 sec.), was dissolved in 0.01 N hydrochloric acid, passed through a resin column (10 mm. $\phi\times100$ mm. of Diaion SK#1, 100—200 mesh), and the column was washed with a sufficient volume of distilled water till the effluent became colorless. Then hydrochloric acid of various concentrations was passed through the column. The ^{51}Cr on the resin was eluted dy this procedure. Elution curve is shown in Fig. 2 in which many peaks appear. As the sample is dissolved in hydrochloric acid, complicated chloro-complexes of chromium may be formed. When the histogram is compared with the elution curves of a few chloro-aquo chromium ions, the first peak in Fig. 2 seems to be ascribed to the dichloro-tetra-aquo, the second to the monochloro-penta-aquo, and the third to the hexa-aquo chromium ion. It is not clear to which chemical forms the fourth and the fifth portion are to be assigned, but they were co-precipitated together with tervalent chromium. Thus 77~83% of the total activity was eluted from the resin in cationic forms.

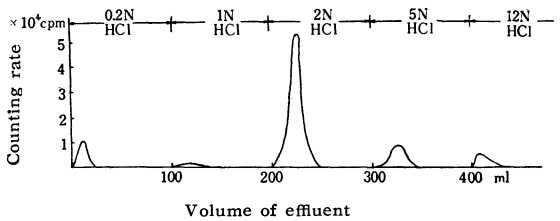


Fig. 2. Elution curve of chromium-51 formed in Palative Fast Blue GGN by hydrochloric acid.

Harbottle[4] investigated the Szilard-Chalmers process of some tervalent chromium salts, and found that about 10% of the neutron-captured atoms are present in sexivalent form. In the present case, whether tervalent chromium of Palatine Fast Blue GGN is oxidized to sexivalent or not was investigated as follows. Pottasium chromate carrier was added to the dye solution which had passed through the cation exchanger, as well as tervalent chromium as hold-back carrier. Lead acetate solution was added to this mixture to precipitate chromate as lead chromate. The activity observed in the procipitates was about 6 to 8% of the total activity. It is considered that this quantity corresponds to that of chromate formed on the present nuclear transformations.

For the preparation of high specific activity ^{51}Cr, it is considered to be convenient to utilize tervalent chromium which is caught by the cation exchanger, because it is difficult to separate the anionic part of chromium from the dye and from the contaminating activities (^{35}S and ^{32}P formed from the sulfonic sulfur).

1) Oak Ridge National Laboratory; "Radioisotopes, Special Material and Services".

2) J. H. Green and A. G. Maddock, *Nature*, **164**, 788 (1949).

3) M. Kahn, A. J. Freedman and E. A. Bryant, AECU-2329 (1949).

4) G. Harbbottle, *J. Chem. Phys.*, **22**, 1038 (1954).

The solution of neutron irradiated dye is passed through the cation exchanger column, and the column is washed with distilled water sufficiently. Tervalent chromium absorbed on the column is eluted by 200 ml. of 5N hydrochloric acid. Then, sulfric acid is added to the effluent and the mixture is dried up. This must be repeated decompose of micro quantities of organic substances. Then the sample is treated with silver peroxide to oxidise tervalent chromium to chromate. The product is sufficiently pure and impure activities were not detected by the inspection of its γ-ray spectrum and decay curve (by the Geiger tube). The yield is 69 to 75%, and the enrichment factor is 915 for 15 hr. irradiation and is 1150 for 5 hr. irradiation. This preparation method of enriched ^{51}Cr is considered to be useful. And the hot-atom chemistry of chromium complexes of diazo-compounds in detail is to be published at hand.

The authors wish to express their acknowledgement to Dr. K. Kimura for his kind encouragement and to Dr. T. Ishimori for his valuable suggestions and to Mr. I. Okubo for his helpful opinions.

Division of Isotope Applications
Japan Atomic Energy
Research Institute
Tokai, Ibaraki

Self-diffusion of Benzene under Pressure

By Hiroyuki HIRAOKA

(Received February 9, 1959)

Most of the works on diffusion in liquids have been made at atmospheric pressure. At atmospheric pressure, however, both the temperature and the density are varying simultaneously and so it is impossible to separate the effects of these two factors on diffusion. There has been no attempt to separate the two effects on self-diffusion of organic liquids except carbon tetrachloride[1] and carbon disulfide[2]. In advance of the present work, diffusion of iodine and sulfur in benzene under pressure was studied[3]. In this communication a study on the self-diffusion of benzene under pressure is presented.

Diffusion was measured by the capillary-cell method. The diffusion cells were accurately calibrated capillaries about 4 cm. in length and 0.02 ml. in volume and were filled with benzene containing carbon-14 sufficient to give 1900 counts per minute in a counting system used. The cells were immersed in a reservoir of pure inactive benzene in a thermostat constant to ± 0.01 °C. Diffusion was allowed to proceed for about 3 days, after which benzen in the cell was transferred into a combustion apparatus by a gas-phase sampling technique and was converted into barium carbonate by wet combustion method. The activity was measured by an α-β-γ proportional counter. Three to six determinations were carried out at each experimental conditions and the maximum deviation occurred was as large as 3.5 per cent from the mean. The results were presented in Table I with Graupner's data[4] at atmospheric pressure.

According to Eyring's theory[5], if the mechanism of activation in diffusion can be assumed identical with that of viscous flow, the relation between self-diffusion coefficient and viscosity in liquids is given by

$$D\eta/\boldsymbol{k}T = \lambda_1/(\lambda_2\lambda_3) \qquad (1)$$

where the common notation is used. The constancy of the values of $D\eta/\boldsymbol{k}T$ is shown in Table I, where at 35°C the values of λ_1 and $(\lambda_2\lambda_3)^{1/2}$, obtained on the assumption that $\lambda_1\lambda_2\lambda_3$ is equal to the mean molecular volume, are also given. The distance between two adjacent layers of graphite is 3.40 Å and the molecular diameter of benzene is 4.96 Å, and thus the values of λ_1 and $(\lambda_2\lambda_3)^{1,2}$ agree fairly well with the known dimensions of the molecule. From the self-diffusion coefficient of carbon-tetrachloloride determined by Hildebrand et al., $\lambda_1 = 2.24$ Å and $(\lambda_2\lambda_3)^{1,2} = 8.48$ Å at 25°C is obtained with the same assumption as used above. Although benzene is particularly amenable to Eyring's theory, because its geometry should lead to diffusion preferentially in the direction of benzene ring plane, it is strange that in the case

1) H. Watts, B. J. Alder and J. H. Hildebrand, *J. Chem. Phys.*, **23**, 659 (1955).
2) R. C. Koeller and H. G. Drickamer, ibid., **21**, 267 (1953).
3) H. Hiraoka, to be published in *J. Chem. Soc. Japan, Ind. Chem. Sec.* (*Kogyo Kagaku Zasshi*), **62** (1959).
4) K. Graupner and E. R. S. Winter, *J. Chem. Soc.*, **1952**, 1145.
5) S. Glasstone, K. J. Laidler and H. Eyring, "The Theory of Rate Processes", McGraw-Hill Co., New York, (1941), p. 477.

Table I
SELF-DIFFIUSION COEFFICIENTS OF BENZENE

	Temp. (°C)									
	15		25		35				45	
Pressure	$D\times10^5$	$D\eta/kT$ $\times10^6$	$D\times10^5$	$D\eta/kT$ $\times10^6$	$D\times10^5$	$D\eta/kT$ $\times10^6$	λ_1	$(\lambda_2\lambda_3)^{1/2}$	$D\times10^5$	$D\eta/kT$ $\times10^6$
(kg/cm²)	$\left(\frac{cm^2}{sec.}\right)$	$\left(\frac{1}{cm^2}\right)$	$\left(\frac{cm^2}{sec.}\right)$	$\left(\frac{1}{cm.}\right)$	$\left(\frac{cm^2}{sec.}\right)$	$\left(\frac{1}{cm.}\right)$	(Å)	(Å)	$\left(\frac{cm^2}{sec.}\right)$	$\left(\frac{1}{cm.}\right)$
1.03	1.83	3.23	2.13	3.12	2.42	2.99	2.12	8.42	2.86	3.00
	1.88[a]		2.15[a]		2.40[a]				2.67[a]	
250	1.47	3.19	1.69	3.02	1.97	2.96	2.09	8.39	2.29	2.93
500			1.39	3.04	1.59	2.92	2.06	8.38	—	—
660									1.64	2.88

a) ref. 4)

of carbontetrachloride λ_1 is much smaller than $(\lambda_2\lambda_3)^{1/2}$. It can not be concluded that the valuse of λ_1 and $(\lambda_2\lambda_3)^{1/2}$ thus calculated are true dimensions in liquid state, as Partington et al.[6] and other investigators did.

The relation between the experimental activation energy of diffusion at a constant volume, E_v, and the experimental activation energy at a constant pressure, E_p, is given by

$$E_v = E_p + (RT^2)(\alpha/\beta)(\partial \ln D/\partial P)_T \quad (2)$$

where α is the isobaric expansion coefficient and β the isothermal compressibility. From the values in Table I the following results are obtained: E_p=2,780 cal./mole, $(RT^2)(\alpha/\beta)(\partial P \ln D/\partial)_T$=2,000 cal./mole, E_r =780 cal./mole. According to Eyring, the increase of internal energy for the activation process, ΔE^*, is given by

$$\Delta E^* = E_v - RT \quad (3)$$

This gives the value ΔE^*=170 cal./mole, which is so small that it is difficult to consider any high potential barrier for diffusion in benzene.

The author wishes to express his appreciation to Dr. Jiro Osugi for his interst in this work.

Department of Chemistry
Faculty of Science
Kyoto University
Sakyo-ku, Kyoto

6) J. R. Partington, R. F. Hudson and K. W. Bagnall, *J. Chem. Phys.*, 55, 77 (1958).

*Studies on Explosion Reaction of Ethylene Mixed with Oxygen or Air. II. On the Explosion Peninsula**

By Masao SUGA

(Received September 22, 1958)

In a previous paper[1], it has been shown that the explosion boundaries of ethylene mixed with oxygen and with air was determined by the "admission method" i. e., by sudden introduction of the premixed gases into a heated and previously evacuated vessel. Also, it has been noticed that the explosion, like that of the other combustible gases[2,3], occurred in a certain region of the pressure, temperature and composition of mixed gases. In this case, there are the first (the lower), the second (the upper) and the third (the thermal) limit in the definite composition and temperature range. The explosion peninsula lies in the range bounded by the first and the second pressure limit of explosion within which pale blue ignitions occurred. On the other hand, the explosion occurred normally with a blue flame which rapidly built up into a bright flash filling the reaction vessel and accompanied by a pulse in pressure. Also, it was apparent that the induction period of the explosion, the color of flame and the propagation velocity of flame were different in the two cases described.

Now the experiment has been made between 550°C and 700°C for mainly 20% ethylene with oxygen in order to observe in detail explosion phenomena in the explosion peninsula and to compare this with normal thermal explosion. The effects of nitrogen and vessel diameter on the explosion limit were studied. They will be briefly discussed.

Experimental

Materials. — The ethylene employed in this experiment was prepared by the dehydration of absolute ethanol and purified by the method described in the previous paper. The oxygen employed was obtained from a commercial cylinder (purity: 99.4%). The oxygen and the air were employed after being purified through a train consisting of two bottles containing a concentrated aqueous solution of sodium hydroxide and concentrated sulfuric acid. Before use, the gases were dried with phosphorus pentoxide.

Apparatus and Procedure. — The apparatus used and the procedure adopted were of the types described in the previous paper. This consisted of an electrically heated reaction vessel into which a gas mixture could be admitted from a separate mixing vessel. Subsequent explosion of the mixture could be observed visually through a small window of mica in the dark room, and a blue filter of 1 mm. thickness whose transmission curve** is shown in Fig. 1 was used to eliminate the red glow of the furnace so that an ignition could be detected. Cylindrical reaction vessels of quartz 15 cm. long and 3 cm. in standard diameter, were used, but the diameter was varied to 4 cm., 2 cm. or 1 cm. as required. The apparatus was evacuated down to $10^{-4}\sim10^{-5}$ mmHg (tested by Gaisler tube) with rotary and "Hücksman's diffusion" pump.

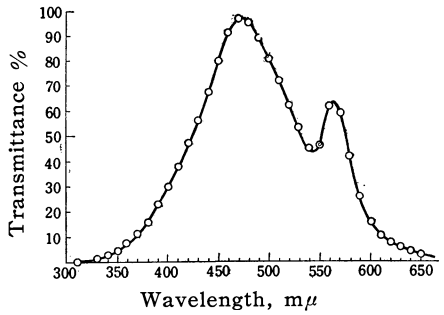


Fig. 1. The transmission curve of a filter.

Results and Consideration

The Explosion Limit.—Isochors for the explosion limits of 20% ethylene with oxygen and of 5% ethylene with air are shown respectively in Fig. 2 and Fig. 3. The evidence of an explosion was judged by observing the appearance of ignition, and usually the observation was continued for twenty minutes in the dark room.

* A part of this investigation was reported at the Annual Meeting of the Chûgoku-Shikoku Branch of the Chemical Society of Japan in Niihama, October 19, 1956.

1) M. Suga, This Bulletin, 31, 515 (1958).

2) B. Lewis and N. von Elbe, "Combustion, Flames and Explosions of Gases", Academic Press, New York (1951), p. 29.

3) K. J. Laidler, "Chemical Kinetics", McGraw-Hill Book Co., Inc., New York (1950), p. 319.

** It was measured with a HITACHI Model EPB-U photo-electric spectrophotometer.

The results of observation were classified as follows:

(1) After the lapse of various induction periods (usually less than 10 sec.), luminous blue flames were observed.

(2) After the lapse of the relatively long induction periods (6 sec.~20 min.), pale blue flames were observed in the dark room.

(3) No flame could be found even in the dark room.

Case 1, 2 and 3 are indicated respectively by ◎, ○ and × in Figs. 2 and 3. Also ⊕ in Fig. 2 indicates the case of the luminous flame propagating into the storage bulb owing to the shorter induction period than 0.8 sec. and the large propagation velocity of flames.

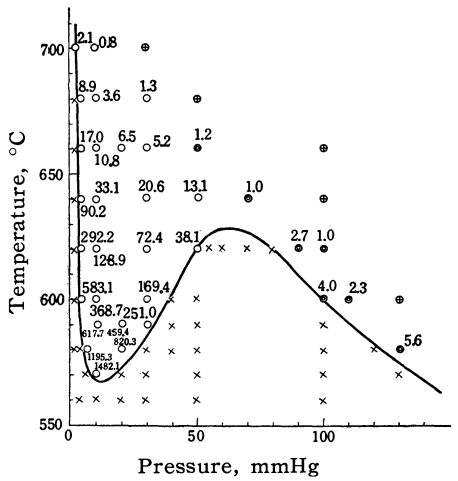


Fig. 2. Explosion limit of 20% ethylene with oxygen. (Induction periods in seconds are indicated by numbers beside observation points.)

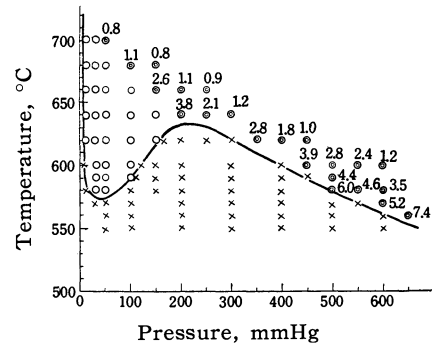


Fig. 3. Explosion limit of 5% ethylene with air. (Induction periods in seconds are indicated by numbers beside observation points and the results of longer induction period will be indicated in Fig. 6).

It is evident from the isochors that the first, the second and the third pressure limit of explosion exist in the explosion limit of ethylene-oxygen and -air mixtures. The first pressure limit of explosion does not seem to depend to a great extent on temperature, but the observation was more or less obscure because of the low admission pressure. The boundary of the first and the second pressure limit of explosion, i. e., the tip of the explosion peninsula, was determined from the results of observation for thirty minutes. The second pressure limit of explosion increases abruptly with increasing temperature, and, on the other hand, the third pressure limit of explosion decreases with increasing temperature.

Fig. 4 shows the isochors for the explosion limits of ethylene-oxygen mixtures. In this case, the explosion peninsula results in various shapes according to the composition of gas mixtures. That is to say, the composition of gas mixture affects the explosion limit considerably, and particularly it was noticed that the explosion peninsula disappears at over 25% ethylene with oxygen.

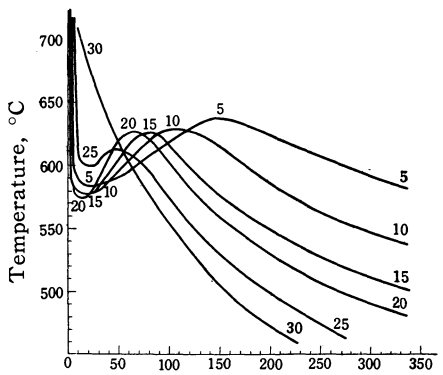


Fig. 4. Isochors for explosion limit of ethylene-oxygen mixtures. curve 5=5%, 10=10%, 15=15%, 20=20%, 30=30% ethylene.

The Effect of Nitrogen in the Air.—As shown in the previous paper, the third pressure limits of explosion for ethylene with oxygen and with air were equivalent to each other in spite of the differences of the propagation velocity of flame, the induction period, etc., so far as the partial pressure of nitrogen was neglected. Also, in order to elucidate the effect of nitrogen, an isochor for explosion limit of 20% ethylene with oxygen is shown and this is plotted with the corresponding points

of the results for explosion limit of 5% ethylene with air, by calculation, subtracting the partial pressure of nitrogen.

This plot is shown by the broken line in Fig. 5. It is concluded that the first and the third pressure limit of explosion are slightly lower, and, the on other hand, the second pressure limit of explosion considerably lower, than the corresponding full line. In other words, nitrogen affects the second pressure limit of explosion, but does not affect the first and the third pressure limit of explosion.

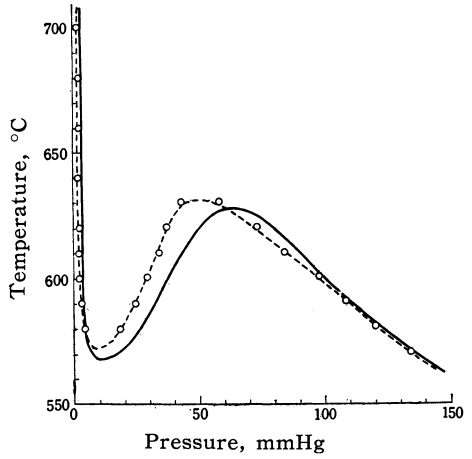


Fig. 5. Effect of nitrogen on isochor for explosion limit of 20% ethylene with oxygen. (Broken line represents the data calculated from the limit of 5% ethylene with air, Fig. 3.)

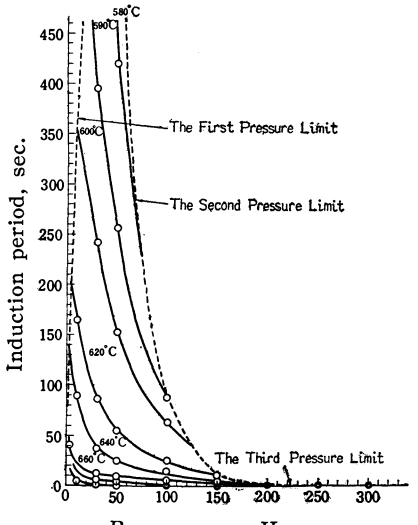


Fig. 6. Relationship between explosion limit pressure and induction period at definite temperatures for 5% ethylene with air.

The Explosion Limit and Induction Period. — The results of the experiment with regard to the induction period are shown by numbers beside the observation points in Figs. 2 and 3. The induction period was measured by a stopwatch. But in cases where the admission time required more than 0.6 sec., the induction period could not always be measured by a stopwatch with high accuracy. Fortunately, induction period is fairly long in the region

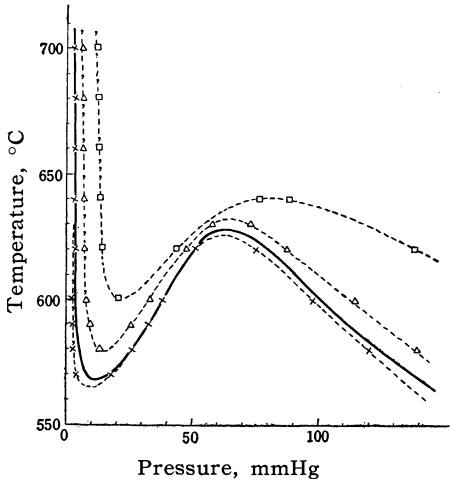


Fig. 7. Effect of reaction vessel diameter on isochor for explosion limit of 20% ethylene with oxygen. Diameter: Full line, 3 cm.; □, 1 cm.; △, 2 cm.; ×, 4 cm.

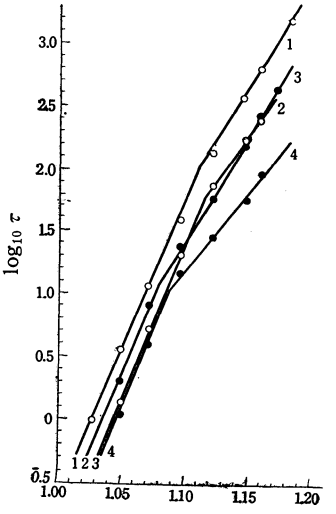


Fig. 8. $\log_{10}\tau$ against $1/T$ curves for the explosion of 20% ethylene with oxygen and 5% ethylene with air.
○; 20% C_2H_4 with O_2, curve 1=10, 2=30 mmHg admission pressure, ●; 5% C_2H_4 with air, curve 3=50, 4=10 mmHg admission pressure.

of the explosion peninsula and is reproducible so far as precautions are taken in accord with standard procedure[1]. Fig. 6 shows the relationship between explosion limit pressure and induction period at various different temperatures for 5% ethylene with air.

The Effect of Reaction Vessel. — For reaction vessels, quartz cylinders of 3 cm. in diameter and 15 cm. in length were usually employed. Quartz cylinders of 4, 2 and 1 cm. in diameter of the same length were also employed in order to compare the effects of the diameter of reaction vessels. The results are indicated in Fig. 7. The decrease of the vessel diameter increaed the first and the third pressure limit, and, on the other hand, lowered the second pressure limit of explosion; i. e., the decrease of the vessel diameter serves invariably to retard the explosion. It is noticed that the second pressure limit of explosion suffers the effect of the surface of the vessel only slightly, and in consequence, the explosion peninsula tends to disappear when the specific surface of the vessel is increased.

The Activation Energy of the Reaction. —In Fig. 8 is shown the relationship between the absolute temperature T and the induction period τ in relation to the results of Fig. 2 and Fig. 6. Every curve bends at the neighborhood of ca. 620°C, but is essentially linear and holds the relationship $\log_{10}\tau = A/T + B$. On the other hand, while this result has no direct relationship with the meaning of kinetics and the adaptability of the former's formula to the latter is questionable, nevertheless the gradient of these lines, A, is thought to be equal to $E/2.303\times R$[4,5]. Thus, values for E, the apparent activation energy, may be as in Table I.

TABLE I. ACTIVATION ENERGIES ESTIMATED FROM THE INDUCTION PERIOD

Curve	A	$E=2.303\times1.987\times A$ (kcal./mol.)
1	15.03	68.77
	22.35	102.27
2	13.77	63.01
	24.30	111.97
3	15.27	69.88
	23.73	108.59
4	13.53	61.91
	23.73	108.59

4) B. P. Mullins, "Spontaneous Ignition of Liquid Fuels", Butterworths Sci. Pub., London (1955).
5) N. Semenoff, *Z. Physik*, **48**, 57 (1928).

Summary

In the previous paper, the explosion limit of ethylene mixed with oxygen and with air by the "admission method" was presented. It was pointed out that the explosion peninsula lies in the region between the first and the second pressure limit of explosion. The results of observation in this region differ from those in thermal explosion.

In the present experiment, the following results have been obtained.

(1) The explosion peninsulas of ethylene-oxygen and ethylene-air mixtures lie approximately in the range of the same temperature and pressure limits as that of carbon monoxide-oxygen mixture[6].

(2) If ethylene concentration exceeds ca. 25% ethylene with oxygen, the explosion peninsula disappears.

(3) The induction period of explosion in the explosion peninsula is relatively longer than those of other thermal explosions.

(4) In the explosion within the explosion peninsula, the apparent activation energy estimated in accordance with Semenoff's theory is of abnormally high value. Merely from these facts, it is difficult to determine the explosion mechanism of ethylene-oxygen mixture, but it is possible for one to assume that the explosion within the explosion peninsula has a different mechanism from other thermal explosions.

If one refers to the studies of Neumann and Serbinoff[7], Norrish and Food[8], and Lewis[2] on the explosion of methane-oxygen mixture, he will find that the explosion peninsula which is observed in the explosion limit of ethylene-oxygen or -air mixtures is not always related to the nature of ethylene itself. In other words, ethylene-oxygen mixture is decomposed into carbon monoxide first in the definite range of temperature and pressure. Furthermore, it is considered that carbon monoxide which is produced and accumulated in slow oxidation of ethylene, i. e., slow reaction, is ignited in the definite condition. Thus, if ethylene concentration is greater than the stoichiometric value crresponding to $C_2H_4+3O_2=2CO+2H_2O$, the oxygen which is required to oxidate this carbon monoxide is insufficient, and therefore the

6) D. E. Hoare and A. D. Walsh, *Trans. Faraday Soc.*, **50**, 37 (1954).
7) M. Neumann and A. Serbinoff, *Phys. Z. Sowjet*, **1**, 536 (1932).
8) R. G. W. Norrish and S. G. Food, *Proc. Roy. Soc.*, **A 157**, 503 (1936).

explosion peninsula disappears. The conclusion is a little too speculative, but it is considered that the explosion peninsula of ethylene-oxygen or -air mixtures originates in the oxidation of carbon monoxide which is accumulated in slow reaction.

The author wishes to express his gratitude to the late Professor R. Kiyama and Dr. J. Ôsugi of the Kyôto University and Professor T. Kôzu for their kind advice and encouragement throughout this work. He is also grateful to Mr. T. Ogura and Mr. Y. Takasuga for their assistance in the observations as a part of the present experiment.

Department of Chemistry
Faculty of Science and Literature
Ehime University, Matsuyama

Dissociation Constants of Some Carboxylic Acids in Mixed Aqueous Solvents

By Motoo YASUDA

(Received October 9, 1958)

The dissociation constants of carboxylic acids were determined by various authors in mixed solvents, such as water-methanol, water-ethanol and water-dioxane mixtures and the relationship between the dissociation constants of the acids and the dielectric constants of the mixed solvents was discussed. As the dissociation of an acid is influenced by the dielectric constant of the solvent, it may be reasonable to suppose that an acid has almost the same acidity, i. e., almost the same dissociation constant in mixed solvents having the same dielectric constant. However, both Speakman[1] and Dondon[2] observed that aqueous dioxane acted as if it had a higher effective dielectric constant than aqueous alcohol of the same bulk dielectric constant. In other words, the values of dissociation constants of several acids in aqueous dioxane were reported to be higher than those determined in aqueous alcohol with the same dielectric constant. The present paper deals with the problem whether a carboxylic acid has really different acidity in various mixed solvents having the same dielectric constant.

Calculation of the Dissociation Constants. — The dissociation of a carboxylic acid in mixed solvents is an equilibrium reaction of the type

$$HA + S \rightleftarrows SH^+ + A^- \qquad (1)$$

where HA is a monobasic acid and S is one of the components of the mixed solvent. Since water has an exceptionally high proton affinity, Eq. 1 may be written as Eq. 2, if the mixed solvent contains a sufficient quantity of water and the concentration of the acid is small.

$$HA + H_2O \rightleftarrows H_3O^+ + A^- \qquad (2)$$

The equilibrium constant of this dissociation, or the dissociation constant of an acid in aqueous mixed solvents should be given by Eq. 3:

$$K = [A^-]\,[H_3O^+] / [HA]\,[H_2O] \qquad (3)$$

where square brackets indicate activity. On the other hand, the strength of an acid in water is usually expressed in terms of the constant K_a, instead of K defined by Eq. 3,

$$K_a = [A^-]\,[H^+] / [HA] \qquad (4)$$

In aqueous solution K_a may be used, for $[H_2O]$ is nearly constant. But this is not true in mixed solvents containing a limited amount of water. Due consideration should be paid to the fact that the activity of water in mixed solvents changes with the molar fraction of organic solvents. Therefore, the constant K defined by Eq. 3 should be used for the estimation of the dissociation of an acid in mixed solvents, in place of K_a defined by Eq. 4.

Furthermore, K_a has a different numerical value in accordance with the unit of concentration used in calculation, whereas

1) J. C. Speakman, *J. Chem. Soc.*, **1943**, 270.
2) M. -L. Dondon, *J. chim. phys.*, **54**, 290, 304 (1957).

K does not depend on the unit of concentration. The present author calculated the values of K from the values of K_a reported by previous workers. But, as the activity of water in mixed solvents containing electrolytes is not known, it was replaced by the concentration of water.

Results and Discussion

1) Benzoic, Adipic and Succinic Acids.— Speakman determined the dissociation constant K_a defined by Eq. 4 of some carboxylic acids in aqueous alcohols and dioxane by using a glass electrode in conjunction with a cell involving liquid-liquid potentials. Some of his results are listed in Table I together with the dielectric constants ε reported by him. As seen in Table I, the values of $pK_a(=-\log K_a)$ in aqueous dioxane are lower than those of pK_a in aqueous alcohol having the same dielectric constant. The present author calculated the values of pK defined by Eq. 3 considering the change in the amount of water in mixed solvents. The values of the first and the second dissociation constant, pK_1 and pK_2, recalculated in this way are listed in Table II.

The values of pK are plotted against $1/\varepsilon$ in Fig. 1. It is seen that all points fall on a straight line. This means that an acid has nearly the same acidity in the medium having the same dielectric constant, at least in the range of the dielectric constant studied.

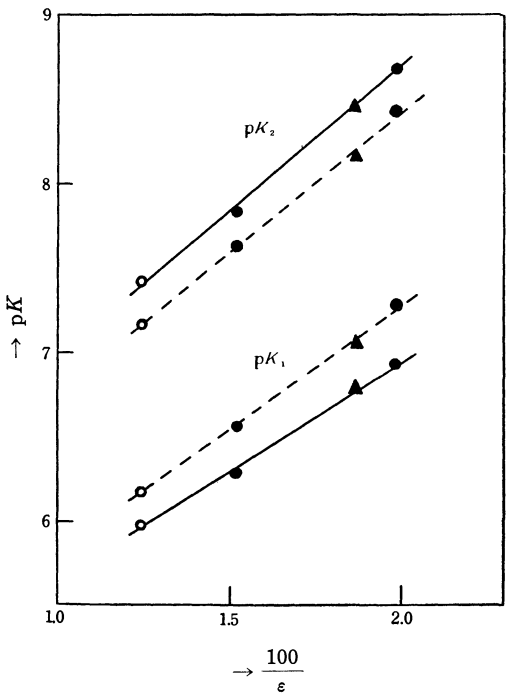


Fig. 1. Variation of pK values with the dielectric constant of the solution. Solid and broken lines indicate succinic and adipic acids, respectively. White and black circles and triangles show values in water, water-alcohol and water-dioxane mixtures, respectively.

TABLE I. VALUES OF pK_a AT 20°C REPORTED BY SPEAKMAN

Solvent % by wt.	ε	Adipic acid		Succinic acid		Benzoic acid
		pK_{a1}	pK_{a2}	pK_{a1}	pK_{a2}	pK_a
Water	80.4	4.43	5.42	4.22	5.67	4.24
25% Ethanol	65.7	4.93	6·00	4.65	6.19	4.83
50% Ethanol	50.4	5.83	6.98	5.48	7.24	5.87
30% Dioxane	53.3	5.45	6.55	5.19	6.84	5.35

TABLE II. RECALCULATED VALUES OF pK AT 20°C

Solvent % by wt.	Adipic acid		Succinic acid		Benzoic acid
	pK_1	pK_2	pK_1	pK_2	pK
Water	6.17	7.16	5.96	7.41	5.98
25% Ethanol	6.55	7.62	6.27	7.81	6.45
50% Ethanol	7.27	8.42	6.92	8.68	7.31
30% Dioxane	7.04	8.14	6.78	8.43	6.94

2) Succinic and Azelaic Acids. — In addition to the work of Speakman, Dondon reported recently the values of dissociation constants of several dibasic acids in water-methanol, water-ethanol and water-dioxane mixtures. A part of her results is shown in Fig. 2. She also reported that the dissociation of acids in aqueous dioxane is larger than in aqueous alcohols with the same dielectric constant. The values of pK_a determined by her in water-dioxane and in water-alcohol mixtures fall on two separate curves when they are plotted against $1/\varepsilon$. The range of the solvent composition studied for succinic acid by Dondon is wider than that by Speakman. She used the molarity basis for the calculation, but Speakman used the molality basis.

Now Dondon's values of pK_a are recalculated to give those of pK_1 and pK_2, which are listed in Table III. The values of density of the aqueous mixed solvents used for calculation were taken from Landolt-Börnstein's Tables[3] and the data

3) Landolt-Börnstein, "Physikalisch-Chemische Tabellen", Verlag J. Springer, Berlin, Hauptwerk (1923), p. 448 and Zweiter Ergänzungsband (1931), p. 287.

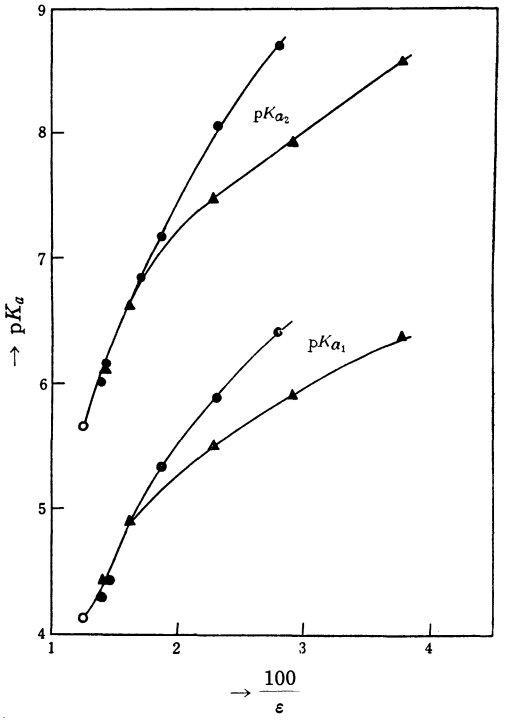


Fig. 2. Variation of pK_a values of succinic acid with the dielectric constant of the solution. White and black circles and triangles show values in water, water-alcohol and water-dioxane mixtures, respectively.

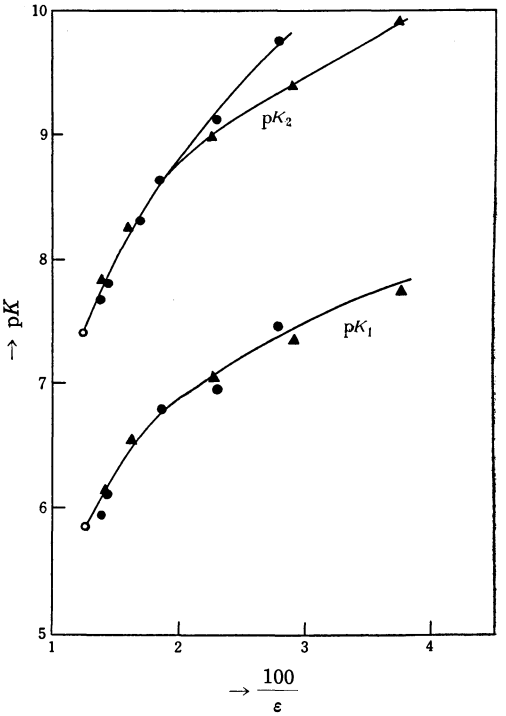


Fig. 3. Variation of pK values of succinic acid with the dielectric constant of the solution. White and black circles and triangles show values in water, water-alcohol and water-dioxane mixtures, respectively.

reported by Dunsmore and Speakman[4]. When the values of pK_1 and pK_2 are plotted against $1/\varepsilon$ (Fig. 3), all points of pK fall on a curve, except the points of pK_2 of succinic acid in the range of ε smaller than 40.

TABLE III. RECALCULATED VALUES OF pK_1 AND pK_2 AT 20°C

Solvent % by vol.	ε	Succinic acid		Azelaic acid	
		pK_1	pK_2	pK_1	pK_2
Water	80.4	5.88	7.41	6.29	7.24
20% Methanol	72.3	5.96	7.68	6.48	7.76
50% Methanol	59.0	6.46	8.31	6.96	8.31
80% Methanol	43.5	6.95	9.10	7.60	8.98
20% Ethanol	70.5	6.12	7.82	6.53	7.86
50% Ethanol	54.0	6.82	8.64	7.49	8.82
80% Ethanol	36.0	7.48	9.75	8.12	9.65
10% Dioxane	71.0	6.15	7.82	6.39	7.77
20% Dioxane	62.0	6.57	8.27	6.67	8.05
40% Dioxane	44.0	7.04	8.99	7.67	9.00
50% Dioxane	34.5	7.34	9.36	8.18	9.57
60% Dioxane	26.5	7.71	9.92	8.80	10.26

4) H. S. Dunsmore and J. C. Speakman, *Trans. Faraday Soc.*, **50**, 236 (1954).

For the irregularity of pK_2 of succinic acid, it is difficult to find the cause. One cause now suspected is the change of the distance between the secondly dissociating proton and the previously dissociated carboxyl group in different mixed solvents.

Although Dondon reported dissociation constants determined in 100% methanol, 100% ethanol and 80% dioxane, these data were not used in the calculation, for the dissociation of an acid in pure organic liquids is different from that shown by Eq. 2 and she reported that the data for 80% dioxane were least reliable.

3) Acetic Acid. — The dissociation constant of acetic acid in mixed aqueous solvents was determined by several authors[5-7]. The same situation as mentioned above was also found for acetic acid. The values of pK_a originally reported and those of pK recalculated for acetic acid are listed in Table IV and

5) T. Shedlovsky and R. L. Kay, *J. Phys. Chem.*, **60**, 151 (1956).

6) A. L. Bacarella, E. Grunwald and H. P. Marshall, *J. Org. Chem.*, **20**, 747 (1955).

7) H. S. Harned and G. L. Kazanjian, *J. Am. Chem. Soc.*, **58**, 1912 (1936).

these values of pK are plotted against $1/\varepsilon$ in Fig. 4. The dielectric constants, ε, of the mixed solvents were calculated by interpolation using the data of Gosting and Albright[8].

As shown in Tables II, III and IV, all the values of pK for acetic, benzoic, succinic, azelaic and adipic acids were calculated using the concentration of water instead of its activity. Nevertheless a carboxylic acid has almost the same dissociation constant in various mixed solvents having the same dielectric constant. The apparently greater acidity of a carboxylic acid in the water-dioxane mixture reported previously is due to the greater concentration of water in this mixture than in the water-alcohol mixture having the same dielectric constant.

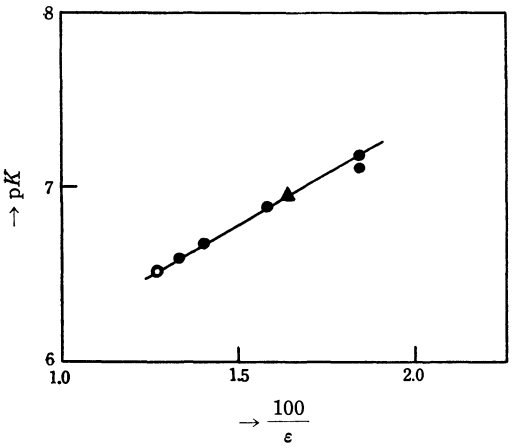


Fig. 4. Variation of pK values of acetic acid with the dielectric constant of the solution. White and black circles and triangle show values in water, water-alcohol and water-dioxane mixtures, respectively.

TABLE IV. THE DISSOCIATION CONSTANT OF ACETIC ACID AT 25°C

Solvent	ε	pK_a	pK
Water	78.5	4.76[5]	6.50
10% Methanol (by vol.)	75.0	4.88[5]	6.58
20% Methanol (by vol.)	71.3	5.02[5]	6.67
40% Methanol (by vol.)	63.2	5.34[5]	6.88
60% Methanol (by vol.)	54.4	5.74[5] 5.81[6]	7.10 7.17
20% Dioxane (by wt.)	60.8	5.29[7]	6.94

Summary

Several authors determined dissociation constants of acids such as benzoic, succinic and azelaic acids in mixed solvents and reported that the dissociation constants determined in aqueous dioxane were higher than those determined in aqueous alcohols having the same dielectric constants. However, if the variation of the amount of water in mixed solvents is taken into consideration in calculating the dissociation constant, an acid has almost the same dissociation constant in various mixed solvents with the same dielectric constant.

The author is greateful to Professor K. Yamasaki and Professor H. Kakihana, who read the manuscript and made helpful comments and criticism.

Chemical Institute, Nagoya University
Chikusa-ku, Nagoya

8) P. S. Albright and L. J. Gosting, ibid., **68**, 1061 (1946).

Interaction Polarization of the Hydrogen Bonded Complexes

By Ko KIMURA and Ryoichi FUJISHIRO

(Received October 20, 1958)

A strong intermolecular interaction such as hydrogen bonding will be expected to give rise to some variation in the charge distribution of the interacting molecules[1]. Hence the dielectric measurement for the system containing hydrogen bonds will give some useful information about the intermolecular association through hydrogen bonding. Hammic, Norris and Sutton[2] investigated the polarization of molecular complexes from this point of view and pointed out[3] that it was not generally practicable to derive both the association constant and the dipole moment of a complex from polarization data alone. Few and Smith[4] also studied this problem, and proposed a method by which both values for a complex were obtained from the dielectric measurement alone. The association constant of a complex derived by them, however, was much lower than the value obtained by other methods such as infrared absorption spectroscopy. Although their analysis is correct, in principle, such a discrepancy may probably result from the difficulty in estimating polarization owing to the solvent effect within the accuracy of 0.1 cc. If an accurate correction for the solvent effect is possible, the method proposed by them will be applied extensively.

This report describes a somewhat different approach from those above mentioned to the interaction polarization of hydrogen bonded complexes such as benzyl alcohol-dioxane and phenol-dioxane in benzene.

Experimental

All materials used in this work were purified by the standard method[5], and dried carefully. The solvent used throughout this work was benzene which was a very "*good solvent*" compared with other non-polar solvents such as cyclohexane or carbon tetrachloride.

Molecular polarizations were determined by measuring dielectric constants ε, refractive indexes n and specific volumes v of the binary or the ternary solutions. The apparatus for the dielectric measurement is almost the same as that generally used; that is to say, the heterodyne beat method. A very stable oscillator is necessary in order to obtain high accuracy, so the circuits devised by Gouriet[6] are employed without any improvement. The beat frequency of both tank circuits was again coupled with a standard tuning fork by making use of the cathode-ray oscilloscope. The dielectric cell was made of nickel and has three coaxial cylindrical electrodes[7], the outer side of which are connected to the ground. The capacity of the cell is about 100 pF. The cell constant was determined by carefully purified and dried benzene. An oil bath was used as a thermostat to minimize the error due to stray capacity. The temperature was kept at 25 ± 0.05°C throughout this work. The refractive index of the solution was measured by a Pulfrich refractometer, and a sodium lamp was used as the light source. The density of the solution was determined by a Lipkin pycnometer.

The calculation of molecular polarization was performed according to Halvelstadt and Kumler's method. For the ternary systems, the amount of the proton acceptor, that is dioxane, was kept constant and the polarization was extrapolated to zero concentration with regard to the proton donor.

Results

The results of the measurements of ε, n^2 and v for the two ternary systems, i.e., benzyl alcohol-dioxane-benzene and phenol-dioxane-benzene, are summarized in Table I together with those for the corresponding binary systems, i.e., benzyl alcohol-benzene and phenol-benzene. Experimentally determined formulae relating ε, n^2 and v to w, respectively, are also included in Table I for each system, where w represents the weight fraction of the proton donor.

1) See the following reviews. C. A. Coulson, *Research*, **10**, 147 (1957); L. Keller, *Repts. Progr. in Phys.*, **15**, 1 (1952).
2) J. W. Smith, "Electric Dipole Moments", Butterworths Scientific Publications, London (1955).
3) J. R. Hulett, J. A. Pegg and L. E. Sutton, *J. Chem. Soc.*, **1955**, 3901.
4) A. V. Few and J. W. Smith, ibid., **1949**, 2781.
5) A. Weissberger, et al., "Organic Solvents", Interscience Publishers, New York (1955).
6) G. G. Gouriet, *Wireless Engineer.*, **72**, 105 (1950).
7) A. W. Weissberger, et al., "Physical Methods of Organic Chemistry III", Interscience Publishers, New York (1954), p. 2293.

TABLE I. DIELECTRIC CONSTANTS, REFRACTIVE INDEXES AND DENSITIES OF THE TERNARY AND THE BINARY SYSTEMS

$w\times10^2$	ε	n^2	v	
Benzyl alcohol-Dioxane-Benzene				
(The weight percentage of dioxane is 31.26)				
0	2.2593	2.1791	1.0895	
0.26	2.2689	2.1795	1.0893	$\varepsilon=2.2593+3.14w$
0.50	2.2766	2.1800	1.0887	$n^2=2.1791+0.167w$
1.49	2.3106	2.1816	1.0873	$v=1.0895-0.146w$
2.18	2.3353	2.1827	1.0863	
Benzyl alcohol-Benzene				
0	2.2725	2.2427	1.1446	
0.51	2.2878	2.2433	1.1434	$\varepsilon=2.2725+3.10w$
0.94	2.3011	2.2439	1.1429	$n^2=2.2427+0.109w$
2.28	2.3431	2.2453	1.1402	$v=1.1446-0.190w$
2.98	2.3666	2.2460	1.1390	
Phenol-Dioxane-Benzene				
(The weight percentage of dioxane is 41.05)				
0	2.2556	2.1578	1.0729	
0.50	2.2781	2.1591	1.0717	$\varepsilon=2.2556+4.26w$
0.99	2.2986	2.1603	1.0710	$n^2=2.1578+0.251w$
2.33	2.3554	2.1640	1.0688	$v=1.0729-0.160w$
3.69	2.4117	2.1671	1.0667	
Phenol-Benzene				
0	2.2725	2.2427	1.1446	
0.29	2.2813	2.2433	1.1439	$\varepsilon=2.2725+2.82w$
0.52	2.2866	2.2437	1.1434	$n^2=2.2427+0.15w$
0.77	2.2944	2.2441	1.1427	$v=1.1446-0.242w$
1.44	2.3131	2.2450	1.1411	

Polarization values calculated from these experimental data are shown in Table II, where p or P is the specific or the molecular polarization, and r or R the corresponding refraction. The values of dipole moment were evaluated on the assumption that $P_{E+A}=[R_D]$ or $P_{E+A}=1.05$ $[R_D]$ and shown in the same table as μ or μ'.

TABLE II. POLARIZATIONS AND DIPOLE MOMENTS OF THE HYDROGEN BONDED COMPLEXES AND THE FREE PROTON DONORS

	Benzyl alcohol -Dioxane	Benzyl alcohol	Phenol-Dioxane	Phenol
p	0.9039 cc.	0.8674	1.0264	0.8993
r	0.2074 cc.	0.3005	0.3009	0.2931
P	97.7 cc.	93.8	96.6	84.9
R_D	32.1 cc.	32.5	28.3	27.6
μ	1.79 D	1.73	1.84	1.67
μ'	1.76 D	1.70	1.82	1.65

Attention was called especially to the association among the proton donors. For example, when the dipole moment of benzyl alcohol was measured in cyclohexane, the value obtained was 1.55 D or so which was a little smaller than 1.70 D[8] of methanol measured in the vapor phase. This fact seems attributable probably to the association of benzyl alcohol in this solvent. On the other hand, we used benzene as a solvent for benzyl alcohol and could obtain almost the same dipole moment as that of methanol in the vapor phase. Infrared absorption spectroscopy showed that the bridged bands were not perceived at concentrations less than ca. 0.01 mol./l. in carbon tetrachloride. Although the dielectric measurements in such a dilute solution are desirable, the change in the dielectric constants within the range of concentrations where the bridged bands are not observed, is not detected by the present apparatus and technique. But it seems probable that the fraction of solutes capable of existing as free molecules without association is more or less altered from one solvent to another. Although we have not ascertained it, it seems appropriate to use benzene as the dispersing solvent to minimize the effect of association of solutes.

For the ternary systems a few remarks must be added. The dielectric constant of the mixed solvent composed of ca. 0.7 benzene and 0.3 dioxane in weight fraction is about 2.26 compared with 2.27 of bezene. Even such a small change in the dielectric constant of the medium may cause the change in polarization due to the solvent effect. Generally speaking, the following factors are considered to contribute to the solvent effect: (1) dielectric constant of the medium, (2) anisotropy of solvent molecules, (3) polarizability of solute molecule and (4) geometrical shape of the solute molecule. The change in polarization by the first factor was estimated as the order of magnitude of 0.1 cc.[9] Contributions of the other factors are difficult to estimate, but will probably lie within the limit of experimental errors. The experiemntal data for the ternary systems were, therefore, employed without any correction for the solvent effect. Molecular polarization obtained by the usual method of extrapolating to zero concentration contains, however, the contributions of both the free molecules and the molecular complexes. In order to divide the observed value into polarization of the free

8) A. A. Maryott and F. Bucklay, *N. B. S. Circular*, **537**, 13 (1953).
9) K. Shogenji, *J. Phys. Soc. Japan*, **12**, 166 (1958).

molecules and that of the molecular complexes, the following procedure was adopted.

Let us consider the equilibrium for the complex formation between molecules A and B. We assume the interaction between A and B to be one to one. The equilibrium constant of this system is

$$K=\frac{x}{(a-x)(b-x)}=\frac{1}{(a-x)(b/x-1)} \quad (1)$$

where a and b are concentrations of molecular species A and B, respectively, in the initial state and x is that of the molecular complex. A is dioxane and B is benzyl alcohol or phenol in the present work. When b is reduced smaller, x also diminishes, and the ratio $f_x=x/b$, i.e., the fraction of the complex in the system approaches to a definite value,

$$\lim_{b\to 0} f_x=\lim_{b\to 0} x/b=aK/(aK+1) \quad (2)$$

since x becomes negligible against a in the denominator of Eq. 1. The formation constants are reported to be about 5,000[10] and 9,400[11] for benzyl alcohol-dioxane and phenol-dioxane complexes, respectively, using mol./cc. as the unit of concentration. Hence f_x is calculated to be 0.942 for the former, and 0.976 for the latter. The contribution of the free proton donor to the observed polarization is, therefore, estimated as $93.8\times 0.058=5.4$ in the former, and $84.6\times 0.024=2.0$ in the latter. If the difference between the observed polarization and the above one is divided by the fraction of the complex, then the value for the true polarization of the complex is obtained as 97.9 cc. for benzyl alcohol-dioxane, and 96.9 cc. for phenol-dioxane. These values are almost the same as those without any correction. It can therefore be concluded that there is no need for this correction when the equilibrium constant is comparatively large and, moreover, the nonpolar proton acceptors exist in large quantities.

Discussion

Perturbation of the proton donor by the proton acceptor and vice versa will be relatively small since the energy of hydrogen bonding is generally about 5 kcal./mol. or so. Hence, the deformation of σ-orbitals or even that of lone pair orbitals not participating in the hydrogen bond but existing in its neighborhood, is completely out of the question in the present treatment as generally believed, whereas in the case of the polarizable π-orbitals their deformation is comparatively large even by a small perturbation. It seems probable therefore that the change in the distribution of π-electrons may be induced by the access of lone pair electrons of a proton acceptor within the range of van der Waals radius. Coulson and Sutton[12] already discussed the hyperpolarizability of benzene and pointed out the importance of this effect in the vicinity of an ion or a dipole. The system of benzyl alcohol-dioxane will not need consideration of the hyperpolarizability as already stated. Contrary to this, the system of phenol-dioxane is supposed to receive a comparatively large effect. It will, therefore, be necessary first to consider the polarizability of the π-electrons of phenol due to the lone pair field of the proton acceptor. To estimate this effect, we try at first to determine the simple molecular orbitals of phenol and those of dimethyl ether, the molecular size of which is presumed to be half as great as a dioxane molecule, and then to evaluate the induced polarization of the π-orbitals of phenol. Then a brief discussion on the delocalization due to hydrogen bonding will be given.

Molecular Orbitals of the π-Electrons of Phenol.—Molecular orbitals of π-electrons of phenol were determined by the use of Matsen's parameter[13]. All the notations used in this section are the same as those of Matsen's paper. According to the molecular symmetry the secular determinant of the seventh order was factored into one of the second and one of the fifth order. All the orbitals obtained by solving these secular determinats are shown in Table III. Orbitals belonging to the symmetry group B_1 are the same as those of benzene, whereas those of A_1 receive a modification as shown in this table. An energy and a moment of each molecular orbital are also tabulated. The calculated π-moment is 1.46 D and its direction is directed toward the benzene ring from the

10) N. D. Coggeshall and E. L. Saier, *J. Am. Chem. Soc.*, **73**, 5414 (1951). Measurements were made at room temperature.

11) H. Tsubomura, *J. Chem. Phys.*, **23**, 2130 (1955). As the values reported were in the range between 9.4 and 9.8 in the unit of mol./l., the lower value of 9.4 was adopted here.

12) C. A. Coulson and L. E. Sutton, *Trans. Faraday Soc.*, **48**, 106 (1952).

13) F. A. Matsen, *J. Am. Chem. Soc.*, **72**, 5243 (1950).

TABLE III. COEFFICIENTS, ENERGIES AND MOMENTS OF THE π-ORBITALS OF PHENOL

B_1:	M.O.	energy	moment
	$\chi_2=\psi_2$	$\alpha+\beta$	10.632 a.u.
	$\chi_4=\psi_4$	$\alpha-\beta$	—

A_1: $\chi_i=c_{i1}\varphi_1+c_{i3}\psi_3+c_{i5}\psi_5+c_{i6}\psi_6+c_{i7}\psi_7$

c_{11}	0.601	c_{13}	0.283	c_{15}	0.107
		c_{16}	0.066	c_{17}	0.736
c_{71}	0.786	c_{73}	−0.370	c_{75}	−0.101
		c_{76}	−0.052	c_{77}	−0.481
c_{31}	0.136	c_{33}	0.880	c_{35}	−0.143
		c_{36}	−0.143	c_{37}	−0.427
c_{51}	0.026	c_{53}	0.055	c_{55}	0.973
		c_{56}	−0.093	c_{57}	−0.202
c_{61}	0.012	c_{63}	0.022	c_{65}	0.066
		c_{66}	0.989	c_{67}	−0.121

M.O.	energy	moment
χ_1	$\alpha+2.494\beta$	3.379
χ_7	$\alpha+1.749\beta$	10.090
χ_3	$\alpha+0.722\beta$	8.369
χ_5	$\alpha-1.116\beta$	—
χ_6	$\alpha-2.050\beta$	—

The total π-moment

$\mu=\mu_1+\mu_7+\mu_2+\mu_3-\mu_c{}^*=0.575$ a.u. $=1.46$ D

* μ_c represents the σ-core moment.

position of the oxygen atom, the positive pole lying at the oxygen nucleus.

Equivalent Orbitals of Dimethyl Ether. —The LCAO SCF MO method developed by Roothaan[14] will give the most reliable results for the electronic structure of a molecule. However, the low symmetry of the molecule of dimethyl ether prevents us from following this procedure. On the other hand, the unique treatment by Pople[15] of some simple molecules with lone pair electrons, such as water or ammonia, seems to express the electronic structures of these molecules quite well, though the results obtained by his method show that the lone pair moment may be overestimated. For example, in the case of water the lone pair moment obtained by Pople's method is about twice as large as that obtained by the LCAO SCF MO method[16]. This defect will be overcome by considering properly the apparent nuclear charge of oxygen as seen later.

Our treatment is similar to that by Pople and the values of the dipole moment used in our calculation are 1.30 D[8] and 0.30 D[2] for an ether molecule and a C–H bond, respectively. For the latter, its direction is assumed to be along the direction of the C–H bond with the negative center at the hydrogen atom. Outer electrons of $2s$ and $2p$ alone were considered explicitly and $1s$ inner electrons of the oxygen atom and the two carbon atoms were treated together with the nucleus as the rigid cores. Thus the nuclear charge of oxygen becomes 6 and that of carbon 1.059 upon the following approximations. For the orbitals of each carbon atom the sp^3 hybridization was a priori assumed. Moreover, to avoid complexity arising from the existence of methyl groups, each methyl group was replaced by a single C–H bond and its charge distribution was assumed to be expressed by point charges located at each nucleus with the distance of 1.09 Å. On these assumptions, the hybridization parameters at the oxygen atom and the coefficients in each bonding orbital were adjusted so as to be reconciled with the observed resultant moment. Such a simplification does not seem to be accompanied by any serious error within the limit of the approximation used here in the determination of wave functions.

TABLE IV. MOLECULAR CONSTANTS AND ATOMIC ORBITALS USED IN THE CALCULATION OF EQUIVALENT ORBITALS OF DIMETHYL ETHER, AND THEIR CALCULATED RESULTS

Molecular constants: Bond distance O-C 1.43Å; Bond angle 111°

Atomic orbitals:

$\phi(2s)=(Z^5/3\pi)^{1/2}\ r\exp(-Zr)$

$\phi(2p)=(Z^5/\pi)^{1/2}\ r\cos\theta\ \exp(-Zr)$

where $Z=2.275$ for the oxygen atom

$Z=1.625$ for the carbon atom

Equivalent orbitals

$\chi(l_1)=\cos\varepsilon_l\phi(O_{2s})+\sin\varepsilon_l\phi(O_{2p_1})$

$\chi(l_2)=\cos\varepsilon_l\phi(O_{2s})+\sin\varepsilon_l\phi(O_{2p_2})$

$\chi(b_1)=\lambda\{\cos\varepsilon_b\phi(O_{2s})+\sin\varepsilon_b\phi(O_{2p_1})\}+\mu\psi(c_1)$

$\chi(b_2)=\lambda\{\cos\varepsilon_b\phi(O_{2s})+\sin\varepsilon_b\phi(O_{2p_2})\}+\mu\psi(c_2)$

where

$\psi(c_i)=1/2\{\phi(c_{i2s})+\sqrt{3}\,\phi(c_{i2p})\}$

Acceptable values for the parameters:

$\lambda=0.665$ $\cos\varepsilon_b=0.367$ $\cos\varepsilon_l=0.508$

$\mu=0.475$ $\sin\varepsilon_b=0.929$ $\sin\varepsilon_l=0.860$

$\beta=110°$ $\gamma=108°$

The calculated total moment:

$M=M_b+M_l+M_m{}^*=-8.89+2.80+7.43=1.34$D

* M_m represents the moment of methyl group.

14) C. C. J. Roothaan, *Rev. Mod. Phys.*, **23**, 69 (1951).

15) A. B. F. Duncan and J. A. Pople, *Trans. Faraday Soc.*, **49**, 218 (1953). See also, *Proc. Roy. Soc.*, **A202**, 323 (1950).

16) F. O. Ellison and H. Shull, *J. Chem. Phys.*, **23**, 2348 (1955); L. Burnelle and C. A. Coulson, *Trans. Faraday Soc.*, **53**, 403 (1957).; W. C. Hamilton, *J. Chem. Phys.*, **26**, 345 (1957).

The molecular constants and the atomic orbitals used in evaluating the necessary integrals are tabulated in Table IV together with the final results thus obtained, where the symbols used are the same as those employed by Pople, et al.[15] Necessary overlap integrals and dipole moment integrals are all found in the tables or the formulae given by Mulliken, et al.[17]

The distinction between the present results shown in Table IV and those by Duncan and Pople lies in the hybridization parameters at the oxygen atom. As pointed out by Pople, this discrepancy originates from the small overlap integral between $\psi(c_1)$ and $\psi(c_2)$ because of the comparatively long distance between the two carbon atoms of an ether molecule, and the larger Z-value of Slater's atomic orbital of carbon.

The Induced Polarization of the π-Electrons of Phenol.—The induced polarization due to the lone pair field was easily calculated by means of the first order perturbation theory based on the equivalent and the molecular orbitals already given. The geometrical configuration of the complex between a proton donating molecule and an accepting one is not clear enough for the present case. However, it is well known that in ice a tetrahedral arrangement prevails and its arrangement has the large electrostatic energy[18] and the large overlap integral which is concerned largely with the delocalization energy[19]. It seems, therefore, probable to assume that the three atoms, O–H···O lie on a straight line, though the thermal motion will, in fact, induce some deviation. Moreover the distance between the oxygen atom of phenol and that of ether is not measured in solution. But according to the relationship proposed by Nakamoto, Margoshes and Rundle[20] between the atomic distance and the shift of the infrared absorption, the distance between the two oxygen atoms was estimated as being about 2.9 Å which is larger than that of ice. For the purpose of comparison, the perturbed wave functions of phenol were calculated in the case of three O···O internuclear distances of 2.7, 2.8 and 2.9 Å, respectively. The following two approximations were employed for this calculation. Firstly, only the interaction between the lone pair electrons of ether and the π-electrons of the oxygen atom of phenol was considered, and the interaction of the lone pair electrons with other π-electrons in the benzene ring of phenol was neglected. Molecular integrals required in this computation were obtained by making use of the formulae described in Roothaan's paper[21]. Secondly, an apparent nuclear charge of the oxygen atom of ether was determined by the point charge approximation. The apparent nuclear charges obtained at the three interatomic distances are as follows:

O···O distance, R	2.7	2.8	2.9
Z'	2.200	2.196	2.192

These large values of the apparent charges look curious, and may probably be due, as already stated, to the effect of overestimation of lone pair moments. It is believed that such a defect will be excluded if the same treatment as that of water by Ellison and Shull[16] is carried out. The extent of the interaction between the apparent nuclear charge of the oxygen atom of ether and the π-electrons of the oxygen atom of phenol was also estimated by Roothaan's formulae as before.

Finally we formulate the calculating procedure for the perturbed wave functions of phenol. The perturbation H' is given by

$$H' = 2\int \frac{\chi(l_i)\chi(l_i)}{r} d\tau - \frac{Z'}{r'}$$

The first term represents a coulombic potential due to the lone pair electrons of ether in the orbital, $\chi(l_i)$ which participates in the hydrogen bond, and the second is that due to the apparent nuclear charge Z' of the oxygen atom of ether. The first-order perturbed wave functions of phenol will then be expressed as

$$\chi_i^{(1)} = \chi_i + \sum_{j \neq i} \frac{H'_{ij}}{E_i - E_j}\chi_j, \quad \begin{pmatrix} i=1,7,3 \\ j=1,7,3,5,6 \end{pmatrix}$$

Values of the π-moments calculated from these orbitals are tabulated in Table V at each internuclear separation.

This table shows that the polarization of the π-orbitals arising from the lone pair field is the order of a magnitude of 0.1 D compared with the value of about 0.2 D given by Hampson and Weissberger[22], who

17) R. S. Mulliken, C. A. Rieke, D. Orloff and H. Orloff, ibid., **17**, 1248 (1949).
18) W. G. Schneider, ibid., **23**, 26 (1955); W. S. Fyfe, ibid., **21**, 2 (1953).
19) H. Tsubomura, This Bulletin, **27**, 445 (1954).
20) K. Nakamoto, M. Margoshes and R. E. Rundle, *J. Am. Chem. Soc.*, **77**, 6480 (1955).
21) C. C. J. Roothaan, *J. Chem. Phys.*, **19**, 1445 (1951).
22) G. C. Hampson and A. Weissberger, *J. Chem. Soc.*, **1936**, 393.

TABLE V. MOMENTS OF THE PERTURBED π-ORBITALS OF PHENOL

At 2.7 Å $\mu=\mu_1+\mu_7+\mu_2+\mu_3+\mu_c$
$=3.704+9.946+10.632+8.250-31.896$
$=0.637$ a.u.$=1.62$ D

At 2.8 Å $\mu=3.647+9.970+10.632+8.277-31.896$
$=0.630$ a.u.$=1.60$ D

At 2.9 Å $\mu=3.615+9.980+10.632+8.92-31.896$
$=0.624$ a.u.$=1.58$ D

The increment of π-moment, $\Delta\mu_\pi$

R in Å	2.7	2.8	2.9
μ in D	0.16	0.14	0.12

estimated the induced moment of the π-electrons due to a polar substituent group by making use of the average polarizability of the molecule. The induced moment decreases almost linearly with the increase of the interatomic distance from 2.7 to 2.9 Å. When we extrapolate it to the distance of 3.5 Å which corresponds to the sum of the van der Waals radii of both the oxygen atom of ether and the O–H of phenol, then the value obtained will be zero. These results show quite well that the theoretical treatment already described is reasonable. But it must be noted that the numerical values thus obtained are those of the interacting molecules which are placed mutually in the fixed configuration.

The Increment of the Dipole Moment Arising from Delocalization.—As is well known, the structures largely contributing to hydrogen bonding are considered as the following three:

[I] O–H O

[II] O^-H^+O

[III] O^-H-O^+

If we suppose that the ratio of the weights of structures I and II is of the same as that in a free state, then the increase of the dipole moment due to hydrogen bonding will be attributable only to the participation of the structure III. Strictly speaking, the transitional structures also must be taken into account. But it is difficult to treat them without making more precise quantum mechanical calculations. Neglecting these transitional structures, we can easily estimate the weight of the structure III from the additional moment observed.

One obstacle remains as yet. That is the direction of the resultant moment of the molecule in the free state. However, in view of the result[16] that the O–H bond moment in a water molecule is not so large as hitherto believed, it is assumed that only the lone pair dipoles make a contribution to the molecular dipole moment of benzyl alcohol. In the case of phenol, the direction of the resultant moment, as usually done, is determined by vectorial combination of dipole moments of both phenol itself and some of *p*-substituted phenols. The result[3] obtained shows that the direction of the resultant vector of phenol makes an obtuse angle of 91° with the O–C bond.

Once the direction of the resultant moment in the free state for benzyl alcohol and phenol, respectively, and the value of the induced moment of phenol in the bonded state are determined, then it is possible to calculate the increment of dipole moment, $\Delta\mu_D$ only due to delocalization.

Firstly, let us discuss the system of benzyl alcohol-dioxane. The bond angle about the oxygen atom of benzyl alcohol was taken to be 110°. Then, the value of $\Delta\mu_D$ obtained from the method mentioned above amounts to 0.10 D. When the interatomic distance between the two oxygen atoms is taken to be 3.0 Å from the shift of the infrared absorption[10], we obtain 14.41 D as the moment referring to the structure III, and its weight is estimated as about 0.7%.

Next, let us consider the system of phenol-dioxane. As the sp^2 hybridization was assumed for the orbitals of the oxygen atom, the bond angle about it was taken to be 120°. The interatomic distance between the two oxygen atoms was estimated as 2.9 Å as already stated. If the value of 0.12 D is used for the induced polarization of the π-electrons as already tabulated, $\Delta\mu_D$ is calculated as 0.21 D. This value corresponds to 1.5% as the weight of the structure III. Although it is qualitatively understood from the viewpoint of acidity that the contribution of the structure III in the latter system is about twice as large as that in the former, further discussion on this point will be given in the forthcoming report together with other data.

Summary

The dielectric measurements for the system of benzyl alcohol-dioxane and that of phenol-dioxane, respectively, were carried out by using benzene as the solvent.

The induced polarization of the π-electrons in the latter system was evaluated based on some assumptions. From these,

the additional moments due to delocalization were estimated and the weights of the structure III were evaluated for both systems.

The authors wish to express their thanks to Professor S. Kawaguchi for his kind inspection and revision of this manuscript, and also Messrs. N. Mataga and K. Nishimoto for their helpful discussions. The cost of this work has been partly defrayed by a Grant from the Ministry of Education.

Institute of Polytechnics
Osaka City University
Kita-ku, Osaka

γ-Hydroxyarginine, a New Guanidino Compound from a Sea-cucumber. I. Isolation and Identification

By Yoshimasa FUJITA

(Received October 28, 1958)

In the course of studies[1] on the extractable naturally occurring guanidino compounds by means of paper chromatography using Makisumi's method[2], the author found an unknown guanidino compound from the extract of a sea-cucumber, *Polycheira rufescens*, and isolated it as a hydrochloride. It was hydrolyzed, though somewhat more slowly than arginine, but completely by the action of arginase, into urea and an unknown amino compound. In 1953, Robin[3] oxidatively prepared γ-guanidinobutyric acid from L-arginine with the action of a homogenate obtained from the hepatopancreas of *Mytilus edulis*. The homogenate from this species appears to contain L-amino acid oxidase only as amino acid oxidase[4]. The isolated compound could also be converted enzymically and chemically into its oxidation products whcih were positive for the Sakaguchi reaction. Further characterizations of the isolated compound and its degradation products led the author to assume the unknown guanidino compound to be γ-hydroxyarginine. Consequently, the unknown amino compound produced from the isolated compound by the action of arginase should be γ-hydroxyornithine.

On the other hand, γ-hydroxyornithine was synthesized according to Tomita's method[5] which was somewhat modified by the author and then transformed into γ-hydroxyarginine by guanidization with S-methylisothiourea. The provisional structures of the isolated guanidino compound and the amino compound produced therefrom were proved to be correct by comparing them on a paper chromatogram with the synthetic γ-hydroxyarginine and γ-hydroxyornithine, respectively.

1) H. Sasaki, Y. Fujita, S. Makisumi and S. Shibuya, *J. Jap. Biochem. Soc.* (*Seikagaku*), **30**, 642 (1958).
2) S. Makisumi, *J. Chem. Soc. Japan, Pure Chem. Sec.* (*Nippon Kagaku Zasshi*), **73**, 737 (1952).
3) Y. Robin, *Bull. Soc. Chim. Biol.*, **35**, 285 (1953).
4) H. Blaschko and D. B. Hope, *Biochem. J.*, **62**, 335 (1956).
5) M. Tomita, *Z. physiol. Chem.*, **158**, 58 (1926).

Experimental

Isolation of the Unknown Guanidino Compound.—The sea-cucumbers used as the material were collected at the tidal zone near the Amakusa Marine Laboratory, the Faculty of Science, Kyushu University. The washed materials (43.5 kg.) removed from their internal organs were chopped in a meat-chopper and introduced into hot water (45 l., 70~80°C) for the purpose of extraction for 2 hr. with stirring. The residue separated from the extract was re-extracted in the same manner. The combined extract, deproteinized with a hot saturated basic lead acetate solution and freed from the lead, was passed through a column of Amberlite IR-120 (H- form). After washing the column with water, the adsorbed fraction was eluted with 2 N aqueous ammonia. The eluate, after removal of the ammonia by evaporation in vacuo, was again passed through a column of Amberlite IR-120 (ammonium form) to adsorb basic substances only. The elution from the washed column was carried out by using the same aqueous ammonia. The eluate freed from the ammonia was made up to 300 ml. with water and neutralized with 6 N hydrochloric acid. The solution, after addition of flavianic acid (50 g.), was heated for 30 min. on a boiling water bath. When the resulting solution was allowed to stand overnight in an

ice-box, a flavianate crystallized out. The flavianate was separated and washed with a small amount of cold water. It consisted almost entirely of the unknown guanidino compound, except for slight contamination with arginine. The product was recrystallized from hot water, until its paper chromatogram showed only one spot with the Sakaguchi or ninhydrin reaction. The purified flavianate was dissolved in hot water (100 ml.), and it was treated with a barium hydroxide solution to remove the flavianic acid moiety in the usual manner. The filtrate freed from the excessive barium was evaporated up to dryness in vacuo. The residue was extracted repeatedly with 50% hot ethanol. The extract, after evaporation to dryness, was dissolved in water (50 ml.), and the resulting solution was brought to pH 6~7 with 1 N hydrochloric acid. It was decolorized with charcoal and concentrated to a syrup in vacuo. The syrup was dissolved in 50% hot ethanol (10 ml.), and then absolute ethanol was added to it until the solution became opalescent. When the solution was kept overnight in a refrigerator, colorless plate crystals of the guanidino compound appeared. The compound was dissolved in a minute amount of 70% hot ethanol and then recrystallized with the addition of absolute ethanol. The yield was about 2.7 g.; m.p. 190~191°C (decomp.); $[\alpha]_D^{23}$ +5.4° (c 2, in 5 N hydrochloric acid).

Anal. Found: C, 31.75; H, 6.95; N, 24.65; Cl, 15.68. Calcd. for $C_6H_{14}N_4O_3 \cdot HCl$: C, 31.79; H, 6.67; N, 24.72; Cl, 15.64%.

It gave the Sakaguchi, the Lieben (iodoform), and ninhydrin reaction, indicating the presence of guanidino, alcoholic hydroxy (on the basis of the hydrogen content, alcoholic hydroxy group is superior to ketonic), and amino groups, respectively.

Enzyme Actions on the Guanidino Compound.—*1. Arginase.*—The arginase used in this experiment was a partially purified beef liver preparation of Step D according to Greenberg[6]. The guanidino compound was incubated to hydrolyze with arginase at pH 9.5 and 35°C for 24 hr. The incubate, after deproteinization with basic lead acetate, was fractionally purified by using Amberlite IR-120 (H- and ammonium forms). Since the purified fraction obtained here showed only one spot on a paper chromatogram with ninhydrin reaction, it was not necessary to carry out further purification. The fraction was decolorized with charcoal and crystallized similarly as in the case of isolation of the guanidino compound. The yield of the recrystallized compound was 280 mg. from 500 mg. of the guanidino compound; m.p. 183°C (decomp.); $[\alpha]_D^{32}$ +21.0° (c 2, in water).

Anal. Found: C, 32.65; H, 6.86; N, 15.2.1 Calcd. for $C_5H_{12}N_2O_3 \cdot HCl$: C, 32.58; H, 7.10; N, 15.17%.

This gave ninhydrin- and iodoform reaction but not the Sakaguchi reaction. The effluent passed through a column of Amberlite IR-120 (H^+ form) was again passed through a column of Amberlite (OH^- form), and from this effluent urea was identified as dixanthylurea and urea nitrate.

2. L-Amino acid oxidase.—The guanidino compound was incubated with the enzyme preparation obtained from the hepatopancreas of *Mytilus edulis* according to Robin's method[3] at pH 6.2 and 35°C for 24 hr. under aeration. The incubate acidified with acetic acid to pH 3~4 was boiled for 10 min. and filtered. To the filtrate (200 ml.) was added 30% hydrogen peroxide (1 ml.) for further oxidation of the keto acid to be produced by oxidative deamination from the guanidino compound, and it was allowed to stand for 15 hr. at room temperature. In this condition the guanidino compound itself is not oxidized at all with hydrogen peroxide. The resulting solution was passed through a column of Amberlite IR-120 (H-form), the column was washed with water, and then the adsorbed oxidation product was eluted from it by using 2 N aqueous ammonia. The eluate was evaporated up to dryness, and the residue was dissolved in 50% hot ethanol. When the solution was cooled in an ice-box, colorless needle crystals of the product appeared. The yield was 100 mg. from 300 mg. of the material; m.p. 238~240°C (decomp.); $[\alpha]_D^{22}$ −15.5° (c 2, in 5 N hydrochloric acid).

Anal. Found: C, 37.26; H, 6.88; N, 26.08. Calcd. for $C_5H_{11}N_3O_3$: C, 37.25; H, 7.11; N, 26.25%.

This compound gave the Sakaguchi and iodoform reaction, but not ninhydrin reaction.

Identification of the Oxidation Product.—*1. Reduction with hydroiodic acid.*—The oxidation product (10 mg.) was heated with hydroiodic acid (d=1.7, 0.5 ml.) for 2 hr. at 140°C in a sealed tube. After removal of the hydroiodic acid, the solution was tested by paper chromatography. On the basis of the result, it was found that the product was reduced to a compound which was identified as γ-guanidinobutyric acid (Table I).

TABLE I. R_f VALUES OF REDUCTION PRODUCT WITH HYDROIODIC ACID AND γ-GUANIDINOBUTYRIC ACID

	Solvent			
	I	II	III	IV
Reduction product	0.55	0.52	0.62	0.43
γ-Guanidinobutyric acid	0.55	0.52	0.62	0.43

One dimensional ascending method. Toyo-Roshi No. 52. Solvent: I, *n*-Butanol : Acetic Acid : Pyridine : Water = 40 : 10 : 10 : 20 (vol. %); II, *n*-Butanol : Acetic Acid : Pyridine : Water=30 : 6 : 24 : 20(vol.%); III, *n*-Butanol : Acetic Acid : Water=40 : 10 : 20 (vol. %); IV, *n*-Propanol : Water=70 : 30 (vol. %).
The R_f values shown in Tables II and III were also obtained by using the same procedures.

2. Comparison with the synthetic γ-guanidino-β-hydroxybutyric acid.—In a preliminary experiment, it was observed paper-chromatographically

6) D. M. Greenberg, "The Enzymes", vol. I, edited by J. B. Sumner and K. Myrbäck, Academic Press Inc., New York (1951), p. 905.

that the naturally occurring guanidino compound was oxidatively degraded with barium permanganate to guanidine and glycocyamine by way of an intermediate which was later proved to be identical with the oxidation product formed by the action of L-amino acid oxidase. The production of glycocyamine led to the conclusion that the alcoholic hydroxy group should situate in β- or γ-, probably γ-position, but not δ-position of the guanidino compound; accordingly, the structure of the enzymatic oxidation product before reduction by hydroiodic acid is to be γ-guanidino-β-hydroxybutyric acid. The conclusion was supported satisfactorily by comparing the paper chromatographic behaviors of the oxidation product with those of the synthetic γ-guanidino-β-hydroxybutyric acid[7,8] (Table II).

TABLE II. R_f VALUES OF OXIDATION PRODUCT WITH OXIDASE AND γ-GUANIDINO-β-HYDROXYBUTYRIC ACID

	Solvent			
	I	II	III	IV
Oxidation product	0.40	0.38	0.48	0.35
γ-Guanidino-β-hydroxybutyric acid	0.40	0.38	0.48	0.35

Synthesis of γ-Hydroxyornithine.—Finely powdered sodium ethyl acetylaminomalonate (24 g.) and γ-phthalimido-β-hydroxypropyl chloride (24 g.) were thoroughly mixed, and the mixture was heated at 140~150°C for 5 hr. with vigorous stirring. To the extremely viscous reaction mixture was added concentrated hydrochloric acid (100 ml.), and it was refluxed for 10 hr. and then allowed to stand overnight. The filtrate removed from the phthalic acid was concentrated in vacuo. Dilution with water and evaporation in vacuo were repeated three times to remove the excess of hydrochloric acid as much as possible. The syrup obtained thus was dissolved in water (200 ml.), and from this solution a basic fraction was separated by using Amberlite IR-120 (H- and ammonium form) in the same manner as described in the isolation procedures for the guanidino compound. The basic fraction, after being passed through a column of finely powdered Amberlite IR-120 (ammonium form, 100~200 mesh, 3 cm. ×40 cm.), was fractionally eluted and collected as follows. The column was washed with water, and the adsorbed substances were developed and eluted with 0.2 N aqueous ammonia. The eluate collected between 350 and 650 ml. was concentrated to a syrup in vacuo. The syrup was dissolved in a small amount of water, and the solution was adjusted to pH 6~7 with 1 N hydrochloric acid, decolorized with charcoal, and again concentrated to a syrup in vacuo. The syrup dissolved in a small amount of 50% hot ethanol was subjected to crystallization in an ice-box with the addition of absolute ethanol. After 2 days, the crystals of γ-hydroxyornithine hydrochloride were obtained. Yield, 8%; m. p. 181~183°C (decomp.).

Anal. Found: C, 32.72; H, 7.30; N, 15.65. Calcd. for $C_5H_{12}N_2O_3 \cdot HCl$: C, 32.53; H, 7.10; N, 15.17%.

Synthesis of γ-Hydroxyarginine.—γ-Hydroxyornithine hydrochloride (370 mg.) and S-methylisothiourea (280 mg.) were dissolved in 1 N sodium hydroxide (5 ml.). The solution which had been left to stand for 5 days at room temperature was passed through a column of Amberlite IR-120 (H- form). After washing the column with water, the adsorbed compounds were eluted with 2 N ammonia. The eluate was evaporated up to dryness in vacuo and the residue was dissolved in water (10 ml.). The solution was heated on a boiling water bath for 30 min. with the addition of flavianic acid (2 g.). On keeping the solution for 2 days in an ice-box, a flavianate of γ-hydroxyarginine crystallized out. The flavianate, after removal of the flavianic acid moiety in the usual manner, was converted into γ-hydroxyarginine hydrochloride. Yield, 57%; m. p. 189~190°C (decomp.).

Anal. Found: C, 31.88; H, 6.76; N, 24.83. Calcd. for $C_6H_{14}N_4O_3 \cdot HCl$: C, 31.79; H, 6.67; N, 24.72%.

Comparison of the Naturally Occurring Guanidino and Amino Compounds with the Synthetic Ones.—The synthetic γ-hydroxyarginine and γ-hydroxyornithine showed the same paper chromatographic behaviors as those of the naturally occurring guanidino compound and the amino compound produced therefrom by the action of arginase as shown in Table III.

TABLE III. R_f VALUES OF NATURALLY OCCURRING GUANIDINO AND AMINO COMPOUNDS AND SYNTHETIC ONES

	Solvent			
	I	II	III	IV
Guanidino compound	0.16	0.19	0.20	0.17
γ-Hydroxyarginine	0.16	0.19	0.20	0.17
Amino compound	0.12	0.15	0.17	0.13
γ-Hydroxyornithine	0.12	0.15	0.18	0.13

Summary

A new guanidino compound was isolated from a sea-cucumber, *Polycheira rufescens*, and identified as γ-hydroxyarginine. γ-Hydroxyornithine and γ-guanidino-β-hydroxybutyric acid produced enzymically from the guanidino compound were also isolated and identified. It was, further, concluded that the new guanidino compound susceptible to arginase and L-amino acid oxidase should be γ-hydroxy-L-arginine, although the configuration of the γ-hydroxy group was not yet decided.

The author wishes to express his cordial thanks to Professor S. Shibuya for his guidance and encouragement, to Assistant

7) M. Tomita, *Z. physiol. Chem.*, **124**, 253 (1923).
8) T. Fukagawa, ibid., **231**, 203 (1935).

Professor N. Izumiya for his advice, and to Messrs. S. Makisumi, S. Ouchi, T. Yamashita, R. Yamada, M. Ono, T. Kamata and Y.Ishikawa for their assistance with the collection of sea-cucumbers. His thanks are also due to the Ministry of Education for financial support of this research.

Laboratory of Biochemistry
Faculty of Science
Kyushu University
Fukuoka

Formation and Aging of Precipitates. XII. Studies on Types of Crystal Growth of Barium Sulfate by Dissolution in Water*

By Kazuyoshi TAKIYAMA

(Received November 4, 1958)

Barium sulfate is one of the sparingly soluble salts and it gradually dissolves in water. The investigation of dissolution of barium sulfate in EDTA solution was reported[1], but hitherto no morphological study has been made. The author previously reported the investigation of growth process of barium sulfate precipitate[2]. The precipitate was purified by the diffusion washing, that is, a drop containing the precipitate was placed on a Formvar film floating on the surface of distilled water for about ten minutes and the soluble matter was made to diffuse through the film into the water below. About ten minutes were suitable for the washing process while, under too long time of washing, the precipitate tended to dissolve in water. The present investigation is intended to study the type of crystal growth of barium sulfate by the dissolution of the crystal under the diffusion washing for a long period.

Sample.—Two kinds of barium sulfate precipitates were used in the dissolution by diffusion washing. One was the oval particles prepared by the method described in the previous paper[3], and the other was the thin rectangular particles prepared by direct mixing of dilute reagents[4].

Experimental.—A drop of the suspension containing the precipitate mentioned above was placed on a thin Formvar film floating on the surface of distilled water. The drop was left for several hours or one day to let ions diffuse from the drop into the water below. The film was then scooped up with a specimen grid for electron microscopy. Both the fresh and the aged precipitates were examined.

Experimental Results and Consideration

Oval Crystal. — The freshly prepared oval particles as shown in Fig. 1a changed to those as shown in Figs. 1b and c after they were treated with water for three hours. The radial arrangement of small particles are observed in each oval particles. It seems that the oval particles, subjected to dissolution, have been formed by the repetition of dendritic growth, the rate of which is rapid and slow alternately, and that the weakly oriented parts around the particles dissolve in water easily while the comparatively stable parts are not easily soluble, thus the radially arranged particles can be observed. Several hours after, the oval particles dissolved in water and changed in appearance as shown in Figs. 2a and c. The particle shown in Fig. 2a has still the original orientation of crystal structure and the orientation of crystal shown in Fig. 2c was disordered, as was proved by electron diffraction pattern shown in Figs. 2b and d.

Oval particles which were aged for about one day in the mother liquid changed in appearance as shown in Figs. 3a and b. In the aging process, the crystal structure of particles, especially that of the surface of particles, seems to become perfect gradually. Thus in the case of an aged particle, the inner part

* The eleventh paper of this series, This Bulletin, **32**, 387 (1959).

1) K. Mukai and K. Goto, *Japan Analyst* (*Bunseki Kagaku*), **6**, 732 (1957).

2) K. Takiyama, This Bulletin, **31**, 950 (1958).

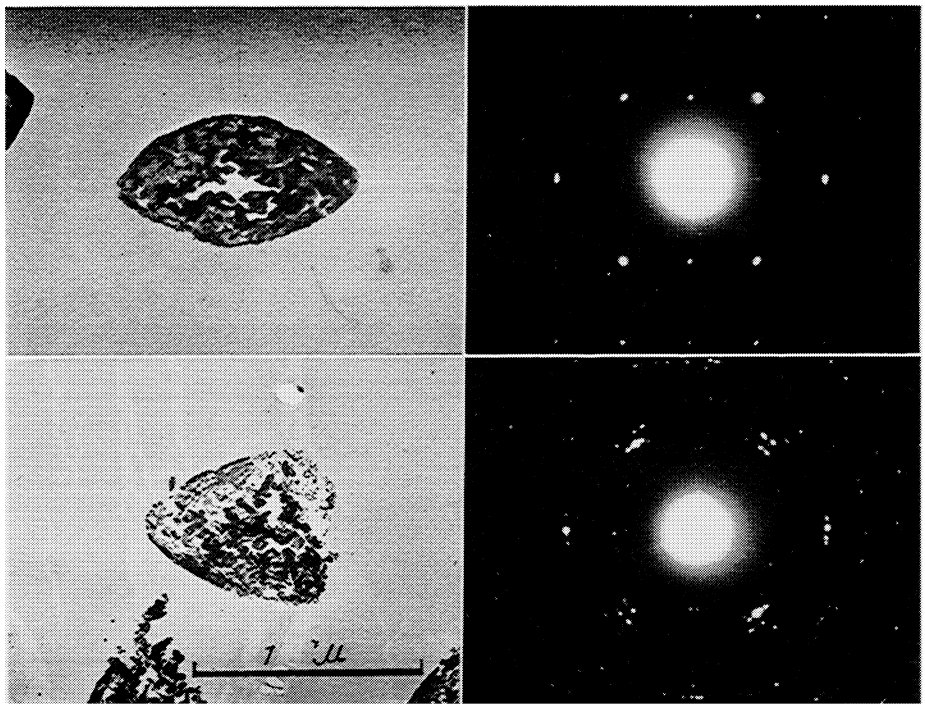
3) K. Takiyama. ibid., **32**, 387 (1959).

4) K. Takiyama, ibid., **27**, 121 (1954); **32**, 68 (1959).



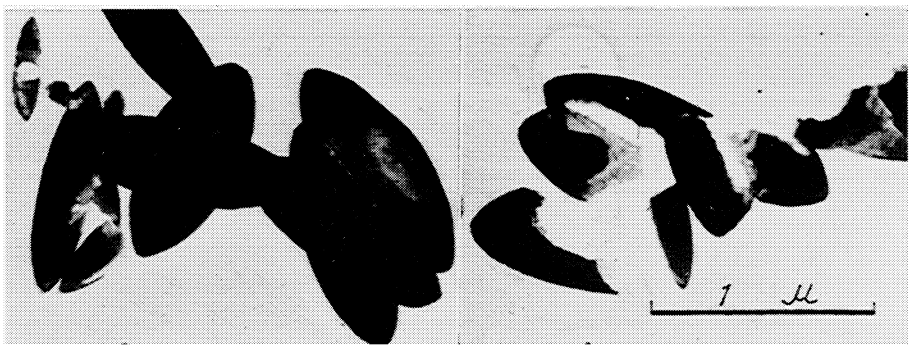
a b e ×30,000

Fig. 1. Dissolution of freshly prepared barium sulfate particles in water.
a: original particles; b, c: after treatment for three hours



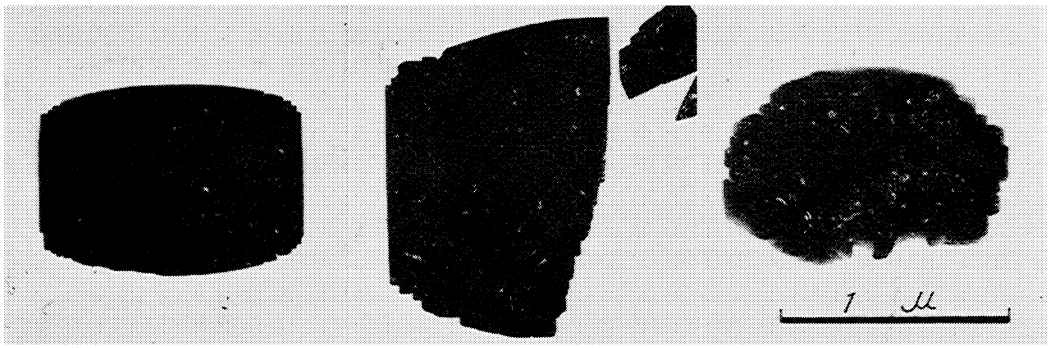
×30,000

Fig. 2. Dissolution of freshly prepared barium sulfate particles by treatment with water for six hours.



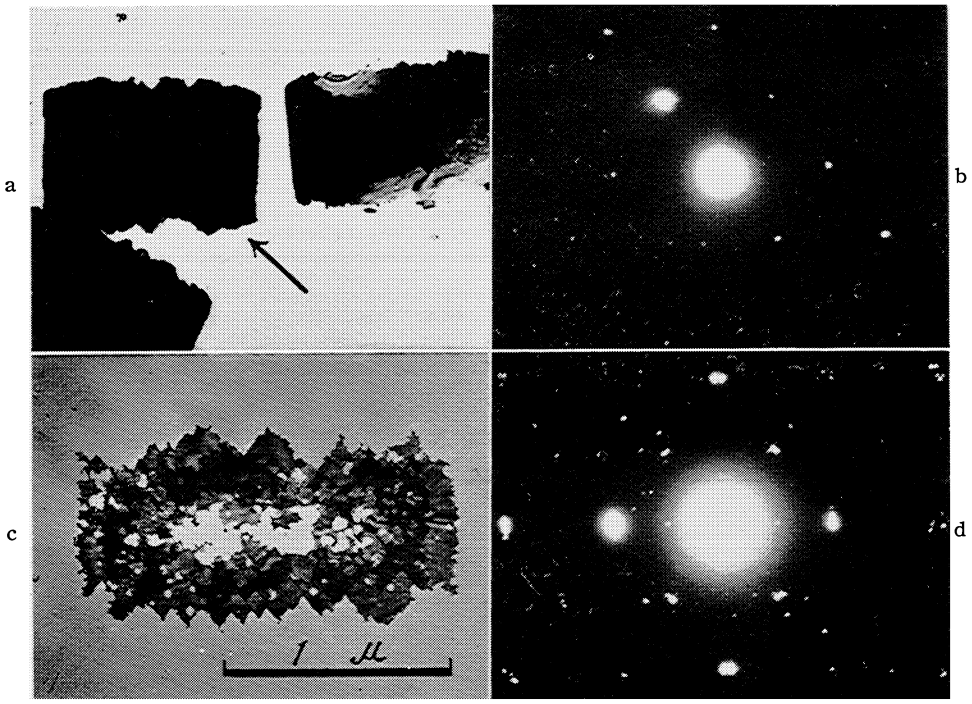
a b ×30,000

Fig. 3. Dissolution of aged barium sulfate particles in water.
a: after treatment for three hours; b: after treatment for six hours



a b c ×30,000

Fig. 4. Dissolution of freshly prepared barium sulfate particles by treatment with water for three hours.



×30,000

Fig. 5. Dissolution of aged barium sulfate particles in water.
a, b: after treatment for six hours
c, d: after treatment for one day

of particle dissolved faster than the surface part which remained undissolved as shown in Fig. 3b.

Rectangular Thin Crystal.—Freshly prepared rectangular particles dissolved from the corner of particles as shown in Fig. 4. The corner of the slightly dissolved particles has many steps as shown in Figs. 4b and c. The rectangular particles are the perfect single crystal as described in the previous paper[4] and their growth seems to agree with the perfect crystal growth theory proposed by Kossel and Stranski[5]. Thus the particles seem to have grown stepwise and to have many steps which are large in some parts. Then weak parts at the surface of particles dissolved quickly and many of these large steps appeared around the particles.

The aged rectangular perfect crystals dissolved in water and gave the figure as shown in Fig. 5. The particles began to dissolve from the side of crystals, that is, from (0 1 0) plane (Fig. 5a), and the inner parts dissolved faster than the surface parts of particles (Fig. 5c). The surface of aged particles seems to become stable by complete orientation of crystal structure during digestion in mother liquid as in the case of oval particles. The particle shown in Fig. 5a (arrow) has a perfect single crystal structure (Fig. 5b) and the single crystal structure of the particle shown in Fig. 5c has begun to decompose (Fig. 5d) as examined by electron diffraction method. The crystal structure of the surface part remained almost perfect even after one day's treatment with water.

5) I. M. Stranski, *Z. phys. Chem.*, **136**, 259 (1928).

Summary

The oval and rectangular crystals of barium sulfate precipitates seem to grow through the dendritic and perfect crystal growth processes, respectively. These particles dissolve in the process of diffusion washing. The oval particles dissolved slightly show the dendrite structure in them, and the rectangular particles dissolved slightly show the large steps around the particles. Thus these particles proved to have grown through dendritic and perfect crystal growth processes, respectively. The surface of the aged particles of both oval and rectangular crystals become stable by digestion in mother liquid; hereby the dissolution rate of inner parts of particles is faster than that of surface parts of them.

The author desires to thank Professor Eiji Suito of Kyoto University for his guidance. He also wishes to express his hearty thanks particularly to Professor Masayoshi Ishibashi of Kyoto University for his continuous advice and encouragement.

Institute for Chemical Research
Kyoto University
Takatsuki, Osaka

Electronic Structures of Naphthalenediols. I. α, α'-*Naphthalenediols*

By Kichisuke NISHIMOTO and Ryoichi FUJISHIRO

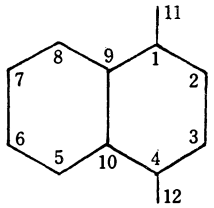
(Received November 4, 1958)

While the electronic structures of substituted benzenes have been studied by many authors, the theoretical investigations of those of substituted naphthalenes have been scarcely ever made[1-4], because of difficulties of the calculation due to low symmetry of these molecules and the presence of many π-electrons to be considered. The spectra of naphthalene mono-derivatives show[5] in general two kinds of characteristic picture depending upon the position of substitution, either β or α positions. In the di-derivatives, two substituents are bonded with rings in two ways, that is, both with the same

1) H. Baba and T. Suzuki, Symposium on the Electronic Structures of Molecules, held at Kyoto, 1958.
2) R. Daudel and M. Martin, *Bull. soc. chim. France*, **1948**, 559; ibid., **1949**, 83.
3) D. Peters, *J. Chem. Soc.*, **1957**, 646, 1993.
4) B. Pullman, *Bull. soc. chim. France*, **1948**, 533.
5) R. A. Friedel and M. Orchin, "Ultraviolet Spectra of Aromatic Compounds", Jone Wiley and Sons, New York, (1951).

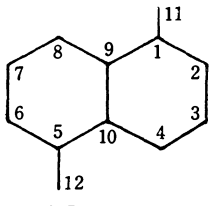
ring and each with the different rings. This seems to lead additional effects on their molecular properties. De Laszlo[6] showed that fourteen isomeric dichloronaphthalenes could be classified spectroscopically as aa, ab and bb compounds. But as pointed out by Daglish[7] in the case of naphthalene di-derivatives having strongly conjugating substituents, such as hydroxyl, amine etc., this classification is an over-simplification of the problem. In the present paper theoretical treatments based on the simple MO theory will be applied to the electronic structures of α,α'-naphthalenediols, such as 1-4, 1-5 and 1-8 diols, in order to establish the effects of substituents on their molecular properties. The electronic structures of β,β'-naphthalenediols will be considered in the next paper.

Method of Calculation.—The method is based on the simple LCAO MO theory with only fourteen $2p\pi$ electrons considered explicitly. The Coulomb and the exchange integrals used are the same as those in the previous paper[8], where the electronic structure of phenol was discussed. All the Coulomb integrals for carbon atoms are taken as equal to α. When the non-uniformity of charge distribution is small, the above assumption may be approximately held. In order to simplify the calculation we make this approximation. The numbering of atoms and the symmetry orbitals for the moleclues are shown in Fig. 1. A, B, A_2 and B_1 in the figure express the irreducible representations, to which each symmetry orbital belongs.



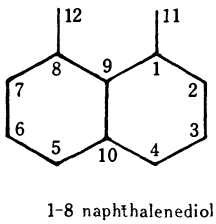
1-4 naphthalenediol

B_1 $\sigma_1=\phi_1+\phi_4$ A_2 $\sigma_7=\phi_1-\phi_4$
$\sigma_2=\phi_2+\phi_3$ $\sigma_8=\phi_2-\phi_3$
$\sigma_3=\phi_5+\phi_8$ $\sigma_9=\phi_5-\phi_8$
$\sigma_4=\phi_6+\phi_7$ $\sigma_{10}=\phi_6-\phi_7$
$\sigma_5=\phi_9+\phi_{10}$ $\sigma_{11}=\phi_9-\phi_{10}$
$\sigma_6=\phi_{11}+\phi_{12}$ $\sigma_{12}=\phi_{11}-\phi_{12}$



1-5 naphthalenediol

A $\sigma_1=\phi_1+\phi_5$ B $\sigma_7=\phi_1-\phi_5$
$\sigma_2=\phi_2+\phi_6$ $\sigma_8=\phi_2-\phi_6$
$\sigma_3=\phi_3+\phi_7$ $\sigma_9=\phi_3-\phi_7$
$\sigma_4=\phi_4+\phi_8$ $\sigma_{10}=\phi_4-\phi_8$
$\sigma_5=\phi_9+\phi_{10}$ $\sigma_{11}=\phi_9-\phi_{10}$
$\sigma_6=\phi_{11}+\phi_{12}$ $\sigma_{12}=\phi_{11}-\phi_{12}$



1-8 naphthalenediol

B_1 $\sigma_1=\phi_1+\phi_8$ A_2 $\sigma_8=\phi_1-\phi_8$
$\sigma_2=\phi_2+\phi_7$ $\sigma_9=\phi_2-\phi_7$
$\sigma_3=\phi_3+\phi_6$ $\sigma_{10}=\phi_3-\phi_6$
$\sigma_4=\phi_4+\phi_5$ $\sigma_{11}=\phi_4-\phi_5$
$\sigma_5=\phi_9$ $\sigma_{12}=\phi_{11}-\phi_{12}$
$\sigma_6=\phi_{10}$
$\sigma_7=\phi_{11}+\phi_{12}$

Fig. 1. Numbering of atoms and symmetry orbitals.

Results and Discussion

(A) MO's and their Polarization.—The calculated MO's and their energies for the naphthalenediols are summarized in Table I.

The comparison of the MO's of the naphthalene[9] and those of diols obtained here makes it clear that the signs of the coefficients at each carbon AO in each MO are unchanged by the introduction of the hydroxy groups. Thus, so far as the mono- and di-derivatives are concerned, it is not too much to say that the effect of substitution brings about some modification of the MO's of parent hydrocarbon, but the extent of these modifications is not so large as to destroy their orbital characteristics. This situation will give a basis to the assumption that in many cases the perturbation theory supplies qualitatively useful results, even if the effect of the substitution amounts to considerable extent. In the naphthalene molecule, φ_1 is totally symmetric for the symmetry operation with respects to the principal axis and has no node of the wave function. For the naphthalenediols, φ_1's of them have still no node, but they are strongly polarized along the direction toward the substituents in a regular manner. If we try to measure the degree of polarization by the value of $C_{1\mu}/C_{1\mu_0}$, where the $C_{1\mu}$ is the square of coefficient at μ-th carbon AO in φ_1 of the diol and the $C_{1\mu_0}$ is that of naphthalene, these values are the greatest at the carbon atoms bonded with a hydroxy group and decrease with the increase in the distance between the μ-th carbon atom and the substituent. For the case of 1-8 diol, the values at the carbon atoms numbered by 1, 2, 3 and 4 in Fig. 1 are 1.367, 0.925, 0.656 and 0.591, respectively. This polarization is similar to the inductive effect which is usually regarded as the polarization of σ-cores

6) H. de Laszlo, *J. Am. Chem. Soc.*, **50**, 892 (1928).
7) C. Daglish, ibid., **72**, 4859 (1950).
8) K. Nishimoto and R. Fujishiro, This Bulletin, **31**, 1036 (1958).
9) B. Pullman and A. Pullman, " Les Theories electroniques de la Chimie organique ", Masson et Cie, Paris, (1952), p. 199.

TABLE I. MO'S AND MO ENERGIES

Symmetry	Orbital energy in β	MO
		1-4-naphthalenediol
B_1	2.4227	$\varphi_1=0.3452\sigma_1+0.2426\sigma_2+0.2386\sigma_3+0.1677\sigma_4+0.4103\sigma_5+0.2619\sigma_6$
A_2	1.9264	$\varphi_2=0.3498\sigma_7+0.1195\sigma_8-0.0962\sigma_9-0.0329\sigma_{10}+0.1524\sigma_{11}+0.5742\sigma_{12}$
B_1	1.8058	$\varphi_3=0.1695\sigma_1+0.2103\sigma_2-0.3111\sigma_3-0.3860\sigma_4-0.1757\sigma_5+0.3877\sigma_6$
B_1	1.3271	$\varphi_4=0.1246\sigma_1+0.381\sigma_2-0.0796\sigma_3-0.2433\sigma_4+0.1377\sigma_5-0.5048\sigma_6$
A_2	1.1082	$\varphi_5=0.1631\sigma_7+0.0774\sigma_8-0.4849\sigma_9-0.2300\sigma_{10}+0.3074\sigma_{11}-0.2914\sigma_{12}$
B_1	1.0000	$\varphi_6=0.4083(\sigma_2+\sigma_4-\sigma_5)$
A_2	0.4321	$\varphi_7=0.4276\sigma_7+0.2986\sigma_8+0.3096\sigma_9+0.2162\sigma_{10}+0.0824\sigma_{11}-0.2803\sigma_{12}$
B_1	−0.6922	$\varphi_8=0.3818\sigma_1-0.2256\sigma_2-0.4607\sigma_3+0.2722\sigma_4+0.0466\sigma_5-0.1219\sigma_6$
A_2	−1.0000	$\varphi_9=-0.4083(\sigma_8-\sigma_{10}-\sigma_{11})$
B_1	−1.3635	$\varphi_{10}=0.4369\sigma_1-0.1846\sigma_2+0.3574\sigma_3-0.1512\sigma_4-0.3361\sigma_5-0.1069\sigma_6$
A_2	−1.6396	$\varphi_{11}=0.2616\sigma_7-0.4090\sigma_8+0.2750\sigma_9-0.4299\sigma_{10}+0.0209\sigma_{11}-0.0584\sigma_{12}$
A_2	−2.3271	$\varphi_{12}=0.3158\sigma_7-0.2379\sigma_8-0.2901\sigma_9+0.2186\sigma_{10}-0.4565\sigma_{11}-0.0578\sigma_{12}$
		1-5-naphthalenediol
A	2.4190	$\varphi_1=0.3362\sigma_1+0.2195\sigma_2+0.1949\sigma_3+0.2519\sigma_4+0.4144\sigma_5+0.2561\sigma_6$
B	1.9945	$\varphi_2=0.3687\sigma_7+0.2472\sigma_8+0.1243\sigma_9+0.0007\sigma_{10}+0.1229\sigma_{11}+0.5219_{12}$
A	1.6212	$\varphi_3=0.1038\sigma_1-0.0407\sigma_2-0.1698\sigma_3-0.2346\sigma_4-0.2106\sigma_5+0.5994\sigma_6$
B	1.5296	$\varphi_4=-0.0084\sigma_7+0.2853\sigma_8+0.4447\sigma_9+0.3951\sigma_{10}-0.1594\sigma_{11}-0.1981\sigma_{12}$
B	1.0034	$\varphi_5=0.2897\sigma_7+0.2877\sigma_8-0.0010\sigma_9-0.2887\sigma_{10}+0.2887\sigma_{11}-0.4082\sigma_{12}$
A	1.0000	$\varphi_6=0.4083(\sigma_2+\sigma_3-\sigma_5)$
A	0.4590	$\varphi_7=0.3696\sigma_1+0.2900\sigma_2-0.2365\sigma_3-0.3985\sigma_4+0.0535\sigma_5-0.2484\sigma_6$
B	−0.7005	$\varphi_8=0.4268\sigma_7-0.2336\sigma_8-0.2632\sigma_9+0.4180\sigma_{10}+0.0296\sigma_{11}-0.1357\sigma_{12}$
B	−1.0000	$\varphi_9=-0.4083(\sigma_8-\sigma_9-\sigma_{11})$
A	−1.3550	$\varphi_{10}=0.3739\sigma_1-0.1062\sigma_2-0.2300\sigma_3+0.4178\sigma_4-0.3362\sigma_5-0.0917\sigma_6$
A	−1.6442	$\varphi_{11}=0.3159\sigma_1-0.4337\sigma_2+0.3972\sigma_3-0.2194\sigma_4-0.0365\sigma_5-0.0703\sigma_6$
B	−2.3269	$\varphi_{12}=0.3129\sigma_7-0.2313\sigma_8+0.2254\sigma_9-0.2931\sigma_{10}-0.4567\sigma_{11}-0.0572\sigma_{12}$
		1-8-naphthalenediol
B_1	2.4249	$\varphi_1=0.3513\sigma_1+0.2219(\sigma_2+2\sigma_5)+0.1868(\sigma_3+2\sigma_6)+0.2312\sigma_4+0.2659\sigma_7$
A_2	1.9360	$\varphi_2=0.3278\sigma_8+0.2662\sigma_9+0.1875\sigma_{10}+0.0969\sigma_{11}+0.5264\sigma_{12}$
B_1	1.7562	$\varphi_3=0.1794\sigma_1-0.0094(\sigma_2+2\sigma_5)-0.1959(\sigma_3+2\sigma_6)-0.3346\sigma_4+0.4903\sigma_7$
A_2	1.4410	$\varphi_4=0.0319\sigma_8+0.3116\sigma_9+0.4172\sigma_{10}+0.2895\sigma_{11}-0.3795\sigma_{12}$
B_1	1.0035	$\varphi_5=0.2977\sigma_1+0.1975(\sigma_2+2\sigma_5)-0.0995(\sigma_3+2\sigma_6)-0.2973\sigma_4-0.4198\sigma_7$
B_1	1.0000	$\varphi_6=0.4083(\sigma_2+\sigma_3-\sigma_5-\sigma_6)$
A_2	0.4666	$\varphi_7=0.3490\sigma_8+0.3283\sigma_9-0.1958\sigma_{10}-0.4197\sigma_{11}-0.2364\sigma_{12}$
A_2	−0.7020	$\varphi_8=0.4332\sigma_8-0.2077\sigma_9-0.2874\sigma_{10}+0.4094\sigma_{11}-0.1378\sigma_{12}$
B_1	−1.0000	$\varphi_9=-0.4083(\sigma_2-\sigma_3-\sigma_5+\sigma_6)$
B_1	−1.3573	$\varphi_{10}=0.3939\sigma_1-0.1557(\sigma_2+2\sigma_5)-0.1826(\sigma_3+2\sigma_6)+0.4035\sigma_4-0.0965\sigma_7$
A_2	−1.6416	$\varphi_{11}=0.2864\sigma_8-0.4255\sigma_9+0.4121\sigma_{10}-0.2511\sigma_{11}-0.0637\sigma_{12}$
B_1	−2.3273	$\varphi_{12}=0.3172\sigma_1-0.2325(\sigma_2+2\sigma_5)+0.2240(\sigma_3+2\sigma_6)-0.2887\sigma_4-0.0581\sigma_7$

caused by the introduction of the polar group into the molecule. But, when we take $\beta_{CO}=0$, this polarization is absent, so far as invoking the simple theory, since the interactions between the $2p\pi$ electrons of the substituents and of the naphthalene ring are impossible in this case. If the polarizations of φ_1's are inductive, it is expected that the value of C_{11}/C_{11_0} for 1-8-diols is the greatest and the smallest for 1-5-diol. Actually, their values are 1,367, 1,319 and 1.251 for 1-8, 1-4 and 1-5-diols, respectively. Although the all MO's for the diols have the same numbers of nodes as those for the corresponding naphthalene MO's, the regular polarizations are not recognized in them except φ_1's. In the light of the above fact, we may except that when the overlap between the electronic cloud of conjugated molecule and that of the attacking molecule is present, the lowest π-orbital of the former will be most sensitive to the influence of the latter. The occupied lowest π-orbital will, therefore, play the most important role for the rearrangement of charge distribution of the molecule produced by the approach of the reagent.

(B) Absorption Spectra. — It is well known that the introduction of the hydroxy group into the α-position of naphthalene causes a very large bathochromic shift in the p-band with some distortion of the fine structure and a rather small shift in the α-band. As mentioned by Daglish[7] and Spruit[10], the spectra of α, α'-diols also have those characteristic features, but these bathochromic shifts in the p-bands are larger in 1–4 derivative and slightly larger in 1–5 compound than that in α-naphthol. Comparison of the energy level diagrams given in Fig. 2

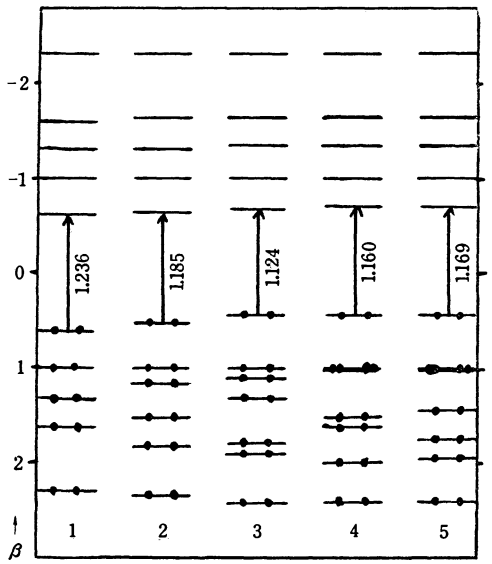


Fig. 2. Energy level diagrams.
1. naphthalene
2. α-naphthol
3. 1-4 naphthalenediol
4. 1-5 naphthalenediol
5. 1-8 naphthalenediol

makes it possible to expect that the spectra of 1–8 diol may be very close to that of 1–5 diol, since the spacing of their levels concerned with the electronic transitions in the near ultraviolet region are very similar to each other. This is the case of Hochstein et al.[11], who reported that the spectroscopic distinction between them was difficult. The energy level diagram of α-naphthol which is calculated by using the same parameters for diols is also given in Fig. 2. The numerical values given in Fig. 2 express the orbital energy differences between φ_7 and φ_8 for the corresponding compounds in the units of β, respectively. The comparison of these values suggests that the wave lengths of absorption corresponding to the $\varphi_7 \rightarrow \varphi_8$ transitions which are closely related to the p-band are in following order; 1–4 diol > 1–5 diol $\simeq$ 1–8 diol $\simeq$ α-naphthol.

The fact that the orbitals having orbital energies of $\pm\beta$ are not affected by the substitution in the α-positions of naphthalene may provide a determining factor for the discussion of electronic transitions concerned with α-bands of α-compounds, because these orbitals are closely connected with them. Experimentally observed distortion of the fine-structure in the p-band will be reasonably attributable to the anharmonicity produced by the ununiform charge distribution and the alteration of the bond orders. The full discussion about the electronic transitions on the ground of the method involving the electronic interaction will be desirable. Here, we will try no further discussion about this problem.

(C) Extra Delocalization Energies and Molecular Diagrams.—Delocalization of the $2p\pi$-electrons of substituents into the naphthalene ring brings the excess of stabilization energies (extra delocalization energies) for the molecule as a whole. These values per one hydroxy group are evaluated to be 0.1807, 0.1851 and 0.1866β for the 1–4, 1–5 and 1–8 diols, respectively. A naive consideration will give larger extra delocalization energy for greater charge migration. Actually, if we plot these values against the magnitudes of the charge migrations from the hydroxy

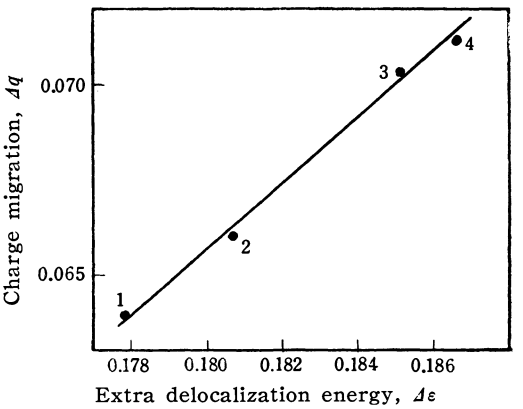


Fig. 3. Relation between the extra delocalization energy of diols and the charge migration in them.
1. phenol
2. 1-4 naphthalenediol
3. 1-5 naphthalenediol
4. 1-8 naphthalenediol

10) C. J. P. Spruit, *Rec. trav. chim.*, **68**, 309 (1949).
11) F. A. Hochstein et al., *J. Am. Chem. Soc.*, **75**, 5457 (1953).

group into the naphthalene ring, a linear relationship is obtained as shown in Fig. 3. It is surprising that a point corresponding to the phenol, which is obtained from our previous paper[9], is also located on this line. This fact gives us an interesting suggestion that the degree of charge migration will be estimated by only the calculation of orbital energies of the molecule. This seems to give a theoretical background to a well-known conception of the electronic theory in organic chemistry that the acidity of the aromatic hydroxy derivatives is closely connected with the magnitude of charge migration. In the case of α-naphthol, the value of extra-delocalization energy is $0.1862\,\beta$. Its magnitude of charge density at the hydroxy group will be, therefore, expected to be comparable with that of 1–8 diol.

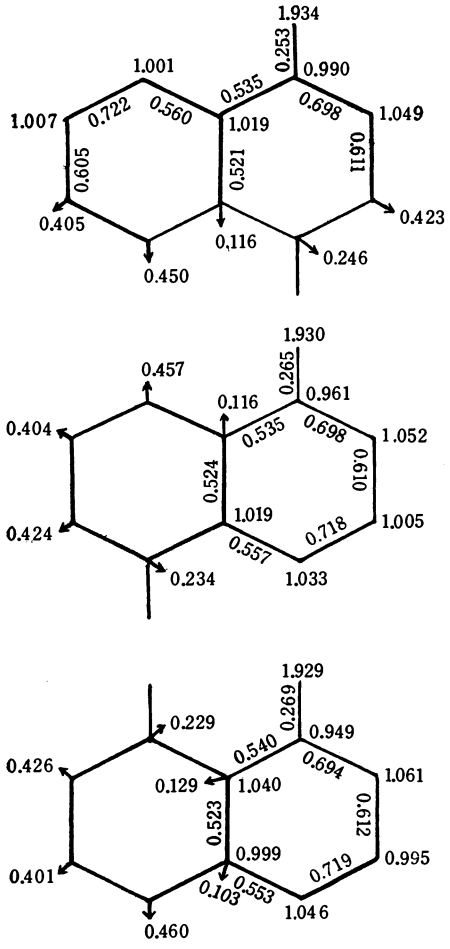


Fig. 4. Molecular diagram.

As seen from the molecular diagrams given in Fig. 4 the charge distributions in the molecules show a sharp difference according to the type of substitution, either two hydroxy groups bonded with the same ring or not. Namely, in the case of 1–4 diol the migrated charges are, for the most part, localized within one ring whereas in those of 1–5 and 1–8 diols they are equally distributed into both rings. In the discussion of the molecular properties, such as reactivity, of the naphthalene di-derivatives this characteristic charge distribution will supply a useful information.

Summary

The simple LCAO MO method was applied to the electronic structures of α,α'-naphthalenediols, using the same parameters as those of phenol based on the ASPMO calculation. The theory proved that

(a) the lowest π-orbital of the molecule would be the most sensitive to the influence of the external molecular field,

(b) the absorption spectra of diols were satisfactorily correlated with their energy level diagrams, and

(c) the extra delocalization energies produced by the charge migrations from the hydroxy groups into the naphthalene ring increased linearly with the increment of the magnitude of charge migrations.

The authors express their gratitude to Mr. N. Mataga for his helpful discussions.

Institute of Polytechnics
Osaka City University
Kita-ku, Osaka

Expansion Formulae of Secular Determinant in Simple LCAO MO Treatment of Aromatic Hydrocarbons

By Kenichi FUKUI, Chikayoshi NAGATA, Teijiro YONEZAWA and Akira IMAMURA

(Received November 17, 1958)

In the LCAO MO treatment of conjugated molecules, it goes without saying that the secular determinant must be known in its expanded form in order to solve it numerically. The use of secular determinant is not necessarily restricted to finding its roots. Coulson and Longuet-Higgins[1] obtained the integral formulae for electronic energy, bond order and various kinds of polarizability in which the integrands were expressed in terms of secular determinants. Also Baba[2] and the present authors[3] pointed out the importance of the coefficients in the expansion of minors of secular determinant for predicting the reactivity of alternant hydrocarbons.

In this paper, we derive several formulae which are useful for expanding the secular determinant of aromatic hydrocarbons. By using these formulae, the secular determinant can be expressed in terms of that of a smaller molecule and the laborious calculation for large molecules can be considerably simplified.

The Expansion Formulae of Secular Determinant for the Aromatic Hydrocarbon.—In the first, the types of "growth" of aromatic hydrocarbons are classified into five as shown in Fig. 1. The first, the third, and the fifth are tentatively named "even growth", and the second, and the fourth "odd growth". Then, an even molecule is formed either by an even growth of an even molecule, or otherwise by an odd growth of an odd molecule, and the formation of an odd molecule results from an odd growth of an even molecule or from an even growth of an odd molecule.

If we put the secular determinants of a molecule before and after the growth as $\Delta(\lambda)$ and $D(\lambda)$, respectively, the expansion formulae for each type are obtained

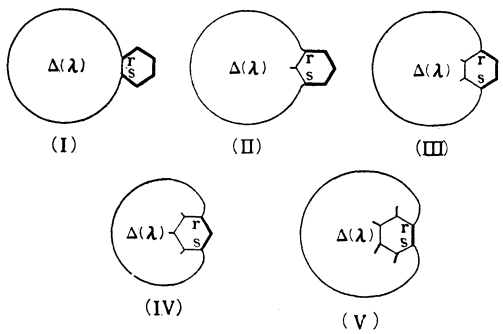


Fig. 1. The types of "growth" of aromatic hydrocarbons are shown. (I) is the first type of growth and (II) is the second type of growth and so on. The thick lines indicate the bonds formed as a result of "growth".

as follows:

For the first type of growth,

$$D(\lambda)=(\lambda^4-3\lambda^2+1)\Delta(\lambda)+\lambda(\lambda^2-2)\{\Delta_{rr}(\lambda)+\Delta_{ss}(\lambda)\}+(\lambda^2-1)\Delta_{rrss}(\lambda)-2(-1)^{r+s+1}\Delta_{rs}(\lambda) \quad (1)$$

For the second type of growth,

$$D(\lambda)=-\lambda(\lambda^2-2)\Delta(\lambda)-(\lambda^2-1)\{\Delta_{rr}(\lambda)+\Delta_{ss}(\lambda)\}-\lambda\Delta_{rrss}(\lambda)+2(-1)^{r+s+1}\Delta_{rs}(\lambda) \quad (2)$$

For the third type of growth,

$$D(\lambda)=(\lambda^2-1)\Delta(\lambda)+\lambda\{\Delta_{rr}(\lambda)+\Delta_{ss}(\lambda)\}+\Delta_{rrss}(\lambda)-2(-1)^{r+s+1}\Delta_{rs}(\lambda) \quad (3)$$

For the fourth type of growth,

$$D(\lambda)=-\lambda\Delta(\lambda)-\Delta_{rr}(\lambda)-\Delta_{ss}(\lambda)+2(-1)^{r+s+1}\Delta_{rs}(\lambda) \quad (4)$$

For the fifth type of growth,

$$D(\lambda)=\Delta(\lambda)-\Delta_{rrss}(\lambda)-2(-1)^{r+s+1}\Delta_{rs}(\lambda) \quad (5)$$

Besides the above types of nuclear growth, the types of branching and bridging also exist in conjugated systems.

1) C. A. Coulson and H. C. Longuet-Higgins, *Proc. Roy. Soc.*, **A191**, 39 (1947).
2) H. Baba, This Bulletin, **30**, 147 (1957).
3) K. Fukui, T. Yonezawa, and C. Nagata, *J. Chem. Phys.*, **26**, 831 (1957).

They are shown in Fig. 2 and are tentatively designated as type 1, 2, ····· , 9. The expansion formulae for them are given as:

For the type 1,

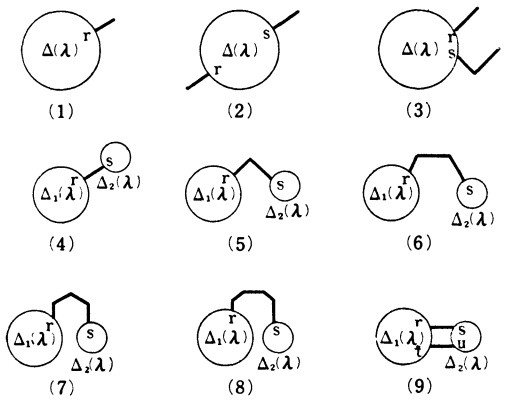


Fig. 2. The types of branching and bridging in conjugated molecules are shown. The thick lines indicate the branches {(1), (2) and (3)} and bridges {(4), (5), (6)·····, (9)} respectively.

$$D(\lambda) = -\lambda\Delta(\lambda) - \Delta_{rr}(\lambda) \tag{6}$$

For the type 2,

$$D(\lambda) = \lambda^2\Delta(\lambda) + \lambda\{\Delta_{rr}(\lambda) + \Delta_{ss}(\lambda)\} + \Delta_{rrss}(\lambda) \tag{7}$$

For the type 3,

$$D(\lambda) = (\lambda^2-1)\{-\lambda\Delta(\lambda) - \Delta_{rr}(\lambda)\} - \lambda^2\Delta_{ss}(\lambda) - \lambda\Delta_{rrss}(\lambda) \tag{8}$$

For the type 4,

$$D(\lambda) = \Delta_1(\lambda)\Delta_2(\lambda) - \Delta_{1rr}(\lambda)\Delta_{2ss}(\lambda) \tag{9}$$

For the type 5,

$$D(\lambda) = -\lambda\Delta_1(\lambda)\Delta_2(\lambda) - \Delta_{1rr}(\lambda)\Delta_2(\lambda) - \Delta_{2ss}(\lambda)\Delta_1(\lambda) \tag{10}$$

For the type 6,

$$D(\lambda) = (\lambda^2-1)\Delta_1(\lambda)\Delta_2(\lambda) + \lambda\{\Delta_{1rr}(\lambda)\Delta_2(\lambda) + \Delta_{2ss}(\lambda)\Delta_1(\lambda)\} + \Delta_{1rr}(\lambda)\Delta_{2ss}(\lambda) \tag{11}$$

For the type 7,

$$D(\lambda) = -\lambda(\lambda^2-2)\Delta_1(\lambda)\Delta_2(\lambda) - (\lambda^2-1)\{\Delta_{1rr}(\lambda)\Delta_2(\lambda) + \Delta_{2ss}(\lambda)\Delta_1(\lambda)\} - \lambda\Delta_{1rr}(\lambda)\Delta_{2ss}(\lambda) \tag{12}$$

For the type 8,

$$D(\lambda) = (\lambda^4-3\lambda^2+1)\Delta_1(\lambda)\Delta_2(\lambda) + \lambda(\lambda^2-2) \times\{\Delta_{1rr}(\lambda)\Delta_2(\lambda) + \Delta_{2ss}(\lambda)\Delta_1(\lambda)\} + (\lambda^2-1)\Delta_{1rr}(\lambda)\Delta_{2ss}(\lambda) \tag{13}$$

For the type 9,

$$D(\lambda) = \Delta_1(\lambda)\Delta_2(\lambda) - \Delta_{1rr}(\lambda)\Delta_{2ss}(\lambda) - \Delta_{1tt}(\lambda)\Delta_{2uu}(\lambda) + \Delta_{1rrtt}(\lambda)\Delta_{2ssuu}(\lambda) - 2(-1)^{r+t+1}\Delta_{1rt}(\lambda)(-1)^{s+u+1}\Delta_{2su}(\lambda) \tag{14}$$

where $\Delta(\lambda)$, $\Delta_1(\lambda)$ and $\Delta_2(\lambda)$ may be secular determinants of any conjugated system. $\Delta_{rr}(\lambda)$, or $\Delta_{ss}(\lambda)$ is the (r, r), or the (s, s) minor and $\Delta_{rrss}(\lambda)$ is the (rs, rs) minor of $\Delta(\lambda)$, and these are obtained by striking off the indicated rows and columns of $\Delta(\lambda)$. The equation of $\Delta_{rs}(\lambda)$ can be obtained according to the theorem proposed by Coulson and Longuet-Higgins[1].

The expansion formulae derived above, are very useful for obtaining secular equations of conjugated molecules, especially of large molecules.

Faculty of Engineering
Kyoto University
Sakyo-ku, Kyoto

Density Matrix in Simple LCAO MO Method

By Kenichi FUKUI, Chikayoshi NAGATA, Teijiro YONEZAWA and Akira IMAMURA

(Received November 17, 1958)

The LCAO MO method has been applied extensively to the explanation of the facts in organic chemical reaction. That is to say, the static method by Coulson and Longuet-Higgins[1], the localization method by Wheland[2] and the frontier electron method by Fukui et al.[3-7] and many other similar methods have been used successfully to explain the reactivity of a number of conjugated molecules.

In this article, the present authors indicate that the theoretical indexes such as electron density, bond order, and various polarizabilities derived by Coulson and Longuet-Higgins[1], can be given also by a novel method which is entirely different from that of the previous authors.

Partial Density Matrix and Hamiltonian Matrix. — First, we define the following two matrices which are most fundamental in the theory. They are referred to as partial density matrix $\mathbf{D}_j$ and Hamiltonian matrix $\boldsymbol{\alpha}$, and are defined respectively as follows:

$$\mathbf{D}_j \equiv \begin{pmatrix} (C_1^j)^2 & C_1^jC_2^j & \cdots\cdots & C_1^jC_n^j \\ C_2^jC_1^j & (C_2^j)^2 & \cdots\cdots & C_2^jC_n^j \\ \cdots\cdots & \cdots\cdots & \cdots\cdots & \cdots\cdots \\ \cdots\cdots & \cdots\cdots & \cdots\cdots & \cdots\cdots \\ C_n^jC_1^j & C_n^jC_2^j & \cdots\cdots & (C_n^j)^2 \end{pmatrix} \quad (1)$$

$$\boldsymbol{\alpha} \equiv \begin{pmatrix} \alpha_1 & \beta_{12} & \cdots\cdots & \beta_{1n} \\ \beta_{21} & \alpha_2 & \cdots\cdots & \beta_{2n} \\ \cdots\cdots & \cdots\cdots & \cdots\cdots & \cdots\cdots \\ \cdots\cdots & \cdots\cdots & \cdots\cdots & \cdots\cdots \\ \beta_{n1} & \beta_{n2} & \cdots\cdots & \alpha_n \end{pmatrix} \quad (2)$$

$$(\beta_{rs}=\beta_{sr})$$

where C_r^j is the coefficient of atomic orbital, ϕ_r, in molecular orbital ψ_j, that is, according to the usual LCAO MO method, ψ_j is expressed as a linear combination of atomic orbitals whose number is n; $\psi_j=\sum_{r=1}^{n} C_r^j\phi_r$. α and β are the Coulomb and the resonance integral, respectively. From Eqs. 1 and 2 the following formulae are easily obtained:

$$\boldsymbol{\alpha}\mathbf{D}_j = \varepsilon_j\mathbf{D}_j \quad (3)$$

$$\boldsymbol{\alpha}\mathbf{D}_j = \mathbf{D}_j\boldsymbol{\alpha} \quad (4)$$

The partial density matrices have the following relations with each other;

$$\mathbf{D}_j=\mathbf{D}_j^2=\mathbf{D}_j^3=\cdots\cdots \quad (5)$$

$$\mathbf{D}_j\mathbf{D}_k = 0 \quad (j\neq k) \quad (6)$$

$$\mathbf{D}_j=\frac{\mathbf{D}_j\boldsymbol{\alpha}\mathbf{D}_j}{\varepsilon_j} \quad (7)$$

$$\mathbf{D}_k\boldsymbol{\alpha}\mathbf{D}_j = 0 \quad (k\neq j) \quad (8)$$

$$\sum_{j=1}^{n}\mathbf{D}_j = \mathbf{E} \quad (9)$$

where $\mathbf{E}$ is unit matrix.

Variation of $\mathbf{D}_j$ leads us to the following relations,

$$\mathbf{D}_j\cdot\delta\mathbf{D}_j+\delta\mathbf{D}_j\cdot\mathbf{D}_j=\delta\mathbf{D}_j \quad (10)$$

$$\mathbf{D}_j\cdot\delta\mathbf{D}_k+\delta\mathbf{D}_j\cdot\mathbf{D}_k=0 \quad (k\neq j) \quad (11)$$

$$\mathbf{D}_j\cdot\delta\mathbf{D}_j\cdot\mathbf{D}_j = 0 \quad (12)$$

$$\mathbf{D}_k\cdot\delta\mathbf{D}_j\cdot\mathbf{D}_k = 0 \quad (k\neq j) \quad (13)$$

$$\mathbf{D}_k\cdot\delta\mathbf{D}_j\cdot\mathbf{D}_l = 0 \quad (l\neq j,\ k\neq j) \quad (14)$$

Perturbation Theory in Density Matrix. — The perturbation theory in density matrix can be constructed in just the same way as in LCAO MO method. When the Hamiltonian matrix $\boldsymbol{\alpha}$ is subjected to perturbation by the amount of $\delta\boldsymbol{\alpha}$, $\mathbf{D}_j$ and ε_j are assumed to become $\mathbf{D}_j+\delta\mathbf{D}_j$ and $\varepsilon_j+\delta\varepsilon_j$, respectively. Then from Eq. 3, the following formulae are obtained.

$$\mathbf{D}_j\cdot\delta\varepsilon_j=\delta\boldsymbol{\alpha}\cdot\mathbf{D}_j+(\boldsymbol{\alpha}-\varepsilon_j)\delta\mathbf{D}_j \quad (15)$$

Multiplying Eq. 15 by $\mathbf{D}_k$ $(k\neq j)$ from the left-hand side, we gain the following relation,

1) C. A. Coulson and H. C. Longuet-Higgins, *Proc. Roy. Soc.*, **A191**, 39 (1947).
2) G. W. Wheland, *J. Am. Chem. Soc.*, **64**, 900 (1942).
3) K. Fukui, T. Yonezawa and H. Shingu, *J. Chem. Phys.*, **20**, 722 (1952).
4) K. Fukui, T. Yonezawa, C. Nagata and H. Shingu, ibid., **22**, 1433 (1954).
5) K. Fukui, T. Yonezawa and C. Nagata, This Bulletin, **27**, 423 (1954).
6) K. Fukui, T. Yonezawa and C. Nagata, *J. Chem. Phys.*, **26**, 831 (1957).
7) K. Fukui, T. Yonezawa and C. Nagata, ibid., **27** 1247 (1957).

$$\mathbf{D}_k\cdot\delta\mathbf{D}_j=\frac{\mathbf{D}_k\cdot\delta\boldsymbol{\alpha}\cdot\mathbf{D}_j}{\varepsilon_j-\varepsilon_k} \tag{16}$$

Similarly, from Eqs. 11 and 16,

$$\delta\mathbf{D}_j\cdot\mathbf{D}_k=\frac{\mathbf{D}_j\cdot\delta\boldsymbol{\alpha}\cdot\mathbf{D}_k}{\varepsilon_j-\varepsilon_k} \tag{17}$$

From Eqs. 16 and 17, using the idempotent nature of $\mathbf{D}_j$ we easily obtain the following formulae:

$$\mathbf{D}_k\cdot\delta\mathbf{D}_j\cdot\mathbf{D}_j=\frac{\mathbf{D}_k\cdot\delta\boldsymbol{\alpha}\cdot\mathbf{D}_j}{\varepsilon_j-\varepsilon_k}\quad(k\neq j) \tag{18}$$

$$\mathbf{D}_j\cdot\delta\mathbf{D}_j\cdot\mathbf{D}_k=\frac{\mathbf{D}_j\cdot\delta\boldsymbol{\alpha}\cdot\mathbf{D}_k}{\varepsilon_j-\varepsilon_k}\quad(k\neq j) \tag{19}$$

From Eqs. 9, 16 and 17,

$$(\mathbf{E}-\mathbf{D}_j)\delta\mathbf{D}_j=\sum_{\substack{k=1\\k\neq j}}^{n}\frac{\mathbf{D}_k\cdot\delta\boldsymbol{\alpha}\cdot\mathbf{D}_j}{\varepsilon_j-\varepsilon_k} \tag{20}$$

$$\delta\mathbf{D}_j(\mathbf{E}-\mathbf{D}_j)=\sum_{\substack{k=1\\k\neq j}}^{n}\frac{\mathbf{D}_j\cdot\delta\boldsymbol{\alpha}\cdot\mathbf{D}_k}{\varepsilon_j-\varepsilon_k} \tag{21}$$

are obtained. These formulae can be transformed to the following formulae by the aid of Eq. 10, that is

$$\delta\mathbf{D}_j\cdot\mathbf{D}_j=\sum_{\substack{k=1\\k\neq j}}^{n}\frac{\mathbf{D}_k\cdot\delta\boldsymbol{\alpha}\cdot\mathbf{D}_j}{\varepsilon_j-\varepsilon_k} \tag{22}$$

$$\mathbf{D}_j\cdot\delta\mathbf{D}_j=\sum_{\substack{k=1\\k\neq j}}^{n}\frac{\mathbf{D}_j\cdot\delta\boldsymbol{\alpha}\cdot\mathbf{D}_k}{\varepsilon_j-\varepsilon_k} \tag{23}$$

After adding Eqs. 22 and 23, we use the relation in Eq. 10, then $\delta\mathbf{D}_j$ is expressed as

$$\delta\mathbf{D}_j=\sum_{\substack{k=1\\k\neq j}}^{n}\frac{\mathbf{D}_j\cdot\delta\boldsymbol{\alpha}\cdot\mathbf{D}_k+\mathbf{D}_k\cdot\delta\boldsymbol{\alpha}\cdot\mathbf{D}_j}{\varepsilon_j-\varepsilon_k} \tag{24}$$

If Eq. 15 is multiplied by $\mathbf{D}_j$ from the left-hand side, the following equation is obtained, that is

$$\mathbf{D}_j\cdot\delta\varepsilon_j=\mathbf{D}_j\cdot\delta\boldsymbol{\alpha}\cdot\mathbf{D}_j \tag{25}$$

Taking the (r, r) element of Eq. 24, we obtain

$$\delta C_r^j=\sum_{\substack{k=1\\k\neq j}}^{n}\frac{C_r^k\sum_t\sum_u C_t^jC_u^k(\delta\alpha)_{tu}}{\varepsilon_j-\varepsilon_k} \tag{26}$$

Similarly, the (r, r) element of Eq. 25 becomes

$$\delta\varepsilon_j=\sum_t\sum_u C_t^jC_u^j(\delta\alpha)_{tu} \tag{27}$$

Now, we define the density matrix $\mathbf{Q}$ as the sum of the partial density matrices, namely,

$$\mathbf{Q}=\sum_{j=1}^{n}\nu_j\mathbf{D}_j=\begin{pmatrix}q_1 & p_{12} & \cdots\cdots & p_{1n}\\ p_{21} & q_2 & \cdots\cdots & p_{2n}\\ \cdots & \cdots & \cdots & \cdots\\ p_{n1} & p_{n2} & \cdots\cdots & q_n\end{pmatrix} \tag{28}$$

where q and p stand for the electron density and the bond order defined by Coulson and Longuet-Higgins and ν_j is the number of electrons in the jth molecular orbital. Then the variation of density matrix is written as

$$\delta\mathbf{Q}=\sum_{j=1}^{n}\nu_j\delta\mathbf{D}_j=\sum_{j=1}^{n}\nu_j\sum_{\substack{k=1\\k\neq j}}^{n}\frac{\mathbf{D}_j\cdot\delta\boldsymbol{\alpha}\cdot\mathbf{D}_k+\mathbf{D}_k\cdot\delta\boldsymbol{\alpha}\cdot\mathbf{D}_j}{\varepsilon_j-\varepsilon_k} \tag{29}$$

If we take the (r, r) and the (r, s) elements of Eq. 29, δq_r and δp_{rs} are obtained respectively.

$$\delta q_r=\sum_{j=1}^{n}\nu_j\sum_{\substack{k=1\\k\neq j}}^{n}\frac{2C_r^jC_r^k\sum_t\sum_u C_t^jC_u^k(\delta\alpha)_{tu}}{\varepsilon_j-\varepsilon_k} \tag{30}$$

$$\delta p_{rs}=\sum_{j=1}^{n}\nu_j\sum_{\substack{k=1\\k\neq j}}^{n}\frac{(C_r^jC_s^k+C_s^jC_r^k)\sum_t\sum_u C_t^jC_u^k(\delta\alpha)_{tu}}{\varepsilon_j-\varepsilon_k} \tag{31}$$

The total π-electron energy E is the sum of the orbital energy ε_j, that is

$$E=\sum_{j=1}^{n}\nu_j\varepsilon_j \tag{32}$$

then, from Eq. 27, is expressed as

$$\delta E=\sum_{j=1}^{n}\nu_j\delta\varepsilon_j=\sum_{j=1}^{n}\nu_j\sum_t\sum_u C_t^jC_u^j(\delta\alpha)_{tu} \tag{33}$$

Relations among Theoretical Indexes.— Differentiating $\delta\varepsilon_j$, δE, and δC_r^j with respect to α and β, we obtain the following relations:

$$\frac{\partial\varepsilon_j}{\partial\alpha_r}=(C_r^j)^2 \tag{34}$$

$$\frac{\partial\varepsilon_j}{\partial\beta_{rs}}=2C_r^jC_s^j \tag{35}$$

$$\frac{\partial E}{\partial\alpha_s}=\sum_{j=1}^{n}\nu_j(C_r^j)^2=q_r \tag{36}$$

$$\frac{\partial E}{\partial\beta_{rs}}=2\sum_{j=1}^{n}\nu_jC_r^jC_s^j=2p_{rs} \tag{37}$$

$$\frac{\partial C_r^j}{\partial\alpha_s}=C_s^j\sum_{\substack{k=1\\k\neq j}}^{n}\frac{C_r^kC_s^k}{\varepsilon_j-\varepsilon_k} \tag{38}$$

$$\frac{\partial C_r^j}{\partial\beta_{st}}=\sum_{\substack{k=1\\k\neq j}}^{n}\frac{C_r^k(C_s^jC_t^k+C_t^jC_s^k)}{\varepsilon_j-\varepsilon_k} \tag{39}$$

These equations coincide with those

derived by Coulson and Longuet-Higgins[1]. Similarly, from Eqs. 30 and 31, the following formulae are obtained and these are nothing but the polarizabilities defined by Coulson and Longuet-Higgins[1].

$$\frac{\partial q_r}{\partial \alpha_s} = \sum_{j=1}^{n} \nu_j \sum_{\substack{k=1 \\ k \neq j}}^{n} \frac{2C_r^j C_r^k C_s^j C_s^k}{\varepsilon_j - \varepsilon_k} \tag{40}$$

$$\frac{\partial q_r}{\partial \beta_{st}} = \sum_{j=1}^{n} \nu_j \sum_{\substack{k=1 \\ k \neq j}}^{n} \frac{2C_r^j C_r^k (C_s^j C_t^k + C_t^j C_s^k)}{\varepsilon_j - \varepsilon_k} \tag{41}$$

$$\frac{\partial p_{rs}}{\partial \alpha_t} = \sum_{j=1}^{n} \nu_j \sum_{\substack{k=1 \\ k \neq j}}^{n} \frac{C_t^j C_t^k (C_r^j C_s^k + C_s^j C_r^k)}{\varepsilon_j - \varepsilon_k} \tag{42}$$

$$\frac{\partial p_{rs}}{\partial \beta_{tu}} = \sum_{j=1}^{n} \nu_j \sum_{\substack{k=1 \\ k \neq j}}^{n} \frac{(C_r^j C_s^k + C_s^j C_r^k)(C_t^j C_u^k + C_u^j C_t^k)}{\varepsilon_j - \varepsilon_k} \tag{43}$$

Faculty of Engineering
Kyoto University
Sakyo-ku Kyoto

Rapid Colorimetric Determination of Selenium by the Tin(II)-Strong Phosphoric Acid Reduction Method

By Toshiyasu KIBA, Ikuko AKAZA and Hiroaki HACHINO

(Received November 18, 1958)

With the increasing demand of the electronic industry for selenium, the element has become critically important, and a rapid and accurate method of detecting and determining the element is badly wanted in the field and in the laboratory. Although selenium occurs widely in many geological formations frequently accompanied with minerals containing sulfur, the amount is so small that chemical analysis of the element is one of the most difficult of techniques. The procedures which have been presented by most investigators are of two parts: decomposition of samples with oxidizing acids, and estimation of the selenium in the solution. However, it is really regrettable that in all the methods the decomposition of the samples is time-consuming and loss of the element is likely to occur during the evaporation of the solution or filtration of the undissolved residue.

Previously the authors devised a new powerful decomposing and reducing agent, tin(II)-strong phosphoric acid[1], by which sulfur in inorganic substances such as ores[2] as well as in organic compounds[3,4] could be taken out as hydrogen sulfide and readily estimated iodimetrically or colorimetrically. A further attempt was made by the present authors to reduce selenates, selenites, and elementary selenium to hydrogen selenide by treatment with the same reagent. As the result of the preliminary experiments it was found that selenium in various forms could be reduced to hydrogen selenide at somewhat higher temperatures than in the case of sulfur. By the powerful decomposing power of the reagent even pyrite can readily and completely be decomposed without any other treatment, and the selenium can be separated as gaseous hydrogen selenide from the sample. The present paper describes the investigation by which a new method for quantitative analysis of selenium is established.

1) T. Kiba et al., This Bulletin, **28**, 641 (1955).
2) T. Kiba, I. Akaza and N. Sugishita, ibid., **30**, 972 (1957).
3) S. Ohashi, ibid., **28**, 645 (1955).
4) T. Kiba, I. Akaza and S. Taki, ibid., **30** 482 (1957).

Experimental

Apparatus —The apparatus used in this study is shown in Fig. 1. It is composed of two parts, a reaction vessel (A) and an absorbing part (B). The reaction vessel (A) is a round-bottomed flask of hard glass having a glass cap fitted to its top and provided with inlet and outlet tubes for hydrogen gas. The absorbing part (B) is composed of two test-tubes 3 cm. in diameter. A gas delivery tube (G) is connected with a piece of rubber tubing (R) to the outlet arm of the reaction vessel (A) and inserted into the absorbing solution. A Kipp's apparatus is employed for the production of hydrogen, which is purified by four gas-washing bottles (not shown in the figure) and introduced in the reaction vessel

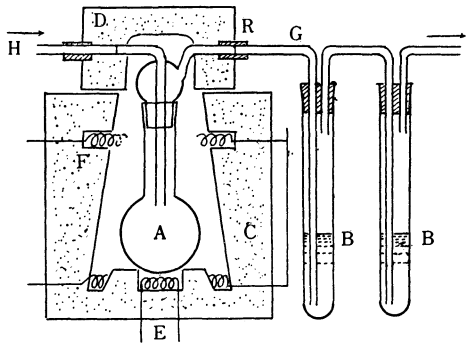


Fig. 1. Apparatus for reduction of selenium and absorption of hydrogen selenide.
A: Reaction vessel, a round-bottomed flask
B: Absorbing vessels
C: Block of diatomaceous earth
D: Cover block of diatomaceous earth
E: Electric heater at the bottom
F: Electric heater around the sides
G: Gas-delivery tube
H: Hydrogen gas introduced into A
R: Short piece of rubber tubing

through the inlet arm. The solution used for the purification of hydrogen is described below.

Reagents. — *Strong phosphoric acid.* — Four hundred grams of commercial orthophosphoric acid of extra pure grade (d=1.7) is placed in a 300 ml. conical beaker, and dehydrated by heating on a 500 W hot plate until a thermometer dipped in the liquid indicates 300°C. If the heating takes too long the liquid will become turbid and viscous and useless for the purpose in view. During the heating, the water vapor and the mist of phosphoric acid coming off should be rapidly removed from the neighborhood of the liquid surface through a glass tube, one end of which is held near the liquid surface, the other end being connected to a suction pump. It saves much time in the dehydration.

Tin(II)-strong phosphoric acid.—Fifty grams of tin(II)-chloride dihydrate of extra pure grade is placed in a 300 ml. conical beaker and on it is poured 250 g. of the strong phosphoric acid prepared as described above. The content is heated to 300°C within about 30 min. in the manner of preparation of strong phosphoric acid. After cooling, the tin(II)-strong phosphoric acid thus obtained, a very viscous and possibly slightly turbid liquid, may be stored in a closed vessel.

Tin(II)-chloride solution.—15% in 9 N hydrochloric acid.

Gum arabic solution.—1% aqueous solution.

Hydrogen gas.—Hydrogen gas produced in the Kipp's apparatus is purified by passing through four gas washing bottles containing respectively, water, 1% potassium permanganate in 10% sodium carbonate solution, 2% vanadium(II) sulfate in 6 N sulfuric acid solution, and 5% barium chloride, and is introduced into the reaction vessel through a glass tube in which a copper net is placed to prevent accidental explosion of the gas.

Standard selenious acid solution. — Elementary selenium is dissolved in concentrated nitric acid and evaporated to dryness, and the selenious acid thus formed is sublimed by gentle heating in another vessel. The sublimate is collected and dissolved in water to make a solution containing 3 mg. of selenium in 1 ml. The solution is diluted to a suitable concentration for the following experiments.

Pyrite ore. — Natural pyrite from the Ogoya Mine near Kanazawa City was ground to 200 mesh size and used as a sample to test the procedure established by the present authors.

Other reagents were all of the pure chemical grade and the utensils were of the ordinary kind for the laboratory.

Procedure.—(1) *Decomposition of samples and evolution of hydrogen selenide.*—Take an accurately measured sample—pipet a solution; weigh a solid—containing selenium and put it into the reaction vessel (A, in Fig. 1). The volume of the vessel should be varied according to the amount of the sample to be analyzed. Evaporate to dryness if the sample is a solution. Pour about 10 to 50 g. of tin(II)-strong phosphoric acid over the sample. Put 5 to 10 ml. of 5 N sodium hydroxide solution into each of the absorbing apparatuses as shown in Fig. 1. Connect all the apparatuses. Pass hydrogen gas very rapidly through the apparatus for five minutes to expel the air from the apparatus. Then reduce the flow of the gas to rate of one bubble per second. Cover the top of the reaction vessel with a block of diatomaceous earth (D) as shown in Fig. 1. Heat the bottom and the sides of the reaction vessel by passing an electric current through nichrome wires placed in the diatomaceous earth blocks (C). The voltage of the current should be regulated by a variable transformer. It is unnecessary to keep the reaction temperature constant, but it should be high enough that the content of the reaction vessel seems to be solidified when cooled after the reaction. After about twenty or thirty minutes the heating is stopped.

Disconnect the absorbing vessels from the gas-outlet arm of the reaction vessel, and transfer the contentin to a 100 ml. Erlenmeyer flask with sufficient washings of the gas-delivery tube. Add 30% hydrogen peroxide solution carefully, drop by drop, since when a relatively large amount of sulfur is present the oxidation takes place explosively. By the above treatment hydrogen selenide is oxidized to selenic acid, and hydrogen sulfide to sulfuric acid. Boil the solution for about ten minutes to decompose the residual hydrogen peroxide completely, and cool the solution by dipping the vessel in running water. Add enough concentrated hydrochloric acid to neutralize the sodium hydroxide and 20 ml. in excess to the solution. Boil the contents for about twenty minutes

with a reflux. By this treatment the selenic acid is reduced to selenious acid, whereas the sulfuric acid remains unchanged.

(2) *Photometric determination of selenium.*—Transfer the content of the flask into a 100 ml. measuring flask, put 4 ml. of gum arabic solution in it, and add water to make the total volume about 95 ml. Place the vessel in a thermostat kept at 45°C, and when the temperature of the liquid has become constant, add 5 ml. of the tin(II) chloride solution and leave the vessel in the thermostat for about twenty minutes. Then, the selenious acid will have been reduced to colloidal elementary selenium having a red color. Add more water till the liquid level comes to the mark, and measure the absorbancy of the solution with a photoelectric colorimeter using a 372 mμ-filter and 10 mm.-cells.

A working curve for the colorimetric measurement should be prepared by carrying out the same procedure with known amounts of selenious acid.

Results and Discussion

Reduction of Selenious Acid by the Tin(II)-Strong Phosphoric Acid.—A definite volume of the standard selenious acid solution was placed in the reaction vessel and the reduction of the acid and the evolution of hydrogen selenide were carried out by the procedure. The recovery of the selenium is satisfactory as shown in Table I, 0.1 to 2.5 mg. of selenium being recovered with relative deviation not exceeding 5%.

TABLE I. RECOVERY OF SELENIUM BY THE METHOD

Se Taken[a]	Number of Experiment	Se Found (Average) mg.	Standard Deviation
0.094	4	0.096	0.004_5
0.305	4	0.308	0.012_3
0.471	4	0.465	0.001_7
1.016	4	0.99	0.05_4
1.52	4	1.48	0.03_6
2.03	4	2.04	0.06_7
2.54	4	2.54	0.05_0

a) Selenium was taken as selenious acid.

TABLE II. RECOVERY OF SELENIUM IN PRESENCE OF SULFUR

Na_2SO_4 Taken g.	Se Taken mg.	Se Found mg.	Recovery of Se %
0.2	0.102	0.103	100.9
0.3	0.305	0.314	102.9
0.2	0.508	0.508	100.0
0.2	1.02	1.00	98.0
0.2	1.52	1.48	97.4
0.2	2.03	1.98	97.5
0.2	2.54	2.47	97.3
0.8	0.508	0.508	100.0

Determination of Selenium in Presence of Sulfur.—As selenium is often accompanied with a larger amount of sulfur, it was deemed necessary that the effect of sulfur on this method be first examined. A mixed solution of sodium sulfate and sodium selenite in various ratios was employed for the test, and the determination of the selenium was done according to the procedure described above. The results are shown in Table II, from which it is confirmed that the presence of forty to two hundred parts of sulfur for one part of selenium does not interfere with the determination of the latter. When still larger amounts of sulfur are present in the sample, larger amounts of the tin(II)-strong phosphoric acid should be employed to decompose the sample and to remove the sulfur as hydrogen sulfide. In such cases, a larger amount of the absorbing solution of sodium hydroxide should be used.

Determination of Selenium in Presence of Sulfur and Iron.—Before the method is applied to the determination of selenium in a sulfur-containing ore such as pyrite, the effect of iron should be first examined by carrying out the procedure with a synthetic sample. The analysis was performed with a mixed solution of iron(III) sulfate and sodium selenite for this purpose. As shown in Table III, iron has no influence on the determination of selenium. So the procedure presented above may safely be applied to the determination of selenium in pyrite.

TABLE III. RECOVERY OF SELENIUM IN PRESENCE OF IRON(III) SULFATE

$Fe_2(SO_4)_3$ Taken	Se Taken mg.	Se Found mg.
0.4	0.102	0.102
0.4	2.54	2.54
0.4	0.508	0.504

Determination of Selenium in Pyrite.—As all the sulfur and the selenium in the ore could be removed as hydrogen sulfide and hydrogen selenide, respectively, all troublesome treatments such as the dissolving of the ore in nitric and hydrochloric acids and the evaporation of the solution were dispensed with by a single treatment with the tin(II)-strong phosphoric acid. The results obtained by this method are tabulated in Table IV, which are in good agreement with the results obtained by the ordinary acid-dissolving

TABLE IV. ANALYSIS OF SELENIUM IN PYRITE

(a) TIN(II)-STRONG PHOSPHORIC ACID REDUCTION METHOD

Pyrite Taken g.	Se Found mg.	Se Found p.p.m.
1.24	0.111	89
1.03	0.093	90
2.05	0.187	91
2.01	0.178	89
3.02	0.271	90
2.99	0.258	86

(b) HYDROCHLORIC-NITRIC ACID DECOMPOSITION METHOD

Pyrite Taken g.	Se Found mg.	Se Found p.p.m.
10.0	0.843	84
10.0	0.860	86
10.0	0.868	87

method. This method takes about two hours, while the usual method takes five or more hours.

Color System of Selenium. — Many methods have been described for the colorimetric determination of minute amounts of selenium, e.g., coloration of elementary selenium by reduction with tin(II) chloride or other reducing agents[5], colorization by pyrrol[6], and by diaminobenzidine[7], but the tin(II) chloride method is considered the simplest. So the method was preferred in this study. To determine the optimum operating wavelength for absorption spectrometry of selenium, an absorbancy-wavelength curve was plotted by means of a spectrophotometer (Hitachi Ltd., Model EPU-2). covering the range between 320 and 500 mμ. The conditions of the experiment were the same as those described in the procedure, The curves obtained are shown in Fig. 2, in which it is seen that remarkable absorption takes place in the ultraviolet region, but the absorbancy of the blank, the solution containing no selenium, increases also in the same region. The authors chose 372 mμ as the optimum wavelength, at which the absorbancy of the blank is scarcely perceptible, and the absorbancy obeys Beer's law when the selenium concentration is from 0.1 to 0.25 mg. in 100 ml. The relation between the amount of the

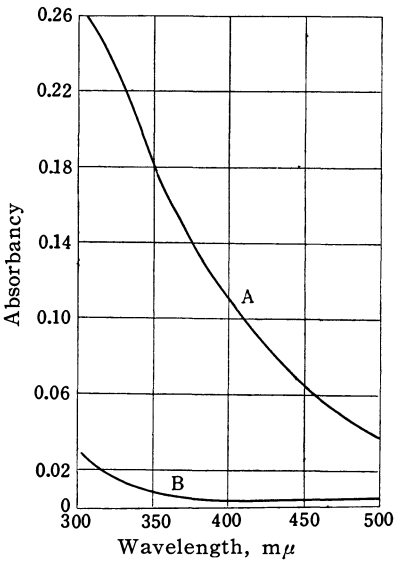


Fig. 2. Spectral absorbance of colloidal selenium.
A: A solution containing 0.6 mg. of selenium, 3 ml. of 15% tin(II) chloride in 9 N hydrochloric acid, and 10 ml. of concentrated hydrochloric acid in 100 ml.
B: The same solution without the selenium.

selenium taken and the absorbancy measured is expressed by the following equation which was computed from twenty-five measurements by the method of least squares

$$x = 3.558\,I$$

where, x is the amount of selenium taken and I the absorbancy measured. A working curve involves a standard deviation of about 1.5%.

Summary

A new procedure for a rapid determination of selenium has been devised by the present authors. Tin(II)-strong phosphoric acid, previously prepared by the authors, has a remarkable decomposing and reducing power, and selenium in various forms can be reduced to hydrogen selenide which is evolved as a gas from samples. Sulfur in various forms is reduced to hydrogen sulfide at the same time. Solid samples such as pyrite can be allowed to decompose rapidly by simple heating with the reagent in an atmosphere of hydrogen. The gas evolved is introduced into an absorbing solution of 5 N sodium hydroxide. Then, a small

5) J. Fidler, *Chem. Listy*, **46**, 221 (1952).
6) S. Hirano, M. Suzuki and T. Noguchi, *J. Chem. Soc. Japan, Ind. Chem. Sec. (Kogyo Kagaku Zasshi)*, **55**, 514 (1952).
7) K. L. Cheng, *Anal. Chem.*, **28**, 1738 (1956).
8) H. Goto et al., *Sci. Repts. Research Inst. Tohoku Univ.*, **A, 4**, 28 (1952);**4**, 121 (1952);**5**, 34 (1953); **7**, 23 (1955).

volume of 30% hydrogen peroxide solution is added. Thus sodium selenate and sodium sulfate are formed in the solution. After adding an excess of concentrated hydrochloric acid and boiling for about twenty minutes with a reflux condenser, the selenic acid is reduced to selenious acid, while the sulfuric acid remains unchanged. The solution is kept at 45°C for several minutes, and solutions of gum arabic and tin(II) chloride are added successively. The red color of the elementary selenium is measured at 372 mμ by a photoelectric colorimeter. The recovery of selenium is uniform even in the presence of large amounts of sulfur and iron. The analysis of selenium in pyrite was carried out by this procedure, and the results were in good agreement with those obtained by other methods.

The expense of the present research was met in part by a Grant for Scientific Research from the Ministry of Education, to which the authors' thanks are due.

Department of Chemistry
Faculty of Science
Kanazawa University
Kanazawa

Crystal Structure of 2-Chloro-1-aza-azulene

By Chihiro TAMURA*, Yoshio SASADA and Isamu NITTA

(Received December 2, 1958)

We have studied several crystal structures of the molecules containing a seven-membered carbon ring, such as tropolone hydrochloride, sodium tropolonate and 1-oxa-azulan-2-one[1-7]. As a part of these serial investigation, the present account deals with the crystal structure of 2-chloro-1-aza-azulene, which Professor T. Nozoe and his collaborators kindly supplied us.

Experimental

Crystal and physical data obtained are: 2-Chloro-1-aza-azulene, C_9H_6NCl, m.p. 72~73°C. Monoclinic, $a=16.00\pm0.07$, $b=7.50\pm0.04$, $c=7.03\pm0.03$ Å, $\beta=113.8\pm0.5$°C.

Absent spectra; $(h\,0\,l)$ when h is odd, $(0\,k\,0)$ when k is odd. Space group; $P2_1/a-{}^5_2C_h$. Four molecules per unit cell. Volume of unit cell; 771.9 Å^3. Density (by flotation); 1.40 g.cm^{-3}. Density (calculated); 1.41 g.cm^{-3}. Linear absorption coefficient for Cu K_α radiation,

$$\mu = 37.5\ \text{cm}^{-1}$$

Total number of electrons per unit cell, $F(0\,0\,0)=336$.

Weissenberg photographs were taken at room temperature around the b and c axes, using Cu K_α radiation. The crystals used, which were cut from a large brown block, were square in cross section with rectangular dimensions:

0.05×0.06 cm. for the b axis rotation,

0.06×0.08 cm. for the c axis rotation.

Intensities were estimated by visual comparison with a calibrated scale. The multiple-film technique was used to correlate strong and weak reflexions, ranging in relative intensities from 8000 to 1 for $(h\,0\,l)$ and from 6000 to 1 for $(h\,k\,0)$ reflexions. Reflexions from 102 and 76 planes were observed out of 135 possible $(h\,0\,l)$'s and 143 $(h\,k\,0)$'s respectively. The corrections for polarization and Lorentz factors were made in the usual way, and that for absorption was omitted.

Results

Structure Determination. — The initial step was intended to locate the chlorine atom by computing Patterson functions $P(uw)$ and $P(uv)$. $P(uw)$ showed three broad peaks, of which two overlapped each other. While the possibility that the one peak is due to the interatomic vector between two chlorines can be excluded by the comparison with $P(uv)$, it was impossible to decide which of the remaining two corresponds to the actual

* Present address, Takamine Laboratory, Sankyo Co., Ltd., Shinagawa, Tokyo.

1) Y. Sasada and I. Nitta, *Acta Cryst.*, **9**, 205 (1956).
2) Y. Sasada, K. Osaki and I. Nitta, ibid., **7**, 113 (1954).
3) Y. Sasada and I. Nitta, This Bulletin, **30**, 62 (1957).
4) Y. Sasada, ibid., **32**, 165 (1959).
5) Y. Sasada, ibid., **32**, 171 (1959).
6) Y. Takaki, Y. Sasada and I. Nitta, to be published.
7) K. Furukawa, Y. Sasada and T. Watanabé, to be published.

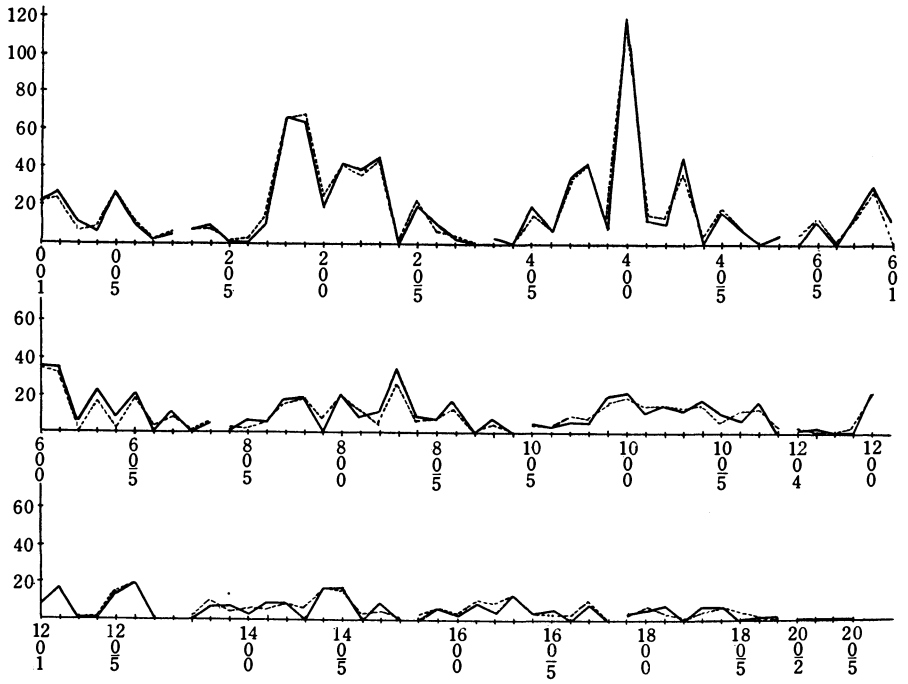


Fig. 1. Observed and calculated structure factors, $F(h\,0\,l)$.
—— $F_{obs.}$, ····· $F_{calc.}$

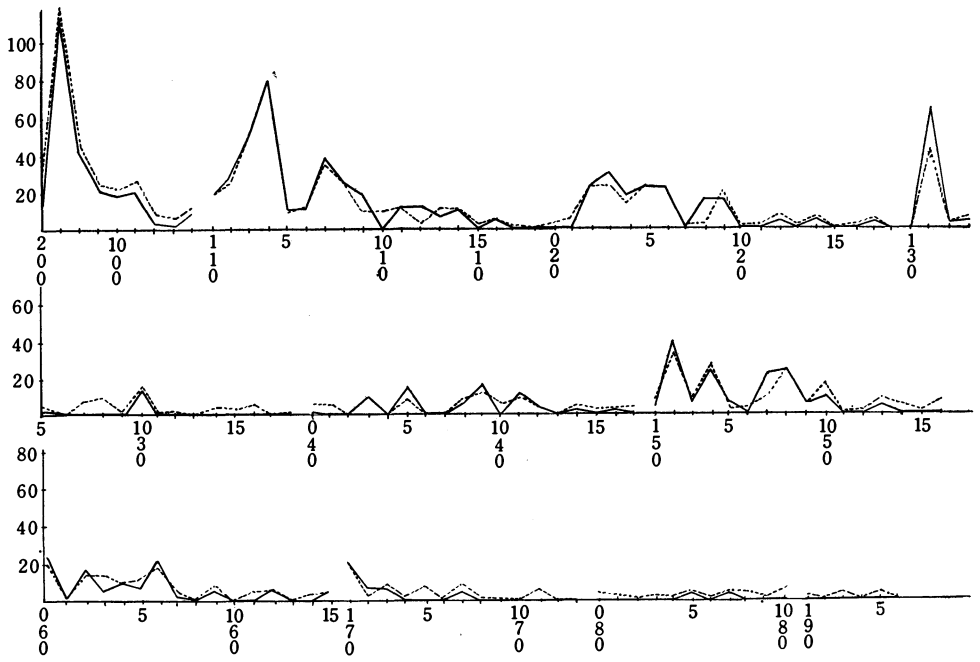


Fig. 2. Observed and calculated structure factors, $F(h\,k\,0)$.
—— $F_{obs.}$, ····· $F_{calc.}$

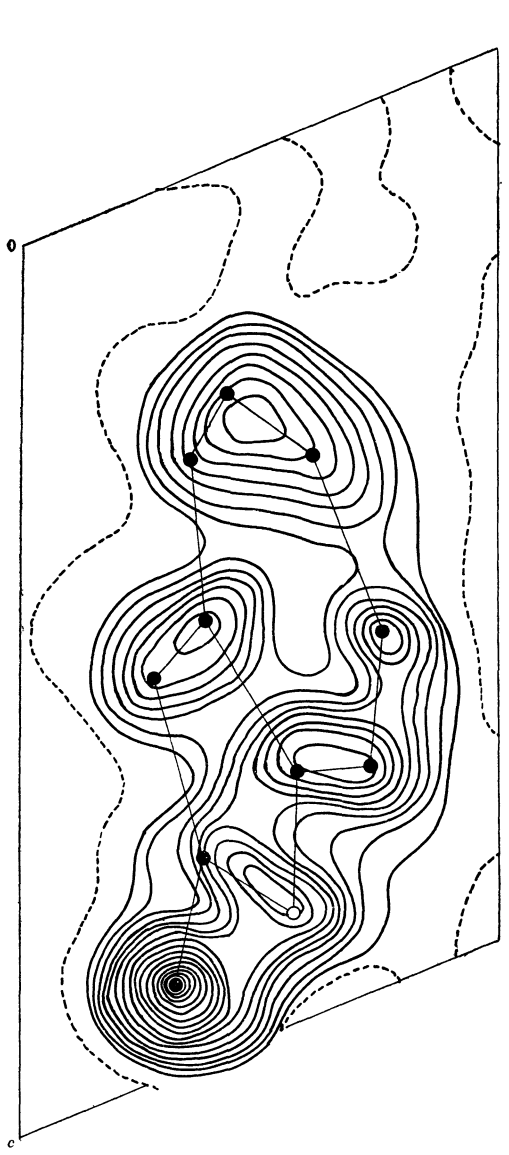


Fig. 3. The final Fourier projection of the electron density along the b axis. Contours at intervals 1 eÅ^{-2}. Contour at 1 eÅ^{-2} is broken.

TABLE I. ATOMIC COORDINATES

Atom	x/a	y/b	z/c
Cl	0.080_5	0.064	0.903
N	0.142	0.401	0.868
C_2	0.097	0.230	0.772
C_3	0.073_5	0.227	0.546
C_4	0.090_5	0.466	0.330
C_5	0.111_5	0.622	0.264
C_6	0.152_5	0.772	0.365
C_7	0.191_5	0.798	0.603
C_8	0.187	0.657	0.758
C_9	0.147	0.494	0.715
C_{10}	0.097	0.390	0.510

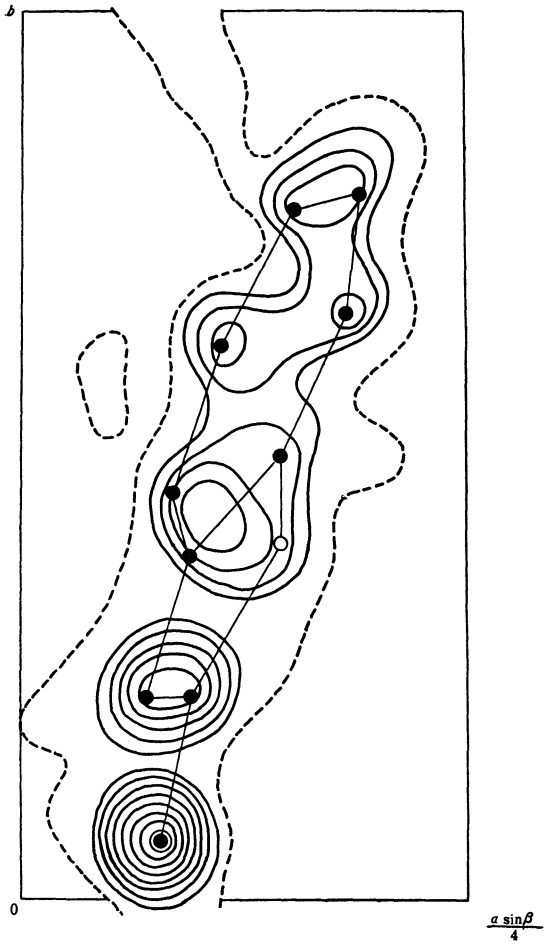


Fig. 4. The final Fourier projection of the electron density along the c axis. Contours at intervals of 2 eÅ^{-2}. Contour at 2 Å^{-2} is broken.

Cl–Cl vector. Therefore, the trial method was applied to $(h\,0\,l)$ first, in order to obtain the x and z coordinates of all atoms. After satisfactory x and z coordinates were determined, y coordinates were estimated by the trial for $(h\,k\,0)$. Refinements of these atomic coordinates were made by successive two-dimensional Fourier and the least square method. The final atomic coordinates of the chlorine, nitrogen and carbon are listed in Table I. Calculated structure factors $F(h\,0\,l)$ and $F(h\,k\,0)$ are shown with broken lines in comparison with observed values (full lines) in Figs. 1 and 2 respectively. In the structure-factor calculations the atomic scattering factors were taken from McWeeny's paper[8], the values for "valence states" being used for carbon. The best B factors were 3.5 and 4.5 Å^2 for $(h\,0\,l)$ and $(h\,k\,0)$

8) R. McWeeny, *Acta Cryst.*, **4**, 513 (1951).

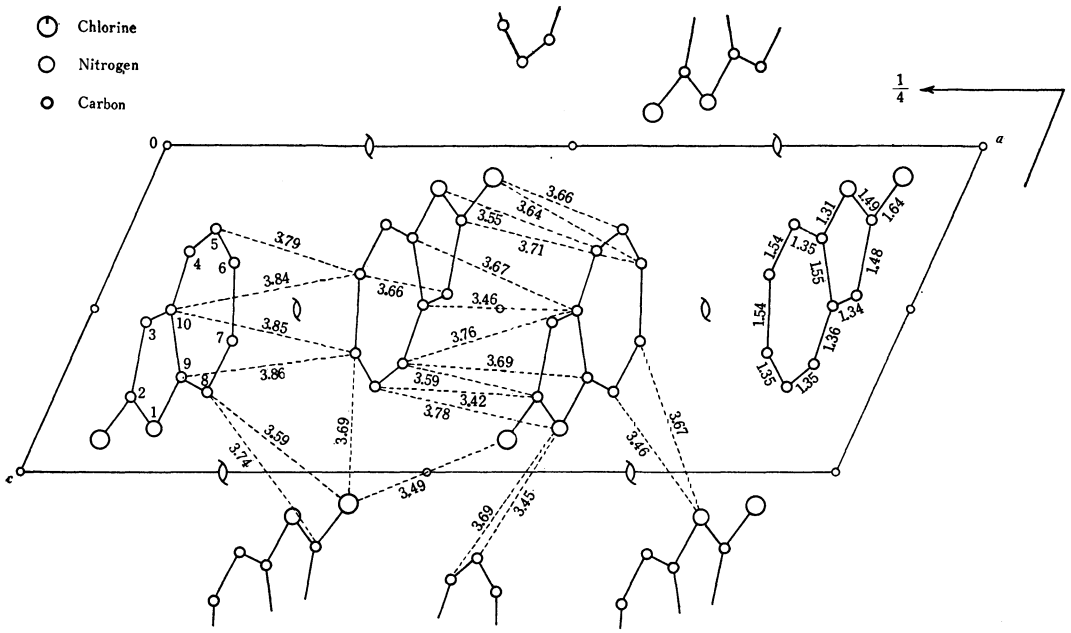


Fig. 5. Arrangement of molecules in the (010) projection, with intra- and intermolecular distances (Å).

respectively. At this stage, R indices become 0.176 for (h 0 l) and 0.231 for (h k 0), if non-observed reflexions are omitted. The electron density projections along the b and c axes are shown in Figs. 3 and 4 respectively.

Description of the Structure.—As the scattering factors modified by thermal coefficients for nitrogen and carbon are hardly different, it is difficult at the earlier stage of analysis to decide which of the atoms, 1 or 3 numbered as shown in Fig. 5 corresponds to the nitrogen. If the atom at 3-position is nitrogen, the R index for (h 0 l) becomes 0.185. On the other hand, if the atom at 1-position is nitrogen, the R index is 0.176 as described in the preceding paragraph. Moreover, the intermolecular distances show that the atom at 1-position has the near approaches to neighboring molecules such as 3.45 and 3.46 Å, which seem unreasonable for the CH–CH contacts. Thus it may be concluded that the atom at the 1-position is nitrogen.

Molecular dimensions (shown in Fig. 5) can not be discussed in detail in view of the rather large standard deviations of the coordinates.

Crystal structure projected along the b axis is shown in Fig. 5. There are no large discrepancies from the ordinarily accepted range of values for the intermolecular approaches. The long and short axes of the molecule make angles of about 50° and 30° with the (0 1 0) plane respectively. An outline of the molecular arrangement in this crystal seems to be of the intermediate type between those in azulene[9] and 1-oxa-azulan-2-one[4,5].

The authors wish to express their sincere thanks to Professor T. Nozoe for supplying the sample and for his continued interest.

Faculty of Science
Osaka University
Kita-ku, Osaka

9) J. M. Robertson, H. M. M. Shearer, G. A. Sim and D. G. Watson, *Nature*, 182, 177 (1958).

*Thermodynamic Studies on Cobalt Complexes. II. Solubility and Standard Free Energy of Formation of $[CoA_6]$-type Salts**

By Motoshichi MORI, Ryokichi TSUCHIYA and Yasuhiro OKANO

(Received August 8, 1958)

Although there are numerous investigations on the cobalt complexes, very few reports[1] have been published on the solubility of these complexes determined at different temperatures, and consequently neither the calculations of the heat of solution have been made nor the discussions from the view point of thermodynamics have been carried on.

In the present study the solubilities of hexamminecobalt(III) complexes in water were determined at various temperatures, and on the basis of these data and from the activity coefficient of hexamminecobalt(III) chloride reported in the preceding paper[2] the heat of solution and the free energy change of the solution were calculated. By using the latter and the standard free energy of formation of the hexamminecobalt(III) ion already known, the standard free energy of formation was calculated for solid hexamminecobalt(III) chloride, bromide, nitrate and perchlorate.

Experimental

Hexamminecobalt(III) chloride was prepared by Bjerrum's method[3]. Hexamminecobalt(III) bromide, nitrate and perchlorate were precipitated from the aqueous solution of the chloride by adding ammonium bromide, nitric acid and perchloric acid, respectively.

Sufficient amount of the sample and water to form the saturated solution was poured into a flask, which was dipped into the thermostat at the desired constant temperature. After the equilibrium of the solution was attained, an aliquot of the solution was taken out through asbestos by a measuring pipette and the solubility was calculated by analyzing the cobalt content of the solution by iodometry[4].

By measuring the specific gravity of the saturated solution by a hydrometer at each temperature the molality m was calculated by means of the following formula,

$$m = 1000C/(1000d - CM)$$

where C is the molar concentration, d, the specific gravity of saturated solution and M, the molecular weight of the solute.

Results

The results obtained for the hexamminecobalt(III) chloride, bromide, nitrate and perchlorate are summarized in Tables I, II, III and IV, respectively.

In the Tables I—IV, $\gamma_\pm$ is the mean activity coefficient of the complex and K is the equilibrium constant of the solution. The methods of the calculation of them are given in the following discussion.

Discussion

Hexamminecobalt(III) Chloride.—When the hexamminecobalt(III) chloride is dissolved into water the change is expressed by,

$$[Co(NH_3)_6]Cl_3(s) = [Co(NH_3)_6]Cl_3(aq.\ a)$$
$$= [Co(NH_3)_6]^{3+}(aq.) + 3Cl^-(aq.)$$

If the activities of the complex salt, the complex cation and the anion in the solution are expressed by $a_{[Co(NH_3)_6Cl_3]}$, $a_{[Co(NH_3)_6]^{3+}}$ and a_{Cl^-} respectively, and the activity coefficients of the complex cation and the anion by $\gamma_{[Co(NH_3)_6]^{3+}}$ and γ_{Cl^-}, the equilibrium constant of the solution, K, is given as follows:

$$K = a_{[Co(NH_3)_6]Cl_3} = a_{[Co(NH_3)_6]^{3+}} \cdot a^3_{Cl^-}$$
$$= (m\gamma_{[Co(NH_3)_6]^{3+}})(3m\gamma_{Cl^-})^3$$
$$= 27m^4\gamma_{[Co(NH_3)_6]^{3+}} \cdot \gamma^3_{Cl^-} \quad (1)$$

When the mean activity coefficient of the salt is expressed by $\gamma_\pm$, the formula 1 is replaced by

$$K = 27m^4\gamma^4_\pm \quad (1')$$

In order to calculate K, it is necessary to know the mean activity coefficient of the hexamminecobalt(III) chloride in each molality. It was obtained by interpolation

* Read at the 11th Annual Meeting of the Chemical Society of Japan, held in April, 1958.

1) J. N. Brönsted and Agnes Petersen, *J. Am. Chem. Soc.*, **43**, 2265 (1921).

2) M. Mori and R. Tsuchiya, *J. Chem. Soc. Japan, Pure Chem. Sec. (Nippon Kagaku Zasshi)*, **79**, 1164 (1958).

3) W. C. Fernelius, "Inorganic Syntheses," Vol. II, (1946), p. 216

4) M. Mori and M. Shibata, *J. Chem. Soc. Japan, Pure Chem. Sec. (Nippon Kagaku Zasshi)*, **75**, 1044 (1954).

TABLE I. SOLUBILITY OF HEXAMMINECOBALT(III) CHLORIDE

Temp.(°C)	Solubility C	Molality m	$1/T\times10^3$	$\gamma_\pm$	$K\times10^5$	log K
10	0.2018	0.2073	3.534	0.1371	1.763	$\bar{5}$.2463
15	0.2336	0.2411	3.472	0.1276	2.417	$\bar{5}$.3833
20	0.2659	0.2758	3.413	0.1194	3.173	$\bar{5}$.5015
25	0.2915	0.3033	3.356	0.1143	3.898	$\bar{5}$.5908
30	0.3289	0.3446	3.300	0.1079	5.159	$\bar{5}$.7126
35	0.3557	0.3741	3.247	0.1045	6.308	$\bar{5}$.7999

TABLE II. SOLUBILITY OF HEXAMMINECOBALT(III) BROMIDE

Temp.(°C)	Solubility C	Molality m	$1/T\times10^3$	$\gamma_\pm$	$K\times10^7$	log K
10	0.04487	0.04503	3.534	0.2749	6.338	$\bar{7}$.8020
15	0.05161	0.05199	3.472	0.2607	9.112	$\bar{7}$.9596
20	0.05916	0.05986	3.413	0.2447	12.43	$\bar{6}$.0944
25	0.06678	0.06788	3.356	0.2304	16.15	$\bar{6}$.2082
30	0.07450	0.07607	3.300	0.2189	20.75	$\bar{6}$.3172

TABLE III. SOLUBILITY OF HEXAMMINECOBALT(III) NITRATE

Temp.(°C)	Solubility C	Molarity m	$1/T\times10^3$	$\gamma_\pm$	$K\times10^7$	log K
10	0.03153	0.03137	3.534	0.3252	2.924	$\bar{7}$.4660
15	0.04129	0.04146	3.472	0.2885	5.526	$\bar{7}$.7424
20	0.05096	0.05138	3.413	0.2620	8.865	$\bar{7}$.9477
25	0.06169	0.06248	3.356	0.2390	13.42	$\bar{6}$.1278
30	0.07103	0.07225	3.300	0.2230	18.29	$\bar{6}$.2622

TABLE IV. SOLUBILITY OF HEXAMMINECOBALT(III) PERCHLORATE

Temp.(°C)	Solubility C	Molality m	$1/T\times10^3$	$\gamma_\pm$	$K\times10^8$	log K
10	0.01344	0.01342	3.534	0.4494	3.570	$\bar{8}$.5526
15	0.01651	0.01652	3.472	0.4189	6.191	$\bar{8}$.7918
20	0.02032	0.02039	3.413	0.3865	10.41	$\bar{7}$.0175
25	0.02539	0.02556	3.356	0.3544	18.17	$\bar{7}$.2595
30	0.03207	0.03240	3.300	0.3205	31.39	$\bar{7}$.4968

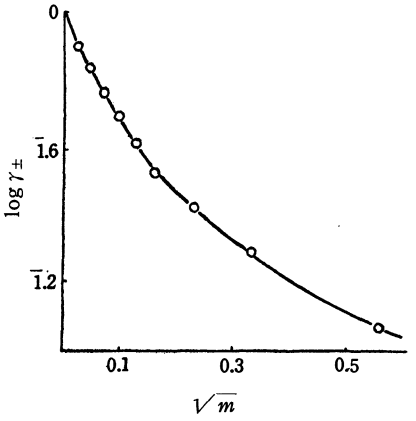


Fig. 1. The mean activity coefficient of hexamminecobalt(III) chloride.

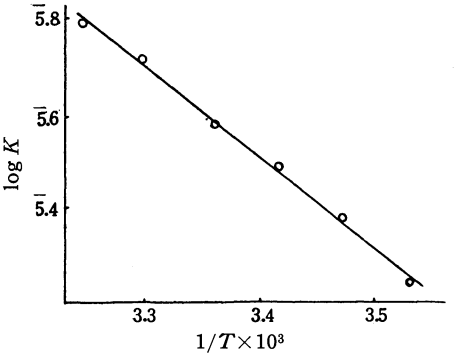


Fig. 2. The relationship between the equilibrium constant and the temperature for hexamminecobalt(III) chloride.

and extrapolation of the curve in Fig. 1 obtained in the preceding paper[2] which gave the relationship between the mean activity coefficient and the molality for hexamminecobalt(III) chloride. The logarithm of K calculated by the formula 1 and given in Table I is plotted against the reciprocal of the absolute temperature in Fig. 2, which shows an almost straight line. By the least square method the equation of this straight line is computed as follows:

$$\log K = 1.8823 - 1873/T \qquad (2)$$

From the inclination of this straight

line or the coefficient of $1/T$, the heat of solution is obtained as $\Delta H=8567$ cal.

As the heat of solution, the value of 9.0 kcal. was determined calorimetrically[5]; this value is in good agreement with our value.

By Kapustinskiĭ[6], the lattice energy of a complex salt was given by,

$$U_{ca}=287.2\frac{\Sigma n\cdot z_1\cdot z_2}{r_1+r_2}\left(1-\frac{0.345}{r_1+r_2}\right) \quad (3)$$

where n is the number of ions dissociated, z_1 and z_2 are the charges of cation and anion, and r_1 and r_2 are the radii of cation and anion, respectively. By Fajans[7], the heat of solution, L, was given by,

$$L = L_1 + L_2 - U_{ca} \quad (4)$$

in which L_1 and L_2 are the heat of hydration of cation and anion. By using these two formulae 3 and 4, the heat of solution of hexamminecobalt(III) chloride is calculated as $\Delta H=13.53$ kcal., which is a little larger than the value, 8567 cal., calculated from the solubility data.

From the heat of formation of solid hexamminecobalt (III) chloride, $\Delta H=-274.1$ kcal.[5], that of the hexamminecobalt(III) ion in unit activity, $\Delta H=-146$ kcal.[8], and that of chloride ion in unit activity, $\Delta H=-40.023$ kcal.[9], given in the literature, the heat of solution of this complex salt can also be calculated as $\Delta H=8031$ cal., which is again in agreement with the value 8567 cal. calculated above.

The standard free energy change of the solution, $\Delta G°$, is computed by the following formula using the value of K given in formula 2,

$$\Delta G° = -RT\ln K = 8567 - 8.61T \quad (5)$$

Values of the standard free energy change of solution at 25°C (298°K), $\Delta G°_{298}=6003$ cal. and the entropy change of solution at 25°C, $\Delta S°_{298}=8.61$ e. u. are obtained; these formulae have never before been found in the literature.

As the standard free energy of formation of the hexamminecobalt(III) ion at 25°C the value of $\Delta G°_{298}=-54.5$ kcal.[10] was already known. By using this value and the heat of formation of this ion, $\Delta H=-146$ kcal.[8], the standard free energy of formation of the ion as the function of temperature is calculated as,

$$\Delta G° = -146000 + 307T \quad (6)$$

From the formulae 5 and 6 and the standard free energy of formation of chloride ion in unit activity, that of hexamminecobalt(III) chloride in the solid state is calculated as

$$\Delta G° = -274660 + 402.9T$$

and the value of $\Delta G°_{293}=-154.55$ kcal. is obtained.

Hexammincobalt(III) Bromide. — The change when the hexamminecobalt(III) bromide was dissolved into water is expressed by,

$$[Co(NH_3)_6]Br_3(s) = [Co(NH_3)_6]Br_3(aq.\ a)$$
$$= [Co(NH_3)_6]^{3+}(aq.) + 3Br^-(aq.)$$

The equilibrium constant of the solution, K, is deduced in the same manner as in the formula 1, if m and $\gamma_\pm$ are replaced by those of the bromide.

If the activity coefficients of the above cation and anion are expressed by γ_+ and γ_-, the mean activity coefficient of the salt, $\gamma_\pm$, is given by $\gamma_\pm=\sqrt[4]{\gamma_+\cdot\gamma_-^3}$. As the activity coefficient of the bromide ion is the same as that of the chloride ion according to Kielland's table[11], the mean activity coefficient of the hexamminecobalt-(III) bromide is assumed to be the same as that of the chloride. Then the value in each molality was obtained by the interpolation of the curve for hexamminecobalt(III) chloride shown in Fig. 1. By using this $\gamma_\pm$ and the molality determined

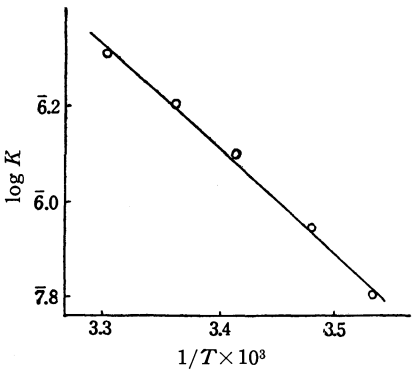


Fig. 3. The relationship between the equilibrium constant and the temperature for hexamminecobalt(III) bromide.

5) K. B. Yatsimirskiĭ and L. L. Pankowa, *Zhur. Obshchei Khim.*, 19, 617 (1949); K. B. Yatsimirskiĭ, "Thermochemie von Komplexverbindungen", Akademie-Verlag, Berlin (1956), p. 162.
6) A. F. Kapustinskiĭ, *Zhur. Obshchei Khim.*, 13, 497 (1943); K. B. Yatsimirskiĭ, "Thermochemie von Komplexverbindungen", Akademie-Verlag, Berlin (1956), p. 14.
7) K. B. Yatsimirskiĭ, ibid., (1956), p. 44.
8) K. B. Yatsimirskiĭ, ibid., (1956), p. 161.
9) F. D. Rossini, D. D. Wagman, W. H. Evans, S. Levine and I. Jaffe, "Selected Values of Chemical Thermodynamic Properties", United States Government Printing Office, Washington, D. C. (1952), p. 21.
10) A. B. Lamb and A. T. Larson, *J. Am. Chem. Soc.*, 42, 2038 (1920).
11) J. Kielland, ibid., 59, 1675 (1937).

from the solubility measurement, the equilibrium constant K given in Table II was calculated.

The plots of $\log K$ against the reciprocal of the absolute temperature are shown as a straight line in Fig. 3, and the equation of the straight line is calculated by the least square method as

$$\log K = 2.1911 - 2378/T \qquad (7)$$

From this equation the heat of solution is obtained as $\Delta H = 10.026$ kcal.

The heat of solution determined calorimetrically is 12.7 kcal.[5] and that calculated by Kapustinskiĭ's formula 3 and Fajans' one 4, is 13.90 kcal., both of which are a little higher than our value, 10.026 kcal. From the heat of formation of hexamminecobalt(III) bromide in the solid state, $\Delta H = -244.5$ kcal.[5], that of the hexamminecobalt(III) ion in unit activity[8] already given and that of the bromide ion in unit activity, $\Delta H = -28.90$ kcal.[12], the heat of solution of the complex bromide is calculated as 11.8 kcal., which is closer to our value 10.026 kcal. than the two former ones, 12.7 and 13.90 kcal.

The standard free energy change of solution is calculated by the formula 7 as

$$\Delta G^\circ = 10026 - 7.56T \qquad (8)$$

and the value of $\Delta G^\circ_{298} = 7772$ cal. and $\Delta S^\circ_{298} = 7.56$ e. u. are obtained.

From the formulae 8 and 6 and the standard free energy of formation of the bromide ion in unit activity, that of hexamminecobalt(III) bromide in the solid state is calculated as

$$\Delta G^\circ = -242726 + 358.09T$$

and the value of $\Delta G^\circ_{298} = -136.12$ kcal. is obtained.

Hexamminecobalt(III) Nitrate.—As the activity coefficient of the nitrate ion is the same as that of the chloride ion according to Kielland's table[11], the mean activity coefficient of the hexamminecobalt(III) nitrate in each molality is obtained in the same way as that for the bromide from Fig. 1, and the equilibrium constant, K, listed in Table III was calculated by the formula 1′.

The plots of $\log K$ against the reciprocal of the absolute temperature are shown in Fig. 4 as a straight line and the equation of the straight line is calculated as

$$\log K = 3.3797 - 2774/T \qquad (9)$$

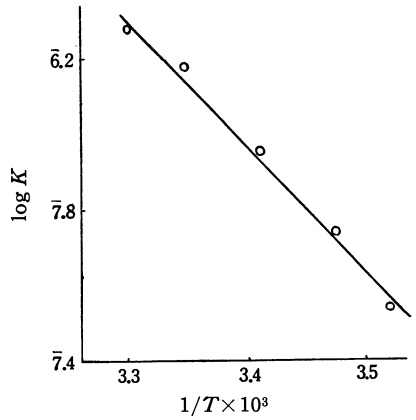


Fig. 4. The relationship between the equilibrium constant and the temperature for hexamminecobalt(III) nitrate.

From this equation, the heat of solution is obtained as $\Delta H = 15.558$ kcal. The value found in the literature[5] is 17.9 kcal. and that which was calculated from the heat of formation of hexamminecobalt(III) nitrate in the solid state, $\Delta H = -311.5$ kcal.[5], that of the hexamminecobalt(III) ion in unit activity[8] already given and that of the nitrate ion in unit activity, $\Delta H = -49.372$ kcal.[13], is 17.384 kcal., both of which are a little higher than our value, 15.558 kcal.

The standard free energy change of solution is calculated by the formula 9 as

$$\Delta G^\circ = 15558 - 25.63T \qquad (10)$$

and the value of $\Delta G^\circ_{298} = 7918$ cal. and $\Delta S^\circ_{298} = 25.63$ e. u. are obtained.

From the formulae 10 and 6 and the standard free energy of formation of the nitrate ion in unit activity, that of hexamminecobalt(III) nitrate in the solid state is calculated as

$$\Delta G^\circ = -309674 + 563.72T$$

and the value of $\Delta G^\circ_{298} = 141.68$ kcal. is obtained.

Hexamminecobalt(III) Perchlorate.—According to Kielland's table[11] the activity coefficient of perchlorate ion is different no more than 0.4% even in the molality of 0.01 from that of the chloride ion. Therefore, the activity coefficient of the hexamminecobalt(III) chloride shown in Fig. 1 was used in the place of that of the perchlorate to calculate the equilibrium constant, K. The values of $\log K$ are plotted against $1/T$ in Fig. 5, and the straight line obtained can be represented by the following equation:

12) F. D. Rossini et al., "Selected Values of Chemical Thermodynamic Properties", United States Government Printing Office, Washington, D. C. (1952), p. 27.

13) F. D. Riossini et al., ibid., (1952), p. 53.

TABLE V. THERMODYNAMIC FUNCTIONS FOR HEXAMMINECOBALT (III) COMPLEXES

Complex salts	Heat of solution	Free energy change of solution	Standard free energy of formation
$[Co(NH_3)_6]Cl_3$	8.567 kcal.	6.003 kcal.	−154.55 kcal.
$[Co(NH_3)_6]Br_3$	10.026	7.772	−136.12
$[Co(NH_3)_6](NO_3)_3$	15.558	7.918	−141.68
$[Co(NH_3)_6](ClO_4)_3$	18.533	9.080	− 71.40

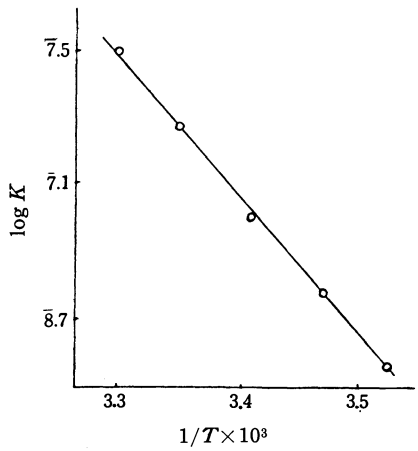


Fig. 5. The relationship between the equilibrium constant and the temperature for hexamminecobalt(III) perchlorate.

$$\log K = 4.0396 - 3226/T \qquad (11)$$

The heat of solution is obtained as $\Delta H=$ 18.53 kcal. The value found in the literature, 22.5 kcal.[14], and that calculated by the equations 3 and 4, 21.54 kcal., are both higher than our value, 18.53 kcal.

The standard free energy change of solution is calculated from 11 as

$$\Delta G^\circ = 18533 - 31.71T \qquad (12)$$

and the value of $\Delta G^\circ_{298}=9080$ cal., and $\Delta S^\circ_{298}=31.71$ e. u. are obtained.

From the formulae 12 and 6 and the standard free energy of formation of the perchlorate ion, that of hexamminecobalt-(III) perchlorate in the solid state is calculated as

$$\Delta G^\circ = - 258763 + 628.96T$$

and the value of $\Delta G^\circ_{298}=-71.46$ kcal. is obtained.

The thermodynamic values obtained for the above four hexamminecobalt(III) salts are summarized in Table V.

As shown in this table, both the heat of solution and the free energy change of the solution become greater in the order of hexamminecobalt(III) chloride, bromide, nitrate and perchlorate. This means that the affinity of these complexes toward water becomes greater in this order. However, the standard free energy of their formation increases in the order of chloride, nitrate, bromide and perchlorate and this means that the thermodynamic stability becomes lower in this order; that is, chloride is the most stable among the above four salts in the solid state.

Summary

The solubilities of hexamminecobalt(III) chloride, bromide, nitrate and perchlorate were measured at 10~35°C. From the solubility measurements the relationships between the equilibrium constant of the solution and the temperature were calculated. The heats of solution calculated from these data agreed approximately with the values given in the literature and those calculated by using formulae of Kapustinskiĭ and Fajans.

The free energy changes of formation of these complexes in the solid state were calculated for the first time. It is concluded from the results that the stability of these salts decreases in the following order:

$[Co(NH_3)_6]Cl_3 > [Co(NH_3)_6](NO_3)_3 > [Co(NH_3)_6]Br_3 > [Co(NH_3)_6](ClO_4)_3$

Department of Chemistry
Faculty of Science
Kanazawa University
Kanazawa

14) A. F. Kapustinskiĭ and K. B. Yatsimirskiĭ, *Zhur. Fiz. Khim.*, 22, 1271 (1948); K. B. Yatsimirsikiĭ, "Thermochemie von Komplexverbindungen", Akademie-Verlag, Berlin (1956), p. 1632.

*Thermodynamic Studies on Cobalt Complexes. III. Thermal Dissociation of Hexamminecobalt(III) Chloride and Chloropentamminecobalt(III) Chloride**

By Motoshichi MORI and Ryokichi TSUCHIYA

(Received September 17, 1958)

Compared with a great number of studies on the reaction of complex salts in the aqueous solution, the investigations on the thermal decomposition of complexes in the solid state are few. These include studies on ammines of cobalt[1,2], nickel[3], platinum[4] and indium[5] and on nitroammines of platinum[6] and cobalt[7,8]. Among these studies the data on dissociation pressure were reported only for cobalt- and nickelammine complexes[1,3] and thermodynamic discussion of them has never been made. For this reason we started the present study and determined the dissociation pressure of hexamminecobalt-(III) chloride and chloropentamminecobalt-(III) chloride. The free energy change of dissociation of the former complex was calculated and the standard free energy of formation of the latter complex was obtained.

Experimental

Hexamminecobalt(III) chloride was prepared by Bjerrum's method[9] and chloropentamminecobalt-(III) chloride, by the method of Jörgensen[10]. The apparatus used for the determination of the dissociation pressure is shown in Fig. 1.

After the sample was put into the reaction vessel, made of heat resistant borosilicate glass, A, the whole apparatus was evacuated. The cocks B and C were closed and the temperature of the electric furnace F was held at the desired constant temperature by an automatic regulator. The dissociation pressure was determined by the manometer M.

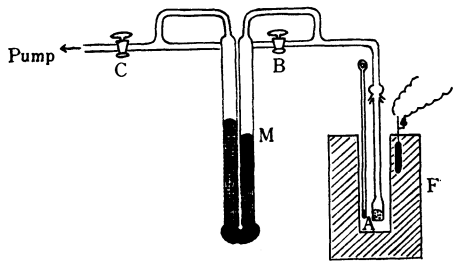


Fig. 1. Apparatus.

Results and Discussion

Dissociation Pressure of Hexamminecobalt(III) Chloride. — The dissociation pressure of hexamminecobalt(III) chloride was measured at several temperatures in the range of 83~173°C. As we found that the decomposition products consist of chloropentamminecobalt(III) chloride and ammonia, but not of cobaltous chloride, the decomposition reaction can be expressed by the following equation,

$$[Co(NH_3)_6]Cl_3(s) = [Co(NH_3)_5Cl]Cl_2(s) + NH_3(g)$$

The values of dissociation pressure determined for hexamminecobalt(III) chloride are listed in Table I.

Biltz[1] reported that the decomposition of hexamminecobalt(III) chloride began at 175~180°C and chloropentamminecobalt-(III) chloride was formed at 216~220°C. Clark et al[2]. reported that the decomposition began at 173°C and ammonium chloride appeared at 181°C. However, we detected the evolution of ammonia at 160°C by passing the decomposition gas into water containing phenolphthalein, and could determine the dissociation pressure at a temperature lower than that pointed out by Biltz[1] and Clark[2].

* Read at the Symposium on Co-ordination Compounds sponsored by the Chemical Society of Japan, held in Nov., 1957.

1) W. Biltz, *Z. anorg. Chem.*, **83**, 177 (1913).
2) G. L. Clark, A. J. Quick and W. D. Harkins, *J. Am. Chem. Soc.*, **42**, 2483 (1920).
3) W. Biltz and B. Fetkenheuer, *Z. anorg. Chem.*, **83**, 163 (1913).
4) A. A. Grinberg and B. V. Ptitzuin, *Izv. Inst. Platin*, **9**, 73 (1932); *Chem. Abstr.*, **27**, 1290 (1933),
5) V. G. Tronev and A. P. Kochetkova, *Khim. Redkikh Elementov, Akad. Nauk S. S. S. R., Inst. Obshchei i Neorg. Khim.*, (1957), No. 3, p. 87; *Chem. Abstr.*, **52**, 2634^b (1958).
6) L. A. Chugaev and S. S. Kil'tuinovich, *Izv. Inst. Platin*, **2**, 70 (1921); *Chem. Abstr.*, **20**, 2961 (1926).
7) A. V. Ablov and N. I. Lobanov, *Zhur. Obshchei Khim.*, **25**, 648 (1955); *Chem. Abstr.*, **49**, 12170^h (1955).
8) A. V. Ablov, E. A. Popa and T. A. Malkova, *Zhur. Neorg. Khim.*, 1,2716 (1956); *Chem. Abstr.*, **50**, 13634^i (1956).
9) W. C. Fernelius, "Inorganic Syntheses", Vol II. McGraw Hill Book Co., Inc., New York, N. Y. (1946), p. 216.
10) S. M. Jörgensen, *Z. anorg. Chem.*, **2**, 281 (1892).

TABLE I. DISSOCIATION PRESSURE OF HEXAMMINECOBALT(III) CHLORIDE

Temp.(°C)	$1/T\times10^3$	Dissociation pressure (mmHg)	$\log p_{mm}$
83	2.808	0.70	−0.1549
92	2.739	1.15	0.0607
102	2.666	1.45	0.1614
114	2.583	2.19	0.3404
124	2.518	2.89	0.4609
129	2.487	3.49	0.5428
133	2.462	3.94	0.5955
138	2.432	4.59	0.6618
143	2.403	5.33	0.7267
149	2.369	6.04	0.7810
153	2.347	6.98	0.8439
158	2.320	7.73	0.8882
162	2.298	8.87	0.9479
168	2.267	10.33	1.0141
173	2.242	12.21	1.0867
176	2.227	14.26	1.1541

Biltz[1] observed 14 mmHg as the dissociation pressure of hexamminecobalt(III) chloride at 174°C, which is relatively close to our value, but he did not measure it at a temperature lower than 174°C. On the other hand, it was found by us that ammonium chloride began to form at about 170°C and the decomposition pressure rapidly increased at higher temperatures.

The logarithm of the dissociation pressure was plotted against the reciprocal of the absolute temperature (Curve a in Fig. 2). The obtained curve is approximately linear except the two points at 173 and 176°C. The equation of the straight line is calculated by the least square method as follows:

$$\log p_{mm} = 5.7705 - 2101.40/T \qquad (1)$$

From this equation the heat of dissociation is obtained as $\Delta H = 9612$ cal.

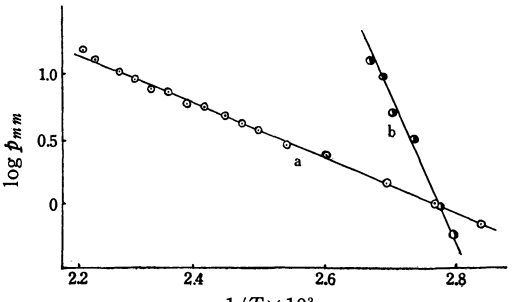


Fig. 2. The relationship between the dissociation pressure and the temperature for
a: hexamminecobalt(III) chloride
b: chloropentamminecobalt(III) chloride.

Biltz[1] obtained the value of about 18 kcal. as the heat of dissociation from his data determined at 174~216°C by means of the Nernst formula, but we recalculated the value of 28 kcal. from his data.

If the value of $\Delta H = 9612$ cal. determined above at the temperature in the range of 83~173°C is assumed to be approximately equal to that at 25°C, it agrees fairly well with the value of 8.56 kcal. calculated from the heats of formation of $[Co(NH_3)_6]Cl_3(s)$, (−274.1 kcal.[11]), $[Co(NH_3)_6Cl]Cl_2(s)$, (−254.5 kcal.[12]) and $NH_3(g)$ (−11.04 kcal.[13]).

The standard free energy change of decomposition calculated by the formula 1 is:

$$\Delta G^\circ = -RT\ln p = 9612 - 13.218T \qquad (2)$$

The values of $\Delta G^\circ_{298} = 5672$ cal. and $\Delta S^\circ_{298} = 13.22$ e. u. are obtained.

The standard free energy of formation of complex salts in the solid state has never been known except that of $[Co(NH_3)_6]Cl_3(s)$, which was calculated by the present authors from the solubility data in the preceding paper[14]. By using this value and the equation 2 the standard free energy of formation of $[Co(NH_3)_5Cl]Cl_2(s)$ in the solid state is calculated to be:

$$\Delta G^\circ = -254008 + 365.99T$$

and the value of $\Delta G^\circ_{298} = -144.90$ kcal. is obtained.

Dissociation Pressure of Chloropentamminecobalt(III) Chloride. — The dissociation pressure of chloropentamminecobalt-(III) chloride was measured by the same apparatus as that shown in Fig. 1. The results are given in Table II.

TABLE II. DISSOCIATION PRESSURE OF CHLOROPENTAMMINECOBALT(III) CHLORIDE

Temp.(°C)	$1/T\times10^3$	Dissociation pressure (mmHg)	$\log p_{mm}$
88	2.769	0.50	−0.3010
93	2.732	1.49	0.1732
96	2.709	3.08	0.4886
99	2.687	5.93	0.7731
101	2.673	9.51	0.9782
103	2.659	12.15	1.0846

11) K. B. Yatsimirskiĭ and L. L. Pankowa, *Zhur. Obshchei Khim.*, **19**, 617 (1949); K. B. Yatsimirskiĭ, "Thermochemie von Komplexverbindungen", Akademie-Verlag, Berlin (1956), p. 162.
12) A. B. Lamb and J. P. Simmons, *J. Am. Chem. Soc.*, **43**, 2188 (1921).
13) F. R. Bichowsky and F. D. Rossini, "Thermochemistry of the Chemical Substances", Reinhold Publishing Corp., New York, N. Y. (1936).
14) M. Mori, R. Tsuchiya and Y. Okano, This Bulletin, **32**, 462 (1959).

Biltz[1] found that chloropentamminecobalt(III) chloride decomposed at 180~220°C, but our results show that the decomposition takes place at a lower temperature. In contrast to hexamminecobalt(III) chloride, the increase of the dissociation pressure of chloropentamminecobalt(III) chloride with the rise of temperature is quite large. In other words, although the dissociation pressure of chloropentamminecobalt(III) chloride is less than that of hexamminecobalt(III) chloride at a temperature lower than 90°C, the thermal dissociation of the former exceeds that of the latter at a temperature higher than 92°C, and the dissociation pressure of the former at 103°C is nearly the same as that of the latter at 173°C. It is concluded from these facts that chloropentamminecobalt(III) chloride is stable at a temperature below 90°C and becomes suddenly unstable at a temperature above 192°C.

The plots of the logarithm of the dissociation pressure against the reciprocal of the absolute temperature give a straight line as shown by the line b in Fig. 2. The equation of the straight line is calculated as follows:

$$\log p_{mm} = 36.4869 - 13288.3/T$$

From this equation as the heat of dissociation the value of $\Delta H = 60.78$ kcal. is obtained. It is in good agreement with the value, 60.84 kcal., which is calculated from the heats of formation of components of the following dissociation reaction,

$$[Co(NH_3)_5Cl]Cl_2(s) = CoCl_2(s) + 1/6\ N_2(g) + NH_4Cl(s) + 11/3\ NH_3(g)$$

$\Delta H_{f[Co(NH_3)_5Cl]Cl_2} = -254.5$ kcal.[12]

$\Delta H_{fCoCl_2} = -77.8$ kcal.[15]

$\Delta H_{fNH_4Cl} = -75.38$ kcal.[13] and

$\Delta H_{fNH_3} = -11.04$ kcal.[13]

The Rate of Thermal Dissociation of Hexamminecobalt(III) Chloride.—The rate of the thermal dissociation of this complex was determined by tracing the pressure change of ammonia produced in the decomposition by the apparatus shown in Fig. 1. The results are shown in Table III and Fig. 3.

The velocity constant k at the time when the dissociation begins to take place is given by the tangent of the velocity curve at zero point in Fig. 3. The plots of logarithm of the velocity constant against the reciprocal of the absolute temperature give a straight line as shown in Fig. 4, from which the value of 17.98

Table III. Rate of dissociation of hexamminecobalt(III) chloride

Temp.(°C)	153	163	173
Time(min.)	Dissociation pressure p mmHg		
3	—	1.05	1.50
5	0.95	1.55	2.35
10	1.65	2.59	3.64
15	2.29	3.14	4.54
20	2.84	3.58	5.18
25	—	3.98	5.53
30	3.14	4.33	5.83
40	3.54	4.98	6.67
50	3.74	5.33	7.32
1(hr.)	3.99	5.58	7.67
1.5	4.44	6.17	9.01
2	4.84	6.47	10.26
2.5	5.13	7.02	10.86
3	5.28	7.42	11.31
4	5.83	—	11.55
k	0.2005	0.3390	0.5220
$\log k$	$\bar{1}.3021$	$\bar{1}.5302$	$\bar{1}.7177$
$1/T\times10^3$	2.347	2.293	2.242

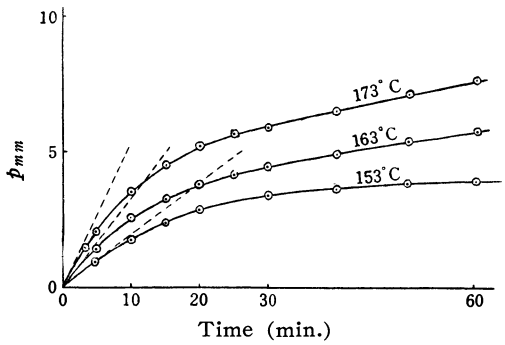


Fig. 3. Rate of dissociation of hexamminecobalt(III) chloride.

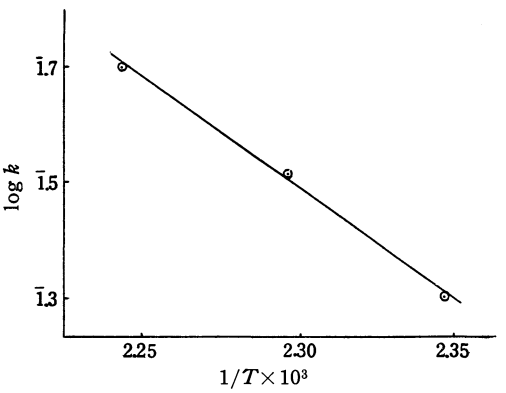


Fig. 4. The relationship between the velocity constant and the temperature for hexamminecobalt(III) chloride.

15) K. Sano, *J. Chem. Soc. Japan, Pure Chem. Sec.* (*Nippon Kagaku Zasshi*), **58**, 370 (1937).

kcal. is obtained as the activation energy of the thermal dissociation of hexamminecobalt(III) chloride.

The Rate of Thermal Dissociation of Chloropentamminecobalt(III) Chloride.— The determination was made by the same method as that used in the above experiment for hexamminecobalt(III) chloride. The results are shown in Table IV and Fig. 5.

The plots of the logarithm of the velocity constant k at the time when the dissociation begins to take place against the reciprocal of the absolute temperature give a straight line as shown in Fig. 6, from which the value of 54.06 kcal. is obtained as the activation energy of the thermal dissociation of chloropentamminecobalt(III) chloride.

TABLE IV. RATE OF DISSOCIATION OF CHLOROPENTAMMINECOBALT(III) CHLORIDE

Temp.(°C)	96	100	103
Time(min.)	Dissociation pressure p mmHg		
2	—	—	0.25
5	—	0.35	0.60
8	—	—	0.90
10	0.40	0.65	1.10
15	—	0.90	1.55
20	0.65	1.10	2.05
25	—	1.30	2.29
30	0.95	1.50	2.49
40	1.10	1.75	3.34
50	1.35	2.00	3.83
1(hr.)	1.44	2.19	4.23
1.5	1.78	2.69	5.78
2	1.93	3.14	6.57
2.5	2.19	3.64	7.42
3	2.45	3.99	8.27
4	2.58	4.29	9.31
k	0.0354	0.0782	0.135
$\log k$	$\bar{2}.5490$	$\bar{2}.8932$	$\bar{1}.1303$
$1/T\times10^3$	2.709	2.680	2.659

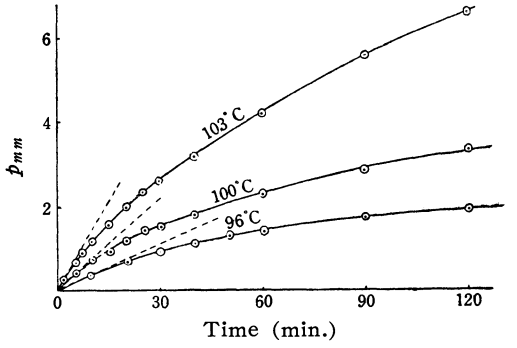


Fig. 5. Rate of dissociation of chloropentamminecobalt(III) chloride.

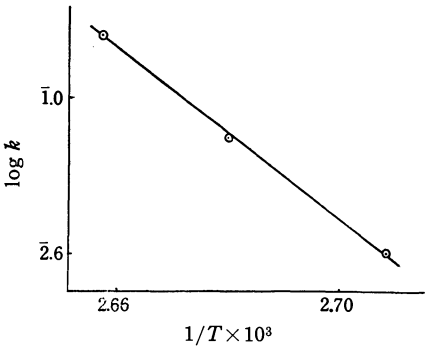


Fig. 6. The relationship between the velocity constant and the temperature for chloropentamminecobalt(III) chloride.

As shown above, the heat of dissociation and the activation energy of chloropentamminecobalt(III) chloride are very high compared with those of hexamminecobalt(III) chloride. These data give an explanation for the fact that chloropentamminecobalt(III) chloride produced in the thermal dissociation of hexamminecobalt(III) chloride does not suffer from further decomposition so far as the latter is present, even if the dissociation pressure of the former is very high.

Summary

1. The thermal dissociation of hexamminecobalt(III) and chloropentamminecobalt(III) chlorides was studied. The heats of dissociation calculated from the the data of dissociation pressure determined are in good agreement with the values calculated from other sources.

2. The free energy change of dissociation of hexamminecobalt(III) chloride was calculated and by combining this value with the standard free energy of formation of that complex previously obtained, the standard free energy of formation of chloropentamminecobalt(III) chloride in the solid state was determined.

3. The rate of the thermal dissociation of hexamminecobalt(III) and chloropentamminecobalt(III) chlorides was determined and the activation energies of the dissociation were calculated.

Department of Chemistry
Faculty of Science
Kanazawa University
Kanazawa

Normal Stress Effects in Polymer Solutions. I. Measurements in a Parallel Plate Instrument

By Mikio TAMURA, Michio KURATA and Tadao KOTAKA

(Received November, 6, 1958)

It is well noted that a visco-elastic fluid under steady shear flow usually generates not only shearing stress but also normal stresses. Thus, the essential requirement for obtaining the complete information for flow behavior of such a fluid is the development of the *goniometry of flow*, or in other words, the development of experimental procedures for the determination of all stress components, i.e., shearing stress and normal stresses[1,2].

In this report, as the first step of the stress-goniometry of flow, we will describe some findings on the normal stress measurements in a parallel plate instrument. Correlations between observed normal pressure and dimension of the instrument, and influences of secondary effects which inevitably arise in the course of measurements will be discussed at some length[3]. Detailed descriptions of the data and their physical interpretations will be published in a subsequent paper[4].

Padden and DeWitt[5], and recently Markovitz and Williamson[6] have suggested that the concentration and temperature dependencies of normal stress should be expressible in terms of "*reduced variables*". These suggestions are tested with the data obtained in our measurements.

Experimental

Instrument and Principles.—A parallel plate instrument used in this study is shown in Fig. 1. The figure itself is self-explanatory. An outer cup containing a test fluid is rotated at a steady speed within the range of 5 to 170 rpm by driving through a pulley and belt system by a 1/2 H. P. induction motor. The rotating bob is held at a distance of one centimeter or less above the cup. The dimensions of two outer cups and three inner bobs used in this study are listed in Table I. When the cup is rotated, the fluid, if it shows the normal stress effect, rises in the manometer tubes mounted on the stationary bob and reaches equilibrium levels. Equilibrium heights of the fluid were read by a travelling microscope. The non-parallelism and the non-concentricity of two plates, especially the former, largely affect the pressure distribution and disturb the quantitative measurements. A con-

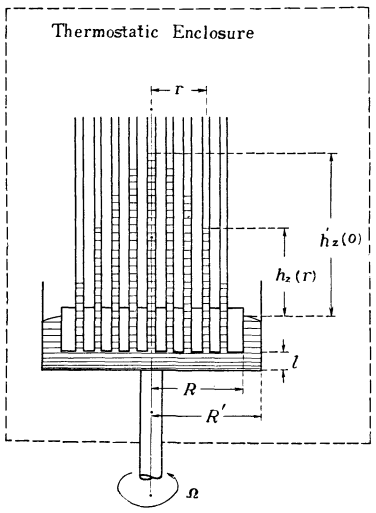


Fig. 1. Schematic diagram of the parallel plate instrument.

TABLE I. DIMENSIONS OF BOBS AND CUPS FOR NORMAL STRESS MEASUREMENTS

	Radius cm.	Manometer tubes		
		Number	Diameter cm.	Spacing cm.
Bob A	5.0	9	0.5	1.0
Bob B	6.5	13	0.2	0.8
Bob C	7.0	15	0.2	0.8
Cup 1	6.0			
Cup 2	8.0			

1) The general review on this subject is obtained in the following article: M. Kurata, "The Weissenberg Effect", in Kobunshi-Jikkengaku-Koza, Vol. V, ed. S. Kambara, Kyoritsu Publishing Co., Tokyo (1958), Chap. 15.

2) See also, A. Jobling and J. E. Roberts, "The Goniometry of Flow and Rupture", in Rheology Vol. II, ed. F. Eirich, Academic Press, New York (1958), Chap. 14.

3) Works of similar nature were developed by Greensmith and Rivlin, but they are different from ours in the standpoint and the approach to the problem. H. W. Greensmith and R. S. Rivlin, *Phil. Trans. Roy. Soc. (London)*, **245**, 399 (1953).

4) T. Kotaka, M. Kurata and M. Tamura, in preparation.

5) F. J. Padden and T. W. DeWitt, *J. Appl. Phys.*, **25**, 1086 (1954).

6) H. Markovitz and R. B. Williamson, *Trans. Soc. Rheology*, **1**, 25 (1957).

dition free from such disturbances is easily attained by making sure that the symmetry in pressure distribution is established and that the pressure values are kept unchanged by clockwise and counterclockwise rotations at the same speed. The temperature at which the measurements were run was roughly controlled within ±1.0°C by a simple thermostatic enclosure.

The normal pressure is correlated to the normal stresses by the relation of force equilibrium in torsional shear flow as follows:

$$-\frac{\partial P_z(r)}{\partial \ln r}=\sigma_{11}-\sigma_{33}+\frac{\partial(\sigma_{22}-\sigma_{33})}{\sigma \ln r} \tag{1}$$

or in the integral form

$$\Delta P_z(r)=P_z(0)-P_z(r)$$
$$=\int_0^r(\sigma_{11}-\sigma_{33})\frac{dr}{r}+\sigma_{22}-\sigma_{33} \tag{2}$$

and

$$P_z(0)-P'=\int_0^R(\sigma_{11}-\sigma_{33})\frac{dr}{r} \tag{3}$$

where $P_z(r)$ denotes the pressure exerted on the stationary bob of radius R at the distance r from the rotating axis, P' denotes the pressure exerted on the fluid in the gap from the outside, σ_{ii} ($i=1,2,3$) denotes the normal stress component parallel to the direction of flow ($i=1$), and perpendicular to the shearing surface ($i=2$), and perpendicular to both ($i=3$), respectively. It should be noted here that in the derivation of the above equations the influences of the centrifugal force, and of disturbances of flow arising from edge effects were all neglected. It is readily seen that, if the state of flow were ideally torsional shear and undesirable disturbances were depressed within the experimental error, the left hand sides of the equations from 1 to 3 should be dependent on the rate of shear, $D=r\Omega/l$, alone. Here r is the distance from the axis, Ω is the angular velocity of rotation and l is the gap between two plates.

Materials.—Solutions of a commercial sodium carboxymethylcellulose (Na-CMC; Harcules, Cellulose Gum Type 70 sp-High) obtained through the courtesy of Dr. H. Inagaki of this University were mainly used in this study. Its molecular weight was about 10^5, and the range of degree of carboxymethylation was from 0.65 to 0.95. The data obtained on the solutions of commercial methylcellulose* (Interchemical, Methocell 4000 cp: $\bar{M}_v\sim10^5$, $D.S.\sim0.92$) in water and polystyrene* (Lustrex Hi-Flow 77, $\bar{M}_v\sim10^5$) in decalin are also described for the sake of comparison.

Results and Discussion

Some Geometrical Studies in a Parallel Plate Instrument.—*$h_z(0)$ vs. Ω Relations: the Centrifugal Force Effect*:—With the combination of bob A and cup 1, we first read $h_z(0)$ against the rotational velocity, Ω, with various gaps, l, on solution of 2g. Na-CMC in 100 ml. water (1.97 wt.%). The results are shown by solid lines in Fig. 2. If the curves of $h_z(0)$ vs. Ω with different l are replotted against the rate of torsion, Ω/l, they fall on a single reduced curve as shown by a broken line in Fig. 2. Close inspection, however, reveals that $h_z(0)$ value begins to deviate below the reduced curve when the rotational speed exceeds about 70~80 rpm irrespective of the gap, l. This tendency should be attributed mainly to the influence of the centrifugal force which repels the fluid outward in a radial direction and also acts as a rotational couple in r-z plane. The exact mathematical treatment of this effect is quite difficult, but in any case, the action of the centrifugal force may lower the $h_z(0)$ values, especially may lower them remarkably at a high velocity. Thus we may conclude that, to eliminate the effect of the centrifugal force, it is preferable to keep the rotational speed below about 70~80 rpm with a cup of this dimension ($R'=6.0$ cm.).

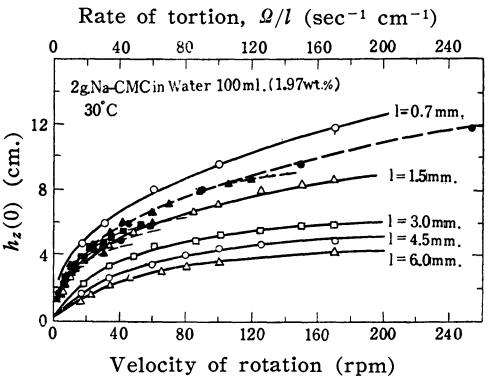


Fig. 2. $h_z(0)$ vs. velocity of rotation (solid lines) and $h_z(0)$ vs. rate of torsion, Ω/l (broken lines); Na-carboxymethylcellulose in water 1.97% at 20°C.

Pressure Distribution on a Stationary Bob: the Edge Effect:—In the derivation of Eqs. from 1 to 3, the influence arising from the side gap was simply replaced by an isotropic term P'. To check the validity of this assumption, measurements were performed with two different combinations of bob A ($R=5.0$ cm.) with cup 1 ($R'=6.0$ cm.), and bob A with cup 2 ($R'=8.0$ cm.) on solutions of Na-CMC-water, and the pressure distributions on the bob were compared. Fig. 3 indicates the pressure distributions, $h_z(r)$, with various velocities.

* Samples of methylcellulose and polystyrene were obtained through the courtesy of Toyo Ink Mfg. Co., Ltd., and Nagase and Co., respectively.

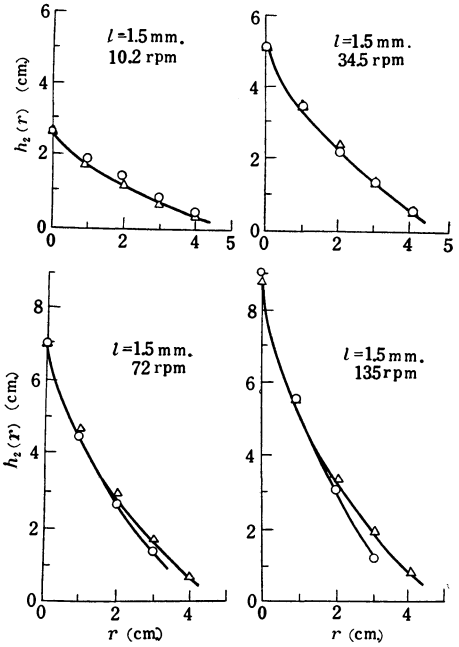


Fig. 3. Pressure distributions on a stationary plate (R=5.0 cm.) with cup 1 (R'=6.0 cm.)···Δ, and cup 2 (R'=8.0 cm.)···0. 1.97wt.%-CMC-water.

It is seen that when the rotational velocity is not so high the pressure distribution, $h_z(r)$, is practically unaffected by the difference in the side gap, but, the higher the velocity becomes (above 70 rpm), the more significant the deviation becomes. The pressure falls more rapidly in the larger cup. The plots of $h_z(0)$ vs. Ω/l, though the data are not shown here, are reduced on a single curve except at high speed and show no indication of edge effect.

Effect Arising from the Finite Size of Accesses of Manometer Tubes.—It might be expected that the presence of holes of manometer tubes on the base of a bob would disturb the flow pattern in their neighbor. Also for the finite size of accesses of manometers, the observed pressure does not represent a value at its center but the average over the area. That the quantitative estimation of this average with a parallel plate instrument is impracticable without the dependence of $h_z(r)$ on r (namely on the rate of shear) has been known. It can be said, however, that when the diameter of holes is larger, their influence is also greater. Actually, in our measurements, for the bob A (diameter of holes is 5 mm.) a slight but appreciable deviation was observed, while for the bob with smaller holes (diameter 2 mm.) no appreciable disturbance was observed. This had also been observed by Greensmith and Rivlin[3]. It is desirable to keep the size of holes as small as possible, but if too small, it becomes time-consuming for the fluid to attain equilibrium positions in each manometer.

The Normal Pressure Gradient $-\partial P_z(r)/\partial \ln r$ *vs. Rate of Shear* D.—Eqs. 1 and 2 indicate that the normal pressure difference, $\Delta P_z(r)$, or the normal pressure

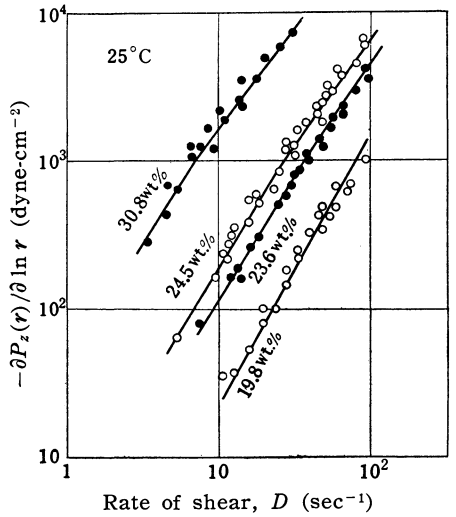


Fig. 4 (a). Normal pressure gradient, $-\partial P_z(r)/\partial \ln r$, as a function of rate of shear, D. Solutions of polystyrene in decalin.

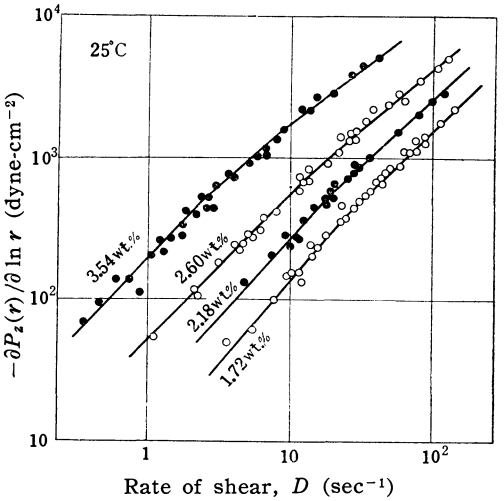


Fig. 4 (b). Normal pressure gradient, $-\partial P_z(r)/\partial \ln r$, as a function of rate of shear, D. Solutions of methylcellulose in water.

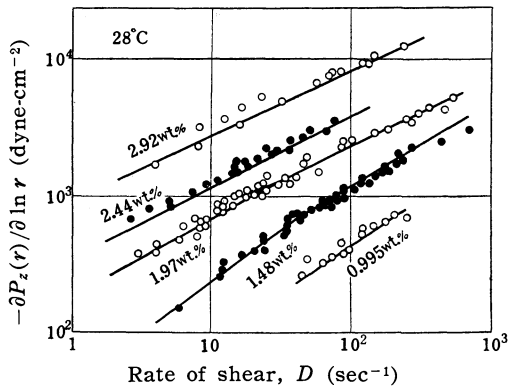


Fig. 4 (c). Normal pressure gradient, $-\partial P_z(r)/\partial \ln r$, as a function of rate of shear, D. Solutions of Na-carboxymethylcellulose in water.

gradient, $-(\partial P_z(r)/\partial \ln r)$**, should be a function of the rate of shear, $D=r\Omega/l$. Fig. 4 indicates the curves of $-\partial P_z(r)/\partial \ln r$ vs. D for three different polymer species, all of which show that the expected relations safely hold. Of course, the data which were beyond the limitations mentioned in the previous subsections were eliminated in the plots.

It should be noticed that the dependences of normal stresses on the rate of shear differ remarkably in each polymer species, which reflect the essential difference in characteristic rheological properties of those polymers. The detailed discussions will be given in our subsequent paper[4].

The Applicability of the Superposition Principle.—It has been suggested that from the normal stress data obtained on solutions of various concentrations and temperatures, a single reduced curve should be obtained by applying the superposition procedure which is currently used for the dynamic data[5,6]. In this case, reduced quantities are defined such as

$$[-\partial P_z(r)/\partial \ln r]_r = [-\partial P_z(r)/\partial \ln r] \cdot [T_0/Tf(c)]$$

and $$D_r = D\eta\, T_0/Tf(c)$$

where T is the absolute temperature, T_0 is a reference temperature, and η is the *zero shear* viscosity of the solution. $f(c)$ is a function of concentration, and was chosen by Padden and DeWitt[5] as $f(c)=c$ and by Markovitz and Williamson[6] as $f(c)=c/c_0$ for $c<c_0$ and $f(c)=c^2/c_0^2$ for $c\geq c_0$. The reduced plot of the data with solutions of methylcellulose in water is shown in Fig. 5, in which $T_0=298$°K and $f(c)=c$. It is seen that the reduction is not so satisfactory, but rather a systematic deviation is observed. Although results are not shown here, another choice of $f(c)$ improves the situation slightly. For another two polymer species, polystyrene in decalin and Na-CMC in water, the reductions are a little better than for methylcellulose in water, but again not so satisfactory.

On the basis of the cross-elasticity theory[4], the normal stresses and the apparent viscosity (=shearing stress/rate of shear) are given as follows:

$$-\frac{\partial P_z(r)}{\partial \ln r} = \sigma_{11}-\sigma_{33} = G\tau^2 D^2 \tag{4}$$

$$\eta = \sigma_{12}/D = G\tau \tag{5}$$

where G and τ are the shear modulus and the relaxation time of the solution, respectively. The superposition procedures are based on the following assumptions: the shear modulus and the relaxation time of the solution are dependent on such concentration and temperature that $G=G_0[Tf(c)/T_0f(c_0)]$ and $\tau=a_Ta_c\tau_0$. Here G_0 and τ_0 are the values of G and τ, respectively, at the reference temperature T_0 and concentration c_0. Introducing these assumptions into Eqs. 4 and 5, we obtain

$$-\frac{\partial P_z(r)}{\partial \ln r} = \frac{Tf(c)}{T_0f(c_0)} G_0\tau_0^2(a_Ta_cD)^2 \tag{6}$$

$$D\eta = \frac{Tf(c)}{T_0f(c_0)} G_0\tau_0(a_Ta_cD) \tag{7}$$

and

$$a_Ta_c = \frac{T_0f(c_0)}{Tf(c)}\frac{\eta}{\eta_0} \tag{8}$$

With the choice of such a reference state that η_0 and $f(c_0)$ are unity and a *zero shear* value for η, the reduced variables indicated before are determined.

It should be mentioned, however, that the above-mentioned definitions of reduced variables implicitly include such a further assumption namely that the reducing factors, $f(c)/f(c_0)$ and a_Ta_c, are independent of the rate of shear. This assumption may be valid in the case of a dynamic measurement if the amplitudes of vibrational motion are sufficiently small. On the other hand, in the steady flow measurements over wide range of rates of shear, this assumption may be improper, or valid only within a limited range of rates of shear, or of concentrations. Actually, the flow curves of polymer solutions

** Many experimental evidences show that the difference of σ_{22} and σ_{33} is nearly zero so it may be considered taht $[-\partial P_z(r)/\partial \ln r]=\sigma_{11}-\sigma_{33}$. See references 1), 2) and 4).

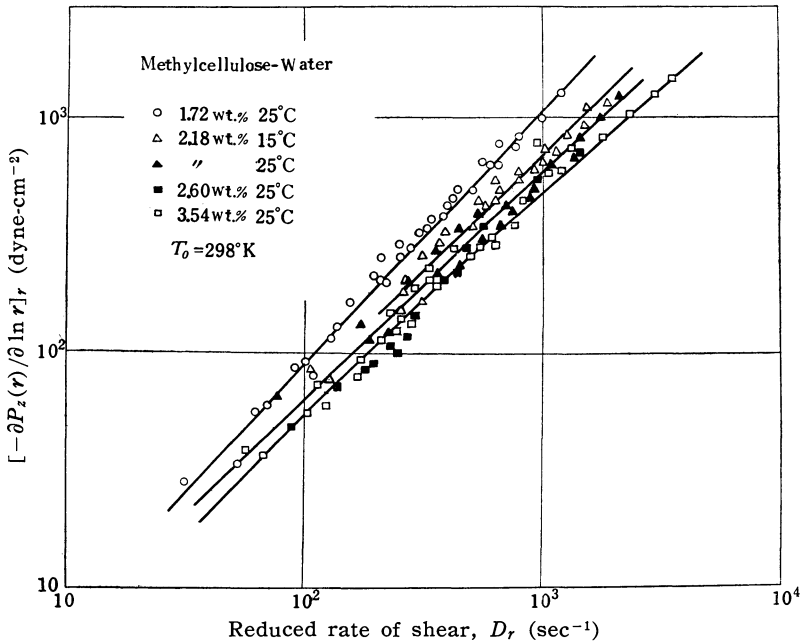


Fig. 5. Reduced normal pressure gradient, $[-\partial P_z(r)/\partial \ln r]_r = -[\partial P_z(r)/\partial \ln r][T_0/Tf(c)]$ vs. reduced rate of shear, $D_r=\eta T_0/Tf(c)$, where $f(c)=c$, T_0=298°K, solutions of methylcellulose in water.

have a distinct S shape[7], which indicates the presence of two different Newtonian regions at low rate of shear and at high rate of shear. In concentrated solutions the initial viscosity, $\eta_{D=0}$, at a low rate of shear increases more rapidly than the fifth or tenth power of the concentration[8], and the final viscosity, $\eta_{D=\infty}$, at a high rate of shear is proportional to the concentration itself[7]. These facts suggest that the whole feature of the flow curve can not be determined by their initial branch. This situation probably reflects also on the normal stresses, therefore, the above-mentioned superposition procedures should be valid only for the data obtained within the limited range of rates of shear and concentrations.

One more remark should be added to the factor T/T_0 of the shear modulus. This factor was derived from the conception of the entropy elasticity of the flexible chain polymer system. But in the case of concentrated solutions, in which the presence of transient junctions due to entanglements or interactions between polymer chains plays an important role and their number itself varies with temperature, the temperature dependence of the modulus of the solution is perhaps more complicated. A correct choice of this factor is a problem for further investigation.

Summary

Results of some geometrical studies of normal stress effects in a parallel plate instrument have been discussed. The parallelism and the concentricity of two plates are necessary conditions for the quantitative measurement. The rotational velocity of a cup should be kept below about 70 rpm for the apparatus with the cup radii about 6~8 cm. to avoid the influence of the centrifugal force. Accesses of manometer tubes with the diameter about 2 mm. cause no appreciable disturbances. The influence of side gap may also be neglected. With these experimental remarks, the normal stresses are obtained as a function of the rate of shear.

The applicability of the concentration-temperature superposition procedures has been tested with the data obtained here. They are partly valid in some limited range of variables.

7) J. G. Brodnyan, F. H. Gaskins and W. Philippoff, *Trans. Soc. Rheology*, 1, 109 (1957).

8) T. G. Fox, S. Gratch and S. Loshaek, "Viscosity Relationships for Polymer in Bulk and in Concentrated Solutions", in Rheology, Vol. I ed. F. Eirich, Academic Press, New York (1956), Chap. 12.

A part of the measurement was performed by Mr. K. Sakamoto, to whom the authors express thanks. The authors are obliged to Professor T. Nakagawa of the University of Tokyo and Dr. M. Yamamoto of this University who attracted our attention to this problem. Thanks are also due to the members of the Research Group on Polymer Science of this University, especially to Professor H. Fujita for his helpful discussions on this problem. This work was supported by a grant-in-aid of the Ministry of Education and by Mitsubishi Paper Mills Co., Kyoto, to both of which we extend our thanks.

Department of Industrial Chemistry
Kyoto University, Sakyo-ku, Kyoto

Studies on the Sapogenins of Dioscorea tokoro Makino. I.[1]* *The Structure of Tokorogenic Acid*

By Katsura MORITA

(Received November 4, 1958)

Steroidal sapogenin from plants belonging to the family *Dioscoreaceae* in Japan was first reported in detail by Tsukamoto et al.[2] Nevertheless, until we reported the isolation of a new sapogenin from *Dioscorea tokoro* Makino, diosgenin had been the sole sapogenin from these plants. In a previous paper[1] we made clear the following points on the new sapogenin: (1) The elementary analyses of the sapogenin and its acetate coincide with those of trihydroxysapogenin and its triacetate. (2) The infrared absorption spectrum (980, 917, 895 and 862 cm^{-1}) shows that the sapogenin has iso-configuration of ring F[3]. (3) Chloroform solution of the sapogenin rapidly consumes bromine and evolves hydrogen bromide fume. (4) 16-Pregnene-x, y, z-triol-20-one triacetate, U.V.λ_{max}^{EtOH}: 240 mμ (ε: 1120), can be derived from the sapogenin by the isomerization to the pseudosapogenin followed by oxidation, hydrolysis and re-acetylation.

Since no trihydroxysapogenin possessing the same physical constants with this had so far been announced, we named this sapogenin "tokorogenin" and started to investigate its chemical structure.

Tokorogenin undergoes oxidation with chromic anhydride in acetic acid to give a dibasic acid "tokorogenic acid" and a small amount of a lactone-like substance, the structure of which has not yet been elucidated. Tokorogenin also undergoes oxidation with periodic acid in an ethanol solution giving a crystalline substance, $C_{34}H_{60}O_6$, which tends to become tokorogenic acid by treatment with aqueous acetic acid and subsequent oxidation with chromic anhydride in the same solvent. The I.R.-absorption spectrum of the periodic-acid oxidation product, however, showed that the substance possessed neither a hydroxyl group nor aldehyde functions, and therefore an acetal structure must be necessarily assigned to this substance.

Lead tetra-acetate also affects tokorogenin in 80% acetic acid, but no crystalline substance could be obtained. Quantitative estimation, however, showed that the oxidizing agent consumed in the reaction was almost equivalent to the value calculated for a glycerol structure.

In view of these results, it is quite reasonable to presume that tokorogenin possesses a glycerol moiety in ring A of steroid nucleus and that the chromic anhydride oxidation of this triol possibly causes elimination of one of its carbon atoms giving tokorogenic acid. It is, therefore, almost certain that tokorogenin must be defined as either spirostan-1, 2, 3-triol (I) or spirostan-2, 3, 4-triol (I') and

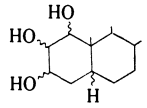
* This is a full paper of the previous communication (K. Morita, *Pharm. Bull.*, **5**, 496 (1957)), and constitutes Part VIII of Nishikawa's paper entitled "Studies in Steroids".

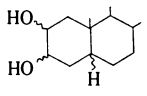
1) M. Nishikawa, K. Morita, H. Hagiwara and M. Inoue, *J. Pharm. Soc. Japan* (*Yakugaku Zasshi*), **74**, 1165 (1954).

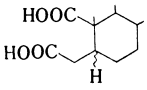
2) T. Tsukamoto and Y. Ueno, ibid., **56**, 802, 939 (1936).

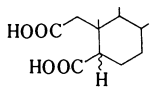
3) C. R. Eddy et al., *Anal. Chem.*, **24**, 1337 (1952).

tokorogenic acid as either 1,3-seco-2-nor-spirostane-1,3-dioic acid (II) or 2,4-seco-3-nor-spirostane-2,4-dioic acid (II′).


(I)


(I′)

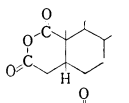
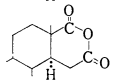
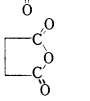

(II)


(II′)

These assumptions are further supported by the fact that tokorogenic acid, on heating with acetic anhydride, forms an anhydride (I.R. λ_{max}^{Nujol}: 5.51, 5.71 μ), for according to the Blanc rule[4] no seven-membered ring anhydride can be formed from the corresponding 1,6-dibasic acids under these conditions. Moreover, the elementary analytical values of tokorogenic acid, its dimethyl ester and the anhydride favor the values calculated for $C_{26}H_{40}O_6$, $C_{28}H_{44}O_6$ and $C_{26}H_{38}O_5$, respectively.

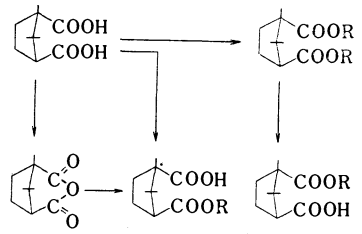
Evidence is also given by the fact that the infrared carbonyl bands of tokorogenic anhydride are typical of the 6-membered ring anhydride as shown in Table I.

TABLE I

Substance	Structure	I.R. max.	Ref. No.
Tokorogenic anhydride (III)		Nujol 5.55, 5.71	5)
3β-Acetoxy-5-etiobilienic anhydride		Nujol 5.55, 5.70	5)
Glutaric anhydride		$CHCl_3$ 5.55, 5.68	6)
Succinic anhydride		Nujol 5.36, 5.61	7)

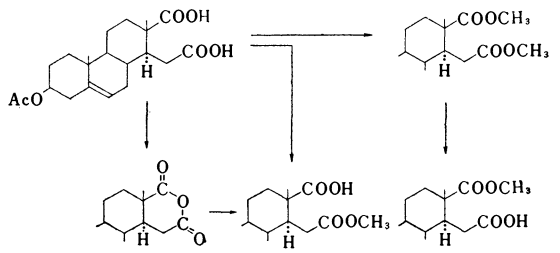
For the determination of the structure of tokorogenic acid, the following facts provide evidence in support of formula II rather than II′: (1) on treatment with methanol and hydrogen chloride tokorogenic acid affords a monomethyl ester (α-monomethyl ester); (2) alkaline hydrolysis of the dimethyl ester gives a different monomethyl ester (β-monomethylester); (3) treatment of the anhydride with one mole of sodium methoxide furnishes the α-monomethyl ester. These results are in complete accord with the earlier observations in the camphoric acid series (Chart 1)[8], where one of the carboxyl groups of the acid is attached to a tertiary carbon atom.

CHART 1



Since the structure II is closely similar to that of etiobilienic acid, which was first prepared from cholesterol by Kuwada[9] in our Laboratories, it can be presumed that etiobilienic acid and its derivatives will undergo reactions similar to those demonstrated in the camphoric acid series (Chart 1). We confirmed that this was true with etiobilienic acid, prepared from 5,16-pregnadien-3β-ol-20-one acetate according to Adams et al.[10]

CHART 2

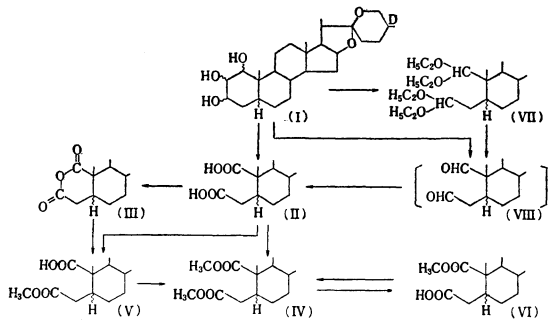


On the basis of these findings and the aforementioned discussion, one is led to conclude that the reactions in the tokorogenic acid series can be best represented by Chart 3; that is, tokorogenic acid must have the structure II, and tokorogenic anhydride III, the α-monoester V, and the β-monoester VI, respectively.

4) L. F. Fieser and M. Fieser, "Natural Products Related to Phenanthrene", 3 Ed., Reinhold Publishing Corporation, New York, N. Y. (1949), p. 130.
5) Presented by the author.
6) H. H. Wasserman and H. E. Zimmerman, *J. Am. Chem. Soc.*, **72**, 5787 (1950).
7) H. M. Randall et al., "Infra-red Determination of Organic Structure" D. Van Norstrand Co., Inc., New York, N. Y. (1949), p. 163.
8) J. W. Brühl, *Ber.*, **25**, 1796 (1892); W. A. Bone et al., *J. Chem. Soc.*, **85**, 534 (1904).
9) S. Kuwada, *J. Pharm. Soc. Japan* (*Yakugaku Zasshi*), **56**, 78 (1936).

It is also evident that the periodic acid oxidation product ($C_{34}H_{60}O_6$) must have a dialdehyde diacetal structure VII and that the structure I has to be assigned to tokorogenin.

CHART 3



Experimental

All melting points are corrected.

Tokorogenic Acid (II). — To a solution of 1.0 g. of tokorogenin I in 90 ml. of glacial acetic acid was added with vigorous stirring a solution of 2.0 g. of chromium trioxide in 20 ml. of 80% acetic acid at room temperature over a period of one hour. The solution was then allowed to stand overnight and the excess of the reagent was destroyed with sodium bisulfite. Partial evaporation gave a difficultly soluble crystalline substance of the solution (135 mg., m.p. 241°C (decomp.); I.R.λ_{max}^{Nujol}: 5.60 μ).

Anal. Found: C, 70.06; H, 8.74. Calcd. for $C_{27}H_{40}O_7$: C, 70.40; H, 8.75%.

The mother liquor was diluted with a large volume of water and extracted with ether, and the ethereal solution was repeatedly washed with water. The ethereal solution was then extracted with alkali and the alkaline solution was acidified and re-extracted with ether. Thorough washing of the solution followed by drying and evaporation furnished a solid residue (II, 470 mg.), which was recrystallized from acetic acid containing water yielding 400 mg. of colorless needles; m.p. 255°C (decomp.), $[\alpha]_D^{23}$ −26.3° (in acetone).

Anal. Found: C, 69.65; H, 9.13. Calcd. for $C_{26}H_{40}O_6$: C, 69.61; H, 8.99%.

Tokorogenic Acid Dimethyl Ester (IV).—A solution of tokorogenic acid II in ether was treated with a slight excess of diazomethane in the same solvent and the solution was immediately evaporated to dryness to give a crystalline dimethyl ester IV. Crystallization from methanol raised the melting point to 158~159°C.

Anal. Found: C, 70.75; H, 9.31. Calcd. for $C_{28}H_{44}O_6$: C, 70.55; H, 9.31%.

Tokorogenic Anhydride (III).—Tokorogenic acid II was heated with acetic anhydride for twenty minutes. After evaporation to a small volume the solution was cooled to give colorless needles of the anhydride III; m.p. 270~273°C, I.R.λ_{max}^{Nujol}: 5.55, 5.71 μ.

Anal. Found: C, 72.47; H, 9.09. Calcd. for $C_{26}H_{38}O_5$: C, 72.52; H, 8.90%.

A small portion of the anhydride III dissolved in methanol containing water and potassium hydroxide was digested for one hour, cooled, and neutralized with hydrochloric acid. Tokorogenic acid (II) was recovered in a good yield.

Tokorogenic Acid α-Monomethyl Ester (V). — a) To a mixture of 80 mg. of tokorogenic acid II and 3 ml. of absolute methanol was added 0.01 ml. of chlorosulfonic acid and the mixture was warmed on a steam bath to ensure complete solution. After being kept at room temperature for two hours the fine needles, which precipitated in the solution, were collected. Recrystallization from methanol afforded the analytical sample, which first melted at 141°C, then soon solidified and finally melted at 184~187°C (sintering 140°C).

Anal. Found: C, 69.88; H, 9.26. Calcd. for $C_{27}H_{42}O_6$: C, 70.10; H, 9.15%.

By the action of diazomethane V gave the dimethyl ester IV.

b) To a solution comprising 5 ml. of methanol and 6 mg. of sodium metal was added 100 mg. of the anhydride III and the mixture warmed on a steam bath for several minutes. The solution was then allowed to stand at room temperature for forty-five minutes. A small quantity of acetic acid was added to this and the solution was evaporated to dryness to give fine needles; m.p. 184~187°C (pre-sintering at 140°C). The sample here obtained did not show depression of melting point on admixture with a specimen prepared according to (a).

Tokorogenic Acid β-Monomethyl Ester (VI).—To a solution of 50 mg. of dimethyl ester IV in 4 ml. of methanol was added 100 mg. of sodium hydroxide dissolved in 1 ml. of water and the solution was refluxed for fifteen minutes on a steam bath and then allowed to stand at room temperature for one hour. The solution was diluted with a large volume of water, extracted with ether and the ethereal solution was discarded. After acidification, the aqueous layer was again extracted with ether and the ethereal solution was washed, dried and evaporated to give a solid substance VI. Recrystallization from methanol afforded colorless thin plates of the β-monomethyl ester VI; m.p. 208~210°C.

Anal. Found: C, 70.18; H, 9.04. Calcd. for $C_{27}H_{42}O_6$: C, 70.10, H, 9.15%.

By the action of diazomethane, the β-monomethyl ester VI gave the dimethyl ester IV melting at 158~159°C, which did not show depression of the melting point on admixture with the sample obtained by the other method.

Periodic Acid Oxidation of Tokorogenin (I).—To a suspension of 500 mg. of tokorogenin I in 10 ml. of absolute ethanol was added 1 g. of periodic acid dissolved in 1 ml. of water. The mixture was stirred vigorously for fifteen minutes and the resulting solution was allowed to stand

10) W. J. Adams et al., *J. Chem. Soc.*, **1956**, 297.

at room temperature for twenty-four hours to give colorless prisms. Recrytallization from methanol afforded 200 mg. of the diacetal VII; m.p. 150~151°C.

Anal. Found: C, 72.86; H, 10.55. Calcd. for $C_{34}H_{60}O_6$; C, 72.80; H, 10.71%.

Three hundred mg. of the diacetal dissolved in 80% acetic acid (40 ml.) was gently warmed on a steam bath for thirty minutes and cooled. To this was added a solution of 0.5 g. of chromic anhydride in 5 ml. of 80% acetic acid in small portions. Working up of the reaction mixture as in the case of tokorogenic acid II led to needles melting at 255°C; yield 190 mg., mixture m.p. with tokorogenic acid II, 255°C.

Lead Tetra-acetate Oxidation of Tokorogenin (I).—To a solution of lead tetra-acetate in 90% acetic acid (40 ml., 0.71 M) was added 444 mg. (1 mmol.) of tokorogenin I and the mixture was stirred vigorously to ensure complete solution. The solution was then allowed to stand at 20°C for two hours and a half. During this time, one ml. of the reaction mixture was taken out at regular intervals, a solution of potassium iodide was added to each of the solutions, and the solution was titrated with 0.1 N sodium thiosulfate with results shown in Table II, which show that tokorogenin consumed about two moles of the reagent.

TABLE II

Time	0.1N $Na_2S_2O_3$ ml.	HIO_4 Consumed m mol.
0 min.	0	0
15 min.	0.47	0.94
30 min.	0.67	1.34
45 min.	0.78	1.56
60 min.	0.81	1.62
90 min.	0.87	1.74
120 min.	0.91	1.82
16 hr.	1.21	2.42

3β-Hydroxy-Δ^5-etiobilienic Acid α-Monomethyl Ester.—a) A solution of 500 mg. of 3β-acetoxy-Δ^5-etiobilienic acid[9] in 30 ml. of methanol containing 0.5 ml. of chlorosulfonic acid was allowed to stand overnight at room temperature. After partial evaporation of the solution in vacuo water was added in small portions to give needles of the α-monomethyl ester. Recrystallization from acetone and water afforded the analytical sample melting at 175~178°C.

b) A solution of 350 mg. of 3β-acetoxy-Δ^5-etiobilienic anhydride[9] in 20 ml. of methanol containing 300 mg. of potassium hydroxide was refluxed on a steam bath for fifteen minutes. After standing at room temperature for thirty minutes a small quantity of acetic acid was added and the solution was evaporated in vacuo to a small volume. Water was added to this and the mixture was extracted with ether and the ethereal solution was extracted with alkali.

After acidification of the alkaline solution, it was extracted with ether, and then ethereal solution washed with water, dried and evaporated to give a syrup. Recrystallization from acetone and water afforded colorless needles melting at 175~178°C; mixed m. p. with the sample prepared according to (a), 175~178°C.

3β-Hydroxy-Δ^5-etiobilienic Acid β-Monomethyl Ester.—A solution of 500 mg. of 3β-acetoxy-Δ^5-etiobilienic acid dimethyl ester[10] in 30 ml. of methanol containing 300 mg. of patassium hydroxide was refluxed on a steam bath for four hours. After evaporation in vacuo a large volume of water was added to this and the mixture was extracted with ether. From the ether solution, 200 mg. of the material melting at 110~112°C was recovered. The aqueous solution, after acidification with diluted hydrochloric acid, was extracted with ether, and the ethereal solution was washed with water, dried and evaporated to give fine needles melting at 214~215°C*.

The β-monomethyl ester, on treatment with diazomethane, gave the dimethyl ester.

Summary

(1) Oxidation of tokorogenin by means of chromic anhydride in acetic acid, periodic acid in ethanol and lead tetra-acetate in aqueous acetic acid led to the conclusion that tokorogenin must have a glycerol moiety in ring A of the steroid nucleus.

(2) Tokorogenic acid, an oxidation product from tokorogenin, forms an anhydride by heating with acetic anhydride and gives rise to a monomethyl ester (α-monoester) by treatment with methanol and hydrogen chloride, while alkaline hydrolysis of the dimethyl ester of the acid furnishes a different monomethyl ester (β-monoester). The same α-monoester also results from tokorogenic anhydride by the action of alkali in a methanol solution.

(3) On the basis of the theoretical considerations and the afore-mentioned observations in the tokorogenic acid series compared with those in the camphoric acid and etiobilienic acid series, it is concluded that tokorogenic acid has to be defined as 1,3-seco-2-nor-spirostan-1,3-dioic acid (II) and hence tokorogenin as spirostan-1,2,3-triol (I).

The author wishes to express his grateful thanks to Dr. Y. Asahina of the University of Tokyo, Dr. S. Kuwada and Dr. T. Matsukawa in our Research Laboratories for their encouragement throughout the work. Thanks are also due to Mr. H. Kamio

* Kuwada[9] assigned the m. p. 176~177°C (sinter. at 169°C) to the same monomethyl ester. Discrepancy between the melting points may would be attributed to the solvents ethanol being used by Kuwada.

for infrared- and ultraviolet-spectral measurements and to Mr. M. Kan for elementary analyses.

Takeda Research Laboratories,
Juso, Higashiyodogawa-ku, Osaka

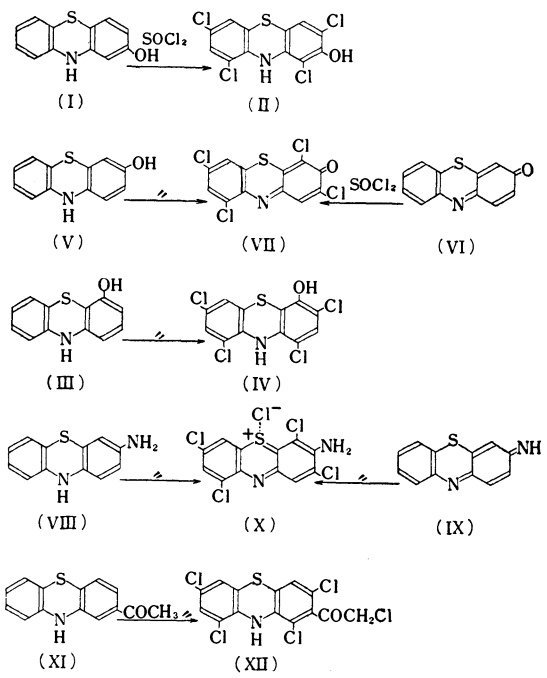
Phenothiazine Derivatives. VI[1]*. Reactions of Some Substituted Phenothiazines with Thionyl Chloride*

By Manabu FUJIMOTO

(Received October 9, 1958)

In Part II[2] of the present series, it was reported that thionyl chloride transforms phenothiazine and its 5-oxide into 1,3,7,9-tetrachlorophenothiazine. Besides the present series, two reports have been published on the nuclear substitutions of phenothiazine derivatives with thionyl chloride. Namely, phenothiazine-1-carboxylic acid gave 3,7,9-trichlorophenothiazine-1-carbonyl chloride[3], and phenothiazine-2-carboxylic acid 1,3,7,9-tetrachlorophenothiazine-2-carbonyl chloride[4].

CHART I



The present paper describes similar substitution reactions of some other phenothiazine derivatives with thionyl chloride.

Mono-substituted Phenothiazines. — As shown in Chart I, the action of thionyl chloride gave 1,3,7,9-tetrachloro-2-hydroxyphenothiazine (II) from 2-hydroxyphenothiazine (I), 2,4,7,9-tetrachloro-3-phenothiazone (VII) from 3-hydroxyphenothiazine (V) and from 3-phenothiazone (VI), and 3-amino-2,4,7,9-tetrachlorophenazathionium chloride (X) from 3-aminophenothiazine (VIII) and from 3-phenothiazime (IX). These three products, II, VII and X, had been obtained by the action of thionyl chloride on 3-hydroxydiphenylamine, 4-hydroxydiphenylamine and 4-aminodiphenylamine, respectively[5]. In Part III[6] of this series it was observed that the reaction of thionyl chloride with diphenylamine to form 1,3,7,9-tetrachlorophenothiazine proceeds through the intermediate formation of phenazathionium chloride and subsequent chlorination. The fact that the substituted phenothiazines and the corresponding diphenylamines gave the same products by the action of thionyl chloride affords support to the above mechanism of the reaction of thionyl chloride with diphenylamine. Thionyl chloride and 4-hydroxyphenothiazine (III) gave a new tetrachloro-4-hydroxyphenothiazine. As it is expected that the hydroxyl group in position 4 of 4-hydroxyphenothiazine will strengthen the 1,3-orienting effect by the imino group, the

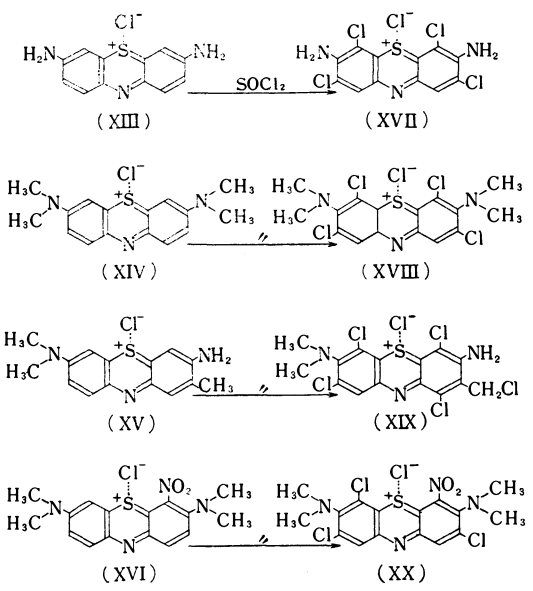
1) Part V: This Bulletin, **32**, 371 (1959).
2) *Pharm. Bull. (Japan)*, **5**, 393 (1957).
3) N. V. Savitskaya and M. N. Shahukina, *Zhur. Obshchei Khim.*, **24**, 152 (1954).
4) A. Burger and J. B. Clements, *J. Org. Chem.*, **19**, 1113 (1954).
5) This Bulletin, **32**, 298 (1959).
6) Ibid., **32**, 294 (1959).

product is assumed with great certainty to be 1,3,7,9-tetrachloro-4-hydroxyphenothiazine (IV).

2-Acetylphenothiazine (XI) gave a pentachloro derivative. A part of the chlorine atoms was found labile giving easily the chloride anion, and thus was present in the side chain. The positions of the chlorine atoms in the ring with the chlorinated acetyl group can not be presumed unequivocally, because the orienting effect by the acetyl group and that by the imino group do not fall on the same positions, but the product can be assumed to be 1,3,7,9-tetrachloro-2-(chloroacetyl)-phenothiazine (XII) in analogy to 1,3,7,9-tetrachlorophenothiazine-2-carbonyl chloride from phenothiazine-2-carboxylic acid[4].

Phenothiazine Dyes[7]. — From among many known phenothiazine dyes, thionine (XIII), methylene blue (XIV), toluidine blue (XV) and methylene green B (XVI) were chosen for the reactions with thionyl chloride.

CHART II



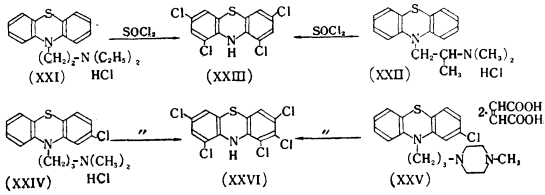
In the order of mention, they gave 3,7-diamino-2,4,6,8-tetrachlorophenazathionium chloride (XVII), 3,7-bis(dimethylamino)-2,4,6,8-tetrachlorophenazathionium chloride (XVIII), 3-amino-1,4,6,8-tetrachloro-2-(chloromethyl)-7-(dimethylamino)-phenazathionium chloride (XIX), and 2,6,8-trichloro-3,7-bis(dimethylamino)-4-nitrophenazathionium chloride (XX), respectively.

7) These dyes are expediently expressed in phenazathionium formulae.

As it is reasonably expected that the amino group and the dimethylamino group in positions 3 and 7 are stronger in the orienting effect than the competing nitrogen atom of position 10, substitution took place presumably in all the positions 2, 4, 6 and 8, unless already substituted. Toluidine blue (XV) gave a pentachloro derivative. It can be assumed by the same reason as stated above that three of the five chlorine atoms are situated at positions 4, 6, and 8. As substitution in position 1 is favored by both the nitrogen atom of position 10 and the methyl group in position 2, one is probably in position 1, and the remaining one in the methyl group to make chloromethyl group. Thus the pentachloro product is considered 3-amino-1,4,6,8-tetrachloro-2-(chloromethyl)-7-(dimethylamino)phenazathionium chloride (XIX).

Phenothiazine Drugs.—Four of the most important phenothiazine drugs were treated with thionyl chloride with results shown in Chart III. The same 1,3,7,9-tetrachlorophenothiazine (XXIII)[2] was obtained from either diethazine (XXI) (2987 R.P.) or promethazine (XXII) (3389 R.P.). In a similar manner, 1,2,3,7,9-pentachlorophenothiazine[2] (XXVI) was derived from chlorpromazine (XXIV) (4560 R.P.) and from prochlorperazine

CHART III



(XXV) (6140 R.P.). As the yields were nearly quantitative, the reaction with thionyl chloride may be useful to the qualitative and quantitative analyses of various phenothiazine drugs.

Experimental

General Procedure of Treatment with Thionyl Chloride.— Thionyl chloride (10 ml.) was added dropwise to 1.0 g. of the compound to be treated, and the mixture was heated gently under reflux for 30 min., when hydrogen chloride and sulfur dioxide were evolved. The cooled mixture was poured onto crushed ice, and the product was collected, dried, and recrystallized.

1,3,7,9-Tetrachloro-2-hydroxyphenothiazine (II) from 2-Hydroxyphenothiazine (I). —Fine powder of chocolate color from chloroform-ethanol, m.p. 202~203°C (decomp.). Yield,

93%. The substance was identified with an authentic sample[5].

1, 3, 7, 9-Tetrachloro-4-hydroxyphenothiazine (IV) from 4-Hydroxyphenothiazine (III).—Fine powder with chocolate color from benzene, m.p. 168~170°C. Yield, 94%. The product IV gives bluish-violet color with sulfuric acid.

Anal. Found: C, 40.67; H, 1.10; N, 4.01. Calcd. for $C_{12}H_5ONCl_4S$: C, 40.82; H, 1.43; N, 3.97%.

2,4,7,9-Tetrachloro-3-phenothiazone (VII) from 3-Hydroxyphenothiazine (V) and from 3-Phenothiazone (VI).—Fine crystals with pinkish tinge from ethanol-benzene, m.p. 145~146°C. Yields, 92% from V and 97% from VI. The product VII gives cobalt-blue coloration with sulfuric acid. The substance showed no depression of the melting point on admixture with an authentic sample[5].

3-Amino-2, 4, 7, 9-tetrachlorophenazathionium Chloride (X) from 3-Aminophenothiazine (VIII) and from 3-Phenothiazime (IX).—Reddish-violet fine powder from chloroform, m.p. 185~186°C. Yields, 89% from VIII and 99% from IX. The substance showed no depression of the melting point on admixture with an authentic sample[5].

1,3,7,9-Tetrachloro-2-(chloroacetyl)phenothiazine (XII) from 2-Acetylphenothiazine (XI).—Green powder, m.p. 145~146°C. Yield, quantitative. Coloration with sulfuric acid is violet. Silver chloride was precipitated on adding silver nitrate to an alcoholic solution of the substance XII.

Anal. Found: C, 37.19; H, 1.93; N, 3.15. Calcd. for $C_{14}H_6ONCl_5S \cdot 2H_2O$: C, 37.37; H, 2.24; N, 3.11%.

3, 7-Diamino-2, 4, 6, 8-tetrachlorophenazathionium Chloride (XVII) from Thionine (XIII).—Bluish-purple fine powder from methanol, m.p. over 360°C. Yield, 99%. The substance gives dark green color with sulfuric acid.

Anal. Found: C, 35.99; H, 1.83; N, 10.54. Calcd. for $C_{12}H_6N_3Cl_5S$: C, 35.90; H, 1.51; N, 10.47%.

2,4,6,8-Tetrachloro-3,7-bis(dimethylamino)-phenazathionium Chloride (XVIII) from Methylene Blue (XIV).—Greenish-blue fine crystals, m.p. over 360°C. Yield, 94%. The substance gives green color with sulfuric acid. When recrystallized from a mixture of dimethylformamide and water, it was transformed into the corresponding phenazathionium hydroxide, which was analyzed.

Anal. Found: C, 43.66; H, 3.28; N, 10.06. Calcd. for $C_{16}H_{15}ON_3Cl_4S$: C, 43.75; H, 3.44; N, 9.57%.

3-Amino-1, 4, 6, 8-tetrachloro-2-(chloromethyl)-7-(dimethylamino)phenazathionium Chloride (XIX) from Toluidine Blue (XV).—Purplish-blue fine powder from acetic acid, m.p. over 360°C. Yield, 96%. It gives reddish-brown color with sulfuric acid.

Anal. Found: C, 37.90; H, 2.72; N, 8.48. Calcd. for $C_{15}H_{11}N_3Cl_6S$: C, 37.68; H, 2.32; N, 8.79%.

2,6,8-Trichloro-3, 7-bis(dimethylamino)-4-nitrophenazathionium Chloride (XX) from Methylene Green B (XVI).—Green fine powder from methanol, m.p. 234~237°C (decomp.). Yield, quantitative. Coloration with sulfuric acid is violet.

Anal. Found: C, 40.88; H, 3.40; N, 12.09. Calcd. for $C_{16}H_{14}O_2N_4Cl_4S$: C, 41.05; H, 3.01; N, 11.97%.

1, 3, 7, 9-Tetrachlorophenothiazine (XXI) from Diethazine (XIX) and from Promethazine (XX).—Yellow needles from benzene, m.p. 234~235°C. Yields, 99% from XIX and 96% from XX. It was identified with an authentic sample[2].

1,2,3,7,9-Pentachlorophenothiazine (XXVI) from Chlorpromazine (XXIV) and from Prochlorperazine (XXV).—Faint-yellow or colorless needles from benzene, m.p. 204~205°C. Yields, 96% from XXIV and 90% from XXV. It was identified with an authentic sample[2].

Summary

Some phenothiazine derivatives including dyes and drugs were treated with thionyl chloride and five new polychlorinated products and six known were obtained.

The author expresses his thanks to Professor Y. Urushibara, the Tokyo, for his helpful guidance throughout this work, to Dr. K. Takeda, Director of the Laboratory, for his permission to conduct this research, and also to the members of the Center of Microanalytical Services, Shionogi and Co., Ltd., for the elementary analyses.

Research Laboratory
Shionogi and Co., Ltd.
Imafuku, Amagasaki

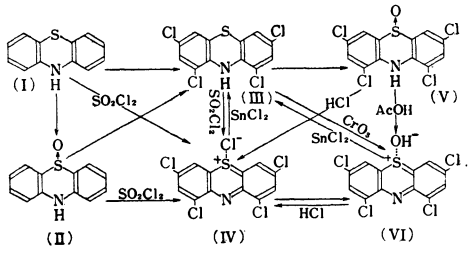
Phenothiazine Derivatives. VII[1]. *Reactions of Phenothiazines with Sulfuryl Chloride and with Chlorosulfonic Acid*

By Manabu FUJIMOTO

(Received October 9, 1958)

In the previous papers of this series, reactions of diphenylamines and phenothiazines with thionyl halides, and of diphenylamine with sulfuryl chloride were described[2]. The present paper deals with the reactions of phenothiazines with sulfuryl chloride and with chlorosulfonic acid.

CHART I



The action of sulfuryl chloride on phenothiazine (I), on phenothiazine 5-oxide (II), and on 1,3,7,9-tetrachlorophenothiazine (III) produced chocolate-colored mixtures which, on treatment with water, gave a highly chlorinated product. The molecular weight of the purified product was found to be 309, and it was analyzed as $C_{12}H_5ONCl_4S$, corresponding to 1,3,7,9-tetrachlorophenazathionium hydroxide (VI).

Brady and Smiles[3] obtained 1,3,7,9-tetrachlorophenazathionium hydroxide(VI) by treating 1,3,7,9-tetrachlorophenothiazine 5-oxide (V) with aqueous sulfuric acid, and they described the substance as a brownish-red powder, decomposing somewhat gradually at 200°C and giving a purple solution in sulfuric acid. The substance obtained by the present author is a fine powder of chocolate color melting at 210~211°C (decomp.) and giving violet coloration with sulfuric acid. We may well be justified in regarding the present substance as identical with the substance of Brady and Smiles.

1) Part VI, This Bulletin, **32**, 480 (1959).
2) Part II, *Pharm. Bull. (Japan)*, **5**, 395 (1957); Part III, IV and VI, This Bulletin, **32**, 294, 296, 480 (1959).
3) O. L. Brady and S. Smiles, *J. Chem. Soc.*, **97**, 1562 (1910).

Without treatment with water, 1,3,7,9-tetrachlorophenazathionium chloride (IV) was obtained as the precursor of the hydroxide VI. Hydrolysis of the purified chloride IV with aqueous sulfuric acid or with ethanolic potassium hydroxide gave the phenazathionium hydroxide VI. Therefore, it was concluded that the treatment of the primary reaction mixtures with water caused a hydrolysis by sulfuric acid which was generated from water and the remaining sulfuryl chloride.

Mutual transformations of the four 1,3,7,9-tetrachlorophenothiazine derivatives, III, IV, V and VI, were further investigated. Reduction of 1,3,7,9-tetrachlorophenathionium chloride (IV) and of the hydroxide VI with stannous chloride gave 1,3,7,9-tetrachlorophenothiazine (III), while the hydroxide VI was produced either by oxidation of the phenothiazine III with chromic anhydride in benzene or by intramolecular rearrangement of 1,3,7,9-tetrachlorophenothiazine 5-oxide (V) in acetic acid. Action of dry hydrogen chloride on the 5-oxide (V) and on the

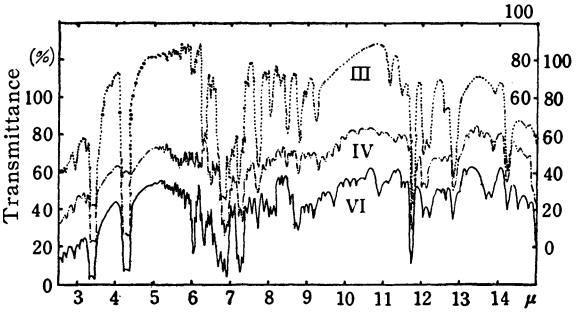


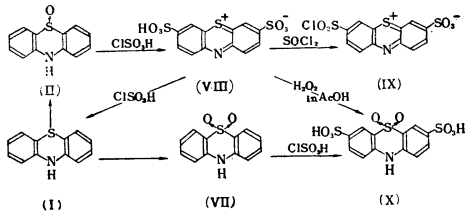
Fig. 1. Infrared spectra in Nujol of 1,3,7,9-tetrachlorophenothiazine (III), 1,3,7,9-tetrachlorophenazathionium chloride (IV), and the hydroxide VI.

phenazathionium hydroxide VI yielded the phenazathionium chloride IV. These transformations demonstrate that the four chlorine atoms are situated at the corresponding positions in the four compounds concerned. The infrared absorptions of

three (III, IV and VI) of the four compounds also indicate that they are similarly substituted (Fig. 1).

Phenothiazine 5,5-dioxide (VII) did not react with sulfuryl chloride, but chlorosulfonic acid transformed it into a disulfonic acid, probably 3,7-disulfophenothiazine 5,5-dioxide (X), as shown in Chart II.

CHART II



The action of chlorosulfonic acid on phenothiazine (I) and on its 5-oxide (II) gave an inner salt VIII of 3,7-disulfophenazathionium hydroxide. The inner salt VIII has converted into the disulfonic acid X by oxidation with 30% hydrogen peroxide in acetic acid, and into the inner salt IX of 3-sulfo-7-(chlorosulfonyl)phenazathionium hydroxide on treatment with thionyl chloride. Thus the sulfo groups and the chlorosulfonyl group in these inner salts are situated at the same positions as in the disulfophenothiazine 5,5-dioxide (X), which were assumed to be 3 and 7 as mentioned above.

Experimental

Reduction of 1,3,7,9-Tetrachlorophenazathionium Chloride (IV) and of 1,3,7,9-Tetrachlorophenazathionium Hydroxide (VI) with Stannous Chloride. — a) A mixture of 1.0 g. of 1,3,7,9-tetrachlorophenazathionium chloride (IV), described below, and 0.8 g. of stannous chloride was dissolved in 20 ml. of acetic acid, and then 1.0 g. of 35% hydrochloric acid was added. The solution was refluxed during 3 hr., and the cooled mass was poured into water. The yellow precipitate was collected, dried, and recrystallized from dioxane. Yellow needles, m. p. 235~236°C. Yield, 96%. The substance was identified with 1,3,7,9-tetrachlorophenothiazine (III) by a mixed melting point determination with an authentic sample[2].

b) Similarly, 1,3,7,9-tetrachlorophenazathionium hydroxide (VI), described below, gave the same tetrachlorophenothiazine (III) in a yield of 94%.

1,3,7,9-Tetrachlorophenazathionium Chloride (IV). — a) Sulfuryl chloride (10 ml.) was added to 1.0 g. of phenothiazine (I), and the mixture was gently refluxed for 30 min. Then the excess of sulfuryl chloride was evaporated under reduced pressure. The product was recrystallized from benzene. 1,3,7,9-Tetrachlorophenazathionium chloride (IV) was obtained in chocolate-colored needles, m. p. 223~224°C (decomp.). Yield, nearly quantitative. It gives purple coloration with sulfuric acid.

Anal. Found: C, 38.95; H, 1.43; N, 3.98. Calcd. for $C_{12}H_4NCl_5S$: C, 38.79; H, 1.09; N, 3.77%.

On treatment with sulfuryl chloride in a similar manner, phenothiazine 5-oxide (II) and 1,3,7,9-tetrachlorophenothiazine (III) gave the same product IV also in nearly quantitative yields.

b) A carbon tetrachloride solution of 1,3,7,9-tetrachlorophenothiazine 5-oxide (V) was saturated with dry hydrogen chloride, the chocolate-colored solution was refluxed for 1 hr., and then the solvent was distilled off. The residue was recrystallized from benzene. 1,3,7,9-Tetrachlorophenazathionium chloride (IV) was obtained quantitatively.

1,3,7,9-Tetrachlorophenazathionium Hydroxide (VI).—a) The reaction mixture resulting from phenothiazine (I) and sulfuryl chloride as described above, was poured into water, and the chocolate-colored product was collected, dried and recrystallized from benzene. 1,3,7,9-Tetrachlorophenazathionium hydroxide (VI) was obtained in chocolate-colored needles, m. p. 210~211°C. Yield, quantitative. It gives violet coloration with sulfuric acid.

Anal. Found: C, 40.49; H, 1.54; N, 4.03; mol. wt. (Rast), 309. Calcd. for $C_{12}H_5ONCl_4S$: C, 40.82; H, 1.43; N, 3.97%; mol. wt., 353.

b) 1,3,7,9-Tetrachlorophenazathionium chloride (IV) (0.2 g.) was dissolved in 5 ml. of sulfuric acid, and then the mixture was poured into 50 ml. of water. A nearly quantitative yield of the same hydroxide VI was obtained.

c) The chloride IV (0.2 g.) was dissolved in 50 ml. of hot ethanol, and a solution of 0.1 g. of potassium hydroxide in 5 ml. of hot ethanol was added. After reflux during 1 hr., the solvent was distilled off, and then the residue was neutralized with 10% hydrochloric acid. Recrystallization of the insoluble part from benzene gave 1,3,7,9-tetrachlorophenazathionium hydroxide (VI).

d) To a solution of 1.0 g. of 1,3,7,9-tetrachlorophenothiazine (III) in 50 ml. of benzene, 1.0 g. of chromic anhydride was added little by little. The mixture was refluxed on a water bath during 3 hr. The solvent was distilled off, and the residue was poured onto crushed ice. The same hydroxide VI was obtained in a quantitative yield.

e) A solution of 1.0 g. of 1,3,7,9-tetrachlorophenothiazine 5-oxide (V) in 30 ml. of acetic acid was refluxed for 1 hr., and the chocolate-colored solution was evaporated in vacuo. The residue was recrystallized from benzene, and 1,3,7,9-tetrachlorophenazathionium hydroxide (VI) was obtained in chocolate-colored fine needles.

Inner Salt VIII of 3,7-Disulfophenazathionium Hydroxide. — Chlorosulfonic acid (10 ml.) was added dropwise to phenothiazine (I),

and the mixture was heated gently under reflux for 30 min., and then the cooled mass was poured onto crushed ice. The precipitate was collected, dried, and recrystallized from benzene. The inner salt VIII of 3,7-disulfophenazathionium hydroxide was obtained in dark reddish-violet powder, m.p. 225~226°C. Yield, 93%. It gives bluish-violet coloration with sulfuric acid.

Anal. Found: C, 36.56; H, 2.39; N, 3.85. Calcd. for $C_{12}H_7O_6NS_3 \cdot 2H_2O$: C, 36.64; H, 2.82; N, 3.56%.

Treatment of phenothiazine 5-oxide (II) with chlorosulfonic acid in a similar manner gave the same product in a yield of 97%.

Inner Salt IX of 3-Sulfo-7-(chlorosulfonyl)phenazathionium Hydroxide.—Thionyl chloride (10 ml.) was added drop by drop to 1.0 g. of the inner salt VIII of 3,7-disulfophenazathionium hydroxide, when hydrogen chloride and sulfur dioxide was evolved. After reflux during 30 min., the mixture was poured into water. The precipitate was collected, dried, and recrystallized from ethyl acetate. The inner salt IX of 3-sulfo-7-(chlorosulfonyl)phenazathionium hydroxide was obtained in dark-violet powder, m.p. 163~164°C. Yield, 0.9 g. (94%). It gives cobalt-blue coloration with sulfuric acid.

Anal. Found: C, 38.70; H, 1.80; N, 3.66. Calcd. for $C_{12}H_6O_5NClS_3$: C, 38.35; H, 1.61; N, 3.73%.

3,7-Disulfophenothiazine 5,5-Dioxide (X).—a) The reaction of phenothiazine 5,5-dioxide (VII) and sulfuryl chloride gave 3,7-disulfophenothiazine 5,5-dioxide (X) as a hygroscopic, dark-green substance. Yield, over 86% of the theory. The substance X is soluble in water, in ethanol, and in methanol. The sodium, potassium, calcium and barium salts are easily soluble in water. Coloration with sulfuric acid is reddish-purple.

b) To a solution of substance VIII in 40 ml. of acetic acid, 1.0 ml. of 30% hydrogen peroxide was added, and the solution was heated on a water bath during 3 hr. Evaporation of the solvent gave the same disulfonic acid X. Yield of the crude product, quantitative.

Summary

Reactions of some phenothiazines with sulfuryl chloride and with chlorosulfonic acid were investigated. With sulfuryl chloride, phenothiazine (I), its 5-oxide (II), and 1,3,7,9-tetrachlorophenothiazine (III) gave the same product, 1,3,7,9-tetrachlorophenazathionium chloride (IV), which yielded the corresponding hydroxide VI by the action of aqueous sulfuric acid and of ethanolic potassium hydroxide. To establish the structural relationship of these substances, mutual transformations were carried out. Treatment of phenothiazine and of its 5-oxide with chlorosulfonic acid gave the inner salt VIII of 3,7-disulfophenazathionium hydroxide, which yielded the inner salt IX of 3-sulfo-7-(chlorosulfonyl)phenazathionium hydroxide by the action of thionyl chloride. Chlorosulfonic acid converted phenothiazine 5,5-dioxide into 3,7-disulfophenothiazine 5,5-dioxide which was obtained also by the oxidation of the inner salt VIII with 30% hydrogen peroxide in acetic acid.

The author expresses his thanks to Professor Y. Urushibara, the University of Tokyo, for his helpful guidance throughout this work, to Dr. K. Takeda, Director of the Laboratory, for his permission to conduct this research, and also to the members of the Center of Microanalytical Services, Shionogi and Co., Ltd., for the elementary analyses and the infrared spectal measurements.

Research Laboratory
Shionogi and Co., Ltd.
Imafuku, Amagasaki

Analysis of Organic Compounds by Flame Spectrometry. I. Determination of Chlorine in Organic Compounds by Band Spectra of Cuprous Chloride*

By Masao MARUYAMA and Setsuya SENO

(Received September 1, 1958)

Analysis by flame spectrometric method has developed around metal elements with low excitation energy and recently its application has gradually been extended to heavy metals. On the other hand, determination of nonmetallic elements has been reported only in a few instances, such as the determination of phosphorus[1] and halogen[2] by indirect method, that of the chloride ion in sea water by band spectrum of cuprous chloride[3], that of organophosphorus compounds[4], and semi-quantitative determination of the fluoride ion by photographic measurement[5].

The present writers re-examined the determination of the chloride ion by the band spectrum of cuprous chloride, based on the so-called Beilstein's reaction, developed by Honma and others[3].

It was thereby learned that a stable band spectrum of cuprous chloride can be obtained similarly even in the case of non-ionized chloride and a rapid determination of chlorine in organic compounds was carried out successfully by the use of an organic solvent, *N*, *N*-dimethylformamide (DMF).

Experimental

Apparatus and Reagents.—Measurement of flame spectrum was made with Beckman Model DU spectrophotometer (with 4300 photomultiplier accessory), with 9200 flame attachment, 4020 atomizer burner, and 92300 spectral energy recording adapter. Hydrogen and oxygen were used for excitation. To obtain a stable low pressure hydrogen flow, a combination of a flow meter, a hydraulic pressure governor, and a damper was placed between the burner and the gas regulator. Brief outline of this apparatus is shown in Fig. 1.

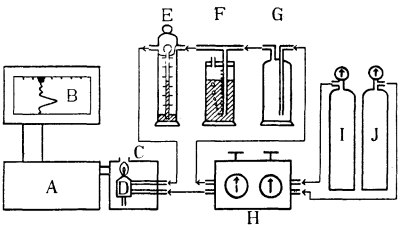


Fig. 1. Schematic diagram of the apparatus.

A Beckman DU spectrophotometer
B Spectral energy recording adapter
C Flame attachment
D Atomizer burner
E Flow meter
F Hydraulic pressure governor
G Damper
H Fuel pressure regulator
I Hydrogen cylinder
J Oxygen cylinder

The reagents used were all commercial reagents of special grade (G.R. grade). The solvent, DMF was dehydrated and distilled, collecting the fraction of b.p. 152~153°C. Standard substance for chloride was the γ-isomer of BHC (hexachlorocyclohexane) of standard quality for polarographic analysis.

Experimental Procedure.—*Preparation of the solvent* (Cu, 0.05 M).—In dehydrated DMF, 12.08 g. of cupric nitrate (trihydrate) was dissolved and 1 cc. of nitric acid was added into this solution to prevent the precipitation of cupric hydroxide or basic cupric chloride and the solution was brought up to 1000 cc.

Preparation of standard chloride solution and sample solution.—In a 100 cc. volumetric flask, 4.848 g. of standard BHC (chloride equivalent, 48.48) was accurately weighed and dissolved in DMF containing 0.05 M of copper to prepare standard 1 M chloride solution. The solution was diluted as required to a concentration of 0.05~0.1 M chloride. Test solutions were prepared by placing a quantity of the sample corresponding to 0.2~1.0 mM of chloride in a 20 cc. volumetric flask and dissolved in DMF containing copper.

Procedure of flame photometric analysis.—For the analysis, a peak of the band spectrum of cuprous chloride at 435.4 mμ was used and the calibration curve was made from the height of the base line to the peak of the spectral curve.

1) W. A. Dippel, C. E. Bricker and N. F. Furman, *Anal. Chem.*, **26**, 553 (1954).
2) O. Menis, H. P. House and T. C. Rains, ibid., **29**, 76 (1957).
3) M. Honma, ibid., **27**, 1656 (1955).
4) O. W. Brite, ibid., **27**, 1815 (1955).
5) R. Ishida, *J. Chem. Soc. Japan, Pure Chem. Sec.* (*Nippon Kagaku Zasshi*), **77**, 241 (1956).

* The gist of this work was presented at the 6th Annual Meeting of the Japan Society for Analytical Chemistry in October, 1957.

Conditions of the measurement were as follows: wavelength, 442 to 428 mμ; slit width, 0.05 mm.; sensitivity, full; oxygen pressure, 1.76 kg./cm² (25 lb./in²) on the fuel pressure gauge; hydrogen pressure, 1st, 0.035 kg./cm² (0.5 lb./in²) on the fuel pressure gauge, 2nd, 10 cm. water column; hydrogen flow rate, 450 cc./min.; scanning speed, 10, on the scale of the instrument; chart speed, 7.62 cm./min. (3 in./min.).

Experimental Results and Discussion

Exeitation of Cuprous Chloride Band Spectrum.—The band spectrum of cuprous chloride emitted in oxy-hydrogen flame has bands at the wave lengths listed in Table I[6].

TABLE I. BAND SPECTRA OF CUPROUS CHLORIDE

Wavelength (mμ)	Relative intensity	Wavelength (mμ)	Relative intensity
526.2_3	6	443.3_8	9
498.2_2	2	441.2_4	8
494.6_2	1	435.3_9	10
488.1_5	4	433.3_2	9
484.6_4	3	428.0_9	9
478.8_5	2	425.8_9	7
475.5_7	1	418.7_9	3
449.3_8	5		

The brightest of these is the band at 435.4 mμ, followed by bands at 443.4, 433.3 and 428.1 mμ; 435.4 mμ was taken as the analytical wavelength.

Honma and others have already examined the cuprous chloride band spectrum of a sample in aqueous solution and found that its measured intensity is low and the slit width must be so wide that hardly any fine structures were observed. It was also pointed out that, in this wavelength region, the cuprous chloride band spectrum is interfered by C_2-Swan band owing to the presence of carbon compounds, and does not make quantitative estimation possible.

The present writers, however, were able to overcome these difficulties by weakening the interfering action of C_2-Swan band by careful adjustment of the fuel gas pressure even in the presence of organic compounds and by markedly increasing the intensity of cuprous chloride band spectrum by the use of a suitable organic solvent in place of water.

In general, organic compounds are sparingly soluble in water and the use of an organic solvent will be the only means of preparing a sample solution for flame photometric analysis.

Dimethylformamide as Solvent for Flame Photometric Analysis and Establishment of Measurement Conditions.—Dimethylformamide (DMF) was chosen as the solvent, which dissolves not only many organic compounds, but also copper compounds to an extent of over 17.5% of cupric nitrate (trihydrate), over 15% of cupric chloride (dihydrate), 1.8% of cupric sulfate, and even a small amount of cupric acetate.

When DMF is used as solvent, the fuel gas pressure, especially the pressure and the flow rate of hydrogen, greatly affect the excitation of the objective cuprous chloride and the interfering C_2- Swan band and cupric oxide spectra. At hydrogen pressure of more than 0.14 kg./cm² (2 lb./in² gauge) the flame becomes very large by inflammation of DMF, attaining a height of over 10 cm., and the emission becomes unstable. The spectral curve obtained in such a case is covered by the C_2-Swan band, cupric oxide and cuprous hydride spectra, and cuprous chloride spectrum are hardly ever distinguishable.

With the decrease of hydrogen pressure, the flame becomes smaller and the effect of interfering spectra lessens gradually, with the appearance of a peak of cuprous chloride band spectrum.

When oxygen pressure is elevated, such as to 1.76 kg./cm² (25 lb./in² gauge), in order to strengthen the spraying of the sample,

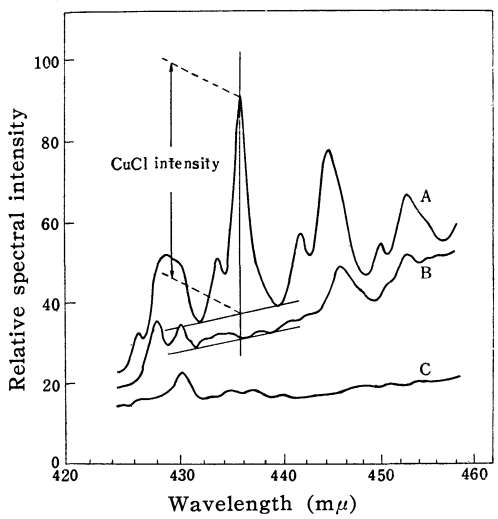


Fig. 2. Spectrum of cuprous chloride.
A (Cu: 0.05 M, Cl: 0.05 M)
B (Cu: 0.05 M)
C (DMF only)
Slit width: 0.05 mm.

6) R. W. B. Pearse and A. G. Gaydon, "Identification of Molecular Spectra", Chapman and Hall, Ltd., London (1950).

and hydrogen pressure is adjusted to about 10 cm. water column, cuprous chloride band spectrum gives a distinguished peak, as indicated in Fig. 2.

The slit width was fixed at 0.05 mm., at which the fine structure of cuprous chloride band spectrum can be observed, and the sensitivity was adjusted accordingly. The relationship between the slit width and the cuprous chloride band spectrum is indicated in Fig. 3.

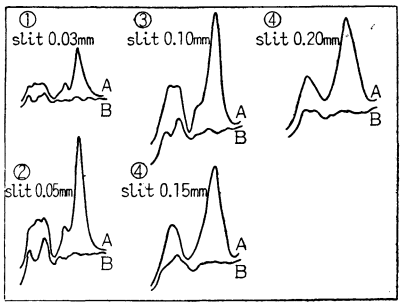


Fig. 3. Effect of slit width on cuprous chloride spectrum.
A (Cu: 0.05 M, Cl: 0.04 M)
B (Cu: 0.05 M)

Preparation of Calibration Curves and Stability of Intensity.—As shown in Fig. 2, a base-line connecting two minima, 431 mμ and 439 mμ, was drawn on a recorded spectral curve, and the height from this line to the top of the peak was taken as the intensity of the cuprous chloride band, whose values were used for preparing the calibration curve.

The concentration of copper affects the stability of the flame and the intensity of the cuprous chloride band and the background. At a low concentration, sufficient intensity can not be obtained; at a high concentration, the background intensity increases and the flame becomes unstable. Examination with various concentrations of copper showed the optimal concentration to be 0.05 M of copper.

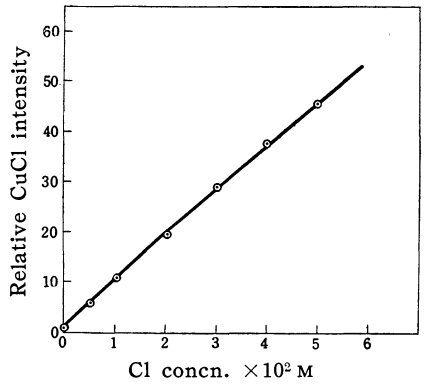


Fig. 4. Calibration curve of chloride.

An example of calibration curve at 0.05 M of copper is indicated in Fig. 4.

In the range of this calibration curve, the intensity becomes most stable in a chloride concentration of 0.02~0.05 M and is available for determination.

Table II gives the stability of cuprous chloride intensity of 0.02 M and 0.05 M chloride concentration.

TABLE II. REPRODUCIBILITY OF CUPROUS CHLORIDE INTENSITY
(concentration of copper: 0.05 M)

Concentration of chloride	
0.02 M	0.05 M
19.8	45.4
19.8	45.6
20.3	45.2
19.5	45.9
18.9	46.1
19.6	45.4
19.9	45.0
19.0	44.9
$\overline{X}=19.6_0$	$\overline{X}=45.4_4$
$\sigma=\pm 0.4_4$	$\sigma=\pm 0.4_0$

Effect of Moisture.—Sample solution absorbs moisture when left in an open vessel in high humidity and its intensity

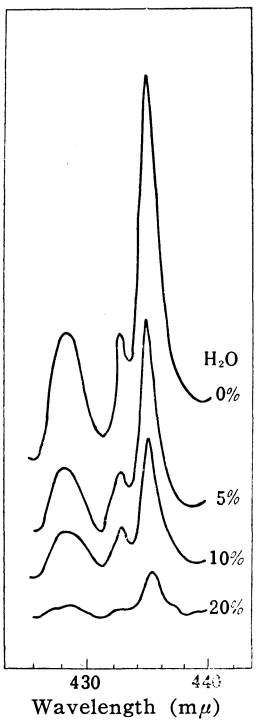


Fig. 5. Effect of moisture on cuprous chloride spectrum.
Cu: 0.05 M, Cl: 0.05 M

TABLE III. DETERMINATION OF VARIOUS ORGANIC CHLORINE COMPOUNDS

Compounds	M.W.	Cl No.	Cl Equivalent	Concn. of Cl (taken)	Concn. of Cl (found)	Recovery %
Chloramphenicol	323.14	2	161.57	0.0257	0.0261	101.5
				0.0398	0.0394	99.0
				0.0514	0.0504	98.1
Monochloroacetic acid	94.50	1	94.50	0.0325	0.0328	100.9
				0.0491	0.0484	98.6
				0.0573	0.0578	100.8
Dichloroacetic acid	128.95	2	64.48	0.0461	0.0469	101.6
				0.0491	0.0501	102.0
Trichloroacetic acid	163.40	3	54.47	0.0237	0.0240	101.3
				0.0418	0.0416	99.6
				0.0474	0.0476	100.5
Chlorobutanol	177.47	3	59.16	0.0227	0.0229	100.9
				0.0454	0.0461	101.6
				0.0428	0.0428	100.0
α-Chloroacetamide	93.52	1	93.52	0.0267	0.0262	98.1
				0.0497	0.0489	98.5
2,4-Dinitrochlorobenzene	202.56	1	202.56	0.0287	0.0290	101.0
				0.0392	0.0380	97.0
				0.0574	0.0582	101.4
Chloramine-T	281.70	1	281.70	0.0237	0.0240	101.3
				0.0338	0.0326	96.5
				0.0474	0.0406	85.6
Procaine hydrochloride	272.77	1	272.77	0.0393	0.0425	108.1
				0.0206	0.0219	106.3
Chloroform	119.39	3	39.80	0.0589	0.0646	109.6
				0.0677	0.0763	112.6
Carbon tetrachloride	153.84	4	38.46	0.0563	0.0725	128.8
				0.0564	0.0717	127.1

will diminish. Hence the determination should be carried out as rapidly as possible after the sample has been transferred to a beaker. The effect of moisture on the spectral curve is shown in Fig. 5.

Determination of Chlorine in Organic Compounds.—Results obtained by the application of the present method to 11 kinds of organic chlorine compounds are shown in Table III.

These results indicate that the amount of chlorine found in solid organic chlorine compounds is approximately 98~102% of the theoretical value, while the value differs greatly from that calculated for liquid organic chlorine compounds, chloramine-T, and procaine hydrochloride. The values are higer by approximately 30% for carbon tetrachloride, and 10% for chloroform, and very arbitrary for chloramine-T.

Such a discrepancy may be due to the change in the intensity of the cuprous chloride band by the characteristic effect of evaporation rate for carbon tetrachloride and chloroform, by the ionic nature of chlorine of procaine hydrochloride, and by the sodium that forms a salt for chloramine-T. However, further detailed examination is still required.

Range of Application.—It is possible to carry out the qualitative and the quantitative determination of chlorine by dissolving organic chlorine compounds in DMF in a chlorine concentration of over 0.005 M and using 2~5 cc. of this solution. It is considered possible that this method can be used as a simple procedure for organic elementary analysis.

Organic compounds containing bromine or iodine can also be determined as in the case of chlorine at approximately the same wavelength region but the band spectra of cuprous bromide or cuprous iodide present less intensity than that of chloride under the same condition.

It is hoped that further research will be made on the determination of compounds containing bromine or iodine.

Summary

Examinations were made on the band spectrum of cuprous chloride based on the Beilstein's reaction in oxy-hydrogen flame. Determination of chlorine in organic chlorine compounds was attempted by using dimethylformamide containing

copper as a solvent and a band peak of 435.4 mμ of cuprous chloride.

In order to decrease the effect of C_2-Swan band that is produced on combustion of organic compounds, and to increase the sensitivity of cuprous chloride band spectrum, combustion gas was maintained at high oxygen pressure; 1.76 kg./cm^2 (25 lb./in^2 gauge), and low hydrogen pressure; 1st, 0.035 kg./cm^2 (0.5 lb./in^2 gauge), 2nd, 10 cm. water column.

γ-BHC was used as the standard and determination was carried out on 11 kinds of organic chlorine compounds, and good results were obtained with samples other than liquid, metal salts, and hydrochlorides. The determinable range for chlorine is 0.005~0.1 M concentration.

Grateful acknowledgment is made to Sankyo Co., Ltd., for permission to publish these data.

Shinagawa Plant, Sankyo Co., Ltd.
Nishi-Shinagawa, Shinagawa-ku, Tokyo

Confirmation of the Formation of Colloidal Particles in Aqueous Cobalt Salt Solution by Radiotracer Electrodialysis

By Tsunetaka SASAKI and Katsuyoshi OSAKA*

(Received October 16, 1958)

It has been pointed out by a series of our experiments[1] as well as of others[1], that polyvalent metallic ions such as aluminum, iron, copper and thorium exhibit remarkable effects in regard to surface-chemical properties, for instance, wettability of paraffin by water and the nature of monomolecular films of fatty acids. Such effects were explained by the assumption that these ions when dissolved in water mainly exist as hydrated polynuclear ions in a region of suitable pH, rather than as simple monomeric ions, as in the case of alkali and alkaline earth metal ions which show no remarkable effects in regard to the surface-chemical properties. Such an assumption of the existence of aggregated ions has also been proposed by Haissinsky[2] to explain a large fluctuation in the published data on the solubility product of one and the same insoluble compound. McGee, Kraus, Milburn and Kohlschütter[3] also offered similar opinions. Thus the existence of the polynuclear structure becomes increasingly convincing. However, all of these experimental evidences are rather indirect in nature. As a more direct evidence of the existence of such polynulear ions, we can also refer to a number of studies upon radiocolloid formation which proved the existence of colloidal particles in extremely dilute solutions of polonium, bismuth, lead, thorium, yttrium, etc.[4] In more concentrated solutions, the formation of aggregated particles were also observed in cobalt salt solution, for instance, by a self-diffusion method[5].

The present authors have also carried out the experiment of radiotracer electrodialysis[6], coupled with an ordinary filtration, to obtain a direct evidence of the formation of colloidal particles in an aqueous cobalt salt solution.

Experimental

(1) Radiotracer Electrodialysis.—The apparatus employed in the experiment was shown in Fig. 1. In this figure, A is a glass U-tube with one end somewhat wider than the other.

* Present address: Kôyô Sangyô Company, Ltd., 1-2 Marunouchi, Chiyoda-ku, Tokyo, Japan.

1) T. Sasaki and R. Matuura, This Bulletin, **24**, 274 (1951); M. Muramatsu and T. Sasaki, ibid., **25**, 21 (1952), **29**, 35(1956); A. Inaba, ibid., **25**, 174(1952); G. A. Wolstenholme and J. H. Schulman, *Trans. Faraday Soc.*, **46**, 475 (1950), **47**, 788 (1951).

2) M. Haissinsky, "Les Radiocolloides", Hermann et Cie, Paris (1934); I. Adler and J. Steigman, *J. Phys. Chem.*, **36**, 493 (1952).

3) C. G. McGee, *J. Am. Chem. Soc.*, **71**, 278 (1949); K. A. Kraus and R. W. Holmberg, *J. Phys. Chem.*, **58**, 325 (1954); R. M. Milburn and W. C. Vosburgh, *J. Am. Chem. Soc.*, **77**, 1352 (1955); H. W. Kohlschütter et al., *Z. anorg. allgem. Chem.*, **248**, 319 (1941); H. W. Kohlschütter, *Kolloid-Z.*, **96**, 237 (1941).

4) J. Schubert and E. E. Conn, *Nucleonics*, **4**, No. 6, 2 (1949).

5) R. Matuura and H. Kimizuka, This Bulletin, **28**, 668 (1955).

6) T. Godlewski, *Kolloid- Z.*, **14**, 229 (1914); F. Paneth, ibid., **13**, 297 (1913).

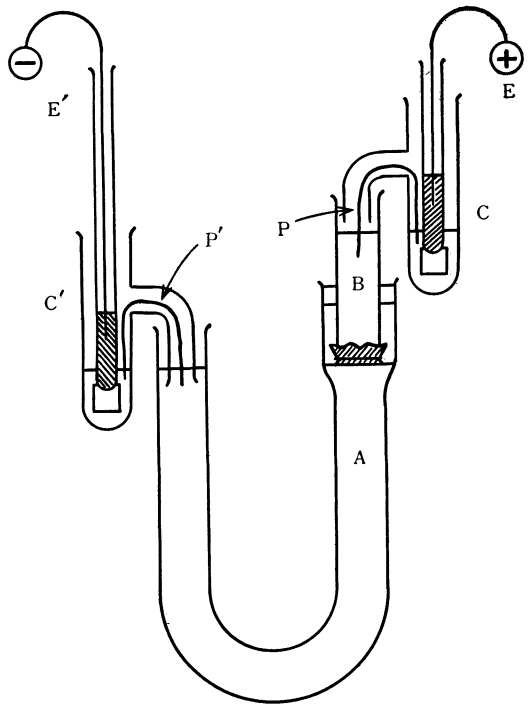


Fig. 1. Electrodialysis cell.

B is a glass cylinder, to the bottom of which a semipermeable cellophane membrane is tightly attached as shown in the figure, with the aid of a rubber ring. The electrode cells C and C' consist of two platinum electrodes E, E' and filter paper bridges P, P'. To carry out an experiment, the tubes A, B and cells C, C' are all filled with the same solution to be studied, that is 10^{-3} mol./l. aqueous solution of cobaltous chloride, with the exception that the solution in B alone is especially tagged with a suitable amount of radioisotope cobalt-60 as a tracer. Hereby, care should be taken that the lower end of the tube B is so placed that it just touches the surface of the solution in A. Now, when we apply D. C. voltage to the electrodes as indicated in Fig. 1, the cobalt ions will move from C to C'. So they will pass through the cellophane membrane downwards, if they are in a state of single ions or relatively small aggregates, while they will not be able to pass through the membrane if they exist as colloidal particles or even larger particles. Thus we can confirm the formation of particles larger than a colloidal size, when we trace the change in concentration of the solution in A.

Now, we have determined a suitable condition for practice from a preliminary experiment. It was evident that the amount dialyzed increased with the increase of applied potential gradient, as well as with the duration of electric current passed, but we performed a 50 volt and 15 minute dialysis*, since prolonged dialysis disturbed the steady condition of the solution to be dialyzed**. After the dialysis, the tube B was removed, 1 cc. of solution in the tube A just below the tube B was taken, heated to dryness in a stainless steel dish, and the radioactivity due to cobalt-60 was measured by a GM counter, as in the usual manner. The permeability was then expressed in c.p.m. Hereby, the GM tube was masked against β-ray and counting was taken only for that due to γ-ray, since the counting due to β-ray fluctuated sensitively for apparently identical geometry of counting arrangement. The cellophane used was a commercial product of a suitable thickness, which was cut in 5×5 cm^2 pieces, and was kept in distilled water for a long time in order to swell the sheets sufficiently for use.

In the course of experiments we found that the permeability of cellophane fluctuated from one sample to another, and also that one and the same sample gradually lost its permeability when used repeatedly. To overcome these undesirable conditions, we used the same membrane only for a couple of measurements, that is, for the permeability measurement of the reference solution containing 10^{-3} mol./l. cobaltous chloride, kept at pH 1, and for the subsequent measurement of the solution to be studied, which was of the same concentration but varying in pH. The control of pH was made using hydrochloric acid and sodium hydroxide.

From the measured permeability, we calculated the relative permeabilty, by the following formula,

$$P_r=\frac{\text{Permeability at pH}=x}{\text{Permeability at pH}=1}$$

The value P_r was used for further discussion. The change of pH due to the electrodialysis was about 0.5 at most.

Before use, cellophane membrane was also examined against pin holes by measuring a leak of Congo red solution through the membrane into pure water for 24 hours, from which we could confirm the fact that the membrane was free from eventual large pores, and also that the

TABLE I. PERMEABILITY OF AQUEOUS COBALT IONS THROUGH CELLOPHANE MEMBRANE

Permeability P_1 at pH=1	Permeability P' at pH=x	P	$P_r=P/P'$
170 cpm	1.0	285 cpm	1.67
173	2.2	92	0.53
146	2.8	52	0.36
163	2.9	97	0.60
188	4.5	104	0.55
169	5.4	119	0.70
136	6.7	50	0.37
148	8.1	44	0.30
144	10.4	0	0

* The distance between the two electrodes is 22 cm.

** The flow of water due to the hydrostatic pressure of water in the tube B was negligible during the period of experiment.

membrane acted as a sieve for particles at least larger than the Congo red molecule. Stock aqueous solution was kept at pH=1 and made up to a desired pH immediately before use. Permeability at varying pH and corresponding P_r values were listed in Table I.

(2) **Filtration.**—Ordinary filtration was carried out to detect the formation of particles coarser than colloidal ones in aqeous solution of cobalt salt. Radioactive cobalt salt solution of the same origin as used in the electrodialysis was filtered under varying pH using fine pore filter paper (Tôyô 5C) and a cobalt content in the filtrate was analyzed by measuring radioactivity due to the aliquot of the filtrate in the same manner as in the preceding experiment. The results were shown in Table II. In this table we showed the amounts of the cobalt ion in solution before and after the filtration by an arbitrary unit of radioactivity of 1 cc. of respective solution which was considered to be proportional to the concentration of cobalt ion. The degree of permeability of cobalt ion was expressed by the ratio F_r of radioactivities in a solution before and after the filtrations as shown in the last column of Table II.

TABLE II. PERMEABILITY OF AQUEOUS COBALT ION THROUGH FILTER PAPER (TÔYÔ 5 C)

pH	Amount of cobalt (cpm) before filtr. (A)	after filtr. (B)	$F_r=(B)/(A)$
2.5	287*	288*	1
6.6	882	874	0.99
8.4	883	774	0.88
8.9	*873*	*772*	*0.88*
9.4	874	336	0.38
10.1	846	15	0.017

* Geometry of the counting arrangement was accidentally different from the rest of the measurements.

Discussion

From Tables I and II, we prepared a diagram showing a pH dependence of permeability of cobalt ions through cellophane membrane and filter paper as shown in Fig. 2. In constructing this diagram, we first plotted P_r against pH, excluding the value at pH 1 which showed an extreme deviation, and obtained a curve which as a whole gave a plateau in the region of pH from 2 to 6. Next, we plotted F_r against pH and a similar curve was obtained. Then we adjusted the units of P_r and F_r axes so that both curves coincided at their plateau portions, assuming that there the complete passage of solute took place for both operations.

Now, in Fig. 2, we can readily recognize that the cobalt ions in the region A pass through both cellophane membrane and

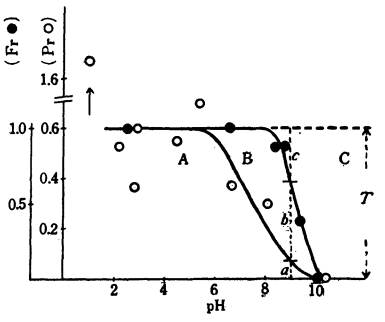


Fig. 2. State of dispersion of aqueous cobalt ion.
A, simple ionic dispersion
B, colloidal dispersion
C, macroscopic aggregation
T, total amount of cobalt in water

filter paper, while those belonging to the region B pass through the filter paper but are retained by the cellophane membrane, and those belonging to the region C are retained both by cellophane membrane and filter paper. Therefore, when we draw an ordinate at a certain pH, a portion a of the ordinate belonging to the region A represents a fraction of an amount of cobalt in the state of A region (simple ionic state), and so on. Thus, in the region of pH from 6 to 10, we confirm the formation of colloidal cobalt particles as those permeable to filter paper but not to cellophane membrane. We can also see the initiation of macroscopic agglomerate formation at pH 8 and precipitation of practically all cobalt ions at pH larger than 10, in the aqueous cobalt salt solution.

Now, from the published data of the solubility product[7], we calculated the minimum pH required to initiate cobaltous hydroxide precipitate in 10^{-3} molar aqueous cobalt salt solution. It was about 6.8, which happened to be situated between pH values of the initiation of colloidal particle formation and macroscopic agglomerate formation. We can conclude from these facts that in the solution studied, there exists a pH region of colloidal particle formation somewhere near the pH, beyond which solubility is exceeded. This conclusion is consistent with the results of a series of our former investigations already mentioned[1].

It must be added that the dissolved state of cobalt ion in aqueous solution changes gradually in the course of time, in a higher pH region as seen from the

7) Landolt-Börnstein, "Physikalisch-chemische Tabellen". I. Erg., Verlag J. Springer, Berlin, (1927), p. 662.

change of color of the solution. So we may expect that the boundary between the A regions and B of Fig. 2 will gradually shift presumably to the left in the course of time. The boundary may also shift according to the nature of the semipermeable membrane used.

Summary

(1) Dissolved state of cobalt ions in 10^{-3} molar aqueous solution of cobaltous chloride, varying in pH, was studied by a radiotracer electrodialysis coupled with an ordinary filtration.

(2) Formation of colloidal particles permeable to filter paper but not permeable to cellophane membrane were confirmed in the solution, in the region of pH from 6 to 10.

(3) Macroscopic precipitates of cobaltous hydroxide began to form at about pH 8 and practically all cobalt ions were precipitated at a pH greater than 10.

(4) The value of pH of insoluble cobaltous hydroxide formation in aqueous 10^{-3} molar cobalt salt solution calculated from the solubility product of cobaltous hydroxide was found to be situated between the pH of the initiation of colloidal particle formation and the pH of the initiation of macroscopic agglomerate formation.

The authors express their hearty thanks to the Deparment of Education for the Scientific Research Expenditure given to T. Sasaki.

Department of Chemistry
Faculty of Science
Tokyo Metropolitan University
Setagaya-ku, Tokyo

The Mannich Base of Troponoid and its Application. I. Synthesis of 5-Hydroxymethyl and 5-Formyltropolone Derivatives

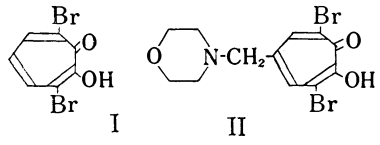
By Shuichi SETO and Kyozo OGURA

(Received October 16, 1958)

Hartwig[1] reported morpholinomethyl derivatives of tropolone, 3-bromotropolone and 5-bromotropolone, and Pauson[2] also gave a brief description on piperidino methyltropolone in his review. However, Mannich reaction of 3,7-dibromotropolone (I) has not been reported. The present authors applied Mannich reaction to I in order to introduce a carbon chain to the 5-position of the tropolone nucleus and obtained 3,7-dibromo-5-morpholinomethyltropolone (II) in a good yield, from which 5-hydroxymethyl and 5-formyl compounds were derived. This paper describes these results.

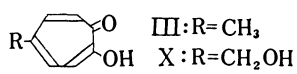
When I was treated with morpholine and formalin in acetic acid, II was obtained as yellow powder. II is sparingly soluble in water and usual organic solvents, produces a hydrochloride difficultly soluble in water when treated with hydrochloric acid and gives a green color to the water layer with ferric chloride. Catalytic hydrogenolysis of II in the presence of palladium-carbon gave 5-methyltropolone (III)[3]. This indicates that the morpholinomethyl group of II has taken 5-position in the tropolone nucleus. 3,7-Dibromo-5-acetoxymethyltropolone (V) was obtained when II was heated with a large excess of acetic acid. If a small quantity of acetic acid is used, bis-(3,7-dibromotropololon-5-yl) methane (IV) is formed as a by-product. IV was also formed when II was treated with formalin and dimethylamine in acetic acid or V was heated in aqueous hydrobromic acid. V was easily hydrolyzed by alkali to give 3,7-dibromo-5-hydroxymethyltropolone (VI). The hydroxymethyl group of VI is readily displaced by other groups. For example, 5-nitro (VII)[4], 5-bromo (VIII)[5]

1) E. Hartwig, *Angew. Chem.*, **66**, 605 (1954).
2) P. L. Pauson, *Chem. Revs.*, **55**, 9 (1955).
3) T. Nozoe, T. Mukai and K. Matsui, *Proc. Japan Acad.*, **27**, 646 (1951).
4) K. Yamane, *J. Chem. Soc. Japan, Pure Chem. Sec.* (*Nippon Kagaku Zasshi*), **76**, 787 (1955); T. Nozoe, Y. Kitahara, K. Doi and T. Arai, *Bull. Chem. Research Inst. of Non-Aqueous Solutions, Tohoku Univ.*, **7**, 13 (1957).
5) T. Nozoe et al., *Proc. Japan Acad.*, **26**, 38 (1950).

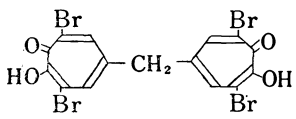


I

II



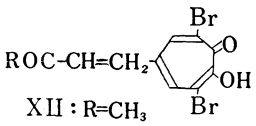
III: R=CH_3
X: R=CH_2OH



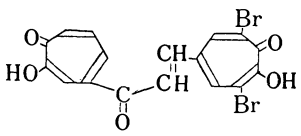
IV



V: R=CH_2OCOCH_3
VI: R=CH_2OH
VII: R=NO_2
VIII: R=Br
IX: R=$N_2C_6H_4CH_3$ (p)
XI: R=CHO



XII: R=CH_3
XIII: R=C_6H_5
XIV: R=C_6H_4OH (2')
XV: R=OH



XVI

and 5-azo (IX)[6] compounds were yielded by the reactions of VI with dinitrogen tetroxide, *N*-bromosuccinimide and diazonium salt respectively.

Sebe and Matsumoto[7] obtained the formyl derivative by oxidizing 3-hydroxymethyltropolone derivatives with activated manganese dioxide. The application of this method to VI gave 3,7-dibromo-5-formyltropolone (XI). Catalytic hydrogenolysis of VI afforded 5-hydroxymethyltropolone (X) which was an unstable substance. Oxidation of X with manganese dioxide gave 5-formyltropolone[8].

3,7-Dibromo-5-formyltropolone (XI) gives an acetal, reacts with various ketonic reagents and produces Schiff's base with aniline. Furthermore, the reactions of XI with acetone, acetophenone, 2-hydroxyacetophenone, malonic acid and 4-acetyltropolone[9] gave 3,7-dibromo-5-(γ-oxobutenyl)tropolone (XII), 3,7-dibromo-5-(γ-phenyl-γ-oxopropenyl)tropolone (XIII), 3,7-dibromo-5-[γ-(2'-hydroxyphenyl)-γ-oxopropenyl]tropolone (XIV), 3,7-dibromo-5-(β-carboxyethenyl)tropolone (XV), and 3,7-dibromo-5-[γ-(tropolone-4'-yl)-γ-oxopropenyl]tropolone (XVI) respectively.

Further experiments of 5-hydroxymethyl and 5-formyltropolone derivatives are in progress.

6) S. Ito, unpublished work.
7) E. Sebe and S. Matsumoto, *Sci. Repts. Tohoku Univ., Ser.* I., **38**, 308 (1954).
8) J. W. Cook et al., *J. Chem. Soc.*, **1952**, 4416.
9) T. Nozoe, K. Takase and M. Ogata, *Chem. and Ind.*, **1957**, 1070.

Experimental[10]

3,7-Dibromo-5-morpholinomethyltropolone (II).—To a stirred mixture of 2 g. of 3,7-dibromotropolone (I), 3 ml. of acetic acid and 2 ml. of morpholine was added 1 ml. of formalin at 70°. The mixture became a clear orange solution and after a few min. a yellow precipitate began to deposit. Thereafter, stirring was continued at 80~90°C for 2 hr. Then 5 ml. of water was added to the cooled reaction mixture. The precipitate, 3,7-dibromo-5-morpholinomethyltropolone (II) was collected and washed with water. Yield, 2.6 g., m. p. 198~200°C.

Anal. Found: C, 38.40; H, 3.55; N, 3.82. Calcd. for $C_{12}H_{13}O_3NBr_2$: C, 38.00; H, 3.43; N, 3.70%. U. V. λ_{max}^{MeOH} (log ε): 268 mμ (4.32), 344 mμ (4.00), 427 mμ (3.92).

Hydrochloride of II; m. p. 225°C (decomp.).

Anal. Found: C, 34.65; H, 3.57; N, 3.35. Calcd. for $C_{12}H_{14}O_3NBr_2Cl$: C, 34.61; H, 3.61; N, 3.36%.

5-Methyltropolone (III).—When 500 mg. of II in aqueous sodium hydroxide was shaken with hydrogen at room temperature in the presence of palladium-carbon, 3 molar equivalents of hydrogen were absorbed. The catalyst was removed by filtration and the filtrate was acidified. A precipitate thereby formed was crystallized from benzene to give 5-methyltropolone (III) as colorless crystals, m. p. 109~110°C, undepressed by admixture with an authentic specimen.

Bis-(3,7-dibromotropolone-5-yl)methane (IV).—To a mixture of 500 mg. of I, 400 mg. of aqueous dimethylamine (40%) and 2 ml. of acetic acid was added 320 mg. of formalin (37%) at 90°C with stirring. After 40 min. the reaction mixture was cooled. Yellow crystals thereby formed

10) Melting points are not corrected.

were collected and washed with a small quantity of methanol. Yield 450 mg., m. p. 225°C (decomp.).

Anal. Found: C, 31.37; H, 1.23. Calcd. for $C_{15}H_8O_4Br_4$: C, 31.48; H, 1.40%. U. V. λ_{max}^{MeOH} (log ε): 272 mμ (4.48), 345 mμ (4.16), 430 mμ (4.07).

When an aqueous solution of ferric chloride was added to a suspension of IV in benzene, a black solid formed at the interface of the benzene and aqueous layers.

Heating of 5-acetoxymethyl compound (V) in aqueous hydrobromic acid under reflux also gave IV.

3,7-Dibromo-5-acetoxymethyltropolone(V). —A suspension of 1 g. of II in 35 ml. of acetic acid was heated at 100°C for 1 hr. and then at 120° for 3 hr. with stirring. The mixture became a yellow solution. When it was cooled, pale yellow needles separated out. The crystals (0.5 g.) were collected. Concentration of the filtrate at 60°C under reduced pressure gave a further crop (0.2 g.). Recrystallization of the combined crystals from ethyl acetate afforded 3,7-dibromo-5-acetoxymethyltropolone (V), m. p. 184~185°C.

Anal. Found: C, 34.66; H, 2.64. Calcd. for $C_{10}H_8O_4Br_2$: C, 34.09; H, 2.27%. U. V. λ_{max}^{MeOH} (log ε): 265 mμ (4.64), 345 mμ (4.14), 425 mμ (4.06).

3,7-Dibromo-5-alkoxymethyltropolone. — Heating of V in methanol under reflux gave 3,7-dibromo-5-methoxymethyltropolone as pale yellow crystals, m. p. 135°C.

Anal. Found: C, 34.08; H, 2.64. Calcd. for $C_9H_8O_3Br_2$: C, 33.33; H, 2.47%.

3,7-Dibromo-5-ethoxymethyltropolone, m. p. 100 °C, was similarly obtained.

Anal. Found: C, 35.19; H, 3.33. Calcd. for $C_{10}H_{10}O_3Br_2$: C, 35.54; H, 2.96%.

3,7-Dibromo-5-hydroxymethyltropolone (VI).—A mixture of 1 g. of V, 5 ml. of 3 N sodium hydroxide and 0.5 ml. of ethanol was heated on a water bath for 5 min. with stirring. After being cooled, the reaction mixture was acidified with 6 N hydrochloric acid and a precipitate thereby formed was collected, washed with water and crystallized from methanol to give 3,7-dibromo-5-hydroxymethyltropolone (VI) as pale yellow needles, m. p. 164~165°C. Yield, 0.8 g.

Anal. Found: C, 31.35; H, 1.79. Calcd. for $C_8H_6O_3Br_2$: C, 30.97; H, 1.93%. U. V. λ_{max}^{MeOH} (log ε): 266 mμ (4.47), 345 mμ (4.12), 425 mμ (4.09).

Reaction of VI with Dinitrogen Tetroxide. —To a solution of 0.1 g. of VI in 40 ml. of chloroform was added 0.5 g. of dinitrogen tetroxide with ice-cooling. After being kept for 30 min. at room temperature, the solvent and excess reagent were removed under reduced pressure. Yellow crystals thereby formed failed to show any depression of m. p. on admixture with an authentic 3,7-dibromo-5-nitrotropolone (VII), m.p. 145~146°C.

Reaction of VI with *N*-Bromosuccinimide. —A mixture of 50 mg. of VI, 30 mg. of *N*-bromosuccinimide and 6 ml. of chloroform was boiled for 2 hr. After removal of succinimide by filtration, the filtrate was evaporated to give 50 mg. of colorless crystals, m. p. 124~125°C, undepressed by admixture with 3,5,7-tribromotropolone (VIII).

Reaction of VI with Diazonium Salt. — To a pyridine solution of 50 mg. of VI was added a solution of diazonium salt prepared from 30 mg. of *p*-toluidine. A red precipitate thereby formed was collected, washed with methanol and crystallized from methanol to give red prisms, m. p. 190~191°C, undepressed by admixture with 3,7-dibromo-(*p*-tolylazo)tropolone (IX).

5-Hydroxymethyltropolone (X). — A suspension of 350 mg. of VI in aqueous sodium hydroxide was shaken with hydrogen at room temperature in the presence of palladium carbon. After absorption of 2 molar equivalents of hydrogen and removal of the catalyst by filtration the filtrate was acidified. A small amount of yellowish brown precipitate thereby formed was removed by filtration and the filtrate was extracted with ethyl acetate. Evaporation of the solvent from the extract afforded 5-hydroxymethyltropolone (X) as colorless needles, m. p. 131~132°C. Yield, 100 mg.

Anal. Found: C, 62.82; H, 5.32: Calcd. for $C_8H_8O_3$: C, 63.15; H, 5.27%. U. V. λ_{max}^{MeOH} (log ε): 233 mμ (4.40), 323 mμ (4.01).

5-Formyltropolone.—A mixture of 50 mg. of X, 5 ml. of acetone and 200 mg. of activated manganese dioxide was stirred for 2 days at room temperature. After removal of excessive manganese dioxide by filtration, the filtrate was concentrated to give a yellow manganese salt which was treated with 6 N hydrochloric acid and extracted with ethyl acetate. Evaporation of the extract left 20 mg. of 5-formyltropolone, m. p. 181°C.

3,7-Dibromo-5-formyltropolone (XI). — A mixture of 1 g. of X, 40 ml. of acetone and 4 g. of manganese dioxide was stirred for 20 hr. at room temperature. The mixture was then separated into a solid A and a filtrate B. Removal of the solvent from filtrate B under reduced pressure afforded a yellowish brown manganese salt. Treatment of the salt with 6 N sulfuric acid yielded a yellow precipitate which was crystallized from benzene to give 3,7-dibromo-5-formyltropolone (XI) as yellow prisms, m. p. 175~176°C. Extraction of solid A with acetone by means of a Soxhlet extractor gave a further crop of manganese salt which was also treated similarly to give XI. Yield, 0.95 g.

Anal. Found: C, 31.39; H, 1.43. Calcd. for $C_8H_4O_3Br_2$: C, 31.17; H, 1.30%. U. V. λ_{max}^{MeOH} (log ε): 260 mμ (4.21), 382 mμ (4.31), 410 mμ (4.33).

Heating of XI with methanol gave the acetal as colorless needles, m. p. 135°C.

Anal. Found: C, 33.58; H, 2.79. Calcd. for $C_{10}H_{10}O_4Br_2$: C, 33.90; H, 2.82%. U. V. λ_{max}^{MeOH} (log ε): 265 mμ (4.43), 350 mμ (4.02), 430 mμ (4.21).

Oxime of XI, yellow needles, m. p. 212~213°C.

Anal. Found: N, 4.21. Calcd. for $C_8H_5O_3NBr_2$: N, 4.35%. U. V. λ_{max}^{MeOH} (log ε): 270 mμ (4.42), 372 mμ (4.43), 433 mμ (4.10).

Semicarbazone of XI, yellow granular crystals, m. p. 249~250°C.

Anal. Found: C, 29.24; H, 2.18; N, 10.72. Calcd. for $C_9H_7O_3N_3Br_2$: C, 29.59; H, 1.92; N, 11.51%. U. V. λ_{max}^{MeOH} (log ε): 273 mμ (4.42), 378

mμ (4.55).

Thiosemicarbazone of XI, orange crystals, m.p. 280~288°C (decomp.).

Anal. Found: C, 28.79; H, 2.13. Calcd. for $C_9H_7O_2N_3SBr_2$: C, 28.35; H, 1.84%. U. V. λ_{max}^{MeOH} (log ε): 289 mμ (4.28), 395 mμ (4.47).

Phenylhydrazone of XI, red needles, m. p. 209~210°C.

Anal. Found: N, 6.97. Calcd. for $C_{14}H_{10}O_2N_2Br_2$: N, 7.04%. U. V. λ_{max}^{MeOH} (log ε): 265 mμ (4.42), 410 mμ (4.58).

2,4-Dinitrophenylhydrazone of XI, red needles, m. p. 257~258°C.

Anal. Found: N, 11.78. Calcd. for $C_{14}H_8O_6N_4Br_2$: N, 11.48%. U. V. λ_{max}^{MeOH} (log ε): 260 mμ (4.41), 440 mμ (4.61).

Schiff's Base of XI. — A mixture of 100 mg. of XI, 1 ml. of aniline and 0.5 ml. of acetic acid was heated on a water bath for 10 min. Deep red crystals thereby formed were recrystallized from methanol. Yield 100 mg., m. p. 209~210°.

Anal. Found: C, 43.61; H, 2.55; N, 3.81. Calcd. for $C_{14}H_9O_2NBr_2$: C, 43.98; H, 2.36; N, 3.67%. U. V. λ_{max}^{MeOH} (log ε): 270 mμ (4.37), 390 mμ (4.40).

Condensation of XI with Acetone. — To a solution of 100 mg. of XI in 1 ml. of acetone was added 0.3 ml. of aqueous sodium hydroxide (10%) with stirring at room temperature. After 2 days, an orange precipitate was collected and acidified with 6 N hydrochloric acid to give a yellow precipitate. Its recrystallization from acetone afforded 100 mg. of 3,7-dibromo-5-(γ-oxobutenyl)tropolone (XII), m. p. 195°C.

Anal. Found: C, 38.19; H, 2.61. Calcd. for $C_{11}H_8O_3Br_2$: C, 37.93; H, 2.30%. U. V. λ_{max}^{MeOH} (log ε): 280 mμ (4.38), 405 mμ (4.56).

Condensation of XI with Acetophenone.— A mixture of 100 mg. of XI, 0.3 ml. of acetophenone and 0.3 ml. of aqueous sodium hydroxide (10%) was stirred for 2 hr. at room temperature. A deep red precipitate thereby formed was collected and acidified with 6 N hydrochloric acid to give a yellow precipitate. Its crystallization from methanol yielded 120 mg. of 3,7-dibromo-5-(γ-phenyl-γ-oxopropenyl)tropolone (XIII), m. p. 200 °C.

Anal. Found: C, 46.16; H, 2.40. Calcd. for $C_{16}H_{10}O_3Br_2$: C, 46.83; H, 2.44%. U. V. λ_{max}^{MeOH} (log ε): 260 mμ (4.14), 288 mμ (4.16), 418 mμ (4.38).

Condensation of XI with 2-Hydroxyacetophenone. — A mixture of 100 mg. of XI, 80 mg. of 2-hydroxyacetophenone, 1 ml. of ethanol, and 0.5 ml. of 6 N sodium hydroxide was stirred on a water bath for 30 min. The mixture became dark red and formed a small quantity of precipitate C. Precipitate C was removed by filtration. Acidification of the filtrate with 6 N hydrochloric acid gave a brown solid. Recrystallization of the solid from methanol afforded 50 mg. of 3, 7-dibromo-5-[γ-(2'-hydroxyphenyl)-γ-oxopropenyl]tropolone (XIV), m. p. 215°C (decomp.).

Anal. Found: C, 45.02; H, 2.60. Calcd. for $C_{16}H_{10}O_4Br_2$: C, 45.11; H, 2.35%. U. V. λ_{max}^{MeOH} (log ε): 260 mμ (4.20), 295 mμ (4.20), 440 mμ (4.54).

Acidification of precipitate C gave XI recovered.

Reaction of XI with Malonic Acid.—A mixture of 100 mg. of XI, 100 mg. of malonic acid, 1 ml. of pyridine and 3 drops of piperidine was heated for 1 hr. at 90°C, for 2 hr. at 100°C and finally for 2 hr. at 120°C. During this time, evolution of carbon dioxide was observed and the mixture turned brown in color. Then the mixture was poured into a mixture of 0.5 g. of ice and 1 ml. of concentrated hydrochloric acid. A brown precipitate thereby formed was crystallized from methanol after decolorization with carbon to give 50 mg. of 3,7-dibromo-5-(β-carboxyethenyl)tropolone (XV), m. p. 195°C.

Anal. Found: C, 34.92; H, 2.01. Calcd. for $C_{10}H_6O_4Br_2$: C, 34.29; H, 1.71%. U. V. λ_{max}^{MeOH} (log ε): 268 mμ (4.39), 380 mμ (4.40).

Condensation of XI with 4-Acetyltropolone.—A mixture of 50 mg. of XI, 40 mg. of 4-acetyltropolone, 0.5 ml. of methanol and 0.5 ml. of aqueous sodium hydroxide (10%) was stirred for 30 min. at room temperature. The mixture turned red in color and deposited a deep red precipitate. The precipitate was collected, acidified with 6 N hydrochloric acid and recrystallized from methanol to give 50 mg. of 3,7-dibromo-5-[γ-(tropolone-4'-yl)-γ-oxopropenyl]tropolone (XVI), m. p. 220°C (decomp.).

Anal. Found: C, 42.93; H, 2.23. Calcd. for $C_{17}H_{10}O_5Br_2 \cdot H_2O$: C, 43.01; H, 2.54%. U. V. λ_{max}^{MeOH} (log ε): 255 mμ (4.24), 430 mμ (4.25).

Summary

Application of the Mannich reaction to 3,7-dibromotropolone gave 3,7-dibromo-5-morpholinomethyltropolone, from which 5-hydroxymethyl and 5-formyl derivatives were derived. It was found that the hydroxymethyl group of 3,7-dibromo-5-hydroxymethyltropolone can be easily displaced, and that 3,7-dibromo-5-formyltropolone has the characteristics of an ordinary aldehyde and reacts with ketones and malonic acid.

For the purpose of this work, 4-acetyltropolone was graciously furnished by Mr. K. Takase (Professor Nozoe's Laboratory, Faculty of Science, Tohoku University). A part of the expenses for the present research was defrayed by Sankyo Co., Ltd. The microanalyses were carried out by Messrs. S. Oyama and S. Azumi and Miss A. Iwanaga. The authors wish to express their sincere gratitude to the above mentioned people.

The Chemical Research Institute of Non-Aqueous Solutions
Tohoku University
Katahira-cho
Sendai

Cesium-137 in the Coastal Waters of Japan

By Noboru YAMAGATA and Shunji MATSUDA

(Received October 20, 1958)

The levels of radioactive cesium-137 in various materials have been analyzed by the authors and their colleagues since May 1957. A part of the results was compiled by Hiyama and presented to the Scientific Committee on the Effects of Atomic Radiation[1]; the full report is to be published in near future. The analytical data from other countries for cesium-137 in various materials are also available in the U.N. Report[2]. However, we have received no information on the level of cesium-137 in sea-water although that of strontium-90 was presented by Bowen in 1957[3]. It is necessary to know the level of the concentration of cesium-137 in oceanic water caused by nuclear fission explosions and also to guess a tolerable discharge rate of radioactive waste, especially for the Japanese people for whom marine products are the principal sources of proteins.

The cumulative ground deposit in Japan of strontium-90 has been shown by Miyake to be about 8 mc/km^2 in June 1957[4], and perhaps this value is also valid for cesium-137, of which the fission yield and the half-life are almost the same. If we consider temporarily that the sea-water is uniformly mixed to the depth of 100 m., then about 80 $\mu\mu$c of cesium-137 is expected to be present in one kilo-liter of sea-water. The sensitivity for cesium-137 measurement was about 100 $\mu\mu$c, and so it was a matter of actual difficulty to deal with kilo-liters of sea-water in the laboratory. Fortunately, domestic salt is commonly produced directly from sea-water in Japan; hence bittern or carnallite of industrial origin could be chosen as the starting material.

The Behavior of Cesium during the Evaporation of Sea-water. — It is a well known fact that cesium and rubidium are enriched in carnallite as compared in sea-water. Jander and Busch found 0.0002% of cesium chloride in Stassfurt carnallite on the average[5]. In the manufacturing process by solar and vacuum evaporation, cesium and rubidium have also been expected to be enriched in bittern and carnallite. The authors performed several experiments by the use of radioactive tracers ^{86}Rb and ^{137}Cs. Small fractions of sodium chloride and potassium chloride were crystallized respectively from their saturated aqueous solution by the isothermal evaporation. Both the activities of the crystal and of the evaporation residue of the initial solution were measured and the logarithmic distribution coefficient λ was calculated from the equation:

$$\lambda \log \frac{\text{NaCl (Total)}}{\text{NaCl(Total)-NaCl(Crystal)}} = \frac{^{137}\text{Cs (Total)}}{^{137}\text{Cs(Total)-}^{137}\text{Cs(Crystal)}}$$

In case of carnallite crystallization, activities were measured for both the initial solution and the mother liquor. The

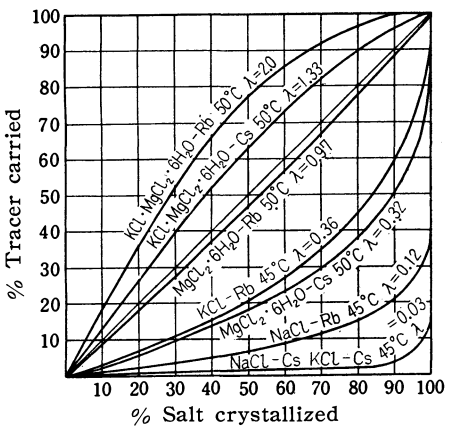


Fig. 1. Efficiency with which the traces of cesium and rubidium are carried by crystallization of several oceanic salts.

1) "Radiological Data in Japan II", edited by Y. Hiyama, Government of Japan, Sept. 1957; U. N. General Assembly A/AC. 82/G/R. 30 (1958).

2) "The Effects of Atomic Radiation", U. N. Report Annex D, A/AC. 82/R. 65/Add. 3 (1958).

3) V. T. Bowen, "Some Geochemical Studies at the Air-Water Interface", presented to the N. R. C. Meteorology Panel, Sept. 25, 1957.

4) Y. Miyake and K. Saruhashi, *Papers in Meteorology and Geophysics*, 8, 242 (1957); U. N. General Assembly, A/AC. 82/R.R. 65/Add. 3 Table XIV (1958).

5) G. Jander and F. Busch, *Z. anorg. u. allg. Chem.*, 187, 165 (1930).

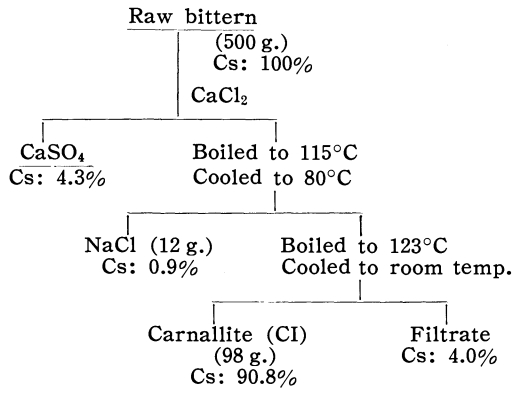


Fig. 2. Loss of cesium in the process of crystallization of carnallite from bittern.

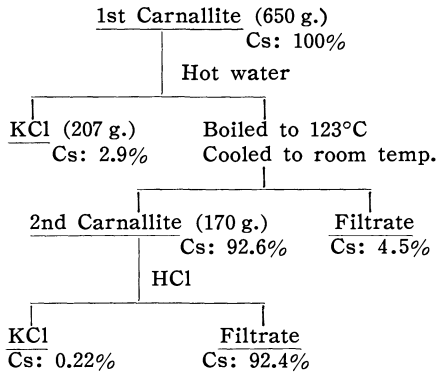


Fig. 3. Loss of cesium in the process of recrystallization of carnallite.

results summarized in Fig. 1[6] are in accord with the fact that cesium and rubidium have been naturally enriched in carnallite, and this nature will be useful for the practical concentration aimed at cesium-137 determination in sea-water. However, as the industrial conditions of carnallite formation greatly differ from the natural, the authors attempted to check the concentration procedure for cesium with a tracer experiment. The procedure and the loss of cesium is schematically shown in Fig. 2; the recovery of cesium is satisfactory.

Recrystallization of Carnallite.—Further enrichment of cesium can be accomplished by fractional recrystallization of carnallite. Halperin and Sambursky applied this method to the determination of rubidium in Dead-Sea carnallites[7]. As easily conceivable from the well-known phase diagram of the system KCl-$MgCl_2$-H_2O, on evaporation of the solution of artificial carnallite which contains a few per cent of sodium chloride, first only sodium and potassium chloride are deposited until the so-called "carnallite point" is reached, where the deposition of carnallite begins. The authors have modified this method for the practical convenience as described below.

A quantity of hot water less than that sufficient for complete dissolving is added to the primary carnallite (CI) and the suspension is cooled with vigorous agitation. Undissolved sodium and potassium chloride are filtered off and the filtrate is boiled until the boiling point reaches 123°C and then cooled to room temperature. The second carnallite (CII) thus obtained is only about one fourth the weight of the primary carnallite and contained 92.6% of the original cesium, so that a fourfold enrichment in concentration of this element can be obtained (Fig. 3).

Another recrystallization of CII resulted in the formation of the third carnallite (CIII) weighing about 600~800 g. which was expected to contain 70~80% of the total cesium originally existing in 50 kg. of bittern. When started from 2.5 kg. of the industrial carnallite sample, only one recrystallization was required to make the mass suitable for the further treatment of cesium separation. The chemical composition of several samples of bittern and carnallite is shown in Table I. An early experiment revealed that only 20 kg. of bittern or 1 kg. of carnallite was sufficient for cesium-137 determination and the later determination were made on this scale.

Separation and Determination of Cesium in Carnallite.—An aliquot of the saturated solution of the final carnallite was reserved for the flame photometric determination of natural cesium and the remainder was made 2.5 N acid with hydrochloric acid after the addition of carrier cesium chloride (100 mg. as Cs). Precipitated potassium chloride was filtered off and to the filtrate was added sodium silicomolybdate solution*) at 60~70°C with constant agitation. After cooling, the precipitate of cesium silicomolybdate was filtered off and washed with 2.5 N hydrochloric acid and then with water. The precipitate was dissolved with the least possible amount of hot 10% solution of sodium hydroxide. The undissolved silica was filtered off and

6) S. Matsuda, *J. Mineral. Soc. Japan* (*Kōbutsugaku Zasshi*), **3**, 523 (1958).
7) A. Halperin and S. Sambursky, *Bull. Research Council of Israel*, **2**, 107 (1952).

* Prepared by the method of Jander and Busch, loc. cited.

TABLE I. CHEMICAL COMPOSITION OF BITTERN AND CARNALLITE

(g./100 g.)

Location	Sample	KCl	NaCl	$MgCl_2$	$MgSO_4$	Total
Onahama	Bittern	3.84	4.03	19.1	6.43	33.4
	CII	18.6	10.7	31.2	0.24	60.7
	CIII	20.7	8.60	33.0	0.19	62.5
Horobetsu	Bittern	3.28	7.92	16.1	3.56	30.9
	CII	19.0	8.67	31.3	0.45	59.4
	CIII	23.5	5.68	31.2	0.19	60.6
Akao	Carnallite	19.1	14.8	32.7	0.45	67.1
	CII	19.4	7.48	31.7	0.39	59.0
Hōfu	Carnallite	23.9	15.5	31.4	0.67	71.5
	CII	20.6	6.87	31.5	0.16	59.1
Tōji	Carnallite	16.4	5.95	30.9	4.95	58.2
	CII	20.5	5.07	32.2	0.42	58.2
Theor. Carnallite $KCl \cdot MgCl_2 \cdot 6H_2O$		26.8	0	34.3	0	61.1

TABLE II. CESIUM-137 CONCENTRATION IN BITTERN AND CARNALLITE

Loc. No.	Location	Sample No.*	Date of Manufacture	^{137}Cs Conc.	$\mu\mu c$**
1	Horobetsu, Hokkaidō	B-1	Oct. 1957	500	± 21
		B-14	Mar. 1958	200	24
2	Watanoha, Miyagi Pref.	B-13	Mar. 1958	1800	46
3	Onahama, Fukushima Pref.	B-2	Aug. 1957	430	17
		B-3	June 1957	290	33
		B-4	Mar. 1958	270	33
4	Asahi, Chiba Pref.	B-8	Mar. 1958	4950	50
5	Kurobe, Toyama Pref.	B-15	Apr. 1958	220	48
6	Kira, Aichi Pref.	B-12	Mar. 1958	2600	60
7	Akao, Hyōgo Pref.	C-3	Oct. 1957	680	20
		C-6	Mar. 1958	450	15
		B-6	Mar. 1958	1300	40
8	Tōji, Okayama Pref.	C-2	Sept. 1957	1450	58
		C-5	Mar. 1958	1650	46
		B-5	Mar. 1958	1500	52
9	Matsunaga, Hiroshima Pref.	B-7	Mar. 1958	1700	48
		C-4	Mar. 1958	1400	31
10	Hōfu, Yamaguchi Pref.	C-1	June 1956	800	40
11	Naruto, Tokushima Pref.	B-10	Mar. 1958	2100	44
12	Takuma, Kagawa Pref.	C-7	Aug. 1957	1800	46
		C-8	Mar. 1958	1200	83
		B-9	Mar. 1958	1500	55
13	Takada, Ōita Pref.	B-11	Mar. 1958	2500	45

* B indicates bittern and C indicates carnallite sample.

** Computed for the basis of 50 kg. bittern.

after the filtrate was made up to about 300 ml. with water, 10% aqueous solution of chloroplatinic acid was added to precipitate the cesium. The precipitate was washed with water and then with ethyl alcohol, dried at 110°C, weighed and mounted for counting.

Radioassay was performed by β-counting by the use of a shielded GM-tube of the mica end-window type and the result was corrected for the absorption and the scattering of cesium chloroplatinate and the chemical yield. Details of the later steps of separation and radiochemical

determination have already been described[8,9]. Contamination of the final precipitate of cesium chloroplatinate with other fission activities, potassium-40, and rubidium-87 is negligibly small[9].

In the determination of natural cesium, it is necessary to take care, not to introduce contamination resulting from the reagents to be used. As there is no evidence of the absence of a trace of cesium in sodium salt, the dipicrylamine has been chosen as the precipitant for potassium. The reagent can easily be purified and a tracer experiment has proved that potassium dipicrylaminate effectively carries down traces of cesium.

An aliquot of the saturated solution of the final carnallite containing approximately 0.1 g. of potassium was diluted to about 50 ml. and treated with magnesium dipicrylaminate solution. The separation of potassium and cesium from the precipitated dipicrylaminate was accomplished in the simple way by the methyl isobutyl ketone extraction, of which the principle was previously reported[10]. The intensity of cesium 852.1 mμ line was measured in the usual way.

Materials and Results

Fifteen samples of bittern and eight samples of carnallite manufactured during June 1956 and April 1958 were collected around Japan. The location and the date of manufacture are shown in Table II and Fig. 4. The outline of manufacture of salt in Japan must be described to serve for the later discussion. The modern system of manufacture is entirely artificial, driven by electric power. Sea-water is pumped up directly into a vacuum evaporator and is never exposed to the open air, so the consideration about atmospheric contamination during the whole production process is unnecessary. The samples of bittern manufactured by this system are B-1, 2, 3, 4, 14 and 15 in Table II. On the other hand, the other samples have been manufactured by the usual salt-field system. In this case, sea-water is exposed to the open air, so that, we must consider the influence of fall-out during production.

The results are shown in Table II. Four

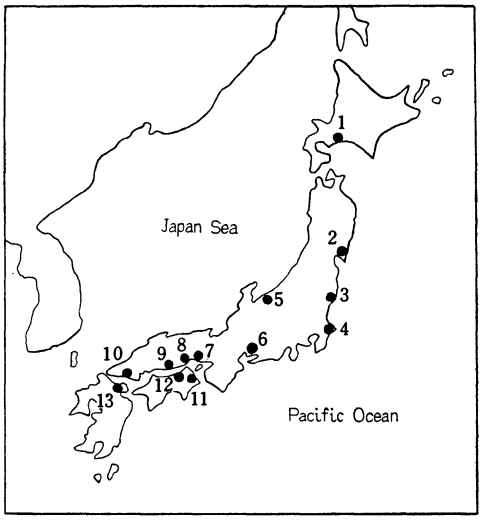


Fig. 4. Locations materials obtained.

kilo-liters of sea-water will produce about 50 kg. of bittern which are equivalent to about 2.7 kg. of carnallite. Values in Table II have been computed on the basis of 50 kg. of bittern. The analytical data for the natural cesium content of several samples are shown in Table III in which the isotopic ratios of cesium-137 and -133 have also been calculated.

The Natural Cesium Content of Sea-water.—Several authors have given surprisingly different values for the cesium content of sea-water. The maximum value is 4.3 μg. whereas the minimum is only 0.002 μg. per liter. The earliest estimate was given by Goldschmidt et al. as 2 μg.[11], although it was not based on actual determination in sea-water. Harada reported values from 0.002 to 0.01 μg.[12] Minami et al. started from about 50 ml. of

TABLE III. ISOTOPIC RATIO OF CESIUM-137 TO -133 IN BITTERN AND CARNALLITE

Sample No.	^{133}Cs mg.	^{137}Cs $\mu\mu$c	^{137}Cs/^{133}Cs $\times 10^9$
B-3	0.21	130	7.7
B-5	0.33	590	22
B-7	0.52	650	16
B-10	0.30	960	40
B-11	0.56	1060	24
B-14	0.26	85	4.1
C-4	0.25	1200	60
C-5	0.22	610	35
C-7	0.33	670	25

8) N. Yamagata et al., *Japan Analyst* (*Bunseki Kagaku*), **7**, 433 (1958).
9) N. Yamagata and T. Yamagata, This Bulletin, **31**, 1063 (1958).
10) N. Yamagata and S. Watanabe, ibid. **30**, 580 (1957).
11) V. M. Goldschmidt et al., *Nachr. Ges. Wiss. Göttingen, Math.-Physik. Klasse*, **1933**, 235.
12) Y. Harada, *J. Chem. Soc. Japan* (*Nippon Kwagaku Kwaisi*), **64**, 1049 (1943); Those values were apparently misabstracted as 2~10 μg./l. in the *Chem. Abstr.*, **41**, 3394 (1947).

sea-water, by use of the cathode layer emission spectroscopy and gave the value of 0.1~1 μg. per liter[13]. Ishibashi and Hara reported values from 3.4 to 4.3 μg.[14] Recently, the most sensitive radioactivation analysis was applied by Smales and Salmon and the value of 0.5 μg. (±10%) per liter was reported[15]. The relative proportions of the major constituents in sea-water are practically constant, although some of the micro-elements of biological activities may fluctuate with time and space. On account of the strongly ionic nature of this element and its biological insignificancy, we can not guess any proper reason for real fluctuations of the concentration of cesium in the open oceans. In fact, the levels of cesium given by Smales and Salmon have been fixed within narrow limits for sea-water from the Atlantic Ocean including a sample of coastal water. The circumstance is considered also valid for the Pacific Ocean and the coastal waters of Japan. On the assumption that the value of 0.5 μg. is correct for the sea waters around Japan, we should like to proceed with the discussions in the following section.

Discussion

The concentration of cesium-137 in samples other than Location No. 1, 3 and 5 is considerably higher by factors of 5 to 10 or more than that in the latter locations; the trend is clear also in the isotopic ratio. The difference may be attributed principally to the contamination by fall-out during production. We can guess the possible contamination as follows. One of the salt-field systems of obtaining the brine from sea-water is the oldest, called the "Irihama" system and the evaporation is effected principally by the sun. For instance, in March 1958, at Watanoha, Miyagi Prefecture (Loc. No. 2), 12 kl. of brine of specific gravity (d_4^{15}=1.125) 16.0° Bé was produced per hectare in two days. Another plan to obtain the brine is a combination of the system of evaporation by the sun and air called the "flowing-down" system. For instance, 120 kl. of sea water is treated per day per hectare by this system. From these figures we can guess the possible contamination of 50 kg. of bittern approximately as 0.3~6 mμc when the fall-out rate of cesium is temporarily assumed to be 0.03~0.3 mc/km^2/month in early 1958.

The above computation indicates that the bittern and the carnallite obtained at the locations other than No. 1, 3 and 5 where salt is produced by the salt-field system are possibly contaminated by fall-out during production to a great extent. Only the results obtained for the bitterns from the locations No. 1, 3 and 5 are reliable to enable us to guess the levels of concentration of cesium-137 in sea-water. On the basis of the approximate figure of the weight of bittern equivalent to the volume of sea water, viz., 50 kg. to 4kl. and of 70% of the over-all yield of cesium, we can compute the concentration of cesium-137 in sea-water approximately to be 70~150 $\mu\mu$c/kl. The values of 160 and 310 $\mu\mu$c/kl. are also derived on the basis that the isotopic ratio of cesium-137 to -133 is 4.1 and 7.7×10^{-9} (Table III) and the cesium-133 content of sea-water is 0.5 μg./l.

The greater part of the domestic salt consumed in Japan comes from sea-salt and an average person takes approximately 15 g. of sodium chloride every day. The average daily intake of cesium-137 by a Japanese in the period from Aug. 1957 to Aug. 1958 is determined by the authors to be 22~56 $\mu\mu$c. The contribution of sea-salt to the total intake of cesium-137 by a person may be roughly computed if the assumption is admitted that the cesium in sea-water moves into the salt during manufacture following the distribution law by the coefficient of 0.03 (Fig. 1). Thus, the weight ratio of Cs/Na in the salt shall be 1.5×10^{-9} as compared with the ratio of 5×10^{-8} in sea-water (calculated from the values, 0.5 μg. of cesium and 10 g. of sodium in one liter). When we take the ratio of cesium-137 to -133 in sea water approximately to be 10^{-8} or 1 mμc of cesium-137 per 1 mg. of cesium-133, 15 g. of sodium chloride shall contain 0.01 $\mu\mu$c of cesium-137. It means that the contribution of sea-salt to the total intake of radioactive cesium-137 by a person is only 10^{-3} or less.

The β-counting equipment used by the authors was a usual mica end-window type GM-counter shielded by lead blocks. Natural background was 10~12 c.p.m. and counting efficiency was 5.3% for cesium-137 by our experimental conditions. About 100 $\mu\mu$c was the minimum amount of cesium-137 to be measured with a standard error of ±10%. Our present program includes the arrangement of a low-level β-counting equipment. With this, only 50~100 liters of sea-water

13) E. Minami, N. Yamagata et al., Read at the Symposium, held by the Chemical Society of Japan for Geochemistry at Nagoya Univ. (1947). Not published.
14) M. Ishibashi and T. Hara, *Bull. Inst. Chem. Res., Kyoto Univ.*, **32**, 248 (1954).
15) A. A. Smales and L. Salmon, *Analyst*, **80**, 37 (1955).

are sufficient for cesium-137 determination. With a slight modification of the separation method direct separation from sea-water will be possible.

The authors thank those who co-operated or assisted in the collection of bittern and carnallite samples, especially Dr. Jirō Sugi and Dr. Kazuo Shimizu at the Central Research Institute, Japan Monopoly Corporation. The authors also thank Mrs. T. Yamagata and Mr. E. Tajima for advice and assistance in the laboratory. Finacially, this work was partly supported by the Ministry of Education.

Kiriu College of Technology
Gunma University
Kiriu

Action of Reducing Agents on Copper Phthalocyanine and its Chlorinated Derivatives

By Masahiro SHIGEMITSU

(Received September 19, 1958)

Although copper phthalocyanine is a very stable organic pigment, it is decomposed by oxidizing agents in its dissolved state in strongly acid solvents. However, it has been considered so far that copper phthalocyanine is stable toward reducing agents. The author examined the action of reducing agents on copper phthalocyanines containing chlorine in the range of naught to sixteen atoms per molecule and found that they were easily attacked by reducing agents, while copper phthalocyanine containing no chlorine was not. When copper phthalocyanine is chlorinated into "copper phthalocyanine green", its color is darkened from bright green to dark green. The cleavage of phthalocyanine nucleus was not caused by reducing agents, although it was caused by oxidizing agents.

Experimental

Materials.—Syntheses of copper phthalocyanine and chlorinated copper phthalocyanines were carried out as follows.

Copper phthalocyanine.—A mixture of phthalic anhydride, urea and cuprous chloride was heated at about 190°C for 3 hr.[1] The reaction product was treated with 5% hydrochloric acid and 2% sodium hydroxide The precipitate was filtered off, washed with water and ethanol, and dried.

Chlorinated copper phthalocyanines.—One part of copper phthalocyanine was dissolved in 6 parts of a eutectic mixture of aluminum chloride and sodium chloride (9:2, by weight, m. p. 145°C) at 150~160°C, and chlorine gas was introduced at a given flow rate and samples were taken out at regular intervals. These samples were washed with 5% hydrochloric acid, 2% sodium hydroxide, water and ethanol, and nine kinds of chlorinated copper phthalocyanine with chlorine content ranging from 2.91% to 44.97% as the degrees of chlorination were prepared. Copper hexadecachlorophthalocyanine (sample XI in Table I) was prepared by chlorinating copper octa-(3,6)-chlorophthalocyanine[2].

The results of chlorine analysis (micro-Carius method) for eleven samples thus prepared are given in Table I.

Methods.—*Particle size reduction.*—The particle size of these samples prepared as above were too large to be used as pigments. Therefore, the particle size of these samples was reduced

TABLE I. CHLORINE CONTENTS OF THE SAMPLES

Sample	Cl	
	%	atom/mol.
I	0.11	0
II	2.91	0.5
III	15.15	1.8
IV	24.05	5.1
V	25.44	5.5
VI	33.71	8.2
VII	39.57	10.6
VIII	42.86	12.1
IX	43.63	12.5
X	44.97	13.2
XI	50.32	16.0

1) M. Shigemitsu, *J. Chem. Soc. Japan, Ind. Chem. Sec.* (*Kogyo Kagaku Zasshi*), **62**, 110 (1959) (presented at the 10th Annual Meeting of Chemical Society of Japan held in April, 1957).

2) M. Shigemitsu, ibid., **62**, 110 (1959) (presented at the Autumnal Joint Meeting of Chemical Societies of Japan, Tokyo, 1957).

by the acid pasting method[3]. One part of the sample (I~V) was dissolved in 5 parts of 98% sulfuric acid, while 1 part of the sample (VI~XI) was dissolved in 3 parts of chlorosulfonic acid. Each solution was poured into 70 parts of ice water with stirring. Fine crystals precipitated were filtered off, washed free from acid with water and dried at about 60°C.

*Treatment by reducing agent, rongalit**. — A mixture of 1 g. of the sample treated as in the above section and 30 cc. of 20% aqueous solution of rongalit was heated at 150~155°C for 20 min. in a stainless steel autoclave equipped with a stirrer. The product obtaind was filtered off, washed with water and dried at about 60°C.

Measurement of the spectral reflectance curves. —One part of the sample treated as in the above section and 1.5 parts of polymerized linseed oil were mixed, made into paste by grinding 400 rounds in a Hoover automatic muller. To one part of this paste were added 70 parts of zinc white paste obtained by grinding 2 parts of zinc oxide with 1.5 parts of polymerized linseed oil. Then the mixed paste was applied 0.5 mm. thick on a coated paper with a "bladeoapplicator" (Gardner Laboratory), and the specimen was dried at room temperature. The spectral reflectance of the specimen prepared thus was measured with a General Electric recording spectrophotometer.

Electron microscopic observation of particle forms and measurement of particle size distributions.—To the samples (VI, VII, VIII, IX and X treated as in the above section was added 0.1% aqueous solution of a non-ionic surface active agent and the pigment was thoroughly dispersed with agitation. A drop of the dispersed solution was placed on a collodion film and dried. The electron microphotographs were taken at 2,000 magnification with an electron microscope of Hitachi Works, and the 20,000 magnification was obtained by enlarging photographs ten times. Three hundreds particles photographed were taken out at random, and particle size distributions were calculated by measuring their shorter and longer diameters.

Results

Variation in Chlorine Content.—Chlorine contents of the samples heated in the aqueous solution of rongalit are given in Table II.

As is clear from Table II, samples I to V do not vary in their chlorine content. But samples VI to X, which have greater chlorine contents, show some decrease in chlorine content by the treatment in rongalit. The greater the chlorine content of the sample, the greater the decrease in the chlorine content by the treatment. However, copper hexadecachlorophthalocyanine (XI) shows somewhat smaller decrease in chlorine content.

TABLE II. VARIATION IN CHLORINE CONTENT

Sample	Cl %: Original sample	Cl %: Sample treated by rongalit
I	0.11	0.12
II	2.91	2.86
III	15.15	15.09
IV	24.05	24.12
V	25.44	25.38
VI	33.71	33.32
VII	39.57	39.15
VIII	42.86	42.41
IX	43.63	43.10
X	44.97	44.30
XI	50.32	49.76

Variation in Color.—The luminosity Y, purity P_e and dominant wavelength λ_D calculated after the C. I. E. coordinate system from the spectral reflectance data are given in Table III.

TABLE III. LUMINOSITY, PURITY AND DOMINANT WAVELENGTH OF THE PIGMENTS

Sample		Y %	P_e %	λ_D mμ
I	original	24.80	48.7	479.0
	treated	22.78	40.3	478.8
II	original	19.07	54.2	478.5
	treated	24.13	48.0	479.4
III	original	18.45	56.0	478.2
	treated	21.62	53.7	478.9
IV	original	19.75	58.3	481.0
	treated	21.87	56.0	481.2
V	original	21.77	54.0	482.2
	treated	23.08	52.0	482.0
VI	original	25.13	49.5	484.8
	treated	23.90	47.3	483.3
VII	original	25.63	46.0	486.9
	treated	21.75	45.5	485.2
VIII	original	26.83	40.3	489.8
	treated	20.48	37.0	486.8
IX	original	26.80	41.0	490.8
	treated	20.07	38.5	487.4
X	original	30.33	37.0	491.4
	treated	20.15	39.0	487.5
XI	original	30.34	36.8	492.6
	treated	22.18	39.1	488.9

It is evident from Table III that the variation of color becomes greater with the increase in the chlorine content and diminishes again in copper hexadecachlorophthalocyanine (XI). The relationship between the luminosity change (ΔY%)

3) H. A. Lubs, "Chemistry of Synthetic Dyes and Pigments", Reinhold Publishing Corp., New York (1955), p. 587.

* addition compound of formalin and sodium hydrosulfite.

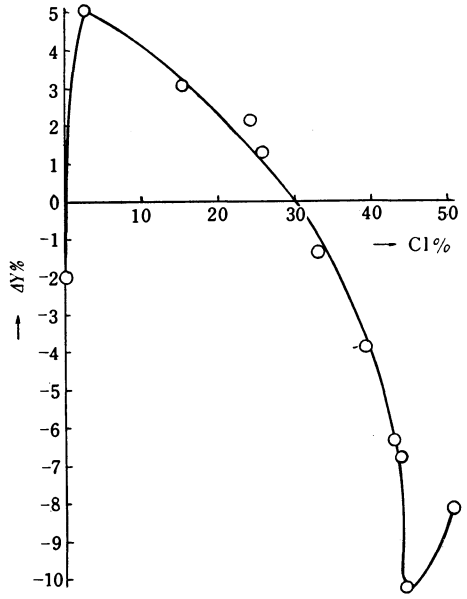


Fig. 1. Relationship between luminosity change and chlorine content.

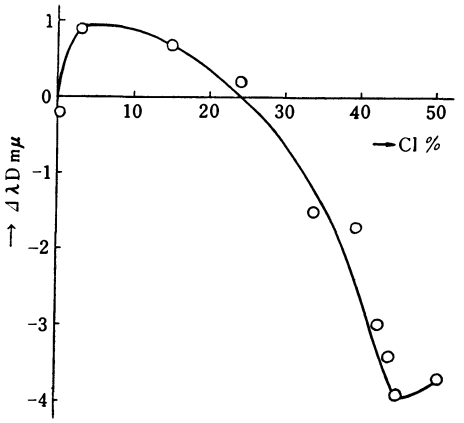


Fig. 2. Relationship between the shift of dominant wavelength and chlorine content.

or shift of dominant wavelength ($\Delta\lambda_D$ mμ) and the chlorine content are shown in Figs. 1 and 2.

It is to be noted that the sample with a greater chlorine content shows a lower brightness in color and shorter dominant wavelength.

Particle Size Distribution of Samples Subject to Remarkable Discoloration.—It is inferred from the above results that darkening of the color of samples treated with reducing agents is accompanied with the change in chemical composition of pigments. However, as the color of pigments, unlike dyes, is largely influenced by the form and the size of particles. particle size distribution of samples subject to remarkable discoloration (VI, VII, VIII, IX and X) was measured. The results are given in Table IV in which d_{mp} denotes the most probable value and d_m the average particle diameter. The value of d_m was calculated from

TABLE IV. PARTICLE SIZE DISTRIBUTION

	Sample	Diameter mμ	d_{mp} mμ	d_m mμ	$\pm\delta$ mμ	Form
VI	original	110~340	207	235	50	leaflet
		225~450	325	337	49	
VI	treated	118~329	213	220	44	〃
		225~452	318	360	59	
VII	original	103~370	208	219	52	〃
		230~480	342	343	44	
VII	treated	110~370	220	223	48	〃
		240~485	350	354	59	
VIII	original	115~320	200	202	45	〃
		220~479	320	337	55	
VIII	treated	112~302	210	201	39	〃
		210~480	335	328	47	
IX	original	120~322	208	207	42	〃
		240~460	345	339	50	
IX	treated	114~330	212	222	44	〃
		250~472	340	347	52	
X	original	121~300	204	216	42	〃
		220~450	330	313	54	
X	treated	110~302	208	217	38	〃
		243~448	315	331	39	

$$d_m = 1/100 \sum_i f_i d_i$$ [4)]

where f is frequency and d particle diameter. "$\pm\delta$" in Table IV denotes deviation, that is, average deviation value from d_m, which was calculated from

$$\Delta = 1/100 \sum_i (d_m - d_i)^2 f_i$$ [4)]

It is obvious from Table IV that variation in form or aggregation of pigment particles did not occur by the treatment of pigments in the aqueous solution of rongalit. Namely, as already described, it was confirmed that the variation of color was due to the change of chemical composition.

Summary

Action of reducing agents on copper phthalocyanine and its chlorinated derivatives was studied, and it was found that, while copper phthalocyanine containing no chlorine did not suffer from discoloration, the color of its polychlorinated derivatives darkened. The discoloration, was most conspicuous when 13 to 14 chlorine atoms per phthalocyanine molecule were contained. The chlorinated copper phthalocyanine become stable towared reducing agents when it was exhaustively chlorinated.

It was confirmed that the darkening of the color of pigments was caused by the change of chemical composition, not by the change of size and form of particles.

The author extends his sincere thanks to Dr. Ryozo Goto, Professor of Kyoto University, for his kind guidance throughout the present study. The author's grateful thanks are also due to Dr. Takahisa Nakamura and Dr. Wataru Ishikawa, Toyo Ink Manufacturing Company, for the valuable advice and much help during the experiments.

Central Research Laboratory
Toyo Ink Mfg. Co.
Sumida-ku, Tokyo

4) E. Suito et al., presented at the 58th Meeting of Electron Microscope Committee of Japan, 1951.

Hydrogen Peroxide Oxidation. I. A New Selenium Dioxide-Catalyzed Synthesis of Carboxylic Acids from Aliphatic Ketones Accompanied by Rearrangement of Alkyl Groups

By Noboru SONODA and Shigeru TSUTSUMI

(Received November 6, 1958)

In the selenium dioxide oxidation of aliphatic carbonyl compounds, α-dicarbonyl compounds are generally obtained, whereas in the presence of hydrogen peroxide the oxidative reaction proceeds quite differently. For instance, selenium dioxide was used as catalyst for hydroxylation of olefins[1,2], and recently the use of selenium dioxide catalyst for the hydrogen peroxide oxidation of acrolein to acrylic acid has been reported by Smith and Holm[3], and the ring contraction of cycloalkanones to cycloalkanecarboxylic acids has also been confirmed by Payne and Smith[4].

We had tried to hydroxylate olefins with hydrogen peroxide in the presence of selenium dioxide catalyst and by using a mixed solvent of *tert*-butyl alcohol and a ketone. It was interesting to note that the oxidation of the ketone, used as solvent, proceeded mainly to form carboxylic acid accompanied by a migration of an alkyl group of the ketone.

For the purpose of elucidating the new reaction mode, acetone, methyl ethyl ketone, methyl *n*-propyl ketone and diethyl ketone were chosen as the starting materials. In the presence of a catalytic

1) M. Mugdan and D. P. Young, *J. Chem. Soc.*, **1949**, 2988.
2) P. Seguin, *Compt. rend.*, **216**, 667 (1943).
3) C. W. Smith and R. T. Holm, *J. Org. Chem.*, **22**, 746 (1957).
4) G. B. Payne and C. W. Smith, ibid., **22**, 1680 (1957).

amount of selenium dioxide, the oxidation of ketones was carried out with a slight excess of hydrogen peroxide in *tert*-butyl alcohol in gentle reflux condition (78~82 °C) for 5~6 hr. At the end of the oxidation the deposition of metallic selenium was observed by which the reaction mixture was colored brownish red, while the hydrogen peroxide completely disappeared. The oxidation products were separated by fractional distillation and analyzed.

When acetone was treated according to the above method, propionic acid, which arose by the shift of either of the methyl carbons to another, was isolated in a yield of 40.7% based on the acetone used. The oxidation of methyl ethyl ketone under similar conditions gave isobutyric acid as the main product in a 27.3% yield and *n*-butyric acid in a 4.8% yield. Both products were formed by the respective migration of the methyl and ethyl groups to the α-carbon atom of the carbonyl group.

$$(CH_3)_2C{=}O \xrightarrow[\textit{tert}\text{-butyl alcohol}]{SeO_2-H_2O_2} CH_3CH_2COOH \quad (1)$$

$$CH_3CH_2(CH_3)C{=}O \longrightarrow CH_3CH_2(CH_3)CHCOOH + CH_3CH_2CH_2COOH \quad (2)$$

All the acids obtained were identified by their physical properties, preparation of the derivatives (*p*-bromophenacyl esters), and their infrared spectra.

When methyl *n*-propyl ketone and diethyl ketone were oxidized under similar conditions to those described above, methyl ethyl acetic acid, which was formed by the respective migration of methyl and ethyl groups to the α-carbon atoms of the carbonyl groups, was isolated in a yield of 22.8% and 32.4%, respectively. The migration of *n*-propyl group of methyl *n*-propyl ketone was also observed, producing *n*-valeric acid in a 5.7% yield.

$$CH_3CH_2CH_2(CH_3)C{=}O \xrightarrow{SeO_2-H_2O_2} CH_3CH_2(CH_3)CHCOOH + CH_3CH_2CH_2CH_2COOH \quad (3)$$

$$CH_3CH_2(CH_3CH_2)C{=}O \longrightarrow CH_3CH_2(CH_3)CHCOOH \quad (4)$$

The above results suggest that similar treatments can be applied to other dialkyl ketones. Thus, the oxidative reactions may be generalized as follows;

$$R{-}CH_2(R')C{=}O \xrightarrow[\textit{tert}\text{-butyl alcohol}]{SeO_2-H_2O_2} R(R')CHCOOH \quad (5)$$

R=H or alkyl R'=alkyl

It is inferable that the main rearrangement in these oxidative reactions is due to the migration of the alkyl group having a smaller number of carbon atoms to the α-carbon atom of the larger alkyl group, and, in consequence, the generated acids have the same number of carbon atoms as the original ketones. On the other hand, the migration of the alkyl group with a larger number of carbon atoms to the smaller one occurs simultaneously in some degree, so that the corresponding isomers are obtainable when unsymmetrical dialkyl ketones are used.

Small amounts of cleavage products were obtained as by-products in all cases. These are listed in Table I.

TABLE I. CLEAVAGE PRODUCTS FROM OXIDATIVE REACTION OF KETONES

Reactants	Products confirmed	Yield
acetone	acetic acid[a]	trace
methyl ethyl ketone	acetic acid	trace
	propionic acid	trace
methyl *n*-propyl ketone	acetic acid[b]	trace
diethyl ketone	acetic acid[a]	trace
	propionic acid	4.1%

(a) The presence of acetic acid was confirmed by the boiling point, the refractive index and the value of neutral equivalent, and the other acids were identified in the form of *p*-bromophenacyl esters.
(b) Propionic acid and *n*-butyric acid are assumed to be present, but were not detected.

These products have apparently formed by the cleavage of the bond between the α-carbon atom and the carbonyl group, although, propionic acid can partly be furnished from oxidation of the solvent; because acetone and methyl alcohol are presumed to be generated from the decomposition of *tert*-butyl hydroperoxide and di-*tert*-butyl peroxide which are produced by the reaction of *tert*-butyl alcohol, used as solvent, with hydrogen peroxide. Actually, the formation of a small amount of aceton was observed (identified as its 2, 4-dinitrophenylhydrazone; the melting point and mixed melting point with authentic sample were 123°C[5]) when the

5) W. Dirscherl and H. Nahm, *Ber.*, **73**, 448 (1940).

selenium dioxide-hydrogen peroxide solution used above was heated without ketones.

The presence of acetic acid and propionic acid in the oxidation products of diethyl ketone indicates that both of the cleavaged groups from one ketone can be oxidized to acids in these reaction systems. In addition, the occurrence of formic acid due to the cleavage of methyl alkyl ketones or oxidation of methyl alcohol produced from solvent may be possible, but it was not detectable.

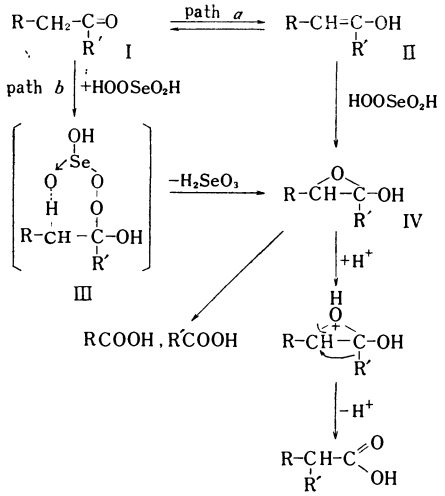
Synthesis of carboxylic acids from ketones by the use of aqueous ammonium polysulfide or a mixture of sulfur and water has been known as Willgerodt-reaction[6], in which aromatic-aliphatic ketones are mainly used as the starting materials, and no change of the carbon skeleton has been observed because of the consecutive reduction and oxidation of the carbon atoms in the aliphatic carbon chain. In the reaction described here the rearrangement of alkyl group occurs apparently and therefore the reaction mode is different from the Willgerodt-reaction. On the other hand, oxidation of ketones accompanying the rearrangement of alkyl group, by peracids or hydrogen peroxide in the presence of acidic catalyst, has been well known as Baeyer-Villiger reaction[7], but in this case the migrating alkyl group becomes the ester group of the resulting carboxylic acid so that the carbon numbers of the generated carboxylic acid are less than those of the starting ketone used. It is of interest to note that the rearrangement by the selenium dioxide-hydrogen peroxide system is applicable to such lower ketones as acetone and methyl ethyl ketone which produce monomeric or polymeric ketone-peroxides under the conditions of Baeyer-Villiger reaction. The ring contraction of cycloalkanones reported by Payne and Smith[4] may be interpreted as one of the rearrangement reactions described here.

Although little evidence was obtained about the mechanism of the rearrangement, the reaction would obviously proceed owing to the peculiar action of the catalyst. It seems to us that selenium dioxide may not affect the reaction directly but a further oxidized form of selenium dioxide by hydrogen peroxide may be the most probable catalytic form. Because α-dicarbonyl compound is not the intermediate[4]; for example, diacetyl was cloven into two molecules of acetic acid under the same reaction conditions and C_4-acid was not obtained.

The oxidation of selenium dioxide with hydrogen peroxide has been reported by several workers[8-10]. Hughes and Martin[9] proposed the formation of peroxyselenious acid in the course of the oxidation of selenium dioxide to selenic acid as shown below.

$$SeO_2 + H_2O_2 \rightleftarrows HOOSeO_2H$$

We investigated[11] previously the fact that the hydroxylation of a double bond was possible by applying the same oxidative method to olefins, and this fact would be elucidated by considering the formation of some kind of peracid in the reaction system. In the present case, the peroxyselenious acid may be formed in *tert*-butyl alcohol solution and may attack ketones in an ionic fashion; thus the following mechanism will be presumed.



Path a indicates that the epoxidation of *enol*-form II by the peroxyselenious acid may occur and addition of proton to the resulting epoxyalcohol IV may cause the migration of an alkyl group. Formation of epoxyalcohol IV will be also expected

6) For a review of this reaction, see (a) M. Carmack, "Organic Reactions", Vol. III, John Wiley and Sons, Inc., New York, N. Y.(1946), p. 83-107; (b) R. Wegler, E. Kühle and W. Schäfer, *Angew. Chem.*, **70**, 351 (1958).

7) For a review of this reaction, see C. H. Hassall, "Organic Reactions", Vol. IX, John Wiley and Sons, Inc., New York, N. Y. (1957), p. 73-106.

8) L. I. Gilbertson and G. B. King, *J. Am. Chem. Soc.*, **58**, 180 (1936).

9) F. J. Hughes and D. S. Martin, Jr., *J. Phys. Chem.*, **59**, 410 (1955).

10) B. Maliňák, *Chem. Listy.*, **50**, 160 (1956); *Chem. Abstr.*, **50**, 3939*a* (1956).

11) The results were presented at the 11th Annual Meeting of the Chemical Society of Japan held in Tokyo, April 3, 1958.

from path b which may include the combination between the α-hydrogen and the oxygen of peroxyselenious acid at the same time of addition of peroxyselenious acid to the carbonyl group. The former path would be more favorable to the latter because of the difficulty of such ring formation III. After the epoxidation, the peroxyselenious acid may become selenious acid which is in equilibrium with selenium dioxide and water (equation 7)[9],

$$H_2SeO_3 \rightleftarrows SeO_2 + H_2O \qquad (7)$$

and the reproduced selenium dioxide will be again oxidized to peroxyselenious acid with hydrogen peroxide (equation 6).

Experimental[12]

Starting Materials.—The ketones and the solvent used in this study were commercial products. Acetone and methyl ethyl ketone were carefully purified by treatment with potassium permanganate solution according to the usual method[13]. The other ketones and *tert*-butyl alcohol, used as the solvent, were purified by fractional distillation prior to their uses. Hydrogen peroxide (30%) and selenium dioxide were from Wako Pure Chemical Industries, Ltd.

Reagent for Oxidation.—A solution containing 150 ml. of 30% hydrogen peroxide and 600 ml. of *tert*-butyl alcohol was dried over 200 g. of anhydrous sodium sulfate overnight. After separating the sodium sulfate, the concentration of hydrogen peroxide in the solution was determined by iodometry. A solution containing 68~69 mg. of hydrogen peroxide per 1 ml. was obtained, and 2 g. of selenium dioxide was dissolved in 500 ml. of the solution (corresponding to about 1 mol. of hydrogen peroxide) with stirring. Selenium dioxide-hydrogen peroxide reagent thus obtained was used in all experiments.

Oxidation of Acetone.—A 1 l. round bottomed flask was charged with 500 ml. of the selenium dioxide-hydrogen peroxide reagent (2 g. of selenium dioxide and 1 mol. of hydrogen peroxide), and 50 g. (0.86 mol.) of acetone was added slowly with stirring. The flask was then fitted with an efficient reflux condenser and was heated on a steam bath. After refluxing (79~81°C) the mixture gently for about 5 hr., the solution became brownish red owing to the deposition of metallic selenium, and the hydrogen peroxide had been completely consumed at this stage. The reaction mixture was allowed to cool to room temperature, the reflux condenser was exchanged for a Widmer-spiral and the distillation was then carried out to remove the remaining acetone-*tert*-butyl alcohol azeotropic mixture. When about 400 ml. of the azeotropic mixture was distilled off, the residue was cooled and the precipitated metallic selenium was filtered off. Ten g. of anhydrous sodium sulfate and 50 ml. of ether were added to the filtrate. After the solution was allowed to stand overnight, it was transferred to a separatory funnel and the water layer was removed and dried over anhydrous sodium sulfate. The ether and the products boiling up to 83°C were distilled off and materials of higher boiling point were fractionated through a 1×40 cm. packed column. The fraction boiling at 139.5~141°C was collected, and 26.0 g. of propionic acid was obtained (40.7% of the theoretical amount based on the quantity of acetone used); n_D^{25} 1.3852, neut. equiv. 74.8; lit.[14] b. p. 140.3°C, n_D^{25} 1.3848. Calcd. for $C_3H_6O_2$: neut. equiv. 74.1.

The infrared spectrum of the acid coincided with that of an authentic sample. *p*-Bromophenacyl ester of the acid was prepared by an usual method[15], m. p. 63.5~64°C, reported[16] 63°C. The mixed melting point with an authentic sample (63.5~64°C) was not depressed.

Anal. Found: C, 48.64; H, 4.23%. Calcd. for $C_{11}H_{11}O_3Br$: C, 48.74; H, 4.09%.

The results of fractional distillation and the characterization of each fraction were listed in Table II.

Table II. Distillation of oxidation products from acetone

Fraction	B. p. °C	Vol. ml.	Characterization n_D^{25}	neut. equiv.
a-1	82~108	6.0	1.3738	90.2
a-2	108~115	2.0	1.3721	69.2
a-3	115~125	0.5	1.3781	78.5
a-4	125~135	0.6	1.3810	83.7
a-5	135~138	o.5	1.3822	80.0
a-6	138~139.5	0.9	1.3844	78.9
a-7	139.5~141	26.0	1.3852	74.8
	residue	1.7(g.)		

Fraction a-1 contained small amount of azeotropic mixture of acids and water. From the value of neutral equivalent, fraction a-2 seemed to contain the carboxylic acid lower than propionic acid. The *p*-bromophenacyl ester of fraction a-2 had melting point of 79~105°C, which indicated presumably the presence of formic acid and acetic acid: reported melting point of *p*-bromophenacyl ester of acetic acid, 85°C[16]; *p*-bromophenacyl ester of formic acid, 135°C[15]. It was presumed from the value of neutral equivalent that fraction a-3 was acetic acid which was contaminated by impurities other than carboxylic acid. Fraction a-4 was also an acid component but was contaminated by impurities. *p*-Bromophenacyl ester of fractions a-5 and a-6 were confirmed to be that of propionic acid

12) The boiling and melting points are uncorrected.
13) A. Weissberger and E. S. Proskauer, "Organic Solvents", Interscience Publishers, Inc., New York, N.Y. (1955).
14) H. U. v. Vogel, "Chemiker Kalender", Springer-Verlag OHG., Berlin (1956).
15) R. L. Shriner, R. C. Fuson and D. Y. Curtin, "The Systematic Identification of Organic Compounds", 4th ed., John Wiley and Sons, Inc., New York, N. Y. (1956).
16) W. L. Judefind and E. E. Reid, *J. Am. Chem. Soc.*, **42**, 1043 (1920).

respectively from their melting points and mixed melting points with an authentic sample. Fraction a-7 was propionic acid, and the residue in the distilling flask consisted mainly of metallic selenium.

Oxidation of Methyl Ethyl Ketone. — To a 500 ml. of the selenium dioxide-hydrogen peroxide reagent (2 g. of selenium dioxide and 1 mol. of hydrogen peroxide) was added 62g. (0.86 mol.) of a methyl ethyl ketone, and the reaction was carried out under gentle reflux condition for 5.5 hr. The reaction mixture was concentrated through a Widmer-spiral to about 150 ml., and conducted in the same manner as described for the oxidation of acetone. The results of the fractional distillation were listed in Table III.

TABLE III. DISTILLATION OF OXIDATION PRODUCTS FROM METHYL ETHYL KETONE

Fraction	B. p. °C	Vol. ml.	Characterization n_D^{25}	neut. equiv.
b-1	102~115	1.0	1.3715	80.7
b-2	115~121	1.0	1.3756	67.7
b-3	121~137	0.4	1.3799	73.0
b-4	137~142	0.5	1.3838	77.4
b-5	142~152	1.2	1.3904	85.5
b-6	152~153.5	1.8	1.3923	88.1
b-7	153.5~156.5	21.2	1.3928	88.9
b-8	156.5~162	2.3	1.3950	89.2
b-9	162~164	4.1	1.3965	88.3
	residue	1.8(g.)		

Fraction b-1 consisted principally of the azeotropic mixture between lower carboxylic acids and water from the standpoint of the values of neutral equivalent and the refractive idex. Fraction b-2 was acetic acid which was identified, from its *p*-bromophenacyl ester m. p. 84~84.5°C; reported[16] m. p. 85°C; the depression of melting point was not shown when the ester was mixed with an authentic sample (m. p. 84.5°C).

Fraction b-3 would be possibly a mixture of acids. Fraction b-4 was identified to be propionic acid from the melting point of its *p*-bromophenacyl ester, m. p. 62.5~63°C, reported[16] m. p. 63°C; the mixed melting point with an authentic sample was not depressed. Fraction b-5 would be a mixture of acids. Fractions b-6 and b-7 were isobutyric acid, 23 g. (27.3% yield of the theoretical amont based on the quantity of methyl ethyl ketone used); the infrared spectrum of the acid coincided with that of an authentic sample; lit.[14] b. p. 154.6°C, n_D^{20} 1.3930; Calcd. for $C_4H_8O_2$, neut. equiv. 88.1.

p-Bromophenacyl ester of the acid was prepared, m. p. 75~75.5C°, reported[16] m. p. 76.2°C. The mixed melting point with an authentic sample (m. p. 75.5°C) was not depressed.

Anal. Found: C, 50.68; H, 4.59. Calcd. for $C_{12}H_{13}O_3Br$: C, 50.55; H, 4.60%.

Fraction b-8 would be obviously a mixture of isobutyric acid and *n*-butyric acid.

Fraction b-9 was *n*-butyric acid, 4.1 g. (4.8% yield based on the quantity of methyl ethyl ketone used); the infrared spectrum of the acid coincided with that of an authentic sample; lit.[14] b. p, 164°C, n_D^{20} 1.3979; Calcd. for $C_4H_8O_2$, neut. equiv. 88.1.

p-Bromophenacyl ester of the acid was prepared, m. p. 62.5°C reported[16] m. p. 63°C. The mixed melting point with an authentic sample (62.5°C) was not depressed.

Anal. Found: C, 50.39; H, 4.70. Calcd. for $C_{12}H_{13}O_3Br$: C, 50.55; H, 4.60%.

Oxidation of Methyl *n*-Propyl Ketone. — To a 250 ml. (1 g. of selenium dioxide and 0.5 mol. of hydrogen peroxide of the selenium dioxide-hydrogen peroxide reagent was added 37 g. (0.43 mol.) of a methyl *n*-propyl ketone, and the mixture was treated under the gentle reflux condition for 6 hr. The reaction mixture was concentrated through a Widmer-spiral to about 70 ml. (when aqueous layer had separated) followed by addition of 5 g. of anhydrous sodium sulfate to saturate the aqueous layer. After separation, the aqueous layer was extracted with 20 ml. of ether. A mixture of the ether extract and the separated organic layer was dried over anhydrous sodium sulfate, and fractional distillation was carried out through the same column described as in the case of acetone. The results of the fractional distillation were listed in Table IV.

TABLE IV. DISTILLATION OF OXIDATION PRODUCTS FROM METHYL *n*-PROPYL KETONE

Fraction	B. p. °C	Vol. ml.	Characterization n_D^{25}	neut. equiv.
c-1	110~117	0.9	1.3733	67.5
c-2	117~122	0.3	1.3752	—
c-3	122~160	1.3	1.3875	81.3
c-4	160~166	0.4	1.3977	97.2
c-5	166~172	1.0	1.4008	101.3
c-6	172~175	3.1	1.4030	103.0
c-7	175~177	7.5	1.4044	103.7
c-8	177~182	1.1	1.4059	102.8
c-9	182~186	2.7	1.4074	104.0
	residue	2.2(g.)		

Fraction c-1 would be a mixture of lower carboxylic acids which consisted mostly of acetic acid. Fraction c-2 was identified as acetic acid from its *p*-bromophenacyl ester, m. p. 84.5°C, reported[16] 85°C; the mixed melting point with an authentic sample was not depressed. Fractions c-3 and c-4 would be a mixture of acids, and a detectable amount of *n*-butyric acid was not obtained. The greater part of fraction c-5 would consist of methyl ethyl acetic acid similar to the next fraction.

Fractions c-6 and c-7 were identified to be methyl ethyl acetic acid, 10.0 g. (22.8% yield of the theoretical amount based on the methyl *n*-propyl ketone used), the infrared spectrum of the acid coincided with that of an authentic sample; lit.[14] b. p. 174°C (reported[15] 176°C), n_D^{20} 1.4051; Calcd. for $C_5H_{10}O_2$, neut. equiv. 102.1.

17) O. T. Schmidt, *Ann.*, *483*, 115 (1930).

p-Bromophenacyl ester of the acid was prepared from the fraction c-7, m. p. 54.5~55°C, reported[15] 55°C; mixed melting point with an authentic sample was not depressed.

Anal. Found: C, 52.34; H, 5.36. Calcd. for $C_{13}H_{15}O_3Br$: C, 52.19; H, 5.06%.

Fraction c-9 was confirmed to be *n*-valeric acid, 2.5 g. (5.7% yield based on the ketone used); the infrared spectrum of the acid coincided with that of an authentic sample; lit.[14] b. p. 186.4°C, n_D^{20} 1.4086; Calcd. for $C_5H_{10}O_2$, neut. equiv. 102.1.

p-Bromophenacyl ester of the acid was prepared; m. p. 73.5~74°C, reported[17] m. p. 74°C; the mixed melting point with an authentic sample was not depressed.

Anal. Found: C, 52.01; H, 5.33. Calcd. for $C_{13}H_{15}O_3Br$: C, 52.19; H, 5.06%.

Oxidation of Diethyl Ketone.—To a 150 ml. (0.6 g. of selenium dioxide and 0.3 mol. of hydrogen peroxide) of selenium dioxide-hydrogen peroxide reagent was added 22.4 g. (0.26 mol.) of diethyl ketone, and the mixture was gently refluxed for 5.5 hr. The resulting reaction mixture was concentrated through a Widmer-spiral to about 50 ml. and was treated according to the same method as described in the case of methyl *n*-propyl ketone. The results of the fractional distillation were listed in Table V.

TABLE V. DISTILLATION OF OXIDATION PRODUCTS FROM DIETHYL KETONE

Fraction	B. p. °C	Vol. ml.	Characterization n_D^{25}	neut. equiv.
d-1	103~112	1.2	—	—
d-2	112~124	0.5	1.3770	68.4
d-3	124~135	0.3	—	—
d-4	135~142	0.8	1.3860	75.4
d-5	142~160	0.6	1.3891	82.8
d-6	160~170	0.5	1.3960	91.0
d-7	170~174	0.8	1.4033	101.5
d-8	174~177	8.0	1.4040	103.1
d-9	177~179	0.3	1.4051	104.8
	residue	1.1(g.)		

Fraction d-1 was an azeotropic mixture of acids and water. Fraction d-2 was a mixture of acids which would consist mainly of acetic acid from the standpoint of the boiling range, the refractive index and the value of neutral equivalent, but the *p*-bromophenacyl ester did not give the constant melting point owing to the presence of the ester of the other acids. Fraction d-3 would be a mixture of acetic acid and propionic acid.

Fraction d-4 was identified to be propionic acid (4.1% yield based on the ketone used); *p*-bromophenacyl ester, m. p. 62.5~63.5°C, reported[16] m. p. 63°C, the mixed melting point with an authentic sample was not depressed. Fractions d-5 and d-6 would be a mixture of acids which were not identified.

Fractions d-7 and d-8 were identified to be methyl ethyl acetic acid, 8.6 g. (32.4% yield based on the quantity of diethyl ketone used); the infrared spectra of these fractions coincided with that of an authentic sample; lit.[14] b. p. 174°C (reported[15] 176°C); n_D^{20} 1.4051; Calcd. for $C_5H_{10}O_2$, neut. equiv. 102.1.

p-Bromophenacyl ester was prepared from the fraction d-8, m. p. 55°C, reported[15] m. p. 55°C; the mixture melting point with an authentic sample was not depressed.

Anal. Found: C, 51.94; H, 5.06. Calcd. for $C_{13}H_{15}O_3Br$: C, 52.19; H, 5.06%.

Oxidation of Diacetyl.—To a 130 ml. (0.52 g. selenium dioxide and 0.26 mol. hydrogen peroxide) of the selenium dioxide-hydrogen peroxide reagent was added 21.5 g. (0.25 mol.) of diacetyl. The mixture was refluxed for 6.5 hr. and then was treated in the same manner as described for the oxidation of acetone. Acetic acid (b. p. 117~119°C) was isolated by distillation and the yield was 10.8 g. (36.0% based on diacetyl used).

Summary

1) Selenium dioxide catalyzed oxidation of aliphatic ketones with hydrogen peroxide gave carboxylic acids which were produced by the rearrangement of the alkyl group as shown by equation 5.

2) Acetone, methyl ethyl ketone, methyl *n*-propyl ketone and diethyl ketone were selected as starting materials. The main rearrangement observed is due to the migration of the alkyl group having a smaller number of carbon atoms to the α-carbon atom of the larger alkyl group, and the migration of the alkyl group with a larger number of carbon atoms to the smaller one also occurs in some degree.

3) The yield of the generated acids were about 30~40% of the theoretical amounts based on the ketones used. Small amounts of cleavage products were obtained as the by-products in all cases. Both of the cleavaged groups from a ketone were oxidized to acids in these reaction systems.

4) The most probable catalytic form seems to be peroxyselenious acid which may be produced by the oxidation of selenium dioxide with hydrogen peroxide (equation 6). Inferential reaction mechanism was discussed.

Department of Applied Chemistry
Faculty of Engineering
Osaka University
Miyakojima-ku, Osaka

Protonation Effects on the Electronic Spectra of Pyrazine

By Shizuyo MATAGA and Noboru MATAGA

(Received October 21, 1958)

In our previous reports[1,2], we have tried to interpret theoretically the characteristics of electronic spectra of hydrogen bonded or protonated nitrogen heterocycles, especially in the case of pyridine. In these reports, semiempirical Hartree-Fock SCF MO's for pyridine interacting with proton have been computed assuming extreme models: (1), there is no transfer of non-bonding electrons on nitrogen toward proton, but bare proton or somewhat shielded proton is located near the nitrogen atom of neutral molecules. In the latter case, the effective charge of proton has been introduced in theory (model I); (2), there is considerable charge transfer from nitrogen atom to proton, leading to covalent binding between them (model II).

The calculated sepectra with model I were in a very good agreement with the experiment. The calculation with model II, however, led to a result which gave rather poor agreement with the experimental values. These results were examined carefully and some discussions on the cause of the superiority of model I and the unsatisfactory result obtained with model II were given.

In the present paper, we shall report another example of our calculations, i.e., the study of the electronic spectra of pyrazinium diion. In this case, the features of spectral change produced by protonation are somewhat different from the case of pyridine.

Method of Calculation

Our method of calculation has already been described in detail elsewhere[2]. Accordingly, the outline of our method will be given briefly as follows.

Model I.—In this case, the complete electronic Hamiltonian may be written as,

$$H=\sum_i H_i^{c\ rel}+\sum_{i<j}^{2m}(e^2/r_{ij}) \tag{1}$$

$$H_i^{core\prime}=H_i^{core}+H_i^P \tag{2}$$

where H_i^P is the electrostatic potential due to proton

$$H_i^P=-\sum_P\frac{Z_{H^+}e^2}{r_{Pi}} \tag{3}$$

In Eq. 2, r_{Pi} is the distance between proton and i-th electron and $Z_{H^+}e$ is the effective charge of proton. In the present calculation it has been assumed to be $Z_{H^+}=1$. The i-th MO may be written in the LCAO form as,

$$\phi_i=\sum_\mu C_{i\mu}\phi_\mu \tag{4}$$

and the eigenvalue equations become as follows in terms of Hartree-Fock SCF MO with neglect of differential overlap,

$$\sum_\nu F_{\mu\nu}C_{i\nu}=\varepsilon C_{i\mu} \tag{5}$$

where

$$F_{\mu\mu}=\alpha_\mu{}'+\frac{1}{2}P_{\mu\mu}\gamma_{\mu\mu}+\sum_{\kappa(\neq\mu)}(P_{\kappa\kappa}-1)\gamma_{\mu\kappa} \tag{6}$$

$$F_{\mu\nu}=B_{\mu\nu}-\frac{1}{2}P_{\mu\nu}\gamma_{\mu\nu} \tag{7}$$

$$\alpha_\mu{}'=\alpha_\mu+V_\mu{}^P \tag{8}$$

$$V_\mu=-\sum Z_{H^+}e^2\int\frac{\phi_\mu{}^2(i)}{r_{Pi}}\mathrm{d}v(i) \tag{9}$$

The meaning of the quantities in these equations other than $V_\mu{}^P$ is the same as before[3-5]. Among the molecular integrals that arise, $V_\mu{}^P$ has been computed theoretically employing the usual Slater $2p\pi$ AO's of nitrogen and carbon atoms, and the others have been evaluated by the same procedure as before[3-5]. Because the interatomic distances in pyrazinium diion necessary for the evaluation of molecular integrals are uncertain, C–C and C–N distances have been assumed to be the same as in neutral molecules and the N–H$^+$ distance has been put to be 1.032 Å, which is the value determined by Bersohn and Gutowsky[6] by means of nuclear

1) N. Mataga and S. Tsuno, *Naturwiss.*, **45**, 333 (1958).
2) S. Mataga and N. Mataga, *Z. physik. Chem. N. F.*, in press.
3) N. Mataga and K. Nishimoto, ibid., **13**, 140 (1957).
4) N. Mataga, This Bulletin, **31**, 453, 459, 463 (1958).
5) N. Mataga, *Z. physik. Chem. N. F.*, **18**, 285 (1958).
6) R. Bersohn and H. S. Gutowsky, *J. Chem. Phys.*, **22**, 651 (1954).

magnetic resonance in the case of ammonium chloride.

Model II.—For the calculation to be made by this by this model, the values of the valence state ionization potential I_{N^+} and electron affinity A_{N^+} of N^+ ion are needed. Using the values of valence state energies above the ground state, which have been taken from Pritchard and Skinner[7], the values of I_{N^+} and A_{N^+} are easily obtained considering the processes,

$N^+(sp_xp_yp_z,\ V_4) \rightarrow N^{++}(sp_xp_y,\ V_3)$ and

$N(sp_xp_yp_z^2,\ V_3) \rightarrow N^+(sp_xp_yp_z,\ V_4)$,

respectively.

With these values the evaluation of molecular integrals has been made in the same manner as before[1-5], and the salf-consistent field calculation has been worked out.

Results and Discussion

The calculated SCF MO's, MO energies, charge and bond orders are collected in Table I.

TABLE I. SCF MO's, MO ENERGIES, CHARGE AND BOND ORDERS OF PYRAZINIUM DIION

Symmetry	ε_i(eV.)	Model I
b_{2u}	−27.0147	$\psi_1=0.3132(\phi_2+\phi_3+\phi_5+\phi_6)+0.5512(\phi_1+\phi_4)$
b_{3g}	−25.4415	$\psi_2=0.2065(\phi_2-\phi_3-\phi_5+\phi_6)+0.6439(\phi_1-\phi_4)$
b_{1g}	−21.4068	$\psi_3=0.5000(\phi_2+\phi_3-\phi_5-\phi_6)$
b_{2u}	−14.1191	$\psi_4=0.3897(\phi_2+\phi_3+\phi_5+\phi_6)-0.4429(\phi_1+\phi_4)$
a_{1u}	−12.0237	$\psi_5=0.5000(\phi_2-\phi_3+\phi_5-\phi_6)$
b_{3g}	− 9.8972	$\psi_6=0.4553(\phi_2-\phi_3-\phi_5+\phi_6)-0.2920(\phi_1-\phi_4)$

$P_{11}=1.4370,\ P_{22}=0.7815,\ P_{12}=0.6112,\ P_{23}=0.6109$

Symmetry	ε_i(eV.)	Model II
b_{2u}	−20.8925	$\psi_1=0.2038(\phi_2+\phi_3+\phi_5+\phi_6)+0.6457(\phi_1+\phi_4)$
b_{3g}	−20.2163	$\psi_2=0.1425(\phi_2-\phi_3-\phi_5+\phi_6)+0.6778(\phi_1-\phi_4)$
b_{1g}	−10.4320	$\psi_3=0.5000(\phi_2+\phi_3-\phi_5-\phi_6)$
b_{2u}	− 4.6592	$\psi_4=0.4566(\phi_2+\phi_3+\phi_5+\phi_6)-0.2882(\phi_1+\phi_4)$
a_{1u}	− 1.1677	$\psi_5=0.5000(\phi_2-\phi_3+\phi_5-\phi_6)$
b_{3g}	0.3512	$\psi_6=0.4792(\phi_2-\phi_3-\phi_5+\phi_6)-0.2015(\phi_1-\phi_4)$

$P_{11}=1.7526,\ P_{22}=0.6237,\ P_{12}=0.4564,\ P_{23}=0.5425$

As shown in Table I, the charge density at nitrogen is increased remarkably by protonation and the features of charge distribution in neutral pyrazine molecule[3] which can be practically regarded as slightly perturbed benzene[5] are lost. With these MO's and MO energies, the electronic spectra of pyrazinium diion are easily calculated. In Table II the calculated spectra are indicated together with the experimental values.

TABLE II. CALCULATED AND OBSERVED SPECTRA OF PYRAZINIUM DIION

Symmetry	Excitation energy (eV.) Calcd. I	Calcd. II	Obsd.[a]	Oscillator strength Calcd. I	Calcd. II	Obsd.
$^1B_{3u}(^1L_b)$	4.2649	3.6205	4.35	0.489	0.723	*
$^1B_{1u}(^1L_a)$	6.3592	6.3130	(6≲)[b]	0.340	0.504	—
$^1B_{1u}(^1B_a)$	8.0161	11.3617	—	0.659	0.286	—
$^1B_{3u}(^1B_b)$	9.3522	14.2097	—	0.720	0.368	—

(a) F. Halverson and R. C. Hirt, *J. Chem. Phys.*, **19**, 712 (1951) and S. Mataga, unpublished.

(b) There is no indication of the existence of other electronic band than ^1L_b below 45 *kK*.

* The observed oscillator strength of pyrazinium diion is uncertain. The oscillator strength of ^1L_b band, however, seems to be two or three times as large as that of neutral molecule.

In contradistinction to the case of protonated pyridine, ^1L_b band is somewhat strengthened as well as shifted to red, while the wave length of ^1L_a band seems to remain almost invariable by double protonation. As shown in Table II, the calculated excitation energy with model I is in good agreement with the experiment. In addition to this, since the calculated oscillator strength of ^1L_b band in neutral pyrazine molecule is 0.162[3], the calculated value in Table II, 0.489, is correct in its order of magnitude in comparison with the calculated value of the neutral molecule. In contrast with the satisfactory results obtained by model I, the calculation with model II leads to the result which is in rather poor agreement with the experiment, that is, the calculated red shift and increase of intensity in the case of ^1L_b band are too great compared with the experiment.

As has already been pointed out in the case of protonated pyridine[1,2], the most predominant factor which leads to the unsatisfactory results with model II may be the neglect of the inductive charge displacement in the σ-core, caused by the transfer of non-bonding electrons on the nitrogen atom toward proton. In the case of model II, the core potential is very deep at nitrogen and is the same as

7) H. O. Pritchard and H. A. Skinner, *Chem. Revs.*, **55**, 745 (1955).

that in the neutral molecule at the carbon atoms. In the case of model I, however, the difference between the core energies at nitrogen and carbon is not so great as in model II and the displacement in σ-core may be appropriately taken into consideration by the formal use of the electrostatic proton potential.

Moreover, the values of $F_{\mu\mu}$'s which may be regarded as an effective electronegativity of μ atom in the molecule[2,3], show the same tendency as the core energies. They are collected in Table III.

TABLE III. VALUES OF α_μ's AND $F_{\mu\mu}$'s

Model	F_{11}	F_{22}	α_1'	α_2'
I	−22.3721	−16.2897	−29.0877	−21.9661
II	−18.3705	−5.0689	−28.72	−11.42

Although the observed spectra can be satisfactorily reproduced by model I as described above, one should not regard model I as the real state of protonated pyrazine. This model represents the electric interaction between proton and π-electrons rather than the electronic interaction between proton and pyrazine. The strong charge transfer interaction between the nitrogen atom in pyrazine and proton may lead to a fairly strong covalent binding between them. Then, the changes in the core energies produced by protonation may be almost completely contributed by the inductive displacement in σ-core. If this is the case, in view of the short range character of the interactions in σ-core, the $(\alpha_\mu' - \alpha_\mu)$ values used in the calculation with model I may be too large. It seems probable that the protonation effect on the core energies may be almost negligible at the nitrogen atom in the opposite side of that proton. However, if we use $(V_\mu^P - 2V_0^P)$'s instead of V_μ^P's of Eq. 9, where V_0^P is the potential energy due to proton at the nitrogen atom in the opposite side of that proton, it is evident that the MO's calculated by model I stay unchanged although the MO energies are lifted by $2|V_0^P|$ uniformly. Thus, the calculation with model I may still be correct even in this case. One might be able to say that the real changes in core energies due to inductive displacement are approximately represented by $(V_\mu^P - 2V_0^P)$ in the case of doubly protonated pyrazine. We shall give a detailed and critical discussion in a later report[8] about such a statement comparing the results obtained with model I with those obtained by an improved model II which employs the self-consistent electronegativity method as developed by Brown and Heffernan[9].

Summary

The protonation effect on the electronic structure and spectra of pyrazine has been studied theoretically employing quantum mechanical calculation. Semi-empirical Hartree-Fock SCF MO's for pyrazine interacting with two protons have been computed with two different methods, respectively.

i) Electrostatic potential due to proton has been added to the core potential in the total electronic Hamiltonian and nuclear attraction integrals which arise owing to the proton potential have been computed theoretically employing the usual Slater $2p\pi$ AO's.

ii) The doubly protonated pyrazine has been replaced by doubly charged pyrazinium ion and molecular integrals have been evaluated semi-empirically using valence state ionization potential and electron affinity of the N^+ atom.

The calculated spectra with method i are in a very good agreement with the experiment. The calculation with method ii has led to a result which is in rather poor agreement with the experimental observation. On the basis of these results, some discussions about the protonation effect on the electronic structure of this molecule have been given.

We are grateful to Professor R. Fujishiro for his encouragement throughout the present study. We also express our appreciation to Mr. T. Kubota of Shionogi Co., Ltd. for his helpful discussions.

Institute of Polytechnics
Osaka City University
Kita-ku, Osaka

8) S. Mataga and N. Mataga, to be published elsewhere.

9) R. D. Brown and M. L. Heffernan, *Trans. Faraday Soc.*, **54**, 757 (1958).

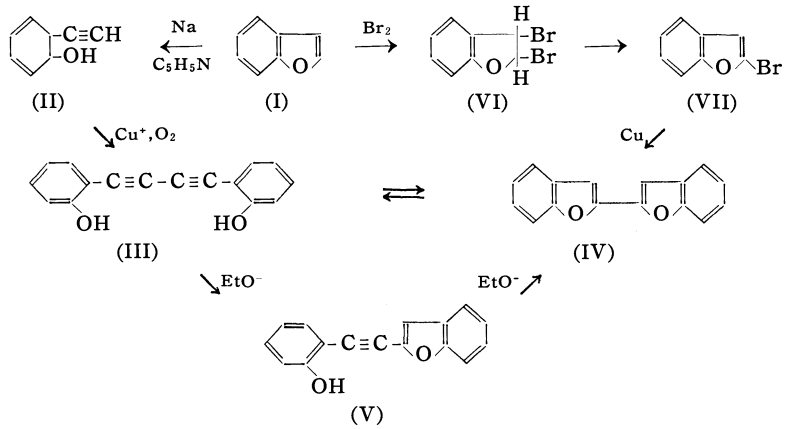
Intramolecular Cyclization of o,o'-Dihydroxydiphenyldiacetylene

By Fumio TODA and Masazumi NAKAGAWA

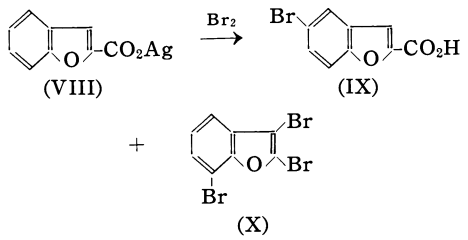
(Received October 21, 1958)

Recently the reactivity of acetylenic bond to the variety of nucleophilic reagents is well recognized, and the formation of furane ring by the intramolecular cyclization of acetylenic glycol[1] and acetylenic phenol[2] has been reported by several investigators. In the course of the studies concerning the synthesis of cyclic acetylenic compounds, the authors found that the nucleophilic addition of the hydroxyl groups in *o,o'*-dihydroxydiphenyldiacetylene (III) to the triple bonds in the same molecule yields benzofurane derivatives. The present paper reports the formation and the structure determination of the benzofurane derivatives thus obtained.

o-Hydroxyphenylacetylene (II) was prepared according to the method of Prey[3] cleaving the furane ring in coumarone I with sodium in pyridine. Oxidative coupling of II was carried out according to the procedure of Sörensen[4] yielding *o,o'*-dihydroxydiphenyldiacetylene (III) in good yield. The physical properties of III were identical with those of the previously reported values[5]. III was heated on a water bath for a few hours with diluted ethanolic sodium ethoxide solution or with aqueous sodium hydroxide solution forming a neutral material in quantitative yield. The U. V. and I. R. spectra of this substance indicate the absence of any acetylenic linkage and hydroxyl group. The presence of ether linkage was recognized from the characteristic absorption at 1250 cm^{-1}. The neutral material yielded III and an unidentified phenolic polymerized material on the treatment with sodium in pyridine at 160~170°C. From these findings the structure of 2,2'-dibenzofuranyl (IV) was assigned to the neutral material. This assignment was confirmed by the mixed melting point determination of the neutral material with a synthetic specimen which was obtained by the Ullmann reaction of 2-bromobenzofurane (VII). VII was prepared by the pyrolytic distillation of 2,3-dibromocoumarane (VI)[6]. The attempt to prepare VII by the Hunsdiecker reaction of silver coumarilate VIII gave an unsatisfactory result. The products were found to be 5-bromocoumarilic acid (IX)[7] and so-called 2,3,7(?)-tribromocoumarone (X)[8].



1) G. Dupont, R. Dulou and L. Audier, *Bull. soc. chim. France*, **1955**, 1078.
2) W. Ried, *Angew. Chem.*, **70**, 273 (1958).
3) V. Prey and G. Pieh, *Monatsh. Chem.*, **80**, 790 (1949).
4) T. Bruun, T. Morthei and N. A. Sörensen, *Acta Chem. Scand.*, **4**, 850 (1950).
5) Y. Odaira, This Bulletin, **29**, 470 (1956).
6) R. Stoermer and B. Kahlert, *Ber.*, **35**, 1633 (1902).
7) R. Stoermer, *Ann.*, **312**, 237 (1900).
8) R. Stoermer and G. Calov, *Ber.*, **34**, 770 (1901).



A phenolic substance and IV was obtained when III in ethanol was refluxed for 1.5 hr. with a small amount of sodium ethoxide. The I. R. spectrum of the phenolic substance showed the characteristic absorption bands of acetylenic bond and hydroxyl group at 2207 cm^{-1} and 3380 cm^{-1} respectively. This substance was converted into IV quantitatively by the action of alkali. It is reasonable to conclude that the structure of the phenolic substance is 2-(*o*-hydroxyphenylethynyl)-benzofurane (V) formed by the half ring closure of III.

Experimental*

o, o'-Dihydroxydiphenyldiacetylene (III).—*o*-Hydroxyphenylacetylene[3] (II, 23.6 g.) was mixed with cuprous chloride (14.5 g.), ammonium chloride (225 g.), concentrated aqueous ammonia 4.0 cc.) and water (572 cc.). The mixture was vigorously stirred at room temperature under an atomosphere of oxygen. The exothermic reaction was completed during the period of 6 hr. with the absorption of theoretical amount of oxygen. The reaction mixture was extracted with ether, washed with water and dried over anhydrous magnesium sulfate. The crude crystals obtained by the evaporation of the solvent were recrystallized from carbon tetrachloride yielding 23 g. (86%) of III, m. p. 142~143°C, colorless needles.

Anal. Found: C, 81.99; H, 4.30. Calcd. for $C_{16}H_{10}O_2$: C, 82.04; H, 4.30%.

U. V. max., 258, 276, 316 and 346 mμ (log ε = 4.13, 3.85, 4.55 and 4.39). I. R. max., 3300, 2180 and 1190 cm^{-1}.

Reaction of III with benzoyl chloride gave dibenzoyl derivative, m. p. 126~126.5°C (from ethanol), colorless needles.

Anal. Found: C, 81.58; H, 4.30. Calcd. for $C_{30}H_{18}O_4$: C, 81.43; H, 4.10%.

U. V. max., 230, 275, 311 and 332 mμ (log ε = 4.91, 4.36, 4.54 and 4.48). I. R. max., 2200, 1744, 1260 and 1240 cm^{-1}.

2, 2'-Dibenzofuranyl (IV) —III (1.0 g.) was dissolved in 30 cc. of 10~20% solution of sodium ethoxide in ethanol or of sodium hydroxide in water. No change was observed after keeping the solution overnight at room temperature. The solution was heated on a water bath for 1~2 hr. causing deposition of crystals. The cooled reaction mixture was filtered. Recrystallization from benzene or ethanol gave IV as colorless needles, m. p. 194.5~195.5°C in quantitative yield.

Anal. Found: C, 81.94; H, 4.47. Calcd. for $C_{16}H_{10}O_2$: C, 82.04; H, 4.30%.

U. V. max., 320 and 338 mμ (log ε = 4.77 and 4.77). I. R. max., 1250 and 1170 cm^{-1}.

Synthesis of 2, 2'-Dibenzofuranyl (IV).—An intimate mixture of 2-bromocoumarone (VII, 1.0 g.) and activated copper bronze (2.5 g.) was heated to 225~240°C in an oil bath for 5 hr. The cooled reaction mixture was transferred to a sublimation apparatus, and was heated to 160~180°C at 20 mmHg. Colorless crystals were obtained as sublimate after removal of the unreacted VII. The crystals were recrystallized from ethanol giving 0.2 g. (40%) of colorless needles, m. p. 194.5~195.5°C. The mixed melting point determination with IV which was derived from III showed no depression.

Anal. Found: C, 82.25; H, 4.33. Calcd. for $C_{16}H_{10}O_2$: C, 82.04; H, 4.30%. I. R. max., 1250 and 1170 cm^{-1}. The I. R. spectra of these two specimens were found as superimposable over the entire region of wave length.

2-(*o*-Hydroxyphenylethynyl)-benzofurane (V).—Heating of III (1.2 g.) in 60 cc. of very diluted ethanolic sodium ethoxide for 1.5 hr. on a boiling water bath resulted in crystallization. Recrystallization from benzene yielded 0.4 g. (33%) of IV, m. p. 194.5~195.5°C. The mother liquor of the recrystallization was concentrated to form crude crystals, which were recrystallized from light petroleum (b. p. 55~75°C) employing active charcoal to give 0.5 g. (41%) of V as colorless needles, m. p. 102.5°C.

Anal. Found: C, 82.24; H, 4.33. Calcd. for $C_{16}H_{10}O_2$: C, 82.04; H, 4.30%.

U. V. max., 250, 298, 318 and 340 mμ (log ε = 3.83, 4.38, 4.44 and 4.45). I. R. max., 3380, 2207 and 1269 cm^{-1}.

V is slightly soluble in aqueous sodium hydroxide. Reaction of V with benzoyl chloride gave monobenzoate, colorless needles, m. p. 117°C.

Anal. Found: C, 81.62; H, 4.27. Calcd. for $C_{23}H_{14}O_3$: C, 81.64; H, 4.17%.

The solution of V (0.1 g.) in ethanolic sodium ethoxide was refluxed for 3 hr., forming colorless crystals in quantitative yield. This was identified as IV by mixed melting point determination with previously obtained IV.

Ring Cleavage of 2, 2'-Dibenzofuranyl (IV).—A mixture of IV (0.4 g.), pyridine (4.0 g.) and sodium (0.3 g.) was refluxed for 3.5 hr. under nitrogen atomosphere. Water was added cautiously to the reaction mixture to decompose the unreacted sodium, and the mixture was extracted with ether. The aqueous layer was acidified with 2 N hydrochloric acid, and extracted with ether. The ethereal extract was washed with 2 N hydrochloric acid and water successively. The dried ether solution was evaporated, and the residue was repeatedly recrystallized from carbon tetrachloride affording a small amount of

* Melting points were not corrected. All U. V. and I. R. spectra were measured employing ethanolic solution and nujol mull respectively.

crystals, m. p. 140~141°C. The mixed melting point of this substance with III showed no depression.

Hunsdiecker Reaction of Silver Coumarilate (VIII). — Bromine (7.5 g.) in dry carbon tetrachloride (20 cc.) was added in one portion on well dried VIII (10.0 g.) at room temperature. Vigorous evolution of gas was observed, and the color of bromine disappeared during the period of 2 hr. The mixture was kept for 3 hr. to complete the reaction. The reaction mixture was extracted with ether, and the extract was washed with aqueous solution of sodium hydrogen carbonate to remove acidic materials. The alkaline solution was neutralized with 2 N hydrochloric acid, and extracted with ether. The ether solution was washed with water and dried. The solvent was removed by distillation and the recrystallization of the residue from aqueous ethanol gave 5 g. (56%) of 5-bromocoumarilic acid (IX), m. p. 256°C as colorless needles. (lit. value m. p. 253°C)[7].

Anal. Found: Br, 33.40. Calcd. for $C_9H_5O_3Br$: Br, 33.19%.

The ether layer which was washed with sodium hydrogen carbonate solution was washed with water and dried. The crude neutral crystals obtained by the evaporation of the solvent were recrystallized from aqueous ethanol yielding 2.0 g. (15%) of colorless needles, m. p. 81~83.5°C.

Anal. Found: Br, 67.07. Calcd. for $C_8H_3OBr_3$: Br, 67.60%.

This would be identical with so-called 2,3,7(?)-tribromocoumarone (X, m. p. 84~85°C) prepared by Stoermer[7,8].

Grateful acknowledgments for supplying coumalin are made to Shiono Perfume Industry Co., Osaka. The authors also wish to express their appreciation to Messrs. T. Shiba and M. Okumiya and Miss K. Koike for performing the elementary analyses.

Department of Chemistry
Faculty of Science
Osaka University
Kita-ku, Osaka

The Formation Constants of Metal Acetate Complexes. I. Polarographic Determination of the Formation Constants of Acetatonickel(II) Complexes

By Nobuyuki TANAKA and Kiyoko KATO

(Received October 20, 1958)

In the course of our studies on the inorganic reactions involving metal complexes[1,2], the necessity for the use of the formation constants of various acetato complexes has been realized. Although many of those constants have been reported[3], they were not determined under the conditions which satisfy our present requirements. They were obtained by various researchers by various methods under various conditions.

In order to determine the formation constants of various acetato complexes under the given conditions, a systematic study has been carried out. The careful considerations of various methods which can be applied to the determination of the formation constants led to the conclusion that none of the methods is satisfactory for the present purpose. The potentiometric methods, which are considered to have the widest applicability, generally include uncertainties due to the estimation of the liquid junction potential and that of the activity coefficients of the ions present. The solubility studies have only a limited applicability. The polarographic method which was applied by Hume and his co-workers[4,5] to their study on the acetatolead(II) complexes is available only when the electrode processes are reversible at the dropping mercury electrode.

In the present paper, the principle of a new method for the determination of the

1) N. Tanaka, K. Kato and R. Tamamushi, This Bulletin, **31**, 283 (1958).
2) Unpublished
3) J. Bjerrum, G. Schwarzenbach and L. G. Sillén, "Stability Constants. Part I. Organic Ligands", The Chemical Society, London (1957), p. 3.
4) D. D. DeFord and D. N. Hume, *J. Am. Chem. Soc.*, **73**, 5321 (1951).
5) E. A. Burns and D. N. Hume, ibid., **78**, 3958 (1956).

formation constants and the application of the method to acetatonickel(II) complexes are presented. The method is similar to that proposed by Schwarzenbach and his co-workers[6-8], but applicable without data of the dissociation and the formation constants concerning the auxiliary complex-forming substance, which Schwarzenbach's method requires.

Theoretical

Let us consider the acetate buffer solution which contains nickel(II) and nitrilotriacetate (NTA) ions[9]. There exist the following equilibria:

$$Ni^{2+} + n\,OAc^- \rightleftarrows Ni(OAc)_n^{(2-n)+} \quad (1)$$

$$Ni^{2+} + X^{3-} \rightleftarrows NiX^- \quad (2)$$

$$NiX^- + H^+ \rightleftarrows NiHX \quad (3)$$

where X^{3-} denotes a tervalent NTA anion. The total concentration of nickel, $\sum[Ni]$, and that of NTA, $\sum[NTA]$, in the solution are given in terms of the ionic and molecular species as follows:

$$\sum[Ni] = [Ni^{2+}] + \sum_1^n [Ni(OAc)_n^{(2-n)+}] + [NiX^-] + [NiHX] \quad (4)$$

$$\sum[NTA] = [NTA]_f + [NiX^-] + [NiHX] \quad (5)$$

where $[Ni^{2+}]$ represents the concentration of hydrated nickel ions and $[NTA]_f$, the sum of the concentrations of uncomplexed NTA. In the polarographic measurement it is impossible to measure separately either the concentration of hydrated nickel ions or that of acetatonickel(II) complexes in an acetate medium. On the contrary, the polarographic diffusion current of nickel corresponds to the sum of the diffusion current due to the hydrated nickel ions and that due to the acetatonickel(II) complexes. If the hydrated nickel ion and the acetatonickel(II) complexes have nearly the same diffusion current constants, the sum of their concentrations can be determined from the polarographic diffusion current, if necessary, after correction.

Then, we write the equation as,

$$[Ni^{2+}]_{app.} = [Ni^{2+}] + \sum_1^n [Ni(OAc)_n^{(2-n)+}] \quad (6)$$

where $[Ni^{2+}]_{app.}$ is the concentration that can be determined from the polarographic diffusion current. Eq. 4 is rewritten as,

$$\sum[Ni] = [Ni^{2+}]_{app.} + [NiX^-] + [NiHX] \quad (7)$$

The concentrations of NiX^-, Ni^{2+} and X^{3-} are given by

$$[NiX^-] = (\sum[Ni] - [Ni^{2+}]_{app.})/\beta \quad (8)$$

$$[Ni^{2+}] = [Ni^{2+}]_{app.}/(1 + \sum_1^n K_{Ni(OAc)_n}[OAc^-]^n) \quad (9)$$

$$[X^{3-}] = [NTA]_f/\alpha \quad (10)$$

$$\alpha = 1 + \frac{[H^+]}{K_{HX}} + \frac{[H^+]^2}{K_{H_2X}K_{HX}} + \frac{[H^+]^3}{K_{H_3X}K_{H_2X}K_{HX}}$$

and $$\beta = 1 + K^H_{NiHX}[H^+]$$

where K_{H_3X}, K_{H_2X} and K_{HX} represent the first, the second and the third dissociation constant of nitrilotriacetic acid, respectively, and $K_{Ni(OAc)_n}$ and K^H_{NiHX} represent the overall formation constant of $Ni(OAc)_n^{(2-n)+}$ and the equilibrium constant of the reaction given by Eq. 3, respectively. The formation constant of NiX^-, consequently, is given as

$$K_{NiX} = \frac{[NiX^-]}{[Ni^{2+}][X^{3-}]} = \frac{\alpha\{\sum[Ni] - [Ni^{2+}]_{app.}\}\{1 + \sum_1^n K_{Ni(OAc)_n}[OAc^-]^n\}}{\beta[Ni^{2+}]_{app.}[NTA]^f} \quad (11)$$

From Eqs. 5 and 7, the concentration of uncomplexed NTA is given as,

$$[NTA]_f = [Ni^{2+}]_{app.} - \sum[Ni] + \sum[NTA] \quad (12)$$

Introducing Eq. 12 into Eq. 11, the relation

$$\frac{\{[Ni^{2+}]_{app.} - \sum[Ni] + \sum[NTA]\}[Ni^{2+}]_{app.}}{\sum[Ni] - [Ni^{2+}]_{app.}} = \frac{\alpha}{\beta K_{NiX}} + \frac{\alpha}{\beta K_{NiX}} \sum_1^n K_{Ni(OAc)_n}[OAc^-]^n \quad (13)$$

is obtained.

When the values of K_{H_3X}, K_{H_2X}, K_{HX}, K_{NiX} and K^H_{NiHX} are known, the formation constants of acetatonickel(II) complexes can be determined with Eq. 13 from the measurements of $[Ni^{2+}]_{app.}$ at n different concentrations of acetate. However, the equilibrium constant K^H_{NiHX} has not been reported and the other constants K_{H_3X},

6) G. Schwarzenbach and E. Freitag, *Helv. Chim. Acta*, **34**, 1492 (1951).
7) G. Schwarzenbach and E. Freitag, ibid., **34**, 1503 (1951).
8) H. Ackermann and G. Schwarzenbach, ibid., **32**, 1543 (1949).
9) Nickel(II) and nitrilotriacetate may be replaced by other metal ions and complex-forming substances.

K_{H_2X}, K_{HX} and K_{NiX} have been determined[6,10,11] in conditions not convenient for our study.

An alternative and better procedure for determining the formation constants of acetatonickel(II) complexes was developed. It is obvious that both α and β in Eq. 13 are constant in the solution of the given pH and the given ionic strength. The values of $[Ni^{2+}]_{app.}$ are determined by the polarographic method at the given pH and ionic strength, but at varied concentrations of acetate. The left-hand side of Eq. 13 is calculated and plotted against the concentration of acetate. If the left-hand side of Eq. 13 is denoted with F_0, it is expressed as,

$$F_0 = \frac{\alpha}{\beta K_{NiX}} + \frac{\alpha}{\beta K_{NiX}} K_{NiOAc}[OAc^-] + \frac{\alpha}{\beta K_{NiX}} K_{Ni(OAc)_2}[OAc^-]^2 + \cdots\cdots \quad (13')$$

From extrapolation of the plot to zero acetate concentration, $\alpha/\beta K_{NiX}$ is obtained. Then we obtain,

$$F_1 = \frac{F_0 - \frac{\alpha}{\beta K_{NiX}}}{\frac{\alpha}{\beta K_{NiX}}[OAc^-]} = K_{NiOAc} + K_{Ni(OAc)_2}[OAc^-] + \cdots\cdots \quad (14)$$

$$F_2 = \frac{F_1 - K_{NiOAc}}{[OAc^-]} = K_{Ni(OAc)_2} + K_{Ni(OAc)_3}[OAc^-] + \cdots\cdots \quad (15)$$

F_1 is plotted against $[OAc^-]$ and the K_{NiOAc} is determined by extrapolating the plot to zero acetate concentration. The further treatment leads to the determinations of $K_{Ni(OAc)_n}$, if higher acetato complexes are present in the solution.

Experimental

Reagents. — The solution of disodium nitrilotriacetate was prepared from the commercial nitrilotriacetic acid (DOTITE NTA), and standardized against the standard solution of copper(II) nitrate by amperometric titration with the same procedure for ethylenediaminetetraacetate[12,13]. The standard solution of nickel nitrate was prepared by dissolving a known amount of pure nickel metal in reagent-grade nitric acid. Commercial guaranteed reagents were used for buffers and supporting electrolytes without further purification.

Apparatus and Procedure. — A Shimadzu RP-2 pen-recording polarograph was used for the measurement of the current-voltage curves. The dropping mercury electrode used had an m value of 1.27 mg./sec. and a drop time t of 3.69 sec. in an air-free 0.1 M potassium chloride solution at 25°C with open circuit.

The sum of the diffusion currents of hydrated nickel ions and acetatonickel(II) complexes were determined in the acetate buffer of pH 3.83±0.01 containing nickel(II) and a slight excess of NTA at 15, 25 and 35°C. The concentration of acetate in the acetate buffer was varied from 0.05 M to 0.20 M. The ionic strength of the solution was adjusted to be 0.2 with potassium nitrate, unless otherwise stated. Polyoxyethylene lauryl ether (LEO) was added as a maximum suppressor by 1×10^{-6} M (at 15°C) or 2×10^{-6} M (at 25° and 35°C) in concentration. The pH of the solution was measured accurately, after the polarographic measurement, with a Hitachi Model EHP-1 pH meter with a glass electrode.

In the preliminary experiment, it was observed that the formation of nickel-NTA complexes nearly completed within 30 minutes under the experimental condition. Therefore, all reaction mixtures were kept in a thermostat for 3 hours to reach the completely equilibrated condition before being subjected to the polarographic measurement.

Results

The polarograms were recorded with the solutions of the same pH containing 1.00×10^{-3} M nickel nitrate, 1.12×10^{-3} M

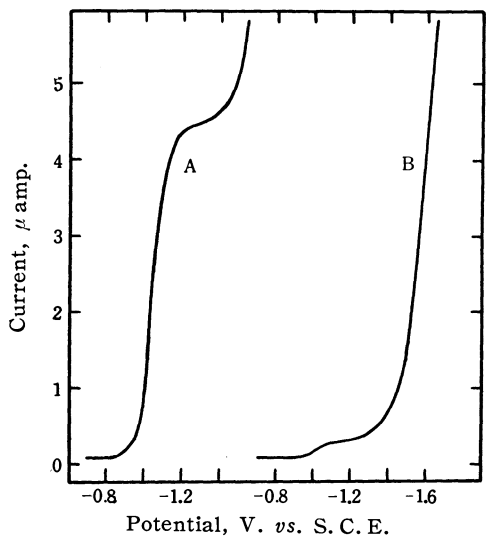


Fig. 1. Polarograms of 1.00×10^{-3} M nickel (II) obtained in the acetate-nitrate media of pH 3.83 at 25°C in the absence (curve A) and in the presence of 1.12×10^{-3} M NTA (curve B). The residual current is not corrected.

10) G. Schwarzenbach, H. Ackermann and H. Ruckstuhl, *Helv. Chim. Acta*, **32**, 1175 (1949).
11) V. L. Hughes and A. E. Martell, *J. Am. Chem. Soc.*, **78**, 1319 (1956).
12) N. Tanaka, M. Kodama, M. Sasaki and M. Sugino, *Japan Analyst (Bunseki Kagaku)*, **6**, 86 (1957).
13) N. Tanaka, I. T. Oiwa and M. Kodama, *Anal. Chem.*, **28**, 1555 (1956).

NTA and various concentrations of acetate. Fig. 1 shows the polarograms obtained in the absence and the presence of a slight excess of NTA. Nickel(II) gives an irreversible wave with the half-wave potential of about −1.05 volts *vs.* S. C. E. in the acetate-nitrate media. (Curve A in Fig. 1). This wave is due to the reductions of the hydrated nickel(II) ions and the acetatonickel(II) complexes. The presence of a slight excess of NTA decreases to a great extent the height of the nickel wave, but does not obliterate the wave completely. A small wave which was followed by the depolarization of the supporting electrolyte is clearly seen in Fig. 1 (Curve B). The limiting current of the wave was found to be proportional to the square root of the effective height of mercury column on the dropping mercury electrode. This clearly showed that the limiting current is diffusion-controlled and is proportional to the concentration of the electroactive species.

The apparent diffusion current constants were determined from the measurement of the diffusion current of nickel(II) at various acetate concentrations at the given ionic strength. In Fig. 2, typical examples

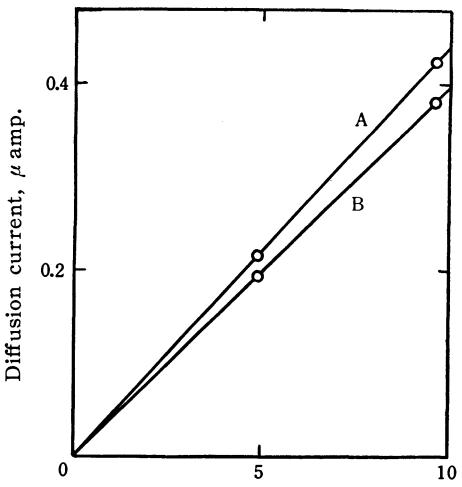


Fig. 2. Relation between diffusion current and concentration of nickel nitrate in acetate buffer solutions of pH 3.83 at 25°C. Acetate concentrations are: A, 0.05 M; B, 0.20 M.

of those measurements are given. The values of $[Ni^{2+}]_{app.}$ of Eq. 6 were calculated with the aid of those diffusion current constants from the limiting currents obtained with reaction mixtures. The results are given in Table I, which indicate that $[Ni^{2+}]_{app.}$ increases with increasing concentration of acetate.

The left-hand side of Eq. 13 was calculated with the values of $[Ni^{2+}]_{app.}$ given in Table I, and was plotted against the acetate concentration. The results are

TABLE I. $[Ni^{2+}]_{app.}$ OBTAINED EXPERIMENTALLY AT VARIOUS TEMPERATURES

Concn. of acetate, M	$[Ni^{2+}]_{app.}\times10^5$, M		
	15°C	25°C	35°C
0.05	3.77	3.86	3.87
	3.80	3.77	3.89
0.10	4.06	4.11	4.23
	4.12	4.19	4.30
			4.30
0.15	4.46	4.42	4.63
	4.33	4.50	4.54
			4.63
0.20	4.78	4.76	4.87
	4.66	4.88	4.83
			4.87

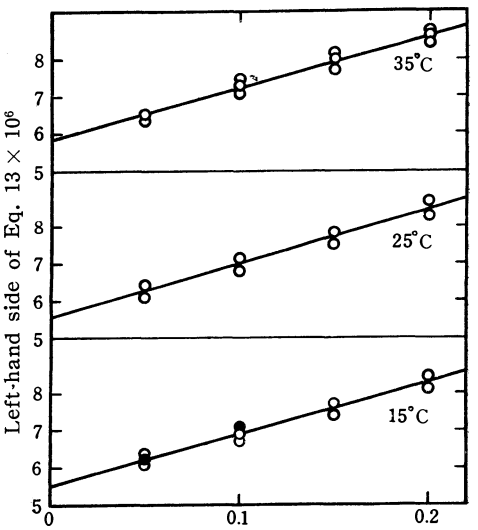


Fig. 3. Relation between the value of left-hand side of Eq. 13 and the concentration of acetate at various temperatures. ○ indicates the values obtained in nitrate media, and ● in perchlorate media.

shown in Fig. 3, where it is clearly seen that there is a linear relation between the values of the left-hand side of Eq. 13 and the concentration of acetate. This indicates conclusively that only one type of acetato complex, $NiOAc^+$, exists in the solution under the experimental condition. From the plots in Fig. 3, the values of

$\alpha/\beta K_{NiX}$ and $\alpha K_{NiOAc}/\beta K_{NiX}$ in Eq. 13′ were determined, the former being given by the intersept at $[OAc^-]=0$ and the latter, by the slope. The experimental results obtained at 25°C were also treated by the least square method, with the result that the probable errors of $\alpha/\beta K_{NiX}$ and $\alpha K_{NiOAc}/\beta K_{NiX}$ were ±1.5% and ±4.1%, respectively. The formation constants of the monoacetatonickel(II) complex at 15°, 25° and 35°C were obtained by dividing the values of $\alpha K_{NiOAc}/\beta K_{NiX}$ by those of $\alpha/\beta K_{NiX}$. These are given in Table II.

TABLE II. FORMATION CONSTANTS OF MONOACETATONICKEL(II) COMPLEX AT VARIOUS TEMPERATURES

Temp., °C	K_{NiOAc}
15	2.6
25	2.6
35	2.4

Discussions

The formation constants of monoacetatonickel(II) complex, K_{NiOAc}, are found to be almost independent of temperature in the range from 15° to 35°C. Jena, Aditya and Prasad[14] studied the acetatonickel(II) complex by the e.m.f. method and reported the thermodynamic formation constant of the monoacetatonickel(II) complex to be 13.5 at 30°C. The formation constant at ionic strength 0.2 was calculated from this value to be 4.5, when the activity coefficient of acetate ions was assumed to be equal to that of monoacetatonickel(II) ions and the activity coefficient of nickel ions was estimated to be 0.33[15]. The resulting value of 4.5 seemed to be in good agreement with the formation constant obtained in this study. Both values were determined by completely different methods and the value obtained by the e. m. f. method involves the uncertainty due to the estimation of the activity coefficient. Fronaeus[16] studied the formation of the complex by means of the ion-exchanger and also by means of the measurement with a quinhydrone electrode and obtained the formation constants of 4.7 and 5.5, respectively, at ionic strength 1.0 (sodium perchlorate) at 20°C. They also seem to support the value obtained in this study.

The experimental solution contained a certain quantity of potassium nitrate, which was added to adjust the ionic strength of the solution. It is expected that the nitrate ion has such a small tendency to form a complex with the nickel(II) ion that it seems unnecessary to consider the effect of the nitrate ion in the present calculation. The confirmation of this was attained in the comparison of the experimental results observed in nitrate and perchlorate media. The perchlorate has been known to have the least complex-forming ability. If an appreciable amount of nitrato complex is formed in the nitrate media, the values of the left-hand side of Eq. 13 obtained at the same concentration of acetate are expected to be larger in the nitrate media than in the perchlorate media. The measurement of $[Ni^{2+}]_{app.}$ was carried out in the solution of which the ionic strength was adjusted with sodium perchlorate instead of potassium nitrate. The value of $[Ni^{2+}]_{app.}$ agreed completely with that obtained in the solution containing nitrate. From this fact it may be concluded that the nitrate ions show least complex-forming tendency and, consequently, the use of nitrate ions requires no correction on the present calculation.

In conclusion it should be noted here that the method for the determination of the formation constant given in this paper may be applicable to the study of other metal complexes of relatively small formation constants. The method is more rigorous than the e. m. f. method, because the latter method requires the estimations of the liquid junction potential and the activity coefficient. The determination of the sum of the concentration of hydrated nickel ions and that of acetatonickel(II) complexes may be carried out by other methods.

Summary

A new method for the determination of the formation constants of metal acetate complexes has been developed. The method is based on the polarographic measurement of the sum of the equilibrium concentrations of hydrated metal ions and metal acetate complexes in the presence of an appropriate auxiliary complex-forming substance. One of the advantages of the method is that no estimation is required in the course of the calculation. The other is that no information of the dissociation and formation constants is

14) P. K. Jena, S. Aditya and B. Prasad, *J. Indian Chem. Soc.*, **30**, 735 (1953).
15) J. Kielland, *J. Am. Chem. Soc.*, **59**, 1675 (1937).
16) S. Fronaeus, *Acta Chem. Scand.*, **6**, 1200 (1952).

required concerning the auxiliary complex-forming substance.

The method is applied to the study of acetatonickel(II) complexes using nitrilotriacetate as an auxiliary ccmplex-forming substance. The results reveal that only monoacetatonickel(II) ions, $NiOAc^+$, exist in the solution containing acetate up to 0.2 M in concentration. The formation constants K_{NiOAc} at ionic strength 0.2 are calculated to be 2.6 at 15°C, 2.6 at 25°C and 2.4 at 35°C.

The authors thank the Ministry of Education for the financial support granted for this research.

Department of Chemistry
Faculty of Science
Tohoku University
Katahira-cho, Sendai

Effects of Protonation on the Electronic Structure and Spectra of Nitrogen Heterocycles

By Shizuyo MATAGA and Noboru MATAGA

(Received October 21, 1958)

In the previous papers[1-3], we have reported detailed theoretical studies about the protonation effects on the electronic spectra of some nitrogen heterocycles. In these reports, the interaction between proton and a nitrogen heterocycle has been treated by various approximations. Among these, the following two are most representative.

i) It has been assumed that there is no transfer of non-bonding electrons on nitrogen toward proton but bare proton is located near the nitrogen atom of neutral molecule. Thus, the electrostatic potential due to proton has been added to the core potential in the total π-electronic Hamiltonian and nuclear attraction integrals which arise owing to this potential have been computed theoretically employing the usual Slater $2p\pi$ AO's.

ii) It has been considered that there is a strong charge transfer from nitrogen atom to proton leading to covalent binding between them and molecular integrals have been evaluated semi-empirically using valence-state ionization potential and electron affinity of N^+ atom.

By means of the semi-empirical Hartree-Fock SCF MO's obtained with these integrals, the electronic spectra of protonated nitrogen heterocycles have been calculated. The calculated spectra by the method i have been in very good agreement with those experimentally obtained. However, the calculation with the method ii has led to a result which is in rather poor agreement with the experimental values. A careful examination of these results has led to the following conclusion. In the case of the later method, the inductive charge displacement in σ-core caused by the charge transfer of non-bonding electrons from nitrogen atom toward proton may not be appropriately accounted, where the core potential is very deep at nitrogen and the same as that in the neutral molecule, at the carbon atoms. In the case of the method i), however, the displacement in σ-core may be appropriately taken into consideration by the formal use of the electrostatic proton potential, which may be the cause of the superiority of this method.

If the unsatisfactory results obtained with the method ii originates from the neglect of the inductive charge displacement in σ-core caused by protonation as described above, one may be able to improve the results by taking into consideration the inductive displacement in σ-core in some appropriate manner. In this respect, we have calculated the electronic structures and spectra of pyridinium ion and pyrazinium diion employing

1) N. Mataga and S. Tsuno, *Naturwiss.*, **45**, 333 (1958).
2) S. Mataga and N. Mataga, *Z. Physik. Chem. N. F.*, in press.
3) S. Mataga and N. Mataga, This Bulletin, **32**, 511 (1959).

the self-consistent electronegativity method proposed by Brown and Heffernan[4] which may be regarded as an improvement of the method ii. Our calculation procedure is essentially the same as that of Brown and Heffernan but a little different from theirs in some details of actual compution procedures. In the present paper, we shall report the results of this calculation with some discussions. In addition, results of some critical studies about the effects of protonation on the core energies and diagonal elements of Fock's Hamiltonian, $F_{\mu\mu}$'s, will be given comparing the present results with previous ones.

Application of Self-Consistent Electronegativity (SCE) Method

In SCE method, it is assumed that Slater's rules for effective charges of atoms are applicable for continuous variation in electron density. Accordingly, for atoms in the first row of the periodic table the relationship is

$$Z_\mu = N_\mu - 1.35 - 0.35\ (\sigma_\mu + P_{\mu\mu}) \qquad (1)$$

where N_μ is the atomic number of μ atom and σ_μ is the number of σ-electrons associated with μ atom in the molecular framework, e.g. 3 for carbon and positively charged nitrogen in pyridinium ion. $P_{\mu\mu}$ is the π-electron density on μ atom. If this variation of Z_μ with $P_{\mu\mu}$ is included in the SCF MO procedure, in addition to the usual functional dependence of the SCF matrix elements upon the charge distribution, the various molecular integrals become functions of $P_{\mu\mu}$ from their dependence on Z_μ. The methods of allowing for this variation are as follows.

Firstly, the form of the relationship between the valence state ionization potential I_μ and Z_μ should be established.

Various valence-state ionization potentials have been calculated from the experimental term values of atomic spectra. If I_μ's are plotted against Z_μ's for the (sp^3, V_4) valence state of the iso-electronic series, C, N^+, O^{2+} and for the (sp^4, V_3) valence state of the iso-electronic series, C^-, N, O^+, respectively, the curves are accurately parabolic:

$$I_\mu(sp^3, V_4) = 3.490\, Z_\mu^2 - 8.541\, Z_\mu + 2.446 \qquad (2)$$

$$I_\mu(sp^4, V_3) = A_\mu(sp^3, V_4) = 3.730\, Z_\mu^2 - 16.285\, Z_\mu + 14.108 \qquad (3)$$

where A_μ is the valence state electron affinity. These equations are used for evaluating I_{C^-} and I_{N^+}. Then, from these eqs., the mono-centric inter-electronic coulomb repulsion integral, $\gamma_{\mu\mu}$, is easily obtained as,

$$\gamma_{\mu\mu}(sp^3, V_4) = I_\mu(sp^3, V_4) - A_\mu(sp^3, V_4) = -0.240\, Z_\mu^2 + 7.743\, Z_\mu - 11.662 \qquad (4)$$

The two-center electronic coulomb repulsion integral, $\gamma_{\mu\nu}$, was evaluated as in our previous works[2,5-7] from the formula,

$$\gamma_{\mu\nu} = e^2/(a_{\mu\nu} + r_{\mu\nu}) \qquad (5)$$

where parameter $a_{\mu\nu}$ has been determined by the equations:

$$a_{\mu\nu} = 2a_{\mu\mu}\cdot a_{\nu\nu}/(a_{\mu\mu} + a_{\nu\nu}) \qquad (6)$$

$$a_{\mu\mu} = 14.3949/\gamma_{\mu\mu} \qquad (7)$$

The other quantities necessary for the calculation are the values of off-diagonal matrix elements of core Hamiltonian, $\beta_{\mu\nu}$. We have used the same values as before[2] for these quantities.

With the parameters described above, SCE LCAO MO's of pyridinium ion and pyrazinium diion have been obtained by the iterative process in which all integrals except $\beta_{\mu\nu}$ depend on the π-electron distribution.

The results are collected in Table I and

TABLE I. SCE MO's AND MO ENERGIES OF PYRIDINIUM ION AND PYRAZINIUM DIION

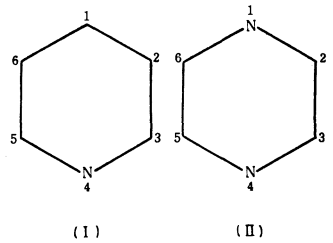
Symmetry	ε_i(eV.)	
Pyridinium ion		
b_2	−18.3382	$\psi_1 = 0.1200(\phi_2+\phi_6) + 0.3272(\phi_3+\phi_5) + 0.0763\,\phi_1 + 0.8667\,\phi_4$
b_2	−13.1857	$\psi_2 = 0.4791(\phi_2+\phi_6) + 0.1121(\phi_3+\phi_5) + 0.6631\,\phi_1 - 0.2758\,\phi_4$
a_2	−11.4409	$\psi_3 = 0.4939(\phi_2-\phi_6) + 0.5059(\phi_3-\phi_5)$
b_2	− 3.3504	$\psi_4 = 0.1846(\phi_2+\phi_6) + 0.4811(\phi_3+\phi_5) - 0.5805\,\phi_1 - 0.3632\,\phi_4$
a_2	− 1.8341	$\psi_5 = 0.5059(\phi_2-\phi_6) - 0.4939(\phi_3-\phi_5)$
b_2	0.6149	$\psi_6 = 0.4711(\phi_2+\phi_6) - 0.3859(\phi_3+\phi_5) - 0.4663\,\phi_1 + 0.2020\,\phi_4$
Pyrazinium diion		
b_{2u}	−19.7914	$\psi_1 = 0.2637(\phi_2+\phi_3+\phi_5+\phi_6) + 0.6007(\phi_1+\phi_4)$
b_{3g}	−18.6618	$\psi_2 = 0.1781(\phi_2-\phi_3-\phi_5+\phi_6) + 0.6607(\phi_1-\phi_4)$
b_{1g}	−12.1179	$\psi_3 = 0.5000(\phi_2+\phi_3-\phi_5-\phi_6)$
b_{2u}	− 5.3902	$\psi_4 = 0.4248(\phi_2+\phi_3+\phi_5+\phi_6) - 0.3729(\phi_1+\phi_4)$
a_{1u}	− 2.6605	$\psi_5 = 0.5000(\phi_2-\phi_3+\phi_5-\phi_6)$
b_{3g}	− 0.7302	$\psi_6 = 0.4672(\phi_2-\phi_3-\phi_5+\phi_6) - 0.2518(\phi_1-\phi_4)$

4) R. D. Brown and M. L. Heffernan, *Trans. Faraday Soc.*, **54**, 757 (1958).

5) N. Mataga and K. Nishimoto, *Z. Physik. Chem. N. F.*, **13**, 140 (1957).

6) N. Mataga, This Bulletin, **31**, 453, 459, 463 (1958).

7) N. Mataga, *Z. Physik. Chem. N. F.*, **18**, 19 (1958).



(I) (II)

Fig. 1. Numbering of atoms in pyridine (I) and pyrazine (II).

the numbering of atoms is indicated in Fig. 1.

The spectra of these ions calculated with these MO's are given in Table II in comparison with the observed values.

TABLE II. CALCULATED AND OBSERVED SPECTRA OF PYRIDINIUM ION AND PYRAZINIUM DIION

Symmetry	Pyridinium ion Excitation energy Calcd.	Obsd.	Calcd. Oscillator strength**
$^1B_1(^1L_b)$	4.7492	4.83	0.346
$^1A_1(^1L_a)$	6.1375	5.50	0.000
$^1A_1(^1B_a)$	7.1336	—	1.108
$^1B_1(^1B_b)$	7.7588	—	0.535

* V. Zanker, *Z. Physik. Chem. N. F.*, **2**, 52 (1954).

** The observed oscillator strengths of pyridinium ion are uncertain. Although ^1L_b band of pyridine is intensified by protonation, the oscillator strength of ^1L_b band may be almost equal to that of ^1L_a band in its order of magnitude, in the case of pyridinium ion.

Symmetry	Pyrazinium diion Excitation energy Calcd.	Obsd.*	Calcd. Oscillator strength**
$^1B_{3u}(^1L_b)$	4.1412	4.35	0.641
$^1B_{1u}(^1L_a)$	6.5108	($6\lesssim$)	0.472
$^1B_{1u}(^1B_a)$	9.5635	—	0.454
$^1B_{3u}(^1B_b)$	11.5009	—	0.624

* F. Halverson and R. C. Hirt, *J. Chem. Phys.*, **19**, 712 (1951) and S. Mataga, unpublished.

** The observed oscillator strength of pyrazinium diion is uncertain. The oscillator strength of ^1L_b band, however, seems to be two or three times as large as that of a neutral molecule. (The calculated oscillator strength of ^1L_b band in the case of pyrazine molecule is 0.162[5]).

The agreement of the calculated spectra with observed values as given in Table II, is not satisfactory. There is not such nice agreement with experiment as seen in the previous calculation[1-3] with method i as described in the introductory part of this paper, and the present result seems to be only a small improvement of the previous calculation[1-3] with the method ii. Accordingly, the present unsatisfactory results may originate from the same circumstance as in the case of the previous calculation with the method ii, i.e., from the insufficient consideration of the inductive charge displacement in the σ-core caused by the transfer of nonbonding electrons on nitrogen atom toward proton. In this respect, some critical discussions about the effects of protonation on the electronic structure of these nitrogen heterocycles will be given in the next section.

On the Inductive Charge Displacement in the σ-Core Caused by the Protonation

In the method i, the electrostatic potential due to proton is simply added to the core Hamiltonian and the diagonal element of Fock's Hamiltonian in terms of AO's has the following form:

$$F_{\mu\mu}=\alpha_\mu+V_\mu^P+\frac{1}{2}P_{\mu\mu}\gamma_{\mu\mu}+\sum_{\kappa(\neq\mu)}(P_{\kappa\kappa}-1)\gamma_{\mu\kappa} \quad (8)$$

where

$$\alpha_\mu=\int\phi_\mu(i)\left\{-\frac{1}{2}\Delta_i^2-V_\mu(i)\right\}\phi_\mu(i)\mathrm{d}v(i)=-I_\mu$$

$V_\mu^P=-e^2\int\sum_P\frac{\phi_\mu^2(i)}{r_{Pi}}\mathrm{d}v(i)$ and r_{Pi} is the distance between proton and i-th electron.

As pointed out before[2,3], the changes in the core energies produced by protonation may be almost completely contributed by the inductive displacement in σ-core. Then, in view of the short range character of the interactions in σ-core, the additional core energy, i.e., V_μ^P, used in the method i may be too large. It seems probable $V_\mu^P=0$ at the atom in the opposite side of proton. However, if we use $(V_\mu^P-V_0^P)$'s instead of V_μ^P's where V_0^P is the additional core energy at the atom in the opposite side of proton, it is evident that, in our approximation, the MO's calculated by method i stay unchanged although the MO energies are lifted by $|V_0^P|$ uniformly. Accordingly, one may be allowed to say that the real changes in core energies due to inductive displacement are represented by $(V_\mu^P-V_0^P)$, because the calculated spectra with method

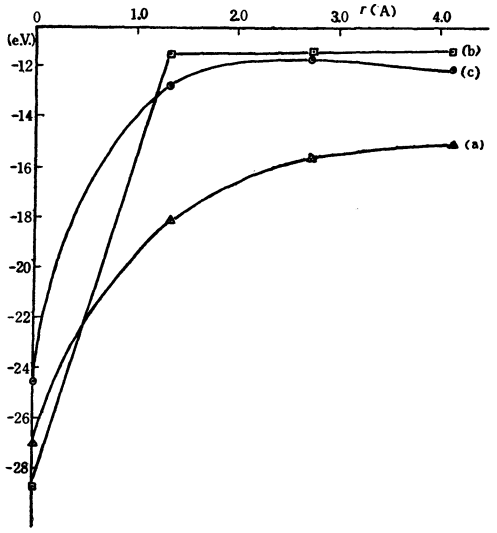


Fig. 2. α_μ's or $(\alpha_\mu+V_\mu{}^P)$ plotted against the distance r along the bonds between the protonated nitrogen and μ-th atom in the case of pyridine. (a) method i, (b) method ii, (c) SCE method.

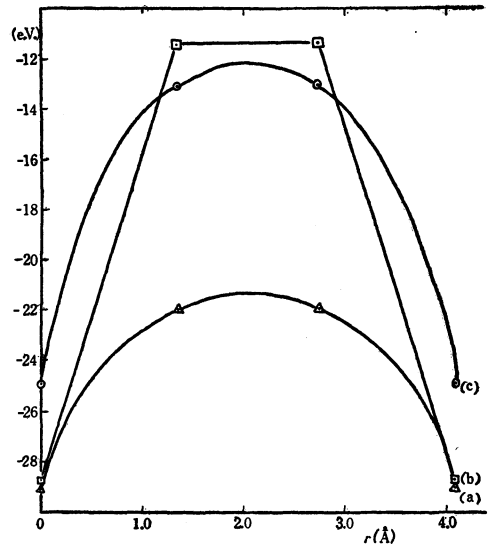


Fig. 3. α_μ's or $(\alpha_\mu+V_\mu{}^P)$ plotted against the distance r along the bonds in the case of pyrazine. (a) method i, (b) method ii, (c) SCE method.

i are in a very good agreement with experiment[1-3].

Now, the circumstance mentioned at the end of the last section is evident from Figs. 2 and 3 where α_μ's in the method ii and SCE method, and $(\alpha_\mu+V_\mu{}^P)$'s in the method i are plotted against the distance along the bonds between protonated atom and μ atom. Moreover, $F_{\mu\mu}$'s which may be regarded as a kind of effective electro-

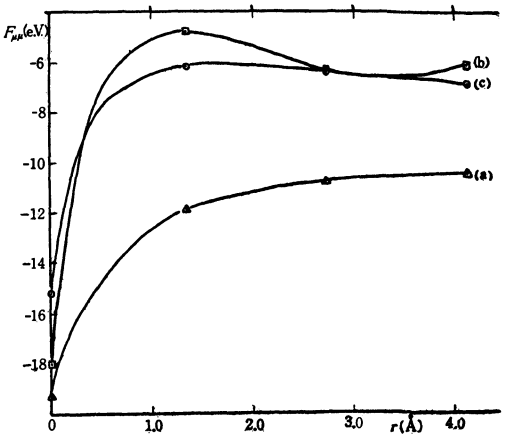


Fig. 4. $F_{\mu\mu}$'s plotted against the distance r along the bonds between the protonated nitrogen and μ-th atom in the case of pyridine. (a) method i, (b) method ii, (c) SCE method.

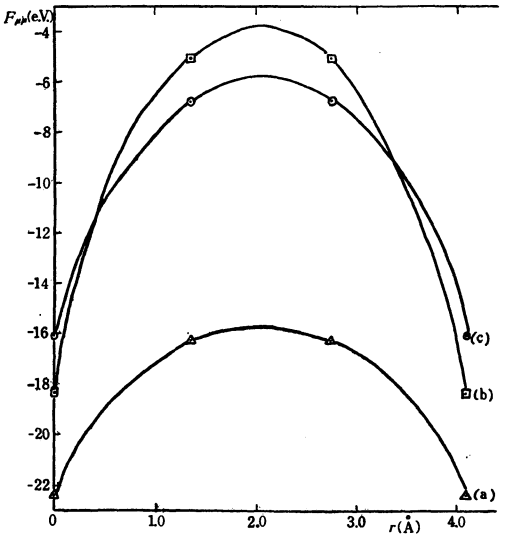


Fig. 5. $F_{\mu\mu}$'s plotted against the distance r along the bonds in the case of pyrazine. (a) method i, (b) method ii, (c) SCE method.

negativity of μ atom in the molecule[2,5] show the same tendencies as α_μ's and $(\alpha_\mu+V_\mu{}^P)$'s, respectively, in Figs. 4 and 5.

In these figures, the results obtained by the SCE method are rather close to the results obtained by the method ii, which may be the most predominant factor that leads to the unsatisfactory prediction of electronic spectra by the former method.

Now, in the case of protonated pyridine, if we put:

$$\alpha_\mu{}'-\theta=(\alpha_4{}'-\theta)/\nu^n \qquad (9)$$

where $\alpha_\mu' = (\alpha_\mu + V_\mu^P)$, θ and ν are parameters to be determined semiempirically and n is the number of bonds between nitrogen and μ atom, then the values of α_μ' plotted in Fig. 2 are well reproduced by this equation putting $\theta = 14.86$ eV. and $\nu = 4$.

If we approximate the distances from nitrogen along the bonds by $r = n \cdot \lambda$ where λ is the average bond distance of pyridine, i.e., 1.38 Å, then Eq. 9 becomes

$$\alpha_\mu' - \theta = (\alpha_4' - \theta)/\nu^{r/\lambda} \quad (10)$$

Actually, Eq. 10 is valid.

Similar equations have been obtained also for $F_{\mu\mu}$'s as follows:

$$(F_{\mu\mu} - 10.50) = (F_{44} - 10.50)/6^n \quad (11)$$

$$\text{or} \quad = (F_{44} - 10.50)/6^{r/1.38} \quad (12)$$

The value of θ in Eqs. 9 and 10 and the corresponding quantity in Eqs. 11 and 12 are very close to α_1' and F_{11}, respectively.

Therefore, these equations may be regarded as representing the inductive displacement caused by protonation and also that the inductive effect due to protonation is practically negligible on the atom which is more than two-bond distance apart from the protonated nitrogen atom.

Then, Eqs. 9 and 10 may be useful in general for the study of the protonation effect on the electronic structure of nitrogen heterocycles, although the behaviour of $F_{\mu\mu}$ may be characteristic of each molecule and Eqs. 11 and 12 can not be used in general. It is customary in the simple MO theory to take into consideration the inductive effect assuming the form of coulomb integral as $\alpha_\mu = \alpha + \delta_\mu \beta$ It has been pointed out[2] that the SCF MO's and charge distributions calculated by the method i are well reproduced with simple MO's obtained using the values of coulomb integrals $\alpha_4 = \alpha + 2.4\,\beta$, $\alpha_3 = \alpha_5 = \alpha + 0.4\,\beta$ and assuming the all resonance integrals are equal to β. Then $\delta_3 = \delta_5 = \delta_4/6$, which is the same relationship as in the case of $F_{\mu\mu}$, i.e., by Eq. 11 $\Delta F_{33} = \Delta F_{55} = \Delta F_{44}/6$, where $\Delta F_{\mu\mu} = (F_{\mu\mu} - 10.50)$

Although, in the case of the protonated pyrazine, we can not obtain the relationship as Eqs. 9—12, because of the higher symmetry of the molecule, the circumstance may be analogous to the case of protonated pyridine.

Summary

The self-consistent electronegativity method has been applied to calculate the electronic structure and spectra of some protonated nitrogen heterocycles. This method may be regarded as an improvement of our method ii which has led to poor agreement with experiment because of the neglect of the inductive displacement in σ-core caused by protonation. The calculated results with the present method, however, are in rather poor agreement with experiment, and it is only a small improvement of the method ii.

Comparing the present results with the previous ones obtained with method i and ii, some discussions about the nature of the protonation effect on the electronic structure of these molecules have been given. In addition, formulae which represent the magnitude of inductive effect on each atom as a function of the distance or number of bonds from the protonated atom have been given.

Institute of Polytechnics
Osaka City University
Kita-ku, Osaka

SHORT COMMUNICATIONS

Photochemical Decomposition of 2,4,6-Trinitrophenyl Amino Acids and Peptides

By Kazuo SATAKE and Tsuneo OKUYAMA

(Received February 9, 1959)

The unstability of dinitrophenyl amino acids to sunlight was already described by Sanger[1], Mills[2], and Blackburn[3]. Akabori et al.[4] also studied the rate of the photochemical decomposition of various dinitrophenyl amino acids by exposure to a tungsten lamp.

Trinitrophenyl (TNP) amino acids and peptides, synthesis of which is going to be published elsewhere, have similar properties to dinitrophenyl derivatives and are also labile photochemically.

A saturated solution of TNP-amino acid in 1 N hydrochloric acid was prepared 20 ml. of the solution was placed in a petri dish (8 cm. in diameter) and exposed to ultraviolet light (Mazda UV-sterilizing lamp) or sunlight. The absorption spectrum of the solution changed gradually to that of picramide. It suggests the formation of picramide by the photochemical decomposition of TNP-amino acids. When the solution showed the absorption spectrum of picramide, it was concentrated to dryness under reduced pressure. The residue was dissolved in a small amount of ethanol and applied to filter paper. The presence of picramide and the absence of free amino acids were verified by means of one-dimensional paper chromatography on Toyo No. 51 filter paper. The solvent systems used were phenol-water (4 : 1, v/v), 1.5 M phosphate buffer (pH 5.6) or butanol saturated with 2 N ammonia.

By further exposure to light (after 24 ~44 hr.), no ninhydrin positive substance was detected by two-dimensional paper chromatography of the concentrated samples, although the decoloration of the solution was observed, indicating the complete decomposition of the TNP-amino acid. A yellow substance, probably resulting from picramide, was then precipitated. Conditions of the two-dimensional paper chromatography were as follows: ascending method, on Toyo No. 51 filter

TABLE I. PHOTODECOMPOSITION OF TNP-AMINO ACIDS AND -PEPTIDES

TNP-compound	Solvent	Photodecomposition products: Ninhydrin positive substance	Photodecomposition products: Recovery of amino acid (%)
TNP-glycine	1 N HCl	none	0
TNP-DL-alanine	1 N HCl	none	0
TNP-L-leucine	1 N HCl	none	0
TNP-L-valine	1 N HCl	none	0
〃	1 N HCl-Dioxane*	valine (?), unknown	—
〃	1 N HCl-Ethanol*	none	0
TNP-glycyl-glycine	1 N HCl	glycine	93
〃	1 N HCl-Dioxane*	glycine, glycyl-glycine, unknown	—
TNP-glycyl-leucine	1 N HCl	leucine	—
TNP-glycyl-DL-valine	1 N HCl	valine	87
TNP-glycyl-DL-serine	1 N HCl	serine	91
TNP-alanyl-DL-asparagine	1 N HCl	asparagine	83
TNP-L-leucyl-L-tyrosine	1 N HCl	tyrosine	92
TNP-glycyl-glycyl-glycine	1 N HCl	glycyl-glycine	—

* 1:1, v./v.

1) F. Sanger, *Biochem. J.*, **45**, 563 (1949).
2) G. L. Mills, ibid., **50**, 707 (1952).
3) S. Blackburn, ibid., **45**, 579 (1949).
4) S. Akabori, T. Ikenaka, Y. Okada and K. Kohno, *Proc. Japan Acad.*, **29**, 509 (1953).

paper, using butanol-acetic acid-water (4 : 1 : 1, v/v) as the first developer and phenol-water (4 : 1, v/v) as the second.

In the cases of TNP-peptides, the similar photochemical decomposition was observed. Only the trinitrophenylated amino-terminal amino acid residue was decomposed photochemically, while the second residue was liberated in a free state.

The liberated amino acid was estimated by the TNP-method, which was composed of the trinitrophenylation of amino acids with picryl sulfonate, followed by the colorimetry at 340 mμ[5]. The recoveries of amino acids were listed on Table I. The amino acid liberation was caused exclusively by the photochemical decomposition of the TNP-amino-terminal amino acid residue, since no amino acid was released by the similar treatment of TNP-peptide without exposure to light, or of free dipeptide with exposure to light.

In the case of TNP-triglycine, glycylglycine was liberated, but no release of glycine could be observed.

These results suggest a probable application for a new method of the stepwise degradation of peptide from the amino terminal. Detail of these studies will be the subject of the future communication.

Department of Chemistry
Faculty of Science
Tokyo Metropolitan University
Fukazawa, Setagaya-ku, Tokyo

5) K. Satake, T. Okuyama and M. Ohashi, unpublished paper.

Ionic Character and Hybridization of Ammonia Molecule

By Yoshifumi KATO*, Utaro FURUKANE and Haruo TAKEYAMA

(Received February 9, 1959)

Townes and Dailey[1] have determined the electronic structure of molecules from the nuclear quadrupole coupling constants. In the present paper, this theory has been applied to the ammonia molecule. On the basis of the theoretical results, together with the experimental value of the dipole moment, some discussion has been made on the ionic character of the N–H bond and the s–p hybridization of the nitrogen atom. The following VB function has been assumed to the ground state of the molecule,

$$\Psi_T = A\left[\Psi_{\mathrm{cov}} + 3\lambda\Psi_{\mathrm{ion1}} + 3\lambda^2\Psi_{\mathrm{ion2}} + \lambda^3\Psi_{\mathrm{ion3}}\right] \quad (1)$$

Here A represents the normalization factor, the coefficient λ is concerned with the magnitude of the ionic character of the N–H bond and the wavefunctions Ψ_{ion1}, Ψ_{ion2}, and Ψ_{ion3} respectively refer to the singly, doubly and triply ionized structure. To each configuration the following electron pair bond functions are assumed:

$$\left.\begin{aligned}
\Psi_{\mathrm{cov}} &= (\mathrm{N}_l)^2(\mathrm{N}_1\mathrm{H}_1)^2(\mathrm{N}_2\mathrm{H}_2)^2(\mathrm{N}_3\mathrm{H}_3)^2 \\
\Psi_{\mathrm{ion1}} &= (\mathrm{N}_l)^2(\mathrm{N}_1)^2(\mathrm{N}_2\mathrm{H}_2)^2(\mathrm{N}_3\mathrm{H}_3)^2 \\
\Psi_{\mathrm{ion2}} &= (\mathrm{N}_l)^2(\mathrm{N}_1)^2(\mathrm{N}_2)^2(\mathrm{N}_3\mathrm{H}_3)^2 \\
\Psi_{\mathrm{ion3}} &= (\mathrm{N}_l)^2(\mathrm{N}_1)^2(\mathrm{N}_2)^2(\mathrm{N}_3)^2
\end{aligned}\right\} \quad (2)$$

Here N_l and N_i ($i=1$, 2 and 3) are the lone pair orbital and the equivalent orbitals on the nitrogen atom and $(\mathrm{N}_i\mathrm{H}_i)^2$ is the normalized bond orbital of the Heitler-London type. When the structure of the ammonia molecule is considered to belong to the symmetry species C_{3v}, N_l and N_i orbitals are expressed as follows:

$$\left.\begin{aligned}
\mathrm{H}_l &= \alpha\mathrm{S} + \sqrt{3}\beta\mathrm{P}_z \\
\mathrm{N}_1 &= \gamma\mathrm{S} + \sqrt{\frac{1}{6}}\delta\mathrm{P}_x + \sqrt{\frac{1}{2}}\delta\mathrm{P}_y + \sqrt{\frac{1}{3}}\varepsilon\mathrm{P}_z \\
\mathrm{N}_2 &= \gamma\mathrm{S} + \sqrt{\frac{1}{6}}\delta\mathrm{P}_x - \sqrt{\frac{1}{2}}\delta\mathrm{P}_y + \sqrt{\frac{1}{3}}\varepsilon\mathrm{P}_z \\
\mathrm{N}_3 &= \gamma\mathrm{S} - \sqrt{\frac{2}{3}}\delta\mathrm{P}_x + \sqrt{\frac{1}{3}}\varepsilon\mathrm{P}_z
\end{aligned}\right\} \quad (3)$$

Here S, P_x, P_y and P_z represent the Slater AO's and the coordinate system was taken as shown in Fig. 1. By considering the orthonormalization conditions for Eq. 3, the number of coefficients to be determined is reduced to only one ε.

The dipole moment and the quadrupole coupling constant are expressed as follows:

$$\mu = e\left(\sum_{i=1}^{3} r_i - \sum_{j=1}^{8} \bar{Z}_j\right), \quad \bar{Z}_j = \int |\Psi_T|^2 Z_j \mathrm{d}v \quad (4)$$

$$eQq = -e^2Q\int |\Psi_T|^2 (3\cos^2\theta_z - 1) r^{-3}\mathrm{d}v \quad (5)$$

$$\approx eQq_{pz}f(\lambda, \varepsilon) \quad (5')$$

* Present address; Osaka Municipal Technical Research Institute, Kita-ku, Osaka.

1) C. H. Townes and B. P. Dailey, *J. Chem. Phys.*, **17**, 782 (1949).

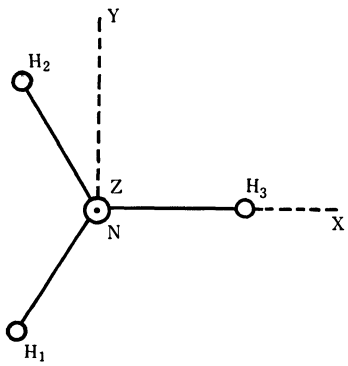


Fig. 1. The coordinate system of NH_3 molecule. Length N-H=1.014 Å. Angle H_i-N-H_j=106° 47' [11].

$$q_{pz} = -e\int|\Psi_{n:2pz}|^2(3\cos^2\theta_z - 1)r^{-3}dv \qquad (6)$$

(e: protonic charge, 4.802×10^{-10} e.s.u.)

We followed the theory of Townes and Dailey that the contribution to the field gradient at the nitrogen nucleus depends exclusively upon the p electrons of the nitrogen atom. Moreover, since we have had no experimental value for eQq_{pz} of the nitrogen atom, we used a value $-11.12\,Mc.$ calculated with the aid of the $2pz$ SCF AO of the ground state ^4S of the nitrogen atom, which was obtained to fit to Hartree-Fock field by Hartree and Hartree[2]. We used the microwave data for the experimental values, $\mu=1.468\,D$ and $eQq=-4.0842\,Mc.$[3], and all the overlap integrals and the dipole moment matrix integrals were evaluated by the ordinary method[4]. These values are tabulated in Table I.

TABLE I. OVERLAP INTEGRAL: $S_{ab}=\int\chi_a\chi_b dv$

DIPOLE MOMENT MATRIX INTEGRAL:

$$M_{ab}=\int\chi_a Z\chi_b dv \text{ (in } a.u.\text{)}.$$

The following abbreviated notations for AO's are used: h_i=(H: 1s), s=(N: 2s), x=(N: 2px), y=(N: 2py) and z=(N: 2pz).

S_{his}	0.510836	M_{hihi}	0.718747
S_{hiz}	0.151483	M_{his}	0.168502
S_{h_1x}	−0.187118	M_{hiz}	0.461132
S_{h_2x}	−0.187118	M_{sz}	0.0866768
S_{h_3x}	0.374235	M_{h_1x}	0.0640552
		M_{h_2x}	0.0640552
		M_{h_3x}	0.128110
		M_{h_1y}	0.111230
		M_{h_2y}	0.111230
		M_{h_3y}	0

The parameters ε and λ were determined as 0.9465 and −0.38, respectively, by the aid of Eqs. 4 and 5′, and the observed values of μ and eQq. The normalized hybrid orbitals of the nitrogen atom then become,

$$\left.\begin{aligned} N_l &= 0.8395S - 0.5434P_z \\ N_1 &= 0.3137S - 0.4082P_x - 0.7071P_y \\ &\quad + 0.4847P_z \\ N_2 &= 0.3137S - 0.4082P_x + 0.7071P_y \\ &\quad + 0.4847P_z \\ N_3 &= 0.3137S + 0.8165P_x + 0.4847P_z \end{aligned}\right\} \qquad (2)$$

TABLE II. RELATIVE WEIGHTS OF VALENCE STRUCTURE IN NH_3 AND S CHARACTER OF THE HYBRID ORBITAL OF N ATOM

Structure		Weight of structure %	
		Present	Syrkin et al.
Covalent form	(I)	14.5	16
Single ionic form	(II)	18.8	13.5
Double ionic form	(III)	2.7	3.9
Triple ionic form	(IV)	0.1	0.3
Transitional	(I)—(II)	33.0	27.3
〃	(I)—(III)	12.5	15
〃	(I)—(IV)	1.6	3
〃	(II)—(III)	14.3	15
〃	(II)—(IV)	1.8	4
〃	(III)—(IV)	0.7	2

	S character %		
	Present	Duncan & Pople	Higuchi
For lone pair orb.	70.5	38.9	71.4
For equivalent orb. (each)	9.8	4.1	3.2

Thus we get the estimates of the ionic character and the s-p hybridization of NH_3 molecule. These are given in Table II, together with the estimated values by other authors. Several views for the orbitals of NH_3[5-8] has been already reported, however we can not always compare those with the present results since those orbitals are almost described in

2) D. R. Hartree and W. Hartree, *Proc. Roy. Soc.* (*London*), **A193**, 299 (1948). This result for $2pz$ function can be approximated in the following analytical form:

$$(3/4\pi)^{1/2}\cos\theta_z r[1.809\,e^{-1.387r}+6.620\,e^{-2.950r}]$$

We calculated q_{pz} by this function.

3) G. R. Gunther-Mohr, R. L. White and A. L. Schawlow, *Phys. Rev.*, **94**, 1184 (1954).

4) For example, M. Kotani et al., "Table of Molecular Integrals", Maruzen Co., Ltd., Tokyo (1955).

5) A. B. F. Duncan and J. A. Pople, *Trans. Faraday Soc.*, **49**, 217 (1953).

6) J. Higuchi, *J. Chem. Phys.*, **24**, 535 (1956).

7) H. Kaplan, ibid., **26**, 1704 (1957).

8) A. B. F. Duncan, ibid., **27**, 423 (1957).

MO and not in Heitler-London type. When we dare to compare, they have some differences from ours as above mentioned. Here Duncan and Pople's orbitals[5] are determined in such a way as the parameters in orbitals are well fitted to the experimental value of the dipole moment of NH_3, and Higuchi's ones[6] are obtained following Roothaan's SCF procedure[9], in which all the electrons in molecule take part in setting up MO, so that the orbitals are considered more accurate than the present and Duncan and Pople's ones. Also, Syrkin et al.[10] have estimated the ionic character of the structure from the base of the additivity of bond moment. On the other hand, our estimations are made taking into consideration the nuclear quadrupole coupling constant besides the dipole moment. However these both estimates may be said to be equal substantially.

Department of Physics, Faculty of Science
Hiroshima University, Hiroshima

9) C. C. J. Roothaan, *Revs. Modern Phys.*, **23**, 69 (1951).
10) Y. K. Syrkin and M. E. Dyatkina, "Structure of Molecules and the Chemical Bond", Butterworths Scientific Publications, London (1950), p. 208.
11) G. Herzberg, "Infrared and Raman Spectra of Polyatomic Molecules", D. Van Nostrand Co., Inc., New York (1945), p. 439.

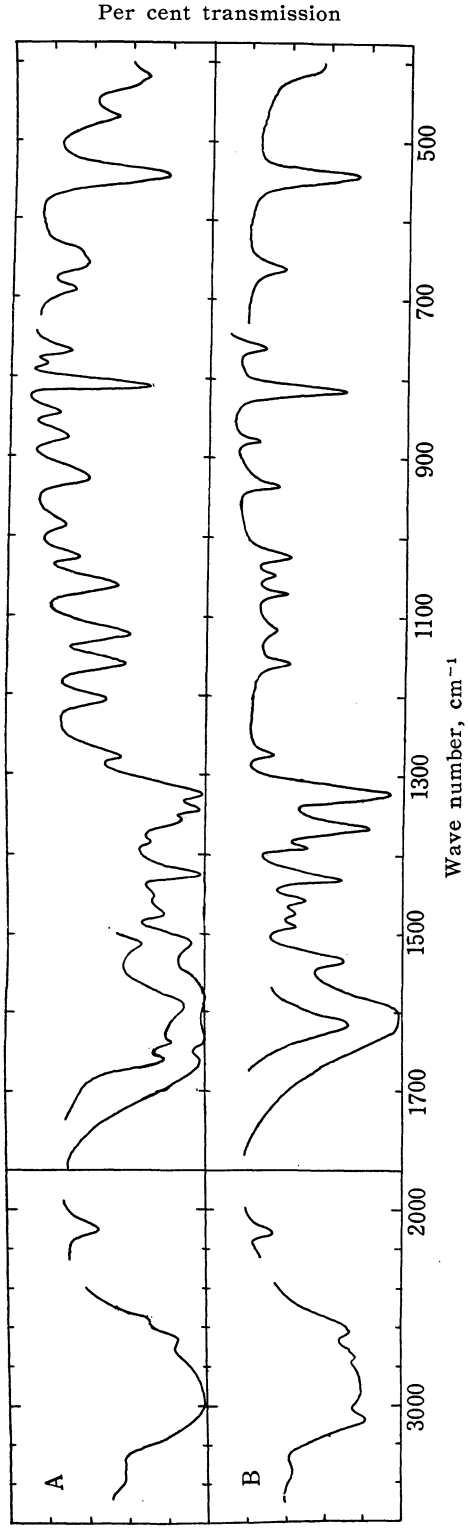


Fig. 1. Infrared absorption spectra of A- and B-forms of DL-α-amino-*n*-butyric acid.

Two Crystalline Forms of DL-α-*Amino-n-butyric Acid*

By Masamichi Tsuboi, Yoichi Iitaka, Shigeko Suzuki and San-ichiro Mizushima

(Received March 19, 1959)

In the course of our infrared studies on amino acids, we have found that there are at least two crystalline modifications in DL-α-amino-*n*-butyric acid,—one of which corresponds to the form already known (hereafter designated as A-form), while the other is a new form (B-form).

A-form is obtained as tabular crystals from the saturated aqueous solution on cooling. While, B-form is obtained as fibrous crystals from the aqueous solution (not necessarily saturated) by adding ethanol. The two forms give different

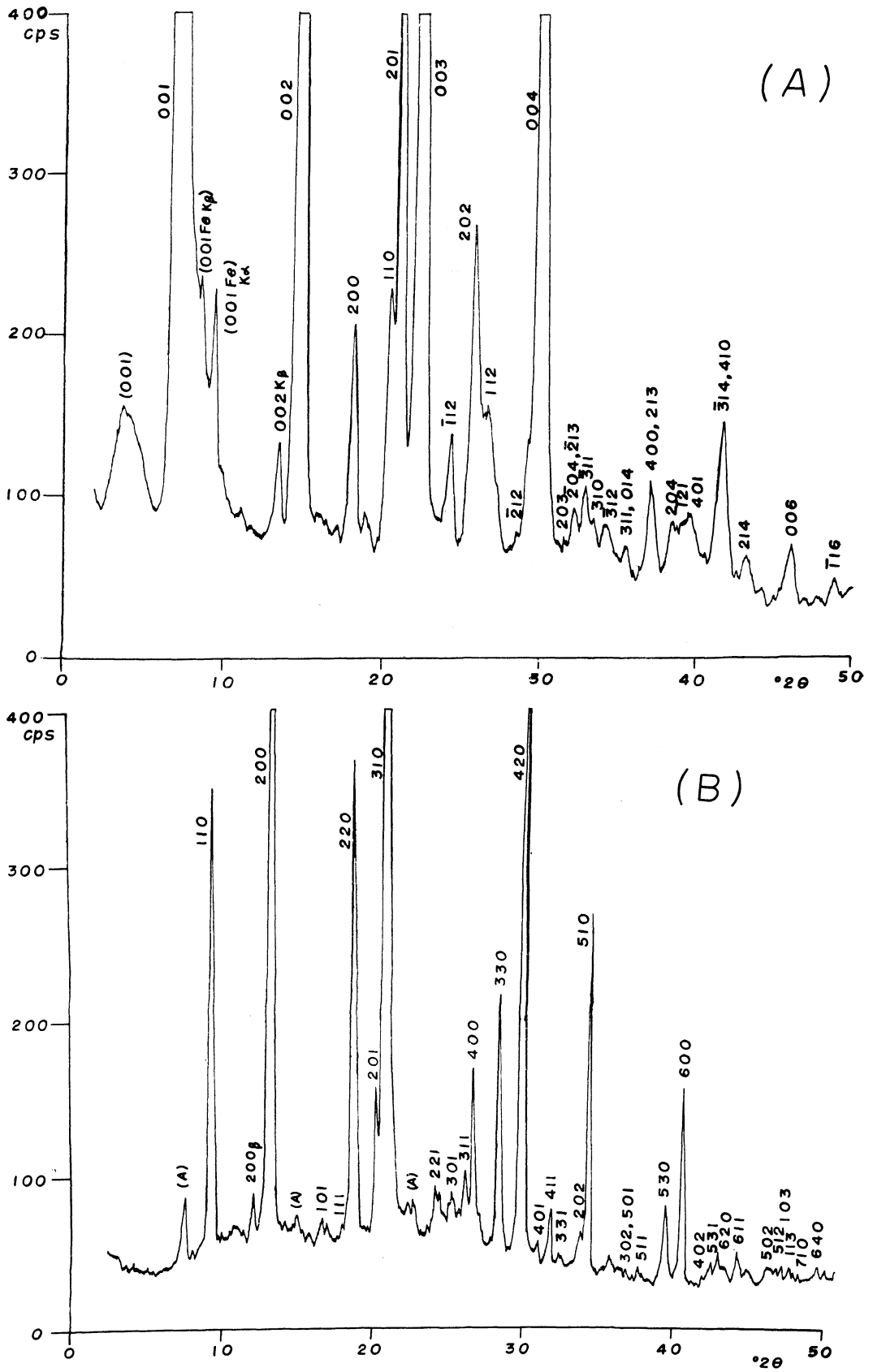


Fig. 2. X-ray powder patterns of A- and B-forms of DL-α-amino-n-butyric acid. Radiation used: CuK, 30 kV., 15 mA., Ni-filtered. (The diffused peak indicated as (0 0 1) for A-form is the continuous spectrum of the X-ray diffracted by the (0 0 1) plane.)

infrared spectra and X-ray powder patterns as shown in Figs. 1 and 2. From the measurements at different temperatures it was found that B-form is transformed into A-form at 195°C, whereas A-form remains unchanged from room temperature to 200°C. Therefore, at room temperature B-form is stable and A-form is metastable, but above 195°C this form becomes stable.

By our X-ray and infrared investigations, A-form is identified as the one, for which Dawson and Mathieson[1] gave the following constants: $P2_1/a$, $a=9.87$ Å, $b=4.80$ Å, $c=12.10$ Å, $\beta=101°$, $Z=4$, and Koegel et al.[2] observed infrared spectrum.

For B-form, it was found, from oscillation and Weissenberg photographs about the axis of the elongation (c-axis) and the axis perpendicular to it (a-axis), that the crystal is tetragonal, with the Laue symmetry of $4/m$, and with the unit cell dimensions: $a=13.38$ Å, and $c=5.85$ Å. Analysis of the photographs showed systematic absence of the reflections for ($h\,k\,0$) planes when $h+k$ is odd, and for ($0\,0\,l$) planes when l is odd; indicating the space group of $P4_2/n$.

As to the molecular configurations of A- and B-forms, it was found probable, from our infrared measurements with plane polarized radiation, that the two forms are rotational isomers to each other[3]. Furhther analysis of the X-ray photographs is now in progress, from which it is hoped to determine accurately the configurations of these isomers.

We wish to thank Sister Mary Marina, for her sending us the infrared spectra of a crystalline DL-α-amino-n-butyric acid which now turned out to be A-form.

Faculty of Science
The University of Tokyo
Hongo, Tokyo

1) B. Dawson and A. McL. Mathieson, *Acta Cryst.*, **4**, 475 (1951).
2) R. J. Koegel, R. A. McCallum, J. R. Greenstein, M. Winitz and S. M. Birnbaum, *Ann. N. Y. Acad. Sci.*, **69**, 94 (1957).
3) S. Mizushima, "Structure of Molecules and Internal Rotation", Academic Press, New York (1954).

A New Very Large Long-period in the X-ray Small-angle Diffraction of Polyethylene Filaments

By Takani Mochizuki

(Received March 25, 1959)

The meridional long-period X-ray diffraction in polyethylene was measured by several authors[1-4]. However the reported long-period spacings are divergent. For instance, a spacing given by Kiessig[2] is 98 Å, whereas that by Statton[3] is 240 Å. These discrepancies might be due to the difference in polyethylene specimens and also their preparations.

This communication is to report that a further large long-period spacing has been observed recently in the meridional small-angle scattering for low-pressure polyethylene filaments.

Polyethylene ("Fortiflex A" of Celanese Corp. of America; Melt index: 0.7) filament specimens were prepared with an extruder at 210°C (Sample A), and stretched at 140°C up to 100% (Sample B), 200% (Sample C) and 300% (Sample D). From the X-ray diffraction photographs, a fairly high orientation of the crystallites was seen for Sample A and a typical uniaxial orientation of the crystallites was observed for Sample D. The small-angle scatterings of X-rays from these samples were

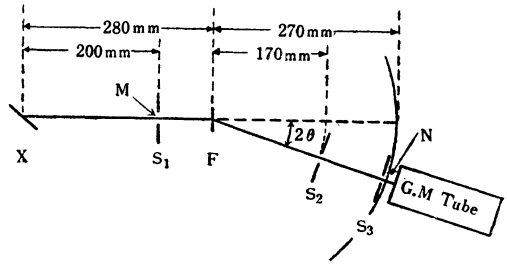


Fig. 1. Schematic diagram of the X-ray diffractometer.
X: X-ray focus
S_1: 1st slit 0.15 mm.
S_2: 2nd slit 0.5 mm.
S_3: 3rd slit 0.1 mm.
F: filament sample
M, N; Soller slit

1) E. P. H. Meibohm and A. F. Smith, *J. Polymer Sci.*, **7**, 449 (1951).
2) K. Hess and H. Kiessig, *Kolloid-Z.*, **130**, 10 (1953).
3) W. O. Statton, *J. Polymer Sci.*, **28**, 423 (1958).
4) I. Sakurada, Y. Nukushina and Y. Tanaka, *Chem. of High Polymers*, **15**, 771 (1958).

measured in the direction parallel to the fiber axis with an X-ray diffractometer having the following slit system, shown in Fig. 1, Cu $K\alpha$ radiation (38 KV. 15 mA) filtered with nickel foil being used.

Curves of the diffracted X-ray intensity are shown Fig. 2. All samples show a very strong and distinct peak of intensity. The center of the peak for Samples A and D is found using Bragg's law to correspond to a spacing of the order of 260 Å and 460 Å, respectively. Such a large long-period of about 460 Å has not been observed previously for synthetic polymers. From the intensity curves of Samples B and C, it seems that two kinds of long-period (260 Å and 460 Å) coexist in these samples.

Further, high-pressure polyethylene ("Tenite #864" of Eastman Chem. Products; Melt index: 0.3) was examined for comparision. Filaments were prepared in the same way as above, and stretched up to 270% at 100°C (Sample E). The intensity curve of the meridional small-angle interference of Sample E is given by the dotted line in Fig. 2, which shows a broad and low intensity peak. The Bragg distance of this peak is calculated to be 177 Å,

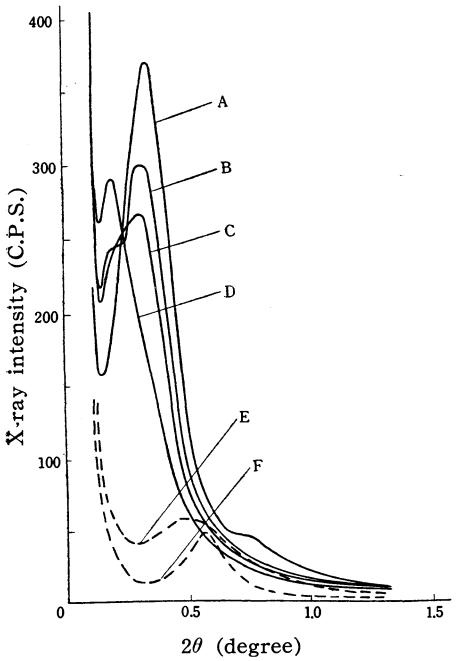


Fig. 2. Intensity curves of small-angle X-ray scattering.
A: original filament
B: 100% stretched filament
C: 200% stretched filament
D: 300% stretched filament
E: high-pressure polyethylene filament
F: polyvinyl alcohol fiber

which is in agreement with the value given by Meibohm and Smith[1] and Sakurada, Nukushina and Tanaka[4].

Some points of interest come to light in this experiment. In the low-pressure polyethylene, a very strong small-angle interference was observed as compared with the intensities obtained for high-pressure polyethylene and polyvinyl alcohol fibers[5]. It seems likely that this marked difference in the intensities might be partly due to the difference between the mean electron densities of the crystalline and amorphous parts, and has something to do with similar difference, shown in Fig. 3, in intensities of the meridional reflections (0 2 0) from both samples[5].

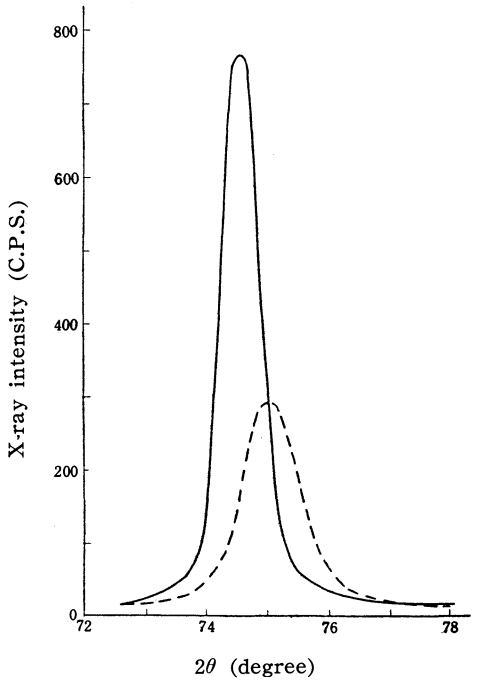


Fig. 3. Intensity curves of (0 2 0) reflection —— polyethylene ------ polyvinyl alcohol

Besides, it is to be noted that the curve A shows a second intensity hump. It corresponds to the second order reflection of the spacing of 260 Å. Such small intensity hump has not been observed in the curves B, C and D, and hence, it seems that the regular fine texture is destroyed by stretching process.

The author expresses his sincere thanks to Professor I. Nitta, Osaka Univercity, for his kind guidance and encouragement

5) The detailed results of polyvinyl alcohol fibers will be reported elsewhere.

throughout this experiments. He is also indebted to Mr. S. Miyazaki for supplying the samples.

Research Laboratory
Kurashiki Rayon Co., Ltd.
Kurashiki

Isotopic Exchange of Zinc Chelate Compounds in an Anhydrous Organic Solvent

By Kazuo Saito and Michiko Tamura

(Received March 31, 1959)

Isotopic exchange of zinc in its complexes has been studied by a few workers with various chelate compounds[1-3]. It is generally agreed that the exchange is rapid, except that of zinc phthalocyanine complex, which has a "fused ring" structure. All these experiments, however, involve the use of water, either as solvent or as separating agent for the two compounds between which the isotopic exchange is to be examined. The present authors are of the opinion that the exchange might be accelerated by water, as is in the case of other metal complexes, and that, when the experiment is carried out in the absence of water, a measurably slow exchange might be expected even for those ions having filled inner *d*-orbitals.

Attempts have been extensively made to separate two chelate compounds of zinc in an anhydrous organic solvent. It was eventually found that pure zinc oxinate is precipitated, when dioxane solution of zinc oxinate and acetylacetonate is treated with a large excess of *iso*-propylether, trichloroethylene or chloroform. The yellow precipitate was spectrophotometrically examined in methanol and found to be free from acetylacetonate. The isotopic exchange was examined with inactive oxinate and acetylacetonate labelled with radioactive zinc-65. A linear relationship was observed, when the counting rate of the photo-multiplier pulse due to photo-electric peak of the γ-ray spectrum (1.114 MeV.) of zinc-65 is plotted against the amount of the labelled compound. In order to avoid the influence of water, all procedures were carried out in a dry box (relative humidity, less than 10%; dew point, below $-14°C$).

It was elucidated that the exchange proceeds instantaneously, even under an anhydrous condition. Since the exchange between zinc acetylacetonate in solution and solid zinc oxinate proceeds slowly, it appears evident that the rapid exchange took place in the homogeneous solution rather than between the solute and the precipitate in the nascent state.

Further work with other chelate compounds is in progress. Details of the study will be published later.

Experimental.—The chelate compounds were prepared by the usual methods and dried at 110°C immediately before use. The organic solvents were refluxed with sodium and distilled with dry apparatus. The presence of water was tested with various reagents, including anhydrous copper sulfate and cobalt chloride, but the results were all negative. It appears as if the water content is less than 0.01%.

Dioxane solution of zinc oxinate (0.000125

Table. Exchange of zinc between oxinate and acetylacetonate

No.	acetylacetonate		oxinate				exchange
	used mg.	c.p.m.	used mg.	recovered mg.	obsvd. c.p.m.	calcd.* c.p.m.	%
1)	32.7	3277	44.2	29.0	1137	1075	106
2)	33.6	2208	44.3	41.7	1062	1039	102
3)	29.3	1966	44.2	40.4	77	1236	7
4)	32.9	2161	44.2	42.0	772	1026	75

1) 2): Both chelates in dioxane; time of exchange, 30 sec.

3) 4): Acetylacetonate, in the mixed solvent; oxinate, solid; time of exchange, 3) 1 hr., 4) 12 hr.

* Calculated on the assumption that a complete exchange has taken place.

1) Don C. Atkins, Jr. and C. S. Garner, *J. Am. Chem. Soc.*, **74**, 3527 (1952).
2) L. Leventhal and C. S. Garner, ibid., **71**, 371 (1949).
3) A. Turco, G. Sordillo and M. Scatena, *Ricerca Sci.*, **25**, 2361 (1955).

mol. in 15 ml.) and that of zinc acetylacetonate (0.000125 mol. in 25 ml.) were mixed (at room temperature, 18°C) and, after 30 sec., *iso*-propylether (ca. 300 ml.) was added. The precipitate was filtered off with a detachable sintered glass filter plate, thoroughly washed with *iso*-propylether, weighed and submitted to γ-ray counting. Precipitation of the oxinate was completed within one hour. (No. 1 and 2 in the table).

Exchange between solid oxinate and acetylacetonate in solution was examined in a mixture (100 ml.) of dioxane and *iso*-propylether (1+3, by volume). About 7 and 75 per cent exchange were observed after one hour and 12 hours, respectively. Since the mixed solvent assumed yellow, the exchange appears to proceed through partial dissolution of the oxinate.

Institute for Nuclear Study
The University of Tokyo
Tanashi, Tokyo

*Crystalline Polymers of Some Nuclear-substituted Styrenes**

By Shunsuke Murahashi, Shun'ichi Nozakura and Hiroyuki Tadokoro

(Received April 9, 1959)

In the preceding paper we pointed out the possible crystallization of poly(*p*-methylstyrene) and poly(*m*-methylstyrene) prepared by Ziegler's catalyst from the observation of infrared spectra and density-measurements[1]. In the present communication, we wish to report that this expectation has been realized by the suitable heat-treatment in both cases and also a newly prepared poly(*p*-trimethylsilylstyrene) has been found to crystallize easily by the same treatment.

These results stand in contrast with the recent observation by Natta that the polymers of *p*-substituted styrene obtained with Ziegler's catalysts are generally amorphous, except for *p*-fluorostyrene, because of a steric hindrance caused by the *p*-substituent in crystallization[2].

Table I. Polymerization of nuclear-substituted styrenes with Ziegler's catalyst at 70°C in 20 ml. of *n*-heptane

Monomer g.	$TiCl_4$ mmol.	$AlEt_3$ mmol.	$AlEt_3$ added after washing mmol.	Time hr.	Conversion %	$[\eta]$[a]	Softening point °C[b]
p-Methylstyrene, 3.7 g.	2.2	2.3	2.5	3.6	43	2.61	130
m-Methylstyrene[c], 3.3 g.	3.2	3.4	3.4	3.5	21	2.52	90
p-Trimethylsilylstyrene[d], 4.3 g.	3.3	3.4	3.4	4.3	13	See Table II	

a) Intrinsic viscosity in toluene at 30°C.
b) Softening points were observed under a microscope.
c) *m*-Methylstyrene was supplied from the Research Laboratory of Dainihon Celluloid Co.
d) *p*-Trimethylsilylstyrene was supplied from the Engineering Laboratory of Mitsubishi Electric Manufacturing Co.

Table II. Fractional extraction of the crude poly(*p*-trimethylsilylstyrene)[a]

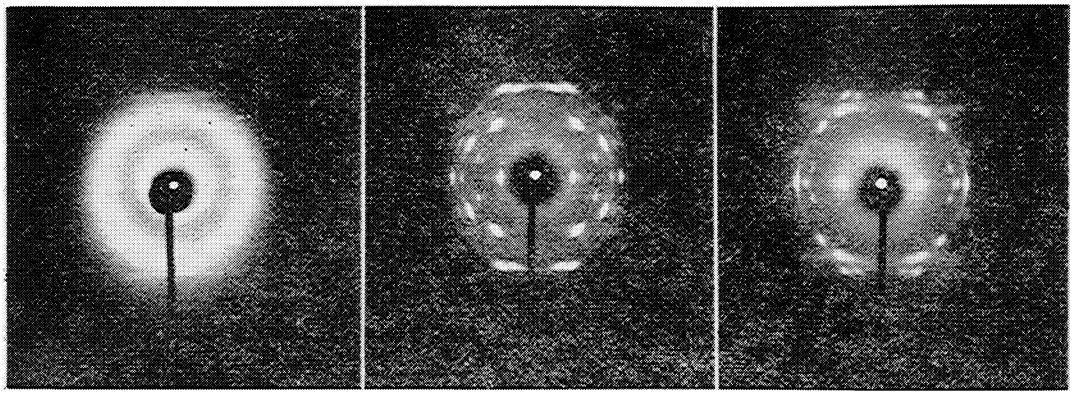
Solvent for extraction	Fraction %	$[\eta]$	Softening p. or m. p. °C[b]	X-ray evidence
Acetone	19	0.35	s. p. 125	Amorphous
Ether	11	0.61	s. p. 145	Partially crystalline
Benzene	70	2.49	m. p. 284	Highly crystalline

a) Hot extraction was carried out using a modified Soxhlet's extractor.
b) Softening points and melting points were observed under a polarized microscope.

* Paper III in a series on "Stereoregular Polymers".

1) H. Tadokoro, S. Nozakura, T. Kitazawa, Y. Yasuhara and S. Murahashi, This Bulletin, **32**, 313 (1959).

2) G. Natta, F. Danusso and D. Sianesi, *Makromol. Chem.*, **28**, 253 (1958).



(a) (b) (c)

Fig. 1. Fiber diagrams of X-ray diffraction patterns.
(a) Poly(*p*-methylstyrene). An extruded filament was drawn at 135°C to about 20 times of the original length and heated for 6 hr. at the same temperature.
(b) Poly(*m*-methylstyrene). Drawn at 90°C to about 20 times and heated for 3 hr. at 100°C.
(c) Poly(*p*-trimethylsilylstyrene). Drawn at 150°C to about 20 times and heated for 0.5 hr. at 200°C.

All the polymerization procedure in this paper was performed by the use of Ziegler's catalysts according to the modified method described in the previous paper[3], i. e., the catalystic solid mass was washed with *n*-heptane prior to polymerization (Table I). The fractional extraction of the crude polymer was carried out in the case of poly(*p*-trimethylsilylstyrene) as shown in Table II.

The fiber diagrams of X-ray diffraction patterns with these polymers are shown in Fig. 1. Poly(*p*-methylstyrene) could be crystallized by the heat-treatment in a stretched state, although its crystallinity was rather low as shown in Fig. 1 (a). On the contrary, the benzene-fraction (Table II) of poly(*p*-trimethylsilylstyrene) was found to be crystallized easily and highly crystalline even in an unoriented state. Poly(*m*-methylstyrene) was more reluctant to crystallize than poly(*p*-trimethylsilylstyrene) in an unoriented sample.

Fiber periods observed are 12.9, 57.0 and 60.4 Å for the polymers of *p*-methyl-, *m*-methyl- and *p*-trimethylsilyl-styrene, respectively. The large values of identity periods of these polymers suggest some complicated nature of the helical structures of these isotactic polymers. The detailed X-ray analysis will be published elsewhere by Nitta and others.

These three polymers are all considered to be isotactic and to have the helical structure of trans-gauche alternate sequence from the inspection of the following infrared data. (1) The 2849 cm^{-1} CH_2 symmetric stretching band has almost no dichroism (or rather weak parallel dichroism), though the 2924 cm^{-1} CH_2 antisymmetric stretching band shows distinguished perpendicular nature, as is in the case of isotactic polystyrene[4]. This dichroic behavior indicates such an inclination of the triangle of the methylene group that the direction of H—H is nearly perpendicular to the fiber axis and the angle between the bisector of the angle H—C—H and the fiber axis is about 54°44′. (2) The four bands in the region of 1400~1100 cm^{-1}, which are considered to be closely associated with the helical structure in the previous paper[1], are also found in the polarized spectra of these three polymers, showing the same dichroic natures as the corresponding bands of the oriented isotactic polystyrene: 1364 (⊥), 1314 (⊥), 1297 (∥) and 1185 cm^{-1} (∥).

Department of Polymer Science
Faculty of Science
Osaka University
Nakanoshima, Kita-ku, Osaka

3) S. Murahashi, S. Nozakura, M. Sumi and K. Hatada, to be published in this Bulletin.

4) H. Tadokoro, N. Nishiyama, S. Nozakura and S. Murahashi, *J. Polymer Sci.*, in press.

*Organic Spot Tests. I. Detection of Acidic Compounds**

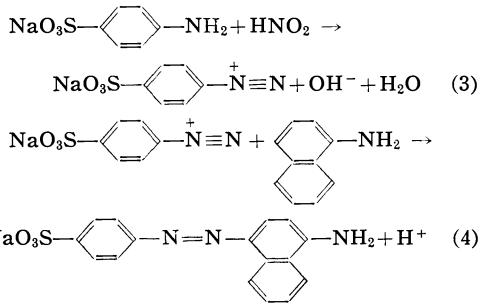
By Yujiro NOMURA

(Received April 11, 1959)

The familiar and sensitive Griess test for nitrites has been found to be used conversely for the detection of very small quantities of acidic compounds. Thus, the mixed solution of sodium sulfanilate, sodium nitrite and α-naphthylamine in dilute alcohol or dioxan produces intense red color on adding a tiny quantity of various acidic compounds. This color reaction depends on the formation of the red azo dye through the following successive reactions:

$$HA \rightleftarrows H^+ + A^- \quad (1)$$

$$NaNO_2 + H^+ \rightleftarrows HNO_2 + Na^+ \quad (2)$$



$$NaO_3S-C_6H_4-NH_2 + HNO_2 \rightarrow NaO_3S-C_6H_4-\overset{+}{N}\equiv N + OH^- + H_2O \quad (3)$$

$$NaO_3S-C_6H_4-\overset{+}{N}\equiv N + C_{10}H_6-NH_2 \rightarrow NaO_3S-C_6H_4-N=N-C_{10}H_6-NH_2 + H^+ \quad (4)$$

The reactions 3 and 4 proceed so rapidly and completely that the equilibria 2 and 1 are shifted toward the right successively. Accordingly, by virtue of the equilibrium disturbance it is possible to detect many organic acids which are not very soluble and are so weak that they do not affect usual dyestuff indicators at all or do indecisively at most.

Reagents.—1) 2.9 g. of sodium sulfanilate $NH_2C_6H_4SO_3Na \cdot 2H_2O$ and 0.7 g. of sodium nitrite are dissolved in 30 cc. of distilled water.

2) 1.8 g. of α-naphthylamine is dissolved in 40 cc. of ethanol or dioxane.

The reagent solution is prepared by mixing two solutions 1) and 2) just prior to use.

Procedure.—A few drops of the reagent solution are placed in a depression of a spot plate. A small amount of the test material (a few crystals or the residue after evaporating a drop of a test solution) is added. Depending on the acidity and solubility of the acid present, a red or orange color appears at once or after a few minutes. A comparison blank test is advisable when dealing with a slight amount of the sample.

Results.—The limits of detection attained with various acids were 25~40 γ. The following compounds were tested.

Immediate intense red color reaction.—Formic acid, acetic acid, propionic acid, butyric acid, isovaleric acid, caproic acid, oxalic acid, malonic acid, succinic acid, adipic acid, fumaric acid, maleic acid, lactic acid, thioglycolic acid, malic acid, citric acid, tartaric acid, benzoic acid, salicylic acid, anthranilic acid, sulfanilic acid, benzenearsonic acid, hippuric acid and picric acid.

Immediate orange to orange-red color reaction.—Caprylic acid, pelargonic acid, capric acid, palmitic acid, stearic acid, oleic acid, elaidic acid, erucic acid, cholic acid, aspartic acid and glutamic acid.

Orange color reaction within a few minutes.—Lauric acid, myristic acid and 12-hydroxyoleic acid.

Negative reaction.—Phenol, cresol, catechol, resorcinol, hydroquinone, ethyl acetate, ethyl benzoate, diethyl malonate, benzoylacetone, ethyl acetoacetate, acetanilide, succinimide and ammonium salts or metal salts of carboxylic and sulfonic acids.

α-Amino acids except aspartic acid and glutamic acid gave no response to the reagent solution. But after digesting with two or three drops of formaline they showed positive reactions. The following amino acids could be detected in this manner: glycine, alanine, cystine, valine, methionine, leucine, isoleucine, phenylalanine, tyrosine, histidine and asparagine.

Department of Chemistry
College of General Education
The University of Tokyo
Meguro-ku, Tokyo

* Presented before 12th Annual Meeting of the Chemical Society of Japan, April 2, 1959.

Purification of Silicontetraiodide by Zone-refining Process

By Hideo BABA, Tadashi NOZAKI and Hidemaro ARAKI

(Received July 12, 1958)

In spite of the superior properties of silicon as a semiconductor material, the electronic devices such as silicon transistors or power rectifiers have not been fully developed. One of the causes of this comes from the fact that the techniques of purification of this material are more difficult than those of germanium. The refining process of silicon would have to choose another direction from that of germanium especially in its chemical purification steps. Moreover, elementary silicon is so chemically active in its molten state that the zone refining can not be carried out in the same way as in the case of germanium. For these reasons, chemical purification is important to obtain a highly pure silicon.

Several methods have been presented for obtaining transistor grade silicon[1-4], but among them, the so called du Pont method is the most predominant in the industrial aspect at present. On the other hand, we expect that the silicon iodide method will be one of the promising ones for improving the purification processes. First of all, the most important problem is the methods of removing impurities in silicontetraiodide. Of course, the usual refining processes such as recrystallization, distillation and sublimation are also applicable in this case, but in addition to them, the zone-refining process, which has been proved excellent for the purification of germanium[5], may be applied to this compound. But the behavior of impurity elements in the iodide during this process has not been made clear. As some elements such as boron, phosphorus and arsenic are removed with difficulty by the zone-refining of elementary silicon[6], it is preferable to remove them from it beforehand. For this reason, we studied the behavior of a trace of boron and phosphorus in silicontetraiodide during the normal freezing and zone-melting of the material.

Recently, Rubin et al. studied the zone-melting of silicontetraiodide and they determined the segregation coefficients of several elements by spectrographic analysis[7]. But as they pointed out, the concentrations of impurities at the top of the charge were too far below the limits of spectrographic detection for some elements to make clear the details of the impurity distribution through the charge.

Experimental Results

Behavior of Phosphorus in Silicontetraiodide.—*a) Preparation of radioactive phosphorus-iodide.*—Radio isotope ^{32}P is conveniently used to trace the behavior of phosphorus during the zone melting process of silicontetraiodide. Phosphorus in silicontetraiodide will not be present in its elemental state but will exist as some iodine compounds such as diphosphorus tetraiodide or phosphorus triiodide. Radio isotope ^{32}P can easily be produced by deuteron radiation. But neither kind of phosphorus, red or yellow, can be irradiated in the cyclotron because of its high vapor pressure. In order to avoid these difficulties, it is preferable to use some phosphorus alloy. Pure copper foil with 99.96% purity and 0.2 mm. thick was vacuum-sealed with red phosphorus in a quartz tube, and was heated at 300°C for about ten hours in a furnace. During this heat treatment, the phosphorus diffused into copper and the surface of the foil turned silver white in color. This alloy was irradiated by deuteron in cyclotron to make it radioactive.

The thus activated Cu—P alloy was treated with toluene containing iodine at its boiling point for about two hours to dissolve out the activated phosphorus, and labeled phosphorusiodide could be obtained. A little portion of activated copper was accompanied with phosphorusiodide in solution forming copper iodide, but the influence of γ rays emitted from ^{64}Cu could be neglected in measuring β rays emitted from ^{32}P using a Geiger counter. Toluene solution containing radioactive phosphorusiodide was added to crystalline siliconiodide and it was dissolved completely by the addition of boiling toluene. Then it was cooled at 0°C for several hours to crystallize out

1) H. V. Wartenberg, *Z. Anorg. allgem. Chem.*, **265**, 186 (1951).
2) D. W. Lyon, C. M. Olsen and E. D. Lews, *J. Elect. Chem. Soc.*, **96**, 359 (1949).
3) H. C. Theuerer, *Bell Tel. Lab. Rec.*, **33**, 327 (1955).
4) F. B. Litton and H. C. Anderson, *J. Elect. Chem. Soc.*, **101**, 287 (1954).
5) W. Pfann, *J. Metals*, **194**, 747 (1952).
6) J. A. Burton, *Physica*, **20**, 845 (1954).
7) B. Rubin, G. H. Moates and J. R. Weiner, *J. Elect. Chem. Soc.*, **104**, 656 (1957).

the silicon iodide contaminated with radioactive phosphorus.

b) Measurement of phosphorus distribution by the radiochemical method. — Segregation Experiments. — The thus prepared silicon iodide was sealed in a quartz tube of 15 mm. diameter and 30 cm. length under reduced pressure. The content was melted by heating uniformly and cooled rapidly so that no segregation of the impurity would occur and was followed by the measurement of the initial distribution of ^{32}P. As shown in Fig. 1, the tracer was distributed uniformly throughout the rod. The content was melted again completely in a furnace which was long enough to melt it uniformly, then the quartz tube was moved down with a speed of 2.2 mm. per minute. The melted silicon iodide was solidified from the top portion outside of the furnace gradually. As a little part of the silicontetraiodide was hydrolyzed by atmospheric moisture, the melted portion of silicon iodide became somewhat turbid. But hydrolyzed products were easily segregated and transferred toward the upper part of the rod.

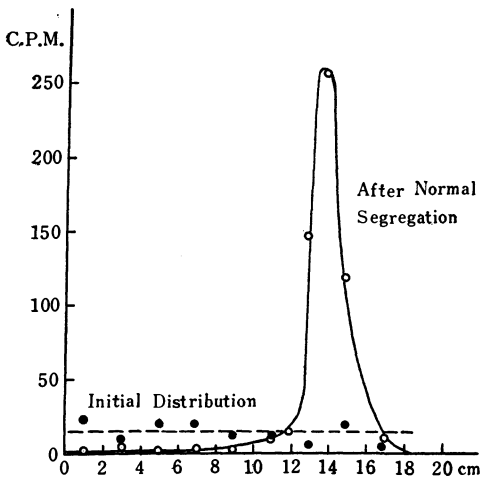


Fig. 1. Distribution of phosphorus after normal freezing.

The distribution of phosphorus after normal segregation could be found by measuring the radioactivity of β-rays emitted from ^{32}P at every 10 mm. length of the rod using a sealing device. The results are shown by curve 2 in Fig. 1 by plotting the counting rate against the distances from the top of the rod.

This method was convenient to carry out the experiment of segregation or zone melting processes, because repetition using the same sample was possible. But the selfabsorption by silicontetraiodide and the absorption by quartz wall made the counting rate less, and when the iodide changed its phase, liquid to solid and vice versa, local strong strength sometimes broke the quartz tube.

These troubles could be avoided by using a quartz boat instead of a tube as shown in Fig. 2. In this case, dried argon gas was introduced gently from the top of the boat to carry the evaporated iodide toward the end of the boat. After normal segregation or zone refining processes, the rod of silicon iodide was taken off from the boat and cut into about ten segments, and each

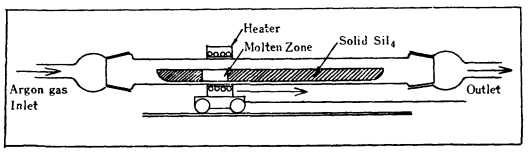


Fig. 2. Zone melting of silicontetraiodide.

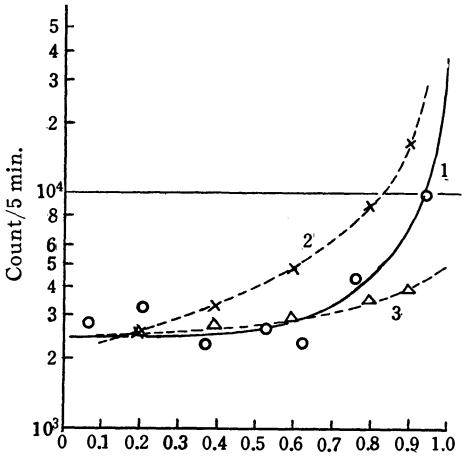


Fig. 3. Distribution of phosphorus in silicontetraiodide after normal segregation.
1. Experimental Result
2. Calculated $k=0.1$
3. 〃 $k=0.8$

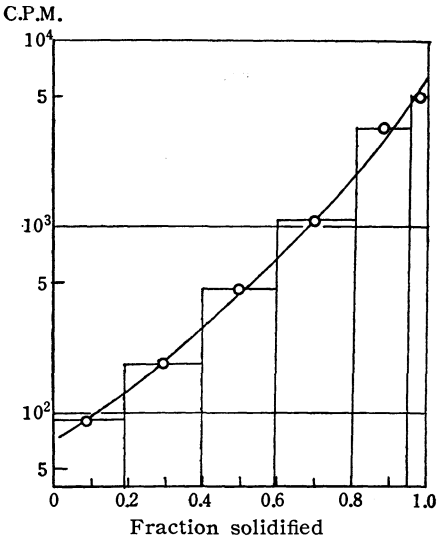


Fig. 4. Distribution of phosphorus after three passes of molten zone.

of them was weighed quickly avoiding the hydrolysis by the atmospheric moisture. Then they were hydrolyzed in a quartz evaporating dish by adding distilled water and dried up on a hot plate. The radioactivity of the samples thus obtained was measured by a Geiger counter.

The results are shown in Fig. 3. Curve 1 indicates the distribution of phosphorus after normal segregation with a velocity of 2.5 mm./min., and Fig. 4 shows the result of zone refining of three passes with a velocity of 0.83 mm./min. In both cases the counts of one gram of hydrolyzed products per five minutes were plotted against a solidified fraction of the iodide bar.

Behavior of Boron in Silicontetraiodide.—*Determination of boron by colorimetric method using curcumin.*—As it is impossible to trace the behavior of boron by using its radioisotope because of its short half life, there is no way but chemical analysis for this purpose. The colorimetric method using curcumin seemed to be the most satisfactory.

Several reports have been published on the determination of boron by this method[8-11]. But some of them have poor reproducibility, because coloring conditions, such as the concentration of the reagents, the time of treating, the evaporation temperature and the dissolving method of formed curcumin-boron complex, affect the results significantly.

Reagents.—*a*) *Curcumin-oxalic acid solution.*—Dissolve 5.0 mg. of crystalline curcumin and 0.5 g. of recrystallized oxalic acid in 50 ml. of redistilled ethanol. This solution was prepared freshly immediately before use and kept cold.

b) *Boron standard solution.*—Dissolve 0.1430 g. of boric acid (extra pure grade) in 500 ml. of redistilled water. Dilute 5.0 ml. portion of this stock solution to 500 ml. (the boron content will be 0.5 γ per ml.).

Standard Reference Curves.—Taking zero to 5.0 ml. of the standard boron solution in quartz evaporating dishes, 1 ml. of hydrochloric acid (1 : 1) and 2 ml. of curcumin oxalic acid solution were added, then they were diluted with distilled water to make the total volume 8 ml. These evaporating dishes were floated on a water bath which was kept at 55±2°C until the contents were dried up. The evaporation could be accelerated by the aid of a gentle air flow on the liquid surface. Ten ml. of ethanol was added to each dish to dissolve the residue, and the solution was transferred to an absorption measurement cell of 10 mm. length. The absorbancy at 540 mμ was measured using a spectrophotometer.

As shown in Fig. 5, curcumin solution itself has absorption maximum at 430 mμ, while boron complex has its maximum at 540 mμ. The curcumin-boron complex is rather stable and no detectable change was observed after several hours as shown in this figure. Beer's law plot is shown in Fig. 6. It was necessary to make

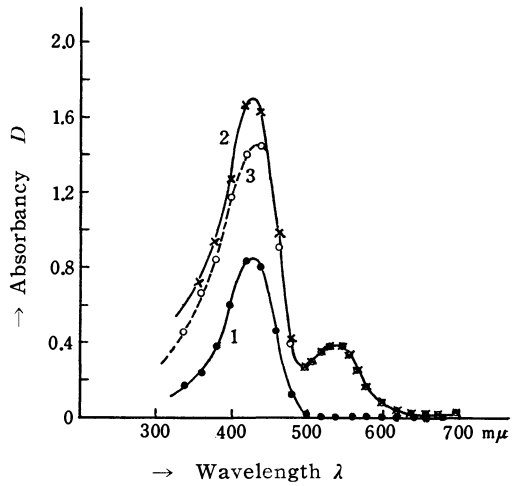


Fig. 5. Light absorption curves of curcumin-oxalic acid solution and curcumin-boron complex.
1. Curcumin solution
2. Curcumin-boron complex (initial absorption)
3. Curcumin-boron complex (after 17 hr.)

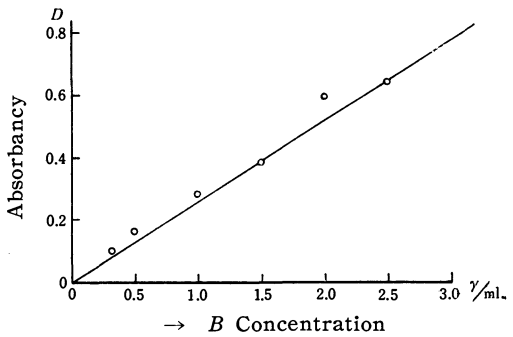


Fig. 6. Beer's law plot of curcumin-boron complex.

blank tests on each sample in order to minimanize the fluctuation of the results.

Determination of Born Distribution in Zonerefined Silicontetraiodide. — Generally, elementary silicon used for iodination experiment contains enough boron in itself, so that a detectable amount of boron should be present in iodide without adding any on purpose. So the hydrolyzed product used for activity measurement of ^{32}P could be used for the determination of boron. About 10 ml. of distilled water was added to the sample and it was heated gently in a quartz evaporating dish to extract the boron into solution as boric acid. Then it was filtered and the precipitate of silicon dioxide on filter paper was washed several times with warm water to remove the boron compound completely. The filtrate was evaporated by heating in a quartz evaporating dish to about 5 ml. Using this solution, boron was determined as described above.

Curve 1 in Fig. 7 shows the distribution of

8) C. C. Luke, *Anal. Chem.*, **27**, 1150 (1955).
9) W. T. Dible, E. Truog and K. C. Berger, ibid., **26**, 418 (1954).
10) H. Kramer, ibid., **27**, 144 (1955).
11) J. H. Yoe and R. L. Grob, ibid., **26**, 1465 (1954).

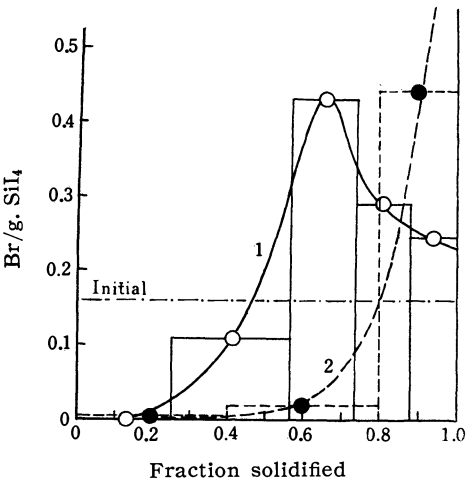


Fig. 7. Distribution of boron after zone refining with different moving speed.
1. Six passes (2.4 mm./min.)
2. Three passes (0.83 mm./min.)

boron after six passes of single zone with a moving speed of 2.4 mm. per min., and curve 2 shows that of three passes with a speed of 0.83 mm./min. In both cases the width of the molten zone was about 20 mm.

Consideration of the Results

Several studies have been reported on the segregation effect of the binary solution of metals. The zone purification method was developed from this principle by Pfann, and the behavior of impurity elements in semiconducting materials has been made clear by many workers. It is well known that the distribution of impurity concentration throughout the ingot after normal segregation is expressed by the equation[5]

$$C = kC_0(1-g)^{k-1} \qquad (1)$$

In this equation, g represents the solidified fraction, C_0 the initial concentration, C the impurity concentration at a point g, and k the distribution constant defined by the ratio of impurity concentration in solid to that in liquid. In the case of segregation of phosphorus in silicontetraiodide this equation may be also applicable. Let k be equal to 0.1 and 0.8, the distributions of phosphorus throughout the iodide bar are represented by curve 2 and 3 respectively in Fig. 3. Comparing these curves with experimental results, it can be said that the results can not be represented by the above equation, but it consists of two different k values. As colloidal silicon dioxide produced by the hydrolysis of tetraiodide has a tendency to adsorb phosphorus as well as some other trace impurities, it is reasonable to consider that a part of phosphorus will be adsorbed by the colloidal silicon dioxide and segregated together. For the reason given above, the beginning portion of the curve shows a large k value corresponding to the distribution constant of phosphorus itself, and the end portion of the curve shows a small k value which corresponds to that of the hydrolyzed product. In this case, the segregation equation can be written as

$$C = C_0\{k_1(1-g)^{k_1-1} + k_2(1-g)^{k_2-1}\} \qquad (2)$$

Curve 1 and 2 in Fig. 8 show the distribution of solute assuming $k=0.1$ and $k=0.8$ respectively. Curve 3 shows the result of calculation from Eq. 2 using $k_1=0.1$ and $k_2=0.8$. C_0 is unity in each case. The resultant curve 3 shows good correspondence with experimental results.

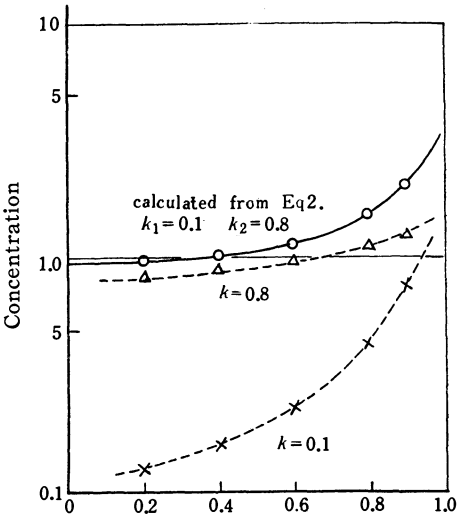


Fig. 8. Resultant distribution calculated from Eq. 2. $k_1=0.1$ $k_2=0.8$

The results of the zone refining process showed a promising effect to remove phosphorus after three passes of single zone, for instance, the concentration could be decreased one tenth of the initial amount at the top portion and the ratio of concentration of phosphorus at the end and the top parts of the bar reached three powers of ten.

As for boron, the results were not so distinct as in the cace of phosphorus, but better refining efficiency could be expected by this process than in the case of its elementary state.

Summary

The behavior of phosphorus and boron as impurity elements in silicon tetraiodide was studied during the normal segregation and zone melting processes. Both of them can be removed efficiently by this process, and it is considered that the colloidal hydrolyzed product suspended in silicon tetraiodide plays a predominant role for segregation because of its high adsorptivity to these elements. The distribution curve of radioactive phosphorus seems to show the influence of this material.

The authors are pleased to express their gratitude to the Director Dr. T. Niimi, and Dr. S. Yanagisawa, Professor of Chemistry at Keio University, for helpful guidance and encouragement during the course of this study.

The Electrical Communication Laboratory
Nippon Telegraph and Telephone
Public Corporation
Musashino-shi, Tokyo

Formation of Tetraazaporphin from Phthalic Anhydride and its Reduced Products

By Masahiro SHIGEMITSU

(Received September 25, 1958)

Phthalic anhydride easily reacts with urea and metallic salts to produce metal phthalocyanine, a kind of tetraazaporphin. Particularly, copper phthalocyanine which is obtained almost quantitatively by the above reaction is one of the most widely used blue organic pigments. But in the case of 3, 4, 5, 6-tetrahydrophthalic anhydride which is the reduced product of phthalic anhydride, the yield of tetraazaporphin is rather small[1].

In the present experiment, the effect of structure of the starting materials on the tetra-azaporphin formation was examined. Phthalic anhydride (I), 3,4,5,6-tetrahydrophthalic anhydride (II), 1,2,3,6-tetrahydro-*cis*-phthalic anhydride (III), hexahydro-*cis*-phthalic anhydride (IV) and 3,6-endomethylene-1,2,3,6-tetrahydro-*cis*-phthalic anhydride (V) were chosen as the examples for the starting materials.

Experimental

Materials.—Phthalic anhydride (I), m. p. 130～131°C. 3,4,5,6-Tetrahydrophthalic anhydride (II) was prepared by reducing phthalic anhydride with sodium-amalgam, m. p. 68～69°C (reported m.p. 68～69°C)[2] (*Anal.* Found: C, 63.09; H, 5.20. Calcd. for $C_8H_8O_3$: C, 63.15; H, 5.26%). 1,2,3,6-Tetrahydro-*cis*-phthalic anhydride (III) was prepared with the aid of Diels-Alder reaction from butadiene and maleic anhydride, m.p. 99～101°C (reported m. p. 99～101°C)[3] (*Anal.* Found: C, 63.08; H, 5.22. Calcd. for $C_8H_8O_3$: C, 63.15; H, 5.26%). Hexahydro-*cis*-phthalic anhydride (IV) was prepared by reducing III with sodium-amalgam, m. p. 33～34°C (reported m. p. 32～33°C)[4] (*Anal.* Found: C, 62.29; H, 6.45. Calcd. for $C_8H_{10}O_3$: C, 62.34; H, 6.49%). 3,6-Endomethylene-1,2,3,6-tetrahydro-*cis*-phthalic anhydride (V) was prepared with the aid of Diels-Alder reaction from cyclopentadiene and maleic anhydride, m. p. 164～165°C (reported m. p. 164～165°C)[5,6] (*Anal.* Found: C, 65.77; H, 4.91. Calcd. for $C_9H_8O_3$; C, 65.84; H, 4.87%).

Methods.—A mixture of 15 g. of phthalic anhydride or its reduced products, cuprous chloride (1/4 mol. of starting materials as shown in Table I), 60 g. of urea, 0.5 g. of ammonium molybdate and 175 g. of nitrobenzene was heated with stirring. Tow model cases will be shown in relation to the experimental conditions. First, the mixture was stirred at room temperature for 30 min., and then heated up to 150°C during ca. 1 hr. at a definite rate, and finally at 150～155°C for 4 hr. In the second example, the mixture was stirred at room temperature for 30 min., and then heated up to 190°C during ca. 2 hr. at a definite rate, and finally at 190～195°C for 3 hr. After the reaction was completed, nitrobenzene was removed by steam distillation

1) G. E. Ficken and R. P. Linstead, *J. Chem. Soc.*, **1952**, 4846.
2) A. von Bayer, *Ann.*, **258**, 199 (1890).
3) L. F. Fieser and E. C. Novells, *J. Am. Chem. Soc.*, **64**, 806 (1942).
4) A. von Bayer, *Ann.*, **258**, 219 (1890).
5) D. Craig, *J. Am. Chem. Soc.*, **73**, 4889 (1951).
6) U. S. Pat. 2,424,948 (1947).

TABLE I. THE CONDITIONS OF REACTION AND THE YIELD OF COLORING MATTERS

Expt.	Starting material (g.)	CuCl (g.)	Temp. (°C)	Rect. prod. color	Rect. prod. wt. (g.)	Coloring matter color	Coloring matter wt. (g.)	Coloring matter yield (%)
1	I, 15.0	2.5	150~155	blue	11.3	blue	11.1	76.0
2	〃 〃	〃	190~195	〃	13.4	〃	13.1	90.5
3	II, 15.0	2.4	150~155	dark brown	9.8	violet blue	0.6	4.1
4	〃 〃	〃	190~195	〃	10.2	〃	0.2	1.4
5	III, 15.0	2.4	150~155	dark brown	11.7	—	—	—
6	〃 〃	〃	190~195	〃	10.6	—	—	—
7	IV, 15.0	2.4	150~155	dark brown	12.4	—	—	—
8	〃 〃	〃	190~195	〃	10.9	—	—	—
9	V, 15.0	2.3	150~155	dark brown	11.2	—	—	—
10	〃 〃	〃	190~195	〃	10.7	—	—	—

and the resulting mixture was heated with 5% hydrochloric acid and then 2% caustic soda, filtered, washed with water and dried at 60~70°C.

When I was used as the starting material, the coloring matter (copper phthalocyanine) was treated with ethanol to remove impurities. In the case of II, the coloring matter (copper tetracyclohexenotetraazaporphin) was extracted from the dark brown product with *o*-dichlorobenzene[7]. In the case of III, IV and V, the coloring matters (tetraazaporphins) could not be obtained by the extraction from the dark brown products with α-chloronaphthalene (good solvent of tetraazaporphins) and *o*-dichlorobenzene.

Coloring matters were formed only in the cases of I and II, both of which were of similar blue shades. Reflectance curves concerning these shades of colors were measured with a recording spectrophotometer (General Electric Co.). Samples were prepared in the following way. One part of copper phthalocyanine obtained from I was dissolved in 3 parts of 98% sulfuric acid at room temperature, and was poured into water. Fine crystals deposited were washed with water free from acid and dried at 60~70°C. One part of β-form copper phthalocyanine here obtained[8] and copper tetracyclohexenotetraazaporphin obtained from II were mixed respectively with 1.5 parts of polymerized linseed oil and were made into paste by grinding 400 rounds in Hoover automatic muller. To 1 part of this paste was added 70 parts of zinc white paste (obtained by grinding 2 parts of zinc oxide in 1.5 parts of polymerized linseed oil), which was applied in 0.5 mm. thickness on a coated paper with a bladeoapplicator (Gardner Laboratory). These were dried at room temperature and used as samples for measuring reflectance curves.

Results and Discussion

Table I shows the relation between the reaction conditions and the reaction products.

As is seen from Experiments 1 and 2 (Table I), the reaction proceeded easily at a reaction temperature of either 150~155°C or 190~195°C when the reaction was conducted with I as the starting material, copper phthalocyanine being obtained in good yield (*Anal.* Found: C, 66.78; H, 2.90; N, 19.38; Cu, 11.00. Calcd. for $C_{32}H_{16}N_8Cu$: C, 66.72; H, 2.78; N, 19.46; Cu, 11.04%). As is shown by Experiments 3 and 4, the use of II as starting material remarkably reduced the yield of the coloring matter (4.1 and 1.4%, respectively). The coloring matter obtained was copper tetracyclohexenotetraazaporphin (*Anal.* Found: C, 65.02; H, 5.54; N, 18.76; Cu,

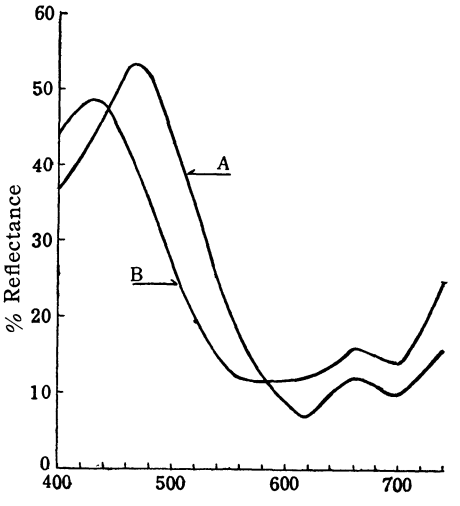


Fig. 1. Reflectance curves of β-form copper phthalocyanine (A) and copper tetracyclohexenotetraazaporphin (B).

7) British Pat., 686,395 (1953).
8) G. von Susich, *Anal. Chem.*, **22**, 425 (1950).

10.67. Calcd. for $C_{32}H_{32}N_8Cu$; C, 64.91; H, 5.41; N, 18.93; Cu, 10.76%).

While copper phthalocyanine slightly dissolves only in α-chloronaphthalene, copper tetracyclohexenotetraazaporphin easily dissolves in *o*-dichlorobenzene and has a color somewhat more reddish than copper phthalocyanine. Their reflectance curves are shown in Fig. 1 and their C. I. E. Notations are given in Table II. In this table, Y denotes luminosity, P_e purity and λ_D dominant wavelength.

TABLE II. C. I. E. NOTATIONS

Sample	Y%	P_e%	λ_D mμ
A	19.10	55.8	475.8
B	17.00	47.0	470.2

A; Copper phthalocyanine (β-form).
B; Copper tetracyclohexenotetraazaporphin.

The dominant wavelength of copper tetracyclohexenotetraazaporphin is shorter by 5.6 mμ than that of β-form copper phthalocyanine with blue color tinged with red.

In the Experiments 5 and 6 where III, which carries the bond in a different position from that in II, was used as starting material; only alkali-soluble dark brown products were obtained, but coloring matters could not be isolated either by α-chloronaphthalene or *o*-dichlorobenzene.

When IV (Experiments 7 and 8) which has no double bond, and V (Experiments 9 and 10) were used as starting materials, only alkali-soluble dark brown products were obtained without formation of tetraazaporphin. Thus, it was confirmed that, when I is reduced and aromaticity is weakened, or when aromaticity is very small as in the case of V, tetraazaporphin can not be produced. However, when the double bond between carbonyl groups is not reduced, tetraazaporphin is produced, though the yield is small.

In Experiments 1 and 2, higher reaction temperature increased the yield of the coloring matter, but, on the contrary, the increase in the temperature decreased the yield in the Experiments 3 and 4. This may be due to the decomposition of II which on heating over approximately 200°C, gives up carbon dioxide and converts into resinous material of m. p. 50~55°C. Fig. 2 shows infrared spectrum of II and Fig. 3 that of its product obtained by heating. These spectra (in potassium bromide pellet) were obtained with Perkin Elmer 12B instrument.

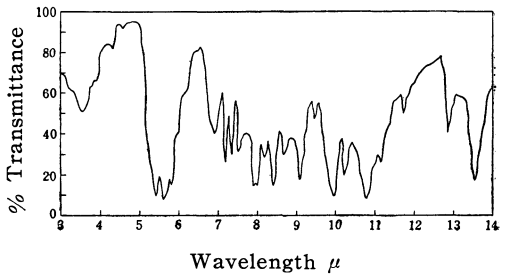


Fig. 2. Infrared spectrum of 3,4,5,6-tetrahydrophthalic anhydride (KBr).

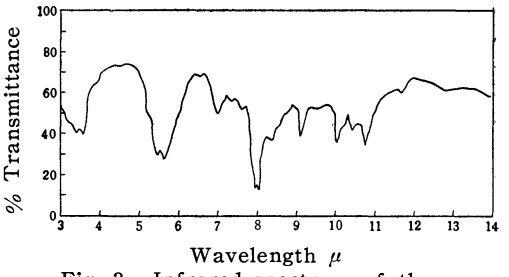


Fig. 3. Infrared spectrum of the product obtained by heating 3,4,5,6-tetrahydrophthalic anhydride (KBr).

In the reaction of II, higher reaction temperature seemed to decrease the yield of the coloring matter and accelerate the conversion into resinous material.

The author gratefully acknowledges the instruction of Dr. Ryozo Goto, Professor of Kyoto University; also Dr. Takahisa Nakamura and Dr. Wataru Ishikawa, Toyo Ink Mfg. Co. The author's thanks are also due to Mr. Ryuichi Kimura, Kyoto University, in measuring the infrared spectra.

Central Research Laboratory
Toyo Ink Mfg. Co.
Sumida-ku, Tokyo

Reduction of Copper Hexadecachlorophthalocyanine

By Masahiro SHIGEMITSU

(Received September 25, 1958)

It was manifest by the previous study[1] that the darkening of chlorinated copper phthalocyanine green by reducing agents was caused, not by variation in forms, but by variation in its crystal structure or in its chemical composition. The degree of discoloration corresponded, though very little, to that of decrease in chlorine content, from which it was inferred that hydrogen atoms had been introduced into phthalocyanine nucleus. If phthalocyanine nucleus is to be reduced, either C=C or C=N bond is considered to be the position of reduction. Whether the position attacked is C=C or C=N is made clear by using the exhaustively chlorinated compound (copper hexadecachlorophthalocyanine, I). Hence the author used I as a sample and studied the mechanism of reduction.

Experimental

Materials. — *Copper hexadecachlorophthalocyanine (I).*—The compound which was synthesized according to the method previously reported[2], was used as chlorinated copper phthalocyanine green. Reducing agent was made to act upon it, which was then oxidized, reprecipitated and heated as follows.

Pulverization.—I was dissolved in chlorosulfonic acid, poured into ice water, and deposited as fine particles. The chlorine content was 50.33% (Calcd. 50.34%) as previously indicated[2].

Reduction.—One gram of I and 30 cc. of 20% aqueous solution of rongalit (addition compound of formalin and sodium hydrosulfite) were placed in a stainless steel autoclave of 50 cc. capacity and heated at 150~155°C for 20 min. The product was filtered off, washed with water and dried. It was dark green particles.

Oxidation of the reduced product.—One gram of the reduced product was added to 80 cc. of 2% sulfuric acid containg 0.2 g. of ceric sulfate and heated at 70~80°C for 1 hr.

Reprecipitation of the reduced product.—One gram of the reduced product was dissolved in 30 g. of chlorosulfonic acid at room temperature and poured into ice water. The precipitate thus obtained was filtered and washed with water.

Heating of the reduced product.—The reduced product was heated at 250~255°C for 3 hr. in a stream of nitrogen.

Methods.—Variation in color observed in the case of reduction of I and of oxidation, reprecipitation and heating of the reduced product was studied by measuring the reflectance curves with a recording spectrophotometer (General Electric Co.). Samples for reflectance-curve measurement were made in the same procedure as previously reported[1]. X-ray diffraction patterns of I and its reduced product were obtained with a recording X-ray diffraction apparatus (Philips Co.) and variation in crystal structure was studied.

Then, elementary analysis of I and its reduced product was conducted. Also, infrared spectra (Nujol) were taken of I, its reduced product, the reoxidized reduced product and the reprecipitated reduced product, using a Perkin Elmer 12B instrument.

Results

Reflectance Curves. — Fig. 1 shows the reflectance curves of I, its reduced product

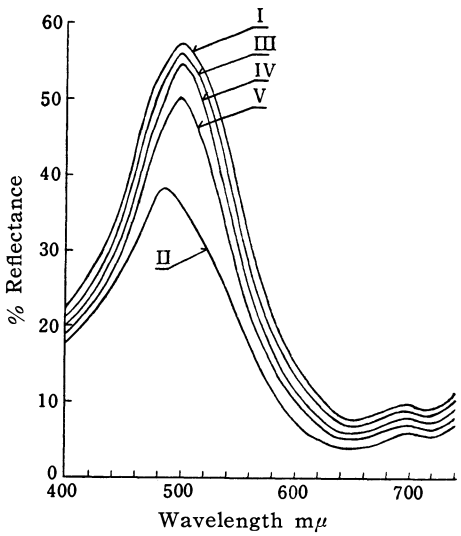


Fig. 1. Reflectance curves of copper hexadecachlorophthalocyanine (I), its reduced product(II), reoxidized reduced product(III), reprecipitated reduced product(IV) and heated reduced product(V).

1) M. Shigemitsu, This Bulletin, **32**, 502 (1959).
2) M. Shigemitsu, *J. Chem. Soc. Japan, Ind. Chem. Sec.* (*Kogyo Kagaku Zasshi*), **62**, 112 (1959) (presented at the Autumnal Meeting of Chemical Society of Japan, Tokyo, 1957).

(II), the reoxidized reduced product(III), the reprecipitated reduced product(IV) and the heated reduced product(V). Table I gives their C.I.E. Notations. In this table, Y denotes luminosity, P_e purity and λ_D dominant wavelength.

TABLE I. C.I.E. NOTATIONS

Sample	Y %	Pe %	λ_D mμ
I	30.34	36.8	492.6
II	22.18	39.1	488.9
III	29.96	37.2	490.8
IV	29.58	37.5	490.2
V	28.41	38.1	489.7

When a reducing agent acted upon I, its luminosity lowered from 30.34 to 22.18% and it darkened in color. When this darkened pigment was heated at 250~255°C for 3 hr. in nitrogen stream, its luminosity increased to 28.41% approaching that of untreated pigment; when being oxidized and reprecipitated, the pigment increased its luminosity to 29.96 and 29.58%, respectively, recovering color of luminosity approaching that of untreated material. Thus the variation in color is of a reversible trend.

X-ray Diffraction Patterns.—Figs. 2 and 3 show the X-ray diffraction patterns of I and its reduced product.

It was made clear by the previous study that the darkening by the action of reducing agent was not due to the change in the form of pigment particles. Now, with the aid of X-ray diffraction method, no change was observed in the crystal structure either. Thus the color change is supposed to be due to the difference in the chemical composition of the compounds in question.

Elementary Analysis.—Results of analysis of I and II are given in Table II.

TABLE II. RESULTS OF ELEMENTARY ANALYSIS

Sample	C %	H %	N %	Cl %	Cu %
I Found	34.10	0.09	9.90	50.33	5.64
I Calcd.	34.09	—	9.94	50.34	5.63
II Found	33.60	1.26	9.80	49.75	5.59
III*	33.67	1.23	9.82	49.71	5.57

*III, Calculated value when fourteen hydrogen atoms were added to I.

I contains no hydrogen, but, on reduction, its hydrogen content increased to 1.26% indicating the addition of fourteen hydrogen atoms.

Infrared Spectra.—Figs. 4, 5, 6 and 7 show infrared spectra of I, II, III and IV. Fig. 8 shows that of copper phthalocyanine containing no chlorine, which was measured by Tyler et al.[3] The lower curve in Fig. 8 denotes the use of Nujol and the upper curve, shown partly, denotes the use of hexachlorobutadiene.

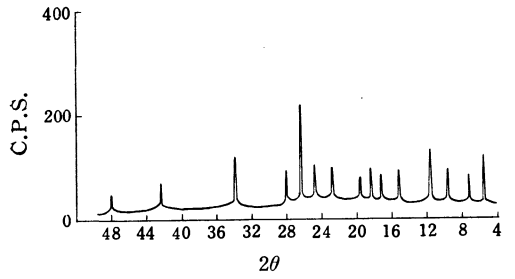


Fig. 2. X-ray diffraction pattern of copper hexadecachlorophthalocyanine (leaflet, fine particle).

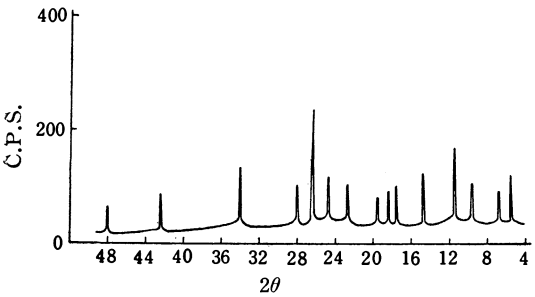


Fig. 3. X-ray diffraction pattern of reduced product of copper hexadecachlorophthalocyanine (leaflet, fine particle).

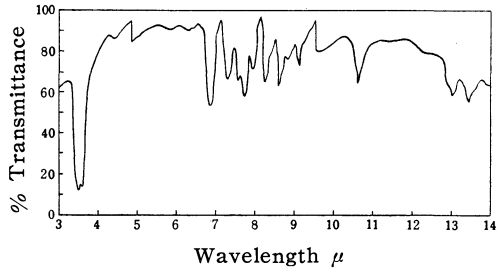


Fig. 4. Infrared spectrum of copper hexadecachlorophthalocyanine.

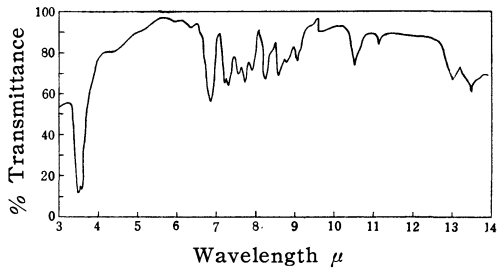


Fig. 5. Infrared spectrum of reduced product of copper hexadecachlorophthalocyanine.

3) J. E. Tyler et al., *Anal. Chem.*, **25**, 393 (1953).

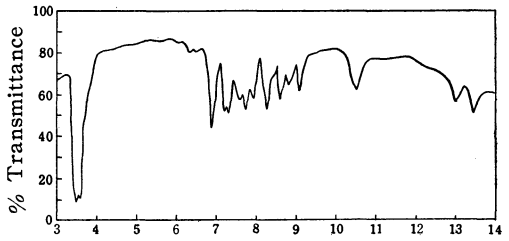


Fig. 6. Infrared spectrum of reoxidized reduced product of copper hexadecachlorophthalocyanine.

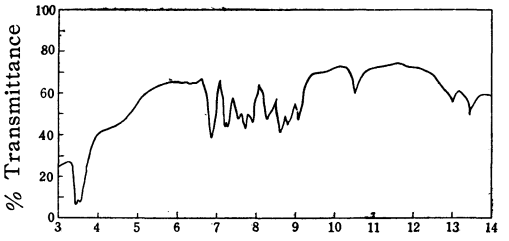


Fig. 7. Infrared spectrum of reprecipitated reduced product of copper hexadecachlorophthalocyanine.

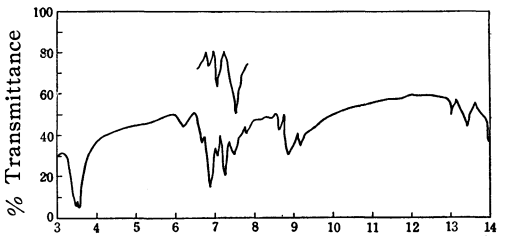


Fig. 8. Infrared spectrum of copper phthalocyanine.

When sixteen hydrogen atoms of copper phthalocyanine were chlorinated to give I, absorption bands at 720 cm^{-1}, 1090 cm^{-1}, 1125 cm^{-1}, 1290 cm^{-1} and 1415 cm^{-1} of copper phthalocyanine disappeared and those at 947 cm^{-1}, 1095 cm^{-1}, 1210 cm^{-1}, 1273 cm^{-1} and 1305 cm^{-1} were exhibited. The absorption band at 1415 cm^{-1} of copper phthalocyanine became even more conspicuous when hexachlorobutadiene was used instead of Nujol.

Discussion

Copper phthalocyanine, I and II are compared (Fig. 9). The absorption band at 1415 cm^{-1} of copper phthalocyanine disappears in I but, when being reduced, the compound shows again the absorption band at 1412 cm^{-1}. Therefore, this absorption band is due to the vibration of

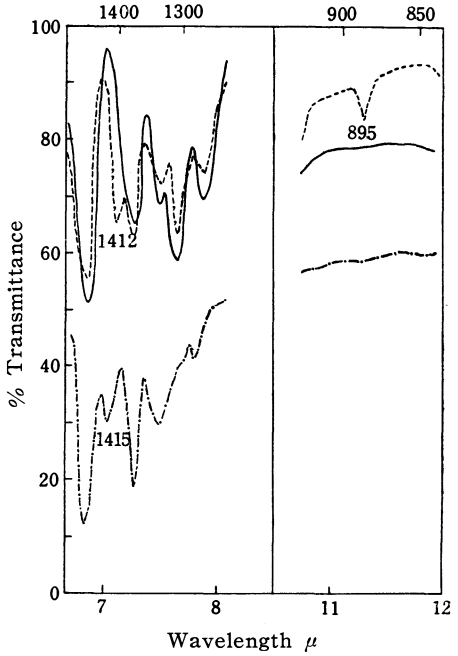


Fig. 9. Comparison of infrared spectra.
—— copper hexadecachlorophthalocyanine.
------ reduced product of copper hexadecachlorophalocyanine.
- - - copper phthalocyanine.

C–H bond of copper phthalocyanine. It is further inferred that, since C–H bending vibration appears in the range of 1475～1300 cm^{-1} [4], this absorption band may be due to the same vibration.

Further, a new absorption band appears at 895 cm^{-1} in II, but no such absorption band in I and copper phthalocyanine. Therefore, this absorption band may be attributed to the addition of hydrogen atoms. The position of the addition of hydrogen atoms is considered to be either C=C or C=N. Actually, the addition seems to proceed at C=N bond of the phthalocyanine nucleus, because the absorption band at 895 cm^{-1} corresponds to N–H bending vibration according to Colthup[4].

Gund[5] describes that cobalt phthalocyanine produces two N–H bonds when reduced. In the present experiment fourteen hydrogen atoms were added to phthalocyanine nucleus. Observing the absorption of C–H and N–H bonds which appeared in II, it is considered that twelve hydrogen atoms add to six C=C bonds and the remaining two hydrogen atoms, as inferred by Gund, produce two N–H bonds.

4) N. B. Colthup, *J. Opt. Soc. Am.*, **40**, 397 (1950).
5) F. Gund, *J. Soc. Dyers and Colourists*, **69**, 671 (1953).

Thus, the chlorination of copper phthalocyanine seems to facilitate hydrogenation at C=C and C=N bonds of phthalocyanine, and the darkening of color occurs as is observed in the reduced vat dyes.

The author gratefully acknowledges the instruction of Dr. Ryozo Goto, Professor of Kyoto University; also Dr. Takahisa Nakamura and Dr. Wataru Ishikawa, Toyo Ink Mfg. Co. The author's thanks are also due to Mr. Seiki Kato, Tokyo Institute of Technology, for his carrying out the X-ray analysis and Mr. Ryuichi Kimura, Kyoto University, for his measuring the infrared spectra.

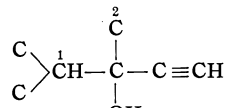
Central Research Laboratory
Toyo Ink Mfg. Co.
Sumida-ku, Tokyo

The Formic Acid Rearrangement of 3,4-Dimethyl-1-pentyn-3-ol and 3-Isopropyl-4-methyl-1-pentyn-3-ol

By Tatsuo TAKESHIMA, Ken NAGAOKA, Masataka YOKOYAMA and Shigeki MORITA

(Received November 4, 1958)

Continuing the study of Rupe reaction of ethynylcarbinols of type I[1], we now show that 3,4-dimethyl-1-pentyn-3-ol (II) and 3-isopropyl-4-methyl-1-pentyn-3-ol (III) on treatment with formic acid afford, in addition to ketone which forms the main product in each case, each corresponding aldehyde (II_b and III_b) in 5* and 6% yield respectively.

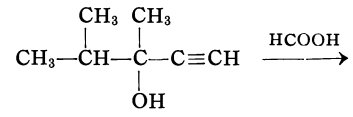


I

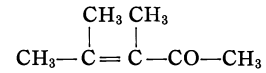
C^1: Tertiary carbon atom.

C^2: Other than secondary carbon atom.

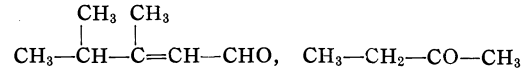
The reaction product from II was separated into three fractions. The main bulk of the low-boiling fraction (fraction 1; 45% yield) consisted of 3,4-dimethyl-3-penten-2-one (II_a)[2]. The high-boiling fraction (faction 3; 5% yield) reacted with carbonyl reagents (consult Table I) and had an unsaturated aldehydic nature. On treatment with phenylhydrazine it gave a product which had a pyrazoline reaction of a coloration different from that in the case of II_a. The hydrogenation product of this fraction also was positive toward Schiff test, the coloration being different from that of the original substance. Thus, together with analyses, 3,4-dimethyl-2-pentenal (II_b) was assigned to the compound. The facts that it is impossible for the geometrical isomer to exist for II_a and also the trend of Rupe reaction are corroborative of the structure.



II



II_a (45%)



II_b (5%)*

The intermediate fraction (fraction 2) consisted of a mixture of II_a and II_b; the quantity of the aldehyde contained diminished on standing. The forerun in the case of the distillation contained a considerable amount of methyl ethyl ketone, which owes its origin possibly to the hydrolytic fission of II_a.

The reaction product of III was distilled and three fractions were collected. The greater part of the low-boiling fraction

1) T. Takeshima, K. Wakamatsu and A. Furuhashi, This Bulletin, 31, 640 (1958).

* The actual yield of the aldehyde seemed to be much more, considering its considerable amount contained in fraction 2.

2) H. Favre and H. Schinz, *Helv. Chim. Acta*, 35, 2388 (1952); F. C. Whitmore et al., *J. Am. Chem. Soc.*, 63, 643 (1941).

TABLE I. REACTION PRODUCTS FROM II

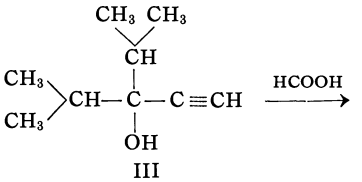
Fraction	B. p., °C	Yield, g. from 20 g. of II	Constituent
Forerun	~133	A small amount	Considerable amt. of methyl ethyl ketone
1	143~151	9	II_a
2	152~159	1.2	II_a, II_b
3	160~164	1.0	II_b

DERIVATIVES OF THE CARBONYL COMPOUNDS

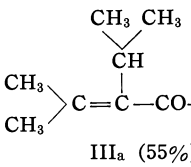
Original Compd.	2,4-Dinitrophenylhydrazone		Semicarbazone	
	M. p., °C	Appearance	M. p., °C	Appearance
II_a	132~133[3]	Lustrous orange plates or long plates	185~187[4] (slow heating) 198~199[4] (rapid heating)	Colorless plates
II_b	205~206	Red plates	163~164 (slow heating) 173~174 (rapid heating)	Colorless plates

(fraction 1; 55% yield) was considered to be 3-isopropyl-4-methyl-3-penten-2-one(III_a) reported by Hickinbottom et al.[5]; it gave no crystalline derivative with common carbonyl reagents**.

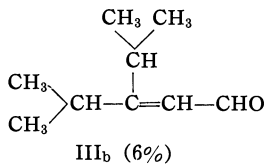
The high-boiling fraction (fraction 3; 6% yield) had an unsaturated aldehydic nature, which gave characteristic derivatives with carbonyl reagents (consult Table II). On treatment with phenylhydrazine, it yielded an oily product which had a pyrazoline reaction of a coloration different from that in the case of III_a. Viewed from these facts together with analyses and also with the course of the reaction, the compound was assigned 3-isopropyl-4-methyl-2-pentenal (III_b). Here also, the absence of geometrical isomer substantiates the structure. Young and Roberts[6] reported the 2,4-dinitrophenylhydrazone of m.p. 151.5~153°C (from ethanol) as the one of III_b without rigid isolation of the original aldehyde which was formed by ozonolysis of crotyldiisopropylcarbinol. However the 2,4-dinitrophenylhydrazone obtained in the present experiment had m.p. 173.5~174°C; its appearance (light red plates) resembled that reported[7] (bright red). Further, III_b was hydrogenated to give a saturated aldehyde which afforded a characteristic 2,4-dinitrophenylhydrazone (consult Table II) and was considered to be 3-isopropyl-4-methylpentanal (IV_b).



III



III_a (55%)



III_b (6%)

The intermediate fraction (fraction 2) which was of a relatively small quantity also contained some III_b.

Experimental

3,4-Dimethyl-1-pentyn-3-ol (II).—The carbinol was prepared from methyl isopropyl ketone according to the usual manner[8]. B. p. 132~133°C.

The Formic Acid Rearrangement of II.—Twenty grams of II was gently refluxed for ca. 1 hr. with 160 g. of ca. 80% formic acid. The reaction mixture was allowed to cool and was worked up in the usual manner[1]. Fractions collected were: forerun up to 133°C, a small amount; (1) b. p. 143~151°C, 9 g., yield 45%; (2) b. p. 152~159°C, 1.2 g.; (3) b. p. 160~164°C, 1 g., yield 5%. All these fractions were colorless when freshly

3) Reported, 132~133°C. See Ref. 2.
4) Reported, 185.5~187.5°C and 194~196°C. See Ref. 2.
5) W. J. Hickinbottom, A. A. Hyatt and M. B. Sparke, *J. Chem. Soc.*, **1954**, 2529.
**Hydrogenation product of III_a which was considered to be 3-isopropyl-4-methyl-2-pentanone (IV_a), on treatment with 2,4-dinitrophenylhydrazine, gave only an oily yellow derivative, the color being apparently different from that in the case of the original ketone.
6) Wm. G. Young and J. D. Roberts, *J. Am. Chem. Soc.*, **67**, 319 (1945).
7) See Ref. 6.
8) Y. R. Naves and P. Ardizio, *Helv. Chim. Acta*, **31**, 2252 (1948).

TABLE II. REACTION PRODUCTS FROM III

Fraction	b. p., °C	Yield, g. from 20 g. of III	Constituent
1	67～71 (19 mm.)	11	III_a
2	72～80 (19 mm.)	1	III_a, III_b
3	85～91 (19 mm.)	1.2	III_b

DERIVATIVES OF THE CARBONYL COMPOUNDS

Original Compd.	2,4-Dinitrophenylhydrazone		Semicarbazone	
	M. p., °C	Appearance	M. p., °C	Appearance
III_a	—	Red oil	Could not be obtained	
IV_a	—	Yellow oil	—	—
III_b	173.5～174[6]	Light red plates	208～210	Colorless micro-needles
IV_b	86～88	Yellow plates	—	—

distilled, hardly soluble in water, had camphor-like odor, instantly decolorized bromine water, and reacted with carbonyl reagents. Fraction 1 especially turned yellowish on standing. Fraction 3 had a less camphoraceous odor and, at the same time, a somewhat stimulative smell.

The lower-boiling fractions seemed, from ammoniacal silver nitrate test, still to contain a small amount of the unreacted original carbinol.

Fraction 1 (3,4-dimethyl-3-penten-2-one, II_a) was treated with phenylhydrazine hydrochloride in ethanolic acetic acid in the usual manner of preparation of pyrazoline. A trace of the reaction mixture thus formed gave a pyrazoline reaction of brownish purple color with sulfuric acid and sodium nitrite; the color was apparently different from that in the case of fraction 3; in the latter case a deep pink-purple color was produced.

Fraction 3 (3,4-dimethyl-2-pentenal, II_b) gave positive test with Schiff reagent (pink-purple color) and reduced ammoniacal silver nitrate. On heating it turned Fehling solution into turbid bluish green[1]. That the greater part of the fraction consisted of II_b was ascertained from the quantity obtained of its 2,4-dinitrophenylhydrazone mentioned below. A considerable amount of the same derivative was also obtained from fraction 2 when the fraction was treated immediately after the distillation; the aldehyde diminished on standing, owing possibly to autoxidation and polymerization.

Fraction 3 was hydrogenated with palladium. The crude oily product was positive toward Schiff test (pink color). The amount was insufficient for rigid purification.

The forerun up to 133°C, which was of a small amount, contained a respectable quantity of methyl ethyl ketone which was obtained in the form of its 2,4-dinitrophenylhydrazone; the derivative had m. p. 116～117°C which was undepressed on admixture with an authentic specimen.

2,4-Dinitrophenylhydrazone of II_a was recrystallized from pyridine-ethanol in lustrous orange plates or long plates, m. p. 132～133°C.

Anal. Found: N, 19.26. Calcd. for $C_{13}H_{16}O_4N_4$: N, 19.17%.

Semicarbazone of II_a was recrystallized from methanol, colorless plates, m. p. 185～187°C (slow heating), 198～199°C (rapid heating).

Anal. Found: N, 24.93. Calcd. for $C_8H_{15}ON_3$: N, 24.83%.

2,4-Dinitrophenylhydrazone of II_b was recrystallized from pyridine-methanol, red plates, m. p. 205～206°C, easily soluble in hot pyridine.

Anal. Found: C, 53.27; H, 5.61; N, 19.17. Calcd. for $C_{13}H_{16}O_4N_4$: C, 53.42; H, 5.52; N, 19.17%.

Semicarbazone of II_b was recrystallized from ethanol, colorless plates, m. p. 163～164°C (slow heating), 173～174°C (rapid heating).

Anal. Found: N, 25.33. Calcd. for $C_8H_{15}ON_3$: N, 24.83%.

3-Isopropyl-4-methyl-1-pentyn-3-ol (III).—Prepared from diisopropyl ketone according to the method used in the preparation of II. B. p. 161～164°C (reported 162～164°C; prepared by the liquid ammonia method)[9]. Yield, ca. 50%.

Diisopropyl Ketone.—A mixture of 80 g. of isobutyric acid and 110 g. of lead monoxide was refluxed for ca. 3 hr. The whole was heated under diminished pressure to remove water produced and the unreacted acid. The porous solid material obtained was then dry-distilled and finally under a diminished pressure. The crude ketone was washed with a concentrated solution of potassium carbonate, dried over calcium chloride, and distilled. B. p. 122～128°;C the greater part distilled out at ca. 125°C. Yield, 35%.

The Formic Acid Rearrangement of III.—Twenty grams of III was refluxed with 160 g. of ca. 80% formic acid for ca. 80 min. and worked up as usual. The product was separated into three fractions: (1) b. p. 67～71°C (19 mm.), 11 g., yield 55%; (2) b. p. 72～80°C (19 mm.), 1g.; (3) b. p. 85～91C° (19 mm.), 1.2 g., yield 6%; residue, a small amount of red oil. All these fractions were colorless, hardly soluble in water, had a camphoraceous odor (fraction 3 was accompanied by a somewhat stimulative smell), and instantly decolorized bromine water. The forerun, b. p. ca. 50～67°C (19 mm.) (ca. 2.7 g.) was somewhat yellowish and seemed still to contain a small quantity of the unreacted carbinol, a few white precipitates being produced with ammoniacal silver nitrate.

9) A. F. Thompson, Jr. et al., *J. Am. Chem. Soc.*, **63**, 186 (1941).

Fraction 1 was believed to be *3-isopropyl-4-methyl-3-penten-2-one* (*III_a*)[5]; its nature coincided with that reported by Hickinbottom et al. They obtained the compound also from III with the aid of Rupe reaction.

Anal. Found: C, 75.87; H, 11.32. Calcd. for $C_9H_{16}O$: C, 77.09; H, 11.50%.

Somewhat greater deviation in the carbon content was due possibly to contamination with a compound enriched in oxygen, perhaps the acid formed on autoxidation of III_b.

This fraction, on treatment with 2,4-dinitrophenylhydrazine, only gave *an oily red derivative; the semicarbazone* could not be obtained. The fraction was refluxed with phenylhydrazine hydrochloride in ethanolic acetic acid, then water was added, and the brown oil separated out gave a pyrazoline reaction of deep bluish violet coloration with sodium nitrite and sulfuric acid.

The same fraction was hydrogenated with palladium to yield an oil of strongly camphoraceous odor, which afforded an oily yellow 2,4-dinitrophenylhydrazone.

Fraction 3 (*3-isopropyl-4-methyl-2-pentenal, III_b*) was positive toward Schiff test (violet color was gradually produced and turned deep pink-purple on standing), and reduced ammoniacal silver nitrate. That the greater part of this fraction consisted of the single compound was ascertained from the quantity obtained of its 2,4-dinitrophenylhydrazone.

The same fraction on being treated with phenylhydrazine in the manner indicated above, gave a brown oil which had a pyrazoline reaction of deep violet coloration.

2,4-Dinitrophenylhydrazone of III_b was recrystallized from pyridine containing a little ethanol, light red plates, m. p. 173.5~174°C (reported m.p. 151.5~153°C)[6]. The derivative became thick deep red prisms or needles when allowed to stand overnight in the acidic reagent (the 2,4-dinitrophenylhydrazine reagent was applied as a methanolic sulfuric acid solution). The melting point of the thick crystals was identical with that of the light red plates, the mixed melting point was undepressed. The light red plates also were converted into the thick crystals on several hours' standing in methanol containing a little sulfuric acid.

Anal. Found: N, 17.52. Calcd. for $C_{15}H_{20}O_4N_4$: N, 17.49%.

Semicarbazone of III_b was recrystallized from methanol, colorless micro-needles, m. p. 208~210°C.

Anal. Found: N, 21.56. Calcd. for $C_{10}H_{19}ON_3$: N, 21.30%.

Hydrogenation Product of III_b (IV).—Half a gram of fraction 3 was hydrogenated in ether with palladium. The reaction product, freed from the ether, was positive toward Schiff test, deep pink color (tinged with purple) being gradually produced. IV was considered to be *3-isopropyl-4-methylpentanal* (*IV*).

2,4-Dinitrophenylhydrazone of IV was recrystallized from pyridine-methanol, yellow plates, m. p. 86~88°C.

Anal. Found: C, 55.67; H, 6.62; N, 17.67. Calcd. for $C_{15}H_{22}O_4N_4$: C, 55.88; H, 6.88; N, 17.38%.

Fraction 2. — The intermediate fraction contained a considerable quantity of III_b as the 2,4-dinitrophenylhydrazone.

The initial distillate of the forerun in the case of fractionation of the rearrangement product, which was collected at ca. 51°C (19 mm.) and weighed 0.2 g., afforded a small amount of 2,4-dinitrophenylhydrazone of yellow plates, m. p. ca. 124°C (from pyridine-methanol). It seemed to be possibly the derivative of acetone produced by hydrolytic fission of III_a; the amount was insufficient for rigid identification.

Summary

The behavior of 3,4-dimethyl-1-pentyn-3-ol (II) and 3-isopropyl-4-methyl-1-pentyn-3-ol (III) toward formic acid was investigated. The carbinols, as in the previous report[1], were chosen as model ones in which the tertiary carbon atom is adjacent to the carbon atom carrying the hydroxyl group. Both carbinols gave a significant quantity of the respective aldehydes. These aldehydes were easily isolated on simple distillation.

II gave 3,4-dimethyl-3-penten-2-one (II_a) in 45% yield and 3,4-dimethyl-2-pentenal (II_b), a new aldehyde, in 5% yield. III gave 3-isopropyl-4-methyl-3-penten-2-one (III_a) in 55% yield and 3-isopropyl-4-methyl-2-pentenal (III_b) in 6% yield. These carbonyl compounds were characterized. III_b was hydrogenated to give 3-isopropyl-4-methylpentanal (IV) as the 2,4-dinitrophenylhydrazone.

Department of Chemistry
Faculty of Science
Ibaraki University
Mito

Studies on the Antitubercular Compounds. XVI. Preparation of Some Derivatives of 2, 1, 3-Benzothiadiazole***

By Isao SEKIKAWA

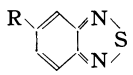
(Received November 19, 1958)

In a previous paper[1] the author has reported the syntheses of several kinds of 4- and 5-substituted 2, 1, 3-benzothiadiazole compound. These compounds have been shown to have no antitubercular activity in vitro. In the present paper, the new compounds listed in Table I and Table II were prepared in order to increase the antibacterial effect of the compounds of this series against *Mycobacterium tuberculosis*. 5-Bromomethyl-2, 1, 3-benzothiadiazole (I) was prepared by bromination of 5-methyl-2, 1, 3-benzothiadiazole with *N*-bromosuccinimide by the usual method, and readily converted into aminomethyl hydrochloride (II) by the Delepine reaction[2].

2, 1, 3-Benzothiadiazole-5-aldehyde (VI) was prepared from I in excellent yields through the hexaminium salt by Sommelet reaction[3]. Reaction of 2, 1, 3-benzothiadiazole with *N*-methylformanilide and phosphorous oxychloride in *o*-dichlorobenzene gave no formyl compound.

VI was readily oxidized into 5-benzothiadiazolecarboxylic acid (III) by the Delepine's method[4] in an alcoholic solution.

TABLE I. 5-SUBSTITUTED 2, 1, 3-BENZOTHIADIAZOLE DERIVATIVES



I	$-CH_2Br$
II	$-CH_2NH_2 \cdot HCl \cdot H_2O$
III	$-COOH$
IV	$-CONHNH_2$
V	$-CONH_2$
VI	$-CHO$

By the oxidation of 5-methyl-2, 1, 3-benzothiadiazole with potassium permanganate, not only methyl group but also benzene nucleus was attacked, so that III could not be obtained. Chlorination of III with thionyl chloride afforded an acid chloride, which was smoothly converted into acid amide V. Acidhydrazide IV was prepared from III by the usual method. Semicarbazone (VII), thiosemicarbazone (VIII), picolinoylhydrazone (IX), nicotinoylhydrazone (X) and isonicotinoylhydrazone (XI) were derived from VI by condensation with semicarbazide, thiosemicarbazide, α-, β- and γ-pyridinecarbohydrazide, respectively.

A detailed report on the antitubercular activity of these compounds will appear elsewhere.

Experimental

I.—A mixture of 4.5 g. of 5-methyl-2, 1, 3-benzothiadiazole, 5.4 g. of *N*-bromosuccinimide and 150 ml. of tetrachloromethane was refluxed for 18 hr. After cooling in ice bath, succinimide was removed by filtration and washed with 50 ml. of tetrachloromethane. After removing tetrachloromethane, the solidified residue was recrystallized from methanol to give 4.9 g. (70%) of lachrymatory white needles, m. p. 89~90°C.

Anal. Found: C, 36.41; H, 2.36. Calcd. for $C_7H_5N_2SBr$: C, 36.70; H, 2.20%.

II.—To a solution of 2.3 g. of I in 22 ml. of chloroform, 1.4 g. of hexamethylenetetramine was added. The mixture was allowed to stand overnight at room temperature, and the hexaminium salt was filtered and washed with 20 ml. of ether; yield 3.5 g., m.p. 182°C (decomp.)

A mixture of 1.2 g. of the hexaminium salt, 3 ml. of concentrated hydrochloric acid and 7 ml. of water was refluxed for 30 min., and the reaction mixture was concentrated to dryness under reduced pressure. The residue was recrystallized from water to give 0.4 g. of white needles, which softened at 235°C, became brown and decomposed at 245~246°C.

Anal. Found: C, 38.24; H, 4.87; H_2O, 8.10. Calcd. for $C_7H_5N_3S \cdot HCl \cdot H_2O$: C, 38.27; H, 4.59; H_2O, 8.20%.

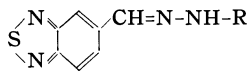
VI.—A mixture of 3 g. of the hexamethylenetetramine salt, 0.1 g. of hexamethylenetetramine and 6 ml. of 50% acetic acid was refluxed

* This paper constitutes a part of a series entitled "Studies on the Antitubercular Compounds", by S. Kakimoto. Paper XV, S. Kakimoto and J. Nishie, *J. Chem. Soc. Japan, Pure Chem. Sec.* (*Nippon Kagaku Zasshi*), **79**, 1403 (1958).

** A part of this study was presented at the Annual Meeting of the Chemical Society of Japan in Tokyo on April 3, 1958.

1) I. Sekikawa, This Bulletin, **31**, 252 (1958).
2) M. Delepine, *Compt. rend.*, **120**, 501 (1895).
3) M. Sommelet, ibid., **157**, 852 (1913).
4) M. Delepine and P. Bonnet, *Bull. soc. chim. France*, (4) **5**, 879 (1909).

TABLE II.



No.	R	m.p. (°C)	Appearance	Formula	Analysis (%) Calcd. C.	H.	H_2O	Found C.	H.	H_2O
VII	$-CO-NH_2$	251~252 d.*	White needles	$C_8H_7ON_5S$	43.43	3.19		43.09	3.37	
VIII	$-CS-NH_2$	228 d.	Yellow needles	$C_8H_7N_5S_2$	40.49	2.97		40.41	3.13	
IX	$-CO-C_5H_4N$ (α)	233~235	Pale yellow needles	$C_{13}H_9ON_5S$	55.11	3.20		55.13	3.51	
X	$-CO-C_5H_4N\cdot 2H_2O$ (β)	216~217	Pale yellow needles	$C_{13}H_{13}O_3N_5S$	48.89	4.10	11.28	48.86	4.43	11.16
XI	$-CO-C_5H_4N\cdot H_2O$ (γ)	218~219	White needles	$C_{13}H_{11}O_2N_5S$	51.82	3.68	5.98	51.63	3.91	6.09

* Decomp.

for 20 min. On cooling, a solid resulted. Recrystallization from methanol afforded 0.6 g. (47%) of white needles, m. p. 94°C.

Anal. Found: C, 51.25; H, 2.56. Calcd. for $C_7H_4ON_2S$: C, 51.21; H, 2.46%.

III.—To a solution of 0.9 g. of VI in 30 ml. of ethanol 2.3 g. of silver nitrate dissolved in 3 ml. of water was added. To the mixture was added 1.5 g. of sodium hydroxide in 10 ml. of water in small portions under stirring.

After being kept overnight, the deposited silver was removed and washed with 10 ml. of water. The solution was acidified with acetic acid to give an orange precipitate which was recrystallized from water to give 0.3 g. of white sandy crystals. It softened at 214°C and melted at 224~225°C.

Anal. Found: C, 46.63; H, 2.57. Calcd. for $C_7H_4O_2N_2S$: C, 46.66; H, 2.24%.

V.—A mixture of 0.4 g. of III and 5 ml. of thionyl chloride was refluxed for 1 hr. The excess of thionyl chloride was removed in a vacuum desiccator. The residue was dissolved in ether, saturated with ammonia and kept at room temperature for 1 hr. After removing ether, the solidified residue was recrystallized from water to give 0.3 g. of white needles, m.p. 202~203°C.

Anal. Found: C, 46.96; H, 3.01. Calcd. for $C_7H_5ON_3S$: C, 46.92; H, 2.81%.

IV.—A mixture of 0.15 g. of III, 3 ml. of absolute ethanol and 0.3 ml. of concentrated sulfuric acid was refluxed for 8 hr. After removing ethanol, the residue was treated with water and neutralized with sodium hydrogen carbonate. The resulting gray solid was heated with 0.1 ml. of hydrazine hydrate (80%) in 5 ml. of ethanol for 8 hr. The mixture was evaporated to dryness and the residue was recrystallized from water to give 0.1 g. of white needles, m.p. 180~181°C (decomp.).

Anal. Found: C, 42.99; H, 3.21. Calcd. for $C_7H_6ON_4S$: C, 43.29; H, 3.11%.

IX.—A mixture of 0.2 g. of VI, 0.16 g. of picolinic acidhydrazide and 5 ml. of ethanol was refluxed for 1 hr. The product was collected and recrystallized from ethanol to give 0.3 g. of yellow needles, m. p. 233~235°C.

Anal. Found: C, 55.13; H, 3.51. Calcd. for $C_{13}H_9ON_5S$: C, 55.11; H, 3.20%.

VII, **VIII**, **X** and **XI** were prepared by analogous methods.

The author wishes to express his gratitude to Professor S. Kakimoto of Hokkaido University for his kind encouragement and advice.

The Research Institute for Tuberculosis
Hokkaido University, Sapporo

The Mechanical Behavior of Swollen Polystyrene, Poly-p-chlorostyrene and their Copolymers in Benzene. I. The Degree of Polymer-solvent Interaction and Thermoelastic Properties

By Kazuyoshi OGINO

(Received November 26, 1958)

In the previous papers[1], the influence of the polymer-solvent interaction upon the mechanical properties of the swollen polymethyl acrylate gels was discussed, and it was shown that the mechanical properties of these gels having various degrees of swelling can be interpreted as the function of the interaction force between polymer chains. The intermolecular force between chain polymers was controlled, however, by giving the different degrees of swelling through the use of several organic solvents of different solvent power.

It is interesting to examine, in the next step, how the mechanical properties of gels in a swelling equilibrium with solvents are influenced by the structural units in a polymer molecule.

In this paper, polystyrene, poly-*p*-chlorostyrene and their copolymers, slightly cross-linked with divinyl benzene, are carried into the swelling equilibrium in benzene, and the mechanical properties of these gels are studied.

At the swelling equilibrium with excess solvent, the following equation holds[2]

$$\ln(1-v_r)+v_r+\mu v_r^2=-\rho V_0 v_r^{1.3}/M_c$$

where v_r is the volume fraction of polymer, ρ the density of pure solvent, V_0 the molar volume of solvent, M_c the average molecular weight of polymer between junction points and μ a parameter which indicates the type and degree of interaction exhibited by the polymer-liquid system.

In the region in which the stress-strain curve is reversible, the force f required to extend a specimen to an extension ratio λ is given by[3]

$$f=2Av_r^{-1/3}(\lambda-\lambda^{-2})(C_1+\lambda^{-1}C_2) \qquad (1)$$

where A is an unstrained area of cross section in the dry state, and C_1 and C_2 are the parameters relating to the mechanical properties of the specimen.

At a high degree of swelling, we can obtain the following relation from statistical consideration,

$$C_1=1/2RTM_c^{-1}$$

From these relations, the next equation follows,

$$-\ln(1-v_r)-v_r-\mu v_r^2=2V_0C_1v_r^{1/3}/RT \qquad (2)$$

Thus, we can estimate the value of C_1 from Eq. 1 by plotting the value of $f\{2A_0(\lambda-\lambda^{-2})\}^{-1}v_r^{1/3}$ against λ^{-1} in the results of the stress-strain measurements, and then can obtain the parameter μ from Eq. 2 using this value of C_1.

On the other hand, the following thermodynamic relations can be deduced.

$$(\partial G/\partial\lambda)_T=fl_0 \qquad (3)$$

$$T(\partial S/\partial\lambda)_T=-Tl_0(\partial f/\partial T)_\lambda \qquad (4)$$

$$(\partial H/\partial\lambda)_T=T(\partial S/\partial\lambda)_T+(\partial G/\partial\lambda)_T \qquad (5)$$

where G is the freee energy, H the enthalpy and S the entropy. From the above relations, we can estimate the change of the thermodynamic functions by measuring initial stresses at various strains and temperatures.

Experimental

Samples.—Commercial monomeric styrene and divinyl benzene were purified by fractional distillation under the reduced pressure after the removal of inhibitor with aqueous alkaline solution.

Benzene was purified by the ordinary method.

p-Chlorostyrene was synthesized in the following way[4]. Purified commercial mono-chlorobenzene reacts with acetyl chloride in the presence of aluminum chloride (Friedel-Crafts' reaction), and the *p*-chloroacetophenone thus obtained was reduced to *p*-chloro-phenylmethylcarbinol by isopropyl alcohol saturated with aluminum isopropylate prepared freshly before

1) K. Ogino, This Bulletin, **31**, 577, 580, 584 (1958).
2) P. J. Flory and J. Rehner, *J. Chem. Phys.*, **11**, 512 (1943); M. L. Huggins, *J. Am. Chem. Soc.*, **64**, 1712 (1942).
3) R. S. Rivlin and D. W. Saunders, *Phil. Trans.*, **A243**, 251 (1951).
4) E. Matui, *J. Chem. Soc. Japan, Ind. Chem. Sec.* (*Kogyo Kagaku Zasshi*), **45**, 1094 (1942).

the reaction. Finally this carbinol was dehydrated by potassium bisulfate in the presence of picric acid[5] under reduced pressure.

Six cc. of styrene, or *p*-chlorostyrene or a mixture of these two monomers was polymerized with about 0.01 cc. of divinyl benzene in bulk in a sealed glass tube by the method described in the previous paper[1].

The polymer block was then cut into several parts about 1 cm. in length by a turning lathe. Care was taken so that the error in the diameter of the specimen was confined within 10^{-3} cm. These polymer rods were then dipped in the excessive amount of benzene, and brought into the swelling equilibrium.

Apparatus. — The apparatus used in this experiment is the same as that used in the previous experiment[1], and is shown in Fig. 1.

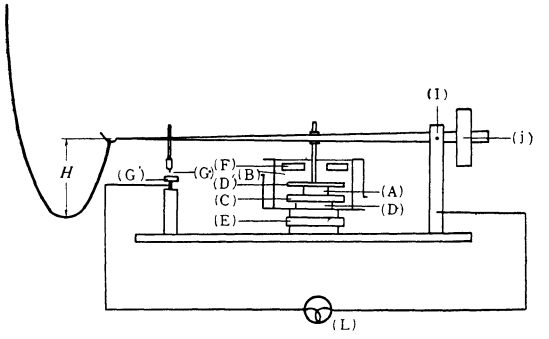


Fig. 1. The apparatus used in this experiment. (A), Specimen; (B), Solvent; (C), Iris; (D), Pressure plate; (E), Screw; (F), Desiccating agent; (G & G'), Contact; (J), Balancing weight.

The specimen in the swelling equilibrium with the solvent is placed between a flat brass block (D) and a pressure plate (D') in the solvent, and is strained vertically to a given extent, by rotating the screw (E) which is graduated to 1/100 mm. The initial stress is measured by the chain (H) using the value of its linear density.

The temperature of the specimen was controlled by circulation of water within the range of ± 0.5°C.

Results and Discussion

The plot of $f\{2A(\lambda-\lambda^{-2})\}^{-1}v_r^{1/3}$ against λ^{-1} at 25°C is shown in Fig. 2, and the values of μ for each polymer are given in Table I.

TABLE I. THE VALUE OF μ IN BENZENE AT 25°C

Polymer	μ
Polystyrene	0.47
Poly-*p*-chlorostyrene	0.49$_5$

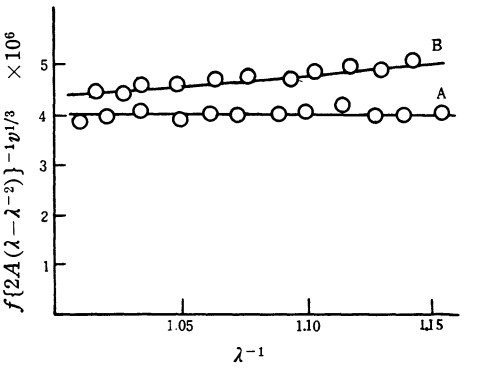


Fig. 2. Diagram of $f\{2A(\lambda-\lambda^{-2})\}^{-1}v_r^{1/3}$ against λ^{-1} for polystyrene-benzene (A) and poly-*p*-chlorostyrene-benzene (B) at 25°C.

The thermodynamic quantities in Eqs. 3, 4 and 5 at 25°C are shown in Figs. 3—6.

The value of μ of 0.47 for the system polystyrene-benzene differs from the value 0.453 by Boyer and Spencer[6] in their study of the stress-strain properties of this system.

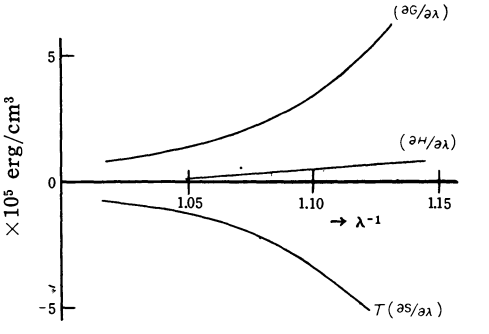


Fig. 3. Thermodynamic relation. Monomer ratio, Styrene 5 : *p*-Chlorostyrene 0

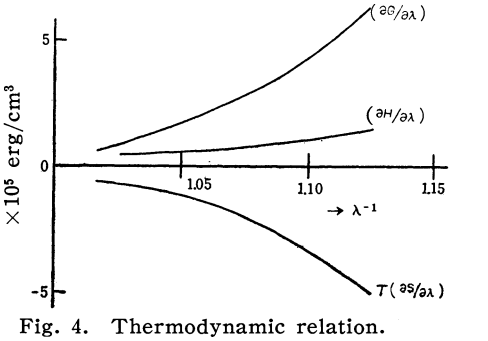


Fig. 4. Thermodynamic relation. Monomer ratio; Styrene 3 : *p*-Chlorostyrene 2

5) H. R. Snyder et al., "Org. Syntheses", Vol. 28, John Wiley & Sons, New York (1948), p. 31.

6) R. F. Boyer and R. S. Spencer, *J. Polymer Sci.*, 3, 97 (1948).

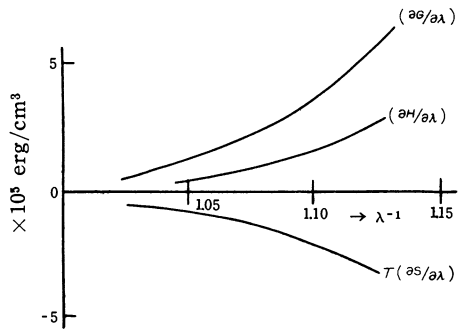


Fig. 5. Thermodynamic relation.
Monomer ratio; Styrene 2 : *p*-Chlorostyrene 3

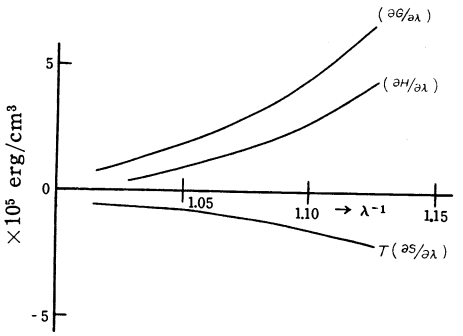


Fig. 6. Thermodynamic relation.
Monomer ratio; Styrene 0 : *p*-Chlorostyrene 5

Such a difference as this is also found among the other workers: Rivlin et al.[7] obtained the value of μ of 0.42 for natural rubber-benzene, and compared it with the value of 0.395 reported by Gee*. These two values were obtained from the stress-strain measurement of swollen rubbers. The measurements were conducted in ways similar to each other. Rivlin et al. considered that the source of the larger value of μ obtained in their investigation might be due to the degradation of the rubber during prolonged swelling in solvent in the determination of v_r.

An alternative source for the discrepancy in the values of μ originates from the effect of cross-linking as mentioned in the previous paper[1].

The fact that the value of μ of poly-*p*-chlorostyrene (0.49_5) is greater than that of polystyrene (0.47) shows that benzene is not so good a solvent for poly-*p*-chlorostyrene as for polystyrene. This may be due to the substituted chlorine atoms, for there appears a large polarity, and greater interaction may arise between long chain molecules. Thus, polymer-polymer contacts increase by the presence of chlorine atoms, and hence μ becomes larger.

The gradient of the curves of $f\{2A(\lambda-\lambda^{-2})\}^{-1}v_r^{1/3}$ against λ^{-1} is identical with C_2. It is well known that[3] the value of C_2 depends on the degree of swelling, v_r, and is found to be independent of the nature of the rubber polymer, the degree of vulcanization, and of the nature of the swelling liquid. It is associated primarily with the existence of secondary network. The experimental data in Fig. 2 shows a good linear relationship for these two polymers, and the gradients of these two lines, or C_2, are nearly equal to zero. But if we compare poly-*p*-chlorostyrene gel with polystyrene gel, the former has a slightly larger positive value of C_2. From this fact, it is reasonable to assume that the larger restriction to the possible configuration of the molecular chain exists in poly-*p*-chlorostyrene gel, and so the interaction force between long chain molecules can be considered to be stronger.

Deutsch, Hoff and Reddish[8] and also Scott and Magat[9] discussed the effect of some polar groups upon the mechanical and dielectric properties, or upon the cohesive energy density of polymer, and their results support the above consideration**.

The strength of intermolecular force between chain molecules is also estimated from the change of thermodynamic functions. The increase of chlorine content in copolymers corresponds to the large contribution of the term $(\partial H/\partial\lambda)$ to $(\partial G/\partial\lambda)$. The function H can be considered as the internal energy, and the large value of a change of this term may be due to the strong interaction between chlorine atoms, i. e., the change of internal energy when a strain increases is increased by the introduction of a stronger intermolecular force. As these systems are in the same solvent and have a nearly equal volume fraction v_r, we can assume that

7) S. M. Gumbrell, L. Mullin and R. S. Rivlin, *Trans Faraday Soc.*, **49**, 1495 (1953).

* Gee has also reported the other value of μ of 0.41 from the vapor pressure measurement. Cf., *Trans. Faraday Soc.*, **42**, 507 (1946).

8) K. Deutsch, E. A. W. Hoff and W. Reddish, *J. Polymer Sci.*, **13**, 565 (1954).

9) R. L. Scott and M. Magat, ibid., **4**, 555 (1949).

** The structural effect upon the melting point or freezing point has been summarized by Uematu. Cf., *J. Chem. Soc. Japan, Ind. Chem. Sec.* (*Kogyo Kagaku Zasshi*), **59**, 750 (1956).

the change of the value of μ or of thermodynamic functions comes from the presence of chlorine atoms.

In the present discussion, the author considered that the effect of chlorine atoms may prevail upon their volume effect in relation to the mechanical properties, and took into account only this effect. But, of course, there must exist some volume effect of this polar group, and this is neglected in the above discussion.

The effect of intermolecular forces upon the other mechanical properties by introducing chlorine atoms is now under study.

In concluding this paper, the author wishes to express his thanks to Professor H. Akamatsu and Assistant Professor T. Nakagawa for the advice and guidance given him during his study.

Department of Chemistry
Faculty of Science
The University of Tokyo
Hongo, Tokyo

New Preparation of Diphenylsilanediol

By Toshio TAKIGUCHI

(Received November 29, 1958)

In separate papers[1,2] the author has described new methods of preparation of diphenylsilanediol (hereafter called diol), in which it has chiefly been aimed at for successful preparation to minimize the polymeric effect of hydrogen chloride produced thereby. In the present communication the author wishes to present some effective methods together with procedural details to prepare diol directly from diphenyldichlorosilane (DPDS). The first is the preparation from the reaction of DPDS with sodium or potassium hydrogen carbonate, the key feature of this method being the hydrolysis of DPDS with water produced by decomposition of the carbonates. The reaction can be represented summarily by the following equation for sodium hydrogen carbonate:

$$(C_6H_5)_2SiCl_2 + 2NaHCO_3 \rightarrow (C_6H_5)_2Si(OH)_2 + 2NaCl + 2CO_2$$

The fairly stable character of this diol has also prompted the second method which is possibly the simplest among the related works[3] and involves the direct hydrolysis of DPDS with a theoretical amount of water dissolved in inert organic solvents followed by complete removal of hydrogen chloride by using some appropriate reagents, e.g., calcium carbonate, sodium carbonate anhydride, calcium hydroxide, aniline or pyridine.

Experimental

Fine powdered inorganic salts in reagent-grades were used after prolonged drying in a vacuum-desiccator. Aniline and pyridine were distilled under reduced pressure after drying over potassium hydroxide. Reagent-grade acetone, benzene, ethyl acetate and ether were used without further purification. Highest-purity DPDS was received from the Shin-etsu Chemical Industrial Company.

(A) From the Reaction with Sodium or Potassium Hydrogen Carbonate. — Each carbonate undergoes reaction entirely similar to that of DPDS; a typical procedure is shown below. 25 g. (0.3 mol.) of sodium hydrogen carbonate and 200 ml. of acetone-benzene were placed in a one liter flask which had been kept in a water bath maintained at 50°C. A 25 g. portion (0.1 mol.) of DPDS dissolved in 50 ml. of acetone was added portion-wise to the flask which was shaken gently during the addition. On adding the silane solution, carbon dioxide was evolved readily and sodium chloride precipitated as fine white crystalline powder. After the addition was complete, the mixture was refluxed gently for 20 min. and then filtered under suction after cooling. On evaporating the filtrate to dryness on a water bath, a white crystalline mass was obtained from

1) "Hydrolysis of Diphenyldichlorosilane in the Presence of Aniline", *J. Chem. Soc. Japan, Ind. Chem. Sec.* (*Kogyo Kagaku Zasshi*), **62**, 601 (1959).
2) "New Simple Preparation of Diphenylsilanediol", *J. Org. Chem.*, in the press.
3) W. Dilthey and F. Eduardoff, *Ber.*, **37**, 1139 (1904); G. Martin, ibid., **45**, 403 (1912); F. S. Kipping, *J. Chem. Soc.*, **101**, 2108 (1912); C. A. Burkhard, *J. Am. Chem. Soc.*, **67**, 2173 (1945); J. F. Hyde and R. C. DeLong, ibid., **63**, 1194 (1941); S. Fukukawa, *Science & Industry, Japan* (*Kagaku to Kogyo*), **30**, 71 (1956).

which 20 g. (93%) of pure diol was obtained by recrystallization from ethyl acetate.

(B) **Direct Hydrolysis Method.**— In a one liter flask, were placed 400 ml. of acetone-benzene and 7 g. (0.4 mol.) of distilled water. After the addition of 51 g. (0.2 mol.) of DPDS to the flask, the mixture was shaken gently for a few minutes. Then, fine powdered calcium carbonate was added portion-wise to the flask which had been preheated at about 50°C, whereby the carbonate decomposed exothermally, evolving carbon dioxide. The addition was continued until the crystal violet indicator (1 drop of 1% ethanol solution) which had been added gradually should acquire a distinct purple color. After the reaction was over, the mixture was treated similarly to A, yielding 39 g. (90%) of white needles.

The use of sodium carbonate in place of calcium carbonate yielded 84% (mean) of diol, while the use of calcium hydroxide gave a considerable amount of uncrystallizable oily product caused by the presumable polymeryzing effect of the hydroxide.

Lastly, the use of aniline[1] or pyridine as hydrogen chloride acceptor gave entirely similar results, whereby the hydrochloride of each base precipitated as fine crystalline powder, the yield of diol being 88~92%.

Some Properties of Diol.—The diol thus obtained has been identified by its infrared absorption data[4] and the interplaner spacing data[1] (by diffractometer). [Found: Si, 12.7; OH/molecule, 1.97 (Karl Fischer titration)[5]; mol. wt., 195~204 (glacial acetic acid)]. The density (measured in aqueous calcium chloride solution of the matched density) was 1.16. The melting point[6] showed a variety of 132~133, 142~144, 147~148, 155 and 158~160°C in spite of all careful measurements. Melting was always accompanied by decomposition and successive fusion always lowered the melting point.

The author gratefully acknowledges the helpful discussions with Dr. F. Hirata in whose laboratory this work was performed.

Department of Applied Chemistry
Kiriu College of Technology
Gunma University
Tenjin-cho, Kiriu

4) W. S. Tatlock and E. G. Rochow, *J. Org. Chem.*, **17**, 1555 (1952).

5) H. Cilman and L. S. Miller, *J. Am. Chem. Soc.*, **73**, 2367 (1951).

6) Measured by using a clean Pyrex capillary tube and at the rate of heating 3~5°C per min., the bath being preheated at about 110°C.

*Dye-sensitized Photopolymerization of Vinyl Compounds. Polymerization of Styrene by Cyanine Dyes. III**

By Ai WATANABE

(Received December 3, 1958)

As reported in the previous papers[1,2], the photopolymerization of styrene occurs when the mixture of styrene and butanol (15 : 1 in volume) involving various cyanine dyes is irradiated by the visible light. The dye, at the same time, is bleached and it was concluded that both these reactions are initiated by a direct interaction between the excited dye molecule and the styrene. Generally speaking, however, the initial processes for the two reactions are not identical, since, for example, the number of kinetic chains for one decomposed dye molecule is a function of temperature. The participation of halogen ion in the reaction is highly plausible because of a marked difference between the rates for pinacyanol-iodide and -chloride. In order to elucidate the photochemical processes in these reactions, it would be desirable to compare the kinetic features of bleaching and polymerization, but only studies on the latter will be reported in this paper. Activation energies for the chain initiation were determined for various dyes and the influence of halogen species was examined. In addition, the following two facts which had been tentatively described in the previous paper[2] were reconfirmed: 1) light promotes only the initiation process of polymerization; 2) the concentration of dye

* Presented before the Ninth Annual Meeting of the Chemical Society of Japan, held at Kyoto, April 1956 and the Tenth Meeting at Tokyo, April 1957.

1) A. Watanabe and M. Koizumi, *J. Inst. Polytech. Osaka City Univ.*, **5C**, 114 (1956); M. Koizumi and A. Watanabe, This Bulletin, **28**, 136 (1955).

2) A. Watanabe and M. Koizumi, *J. Inst. Polytech. Osaka City Univ.*, **5C**, 124 (1956); A. Watanabe and M. Koizumi, This Bulletin, **28**, 141 (1955).

does not affect the rate in the region of $6.3\times10^{-6}\sim19\times10^{-6}$ mol./l.

Experimental

Material.—Styrene and *n*-butanol were purified in the same way as in the previous paper[1]. Isocyanine iodide, pinacyanol iodide and kryptocyanine iodide were granted by the late Dr. T. Ogata of the Institute of Physical and Chemical Research, Tokyo. All the other dyes except the above three were kindly supplied by the Japanese Research Institute for Photosensitizing Dyes, Co., Ltd. in Okayama.

Apparatus and Experimental Procedure.—The apparatus employed and the experimental procedure are mostly identical with the previous ones[1], but the dilatometric technique was adopted to follow the course of polymerization. The type of dilatometer was almost the same as used by Nakatsuka[3] except that a drum-type reaction cell of about 5 cc. in capacity was made of quartz and connected to a tube of hard glass. The reaction cell was arranged so as to let the parallel light beam illuminate the whole plane surface of the drum. Matsuda color filters were used; V-O 2 for pinacyanol, kryptocyanine and isocyanine, and V-Y 1 for trimethinthiocyanine.

One volume of *n*-butanol solution of dye was mixed with 15 volumes of styrene and the mixture was extensively evacuated. The concentration of the dye is always 1.2×10^{-5} mol./l. unless otherwise cited.

The extent to which the polymerization proceeded was calculated from the volume contraction, as performed by Burnett[4] employing the data of density for monomer and polymer reported by Patnode and Scheiber[5]. The average degree of polymerization was determined as in the previous paper[1].

Experimental Results

The Characteristics of the Bleaching Reaction.—The absorption spectra of various dyes employed are shown in Figs. 1 and 2. To avoid the overlapping of curves, the plot of $\log I_0/I$ is suitably displaced for some dyes, the magnitude of displacement being given by X. It is evident from these figures that in the butanol solution the position of absorption maximum is not affected by the kind of halogen, but in the styrene-butanol solution the maximum is more or less displaced to the longer wavelengths, the magnitude of shift being slightly different according to the species of dye and halogen.

The butanol solution of each dye does not bleach practically at 60°C even after

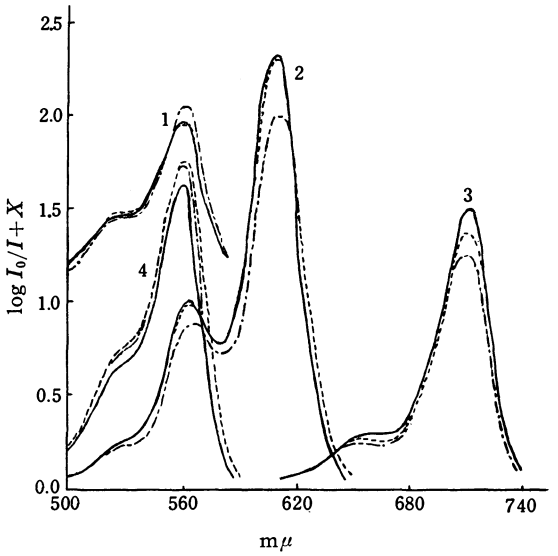


Fig. 1. Absorption spectra of cyanine dyes in *n*-butanol. Thickness of the cell, 1 cm.; 1.2×10^{-5} mol./l. (1, 2 and 4), 6.3×10^{-6} mol./l. (3). 1, isocyanine ($X=1$); 2, pinacyanol ($X=0$); 3, kryptocyanine ($X=0$); 4, trimethinthiocyanine ($X=0$). ——, iodide; ------, bromide; —·—, chloride.

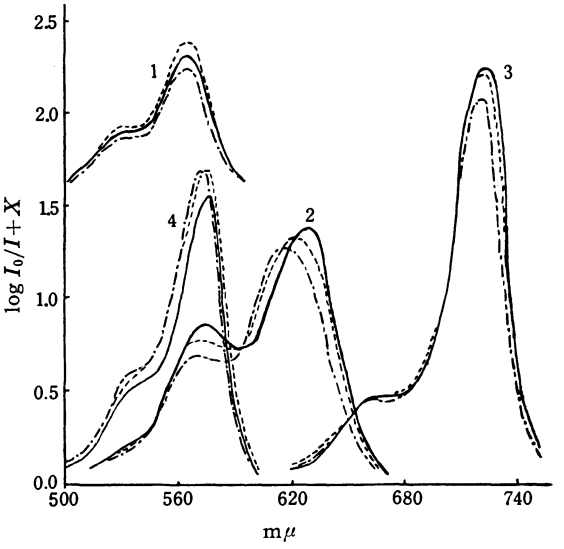


Fig. 2. Absorption spectra of cyanine dyes in styrene and *n*-butanol (15:1 in vol.). Thickness of the cell, 1 cm.; 1.2×10^{-5} mol./l. 1, isocyanine ($X=1.5$); 2, pinacyanol ($X=0$); 3, kryptocyanine ($X=0$); 4, trimethinthiocyanine ($X=0$). ——, iodide; ------, bromide; —·—, chloride.

illumination by the visible light for 6 hr. In the styrene-butanol solution, bleaching does not take place in the dark

3) K. Nakatsuka, S. Wada and M. Koizumi, *Chem. High Polymers (Kôbunshi Kagaku)*, **14**, 609 (1957).
4) G. M. Burnett, *Trans. Faraday Soc.*, **46**, 772 (1950).
5) W. Patnode and W. J. Scheifer, *J. Am. Chem. Soc.*, **61**, 3449 (1939).

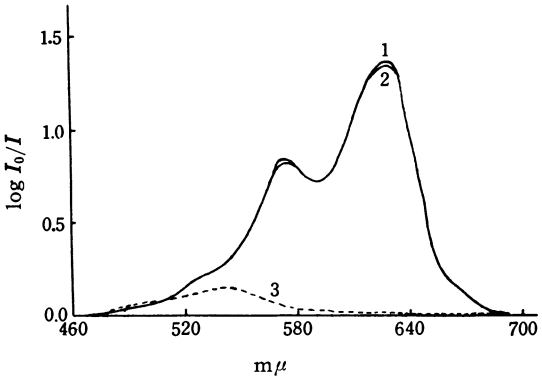


Fig. 3. Absorption spectra of pinacyanol iodide. 1, original sample; 2, after the reaction in dark for 2.5 hr. at 60°C; 3, after the reaction in light for 2.5 hr. at 60°C.

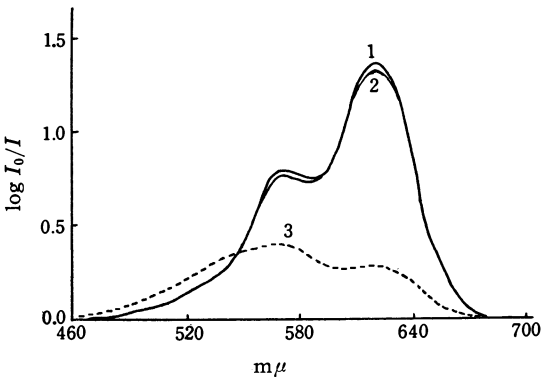


Fig. 4. Absorption spectra of pinacyanol bromide. 1, original sample, 2, after the reaction in dark for 5 hr. at 60°C; 3, after the reaction in light for 5 hr. at 60°C.

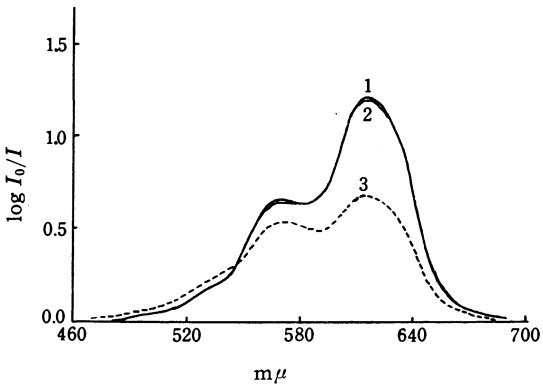


Fig. 5. Absorption spectra of pinacyanol chloride. 1, original sample; 2, after the reaction in dark for 5 hr. at 60°C; 3, after the reaction in light for 5 hr. at 60°C.

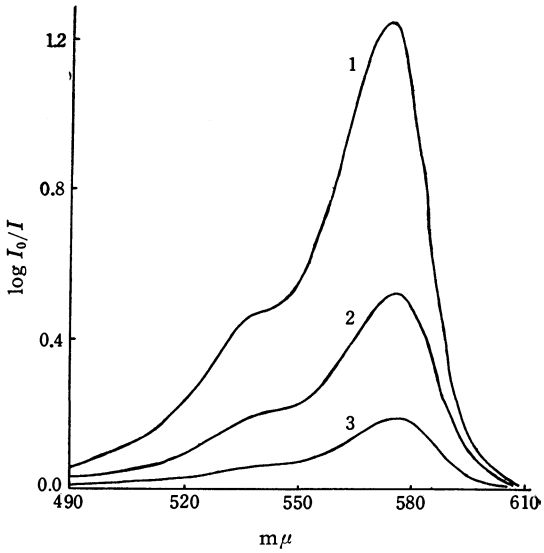


Fig. 6. Absorption spectra of illuminated trimethinthiocyanine. 1, chloride (60°C, 5 hr.); 2, bromide (60°C, 5 hr.); 3, iodide (60°C, 1 hr.).

(or does very slightly perhaps because of the dissolved oxygen or some impurities), but when illuminated, the bleaching occurs and at the same time the polymerization is promoted. The only curious exception is kryptocyanine bromide which is photobleached without inducing the polymerization, but retarding it very slightly at 60°C. Some of the absorption curves after the reaction for several hours are shown in Figs. 3, 4, 5 and 6. In case of pinacyanol, a new small absorption band appears in the visible region. So does it with isocyanine. In case of trimethinthiocyanine or kryptocyanine, the absorption curves merely decline over the whole visible region.

Effect of the Concentration of Dye.— Though it is a natural expectation that the rate of photochemical initiation is proportional to the intensity of light absorbed, there is some doubt about it under the present experimetal condition, since the dye of about 10^{-5} mol./l. in concentration absorbs nearly all the light and the distribution of the excited molecule in the system is not uniform. Hence it is desirable to check whether such a state of affairs does influence the rate or not. In the previous report it was perceived that the rate of polymerization is independent of the concentration of pinacyanol iodide in the range of $6\sim20\times10^{-6}$ mol./l. at 60°C, but this was not necessarily

conclusive since the styrene then used was not so carefully purified. Therefore the analogous experiment was repeated with more caution at 40°C. The results are tabulated in Table I. It is quite certain from Table I that the rate is completely independent of the dye concentration. In view of the absorbance of the dye the effective light is almost completely absorbed and the rate is not influenced by

TABLE I. EFFECT OF PINACYANOL IODIDE CONCENTRATION AT 40°C

Expt. no.	Dye concn. (10^{-6} mol./l.)	Relative rate (mm./hr.)
1	6.3	1.60
2	6.3	1.70
3	6.3	1.50
4	12	1.65
5	12	1.70
6	12	1.65
7	19	1.55
8	19	1.60

the dye concentration under the light intensity employed, but is determined by the quantity of excited dye produced in the whole system in a unit time.

The Relation between the Average Degree of Polymerization and the Overall Rate.—In the previous report[2], a test was made to see whether the irradiation only induces the chain initiation or also affects other steps such as propagation or termination. Using many data for several cyanine dyestuffs under various experimental conditions, the reciprocal of $\bar{P}_L$ (the average degree of polymerization for the polymer produced in the irradiated region of the reaction cell) was plotted against the overall rate V (the quantity of polymer produced in the irradiated region in a unit time). An approximately linear relationship was obtained supporting the view that the light only promotes the initiation process. But the points of data were not so satisfactory showing some scattering and it seemed desirable to repeat it again. In the present experiments, the solution of pinacyanol iodide of 1.2×10^{-5} mol./l. in concentration was used at 60°C and the intensity of light was varied by means of gauze wires. The results obtained by a similar treatment as in the previous paper are shown in Fig. 7. In this figure $\bar{P}_D$ is the average degree of polymerization in the dark part. The data are still distributed with some randomness, but in view of the fact that the value of $\bar{P}_D$ employed for the evaluation of

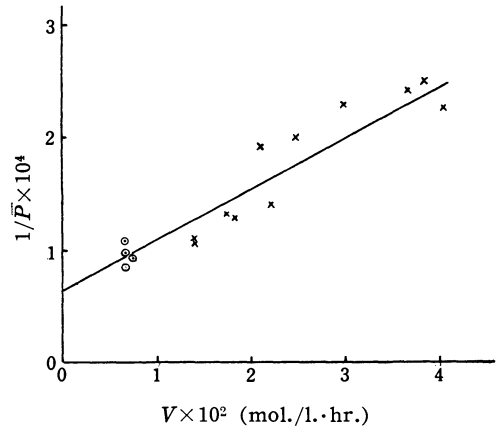


Fig. 7. Variation of the average degree of polymerization with the overall rate. ⊙, in dark; ×, in light.

$\bar{P}_L$ was a mean of many data in the dark, and further taking into account the poor reproducibility of the experiment the linearity can be regarded to hold.

Activation Energy. — The energy of activation was determined from rate measurements between 20° and 60°C under illumination and between 40° and 60°C in the dark using the dye solution of 1.2×10^{-5} mol./l. in concentration. The rate of photochemical reaction V_p was determined from the expression $V_p=\sqrt{V_l^2-V_d^2}$, where V_d is the rate of thermal reaction in the illuminated space and V_l is the total rate under illumination. The relation between $\log V_p$ and $1/T$ for various dyes is shown in Figs. 8, 9 and 10, where V_p are represented in per cent per hour. In case of pinacyanol iodide, V_p shows an abnormally high value at 50° and 60°C, but these are excluded from the calculation of

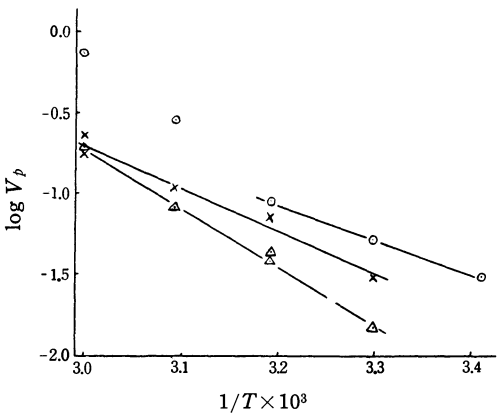


Fig. 8. Arrhenius plot for photopolymerization. ⊙, pinacyanol iodide; ×, pinacyanol bromide; △, pinacyanol chloride.

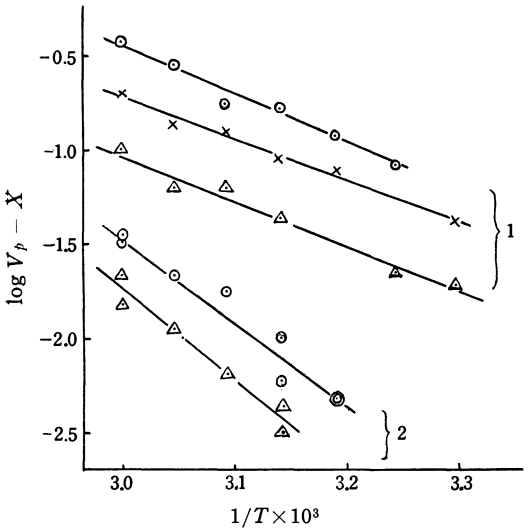


Fig. 9. Arrhenius plot for photopolymerization. 1, isocyanine (⊙, iodide (X=0); ×, bromide (X=0); △, chloride (X=0.4)); 2, kryptocyanine (⊙, iodide (X=1); △, chloride (X=1)).

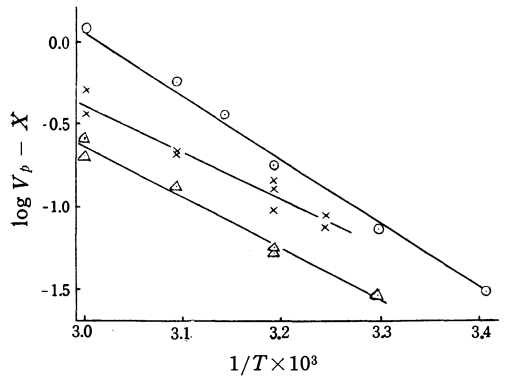


Fig. 10. Arrhenius plot for photopolymerization. Trimethinthiocyanine; ⊙, iodide (X=0); ×, bromide (X=0); △, chloride (X=0.3).

activation energy for the following reason. In the course of decomposition, this dye is transformed into a stable intermediate with a new visible absorption band, which is further decomposed by light absorption at 60°C accompanied with the induced polymerization. The above mentioned decomposition of the intermediate is far more rapid for iodide than for bromide or chloride as is evident from the Figs. 3, 4 and 5. Hence the polymerization induced by the decomposition of the intermediate is remarkable only for pinacyanol iodide at higher temperatures, while for bromide and chloride, in which similar intermediates are also produced, this secondarily induced polymerization is negligible at least in the initial stage of reaction due to their much lower rates of decomposition**. In case of isocyanine a new small peak also appears in the shorter wavelength region but the filter V-O 2 in this case does not transmit the light corresponding to the absorption of the intermediate, hence the polymerization due to its destruction will not take place. In case of kryptocyanine or trimethinthiocyanine the absorption declines monotonously in the whole visible region and the above considerations need not be taken into account. The values of the activation energy for the overall reaction thus evaluated are tabulated in Table II. By making use of Bamford's values[6] of activation energies for chain growth and chain termination (E_p=6.5 kcal./mol., E_t=2.8 kcal./mol.), the activation energy for initiation E_i can be calculated from the relation $E_i=2E-2E_p+E_t$. They are also included in Table II. Although the errors of these values are rather large owing to the poor reproducibility of experiments, some features can be seen and semi-quantitative discussions will be given below on the basis of these data.

TABLE II. ACTIVATION ENERGY (kcal./mol.)

Dye	Dark-reaction		Photo-reaction	
	E	E_i	E	E_i
No dye	22.9	35.6		
Pinacyanol iodide	—	—	10.4	10.6
Pinacyanol bromide	21.6	33.0	12.1	14.0
Pinacyanol chloride	22.6	35.0	16.9	23.6
Kryptocyanine iodide	22.6	35.0	20.6	31.0
Kryptocyanine chloride	22.0	33.8	22.4	34.6
Isocyanine iodide	18.3	26.4	11.7	13.2
Isocyanine bromide	—	—	10.5	10.8
Isocyanine chloride	15.8	21.4	11.0	11.8
Trimethinthiocyanine iodide	—	—	17.4	24.6
Trimethinthiocyanine bromide	—	—	12.8	15.4
Trimethinthiocyanine chloride	22.0	33.8	14.2	18.2

Discussion

If the irradiation only promotes the

** Filter V-O 2 transmits the light including the absorption maximum of the intermediate as well as the two absorption peaks of the original dye.

6) C. H. Bamford and M. J. S. Dewar, *Proc. Roy. Soc.*, **A192**, 309 (1948).

chain initiation, then the following linearity between the reciprocal of $\bar{P}_L$ and V must hold as derived in a previous paper[2].

$$1/\bar{P}_L = k_t V/2\,k_p^2\,[M]^2 + (R_{tr\cdot M}[M] + k_{tr\cdot S}[S])/k_p[M] \quad (1)$$

where k_p, $k_{tr\cdot M}$, $k_{tr\cdot S}$ and k_t are the rate constants for propagation, monomer transfer, solvent transfer and termination, respectively, and $[M]$ and $[S]$ denote the concentrations of the monomer and the solvent, respectively. Under the present experimental conditions $k_{tr\cdot S}[S]$ can be neglected against $k_{tr\cdot M}[M]$, hence from the intercept and the inclination of the straight line in Fig. 7, $k_{tr\cdot M}/k_p$ and k_t/k_p^2 can be evaluated, to be 6×10^{-5} and 2.1×10^3 mol. l^{-1} sec., respectively. The value of $k_{tr\cdot M}/k_p$ obtained above shows an excellent coincidence with that reported by Mayo et al.[7] As for the value of k_t/k_p^2, Bamford's data[6], $k_t=4.6\times10^6$ l. mol^{-1} sec^{-1} and $k_p=60$ l. mol^{-1} sec^{-1} at 60°C, give $k_t/k_p^2=1.28\times10^3$ mol. l^{-1} sec., while Matheson's values[8], $k_t=7.2\times10^7$ l. mol^{-1} sec^{-1} and $k_p=176$ l. mol^{-1} sec^{-1}, give $k_t/k_p^2=2.32\times10^3$ mol. l^{-1} sec. and the present value is about the same as the Matheson's one. From the agreement of these constants it is certain that the irradiation only induces the chain initiation process and does not affect either the propagation nor the termination process. Thus there is no doubt that the mechanism of the photochemical initial process may be discussed on the basis of the values of E_i tabulated in Table II.

Table II indicates that mere interchange of the halogen often results in a marked change in E_i-value and it can be concluded that the halogen ion plays an essential rôle in the primary photoprocess. Next, broadly speaking, a tendency is noted that the larger the frequency of absorbed light, the smaller is the value of E_i. In the following, some considerations will be given about these results more closely.

From the fact that bleaching does not occur in the absence of monomer, there is no doubt that the photochemical process takes place between the excited dye and the monomer. Further the chain initiation of polymerization is considered to be induced by a radical, since the quantitative aspects of polymerization such as the values of k_t/k_p^2 and $k_{tr\cdot M}/k_p$ coincide with the data for the well-established radical polymerization. Of course, a detailed description of the photochemical primary process is beyond the scope of the present stage of investigation, but some consideration about it will be helpful for further investigation.

As regards the formation of the radical, it seems natural to suppose that in the course of attack of a styrene molecule on dye, an electron-transfer occurs, the electron of a halogen anion being transferred to a dye cation. Then, the styrene molecule may seize a halogen atom and the two radicals produced may sometimes both induce the chain-initiation, or otherwise the dye-radical produced may decompose of itself.

It will be described in the following how the above idea is materialized and how it can explain the present results. Firstly, according to the above idea, the photochemical primary process may be pictured as follows:

$$\underset{\text{Initial state}}{D^+{}^*\cdots X^-} + M \rightarrow \underset{\text{Activated state}}{D\cdots X\cdots M} \rightarrow \underset{\text{Final state}}{D\cdot + MX\cdot}$$

where D^+ and X^- are a dye cation and a halogen anion, respectively. The activated state would have a configuration in which an electron is transferred from X^- to D^+ and a bond is partially formed between X and M, these two processes chiefly determining the energy of the activated state.

In case of a common D, a) the ease of electron transfer would be in the order, $I > Br > Cl$, while b) the energy decrease due to $X-M$ partial bond formation would be in the reversed order $Cl > Br > I$. If a styrene molecule is separated from $D\cdots X$ in the activated state, then a) would be a chief factor in determining the activation energy. On the contrary, when a styrene molecule is in close proximity to X, the activation energy would depend largely on b). Such would be the reason why the influence of halogen on activation energy is different in each dye.

In case of different D, the maximum of absorption differs and at the same time the tendency of electron transfer would also do so. Roughly speaking, these two factors would commonly act in the same direction for the following reason. The longer the wavelength of the absorption maximum which in many cases is caused by the longer chain of conjugation, the higher the highest occupied level

7) F. R. Mayo, R. A. Gregg and M. S. Matheson, *J. Am. Chem. Soc.*, **73**, 1691 (1951).
8) M. S. Matheson, E. E. Auer, E. B. Bevilacqua and E. J. Hart, ibid., **73**, 1700 (1951).

(or the lowest vacant level) lies and an electron is expected to transfer from X^- to D^+ with more difficulty. Thus it is expected that activation energy becomes greater as the absorption band is situated in the longer wavelength. This expectation is in accord with a general trend of the results.

The above qualitative discussion can be stated in much clearer form for an ideal case in which only the electron transfer

$$(D^+X^-)^* \rightarrow D \cdot X \cdot$$

is essential. It would be convenient to discuss this problem in terms of potential energy curves drawn against the distance between D and X. In Fig. 11, 1 is a

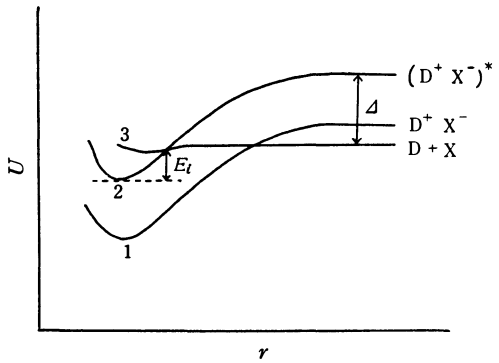


Fig. 11. Potential energy diagram.

potential energy curve of a dye in the ground state which is chiefly determined by the coulombic attraction between the solvated ions. 2 is the one of the excited dye, and 3 is a curve for the system after the electron is transferred from a halogen anion to a dye cation. The relative positions of the three curves are arbitrarily chosen but this does not essentially affect the discussion. Now at a larger distance, the energy difference between 2 and 3, Δ, is given by the equation

$$\Delta = I_D - A_X + h\nu - S \qquad (2)$$

where I_D is the ionization potential of a dye radical, A_X, the electron affinity of a halogen atom, $h\nu$, the energy of an absorbed quantum and S, a correction term related with the energy of solvation.

If the potential minimum in 1 and 2 is given by $e^2/\varepsilon r_X$ where r_X is the D–X distance in the minimum and ε is the effective dielectric constant, then the energy of activation is given by the following equation,

$$E_i = e^2/\varepsilon r_X - \Delta$$
$$= e^2/\varepsilon r_X - I_D + A_X - h\nu + S \qquad (3)$$

For a series of cyanine dyes with various halogens, E_i is determined by the value of

$$(e^2/\varepsilon r_X + A_X + S_X) = \delta_X$$

A_X for iodine, bromine and chlorine is respectively $72 < 81 < 87$ kcal./mol.[9] and S_X is most certainly in the same order. $e^2/\varepsilon r_X$ cannot always be determined by the size of a free ion, but may depend rather on the degree of solvation. In the former case it is in the order Cl > Br > I while in the latter case it might be reversed. If the magnitude of δ_X is mainly determined by $A_X + S_X$ then the activation energy will be in the order Cl > Br > I. Such would be the case for pinacyanol. The fact that there is no great difference in the values of E_i for isocyanine and kryptocyanine might be due to the participation of X–M bond energy in the activated state or to the contribution of $e^2/\varepsilon r_X$ in the inverse order depending on the structure of dye. In this connection, it seems suggestive that for trimethinthiocyanine and pinacyanol for which halogen anion can be placed naturally in between two N atoms, the value of E_i is much dependent on X, while for isocyanine and kryptocyanine for which halogen ion has to be situated in the neighborhood of one N atom apart from the other, the value of E_i is scarecely dependent at all on X. But it is a problem for the future why in the former pair, trimethinthiocyanine and pinacyanol, the effect of halogen is roughly in the inverse order.

Eq. 3 can also give a plausible interpretation of the results for various dyes with common X. With larger ν, I_D perhaps will also become larger, especially in cases when ν is largely dependent on the length of the chain and this causes E_i to become smaller. This is a general tendeny already mentioned.

Although a conclusive statement must await further investigation, the general feature of scheme would be as pictured above.

Summary

Extensive studies on the photopolymerization of styrene by virtue of cyanine dyes were performed and it was reconfirmed

9) A. Eucken and Landolt-Börnstein, "Zahlenwerte und Funktionen", I. Band, 1. Teil, Springer-Verlag, Berlin (1950), p. 213.

that only the chain initiation is promoted by the direct interaction between the excited dye and the styrene molecule. Activation energies for the photochemical initiation process were experimentally determined for several dyes of iodide, bromide and chloride. In general the activation energy depends on the kind of halogen ion and from this result it was concluded that halogen ion plays an essential rôle in the reaction. A general tendency was observed that the activation energy diminishes as the wavelength of absorption maximum of dyes becomes shorter. A plausible scheme for the chain initiation process was given, in which an electron transfer from X^- to D^+ is involved in the process of activation.

The author expresses her cordial thanks to Professor M. Koizumi of Tohoku University for his helpful discussions and to Professor R. Fujishiro and Professor S. Kawaguchi for their encouragement. She is also grateful to Dr. M. Banno of the Japanese Research Institute for Photosensitizing Dyes, Co., Ltd. in Okayama and to the late Dr. T. Ogata of the Institute of Physical and Chemical Research in Tokyo for their kind favors with dye samples. The cost of the present research has been partly defrayed from the Scientific Research Grant from the Ministry of Education.

Institute of Polytechnics
Osaka City University
Minami-ogi-machi, Kita-ku, Osaka

Oxidative Cleavage of 1-Phenyl-dialin with Peracetic Acid

By Yoshinobu ODAIRA and Shigeru TSUTSUMI

(Received December 4, 1958)

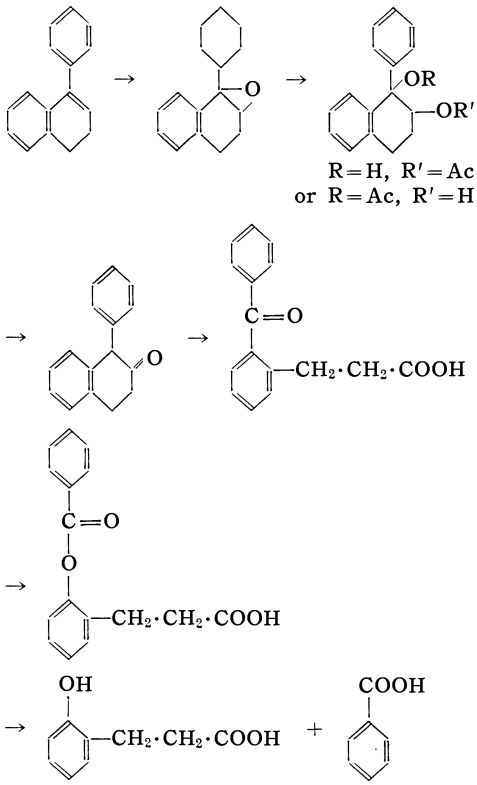
The present authors, recently, have carried out an extensive study on the oxidative cleavage of various compounds with peracetic acid, and it has been found that the hydroaromatic ring was readily dehydrogenated by peracetic acid. Our previous reports[1] indicated that the oxidative cleavage of dialin proceeded in two different reactions in an initial stage; the one was epoxidation and the other, dehydrogenation. On the contrary, the oxidative cleavage of 1-alkyl-dialin (4-alkyl-Δ^1-dialin) was shown to proceed by a predominant epoxidation with no dehydrogenation owing to the influences of alkyl groups.

In order to investigate the substituent-effects of phenyl group, the oxidative cleavage of 1-phenyl-dialin (4-phenyl-Δ^1-dialin) was carried out with peracetic acid. A mixture of 1-phenyl-dialin, ammonium molybdate and glacial acetic acid was heated at 40°C, and then 30% hydrogen peroxide solution was added. After the addition was completed, the reaction mixture was still maintained at the same temperature for further 12 hr.

From the neutral part, melilotine and 1-phenyl-tetralone-2 were isolated, and the presence of monoacetate of 1, 2-dihydroxy-1-phenyl-tetralin was confirmed, but unreacted 1-phenyl-dialine was not found. Moreover, the products obtained from the acidic part were benzoic acid, melilotic acid and the benzoate of melilotic acid. The benzoate of melilotic acid was confirmed by elementary analysis, infrared spectrum measurement and hydrolysis. In the ultraviolet spectrum of the compound in 95% ethanol, the maximum absorption is present in 263 mμ ($\log \varepsilon$ 3.45) and 272 mμ ($\log \varepsilon$ 3.35). It is very interesting to note that no product formed by dehydrogenation was isolated.

From these results and also by analogy with the case of 1-alkyl-dialin, it was concluded that the reaction of peracetic acid with 1-phenyl-dialin proceeded by a predominant epoxidation with no dehydrogenation, followed by the oxidative cleavage. Although *o*-carboxyethyl-benzophenone could not be isolated, it might be considered to be the precursor of the benzoate of melilotic acid. Thus the essential steps in the reaction were as follows;

1) Y. Odaira and S. Tsutsumi, *Technol. Repts. Osaka Univ.*, 8, 455 (1958).



In order to obtain further evidence for the above sequence, an authentic 1-phenyl-tetralone-2 was oxidized with peracetic acid and the benzoate of melilotic acid, benzoic acid and melilotic acid were isolated in good yields as the oxidation products.

Compared with the case of 1-alkyl-dialin, it is very interesting that the Baeyer-Villiger reaction occurred because of the effect of phenyl substituent in this case.

It is generally accepted that, in the cleavage of unsymmetrical diaryl ketones[2] by the Baeyer-Villiger oxidation, the migrating group is normally the more electron-releasing one. For example, treatment of *p*-methyl-benzophenone with peracetic acid gives benzoic acid and *p*-cresol; that is, *p*-tolyl group migrates more readily than phenyl group. On the other hand, the oxidation of *o*-methyl-benzophenone with peracetic acid[3] leads to the mixture of *o*-tolylbenzoate (12%) and phenyl-*o*-toluate (38%). Therefore, it is obvious that the ortho-effect can even overcome, to some extent, an electronic effect in the opposite direction (*o*-tolyl vs. phenyl).

In the series $Ph\cdot(CH_2)_n\cdot COOH$ it was found that, whereas the absorption band of benzoic acid is at 268 mμ (ε 1780), the ω-phenyl fatty acids from phenyl-butyric acid upwards have the absorption maximum at 260 mμ with greatly reduced intensity (ε ca. 200), and that this absorption is almost identical in every respect with that of a mixture of ethylbenzene and acetic acid[4]. Moreover, *o*-toluic acid and *o*-carboxyethyl-benzoic acid have the same maximum band at 278 mμ ($\log\varepsilon$ 3.15 and 3.08, respectively).

From the above ultraviolet spectra results, it may be assumed that no resonance between carboxyl group and benzoyl group in the molecule of *o*-carboxyethyl-benzophenone exhibits, and the compound will be considered as identical with *o*-methyl-benzophenone from the electronic point of view. If the above concept is true, phenyl group should migrate more easily than *o*-carboxyethyl-phenyl group owing to the ortho-effect, and one would expect the stronger retarding effect of *o*-carboxyethyl group, since this group is bulkier than methyl group. Actually, the reverse result was obtained in our experiments; namely, only the benzoate of melilotic acid was isolated and the migration of *o*-carboxyethyl-phenyl group occurred predominantly.

A more plausible explanation of such an abnormal phenomenon appears to be the steric assistance caused by steric interference of *o*-carboxyethyl group. Further discussion of the problem of the steric assistance in the Baeyer-Villiger reaction now requires more detailed experiments.

Experimental

Reagent.—1-Phenyl dialin, (b. p. 178~180°C/12 mmHg; $n_D^{20.5}$ 1.6323), was prepared from tetralone-1 according to the procedure of Weiss[5] in 55% yield. Ultraviolet absorption spectrum: λ_{max} 227.5 mμ, $\log\varepsilon$ 4.26; 265.0 mμ, $\log\varepsilon$ 3.92; λ_{min} 248.0 mμ, $\log\varepsilon$ 3.84 (*iso*-octane). Infrared absorption spectrum: ν_{max} 1500, 1600 cm^{-1} (aromatics), 827 cm^{-1} ($CR_1R_2=CHR_3$); no OH band.

Oxidative Cleavage of 1-Phenyl-dialin.—A mixture of 1-phenyl-dialin (15 g.), ammonium molybdate (0.13 g.) and glacial acetic acid (240 cc.) was heated at 40°C, and then 30% hydrogen peroxide solution (30 cc.) was slowly added with stirring in the course of 2 hr. After the addition, the solution was maintained at the same temperature with continued stirring for another 12 hr. To the above solution was added hot water (350 cc.) with stirring to decompose most of unreacted peracetic acid and allowed to stand

2) C. Hassall, *Org. Reactions*, **9**, 73 (1957).
3) W. Saunders, *J. Am. Chem. Soc.*, **77**, 4679 (1555).
4) P. Ramart-Lucas, *Bull. soc. chim.*, **10**, 13 (1943).
5) R. Weiss, *Org. Syntheses*, **24**, 84 (1944).

for 2 days. The reaction mixture was concentrated as completely as possible on a steam bath under reduced pressure (40°C/20 mmHg).

The orange residue obtained was dissolved in ethyl ether (350 cc.), the ethereal layer was extracted with three 200 cc. portions of 10% aqueous sodium bicarbonate and divided into the ethereal layer (I) and the sodium bicarbonate solution (II). The ethereal layer (I) was washed with water and dried over anhydrous sodium sulfate. After evaporation, 5.5 g. of the yellowish residual oil was distilled under reduced pressure. The product, on fractionation, gave: (i) b. p. 120~140°C/6 mmHg (0.5 g., n_D^{28} 1.5560); (ii) b. p. 180~195°C/6 mmHg (2.7 g., n_D^{28} 1.6080); and (iii) dark orange residue (2.0 g.).

The fraction i, having the perfume like coumarine, showed the presence of lactone group (ν_{max} 1786, 1754 cm^{-1}) and ortho-substitution (ν_{max} 757, 746 cm^{-1}) in the infrared spectrum, and gave 0.32 g. of melilotic acid, m. p. 82~83°C, by hydrolysis with 25% potassium carbonate.

Melilotic acid obtained showed no melting point depression by mixing with the authentic melilotic acid prepared from coumarine. From these facts, the above fraction i was determined as melilotine.

The fraction ii gave a positive Brady's test and showed the presence of carbonyl group in the infrared spectrum. Oxime of the fraction ii was obtained as colorless needles, m. p. 184~185°C.

Anal. Found: N, 5.97. Calcd. for $C_{16}H_{15}ON$: N, 5.90%.

Lit. b. p. 156~158°C/1 mmHg (n_D^{24} 1.6089) for 1-phenyltetralone-2; m. p. 184~185°C for oxime of 1-phenyltetralone-2.

From these facts, the carbonyl compound obtained in the fraction ii was confirmed to be 1-phenyl-tetralone-2. A mixture of the fraction iii and 30% sulfuric acid (15 cc.) was heated under reflux for 3.5 hr. After cooling, the reaction mixture was treated in the usual ways and gave 0.8 g. of brown oil. The oxime obtained from the above oil melted at 184~185°C and weighed 0.34 g. Since the oxime was identified as the oxime of 1-phenyl-tetralone-2, it might be considered that monoacetate of 1,2-dihydroxy-1-phenyl-tetralin was contained in the fraction iii, the yield calculated from the oxime obtained was 0.402 g.

The above sodium bicarbonate solution II was acidified with dilute hydrochloric acid and saturated with sodium chloride and extracted with ethyl ether. The ethereal extract was washed with water and dried over anhydrous sodium sulfate. After the solvent was evaporated, 10.7 g. of crude acid was isolated. The crude acid was distilled under reduced pressure. The product, on fractionation, gave: i b. p. 125~200°C/7 mmHg (3.2 g.); and ii brown viscous residue.

The fraction i was recrystallized from water to 1.1 g. of colorless needles, m. p. 121°C. *p*-Bromo-phenacyl-ester of this crystal was obtained as colorless needles, m.p. 119°C. Since this crystal showed no melting point depression by mixing with pure benzoic acid, and the infrared spectrum of this crystal was in good agreement with that of pure benzoic acid, the above crystal was confirmed to be benzoic acid.

The above recrystallization mother liquor was extracted with ethyl ether and dried over anhydrous sodium sulfate. After the solvent was evaporated, the yellowish residual oil was distilled, giving a colorless oil, b. p. 265~275°C. Hydrolysis of this oil with 25% potassium carbonate gave 0.45 g. of colorless needles, m. p. 82~83°C, identified as melilotic acid by mixed fusion.

The fraction ii, a brown viscous residue, was dissolved in benzene-light petroleum ether (1 : 1) and chromatographed by passing the solution through a silica-gel column. The column was then eluted with benzene and evaporation of benzene from the effluent left 3.3 g. of colorless crystals, m. p. 144~145°C. Recrystallization from benzene afforded colorless needles, m. p. 145.5°C.

Anal. Found: C, 70.96; H, 5.47. Calcd. for $C_{16}H_{14}O_3$: C, 71.10; H, 5.22%.

Infrared analysis showed the absence of diarylketone group and hydroxyl group, whereas the presence of the hydroxyl stretching vibration of carboxyl group (ν_{max} 2700 cm^{-1}) and carbonyl group (ν_{max} 1730, 1706 cm^{-1}). *p*-Bromo-phenacyl-ester of the above crystals was obtained as colorless needles, m. p. 166~167°C.

In the ultraviolet spectrum of the above crystals, m. p. 145.5°C, the maximum absorption lies at 263 mμ (log ε 3.447) and 272 mμ (log ε 3.555) in 95% ethanol.

Moreover, hydrolysis of 2 g. of the above substance by sodium-alcoholat gave 0.78 g. of benzoic acid and 0.86 g. of melilotic acid. From these facts, the above substance was identified to be the benzoate of melilotic acid.

Oxidative Cleavage of 1-Phenyl-tetralone-2.—A mixture of 1-phenyl-tetralone-2 (2.5 g.), ammonium molybdate (0.02 g.) and glacial acetic acid (40 cc.) was heated at 40°C, and then 30% hydrogen peroxide solution (50 cc.) was slowly added with stirring. After the addition, the reaction mixture was kept at the same temperature with continued stirring for 14 hr. The reaction mixture was treated in the usual ways. Remaining 1-phenyl-tetralone-2, the benzoate of melilotic acid, benzoic acid and melilotic acid were obtained, and the yields were 1.6 g., 12 mg., 0.25 g. and 0.22 g., respectively.

Department of Chemical Technology
Faculty of Engineering
Osaka University
Miyakojima-ku, Osaka

Intramolecular Interaction between Hydroxyl Group and π-Electrons. II[1]*. Limitation of the Interaction by Chain-length in ω-Hydroxy-1-alkenes**

By Michinori Ōki and Hiizu Iwamura

(Received December 16, 1958)

Recent studies on the intermolecular interaction between the hydroxyl group and aromatic nucleus have led some authors to examine the O–H stretching absorption band in the infrared region with compounds which are considered to possess possible intramolecular interaction between the hydroxyl group and aromatic nucleus. The first of these examples was found by Trifan and his co-workers in α-hydroxyethylferrocene and β-phenylethyl alcohol[2]. However, the phenomenon, splitting of the O–H stretching band, had been known for some years, although those authors who investigated the matter were not quite aware of the cause. That is to say, O–H stretching bands were found by Wulf[3] in 2-hydroxybiphenyl, by Fox and Martin[4] in benzyl alcohol and by Barnard and his collaborators[5] in cumene α-hydroperoxide.

Quite recently Goldman and Crisler[6] have also reported the existence of two O–H stretching bands in the first overtone vibrational region in some β-phenylethyl alcohol derivatives, but these examples mentioned here are all limited to the participation of an aromatic nucleus in the interaction as a hydrogen acceptor. Therefore, the authors felt that it was necessary to know whether a conjugated π-electron system, such as an aromatic ring, is really indispensable to this interaction and carefully investigated the O–H stretching absorption of ω-hydroxy-1-alkenes.

Although the only known example of the intermolecular interaction between the hydroxyl group and isolated double bond was the result of Lüttke and Mecke[7] who found it in cyclohexene and phenol, it turned out to be true that the intramolecular interaction between the hydroxyl group and π-electrons of an isolated double bond does exist, the result being in agreement with that obtained by Baker and Shulgin[8] who published a paper on the interaction in *o*-propenylphenol and *o*-allylphenol during the preparation of this paper.

Experimental

Measurement and Calculation. — The infrared absorption was measured with a Perkin Elmer Model 112-G Double Pass High Precision Grating Infrared Spectrometer[9], the spectral slit width being 1.0 cm^{-1} in the region required. Eastman-Kodak spectro grade or redistilled carbon tetrachloride was used as a solvent. A quartz absorption cell 2 cm. in length was used and the concentration of the solution was 0.0025～0.0032 mol./l. at which dilution the association of the solute is negligible. The temperature was 28.0～28.5°C.

The integrated intensities of the two bands were calculated according to the equations

$$A = \pi/2 \cdot \Delta\nu_{1/2} \cdot \log_e (I_0/I)_{max}$$

$$\log_e (I_0/I) = a/[(\nu-\nu_0)^2+b^2]$$

$$a/b^2 = \log_e (I_0/I)_{max}$$

$$2b = \Delta\nu_{1/2}$$

given by Ramsay[10], where A is the integrated intensity, $\Delta\nu_{1/2}$ the half-width, ν_0 the amount expressed by wave number at the band center and a and b are parameters. Because of the presence of two bands, four parameters had to be used.

Materials.—Allyl alcohol obtained from a commercial source was purified by redistillation using

1) Part I: M. Ōki, H. Iwamura and Y. Urushibara, This Bulletin, **31**, 769 (1958).

* Added in proof: After the submission of this article P. von Schleyer, D. S. Trifan and R. Bacskai have reported in a brief note that they observed two O-H stretching absorptions with allyl alcohol and 3-buten-1-ol [*J. Am. Chem. Soc.*, **80**, 6691 (1958)].

2) D. S. Trifan, J. L. Weinmann and L. P. Kuhn, *J. Am. Chem. Soc.*, **79**, 6566 (1957).

3) O. R. Wulf, ibid., **58**, 2290 (1936).

4) J. J. Fox and A. E. Martin, *Trans. Faraday Soc.*, **36**, 897 (1940).

5) D. Barnard, K. R. Hargrave and G. M. G. Higgins, *J. Chem. Soc.*, **1956**, 2845.

6) I. M. Goldman and R. O. Crisler, *J. Org. Chem.*, **23**, 751 (1958).

7) W. Lüttke and R. Mecke, *Z. Electrochem.*, **53**, 241 (1949).

8) A. W. Baker and A. T. Shulgin, *J. Am. Chem. Soc.*, **80**, 5358 (1958).

9) For calibration of the wave number, see: S. Mizushima et al., *J. Japan. Chem.* (*Kagaku no Ryoiki*), Extra Ed., No. 28, Nankodo, Tokyo (1957) p. 1.

10) D. A. Ramsay, *J. Am. Chem. Soc.*, **74**, 72 (1952).

carbon tetrachloride for removal of water[11], b.p. 96.0~96.3°C. 3-Buten-1-ol and 5-hexen-1-ol were prepared by action of formaldehyde on the corresponding alkenylmagnesium bromides and the physical constants were as follows: 3-buten-1-ol b. p. 113~113.5°C, $n_D^{26.5}$ 1.4185 (lit.[12] b. p. 112~114°, n_D^{25} 1.4189): 5-hexen-1-ol, b.p. 72.0~72.2°C/19.5mm., n_D^{30} 1.4353 (lit.[13] b.p. 155.6~156.0°C/718 mm., n_D^{20} 1.4364). 4-Penten-1-ol and 10-undecen-1-ol were prepared by lithium aluminum hydride reduction of the corresponding carboxylic acids and the following physical constants were obtained: 4-penten-1-ol, b. p. 63°C/3.0 mm., n_D^{21} 1.4292 (lit.[14] n_D^{20} 1.4299); 10-undecen-1-ol, b. p. 95.5~96°C /3.5 mm., n_D^{20} 1.4462 (lit.[15] n_D^{19} 1.4506).

Results and Discussion

The actual O–H stretching absorption curves of the alcohols are shown in Fig. 1 and the data of the two bands divided by the Ramsay's equations are given in Table I, in which, for the convenience of the discussion, the bands are named I and II rather than interacted and free.

As is seen from Fig. 1, the only example which showed two distinct bands is 3-buten-1-ol which can undoubtedly be said to possess intramolecular interaction between the hydroxyl group and π-electrons of the double bond.

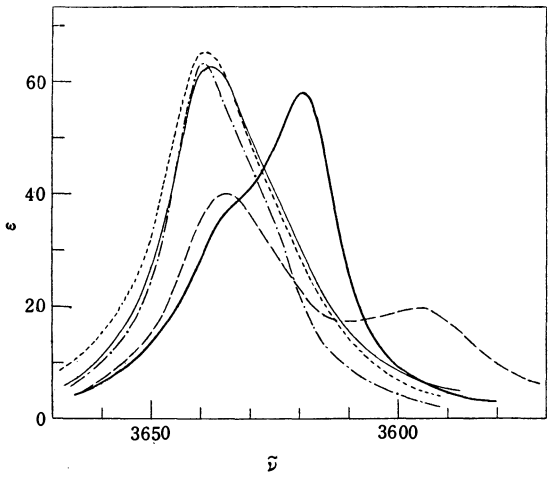


Fig. 1. ν_{O-H} absorption of ω-hydroxy-1-alkenes.
—— allyl alcohol, ---- 3-buten-1-ol,
—— 4-penten-1-ol, ····· 5-hexen-1-ol,
-·-· 10-undecen-1-ol

TABLE I. O–H STRETCHING ABSORPTION BANDS OF ω-HYDROXY-1-ALKENES

$[CH_2=CH(CH_2)_nOH]$

n		ν_{max} (cm^{-1})	$\Delta\nu^a_{1/2}$ (cm^{-1})	$A\times10^{-4}$ (mol.$^{-1}$·liter·cm^{-2})	$\Delta\nu_{max}$ (cm^{-1})
1	I	3619.4	16.4	2.87	15.4
	II	(3634.8)	(23.4)	(2.29)	
2	I	3596.1	32.2	1.93	39.1
	II	3635.2	24.0	3.27	
3	I	(3624.5)	(24.0)	(1.76)	14
	II	3638.3	20.8	4.03	
4	I	(3626.0)	(17.2)	(1.15)	13
	II	3639.2	20.8	4.45	
9	I	(3628.5)	(18.8)	(1.78)	12
	II	3640.0	15.8	2.94	

The lower homolog of 3-buten-1-ol, allyl alcohol, was spectroscopically studied by Flett[16] in its O–H stretching region and reported to have a single band at 3620 cm^{-1}. However, the present authors' result with the instrument of high resolution shows that allyl alcohol possesses two bands at 3619.4 cm^{-1} and 3634.8 cm^{-1}, the latter corresponding to the normal vibration of aliphatic primary alcohols and is reminiscent of the result obtained by Fox and Martin[4] with benzyl alcohol. Since this kind of curve for O–H stretching vibration is obtained only with allyl alcohol or benzyl alcohol, the band at ca. 3620 cm^{-1} may be attributed to the interaction between π-electrons and the hydroxyl group.

Comparison of the curves for allyl alcohol and 3-buten-1-ol reveals that the number of internally interacted molecules is greater in allyl alcohol than in 3-buten-1-ol, provided that the absorption intensity of a molecule is equal in both free and interacted forms. This assumption is based on the fact that the sum of two integrated intensities is almost the same in the two compounds. This phenomenon seems to be rather striking, because it is a common concept that the difference in wave number corresponds to the energy[17], but can be explained in either of the following two ways. Firstly, the interactions occurring in allyl alcohol and in 3-buten-1-ol may be different in nature and, secondly, unfavorable entropy change in 3-buten-1-ol may limit the number of the internally interacted molecules, in spite of the greater stabilization in energy term. Although, as far as the present data are concerned, it is not clear which is the real cause, the accumulated data

11) O. Kamm and C. S. Marvel, "Org. Synth.", Coll. Vol. I. John Wiley & Sons, Inc., New York (1948), p. 43.
12) E. D. Amstutz, *J. Org. Chem.* **9**, 310 (1944).
13) V. P. Gol'mov, *Zhur. Obshcheĭ Khim.*, **22**, 2132 (1952); *Chem. Abstr.*, **48**, 1240 (1954).
14) M. S. Kharash and C. F. Fuchs, *J. Org. Chem.*, **9**, 359 (1944).
15) P. Chuit, F. Boelsing, J. Hausser and G. Malet, *Helv. Chim. Acta*, **9**, 1074 (1926).
16) M. St. C. Flett, *Spectrochim. Acta*, **10**, 210 (1957).
17) See, e.g., R. M. Badger and S. H. Bauer, *J. Chem. Phys.*, **5**, 839 (1937).

in this laboratory suggest that the former is the preferable cause.

Higher homologs of 3-buten-1-ol, 4-penten-1-ol and 5-hexen-1-ol, possess an unsymmetric band, fatter at the smaller wave number side, and the band can be divided into two, assuming that the band is an overlapping of two symmetric bands which are expressed by the Lorentz function. The smaller peaks (band I) at ca. 3625cm^{-1} may be attributed to the presence of the hydroxyl group and π-electrons interaction but the minor peak (band I) also appears in 10-undecen-1-ol in which the intramolecular interaction is improbable in respect of the entropy increase. Moreover, these three curves are quite similar and suggest that the minor peaks do not represent the intermolecular interaction, since it is not plausible to consider that the same extent of intramolecular interaction between the hydroxyl group and π-electrons exists in these three compounds. In other words, this kind of interaction can not be found in higher homologs than 4-penten-1-ol. The origin of the minor peaks (bands I of 4-penten-1-ol, of 5-hexen-1-ol and of 10-undecen-1-ol) will be dealt with in the following paper.

It may seem to be rather strange that the interaction takes place up to 3-buten-1-ol in the homologs studied, in contrast with the finding of Baker and Shulgin who reported the existence of the interaction both in *o*-propenylphenol and *o*-allylphenol, the latter being an analog of 4-penten-1-ol. But the explanation can be given by considering the difference in proton donating ability of phenolic and alcoholic hydroxyl groups and the favorable structure of the phenols in which O–C–C–C bonds are fixed *cis*. The representative cases are under investigation.

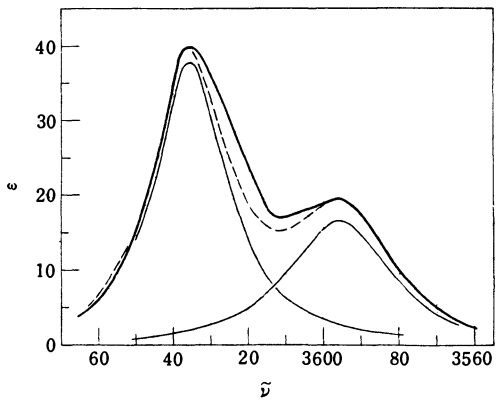


Fig. 2. ν_{O-H} absorption of 3-buten-1-ol.
—— observed curve
—— divided bands
---- calculated curve

It might also be mentioned here that, as shown in Fig. 2, the calculated band area of 3-buten-1-ol does not quite agree with the observed one. Namely, the computed value is always lower than the observed one at the valley of the band for 3-buten-1-ol, while that for the others

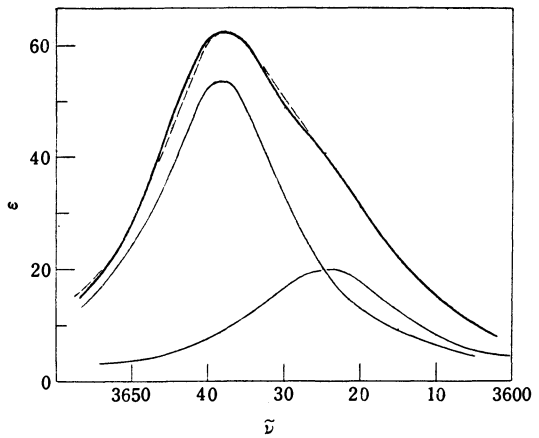


Fig. 3. ν_{O-H} absorption of 4-penten-1-ol.
—— observed curve
—— divided bands
---- calculated curve

agree, as shown in Fig. 3 (taking 4-penten-1-ol as an example). The cause of the disagreement is unknown but is quite understandable if one considers that another absorption band exists in this compound at about 3626 cm^{-1} corresponding to those in the higher homologs.

In closing, the authors would like to mention the terminology of this interaction. Although many authors[2,6,8] used "hydrogen bonding", "interaction" is the present authors' choice, since the definition of the hydrogen bonding was discussed at the international symposium[18] on the hydrogen bonding and an agreement that the interaction between a hydrogen donating group and an electron pair of an atom was hydrogen bonding, was reached. The interaction discussed here undoubtedly resembles the hydrogen bonding, but is still distinguishable from the hydrogen bonding because of the participation of the π-electrons of a double bond which are not on the same atom, although they overlap.

Summary

Infrared absorption was measured with

18) See: *Angew. Chem.*, **67**, 755 (1957).

five ω-hydroxy-1-alkenes in the 3 μ region, using an instrument of high resolution and the following results were obtained.

1) Intramolecular interaction between the hydroxyl group and π-electrons was found in allyl alcohol and in 3-buten-1-ol.

2) Interactions which occur in allyl alcohol and in 3-buten-1-ol may be of a different kind.

3) Higher homologs also possess two O–H stretching absorption bands but these bands can not be associated with the intramolecular interaction.

The authors are indebted to Professors Y. Urushibara and T. Shimanouchi for their valuable advice and encouragement and to Mr. I. Suzuki for his technical assistance throughout this work. A part of the cost was defrayed from the Grant in Aid for Fundamental Scientific Research of the Ministry of Education, for which the authors' thanks are due.

Department of Chemistry
Faculty of Science
The University of Tokyo
Hongo, Tokyo

Analysis of the Multi-azeotropes in Terms of the Zeroth Approximation

By Ikuho YAMADA, Takatoshi YOSHIDA and Osamu KAWASE

(Received October 3, 1958)

Theoretical and experimental studies on the binary azeotropes, characterized by a maximum or a minimum in vapor pressure curves, have been made by many investigators. Among them, the theoretical studies of Prigogine[1], Mashiko[2] and Ikari[3], in terms of strictly regular solutions are viewed with interest.

However, most of these studies have dealt only with the case of binary systems. We shall report here the results obtained in the theoretical study of multi-azeotropes in the zeroth approximation by extending the method of Prigogine and Mashiko.

Theoretical Equation of the Vapor-liquid Equilibrium in Terms of the Zeroth Approximation.—The authors[4] have already published the theoretical equations of the vapor-liquid equilibrium in multi-component systems at the zeroth approximation.

Rewriting, now, the final result of activity coefficient γ_i of i-th component, the following equation is given

$$\boldsymbol{R}T \ln \gamma_i = \sum_{p=1}^{n}(1-x_i)x_p\omega_{ip}(i\neq p) - \sum_{p,q=1}^{n} x_p x_q \omega_{pq}\begin{pmatrix} p\neq q \\ p,q\neq i \end{pmatrix} \qquad (1)$$

where x is mole fraction of component of subscription $1, 2, \cdots\cdots, i, \cdots\cdots, n$ in liquid phase, ω the inter-molecular exchange energy in different molecules, $\boldsymbol{R}$ the gas constant and T the absolute temperature in the equilibrium state.

Taking as an example the case of a binary solution, Eq. 1 becomes as follows:

$$\begin{cases} \boldsymbol{R}T \ln \gamma_1 = (1-x_1)x_2\omega_{12} \\ \boldsymbol{R}T \ln \gamma_2 = (1-x_2)x_1\omega_{12} \end{cases} \qquad (2)$$

which is the same as given by Guggenheim[5].

Condition of the Azeotropic Formation in Multi-component System.—The activity coefficient of the i-th component in liquid phase is given by

$$\gamma_i = \pi y_i / p_i^\circ x_i \qquad (3)$$

where π is the total pressure, y the mole fraction in vapor phase and p° the vapor pressure of pure component at temperature T.

At an azeotropic point, $y_i = x_i$ and by the Clausius-Clapeyron's equation, $\ln \gamma_i$ is expressed as

$$\boldsymbol{R} \ln \gamma_i = \Delta H_i (1/T - 1/T_i^\circ) \qquad (4)$$

where ΔH is the heat of vaporization of

1) I. Prigogine and R. Defay, "Chemical Thermodynamics", Translated by D. H. Everett, Longmans, London, (1954), p. 450.
2) Y. Mashiko, *Rep. Gov. Chem. Ind. Res. Inst. Tokyo*, **52**, 158 (1957).
3) A. Ikari, *J. Chem. Soc. Japan, Ind. Chem. Sec.* (*Kogyo Kagaku Zasshi*), **60**, 1375 (1957).
4) I. Yamada, will be published in *Chem. Eng. Japan*.
5) E. A. Guggenheim, "Mixtures", Oxford University Press (1952), p. 32.

TABLE I. EXAMPLES OF AZEOTROPIC RELATIONS IN TERNARY AZEOTROPES

Components of system	Boiling point (B. P.)	B. P. difference	$\omega_{ij}/\Delta S_i$	$\omega_{ij}/\Delta S_j$	Azeotropes
Ethanol (1)		$\Delta_{12}=$ 2.2	69.4	53.6	
—Cyclohexane (2)	62.1°C	$\Delta_{32}=$ 19.2	97.4	115.9	exist
—Water (3)		$\Delta_{13}=-21.4$	26.0	28.2	
iso-Propanol (1)		$\Delta_{12}=-$ 1.2	68.7	50.7	
—Cyclohexane (2)	63.8°C	$\Delta_{32}=$ 19.2	93.5	111.3	exist
—Water (3)		$\Delta_{13}=-17.5$	37.3	42.4	
Allylalcohol (1)		$\Delta_{12}=-16.3$	94.7	73.0	
—Cyclohexane (2)	65.2°C	$\Delta_{32}=$ 19.2	90.0	107.2	exist
—Water (3)		$\Delta_{13}=-$ 2.9	25.1	27.4	
Ethanol (1)		$\Delta_{12}=$ 1.8	55.4	71.5	
—Benzene (2)	64.8°C	$\Delta_{32}=$ 19.8	106.9	129.8	exist
—Water (3)		$\Delta_{13}=-21.6$	49.8	53.0	
iso-Propanol (1)		$\Delta_{12}=-$ 1.7	65.7	48.5	
—Benzene (2)	65.3°C	$\Delta_{32}=$ 19.7	89.7	104.6	exist
—Water (3)		$\Delta_{13}=-18.5$	31.6	27.8	
Allylalcohol (1)		$\Delta_{12}=-17.3$	109.1	79·6	
—Benzene (2)	67.8°C	$\Delta_{32}=$ 19.8	85.6	101.8	exist
—Water (3)		$\Delta_{13}=-$ 2.5	42.7	42.7	
Methanol (1)		$\Delta_{12}=$ 8.2	−6.1	−6.9	
—Acetone (2)	61.7°C	$\Delta_{32}=$ 35.3	31.2	31.1	none-exist
—Water (3)		$\Delta_{13}=-43.5$	64.8	57.6	

B. P. shows the azeotropic point under 1 atm.

pure component and T° is the boiling point under the pressure π.

From Eqs. 1 and 4, the following expressions for the i- and j-th components can be deduced by substituting ΔS for $\Delta H/T$

$$\Delta S_i(T_i^\circ - T) = \sum_{p=1}^{n}(1-x_i)x_p\omega_{ip}(i\neq p) - \sum_{p.q=1}^{n}x_px_q\omega_{pq}\begin{pmatrix}p\neq q\\ p.q\neq i\end{pmatrix} \quad (5)$$

$$\Delta S_j(T_j^\circ - T) = \sum_{p=1}^{n}(1-x_j)x_p\omega_{jp}(j\neq p) - \sum_{p.q=1}^{n}x_px_q\omega_{pq}\begin{pmatrix}p\neq q\\ p.q\neq j\end{pmatrix} \quad (6)$$

and

$$T_i^\circ - T_j^\circ = \left\{\sum_{p=1}^{n}(1-x_i)x_p\omega_{ip}(i\neq p) - \sum_{p.q=1}^{n}x_px_q\omega_{pq}\begin{pmatrix}p\neq q\\ p.q\neq i\end{pmatrix}\right\}\Delta S_i^{-1} - \left\{\sum_{p=1}^{n}(1-x_j)x_p\omega_{jp}(j\neq p) - \sum_{p.q=1}^{n}x_px_q\omega_{pq}\begin{pmatrix}p\neq q\\ p.q\neq j\end{pmatrix}\right\}\Delta S_j^{-1} \quad (7)$$

When $x_j=1$, Eq. 7 shows a maximum and when $x_i=1$, a minimum, so that the following relation should hold.

$$-\omega_{ij}/\Delta S_j \leqq T_i^\circ - T_j^\circ \leqq \omega_{ij}/\Delta S_i \quad (8)$$

Hence, in the case of multi-azeotropes, the same relation as Eq. 7 should hold for all such combinations made of n components.

In the case of binary azeotropes, Eq. 8 takes the form given by Mashiko[6]. Table I shows the azeotropic relations from the given data[7], and the values of ω_{ij} are calculated from Eq. 1 for ternary systems.

Constancy of ω_{ij}.—The theoretical equations of the vapor-liquid equilibrium in multicomponent systems on the zeroth approximation have been derived by assuming that the molecular configurations have pairs in the liquid phase and intermolecular exchange energy between molecules i and j are independent of each other. If these assumptions are correct ω_{ij} should have a constant value for any pair of components.

ω_{ij} can be obtained by solving Eq. 1 for a given set of values of T, x_i and γ_i, i being $1, 2, \cdots\cdots, n$.

In the case of ternary azeotropes, the following solution can be obtained

$$\omega_{12}\Delta = \boldsymbol{M}$$

where

6) M. Mashiko, *Rep. Gov. Chem. Ind. Res. Inst. Tokyo*, **52**, 160 (1957).

7) L. H. Horsley, *Anal. Chem.*, **19**, 508 (1947); **21**, 831 (1949).

$$\Delta = \begin{bmatrix} (1-x_1)x_2 & -x_2x_3 & (1-x_1)x_3 \\ (1-x_2)x_1 & (1-x_2)x_3 & -x_1x_3 \\ -x_1x_2 & (1-x_3)x_2 & (1-x_3)x_1 \end{bmatrix}$$

and

$$\boldsymbol{M} = \begin{bmatrix} \Delta H_1(1-T/T_1^\circ) & -x_2x_3 & (1-x_1)x_3 \\ \Delta H_2(1-T/T_2^\circ) & (1-x_2)x_3 & -x_1x_3 \\ \Delta H_3(1-T/T_3^\circ) & (1-x_3)x_2 & (1-x_3)x_1 \end{bmatrix}$$

By plotting Δ vs. $\boldsymbol{M}$, a linear relation is obtained for several ternary systems as shown in Figs. 1—3.

Temperature Effect upon Azeotropic Compositions.—Taking the difference between $\ln\gamma_i$ and $\ln\gamma_{i+1}$ for all i's in Eq. 1, all second order terms $x_px_q\omega_{pq}$ cancel each other and the following equation can be obtained.

$$\Delta H_i(1-T/T_i^\circ) - \Delta H_{i+1}(1-T/T_{i+1}^\circ) = (x_{i+1}-x_i)\omega_{i\,i+1} + \sum_{p=1}^{n}(\omega_{ip}-\omega_{j+p})x_p \qquad (p \neq i, i+1) \quad (12)$$

where $i=1,2,\cdots\cdots,n-1$

As $\sum x=1$, Eq. 12 becomes

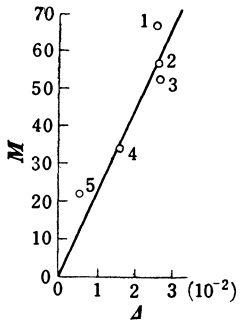
$$\begin{bmatrix} 1 \\ \Delta\phi_{1\,2} \\ \vdots \\ \Delta\phi_{i\,j+1} \\ \vdots \\ \Delta\phi_{n-1,n} \end{bmatrix} = \begin{bmatrix} 1 & 1 & \cdots\cdots & 1 & 1 & \cdots\cdots & 1 \\ -\omega_{1\,2} & \omega_{1\,2} & \cdots\cdots & (\omega_{1\,i}-\omega_{2\,i}) & (\omega_{1\,i+1}-\omega_{2\,i+1}) & \cdots\cdots & \vdots \\ \vdots & \vdots & & \vdots & \vdots & & \vdots \\ (\omega_{1\,i}-\omega_{1\,i+1}) & (\omega_{2\,i}-\omega_{2\,i+1}) & \cdots\cdots & -\omega_{i\,i+1} & \omega_{i\,i+1} & \cdots\cdots & (\omega_{i\,n}-\omega_{i+1\,n}) \\ \vdots & \vdots & & \vdots & \vdots & & \vdots \\ (\omega_{1\,n-1}-\omega_{1\,n}) & (\omega_{2\,n-1}-\omega_{2\,n}) & \cdots\cdots & (\omega_{i\,n-1}-\omega_{i\,n}) & (\omega_{i+1\,n-1}-\omega_{i+1\,n}) & \cdots\cdots & \omega_{n-1\,n} \end{bmatrix} \begin{bmatrix} x_1 \\ x_2 \\ \vdots \\ x_i \\ \vdots \\ x_n \end{bmatrix} \qquad (13)$$

where

$$\Delta\phi_{i\,i+1} = \Delta H_i(1-T/T_i^\circ) - \Delta H_{i+1}(1-T/T_{i+1}^\circ)$$

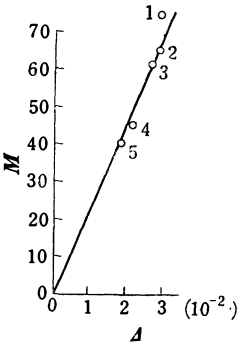
Consequently, x's can be expressed by linear functions of T for given values ω_{ij}'s, ΔH_i's and T_i°'s.

For binary azeotropes, the following results can be given.



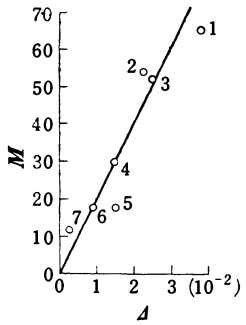
Alcohols
1 ethanol
2 *t*-butanol
3 propanol
4 allyl alcohol
5 *sec*-butanol

Fig. 1. Carbontetrachloride-water-alcohol system.



Alcohols
1 ethanol
2 *iso*-propanol
3 *t*-butanol
4 allyl alcohol
5 propanol

Fig. 2. Cyclohexane-water-alcohol system.



Alcohols
1 ethanol
2 *iso*-propanol
3 *t*-butanol
4 propanol
5 allyl alcohol
6 *sec*-butanol
7 hexanol

Fig. 3. Benzene-water-alcohol system.

$$\begin{bmatrix} 1 \\ \Delta H_1(1-T/T_1^\circ) - \Delta H_2(1-T/T_2^\circ) \end{bmatrix} = \begin{bmatrix} 1 & 1 \\ -\omega & \omega \end{bmatrix} \begin{bmatrix} x_1 \\ x_2 \end{bmatrix} \qquad (14)$$

Consequently

$$2x_1 = 1 - \{\Delta H_1(1-T/T_1^\circ) - \Delta H_2(1-T/T_2^\circ)\}\omega^{-1} \qquad (15)$$

$$2x_2 = 1 + \{\Delta H_1(1-T/T_2^\circ) - \Delta H_2(1-T/T_2^\circ)\}\omega^{-1} \qquad (16)$$

Eqs. 15 and 16 agree with those given by Prigogine[8].

Breaking Point of Azeotropes. — When x_i obtained by solving Eq. 13 is equal to zero or unity, the multi-azeotropes are broken; these points are predicted by solving the equation for $i=1,2,\cdots\cdots,n$.

8) I. Prigogine and R. Defay, "Chemical Thermodynamics", Translated by D. H. Everett, Longmans, London, (1954), p. 462.

The closest value to initial T obtained for each may be considered as the break point.

Prediction of Azeotropic Temperature.— Substituting Eq. 4 and x_i given by Eq. 13 into Eq. 1, the azeotropic temperature can be predicted by solving the second-order equation in respect to T for given values of ω_{ii}, T_i°, ΔH and $\boldsymbol{R}$.

Summary

Assuming the zeroth approximation for the vapor-liquid equilibrium in multi-component systems the authors have analyzed multi-azeotropes, and the following results have been obtained.

1) For the condition of azeotropic formation in multi-component systems, Eq. 8 should hold for all combinations of n components.

2) The constancy of ω_{ij} is shown as Figs. 1 to 3.

3) Azeotropic composition effect upon temperature is given by solving Eq. 13, and the breaking temperatures are obtained by substituting $x_i=1$ or 0 into Eq. 13.

4) Azeotropic temperature can be deduced from Eqs. 2, 4 and 13.

Nagoya Institute of Technology
Gokiso-cho, Showa-ku, Nagoya

Polarography of Tetracyano- and Dithiooxalato-Nickelate(II) Complexes[1]

By Nobufumi MAKI, Shigeo KIDA* and Ryutaro TSUCHIDA

(Received October 10, 1958)

There have been no reports on the polarographic reduction of dithiooxalatonickelate(II) complex, although some studies have been reported for tetracyanonickelate(II) complex by several authors[2-8]. For instance, Hume et al.[6] studied the polarographic behavior of the tetracyanonickelate(II) ion and found that the ion, $[Ni(CN)_4]^{2-}$, is irreversibly reduced in one step and the wave corresponds to a two-electron reduction of the ion to metal. They also found that the univalent nickel complex ion, $[Ni_2(CN)_6]^{4-}$, is oxidized, but not reduced polarographically.

Recently, Vlček[7,8] studied the mechanism of the electrochemical reduction of the ion, $[Ni(CN)_4]^{2-}$, in further detail and obtained the following results. The electrochemical reduction of the ion, $[Ni(CN)_4]^{2-}$, proceeds principally by the acceptance of two electrons. The reduction product of the two-electron reduction may be either metallic nickel or a complex of zero-valent nickel, $[Ni(CN)_4]^{4-}$, the latter of which is very unstable in solution and is immediately oxidized to univalent nickel with evolution of hydrogen and simultaneous formation of the deep red ion, $[Ni_2(CN)_6]^{4-}$.

$$2[Ni(CN)_4]^{4-} + 2H_2O = [Ni_2(CN)_6]^{4-} + 2CN^- + 2OH^- + H_2$$

The ion, $[Ni_2(CN)_6]^{4-}$, is also oxidized to $[Ni(CN)_4]^{2-}$, though the rate is very small. The increase of the current in solution with a high concentration of the cyanide ion was explained as being due to the regeneration of bivalent nickel from the product of the electrode reaction.

The present paper deals with the polarography of the tetracyano- and dithiooxalato-nickelate(II) ions. The main purpose of this study is to examine polarographically whether the mixed complex is formed or not in the solution when the two kinds of ion, $[Ni(CN)_4]^{2-}$ and $[Ni(C_2S_2O_2)_2]^{2-}$, were mixed together.

1) Partly presented at the Symposium on Co-ordination Compounds, Tokyo, November 15, 1958.

* Present address: Department of Chemistry, Wakayama University, Masago-cho, Wakayama.

2) N. V. Emelianova, *Rec. trav. chim.*, **44**, 529 (1925).

3) G. Sartori, *Gazz. chim. ital.*, **66**, 688 (1936).

4) J. P. Hochstein, *J. Gen. Chem. U. S. S. R.*, **7**, 2488 (1937).

5) V. Caglioti, G. Sartori and P. Silvestroni, *Atti accad. natl. Lincei, Classe Sci. fis. mat. nat.*, **3**, 448 (1947).

6) D. N. Hume and I. M. Kolthoff, *J. Am. Chem. Soc.*, **72**, 4423 (1950).

7) A. A. Vlček, *Collection Czechoslov. Chem. Communs.*, **22**, 948 (1957).

8) A. A. Vlček, ibid., **22**, 1736 (1957).

Experimental

Apparatus.—A Yanagimoto model 104 polarograph with a sensitivity of galvanometer (2×10^{-9} μA/mm./m.) was used. For the determination of the half-wave potentials, the method previously described was employed[9]. An H-type cell with a saturated calomel electrode was used. The capillary used had a rate of flow of mercury, 0.635 mg./sec., and a drop time of 4.16 sec. in the solution of 1 F potassium chloride at an open circuit with a mercury head of 66.5 cm. The capillary was connected with a mercury reservoir by a tube of polyvinyl chloride. All the measurements were made at 28±0.1°C, the temperature being maintained by a water thermostat. The reversibilities of the electrode reactions were tested by determining the slope of $\log i/(i_d-i)$ vs. potential. Slopes of the log plots indicated irreversible reduction throughout.

Material. — The complex compounds studied were prepared by the following methods.

1. *Tetracyanonickelate(II) complx*, $K_2[Ni(CN_4]\cdot H_2O$. — Pure potassium tetracyanonickelate(II) complex was prepared in the usual way by dissolving freshly precipitated nickel cyanide in potassium cyanide and evaporating the filtered solution. On recrystallization from hot water, an orange crystalline product was obtained.

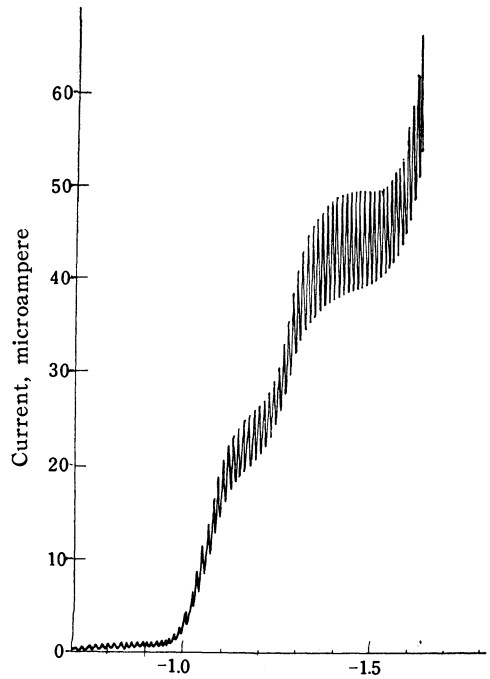
2. *Dithiooxalatonickelate(II) complex*, $K_2[Ni\cdot(C_2S_2O_2)_2]$[10,11]. — Concentrated aqueous solutions of nickel sulfate (2 g. in 10 ml.) and potassium dithiooxalate (2 g. in 4 ml.) were mixed at room temperature; a deep purple solution was at once produced, from which small, almost black crystals separated. The product prepared in this way is contaminated by the remaining simple salt and may be purified by recrystallization from hot water. After dissolving the crystals in water at 40°C, one-half its volume of the saturated solution of potassium nitrate was added to the solution, from which the large iridescent bipyramidal crystals separated again on cooling. The crystals were filtered and washed several times with water and ethanol; then they were transferred to a vacuum desiccator to remove the remaining ethanol.

The complex compounds used were checked for purity by the comparison of the ultraviolet absorption spectra. Each solution for electrolysis was made freshly from the dry crystalline nickelate-(II) complexes before use. The solutions were mainly 0.005 F or 0.01 F with respect to the complex ion studied. In order to remove the dissolved oxygen, a vigorous stream of nitrogen which was purified from oxygen by means of an alkaline solution of pyrogallol was passed through the cell solution for an hour prior to each electrolysis, preventing the evaporation.

In order to examine the formation of the mixed complex, two kinds of solution of the same concentration for each ion were mixed together after the removal of the dissolved oxygen. After mixing, a stream of nitrogen was passed further for about ten minutes. Each polarographic run was completed within ten minutes. The maximum suppressor, Tween-80**, was added to the solution, which was enough to suppress the maxima of both the waves of the ions, $[Ni(CN)_4]^{2-}$ and $[Ni(C_2S_2O_2)_2]^{2-}$. (0.0032% Tween-80). The supporting electrolyte used was 1 F potassium chloride.

Results and Discussion

The dithiooxalatonickelate(II) complex ion, $[Ni(C_2S_2O_2)_2]^{2-}$, is reduced irreversibly in two steps at the dropping mercury electrode in the solution of 1 F potassium chloride, as is shown in Fig. 1. The waves have a maximum at around −1.1 V. (vs. S. C. E.), which could easily be suppressed in the presence of 0.0032% Tween-80. The ratio of the height of the first wave to that of the second is approximately 1 : 1. This ratio is independent



Applied potential, volt vs. S. C. E.

Fig. 1. The polarogram of $[Ni(C_2S_2O_2)]^{2-}$ obtained at the concentration of 0.005 F in the presence of 0.0032% Tween-80. Supporting electrolyte; 1 F KCl. Temp., 28°C. Sensitivity; 0.400 μA/mm., Damping; 200. $E_{1/2}$ of 1st wave = −1.03 V., $E_{1/2}$ of 2nd wave = −1.25 V. vs. S. C. E.

9) N. Maki, Y. Shimura and R. Tsuchida, This Bulletin, **30**, 909 (1957).
10) H. O. Jones and H. S. Tasker, *J. Chem. Soc.*, **95**, 1904 (1909).
11) E. G. Cox, W. Wardlaw and K. C. Webster, ibid., **1935**, 1475 (1935).

** Polyoxyethylene sorbitan mono-oleate (Atlas Powder Co., in U. S. A.).

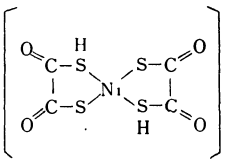
TABLE I. THE HALF-WAVE POTENTIALS AND THE CURRENT VALUES OF THE WAVES OF DITHIOOXALATONICKELATE(II) ION, $[Ni(C_2S_2O_2)_2]^{2-}$

Concn. of the ion (F)	$E_{1/2}$ of the 1st wave (V.)	$E_{1/2}$ of the 2nd wave (V.)	Total height of the waves (μA)
10^{-2}	−1.03	−1.25	80.0
5×10^{-3}	−1.03	−1.25	41.0
10^{-3}	−1.10	−1.31	20·8

1) The data obtained in the presence of 0.0032% Tween-80.
2) Supporting electrolyte; 1 F KCl.
3) Potential unit; V. vs. S. C. E., Temp., 28°C.
4) Characteristics of the capillary used; $m=0.635$ mg./sec., $t=4.16$ sec.

of the concentration of the complex ion. The limiting current for the unit concentration of the ion, i_l/c, becomes greater with the decreasing concentration of the ion. Table I shows the relation between the current value and the concentration. The fact that the heights of the waves of dithiooxalato complex are significantly greater than those of the usual nickel(II) complexes, such as $[Ni(CN)_4]^{2-}$, may well be explained as being due to the following reason. Namely, a part of the dithiooxalato complexes is considered to be present in solution as a form of the complex having protons to the sulfur atom.

For instance;



Hence, at the reduction potential of the complex, the hydrogen ion liberated from the complex is coreduced and contributes to the limiting current of the nickelate(II) complex. In conjunction with this consideration, the fact that the ratio of the height of the first wave to that of the second is always approximately 1:1 supports the idea that the dithiooxalatonickelate(II) complex might perhaps be reduced to the nickel(0) state in two steps. However, it appears desirable to delay further speculation on possible mechanisms of the reduction until more evidence, such as the data in buffer solution, is available. Concerning this point, further study is to be carried out in more detail and to be reported later.

On the other hand, the tetracyanonickelate(II) ion, $[Ni(CN)_4]^{2-}$, is reduced irreversibly in one step at the dropping mercury electrode in 1 F potassium chloride supporting electrolyte. (Fig. 2). The height of the wave is roughly proportional to the concentration of the complex ion. According to the results obtained by Vlček[7,8] and Hume et al.[6], the wave, corresponding to a gain of two electrons, represents the reduction for nickel(II) to nickel(0). In the solution of 1 F potassium chloride the wave of this ion indicated the maximum, which could be suppressed in the presence of 0.0016% Tween-80. In the solution of 0.5 F potassium sulfate it was very difficult to diminish the oxygen waves, which appeared at around −0.55 and −0.85 V. (vs. S. C. E.). Accordingly, the solution of 1 F potassium chloride was used as a supporting electrolyte to examine the formation of the mixed complex.

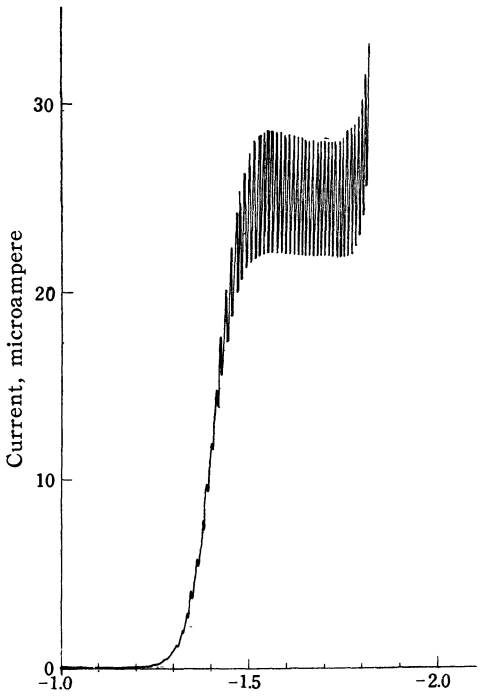
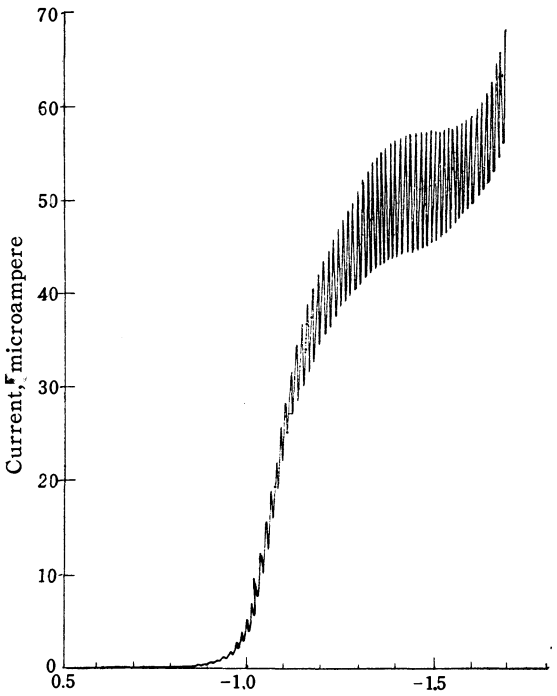


Fig. 2. The polarogram of $[Ni(CN)_4]^{2-}$ obtained in the solution of 1 F KCl at the concentration of 0.005 F in the presence of 0.0016% Tween-80. Sensitivity; 0.200 μA/mm., Damping; 200. $E_{1/2}=-1.38_5$ V. vs. S. C. E. $i_d=25.3$ μA.

In order to confirm the formation of the mixed complex, the solution of tetracyanonickelate(II) ion, $[Ni(CN)_4]^{2-}$, and of dithiooxalatonickelate(II) ion, $[Ni\cdot(C_2S_2O_2)_2]^{2-}$, are mixed together at each concentration of 10^{-2} F in the presence of

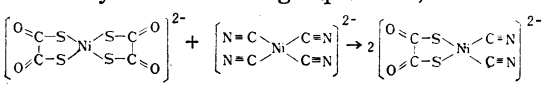
0.0032% Tween-80 after the removal of the dissolved oxygen. The polarogram of the mixed solution was taken within about a quarter of an hour after mixing. If the reaction between the complex ions, $[Ni(CN)_4]^{2-}$ and $[Ni(C_2S_2O_2)_2]^{2-}$, takes place, it is expected that the new reduction wave of the mixed complex ion, $[Ni(C_2S_2O_2)(CN)_2]^{2-}$, is obtained. This is neither the wave of the ion, $[Ni(CN)_4]^{2-}$, nor that of the ion, $[Ni(C_2S_2O_2)_2]^{2-}$. In fact, both the waves of the original ions, $[Ni(CN)_4]^{2-}$ and $[Ni(C_2S_2O_2)_2]^{2-}$, almost disappeared and a new well-defined wave was obtained near the potential between the waves of the original ions. This fact may be regarded as a proof for the formation of the mixed complex ion, $[Ni(C_2S_2O_2)(CN)_2]^{2-}$, in the solution. (Fig. 3).



Applied potential, volt vs. S. C. E.

Fig. 3. The polarogram of the mixture of $[Ni(CN)_4]^{2-}$ and of $[Ni(C_2S_2O_2)_2]^{2-}$ at the equal concentration of 0.01 F for each complex ion obtained in the presence of 0.0032% Tween 80. The supporting electrolyte; 1 F KCl. $E_{1/2}$ of the wave $=-1.06$ V. vs. S. C. E. $i=47.6$ μA. Sensitivity; 0.400 μA/mm., Damping; 200.

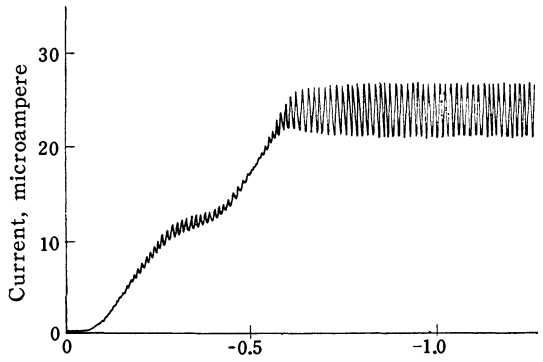
It is considered that the reaction proceeds by the following equation;



The reaction was so fast that the progress of the reaction could not be detected nor traced by the classical polarographic method. The results obtained here are also supported by those of the spectrochemical study obtained by Kida[12].

The mixed complex ion, $[Ni(C_2S_2O_2)\cdot(CN)_2]^{2-}$, gives the irreversible wave of one step in the presence of 0.0032% Tween-80 in the solution of 1 F potassium chloride. The current is roughly proportional to the square root of the height of the mercury column. The straight line plot, however, does not pass through the origin but gives a negative intercept on the current axis. The height of the wave was not proportional to the concentration of the original ions. The half-wave potential of the wave shifts to the positive direction of potential with the decreasing concentration of the original ions.

For the same purpose as in the case of the dithiooxalatodicyanonickelate(II) complex, the polarogram of the mixed solution of the ions, $[Cu\ en_2^{***}]^{2+}$ and $[Cu\ ox_2^{***}]^{2-}$, was taken at equal concentration of both



Applied potential, volt vs. S. C. E.

Fig. 4. The polarogram of the mixed solution of $[Cu\ ox_2]^{2-}$ and $[Cu\ en_2]^{2+}$ obtained in the presence of 0.0032% Tween-80. The supporting electrolyte used is 0.5 F $NaClO_4$. The mixed solution was prepared by mixing the solution of the same amount of $[Cu\ ox_2]^{2-}$ and of $[Cu\ en_2]^{2+}$ at each concentration of 0.005 F at 25°C. The half-wave potentials of both the waves were quite the same as those of the original ions, $[Cu\ ox_2]^{2-}$ and $[Cu\ en_2]^{2+}$.
$E_{1/2}$ of $[Cu\ ox_2]^{2-}=-0.14_5$ V. vs. S.C.E.
$E_{1/2}$ of $[Cu\ en_2]^{2+}=-0.49$ V. vs. S.C.E.
While the height of the wave becomes one half, since one is diluted to double by another.

12) S. Kida, This Bulletin, **29**, 805 (1956).
*** The following abbreviation was used; en=ethylenediamine, ox=oxalate.

the ions in the presence of 0.0032% Tween-80. (Fig. 4). In this case, however, the reduction waves obtained were only those of the original ions, $[Cu\,en_2]^{2+}$ and $[Cu\,ox_2]^{2-}$, and the wave of the mixed complex, [Cu en ox], could not be found, though the presence of this was verified by Kida[12] and DeWitt et al.[13] Namely, the percentage of the mixed complex formed in the solution is calculated to be 64%**** when equal amounts of both the ions, $[Cu\,en_2]^{2+}$ and $[Cu\,ox_2]^{2-}$, were mixed together at room temperature. This fact is explained as being due to the presence of the fast equilibrium among these complexes, $[Cu\,en_2]^{2+}$, $[Cu\,ox_2]^{2-}$ and [Cu en ox]. In other words, at the reduction potential of the ions, $[Cu\,en_2]^{2+}$ and $[Cu\,ox_2]^{2-}$, the equilibrium shifts very fast to the direction for supplying these ions. Further, in the equilibrium of the system,

$$[Ni(C_2S_2O_2)_2]^{2-} + [Ni(CN)_4]^{2-} \rightleftarrows 2\,[Ni(C_2S_2O_2)(CN)_2]^{2-}$$

its rate is very small. Consequently, the reduction wave of the mixed complex can be found. This fact suggests that the coordinating bond of these complexes has a considerable covalent character, in spite of the fact that the exchange reaction of tetracyanonickelate(II) ion with radioactive cyanide in solution is very fast[14].

13) R. DeWitt and J. Watters, *J. Am. Chem. Soc.*, **76**, 3810 (1954).
14) F. A. Long, ibid., **73**, 537 (1951).
**** The influence of temperature on the percentage is considered to be small.

Summary

1. It was verified polarographically that the reaction between the ions, $[Ni(CN)_4]^{2-}$ and $[Ni(C_2S_2O_2)_2]^{2-}$, takes place and the mixed complex ion, $[Ni(C_2S_2O_2)(CN)_2]^{2-}$, is formed in solution. The rate of the reaction was so great that the progress of the reaction could not be traced by the usual polarographic method. Meanwhile the wave of the oxalato-ethylenediamine copper(II) complex, [Cu en ox], the presence of which in solution had been verified spectrophotometrically, was not detected polarographically. That is to say, the polarographic method can be applied to detect the formation of the mixed complex, the coordinating bonds of which have a considerable covalent character, such as $[Ni(C_2S_2O_2)(CN)_2]^{2-}$, but can not be applied to detect the mixed complex having ionic bonds.

2. The ion, $[Ni(C_2S_2O_2)_2]^{2-}$, is reduced irreversibly in two steps at the dropping mercury electrode in the presence of 0.0032% Tween-80, when 1 F potassium chloride solution was used as a supporting electrolyte. The heights of the two waves are not proportional to the concentration of the ion. The height of the wave for the unit concentration of the ion increases with the decreasing concentration of the ion.

Department of Chemistry
Faculty of Science
Osaka University
Kita-ku, Osaka

The Kinetics of the Complex-forming Reaction between Nickel(II) and Ethylenediaminetetraacetate

By Nobuyuki TANAKA and Yasuhiko SAKUMA*

(Received December 8, 1958)

Although there are a number of papers concerning the inorganic reactions involving metal complexes, few of them deal with the kinetics of the complex-forming reactions between metal ions and organic ligands. Several investigations in which the dissociation reactions, the substitution reactions or the exchange reactions involving metal-ethylenediaminetetraacetate complexes were dealt with have given some information of the complex-forming reactions between the metal and ethylenediaminetetraacetate (EDTA)[1-5]. Those reactions, which are reactions of copper(II)[3], cadmium II)[2], lead(II)[5], nickel (II)[4], and iron(II)[1] with EDTA, proceed so rapidly that the direct measurement of the concentration-time relation by the conventional techniques seems to be difficult.

Recently, a rotated dropping mercury electrode (RDME) has been developed, which has a current sensitivity some ten times as great as that of the conventional dropping mercury electrode[6-12]. In this investigation, the rate of the complex-forming reaction between nickel(II) and EDTA was followed by measuring the limiting current of nickel(II) at the RDME. The mechanisms of the reaction and the rate constant for each reaction path are presented in this paper.

* Present address, Research Laboratory, Mitsubishi Rayon Co., Ltd., Otake, Hiroshima Prefecture.

1) S. Jones and F. A. Long, *J. Phys. Chem.*, **56**, 25 (1952).
2) N. Tanaka, R. Tamamushi and M. Kodama, *Z. physik. Chem. (Frankfurt)*, **14**, 141 (1958).
3) N. Tanaka, K. Kato and R. Tamamushi, This Bulletin, **31**, 283 (1958).
4) C. M. Cook, Jr. and F. A. Long, *J. Am. Chem. Soc.*, **80**, 33 (1958).
5) N. Tanaka and K. Kato, unpublished.
6) W. Stricks and I. M. Kolthoff, *J. Am. Chem. Soc.*, **78**, 2085 (1956).
7) N. Tanaka, *J. Japan. Chem. (Kagaku no Ryoiki)*, **10**, 814 (1956).
8) N. Tanaka and T. Koizumi, This Bulletin, **30**, 303 (1957).
9) Y. Okinaka and I. M. Kolthoff, *J. Am. Chem. Soc.*, **79**, 3326 (1957).
10) I. M. Kolthoff and Y. Okinaka, *Anal. Chim. Acta*, **18**, 83 (1958).
11) N. Tanaka, T. Koizumi, T. Murayama, M. Kodama and Y. Sakuma, ibid., **18**, 97 (1958).
12) I. M. Kolthoff, Y. Okinaka and T. Fujinaga, ibid., **18**, 295 (1958).

Theoretical

Let us consider a complex-forming reaction of nickel(II) with ethylenediaminetetraacetate (EDTA) in sodium acetate-acetic acid buffers which contain 0.1 M acetate. At pH of the acetate buffer, EDTA exists mainly in the form of H_2Y^{2-} and partly in the forms of H_3Y^- and HY^{3-}, where Y^{4-} denotes the completely dissociated EDTA anion. These species are in equilibrium given in Eqs. 1 and 2.

$$H_3Y^- \rightleftarrows H_2Y^{2-} + H^+ \quad (1)$$

$$H_2Y^{2-} \rightleftarrows HY^{3-} + H^+ \quad (2)$$

Nickel(II) forms acetato complexes in a solution containing acetate ions. It has been found that the monoacetatonickel(II) ion is a predominant species of acetato complexes unless the concentration of acetate exceeds 0.2 M[13]. The monoacetatonickel(II) and the hydrated nickel ions are in equilibrium according to the equation,

$$Ni^{2+} + OAc^- \rightleftarrows NiOAc^+ \quad (3)$$

The reaction between nickel(II) and EDTA may proceed through various reaction paths. Among three ionic species of EDTA mentioned above, H_3Y^- is considered to be the least favorable to react with nickel(II). The rate of the reaction between nickel(II) and H_3Y^- seems to be much smaller than those between nickel (II) and other ionic species of EDTA. From these considerations, the following reaction paths are assumed:

$$Ni^{2+} + HY^{3-} \xrightarrow{k_{1a}} NiHY^- \quad (4)$$
$$NiHY^- \rightleftarrows NiY^{2-} + H^+$$

$$Ni^{2+} + H_2Y^{2-} \xrightarrow{k_{2a}} NiH_2Y \quad (5)$$
$$NiH_2Y \rightleftarrows NiHY^- + H^+ \rightleftarrows NiY^{2-} + 2H^+$$

$$NiOAc^+ + HY^{3-} \xrightarrow{k_{1b}} NiHY^- + OAc^- \quad (6)$$
$$NiHY^- \rightleftarrows NiY^{2-} + H^+$$

13) N. Tanaka and K. Kato, This Bulletin, **32**, 516 (1959).

$$NiOAc^+ + H_2Y^{2-} \xrightarrow{k_{2b}} NiH_2Y + OAc^- \quad (7)$$
$$NiH_2Y \rightleftarrows NiHY^- + H^+ \rightleftarrows NiY^{2-} + 2H^+$$

From reactions 4 and 5, the rate of the decrease of $[Ni^{2+}]$ is expressed as,

$$-\frac{d[Ni^{2+}]}{dt} = k_{1a}[Ni^{2+}][HY^{3-}] + k_{2a}[Ni^{2+}][H_2Y^{2-}]$$
$$= \left\{k_{1a}\frac{K_{H_2Y}}{[H^+]} + k_{2a}\right\}[Ni^{2+}][H_2Y^{2-}] \quad (8)$$

where K_{H_2Y} represents the dissociation constant of H_2Y^{2-} ($= [HY^{3-}][H^+]/[H_2Y^{2-}]$). From reactions 6 and 7 the rate of the decrease of $[NiOAc^+]$ is expressed as,

$$-\frac{d[NiOAc^+]}{dt} = k_{1b}[NiOAc^+][HY^{3-}] + k_{2b}[NiOAc^+][H_2Y^{2-}]$$
$$= \left\{k_{1b}\frac{K_{H_2Y}}{[H^+]} + k_{2b}\right\}[NiOAc^+][H_2Y^{2-}] \quad (9)$$

The quantity of nickel(II) that is determined polarographically in acetate buffer is not the quantity of the hydrated nickel(II) ion, but the sum of those of the monoacetato- and the hydrated nickel ions[13]. If the sum is denoted by $[Ni^{2+}]_{app.}$,

$$[Ni^{2+}]_{app.} = [Ni^{2+}] + [NiOAc^+] \quad (10)$$

Therefore, the rate of the decrease of nickel(II) that is followed by the polarographic method is given as,

$$-\frac{d[Ni^{2+}]_{app.}}{dt} = -\frac{d\{[Ni^{2+}] + [NiOAc^+]\}}{dt}$$
$$= -\left\{\frac{d[Ni^{2+}]}{dt} + \frac{d[NiOAc^+]}{dt}\right\} \quad (11)$$

As for the EDTA present in the acetate buffer, the total concentratration of uncomplexed EDTA, $[EDTA]_f$, is represented by

$$[EDTA]_f = [HY^{3-}] + [H_2Y^{2-}] + [H_3Y^-] \quad (12)$$

From Eq. 12, $[H_2Y^{2-}]$ is given as

$$[H_2Y^{2-}] = \frac{[EDTA]_f}{\frac{[H^+]}{K_{H_3Y}} + 1 + \frac{K_{H_2Y}}{[H^+]}} \quad (13)$$

where K_{H_3Y} is the dissociation constant of H_3Y^- ($= [H_2Y^{2-}][H^+]/[H_3Y^-]$). The concentration of $NiOAc^+$ is written with the formation constant (K_{NiOAc}) and the concentrations of Ni^{2+} and OAc^-,

$$[NiOAc^+] = K_{NiOAc}[Ni^{2+}][OAc^-] \quad (14)$$

Introducing Eq. 14 into Eq. 10, $[Ni^{2+}]$ is given by

$$[Ni^{2+}] = \frac{[Ni^{2+}]_{app.}}{1 + K_{NiOAc}[OAc^-]} \quad (15)$$

Introducing Eqs. 8 and 9 into Eq. 11 and substituting Eq. 14 for $[NiOAc^+]$, we obtain

$$-\frac{d[Ni^{2+}]_{app.}}{dt} = \left[\left\{k_{1a}\frac{K_{H_2Y}}{[H^+]} + k_{2a}\right\} + \left\{k_{1b}\frac{K_{H_2Y}}{[H^+]} + k_{2b}\right\}K_{NiOAc}[OAc^-]\right][Ni^{2+}][H_2Y^{2-}] \quad (16)$$

Replacing $[H_2Y^{2-}]$ and $[Ni^{2+}]$ by the expressions given in Eqs. 13 and 15, respectively, and rearranging the resulted equation, Eq. 17 is obtained. Eq. 17 represents the overall rate expression for the complex-forming reaction between nickel(II) and EDTA whose reaction mechanisms are given by Eqs. 4 to 7. If $[H^+]$ and $[OAc^-]$ are not varied while the reaction proceeds, Eq. 17 can be written as

$$-\frac{d[Ni^{2+}]_{app.}}{dt} = k_{app.}[Ni^{2+}]_{app.}[EDTA]_f \quad (18)$$

where $k_{app.}$ means an apparent rate constant and corresponds to Eq. 19. The magnitude of $k_{app.}$ is dependent on both pH and the acetate concentration of the solution.

Experimental

Reagents.—A stock solution of disodium ethylenediaminetetraacetate was prepared by dissolving the commercial guaranteed reagent, and

$$-\frac{d[Ni^{2+}]_{app.}}{dt} = \frac{\{k_{1a} + k_{1b}K_{NiOAc}[OAc^-]\}\frac{K_{H_2Y}}{[H^+]} + \{k_{2a} + k_{2b}K_{NiOAc}[OAc^-]\}}{\{1 + K_{NiOAc}[OAc^-]\}\left\{\frac{[H^+]}{K_{H_3Y}} + 1 + \frac{K_{H_2Y}}{[H^+]}\right\}}[Ni^{2+}]_{app.}[EDTA]_f \quad (17)$$

$$k_{app.} = \frac{\{k_{1a} + k_{1b}K_{NiOAc}[OAc^-]\}\frac{K_{H_2Y}}{[H^+]} + \{k_{2a} + k_{2b}K_{NiOAc}[OAc^-]\}}{\{1 + K_{NiOAc}[OAc^-]\}\left\{\frac{[H^+]}{K_{H_3Y}} + 1 + \frac{K_{H_2Y}}{[H^+]}\right\}} \quad (19)$$

standardized against the standard copper(II) solution by amperometric titration using a dropping mercury electrode as an indicator electrode[14]. The copper(II) solution was prepared by dissolving recrystallized copper(II) sulfate, and its concentration was determined by electrogravimetry at constant potential by means of a Yanagimoto automatic potentiostat. The standard solution of nickel nitrate was obtained in the following way[15]. The alcoholic solution of dimethylglyoxime was added to the dilute solution of guaranteed nickel(II) nitrate. The precipitates were filtered and dissolved in guaranteed nitric acid. The nickel(II) solution obtained was made ammoniacal and subjected to the electrolysis. The nickel metal deposited was weighed accurately, dissolved in guaranteed nitric acid and diluted to the desired concentration with redistilled water. The concentration of nickel(II) of the solution was determined with the standard EDTA solution by amperometric trtration[16]. The concentration obtained was in good agreement with that determined by electrogravimetry.

Acetic acid-sodium acetate buffers were prepared with guaranteed sodium carbonate and acetic acid. Polyoxyethylene lauryl ether (LEO) with a mean molecular weight of 862 was used for a maximum suppressor. Other chemicals used were of guaranteed reagent grade.

Apparatus and Procedure.—The rate of the reaction between nickel(II) and EDTA was followed by measuring the change of the polarographic diffusion current of the nickel(II) with time. The current-time curves were recorded with a Yanagimoto Model PB-4 pen-recording polarograph using a rotated dropping mercury electrode (RDME)[6-12].

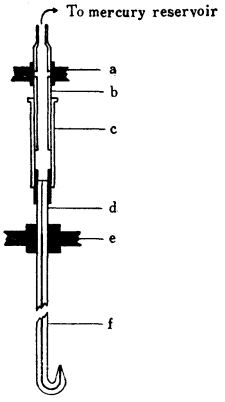


Fig. 1. Assembly of the RDME: a, fixed holder; b and c, inner and outer tubes of a 2 ml. syringe; d, capillary; e, holder of rotating apparatus; f, end tube.

14) N. Tanaka, M. Kodama, M. Sasaki and M. Sugino, *Japan Analyst* (*Bunseki Kagaku*), **6**, 86 (1957).
15) F. P. Treadwell and W. T. Hall, "Analytical Chemistry", Vol. 2, 9th ed., John Wiley and Sons, Inc., New York (1952), p. 193.
16) R. Přibil and B. Matyska, *Collection Czechoslov. Chem. Communs.*, **16**, 139 (1951).

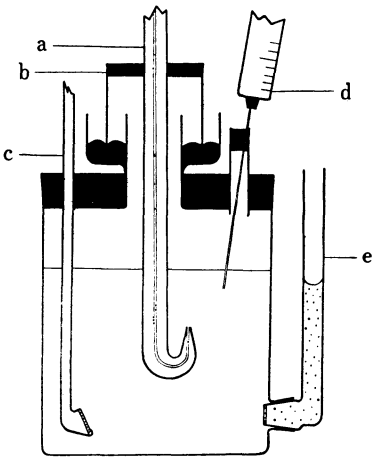


Fig. 2. Electrolysis cell: a, RDME; b, mercury seal; c, N_2 gas disperser; d, syringe; e, KNO_3-agar bridge.

In Fig. 1 is shown the RDME used in this study, which was similar to that reported by Okinaka and Kolthoft[9], being driven by means of a synchronous motor (Type A, provided with gears for speeds of 100, 150, 200 and 300 r.p.m., constructed by Yanagimoto Co., Ltd.). The electrode had an m value of 25.43 mg./sec. and a drop time of 2.95 sec. at 100 r.p.m., being measured at −0.60 volt vs. S.C.E. in air-free 0.2 M potassium nitrate solution containing 5×10^{-6} M LEO at 51.2 cm. of mercury head at 25°C.

The electrolysis cell in which the reaction took place was of a beaker-type of 100 ml. capacity as shown in Fig. 2. The cell was connected to a saturated calomel electrode through a potassium nitrate agar bridge. Special precautions were taken against the intrusion of atmospheric oxygen into the electrolysis cell during the measurement. A mercury seal was attached for this purpose. (See Fig. 2). The nitrogen gas was introduced into the solution through a gas disperser before and also during the measurement. The current measurement with the RDME was not disturbed by bubbling the gas through the solution. The rate of the flow of nitrogen gas was kept constant, being controlled by means of a flow-meter. The fluctuation of the residual current due to the change of the oxygen concentration was controlled within 0.05 microampere.

All kinetic measurements were made in acetate buffers of pH 3.8 to 5.2 at 0°C. The acetate concentrations were varied from 0.02 M to 0.1 M. The ionic strength was adjusted to be 0.2 with potassium nitrate. LEO was added as a maximum suppressor by 5×10^{-6} M in concentration. The pH of the solution was measured with a Hitachi Model EHP-1 pH meter, immediately after the measurements of current-time curves, within the accuracy of 0.02 pH unit.

The reaction was initiated by adding the air-free solution of the equivalent EDTA into the deaerated nickel(II) solution in the electrolysis

cell with the aid of a calibrated 1 ml. syringe. Since the RDME was driven and the nitrogen gas was bubbled throughout the measurement, reproducible current-time curves were able to be obtained immediately after the injection of the EDTA solution.

Results

A typical polarogram of nickel(II) which was obtained with 2×10^{-4} M Ni(II) in acetate buffer of pH 4.6 with the RDME is shown in Fig. 3. Although the limiting current plateau of the polarogram is not well-defined, the proportionality was found between the concentration of nickel(II) and the current that was measured at −1.35 V. vs. S.C.E. and corrected for the residual current, unless the concentration of nickel(II) exceeded 5×10^{-4} M. Therefore, current-time curves of the reaction mixtures were recorded at this potential. Typical examples of the current-time curves are reproduced in Fig. 4. Those curves were recorded at varied pH's with reaction mixtures in which the initial concentrations of nickel(II) and EDTA were each 1.00×10^{-4} M and the concentration of acetate was 0.1 M. It is expected from Eq. 18 that a plot of the reciprocal of $[Ni^{2+}]_{app.}$ against time gives a straight line with a slope of k_{app}. Some of the plots are given in Fig. 5, from which the values of $k_{app.}$ were determined.

The current-time curves were obtained

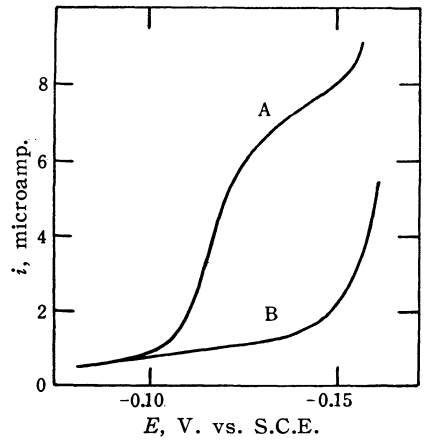


Fig. 3. Current-voltage curves of 2×10^{-4} M Ni(II) (curve A) and Ni(II)-EDTA (curve B) obtained at 0°C in acetate buffer-potassium nitrate solution of pH 4.6 and ionic strength 0.2 containing 0.1 M acetate and 5×10^{-6} M LEO.

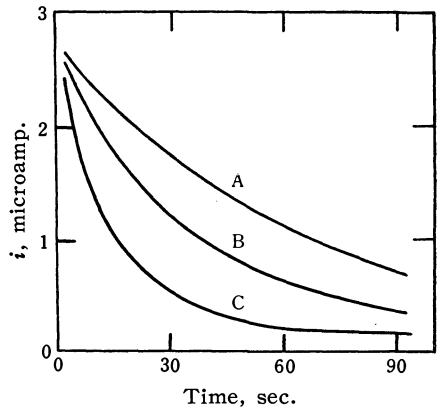


Fig. 4. Limiting current-time relation of the reaction between nickel(II) and EDTA, measured at −1.35 V. vs. S.C.E. at 0°C in acetate buffer-potassium nitrate solution of ionic strength 0.2 containing 0.1 M acetate and 5×10^{-6} M LEO, at pH 3.9 (curve A), pH 4.4 (curve B) and pH 5.0 (curve C). Initial concentrations of nickel(II) and EDTA are each 1.00×10^{-4} M.

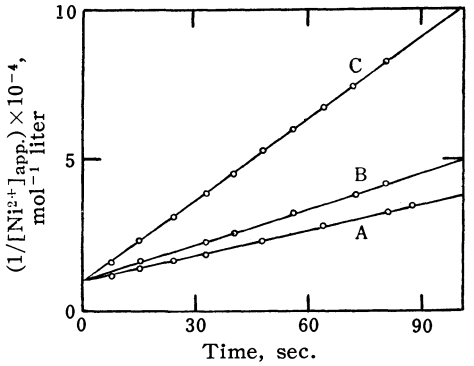


Fig. 5. Relation between the reciprocal nickel concentration and the time. Plots A, B and C are obtained from curves A, B and C in Fig. 4, respectively.

TABLE I. TYPICAL EXAMPLES OF THE RATE MEASUREMENT*

pH(0°C)	$[H^+]\times10^4$, mol./l.	$\frac{[H^+]}{K_{H_3Y}}$	$\frac{K_{H_2Y}}{[H^+]}$	$k_{app.}\times10^{-2}$, $(mol./l.)^{-1}$ sec^{-1}
4.03	1.197	0.06	0.00	3.02
4.09	1.044	0.05	0.00	3.18
4.14	0.928	0.04	0.01	3.26
4.55	0.361	0.02	0.01	4.54
4.72	0.244	0.01	0.02	5.43
4.94	0.148	0.01	0.03	6.70
5.01	0.125	0.01	0.04	7.60
5.16	0.089	0.00	0.06	10.0_0
5.21	0.079	0.00	0.07	10.3_3
5.26	0.071	0.00	0.08	11.2_5

* The solutions contain 0.05 M acetate. The initial concentrations of nickel(II) and EDTA are each 1.00×10^{-4} M.

at varied pH's in the range of pH 3.8 to 5.2 and at three different concentrations of acetate. It was found that the analysis of the current-time curves which were obtained with different initial concentrations of the reactants but at the same pH and acetate concentration gave the same $k_{app.}$ This fact confirmed that the reaction in question is of second order.

The magnitudes of $k_{app.}$ were determined at varied pH's and at three different concentrations of acetate. Examples of the experimental results which were obtained at 0.05 M acetate are given in Tabele I. From Eq. 19,

$$\alpha\beta k_{app.} = \{k_{1a} + k_{1b}K_{NiOAc}[OAc^-]\}\frac{K_{H_2Y}}{[H^+]} + \{k_{2a} + k_{2b}K_{NiOAc}[OAc^-]\}$$
$$= k_1\frac{K_{H_2Y}}{[H^+]} + k_2 \qquad (20)$$
$$\alpha = \frac{[H^+]}{K_{H_3Y}} + 1 + \frac{K_{H_2Y}}{[H^+]}$$
$$\beta = 1 + K_{NiOAc}[OAc^-]$$
$$k_1 = k_{1a} + k_{1b}K_{NiOAc}[OAc^-]$$
$$k_2 = k_{2a} + k_{2b}K_{NiOAc}[OAc^-]$$

are obtained. Eq. 20 indicates that a plot of the values of $\alpha\beta k_{app.}$ against the reciprocal of the hydrogen ion concentration should give a straight line, if $k_{app.}$'s were determined at the same concentration of acetate. The plots with the observed values of $k_{app.}$ gave the straight lines as shown in Fig. 6. The slope gave the value of $k_1K_{H_2Y}$ in Eq. 20 and the intercept at $1/[H^+]=0$, that of k_2. The relation between $\alpha\beta k_{app.}$ and the reciprocal of the hydrogen ion concentration was also treated by the method of least squares. The mean values and the probable errors of k_1 and k_2 were calculated as given in Table II.

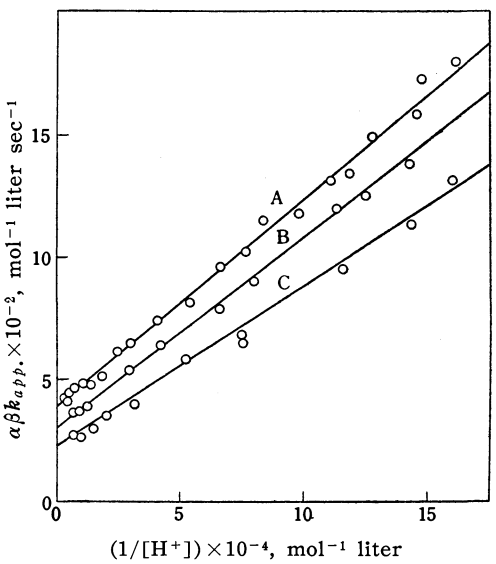


Fig. 6. Relations between $\alpha\beta k_{app.}$ and $1/[H^+]$ obtained at 0°C in acetate buffer-potassium nitrate solution of ionic strength 0.2 at acetate concentrations 0.10 M (curve A), 0.05 M (curve B) and 0.02 M (curve C).

TABLE II. OBSERVED VALUES OF k_1 AND k_2

Concn. of acetate, M	$k_1\times10^{-4}$, mol^{-1} liter sec^{-1}	$k_2\times10^{-2}$, mol^{-1} liter sec^{-1}
0.10	$1.73\pm0.01_6$	$3.89\pm0.06_7$
0.05	$1.41\pm0.01_8$	$2.95\pm0.15_3$
0.02	$1.18\pm0.00_9$	$2.42\pm0.07_6$

The hydrogen ion concentration used in this calculation was derived from the pH observed and the activity coefficient of the hydrogen ion. The pH of the solution was measured at 25°C and corrected for temperature to be reduced to the value at 0°C. The activity coefficient of the hydrogen ion was calculated to be 0.78 at 0°C and ionic strength 0.2 according to Kielland[17]. The third dissociation constant of EDTA, K_{H_2Y}, which was determined by Schwarzenbach and Ackermann[18] at 20°C and $\mu=0.1$, was used after correction for ionic strength and temperature. The ion size parameters of H_2Y^{2-} and HY^{3-} were assumed to be the same as that of suberic acid given by Kielland[17]. The temperature correction for K_{H_2Y} was made with the aid of the ΔH value reported by Carini and Martell[19]. The resulted value of K_{H_2Y} was $10^{-6.27}$. On the other hand, there has been no publication concerning the temperature coefficient of K_{H_3Y}. In this calculation, therefore, the value of $10^{-2.67}$, which was obtained by Schwarzenbach and Ackermann[18] at 20°C and $\mu=0.1$, was used without further correction. Since this constant is concerned only with the calculation of α, in which the contribution of the term $[H^+]/K_{H_3Y}$ does not exceed 10% under the present condition, the use of K_{H_3Y} without correction seems to introduce no significant error into the calculation of the rate constant.

17) J. Kielland, *J. Am. Chem. Soc.*, **59**, 1675 (1937).
18) G. Schwarzenbach and H. Ackermann, *Helv. Chim. Acta*, **30**, 1798 (1947).
19) F. F. Carini and A. E. Martell, *J. Am. Chem. Soc.*, **75**, 4810 (1953).

The formation constant of the monoacetatonickel(II) complex, K_{NiOAc}, was determined to be 3.0 at 0°C, by extrapolating the values obtained at 15°, 25° and 35°C in the solution of ionic strength 0.2[13].

From k_1 and k_2 in Table II, the values of k_{1a}, k_{1b}, k_{2a} and k_{2b} were calculated as given in Table III.

TABLE III. RATE CONSTANTS OF VARIOUS NICKEL(II)-EDTA REACTIONS

Reaction	Rate constant, mol^{-1} liter sec^{-1}
$Ni^{2+}+HY^{3-} \xrightarrow{k_{1a}} NiHY^-$	$1.0_6\times10^4$
$NiOAc^+ + HY^{3-} \xrightarrow{k_{1b}} NiHY^- + OAc^-$	$2.2_5\times10^4$
$Ni^{2+}+H_2Y^{2-} \xrightarrow{k_{2a}} NiH_2Y$	$2.0_4\times10^2$
$NiOAc^+ + H_2Y^{2-} \xrightarrow{k_{2b}} NiH_2Y + OAc^-$	$6.0_4\times10^2$

Discussion

The complex-forming reaction of nickel with ethylenediaminetetraacetate was found to proceed through four different reaction paths given in Eqs. 4 to 7 in acetate buffers of pH 3.8 to 5.2. The rate constants of those four elementary reactions were determined. It seems reasonable that the reactions involving HY^{3-} species are much faster than those involving H_2Y^{2-}.

On the other hand, the effect of acetate ions on the reaction rate was rather unexpected. The previous studies on the displacement reactions involving metal-EDTA complexes indicated that the reaction rate decreased with increasing concentration of acetate[20,21]. The rate of the complex-forming reaction between nickel (II) and EDTA, however, was found to decrease with decreasing concentration of acetate. The rate constants of the reactions involving the monoacetatonickel(II) ions were nearly twice as great as those of the corresponding reactions involving the hydrated nickel ions. A similar phenomenon was reported by Wilkins[22], who studied the exchange reaction involving the nickel(II)-2,3-diamino-2,3-dimethylbutane complex and observed the faster reaction rate in the presence of ammonium acetate. Although the effect of acetate on the nickel-EDTA reaction is not completely solved at the present moment, it may not be unreasonable to consider the decrease of the activation energy of the reaction as being due to the acetate co-ordinated.

It seems interesting to compare the rate constants obtained in this study with those obtained by Cook and Long[4]. They studied the exchange reaction between nickel(II) and nickel(II)-EDTA complexes with the aid of the radioactive isotope at 25°C and ionic strength 0.1, and determined the rate constants of several reaction paths including the following:

$$NiY^{2-} + H^+ \rightleftarrows Ni^{2+} + HY^{3-} \quad (21)$$

$$NiHY^- + H^+ \rightleftarrows Ni^{2+} + H_2Y^{2-} \quad (22)$$

The reactions given by Eqs. 21 and 22 correspond to the reverse of those given by Eqs. 4 and 5, respectively. The equilibrium constants of reactions 21 and 22,

$$K(\text{Eq. 21}) = [Ni^{2+}][HY^{3-}]/[NiY^{2-}][H^+] = 1/K_{NiY}K_{HY}$$

$$K(\text{Eq. 22}) = [Ni^{2+}][H_2Y^{2-}]/[NiHY^-][H^+] = 1/K_{NiY}K^{H}_{NiHY}K_{HY}K_{H_2Y}$$

were calculated, where K_{NiY} represents the formation constant of NiY^{2-}, K_{HY} and K_{H_2Y} the dissociation constants of HY^{3-} and H_2Y^{2-}, respectively, and K^{H}_{NiHY} the equilibrium constant of the reaction,

$$NiY^{2-} + H^+ \rightleftarrows NiHY^-$$

The values of K_{HY}, K_{H_2Y}, K_{NiY} and K^{H}_{NiHY} which were determined by Schwarzenbach and his co-workers[18,23] at 20°C and $\mu=0.1$ were used without further correction. With the equilibrium constants obtained and the rate constants given by Cook and Long, the rate constants for the reverse reactions of Eqs. 21 and 22 were calculated and compared with k_{1a} and k_{2a} as shown in Table IV.

Unfortunately, Cook and Long did not take into account the effect of the acetate

TABLE IV. COMPARISON OF THE RATE CONSTANTS

Reaction	Rate constant, mol^{-1} liter sec^{-1}: Calculated from data at 25°C given by Cook and Long[4]	Observed at 0°C in this study
$Ni^{2+}+HY^{3-} \longrightarrow NiHY^-$	3.0×10^5	$1.0_6\times10^4$
$Ni^{2+}+H_2Y^{2-} \longrightarrow NiH_2Y$	8.1×10^2	$2.0_4\times10^2$

20) H. Ackermann and G. Schwarzenbach, *Helv. Chim. Acta*, **35**, 485 (1952).
21) N. Tanaka and K. Kato, unpublished.
22) R. G. Wilkins, *J. Chem. Soc.*, **1957**, 4521.
23) G. Schwarzenbach, R. Gut and G. Anderegg, *Helv. Chim. Acta*, **37**, 937 (1954).

on the reaction mechanisms and gave no information of the concentration of acetate present in their reaction mixtures. Therefore, the rate constants given by those authors do not exactly correspond to those given in this study. Nevertheless, it may be concluded that the results obtained in both investigations are in reasonable agreement.

Bjerrum and Poulsen[24] studied the kinetics of the formation of nickel(II) and copper(II) complexes of ethylenediamine in methanol at 0°C. They found that copper(II) complexes are more labile than the corresonding nickel(II) compounds. The rate constants of the formation of $Ni(en)^{2+}$ was 2.5×10^{4} mol^{-1} liter sec^{-1} and that of $Cu(en)^{2+}$, 5×10^{11} mol^{-1} liter sec^{-1}, where en denotes ethylenediamine.

Recent studies[3,5] in this laboratory revealed that the rate constants of the formation of copper(II) and lead(II) complexes of EDTA through the reaction

$$M^{2+}+HY^{3-} \rightleftarrows MY^{2-}+H^{+}$$
$$(M=Cu \text{ or } Pb)$$

range from 10^{9} to 10^{11} mol^{-1} liter sec^{-1} at room temperature. The slower rate of the formation of nickel(II)-EDTA complexes is apparent as in the case of the formation of nickel-ethylenediamine complexes.

Summary

The complex-forming reaction of nickel (II) with ethylenediaminetetraacetate (EDTA) was found to proceed in acetate buffers of pH 3.8 to 5.2 through four different reaction paths,

$$Ni^{2+}+HY^{3-} \xrightarrow{k_{1a}} NiHY^{-}$$
$$NiOAc^{+}+HY^{3-} \xrightarrow{k_{1b}} NiHY^{-}+OAc^{-}$$
$$NiHY^{-} \rightleftarrows NiY^{2-}+H^{+}$$
$$Ni^{2+}+H_2Y^{2-} \xrightarrow{k_{2a}} NiH_2Y$$
$$NiOAc^{+}+H_2Y^{2-} \xrightarrow{k_{2b}} NiH_2Y+OAc^{-}$$
$$NiH_2Y \rightleftarrows NiHY^{-}+H^{+} \rightleftarrows NiY^{2-}+2H^{+}$$

The change in the polarographic diffusion current of nickel(II) at the rotated dropping mercury electrode was utilized to follow the decrease of the nickel(II) concentration in the reaction mixture after the initiation of the reaction. The rate constants of the reaction paths were determined at 0°C and ionic strength 0.2, with the results:

$k_{1a}=1.0_6\times10^{4}$ mol^{-1} liter sec^{-1}
$k_{1b}=2.2_5\times10^{4}$ 〃
$k_{2a}=2.0_4\times10^{2}$ 〃
$k_{2b}=6.0_4\times10^{2}$ 〃

These constants are much smaller than those of the corresponding reactions between copper(II) and EDTA.

The authors thank the Ministry of Education for the financial support granted for this research.

Department of Chemistry
Faculty of Science
Tohoku University
Katahira-cho, Sendai

24) F. Basolo and R. G. Pearson, "Mechanisms of Inorganic Reactions", John Wiley & Sons, Inc., New York (1958), p. 204.

*Cation Arrangement in Lithium Ferrospinel-Lithium Aluminospinel Solid Solution**

By Eizo KATO**

(Received September 25, 1958)

A cation arrangement in a spinel structure shows how some cations of different valencies are distributed at tetrahedral interstices of the 8-fold position or octahedral ones of the 16-fold position in a spinel lattice, and it has given very interesting subjects concerning a correlation between crystal structure and physico-chemical properties. From the crystallographic aspect a spinel structure is specified into a normal and an inverse type by some difference of the cation arrangement, and only the ferrospinel of inverse structure can reveal ferromagnetism. These fruitful works in solid state physics were presented by Verwey and his co-workers' experiments[1] and by Néel's theory[2].

Cation arrangement in 2—3 ferrospinel*** solid solution, e.g., nickel-zinc ferrospinel, has been studied not only from the scientific aspect but also in reference to the improvement of magnetic materials[3]. At present the arrangement of trivalent cations is aimed at which is studied in nickel ferro-aluminospinel[4] and other ferro-aluminospinel solid solutions[1]. In the previous paper[5] LFS-LAS solid solution was found to show an order-disorder transition, in addition to showing properties seen in other ferro-aluminospinel solid solutions. On purpose to know correlations between the cation arrangements and other physico-chemical properties, X-ray diffraction intensities were measured and simple magnetic measurements were also carried out.

Experimental

Specimens.—Specimens were synthesized and heat-treated by the method mentioned already[5]. Specimen codes were A (=LAS), B, C, P, R, Q, D, E and F (=LFS), according to each chemical composition as is shown in Table I. The subscript "L" or "H" was supplied behind the code name of a specimen to show whether it was of ordered or disordered phase.

Apparatus.—X-ray diffraction intensities were measured by Norelco X-ray diffractometer with Co K_α radiation.

Magnitude of magnetization was determined by means of the measurement of distances at which small rods of a sample with dimensions (ca. 0.2 mm. diameter, ca. 3 mm. length) can be attracted by a magnet so as to give a definite attractive force.

Results and Discussion

A general expression of the cation arrangement in LFS-LAS solid solution, $LiFe_pAl_{(5-p)}O_8$, is as follows:

$$[Li_xFe_yAl_{(2-x-y)}]_{tet}\,[Li_{(1-x)}Fe_{(p-y)}Al_{(3+x+y-p)}]_{oct}O_8$$

where subscript "tet" means the tetrahedral site and "oct" the octahedral site. x and y are the numbers of lithium ions and ferric ions, respectively, located in the tetrahedral site. Then, the average atomic scattering factor for the cation mixture existing in the tetrahedral or the octahedral site, i.e., $\langle f_{tet}\rangle$ or $\langle f_{oct}\rangle$, is written as

$$2\langle f_{tet}\rangle = xf_{Li} + yf_{Fe} + (2-x-y)f_{Al}$$

$$4\langle f_{oct}\rangle = (1-x)f_{Li} + (5-y)f_{Fe} + (3+x+y-p)f_{Al}$$

where f_{Li} is the atomic scattering factor of lithium ion, f_{Fe} of ferric ion and f_{Al} of aluminum ion.

A cation arrangement in LFS is shown as $[Li_xFe_{(2-x)}]_{tet}\,[Li_{(1-x)}Fe_{(3+x)}]_{oct}O_8$, and $\langle f_{tet}\rangle$ and $\langle f_{oct}\rangle$ are written as

---

* Lithium ferrospinel and lithium aluminospinel are abbreviated to LFS and LAS, respectively, in the following.

** Present address: Idemitsu Kōsan Co., Ltd., Chuō-ku, Tokyo.

1) For instances, E. J. W. Verwey and E. L. Heilmann, *J. Chem. Phys.*, **15**, 174 (1947); E. J. W. Verwey, P. W. Haayman and F. C. Romeijn, ibid., **15**, 181 (1947); E. J. W. Verwey, P. B. Braun, E. W. Gorter, F. C. Romeijn and J. H. van Santen, *Z. physik. Chem.*, **198**, 6 (1951).

2) L. Néel, *Ann. phys.*, [12], **3**, 137 (1948).

*** 2—3 spinel means the spinel with di- and tri-valent cations.

3) For instance, R. L. Harvey, I. J. Hegyi and H. W. Leverenz, *RCA Rev.*, **11**, 321 (1950).

4) E. W. Gorter, *Nature*, **173**, 123 (1954); J. S. Smart, *Phys. Rev.*, **94**, 847 (1954).

5) E. Kato, This Bulletin, **32**, 51 (1959).

$$2\langle f_{tet}\rangle = xf_{Li} + (2-x)f_{Fe}$$
$$4\langle f_{oct}\rangle = (1-x)f_{Li} + (3+x)f_{Fe}$$

The same procedure is available in case of LAS. Values of the structure amplitude for reflections were calculated through the above expressions.

Integrated intensity P, which is estimated from structure amplitude F, is proportional to diffractometric peak area A, i. e.,

$$\frac{A_{hkl}}{A_{lmn}} = \frac{P_{hkl}}{P_{lmn}} = \frac{[mF^2(1+\cos^2 2\theta)\ \mathrm{cosec}^2\theta\ \sec\theta]_{hkl}}{[mF^2(1+\cos^2 2\theta)\ \mathrm{cosec}^2\theta\ \sec\theta]_{lmn}}$$

where $h\,k\,l$ and $l\,m\,n$ show Miller's indices for two arbitrary reflections, m=multiplicity and θ=Bragg angle. By measurements of X-ray diffraction intensities for the fundamental reflections, which appear regardless of the existence of a superstructure in the crystal lattice, the cation arrangements can be determined not only in the disordered phase but also in the ordered phase by the above procedures. In order to estimate the cation arrangements in LFS, LAS and LFS-LAS solid solution, reflections 220, 311 and 400 were chosen. The values of the peak area are listed in Table I.

The cation arrangements in LFS and LAS**** are listed in Table II. In this table $[Fe_{2.0}]_{tet}[Li_{1.0}Fe_{3.0}]_{oct}O_8$ was given at both the ordered phase (FL) and the disordered phase (FH) of LFS, which agree with Braun's report[6]. At the ordered phase of LAS, AL, the cation arrangement is expressed in $[Li_{0.3}Al_{1.7}]_{tet}[Li_{0.7}Al_{3.3}]_{oct}O_8$ which also agrees with $[Li_{1/3}Al_{5/3}]_{tet}[Li_{2/3}Al_{10/3}]_{oct}O_8$ given by Verwey[3]. The error in x measurement decreases with increase in peak area, and the accuracy of x was estimated to range within ± 0.05 for LFS and within ± 0.1 for LAS.

To determine the cation arrangement in LFS-LAS solid solutions[7], it is necessary to assume an adequate value for x, because x and y are variables dependent on each other for any kind of reflection. The following postulations are offered;

1) In LAS a partition of lithium ions to the tetrahedral and to the octahedral site is proportional to that of aluminum ions. In LFS, lithium ions are located only in the octahedral site. In any LFS-LAS solid solution, it is assumed that the partitions of lithium and aluminum ions have the same value regardless of distribution of ferric ions, i. e.,

$$x/(1-x) = (2-x-y)/(3+x+y-p)$$

2) A structural parameter u for oxygen ion has near values both for LFS and for LAS, and u value is almost free in the calculations of structural amplitude in this case. Therefore, u in the solid solutions is assumed to have additive property.

The values of x and y are shown in Table I, and the resultant cation arrangements are listed in Table II. Though numerous errors may be found in the determination of x and y, qualitative conclusions can be proved from experiments of a series of specimens. Lithium ions and ferric ions are located in the different site in the ordered lattice of LFS. In LAS and LFS-LAS solid solution, lithium ions are insufficient in number to be arranged in their proper lattice points (the lithium sites), wherein lithium ions enter for the ordered state of LFS. It is expected that the lithium sites in LAS and LFS-LAS solid solution are occupied by all of the lithium ions in question and the remnants by a few aluminum ions or ferric ions divided into the octahedral site, because the diffraction intensities of LAS and of LFS-LAS solid solution have the same result as that of LFS. Therefore, the crystal structures of low-temperature forms of LAS and of LFS-LAS solid solutions may be considered as those of a sort of disordered state. The lattice points, where aluminum ions are exchanged for ferric ions, are mainly

AL→BL and QL→DL→EL at the tetrahedral site,

BL→CH→PH→RH→QL and EL→FL at the octahedral site.

In the previous paper[5], I have reported the distinction in physical properties between LFS-LAS solid solutions of iron-rich composition (above 68 mol. % LFS) and those of an aluminum-rich one (below 20 mol. % LFS). No change takes place in the cation arrangement at the octahedral site in spite of the change from AL to BL. It is considered that this fact makes the aluminum-rich solid solution stable in ordered state. The manner is similar for the cation exchange in the tetrahedral site from EL to FL. It is

---

**** As for structural parameter, u, following values were used; LFS: $u=0.382$[6]; LAS: $u=0.385$[1].

6) P. B. Braun, *Nature*, **170**, 1123 (1952).

7) For evaluating x and y, conditions to be satisfied are,
(i) $5\geqq p\geqq 0$ (ii) $p+1\geqq x+y\geqq p-3$, $2\geqq x+y\geqq 0$
(iii) $1\geqq x\geqq 0$ (iv) $p\geqq y\geqq p-4$, $2\geqq y\geqq 0$

TABLE I. DIFFRACTOMETRIC PEAK AREAS AND THE VALUES FOR x AND y

Specimen code	Composition, p	Peak area			x	y
		A_{220}	A_{311}	A_{400}		
AL	0	308	831	516	0.2_8	—
BL	1	696	1232	357	0.2_2	0.8_8
CH	1.5	723	1471	473	0.2_7	0.7_8
PH	2	710	1565	485	0.2_8	0.8_8
RH	2.5	865	1791	481	0.2_5	1.0_8
QL	3	815	1673	485	0.3_0	1.1_0
DL	3.5	724	1570	350	0.2_2	1.4_8
DH	3.5	642	1518	450	0.3_3	1.1_5
EL	4	956	2358	434	0.0_8	1.8_2
FL*	5	798	2036	—	-0.0_2	—
FH*	5	767	1902	—	-0.0_6	—

* Peak areas are given from the previous paper[5].

TABLE II. CATION ARRANGEMENT IN LFS-LAS SOLID SOLUTION

Specimen code	Tetrahed. lattice point	Octahed. lattice point
AL	$Li_{0.3}$ $Al_{1.7}$	$Li_{0.7}$ $Al_{3.3}$
BL	$Li_{0.2}$ $Fe_{0.9}$ $Al_{0.9}$	$Li_{0.8}$ $Fe_{0.1}$ $Al_{3.1}$
CH	$Li_{0.3}$ $Fe_{0.8}$ $Al_{0.9}$	$Li_{0.7}$ $Fe_{0.7}$ $Al_{2.6}$
PH	$Li_{0.3}$ $Fe_{0.9}$ $Al_{0.8}$	$Li_{0.7}$ $Fe_{1.1}$ $Al_{2.2}$
RH	$Li_{0.2}$ $Fe_{1.1}$ $Al_{0.7}$	$Li_{0.8}$ $Fe_{1.4}$ $Al_{1.8}$
QL	$Li_{0.3}$ $Fe_{1.1}$ $Al_{0.6}$	$Li_{0.7}$ $Fe_{1.9}$ $Al_{1.4}$
DL	$Li_{0.2}$ $Fe_{1.5}$ $Al_{0.3}$	$Li_{0.8}$ $Fe_{2.0}$ $Al_{1.2}$
DH	$Li_{0.3}$ $Fe_{1.2}$ $Al_{0.5}$	$Li_{0.7}$ $Fe_{2.3}$ $Al_{1.0}$
EL	$Li_{0.1}$ $Fe_{1.8}$ $Al_{0.1}$	$Li_{0.9}$ $Fe_{2.2}$ $Al_{0.9}$
FL, FH	$Fe_{2.0}$	$Li_{1.0}$ $Fe_{3.0}$

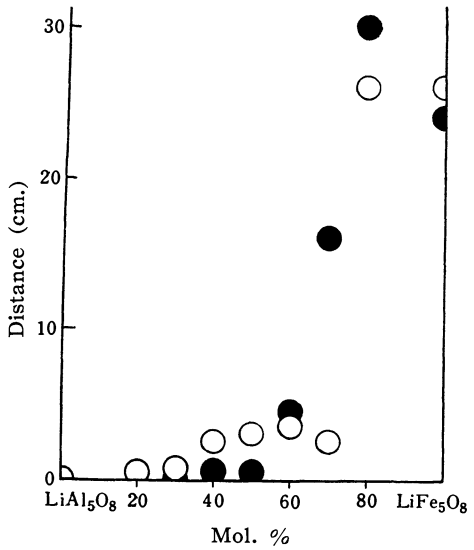


Fig. 1. Magnetization vs. chemical composition.
○: ordered phase
●: disordered phase

difficult at present to resolve physical changes in view of the cation arrangement.

Magnetism in a ferrospinel is explained by the theory of ferrimagnetism. Only ferric ions contribute to spontaneous magnetization in LFS-LAS solid solution, and the magnitude of magnetization is related both with the difference between numbers of ferric ions at the tetrahedral and at the octahedral site and with an interaction between cations at the tetrahedral and octahedral site (the latter relating to numbers of ferric ions located in two kinds of lattice point). Fig. 1 shows the relative magnitude of magnetization of LFS-LAS solid solutions at room temperature, measured by the distances capable of attracting specimens by a magnet, as a function of the chemical composition. The observed magnitudes of magnetization qualitatively agree with magnitudes presumed from the cation arrangement.

Now, a quenching effect of LFS-LAS solid solution will be discussed. In specimens C, P and R, magnitudes of magnetization in disordered phase were smaller than those in ordered phase. C, P and R in ordered phase were mixtures of two phases which roughly corresponded to B and D, so that magnetization of specimens was suitable to the resultant magnetization of two phases. When the configurational free energy of crystal lattice is scarcely changed by any cation arrangement, cations, owing to thermal agitation at high temperature, incline to be statistically distributed[8] rather than to be located in the most stable state. In CH, PH, RH, high-temperature form of E and FH, their statistical structures are not recognized. On the other hand, in D, the cation

8) "Statistical distribution" means that cations are distributed over all cation sites at random, while "disordered" phase as for ferrospinel indicates a phase in statistical distribution over the octahedral site alone.

arrangement in disordered phase differs from that in ordered phase, and its statistical distribution at a high temperature is recognized from magnetic measurements as well as from X-ray studies. In Q also, the magnetization in ordered phase results in the near magnitude to that in a disordered one, and the statistical distribution is demonstrated. Briefly summarizing, LFS-LAS solid solution gave different cation arrangements within the ordered and the disordered phase in general, but the possibility of the statistical distribution, as is shown in magnesium and cupric ferrospinels, can not yet be determined.

The author is indebted to Mr. Kazuo Sasaki of Osaka City University for his assistance in X-ray measurements.

Institute of Polytechnics
Osaka City University
Kita-ku, Osaka

The Mechanism of Reductive Cleavage Reaction of 2, 3-Dimethyl-3-cyanomethylindolenine

By Masao NAKAZAKI

(Received December 1, 1958)

Hoshino and Tamura[1] observed the unexpected formation of 2, 3-dimethylindole(II) by the reduction of 2, 3-dimethyl-3-cyanomethylindolenine(Ia) with sodium and ethanol.

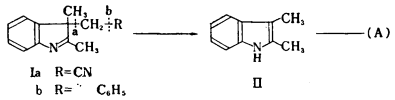


Fig. 1

Recently, we have reported[2] a conversion of 3-alkyl-2, 3-dimethylindolenines into 2, 3-dimethylindole by means of acid, and proposed a mechanism which could not be applied to the explanation of the mechanism of Hoshino's reaction mentioned above.

In some cases, the reductive cleavage of $-CH_2CN$ to CH_3 was reported[3]; however, a search of the literature failed to find analogous reaction[4] to Hoshino's reductive cleavage by the action of sodium and ethanol.

The study of elucidation of the mechanism of this novel reductive cleavage reaction was undertaken with the hope that this might lead to some bits of information which would be able to be applied to the structure determination of the indole alkaloids.

The simplest, but not so attractive, explanation would be the hydrogenolysis of bond a (Fig. 1). Since in many instances, a benzyl group is noticed to be split off very easily under various reductive conditions, 2,3-dimethyl-3-benzylindolenine(Ib) was treated with sodium and ethanol as a model experiment. But, as would be expected, 2, 3-dimethyl-3-benzylindoline, instead of II, was obtained from the reaction mixture, simply as the result of the reduction of indolenine double bond.

To examine another possible route, which would be initiated by an attack of ethoxide anion (Fig. 2. mechanism B), Ia was treated with sodium ethoxide in ethanolic solution.

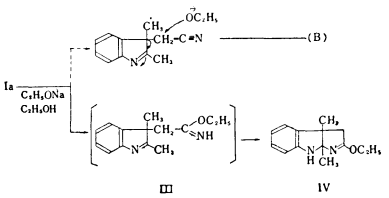


Fig. 2

It was unsuccessful to detect any trace of II, but a crystalline compound, m. p. 148~

1) T. Hoshino and K. Tamura, *Ann.*, **500**, 46 (1933).

2) M. Nakazaki, S. Isoe and K. Tanno, *J. Chem. Soc. Japan, Pure Chem. Sec.* (*Nippon Kagaku Zasshi*), **76**, 1262 (1955).

3) J. J. Bloch, *Chem. Zentr.*, III, 609 (1919); see also R. B. Wagner and H. D. Zook, "Synthetic Organic Chemistry", John Wiley and Sons, Inc., New York (1953), p. 659.

4) In the case of indole compounds, the vulnerability of bond b (Fig. 1) is noticed, e. g., F. C. Uhle and L. S. Harris, *J. Am. Chem. Soc.*, **79**, 103 (1957); H. R. Snyder and D. S. Mattson, ibid., **79**, 2217 (1957); E. Lecte and L. Marion, *Can. J. Chem.*, **31**, 775 (1953).

149°C, was isolated, the molecular formula of which corresponded to Ia plus one molecule of ethanol. This compound could be prepared also by the action of ethanolic hydrochloric acid onto Ia, and was given the structure IV by the observation of I. R. (see, experimental part) and U. V. spectrum (Fig. 7).

The failure of the conversion of Ia into II only by means of sodium ethoxide indicated that course B must be ruled out, and the reductive condition seems to be imperative for the change Ia→II.

The fact that it was found possible for the compound IV, in turn, to afford II by the action of potasium and *tert*-butanol, led to the conclusion that Ia is not the only compound capable of undergoing Hoshino's reaction. This was confirmed further by the isolation of II, when sodium was added to the ethanolic solution of the indolenine ester V, prepared from Ia by the alcoholysis with ethanol and concentrated sulfuric acid.

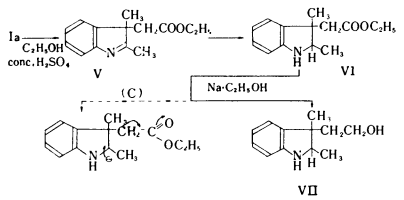


Fig. 3

The complexity encountered in the case of Ia suggested that the compound V appeared to be more suitable than Ia for the further study of Hoshino's reaction[5]. Having two reducible groups in the molecule, at the initial stage of the reaction, the compound V would be attacked by a reduction reagent either on the indolenine nucleus or on the side chain.

If the former is the case, the intermediate compound will be the compound VI which would give II, according to the mechanism C shown on Fig. 3. But VI, prepared by catalytic hydrogenation[6] of V with platinum oxide in acetic acid failed to afford II with sodium ethoxide or potassium *tert*-butoxide[7]. The reduction of VI with sodium and ethanol did not afford II either, but an alcohol VII was the sole product isolable from the reaction mixture. This alcohol was proved to be identical with the one prepared from VI by the lithium aluminum hydride reduction.

Thus, mechanism C had to be abandoned, and another conceivable route in which the reduction reagent would attack the side chain first was to be sought. To examine this possibility, an attempt was made to prepare the possible intermediate IX.

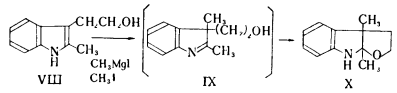


Fig. 4

The reaction of the Grignard complex of VIII with methyl iodide afforded a crystalline product, m. p. 51.5~52.5°C, to which the structure X[8] was assigned because of the lack of OH band but the presence of NH band in its I. R. spectrum, coupled with its indoline type absorption in the U. V. region (Fig. 7). This material again failed to give II, under the Hoshino's condition.

These observations lead one to conclude that: 1. the compounds of the general structure XI[9] (Fig. 5, where X is electronegative atom, such as oxygen or nitrogen.), furnish 2,3-dimethylindole with sodium and alcohol; 2. reduction reagent attacks simultaneously[10] the unsaturated bond of indolenine nucleus and the one on the side chain.

The most plausible mechanism, D, is shown on Fig. 5. A 1,4-biradical XII,

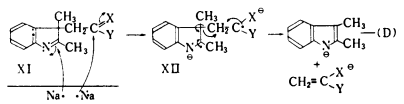


Fig. 5

5) Upon catalytic hydrogenation, V gave the compound VI as the result of the hydrogenation of the indolenine double bond, but in the case of Ia the side chain also would be reduced at the same time.

6) H. L. Holmes, H. T. Openshaw and R. Robinson, *J. Chem. Soc.*, **1946**, 910.

7) The formation of a small amount of *tert*-butyl ester by *tert*-butanolysis was presumed by effervescence of the crude picrate of recovered ester observed at its melting point.

8) T. Hoshino and K. Shimodaira (*Ann.*, **520**, 19 (1935)) succeeded in preparing the first compound which has the same skeleton as X, but they could decide whether their compound has the skeleton IX or X. Since our compound was established to have the structure X (3a, 8a-dihydro-3a,8a-dimethyl-2-furo [2.3-b] indole), their compound is 3a, 8a-dihydro-3a-methyl-2-furo [2.3-b] indole. See the nomenclature in "The Ring Index", by A. M. Patterson and L. T. Capell, Reinhold Pub. Corp., (1940), p. 198.

9) Under the reaction condition, the compound IV would be safely assumed to be converted back to III, which would be cleaved to give II. This causes a shift of equilibrum, and eventually all of IV would be transformed to II.

10) Though not necessarily at the very same instance, the reduction of one of two functional groups should not exceed the other, otherwise it would give either VI or X which can not give II.

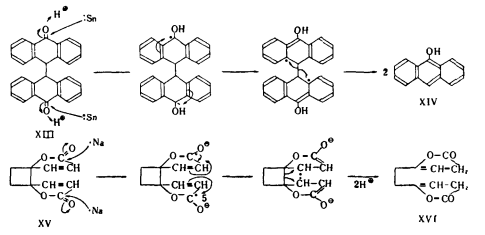


Fig. 6

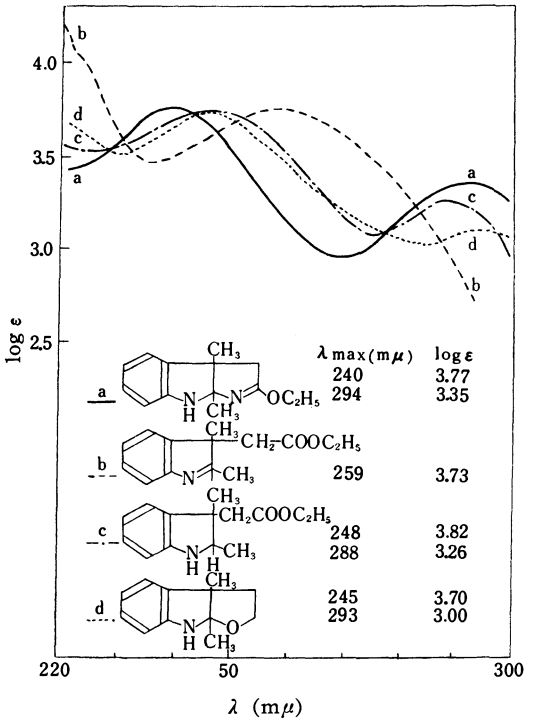


Fig. 7

which is caused by a nucleophilic attack[11] of the electron from sodium, is unstable[12] and suffered cleavage of bond a by the electron migration as indicated with arrows, resulting in end products.

According to this mechanism, in the case of Ia, the side chain split off is probably acetonitrile, which would be reduced further to give ethylamine. The actual isolation of ethylamine as the form of ethyloxamide from the reaction mixture of Hoshino's reaction of Ia, will support this mechanism.

The reductive cleavage of dihydrodianthrone(XIII) to anthrone(XIV)[13] with tin and acetic acid containing hydrochloric acid, and the conversion of anemonine (XV) into dihydroanemonine(XVI)[14] with sodium amalgam and acetic acid in methanolic solution appear to follow the analogous reaction pattern. (Fig. 6).

The driving force of the reaction could be sought in the steric strain of cyclobutane ring in the case of XV, and the tendency to aromatize into stable indole structure would play an important rôle in promoting Hoshino's reaction.

Experimental[15]

2, 3-Dimethyl-3-cyanomethylindolenine(Ia). —Ia was prepared following Hoshino and Tamura's procedure[1]. Attempts were made to improve the yield by using methyl bromide in place of the ethyl iodide used in their synthesis or employing "reversed Grignard synthesis". The best result was obtained when chloroacetonitrile was added rather rapidly. Grignard solution prepared from 1.2 g. of magnesium and 8.0 g. of methyl iodide in 30 cc. of absolute ether was cooled and 7.3 g. of 2, 3-dimethylindole in 35 cc. of ether was added dropwise onto it.

After the generation of methane subsided, the reaction mixture was stirred for 10 min. at room temperature and refluxed on a water bath for another 30 min. When 4.0 g. of chloroacetonitrile[16] was added during 5 min. into the cooled solution, a yellow viscous precipitate was observed on the wall of the reaction vessel.

After the solution was allowed to stand for 20 min. at room temperature, it was refluxed for 30 min. The Grignard complex was decomposed by the addition of 6 g. of acetic acid and 200 cc. of ice water, and the reaction mixture was thoroughly extracted with ether. Basic material was extracted by shaking with 2 N hydrochloric acid solution from the combined ether extract, and was precipitated from the solution as yellow oil by the addition of excess of 4 N sodium hydroxide solution. The oil was extracted with ether, and the ether extract was washed with water and dried over magnesium sulfate. Evaporation of

11) As for the action of sodium on organic compounds, see an excellent article by A. J. Birch, *Quart. Rev.*, **4**, 69 (1950).

12) R. C. Fuson, "Advanced Organic Chemistry", John Wiley and Sons, New York (1953), p. 72.

13) E. de Barry Barnett and M. A. Mathews, *J. Chem. Soc.*, **123**, 380 (1923).

14) Y. Asahina and R. Fujita, *J. Pharm. Soc. Japan* (*Yakugaku Zasshi*), **448**, 471 (1919); ibid., **455**, 1 (1920). The position of the double bonds of dihydroanemonine (XVI) deduced by this mechanism agrees with the one established by their experimental results.

15) All melting points are uncorrected. All U. V. spectra were measured with an EPS-2 Hitachi Autorecording Spectrophotometer and I. R. spectra on a Perkin Elmer Model 12C. The analyses were performed in the microanalytical laboratory of the Institute of Polytechnics, Osaka City University.

16) Since trimethylbenzene recommended as solvent is not easily accessible, the procedure described in "Organic Syntheses" (Vol. **30**, 22 (1950)) was simplified as follows. An intimate mixture of finely powdered chloroacetamide (1 mol.) and phosphorus pentoxide (2.5 mol.) was placed in oil bath heated at 200~220°C beforehand, and the resulting chloroacetonitrile was distilled off at 80~100 mm. collected in a receiver chilled by a freezing mixture. Purification by further distillation gave a yield of 76%. ("Organic Syntheses": 61~70%).

the solvent furnished a yellow viscous residue which gave 2.6 g of Ia (28% yield), b. p. 140~145°C/1 mm. (literature[1]: b. p. 150°C/1 mm., 15% yield).

This compound has a characteristic odor of indolenine compound and solidified on standing to give m. p. 75~76°C after sublimation in vacuo.

Anal. Found: C, 78.41; H, 6.69; N, 15.17. Calcd. for $C_{12}H_{12}N_2$: C, 78.23; H, 6.57; N, 15.21%.

The picrate was recrystallized to give yellow crystals, m. p. 175~178°C. (literature[1]: 177~178°C).

Anal. Found: N, 16.99. Calcd. for $C_{12}H_{12}N_2 \cdot C_6H_3O_7N_3$: N, 16.94%.

2,3-Dimethyl-3-benzylindoline.—To a stirred solution of 1.8 g. of Ib in 25 cc. of absolute ethanol, 2.1 g. of sodium was added in five portions. After the sodium disappeared, water was added and the reaction mixture was extracted with ether. The ether extract gave, after removal of the solvent, 1.8 g. of crystals which melted at 80~82°C after recrystallization from ethanol-water. I. R. spectrum[17]: 3.10 μ (NH). U. V. spectrum[17]: λ_{max} 273 mμ (log ε 3.35) in ethanol.

Anal. Found: C, 85.86; H, 8.10. Calcd. for $C_{17}H_{19}N$: C, 86.03; H, 8.07%.

The picrate was recrystallized to yield yellow needles, m. p. 177~179°C.

Anal. Found: C, 58.86; H, 4.87. Calcd. for $C_{17}H_{19}N \cdot C_6H_3O_7N_3$: C, 59.22; H, 4.75%.

1,2-Dehydro-2-ethoxy-9-methyldinordesoxyeseroline (IV).—*By the action of ethanolic hydrochloric acid on Ia.*—A solution of 4.35 g. of Ia in 45 cc. of absolute ethanol was cooled at −10°C, and saturated with dry hydrogen chloride. After the solution was kept at room temperature overnight, ethanol was removed by distillation in vacuo, and the residue was neutralized with 5% sodium carbonate solution to afford crystals, m. p. 151~152°C (4.2 g.) after recrystallization from water-ethanol. I. R. spectrum: 3.2 μ (NH), 6.33 μ (CN). U. V. spectrum: λ_{max} 240 mμ (log ε 3.77), 294 mμ (log ε 3.35) in methanol.

Anal. Found: C, 72.85; H, 7.70; N, 12.25. Calcd. for $C_{14}H_{18}ON_2$: C, 73.01; H, 7.80; N, 12.17%.

The picrate was recrystallized to give yellow needles, m. p. 174~175°C.

Anal. Found: C, 52.95; H, 4.96; N, 15.09. Calcd. for $C_{14}H_{18}ON_2 \cdot C_6H_3O_7N_3$: C, 52.28; H, 4.61; N, 15.25%.

By the action of sodium ethoxide on Ia.—To a solution of sodium ethoxide prepared from 0.2 g. of sodium and 20 cc. of absolute ethanol, 0.38 g. of Ia was added with 1 cc. of ethanol. After the solution was refluxed for 1 hr., the reaction mixture was subjected to steam distillation, but 2,3-dimethylindole could not be detected in the steam distillate.

The residue of the steam distillation afforded a pale yellow precipitate which was purified by recrystallization from ethanol-water to give crystals, m. p. 148~149°C, undepressed m. p. on admixture with that prepared by the method described above.

Reductive Cleavage of IV with Potassium and *tert*-Butanol.—To a solution of 0.8 g. of IV in 30 cc. of *tert*-butanol, 1.8 g. of potassium was added in small portions. After the solution was refluxed on a water bath for 2 hr., the reaction mixture was subjected to steam distillation. The crystals which separated on the condenser weighed 0.2 g., and melted at 101~104°C after recrystallized from petroleum ether (b. p. 50~70°C). This compound was proved identical with 2,3-dimethylindole by the mixed m. p. (101~103°C) with an authentic specimen (m. p. 104~105°C).

Anal. Found: C, 82.81; H, 7.42; N, 9.41. Calcd. for $C_{10}H_{11}N$: C, 82.72; H, 7.64; N, 9.65%.

Ethyl 2,3-Dimethylindolenine-3-acetate (V).—Ia (4.6 g.) was ethanolyzed by boiling with 20 cc. of 94% ethanol and 10 cc. of concentrated sulfuric acid for 8 hr. The cooled reaction mixture was poured onto a stirred solution of 40g. of sodium carbonate in 100 cc. of water and 100 cc. of ether which formed an upper layer. The ether extract, after being washed with water and dried over magnesium sulfate, was concentrated to give a yellow brown liquid which was distilled to afford 4.2 g. of pale yellow viscous oil with green-yellowish fluorescence, b. p. 120~130°C/6 mm. I. R. spectrum: 5.75 μ (ester carbonyl), 6.30 μ (indolenine C=N). U. V. spectrum: λ_{max} 259 mμ (log ε 3.75), λ_{min} 235 mμ (log ε 3.49) in ethanol.

Anal. Found: N, 6.01. Calcd. for $C_{14}H_{17}O_2N$: N, 6.06%.

The picrate was recrystallized to furnish yellow needles, m. p. 141~143°C.

Anal. Found: C, 52.47; H, 4.61; N, 12.22. Calcd. for $C_{14}H_{17}O_2N \cdot C_6H_3O_7N_3$: C, 52.17; H, 4.38; N, 12.17%.

Reductive Cleavage of V.—To a solution of 0.589 g. of V in 13 cc. of absolute ethanol, 1.0 g. of sodium was added in three portions as rapidly as the capacity of the condenser allowed, and after the disappearence of sodium the solution was heated on a water bath for 30 min. To the reaction mixture, 20 cc. of water was added and ethanol was removed to give a turbid solution from which a crystalline material (0.14 g.) precipitated. After recrysallization from petroleum ether (b. p. 50~70°C), this crystal showed m. p. 97~100°C, the identity of which with 2,3-dimethylindole was established by mixed m. p. determination with an authentic sample. Its picrate melted at 152~153°C alone and admixed with an authentic specimen.

Ethyl 2,3-Dimethylindoline-3-acetate (VI).—On catalytic hydrogenation of V (2.1 g.) with 69 mg. of platinum oxide in 10 cc. of acetic acid, the theoretical hydrogen up-take was completed after 2 hr. After the catalyst was filtered, the filtrate was poured onto a solution of 20 g. of sodium carbonate in 150 cc. of water, and extracted with ether. The ether extract,

17) Cf. M. Nakazaki and S. Isoe, *J. Chem. Soc. Japan, Pure Chem. Sec.* (*Nipon Kagaku Zasshi*), **76**, 1161 (1955).

18) After the nomenclature of "The Ring Index", p. 196, this can be named as 3a, 8a-dihydro-1,2-dehydro-2-ethoxypyrrolo [2.3-b] indole.

after removal of the solvent, afforded a pale yellow oil, which gave 1.64 g. of (78% yield) VI, b. p. 153~154°C/6 mm. No fluorecence was observed. I. R. spectrum: 2.95 μ (NH), 5.76 μ (ester carbonyl). U. V. spectrum: λ_{max} 288 mμ (log ε 3.26), 248 mμ (log ε 3.82) in ethanol.

Anal. Found: C, 70.96; H, 8.24; N, 5.84. Calcd. for $C_{14}H_{19}O_2N$: C, 72.07; H, 8.21; N, 6.00%.

The picrate was recrystallized from ethanol to give yellow needles, m. p. 153°C.

Anal. Found: C, 51.95; H, 4.85; N, 12.12. Calcd. for $C_{14}O_{19}O_2N \cdot C_6H_3O_7N_3$: C, 51.95; H, 4.80; N, 12.12%.

The Action of Potassium *tert*-Butoxide on VI.—To a solution of potassium *tert*-butoxide prepared from 0.08 g. of potassium and 6 cc. of *tert*-butanol, a solution of 0.33 g. of VI in 2 cc. of *tert*-butanol was added. After the reaction mixture was heated for 1 hr. on a water bath, the solvent was removed under reduced pressure. After the residue was dissolved in water and saturated with sodium chloride, the solution was extracted with ether. The ether extract was shaken with 2 N hydrochloric acid solution to separate neutral and basic fractions. From the ether layer, after the usual work-up, there could not be detected anything but a faint smell of *tert*-butanol. The hydrochloric acid solution was made strongly basic, and the separated oily material was extracted with ether. The ether extract gave, after evaporation of the solvent, 0.25 g. of liquid which was converted into picrate directly. The crude picrate melted at 145~151°C with a little effervescence, but after two more recrystallizations from ethanol, its m. p. was 152~153°C and proved identical with the picrate of VI.

The Action of Sodium on the Ethanolic Solution of VI.—To a solution of 0.47 g. of VI in 9 cc. of absolute ethanol, 0.7 g. of sodium was added in three portions. After the sodium disappeared, the solvent was removed on a water bath, and water was added to the residue. The basic and neutral fractions were separated as mentioned above. From the neutral fraction, no 2,3-dimethylindole was found. The basic fraction gave 0.221 g. of a pale yellow liquid which afforded a yellow prismatic picrate melting at 152~154°C after recrystallization from ethanol. The mixed m. p. with the picrate of VII (m. p. 151~153°C) was 151~154°C.

Anal. Found: C, 51.84; H, 5.16; N, 13.23. Calcd. for $C_{12}H_{17}ON \cdot C_6H_3O_7N_3$: C, 51.42; H, 4.80; N, 13.33%.

β-(2, 3-Dimethylindolinyl)-ethanol (VII).—To a suspension of 0.15 g. of lithium aluminum hydride on 20 cc. of absolute ether, a solution of 0.909 g. of VI in 10 cc. of ether was added dropwise over a period of 30 min. After the reaction mixture was heated on a water bath for 1 hr., the excess of the reduction reagent was destroyed by the addition of ethyl acetate, and the resulting white voluminous precipitate was dissolved in 2N sodium hydroxide. Continuous extraction with ether (10 hr.) gave, after removal of the solvent, 0.635 g. of a viscous liquid, which was distilled at 136~145°C (air bath temperature) under 3 mm. to yield 0.53 g. of viscous oil. This solidified to give colorless needles, m. p. 100~101°C, after recrystallization from ethanol-petroleum ether.

Anal. Found: C, 75.63; H, 9.14; N, 7.38. Calcd. for $C_{12}H_{17}ON$: C, 75.35; H, 8.96; N, 7.32%.

The picrate was recrystallized to produce yellow crystals, m. p. 151~153°C.

2-Methyltryptophol (VIII).—To a slurry of 1.75 g. lithium aluminum hydride in 130 cc. of absolute ether, a mixture of 10 g. of ethyl 2-methylindole-3-acetate[19] in 50 cc. of ether was added dropwise at such a rate as to keep the ether boiling.

Stirring and refluxing was continued for 30 min., and 15 cc. of ethyl acetate was added to destroy the excess of the reduction reagent followed by the addition of dilute sulfuric aid. The aqueous layer was thoroughly extracted with ether, and ether extract was washed with water and dried over anhydrous magnesium sulfate. After the removal of the solvent, the ether extract gave a viscous liquid, which was purified by distillation in vacuo resulting in 6.0 g. of liquid (75% yield), b. p. 143~144°C/10^{-3} mm.[20]

3a, 8a-Dihydro-3a, 8a-dimethyl-2-furo(2.3-b)-indole (X).—A solution of 5 g. of VIII in 30 cc. of ether was added dropwise onto a stirred cold Grignard solution prepared from 2.08 g. of magnesium and 15.3 g. of ethyl iodide in 15 cc. of ether.

After being kept at room temperature for about 20 min., the reaction mixture was refluxed on a water bath for 1 hr. To this solution 9.3 g. of methyl iodide was added during 3 hr., and the mixture was kept at room temperature overnight. The Grignard complex was decomposed with acetic acid and water, and extracted with ether. From the ether extract the basic material was transferred into 1 N hydrochloric acid. The oily material, liberated by the addition of 2 N sodium hydroxide solution to the hydrochloric acid extract, was again extracted with ether. Distillation of the residue, after evaporation of ether, at a reduced pressure gave 0.94 g. of viscous oil, b. p. 125~126°C/5 mm.

This compound solidified gradually, and recrystallization from petroleum ether (b. p. 50~70°C) gave prismatic crystals, m. p. 51.5~52.5°C. I. R. spectrum: 3.00 μ (NH). U. V. spectrum: λ_{max} 245 mμ (log ε 3.7), 293 mμ (log ε 3.0).

Anal. Found: C, 76.29; H, 8.26. Calcd. for $C_{12}H_{15}ON$: C, 76.15; H, 7.99%.

The picrate gave yellow prisms from ethanol, m. p. 137~139°C.

Anal. Found: C, 52.01; H, 4.61; N, 13.39. Calcd. for $C_{12}H_{15}ON \cdot C_6H_3O_7N_3$: C, 51.67; H, 4.34; N, 13.39%.

The Action of Sodium on the Ethanolic Solution of X.—One gram of sodium was added in three portions to a solution of 0.26 g. of X in

19) M. V. Bulloch and S. W. Fox, *J. Am. Chem. Soc.*, **73**, 5156 (1951).

20) T. Hoshino and K. Shimodaira, *Ann.*, **520**, 19 (1935) prepared this alcohol by the Bouveault-Blanc reduction in a yield of 32%, b. p. 198°C/3.5 mm. and m. p. 55~56°C.

20 cc. of absolute ethanol. After the reaction was complete, water was added to the reaction mixture and saturated with sodium chloride. The solution was thoroughly extracted with ether, but the test of 2,3-dimethylindole was negative on the small amount of residue remaining after removal of the solvent.

Reductive Cleavage of Ia. Isolation of Ethylamine.—In a 100 cc. three-necked flask, provided with an inlet tube for dry nitrogen, a reflux condenser carrying a glass tubing which reached the bottom of a Erlenmeyer flask containing 10 cc. of 4 N hydrochloric acid solution, and an inlet tude for sodium, were placed 2.09 g. of Ia and 45 cc. of absolute ethanol. While nitrogen from a cylinder was passed through the flask, 3.5 g. of sodium was added in five portions as rapidly as the capacity of the condenser allowed. Volatile material was swept with nitrogen gas into the hydrochloric acid solution. After completion of the reaction, cooling water for the condenser was cut off, and about 5 cc. of ethanol was distilled through the condenser into the Erlenmeyer flask contaning the acid solution. Another 15 cc. of ethanol was distilled into the same receiver by the usual downward distillation.

Water was added to the residue which remained in the three-necked flask and the turbid solution was distilled with steam. From the distillate, 0.5 g. of 2, 3-dimethylindole was obtained, and identified by mixed m. p. determination with an authentic sample and as in the form of picrate.

The hydrochloric acid solution containing the basic material, was concentrated in vacuo to give a crystalline product which was soluble completely in absolute ethanol. The amine generated by the addition of 10 cc. of 4 N sodium hydroxide solution onto the above mentioned amine hydrochloride, was distilled with water into a flask containing 0.2 g., of diethyl oxalate and 1 cc. of water. The crystals separated from the cold solution, were washed with a small amount of cold water and dried in a desiccator to give 10 mg. of colorless needles, m. p. 178~179°C, which did not depress the mixed m. p. with an authentic sample of ethyloxamide (m. p. 178~180°C[21]). Their I. R. spectra could overlap in every respect.

Anal. Found: C, 50.28; H, 8.85: N, 19.40. Calcd. for $C_6H_{12}O_2N_2$: C, 49.98; H, 8.39; N, 19.43%.

On a control experiment using the same method, 65 mg. of ethyloxamide was isolated by the reduction of 600 mg. of acetonitrile with sodium-ethanol.

The author is very gratiful to Messrs. Kohei Tanno, Masaru Tamura and Munesuke Sato for their skillful technical assistance.

Institute of Polytechnics
Osaka City University
Kita-ku, Osaka

21) S. P. Mulliken, "A Method for the Indentification of Pure Organic Compounds," Vol. II, John Wiley Inc., New York (1922), p. 132.

Indirect Complexometric Titration of Beryllium with Ethylenediaminetetraacetic Acid

By Seizo MISUMI and Tomitsugu TAKETATSU

(Recived December 19, 1958)

Ethylenediaminetetraacetic acid (EDTA) has been used for volumetric determination of various metal ions, but it can not be used for a direct titration of the beryllium ion nor for that of the sodium and the potassium ion because these metal ions do not form stable EDTA complexes. Flaschka[1] reported the indirect titration method for sodium, and Pilleri[2] and one of the present authors[3] that for potassium. Pirtea and Mihail[4] reported that beryllium was determined gravimetrically, producing the precipitate $[Co(NH_3)_6]\cdot[(H_2O)_2Be_2(CO_3)_2(OH)_3]\cdot 3H_2O$, by adding saturated hexammine cobaltic trichloride solution (Luteo salt) to beryllium carbonate solution. We studied the determination of beryllium ion concentration by volumetrically measuring the cobalt content in this precipitate. This method was proved to be quantitative and it was possible to separate and determine beryllium from iron (III), aluminum

1) H. Flaschka, *Mikrochemie ver. Mikrochim. Acta*, **39**, 391 (1952).
2) R. Pilleri, *Z. anal. Chem.*, **157**, 1 (1957).
3) T. Taketatsu, *J. Chem. Soc. Japan, Pure Chem. Sec.* (*Nippon Kagaku Zasshi*), **76**, 756 (1957).
4) T. I. Pirtea and G. Mihail, *Z. anal. Chem.*, **159**, 205 (1958).

and magnesium by using EDTA as a masking agent.

Experimental

Reagents.—Standard beryllium solution was prepared by dissolving the nitrate salt in distilled water and the concentration was determined gravimetrically as the oxide. The content (BeO) was 1.95 mg./ml.

Standard EDTA solution was obtained by dissolving the pure disodium salt of ethylenediaminetetraacetic acid dihydrate (Research Laboratory, Dojindo & Co., Ltd.) in distilled water. The concentration was determined by titrating standard zinc chloride solution with Eriochrome black T as indicator. The concentration was 0.01016 mol.

Hexammine cobaltic trichloride (Luteo salt) solution was prepared by Fernelius's method[5] and the supernatant liquid of the saturated solution was used in this experiment.

All other chemicals used were analytical reagent grades.

General Procedure.—An excess of ammonium carbonate was added to about 10 ml. of a slightly acidic solution containing 0.70 to 3.50 mg. of beryllium; a precipitate of basic beryllium carbonate was formed, which was then dissolved completely by stirring for a time. To this clear solution was added a few milliliters of saturated Luteo salt solution and an orange yellow precipitate[4] was obtained by stirring the solution. The solution containing the precipitate was stirred occasionally by a magnetic stirrer for several hours to make the precipitation complete. The precipitate was then filtered with a glass filter (1G. No. 4) and washed 2 to 3 times successively with 2 to 3 ml. of the following solutions: 0.2% Luteo salt solution, a mixture of ethanol and water (60 ml. +40 ml.) containing 2 to 3 drops of 0.2% Luteo salt solution, and absolute ethanol. The percipitate on the glass filter was dissolved in a small amount of 0.1 N hydrochloric acid. To decompose the Luteo salt in the solution obtained, one gram of sodium hydroxide was added to the solution and then the solution was boiled till the black-brown precipitate of cobalt (III) hydroxide was obtained. The solution containing the precipitate was acidified by adding hydrochloric acid and boiled to dissolve the cobalt hydroxide. By this procedure the valency of cobalt was reduced to II from III with hydrochloric acid and a solution containing cobalt (II) and beryllium ions was obtained. After the solution cooled, a small amount of malic acid was added to the solution and it was neutralized with aqueous ammonia (1:1, by volume). The cobalt in the solution was titrated with the standard EDTA solution by adding 0.2 g. of Murexide as indicator. The point at which the indicator attained its maximum violet color was as the end point.

1 ml. of 0.01 mol. EDTA solution
≡0.1803 mg. of berlliyum.

These procedures were carried out at 20~25°C except for boiling purposes.

Results and Discussion

In the general procedure described above, the following factors were specially considered; effects of the amount of ammonium carbonate, Luteo salt and malic acid, and of time allowed for the formation of the precipitate II*.

1) Relation between Ammonium Carbonate Added and the Time Required to Dissolve Basic Beryllium Carbonate.—When an excess of ammonium crabonate was added to about 10 ml. of solution containing 1.40 mg. of beryllium, basic beryllium carbonate was precipitated at first, but the precipitate was dissolved gradually by stirring, because beryllium carbonate complex was produced. The relation between the amount of ammonium carbonate added and the time required for dissolving the precipitate was studied and the results are shown in Table I. It is shown that the more the amount of ammonium carbonate, the shorter the time required for the dissolving of the precipitate.

TABLE I. RELATION BETWEEN THE AMOUNT OF AMMONIUM CARBONATE AND APPROXIMATE TIME REQUIRED TO DISSOLVE BASIC BERYLLIUM CARBONATE

Ammonium carbonate added, g.	Time for dissolving the precipitate, min.
0.5	>60
1.0	25~30
1.5	10~20
2.0	7~ 8
2.5	5~ 7
3.0	3~ 5
4.0	1~ 2

2) Effect of Luteo Salt Added.—To determine the optimum amount of Luteo salt added, various volumes of saturated Leuteo salt solution were added to the beryllium carbonate complex solution. In this case, all other conditions were kept constant. The results are shown in Table II.

It was found that the amount of the reagent added did not affect the determination of beryllium within the range 1 to 8 ml.

5) W. C. Fernelius," Inorganic Syntheses ", Vol. II, McGraw Hill Book Co., Inc., New York (1946), p. 217.

* The precipitate II means $[Co(NH_3)_6][(H_2O)_2Be_2(CO_3)_2(OH)_3]\cdot 3H_2O$

TABLE II. EFFECT OF LUTEO SALT ADDED

Be taken, mg.	Saturated Luteo salt solution added, ml.	Vol. of 0.01016 mol. EDTA titrated, ml.	Be found, mg.	Error, mg.
1.40	1.0	7.72	1.41	+0.01
1.40	2.0	7.79	1.43	+0.03
1.40	4.0	7.61	1.39	−0.01
1.40	5.0	7.72	1.41	+0.01
1.40	8.0	7.65	1.40	±0.00

3) Relation between the Amount of the Precipitate and That of Ammonium Carbonate Added.—Since the amount of ammonium carbonate added had an effect on the formation of the precipitate II., the relation between the amount of the precipitate formed and that of ammonium carbonate added was studied at various time intervals after Luteo salt was added. The results are shown in Fig. 1.

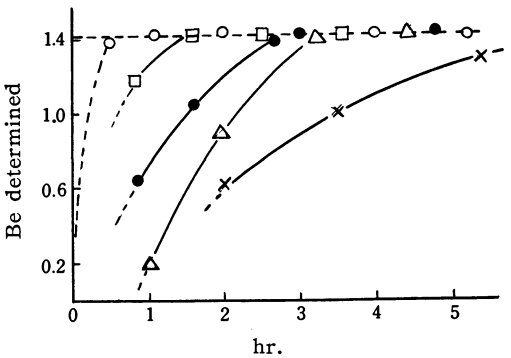


Fig. 1. Relation between beryllium determined v.s. time at various concentrations of ammonium carbonate added.

	Ammoium carbonate
—○—○—	1.0 g
—□—□—	1.5 g
—●—●—	2.0 g
—△—△—	3.0 g
—×—×—	4.0 g

When a small amount of ammonium carbonate had been added to the initial beryllium solution, the precipitate II was formed quantitatively as soon as Luteo salt was added. On the other hand, a longer time was necessary for the formation of the precipitate II with increase in the amount of ammonium carbonate. However, as it is convenient for the dissolution of the precipitate of basic beryllium carbonate to add a greater amount of ammonium carbonate as described above, 1.5 to 2.0 g. of ammonium carbonate was used in this experiment.

4) Effect of Malic Acid on the Titration of Cobalt. — When the titration of cobalt was carried out in an ammonium alkaline solution by using Murexide as indicator, beryllium precipitated as its hydroxide and the results, therefore, proved inaccurate. Since the hydroxide does not precipitate in general in the presence of malic acid, the effect of malic acid on the titration of cobalt was studied. The results are shown in Table III.

TABLE III. EFFECT OF MALIC ACID ADDED

Co taken, mg.	5% malic acid added, ml.	Vol. of 0.01016 mol. EDTA titrated, ml.	Co found, mg.	Error, mg.
3.64	0	6.08	3.64	±0.00
3.64	2	6.08	3.64	±0.00
3.64	4	6.08	3.64	±0.00
3.64	5	6.07	3.63	−0.01
3.64	10	6.05	3.62	−0.02

It is evident that the addition of 2 to 10 ml. of 5% malic acid solution did not give an error in the titration. But larger amounts of malic acid showed negative errors. Therefore, 2 ml. of 5% malic acid were used.

The results obtained from the titration of cobalt (3.64 mg.) with standard EDTA solution in the presence of 0.70 to 3.50 mg. of beryllium and 2 ml. of 5% malic acid are shown in Table IV. It was found that beryllium gives no effects in the titration of cobalt.

TABLE IV. TITRATION OF COBALT IN THE PRESENCE OF BERYLLIUM

Co taken, mg.	Be added, mg.	Vol. of 0.01016 mol. EDTA titrated, ml.	Co found, mg.	Error, mg.
3.64	0.70	6.08	3.64	±0.00
3.64	1.40	6.07	3.63	−0.01
3.64	1.40	6.09	3.65	+0.01
3.64	2.10	6.08	3.64	±0.00
3.64	3.50	6.07	3.63	−0.01

The optimum conditions for the general procedure were concluded as follows: the amount of ammonium carbonate added, 1.5 to 2.0 g.; the volume of saturated Luteo salt solution added, 2 ml.; the time allowed for the precipitate II to form, about 3 hr. after Luteo salt was added; the volume of 5% malic acid added, 2 ml.

5) Determination of Various Concentrations of Beryllium under the Optimum Conditions. — Various concentrations of

beryllium were determined by following the general procedure under the optimum conditions and the results are shown in Table V. Thus, it was concluded that the indirect titration of beryllium was satisfactorily carried out.

TABLE V. DETERMINTION OF VARIOUS CONCENTRATIONS OF BERYLLIUM AT THE OPTIMUM CNDITIONS

Be taken, mg.	Vol. of 0.01016 mol. EDTA titrated, ml.	Be found, mg.	Error, mg.
0.70	3.90	0.71	+0.01
0.70	3.84	0.70	±0.00
1.40	7.63	1.40	±0.00
1.40	7.68	1.41	+0.01
2.10	11.36	2.08	−0.02
3.50	19.02	3.48	−0.02

6) The Determination in the Presence of Iron (III), Aluminum and Magnesium. — After EDTA solution (0.1 mol., 5 ml.) and ammonium chloride (0.5 g.) were added to the sample solution containing iron(III), aluminum and magnesium, aqueous ammonia (1 : 1, 1 ml.) was added to the solution. At that time only beryllium hydroxide was precipitated. Then, 2 g. of ammonium carbonate was added to the solution and beryllium hydroxide was dissolved by stirring. The subsequent determination of beryllium was carried out by the procedure described above. In this case, iron, aluminum and magnesium were completely separated from beryllium when the precipitate II was formed and filtered. The results are shown in Table VI.

It is shown that the determination of berylium in the presence of these metals was carried out satisfactiorily. Therefore, this procedure is considered useful for a practical analysis of beryllium.

TABLE VI. DETERMINATION OF BERYLLIUM IN THE PRESENCE OF IRON(III), ALUMINUM AND MAGNESIUM

Be taken, mg.	Other metals added.	mg.	Vol. of 0.01016 mol. EDTA titrated, ml.	Be found, mg.	Error, mg.
1.40	Fe^{3+}	2.0	7.70	1.41	+0.01
1.40	Fe^{3+}	4.0	7.60	1.39	−0.01
1.40	Fe^{3+}	8.0	7.58	1.39	−0.01
1.40	Al^{3+}	1.7	7.64	1.40	±0.00
1.40	Al^{3+}	3.4	7.60	1.39	−0.01
1.40	Al^{3+}	6.8	7.55	1.38	−0.02
1.40	Mg^{2+}	2.1	7.65	1.40	±0.00
1.40	Mg^{2+}	8.3	7.69	1.41	+0.01

Summary

When Luteo salt was added to beryllium carbonate complex solution, the precipitate $[Co(NH_3)_6][(H_2O)_2Be_2(CO_3)_2(OH)_3]\cdot 3H_2O$ was obtained. In this experiment, the indirect determination of beryllium was tried by the titration of the cobalt content in the precipitate with EDTA. The following procedures were examined mainly; the formation of the precipitate II, the decomposition of the precipitate and titration of cobalt in the presence of beryllium. In the optimum conditions, 0.70 to 3.50 mg. of beryllium were determined quantitatively. This method could be applied to separation and determination of beryllium from iron(III), aluminum and magnesium by using EDTA as a masking agent.

Department of Chemistry
Faculty of Science
Kyusyu University
Hakozaki, Fukuoka

Molecular Rotations of Glucides in Relation to their Structures. VII.[1] *Internal Conformation of $O^{1\alpha}$—C^m Bond in $(OCH_3)^{1\alpha}$ of Methyl α-D-Xylopyranoside and of Methyl β-L-Arabinopyranoside in Aqueous Solutions*[2]

By Shukichi YAMANA

(Received October 21, 1958)

Although the internal conformation of $O^{1\alpha}$—C^m bond[3] in $(OCH_3)^{1\alpha}$ of methyl α-D-xylopyranoside[5,6] or of methyl β-L-arabinopyranoside[6,7] in crystalline state has been studied from the standpoint of X-ray analysis, those in the aqueous solutions have not yet been determined owing to the lack of a suitable method. (Fig. 1)

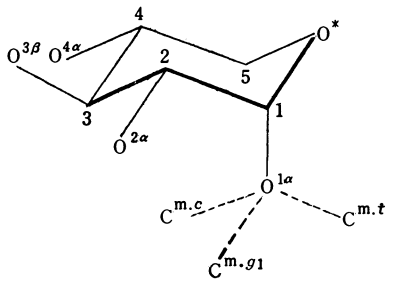


Fig. 1. Perspective drawing of the molecular model of methyl α-D-xylopyranoside: *t—trans* ($\phi_{1\alpha}=0°$), *g1—gauche* 1 ($\phi_{1\alpha}=120°$), *c—cis* ($\phi_{1\alpha}=180°$).

Hudson empirically observed the existence of a certain quantitative relationship between the structure of methyl glycosides and their molecular rotations, $[M]_D^{20}(W)$[8], but no one has attempted to utilize these $[M]_D^{20}(W)$ values for the determination of the internal conformation of their $O^{1\alpha}$—C^m bonds. Recently, the present author succeeded in presuming the internal conformation of C^6—O bond in D-mannopyranose in its aqueous solution by using $[M]_D^{20}(W)$ values of some glucides[9]. By a similar method, the internal conformation of $O^{1\alpha}$—C^m bond in $(OCH_3)^{1\alpha}$ of methyl α-D-xylopyranoside and of methyl β-L-arabinopyranoside in aqueous solutions has been presumed in this article.

Molecular Model and Data Used.—As the molecular model, the one proposed by McDonald and Beevers was used. The values of bond lengths and valency angles concerning the side chain are assumed as follows; $O^{1\alpha}$—C^m is 1.421 Å[a] and $\angle C^1O^{1\alpha}C^m$ is a tetrahedral angle (109° 28′). The unit groups in the glucide molecules under discussion and their corresponding molecular rotations are given in Table I.

As the optical data for OH, CH_3 and H, the values used in the previous papers[1,4]

TABLE I

Name	Unit groups	$[M]_D^{20}(W)$	Lit.
methyl α-D-xyloside	$[(OCH_3)^{1\alpha}$,[10] $(OH)^{2\alpha}$, $(OH)^{3\beta}$, $(OH)^{4\alpha}$, Ring]	252.6°	(b)
methyl β-L-arabinoside	$[(OCH_3)^{1\alpha}$, $(OH)^{2\alpha}$, $(OH)^{3\beta}$, $(OH)^{4\beta}$, Ring]	403.0°	(c)
α-D-xylose	$[(OH)^{1\alpha}$, $(OH)^{2\alpha}$, $(OH)^{3\beta}$, $(OH)^{4\alpha}$, Ring]	140.5°	(b)
β-L-arabinose	$[(OH)^{1\alpha}$, $(OH)^{2\alpha}$, $(OH)^{3\beta}$, $(OH)^{4\beta}$, Ring]	286.1°[11]	(c)

1) Part VI; S. Yamana, This Bulletin, **31**, 564 (1958).
2) Reported at the Symposium on the Structural Chemistry, held on October 13, 1958, at Kyoto, under the auspices of the Chemical Society of Japan.
3) $O^{1\alpha}$ means the O atom which combines with C^1-atom of the aldopyranose-ring in α-orientation, and so on. (Cf. the foot-note *5 in the previous paper[4]). C^m means the C atom in methyl group. Then, $O^{1\alpha}$—C^m bond is the O—C bond in $(OCH_3)^{1\alpha}$. (Ref. Fig. 1).
4) S. Yamana, This Bulletin, **30**, 203 (1957).
5) E. G. Cox, *J. Chem. Soc.*, **1932**, 2535.
6) H. Braekken, C. J. Koren and N. A. Sörensen, *Z. Krist.*, **88**, 205 (1934).
7) E. G. Cox and T. H. Goodwin, **85**, 462 (1933); E. G. Cox, T. H. Goodwin and (Miss) A. I. Wagstaff, *J. Chem. Soc.*, **1935**, 978.
8) C. S. Hudson, *J. Am. Chem. Soc.*, **31**, 66 (1909).
9) S. Yamana, This Bulletin, **30**, 920 (1957).
a) D. G. Burkhard and D. M. Dennison. *Phys. Rev.*, **84**, 408 (1951).
10) The internal conformation of $O^{1\alpha}$—C^m bond in $(OCH_3)^{1\alpha}$ of methyl α-D-xyloside is the same as that of methyl β-L-arabinoside. Concerning this information, refer to "**Method Proposed**" in this article.
b) F. J. Bates and Associates, "Polarimetry, Saccharimetry and the Sugars", United States Government Printing Office, Washington (1942), p. 759.
c) Ibid., p. 708.
11) Hudson's datum is 303.3°. (Ref. the foot-note *12 in the previous paper[12].)
12) S. Yamana, This Bulletin, **31**, 558 (1958).

are again adopted in this article. In order to simplify the calculations, the optical centers of OH and CH_3 groups are assumed to be located at O and C atoms, respectively[13]. Accordingly, the value of ζ_{CH_3} becomes 0.2880 $(3/n^2+2)^{1/2}$ [14]. The refractive indices of the aqueous solutions of these methyl glycosides are presumed to be nearly equal to 1.34[15].

Method Proposed.—If the orientation of $(OH)^4$ in methyl β-L-arabinopyranoside is changed from β to α, methyl α-D-xylopyranoside is obtained[16]. But, throughout the course of this process, the distance between $(CH_3)^{\leftarrow 1\alpha}$ [17] and $(OH)^4$ is so much larger[18] than those between $(CH_3)^{\leftarrow 1\alpha}$ and the other atoms (than $(OH)^4$) in the same molecules, that the orientation-change of $(OH)^4$ should not cause any influence on the internal conformation of $O^{1\alpha}$—C^m bond. In other words, the internal conformation of $O^{1\alpha}$—C^m bond in $(OCH_3)^{1\alpha}$ of methyl α-D-xylopyranoside is said to be the same as that of methyl β-L-arabinopyranoside in their aqueous solutions. Then, the unit groups which can couple with $(OH)^4$ dynamically in the molecules of methyl α-D-xylopyranoside and of methyl β-L-arabinopyranoside are $(OCH_3)^{1\alpha}$, $(OH)^{2\alpha}$, $(OH)^{3\beta}$ and Ring[16]. Therefore, Yo. Diff.[20] between these two methyl glycosides is given by the following equation,

$$\{(4\alpha)-(4\beta)\}\lambda\{(OCH_3)^{1\alpha}+(2\alpha)+(3\beta)+R\}^{21)}=(4\alpha)\lambda(OCH_3)^{1\alpha}+(4\alpha)\lambda(2\alpha)+(4\alpha)\lambda(3\beta)+(4\alpha)\lambda R\}-\{(4\beta)\lambda(OCH_3)^{1\alpha}+(4\beta)\lambda(2\alpha)+(4\beta)\lambda(3\beta)+(4\beta)\lambda R\}\equiv I$$

Similarly, Yo. Diff. between α-D-xylopyranose and β-L-arabinopyranose is given by,

$$\{(4\alpha)-(4\beta)\}\lambda\{(1\alpha)+(2\alpha)+(3\beta)+R\}=\{(4\alpha)\lambda(1\alpha)+(4\alpha)\lambda(2\alpha)+(4\alpha)\lambda(3\beta)+(4\alpha)\lambda R\}-\{(4\beta)\lambda(1\alpha)+(4\beta)\lambda(2\alpha)+(4\beta)\lambda(3\beta)+(4\beta)\lambda R\}\equiv J$$

Accordingly, $I-J$ [22] $=\{(4\alpha)\lambda(OCH_3)^{1\alpha}-(4\beta)\lambda(OCH_3)^{1\alpha}\}-\{(4\alpha)\lambda(1\alpha)-(4\beta)\lambda(1\alpha)\}=(4\alpha)\lambda(OCH_3)^{1\alpha}-(4\beta)\lambda(OCH_3)^{1\alpha}\}-\{(4\alpha)\lambda(OH)^{1\alpha}-(4\beta)\lambda(OH)^{1\alpha}\}$ [23] (1)

$(OCH_3)^{1\alpha}$ may be considered to occur by replacing $H^{\leftarrow 1\alpha}$-atom[25] in $(OH)^{1\alpha}$ by $CH_3{}^{\leftarrow\alpha}$ group. And because of the small polarizability of $H^{\leftarrow 1\alpha}$, $(4\alpha)\lambda H^{\leftarrow 1\alpha}\simeq 0$ and $(4\beta)\lambda H^{\leftarrow 1\alpha}\simeq 0$. Therefore, Eq. 1 can be simplified as below;

$$I-J=[(4\alpha)\lambda\{O^{1\alpha}+(CH_3)^{\leftarrow 1\alpha}\}-(4\beta)\lambda\{O^{1\alpha}+(CH_3)^{\leftarrow 1\alpha}\}]-[(4\alpha)\lambda\{O^{1\alpha}+H^{\leftarrow 1\alpha}\}-(4\beta)\lambda\{O^{1\alpha}+H^{\leftarrow 1\alpha}\}]\simeq(4\alpha)\lambda(CH_3)^{\leftarrow 1\alpha}-(4\beta)\lambda(CH_3)^{\leftarrow 1\alpha}$$ [26]

The value of this $\{(4\alpha)\lambda(CH_3)^{\leftarrow 1\alpha}-(4\beta)\lambda(CH_3)^{\leftarrow 1\alpha}\}$ was calculated by PM-method[27] as a function of $\phi_{1\alpha}$[19]. These values, $[\mu]_{D\ obs}^{20}$ for $(I-J)$ are shown in Table II.

The corresponding observed value of $(I-J)$, given by $[\{([M]_D^{20}(W)$ of methyl α-D-xylopyranoside) minus $([M]_D^{20}(W)$ of

13) In Eq. 5 of the previous paper[1], ζ_{CH3} was calculated as 0.1962 $(3/n^2+2)^{1/2}$ on the supposition that the optical center of CH_3 group is located at the center of mass of ^rC—(CH_3) bond (cf. the foot-note *13 of the previous paper[12].) But here, since CH_3 group combines with O atom instead of ^rC-atom, the above value of ζ_{CH3} is hardly adoptable.

14) According to Hudson's data of L-arabinoses, $\zeta_{CH3}=0.6206(3/n^2+2)^{1/2}$. (Ref. the foot-note *31 in the previous paper[1]).

15) The refractive index (n) of an aqueous solution of methyl glycoside is 1.33~1.35[d]. When the value of n changes by 0.01, $(n^2+2/3)$ changes by $\partial/\partial n(n^2+2/3)\delta n\simeq 0.007$. The magnitude of this value of $(n^2+2/3)$-change is very small and may be neglected on comparison with that of $(n^2+2/3)\simeq 1.265$. On the other hand, $[\mu]_{D\ obs}^{20}$ contains the factor n in itself only in the form of $(n^2+2/3)$. (Ref. "**Theoretical Formulae**" in the previous paper[4].) Then, $[\mu]_{D_{obs}}^{20}$, resulting from the dynamical coupling between two definite unit groups may be considered to be constant in that range of $n=1.33\sim1.35$.

d) "International Critical Tables of Numerical Data", Vol. 7. p. 69.

16) Ref. Table I in this article.

17) $(CH_3)^{\leftarrow 1\alpha}$ indicates the CH_3 group which combines with $O^{1\alpha}$-atom, and so on. Therefore, $(CH_3)^{\leftarrow 1\alpha}$ is the CH_3 group in $(OCH_3)^{1\alpha}$. (Ref. Fig. 1).

18) Since C^1- and C^4-atoms are situated nearly on the opposite ends of a diameter of the aldopyranose-ring together, the distances between C^m-atom[3] in $(CH_3)^{\leftarrow 1\alpha}$ and the O atom in $(OH)^4$ are shown below:

	longest	shortest
$(OH)^{4\alpha}$	5.91 Å (at $\phi_{1\alpha}$[19]$=60°$)	3.63 Å (at $\phi_{1\alpha}=240°$)
$(OH)^{4\beta}$	5.60 Å (at $\phi_{1\alpha}=60°$)	4.23 Å (at $\phi_{1\alpha}=240°$)

19) The author defined an angle $\phi_{1\alpha}$ which determines the internal conformation of $O^{1\alpha}$—C^m bond as follows; (i) $\phi_{1\alpha}$ is zero at the situation where C^m— and C^2-atoms are in *trans* position each other. (ii) The value of rotation in the positive direction increases with the distance between C^*- and C^m-atoms. (Fig. 1).

20) Yo. Diff. is an abbreviated symbol of "yomeric difference". This is $[M]_D^{20}(W)$-change of a glucide, caused by the orientaionchange of $(OH)^4$ from β to α. (ref. the foot-note *10 in the previous paper[1].)

21) Ref. the foot-note *12 in the previous paper[1].

22) J is adopted only for the purpose of canceling the terms concerning the aldopyranose-ring, R, in I.

23) Ref. the foot-note *10 in the previous paper[24].

24) S. Yamana, This Bulletin, **30**, 916 (1957).

25) $H^{\leftarrow 1\alpha}$ means the H atom which combines with $O^{1\alpha}$-atom. (Cf. the foot-note 17 in this article).

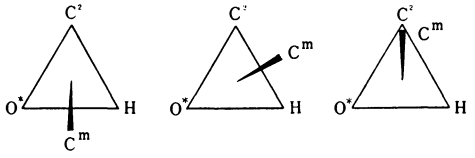
26) In other expressions, $(OCH_3)^{1\alpha}\simeq(OH)^{1\alpha}+(CH_3)^{\leftarrow 1\alpha}$ $\therefore$ Eq. $1=[(4\alpha)\lambda(OCH_3)^{1\alpha}-(4\beta)\lambda(OCH_3)^{1\alpha}]-[(4\alpha)\lambda(OH)^{1\alpha}-(4\beta)\lambda(OH)^{1\alpha}]\simeq[(4\alpha)\lambda\{(OH)^{1\alpha}+(CH_3)^{\leftarrow 1\alpha}\}-(4\beta)\lambda\{(OH)^{1\alpha}+(CH_3)^{\leftarrow 1\alpha}\}]-[(4\alpha)\lambda(OH)^{1\alpha}-(4\beta)\lambda(OH)^{1\alpha}]=(4\alpha)\lambda(CH_3)^{\leftarrow 1\alpha}-(4\beta)\lambda(CH_3)^{\leftarrow 1\alpha}$

27) Ref. the foot-note *17 in the previous paper[12].

TABLE II. $\sum[\mu]^{20}_{Dobs}$ FOR THE DIFFERENCE BETWEEN TWO YOMERIC DIFFERENCE *I* AND *J*, AS A FUNCTION OF $\phi_{1\alpha}$

$\phi_{1\alpha}$	Isbell and Pigman's data of L-arabinoses	Hudson's data[14] of L-arabinoses
0	5.7	12.2
20	4.5	9.7
40	2.8	5.9
60	1.3	2.8
80	−1.4	−3.0
100	−3.3	−7.2
120	−4.9	−10.5
140	−5.7	−12.3
160	−5.5	−11.9
180	−4.2	−9.1
200	−2.1	−4.6
220	−0.4	−0.8
240	0.0	0.1
260	−0.2	−0.4
280	0.7	1.5
300	2.8	6.1
320	4.9	10.5
340	5.9	12.6

methyl β-L-arabinopyranoside)} minus {([M]$^{20}_{D}$(W) of α-D-xylopyranose) minus ([M]$^{20}_{D}$(W) of β-L-arabinopyranose)}], becomes −4.8 on the basis of the Isbell and Pigman's data of L-arabinoses or 12.4 on the basis of the Hudson's data of L-arabinoses[16]. The former value coincides with the calculated value when $\phi_{1\alpha}$ is 120° or 180° as seen in the second column of Table II and the latter value coincides with that when $\phi_{1\alpha}$ is 0° as seen in the third column of Table II. It follows from this result that there are three possible internal conformations of $O^{1\alpha}$—C^m bond as figured in Fig. 2.



trans $\phi_{1\alpha}=0°$ (Hudson) | *gauche* 1 $\phi_{1\alpha}=120°$ (Isbell and Pigman) | *cis* $\phi_{1\alpha}=180°$ (Isbell and Pigman)

Fig. 2. Internal conformation along $O^{1\alpha}$—C^1 axis.

Discussion of the Results

Among the above three possibilities, it seems difficult for a *cis* form to exist owing to the repulsion between C^2-atom and $(CH_3)^{\leftarrow 1\alpha}$. The internal conformation under consideration, therefore, should be either a *trans*- or a *gauche* 1 form.

C^5—O*—C^1—$O^{1\alpha}$—C^m moiety in methyl α-D-xylopyranoside (Ref. Fig. 1) and also in methyl β-L-arabinopyranoside, is considered to be a kind of polyoxymethylene-chain. The internal conformation of a polyoxymethylene-chain along its C—O axis has been investigated by the methods of measuring the dipole moment, infrared spectrum, etc.[28,29] And it has been concluded that the most stable form of —C—O—C—O—C— chain is a *gauche* type[30]. From these facts, O*—C^1—$O^{1\alpha}$—C^m moiety in the methyl glycoside under discussion is likely to exist in the conformation which corresponds to $\phi_{1\alpha}=0°$. This leads to the following anticipation.

The position of the minimal potential of $O^{1\alpha}$—C^m bond corresponds to $\phi_{1\alpha}=0°$. (Anticipation 1)

On the other hand, C^2—C^1—$O^{1\alpha}$—C^m moiety in metyl α-D-xylopyranoside and in methyl β-L-arabinopyranoside is a kind of polyethyleneglycol-chain. Because of the non-polar property of its C—C bond and of the steric repulsion between two C-atoms in —C—C—O—C— chain, —C—C—O—C— along its C—O axis is strongly expected to be more stable in a *trans* form than in a *gauche* form. This produces the conclusion that the conformation under discussion would be more advantageous at $\phi_{1\alpha}=0°$ than at $\phi_{1\alpha}=120°$. In other words,

$O^{1\alpha}$—C^m bond has a tendency to keep the position corresponding to $\phi_{1\alpha}=0°$ rather than that corresponding to $\phi_{1\alpha}=120°$. (Anticipation 2)

This anticipation is consistent with Anticipation 1. Therefore, concerning [M]$^{20}_{D}$ (W) of L-arabinoses, Hudson's data seem to be more reliable than Isbell and Pigman's data[31].

28) T. Uchida, Y. Kurita and M. Kubo, *J. Polymer Sci.*, **19**, 365 (1956).

29) A. R. Philpotts, D. O. Evans and N. Sheppard, *Trans. Faraday Soc.*, **51**, 1051 (1955).

30) Notice that the shape of a polyoxymethylene-chain shown by the word "*gauche* type" in this case is not the same as that of O*—C^1—$O^{1\alpha}$—C^m corresponding to the internal conformation of $O^{1\alpha}$—C^m bond of a *gauche* type in Figs. 1 and 2. O*—C^1—$O^{1\alpha}$—C^m moiety in Figs. 1 and 2 can become a *gauche* type of polyoxymethylene-chain when $\phi_{1\alpha}$ is 0° and become a *trans* type of polyoxymethylene-chain when $\phi_{1\alpha}$ is 120°. (Ref. Fig. 3).

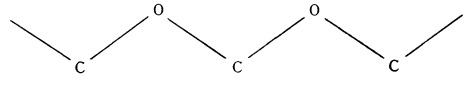


Fig. 3. Polyoxymethylene-chain of *trans* type.

31) If Isbell and Pigman's data are correct, it must be concluded that the internal conformation of $O^{1\alpha}$—C^m bond corresponds to $\phi_{1\alpha}=120°$. In this case, a kind of the attractive force should be considered between $O^{2\alpha}$-atom and C^m-atom (strictly speaking, the H atom which is combined with C^m-atom).

Summary

By the author's new method, the internal conformation of $O^{1\alpha}—C^{m}$ bond in $(OCH_3)^{1\alpha}$ of methyl α-D-xylopyranoside and of methyl β-L-arabinopyranoside in aqueous solutions was presumed. At the same time, Isbell and Pigman's data and Hudson's data of $[M]_D^{20}(W)$ of L-arabinoses were discussed.

The author wishes to express his sincere gratitude to Professor S. Tanaka (Kyoto University) and Professor T. Yamamoto (Kyoto University) who is studying in the University of Oregon for their special interests in this series of research.

Department of Chemistry
Kyoto Gakugei University
Fushimi-ku, Kyoto

On the Intramolecular Charge Transfer Spectra and Structure of Isomeric Aminopyridines

By Noboru MATAGA and Shizuyo MATAGA

(Received November 6, 1958)

In a series of papers, we have reported detailed theoretical studies on the electronic structure and the nature of electronic transitions of nitrogen heterocycles[1-5]. The detailed Hartree-Fock SCF study has been made only for nitrogen heterobenzenes such as pyridine[1], pyrazine[1], *sym*-triazine[1] and *sym*-tetrazine[2]. In addition, some extensions to larger molecules such as quinoline[3,5], isoquinoline[3,5], phthalazine[5], quinoxaline[5], acridine[4,5] and phenazine[4,5] have been made on the basis of the results obtained for nitrogen heterobenzenes, employing the perturbation method based on the Hartree-Fock SCF theory. Thus a theoretical ground for the classification and interpretation of the electronic spectra of nitrogen heterocycles has been given. As an extension of these investigations, we have studied the electronic structure and the spectra of some substituted nitrogen heterocycles. Among these, we have taken up the isomeric aminopyridines. There have been some disputes concerning the molecular forms of these molecules, especially 2- and 4- aminopyridines, i. e., imine-enamine tautomerism[6]. However, the possibility of the existence of imino-form was rejected by Anderson and Seeger[7] by spectral studies of these and related molecules and also Angyal and Angyal[8] reported that these compounds exist predominantly in the amino-form by critically surveying the foregoing data and arguments and also by the measurement of pK_a values of these molecules and related ones. Nevertheless, there seem to remain some ambiguities about this problem, even now. Morita[9] has calculated the electronic spectra of 4-aminopyridine by a method analogous to Dewar and Paoloni[10], assuming various models with respect to the molecular forms of this molecule. However, no definite conclusion about the form of this molecule has been derived from his calculation. We have tried to make clear the interrelation among the isomeric aminopyridines and their relation to aniline, pyridine and benzene, with respect to the electronic structure and spectra. We have assumed the amino-form of these isomers and attempted to interpret the observed spectra. It will be expected that some contributions to the problem of the tautomerism of these molecules will be made also by such a study even if it is by an indirect method.

1) N. Mataga and K. Nishimonto, *Z. physik. Chem. N. F.*, **13**, 140 (1957).
2) N. Mataga, This Bulletin, **31**, 453 (1958).
3) N. Mataga, ibid., **31**, 459 (1958).
4) N. Mataga, ibid., **31**, 463 (1958).
5) N. Mataga, *Z. physik. Chem. N. F.*, **18**, 285 (1958).
6) See, for example, E. A. Steck and G. W. Ewing, *J. Am. Chem. Soc.*, **70**, 3397 (1948).
7) L. C. Anderson and N. V. Seeger, ibid., **71**, 340 (1949).
8) S. J. Angyal and C. L. Angyal, *J. Chem. Soc.*, **1952**, 1461.
9) T. Morita, presented at the "Symposium on the Electronic States of Molecules", held by Chem. Soc. Japan and Phys. Soc. Japan on october 13, 1958.
10) M. J. S. Dewar and L. Paoloni, *Trans. Faraday Soc.*, **53**, 261 (1957).

Method

Previously, Tsubomura[11] has studied the electronic spectra of substituted pyridines by the electron migration theory of Sklar and Herzfeld[12]. The general features of the substituted pyridine spectra have been well comprehended by his study. As pointed out by Goodman and Shull[13] in the case of substituted benzene spectra, however, for certain very strongly conjugating substituents, e. g., $-NH_2$, such a simplified perturbation method may be essentially invalid, and a more rigorous method will be needed. In the present study we have used the method developed by Longuet-Higgins and Murrell[14] for the study of the composite system. An excellent treatment based on an analogous idea has been developed independently by Nagakura and Tanaka[15]. Hereafter the outline of the method will be mentioned briefly.

Generally speaking, the electron transfer states are of two kinds, according as the electron is transferred from pyridine to the substituent or from the substituent to pyridine. In the present case, however, the substituent is a fairly strong electron donor and accordingly the configuration in which the electron is transferred from pyridine to the substituent will have a very high energy compared with the opposite case and may be neglected.

With this approximation, the problem is reduced to an evaluation of the interaction between the locally excited states of pyridine and one set of electron transfer states in which the electron is transferred from the substituent to pyridine.

If the SCFMO's of pyridine are written $\phi_1 \cdots\cdots \phi_p$ and those of the substituent $\theta_1 \cdots\cdots \theta_s$, then the energy of the electron transfer configuration $\chi_{s\to k}$ where one electron is transferred from an occupied orbital θ_s to an unoccupied orbital ϕ_k, is given by

$$E(\chi_{s\to k}) = \varepsilon_k - \varepsilon_s - \int \theta_s^2(i) \frac{e^2}{r_{ij}} \phi_k^2(j) \mathrm{d}v(i) \mathrm{d}v(j) \quad (1)$$

where ε_k and ε_s are SCFMO energies of ϕ_k and θ_s, respectively, and ϕ_k's are linear combinations of $2p\pi$ AO's $\phi_1 \cdots\cdots \phi_p$ of carbon or nitrogen

$$\phi_k = \sum_\mu c_{k\mu} \phi_\mu \quad (2)$$

Now, in actual computation, ε_s will be given, to a good approximation, by the ionization potential of ammonia. The difference of the observed[16] and calculated[17] values of electron affinity of benzene, $\Delta A = A_{\text{benz}}^{\text{obs}} - A_{\text{benz}}^{\text{calc}}$ has been added to the calculated values of ε_k's.

With neglect of differential overlap, the integral in 1 is reduced to

$$\sum_\mu \gamma_{s\mu} = \sum_\mu \int \theta_s^2(i) \frac{e^2}{r_{ij}} \phi_\mu^2(j) \mathrm{d}v(i) \mathrm{d}v(j) \quad (3)$$

These integrals have been replaced by the interaction energy of point charges centered on the substituent and on the μ atom, taking the length of bond joining the substituent and pyridine to be 1.46 Å. The matrix elements of the interaction between the various configurations have been evaluated from the following formulae,

$$(\chi_{s\to k} | \boldsymbol{H} | \chi_{j\to l}) = -\delta_{kl} \int \theta_s(i) H(i) \phi_j(i) \mathrm{d}v(i) \quad (4)$$

$$(\chi_{s\to k} | \boldsymbol{H} | \chi_0) = \sqrt{2} \int \theta_s(i) H(i) \phi_k(i) \mathrm{d}v(i) \quad (5)$$

$$(\chi_{s\to k} | \boldsymbol{H} | \chi_{s\to l}) = -(sk|G|sl) = -\int \theta_s^2(i) \frac{e^2}{r_{ij}} \phi_k(j) \phi_l(j) \mathrm{d}v(i) \mathrm{d}v(j) \quad (6)$$

The integral $\int \theta_s(i) H(i) \phi_j(i) \mathrm{d}v(i)$ can be reduced to $c_{jr} \int \theta_s(i) H(i) \phi_r(i) \mathrm{d}v(i)$ the substitutent being attached to carbon atom 'r'.

We have used a reasonable value for $\beta_{RS} = \int \theta_s(i) H(i) \phi_r(i) \mathrm{d}v(i) = -1.6$ eV. which is the same value as that used by Murrell[14] for the study of aniline. The wave functions and energies above the ground state of locally excited states of pyridine to be used in the present calculation are as follows[15]:

11) H. Tsubomura, *J. Chem. Soc. Japan, Pure Chem. Sec.* (*Nippon Kagaku Zasshi*), **78**, 293 (1957).
12) A. L. Sklar, *J. Chem. Phys.*, **7**, 987 (1939); K. F. Herzfeld, *Chem. Revs.*, **41**, 233 (1947); H. Baba and S. Nagakura, *J. Chem. Soc. Japan, Pure Chem. Sec.* (*Nippon Kagaku Zasshi*), **72**, 72 (1951).
13) L. Goodman and H. Shull, *J. Chem. Phys.*, **27**, 1388 (1957).
14) H. C. Longuet-Higgins and J. N. Murrell, *Proc. Phys. Soc.*, A**68**, 601 (1955); J. N. Mureell, ibid., **68**, 969 (1955).
15) S. Nagakura and J. Tanaka, *J. Chem. Phys.*, **22**, 236 (1954); S. Nagakura, ibid., **23**, 1441 (1955); J. Tanaka, S. Nagakura and M. Kobayashi, ibid., **24**, 311 (1956); J. Tanaka and S. Nagakura, ibid., **24**, 1274 (1956).
16) Blackedge and Hush, quoted in N. S. Hush and J. A. Pople, *Trans. Faraday Soc.*, **51**, 600 (1955).
17) N. Mataga, K. Nishimoto and S. Mataga, This Bulletin, **32**, 395 (1959).

	E (eV.)
$\Psi(L_b)=0.8202\chi_{3\to4}-0.5720\chi_{2\to5}$	5.009
$\Psi(L_a)=0.8688\chi_{3\to5}+0.4951\chi_{2\to4}$	6.248
$\Psi(B_a)=0.4951\chi_{3\to5}-0.8688\chi_{2\to4}$	7.229
$\Psi(B_b)=0.5720\chi_{3\to4}+0.8202\chi_{2\to5}$	7.159

Results and Discussion

The interactions which occur between the various electronic states are shown in Table I.

As shown in Table I, in the case of 4-amino-pyridine, the seventh order matrix splits off into fourth and third order matrices, owing to the c_{2v} symmetry of the molecule.

Now, the wave functions and energies of the electronic states of 4-amino-pyridine are easily obtained as shown in Table II by solving the secular equations. In Table II, the corresponding quantities for aniline* are also indicated for the purpose of comparison.

TABLE I. THE MATRIX ELEMENTS OF THE INTERACTIONS BETWEEN THE ELECTRONIC STATES DUE TO THE CHARGE TRANSFER

2-Amino-pyridine

χ_0	L_b	L_a	B_a	B_b	$\chi_{s\to4}$	$\chi_{s\to5}$
0	0	0	0	0	−0.765	1.138
	5.009	0	0	0	0.652	0.166
		6.248	0	0	−0.144	0.691
			7.229	0	0.252	0.394
				7.159	0.455	−0.238
					5.554	0.696
						5.286

3-Amino-pyridine

χ_0	L_b	L_a	B_a	B_b	$\chi_{s\to4}$	$\chi_{s\to5}$
0	0	0	0	0	−0.617	−1.125
	5.009	0	0	0	0.660	−0.330
		6.248	0	0	0.286	0.699
			7.229	0	−0.502	0.398
				7.159	0.460	0.474
					5.593	−0.405
						5.313

4-Amino-pyridine

χ_0	L_a	B_a	$\chi_{s\to4}$
0	0	0	1.333
	6.248	0	0.484
		7.229	−0.850
			4.643

L_b	B_b	$\chi_{s\to5}$
5.009	0	−0.559
	7.159	0.802
		6.221

TABLE II. THE WAVE FUNCTIONS AND ENERGIES OF THE ELECTRONIC STATES OF 4-AMINO-PYRIDINE AND ANILINE

4-Amino-pyridine

Energy (eV.)		χ_0	L_a	B_a	$\chi_{s\to4}$
−0.364	Ψ_0	0.963	0.019	−0.029	−0.263
4.609	$\Psi_{\mathrm{I}}(A_1)$	0.255	−0.261	0.286	0.885
6.352	$\Psi_{\mathrm{II}}(A_1)$	0.043	0.954	0.198	0.205
7.522	$\Psi_{\mathrm{III}}(A_1)$	0.057	0.122	−0.934	0.322
		L_b	B_b	$\chi_{s\to5}$	
4.750	$\Psi_{\mathrm{I}}(B_1)$	0.898	−0.138	0.416	
5.990	$\Psi_{\mathrm{II}}(B_1)$	0.425	0.511	−0.746	
7.651	$\Psi_{\mathrm{III}}(B_1)$	0.109	−0.846	−0.519	

Aniline

		χ_0	L_a	B_a	$\chi_{s\to4}$
−0.297	Ψ_0	0.972	−0.022	0.020	0.221
5.185	$\Psi_{\mathrm{I}}(A_1)$	0.192	0.550	−0.282	−0.762
6.404	$\Psi_{\mathrm{II}}(A_1)$	0.078	−0.793	−0.460	−0.384
7.315	$\Psi_{\mathrm{III}}(A_1)$	0.084	−0.250	0.839	−0.471
		L_b	B_b	$\chi_{s\to5}$	
4.704	$\Psi_{\mathrm{I}}(B_1)$	0.942	−0.092	0.316	
6.348	$\Psi_{\mathrm{II}}(B_1)$	0.296	0.702	−0.646	
7.588	$\Psi_{\mathrm{III}}(B_1)$	0.169	−0.704	−0.689	

As shown in Table II, in both 4-amino-pyridine and aniline, $\Psi_{\mathrm{I}}(B_1)$ is mainly contributed by L_b of pyridine and benzene, respectively, and accordingly the band due to the transition to this state may be regarded as a slightly modified L_b band in both of these molecules.

Contrary to this, $\Psi_{\mathrm{I}}(A_1)$ is mainly contributed by $\chi_{s\to4}$. Although the contribution of L_a to this state is still fairly great in the case of aniline, it becomes less prominent in the case of 4-amino-pyridine, and the contribution of $\chi_{s\to4}$ becomes more predominant (~80%). Therefore, the band due to the transition to this state in the case of 4-amino-pyridine may be called an intramolecular charge transfer band according to the naming of Nagakura and Tanaka[15].

Such a clear-cut classification of band character, however, does not hold in the case of the other isomers, various configurations being mixed in each state.

Now, whereas the MO ϕ_5 has the nodal plane through the C_2 axis of pyridine, the coefficient of AO at nitrogen has fairly great value in the MO ϕ_4. Accordingly, the increase of π-electron density or ring nitrogen caused by the substitution of an amino group for hydrogen may be determined by the degree of contribution of $\chi_{s\to4}$ to the ground state. This contribution is the greatest in the case of 4-amino-pyridine and the smallest in the case of

* The wave functions and energies of elctronic states of aniline collected in Table II are slightly different from those calculated by Murrell[14] because, in the present work, our parameters[1-5] have been used to calculate the wave functions and energies of benzene.

18) H. C. Longuet-Higgins, *J. Chem. Phys.*, 18, 275 (1950).

TABLE III. THE WEIGHT (%) $\chi_{s\to4}$ IN THE GROUND STATE WAVE FUNCTIONS OF ISOMERIC AMINOPYRIDINES

	% weight of $\chi_{s\to4}$	pK_a at 20°C
4-Amino-pyridine	6.9	9.17
2-Amino-pyridine	2.3	6.86
3-Amino-pyridine	1.4	5.98

3-amino-pyridine as shown in Table III. This is in accordance with the conclusion obtained by the qualitative discussion of resonance theory. In addition, this is in good correspondence with the experimental pK_a values as indicated in Table III, if it is allowed to be assumed that pK_a is proportional to the π-electron density on ring nitrogen[18],**. In Table IV, the calculated and observed spectra are compared, where only the two bands which originate from the transitions to the lowest and second lowest excited states are shown, because of the lack of experimental values for the other states.

TABLE IV. CALCULATED AND OBSERVED SPECTRA OF ISOMERIC AMINO-PYRIDINES

Excitation energy (eV.)		Obsd. intensity[a] (ε_{max})
Calcd.	Obsd.[a]	
	2-Amino-pyridine	
4.865	4.20	4000
5.266	5.26	12000
	3-Amino-pyridine	
4.845	4.13	3000
5.137	5.18	10000
	4-Amino-pyridine	
5.114	~4.6	weak
4.973	5.1	14000

a) Ref. 6.

In Table IV, we have assigned the 5.114 eV. band of 4-amino-pyridine to the observed lowest energy band because, according to the calculated result, this band can be regarded as a slightly modified L_b band and consequently is likely to be weak. Contrary to this, the 4.973 eV. band is likely to be strong since it is the intramolecular charge transfer band. Accordingly we have assigned this band to the observed strong band at 5.1 eV.

It is evident from Table IV that the calculated two excitation energies in the case of 4-amino-pyridine are close to each other, while those in the case of the other isomers are more separated. This theoretical prediction is in qualitative or semiquantitative agreement with the experimental observation. Eventually, the general features of electronic spectra and structure of the isomeric amino-pyridines are well comprehended by the present calculation assuming the amino-form of these molecules.

Summary

The electronic spectra and structure of isomeric amino-pyridines have been studied theoretically employing the general method for the study of a composite system. The calculated results correspond satisfactorily with the experiment, in general, and the nature of electronic transitions in these molecules has been made clear. Thus it is evident that there is no difficulty in assuming the amino-form of these molecules in interpreting theoretically their electronic spectra and structure.

We are grateful to Dr. S. Nagakura of the University of Tokyo, Mr. T. Morita of Tokyo Metroporitan University and Mr. T. Kubota of Shionogi Co., Ltd. for their fruitful discussions.

Institute of Polytechnics
Osaka City University
Minamiogimachi, Kita-ku
Osaka

** Of course, this is no more than a limited and very approximate treatment as pointed out elesewhere[a].

a) S. Mataga and N. Mataga, *Z. physik. Chem. N. F.*, in press; S. Tsuno and N. Mataga, *Busseiron Kenkyu*, 3, Ser. 2, 665 (1958).

The Aconite Alkaloids. XXVIII.[1] *The Isolation of a New Alkaloid, Sachaconitine, from Aconitum Miyabei, Nakai*

By Harusada SUGINOME, Nobukatsu KATSUI and Gen HASEGAWA

(Received September 4, 1958)

In a previous paper of this series[2], it was reported that two alkaloids, miyaconitine, $C_{23}H_{29}O_6N$, and miyaconitinone, $C_{23}H_{27}O_6N$, had been isolated from the roots of Aconitum Miyabei, Nakai. The present paper describes the isolation and the characterization of a new alkaloid, sachaconitine, which was obtained, in addition to the above-mentioned alkaloids, from the same material.

In the isolation of miyaconitine and miyaconitinone[2], they were crystallized from fraction III[3] and their mother liquors still contained appreciable amounts of basic substances.

The amorphous base obtained from the mother liquors was dissolved in 1 N-acetic acid and 10 % aqueous sodium carbonate was added to the solution. The precipitate was filtered off, and the filtrate was extracted with ether. The extracted base was then converted into the perchlorate. The crystalline perchlorate is easily soluble in alcohol and in hot water. From alcohol it crystallized in needles, m. p. 188~189°C, $[\alpha]_D$ −23.72° and from water its trihydrate crystallized in prisms, m. p. 180~185°C after softening at 100°C.

The composition, $C_{23}H_{37}O_4N \cdot HClO_4$, compares favorably with the analytical results; the formula was ascertained by analyses of acid oxalate, m. p. 182~183°C, aurichloride, m. p. 198~199°C, free base, m. p. 129~130°C, $[\alpha]_D$ −13.08°, and the diacetyl derivative, m. p. 114~116°C, $[\alpha]_D$ −10.87°.

It appears that this alkaloid has not yet been described, and the name "sachaconitine" was given to the new alkaloid. The analyses do not discriminate between H_{37} and H_{39} in the composition. Though the analytical result of diacetyl sachaconitine favors the latter, the formula with H_{37} seems more probable since it brings sachaconitine into line with other aconite alkaloids for reasons described below.

The base is stable against alkali and acid and thus contains no ester group. Acetylation of the base with acetyl chloride yielded a diacetyl compound which gave the original base on saponification. The presence of two methoxyl groups was confirmed by the Micro-Zeizel methoxyl determination. Hence the base contains two hydroxyl and two methoxyl groups.

The base gave ethyl iodide in the Herzig-Mayer *N*-alkyl determination and acetaldehyde on oxidation with permanganate, similarly to other aconite alkaloids containing an *N*-ethyl group, for example, lycoctonine[4-6], delpheline[7], and aconitine[8]. Coockson and Trevett[7] and Abubakirov and Yunusov[9] succeeded in confirming the presence of a simple *N*-alkyl group by converting de-ethyl derivatives (nor-compounds) into the corresponding alkaloids. It appears, therefore, that the new alkaloid also contains a simple *N*-ethyl group.

On the other hand, it has been reported[10] that atisine with an oxazolidine ring[11] gave also ethyl iodide in the *N*-alkyl determination by the same method. But sachaconitine contains two methoxyl and two hydroxyl groups, and no more oxygen atoms to make such a ring.

The base was not hydrogenated with platinum oxide in acidic solution. The ultraviolet spectrum of the base showed only end absorption (Fig. 1) quite similarly

1) Part XXVII, S. Furusawa, This Bulletin, **32**, 399 (1959).

2) H. Suginome, S. Furusawa, Y. Chiba and S. Kakimoto, *J. Fac. Sci., Hokkaido Univ., Ser. III. Chem.*, **4**, 1 (1950).

3) Fraction I is the part readily precipitable with aqueous ammonia. The mother liquor from fraction I is shaken with chloroform and then the resulting chloroform extract is treated with 1N-hydrochloric acid. Then the material obtained from chloroform solution is called fraction II and the part precipitated with ammonia from the acidic solution is called fraction III.

4) H. Suginome and K. Ohno, *J. Fac. Sci., Hokkaido Univ., Ser. III. Chem.*, **4**, 36 (1950).

5) M. S. Rabinovich and R. A. Konovalova, *J. Gen. Chem. (U. S. S. R.)*, **19**, 1387 (1949).

6) J. A. Goodson, *J. Chem. Soc.*, **1945**, 145.

7) R. C. Cookson and M. E. Trevett, ibid., **1956**, 2689.

8) R. Majima and K. Tamura, *Ann.*, **526**, 116 (1936).

9) N. K. Abubakirov and S. Yu. Yunusov, *J. Gen. Chem. U. S. S. R.* **27**, 733 (1954).

9) C. F. Huebner and W. A. Jacobs, *J. Biol. Chem.*, **170**, 515 (1947); **174**, 1001 (1948).

11) S. W. Pelletier and W. A. Jacobs, *J. Am. Chem. Soc.*, **76**, 4496 (1954).

to lycoctonine[12] possessing no unsaturation.

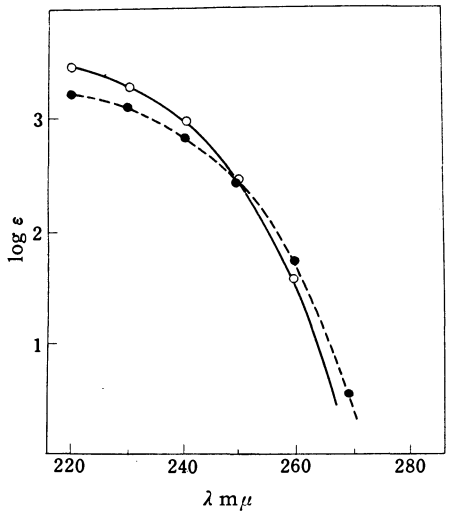


Fig. 1
Sachaconitine —○—○—
Lycoctonine ---●---●---

The above results relate the formula $C_{23}H_{37}O_4N$ of sachaconitine to other aconite alkaloids possessing the $C_{19}H_{29}N$ skeleton which is believed to be the fundamental base as pointed out by Suginome and Ohno[4], by Stern[13] and by Edwards and Marion[12]. Accordingly the formula can be extended as follows:

$$C_{19}H_{24}\begin{cases}(OCH_3)_2\\(OH)_2\\N-C_2H_5\end{cases}$$

The three alkaloids, miyaconitine, miyaconitinone and sachaconitine, were thus isolated from fraction III; they had no toxicity. In general, toxic bases containing an acyl and an aroyl group in aconite roots have been obtained from fraction I[3].

In attempts to isolate a crystalline substance from the amorphous base from the same roots, the fourth alkaloid, $C_{33}H_{45}O_9N$, m. p. 167~168°C, $[\alpha]_D$ +20.1° was isolated from fraction I. It agrees with delphinine in the composition but not in physical constants. Thus the name "base D" was assigned tentatively to this alkaloid. The investigation concerning the identification of "base D" with delphinine will be reported in a later paper.

12) O. E. Edwards and Leo Marion, *Can. J. Chem.*, **30**, 627 (1952).
13) E. S. Stern, "The Aconitum and Delphinium Alkaloids" in "The Alkaloids", Vol. IV, edited by R. H. F. Manske and H. L. Holmes, Academic Press Inc., New York (1954), p. 275.

Experimental

Isolation of Sachaconitine Perchlorate.— The residue of evaporation of the mother liquors from crystallization of miyaconitine and miyaconitinone perchlorate was converted into the free base by the usual method of treatment with chloroform and alkali. Amorphous basic material (14 g.) thus obtained was neutralized with 10% acetic acid and diluted with water. To the diluted solution 30% aqueous sodium carbonate was added until no more precipitate was produced. The precipitate was filtered off, but not examined.

The filtrate was subjected to continuous extraction with ether. Miyaconitinone remaining in the crude material separated out in prisms in 1 hr. Without removing it, extraction was continued further for 40 hr.

The extract, after being separated from miyaconitinone and dried over anhydrous sodium sulfate, was evaporated under reduced pressure to yield 7.5 g. of an amorphous material. This material was again neutralized with 0.1 N-hydrochloric acid and to the resulting solution 30% aqueous sodium perchlorate was added in small portions. On addition of the perchlorate the solution first became turbid but soon turned clear on stirring with further portions of the perchlorate solution. When turbidity was no longer noticed, the resulting solution was warmed on a steam bath until it became clear, treated with charcoal and filtered while hot. The perchlorate of the base separated as an oil on cooling the solution. The aqueous layer was decanted off and the oil was allowed to stand at room temperature overnight to give a gum containing some crystals which could not be separated. The gum was dissolved in a small amount of methanol and the solution was diluted with water until faint cloudiness remained. Concentration of the solution at room temperature gave 5 g. of crude sachaconitine perchlorate.

Sachaconitine perchlorate is easily soluble in alcohol and in hot water, and slightly soluble in cold water. From alcohol it crystallized in needles, m. p. 188~189°C, $[\alpha]_D^{20}$ −23.72° (C, 1.79 in alc.), and from water the trihydrate crystallized in plates, m. p. 188~189°C after softening at 100°C. The trihydrate gave the same m. p. and $[\alpha]_D$ after being dried over P_2O_5 under reduced pressure.

Anal. Found (anhydrous): C, 56.06; H, 7.70; N, 2.47; Cl, 7.34. Calcd. for $C_{23}H_{37}O_4N\cdot HClO_4$: C, 56.09; H, 7.72; N, 2.84; Cl, 7.21. Calcd. for $C_{23}H_{39}O_4N\cdot HClO_4$: C, 55.91; H, 8.16; N, 2.84; Cl, 7.18. Found (trihydrate): H_2O, 9.88. Calcd. for $C_{23}H_{37}O_4N\cdot HClO_4\cdot 3H_2O$: H_2O, 9.89%.

Sachatonitine. — The solution of the perchlorate in water was warmed to 50~60°C, and basified with aqueous sodium carbonate. The free base separated out as a resin, which soon solidified on cooling. Colorless plates from alcohol, m. p. 129~130°C, $[\alpha]_D^{20}$ −13.08° (C, 2.35 in 95% alc.).

Anal. Found: C, 70.35; H, 9.39; N, 3.59%. Calcd. for $C_{23}H_{37}O_4N$: C, 70.58; H, 9.46; N, 3.55%. Calcd. for $C_{23}H_{39}O_4N$: C, 70.19; H, 9.99; N, 3.56%.

The ultraviolet spectrum of the base showed only end absorption (Fig. 1).

The base was subjected to the Micro-Zeizel methoxyl, and the Herzig-Meyer *N*-alkyl determinations.

Anal. Found: CH_3O-, 15.91; C_2H_5-, 7.02. Calcd. for $C_{19}H_{26}O_2(OCH_3)_2 \cdot N \cdot C_2H_5$: CH_3O-, 15.85; C_2H_5-, 7.42%. Calcd. for $C_{19}H_{28}O_2(OCH_3)_2 \cdot N \cdot C_2H_5$: CH_3O-, 15.77; C_2H_5-, 7.38%.

The base (100 mg.) was submitted to the conventional Herzig-Meyer *N*-alkyl determination; the gases which evolved during pyrolysis of the hydroiodide were passed into a cold solution of trimethylamine in alcohol. The ethanol-soluble salt, ethyltrimethyl-ammonium iodide, was obtained from the trimethylamine solution.

Anal. Found: I, 59.27. Calcd. for $C_5H_{14}NI$: I, 59.04%.

The base absorbed no hydrogen in the presence of PtO_2 in acetic acid solution.

A solution of sachaconitine in 1N-potassium hydroxide in 50% aqueous methanol was refluxed on a steam bath for 30 min. From the resulting reaction mixture no acidic substance was detected, but unchanged sachaconitine was recovered.

Estimation of Acetaldehyde.—To a cold solution of 400 mg. of sachaconitine in 3 cc. of 1N-sulfuric acid, 15 cc. of 2% aqueous potassium permanganate was added dropwise in the course of 3 hr. After standing overnight, the manganese dioxide was filtered off and washed twice with water. The combined filterate and washings were distilled into a receiver containing 50 cc. of a slightly alkaline solution of 280 mg. of dimedone. Acidification with hydrochloric acid gave 73 mg. of acetaldehyde-dimedone, m. p. 139~140°C. It showed no depression of the melting point on admixture with an authentic specimen.

Sachaconitine Aurichloride. — The compound, prepared from the base and auric chloride, crystallized from a mixture of acetone and ether in prisms, m. p. 197~198°C (decomp.).

Anal. Found: Au, 26.88. Calcd. for $C_{23}H_{37}O_4N \cdot AuCl_3 \cdot HCl$: Au, 26.96%. Calcd. for $C_{23}H_{39}O_4N \cdot AuCl_3 \cdot HCl$: Au, 26.88%.

Sachaconitine Acid Oxalate.—The compound, prepared from the base and oxalic acid, crystallized from absolute alcohol in needles, m. p. 182~183°C, $[\alpha]_D^{20}$ −29.71° (C, 0.69 in 70% alc.)

Anal. Found: C, 61.70; H, 8.16. Calcd. for $C_{23}H_{37}O_4N \cdot C_2H_2O_4$: C, 62.35; H, 8.16. Calcd. for $C_{23}H_{39}O_4N \cdot C_2H_2O_4$: C, 62.09; H, 8.55%.

Sachaconitine Hydrochloride.—Dried hydrogen chloride was passed into a solution of the base in anhydrous acetone to produce a white precipitate. Reprecipitation by adding acetone to a very concentrated alcoholic solution of the precipitate gave sachaconitine hydrochloride in colorless needles, m. p. 203~204°C, $[\alpha]_D^{20}$ −30.43° (C, 0.78 in 95% alc.). No satisfactory analytical data have been found because of the extremely hygroscopic property of this compound.

Diacetylsachaconitine.—The base (1 g.) was treated with 4 g. of acetyl chloride in a sealed tube at room temperature for 5 days. The excess of the reagent was distilled off under reduced pressure and water was added. The aqueous solution was basified and extracted with chloroform. The residual product, obtained by evaporation of the chloroform, was crystallized from aqueous alcohol to give 400 mg. of plates, m. p. 114~116°C, $[\alpha]_D^{20}$ −10.87° (C, 1.70 in 95% alc.).

Anal. Found: C, 68.03, H, 8.92, N, 3.12. Calcd. for $C_{22}H_{35}O_2N \cdot (OCOCH_3)_2$: C, 68.18; H, 8.69; N, 2.95%. Calcd. for $C_{23}H_{37}O_2N \cdot (OCOCH_3)_2$: C, 67.89; H, 9.07; N, 2.93%.

On saponifying diacetylsachaconitine with alkali sachaconitine was regenerated.

Isolation of "Base D". — Fraction 1[3] (10 g.) was refluxed with 100 cc. of ether for 30 min. on a steam bath and the ether insoluble residue was again refluxed with 50 cc. of fresh ether. Complete removal of the solvent from the combined extracts gave 8 g. of amorphous yellow powder, which was neutralized with 1N-acetic acid and diluted to 100 cc. with water. To the resulting solution powdered sodium bicarbonate was added in small portions until no further precipitation was noticed. After being left to stand for 30 min., the resinous precipitate (Ia) was filtered off. From the filtrate a precipitate (Ib) was obtained on adding 50 cc. of 20% aqueous sodium carbonate, and another (Ic) on adding ammonia. No crystallizable alkaloids were obtaind from Ia and Ic. The fractional precipitation of Ib with sodium bicarbonate and carbonate was repeated twice; then 5 g. of powder precipitating with sodium carbonate was obtained. This material was dissolved in alcohol and the solvent was allowed to evaporate at room temperature, because heating of the solution caused crystallization with difficulty. Thus 2.5 g. of the crystalline "base D" was deposited from the alcoholic solution.

"Base D" is readily soluble in alcohol, chloroform and ether and insoluble in petroleum ether. It was recrystallized from a mixture of ether and petroleum ether in needles, m. p. 167~168°C, $[\alpha]_D^{20}$ +20.10° (C, 2.05 in 95% alc.).

Anal. Found: C, 66.13; H, 7.54; N, 2.23. Calcd. for $C_{33}H_{45}O_9N$: C, 66.09; H, 7.56; N, 2.34%.

Department of Chemistry,
Faculty of Science
Hokkaido University
Sapporo

Studies on Copper Phthalocyanine and its Chlorinated Derivatives Based upon the X-ray Diffraction Patterns

By Masahiro SHIGEMITSU

(Received August 13, 1958)

The molecular structure of copper phthalocyanine was first investigated by R. P. Linstead et al.[1] and later J. M. Robertson[2] studied its crystal structure by means of X-ray diffraction. He had only one form of copper phthalocyanine —namely, the α-form. This was prepared by sublimation as large needle crystal unsuited for pigment use. In order to reduce the particle size of copper phthalocyanine, the needle pigment is dissolved in concentrated sulfuric acid, and then is precipitated in fine particles by adding the acid solution to a large quantity of water with agitation. The first commercial pigment is the fine particles thus obtained. G. von Susich[3] showed that copper phthalocyanine conditioned in the above manner had a different X-ray diffraction pattern from that of the sublimed product studied by J. M. Robertson. Here the J. M. Robertson form is called α-form, because historically this crystal form was the first to be identified, and the first commercial pigment form is called β-form.

The copper phthalocyanine and lowly chlorinated copper phthalocyanines (containing chlorine atoms not more than six) are mostly used in blue pigments, while the highly chlorinated copper phthalocyanines (containing about 14 chlorine atoms) in green pigments. As to polymorphism of chlorinated copper phthalocyanines, D. N. Kendall[4], on the basis of infrared absorption measurement, reported that there were also two forms of crystal structures, α- and β-forms, in copper monochlorophthalocyanine (no mention is made of position of chlorine atom), whereas only one form of crystal structure was identified in highly chlorinated copper phthalocyanine green.

The author worked out X-ray diffraction patterns on twelve samples, six in needle forms and six in granular ones, of the following compounds; copper phthalocyanine, copper tetra-(3)-chlorophthalocyanine, copper tetra-(4)-chlorophthalocyanine, copper octa-(3, 6)-chlorophthalocyanine, copper octa-(4, 5)-chlorophthalocyanine and copper hexadecachlorophthalocyanine; the polymorphism was hereby investigated with copper phthalocyanine and its chlorinated derivatives.

Experimental

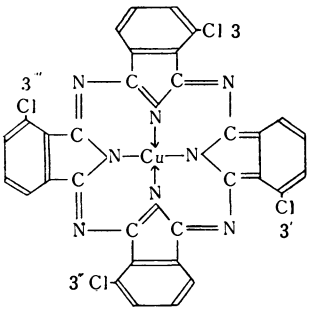
Materials.—Two forms of crystals, needle and granular forms, of copper phthalocyanine derivatives of different chlorine contents were synthesized as follows.

(1) *α-Form (I) and β-form (II) copper phthalocyanines.*—Synthesis of copper phthalocyanine was carried out following the method described in Ref. 5. From the product, then, α- and β-form crystals were obtained by the following procedure. First, copper phthalocyanine was put into a quartz glass tube, heated up to 550~580°C in an electric furnace, making the needle crystal of I sublime. α-Form crystal thus obtained was dissolved in 98% sulfuric acid of 20 times in weight at room temperature and allowed to stand 4 hr. Then, poured into ice water, granular II was formed, and separated through filtration. By chlorine analysis, it was found that there was just a trace of chlorine content, that is, 0.11%. Micro-Carius method was applied in all the following chlorine analyses.

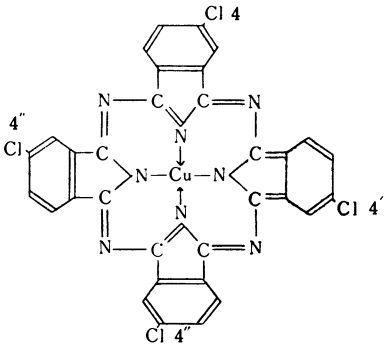
Granular I of a size which seemed to be suitable for pigment was prepared by the method described in Ref. 6. Namely, 100 cc. of acetone, 1.2 kg. of steel shots of approximately 3 mm. in diameter and 5 g. of I in needle form which was obtained by sublimation were put into a porcelain pot of 500 cc. capacity and pulverized at 100 r. p. m. for 72 hr.; the product was granular I in brilliant greenish blue.

(2) *Copper tetra-(3)-chlorophthalocyanine (III) and copper tetra-(4)-chlorophthalocyanine (IV).*—

1) R. P. Linstead et al., *J. Chem. Soc.*, **1934**, 1036.
2) J. M. Robertson, ibid., **1935**, 615; ibid., **1936**, 1195; ibid., **1937**, 219.
3) G. von Susich, *Anal. Chem.*, **22**, 425 (1950).
4) D. N. Kendall, ibid., **25**, 382 (1953).
5) M. Shigemitsu, *J. Chem. Soc, Japan, Ind. Chem. Sec. (Kogyo Kagaku Zasshi)*, **62**, 110 (1959) (presented at the 10th Annual Meeting of the Chemical Society of Japan held in April, 1957).
6) U. S. Pat. 2,556,726 (1951); U. S. Pat. 2,556,727 (1951); U. S. Pat. 2,556,728 (1951); U. S. Pat. 2,556,730 (1951).
7) M. Shigemitsu, *J. Chem. Soc. Japan, Ind. Chem. Sec. (Kogyo Kagaku Zasshi)*, **62**, 112 (1959) (presented at the Autumnal Joint Meeting of Chemical Society of Japan with other Societies, Tokyo, 1957).

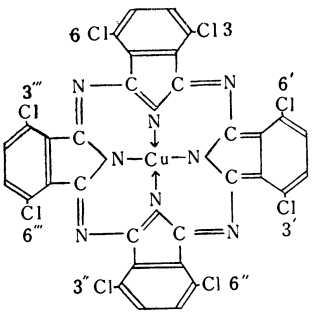


Copper tetra-(3)-chlorophthalocyanine

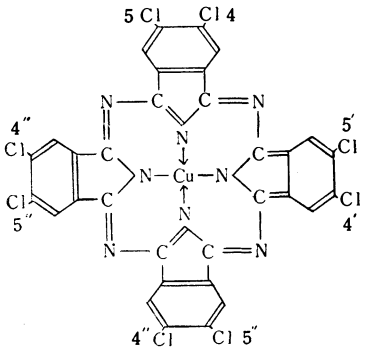


Copper tetra-(4)-chlorophthalocyanine

Fig. 1



Copper octa-(3, 6)-chlorophthalocyanine



Copper octa-(4, 5)-chlorophthalocyanine

Fig. 2

III and IV were prepared by condensing 3- and 4-monochlorophthalic anhydrides (see below) respectively with urea and copper in trichlorobenzene. From the mixture of monochlorophthalic anhydrides prepared following the method in Ref. 7, separated 3-monochlorophthalic anhydride, m. p. 121~122°C (reported m. p. 122°C)[8] (*Anal.* Found: Cl, 19.40%) and 4-monochlorophthalic anhydride, m. p. 97~98°C (reported m. p. 98°C°[8]) (*Anal.* Found: Cl, 19.44%) by repeating recrystallization with toluene-ethanol (1 : 1) solvent. The chlorine contents in III and IV derived from these 3- and 4-monochlorophthalic anhydrides were 19.72% and 19.80%, respectively.

Both of III and IV prepared in this way were of needle crystals. To convert them into granular forms, they were dissolved in 98% sulfuric acid of 20 times in weight at room temperature, allowed to stand for 4 hr. and poured into ice water.

Since chlorinated copper phthalocyanines do not sublime, it is impossible to obtain the needle crystals by sublimation, but they can be obtained by condensing various chlorophthalic anhydrides together with urea and copper in trichlorobenzene. Therefore, this method was adapted later in obtaining the needle crystals of various chlorinated copper phthalocyanines.

8) V. Villiger, *Ber.*, **42**, 3532 (1909).

(3) *Copper octa-(3, 6)-chlorophthalocyanine (V) and copper octa-(4, 5)-chlorophthalocyanine (VI).* —V which was synthesized following the method described in Ref. 7 was taken up; it showed a chlorine content of 33.21% and was of needle crystal.

VI was synthesized by condensing 4, 5-dichloro phthalic anhydride (see below) together with urea and copper in trichlorobenzene; it showed a chlorine content of 33.23% and was of needle crystal. 4, 5-Dichlorophthalic anhydride, m. p. 185~186.5°C (reported m. p. 185~187°C)[8] (*Anal.* Found: Cl, 32.60%) was separated from the mixture of dichlorophthalic anhydrides[7] with toluene-ethanol (1:1) solvent.

To convert them into granular forms, they were dissolved in chlorosulfonic acid of 20 times in weight at room temperature, allowed to stand 4 hr. and poured into ice water.

(4) *Copper hexadecachlorophthalocyanine (VII).* —Needle-formed VII synthesized following the method described in Ref. 7, with chlorine content of 50.33%, was used. Granular VII was prepared by dissolving needle-formed VII in chlorosulfonic acid of 30 times in weight at room temperature, allowing it to stand for 4 hr. and then pouring it into ice water.

Methods.—(1) *Observation of pigment forms.* —Two types of samples were prepared as follows. One was made first by washing with water the

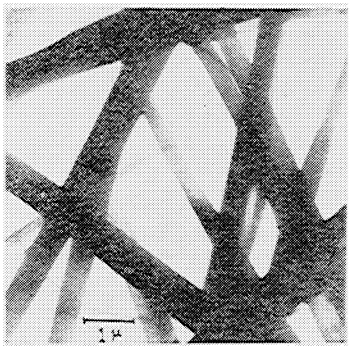


Fig. 3. α-Form copper phthalocyanine (I) (needle form)

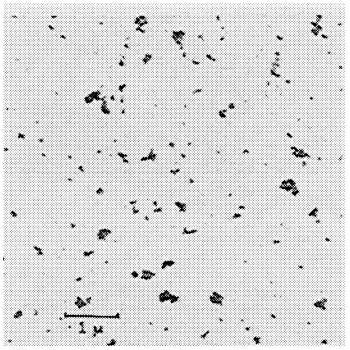


Fig. 4. β-Form copper phthalocyanine (II) (granular form)

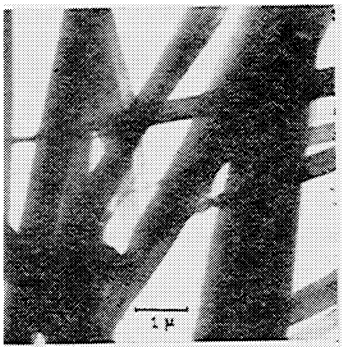


Fig. 5. Copper tetra-(3)-chlorophthalocyanine (III) (needle form)

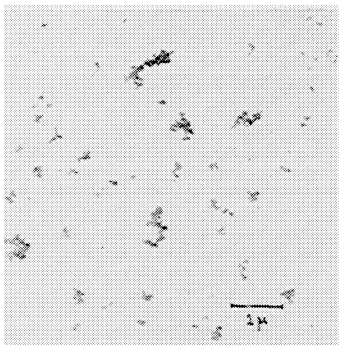


Fig. 6. Copper tetra-(3)-chlorophthalocyanine (III) (granular form)

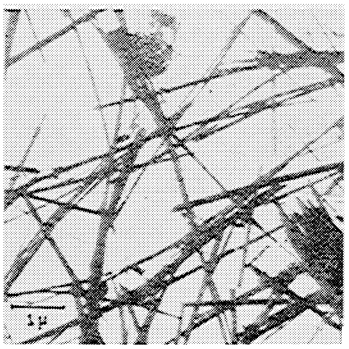


Fig. 7. Copper tetra-(3)-chlorophthalocyanine (III) (boiled for 10 hr. in trichlorobenzene)

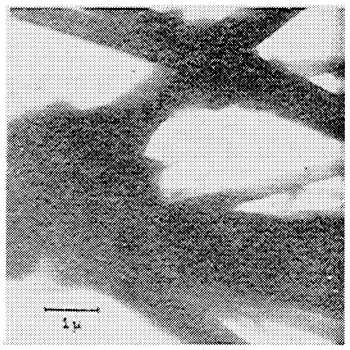


Fig. 8. Copper tetra-(4)-chlorophthalocyanine (IV) (needle form)

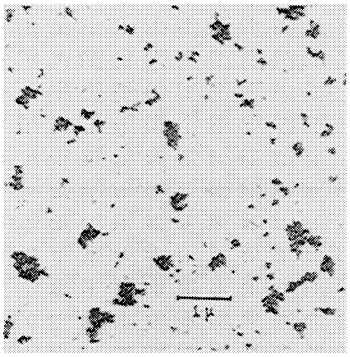


Fig. 9. Copper tetra-(4)-chlorophthalocyanine (IV) (granular form)

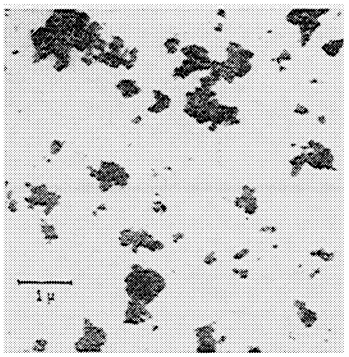


Fig. 10. Copper tetra-(4)-chlorophthalocyanine (IV) (boiled for 10 hr. in trichlorobenzene)

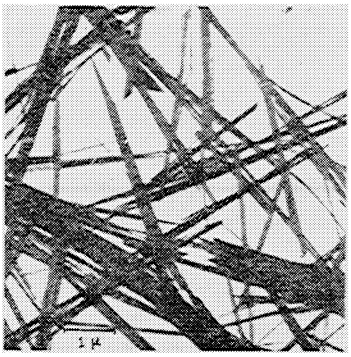


Fig. 11. Copper octa-(3, 6)-chlorophthalocyanine (V) (needle form)

granular pigments reprecipitated from the solution in 98% sulfuric acid of chlorosulfonic acid, and then placing and drying a drop of pigment suspension in water upon the collodion film of sample holder. The other was prepared first by drying the pigments obtained in any way other than by reprecipitation and then by sprinkling them over the collodion film of sample holder. The author photographed them with an electron microscope (Hitachi Works) at 2,000 direct magnification. The pictures were enlarged again by 10,000 times, and by means of these enlargements, their forms were closely examined.

(2) *Changes in pigment shade accompanied by being heated in trichlorobenzene.*—Granular pigments prepared by reprecipitation were heated in the boiling trichlorobenzene (b. p. 200~210°C) of 100 times in weight for 10 hr, and then filtered. After the sticking trichlorobenzene was eliminated by washing with ethanol, they were

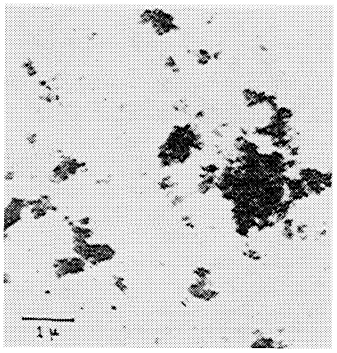


Fig. 12. Copper octa-(3,6)-chlorophthalocyanine (V) (granular form)

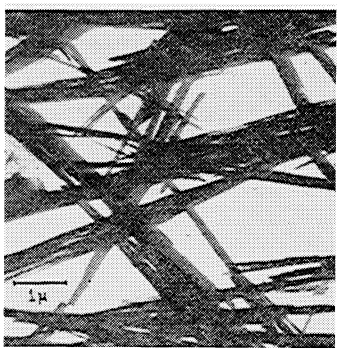


Fig. 13. Copper octa-(4,5)-chlorophthalocyanine (VI) (needle form)

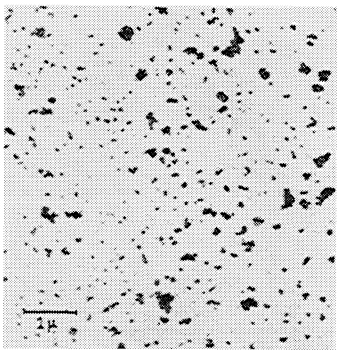


Fig. 14. Copper octa-(4,5)-chlorophthalocyanine (VI) (granular form)



Fig. 15. Copper hexadecachlorophthalocyanine (VII) (needle form)

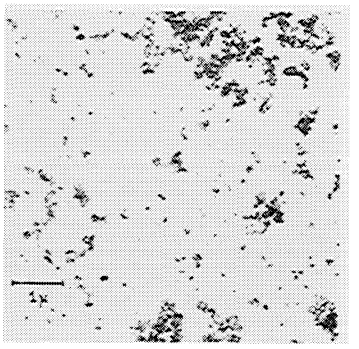


Fig. 16. Copper hexadecachlorophthalocyanine (VII) (granular form)

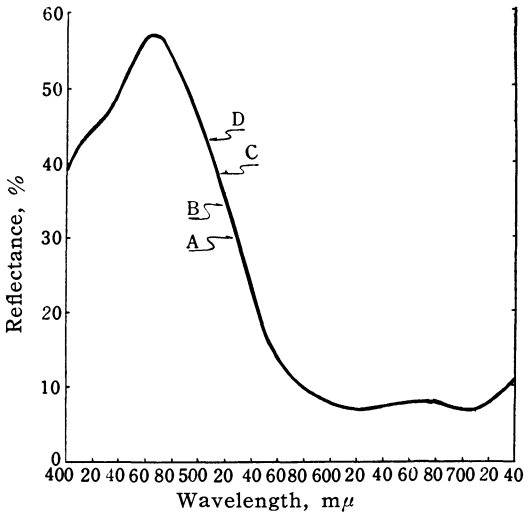


Fig. 17. α-Form copper phthalocyanine (I), (granular form):
A, untreated; B, stood for 5 days;
C, boiled for 1 hr.; D, boiled for 10 hr.

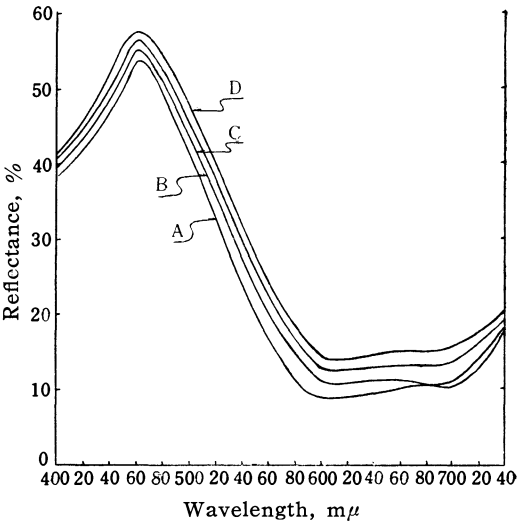


Fig. 18. β-Form copper phthalocyanine (II), (granular form):
A, untreated; B, stood for 5 days;
C, boiled for 1 hr.; D, boiled for 10 hr.

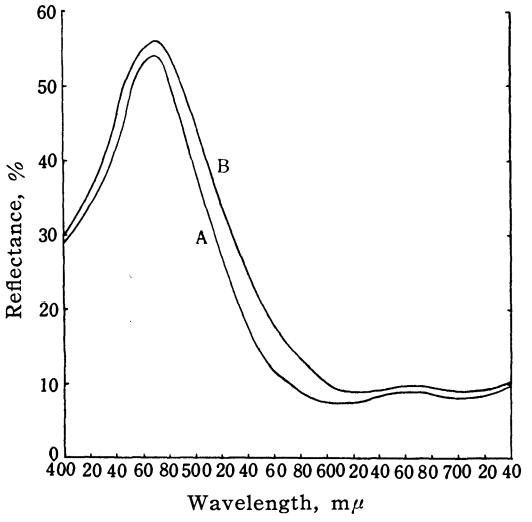


Fig. 19. Copper tetra-(3)-chlorophthalocyanine (III), (granular form):
A, untreated; B, boiled for 10 hr.

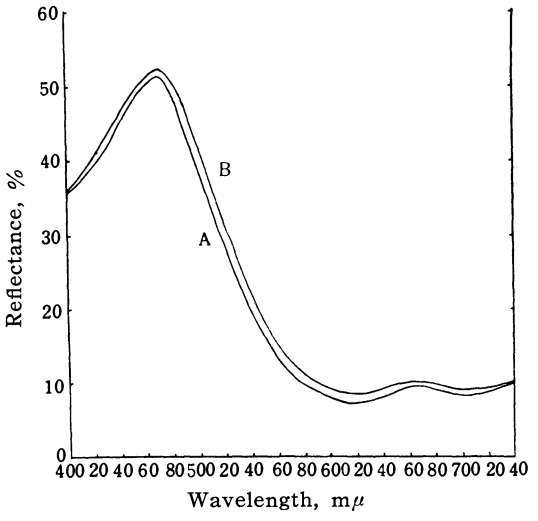


Fig. 20. Copper tetra-(4)-chlorophthalocyanine (IV), (graunlar form):
A, untreated; B, boiled for 10 hr.

dried at about 60°C. The pigments thus obtained and the original untreated ones were mixed respectively with polymerized linseed oil of 1.5 times in weight and were made into paste by grinding 400 rounds in a Hoover automatic muller. To 1 part of each paste was added 70 parts of zinc white paste (obtained by grinding 2 parts of zinc oxide with 1.5 parts of polymerized linseed oil), which was applied 0.5 mm. in thickness on a coated paper with a bladeoapplicator (Gardner Laboratory). These were dried at room temperature, their reflectance curves were obtained with a recording spectrophotometer (General Electric Co.), and calculation was thereby conducted.

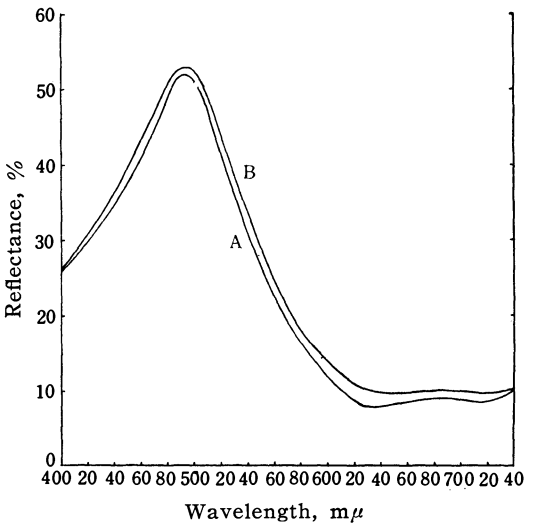


Fig. 21. Copper octa-(3, 6)-chlorophthalocyanine (V), (granular form):
A, untreated; B, boiled for 10 hr.

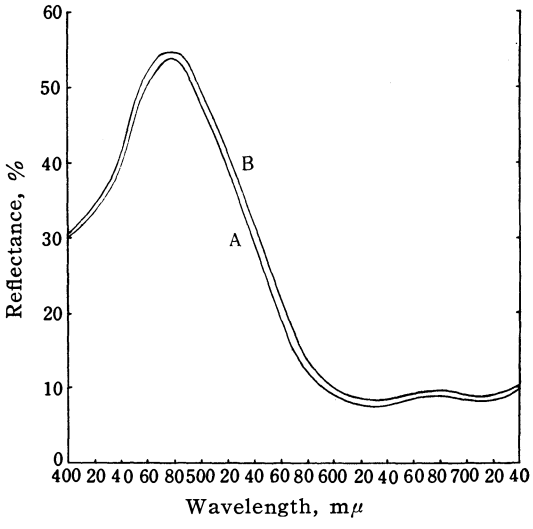


Fig. 22. Copper octa-(4, 5)-chlorophthalocyanine (VI), (granular form):
A, untreated; B, boiled for 10 hr.

(3) *Crystal structures of pigments.*—The X-ray diffraction patterns of each pigment were obtained with a recording X-ray diffraction apparatus (Philips Co.).

Results. — (1) *Forms of pigments.* — Photos taken with an electron microscope are shown (Fig. 3 to Fig. 16). Fig. 3 shows I obtained by sublimation, while Figs. 5, 8, 11, 13 and 15 show chlorinated copper phthalocyanines obtained by synthesis in trichlorobenzene; they are all in needle forms. Figs. 4, 6, 9, 12, 14 and 16 show II and chlorinated copper phthalocyanines, all in granular forms, obtained by dissolving the needle crystals in 98% sulfuric acid or chlorosulfonic

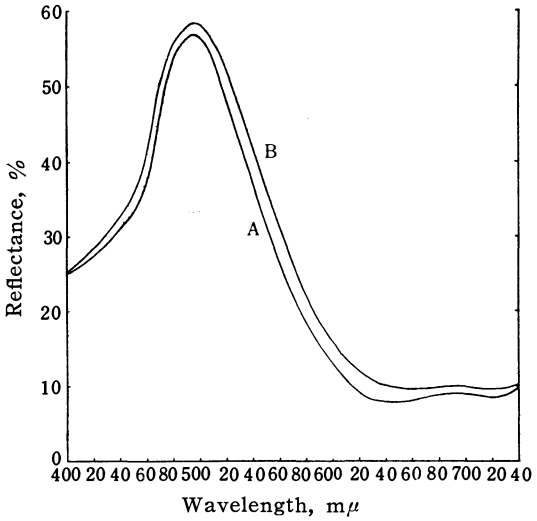


Fig. 23. Copper hexadecachlorophthalocyanine (VII), (granular form):
A, untreated; B, boiled for 10 hr.

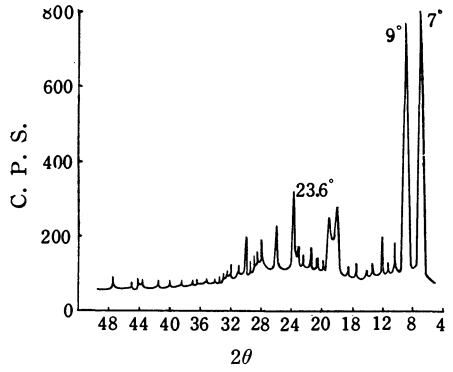


Fig. 24. α-Form copper phthalocyanine (I), (needle form)

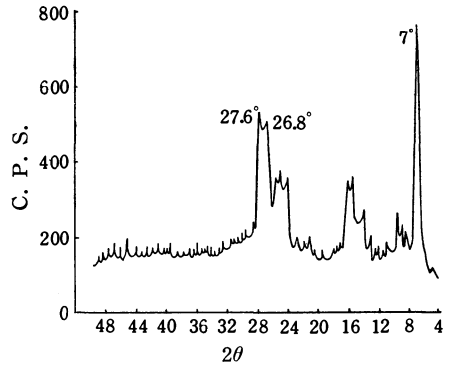


Fig. 25. β-Form copper phthalocyanine (II), (graunlar form)

acid and pouring them into ice water.

Fig. 7 shows the needle crystal prepared by boiling the granular III (Fig. 6) in trichlorobenzene for 10 hr. This change resembles the transformation of granular II into needle-formed I, which appears when the former is heated in organic solvents[9,10]. However, no change can be detected in case IV (Fig. 9) when it is heated in the boiling trichlorobenzene for 10 hr, as is manifested from Fig. 10.

It is known that, when a small amount of chlorine is introduced by the direct chlorination of copper phthalocyanine, a compound can be obtained which does not show any crystal growth in organic solvents[11]. In this case, chlorine is first substituted at the 4- or 5-position of phthalocyanine nucleus[7,12]. Meanwhile, according to Bansho et al.[13], no crystal growth takes place in the case of chlorinated copper phthalocyanine obtained from the direct chlorination or 4-monochlorophthalic anhydride. These facts are in good harmony with the results by the author.

As to copper octachlorophthalocyanines, on the other hand, no difference is formed any more in the crystal growth; independently of the positions which are occupied by chlorine atoms, 3,6- or 4,5-positions of phthalocyanine nucleus, no crystal growth takes place even in case copper octachlorophthalocyanines are boiled in trichlorobenzene for 10 hr. The case of granular VII is also quite the same.

(2) *Changes in pigment shade.* — Reflectance curves obtained with a recording spectrophotometer are shown (Fig. 17 to Fig. 23). Table I gives the data of these curves expressed in terms of C. I. E. Notation. In this table, *Y* denotes luminosity, *Pe* purity and λ_D dominant wavelength.

It is evident from Fig. 17, that granular I, even though boiled in trichlorobenzene for 10 hr.,

TABLE I. C. I. E. NOTATION

Sample	Reflectance curve	*Y* %	*Pe* %	λ_D mμ
A	Fig. 17	20.7	56.0	480.7
B		20.7	56.0	480.7
C		20.7	56.0	480.7
D		20.7	56.0	480.7
A	Fig. 18	19.1	55.0	475.8
B		23.4	52.0	478.8
C		24.2	51.0	479.7
D		25.2	49.6	479.8
A	Fig. 19	19.7	58.4	481.5
B		21.6	54.2	484.2
A	Fig. 20	18.4	56.1	478.3
B		18.5	56.0	478.7
A	Fig. 21	25.2	49.6	485.0
B		25.5	48.8	485.9
A	Fig. 22	21.6	55.8	482.5
B		21.9	55.6	482.7
A	Fig. 23	30.3	36.8	492.6
B		31.2	35.7	494.5

9) FIAT Report, No. 1313, 3, 446 (1948).
10) U. S. Pat. 2,486,351 (1949).
11) U. S. Pat. 2,615,026 (1952); U. S. Pat. 2,618,642 (1952).
12) R. P. Linstead et al., *J. Chem. Soc.*, **1939**, 1820.
13) Y. Bansho et al., *J. Chem. Soc. Japan, Ind. Chem. Sec.* (*Kogyo Kagaku Zasshi*), **59**, 67 (1956).

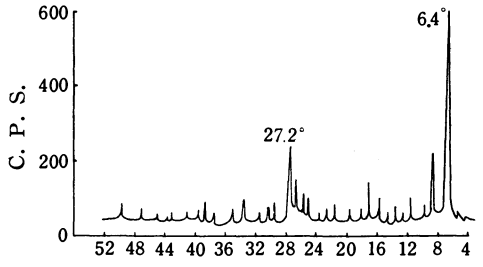


Fig. 26. Copper tetra-(3)-chlorophthalocyanine (III), (needle form)

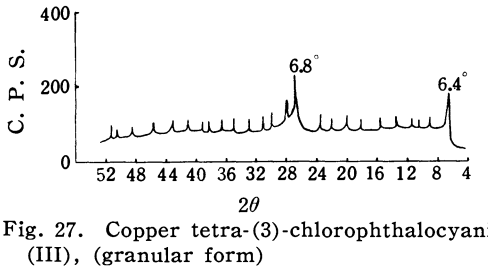


Fig. 27. Copper tetra-(3)-chlorophthalocyanine (III), (granular form)

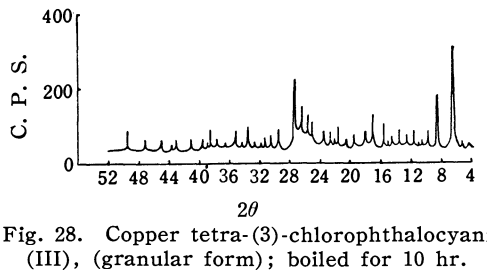


Fig. 28. Copper tetra-(3)-chlorophthalocyanine (III), (granular form); boiled for 10 hr.

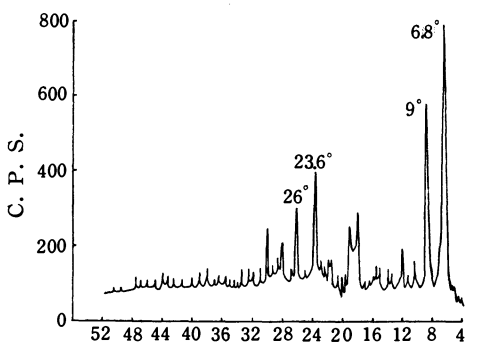


Fig. 29. Copper tetra-(4)-chlorophthalocyanine (IV), (needle form)

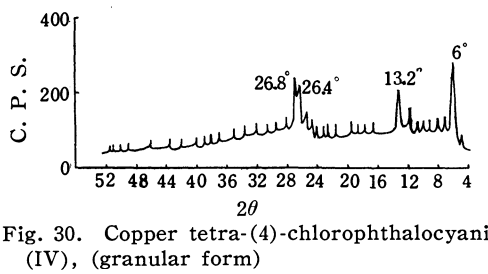


Fig. 30. Copper tetra-(4)-chlorophthalocyanine (IV), (granular form)

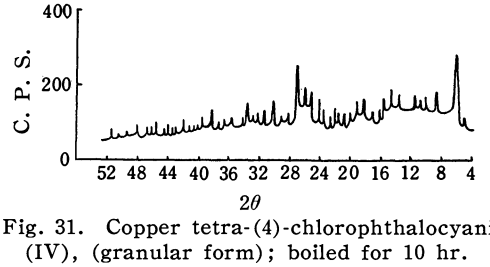


Fig. 31. Copper tetra-(4)-chlorophthalocyanine (IV), (granular form); boiled for 10 hr.

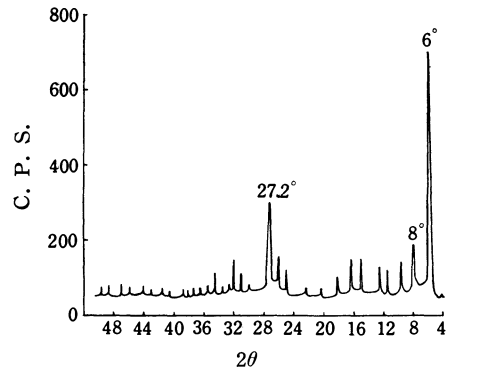


Fig. 32. Copper octa-(3, 6)-chlorophthalocyanine (V), (needle form)

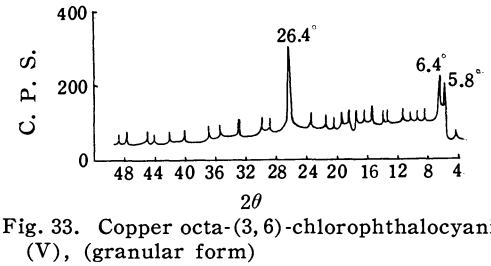


Fig. 33. Copper octa-(3, 6)-chlorophthalocyanine (V), (granular form)

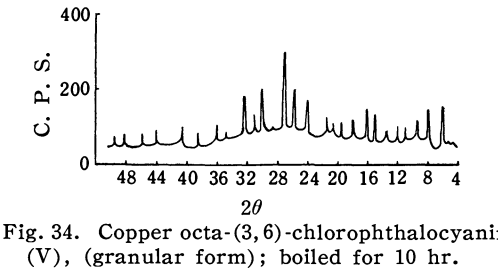


Fig. 34. Copper octa-(3, 6)-chlorophthalocyanine (V), (granular form); boiled for 10 hr.

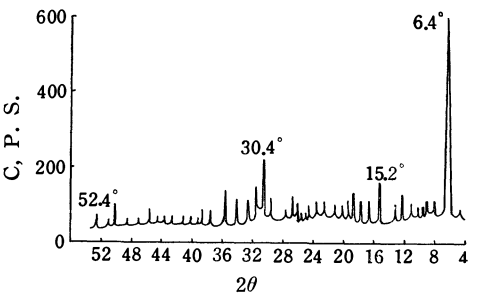


Fig. 35. Copper octa-(4, 5)-chlorophthalocyanine (VI), (needle form)

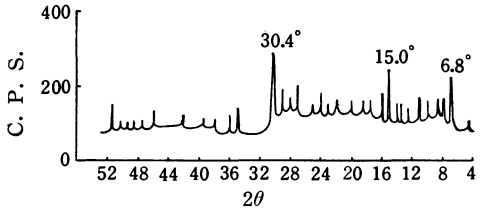


Fig. 36. Copper octa-(4, 5)-chlorophthalocyanine (VI), (granular form)

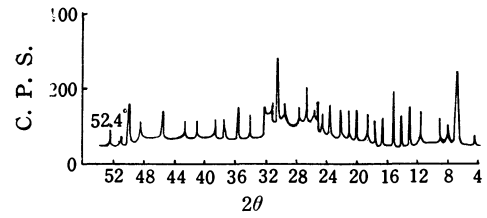


Fig. 37. Copper octa-(4, 5)-chlorophthalocyanine (VI), (granular form); boiled for 10 hr.

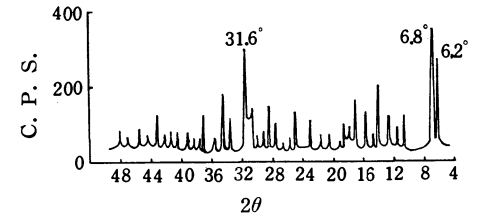


Fig. 38. Copper hexadecachlorophthalocyanine (VII), (needle form)

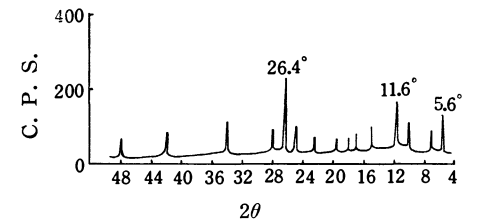


Fig. 39. Copper hexadecachlorophthalocyanine (VII), (granular form)

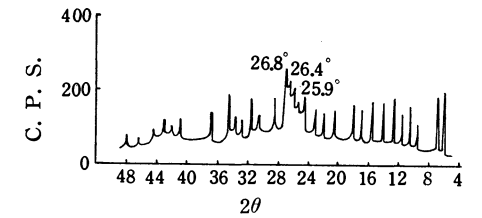


Fig. 40. Copper hexadecachlorophthalocyanine (VII), (granular form); boiled for 10 hr.

causes neither crystal growth nor color change, while in the case of granular II the crystal grows with remarkable change of shade, as shown in Fig. 18. As to the shade, its dominant wavelength shifts to the longer wavelength side by 4 mμ, that is, yellowishness increases.

Granular III grows into needle crystal and, as is clear from Fig. 19, changes in its shade. With a shift of its dominant wavelength by 2.7 mμ, it increases in yellowishness. On the contrary, its isomer, granular IV causes no crystal growth and scarcely changes at all in its shade, as shown in Fig. 20.

Though granular V causes no crystal growth, it changes in shade to some extent, its dominant wavelength making a shift to the longer wavelength side by 0.9 mμ just as illustrated in Fig. 21. On the contrary, its isomer, granular VI causes no crystal growth and scarcely changes in its shade at all, as shown in Fig. 22. It can be said that the effect of chlorine atoms at 3,6- or 4,5-positions on the color change is the same as far as tetrachloro- and octachloro-compounds are concerned.

Fig. 23 shows the color change of granular VII. As the degree of chlorination becomes higher, the color change caused by heating in trichlorobenzene tends to diminish, but even VII exhaustively chlorinated changes its shade to some extent and its dominant wavelength shifts to the longer wavelength side by 1.9 mμ with an increase in yellowishness. However, there is no such crystal growth here as is observed in the case of granular II and III.

Compared with the chlorine atoms of 4,5-positions, those of 3,6-positions have scarcely any power of checking the crystal growth in organic solvents, but they are very powerful in shifting their dominant wavelength to the longer wavelength side. The dominant wavelengths of granular III and its isomer, granular IV are 481.5 mμ and 478.3 mμ respectively, which show that chlorine atom of 3-position is more influential in making an increasing of yellowishness than that of 4-position. This is also the case with granular V and its isomer, granular VI. That is, the former has a dominant wavelength of 485.0 mμ while the latter one of 482.5 mμ.

(3) *X-ray diffraction patterns of pigments.*— X-ray diffraction patterns obtained with a recording X-ray apparatus are shown (Fig. 24 to Fig. 40).

Fig. 24 shows the needle-formed I prepared by sublimation and Fig. 25 shows the granular II prepared from the solution of I in 98% sulfuric acid through reprecipitation method. What is common to both of them is the line of 7°, but they have nothing in other respects. I has the second and third strongest lines at 9° and 23.6°, but II has them at 27.6° and 26.8°; this indicates that there is a great difference between the two forms.

Figs. 26 and 27 show respectively III in needle form as well as in granular form. Fig. 28 shows granular III boiled in trichlorobenzene for 10 hr. The line of 6.4° is the only point in

common to Figs. 26 and 27. When the granular product is boiled in trichlorobenzene, its diffraction pattern changes as shown in Fig. 28, approaching that of the needle product (Fig. 26). This phenomenon perfectly coincides with the shade change exhibited by reflectance curves and the form change exhibited by electron microscopic photos.

Figs. 29 and 30 show respectively IV in needle form as well as in granular form. Fig. 31 shows the granular IV boiled in trichlorobenzene for 10 hr. What is common to Figs. 29 and 30 is the neighborhood of 6°. In the needle product, the second, third and fourth strongest lines are found at 9°, 23.6°, and 26°, but in the granular product they are at 26.8°, 26.4° and 13.2°, no similarity being found between the two forms. The granular product, if boiled in trichlorobenzene, changes to some extent and, judging from the diffraction pattern (Fig. 29), approaches the needle product, as shown in Fig. 31.

The X-ray diffraction pattern of needle-formed IV (Fig. 29) closely resembles that of needle-formed I (Fig. 24), but needle-formed III (Fig. 26) differs from needle-formed I. Granular IV (Fig. 30) and granular III (Fig. 27) show different patterns as is the case with the needle forms. Between III and IV, no similarity is found either in needle forms or in granular forms.

Figs. 32 and 33 show respectively V in needle form as well as in granular form. Fig. 34 shows the granular V boiled in trichlorobenzene for 10 hr. In Fig. 32 the strongest line is at 6° and the second and third strongest lines at 27.2° and 8° respectively. In Fig. 33 such lines are at 26.4°, 6.4° and 5.8° respectively, but no similarity is found between the two forms. When the granular product is boiled in trichlorobenzene, a diffraction pattern very similar to the needle form (Fig. 32) is obtained as shown in Fig. 34.

Figs. 35 and 36 show respectively VI in needle form as well as in granular form. Fig. 37 shows the granular VI boiled in trichlorobenzene for 10 hr. In Fig. 35 the strongest line is at 6.4° and the second and third strongest lines at 30.4° and 15.2°. In Fig. 36 such lines are at 30.4°, 15° and 6.8° respectively. Though there is no similarity between the two forms, their X-ray diffraction patterns are considerably closer to each other than those of I, II, III, IV and V. The granular product has no line at 52.4° which is in the case of the needle product. But, when it is boiled in trichlorobenzene, 52.4° line appears and the tendency of approaching the X-ray diffraction pattern of the needles product (Fig. 35) is also recongnized. On the other hand, no similarity is found between V and VI; this fact reminds us of the relation of III to IV. Thus, the influence of the position of chlorine upon the crystal structure is quite evident.

Figs. 38 and 39 show respectively VII in needle form as well as in granular form. Fig. 40 shows the granular VII boiled in trichlorobenzene for 10 hours. In Fig. 38 the strongest line at 6.8° and the second and third strongest lines at 31.6° and 6.2°. In Fig. 39 such lines are at 26.4°, 11.6° and 5.6° respectively. Thus there is no similarity between the two forms. When the granular product is boiled in trichlorobenzene, the strongest line is at 26.8° and the second and third strongest lines at 26.4° and 25.9°, showing a tendency of approaching the X-ray diffraction pattern of the needle product, just as in the case already described.

Discussion

(1) Polymorphism of Copper Phthalocyanine and its Chlorinated Derivatives.—It has been obvious that copper phthalocyanine and copper monochlorophthalocyanine have two forms of crystal structures. The author could make it clear that, chlorinated copper phthalocyanine have two form of crystal structures, no matter how large or small the chlorine contents may be.

This fact must be verified for copper phthalocyanines that their chlorine numbers ranges from naught to sixteen. These chlorinated copper phthalocyanines are to be obtained from mono-, di- and trichlorophthalic anhydrides with chlorine atoms at definite positions and tetrachlorophthalic anhydride. But it becomes difficult for chlorinated derivatives of phthalic anhydride to react as the chlorine contents grow larger. To cite an example of the experiments by the author, in the formation of phthalocyanine from tetrachlorophthalic anhydride, dechlorination reaction occurred and copper hexadecachlorophthalocyanine the author aimed at was not obtained. Meanwhile, phthalocyanine formation was run on the mixture of a given amount of chlorinated phthalic anhydrides, but it was not confirmed whether they reacted uniformly or singly. Consequently, this experiment was discontinued and examination was done with the six kinds of samples listed above. The aimed object was satisfactorily achieved by the results with them.

(2) Crystal Growth of Chlorinated Copper Phthalocyanines.—It is known that the introduction of chlorine atoms into copper phthalocyanine can prevent the crystal growth in organic solvents. Particularly, no crystal growth is recognizable in copper phthalocyanine green with a large chlorine content, but the position of chlorine atom plays an important role in crystal growth of lowly chlorinated compounds. Namely, chlorine atom at 4-position gives forth a very great action

in suppressing the crystal growth but the one at 3-position gives hardly any effect.

When more than eight chlorine atoms are contained, crystal growth is not usually recognized. But, if boiled in such high boiling point organic solvent as trichlorobenzene, all the X-ray diffraction patterns of the products where no crystal growth is recognized tend to approach those of the needle products. This phenomenon is similar to the transformation of unstable β-form copper phthalocyanine into stable α-form by heating the former in organic solvents.

The author gratefully acknowledges the instruction of Dr. Ryozo Goto, Professor of Kyoto University, Dr. Teruichiro Kubo, Professor of Tokyo Institute of Technology, Dr. Takahisa Nakamura and Dr. Wataru Ishikawa, Toyo Ink Mfg. Co. The author's thanks are also due to Mr. Seiki Kato, Tokyo Institute of Technology, for carrying out the X-ray analysis.

Central Research Laboratory
Toyo Ink Mfg. Co.
Sumida-ku, Tokyo

Study on Zinc Oxide-Chromium Oxide Catalyst. IV. Dependency of Catalytic Activity on Catalyst Structure

By Yoshisada OGINO, Masaaki OBA and Hiroshi UCHIDA

(Received November 13, 1958)

Our previous paper[1] reported that chromium oxide in a catalyst for methanol synthesis played two roles of promoting actions, intercrystalline on the one hand, and intracrystalline on the other hand. For the purpose of understanding the promoting actions from a structural viewpoint of the catalyst, this study has been made, and presents results on catalyst structures such as the crystal- and the macroscopic geometrical structure. On the basis of available data, the relationship between the catalytic activity and the catalyst structure is considered.

Taking the information thus obtained into consideration, we have attempted to prepare a catalyst of the higher activity for the methanol synthesis.

Experimental

Specimens of the same catalysts as described in our previous paper have been used in the present study. The catalysts were divided into three groups, catalysts A, B, and a catalyst S. A catalyst of the first group was a direct preparation from a paste of zinc oxide powder kneaded with a chromic acid solution, while one of the second group was produced from the solid matter remaining after washing of the paste with acetone. This last was prepared from a residue obtained by treating a reduced preparation of catalyst B with nitric acid. Table I shows Cr/Zn ratio determined for each catalyst, with its denotation. The previous paper[1] reported their catalytic activities for the methanol synthesis and decomposition, together with specific surface areas after reduction.

Part of the catalysts, both the raw and the reduced ones, were subjected to an X-ray study by means of a Geiger-counter spectrometer using filtered copper K_α ray.

Experimental data for the specific surface areas were supplemented with those determined on the raw catalysts by the BET method. From an extent of the surface area S, an average diameter d of particles in the catalyst granules was calculated by the aid of the relation of $d=6/(\rho S)$, where ρ was a catalyst density determined by the water-displacement method. Moreover, pore size distributions in three reduced preparations of the catalysts were determined by applying Barret's method[2] to nitrogen desorption isotherms at $-195°C$.

Experimental Results

Crystal Structure from X-ray Diagram. —Catalyst structures as revealed by X-ray diagrams are listed in Table II. Even the raw catalysts of a very low chromic

1) Y. Ogino, M. Oba and H. Uchida, This Bulletin, **32**, 284 (1959).

2) E. P. Barret, L. G. Joyer et al., *J. Am. Chem. Soc.*, **73** 373 (1951).

TABLE I. CHEMICAL COMPOSITION OF THE CATALYST

Catalyst	A-0	A-1	A-2	A-3	A-4	A-5	A-6
Cr/Zn ratio	0	0.05	0.10	0.18	0.25	0.33	0.40
Catalyst	—	B-1	B-2	—	B-4	B-5	B-6
Cr/Zn ratio	—	0.05	0.09	—	0.23	0.31	0.36
Catalyst	A-7	A-8	A-9	A-10	A-11		
Cr/Zn ratio	0.50	0.67	1.00	1.10	1.50		
Catalyst	B-7	B-8	B-9	B-10	B-11		
Cr/Zn ratio	0.38	0.47	0.50	0.50	0.50		

TABLE II. CRYSTALLITES IN RAW CATALYSTS FROM X-RAY DIAGRAMS

Catalyst	Crystallites	Catalyst	Crystallites
A-2	ZnO(s), II_β, II_α, III_β	B-2	ZnO(s), II_β, II_α, III_β
A-6	I_β	B-4	ZnO(w), II_β, II_α, III_β
A-7	I_β	B-5	ZnO(very w), II_β(b)
A-9	complicated pattern	B-7	I_β
A-10	probably of Zn bichromate	B-8, -9, B-11	I_β

s, strong: w, weak: b, broad.

acid content (catalysts A-2, B-2) give diffraction patterns of zinc-hydroxychromates, such as III_β, II_α and II_β besides the strong pattern of zinc oxide[3]. As the chromic acid content increases, the pattern due to I_β begins to appear in place of the foregoing hydroxychromates, and that due to zinc oxide becomes weaker, disappearing finally (catalysts B-4, -5). The diagrams taken of catalysts B-7, -8, -9 and -11 of the highest chromic acid content (Cr/Zn ratio of 0.5) among the catalysts of to B series show only the sharp pattern due I_β, whereas the one taken of catalyst A-7 of the same Cr/Zn ratio gives, besides the above, a complicated pattern, which appears stronger in the diagram taken of catalyst A-8. The complicated one seems to refer to zinc bichromate, and presumably comes from the solid layer of a much higher chromic acid content which the liquid in the paste has left behind on the original solid particles (refer to 1).

The crystal structure of the catalyst is appreciably altered by reduction. Although the diagrams taken of the raw catalysts give patterns of various kinds of zinc-hydroxychromates and bichromate, those taken of the reduced catalysts give only two kinds of patterns referring to zinc oxide and zinc chromite spinel. Within a range of Cr/Zn ratio less than 0.5, the pattern of zinc oxide becomes the weaker and the broader for the increaing Cr/Zn ratios, whereas that of zinc chromite maintains a definite degree of broadening, notwithstanding the fact that the intensity is increasing. Catalyst A-10 of a high Cr/Zn ratio gives much sharper patterns of both kinds, and catalyst S, though it has a Cr/Zn ratio (1.6) a little less than the stoichiometric ratio (2) of zinc chromite spinel, gives the pattern due to zinc chromite spinel alone[5].

Rough calculations of linear dimensions D of zinc oxide and zinc chromite spinel crystallites have been made by the aid of Scherrer's formula, $D=k\lambda/\beta\cos\theta$, where k is a constant approximately 0.9, λ is wave length of an X-ray, β is diffraction breadth of a line, and θ is Bragg angle. In the calculation, respective (102) and (400) reflections of zinc oxide and zinc chromite spinel were employed.

In Fig. 1 linear dimensions of crystallites of zinc oxide and zinc chromite spinel are plotted as a function of Cr/Zn ratio, respectively. As Cr/Zn ratio increases, the crystallite size of zinc oxide which originally was as large as 500 Å in linear dimension diminishes rapidly. In this respect, the crystallites of zinc chromite spinel contrast sharply with the above, the linear dimension being kept within a narrow range of 60~100 Å. With an addition of the further increasing amounts

3) By Feitknecht et al.[4], the diffraction patterns as well as chemical formulae of zinc-hydroxychromates were given. The formulae are as follows:
III_β: $ZnCrOr_4\cdot 3Zn(OH)_2\cdot 4Zn(OH)_2$, II_α: $ZnCrO_4\cdot 2.5Zn(OH)_2\cdot 2H_2O$, II_β: $ZnCrO_4\cdot 2.5Zn(OH)_2$, I_β: $ZnCrO_4\cdot Zn(OH)_2$

4) W. Feitknecht and L. Hugi-Carmes, *Helv. Chim. Acta.*, **37**, 2107 (1954).

5) Our results have revealed more kinds of zinc-hydroxychromates than those found by Kawamura et al.[6] with their catalysts, which they prepared by a little different procedure from ours.

6) M. Kawamura, T. Irie, Y. Shiraishi et al., *J. Chem. Soc. Japan, Ind. Chem. Sec.* (*Kogyo Kagaku Zasshi*), **60**, 162 (1957).

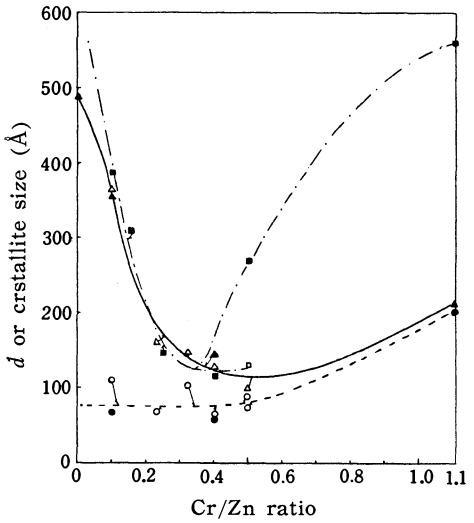


Fig. 1. Average particle diameter and crystallite size as function of Cr/Zn ratio.
—·—·—, average particle diameter: ——, size of ZnO crystallite: ·····, size of zinc chromite spinel crystallite. ●▲■, catalyst A: ○△□, catalyst B.

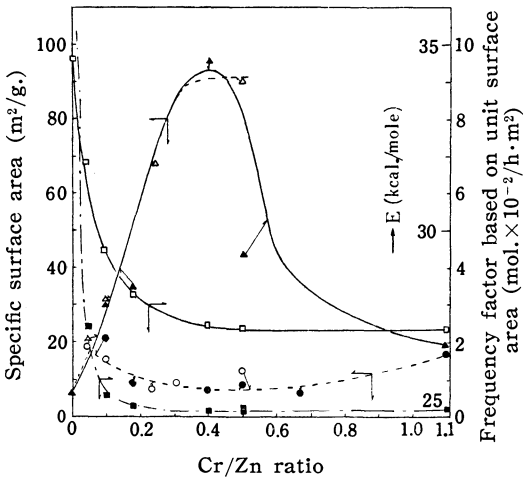


Fig. 2. Specific surface area, activation energy, and frequency factor as function of Cr/Zn ratio.
specific surface area: ●, raw catalyst (catalyst A), ○, (B), ▲, reduced catalyst (A), △, (B). □, activation energy for the synthesis, ■, frequency factor

of chromic acid beyond a Cr/Zn ratio of 0.5, the crystallites of both kinds grow to quite large ones.

Specific Surface Area and Average Size of Particles. — Specific surface areas of the raw catalysts as well as those of the reduced ones are shown as the function of Cr/Zn ratio in Fig. 2. Change in the areas of the former is small, the areas ranging from 7 to 20 $m^2/g.$, while the one in the area of the latter gives a remarkable peak at a Cr/Zn ratio of about 0.4～0.5, where the areas are five to ten times larger than those of the corresponding raw catalysts.

Granules of the raw catalysts are built up of particles as large as 1000～3000 Å in diameter. After reduction, the average size of the particles diminishes more or less remarkably according to chromic acid contents in the catalysts. Fig. 1 presents also the relationship between them. It shows that in a range of Cr/Zn ratio, less than 0.4, an average size of the particles is approximatly equal to the size of zinc oxide crystallites, and that in a range of higher Cr/Zn ratio, the particles are of much larger size than the crystallites of zinc oxide as well as zinc chromite spinel. The latter fact indicates that a particle is made up of a number of crystallites.

The growth of the particles as well as the crystallites, appearing in the catalysts of higher Cr/Zn ratios than 0.5, may be ascribed to thermal sintering[7] due to the glowing phenomenon that was once pointed out by Kawamura et al.[8] The glow has been found actually in the catalyst bed

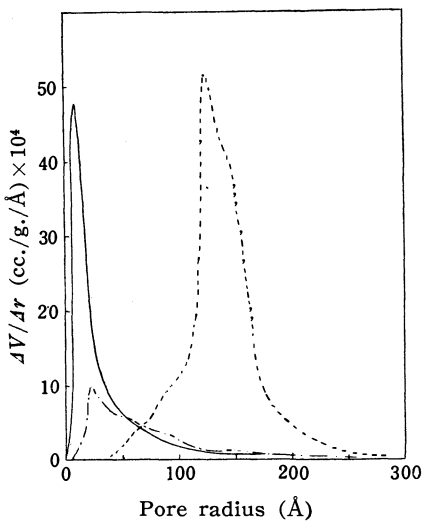


Fig. 3. Pore size distribution.
——, catalyst A-6: —·—·—, A-2: ····, A-10.

7) An assumption is also possible that crystallites of zinc chromite spinel are apt to aggregate with each other to become a large one, since there are not such a large number of zinc oxide crystallites as would be sufficient to prevent the aggregation. However, the assumption can not explain the simultaneous growth of zinc oxide crystallites.

8) M. Kawamura and T. Irie, *J. Chem. Soc. Japan, Ind. Chem. Sec.* (*Kogyo Kagaku Zasshi*), **60**, 166 (1957).

during reduction tending to appear more readily in the catalysts of the higher Cr/Zn ratios. It necessarily accompanies the growth to a greater extent.

Pore Size Distribution.--The results are shown in Fig. 3. Volumes of pores smaller than 300 Å in radius are 0.0588, 0.1178 and 0.2814 cc./g. for catalysts A-2, -6 and -10, respectively. A greater pore volume is not always associated with a larger extent of specific surface area, but the greater pore volume of extremely small pores with the larger extent of specific surface area.

Discussion

Intercrystalline Promoting Action of Chromium Oxide. — The intercrystalline promoter is a structural one responsible for production of a high-area structure. In this study, experimental evidences have been presented that a marked increase in the specific surface area takes place after reduction of the catalyst, and that well-grown particles of zinc-hydroxychromates in the raw catalysts disintegrate after reduction into extremely fine particles, which are often as small as the individual crystallites of zinc oxide and zinc chromite spinel[9], provided that scarcely any glow phenomenon has occurred during reduction. It has thus appeared that the formation of large particles of zinc-hydroxychromates in the raw catalysts is a requisite necessary for production of the extremely fine particles in the reduced catalysts, namely for the intercrystalline promotion of the activity by a chromic acid addition.

This picture[10] of structures of the raw and the reduced catalysts is consistent with the observations made by Matsui[12] on preparations of zinc-hydroxychromate II_β and its thermal decomposition products under an electron microscope. In his observations, the crystallites (100~500 Å, 500~600 Å in diameter for zinc chromite spinel and zinc oxide, respectively) were much larger in size than the ones defined in the present study. This may have been due mainly to a higher temperature (500°C), at which zinc-hydroxychromate II_β was decomposed, than to the reduction temperature in our study.

Compensation Effect in Catalytic Reactions[13].—We have found that catalyst S consists of zinc chromite spinel alone, and that a surface of the reduced zinc oxide-chromium oxide catalysts contains only two kinds of crystallites, crystallites of zinc oxide and zinc chromite spinel. As a consequence of the findings, we can expect according to the statement by Cremer[14] the compensation effect at the catalytic reactions on a series of the catalysts, under a reasonable assumption that crystallites of the different kinds simultaneously act as sites of a catalytic reaction[15]. On the other hand, the findings lead to the following expression of the intracrystalline promoting action of chromium oxide[1]; namely both the activation energy and the frequency factor based on unit surface area simultaneously fall with increasing proportions of zinc chromite spinel in the surface, the highest levels being thore of zinc oxide and the lowest levels being those of zinc chromite spinel (refer to Fig. 2). The expression coincides with the concept of the compensation effect by Cremer.

According to the aforegoing concept, an overall rate constant, k, is given by

$$k = F_1 A_1 \exp(-E_1/RT) + F_2 A_2 \exp(-E_2/RT) \quad (1)$$

where F is a fraction of the surface, subscripts 1 and 2 mean zinc oxide and zinc chromite spinel, respectively, and hence F_1 and F_2 stand for fractions of the surface occupied by zinc oxide and zinc chromite spinel, respectively. E is an activation energy, and A is a frequency factor based on unit surface area. Moreover, the finding in this study presents the following relationship,

$$F_1 + F_2 = 1 \quad (2)$$

As each value of A_1, A_2, E_1 and E_2 has already been known (refer to 1), F_1 and F_2 for any catalyst of the series can be evaluated from Eq. 1 and 2 by employing a value of k at a high temperature.

9) Comparatively large values of both the zinc oxide crystallite size and the average particle size determined for the catalysts of low Cr/Zn ratios are due to the presence of original large crystals of zinc oxide which have not been brought to a reaction with chromic acid.

10) The picture dose not exactly agree with the one for our previous catalysts[11], which were prepared by a somewhat different procedure from the present one.

11) H. Uchida and Y. Ogino, This Bulletin, **29**, 587 (1956).

12) T. Matsui, *J. Research Inst. Catalysis, Hokkaido University*, **4**, 109 (1956).

13) In this study the reactions include the methanol synthesis and decomposition.

14) E. Cremer, "Advances in Catalysis", Vol. VII, Rheinhold Publishing Corporation, New York (1956), p. 85.

15) According to the statement by Cremer, the compensation effect can be expected at the catalytic reactions on a series of the catalysts whose surface contains different activation energies, and in which the proportions of the sites are shifted with the chemical composition.

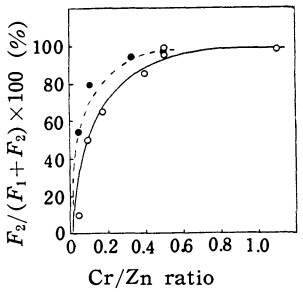


Fig. 4. Fraction of surface occupied by zinc chromite spinel as function of Cr/Zn ratio.
○, calculated from rate constant of synthesis, ●, calculated from rate constant of decomposition.

The results are shown in Fig. 4 as plots of $F_2/(F_1+F_2)$ vs. Cr/Zn ratio. This suggests migration of chromium ions from the particle interior into the surface taking place during reduction of the catalyst, but we can say nothing decisive in this respect as yet.

Attempt to Prepare Catalyst of Higher Catalytic Activity.—From the result that zinc chromite spinel yielded the lowest activation energy of the synthesis, it occurred to us first that a catalyst made of the spinel would be expected to give high activity, if it were provided with a large extent of surface area. However, an addition of chromic acid excessive to the amount corresponding to I_β always caused considerable decline in the surface area due to glowing in reduction. In this connection, we have made various efforts, e.g., reduction processes in hydrogen containing appropriate amounts of steam, to carry out the reduction without the glowing, but with no success. Another procedure, the simultaneous precipitation of hydroxides of zinc and chromium from a mixed solution of the nitrates with ammonia, yielded a catalyst of the desired chemical composition, but scarcely any evidence of zinc chromite spinel has been found unless the precipitate was heated at temperatures higher than 600°C[16]. The heating reduced the activity to a large extent, and we were unsuccessful in putting our first expectation into practice.

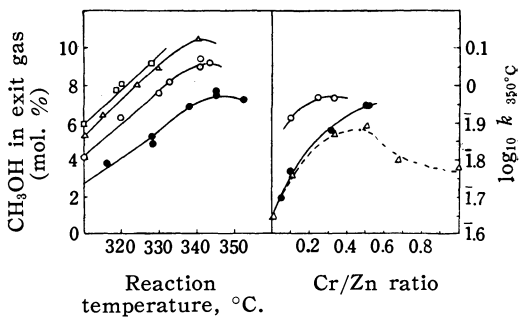
Our results[1] furthermore demonstrate that the specific catalytic activity, i. e., the activity based on unit surface area, for the methanol synthesis is increased appreciably by an addition of a small amount of chromic acid to such a level that is only a little lower than that of zinc chromite spinel. Natta[17], on the other hand, pointed out that zinc oxide produced by decomposition of zinc acetate was of a smaller crystallite size, and consequently showed higher activity than the usual ones. In view of the facts, it can next be expected that a catalyst of even a low chromic acid content may give higher activity, when it happens to have contained zinc acetate in the raw material. In producing a catalyst along with this expectation, the amount of chromic acid should be kept so low as not to provoke glowing during reduction, and hence a paste of the rather small Cr/Zn ratio of 0.25 has been chosen as a starting material, during the kneading of which appropriate amounts of acetic acid are added[18].

The results are given in Table IV, and Figs. 5A and 5B. A comparison of the

TABLE III. INCREASE IN SPECIFIC SURFACE AREA BY ACETIC ACID ADDITION

Catalyst	A-4	A-41	A-411	A-4111
CH_3COOH/ZnO (mol. ratio)	0	1/6	1/2	5/6
Specific surface area, m^2/g.	80	76	98	111
$k^{a)}\cdot 10^2$	6.9	10.1	12.4	14.2
$k/WS^{b)}\cdot 10^5$	7.75	10.5	10.0	8.3

a) a rate constant of the synthesis based on 10 cc. of the catalyst at 330°C.
b) the rate constant based on unit surface area.



Figs. 5A and 5B. Effect of acetic acid addition on catalytic activity.
A, synthesis. (left).
●, catalyst A-4, ○, A-41, △, A-II, □, A-4III.
B, decomposition. (right).
○, catalyst after acetic acid addition.
△, catalyst A, ●, catalyst B.

16) Even though the catalyst had not been heated at high temperatures, it could not give such a high activity for the methanol synthesis as the one obtainable with the catalyst in this study.

17) G. Natta, "Catalysis", Vol III, Rheinhold Publishing Corporation, New York (1955), p. 349.

18) By an acetic acid addition, the more violent glowing comes to take place.

table with the figures indicates a nearly parallel increase in the activities to the increasing extent of surface area. The figures disclose that the activity for decomposition rises more remarkably than the synthetic activity does. This leads to a premise that the addition of acetic acid does not result in surface enlargement of zinc chromite spinel, but results in that of zinc oxide whose synthetic activity is apt to decline rapidly with time (refer to 1). The premise can be confirmed from a constant value, 28.8 kcal./mol., of the activation energy of the synthesis independent of amounts of acetic acid added.

Summary

So far as catalysts made from pastes of zinc oxide powders kneaded with chromic acid solutions are considered, granules in the reduced ones are built up of extremely fine particles which usually are as small as individual crystallites of zinc chromite spinel as well as zinc oxide. The fine particles appear by way of the large particles of zinc-hydroxychromates in the raw catalysts. However, once the raw catalyst comes to contain a greater amount of chromic acid than that corresponding to zinc-hydroxychromate I_β, the granules in the reduced one are composed of the larger particles, an individual one of which is an assembly of a number of the crystallites.

On the basis of the results available on the catalyst structures, the intracrystalline promoting action of chromium oxide can be explained from Cremer's viewpoint of the compensation effect. The catalytic activity can be increased by adding an appropriate amount of acetic acid into the paste, the increase being nearly parallel to an increasing extent of the specific surface area. The increase by the addition, however, is expected only with the catalyst produced from the paste of a low chromic acid content.

The authors wish to express their sincere thanks to Messrs. S. Kato and M. Taniguchi of Tokyo Institute of Technology for their taking X-ray diagrams.

Government Chemical Industrial Research Institute, Tokyo
Shibuya-ku, Tokyo

The Normal Vibrations of Methanesulfonate Ion

By Kuniaki FUJIMORI

(Received October 28, 1958)

In the preceding paper[1] the infrared spectra of *n*-alkane-1-sulfonates were investigated and it was found that two S-O stretching vibrations and C-S stretching vibration were in the rock salt region.

In this paper the normal vibrations of the methanesulfonate ion were calculated, assuming the Urey-Bradley's field as the intra-molecular potential. This calculation was treated as a five-body problem, supposing the methyl radical to be one particle.

Calculation of Normal Vibration

Molecular Shape.—It was assumed that the methyl radical was one particle and the molecular shape of the methanesulfonate ion was similar to that of chloroform, i. e., this ion had the symmetry property of C_{3v}. This assumption is not reckless under the first order approximation[2].

Intra-molecular Potential. — As intra-molecular potential, the following Urey-Bradley's field[3] is assumed

$$V=\sum V_{r_i}+\sum_{i>j} V_{\alpha_{ij}}+\sum_{i>j} V_{q_{ij}}$$

where

$$V_{r_i}=K'_i r_i \Delta r_i+\frac{1}{2}K_i(\Delta r_i)^2$$

$$V_{\alpha_{ij}}=H'_{ij} r^2 \Delta\alpha_{ij}+\frac{1}{2}H_{ij}(r_{ij}\Delta\alpha_{ij})^2$$

1) K. Fujimori, This Bulletin, in press.

2) A. Simon and H. Kriegsmann, *Chem. Ber.*, **89**, 1718 (1956).

3) H. C. Urey, C. A. Bradley, *Phys. Rev.*, **38**, 1969 (1931).

$$V_{q_{ij}}=F'_{ij}q_{ij}\Delta q_{ij}+\frac{1}{2}F_{ij}(\Delta q_{ij})^2$$

and

K_i and K'_i: stretching force constants
H_{ij} and H'_{ij}: bending force constants
F_{ij} and F'_{ij}: repulsive force constants
r_i: distance between the central atom and the i-th atom
q_{ij}: distance between non-bonded atoms
r^2_{ij}: equals r_ir_j
α_{ij}: valence angle.

G and F Matrixes.—The G and F marixes of this molecule were made by Wilson's method[4] and were factored by symmetry property of C_{3v}[5]. The following elements were obtained.

a) A_1 type vibration (totally symmetric vibration).—i) Elements of G matrix

$$g_{11}=\mu_S+\mu_R \qquad g_{22}=-\frac{1}{3}\mu_S+\mu_O$$
$$g_{12}=-\frac{1}{\sqrt{3}}\mu_S \qquad g_{23}=\frac{4}{3}\mu_S$$
$$g_{13}=-\frac{4}{\sqrt{3}}\mu_S \qquad g_{33}=\frac{16}{3}\mu_S+2\mu_O$$

ii) Elements of F matrix

$$f_{11}=K_{S-R}+3t^2_{R-O}F'_{R-O}+3s^2_{R-O}F_{R-O}$$
$$f_{12}=\sqrt{3}\,(-t_{O-R}t_{R-O}F'_{R-O}+s_{R-O}s_{O-R}F_{R-O})$$
$$f_{13}=\frac{\sqrt{3}}{2}(t_{R-O}s_{O-R}F'_{R-O}+t_{O-R}s_{R-O}F_{R-O})$$
$$f_{22}=K_{S-O}+t^2_{O-R}F'_{R-O}+s^2_{O-R}F_{R-O}+4s^2_{O-O}F_{O-O}$$
$$f_{23}=\frac{1}{\sqrt{2}}\{(t_{O-R}s_{R-O}F'_{R-O}+t_{R-O}s_{O-R}F_{R-O})\sigma-2t_{O-O}s_{O-O}(F'_{O-O}+F_{O-O})\}$$
$$f_{33}=\frac{1}{2}\{(H_{R-S-O}-s_{R-O}s_{O-R}F'_{R-O}+t_{R-O}t_{O-R}F_{R-O})\sigma+(H_{O-S-O}-s^2_{O-O}F'_{O-O}+t^2_{O-O}F_{O-O})\}+\frac{3}{\sqrt{8}}\kappa/r^2_{S-O}$$

b) E type vibration (doubly degenerated vibration).—i) Elements of G matrix

$$g_{11}=\frac{4}{3}\mu_S+\mu_O$$
$$g_{12}=-\frac{\sqrt{2}}{3}\left(\frac{3}{\sigma}+1\right)\mu_S$$
$$g_{13}=\frac{4\sqrt{2}}{3}\mu_S$$
$$g_{22}=\mu_O+\left(\frac{1}{\sigma}\right)^2\mu_R+\frac{1}{6}\left(\frac{3}{\sigma}+1\right)^2\mu_S$$
$$g_{23}=-\frac{2}{3}\left(\frac{3}{\sigma}+1\right)\mu_S+\frac{1}{2}\mu_O$$
$$g_{33}=\frac{8}{3}\mu_S+\frac{5}{2}\mu_O$$

ii) Elements of F matrix

$$f_{11}=K_{S-O}+t^2_{O-R}F'_{R-O}+s^2_{O-R}F_{R-O}+3^2t_{O-O}F'_{O-O}+s^2_{O-O}F_{O-O}$$
$$f_{12}=(t_{O-R}s_{R-O}F'_{R-O}+t_{R-O}s_{O-R}F_{R-O})\sigma$$
$$f_{13}=-t_{O-O}s_{O-O}(F'_{O-O}+F_{O-O})$$
$$f_{22}=(H_{O-S-R}-s_{R-O}s_{O-R}F'_{R-O}+t_{R-O}t_{O-R}F_{R-O})\sigma+\left(\frac{1}{\sqrt{8}}\right)\kappa/r^2_{S-O}$$
$$f_{23}=-\frac{\sqrt{2}}{2}\kappa/r^2_{S-O}$$
$$f_{33}=(H_{O-S-O}-s^2_{O-O}F'_{O-O}+t^2_{O-O}F_{O-O})+\frac{1}{\sqrt{8}}\kappa/r^2_{S-O}$$

where the following notations are used;

κ(intra-molecular tension)
$$=-(K'_ir^2_{ij}+F'_{q_{ij}}r_{ij}q_{ij}\sqrt{t_{ij}t_{ji}})$$
$\sigma=r_{R-S}/r_{S-O}$, $s_{ij}=(r_i-r_j\cos\alpha_{ij})/q_{ij}$
$s_{ji}=(r_j-r_i\cos\alpha_{ij})/q_{ij}$, $t_{ij}=r_j\sin\alpha_{ij}/q_{ij}$
and $t_{ji}=r_i\sin\alpha_{ij}/q_{ij}$

and μ_S, μ_O and μ_R are reciprocals of atomic weights for sulfur, oxygen and the methyl radical, respectively.

Constants Used in Calculation.—*a) Nuclear distances.*—

S–O : 1.50 A[6]
S–R : 1.80 A*

b) Valence angles.—Valence angles for O–S–O and R–S–O are assumed to equal the tetrahedral one, that is 109°28′.

c) Force constants.—K_{S-O}, H_{O-S-O} and F_{O-O} are taken from those for sulfate ion[8], and K_{R-S} is taken from H_{Me-S} of dimethyl sulfide[9]. H_{R-S-O} is taken from the mean of H_{O-S-O} for sulfate ion and $H_{CH_2-S-CH_2}$ for diethyl sulfide[9]. F_{R-O} is taken from the mean of F_{O-O} for sulfate ion and F_{Me-Me} for tetramethyl silane[8]. $\kappa_{MeSO^-_3}$ is taken

4) E. B. Wilson, *J. Chem. Phys.*, **7**, 1047 (1939); **9**, 76 (1941).
5) T. Shimanouchi, *Bulletine Inst. Phys. Chem. Research Tokyo (Riken Iho)*, **21**, 825 (1942).
6) A. Simon and H. Kriegsmann, *Z. Phys. Chem.*, **209**, 369 (1955).
* Summation of Pauling's covalent radii of single carbon and sulfur[7].
7) L. Pauling, "The Nature of the Chemical Bond", Cornell Univ. Press, Ithaca, N. Y. (1940), p. 164.
8) T. Shimanouchi, *J. Chem. Soc. Japan, Pure Chem. Sec. (Nippon Kagaku Zasshi)*, **74**, 226 (1953).
9) M. Hayashi, ibid., **77**, 1962 (1956).

from the mean of $\kappa_{SO_4^{2-}}$ and $\kappa_{Si(CH_3)_4}$[8]. F' is assumed to be $-1/10\ F$[8]. In Table I values of these force constants are given.

TABLE I. FORCE CONSTANTS

F. C.	(dyn./cm.)$\times 10^5$	F. C.	(dyn./cm.)$\times 10^5$
K_{S-O}	6.01	F'_{O-O}	−0.076
K_{S-R}	3.01	F_{O-R}	0.397
H_{O-S-O}	0.43	F'_{O-R}	−0.0397
H_{O-S-R}	0.294	κ	0.328*
F_{O-O}	0.76		

* Unit is (dyn./cm.)$\times 10^{-11}$.

Results, Assignment and Comparison with Observed Data

As the results of calculation, the following values were obtained:

$\nu_1 = 788\ cm^{-1}$ $\nu_2 = 1002\ cm^{-1}$ $\nu_3 = 538\ cm^{-1}$

$\nu_4 = 1081\ cm^{-1}$ $\nu_5 = 537\ cm^{-1}$ $\nu_6 = 367\ cm^{-1}$

Of these vibrations ν_1, ν_2 and ν_3 are totally symmetric and ν_4, ν_5 and ν_6 are doubly degenerated.

These values are compared with the results of Raman spectra of potassium methanesulfonate in aqueous solution studied by Simon and Kriegsmann[6]. Relatively strong lines which could not be considered as C-H stretching and C-H deformation vibrations, are as follows: 348 cm^{-1}(5b), 533 cm^{-1}(2), 560 cm^{-1}(4), 789 cm^{-1}(8), 1054 cm^{-1} (10) and 1184 cm^{-1} (2b). (Number in brackets are intensities of Raman lines.)

They attributed the lines at 789, 1054 and 1184 cm^{-1} to ν_1 (C-S stretching vibration), ν_2 (S-O stretching totally symmetric vibration) and S-O stretching antisymmetric vibration, respectively.

By comparing the author's calculation with observed infrared spectra[1], the assignments can be made as indicated in Table II.

The agreement between the calculated and the observed frequencies is satisfactory except for S-O stretching vibration. The reason will be attributed to the fact that the S-O stretching force constant is taken from that of sulfate ion.

TABLE II. COMPARISON OF CALCULATED AND OBSERVED VALUES (in cm^{-1})

Assignment	Raman	I. R.	Calcd. I	Calcd. II
C-S Stretching	789	789	788	789
S-O Stretching	1054	1060	1002	1055
Deformation	533		538	536
S-O Stretching	1184	1192	1080	1182
R-S-O Deformation	560		537	557
O-S-O Deformation	348		367	349

The force constants were corrected as indicated in Table III, using the trial and error method combined with the method of least squares[10]. If the calculation of normal vibration is done again using these corrected force constants, the agreement between the calculated and observed values becomes much more satisfactory. The calculated values are indicated in Table II as "Calcd. II".

TABLE III. CORRECTED FORCE CONSTANTS

F. C.	(dyn./cm.)$\times 10^5$	F. C.	(dyn./cm.)$\times 10^5$
K_{S-O}	7.31	F'_{O-O}	−0.065
K_{S-R}	3.05	F_{O-R}	0.34
H_{O-S-O}	0.552	F'_{O-R}	−0.034
H_{O-S-R}	0.26	κ	0.328*
F_{O-O}	0.65		

* Unit is (dyn./cm.)$\times 10^{-11}$.

The author wishes to express his indebtedness to Dr. A. Kotera, Professor of Tokyo University of Education, and Dr. T. Shimanouchi, Professor of the University of Tokyo, under whose kind direction this work was performed. And the author wishes to thank Mr. Y. Akai, Chief of Research Section of Funakawa Refinery, for his encouragement of this research.

Nippon Mining Co., Funakawa Refinery
Oga-shi, Akita-ken

10) D. E. Mann, T. Shimanouchi, J. H. Meal and L. Fano, *J. Chem. Phys.*, 27, 43 (1957).

The Role of the Cationic Group in Anionic Detergents

By Maresuke KASHIWAGI and Heihachi EZAKI

(Received November 6, 1958)

It seems that sodium salt of alkyl sulfate has been extensively studied, while little data are known concerning organic salts of alkyl sulfate. It is therefore thought to be of interest to investigate the effect of the substitution of the cationic group attached to the hydrophilic portion of the detergent molecule. Such effcts should be studied both surface-chemically and from the viewpoint of bulk properties.

Materials used for those investigations were, as sulfate type, triethanolamine dodecyl sulfate (TDS), morpholine DS (MDS), pyridine DS (PDS), and sodium DS. As sulfonate type, triethanolamine alkyl benzene sulfonate (TABS) and sodium salt of the same sulfonate (SABS) were used.

Experimental

Materials.—All dodecyl sulfates were synthesized from dodecyl alcohol, chlorosulfonic acid and the corresponding base. The way of synthesis and the identification of product was given in detail previously[1].

Alkyl benzene, the raw material for the sulfonated detergent was the product of Oronite Chemical Co. and was redistilled at 130~136°C/3 mmHg. It was sulfonated with pure chlorosulfonic acid, at an equimolar ratio assuming the alkyl chain of the alkane to be mainly isododecyl, and neutralized either with aqueous sodium hydroxide or triethanolamine. The analysis of SABS showed that the amounts of unreacted alkane and inorganic material were less than 1.5%, respectively.

Measurements.—Monolayer experiments were carried out with the use of a Wilhelmy-type surface balance and surface tension was measured with DuNuoy's instrument. Foaming power was measured, at 40°C throughout, by Ross-Miles method[2,3], apparent viscosity was measured, at 30°C, with a modified Couette type rotational viscometer. Because of their extremely high solubility, the yield of TDS and PDS decreased considerably in the process of purification and we could not carry out whole-scale solubility measurements. Therfore, a Kraft point conventionally determined by dye color change[4] was adopted as a measure of solubility, since this method requires only a very small amount of the sample. It appeared that the Rhodamine 6G used for this purpose fortunately gave a clear color change at the K. P.

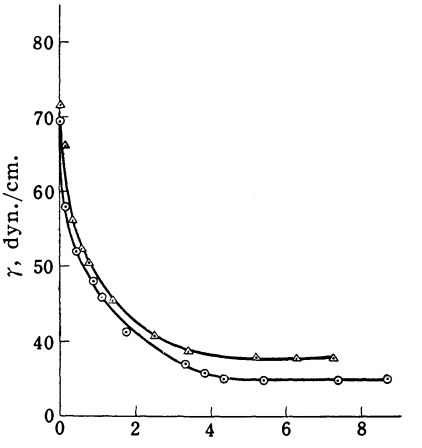


Fig. 1. Surface tension of organic DS.
—⊙— MDS 40°C
—△— TDS 33°C

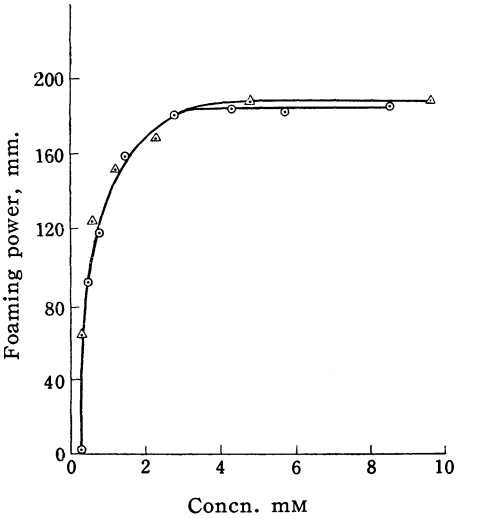


Fig. 2. Foaming power of TDS and MDS.
—⊙— MDS
—△— TDS 40°C

1) M. Kashiwagi, This Bulletin, **31**, 667 (1958).
2) M. Kashiwagi, ibid., **29**, 193 (1957).
3) M. Kashiwagi, ibid., **30**, 572 (1957).
4) K. Ino, *J. Chem. Soc. Japan, Pure Chem. Sec.* (*Nippon Kagaku Zasshi*), **79**, 165 (1958).

Results

1) **Substitution of the Cationic Group in Sulfate Portion.**—(*A*) *Surface Chemical Properties.* — (*1*) *Surface area.* — Surface areas of MDS, TDS and PDS on the substrate of 25% ammonium sulfate are calculated from $F-A$ curve and a surface equation of their state[5] developed by Pethica, $F(A-A_0)=nkt$, where A_0 refers to the surface co-area of the hydrophilic group in the molecule and n is a constant. A_0 is thus calculated to be 34 Å²/mol., identical for all three DS', between the surface areas of 70 Å²/mol. and 40 Å²/mol. and, at 40 Å²/mol., changes to 17 Å²/mol. which corresponds to the cross-sectional area of the hydrocarbon chain. Those values of A_0 are in excellent agreement with those of SDS[5]. The reason for this coincidence is now ascribed to the shielding effect of ammonium ions fully present in bulk phase since the colloidal electrolyte of the detergent may be considered to be equally accessible to both ammonium and organic cations.

(*2*) *Surface tension.* — Surface tension vs. concentration curves of both TDS and MDS are shown in Fig. 1, from which values of CMC are determined to be 0.004 M for both detergents. The CMC value of SDS is known to be about 0.007 M[6]. This value (0.004 M) is the same in the order of magnitude, but somewhat smaller than that of SDS. This small discrepancy may be ascribed both to the relatively large size of the counter ion[7,8] and the greater ions degree of hydration of these ions[9].

(*3*) *Foaming power.*—Foaming power vs. concentration curves of TDS and MDS are shown in Fig. 2, from which values of CMC for both detergents can be determined[2] to be 0.004 M and 0.003 M respectively. These values of CMC can be considered to be in good agreement with the values from surface tension measurements, as appeared in Fig. 1. Anyway, those two salts of DS exhibit approximately the same degree of foaming power, and moreover this in turn proves to be nearly equal to the foaming power of 186 mm. shown by aqueous SDS at its CMC.

(*B*) *Bulk Properties.* — (*1*) *Solubility.* — Solubility values of organic salts of DS, except for MDS, are found to be much higher than those of SDS. Solutions of both TDS and PDS at 30% remainded perfectly transparent even at 0°C, while MDS alone has very small solubility at 0°C, evidently much less than its CMC (i. e., less than 0.15%). The kraft points (K. P.) of both TDS and PDS are found to be less than 0°C, whereas the K. P. of MDS is found to be 30°C, compared with 10°C of SDS[10]. Thus a striking difference in solubility by the nature of the cationic group is observed as estimated from K. P. data.

(*2*) *Viscosity.*—Viscosity values of TDS and SDS at 30°C are listed in Table I. It is clear that SDS exhibits much higher viscosity than organic DS.

Table I. Viscosity of TDS and SDS at 30°C

	10%	20%	30%
TDS	1.5 c. poise	3	5
SDS	4.5	8.5	820

(II) Substitution of the Cationic Group in Sulfonate Portion.—Foaming power of TABS in a standard condition (0.25%, 40°C) is 193 mm., while that of SABS under the same conditions is found to 196 mm. in the Ross-Miles unit. Those values nearly equal each other. The relation is, however, quite different in solubility. TABS dissolves in the amount of 80%, at 0°C, while the solubility of SABS is found to be less than 10% at 20°C. Viscosity values at 30°C are 7 cp. at 30%, 2.5 cp. at 20%, and 1.4 cp. at 10% solutions for TABS, while the viscosity of SABS is found to be 5 cp. at 10% solution. Once again those data may be interpreted as an indication that the substitution of the cationic group in sulfonate portion does not virtually change surface chemical properties, but it does change the bulk properties.

Discussion

The results thus obtained are summarized in Table II. The value of CMC obtained for TDS and MDS, as they appeared in Table II, are in the same order but smaller than that of SDS. It has been shown that the value of CMC decreases when the counter ion becomes very large[7], or the degree of hydration of the counter ion decreases[8,9]. The

5) B. A. Pethica, *Trans. Faraday Soc.*, **50**, 413 (1954).
6) E. G. Goette, *J. Colloid Sci.*, **4**, 459 (1949).
7) A. Cushman A. P. Brady and J. W. McBain, ibid., **3**, 425 (1948).
8) K. Meguro and T. Kondo, private communications.
9) K. Meguro et al., *J. Chem. Soc. Japan, Pure Chem. Sec.* (*Nippon Kagaku Zasshi*), **77**, 1236 (1956).
10) E. Hutchinson, *J. Phys. Chem.*, **58**, 1126 (1954).

second factor would be less effective, because CMC values of potassium, sodium and lithium salts of DS are fairly close (7~10 mM)[9].

According to Klevens, these differences may be due to minor differences in the degree of ionization of the micelles, for it has been observed that the presence in small amounts of unionized additives (unreacted alcohol for example) will markedly decrease the CMC, whereas the use of an ionized additive of an equivalent chain length and the same charge will result in little change[11]. This is true of uni-univalent electrolytes. As for a polyvalent electrolyte, valence of cation may follow the Schulz-Hardy rule in decreasing CMC[12].

TABLE II. PROPERTIES OF VARIOUS SALTS OF DODECYL SULFATE

Surface properties

	TDS	PDS	MDS	SDS
Surface area of hydrophilic group on 25% $(NH_4)_2SO_4$	34Å²/mol.	34	34	34
Foaming power (0.25%, 40°C)	188 mm.	—	184	186
CMC	4mM		3~4	7

Bulk properties

	TDS	PDS	MDS	SDS
Kraft P.	less than -5°C	less than 0°C	30°C	10°C
Estimated solubility grade	1	2	4	3
Viscosity	low	low	low	high

Summary

Various salts of dodecyl sulfate (DS) and alkylbenzene sulfonate have been investigated surface-chemically and from the viewpoint of their bulk properties. It was shown that these organic salts of DS occupy the same surface area as that of SDS, on the substrate of concentrated anmonium sulfate, independent of the nature of the cationic group attached to the sulfate anion. CMC values determined by two different methods (i. e., surface tension and foaming power) show practically the same value. These results are approximately in accord with the known principle that the number of carbon atoms in the molecule of the normal straight chain colloidal electrolyte of one particular class is the determining factor for the value of CMC, although a slight but definite shift in CMC value is observed with variation in substituting group. On the other hand, bulk properties such as viscosity and solubility are influenced remarkably by the substitution of cationic group in anionic detergents.

The author wishes to thank Professor R. Matsuura of Kyusyu University for his kind advice.

Mitsuwa Chemical Laboratory
Terajima-machi, Sumida-ku
Tokyo

11) H. B. Klevens, ibid., **14**, 742 (1946).
12) H. Lange, *Kolloid-Z.*, **121**, 16 (1951).

Polymerization of Aminoacetonitrile

By Hidesaburo HANAFUSA* and Shiro AKABORI

(Received October 28, 1958)

If the protein is absolutely essential for all living things, the non-enzymic formation of protein must have been prerequisite for the origination of life.

In 1936 Oparin[1] postulated that α-amino acids could have been formed non-biologically from hydrocarbons, ammonia and hydrogen cyanide at the age of the earth when atmosphere contained these substances in high concentrations. Bernal[2] emphasized the role played by ultraviolet light in the formation of organic compounds at a certain stage of the evolution of the earth. He also suggested that life

* Present Address: The Research Institute for Microbial Deseases, Osaka Univ., 3, Doshima Nishimachi, Osaka.

1) A. I. Oparin, "The Origin of Life", Macmillan Co. N. Y. (1936).

2) J. D. Bernal, "Physical Basis of Life", Routledge and Kegan Paul Ltd., London (1951).

might have originated on the surface of clay which accumulated large amounts of organic substances. Oparin's hypothesis has received strong experimental support from the recent work of Miller[3].

It has generally been accepted that the first proteins or fore-proteins were non-biologically formed by the polycondensation of preformed free amino acids. This belief is solely based on the fact that proteins in the present-day organisms are synthesized via free amino acids. Such non-biological formation of polypeptides and proteins, however, seems to be very difficult owing to the requirement of free energy, though Bresler[4] reported the reconversion of tryptic hydrolysates to the original proteins under an extremely high pressure.

In 1955 Akabori proposed[5] a hypothesis concerning the origin of the fore-protein and speculated that it must have been produced through reactions consisting of the following three steps.

I) $CH_2O + NH_3 + HCN \rightarrow NH_2—CH_2—CN + H_2O$

II) $n(NH_2—CH_2—CN) \rightarrow (—NH—CH_2—C(=NH)—)_n$

$\xrightarrow{+H_2O} (—NH—CH_2—CO—)_n + NH_3$

III) $(—NH—CH_2—CO—)_n \rightarrow (—NH—CH(R)—CO—)_n$

The first step is the formation of aminoacetonitrile from formaldehyde, ammonia and hydrogen cyanide. The second is the polymerization of aminoacetonitrile on a solid surface, probably in the state adsorbed on clay, followed by the hydrolysis of the polymer to polyglycine and ammonia. The third step is the introduction of side chains into polyglycine by the reaction with aldehyde or with unsaturated hydrocarbons. The reaction in the first step is well known as Strecker's reaction. Akabori and co-workers[6] reported some experimental results on the possibility of the third step.

The present paper deals with experiments concerning the second step in the formation of the fore-protein, that is the polymerization of aminoacetonitrile. Although acetamidine is formed from ammonia and acetonitrile in methanol solution, the condensation of primary amine with nitrile has been known very little. In the synthesis of purine derivatives, Traube[7] synthesized diamino thiopyrimidine by the condensation of thiourea and malonitrile. In this reaction sodium ethoxide was used as catalyst, and the anhydrous condition had been kept in the course of reaction.

Aminoacetonitrile prepared by the usual method was heated at 120~140°C for 3~5 hr. in the presence of clay, which was used as adsorbent of the nitrile and seemed to play a role as catalyst in this reaction. The product was extracted with water, dilute hydrochloric acid and sodium hydroxide solution. The presence of glycyl-glycine and glycyl-diglycine in extract and partial hydrolysate of extraction residue was confirmed by paper and column chromatography.

Experimental

Materials.—*Aminoacetonitrile sulfate;* According to Anslow and King's method[8] aminoacetonitrile sulfate was obtained, m. p. 164°C (decomp.). *Kaolin;* Commercial "Kaolin" was refluxed with hot water. After 2 hr., it was centrifuged, washed with distilled water and dried in an air bath. Kaolin treated with concentrated hydrochloric acid was used in some cases. *Other clays;* Japanese acid clay and bentonite were treated in the same way as kaolin. *Glycyl peptides;* Gly-Gly** and Gly-Gly-Gly** were synthesized in our laboratory and the purity was confirmed on paper chromatogram.

Procedures.—Several procedures were tried for polymerization of aminoacetonitrile. A typical method is the following.

One gram of amino acetonitrile sulfate was mixed with 20 times of kaolin and heated at 130~135°C for five hours. To heat uniformly, the mixture was taken in a wide bottomed flask and kept in an air bath at 130°C. As the liberation of ammonia was detected in the course of reaction, the top of flask was connected with a small tube of Dowex-50 (H-form). The reaction mixture, being of violet-grey color, was extracted with each 30 ml. of water, N/10 hydrochloric acid and N/10 sodium hydroxide successively in the cold (see Fig. 1). The pH of the water extract was about 5.5, and each of extracts showed a strong positive biuret reaction. A part of the residue was hydrolyzed with N/10 hydrochloric acid at 100°C for 1 hr. (KB) and another part was

3) S. L. Miller, *Science*, **177**, 528 (1953); *J. Am. Chem. Soc.*, **77**, 2351 (1955); *Biochim. et Biophys. Acta*, **23**, 480 (1957).

4) E. S. Bresler et al., *Izvest. Akad. Nauk, SSSR, Ser. Biol.*, **13**, 392 (1949).

5) S. Akabori, *Kagaku (Science in Japan)*, **25**, 54 (1955).

6) S. Akabori, K. Okawa and M. Sato, This Bulletin, **29**, 608 (1956).

7) W. Traube, *Ann. Chem.*, **331**, 64 (1904).

** Glycine, glycyl-glycine and glycyl-diglycine are abbreviated as Gly, Gly-Gly, Gly-Gly-Gly, respectively.

8) W. K. Anslow and H. King, *J. Chem. Soc.*, **1929** 2463.

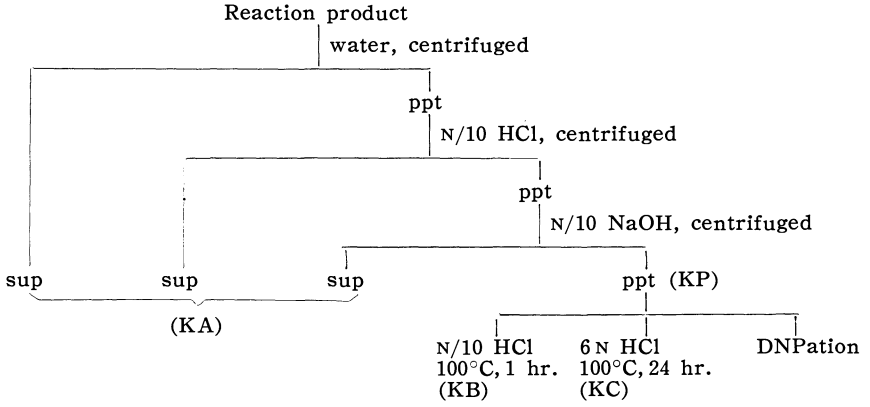


Fig. 1. The Scheme of extraction of reaction product

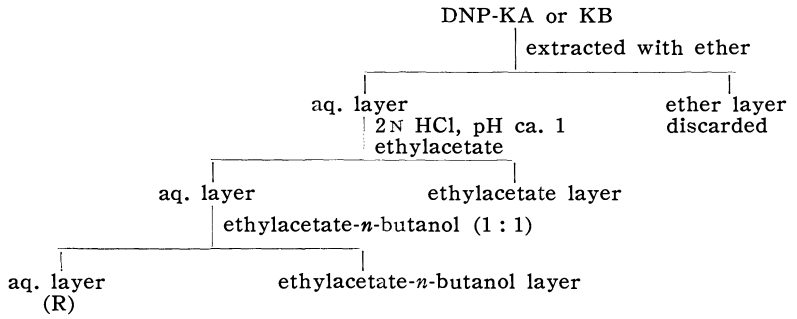


Fig. 2. Procedure for the extraction of DNP-peptides.

hydrolyzed with 6 N hydrochloric acid at 100°C for 24 hr. (KC). For the purpose of the hydrolysis of imino group of polymerized product, combined extract (KA) was refluxed at pH 1 for 1 hr. After neutralization the component of each fraction was examined by paper chromatography and by paper and column chromatography after dinitrophenylation.

The Component of Product. — After concentration, an aliquot of each fraction was chromatographed on filter paper using 80% phenol as solvent. From this paper chromatogram, it was found that each fraction contained glycine, and KA and KC contained also glycyl peptide, probably Gly-Gly and Gly-Gly-Gly. These findings were confirmed by dinitrophenylation technique. This method is excellent for the reason that non-peptide basic substance which is ninhydrin positive can be separated from dinitrophenylated (DNP-) glycyl peptide. After each fraction was dinitrophenylated by the usual method, DNP-peptides were extracted with ethylacetate and *n*-butanol as shown in Fig. 2. Ethylacetate extract and ethylacetate-*n*-butanol extract were combined and dried in vacuo. After removing dinitrophenol by sublimation using cold-finger condenser[9], a part of this DNP-peptide fraction was subjected to one-dimensional chromatography on filter paper using *n*-butanol saturated with 1% ammonia as solvent. Several spots of R_f values 0.30, 0.17, 0.11 and lower ones were obtained; the first three spots were identified as DNP-derivatives of Gly, Gly-Gly and Gly-Gly-Gly in comparison with standard samples. Another part of the DNP-peptide fraction was chromatographed on a buffered celite column by a partly modified Perrone's method[10]. The solvent system used was ethylacetate-0.5 M phosphate buffer (1:1). After 10 parts of celite were mixed with 6.6 parts of the lower layer of the solvent mixture, celite was poured into the column of 20 cm. high and 2 cm. in diameter with the upper layer of solvent and packed with glass rod compactly. The upper half of the column was bufferized to pH 5.5 and the lower half to pH 6.4. Samples were charged on the column and developed with the upper layer of the solvent mixture of pH 5.5. DNP-Gly, DNP-Gly-Gly and DNP-Gly-Gly-Gly were separated each other forming sharp bands. The bands corresponding to DNP-Gly-Gly and DNP-Gly-Gly-Gly were cut off and eluted with ethanol acidified by small quantity of hydrochloric acid. The eluates were dried up and dissolved in 1% sodium bicarbonate. The optical densities were measured photometrically. After measurement, such DNP-peptides were hydrolyzed with 6 N hydrochloric acid for 5 hr. and DNP-derivative was removed by ethylacetate extraction. Aqueous layer was redinitrophenylated, extracted again with ethylacetate, separated by column chromatography and the quantity of DNP-Gly was measured. If the molecular extinction coefficients of dinitrophenyl

9) G. L. Mills, *Biochem. J.*, **50**, 707 (1952).

10) J. L. Perrone, *Nature*, **167**, 513 (1951).

amino acid and peptide are the same, the ratio of optical density of DNP-derivative before and after acid hydrolysis must indicate the length of the peptide. These ratios were 1:1.07 and 1:2.23 respectively for the two DNP-peptides, and were agreed with the expected value for DNP-Gly-Gly and DNP-Gly-Gly-Gly.

Residual aqueous layer (R) in Fig. 2, the yellow color of which shows the presence of unextracted DNP-derivatives, was hydrolyzed with 1 N hydrochloric acid at 100°C for 2 hr. By the same procedure for DNP-peptides, newly formed extractable DNP-derivatives were taken into ethylacetate-*n*-butanol layer. From this fraction, also, DNP-Gly-Gly and DNP-Gly-Gly-Gly were obtained. This fact shows that the extracts (KA and KB) might contain the longer glycyl peptide. From the procedures described above it was found that the reaction products contain many non-peptide compouds, for example, on the celite column chromatography there appeared DNP-derivatives which have an absorption maximum at 365~380 mμ and do not yield DNP-Gly by hydrolysis. Further, the first extracted solution of reaction product (KA) produces a black colloidal substance on standing at room temperature for 24 hr., and this substance precipitates on acidification.

In order to study the possibility that the polymerized substance remains in the residue as an adsorbed form, determination of nitrogen content of the residue and estimation of mean chain length of peptides were tried using micro-Kjeldahl method and dinitrophenylation technique. Nitrogen distribution in the process of reaction and extraction was shown in Table I. From these data obtained it seems reasonable to assume that not only the expected reaction, i. e., polymerization of aminoacetonitrile, but also the

Table I. Nitrogen distribution in the process of reaction and extraction

	mg. N	%
Starting material	540	100
After reaction period	376	70
Extract (KA)	149	28
Residue (KP)	29	5.3

reaction liberating nitrogen as ammonia or volatile form may take place. Nitrogen content of the residue was lower than expected, but this value varied from one reaction to another between 4~20 per cent. In order to determine the mean chain length of adsorbed polymer, the same procedure as used in the confirmation of two bands on the celite chromatogram was applied to the residue (KP) after refluxing at pH 1 for one hour.

The result of this experiment shows that the mean chain length of adsorbed substance is 1.8. However, it is hard to say that the reaction product involves long-chain, high molecular polyglycine although the residue might adsorb still low molecular peptide and contain the not-straight chain compound as diketopiperazine which produces DNP-Gly by hydrolysis and dinitrophenylation.

The presence of diketopiperazine in the reaction product was supposed by the qualitative test using picrate[11] and the different content of diglycine of the solution with and without alkaline treatment of the hot water extract of reaction product.

Change of Condition.—If the presence of the clay such as kaolin is advantageous for the proposed reaction, one of the effects must be the adsorption of starting material. The degree of adsorption of aminoacetonitrile on several kinds of clay was determined by the following way. The solution of 200 mg. of aminoacetonitrile sulfate in 4 ml. of water was mixed with 1 g. of clay; after shaking the suspension was allowed to stand overnight at 5°C and filtered. The concentration of free aminoacetonitrile in the filtrate and the control solution (without clay) was measured by ninhydrin reaction[12], which is used generally for the determination of amino acid. By a preliminary test it was confirmed that the aminoacetonitrile was not hydrolyzed in the process of determination and could be determined quantitatively, though the color yield is very low. As shown in Table II, the nitrile was adsorbed most

Table II. The degree of adsorption of aminoacetonitrile on the clay

A. pH 4.5

	Adsorption %
Control	0
Kaolin	3.7
Silicic acid	0
Bentonite	27.0
Silica gel	1.0
Japanese acid clay	37.8

B. Adsorption of Japanese acid clay at different pH

pH	Adsorption %	pH	Adsorption %
4.6	37.8	6.8	54.0
4.6	40.0	7.5	45.0
5.5	51.4	8.7	36.5

on Japanese acid clay and at pH 7. This pH coincides with that of the solution of aminoacetonitrile sulfate neutralized with sodium hydroxide solution.

In an effort to study the effect of adsorption on the reactivity, aminoacetonitrile in an adsorbed state was used as starting material. After adsorption, as described above, Japanese acid clay was filtered, dried and heated at 130°C for 3 hr. in the same way as the typical method. In this case, yield of peptides was slightly high, but black colloidal material was produced abundantly at the same time. It may be concluded from the above fact that the adsorption on the clay

11) M. Frankel and E. Katchalski, *J. Am. Chem. Soc.*, **64**, 2264 (1942).

12) S. Moore and W. H. Stein, *J. Biol. Chem.*, **176**, 367 (1948).

activates the starting material to some extent but the effect is not specific for peptide synthesis.

When bentonite, silicic acid, silica gel and alumina were used as adsorbent, the yields of peptides were poor. Kaolin and Japanese acid clay treated with concentrated hydrochloric acid did not adsorb the aminoacetonitrile.

The effect of temperature was investigated between 100~150°C; below 120°C the reaction did not occur, and above 150°C the decomposition was predominant.

When methylene aminoacetonitrile was used instead of aminoacetonitrile as starting material, many spots appeared on the paper chromatograms of the extract of reaction product, but Gly-Gly-Gly could not be detected. In this case, the extracted solution (corresponding to KA) gave positive biuret reaction, but since several positive compounds besides poly-peptide have been known, biuret test is not suitable to such solutions which involve various unknown substances similarly as the test of diketopiperazine by picrate.

As cited in the introduction of this paper, diaminopyrimidine was synthesized from thiourea and malonitrile in ethanol in the presence of sodium ethoxide by Traube. If aminoacetonitrile reacts analogously, diimino-piperazine may be obtained from two molecules of aminoacetonitrile to yield diketopiperazine and diglycine by hydrolysis.

Four grams of aminoacetonitrile sulfate was suspended in 10 ml. of ethanol. To this suspension, 20 ml. of ethanol dissolving 1.4 g. of sodium was allowed to run from a dropping funnel under stirring. Two aliquots of the mixture were heated to 40°C and to boiling point, respectively, for 3 hr. In each case, the product was neutralized, dried in vacuo, and dissolved in 1 N sodium hydroxide. After 1 hr. the product was neutralized again, dried and subjected to paper chromatography. Only a trace of glycyl-glycine was observed, and here again the black colloidal substance appeared in the solution of the product.

Discussion

As aminoacetonitrile has a bifunctional group and an active methylene group, it may be reactive and be able to cause various reactions simultaneously. These characteristics are a strong point as well as a weak point in the case of polymerization which was tried. From the result of investigation, it was obvious that peptides were formed from aminoacetonitrile, but the presence of high polymer which might be firmly adsorbed on the clay was not confirmed. If the conditions may be found, in which polypeptide synthsis is promoted while the side reaction and decomposition are suppressed, poly-glycine should be yielded more easily. Because the heat reaction of aminoacetonitrile without clay was unsuccessful, the solid surface of clay seems to play a certain role in this reaction as in the case of activation of the methylene group of polyglycine[6].

In some cases, the formation of only glycyl-glycine was observed in the typical reaction procedure. Though it is hard to explain, this phenomenon suggests that the reaction proceeds in two directions, the one toward diketopiperazine formation and the other toward polyglycine formation similarly as the polymerization of glycine ethyl ester.

Summary

Aminoacetonitrile sulfate was heated with kaolin and/or Japanese acid clay at 120~140°C for 5 hr. The presence of glycyl-glycine and glycyl-diglycine in the extract and the partial hydrolysate of this reaction product was confirmed by paper and column chromatography.

Department of Chemistry
Faculty of Science
Osaka University, Osaka

Phase Transition of Li_2O-Fe_2O_3 System. III. Long-range Order in Lithium Ferrite and Lithium Ferrospinel

By Eizo KATO*

(Received July 22, 1958)

In the previous papers[1,2], the thermal and the electric properties of lithium ferrite and lithium ferrospinel were studied from the viewpoint of an order-disorder transition. Then the anomalous phenomena in these properties were observed at the transition.

The order-disorder transition in binary alloys has been widely studied by the statistical thermodynamics[3]. In order to specify the degree of order for the arrangement of atoms, two kinds of order parameters are defined. One is a long-range parameter introduced by Bragg and Williams, and the other is a short-range order parameter introduced by Bethe. When the former parameter is present, some super-stucture reflections appear in an X-ray diffraction. At the transition temperature, this parameter vanishes and the latter parameter remains in a diffuse scattering of X-rays.

The long-range order parameter in a substitutional transition, which was defined by Buerger[4], has not yet been measured except of binary alloys. As the first example of an extension of the transition theory for binary alloys to more complex crystals, temperature dependencies of the long-range order parameter for lithium ferrite and lithium ferrospinel were measured by an X-ray powder method.

Diffraction Theory of Long-range Order

The long-range order parameter S may be written as

$$S=(r_\alpha-p_A)/(1-p_A)=(r_\beta-p_B)/(1-p_B) \quad (1)$$

where r_α is the fraction of α site occupied by A ions and p_A is the fraction of A ions in the crystal, and so forth. S is, of course, defined so that it may be unity for the perfectly ordered state and zero for the perfectly disordered one. When the crystal is of AB type or of AB_3 type, S is given from Eq. 1.

$$S=2r_\alpha-1=2r_\beta-1 \quad \text{for AB type} \quad (2a)$$

and

$$S=(4r_\alpha-1)/3=4r_\beta-3 \quad \text{for } AB_3 \text{ type} \quad (2b)$$

Let us consider the order-disorder equilibrium, in which two kinds of ions in the crystal contribute to the transition, i.e.,

$$A_aB_bL_l\cdots\cdots N_n \rightleftarrows (A_aB_b)L_l\cdots\cdots N_n$$

where A_a means that a A ions are at the definite equivalent points, and so forth and (A_aB_b) means that a A ions and b B ions are randomly distributed to the points. According to the method used for binary alloys, the expression for the structure amplitude of any state is

$$F=[f_Ar_\alpha+f_B(1-r_\alpha)]G_\alpha + [f_Br_\beta+f_A(1-r_\beta)]G_\beta+\sum_L F_L \quad (3)$$

where f_A is the atomic scattering factor for A ion, f_B that for B ion, G_α and G_β are the geometrical structure factors referring only to the positions of α site and β site respectively, and $\sum_L F_L$ is the sum of structure amplitudes as to L,……, N ions which are independent of the transition. When A_aB_b is AB or AB_3, Eq. 3 is rewritten by introducing Eq. 2,

$$F=S(f_A-f_B)/2\cdot(G_\alpha-G_\beta) + (f_A+f_B)/2\cdot(G_\alpha+G_\beta)+\sum_L F_L \quad \text{for AB} \quad (4a)$$

and

$$F=S(f_A-f_B)/4\cdot(3G_\alpha-G_\beta) + (f_A+3f_B)/4\cdot(G_\alpha+G_\beta)+\sum_L F_L \quad \text{for } AB_3 \quad (4b)$$

For simplicity, both cases are expressed by a single form as

$$F=SF_{ss}+F_{fund} \quad (5)$$

where the subscript *ss* means the superstructure reflection and *fund* the funda-

---

* Present address; Idemitsu Kōsan Co., Ltd., Chuō-ku, Tokyo.

1) E. Kato, This Bulletin, 31, 108 (1958).

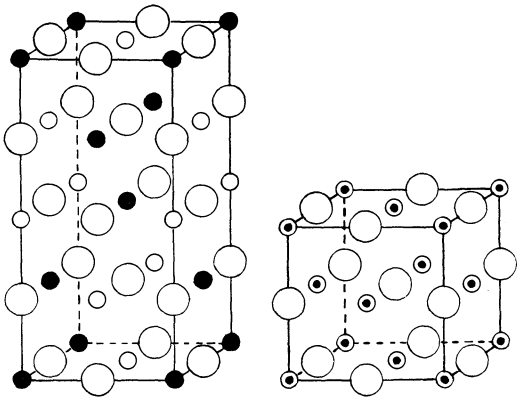
2) E. Kato, ibid., 31, 113 (1958).

3) See, for instances, S. Siegel, "Phase Transformations in Solids", Wiley, New York (1951), p. 366; T. Muto and Y. Takagi, "Solid State Physics", Vol. 1, Academic Press, London (1955), p. 193.

4) M. J. Buerger, "Phase Transformations in Solids", Wiley, New York (1951), p. 183.

5) Z. W. Wilchinsky, *J. Appl. Phys.*, 15, 806 (1944); D. T. Keating and B. E. Warren, ibid., 22, 286 (1952).

mental reflection. SF_{ss} and F_{fund} correspond respectively to the first term and the rest two terms in Eq. 4.



(ordered lattice) (disordered lattice)

Fig. 1. Crystal structures of lithium ferrite.
○ Li^+ ion ● Fe^{3+} ion ○ O^{2-} ion
⊙ $\frac{1}{2}$ ($Li^+ + Fe^{3+}$)

The above-mentioned procedures were applied to the transition between $D_{4h}^{19} - I4/amd$ and $O_h^5 - Fm3m$ in lithium ferrite, and to that between $O^6 - P4_33$ and $O_h^7 - Fd3m$ in lithium ferrospinel. The crystal structures of lithium ferrite are shown in Fig. 1, where oxygen ions are at the same equivalent point in either the perfectly ordered or the perfectly disordered state. The crystal structures of lithium ferrospinel are shown in Fig. 2, where the equivalent points of ferric ions (small shaded circles) at the tetrahedral sites of the eightfold position are the same in either state, and the structural parameter of oxygen ions (large circles) is 0.382[6] at the perfectly ordered state and 0.382 ± 0.005[7] at the perfectly disordered state. Under the following postulations,

(1) oxygen ions in lithium ferrite, and oxygen ions and tetrahedrally-coordinated ferric ions in lithium ferrospinel are independent of the transition mechanism,

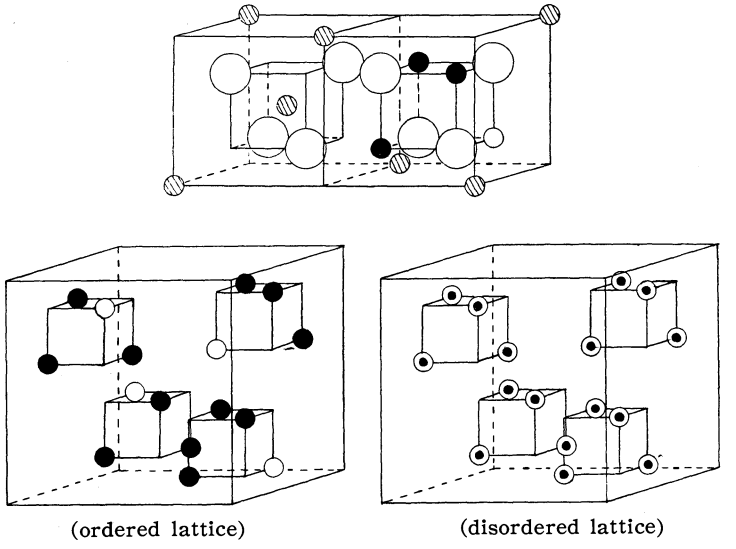
(2) the migrating ions, i.e., all the cations in lithium ferrite or the octahedrally-coordinated cations in lithium ferrospinel, occupy the equivalent points invariable at any state of the transition,

the structure amplitudes of the superstructure reflection can be calculated from Eq. 4 as follows:

For lithium ferrite

$$|F_{ss}| = 2\sqrt{2}\,(f_{Fe} - f_{Li}),\quad h+k=2n+1,\quad l=m+1/2\ \ (L=2l=2m+1) \tag{6a}$$

and for lithium ferrospinel



(ordered lattice) (disordered lattice)

Fig. 2. Crystal structures of lithium ferrospinel. Above: One-fourth of a unit cell of the ordered lattice. Below: Total unit cell showing the tetrahedrons of $LiFe_3$.
◍: Fe^{3+} ion at the tetrahedral site ○: Li^+ ion at the octahedral site
●: Fe^{3+} ion at the octahedral site ⊙: $\frac{1}{4}$ ($Li^+ + 3Fe^{3+}$) ○: O^{2-} ion

6) P. B. Braun, *Nature*, **170**, 1123 (1952).
7) F. de Boer, J. H. van Santen and E. J. W. Verwey, *J. Chem. Phys.*, **18**, 1032 (1950).

$$\left.\begin{array}{l} |F_{ss}|=2(f_{Fe}-f_{Li}),\ h,k,l: \\ \quad \text{one even and two odd} \\ 2\sqrt{2}\,(f_{Fe}-f_{Li}),\ h,k,l: \\ \quad \text{one odd, one } 4n, \text{ one } 4m+2 \end{array}\right\} \quad (6b)$$

where f_{Li} is the atomic scattering factor for lithium ion and f_{Fe} that for ferric ion. Here, in lithium ferrite, l indicates the third index of a plane which refers to the cubic unit cell in the perfectly disordered state and L that referred to the tetragonal one in the perfectly ordered state, the latter cell being double of the former along c direction.

Experimental and Results

Specimens.—Lithium ferrite and lithium ferrospinel were prepared by the same method as in the previous papers[1,2]. The probes for X-ray measurements were made by quenching in water after heating for a necessary time at the definite temperatures which were listed in Tables I and II.

TABLE I. ANNEALING TIMES, TEMPERATURE AND VALUES OF S FOR SAMPLES OF LITHIUM FERRITE

Temp. (°C)	Annealing time (days)	Peak area $A_{10\frac{1}{2}}$	Peak area A_{200}	S
518	20	4263	2798	0.92
554	21	4928	3017	0.95
587	28	0	—	0
598	28	0	—	0
616	30	0	—	0
627	27	0	—	0
642	15	0	—	0
650	34	0	—	0
661	11	0	—	0

$A_{10\frac{1}{2}}$ in the range of 616~661°C were measured by the film method.

TABLE II. ANNEALING TIMES, TEMPERATURE AND VALUES OF S FOR SAMPLES OF LITHIUM FERROSPINEL

Temp. (°C)	Annealing time (hr.)	Peak area A_{210}	Peak area A_{220}	S
448	53	636	1831	0.95
542	61	688	1839	0.98
652	60	665	1910	0.95
708	64	635	1805	0.96
721	95	623	1816	0.94
744	140	194	1784	0.53
765	24	0	—	0
802	25	0	—	0

Apparatus.—The X-ray reflection intensity was measured by a Norelco diffractometer with filtered Co K_α radiation.

Procedures.—From the observed integrated intensities of a super-structure reflection and a fundamental reflection, S is computed by the following formula,

$$S^2=\left(\frac{P_{ss}}{P_{fund}}\right)\frac{F_{fund}^2[m(1+\cos^2 2\theta)\operatorname{cosec}^2\theta\sec\theta]_{fund}}{F_{ss}^2[m(1+\cos^2 2\theta)\operatorname{cosec}^2\theta\sec\theta]_{ss}}$$

where P: integrated intensity
m: multiplicity
θ: Bragg angle of the reflection

since $F_{ss}=0$ on the fundamental reflection and $F_{fund}=0$ on the super-structure reflection. The integrated intensity is proportional to the area A under the peak curve traced by diffractometer for the reflection, i.e.,

$$P_{ss}/P_{fund}=A_{ss}/A_{fund}$$

Lithium Ferrite.—The super-structure line $10\frac{1}{2}$ [8] and the fundamental line 200 were chosen. The final results are listed in Table I.

Lithium Ferrospinel.—The super-structure line 210 and the fundamental line 220 were chosen, and 0.382 was adopted for the value of structural parameter of oxygen ion. The final results are listed in Table II.

Discussion

The statistical theory[9] for the order-disorder transition has been studied on binary alloys. In the simplest case, the approximation is given by Bragg and Williams in which the effect of the nearest neighbors is neglected. Considering the nearest neighbor interaction only, the first approximation is derived from the Bethe's method. Although it may not always be valid to apply the theory for the order-disorder transition in binary alloys to such complex crystals as lithium ferrite and lithium ferrospinel it can be permitted, for the sake of simplicity, to make a trial as follows. Namely, if we neglect the ions which have no direct contribution to the transition, the remaining lattice constructed by the migrating ions alone belongs to the binary system to which the theory may be applied. This lattice is conveniently named a simplified lattice.

The simplified lattice of lithium ferrite belongs to AB type and its disordered lattice is a face-centered cubic. Comparison of the experimental results for lithium ferrite with the curves calculated by the zeroth approximation and the first one for AuCu[10], which is one of binary alloys

8) Here is represented the index of the plane referred to the disordered lattice.

9) See, for instance, E. A. Guggenheim, "Mixtures", Oxford Univ. Press, London (1952), p. 101.

10) The theory gives the following results: from the zeroth approximation $T/T_c=S/\tanh^{-1}S$, where T_c is the transition temperature; from the first approximation in which all combinations of the quadruplets of sites are considered, the value of S jumps from random value zero to the value $S=0.9828$ at T_c[9].

of face-centered cubic type, is shown in Fig. 3[11]. The experimental results are in qualitative agreement with the curve by the first approximation for AuCu. Comparing the crystal structures of the simplified lattice of lithium ferrite with those of AuCu lattice, both lattices have similar structure in disordered phase. The ordered AuCu lattice is pseudo-cubic (tetragonal but the axial ratio is 1.08 : 1.08 : $\sqrt{2}$), while the ordered lattice of lithium ferrite is a tetragonal one which is double the size of cubic lattice in the disordered state along c axis as is seen in Fig. 1. However, the number of the nearest neighbor is 12 in either lattice although the relative arrangement of A and B atoms on these 12 positions around the centered atom is different in both lattices. Hence under such a rough assumption as neglecting oxygen ions as mentioned above, lithium ferrite can be approximated to be LiFe as AuCu with respect to its transition.

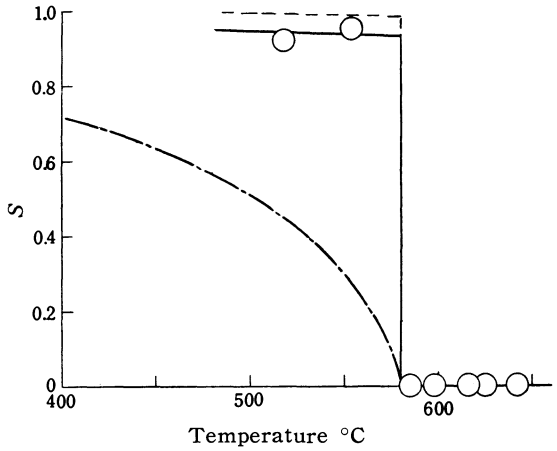


Fig. 3. Variation of long-range parameter for lithium ferrite, experimental and theoretical.
-○-: experimental
- · -: zeroth approximation
------: first approximation

On the other hand, the simplified lattice of lithium ferrospinel belongs to AB_3 type, the typical example of which is $AuCu_3$ (face-centered cubic type). Comparison of the experimental results for lithium ferrospinel with the curves calculated by the zeroth and the first approximation for $AuCu_3$[12] is shown in Fig. 4, where it is found that the experimental results are in good agrreement with the curve calculated by the first approximation. It is noted here that the groups of $AuCu_3$ are arranged side by side along the three directions while those of $LiFe_3$ are arranged tetrahedrally as is seen in Fig. 2, as a result of which the number of the first neighbors is 12 in $AuCu_3$ but 6 in $LiFe_3$[13]. In the present stage the effect of the number of the first neighbor is not ascertained.

In conclusion, it is very interesting that

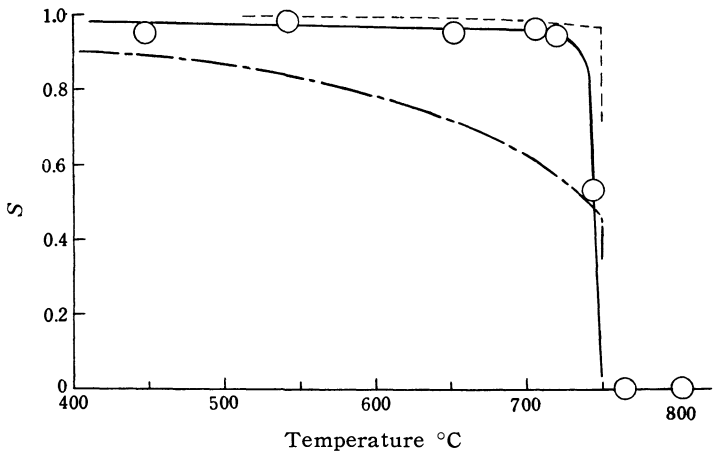


Fig. 4. Variation of long-range order parameter for lithium ferrospinel, experimental and theoretical.
-○-: experimental, - · -: zeroth approximation, ------: first approximation

11) Here T_c is conveniently assumed to be 580°C.

12) The theory gives the following results: from the zeroth aproximation $T/T_c=\frac{4.88\ S}{\ln\{1+16S/3(1-S)^2\}}$; from the first approximation in which all combinations of the quadruplets of sites are considered, the value of S jumps from the random value zero to the value $S=0.9557$ at T_c[9].

13) It may be shown that T_c can not exist in the case of six nearest neighbors (private communication from R. Fujishiro).

in spite of such a rough assumption as ignoring serveral ions having no direct contribution to the transition, statistical theory for order-disorder transition in binary alloys can be approximately applied to estimation of the long-range order parameter in such complex crystals as lithium ferrite and lithium ferrospinel. Moreover, it is emphasized that in the present stage where we have no theory including the effect of all ions in the complex crystal, the assumption of the simplified lattice which can reduce the complex system to a binary one is very useful in treating the order-disorder phenomena.

Transition Temperature of Lithium Ferrite.—As is shown in Fig. 3 the long-range order in lithium ferrite vanishes at 554~587°C[14]. In the previous paper[1] it was found that the anomalous thermal expansion took place at 660°C in the case of ascending temperature and no change was measured down to 550°C in the case of descending temperature. In both the differential thermal analysis and the electric measurement a change was recognized in the vicinity of 660°C. This discrepancy between the observed transition temperatures by X-ray method and those by others is due to the fact that the samples used in the X-ray method were annealed for a long time (20~30 days), while the dilatometry was measured under the non-equilibrium condition, because of its sluggish transition.

Transition Temperature of Lithium Ferrospinel.—The value of the transition temperature for lithium ferrospinel was decided to be 750±1°C from the dilatometry. This value was also given from the differential thermal analysis and the measurement of d.c. electric resistance. The diffractometric curves used for the determination of the transition temperature are shown in Fig. 5, where the superstructure lines 210 and 211 are as yet prominent at 744°C, but very faint at 747°C

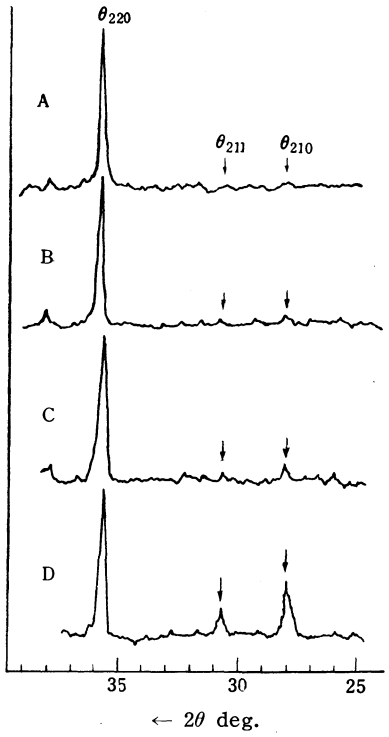


Fig. 5. Diffractometric curves for some samples of lithium ferrospinel in the neighborhood of the transition temperature.
A: 756°C, B: 747°C, C: 744°C, D: 721°C

and disappear completely at 756°C. Hence the probable value of the transition temperature can be estimated to be 750°C in good agreement with the value determined by other physical methods.

The author wishes to express his appreciation to Professor S. Nagaura for his encouragement during this work. He is also indebted to Professor R. Fujishiro for his kind instruction on the statistical treatment and to Professor Y. Saito for his suggestion on X-ray diffraction theory.

Institute of Polytechnics
Osaka City University
Kita-ku, Osaka

14) By R. Collongues (*Bull. soc. chim. France*, 1957, 261) the ordered phase was found at 600°C for a sample annealed for 25 days.

*Preparation of Chloropolysilane from the Copper-catalyzed Reaction of Silicon Metal and Hydrogen Chloride**

By Isao SHIIHARA and Jun IYODA

(Received November 13, 1958)

The copper-catalyzed reaction of silicon metal powder with hydrogen chloride by the flow method was studied in order to find a convenient preparative method for chloropolysilanes, and to elucidate the mechanism of this reaction which seems to have a close relationship with the so-called direct method of preparing alkylchlorosilanes. Hitherto, the conventional way to prepare chloropolysilanes has been to use a binary alloy such as magnesium-silicon[1,2] or ferrosilicon[1] so as to smooth the reaction of silicon and chlorine, and to work at a temperature as low as possible. However, the yields were not satisfactory.

The present investigation was carried out with several kinds of silicon-copper powder mixtures, varying the species of silicon metal, the reaction temperature, the flow velocity of reactant gas, and the ratio of copper powder to silicon. Under the optimum conditions, the yield of chloropolysilane was found to reach 30 wt. % based on the amount of hydrogen chloride. The preferable species of metallic silicon were those which contained aluminum as a main impurity.

Experimental

Materials. — *Metallic silicon of commercial grade.*—Three species of metallic silicon which contained aluminum (Samples A and C) and iron (Sample B), respectively, as main impurities were used in these experiments after being crushed and pulverized into minus 80 mesh. The analytical values of each sample were as follows:

Sample	Exptl. run No.	Fe%	Al%	Ca and Mg%	Particle size (mesh)
A	1, 4, 5, 7	2.70	1.60	0.2	80～150
B	2, 3	7.94	0.42	—	80～120
C[3]	6, 8	trace	0.52	—	120～170

Silicon-aluminum and silicon-calcium alloys. — An alloy having the composition Si:Al=8:2 was prepared by melting 98% silicon and aluminum block in a sealed graphite crucible. Another was a commercial silicon-calcium alloy. Both were crushed and pulverized into minus 80 mesh. The analytical values of the two alloys were as follows:

Sample	Si%	Al%	Fe%	Cu%	Ca%	Particle size (mesh)
Si-Al alloy	80.6	17.2	1.02	0.01	—	80～120
Si-Ca alloy	27.3	—	—	—	68.6	80～120

Copper powder.—Finely pulverized copper for catalyst, prepared by the Fukuda Metal Plate and Powder Mfg. Co., and known as "3L3" (Purity: >98%; size minus 200 mesh[4]), was used.

Hydrogen chloride. — It was prepared in the usual way by the reaction of ammonium chloride and sulfuric acid, washed and dried by concentrated sulfuric acid, and reserved in a 20 l. glass bottle tank which was sealed by concentrated sulfuric acid. The gas was made to flow by the pressure of the sealed liquid head and was measured by its volume (Fig. 1).

Apparatus and Experimental Procedure.— The whole apparatus is shown in Fig. 1. About 20～200 g. of contact mass was charged into a reaction tube of 3 cm. diameter and 1 m. length in an electric furnace. After replacing the air in the apparatus with nitrogen, it was heated to about 150°C in order to dry off the absorbed water and cooled. Then the temperature was raised again from room temperature at the rate of 4～5°C/min. while passing hydrogen chloride at the rate of 8 l./hr. The initiation of the reaction was observed by sudden rise of temperature, change in volume of evolved hydrogen gas, and fuming in the adapter part which was due to the generation of aluminum chloride or chlorosilanes. As explained in our former report[5], the temperature at which this initiation occurred was designated as initiation temperature, or I.T. as abbreviated. Once the reaction occurred, the contact mass was activated and thus the succeeding reaction could proceed at a somewhat lower temperature. Accordingly the reaction tube was cooled to room temperature and then re-heated gradually in order to determine the actual

* Presented before the Symposium on the organosilicon and organometallic compounds held at Osaka under auspices of Kinki Chemical Industries Association, Oct. 15, 1957.

1) W. C. Schumb and E. L. Gamble, "Inorganic Synthesis", (H. S. Booth, Editor in Chief), McGraw-Hill Book Co., Inc., New York (1939), p. 42.

2) W. L. Walton, U. S. Pat. 2,602,728 (1952).

3) A powder of silicon-aluminum alloy was treated with dilute hydrochloric acid and washed with water and dried.

4) −200～+250 mesh 9%; −250～+325 mesh 15%, −325 mesh 76%; covering power 1900 cm²/g.

5) I. Shiihara and J. Iyoda, *J. Chem. Soc. Japan, Ind. Chem. Sec.* (*Kogyo Kagaku Zasshi*), **60**, 1388 (1957).

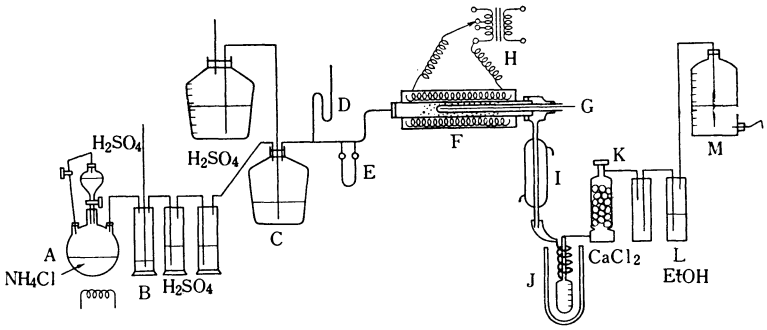


Fig. 1. Reaction apparatus for Si(Cu)+HCl gas.
A: HCl generator B: Drying bottle and prevention of backflow
C: Storage and measuring bottle of HCl gas D: Manometer
E: Flowmeter F: Reaction tube and electric furnace
G: Thermocouple H: Transformer I: Water condenser
J: Dry Ice condenser K: Prevention of moisture and backflow
L: Absorption bottle of HCl M: Mariotte bottle.

starting point of reaction, or R.T. as abbreviated. After the confirmation of R.T., the reaction was carried out by making hydrogen chloride flow under the appropriate conditions. The condensates, both in the water-cooled receiver and in the Dry Ice trap, were combined and distilled through a Widmer column and separated into trichlorosilane, silicon tetrachloride and residue with a high boiling point. The residual contact masses were analyzed by the usual methods as to metallic silicon, volatile silicon component on treating with hydrofluoric acid, copper and chlorine. In each experiment, the unreacted hydrogen chloride and volatile chlorosilane in the effluent gas were absorbed in ethanol and the amount of acidic chlorine was measured by titration and silica by weight. Thus insoluble gas was accumulated as hydrogen in a Mariotte bottle and measured.

Results

Effect of the Other Metallic Ingredients in Silicon Metal.—In our previous experiments it was found that the species of silicon metal have a direct influence upon the so-called direct method of preparing methylchlorosilanes. Accordingly, in order to investigate the effect of ingredients in silicon metal, three representative species of silicon metal powder (Samples A, B and C) and silicon-calcium were chosen as contact masses in the present experiments. Because of the prominent catalytic action of copper in the reactions, experiments were conducted with special addition of 3 wt. % copper powder with three kinds of silicon metals. In the case of chips of silicon-calcium alloy no catalyst was used because of the great reactivity of the alloy at lower temperatures, i.e., about 150°C.

A summary of experimental results is shown in Table I. It was found that Sample A—fairly rich in aluminum ingredient—was the best contact mass among the four species tested, and showed its optimum temperature of 215°C for forming the best yield of chloropolysilanes. In silicon-calcium, the product was found to be almost exclusively chloromonosilane, although the R.T. was as low as 150°C.

Influence of Elapse of Reaction Time.—It was found that with long reaction runs the yield of chloropolysilane gradually increased as the reaction time increased. An example with the silicon Sample A is shown in Table III.

The flow rate of hydrogen chloride in the run was almost equal from beginning to end, i.e., 8 l./hr. It seems that the higher molecular weight polysilane derivatives which were produced on the contact mass as intermediates would increase as the elapse of reaction time, just as it will be shown in the case of the contact mass of high copper ratio. From these intermediates some lower series of chloropolysilanes, such as di- or trisilane, might be split out.

Effect of the Copper Catalyst.—As was known in many previous experiments, the reaction of silicon metal or silicon alloy with hydrogen chloride was promoted when a small per cent of copper was added as catalyst.

Copper enables this reaction to proceed even at 215°C; without the copper catalyst

TABLE I. EFFECT OF THE OTHER METALLIC INGREDIENTS IN SILICON METAL

Contact masses	Run No.	Reacn. temp.	Reacn. time	HCl used	Liquid product	Yield	Absorption in EtOH		Distillation analysis				
							HCl	SiO_2	H_2SiCl_2	$HSiCl_3$	$SiCl_4$	High b.p. materials	Loss
		(°C)	(hr.)	(g.)	(g.)	(%)	(g.)	(g.)	(%)	(%)	(%)	(%)	(%)
Si (A) (Al rich)	H-1-(10)	215	6	85.2	102	119	7.55	0.1	0	35.5	24.0	37.5	3
200 g.	H-4-(4)	170	6	79.6	42	52.7	35.6	2.0	0	58.5	13.6	23.4	4.5
Cu 6 g.	H-4-(6)	275	6	90.0	107.5	111	4.25	1.7	0	65.7	21.9	8.6	3.8
	H-4-(9)	180	6.5	86.1	56	65.0	35.0	2.8	0	86.5	13.4	26.8	3.4
Si (B) (Fe rich)	H-2-(4)	215	6	97.3	93	95.7	20.4	1.1	0	57.3	18.3	23.1	1.3
200 g.	H-2-(8)	355	6	92.0	78.5	85.2	29.8	0.7	0	63.2	25.7	8.7	2.4
Cu 6 g.	H-3-(6)	275	7	107	131	112	1.2	0.3	0	60.8	23.2	12.7	3.3
Si (C) (HCl aq. treated) 107 g. Cu 3.3 g.	H-8	275	5	111.8	97	86.8	27.0	0.5	5.8	65.6	13.2	12.2	3.2
Si—Ca* 1.1 kg.	previously performed	150	6.5	144.2	87	61.2	—	—	0	41.7	52.5	2.8	3.0

* 2～3 mm. chip was used.

TABLE II. THE EFFECT OF ADDITION RATIO OF COPPER CATALYST TO SILICON METAL

Contact mass	Run No.	Cu added ratio	Reacn. temp.	Reacn. time	HCl used	Liquid product	Yield	Absorption in EtOH		Distillation analysis			
								HCl	SiO_2	$HSiCl_3$	$SiCl_4$	High b.p. materials	Loss
		(%)	(°C)	(hr.)	(g.)	(g.)	(%)	(g.)	(g.)	(%)	(%)	(%)	(%)
	H-1-1	3	300	3	40.2	43.5	10.8	1.34	0.11	40.4	28.7	25.6	5.3
	H-4-7	3	270	6	86.5	100.5	115.5	4.1	2.3	66.3	20.1	6.5	7.1
	H-4-4	3	215	5	71.4	59	82.6	15.6	3.5	33.9	21.9	36.5	5.9
Si (A)	H-7-5	10	300	2.5	53.6	8	15	40.0	9.8	(10.9 g.)*			
	H-7-4	10	215	2	33.4	3.5	11	39.0	4.4	(4.9)*			
	H-5-2	20	300	2	65.5	61	93.1	20.4	2.7	37.7	26.4	6.6	34.3
	H-5-6	20	215	2.3	40.3	1	2.5	34.9	11.8	(13.2)*			

* As H_3SiCl calculated from absorbed SiO_2 in ethanol (g.).

TABLE III. THE INFLUENCE OF ELAPSE OF REACTION TIME

Contact mass	Cu added ratio	Time elaspe	Reacn. temp.	Reacn. time	HCl	Liquid product	Yield	Absorption in EtOH		Distillation analysis			
								HCl	SiO_2	$HSiCl_3$	$SiCl_4$	High b.p. materials	Loss
	(%)	(hr.)	(°C)	(hr.)	(g.)	(g.)	(%)	(g.)	(g.)	(%)	(%)	(%)	(%)
Si (A)	3	12	215	3	55.4	57	103	10.2	0.05	47.7	16.5	29.4	6.4
		22	215	6	45.6	58	127	7.5	0.07	35.5	24	37.5	3
		34	215	6	92.5	94	102	19.1	2.4	34.6	22.7	40.0	2.7

TABLE IV. i. YIELDS OF CHLOROPOLYSILANE AND DISTILLATION ANALYSIS OF THEM

Contact masses	Run No.	Mean reacn. temp.	Reacn. time	HCl used	Liquid product	Yield (HCl based)	Chloropoly-silane		Distillate to b.p. 180°C (disilane fracn.)		Residual liq. (trisilane fracn.)		Loss
		(°C)	(hr.)	(g.)	(g.)	(%)	(g.)	(%)	(g.)	(%)	(g.)	(%)	(%)
Si (A)	H-1	210	69.3	1053	860	82	248	28.8	202	81.5	42.7	17.2	1.3
Si (A)	H-4	210	68.2	937.4	783	83.4	181.5	23.2	154	85.0	25.5	14.1	0.9
Si (B)	H-2	210	60.0	933.8	813.5	87	150	18.5	123	82.2	25.0	16.1	1.7
Si (B)	H-3	210	47.1	697.5	767	110	62	8.1	52	83.9	8.9	14.3	1.8

ii. REDISTILLATION OF DISILANE FRACTION

Charge: H-1 168.5 g.						
B.p. (°C)	~75	120~143	143~148	148~149	Residue	Loss
Fracn. %	8.6	12.7	5.3	65.1	5.9	1.5
Cl %		80.5		80.0		
Charge: H-4 101 g.						
Fracn. %	7.0	19	12	46	16	0

iii. REDISTILLATION OF TRISILANE FRACTION[a)]

Charge: 86 g.					
B.p. (°C)	~145	145~190	213~215	215~115[b)]	gel residue
Fracn. %	10.5	2.6	35.5	32.5	19.7
Cl %	78.3				

a) The fact that the total sum of this distillation fraction and residue was over 100% and other distillation losses of chloropolysilane were very small, was reasonably explained by the ease of oxidation of chloropolysilane.

b) Violent thermocracking was occurred.

TABLE V. PHYSICAL CONSTANT OF SOME CHLOROMONOSILANES AND CHLOROPOLYSILANES

	Compound	Formula	Mol. wt.	B.p. (°C)	M.p. (°C)	D_{20}^{10}	Cl%
Monosilanes	Silicon tetrachloride	$SiCl_4$	170.0	57.5	−70	1.48	83.5
	Silicochloroform	$HSiCl_3$	135.5	31.5	−128.2	1.34	78.5
	Dichloromonosilane	H_2SiCl_2	102.1	8.0		—	69.6
Disilanes	Hexachlorodisilane	Si_2Cl_6	269.2	149	2.5	1.47	79.3
	Pentachlorodisilane	HSi_2Cl_5	234.5	125			75.6
Trisilanes	Octachlorotrisilane	Si_3Cl_8	367.9	215	−67	1.56	77.1
	Heptachlorotrisilane	HSi_3Cl_7	333.5	unknown		—	74.4

TABLE VI. REACTION OF THE CHLOROPOLYSILANES $H_nSi_mCl_{2m+2-n}$ AND COPPER POWDER

Expt. No.	Samples of chloro-polysilanes	(g.)	Catalyst	(g.)	H_2 generated (cc.)	Reacn. time (min.)
1		3.729	Cu powd.	0.5	2.8	20
2	Disilane fracn.	2.440	$Cu+AlCl_3$	0.5+0.5	16.9	10
3	B.p. 120~143°C in Table IV	2.570	CuCl	0.5	0	10
4		2.570	$CuCl+AlCl_3$	0.5+0.5	0.4	10
5		6.859	$HCl+AlCl_3$	0.5	ca. 60	15
6	Si_2Cl_6 b.p. 143~148°C	15.0	$Cu+AlCl_3$	0.5+0.5	4.0	10
7	H-3 residual contact mass	5.0	$Cu+AlCl_3$	0.5+0.5	7.4	10

TABLE VII. ANALYTICAL RESULTS OF THE RESIDUAL MASSES IN EACH RUN

Run No.	H-1	H-2	H-3	H-4	H-5-2	H-5-6
Residual wt.(g.)	33	60	43	35.08	116	55[a]
Si species	A	B	B	A	A	A
Ignition loss (%)	46.97	48.43	2.19	35.40	−3.50[b]	−6.74[b]
SiO_2[c] (%)	16.10	12.43	29.83	57.11	7.43	6.61
Si (%)	6.91	4.10	23.88	0	62.82	56.48
Fe (%)	11.76	18.33	26.67	11.42	2.35	4.24
(Recovery)[d] (%)	(71.7)	(69.7)	(72.8)	(74.2)	(100)	(86.4)
Cu (%)	15.21	7.18	11.14	18.05	19.75	24.20
(Recovery)[d] (%)	(83.7)	(71.8)	(80.2)	(106.0)	(95.4)	(93.8)
Cl (%)	34.62	37.10	2.19	3.69	1.74	0.55
Total (%)	84.60	79.14	93.71	90.27	94.09	92.08

a) 37 g. was sampling out at intervals.
b) When the content of chlorine and volatile silicon hydrides in contact masses was small, this value often became a negative value because of the increase of weight caused perhaps by oxydation of the contact mass in air.
c) This value was calculated so as to take the weight difference after and before the treatment of HF solution as silica, but presumable some Si—Cl and Si—H might be remained even if they were ignited in air.
d) % of recovery to the starting contact masses.

it was necessary to raise the temperature to 300°C[6] in order to get a sufficient yield of liquid product. This effect makes it possible to get chloropolysilane and silicon-hydrides in more satisfactory yield, which are both unstable at temperatures higher than 250°C, the temperature used in the hitherto-performed procedures.

As to the amount of the copper added to the silicon metal, it was remarkable that it showed optimum at 1~3 wt. % copper content, and the increased ratios of copper, for instance 10% or 20%, yielded less liquid chlorosilane (Table II). This was due to the formation of monochloromonosilane which could not be condensed in a Dry Ice-acetone trap but was absorbed in alcohol. The reason for the formation of a small amount of chloropolysilanes may be the smaller reactivity of some higher molecular weight cupropolysilanes which might be formed by the reaction of Eq. E proposed in the discussion part of this report. These compounds

6) F. C. Whitmore, *J. Am. Chem. Soc.*, **69**, 2108 (1947).

might be produced proportionally to the amount of copper, and would not be able to accept further cleavage reaction of hydrogen chloride and remained as solid materials on contact mass. Moreover, the life of contact mass was defined as the interval of the time in which the contact mass is active and forms the liquid product; then the life of the contact mass having a large amount of copper was very short. For instance, 10% and 20% copper masses, have lives of 6.9 and 7.8 hr. respectively as compared to the longer time of 3% copper (Table IV).

Composition of the Chloropolysilanes Condensates.—The contact masses have their own lives and lose their reactivity toward hydrogen chloride at the step where a considerably large amount of silicon component still remains in the residual contact masses (see Table VII). The total figures of a few runs are shown in Table IV. The mean yield of the liquid product was 800 g. from 200 g. silicon metals, and the yields of chloropolysilanes were found to be 8.1~28.8 wt. % as the high boiling residue in the crude product. Distillation analysis was carried out for several intervals of the run in order to investigate the change of the compositions of the crude chlorosilanes with elapse of reaction time (see Table III); however, the distillation of a high boiling point fraction was performed with the gathered sample of several runs. The physical constants of some chlorosilanes and chloropolysilanes of this experiment are shown in Table V. Upon distillation of these chloropolysilanes, the chlorodisilane fraction was found to be 80~85 wt. % and the higher fraction, chlorotrisilane, was found to be 14~17 wt. % based on the charged crude chloropolysilanes. The fraction of trisilane was found to be accompanied by some iron compound, and darkened after some elapse of time. This impurity finally deposited as a brown coagulate of ferric oxychloride, and the upper trisilane distillate became a colorless, transparent liquid. The residual gel substance which was obtained after distilling trisilane was brownish black, generated some hydrogen by hydrolysis in water, violently evolved hydrogen by cleavage in alkaline solution, burned in air with a red flame, and left white ashes. This must have been impure higher chloropolysilanes and did not contain any copper component although it had silicon, iron, aluminum and chlorine in it.

Naturally, it was expected that these chloropolysilanes would possibly have silicon hydride bonds in their molecules arising from the hydrogen atom of hydrogen chloride, contrary to the hitherto-used preparative methods in which chlorine and silicon alloys were used as starting materials. Among the series of $H_nSi_m \cdot Cl_{2m+2-n}$[7], both pentachlorodisilane HSi_2Cl_5 and heptachlorotrisilane HSi_3Cl_7, which were expected to be formed but unknown in literature, were found only in traces in the produced chloropolysilanes and moreover, judging from its boiling point and its hydrogen analysis (Table VI), it was found that the chlorodisilane fraction was rather pure hexachlorodisilane and the chlorotrisilane fraction was also octachlorotrisilane.

As to the hydrogen analysis of the chloropolysilane, there has been no adequate method hitherto[8], but the authors have found that silicon hydride bonds are reactive with metallic copper, especially in the presence of small amounts of anhydrous aluminum chloride when their reactions are carried out in liquid phase.

Therefore, this analysis was performed by the apparatus shown in Fig. 2 in which the polysilanes containing hydrogen were treated with copper powder and $AlCl_3$ in

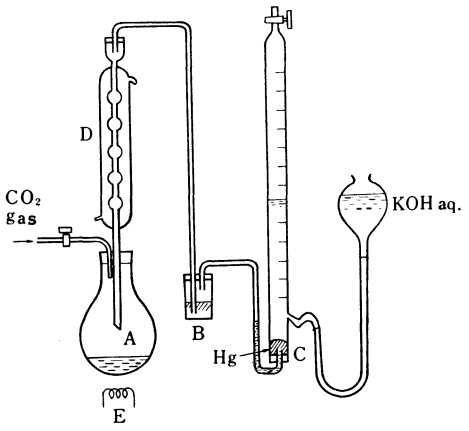


Fig. 2. Apparatus for analysis of Si-H containing chloropolysilane.
A: Reaction bottle
B: Washing bottle with C_2H_5OH
C: Gas burette with KOH aq. and Hg
D: Reflux condenser
E: Heater

7) R. Schwarz, *Z. anorg. u. allgem. Chem.*, **235**, 247 (1938).

8) V. G. Fritz, Ibid., **280**, 135 (1955).

a bottle A. The method devised was almost analogous to that of Dumas' nitrogen analysis, i.e., the evolved hydrogen was carried by carbon dioxide and the hydrogen produced gathered in a gas burette on potassium hydroxide solution and measured. The results of this hydrogen analysis are shown in Table VI. This method was confirmed previously with the known silicon-hydride containing substance, for instance, with Ph_3SiH, and showed a fairly good agreement. The occurrence of silicon-copper bond which was made by the reaction of silicon hydride and copper may be recognized by the change of metallic copper to gray metallic silicon color. It was also known that the liberated gas was hydrogen. The contents of silicon hydride in these chloropolysilanes were proved to be very small according to this analysis.

One must be careful in treating chloropolysilanes, because they are apt to form certain dangerous materials. When hydrolyzed in air, they form compounds which exqlode with slight friction or shock. These chloropolysilanes have a flammable nature although they consist only of silicon and chlorine.

Composition of the Residual Reaction Mass.—The final residual masses which were left after reaction had an appearance of very voluminous light powder possessing no metallic lustre like starting silicon, and were caqable of burning in air when ignited, revealing a very brilliant blue flame by burner test.

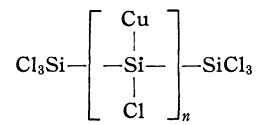
The results of chemical analysis are shown in Table VII. The amounts of hydrogen evolved on treating the residues with alkali solution are given in Table VIII.

TABLE VIII. HYDROGEN GENERATION ON TREATING THE RESIDUAL MASSES WITH 10% SODIUM HYDROXIDE SOLUTION

Sample	(g.)	H_2 evolved (m mol./g.)	SiO_2 (g.)	Si%	H/Si atom ratio
H-2	0.1240	2.00	0.0114	4.30	2.61
H-2	0.1280	1.85	0.0160	5.65	1.78
H-3	0.1330	5.75	0.0412	14.50	2.23
H-3	0.0950	5.34	0.0351	17.20	1.74
H-4	0.1570	3.20	0.0461	13.70	1.31

These facts led to the conclusion that the remainder may be the higher molecular weight chloropolysilanes and that some chloropolysilanes, especially those which have much silicon-copper bond in them, could not be cleaved by hydrogen chloride even if the copper catalyst were present, and so the reaction ceased.

If it was supposed that all iron was converted into ferrous chloride and copper remained as metal[9], the residual number of chlorine atoms of the final contact masses in H-1 and H-2 would be almost equal to the number of the silicon atoms, and the hydrogen atoms generated by alkali solution would be also twice as much as the silicon atoms (Table VIII). As the final reaction temperature, rather high temperatures, say 475°C for H-1, 460°C for H-2, were applied, and so it may be reasonably considered that all the iron changed to ferrous chloride, and in the final stage of this reaction almost every silicon atom has one chlorine atom linked to it, and the silicon atoms are linked to each other with silicon-silicon bonds. Thus, the proposed structure of these chloropolysilanes is as follows:



However, the contact mass in the reaction course was thought to contain much more silicon hydride bond than the final structure proposed above, because samples H-3 and H-5 in the reaction were of a more flammable nature than that of H-1, H-2 and H-4 of the final stages. The amount of silicon hydride bond in the former contact masses was measured by the generation of hydrogen with copper and aluminum chloride and found to be high (Table VI).

I. T. and R. T. Measurements.—Many I. T. and R. T. measurements were performed at the beginning of each run and with the special contact mass species. The results of observations are listed in Table IX, and also some examples of the graph with I. T. and R. T. measurements are shown in Fig. 3. The sudden rise in the temperature curve in comparison with the blank curve[10] showed the occurrence

9) The forms of iron and copper componet were found by extracting H-1, H-2 residual contact masses with dimethylformamide. Their salts are both soluble in this solvent, but the extracted ones were almost ferrous chloride and not cuprous chloride.

10) The blank curves were figured separately by measuring temperature versus time at several voltages in an electric furnace. Nitrogen gas was passed at the rate of 8 l./hr. (the same as that of hydrogen chloride) into the reaction tube containing the same amount of contact mass as in the actual measurements. This was repeated several times and each time the same curve was obtained. Thus, this curve could be considered as a blank.

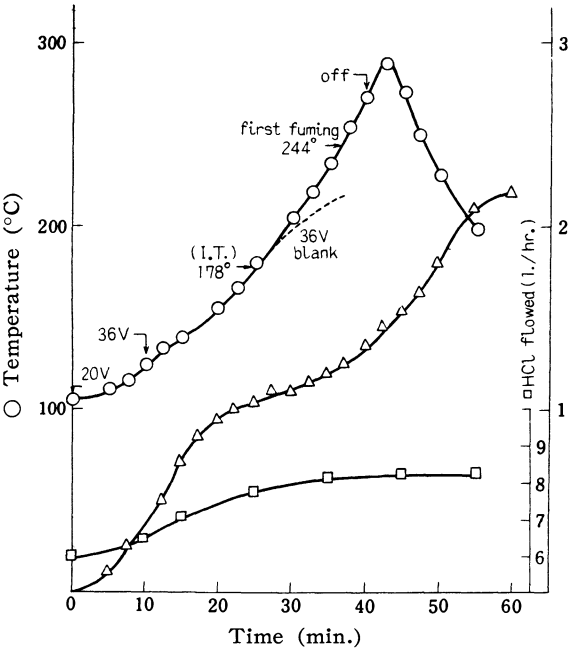


Fig. 3a. An example of the graph with I.T. measurement (H-3-1).

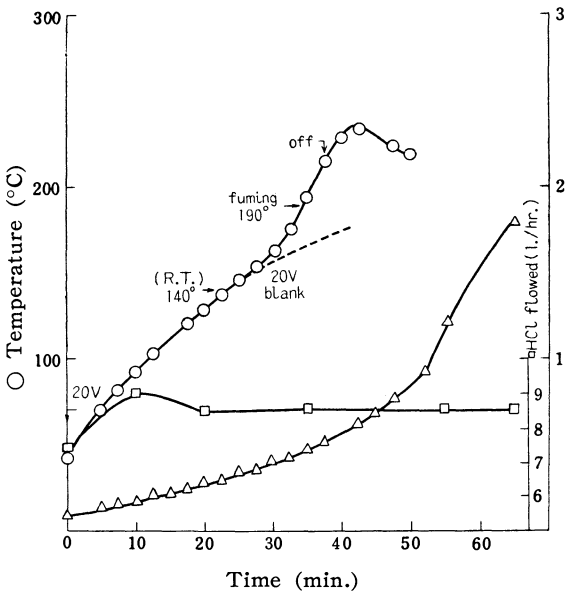


Fig. 3b. An example of the graph with R.T. measurement (H-3-2).

of the reaction about the contact mass. At this critical point, usually some gas evolution, or rate change of gas generation, or fuming caused by the product in the adaptor part were also present, and these could be also considered the evidence of the reaction occurrence, but these

TABLE IX. I.T. AND R.T. OF THE REACTION OF SOME SILICON CONTACT MASSES WITH HCl UNDER ATMOSPHERIC PRESSURE

Silicon materials	Catalyst (%)	I.T. (°C)	R.T. (°C)
Si (A)		205	103, 172, 223, 298
Si (A)	Cu(3)	180	105, 146
Si (A)	Cu(10)	230	186
Si (A)	Cu(20)	236	119, 197
Si (B)		190	105
Si (B)	Cu(3)	178	106, 140, 218
Si (C)	Cu(3)	265	52, 172
Si—Al(8:2)		205	56
Si—Al(8:2)	Cu(5)	180	50
Si—Ca(3:7)		145, 180	100, 176
Si—Ca(3:7)	Cu(3)	165, (65)*	122, (85)*

* It appears as shoulder.

phenomena often had time lags and the precise points could not be determined by them. Therefore, only the temperature curve was chosen for determining the precise value. It was found from many observations that the I. T. value is not always the same in a contact mass, sometimes as much as 10°C difference, although it is always higher than R. T. The I. T. values obtained in the present experiment seemed to originate mainly from the composition of the materials or alloys of the contact masses tested, even though these values fluctuated somewhat with the changes of the particle surfaces. As to the R. T. value, there are more than two values for some samples of silicon metal or alloy. Moreover, as was seen in many observations, the 50, 105, 145 and 170°C points are prominent and sometimes common to the same kind of contact mass species. They seemed to correspond to the R. T. as shown in the following reaction Eqs. A, B, C and D.

$$\text{Al (in solid phase Si—Al)} + \text{HCl} \xrightarrow{50^\circ\text{C}} \text{AlCl}_3 + \text{H}_2 \quad \text{(A)}$$

$$\text{Fe (in solid phase Si—Fe)} + \text{HCl} \xrightarrow{105^\circ\text{C}} \text{FeCl}_2 + \text{H}_2 \quad \text{(B)}$$

$$\equiv\text{Si—Al}= \text{(in solid phase Si—Al)} + \text{HCl} \xrightarrow{145^\circ\text{C}} \equiv\text{Si—H} + =\text{AlCl} \quad \text{(C)}$$

$$\equiv\text{Si—}\underset{\displaystyle|}{\overset{\displaystyle|}{\text{Si}}}\text{—H} + \text{HCl} \xrightarrow[\text{AlCl}_3 \text{ present as catalyst}]{170^\circ\text{C}} \equiv\text{Si—H} + \underset{\displaystyle|}{\overset{\displaystyle|}{\text{ClSi}}}\text{H} \quad \text{(D)}$$

The following is a brief explanation to substantiate this relation. As is seen in

Table IX, Si (C)[11] and Si—Al alloy have almost the same R. T. at 50°C, as in the case of the metallic aluminum and hydrogen chloride reaction[12]. Therefore, Eq. A, which mainly concerns the presence of metallic aluminum in the contact mass, was given for the 50°C value. By the same speculation, 105°C value corresponding to the iron component which exists as the other main impurity in most silicon metal or silicon alloys, is indicated by Eq. B[13], the 145°C value has been assigned to Eq. C[5] by the authors. In almost all the reactions the forming of chlorosilane actually began at 170°C. Thus it was plausible that Eq. D was adequate for this R. T. value.

It was very interesting and important that when a small amount of anhydrous aluminum chloride was added to the contact masses as mixture or as vapor, the I. T.'s of these reactions were depressed close to the R.T.'s of their own. The fact that the commercial silicon Si(A)—fairly rich in aluminum ingredient—had a good yield of liquid product (Table I), might be proved by the above effect of aluminum chloride. Because in this reaction system the aluminum chloride could be easily derived from the reactions shown as Eqs. A and C. However, the remarkable effect of copper to each contact mass could not be understood from the results of I. T. and R. T. Unexpectedly the copper was reasonably considered only to promote the rate of this reaction.

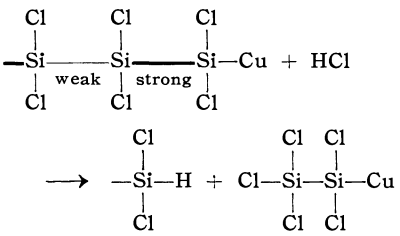
Discussion

The results of this experiment mentioned above and an assumption which will be proposed afterward afford the following reaction mechanism of the formation of chloropolysilane, i.e., the activation and main course stages for the reaction between commercial silicon and hydrogen chloride which gave monosilanes were explained as the formulae A, B, C and D mentioned above, but by those mechanisms alone no important part of the mechanism of forming chloropolysilane using copper catalyst could be explained. It might be reasonable to assume that copper combines with Si—H bond on the silicon mass which is formed as an intermediate of the C or D reactions (see Table VI):

$$\equiv SiH + Cu \xrightarrow[AlCl_3 \text{ catalyst}]{150^\circ C} \equiv Si—Cu + 1/2\ H_2 \qquad (E)$$

Hence, the co-catalytic action of aluminum chloride, produced by A and C reactions in the above reaction, is seen in the comparison of the experiments No. 1 and 2 in Table VI. Therefore, apart from the before mentioned I. T. depressing effect of aluminum chloride, it is preferable to use commercial silicon metal which has a small amount of aluminum as impurity or the vapor of aluminum chloride purposely conducted to the reaction zone of the pure silicon metal.

The authors have proposed the following assumption for the catalytic action of copper, i.e., the silicon-silicon bond which is adjacent to the silicon-copper bond formed by E reaction is difficult to be cleaved by hydrogen chloride as was shown in the above-mentioned results and the supposed cleavage is as follows:



This assumption may also facilitate the understanding of the mechanism of the chlorodisilane formation, and the catalytic action of copper for the present reaction. This unequalness of silicon-silicon bond strength may well be explained by the unequal electron density on the silicon atoms like the alternative strength-change theory of carbon bonds proposed by Ingold. If this assumption is correct at all, the reasons for the large yield of chlorodisilane in the main course of reaction by addition of a few per cent of copper and its sharply diminished formation at the final stage of the reaction may also be plausible. Hence, the copper content at the surface of the contact mass at the final stage may become so high that the copper atoms can be distributed enough through the adjacent silicon atoms.

11) As was mentioned Si (C) was originated from the Si-Al alloy. It was somewhat curious that Si (A), Si (B) which had more aluminum content than Si (C) did not show this 50°C R. T. value. However, this may be explained by the fact that iron masked the free aluminum character, perhaps by forming some kind of alloy.

12) J. Iyoda and I. Shiihara, *J. Chem. Soc. Japan, Ind. Chem. Sec.* (*Kogyo Kagaku Zasshi*), in press.

13) Generally speaking, the iron component in a silicon alloy must form some intermetallic compounds with silicon, but here in these contact masses, part of it combined with aluminum, forming some kind of easily reactive alloy.

The reaction between a typical silicon-copper bond and hydrogen chloride is shown as follows:

$$\equiv Si—Cu + HCl \longrightarrow \equiv Si—H + CuCl \qquad (F)$$

This reaction can also explain the formation of much H_3SiCl when a large amount of copper is added as catalyst. However, the reason for the meager existence of Si—H bond in chloropolysilane product seems to be plausible when the hydrogen chloride exchange reaction with some species of compounds on contact mass is assumed. A typical reaction can be considered:

$$Cu—\overset{Cl}{\underset{Cl}{Si}}—\overset{Cl}{\underset{Cl}{Si}}—H + HCl \xrightarrow{AlCl_3} Cu—\overset{Cl}{\underset{Cl}{Si}}—\overset{Cl}{\underset{Cl}{Si}}—Cl + H_2 \qquad (G)$$

The reverse reaction of F about the Si—H in the above compound is excluded from the results of experiments No. 3 and 4 in Table VI, and the possibility of E reaction of the Si—H is also taken to be small, since the chance of Si—H in this compound fixed on contact mass coming in contact with copper metal is supposed to be slight.

Also, the reaction of silicon and cuprous chloride is excluded under the reaction temperature of this experiment as 215°C, which is far from the R.T. value[14] (295°C) of this reaction.

$$\equiv Si—Si\equiv + CuCl \xrightarrow{R.T.\ 295°C} \equiv Si—Cu + \equiv Si—Cl \qquad (H)$$

Therefore, cuprous chloride produced by F reaction may be reduced[15] mainly by hydrogen formed by E and G reactions.

$$2CuCl + H_2 \longrightarrow 2Cu + 2HCl \qquad (I)$$

And so regenerated metallic copper can be recycled to E reaction.

Summary

The copper catalyzed reaction of silicon metal powder with hydrogen chloride by flow method was studied in order to find a convenient preparative method of chloropolysilane, and also to elucidate the mechanism of this reaction.

This reaction was found to start at about 170~230°C, and once the reaction occurred, the contact mass is activated and the reaction takes place even at 170°C. When the most adequate conditions were adopted, chloropolysilanes were obtained in the condensate as efficiently as 30 wt.% yield based on hydrogen chloride.

As to the mechanism of the reaction, it seems to be plausible that the first step of the reaction is an attack of hydrogen chloride on aluminum which is usually present in the commercial silicon metal. The second step is the reaction between silicon hydride, which is derived from the first step reaction upon the silicon contact mass and metallic copper forming the silicon-copper bonding. The third step is the cleavage reaction of copper-activated silicon by hydrogen chloride to produce chlorosilanes under the presence of aluminum chloride. The aluminum chloride is also derived from the first step reaction, and copper is regenerated in metal form which can circulate among the latter two reaction steps as long as the effective silicon component is present.

The authors are indebted to Mr. S. Hara of their Institute for the analyses of residual masses, and to Mr. H. Takahashi of their laboratory for the analysis of siliconhydride.

Osaka Industrial Research Institute
Nishi-2-Chome, Daini
Oyodo-ku, Osaka

14) Details will be published before long. About the formation of Si-Cu bond presented before the 7th Annual Meeting of Chem. Soc. of Japan, April 3, 1954, Paper No. 7075 by Shiihara.

15) M. Rubalkin, *J. Russ. Phys. Chem.*, **21**, 155 (1889).

The Study of the Adsorption of Detergents at a Solution-Air Interface by Radiotracer Method. III. The Effect of Inorganic Electrolytes on the Adsorption of Sodium Dodecyl Sulfate

By Ryohei MATUURA, Hideo KIMIZUKA and Katsumasa YATSUNAMI

(Received November 17, 1958)

Roe and Brass[1], Nilsson[2] and Salley et al.[3] have checked the Gibbs adsorption equation with potassium palmitate, sodium dodecyl sulfate and Aerosol OTN in the presence of potassium hydroxide, sodium chloride and Aerosol OT, respectively. They have obtained the result that the adsorption of detergent at the air-solution interface takes place in accordance with the Gibbs adsorption equation. It was suggested also through the observation of the change with time in surface tension of detergent solution that the addition of excess electrolytes increases the adsorption rate of surface active ion[4].

However, the adsorption isotherm and adsorption rate for the detergent solution in the presence of various electrolytes, especially in the presence of the salts containing no common ion with the detergent, has not yet been measured directly. In the present study, we have succeeded by the aid of the radiotracer method in measuring directly the adsorption of dodecyl sulfate ion (abbreviated as DS^-) at the solution-air interface from the solutions containing sodium dodecyl sulfate (abbreviated as SDS) and excess inorganic electrolytes. The surface tension of the solution has been measured and the Gibbs adsorption equation has been checked.

Experimental

Materials. — The radioactive SDS used was synthesized as described in the preceding paper[5]. Of the inorganic electrolytes, manganous and aluminum chlorides were those of extra pure reagents and purified by recrystallization, while sodium, potassium and magnesium chlorides were those of guaranteed reagents and used without further purification. For the preparation of the solution under investigation, SDS was dissolved in the aqueous solution of respective inorganic electrolyte with a given concentration.

Method.—The procedure used for the measurement of the surface excess of DS^- was the same as described in the preceding paper[5,6]. The surface count of radioactive sodium sulfate solution was taken as the same as that of the bulk of radioactive SDS solution, both containing excess of salts.

The surface tension measurement was carried out by means of the du Noüy tensiometer. The temperature of the experiment was maintained at 29±1°C.

Results and Discussion

It was found that the adsorption of DS^- in the presence of excess salts with or without common ions was so rapid that

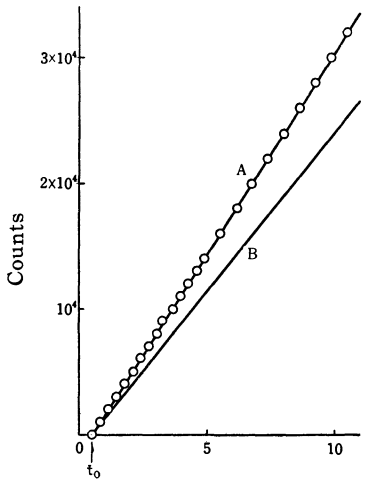


Fig. 1. Count vs. time relation for the solution A containing 5.543×10^{-4} mol./l. SDS and 0.3 N NaCl and the solution B containing 5.543×10^{-4} mol./l. Na_2SO_4 and 0.3 N NaCl, 29±1°C.

1) C. P. Roe and P. D. Brass, *J. Am. Chem. Soc.*, **76**, 4703 (1954).
2) G. Nilsson, *J. Phys. Chem.*, **61**, 1135 (1957).
3) H. Sobotka, "Monomolecular Layers", The American Association for Advancement of Science, Washington, D. C. (1954), p. 81.
4) N. K. Adam and H. L. Shute, *Trans. Faraday Soc.*, **34**, 758 (1938); K. S. G. Doss, *Kolloid-Z.*, **86**, 205 (1939); G. C. Nutting, F. A. Long and W. D. Harkins, *J. Am. Chem. Soc.*, **62**, 1946 (1940).
5) R. Matuura, H. Kimizuka, S. Miyamoto and R. Shimozawa, This Bulletin, **31**, 532 (1958).
6) R. Matuura, H. Kimizuka, S. Miyamoto, R. Shimozawa and K. Yatsunami, ibid., **32**, 404 (1959).

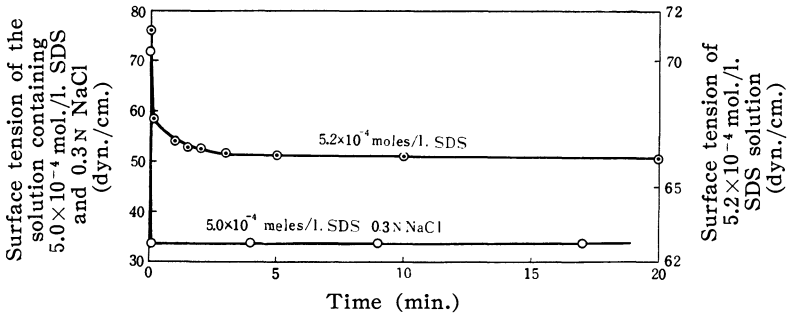


Fig. 2. Effect of the presence of sodium chloride on the surface tension of SDS solution, 29±1°C.

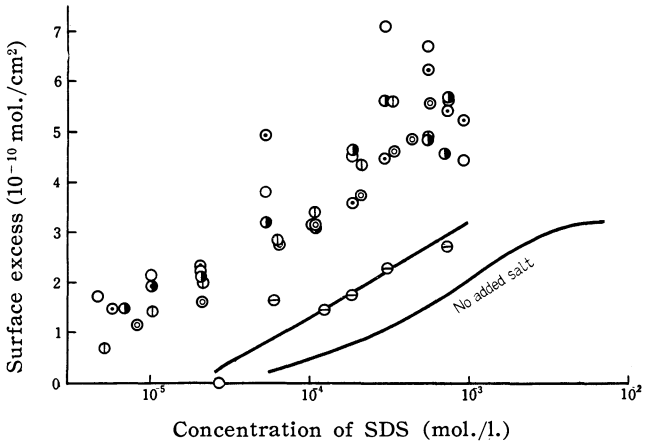


Fig. 3. Effect of addition of sodium chloride on the adsorption of DS^-, 29±1°C.
⊖ 0.01 N NaCl, ◎ 0.1 N NaCl, ◐ 0.2 N NaCl, ◑ 0.3 N NaCl, ⊙ 0.5 N NaCl, ○ 1.0 N NaCl.

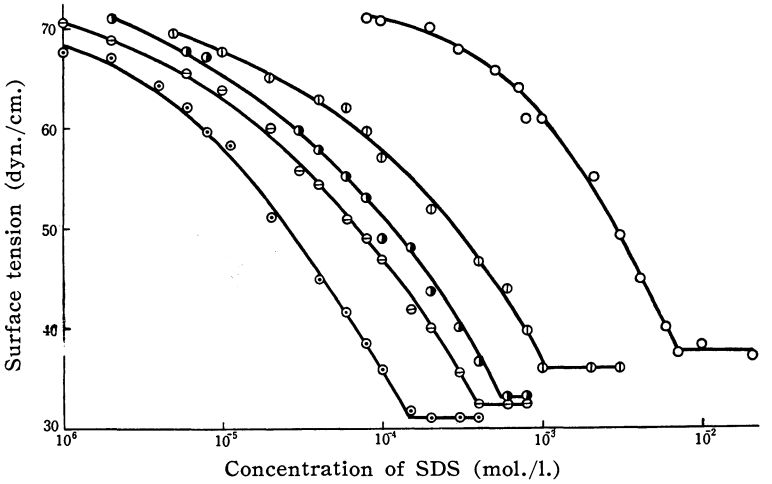


Fig. 4. Effect of added sodium chloride on the surface tension of SDS solution, 29±1°C. Numericals in this figure show the concentration of sodium chloride in N.
○ no added NaCl, ◐ 0.1 N NaCl, ◑ 0.3 N NaCl, ⊖ 0.5 N NaCl, ⊙ 1.0 N NaCl.

the equilibrium was attained within one minute, while without added salts it took several minutes or more to reach the adsorption equilibrium at the solution-air interface as was reported in the preceding paper[6]. Fig. 1 is an example of counts vs. time relation of SDS solution (concentration is 5.543×10^{-4} mol./l.) containing 0.3 N sodium chloride. t_0 in Fig. 1 is the starting time of counting. It is seen that a linear relation is held between count and time, showing that the adsorption has already reached equilibrium at the starting time (t_0) of counting. It has already been known that the presence of inorganic salts makes faster the attainment of equilibrium of surface tension of the detergent solution[4]. In the present study, the effect of the presence of sodium chloride on the change with time of surface tension of SDS solution was also measured by means of the Wilhelmy plate method. Fig. 2 shows an example of the effect of the presence of sodium chloride on the rate of surface tension lowering. It may easily be seen that the presence of salt not only makes faster the attainment of equilibrium of surface tenstion, but also lowers the surface tension value. Furthermore, it may be pointed out that in the presence of salt the surface tension almost reaches equilibrium even at the starting time of experiment. The present experiment, therefore, clearly shows that the rapid rate of surface tension lowering actually corresponds, as might be expected, to the rapid rate of adsorption at least qualitatively. However the rate of adsorption was too rapid to measure precisely and so the quantitative relation between the surface tension lowering and the adsorption before reaching equilibrium could not be determined in the present study. The results and discussions below therefore are concerned only with the equilibrium state of adsorption and surface tension.

First the effect of sodium chloride of various concentrations on the adsorption of DS^- was measured and the result is shown in Fig. 3. It is obvious that the presence of excess sodium chloride increases the adsorption of DS^- considerably. Here it is to be noted that, although below 0.1 N of sodium chloride the adsorption of DS^- increases with the concentration of the salt, above 0.1 N of sodium chloride the values of surface excess of DS^- fall within a range almost independent of the concentration of the salt. On the contrary, the surface tension of SDS solution containing sodium chloride decreases regularly with the concentration of the salt up to 1 N, as shown in Fig. 4.

When the Gibbs adsorption equation for the solution of surface active electrolyte is written in the form

$$\Gamma = -\frac{1}{nRT}\frac{\partial\gamma}{\partial \ln C}$$

where Γ is the surface excess, γ, surface tension, C, concentration of the detergent and R and T are gas constant and temperature, respectively. n is expected, from theoretical considerations, to be unity in the presence of large excess of salts

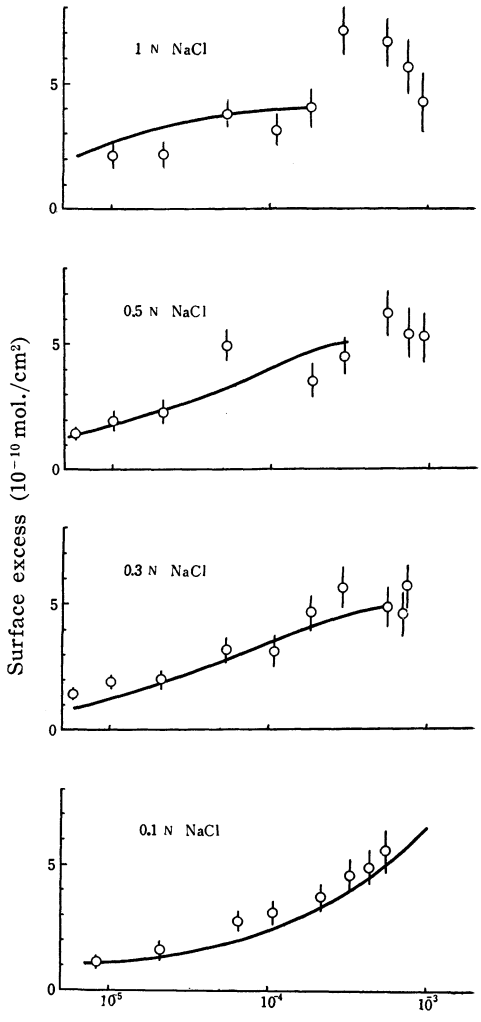


Fig. 5. Adsorption of DS^- from SDS solution containing sodium chloride. Full lines represent calculated relations from surface tension vs. logarithmic concentration curves by using the Gibbs adsorption equation of $n=1$.

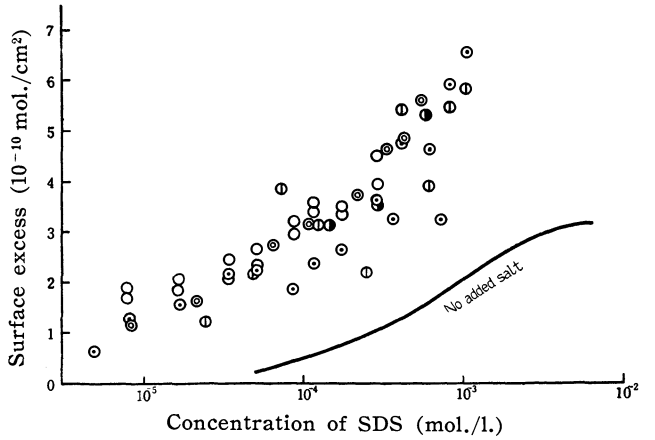


Fig. 6. Effect of added electrolytes on the adsorption of DS^-, 29±1°C. Concentration of electrolytes are all 0.1 N.
◎ NaCl, ◑ KCl, ⊙ $MgCl_2$, ◫ $MnCl_2$, ○ $AlCl_3$.

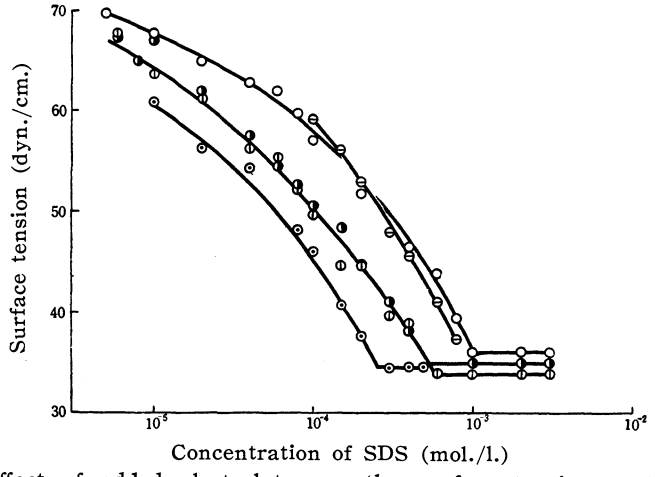


Fig. 7. Effect of added electrolytes on the surface tension of SDS solution, 29±1°C. Concentrations of electrolytes are all 0.1 N.
○ NaCl, ⊖ KCl, ◑ $MgCl_2$, ◫ $MnCl_2$, ⊙ $AlCl_3$.

or alkalis[5]. From the data in Fig. 4 we can calculate Γ of DS^- in the presence of sodium chloride and check the Gibbs equation*. The results are shown in Fig. 5 for various concentrations of sodium chloride. From these figures it is reasonable to conclude that the Gibbs adsorption equation of $n=1$ is a fair expression for the adsorption of DS^- below cmc in the presence of sodium chloride.

Next the effect of various inorganic electrolytes having no common ion with the detergent was measured. Some salts made precipitates even in the dilute solution of the detergent and so the kinds of salts investigated were limited. The salts used in the present experiment were potassium chloride, magnesium chloride, manganous chloride and aluminum chloride and SDS was dissolved in the aqueous solution of each electrolyte of the concentration of 0.1 N. The relation between the surface excess of DS^- and SDS concentration in the presence of 0.1 N inorganic electrolytes is shown in Fig. 6. From this figure we can see that the presence of excess of inorganic salts makes considerable increase in the adsorption of the detergent, regardless of the type of the salts added.

* Strictly speaking, the concentration in the Gibbs equation should be replaced by the activity. However it may not cause serious errors to use concentration instead of activity *below cmc* of the detergent even in the presence of excess salt as in the present experiment[2,3].

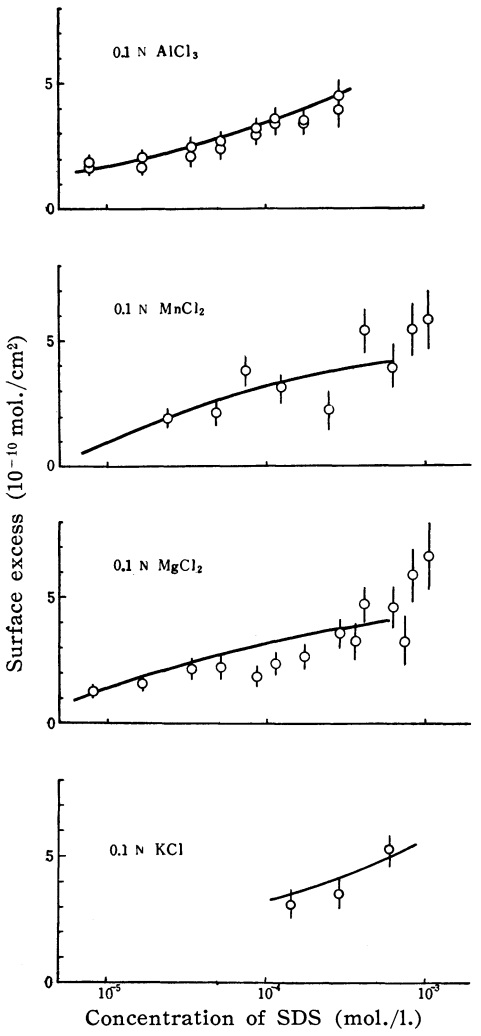


Fig. 8. Adsorption of DS^- from SDS solution containing 0.1 N excess of salt. Full lines represent calculated relations from surface tension vs. logarithmic concentration curves by using the Gibbs adsorption equation of $n=1$.

The surface tension vs. concentration relation of these systems is shown in Fig. 7. It is interesting to note that the surface tension decreases regularly with the valency of cation of added salts, while the surface excess shows no such regular relations.

Using the data in Fig. 7, the surface excess was calculated by the Gibbs equation putting $n=1$ and compared with the observed value. The results are plotted in Fig. 8. From these results it will be possible to say that the Gibbs equation of $n=1$ represents approximately the experimental values of surface adsorption of DS^- even in the presence of inorganic salts having no common ions with the detergent.

Summary

The direct measurement of the adsorption of ^{35}S labelled dodecyl sulfate ion at the solution surface and the measurement of the surface tension were carried out on the aqueous solutions of sodium dodecyl sulfate containing a given concentration of an excess salt. The salt concentrations studied were 0.01, 0.1, 0.3, 0.5 and 1 N for sodium chloride, and 0.1 N for potassium-magnesium, manganous and aluminum chlorides.

1. The adsorption of dodecyl sulfate ion reaches equilibrium within one minute for all the systems under investigation.
2. The presence of excess of salt gives rise to the remarkable increase in the adsorption of dodecyl sulfate ion, but at the concentrations of excessive salts of about 0.1 N or more, the effects of the concentration and nature of the salts on the adsorption of dodecyl sulfate ion are not so appreciable.
3. The adsorption of dodecyl sulfate ion was well expressed by the Gibbs adsorption equation of $n=1$ for the systems under investigation.

In conclusion the authors express their hearty thanks to Professor T. Sasaki of Tokyo Metropolitan University for his kind advice and encouragement in the course of this study. The cost of this study was defrayed from the Chemical Research Grant of the Ministry of Education, to which the authors' thanks are also due.

Department of Chemistry
Faculty of Science
Kyusyu University
Fukuoka

SHORT COMMUNICATIONS

Polymerization of Methyl Methacrylate Initiated by a Combined Action of Di-p-tolyl Disulfoxide, Dimethylaniline and Oxygen in Air

By Ryoichi UEHARA

(Received February 27, 1959)

The effects of *p*-toluenesulfinic acid (TSA) upon polymerization of vinyl monomers have been noted by Hagger[1] and Bredereck[2]. In a previous paper by the present author[3], results of studies on the kinetics of the polymerization of methyl methacrylate (MMA) initiated by the system of TSA, dimethylaniline (DMA) and oxygen in air have been reported. The polymerization was initiated at room temperature by means of this system. TSA is not so stable even at room temperature, and by being left in air changes into *p*-toluenesulfonic acid (TSOA), di-*p*-tolyl disulfoxide(DTDS) and water through the following reaction[4]:

$$3CH_3C_6H_4SO_2H = CH_3C_6H_4SO_3H + (CH_3C_6H_4SO)_2 + H_2O$$

Owing to this deterioration, the activity of TSA as a component of the initiating system of the room-temperature polymerization of MMA is reduced gradually[5]. The present author has examined the effects of TSOA and DTDS upon the polymerization of MMA at various temperatures, and found that the polymerization was initiated by a combined action of DTDS, DMA and oxygen in air at above 60°C. TSOA could not initiate the polymerization in combination with DMA and oxygen. It has been found by the present author that several compounds related to TSA, e.g., *p*-tolyl methyl sulfone[6] and di-*p*-tolylsulfonylhydroxylamine[6], initiated the polymerization of MMA in combination with DMA and oxygen. DTDS is a new material which belongs to this group of compounds. In the present communication, some results of experiments are given. The nature of the effects of the polymerization-initiating system will be discussed in future.

In Table I, per cent conversions after 1 hr. at various temperatures are given (DTDS 2.34×10^{-2} mol./l. and DMA 2.58×10^{-2} mol./l. in air). For the initiation of the polymerization, the coexistence of the three components of the initiating system was necessary. Namely, in the cases when MMA was heated at 70°C with DTDS 2.51×10^{-2} mol./l. and DMA 2.52×10^{-2} mol./l. in the atmosphere of nitrogen or with DTDS 2.48×10^{-2} mol./l. alone in air, no polymerization took place, and when DMA 2.52×10^{-2} mol./l. alone was employed in air, only trace of polymethyl methacrylate (PMMA) was obtained after 3 hr. at 70°C. In Fig. 1, per cent conversions of the bulk polymerization of MMA at 70°C in air (DTDS 2.16×10^{-2} mol./l. and DMA 2.20×10^{-2} mol./l.) are plotted against the time of polymerization. A time conversion curve of the polymerization by means of benzoyl peroxide (BPO, 2.0×10^{-2} mol./l.) in nitrogen is shown by the dotted line in the figure. From the beginning of

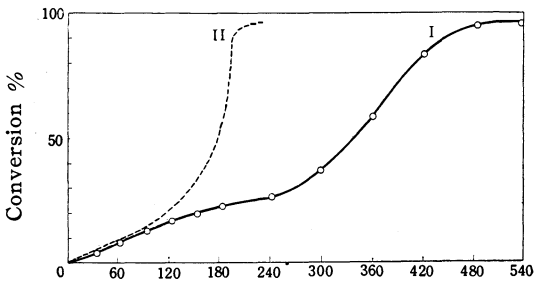


Fig. 1. Time versus conversion curve of bulk polymerization of MMA at 70°C in air. I, DTDS 2.16×10^{-2} mol./l. and DMA 2.20×10^{-2} mol./l. II, BPO 2.0×10^{-2} mol./l. (under nitrogen).

1) O. Hagger, *Helv. Chim. Acta*, **31**, 1629 (1948).
2) H. Bredereck et al., *Ber.*, **89**, 731 (1956).
3) R. Uehara, Submitted to this Bulletin for publication., **32**, No. 9 or 10 (1959).
4) C. Pauly and R. Otto, *Ber.*, **10**, 2128 (1877).
5) C. E. Schildknecht, "Polymer Processes", Interscience, New York, (1956), p. 61.
6) R. Uehara, Submitted to this Bulletin for publication, **32**, No. 9 or 10 (1959).

the polymerization until the conversion reached to 15%, the rate of polymerization initiated by the system of DTDS, DMA and oxygen was only slightly smaller than that of the polymerization by BPO. After this period, the polymerization initiated by the system of DTDS, DMA and oxygen proceeded at a moderate rate and somewhat acceleratively in the final period, while the polymerization by BPO run quite acceleratively and almost explosively at the final stage. In the polymerization initiated by the system of DTDS, DMA and oxygen, the conversion reached to 90% after 450 min. from the beginning of the reaction, but in case of the polymerization by BPO the conversion reached to the same extent after 190 min. In the bulk polymerization of MMA, gelation of the reacting system occurs when the conversion reaches to 20~30%. So, it is very probable that the polymerization initiated by the system of DTDS, DMA and oxygen does not proceed so acceleratively owing to the fact that the rate of diffusion of oxygen from air into the reacting system is reduced due to the gelation. On the other hand, DTDS alone did not affect upon the polymerization of MMA initiated by BPO under nitrogen, i. e., per cent conversion after 1 hr. and the degree of polymerization (DP) of PMMA were not changed by the addition of DTDS (Table I).

TABLE I. RESULTS OF THE BULK POLYMERIZATION OF METHYL METHACRYLATE

Atmosphere	Initiator (mol./l. × 10^2)	°C	% Conversion after 1 hr.	DP
Air	[DTDS (2.34) DMA (2.58)]	40	0	
Air	[DTDS (2.34) DMA (2.58)]	50	1.5	
Air	[DTDS (2.34) DMA (2.58)]	60	3.7	4900
Air	[DTDS (2.34) DMA (2.58)]	70	8.7	2850
Air	[DTDS (2.34) DMA (2.58)]	80	17.4	1390
Air	DTDS (2.48)	70	0*	
Air	DMA (2.52)	70	trace*	
Nitrogen	[DTDS (2.51) DMA (2.52)]	70	0*	
Nitrogen	BPO (2.0)	70	10.3	3900
Nitrogen	[BPO (2.0) DTDS (2.51)]	70	10.9	3780

* After 3 hr.

Experimental — DTDS was prepared by heating TSA (20 g.) with water (60 cc.) in a boiling water bath. TSA was dissolved and then an oily material separated gradually. After 5 hr., the oil was washed with 5% aqueous sodium hydroxide and pure water, and cooled. Crude DTDS was recrystallized three times from a mixture of methanol and ether (1 : 1 by volume), and pure DTDS (6.5g.) was obtained, m.p. 78.5°C. Purification of MMA and DMA have been mentioned in a previous paper[7]. The polymerization in air and under nitrogen were carried out respectively in open test tubes[3] and sealed tubes[7]. DTDS and DMA were dissolved in MMA cooled in an ice-salt bath. The solution (5 cc.) was placed in a test tube and heated with shaking. Per cent conversion of the polymerization was estimated from the weight of PMMA. Details of the procedures have been given previously[7]. DP of PMMA was calculated from the intrinsic viscosity in chloroform by using the equation of Sakurada[8].

Tama Kagaku Kogyo Co.
2—28 Minamirokugo
Ota-ku, Tokyo

7) R. Uehara, This Bulletin, 31, 685 (1958).
8) I. Sakurada, *Chem. High Polymers* (*Kobunshi Kagaku*), 2, 253 (1945).

On the Concentration Potential

By C. V. Suryanarayana and
V. K. Venkatesan*

(Received April 2, 1959)

Vaidhyanathan[1] is in great error in his 'Remarks on the composition potential' in regard to a quantity defined by us[2] recently. We defined a quantity C_p as the ratio of the mole fraction of the solute at any given molal concentration to that at saturation at the same temperature. Precisely we called this ratio C_p, the concentration potential and not the composition potential as he states in his remarks. What is most amusing is that Vaidhyanathan imagines that we have stated the above ratio as being a truly thermodynamic potential. We have not done so. A careful perusal of our paper (loc. cit.) shows that the wording is as follows:

"The concentration potential newly conceived herein is a truly thermodynamic *concept of concentration* dependent only on

* Present address: Central Electrochemical Research Institute, Karaikudi, India.

1) V. S. Vaidhyanathan, This Bulletin, **32**, 99 (1959).

2) C. V. Suryanarayana and V. K. Venkatesan, ibid. **31**, 442 (1958).

the initial and final states of stability of a solution and independent of any arbitrary scale of concentration or the nature of both the solvent and the solute". The *concept* is a thermodynamic one as explained by the rest of the above sentence but definitely it can never even imply that the ratio called by us 'concentration potential' is ever a thermodynamic potential at all.

We must point out incidentally that the definition of thermodynamic potentials given naively by Vaidhyanathan is in serious error. He states: "The potentials that can be defined as 'thermodynamic potentials' and which conform to this statement are the Gibbs and Helmholtz functions, energy, enthalpy, entropy and the chemical potential and they alone". Excepting the last mentioned chemical potential which is the derivative of the Gibbs free energy with respect to the number of moles of the species at constant temperature and pressure all the other functions are extensive properties and are not called thermodynamic potentials merely by themselves. They have of course the properties of exact differentials. Thermodynamic potentials are always intensive[3] (expressed per mol.) especially for the chemist when dealing with solutions. Further what he states in the first part of his last para has either no purpose or contradicts the last part of his first para and hangs loosely.

What may be really a pertinent question is the reason why we have called the newly defined ratio a concentration potential. An answer to this is due to appear elsewhere (under publication), and is briefly as follows. When we picture what happens when a soluble solid solute is added to a solvent, we can imagine its dissolution at any instant giving in the vicinity of the solute a successive series of layers of solutions, the most concentrated one being nearest the solid and the least concentrated one the pure solvent itself. The most concentrated one is the saturation concentration and the lowest concentration is zero. In between, there is to be imagined a concentration gradient. It is so clear that the saturation concentration has a directive influence on the concentration gradient. Our main purpose in defining this new ratio is to indicate the soundness of comparing a physical property of solutions of two different solutes in a given solvent at identical gradients and not at identical arbitrary concentrations as is being done so far. In this context any arbitrary concentration between the saturation and zero values has been visualized as better represented by the ratio of mole fraction to that at saturation and called the concentration potential due to its relation to the above mentioned gradient. Any arbitrary concentration for a salt must occur in the concentration gradient given in the above picture of the dissolution of the same salt. The situation is similar to the well-known classical law of corresponding states. But it is too early to predict the usefulness of the newly defined ratio, especially whether equally important generalizations will accrue out of the use of C_p. Of course, C_p has the properties of an exact differential between the limits of zero concentration and saturation.

Again Vaidhyanathan states that apart from the fact that C_p is an intensive variable and is dimensionless, no other thermodynamic significance can be attributed to it. We should say that the above reasons are not enough to say that no other thermodynamic significance can be attributed to it. An understanding of the thermodynamic significance of the saturation state of a solution will be the final deciding factor in assessing the thermodynamic significance of the concentration potential defined by us. A perusal through Walden[4], van Laar[5], and Ricci and Davis[6] indicates enough thermodynamic importance of the saturated state.

In this back ground, though we should have no objection to call the concentration potential by any other name for any good reasons, we fail to see why it should not be called so as at present.

Physico-Chemical Laboratory
Annamalai University
Annamalainagar
South India

3) E. A. Guggenheim, "Thermodynamics", North Holland Publ. Co., Amsterdam, (1957).

4) P. Walden, *Z. physik. Chem.*, **54**, 129, **55**, 683 (1906).
5) J. J. van Laar, ibid., **58**, 567; **59**, 212 (1907).
6) J. E. Ricci and J. W. Davis, *J. Am. Chem. Soc.*, **62**, 407 (1940).

A Transannular Beckmann Rearrangement in Liquid Sulfur Dioxide

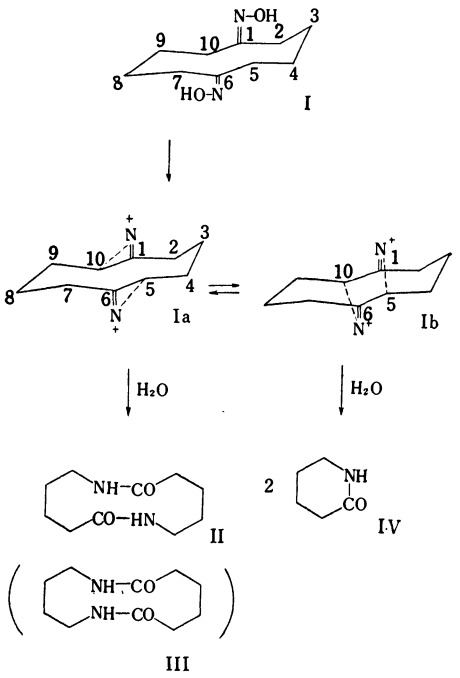
By Niichiro Tokura, Ritsuro Tada and Kunio Suzuki

(Received April 15, 1959)

In medium sized alicyclic compounds, transannular reactions have often been observed[1-3]. This communication is concerned with an abnormal Beckmann rearrangement, the nature of which should be attributed to a novel transannular type of reaction.

When cyclodecane-1,6-dione dioxime (I) reacted with sulfur trioxide in liquid sulfur dioxide at room temperature for twelve hours, followed by elimination of sulfur dioxide by evaporation and addition of ice water to the reaction residue, a hitherto unreported cyclic oligomer of δ-valerolactam, 1,7-diaza-6,12-dioxocyclododecane (II) (yield 75%), separated out as fine crystals, m.p.(purified by sublimation) 264~266°C (Found: N, 13.9%. Calcd. for $C_{10}H_{18}O_2N_2$: N, 14.1%; mol. wt. Found: 215. Calcd. 198; ninhydrin test, negative[4]; I. R. ν_{max}^{KBr}: 1650 (CO), 3280 (NH) cm^{-1}). The I. R. spectrum of II closely resembles the spectra of cyclic oligomers of ε-caprolactam[4]. As we could find no diamine or dicarboxylic acid in the acid hydrolyzed product of II, absence of III (another possible product of rearrangement) in the reaction mixture was proved.

However, when the reaction was carried out with thionyl chloride in place of sulfur trioxide in liquid sulfur dioxide similarly as described above, followed by extraction with chloroform and evaporation of the solvent, I afforded a brown viscous nitrogen-containing liquid (27%), the structure of which was difficult to be identified. The residual solution after the extraction was made slightly alkaline with sodium hydroxide and again extracted with chloroform. The chloroform solution was condensed and the residue was subjected to distillation in vacuo. A yellow oil(IV) b.p. 90~93°C(2mmHg) was obtained. IV was identified as δ-valerolactam (33%),



n_D^{17}=1.5339 (Found: N, 13.8%. Calcd. for C_5H_9ON: N, 14.1%, N-(4-carboxyl butyl) phthalimide, m. p. and mixed m. p. with an authentic specimen, 117.5~118.5°C[5]). Its I. R. spectrum also coincided with that of IV described in the literature[6]. That δ-valerolactam (IV) was not a secondary product derived from II was demonstrated when II reacted in liquid sulfur dioxide with thionyl chloride at room temperature. No appreciable formation of IV was observed.

As the distances between the nitrogen atoms and carbon atoms (C_5 and C_{10}) are sufficiently close to permit an equilibrium state between the structures Ia and Ib, the latter being favored by thionyl chloride, the completion of the rearrangement, involving cleavage of C_1-C_{10} and C_5-C_6 linkages, gives rise to formation of IV. In such a case, a transannular Beckmann rearrangement is the most plausible explanation for the formation of IV from I in liquid sulfur dioxide.

The authors wish to thank the Befu Chemical Industries Co. for the donation of liquid sulfur dioxide.

The Chemical Research Institute of Non-aqueous Solutions, Tohoku University Katahira-cho, Sendai

1) P. A. Plattner and J. Hulstkamp *Helv. Chim. Acta*, **27**, 220 (1944).
2) A. C. Cope, S. W. Fenton and C. F. Spencer, *J. Am. Chem. Soc.*, **74**, 5885 (1952).
3) V. Prelog, K. Schenker and W. Kunig, *Helv. Chim. Acta*, **36**, 471 (1953).
4) H. Zahn et al., *Angew. Chem.*, **68**, 231 (1956).
5) M. Taniyama et al., *J. Chem. Soc. Japan, Ind. Chem. Sec.* (*Kogyo Kagaku Zasshi*), **59**, 545 (1956).
6) W. Schneider, *Ann*, **590**, 155 (1954).

NMR Spectra of Formals, Acetals and the Related Compounds

By Kenkichi NUKADA and Utako MAEDA

(Received April 22, 1959)

It is interesting to study the NMR spectra of formals (R_1-O-CH_2-O-R_2), acetals (R_1-O-CH(CH_3)-R_2) and the related compounds (H-C(OR)$_3$ and R-(O-CH_2-CH_2)$_n$-OR), as these compounds contain functional groups such as CH_3-O, CH_3-CH_2-O, O-CH_2-CH_2-O, O-CH_2-O, H-C(O)(O)-CH_3, etc. It is quite difficult, or sometimes perfectly impossible, to identify some of these functional groups by the infrared spectroscopy[1]. We have tried to identify them by the high resolution NMR spectroscopy[2]. JNM-3 (Japan Electron Optics Laboratory Co.) and 4300-B (Varian Associates) spectrometers were used.

Fig. 1 shows the NMR spectra of benzene solutions of several compounds except dimethyl acetal (CH_3-O-CH(CH_3)-O-CH_3), acetal (C_2H_5-O-CH(CH_3)-O-C_2H_5) and diethylene-glycol diethyl ether (C_2H_5-(O-CH_2-CH_2)$_2$-O-C_2H_5). The spectra of these three compounds were obtained in pure liquid phase and reference bands are shown with arrows on the peaks of each spectrum. The unit of abscissa means the chemical shift from the signal of benzene protons. The tentative assignments are shown on the tops of each peak.

TABLE I. THE VALUES OF CHEMICAL SHIFTS OF FUNCTIONAL GROUPS

Type of group	Chemical shift from benzene protons ($\times 10^{-7}$)
H-C(O)(O)(O)	21.3
(H)-C(O)(O)-CH_3	27.5
O-CH_2-O	27.8±1.0
O-CH_2-C	37.8±2.0
CH_3-O	40.3±0.8
(CH_3)-C(O)(O)-H	62±2
(CH_3)-CH_2-O	61±3

1) K. Nukada, *J. Chem. Soc. Japan. Pure Chem. Sec.* (*Nippon Kagaku Zasshi*), in press.

2) Chamberlain reported the NMR spectra of several hundreds of compounds including some ethers and alcohols, but in his paper those of above-mentioned compounds have not been reported. (N. F. Chamberlain, *Anal. Chem.*, 31, 56 (1959)).

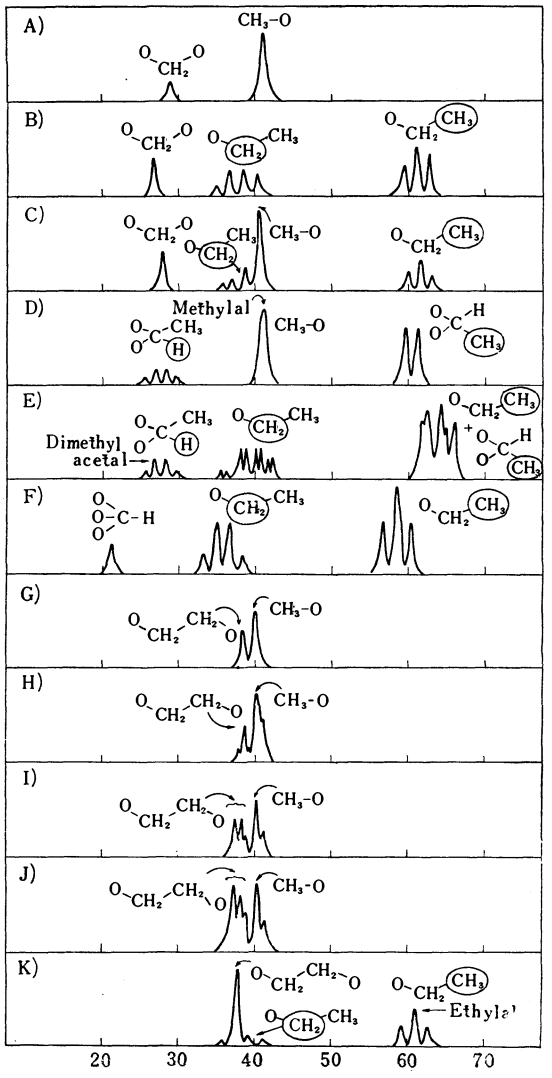


Fig. 1. Proton magnetic resonance spectra of formals, acetals and the related compounds.

A. Methylal. ($CH_3OCH_2OCH_3$)
B. Ethylal. ($CH_3CH_2OCH_2OCH_2CH_3$)
C. Methyl-ethyl formal. ($CH_3CH_2OCH_2OCH_3$)
D. Dimethyl acetal. ($CH_3OCH(CH_3)OCH_3$)
E. Acetal. ($CH_3CH_2OCH(CH_3)OCH_2CH_3$)
F. Orthoformic acid ethyl ester. ($CH(OCH_2CH_3)_3$)
G. Ethylene glycol dimethyl ether. ($CH_3OCH_2CH_2OCH_3$)
H. Diethylene glycol dimethyl ether. ($CH_3(OCH_2CH_2)_2OCH_3$)
I. Triethylene glycol dimethyl ether. ($CH_3(OCH_2CH_2)_3OCH_3$)
J. Tetraethylene glycol dimethyl ether. ($CH_3(OCH_2CH_2)_4OCH_3$)
K. Diethylene glycol diethyl ether. ($CH_3CH_2(OCH_2CH_2)_2OCH_2CH_3$)

We wish to express our sincere thanks to Dr. Y. Mashiko of this Institute, Dr. S. Hattori of Kanazawa University and Dr. T. Seki of Japan Electron Optics Laboratory Co. for their kind advice and to Dr. H. Honda and Dr. K. Nagata of the Resources Research Institute who kindly measured a part of spectra.

Government Chemical Industrial Research Institute of Tokyo
Hatagaya Honmachi,
Shibuya-ku, Tokyo

A New Compound of Tin(IV) with 8-Quinolinol and its Use in Gravimetric Analysis

By Hiroshi Hamaguchi, Nagao Ikeda and Kazuya Osawa

(Received May 8, 1959)

Shiba[1] reported that tin(II) was precipitated with 8-quinolinol (oxine) from dilute ammoniacal solution. As to the oxinate of tin(IV), Gentry and Sherrington[2] found that tin(IV) was extractable by oxine chloroform solution. They estimated the formula of the extractable oxinate of tin to be $Sn(C_9H_6NO)_4$. No report has been published, however, on the formation of a stable precipitate of oxine compound of tin(IV).

According to the present authors' experiments, tin(IV) is precipitated quantitatively from 0.2 N hydrochloric acid solution by adding oxine solution, but at the other concentrations of hydrochloric acid, the precipitation is not complete, as is shown in Fig. 1.

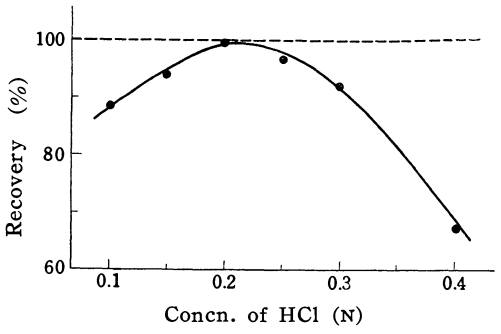


Fig. 1. Effect of hydrochloric acid concentration on the precipitation of tin(IV) oxinate.

The color of the precipitate is brilliant yellow. The compound is stable against heating at least up to 360°C. It is insoluble in mineral acid or alkaline solutions except for concentrated sulfuric acid. It is also insoluble in ordinary organic solvents. The chemical composition of the precipitate is as follows:

Anal. Found: Sn, 24.9; Cl, 15.2; C, 45.05; H, 2.63; N, 5.68*. Calcd. for $SnCl_2(C_9H_6NO)_2$; Sn, 24.8; Cl, 14.8; C, 45.2; H, 2.54; N, 5.87%.

The ionic species of tin(IV) in 0.2 N hydrochloric acid solution was examined by the aid of ion-exchange resin (Dowex 50), and it was found the charge of the species to be +2, which seems to justify the above mentioned chemical composition of the compound.

The application of this compound to the gravimetric determination of tin was then examined. The recommended procedure is the following.

Adjust the acidity to 0.2 N hydrochloric acid. Add the same volume of 2% oxine solution**. Keep the solution at 70~90°C for 1.5~2 hr. Filter with a glass filter, wash with 3 N hydrochloric acid, dry at 110~120°C and then weigh as $SnCl_2(C_9H_6NO)_2$.

Table I. Determination of tin as oxinate

Sn taken (mg.)	Sn oxinate (mg.)	Sn found (mg.)	Error (mg.)
1.00	3.5	0.87	0.13
1.99	8.0	1.99	0.00
2.99	11.9	2.96	0.03
4.98	19.2	4.77	0.21
9.96	39.5	9.81	0.15

Some results are shown in Table I. No metallic salt except molybdenum interferes. Bismuth and antimony should be absent because of their hydrolysis in the condition of the procedure. Presence of nitrate or phosphate leads to the hydrolysis of stannic ions. The precipitate of oxinate is not formed under the presence of tartrate.

1) Y. Shiba, *Repts. Gov. Ind. Research Inst. Tokyo*, **27**, No. 8, 12 (1932).
2) C. Gentry and L. Sherrington, *Analyst*, **75**, 17 (1950).

* The analyses of carbon, hydrogen and nitrogen were carried out at the Institute of Physical and Chemical Research.

** The oxine solution: Dissolve 6 g. of oxine in 5 ml. of concentrated hydrochloric acid, and dilute to 300 ml. with distilled water.

The authors wish to express their sincere thanks to Dr. Rokuro Kuroda for his helpful advice.

Department of Chemistry
Faculty of Science
Tokyo University of Education
Koishikawa, Tokyo

*Chemical Shifts of the Proton Magnetic Resonance in Alkylhydroperoxides**

By Shizuo FUJIWARA, Mikio KATAYAMA and Shinichi KAMIO**

(Received May 12, 1959)

Chemical shifts of the proton magnetic resonance in alkylhydroperoxides were measured in order to obtain the NMR informations of these compounds which have not been reported. The samples are listed in Table I with their characteristic data. All of them except *tert*-butylhydroperoxide were synthesized by one of us (S. K.) according to the methods reported by Williams and Mosher[1]. The *tert*-butylhydroperoxide was obtained commercially from the International Chemical Company.

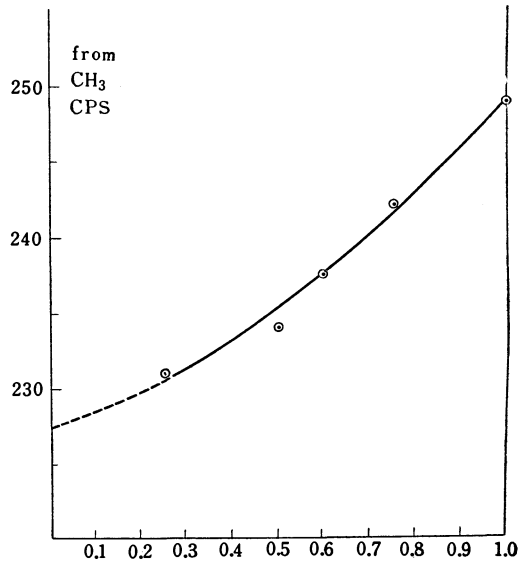
TABLE I. SAMPLES OF NMR MEASUREMENTS

n-Propyl hydroperoxide	35°C/20 mm.	$n_D^{25}=1.3890$
n-Butyl hydroperoxide	28~29°C/5 mm.	$n_D^{20}=1.4057$
sec-Butyl hydroperoxide	41~42°C/11 mm.	$n_D^{20}=1.4050$
n-Amyl hydroperoxide	41~42°C/4 mm.	$n_D^{20}=1.4146$
n-Octyl hydroperoxide	64~66°C/0.7 mm.	$n_D^{20}=1.4311$

tert-Butylhydroperoxide was obtained commercially.

The apparatus used for the measurements of the chemical shifts is the one constructed in this laboratory using the permanent magnet manufactured by the Indiana Steel Company and the resonant frequency is about 27.030 Mc. (H_0=6300 gauss). The chemical shift of the OOH proton resonance in each compound was measured as the separation from CH_3 signal appearing as the peak in the highest field on the recorded charts taking the cyclohexane and benzene mixture (0.28 g. +0.30 g.) as the reference to show the separation of 227 cps. at 40 Mc.

According to the results of the measurements, the resonant positions for the OOH protons are in the field lower than those for CH_3 by about 245 (±5) cps., being close to the value for COOH proton in aliphatic acid, 267 (±3) cps. for *n*-butylric acid, or about 280~230 cps.[2], and less shielded than the OH protons in alcohols which were measured as 120 (±5) cps. or 120~100 cps[2]. The propylhydroperoxide showed a very small value of 222 (±5) cps., and this was assumed to be due to the decomposition of the compound. The figures showing the variations of the observed data are due to the overlapping and the incomplete separation of the signals of CH_3 and CH_2's.



Mol. fraction of *n*-butyl HPO in CCl_4

Fig. 1

In order to investigate the effects of the decomposition of the samples, the concentration dependence of the shifts were measured for the carbon tetrachloride solutions of the *n*-butylhydroperoxide.

* Presented before the 12th Annual Meeting of the Chemical Society of Japan in April, 1959.

** Railway Technical Research Institute, Japanese National Railways, Minato-ku, Tokyo, Japan.

1) H. R. Williams and H. S. Mosher, *J. Am. Chem. Soc.*, 76, 2984 (1954).

2) These values were obtained from Fig. 6 in the article given by N. F. Chamberlain, *Anal. Chem.*, 31, 56 (1959).

The results are as shown in Fig. 1, it is seen that the OOH signal is shifted to the lower field with the increase of the concentration of the hydroperoxide, and this result will be interpreted in terms of the destruction of the structures of associated molecules as in the cases of other hydrogen-bonded liquids[3,4]. The susceptibility corrections are not made in the results of Fig. 1. Since the concentration dependence is so large that the results of the measurements with one another shifts are to be compared to each other at the same conditions of concentration. As the hydroperoxides are unstable and, moreover, it is rather difficult to determine their concentrations, we made the measurements immediately after the preparation of the samples. Hence, the results of Fig. 1 are assumed to refer to those for the actually pure hydroperoxides which are not so much different from one another in the concentration. It is also noted that α-CH_2 protons in all the samples fall in almost same position of about 79 ($\pm$1) cps. away from CH_3. Since the α-CH_2 protons in alcohols with the same carbon number as the samples showed the value of 65 ($\pm$2) cps., we notice that α-CH_2 protons in hydroperoxides are less shielded than those in alcohols as well as OOH protons. In comparison with aliphatic acids, the COOH protons which are expected to be away from CH_3 by about 275~230 cps.[2] are, as noted above, very close to the OOH protons in hydroperoxides, while α-CH_2 protons in acids are only 35 cps.[2] away from CH_3 and more shielded than those in hydroperoxides and in alcohols. Therefore, it is a quite interesting problem to investigate the chemical characters of alcohols, hydroperoxides and acids from the viewpoint of structures and of electronic distributions of OH, OOH and COOH groups.

3) J. T. Arnold and M. E. Packard, *J. Chem. Phys.*, **19**, 1608 (1951).
4) L. W. Leeves and W. G. Schneider, *Trans. Faraday Soc.*, **54**, 314 (1958).

University of Electro-Communications
Chōfu, Tokyo

The Roles of Prolyl Residue in Polypeptide Monolayers. II. On the Surface Viscosity and Types of Monolayers

By Shoichi IKEDA and Toshizo ISEMURA

(Received November 17, 1958)

In the preceding paper[1] we have described the effects of prolyl residue in polypeptide monolayers revealed in the surface pressure and potential behavior and deduced their roles in the chain configuration, chain flexibility and intrachain interaction in the polypeptide monolayers. It was found that, as for the polypeptides examined, the presence of prolyl residues makes the monolayers more expanded as their content becomes increased, in spite of the peptide carbonyl groups having the same orientation at the interface. (However, the carbonyl groups in poly-L-proline film are oriented in a different manner.) This expanded nature of monolayer was attributed to the flexible chain configuration of polypeptide arising mainly from the decrease in number of hydrogen bonds. Conversely, the ordinary non-electrolytic polypeptide forms a monolayer of condensed type due to its rigidly held configuration with the strong intrachain hydrogen bonds.

In the study of monolayer the measurement of surface viscosity also gives information concerning its structure and other characteristics. Cumper and Alexander[2], and also Isemura and Hamaguchi[3] established the β-configuration in monolayers of non-electrolytic polypeptides from the surface viscosity measurement. Later, it was noticed[4] that in the monolayer of an amphoteric polypeptide the surface viscosity rises even at the area of low surface pressure if the pH of the aqueous subphase is near the isoelectric point, while the surface viscosity rises at the area of high surface pressure on either side of this pH. Generally, the former behavior appears to be observed in the monolayer of condensed type and the latter in that of expanded type. Such aspects of surface viscosity may be expected in the monolayers of polypeptides with the various proportions and arrangements of prolyl residues and may be related to their chain configuration, chain flexibility and intrachain hydrogen bonding.

In this paper we will report the results of surface viscosity measurements for poly-DL-alanine, poly-L-prolyl-L-leucylglycine and copoly-1:1:1-(L-proline, L-leucine, DL-alanine) and give a further confirmation of inferences obtained from the surface pressure and potential measurements.

Experimental

Materials.—The polypeptide samples were poly-DL-alanine, poly-L-prolyl-L-leucylglycine and copoly-1 : 1 : 1-(L-proline, L-leucine, DL-alanine) which were the same as those reported in the preceding paper[1]. Their degrees of polymerization and spreading solvents were as follows:

	D. P.	Spreading solvent dichloroacetic acid-benzene
Poly-DL-alanine	300	1 : 9
Poly-L-prolyl-L-leucylglycine	13	1 : 4
Copoly-1:1:1-(L-proline, L-leucine, DL-alanine)	129	1 : 4

Methods.—The lower portion of surface pressure was measured by a surface balance of float type and the higher portion (for the other two polypeptides) by a surface balance of hanging plate type. The surface pressures measured by these two balances were ascertained to be identical in the cases of the latter two polypeptides.

Surface viscosity was measured by the damped rotatory oscillation of a disk, utilizing the relation

$$\eta=\frac{2.303I\cdot\Delta\lambda}{2\pi P}\left(\frac{1}{a^2}-\frac{1}{b^2}\right)$$

where I is the moment of inertia of the disk, P the period of oscillation, $\Delta\lambda$ the difference between logarithmic decrements of oscillation in the presence of film and in its absence, a the radius of disk and b the distance between the center of disk and the edge of trough. Usually an outer edge concentric with the disk is put on the aqueous surface in order to calculate surface viscosity by means of the above formula, but its

1) T. Isemura and S. Ikeda, This Bulletin, **32**, 178 (1959).
2) C. W. N. Cumper and A. E. Alexander, *Trans. Faraday Soc.*, **46**., 235 (1950).
3) T. Isemura and K. Hamaguchi, This Bulletin, **27**, 125 (1954).
4) T. Isemura and K. Hamaguchi, ibid,. **27**, 339 (1954).

use makes the reproducibility of measurement unsatisfactory for the monolayer of condensed type such as poly-DL-alanine, because it is difficult for it to flow into the annular region under high compression and it makes a heterogeneous film. It was found that substantially equal values of surface viscosity can be obtained for monolayers of expanded type such as copoly-1 : 1 : 1-(L-proline, L-leucine, DL-alanine) whether the concentric edge is put on or not. Hence, all the measurements were carried out on the surface without concentric edge. In the present apparatus, I was measured to be 43.45 g. cm^2, P 7.50 sec., a 1.28 cm. and b 7.00 cm. and the measurable range of surface viscosity was 10^{-3} to 2×10^{-1} surface poise, where the flow was Newtonian.

To regulate the temperature, a glass serpentine coil was put in the trough, through which water at constant temperature was passed from a thermostat.

Results

The surface pressure-area (Π-A) and surface viscosity-area (η-A) curves of poly-DL-alanine are shown in Fig. 1. The monolayer is of condensed type. Surface

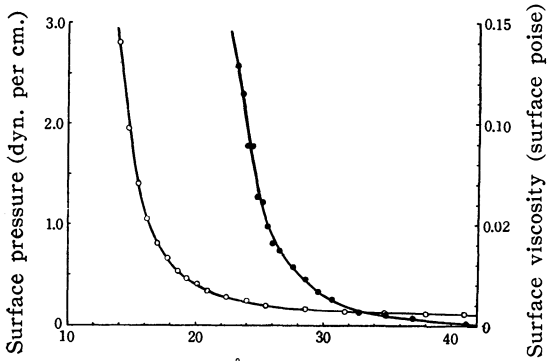


Fig. 1. The surface pressure-area (○) and surface viscosity-area (●) curves of poly-DL-alanine at 9°C.

viscosity begins to rise at the area of 42 Å^2 per residue and gelates at 22 Å^2 per residue and at the surface pressure lower than 0.3 dyn. per cm. Surface viscosity of poly-DL-alanine could be readily measured at room temperature. It appears to be slightly affected by temperature and to increase with the rise of temperature. However, its temperature dependence was not reproducible.

The Π-A and η-A curves of polyl-L-prolyl-L-leucylglycine and copoly-1 : 1 : 1-(L-proline, L-leucine, DL-alanine) are shown in Figs. 2 and 3, respectively. Both films are of expanded type. While their close-packed areas are 57 and 46 Å^2 per three amino acid residues, respectively, both surface

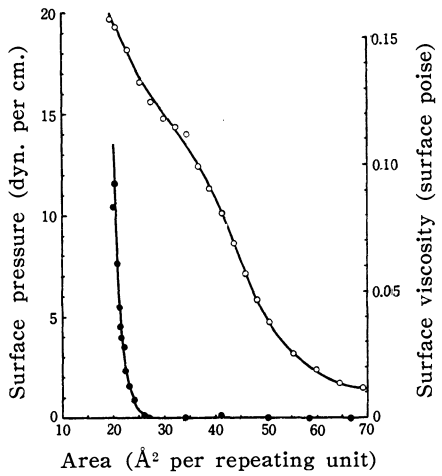


Fig. 2. The surface pressure-area (○) and surface viscosity-area (●) curves of poly-L-prolyl-L-leucylglycine at 16.7°C.

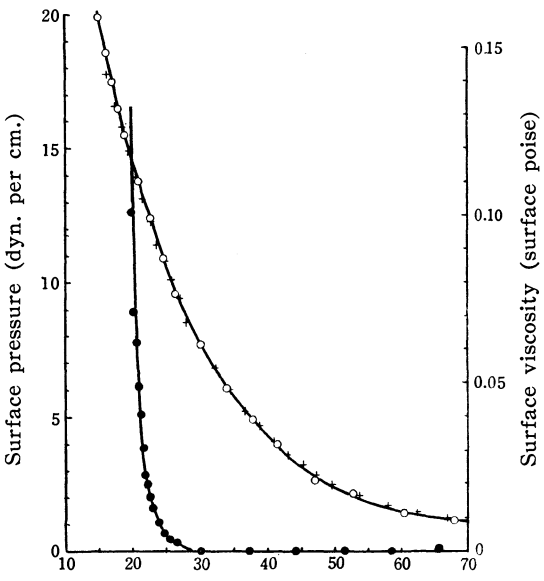


Fig. 3. The surface pressure-area curve (○, at 10.8°C; +, at 26.4°C) and the surface viscosity-area curve (●, at 16.7°C) of copoly-1:1:1-(L-proline, L-leucine, DL-alanine).

viscosities rise at the area less than about 29 Å^2 per three amino acid residues. The corresponding surface pressures range over 15 to 21 dyn. per cm. for the former polypeptide and over 10 to 16 dyn. per cm. for the latter, as the latter film is more expanded than the former. Thus these two polypeptides show almost the same behavior in surface viscosity, irrespective of their different behaviors in surface pressure.

It should be added here that surface

viscosities of these two polypeptides rise at such a small area that films can not occupy an area large enough to spread as complete monolayers. They were initially spread on the surface with an area therefore of about 80 Å^2 per three amino acid residues which is not a sufficiently large area compared with the close-packed areas, and the *Π-A* curves in Figs. 2 and 3, therefore, shift to a smaller area than those obtained when spread on larger areas. The film of copoly-1 : 1 : 1-(L-proline, L-leucine, DL-alanine) was readily compressed even in the high surface pressure region, but the film of poly-L-prolyl-L-leucylglycine required some minutes after compression to establish the final surface pressure.

Surface viscosities of poly-L-prolyl-L-leucylglycine and copoly-1 : 1 : 1-(L-proline, L-leucine, DL-alanine) were found to be markedly dependent of temperature. They were quite reproducible and, to some extent, reversible for compression and expansion. The variation of *η-A* curves with temperature are shown in Figs. 4 and 5, for the respective polypeptide. The higher the temperature is, the lower is the surface viscosity. Both values of surface viscosity and their temperature dependence are almost identical for these two polypeptides. However, as illustrated in Fig. 3, surface pressure was not changed by temperature.

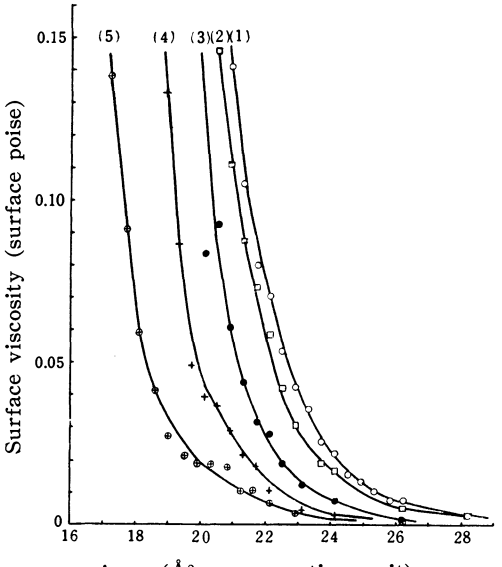


Fig. 4. The variation of surface viscosity-area curves of poly-L-prolyl-L-leucylglycine with temperature. Curves (1) 6.9°, (2) 10.0°, (3) 16.7°, (4) 21.5° and (5) 30.4°C.

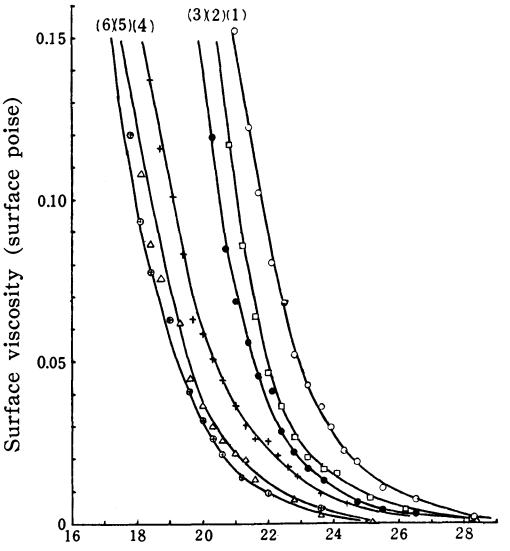


Fig. 5. The variation of surface viscosity-area curves of copoly-1 : 1 : 1-(L-proline, L-leucine, DL-alanine) with temperature. Curves (1) 4.7°, (2) 10.7°, (3) 16.7°, (4) 20.5°, (5) 25.6° and (6) 29.9°C.

Discussion

Surface Viscosity as a Function of Surface Pressure. — It was noticed that surface viscosity of poly-DL-alanine film is already high at the area where surface pressure is sufficiently low and surface viscosities of the other two polypeptide films are detected at the area where surface pressures are considerably high. In other words, surface viscosity of condensed film is actually measured for the monomolecular layer, but that of expanded film is presumably for folded monolayer. Such a difference in surface viscosity was already pointed out by Isemura and Hamaguchi[4] for the film of an electrolytic copolypeptide. It may be attributed to

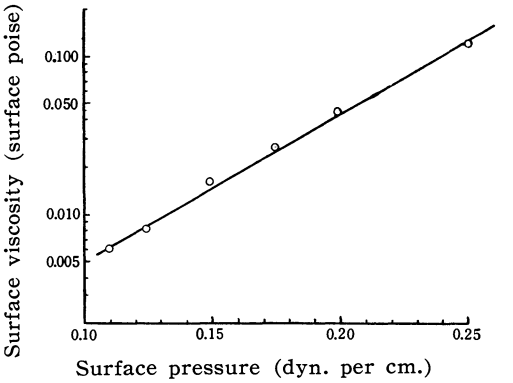


Fig. 6. The log *η-Π* curve of poly-DL-alanine.

the difference in chain configurations of spread polypeptides.

The monolayer of poly-DL-alanine is of condensed type. It was found that for the condensed films of fatty acids[5] and their mixtures[6] the logarithm of surface viscosity is in a linear relation to surface pressure. As shown in Fig. 6, the poly-DL-alanine monolayer follows the same relation as fatty acid films over the region of temperature, 8 to 12°C, and of area, 24 to 34 Å^2 per residue, although the surface pressure at which surface viscosity was measured is much lower. This relation is expressed by

$$\log \eta = \log K + c\Pi \qquad (1)$$

where $\log K$ and c are constants, the values of which are shown in Table I.

TABLE I

	$\log K$	c	B
Poly-DL-Ala	-3.2_3	9.24	0
Poly-L-Pro-L-Leu-Gly	−22.5	0.46	3560
Copoly-(L-Pro, L-Leu, DL-Ala)	−17.3	0.33	3370

On the other hand, poly-L-prolyl-L-leucylglycine and copoly-1 : 1 : 1-(L-proline, L-leucine, DL-alanine) give monolayers of expanded type. It was observed[7] that for the expanded monolayer of polyvinyl acetate the logarithm of surface viscosity changes also linearly with surface pressure at constant temperature. Joly[8] has tabulated the values of surface viscosity as a function of surface pressure for various protein films. These films are probably of expanded type, as they are spread on 0.01 N hydrochloric acid and will be ionized completely. If these values are plotted on a semilogarithm scale, again linear relations are obtained, particularly for the film of gliadin. As shown in Figs. 7 and 8, the films of the two polypeptides also follow the linear relation over the region of temperature, 5 to 30°C, and of area, 21 to 24 Å^2 per three amino acid residues. The relation is written as

$$\log \eta = \log \mu + c\Pi \qquad (2)$$

where c is a constant but $\log \mu$ is a function of temperature, as seen in Table II. Further, the temperature dependence of $\log \mu$ is found to be given by

$$\log \mu = \log K + B/T \qquad (3)$$

where $\log K$ and B are constants, the

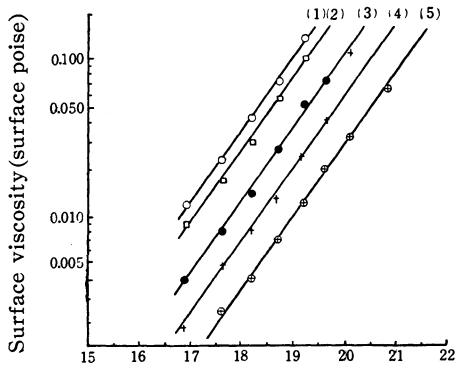


Fig. 7. The $\log \eta$-Π curves of poly-L-prolyl-L-leucylglycine at various temperatures. Curves (1) 6.9°, (2) 10.0°, (3) 16.7°, (4) 21.5° and (5) 30.4°C.

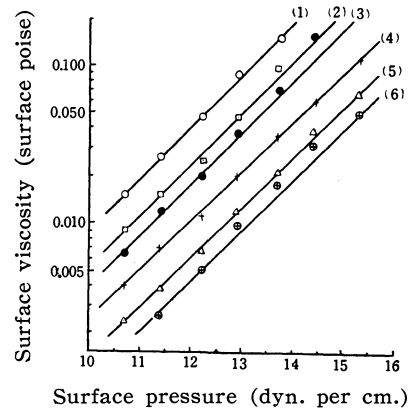


Fig. 8. The $\log \eta$-Π curves of copoly-1 : 1 : 1-(L-proline, L-leucine, DL-alanine) at various temperatures. Curves (1) 4.7°, (2) 10.7°, (3) 16.7°, (4) 20.5°, (5) 25.6° and (6) 29.9°C.

TABLE II

Poly-L-Pro-L-Leu-Gly			
T (°C)	$\log \mu$	c	
30.4	−10.80	0.46_4	
21.5	−10.54	0.45_7	$\log K = -22.7_0$
16.7	−10.21	0.46_3	$B = 3610$
10.0	−9.89	0.46_1	
6.9	−9.76	0.46_6	
Copoly-(L-Pro, L-Leu, DL-Ala)			
T (°C)	$\log \mu$	c	
29.9	−6.29	0.32_4	
25.6	−6.09	0.32_2	
20.5	−5.80	0.31_7	$\log K = -17.2_7$
16.7	−5.76	0.33_3	$B = 3340$
10.7	−5.48	0.32_0	
4.7	−5.42	0.33_5	

5) G. E. Boyd and W. D. Harkins, *J. Am. Chem. Soc.*, **61**, 1188 (1939).
6) G. E. Boyd and F. Vaslow, *J. Colloid Sci.*, **13**, 275 (1958).
7) T. Isemura and K. Fukuzuka, *Mem. Inst. Sci. Ind. Res., Osaka Univ.*, **13**, 137 (1956).
8) M. Joly, "Surface Chemistry", But-terworths Scientific Publications, London (1949), p. 157.

values of which are also shown in Table II.

Surface Viscosity as a Function of Temperature. — As mentioned before, surface viscosity of poly-DL-alanine monolayer scarcely varies with temperature but tends to increase slightly as temperature is raised. This appears to be a general aspect of the monolayer of condensed type.

For the films of poly-L-prolyl-L-leucylglycine and copoly-1 : 1 : 1-(L-proline, L-leucine, DL-alanine) surface viscosities diminish as temperature rises and it was found that plots of logarithm of surface viscosity against the inverse of temperature are linear over the region of temperature, 5 to 30°C, and of areas, 21 to 24 Å^2 per three amino acid residues, as illustrated in Figs. 9 and 10. That is, the relation is fitted to the Andrade equation

$$\log \eta = \log \nu + B/T \qquad (4)$$

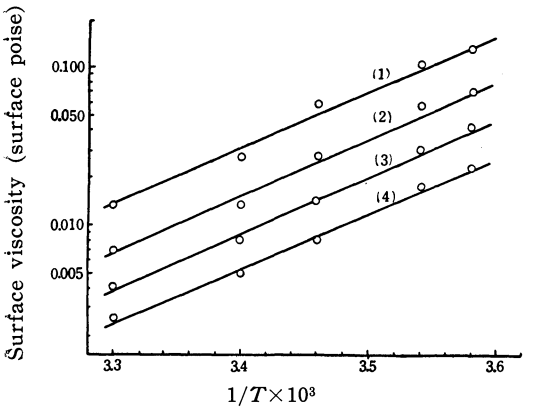


Fig. 9. The $\log \eta - 1/T$ curves of poly-L-prolyl-L-leucylglycine at various areas (at various surface pressures). Curves (1) 21.0 Å^2, (2) 22.0 Å^2, (3) 23.0 Å^2 and (4) 24.0 Å^2.

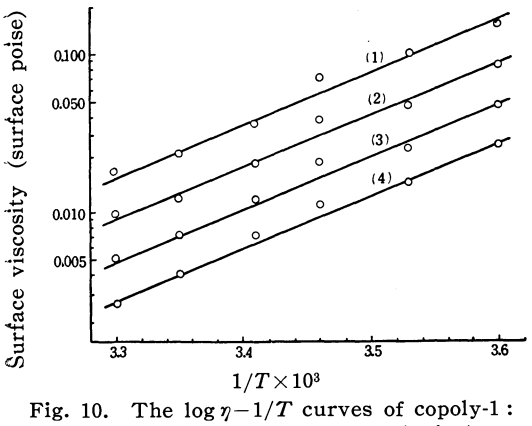


Fig. 10. The $\log \eta - 1/T$ curves of copoly-1 : 1 : 1-(L-proline, L-leucine, DL-alanine) at various areas (at various surface pressures). Curves (1) (21.0Å^2, (2) 22.0 Å^2, (3) 23.0 Å^2 and (4) 24.0 Å^2.

TABLE III

Poly-L-Pro-L-Leu-Gly

Π (dyn./cm.)	$\log \nu$	B	
19.2	−13.61	3520	
18.7	−13.92	3580	$\log \nu = -22.4_8$
18.2	−14.12	3610	$c = 0.46$
17.6	−14.38	3500	

Copoly-(L-Pro, L-Leu, DL-Ala)

Π (dyn./cm.)	$\log \nu$	B	
13.7	−12.88	3320	
12.9	−13.14	3370	$\log \nu = -17.3_0$
12.4	−13.41	3390	$c = 0.32$
11.4	−13.66	3390	

where B is a constant but $\log \nu$ depends on surface pressure. This has already been established for films of polyvinyl acetate[9] and 6-nylon[10], although the dependence of $\log \nu$ on surface pressure is not explicitly indicated. The values of B and $\log \nu$ are given in Table III. It can be seen that $\log \nu$ is represented by

$$\log \nu = \log K + c\Pi \qquad (5)$$

as a function of surface pressure, where both $\log K$ and c are constants the values of which are also shown in Table III.

From the data given in Tables II and III, numerical coincidences may be noticed between $\log K$ in Eqs. 3 and 5, between c in Eqs. 2 and 5 and between B in Eqs. 3 and 4. Consequently, the surface viscosity equation is reduced to

$$\log \eta = \log K + c\Pi + B/T \qquad (6)$$

for the films of poly-L-prolyl-L-leucylglycine and copoly-1 : 1 : 1-(L-proline, L-leucine, DL-alanine). Values of constants are listed in Table I. The values of B for these two polypeptides are found to be almost equal to each other, which should be the necessary condition for the equal temperature coefficient of surface viscosity.

Configuration and Flexibility of Polypeptide Chains. — In comparing the close-packed area with the area where surface viscosity was measured, it will be evident that surface film in this region corresponds to liquid or melt in bulk rather than to dilute solution, and accordingly, surface viscosity to viscosity of liquid or melt. It is generally accepted that a transition takes place at the glass temperature or the second-order transition temperature for polymers, below which the segmental motion becomes frozen-in. The segmental motion is exhibited in the behavior of

9) T. Isemura and K. Fukuzuka, *Mem. Inst. Sci. Ind. Res., Osaka Univ.*, 14, 169 (1957).
10) K. Inokuchi, This Bulletin. 28, 453 (1955).

melt viscosity[11]. At the transition temperature melt viscosity decreases markedly with the rise of temperature. While above the transition temperature melt viscosity alters with temperature in such a way as expressed by the Andrade equation, below that temperature it is not influenced by temperature very much but rather depends on other complicated factors[12]. The temperature at which such freezing-in of the segmental motion will occur depends on the structural factors such as inter- or intrachain interaction, chain flexibility or steric effect. Then at a given temperature a polymer will behave as liquid or glass whether that temperature is higher or lower than the glass temperature. This idea can be adequately applied to explain the observed behavior of surface viscosity of monolayer. Thus the monolayers of expanded type and condensed type might be correlated reasonably with a melt and glassy state in bulk, respectively. In other words, a spread polymer which gives a film of expanded type will behave as an ordinary liquid at the temperature where film properties are measured, since the segmental interaction is weak and the molecular chain is flexible; also the segmental motion of a spread polymer in a film of condensed type is inhibited at that temperature, since the chain is rigidly held owing to the strong segmental interaction. The difference is revealed most distinctly in surface viscosity behavior.

Eyring et al.[13,14] derived the surface viscosity equation by a simple analogy with liquid viscosity, regarding monolayer as a two-dimensional liquid. According to them, surface viscosity is expressed by

$$\eta = \frac{\boldsymbol{h}}{A_f} \exp\left(\frac{\Delta F^{\ddagger}}{\boldsymbol{k}T}\right) \tag{7}$$

where $\boldsymbol{h}$ is the Planck constant, $\boldsymbol{k}$ the Boltzmann constant and A_f is the area occupied by a unit of flow. The free energy of activation for flow per unit, $\Delta F^{\ddagger}$, is given by

$$\Delta F^{\ddagger} = \Delta E^{\ddagger} + \Pi \Delta A^{\ddagger} - T\Delta S^{\ddagger} \tag{8}$$

where $\Delta E^{\ddagger}$ and $\Delta S^{\ddagger}$ are the energy and the entropy of activation per unit, respectively, and $\Delta A^{\ddagger}$ is the increment of area in the activated state over that of the initial state. Substituting Eq. 8 into Eq. 7, the final equation becomes

$$\ln \eta = \ln \frac{\boldsymbol{h}}{A_f} - \frac{\Delta S^{\ddagger}}{\boldsymbol{k}} + \frac{\Delta A^{\ddagger}}{\boldsymbol{k}T}\pi + \frac{\Delta E^{\ddagger}}{\boldsymbol{k}T} \tag{9}$$

This equation has the same form as Eqs. 1 and 6. From their comparison it can be seen that

$$\Delta E^{\ddagger} = 2.303\,\boldsymbol{k}B \tag{10}$$

$$\Delta A^{\ddagger} = 2.303\,\boldsymbol{k}Tc \tag{11}$$

$$\frac{\boldsymbol{h}}{A_f} \exp\left(-\frac{\Delta S^{\ddagger}}{\boldsymbol{k}}\right) = K \tag{12}$$

Thus $\Delta E^{\ddagger}$ and $\Delta A^{\ddagger}$ may be calculated from the data in Table I. Although the value of $\Delta S^{\ddagger}$ can not be determined uniquely from a single experimental value of log K, its approximate value may be assigned, as it is not very sensitive for the choice of values of A_f. Table IV shows these data for the polypeptide films studied in the present investigation.

TABLE IV

	$\Delta E^{\ddagger}$ (kcal./mol.)	$\Delta A^{\ddagger}$ (Å^2)	$\Delta S^{\ddagger *}$ (e. u.)
Poly-DL-Ala	0	8000	$-110 \sim -120$
Poly-L-Pro-L-Leu-Gly	16.3	420	$-21 \sim -29$
Copoly-(L-Pro, L-Leu, DL-Ala)	15.4	300	$-45 \sim -50$

* Values when A_f is assumed to be 10 Å^2 to $\Delta A^{\ddagger}$

For the monolayer of poly-DL-alanine, $\Delta E^{\ddagger}$ was found to be nearly zero. This suggests that the flow mechanism is different from that in liquid state and the polypeptide molecules flow under shear by breaking the entanglement or linkages such as van der Waals or hydrogen bonds between them. This may be expected from the discussion above that such a flow occurs for the film of polypeptide in which the segmental interaction is strong and the rigidity of the chain is high. This result is consistent with that deduced for the condensed nature of this film in the previous paper[1]. Further support is provided by estimating the value of $\Delta A^{\ddagger}$, which was found to be about 8000 Å^2 per flow unit. Since the close-packed area of poly-DL-alanine is 15 Å^2 per residue, the area obtained above is occupied by about 500 residues. Taking account of the ambiguity concerning the degree of polymerization of material, 300, it may be roughly assumed that a unit of flow is composed of a poly-DL-alanine molecule. In addition, a large

11) T. Alfrey, G. Goldfinger and H. Mark, *J. Appl. Phys.*, **14**, 700 (1943); E. Jenkel, *Kolloid-Z.*, **120**, 160 (1951).
12) K. Ueberreiter and H. J. Orthmann, ibid., **126**, 140 (1952).
13) E. J. Moore and H. Eyring, *J. Chem. Phys.*, **6**, 391 (1938).
14) S. Glasstone, K. J. Laidler and H. Eyring, "The Theory of Rate Processes", McGraw-Hill Co., New York (1941), p. 561.

negative value for $\Delta S^{\ddagger}$, -120 e. u., was assigned to the polypeptide. In view of the deduction concerning dependence of the entropy of activation for flow in bulk on chain length of polymers[15] and the result on surface viscosity of polyvinyl acetate[7], the entropy of activation for flow in film might be scarcely influenced by the degree of polymerization of polymers, that is, the term involving the degree of polymerization contributes to the entropy only a few e. u. Then the large negative value for $\Delta S^{\ddagger}$ should be characteristic of the monolayer of poly-DL-alanine. It might be attributed to the highly disordered configuration of flow unit or molecule of poly-DL-alanine at the interface. Probably the spread molecule is coiled and held together in monolayer.

On the other hand, for the films of poly-L-prolyl-L-leucylglycine and copoly-1 : 1 : 1-(L-proline, L-leucine, DL-alanine) values of $\Delta E^{\ddagger}$ are not zero but 16.3 and 15.4 kcal. per mole, respectively, and nearly equal to each other. These are of comparable order of magnitude with those reported, namely, 12.7 kcal. per mole for the film of polyvinyl acetate[9] and 6.4 kcal. per mole for the film of 6-nylon[10], although the sizes of their unit of flow will be different from one another. But the larger values for these two polypeptides than the other might come from the additional energy necessary for breaking (more) hydrogen bonds when units of flow move. The values of $\Delta A^{\ddagger}$ were 420 and 300 $Å^2$ per three amino acid residues, respectively. The size of flow units can not be estimated in the same way as above, as the viscous flow takes place at such small areas that they do not always correspond to a monomolecular layer. The polypeptide chains are probably in a folded configuration partly submerged into the aqueous subphase in these areas. The small negative values of $\Delta S^{\ddagger}$, -25 and -50 e. u., respectively, would be an indication of the relatively regular configuration of chains. Both the mechanism of flow through the activation process and the regular folding of chains under compression favor the weak interaction and the flexibility of chains. This supports the results obtained in the previous paper[1].

All the differences in surface viscosity behavior between poly-DL-alanine and the other two polypeptides are based on the types of monolayers, namely, the nature of condensation and expansion of films. The types of monolayers depend on the structural factors defined by the proportion and arrangement of prolyl residues in polypeptide chains. But the surface viscosities and their temperature dependences were found to be equal to each other for poly-L-prolyl-L-leucylglycine and copoly-1 : 1 : 1-(L-proline, L-leucine, DL-alanine), which will originate from their identical chain configurations, irrespective of their different amino acid sequences in chains. The fact that the surface pressure of the former polypeptide is higher than that of the latter and shows some time effect. will mean that the former chain folds itself by compression with greater difficulty, as described in the preceding paper[1].

Summary

To investigate the roles of prolyl residue in polypeptide monolayers, surface viscosity was measured for the monolayers of poly-DL-alanine, poly-L-prolyl-L-leucylglycine and copoly-1 : 1 : 1-(L-proline, L-leucine, DL-alanine).

For the monolayer of poly-DL-alanine which is of condensed type, the surface viscosity was found to rise at the area larger than the close-packed area and scarcely to be dependent of temperature. This result was correlated with that observed in the glassy state of polymers in bulk and interpreted by assuming that the polypeptide chain is rigid owing to the strong interaction. For the films of the other two polypeptides which are of expanded type appreciable surface viscosities were manifested at the areas much smaller than their close-packed areas and temperature exerted marked influence on surface viscosities. Their chain configurations were considered to be flexible owing to the weak interaction, since the flows in films occur as in melt of polymers in bulk.

Further evidence for this inference was obtained from the results on dependences of surface viscosity on surface pressure and temperature. The dependences were found to follow Eyring's equation of surface viscosity. It was found that in the monolayer of poly-DL-alanine a unit of flow is roughly composed of a molecule and its chain is rather coiled at the interface, but the chains of the other two polypeptides are in a regularly folded configuration partly submerged into the

15) W. Kauzmann and H. Eyring, *J. Am. Chem. Soc.*, **62**, 3113 (1940). See also Ref. 14, p. 501.

aqueous phase when compressed, as they are flexible.

The difference in surface viscosity behavior between poly-DL-alanine and the other two polypeptides was related to the condensed and expanded nature of films, which is defined by the content and distribution of prolyl residues in polypeptide chains. It was, however, observed that poly-L-prolyl-L-leucylglycine and copoly-1 : 1 : 1-(L-proline, L-leucine, DL-alanine) exhibit the same surface viscosity behavior, irrespective of their different distribution of prolyl residues in chains, while the former has a higher surface pressure than the latter.

All the results obtained were found to confirm the view deduced from the surface pressure and potential measurements.

The authors are indebted to Dr. H. Tani and Dr. S. Sakakibara of the Faculty of Science, Osaka University, to Dr. J. Kurtz of the Weizmann Institute of Science in Israel and to Professor J. Noguchi of Kanazawa University for the supply of valuable samples. This work was partly supported by a grant given by the Ministry of Education, to which the authors' thanks are also due.

Institute of Scientific and Industrial Research, and Institute for Protein Research
Osaka University, Sakai, Osaka

Role of Dielectric Constant at the Miscibility Point in the Ternary System 2-Propanol-Water and Carbon Tetrachloride

By C. V. SURYANARAYANA and K. M. SOMASUNDARAM

(Received December 26, 1958)

Two liquids are known[1] to be miscible in all proportions when both are sufficiently alike to obey Raoult's law. Only when the internal forces are quite unlike, separation of two liquid phases is known to occur. The fundamental question underlying all problems relating to solubility is the nature and the strength of intermolecular forces. The thermodynamic condition for equilibrium in any system is that the total free energy should be a minimum. If separation into two layers minimises the free energy of the system, it will happen so. Deviations from ideal behavior occur either owing to lowering the temperature or by choosing components more unlike in attractive forces. Either of these changes, when pursued far enough, can bring about a separation into two liquid phases.

A new outlook is developed in the following investigations. The work of Coomber[2] and McC. Lewis[3] shows that dielectric constant of a liquid system is related to its internal pressure. To an inhomogeneous mixture of two liquids progressive addition of a third component which happens to mix with both the liquids entails in a distribution of the added component between the two layers. With successive additions of the third component there is to be expected, as a result of the distribution between the two phases a progressive variation of the physico-chemical properties in the two layers. Just at the miscibility point these properties in the respective layers should tend to a limit at which the phase boundary just disappears forming a homogeneous system. Since internal pressure is connected with the dielectric constant (loc. cit.), at the transition when the phase boundary disappears, we may expect a quantitative relationship among the values of dielectric constant of the solution and those of the three pure components. The ternary system 2-propanol–water–carbon tetrachloride has been studied from the above point of view. We have reported[4] earlier our results on the ternary system 1-propanol–water–toluene.

1) E. Washburn, *Trans. Am. Electrochem. Soc.*, **22**, 330 (1912).
2) D. I. Coomber, *Trans. Faraday Soc.*, **35**, 304 (1939).
3) W. C. McC. Lewis, *Phil. Mag.*, **28**, 104, (1914).
4) K. M. Somasundaram and C. V. Suryanarayana, This Bulletin, **31**, 838 (1958).

TABLE I. 2-PROPANOL-WATER-CARBON TETRACHLORIDE

Mole fraction			Density	Viscosity in centipoises	Dielectric constant
2-Propanol x_1	Water x_2	CCl_4 x_3			
0.4397	0.2385	0.3222	1.1650	1.047	8.09
0.4345	0.3362	0.2291	1.0810	1.114	10.80
0.4101	0.4149	0.1752	1.0480	1.223	13.50
0.3853	0.4788	0.1355	1.0170	1.319	16.05
0.3431	0.5584	0.0986	0.9940	1.452	20.52
0.3057	0.6323	0.0622	0.9625	1.570	24.87
0.2844	0.6591	0.0565	0.9636	1.629	28.01
0.2349	0.7283	0.0364	0.9515	1.723	33.00
0.1939	0.7872	0.0188	0.9380	1.672	40.70

TABLE II

$\sum_3 P_3x_3$	$P_{1,2,3}$	% deviation from the mean value	$\sum_3 L_3x_3$	$L_{1,2,3}$	% deviation from the mean value
42.211	48.48	6.911	0.6946	0.7030	0.6009
40.948	47.73	7.647	0.7572	0.7656	0.5516
39.190	45.45	7.396	0.7967	0.8065	0.6113
37.545	43.14	6.937	0.8259	0.8337	0.4700
35.112	39.97	6.471	0.8559	0.8666	0.6212
32.913	36.32	4.920	0.8847	0.8886	0.2200
31.811	35.26	5.142	0.8908	0.9003	0.5304
29.196	31.54	3.860	0.9097	0.9141	0.2413
27.010	28.49	2.667	0.9264	0.9298	0.1832

TABLE III. 2-PROPANOL-WATER

Mole fraction		Density	Viscosity in centipoises	Dielectric constant
2-Propanol x_1	Water x_2			
—	1.0000	0.9941	0.7225	72.94
0.0232	0.9770	0.9813	0.947	71.00
0.0514	0.9486	0.9692	1.248	66.25
0.0956	0.9044	0.9499	1.639	58.22
0.1578	0.8422	0.9226	1.954	49.72
0.1914	0.8086	0.9097	2.040	45.98
0.2619	0.7381	0.8857	2.116	38.62
0.3526	0.6474	0.8618	2.095	32.47
0.4829	0.5171	0.8354	1.938	26.51
0.6797	0.3203	0.8072	1.699	20.70
0.8819	0.1183	0.7866	1.529	18.35
1.0000	—	0.7736	1.550	17.50

TABLE IV

$\sum_2 P_2x_2$	$P_{1,2}$	% deviation from the mean value	$\sum_2 L_2x_2$	$L_{1,2}$	% deviation from the mean value
—	17.42	—	—	0.9610	—
18.551	18.57	0.0512	0.9586	0.9590	0.0209
19.908	19.90	0.0201	0.9552	0.9559	0.0366
22.051	22.05	0.0023	0.9503	0.9504	0.0053
25.070	25.17	0.1991	0.9432	0.9419	0.0690
26.690	26.86	0.3174	0.9393	0.9376	0.0906
30.130	30.38	0.4130	0.9317	0.9262	0.2960
34.510	34.77	0.3753	0.9212	0.9128	0.4580
40.825	41.05	0.2748	0.9065	0.8948	0.6204
50.368	50.12	0.2468	0.8843	0.8680	0.9303
60.274	59.73	0.4533	0.8617	0.8523	0.5484
—	65.91	—	—	0.8484	—

TABLE V. 2-PROPANOL-CARBON TETRACHLORIDE

Mole fraction		Density	Viscosity in centipoises	Dielectric constant
2-Propanol x_1	CCl_4 x_2			
—	1.0000	1.5652	0.7942	2.205
0.1721	0.8279	1.4500	0.8910	2.84
0.3180	0.6820	1.3460	0.8742	3.84
0.4248	0.5752	1.2680	0.8710	5.09
0.5556	0.4444	1.1680	0.8828	7.04
0.6238	0.3762	1.1110	0.9042	8.60
0.8251	0.1749	0.9389	1.0300	13.10
0.8748	0.1252	0.8919	1.0510	14.30
0.9326	0.0674	0.8390	1.1090	15.68
0.9623	0.0377	0.8168	1.1350	16.27
1.0000	—	0.7736	1.5500	17.80

TABLE VI

$\sum_2 P_2x_2$	$P_{1,2}$	% deviation from the mean value	$\sum_2 L_2x_2$	$L_{1\,2}$	% deviation from the mean value
—	28.66	—	—	0.2865	—
34.66	36.13	2.077	0.3832	0.3802	0.393
40.19	44.79	5.413	0.4654	0.4863	2.196
44.20	51.87	7.984	0.5252	0.5769	4.690
49.13	57.66	7.989	0.5988	0.6680	5.463
51.69	61.49	8.660	0.6367	0.7169	5.926
59.29	65.24	4.779	0.7499	0.8013	3.313
61.15	65.69	3.582	0.7777	0.8160	2.403
63.36	65.73	1.836	0.8105	0.8305	1.219
64.48	65.12	0.491	0.8272	0.8358	0.517
—	65.91	—	—	0.8484	—

Experimental

Preparation of solutions, measurements of dielectric constant, density and viscosity were done as given in our previous paper (loc. cit., this bulletin).

Purification of the Components.—E. Merck's purest 2-propanol was refluxed[5,6] with an excess of freshly burnt calcium oxide and distilled. The distillate was dried over small pieces of magnesium ribbon and fractionally distilled. The fraction boiling at 82.4°C was collected and stored in a pyrex bottle. E. Merck's pro analysi carbon tetrachloride was distilled, the distillate boiling at 76.8°C was collected and stored in a Pyrex bottle. Conductivity water was distilled once more in a Pyrex outfit and this was preserved free from carbon dioxide. A dielectric constant check was made now and then. This was used throughout the investigation.

All the experiments were performed at 35°C. Results obtained are given in Tables I to VI.

Discussion

In our previous publication in this bulletin[4] on the ternary system 1-propanol-water-toluene we had derived the equation

$$\sum_k L_k x_k = L_{1,2\ldots k} \qquad (1)$$

where L_k is the volume polarization of the k-th component, $L_{1,2\ldots k}$, that of the mixture of k components and x_k, the mole fraction. This derivation was made on the usual assumption of isomegethic solutions as done in some theories of solutions which means that

$$\bar{v}_1 = \bar{v}_2 = \cdots\cdots = \bar{v}_k \qquad (2)$$

On this assumption,

$$V_k = \frac{v_k}{\sum v_k} = \frac{n_k \cdot \bar{v}_k}{\sum n_k \cdot \bar{v}_k} = \frac{n_k}{\sum n_k} = x_k$$

But the above assumption 2 is not correct with real solutions. We rarely meet with solutions wherein the molecules of the components have the same molar volume. We shall now consider the consequences of this assumption.

Turning to the experimental values, Table II shows that Eq. 1 holds excellently well at the point of disappearance of the phase boundary, whereas the well known equation.

$$\sum_k P_k \cdot x_k = P_{1,2\ldots k} \qquad (3)$$

fails thoroughly.

5) A. I. Vogel, "Practical Organic Chemistry", Longmans, 2nd Ed., London (1951), p. 168.
6) A. A. Maryott, *J. Am. Chem. Soc.*, **63**, 3079 (1941).

Comparison of Tables IV and VI shows that in the case of 2-propanol–water system both Eq. 1 and 3 hold excellently, whereas with 2-propanol–carbon tetrachloride system both the Eq. 1 and 3 are inapplicable. Akerlöf[7] determined the dielectric constants of mixtures of 2-propanol–water at 25°C. Our data in Table III were collected at 35°C.

In this laboratory[8] the general observation made was that in about thirteen ternary systems investigated so far, Eq. 3 fails thoroughly while Eq. 1 succeeds just at the point of disappearance of the phase boundary. Further in polar-polar binary mixtures both Eqs. 1 and 3 are applicable, whereas in polar-nonpolar binary combinations both Eqs. 1 and 3 fail. From these observations one conclusion can be drawn, that Eq. 1 is in now way better than Eq. 3 in general but the former seems to be holding excellently at the transition of disappearance of the phase boundary.

We have pointed out above that the derivation of Eq. 1 assumes that the molar volumes of the participating species of molecules must be the same, which is not really so, as far as the three components 2-propanol, water and carbon tetrachloride are concerned. Even then, if Eq. 1 should hold good specially at the transition of disappearance of the phase boundary, one has to conclude that at the transition when the two phases should disappear, conversely one should obtain the condition that the molar volumes of the different species of molecules must be the same. That means condition 2 is satisfied at the transition. This may perhaps mean that for two phases to become homogeneous condition 2 is to be satisfied.

Let us examine the implication of condition 2 being satisfied at the transition of the disappearance of the phase boundary. Usually we obtain the molar volume of a substance by dividing the molecular weight by the macroscopic bulk density. The molar volume thus obtained is actually due to the molecules as well as the voids. Obviously such a computation is no indication of the actual size of the molecules. Molar volume thus obtained may be written as $(V_{ma}+\phi_v)$, where V_{ma} is the actual volume due to the molecules and ϕ_v that due to the voids. In this context, if Eq. 1 holds good at the transition of the disappearance of the phase boundary, by converse the condition

$$(V_{ma}+\phi_v)_1=(V_{ma}+\phi_v)_2=(V_{ma}+\phi_v)_3 \quad (4)$$

is valid. Of course ϕ_v is a characteristic constant for a given liquid at a particular temperature. In other words satisfaction of condition 4 seems to be a precondition for liquid-liquid miscibility. Relation 4 seems to imply that just at the transition when a phase boundary disappears to form a homogeneous system, there seems to be occurring an equipartition of space by the different species of molecules, irrespective of their sizes, constituting the homogeneous system resulting from the disappearance of the phase boundary. For a successful theory of liquid–liquid miscibility the future seems to revolve on a thorough understanding of the ϕ_v factor in Eq. 4 in all its qualitative and quantitative aspects.

In the binary system 2-propanol-carbon tetrachloride the viscosity variation is anomalous. A plot of viscosity against mole per cent of 2-propanol shown in the graph exhibits a minimum at about 45 mole per cent of 2-propanol. Sugden[9] explained a similar phenomenon of negative viscosity in aqueous solutions as due to the strong dipole action of one of the constituents in the solution having the effect of depolymerizing the associated molecules of the other constituent entailing in a decrease of viscosity. But in this binary system carbon tetrachloride molecule is not a dipole. Sometimes a shortening of the length of the associated polymers is given as an explanation for lowering of viscosity. But then this presupposes a length of the associated polymer of the alcohol more than that due to two molecules. Of course, we can not assume a long chain formation of a compound between 2-propanol and carbon tetrachloride. The situation, therefore, leaves us in doubt as to what is the causative factor for such a decrease in viscosity.

Summary

To understand why a heterogeneous system of two immiscible liquids so exists without mixing we have made a new approach of studying the physical properties of the system just at the transition of the disappearance of the phase

7) G. Akerlöf, ibid., **54**, 4125 (1932).
8) K. M. Somasundaram, Ph. D. thesis, Annamalai University (1958).
9) J. N. Sugden, *J. Chem. Soc.*, **1926**, 183.

boundary after the addition of an optimum amount of a third component which is freely miscible with the two heterogeneous components thus resulting in the formation of a ternary system. At the transition of the disappearance of the phase boundary we have found that $\sum_3 L_3 x_3 = L_{1,2,3}$, wherein L represents volume polarization and x the mole fraction, holds good. The implications of the validity of the above equation have been discussed.

Physico-Chemical Laboratory
Annamalai University
Annamalainagar
South India

*Stereoregular Polymers. II. Polymerization of Alkenyltrimethylsilanes with Ziegler Catalyst**

By Shunsuke MURAHASHI, Shun'ichi NOZAKURA and Masao SUMI

(Received November 17, 1958)

Isotactic polymers of normal α-olefins have been known to have a maximum melting point at polypropylene (165°C), a minimum value at polyhexene-1 (−55°C), and after that show a gradual increase of melting points with the higher members[1,2]. On the other hand, isotactic polymers of branched α-olefins, which are shown in Table I by the general formulae II and III, have considerably higher melting points than those of the corresponding polymers of normal olefins.

The present study was undertaken to see if (i) the polymerization of alkenyltrimethylsilanes with Ziegler catalyst could lead to crystalline polymers and (ii) the similar melting behaviors could be expected in the case of polyalkenyltrimethylsilane having the same structure of monomer as type III of branched olefins.

A survey of the literature of the subject reveals that the polymers of alkenyltrimethylsilanes hitherto obtained are all liquid polymers of low molecular weight. Kanazashi[3] studied the polymerization of vinyltrimethylsilane with peroxide catalysts at 120°C and with Friedel-Crafts catalysts at 150°C, and obtained oily polymer in the former case and no polymer in the latter case. Polymerization of allyltrimethylsilane was attempted by Sommer[4] with Friedel-Crafts catalysts and also by Petrov[5] and Polyakova[6] at 130°C under a high pressure in the presence of peroxide catalysts. However, in both the cases the product was viscous liquid polymers. Polymerization of 3-butenyltrimethylsilane was also carried out by the latter author[6] to yield only a viscous liquid.

The present authors have prepared three alkenyltrimethylsilanes of the general formula $CH_2=CH(CH_2)_nSi(CH_3)_3$ ($n=0, 1$ and 2), i. e., vinyl-, allyl-, and 3-butenyltrimethylsilane, and subjected them to polymerization by means of Ziegler catalyst. It was found from the experiments that the alkenyltrimethylsilanes could polymerize to high polymeric products having high melting points and, furthermore, the polymers were proved to be highly crystalline by X-ray investigation**.

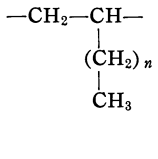
Polymerization. — Polymerization was carried out in *n*-heptane in the presence of Ziegler catalyst, that is, triethylaluminum and titanium tetrachloride. Considering the question from the results of the preceding paper[7], a method which had given a good yield of isotactic polystyrene was adopted in the present study;

* Presented at the 11th Meeting of Chem. Soc. of Japan in Tokyo, April 4, 1958. A brief description of this work was published in *Annual Report of the Institute of Fiber Research (Japan)* (*Sen'ikagaku Kenkyusho Nenpo*), 11, 23 (1958).

1) F. P. Reding, *J. Polymer Sci.*, **21**, 547 (1956).
2) G. Natta, *Angew. Chem.*, **68**, 393 (1956).
3) M. Kanazashi, This Bulletin, **28**, 44 (1955).
4) L. H. Sommer, L. J. Tyler, F. C. Whitmore, *J. Am. Chem. Soc.*, **70**, 2872 (1948).
5) A. D. Petrov et al., *Doklady Akad. Nauk S. S. S. R.*, **99**, 785 (1954).
6) A. M. Polyakova, et al., *Izvest. Akad. Nauk S. S. S. R., Otdel Khim. Nauk*, **1956**, 978.

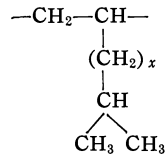
** Quite recently Natta and his collaborators have presented a letter and we have learned that they succeeded to prepare the crystalline polymers of allylsilane and of allyltrimethylsilane. G. Natta et al., *J. Polymer Sci.*, **31**, 181 (1958).

TABLE I. MELTING POINTS OF ISOTACTIC POLY-α-OLEFINS



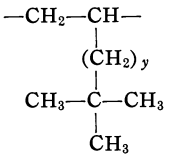
(I)

n	m. p., °C
0	165, 165*
1	128, 120*
2	80, 70*
3	−55*
4	−40*
5	−38*
9	45*
15	70*



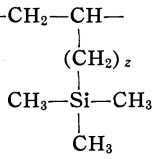
(II)

x	m. p., °C
0	245, 300*
1	205, 235*
2	130



(III)

y	m. p., °C
1	320



(IV)

z	m. p., °C
0	340
1	258
2	206

The values with asterisks are reported by Reding[1] and the others except the type IV are reported by Natta[2]. The values of type IV are presented by the present authors.

TABLE II. POLYMERIZATION OF ALKENYLTRIMETHYLSILANES WITH ZIEGLER CATALYSTS AT 70°C[a]

$AlEt_3$, g.	$TiCl_4$, g.	Monomer	Wt., g.	Polymn. time, hr.	Conversion, %
0.66	0.47	Vinyltrimethylsilane	2.77	5.5	2.4
0.44	0.27	Allyltrimethylsilane	5.54	9.0	30.2
0.34	0.23	3-Butenyltrimethylsilane	2.76	6.0	44.6

a) Twenty ml. of *n*-heptane were used as a solvent in each run.

TABLE III. SEPARATION OF CRYSTALLINE POLYMERS FROM CRUDE POLYMERS

Polymer	Extracting solvent	Fraction, %	Analysis of fractions C, % Found	C, % Calcd.	H, % Found	H, % Calcd.	Si, % Found	Si, % Calcd.
Polyvinyltrimethylsilane	Hot toluene	Extract, 44	80.26	85.6[a]	12.49	14.4[a]		
		Residue, 55	58.94	59.91	11.83	12.07	29	28.02
Polyallyltrimethylsilane	Toluene	Extract, 23	64.89	63.14	12.70	12.69	23.03	24.59
		Residue, 72	63.70		12.43		24.19	
Poly-3-butenyltrimethylsilane	Hot ether	Extract, 26	65.93	65.57	12.48	12.49	21.20	21.90
		Residue, 70	65.90		12.66		21.47	

a) Calcd. for $(C_2H_4)_n$, polyethylene.

that is, the catalysts were prepared without stirring and polymerizations were carried out also without stirring.

The conversions of both allyl- and 3-butenyltrimethylsilane were moderately high, but the conversion of vinyltrimethylsilane was very low (Table II).

Separation of Crystalline Polymers. — In the polymerizate of vinylmethylsilane, the existence of polyethylene was recognized from the analytical data and X-ray diffraction pattern. The separation of the polyethylene was effected by extraction with hot toluene. The occurrence of the polyethylene is considered to be due to the polymerization of ethylene which evolved during the preparition of the heterogeneous catalyst[7]. Polyvinyltrimethylsilane is insoluble in most organic solvents.

The amorphous polymer in the polymerizate of allyltrimethylsilane could be separated from the crystalline part by extraction with toluene. It was found that the crystalline part is soluble only in hot high-boiling solvents such as α-methylnaphthalene and dioctylphthalate.

In the case of 3-butenyltrimethylsilane, the separation of amorphous polymer was effected by hot extraction with ether, and also the extraction with cold *n*-heptane was found to be effective, wherein the

7) S. Murahashi, S. Nozakura, M. Sumi and K. Hatada, This Bulletin, in press.

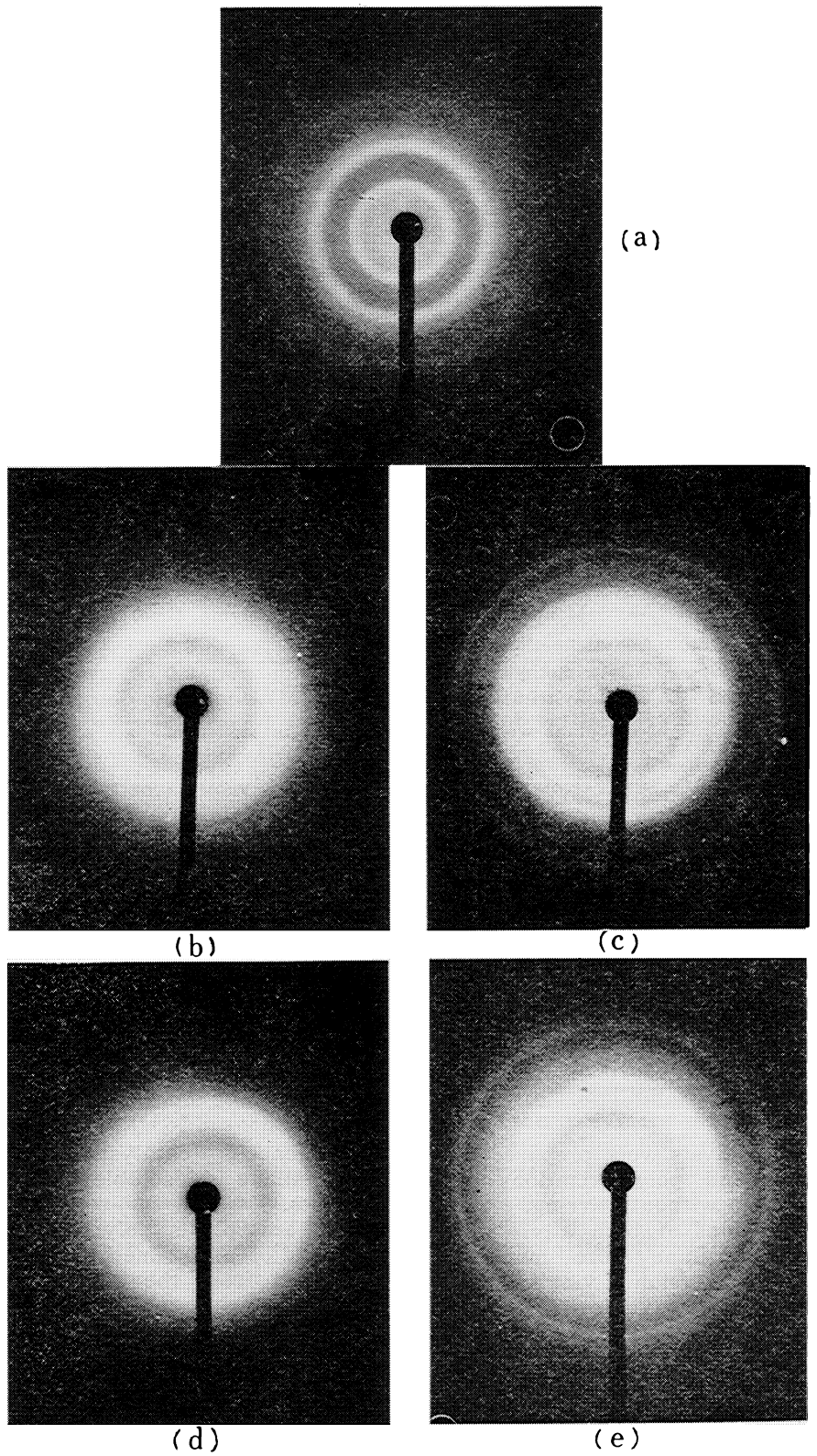


Fig. 1. X-ray diffraction patterns of polyalkenylsilanes.
(a) Polyvinyltrimethylsilane, the insoluble part in hot toluene.
(b) Polyallyltrimethylsilane, the soluble part in toluene.
(c) Polyallyltrimethylsilane, the insoluble part in toluene.
(d) Poly-3-butenyltrimethylsilane, the soluble part in hot ether.
(e) Poly-3-butenyltrimethylsilane, the insoluble part in hot ether.

TABLE IV. SOME PROPERTIES OF POLYALKENYLTRIMETHYLSILANES

Polymer		m. p., °C	*Tg*, °C	Density[a]	Appearance
Polyvinyltrimethylsilane		340[b]	—	0.95	White powder
Polyallyltrimethylsilane	amorph.	—	114	—	Soft solid
	cryst.	258	—	0.895	Hard and brittle
Poly-3-butenyltrimethylsilane	amorph.	—	132	—	Soft solid
	cryst.	206	—	0.889	Hard and brittle

a) Measured at room temperature by flotation method.
b) Upon being heated on a free flame in a nitrogen atmosphere the polymer decomposed to a volatile liquid.

crystalline part was insoluble. It was found to be soluble in decalin and hot tetralin. The experimental results of extraction and the analytical data of both the amorphous and crystalline fractions were summarized in Table III.

Physical Properties.—The X-ray photograph of the extraction residue of polyvinyltrimethylsilane showed a sharp Debye reflection, indicating the highly crystalline nature of the polymer. The photographs of the fractions of polyvinyl-, polyallyl-, and poly-3-butenyltrimethylsilane were presented in Fig. 1. In all the cases the residual part of solvent extraction showed marked crystalline patterns, while the extracts showed only minor extents of crystallinity. From the crystalline part of poly-3-butenyltrimethylsilane an extruded filament was obtained, which could be drawn at 100°C to several times of its original length, and gave a fine X-ray fiber diagram. From the analysis of the fiber diagram, a helical structure containing three monomeric units per identity period was established as follows***.

Rhombic $\begin{cases} a=10.97\ \text{Å} \\ b=20.02\ \text{Å} \\ c=6.46\ \text{Å (fiber axis)} \end{cases}$

No. of monomeric unit in unit cell=6

ρ(X-ray)=0.902 g./cm^3

ρ(obsd.)=0.889 g./cm^3

The crystalline polymers of other monomers than 3-butenyltrimethylsilane considered to be isotactic by analogy to the case of poly-3-butenyltrimethylsilane, but their fiber diagrams could not be obtained because of the difficulty of drawing.

Melting points and glass transition temperatures were determined dilatometrically on the amorphous as well as the crystalline parts of the polymers. The results and other properties are shown together in Table IV. As was expected, the melting points of the crystalline parts are very high in all cases and the polymer with the larger branch has the lower melting points. Particularly, the first member of this series, polyvinyltrimethylsilane has an extremely high melting point and was completely insoluble in all organic solvents examined.

Experimental

Monomers. — Vinyltrimethylsilane was synthesized through two different ways. One is the methylation of vinyltrichlorosilane by methylmagnesium bromide[8]. Refluxing the ethereal reaction mixture for 6 hr. gave 58% of the product, b. p. 55.0~55.2°C. The other way is the Wurtz-Wittig's reaction between trimethylchlorosilane and vinylchloride[9]. The yield was 55.6% based on trimethylchlorosilane used, b. p. 55.0~55.2°C.

Allyltrimethylsilane was also synthesized through two alternating methods. One is the methylation of allyltrichlorosilane**** by methylmagnesium bromide[10] and the other is the reaction of allylmagnesium bromide on trimethylchlorosilane[5]. The former yielded 53% of allyltrimethylsilane calculated from allyltrichlorosilane used and the latter yielded only 19.3% of the product after refluxing the ethereal solution for 8.5 hr.

3-Butenyltrimethylsilane was synthesized according to Petrov's method: that is the reaction between allylbromide and trimethylsilylmethylmagnesium chloride[5]. After refluxing the ether solution for 5 hr., 35.2% of the product was obtained, b. p. 118.5~111.7°C.

Materials.—Triethylaluminum was the product of Mitsui Chem. Ind. Co. Thirty percent solution in *n*-heptane was prepared in a modified Schlenk's apparatus and separated in small portions into sealed ampoules.

*** Details of the structural annalysis of the polymer will be published elsewhere by Mr. Y. Chatani of Nitta's laboratory. We are very grateful to him for the X-ray data.

8) R. Nagel and H. W. Post, *J. Org. Chem.*, 17, 1379 (1952).
9) M. Kanazashi, This Bulletin, 26, 493 (1953).
**** Allyltrichlorosilane was kindly offered by Dr. R. Okawara at Faculty of Engineering, Osaka University.
10) C. A. Burkhard, *J. Am. Chem. Soc.*, 72, 1078 (1950).

Titanium tetrachloride was the product of Osaka Titanium Co. and 21% solution in *n*-heptane was used.

n-Heptane was purified by shaking with fuming sulfuric acid, washing with water and aqueous sodium hydroxide, and was dried over calcium chloride, distilled and stored over sodium chips.

Polymerization. — Polymerization was carried out in the same apparatus as in the preceding paper[7]. The solution of $AlEt_3$ was added first to *n*-heptane and mixed thoroughly, and the solution of $TiCl_4$ was dropped slowy along the wall of the vessel without stirring. The solid brown mass was observed to form at the bottom of the flask. Finally the monomer was added and the polymerization was carried out without stirring.

Polymerization was stopped by adding 2 ml. of methanol and 0.3 ml. of concentrated hydrochroric acid, and the reaction mixture was poured onto about 100 ml. of methanol. After being kept overnight, the polymer was collected and washed thoroughly with methanol. The results of polymerization were given in Table II.

Separation of Crystalline Polymers from Crude Products. — When the crude polyvinyltrimethylsilane was extracted with hot toluene, a precipitate was obtained from the cooled extract. The precipitate was ascertained to be polyethylene from the analytical data and X-ray powder pattern. The insoluble part was nearly pure polyvinyltrimethylsilane.

Crude polyallyltrimethylsilane was refluxed gently with a large volume of toluene for several hours. After being cooled, the insoluble part was separated from the solution by a centrifuge. The intrinsic viscosity of the amorphous part in toluene was 0.087 at 30°C.

In the case of poly-3-butenyltrimethylsilane, the separation was effected by hot extraction with ether using a modified Soxhlet apparatus. The separation could also be done by cooling the hot solution of the crude polymer in *n*-heptane; only the crystalline polymer was precipitated when being cooled, while the amorphous polymer still remained in solution. Intrinsic viscosities of the amorphous and the crystalline part in decalin were 0.169 and 1.21 at 30°C, respectively.

Analysis of Silicon. — Analysis of silicon in the polymers was carried out by wet digestion using fuming sulfuric acid in a platinum crucible. The ignited silica was ascertained by treating with 60% hydrofluoric acid.

Properties. — Melting points and glass transition temperatures were determined dilatometrically. The polymer was melted in vacuum to form a small rod prior to measurement.

Density was measured by the flotation method at room temperature using the mixtures of carbon tetrachloride and alcohol.

Summary

Vinyl-(I), allyl-(II), and 3-butenyl-trimethylsilane(III) were polymerized at 70°C in *n*-heptane with the heterogeneous catalyst of Ziegler's type. The monomer I gave only a small yield of polymer, while the monomers II and III gave moderate amounts of polymers.

The amorphous and crystalline polymers of these monomers were separated by extraction with appropriate solvents. As regards the crystalline polymers, solubility property, density, dilatometrical melting point, and X-ray spectra were described. Glass transition temperatures of the amorphous polymers are also determined.

The authors wish to thank Mitsui Chemical Industry Co. for the supply of triethyltitanium aluminum and Osaka Titanium Co. for tetrachloride.

Department of Chemistry
Faculty of Science
Osaka University
Kita-ku, Osaka

Absorption Spectra of Dyes. III[1]. *On the Composition of Complexes Formed in Mixtures of Chlorazol Sky Blue FF and p-Nitroaniline→γ Acid in Aqueous Solution**

By Teruaki KOBAYASHI, Yoshié TANIZAKI and Noboru ANDO

(Received November 22, 1958)

The fact that complexes are formed between some kinds of dyes in aqueous solution has been revealed by means of spectroscopic measurements[2-4], and the mixtures of some direct dyes have been measured qualitatively in order to investigate the composition of the complexes formed[3,4].

The authors reported in the previous paper[1] that the mixtures of Chlorazol Sky Blue FF and some acid dyes, *p*-X-aniline→γ acid (X=H, CH_3, OCH_3, Cl or NO_2), did not show additive spectra in aqueous solution at room temperature, and that, of these mixtures, a pair of Chlorazol Sky Blue FF and *p*-nitroaniline →γ acid underwent the greatest change in spectrum. In the present paper the authors selected the combination of Chlorazol Sky Blue FF with *p*-nitroaniline→γ acid and investigated its spectrum at 620 mμ where the most remarkable change was seen in the whole region measured, in order to obtain some information about the composition of the complexes formed.

Experimental

Materials.—All the dyes used are the same as those used in the previous paper[1].

Preparation of Samples.—The dye solutions were prepared by using conductivity water whose specific conductivity was about 3.5×10^{-7} mho. All of the concentrations were determined by weight.

Absorption Spectra.—All the absorption spectra of the dyes in aqueous solution were measured by means of the Shimadzu QB-50 or QR-50 spectrophotometer at room temperature. Absorption cells were about 0.2 to 5 cm. thick.

Results

Hereafter Sky Blue will stand for Chlorazol Sky Blue FF, and NO_2-α for the acid dye made by coupling diazotized *p*-nitroaniline with γ acid in acid, and NO_2-β for the same in alkali.

It has already been shown[1] that the absorption spectrum of the mixture of Sky Blue and NO_2-α or NO_2-β in aqueous solution does not coincide with the sum of the spectra of individual dye, and this non-additivity is the most remarkable in the neighborhood of 620 mμ in wavelength. This spectral change is characterized by a marked decrease in optical density, with a slight shift of absorption maxima to longer wavelengths. For example, the absorption spectra of solutions containing

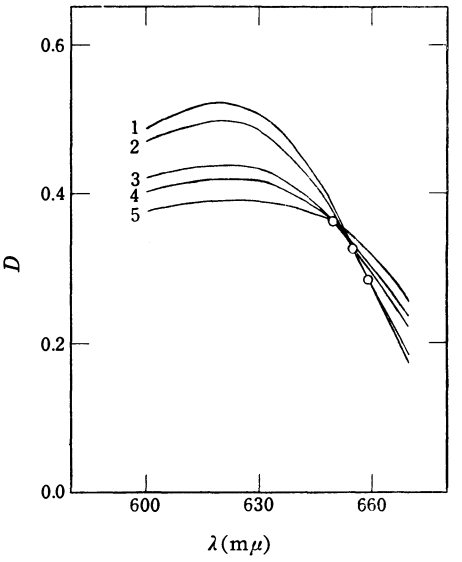


Fig. 1. Absorption spectra of mixtures of Sky Blue and NO_2-α in aqueous solution at room temperature. The concentration of Sky Blue is 1.41×10^{-5} mol./l., and that of NO_2-α is $1=2.72\times10^{-6}$, $2=6.98\times10^{-6}$, $3=2.11\times10^{-5}$, $4=3.51\times10^{-5}$ and $5=8.36\times10^{-5}$ mol./l. The absorption of NO_2-α alone is subtracted from each curve.

1) Part II of this series, Y. Tanizaki, T. Kobayashi and N. Ando, This Bulletin, **32**, 119 (1959).

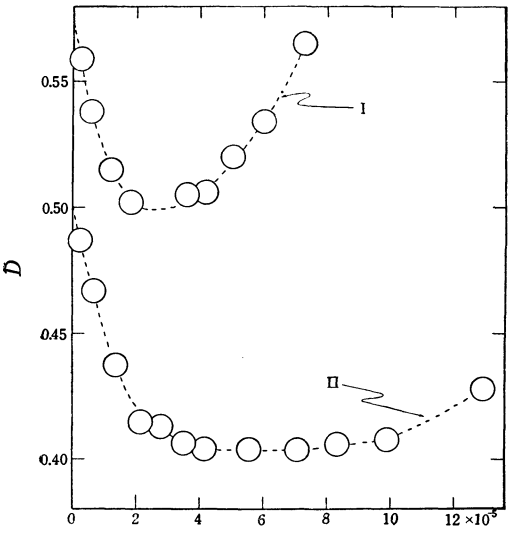
* This was represented before the 11th Annual Meeting of the Chemical Society of Japan, April 1958.

2) S. M. Neale and W. A. Stringfellow, *J. Soc. Dyers Col.*, **59**, 241 (1943).

3) D. R. Lemin and T. Vickerstaff, *Trans. Faraday Soc.*, **43**, 491 (1947).

4) A. N. Derbyshire and R. H. Peters, *J. Soc. Dyers Col.*, **72**, 268 (1956).

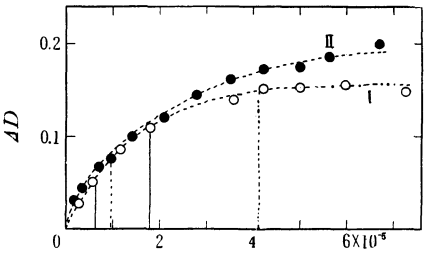
a given amount of Sky Blue and different amounts of NO_2-α are illustrated in Fig. 1, in which each absorption of NO_2-α alone is subtracted from that of the corresponding mixture. The figure shows that the spectra obviously indicate no isobestic point and the intersections of the adjacent curves are gradually shifted to shorter wavelengths. Therefore, it is clear that the formation of only a 1:1 complex does not adequately explain the data over the whole concentration range measured. Plotting the observed optical density, D, of this mixture at 620 mμ in relation to the concentration of NO_2-α, we obtain the curves as shown in Fig. 2, where the concentrations of Sky Blue indicated by the curves I and II are 6.02×10^{-6} and 1.41×10^{-5} mol./l., respectively. Inspection of these curves shows that in either case the optical density decreases with the concentration of NO_2-α to the amount about four times as great as that of Sky Blue, and then increases with the further increase of NO_2-α. The same



[NO_2-α], mol./l.

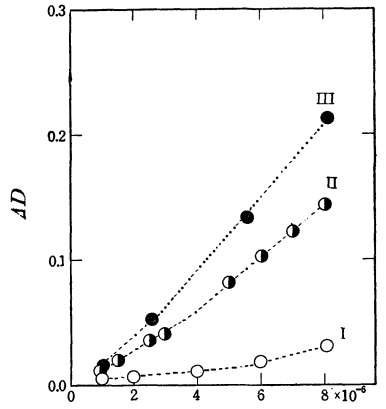
Fig. 2. The relation between the observed optical density of the combination of Sky Blue with NO_2-α and the concentration of NO_2-α at 620 mμ.

	The concentration of Sky Blue (mol./l.)	Cell (cm.)
I	6.02×10^{-6}	1
II	1.41×10^{-5}	0.399



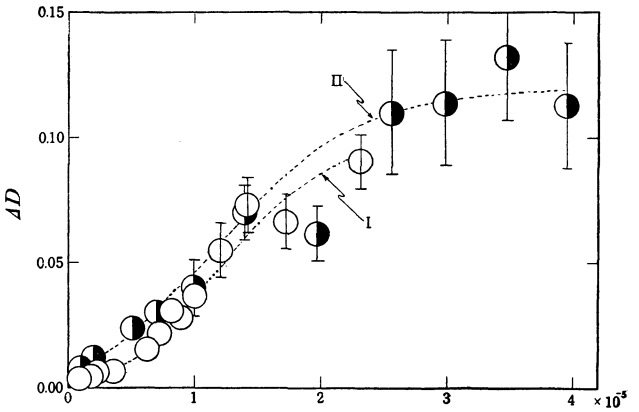
[A], mol./l.

Fig. 3. The relation between the difference in density, ΔD, and the concentrations of the acid dyes at 14~16°C. 1 cm. cell, λ=620 mμ. I: The mixture of NO_2-α and Sky Blue of 6.02×10^{-6} mol./l. II: The mixture of NO_2-β and Sky Blue of $7.15\times^{-6}$ mol./l.



[Blue], mol./l.

Fig. 4. The relation between the difference in density, ΔD, of the combination of Sky Blue with NO_2-α and the concentration of Sky Blue at 14~16°C. 1 cm. thick, λ=620 mμ. The concentration of NO_2-α is $I=2.00\times10^{-6}$, $II=2.02\times10^{-5}$ and $III=6.41\times10^{-5}$ mol./l.



[Blue], mol./l.

Fig. 5. The relation between the difference in density, ΔD, of the combination of Sky Blue with NO_2-α and the concentration of Sky Blue at 20~22°C. 1 cm. thick, λ=620 mμ. The concentration of NO_2-α is $I=4.0\times10^{-6}$ and $II=5.97\times10^{-6}$ mol./l.

tendency was also observed in the mixture of Sky Blue and NO_2-β.

Now, let us consider the difference between the sum of densities of its components and that of the mixture, ΔD. The relation between ΔD and the concentration of NO_2-α or of NO_2-β for a given concentration of Sky Blue is shown in Fig. 3. Both the curves in the figure curve upwards in the whole region and are inclined to approach certain values.

On the other hand, corresponding series of measurements were also carried out with mixtures containing various amounts of Sky Blue and given amounts of NO_2-α, and the results are shown in Figs. 4 and 5. Here celles were selected so as to make values of density fall in 0.3 to 0.7, but all the observed values were converted into those for 1 cm. cell. Similarly, Fig. 4 indicates the relation between ΔD at 620 mμ and the concentration of Sky Blue, where the curves I, II and III correspond to the concentration of NO_2-α 2.00×10^{-6}, 2.02×10^{-5} and 6.41×10^{-4} mol./l., respectively. Fig. 5 shows the same relation as that in Fig. 4, but the curves I and II correspond to the concentrations of NO_2-α, 4.0×10^{-6} and 5.97×10^{-6} mol./l. The optical densities were measured at about 21°C unlike the former case (at about 15°C). It will be seen at once from these curves that the higher the concentration of acid dye, the more remarkable the difference (Figs. 4 and 5), and that each curve bends downwards and upwards relatively to the low and high concentrations of Sky Blue, respectively (Fig. 5). Moreover, its point of inflexion moves towards a smaller value of concentration of Sky Blue in accordance with an increase in that of NO_2-α. These are distinctly different from the case of the curves of ΔD-concentration of NO_2-α or ΔD-concentration of NO_2-β.

Discussion

Lemin and Vickerstaff[3] showed by the spectroscopic measurement that Chlorazol Sky Blue FF and Durazol Red 2B formes a 1:1 complex in aqueous solution at room temperature. On the other hand, Derbyshire and Peters[4] examined the mixture of Chlorazol Sky Blue FF and Chrysophenine G in aqueous solution by the spectroscopic and calorimetric measurements and concluded that the formation of a 1:1 complex occurs to an appreciable extent even at 90°C, while higher complexes are formed to a certain extent in the presence of an excess of Chrysophenine G. Now, as for the present case, it was stated in the last section that the formation of a 1:1 complex does not explain all the spectral change, judging from the fact that the absorption spectra of solutions containing Sky Blue and NO_2-α showed no isosbestic point anywhere over the region measured (Fig. 1).

The fact that most direct dyes aggregate more or less in aqueous solution and that this aggregation is increased by adding neutral salts has been confirmed by measuring conductivity, absorption spectra, etc.[5] And it has also been recognized that the absorption spectrum of Sky Blue in aqueous solution does not obey Beer's law[3]. In addition, it can safely be considered as a matter of course that another dye added to Sky Blue solution exerts such a salt effect on this dye. In spite of these facts, however, it will be assumed here that the effect of the self-aggregation of the individual dye, which is induced by its increased concentration or by the addition of another dye, can be disregarded as compared with the effect of the complex formation, because the change in optical density of either component caused by increasing its concentration was of comparatively small magnitude compared with that produced by mixing**. Further the change in density of Sky Blue produced by the salt effect of the acid dyes can also be disregarded on account of the fact that an addition of sodium

TABLE I. VARIATION OF MOLAR EXTINCTION COEFFICIENT OF CHLORAZOL SKY BLUE FF IN AQUEOUS SOLUTION AT ROOM TEMPERATURE
1 cm. thick, $\lambda=620$ mμ

Solution (mol./l.)	Molar extinction coefficient
5.10×10^{-6}	$9.3_9\times10^4$
9.97×10^{-6}	9.5_2 〃
1.99×10^{-5}	9.3_0 〃
2.99×10^{-5}	9.3_0 〃
3.97×10^{-5}	9.1_1 〃

5) C. Robinson and J. L. Moilliet, *Proc. Roy. Soc.* (*London*), **A143**, 630 (1934); E. Valkó, *Trans. Faraday Soc.*, **31**, 230 (1935); C. Robinson, *Proc. Roy. Soc.* (*London*), **A148**, 681 (1935); N. Ando, *J. Chem. Soc. Japan, Pure Chem. Sec.* (*Nippon Kagaku Zasshi*), **64**, 1192, 1431 (1943); Y. Tanizaki and N. Ando, ibid., **78**, 343 (1957).

** The variation of the molar extinction coefficient of Sky Blue with respect to its concentration is shown in Table I. The measurement was carried out at 620 mμ over a range of concentration up to 3.97×10^{-5} mol./l. This table shows that the deviation from Beer's law is negligible. On the other hand, the aggregation of the acid dye itself, even if it occurs, could be disregarded, because its absorption at 620 mμ is very small.

TABLE II. OPTICAL DENSITY OF CHLORAZOL SKY BLUE FF (6.66×10^{-6} mol./l.) IN SODIUM CHLORIDE SOLUTION AT ROOM TEMPERATURE
1 cm. thick, $\lambda=620$ mμ

Sodium chloride (mol./l.)	Optical density
0	0.62_3
5.23×10^{-6}	0.61_6
1.00×10^{-5}	0.62_1
5.02×10^{-5}	0.61_6
1.02×10^{-4}	0.62_3

chloride to Sky Blue solution, in a range of concentrations comparable to those of the acid dyes used here, showed no significant change in optical density of Sky Blue***. Based on these assumptions, the observed result will be discussed as follows.

Now, in order to investigate the composition of the complexes formed, let us suppose m mol. of Sky Blue, B, and n mol. of any acid dye, A, have produced one mole of complex, C, in solution, that is,

$$m\mathrm{B} + n\mathrm{A} \rightleftarrows \mathrm{C}$$

According to the law of mass action, we can rewrite this as follows:

$$K=[\mathrm{C}]/([\mathrm{B}]-m[\mathrm{C}])^m([\mathrm{A}]-n[\mathrm{C}])^n \quad (1)$$

where [C], [B] and [A] mean the concentration in mol./l. of the complex and the initial concentrations of Sky Blue and the acid dye, respectively; and K is the equilibrium constant. When the absorption layer is regarded as unity, the observed optical density, D_{obs}, at any wavelength of a mixture will be

$$D_{obs}=([\mathrm{B}]-m[\mathrm{C}])\varepsilon_B + ([\mathrm{A}]-n[\mathrm{C}])\varepsilon_A + [\mathrm{C}]\varepsilon_C$$

where ε_B, ε_A and ε_C signify the molar extinction coefficients of Sky Blue, the acid dye and the complex, respectively. On the other hand, the sum of optical densities of the components, D_{sum}, is

$$D_{sum}=[\mathrm{B}]\varepsilon_B+[\mathrm{A}]\varepsilon_A$$

so the difference, ΔD, becomes

$$\Delta D=(m\varepsilon_B+n\varepsilon_A-\varepsilon_C)[\mathrm{C}] \quad (2)$$

Since the molar extinction coefficients may be assumed to be unvarying, ($m\varepsilon_B+n\varepsilon_A-\varepsilon_C$) can be described as a constant, k, provided that m and n are not changed in the entire concentration range of the dyes. As [C] is a function of [B] and [A] (Eq. 1), ΔD can be expressed as a function of them. According to the usual method[3], K and k can be determined. A calculated value of K by making use of the observed values of optical density indicated by full lines in Fig. 3 was 8.0×10^4 for the mixture of Sky Blue and NO_2-α when $m=n=1$. K values calculated by various observed optical densities were not so different from one another. Now, in order to investigate the relation between ΔD and the concentration of NO_2-α, curves were drawn in accordance with Eq. 2. The results are shown in Fig. 6, in which the full lines indicate the calculated ones

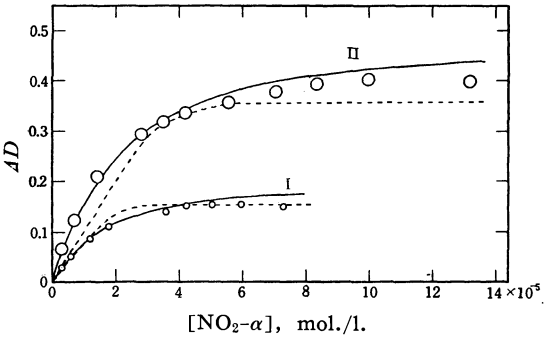


Fig. 6. The comparison between the differences observed and calculated by Eq. 2 for the mixtures of Sky Blue and NO_2-α at 15°C. 1 cm. thick, $\lambda=620$ mμ. The concentration of Sky Blue is I $=6.02\times10^{-6}$ and II $=1.41\times10^{-5}$ mol./l. The full lines signify calculated 1 : 1 curves ($K=8.0\times10^4$), the dotted lines 1 : 2 curves ($K=7.1\times10^{10}$) and the circles the corresponding observed values.

and the circles the corresponding observed values. From the figure it will be seen at once that the curves of $m=n=1$, namely of a 1 : 1 complex, suit the observed values comparatively well. A minute observation shows, however, that the calculated values are somewhat greater than the observed ones where the concentration of NO_2-α is higher than that of Sky Blue. As Derbyshire and Peters reported[4], while Chlorazol Sky Blue FF and Chrysophenine G form a 1 : 1 complex in aqueous solution, they form higher complexes richer in Chrysophenine G in presence of an excess of this dye. If this happens in the present case and higher complexes richer in the acid dye are formed, a curve of $m=1$ and $n=2$,

*** As is shown in Table II, the effect of sodium chloride on Sky Blue solution in a range of concentrations comparable to those of the acid dyes used here is not so great as can be observed, so we leave the salt effect by the acid dye out of consideration.

namely of a 1:2 complex, should fit the observed values better than the 1:1 curve in the higher concentration region of the acid dye. The 1:2 curves ($K=7.1\times10^{10}$ which was calculated by making use of the observed values of optical density shown by the dotted lines in Fig. 3) are indicated by the dotted lines in Fig. 6. These curves differ extremely from the observed ones in the region where the 1:1 curve was rather suitable, but they are more suitable in the higher concentration range of the acid dye where the 1:1 complex curve has not fitted well. These facts suggest that a 1:1 complex is formed first and then higher complexes richer in the acid dye are formed with an increase of its concentration. If this is the case, the region of low concentration of the acid dye in the mixtures containing a given amount of Sky Blue should correspond to that of high concentration of Sky Blue in the mixtures containing a given amount of the acid dye. Actually, the curves of ΔD-concentration of Sky Blue (Figs. 4 and 5) are obviously different in shape from the curves of ΔD-concentration of NO_2-α, and become similar to the 1:1 curve in a region of high concentration of Sky Blue. Probably all the experimental results would be explained by a combination of a 1:1, a 1:2 and other complexes, or by a combination of several complexes different in their compositions. Exactly the same result has been obtained in the mixture of Sky Blue and NO_2-β. It is concluded here that one kind of complex does not explain all the exprimental data, and the comparison between the calculated and observed curves shows that a 1:1 complex occurs to a greater extent over a range of relatively low concentration of acid dye and that higher complexes richer in the acid dye may be formed in the presence of an excess of it.

Summary

1. The change in spectrum at 620 mμ of the mixture of Chlorazol Sky Blue FF and *p*-nitroaniline→γ acid in aqueous solution was measured in detail at room temperature, by varying the concentration of the component dyes.

2. On the assumption that the spectral change is due to the complex formation, the composition of complexes was discussed by comparing the observed and the calculated difference in optical density.

3. It may be supposed that a 1:1 complex occurs to a great extent over a range of low concentration of *p*-nitroaniline→γ acid as compared with that of Chlorazol Sky Blue FF, and that higher complexes are formed in the presence of an excess of the acid dye.

Laboratory of Physical Chemistry
Tokyo Institute of Technology
Meguro-ku, Tokyo

Absorption Spectra of Dyes. IV[1]. *Absorption Spectra of Mixtures of Chlorazol Sky Blue FF and Dyes Prepared from Sulfanilic Acid and Cresidine*

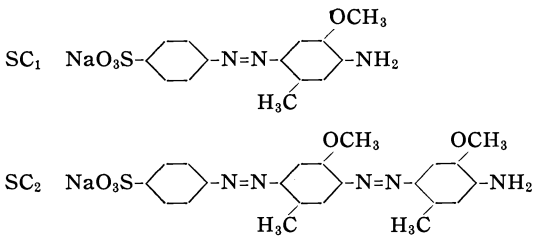
By Teruaki KOBAYASHI, Yoshié TANIZAKI and Noboru ANDO

(Received December 19, 1958)

In the previous papers the authors have reported that binary mixtures of Chlorazol Sky Blue FF and certain monoazo acid dyes in aqueous solution show non-additivity in absorption spectrum at room temperature, explained qualitatively the spectral change assuming the formation of loose complexes[2], and then discussed their compositions[1]. In the present paper, absorption spectra of the binary mixtures in aqueuos solution of Chlorazol Sky Blue FF, as the one component, and dyes prepared from sulfanilic and cresidine, as the other, were analyzed, and the result obtained was examined.

Experimental

Dyes.—Chlorazol Sky Blue FF (called Sky Blue) is the same as used before[1,2]. SC_1 and SC_2 will signify the dye obtained by coupling diazotized sulfanilic acid with cresidine and that obtained by coupling diazotized SC_1 with cresidine. Their structures are as follows:



Both of them are carefully prepared from purified intermediates. SC_1 was purified by the recrystallization from water and SC_2 by the Robinson and Mills' method until no change in spectrum was observed. It was noticed that the solubility of SC_2 in water is extremely dependent on pH, and that its flocculent precipitate was easily produced by carbon dioxide from the air. The dye solutions, therefore, were once heated in order to remove carbon dioxide.

Measurements of Absorption Spectra.—All the absorption spectra of the dyes in aqueous solution were measured by means of the Shimadzu QR-50 spectrophotometer at room temperature. Absorption cells used were 0.2, 0.5 and 1 cm. thick. All the experimental values were converted into those corresponding to 1 cm. cell.

Results

The absorption spectrum of a mixture of Sky Blue (7.44×10^{-6} mol./l.) and SC_1 (3.58×10^{-5} mol./l.) is shown by a full line in Fig. 1, together with each spectrum of Sky Blue (curve I) and of SC_1 (curve II). The sum (curve III) of curves I and II coincides completely with the observed one (curve IV) in the whole region measured. The additivity in spectrum, however, does not come into being in the mixtures containing a great excess of SC_1. The results are given in Fig. 2, where the dotted line shows the absorption spectrum of Sky Blue alone (7.42×10^{-6} mol./l.) and curves I and II those of mixtures containing Sky Blue and SC_1 49.4 and 137 times as much as Sky Blue, respectively. In this wavelength region, SC_1 does not absorb light. As this change in spectrum is similar to that of certain benzidine disazo dyes like Sky Blue caused by the salt effect[3], it is supposed that it may be due to the self-aggregation of Sky Blue. Then the variation in optical density at 620 mμ of Sky Blue (7.42×10^{-6} mol./l.) in sodium chloride solution was examined, in order to investigate whether or not the change

TABLE I. VARIATION OF OPTICAL DENSITY OF CHLORAZOL SKY BLUE FF (7.42×10^{-6} mol./l.) IN SODIUM CHLORIDE SOLUTION AT 27°C. 1 cm. cell, $\lambda=620$ mμ

Sodium chloride (mol./l.)	Ratio of sodium chloride to Sky Blue	Optical density
0	0	0.73_4
4.05×10^{-4}	54.6	0.73_1
1.01×10^{-3}	136	0.73_0
1.05×10^{-2}	1415	0.70_9

1) Part III of this series, T Kobayashi, Y Tanizaki and N. Ando, This Bulletin, **32**, 675 (1959).

2) Y. Tanizaki, T. Kobayashi and N. Ando, ibid., **32**, 119 (1959).

3) Y. Tanizaki and N. Ando, *J. Chem. Soc. Japan, Pure Chem. Sec.* (*Nippon Kagaku Zasshi*), **78**, 343 (1957).

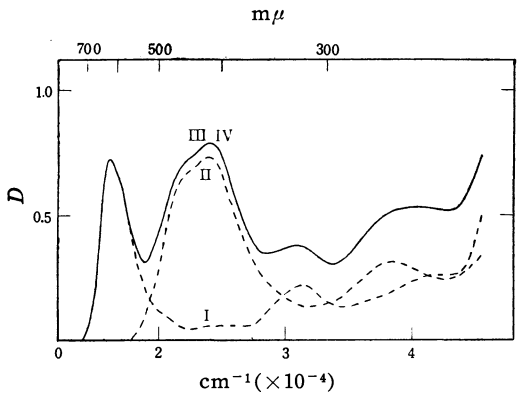


Fig. 1. Absorption spectra of Sky Blue, SC_1 and their mixture in aqueous solution at room temperature (27°C). 1 cm. cell.
I: Sky Blue (7.44×10^{-6} mol./l.)
II: SC_1 (3.58×10^{-5} mol./l.)
III: Sum of curves I and II
IV: Mixture

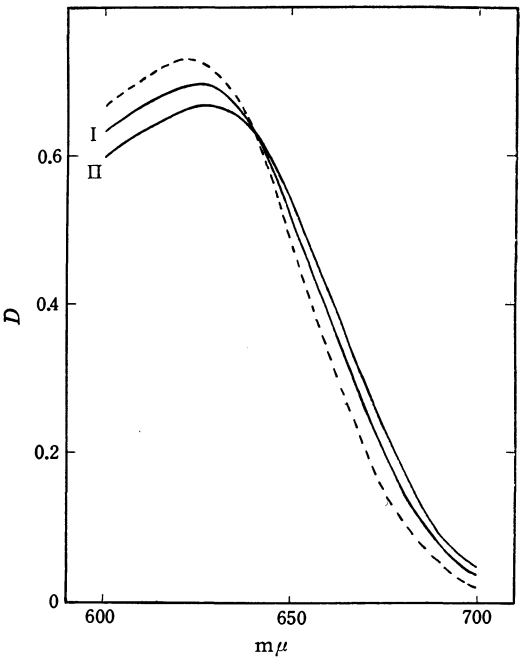


Fig. 2. Absorption spectra of mixtures of Sky Blue (7.42×10^{-6} mol./l.) and SC_1 in aqueous solution at room temperature (27°C). 1 cm. cell.
Dotted line: Sky Blue alone
I: The ratio of concentrations of Sky Blue and SC_1 is 49.4
II: The ratio is 137

is due to the salt effect of SC_1. The results are shown in Table I. It shows clearly that no significant departure from Beer's law is observed, even though the amount of sodium chloride becomes 140 times as much as that of Sky Blue. Therefore, we must consider that the spectral change shown in Fig. 2 is not due to the self-aggregation of Sky Blue caused by the salt effect of SC_1 added, but due to the interaction between the two dyes. It will be seen that the spectra pass through an isosbestic point at about 640 mμ, where the absorption of SC_1 does not appear (Fig. 1). This suggests that one Sky Blue molecule interacts with SC_1 molecules, or that $1:n$ complexes are formed. But the number n of SC_1 component in one complex molecule has not been known. These results mean that even if the additive spectrum appears in an equimolar or nearly equimolar mixture, the spectrum of the same mixture will often become non-additive with an increase of one component, and the interaction between the two components will occur.

The absorption spectrum of a mixture of Sky Blue and SC_2 is given in Fig. 3, where curves I and II show each absorption spectrum of Sky Blue and of SC_2, curve III the sum of them, and curve IV the observed one of the mixture. Inspection of them shows that the observed curve is weaker in intensity than the resultant curve both in the neighborhood of 620 mμ (the first band of Sky Blue) and at absorptions in the ultraviolet region, but stronger in the neighborhood of the first band of SC_2 (505 mμ).

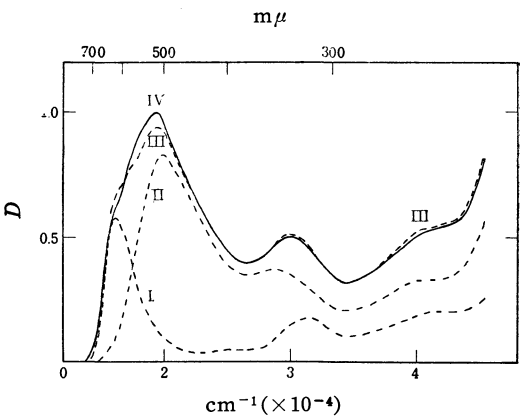


Fig. 3. Absorption spectra of Sky Blue, SC_2 and their mixture in aqueous solution at room temperature (30°C). 1 cm. cell.
I: Sky Blue (5.90×10^{-6} mol./l.)
II: SC_2 (3.01×10^{-5} mol./l.)
III: Sum of curves I and II
IV: Mixture

This spectral change was more systematically examined by varying the concentration of SC_2 and keeping that of Sky

Blue constant (5.90×10^{-6} mol./l.). The results are shown in Fig. 4, in which each absorption of SC_2 is subtracted from the corresponding observed curve. The curves in the figure pass through a well-defined isosbestic point at about 650 mμ; this means that one Sky Blue molecule interacts with a molecule or molecules of SC_2.

On the other hand, the relation between the concentration of SC_2 added and the

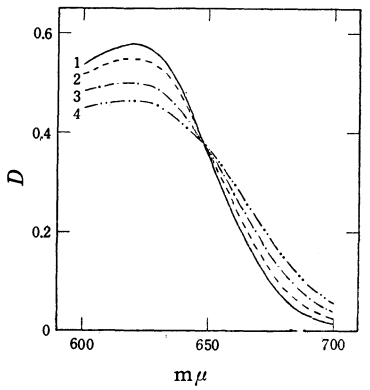


Fig. 4. Absorption spectra of mixtures of Sky Blue and SC_2 in aqueous solution at room temperature (30.5°C), where each absorption of SC_2 is subtracted from the corresponding mixture curve. 1 cm. cell. Concentration of SC_2 is 1: zero, 2: 6.08×10^{-6}, 3: 3.01×10^{-5} and 4: 1.20×10^{-4} mol./l. that of Sky Blue is 5.90×10^{-6} mol./l;

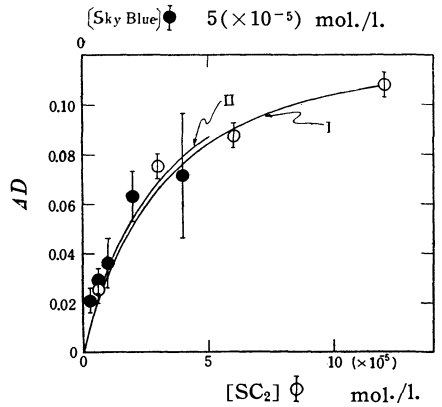


Fig. 5. The relation between the difference in density, ΔD, of the combination of Sky Blue with SC_2 and the concentration of SC_2 or of Sky Blue. 1 cm. cell, $\lambda=620$ mμ. $K=3.8\times10^4$ (at 30.5°C).
I: Calculated difference when the concentration of Sky Blue is constant (5.90×10^{-6} mol./l.); the white circles are corresponding observed values at 30.5°C.
II: Calculated difference when the concentration of SC_2 is constant (6.07×10^{-6} mol./l.); the black circles are representing observed values at 28.2°C.

difference between the sum of optical densities of the components and that of the mixture, ΔD, at 620 mμ is plotted by white circles in Fig. 5. Now, if a 1:1 complex is assumed to be formed in the solution, and if the mass action law is applied to it, an equilibrium constant, K, will be obtained by the method mentioned before[1]. Thus the obtained value of K was 3.8×10^4 at 30.5°C. Here were used the observed values of ΔD, when the concentrations of Sky Blue and of SC_2 are 5.90×10^{-6} mol./l. and up to 1.20×10^{-4} mol./l., respectively. Curve I in the figure was drawn by making use of this value of K. It will be seen at once from the figure that the observed values (white circles) well fit the calculated curve; this means the formation of a 1:1 complex. If a 1:1 complex is formed, the curve of ΔD should show the same feature when the concentration of Sky Blue is varied, while that of SC_2 is kept constant, because of the symmetry of the equation. The curve of ΔD-concentration of Sky Blue is also shown in Fig. 5, where the black circles denote the observed values and curve II the calculated. These two also well fit each other within an experimental error. Therefore, the formation of a 1:1 complex of Sky Blue and SC_2 would well explain all the results obtained.

The absorption spectrum of the 1:1 complex of Sky Blue and SC_2 will, therefore, be obtained experimentally by making use of the equilibrium constant*.

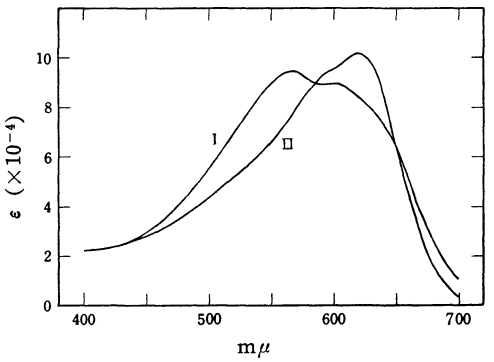


Fig. 6. Absorption spectrum of the 1:1 complex of Sky Blue and SC_2.
I: Complex
II: Sum of absorptions of the components (both 2.9×10^{-6} mol./l.)

* If the equilibrium constant is known, the concentration of the complex corresponding to given amounts of the components can be calculated and then that of the components free from the complex formation will be known. Therefore, the absorption of the complex will be obtained by subtracting absorptions of the free components from that of the mixture.

The absorption spectrum of the complex (curve I) obtained from the experimental results shown in Fig. 3 is indicated in Fig. 6, together with the sum of those of the components (curve II). The figure shows clearly that the absorption of the complex is weaker in intensity than that indicated by the resultant curve at the first absorption band of Sky Blue (620mμ), but stronger at that of SC_2.

Discussion

It has been reported before[1] that Sky Blue and certain monoazo acid dyes (*p*-nitroaniline $\rightarrow\gamma$ acid) form higher complexes richer in the acid dyes in presence of an excess of these dyes, when mixed in water[4]. Though SC_1 and *p*-nitroaniline $\rightarrow\gamma$ acid are both monoazo acid dyes, only the former shows an isosbestic point in spectra when mixed with Sky Blue (Fig. 2). It seems that such a difference has relation to the fact that the substantivity of dyes increases with the length of the conjugated double bonds chain connecting their auxochromes[5], and that at the same time they come to associate with themselves easily[6].

According to measurements of the conductivity of SC_1 and SC_2[6], the association of SC_1 with itself is not noticed over a range of concentrations $(3\sim60)\times10^{-4}$ mol./l., while the formation of ion-micelles of SC_2 is clearly observed. From these results, Ando considered, according to the substantivity theory, that the length of the conjugated double bonds was closely related to the aggregation of SC_1 and SC_2**. It has also been known that, of dyes with various substituents, similar to Congo Red in constitution, those which have the stronger substantivity show the greater spectral change caused by their association[3]. Therefore, though it is impossible to explain briefly the fact that a larger quantity is needed for SC_1 than for SC_2 to cause a change in spectrum when mixed with Sky Blue***, it may be said that this is partly due to the difference in the substantivity of SC_2 and of SC_1.

Derbyshire and Peters[7] obtained experimentally the absorption spectrum of a 1 : 1 complex of Sky Blue and Chrysophenine G. To be compared with the present result (Fig. 6, curve I), their spectra are shown in Fig. 7, in which curve I shows the absorption of the 1 : 1 complex and curve II the sum of those of the components. Inspection of these figures shows that the absorption of each mixture corresponding to the first band of the dye combined with Sky Blue shifts to longer wavelengths with an increase in intensity. On the other hand, the absorption corresponding to the peak of the first band of Sky Blue (620 mμ) shifts to longer wavelengths, with a peak getting more distinct, in the complex of Chrysophenine G, while it disappears in the complex of SC_2. Derbyshire and Peters[7] consider that Sky Blue and Chrysophenine G can approach in parallel with each other and form a complex, because while Sky Blue has its charged groups at the ends of the linear molecule, the corresponding groups of Chrysophenine G are near the centre, so the repulsion between them is small. On the other hand, if SC_2, which has its charged group at an end of the molecule, forms a complex in parallel with Sky Blue, it may be repelled by the charged groups of Sky Blue. The difference between the spectra of the two complexes and their stabilities may be related to the fact just mentioned. Further, the fact

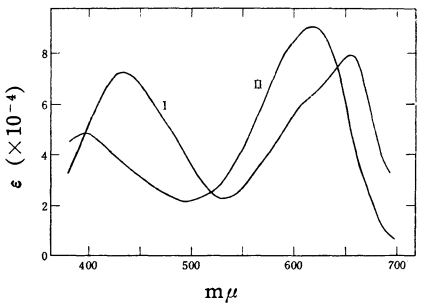


Fig. 7. Absorption spectrum of the 1 : 1 complex of Sky Blue and Chrysophenine G (quoted from the result of Derbyshire and Peters).
I: Complex
II: Sum of absorptions of the components

4) This fact has been recently confirmed by dyeing measurements from mixtures of the same pairs of dyes. [Y. Horiki, Y. Tanizaki and N. Ando, This Bulletin, to be published.]

5) E. Schirm, *J. prakt. Chem.*, **144**, 69 (1935).

6) N. Ando, *J. Chem. Soc. Japan, Pure Chem. Sec.* (*Nippon Kagaku Zasshi*), **64**, 1305 (1943).

** The number of sulfonic groups per molecular weight of SC_2 is smaller than that of SC_1, and the former is more insoluble in water. This may be one of the reason why SC_2 more easily associates with itself.

*** If a complex is formed from two dyes, the extent of the change in spectrum of the mixture also depends on wavelengths of corresponding absorptions of the component dyes and the relative direction of their transitions (Ref. 2).

7) A. N. Derbyshire and R. H. Petes, *J. Soc. Dyers Col.*, **72**, 268 (1956).

that the increasing order of length of the conjugated chain connecting the auxochromes is SC_2 <Sky Blue<Chrysophenine G may also be related to the difference between the spectra, according to the following reason. The first absorption band of a dye has close relation to the electron donating power of its auxochromes containing lone paired electrons[8], which are more easily affected by outer conditions than other π electrons under consideration. It will be seen that if both of the components approach in parallel with each other to form a complex, the auxochromes at both ends of Sky Blue get out of place from the π electron system of SC_2 or only one of them approaches it, though they draw near that of Chrysophenine G.

From the above discussion, it may be considered that the pair of Chrysophenine G and Sky Blue has a smaller intermolecular distance in a complex than that of SC_2 and Sky Blue. The amount of delocalization energy of π electrons between two components in a complex formed from molecules containing no lone pair electrons has been estimated[9]. If this idea can be applied to the present discussion, it will turn out that the pair of Chrysophenine G and Sky Blue is more stable than that of SC_2 and Sky Blue, and that the spectral change of the former is also larger; that is, in case of the former the electron transition corresponding to the first absorption band of Sky Blue will change more remarkably with larger intermolecular charge transfer (probably through auxochromes) than in case of the latter. Thus the character of the absorption spectra of the complexes can be explained qualitatively.

The above discussion will be applied to the difference between spectral characters of the pairs of SC_1 and Sky Blue and of SC_2 and Sky Blue.

8) J. Tanaka and S. Nagakura, *J. Chem. Soc. Japan, Pure Chem. Sec.* (*Nippon Kagaku Zasshi*), **78**, 1200 (1957).
9) K. E. Shuler, *J. Chem. Phys.*, **20**, 1865 (1952).

Summary

1. The absorption spectra of the binary mixtures in aqueous solution of Chlorazol Sky Blue FF and sulfanilic acid → cresidine and sulfanilic acid → cresidine → cresidine were measured at room temperature.

2. The mixture of Chlorazol Sky Blue FF and sulfanilic acid → cresidine shows the additive spectrum when the ratio of the two dyes is about 1:5 but the non-additive one when it is about 1:40. From this fact the authors pointed out that even if an equimolar or nearly equimolar mixture shows the additive spectrum, it often exhibits the additive one with a relative increase of one component, due to the interaction between the components. That the spectra of the mixture pass through an isosbestic point means that a Sky Blue molecule interacts with n molecules of sulfanilic acid → cresidine (n is unknown).

3. It was indicated that the mixture of Chlorazol Sky Blue FF and sulfanilic acid → cresidine → cresidine showed the non-additive spectrum, and that this was well explained by assuming the formation of a 1:1 complex over the range of concentrations measured.

4. The authors discussed qualitatively the characters of the spectra and the stability of these complexes, comparing them with the complex of Sky Blue and Chrysophenine G, etc.

The intermediates used were presented by the Sumitomo Kagaku Kogyo Co. Ltd. through Dr. S. Arikawa and Dr. M. Okazaki. The authors wish to express their gratitude to them.

Laboratory of Physical Chemistry
Tokyo Institute of Technology
Meguro-ku, Tokyo

The Volume Change on Neutralization of a Strong Acid with a Strong Base[1]

By Akira TSUJIOKA

(Received November 23, 1958)

A method of calculation has been proposed by which we may evaluate the changes of volume on neutralization of various acids and bases at a constant temperature. The values of volume change fraction on neutralization of hydrochloric acid with sodium hydroxide solution at 20°C have been calculated. These calculated values have shown a good agreement with the observed ones. We have, on the other hand, shown that the volume change fraction of the reaction between a strong acid and a strong base of equal concentrations is represented by a simple function of the initial concentration.

It was noticed in an early period that there is an expansion on the neutralization of a strong acid with a strong base[2], but there are only a few data[3]. In particular, there are few data regarding the volume change on neutralization of an acid and a base of unequal concentrations. No investigation has as yet been made to correlate quantitatively the change of volume with concentration. Therefore we devised a method of calculation by which still more data can easily be provided, and then derived the relationship between the volume change on neutralization and the concentration of an acid or a base.

Now, if the density of a salt solution produced by neutralization is obtained, the volume change which occurs in this case can readily be evaluated. Then we have evaluated the density of the salt solution from the density table. That is, the weight per cent concentration of the resulting salt solution can be evaluated from the initial concentrations, so the density of this solution may be obtained by interpolation from the density table. The densities of electrolyte solutions have been fully known at intervals of one or two per cent concentration, so this interpolation does not cause any appreciable errors, as will be dealt with later.

The method mentioned above can be applied to the neutralization not only of a strong acid and a strong base, but also of both weak electrolytes or a strong electrolyte and a weak one.

Calculations

In considering the volume changes on neutralization of various acids and bases, we shall deal with both 1-1 strong electrolytes. In the other cases, we may deal with them in the manner described below.

If V_a ml. of a C_a mol./l. acid (the density, d_a) is neutralized with V_b ml. of a C_b mol./l. solution of a base (the density, d_b) at constant temperature, the volume change can be calculated as follows.

The weight per cent concentration of the resulting salt solution, denoted by a, is represented by the equation,

$$a = M_s/10(d_a/C_a + d_b/C_b) \tag{1}$$

where M_s is the molecular weight of the salt. If the density of this solution is denoted by d_s, the apparent molar volume of the acid by Φ_a, that of the base by Φ_b and that of the salt by Φ_s, these apparent molar volumes are defined by the following equations, respectively.

$$\Phi_a = \{1000 - (1000d_a - C_aM_a)/d_w\}/C_a \tag{2}$$

$$\Phi_b = \{1000 - (1000d_b - C_bM_b)/d_w\}/C_b \tag{3}$$

$$\Phi_s = 1000(d_a/C_a + d_b/C_b)(1/d_s - 1/d_w) + M_s/d_w \tag{4}$$

where d_w is the density of water, M_a, the molecular weight of the acid and M_b, that of the base.

Then it may be presumed that the volume change on neutralization is due to the change in the apparent molar volume of the solute, so that the volume change denoted by ΔV ml. is given by

1) A part of this paper was presented at the 11th Annual Meeting of the Chemical Society of Japan, held in Tokyo in April, 1958.

2) J. R. Partington, "An Advanced Treatise on Physical Chemistry", Vol. 2, 1st Ed., Longmans, Green and Co., London (1951), p. 33.

3) J. D'Ans and E. Lax, "Taschenbuch für Chemiker und Physiker", 2nd Ed., Springer Verlag, Berlin (1949), p. 821; Landolt-Börnstein, "Physikalisch-Chemische Tabellen", Erg. B. II, Springer Verlag, Berlin (1931), p. 274.

$$\Delta V=(\Phi_s+\Phi_w-\Phi_a-\Phi_b)C_aV_a/1000 \quad (5)$$

where Φ_w is the apparent molar volume of water, equal to M_w/d_w (M_w is the molecular weight of water). In Eq. 5, ΔV has been defined as a positive value when there is an expansion in total volume.

On the other hand, ΔV may be directly represented by means of the equation,

$$\Delta V=(d_aV_a+d_bV_b)/d_s-(V_a+V_b) \quad (6)$$

We may choose between Eqs. 5 and 6 to evaluate ΔV, because substitution of Eqs. 2, 3 and 4 into Eq. 5 gives Eq. 6.

Neutralization at Equal Concentrations. —The equations by which we may evaluate the volume change on neutralization of a C mol./l. acid, which occupies a volume V ml., with a base of an equal concentration can be derived by replacing V_a and V_b in Eqs. 5 and 6 by V, and C_a and C_b in Eqs. 1—5 by C.

The weight per cent concentration of the resulting salt solution is obtained by

$$a^*=M_sC/10(d_a+d_b) \quad (7)$$

Therefore, in the case of neutralization of an acid with a base of equal concentration, the increase in total volume is

$$\Delta V^*=(\Phi_s^*+\Phi_w-\Phi_a-\Phi_b)CV/1000 \quad (8)$$

where

$$\Phi_s^*=1000(d_a+d_b)(1/d_s^*-1/d_w)/C+M_s/d_w$$

or by an alternative formula (using Eq. 6).

$$\Delta V^*=\{(d_a+d_b)/d_s^*-2\}V \quad (9)$$

The subscripts refer to salt, water, acid and base, respectively, and the asterisk indicates that the salt concentration is a^* %.

Then replacing $(\Delta V^*/2V)\times10^3$ by Ψ in Eqs. 8 and 9, we have

$$\Psi=(\Phi_s^*+\Phi_w-\Phi_a-\Phi_b)C/2 \quad (10)$$

$$\Psi=\{(d_a+d_b)/2d_s^*-1\}\times10^3 \quad (11)$$

Now we will for convenience' sake call Ψ, which represents the rate of change of the volume upon neutralization, "Volume Change Fraction". The numerical value of Ψ represents the change in the total volume observed on mixing the acid, which amounts to 500 ml., with an equi-volume of the base, of which the concentration is equal to that of the acid. The value of Ψ has the same sign as ΔV^*, so it is positive when the total volume expands on mixing the two solutions.

Results and Discussion

The values of volume change fraction on neutralization of a hydrochloric acid with a sodium hydroxide solution of equal concentration at 20°C have been calculated by the method mentioned in the previous section.

The weight per cent concentration of the resulting sodium chloride solution has been evaluated by Eq. 7, so the density of this solution has been obtained by interpolation from the density data of the "International Critical Tables"[4].

Therefore, the value of Ψ has been calculated by Eq. 11. The results obtained here are shown in Table I. In this table the values of the fifth column are those observed by Saslawsky et al.[5] and those in the last column are those calculated by Eq. 24, which will be derived later.

In Table II are shown volume changes

TABLE I. VOLUME CHANGE FRACTIONS ON NEUTRALIZATION OF HYDROCHLORIC ACID WITH SODIUM HYDROXIDE AT 20°C

Initial concn.	Final concn.	Density of NaCl. aq.	Volume change fraction		
C (mol./l.)	a^* (%)	d_s^*	$\Psi_{calc.}$	$\Psi_{obs.}$	$\Psi_{eq.(24)}$
1	2.841	1.01849	10.02	9.8	9.9
2	5.530	1.03787	18.16	18.0	18.2
3	8.093	1.05658	25.37	25.1	25.5
4	10.544	1.07475	31.74	31.8	31.9
5	12.895	1.09246	37.42	37.6	37.7
6	15.159	1.10975	42.51	42.8	42.8
7	17.346	1.12677	46.91	47.2	47.3
8	19.459	1.14349	50.80	51.3	51.3
9	21.514	1.16002	54.14	54.6	54.8
10	23.504	1.17632	57.02	57.3	57.8
11	25.448	1.19254	59.35	59.0	60.4

4) "International Critical Tables", Vol. III, McGraw-Hill Book Co., New York (1928), p. 79.

5) J. J. Saslawsky aad E. G. Standel, *Z. anorg. Chem.*, **186**, 171 (1930).

TABLE II. VOLUME CHANGES ON NEUTRALIZATION OF HYDROCHLORIC ACID WITH SODIUM HYDROXIDE OF UNEQUAL CONCENTRATION AT 20°C

HCl		NaOH		NaCl		Vol. change	Vol. change per mole
Concn.(mol./l.) C_a	Vol.(l.) V_a	Concn.(mol./l.) C_b	Vol.(l.) V_b	Concn. (%) a	Density d_s	ΔV ml.	
1	1	2	0.5	3.756	1.02505	18.17	18.17
2	0.5	1	1	3.753	1.02503	19.68	19.68
2	1	4	0.5	7.266	1.05052	31.63	15.82
4	0.5	2	1	7.246	1.05038	35.93	17.97
4	1	8	0.5	13.725	1.09876	50.46	12.62
8	0.25	2	1	8.582	1.06019	34.97	17.49
8	0.5	4	1	13.628	1.09802	62.58	15.65
8	0.75	6	1	16.983	1.12392	84.88	14.15

on neutralization at unequal concentrations, which are calculated by Eqs. 1 and 6.

The Degree of Inaccuracy in Ψ.—Whether or not the values of Ψ in Table I and ΔV^* in Table II are nearly the same as those obtained by a strict experiment depends upon the extent to which an error is made in evaluating the density of the resulting solution by interpolation. Therefore, we will discuss the error in density caused by interpolation[6].

In the case of sodium chloride, the maximum error in density caused by interpolation at intervals of four per cent concentration is 0.007~0.015 per cent in each range of concentration. It is proved by a mathematical calculation that the error in density caused by interpolation at intervals of two per cent concentration is less than one fourth of that at intervals of four per cent concentration, so that it would be rightly considered that the maximum of the errors which would be expected by interpolation at intervals of two per cent concentration is less than 0.004 per cent. If the density data are given at intervals of one per cent concentration, it is needless for us to consider the error in density caused by interpolation.

On the other hand, an error of 0.001 per cent in density would cause an inaccuracy of about 0.01 in Ψ. It is derived from Eq. 11 or deduced from the inaccuracy in Φ (cf. Eq. 10)[7]. Therefore, each of the calculated values of Ψ in Table I may be slightly less than the corresponding true value of Ψ, but the difference between the two does not exceed 0.04.

It is of course true that the above-mentioned discussion can be applied not only to Ψ in Table I, but also to ΔV^* in Table II.

Further, densities of the solutions of acids and bases at 20°C shown in Table III have been evaluated by the following equations, which have been suggested by Root[8].

$$d_{HCl} = 0.99823 + 0.01870\,C - 0.00087\,C^{3/2} \quad (12)$$

$$d_{NaOH} = 0.99823 + 0.04744C - 0.00454C^{3/2} \quad (13)$$

where C is the concentration in mol./l. of the electrolyte solution. These equations have been derived by using the values of Φ^0 and S_v for each electrolyte shown in Table IV.

TABLE III. DENSITIES OF HYDROCHLORIC ACIDS AND SODIUM HYDROXIDE SOLUTIONS AT 20°C

Concn. (mol./l.)	Density	
C	d_{HCl}	d_{NaOH}
1	1.01606	1.04113
2	1.03317	1.08027
3	1.04981	1.11696
4	1.06607	1.15167
5	1.08200	1.18467
6	1.09769	1.21615
7	1.11302	1.24623
8	1.12814	1.27502
9	1.14304	1.30261
10	1.15772	1.32906
11	1.17219	1.35444

TABLE IV. VALUES OF THE PARAMETERS OF EQS. 14, 15 AND 16 AT 20°C

Electrolyte	Φ^0	S_v
HCl	17.80	0.87
NaOH	−7.45	4.55
NaCl	15.82	2.32

6) It has been fully discussed in "Changes of Volume of Mixing Electrolytic Solutions with Water", presented at the 10th Annual Meeting of the Chemical Society of Japan, held in Tokyo in April, 1957; A. Tsujioka, *Proc. of Faculty of Eng., Keio Univ.*, **10**, 47 (1957).

7) H. S. Harned and B. B. Owen, "The Physical Chemistry of Electrolytic Solutions", 2nd Ed., Reinhold Publishing Co., New York (1950), p. 251.

8) W. C. Root, *J. Am. Chem. Soc.*, **55**, 850 (1933).

At this point, therefore, the errors other than those caused by interpolation would be introduced in the values of Ψ and ΔV^* shown in Tables I and II, because they were evaluated by using the data in Table III. In conclusion, the values of Ψ and ΔV^* shown in Tables I and II appear to leave more or less room for doubt at 2 places of decimals. Nevertheless, the agreement between our data and Saslawsky's data has been found very satisfactory in Table I.

Relationships between the Volume Change Fraction and the Concentration.— Since the discovery by Masson[9] that the apparent molar volume of a dissolved salt is a linear function of the square root of the volume concentration, several investigators[10,11] have made extensive tests of the applicability of this relationship. It was found valid for a number of electrolytes over a surprisingly large concentration range. In the range of high dilution, however, the apparent molar volumes Φ_v of strong electrolytes in solution confirm the limiting law derived from the Debye-Hückel theory[12,13]. That is, the function $\Phi_v - S_v C^{1/2}$ is linearly related to the volume concentration C, where S_v is the universal limiting slope. (The experimental limiting slopes determined from the results above 0.25 N are specific[14].)

Therefore, the following Masson's linear relationships hold over a wide range of concentration except at high dilution.

$$\Phi_a = \Phi_a^0 + S_a\sqrt{C} \tag{14}$$

$$\Phi_b = \Phi_b^0 + S_b\sqrt{C} \tag{15}$$

$$\Phi_s^* = \Phi_s^0 + S_s\sqrt{C_s^*} \tag{16}$$

where Φ_a^0, Φ_b^0, Φ_s^0, S_a, S_b and S_s are constants, and C_s^* is the concentration in mol./l. of the salt solution, of which the concentration has been denoted by a^* % in the above section, obtained on neutralization of an acid with a base of equal concentration, C mol./l. Accordingly Eq. 10 for Ψ can be reduced to

$$\Psi = \{(\Phi_s^0 + \Phi_w - \Phi_a^0 - \Phi_b^0) + S_s\sqrt{C_s^*} - S_a\sqrt{C} - S_b\sqrt{C}\}C/2 \tag{17}$$

The resulting salt solution has a volume $(2V + \Delta V^*)$ ml., as has been indicated in the previous section. Hence the following equation:

$$C_s^* = C/2(1 + 10^{-3}\cdot\Psi) \tag{18}$$

Where Ψ, equal to $(\Delta V^*/2V)\times 10^3$, is the volume change fraction. Substituting Eq. 18 in Eq. 17 and then putting it in order by the binomial formula, we find the following equation.

$$\Psi = [(\Phi_s^0 + \Phi_w - \Phi_a^0 - \Phi_b^0) + (S_s\sqrt{2C}/2) \times\{1 + \sum_{r=1}^{\infty}\binom{-1/2}{r}(10^{-3}\cdot\Psi)^r\} - S_a\sqrt{C} - S_b\sqrt{C}\,]C/2 \tag{19}$$

In this equation, the terms $\sum_{r=1}^{\infty}\binom{-1/2}{r}(10^{-3}\cdot\Psi)^r$ are small and can usually be ignored[15], so that we may write,

$$\Psi = \{(\Phi_s^0 + \Phi_w - \Phi_a^0 - \Phi_b^0) + (S_s\sqrt{2C}/2)(1 - \Psi/2000) - S_a\sqrt{C} - S_b\sqrt{C}\}C/2 \tag{20}$$

Solving this equation with respect to Ψ, we may readily derive the following equation.

$$\Psi = \{(\Phi_s^0 + \Phi_w - \Phi_a^0 - \Phi_b^0) + \sqrt{C}(\sqrt{2}S_s/2 - S_a - S_b)\}(1 - \sqrt{2}S_sC^{3/2}/8000)C/2 \tag{21}$$

Consequently we obtain the following equation for Ψ.

$$\Psi = K_1C + K_2C^{3/2} - K_3C^{5/2} - K_4C^3 \tag{22}$$

where
$$K_1 = (\Phi_s^0 + \Phi_w - \Phi_a^0 - \Phi_b^0)/2$$
$$K_2 = (\sqrt{2}S_s - 2S_a - 2S_b)/4$$
$$K_3 = (\sqrt{2}S_s/8000)K_1$$
$$K_4 = (\sqrt{2}S_s/8000)K_2$$

In most cases K_3 and K_4 are small and can be ignored, so that Eq. 22 is approximately represented by means of the following equaiion.

$$\Psi = K_1C + K_2C^{3/2} \tag{23}$$

As an example, we shall deal with the reaction between a hydrochloric acid and a sodium hydroxide solution. Values of the parameters of Eqs. 14, 15 and 16 at 20°C obtained by the present writer are shown in Table IV[16]. The limiting law of the apparent molar volume has been

9) D. O. Masson, *Phil. Mag.*, 8, 218 (1929).
10) W. Geffcken and D. Price, *Z. physik. Chem.*, **B26**, 81 (1934).
11) A. F. Scott, *J. Phys. Chem.*, **35**, 2315 (1931).
12) B. B. Owen and S. R. Brinkley, Jr., *Ann. N. Y. Acad. Sci.*, **51**, 753 (1949).
13) O. Redlich and J. Bigeleisen, *J. Am. Chem. Soc.*, **64**, 758 (1942).
14) See Ref. 7, p. 523.
15) The largest one of these terms, $\binom{-1/2}{2}(10^{-3}\cdot\Psi)^2$, is generally less than 0.001. So it would be rightly considered that the contribution of these terms to the value of Ψ does not exceed 0.1 per cent.
16) These values were not evaluated from data at high dilution.

confirmed for aqueous solutions of sodium chloride up to 0.75 N and of hydrochloric acid up to 0.2 N[12,13]. Therefore the empirical equations, which will be derived below, should not be extrapolated to lower concentrations. Again for aqueous solutions of a few acids (i. e., perchloric acid and sulfuric acid) the apparent molar volume show an unusual dependence on the concentration[17-19].

It appears to be the same for aqueous solutions of hydrogen halides[20]. For hydrochloric acid, however, this deviation from Masson's rule is negligibly small[21,22], so we have not taken it into consideration.

By using the data in Table IV, the coefficients K_1, K_2, K_3 and K_4 in Eq. 22 have been calculated as follows.

$$K_1=11.76,\ K_2=-1.89,\ K_3=4.8\times10^{-3},$$
$$K_4=-7.7\times10^{-4}$$

In this case, therefore, we obtain

$$\Psi=11.76\,C-1.89\,C^{3/2} \qquad (24)$$

The correctness of this equation has been found very satisfactory in Fig. 1 and Table I. In Fig. 1, values of $2\Psi/C$ have been plotted against the square root of the concentration. The numerical value of $2\Psi/C$ represents the volume change in ml. on neutralization of an acid and a base of equal concentrations, C mol./l., which occupy the equal volume, v ml.,

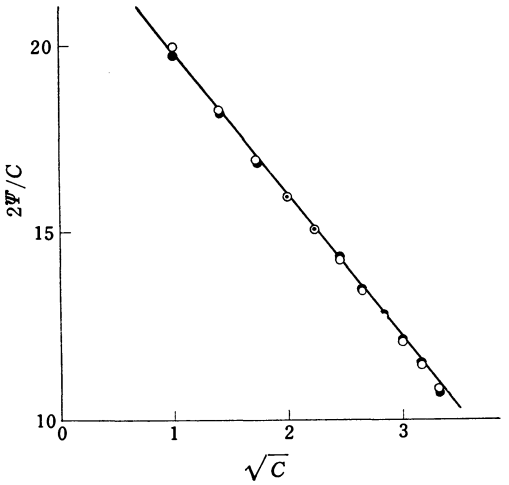


Fig. 1. Dependence of the volume change per mol., on neutralization of hydrochloric acid with sodium hydroxide of equal concn., upon concentration, at 20°C.
——, Calculated by Eq. 24, i.e., $2\Psi/C=23.52-3.78\sqrt{C}$;
○, Tsujioka's data; ●, Saslawsky's data

where v is the volume of the solution, expressed in ml., containing one mole of the solute[23].

On the other hand, in the case of volume changes on neutralization of acids and bases of unequal concentrations, it has been shown in Table II that the expansion in total volume on neutralization gets larger as the range of concentration gets lower, and that the volume change which occurs when hydrochloric acid is more concentrated than sodium hydroxide is larger than that in the reverse case, and so on. These facts, together with the discussion of Eq. 24, may be explained by considering the volume change on dilution. It will be reported in this bulletin shortly.

The Chemical Laboratory, Keio University
Hiyoshi, Yokohama

17) J. Bigeleisen, *J. Phys. and Colloid Chem.*, **51**, 1369 (1947).
18) H. E. Wirth and F. N. Collier, Jr., *J. Am. Chem. Soc.*, **72**, 5292 (1950).
19) I. M. Klotz and C. F. Eckert, ibid., **64**, 1878 (1942).
20) A. Tsujioka, *J. Chem. Soc. Japan, Pure Chem. Sec.* (*Nippon Kagaku Zasshi*), in contribution.
21) H. E. Wirth, *J. Am. Chem. Soc.*, **62**, 1128 (1940).
22) T. F. Young and M. B. Smith, *J. Phys. Chem.*, **58**, 716 (1954).
23) Then C is equal to $10^3/v$, and the volume change fraction Ψ is equal to $(\Delta v/2v)\times10^3$, as has been defined in the previous section, where Δv is the volume change in ml. on neutralization. Therefore it follows that $\Delta v=2\Psi/C$.

Reactions of Active Methylene Compounds. VI. A New Synthesis of Coumestrol, 6,7'-Dihydroxycoumarino (3',4':3,2) coumarone

By Yoshiyuki KAWASE

(Received December 13, 1958)

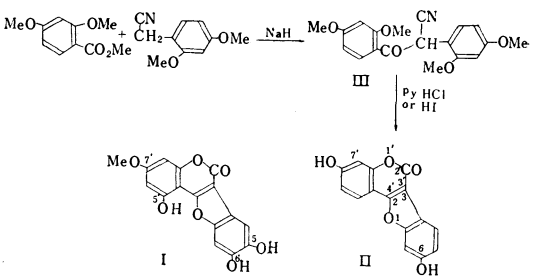
It has been reported that naturally occurring wedelolactone[1] (I) and coumestrol[2] (II) are 5,5',6-trihydroxy-7'-methoxy and 6,7'-dihydroxy derivatives of coumarino (3',4':3,2) coumarone, respectively.

The synthesis of coumarino (3',4':3,2) coumarones has been achieved by the action of hydrobromic acid[3] or pyridine hydrochloride[4] on 3-(2'-methoxyphenyl)-4-hydroxycoumarin derivatives; wedelolactone trimethylether[3,4], from which wedelolactone[5] was derived, was prepared by this method, and coumestrol has recently been synthesized by the action of aniline hydrochloride or hydriodic acid on 3-(2',4'-dimethoxyphenyl)-4,7-dihydroxycoumarin[6].

Another synthetic route to coumarino-(3',4':3,2) coumarone was reported by Chatterjea and Roy, which involves the action of hydrobromic acid on 2-methoxybenzoyl-2-methoxyphenylacetonitrile[7].

The author also has achieved independently the synthesis of 3-phenyl-4-hydroxycoumarins[8] and coumarino (3',4':3,2) coumarones[9] from methoxy derivatives of benzoyl-phenylacetonitrile or corresponding ester by the action of hydrobromic or hydriodic acid or pyridine hydrochloride or anhydrous aluminum chloride.

Now, the synthesis of coumestrol has been carried out by the action of pyridine hydrochloride or hydriodic acid on 2,4 dimethoxybenzoyl-2,4-dimethoxyphenylacetonitrile (III). The acetate of coumestrol thus obtained, m.p. 227~228°C (uncorrected), was identical with the sample, m.p. 227~228°C (uncorrected), which was kindly sent by Dr. Emerson.



Experimental[10]

Ester Condensation.—To a solution of methyl 2,4-dimethoxybenzoate (3.5 g.) and 2,4-dimethoxyphenylacetonitrile (3 g., prepared by azlactone-method[11]) in anhydrous benzene (100 cc.), sodium hydride (ca. 0.6 g.) was added, and the mixture was heated on an oil bath (ca. 95~100°C) for 4 hr. under anhydrous condition, most of the benzene having been distilled off in the meantime. After being well cooled, the mixture was treated with a small amount of ethanol to destroy the excessive sodium hydride, and then diluted with water. Insoluble starting materials being extracted with ether (from the residue of the ether solution, 1.5 g. of the nitrile was recovered through crystallization from methanol), the alkaline solution was acidified and the separated product was collected, washed with aqueous sodium bicarbonate solution and recrystallized from ethanol to give III in colorless needles, m.p. 97~98°C; yield 2.4 g. or 40% (yield was raised to 70% when recovery of the nitrile was taken into account).

Anal. Found: C, 67.01; H, 5.72; N, 4.25. Calcd. for $C_{19}H_{19}O_5N$: C, 66.85; H, 5.61; H, 4.10%.

Coumestrol.—(*a*) *By pyridine hydrochloride.*—A mixture of III (0.7 g.) and anhydrous pyridine hydrochloride (3.5 g.) was refluxed for 40 min.

1) T. R. Govindachari et al., *J. Chem. Soc.*, **1956**, 629; ibid., **1957**, 545.
2) E. M. Bickoff et al., *Science*, **126**, 969 (1957); *J. Agr. Food Chem.*, **6**, 536 (1958); *J. Am. Chem. Soc.*, **80**, 3969 (1958).
3) W. J. Bowyer, A. Robertson and W. Whalley, *J. Chem. Soc.*, **1957**, 542.
4) T. R. Govindachari et al., ibid., **1957**, 548.
5) N. R. Krishnaswamy and T. R. Seshadri, *J. Sci. Ind. Research (India)*, **16B**, 268 (1957); [*Chem. Abstr.*, **52**, 376 (1958)].
6) O. H. Emerson and E. M. Bickoff, *J. Am. Chem. Soc.*, **80**, 4381 (1958).
7) J. N. Chatterjea and S. K. Roy, *J. Indian Chem. Soc.*, **34**, 98 (1957); [*Chem. Abstr.*, **51**, 16445 (1957)]; cf. J. N. Chatterjea and S. K. Roy, *J. Indian Chem. Soc.*, **34**, 155 (1957); [*Chem. Abstr.*, **52**, 1987 (1958)].
8) Y. Kawase, This Bulletin, **31**, 440 (1958); ibid., **32**, 9, 11 (1959); *Experientia*, **14**, 435 (1958).
9) A report will appear in this bulletin afterwards.
10) Melting points are uncorrected.
11) P. C. Mitter and S. S. Maitra, *J. Indian Chem. Soc.*, **13**, 236 (1936).

on an oil bath (ca. 220~230°C) in a carbon dioxide atmosphere under anhydrous condition. The cooled mixture was warmed with dilute hydrochloric acid on a steam bath for 30 min. The separated precipitates were crystallized from ethanol to give light brown microcrystals (m. p. of this was very high); yield ca. 0.2 g.

Anal. Found: C, 67.35; H, 3.18. Calcd. for $C_{15}H_8O_5$: C, 67.17; H, 3.01%.

The acetate prepared by pyridine-acetic anhydride method was colorless needles (from acetic acid), m. p. 227~228°C, and was identical with the sample from Dr. Emerson, m. p. 227~228°C (corrected m. p. is reported to be 235~236°C).

Anal. Found: C, 64.51; H, 3.59. Calcd. for $C_{19}H_{12}O_7$: C, 64.77; H, 3.43%.

(*b*) *By hydriodic acid.* — A mixture of III (0.8 g.), hydriodic acid (d=1.7, 15 cc.), acetic acid (7.5 cc.) and acetic anhydride (7.5 cc.) was refluxed for 2 hr. on an oil bath (ca. 140°C) under a carbon dioxide atmosphere. The cooled solution was diluted with dilute aqueous sodium bisulfite solution, and the precipitates were crystallized from ethanol to give a red product (ca. 0.1 g.), the acetate, m. p. 225.5~226.5°C, which was identical with the other sample.

The author wishes to express his hearty thanks to Professor K. Fukui for his helpful advice, to Dr. O. H. Emerson of the United States Department of Agriculture for the sample of coumestryl acetate, and the members of the Agricultural Department of Kyoto University for microanalyses.

Faculty of Literature and Science
Toyama University
Hasumachi, Toyama

Syntheses of Chlorinated Copper Phthalocyanines from Chlorophthalic Anhydrides

By Masahiro SHIGEMITSU

(Received December 16, 1958)

As a method of synthesis of copper phthalocyanine, the urea-method[1] resorting to the condensation of phthalic anhydride, urea and copper salts prevails. Chlorinated copper phthalocyanines can be obtained by the use of chlorophthalic anhydrides instead of phthalic anhydride. However, since chlorinated copper phthalocyanines are manufactured by chlorinating copper phthalocyanine, little work has been done upon the syntheses of them from chlorophthalic anhydrides.

The author carried out the syntheses of chlorinated copper phthalocyanines by the urea-method, using chlorophthalic anhydrides instead of phthalic anhydride and studied the effect given by the chlorine atoms of starting materials.

Experimental

Materials.—*Phthalic anhydride* (I).—Commercial phthalic anhydride was used with further purification (m. p. 130~131°C).

Monochlorophthalic anhydrides. — By the improved V. Villiger's method[2,3], phthalic anhydride was chlorinated with chlorine gas at 50~55°C in an iron closed vessel, using oleum as solvent and iodine as catalyst. From the mixture of monochlorophthalic anhydrides thus prepared, were separated 3-monochlorophthalic anhydride (II), m. p. 121~122°C (reported m. p. 122°C[4]) (*Anal.* Found: Cl, 19.47%) and 4-monochlorophthalic anhydride (III), m. p. 97~98°C (reported m. p. 98°C[4]) (*Anal.* Found: Cl, 19.44%) by repeating recrystallization with toluene-ethanol (1 : 1) solvent.

Dichlorophthalic anhydrides. — From the mixture of dichlorophthalic anhydrides prepared by the same procedure as above, were separated 3,4-dichlorophthalic anhydride (IV), m. p. 120~121°C (reported m. p. 120~121°C[4]) (*Anal.* Found: Cl, 32.68%), 3,6-dichlorophthalic anhydride (V), m. p. 190~191°C, (reported m. p. 190~191°C[4]) (*Anal.* Found: Cl, 32.71%) and 4,5-dichlorophthalic anhydride (VI), m. p. 185.5~186.5°C (reported m. p. 185~187°C[4]) (*Anal.* Found: Cl, 32.66%) with toluene-ethanol (1:1) solvent.

1) U. S. Pat. 2,197,458 (1940).

2) V. Villiger, *Ber.*, **42**, 3538 (1909).

3) M. Shigemitsu, *J. Chem. Soc. Japan, Ind. Chem. Sec.* (*Kogyo Kagaku Zasshi*), **62**, 110 (1959). (Presented at the Autumnal Joint Meeting of Chemical Society of Japan with other Societies, Tokyo, 1957).

4) V. Villiger, *Ber.*, **42**, 3532 (1909).

Trichlorophthalic anhydrides.—From the mixture of trichlorophthalic anhydrides prepared by the same procedure as above, were separated 3,4,6-trichlorophthalic anhydride (VII), m. p. 147.5~148.5°C (reported m. p. 148°C[5]) (*Anal.* Found: Cl, 42.19%) and 3,4,5-trichlorophthalic anhydride (VIII), m. p. 155.5~156.5°C (reported m. p. 157°C[6]) (*Anal.* Found: Cl, 42.20%) with toluene-ethanol (1:1) solvent.

Tetrachlorophthalic anhydride (IX).—By N. Juvalta's method[7], phthalic anhydride was chlorinated with chlorine gas at 50~60°C and thereafter 200°C in oleum, using iodine as catalyst, and the product was recrystallized with toluene-ethanol (1:1) solvent; m. p. 255~256.5°C (reported m. p. 255~256.5°C[8]) (*Anal.* Found: Cl, 49.22%).

Methods.—Into a three-necked flask of 300 cc. capacity equipped with a stirrer, a thermometer and a reflux condenser were placed 4 : 20 : 1 mol. ratio mixture of phthalic anhydride or its chlorinated derivatives, urea and cuprous chloride as indicated in Table I, and 150 g. of trichlorobenzene used as solvent.

The mixture was stirred at room temperature for 30 min., and then heated to 175°C for 1 hr. at a uniform rate and finally at 175~180°C for 3 hr. After the reaction was complete, trichlorobenzene was removed by steam distillation and the product was heated with 5% hydrochloric acid and then with 2% caustic soda, filtered, washed with water and ethanol and dried at 95~100°C.

In the case of tetrachlorophthalic anhydride, the reaction was conducted with the addition of ammonium molybdate[9], boric acid[1], zirconium tetrachloride[10] and titanium tetrachloride[10] as catalysts of condensation.

Results and Discussion

Results of condensation of phthalic anhydride or its chlorinated derivatives with urea and cuprous chloride are given in Table I.

Phthalic anhydride easily reacts with urea and cuprous chloride and forms copper phthalocyanine. However, when the chlorine content of phthalic anhydride increases, the yield of the product decreases.

The yields obtained in Experiments 3, 6 and 8 are all larger than those obtained in Experiments 2, 5 and 7. Experiment 4 shows the yield between those obtained in Experiments 5 and 6. It is recognized from the above experiments that chlorinated copper phthalocyanines are formed from chlorophthalic anhydrides more easily when chlorine atoms are in 4,5-positions of phthalic anhydride than when they are in its 3,6-positions.

Although copper hexadecachlorophthalocyanine should be obtained in Experiment 9, the chlorine content of the product coincides with that of copper dodecachlorophthalocyanine. The author further studied this matter as follows.

Ammonium molybdate, boric acid, zirconium tetrachloride and titanium tetrachloride are used as catalysts to increase the yield of phthalocyanine formed in

TABLE I. CONDENSATION OF PHTHALIC ANHYDRIDE OR ITS CHLORINATED DERIVATIVES WITH UREA AND CUPROUS CHLORIDE

Expt.	Starting material	Urea	Cuprous chloride	Product				
				Wt.	Yield	Cl (%)		
						Found	Calcd.	
	(g.)	(g.)	(g.)	(g.)	(%)			
1	I, 10.0	19.3	1.7	A, 8.6	89	0.09	0	($C_{32}H_{16}N_8Cu$)
2	II, 10.0	13.7	1.4	B, 7.4	76	19.76	19.87	($C_{32}H_{12}N_8Cl_4Cu$)
3	III, 10.0	13.7	1.4	C, 8.3	85	19.80	〃	〃
4	IV, 10.0	11.6	1.2	D, 7.3	75	33.19	33.24	($C_{32}H_8N_8Cl_8Cu$)
5	V, 10.0	11.6	1.2	E, 6.9	70	33.22	〃	〃
6	VI, 10.0	11.6	1.2	F, 7.8	80	33.18	〃	〃
7	VII, 10.0	9.9	1.0	G, 5.9	60	42.98	43.02	($C_{32}H_4N_8Cl_{12}Cu$)
8	VIII, 10.0	9.9	1.0	H, 6.8	69	43.01	〃	〃
9	IX, 10.0	8.8	0.9	I, 4.1	42	43.04	50.34	($C_{32}N_8Cl_{16}Cu$)

A, Copper phthalocyanine.
B, Copper tetra-(3)-chlorophthalocyanine.
C, Copper tetra-(4)-chlorophthalocyanine.
D, Copper octa-(3,4)-chlorophthalocyanine.
E, Copper octa-(3,6)-chlorophthalocyanine.
F, Copper octa-(4,5)-chlorophthalocyanine.
G, Copper dodeca-(3,4,6)-chlorophthalocyanine.
H, Copper dodeca-(3,4,5)-chlorophthalocyanine.
I, To be discussed later.

5) C. Graebe and S. Rostowzew, ibid., **34**, 2108 (1901).
6) Ad. Claus and H. Kautz, ibid., **18**, 1370 (1885).
7) D. R. Pat. 50,177 (1889).
8) D. S. Pratt and G. A. Perkins, *J. Am. Chem. Soc.*, **40**, 204 (1918).
9) U. S. Pat. 2,214,477 (1940).
10) U. S. Pat. 2,549,842 (1951).

TABLE II. CONDENSATION OF TETRACHLOROPHTHALIC ANHYDRIDE WITH UREA AND CUPROUS CHLORIDE

Expt.	IX	Urea	Cuprous chloride	Catalyst	Product		
	(g.)	(g.)	(g.)	(g.)	Wt. (g.)	Yield (%)	Cl (%)
10	10.0	8.8	0.9	A, 0.5	4.6	47	43.25
11	10.0	8.8	0.9	B, 0.5	4.9	50	43.51
12	10.0	8.8	0.9	C, 0.5	5.9	60	45.95
13	10.0	8.8	0.9	D, 0.5	5.4	55	44.73

A, Ammonium molybdate. B, Boric acid.
C, Zirconium tetrachloride. D, Titanium tetrachloride.

urea-method. Using these compounds as catalysts and under the reaction conditions in Table I, IX was condensed with urea and cuprous chloride. The results are given in Table II.

In Table II, the yield in Experiment 12 is the largest, but it is only 60%. The larger the yield, the larger the chlorine content is. However, all the chlorine contents in Table II are smaller than that of copper hexadecachlorophthalocyanine and close to that of copper dodecachlorophthalocyanine.

As it was considered that dechlorination reaction might possibly occur in the formation of phthalocyanine, the product obtained in Experiment 9 (Table I) was examined. Based on the method in Ref. 11, 3 g. of the product was decomposed by oxidation with ceric sulfate, which gave 2.0 g. of 3,4,5-trichlorophthalic anhydride, m. p. 156~157°C (reported m. p. 157°C[6]) (*Anal.* Found: Cl, 42.17%). It was evident from the above experiments that the chlorine atom at 6-position of IX separated and condensed with urea and cuprous chloride.

11) R. P. Linstead el al., *J. Chem. Soc.*, **1939**, 1823.

Summary

Syntheses of chlorinated copper phthalocyanines from various chlorophthalic anhydrides were conducted. Formation of phthalocyanine depends upon the contents and positions of chlorine atoms of chlorophthalic anhydrides.

The author extends his sincere thanks to Dr. Ryozo Goto, Professor of Kyoto University, for his kind guidance. Thanks are also due to Dr. Takahisa Nakamura and Dr. Wataru Ishikawa, Toyo Ink Manufacturing Company, for their help.

Central Research Laboratory
Toyo Ink Mfg. Co.
Sumida-ku, Tokyo

Color Characteristics of Copper Phthalocyanine and its Chlorinated Derivatives

By Masahiro SHIGEMITSU

(Received December 16, 1958)

Copper phthalocyanine pigments range in shade from blue to green, and are very strong and bright. Arranged in order of increasing greenness or of decreasing redness, they are listed as follows:

(1) Copper phthalocyanine (β-form)
(2) Copper phthalocyanine (α-form)
(3) Copper semichlorophthalocyanine
(4) Copper polychlorophthalocyanine

They are used as coloring matters dispersed in various vehicles such as polymerized linseed oil, nitrocellulose and miscellaneous synthetic resins.

In order to study the effects of the crystal structures, the numbers and positions of chlorine atoms and the pigment contents on the variation of color, the author formulated coloring matter with polymerized linseed oil used as the vehicle, and measured the reflectance curves.

Experimental

Materials.—*α-Form* (I) *and β-form* (II) *copper phthalocyanines.* — A mixture of phthalic anhydride, urea and cuprous chloride was heated in trichlorobenzene at about 190°C for 3 hr[1]. The reaction product was treated with 5% hydrochloric acid and 2% caustic soda, filtered off, washed with water and ethanol, and dried.

The crystal structure of copper phthalocyanine thus prepared was α-form (I)[2,3]. It was pulverized in a ball mill by the method described in Ref. 4.

To transform it into β-form (II), it was dissolved in 98% sulfuric acid, poured into water and deposited as fine crystals[5].

Copper octa-(4,5)-chlorophthalocyanine (III) *and copper octa-(3,6)-chlorophthalocyanine* (IV).— First, from the mixture of dichlorophthalic anhydrides prepared by chlorinating phthalic anhydride in oleum by the improved V. Villiger's method[6,7], 4,5-dichlorophthalic anhydride, m. p. 185.5～186.5°C (reported m. p. 185～187°C[8]) (*Anal.* Found: Cl, 32.66%) and 3,6-dichlorophthalic anhydride, m. p. 190～191°C (reported m. p. 190～191°C[8]) (*Anal.* Found: Cl, 32.71%) were separated with toluene-ethanol (1:1) solvent.

III (*Anal.* Found: Cl, 33.21%) and IV (*Anal.* Found: Cl, 33.23%) were synthesized respectively from 4,5- and 3,6-dichlorophthalic anhydrides by the urea-method[1]. They were respectively dissolved in chlorosulfonic acid and poured into ice water and reprecipitated as fine crystals.

Copper hexadecachlorophthalocyanine (V). — V was prepared by chlorinating copper octa-(3,6)-chlorophthalocyanine (*Anal.* Found: Cl, 50.33%)[7]. It was dissolved in chlorosulfonic acid, poured into ice water and reprecipitated as fine crystals. Particle size distributions of these materials were obtained with an electron microscope[9]. The diameters of these particles were 200～400 mμ and the mean value was about 250 mμ.

Methods.—A mixture of an equal quantity of each pigment and polymerized linseed oil was made into paste (A) by grinding 400 rounds in a Hoover automatic muller. A mixture of an equal quantity of aluminum hydroxide and polymerized linseed oil was made into paste (B) as above. A and B were mixed and pastes of each pigment, having pigment contents of 30, 25, 20, 15, 10, 7.5 and 5%, respectively, were prepared. These were applied 0.5 mm. in thickness on coated papers with a bladeoapplicator (Gardner Laboratory) and dried at room temperature. Reflectance curves of these samples were measured with a recording spectrophotometer (General Electric Co.) and C. I. E. Notations were obtained.

Results

Tables I, II, III, IV and V show the C. I. E. Notations of I, II, III, IV and V. In these tables, *Y* denotes luminosity, *Pe* purity and λ_D dominant wavelength.

TABLE I. C. I. E. NOTATIONS OF COPPER PHTHALOCYANINE (α-form)

Pig. cont. %	*Y* %	*Pe* %	λ_D mμ
30	8.42	50.2	465.5
25	9.10	51.0	466.0
20	10.62	51.8	470.2
15	12.40	51.0	471.9
10	16.60	49.1	475.4
7.5	18.28	47.1	476.4
5	25.08	40.2	478.2

TABLE II. C. I. E. NOTATIONS OF COPPER PHTHALOCYANINE (β-form)

Pig. cont. %	*Y* %	*Pe* %	λ_D mμ
30	7.64	50.0	463.0
25	8.52	52.5	464.1
20	9.44	52.0	466.2
15	10.37	51.2	469.4
10	15.10	47.5	472.4
7.5	17.49	44.8	474.8
5	23.18	38.4	476.2

TABLE III. C. I. E. NOTATIONS OF COPPER OCTA-(4,5)-CHLOROPHTHALOCYANINE

Pig. cont. %	*Y* %	*Pe* %	λ_D mμ
30	9.86	49.7	466.4
25	10.85	49.8	468.5
20	12.59	49.2	470.6
15	14.29	47.0	474.4
10	18.29	43.5	478.5
7.5	20.43	40.6	480.8
5	27.15	33.4	482.4

TABLE IV. C. I. E. NOTATIONS OF COPPER OCTA-(3,6)-CHLOROPHTHALOCYANINE

Pig. cont. %	*Y* %	*Pe* %	λ_D mμ
30	10.45	49.2	474.0
25	11.05	48.0	474.4
20	13.17	46.0	476.2
15	15.00	43.1	479.1
10	19.25	38.4	482.1
7.5	23.62	33.5	484.0
5	30.24	31.5	486.1

1) U. S. Pat. 2,197,458 (1940).
2) J. M. Robertson, *J. Chem. Soc.*, **1935**, 615; ibid., **1936**, 1195; ibid., **1937**, 219.
3) M. Shigemitsu, This Bulletin, **32**, 607 (1959).
4) U. S. Pat. 2,556,726 (1951); U. S. Pat. 2,556,727 (1951); U. S. Pat. 2556,728 (1951); U. S. Pat. 2,556,730 (1951).
5) G. von Susich, *Anal. Chem.*, **22**, 425 (1950).
6) V. Villiger, *Ber.*, **42**, 3538 (1909).
7) M. Shigemitsu, to be published in *J. Chem. Soc. Japan, Ind. Chem. Sec.* (*Kogyo Kagaku Zasshi*), **62**, 112 (1959), (presented at the Autumnal Joint Meeting of Chemical Society of Japan with other Societies, Tokyo, 1957).
8) V. Villiger, *Ber.*, **42**, 3532 (1957).
9) E. Suito et al., presented at the 58th Meeting of Electron Microscope Committee of Japan, 1951.

TABLE V. C. I. E. NOTATIONS OF COPPER HEXADECACHLOROPHTHALOCYANINE

Pig. cont. %	*Y* %	*Pe* %	λ_D mμ
30	10.14	49.4	479.0
25	10.45	46.3	479.2
20	12.50	42.9	480.5
15	15.06	39.1	483.0
10	20.84	34.4	486.8
7.5	25.56	30.5	489.3
5	34.24	28.5	492.0

In all cases, luminosities and dominant wavelengths decreased as the pigment contents increased, but variations of purities differed depending upon the kinds of pigments. I and II gave the maximum purities when their pigment contents were 20 and 25% respectively. On the other hand, purities of IV and V increased as their pigment contents increased. III showed a tendency similar to I and II. Fig. 1 shows the relation between purities and luminosities.

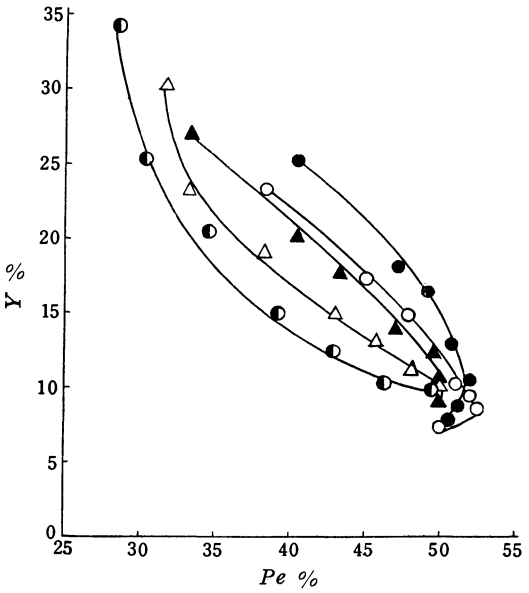


Fig. 1 Relation between purity and luminosity.
-●- Copper phthalocyanine (β-form).
-○- Copper phthalocyanine (α-form).
-▲- Copper octa-(4, 5)-chlorophthalocyanine.
-△- Copper octa-(3, 6)-chlorophthalocyanine.
-◐- Copper hexadecachlorophthalocyanine.

The purity of II was higher than that of I. The luminosities of I and II increased and decreased from the points of maximum purities with the variations in their purities, and the tendency in II was more conspicuous than in I. On the other hand, the luminosities of IV and V decreased with the increase in their purities.

Summary

The variation of color of copper phthalocyanine and its chlorinated derivatives in polymerized linseed oil was investigated.

The β-form of copper phthalocyanine is more conspicuous than the α-form in their variation of color.

Chlorine atoms at 3, 6- or 4, 5-positions of phthalocyanine nucleus give very different actions according to their variations of color, even if their chlorine contents are the same.

The author extends his sincere thanks to Dr. Ryozo Goto, Professor of Kyoto University, for his kind guidance. Thanks are also due to Dr. Takahisa Nakamura and Dr. Wataru Ishikawa, Toyo Ink Manufacturing Co., for their help.

Central Research Laboratory
Toyo Ink Mfg. Co.
Sumida-ku, Tokyo

Hydrothermal Reaction of Aluminumtrihydroxides

By Goro YAMAGUCHI and Kenichi SAKAMOTO

(Received December 17, 1958)

Recently, many studies of thermal transformation of the aluminumtrihydroxides have been reported[1] and we have got details of the mechanism of thermal change. Moreover, there are many experiments dealing with the digesting of gibbsite in an autoclave, but there is no consistent theory of the mechanism of the digesting reaction. The present authors studied and tried to explain the mechanism of hydrothermal reaction of aluminumtrihydroxides. Details are shown as follows.

Experimental

· Materials. — The aluminumtrihydroxides employed in this experiment were gibbsite and bayerite. The gibbsite was a commercial product. It was washed with pure water. Ignition loss was 34.40%. The bayerites were prepared by three methods. The details of the methods had already been reported by the authors[2]. Three bayerites are named bayerite-*a*, -*b* and -*c*. In this study, the *a* was prepared by aging alumina-gel in ammonia water, the *b* was precipitated from sodium aluminate solution by means of a current of carbon dioxide, and the *c* was prepared by auto-precipitation from sodium aluminate solution. The main impurity was sodium oxide of 0.10~0.50%. The crystallinities of bayerites were quite different according to their processes of preparation. They were identified by X-ray analysis.

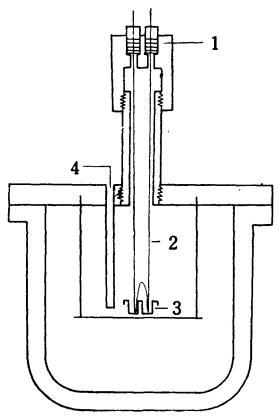


Fig. 1. Diagram of autoclave for DTA in saturated vapor.
(1) Teflon packing, (2) double thermocouples, (3) sample holders, (4) thermometer.

Apparatus and Procedure.—The authors devised an apparatus for differential thermal analysis in saturated vapor. The diagram is shown in Fig. 1. Air-tightness of the part 1 is kept by packing many thin Teflon sheets. This part is cooled in runs to protect the Teflon packings from thermal damage. Sample holders are silica vessels with 1 cm. diameter and 1.5 cm. depth.

The sample was about 1.5 g. in weight, and soaked with 1.5 cc. of water or alkali solutions of various concentrations. In some cases samples were mixed with boehmite. The reaction products were checked by X-ray diffraction.

TABLE I. GIBBSITE

The concn. of alkali added (%)	The contents of boehmite added (%)	Peak temp. (°C)	The breadth
—	—	218	5
0.5	—	217	6
5.0	—	212	8
20.0	—	207	8
—	5	210	9
—	10	205	9
—	20	203	10
—	30	200	17
	Bayerite-*a*		
—	—	190	14
0.5	—	167	14
5.0	—	153	12
20.0	—	145	10
—	30	185	13
	Bayerite-*b*		
—	—	205	8
0.5	—	202	10
5.0	—	192	11
20.0	—	190	11
—	30	194	11
	Bayerite-*c*		
—	—	206	6
0.5	—	200	8
5.0	—	187	10
20.0	—	185	9
—	30.0	194	6

1) A. S. Russell et al., Technical Paper No. 10, Aluminum Company of America, Pittsburgh, Pennsylvania (1956).
2) G. Yamaguchi, K. Sakamoto and K. Shirasuka, *J. Chem. Soc. Japan, Ind. Chem. Sec.* (*Kogyo Kagaku Zasshi*), **61**, 307 (1958).

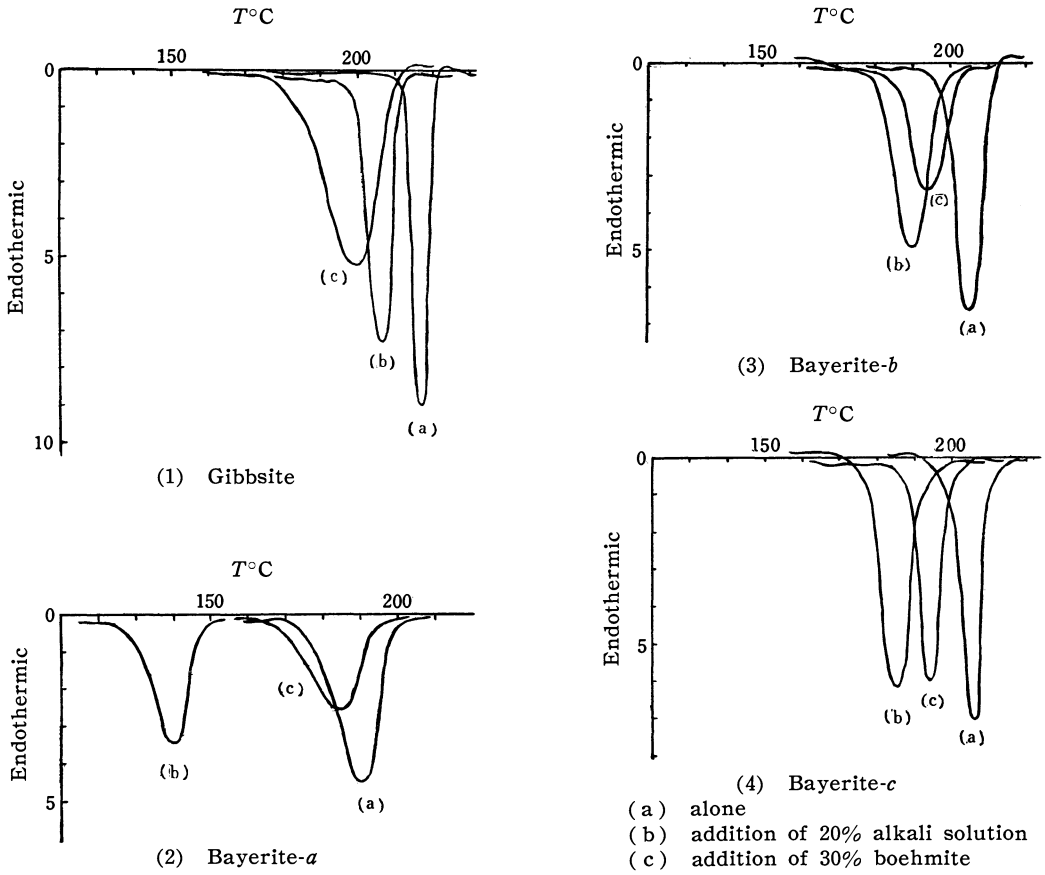


Fig. 2. DTA-curve of aluminumtrihydroxides.

Result

The results of the differential thermal analysis were shown in Fig. 2 and Table I. Gibbsite decomposes endothermally into boehmite. When gibbsite is immersed in alkali solution the peak temperature shifts to a lower point and the breadth at the half value of the endothermic peak becomes greater. The fall in peak temperature and the widening in breadth are very striking at the mixture of gibbsite and boehmite. In the case of 30%-boehmite, the peak temperature lowers to 200°C and the breadth becomes as wide as 17°C. These facts indicate that the alkalinity and the existence of boehmite lower the transformation temperature, that is, accelerate the transformation velocity.

About bayerites, it is clear that they have different stabilities according to the process of preparation. The bayerite-*a* exhibited the lowest peak temperature, and the temperature at the beginning of the transformation is also low. The peak temperature of DTA-curve is lowered remarkably by the addition of alkali. This indicates that this type of bayerite dissolves faster than it does in water. On the other hand, boehmite has only a little effect on the transformation of bayerite-*a*. Bayerite-*b* and -*c* showed similar characters. Added alkali lowers the peak temperature of these two bayerites, and makes the breadth wider. Boehmite lowers also the peak temperature of these bayerites, but has a different effect upon their width. The width of DTA-curve for bayerite-*c* is not effected by the addition of boehmite but the width for bayerite-*b*, becomes wider.

Consideration

Bauermeister and Fulda[3] and also Ginsberg and Koester[4] reported that the transformation of gibbsite to boehmite in an autoclave was accelerated by a small amount of alkali being added. Their

3) B. Bauermeister and W. Fulda, *Aluminum*, **25**, 97 (1953).
4) H. Ginsberg and M. Koester, *Z. anorg. u. allgem. Chem.*, **271**, 41 (1952).

results agree with the present results. Further Russell and his co-workers[5] reported that gibbsite transformed quickly to boehmite in a concentrated alkali solution. Bauermeister explained the transformation from gibbsite to boehmite as a dissolution change, but Ginsberg, and also Sato[6] supposed this reaction to be solid-decomposition. Now, the authors support the resolution reaction through which the transformation proceeds. This reaction consists of two steps ; the dissolution of trihydroxides and the crystallization of boehmite. We can represent this reaction as follows :

$$Al(OH)_3 + (OH)^- \rightarrow Al(OH)_4^-$$

$$Al(OH)_4^- \rightarrow AlO(OH) + (OH)^- + H_2O$$

Thus, we can understand the effect of boehmite as the seed of the crystallization of boehmite. In this region boehmite is very stable, so it is unnatural to suppose that this boehmite reacts directly with aluminumtrihydroxide. This is quite analogous to the effect of gibbsite-seed in the Bayer-process.

About bayerites, it was found that their stabilities were quite different according to the process of their preparation. Also in reference to X-ray diffraction data, it is sure that stabilities of bayerites correspond to their crystallinities. So, the properties which bayerite-*a* exhibited, i.e., the low temperature of the beginning of the transformation and the broad width of the DTA-curve, are attributed to its poor crystallinity. This bayerite was prepared by aging an alumina gel in ammonia solution. So it is supposed that this bayerite consisted of components with different crystallinities. The stability of the composition with poor crystallinity is very small, so this part begins to change into boehmite at temperature as low as 165°C. When alkali solution was added to this bayerite the peak temperature lowered remarkably. This is explained as follows: The part with poor crystallinity dissolves faster in alkali solution than in water, then boehmite crystallizes quickly from this aluminate solution, so this boehmite acts as the seed for the following crystallization. Therefore, the peak temperature fell remarkably, and the width of the DTA-curve remained as before.

Finally, it is emphasized that the transition of aluminumtrihydroxides in saturated vapor does not proceed as an equilibrium transition but as the change from an unstable system to a stable one. This means that the transition velocity at the equilibrium state is very slow and the first phase exists unchanged. A sufficiently high temperature is necessary for rapid change of aluminumtrihydroxides. When this condition is fulfilled, the transition proceeds quickly and shows a sharp endothermic peak of DTA-curve. This was realized in the thermal analysis of trihydroxides without alkali and boehmite (Fig. 2). In this case, the endothermic peak is very sharp and seems to be the peak of a monovariant reaction. But this is attributed to the large velocities of dissolution of aluminumtrihydroxides and of crystallization of boehmite.

In general the change of the Gibbs free energy of any reaction is represented by the next formula

$$\Delta G = \Delta H - T\Delta S$$

In this experiment, the chemical change proceeds as follows :

$$Al(OH)_3 + (OH)^- \rightarrow Al(OH)_4^-$$

$$Al(OH)_4^- \rightarrow AlO(OH) + (OH)^- + H_2O$$

in short

$$Al(OH)_3 \rightarrow AlO(OH) + H_2O$$

Under this condition, of course, ΔG must be negative. ΔH was found to be positive, and the entropy change is positive, because entropy increases at dehydration reaction. When this entropy term overcomes the enthalpy term, then the reaction proceeds. Russell and his co-workers studied the equilibrium constants to form aluminate ion from gibbsite and boehmite and found the transition temperature from gibbsite to boehmite in pure water to be 27°C. Also they found that the trihydrates transformed rapidly to α-monohydrate at solution temperatures above 100°C. This is consistent with the present results.

Summary

In saturated vapor, the aluminumtrihydroxides dissolve in the water and the velocity of dissolution of the trihydroxides becomes larger as the temperature rises. When this solution is supersaturated over the solubility of boehmite, transformation proceeds. The alkalinity and the boehmite added to the hydroxides accelerate

5) A. S. Russell et al., *J. Metal*, **7**, 1123 (1955).
6) T. Sato, Abstracts of the 11th Annual Meeting of Chemical Society of Japan, 296 (1958).

the transition. The former makes easy the dissolution of trihydroxides, and the latter acts as the seed and accelerates the velocity of the crystallization of boehmite.

Department of Applied Chemistry
Faculty of Engineering
The University of Tokyo
Hongo, Tokyo

A Convenient Method for the Calculation of the π-Electronic Structures of Aromatic Derivatives

By Kichisuke NISHIMOTO and Ryoichi FUJISHIRO

(Received January 12, 1959)

Theoretical investigations about the π-electronic structures of the aromatic derivatives based on the LCAO MO method have been carried out by many authors[1]. According to the results obtained by them, the molecular properties have been well correlated with their π-electronic structures, if the parameters appearing in the method have been properly chosen. But the actual calculation of the π-electronic structure of the molecule by means of the MO method is in general rather laborious. Therefore, it will be very convenient if one can find the method by which the calculation is simplified. In this paper we shall provide a convenient method using the set of vacant orbitals for the calculation and apply this method to the calculation of the molecular diagrams of the benzene hydroxy derivatives. In later discussions, we shall refer to this method as the "VO method" (vacant orbital method).

Method

The method is based on the framework of LCAO MO approximation, neglecting the differential overlap. When the molecule contains $2p\pi$ atomic orbitals (AO) in number of n, the molecular orbitals (MO), φ_i, are expressed by the linear combination of these AO's as follows:

$$\varphi_i = \sum_{\mu}^{n} \phi_\mu c_\mu \qquad (1)$$

where ϕ_μ is the μ-th $2p\pi$AO and c_μ is the coefficient to be determined by the variational method. When the following matrix notations which are the same as in Roothaan's paper[2] are used

$$\boldsymbol{\Phi} = (\varphi_1 \varphi_2 \cdots\cdots \varphi_n)$$

$$\boldsymbol{\phi} = (\phi_1 \phi_2 \cdots\cdots \phi_n)$$

$$\mathbf{C} = \begin{pmatrix} c_{11} & c_{12} & \cdots\cdots & c_{1n} \\ c_{21} & c_{22} & \cdots\cdots & c_{2n} \\ \vdots & \vdots & & \vdots \\ c_{\mu 1} & c_{\mu 2} & \cdots\cdots & c_{\mu n} \\ \vdots & \vdots & & \vdots \\ c_{n1} & c_{n2} & \cdots\cdots & c_{nn} \end{pmatrix}$$

we may write then for Eq. 1

$$\boldsymbol{\Phi} = \boldsymbol{\phi}\mathbf{C}$$

If we multiply the right-hand side by $\boldsymbol{\Phi}^*$ and the left-hand side by $\boldsymbol{\phi}^*\mathbf{C}^*$, then the following relation may be obtained,

$$\mathbf{C}^*\mathbf{C} = \mathbf{E}$$

or

$$\sum_{\mu}^{n} c_{\mu i}^* c_{\mu i} = 1 = \sum_{\mu}^{occ} c_{\mu i}^* c_{\mu i} + \sum_{\mu}^{vac} c_{\mu i}^* c_{\mu i}$$

$$\sum_{\mu}^{n} c_{\mu i}^* c_{\nu i} = 0 = \sum_{i}^{occ} c_{\mu i}^* c_{\nu i} + \sum_{i}^{vac} c_{\mu i}^* c_{\nu i} \qquad (2)$$

where $\sum_{i}^{occ}$ and $\sum_{i}^{vac}$ mean the summation over the set of occupied orbitals and that of vacant orbitals, respectively. According to the definitions, the charge density q_μ and the bond order $p_{\mu\nu}$ may be written as,

$$2\sum_{i}^{occ} c_{\mu i}^* c_{\mu i} = q_\mu$$

$$2\sum_{i}^{occ} c_{\mu i}^* c_{\nu i} = p_{\mu\nu}$$

1) See, e.g., B. Pullman and A. Pullman, "Les Theories Electroniques de la Chimie Organique", Masson et Cie, Paris (1952).

2) C. C. J. Roothaan, *Rev. Modern Phys.*, **23**, 69 (1951).

It is convenient to introduce q^v_μ and $p^v_{\mu\nu}$ as the corresponding quantities for the set of vacant orbitals, that is,

$$2\sum_i^{vac} c^*_{\mu i}c_{\mu i}=q^v_\mu$$

$$2\sum_i^{vac} c^*_{\mu i}c_{\nu i}=p^v_{\mu\nu}$$

Using these quantities, Eq. 2 can be rewritten as

$$(q_\mu-1)=-(q^v_\mu-1)$$

$$p_{\mu\nu}=-p^v_{\mu\nu} \qquad (3)$$

$(q_\mu-1)$ represents the net charge at the position of the μ-th carbon atom belonging to the parent hydrocarbon system. As seen in Eq. 3, the set of vacant orbitals may become a mirror image of that of occupied orbitals. For the case of substituents which have only the lone pair orbitals, such as OH, NH_2, Cl, etc., the net charge must be expressed by $(q_\mu-2)$ instead of $(q_\mu-1)$. Therefore, in this case $-q^v_\mu$ may directly measure the net charge at the substituent. Using the relation 3, the calculation of the molecular diagram of the aromatic derivative may be considerably simplified, because

(1) the number of vacant orbitals is always less than that of occupied orbitals, and

(2) the vacant orbital and their energies differ only slightly from those of the reference system, since the large differences in orbital energies between the occupied and the vacant orbitals in the reference system may restrict the deformation of the vacant orbitals by conjugation to small extent. Here, we call the system in which the interactions between the parent hydrocarbon system and the substituents do not take place, as the reference system.

Pople's method for the LCAO SCF MO calculation tells us that the matrix elements of the Hartree-Fock Hamiltonian can be expressed by q_μ's, $p_{\mu\nu}$'s and the fundamental atomic integrals. Therefore, the SCF calculation based on his method may substantially expedited by the use of VO method, because

(1) the calculations of q_μ's and $p_{\mu\nu}$'s are easily carried out, and

(2) the rapid convergence to the SCF MO's may be expected, since the vacant orbitals may differ only slightly from those of the reference system.

When the square of the coefficient of the carbon atom to be bonded with the substituent in the lowest vacant orbital (frontier orbital) of the parent hydrocarbon system has considerably large value, the deformation for the lowest vacant orbital by conjugation may be greater than for others. Thus, in this case the frontier orbital will make the greatest contribution to the mirror image relations. Actually, it is well known[3] in many cases that the frontier orbital theory provides satisfactory information for the discussion of chemical reactions.

Next, we shall show a mirror image relation of orbital energies. The energy, ε_i, of the φ_i is determined by the solution of the secular determinant of n-th degree, that is,

$$\det|H_{\mu\nu}-\delta_{\mu\nu}\varepsilon|=0$$

where $H_{\mu\nu}$ is the matrix element of the Hamiltonian, which is expressed by

$$H_{\mu\nu}=\int\phi^*_\mu H\phi_\nu\,dv$$

where H is the (effective or Hartree-Fock) Hamiltonian operator. According to the algebraic theory, the total sum of roots is equal to the negative value of the coefficient of ε^{n-1} term in the development of the secular determinant in terms of ε, that is,

$$\sum_i^n\varepsilon_i=\sum_\mu^n H_{\mu\mu}=\sum_i^{occ}\varepsilon_i+\sum_i^{vac}\varepsilon_i \qquad (4)$$

From this equation we obtain

$$2\sum_i^{occ}\varepsilon_i-\sum_\mu^n H_{\mu\mu}=-(2\sum_i^{vac}\varepsilon_i-\sum_\mu^n H_{\mu\mu}) \qquad (5)$$

For many purposes, only the extra delocalization energy, $\Delta\varepsilon$, arising from the delocalization of the $2p\pi$ electrons by substitution may be important. $\Delta\varepsilon$ is defined as follows:

$$\Delta\varepsilon=2(\sum_i^{occ}\varepsilon_i-\sum_i^{occ}\varepsilon^0_i) \qquad (6)$$

where ε^0_i is the orbital energy in the reference system. Similar relation to Eqs. 4 and 5 may also be obtained for the case of reference system, that is,

$$\sum_i^n\varepsilon^0_i=\sum_\mu^n H^0_{\mu\mu}=\sum_i^{occ}\varepsilon^0_i+\sum_i^{vac}\varepsilon^0_i$$

$$2\sum_i^{occ}\varepsilon^0_i-\sum_\mu^n H^0_{\mu\mu}=-(2\sum_i^{vac}\varepsilon^0_i-\sum_\mu^n H^0_{\mu\mu}) \qquad (7)$$

3) K. Fukui, T. Yonezawa and H. Shingu, *J. Chem. Phys.*, **20**, 722 (1952); K. Fukui, T. Yonezawa, C. Nagata and H. Shingu, ibid., **22**, 1433 (1954); K. Fukui, T. Yonezawa and C. Nagata, This Bulletin, **27**, 423 (1954).

TABLE I. MO'S AND MO ENERGIES

Orbital energy in β	MO
	Benzene
-2	$\varphi_1^v=1/\sqrt{6}\,(\phi_1-\phi_2+\phi_3-\phi_4+\phi_5-\phi_6)$
-1	$\varphi_2^v=1/\sqrt{12}\,(2\phi_1-\phi_2-\phi_3+2\phi_4-\phi_5-\phi_6)$
-1	$\varphi_3^v=1/\sqrt{4}\,(\phi_2-\phi_3+\phi_5-\phi_6)$
	Catechol
-2.0497	$\varphi_1^v=0.3978(\phi_1-\phi_4)-0.4365(\phi_2-\phi_3)-0.3790(\phi_6-\phi_5)+0.0861(\phi_7-\phi_8)$
-1.0897	$\varphi_2^v=0.0462(\phi_1-\phi_4)+0.4651(\phi_2-\phi_3)-0.5155(\phi_6-\phi_5)-0.1256(\phi_7-\phi_8)$
-1.0346	$\varphi_3^v=0.5663(\phi_1+\phi_4)-0.3076(\phi_2+\phi_3)-0.2783(\phi_6+\phi_5)+0.0849(\phi_7+\phi_8)$
	Resorcinol
-2.0480	$\varphi_1^v=0.4125\phi_1-0.4224(\phi_2+\phi_6)+0.3943(\phi_3+\phi_5)-0.3850\phi_4+0.0833(\phi_7+\phi_8)$
-1.0987	$\varphi_2^v=0.5129(\phi_2-\phi_6)-0.4668(\phi_3-\phi_5)-0.1381(\phi_7-\phi_8)$
-1.0313	$\varphi_3^v=0.5258\phi_1-0.2711(\phi_2+\phi_6)-0.3389(\phi_3+\phi_5)+0.5791\phi_4+0.0752(\phi_7+\phi_8)$
	Hydroquinone
-2.0475	$\varphi_1^v=0.4180(\phi_1-\phi_4)-0.3990(\phi_2-\phi_3-\phi_5+\phi_6)-0.0826(\phi_7-\phi_8)$
-1.1269	$\varphi_2^v=0.5748(\phi_1+\phi_4)-0.2702(\phi_2+\phi_3+\phi_5+\phi_6)-0.1532(\phi_7+\phi_8)$
-1.0000	$\varphi_3^v=0.5000(\phi_2-\phi_3+\phi_5-\phi_6)$
	Phloroglucinol
-2.0698	$\varphi_1^v=0.4111(\phi_1+\phi_3+\phi_5)-0.3973(\phi_4+\phi_2+\phi_6)-0.0806(\phi_7+\phi_8+\phi_9)$
-1.0987	$\varphi_2^v=0.2961(2\phi_1-\phi_3-\phi_5)+0.2695(2\phi_4-\phi_2-\phi_6)-0.0797(2\phi_7-\phi_8-\phi_9)$
-1.0987	$\varphi_3^v=0.5129(\phi_3-\phi_5)-0.4668(\phi_2-\phi_6)-0.1381(\phi_8-\phi_9)$
	2, 3, 5, 6-Tetrahydroxybenzene
-2.0923	$\varphi_1^v=0.3909(\phi_1-\phi_4)-0.4090(\phi_2-\phi_3-\phi_5+\phi_6)+0.0797(\phi_7-\phi_8-\phi_9+\phi_{10})$
-1.1827	$\varphi_2^v=0.4838(\phi_2-\phi_3+\phi_5-\phi_6)-0.1261(\phi_7-\phi_8+\phi_9-\phi_{10})$
-1.0664	$\varphi_3^v=0.5571(\phi_1+\phi_4)-0.2971(\phi_2+\phi_3+\phi_5+\phi_6)+0.0810(\phi_7+\phi_8+\phi_9+\phi_{10})$

We may now define $\Delta\varepsilon^v$ as follows:

$$\Delta\varepsilon^v=2\left(\sum_i^{vac}\varepsilon_i-\sum_i^{vac}\varepsilon_i^0\right) \tag{8}$$

Then the following expression may be derived from above equations,

$$\Delta\varepsilon-\sum_i^n(H_{\mu\mu}-H_{\mu\mu}^0)=-\left[\Delta\varepsilon^v-\sum_\mu^n(H_{\mu\mu}-H_{\mu\mu}^0)\right] \tag{9}$$

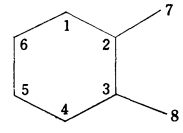
When $H_{\mu\mu}=H_{\mu\mu}^0$, which is the case in the simple LCAO MO treatment neglecting the inductive effect, Eq. 9 becomes

$$\Delta\varepsilon=-\Delta\varepsilon^v$$

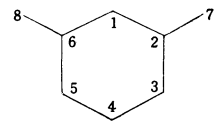
Thus the mirror image relation of orbital energies is established.

Calculation of the Molecular Diagrams

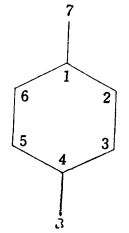
We shall apply VO method to the calculation of the molecular diagrams of benzene hydroxy derivatives. The method is based on the framework of simple LCAO AO method neglecting the inductive effect. The parameters used are the same as those of phenol[4]. All the hydroxy derivatives have only three vacant orbitals, since the reference systems have



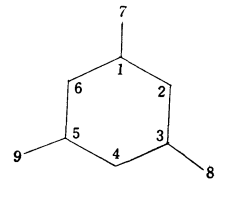
Catechol



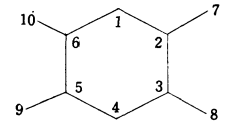
Resorcinol



Hydroqinone



Phloroglucinol



2, 3, 5, 6-Tetrahydroxy benzene

Fig. 1. Numbering of atoms.

4) K. Nishimoto and R. Fujishiro, This Bulletin, 31, 1036 (1958).

only three vacant orbitals, respectively. Therefore, the calculation based on the VO method is an easier task than that employing the set of occupied orbitals. The numbering of atoms is shown in Fig. 1. The calculated vacant MO's, ϕ_i^v, and their energies are collected in Table I, with those of a benzene molecule. Comparison of ϕ_1^v's of hydroxy derivatives with that of benzene indicates that the former are polarized regularly along the direction toward the substituent; but their magnitudes are rather small. On the other hand, the frontier orbitals, φ_2^v and φ_3^v, seem to reflect roughly the characters of the ground states of the molecules. The molecular diagrams calculated are given in Fig. 2. When we try to plot the magnitude of the charge migration, Δe, from the substituents into the benzene ring, against the extra delocalization energy, $\Delta\varepsilon$, a linear relationship is obtained as shown in Fig. 3.

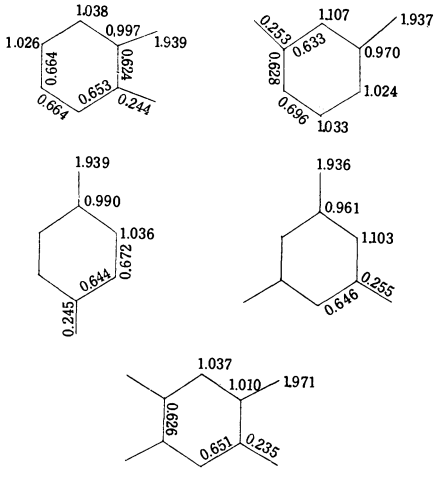


Fig. 2. Molecular diagrams.

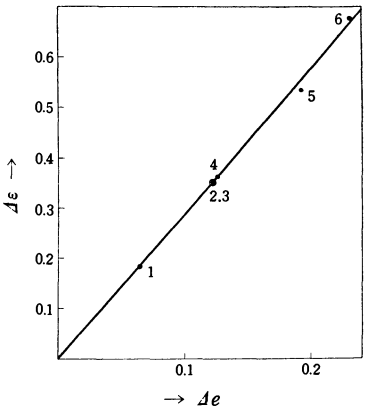


Fig. 3. Relation between $\Delta\varepsilon$ and Δe for benzene hydroxy derivatives.
1. Phenol
2. Catechol
3. Hydroquinone
4. Resorcinol
5. Phloroglucinol
6. 2, 3, 5, 6-Tetrahydroxy benzene

Summary

It was shown that the set of vacant orbitals of the conjugated system would be a mirror image of that of occupied orbitals. Using this relation the calculations of the π-electronic structures of the aromatic derivatives are considerably simplified. As an example, the molecular diagrams of the benzene hydroxy derivatives were calculated.

Department of Chemistry
Institute of Polytechnics
Osaka City University
Kita-ku, Osaka

Isomerism and Polymorphism of Cinnamic Acids and Deuterated Allocinnamic Acids

By Minoru HIROTA and Yoshiyuki URUSHIBARA

(Received January 17, 1959)

Since the three polymorphic forms of allocinnamic acid were found and studied by Liebermann[1], by Paal[2], and by Biilmann[3], they have been the subject of many researches[4] including those on the dipole moment[5], the infrared absorption[6], other physical properties, and the transition between them[7].

In the course of the studies of the polymorphic behaviors of the compounds with group $C_6H_5CH=CHCO$[8], deuterated allocinnamic acids have been investigated in comparison with the ordinary allocinnamic acid, the powder X-ray diffraction and ultraviolet absorption spectra of α,β-d_2-allocinnamic acid and *O*-*d*-allocinnamic acid being measured. The X-ray diffraction patterns of the *O*-*d*-allocinnamic acid showed an expansion of the crystal lattice. No remarkable difference was found among the ultraviolet absorptions of three polymorphic forms of allocinnamic acid. In an experiment of catalytic hydrogenation of phenylpropiolic acid to allocinnamic acid, a new polymorphic form, m. p. 120°C, of (*trans*-)cinnamic acid was obtained by chance, and its transition to the stable form, m. p. 133°C, was observed.

Experimental

Partial Hydrogenation of Phenylpropiolic Acid.—Phenylpropiolic acid was prepared from commercial cinnamic acid according to the method of "Organic Syntheses"[9,10], and catalytically hydrogenated to allocinnamic acid. Palladium catalysts, e. g., Pd-$BaSO_4$[11] Pd-poly(vinyl alcohol)[12] and Pd-Na protalbinate[13], and the Urushibara catalysts[14,15], e. g., U-Ni-B and U-Co-A, were used in the partial hydrogenation and the latter catalysts were found useful for the purpose. The U-Ni-B catalyst gave the purest allocinnamic acid, while the palladium catalysts yielded hardly crystallizable products which had to be purified through the aniline salt[16]. The results of the catalytic hydrogenation with various catalysts are summarized in Table I.

The 58°-form[17] of allocinnamic acid was prepared by recrystallization of the hydrogenation products, the 68°-form through the aniline salt and the 42°-form by cooling suddenly the melt of the 58°-form or 68°-form in dry ice.

Preparation of Deuterated Allocinnamic Acids.—α,β-d_2-Allocinnamic acid was prepared by the catalytic deuteration of sodium phenylpropiolate with deuterium in a solution in 99.7% heavy water produced by the Norsk Hydro-Elektrisk Kvaelstofaktieselskab, Norway. The deuterium was generated by the electrolysis of the heavy water by using anhydrous sodium sulfate as the electrolyte, platinum electrodes, and an electric current of density 0.02~0.03 amp./cm^2 and 6~8 V. Palladium on barium sulfate, which was chosen on account of its small content of exchangeable hydrogen, was first deuterated in the heavy water and then employed for the catalytic deuteration. It was presumed without any determination that the α,β-d_2-allocinnamic acid contained nearly 100% deuterium in the α and β positions.

In order to deuterate the carboxylic hydrogen, allocinnamic acid was recrystallized once from 47.4% D_2O and then from 99.7% D_2O. The deuterium content of allocinnamic acid deuterated in this way was determined to be 80±5% of the carboxylic hydrogen.

Measurements of Absorption Spectra.—Ultraviolet absorptions were measured in ethanolic solution in the range of wavelengths 2100~4000 Å with a Beckman Model DU spectrophotometer. Infrared absorptions were measured with a Baird Model B infrared recording spectrophotometer in

1) C. Liebermann, *Ber.*, **23**, 515 (1890); **25**, 91 (1892).
2) C. Paal and W. Hartmann, ibid., **42**, 3931 (1909).
3) E. Biilmann, ibid., **43**, 573 (1910).
4) Cf. C. Weygand and H. Baumgärtel, ibid., **65**, 693 (1932); A. W. K. De Jong, *Rec. Trav. Chim. Pays-Bas*, **51**, 397 (1932).
5) F. Eisenlohr and W. Hass, *Z. physik. Chem.*, **A173**, 249 (1935).
6) J. Guy, *Ann. Phys.*, (12), **4**, 704 (1949).
7) F. Eisenlohr and A. Metzner, *Z. physik. Chem.*, A, **178**, 339 (1937).
8) F. Iimura, *J. Chem. Soc. Japan, Pure Chem. Sec.* (*Nippon Kagaku Zasshi*), **77**, 1851 (1956).
9) T. W. Abbott, "Organic Syntheses", Col. Vol. 2, John Wiley & Sons, New York (1948), p. 515.
10) T. W. Abbott and D. Althousen, ibid., Col. Vol. 2, (1948), p. 270.
11) R. Mozingo, ibid., Vol. 26, (1946), p. 77.
12) L. D. Rampino and F. F. Nord, *J. Am. Chem. Soc.*, **63**, 2745 (1941).
13) C. Paal and C. Amberger, *Ber.*, **38**, 1398 (1905).
14) Y. Urushibara and S. Nishimura, This Bulletin, **27**, 480 (1954).
15) Y. Urushibara, S. Nishimura and H. Uehara, ibid., **28**, 446 (1955).
16) C. Liebermann, *Ber.*, **27**, 2037 (1894).
17) "58°-Form" denotes the polymorphic form melting at 58°C and so on.

TABLE I. PARTIAL HYDROGENATION OF PHENYLPROPIOLIC ACID WITH VARIOUS CATALYSTS*

Catalyst	Conditions of hydrogenation	Forms of cinnamic acid obtained
U-Ni-B	Na salt in water	*cis*-58°**
U-Ni-A	Acid in ethanol	*cis*-58°
U-Co-A	Na salt in water	*cis*-58°, *cis*-68°
U-Co-A, then U-Ni-A	Acid in ethanol	*trans*-120°
U-Co-B	Na salt in water	*cis*-58°**
Pd-Na protalbinate (colloidal)	Na salt in water	Oil, *cis*-68° through aniline salt
Pd-charcoal	Na salt in water	Oil, *cis*-68° by recrystallization
Pd-$BaSO_4$	Na salt in water	*cis*-58°
Pd-poly(vinyl alcohol) (colloidal)	Na salt in water	Oil (*cis*-58°)**
U-Ni-B and active charcoal	Na salt in water	*cis*-68°, *cis*-58°

* Hydrogenation was stopped when one mole of hydrogen was absorbed.
** Phenylpropionic acid was obtained.

Nujol and in carbon tetrachloride solution when necessary.

Measurements of X-ray Diffraction Patterns. — The powder method was used with a Norelco X-ray diffractometer. The identity and the difference among polymorphic forms were determined by the diffraction patterns, the diffraction angles being mainly taken into consideration for the identification and the intensity of the diffracted beams being only auxiliarily respected.

Results and Discussion

Ultraviolet Absorption.—Guy[18] observed that polymorphic forms of allocinnamic acid give different infrared spectra especially in the finger print region, and Urushibara, Iimura and Ikeda[8,19] showed that polymorphic forms of chalcones differ not only in infrared but also in ultraviolet spectra. The ultraviolet absorptions of cinnamic acid and allocinnamic acid have been reported with no notice of any difference in polymorphic forms[20].

TABLE II. ULTRAVIOLET ABSORPTION SPECTRA OF CINNAMIC ACIDS IN ETHANOL

	Form	λ_{max}(Å)	ε_{max}
Cinnamic acid	133°	2730	20500
(*trans*)	120°	2725	19000
Allocinnamic acid	58°	2670	9500
(*cis*)	68°	2660	9800
	42°	2630~2650	ca.10000

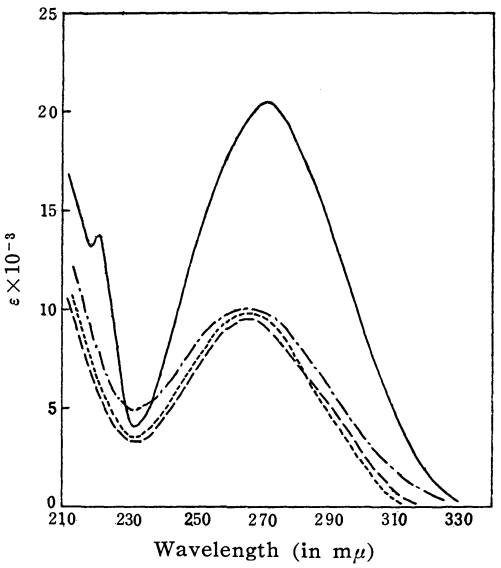


Fig. 1. The ultraviolet spectra of cinnamic acids.
Cinnamic acid 133°-form ————
Allocinnamic acid 42°-form —·—·—
58°-form ·····
68°-form ————

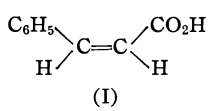
Ultraviolet absorption spectra in ethanol were measured with all the polymorphic forms of cinnamic acid and of allocinnamic acid with the results shown in Table II and Fig. 1. The three forms of allocinnamic acid gave similar absorption curves with no remarkable differences in either the locations or the intensities of the absorption maxima. Moreover, cinnamic acid and allocinnamic acid absorbed almost the same wavelength but the intensity of the former was roughly twice as strong as the latter.

18) J. Guy, *Ann. Phys.*, (12), **4**, 704 (1949).
19) Y. Urushibara, F. Iimura and K. Ikeda, *J. Chem. Phys.*, **22**, 1943 (1954); **23**, 759 (1955); F. Iimura, *J. Chem. Soc. Japan, Pure Chem. Sec.* (*Nippon Kagaku Zasshi*), **77**, 1846 (1956).
20) A. E. Gilam and E. S. Stern, "Introduction to Electronic Absorption Spectroscopy in Organic Chemistry", Edward Arnold Ltd., London (1954); H. M. Hershenson, "Ultraviolet and Visible Absorption Spectra, Academic Press Inc., New York (1956), p. 233.

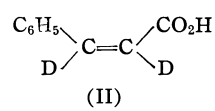
Braude and his co-workers[21-23] have extensively studied the relations between the ultraviolet spectra and the steric hindrance in conjugated systems and concluded that, when the steric hindrance is not so large as to prevent the conjugation, the sterically hindered *cis*-isomer gives an absorption maximum almost at the same location as the unhindered *trans*-isomer but having a remarkably lower intensity. The appearance of polymorphism in a molecule with a partially hindered conjugated system is caused by the existence of metastable, rotationally hindered, forms conditioned by both the steric hindrance and the π-electron interaction between two parts of the molecule[24,25]. The interpretation that the polymorphism of cinnamic acids is based on such causes is supported by the different infrared spectra of the polymorphic forms.

The ultraviolet spectra of the deuterated allocinnamic acids revealed no isotope effect in any polymorphic forms.

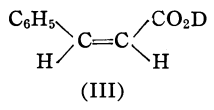
Polymorphism of Deuterated Allocinnamic Acids.—Measurements of the powder X-ray diffraction with α,β-d_2-allocinnamic acid (II) and *O*-*d*-allocinnamic acid (III) in comparison with the ordinary allocinnamic acid (I) showed that the diffraction patterns of the polymorphic forms of *O*-*d*-allocinnamic acid deviate from those of the corresponding forms of the other



(I)



(II)

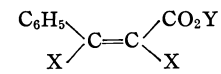


(III)

two, respectively. The deviations are comparatively remarkable, though small, in the two polymorphic forms melting at 58°C and at 68°C, and noticeably in the direction of smaller diffraction angles, suggesting a lattice expansion caused by deuteration. Deviations observed in the 42°-form permit to conclude neither a lattice expansion nor a lattice contraction.

The lattice expansion observed in the two forms of *O*-*d*-allocinnamic acid is supposed to be due to the deuterium bond which is weaker than the hydrogen bond in the corresponding forms of the ordinary allocinnamic acid. Such an isotope effect is known in oxalic acid[26] and other compounds[27] and explained on the basis of the weaker deuterium bond.

TABLE III. THE MELTING POINTS OF ALLOCINNAMIC ACIDS



Form	I X=Y=H	II X=D, Y=H	III X=H, Y=D
68°	67.5~68.0°	67.0~68.0°	66.5~67.0°
58°	57.5~58.5°	55.0~57.5°	54.5~55.0°
42°	41.0~42.5°		41.5~42.0°

Some forms of the deuterated allocinnamic acids melted lower than the corresponding forms of the ordinary allocinnamic acid, as shown in Table III, and, since the melting point of either the 58°-form or the 68°-form of the ordinary allocinnamic acid was lowered by recrystallization from heavy water, it can be concluded that the lowering of the melting points of *O*-*d*-allocinnamic acid is connected with the lattice expansion.

Formation and Properties of the Metastable Form, m. p. 120°C, of Cinnamic Acid.—The new form of (*trans*-)cinnamic acid was obtained in an experiment to prepare allocinnamic acid from phenylpropiolic acid. The experimental sequence was as follows: When phenylpropiolic acid was hydrogenated with the U-Co-A catalyst, the reaction was too slow to be completed. Then U-Ni-A was added with an intension of finishing the partial hydrogenation to allocinnamic acid. After being left to stand for a day, the product was isolated from the reaction mixture, but it melted at 120°C and did not coincide with any form of allocinnamic acid. The product proved a new form of (*trans*-)cinnamic acid, since it gave an infrared absorption in solution quite similar to that of the known form (m. p. 133°C) of cinnamic acid except for a slight difference in the finger print region, and an ultraviolet absorption also similar to that of the 133°-form of cinnamic acid (120°-form: λ_{max} 2725 Å, ε_{max} 19000; 133°-form: λ_{max} 2730 Å, ε_{max} 20500). On the other hand,

21) E. A. Braude et al., *J. Chem. Soc.*, **1949**, 1890.
22) E. A. Braude and F. Sondheimer, ibid., **1955**, 3754.
23) E. A. Braude and C. J. Timmons, ibid., **1955**, 3766.
24) B. Eistert, F. Weygand and E. Csendes, *Ber.*, **84**, 745 (1951).
25) B. Eistert, F. Weygand and E. Csendes, ibid.. **85**, 164 (1952).
26) M. J. Robertson and A. R. Ubbelhde, *Proc. Roy. Soc.*, **A170**, 222 (1939).
27) Benzoic acid, succinic acid, sodium bicarbonate, etc.

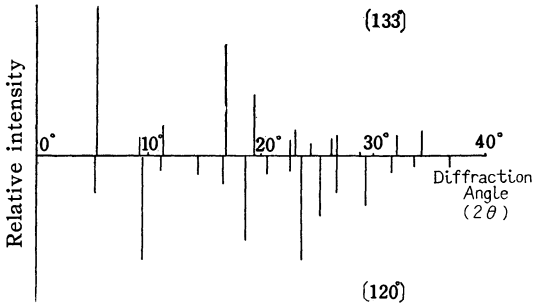


Fig. 2. The X-ray diffraction patterns of the 120°-form and the 133°-form of (*trans*-)cinnamic acid.

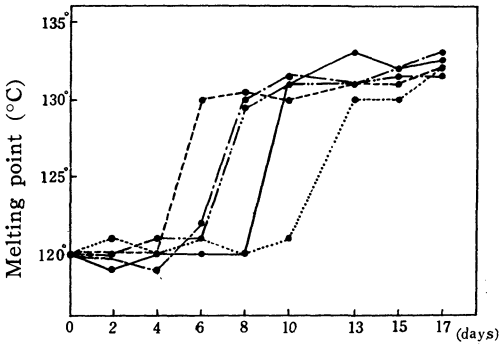


Fig. 3. Changes of the melting points of the 120°-form of cinnamic acid.

the X-ray diffraction pattern of the 120°-form is clearly different from that of the stable 133°-form of cinnamic acid, as shown in Fig. 2.

The formation of the new form of cinnamic acid in the hydrogenation of phenylpropiolic acid is explained by assuming that the allocinnamic acid formed by the catalytic hydrogenation was isomerized to a metastable form of the *trans*-isomer during its contact with the catalyst. The 120°-form was transformed into the 133°-form in one week or two, when it was kept in a dark place at room temperature. All attempts to repeat the preparation of the metastable form failed and the *cis*-isomer was always obtained instead. Further, it was observed that the transition of the metastable form to the stable form occurred abruptly when it once started by chance. Namely, when five portions of the metastable form were kept in a dark place at about 15°C, the melting points of these portions, determined every second or third day, changed suddenly but at different times, as shown in Fig. 3.

The authors wish to acknowledge their indebtedness to the late Dr. Iimura, and to express their thanks to Dr. Ōki and to Dr. Kobayashi, for their helpful discussions, to Dr. Nishimura and Dr. Sugimori for catalytic hydrogenation, and to Dr. Hayashi for measurements of the infrared spectra.

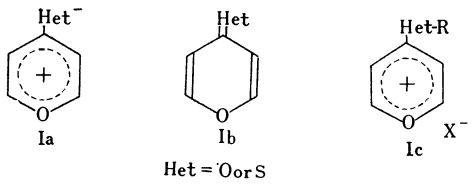
Department of Chemistry
Faculty of Science
The University of Tokyo
Hongo, Tokyo

Non-benzenoid Aromatic Heterocycles. I. Reactions of 4-Pyrone, 4-Thiopyrone, and their Pyrylium Salts with Active Methylene Compounds

By Masaki OHTA and Hiroshi KATO

(Received January 9, 1959)

It has been widely accepted that the -O- group is equivalent to the -CH=CH- group, thus 4-pyrone and 4-thiopyrone can be regarded as heterocyclic tropone analogues. The physical and chemical properties of these compounds can be more adequately explained in terms of formula Ia than in terms of the conventional formula Ib. In the same sense the pyrylium salts Ic derived from them can be considered as heterocyclic tropylium salt analogues.



In this respect, it is of interest to study some of their reactions. The concept that the carbonyl group of 4-pyrone behaves anomalously and does not react with most carbonyl reagents had long been accepted until Woods' report[1], where he has shown that 2,6-dimethyl-4-pyrone(II) undergoes condensation with malonitrile by refluxing in acetic anhydride. The present authors have tried further the condensation of II and 2,6-dimethyl-4-thiopyrone(III) with active methylene compounds aiming to show, to what extent the carbonyl or thiocarbonyl group of these compounds is active, and to distinguish the difference between these two compounds. 2,6-Dimethyl-4-pyrone(II) reacted with malonitrile, ethyl cyanoacetate, or rhodanine to give the corresponding condensation product IV~VI under the condition reported by Woods, but it failed to react with diethyl malonate, acetylacetone, cyclopentadiene, or nitromethane. Just the same result was obtained when III was treated with the above-cited compounds; this fact indicates essentially the same carbonyl character of these two compounds. The fact that the same condensation products are obtained starting from II or III unequivocally proves the structures of the condensation products. It is noteworthy that the condensation is not effected by the usual catalysts, e.g., sodium ethoxide or *tert.*-butoxide, sodium acetate, or piperidine. This fact suggests anomalous character of pyrone carbonyl group.

Woods reported that IV was hydrolyzed to the corresponding dicarboxylic acid, but in the authors' experiment, the corresponding nitrile-amide VII was the sole product. In this connection, it is worthy of note that malonic acid reacted with II or III by gently warming in acetic anhydride, but the reaction was accompanied by decarboxylation, and the product obtained in each case was black unpurifiable powder.

Recently, Dimroth et al.[2] have reported that 2,4,6-trialkylpyrylium borofluorides or perchlorates, when treated with potassium *tert*-butoxide in nitromethane, give the corresponding nitrobenzene derivatives. As 4-methoxy- or 4-methylmercaptopyrylium perchlorate, derived from II or III respectively, is structurally similar to trialkylpyrylium salts, the present authors predicted the reaction of the same type. This occurred as expected, and when 4-methoxy-2,6-dimethylpyrylium perchlorate (VIII) was treated with nitromethane and sodium *tert*-butoxide, 4-methoxy-2,6-dimethylnitrobenzene(IX)* was obtained. This compound IX was converted into 3,5-dimethyl-4-nitrophenol(X)* by refluxing

1) L. L. Woods, *J. Am. Chem. Soc.*, **80**, 1440 (1958).

2) K. Dimroth and D. Bräuniger, *Angew. Chem.*, **68**, 519 (1956); K. Dimroth, G. Bräuniger and G. Neubauer, *Chem. Ber.*, **90**, 1634 (1957); K. Dimroth, G. Neubauer, H. Möllenkamp and G. Oosterloo, ibid., **90**, 1668 (1957).

* Rowe et al.[3] prepared X in 2.4% yield by nitrating 3,5-dimethylphenol, and X was converted into IX by dimethyl sulfate.

3) F. M. Rowe, S. H. Bannister, R. R. Seth and R. C. Storey, *J. Soc. Chem. Ind.*, **49**, 469 (1930); *Chem. Abstr.*, **25**, 930 (1931).

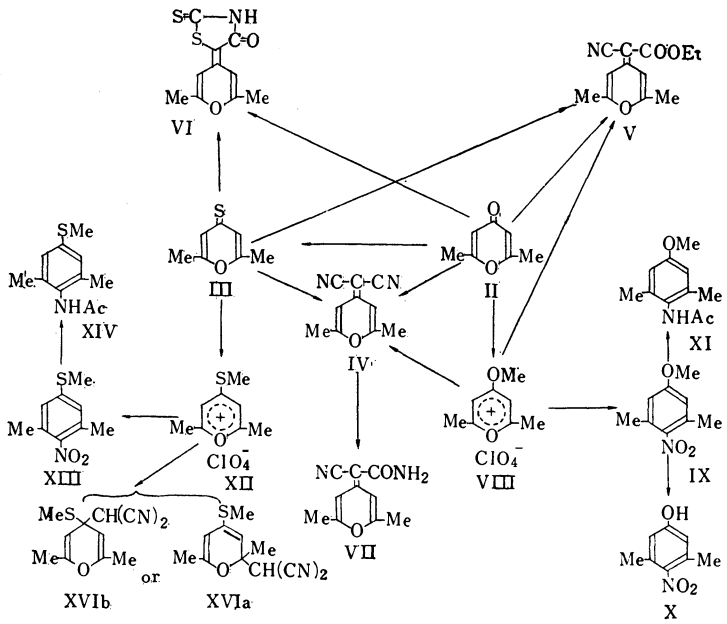
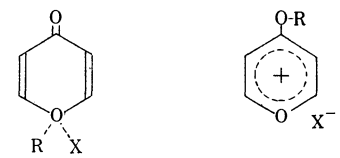


Fig. 1. Reactions of 2,6-dimethyl-4-pyrone and their derivatives with active methylene compounds.

with hydrobromic acid, and to 2,6-dimethyl-*p*-anisidine** by reduction with zinc and hydrochloric acid, which was identified as its acetyl derivative XI. Similarly, 4-methylmercapto-2,6-dimethylpyrylium perchlorate(XII) gave 4-methylmercapto-2,6-dimethylnitrobenzene(XIII) by the reaction with nitromethane and sodium *tert*-butoxide. This compound XIII was reduced, by zinc and hydrochloric acid to the corresponding amine, which was identified as an acetyl derivative(XIV)***. As Dimroth et al. have pointed out, these reactions are of value as a convenient preparatory method of the otherwise unobtainable or not easily accessible compounds. Moreover, the results of these reactions clearly reject the structure XVa which was once proposed for the salts****, and add an unambiguous proof of the widely accepted structure XVb.



XVa XVb

Dimroth et al.[6] have briefly reported that the reaction of 2,4,6-trialkylpyrylium salts with ethyl cyanoacetate leads to benzonitrile derivatives. The present authors have expected the reaction of the same type with VIII, but in this case, the condensation at the position 4 of the salt VIII occurred, and gave exclusively 4-(ethoxycarbonylcyanomethylene)-2,6-dimethyl-4H-pyrane(V). Similarly, when VIII was treated with malonitrile, 4-(dicyanomethylene)-2,6-dimethyl-4H-pyrane (IV) was obtained. In the case of XII, the splitting up of methyl mercaptan did not occur, and the compound of the type XVIa or XVIb was obtained.

These reactions can be interpreted if the reaction mechanism shown in Fig. 2 is taken into account.

In Fig. 2, the key steps which determine the reaction routes are assumed to be steps A, B, C and D. The reactions with nitromethane take place smoothly by way of the steps A and C, but in the reaction with ethyl cyanoacetate, the step

** Bamberger et al.[4] prepared this compound by treating 2,6-dimethylphenylhydroxylamine with methanol in the presence of sulfuric acid.

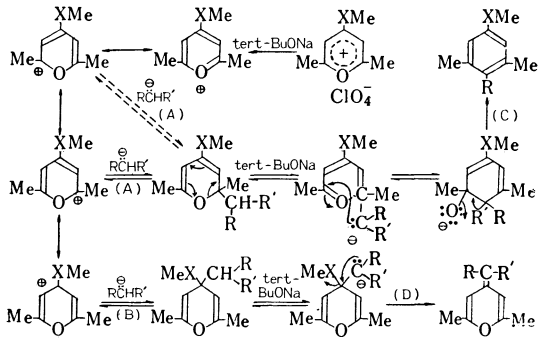
4) E. Bamberger, *Ber.*, **36**, 2028 (1903).

*** This compound was prepared by Kloosterziel et al.[5], starting from 2,6-xylidine via thiocyano compound followed by reduction with lithium aluminum hydride and methylation.

**** Cf., for example, J. N. Collie and T. Tickle, *J. Chem. Soc.*, **1899**, 710; F. Kehrmann and A. Duttenhöfer, *Ber.*, **39**, 1299 (1906).

5) H. Kloosterziel and H. J. Backer, *Rec. trav. chim. Pays-Bas*, **72**, 655 (1953).

6) K. Dimroth and G. Neubauer, *Angew. Chem.*, **69**, 95 (1957).



X = O or S

Fig. 2. Mechanism of the condensation reaction.

D (demethoxylation) is more favorable than the step C (decarbethoxylation), and the reaction leads to the condensation at the position 4. The same reaction mechanism can be assumed to the reaction with malonitrile. In the case of trialkylpyrylium salts, the step D corresponds to dealkylation which is hindered, thus the reaction proceeds thoroughly via the step C to give benzonitrile derivatives, as is observed in Dimroth's report.

As 4-pyrone perchlorate is believed to possess the structure of the pyrylium salt type, the reaction between this compound and malonitrile was tried in hopes of effecting a condensation reaction, but when 2,6-dimethyl-4-pyrone perchlorate was treated with malonitrile and sodium *tert*-butoxide, free 2,6-dimethyl-4-pyrone was obtained.

Experimental

2,6-Dimethyl-4-pyrone (II)[7].—Dehydroacetic acid (100 g.) was refluxed in concentrated hydrochloric acid (400 ml.) for an hour, and the solution was boiled for two hours to concentrate, and finally concentrated nearly to dryness under reduced pressure. The residue was dissolved in water, and the solution was washed with benzene, saturated with potassium carbonate and extracted with chloroform. The extract, after being dried with potassium carbonate, was evaporated and the residue was collected. Yield, 71 g. (97%); m. p. 130°C. The product was pure enough for use in the subsequent experiments.

2,6-Dimethyl-4-thiopyrone (III).—This compound was prepared by King's method[8].

Condensation of II or III with Active Methylene Compounds.—2,6-Dimethyl-4-pyrone (II) (1 g.) or -thiopyrone (III) (0.5 g.) and 1 mol. each of active methyl or methylene compounds were refluxed in acetic anhydride for an hour. Solvent was removed under reduced pressure, and the residue was collected, washed with ether and recrystallized.

The following results were obtained (Yield A refers that from II and Yield B that from III):
Malonitrile: pale yellow needles (from ethanol), m. p. 191°C[9]. Yield A, 90%; B, 33%.
Ethyl cyanoacetate: pale yellow needles (from ethanol), m. p. 184°C. Yield A, 31%; B, 44%.

Anal. Found: C, 65.51; H, 6.10; N, 6.67. Calcd. for $C_{12}H_{13}O_3N$ (V): C, 65.74; H, 5.98; N, 6.39%.

Rhodanine: yellow needles (washed with benzene and recrystallized from acetone), m. p. 260°C. Yield A, 32%; B, 59%.

Anal. Found: C, 49.93; H, 4.12; N, 5.17. Calcd. for $C_{10}H_9O_2NS_2$ (VI): C, 50.21; H, 3.79; N, 5.86%.

The products obtained from III were identified by their melting points, and by the failure of m. p. depressions on admixture with the specimens prepared from II.

These condensations could not be effected by sodium ethoxide or *tert*-butoxide, sodium acetate, or piperidine as catalyst.

In the case of diethyl malonate, acetylacetone, cyclopentadiene, or nitromethane, the reaction occurred neither with II nor with III, and the starting material was recovered unchanged.

When malonic acid (3 g.) was gently warmed in acetic anhydride (15 ml.) with II or III (3 g. each) a marked evolution of gas was observed and black unpurifiable powder (3 g.) was obtained after removal of the solvent. This substance was soluble in aqueous solution of sodium bicarbonate, but insoluble in most solvents.

Hydrolysis of IV.—A suspension of IV (7 g.) in a mixture of concentrated hydrochloric acid (40 ml.) and ethanol (40 ml.) was refluxed for twenty-four hours and then poured into water. The precipitate was collected and recrystallized from ethanol giving pale yellow amorphous powder with green fluorescence. (5 g.) m. p. 252°C (decomp.).

Anal. Found: C, 62.61; H, 5.35; N, 14.42. Calcd. for $C_{10}H_{10}O_2N_2$ (VII): C, 63.15; H, 5.30; N, 14.73%.

No dicarboxylic acid was obtained when refluxing was prolonged for another thirty hours.

4-Methoxy-2,6-dimethylpyrylium Perchlorate (VIII).—This compound was prepared by Baeyer's method[10].

4-Methylmercapto-2,6-dimethylpyrylium Perchlorate (XII).—This compound was prepared by Arndt's method[11].

4-Methoxy-2,6-dimethylnitrobenzene (IX).—A hot solution of sodium *tert*-butoxide (0.47 g. of metallic sodium in 30 ml. of *tert*-butanol) was added into a solution of VIII (2.4 g.) in nitromethane (10 ml.) under stirring and reflux. After refluxing for an hour, the mixture was

7) This is a modification of the procedure reported by Cornubert et al. (*Bull. soc. chim. France*, **1950**, 40) and by King et al.[8]
8) L. C. King et al., *J. Am. Chem. Soc.*, **73**, 300 (1951).
9) Woods[1] reports the m. p. 190~192°C.
10) A. Baeyer, *Ber.*, **43**, 2337 (1910).
11) F. Arndt and P. Nachtwey, ibid., **59**, 446 (1926).

poured into dilute hydrochloric acid (200 ml. containing 2 ml. of concentrated hydrochloric acid) and the solution was extracted with chloroform. The extract was dried with potassium carbonate, the viscous oily residue which remained after removal of the solvent was distilled under reduced pressure, and the fraction distilling at 129°C/8 mmHg was collected; it soon solidified to pale yellow needles (1 g.), m. p. 50°C [12].

Anal. Found: C, 59.68; H, 6.43; N, 7.67. Calcd. for $C_9H_{11}O_3N$ (IX): C, 56.66; H, 6.12; N, 7.73%.

4-Methylmercapto-2, 6-dimethylnitrobenzene (XIII). — A hot solution of sodium *tert*-butoxide (0.32 g. of metallic sodium in 30 ml. of *tert*-butanol) was added to a solution of XII (1.7 g.) in nitromethane (8 ml.), and was treated by essentially the same method as described above. A fraction which was distilled at 148～149°C/8 mmHg was collected, and it solidified to yellow needles (0.6 g.), m. p. 62～63°C.

Anal. Found: N, 7.39. Calcd. for $C_9H_{11}O_2NS$ (XIII): N, 7.10%.

3, 5-Dimethyl-4-nitrophenol (X).—A solution of IX (0.5 g.) in a mixture of hydrobromic acid (48%, 10 ml.) and acetic acid (5 ml.) was refluxed for three hours and the reaction mixture was extracted with chloroform. Removal of the solvent left yellow residue, which was recrystallized from ethanol giving yellow plates (0.4 g.), m. p. 107～108°C [13].

Anal. Found: N, 8.34. Calcd. for $C_8H_9O_3N$ (X): N, 8.38%.

***N*-Acetyl-2, 6-dimethyl-*p*-anisidine (XI).** — To a solution of IX (1 g.) in a mixture of hydrochloric acid (10%, 20 ml.) and acetic acid (10 ml.) was added zinc dust (5 g.) portionwise under warming. After two hours, the mixture was extracted with chloroform, and the residue, left after removal of the solvent, was warmed with acetic anhydride. After removal of the solvent, the residue was recrystallized from ethanol giving colorless plates (0.8 g.), m. p. 178°C.

Anal. Found: N, 7.22. Calcd. for $C_{11}H_{15}O_2N$ (XI): N, 7.25%.

12) Rowe et al.[3] report the m. p. 53°C.
13) Rowe et al.[3] report the m. p. 107～108°C.

***N*-Acetyl-4-methylmercapto-2, 6-dimethylaniline (XIV).**—Treatment of XIII (0.4 g.) by the same procedure as described above gave white needles (0.4 g.), m. p. 155～156°C [14].

Anal. Found: N, 6.80. Calcd. for $C_{11}H_{15}ONS$ (XIV): N, 6.69%.

Reaction of VIII with Ethyl Cyanoacetate. —A solution of VIII (2.4 g.) in a mixture of ethyl cyanoacetate (10 ml.) and *tert*-butanol (10 ml.) was treated by the same method as described in the reaction with nitromethane. Distillation gave solid distillate, which on recrystallization from ethanol gave orange leaflets (0.7 g.), m. p. 185°C. (Found: N, 6.35%). No melting point depression occurred when admixed with the authentic specimen V prepared by the condensation of II with ethyl cyanoacetate.

Reaction of VIII with Malonitrile.—A solution of VIII (2.4 g.) in a mixture of malonitrile (3 g.) and *tert*-butanol (15 ml.) was treated as described above. After refluxing for an hour, the mixture was poured into dilute hydrochloric acid and the yellow precipitate which separated out was collected. Yield, 1.7 g., m. p. 189°C. (Found: N, 15.99%.). No melting point depression occurred when admixed with the authentic specimen IV[1].

Reaction of XII with Malonitrile. — Into a suspension of XII (2.6 g.) in a mixture of malonitrile (1 g.) and *tert*-butanol (30 ml.) was added a hot solution of sodium *tert*-butoxide (0.47 g. of metallic sodium in 30 ml. of *tert*-butanol) under stirring and reflux. After refluxing for an hour, the mixture was poured into dilute hydrochloric acid and the precipitate which separated out was collected and recrystallized from ethanol giving yellow plates; m. p. 132～133°C.

Anal. Found: C, 60.14, N, 5.54; H, 12.87. Calcd. for $C_{11}H_{12}ON_2S$ (XVI): C, 60.00; H, 5.49; N, 12.72%.

The authors are indebted to Mr. Asaji Kondo for performing the microanalyses.

Laboratory of Organic Chemistry
Tokyo Institute of Technology
Meguro-ku, Tokyo

14) Kloosterziel et al.[5] report the m. p. 156.7～157.5°C.

Synthesis of 1,8(9)-p-Menthadien-10-yl-carbinol

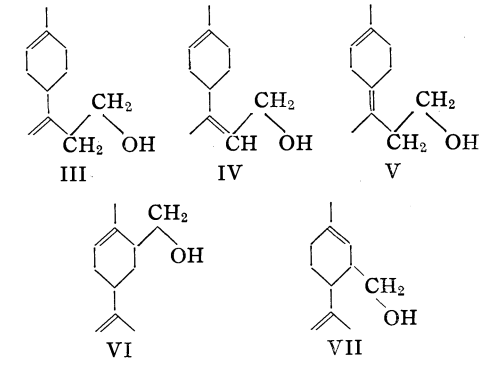
By Kyoichi SUGA, Juichi ISHII and Shoji WATANABE*

(Received January 17, 1959)

The addition of formaldehyde to olefines is known as Prins reaction[1]. For the first time Ladenberg[2] discovered that formaldehyde can be added to terpenes and Kriewitz[3] researched this reaction with β-pinene. Lombard[4] obtained alcohol (IV) from *d*-limonene, using zinc chloride as a catalyst. The present authors investigated the addition reaction of *d*-limonene and formaldehyde, and prepared a limonenylcarbinol in high yields (30%), the structure of which was proved to be 1,8(9)-*p*-menthadien-10-yl-carbinol (III).

d-Limonene(I) and paraformaldehyde(II) scarcely reacted at all when the mixture was agitated in the presence of zinc chloride for 3 hr. at about 80°C; neither aluminum chloride nor ferric chloride in place of zinc chloride gave good results. When a mixture of one mol. each of I and II was heated for 12 hr. at 200~220°C in a sealed tube, a yellow viscous oil was obtained (yield, 11%). It gave a phenylurethan, m. p. 54~55°C, which was analyzed as the phenylurethan derived from an alcohol, $C_{11}H_{18}O$. As this procedure did not give satisfactory yields, a mixture of I, II and acetic anhydride was heated in an autoclave, and a limonenylcarbinyl acetate was obtained in a yield of 30%. The use of 0.5 mol. or more of acetic anhydride per one mol. of I, the reaction temperature 180~190°C, and the reaction time 4~5 hr., gave the best result. A limonenylcarbinol was prepared by the saponification of the acetate. The acetate could not be saponified by the action of 20% aqueous or alcoholic potassium hydroxide at 100°C, but the carbinol was produced almost quantitatively by heating the acetate with 20% aqueous potassium hydroxide for 3~4 hr. at 180~190°C in an autoclave. The carbinol is a colorless liquid and it smells like cineol. The analysis of its phenylurethan, m. p. 56~57°C, indicated that the alcohol was a limonenylcarbinol. The velocity of esterification of phenylacetic acid with the carbinol showed that the carbinol was a primary alcohol.

In the addition of formaldehyde to terpenes or other compounds[5], formaldehyde adds usually at an end methylene group[6] or an active methylene group[9] adjacent to a double bond. Thus it is considered that the limonenylcarbinol possesses one of structures III, IV, V, VI and VII.



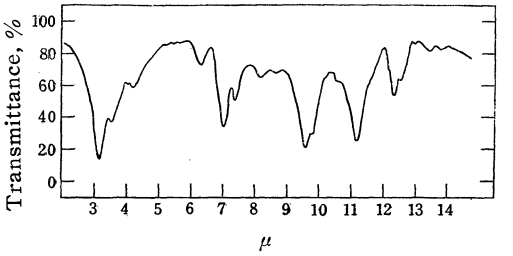


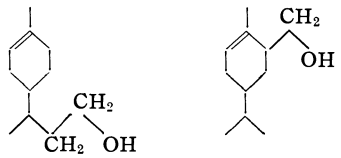
Fig. 1. The infrared absorption spectrum of the limonenylcarbinol(III).

The infrared absorption spectrum (Fig. 1) indicates the presence of a primary alcohol group (absorption peak at 9.6 μ) and an end methylene group (strong band at 11.25 μ), which excludes IV and V.

* Present address: Faculty of Technology, Chiba University, Iwase, Matsudo-shi, Chiba.

1) H. J. Prins, *Proc. Acad. Sci. Amsterdam*, **22**, 51 (1919), *J. Chem. Soc.*, 118, 42 (1920).
2) A. Ladenberg, *Ber.*, **31**, 289 (1898).
3) O. Kriewitz, ibid., **32**, 57 (1899).
4) R. Lombard, *Bull. soc. chim. France*, No. **10**, C 24 (1953), No. 11, C 1216 (1954).
5) E. E. Swissmann and R. A. Mode, *J. Am. Chem. Soc.*, **79**, 3447 (1957).
6) For example, β-pinene[7], 8(9)-*p*-menthene[4] and methylenecyclohexene[8].
7) J. P. Bain, *J. Am. Chem. Soc.*, 68, 638 (1946).
8) E. Arundale and L. A. Mikeska, *Chem. Revs.*, **51**, 505 (1952).
9) For example, carvomenthene[10].
10) H. Yonetani and H. Yamabe, *Reports of Campho1 Chemists' Society* (*Shono Gijitsu Kyokai Kogi*), **20**, 109 (1955).

The optical activity ($[\alpha]_D^{10}$ +37.2) also makes V improbable. Formula III was concluded from the comparison of the infrared spectrum of the product(VIII), prepared by catalytic hydrogenation of the end methylene group of the carbinol, with that of 1(2)-*p*-menthen-6-yl-carbinol (IX) which was prepared from 1(2)-*p*-menthene and paraformaldehyde. The 1(2)-*p*-menthen-6-yl-carbinol (IX) showed remarkable doublet absorption peaks[11] at 7.2 μ (1390 cm^{-1}) and 7.3 μ (1370 cm^{-1}), and



VIII IX

medium absorption peaks at 8.55 μ (1170 cm^{-1}) and 9.05 μ (1150 cm^{-1})[12] owing to an isopropyl radical (Fig. 2). On the other hand, the hydrogenation product from the limonenylcarbinol gave the strong single band of a methyl group at 7.25 μ, but no absorptions of an isopropyl group at 8.55 μ and 9.05 μ (Fig. 3). These results suggest the structure of 1,8(9)-*p*-menthadien-10-yl-carbinol (III) for the limonenylcarbinol.

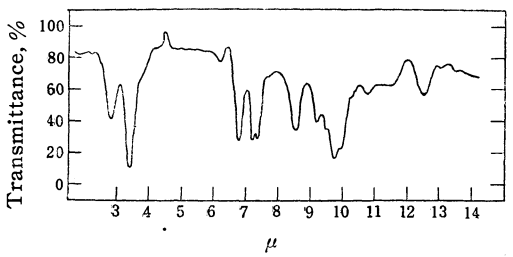


Fig. 2. The infrared absorption spectrum of 1(2)-*p*-menthen-6-yl-carbinol (IX).

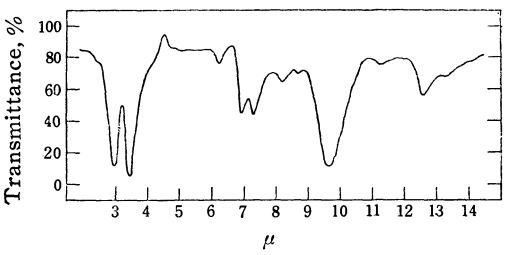


Fig. 3. The infrared absorption spectrum of 1(2)-*p*-menthen-10-yl-carbinol (VIII).

11) It was reported that the doublet absorption peaks of the isopropyl group are at 1362 cm^{-1} and 1378 cm^{-1}.

12) H. L. McMurry and V. Thornton, *Anal. Chem.*, **24**, 318 (1952).

Experimental

***d*-Limonene(I).**—Commercial *d*-limonene was distilled with a rectifying column. B. p. 64～65°C/15 mmHg; d_4^{15} 0.8494; n_D^{15} 1.4756; $[\alpha]_D^{10}$ +113°.

Reaction in a Sealed Tube. — A mixture of 20 g. (0.15 mol.) of I, 4.5 g. (0.15 mol.) of II and 10 g. of ethanol was sealed in a hard glass tube, and heated at 200～220°C for 12 hr. in an electric furnace. The reaction mixture was poured into water and extracted with ether, and the ethereal solution was washed with water and dried over anhydrous sodium sulfate. By fractional distillation, 14 g. of I and 2.8 g. of the limonenylcarbinol were obtained. B. p. 102～105°C/4 mmHg; d_4^{8} 0.9612; n_D^{12} 1.5069. Yield, 11%.

Phenylurethan.—It was prepared as usual and recrystallized from methanol. Colorless needles, m. p. 54～55°C.

Anal. Found: N, 4.79; Calcd. for $C_{18}H_{23}O_2N$: N, 4.91%.

Limonenylcarbinyl Acetate (1,8(9)-*p*-Menthadien-10-yl-carbinyl Acetate).—A mixture of 45.3 g. (0.333 mol.) of I, 10 g. (0.333 mol.) of II and 20 g. (0.196 mol.) of acetic anhydride was heated at 180～190°C for 4～5 hr. in an autoclave. The reaction mixture was washed with water and dried over anhydrous sodium sulfate. Fractional distillation gave 20.5 g. of the crude acetate. B. p. 96～106°C/4 mmHg Yield, 29.6%. It was redistilled for characterization. B. p. 103～107°C/5 mmHg; d_4^{28} 0.9618; n_D^{28} 1.4790; molecular refraction 61.38 (Calcd. for $C_{11}H_{17}O\cdot COCH_3$, F_2, 60.75).

Limonenylcarbinol (1,8(9)-*p*-Menthadien-10-yl-carbinol).—A mixture of 13 g. of the crude acetate and 6 g. of potassium hydroxide (20% aq. solution) was heated at 180°C for 4 hr. in an autoclave. After cooling, the reaction mixture was extracted with ether, and the extracts were washed with water and dried over anhydrous sodium sulfate. Fractional distillation gave 10 g. of the limonenylcarbinol in a yield of 96%. B. p. 102～106°C/4 mmHg; d_4^{17} 0.9603; n_D^{17} 1.5020; molecular refraction 51.04 (Calcd. for $C_{10}H_{15}CH_2OH$, F_2, 51.39) $[\alpha]_D^{10}$ +37.2.

Phenylurethan.—It was prepared as usual and recrystallized from methanol. Colorless needles, m. p. 56～57°C.

Anal. Found: N, 4.86. Calcd. for $C_{18}H_{23}O_2N$: N, 4.91%.

Velocity of Esterification of Phenylacetic Acid with the Limonenylcarbinol.—The nature of the hydroxyl group of the limonenylcarbinol was determined by Murahashi's method[13]. A small amount of the carbinol was heated with phenylacetic acid at 150°C for an hour in a sealed glass tube. The initial rate of esterification in an hour was found 63% showing the carbinol is a primary alcohol.

1(2)-*p*-Menthen-10-yl-carbinol (VIII). — In methanol solution 3.93 g. of the limonenylcarbinol was hydrogenated with Pd-$BaSO_4$ containing 3%

13) E. Funakubo, "Identification of Organic Compounds, I" (Yuki Kagobutsu Kakuninho I), Yokendo, Tokyo (1951), p. 11.

Pd, and absorbed 583 cc. of hydrogen (760 mmHg, 20°C) to give 3.0 g. of VIII. B. p. 100~103°C/4.5 mmHg; n_D^{13} 1.4923.

***d*-Limonene Hydrochloride**[14,15].—In a 200 cc. three-necked flask equipped with a mechanical stirrer, a thermometer and a gas inlet tube, 100 g. of I was placed. The flask was cooled to −5°C in an ice-salt freezing mixture. Anhydrous hydrogen chloride was passed into the solution for 2 hr. The reaction mixture turned deep purple in color and sticky. It was washed with water, dried over anhydrous sodium sulfate and fractionally distilled to give a fraction of b.p. 65~68°C/4 mmHg. By redistillation 84 g. of *d*-limonene hydrochloride was obtained. B. p. 73~75°C/5 mmHg; n_D^{12} 1.4850.

1(2)-*p*-Menthene[14,16]. — Sodium (40 g.) was added gradually in an hour to a mixture of 40 g. of *d*-limonene hydrochloride and 200 g. of absolute ethanol with ice cooling. After sodium ethylate was decomposed with water, the product was extracted with ether and the ethereal solution was washed with water and dried over anhydrous sodium sulfate. By fractional distillation, 22 g. of 1(2)-*p*-menthene was obtained. B. p. 50~54°C/3.5 mmHg; n_D^{12} 1.4766.

1(2)-*p*-Menthen-6-yl-carbinol (IX). — To a mixture of 12 g. of 1(2)-*p*-menthene, 3 g. of II, 17 g. of 95% acetic acid and 4 g. of ether, cooled to −2°C, a mixture of 7 g. of 95% acetic acid and 2.5 g. of 98% sulfuric acid was added, and the mixture was agitated for 5 hr. After being allowed to stand overnight, it was extracted with ether and the ethereal solution was washed with aqueous sodium bicarbonate and with water, dried over anhydrous sodium sulfate, and fractionally distilled to give 3 g. af 1(2)-*p*-menthen-6-yl-carbinyl acetate. B. p. 90~100°C/4 mmHg; n_D^6 1.4860.

A mixture of 3 g. of the acetate, 4 g. of potassium hydroxide, 40 cc. of methanol and 1 cc. of water, was refluxed on a warm water bath for 3 hr. The product was extracted with ether, and the ethereal solution was washed with water and dried over anhydrous sodium sulfate. Evaporation of the ether and fractional distillation gave 2 g. of the carbinol (IX). B. p. 95~97°C/3 mmHg; n_D^9 1.4896.

The authors are indebted to Shonan Aromatic Perfumery Co., Ltd. for *d*-limonene and to Mr. A. Matsuda for technical assistance.

Department of Applied Chemistry
Faculty of Technology
Chiba University
Matsudo-shi, Chiba

14) F. W. Semmler, *Ber.*, **36**, 1036 (1903).
15) H. Katsuragi, *Koryo*, No. **24**, 25 (1953).
16) F. W. Semmler, *Ber.*, **40**, 2959 (1907).

Distribution of Neptunium between TBP and Some Mineral Acids

By Tomitaro ISHIMORI and Eiko NAKAMURA

(Received January 20, 1959)

Tri-*n*-butyl phosphate*, an excellent solvent which plays an important role in the Purex process, attracts the attention of chemists. For example, the distribution of plutonium was studied by McKay et al.[1] in the TBP-nitric acid system. Peppard et al.[2-5] are aggressively studying the behaviors of both actinides and lanthanides in TBP-mineral acid systems.

Although the extraction of neptunium with TBP has caused deep concern in connection with the isolation of the element[6,7], systematic studies on the behavior of the element are not known. Besides, the existence of three kinds of oxidation states of the element, (IV), (V) and (VI) makes the study complicated.

In the present paper, extraction of neptunium with TBP is studied systematically with the emphasis on its oxidation states.

* Tri-*n*-butyl phosphate is denoted by "TBP" in the present paper.

1) G. F. Best, H. A. C. McKay and P. R. Woodgate, *J. Inorg. & Nucl. Chem.*, **4**, 315 (1957).

2) D. F. Peppard, G. W. Mason and J. L. Maier, ibid., **3**, 215 (1956).

3) D. E. Peppard, S. W. Moline and G. W. Mason, ibid., **4**, 344 (1957).

4) D. F. Peppard, W. J. Driscoll, R. J. Sironen and S. McCarty, ibid., **4**, 326 (1957).

5) D. F. Peppard, G. W. Mason, J. L. Maier and W. J. Driscoll, ibid., **4**, 334 (1957).

6) H. A. C. Mckay, "First United Nations International Conference on the Peaceful Uses of Atomic Energy", Vol. VII, P/441, United Nations Publication, New York (1956).

7) E. K. Hyde, ibid., Vol. VII, P/728.

Experimental

Sources of Materials.—Neptunium-239 tracer is prepared from uranyl nitrate hexahydrate irradiated by JRR-1 reactor for 2 hr. After cooling several hours, the irradiated uranyl salt is converted into chloride and dissolved in 0.5 M hydrochloric acid solution. After reduction by a small amount of granulated zinc**, neptunium is extracted by about 5% TTA***-benzene. After rinsing with a small portion of 0.5 M hydrochloric acid solution, the benzene layer is contacted with >3 N hydrochloric, nitric, perchloric or sulfuric acid according to preference. Neptunium is thus obtained as acid solution. The TTA which might go into the tracer solution is removed by contact with benzene. The radiochemical purity of the tracer is checked by both gamma spectrometry and the decay measurement. Separation from fission products is excellent. But a small remaining amount of uranium was still found by a color reaction with hydrogen peroxide.

Protactinium-233 is isolated from irradiated thorium nitrate by solvent extraction. Irradiation is carried out in conditions similar to those mentioned above. Protactinium is separated from thorium by contacting concentrated nitric acid solution with 10% TBP-toluene. In this separation protactinium is extracted into the organic phase leaving thorium in the aqueous phase. After washing with concentrated nitric acid, protactinium is recovered by shaking with water. The resultant solution of protactinium-233 gives no precipitate by adding aqueous ammonia, showing that practically thorium does not remain. The radiochemical purity of protactinium-233 thus prepared is checked again by both γ-spectrometry and the measurement of the decay curve.

Hafnium-181 received from Oak Ridge National Laboratory is used without further purification.

Thorium-234 is prepared according to Dyrssen's[8] method. The radiochemical purity is checked by determining its half life of 24.1 days.

Determination of Distribution Ratios. — In the determination of the distribution ratio, *Kd*, of a specific nuclide, defined as the concentration of nuclide in the organic phase divided by that of nuclide in the aqueous phase of two equilibrated liquid phases, a portion of aqueous acid of the indicated concentration containing a radioactive nuclide is equilibrated against a portion of solvent which is previously pre-equilibrated with respect to the corresponding barren aqueous acid. Every contact is carried out on a milliliter scale. For example, a 2.5 ml. portion of 10.1 M nitric acid containing approximately 10^5 cpm neptunium-239 is equilibrated with a 2.5 ml. portion of undiluted TBP which was previously contacted with three successive equal-volume portions of barren 10.1 M nitric acid. All solvent pre-equilibrations are made immediately before the use to avoid any complications arising from solvent hydrolysis. Aliquots of each phase are pipetted into small glass tubes for gamma counting. Gamma counting is made by means of Philips' scintillation counter with bed type head. Scrubbings are carried out both for aqueous and organic phases, if necessary. The *Kd* values are calculated dividing cpm of the organic phase by that of the aqueous phase after making a correction for natural counting.

Results and Discussion

Nitric Acid-TBP System. — Nitric acid solution of neptunium tracer prepared as mentioned above contains both neptunium (IV) and (V). The relative abundance between neptunium(IV) and (V) varies according to the treatment of the tracer solution. The freshly prepared solution contains only a very small amount of neptunium(V), whereas standing for a few days or warming in boiling water makes neptunium(V) rich.

Nitric acid solution containing both neptunium(IV) and (V) is contacted with TBP. The resultant organic or aqueous

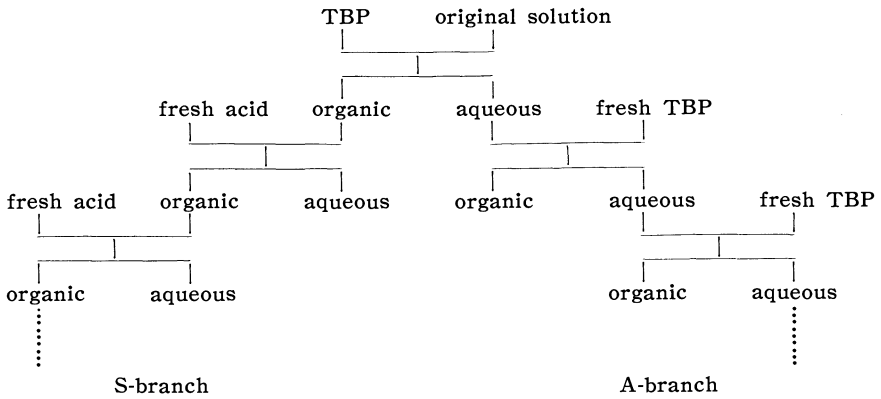


Fig. 1. The extraction scheme of neptunium.

** In order to avoid reduction of uranyl ion, reduction with zinc should be carried out at room temperature for only a few minutes.

*** Thenoyltrifluoroacetone

8) D. Dyrssen, *Svensk. Kem. Tid.*, **62**, 153 (1950).

phases are scrubbed with fresh acid solution or TBP, respectively. Scrubbings are carried out as shown in Fig. 1, until *Kd* values become practically constant, keeping the acidity of aqueous solution the same all through the procedures. Thus two values of *Kd*, Kd^{IV} and Kd^{V}, are obtained from S- and A-branches of the scrubbing scheme. Species which give Kd^{IV} and Kd^{V}, are assigned to neptunium (IV) and (V) respectively by the chemical behaviors against zinc, potassium bromate or TTA-benzene, to be mentioned below.

(*a*) *Oxidation with potassium bromate.* — The species which gives Kd^{IV} can not be oxidized with potassium bromate. At 0.5 N nitric acid Kd^{IV} value is 2.5. After adding the oxidant and scrubbing with a few portions of fresh acid, the *Kd* value remains almost constant, 2.7, showing that the species which gives Kd^{IV} is not practically oxidized.

On the other hand, Kd^{V} which is about 0.026 at 1 N nitric acid becomes about 16.3 after oxidation with potassium bromate and scrubbing with fresh acid solution. This change shows that the species which gives Kd^{V} is easily oxidized by potassium bromate. Besides that, the new third *Kd* value is also different from Kd^{IV} value of the same acidity. Accordingly this third value is supposed to be assigned to the hexavalent state. It is well known that neptunium(V) is easily oxidized by potassium bromate to neptunium(VI) state, whereas neptunium(IV) is not[9].

(*b*) *Reduction with zinc metal.* — Kd^{IV} value (6.92 at about 1 N) remains almost the same after adding zinc and heating on a water bath, whereas Kd^{V} value (0.026 at 1 N) becomes 7.8 after reduction with zinc metal****. This value almost coincides with that of Kd^{IV} at the same acidity, showing that the species which gives Kd^{V} is reduced to another species which gives Kd^{IV}.

(*c*) *Extraction with TTA.* — The comparison of extraction behaviors of the two species are given in Table I. The difference shown in the table again shows that the species which gives high Kd^{IV} in TBP-nitric acid system has high *Kd* in TTA extraction and is assigned to tetravalent[10], whereas another species which gives low Kd^{V} in TBP-nitric acid system has low *Kd* in TTA extraction and is assigned to quinquevalent[10].

TABLE I. THE BEHAVIOR OF NEPTUNIUM ON TTA EXTRACTION AT 1 N NITRIC ACID

Concn. of TTA in benzene (%, w/v)	*Kd* for the species which gives Kd^{IV} in TBP-HNO_3 system	*Kd* for the species which gives Kd^{V} in TBP-HNO_3 system
5.0	4.11	0.017
2.5	0.95	0.021
1.25	0.31	0.011

The variation of Kd^{IV} or Kd^{V} caused by changing the acidity of aqueous phase is shown in Fig. 2. In Fig. 3 acid dependences of neptunium(IV) and (V) are compared with those of hafnium(IV), thorium(IV), protactinium(V) and plutonium(IV). The thorium line is written according to Peppard et al.[2] and that of plutonium(IV) is rewritten based upon the values of McKay et al.[1] The behavior of neptunium(IV) shows strong similarity to that of plutonium(IV). However, *Kd* value of neptunium(IV) always lies below that of plutonium(IV) at the same acidity. *Kd* values of neptunium(IV) and thorium are almost the same at acidities less than 10 N. But the neptunium(IV) curve shows a maximum at about 9 N while that foi

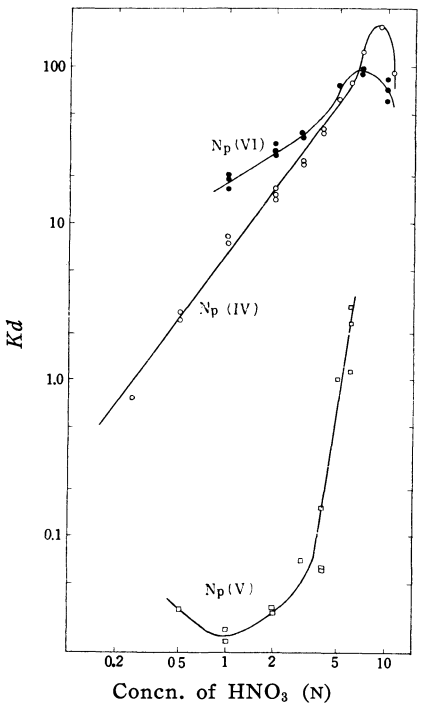


Fig. 2. The *Kd* values of neptunium in HNO_3-100% TBP.
—●— Np(VI) —○— Np(IV) —□— Np(V)

9) G. T. Seaborg and J. J. Katz, "The Chemistry of the Actinide Elements", Methuen and Co., Ltd., London (1957), p. 231.

**** The solution gives *Kd*=0.064 after heating on a water bath without zinc.

10) F. L. Moore, *Anal. Chem.*, **29**, 941 (1957).

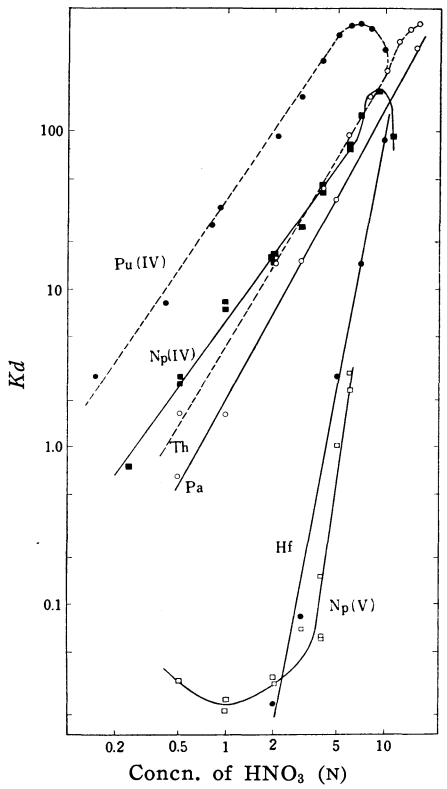


Fig. 3. The *Kd* values of neptunium, plutonium, thorium, protactinium and hafnium.
—●— Pu(IV) —■— Np(IV) —●— Hf
---○--- Th —□— Np(V) —○— Pa

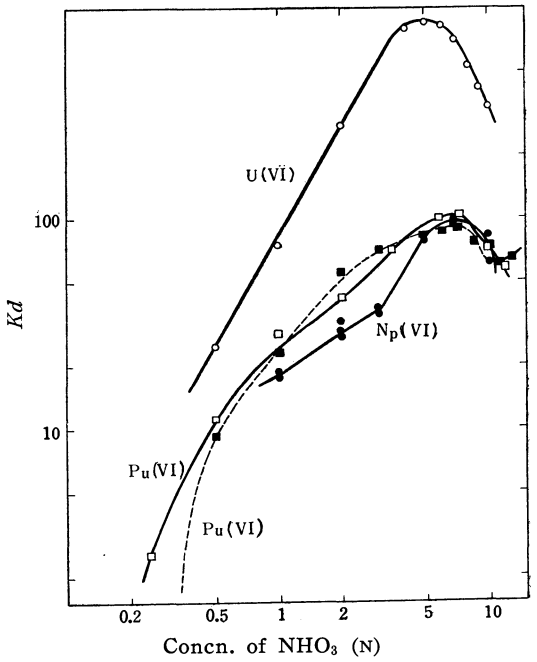


Fig. 4. The *Kd* values in HNO_3-100% TBP system.
—○— U(VI) —□— Pu(VI)
—●— Np(VI) —■— Pu(VI)

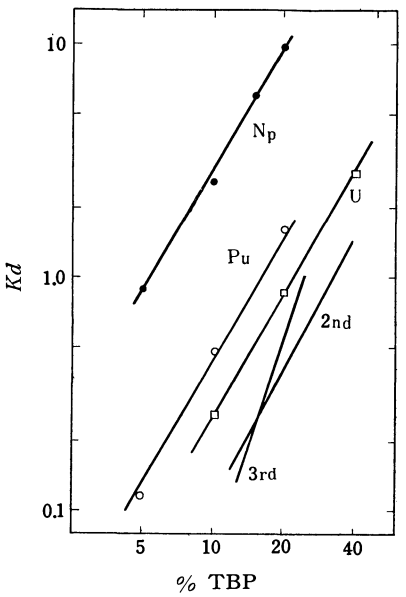


Fig. 5. The solvent dependence of *Kd* values in HNO_3-100% TBP system.
—●— Np(VI) at 10 N HNO_3
—○— Pu(VI) at 11.5 N HNO_3
—□— U(VI) at 0.27 N HNO_3

thorium does not. Hafnium shows a quite different behavior from that which neptunium(IV) does.

The behavior of neptunium(V) resembles that of hafnium(IV) more than that of protactinium(V).

As mentioned already neptunium(VI) is prepared easily by oxidation of neptunium (V) with potassium bromate and scrubbing of TBP phase with fresh acid solution in order to remove neptunium(V). Alternatively ceric ammonium nitrate works well as the oxidant in this case. The acid dependence of *Kd* value for neptunium(VI) is also given in Fig. 2. A comparison of *Kd* values for uranium(VI), neptunium(VI) and plutonium(VI) is also seen in Fig. 4. Naito[11] gave *Kd* values for macro amounts of uranium in 20% TBP in carbon tetrachloride-nitric acid system. He also found second power dependence of *Kd* in this system. Accordingly the present authors rewrite uranium (VI) curve of Fig. 4 multiplying Naito's *Kd* value with the factor of 25 in order to make it represent *Kd* values for 100% TBP-nitric acid solution system. Broken plutonium(VI) curve of Fig. 4 is rewritten

in a similar way correcting the values of McKay et al.[1] which were obtained with diluted TBP. The other plutonium(VI) curve represents values obtained by one of the present authors. As is known very well, correction with solvent dependence is not so satisfactory. Besides that, there might be some differences between behaviors of macro and micro amounts of actinide elements. Therefore, the comparison with each other of 3 curves in Fig. 4 will not be valid for a strict discussion. But it is remarkable that all of them show a maximum *Kd* value at about 6 or 7 N.

Solvent dependence of *Kd* value for neptunium is checked at 10 N nitric acid. As shown in Fig. 5, neptunium(VI) shows second power dependence. The figure shows also second power solvent dependences of uranium(VI) and plutonium(VI) according to the values obtained by Naito for uranium[11] and Mckay et al. for plutonium[1]. Here again strong similarity is shown among hexavalent uranium, neptunium and plutonium.

Hydrochloric Acid-TBP System. — Neptunium(VI) prepared by oxidizing neptunium(IV) and (V) with potassium chlorate and heating in boiling water shows *Kd* values as shown in Fig. 6. *Kd* values of uranium obtained by using uranium-233 as the tracer in the form of uranyl chloride are also show in the same figure in order to compare them with those for neptunium(VI). The acid dependences of these two elements are very similar in the shape indicating strong similarity in the chemical behaviors of these two species. However, neptunium(VI) is more extractable than uranium(VI) all through the acidity range investigated.

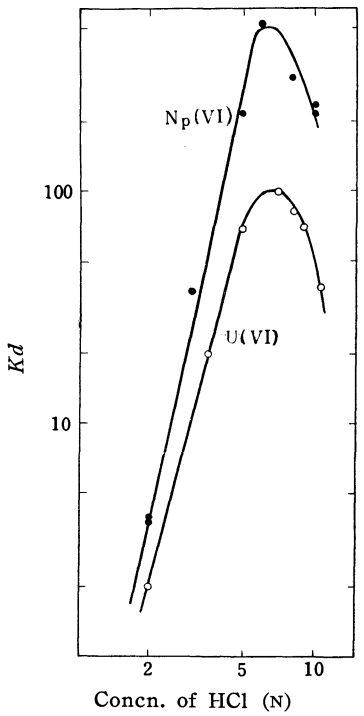


Fig. 6. The acid dependence of *Kd* values for neptunium and uranium.
—●— Np(VI) —○— U(VI)

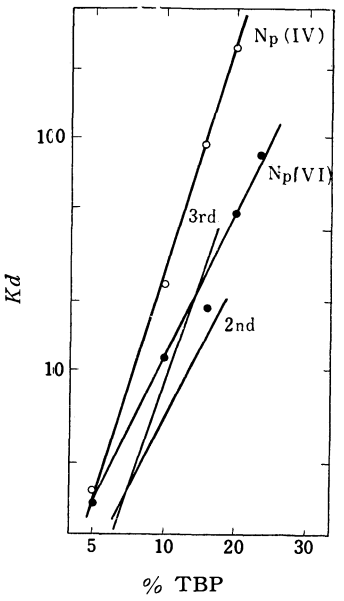


Fig. 7. The *Kd* values in diluted TBP-HCl system.
—●— Np(VI) at 6 N HCl
—○— Np(IV) at 8 N HCl

The solvent dependence of *Kd* for neptunium is studied at 6 N hydrochloric acid and found to be of second power as is seen in Fig. 7. Diluent used is toluene and TBP concentration is shown in volume per cent.

Neptunium(V) is prepared in hydrochloric acid solution by reducing neptunium(VI) with hydrazine sulfate. On the other hand, a solution of neptunium (IV) is prepared by recovering neptunium from TTA-benzene with hydrochloric acid (>3 N) and then treating it with hydroxylamine hydrochloride, granulated zinc or ascorbic acid in order to reduce neptunium(V) which comes into the solution in very small amount. Fig. 8 shows acid dependences of *Kd* values for both neptunium(V) and (IV) as well as those for hafnium, thorium and protactinium. The

11) K. Naito, In press.

neptunium(V) line is quite different from that of protactinium(V). In the range of 9~4 N, *Kd* of neptunium(IV) shows almost the same slope as those of thorium(IV) and hafnium(IV). It is notable that the acid dependence of neptunium(IV) shows a maximum at about 8 N.

The solvent dependence of *Kd* values for neptunium(IV) is studied at 8 N using toluene as the diluent. The result shows third power dependence as given in Fig. 7.

Sulfuric Acid-TBP System.—Neptunium (VI) in sulfuric acid solution is prepared by oxidation of the mixture of neptunium (IV) and (V) with ceric sulfate, while neptunium (V) is prepared by reducing neptunium (VI) with hydrazine sulfate. Variation curves of *Kd* values for both neptunium (V) and (VI) caused by the variation of the acidity in aqueous phases are given in Fig. 9. Extraction can not be carried out in the acidity range over about 20 N, because TBP becomes miscible with aqueous phase at such high acidity. Generally *Kd* values for both neptunium(V) and (VI) are small, their highest values being only about 2.5. The acid dependence of *Kd* values for protactinium is shown in Fig. 9 in order to compare it with that for neptunium(V).

Neptunium(IV) is prepared by contacting sulfuric acid solution with TTA-benzene which contains neptunium. In order to prevent contamination of neptunium (V), the resultant acid solution is treated

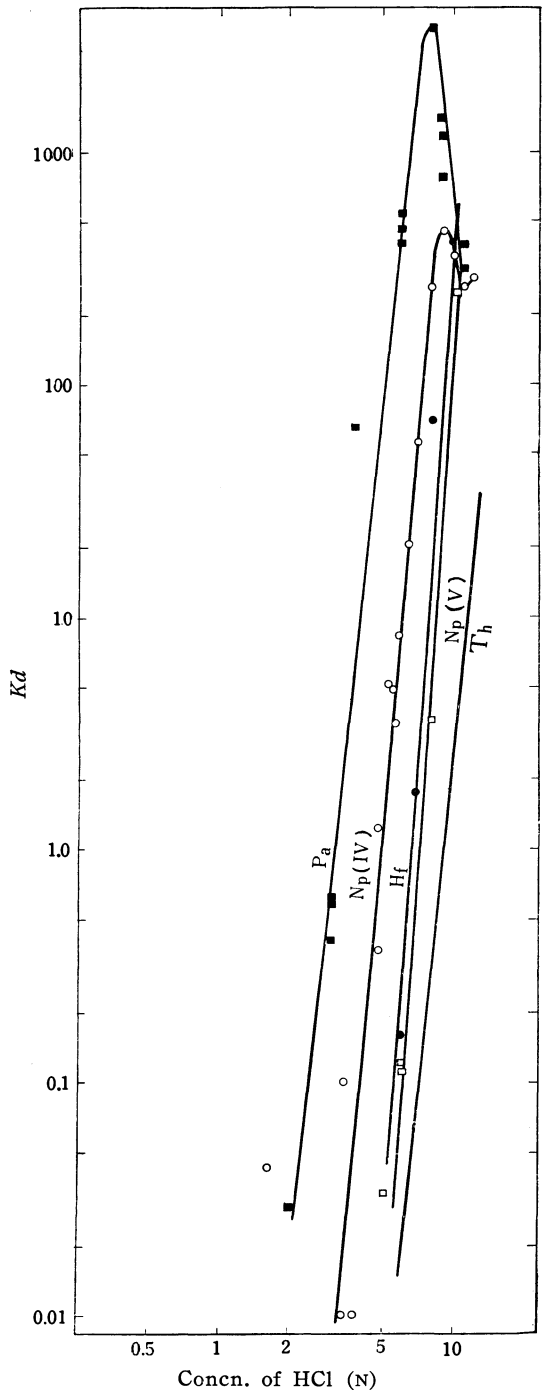


Fig. 8. The *Kd* values in HCl-100% TBP system.
—○— Np(IV) —□— Np(V) —— Th
—●— Hf —■— Pa

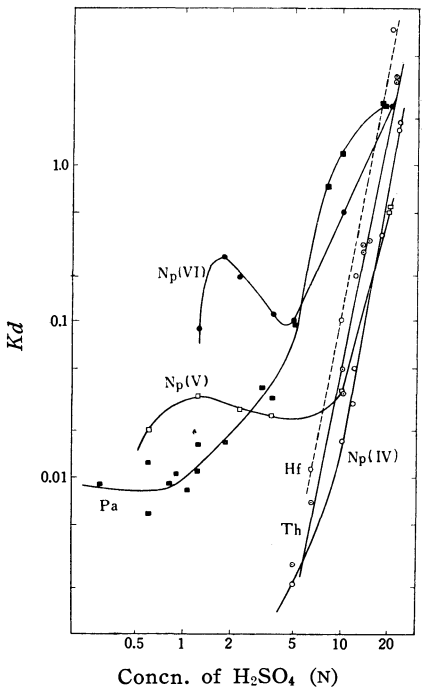


Fig. 9. The *Kd* values in H_2SO_4-100% TBP system.
—●— Np(VI) —■— Pa ---○--- Hf
—○— Np(IV) —□— Np(V) —⊙— Th

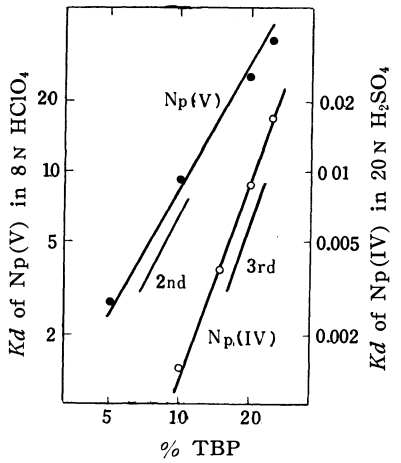


Fig. 10. The *Kd* values in diluted TBP-$HClO_4$ or H_2SO_4 system.
—●— Np(V) at 8 N $HClO_4$
—○— Np(IV) at 20 N H_2SO_4

with hydroxylamine hydrochloride and ferrous sulfate or 0.1 M hydroquinone and potassium iodide at higher acidities, while it is treated with granulated zinc at lower acidities. Acid dependence of *Kd* values for neptunium(IV) can also be seen in Fig. 9 where those for hafnium and thorium are added for comparison. These three curves resemble each other considerably. It is noted that in the range of lower acidities neptunium (IV) gives lower *Kd* values than neptunium(V) does.

The solvent dependence of *Kd* values for neptunium(IV) is studied at 20 N sulfuric acid and found as a third power. (Fig. 10).

Perchloric Acid-TBP System.—Perchloric acid (>3 N) solution obtained by contacting with neptunium solution in TTA-benzene contains only neptunium(V). This assignment is based on the following experiments:

(a) 3.4 N perchloric acid containing neptunium(V) is contacted with almost equal volume of TBP pre-equilibrated with 9 N hydrochloric acid. The resultant organic phase is equilibrated with many portions of 9 N hydrochloric acid successively. In this way, the system is converted to hydrochloric acid-TBP system. Finally *Kd* value approaches that of neptunium(V) at 9 N hydrochloric acid. (b) By oxidation with silver peroxide this species becomes another species which could be assigned to neptunium(VI).

The acid dependences of *Kd* values for both neptunium(V) and (VI) are given in Fig. 11 as well as that of protactinium.

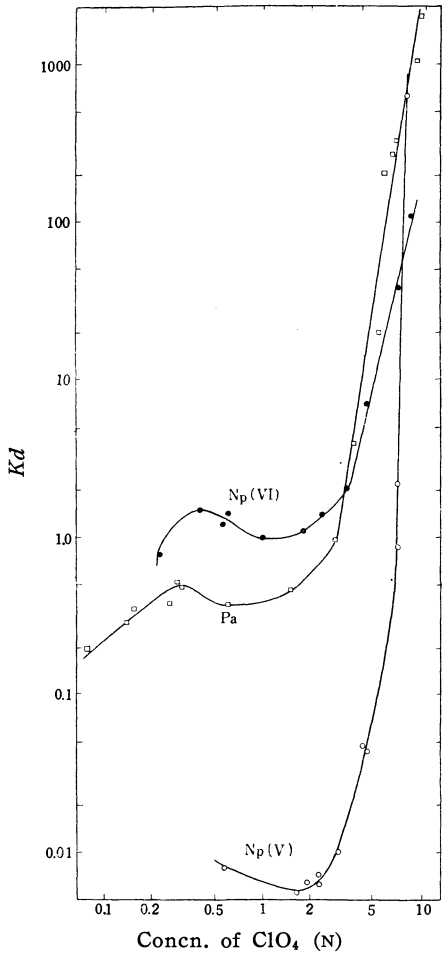


Fig. 11. The *Kd* values of neptunium and protactinium in $HClO_4$-100% TBP system.
—●— Np(VI) —□— Pa —○— Np(V)

It is characteristic that the neptunium(V) curve shows very rapid increase in *Kd* at the range of 3~8 N acidity. As will be shown later, this can be utilized for isolation of neptunium from irradiated uranyl nitrate.

As 8 N perchloric acid, the solvent dependence of *Kd* values for neptunium(V) is studied. The result is shown in Fig. 10.

The Reduction of neptunium(V) with hydroquinone and potassium iodide, hydrogen peroxide, granulated zinc or 3% zinc amalgam is not successful. Accordingly *Kd* values which could be assigned to the tetra-positive state can not be found.

Isolation of Neptunium from Irradiated Uranyl Nitrate. — As Fig. 11 shows, *Kd* for neptunium(V) in perchloric acid-TBP system varies from 800 at 8 N to 0.006 at 2 N. This is utilized in the isolation of

neptunium without introducing any other reagent.

Procedure. — Neutron irradiated uranyl nitrate hexahydrate is dissolved in a small volume of concentrated perchloric acid. The solution is heated under an infrared lamp in order to expel nitric acid. The residue is taken up by a few ml. of concentrated perchloric acid and the resultant solution is heated by dipping in boiling water for about 10 min. After cooling, it is shaken with 100% TBP. The organic phase contains neptunium(V) and uranium, while most of the fission products remain in the aqueous phase. The separated organic phase is shaken with 3 portions of 2 N perchloric acid. The resultant aqueous phase contains neptunium(V) and a small amount of uranium, while a large amount of uranium remains in organic phase. The resultant aqueous phase is washed with benzene in order to remove TBP, dried up under the infrared lamp, and dissolved into concentrated perchloric acid. The whole procedure is repeated as shown in Fig. 12.

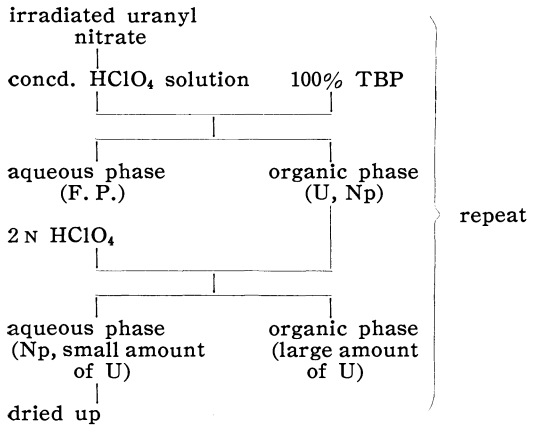


Fig. 12. Scheme for isolation of Np.

The yield of neptunium is 99%, and the decontamination of fission products is excellent. A very small amount of uranium remains.

Summary

Neptunium-239 is used as the tracer for studies on solvent extraction behaviors of neptunium in the following system:

1. Nitric acid solution and TBP.
2. Hydrochloric acid solution and TBP.
3. Sulfuric acid solution and TBP.
4. Perchloric acid solution and TBP.

Kd values are measured by combinations of scrubbing techniques and chemical treatments. In nitric, hydrochloric and sulfuric systems, neptunium gives three kinds of *Kd*, distribution ratio which could be assigned to oxidation states of (IV), (V) and (VI). On the other hand, in the perchloric system neptunium does not show *Kd* value which should be assigned to the oxidation state(IV).

Some of these results are compared with those of uranium, plutonium and other elements. In the nitric system, neptunium(VI) shows an acid dependence of *Kd* value similar to those of uranium (VI) and plutonium(VI). *Kd* values of neptunium(IV) and plutonium(IV) vary in almost the same way against the acid concentration of nitric acid. There is also a strong similarity between acid dependences of uranium(VI) and neptunium (VI) in the hydrochloric system.

Behavior of neptunium(V) are compared with those of protactinium.

Finally a simple method for isolation of neptunium from irradiated uranyl salt is stated.

The authors wish to express their sincere thanks to Dr. Kenjiro Kimura who afforded them convenience for this study in many ways.

Chemistry Division, Tokai Laboratory
Japan Atomic Energy
Research Institute
Tokai, Ibaraki

Spectrochemical Study of Microscopic Crystals. XIX[1] *The Structure and Absorption Spectra of Fremy's Salt*

By Shoichiro YAMADA and Ryutaro TSUCHIDA

(Received February 4, 1959)

In the nineteenth century, Fremy[2] isolated an interesting compound having an empirical formula of $ON(SO_3)_2K_2$, which is violet-blue in solution and yellow in the crystalline state. This phenomenon, which has been studied by a number of investigators[3,4] was eventually understood on the assumption that the compound might consist of monomeric ions in solution and of dimeric ions in the crystalline state[5-7]. Aside from the electronic structure of the monomeric ion involving a queer type of bonding, the structure of the dimeric ion was often discussed by the earlier investigators, but still remains in dispute. Although the compound has been studied from various sides, no spectral data have so far been reported. In an attempt to elucidate the structure of Fremy's salt, we have carried out a spectroscopic study with this salt and related compounds.

Experimental

Materials. — Potassium peroxylamine disulfonate, $K_2(O_3S)_2NO$, was prepared by the method of Haga[8] with slight modification. To a solution of 17.5 g. of sodium nitrite in 50 ml. of water were added 100 g. of crushed ice, a solution of 25 g. of sodium hydrogen sulfite in 50 ml. of water under continuous stirring, and finally 10 ml. of glacial acetic acid. After a few minutes the reaction mixture was rendered alkaline by the addition of 7 ml. of concentrated aqueous ammonia (*d*, 0.880), and then a solution of 6.3 g. of potassium permanganate in 200 ml. of water was added under stirring. The precipitate of manganese dioxide which was at once formed was removed by filtration. To the violet-colored filtrate was added 250 ml. of a saturated solution of potassium chloride. Orange-yellow crystals which precipitated were filtered by suction, and washed successively with a 5% solution of potassium hydroxide, ethanol and acetone. Recrystallization from water yielded orange-yellow crystals of Fremy's salt, which showed the typical reactions of Fremy's salt. Thus the crystals were dissolved in water to give a blue-violet solution, from which the orange-yellow crystals separated again on concentration. Potassium peroxylamine disulfonate thus prepared was found to form blue-colored mixed crystals with potassium hydroxylamine disulfonate, which was prepared in colorless crystals according to the method of Rollefson and Oldershaw[8].

The mixed crystals were prepared in the following way. Into 45 ml. of a 5% solution of potassium hydroxide were added 1 g. of potassium hydroxylamine disulfonate and 0.5 g. of potassium peroxylamine disulfonate at 45°C. The solution was filtered and cooled with crushed ice. After twenty hours large mixed crystals which were blue in color began to separate together with the crystals of potassium peroxylamine disulfonate. The blue mixed crystals were picked up from the mixture mechanically. Accurate determination of the $K_2(O_3S)_2NO$ content in the mixed crystal was not made, but approximate estimation from the intensity of the "NO band" showed it to be only a few per cent. The value seems to agree well with those reported earlier[5].

Measurements.—Quantitative dichroism measurements in the visible and ultra-violet regions were carried out at room temperature by Tsuchida and Kobayashi's microscopic method[9].

Absorption spectra of the compounds in aqueous solution were determined at room temperature by a Beckman DU spectrophotometer.

Infrared absorption spectra of the compounds in Nujol mulls and in potassium bromide discs were determined in the rock salt region by a Hilger H 800 infrared spectrophotometer.

The notations in the present paper are the same as those used in the former papers of this series.

Results and Discussion

Visible and Ultra-violet Absorption Spectra.—The mixed crystal formed from $K_2(O_3S)_2NOH$ and $K_2(O_3S)_2NO$ shows an absorption band at 52×10^{13}/sec., as seen

1) Part XVIII of this series, S. Yamada and R. Tsuchida, This Bulletin, **31**, 813 (1958).
2) E. Fremy, *Ann. chim. phys.*, **15**, iii, 408 (1845).
3) F. Raschig, *Ann.*, **241**, 223 (1887).
4) A. Claus, ibid., **158**, 205 (1871).
5) A. Hantzsch and W. Semple, *Ber.*, **28**, 2744 (1895).
6) T. Haga, *J. College of Sci. Imp. Univ. Tokyo*, **19**, No. 15 (1904); T. Haga and E. Divers, *J. Chem. Soc.*, **77**, 440 (1900).
7) R. W. W. Asmussen, *Z. anor. allgem. Chem.*, **212**, 316 (1933).
8) T. Haga, *J. Chem. Soc.*, **85**, 78 (1904); G. K. Rollefson and C. F. Oldershaw, *J. Am. Chem. Soc.*, **54**, 977 (1932).
9) R. Tsuchida and M. Kobayashi, "The Color and the Structure of Metallic Compounds", Zoshindo, Osaka (1944), p. 180 (in Japanese).

in Fig. 1. It has been found by the present measurements that for the band at 52×10^{13}/sec. the A-absorption in Fig. 1 is at least ten times stronger than the B-absorption. The difference in intensity between the two absorptions was so great that exact determination of the dichroic ratio could not be made.

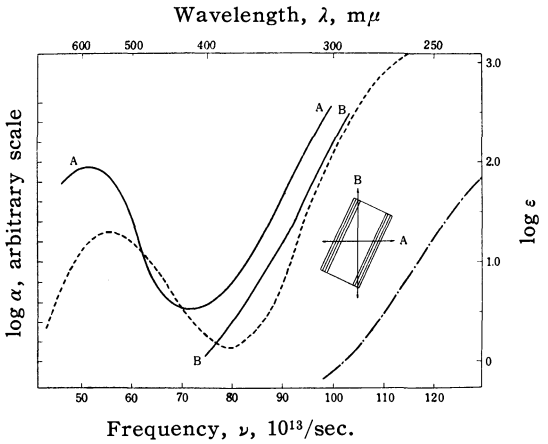


Fig. 1. Absorption spectra of a mixed crystal from $K_2(O_3S)_2$ NO and $K_2(O_3S)_2$·NOH, and its components: the mixed crystal in the solid state, ——: $K_2(O_3S)_2$·NO in 5% KOH solution, ----: $K_2(O_3S)_2$·NOH in water, ·—·—.

Comparison of the absorption spectrum of the mixed crystal with the spectra of $K_2(O_3S)_2NOH$ and $K_2(O_3S)_2NO$ in solution (Fig. 1) reveals that the band at 52×10^{13}/sec. of the mixed crystal in the solid state may evidently be ascribed to the component, $K_2(O_3S)_2NO$, since the other component has no absorption in the neighborhood of this absorption band. It is presumed, in a similar way, that the state of the peroxylamine disulfonate ion in the mixed crystal is similar to that of Fremy's salt in water. Previously Asmussen[7] concluded from magnetic measurements that $K_2(O_3S)_2NO$ in aqueous solution consists largely of monomeric ions; the three-electron bond is usually assumed to be involved in the bonding within the NO-group of the monomer. Therefore, it may be certain that Fremy's salt exists as a monomeric form when incorporated into the mixed crystal with $K_2(O_3S)_2NOH$. Thus the band at 52×10^{13}/sec. of the mixed crystal may be ascribed to the $(O_3S)_2NO^{2-}$ ions under the effect of the field by the surrounding ions. The band is, therefore, regarded as due primarily to the NO-group in the monomeric ion under small perturbation from the surrounding ions, although the bonding around the NO-group should not be considered, in a strict sense, to be isolated from the other part of the ion. The present measurements show that *the NO-band, in which the three-electron bond may be involved, is highly polarized.*

The effects of solvents upon the absorption band have also been examined. Formerly the "nitroso-band" at about 700 mμ of nitroso-derivatives and the band at about 350 mμ of a nitrite ion were reported to undergo a "blue solvent effect"[10]. This fact was then assumed to show that both the bands were due to $n-\pi^*$ transitions. On the contrary, the present measurements indicate that the absorption band at about 55×10^{13}/sec. (540 mμ) of the $ON(SO_3)_2^{2-}$ ion is displaced to longer wavelengths on changing a solvent from ethanol to water. The "red shift" of the band seems to show that the band may originate from a $\pi-\pi^*$ transition[10], although the intensity of the band is rather small for this type of transition. This appears to be consistent with the electronic structure of the NO group having a sort of three-electron bond, since the absorption band in question may originate from a transition of one of the three bonding electrons to an excited level.

It was reported earlier that the above mentioned bands, ascribed to the $n-\pi^*$ transition, were polarized perpendicularly to the plane of the NO-group in nitrosobenzene and its derivatives[11] or to the plane of an NO_2^- ion[12]. As for the band of the monomeric ion of $ON(SO_3)_2^{2-}$, which possibly originates from a $\pi-\pi^*$ transition and may be different in its origin from the above mentioned bands, we are inclined to regard it likely that the polarization of the band would be along the plane of the NO-group. Thus the A-absorption in Fig. 1 may correspond to the electric vector along the NO-group, and the B-absorption to the electric vector perpendicular to the NO-group. In order to confirm this suggestion, however, further study seems to be desirable.

Infrared Absorption Spectra. — Results of the present measurements are shown in Table I. Tentative assignment of the

10) H. McConnell, *J. Chem. Phys.*, **20**, 700 (1952); M. Kasha, *Discussions Faraday Soc.*, **9**, 14 (1950), etc.
11) K. Nakamoto and K. Suzuki, *J. Chem. Phys.*, **20**, 1971 (1952).
12) W. G. Trawick and W. H. Eberhardt, ibid., **22**, 1462 (1954); J. W. Sidman, *J. Am. Chem. Soc.*, **78**, 2911 (1956).

TABLE I. INFRARED ABSORPTION SPECTRA OF FREMY'S SALT AND RELATED COMPOUNDS IN THE SOLID STATE

Tent. Assign.	Mixed crystal $K_2(O_3S)_2NOH+K_2(O_3S)_2NO$*	$K_2(O_3S)_2NOH$	(presumed) $K_2(O_3S)_2NO$	$K_4[(O_3S)_2NO]_2$
O-N-SO_3	870 m	870 m	860~870 m	850 m
H-O-N	980 m	945 m		
SO_3	1030 s	1030 s		
SO_3	1050 s		1050 s	1050 s
SO_3	1085 m	1070 m	1080 m	1070 s
SO_3	1260 s	1255 s		
SO_3	1285 s		1285 s	1290 s
NO-str.	1620 m		1620 s	1260 s

* A very small amount as compared with the other component.
s: strong, m: medium intensity.

observed absorption bands to particular group-vibrations was made using the assignment by Drago[13] for $K_2(O_3S)(NO)_2$ and by Griffith and others[14] for Fremy's salt. Griffith and others have also reported the infrared absorption spectrum with Fremy's salt[15]. Unfortunately they did not state whether the measurements refer to the compound in the solid state, or in aqueous solution. Their measurements were probably made in the solid state in which the compound consists of the dimeric form, since their data agree with ours for the $[(O_3S)_2NO^{2-}]_2$ ion. They have not presented any detailed discussion about the infrared spectrum or the structure of the dimer, but mentioned the compound as having an N-N linkage. It seems, however, that no reports have appeared which may be regarded to establish the structure of the dimeric ion with certainty, as far as literatures accessible to us are concerned.

The infrared absorption bands of the monomeric $ON(SO_3)_2^{2-}$ ion were determined by comparing an absorption spectrum of the mixed crystal from Fremy's salt and potassium hydroxylamine disulfonate with the spectrum of the latter alone. Although some effects, such as hydrogen bonds, which possibly exist in the mixed crystal, are liable to complicate the spectrum and make the exact assignment of the absorption bands difficult, the interpretation of the absorption spectrum of $K_2(O_3S)_2NO$ has been possible. In a strict sense, the infrared absorption bands are not to be ascribed to particular groups within a molecule, but to a molecule or an ion as a whole. Nevertheless, the discussion, as is given here, may be correct for the nature and the purpose of the present work.

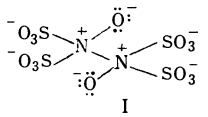
The vibrations which are ascribed to the $(O_3S)_2NO^{2-}$ ion in the mixed crystal are given in Table I, where the vibrations due to the sulfonate groups are added together, since the ion would certainly show the vibrations of the sulfonate groups. A rather strong band at 1620 cm^{-1} of the monomeric $(O_3S)_2NO^{2-}$ ion may be due possibly to an NO-stretching vibration. This assignment is regarded as reasonable, in view of the NO-frequencies which were formerly reported for other compounds: nitroalkyls[16] 1560~1500 and 1350~1300 cm^{-1}, dimeric nitrosomethane[17] 1282 cm^{-1}, nitrosamine 1455 cm^{-1} in a monomeric form and 1310 cm^{-} in a dimeric form[18]. Thus the rather high frequency of the NO-vibration for the monomeric $(O_3S)_2$ NO^{2-} ion is found to correspond to comparatively high bond-order of the NO-linkage, being in agreement with the assumption of the three-electron bond.

The Structure of the Dimeric Form of Fremy's Salt. — The structure of the dimeric form of Fremy's salt has formerly been examined by a number of investigators. Hantzsch and Semple[5] assumed that the violet-blue and the yellow form are, respectively, the monomeric and the dimeric form of Fremy's salt, comparing the relation between them to that between nitrogen dioxide and dinitrogen tetroxide. Investigating chemical property of Fremy's salt in aqueous solution, Haga and Divers[6] proposed a structure, $K_4(O_3S)_2NO\cdot ON(SO_3)_2$, for the monomeric form of Fremy's

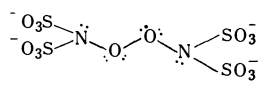
13) R. S. Drago, ibid., **79**, 2049 (1957).
14) W. P. Griffith, J. Lewis and G. Wilkinson, *J. Inorg. Nucl. Chem.*, **7**, 38 (1958).
15) They denote Fremy's salt as $K(O_3S)(NO)_2$, but the compound should be represented by an empirical formula of $K_2(O_3S)_2NO$, as has usually been adopted for the compound.
16) L. J. Bellamy, "The Infrared Spectra of Complex Molecules", Methuen and Co., London (1954).
17) B. G. Gowenlock and J. Trotman, *J. Chem. Soc.*, **1955**, 4190.
18) R. n. Haszeldine and B. J. H. Mattinson, ibid., **1955**, 4172.

salt in solution and double the formula for the dimeric form. Much later, Asmussen[7] investigated the compound magnetochemically only to reaffirm Hantzsch and Semple's hypothesis, and regarded that Fremy's salt in aqueous solution exists as an equilibrium mixture consisting of a monomeric form in most part and a dimeric form in a very small amount. Neither Asmussen nor Hantzsch and Semple, however, presented a structural formula for the dimer after all. The structures, as proposed long ago for the dimer of Fremy's salt by Rasching[3] and by Claus[4], are not quite satisfactory, in view of insufficient materials available as well as because of poor knowledge at that time about the chemical bonds in general. Thus the problem of the structure of the dimer is not to be regarded as settled, but reexamination of the structure seems to be most desirable.

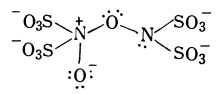
Examination of the possible electronic structures seems to indicate that the following three configurations (Fig. 2) may most probable for the dimer, the structures with resonance which involves the sulphonate-groups being omitted.



I



II



III

Fig. 2. Possible configurations for the dimeric form of Fremy's salt.

Examination of the steric requirements using molecular models shows that structure I seems to be very difficult, although it might not be quite impossible. Thus crowding of one oxygen atom and two sulfonate-groups around the nitrogen atom would hinder dimerization through an N–N linkage. Structure III is also difficult sterically, although this may not be impossible. On the other hand, structure II suffers no steric hindrance. Structure II, therefore, seems to be most probable from this standpoint.

The present measurements of UV spectra show that the electronic state of the dimer deviates greatly from the state of the monomer, since the UV absorption spectrum of Fremy's salt in the crystalline state is quite different from that of the monomer (Fig. 3). Thus the absorption band at about 55×10^{13}/sec., which is due primarily to the NO-group in the monomer, disappears with the dimer. Instead, the latter shows a few absorption

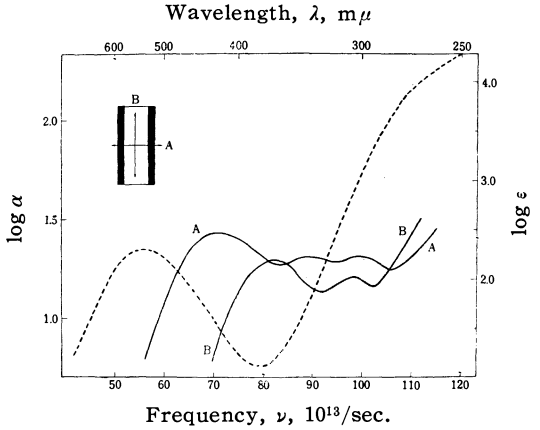


Fig. 3. Absorption spectra of Fremy's salt in the crystalline state (——) and in aqueous solution (----).

bands in the visible region and its neighborhood. If the dimer were represented by structure I, it would not exhibit an absorption band in the visible region, as is readily expected from absorption spectra of its related compounds. Previous data indicate that the dimer of nitrosomethane, which has a configuration similar to structure I, shows an absorption band at about 280 mμ (107×10^{13}/sec.) but no absorption band in the visible region, much less the "nitroso-band" at about 650 mμ (46×10^{13}/sec.). Since inspection of the structural formulae shows that structure I might involve N–O bonds with lower bond order than that of the N–O bond in the dimer of nitrosomethane, the ion represented by structure I would not show an absorption band in the neighborhood of the visible region. In fact, the present measurements indicate that the dimer of Fremy's salt has a few absorption bands in this wavelength range. Structure I, therefore, is rejected on the basis of the UV absorption spectra as well as of the steric requirements.

Absorption spectra of the compounds

which are somewhat similar to the compound represented by structure II have previously been studied. Thus Kortüm and Finckh[19] reported absorption spectra of sodium nitrite, pernitrite, hyponitrite and related compounds in solution, which were found to display absorption bands in the comparatively long wavelength region. Structure II, therefore, may not be inconsistent with the present observation that the compound in question displays absorption bands in the visible region and its neighborhood. Structure III, however, may not be excluded from the visible and ultra-violet spectrum alone.

The above discussion on the structure of the dimer of Fremy's salt is corroborated by the infrared absorption spectra. It is seen in Table I that the monomeric ion of $(O_3S)_2NO^{2-}$ shows a strong band at about 1620 cm^{-1} which is due to the N–O stretching vibration, whereas the dimeric ion shows the corresponding bands at 1260 cm^{-1}. Structure III would show the corresponding bands of high intensity due to the N–O stretching vibrations at wavenumbers smaller than the vibration of the monomer. Thus, at least a few absorption bands due to the N–O stretching vibrations might be observed in the infrared spectrum for structure III, since three kinds of the NO-groups are involved in this structure and those vibrations are all infrared active. The fact that there is observed only one absorption band of this sort for the dimer is not consistent with structure III, although a possibility might remain that some of the absorption bands would be hidden under strong bands due to the sulfonate groups.

On the contrary, structure II has only one kind of N–O bond, and the symmetric vibration due to the NO groups is infrared inactive. Only the symmetric vibration is infrared active, and may be regarded as corresponding to the band at 1260 cm^{-1}. Thus the infrared spectrum may be reconciled in a satisfactory way with structure II. Further evidence for this conclusion may be obtained by complete analysis of the infrared absorption spectra, which, however, requires data of the Raman spectrum with this compound. The determination of it would be enlightening in this respect. Based on the infrared spectrum alone, structure I might also be possible, but this structure has been shown in the preceding part of the present paper to be inconsistent with the UV spectra and steric requirements.

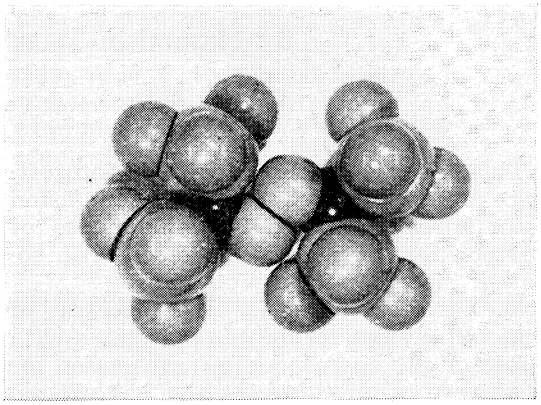


Fig. 4. Stuart model of $(O_3S)_2NO\cdot ON(SO_3)_2^{4-}$.

All the above materials combined seem to favour most strongly structure II having an O–O linkage. — A Stuart model representing structure II is shown in Fig. 4. This conclusion on the structure of the dimer seems to be noteworthy, since it is known that most nitroso-derivatives tend to form dimers involving a linkage of an N–N type.

Summary

Absorption spectra in the visible and ultra-violet region have been determined at room temperature by Tsuchida and Kobayashi's microscopic method with crystals of Fremy's salt and related compounds. Infrared absorption spectra have also been measured with these compounds.

The results of the measurements are discussed in relation to the structure of the compounds. A steric condition, visible and ultra-violet absorption spectra and infrared spectra are found to be in best agreement with a structure having a peroxide grouping.

The present authors wish to thank the Ministry of Education for a grant-in-aid, Mr. H. Nakamura for experimental assistance, and Mr. Ishikawa for infrared spectra.

Department of Chemistry, Faculty of Science, Osaka University
Nakanoshima, Osaka

19) G. Kortüm and B. Finckh, *Z. physik. Chem.*, B48, 32 (1941).

On the Difference between L-Forms and the Corresponding DL-Forms of Amino Acids in their Solid-State Infrared Spectra

By Masamichi TSUBOI and Tadao TAKENISHI

(Received February 6, 1959)

This paper is concerned with an interesting fact which led us to a conclusion that there are three different modes of composition of D- and L-molecules in so-called racemates of amino acids.

We have compared infrared spectra[1] of optically active forms in solid states with those of the corresponding racemates for a variety of amino acids, and have found that these results of the comparisons are grouped in three classes, A, B and C, as given below. It is remarkable that the distinction between these classes is sharp and that there is none intermediate between them.

(A) In class A, *the spectra of the L- and DL-forms are identical.*—Examples[1]: threonine, histidine hydrochloride monohydrate. Here, every band of the DL-form is observed at the same position with the same relative intensity as the corresponding band of the L-form, within the limits of experimental error.

(B) In class B, *the spectra of the L- and DL-forms are a little different from each other.*—Examples[1]: tyrosine (see Fig. 1), alanine, leucine, phenylalanine, asparagine, tryptophan. Here, as illustrated in Fig. 1, some of the bands of the DL-form are observed at different positions and/or with different relative intensities from the corresponding bands of the L-form, but all the bands of the DL-form are observed within 20 cm^{-1} from the corresponding bands of the L-form. Sometimes a band of the L-form splits into two in the DL-form, or a band of the DL-form splits into two in the L-form. But the splitting is mostly observed within a distance of 20 cm^{-1}.

(C) In class C, *the spectra of the L- and DL-forms are greatly different from each other.*—Examples[1]: aspartic acid (see Fig. 2), valine, isoleucine, serine, methionine, proline, lysine hydrochloride. Here, as illustrated in Fig. 2, many of the bands of the DL-form have no corresponding bands within 20 cm^{-1} in the spectrum of the L-form; and/or many of the bands of

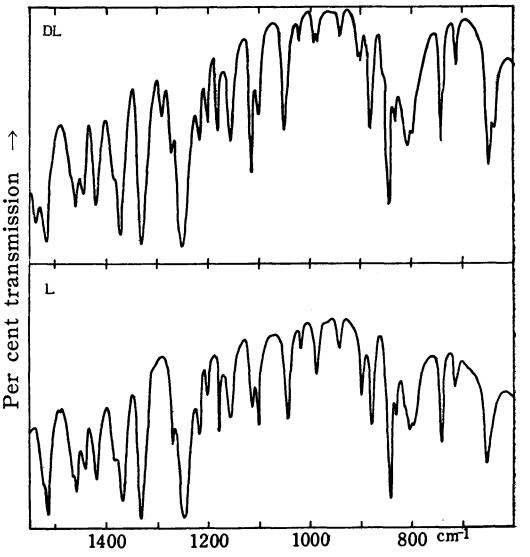


Fig. 1. Infrared spectra of DL- and L-forms of tyrosine in KBr disks.

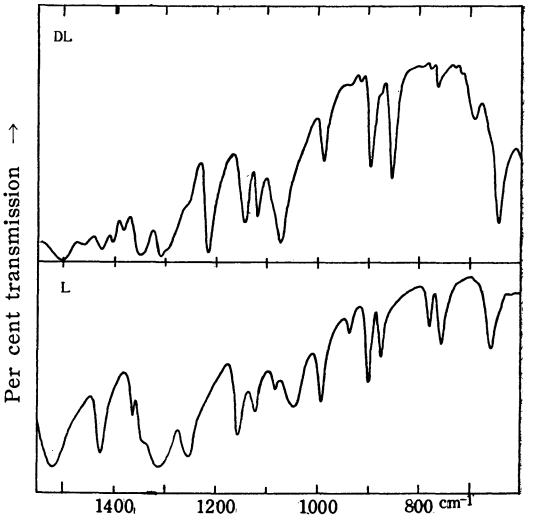


Fig. 2. Infrared spectra of DL- and L-forms of aspartic acid in KBr disks.

1) For the infrared spectra observed, see M. Tsuboi and T. Takenishi, *J. Japanese Chemistry* (*Kagaku-no-Ryoiki*), *Zokan*, No. 7, Nankodo Co. (1959).

the L-form have no corresponding bands within 20 cm^{-1} in the spectrum of the DL-form.

The comparisons of the infrared spectra in the solid states of optically active forms with those of the corresponding racemates have also been made by several authors[2-6] for several amino acids. All of these results, so far as is known to us, are grouped, without exception, in the same way as above.

From the above, we are led to consider that the three classes correspond to three different modes in which the D- and L-forms compose the DL-forms in solid states. Thus, in class A, the DL-form is merely a racemic mixture of the D- and L-forms; in class B, the crystal of the DL-form has a lattice composed of the D- and L-molecules, but the composing molecules are essentially identical in configuration with the molecules in the crystal lattice of the active forms; and in class C, the molecules composing the DL-form take different configurations from those in the D- and L-forms.

In the case where the crystal lattice of a racemate is composed of D- and L-molecules, the crystalline force field in it must of course be different from that in the lattice of the optically active crystal which is formed solely by the D- or L-molecules. This difference in the force field must be essentially of the same degree as that between different polymorphic forms of an ionic crystal[7], and must cause just as much difference in spectra as actually observed in class B.

On the other hand, no spectral difference is expected between a mechanical mixture of the D- and L-crystals and its component crystals, because all factors influencing the molecular and lattice vibrations must be exactly identical in the D- and L-crystals, as well as in their mixtures. Then, it may be concluded that the DL-form in class A is a mechanical mixture of the D- and L-crystals. For threonine, one of the examples for class A, Shoemaker et al.[8] reached, from X-ray examinations, a conclusion consistent with the above.

Considered on the basis of the accumulated knowledge on the internal rotations around the C–C and other single bonds[9,10] many of the amino acid molecules are expected to form rotational isomers with small energy differences. For such amino acids, the different crystalline force fields between the DL- and L-forms may result in occurrence of different rotational isomers[11]. Between these rotational isomers a great difference is expected in their infrared spectra. The great spectral difference actually observed in class C may be attributed to such rotational isomerism.

We wish to express our sincere thanks to Professor San-ichiro Mizushima, Dr. Takehiko Shimanouchi and Dr. Haruomi Oeda for their kind encouragements and valuable suggestions.

Department of Chemistry
Faculty of Science
The University of Tokyo
Hongo, Tokyo (M.T.)

Central Research Laboratory
Ajinomoto Company
Kawasaki, Knagawa (T.T.)

2) N. Wright, *J. Biol. Chem.*, **120**, 641 (1937).
3) N. Wright, ibid., **127**, 137 (1939).
4) G. B. B. M. Sutherland, *Discussions Faraday Soc.*, **9**, 319 (1950).
5) H. Brockman and H. Musso, *Chem. Ber.*, **89**, 241 (1956).
6) R. J. Koegel, R. A. McCallum, J. P. Greenstein, M. Winitz and S. M. Birnbaum, *Ann. N. Y. Acad. Sci.*, **69**, 94 (1957).
7) See, for example, M. Tsuboi, T. Onishi, I. Nakagawa, T. Shimanouchi and S. Mizushima, *Spectrochim. Acta*, **12**, 253 (1958).
8) D. P. Shoemaker, J. Donohue, V. Schomaker and R. B. Corey, *J. Am. Chem. Soc.*, **72**, 2328 (1950).
9) S. Mizushima, "Structure of Molecules and Internal Rotation", Academic Press, New York (1954).
10) M. Hayashi, T. Shimanouchi and S. Mizushima, This Bulletin, **29**, 802 (1956).
11) See, for example, J. Trommel and J. M. Bijvoet, *Acta Cryst.*, **7**, 703 (1954); A. McL. Mathieson, ibid., **5**, 332 (1952); M. Tsuboi, T. Takenishi and Y. Iitaka, This Bulletin, **32**, 305 (1959); M. Tsuboi, Y. Iitaka, S. Suzuki and S. Mizushima, ibid., **32**, 529 (1959).

Studies on the Graphitization. III. The Sub-Structure of Heat-Treated Coke*

By Haruo KURODA

(Received January 29, 1959)

Carbons made by carbonizing organic substances at a temperature lower than 1000°C are made up of minute crystallites of non-graphitic structure and disordered phase consisting of carbon, hydrogen and oxygen. The heat-treatment at a higher temperature causes in carbons the decrease of disordered phase and the crystallite growth as well as the improvement of the stacking order of the layer lattice in crystallites.

The progress of the structural change in the heat-treatment differs greatly depending on the characters of carbons even if they are heat-treated under the similar conditions. The crystal structure of carbons can be well defined by the analysis of their X-ray diffraction pattern[1]. Graphitization has been discussed hitherto mainly based on the knowledge concerning the crystal structure. The difference in graphitizability, however, can not be explained by comparing the crystal structure alone.

In the previous papers[2], we pointed out that the particular features in graphitization of carbon blacks are due to the substructure of carbon black particles. It might be natural that the graphitizability of carbon is strongly influenced by the character of crystallite boundaries, alignment of crystallites or other similar aspects of its structure which we shall call micro-structure distinguished from crystal structure. From such a point of view, we investigated the micro-structure and its change after heat-treatments in petroleum coke, which is known to be one of the well-graphitizable carbons.

Experimental and Results

Heat-Treatment and Crystal Structure.— Petroleum coke of Great Lake Co. was heat-treated in vacuo at several temperatures from 1000°C to 3000°C. X-ray diffraction was studied using a commercial X-ray diffractometer, with Cu K_α radiation. Diffractometer records of 10 diffraction are reproduced in Fig. 1. As seen in this figure, the raw coke has non-graphitic structure, and the improvement of the stacking order of layer lattice starts at a temperature around

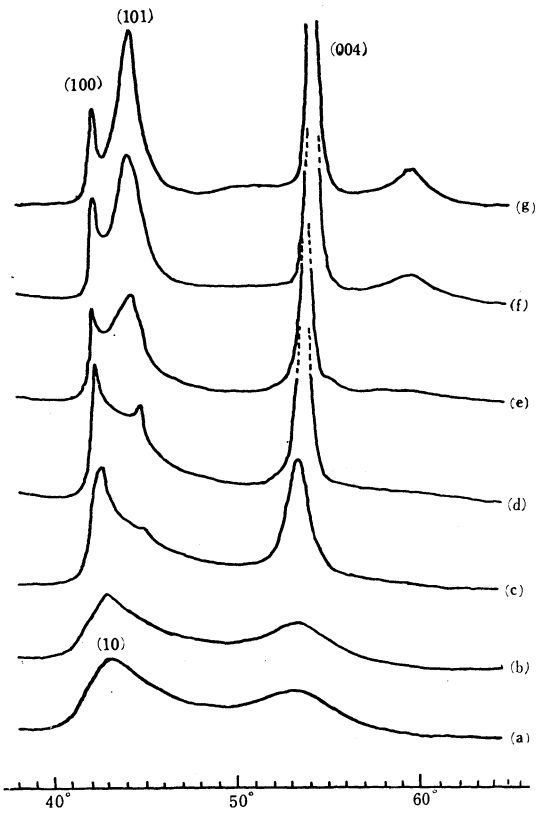


Fig. 1. X-ray diffraction pattern of petroleum coke. The effect of heat-treatment on the profile of (10) diffraction peak. (Cu K_α, Ni-filtered). (a) Raw state. (b) 1400°C. (c) 1850°C. (d) 1900°C. (e) 2040°C. (f) 2500°C. (g) 3000°C.

* This work is a part of a research project on carbons, supported by the 117 Committee in Nippon Gakujutsu Shinkokai, directed by Prof. H. Akamatu. Part I, This Bulletin, **29**, 574 (1956); Part II, ibid., **32**, 142 (1959).

1) J. Biscoe and B. E. Warren, *J. Appl. Phys.*, **13**, 364 (1942); C. E. Houska and B. E. Warren, ibid., **25**, 1503 (1954); R. E. Franklin, *Acta Cryst.*, **3**, 107 (1950); *Proc. Roy. Soc.* (*London*), **A209**, 196 (1951); H. Akamatu, H. Inokuchi, H. Takahashi and Y. Matsunaga, This Bulletin, **29**, 574 (1956).

2) H. Kuroda and H. Akamatu, "Proceeding of the 3rd Conference on Carbon", Pergamon Press, New York (1958), p. 381; This Bulletin, **32**, 142 (1959).

1900°C. When H.T.** is 2500°C, the observed value of layer spacing is 3.365 Å. This indicates that nearly 65% of layers are in graphitic orientation. It becomes 3.351 Å after the heat-treatment at 3000°C.

The crystallite sizes determined from the breadth of diffraction peak are given in Table I. At lower temperatures crystallite size increases only a little. The rapid growth starts at a temperature around 1900°C.

TABLE I. GROWTH OF CRYSTALLITE DIMENSION IN PETROLEUM COKE WITH HEAT-TREATMENT

H.T. (°C)	L_a (Å)	L_c (Å)
Original	38	37
1400	40	38
1550	42	49
1720	87	71
1850	110	93
2040	276	180
2500	392	202
3000	444	213

Grains of Coke Powder.—After the heat-treatment, coke was milled into a fine powder and observed under the electron microscope***. Minute flaky grains can be observed with the raw coke as shown in Fig. 2. They have a jagged outline and the appearance of the granular structure. Most of them are of several microns in transverse direction and less than 1000 Å in thickness. The granular appearance is removed by the heat-treatment. When H.T. is higher than 2000°C, it entirely disappears. After the heat-treatment with high H.T., the stepwise variation of electron transmission is seen at edges of grains. It can be found also at the inner part of grains when its thickness is very small. These facts indicate that each grain is a bundle of many thin lamellae. The thickness of one lamella seems to be in the order of 200~300 Å.

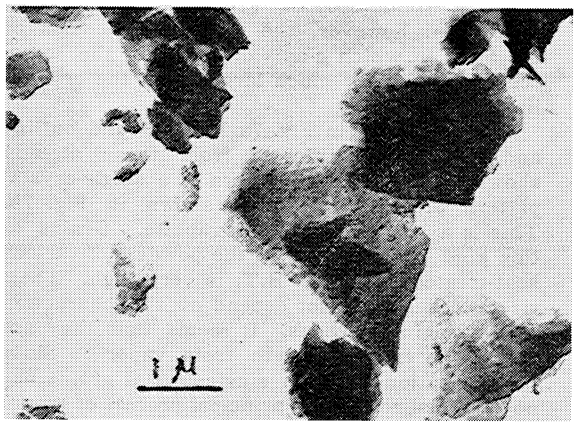


Fig. 2. Electron micrograph of coke grains, (raw state). (shadowed with Ge)

** The temperature of heat-treatment is abbreviated to H. T.

*** Electron microscopic studies were made using Hitachi Electron Microscope, Model 10-A.

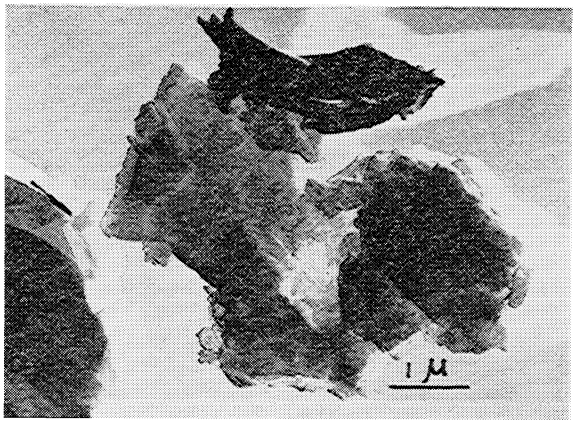
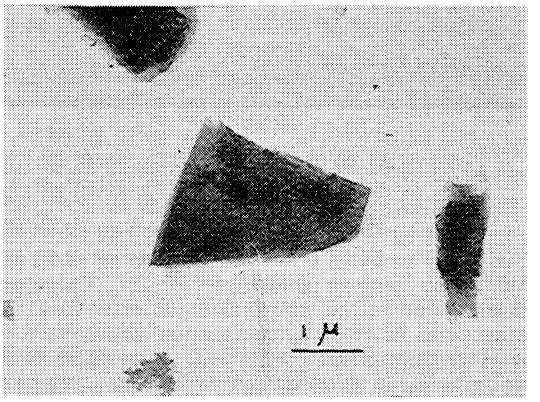


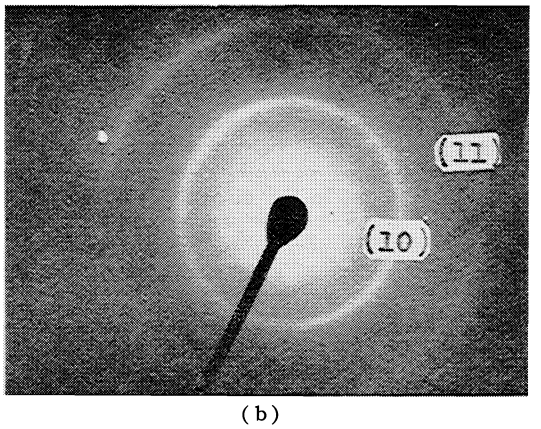
Fig. 3. Electron micrograph of coke grains, (H.T., 2500°C). (shadowed with Ge)

As can be seen in Figs. 3 and 6, in every coke grain are sub-boundaries, which are dividing it into smaller grains.

The electron diffraction pattern corresponding to each grain was studied by the method of selected-area electron diffraction. One of the typical results with the raw coke is given in

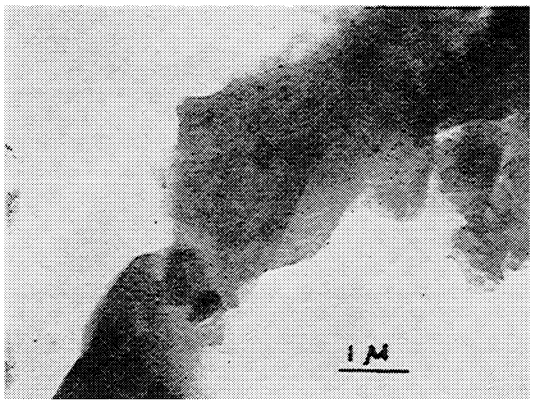


(a)

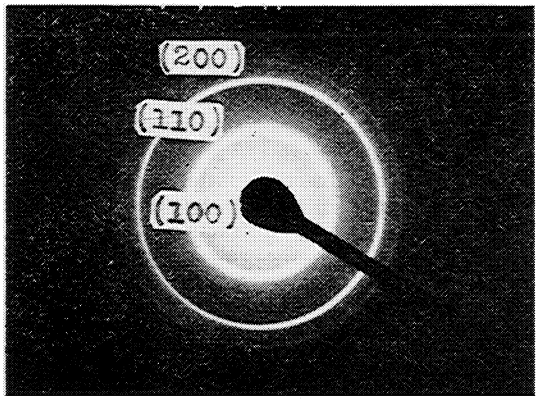


(b)

Fig. 4. A coke grain, (raw state): (a) electron micrograph, (b) selected-area electron diffraction.

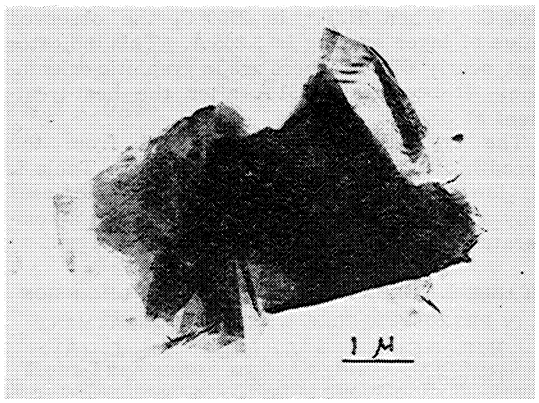


(a)

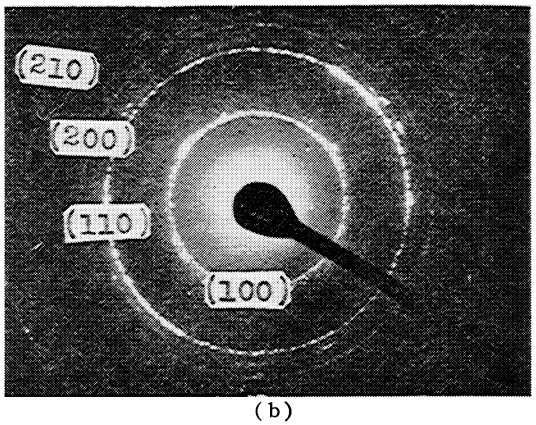


(b)

Fig. 5. A coke grain, (H.T., 1850°C): (a) electron micrograph, (b) selected-area electron diffraction.



(a)



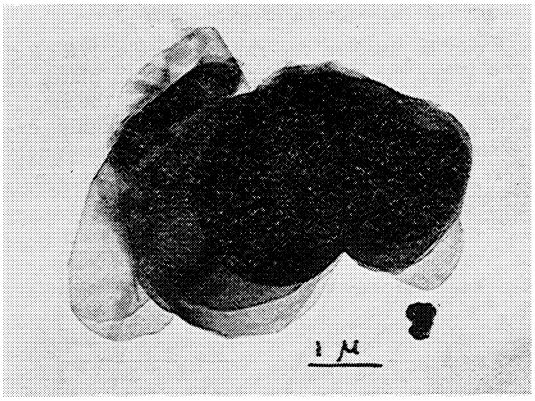
(b)

Fig. 6. A coke grain, (H.T., 3000°C): (a) electron micrograph, (b) selected-area electron diffraction.

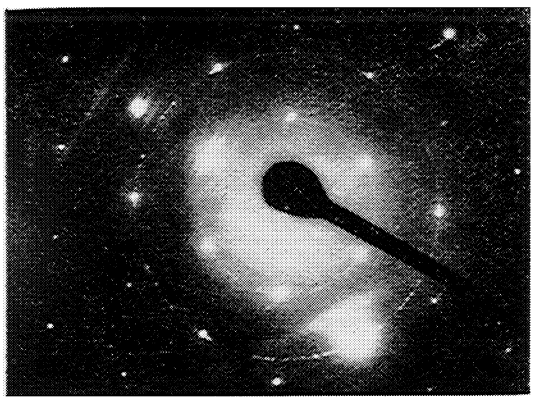
Fig. 4. The flaky grain in Fig. 4a gives a diffuse diffraction pattern shown in Fig. 4b. The spacings related to the two halos indicate that the inner one is (100) diffraction and the outer one is (110) diffraction. (002) and (004) diffractions are missing in this diffraction pattern. They are always either missing or very weak in every selected-area electron diffraction pattern of the grain of the raw coke. After heat-treatment, diffraction rings become clear and sharp as seen in Figs. 5 and 6. In both of them, diffraction rings correspond to (100), (110),(200), (210) and (300) diffractions, respectively. Most of the grains give such a polycrystalline diffraction pattern consisting of ($h\,k\,0$) diffractions alone. c-axis should be in the direction parallel to the incident electron beam, hence parallel to the direction that is normal to the surface of the grains, in order to give such diffraction patterns. Thus each coke grain is a group of many crystallites with a preferential orientation of c-axis. In Fig. 5a diffraction rings have homogeneous intensity distribution in all directions, hence a-axis direction is quite random in the plane of the grain. In Fig. 6b however, diffraction rings split into many spots. Many grains give such a pattern if H.T. is 2500~3000°C. There are some grains which give a diffraction pattern like that of a single crystal. They seem to be a quasi-single crystal. As shown in Table I, the crystallite size along a-axis determined from X-ray diffraction is only 400~500Å, even if H. T. is around 3000°C. From the selected-area diffraction, however, the average dimension of the area, in which a-axis direction is the same, seems to be very much larger than the crystallite size.

A grain shown in Fig. 7a has a round outline and looks quite different from those already shown. Its diffraction pattern is a single-crystal pattern with Kikuchi-lines as shown in Fig. 7b. This is a single crystal of graphite. Grains of this kind can be found in the powders of various heat-treated carbons if H.T. is very high. Their size and shape do not depend on the characters of the original carbons. It seems that they are due to the crystal growth from vapor[3]. Since the formation of such single-crystal grains has no essential role in the principal process of graphtiization, we shall not further discuss it in this paper.

3) The growth of graphite crystals by the dislocation mechanism was observed and discussed by T. Tsuzuku, *Tanso* (*Carbons*), **5**, 2 (1955); T. Tsuzuku and T. Komoda, *Acta Cryst.*, **9**, 90 (1956).



(a)



(b)

Fig. 7. A single-crystal grain: (a) electron micrograph, (b) selected-area electron diffraction.

Structure of Coke Grains.—If the direction of the incident electron beam is parallel to the texture axis, we can not find any difference between ($h\ k$) two-dimensional diffraction and ($h\ k\ 0$) diffraction. This is the case in the diffraction patterns shown above. We studied the oblique diffraction pattern of coke grains in order to know their structure.

If coke grains have the textured polycrystalline structure, they should give oblique texture patterns[4]. The reciprocal lattice of non-graphitic structure consists of a series of (0 0 1) points along c-axis and ($h\ k$) lines parallel to it. Hence a grain should give an oblique pattern consisting of continuous ellipses if crystallites in it have non-graphitic structure. As the stacking order of layer lattice is improved, the structure factor has a periodic variation on each ($h\ k$) line in the reciprocal lattice. Thus the stacking order in the crysallites can be known from the intensity variation on the elliptical pattern in the oblique texture pattern.

Fig. 8 is one of the diffraction patterns obtained with the raw coke. The long arc-patterns are (10) and (11) diffractions and the short ones are (002) and (004) diffractions. It can be seen from this diffraction pattern that the direction of the texture axis, c-axis, has fluctuation around that which is normal to the surface of the grain. Most of the grains in the raw coke give such diffraction patterns. This is the case also in the heat-treated coke if H.T. is low. The fluctuation of c-axis direction decreases as H.T. is raised, and it almost disappears when H.T. is higher than 1850°C. The indication of the improvement of the stacking order, however, is not observed with the grains which have appreciable fluctuation of c-axis direction. The improvement of the crystallite alignment seems to proceed in advance of the change in the stacking order.

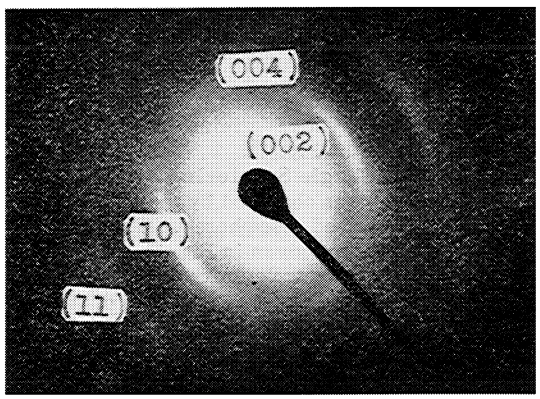


Fig. 8. An oblique pattern of a coke grain, (raw state). The oblique angle is larger than 80°.

In the X-ray diffraction pattern, the modulation of two-dimensional diffraction peak appears when H.T. is around 2000°C. The indication of the change in the stacking order can be observed also in electron microdiffraction from H.T. around 1900°C. One of the typical diffraction patterns corresponding to the earlier stage of graphitization is shown in Fig. 9. As H.T. is raised, the diffraction pattern becomes that of the textured polycrystalline structure of graphite. Some grains

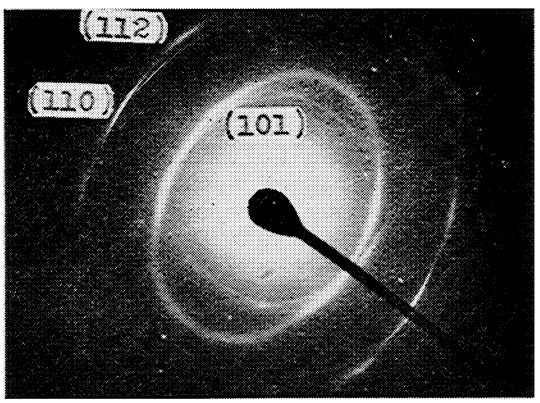


Fig. 9. An oblique pattern of a coke grain, (H.T., 1850°C). The oblique angle is 43°.

4) Z. G. Pinsker, "Electron Diffraction", Butterworths Scientific Publications, London (1953), p. 93.

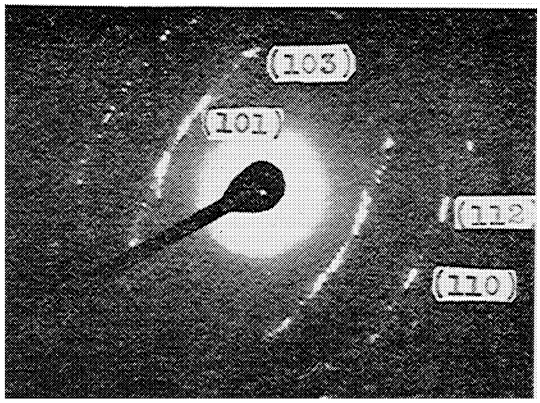


Fig. 10. An oblique pattern of a coke grain, (H.T., 2500°C). The oblique angle is 62°.

give a single crystal pattern. A typical diffraction pattern for coke grains heat-treated at 3000°C is shown in Fig. 10.

X-ray Small-Angle Scattering.—X-ray small-angle scattering was observed by the experimental procedures described elsewhere[5]. The observed intensity curves are given in Fig. 11. The small-angle scattering of petroleum coke is very weak, and, as H.T. is raised, the gradient of the intensity curve becomes very steep. It is difficult to make an accurate measurement when H.T. is high. As can be seen from Fig. 12, the intensity is nearly proportional to $h^{-2.3}\sim h^{-2.5}$ throughout the observed range of scattering angle. Such a relation can not be expected if the system is made up of spherical particles. The result seems to suggest that the structural units responsible for the observed scattering are thin plates.

Kratky and Porod[6] have derived an approximate formula for the scattering function of a thin disk of thickness $2H$ and diameter $2R$****.

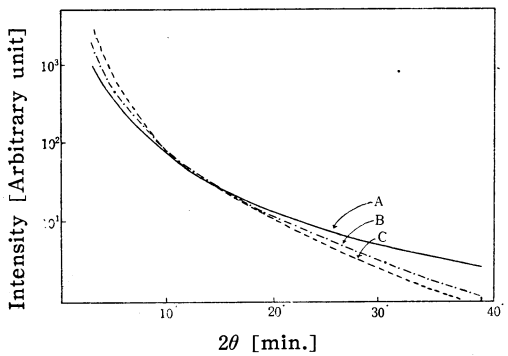


Fig. 11. Intensity curves of X-ray small-angle scattering: (A) raw state, (B) H.T., 1725°C, (C) H.T., 1850°C.

5) H. Kuroda, *J. Chem. Soc. Japan, Pure Chem. Sec.* (*Nippon Kagaku Zasshi*), **77**, 1298 (1956); *J. Colloid Sci.*, **12**, 496 (1957).
6) O. Kratky and G. Porod, ibid., **4**, 35 (1949).
**** $h=4\pi\sin\theta/\lambda$ and n is the number of electrons in the particle.

$$\overline{F^2(h)} = (2n^2/h^2R^2)\exp(-h^2H^2/3)$$

This can be used in the range of angle, $1/R<h<1/H$. When the system consists of thin plates of different sizes and random orientation, the small-angle scattering intensity might be roughly expressed by the following formula at the angle where h is large with respect to $1/\bar{R}$ but small with respect to $1/\bar{H}$.

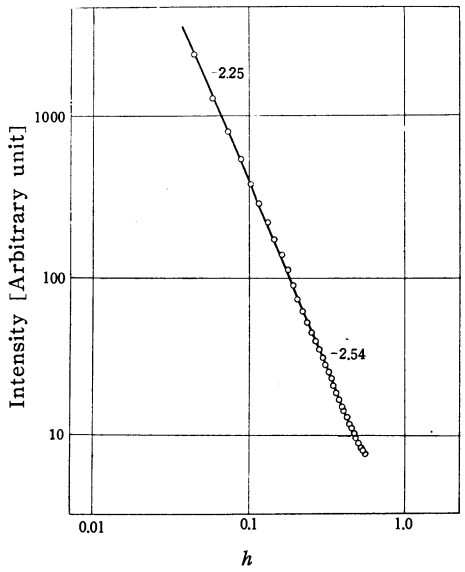


Fig. 12. Plot of $\log I(h)$ versus $\log h$, (raw state). The numbers on the curve indicate the inclination.

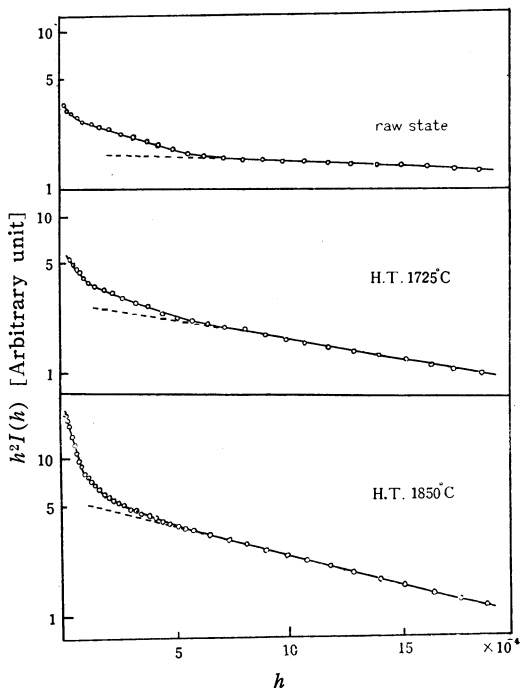


Fig. 13. Plot of $\log h^2I(h)$ versus h^2.

$$h^2I(h) = \text{const} \sum M(H_i) H_i \exp(-h^2H_i^2/3)$$

where $M(H_i)$ is the mass-fraction of plates with thickness of $2H$, and $\bar{R}$, $\bar{H}$ are the average value of R and H, respectively.

The curves of $\log h^2I(h)$ versus h^2 are shown in Fig. 13. There is a wide linear part in each curve. The value of $2H$ corresponding to the inclination of this part is given in Table II. They are of the same magnitude with crystallite size.

TABLE II. VALUES OF $2H$

H.T. (°C)	Range of the linear part (h)	Inclination of the linear part	$2H$ (Å)	L_c (Å)
Original	$>7.3\times10^{-4}$	3.48×10^2	49	37
1720	$>5.8\times10^{-4}$	10.72×10^2	86	71
1850	$>5.1\times10^{-4}$	14.51×10^2	100	93

$2H$ was calculated assuming that the inclination is equal to $-0.434H^2/3$.

Although we are not sure whether the structural units responsible for the observed small-angle scattering are the groups of crystallites or the voids between them, the results seem to suggest that petroleum coke has some kind of lamellar units in its structure even in the raw state and after heat-treatment at low temperatures.

Discussion

It has been found that petroleum coke can be disintegrated into minute flaky grains. When H.T. is high, it has been observed that each coke grain is made up of smaller grains or lamellae in which carbon crystallites are aligned so as to make their c-axes normal to the plane of the lamella. When H.T. is low, the lamellar structure can not be seen, but the alignment of crystallites is already not at random, c-axis direction being nearly perpendicular to the surface of grain. X-ray small-angle scattering suggests also the presence of lamellar units in the structure of petroleum coke.

It has been frequently presumed hitherto as the structural model for cokes that carbon crystallites are randomly linked to one another with chain-like molecules in disordered phase. Such a model, however, is not satisfactory for petroleum coke, since it is disintegrated into grains as mentioned above, and it must be made up of lamellar groups of crystallites with the preferential orientation concerning c-axis.

As mentioned already, the textured structure can be found even in the raw coke. It seems to have been formed during the carbonization process. If each crystallite is separated from the neighboring ones by a large amount of disordered phase, it might be difficult to form a large group of crystallites in which c-axis direction is nearly the same. The textured structure will be explained if we presume that there is a comparatively small amount of disordered phase between neighboring crystallites.

It has been known that the disordered phase is made up of mainly aliphatic C–C bonds, C–H bonds, C–O, bonds etc. Since these chemical bonds are thermally unstable compared with aromatic C–C bond, they can be broken at a lower temperature which can not provide a sufficient energy to break up residual bonds of aromatic character. Thus, when H.T. is low, the crystallite growth will proceed solely at the expense of disordered phase. This will cause only a slight increase of crystallite size. This is actually the case as seen in Table I. The crystallite alignment, however, is to be improved well in this stage. At the extreme of the crystallite growth of this mechanism, there should be only a very narrow disordered region or slight structural defects between the neighboring crystallites. The remaining residual bonds might be of aromatic character at this stage. If H.T. is high enough to provide sufficient energy to break them up, the rapid growth will proceed by the condensation of the neighboring crystallites. Actually it starts at a temperature around 2000°C which is known to be a temperature at which the plastic deformation can occur in various carbons. If we presume such a mechanism of crystal growth, the structural change in petroleum coke will be explained well.

In a carbon black particle, c-axis direction of crystallites is considered to be nearly normal to the surface of the particle. When crystallite grows well, a carbon black particle becomes polyhedrone. If the crystallite size increases too much, a stress will be created in the particle. As has been shown in the previous papers, this situation sometimes causes the disintegration of carbon black particle into smaller units. There is no situation like this in the crystallite growth in petroleum coke if it proceeds within each textured polycrystalline group.

The micro-structure pictured in this paper is not to be considered as the special one that can be found only in petroleum coke. The similar structure can be found widely in soft cokes. In hard cokes, the

textured polycrystalline group does not exist, or, if it exists, the crystals are of small dimension. The large difference in graphitizability seems to be due to such a situation.

The author wishes to express his thanks to Professor H. Akamatu for his kind direction, and to Dr. H. Takahashi for his valuable advice. He is also indebted to Mr. S. Sakata for his kind help in the experiment.

Department of Chemistry
Faculty of Science
The University of Tokyo
Hongo, Tokyo

Theoretical Study on the Mechanism of the Aromatic Substitution[1)]

By Saburo NAGAKURA and Jiro TANAKA

(Received July 30, 1958)

As is well known, the mechanism of aromatic substitution may be regarded as one of the most typical problems to which the quantum mechanical theory has been applied with success. Since 1940, a number of notable theoretical papers on this subject have already been published by several authors[2-8)]. In these papers, some quantum mechanical concepts useful for interpreting chemical reactivity of the aromatic molecule have been introduced. They are such concepts as π-electron density, free valency, localization energy, frontier electron density, etc.[9)] By means of them, one has succeeded in explaining the orientation rule observed with some aromatic substitution reactions. It seems hasty, however, to consider that all the problems in this field have been settled completely. In fact, one can easily find some facts which can hardly be interpreted by any theory presented hitherto. For instance, the facts that the aliphatic hydrocarbon like methane is generally less susceptible to the electrophilic substitution than the aromatic hydrocarbon is, and that the silver cation is difficult to cause the substitution reaction with benzene while the nitronium cation is well known as a typical reagent for it, are not thought to be explained satisfactorily by the previous theories.

In the present paper, it is undertaken to study the mechanism of the aromatic substitution with reference to the relative heights of energy levels of the reagent to those of the aromatic molecule. From the consideration of these energy levels, it is concluded that a large electron transfer necessarily occurs from the aromatic molecule towards the reagent and in the reverse direction for the electrophilic and the nucleophilic substitution, respectively. On the basis of this electron transfer mechanism, conditions necessary for causing the aromatic substitution are reasonably introduced. It is shown, moreover, that the orientation in the aromatic substitution can properly be predicted by the free valency values evaluated with the aromatic cation, the neutral molecule and the anion for the electrophilic, the radical and the nucleophilic substitution, respectively.

1) Preliminary reports on this work have been published in *J. Chem. Phys.*, **22**, 563 (1954) and *J. Chem. Soc. Japan, Pure Chem. Sec.* (*Nippon Kagaku Zasshi*), **75**, 933 (1954).

2) T. Ri and H. Eyring, *J. Chem. Phys.*, 8, 433 (1940).

3) G. W. Wheland, *J. Am. Chem. Soc.*, **64**, 900 (1942).

4) M. J. S. Dewar, *J. Chem. Soc.*, **1949**, 463.

5) C. A. Coulson and H. C. Longuet-Higgins, *Proc. Roy. Soc.*, **A191**, 39; **A192**, 16 (1947).

6) K. Fukui, T. Yonezawa and H. Shingu, *J. Chem. Phys.*, **20**, 722 (1952); K. Fukui, T. Yonezawa and C. Nagata, This Bulletin, **27**, 423 (1954).

7) R. S. Mulliken, *J. Phys. Chem.*, **56**, 801 (1952).

8) On this problem various excellent reviews have already been published. Some of them are as follows:
(a) C. A. Coulson, *Research*, **4**, 307 (1951).
(b) K. Higasi, *Monograph Ser. Research Institute of Applied Electricity, Hokkaido University*, **No. 4**, 307 (1951).
(c) R. D. Brown, *Quart. Revs.*, **6**, 63 (1952).

9) Some of these concepts are in intimate relations to one another. This problem has been discussed by Baba and also by Fukui et al. (cf. H. Baba, This Bulletin, **30**, 147, 154 (1957); K. Fukui, T. Yonezawa and C. Nagata, *J. Chem. Phys.*, **26**, 831 (1957)).

Determination of Energy Level Diagrams of Some Reagents and Aromatic Molecules

According to the authors' method described in the previous papers[10], the highest occupied (H) and the lowest vacant (V) orbital of a certain molecule can be determined by the aid of the experimental data on the ionization potential and the near ultraviolet absorption spectrum. The same method was applied to the determination of orbital energies of the neutral molecules and radicals considered in the present paper. Concerning electrophilic reagents, such as the nitronium (NO_2^+), chlorine (Cl^+), bromine (Br^+), iodine (I^+), and hydrogen cations[11], the lowest vacant orbital was set equal to the ionization potential of the corresponding neutral molecule or atom. On the other hand, the highest occupied orbital of the nucleophilic reagent, such as hydroxyl (OH^-) or chlorine (Cl^-) anion, was estimated from the electron affinity of the corresponding neutral radical or atom. The results thus obtained are shown in Fig. 1, where energy levels of the silver cation (Ag^+) and the iodine molecule are also given for the purpose of comparison. It is worthy of notice that both of them can form the stable charge transfer complex with the aromatic molecule[12-14] but are difficult to cause the substitution reaction.

Consideration of the Reaction Mechanism from Energy Level Diagrams[15]

First of all, let us consider the electrophilic substitution. It is evident from Fig. 1 that the lowest vacant orbital (hereafter abbreviated to V) of the typical electrophilic reagent lies definitely below the highest occupied orbital (hereafter abbreviated to H) of the aromatic molecule which is susceptible to the substitution reaction. On the other hand, the V orbitals of the silver cation and the iodine molecule, which can not act as the electrophilic reagent for the substitution, are apparently higher than the H orbitals of the aromatic molecules. This remarkable fact suggests that it may be necessary for the occurrence of the electrophilic substitution that the V orbital of the reagent is considerably lower than the H orbital of the aromatic molecule. Under this assumption, moreover, the fact that the simple aliphatic hydrocarbon like methane is attacked with difficulty by the electrophilic reagent can readily be understood. As is shown in Fig. 1, the H orbital of methane which exists at -13.0 eV. is clearly lower than or almost equal to the V orbitals for most electrophilic reagents. In this case, therefore, it is difficult to fulfil the necessary condition for causing the electrophilic substitution.

The above-mentioned fact probably gives an interesting suggestion concerning the mechanism of the electrophilic substitution. According to Mulliken's theory relevant to the intermolecular charge transfer phenomenon, the electron transfer occurs to some extent from a donor towards an acceptor when these two components approach each other[14]. For example, in the case of the molecular complex between benzene (electron donor) and iodine (electron acceptor), the magnitude of this electron transfer was estimated by Mulliken to be about 3%. On the basis of the molecular energy level diagrams shown in Fig. 1, this intermolecular charge transfer phenomenon can approximately be represented by the interaction of the H orbital of the electron donor with the V orbital of the electron acceptor. The simple LCMO treatment on this interaction leads to a qualitative conclusion that the magnitude of the electron transfer increases as the V orbital becomes lower or the H orbital higher if the resonance integral between these two orbitals remains almost constant. In fact, in the

10) S. Nagakura and J. Tanaka, *J. Chem. Phys.*, **22**, 236 (1954); S. Nagakura, ibid., **23**, 1441 (1955); J. Tanaka, S. Nagakura and M. Kobayashi, ibid., **24**, 311 (1956).

11) The reagent ion in solution is undoubtedly stabilized by the orientation of surrounding solvent molecules. In the present state of the study, however, it is difficult to make quantitative discussion on the solvation energy of the ion under actual conditions of reaction. Therefore, the effect of the solvent upon the orbital energies of the ion was not taken into account in the present treatment.

12) H. A. Benesi and J. H. Hildebrand, *J. Am. Chem. Soc.*, **71**, 2703 (1949).

13) L. J. Andrews and R. M. Keefer, ibid., **71**, 3644 (1949); **72**, 3113 (1950).

14) R. S. Mulliken, ibid., **72**, 600 (1950); **74**, 811 (1952); *J. Phys. Chem.*, **56**, 801 (1952).

15) The description in this chapter is an extention of the basic idea mentioned in the preliminary papers published in 1954[1]. The present authors' view on the importance of the electron transfer in the aromatic substitution is based on the energy level diagrams of the reagent and the aromatic molecule, which are determined by the use of the experimental data on the ionization potential and the near ultraviolet absorption spectrum. On the other hand, Fukui et al. have discussed a similar problem from the purely theoretical point of view and derived the equations representing the dependence of the electron density on the reagent upon the Coulomb and resonance integrals (K. Fukui, T. Yonezawa and C. Nagata, *J. Chem. Phys.*, **27**, 1247 (1957).

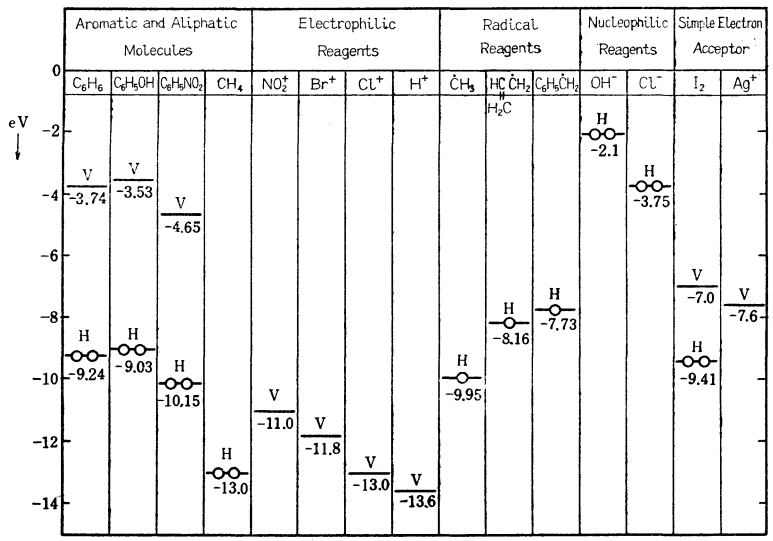


Fig. 1. Energy level diagrams for some reagents, and aromatic and aliphatic molecules.

The ionization potentials necessary for determining these diagrams were taken from the following references:

Benzene: W. C. Price and R. W. Wood, *J. Chem. Phys.*, 3, 439 (1935).

Phenol and nitrobenzene: J. D. Morrison and A. J. C. Nicholson, ibid., **20**, 1221 (1952) and private communication from Dr. Morrison.

Iodine: J. D. Morrison, ibid., **19**, 1305 (1951).

Methane: R. E. Hornig, ibid., **16**, 105 (1948).

Nitrogen dioxide: E. C. G. Stueckelberg and H. D. Smyth, *Phys. Rev.*, **36**, 478 (1930).

Hydrogen, chlorine, bromine and silver atoms: Landolt-Börnstein, "Physikalische-Chemische Tabellen", 6-Auflage, I Band, 1. Teil, Springer-Verlag, Berlin (1951), p. 211.

Methyl, allyl and phenyl radicals: F. P. Lossing, K. U. Ingold and I. H. S. Henderson, *J. Chem. Phys.*, 22, 621 (1954).

Electron affinities for hydroxyl group and chlorine atom are taken from Landolt-Börnstein, "Physikalische-Chemische Tabellen", 6-Auflage, I Band, 1. Teil, Springer-Verlag, Berlin (1951).

case of the iodine complex with triethylamine whose H orbital is much higher than that of benzene[16], the extent of the electron transfer certainly exceeds 50% as is revealed from the big dipole moment (11.3D)[17].

Applying the above consideration on the electron transfer to the system consisting of the aromatic molecule and the electrophilic reagent, one may be led to the conclusion that there necessarily occurs an extremely large electron transfer from the former towards the latter, because in this system the V orbital of the reagent is extraordinarily low and even lower than the H orbital of the aromatic molecule as mentioned above. This means that the electrophilic substitution proceeds passing through a stage at which the reagent cation robs almost one electron from the aromatic molecule and consequently the former changes nearly to the neutral radical and the latter nearly to the cation. On the present study of situation, it is difficult to ascertain whether or not this stage corresponds to the so-called transition state, namely the highest point in the potential energy curve for the reaction. According to our opinion, however, it is probably just before the transition state assumed by Wheland[2]. In other words, the above-mentioned large electron transfer may be accompanied by changes of the hybridizations and geometrical configurations in both the reagent and the aromatic molecule, and then a new σ bond may be formed between the former and a carbon atom of the latter

16) The ionization potential of triethylamine was determined as 7.50 eV. by Watanabe (K. Watanabe, *J. Chem. Phys.*, **26**, 542 (1957), whereas the ionization potential of benzene is 9.24 eV.

17) S. Nagakura, *J. Am. Chem. Soc.*, **80**, 520 (1958); H. Tsubomura and S. Nagakura, *J. Chem, Phys.*, **27**, 819 (1957).

(Wheland's activated complex, type II)[18]. This view is schematically shown in Fig. 2. In this figure, stages B and C correspond to the electron transfer state and Wheland's transition state, type II, respectively.

Spectrophotometric studies by Reid[19] and also by Gold and Tye[20] show that the aromatic carbonium ion $(ArH)^+$ can be formed by the interaction of the aromatic molecule with proton under suitable conditions. This kind of ion, which is called $b\pi$, $h\sigma$ inner complex and σ-complex by Mulliken[7] and by Brown[21], respectively, may be thought to take a structure similar to that of Wheland's activated complex, type II. Hence, the present theory may be said to clarify the necessary conditions for forming the inner complex.

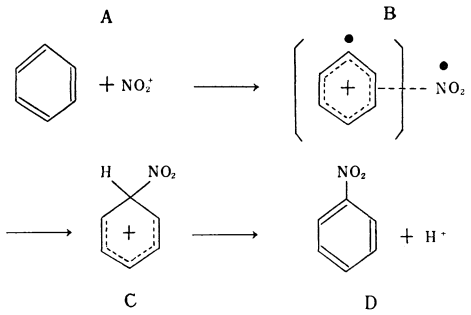


Fig. 2. Schematic diagram depicting the process of the substitution reaction between benzene and nitronium cation.

Let us now turn to the nucleophilic substitution. As is clearly seen from Fig. 1, the H orbital of the nucleophilic reagent is generally very high and may be regarded as comparable to the V orbital of the aromatic molecule. It is inferred from this that in this case a large electron transfer occurs from the reagent towards the aromatic molecule, and consequently the reaction takes place passing through the state in which the reagent becomes a nearly neutral radical and the aromatic molecule becomes an anion.

On the other hand, in the case of the radical substitution one may not expect such a large electron transfer as in the case of the heterolytic substitution, because unpaired electron levels of most radicals lie in an intermediate position between the H and the V orbitals of the aromatic molecule[22]. Thus in our opinion, the distinction between the heterolytic (electrophilic and nucleophilic) and homolytic (radical) substitutions is made in terms of the magnitude of the electron transfer between the reagent and the aromatic molecule. Furthermore, it is sure that in the electrophilic and the nucleophilic substitutions the directions of electron transfer are opposite to each other.

The present theory seems to have intimate relations with that presented by Weiss[23]. In 1946, Weiss emphasizes almost intuitively the importance of the electron transfer in many kinds of organic reactions. However, the grounds for his insistence concerning the aromatic substitution seem to be indefinite. The present theory has an advantage in that the necessity of a large electron transfer is reasonably concluded from the consideration of energy level diagrams of the reagent and the aromatic molecule.

Now, some consideration will be taken of the orientation in the aromatic substitution reaction, namely, the relative rate of substitution on various positions of the aromatic molecule. According to the present authors' view, in the heterolytic substitution the electron transfer takes place and consequently the reagent ion may be thought to attack the substrate as the radical. In other words, after the occurrence of the electron transfer, the mechanism of the heterolytic substitution may be regarded as similar to that of the homolytic substitution. Moreover, as is

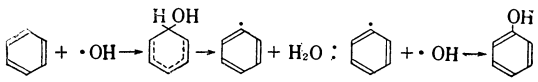
18) The authors wish to express their sincere thanks to Professor Mulliken at Chicago and Professor Coulson at Oxford for their kindness in giving helpful suggestions on this respect. According to the present authors' opinion, Wheland's transition state, type II, corresponds to a basin in the potential energy curve for the substitution reaction.

19) C. Reid, *J. Am. Chem. Soc.*, **76**, 3264 (1954).

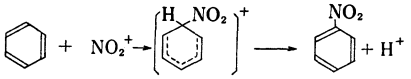
20) V. Gold and F. L. Tye, *J. Chem. Soc.*, **1952**, 2184.

21) H. C. Brown and J. D. Brady, *J. Am. Chem. Soc.*, **74**, 3570 (1952).

22) It is doubtful if the radical and the nucleophilic substitution proceed completely parallel to the electrophilic substitution. For example, the substitution of the hydroxyl radical for the hydrogen atom of benzene is considered to take place through the following procedures (G. Stein and J. Weiss, *J. Chem. Soc.*, **1949**, 3245):



This mechanism is apparently different from that of the electrophilic substitution such as



However, both reactions pass commonly through Wheland's type II transition state where the attacked point is clearly determined. Therefore, it seems reasonable to consider that concerning the orientation rule parallel treatment can be applied to the three types of aromatic substitution reactions.

23) J. Weiss, *Trans. Faraday Soc.*, **42**, 116 (1946).

well known, in the homolytic substitution the concept of free valency is very useful for explaining the orientation rule[8a,24,25]. Hence, it is quite natural to consider that the orientation in the electrophilic and nucleophilic substitutions can be predicted on the basis of the free valency value of the aromatic cation and of the anion, respectively.

Calculation of the Free Valency and Consideration of the Results

Free valency of the r-th atom(F_r) can be evaluated with the aid of the following equation:

$$F_r = F_{\max} - \sum_s p_{rs}$$

where $F_{\max}$ is the maximum value of the total π bond order of the carbon atom and estimated at $\sqrt{3}$[24], and p_{rs} is the π bond order of the r-s bond, where s denotes the adjacent atom to the r-th one. The value of p_{rs} can be calculated by the aid of the following equation:

$$p_{rs} = \sum_i n_i C_{ri} C_{si}$$

Here C_{ri} is the coefficient of the r-th atomic orbital in the i-th molecular orbital and n_i is the number of π-electron occupying it. The calculation of C_{ri} was made on the basis of the usual LCAO method under the assumption of orthogonality between adjacent $2p\pi$ atomic orbitals. Moreover, it was assumed that one electron is removed from the highest occupied orbital and is added to the lowest vacant one for the cation and the anion, respectively. In molecules containing hetero-atoms, evaluated values of free valency are rather sensitive to the assignment of the Coulomb and resonance integrals[26]. In the present calculation, the Coulomb integral for the hetero-atom was estimated with reference to its electronegativity and the resonance integral was set proportional to the corresponding overlap integral. By employing the self-consistent procedure which was certified to be useful for calculating the electron density for various molecules such as acetamide[27], tropolone[28], furan, pyrrole and thiophene[29], it was proved that the dependence of free valency upon the assignment of the Coulomb integral decreases considerably. The C_{ri} values for aniline, nitrobenzene, benzaldehyde and chlorobenzene were evaluated by the use of this iterative procedure. The C_{ri} values for phenol were calculated by Tsubomura[30]. The free valency values finally obtained in the present study are given in Tables I—III. In these tables, observed orientation rules are also given for the purpose of comparison.

It is seen from these tables that free valency values calculated for the aromatic cation, neutral molecule and anion can explain without contradiction the orientation observed with the electrophilic, radical and nucleophilic substitutions, respectively. Especially, it is worth notice that the free valency values calculated for the cations of the so-called o-, p-directing monosubstituted benzene molecules generally decrease in the order of $p > o > m$. This order is in complete accordance with the experimental results on the electrophilic substitution.

It is known that in some monosubstituted benzene molecules such as toluene[31] and styrene the radical substitution takes place in the side chain. In the case of styrene, this fact is coincident with the theoretical conclusion as is shown in Table II. The free valency of the carbon atom in the substituent group of benzaldehyde is also great compared with that of each atom in the benzene ring. This predicts the possibility that this molecule may be attacked on the carbon atom of the substituent group by the radical reagent.

The only exception in which the order of the free valency values does not agree with that of the observed reactivities in various positions is the case of radical substitution of biphenyl. In this case, free valencies decrease in the order of $2 > 4 > 3$, while the 4-position is most reactive from the experimental point of view. This descrepancy may be due to steric hindrance in the 2-position.

Such a satisfactory agreement between theoretical and experimental results as is seen from Tables I—III seems to support our view that at some stage of the heterolytic substitution reaction a large electron transfer takes place between the aromatic

24) H. H. Greenwood, ibid., **48**, 677 (1952).
25) F. H. Burkitt, C. A. Coulson and H. C. Longuet-Higgins, ibid., **47**, 553 (1951).
26) C. M. Moser, *J. Chem. Soc.*, **1953**, 1073.
27) S. Nagakura, This Bulletin, **25**, 164 (1952).
28) Y. Kurita and M. Kubo, ibid., **24**, 13 (1951).
29) S. Nagakura and T. Hosoya, ibid., **25**, 179 (1952).

30) The authors wish to express their thanks to Dr Tsubomura for his kindness in giving them information on these values.
31) J. H. Merz and W. A. Waters, *J. Chem. Soc.*, **1949**, 2427.

TABLE I. FREE VALENCY VALUES CALCULATED WITH VARIOUS AROMATIC CATIONS

Parent molecule	Free valency					Orientation	
						Theoretical	Experimental
	o	*m*	*p*				
Toluene	0.502	0.454	0.697			$p > o > m$	$p > o > m$
Aniline	0.494	0.395	0.495			$p > o > m$	$p > o > m$
Phenol	0.497	0.431	0.622			$p > o > m$	$p > o > m$
Chlorobenzene	0.472	0.405	0.488			$p > o > m$	$p > o > m$
Nitrobenzene	0.694	0.884	0.472			$m > o > p$	$m > o > p$
	o	*m*	*p*				
Styrene	0.502	0.407	0.518			$\beta > \alpha > p > o > m$	β
	α	β					
	0.517	1.055					
	α	β					
Naphthalene	0.545	0.447				$\alpha > \beta$	$\alpha > \beta$
	2	3	4				
Biphenyl	0.500	0.409	0.523			$4 > 2 > 3$	$4 > 2 > 3$
	1	2	3				
Phenanthrene	0.376	0.06	0.541			$9 > 4 > 3 > 1 > 2$	9
	4	9					
	0.768	0.814					

The experimental results given in this table are taken from the following references:

C. K. Ingold, "Structure and Mechanism in Organic Chemistry", G. Bell and Sons, Ltd., London (1953).

F. Bell, J. Kenyon and P. H. Robinson, *J. Chem. Soc.*, **1926**, 1239.

G. M. Badger, "The Structures and Reactions of the Aromatic Compounds", Cambridge University Press, London (1954).

TABLE II. FFEE VALENCY VALUES CALCULATED WITH VARIOUS AROMATIC MOLECULES

Molecule	Free valency					Orientation	
						Theoretical	Experimental
	o	*m*	*p*				
Toluene	0.412	0.398	0.402			$o > p > m$	$o > p > m$
Aniline	0.433	0.396	0.415			$o > p > m$	—
Phenol	0.400	0.387	0.396			$o > p > m$	$o > p > m$
Chlorobenzene	0.420	0.389	0.409			$o > p > m$	$o > p > m$
Nitrobenzene	0.444	0.428	0.472			$p > o > m$	$p > o > m$
	o	*m*	*p*	α	β		
Benzaldehyde	0.438	0.396	0.457	0.870[a]	—	$\alpha > p > o > m$	—
Styrene	0.448	0.396	0.412	0.412	0.821	$\beta > o > \alpha = p > m$	β
	2	3	4				
Biphenyl	0.437	0.396	0.412			$2 > 4 > 3$	$4 > 2 > 3$

The experimental results given in this table are taken from the following references:

D. H. Hey and G. H. Williams, *Discussions Faraday Soc.*, **14**, 216 (1953).

J. I. G. Gadogan, D. H. Hey and G. H. Williams, *J. Chem. Soc.*, **1954**, 794.

O. Simamura and T. Migita, This Bulletin, **27**, 228 (1954).

O. Simamura and T. Inukai, ibid., **28**, 444 (1955).

T. Suehiro, *J. Chem. Soc. Japan, Pure Chem. Sec.* (*Nippon Kagaku Zasshi*), **72**, 301 (1951). (The experimental result on phenol referred to above is taken from this paper which is concerned with anisole).

a) This value was evaluated under the assumption that the π bond order for the C=O bond may be obtained with the aid of the same equation as for the C=C bond.

TABLE III. FREE VALENCY VALUES CALCULATED WITH NITROBENZENE AND CHLOROBENZENE ANIONS

Parent molecules	Free valency			Orientation	
				Theoretical	Experimental[a]
	o	*m*	*p*		
Nitrobenzene	0.436	0.427	0.448	$p > o > m$	$p > o > m$
Chlorobenzene	0.669	0.648	0.409	$o > m > p$	$o > m > p$

The experimental results given in this table are taken from the following reference:
J. F. Bunnett and R. E. Zahler, *Chem. Revs.*, **49**, 273 (1951).

a) The orientation rules for nitrobenzene and chlorobenzene were deduced from the experimental results on dinitrobenzene and chloronitrobenzene, respectively, because it is difficult to replace a hydrogen atom of benzene directly by nucleophilic reagents such as Cl^- and OH^-.

TABLE IV. THE RELATIVE RATES OF RADICAL SUBSTITUTIONS IN *o*-, *m*- AND *p*-POSITIONS OF NITROBENZENE AND BENZOIC ACID

Molecule	Radical	Relative rate (%)		
		o	*m*	*p*
Nitrobenzene	OH[a]	35.5	29.0	35.5
Nitrobenzene	C_6H_5[b]	43.1	7.50	49.4
Benzoic acid	OH[c]	40.0	40.0	20.0
Benzoic acid	OH[d]	29.4	11.8	58.9
Benzoic acid ester	C_6H_5[e]	44.1	8.30	47.5

a) H. Loebl, G. Stein and J. Weiss, *J. Chem. Soc.*, **1950**, 2704.
b) D. H. Hey and G. H. Williams, *Discussions Faraday Soc.*, **14**, 216 (1953).
c) H. G. C. Bates, M. G. Evans and N. Uri, *Nature*, **166**, 869 (1950).
d) H. Loebl, G. Stein and J. Weiss, *J. Chem. Soc.*, **1951**, 405.
e) O. Simamura, T. Inukai and T. Migita, unpublished data.

molecule and the reagent, and consequently the orientation in the substitution can be determined by free valency values of the aromatic cation, neutral molecule and anion for the electrophilic, radical and nucleophilic substitutions, respectively.

Finally it may be necessary to add a note on the reaction between the OH radical and the aromatic molecule. According to the measurement by Robertson[32], the ionization potential of the OH radical is determined as 13.75 eV. This means that the energy of its unpaired electron orbital is fairly low and a large electron transfer from the aromatic molecule may be expected for this radical as well as for the electrophilic reagent. From this it is inferred that the orientation rule for this radical becomes somewhat similar to that for the electrophilic reagent. In this respect, it seems interesting that in the radical substitution of nitrobenzene and of benzoic acid, the ratio of *m*-derivative to *o*- or *p*-derivative is conspicuously greater for the hydroxyl radical than for the phenyl radical (cf. Table IV). One of possible explanations for this is presumably that the hydroxyl radical partly possesses the characteristic of the electrophilic reagent.

32) A. G. B. Robertson, *Trans. Faraday Soc.*, **48**, 228 (1952).

Summary

The mechanism of the aromatic substitution was studied on the basis of the energy level diagrams determined for both the aromatic molecule and the reagent. From the consideration of the relative heights of the highest occupied and lowest vacant orbitals of the former to those of the latter, it was deduced that a large electron transfer occurs at some stage of the reaction from the aromatic molecule towards the reagent for the electrophilic substitution and in the reverse direction for the nucleophilic substitution.

In connection with this electron transfer mechanism, it was expected that the orientation rule observed with the aromatic substitution can be explained by free valency values of the aromatic cation,

neutral molecule and anion for the electrophilic, radical and nucleophilic substitutions respectively. It was shown that this expectation is fully satisfied for various aromatic substitutions.

The authors wish to express their sincere thanks to Professor K. Higasi and Professor O. Simamura for their kind advice. Their thanks are also due to Assistant Professor H. Baba and Mr. Y. Mizuno for their helpful discussion.

The Institute for Solid State Physics
The University of Tokyo
Komaba-cho, Meguro-ku, Tokyo

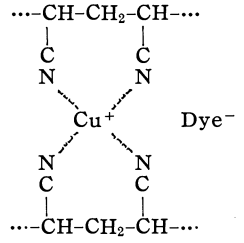
*The Crystal Structure of Bis(succinonitrilo)copper(I) Nitrate**

By Yukio KINOSHITA, Ikuo MATSUBARA and Yoshihiko SAITO**

(Received January 25, 1959)

It is well known that cuprous ion plays an important role in the dyeing of polyacrylonitrile fibers with anionic dyes; cuprous ion is readily absorbed by the fibers which then acquire an almost unlimited affinity for anionic dyes, which ordinarily can not be applied to this class of fibers.

Blaker et al.[1] suggested that the high affinity of cuprous ion for polyacrylonitrile is due to the inherent capability of nitrile groups in the fibers to absorb cuprous ion through formation of complexes analogous to those described by Morgan[2] for simple nitriles. These complexes, which may act as positive sites for fixation of dye anions, are considered to be of the type,



To verify this hypothesis, Rath et al.[3] have prepared similar complexes from nitriles of aliphatic dibasic acids. It would be of interest to determine the crystal structures of these compounds, since they would shed light on the mechanism of the dyeing.

The crystal structure of bis(succinonitrilo) copper (I) nitrate, $[Cu(NC-CH_2-CH_2-CN)_2]NO_3$, has been determined as a part of a program to establish the configurations of these complexes. Furthermore, the infrared spectrum of this complex has been investigated in relation to the crystal structure.

Experimental

Bis(succinonitrilo)copper(I) nitrate was prepared according to the directions of Morgan[2] by dissolving silver nitrate into succinonitrile at 60°C and adding an excess of copper powder. After black spongy silver was deposited, the mixture was filtered while warm and the filtrate was extracted with a mixture of ether and alcohol. On cooling, the clear extract deposited colorless crystals. This compound shows no definite melting point.

Anal. Found: C, 33.24; H, 2.99; N, 24.85; Cu, 22.12. Calcd. for $C_8H_8N_5O_3Cu$: C, 33.63; H, 2.82; N, 24.51; Cu, 22.24%.

Rotation and Weissenberg photograph showed the crystal to be monoclinic with

$a=11.62\pm0.03$Å, $b=5.31\pm0.01$Å, $c=9.53\pm0.03$Å, $\beta=98.8°\pm0.2°$.

Systematically absent reflections were $(h\,0\,l)$ for h odd, which indicated space groups $P2/a$ or Pa. The statistical method of Howells, Phillips and Rogers[4], when applied to the $h\,0\,l$ data, indicated the presence of a center of symmetry, which enabled us to adopt the space group $P2/a$ for the crystal. The density, determined by floatation, was found to be 1.634 g./cc., while

* Presented in part at the Symposium on the Chemistry of Complex Compounds, Tokyo, November 16, 1958.

** Institute of Polytechnics, Osaka City University, Kita-ku, Osaka.

1) R. H. Blaker, S. M. Katz, J. F. Laucius, W. R. Remington and H. E. Schroeder, *Discussions Faraday Soc.*, No. **16**, 210 (1954).

2) H. H. Morgan, *J. Chem. Soc.*, **123**, 2901 (1923).

3) H. Rath, H. Rehm, H. Rummler and E. Specht, *Melliand Textilber.*, **38**, 431, 538 (1957).

4) E. R. Howells, D. C. Phillips and D. Rogers, *Acta Cryst.*, **3**, 210 (1950).

that calculated assuming two formula units per cell was 1.633 g./cc.

Intensity data were obtained by visual estimation of *a*-, *b*- and *c*-axis zero-layer Weissenberg photographs taken with Cu $K\alpha$ radiation. A multiple-film technique was used and the intensity was corrected for geometrical and polarization factors. The final set of data consisted of 122 ($h\,0\,l$), 66 ($h\,k\,0$) and 54 ($0\,k\,l$) terms of measurable amplitudes. Absorption corrections were not made, but errors were minimized by selecting small and as well-formed crystals as were available.

The infrared absorption spectra of bis(succinonitrilo)copper(I) nitrate and succinonitrile in the wavelength region from 2 to 15 microns were obtained with a Perkin-Elmer model 21 spectrophotometer (with NaCl optics).

Structure Determination

Space group $P2/a$ contains fourfold general point positions. Since the unit cell contains only two formula units, the copper atom and the nitrate ion must lie either on a twofold symmetry axis or on a center of symmetry. The latter can be excluded since a tetrahedral coordination of a cuprous ion and trigonal configuration of a nitrate ion are to be expected. The copper atom and the central nitrogen atom(N_1) of the nitrate ion, therefore, must lie on twofold axes. The Patterson function was computed for the *b*-axis projection, which could be solved without difficulty, because of the occurrence of the copper atoms on special positions. Approximate *x*- and *z*-coordinates of all the lighter atoms were obtained at once.

A Fourier synthesis of the electron density projected along the *b*-axis was computed and this enabled all the *x*- and *z*-coordinates to be fixed. The Patterson function for the *a*- and *c*-axis projection could be solved successfully by trial

TABLE I. FINAL ATOMIC COORDINATES

Atom	*x*/*a*	*y*/*b*	*z*/*c*
Cu	0.250	−0.110	0.000
O_1	0.250	−0.359	0.500
O_2	0.155	−0.015	0.487
N_1	0.250	−0.123	0.500
N_2	0.340	0.108	0.143
N_3	0.153	−0.331	0.108
C_1	0.385	0.247	0.225
C_2	0.455	0.427	0.330
C_3	0.028	−0.607	0.262
C_4	0.100	−0.450	0.175

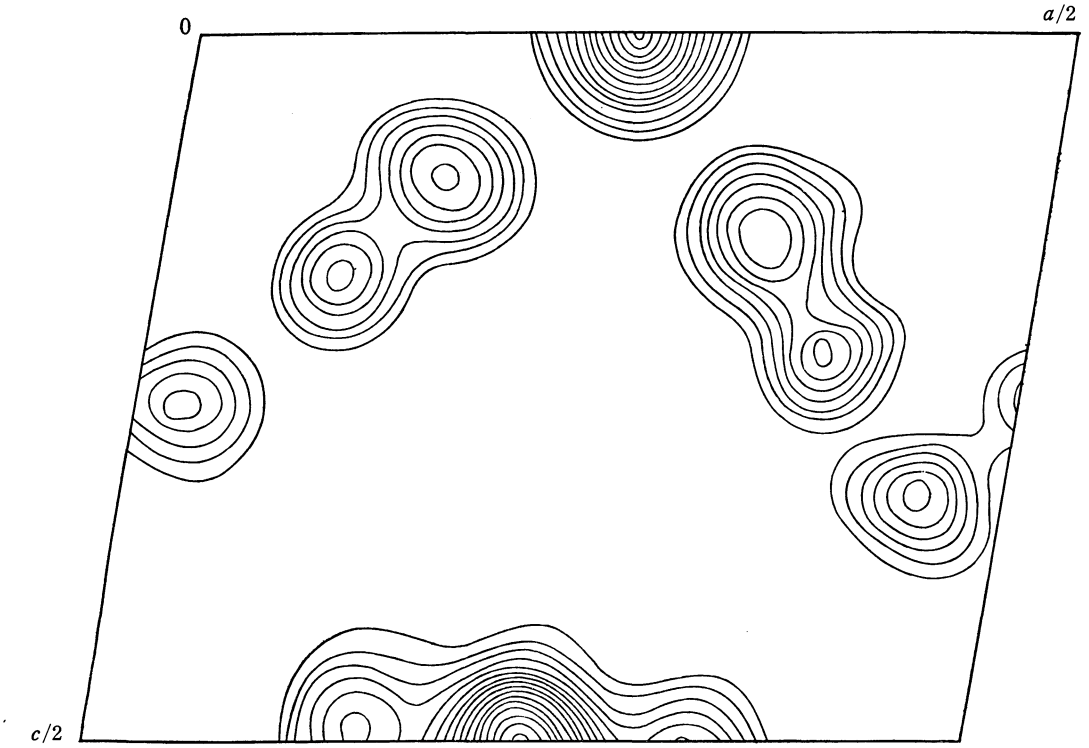


Fig. 1. Final Fourier projection of electron density along [0 1 0]. Contours are drawn at intervals of 3 eÅ^{-2} for copper and those for other atoms are at intervals of 1 eÅ^{-2}, the lowest being 2 eÅ^{-2}.

TABLE II. COMPARISON OF OBSERVED AND CALCULATED STRUCTURE FACTORS

Index	$F_o/4$	$F_c/4$	Index	$F_o/4$	$F_c/4$	Index	$F_o/4$	$F_c/4$
200	15.7	−15.8	601	6.1	− 5.6	$40\bar{1}$	2.6	+ 3.7
400	3.7	+ 3.5	602	7.3	− 6.9	$40\bar{2}$	17.5	+17.1
600	6.1	− 4.7	603	5.0	− 3.9	$40\bar{3}$	13.5	+14.2
800	9.8	+ 8.7	604	7.2	− 6.3	$40\bar{4}$	10.6	+ 9.6
1000	6.7	− 7.4	605	10.0	− 8.8	$40\bar{5}$	5.3	+ 4.4
1200	2.9	+ 3.2	606	6.1	− 5.1	$40\bar{6}$	7.0	+ 6.1
1400	2.6	− 2.3	607	<1.2	+ 0.2	$40\bar{7}$	4.8	+ 3.8
			608	1.1	− 1.5	$40\bar{8}$	8.1	+ 6.9
010	5.1	+ 5.6	609	2.2	− 1.7	$40\bar{9}$	2.4	+ 2.2
020	7.3	+ 7.4	6010	1.5	− 1.4	$40\bar{1}\bar{0}$	<1.1	+ 1.2
030	<0.9	+ 0.6				$40\bar{1}\bar{1}$	<0.9	+ 0.9
040	7.1	− 6.2	801	5.1	+ 4.3	$40\bar{1}\bar{2}$	1.2	+ 1.7
050	2.6	− 2.1	802	6.8	+ 6.0			
060	1.4	− 1.4	803	2.4	+ 1.8	$60\bar{1}$	4.0	− 5.4
			804	5.6	+ 5.1	$60\bar{2}$	7.2	− 6.5
001	7.2	+ 8.5	805	<1.2	− 0.2	$60\bar{3}$	13.9	−12.7
002	10.3	+11.0	806	2.3	+ 3.0	$60\bar{4}$	12.6	−10.9
003	6.4	− 6.7	807	2.6	+ 2.5	$60\bar{5}$	4.4	− 5.6
004	13.1	+14.3	808	2.4	+ 3.0	$60\bar{6}$	6.7	− 5.1
005	1.2	− 0.6	809	0.6	+ 0.4	$60\bar{7}$	4.4	− 4.5
006	12.0	+11.5				$60\bar{8}$	1.2	− 0.7
007	3.6	+ 2.5	1001	1.7	− 1.8	$60\bar{9}$	<1.2	− 1.1
008	7.2	+ 7.2	1002	6.8	− 5.7	$60\bar{1}\bar{0}$	1.8	− 2.1
009	2.9	+ 2.2	1003	2.4	− 1.5	$60\bar{1}\bar{1}$	0.8	− 1.5
0010	2.5	+ 2.6	1004	2.3	− 2.6			
0011	<0.9	+ 0.5	1005	<1.1	+ 0.8	$80\bar{1}$	4.7	+ 4.3
0012	1.8	+ 2.1	1006	1.9	− 2.0	$80\bar{2}$	7.1	+ 6.2
			1007	1.2	− 0.6	$80\bar{3}$	<1.1	+ 1.5
201	7.6	− 7.0				$80\bar{4}$	10.1	+ 8.7
202	26.9	−28.7	1201	1.6	+ 1.3	$80\bar{5}$	9.7	+ 7.9
203	3.4	− 3.9	1202	2.9	+ 3.5	$80\bar{6}$	3.4	+ 2.9
204	10.4	− 9.8	1203	<1.0	+ 0.4	$80\bar{7}$	1.2	− 0.8
205	5.1	− 5.0	1204	1.2	+ 1.5	$80\bar{8}$	2.0	+ 2.1
206	7.1	− 6.4	1205	1.3	+ 0.9	$80\bar{9}$	1.1	+ 1.8
207	3.9	− 3.2				$80\bar{1}\bar{0}$	1.8	+ 1.8
208	6.1	− 4.9	1401	1.4	− 1.6	$80\bar{1}\bar{1}$	1.4	+ 1.7
209	<1.2	− 1.3	1402	<0.5	− 0.4			
2010	<1.0	− 1.3				$100\bar{1}$	2.1	− 1.5
2011	0.8	− 1.3	$20\bar{1}$	11.2	−10.1	$100\bar{2}$	6.5	− 6.2
			$20\bar{2}$	24.7	−24.7	$100\bar{3}$	2.9	− 2.2
401	0.7	+ 1.9	$20\bar{3}$	6.5	+ 5.8	$100\bar{4}$	2.7	− 3.3
402	8.6	+ 7.5	$20\bar{4}$	11.2	−11.5	$100\bar{5}$	<1.2	+ 1.0
403	18.0	+16.8	$20\bar{5}$	2.1	− 1.9	$100\bar{6}$	4.1	− 4.9
404	14.8	+13.3	$20\bar{6}$	11.8	−11.6	$100\bar{7}$	1.1	− 1.9
405	5.7	+ 4.9	$20\bar{7}$	4.0	− 3.1	$100\bar{8}$	2.0	− 2.3
406	6.0	+ 4.4	$20\bar{8}$	6.0	− 6.5	$100\bar{9}$	1.7	− 1.0
407	4.8	+ 3.8	$20\bar{9}$	3.4	− 2.3	$100\bar{1}\bar{0}$	1.9	− 2.0
408	<1.2	+ 0.5	$20\bar{1}\bar{0}$	5.7	− 5.4			
409	<1.1	+ 0.9	$20\bar{1}\bar{1}$	<0.9	+ 0.1			
4010	2.5	+ 2.0	$20\bar{1}\bar{2}$	<0.6	− 0.1			
4011	1.3	+ 1.7						

TABLE II. (continued)

Index	$F_o/4$	$F_c/4$	Index	$F_o/4$	$F_c/4$	Index	$F_o/4$	$F_c/4$
$120\bar{1}$	2.3	+ 2.6	710	6.5	− 6.4	021	4.1	− 3.9
$120\bar{2}$	3.9	+ 4.3	720	4.0	− 3.7	022	5.2	+ 4.9
$120\bar{3}$	<1.1	− 0.9	730	7.5	− 8.2	023	1.7	− 0.8
$120\bar{4}$	1.1	+ 1.8	740	<1.2	+ 0.5	024	3.6	+ 2.6
$120\bar{5}$	<1.1	+ 0.2	750	<1.0	+ 0.8	025	<0.9	− 0.8
$120\bar{6}$	1.9	+ 2.8	760	<0.5	+ 1.3	026	5.8	+ 5.2
$120\bar{7}$	2.4	+ 1.8				027	2.1	+ 0.8
$120\bar{8}$	2.5	+ 3.1	810	4.1	+ 4.0	028	<1.1	+ 0.3
			820	<1.2	− 0.4	029	<1.0	− 1.2
$140\bar{1}$	<0.8	− 0.2	830	1.8	− 1.2	0210	<0.9	+ 0.2
$140\bar{2}$	0.8	− 0.8	840	1.2	− 2.2	0211	<0.6	+ 0.4
$140\bar{3}$	1.6	− 1.4	850	1.3	− 1.5			
$140\bar{4}$	1.0	− 1.8				031	6.9	− 6.2
$140\bar{5}$	<0.6	− 0.9	910	3.5	+ 3.0	032	<0.8	+ 0.7
$140\bar{6}$	<0.4	− 1.4	920	3.8	+ 4.1	033	4.7	− 5.1
			930	1.2	+ 1.6	034	1.4	− 0.4
110	11.7	+10.7	940	1.6	+ 2.0	035	5.7	− 5.7
120	4.6	+ 4.4	950	0.8	− 1.1	036	2.6	− 2.4
130	8.5	+ 8.2				037	3.4	− 2.6
140	3.4	+ 3.1	1010	3.4	− 3.9	038	<1.0	+ 0.4
150	2.2	− 1.9	1020	1.3	− 1.4	039	<0.9	− 0.8
160	1.4	− 1.2	1030	<1.2	− 0.4	0310	<0.7	+ 0.1
			1040	2.4	+ 2.6			
210	19.2	−20.4	1050	0.5	+ 1.0	041	4.8	− 5.3
220	<0.8	− 0.3				042	4.8	− 4.1
230	2.4	+ 1.6	1110	2.9	− 3.5	043	4.4	− 3.9
240	5.0	+ 5.0	1120	<1.2	− 0.9	044	2.6	− 2.1
250	4.2	+ 4.1	1130	<1.1	− 1.3	045	<1.1	− 1.3
260	<1.0	− 0.2	1140	0.8	− 0.9	046	3.6	− 2.5
						047	2.4	− 3.1
310	15.0	−14.6	1210	2.7	+ 2.8	048	2.7	− 2.3
320	7.9	− 8.3	1220	1.1	+ 0.8	049	1.0	− 0.8
330	6.2	− 6.6	1230	0.9	− 0.3			
340	1.7	− 1.5	1240	<0.4	− 1.4	051	4.0	− 4.7
350	1.7	+ 1.3				052	3.7	− 2.9
360	<1.0	+ 1.0	1310	1.0	+ 1.3	053	1.5	− 1.7
			1320	0.9	+ 1.1	054	<1.0	− 0.3
410	4.4	+ 3.0	1330	1.1	+ 1.2	055	1.7	− 2.2
420	1.2	+ 1.1				056	1.5	− 1.5
430	3.5	− 3.9	1410	<0.7	− 0.2	057	1.8	− 1.9
440	5.9	− 6.9	1420	<0.6	− 0.2	058	<0.6	− 1.1
450	1.7	− 1.8						
460	0.9	− 1.0	011	4.2	+ 4.0	061	1.3	− 1.2
			012	20.9	+20.8	062	<0.8	+ 0.8
510	6.0	+ 6.0	013	<0.6	+ 0.8	063	1.2	− 1.4
520	12.5	+13.5	014	10.5	+ 9.1	064	<0.7	− 0.7
530	2.9	+ 3.9	015	5.3	+ 4.0	065	1.0	− 1.4
540	2.2	+ 1.7	016	7.7	+ 6.4			
550	1.2	− 1.3	017	4.2	+ 3.0			
560	<1.1	− 1.7	018	5.3	+ 4.5			
			019	1.8	+ 1.2			
610	1.3	− 1.0	0110	2.1	+ 1.8			
620	<1.0	+ 0.4	0111	<0.8	+ 0.1			
630	3.9	+ 4.9	0112	<0.3	+ 0.4			
640	3.0	+ 2.9						
650	1.6	+ 2.0						
660	<0.7	+ 1.1						

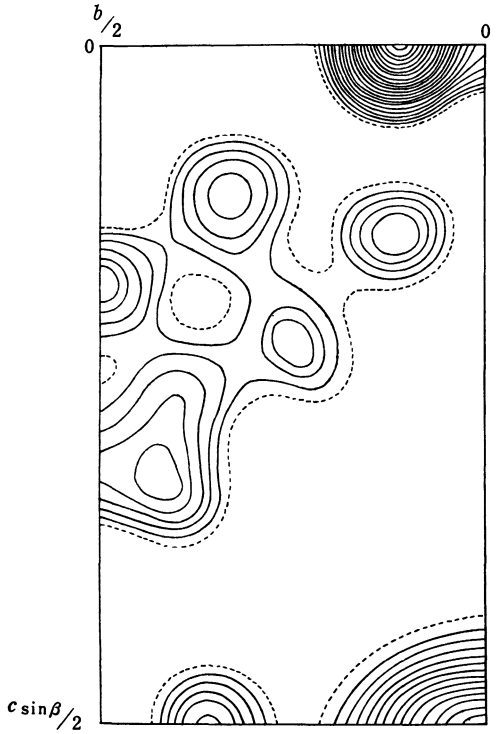


Fig. 2. Final Fourier projection of electron density along [1 0 0]. Contours are drawn at intervals of 2 eÅ^{-2} for copper and nitrate group except O_1. Those for other atoms are at intervals of 1 eÅ^{-2}, the lowest being 2 eÅ^{-2} (broken).

studies with models having suitable interatomic distances and bond angles. Approximate y-coordinates of all the atoms were thus obtained. Fourier projections of the electron density along [1 0 0] and [0 0 1] were then computed. Fourier refinements were repeated as usual. The final projections along [0 1 0] and [1 0 0] are shown in Figs. 1 and 2, respectively.

The final set of parameters is listed in Table I. This gave the reliability index $R=\Sigma||F_o|-|F_c||/\Sigma|F_o|$ of 0.124, 0.106 and 0.134 for $(h\,0\,l)$, $(h\,k\,0)$ and $(0\,k\,l)$, respectively. A mean isotropic temperature factor with B=4.0 Å^2 was found to be satisfactory for the three equatorial zones. Observed and calculated structure factors are shown in Table II.

Calculation of the structure factors as well as that of the electron density was carried out with Remington Rand UNIVAC 120 electronic computer quite effectively.

Description of the Structure

The interatomic distances and the bond angles calculated on the basis of the above parameter values are given in Table III. Calculation of the standard deviation of atomic coordinates by Cruickshank's

TABLE III. INTERATOMIC DISTANCES AND BOND ANGLES

Cu—N_2	1.96 Å	∠CuN_2C_1	175°
Cu—N_3	2.02	∠CuN_3C_4	177
C_1 —N_2	1.14	∠$N_2C_1C_2$	175
C_4 —N_3	1.14	∠$N_3C_4C_3$	180
C_1 —C_2	1.53	∠$C_1C_2C_3$	113
C_3 —C_4	1.52	∠$C_4C_3C_2$	107
C_2 —C_3	1.49	∠$O_1N_1O_2$	118
N_1—O_1	1.25	∠$O_2N_1O_2'$	125
N_1—O_2	1.23		

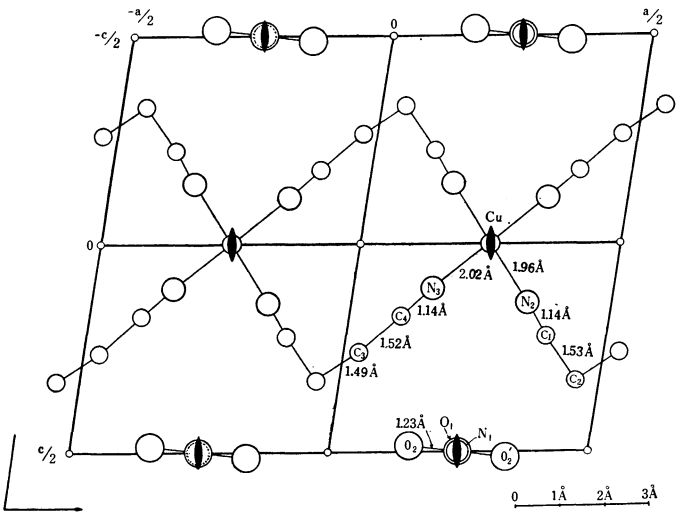


Fig. 3. Projection of the structure along [0 1 0].

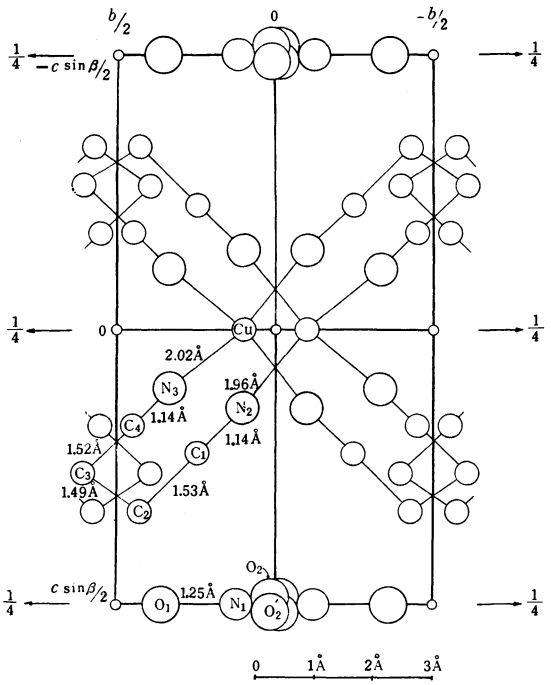
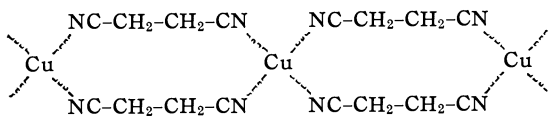


Fig. 4. Projection of the structure along [1 0 0].

method[5] for each projection gives 0.025Å for the resolved carbon and nitrogen atoms. This suggests a standard deviation of about ±0.04 Å in the Cu-N bond length determination.

The projections of the structure of bis-(succinonitrilo)copper (I) nitrate along [0 1 0] and [1 0 0] are shown in Figs. 3 and 4, respectively.

It is evident from the figures that the structure consists of nitrate ions and a polymeric chain of the composition,



which runs parallel to the *a*-axis. A copper atom is surrounded tetrahedrally by four nitrogen atoms with Cu-N distances of 1.96 and 2.02 Å. A succinonitrile molecule in the complex takes a *gauche* configuration with respect to the central C_2-C_3 bond, the azimuthal angle of internal rotation being 127° with the *trans* position taken as the origin. The observed C-N distance of 1.14 Å is, within the limits of error, close to the value expected for triple C-N bond length. The N-C-C bond as well as the Cu-N-C bond is found to be approximately linear. It is possible accordingly that the bond character in the C-N group may be expressed as C≡N.

The nitrate ion exists on a twofold symmetry axis. The shape and size of the ion is as listed in Table III. These data are in good agreement with those obtained for other crystals.

Infrared Spectrum as Related to the Configuration of the Ligand Molecule

The vibrational spectrum of the free succinonitrile molecule was investigated by Fitzgerald and Janz[6], who concluded that this molecule exists as an equilibrium mixture of two rotational isomers, *trans* and *gauche*, the latter being the more stable configuration. Nakagawa and Tokumaru[7] also studied the vibrational spectrum of this substance and reached a similar conclusion. In considering the infrared spectrum of the complex compound it was first assumed that the interaction forces between ligand molecules are so small that the main features of the spectrum may be explained from consideration of an isolated succinonitrile molecule. The infrared spectra of bis-(succinonitrilo)copper(I) nitrate and free succinonitrile are shown in Fig. 5. In Table IV are listed the vibrational frequencies and the assignments for the infrared absorption bands of these substances in the region 1300~700 cm^{-1}. In fact, all the main bands of the complex in this region may be assigned to the vibrations of the

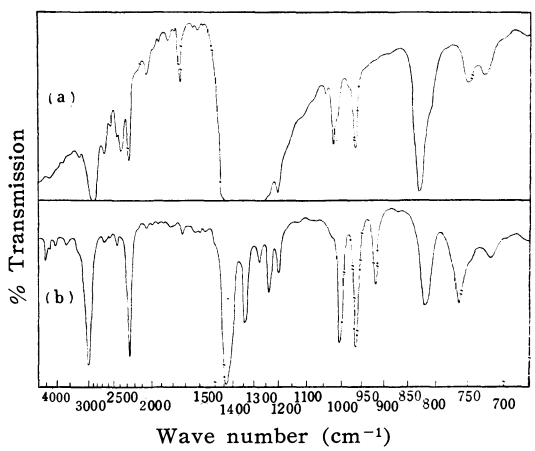


Fig. 5. Infrared spectra of (a) complex and (b) free succinonitrile.

5) D. W. J. Cruickshank, *Acta Cryst.*, 2, 65 (1949).

6) W. E. Fitzgerald and G. J. Janz, *J. Molec. Spectroscopy*, 1, 49 (1957).

7) I. Nakagawa, Private communication.

TABLE IV. INFRARED BANDS OF COMPLEX AND FREE SUCCINONITRILE

Wave numbers in cm^{-1}

Free[a]	Complex[b]	Assignments[c]			
1335	?	*gauche*	CH_2	wag	*B*
1271	—	*trans*	CH_2	wag	B_u
1231	1242	*gauche*	CH_2	wag	*A*
1198	1202	*gauche*	CH_2	twist	*A*
1020	1021	*gauche*	C-C	stretch	*A*
1001	1010	*gauche*	C-CN	stretch	*B*
962	965	*gauche*	CH_2	rock	*A*
917	—	*trans*	C-C	stretch	B_u
818	825	*gauche*	CH_2	rock	*B*
813	813	*gauche*	C-CN	stretch	*A*
761	—	*trans*	CH_2	rock	A_u

a) Solid film
b) In Nujol
c) Based on Nakagawa and Tokumaru's results

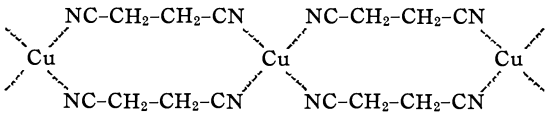
gauche configuration of succinonitrile, which is in complete agreement with the X-ray results.

The spectral features in the nitrile absorption region show strong evidence of tetrahedral coordination of the nitrile groups to the copper sp^3 orbitals; the complex compound shows two intense bands with peaks at 2278 cm^{-1} and 2381 cm^{-1}, instead of the one at 2257 cm^{-1} corresponding to the C≡N stretching vibration of the free succinonitrile. These two bands are certainly to be assigned to the C≡N stretching modes characteristic to the tetrahedral configuration of the complex compound, although the vibrational shifts towards higher frequencies with respect to the free nitrile may require further considerations.

The intense bands at 830 cm^{-1} and near 1380 cm^{-1} and a weak band at 749 cm^{-1} are assigned to the vibrations of the nitrate ion. A weak band at 1042 cm^{-1} may correspond to an infrared inactive frequency for the nitrate ion which is considered to become active because of the breakdown of the selection rule in the crystalline field.

Summary

The crystal structure of bis(succinonitrilo)copper(I) nitrate has been determined by two dimensional Fourier method. It is monoclinic $P2/a$ with two formula units in a cell of dimensions: $a=11.62\pm0.03$ Å, $b=5.31\pm0.01$ Å, $c=9.53\pm0.03$ Å and $\beta=98.8°\pm0.2°$. The crystal consists of nitrate ions and polymeric chains of the following composition:



These chains run parallel to the a-axis. A succinonitrile molecule takes a *gauche* form with respect to the central C_2–C_3 bond. A copper atom is surrounded tetrahedrally by four nitrogen atoms with Cu–N distances of 1.96 and 2.02 Å. These facts are in close agreement with infrared spectral observations.

All the atoms in the group Cu–N–C–C lie almost on a straight line. This fact and the observed C–N distance of 1.14 Å suggest that the bond character in the C–N group may essentially be expressed as C≡N.

The authors wish to express their hearty thanks to Dr. K. Hoshino and Dr. K. Kato of the Central Research Laboratories of Toyo Rayon Co., Ltd. for their kind encouragement in the course of this study. They also wish to thank Mr. K. Yoshida of Toyo Rayon Co., Ltd. for carrying out the mechanical computations.

Central Research Laboratories
Toyo Rayon Co., Ltd.
Otsu, Shiga

Electron Diffraction Investigation on the Molecular Structure of n-Butane

By Kôzo KUCHITSU

(Received December, 27, 1958)

The structural parameters of normal hydrocarbons have not yet been thoroghly studied[1], except the simplest ones, methane[2] and ethane[3-5], though there are many investigations on their halogen derivatives[6]. The results which have so far been obtained, except the above two, are on propane by Pauling and Brockway[7], C-C=1.54±0.02A, and ∠C-C-C=111.5°±3°, and on *n*-butane by Wierl[8], C-C=1.51± 0.05A. As the technique has since been developed, more accurate results are expected to be given in the determination of the C-C distances and the C-C-C valence angles. Furthermore, the position of hydrogen atoms may be located with considerable accuracy, because these molecules do not include heavier atoms than carbon. Accordingly, it seems worth while to investigate the structure of *n*-butane.

Various spectroscopic and thermodynamic studies have shown that rotational isomers exist in the normal paraffins higher than propane[6]. As for *n*-butane, it was first noticed by Kohlrausch and Köppl[9] in their study of the Raman spectra. It was soon confirmed by Mizushima, Morino and Nakamura[10] in their study of the Raman spectra in the liquid and solid. They found that two forms exist in the liquid whereas only the *trans* form remains in the solid. The energy difference between the isomers was measured by Szasz and his co-workers in the liquid phase[11,12]. They obtained from the measurement of the temperature dependence of the Raman intensity the value of 770±90 cal./mol.[11], or 760±100 cal./mol.[12] (the *trans* form being the more stable). This result is in good agreement with the value of 800 cal./mol. which was estimated by Pitzer[13] from the entropy of *n*-butane[14] and used in the studies of the thermodynamic functions of hydrocarbons. Thus the rotational isomerism seems to be well established in the liquid phase, but no experimental evidence concerning the energy difference in the vapor is so far available[12]. While it seems probable that the magnitude is nearly the same as in the liquid because of the nonpolar nature of the molecule, the infrared spectrum of the vapor of *n*-butane was interpreted by Gates[15] in terms of a single form. However, as pointed out by Axford and Rank[16], his interpretation seems to rest on a rather insecure foundation and a further study on this point will make the situation clear. In the present study it is confirmed that two isomers exist, the *trans* and the *gauche* forms, in the vapor of *n*-butane, the energy difference being nearly equal to that in the liquid.

Experimental

The electron diffraction instrument used in this study was designed by Morino, Kimura and Iwasaki[17]. The details of the apparatus and procedure were reported previously[18-20]. Diffraction photographs were taken through an r^3-sector

1) M. H. Jellinek, "Physical Chemistry of Hydrocarbons," Vol. I, Chap. 2, Academic Press Inc., New York (1950).
2) G. Herzberg, "Infrared and Raman Spectra of Polyatomic Molecules", D. Van Nostrand Co., Inc., New York (1945).
3) G. E. Hansen and D. M. Dennison, *J. Chem. Phys.*, **20**, 313 (1952).
4) K. Hedberg and V. Schomaker, *J. Am. Chem. Soc.*, **73**, 1482 (1951).
5) A. Almenningen and O. Bastiansen, *Acta Chem. Scand.*, **9**, 815 (1955).
6) S. Mizushima, "Structure of Molecules snd Internal Rotation", Academic Press Inc., New York (1954).
7) L. Pauling and L. O. Brockway, *J. Am. Chem. Soc.*, **59**, 1223 (1937).
8) R. Wierl, *Ann. Physik*, **13**, 453 (1932).
9) K. W. F. Kohlrausch and F. Köppl, *Z. phys. Chem.*, **B26**, 209 (1934).
10) S. Mizushima, Y. Morino and S. Nakamura, *Sci. Papers Inst. Phys. Chem. Research (Tokyo)*, **37**, 205 (1940).
11) G. J. Szasz, N. Sheppard and D. H. Rank, *J. Chem. Phys.*, **16**, 704 (1948).
12) N. Sheppard and G. J. Szasz, ibid., **17**, 86 (1949).
13) K. S. Pitzer, ibid., **5**, 473 (1937).
14) K. S. Pitzer, ibid., **8**, 711 (1940); *J. Am. Chem. Soc.*, **63**, 2413 (1941).
15) D. M. Gates, *J. Chem. Phys.*, **17**, 393 (1949).
16) D. W. E. Axford and D. H. Rank, ibid., **18**, 51 (1950).
17) Y. Morino, M. Kimura and M. Iwasaki, The Sixth Annual Meeting of the Chemical Society of Japan (1953).
18) T. Ino, *J. Phys. Soc. Japan*, **8**, 92 (1953).
19) Y. Morino and K. Kuchitsu, *J. Chem. Phys.*, **28**, 175 (1958).
20) Y. Morino, K. Kuchitsu and E. Hirota, "Electron Diffraction by Gas", Maruzen Co., Tokyo (1957).

(in the case of the shorter camera length, 11.8 cm.) or an r^2-sector (in the case of the longer camera length, 27.9 cm.). The sectors were carefully cut to fit the proper shape within a hundredth of a millimeter[21]. They were mounted on a ball-bearing race and rotated rapidly during the exposure. In taking the diffraction photographs particular care was taken in regard to the constancy of the electron wavelength, the reducing of the extraneous scattering, and a good localization of the sample vapor.

The electron beam was focused to a spot of about 0.1 mm. in diameter. The fluctuation or the drift of the accelerating voltage was regulated within 0.1%. The wavelength of the beam was determined to be about 0.0556Å by a transmission pattern of gold foil. In order to reduce the extraneous scattering, a beam stopper of a shape similar to that described by Brockway[22] or Bastiansen[23] was mounted at the center of the sector[21]. The effect of the stopper on reducing the extraneous background was clearly seen on the photometer trace; the blank line of the photometer curve was nearly on the same level as the center line screened by the stopper, illustrating the fact that the extraneous background was not significant. Further evidence was given by a "blank test"[24] (taking photographs under the same condition as the experiment but without a sample jet), or by the "shadow test"[24] (taking photographs with the sample jet through a non-rotating sector) showing that there was no appreciable extraneous scattering caused by the main beam, nor by the scattering on the edge of the sector, of the slit, and of the nozzle aperture.

A "Research Grade" sample of *n*-butane of Phillips Petroleum Company was kindly furnished by Mr. T. Takatani of the Hitachi Central Research Laboratory. The sample (gas at room temperature) was introduced into a glass container of about 1 liter and the pressure was kept at about 20 mmHg. A liquid air trap was placed just over the nozzle to prevent the sample from diffusing through the camera. The flowing rate of the sample gas was carefully controlled, and diffraction photographs were taken with a long exposure time (a few minutes)[23,25]. A set of three photographs of different exposures were taken successively and developed at one time in the same bath. Two of the better photographs among them were used for the density-intensity calibration.

The photographs were scanned by a Riken B-type recording microphotometer of Nagoya University to measure the optical density as a function of the radius[18]. The photographic plate was rotated rapidly about the center of the pattern while being scanned by the photometer.

The measurement of the photometer curves was carried out with a Riken two-dimensional comparator in the interval of $\Delta q=0.5$. Optical densities thus measured were converted into relative intensities either by Karles' method[26] or by Bartell's method[27] by using the set of two density curves. The resulting intensity curves were averaged respectively for each set. The agreement between the calibration curves obtained by either method was satisfactory. The curves obtained in both procedures were used in the analysis described below.

The averaged intensity curve was multiplied by $q^{1/2}$ to accentuate the molecular oscillations, and a smooth background line I_B was drawn through the curve. After a few steps of redrawing of the line, a reasonable background which satisfies Karles' criterion[24,26], that is, no fluctuation (0.0 through 0.7Å) and non-negativeness of the baseline of the radial distribution curve was obtained. The corresponding molecular intensity curve $qM(q)$ was readily calculated by using the following equation[26]:

$$qM(q)=q(I/I_B-1) \tag{1}$$

The above procedures were repeated one by one for the three sets of plates taken with the shorter camera length, and finally five molecular intensity curves shown in Fig. 1 were obtained: two from the curves calibrated by Karles' procedure, two by Bartell's procedure, and one for which the density is nearly linear so that the same molecular intensity curve was obtained by both calibrations. The average deviations of the peak positions and intensities, listed in Table I,

TABLE I. AVERAGE DEVIATIONS OF THE PEAK POSITIONS AND INTENSITIES FOR FIVE OBSERVED MOLECULAR INTENSITY CURVES

Peak		Peak position[a]		Peak intensity[b]	
Max.	Min.	Average	Average dev.	Average	Average dev.
3		18.18	0.08	1.37	0.06
	3	23.02	0.06	−0.22	0.04
4		28.18	0.06	1.12	0.06
	4	35.07	0.04	−2.95	0.14
5		41.08	0.02	3.05	0.18
	5	50.19	0.07	−1.70	0.08
6		56.55	0.04	2.10	0.10
	6	61.31	0.05	−1.28	0.05
7		67.84	0.06	0.80	0.04
	7	75.14	0.09	−0.79	0.03
8		80.92	0.14	1.08	0.02
	8	87.60	0.16	−0.93	0.04
9		95.03	0.14	0.89	0.04
Average		—	0.08	—	0.07

a) in q-unit.
b) in absolute unit.

21) S. Shibata, Symposium on the Diffraction of X-ray and Electrons (1955).
22) L. O. Brockway and L. S. Bartell, *Rev. Sci. Instr.*, **25**, 569 (1954).
23) O. Bastiansen, O. Hassel and E. Risberg, *Acta Chem. Scand.*, **9**, 232 (1955).
24) I. L. Karle and J. Karle, *J. Chem. Phys.*, 18, 963 (1950).
25) O. Bastiansen, L. Hedberg, and K. Hedberg, ibid., **27**, 1311 (1957).
26) J. Karle and I. L. Karle., ibid., 18, 957 (1950).
27) L. S. Bartell and L. O. Brockway, *J. Appl. Phys.*, **24**, 656 (1957).

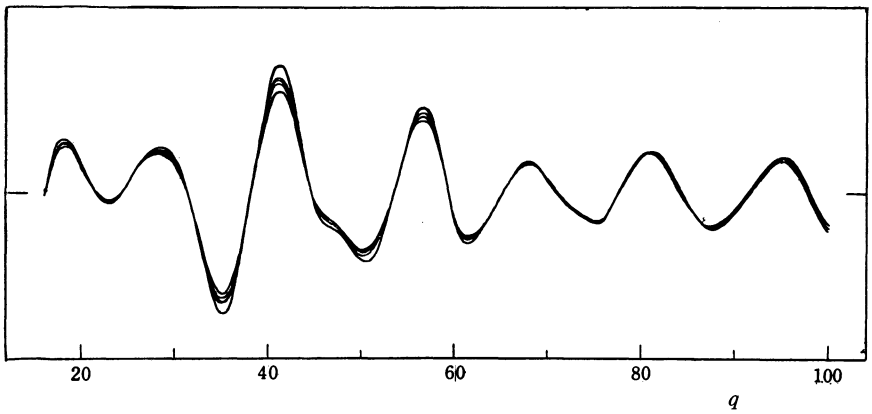


Fig. 1. Experimental molecular intensity curves for *n*-butane. Five experimental intensity curves are given in the same coordinate. The maximum average deviations among these intensities (near $q=40$) amounts to about 6%.

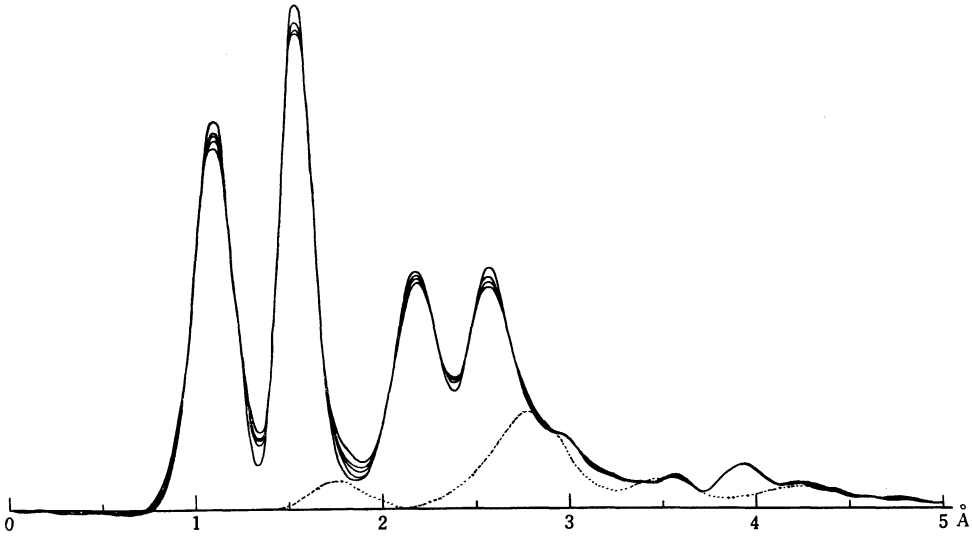


Fig. 2. Experimental RD curves. The RD curves computed from the five experimental intensity curves (Fig. 1) are illustrated in the same scale. The average deviations at the larger peaks are 1~2%. The dotted line denotes a minor contribution from the atomic pairs including hydrogen computed by use of a self-consistent model (see text). It is seen that the curves are non-negative everywhere within the experimental uncertainty.

are important measures for estimating the experimental errors of the structure analysis.

Analysis of the Radial Distribution Curve

Procedure.—Modified radial distribution curves[28] (they will be abbreviated as RD curves) were calculated from the molecular intensity curves, changing the Fourier integral into summation[29,30],

$$f(r)=\sum_{q=1}^{100} qM_c(q)\sin(\pi qr/10)\exp(-b\pi^2q^2/100) \quad (2)$$

where $qM_c(q)$ is the observed molecular intensity corrected for the non-nuclear scattering. Since the experimental intensity extends to $q=100$, a constant b was chosen to be 0.002333 to make the summation converge rapidly.

The summation was performed by the use of a punched-card machine[29]. The detail of the computation was given elsewhere[31]. Near the end of the study, a

28) Y. Morino and E. Hirota, *J. Chem. Phys.*, 28, 185 (1958).
29) P, A. Shaffer, V. Schomaker and L. Pauling, ibid., 14, 648, 659 (1946).
30) T. Ino, *J. Phys. Soc. Japan*, 12, 495 (1957).
31) Y. Morino and K. Kuchitsu, *X-Rays*, 8, 37 (1954).

TABLE II. SELF-CONSISTENT ANALYSIS FOR THE STRUCTURE (in Å unit)

Atomic pair	A		B		C	
	Distance	Mean amplitude	Distance	Mean amplitude	Distance	Mean amplitude
C-H	1.090	0.078	1.092	0.0830	1.092	0.0823
C-C	1.540	0.050	1.540	0.0534	1.539	0.0530
C-H (nonbonded)	2.163	0.110	2.178	0.1075	2.179	0.1005
C-C (nonbonded)	2.515	0.070	2.552	0.0739	2.553	0.0726
C-C (*gauche*)	2.949	0.160	(3.047)[a]	(0.160)[a]	3.12	0.125
C-C (*trans*)	3.876	0.070	3.906	0.0749	3.914	0.065

A: The model assumed at the first stage.
B: Result of the first analysis.
C: Result of the second analysis.
a) The *gauche* distance and its mean amplitude could not be measured accurately in the first analysis. Therefore, the values in brackets were used as the basis of the second analysis. The distance was calculated by using the result of the first analysis and the assumption that the azimuthal angle was 60°.

parametron digital computor became available at Department of Physics of the University of Tokyo. Some of the calculations were carried out by the use of this machine[32].

The RD curves thus obtained for the five molecular intensity curves are illustrated in Fig. 2; the agreement is satisfactory. A detailed analysis was made for the averaged RD curve.

Care was taken in the analysis in regard to the following points: a) the structure assumed in the analysis, b) a correction for the non-nuclear scattering, and c) minor contributions of hydrogen terms.

a) In the calculation of the RD curve, the inner region ($q=0\sim15$) of the molecular intensity curve was spliced by a theoretical intensity curve $qM_c(q)$ computed with an assumed model*. The model listed in the first column A of Table II was assumed at the first stage; in this model all angles were assumed to be tetrahedral and the mean amplitudes calculated theoretically (see section V) were used**. The result of the first analysis was used to calculate the second RD curve, and as shown in the second B and the last column C of the table the second-stage parameters were made self-consistent with the final result of the analysis.

TABLE III. SELF-CONSISTENT ANALYSIS FOR THE FRACTIONS OF THE ISOMERS

Series		A	B	C	D
I	*trans*	100%	65%	67%	65%
II	〃	0%	48%	57%	61%

Besides the assumptions on the structural parameters, assumptions had to be made for the rotational isomers, i.e., the configurations and the fractions of the isomers[19]. It was found that the shape of the RD curve beyond 2.3Å is sensitive to these assumptions, though they had no appreciable effect on the inner part of the RD curve. A method of analysis similar to that used by Iwasaki[33] was applied as follows. The process is shown in Table III. Theoretical curves were calculated first for 100% *trans* form (azimuthal angle 180°) (Series I), and for 100% *gauche* form (azimuthal angle assumed to be 60°) (Series II). The frame structure was based on the model C of Table II. The area under the *trans* C–C peak in the resulting RD curve was compared with the theoretical value and the fraction of the *trans* form was estimated from the ratio (IB and IIB). A theoretical curve of the mixture of two isomers in this fraction was then spliced to the experimental curve and the same analysis was carried out. This procedure was repeated until a self-consistent result for

32) Y. Morino, K. Kuchitsu and M. Shibuya, Symposium on Structural Chemistry, Kyoto, Japan, Oct. 1958.

* The contribution of the theoretical molecular intensity curve spliced in the inner region ($q=0\sim15$) to the RD curve is such a slowly fluctuating function that slight changes in the parameters have no essential influences on either the peak positions or the peak widths, though there may be considerable changes in the peak areas. Account was taken of this point for estimating the errors.

** The hydrogen atoms in the methyl groups were assumed to be at the staggered configuration in euqilibrium with respect to the hydrogen and carbon atoms in the methylene groups. See L. G. Smith, *J. Chem. Phys.*, **17**, 179 (1949), Refs. 4 and 5 for ethane, Ref. 50 for ethyl chloride, and K. S. Pitzer, ibid., **12**, 310 (1944), for propane.

33) M. Iwasaki, S. Nagase and R. Kojima, This Bulletin, **30**, 230 (1957).

the fraction of the isomers was obtained (C and D). Since both series gave nearly the same values, the fraction of the *trans* form was thus found to be 60~65% in this analysis. The area under the *gauche* peak in the final RD curve was found to be about 35~40% of the theoretical maximum value (that is, the area which could be expected if the *gauche* form only were present), also in agreement with this result.

In conclusion, the model used for calculating the final RD curve was made sufficiently self-consistent, so that the result of the following RD analysis is essentially free from any arbitrary assumptions.

b) A correction for the non-nuclear scattering was made by using the method of Bartell[34]. A minor correction term $\Delta M(q)$ was subtracted from the observed molecular intensity $qM(q)$ to obtain $qM_c(q)$. The function $\Delta M(q)$, which is defined as

$$\Delta M(q) = qM(q) - qM_c(q)$$
$$= \sum_{i,j}{}' (c_{ij}/r_{ij})(\mu_{ij}-1)\exp(-l^2_{ij}s^2/2)\sin sr_{ij} \quad (3)$$

where

$$\mu_{ij} = c_{ij}/c_{ij}$$
$$c_{ij} = (Z_i - f_i)(Z_j - f_j)/\sum[(Z_i - f_i)^2 + S_i]$$

and

$$c_{ij} = Z_iZ_j/(\sum Z_i^2 + Z_i)$$

was calculated theoretically on the base of an assumed model. As in the former case a), the structure first assumed was that listed in the first column of Table II; and then ΔM was calculated again by using the second column of the same table. The elastic scattering factors for carbon and hydrogen atoms, $f(s)$, were taken from the tables of Viervoll and Ögrim[35], McWeeny[36], and Berghuis[37]. For the inelastic scattering factor of carbon, $S_C(s)$, Bewilogua's function[38] was used; as pointed out in his paper, this function which is based on the Thomas-Fermi model is still a good approximation for carbon. The *S*-function for hydrogen, $S_H(s)$, is approximated by $S_H(s) = 1 - [f_H(s)]^2$ after the argument of Mott and Massey[39]. In order to make the magnitude of the ΔM-function smaller, the value Z_H in Eq. 3 was put equal to 1.25. It seems probable that uncertainties in these factors have a negligible effect on the final result as compared with the experimental errors.

c) As there are many non-equivalent C–C, C–H and H–H distances in *n*-butane, (twenty-seven in the *trans* form, and thirty-five in the *gauche* form), thorough analysis of all distances is obviously too

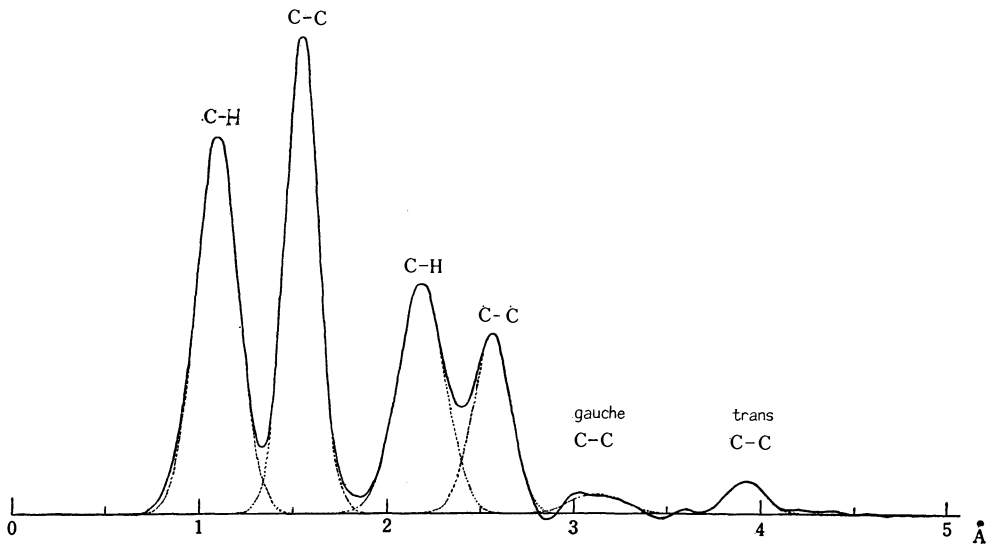


Fig. 3 Analysis of the average RD curve. The minor contribution illustrated in Fig. 2 is subtracted from the total curve. The dotted curves denote the best-fit Gaussian curves. The peaks represent (from left to right) the C–H, C–C, nonbonded C–H, nonbonded C–C, *gauche* C–C, and *trans* C–C distances, respectively.

34) L. S. Bartell, L. O. Brockway and R. H. Schwendeman, *J. Chem. Phys.*, **23**, 1854 (1955).
35) H. Viervoll and O. Ögrim, *Acta Cryst.*, **2**, 277 (1949).
36) R. McWeeny, ibid., **4**, 513 (1951).
37) J. Berghuis, et al., ibid., **8**, 478 (1955).
38) L. Bewilogua, *Physik. Z.*, **32**, 740 (1931).
39) N. F. Mott and H. S. W. Massey, "The Theory of Atomic Collisions", Oxford Univ. Press, London (1949).

complicated to be feasible. However, the structure of this molecule is principally determined by four main structure parameters, i.e., the C–H (average), C–C (average), C—H (average), and C—C distances. Since the contribution from these distances are exceedingly greater than that from the other distances, it is advantageous to subtract the minor contributions from the total RD, leaving the contributions from the principal parameters, which can then be analyzed uniquely. The minor contributions calculated by use of a self-consistent model are illustrated in Fig. 2 as a dotted line. The same procedure of obtaining such a self-consistent model as that discussed in a and b was undertaken. Tables II and III show that for the procedures a, b and c the model was simultaneously made self-consistent in two steps. The result is shown in Fig. 3.

Least-square Analysis of the Main Peak*.—The peak at 1.1Å in the RD curve (Fig. 3) corresponds to the C–H distance. The center of gravity which is equal to the mean distance was readily determined. The peak was found to be symmetrical with respect to the center, and accordingly, the curve could be fitted to a Gaussian function**.

The Gaussian function to be fitted is

$$y=y_0\exp(-Hx^2),\quad x=r-r_g \tag{4}$$

where r_g is the center of gravity. By taking the logarithm of both sides, the following linear equation is obtained.

$$Y=q-pX \tag{5}$$

where

$$X=x^2,\quad Y=\log_{10} y,\quad p=H\log_{10} e$$
$$\text{and}\quad q=\log_{10} y_0 \tag{6}$$

About ten sets of the observed values X_i's and Y_i's were used to determine the parameter p, under the condition that

$$\sum_i (\mathrm{d}y_i)^2=(\log_{10} e)^{-2}\sum_i y_i^2(\mathrm{d}Y_i)^2=\text{minimum} \tag{7}$$

Solving the equation for p,

$$p=\frac{[\sum y_i^2X_i]\,[\sum y_i^2Y_i]-[\sum y_i^2]\,[\sum y_i^2X_iY_i]}{[\sum y_i^2]\,[\sum y_i^2X_i^2]-[\sum y_i^2X_i]^2} \tag{8}$$

The parameter is related to the mean amplitude as

$$p=\log_{10} e/(4b+2l^2) \tag{9}$$

and

$$l=(\log_{10} e/2p-2b)^{1/2} \tag{10}$$

Since the standard error of the parameter p is given by

$$\sigma_p^2=\frac{[\sum y_i^2]}{[\sum y_i^2]\,[\sum y_i^2X_i^2]-[\sum y_i^2X_i]^2}\cdot\frac{\sum(\mathrm{d}y_i)^2}{n-2} \tag{11}$$

the standard error of the parameter l is readily obtained as*

$$\sigma_l=-\frac{\log_{10} e}{4lp^2}\sigma_p \tag{12}$$

The second peak at 1.54Å corresponds to the C–C distance. Because of the separation of 0.45Å between the C–H and C–C distances, a similar least-square analysis could be made with no ambiguity. The peaks for the non-bonded C–H and C–C distances are in a slightly closer separation. However, they were resolved by using the left side of the C–H peak, and the same procedure was applied. The results are listed in Table IV.

In the region beyond 3Å, two peaks

TABLE IV. RESULT OF THE LEAST-SQUARE ANALYSIS OF THE MRD CURVE

	$r_g(1)$[a]	Apparent mean amplitude	Area[b]
C–H (average)	1.092	0.084_6	0.987
C–C (average)	1.539	0.054_0	0.994
C–H (average)	2.179	0.103_2	0.970
C–C	2.553	0.074_8	1.060
C–C *trans*	3.914	0.069_6	0.590[c]

∠C-C-H (average) = 110°40′[d]

∠C-C-C = 112°6′

a) in Å unit

b) the ratio with respect to the theoretical absolute value

c) to be regarded as the fraction of the *trans* isomer

d) the value derived from $r_g(1)$ by Eq. 24

* The least-square analysis of RD curve has been reported recently by Bastiansen and Cyvin (O. Bastiansen and S. J. Cyvin, *Acta Chem. Scand.*, 11, 1789 (1957).). For a similar treatment of a $\sigma(r)$ curve, see the paper by Cruickshank et al. (D. W. J. Cruickshank and H. Viervoll, *Acta Chem. Scand.*, 3, 560 (1949).).

** The middle points of the curve at various peak heights were constant to a third decimal place of an angstrom. Strictly speaking, an $f(r)$ peak is expressed as

$$f(r)=\frac{c(\pi H)^{1/2}}{2r_e}\exp(-Hx^2)(1+ax+bx^2+cx^3+\cdots\cdots),\quad x=r-r_e$$

showing a slight distortion in trems of the parameters of anharmonicity and of the perpendicular amplitudes. However, the distortion is often so small that the curve can be interpreted as Gaussian. As will be shown later, the mean amplitude for $f(r)$ curve is almost the same as that for the probability distribution.

* The standard error is about 1%, being considerably smaller than the random errors estimated in section IV B.

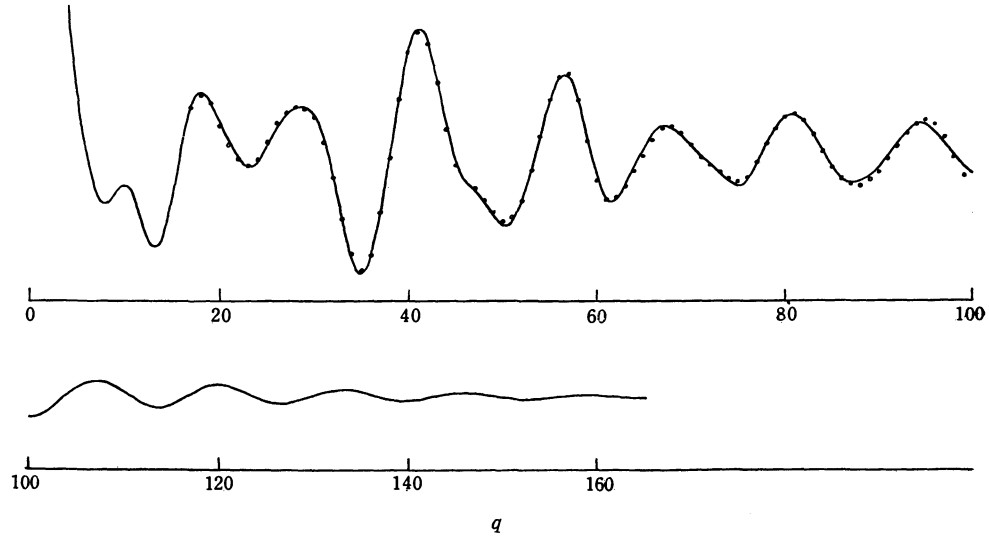


Fig. 4. Comparison of the observed and calculated molecular intensity curves. The solid line denotes the theoretical intensity calculated from the result of the MRD analysis (Table IV). The dots are the averaged experimental molecular intensity. These intensities fit within the experimental uncertainty illustrated in Fig. 1. The theoretical curve is extended beyond $q=100$, and is used in the UMRD analysis.
—— calculated ○ observed

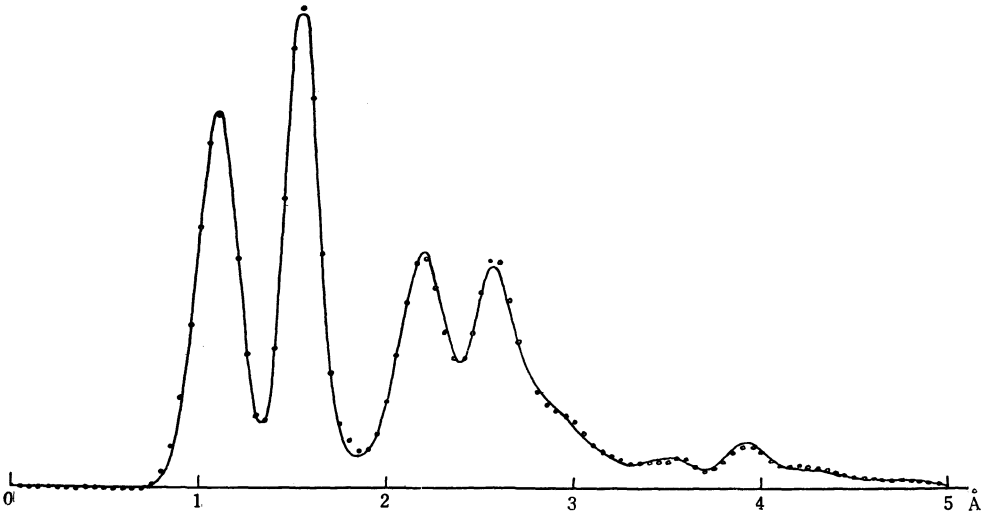


Fig. 5. Comparison of the observed and theoretical RD curves. The solid line represents the theoretical RD curve based on the result of the analysis assuming Gaussian distribution. The dots are the experimental MRD curve.
—— theoretical ○ observed (average)

appeared at 3.1Å and 3.9Å, corresponding to the *gauche* and the *trans* C–C distances, respectively. It affords a definite evidence for the rotational isomerism in this molecule. As the shape of the latter peak is practically Gaussian, the same procedure was applied, whereas only approximate values for the distance and its mean amplitude were estimated from the former peak. A theoretical intensity curve and an RD curve were calculated by the use of the result listed in Table IV. The agreement with the experimental curve is satisfactory, as shown in Figs. 4, 5 and Table V. The average index of resolution is about 99%.

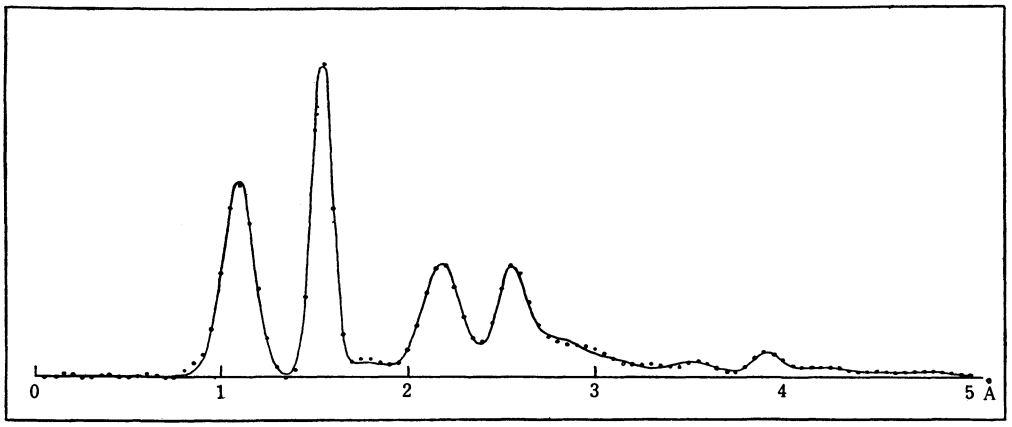


Fig. 6. Unmodified RD curve.
—— starting model (theoretical) ○ observed

TABLE V. COMPARISON OF THE OBSERVED AND THE CALCULATED INTENSITY CURVES

Max.	Min.	Peak position		Peak intensity	
		q_{calc}	q_{calc}/q_{obs}	I_{calc}	I_{obs}/I_{calc}
3		18.0	(0.990)	1.41	0.977
	3	23.1	1.004	−1.20	1.085
4		28.8	(1.022)	1.20	0.937
	4	34.9	0.995	−3.03	0.974
5		41.2	1.003	3.15	0.970
	5	50.0	0.996	−1.77	0.964
6		56.5	0.999	1.99	1.056
	6	61.4	1.001	−1.35	0.948
7		67.2	(0.991)	0.80	1.011
	7	75.3	1.002	−0.90	0.876
8		80.8	0.999	1.18	0.912
	8	87.2	0.996	−0.85	1.099
9		94.5	0.995	0.81	1.096
Average		—	0.998_8	—	0.993
Average Deviation		—	0.003	—	0.059

Unmodified Radial Distribution Curve.—By the same procedure as that described by Morino and Hirota[28], an unmodified radial distribution curve (UMRD), Eq. 13, was calculated for a further refinement of the analysis:

$$f(r)=\sum_{q=0}^{\infty}[w(q)qM_c(q)_{obs}+(1-w)qM_c(q)_{calc}]\times\sin\frac{\pi}{10}qr \qquad (13)$$

where $qM_c(q)_{obs}$ is the observed molecular intensity corrected for the non-nuclear scattering[34] and $qM_c(q)_{calc}$ is the calculated intensity based on the result of the analysis of the modified RD curve (Table IV and Fig. 4). The weight function $w(q)$ was so chosen that $w(q)\propto\exp[-c\Delta(q)^2]$, where $\Delta(q)$ is the amount of fluctuation among the observed intensity curves at a point q (Fig. 1), and c is a constant. The value $w(q)$ fluctuates somewhat irregularly with q between 100 and 80% for most of the experimental region ($q=17\sim95$), and is zero for the inner and outer parts. The UMRD curve is shown in Fig. 6. The analysis was carried out in the same way as that of the MRD curve (item 2). The results are given in Table VI and Fig. 6.

Estimation of the Errors in the Measurement of Interatomic Distances.—For the estimation of errors in the interatomic distances, sources of systematic errors in the scale factor and other errors in the observed RD curve must be considered. The main sources of systematic errors may be as follows.

a) The uncertainty in the scale-magnification ratio on the microphotometer trace, which is estimated to be about 0.1%.

b) The uncertainty in the camera length: it comes mainly from the difference between the position of the scattering center of the sample and that of the reference, and from the uncertainty in the position of the photographic plate. This error is about 0.1%.

c) The errors involved in the measurement of $L\lambda$: the product of the camera length L and the wavelength λ is determined by the measurement of the transmission pattern of gold foil. The standard error of the measurement is about 0.1%.

d) The drift of the wavelength: since a few minutes were required for exposure, the drift of the wavelength may be a cause of systematic error. In this experiment, however, the drift was controlled to within 0.05% by use of voltage stabilizers.

e) Errors in the determination of the

center in the photometric trace: they will cause error of less than 0.05%*. Assuming that these errors occur independently, a standard error in the scale factor is estimated to be about 0.2%.

f) A finite size of the light beam in the photometry: if the light beam has the rectangular shape of $a \times b$ on the photographic plate which is being measured (a being measured in the radial, and b in the perpendicular direction), the location of a halo of radius R on the plate suffers an inward shift of about $b^2/24R$. Since $a \times b = 0.1\,\text{mm.} \times 1\,\text{mm.}$ in this experiment, this shift has a uniform dependence on q, which is about 0.1% at $q=20$, and 0.01% at $q=60$. The correction was made for this effect though the magnitude is not important compared with other random errors.

For the standardization of the absolute scale factor, an analysis of carbon tetrachloride was made to check the apparatus and the method of analysis[19]. The C–Cl distance (the center of gravity of the $f(r)$ curve) was found to be 1.766Å, in good agreement with the results reported in the literature[34,40] within the experimental error.

Other errors were estimated from the variance of the results of the analyses for each of the five experimental RD curves, by using the standard statistical method on the assumption that this variance was caused by random errors. For the non-bonded peaks, possible sources of errors caused by the processes a, b and c stated in item 1 and the process of the decomposition of the composite peaks were also taken into account, the results of the above estimation are given in Table VI.

The Meaning of the Values Measured.— It is important to define clearly the meaning of the distances determined in this analysis, as pointed out by Bartell[41]. While the distance obtained above is the "center of gravity" or the "mean distance" of the $f(r)$ curve, it seems useful to correlate it to the $r_g(0)$ value, or the center of gravity of the probability distribution curve $P(r)$.

Including the anharmonicity in molecular vibrations[41] and the correction for the perpendicular amplitude, $P(r)$ may be expanded as (See f on page 756)

$$P(x) = (h/\pi)^{1/2} \exp(-hx^2) \times (1 + \alpha x + \beta x^2 + \gamma x^3 + \cdots\cdots) \tag{14}$$

where

$$x = r - r_e, \quad h = 1/2 < \Delta z^2 > \tag{15}$$

Then the mean value of the distance, $r_g(0)$, is expressed as

$$r_g(0) = \frac{\int_0^\infty r P(r)\,dr}{\int_0^\infty P(r)\,dr} = \frac{\int_{-\infty}^\infty (r_e + x) P(x)\,dx}{\int_{-\infty}^\infty P(x)\,dx}$$

$$= r_e + \alpha l^2 + \left(3\gamma - \frac{3}{2}\alpha\beta\right) l^4 + \cdots\cdots \tag{16}$$

where l^2 is the mean square amplitude, $< \Delta z^2 >$. On the other hand, the center of gravity of $f(r)$ is written by using the relation between $P(r)$ and $f(r)$,

$$f(r) = (\pi/16b)^{1/2} \int_{-\infty}^\infty [P(\rho)/\rho] \times \exp[-(r-\rho)^2/4b]\,d\rho \tag{17}$$

as

$$r_g(f) = \frac{\int_0^\infty r f(r)\,dr}{\int_0^\infty f(r)\,dr} = \frac{\int_0^\infty P(r)\,dr}{\int_0^\infty (P(r)/r)\,dr} \tag{18}$$

Therefore, it is equal to the center of gravity of the $P(r)/r$ curve, $r_g(1)$. By using Eq. 14, the difference between the above two is approximated by

$$r_g(0) - r_g(1) \cong \frac{l^2}{r_e} + \cdots\cdots \tag{19}$$

It amounts to a few thousandth of an angstrom; the second term is of the order of 10^{-5}Å. If a Morse-type potential function for the ground state of a diatomic molecule is assumed, as done by Bartell[41], the constants in Eq. 14 are in the following approximate relations,

$$\alpha = a, \quad \beta = 0, \quad \gamma = ah/3 \tag{20}$$

where a is a parameter of the Morse potential function, and Eqs. 16 and 19 agree with his expression (Eq. 4 of his paper). On the other hand, the center of gravity of the $rf(r)$ curve is given by

$$r_g(rf) = r_g(0) + 2b/r_g(1) \tag{21}$$

the difference being dependent on the damping factor b. The distance $r_g(0)$ can be obtained either from Eq. 19 or from 21. It is also obtained from the UMRD curve. The values of $r_g(0)$ obtained in this way are given in Table VI.

* The error due to an imperfect centering of the photographic plate during the scanning by the photometer is negligible, being of the order of a few ten thousandth of an angstrom, since the center was adjusted to within 5/100 mm. The error due to the deviation of the electron beam from the correct center of the sector during the exposure (which was within 5/100 mm.) is also negligible.

40) I. L. Karle and J. Karle, *J. Chem. Phys.* **17**, 1052 (1949).

41) L. S. Bartell, ibid., **23**, 1219 (1955).

TABLE VI. THE MEAN DISTANCES[a] AND ANGLES[b]

	MRD	UMRD	Standard error
C-H (average)	1.098	1.100	0.003
C-C (average)	1.540	1.539	0.003
C-H (nonbonded average)	2.182	2.181	0.005
C-C (nonbonded)	2.554	2.554	0.005
C-C (*gauche*)	3.12	3.13	0.02
C-C (*trans*)	3.913	3.911	0.009
∠C-C-H (average)	110°32′	110°22′	15′
∠C-C-C	112° 1′	112° 9′	9′

a) $r_g(0)$ in Å unit
b) the "mean angle" derived from $r_g(0)$ by Eq. 24

The mean square amplitude af a distance is defined by*

$$l^2(0)=\left[\int_0^\infty r^2P(r)\mathrm{d}r\right]\Big/\left[\int_0^\infty P(r)\mathrm{d}r\right]-[r_g(0)]^2 \tag{22}$$

whereas the mean square amplitude obtained from the radial distribution curve is

$$l^2(f)=\left[\int_0^\infty r^2f(r)\mathrm{d}r\right]\Big/\left[\int_0^\infty f(r)\mathrm{d}r\right]-[r_g(1)]^2 \tag{23}$$

A simple calculation using Eqs. 14 and 17 shows that the latter is equal to the mean square amplitude for the $P(r)/r$ curve, $l^2(1)$, plus $2b$, and the difference between $l^2(0)$ and $l^2(1)$ is only a minor correction as compared with the experimental error. (See f on page 756).

Determination of Valence Angles.—Following the above argument, the "mean angle" may be defined as the angle α derived by the following equation

$$\cos\alpha=(r_A^2+r_B^2-r_C^2)/(2r_Ar_B) \tag{24}$$

where r_A, r_B, and r_C are the mean values of the respective distances. The standard error of the angle is readily calculated to be

$$\sigma_\alpha=\left\{\left(\frac{1}{r_B}-\frac{\cos\alpha}{r_A}\right)^2\sigma_{r_A}^2+\left(\frac{1}{r_A}-\frac{\cos\alpha}{r_B}\right)^2\sigma_{r_B}^2+\left(\frac{r_C}{r_Ar_B}\right)^2\sigma_{r_C}^2\right\}^{1/2}\Big/\sin\alpha \tag{25}$$

The systematic error of the scale factor, 0.2%, is not included in σ_r's, because it has no effect on the angle. The result is given in Table VI.

Discussion Concerning the Longer Distances.—The *trans* C-C distance is calculated from the C-C distance $r_g(0)$ and the C-C-C angle assuming that the four carbon atoms are coplanar; it was found to be 3.926±0.003Å. On the other hand, the observed distance was 3.911±0.004Å*. The shortening, 0.015±0.005Å, can be interpreted as "significant", according to Cruickshank's definition[42]. It is likely that the shift is caused by a hindered rotation of the ethyl groups around the C-C axis taking the equilibrium position on the plane. The shift due to this effect was calculated theoretically by Karle and Hauptman[43]. It is calculated in a similar manner that the shift is 0.0120Å when the barrier V_0 is equal to 3.6 kcal./mol., and 0.0155Å when it is equal to 3.0 kcal./mol., in satisfactory agreement with the experimental shift. It is therefore inferred that the barrier height lies close to these values, in agreement with the value estimated by Pitzer, 3.6 kcal./mol.[14]

The azimuthal angle of the *gauche* form was calculated from the *gauche* C-C distance R_g(3.13±0.01Å) to be 67.5°±1.1°. The angle is thus nearly 60° as was usually assumed but possibly a little larger than that.

Estimation of Errors in the Mean Amplitude

The mean amplitudes listed in Table IV include both systematic and random errors. They were either corrected or estimated as shown in the following table.

A. Systematic errors
  Experimental
    a) effect of finite sample size: corrected,
    b) multiple or extraneous scattering: negligible,
    c) density-intensity calibration: estimated,
  Theoretical
    d) failure of Born approximation: corrected,
    e) effect of the possible difference in length between non-equivalent bonds: estimated,
    f) effect of perpendicular amplitude and of anharmonicity: negligible,
    g) effect of series termination: negligible, (in the case of MRD)
B. Random errors*

* The definition corresponds to u_a used by A. Reitan (Ref. 53).

* The error of the scale factor is not included in this comparison.

42) D. W. J. Cruickshank, *Acta Cryst.*, 2, 65 (1949).

43) J. Karle and H. Hauptman, *J. Chem. Phys.*, 18, 875 (1950).

* Errors which could not be treated as systematic errors were simply regarded as random errors though they might not be purely random in a strict sense.

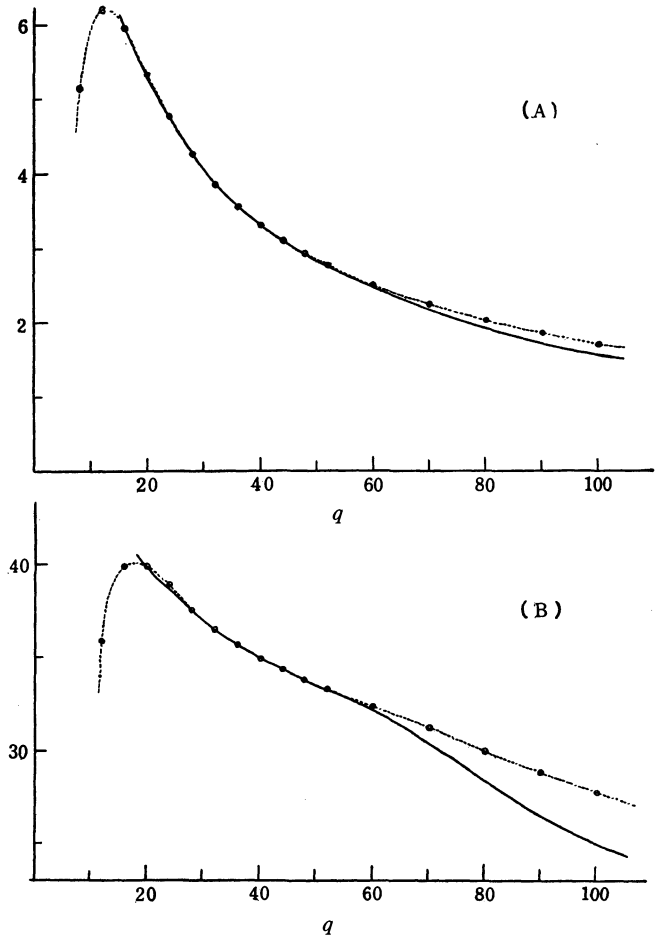


Fig. 7. Comparison of the background lines. Soild line: experimental; and dotted line: theoretical. The ordinate scales are adjusted in such a way that two curves coincide at $q=40$. (A) The background line obtained by use of an r^3-sector. (B) The curves shown in A are multiplied by $q^{1/2}$ to accentuate the difference; it amounts to about 10% at $q=100$.

Experimental: treated with a simple statistical method,
Computational: estimated.

These errors will be discussed as follows.

A. Systematic Errors.—*a) Effect of finite sample size.*—This effect was extensively studied by Karle[24], and also Harvey et al.[44] It is easily estimated if the distribution of the sample gas around the nozzle is known. The shape of the background line was found to be useful in this case for estimating the distribution. In Fig. 7 is shown a comparison of the observed background line with the calculated curve based upon the assumption that the diffracting molecules are located at an infinitesimal volume. The agreement is good in the inner region, whereas the deviation of the observed curve is clearly recognized beyond $q=60$. The nozzle used in this experiment is illustrated in Fig. 8. If this effect is attributed to the "screening" of the electrons at the nozzle edge, the distribution is estimated with the following simple assumptions:

1) The decrease in the observed background compared with the theoretical background is essentially caused by process in which a small fraction of the electrons scattered by the sample hit the wall of nozzle and do not reach the photographic plate (Fig. 8).

2) Since the beam diameter is much less than the nozzle aperture, a one-dimensional distribution of the sample gas, the area being normalized, is considered. Then the decrease is determined by the area of the shadowed region in Fig. 8.

44) R. B. Harvey, F. A. Keidel and S. H. Bauer, *J. Appl. Phys.*, **21**, 860 (1950).

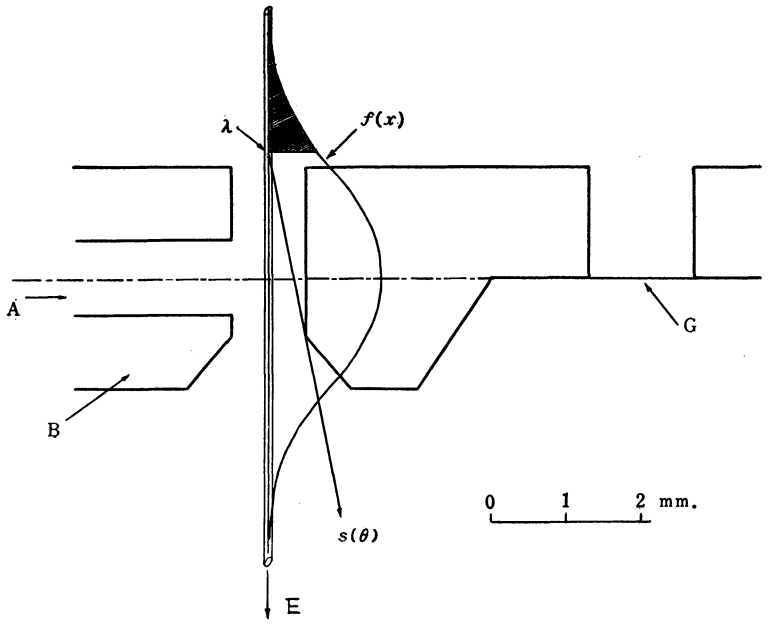


Fig. 8. "Screening effect" of the nozzle. An enlarged cross section of the drum-type nozzle is illustrated. A: gas inlet; B: nozzle body; E: electron beam (the cylinder represents a rough measure of the diameter); $f(x)$: normalized one-dimensional distribution of the gas; G: gold foil used as the reference. It is assumed that the electrons scattered at the point farther than the critical point $\lambda(\theta)$ (shaded region) in the direction of $s(\theta)$ are completely screened by the wall of the nozzle and do not reach the photographic plate, and that the scattered intensity undergoes a fractional decrease proportional to the shaded area.

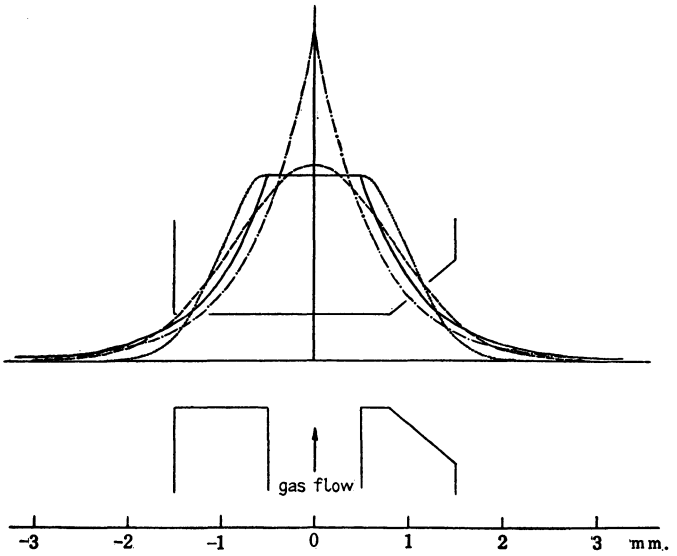


Fig. 9. Distribution functions of the gas spreading. It is assumed that they are symmetrical across the center of the nozzle inlet, and the areas are normalized. Solid line : flat and exponential; dotted line: flat and Gaussian; chain line: exponential; and broken line: Gaussian. It is seen that the distributions are all practically zero outside the nozzle.

3) The distribution is symmetrical across the center of the nozzle inlet.

In additon to these assumptions, the following simple analytical functions were assumed for the distribution, and parameters were determined to reproduce the experimental fractional decrease. The shapes of the distribution functions assumed are:

Exponential:

$$f(x)=\frac{1}{2}\rho\exp(-\rho|x|),\quad \rho=1.593 \tag{26}$$

Gaussian:

$$f(x)=(\sigma/\pi)^{1/2}\exp(-\sigma x^2),\quad \sigma=0.700 \tag{27}$$

Flat and exponential:

$$f(x)=c,\quad |x|\leq x_0,\quad c=0.45$$
$$f(x)=c\ \exp(-\alpha|x|),\ |x|>x_0,\ \alpha=1.636 \tag{28}$$

and Flat and Gaussian:

$$f(x)=c,\quad |x|\leq x_0,\quad c=0.45$$
$$f(x)=c\exp(-\beta x^2),\ |x|>x_0,\ \beta=2.103 \tag{29}$$

where x is the distance in millimeters measured from the center of the nozzle inlet, and $x_0=0.5$ mm. is the radius of the inlet. The distribution is illustrated in Fig. 9. It is seen that the density is practically zero outside the nozzle, though the localization is somewhat poorer than that of Karles' nozzle estimated in their paper[24].

The distribution function being assumed, the damping of the molecular intensity (a contribution of a particular atomic pair whose equilibrium distance is r) caused by the spreading of the sample is calculated by the following integration:

$$M=\int_{-\infty}^{\infty}M(s)f(x)\mathrm{d}x=\int_{-\infty}^{\infty}(\text{const.})\times\exp\left(-\frac{l^2}{2}s^2\right)\frac{\sin sr}{sr}f(x)\mathrm{d}x \tag{30}$$

where s is a function of the camera length L, which is the sum of L_0+x, L_0 being the camera length referred to the nozzle center. This may be expressed as:

$$s(x)=\frac{2\pi R}{\lambda}\frac{1}{(L_0+x)}\left[1-\frac{3}{8}\frac{R^2}{(L_0+x)^2}\right]$$
$$=\frac{2\pi R}{\lambda L_0}\left(1-\frac{3R^2}{8L_0^2}\right)\left(1-\gamma\frac{x}{L_0}\right) \tag{31}$$
$$=s_0\left(1-\gamma\frac{x}{L_0}\right)$$

$$\gamma=1-\frac{3R^2}{4L_0^2}\sim 1-7\times10^{-5}s_0^2 \tag{32}$$

where R is the radius on the photographic plate. Substituting Eq. 31 into 30 and remembering that $f(x)$ is assumed to be a symmetrical function of x, Eq. 30 is transformed into Eq. 33 giving the damping of the molecular intensity:

$$M/M_0=\int_{-\infty}^{\infty}f(x)\cos\alpha x\mathrm{d}x,\ \alpha=\gamma s_0 r/L_0 \tag{33}$$

where $M_0(s_0)$ refers to L_0 (the molecular intensity scattered by a point source).

TABLE VII. CORRECTION AND ESTIMATION OF ERRORS IN THE MEAN AMPLITUDES

		C-H_{av}	C-C_{av}	C-H_{av}	C-C	C-C_{trans}
Systematic errors (%)						
(a) Finite sample size	cor	+0.5	+2.1	+1.0	+3.0	+7.2
(b) Multiple or extraneous scattering	neg	—	—	—	—	—
(c) *D-E* calibration[a]	est	$<\pm3$	$<\pm5$	$<\pm4$	$<\pm3$	$<\pm3$
(d) Born approximation	cor	+2.3	—	+1.6	—	—
(e) Non-equivalent bonds	est	$<+0.2$	$<+1.6$	$<+0.4$		
(f) Perpendicular amplitude and anharmonicity	neg	—	—	—	—	—
(g) Series termination (in the case of MRD)	neg	—	+0.7	—	—	—
Random errors (%)	est	$\sim\pm4$	$\sim\pm3.5$	$\sim\pm4$	$\sim\pm8$	$\sim\pm7$
Total standard errors[b] (%)	est	$\sim\pm5$	$\sim\pm5$	$\sim\pm5$	$\sim\pm9$	$\sim\pm9$
Apparent mean amplitude (UMRD)		0.085_5	0.053_7	0.100_1	0.080_0	0.072_9
Corrected mean amplitude (A)		0.083_1	0.052_6	0.097_5	0.077_6	0.067_7
Standard error (A)		0.004	0.003	0.005	0.007	0.007

cor: corrected; est: estimated; neg: negligible

a) The meaning of the symbol $<\pm$ is that the sign may be positive or negative, but that the absolute value should not exceed the given figure.

b) The uncertainties involved in the corrections a and d are estimated to be $\pm70\%$ of the correction values.

On calculating the damping function (Eq. 33) analytically using Eq. 26 through 29 for $f(x)$*, it was found that all assumed distributions give nearly the same result, and it can be expressed in a good approximation in the form

$$M/M_0=\exp(-\varepsilon s^2) \tag{34}$$

An apparent increase in the mean amplitude is accordingly given by

$$(l+\Delta l)^2=l^2+2\varepsilon, \quad \Delta l\sim\varepsilon/l \tag{35}$$

The percentage correction for each interatomic distance is given in Table VII. It should be noted that the parameter ε is a function of r, and that the correction is greater for the longer distance, and for the harder distance (i.e., the distance which has a smaller mean amplitude), as already pointed out[24,44].

b) Effect of multiple or extraneous scattering.—This effect was considered to be negligible in view of the following argument.

1) No appreciable extraneous scattering was found to be present, as stated in the experiment part.

2) Care was taken in the experiment to reduce the sample pressure during the exposure[25]; the flow rate was sufficiently "slow" in the sense discussed by Harvey et at.[44] to avoid the multiple scattering.

3) The observed background line agrees well with the theoretical form, showing no appreciable multiple scattering present (Fig. 7).

4) The index of resolution is nearly unity, which affords another point of support.

5) It was shown by Karle[24] theoretically that even if a considerable amount of multiple scattering were present, it would raise the background uniformly and decrease the molecular intensity also in a uniform manner. Consequently it does not change the damping factor of the molecular term significantly.

c) Uncertainty in the density-intensity calibration curve. — This effect may be estimated in the following way. Suppose the calibration function $E(D)$, in which E and D denote the intensity and density, respectively, is obtained experimentally instead of the true function $E^0(D)$ which is unknown. Since the functions E^0 and E are both uniform functions of D, their ratio may be expanded as

$$E(D)/E^0(D)=c(1+\alpha D+\beta D^2+\cdots\cdots) \tag{36}$$

If the maximum or the minimum point of the intensity curve and the background intensity of the same point are denoted by E_1 and E_2 respectively, and the densities which correspond to E_1 and E_2 on the $D-E$ curve by D_1 and D_2, the fractional error R in the molecular intensity obtained from Eq. 1 is given by

$$\begin{aligned} R&=\left\{\frac{E_1^0(1+\alpha D_1+\beta D_1^2)}{E_2^0(1+\alpha D_2+\beta D_2^2)}-1\right\}\Big/\left\{\frac{E_1^0}{E_2^0}-1\right\} \\ &=1+\frac{E_1^0}{E_1^0-E_2^0}\{\alpha(D_1-D_2) \\ &\quad+(2\beta-\alpha^2)D_2(D_1-D_2)\} \end{aligned} \tag{37}$$

Since D is nearly proportional to E,

$$R\sim1+\alpha D_1+(2\beta-\alpha^2)D_1D_2 \tag{38}$$

On the other hand, the experimental measure of the uncertainty in the $D-E$ curve may be estimated 1) by the variance of the slope of the observed background lines, and 2) by the difference between the $D-E$ curve obtained by Karles' method and that obtained by Bartell's method using the same density curves.

It was found that the magnitude of the parameters α or β is about ±0.05. Since the maximum density in this experiment was about 0.8, the upper limit of the error in the molecular intensity was estimated to be 10%. Possible error in the mean amplitude caused by this effect is accordingly estimated for each distance by fitting roughly to an exponential function, and listed in Table VII.

d) Failure of Born approximation. — It is well known that the theoretical expression 4 for the scattering of electrons by molecules is derived by Born approximation, which is not always justified[39]. The failure of Born approximation was first pointed out by Schomaker and Glauber[45,46], and discussed by Hoerni and Ibers[47]. The effect on the mean amplitude, an apparent increase, was discussed by Bartell and

* For example, the use of Eq. 26 gives

$$M/M_0=\rho^2/(\alpha^2+\rho^2)$$

and the use of Eq. 27 gives

$$M/M_0=\exp[-\alpha^2/(4\sigma)]$$

The latter formula corresponds to Eq. 13 of Karles' paper[24]. More strictly, the upper limit of the integral 30 should be the cut-off point, λ, shown in Fig. 8, which is a function of s. A detailed calculation shows, however, that the molecular term assumes an additional factor and a phase shift which are both of a negligible order of magnitude.

45) V. Schomaker and R. Glauber, *Nature*, **170**, 291 (1952).
46) R. Glauber and V. Schomaker, *Phys. Rev.*, **89**, 667 (1953).
47) J. A. Hoerni and J. A. Ibers, ibid., **91**, 1182 (1953).

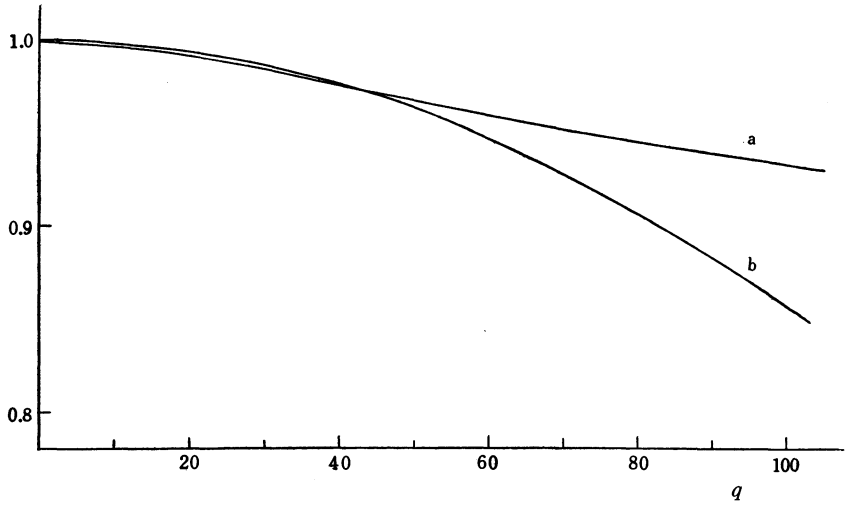


Fig. 10. Approximation of the phase shift $\cos \Delta\eta$ by an exponential function. a) $\cos \Delta\eta$ for the C-H pair; and b) $\exp(-\delta s^2/2)$ where $\delta=3.096\times10^{-4}$. The deviation is about 7% at $q=100$.

Brockway[48,34]. In the following a similar correction for this effect is carried out.

The expression is given by

$$sM(s)=\sum_{i,j}{}'(c_{ij}/r_{ij})\exp\left(-\frac{l_{ij}^2}{2}s^2\right)\times\cos\Delta\eta_{ij}\sin sr_{ij} \quad (39)$$

$$\Delta\eta_{ij}=\eta_i(s)-\eta_j(s) \quad (40)$$

The C-H pairs are the only objects to be considered for this molecule, since the phase shift $\Delta\eta$ appears only for a pair of different atoms. The phase function $\eta(s)$ was calculated and tabulated by Ibers and Hoerni[49]. Since the values are based on the Thomas-Fermi model, they may naturally be a poor approximation for carbon and hydrogen. According to their argument[49], however, the phase shift $\Delta\eta$ is probably reliable, and in addition, the magnitude of η for hydrogen is very small. The Eq. 13 of their paper is available to convert the values to η for the accellerating voltage used in this experiment.

The damping function $\cos\Delta\eta_{C-H}$ was approximated by an exponential form, as discussed by Bartell,

$$\cos\Delta\eta_{C-H}(s)\sim\exp(-\delta s^2/2) \quad (41)$$

the value δ being derived numerically in the following average, taking the damping function (including the artificial temperature factor) as a weight $w(s)$

$$\int w(s)\,[\cos\Delta\eta-\exp(-\delta s^2/2)]\,ds=0 \quad (42)$$

$$w(s)=\exp\left(-\frac{l^2_{C-H}}{2}s^2\right)\exp(-bs^2) \quad (43)$$

The value thus obtained is

$$\delta=3.096\times10^{-4}\ \text{Å}^2 \text{ for bonded C-H,}$$

and $\delta'=3.431\times10^{-4}$ Å^2 for non-bonded C-H.

The maximum deviations of the exponential functions from the cosine functions were about 7% (Fig. 10). These deviations were further corrected by introducing a δM-function in a way similar to that discussed in the case of non-nuclear scattering[34],

$$\delta M(s)=M_{C-H}(s)\{1-\cos\Delta\eta/\exp(-\delta s^2/2)\}+M'_{C-H}(s)\{1-\cos\Delta\eta/\exp(-\delta' s^2/2)\} \quad (44)$$

The order of magnitude of this function is less than 1% of the molecular intensity, and therefore it barely contributes to the RD curve.

The percentage correction for this effect to the mean amplitude is given in Table VII.

e) Effect of the possible difference in the distances between non-equivalent bonds. — It should be noted that the C-H, C-H (non-bonded), and C-C distances observed are the average values of the two respective non-eqivalent distances, i.e., C-H (methyl) and C-H (methylene), and C-C (end) C-C (central). Should these distances differ slightly, as may be the case, observed mean amplitudes will show apparent increase.

This effect is readily treated as follows. Suppose there are two Gaussian peaks 1 and 2 (peak positions r_1 and r_2, and peak

48) L. S. Bartell and L. O. Brockway, *Nature*, 171, 978 (1953).
49) J. A. Ibers and J. A. Hoerni, *Acta Cryst.*, 7, 405 (1954).

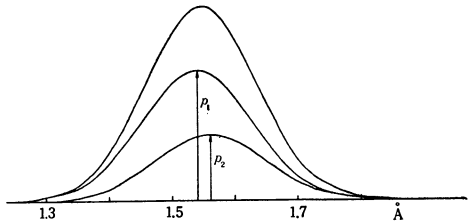


Fig. 11. A composite peak of non-equivalent C-C distances. The peak is slightly broader than each of the component peaks.

heights p_1 and p_2, respectively) close together (Fig. 11). Their mean amplitudes are assumed to be the same, l. The composite peak will then be given by

$$P=p_1\exp\{-H(r-r_1)^2\}+p_2\exp\{-H(r-r_2)^2\} \quad (45)$$
$$H=(2l^2+4b)^{-1}$$

If the origin of the distance r is chosen at the center of gravity, the composite peak is expresed as

$$P=\exp(-Hr^2)\,[\sum P_i\exp(2Hr_ir)] \quad (46)$$
$$P_i=p_i\exp(-Hr_i^2), \qquad i=1,2 \quad (47)$$

The term in the bracket being expanded,

$$\sum_{1,2} P_i\exp(2Hr_ir) = (P_1+P_2)+2H^2rp_1r_1(r_1^2-r_2^2) + 2H^2r^2(P_1r_1^2+P_2r_2^2) \quad (48)$$

The second term is about a small percentage of the third term and does not affect the width. Therefore, the peak is expressed as a Gaussian function to a good approximation:

$$P=(P_1+P_2)\exp(-H'r^2) \quad (49)$$

where

$$H'=H-2H^2(P_1r_1^2+P_2r_2^2)/(P_1+P_2) \quad (50)$$

The coefficient H is related to l in Eq. 45, so that the apparent increase in l is calculated by Eq. 50.

The splittings of the distances are definitely too small to be detected in this experiment; the only available references seem to be the splitting of the C-H distances in ethyl chloride estimated in the microwave spectroscopy[50],

C-H(methyl) = 1.110Å

C-H(methylene) = 1.101Å

and the plausible values predicted by Glockler from the consideration of bond-energy data[51],

C-H(methyl) = 1.097Å

C-H(methylene) = 1.0985Å

C-C(end) = 1.559Å

C-C(central) = 1.564Å (in *n*-butane)

The maximum possible percentage apparent increases listed in Table VII are calculated by inserting in Eq. 50 the value:

r_1-r_2(C-H bonded) = 0.01Å

r_1-r_2(C-H non-bonded) = 0.02Å

and r_1-r_2(C-C bonded) = 0.02Å

It is seen that this effcet is possibly negligible.

f) The effect of perpendicular amplitude and of anharmonicity. — The probability distribution function of an interatomic distance including both parallel and perpendicular amplitudes was derived by Morino and Hirota[52]

$$P(r)=(h/\pi)^{1/2}\exp(-hx^2)\times(1+c_1x+c_3x^3+\cdots\cdots) \quad (51)$$

where

$$h=1/2<\Delta z^2>, \qquad x=r-r_e$$

and

$$c_1=(h/r_e)\,[<\Delta x^2>+<\Delta y^2>-6h(<\Delta z\Delta x>^2+<\Delta z\Delta y>^2)] \quad (52)$$
$$c_3=(4h^3/r_e)\,[<\Delta z\Delta x>^2+<\Delta z\Delta y>^2] \quad (53)$$

On the other hand, the following $P(r)$-function including anharmonic vibration was given by Bartell[41] and by Reitan[53].

$$P_{anh}(r)=(h/\pi)^{1/2}\exp(-hx^2)\times(1+a_1x+a_2x^2+a_3x^3+\cdots\cdots) \quad (54)$$

Since these effects introduce only slight modifications on the Gaussian distribution, the combined effect may be written in the first approximation,

$$P(x)=(h/\pi)^{1/2}\exp(-hx^2)(1+c_1x+c_3x^3)\times(1+a_1x+a_2x^2+a_3x^3) \quad (55)$$
$$=(h/\pi)^{1/2}\exp(-hx^2)\times(1+\alpha x+\beta x^2+\gamma x^3+\cdots\cdots) \quad (14)$$

The mean square amplitude for this distribution is readily calculated as

$$l^2(0)=<\Delta z^2>+\left(2\beta-\frac{3}{2}\alpha^2\right)(<\Delta z^2>)^2 \quad (56)$$

$l^2(0)$ can be obtained from $l^2(f)$ by the equation,

50) R. S. Wagner and B. P. Dailey, *J. Chem. Phys.*, **23**, 1355 (1955).
51) G. Glockler, ibid., **17**, 747 (1949).
52) Y. Morino and E. Hirota, ibid., **23**, 737 (1955).
53) A. Reitan, *Acta Chem. Scand.*, **12**, 131, 785 (1958).

$$l^2(0)=l^2(f)-2b+\left[\frac{1}{2}\alpha^2+\frac{3\alpha}{2r_e}-3\alpha\beta r_e+4\beta+4\beta^2 r_e^2-\frac{1}{r_e^2}\right]l^4+\cdots\cdots \quad (57)$$

It is to be noted that a minor fractional correction is of the order of $l^2/2r_e^2$, which is less than 0.5%. Thus the effect of anharmonicity or the perpendicular amplitude are regarded as negligible, at least in obtaining the mean amplitude defined in Eq. 56.

Care should be taken, however, in the comparison of the amplitudes observed in this way with that calculated from the vibrational data. For the influence of anharmonicity on the mean amplitudes, interesting discussions were made by Reitan[53]. According to his calculation, apparent mean amplitudes of O-H and H-H bonds in water molecule based on the harmonic approximation are about 5% smaller than those which include the anharmonic effect. For heavier molecules such as Br_2, the correction was shown to be negligible.

g) Effect of series termination. — The MRD function was computed by use of Eq. 2 taking the upper limit of the integral as q_{max} instead of infinity. According to Waser and Schomaker[54], an exponential damping function $\exp(-bs^2)$ was adopted in the present analysis for the modification of the RD, the factor b being chosen following the usual convention that $\exp(-bs_{max}^2)=0.1$.

Since the intensity curve multiplied by the damping factor is given by a sum of the contribution of the component terms,

$$sM(s)=\sum_n sM_n(s)=\sum_n (c_n/r_n)\times\exp(-s^2/4H_n)\sin sr_n \quad (58)$$

the Fourier inversion is also expressed as a sum,

$$f(r)=\sum_n\int_0^\infty sM_n(s)\sin sr\,ds-\sum_n\int_{s_{max}}^\infty sM_n(s)\sin sr\,ds=f_0(r)-f'(r) \quad (59)$$

The RD function actually obtained is the sum of $f_0(r)$, the true RD function, and $-f'(r)$, additional ripples. Taking out the n-th contribution to $f'(r)$, and using Eq. 58, $f'_n(r)$ is given by

$$f'_n(r)=(c_n/2r_n)\left\{\int_{s_{max}}^\infty \cos s(r_n-r)\times\exp(-s^2/4H_n)ds-\int_{s_{max}}^\infty \cos s(r_n+r)\exp(-s^2/4H_n)ds\right\} \quad (60)$$

where the second term is usually negligible. At the center of the RD peak, i.e., $r=r_n$, the function $f'_n(r)$ has its maximum value, which is expressed in terms of the error integral, $\Phi(s_{max}/\sqrt{2H_n})$. Elsewhere, $f'_n(r)$ reveals itself as a ripple of the period of slightly less than $2\pi/s_{max}$. It is obviously symmetrical across the center of the peak and damps slowly as $|r-r_n|$ increases.

In the present example, $s_{max}=10\pi$, $H_n\sim 66$ for the C-C bond which has the smallest damping factor, and $H_n\sim 50-30$ for the other bonds. By the evaluation of the error integral, it was found that the maximum magnitude of f'_n is about 0.6% of the peak height for the C-C peak, and less than 0.1% for the others. The effect is thus unquestionable except for the C-C peak, and even in that case, it causes a slight symmetrical distortion of the C-C peak itself and an apparent increase of about 0.7% in its mean amplitude. A shift of the distance r_g of the adjacent peaks due to this effect amounts to only a few ten thousandth of an angstrom.

A similar, but more extensive discussion was carried out by Morimoto in his recent RD analysis of evaporated crystallites[55]. The result is in agreement with the estimation described above.

B. Random Errors.—The main origins of experimental random errors are 1) errors introduced in the photographic process (exposure, development, etc.), 2) errors of the microphotometry, 3) errors of the measurement of the photometer curve, and 4) errors introduced in the failure of drawing a proper background line, etc.

These errors are included in the molecular intensity and, being Fourier inverted, reveal themselves as random fluctuations or "ghosts" in the RD curve, which cause errors in the measurement of mean amplitudes.

The following features may be used as the measures of these fluctuations.

1) Fluctuations of the baseline in the regions where no interatomic distance should exist: as shown previously, there are no appreciable fluctuations in the baseline from 0 through 0.7Å (Fig. 3). Beyond 2.8Å of the RD curve, however, there

54) J. Waser and V. Schomaker, *Revs. Modern Phys.*, **25**, 671 (1953).

55) H. Morimoto, *J. Phys. Soc. Japan*, **13**, 1015 (1958).

appear small fluctuations, which probably come from the experimental errors together with the computational errors.

2) Difference among RD curves illustrated in Fig. 2, obtained by the independent procedure: the maximum deviation amounts to a small percentage of the peak height.

3) The standard errors given in the least-square analysis of the mean RD curve (Eq. 12): they were found to be about 1% of the mean amplitudes.

4) Deviations of the areas of the RD peaks from the theoretical values: the ratios listed in Table IV show that the deviations amount to a small percentage.

In order to estimate the random errors in the mean amplitudes, it seems possible to make use of one of the following methods:

1) Use of the variance in the results of the least-square analysis of the individual RD curves, which may correspond to the "mean square deviation between classes",

2) Use of the square sum of the residuals in the process 1, which may correspond to the "mean square deviation within classes",

3) Use of the difference among the RD curves to estimate the standard error at each point of the peak.

Each method was used in the present estimation together with Eqs. 11 and 12. Errors introduced in the computational process were also taken into account. Important ones among them would be 1) errors in the computation (rounding-up errors, etc.), 2) improper assumptions used in the analysis (structure, scattering factors, etc.), 3) ambiguity in the decomposition of the composite peak, and 4) improper correction for various systematic errors. A plausible estimation was made utilizing the experience in the self-consistent analysis described above. As for the effect 4, the corrections for systematic errors were considered to include ±70% uncertainties.

The results of the estimation of random errors are listed in Table VII. In the last row of the table are listed the mean amplitudes for which suitable corrections have been made, with their total standard errors which include all errors estimated in the above consideration.

Calculation of the Mean Amplitudes

In order to correlate the observed mean amplitudes to be spectroscopic data, a calculation of the mean amplitudes was carried out. Because of the lack of knowledge of the force constants, a simple and approximate treatment was made.

First the skeleton vibrations were considered by assuming a methyl or a methylene group as a particle for the *trans* and the *gauche* forms. The Wilson's G and F matrices for the *trans* form given as follows[56,58].

$$\begin{array}{lll} & \text{G} & \text{F} \\ \text{A}: & \begin{bmatrix} 2\mu_0 & & \\ 2\mu_0\cos\varphi & \mu_0+\mu & \\ -\sqrt{2}\rho_0\mu_0\sin\varphi & -2\rho_1\mu_0\sin\varphi & \rho_0^2(\mu_0+\mu)+4\mu_0(\rho_1^2-\cos\varphi) \end{bmatrix} & \begin{bmatrix} K_0+2a_0F & & \\ \sqrt{2}cF & K_1+a_1F & \\ \sqrt{2}\rho_1d_0F & \rho_0d_1F & H+bF \end{bmatrix} \\ \text{B}: & \begin{bmatrix} \mu_0+\mu & \\ 0 & \rho_0^2(\mu_0+\mu) \end{bmatrix} & \begin{bmatrix} K_1+a_1F & \\ \rho_0d_1F & H+bF \end{bmatrix} \end{array} \quad (61)$$

TABLE VIII. COMPARISON OF THE NORMAL FREQUENCIES FOR THE TRANS FORM

		Skeleton vibration	Observed (cm^{-1})			Calculated (cm^{-1})	
			a	b	c	A set	B set
A_g	ν_1	stretching	1059	1058	1056	1075	1068
	ν_2	mixed	837	835	833	835	909
	ν_3	deformation	425	432	(319?)	432	374
B_u	ν_4	stretching	—	970?	956.4	955	993
	ν_5	deformation	—	?	215.0	295	277

a: Ref. 60, b: Ref. 11, c: Refs. 9 and 15.

56) E. B. Wilson, Jr., *J. Chem. Phys.*, **7**, 1047 (1939); **9**, 76 (1941).

57) E. B. Wilson, Jr., J. C. Decius, and P. C. Cross, "Molecular Vibrations" McGraw-Hill, New York (1955).

TABLE IX. CALCULATED VALUES FOR THE MEAN AMPLITUDES (skeleton) (in Å unit)

Atomic pair	Observed (UMRD)	Calculated			
		trans Form		*gauche* Form	
		A set	B set	A set	B set
C-C (CH_2-CH_2)	$0.052_6\pm0.003$	0.048_7	0.049_8	0.049_1	0.049_9
C-C (CH_2-CH_3)		0.051_6	0.048_9	0.051_3	0.049_0
C-C (nonbonded)	$0.077_6\pm0.007$	0.069_2	0.079_4	0.068_2	0.078_2
C-C (*gauche*)	0.136	—	—	0.161_1	0.169_1
C-C (*trans*)	$0.067_7\pm0.007$	0.070_4	0.079_2	—	—

where the symbols have their usual meaning[57,59]. Two different sets of Urey-Bradly force constants were taken. One set A is that given by Shimanouchi[60], which was selected to the fit to Raman spectra of *n*-butane,

$K_0=4.0$, $K_1=3.2$, $H=0.11$, $F=0.96$ and $F'=0$

The other set B is that reported as the force constants of methyl and methylene groups[59], and taken by Hayashi in his calculation of the normal vibration of *n*-pentane molecule as a five-body problem[61].

$$K_0=3.7,\quad K_1=4.0,\quad H=0.20,\quad F=0.33$$
$$\text{and } F'=-0.1F$$

These force constants being inserted in Eq. 61, it is an easy and straightforward computation to obtain the normal frequencies[56,57] and the mean amplitudes[62,63]. A comparison of the frequencies for the *trans* form is given in Table VIII. The assignment of the skeleton frequencies was made by several authors[11,15,60,64], and there seems to be no difficulty except in the lowest B_u (bending) mode*. Although the band 215.0 cm^{-1} observed in the far infrared spectra was assigned to this mode by Gates, and no other band was found between 400 and 170 cm^{-1}, it seems likely that this mode has a little higher frequency. The agreemment of the calculated frequencies with the observed is much better for the A-set. Accordingly, the mean amplitudes calculated with the A-set may be the more reliable.

For the mean amplitudes of the *gauche* form the barrier against the torsional motion was assumed to be 3.6 kcal./mol.[14] An approximate method[63] was applied. These results are shown in Table IX. The larger amplitude obtained for the *gauche* C–C distance as compared with the *trans* C–C is just as expected.

For the mean amplitudes of the distances including hydrogen atoms, methyl groups were approximated by chlorine atoms, that is, the mean amplitudes of the H–H and C–H atom pairs in 1,2-dichloroethane were calculated, be cause the L matrices for this molecule calculated by Nakagawa[65] were available. Although this approximation apparently seems drastic, past experience on the calculation of mean amplitudes assures that it will give sufficiently correct values for this purpose[63]. The results obtained are listed in Table X. The mean amplitude of the C–C distance agrees with the previous values given in Table IX.

TABLE X. COMPARISON OF THE OBSERVED AND CALCULATED MEAN AMPLITUDES (FOR PAIRS INCLUDING HYDROGEN) (in Å unit)

Pairs	Observed	Calculated
(C-C)	$0.052_6\pm0.003$	0.050_3
C-H	$0.083_1\pm0.004$	0.078_3
C-H (nonbonded)	$0.097_5\pm0.005$	0.109_7
H-H (nonbonded)	—	0.126_8
H-H (*trans*)	—	0.128_2
H-H (*gauche*)	—	0.156_8

The comparison of the calculated amplitudes with the observed values is given in Table IX and X. The agreement is satisfactory, taking account of the experimental error, and of the uncertainty in the theoretical values (possibly a small

58) J. C. Decius, *J. Chem. Phys.*, **16**, 1025 (1948).
59) S. Mizushima, T. Shimanouchi, I. Nakagawa and A. Miyake, ibid., **21**, 215 (1953).
60) T. Shimanouchi, *Sci. Papers Inst. Phys. Chem. Research (Tokyo)*, **40**, 467 (1943); *Bull. Inst. Phys. Chem. Research (Tokyo)*, **23**, 371 (1944).
61) M. Hayashi, *J. Chem. Soc. Japan, Pure Chem. Sec. (Nippon Kagaku Zasshi)*, **78**, 222 (1957).
62) Y. Morino, K. Kuchitsu and T. Shimanouchi, *J. Chem. Phys.*, **20**, 726 (1952).
63) Y. Morino, K. Kuchitsu, A. Takahashi and K. Maeda, ibid., **21**, 1927 (1953).
64) R. S. Rasmussen, ibid., **16**, 712 (1948).
* Although Gates (Ref. 15) assigned the Raman line 319 cm^{-1} to the lowest A_g mode, this line should be assigned to the same mode of the *gauche* form (Ref. 16). The valence force constants determined by Gates are therefore not very reliable.
65) I. Nakagawa, *J. Chem. Soc. Japan., Pure Chem. Sec. (Nippon Kagaku Zasshi)*, **74**, 848 (1953); **75**, 60 (1954).

percentage), caused by the approximate nature of the calculation, the uncertainty in the force constants, and the neglect of anharmonicity in the vibration.

Analysis of the Intensity in the Small-angle Region

The intensity curve in a small-q region was analyzed for the purpose of obtaining further information on the rotational isomerism. The detail of the method was described in a previous paper[19,66].

Diffraction photographs were taken at the longer camera length through an r^2-sector with a multiple-layer stopper of the same type as that used by Bastiansen[23]. The density measured was converted into the intensity by Karles' procedure[26]. Independent observations gave good agreement with one another.

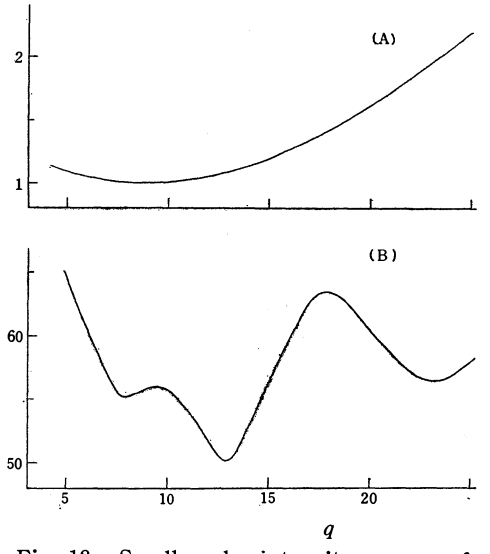


Fig. 12. Small-angle intensity curve of *n*-butane. (A) $f(q)$ curve; and (B) $f(q)I(q)$ curve.

The intensity $I(q)$ was multiplied by a smooth function $f(q)$ (Fig. 12) to make the background line nearly flat, where

$$f(q)=1+0.0054(q-9)^2+3\times10^{-6}(q-9)^4 \quad (62)$$

A background function $I_b(q)$ was calculated by the following equation,

$$I_b(q)=f(q)I(q)/(1+cM(q)_{\mathrm{calc}}) \quad (63)$$

where $M(q)_{\mathrm{calc}}$ is the theoretical molecular intensity divided by q, and c is the index of resolution[34,44]. A criterion that I_b should be a smooth function of q can be used to select a reasonable model[19].

The frame structure and the mean amplitudes determined by the analysis described on pages 750~757 was used to compute the theoretical molecular intensity, together with the same assumption discussed in *procedure* of that section. Two parameters of the rotational isomerism, the *gauche* azimuthal angle ϕ and the fraction of the *trans* form n_t, were varied systematically. The index of resolution was estimated to be 0.90±0.10.

It was found that when n_t was assumed to be less than 30% or more than 70%, the I_b functions (Fig. 13) showed such large fluctuations irrespective of the choice of angle ϕ, that the existence of both rotational isomers was definitely confirmed. It gives an independent support to the conclusion of the RD analysis.

For the estimation of the parameters and their limits, the maximum possible ripples caused by experimental errors or by theoretical uncertainties were regarded as about 1% of the I_b function*. The result of the analysis is

$$\phi=65°\pm10°, \text{ and } n_t=65\sim35\%$$

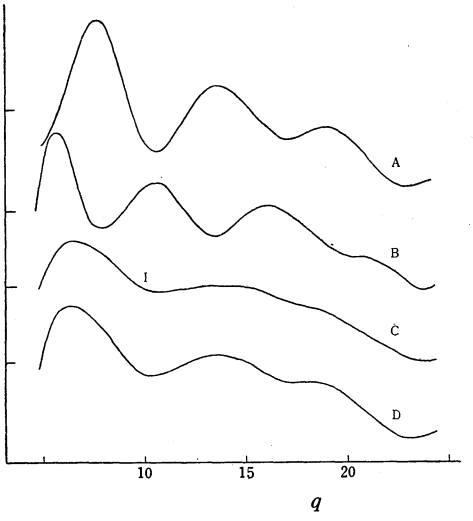


Fig. 13. I_b functions of *n*-butane for models (A) *trans* 100%; (B) *gauche* ($\phi=65°$) 100%; (C) a mixture of *trans* and *gauche* ($\phi=65°$) in 1:1; and (D) a mixture of *trans* and *gauche* ($\phi=50°$) in 1:1. The index of resolution is 0.90. The curve C is in the acceptable region. The vertical line denotes the amplitude of a one per cent fluctuation of the I_b curve.

66) K. Kuchitsu, This Bulletin, **30** 391, 399 (1957).

* This estimation was based on a similar argument given in the previous paper on *n*-propyl chloride (Ref. 19), but a larger value should be taken for the uncertainty in this case, since the contribution of the internal rotation is less (being about 20% of the total intensity), and the uncertainty of the assumptions is more serious (particularly for the position of the hydrogen atoms).

TABLE XI. COMPARISON OF THE STRUCTURES OF RELATED MOLECULES

Molecule	Ethane			Propane	Butane	
Method	Infrared	E.D.	E.D.	E.D.	E.D.	E.D.
C-H(A)	1.102	1.114±0.027	1.107	(1.09)	1.100±0.003	1.107_5 ±0.005
C-C(A)	1.543	1.536±0.016	1.536	1.54±0.02	1.53_9 ±0.003	1.533 ±0.003
∠C-C-H	109°37′	110.5°±3.5°	109°32′	—	110°22′±15′	110.5°±0.7°
∠C-C-C	—	—	—	111.5°±3°	112°9′±9′	112.4°±0.4°
Reference	3	4	5	7	Present work	72

E.D.: electron diffraction investigation.

which is consistent with the result on pages 750~757 within the limit of uncertainty.

Discussion

The C–H and C–C distances were obtained with accuracies of better than 0.01Å (Table VI). These distances are the average values of two non-equivalent distances, but they may not differ more than 0.01Å. It is seen that the values are close to the "normal" bond lengths[67] accepted generally: C–H=1.09Å, and C–C=1.54Å. This result therefore gives some support for these standard values.

The average C–C–H angle was found to be slightly larger than the tetrahedral angle. The structures of methyl groups have been obtained by means of microwave spectroscopy for a number of simple molecules[68]; the angles C–C–H differ slightly from one molecule to another around the tetrahedral angle.

The structural data for normal paraffins comparable with the present result are those for ethane and propane (Table XI). The spectroscopic value r_0 is slightly different from $r_g(0)$ (probably about 0.01Å or less), and the values given by electron diffration may be $r_g(1)$, although not stated explicitly. The general agreement shows that there may be no conspicuous difference between the structures of these hydrocarbons.

It was confirmed that the angle C–C–C is definitely larger than tetrahedral (112°9′). A similar but not so accurate result was obtained in propane (111.5°±3.5°)[7]. It is interesting to note that a similar fact was known for higher normal paraffin crystals studied by the X-ray diffraction; it was first noticed by Bunn[69], and confirmed in a recent study of Shearer and Vand[70], who found that ∠C–C–C=112°1′± 21′ for $C_{36}H_{74}$. This fact is consistent with the earlier theoretical prediction of Ingold[71] based on organic reactions.

As for the rotational isomerism, it was definitely confirmed that there are two isomers, the *trans* and the *gauche* forms, in the gaseous phase. The fractions of these forms were found to be about 60% for the *trans* form and about 40% for the *gauche* form. Since the complete assignment of the vibrational frequencies is not available at present, the partition functions can not be calculated. If the ratio of the functions is assumed to be unity, (the statistical weight for the *gauche* form being 2), then the energy difference between the two forms is about 650 cal./mol., the *trans* form being the more stable. This value is close to that of liquid *n*-butane[11,12], as expected. The azimuthal angle of the *gauche* form was found to be slightly larger than 60°. The effect of hindered internal rotation around the *trans* position was observed in the shift of the *trans* C–C distance. An evaluation of the barrier height gave a rough but reasonable order of magnitude for this value.

A precise measurement of the structure of *n*-butane has been made by Bartell[72]. His result is in satisfactory agreement with the present result, except slight discrepancies in atomic distances (less than 0.7%) which may be partly due to uncertainties in the scale factor.

Summary

The molecular structure of *n*-butane has been investigated by means of the sector-microphotometer method of electron diffraction. The least-square analysis of the radial distribution curve has been carried out both for modified and unmodified curves giving the internuclear

67) L. Pauling, "The Nature of the Chemical Bond", Cornell University Press, Ithaca, N. Y. (1940), p. 160.
68) W. Gordy, W. V. Smith and R. F. Trambarulo, "Microwave Spectroscopy", John Wiley and Sons, Inc., New York (1953). C. H. Townes and A. L. Shawlow, "Microwave Spectroscopy" McGraw-Hill, New York (1955).
69) C. W. Bann, *Trans. Faraday Soc.*, **35**, 482 (1939).
70) H. M. M. Shearer and V. Vand, *Acta Cryst.*, **9**, 379 (1956).
71) C. K. Ingold, *J. Chem. Soc.*, **1921**, 305.
72) L. S. Bartell, private communication (1958).

distances as well as their mean amplitudes and the bond angles. The estimation of experimental standard errors has been made by examining various sources of errors. Important results are the following:

a) The average distance of the C–C bonds is 1.539±0.003Å.

b) The angle C–C–C is 112°9′±9′, is considerably greater than the tetrahedral angle.

c) The position of hydrogen atoms is located with considerable accuracy; C–H =1.100±0.003Å and ∠C–C–H=110°22′±15′.

d) The mean amplitudes measured are in agreement with the calculated values within the limit of error.

e) The existence of rotational isomers, the *trans* and the *gauche* forms, are confirmed. The structure and the fraction of the isomers are determined. The result is consistent with the spectroscopic results.

The author wishes to express his sincere gratitude to Professor Yonezo Morino for his kind guidance and encouragement throughout this work. He is also indebted to Mr. H. Morimoto of Nagoya Univesity and to Dr. M. Iwasaki of the Government Industrial Research Institute of Nagoya for their help in the microphotometry, to Mr. R. Tsunoda in the Division of Health and Welfare Statistics, Welfare Ministries Secretariat for the use of the punched cards machines, and to Mr. T. Takatani of Hitachi Central Research Laboratory for his kind supply of the *n*-butane sample. This research was financially supported by the Scientific Grant from the Ministry of Education.

Department of Chemistry
Faculty of Science
The University of Tokyo
Hongo, Tokyo

SHORT COMMUNICATIONS

Far Infrared Spectrum of Gaseous Formic Acid

By Kozo HIROTA and Yasuo NAKAI

(Received April 20, 1959)

Since the first report of Bonner and Kirby-Smith[1] on a Raman line of formic acid, low frequency vibrations of the acid have not been studied till recently. However, it is interesting to investigate the vibrational bands in relation to the anomalous band features of OH groups due to hydrogen bonding found in both near infrared and infrared regions[2]. Sato and Nagakura explained their results by the motion of the proton in the double minimum potential. Oshida, Ooshika and Miyasaka[3] also explained these phenomena theoretically by the same model, and predicted appearance of new bands in the far infrared region. However, though Pitzer et al.[4] observed two bands of gaseous formic acid at 237 cm^{-1} and 160 cm^{-1}, they ascribed[5] them to the intermolecular vibrations between the two monomers making up formic acid dimer by hydrogen bonding.

In the course of studies[6] on chemisorption of gaseous formic acid HCOOH to the silver surface, the present authors also found two bands independently[7]. In connection to this measurement they extended their research over the region 85~300 cm^{-1} not only on formic acid HCOOH but also on formic acid-d HCOOD, and found some new knowledge, the essential point of

1) L. Bonner and J. B. Kirby-Smith, *Phys. Rev.*, **57**, 1078 (1940).
2) Y. Sato and S. Nagakura, *Sci. of Light*, **4**, 120 (1955); *J. Chem. Soc. Japan, Pure Chem. Sec.* (*Nippon Kagaku Zasshi*), **76**, 1007 (1955): Y. Sato, ibid., **79**, 358, 1384 (1958).
3) I. Oshida, Y. Ooshika and R. Miyasaka, *J. Phys. Soc. Japan*, **10**, 849 (1955).
4) R. C. Millikan and K. S. Pitzer, *J. Am. Chem. Soc.*, **80**, 3515 (1958).
5) T. Miyazawa and K. S. Pitzer, ibid., **81**, 74 (1959).
6) K. Hirota, K. Kuwata and Y. Nakai, This Bulletin, **31**, 861 (1958).
7) K. Hirota and Y. Nakai, *J. Chem. Soc. Japan, Pure Chem. Sec.* (*Nippon Kagaku Zasshi*), **80**, 709 (1959).

which will be reported.

Formic acid of chemically pure grade (Edogawa Kagaku Kogyo Co.) was repeatedly vacuum-distillated, crystallized, and dehydrated with unhydrous copper sulfate. Formic acid-d was prepared by the reaction of sodium formate, whose degree of purity was the same as formic acid, with sulfuric acid-d D_2SO_4 (36%). Method of purification was the same as described on formic acid. It was confirmed that formic acid-d thus obtained does not include H_2O and HCOOH so much as can be detected by use of the NMR method (Apparatus: Varian V 4300 B).

The spectrometer made by Yoshinaga et al.[8], Engineering Faculty of Osaka University, was used. During the measurement, the apparatus was kept constant at 21°C, while the pressure of the acid in the measuring cell was about 30 mmHg. Gratings, light sources, reststrahlen filter and width of slits were changed according to the spectrum range as shown in Table I.

TABLE I

Wave number (cm^{-1})	Light source	Reststrahlen filter	Slit width (mm.)
300～190	Pt-source	NaCl	0.36
190～155	Hg lamp	NaCl	0.50
160～130	〃	KCl	0.47
140～105	〃	KBr	0.68
110～ 85	〃	KBr	1.30

The experimental results are shown in Figs. 1 and 2 and in Table II, where the data of Pitzer[4] and Simova[9] are compared for the sake of discussion. However, Simova's values seem to be of less confidence, because they were estimated from the combination bands of a Raman line.

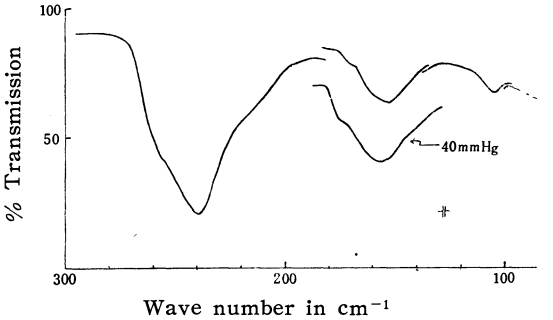


Fig. 1. Far infrared spectrum of HCOOH
Pressure 30 mmHg; Temp. 21°C.

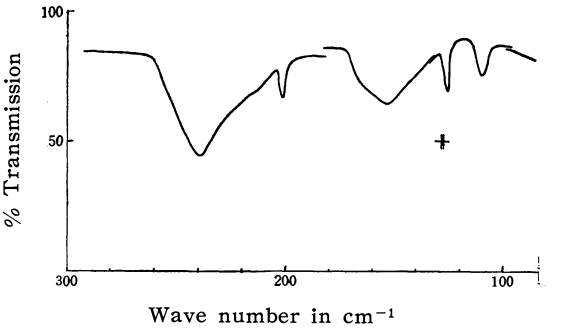


Fig. 2. Far infrared spectrum of HCOOD
Pressure 30 mmHg; Temp. 21°C.

TABLE II. FAR INFRARED BANDS OF FORMIC ACID (cm^{-1})

The present work		Pitzer	Simova	Other researchers
HCOOH	HCOOH	HCOOH	HCOOH	HCOOH
ca. 270 (sh.)				
240±5 (vs)	240±5 (vs)	237	230	232[a]
	202 (m)		200	
175 (sh.)			170	
155 (s)	155 (s)	160		
			145	
	126 (m)			
109 (m)	111 (m)			110[b]

a) Cf. G. Herzberg, "Infrared and Raman Spectra", D. Van Nostrand Co., New York (1945).

b) L. M. Sverklow, *Izv. AN. USSR*, 17, 567 (1953).

The important point obtained from the present data is as follows. Strong bands are observed at 240 cm^{-1} and 155 cm^{-1} in both acids, but it is noteworthy that their feature differs markedly; i.e., (a) in case of HCOOH the 240 cm^{-1} band is broad and begins at 278 cm^{-1}, making a sharp contrast with the beginning at ca. 258 cm^{-1} in case of HCOOD, and (b) small bands can be detected at ca. 270 cm^{-1} and 175 cm^{-1} as shoulders of the 240 cm^{-1} and 155 cm^{-1} bands, respectively, in case of HCOOH. These shoulders become conspicuous if the pressure of formic acid is increased to ca. 40 mmHg as shown in Fig. 1. The second point to be mentioned is appearance of sharp bands at 202 cm^{-1} and 126 cm^{-1} in case of HCOOD. Besides, a new band is observed at ca. 110 cm^{-1} in both acids. Their nature, however, will not be discussed in the present note*),

8) Y. Yoshinaga, S. Fujita, S. Minami, A. Mitsuishi, R. A. Oetjen and Y. Yamada, *J. Opt. Soc. Am.*, 48, 311 (1958).

9) P. Simova, *Izv. Bulgar. Akad. Nauk. Otdel. Fiz. Mat. i Tekh., ser. Fiz.*, 2, 107 (1951).

*) Their frequency is too high if they are the lowest infrared active band predicted by Miyazawa and Pitzer.

except to mention that a Raman line has been observed in the neighborhood of this band (110 cm^{-1}).

The strong and broad bands at 240 cm^{-1} and 155 cm^{-1} seem to correspond to those at 238 cm^{-1} and 160 cm^{-1} observed by Pitzer et al. and can be assigned to the bands produced by the intermolecular vibration between the two monomers making up formic acid dimer as already done by Miyazawa and Pitzer. They may be two higher frequency bands of the three infrared active ones which are expected from the symmetry of the dimer (C_{2h}). It is necessary, therefore, to introduce another cause in order to explain the appearance of two bands of the similar form at 270 cm^{-1} and 175 cm^{-1} in case of HCOOH. Taking the fact into consideration that the ratio of their wave number to that of the sharp bands at 202 cm^{-1} and 126 cm^{-1} in case of HCOOD nearly equals $\sqrt{2}$, respectively, it may presumably be reasonable to assign them to the bands due to the motion of the proton in the double minimum potential, as proposed several years ago[2,3,10].

In conclusion, the present authors express their sincere thanks to Professor H. Yoshinaga and the members of his laboratory (Dr. S. Fujita, Dr. Y. Yamada and Dr. A. Mitsuishi) without whose assistance the present research could not be carried out, and they are much indebted to Professor S. Nagakura of the University of Tokyo and also to Associate Professor S. Seki of Osaka University for helpful discussion of the problem here considered.

Department of Chemistry
Faculty of Science
Osaka University
Kita-ku, Osaka

10) *Discussions Faraday Soc.*, **9**, 210–212 (1950).

Poly-p-halostyrenes. I. Preparation of Crystalline Poly-p-chlorostyrene

Kazuo NAGAI, Masamichi KOBAYASHI and Eiichi NAGAI

(Received May 12, 1959)

Recently Natta et al. reported[1] that while some substituted polystyrenes prepared by Ziegler catalyst were crystalline, others were amorphous. To the contrary of Natta et al.'s results that poly-*p*-chlorostyrene is not crystalline, we find that a small part of poly-*p*-chlorostyrene prepared by Ziegler catalyst is crystalline.

p-Chlorostyrene (4.4 g.) prepared by an usual method[2], enclosed in a glass tube with $Al(C_2H_5)_3$ (0.53 g.), $TiCl_4$ (0.18 g.) and *n*-heptane (20 cc.) is polymerized at 70°C

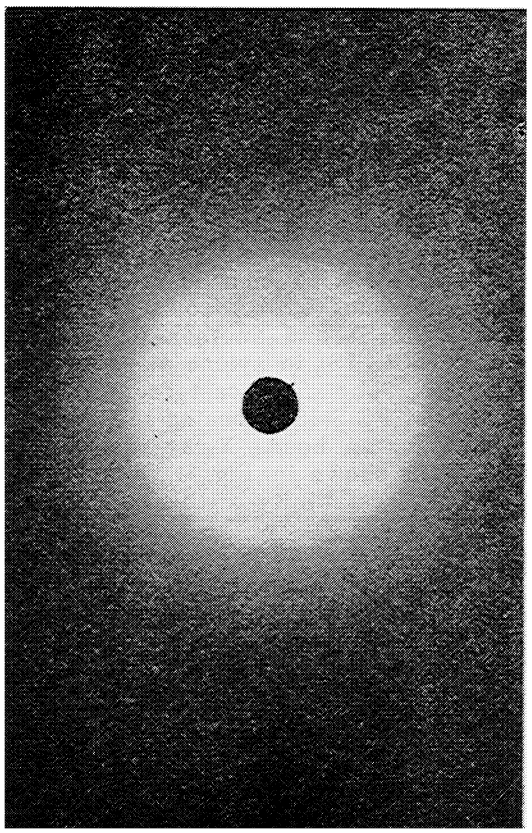


Fig. 1. X-ray diagram of poly-*p*-chlorostyrene (PClS-IS)

1) G. Natta, F. Danusso and D. Sianesi, *Makro. Mol. Chem.*, **28**, 253 (1958).
2) R. Adams and C. R. Noller, "Organic Syntheses", Vol. 5, John Wiley & Sons, New York (1925), p. 17; W. Kern and D. Braun, *Makro. Mol. Chem.*, **27**, 23 (1958).

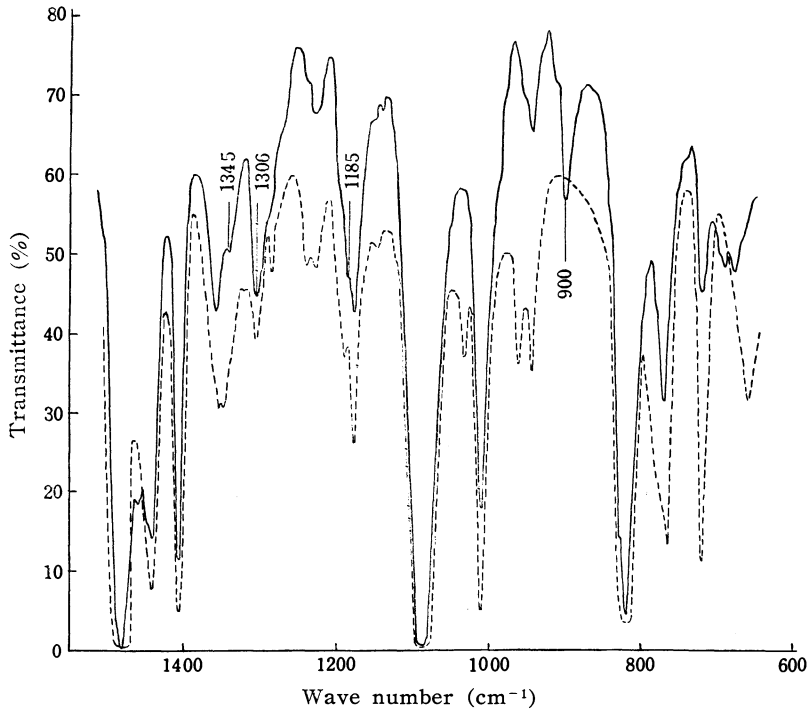


Fig. 2.

for about 10 hr. The product washed by hot ethanol and then boiled in water is dissolved in boiling xylene and the solution is filtered to separate from titanium oxide. By centrifuging this solution kept at room temperature the polymer is devided into two parts; one (2.20 g.) soluble (refered as to PClS-S) and another (0.13 g.) insoluble (PClS-IS) in xylene at room temperature. The film cast from toluene solution of PClS-IS is heated in silicon oil at 160°C for an hour. X-ray diagram of this film is shown in Fig. 1, manifesting moderate crystallinity of this sample.

In Fig. 2 are shown the infrared spectroscopic data of PClS-IS (full line) and radically polymerized poly-*p*-chlorostyrene (PClS-At) (dashed line), both previously heated at 160°C for an hour. It is expected that in the crystalline region and in the amorphous region, so far as the short portion of the polymer chain is concerned, the skeletal chain of PClS-IS has a helical structure, although whether 3-fold helix as in the case of polystyrene is still kept or not is not obvious, owing to the steric effects of chlorine atoms. Recently Tadokoro et al.[3,4] showed that the absorption bands ascribed to deformation vibrations of CH_2 and CH groups of the skeletal carbon chain, and to C–C stretching vibration were affected by the configurations of the skeletal chain, and bands at 1364, 1314, 1297 and 1185 cm^{-1} of isotactic polystyrene and *p*-deuterostyrene were assumed to be characteristic to 3-fold helical structure. Moreover, in our investigations on the infrared spectroscopy of the crystalline poly-*p*-fluorostyrene, we found[5] the bands at 1330 and 1302 cm^{-1} as to be charasteristic to the helical structure of the skeletal chain. From these results, the bands 1345, 1306 and 1185 cm^{-1} of PClS-IS are assumed to be characteristic to the helical structure. A band at 900 cm^{-1} probably corresponds to crystallization sensitive band. The spectroscopic data of PClS-S are almost similar to those of PClS-At. Investigations are in progress on the bands appearing at near 700 cm^{-1} and longer wavelength region.

We thank Mr. S. Kuribayashi for his preparation of X-ray diagram.

The Osaka Industrial Research Institute
Daini-Nishi 2-Chome, Oyodo-ku, Osaka

3) H. Tadokoro, S. Nozakura, T. Kitazawa, Y. Yasuhara and S. Murahashi, This Bulletin, **32**, 313 (1959).
4) S. Murahashi, S. Nozakura and H. Tadokoro, This Bulletin, **32**, 534 (1959).
5) K. Nagai, M. Kobayashi and E. Nagai, Presented at the 8th Annual Meeting of the Society of Polymer Science of Japan, held in Tokyo, May, 1959.

On the Magnetic Susceptibility of Hexabenzocoronene and Triphenylene

By Hideo Akamatu
and Minoru Kinoshita

(Received May 15, 1959)

Hexabenzocoronene is an extremely stable, pale yellow hydrocarbon. Clar and Ironside suggested that it contains exclusively benzenoid rings interlinked by quasi-single bonds[1]. Afterwards, however, they found an asymmetric effect of the electronic interaction between benzenoid rings, and proposed a formula of hexabenzocoronene consisting of a triphenylene complex and 4 benzenoid rings[2]. Magnetic susceptibility of hexabenzocoronene would be interesting for these points of view, as the effect of the aromatic conjugation should reflect on its value. We measured the magnetic susceptibility of hexabenzocoronene and triphenylene; the samples were provided by C. T. Ironside and M. Zander, respectively.

The purification of the specimens was made by sublimation in vacuo at about 490°C for hexabenzocoronene, and at about 120°C for triphenylene. The magnetic measurement was made by the Gouy method at room temperature. The observed values are as follows. Hexabenzocoronene (M.W. 522.6, density 1.57[3]) :

$-\chi_g \times 10^6 = 0.662 \pm 0.002$ per gram,

$-\chi_M \times 10^6 = 346.0$ per mole.

Triphenylene (M.W. 228.3, density 1.30).

$-\chi_g \times 10^6 = 0.686 \pm 0.001$ per gram,

$-\chi_M \times 10^6 = 156.6$ per mole.

The magnetic susceptibilities of related compounds are as follows.

Phenanthrene :

$-\chi_g \times 10^6 = 0.718$; $-\chi_M \times 10^6 = 127.9$

Benzene :

$-\chi_g \times 10^6 = 0.712$; $-\chi_M \times 10^6 = 55.6$

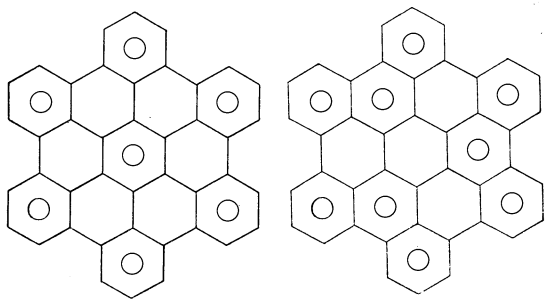
Atomic susceptibility of hydrogen ;

$-\chi_M(\mathrm{H}) \times 10^6 = 2.93$

Hexabenzocoronene can be presumed as being made of seven benzenoid rings interlinked by quasi-single bonds (Formula 1), or consisting of triphenylene and four benzenoid rings. The expected value of each formula will be respectively,

$$-\chi_M \times 10^6 = 7\chi_M(\text{Benzene}) - 24\chi_M(\text{H}) = 318.9$$

$$-\chi_M \times 10^6 = \chi_M(\text{Triphenylene}) + 4\chi_M(\text{Benzene}) - 18\chi_M(\text{H}) = 326.3$$



Formula (1) Formula (2)

Fig. 1. Hexabenzocoronene

The observed value is higher than those of anticipated formulae. The other formula which is conceivable consists of three phenanthrene rings connected by contact bonds (Formula 2). This leads to the expected value as,

$$-\chi_M \times 10^6 = 3\chi_M(\text{Phenanthrene}) - 12\chi_M(\text{H}) = 348.5 \; ; \quad -\chi_g \times 10^6 = 0.667$$

This value is very near to the observed one. It is likely that a small effect of the electronic interaction takes place between benzenoid rings, its amount is in the same order as the aromatic conjugation in phenanthrene molecule.

The mean susceptibility of triphenylene was measured by Honda and Ōuchi[4]. Their observed value is $\chi_g = -0.685 \times 10^{-6}$, which is in good agreement with the present result. From the observed susceptibility and using the empirical formula[5], the principal diamagnetic susceptibilities of triphenylene molecule can be estimated as $K_1 = -95.6 \times 10^{-6}$ and $K_3 = -278.6 \times 10^{-6}$, where K_1 is in the plane of molecule and K_3 is perpendicular to it. This leads to the diamagnetic anisotropy of $\Delta K = -183.0 \times 10^{-6}$. This value is 3.4 times of the diamagnetic anisotropy of benzene, ΔK (Benzene) $= -54 \times 10^{-6}$. The molecular

1) E. Clar and C. T. Ironside, *Proc. Chem. Soc.*, **1958**, 150.
2) E. Clar, C. T. Ironside and M. Zander, *J. Chem. Soc.*, **1959**, 142; E. Clar, *Tetrahedron*, **5**, 98 (1959); Private communication.
3) A. Halleux, R. H. Martin and G. S. D. King, *Helv. Chim. Acta*, **41**, 1177 (1958).
4) H. Honda and K. Ōuchi, *Reports of the Resources Research Institute, Japan*, No. 1, 8, (1952).
5) H. Akamatu and Y. Matsunaga, This Bulletin, **26**, 364 (1953); **29**, 800 (1956).

orbital calculation[6], however, gave 4.08 for this ratio, which is too large compared with the above value.

Our estimated values of the principal diamagnetic susceptibility are likely to be reasonable from the following reason. Triphenylene crystal is orthorhombic, and its principal susceptibilities along the crystal axes were measured by Banerjee and Guha[7]. Their observed values are $\chi_a = -150.1 \times 10^{-6}$, $\chi_b = -149.5 \times 10^{-6}$ and $\chi_c = -174.2 \times 10^{-6}$. Using these values combined with the above values for K_1 and K_3, we can estimate the orientation of the molecule to the crystal axes. The procedure has been given by Lonsdale and Krishnan[8]. This gives the result that the plane of molecule makes the angle of 50°20′ to the *ab*-plane. This value is in good agreement with the observed angle, 50°30′, by Klug[9] who made the X-ray crystal analysis of triphenylene.

The authors wish to express their thanks to Dr. E. Clar and his school who provided them with the samples of hexabenzocoronene and triphenylene.

Department of Chemistry
Faculty of Science
The University of Tokyo
Hongo, Tokyo

Added in Proof:

E. Clar proposed* the other possible formula for hexabenzocoronene, after we had made our communication. He suggested that the induced sextet in the center ring of triphenylene may rotate or oscillate through the ring system of hexabenzocoronene, as if the Formulae 1 and 2 are overlapping with each other. In this case, the induced sextet in triphenylene (the center ring) has magnetic susceptibility of

$$\chi_M(\text{Triphenylene}) - 3[\chi_M(\text{Benzene}) - 2\chi_M(\text{H})] = -7.4 \times 10^{-6}$$

Three times this value (-22.2×10^{-6}) added to the value for Formula 1, it leads to -341.1×10^{-6} which is near to the observed value.

6) G. Berthier, M. Mayot, A. Pullman and B. Pullman, *J. Physique Rad.*, **13**, 15 (1952).
7) S. Banerjee and A. C. Guha, *Z. Krist.*, **96**, 107 (1936).
8) K. Lonsdale and K. S. Krishnan, *Proc. Roy. Soc.*, **A156**, 597 (1936).
9) A. Klug, *Acta Cryst.*, **3**, 165 (1950).
* Private communication.

Isodelphinine, a New Alkaloid from Aconitum miyabei, Nakai

By Nobukatsu KATSUI

(Received May 26, 1959)

Recently a third new alkaloid, sachaconitine, and a fourth probably new alkaloid (I)[1], base D, having the same empirical formula, $C_{33}H_{45}O_9N$, as that of delphinine (II)[2] but different m.p. and $[\alpha]_D$, were isolated from Aconitum *miyabei*, Nakai. As described below, I has the same empirical formula and the same functional groups as II, but differs distinctly from II as shown by the mixed m. p. and infrared spectra. Thus the name isodelphinine was assigned to I. This substance, m. p. 167~168°C, $[\alpha]_D^{20}$ + 20.1°, gave a perchlorate, m. p. 171~172°C, $[\alpha]_D^{20}$ −2.38°. (*Anal.* Found: C, 56.35; H, 4.97; Cl, 4.87. Calcd. for $C_{33}H_{45}O_9N \cdot HClO_4$: C, 56.55; H, 5.19; Cl, 5.06%). The aurichloride crystallized from chloroform-ethanol in prisms, m. p. 228~229°C. (*Anal.* Found: Au, 20.96. Calcd. for $C_{33}H_{45}O_9N \cdot HAuCl_4$: Au, 20.94%). Other salts of I, for example, acid oxalate or hydrochloride, did not crystallize although the corresponding salts of II had been obtained[3] as crystals.

On acetylation with acetyl chloride I gave a monoacetate, m.p. 188~190°C. (*Anal.* Found: C, 65.43; H, 6.81. Calcd. for $C_{35}H_{47}O_{10}N$: C, 65.55; H, 6.76%). Saponification of I gave benzoic acid which was identified with an authentic sample, and acetic acid which was confirmed as silver salt. (*Anal.* Found: Ag, 64.49. Calcd. for $C_2H_3O_2Ag$: Ag, 64.67%). The presence of four methoxyl groups was determined by the micro-Zeizel determination. (*Anal.* Found: OCH_3, 20.11. Calcd. for $C_{29}H_{33}O_5N \cdot 4(OCH_3)$: OCH_3, 20.63%). In the Herzig-Meyer *N*-alkyl determination, I gave methyl iodide which was confirmed as tetramethylammonium iodide. (*Anal.* Found: I, 67.46. Calcd. for $(CH_3)_4 \cdot NI$: I, 67.86%).

Above evidences show that the formula of I may be extended as follows in the same way as that of II:

1) H. Suginome, N. Katsui and G. Hasegawa, This Bulletin, **32**, 604 (1959).
2) R. H. F. Manske and H. L. Holmes, "The Alkaloids", Vol. IV, Academic Press Inc., New York (1954), p. 275.
3) T. Walz, *Arch. Pharm.*, **260**, 9 (1922); W. A. Jacobs and L. C. Craig, *J. Biol. Chem.*, **127**, 301 (1939).

$$C_{19}H_{21}\begin{cases}(OCH_3)_4\\OH\\OCOCH_3\\OCOC_6H_5\\N\text{-}CH_3\end{cases}$$

The infrared spectra of I and II were quite similar except for the region due to ester carbonyl groups : compound I showed two bands at 1720 cm^{-1} and 1702 cm^{-1}, whilst II one band[4] at 1720 cm^{-1}.

On the basis of the same extended formula and the resemblant spectra, it may be reasonable to consider that I possesses a skeletal formula closely related to that of II. Furthermore, the same ring structure has been suggested for several alkaloids[5] of two genera, Aconitum and Delphinium, in which oxygen atoms are similarly located although the substituents are different. And then it may be considered that the substituents of I and II are also similarly located. On the other hand, it is well known[6] that the benzoyl group in II covers a secondary hydroxyl group which is vicinal to a free *tert* hydroxyl group.

If above consideration is correct, a simple explanation of the difference in infrared spectra of I and II may be that the free hydroxyl and the benzoyl group have *trans* orientation in II against *cis* in I.

In the *cis* orientation, an ester carbonyl band displacement[7] to lower frequencies due to hydrogen bonding is considerable. An experiment to clarify the relation of I and II is in progress and will be reported in a later paper.

The author is grateful to Professor Harusada Suginome, President of Hokkaido University, for his unfailing kindness in encouraging this work, and to Dr. S.W. Pelletier for his courtesy in sending the sample of delphinine.

Department of Chemistry
Faculty of Science
Hokkaido Univerity, Sapporo

4) Schneider has reported that the spectrum of II showed one band due to two ester groups at 5.78 μ, *Ann.*, **590**, 155 (1954).

5) R. C. Cookson and M. E. Trevett, *J. Chem. Soc.*, **1956**, 3121; R. Anet, D. W. Clayton and L. Marion, *Can. J. Chem.*, **35**, 397 (1957); F. Sparatore, R. Greenhalgh and L. Marion, *Tetrahedron*, **4**, 157 (1958); O. E. Edwards, L. Marion and K. H. Palmer, *Can. J. Chem.*, **36**, 1097 (1958); E. Ochiai, T. Okamoto and M. Kaneko, *Chem. Pharm. Bull. Japan*, **6**, 730 (1958).

6) W. A. Jacobs and Y. Sato, *J. Biol. Chem.*, **180**, 479 (1949); K. Wiesner, F. Bickehaupt and Z. Valenta, *Tetrahedron*, **4**, 418 (1958).

7) R. N. Jones, P. Humphries, F. Herling and K. Dobriner, *J. Am. Chem. Soc.*, **74**, 2820 (1952).

Visible Absorption Spectra of Colored Solutions Produced by Adding Alkali to Nitro-, Dinitro-, and Trinitro-substituted Benzenes in Acetone

By Takehiro Abe

(Received May 28, 1959)

In the course of my visible absorption studies on the color reactions of polynitrobenzenes with alkali, it has been found that nitrobenzene, *o*-, *m*-, and *p*-dinitrobenzene, and 1,3,5-trinitrobenzene, all in acetone give intense absorption bands at the visible region when they are treated with a few drops of dilute aqueous solution of sodium hydroxide at room temperature, as shown in Fig. 1. Dinitrobenzenes slowly yield reddish-violet colors. Trinitrobenzene at once gives a red color, while a red color can be observed by standing the nitrobenzene solution containing sodium hydroxide (in a brown desiccator to avoid light) for a long time. These red colors show the maximum

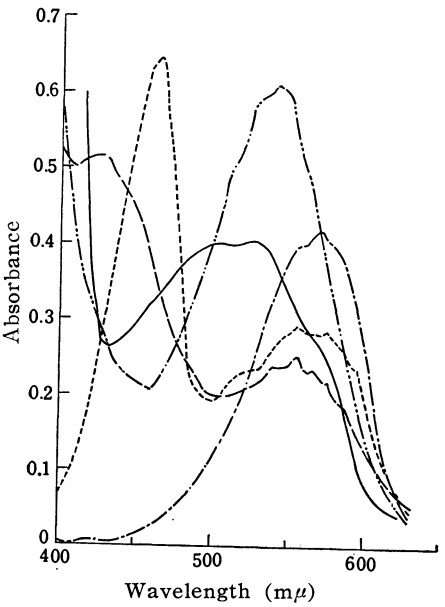


Fig. 1. Absorption spectra of the colored solutions produced by adding a few drops of dilute sodium hydroxide solution to nitrobenzene (——), *o*-dinitrobenzene(—·—), *m*-dinitrobenzene (—··—), *p*-dinitrobenzene (—···—), and 1,3,5-trinitrobenzene (----), in acetone at room temperature.

absorption bands at longer wavelengths as compared with the maximum absorption bands observed for the solutions that are obtained by adding sodium hydroxide into aqueous solutions of polynitrobenzenes[1]. There is no simple relation between numbers of nitro group and the positions of the absorption maxima, although the aromatic nitro compounds show the absorption bands at longer wavelengths in the aqueous solutions of sodium hydroxide as the number of nitro group increases[1].

The absorption curve of the red-colored solution produced by treating trinitrobenzene in acetone with sodium hydroxide solution, giving the intense maximum absorption band at about 460 mμ and several bands at 510~590 mμ, is greatly different from that of the red complex of trinitrobenzene with ammonium hydroxide[2]. Fig. 2 shows the absorption curves of the red solutions produced by adding a few drops of dilute sodium hydroxide solution, of dilute calcium hydroxide solution, or of concentrated ammonia water into the acetone solutions of 1,3,5-trinitrobenzene. It may be known from Fig. 2 that the absorption curves of the colored solutions produced by treating with strong alkalies (sodium hydroxide and calcium hydroxide) is different from that of the red solution obtained by addition of a weak alkali (ammonia). The maximum absorption band of the red complex of trinitrobenzene with ammonium hydroxide lies at the longer wavelength in acetone than in ethanol and in water[2].

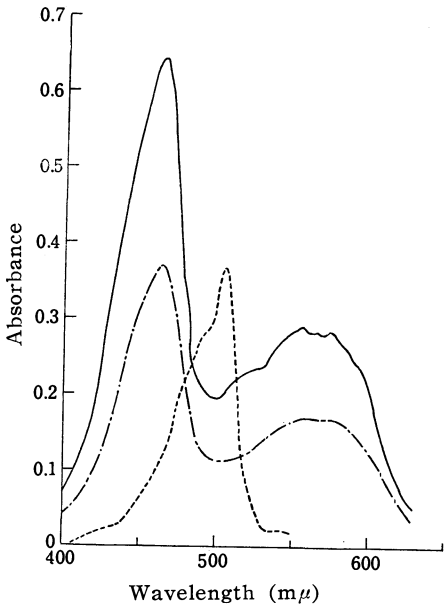


Fig. 2. Absorption spectra of the colored solutions produced by adding a few drops of dilute sodium hydroxide solution (——), of dilute calcium hydroxide solution (—·—), and of concentrated ammonia water (----) to 1,3,5-trinitrobenzene in acetone at room temperature.

Although weak alkali and strong alkali give different absorption curves, all the above red colors seems possibly to be owing to formation of the same transition complexes of Meisenheimer's type as the intermediates presented for the color reactions of trinitrobenzenes and dinitrobenzens with alkalies[1-8].

The author is particularly indebted to Professor Y. Nomura for his suggestion and encouragement through this work.

Department of Chemistry
Defense Academy
Yokosuka

1) A. Abe, This Bulletin, **31**, 904 (1958); **32**, 339 (1959).
2) T. Abe, ibid., to be published.
3) J. Meisenheimer, *Ann.*, **323**, 205, 214, 241 (1902).
4) D. L. Hammick and R. Foster, *J. Chem. Soc.*, **1954**, 2153.
5) R. Schaal, *Compt. rend.*, **239**, 1036 (1954).
6) R. Foster, *Nature*, **175**, 746 (1955).
7) J. B. Ainscough and E. F. Caldin, *J. Chem. Soc.*, **1956**, 2528.
8) S. Nagakura and S. Oosawa, Presented at the 12th Annual Meeting of the Chemical Society of Japan, held at Kyoto in April, 1959.

*On the Mechanism of Oxidation by Cuprous Chloride, Pyridine and Air. I. The Properties of the Reaction**

By Keizō KINOSHITA

(Received September 30, 1958)

It was previously reported that by aerial oxidation catalyzed by cuprous chloride in a pyridine solution, benzoin was primarily converted into benzil, which was further oxidized to benzoic acid almost quantitatively[1]. In this reaction, "oxidant A", a product of aerial oxidation of cuprous chloride pyridine complex, is considered to be the actual oxidant[2]. On the other hand, with cupric chloride as a catalyst, no benzoic acid is obtained, although benzoin is converted into benzil almost quantitatively[1].

$$\underset{\text{Benzoin}}{C_6H_5CHOHCOC_6H_5} \xrightarrow[\text{Air}]{Cu_2Cl_2+\text{Pyridine}} 2C_6H_5COOH \quad (1)$$

$$C_6H_5CHOHCOC_6H_5 \xrightarrow[\text{Air}]{CuCl_2+\text{Pyridine}} \underset{\text{Benzil}}{C_6H_5COCOC_6H_5} \quad (2)$$

Terent'ev et al.[3] reported that by aerial oxidation catalyzed by cuprous chloride in a pyridine solution, aromatic amines were converted into the corresponding azo compounds, but that with cupric chloride as a catalyst, these azo compounds were never obtained.

$$2C_6H_5NH_2 \xrightarrow[\text{Air}]{Cu_2Cl_2+\text{Pyridine}} C_6H_5N=NC_6H_5 \quad (3)$$

This paper describes the properties of these reactions.

Experimental

Materials.—Benzil was prepared by oxidation of benzoin with nitric acid, and recrystallized from alcohol, m.p. 94~95°C[4]. Aniline (b.p. 184~185°C) was redistilled immediately before use. Cuprous chloride was prepared by reduction of cupric chloride with sodium sulfite[5], washed with acetone and dried.

(1) Aerial Oxidation of Aniline Catalyzed by Cuprous Chloride in a Pyridine Solution.—A mixture of aniline (2.0 g., 2.2/100 mol.), cuprous chloride (2.0 g., 1/100 mol.) and pyridine (50 cc.) was stirred in a stream of air for 5 hr. at room temperature. The resulting mixture was acidified with 6N-H_2SO_4, and extracted with ether (500 cc.). After removal of the ether, the residue was extracted with light petroleum (b.p. 40~60°C), and chromatographed on activated alumina (Wako Pure Chemical Industries, Ltd.). Azobenzene (1.2 g., 60%) was obtained; m.p. 67~68°C. (Lit. 68°C). It was identified with azobenzene by a mixed melting point determination and an analysis.

Anal. Found: C, 79.27; H, 5.57; N, 15.36. Calcd. for $C_{12}H_{10}N_2$: C, 79.12; H, 5.49; N, 15.38%.

(2) Oxidation of Aniline in the Absence of Air.—Cuprous chloride (8.0 g., 4/100 mol.) in pyridine (100 cc.) was oxidized with air for 3 hr. at room temperature. A mixture of aniline (2.0 g., 2.2/100 mol.) and "oxidant A" thus prepared, was stirred for 5 hr. at room temperature in a stream of nitrogen. The resulting mixture was acidified with 6N-H_2SO_4 and extracted with ether. White precipitate remained. From the ether solution, azobenzene (0.5 g.) was obtained as in Experiment 1; m.p. 67~68°C, its melting point was not depressed on admixing with an authentic sample. A trace of red substance remained on top of the activated alumina.

The color of the aqueous layer was at first pale blue, but after the solution was kept in air its color turned to darker blue. The white precipitate was dissoluble in an aqueous ammonia solution. The color of the ammonia solution kept in air turned to blue. These results suggest that cuprous chloride was produced during the oxidation of aniline.

(3) Attempted Aerial Oxidation of Aniline in the Presence of Acetic Acid.—A mixture of aniline (2.0 g., 2.2/100 mol.), cuprous chloride (2.0 g., 1/100 mol.), acetic acid (1.8 g., 3/100 mol.) and pyridine (100 cc.) was treated as in Experiment 1. A trace of red substance remained on top of the activated alumina, and no other neutral substance was obtained. The color of the aqueous solution was blue.

(4) Reaction of Cupric Chloride Pyridine Complex with Potassium Hydroxide.—(a) Cupric chloride (3.4 g., 2/100 mol.) was refluxed in pyridine (50 cc.) until all the precipitate was turned into blue needles. Potassium hydroxide (1.1 g., 2/100 mol.) in methyl alcohol (50 cc.) was added dropwise under stirring to the cooled pyridine solution of cupric chloride pyridine

* The present work was presented partly at the Symposium on the Mechanism of Organic Chemical Reaction of the Chemical Society of Japan, held at Osaka in October, 1955, and partly at the similar symposium of the same society, held at Nagoya in October, 1957.

1) K. Kinoshita, *J. Chem. Soc. Japan, Pure Chem. Sec.* (*Nippon Kagaku Zasshi*), **75**, 48 (1954).

2) K. Kinoshita, ibid., **75**, 173 (1954).

3) A. P. Terent'ev et al., *Doklady Akad. Nauk U. S. S. R.*, **1955**, 91—93. [*Chem. Abstr.*, **50**, 4807 (1956).]

4) R. Adams, "Organic Syntheses", Vol. I, John Wiley & Sons, Inc., New York (1921), p. 25.

5) W. C. Ferdnelius, "Inorganic Syntheses", Vol. II, McGraw-Hill, New York (1946), p. 1.

complex. The color of the resulting mixture was green.

(b) When potassium hydroxide (1.1 g., 2/100 mol.) in methyl alcohol (50 cc.) was added to the copper complex prepared in Experiment 4a, pale blue precipitate was formed from the green solution.

(5) Oxidation of Benzil with the Copper Complex Prepared in Experiment 4.—(a) A mixture of benzil (2.0 g., 1/100 mol.) and the copper complex prepared in Experiment 4a was stirred at 30°C for 2 hr. in a stream of air. The resulting mixture was acidified with 6N-H_2SO_4, and extracted with ether (500 cc.). The ethereal layer was extracted with aqueous sodium carbonate solution. After removal of the ether, the residue was benzil (0.7 g., 35%); this melted at 94~95°C alone or with an authentic sample of benzil. The aqueous layer was acidified by 6N-H_2SO_4 and extracted with ether. After removal of the ether, the residue was sublimed to give benzoic acid (1.4 g., 57%), m.p. 121~122°C; its melting point was not depressed on admixing with an authentic sample.

(b) A mixture of benzil (1.0 g., 1/200 mol.) and the copper complex prepared in Experiment 4b was treated as in Experiment 5a. Benzil (0.9 g., 90%) was recovered; m. p. 94~95°C, its melting point was not depressed with an authentic sample. No benzoic acid was obtained.

(c) When diethylamine (10 g., excess) was added to the copper complex prepared in Experiment 4a, the color of the solution did not change. A mixture of benzil (1.0 g., 1/200 mol.) and the resulting copper complex was treated as in Experiment 5a. Benzoic acid (1.1 g., 90%) was obtained; m. p. 121~122°C, its melting point was not depressed on admixing with an authentic sample. No benzil was recovered.

(d) When trimethylamine hydrochloride (3.9g., 3/100 mol.) was added to the copper complex prepared in Experiment 4a, blue needles appeared, and trimethylamine was separated. The mixture of benzil (1.0 g., 1/200 mol.) and the resulting copper complex was treated as in Experiment 5a. Benzil (0.9 g., 90%) was recovered; it melted at 94~95°C alone or with an authentic sample of benzil. No benzoic acid was obtained.

(6) Oxidation of Aniline in the Presence of Methyl Alcohol.—(a) A mixture of aniline (2.0 g., 2.2/100 mol.) and the copper complex described in Experiment 4a [prepared from $CuCl_2 \cdot 2H_2O$ (3.4 g.), KOH (1.1 g.), methyl alcohol (10 cc.) and pyridine (50 cc.)] was treated as in Experiment 1. Azobenzene (0.9 g., 45%) was obtained; it melted at 67~68°C alone or with an authentic sample of azobenzene.

(b) A mixture of aniline (2.0 g., 2.2/100 mol.), cuprous chloride (2.0 g., 1/100 mol.), methyl alcohol (100 cc.) and pyridine (50 cc.) was treated as in Experiment 1. Azobenzene (0.1 g., 5%) was obtained; it melted at 67~68°C alone or with an authentic sample of azobenzene.

(7) Effect of Bases on "Oxidant A".—(a) Cuprous chloride (2.0 g., 1/100 mol.) in pyridine (50 cc.) was oxidized with air at room temperature for 2 hr.

(b) When potassium hydroxide (1.1 g., 2/100 mol.) in methyl alcohol (50 cc.) was added to the copper complex prepared in Experiment 7a, brown precipitate appeared. Its mixture with benzil (1.0 g., 1/200 mol.) was treated as in Experiment 5a. The same results as in Experiment 5b were obtained.

(c) When diethylamine (10 g., excess) was added to the copper complex prepared in Experiment 7a, no color change occurred. A mixture of benzil (1.0 g., 1/200 mol.) and the resulting copper complex, was treated as in Experiment 5a. The same results as in Experiment 5c were obtained.

(d) When trimethylamine hydrochloride (3.9 g., 3/100 mol.) was added to the copper complex prepared in Experiment 7a, blue needles were formed, and trimethylamine was separated. A mixture of benzil (1.0 g., 1/200 mol.) and the resulting copper complex, was treated as in Experiment 5a. The same results as in Experiment 5d were obtained.

Results and Discussion

By aerial oxidation catalyzed by "oxidant A", aniline is converted into azobenzene in a yield of about 60%. Through the treatment of aniline with "oxidant A" in the absence of air, azobenzene and cuprous chloride are obtained (Table I). These results suggest that "oxidant A" is the actual oxidant in the aerial oxidation of aniline catalyzed by cuprous chloride in a pyridine solution. Similar facts were found in the oxidative cleavage of benzil under the similar condition[2].

TABLE I. OXIDATION OF ANILINE BY CUPROUS CHLORIDE, PYRIDINE AND AIR

Catalyst	Cu_2Cl_2 in the catalyst g. (mol.)	Pyridine cc.	Azobenzene g. (%)
Oxidant A*	8.0 (4/100)	100	0.5**
Cu_2Cl_2	2.0 (2/200)	50	1.2 (60)
Oxidant A	1.0 (1/200)	50	1.2 (60)
Oxidant A	2.0 (2/200)	50	1.2 (60)
Oxidant A	3.0 (3/200)	80	1.2 (60)
Oxidant A	4.0 (4/200)	100	1.2 (60)

Aniline (2.0 g., 2.2/100 mol.) was treated.
* Nitrogen atomosphere.
** Cuprous chloride was obtained.

In the presence of an excess of acidic substance "oxidant A" has no longer its catalytic activity (Table II). The oxidation of benzil is stopped after a definite amount of benzil is oxidized[2], because the produced benzoic acid retards the reaction. On the other hand, "oxidant A" keeps its catalytic activity during the

aerial oxidation of aniline, because acidic substance is hardly produced in the reaction.

TABLE II. EFFECT OF ACIDIC SUBSTANCE

Cu_2Cl_2 g. (mol.)	Acidic substance g. (mol.)	Azobenzene g.
2.0 (1/100)	Acetic acid 1.8 (3/100)	0
2.0 (1/100)	Ammonium chloride 1.6 (3/100)	0
2.0 (1/100)	Trimethylamine hydrochloride* 3.9 (3/100)	0

Aniline (2.0 g., 2.2/100 mol.) was treated in pyridine (100 cc.).
* Trimethylamine was separated.

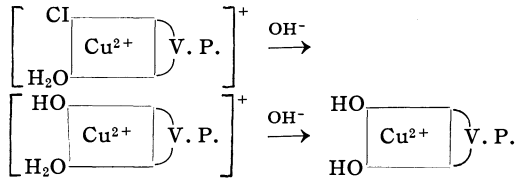
Another catalyst for benzil is obtained from reaction of cupric chloride pyridine complex with a methyl alcohol solution of potassium hydroxide — not with its aqueous solution. With a methyl alcohol solution of potassium hydroxide, cupric chloride pyridine complex—blue needles —turns to a greenish solution, as far as the molar ratio of cupric chloride to potassium hydroxide reaches 1 : 1.5. Benzil is oxidized to benzoic acid by aerial oxidation catalyzed by this greenish cupric complex—"oxidant B". The amount of oxidized benzil apparently increases in accordance with the amount of added potassium hydroxide (Table III).

TABLE III. OXIDATION OF BENZIL BY "OXIDANT B" AND AIR

$CuCl_2 \cdot 2H_2O$* g. (mol.)	KOH g. (mol.)	Benzoic acid g. (%	Sample (recovered) g. (%)
3.4 (2/100)	0	0	1.8 (90)
3.4 (2/100)	0.6 (1/100)	0.6 (25)	1.4 (70)
3.4 (2/100)	1.1 (2/100)	1.4 (58)	0.7 (35)
3.4 (2/100)	1.7 (3/100)	2.0 (82)	0.3 (15)

Benzil (2.0 g., 1/100 mol.) was treated.
* Cf. Experiment 4a.

The following change was postulated in the reaction of dichloro-(2-vinyl pyridine)-copper(II) with potassium hydroxide[6] (Reaction 4). It was reported that by reaction of an aqueous cupric salt pyridine complex solution with equimolar potassium hydroxide, a solution of hydroxy cupric salt pyridine complex ion [I] was produced[7] (Reaction 5). All this seems to lead to the conclusion that "oxidant B" is hydroxy cupric chloride pyridine complex.



(4)

$$2\,Cu^{2+} + 4\,Py + 2\,OH^- \rightleftarrows Py_2Cu(OH)_2CuPy_2^{2+} \quad [\mathbf{I}] \qquad (5)$$

(V. P.: Vinyl pyridine, Py: Pyridine).

By aerial oxidation catalyzed by "oxidant B", aniline is converted into azobenzene, although the yield of azobenzene is decreased in the presence of an excess of methyl alcohol. The aerial oxidation of aniline catalyzed by "oxidant A" is also retarded by an excess of methyl alcohol (Table IV).

TABLE IV. EFFECT OF METHYL ALCOHOL ON THE AERIAL OXIDATION OF ANILINE

Copper salt in the catalyst* g. (mol.)		KOH in the catalyst g. (mol.)	Methyl alcohol cc.	Azobenzene g. (%)
Cu_2Cl_2	2.0 (1/100)	0	100	0.1 (5)
$CuCl_2 \cdot 2H_2O$	3.4 (2/100)	0	20	0
	3.4 (2/100)	1.1 (2/100)	100	0
	3.4 (2/100)	1.1 (2/100)	20	0.3 (15)
	3.4 (2/100)	1.1 (2/100)	10	0.9 (45)

Aniline (2.0 g., 2.2/100 mol.) was treated.
* Pyridine (50 cc.) was used as a solvent.

When equimolar potassium hydroxide in methyl alcohol is added "oxidant A" or "oxidant B", these complexes are destroyed and their catalytic activity is lost. However, when "oxidant A" or "oxidant B" is treated with excessive diethylamine or benzylamine, they keep their color and their catalytic activity. Through the reaction between trimethylamine hydrochloride and "oxidant A" or "oxidant B", trimethylamine separates. The resulting complexes no longer have their catalytic activity. This fact suggests that "oxidant A" and "oxidant B" have stronger basicity than trimethylamine (Ref. 7).

All the phenomena described above suggest that there is a remarkable resemblance between "oxidant A" and "oxidant B".

Summary

(1) By aerial oxidation of aniline catalyzed by cuprous chloride in a pyridine solution, azobenzene of about 60% is

6) J. F. Pudivin et al., *J. Am. Chem. Soc.*, **78**, 2104 (1956).
7) D. L. Leussing et al., ibid., **79**, 4270 (1957).

produced. In this reaction, the actual oxidant may be considered "oxidant A" which is produced by aerial oxidation of cuprous chloride pyridine complex.

(2) Hydroxy cupric chloride pyridine complex, a reaction product of cupric chloride pyridine complex with a methyl alcohol solution of potassium hydroxide, has a similar catalytic activity.

(3) These two complexes are to be considered strong bases.

(4) These two complexes have a remarkable resemblance to each other.

The author wishes to express his sincere gratitude to Professor Ryozo Goto for his invaluable advice and unfailing encouragement of this work.

Laboratory of Chemistry
School of General Studies
Kyoto University
Sakyo-ku, Kyoto

*On the Mechanism of Oxidation by Cuprous Chloride, Pyridine and Air. II. The Mechanism of Formation of Azobenzene from Aniline**

By Keizō KINOSHITA

(Received September 30, 1958)

Terent'ev et al.[1] reported that when aerial oxidation of aniline was carried out in a pyridine solution catalyzed by cuprous chloride, azobenzene was obtained in a good yield. In Part I of this series, the details of this reaction were studied and it was considered that the actual oxidant of this oxidation was "oxidant A" obtained by aerial oxidation of cuprous chloride pyridine complex[2]. In this paper, the mechanism of this reaction is discussed.

Experimental

Materials.—Aniline (b. p. 184~185°C), *o*-toluidine (b. p. 199~200°C) and *o*-anisidine (b. p. 225°C) were redistilled immediately before use. Extra chemical pure grade *p*-toluidine (m. p. 44~45°C) and *p*-anisidine (m. p. 56~57°C) were used. Cuprous acetate pyridine complex was prepared as follows. When cupric acetate (3.8 g., 2/100 mol.) in pyridine (50 cc.) was refluxed for 2 hr., deep blue crystals were formed (cupric acetate pyridine complex). A mixture of metallic copper (0.5 g. excess) and the above pyridine solution of cupric acetate pyridine complex was stirred at 60°C in a stream of nitrogen until the color of the solution was turned to dark yellow.

(1) Attempted Aerial Oxidation of Aniline Catalyzed by the Copper Acetate Complexes.—(a) A mixture of aniline (2.0 g., 2.2/100 mol.) and the above-mentioned cuprous acetate pyridine complex in pyridine was stirred for 5 hr. at 30°C in a stream of air. The resulting mixture was acidified with 6N-H_2SO_4, and extracted with ether (500 cc.). After removal of the ether, a trace of residue was obtained. The residue was dissolved with light petroleum (b. p. 40~60°C) and chromatographed on activated alumina (Wako Pure Chemical Industries, Ltd.). All the substance remained on top of the activated alumina. No azobenzene was obtained. The color of the aqueous layer was blue.

(b) Potassium hydroxide (1.1 g., 2/100 mol.) in methyl alcohol (10 cc.) was added to a cupric acetate pyridine complex in pyridine (described in the preparation of cuprous acetate pyridine complex). A mixture of aniline (2.0g., 2.2/100 mol.) and the resulting copper complex was stirred at 80°C for 5 hr. in a stream of air. The resulting mixture was treated as in Experiment 1a. The same results as in Experiment 1a were obtained.

(2) Oxidation of Substituted Anilines.—(a) A mixture of *p*-toluidine (2.2 g., 2/100 mol.), cuprous chloride (2.0 g., 1/100 mol.) and pyridine (50 cc.) was stirred for 5 hr. at room temperature in a stream of air. The resulting mixture was acidified with 6N-H_2SO_4, and extracted with ether (500 cc.). After removal of the ether, the residue was dissolved with benzene, and chromatographed on activated alumina. 4,4'azotoluene (2.0 g., 90%) was obtained; m. p. 142~143°C (Lit. 143°C). It was identified with 4,4'azotoluene by a mixed melting point determination and an analysis.

Anal. Found: C, 80.10; H, 6.92; N, 13.16.

* The present work was presented at the Symposium on the Mechanism of Organic Chemical Reaction of the Chemical Society of Japan, held at Nagoya in October, 1957.

1) A. P. Terent'ev et al., *Doklady Akad. Nauk, U. S. S. R.*, **1955**, 91—93. [*Chem. Abstr.*, **50**, 4807 (1956).]

2) K. Kinoshita, Part I of this series in This Bulletin, **32**, 777 (1959).

Calcd. for $C_{14}H_{14}N_2$: C, 80.00; H, 6.66; N, 13.33%.

A trace of black substance remained on top of the activated alumina.

(b) A mixture of *p*-anisidine (2.5 g., 2/100 mol.), cuprous chloride (2.0 g., 1/100 mol.) and pyridine (50 cc.) was treated as in Experiment 2a. 4,4'Azoanisol (2.2 g., 88%) was obtained; m. p. 162~163°C (Lit. 163°C). It was identified with 4,4'azoanisol by a mixed melting point determination and an analysis.

Anal. Found: C, 69.54; H, 5.96; N, 11.47. Calcd. for $C_{14}H_{14}O_2N_2$: C, 69.42; H, 5.78; N, 11.57%.

A trace of black substance remained on top of the activated alumina.

(c) A mixture of *o*-toluidine (2.2 g., 2/100 mol.), cuprous chloride (2.0 g., 1/100 mol.) and pyridine (50 cc.) was treated as in Experiment 2a. The resulting mixture was acidified with 6N-H_2SO_4, and extracted with ether (500 cc.). After removal of the ether, the residue was distilled with steam; then a large amount of substance remained in the vessel. From the distillate 2,2'-azotoluene (0.3 g., 14%) was obtained; m. p. 54~55°C (Lit. 55°C). It was identified with 2,2'-azotoluene by a mixed melting point determination and an analysis.

Anal. Found: C, 79.93; H, 6.89; N, 13.19. Calcd. for $C_{14}H_{14}N_2$: C, 80.00; H, 6.66; N, 13.33%.

The aqueous layer was dark violet.

(d) A mixture of *o*-anisidine (2.5 g., 2/100 mol.), cuprous chloride (2.0 g., 1/100 mol.) and pyridine (50 cc.) was treated as in Experiment 2a. 2,2'-Azoanisol (0.4 g., 16%) was obtained; m. p. 153~154°C (Lit. 153°C). It was identified with 2,2'-azoanisol by a mixed melting point determination and an analysis.

Anal. Found: C, 69.41; H, 5.98; N, 11.44. Calcd. for $C_{14}H_{14}O_2N_2$: C, 69.42; H, 5.78; N, 11.57%.

A large amount of substance remained on the activated alumina. There were some substances which did not dissolve in ether. The color of the aqueous layer was dark violet.

(3) Oxidation of Hydrazobenzene. — Cuprous chloride (2.0 g., 1/100 mol.) in pyridine (50 cc.) was oxidized with air for 2 hr. at room temperature. When hydrazobenzene (2.0 g., 1.1/100 mol.) was added to the resulting copper complex, the color of the solution was turned to yellow. The yellow solution was stirred for 1 hr. at room temperature in a stream of air. From the resulting mixture azobenzene (1.9 g., 95%) was obtained; melted at 67~68°C alone or with an authentic sample of azobenzene.

(4) Competitive Oxidation of Aniline and *p*-Anisidine.—A mixture of aniline (3.6 g., 4/100 mol.), *p*-anisidine (5.0 g., 4/100 ml.), cuprous chloride (1.0 g., 1/200 mol.) and pyridine (50 cc.) was stirred at room temperature in a stream of air. The resulting mixture was acidified with 6N-H_2SO_4 and filtered. The residue was continuously extracted for 24 hr. with light petroleum (b. p. 40~60°C, 100 cc.). A trace of black substance remained. From the extract 4,4'azoanisol was separated; this melted at 163~164°C alone or with an authentic sample of 4,4'azoanisol. When the reaction was carried out for 30 min. and 60 min., the obtained 4,4'azoanisol amounted to 1.2 g. and 2.3 g. respectively, and the residues, after removal of the mother liquor, were 0.1 g. and 0.2 g., respectively.

Results and Discussion

Since it was reported that the chlorine ion in cupric chloride complexes was easily substituted[3], chlorine ion in "oxidant A" I may also be substituted by aniline or methyl alcohol (Reactions 1 and 2). On the other hand, acetate ion in cupric acetate complexes may not be substituted easily by the above compounds (Ref. 3).

$$\underset{}{C_6H_5NH_2} + \underset{}{Cu(II)\text{-}Cl} \rightleftarrows \underset{II}{[C_6H_5NH_2Cu(II)]^+Cl^-} \quad (1)$$
$$\quad\quad\quad

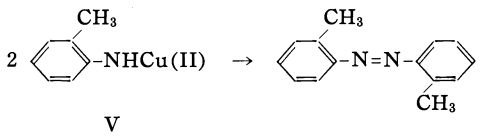
$$\underset{\text{II}}{[\text{Cu(II)-NH}_2\text{C}_6\text{H}_5]^+\text{Cl}^-} \rightarrow \underset{\text{I}}{\text{Cu(II)-Cl}} + \underset{\text{III}}{\text{NHC}_6\text{H}_5} \quad (3)$$

By aerial oxidation of an equimolar mixture of aniline and *p*-anisidine catalyzed by a small amount of cuprous chloride, 4,4'azoanisol is selectively obtained in the early stage of this reaction (Experiment 4). This result suggests that IV reacts with another IV to produce 4,4'azoanisol (Reaction 4), because the reaction between IV and free amines, may accompany 4-methoxy azobenzene with 4,4'azoanisol, even in the early stage of this reaction.

$$2\ \underset{\text{IV}}{(p\text{-})\text{CH}_3\text{OC}_6\text{H}_4\text{NH-Cu(II)}} \rightarrow (p\text{-})\text{CH}_3\text{OC}_6\text{H}_4\text{N=NC}_6\text{H}_4\text{OCH}_3(p\text{-}) \quad (4)$$

By aerial oxidation catalyzed by cuprous chloride in a pyridine solution, *p*-toluidine and *p*-anisidine are converted into the corresponding azo compounds almost quantitatively, while *o*-toluidine and *o*-anisidine are converted into the corresponding azo compounds only in a poor yield, although many other products are formed besides the azo compounds (Table II).

It was reported that the yield of azo compounds from substituted anilines were hardly affected at all by the position of the substituents in these amines, if these azo compounds were produced from the dimerisation of intermediate free radicals[5,6]. On the other hand, the steric hindrance of ortho substituent in V may interfere with the approach of two nitrogen atoms to decrease the yield of 2,2'-azotoluene,



V (5)

if 2,2'azotoluene is produced from a reaction of V with another V, (Reaction 5). The experimental results prove this to be valid.

Hydrazobenzene is converted into azobenzene almost quantitatively, by aerial oxidation catalyzed by "oxidant A" in a pyridine solution (Experiment 3). Accordingly, it is reasonable to assume that III is converted primarily into hydrazobenzene, which is further oxidized to azobenzene[5,6].

$$2\ \underset{\text{III}}{\text{C}_6\text{H}_5\text{NH-Cu(II)}} \rightarrow \text{C}_6\text{H}_5\text{NH-NHC}_6\text{H}_5 \rightarrow \text{C}_6\text{H}_5\text{N=NC}_6\text{H}_5 \quad (6)$$

In a pyridine solution, it was reported that cuprous salts and complexes increased in their stability[7]. Consequently, the activated complex may be as VI[8]. By the reaction of VI with another VI, hydrazobenzene and cuprous complex are produced. Hydrazobenzene is further oxidized to azobenzen (Reaction 7).

$$\underset{\text{III}}{\text{C}_6\text{H}_5\text{NH-Cu(II)}} \rightleftarrows \underset{\text{VI}}{[\text{Cu(I)-}\dot{\text{N}}\text{HC}_6\text{H}_5]}$$

$$2\ [\text{Cu(I)-}\dot{\text{N}}\text{HC}_6\text{H}_5] \rightarrow \text{C}_6\text{H}_5\text{NH-NHC}_6\text{H}_5 + 2\ \text{Cu(I)}$$

$$\text{C}_6\text{H}_5\text{NH-NHC}_6\text{H}_5 \rightarrow \text{C}_6\text{H}_5\text{N=NC}_6\text{H}_5 \quad (7)$$

TABLE II. OXIDATION OF SUBSTITUTED ANILINES

Amine g.(mol.)	Cu_2Cl_2 g.(mol.)	Time (hr.)	Azocompound g. (%)
p-Toluidine 2.2(2/100)	2.0(1/100)	5	4,4'Azotoluene 2.0 (90)
p-Anisidine 2.5(2/100)	2.0(1/100)	5	4,4'Azoanisol 2.2 (88)
o-Toluidine 2.2(2/100)	2.0(1/100)	5	2,2'Azotoluene 0.3 (14)
o-Toluidine 4.4(4/100)	4.0(2/100)	6	2,2'Azotoluene 0.8 (18)
o-Toluidine 8.8(8/100)	8.0(4/100)	8	2,2'Azotoluene 1.7 (20)
o-Anisidine 2.5(2/100)	2.0(1/100)	5	2,2'Azoanisol 0.4 (16)
p-Toluidine 1.1(1/100)	2.0(1/100)*	5	4,4'Azotoluene** 0.5
o-Anisidine 2.5(2/100)	4.0(2/100)*	20	2,2'Azoanisol** 0.2

* "Oxidant A" was used.
** Absence of air.

Summary

(1) Attempted aerial oxidation of aniline, catalyzed by cuprous acetate pyridine complex, is unsuccessful even at 80°C.

(2) By the aerial oxidation of equimolar mixture of aniline and *p*-anisidine, catalyzed by a small amount of cuprous chloride, 4,4'azoanisol is selectively obtained in the early stage of this reaction.

(3) By the aerial oxidation catalyzed by cuprous chloride in a pyridine solution, the yields of the azo compounds, which are produced from *p*-toluidine and *p*-anisidine, are almost quantitative. On

5) K. H. Pausacker, *J. Chem. Soc.*, **1953**, 1989.
6) K. H. Pausacker et al., ibid., **1954**, 4003.
7) J. E. B. Landles, ibid., **1942**, 802.
8) R. E. Connick, *J. Phys. Chem.*, **56**, 21 (1952). In this remark, he described the activated complex in which oxidized cyanide ion was combined with $[Cu(CN)_3]^{2-}$ in the oxidation of cyanide ion with cupric ion.

the other hand, the yields of the azo compounds, which are produced from *o*-toluidine and *o*-anisidine, are very poor.

(4) In this reaction, it is postulated that an intermediate [Cu(II)–NHC_6H_5] is initially formed, and that hydrazobenzene and cuprous complex are produced by the bimolecular reaction of this intermediate.

(5) Hydrazobenzene is converted into azobenzene almost quantitatively under the same condition as aniline is oxidized.

The author wishes to express his sincere gratitude to Professor Ryozo Goto for his invaluable advice and unfailing encouragement of this work.

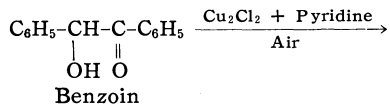
Laboratory of Chemistry
School of General Studies
Kyoto University
Sakyo-ku, Kyoto

*On the Mechanism of Oxidation by Cuprous Chloride, Pyridine and Air. III. On the Mechanism of Oxidative Cleavage of Benzil, α-Methyl Benzoin and Hydrobenzoin**

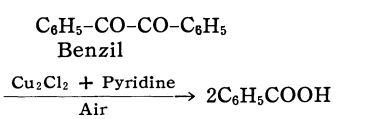
By Keizō KINOSHITA

(Received September 30, 1958)

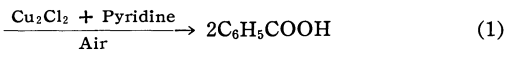
An earlier work reported that by aerial oxidation catalyzed by cuprous chloride in a pyridine solution, benzoin, benzil, α-methyl benzoin and hydrobenzoin were oxidized to break down as follows[1].



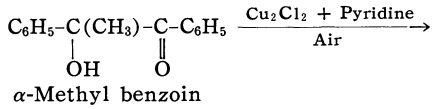
Benzoin



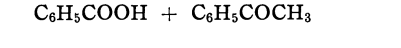
Benzil



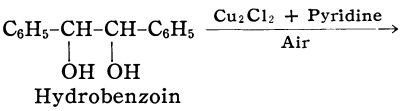
(1)



α-Methyl benzoin



(2)



Hydrobenzoin



(3)

It was also discovered that in these reactions, the actual oxidant was " oxidant A " which was produced by aerial oxidation of cuprous chloride pyridine complex[2]. In this paper, the mechanism of oxidative cleavage of the above compounds is discussed.

Experimental

Materials.—Benzil was prepared by oxidation of benzoin with nitric acid, and recrystallized from alcohol, m.p. 94～95°C[4]. α-Methyl benzoin was prepared by reaction of benzil with methyl magnesium iodide, and recrystallized from ligroin (b.p. 80～100°C), m.p. 90～91°C[5]. Hydrobenzoin was prepared by reduction of benzoin with aluminum *iso*-propylate, and recrystallized from aqueous alcohol, m.p. 135～136°C[6].

(1) Preparation of Catalysts.—(a) " Oxidant A ": Cuprous chloride (4.0 g., 2/100 mol.) in pyridine (50 cc.) was oxidized with air for 2 hr. at room temperature.

(b) " Oxidant B ": Potassium hydroxide (2.2 g., 4/100 mol.) in methyl alcohol (50 cc.) was added with stirring to cupric chloride pyridine complex (prepared from $CuCl_2 \cdot 2H_2O$ (6.8 g., 4/100 mol.) and pyridine (50 cc.)).

(c) " Oxidant C ": Cuprous acetate pyridine complex[3] (prepared from $Cu(OAc)_2 \cdot H_2O$ (3.8 g., 2/100 mol.) and pyridine (50 cc.)), was oxidized with air for 2 hr. at room temperature.

(d) " Oxidant D ": Potassium hydroxide

* The present work was presented at the Symposium on the Mechanism of Organic Chemical Reaction of the Chemical Society of Japan, held at Sendai in October, 1956.

1) K. Kinoshita, *J. Chem. Soc. Japan, Pure Chem. Sec.* (*Nippon Kagaku Zasshi*), **75**, 48 (1954).

2) K. Kinoshita. ibid., **75**, 175 (1954).

3) K. Kinoshita, Part II of this series in This Bulletin, **32**, 780 (1952).

4) R. Adams, "Organic Synthesis", Vol. I, John Wiley & Sons, Inc., New York (1921), p. 25.

5) R. Nodzu et al., *J. Chem. Soc. Japan* (*Nippon Kagaku Kaishi*), **59**, 1237 (1938).

6) H. Lunde, *Ber.*, **70**, 1520 (1937).

(2.2 g., 4/100 mol.) in methyl alcohol (50 cc.) was added with stirring to cupric acetate pyridine complex (prepared from $Cu(OAc)_2 \cdot H_2O$, (7.6 g., 4/100 mol.) and pyridine (50 cc.)).

(2) Oxidation of Benzil.—(a) When methyl alcohol (50 cc.) was added to "oxidant A", the color of the solution turned to green. A mixture of benzil (2.0 g., 1/100 mol.) and the greenish solution was stirred at 30°C for 2 hr. in a stream of air. The resulting mixture was acidified with 6N-H_2SO_4, and extracted with ether (500 cc.). The ethereal layer was washed with water and extracted with aqueous sodium carbonate solution. After removal of the ether, a trace of the substance remained. The sodium carbonate solution was acidified with 6N-H_2SO_4, and extracted with ether (500 cc.). After removal of the ether, the residue was sublimed to give benzoic acid (2.1 g., 86%); it melted at 121~122°C alone or with an authentic sample of benzoic acid.

The same results were obtained with "oxidant C" or "oxidant D" in place of "oxidant A".

(b) When trimethylamine hydrochloride (7.8 g., 6/100 mol.) was added to "oxidant C or D", trimethylamine was separated, and dark blue needles appeared. The mixture of benzil (2.0 g., 1/100 mol.) and the resulting complex was treated as above. No benzoic acid was obtained. Benzil 1.8 g., 90%) was recovered; it melted at 94~95°C alone or with an authentic sample of benzil.

(3) Oxidation of Hydrobenzoin.—(a) A mixture of hydrobenzoin (2.0 g., 1/100 mol.), methyl alcohol (10 cc.) and "oxidant A" (prepared from Cu_2Cl_2 (2.0 g., 1/100 mol.)) was stirred at 30°C for 4 hr. in a stream of air. The resulting mixture was acidified with 6N-H_2SO_4, and extracted with ether (500 cc.). The ethereal layer was washed with water, and extracted with aqueous sodium carbonate solution. After removal of the ether, the residue was treated with aqueous sodium hydrogen sulfite solution. The mixture was filtered. The precipitate was washed with water and dried. Hydrobenzoin (1.3 g., 65%) was recovered; m.p. 135~136°C, its melting point was not depressed on admixing with an authentic sample. From the sodium hydrogen sulfite solution, benzaldehyde phenyl hydrazone (0.8 g., 20%) was obtained; m.p. 155~156°C (Lit. 156°C). It was identified with benzaldehyde phenyl hydrazone by a mixed melting point determination and an analysis.

Anal. Found: C, 79.36; H, 6.38; N, 14.32. Calcd. for $C_{13}H_{12}N_2$: C, 79.59; H, 6.12; N, 14.28%.

From the sodium carbonate solution, a trace of benzoic acid was obtained. It was identified by converting it into salicylic acid[7].

(b) A mixture of hydrobenzoin (2.0 g., 1/100 mol.) and "oxidant C or D" was stirred for 4 hr. in a stream of air. Although the oxidation was attempted at 30, 60 and 80°C, no oxidation products were obtained, and hydrobenzoin (1.8 g., 90%) was recovered; it melted at 135~136°C alone or with an authentic sample of hydrobenzoin.

(4) Reaction of Cupric Chloride with Hydrobenzoin in the Presence of Potassium Hydroxide. — When cupric chloride (1.7 g., 1/100 mol.) in methyl alcohol (20 cc.) was added to a mixture of hydrobenzoin (4.0 g., 2/100 mol.), potassium hydroxide (2.8 g., 5/100 mol.), pyridine (20 cc.) and methyl alcohol (20 cc.), a deep blue solution was formed. When ethylene glycol was used in place of hydrobenzoin, a similar result was obtained. But in the absence of such glycols, brown precipitate appeared. Even after this deep blue solution was kept for 24 hr. room temperature, cuprous oxide did not appear.

(5) Oxidation of α-Methyl Benzoin.—(a) A mixture of α-methyl benzoin (2.0 g., 0.8/100 mol.), "oxidant A" and methyl alcohol (50 cc.) was stirred at 30°C for 4 hr. in a stream of air. The resulting mixture was acidified with 6N-H_2SO_4, and extracted with ether (500 cc.). The ethereal layer was washed with water, and extracted with aqueous sodium carbonate solution. After removal of the ether, the residue was treated with aqueous semicarbazide hydrochloride and sodium acetate solution. The resulting mixture was filtered and washed with benzene. The residue was pure acetophenone semicarbazone (0.6 g., 40%); m. p. 197~198°C (Lit. 198°C). It was indentified with acetophenone semicarbazone by a mixed melting point determination and an analysis.

Anal. Found: C, 61.15; H, 6.52; N, 23.72. Calcd. for $C_9H_{11}ON_3$: C, 61.00; H, 6.25; N, 23.72%.

After removal of the benzene, the residue was recrystallized from ligroin (b. p. 80~100°C). α-Methyl benzoin (0.7 g., 35%) was recovered; m.p. 90~91°C, its melting point was not depressed on admixing with an authentic sample. From the sodium carbonate solution, benzoic acid (0.5 g., 50%) was obtained; it melted at 121~122°C alone or with an authentic sample of benzoic acid.

(b) A mixture of α-methyl benzoin (2.0 g., 0.8/100 mol.) and "oxidant C or D", was stirred for 4 hr. in a stream of air. Although the oxidation was attempted at 30, 60 and 80°C, no oxidation products were obtained, and α-methyl benzoin (1.7 g., 85%) was recovered, m.p. 90~91°C; its melting point was not depressed on admixing with an anthentic sample.

Results and Discussion

Cuprous acetate pyridine complex has a similar catalytic activity as cuprous chloride pyridine complex for aerial oxidation of benzil. Hydroxy cupric acetate pyridine complex (Experiment 1d) has a similar activity as cuprous acetate pyridine complex for these reactions (Experiment 2a). Furthermore, the oxidation of benzil is hardly retarded at all by an excess of methyl alcohol (Table I).

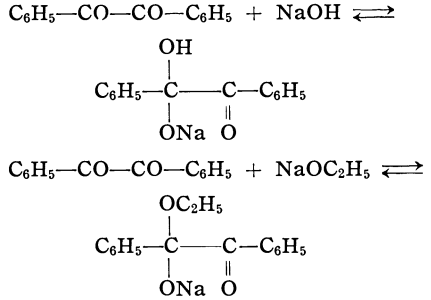
7) H. Meyer, "Nachweis und Bestimmung Organischer Verbindungen", Julius Springer, Wien (1933), p. 314.

TABLE I. EFFECT OF METHYL ALCOHOL ON THE OXIDATION OF BENZIL

Catalyst	Copper salt in the catalyst	Methyl alcohol	Benzoic acid
	g.	cc.	g. (%)
Oxidant A*	Cu_2Cl_2, 4.0	50	2.1 (86)
Oxidant A*	Cu_2Cl_2, 4.0	100	2.1 (86)
Oxidant B*	$CuCl_2 \cdot 2H_2O$, 6.8	50	2.0 (82)
Oxidant B*	$CuCl_2 \cdot 2H_2O$, 6.8	100	2.0 (82)

Benzil (2.0 g.) was treated.
* Cf. Experiment 1.

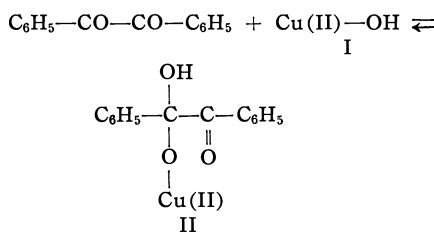
It was reported that strong bases were capable of combining to the keto group of benzil in alcohol[5,8]. (Reactions 4 and 5).



(4)

(5)

"Oxidant A, B, C** and D**" are belived to be strong bases[9]. Since "oxidant B" I is considered to have hydroxy group[9], it can also combine with benzil at its keto group to form II —— this addition reaction seems not to be easily retarded with an excess of methyl alcohol. Since "oxidant A" and "oxidant B" bear a remarkable resemblance, a similar intermediate may be produced by reaction of benzil with "oxidant A".



(6)

An attempt to oxidize hydrobenzoin by aerial oxidation catalyzed by "oxidant C" or "oxidant D" is unsuccessful even at 80°C. (Experiment 3b), although it is oxidized to benzaldehyde by aerial oxidation catalyzed by "oxidant A" or "oxidant B". Furthermore, an excess of methyl alcohol retards the oxidation (Table II).

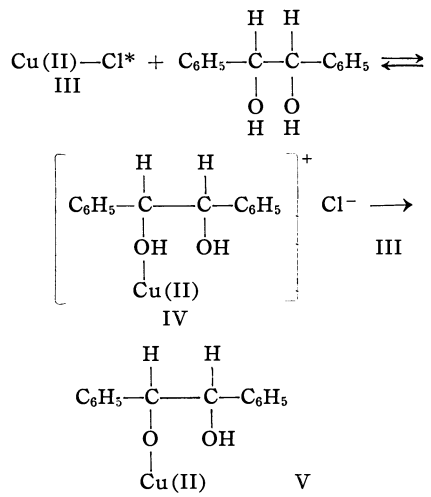
8) A. Lachmann, *J. Am. Chem. Soc.*, **45**, 1509 (1923).
** Cf. Experiment 1.
9) K. Kinoshita, Part I of this series in This Bulletin, **32**, 777 (1959).

TABLE II. EFFECT OF METHYL ALCOHOL ON THE OXIDATION OF HYDROBENZOIN

Catalyst	Methyl alcohol	Benzaldehyde	Benzoic acid	Sample (Recovered)
	cc.	g. (%)	g. (%)	g. (%)
Oxidant A*	0	1.0 (50)	0.1 (4)	0.6 (30)
Oxidant A*	10	0.4 (20)	trace	1.3 (65)
Oxidant A*	50	0.2 (10)	trace	1.5 (75)
Oxidant B**	10	0.5 (25)	trace	1.1 (55)
Oxidant B**	50	trace	trace	1.7 (85)

Hydrobenzoin (2.0 g.) was treated.
* Cu_2Cl_2, 2.0 g. ** $CuCl_2 \cdot 2H_2O$, 1.7 g.

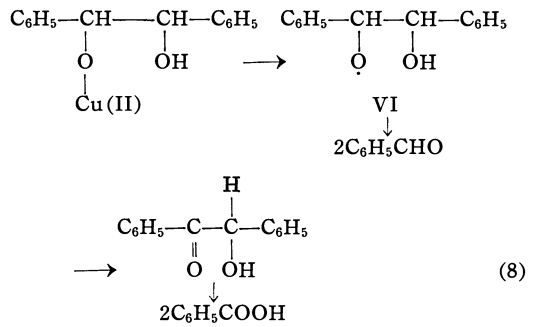
These results are similar to those obtained in the aerial oxidation of aniline[3]. Thus a similar intermediate to that postulated in the oxidation of aniline, may be produced (Reaction 7) (Ref. 3).



(7)

* Cu(II)-Cl stands for "oxidant A".

If V is converted directly into benzaldehyde, a free racidal such as VI would appear in this reaction.



(8)

On the one hand, VI seems to be converted into benzaldehyde. On the other hand, VI seems to be converted into benzoin, which is further oxidized to benzoic acid. Thus, if VI appears in this reaction, a good amount of benzoic acid may be

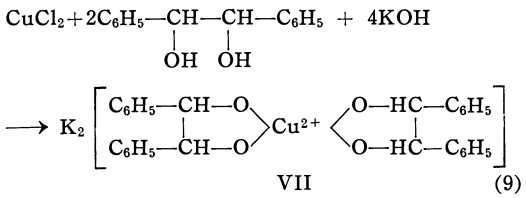
obtained. Since this assumption is not supported by the experimental results[1], it is postulated that such a free radical as VI hardly ever appears in this reaction. Moreover, if VI were intermediate, the stability of benzyl alcohol to "oxidant A" (Ref. 2) would be inexplicable.

Deep blue color is developed upon the addition of cupric chloride—methyl alcohol solution—to a mixture of hydrobenzoin and potassium hydroxide—pyridine-methyl alcohol solution (Experiment 4). For the following reason (1—3), this complex seems to be a chelate compound such as VII.

(1) In the absence of hydrobenzoin, this complex is never formed.

(2) In the presence of ethylene glycol in place of hydrobenzoin, a similar complex is formed.

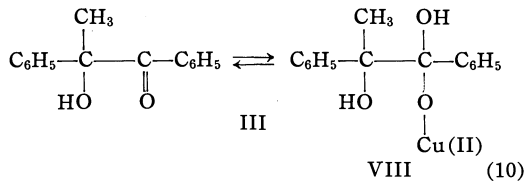
(3) It was reported that *bis*-glycolatocopper(II) complex was produced upon the addition of cupric nitrate to aqueous erythritol anhydride solution in the presence of sodium hydroxide[10].



VII (9)

Cuprous oxide does not appear even after 24 hr. from this deep blue solution and the formation of chelate compounds such as VII seems to have no effect upon the oxidation of hydrobenzoin.

Because strong bases can combine with the keto group of α-methyl benzoin in alcohol[5,11], an intermediate VIII may be produced by the reaction of α-methyl benzoin with "oxidant A" (Reaction 10).



III VIII (10)

However, α-methyl benzoin is not oxidized in aerial oxidation catalyzed by "oxidant C" or "oxidant D" (Experiment 5b). Furthermore, the oxidation of α-methyl benzoin is retarded by an excess of methyl alcohol (Table III).

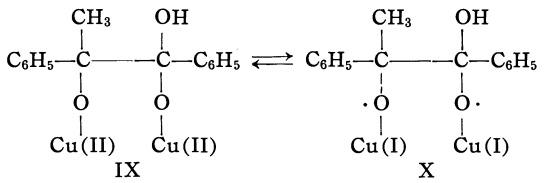
TABLE III. EFFECT OF METHYL ALCOHOL ON OXIDATION OF α-METHYL BENZOIN

Catalyst	Methyl alcohol	Benzoic acid	Aceto-phenone	Sample (Recovered)
	cc.	g. (%)	g. (%)	g. (%)
Oxidant A*	0	0.8 (80)	0.8 (80)	0.1 (5)
Oxidant A*	50	0.5 (50)	0.4 (40)	0.7 (35)
Oxidant A*	100	0.2 (20)	0.2 (20)	1.3 (65)
Oxidant B**	50	0.5 (50)	0.5 (50)	0.6 (30)
Oxidant B**	100	trace	trace	1.7 (85)

α-Methyl benzoin (2.0 g.) was treated.
* Cu_2Cl_2, 4.0 g. ** $CuCl_2 \cdot 2H_2O$, 6.8 g.

These results suggest that the hydroxy group of α-methyl benzoin in VIII must be combined with "oxidant A" to form IX.

The oxidative cleavage of IX probably takes place through activated complex X (Ref. 3). As two unpaired electrons are located on both oxygen atoms of α-methyl benzoin respectively in X, it causes a cleavage of α-methyl benzoin (Reaction 11)***.



IX X

$\longrightarrow C_6H_5COCH_3 + C_6H_5COOH + 2Cu(I)$ (11)

Benzil or hydrobenzoin may be oxidized under the same mechanism as described above.

In Part II, the mechanism of the formation of azobenzene in aerial oxidation of aniline catalyzed by cuprous chloride, was discussed[3]. It is believed that the copper-nitrogen linkage in oxidative dimerisation of aniline, is similarly situated to the copper-oxygen linkage in oxidative cleavage of α-methyl benzoin. Thus, the oxidative dimerisation of aniline and oxidative cleavage of α-methyl benzoin, are carried out through similar mechanism.

Summary

(1) Benzil is oxidized by aerial oxidation catalyzed by "oxidants A, B, C and D".

(2) α-Methyl benzoin or hydrobenzoin is oxidized by aerial oxidation catalyzed by "oxidants A and B" only. This reac-

10) H. B. Jonassen et al., *J. Am. Chem. Soc.*, **77**, 2667 (1955). Ref. L. Segal et al., ibid., **78**, 273 (1955): N. V. Sidgwick, "The Chemical Elements and their Compounds", Vol. I, Oxford University Press, London (1950), p. 171; W. Traube et al., *Ber.*, **69**, 2655 (1936).

11) D. B. Sharp et al., *J. Am. Chem. Soc.*, **74**, 5643 (1952).

*** Bawn et al. reported that the biradical with the structure ·CH-CH_2-CH_2-CH· has a strong tendency to break up the linkage between C(2) and C(3); E. H. Bawn et al., *Trans. Faraday Soc.*, **35**, 889 (1939).

tion is retarded by methyl alcohol.

(3) The mechanism of oxidative cleavage of benzil, α-methyl benzoin and hydrobenzoin, is described. It is also considered that the oxidative cleavage of benzil, α-methyl benzoin and hydrobenzoin, and the oxidative dimerisation of aniline[3] are carried out through similar mechanism.

The author wishes to express his sincere gratitude to Professor Ryozo Goto for his invaluable advice and unfailing encouragement of this work.

Laboratory of Chemistry
School of General Studies
Kyoto University
Sakyo-ku, Kyoto

Mild Oxidation of Alicyclic Secondary Amines. I. On Formation of Isonitrone from Perhydroquinoline Series

By Nobukatsu KATSUI and Yoshiyuki ICHINOHE

(Received October 28, 1958)

In recent years, a few papers concerning the nitrones of alicyclic secondary amines, especially piperidine[1,2] and pyrrolidine[3], have been reported. But the obtaining of isonitrone from alicyclic scondary amine has not yet been described. This paper reports on some of the isonitrones obtained from polycyclic compounds in the alicyclic secondary amine series.

Oxidation of *trans*-decahydroquinoline (I) with silver oxide in 30%-methanol solution at a temperature of 30~40°C gave a product, $C_9H_{15}ON$*, m.p. 280~282°C (IV). This product is different from a compound obtained by Witkop[5] from an air oxidation of I. Also from *cis*-decahydroquinoline (II), the same compound IV was obtained under the same condition. This compound was moreover formed by the treatment of I and II with 30%-hydrogen peroxide, perbenzoic acid, or with *N*-bromosuccinimide (NBS) although accompanied by the known hydroperoxide (XIV)[6].

This new substance (IV) was easily soluble in a polar solvent, but not in a non-polar one. In the infrared spectrum (in Nujol) of IV, the NH-stretching band at 2.96 μ which had been observed in that of *trans*-decahydroquinoline (I), disappeared. This compound IV had no unsaturated nature** and did not react with phenylisocyanate. It was reduced with sodium borohydride, sulfurous acid or with acidic potassium iodide, giving I in all cases.

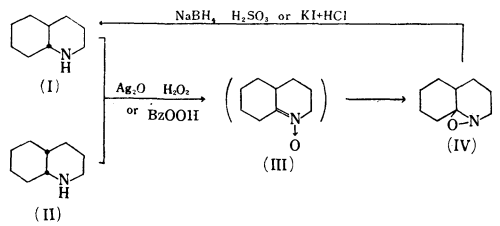


Fig. 1

When α-perhydroacridine (*trans-syn-trans*) (V)[7] was treated with 30%-hydroperoxide at room temperature for a week, it gave a crystalline product, $C_{13}H_{21}ON$*, (sublimed with decomposition at near 320°C) (VI). On the other hand, α-perhydrophenanthridine (*trans-anti-trans*) (VII)[8] reacted with silver oxide at a temperature of 90~100°C, producing a new

1) J. Thesing and H. Mayer, *Ber.*, **89**, 2159 (1956).
2) J. Thesing and H. Mayer, *Ann.*, **609**, 46 (1957).
3) R. F. C. Brown, V. M. Clark and Sir A. Todd, *Proc. Chem. Soc.*, **1957**, 97.
* It is well known that aromatic amine oxides do not appear to form definite hydrates[4a]. Henry and Leete[4b] have recently reported that gramine oxide has hydrogen peroxide of crystallization which is determined by iodometry. These new compounds, IV, VI and VIII, had hydrogen peroxide determined by the same method (described in experimental part).
4a) T. W. J. Taylor and W. Baker, "The Organic Chemistry of Nitrogen by Sidgwick", Oxford University Press, London (1937), p. 167.
4b) D. W. Henry and E. Leete, *J. Am. Chem. Soc.*, **79**, 5254 (1957).
5) B. Witkop, *Experientia*, **10**, 419 (1954).
6) L. A. Cohen and B. Witkop, *J. Am. Chem. Soc.*, **77**, 6575 (1955).

** The compound IV gave a negative test to bromine or tetranitromethane and decolorized only permanganate.
7) T. Masamune and S. Wakamatsu, *J. Chem. Soc. Japan, Pure Chem. Sec. (Nippon Kagaku Zasshi)*, **77**, 1145 (1956); *J. Fac. Sci. Hokkaido Univ. Ser. III. Chem.*, **5**, 47 (1957).
8) T. Masamune and Y. Kubota, *J. Chem. Soc. Japan, Pure Chem. Sec. (Nippon Kagaku Zasshi)*, **77**, 1468 (1956).

substance, $C_{13}H_{21}ON$*, (sublimed with decomposition at near 325°C) (VIII), although it did not react with hydrogen peroxide. Both compounds, VI and VIII, showed extreme susceptibility to reduction as well as IV, and the infrared absorption spectrum similar to that of IV. On the basis of these data, it seems reasonable to assume that these two products were derived by the reaction of the same type as that which occurred in decahydroquinoline.

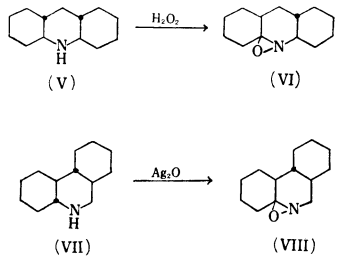


Fig. 2

In order to confirm the constitution of IV, VI and VIII, the compound IV was mainly examined since many oxidation products of decahydroquinoline have already been prepared and characterized in detail. *cis*-*N*-Benzoyldecahydroquinoline could be recovered unchanged after attempting silver oxide oxidation of it under various conditions, hence it would be expected that basic nitrogen is concerned in this reaction. On the other hand, the same product (IV) was obtained not only from *trans*(I), but also from *cis*(II) as described above. Therefore, it is considered that this reaction involves change in the nitrogen $C_{(9)}$ atoms.

As to the conversion of the bond between nitrogen and $C_{(9)}$ atom in decahydroquinoline, four possibilities are considered. The first is the formation of an *N*-hydroxyl derivative corresponding to that obtained from piperidine (IX)[9]. The second is the formation of a dimer corresponding to that produced from *N*-hydroxyl piperidine (X)[1]. The third is the formation of a nitrone and the fourth is the formation of an isonitrone***.

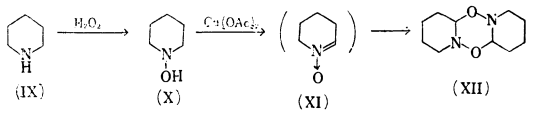


Fig. 3

(i) The new compounds, IV, VI and VIII, had no characteristic absorption of the hydroxyl group in the infrared spectra and IV did not react with phenylisocyanate as has been above mentioned. Therefore, no *N*-hydroxyl group is present in these compounds.

(ii) 1,4,2,5-Dioxa-diazine ring formed in the dimer (XII) has been reduced only by catalytic hydrogenation giving X, but not so with lithium aluminum hydride or with sulfurous acid. On the contrary, these compounds, IV, VI and VIII, were readily reduced with sodium borohydride or even with acidic potassium iodide. Hence the dimer as mentioned under the second possibility is not considered.

(iii) The new compounds, IV, VI and VIII, are similar to a nitrone in physical properties (i.e., in higher melting point or insolubility to non-polar solvents, etc.). These compounds however showed no ultraviolet absorption maxima at near 220~230 mμ[3,11,12] and no infrared absorption band at 6.25μ[12] probably due to the CN-double bond of nitrone. Therefore, it is not needful to consider the structure of nitrone for these compounds.

(iv) On the basis of these considerations three of the four possibilities described above are excluded; then the fourth is the most reasonable. It has been reported that isonitrone is readily reduced by acidic potassium iodide[11-13] and these compounds, IV, VI and VIII, also were reduced by the reagent as above mentioned. These compounds formed stable chloroplatinates although they did not form stable salts with some of the usual acids. The compound IV showed instability to any acidic reagent**** and to alkaline potassium ferricyanate[14]. As shown by these chemical behaviors, these new compounds were considered to be analogous with isonitrone. Krimm[12] reported recently that a characteristic band of isonitrone appears at near 7μ in the infrared

9) R. Wolffenstein, *Ber.*, **25**, 2777 (1892).

*** The isonitrone has a three membered ring consisting of nitrogen, oxygen and carbon atoms, and was recently named by Krimm[10]. Although the presence of this ring has been discussed for a long time, it has recently been synthesized from the Schiff base by means of hydrogen peroxide or peracetic acid. Emmons[11] suggested the name "oxazirane" for this compound.

10) H. Krimm and K. Hammann, cf. *Chem. Abstr.*, **51**, 3656 (1957).

11) W. D. Emmons, *J. Am. Chem. Soc.*, **78**, 6208 (1956).

12) H. Krimm, *Ber.*, **91**, 1057 (1958).

13) L. Horner and E. Jürgens, ibid., **90**, 2184 (1957).

**** When IV was treated with acetic anhydride it gave oily products which could not yet be characterized.

14) Oxidation of IV with alkaline potassium ferricyanate gave a neutral product, m. p. 56~57°C, which has not been characterized.

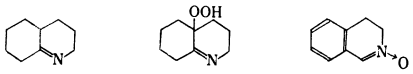
spectrum. Similar absorption was observed in these compounds, IV, VI and VIII. However, the settlement of the absorption[15] (due to near 7μ) will be deferred until more evidences are available on the various isonitrones.

In the course of the oxidation of decahydroquinoline, two pathways are considered reasonable.

i) Carbinol amine (as initial intermediate) is converted to the Schiff base by dehydration and then is further changed to isonitrone by the addition of oxygen.

ii) *N*-Hydroxyl amine (as initial intermediate) is converted to nitrone by dehydrogenation and then changed to isonitrone.

In the first case, the formation of carbinol amine has usually been observed in a reaction of tertiary amine with silver oxide[16a,b] or NBS reagent[16b]. It has been reported that the formed C(OH)–NH group is readily dehydrated to C=N-group[17]. Cohen and Witkop[6] have reported that 10-hydroperoxy-$\Delta^{1(9)}$-octahydroquinoline (XIV) is formed by the oxidation of $\Delta^{1(9)}$-octahydroquinoline (Schiff base) (XIII). Moreover, isonitrones have been obtained directly by oxidation of the Schiff base[10,11]. Accordingly, it is considered that the reaction of decahydroquinoline with silver oxide or NBS may proceed through the Schiff base stage (XIII) since the isonitrone (IV) was produced together with the hydroperoxide (XIV) in NBS oxidation as above mentioned.



(XIII) (XIV) (XV)

Fig. 4

In the second case, the formation of *N*-hydroxyl amine has commonly been observed in an oxidation of secondary amine with hydrogen peroxide[9] or perbenzoic acid[18]. It has been reported that further oxidation of *N*-hydroxylamine led to the corresponding nitrone by dehydrogenatian. If the nitrone (III) arose from the reaction of decahydroquinoline with hydrogen peroxide or perbenzoic acid, it has no stability because there is no conjugated double bond with nitrone group as shown in 3,4-dihydroisoquinoline-*N*-oxide (XV)[2]. Consequently, the nitrone (III) is converted to the corresponding isonitrone (IV). In this case, no formation of a dimer will result from a steric effect, although that point is not sure.

Further study of the other compounds related to isonitrone derived from alicyclic secondary amine series is in progress.

Experimental

Formation of Isonitrone (IV) from *trans*-Decahydroquinoline (I).—(i) *Oxidation with silver oxide.*—To a solution of 1 g. of *trans*-decahydroquinoline in 20 cc. of 30% aqueous methanol, silver oxide which was freshly prepared from 5 g. of silver nitrate was added. When the resulting suspension was warmed at 30~40°C, a silver mirror gradually formed. After 6 hr. the mixture was cooled and filtered. The methanol of the filtrate was removed under reduced pressure and the resulting aqueous solution was extracted with chloroform after being made alkaline with sodium hydroxide solution. Drying and concentration of the extract left a residue, from which 170 mg. of the product crystallized readily after the addition of ether. Unreacted *trans*-decahydroquinoline could be removed readily by means of addition of ether followed by filtration because of its great solubility in the solvent. The product insoluble in ether was recrystallized from a mixture of ethanol and ether as white needles, m.p. 280~282°C. This substance was readily soluble in polar solvents, i.e., alcohol, water or chloroform, but insoluble in non-polar solvents, i.e., ether, benzene or tetrahydrofurane. It could also be purified by sublimation at 200°C at 5 mm. and had hygroscopic property under high moisture, but did not show any change in the melting point even in that case. It could be heated over its melting points, and recovered unchanged. It formed an aurichloride, m.p. 126~127°C, and a chloroplatinate, m.p. 176~177°C.

In the infrared absorption spectrum (in Nujol) the substance showed peaks at 7.32, 7.46, 7.61, 7.80, 7.94, 8.27, 9.36, 9.53, 10.27, 10.35, 10.48, 10.81, 11.06, 11.30, 11.57, 11.86 and 12.04 μ.

Anal. Found: C, 60.72; H, 9.58; N, 7.43; H_2O_2, 13.70. Calcd. for $C_9H_{15}ON \cdot {}^3/_4\ H_2O_2$: C, 60.48; H, 9.31; N, 7.84; H_2O_2, 14.27%.

ii) *Oxidation with hydrogen peroxide.*—When a suspension of 1 g. of *trans*-decahydroquinoline in 20 cc. of 30%-hydrogen peroxide solution was left at room temperature, *trans*-decahydroquinoline dissolved during the course of the reaction and a deep orange-yellow color gradually developed. After 3 days the reaction mixture was made alkaline with concentrated ammonium hydroxide solution under cooling with water. The alkaline

15) It has been reported that the N-O-stretching vibration in amine oxide shows at near 10.6~10.8μ [R. Mathis Noel et al. *Compt rend.*, **242**, 1873 (1956)], and the characteristic absorption of grouping -O-C-N in oxazolidine ring displays at 8.63, 8.92 and 9.06μ, respectively [E. D. Bergmann, *Chem. Rev.*, **53**, 326 (1953)].

16a) H. Suginome and K. Ohno, *J. Fac. Sci. Hokkaido Univ. Ser. III Chem.*, **4**, 36 (1950).

16b) O. E. Edwards, F. H. Clarke and B. Douglas, *Can. J. Chem.* **32**, 235 (1954).

17) D. H. R. Barton, *J. Chem. Soc.*, **1953**, 1027.

18) M. A. T. Rogers, ibid., **1955**, 769.

solution obtained was extracted with chloroform in as short a time as possible; the extract was washed with water and then dried with sodium sulfate. The residue that remained after evaporation of the solvent crystallized on the addition of ether. The product (185 mg.) was recrystallized from a mixture of ethanol and ether and melted at 280~282°C. It was proved to be identical (mixed melting point and comparison of infrared absorption spectra) with the product from the silver oxide oxidation.

iii) *Oxidation with perbenzoic acid.*—A solution of 100 mg. of *trans*-decahydroquinoline in 100 cc. of chloroform was treated with 150 mg. of perbenzoic acid for a day at room temperature. After this treatment, the chloroform solution afforded 13 mg. of a product which melted at 280~282°C after recrystallization and was proved to be identical also with the product obtained by the oxidation with silver oxide.

iv) *Oxidation with N-bromosuccimide (NBS).*—A solution of 1 g. of *trans*-decahydroquinoline in 40 cc. of acetone containing 10 cc. of water was treated with 1.28 g. of NBS overnight in an atmosphere of nitrogen at room temperature. The solution was then refluxed in a stream of nitrogen for 20 min. After removal of the acetone under reduced pressure the aqueous solution was extracted with ether. The ethereal extract was subjected successively to drying, removal of the solvent and distillation in vacuo. The distillate obtained at 52~53°C at 5 mmHg consisted mainly of unreacted *trans*-decahydroquinoline. The distillate obtained above the temperature of 52~53°C deposited as needle crystals on being allowed to stand in an ice box cooled at −5°C. Separation by filtration and recrystallization from ethyl acetate led to a product which melted at 96~98°C, and was positive to the starch-potassium iodide test. Its crystal form changed from needle to plate on standing. From these properties the product appeared to be identical with 10-hydroperoxy-$\Delta^{1(9)}$-octahydroquinoline, but it was necessary to carry out a further investigation for the identification because of the shortage of the material. On standing for several weeks the mother liquor of the above crystals deposited a further amount of crystals. This compound had m.p. 280~282°C after recrystallization from a mixture of ethanol and ether. It showed no depression on admixture with isonitrone (IV) obtained by the oxidation with silver oxide.

Formation of Isonitrone (IV) from *cis*-Decahyhdroquinoline (II).—When *cis*-decahydroquinoline was treated with silver oxide or hydrogen peroxide under the same conditions as *trans*-decahydroquinoline was, it produced the same isonitrone (IV) which was confirmed by the mixed melting point method and the comparison of infrared spectra.

Action of Silver Oxide on *cis*-*N*-Benzoyl-decahydroquinoline.—*cis*-*N*-Benzoyl-decahydroquinoline was nearly inert to the reagent at 30~40°C under the conditions as described under oxidation of *trans*-decahydroquinoline. Furthermore, the compound proved to be inert to silver oxide even at 80~90°C in aqueous methanol.

Reduction of Isonitrone (IV).—i) *Reduction with sodium borohydride.*—A solution of 10 mg. of sodium borohydride in 2 cc. of methanol was added to a solution of 40 mg. of isonitrone (IV) in 2 cc. of methanol under cooling with water. After having been heated for 30 min. on a steam bath, the solution was concentrated to near dryness under reduced pressure. The residue was then taken up in ether, washed with water, dried and evaporated to dryness. There were thus obtained 34 mg. of crystals which were recrystallized from petroleum ether, m.p. 46~48°C, and proved identical with *trans*-decahydroquinoline[19] by mixed melting point not only as free base but also as hydrochloride.

ii) *Reduction with sulfurous acid.*—Sulfur dioxide was saturated into a solution of 50 mg. of isonitrone (IV) in 5 cc. of water under cooling with water. After being kept for two days the resulting solution was alkalized with sodium carbonate solution and extracted with chloroform. After drying, evaporation of the extract left a residue which crystallized on standing for a few hours, giving 23 mg. of the product. On recrystallization from petroleum ether the product melted at 46~48°C and was proved identical with *trans*-decahydroquinoline.

iii) *Reduction with acidic potassium iodide.*—To a solution of 82 mg. of isonitrone (IV) in 1 cc. of 2 N-hydrochloric acid was added 1 cc. of an aqueous solution saturated with potassium iodide. On standing at room temperature iodine was gradually separated. After being kept overnight the mixture was concentrated to a syrup in a desiccator under reduced pressure and methanol was then added. Evaporation of the methanolic solution from which inorganic salt was removed by filtration left 12 mg. of a product. On washing with ether and recrystallization from a mixture of ethylacetate and chloroform, the product melted at 274~278°C and showed no depression of the melting point by admixture with *trans*-decahydroquinoline hydrochloride.

Action of Phenylisocyanate on Isonitrone (IV).—Isonitrone (IV) did not react with phenylisocyanate in dioxane on treatment for 16 hr. at room temperature.

Oxidation of α-Perhydroacridine with Hydrogen Peroxide.—A half g. of α-perhydroacridine was treated with an excess of 30% hydrogen peroxide solution at room temperature for a week. The reaction mixture gradually colored orange-yellow. The solution was made alkaline with sodium hydroxide solution under cooling with cold water and extracted with chloroform as quickly as possible. The resulting chloroform extract was washed once with water, then dried (sodium sulfate) and concentrated to dryness. On treatment with ether, the crystals could be separated into soluble and insoluble parts for the solvent. The soluble

19) Cohen and Witkop[5] and Leonard et al. (*J. Am. Chem. Soc.*, 78, 3463 (1956)) reported that derivatives of $\Delta^{1(9)}$-octahydroquinoline were reduced to the *trans*-form of decahydroquinoline in good yields by lithium aluminum hydride reduction.

part was unchanged amine. The insoluble part was recrystallized from a mixture of chloroform-ethanol as thin plates, giving 230 mg. of the product, isonitrone (VI), which sublimed with decomposition at near 320°C. This isonitrone was completely insoluble in a non-polar solvent, less soluble in water and alcohol, and more soluble in chloroform. The VI formed a chloroplatinate, m. p. 248~250°C (decomp.) In the infrared absorption spectrum (in Nujol) the substance showed peaks at 7.32, 7.46, 7.61, 7.80, 7.96, 8.17, 8.27, 8.46, 9.12, 9.56, 9.72, 10.09, 10.35, 10.50, 10.81, 11.04 and 11.91 μ.

Anal. Found: C, 67.36; H, 10.10. Calcd. for $C_{13}H_{21}ON \cdot 3/4H_2O_2$: C, 67.06; H, 9.74%.

Oxidation of α-Perhydrophenanthridine (VII) with Silver Oxide.—A mixture of 0.5 g. of α-perhydrophenanthridine and silver oxide (freshly prepared from 2 g. of silver nitrate) in 3 cc. of methanol and 30 cc. of water was refluxed at 90~100°C on a steam bath for 3 hr. A silver mirror was gradually formed. The solids were removed by filtration and washed thoroughly with hot methanol. After removal of methanol from the combined filtrate and washings, the aqueous solution was made alkaline with sodium hydroxide solution, filtered and extracted with chloroform. On evaporation of the solvent after drying, the chloroform extract afforded crystals. Since the unchanged base (VII) was readily soluble in ether, it could be separated from the reaction product by the addition of ether. The insoluble ether part was recrystallized from a mixture of ethanol and ether as needles giving 318 mg. of the product, which sublimed with decomposition at near 325°C. The property of solubility in a polar solvent was closely like that of isonitrone (IV). This product (VIII) formed a chlorofolatinate; m.p. 228~229°C (resolidified at 121°C). In the infrared absorption spectrum (in Nujol) the substance showed peaks at 7.32, 7.46, 7.61, 7.78, 7.80, 8.17, 8.27, 8.44, 9.12, 9.58, 9.72, 10.02, 10.09, 10.35, 10.52, 10.81, 11.04 and 11.91 μ.

Anal. Found: C, 66.80; H, 9.79; H_2O_2, 11.26. Calcd. for $C_{13}H_{21}ON \cdot 3/4H_2O_2$: C, 67.06; H, 9.74; H_2O_2, 10.96%.

Reductions of Isonitrone, VI and VIII, with Sodium Borohydride.—The isonitrones, VI and VIII, were respectively reduced to the original bases, V and VII with sodium borohydride in a good yield by the same treatment as described under the reduction of isonitrone (IV).

The present research was conducted under the supervision of Professor Harusada Suginome, President of Hokkaido University. The authors are also deeply indebted to Mr. Tadashi Masamune for his interest and advice and for supplying the material.

Department of Chemistry
Faculty of Science
Hokkaido University
Sapporo

Studies on the Sapogenins of Dioscorea tokoro Makino. II[1]. *The Structure of Tokorogenin*

By Katsura MORITA

(Received November 4, 1958)

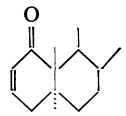
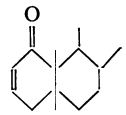
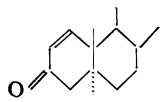
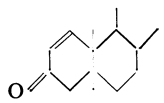
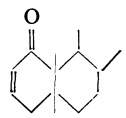
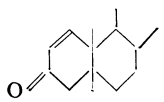
Although it was postulated that the three hydroxyl groups in tokorogenin are situated at positions 1, 2 and 3 of the steroid nucleus[2], their configuration and the nature of the A/B ring junction still remained unclarified. To make these points clear it was most desirable to establish a correlation of tokorogenin with a known sapogenin, which has been done as described in the present paper.

In the presence of a small amount of chlorosulfonic acid tokorogenin reacted with acetone and with cyclohexanone to give an isopropylidenetokorogenin (tokorogenin acetonide) and a cyclohexylidenetokorogenin, respectively. On treatment with pyridine and *p*-toluenesulfonyl chloride, the isopropylidenetokorogenin gave a tosylate, which on heating in 80% acetic acid solution furnished tokorogenin monotosylate. When the monotosylate was further treated with alkali in methanol, a crystalline, substance, soluble with difficulty, was obtained and analyzed as $C_{27}H_{42}O_4$. It was presumed to be an oxido-spirostanol,

1) This is a full paper of the previous communication (K. Morita, *Pharm. Bull.*, **5**, 494 (1957).), and constitutes Part IX of Nishikawa's paper entitled "Studies in Steroids". Part VIII: (K. Morita, This Bulletin, **32**, 476 (1959)).

2) Studies on the Sapogenins of *Dioscorea tokoro* Makino. I. (K. Morita, This Bulletin, **32**, 476 (1959).)

TABLE I

Chromophor	Substance	U. V. Spectra Max.	Log	Solvent	Ref. No
	5α-Cholest-2-en-1-one	224; 333	3.90; 1.75	C_2H_5OH	7)
	Methyl 1-keto-5β-eti-2-enate	225; 333	3.93; 1.96	C_2H_5OH	7), 8)
	Methyl 3-keto-5α-eti-1-enate	230; 323	4.07; 1.62	C_2H_5OH	7)
	Methyl 3-keto-5β-eti-1-enate	230; 323	4.12; 1.59	C_2H_5OH	9)
	25D-5β-Spirost-2-en-1-one (VII)	225; —	3.89; —	C_2H_5OH	*
	25D-5β-Spirost-1-en-3-one	232.5; —	3.99; —	C_2H_5OH	**

* This paper ** The subsequent report (Part III)

7) F. Sallman and Ch. Tamm, *Helv. Chim. Acta*, **39**, 1340 (1956).
8) W. Schlegel and Ch. Tamm, ibid., **40**, 160 (1957).
9) W. Schlegel, Ch. Tamm and T. Reichstein, ibid., **38**, 1013 (1955).

anhydrotokorogenin, from the reaction sequence. The anhydrotokorogenin gave a monoacetate and infrared absorption spectra exhibiting no characteristic band of the carbonyl group. It is, therefore, evident that the substance possesses a hydroxyl an oxido group. Oxidation of the anhydrotokorogenin with chromic anhydride-pyridine furnished a ketone, anhydrotokorogenone.

In the light of the structure of tokorogenin suggested in the previous paper[2] and the reaction sequence described above, the anhydrotokorogenone is either 2,3-oxido-spirostan-1-ol or 1,2-oxido-spirostan-3-ol. Since such an α,β-oxido-ketone has been known to undergo reduction with chromous chloride[3] giving the corresponding α,β-unsaturated ketone, the reaction was applied to the anhydrotokorogenone. As expected, anhydrotokorogenone gave an α,β-unsaturated ketone, which showed a specific U. V. absorption band at 225 mμ.

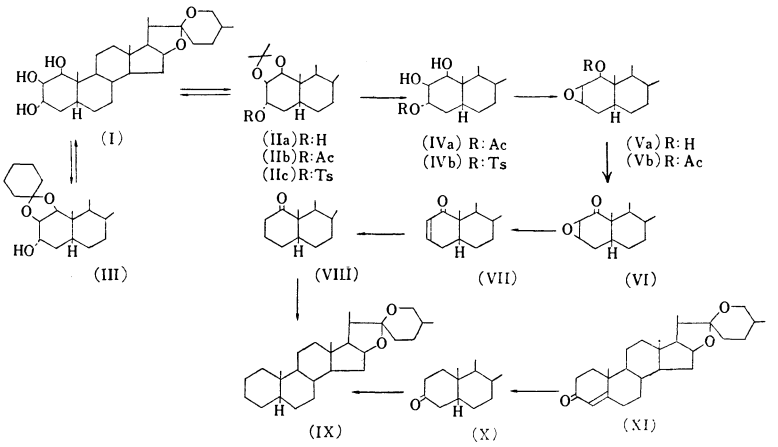
Catalytic hydrogenation of the α,β-unsaturated ketone furnished a saturated ketone, which showed marked depression of the melting point on admixture with smilagenone (X)[4]. Finally, the product from the Huang-Minlon reduction[5] of the saturated ketone proved to be identical with 25D-5β-spirostan (IX), prepared from smilagenone (X) by the known method[6]. The identity was established by the mixed melting point and the infrared absorption spectra.

The above reactions correlate tokorogenin with the known 25D-5β-spirostan (IX), and show that tokorogenin is an isosapogenin. Since the saturated ketone was not identical with smilagenone (X) as mentioned above, the structure 25D-5β-spirostan-1-one (VIII) has to be assigned to the saturated ketone from tokorogenin, and accordingly 25D-5β-spirost-2-en-1-one

3) W. Cole and P. L. Julian, *J. Org. Chem.*, **19**, 131 (1954).

4) The sample of smilagenone (X) was synthesized from diosgenin by Oppenauer oxidation followed by catalytic hydrogenation. C. Djerassi, R. Yashin and G. Rosenkranz, *J. Am. Chem. Soc.*, **74**, 422 (1952).
5) Huang-Minlon, ibid., **71**, 3301 (1949).
6) C. Djerassi and J. Fishman, ibid., **77**, 4291 (1955).

Chart 1



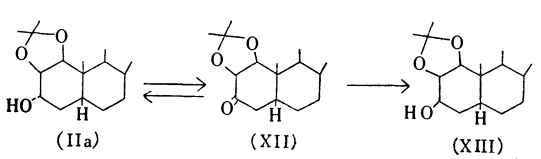
(VII) to the α,β-unsaturated ketone. These conclusions are further supported by the ultraviolet absorption spectrum of the α,β-unsaturated ketone (VII) which is in complete accord with those of known Δ^2-1-ketosteroids as shown in Table. I.

Thus, it is reasonable to assign the structure of $2\xi,3\xi$-oxido-25D-5β-spirostan-1-one to anhydrotokorogenone and that of $2\xi,3\xi$-oxido-25D-5β-spirostan-1ξ-ol to anhydrotokorogenin. Since the two hydroxyl groups in positions 1 and 2 in tokorogenin take part in the formation of the acetonide and therefore are *cis*-oriented, and the third in position 3 is *trans* to the other two, tokorogenin is either $1\alpha,2\alpha,3\beta$-triol or $1\beta,2\beta,3\alpha$-triol.

From the above arguments and on the basis of the assumption that the configuration of the hydroxyl group in position 3 of tokorogenin is α, all the reactions can be represented by the scheme shown in Chart 1.

Evidence for the α-configuration of the 3-hydroxyl group is given by the following experiment: Treatment of isopropylidenetokorogenin (IIa) with chromic anhydride-pyridine furnished isopropylidenetokorogenone (XII). Reduction of the ketone (XII) with lithium aluminum hydride gave a mixture of isopropylidenetokorogenin (IIa) and its C_3-epimer (XIII), which were separated by careful chromatography on Florisil, the latter being eluted first and then the former.

Chart 2



It has been generally accepted[8] that when a mixture of two epimeric steroidal alcohols is chromatographed, the one having an axial hydroxyl group moves more rapidly than the other. The above experiment, therefore, suggests that the 3-hydroxyl group in isopropylidenetokorogenin (IIa) is α-oriented (equatorial). In this way the structure of tokorogenin has been determined to be 25D-5β-spirostan-1β, $2\beta,3\alpha$-triol (I).

Experimental

Isopropylidenetokorogenin (Tokorogenin Acetonide) (IIa).—a) A suspension of 1 g. of tokorogenin (I) in 100 ml. of acetone containing 0.1 ml. of chlorosulfonic acid was vigorously stirred at room temperature for sixty minutes. When tokorogenin was dissolved and the acetonide was completely precipitated, the precipitates were collected, washed with ethanol and dried, m. p. 290~295°C. Yield, 1.0 g.

For analysis the substance was recrystallized from a large volume of hot methanol or dimethylformamide, m. p. 309~312°C.

Anal. Found: C, 73.50; H, 9.90. Calcd. for $C_{30}H_{48}O_5$: C, 73.73; H, 9.90%.

b) A solution of 100 mg. of tokorogenin in 100 ml. of acetone containing 50 mg. of *p*-toluenesulfonic acid was boiled under reflux for three hours and the solution was allowed to stand at room temperature overnight to separate fine needles of tokorogenin acetonide, m.p. 300~305°C, mixed m. p. with the above specimen, 305~309°C. When the acetonide was boiled in 80% acetic acid for several minutes and the solution was cooled, tokorogenin was precipitated in colorless needles melting at 273~275°C.

Cyclohexylidenetokorogenin (III).—Tokorogenin in cyclohexanone was treated with a few drops of chlorosulfonic acid under the conditions

described in the case of the acetonide. Recrystallization of the crude product from methanol furnished III melting at 288~290°C.

Anal. Found: C, 74.91; H, 10.04. Calcd. for $C_{33}H_{52}O_5$: C, 74.96; H, 9.91%.

When the cyclohexylidene compound (III) was boiled in ethanol containing a few drops of hydrochloric acid for one hour, tokorogenin was recovered.

Isopropylidenetokorogenin Acetate (IIb). — Isopropylidenetokorogenin (IIa) was acetylated by the usual means with pyridine and acetic anhydride to give the acetate (IIb), m. p. 207~208°C.

Anal. Found: C, 72.42; H, 9.70. Calcd. for $C_{32}H_{50}O_6$: C, 72.41; H, 9.50%.

Tokorogenin Monoacetate (IVa).—Isopropylidenetokorogenin acetate (IIb) was boiled in 80% acetic acid and the solution was cooled to separate colorless needles of tokorogenin monoacetate (IVa). The analytical sample recrystallized from methanol melted at 237~239°C.

Anal. Found: C, 70.75; H, 9.61. Calcd. for $C_{29}H_{46}O_6$: C, 70.98; H, 9.45%.

Isopropylidenetokorogenin Tosylate (IIc). —To a solution of 2.3 g. of isopropylidenetokorogenin (IIa) in 80 ml. of pyridine 5 g. of *p*-toluenesulfonyl chloride was added and the mixture was kept at 50°C for one hour and then at room temperature for two days. Then a large volume of water was added and the precipitate of the crude tosylate (IIc) was filtered, washed with water, and dried. Recrystallization from ether afforded colorless platelets melting at 198°C followed by immediate decomposition to a tar. Yield, 2.0 g.

Anal. Found: C, 68.94; H, 8.63. Calcd. for $C_{37}H_{54}O_7S$: C, 69.13; H, 8.47%.

Tokorogenin Monotosylate (IVb).—A suspension of 500 mg. of isopropylidenetokorogenin tosylate (IIc) in a small volume of 80% acetic acid was heated on a steam bath for twenty minutes till the solution became clear. The solution was then cooled to furnish colorless needles, m. p. 192°C (decomp.). Yield, 370 mg.

Anal. Found: C, 67.28; H, 7.96. Calcd. for $C_{34}H_{50}O_7S$: C, 67.75; H, 8.36%.

2β, 3β-Oxido-25D-5β-spirostan-1β-ol (Anhydrotokorogenin) (Va).—A methanol solution of 2.0 g. of potassium hydroxide was added to a solution of 1.0 g. of tokorogenin monotosylate (IVb) in 80 ml. of methanol and the solution was boiled under reflux for one hour and cooled. The hardly soluble crystalline solid was collected, washed with methanol, and dried, m. p. 237~239°C. Yield, 500 mg.

Anal. Found: C, 75.44; H, 9.88. Calcd. for $C_{27}H_{42}O_4$: C, 75.31; H, 9.83%.

2β, 3β-Oxido-25D-5β-spirostan-1β-ol Acetate (Vb). — A portion of 2β,3β-oxido-25D-5β-spirostan-1β-ol (Va) was acetylated by the usual means with pyridine and acetic anhydride to furnish the acetate (Vb) as colorless prisms melting at 246~249°C.

Anal. Found: C, 73.51; H, 9.49. Calcd. for $C_{29}H_{44}O_5$: C, 73.69; H, 9.38%.

2β, 3β-Oxido-25D-5β-spirostan-1-one (Anhydrotokorogenone) (VI). — To a solution of 800 mg. of 2β,3β-oxido-25D-5β-spirostan-1β-ol (Va) in 50 ml. of pyridine was added with vigorous stirring 1.0 g. of chromic anhydride in small portions. The reaction mixture was gradually heated to 40°C and was kept at this temperature for three hours and then at room temperature for twenty-four hours. Water was added and the mixture was extracted with ether. The ethereal solution was thoroughly washed and dried, and evaporation afforded 700 mg. of needles, m. p. 238~239°C, I. R. in Nujol λ_{max} 5.86 μ (1-c=o).

Anal. Found: C, 75.35; H, 9.40. Calcd. for $C_{27}H_{40}O_4$: C, 75.66; H, 9.41%.

25D-5β-Spirost-2-en-1-one (VII).—To a suspension of 650 mg. of 2β,3β-oxido-25D-5β-spirostan-1-one (VI) in 5 ml. of acetic acid was added 20 ml. of a chromous chloride solution[10] at one time with vigorous stirring in nitrogen stream. The oxide (VI) dissolved immediately and soon 25D-5β-spirost-2-en-1-one (VII) was precipitated. Water was added and the mixture was extracted with ether. The ethereal solution was thoroughly washed and dried and evaporation furnished colorless needles, m. p. 222~223°C. Yield, 320 mg.; U. V. in EtOH λ_{max} 225 mμ (ε: 7690).

Anal. Found: C, 78.54; H, 9.51. Calcd. for $C_{27}H_{40}O_3$: C, 78.59; H, 9.77%.

25D-5β-Spirostan-1-one (VIII).—A solution of 300 mg. of 25D-5β-spirost-2-en-1-one (VII) in 50 ml. of methanol was subjected to catalytic hydrogenation over 1 g. of 5% palladium-charcoal catalyst. When 16 ml. of hydrogen was absorbed in five minutes the catalyst was removed and the filtrate was evaporated to give colorless prisms, m. p. 183~184°C. Yield, 220 mg.

Anal. Found: C, 78.17; H, 10.00. Calcd. for $C_{27}H_{42}O_3$: C, 78.21; H, 10.21%.

25D-5β-Spirostan (IX). — a) A mixture of 150 mg. of 25D-5β-spirostan-1-one (VIII), 5 ml. of diethylene glycol and 0.2 ml. of 80% hydrazine hydrate was heated to 160~170°C till the solution became clear. Potassium hydroxide (300 mg.) was added to the solution and the temperature was gradually raised to 200°C and kept there for two hours. After cooling, water was added and the mixture was extracted with petroleum ether. Evaporation of the thoroughly washed and dried extract furnished a crystalline solid. Recrystallization from methanol containing ether afforded colorless platelets, m. p. 136~137°C. Yield, 98 mg.

Anal. Found: C, 80.62; H, 11.05. Calcd. for $C_{27}H_{44}O_2$: C, 80.94; H, 11.07%.

b) Smilagenone (X) was subjected to the same treatment as the above to give 25D-5β-spirostan (IX).

Comparison of the I. R.-spectra and mixed melting point determination with the two specimens showed that they were in complete accord in all respects.

25D-5β-Spirostan-1β, 2β-diol-3-one Acetonide (Tokorogenone Acetonide) (XII).— To a solution of 1 g. of tokorogenin acetonide (IIa) in

10) A solution of chromous chloride was prepared by the method of Cole and Julian[3].

150 ml. of pyridine was added 700 mg. of chromic anhydride in small portions with vigorous agitation. Temperature was kept at 45~50°C for forty hours, and stirring was continued throughout this time. After cooling, the mixture was diluted with a large volume of water and extracted with ether. The ether solution was thoroughly washed, dried and evaporated. Recrystallization of the residue from methanol yielded colorless needles melting at 225~228°C. Yield, 800 mg. The analytical sample recrystallized from the same solvent melted at 229~231°C. I. R. in Nujol, λ_{max} 5.80 μ (3-c=o).

Anal. Found: C, 73.98; H, 9.29. Calcd. for $C_{30}H_{46}O_5$: C, 74.03; H, 9.53%.

Lithium Aluminum Hydride Reduction of 25D-5β-Spirostan-1β, 2β-diol-3-one Acetonide (Tokorogenone Acetonide) (XII).—A solution of 300 mg. of $LiAlH_4$ in 50 ml. of anhydrous ether was added in small portions to a solution of 200 mg. of 25D-5β-spirostan-1β,2β-diol-3-one acetonide (XII) in 150 ml. of the same solvent. After being left to stand overnight at room temperature, the reaction mixture was poured into ice-water and extracted with methylene chloride. The organic layer was washed with water, dried, and evaporated to give a crystalline solid, which was re-dissolved in methylene chloride and subjected to careful chromatography on Florisil.

Fraction 1 (30 ml., CH_2Cl_2),
needles, 20 mg., m. p., 204~206°C
Fraction 2 (30 ml., CH_2Cl_2),
needles, 50 mg., m. p., 208~210°C
Fraction 3 (30 ml., CH_2Cl_2),
needles, 35 mg., m. p., 210~240°C
Fraction 4 (30 ml., CH_2Cl_2),
needles, 35 mg., m. p., 295~300°C
Fraction 5 (50 ml., CH_2Cl_2)

Fraction 6 (50 ml., ether)

The substances from Fractions 1 and 2 were the same and did not show depression of m. p. on admixture. They were combined and recrystallized to give an analytical sample, m. p. 208~210°C.

Anal. Found: C, 73.77; H, 9.67. Calcd. for $C_{30}H_{48}O_5$: C, 73.73; H, 9.90%.

As already discussed it is 25D-5β-spirostan-1β, 2β,3β-triol 1,2-acetonide (XIII).

The substance from Fraction 4 proved to be identical with tokorogenin acetonide (IIa), and the substance from Fraction 3 is, therefore, very likely a mixture of IIa and XIII.

Summary

(1) The correlation of tokorogenin (I) with the known steroid, 25D-5β-spirostan (IX), was established: Tokorogenin formed an acetonide (IIa), which could be tosylated and then hydrolyzed to give tokorogenin monotosylate (IVb). On treatment with alkali, IVb was led to anhydrotokorogenin (Va), which on oxidation with Py.-CrO_3 and subsequent reduction with $CrCl_2$ gave rise to an α,β-unsaturated ketone (VII). Catalytic hydrogenation of VII followed by the Huang-Minlon reaction furnished 25D-5β-spirostan (IX).

(2) In order to determine the configuration of the hydroxyl group at C_3, IIa was oxidized with Py.-CrO_3 and the product was reduced with $LiAlH_4$ to give a mixture of IIa and XIII. Careful chromatography of the mixture revealed that the substance eluted first was XIII, while the second which eluted from the column was IIa, thus leaving only the structural possibility of 25D-5β-spirostan-1β,2β,3α-triol (I) to tokorogenin.

The author wishes to express his grateful thanks to Dr. Y. Asahina of the University of Tokyo, Dr. S. Kuwada and Dr. T. Matsukawa of Takeda Research Laboratories, for their encouragement throughout the work. Thanks are also due to Mr. H. Kamio for infrared- and ultraviolet-spectral measurements and to Mr. M. Kan for elementary analyses.

Takeda Research Laboratories
Juso, Higashiyodogawa-ku
Osaka

Studies on the Sapogenins of Dioscorea tokoro Makino. III[1]. *Synthesis of Isorhodeasapogenin and Some Reactions of Tokorogenin*

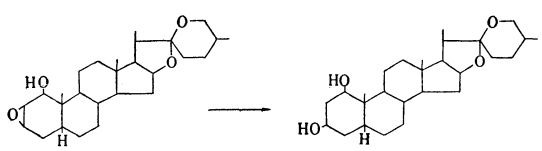
By Katsura MORITA

(Received November 4, 1958)

In order to obtain further information concerning the configuration of the hydroxyl groups in tokorogenin, the following reactions were investigated.

Reduction of anhydrotokorogenin (I) with lithium aluminum hydride in anhydrous ether caused ring-opening of the oxide giving a new dihydroxysapogenin, desoxytokorogenin. Since this dihydroxysapogenin neither formed an acetonide nor suffered oxidation by means of periodic acid and lead tetraacetate, the two hydroxyl groups in this substance have to be located at carbon atoms C_1 and C_3. As lithium aluminum hydride reduction of an oxide in the cyclohexane series is known to result in formation of an axial hydroxyl bond[2], the configuration of the hydroxyl group in position 3 of desoxytokorogenin must be β; that is, the structure of 25D-5β-spirostan-1β, 3β-diol (II) has to be assigned to this substance.

Chart 1

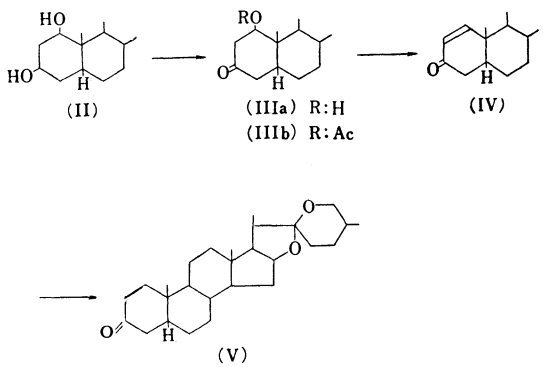


(I) (II)

Further evidence for the structure of desoxytokorogenin (II) is given by the following reaction sequence:

Desoxytokorogenin (II) was oxidized with *N*-bromoacetamide to 25D-5β-spirostan-1β-ol-3-one (IIIa), which was acetylated and then treated with activated alumina giving 25D-5β-spirost-1-en-3-one (IV)[3]. The U.V.-absorption spectrum of this substance (IV) showed a good identity with those of known Δ^1-3-ketosteroids[4]. Upon catalytic hydrogenation over $Pd/CaCO_3$ IV yielded smilagenone (V)[5].

Chart 2



(II) (IIIa) R:H (IIIb) R:Ac (IV) (V)

Some years ago, Nawa[6] isolated a new dihydroxysapogenin, rhodeasapogenin, from *Rhodea japonica* Roth. and suggested that it was 25L-5β-spirostan-2β, 3α-diol on the basis of various reactions, none of which led to a known steroid. Djerassi[7] attempted the oxidation of isorhodeasapogenin, an acid isomerization product of rhodeasapogenin, with chromic anhydride with the aim of obtaining a dibasic acid, isorhodeasapogenic acid, which he supposed to be identical with one of his four 2, 3- and 3, 4-seco-sapogenic acids. Unfortunately, the acid obtained by Djerassi was identical with none of his four sapogenic acids.

Quite recently, Takeda et al.[8] isolated a new dihydroxysapogenin, yonogenin, from *Dioscorea tokoro* Makino and defined its structure as 25D-5β-spirostan-2β, 3α-diol, which was the very one suggested

1) This is a full paper of the previous commuication (K. Morita, *Pharm. Bull.*, **5**, 496 (1957).), and constitutes Part X of Nishikawa's paper entitled "Studies in Steroids". Part IX: K. Morita, This Bulletin, **32**, 791 (1959).

2) M. S. Newman, "Steric Effects in Organic Chemistry", John Wiley & Sons, Inc., New York (1956), p. 130.

3) A similar reaction sequence was reported by W. Schlegel et al. (*Helv. Chim. Acta*, **38**, 1013 (1955).), who synthesized methyl 3-oxo-1-etienate from methyl 1β,3β-dihydroxyetianate.

4) See Table I in the foregoing paper (Part II) of this series.

5) The sample of smilagenone was synthesized from diosgenin by Oppenauer oxidation followed by catalytic hydrogenation.

6) H. Nawa, *J. Pharm. Soc. Japan* (*Yakugaku Zasshi*), **73**, 1192 (1953).

7) C. Djerassi and J. Fishman, *J. Am. Chem. Soc.*, **77**, 4291 (1955).

8) K. Takeda, T. Okanishi and A. Shimaoka, *J. Pharm. Soc. Japan* (*Yakugaku Zasshi*), **77**, 822 (1957).

for isorhodeasapogenin. The present author also isolated the sapogenin from the same plant and confirmed that yonogenin was not identical with isorhodeasapogenin[9].

In the course of the present investigations it was noticed that the melting points of desoxytokorogenin (II) and its diacetate were similar to those of isorhodeasapogenin and its diacetate, respectively. Similarly, the melting points of tokorogenic acid[10] and its dimethyl ester[10] were found to be in close proximity to those of isorhodeasapogenic acid and its dimethyl ester, respectively.

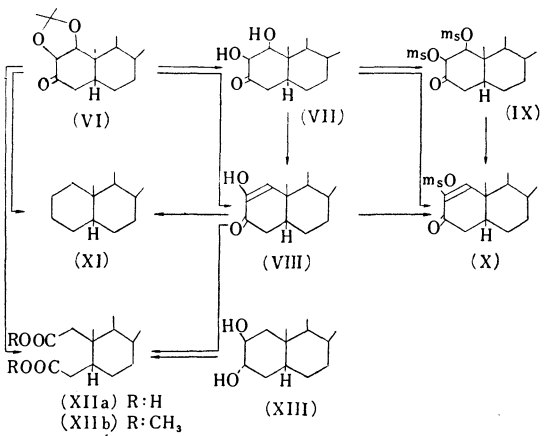
Most of the evidence for a glycol structure of rhodeasapogenin had been sought by Nawa in the fact that the sapogenin underwent ready oxidation to a dibasic acid, rhodeasapogenic acid, but it seemed probable that desoxytokorogenin (II) would be able to undergo oxidation with the same reagent to an intermediate 1,3-diketone, which would enolize and suffer further oxidation to a dibasic acid, namely, tokorogenic acid. Comparison of the I.R.-spectra and determination of the mixed melting points proved that desoxytokorogenin (II) is identical with isorhodeasapogenin, and tokorogenic acid with isorhodeasapogenic acid. Basing on these findings, Nawa has recently corrected all the structural assignments of rhodeasapogenin and its derivatives[11].

When tokorogenone acetonide (VI) was heated with acetic acid and water, tokorogenone (VII) was obtained. Tokorogenone (VII), on heating with alkali in methanol solution, lost 1 mol. of water to give a diosphenol (VIII), $C_{27}H_{40}O_4$, U. V. λ_{max} in EtOH: 269.5 mμ (ε: 6900). Direct conversion of tokorogenone acetonide (VI) into the diosphenol (VIII) could also be effected by the action of alkali at 100°C.

Stiller et al.[12] reported that selenium dioxide oxidation of cholestanone gave a mixture of cholest-1-en-2-ol-3-one (diosphenol A) and cholest-3-en-3-ol-2-one (diosphenol B). They also demonstrated that in equilibrium diosphenol A predominated in alkaline medium, while diosphenol B in acidic solution. The diosphenol (VIII) from tokorogenone (VII), however, was transformed in a mineral acid solution into an unidentified isomeric substance ($C_{27}H_{40}O_4$), from which the diosphenol (VIII) could no longer be recovered by any means. This discrepancy seems to be due to the fact that cholestanone and its diosphenols are 5α-steroids (allo-series) while tokorogenone (VII) and its diosphenol (VIII) are 5β-steroids (normal-series).

Tokorogenone (VII), on treatment with mesyl chloride and pyridine, gave a mixture of a dimesylate (IX) and an enol mesylate (X). The latter (X) was yielded also by heating the former (IX) with pyridine or with sodium iodide in acetone, and by treating the diosphenol (VIII) with mesyl chloride and pyridine. These reactions unambiguously show that the diosphenol (VIII) has to be defined as 25D-5β-spirost-1-en-2-ol-3-one.

Chart 3



It is interesting to note that the Huang-Minlon reduction of the diosphenol (VIII) as well as of tokorogenone acetonide (VI) gave 25D-5β-spirostan (XI), while the reduction of the acid isomerization product of the diosphenol (VIII) did not lead to XI.

The diosphenol (VIII) suffered oxidation with hydrogen peroxide and alkali at room temperature to give samogenic acid (XIIa)[7]. The same acid was prepared also from yonogenin by the known method, and the identity of both specimens was established by the mixed melting point determination and by the comparison of their I.R.-spectra.

Experimental

25D-5β-Spirostan-1β,3β-diol (Desoxytokorogenin) (II).—A solution of 400 mg. of 2β,3β-oxido-25D-5β-spirostan-1β-ol (anhydrotokorogenin) (I) in 50 ml. of anhydrous ether was added to a solution of 1.5 g. of lithium aluminum hydride in 60 ml. of the same solvent through a dropping

9) A sample of yonogenin was kindly given by Dr. Takeda[8] and that of isorhodeasapogenin by Dr. Nawa[6] in Takeda Research Laboratories. The mixture of these specimens melted at a temperature lower than that of either.

10) See previous paper (Part I) in this series.

11) H. Nawa, *Chem. & Pharm. Bull.*, **6**, 255 (1958).

12) E. T. Stiller and O. Rosenheim, *J. Chem. Soc.*, **1938**, 353.

funnel with stirring. The reaction mixture was stirred for two hours at room temperature and poured into a large volume of ice-water, 10% sulfuric acid was added, and the mixture was extracted with ether. The ether solution was thoroughly washed, dried, and evaporated to give colorless needles, m. p. 236~238°C. Yield, 310 mg. Recrystallization from methanol raised the m. p. to 240~242°C.

Anal. Found: C, 74.82; H, 10.46. Calcd. for $C_{27}H_{44}O_4$: C, 74.96; H, 10.25%.

On admixture with a sample of isorhodeasapogenin the melting point of the diol (II) was not depressed. The infrared spectra also established the identity of the two specimens.

Treatment of the diol (II) with acetic anhydride and pyridine at room temperature for twenty-four hours furnished the diacetate, m. p. 207~209°C.

Anal. Found: C, 72.12; H, 9.64. Calcd. for $C_{31}H_{48}O_6$: C, 72.06; H, 9.36%.

The substance thus obtained showed a good identity with isorhodeasapogenin diacetate in all respects.

25D-5β-Spirostan-1β-ol-3-one (IIIa).—25D-5β-Spirostan-1β, 3β-diol (II) (200 mg.) was added to a solution of 139 mg. of *N*-bromoacetamide in 20 ml. of 90% acetone and the mixture was warmed on a steam bath for a short time to clear the solution. After one hour, a portion of the solution was titrated with 1/10-N sodium thiosulfate solution and potassium iodide and it was indicated that the reaction proceeded stoichiometrically. A large volume of water was added and the mixture was extracted with ether. The ethereal solution was washed, dried and evaporated to dryness. Recrystallization of the residue from methanol afforded colorless needles melting at 232~233°C (decomp.).

Anal. Found: C, 74.96; H, 9.63. Calcd. for $C_{27}H_{42}O_4$: C, 75.31; H, 9.83%.

25D-5β-Spirostan-1β-ol-3-one Acetate (IIIb).—25D-5β-Spirostan-1β-ol-3-one (IIIa) (70 mg.) was acetylated with acetic anhydride and pyridine to give colorless needles of the acetate (IIIb), m. p. 200~201°C.

Anal. Found: C, 73.66; H, 9.31. Calcd. for $C_{29}H_{44}O_5$: C, 73.69; H, 9.38%.

25D-5β-Spirost-1-en-3-one (IV).—A solution of 70 mg. of IIIb was passed through unwashed alumina to furnish 50 mg. of platelets melting at 191~192°C. U. V. λ_{max} in EtOH: 232.5 mμ (ε: 9700).

Anal. Found: C, 78.55; H, 9.63. Calcd. for $C_{27}H_{40}O_3$: C, 78.59; H, 9.77%.

25D-5β-Spirostan-3-one (Smilagenone) (V).—A solution of 35 mg. of 25D-5β-spirost-1-en-3-one (IV) in 30 ml. of methanol was subjected to catalytic hydrogenation over 5% palladium-charcoal catalyst in an atmospheric pressure. The solution rapidly took up 1.6 ml. of hydrogen and the reaction almost stopped. The catalyst was removed and the filtrate was concentrated under diminished pressure to give colorless platelets. Recrystallization from methanol afforded the pure material melting at 183~184°C.

The sample here obtained showed no depression of the melting point on admixture with an authentic specimen prepared from diosgenone by the known method[5].

25D-5β-Spirostan-1β, 2β-diol-3-one (Tokorogenone) (VII). — 25D-5β-Spirostan-1β, 2β-diol-3-one acetonide (VI) (100 mg.) in 3 ml. of 80% acetic acid was heated on a steam bath for forty minutes. The resulting solution was evaporated under diminished pressure to give a crystalline solid (VII), which upon recrystallization from methanol afforded thin plates melting at 224~227°C. Yield, 60 mg.

Anal. Found: C, 72.54; H, 9.57. Calcd. for $C_{27}H_{42}O_5$: C, 72.65; H, 9.42%.

A small portion of the diol (VII) was acetylated with acetic anhydride and pyridine by the usual means. Recrystallization of the crude acetate from methanol furnished colorless needles, m. p. 223~226°C.

Anal. Found: C, 70.10; H, 8.59. Calcd. for $C_{31}H_{46}O_7$: C, 70.16; H, 8.74%.

25D-5β-Spirostan-1β,2β-diol-3-one Dimesylate (IX) and 25D-5β-Spirost-1-en-2-ol-3-one Mesylate (X).—a) Mesyl chloride (1 ml.) was added to a solution of 500 mg. of 25D-5β-spirostan-1β, 2β-diol-3-one (VII) in 10 ml. of pyridine at 0°C and the solution was allowed to stand at room temperature in a dark place for three days. A large volume of water was added and the mixture was extracted with ether. The ether solution was thoroughly washed with water, dried and evaporated to furnish almost colorless needles of the dimesylate (IX), m. p. 223°C (decomp.). Yield, 340 mg.

Anal. Found: C, 57.71; H, 7.66. Calcd. for $C_{29}H_{46}O_9S_2$: C, 57.78; H, 7.69%.

The mother liquor from the above dimesylate (IX) was further concentrated and left overnight to give different crystals, m. p. 222~223°C. Yield, 120 mg. The substance here obtained showed a marked depression of the melting point on admixture with the dimesylate (IX). On the basis of the ultraviolet absorption spectrum and elementary analyses structure X was assigned to this substance. U. V. λ_{max} in EtOH: 238.5 mμ (ε: 7100).

Anal. Found: C, 66.10; H, 8.20. Calcd. for $C_{28}H_{42}O_6S$: C, 66.38; H, 8.36%.

b) A solution of 200 mg. of 25D-5β-spirostan-1β, 2β-diol-3-one dimesylate (IX) in 8 ml. of acetone containing 500 mg. of sodium iodide was heated in a sealed tube at 120°C for twenty-four hours. After cooling, the reaction mixture was diluted with water and extracted with ether. The ethereal solution was washed with water and then with sodium thiosulfate solution, dried, and evaporated to furnish colorless crystals, m. p. 222~223°C.

c) A portion of 25D-5β-spirost-1-en-2-ol-3-one (VIII) dissolved in pyridine was treated with mesyl chloride by the usual means. Dilution of the reaction mixture with water followed by washing, drying and evaporation afforded the same mesylate, m. p. 222~223°C.

25D-5β-Spirost-1-en-2-ol-3-one (Diosphenol) (VIII).—a) A solution of 25D-5β-spirostan-1β,2β-

diol-3-one (VII) (70 mg.) in 5 ml. of methanol containing 500 mg. of potassium hydroxide was boiled on a steam bath for thirty minutes. After cooling and diluting with a large volume of water, the mixture was extracted with methylene chloride. The organic layer was then washed, dried, and evaporated to give colorless needles. Recrystallization from methanol afforded the analytical sample, m. p. 227~228°C. Yield, 40 mg. U. V. λ_{max} in EtOH: 269.5 mμ (ε: 6900).

Anal. Found: C, 75.49; H, 9.37. Calcd. for $C_{27}H_{40}O_4$: C, 75.66; H, 9.41%.

b) A portion of 25D-5β-spirostan-1β, 2β-diol-3-one acetonide (VI) was treated with potassium hydroxide as described and the resulting solution was worked up as above to give the same diosphenol (VIII); mixed melting point with the specimen from a, 227~228°C.

Acid Isomerization of 25D-5β-Spirostan-1β, 2β-diol-3-one (VII), 25D-5β-Spirostan-1β, 2β-diol-3-one Acetonide (VI) and 25D-5β-Spirost-1-en-2-ol-3-one (VIII).—a) A solution of 70 mg. of 25D-5β-spirostan-1β, 2β-diol-3-one (VII) in 5 ml. of methanol containing 0.2 ml. of concentrated hydrochloric acid was boiled under reflux for thirty minutes. After concentration under reduced pressure, water was added and the mixture was extracted with methylene chloride. Thorough washing with water followed by drying and evaporation furnished a crystalline solid, m. p. 245~248°C. Recrystallization from methanol raised the m. p. to 254~255°C. The ultraviolet absorption spectrum of this substance showed a slight shift to a lower wavelength than that of the alkali isomerization product VIII, i. e., U. V. λ_{max} in EtOH: 267 mμ (ε: 5700), no hydroxyl absorption bands being noticed.

Anal. Found: C, 75.49; H, 9.37. Calcd. for $C_{27}H_{40}O_4$: C, 75.66; H, 9.41%.

b) 25D-5β-Spirostan-1β, 2β-diol-3-one acetonide (VI) was subjected to acid isomerization under the conditions described above. The crude product after recrystallization from methanol showed the same melting point as that of the specimen from a.

c) A solution of 70 mg. of 25D-5β-spirost-1-en-2-ol-3-one (VIII) in 5 ml. of methanol containing 0.2 ml. of concentrated hydrochloric acid was boiled under reflux for thirty minutes. Working up of the reaction mixture by the same procedure as described in a and b yielded fine needles melting at 254~255°C.

All the specimens from a, b and c were confirmed to be identical with one another by mixed melting point determination.

25D-5β-Spirostan (XI).—25D-5β-Spirostan-1β, 2β-diol-3-one acetonide (VI) (500 mg.) was dissolved in 20 ml. of diethylene glycol containing 1 ml. of 80% hydrazine hydrate and 2.0 g. of potassium hydroxide. The mixture was heated at 200°C in an oil bath for three hours. After cooling, the reaction mixture was diluted with a large volume of water and extracted with ether. The ethereal solution was washed with water, dried, concentrated, and chromatographed on Florisil. 25D-5β-Spirostan (XI) was eluted from the column by petroleum ether and recrystallization from methanol-petroleum ether gave the analytical sample melting at 136~137°C. Identity of the substance here obtained was confirmed by comparison of the I. R.-spectra and the mixed melting point determination with an authentic specimen. When 25D-5β-spirostan-1β, 2β-diol-3-one (VII) and 25D-5β-spirost-1-en-2-ol-3-one (VIII) were subjected to the same reaction, 25D-5β-spirostan (XI) was obtained.

Samogenic Acid (XIIa).—Thirty per cent hydrogen peroxide (1 ml.) was added to a solution of 300 mg. of 25D-5β-spirost-1-en-2-ol-3-one (diosphenol) (VIII) in 5 ml. of methanol containing 200 mg. of potassium hydroxide and the solution was left standing at room temperature for one hour. A large volume of water was added, the resulting clear solution was extracted once with ether, and the ether solution was discarded. The aqueous solution was acidified and extracted with ether and the ethereal solution was washed with water, dried and evaporated to give a crystalline solid. Recrystallization of the solid from methanol furnished colorless thin plates melting at 271~273°C. Yield, 200 mg.

By the action of diazomethane, the acid (XIIa) afforded the dimethyl ester (XIIb), m. p. 147~148°C, $[\alpha]_D^{31}$: −28° (*c*; 0.5% in $CHCl_3$).

Summary

(1) Reduction of anhydrotokorogenin with lithium aluminum hydride led to a new dihydroxysapogenin, desoxytokorogenin; the structure 25D-5β-spirostan-1β, 3β-diol was assigned on the basis of various reactions and theoretical considerations.

(2) Desoxytokorogenin, 25D-5β-spirostan-1β, 3β-diol, was incidentally found to be identical with isorhodeasapogenin, the structure of which had so far been left unclarified.

(3) Identity of tokorogenic acid with isorhodeasapogenic acid was also confirmed.

(4) Tokorogenin was correlated with samogenic acid and yonogenin via a diosphenol, 25D-5β-spirost-1-en-2-ol-3-one, whose structure was unambiguously established.

The author wishes to express his grateful thanks to Dr. Y. Asahina of the University of Tokyo, Dr. S. Kuwada and Dr. T. Matsukawa of Takeda Research Laboratories for their encouragement throughout the work. Thanks are also due to Dr. K. Takeda of Shionogi Research Laboratories for the gift of a sample of yonogenin, to Mr. H. Kamio for infrared- and ultraviolet-spectral measurements and to Mr. M. Kan for elementary analyses.

Takeda Research Laboratories
Juso, Higashiyodogawa-ku,
Osaka

Studies on the Sapogenins of Dioscorea tokoro Makino. IV[1]. *The Contents of Tokorogenin, Yonogenin and Diosgenin*

By Katsura MORITA

(Received November 4, 1958)

Until recently, three steroids of natural origin possessing a hydroxyl group in position 1 had been announced. They are ouabagenin[2], acovenosigenin A[3], both being cardiac aglycones, and ruscogenin[4], a steroidal sapogenin isolated quite recently by C. Sannié et al. from *Ruscus aculeatus* L. and defined by Benn et al.[5] as 25D-spirost-5-en-1ξ, 3β-diol. Tokorogenin and rhodeasapogenin[6] are further additions to the examples of 1-hydroxylated steroids of natural origin. Tokorogenin is the only known steroid possessing a glycerol moiety in ring A, its structure having been defined by the author as 25D-5β-spirostan-1β, 2β, 3α-triol.

As described in a previous paper[7], tokorogenin was isolated from the rhizomes of *D. tokoro* Makino in a poor yield compared with diosgenin, which had been regarded as the sole steroidal sapogenin in the same plant. In the course of the present investigation, however, it was noticed that the rhizomes of *D. tokoro* Makino collected at Gotenba in Shizuoka Prefecture yielded extraordinarily large amounts of tokorogenin and a new sapogenin[8] and a minute quantity of diosgenin, compared with those collected in other places. No difference in appearance could be found between the rhizomes and the plants collected at Gotenba and those from other places.

In the light of these findings it was presumed that the rhizomes of *D. tokoro* Makino from certain districts other than Gotenba might be an excellent source of tokorogenin or other sapogenins, and the author started investigations on the sapogenin contents in the same plant species from various districts in Japan.

For this purpose, dried and sliced rhizomes collected at various sites were subjected to digestion with 1.2-N hydrochloric acid for six hours followed by drying and extraction with ether in a Soxhlet apparatus. The ether extract separated a voluminous jelly comprising tokorogenin, yonogenin and other unknown impurities. The jelly yielded rather impure tokorogenin and yonogenin by chromatographic purification on Florisil, while the mother liquor yielded almost pure diosgenin.

Since the above procedure was rather troublesome and unsuitable for rapid estimation with many samples, the following process was used: The ether extract was evaporated to dryness, and the residue was dissolved in methylene chloride and chromatographed on Florisil to give a diosgenin fraction and a yonogenin-tokorogenin fraction; both fractions were then evaporated and weighed to find roughly the amount of diosgenin and the total amount of other sapogenins. The results are summarized in Table I, which shows that the amount of diosgenin and that of other sapogenins vary markedly according to the site of collection of the rhizomes. It is especially noteworthy that the rhizomes collected even in neighboring villages (No. 21—No. 25) in Gotenba showed considerable differences in their sapogenin contents.

In order to obtain further information on these points, similar experiments were carried out with the rhizomes cultivated in the Experimental Farm of our company[9], each sample being prepared from one plant and by the same process.

A methanol extract of a rhizome was

1) This communication is Part XI of Nishikawa's paper entitled "Studies in Steroids". Part X; K. Morita, This Bulletin, **32**, 796 (1959).

2) C. Mannich and C. Siewert, *Ber.*, **75**, 737 (1942); Ch. Tamm, G. Volpp and C. Baumgartner, *Helv. Chim. Acta*, **40**, 1469 (1957).

3) W. Schlegel, Ch. Tamm and T. Reichstein, ibid., **38**, 1013 (1955).

4) C. Sannié and H. Lapin, *Bull. soc. chim. France*, **1955**, 1556.

5) W. R. Benn, F. Colton and R. Pappo, *J. Am. Chem. Soc.*, **79**, 3920 (1957).

6) The previous papar (Part III) of this series; H. Nawa, *Chem. & Pharm. Bull.*, **6**. 255 (1958).

7) M. Nishikawa, K. Morita, H. Hagiwara and M. Inoue, *J. Pharm. Soc. Japan* (*Yakugaku Zasshi*), **74**, 1165 (1954).

8) This sapogenin was thereafter shown to be identical with yonogenin: K. Takeda, T. Okanishi and A. Shimaoka, ibid., **77**, 822 (1957).

9) Cultivation of the plants in the Experimental Farm was started from the rhizomes collected in the neighborhood of Gotenba and other places, and has been continued for more than three years.

TABLE I

Expt. No.	Collection site	♀ ♂	Diosgenin (%)	Yonogenin & tokorogenin (%)
1	Kongosan (Osaka)	—	1.4	0.5
2	Tachikawa (Chiba)	—	3.2	0.7
3	Mishima (Shizuoka)	—	2.5	1.0
4	Yamakita (Shizuoka)	—	1.0	1.0
5	Nagano (Nagano)	—	2.8	0.8
6	Jubuin (Kyushu)	—	2.0	0.6
7	Miyanohara (Kyushu)	—	2.7	0.8
8	Mutobe (Kyoto)	—	2.7	0.7
9	Sado (Niigata)	—	1.9	0.5
10	Suginosawa (Niigata)	—	4.1	1.6
11	Katsuyama (Fukui)	♀	2.4	1.6
12	Katsuyama (Fukui)	♂	2.0	0.6
13	Hakusanshita (Ishikawa)	♀	2.0	0.7
14	Hakusanshita (Ishikawa)	♂	2.2	0.6
15	Takarazuka (Hyogo)	♀	1.2	0.6
16	Takarazuka (Hyogo)	♂	1.3	1.7
17	Shinjuku (Tokyo)	♀	3.8	1.4
18	Shinjuku (Tokyo)	♂	3.0	1.4
19	Gotenba (Shizuoka)	♀	0.4	1.8
20	Gotenba (Shizuoka)	♂	0.6	2.8
21	Gotenba-Nagahara (Shizuoka)	—	1.4	2.3
22	Gotenba-Taniga (Shizuoka)	—	1.1	1.4
23	Gotenba-Oyama (Shizuoka)	—	0.2	2.6
24	Gotenba-Ueno (Shizuoka)	—	0.3	2.9
25	Gotenba-Subashiri (Shizuoka)	—	2.5	1.9

TABLE II

Expt. No.	Diosgenin (%)	Yonogenin (%)	Tokorogenin (%)	Expt. No.	Diosgenin (%)	Yonogenin (%)	Tokorogenin (%)
1	<0.1	0.7	0.8	26	1.1	0.2	0.3
2	<0.1	0.5	0.7	27	0.9	0.1	0.2
3	<0.1	0.6	0.8	28	0.1	0.5	0.6
4	<0.1	0.5	0.6	29	<0.1	0.7	0.8
5	<0.1	1.4	0.8	30	<0.1	0.4	0.6
6	<0.1	0.7	0.8	31	1.5	0.2	0.2
7	0.8	0.2	0.3	32	0.1	0.5	0.5
8	0.1	0.3	0.7	33	0.1	0.5	0.6
9	1.1	0.1	0.2	34	<0.1	0.6	0.7
10	0.7	0.2	0.1	35	<0.1	0.2	0.4
11	<0.1	0.9	0.6	36	<0.1	0.3	0.4
12	0.1	0.7	0.6	37	<0.1	0.5	0.7
13	0.1	0.7	0.7	38	<0.1	0.8	0.9
14	0.1	0.6	0.6	39	2.1	0.2	0.3
15	0.1	1.3	0.8	40	2.3	0.2	0.3
16	0.2	1.0	1.0	41	0.1	0.3	0.6
17	1.3	0.2	0.2	42	<0.1	1.0	0.7
18	0.2	0.6	0.7	43	1.9	0.2	0.3
19	1.1	0.1	0.3	44	1.3	0.2	0.3
20	1.7	0.2	0.3	45	2.1	0.2	0.3
21	1.0	0.2	0.3	46	<0.1	0.7	0.8
22	*1.1*	*0.1*	*0.2*	47	0.1	0.7	0.7
23	1.3	0.2	0.2	48	0.2	0.8	0.7
24	0.2	1.0	0.6	49	0.2	0.7	0.8
25	0.3	0.7	0.7	50	0.1	0.5	0.7

TABLE II (Continued)

Expt. No.	Diosgenin (%)	Yonogenin (%)	Tokorogenin (%)	Expt. No.	Diosgenin (%)	Yonogenin (%)	Tokorogenin (%)
51	<0.1	0.8	1.0	106	1.8	<0.1	<0.1
52	<0.1	0.2	1.1	107	0.8	<0.1	<0.1
53	0.1	1.0	1.0	108	1.2	<0.1	<0.1
54	<0.1	1.1	1.0	109	1.0	<0.1	<0.1
55	0.1	0.7	1.0	110	0.9	<0.1	<0.1
56	1.3	0.2	1.3	111	1.0	<0.1	<0.1
57	<0.1	0.5	1.8	112	0.6	<0.1	<0.1
58	<0.1	0.8	1.1	113	1.0	<0.1	<0.1
59	0.1	0.5	1.9	114	1.5	0.1	0.2
60	0.2	0.7	0.7	115	1.8	<0.1	0.2
61	1.2	0.2	0.3	116	0.2	1.0	0.6
62	0.1	0.5	0.8	117	2.3	0.2	0.3
63	0.2	0.9	0.8	118	0.2	0.5	0.6
64	0.2	0.7	0.8	119	0.2	0.6	0.7
65	0.1	0.8	0.8	120	2.0	0.1	0.2
66	0.2	0.7	0.8	121	0.3	0.7	0.6
67	0.1	0.7	0.8	122	2.3	0.3	0.2
68	0.2	0.6	0.6	123	1.7	0.1	0.2
69	0.1	0.6	0.6	124	2.1	0.2	0.3
70	0.1	0.8	0.6	125	1.2	0.1	0.2
71	<0.1	0.8	0.9	126	1.1	0.1	0.1
72	<0.1	0.7	1.1	127	2.1	0.2	0.2
73	<0.1	0.8	0.9	128	1.4	0.1	0.2
74	0.1	0.9	0.9	129	0.3	0.4	1.1
75	<0.1	0.6	1.0	130	0.2	0.4	1.0
76	0.1	0.6	0.9	131	0.3	0.8	0.8
77	0.2	0.8	1.5	132	0.1	0.4	1.2
78	<0.1	0.7	0.8	133	0.3	1.1	1.4
79	<0.1	1.1	1.0	134	0.3	0.9	1.7
80	0.3	0.5	0.8	135	0.2	0.8	1.6
81	0.3	1.0	1.2	136	0.2	0.9	1.3
82	0.2	1.6	1.1	137	0.2	1.2	1.4
83	0.1	0.3	1.1	138	0.2	0.8	1.0
84	0.2	1.3	1.1	139	1.6	0.1	0.2
85	2.2	0.2	0.4	140	0.2	0.6	0.7
86	<0.1	0.6	1.1	141	1.4	0.1	0.2
87	<0.1	1.2	1.1	142	0.2	0.9	0.7
88	0.4	0.1	<0.1	143	1.6	0.2	0.2
89	0.6	<0.1	<0.1	144	1.8	0.1	0.2
90	0.9	<0.1	<0.1	145	0.2	0.6	0.7
91	0.6	<0.1	<0.1	146	0.2	0.5	0.8
92	0.9	<0.1	<0.1	147	1.7	0.1	0.3
93	0.8	0.3	<0.1	148	0.2	0.7	1.0
94	0.7	<0.1	<0.1	149	1.3	0.1	0.2
95	1.1	<0.1	<0.1	150	1.4	0.1	0.3
96	1.1	0.1	<0.1	151	1.2	0.1	0.2
97	0.7	0.1	<0.1	152	0.3	1.0	0.9
98	0.8	0.1	<0.1	153	0.1	0.6	0.6
99	0.9	<0.1	<0.1	154	1.7	0.2	0.2
100	0.8	<0.1	<0.1	155	1.1	0.9	0.8
101	0.8	<0.1	<0.1	156	0.3	1.0	0.9
102	0.7	<0.1	<0.1	157	0.2	0.7	0.9
103	0.9	<0.1	<0.1	158	1.2	0.2	0.2
104	1.0	<0.1	<0.1	159	0.3	0.8	0.9
105	1.3	<0.1	<0.1	160	1.0	0.3	0.7

hydrolyzed with ethanolic hydrochloric acid[10], extracted with methylene chloride, chromatographed on Florisil and finally subjected to the colorimetric estimation of the three sapogenins by means of Yamagishi's method[11]. The results of the analyses tabulated in Table II reveal that the plants containing diosgenin as the major ingredient contain very small amounts of tokorogenin and yonogenin or lack them, while those containing large amounts of tokorogenin and yonogenin give only minute yields of disogenin or lack it. These findings are very interesting in view of the fact that the structures of tokorogenin and yonogenin are closely related (5β,2β-OH, 3α-OH), while diosgenin is considerably different from these two sapogenins (Δ^5, 3β-OH). In this connection it is also interesting to point out that the Shionogi's workers have isolated the fourth sapogenin, kogagenin, from the vines and leaves of the same plant[8] and suggested a structure of 25D-spirostan-1β, 2β,3α,5β-tetrol for the new sapogenin[12].

Experimental

Improved Isolation of Diosgenin, Yonogenine and Tokorogenin from the Rhizomes of *D. tokoro* Makino (Collected at Gotenba). —Dried rhizomes (1 kg.) collected at Gotenba was gently heated with 4.6 l. of 1,2-N hydrochloric acid for six hours and the hydrolyate was centrifuged, and the solid was washed with water and dried to give 186 g. of a dark brown cake. The cake was then extracted with petroleum benzine in a large Soxhlet apparatus for five hours, whereby diosgenin separated out as a white crystalline solid during the extraction. Ether was then substituted for petroleum benzine and extraction was continued for twenty more hours to give voluminous precipitation of dark brown jelly, which was filtered, washed with ether and dried. It weighed 18.7 g.

TABLE III

Sample	Content		
	Diosgenin (%)	Yonogenin (%)	Tokorogenin (%)
Dried rhizomes 1 kg.	0.82	0.63	0.50
Acid hydrolysate 186 g.	4.32	3.1	2.6
Jelly 18.7 g.	—	30	24

10) Hydrolysis was carried out by Marker's standard method.

11) M. Yamagishi and I. Nakamura, *Chem. & Pharm. Bull.*, **6**, 421 (1958).

12) At the Meeting of Organic Chemistry of Naturally Occurring Substances, October 18, 1958.

The analytical data shown in Table III[13] indicate that the procedure described above is satisfactory for the separation of diosgenin and a mixture of tokorogenin and yonogenin from the rhizomes.

For the separation of tokorogenin from yonogenin, the jelly (18.7 g.) was acetylated with pyridine-acetic anhydride and the acetylated mixture dissolved in ether was repeatedly washed with dilute aqueous alkali until washings became colorless. After the ether solution was dried and evaporated, the residue was redissolved in hot ethanol and treated with charcoal. Upon the solution was cooled tokorogenin triacetate was precipitated as almost colorless leaflets melting at 250~255°C. For analysis the crude material (m. p. 250~255°C) was dissolved in methylene chloride and the solution was passed through a column of Florisil, and concentration of the solution and recrystallization of the residue from ethanol raised the m. p. to 260~263°C. Yield, 4.7 g. The mother liquor, after hydrolysis with methanol and alkali, was poured into water and extracted with ether. The ether solution was washed with water, dried and evaporated to dryness. Chromatography of a portion of the residue on Florisil furnished yonogenin from methylene chloride-ethyl acetate (4 : 1) eluates and a small amount of tokorogenin from ethyl acetate eluates. After recrystallization from hot ethanol[14] the sample of yonogenin melted at 238~240°C and was identified with an authentic sample.

Yonogenin Acetate. — A small portion of yonogenin was acetylated with pyridine and acetic anhydried to give colorless needles of the diacetate, m. p. 213°C, $[\alpha]_D^{17}$ −17° (c=1.0%, $CHCl_3$). The sample showed no depression of m. p. on admixture with an authentic specimen.

Hydrolysis of the diacetate with alkali and methanol led to needles of the free sapogenin melting at 238~240°C.

Summary

(1) Improved isolation of tokorogenin, yonogenin and diosgenin from the rhizomes of *D. tokoro* Makino collected at Gotenba is described.

(2) The sapogenin contents in rhizomes of *D. tokoro* Makino collected in various districts in Japan were examined by means of chromatography.

(3) The sapogenin contents in rhizomes of cultivated plants of *D. tokoro* Makino were examined and it was found that the plants containing diosgenin as the major ingredient contain very small amounts of tokorogenin and yonogenin or lack them, while those containing large amounts of tokorogenin and yonogenin give only minute yields of diosgenin or lack it.

13) Analyses were carried out by Yamagishi's colorimetric method[7].

14) A solution of yonogenin in organic solvents showed strong tendency to form a gel.

The author wishes to express his grateful thanks to Dr. Y. Asahina of the University of Tokyo, Dr. S. Kuwada and Dr. T. Matsukawa of Takeda Research Laboratories for their encouragement throughout the work. Thanks are also due to Dr. K. Takeda of Shionogi Research Laboratories for the gift of a sample of yonogenin, to Dr. S. Yamagishi and Mr. I. Nakamura for the analyses of the sapogenins, to Dr. T. Watanabe for the collection of the plants, and to Mr. R. Hatta of their Experimental Form in Kyoto for the growing of the plants.

Takeda Research Laboratories
Juso, Higashiyodogawa-ku
Osaka

On the Crystal Growth of Zinc Sulfide Phosphor

By Yoshiro ŌTOMO

(Received November 12, 1958)

When zinc sulfide is fired, usually the flux is to be used, which 1) protects the phosphor from oxidation[1], 2) acts as the co-activator[2-4] and 3) promotes its crystallization. Concerning those functions, there have been few detailed reports on 3), the crystallization of the phosphor.

The author has made observations with an electron microscope on the process of crystallization of the phosphor, with and without flux — here, 2 wt. % of sodium chloride has been added — and, at the same time, he has determined the sizes and the forms of crystals, using a NORELCO X-ray diffractometer. It is found that, before firing, the raw material of zinc sulfide is a large aggregate of crystallites of β-form with 8% of α-form of the same material, and through firing, the process of crystal growth is much affected by the addition of flux. Also, he has discussed the effect of flux on the size of the grown crystals, the forms of crystals and their transition velocities.

Experimental Results and Discussion

The Crystal Growth and the Electron Microscope Observation.—A special replica method was used for the electron microscope observation. The phosphor powder was scattered on rock salt and Pt-Pd metal was evaporated on it obliquely from one direction. Carbon was then evaporated to cover the Pt-Pd metal and the phosphor crystal. After those procedures, rock salt was dissolved in water and zinc sulfide was dissolved in 6 N-hydrochloric acid. Thus, the Pt-Pd metal covered with carbon film was left, and was put on the mesh as a sample.

The base material of zinc sulfide phosphor was precipitated through the reaction of hydrogen sulfide gas with the solution of zinc sulfate. The precipitate was washed with de-ionized water and dried at room temperature. The precipitate was observed by the electron microscope and was found to be a large aggregate of needle-like crystallites, as is demonstrated in Fig. 1. In order to see the crystal structure of the aggregate, a NORELCO X-ray diffractometer was used and $10\bar{1}0$, 0002 and $10\bar{1}1$ patterns, the strongest patterns of α-form crystal, and 111 pattern, the strongest pattern of β-form, were checked. It was found that the raw material of zinc sulfide was not amorphous but consisted of nearly perfect crystals of β-form containing approximately 8% of α-form.

Assuming that they are perfect β-form crystals, the mean diameter of the crystals, d, is obtained from the half-peak breadth, B, of the 111 diffraction pattern, using

$$B = K\lambda/d\cos\theta \qquad (1)$$

where λ is the wavelength of X-ray and θ is the angle of diffraction. For $K \approx 1$, the diameter of the unfired zinc sulfide crystal, d, is evaluated to be about 150 Å from our X-ray diffraction measurements.

1) K. Takagi, *J. Chem. Soc. Japan, Ind. Chem. Sec.* (*Kogyo Kagaku Zasshi*), **61**, 959 (1958).
2) F. A. Kröger and J. Dikhoff, *Physica* XVI, 297 (1950).
3) F. A. Krgöer, ibid., XXII, 637 (1956).
4) F. E. Williams, *J. Opt. Soc. Am.*, **47**, 869 (1957).

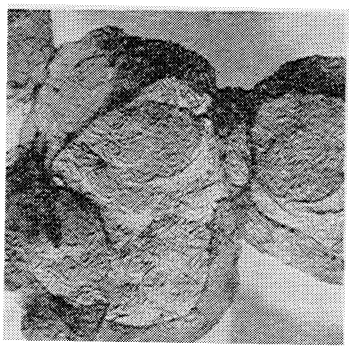


Fig. 1. Unfired ZnS: Ag.
Electron micrograph×5,000

In Figs. 2a and 2b, the processes of crystal growth during the firing of the precipitated zinc sulfide are shown. The processes of crystalization of the samples added with or without the flux of 2 wt. % of sodium chloride were investigated with an electron microscope. In both cases, no difference is observed up to 400°C and a slight change in the crystalline state is observed at 500°C in case of a sample with 2 wt. % of sodium chloride. At 600°C, the crystallites of zinc sulfide have grown together considerably in both cases, and, at 700°C, perfectly grown crystallites were observed with 2 wt. % of sodium chloride. But without flux, the rapid crystal growth is seen at temperatures between 800 and 900°C. However, the difference between the two cases is not only in the speed of crystal growth, but also in some other aspects of growing processes. Considerations on the later aspects are given below.

For the modes of crystal growth of such sulfides, two processes are mainly considered; the one, through the screw dislocation and the other, the surface nucleation[5].

The zinc sulfide molecule, which is adsorbed on the step of the crystal, diffuses towards the kink and forms a part of the crystal lattice, pushing the step out and making the crystal larger. The diffusion length, l_d, of zinc sulfide is given by

$$l_d=\sqrt{D\tau}$$

where D is the diffusion constant and τ is the lifetime of the molecule adsorbed on the surface.

By the addition of 2 wt. % of sodium chloride the diffusion is made more active, and D becomes larger. And, through the interaction with the flux, there will be more possibilities of forming kinks at the surface of crystals, and the mean distance, l_k, between kinks will become smaller. Hence, the relationship

$$l_d \gg l_k$$

will be satisfied easily and the growth of the steps at crystal surfaces will become independent of the crystal symmetry, resulting in the circular step-wise crystals. Such cases are given in Fig. 2a; one for the sample fired at 700°C and another for that fired at 1000°C. Without flux, the diffusion of zinc sulfide molecules along the crystal surfaces is not active, and D becomes smaller. Also, the kinks at the surfaces are not formed so easily, and l_k becomes larger.

Hence, the relationship, $l_d \gg l_k$, is no longer satisfied, resulting in the considerable influence of crystal symmetries on the growth of steps at the surfaces and the anisotropic crystal growth. Some examples are given in Fig. 2b. For the firing at temperatures above 900°C, the straight step, perpendicular to the direction of crystal growth, is seen clearly. At 1100°C, the α-form crystal of zinc sulfide is observed, especially along (0001) crystal surface, which is developed as pyramids.

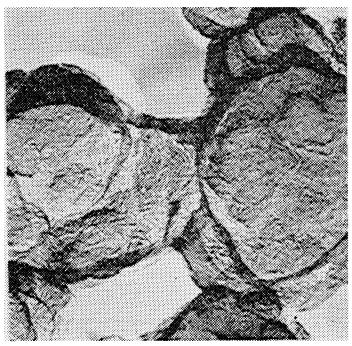
Relationship between the Firing Condition and the Diameter of Crystals.—The half-peak breadth of the X-ray diffraction pattern was corrected for the characteristic width of the instrument, and the crystal sizes of various zinc sulfide phosphors were obtained by using Eq. 1.

The results are given in Fig. 3. In this diagram, the solid line shows the diameter of crystals without flux and the dotted line shows that with 2 wt. % of sodium chloride as flux. For both cases, up to 400°C, little crystal growth is observed and no difference can be seen compared with the material before firing. At about 500°C, the crystal growth begins and, at 600°C, it becomes extremely rapid. When the flux is added, the growth, at temperatures around 600°C, is especially remarkable. Those results show a rather good correspondence with the behaviors of crystal growth shown in Fig. 2.

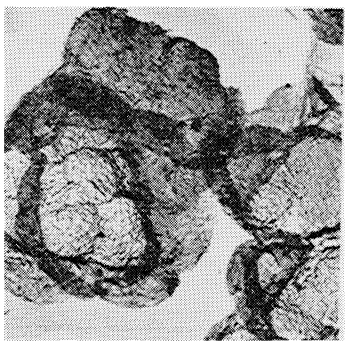
Comparison between the measured crystal diameters obtained through the X-ray diffraction method and the electron microscope is made below.

In Fig. 2b, the picture of the sample fired, without flux, at 800°C shows that the diameter of the crystal agrees with that obtained by X-ray diffraction which

5) D. C. Reynolds and L. C. Greene, *J. Appl. Phys.*, **29**, 559 (1958).



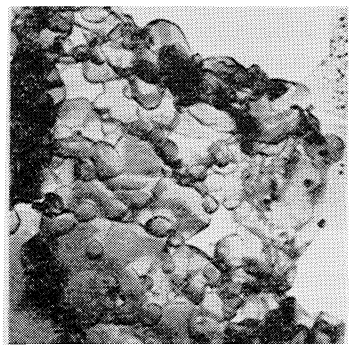
400°C×3*h*



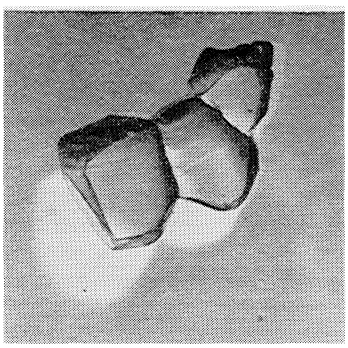
500°C×3*h*



600°C×3*h*

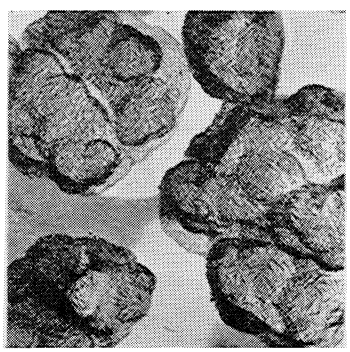


700°C×3*h*



1000°C×3*h*

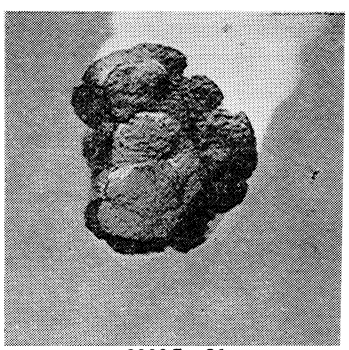
Fig. 2a. ZnS: Ag phosphor (with added 2 wt. % NaCl as flux).
Electron micrograph×5,000



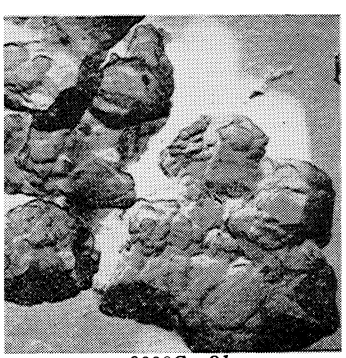
500°C×3*h*



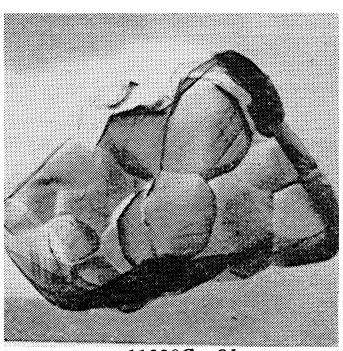
600°C×3*h*



800°C×3*h*



900°C×3*h*



1100°C×3*h*

Fig. 2b. ZnS: Ag phosphor (without flux).
Electron micrograph×5,000

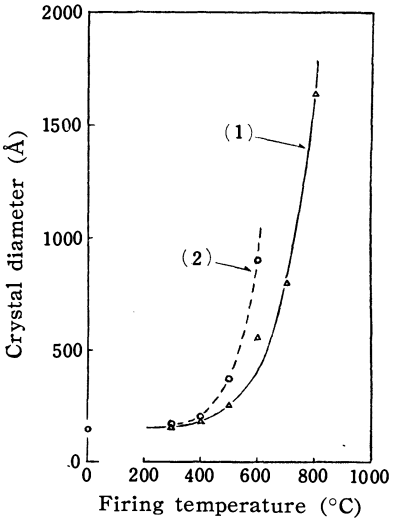


Fig. 3. Relationship between the firing temperature and the diameter of crystals;
(1) without flux, (2) with added 2 wt. % NaCl as flux.

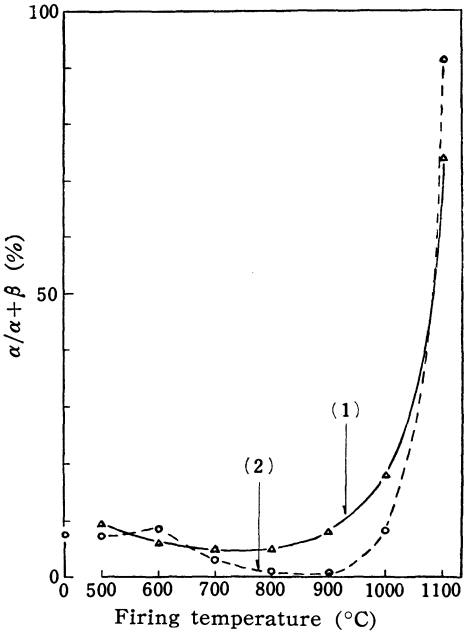


Fig. 4. Relationship between the firing temperature and the crystal form of ZnS: Ag phosphor;
(1) without flux, (2) with 2 wt.% NaCl as flux.

is about 0.2 μ. This is also true for the sample fired by 600°C. However, for the sample fired at 600°C with flux, as shown in Fig. 2a, the diameter is 0.1 μ from X-ray diffraction and is 0.3~0.4 μ from the electron microscope experiment. The disagreement is probably due to the growth of thin plate-like crystals under this particular condition.

Relationship between the Firing Temperature and the Crystal Forms.—The transition of the crystal forms of zinc sulfide takes place at about 1020°C[6]. It is known that, below 1050°C, the β-form is stable and, above 1100°C, the hexagonal α-form is stable[7]. However, from our experiments the situation seems to be a little more complicated.

In Fig. 4, the ratio of the amount of α-form to that of β-form in crystal was given, which was obtained by comparing the strengths of the strongest diffraction patterns, $10\bar{1}0$, 0002 and $10\bar{1}1$ of α-form, with that of β-form, 111. The measurements were made for zinc sulfide phosphors fired for three hours at various temperatures ranging from 500°C to 1100°C, with the raw material containing 8% of α-form.

As is seen in Fig. 4, the amount of α-from in the material without flux decreases as the firing temperature increases, and the transition from α-from to β-form is observed. However, at about 900°C, the content of α-form begins to increase again and becomes 18% at 1000°C and 73% at 1100°C. For the sample with the flux of 2 wt. % of sodium chloride, the α-form begins to decrease at about 700°C. Almost all of the α-form changes into β-form at 800°C, and the amount of α-form becomes nearly equal to zero. As the temperature increases, the α-form appears again at about 1000°C and more than 90% of α-form is found at 1100°C.

The above results show the fact that the transition velocity of crystal forms is much influenced by the existence of the flux and that the transition, α-form $\leftrightarrow$ β-form, becomes easier with 2 wt. % of sodium chloride, but is difficult without it.

The increase of α-form is observed at 600°C for the sample with 2 wt. % of sodium chloride, but the same phenomenon appears in the cases with fluxes other than sodium chloride. The explanation of this is not given yet, and the author is planning to check whether it originates from the existence of some meta-stable state which promotes the formation of α-state, because of some critical temperature to stimulate the sudden crystallization, or whether it is due to the existence of a

6) E. T. Allen and J. L. Crenshaw, *Am. J. Science*, **34**, 341 (1912).
7) R. H. Bube, *J. Chem. Phys.*, **20**, 708 (1952).

state where the α-form is essentially stable.

Influence of Time of Firing.—Fig. 5 gives the relationships among the time of firing, the crystal forms and the intensity of luminescence. At firing temperature of 1000°C, there is not much difference in crystal forms between the sample fired for ten minutes and that fired for three hours, and the former shows a considerably better luminescence intensity. This fact implies that the crystallization has taken place during the firing for a short period. At firing temperature of 800°C, the amount of α-form decreases with the time of firing and the greater part of the crystals are of β-form after firing for thirty minutes. The intensity of luminescence shows a similar tendency and attains the limiting value in thirty minutes.

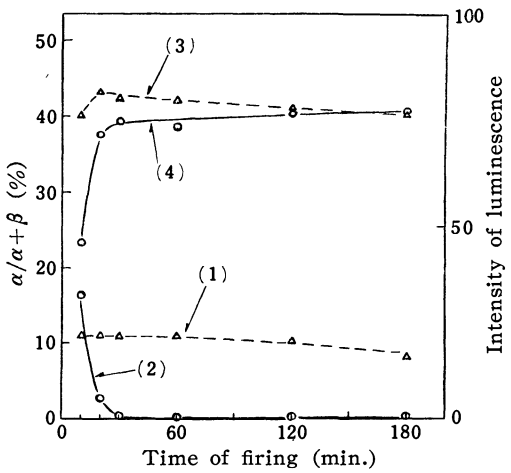


Fig. 5. Relationships among the time of firing, the crystal forms and the intensity of luminescence.
(ZnS: Ag added 2 wt. % NaCl as flux.)
(1) Content of α-form (fired at 1000°C).
(2) Content of α-form (fired at 800°C).
(3) Intensity of luminescence (fired at 1000°C; 12 kV. C.R. excitation).
(4) Intensity of luminescence (fired at 800°C; 12 kV. C.R. excitation).

Those facts imply that the complete change from α-form into β-form is finished within ten minutes when fired at 1000°C and after thirty minutes when fired at 800°C, both with 2 wt.% of sodium chloride as flux.

Summary

(1) The zinc sulfide, before firing, is a large aggregate of crystallites with the crystal diameter of about 150 Å and contains about 8% of α-form.

(2) The crystal growth of zinc sulfide phosphor takes place at about 500°C regardless of whether there is flux or not, but the rate of the growth is much affected by the flux. Without flux, the crystal grows as step-wise piled layers, but, with flux, it grows isotropically showing no influence from the crystal symmetry. Concerning the above difference, there has been discussion, taking into account the density of kinks at the step-wise surfaces of crystals and the change of diffusion constant of zinc sulfide molecules adsorbed at the surfaces.

(3) The transition, α-form $\leftrightarrow$ β-form, of zinc sulfide phosphor is rather easy, but becomes difficult without flux. Also, the transition is completed in thirty minutes of firing at 800°C with the flux of 2 wt.% of sodium chloride, but it is completed within ten minutes of firing at 1000°C.

(4) It is probable that there is a metastable state of α-form at about 600°C, but it requires further consideration.

The author wishes to express his thanks to Mr. T. Mitsuishi and Mr. H. Nagasaki for their cooperation in the X-ray diffraction measurements and the electron microscope experiments.

Central Research Laboratory
Hitachi Co., Ltd.
Kokubunji, Tokyo

Recombination of Hydrogen Atoms on Various Transition Metal Surfaces

By Kazuo NAKADA

(Received January 20, 1959)

Apart from the well-known research of Bonhoeffer[1], in which the order of recombination activity of metals was found to be in good accordance with the series of hydrogen over-voltage, comparison of the relative activities of various kinds of metals for the recombination of hydrogen atoms was made by Katz et al.[2] However, our present knowledge about the recombination activity of transition metals is not sufficient for the detailed discussion.

From the works just cited, it is immediately noticed that the transition metals have the highest activity among all sorts of metals, noble metals follow them, and polyvalent metals have much lower activity as compared with the former two. However, it is not yet well understood why such a distinct change in activity appears when metal species are altered, even though it might be inferred that different electronic band structures are responsible for the difference in activity.

In order to examine the dependence of recombination activity principally on the *d*-band hole, the comparison of activities was made for several transition metals available for us.

We further attempted to obtain the information about the correlation between the work function and the recombination coefficient, which had attracted our attention ever since Suhrmann[3] had made clear many years ago the linearity between them, for it seems to be open to question whether the exact linearity would hold over all kinds of metals at all.

Trapnell et al.[4] intended to interpret the origin of different activities in terms of the so-called Pauling's *d*-character. It is another aim of the present work to make clear in what manner the *d*-character can be related to the catalytic activity.

1) K. F. Bonhoeffer, *Z. physik. Chem.*, **113**, 199 (1924).
2) S. Katz, G. B. Kistiakowsky and R. F. Steiner, *J. Am. Chem. Soc.*, **71**, 2258 (1949).
3) R. Suhrmann and H. Csesch, *Z. physik. Chem.*, **B28**, 215 (1935).
4) K. G. Pickup and B. M. W. Trapnell, *J. Chem. Phys.*, **25**, 182 (1956).

Experimental

In order that the place where the recombination proceeds was confined to the metal surface concerned, a method adequate to be called "an effusion method" was adopted here instead of the usual flow method.

The relative activities of Ta, W, Mo, Ti, Co and Cr were determined with respect to Ni. In the series of Fe, Cr, Mn and Cu, Cu was chosen as a standard of comparison. In another series of Ti, Zr and Th, Ti was adopted as a standard metal. U was compared only with Mo.

Samples.—Most metal samples used were in the form of a circular disk (15 or 20 mm. in diameter and 0.1~0.3 mm. thick), but Ti and Zr were ribbon-like foil. Fe and Mn were electrically plated on one side of copper plate, while Cr was evaporated on copper plate in a vacuum.

Two kinds of metals, one of which was chosen as the standard metal, were stuck together back to back by soldering or spot welding or, in unavoidable cases, by means of synthetic resin adhesives. Their surfaces were polished with 06 emery papers, but no other treatment like chemical etching or electropolishing was done at all.

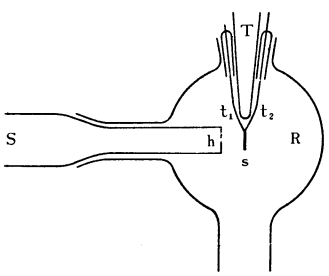


Fig. 1. Main part of apparatus.
S: The side tube of discharge tube
R: The reaction chamber
h: A small circular hole
t_1, t_2: Pt/Pt−Rh thermocouple
s: The sample
T: The top tube inside of which the city water was allowed to flow.

Apparatus and Procedure.—Only the main part of apparatus, made of hard glass, was shown in Fig. 1. Hydrogen atoms were produced in a Wood's discharge tube. The electric discharge was carried out by an alternating current from 5 kW. transformer giving up to 4000 V. The voltage across the electrodes was of the order of 1000~1500 V.

The hydrogen gas including hydrogen atoms was allowed to effuse into the reaction chamber (B) through a small circular hole (h) provided at the end of the side tube (S). In this chamber the sample metal disk was hung by molybdenum wire (0.3 mm. in diameter) at the front of the hole. This chamber was strongly pumped off by an oil diffusion pump backed by a rotary oil pump, but could not be evacuated to less than 5×10^{-4} mmHg on account of leakage gas from the hole.

Even such a non-high vacuum seems to be sufficiently good to ensure that the reaction gas reaches the catalyzing metal surface not by diffusion but rather by effusion, considering the much shorter distance between the sample surface and the hole than the mean free path at the vacuum of 10^{-3} mmHg.

The temperature rise of the sample caused by recombination heat liberating on it was followed by measuring the electromotive force of Pt/Pt-Rh thermocouple attached to the sample by use of a K-type potentiometer. The sample metal disk could be allowed to turn over by virtue of the ground glass joint. Inside the tube (T), in the bottom of which molybdenum lead was sealed, the city water was allowed to flow in order to diminish the effect of the drift of room temperature on the measurements. This procedure was useful to eliminate the error resulting from temperature variation, because the drift of city water temperature was smaller than that of room temperature by a factor of about 5.

Hydrogen. — Commercial cylinder hydrogen was used. The gas was allowed to bubble through a saturated solution of sodium hydroxide. After being dried with sulfuric acid, it was passed over the platinized asbestos (ca. 400°C), and dried again over the phosphoric pentoxide. Hydrogen thus dried was sent to 3 l. flask equipped with a manostat capable of keeping the pressure constant within 0.1 mmHg.

Hydrogen was allowed to diffuse into the discharge tube through a capillary. At this stage the pressure was lowered enough to permit the electric discharge.

In order to keep the catalytic action of discharge tube wall as constant as possible, hydrogen at a pressure of about 150 mmHg was saturated with water vapour on the saturated solution of sodium hydroxide.

Result. — The electromotive forces of two thermocouples, one of which was attached to the sample and the other was immersed in a city-water stream, was read simultaneously for the intervals of 5 min. over the range of 1 to 2 hr. before and during the course of electric discharge. The values averaged over all the reads are taken as expressing the temperatures of the sample and the city-water. The difference of these temperatures varied before and after the discharge was switched on. This variation of temperature difference was adopted as the rise of temperature due to the recombination heat.

At first the temperature rise for the metal aimed at was determined, then the same procedure was applied to the standard metal of another side. The ratio of the former to the latter was adopted as a measure of the recombination coefficient. The values thus determined were summarized as follows:

a) for the case when nickel was adopted as a standard metal, Co(118), Ni(100), Ta(88), Mo(86), W(84), Ti(83) and Cr(71):

b) for the case when copper was a standard metal, Fe(167), Cr(120), Mn(111) and Cu(100).

The latter case could be converted into the former case as given below:

Fe(99), Cr(71), Mn(66), and Cu(59).

In the series of Ti, Zr and Th, the order of activity was determined as follows:

$$Zr>Ti>Th$$

From the comparison of U with Mo, the relation

$$Mo>U$$

was obtained.

Discussion

In this section, present results have been discussed from several points of view through comparison of activity with physical properties. At first we confine ourselves to metals belonging to the first long period of the periodic table.

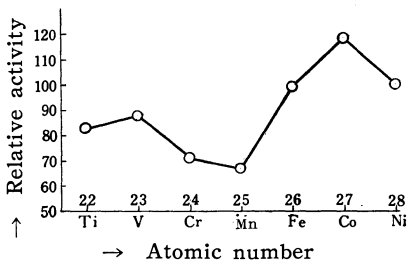


Fig. 2. The dependence of relative activity on atomic number, where Ta is taken in place of V.

In Fig. 2 is given the dependence of the recombination activity on atomic number, where tantalum is used in place of vanadium. It is perceived that this plot has two peaks at group V and group VIII. On the other hand, if the cohesive energy[5] is plotted against the atomic number, Fig. 3 curve a is obtained. It is noticed that this plot has also two peaks at the same positions. When other physical properties, e. g., the effective electron number per atom[6], density of states per eV. per atom[7], etc., are plotted against the atomic number, plots similar to the above are obtained as shown in Fig. 3 curve b. From the resemblance of these plots to the plot in

5) C. Kittel, "Introduction to Solid State Physics", John Wiley & Sons, New York (1956), p. 99.
6) Ibid., p. 132.
7) Ibid., p. 259.

Fig. 2, it is suggested that these physical properties are more or less related to the catalytic activity.

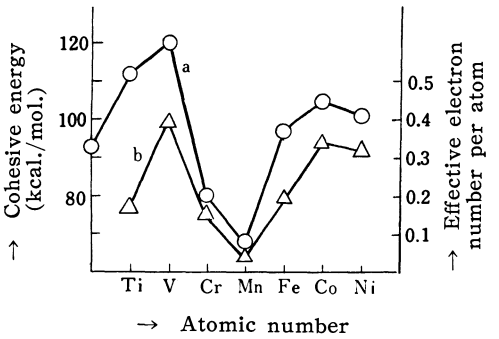


Fig. 3. Curve a, plot of cohesive energies versus the atomic number and curve b, plot of the effective electron number versus the same.

Let us consider a little further the correlation of activity with the cohesive energy. From the resemblance between the plot of cohesive energy versus the atomic number and that of activity versus the same, it is suggested that the bond strength of chemisorption which can be evaluated by an approximate method stated just below, may have an important connection with the catalytic activity. Recently, a method for evaluating the bond strength of chemisorption approximately by use of the experimental heat of sublimation and the electronegativity had been presented by Eley[8]. More recently, a somewhat different method was offered by Stevenson[9], in which the work function was used instead of the value of dipole moment in evaluating the ionic contribution.

If the semi-empirical values of bond strength of chemisorption evaluated by the above two kinds of methods are taken, plots quite similar to the relation between cohesive energy and atomic number must be obtained. From this fact, the conclusion may be drawn that metals having strong bond strength of chemisorption should have high activity. However, the statement given below has made such a view less convincing.

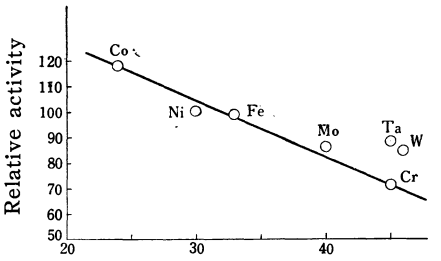


Fig. 4. The dependence of the relative activity on the experimental heat of chemisorption, where the data are taken from Stevenson's report.

Alternatively, if the recombination activities are plotted against the data on the experimental heat of chemisorption quoted by Stevenson, it is found that almost all points fall on a straight line aside from the slight upward deviation of tantalum and tungsten as shown in Fig. 4. From this fact, it is suggested that metals with strong bond strength of chemisorption are less active in contrast to the above statement deduced from the comparison of the dependence of cohesive energy on atomic number with that of activity on the same.

In order for the surface recombination to proceed, if the Rideal mechanism is assumed, hydrogen atoms need be chemisorbed first on bare metal surface and yet their bonds must have moderate strength to be ready to break on the attack of a chemisorbed layer by hydrogen atoms from the gas phase so as to reproduce hydrogen molecules, for it is supposed that the activation energy for the latter process can be approximated to be proportional to the chemisorption bond strength[10].

Obviously, the reason why polyvalent metals have low activity comes from the fact that the Brillouin zone is almost fully filled and, accordingly, only a few sites can be used for hydrogen atom chemisorption. On the contrary, in the case of transition metals with unfilled *d*-orbitals capable of supplying ample sites for the appreciable adsorption to occur, it seems likely that the bond strength of chemisorption may play a more important role in

8) D. D. Eley, *Discussions Faraday Soc.*, 8, 34 (1950).

9) D. R. Stevenson, *J. Chem. Phys.*, **23**, 203 (1955).
The surface M-H bond can be calculated from Pauling's equation
$E(\mathrm{M-H})=1/2\{E(\mathrm{M-M})+E(\mathrm{H-H})\}+23.06(x_{\mathrm{M}}-x_{\mathrm{H}})^2$
where $E(\mathrm{M-M})$ is one sixth of the experimental sublimation energy and $E(\mathrm{H-H})$ is the dissociation energy of hydrogen molecule. The difference of electronegativity, $x_{\mathrm{M}}-x_{\mathrm{H}}$, can be approximated as equal to the dipole moment of the bond in debyes, the values of which are known from the data on contact potential.

10) S. Glasstone, K. J. Laidler and H. Eyring, "The Theory of Rate Process", McGraw-Hill Book Co., New York (1941), p. 152.
In the three-atom reaction AB+C→A+BC, the activation energy can be approximated to be 0.055D′, where D′ is the dissociation energy plus zero point energy of AB molecule.

determining the catalytic activity than the number of sites. The correlation between the experimental heat of chemisorption and recombination activity may be understood, in a sense, in terms of different bond strength of chemisorption.

Even though it is not known at what degree of coverage recombination would proceed in the present experimental condition, the above slight deviation in the case of tantalum and tungsten might be attributed in part to such a character of adsorption as that when the heat of chemisorption of hydrogen on them decreases more markedly with increasing coverage than the case of nickel and iron[11].

However, there seems to be another explanation of the origin of low activities of some transition metals (e.g., Ti, Zr and Th). The transition metals can be grouped into two main classes[12], because of wide diversity of their behavior for hydrogen absorption. Namely, metals of group A absorb hydrogen endothermically and those of group B exothermically. As a whole, it is permissible to say that the former just corresponds to the more active group, and the latter to the less active group. Though it is not clear to what extent the parallelism between hydrogen absorption and adsorption would be preserved, some kinds of resemblance between them may be excepted to exist concerning the state of hydrogen atoms in and on metals. With this in mind, the different activities of group A and B metals can be explained in the following way: In the case of group B metals a hydride layer on which hydrogen atoms are adsorbed with difficulty, would be formed. Contrary to this, in the case of group A the usual monoatomic chemisorbed layer of hydrogen is formed serving as the intermediate compound of this recombination reaction.

Next, let us examine how the physical properties, e.g., work function, *d*-character and surface potential of chemisorbed hydrogen atom layer, may correlate to recombination activity.

In view of Suhrmann's old work it is permissible to say that the larger the work function, the higher the activity. As shown in Fig. 5 curve a, the values of work function[13] of the first long period metals show a tendency to increase with

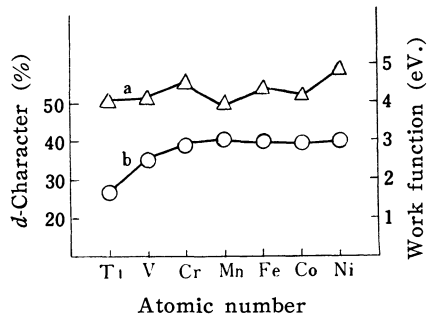


Fig. 5. Curve a, plot of the work function versus the atomic number and curve b, plot of the *d*-character versus the same.

the atomic number, despite the existence of rather complex ups and downs. Such a tendency as that where both catalytic activity and work function increase with the atomic number seems to support Suhrmann's view in the limited sense. However, this view may be, if anhything, an approximation, considering the fact that with respect to recombination activity, for example, the relation Ni<Co, Ti<Zr, and W<Mo was obtained by the present author, while the opposite relation holds for the work function.

Trapnell et al.[14] predicted that the *d*-character, which was defined by Pauling, might play an important role in the present reaction. From the present author's result it can be said that metals with large *d*-character have, on the whole, high activity. However, the monotonous increase of *d*-character with atomic number, as shown in Fig. 5 curve b is not adequate to explain the existence of two peaks in the activity-atomic number plot.

So long as the data[15] available up to date are concerned, metals can be roughly classified into two groups according to the magnitude of the absolute values of surface potential of chemisorbed hydrogen layer. The first group metals corresponding to the higher value, to which W (−0.48 or −0.65 V.) and Ta (−0.9, −1.2 or −0.43 V.) belong, have lower activity than the second corresponding to the lower value, to which Fe (−0.19 or −0.47 V.), Ni (−0.1 or −0.12 V.) and Co (0.06 V.) belong. This is naturally accepted from the statement given before, considering the fact that metals corresponding to large surface potential values have generally large experimental chemisorption heats. Accordingly, there seems to be no direct connection between

11) O. Beeck, *Discussions Faraday Soc.*, 8, 118 (1950).
12) S. Dushman "Scientific Foundation of Vacuum Techniques", John Wiley & Sons, New York (1949), p. 553.
13) H. B. Michaelson, *J. Appl. Phys.*, 21, 536 (1950).
14) Loc. cit.
15) J. J. Broeder, L. L. van Reijen, W. M. H. Sachtler and G. C. A. Schuit, *Z. Elektrochem.*, 60, 838 (1956).

the degree of polarization of chemisorbed hydrogen atom and recombination activity.

Our attempt to explain the different recombination activities in terms of any one of physical properties proves less successful. This is probably because there is no strict theory capable of connecting the activity to the physical properties. At any rate, it is apparent that many more quantitative experiments remain to be done before a systematic account can be given concerning the origin of different activities of transition metals for this recombination reaction.

Summary

A study has been made of surface recombination of hydrogen atoms on various transition metals.

Hydrogen atoms were produced in the electric discharge tube by use of an alternating current. In order to prevent the reacting gas from reaching the undesired part of the sample, a method which may be called "an effusion method" was adopted here. The relative activity of two kinds of metal plates, stuck together by the solder or some such material, was determined, comparing the temperature rises of the sample by means of alternative exposure of each side surface to the reacting gas.

The following results were obtained:

a) Co> Fe> Ni> Ta> Mo> W> Ti> Cr > Mn> Cu

b) Zr> Ti> Th

c) Mo> U

These orders of activity were examined from several points of view through the comparison of recombination activity with the work function, the *d*-character, the experimental heat of chemisorption, etc.

The present results are still fragmentary but may suffice to show a qualitative trend.

The author wishes to express his gratitude to Professor S. Shida for his kind encouragement and to Mr. I. Yasumori for his helpful advice.

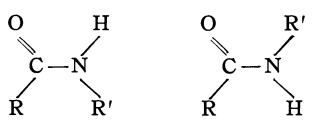
Laboratory of Physical Chemistry
Tokyo Institute of Technology
Meguro-ku, Tokyo

On the Reactivity of Amide Group of ε-Caprolactam Derivatives

By Naoya OGATA

(Received January 28, 1959)

The bond between carbon and nitrogen of an amide has appreciably double bond character due to resonance[1], and the configuration of amide linkage tends to be a planer structure and two configurations of *cis* and *trans* forms are possible as follows:



cis form *trans* form

ε-Caprolactam is the *cis* form[2], while monosubstituted acid amide RNHCOR′ is the *trans* form[3]. It was ascertained[4] that ε-caprolactam caused an amide interchange reaction with a *trans* amide and the reaction rate of ε-caprolactam with its ring oligomers became faster with the enlargement of the ring. When it is compared with the polymerization of ε-caprolactam, the equilibrium between ring and chain structures shifts to the ring form in the case of the polymerization of substituted ε-caprolactam such as γ-methyl-ε-caprolactam, and *N*-methyl-ε-caprolactam is too stable to polymerize[5]. Therefore, this study was undertaken in order to elucidate the difference in reactivity of amide group of ε-caprolactam derivatives.

1) G. W. Wheland, "Resonance in Organic Chemistry", John Wiley & Sons, Inc., New York (1955), p. 109.
2) M. Tsuboi, This Bulletin, **22**, 215 (1949).
3) S. Mizushima et al., *J. Am. Chem. Soc.*, **72**, 3490 (1950).
4) N. Ogata, Contributed to the *Makromoleculare Chemie*.
5) H. Yumoto, K. Ida and N. Ogata, This Bulletin, **31**, 249 (1958).

Experimental

1. Determination of the Dipole Moment of Amides.—The dipole moment of ε-caprolactam, γ-methyl-ε-caprolactam and *N*-methyl-ε-caprolactam was determined in benzene solution at 25°C, as shown in Table I. The molecular polarization of ε-caprolactam or γ-methyl-ε-caprolactam decreased with the increase of the concentration but that of *N*-methyl-ε-caprolactam was almost constant, as shown in Fig. 1.

TABLE I. THE DIPOLE MOMENT OF ε-CAPROLACTAM DERIVATIVES

Sample	Dipole moment (D)
ε-Caprolactam	3.88
γ-Methyl-ε-caprolactam	5.48
N-Methyl-ε-caprolactam	4.23

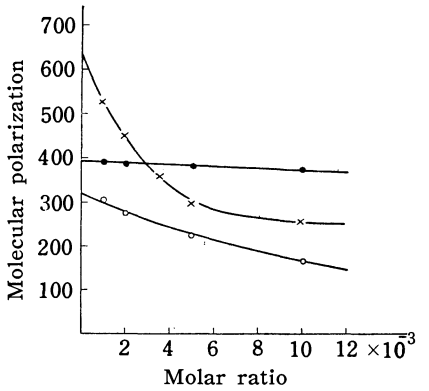


Fig. 1. The molecular polarization of ε-caprolactam derivatives.
● *N*-Methyl-ε-caprolactam
× γ-Methyl-ε-caprolactam
○ ε-Caprolactam

TABLE II. THE RATE OF HYDROLYSIS OF ε-CAPROLACTAM

Temp. (°C)	Concn. of H_2SO_4 (N)	Reaction time (hr.) 1/6	1/3	1/2	1	2	3	5	7	8
60	1.0	—%	—%	—%	4.9%	6.7%	11.4%	15.1%	21.2%	—%
60	2.0	—	—	—	8.2	12.9	19.4	32.7	42.9	—
80	1.0	—	—	13.1	21.0	34.7	43.3	59.5	67.1	—
80	2.0	10.9	15.0	16.0	38.0	56.9	78.9	88.0	—	—
100	0.5	—	—	24.9	40.8	49.2	56.1	63.3	—	—
100	1.0	21.7	32.9	44.9	66.3	87.3	93.2	97.5	—	100.0
100	1.5	28.2	56.8	60.2	80.6	100.0	—	—	—	—
100	2.0	35.3	60.2	64.7	86.5	100.0	—	—	—	—

TABLE III. THE RATE OF HYDROLYSIS OF RING OLIGOMERS
(Concentration of sulfuric acid, 3 N)

Ring oligomer	Temp. (°C)	Reaction time (hr.) 2	4	6	8	10	15	20
dimer	78	—%	—%	—%	5.2%	—%	8.8%	12.0%
	100	—	6.8	9.7	—	21.6	29.6	25.5
trimer	78	—	6.1	8.4	12.4	—	—	—
	100	18.0	32.0	38.0	42.3	—	—	—
tetramer	78	—	5.4	7.7	11.9	—	—	—
	100	20.0	28.5	34.0	39.0	—	—	—

TABLE IV. THE RATE OF HYDROLYSIS OF *N*-METHYL-ε-CAPROLACTAM

Temp. (°C)	Concn. of H_2SO_4 (N)	Reaction time (hr.) 1	2	3	4	5	7.5	10	15	20	30
80	3.0	1.8%	4.4%	6.3%	—%	12.9%	15.5%	18.5%	—%	—%	—%
90	3.0	—	10.2	—	17.2	21.7	31.5	40.1	—	—	—
100	1.0	9.4	16.0	19.7	24.0	27.6	—	40.3	—	—	—
100	2.0	10.8	18.0	27.4	34.9	40.5	—	60.8	—	—	—
100	3.0	12.3	23.5	30.3	36.5	43.9	57.6	67.9	75.8	82.2	89.8
100	5.0	8.4	18.0	26.1	38.6	46.7	—	100.0	—	—	—

2. Determination of the Reaction Rate of Hydrolysis.—ε-Caprolactam, *N*-methyl-ε-caprolactam or ring oligomers of ε-caprolactam which were obtained by repeated recrystallizations of the water extract of poly-ε-capramide, at the amount of 10^{-2} mol., was heated in 20 ml. of sulfuric acid in sealed glass tubes and then the solution was neutralized quickly. The quantities of ε-aminocaproic acid formed in the case of ε-caprolactam or its ring oligomers could be determined by the formol titration method but the quantitative determination of *N*-methyl-ε-aminocaproic acid was possible by neither the formol titration nor the method using an ion exchange resin. *N*-methyl-ε-aminocaproic acid could be quantitatively determined in the mixed solvent of ethanol and 30% formalin (1:1). The neutralized solution of *N*-methyl-ε-aminocaproic acid was filled up to 50 ml. and 10 ml. of the solution were dried and then the residue was dissolved in 10 ml. of ethanol and 30% formalin. The solution was titrated by 0.1 N sodium hydroxide solution with phenolphthalein as an indicator. These results are shown in Tables II, III and IV.

The hydrolysis of lactam in the presence of large quantities of water is the first order reaction and the rate constant is calculated by the following equation, where a designates the mole of amide and x the mole of amino acid formed at t hr.

$$k=2.303/t\cdot\log a/(a-x) \qquad (1)$$

The rate constants, which are shown in Table V, are proportional to the concentration of sulfuric acid, as shown in Figs. 2 and 3.

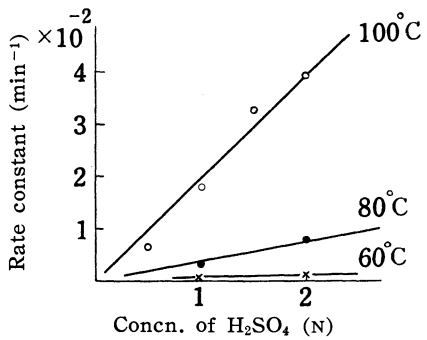


Fig. 2. The rate constant of hydrolysis of ε-caprolactam.

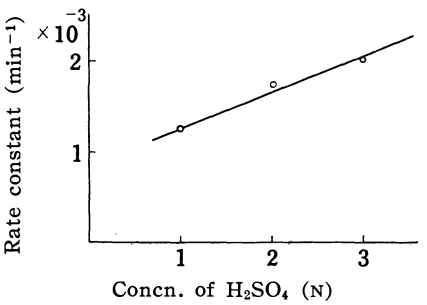


Fig. 3. The rate constant of hydrolysis of *N*-methyl-ε-caprolactam at 100°C.

TABLE V. THE RATE CONSTANT OF HYDROLYSIS OF ε-CAPROLACTAM DERIVATIVES

Sample	Temp. (°C)	Concentration of H_2SO_4 (N)	Rate constant (min^{-1})
ε-Caprolactam	60	1.0	0.6×10^{-3}
		2.0	1.3×10^{-3}
	80	1.0	3.5×10^{-3}
		2.0	8.0×10^{-3}
	100	0.5	6.4×10^{-3}
		1.0	18.1×10^{-3}
		1.5	33.2×10^{-3}
		2.0	39.4×10^{-3}
N-Methyl-ε-caprolactam	80	3.0	0.38×10^{-3}
	90	3.0	0.84×10^{-3}
	100	1.0	1.23×10^{-3}
		2.0	1.73×10^{-3}
		3.0	2.00×10^{-3}
Ring dimer	78	3.0	0.11×10^{-3}
	100	3.0	0.25×10^{-3}
Ring trimer	78	3.0	0.26×10^{-3}
	100	3.0	1.15×10^{-3}
Ring tetramer	78	3.0	2.33×10^{-3}
	100	3.0	13.75×10^{-3}

3. Determination of Infrared Spectrum.—The infrared spectrum of ε-caprolactam, ring-dimer, -trimer and -tetramer, which is shown in Figs. 4, 5, 6 and 7, was measured in a potassium bromide disc with a Hitachi model EPI-2 spectrophotometer, with a rock-salt prism. The absorption band of N-H of ε-caprolactam appears at 3215 and 3077 cm^{-1}, while that of ring-dimer at 3279 and 3077 cm^{-1}. The absorption band of CO of ε-caprolactam appears at 1650 cm^{-1}, while that of ring-dimer at 1639 cm^{-1}. The spectrum of ring-dimer shows absorption maximum at 1555 cm^{-1}, which is not found in ε-caprolactam. The absorption bands of N-H of ring-trimer and -tetramer appear at 3289 and 3077 cm^{-1} and the spectra come to resemble that of poly-ε-capramide (Fig. 8).

When dry hydrogen chloride was introduced into carbon tetrachloride solution of ε-caprolactam, a white crystal was precipitated. This crystal was decomposed easily in the air, evolving hydrogen chloride. It was filtered off in dry hydrogen chloride atomosphere and dried, and then its infrared spectrum was measured, in a potassium bromide disc, which is shown in Fig. 9. The absorption bands of N-H at 3215 and 3077 cm^{-1} disappear and new ones appear at 2730, 2500 and 2398 cm^{-1}. The absorption band of N-H of dibutylamine $(C_4H_9)_2N$-H appears only at 3311 cm^{-1}, while that of its hydrochloride at 2564, 2463 and 2398 cm^{-1}. Therefore, these new bands are estimated to be the absorption of N-H of the reaction product which was produced by adding hydrogen chloride to the nitrogen atom of ε-caprolactam. The absorption band of CO of the

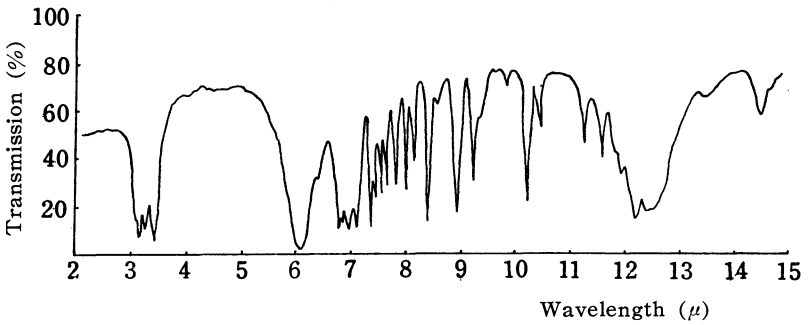


Fig. 4. The infrared spectrum of ε-caprolactam (KBr disc).

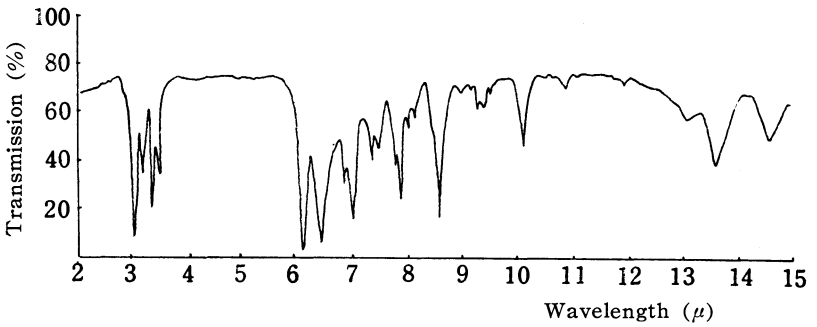


Fig. 5. The infrared spectrum of ring dimer (KBr disc).

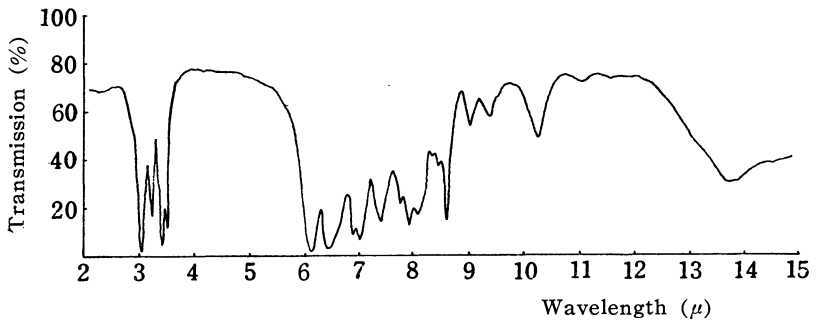


Fig. 6. The infrared spectrum of ring trimer (KBr disc).

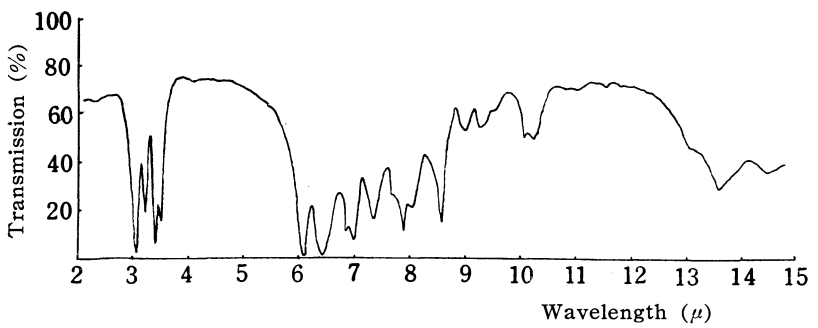


Fig. 7. The infrared spectrum of ring tetramer (KBr disc).

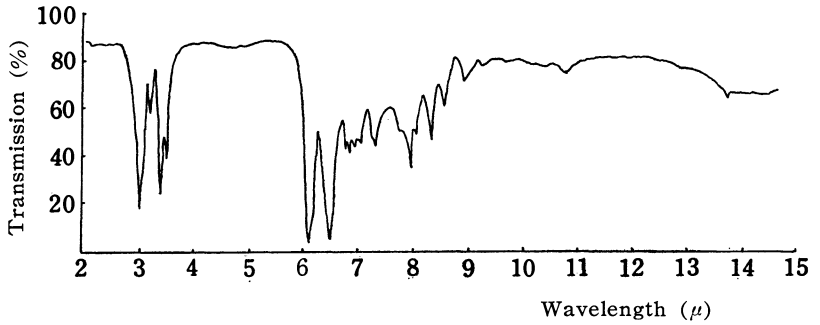


Fig. 8. The infrared spectrum of poly-ε-capramide (KBr disc).

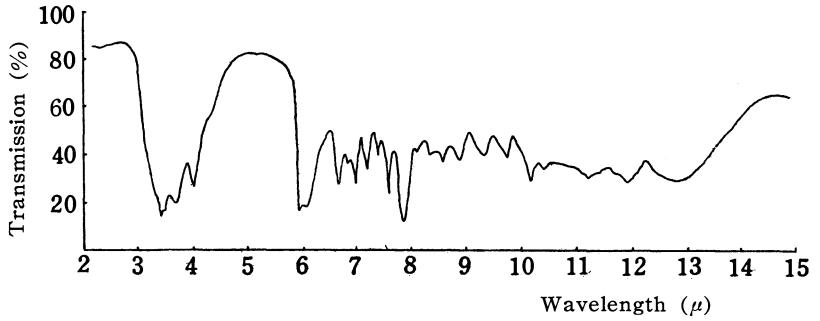


Fig. 9. The infrared spectrum of the reaction product of ε-caprolactam with hydrogen chloride (KBr disc).

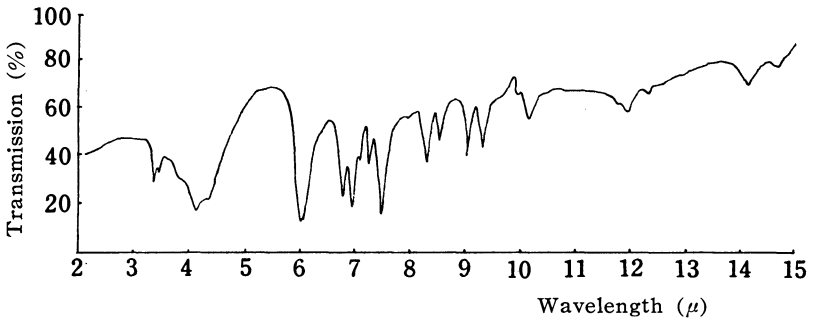


Fig. 10. The infrared spectrum of the reaction product of *N*-methyl-ε-caprolactam with hydrogen chloride (KBr disc).

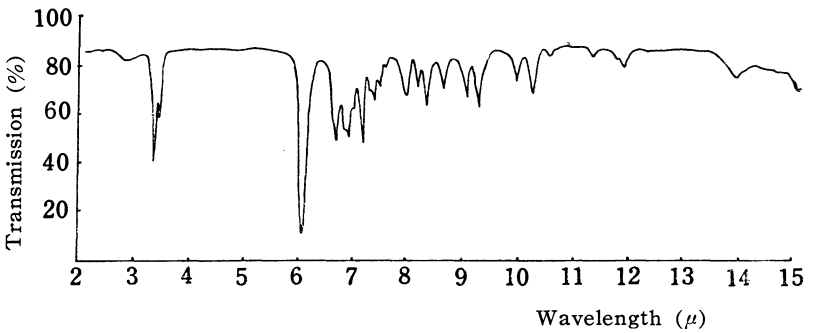


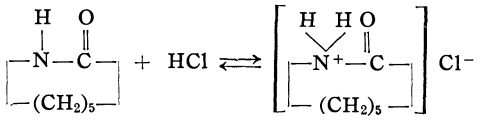
Fig. 11. The infrared spectrum of *N*-methyl-ε-caprolactam (liquid).

reaction product shifts from 1650 to 1681 cm^{-1}.

When dry hydrogen chloride was introduced into carbon tetrachloride solution of *N*-methyl-ε-caprolactam, a white crystal was precipitated but it dissolved again by the further introduction and *N*-methyl-ε-caprolactam was floated on carbon tetrachloride. The infrared spectrum of the crystal formed at first was measured in a potassium bromide disc, which is shown in Fig. 10. A new broad absorption appears at 2398 cm^{-1} which is tentatively assigned to the N-H band of the addition product of *N*-methyl-ε-caprolactam. The absorption band of CO of *N*-methyl-ε-caprolactam appears at 1645 cm^{-1}, which is shifted to the lower frequency than that of normal carbonyl compound, as shown in Fig. 11.

Discussion

ε-Caprolactam forms an addition compound with hydrogen chloride in carbon tetrachloride solution as follows

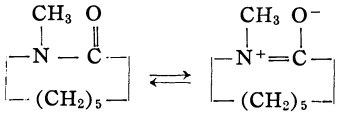


The ring opening reaction of ε-caprolactam in the presence of the ammonium cation[6] is presumed to be caused by the addition of the ammonium cation to the amide group.

The rate constant of hydrolysis of *N*-methyl-ε-caprolactam is about one twentieth of that of ε-caprolactam. The activation energy of hydrolysis of ε-caprolactam is calculated from the temperature dependence of the rate constants to be 20 kcal./mol., while that of *N*-methyl-ε-caprolactam 22 kcal./mol.

Since the molecular polarization of *N*-methyl-ε-caprolactam is almost constant with the increase of concentrations, it is expected that molecules do not associate at all. However, the absorption of CO in its infrared spectrum appears in much lower frequency than that of carbonyl compounds (about 1700 cm^{-1}). The dipole moment of *N*-methyl-ε-caprolactam is larger than that of ε-caprolactam.

From these results as stated above, it is expected that the amide linkage of *N*-methyl-ε-caprolactam has considerably ionic character due to resonance by the effect of methyl group as shown below and the stability of ring structure increases.



The rate constant of hydrolysis of ring-dimer is remarkably smaller than that of ε-caprolactam and that of ring-oligomers becomes faster as the ring becomes larger. It is ascertained[2,7] that the absorption of N-H of the *trans* or the *cis* amide appears in the 3370 to 3290 cm^{-1} or the 3240 to 3170 cm^{-1} regions in the infrared spectrum. The infrared spectrum of ring dimer, in the crystalline state, shows absorption maxima at 3279 and 3077 cm^{-1} and the configuration is expected to be not *cis*-[8] but *trans*- form. As the absorption band of CO of ring dimer appears in lower frequency than that of ε-caprolactam, ring-trimer or -tetramer, the low reactivity of ring dimer can be explained from the expectation that two amide groups are particularly favorable for the formation of two intramolecular hydrogen bonds and its structure is presumed to be as shown in Fig. 12. As amide groups lie too far apart to form the intramolecular hydrogen bond with the enlargement of the ring, the reactivity of ring oligomers becomes larger.

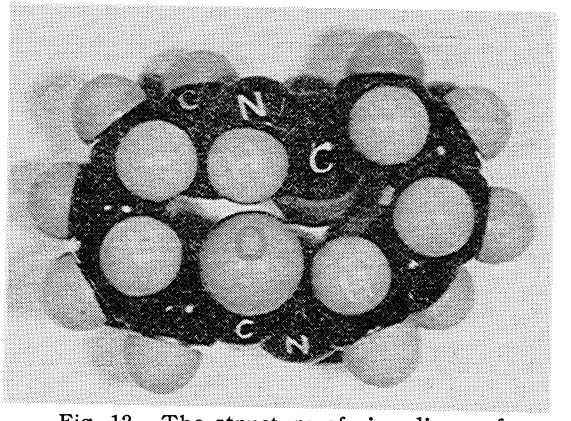


Fig. 12. The structure of ring dimer of ε-caprolactam.

Summary

The dipole moments, infrared spectra and rate constants of hydrolysis of ε-caprolactam derivatives have been determined in order to elucidate the difference in reactivity. The great stability of *N*-methyl-ε-caprolactam is expected, due to the increase of reasonance of amide linkage. Ring dimer of ε-caprolactam is stable for hydrolysis due to the strong intramolecular hydrogen bonds and the reactivity

6) H. Yumoto and N. Ogata, *Makromol. Chem.*, **25**, 71 (1958).
7) T. Miyazawa, T. Shimanouchi and S. Mizushima, *J. Chem. Phys.*, **24**, 408 (1950).
8) P. H. Hermans, *Nature*, **177**, 126 (1956).

of ring oligomers of ε-caprolactam increases as the ring becomes larger.

The author wishes to thank Dr. K. Hoshino and Dr. H. Kobayashi who instructed him in these studies and permitted the publication. He also thanks Mr. M. Nakata et al. who collaborated with him in experiments.

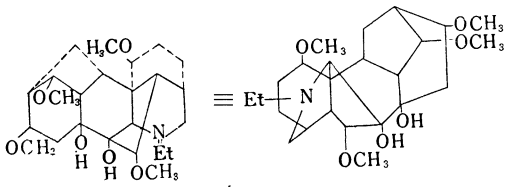
Research Department
Toyo Rayon Co., Ltd.
Minato-ku, Nagoya

The Aconite Alkaloids. XXIX. Some Oxidation Products of Lycoctonine*

By Harusada SUGINOME, the late Shigehiko IMATO, Shozo YAMADA** and Nobukatsu KATSUI

(Received September 4, 1958)

The total structure of de-(hydroxymethylene)-lycoctonine (I) was determined by Przybylska and Marion[1] by X-ray crystallographic method, and that of lycoctonine (II) was proposed by Edwards, Marion and Stewart[2] on the basis of chemical evidences for the location of the hydroxymethylene group.



(I)

Fig. 1.

Most of the reactions and products have been interpreted[2,3] on the basis of these formulae; some of them are indicated in Fig. 2.

Since two new oxidation products from lycoctonine have been obtained, the present authors wish to report several arguments concerning their chemical properties and their relationship to other lycoctonine derivatives.

Oxidation of lycoctonam (III)[4] with chromic anhydride in N sulfuric acid solution gave three compounds, lycoctonamic acid (IV)[4], formic acid and a new neutral

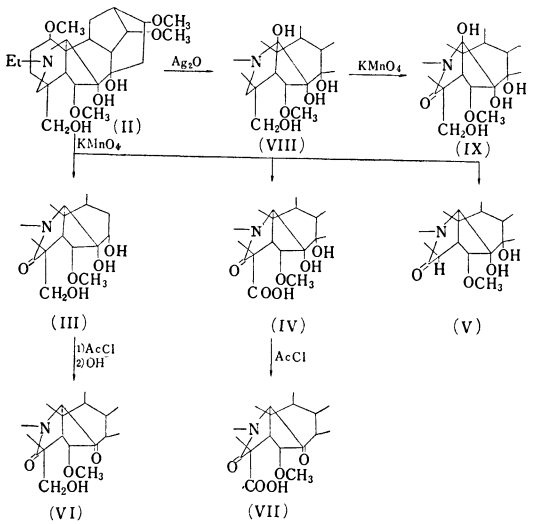
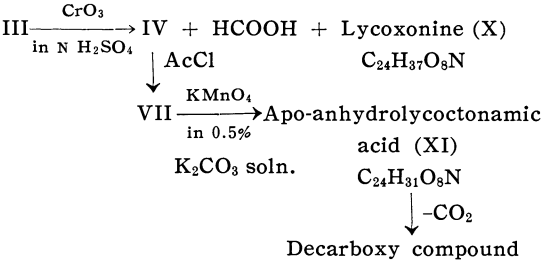


Fig. 2.

product, lycoxonine (X), $C_{24}H_{37}O_8N \cdot 4H_2O$, m. p. 80~83°C, $[\alpha]_D$ +40.8°.



* Part XXVIII, H. Suginome, N. Katsui and G. Hasegawa, This Bulletin, **32**, 604 (1959).

** Present address: Osaka Municipal Hygienic Laboratory, Kitaōgi-machi, Kita-ku, Osaka.

1) M. Przybylska and Léo Marion, *Can. J. Chem.*, **34**, 185 (1956).

2) O. E. Edwards, Léo Marion and D. K. R. Stewart, ibid., **34**, 1351 (1956).

3) O. E. Edwards, Léo Marion and K. H. Palmer, *J. Org. Chem.*, **24**, 1372 (1957).

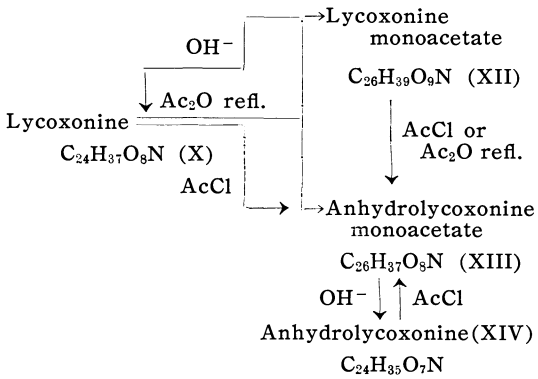
4) O. E. Edwards and Léo Marion, *Can. J. Chem.*, **30**, 627 (1952). These compounds had been isolated independently in these laboratories. (A report on them was read before the Annual Meeting of the Chemical Society of Japan, held in Tokyo, April, 1949, and the Meeting of the Hokkaido Branch of the Chemical Society of Japan, held in Sapporo, July, 1949). The names oxolycoctonine, L-acid and anhydro-L-acid were assigned for III, IV and VI, respectively.

On oxidation of anhydrolycoctonamic acid (VII)[4] with potassium permanganate in 0.5 per cent potassium carbonate solution, a new acid, apo-anhydrolycoctonamic acid (XI), $C_{24}H_{31}O_8N$, m. p. 183~184°C, $[\alpha]_D$+37°, was yielded.

Lycoxonine (X) contains an *N*-ethyl and four methoxyl groups as does lycoctonam (III). In the infrared spectra of both compounds no decisive difference could be detected in the hydroxyl region because of the broad absorption. On the other hand, the bands due to lactam carbonyl were distinctly different (lycoxonine showed at 1631 cm^{-1} and lycoctonam at 1618 cm^{-1}). The same shift has been observed[4] between lycoctonam and the compounds in which the primary hydroxyl group has been acetylated or replaced by hydrogen. Since, from the above observations, the properties of the primary hydroxyl group were considered to be different, the acetylation of lycoxonine was examined.

Lycoxonine was acetylated with acetyl chloride at room temperature yielding anhydrolycoxonine monoacetate (XIII), m. p. 232~234°C, $[\alpha]_D$+37.8°, or with acetic anhydride under reflux yielding the same anhydro monoacetate (XIII) and lycoxonine monoacetate (XII), m. p. 222~225°C. The compound XIII gave anhydrolycoxonine (XIV), m. p. 160~162°C, by hydrolysis.

However, lycoxonine is not acetylated on treatment with acetic anhydride and pyridine at room temperature, but lycoctonam (III) or other lycoctonine derivatives containing original the primary hydroxyl group have been readily acetylated[4] under the same conditions. Thus the formation of anhydro monoacetate (XIII) indicates the existence of the original glycol system and at least another hydroxyl group in lycoxonine (X). However, the hydroxyl group to be acetylated in lycoxonine is no longer the original primary one in view of the difficulty of acetylation.



This interpretation is in concordance not only with the properties of lycoxonine (whilst lycoctonam has been oxidized readily, lycoxonine is stable), but also with the observation of the infrared spectra of anhydrolycoxonine (XIV) and anhydrolycoctonam (VI) (the latter compound is derived from lycoctonam (III) by pinacolic dehydration). The absorption band at 3413 cm^{-1}, characteristic of the hydroxyl in compound VI, disappeared and a new band at 3534 cm^{-1} appeared in compound XIV. From the above results of acetylation, oxidation, and examination of spectra and compositions, it may be concluded that the properties of lycoxonine (X) are probably consistent with a structure in which the hydroxymethylene of lycoctonam (III) has been removed and a hydroxyl group has been produced.

It has been reported[2-4] that the substituent group, which is located at the bridgehead of the azabicyclo [3,3,1]-nonane system in the skeleton of lycoctonine, is readily removed. For example, de-(hydroxymethylene)-lycoctonam (V) has been formed during the permanganate oxidation of lycoctonine, and it has been obtained also by decarboxylation of lycoctonamic acid (IV). Thus, on the basis of the ready removal of the hydroxymethylene group, it may be considered that compound V is an intermediate in the formation of lycoxonine from lycoctonam. If this consideration is correct, the formation of formic acid during the oxidation will be explained by the analogous mechanism which has been suggested by Edwards, Marion and Stewart[2].

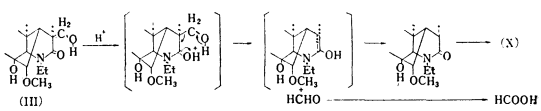


Fig. 3.

However, on the same treatment with chromic anhydride in N-sulfuric acid solution, de-(hydroxymethylene)-lycoctonam (V) is very stable against the reagents. On more vigorous treatment of lycoctonam (III) with the acid only, the hydroxymethylene group is left intact while lycoctonam undergoes extensive change[5]. It is, therefore, unlikely that de-(hydroxymethylene)-lycoctonam (V) is an intermediate. An attempt was made to determine the location of the new hydroxyl

5) O. E. Edwards, Léo Marion and R. A. McIvor, *Can. J. Chem.*, **32**, 708 (1954).

group, but decisive conclusions have not yet been obtained.

Recently an interesting compound, which may be related to the change from lycoctonam to lycoxonine, has been reported by Edwards, Marion and Stewart[2]. This compound was obtained by the action of lead tetraacetate on hydroxylycoctonam (VIII). It was suggested that it had a structure in which the hydroxymethylene group of compound VIII had been replaced by a new hydroxyl group and the glycol system had been cleaved.

Therefore, except for the cleavage of glycol, the properties of this compound appear to be closely analogous to those of lycoxonine. The same investigators[2] suggested in addition that it is difficult to demonstrate whether the skeleton of hydroxylycoctonine[6] (VIII) is or is not the same as that of lycoctonine. Hence, it is of interest to compare the action of chromic anhydride upon lycoctonam (lycoctonine skeleton) with that upon hydroxylycoctonam (hydroxylycoctonine skeleton), and to investigate whether the new hydroxyl group in lycoxonine is or is not located at the same position as that of the compound obtained by the above workers.

On treatment of hydroxylycoctonam (IX) with chromic anhydride in N sulfuric acid solution, two acids, Y-acid, m. p. 193~195°C, and C_I-acid, m. p. 220~222°C, and two neutral compounds, Y, m. p. 177~180°C, and Z, m. p. 226~227°C, were obtained. The properties of these compounds will be reported later.

The new acid, apo-anhydrolycoctonamic acid (XI), obtained by alkaline permanganate oxidation of anhydrolycoctonamic acid (VII), still contains an *N*-ethyl group. It shows the lactam band at 1597 cm^{-1} in the infrared spectrum, and gives a decarboxy-compound, m. p. 105~110°C. These evidences have been observed[4] analogously as in the case of the starting acid (VII), but the apo-acid (XI) contains only three methoxyl groups while the starting acid contains four.

In the ultraviolet spectrum the apo-acid (XI) shows the maximum at 305 mμ (log ε 2.07) which is usual in position but unusual in intensity; the maximum of dehydro-compounds from lycoctonine has been shown at 305 mμ (log ε 1.89). In addition, an oxime of the decarboxy-compound derived from the apo-acid shows the ultraviolet maximum still at 305 mμ, but the intensity is usual (log ε 1.85).

From the above observations, the conversion of anhydro-lycoctonamic acid (VII) to apo-anhydrolycoctonamic acid (XI) seems to involve the loss of one methoxyl and the formation of one carbonyl group. The detection of the produced carbonyl group was unsuccessful in the infrared spectrum, but the above consideration is supported by the chemical evidence that, whilst the starting acid VII is resistant to carbonyl reagents, the apo-acid consumes bromine quickly although the starting acid does not. The decarboxy compound from the apo-acid gave a 2,4-dinitrophenylhydrazone, m. p. 221~222°C, and an oxime, m. p. 140~142°C.

In the apo-acid (XI), the location of the removed methoxyl and the newly produced carbonyl group have not yet been determined. However, it is sure that the carbonyl group in anhydrolycoctonamic acid (VII) exerted some effects upon this conversion, because the analogous conversion was not observed in lycoctonamic acid (IV).

Experimental

Lycoctonam (III).—To a solution of 1 g. of lycoctonine in 70 cc. of acetone containing 7 cc. of water, was added 0.6 g. of powdered potassium permanganate in small quantities at room temperature; the resulting solution was left at room temperature overnight. After filtration of manganese dioxide, the filtrate was evaporated to syrup under reduced pressure. When the syrup was further concentrated in a desiccator, crystalline lycoctonam was separated. A further amount was deposited by the addition of ether. Thus 0.7 g. of crystal was obtained. This substance was recrystallized from ethyl acetate in needles, m. p. 95~98°C, $[\alpha]_D^{14}$ +67.5° (C, 1.10 in water).

Anal. Found: C, 58.05; H, 8.24; N, 2.74; H_2O, 6.94. Calcd. for $C_{25}H_{39}O_8N \cdot 2H_2O$: C, 58.01; H, 8.37; N, 2.71; H_2O, 6.96%.

In the infrared spectrum in Nujol, this compound showed broad bands at 3367, 3401 and 3460 cm^{-1} in the region of hydroxyl group. This compound was identical with lycoctonam, obtained in the same way as reported by Edwards and Marion[4].

Oxidation of Lycoctonam with Chromic Acid.—To a solution of 4 g. of lycoctonam in

6) It was reported in a previous paper[7] that hydroxylycoctonine was obtained from lycoctonine on oxidation with Ag_2O; Cookson and Trevett[8] reported that they had obtained also the same compound by means of lead tetraacetate. The present authors found that this compound was produced by treatment not only with the above reagents but also with potassium ferricyanide.

7) H. Suginome and K. Ohno, *J. Fac. Sci., Hokkaido Univ., Ser. III. Chem.*, **4**, 36 (1950).

8) R. C. Cookson and M. E. Trevett., *Chem. & Ind.*, **1956**, 276.

100 cc. of N sulfuric acid was added a solution of chromic anhydride in a small volume of water with ice-cooling. When the resulting solution was left at room temperature overnight, an acidic product a was separated in needles. After filtration of the acid a, the filtrate was extracted with chloroform. The chloroform extract containing the acidic and neutral materials was shaken with diluted aqueous ammonia. On evaporation the chloroform solution gave 1.15 g. of the neutral product, lycoxonine (see below).

When the aqueous ammonia layer was acidified with dilute sulfuric acid, an acidic product b was obtained. Thus the combined acidic product, a and b, weighed 1.45 g. After recrystallization from aqueous ethanol, this acid was confirmed to be identical with lycoctonamic acid (IV)[4], m. p. 200~203°C, after softening at 95~100°C, $[\alpha]_D^{14}$+94.2° (C, 1.66 in ethanol).

Estimation of Formic Acid Formed during Oxidation. — Lycoctonam was oxidized with chromic anhydride in the same way as described above. After being kept overnight, the major amount of the solution was distilled. When the distillate was just neutralized with 0.05 N sodium hydroxide and evaporated to dryness, crystals were obtained which decomposed at 250~253°C (authentic sodium formate decomposed at 255°C). The acidic material was confirmed to be formic acid by the chromotropic acid test after it was reduced to formaldehyde.

Lycoxonine (X).— This compound was obtained as described under oxidation of lycoctonam. It crystallized from water as a tetrahydrate in rhombic forms. After recrystallization it melted at 80~83°C and had $[\alpha]_D^{13}$+40.8° (C, 1.66 in ethanol). In the infrared spectrum in Nujol, lycoxonine showed the broad band at 3448 cm^{-1} in the region of hydroxyl group.

Anal. Found: C, 53.75; H, 8.48; H_2O, 13.52. Calcd. for $C_{24}H_{37}O_8N \cdot 4H_2O$: C, 53.42; H, 8.41; H_2O, 13.35%.

This compound was subjected to the Micro-Zeisel methoxyl, Herzig-Meyer *N*-alkyl and Ginger *C*-methyl[9] determinations.

Anal. Found: C_2H_5, 4.83; OCH_3, 23.20, CH_3, 2.45. Calcd. for $C_{18}H_{28}O_8N(CH_2 \cdot CH_3)(OCH_3)_4$: C_2H_5, 5.36; 4-OCH_3, 23.00; CH_3, 2.78%.

De-(hydroxymethylene)-lycoctonam (V).— Since this compound could not be isolated directly from the oxidation products of lycoctonine, the present authors obtained it by pyrolysis of lycoctonamic acid in the same manner as described in Edwards and Marion's report[4]. The compound obtained was recrystallized from water as a trihydrate, m. p. 110~113°C.

The melting point and the form of the trihydrate were not in agreement with the above report[4]. However, the derivatives of this compound, de-(hydroxymethylene)-lycoctonine perchlorate and anhydro-de-(hydromethylene)-lycoctonam, were well in agreement with those of the same report.

Upon subjection to the same treatment with chromic anhydride as described under oxidation of lycoctonam, this compound V did not react for more than three days.

Acetylation of Lycoxonine.—(i) Lycoxonine tetrahydrate (0.5 g) was treated with 2 cc. of acetyl chloride in a sealed tube at room temperature overnight. Excessive reagent was removed under reduced pressure, and water was added. On standing, the resulting aqueous mixture gave 0.2 g. of a crystalline product, anhydrolycoxonine monoacetate (XIII). It was recrystallized readily from ethanol in rosette forms, m. p. 225~230°C, $[\alpha]_D^{15}$+37.8° (C, 3.30 in ethanol). The ultraviolet absorption spectrum showed the maximum at 305 mμ (log ε 1.85).

Anal. Found: C, 63.38; H, 7.72; N, 2.67. Calcd. for $C_{24}H_{34}O_6N(OCOCH_3)$: C, 63.52; H, 7.59; N, 2.85%.

(ii) Anhydrous lycoxonine (0.1 g.), obtained by drying the hydrate under reduced pressure over phosphorous pentoxide, was treated with 1 cc. of acetic anhydride and 0.5 cc. of pyridine in a sealed tube at room temperature, but lycoxonine was recovered unchanged after more than 80 hr.

(iii) A solution of 0.5 g. of anhydrous lycoxonine in 0.7 g. of acetic anhydride was refluxed for 3 hr. and the solution was then concentrated to a syrup in a desiccator under reduced pressure. When a small amount of water was added to the resulting syrup, a crystalline product was obtained. This product could be separated into two parts by treating it with hot water. The first part was insoluble in hot water whilst the second was readily soluble. The insoluble material was identical with anhydrolycoxonine monoacetate which was obtained by acetyl chloride treatment (i). The readily soluble material was lycoxonine monoacetate (XII); it was recrystallized from water in prisms, m. p. 222~225°C.

Anal. Found: C, 61.35; H, 7.78; $OCOCH_3$, 10.43. Calcd. for $C_{24}H_{36}O_7 \cdot (OCOCH_3)$: C, 61.28; H, 7.71; $OCOCH_3$, 10.02%.

Lycoxonine monoacetate gave anhydrolycoxonine monoacetate upon further treatment with acetyl chloride or acetic anhydride as described above.

Anhydrolycoxonine (XIV).—Anhydrolycoxonine monoacetate was saponified by 50% potassium hydroxide in aqueous methanol on a steam bath for 30 min. The solution was neutralized with dilute hydrochloric acid and evaporated under reduced pressure to dryness. The resulting residue was extracted with ethanol. When the alcoholic solution was evaporated at room temperature, anhydrolycoxonine was separated in plates. After recrystallization from aqueous ethanol, it melted at 160~162°C and showed the maximum at 305 mμ (log ε 1.85) in ultraviolet spectrum.

Anal. Found: C, 64.38; H, 7.90; N, 3.21. Calcd. for $C_{24}H_{35}O_7N$: C, 64.12; H, 7.85; N, 3.12%.

Anhydrolycoctonamic Acid (VII).—Lycoctonamic acid (1 g.) was treated with 4 cc. of acetyl chloride in a sealed tube overnight. After evaporation of excess of the reagent, water was

9) L. G. Ginger, *J. Biol. Chem.*, **156**, 453 (1944).

added to the resulting residue. Then, 0.5 g. of an amorphous material was obtained, which crystallized readily from ethanol in prisms, m. p. 177~178°C, $[\alpha]_D^{13}$+52.8° (C, 1.00 in ethanol), λ_{max} 305 mμ (log ε 1.87). This product was identical with anhydrolycoctonamic acid reported by Edwards and Marion[4].

Anal. Found: C, 62.47; H, 7.38. Calcd. for $C_{25}H_{35}O_8N$: C, 62.87; H, 7.39%.

Apo-anhydrolycoctonamic Acid (XI).—To a solution of 0.5 g. of anhydrolycoctonamic acid in 100 cc. of water containing 0.5 g. of potassium carbonate, 0.3 g. of powdered potassium permanganate was added in portions at room temperature. The potassium permanganate was consumed very slowly in three days.

The manganese dioxide was filtered off and washed with 0.1% potassium carbonate solution. When the combined filtrate and washings were acidified with diluted sulfuric acid, apo-anhydrolycoctonamic acid was obtained. Yield, 0.19 g. It was recrystallized from ethanol in thin plates, m. p. 183~184°C, $[\alpha]_D^{13}$+37° (C, 1.00 in ethanol). This acid was considerably less soluble in ethanol than anhydrolycoctonamic acid. The ultraviolet spectrum of this acid showed the maximum at 305 mμ (log ε 2.07).

Anal. Found: C, 62.14; H, 6.69; OCH_3, 20.20. Calcd. for $C_{24}H_{31}O_8N$: C, 62.45; H, 6.77; 3-OCH_3, 20.17%.

On oxidation in the same way as described above, lycoctonamic acid was not affected.

The apo-acid decolorized one mole of bromine within 30 min. in acetic acid, while anhydrolycoctonamic acid did not do so within 24 hr.

Decarboxy Compound of Apo-anhydrolycoctonamic Acid.—(i) On treatment of apo-anhydrolycoctonamic acid in the same way as reported by Edwards and Marion[4], no crystalline product was isolated.

(ii) A solution of 40 mg. of the apo-acid in 0.3 cc. of acetic anhydride was refluxed for 3 hr. The solution was poured into 10 cc. of water, and the resulting aqueous solution was extracted with chloroform. After being washed with diluted potassium hydroxide and then with water, the chloroform extract was evaporated to dryness. When ether was added to the residue, crystals were deposited from the ether solution in prisms. The substance was recrystallized from water as a polyhydrate, which melted at 110~113°C after softening at 100°C.

Formation of Oxime and 2,4-Dinitrophenylhydrazone from the Decarboxy Compound.—(i) To a solution of 40 mg. of the decarboxy compound in 1 cc. of ethanol was added a solution of 40 mg. of hydroxyl amine hydrochloride in 0.4 cc. of water containing 40 mg. of potassium carbonate; the resulting solution was warmed on a steam bath for 4 hr. When the alcoholic solution was concentrated under reduced pressure, the oxime of the decarboxy compound was separated in needles, m. p. 140~142°C. In the ultraviolet spectrum, this oxime showed the maximum at 305 mμ (log ε 1.85).

Anal. Found: N, 6.54. Calcd. for $C_{23}H_{32}O_6ON$: N, 6.48%.

(ii) To a solution of 20 mg. of the decarboxy compound in 2 cc. of ethanol was added four drops of the solution of 0.5 g. of 2,4-dinitrophenylhydrazine and 1 cc. of 90% sulfuric acid in 7 cc. of ethanol. When the resulting solution was allowed to stand at room temperature for several hours, it deposited 2,4-dinitrophenylhydrazone of the decarboxy compound in yellow needles, m. p. 221~222°C.

Anal. Found: N, 11.54. Calcd. for $C_{29}H_{35}O_9N_5$: N, 11.72%.

On treatment of anhydro-de-(hydroxymethylene)-lycoctonam with either of the above reagents, the starting compound was recovered without change.

Hydroxylycoctonine (VIII).—A solution of lycoctonine in 20 cc. of methanol was mixed with a solution of 1.2 g. of potassium hydroxide in 20 cc. of methanol. Then, a solution of 5.4 g. of potassium ferricyanide in 25 cc. of water was added to the above alcoholic solution and cooled in water. Then the resulting solution was left at room temperature overnight. After evaporation of the methanol under reduced pressure, the solution was extracted with chloroform. The chloroform extract was evaporated to dryness after being washed with water and then dried with anhydrous sodium sulfate. When ether was added to the resulting residue, 2 g. of the product was obtained. It crystallized readily from ethyl acetate in little buttons. After recrystallization from the same solvent, the compound melted at 152~154°C and did not depress the melting point of an authentic hydroxylycoctonine, prepared by silver oxide oxidation[7].

Hydroxylycoctonam (IX).—This compound was obtained by treatment analogous to that reported by Edwards and Marion[10]. To a solution of 5.32 g. of hydroxylycoctonine in 400 cc. of water was added 3.45 g. of powdered potassium permanganate in small portions at room temperature. After the addition of the entire amount of the oxidant, the reaction mixture was left at room temperature overnight, and the resulting manganese dioxide was filtered off. The filtrate was extracted with chloroform, and the resulting extract was washed with diluted hydrochloric acid and then with water. When the washed chloroform solution was evaporated, a resinous material remained. This material was crystallized by the addition of acetone-ether. It was recrystallized from acetone as a monohydrate, m. p. 200~203°C.

Anal. Found: C, 58.31; H, 7.98. Calcd. for $C_{25}H_{39}O_9N \cdot H_2O$: C, 58.24; H, 8.01%.

Oxidation of Hydroxylycoctonam (IX) with Chromic Anhydride.—In 10 cc. of 5% sulfuric acid solution, 0.51 g. of hydroxylycoctonam was treated with 0.4 g. of chromic anhydride in just the same way as described under oxidation of lycoctonam. The oxidation of this compound was slower than that of lycoctonam, and required more than a week. After reducing the oxidant

10) O. E. Edwards and Léo Marion: *Can. J. Chem.* **32**, 1146 (1954).

the solution was extracted with chloroform, and the extract was shaken with dilute aqueous ammonia. When the chloroform layer was evaporated, there remained resinous products a. Yield, 0.20 g. (see below).

The aqueous layer was acidified with dilute hydrochloric acid and then extracted with chloroform. On evaporation of the solvent, the chloroform extract gave acidic products which were crystallized by the addition of ether. These products were separated into two acids, one readily soluble in acetone and the other less soluble. The readily soluble acid was recrystallized from acetone-ethanol in prisms melting at 220~222°C (decomp.) after softening at 200°C. This acid was named C_1-acid. The less soluble acid was crystallized from hot water in plates, melting at 193~195°C. This acid was named Y-acid.

The neutral product a was separated into two parts, one insoluble in benzene and the other soluble. The insoluble part crystallized from acetone in small buttons, which weighed 80 mg. each and melted at 177~180°C after recrystallization from acetone. This neutral product was named Y. The benzene-soluble part, weighing 100 mg., was subjected to chromatography on alumina. Elution with 5% methanol in benzene gave a product which crystallized from acetone in rhombic forms, m. p. 226~227°C. This product was named Z.

Department of Chemistry
Faculty of Science
Hokkaido University, Sapporo

The Aconite Alkaloids. XXX. On Lucidusculine*

By Harusada SUGINOME, Takashi AMIYA and Takeo SHIMA

(Received November 15, 1958)

Lucidusculine, $C_{24}H_{35}O_4N$, was previously isolated from the roots of *Aconitum luciduscului* Nakai by R. Majima and S. Morio[1,2], and studied by H. Suginome and his collaborators[3-5]. Lucidusculine is a monoacetate of a trihydric amino alcohol, luciculine, $C_{22}H_{33}O_3N \cdot H_2O$[2,5], which was obtained by hydrolysis of the former. The presence of an *N*-ethyl group was confirmed by the formation of mesoluciculine, $C_{21}H_{31}O_3N \cdot H_2O$[5], on Hofmann degradation of luciculine. Further, as lucidusculine absorbed one mole of hydrogen on catalytic hydrogenation, it was assumed that the base has one double bond[4].

On the basis of the above results, the partial structure of lucidusculine was previously represented as:

$$C_{20}H_{25} \begin{cases} (OH)_2 \\ OCOCH_3 \\ >N-C_2H_5 \\ 1\,F \end{cases}$$

Luciculine shows absorption peaks in the infrared spectrum at 6.09 and 11.27 μ and lucidusculine diacetate[4] shows peaks at 6.08 and 11.32 μ. Nevertheless, dihydrolucidusculine diacetate shows no peak near the above-mentioned region[6]. These data suggest the presence of a terminal methylene group in each of luciculine and lucidusculine diacetate, which is also supported by the isolation of formaldehyde as the dimedone complex in ozonolysis experiment with lucidusculine and lucidusculine diacetate. Further, mesoluciculine gave 0.45 mol. of acetic acid on Kuhn-Roth oxidation, while dihydromesoluciculine[7] yielded 0.92 mol. of acetic acid on the same oxidation. The difference (0.47 mol.) can be explained by the following scheme:

$$\underset{\text{Mesoluciculine}}{>C=CH_2} \xrightarrow{H_2} \underset{\text{Dihydromesoluciculine}}{>CH-CH_3}$$

From these results and the biogenesis of the aconite alkaloids[8], the formula of

* The report, "Aconite Alkaloids. On Pyrolytic Products of Aconitine, Oxonitine, and their Derivatives", printed in This Bulletin, **31**, 658 (1958), constitutes Part XXXI. Part XXIX: H. Suginome, S. Imato, S. Yamada and N. Katsui, This Bulletin, **23**, 819 (1959).

1) R. Majima and S. Morio, *Proc. Imp. Acad. Tokyo*, **7**, 351 (1931).

2) R. Majima and S. Morio, *Ber.*, **65**, 559 (1932).

3) H. Suginome and F. Shimanouchi, *Ann.*, **545**, 222 (1940).

4) H. Suginome, S. Kakimoto and J. Sonoda, *J. Fac. Sci., Hokkaido Univ., Ser. III. Chem.*, **4**, 25 (1950).

5) H. Suginome and S. Umezawa, ibid., 44.

6) T. Amiya, unpublished work.

7) H. Suginome and S. Umezawa, *J. Fac. Sci., Hokkaido Univ., Ser., III. Chem.*, **4**, Supplement, 74 (1952).

8) R. H. F. Manske, H. L. Holmes, "The Alkaloids", Vol. IV, Academic Press, Inc., New York (1954), p. 280.

lucidusculine may be extended further as follows:

$$C_{18}H_{23}\begin{cases}(OH)_2\\OCOCH_3\\>N-C_2H_5\\>C=CH_2\end{cases}$$

Lucidusculine is assumed to have a hexacyclic structure based on the skeletal formula $C_{19}H_{29}N$[3].

Amiya and Nagaoka previously isolated lucidusculine and jesaconitine from the roots of *Aconitum* species from Shoya, Hidaka in Hokkaido[9]. Extraction with ethanol and the following treatment were done in the same way as in the case of other aconite roots[10], and these two alkaloids were isolated from the water-insoluble portion. Now, quantitative separation of these alkaloids from mother-roots and from daughter-roots of the above-mentioned *Aconitum* plants by Ochiai's chromatographic method[11] was tried. As a model experiment, aconitine, jesaconitine and lucidusculine were dissolved in chloroform which was saturated with concentrated ammonia water[12], the solution was passed through a column of alumina, and the column was eluted with chloroform-ammonia water, followed by acetone and then methanol. The residue from the chloroform-ammonia water elute was found to be composed of aconitine and jesaconitine and that from the acetone elute was composed of lucidusculine only. Thus, the same procedure was applied to the above-mentioned water-insoluble portions with results as follows:

Weights of dried roots	Water-insoluble portions	Crystalline alkaloids	
Mother-roots 4.5 kg.	4.4 g.	Jesaconitine	0.4 g.
		Lucidusculine	0.2 g.
Daughter-roots 4.5 kg.	20.5 g.	Jesaconitine	1.4 g.
		Lucidusculine	0.8 g.

Experimental

Ozonolysis of Lucidusculine.—Lucidusculine (95 mg.) was ozonized in 20 ml. of chloroform-acetic acid (1 : 1 by volume) at −25～−35°C with three moles of ozone. The solution was hydrogenated with 5% palladium-carbon for 15 min. After removal of the palladium-carbon, dimedone (75 mg.) was added to the solution. After standing overnight, the solvents were completely evaporated in vacuo. To the residue, 10% sodium hydroxide solution (5 ml.) was added. When the solution was washed with chloroform and acidified with hydrochloric acid, the crystalline dimedone-formaldehyde complex was separated. It was extracted with chloroform and the chloroform solution was evaporated in vacuo to give a crystalline residue. Recrystallization from ethanol yielded 10 mg. of the dimedone-formaldehyde complex, which melted at 190°C and showed no depression of the melting point on admixture with an authentic specimen.

Ozonolysis of Lucidusculine Diacetate.—Lucidusculine diacetate (350 mg.) was ozonized and treated in the same way. Thus, 65 mg. of the dimedone-formaldehyde complex was obtained.

Kuhn-Roth Oxidation.—Mesoluciculine and dihydromesoluciculine were oxidized by L. G. Ginger's method[13]. The results were as follows:

Mesoluciculine: *Anal.* Found: (C)-CH_3, 1.84 (0.45 mol.). Calcd. for $C_{21}H_{31}O_3N\cdot H_2O$: 1 (C)-$CH_3$, 4.13%.

Dihydromesoluciculine: *Anal.* Found: (C)-CH_3, 3.71 (0.92 mol.). Calcd. for $C_{21}H_{33}O_3N\cdot 1.5H_2O$: 1 (C)-$CH_3$, 4.01%.

Model Experiment of Separation.—Lucidusculine, aconitine and jesaconitine (100 mg. each) were dissolved in 10 ml. of chloroform-ammonia water, the solution was passed through a column (1.4 cm. in diameter) of 90 g. of alumina, and the column was eluted with 280 ml. of chloroform-ammonia water, 100 ml. of acetone and 100 ml. of methanol in succession. The chloroform-ammonia water elute gave 200 mg. of a residue. The solution of the residue (0.661 mg.) in methanol (10 ml.) gave an ultraviolet absorption spectrum, λ 220 mμ (E 0.69)[14], λ_{max} 232 mμ (E 0.91), λ_{min} 245 mμ (E 0.78) and λ_{max} 259 mμ (E 1.10). The solution of 0.323 mg. of aconitine and 0.323 mg. of jesaconitine in 10 ml. of methanol showed an identical ultraviolet spectrum[15]. The acetone elute gave 100 mg. of lucidusculine melting at 170°C alone and on admixture with an authentic specimen.

Isolation of Alkaloids.—The dried roots were divided into mother-roots and daughter-roots.

Isolation of alkaloids from mother-roots.—The mother-roots (4.5 kg.) were ground and percolated with ethanol. The percolate was treated as in the case of other aconite roots[10]. The water-insoluble portion (4.4 g.) was dissolved in 10 ml. of chloroform-ammonia water and the solution was passed through a column (1.4 cm. in diameter) of 90 g. of alumina, and the column was

9) T. Amiya and I. Nagaoka, Read before the 5th Annual Meeting of the Chemical Society of Japan, held in Tokyo, April, 1952, and the 6th Annual Meeting of the Chemical Society of Japan, held in Kyoto, April, 1953. The plants were collected by I. Nagaoka and the late T. Ichihashi in Sepetember, 1944.

10) H. Suginome, S. Furusawa, Y. Chiba and S. Kakimoto, *J. Fac. Sci., Hokkaido Univ., Ser. III. Chem.*, **4**, 1 (1950).

11) E. Ochiai, T. Okamoto, T. Sugasawa, H. Tani and S. Hung, *J. Pharm. Soc. Japan* (*Yakugaku Zasshi*), **72**, 816 (1952).

12) This solvent is designated as "chloroform-ammonia water".

13) L. G. Ginger, *J. Biol. Chem.*, **156**, 453 (1944).

14) $E=\log_{10} I_0/I$.

15) A. E. Gillam, E. S. Stern, "An Introduction to Electronic Absorption Spectroscopy in Organic Chemistry", Edward Arnold Publishers, Ltd., London, (1954), p. 185; E. Ochiai, T. Okamoto and S. Sakai, *J. Pharm. Soc. Japan* (*Yakugaku Zasshi*), **75**, 545 (1955).

eluted with 280 ml. of chloroform-ammonia water, next with 100 ml. of acetone and then with 70ml. of methanol. The basic substance was obtained from the entire amount of the chloroform-ammonia water elute. It was purified as perchlorate by recrystallization from ethanol and 0.5 g. of pure perchlorate was obtained, m. p. 220~230°C (decomp.). The base (0.670 mg.) liberated from the perchlorate by means of ammonia water was dissolved in 10 ml. of methanol. The solution showed ultraviolet absorption, λ 220 mμ (E 0.55), λ_{min} 225 mμ (E 0.44) and λ_{max} 259 mμ (E 1.44). The solution of 0.130 mg. of aconitine and 0.540 mg. of jesaconitine in 10 ml. of methanol showed an identical ultraviolet spectrum. The spectral observations and the experiments mentioned below indicate that jesaconitine is contained in the material in an amount of about 80%[15,16].

The remaining portion of the free base was extracted with ether in a Soxhlet extractor for 3 hr.; and the extracted base was transformed into the perchlorate. The salt yielded 0.1 g. of the salt of "jesaconitine-rich base" upon recrystallization from ethanol. The purified salt had m. p. 230°C (decomp.), $[\alpha]_D^{25}$ −12.6° (methanol). The jesaconitine-rich base (0.673 mg.) prepared from the above salt was dissolved in 10 ml. of methanol. The solution showed ultraviolet absorption, λ 220 mμ (E 0.50), λ_{min} 225 mμ (E 0.32) and λ_{max} 259 mμ (E 1.79). The solution of 0.060 mg. of aconitine and 0.615 mg. of jesaconitine in 10 ml. of methanol showed an identical ultraviolet spectrum. The salt of the jesaconitine-rich base was analyzed.

Anal. Found: C, 53.72; H, 6.44; N, 2.06. Calcd. for $C_{35}H_{49}O_{12}N \cdot HClO_4$[17]: C, 54.15; H, 6.49; N, 1.80%.

After evaporation of the acetone elute in vacuo, the residue yielded 0.2 g. of lucidusculine by recrystallization from ethanol, m. p. 170°C with no depression on admixture with an authentic specimen.

Isolation of alkaloids from daughter-roots. — The water-insoluble portion (20.5 g.) from 4.5 kg. of the daughter-roots was treated in the same way as in the case of the mother-roots. The basic substance was obtained from the entire portion of the chloroform-ammonia water elute. The perchlorate of the base was recrystallized from ethanol. The free base liberated from the perchlorate was neutralized with 0.77 N hydrobromic acid. The solution of the resulting hydrobromide gave 0.08 g. of a crystalline material on standing[18]. The free base (0.665 mg.) prepared from the hydrobromide was dissolved in 10 ml. of methanol. The solution showed ultraviolet absorption, λ_{max} 232 mμ (E 0.90), λ_{min} 245 mμ (E 0.71) and λ_{max} 259 mμ (E 1.03). The solution of 0.356 mg. of aconitine and 0.309 mg. of jesaconitine in 10 ml. of methanol gave an identical ultraviolet spectrum.

The mother liquor from the hydrobromide was treated with ammonia water, yielding 1.7 g. of the free base. The solution of the free base (0.667 mg.) in 10 ml. of methanol showed ultraviolet absorption, λ 220 mμ (E 0.55), λ_{min} 225 mμ (E 0.44) and λ_{max} 259 mμ (E 1.53). The solution of 0.120 mg. of aconitine and 0.545 mg. of jesaconitine in 10 ml. of methanol showed an identical ultraviolet spectrum.

The spectral observations and the experiments described below indicate that jesaconitine was contained in an amount of about 80%.

The remaining portion of the above free base was extracted with ether in a Soxhlet extractor for 3 hr.; and the extracted base was transformed into the perchlorate. The crude perchlorate yielded 0.2 g. of the perchlorate of a jesaconitine-rich base upon recrystallization from ethanol. The purified perchlorate had m. p. 230°C (decomp.), $[\alpha]_D^{25}$ −14.8°C (methanol). The solution of jesaconitine-rich base (0.673 mg.), prepared from a part of the perchlorate, in 10 ml. of methanol showed ultraviolet absorption, λ 220 mμ (E 0.50), λ_{min} 225 mμ (E 0.32) and λ_{max} 259 mμ (E 1.79). The solution of 0.060 mg. of aconitine and 0.615 mg. of jesaconitine showed an identical ultaviolet spectrum. The purified perchlorate was analyzed.

Anal. Found: C, 53.92; H, 6.50; N, 1.91. Calcd. for $C_{35}H_{49}O_{12}N \cdot HClO_4$: C, 54.15; H, 6.49; N, 1.80%.

Hydrolysis of the ether-insoluble portion (1.1 g.) of the above base gave 50 mg. of anisic acid and 300 mg. of aconine hydrochloride, which melted at 176°C and was analyzed.

Anal. Found. C, 52.65; H, 8.16; N, 2.43. Calcd. for $C_{25}H_{41}O_9N \cdot HCl \cdot 2H_2O$: C, 52.48; H, 8.04; N, 2.45%.

The acetone elute gave 0.8 g. of lucidusculine as in the case of the mother-roots, m. p. 170°C with no depression on admixture with an authentic specimen.

Summary

1. In lucidusculine the presence of a double bond had previously been assumed. Further, on the basis of observations of the infrared spectra of luciculine, lucidusculine diacetate and dihydrolucidusculine diacetate, the presence of a terminal methylene group in lucidusculine was suggested.

Kuhn-Roth oxidation of mesoluciculine and of dihydromesoluciculine and ozonolysis of lucidusculine and of lucidusculine diacetate supported the suggested presence of a terminal methylene group. These results and the biogenesis of the aconite

16) On account of the the existence of the benzoyl ester of an alkaloidal amino alcohol, aconitine was assumed to be present.

17) If the salt is composed of 1 mol. of jesaconitine and 1/10 mol. of aconitine, the calculated values are: C, 54.19; H, 6.44%.

18) The benzoyl ester of an alkaloidal amino alcohol may be aconitine; this seems to be supported by the fact that the crystalline hydrobromide of the ester alkaloid is slighthly soluble in water.

alkaloids show that the double bond in lucidusculine belongs to a terminal methylene group.

2. The roots of *Aconitum* species from Shoya, Hidaka in Hokkaido, were divided into mother-roots and daughter-roots; the water-insoluble basic portions were obtained from both; lucidusculine and jesaconitine were isolated by the chromatographic method.

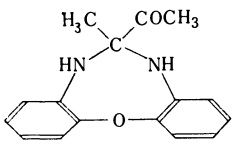
Depatment of Chemistry
Faculty of Science
Hokkaido University
Sapporo

On the Structure of Condensation Products of o-Aminophenols with α-Dicarbonyl Compounds. I

By Ichiro MURASE

(Received December 11, 1958)

The condensation reaction between *o*-aminophenol and diacetyl was first carried out by Kehrmann in 1895, who tentatively suggested for the condensation product the eight-membered ring structure containing a diphenyl ether bond as shown in the formula A[1].



(A)

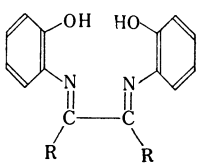
Recently, Bayer assigned Schiff base structures to the compounds obtained by the condensation of *o*-aminophenol with glyoxal and diacetyl and reported that glyoxal bis-(2-hydroxy anil) gave chelates with copper, nickel, cobalt, etc., but diacetyl bis-(2-hydroxy anil) did not form a metal chelate[2].

The present investigation was undertaken in order to confirm the structure of these condensation products.

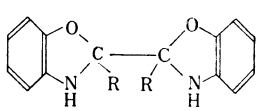
o-Aminophenol smoothly condensed with glyoxal and with diacetyl by heating the mixture in an aqueous or alcoholic solution. The product I from glyoxal was colorless needles, m. p. 210°C*, and the product II from diacetyl was colorless plates, m. p. 241°C**.

The Schiff base structure is represented as the formula B.

It was confirmed in some cases that condensation products of β-aminoalcohols and carbonyl compounds are oxazolidine or equilibrium mixtures of the Schiff base with the former[3]. Along with these facts, the alternative structure of I and II is bibenzoxazoline (C).



(B)



R : H (I)
R : CH_3 (II)

(C)

Only a few instances of benzoxazoline structure were reported concerning the condensation products of *o*-aminophenols and carbonyl compounds[4], but their structures were not always confirmed exactly. It has been accepted that the benzoxazole owes its formation to pyrolysis of the benzoxazoline primarily formed in the condensation of *o*-aminophenol with ketone[5].

1) F. Kehrmann, *Ber.*, **28**, 343 (1895).
2) E. Bayer, *Ber.*, **90**, 2325 (1957).
* According to Bayer, the melting point of the product I is 204°C.
** The melting point of II is 227°C according to Bayer, but Kehrmann reported it as being 239~240°C.
3) G. E. McCasland and C. Horswill, *J. Am. Chem. Soc.*, **73**, 3923 (1951); H. R. Nace and M. H. Gollis, ibid., **74**, 5189 (1952); J. Metzger and A. Pacault, *Rec. trav. chim.*, **71**, 259 (1952); E. P. Goldberg and H. R. Nace, *J. Am. Chem. Soc.*, **75**, 6260 (1953); E. D. Bergmann, E. Gil-Av and S. Pinchas, *Rec. trav. chim.*, **71**, 168 (1952); *J. Am. Chem. Soc.*, **75**, 358 (1953); H. R. Nace and E. P. Goldberg, ibid., **75**, 3646 (1953).
4) A. Hantzsch, *Ber.*, **16**, 1948 (1883); Schroeter et al., *Ann.*, **426**, 83 (1922); F. Sachs and W. Brunetti, *Ber.*, **40**, 3234 (1907); L. Calatis, ibid., **66**, 1774 (1933).
5) Elderfield, "Heterocyclic Compound", Vol. 5, John Wiley & Sons, Inc., New York, (1957), p. 431.

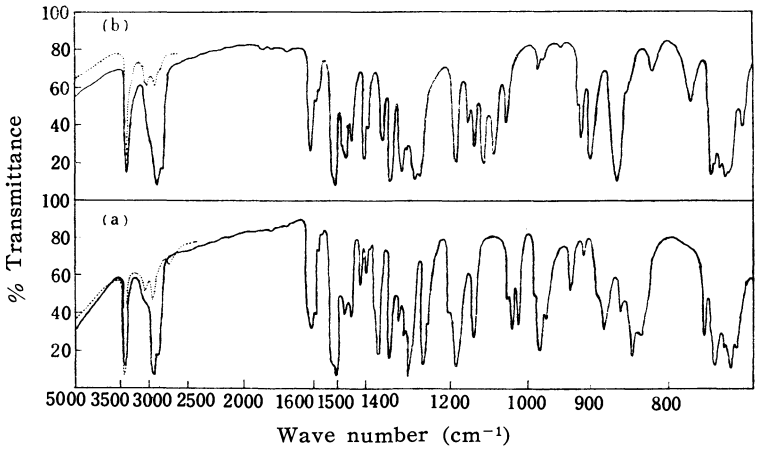


Fig. 1. Infrared spectra of the compounds. I : a and II : b, —— Nujol mull, ····· hexachlorobutadiene mull.

TABLE I. INFRARED ABSORPTION SPECTRA OF I, II AND RELATED SCHIFF BASES NEAR 3000 cm^{-1} AND 1600 cm^{-1} REGION

I	II	Diacetyl dianil	Glyoxal bis-(4-hydroxy anil)	Glyoxal bis-(4-dimethyl-amino anil)	Salicyl-idene *o*-amino-phenol	Bissalicyl-aldehyde ethylene-diimine	Assignment
3378	3358						NH stretching
		1631	1610	1605	1631	1631	Conjugated C=N
1613	1613						
1600	1587	1587	1595		1619	1613	Phenyl ring
1585	1580	1577	1580	1567	1597	1582	
1499	1497	1490	1513	1517	1531	1506	

Eventually, a Schiff base structure or an oxazoline structure will be the only choice offered for the determination of the structure of the condensation products of *o*-aminophenol with glyoxal and diacetyl. The following investigations led to the conclusion that the structures of these are not so much a Schiff base type as an oxazoline type.

Behaviors to Mineral Acid and Aqueous Alkali.—I and II are insoluble in dilute mineral acids and stable to such an extent that they are not hydrolyzed after standing overnight at room temperature with 3 N hydrochloric acid, but hydrolyzed by heating with 6 N hydrochloric acid; thus they were gradually hydrolyzed and *o*-aminophenol hydrochloride was obtained quantitatively. I and II were not only insoluble in dilute aqueous alkali, but also stable at room temperature. On heating them with a ten per cent aqueous sodium hydroxide solution, *o*-aminophenol was obtained and identified as the *N*-acetyl derivative.

Spectroscopic Investigation. — Infrared and ultraviolet absorption spectra of I and II are shown In Figs. 1 and 2 respectively***. The assignment of the infrared absorption bands and the ultraviolet absorption maxima are summarized and compared with those of the related Schiff bases in Tables I and II, respectively.

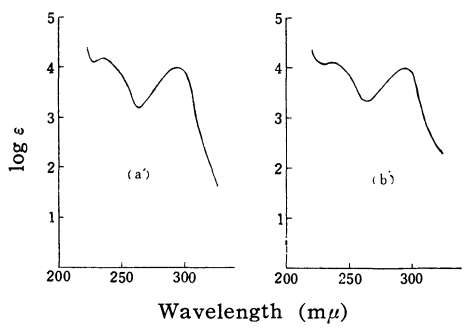


Fig. 2. Absorption curve of the compounds I (a') and II (b'), (ethanol solution).

*** The infrared spectra were obtained with a Perkin-Elmer Model 21 and an Oyōkōken D-201 spectrometer using NaCl prism. Ultraviolet spectra were obtained with a Beckman Model DK-2 spectrometer.

TABLE II. THE ULTRAVIOLET ABSORPTION SPECTRA OF I, II AND RELATED SCHIFF BASES IN ETHANOL

Compound	λ (mμ)	ε	λ (mμ)	ε	λ (mμ)	ε
I	236	14340	294	9880		
II	236	13200	293	9880		
Diacetyl dianil	227	40700			332	4360
Glyoxal bis-(4-hydroxy anil)	244	13200	296	8300	383	23980
Glyoxal bis-(4-dimethyl-amino anil)	253	15760	318	5700	450	37200

If the Schiff base structure (B) is adopted, the bands in the 3000 cm^{-1} region of infrared are assigned to OH vibration, 1613 cm^{-1} being a C=N vibration shifted by the strong conjugation in the same manner as in the case of the Schiff bases quoted.

Intermolecular hydrogen bondings, however, should be present in this case; a hydrogen bonding causes a shift of the OH stretching band to the lower frequency and broadening of the band[6]. From these circumstances, the shape and the position of these bands (Fig. 1) are more plausibly explained to correspond to the NH vibration. Furthermore, the ultraviolet absorption spectra of I and II (Fig. 2) are closely related to that of *o*-aminophenol itself (λ_{max} 232 mμ, ε_{max} 7240; λ_{max} 286 mμ, ε_{max} 4270)[7], thus the presence of the chromophore, such as conjugated azomethine linkages which cause a bathochromic effect, should be discounted.

It is well known that a compound having an anilino structure has an infrared absorption band near 1600 cm^{-1} region[8]. From the investigations of indolenine derivatives, Witkop and Patrick[9] have quoted a band at 1613 cm^{-1} as being typical of the structure C_6H_5–NH–$\overset{|}{\underset{|}{C}}$–. Since the structure of bibenzoxazoline (C) resembles that of indolenine and an absorption similar to that of the latter is present at 1613 cm^{-1}, the author concluded the absorption to be caused by the same structural element, and at least shouldered bands are regarded as phenyl ring vibrations; it is not completely clear whether this absorption arises from an NH deformation or from a phenyl ring.

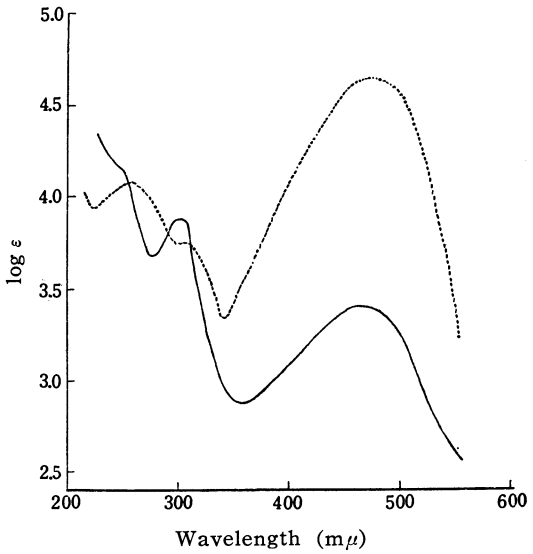


Fig. 3. Absorption curve of the compound I+KOH: —— and glyoxal bis-(4-hydroxy anil)+KOH: ·····.

Although compound I was insoluble in aqueous alkali, a reddish yellow color was produced when an excess of potassium hydroxide was added to its ethanol solution, and another absorption maximum was observed at 467 mμ (ε, 2445) as shown in Fig. 3.

In the case of glyoxal bis-(4-hydroxy anil), the absorption maximum shifted from 367 mμ to 470 mμ when potassium hydroxide was added. The explanation of this phenomenon is that when a proton acceptor such as a hydroxyl ion is present in the ethanol solution, bibenzoxazoline (C′) tautomerizes to Schiff base B′ under ring opening. The above consideration is tenable in view of the fact that oxazolidine tautomerizes to Schiff base resulting in an equilibrium mixture of the two structures[3].

The curve in Fig. 4 means that the Schiff base is produced as a result of tautomerism and the solution reaches an equilibrium. The curve comes up again after standing for a long time, because hydrolysis sets in.

The formation of a metal chelate I is also explained by the tautomeric change.

6) L. J. Bellamy, "The Infrared Spectra of Complex Molecules", John Wiley & Sons, Inc., New York, (1954), p. 86.
7) R. A. Friedel, M. Orchin, "Ultraviolet Spectra of Aromatic Compounds", John Wiley & Sons, Inc., New York, (1951).
8) Reference 6, p. 219.
9) B. Witrop and J. B. Patrick, *J. Am. Chem. Soc.*, **73**, 713 (1951).

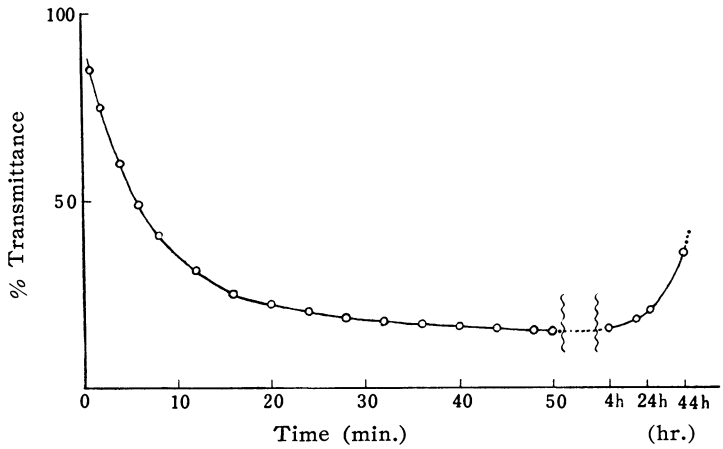


Fig. 4. Variation of the transmittance of the absorption maximum of I in ethanol (about 1/2000 mol.) at 470 mμ after the addition of potassium hydroxide.

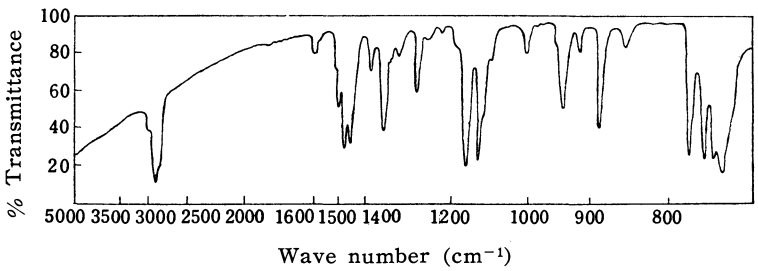


Fig. 5. Infrared spectrum of 2,2'-bibenzoxazole (Nujol mull).

When metal acetate has been added to the solution, an acetate ion acts as a proton acceptor and an anion of Schiff base is produced in the same manner as in the case of potassium hydroxide. The structure of a metal chelate thus formed, has been represented by Bayer as an ionic one of glyoxal bis-(2-hydroxy anil).

Compound II failed to give a new absorption band at a visible region on addition of potassium hydroxide to its ethanol solution. Accordingly, II lacks the feature of tautomerism in contrast with I, and the inability to form a metal chelate is well understood.

Chemical Properties.—Methylation of I and II was attempted using sodium amide and methyl iodide in dioxane or diazomethane in ether, but only an unchanged material was recovered.

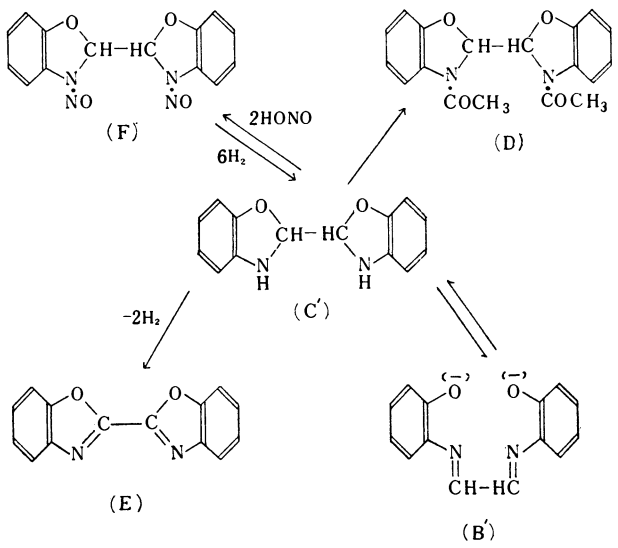
By the acetylation of I with acetic anhydride, a crystalline diacetyl derivative was obtained, m. p. 263~265°C. It was not hydrolyzed by acid or alkali and the infrared spectrum showed absorptions at 1670 cm^{-1} (C=O stretching) and 1587 cm^{-1} (phenyl ring) and no absorption was observed in the 3000 cm^{-1} region. Thus, the diacetyl derivative proved to be *N,N'*-diacetyl-2,2'-bibenzoxazoline(D).

When the dilute solution of I in acetone was carefully treated with potassium permanganate, a dehydrogenation product was obtained in pale yellow prisms, m. p. 257°C. It was confirmed to be 2,2'-bibenzoxazole (E) from mixed melting point test with the authentic sample[10] prepared by the oxidative condensation of benzoxazole with copper acetate. 2,2'-Bibenzoxazole was also obtained by the oxidation of I with lead dioxide in benzene. The infrared absorption pattern (Fig. 5) of the dehydrogenation product was quite identical with that of the authentic sample.

Similar oxidation did not proceed in the case of II under the same conditions.

By the nitrosation of I, yellow dinitroso derivative (F) was obtained. It has no absorption band near 3000 cm^{-1} of infrared; the substitution of nitroso group occurred at imino hydrogen in the bibenzoxazoline (C'). By the catalytic hydrogenation of

10) D. R. Pat., 650,050 (1936); *Chem. Zentr.*, **1937**, II, 4395.



F, six moles of hydrogen were absorbed and I was reproduced.

The above reactions are summarized in the following schema.

Thus, the most reasonable conclusion to be drawn from the available data is that the condensation product of *o*-aminophenol with glyoxal is 2,2'-bibenzoxazoline and with diacetyl is 2,2'-dimethyl-2,2'-bibenzoxazoline as shown in the formula C. Bayer's investigation concerning the structure of metal chelates would be supported along with the consideration that 2,2'-bibenzoxazoline tautomerizes to glyoxal bis-(2-hydroxy anil).

Condensation products of many other *α*-dicarbonyl compounds with *o*-aminophenol derivatives and their structures will be reported in the subsequent paper.

Experimeatal

2, 2'-Dimethyl-2, 2'-bibenzoxazoline. — Prepared from *o*-aminophenol and diacetyl according to Kehrmann's method. Colorless plates, m. p. 241°C. The substance afforded a deep reddish violet color when dissolved in concentrated sulfuric acid. The aqueous alcoholic solution did not show the color reaction with ferric chloride.

Anal. Found: C, 71.97; H, 6.22; N, 10.52. Calcd. for $C_{16}H_{16}N_2O_2$: C, 71.67; H, 6.01; N, 10.44%.

2, 2'-Bibenzoxazoline.—To a solution of 10 g. of *o*-aminophenol in 90 ml. of hot ethanol, 15 g. of 30% aqueous glyoxal was added and gently refluxed for thirty minutes. The mixture became dark brown and the crystals separated out. The crystals collected after being cooled were washed with ethanol to give almost colorless ones. Recrystallization from ethanol using a Norit gave colorless needles, m. p. 210°C. Yield, 6 g.

2,2'-Bibenzoxazoline is soluble in methanol, benzene and dioxane and insoluble in water and chloroform. The substance afforded a deep green color when dissolved in concentrated sulfuric acid.

Anal. Found: C, 70.34; H, 4.86; N, 11.30. Calcd. for $C_{14}H_{12}N_2O_2$: C, 69.99; H, 5.03; N, 11.66%.

Acetylation of 2, 2'-Bibenzoxazoline : *N, N'*-Diacetyl-2-2'-bibenzoxazoline. — A solution of 0.5 g. of 2,2'-bibenzoxazoline in 20 ml. of acetic anhydride was gently refluxed for ca. 2 hr. The reaction mixture became dark brown. The solvent was removed under reduced pressure, and the resulting dark brown tarrish residue was treated with a small amount of benzene, filtered, and the remaining crystals were washed with benzene and methanol, and recrystallized from dilute acetic acid. Colorless crystals, m. p. 263~265°C, were obtained in a poor yield.

This diacetyl derivative is slightly soluble in benzene and soluble in dioxane and afforded a red color in warm concentrated sulfuric acid.

Anal. Found: C, 66.17; H, 4.97; N, 8.67. Calcd. for $C_{18}H_{16}N_2O_4$: C, 66.65; H, 4.97; N, 8.67%.

Potassium Permanganate Oxidation of 2, 2'-Bibenzoxazoline : 2, 2'-Bibenzoxazole.—To a solution of 0.5 g. of 2,2'-bibenzoxazoline in a mixture of 250 ml. of pure acetone and 50 ml. of water, 0.5 g. of potassium permanganate in 100 ml. of acetone was added dropwise with stirring and gentle boiling. The addition required ca. 3 hr. and the reaction mixture was boiled for an additional 1 hr. After being kept overnight, the reaction mixture was filtered and the filtrate was concentrated under reduced pressure. The yellowish brown residue was recrystallized twice from dioxane and then from chlorobenzene to give pale yellow prisms, m. p. 257°C.

Anal. Found: C, 71.27; H, 3.52; N, 11.60. Calcd. for $C_{14}H_8N_2O_2$: C, 71.18; H, 3.41; N, 11.86%.

Lead Dioxide Oxidation of 2, 2'-Bibenzoxazoline : 2, 2'-Bibenzoxazole. — To a solution of 2, 2'-bibenzoxazoline in 80 ml. of hot benzene, was added 20 g. of lead dioxide. The mixture was refluxed for ca. 6 hr. and turned dark brown. The hot mixture was filtered and the solvent was distilled off. The reddish brown residue was treated with alcohol, dried and dissolved in 20 ml. of benzene. The benzene solution was chromatographed over commercial activated alumina and developed with the same solvent. The first fraction which was obtained almost unabsorbed amounted to ca. 100 ml.; the solvent was removed by evaporation, the pale yellow residue was treated with hot alcohol and recrystallized twice from dioxane to give pale yellow crystals, m. p. 256°C. Mixed melting point with the authentic sample showed no depression.

Nitrosation of 2, 2'-Bibenzoxazoline. — A mixture of 1 g. of 2, 2'-bibenzoxazoline in 130 ml. of benzene and 1.1 g. of sodium nitrite in 20 ml. of water was warmed at 50°C and stirred vigorously. To the mixture, 10 ml. of 1 N hydrochloric acid was gradually added; then the benzene layer became yellow. The benzene layer which separated was washed with water and dried over anhydrous sodium sulfate. The solvent was distilled off under reduced pressure and the residue was recrystallized from ca. 150 ml. of alcohol to yield yellow needles, m. p. 157°C (decomp.).

This dinitroso derivative was not hydrolyzed even by boiling with dilute mineral acid or aqueous alkali, but dissolved in concentrated sulfuric acid with a green color and evolution of nitrogen monoxide (potassium iodide starch paper test).

Anal. Found: C, 56.36; H, 3.47; N, 18.13; mol. wt. (cryoscopic method, benzene), 301. Calcd. for $C_{14}H_{10}N_4O_4$: C, 56.39; H, 3.36; N, 18.77%; mol. wt., 298.27.

Hydrogenation of *N*, *N'*-Dinitroso-2, 2'-bibenzoxazoline. — A solution of 0.1 g. of the dinitroso compound in ca. 50 ml. of alcohol was hydrogenated using Adams catalyst at atmospheric pressure and room temperature. The yellow solution became colorless on absorption of a slight excess of hydrogen. The catalyst was filtered and the filtrate was evaporated under reduced pressure. The remaining crystals were recrystallized from alcohol, colorless plates, m. p. 209°C (decomp.). The substance was identical with 2, 2'-bibenzoxazoline. From the gas in the hydrogenation vessel, ammonia was detected (Nessler's reagent).

Glyoxal Bis-(4-hydroxy anil).—To a solution of 1 g. of freshly recrystallized *p*-aminophenol in a small amount of 80% alcohol, was added 1.2 g. of 30% aqueous glyoxal, and the mixture was heated on a water bath for several minutes. Then, crystals were separated out and the mixture was cooled and filtered. Recrystallization from a large amount of alcohol gave yellow needles, m. p. 212~213°C (decomp.).

Anal. Found: C, 70.04; H, 5.10; N, 11.47. Calcd. for $C_{14}H_{12}N_2O_2$: C, 69.99; H, 5.03; N, 11.66%.

The author wishes to express his thanks to Professor Tokuichi Tsumaki and Professor Takeichi Nishikawa for their exceedingly kind direction of this work. The author also thanks Dr. Yo Ueda and Mr. Hiroshige Yano of the Department of Pharmacy for their measurement of infrared and ultraviolet spectra and Mr. Michio Shido and Miss Sachiko Indo for microanalysis.

General Education Department
Kyushu University
Otsubo-machi, Fukuoka

Polarographic Studies of Metallic Complexes. V[1]. *Tetrammine Series of Cobalt(III) Complexes*[2]

By Nobufumi MAKI, Yoichi SHIMURA and Ryutaro TSUCHIDA

(Received December 24, 1958)

In the earlier papers of this series[1,3] the orders of the polarographic stability were determined for cobalt(III) complexes of pentammine and bisethylenediamine series, $[Co(NH_3)_5X]$, $[Co\ en_2X_2]$ or $[Co\ en_2Y]$. For the same purpose, the comparison of the half-wave potentials of the first waves has been carried out for the cobalt(III) complexes of tetrammine series, $[Co(NH_3)_4X_2]$ or $[Co(NH_3)_4Y]$, which has been briefly reported in the present paper. Some studies[4-10] were found in literature for the hexammine and the tetrammine cobalt(III) complexes of $[Co(NH_3)_4X_2]$ type, but few reports were found on the $[Co(NH_3)_4Y]$ type[10].

Experimental

A Yanagimoto model 104 polarograph similar to that previously described[1] was used to obtain the polarograms. The rate of flow of mercury, m, and the drop time, t, of the dropping mercury electrode were 0.635 mg./sec. and 6.92~7.32 sec., respectively, being measured in the solution of 0.1 F potassium chloride or 0.5 F potassium sulfate at an open circuit with a mercury head of 66.5 cm. A saturated calomel electrode (S.C.E.) was used for a reference electrode and connected to the cell solution through an agar bridge. The cell temperature was maintained at 25±0.1°C by means of a water thermostat. For accurate evaluation of curves and half-wave potentials the method previously described[10] was used. The oxygen dissolved in solution was expelled by passing a stream of nitrogen through the cell solution for an hour prior to each electrolysis. The reversibilities of the electrode reactions were examined by determining the slopes of $\log i/(i_d-i)$ vs. potential. The slopes of the log plots indicated irreversible reduction throughout.

The complex compounds studied were prepared by the methods described in literature. (The references are given in Tables I and II.) Each solution for electrolysis was made freshly from the dry crystalline cobalt(III) complexes before use and the polarographic measurements were made as soon as possible after the removal of oxygen. The concentration of the solution was 0.001 gram complex ion per litre. No maximum suppressor was used for the purpose of comparing the half-wave potentials of the complexes with one another. The presence of the maximum suppressor causes the lowering of the diffusion current and the shift of the half-wave potential to the negative direction. For instance, the half-wave potential of the first wave of the complex,

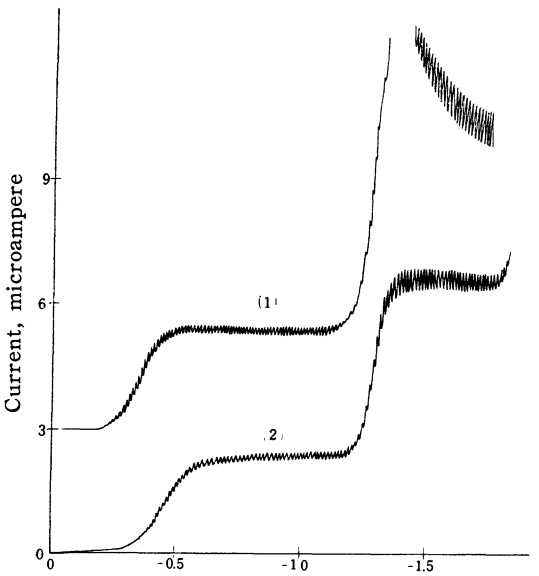


Fig. 1. The polarograms of alaninato-tetramminecobalt(III) complex, $[Co(NH_3)_4 alan]SO_4$, obtained in 0.5 F K_2SO_4 solution at the concentration of 0.001 F.
1. In the absence of the maximum suppressor.
   $E_{1/2}$ of 1st wave $= -0.32$ V.
2. In the presence of 0.0032% Tween-80.
   $E_{1/2}$ of 1st wave $= -0.44_5$ V.
   $E_{1/2}$ of 2nd wave $= -1.28_3$ V.

1) Part IV of this series; N. Maki, Y. Shimura and R. Tsuchida, This Bulletin, **32**, 150 (1959).
2) Partly presented at the Eleventh Annual Meeting of the Chemical Society of Japan, Tokyo, April 6, 1958.
3) N. Maki, Y. Shimura and R. Tsuchida, This Bulletin, **32**, 23 (1959).
4) J. B. Willis, J. A. Friend and D. P. Mellor, *J. Am. Chem. Soc.*, **67**, 1680 (1945).
5) H. F. Holtzclaw, Jr., ibid., **73**, 1821 (1951).
6) H. F. Holtzclaw, Jr. and D. P. Sheetz, ibid., **75**, 3053 (1953).
7) H. F. Holtzclaw, Jr. *J. Phys. Chem.*, **59**, 300 (1955).
8) H. A. Laitinen, J. C. Bailar, H. F. Holtzclaw, Jr. and J. V. Quagliano, *J. Am. Chem. Soc.*, **70**, 2999 (1948).
9) H. A. Laitinen, A. J. Frank and P. Kivalo, ibid., **75**, 2865 (1953).
10) N. Maki, Y. Shimura and R. Tsuchida, This Bulletin, **30**, 909 (1957).

TABLE I. HALF-WAVE POTENTIALS OF COBALT(III) COMPLEXES OF $[Co(NH_3)_4X_2]$ TYPE

Complex	Supporting electrolyte 0.5 F K_2SO_4			Supporting electrolyte 0.1 F KCl		
	$E_{1/2}$ of the 1st wave Co(III)→Co(II)	$E_{1/2}$ of the wave of aquated species Co(III)→Co(II)	$E_{1/2}$ of the 2nd wave Co(II)→Co(0)	$E_{1/2}$ of the 1st wave Co(III)→Co(II)	$E_{1/2}$ of the wave of aquated species Co(III)→Co(II)	$E_{1/2}$ of the 2nd wave Co(II)→Co(0)
$NH_4[Co(NH_3)_4(SO_3)_2]\cdot 3H_2O$[11]	−0.63		——**	−0.57		−1.25
cis-$[Co(NH_3)_4(OH_2)_2]_2(SO_4)_3\cdot 3H_2O$[12]	-0.48_5		——**	-0.40_2		−1.25
$[Co(NH_3)_6](ClO_4)_3$[13]	-0.43_8		−1.28	-0.23_5		*prewave*
trans-$[Co(NH_3)_4(NO_2)_2]ClO_4$[14]	-0.20_7*		-1.28_1*	−0.21		
cis-$[Co(NH_3)_4(NO_2)_2]ClO_4$[14]	-0.04_3*		-1.28_3*	-0.04_8		
trans-$[Co(NH_3)_4Cl_2]Cl$[15]	+	−0.42	——**	+	−0.40	——**
cis-$[Co(NH_3)_4Cl_2]Cl$[16]	+	−0.42	——**	+	−0.40	——**
$[Co(NH_3)_4(IO_3)_2]IO_3\cdot HIO_3$[17]	+		*hydrogen wave*	+		*hydrogen wave*

The concentration of complex: 0.001 gram complex ion per litre. Potential unit: V. vs. S.C.E. Temp.: 25°C.

* The data quoted from J. B. Willis, J. A. Friend and D. P. Mellor, *J. Am. Chem. Soc.*, **67**, 1680 (1945).

** Maximum wave

TABLE II. HALF-WAVE POTENTIALS OF TETRAMMINE COBALT(III) COMPLEXES CONTAINING ONLY ONE CHELATE RING

Complex	Supporting electrolyte 0.5 F K_2SO_4		Supporting electrolyte 0.1 F KCl	
	$E_{1/2}$ of the 1st wave Co(III)→Co(II)	$E_{1/2}$ of the 2nd wave Co(II)→Co(0)	$E_{1/2}$ of the 1st wave Co(III)→Co(II)	$E_{1/2}$ of the 2nd wave Co(II)→Co(0)
$[Co(NH_3)_4en]_2(SO_4)_3\cdot 4H_2O$[18]	−0.44	——*	−0.27	——*
$[Co(NH_3)_4gly]SO_4\cdot H_2O$[19]	-0.40_5	——*	-0.23_4	——*
$[Co(NH_3)_4CO_3]_2SO_4\cdot 3H_2O$[20]	−0.37	−1.28	-0.30_5	−1.24
$[Co(NH_3)_4alan]SO_4$[19]	−0.32	——*	-0.20_5	——*
$[Co(NH_3)_4ox]Cl$[21]	-0.29_5	——*	−0.19	——*
$[Co(NH_3)_4leuc](ClO_4)_3$[22]	-0.25_5	——*	——*	——*
$[Co(NH_3)_6](ClO_4)_3$[13]	-0.43_8	*prewave*	-0.23_5	*prewave*

The concentration of complex: 0.001 gram complex ion per litre. Potential unit: V. vs. S.C.E. Temp.: 25°C.

* Maximum wave

$[Co(NH_3)_4alan^*]SO_4$, shifts towards the negative direction by -0.12_5V. (vs. S.C.E.) in the presence of 0.0032% Tween-80**, as is shown in Fig. 1.

The supporting electrolytes used are 0.1 F potassium chloride and 0.5 F potassium sulfate.

Results and Discussion

In Tables I and II are shown the half-wave potentials of the cobalt(III) complexes of tetrammine series.

All the compounds are reduced irreversibly in two steps at the dropping mercury electrode in 0.1 F potassium chloride or 0.5 F potassium sulfate except the complexes which aquate easily in solution. The ratio of the height of the first wave to that of the second is approximately 1:2. The heights of the first and the second waves are roughly proportional to the concentration of the complex ion at the concentration of $5\times10^{-3}\sim10^{-4}$ gram complex ion per litre. Consequently, it is considered that the first wave, corresponding to a gain of one electron, represents the reduction to cobalt(II) state and the second, corresponding to two electrons, represents the reduction to the metal. The half-wave potentials of the latter are always close to that of the hexaquocobalt(II) ion, $[Co(OH_2)_6]^{2+}$. ($E_{1/2}=-1.428$ V. vs. S.C.E. in 0.5 F K_2SO_4 solution[4].)

The reduction processes of tetrammine cobalt(III) complexes are considered as follows:

$$[Co(NH_3)_4X_2]^{(3-2n)+}+e^- \rightarrow [Co(NH_3)_4X_2]^{(2-2n)+}$$

$$[Co(NH_3)_4X_2]^{(2-2n)+}+mH_2O \xrightarrow[\text{rapidly}]{} \begin{cases} [Co(OH_2)_6]^{2+}+2X^{n-}+4NH_3 \\ [Co(OH_2)_5X]^{(2-n)+}+X^{n-}+4NH_3 \\ [Co(OH_2)_4X_2]^{(2-2n)+}+4NH_3 \\ \text{etc.} \end{cases}$$

$$\begin{cases} [Co(OH_2)_6]^{2+}+2e^- \rightarrow Co+6H_2O \\ [Co(OH_2)_5X]^{(2-n)+}+2e^- \rightarrow Co+5H_2O+X^{n-} \\ [Co(OH_2)_4X_2]^{(2-2n)+}+2e^- \rightarrow Co+4H_2O+2X^{n-} \\ \text{etc.} \end{cases}$$

From the above scheme of the reduction it may be seen that the first step in the polarographic reduction of these cobalt(III) complexes corresponds to the disruption of the complexes, so its half-wave potential may be regarded as a measure of the stability against the polarographic reduction.

The polarographic stability of the cobalt(III) complexes of tetrammine series increases in the following order of the ligands; for the complexes of $[Co(NH_3)_4X_2]$ type,

$$IO_3^-,\ Cl^- < NO_2^- < NH_3 < OH_2 < SO_3^{2-}$$

(supporting electrolyte; 0.5 F K_2SO_4)

and for the complexes of $[Co(NH_3)_4Y]$ type,

$$leuc^- < ox^{2-} < alan^- < CO_3^{2-} < gly^- < en$$

(supporting electrolyte; 0.5 F K_2SO_4)

The order of the stability for the latter type was found to be altered between carbonate and ethylenediamine in the supporting electrolyte of 0.1 F potassium chloride.

$$leuc^- < ox^{2-} < alan^- < gly^- < en < CO_3^{2-}$$

(supporting electrolyte; 0.1 F KCl).

No special relation between the orders of the polarographic stability and that of the spectrochemical series could be found.

The half-wave potentials of the first waves for the complexes of the tetrammine series, $[Co(NH_3)_4X_2]$ or $[Co(NH_3)_4Y]$, exhibit always less negative values than those of the corresponding complexes of bisethylenediamine series, $[Co\ en_2X_2]$ or $[Co\ en_2Y]$, as is shown in Table III. This means that the two ethylenediamine chelate rings have the ability of forming the more stable cobalt(III) complexes against the polarographic reduction than the coordination of the corresponding four ammonia ligands. The result is quite in agreement with that obtained in the previous paper[10].

Fig. 2 shows the polarograms of *cis*-diaquotetramminecobalt(III) ion, $[Co(NH_3)_4(OH_2)_2]^{3+}$, in neutral supporting electrolyte. The slope of the tangent at the half-wave potential of the first wave is very small and the current rising gradually near the zero potential just like a residual current was observed as well as in the case of

* The following abbreviations are used; gly, $NH_2CH_2COO^-$; alan, $NH_2CH(CH_3)COO^-$; leuc, $(CH_3)_2CHCH_2CH(NH_2)COO^-$; ox, $(COO)_2^{2-}$; en, $NH_2CH_2CH_2NH_2$.

** Polyoxyethylene sorbitane monooleate.

11) A. Werner and H. Grüger, *Z. anorg. Chem.*, **16**, 398 (1898).
12) S. M. Jörgensen, ibid., **2**, 279 (1892).
13) M. Linhard, *Z. Elektrochem.*, **50**, 224 (1944).
14) S. M. Jörgensen, *Z. anorg. Chem.*, **17**, 455 (1898).
15) S. M. Jörgensen, ibid., **14**, 404 (1897).
16) C. Duval, *Compt. rend.*, **182**, 636 (1926).
17) N. I. Lobanov, *Obschei Neorg. Khim., Akad. Nauk S. S. S. R.*, **28**, 277 (1954), *Chem. Abstr;* **49**, 14555e.
18) Y. Shimura, This Bulletin, **31**, 311 (1958).
19) Y. Shimura, ibid., **31**, 173 (1958).
20) S. M. Jörgensen, *Z. anorg. Chem.*, **2**, 279 (1892).
21) S. M. Jörgensen, ibid., **11**, 416 (1896).
22) Y. Shimura, This Bulletin, **31**, 315 (1958).

TABLE III. COMPARISON OF THE HALF-WAVE POTENTIALS OF THE FIRST WAVES IN THE COBALT(III) COMPLEXES OF BISETHYLENEDIAMINE SERIES AND OF THE CORRESPONDING TETRAMMINE SERIES

Complex	Supporting electrolyte 0.5 F K_2SO_4 $E_{1/2}$ of the 1st wave Co(III)→Co(II)	Supporting electrolyte 0.1 F KCl $E_{1/2}$ of the 1st wave Co(III)→Co(II)
[Co en$_2$CO$_3$]Cl·H$_2$O	−0.45$_5$	−0.40
[Co(NH$_3$)$_4$CO$_3$]$_2$SO$_4$·3H$_2$O	−0.37	−0.30$_5$
[Co en$_2$ gly]Cl$_2$·H$_2$O	−0.41	−0.36
[Co(NH$_3$)$_4$gly]SO$_4$	−0.40$_5$	−0.23$_4$
[Co en$_2$ox]Cl	−0.31	−0.32
[Co(NH$_3$)$_4$ox]Cl	−0.29$_5$	−0.19
[Co en$_2$leuc](ClO$_4$)$_2$	−0.30$_5$	−0.33$_5$****
[Co(NH$_3$)$_4$leuc](ClO$_4$)$_2$	−0.25$_5$	——*
cis-[Co en$_2$(OH$_2$)$_2$](NO$_3$)$_3$	−0.50	−0.42
cis-[Co(NH$_3$)$_4$(OH$_2$)$_2$]$_2$(SO$_4$)$_3$·3H$_2$O	−0.48$_5$	−0.40$_2$
trans-[Co en$_2$(NH$_3$)$_2$]Cl$_3$·H$_2$O	−0.45	−0.31
cis-[Co en$_2$(NH$_3$)$_2$](ClO$_4$)$_3$	−0.45	−0.31
[Co(NH$_3$)$_6$](ClO$_4$)$_3$	−0.43$_8$	−0.23$_5$
trans-[Co en$_2$(NO$_2$)$_2$]Cl	−0.26	−0.27***
trans-[Co(NH$_3$)$_4$(NO$_2$)$_2$]ClO$_4$	−0.20$_7$**	−0.21
cis-[Co en$_2$(NO$_2$)$_2$]ClO$_4$	−0.25	−0.24***
cis-[Co(NH$_3$)$_4$(NO$_2$)$_2$]ClO$_4$	−0.04$_3$**	−0.04$_8$

The data for the cobalt(III) complexes of bisethylenediamine series were quoted from N. Maki, Y. Shimura and R. Tsuchida, This Bulletin, 32, 150 (1959). The concentration of complex: 0.001 gram complex ion per litre. Potential unit: V. vs. S.C.E.

* Maximum wave

** The data quoted from J. B. Willis, J. A. Friend and D. P. Mellor, *J. Am. Chem. Soc.*, 67, 1680 (1945).

*** The data adopted from H. F. Holtzclaw, Jr. and D. P. Sheetz, ibid., 75, 3053 (1953).

**** The data obtained in the presence of 0.0016% Tween-80.

diaquobisethylenediaminecobalt(III) complex[1] and could not be diminished only by the removal of the oxygen dissolved in solution. In perchloric acid, on the other hand, the first wave becomes steeper as is shown in Fig. 3. The reason for this is considered to be quite similar to the case of *cis*-diaquobisethylenediaminecobalt(III) complex. Namely, in neutral aqueous solution, the hydroxytetramminecobalt(III) ions are formed by the following ligandolysis.

$$[Co(NH_3)_4(OH_2)_2]^{3+} \rightleftarrows [Co(NH_3)_4(OH_2)(OH)]^{2+} + H^+$$

$$[Co(NH_3)_4(OH_2)(OH)]^{2+} \rightleftarrows [Co(NH_3)_4(OH)_2]^{+} + H^+$$

The monohydroxymonoaquo complex ions formed here polymerize to the various kinds of the polynuclear cobalt(III) complex with the lapse of time, as was verified by the spectrochemical studies of Rasmussen et al.[23]

For instance,

$$2\ cis\text{-}[Co(NH_3)_4(OH_2)(OH)]^{2+} \rightarrow \left[(NH_3)_4Co\begin{matrix}OH\\OH\end{matrix}Co(NH_3)_4\right]^{4+} + 2H_2O$$

Accordingly, in neutral solution the several kinds of these cobalt(III) complexes having similar structures are considered to be reduced almost at the same time.

The above mechanism well explains the fact that the overlapped waves of small slope are obtained for the diaquotetramminecobalt(III) complex. In perchloric acid, on the other hand, the above equilibrium is markedly shifted to the left hand due to the presence of an overwhelming hydrogen ion. Hence, the polymerization is quite inhibited and only the original ion is present in solution. Consequently, the wave of steep slope was obtained.

23) S. E. Rasmussen and J. Bjerrum, *Acta Chem. Scand.*, 9, 735 (1955).

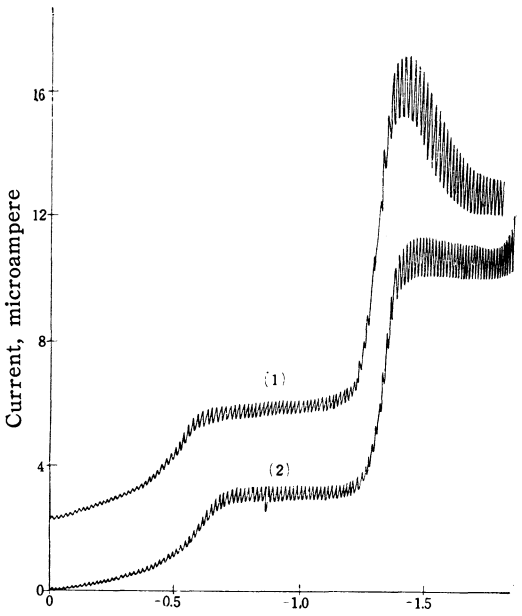


Fig. 2. The polarograms of *cis*-diaquotetramminecobalt(III) complex, $[Co(NH_3)_4(OH_2)_2](SO_4)_3 \cdot 3H_2O$, obtained at the concentration of 0.001 gram complex ion per litre in 0.5 F K_2SO_4 solution.
1. In the absence of the maximum suppressor.
2. In the presence of 0.0032% Tween-80.
Sensitivity: 0.08 μA/mm. Damping: 200.

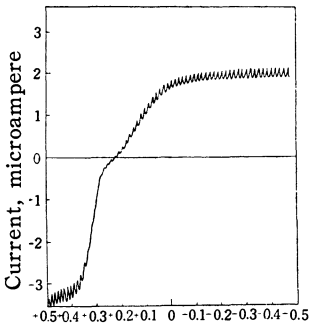


Fig. 3. The polarogram of *cis*-diaquotetramminecobalt(III) ion, $[Co(NH_3)_4(OH_2)_2]^{3+}$, obtained in 1 F perchloric acid at the concentration of 0.001 gram complex ion per litre.

The wave of *cis*- or *trans*-dichlorotetramminecobalt(III) ion which appeared at around −0.42 V. (vs. S.C.E.) is considered to correspond to the reduction of the aquated species such as $[Co(NH_3)_4(OH_2)Cl]^{2+}$ and $[Co(NH_3)_4(OH_2)_2]^{3+}$, since the half-wave potential is in proximity to that of diaquotetramminecobalt(III) ion. ($E_{1/2}$= −0.40$_2$ V. vs. S.C.E. in 0.1 F KCl). Judging from the wavelet, the reduction wave of the original ion is believed to be in the positive region of potential.

As to the wave of diiodatotetramminecobalt(III) complex, $[Co(NH_3)_4(IO_3)_2]IO_3 \cdot HIO_3$, the half-wave potential of the first wave is in the positive region of potential and the second wave is covered by the reduction wave of the hydrogen ion liberated from iodic acid.

Summary

1. All the cobalt(III) complexes of tetrammine series, $[Co(NH_3)_4X_2]$ or $[Co(NH_3)_4Y]$, were reduced irreversibly in two steps at the dropping mercury electrode. The first wave, corresponding to a gain of one electron, represents the reduction of Co(III)→Co(II) and the second, corresponding to two electrons, represents the reduction of Co(II)→Co(0).

2. The polarographic stability of the cobalt(III) complexes of tetrammine series are ranked in the following order of the ligand; for the complexes of $[Co(NH_3)_4X_2]$ type,

IO_3^-, $Cl^- < NO_2^- < NH_3 < OH_2 < SO_3^{2-}$

(supporting electrolyte; 0.5 F K_2SO_4),

and for the complexs of $[Co(NH_3)_4Y]$ type,

$leuc^- < ox^{2-} < alan^- < CO_3^{2-} < gly^- < en$

(supporting electrolyte; 0.5 F K_2SO_4).

3. The half-wave potentials of the reduction step of Co(III)→Co(II) for all the tetrammine cobalt(III) complexes exhibit always more positive values than those of the corresponding bisethylenediamine cobalt(III) complexes.

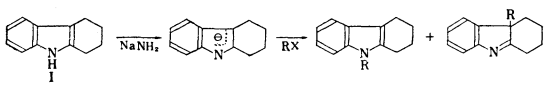
Department of Chemistry
Faculty of Science
Osaka University
Nakanoshima, Osaka

Alkylation of 2,3-Dimethylindole in Liquid Ammonia

By Masao NAKAZAKI

(Received February 9, 1959)

In the previous paper[1], formation of both 9-alkyltetrahydrocarbazoles (IIa, b, c) and 11-alkyltetrahydrocarbazolenines (IIIa, b, c) by the alkylation of tetrahydrocarbazole(I) in liquid ammonia with sodium amide and alkyl halides was reported. But, when isopropyl iodide was employed as alkylation reagent, 11-isopropyltetrahydrocarbazolenine (IIId) was a sole product isolated. These 11-alkyltetrahydrocarbazolenines could be also prepared by the Grignard synthesis, contrary to the negative result of Witkop[2].



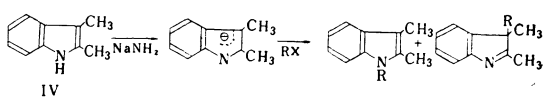
II a, R=CH_3 III a, R=CH_3
b, R=CH_2-CH=CH_2 b, R=CH_2-CH=CH_2
c, R=$CH_2C_6H_5$ c, R=$CH_2C_6H_5$
d, R=$CH(CH_3)_2$

When these experiments had been completed, Patts and Saxton[3] published a paper in which they reported formation of *N*-methyl derivatives in excellent yield from various indole derivatives by the alkylation with sodium amide and methyl iodide in liquid ammonia.

Beside indole itself, all compounds they tried were 2- or 3-monosubstituted indole, and no 2,3-disubstituted indole was subjected to their alkylation method.

Since tetrahydrocarbazole is a 2,3-disubstituted indole, and affords both 9- and 11-alkyl derivatives by the alkylation in liquid ammonia, 2,3-dimethylindole can be expected to give indolenine derivatives by this method.

When the same procedure used in the alkylation of tetrahydrocarbazole was employed, 2,3-dimethylindole gave *N*-methyl derivative (Va) accompanied by a small amount of 2,3,3-trimethylindolenine (VIa), but using allyl bromide and benzyl chloride there were found *N*-alkyl (Vb, c) and indolenine derivatives (VIb, c) in about the same amount.



V a, R=CH_3 VI a, R=CH_3
b, R=$CH_2C_6H_5$ b, R=$CH_2C_6H_5$
c, R=CH_2-CH=CH_2 c, R=CH_2-CH=CH_2
d, R=$CH(CH_3)_2$

Isopropyl bromide failed to afford *N*-isopropyl derivative and a small amount of 2,3-dimethyl-3-isopropylindolenine (VId) was the only prduct isolated. These results are exactly parallel to the one observed in the case of the alkylation of tetrahydrocarbazole in liquid ammonia.

The structures of all indolenine compounds provided by the alkylation in liquid

TABLE I

	Methyl iodide		Benzyl chloride		Allyl bromide		Isopropyl bromide	
Product	Va	VIa	Vb	VIb	Vc	VIc	*	VId
M. p.			59～60	48～49				
B. p. (mmHg)	117～120 (6)	113 (21)	110～115 (1.5)		159～161 (16)	128～132 (12)		100～110 (11)
M. p.** of picrate	148～149 B	158～160 Y	98～99 B	138～141 Y	86 B	156～157 Y		173～174 Y

* Could not be obtained by the alkylation in liquid ammonia or by the Grignard synthesis.

** Picrates of *N*-alkyl derivatives are brown black needles (B), and picrates of indolenines are yellow (Y).

1) M. Nakazaki and S. Isoe, *J. Chem. Soc. Japan, Pure Chem. Sec.* (*Nippon Kagaku Zasshi*), **76**, 1159 (1955).
2) B. Witkop, *J. Am. Chem. Soc.*, **72**, 614 (1950).
3) K. T. Patts and J. E. Saxton, *J. Chem. Soc.*, **1954**, 2641. In our independent work, indole was found to give *N*-benzyl and *N*-allylindole in liquid ammonia with sodium amide and benzyl chloride and allyl bromide, respectively.

ammonia, were confirmed by the comparison with the specimens prepared by the Grignard synthesis, and their properties were shown in Table I, together with the one of *N*-alkyl-2,3-dimethylindoles.

Since 2,3-disubstituted indoles, as this experiment clearly shows, must be expected to give a considerable amount of indolenine derivatives even when methyl iodide is employed in the alkylation in liquid ammonia, adequate caution should be paid at the application of this alkylation method to the structure determination or the synthesis of indole alkaloids and the related compounds[4].

Experimental

N-Methyl-2,3-dimethylindole (Va) and 2,3,3-Trimethylindolenine (VIa). — *Alkylation in liquid ammonia.*—To 150 cc. of liquid ammonia collected in a three-necked flask chilled in a dry ice-acetone bath, 0.05 g. of ferric nitrate was added followed by the addition of 0.8 g. of sodium. After the blue color disappeared, a solution of 5 g. of 2,3-dimethylindole in 20 cc. of ether was added dropwise with stirring. After a mixture of 5 g. of methyl iodide and 5 cc. of ether was added over 20 min., the cooling bath was removed and the flask was allowed to stand overnight at room temperature to evaporate the ammonia off. Water was added to the residue left in the flask, and the oil separated was extracted with ether.

The ether extract was washed with water to neutral, and dried over anhydrous magnesium sulfate. After removal of the solvent, yellow residue was distilled under reduced pressure.

A forerun (1 g.) which boiled below 117°C at 6 mmHg and had a smell reminiscent of jasmine was dissolved in ether.

The basic fraction extracted with 4 N hydrochloric acid was liberated by the addition of 2 N sodium hydroxide solution and taken up in ether. An pale yellow oil (0.5 g.) obtained after removal of the ether, was converted into picrate which melted at 158°C after recrystallization from ethanol. The mixed melting point with the picrate of 2,3,3,-trimethylindolenine (m. p. 158~160°C) prepared by the Grignard synthesis was 158~161°C.

The main fraction boiling at 117~120°C/6 mmHg, weighed 3.2 g. (58% yield).

Anal. Found: C, 82.80; H, 8.29; N, 8.80. Calcd. for $C_{11}H_{13}N$: C, 82.97; H, 8.24; N, 8.80%.

The picrate was recrystallized from benzene to yield brown-black needles, m. p. 148~149°C. (literature[5]): m. p. 150°C). The mixed m. p. with the picrate of 2,3-dimethylindole (m. p. 152~153°C) was 140~143°C.

Grignard synthesis.—2,3,3-Trimethylindolenine was prepared following Hoshino's procedure[6], b. p. 113°C/21 mmHg. The picrate was recrystallized to give yellow needles melting at 158~160°C (literature[6]: m. p. 160~161°C).

N-Benzyl-2,3-dimethylindole (Vb) and 2,3-Dimethyl-3-benzylindolenine (VIb).—*Alkylation in liquid ammonia.*—Into a solution of sodium amide prepared from 200 cc. of liquid ammonia, 0.05 g. of ferric nitrate and 0.78 g. of sodium, a mixture of 5 g. of dimethylindole in 10 cc. of ether was added followed by the addition of 4 g. of benzyl chloride in 10 cc. of ether with stirring. After being kept overnight at room temperature in order to evaporate the ammonia, the residue was extracted with ether, and a basic fraction was extracted with 2 N hydrochloric acid. The basic fraction was liberated by the addition of 4 N sodium hydroxide solution to the hydrochloric acid solution, and extracted with ether. The ether layer, after being washed with water and dried, was evaporated to afford a viscous liquid which solidified gradually (1.80 g.). A small amount was sublimed to give crystals, m. p. 48~49°C. This was found identical with 2,3-dimethyl-3-benzylindolenine prepared by the Grignard synthesis[7] by mixed m. p. determination.

The picrate was recrystallized from ethanol to yield yellow needles, m. p. 138~140°C. The mixed melting point with the picrate prepared from the indolenine synthesized by the Grignard synthesis[7] was 138~141°C.

The natural fraction. — The ether layer freed of the indolenine was washed with water and dried. The solvent was removed to give 5.74 g. of a brown viscous liquid which solidified when allowed to stand at room temperature overnight. After 1.4 g. of dimethylindole (m. p. 94~97°C. picrate: m. p. 153~154°C, identified by mixed m. p. determinations) was recovered by sublimation at 3 mmHg, the residue was distilled in vacuo. A pale yellow fraction boiling at 110~115°C/1.5 mmHg was collected (1.7 g.) and recrystallized from methanol to give large needles, m. p. 59~60°C.

Anal. Found: C, 86.74; H, 7.32. Calcd. for $C_{17}H_{17}N$: C, 86.77; H, 7.28%.

The picrate was recrystallized to give brown black needles, m. p. 98~99°C.

Anal. Found: C, 59.79; H. 4.60; N, 12.20. Calcd. for $C_{23}H_{20}O_7N_4$: C, 59.88; H, 4.34; N, 12.06%.

N-Allyl-2,3-dimethylindole (Vc) and 2,3-Dimethyl-3-allylindolenine (VIc).—*Alkylation in liquid ammonia.* — To a solution of sodium amide prepared from 200 cc. of liquid ammonia, 0.05 g. of ferric nitrate and 1.2 g. of sodium, 7.0 g. of dimethylindole was added with 20 cc. of ether followed by the addition of a mixture of 7.7 g. of allyl bromide and 10 cc. of ether. The basic and neutral fractions were separated by the procedure described above.

4) M. F. Bartlett, D. F. Dickel and W. I. Taylor., *J. Am. Chem. Soc.*, **80**, 126 (1958), in which is obtained the only *N*-methylibogaine from iboganine (a 2,3-disubstituted indole) following the procedure of Patts and Saxton.

5) J. Degen, *Ann.*, **236**, 162 (1886).

6) T. Hoshino, ibid., **500**, 35 (1932).

7) M. Nakazaki, S. Isoe and K. Tanno, *J. Chem. Soc. Japan, Pure Chem. Sec.* (*Nippon Kagaku Zasshi*), **76**, 1262 (1955).

The basic fraction boiled at 128~132°C/12 mmHg and weighed 3.82 g. This 2,3-dimethyl-3-allylindolenine (VIc) was very sensitive to air oxidation and rapidly turned brown at the surface, but was able to be kept a little while in a refrigerator in a sealed bottle.

Anal[8]. Found: C, 82.75; H, 8.32; N, 7.06. Calcd. for $C_{13}H_{15}N$: C, 84.28; H, 8.16; N, 7.56%.

The picrate was recrystallized from ethanol to give yellow needles, m. p. 156~157°C, and it was found identical with the picrate of 2,3-dimethyl-3-allylindolenine prepared by the Grignard synthesis (vide infra).

The neutral fraction boiled at 159~160°C/16 mmHg and weighed 3.22 g.

Anal. Found: C, 84.11; H, 8.38; N, 7.35. Calcd. for $C_{13}H_{15}N$: C, 84.28; H, 8.16; N, 7.56%.

The picrate was recrystallized from ethanol to give brown black needles, m. p. 86°C.

Anal. Found: C, 54.85; H, 4.34; N, 13.37. Calcd. for $C_{19}H_{18}O_7N_4$: C, 55.07; H, 4.38; N, 13.52%.

Grignard synthesis.—To a Grignard compound prepared from 11.1 g. of methyl iodide and 1.9 g. of magnesium in 20 cc. of ether, a solution of 7.0 g. of dimethylindole in 20 cc. of ether was added dropwise over a period of 25 min. After generation of methane subsided, 7.7 g. of allyl bromide was added slowly over 20 min., and stirred for one additional hour. The ether layer was separated, after the Grignard complex was decomposed by the addition of 4 cc. of acetic acid with 15 cc. of water, and the aqueous layer was extracted thoroughly with ether. The combined ether extracts were shaken with 2 N hydrochloric acid to extract the basic fraction.

The oil which separated from the hydrochloric acid solution by being made alkaline was extracted with ether. After removal of the solvent, the residual liquid was distilled in vacuo to give a liquid which had a camphor-like smell, b. p. 80~90°C/2 mmHg, weighed 4.05 g.

2,3-Dimethyl-3-allylindolenine was found quickly to turn brown in color by air oxidation.

Anal[8]. Found: C, 82.86; H, 8.41; N, 6.95. Calcd. for $C_{13}H_{15}N$: C, 84.28; H, 8.16; N, 7.56%.

The picrate was recrystallized from ethanol to give yellow crystals, m. p. 157~158°C.

Anal. Found: C, 55.22; H, 4.60; N, 13.54. Calcd. for $C_{19}H_{18}O_7N_4$: C, 55.07, H, 4.38; N, 13.52%.

2,3-Dimethyl-3-isopropylindolenine (VId). —*Alkylation in liquid ammonia.*— To a solution of sodium amide prepared from 250 cc. of liquid ammonia, 0.1 g. of ferric nitrate and 1.5 g. of sodium in a 3-necked flask chilled in a dry ice-acetone bath, 7.0 g. of dimethylindole was added with 20 cc. of ether, followed by the addition of 7.5 g. of isopropyl bromide over 20 min. with stirring. The cooling bath was removed and the reaction mixture was allowed to stand at room temperature overnight to evaporate the ammonia. Following the same procedure described above, the basic and neutral fractions were separated. The basic fraction boiled at 100~110°C/11 mmHg, weighed 0.2 g. This compound was noticed to have a characteristic indolenine smell.

Anal. Found: C, 82.62; H, 9.59; N, 7.92. Calcd. for $C_{13}H_{17}N$: C, 83.37; H, 9.15; N, 7.48%.

The picrate was recrystallized to give yellow crystals, m. p. 173~174.5°C.

Anal. Found: C, 55.00; H, 5.08; N, 13.92. Calcd. for $C_{19}H_{20}O_7N_4$: C, 54.80; H, 4.84; N, 13.46%.

The neutral fraction weighed 7.9 g., and from it 4.6 g. of dimethylindole was recovered by sublimation. But attempts to isolate *N*-isopropyl derivative from the viscous residue in the form of picrate failed, and the picrate of dimethylindole was the only material traceable.

Grignard synthesis.— To a Grignard solution prepared from 1.9 g. of magnesium and 11.1 g of methyl iodide in 20 cc. of ether, a mixture of 7.0 g. of dimethylindole in 10 cc. of ether was added dropwise.

After the evolution of methane subsided, 7.9 g. of isopropyl bromide was added over a period of 30 min. with stirring and cooling in an ice bath. After being kept at room temperature for 2 hr., the Grignard complex was decomposed by the addition of 4 cc. of acetic acid and 15 g. of ice. The basic and neutral fractions were separated by the same procedure described above.

The basic fraction was distilled in vacuo to give a liquid which boiled at 75~90°C/10 mmHg. Yield, 0.7 g.

The picrate was recrystallized to afford yellow crystals, m. p. 173~175°C which melted at 172~173°C when admixed with the picrate of 2,3-dimethyl-3-isopropylindolenine prepared by the alkylation of dimethylindole in liquid ammonia. From the neutral fraction, only dimethylindole was recovered.

The authors is very grateful to Mr. Muneo Sato for his enthusiastical technical assistance.

Department of Chemistry
Institute of Polytechnics
Osaka City University
Kita-ku, Osaka

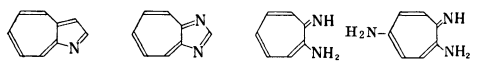
8) This rather poor result may be due to the sensitivity of the indolenine to air oxidation.

Benzoylation of 1,3-Diazaazulene[1]

By Ichiro MURATA

(Received February 6, 1959)

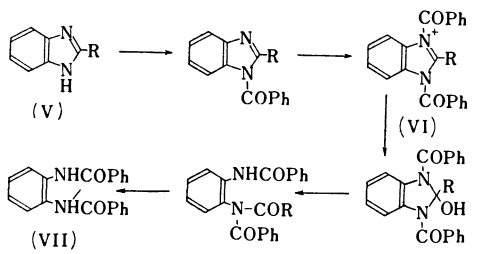
In 1949, Nozoe[2] predicted the possibility that the so-called 2-aminotropoimine and azaazulenes, which may be considered as the nitrogen homolog of tropolone and azulene respectively, are stable enough to exist. Later studies have confirmed their presence by the syntheses of azaazulenes such as 1-azaazulene (I)[3] and 1,3-diazaazulene (II)[4].



(I) (II) (III) (IV)

However, the only derivative of 2-aminotropoimine (III) known to date is 2,5-diaminotropoimine (IV)[5] obtained by the reduction of 5-nitrosotropolone dioxime (*p*-tropoquinone trioxime)[6].

In a sense, 1,3-diazaazulene (II) may be considered as a seven-membered ring homolog of benzimidazole (V). From such a view point, the cleavage reaction of an imidazole ring by the Schotten-Baumann method, known as the Bamberger reaction[7,8] in imidazole compounds, was applied to II.



Scheme 1.

The Bamberger reaction is considered to poceed as indicated in Scheme 1, starting with benzoylation, followed by the formation of a quaternary base (VI) by the presence of excess benzoyl chloride and the cleavage of the base by the action of alkali hydroxide, forming *o*-phenylenediamine dibenzoate (VII)[8].

II differs from the imidazole ring in not possessing an N-H group that could be benzoylated. However, since II easily forms a methiodide[4], the possibility of its ring fission may be considered and examination of this reaction was made.

A solution of II dissolved in 4 molar equivalents of sodium hydroxide solution, and chilled in ice, was added with 4 molar equivalents of benzoyl chloride, the mixture was shaken thoroughly, and allowed to stand overnight. This was extracted with chloroform and the brown oil obtained from the extract was separated and purified by alumina chromatography, from which yellow scales (VIII), m. p. 157 ~158°C, and pale yellow needles (IX), m. p. 94~95°C, were obtained besides recovery of the starting II.

By exactly the same procedure, the reaction of 6 molar equivalents of sodium hydroxide and 4 molar equivalents of benzoyl chloride gave a small amount of pale yellow prisms (X), m. p. 158°C, besides VIII and recovery of II.

When this reaction was carried out at 70~72°C, the kind and amount of the products obtained were different, as indicated in Table I.

The reaction of II and benzoyl chloride

TABLE I. REACTION OF 1,3-DIAZAAZULENE AND BENZOYL CHLORIDE

Molar ratio			Temp.	Product (%)			
II	NaOH	C_6H_5COCl	(°C)	VIII	IX	X	II
1	4	4	0	25	30	—	37
1	6	4	0	30	—	5	40
1	4	4	70~72	—	60	—	15
1	6	4	70~72	—	—	62	14

1) Presented at the Local Meeting of Tohoku District of the Chemical Society of Japan, held at Yonezawa, June 25, 1956.

2) T. Nozoe, *Science of Drugs* (*Yakugaku*), **3**, 191 (1949); T. Nozoe, *Science Repts. Tohoku Univ.*, **I**, **34**, 225 (1950).

3) T. Nozoe, S. Seto, S. Matsumura and T. Terasawa, *Chem. and Ind.*, **1954**, 1357.

4) T. Nozoe, T. Mukai and I. Murata, *J. Am. Chem. Soc.*, **76**, 3352 (1954).

5) T. Nozoe, M. Sato, S. Ito, K. Matsui and T. Matsuda, *Proc. Japan Acad.*, **29**, 565 (1953); T. Nozoe and S. Ito, unpublished data.

6) T. Nozoe and S. Seto, *Proc. Japan Acad.*, **27**, 188 (1951).

7) E. Bamberger, *Ann.*, **273**, 267 (1893); E. Bamberger, B. Berle, ibid., **273**, 342 (1893).

8) A. Weissberger, "The Chemistry of Heterocyclic Compounds, Imidazole and its Derivatives", Part I, Interscience Publishers, New York (1953), p. 48, 273.

afforded, according to conditions of the reaction, VIII and IX or X. Examinations were made on the structure of these three products.

VIII and X show the same melting point but a distinct depression of the melting point occurs on their admixture and they show different degrees of solubility, color, and crystal form. The ultraviolet absorption spectra[9] of the two compounds, shown in Fig. 1, are also entirely different. Elementary analytical values of X correspond to the molecular formula of $C_{14}H_{10}N_2$, not containing any oxygen. It easily forms a picrate of m. p. 210°C, a styphnate of m. p. 231°C (decomp.), and a hydrochloride of m. p. 210°C (decomp.), whose analytical values also agree with those calculated for a salt of the foregoing composition.

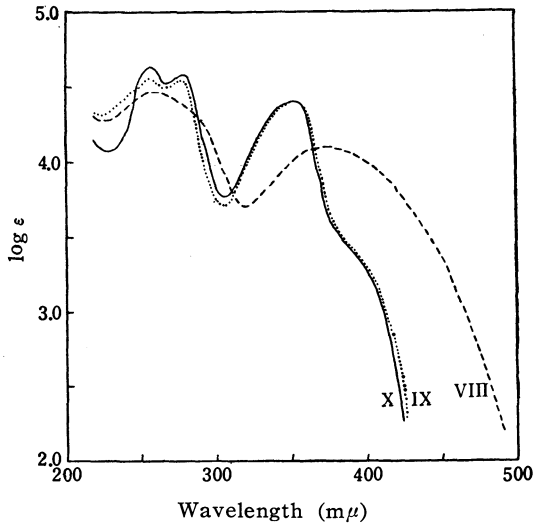


Fig. 1. U. V. absorption spectra of VIII, IX and X in methanol.

The infrared absorption spectrum[10] of X (Fig. 2) exhibits an absorption band at 1604 cm^{-1}, corresponding to the C=N stretching vibration or ring vibration (1602 cm^{-1}) in 1,3-diazaazulene, and absorption bands at 717 and 686 cm^{-1} due to the C-H out-of-plane vibration of mono-substituted benzene. These facts suggest that X is a phenyl derivative of II.

Oxidation of X with potassium dichromate in diluted sulfuric acid affords 2-phenylimidazole-4,5-dicarboxylic acid(XI)[11] of m. p. 264°C (decomp.), and its decarboxylation gives 2-phenylimidazole (XII)[11] of m. p. 143°C, which showed no depression on admixture with XII synthesized from tartaric acid. The ultraviolet absorption spectra of these two compounds were also identical. It follows, therefore, that the structure of X is 2-phenyl-1,3-diazaazulene.

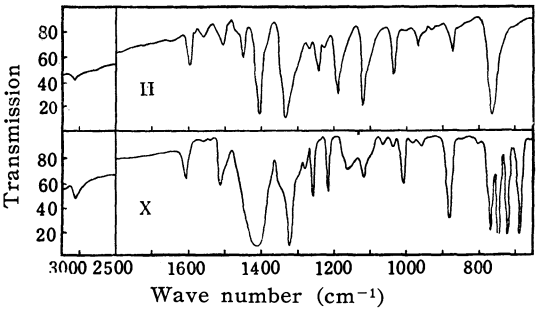


Fig. 2. I. R. absorption spectra of II and X in KBr.

IX is converted into X merely by mild treatment with dilute alkali and liberates one molar equivalent of benzoic acid during this course. The ultraviolet spectrum (Fig. 1) of IX is almost identical with that of X except for the absorption at around 230 mμ[12]. Since the heating of X with an equivalent amount of benzoic acid in ethanol results in quantitative formation of IX and from the analytical

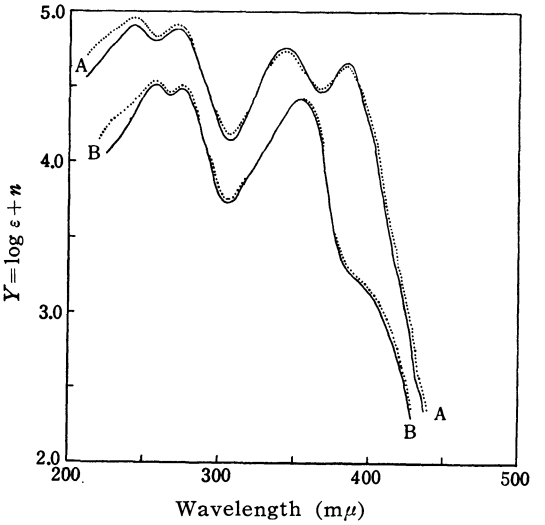


Fig. 3. U. V. Absorption spectra
—— X ····· VIII
A, in 0.1N HCl ($Y=\log\varepsilon+0.5$)
B, in 0.1N NaOH ($Y=\log\varepsilon+0$)

9) Measured by the Beckman Model DU Spectrophotometer.

10) I. R. spectra are measured using Perkin-Elmer Model 21 double beam spectrophotometer by Mr. Y. Ikegami of this Institute, to whom the author is deeply indebted.

11) R. G. Fargher and F. L. Pyman, *J. Chem. Soc.*, **115**, 217 (1919).

12) This is considered to have appeared by the overlapping of the K-band of benzoic acid. Cf. A. E. Gillam and E. S. Stern, "An Introduction to Electronic Absorption Spectroscopy in Orgaic Chemistry", Edward Arnold Publishers, London (1954), p. 126.

values of IX, it is assumed that IX is a benzoic acid salt of X.

Analytical values of VIII agree with $C_{21}H_{16}O_2N_2$. Its mild treatment with dilute acid or alkali affords X from the basic portion and one molar equivalent of benzoic acid from the acid portion. The ultraviolet spectrum of VIII (Fig. 1) shows an entirely different curve from those of IX and X, but its spectrum in acid and alkaline solvents (Fig. 3) shows a curve extremely similar to the absorption of X in acid and alkaline media with the exception of the absorption at around 230 mμ[12].

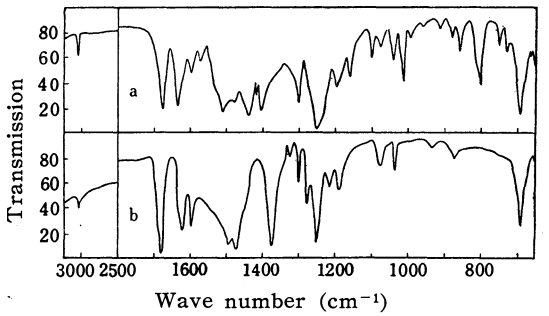
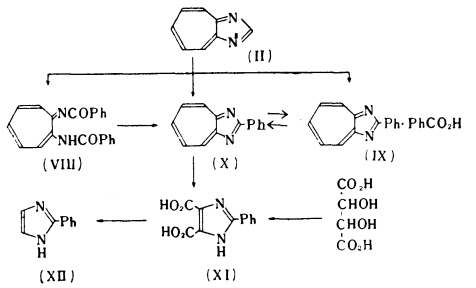


Fig. 4. I. R. absorption spectra of VIII.
a, in KBr-pellet; b, in CCl_4 soln.

In the infrared absorption spectrum of VIII (Fig. 4), there are absorptions considered to be the C=O stretching vibration of secondary amide[13] at the wave number[15] of 1683 (1676), the N-H deformation vibration at 1492 (1515), the N-H strectching vibration at (3290), and the C=O stretching vibration of tertiary amide at 1622 (1630).



Scheme 2.

The foregoing results suggest that VIII is 2-aminotropoimine dibenzoate formed by the ring-cleavage of II. These changes are presented in Scheme 2.

Attempts were made to remove the benzoyl group from VIII by hydrolysis and to obtain the parent structure, 2-aminotropoimine (III), but the attempts failed because of the extreme facility with which VIII underwent cyclization[16] and its facile conversion to X under the conditions for hydrolysis.

Experimental[17]

Reaction of 1,3-Diazaazulene (III) and Benzoyl Chloride.—a) To a solution of 300 mg. (2.3 mmol.) of II dissolved in a solution of 370 mg. (9.2 mmol.) of sodium hydroxide in 8 cc. of water, 1.29 g. (9.2 mmol.) of benzoyl chloride was added in one lot, under ice cooling, and the mixture was stirred thoroughly. This treatment is accompanied by a considerable generation of heat and the mixture must be chilled efficiently. When yellowish brown clay-like substance began to separate out on the wall of the vessel, the mixture was allowed to stand overnight and extracted with chloroform, from which 1.02 g. of brown oily substance was obtained. This oil was dissolved in 2 cc. of mixture of benzene and petroleum ether (1 : 1), and the solution was passed through a column (10×150 mm.) of alumina. The column was eluted with petroleum ether and 80 mg. of yellow crystals, m. p. 146~151°C, was obtained. Four recrystallizations from ethanol afforded 2-aminotropoimine dibenzoate (VIII) as yellow scaly crystals, m. p. 157~158°C.

Further elution of the alumina column with mixture of benzene and petroleum ether (1 : 1) afforded 90 mg. of pale yellow oil which was crystallized from cyclohexane to crystals of m. p. 91~92°C. Recrystallization from benzene-cyclohexane mixture afforded 2-phenyl-1,3-diazaazulene benzoic acid salt (IX) as pale yellow needles, m. p. 94~95°C.

Further elution of the column with benzene, followed by elution with ethanol, gave dark brown oil from both. These products were derived to respective picrates and decomposed by dilute hydrochloric acid, from which 110 mg. of unchanged II was recovered.

b) To a solution of 500 mg. (3.8 mmol.) of II dissolved in a solution of 915 mg. (22.8 mmol.) of sodium hydroxide in 16 cc. of water, 2.13 g. (15.2 mmol.) of benzoyl chloride was added and reacted as in a). Purification through a column (10×180 mm.) of alumina was carried out similarly and 140 mg. of VIII from the fraction eluted with petroleum ether and 25 mg. of yellow crystals,

13) Absorption of 2-benzoylaminotropone[14] as the secondary amide with unsaturated seven-membered ring was as follows: 1685 (1678), 1502 (1513), 3270 (3275); these values were read by the author.

14) T. Nozoe, S. Seto, H. Takeda, S. Morosawa and K. Matsumoto, *Science Repts. Tohoku Univ.*, **I**, **36**, 126 (1952).

15) Measurements were made by the KBr-pellet method. Values in parentheses are of those measured as CCl_4 solution.

16) It has been also known that *o*-phenylenediamine dibenzoate also undergoes facile dehydration and cyclization to 2-phenylbenzimidazole. Cf. O. Gerngross, *Ber.*, **46**, 1913 (1913).

17) All melting points are uncorrected. Petroleum ether used in this work was of b. p. 40~60°C. The microanalyses were carried out by Mr. S. Ohyama and Miss A. Iwanaga, to whom the author's deep gratitude is hereby expressed.

m. p. 142~153°C, from a fraction eluted with benzene-petroleum ether were obtained. Recrystallization of the latter from benzene-petroleum ether mixture afforded 2-phenyl-1, 3-diazaazulene (X) as yellow prisms, m. p. 158~159°C.

c) A solution of 830 mg. (6.34 mmol.) of II dissolved in a solution of 1.02 g. (25.5 mmol.) of sodium hydroxide in 26 cc. of water was heated to 70~72°C on a water bath and 3.57 g. (25.5 mmol.) of benzoyl chloride was added in one lot with stirring. The mixture was maintained at this temperature for 1 hr., cooled, and extracted with chloroform. The oily substance obtained from this extract was purified by chromatography and 510 mg. of IX was obtained besides recovery of 155 mg. of II.

d) A solution of 850 mg. (6.5 mmol.) of II dissolved in a solution of 1.56 g. (39 mmol.) of sodium hydroxide in 27 cc. of water was reacted with 3.64 g. (26 mmol.) of benzoyl chloride as in c) and 520 mg. of X and 120 mg. of II were obtained.

2-Aminotropoimine Dibenzoate (VIII).—*Anal.* Found: C, 76.89; H, 4.80; N, 8.76. Calcd. for $C_{21}H_{16}O_2N_2$: C, 76.81; H, 4.91; N, 8.53%.

2-Phenyl-1, 3-diazaazulene Benzoic Acid Salt (IX).—*Anal.* Found: C, 76.28; H, 4.71; N, 8.56. Calcd. for $C_{14}H_{10}N_2 \cdot C_7H_6O_2$: C, 76.81; H, 4.91; N, 8.53%.

2-Phenyl-1, 3-diazaazulene (X).—*Anal.* Found: C, 78.05; H, 5.06; N, 13.37. Calcd. for $C_{14}H_{10}N_2 \cdot \frac{1}{2} H_2O$: C, 78.12; H, 5.15; N, 13.02%.

Found (in a sample dried over P_2O_5 at 50°C/10 mmHg): C, 81.28; H, 4.95; N, 13.82. Calcd. for $C_{14}H_{10}N_2$: C, 81.53; H, 4.89; N, 13.58%.

a) Hydrochloride of X: Pale yellow prisms, m. p. 210°C (blacken) as recrystallized from ethanol.

Anal. Found: N, 11.47. Calcd. for $C_{14}H_{10}N_2 \cdot HCl$: N, 11.53%.

b) Picrate of X: Pale yellow, silky needles, m. p. 209~210°C, as recrystallized from water.

Anal. Found: C, 55.12; H, 3.43; N, 16.17. Calcd. for $C_{14}H_{10}N_2 \cdot C_6H_3O_7N_3$: C, 55.18; H, 3.01; N, 16.09%.

c) Styphnate of X: yellow silky needles, m. p. 231°C (decomp.), as recrystallized from 50% ethanol.

Anal. Found: C, 52.87; H, 3.24; N, 15.31. Calcd. for $C_{14}H_{10}N_2 \cdot C_6H_3O_8N_3$: C, 53.22; H, 2.90; N, 15.52%.

d) Benzoic acid salt (IX) of X: A solution of 50 mg. of X and 20 mg. of benzoic acid dissolved in 1 cc. of ethanol was heated for a few minutes, ethanol was evaporated, and the residue was recrystallized from benzene-petroleum ether mixture to pale yellow needles, m. p. 93~94°C, which showed no depression on admixture with IX.

Oxidation of X with Potassium Dichromate.—A solution of 150 mg. of X and 490 mg. of potassium dichromate dissolved in 12 cc. of 6 N sulfuric acid was heated on a water bath for 45 min. and the mixture was allowed to stand for 3 days at room temperature. The crystals that separated out were collected by filtration and 55 mg. of XI, m. p. 263~264°C (decomp.), was obtained. This XI was sublimed under diminished pressure to effect decarboxylation and 30 mg. of colorless crystals, m. p. 138~140°C, was obtained which showed no depression in the melting point on admixture with 2-phenylimidazole (XII), synthesized from tartaric acid[18].

Hydrolysis of VIII.—a) A mixture of 200mg. of VIII in 1.5 cc. of 2 N sulfuric acid was heated on a water bath for a few minutes, by which time the crystals dissolved to form an orange solution. This solution was extracted with chloroform and 50 mg. of crystals; m. p. 111~120°C, was obtained. Recrystallization from petroleum ether raised the melting point to 119~120°C, undepressed by admixture with benzoic acid. The aqueous layer separated after chloroform extraction was made weakly alkaline with sodium hydrogen carbonate and extracted with chloroform, from which 125 mg. of crystals melting at 156~157°C, identified with X, was obtained.

b) A mixture of 50 mg. of VIII dissolved in 1 cc. of ethanol and 0.5 cc. of 2 N sodium hydroxide solution was refluxed on a water bath for 5 min., ethanol was evaporated, and the residual solution was diluted with water. This was extracted with chloroform and 20 mg. of X was obtained from the extract. Extraction of the aqueous layer after acidification afforded 10 mg. of benzoic acid.

The author takes this opportunity to express his deep gratitude to Professor Tetsuo Nozoe for his unfailing guidance and to Assistant Professor Toshio Mukai for much helpful advice.

The Chemical Research Institute of Non-Aqueous Solutions
Tohoku University
Katahira-cho, Sendai

18) Ultraviolet absorption spectra of the sample and synthesized product were in good agreement, both showing λ_{max}^{MeOH} 269 mμ (log ε 4.20) and λ_{min}^{MeOH} 230 mμ (log ε 3.37).

The Kinetic Study of Surface-chemical Reactions at Extremely Low Pressures. II. The Thermal Reaction between Water Vapor and a Tungsten Filament. Part II

By Takuya HAMAMURA

(Received August 15, 1958)

It has been shown previously[1] by a hot filament method that the major part of water molecules impinging on the hot surface of tungsten filament rebound without reaction even at high temperatures. These results, however, were not free from the end effect of the filament, since it was kept cooler at the both ends, where it was joined with leads which were much thicker than the filament and hence practically not heated at all by an electric current; the reaction probability* determined directly from the observed rate of reaction is, in consequence, an average one being smaller than that at the middle portion. The present paper is concerned with the elimination of the effect of the above-mentioned end losses.

Several devices[2] have been reported for the elimination of end losses, e. g., to heat the leads with auxiliary heaters attached to them or to heat the filament from outside of the vessel by an electric furnace, but the former is complicated in structure and the latter is not suitable for the present purpose. The use of a long filament often employed for this purpose is not appropriate to the flow method, since the pressure difference along the filament becomes too large at a high rate of reaction.

Two-filament Method. — In the present work, two filaments differing in length are used and the end effect of the longer filament is compensated with that of the shorter one. Two filaments, one longer (main) and the other shorter (compensating), of the same diameter and material are mounted in the vessel and heated one by one with the same current to obtain the reaction probabilities separately. Then, the reaction probability free from the end effect is obtained as follows. Let L_m and L_c denote the lengths of the two filaments ($L_m > L_c$) and k_m and k_c the respective reaction probabilities. Dividing the main filament into two end portions $L_c/2$ in length each and the middle portion $L_m - L_c$ in length, the reaction probability k_m can be expressed as a weighted mean of the probability k'_c at the end portions and k' at the middle portion. Then, k' is given by

$$k' = (k_m L_m - k'_c L_c)/(L_m - L_c) \qquad (8)^{**}$$

When the two filaments are heated with the same current, the end portions of the longer one will attain the same distribution of temperature as that along the compensating filament, and the middle portion at a uniform temperature provided that the filaments are long enough. Therefore, k'_c is equal to k_c if the reaction probability is independent of the pressure of water vapor, and is equal to k_c at the same partial pressure of water vapor as that under which k_m is obtained if the probability depends upon the pressure. Therefore, if k_c is obtained at various pressures P of water vapor and plotted against P, k'_c is obtained graphically, and hence k', the reaction probability free from the end losses, can be evaluated by Eq. 8. Although the two filaments are heated under the same initial pressure, the partial pressure while the respective filament is being heated is not the same, owing to the difference in the reacting areas of the filaments.

Experimental

Apparatus. — The apparatus was essentially the same as that of the previous paper. Only the changed points will be described below.

A reaction vessel was 7.0 cm. in diameter and 30 cm. in length. In it two tungsten filaments each 0.114 mm. in diameter and 128 mm. and 81 mm. long, respectively, were mounted perpendicular to the axis of the vessel at a distance of 5 cm. from each other. The distributions of

1) N. Sasaki and T. Hamamura, This Bulletin, **29**, 365 (1956).

2) L. B. Thomas and R. E. Brown, *J. Chem. Phys.*, **18**, 1367 (1950).

* The probability of reaction of water molecule with the filament for a single collision.

** Eqs., Figs. and Tables are numbered following consecutively those of the previous paper (Ref. 1).

temperature along the filaments were previously determined by the method of Langmuir and others[3]. The tungsten filaments used were taken from the same spool as that used in the previous experiments and pretreated in a similar manner. A Pirani gauge having a sensitivity of 1.42×10^{-5} mmHg for hydrogen was attached to the glass balloons in place of McLeod manometer M_3. The wall in front of the filaments was protected from the blue deposit of reaction product by a glass tube containing an iron rod which was hung in the vessel with a thin wire and shifted by a solenoid only when the temperature was measured by an optical pyrometer.

Procedure.—Procedures of evacuating the apparatus, degassing the filaments and introducing water vapor into the vessel have been described previously[1]. When the flow of water vapor became stationary, the main filament was heated and the temperature was measured with an optical pyrometer. As the reaction proceeded the pressure in the glass balloons increased gradually and this increase was measured with the Pirani gauge, every two minutes for sixteen minutes. The filament was then cooled and the balloons were evacuated. After this treatment, the compensating filament was heated with the same current and the pressure increase was measured similarly for the same time. The pressure increase gave the rate of reaction, and hence k_m[4] and k_c were evaluated by Eq. 7 and P by Eq. 6. Variations of k_m and k_c with P at a definite temperature were determined by a series of the experiments carried out by heating the filaments with a fixed current under various initial pressures of water vapor.

The temperature of the vessel remained at room temperature throughout the experiments, the effect of the heated filament being negligible at its highest temperature.

Results and Discussion

The experiments were carried out at temperatures from 1430 to 1940°K and initial pressures of water vapor from 12×10^{-5} to 125×10^{-5} mmHg. Values of k_m and k_c obtained were plotted against P in a log–log plot, respectively. Some of them are shown in Fig. 5.

From these plots, values of k_m and k'_c at a definite pressure were obtained, and the probability k' free from the end losses was evaluated by Eq. 8. Values of k_m, k'_c and k' at 60×10^{-5} mmHg pressure of water vapor thus obtained are given in Table II. Plots of $\log k'$ vs. $1/T\times10^3$ at 30×10^{-5} and 60×10^{-5} mmHg of water vapor are given in Fig. 6. Humps observed in the curves in the vicinity of 1700°K were not observed in the previous experiments, perhaps because of insufficient points of observation. No hysteresis was observed in the whole range of temperatures. The apparent heat of activation at 60×10^{-5} mmHg of water vapor is plotted against the filament temperature in Fig. 7.

Plots of $\log k'$ vs. $\log P$ at various temperatures are also shown in Fig. 5. It is evident that the elimination of end losses is significant especially at lower temperatures. It was found from this figure that the reaction probability decreased with increase of the pressure of water vapor. Although this decrease seemed to be

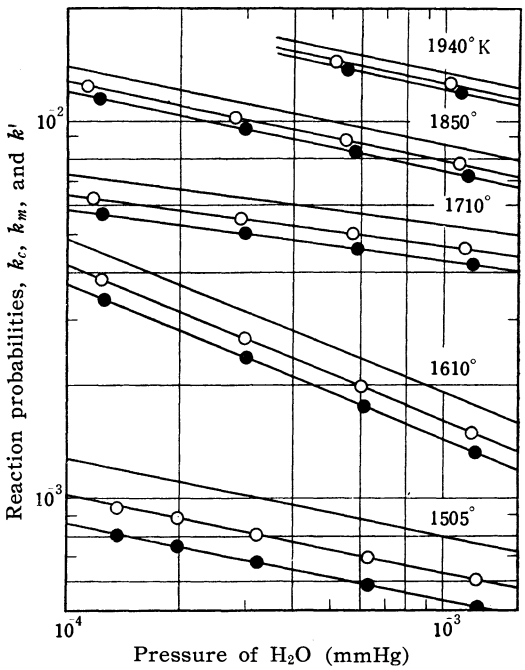


Fig. 5. Effect of pressure of water vapor on the reaction probabilities, k', k_m and k_c.
—— k', —○— k_m, —●— k_c

TABLE II. REACTION PROBABILITIES AT 60×10^{-5} mmHg PRESSURE OF WATER VAPOR

Temp. of filament (°K)	k_m	k_c	k'
1430	$3.3_4\times10^{-4}$	$2.6_3\times10^{-4}$	$4.5_7\times10^{-4}$
1470	$5.1_6\times10^{-4}$	$4.2_0\times10^{-4}$	$6.8_2\times10^{-4}$
1505	$7.0_2\times10^{-4}$	$5.9_1\times10^{-4}$	$8.8_4\times10^{-4}$
1560	$1.2_2\times10^{-3}$	$1.0_6\times10^{-3}$	$1.4_9\times10^{-3}$
1610	$1.9_8\times10^{-3}$	$1.7_6\times10^{-3}$	$2.3_4\times10^{-3}$
1675	$4.0_8\times10^{-3}$	$3.6_7\times10^{-3}$	$4.7_9\times10^{-3}$
1710	$4.9_8\times10^{-3}$	$4.5_7\times10^{-3}$	$5.7_0\times10^{-3}$
1760	$5.3_2\times10^{-3}$	$4.9_4\times10^{-3}$	$5.9_8\times10^{-3}$
1850	$8.7_3\times10^{-3}$	$8.2_5\times10^{-3}$	$9.5_6\times10^{-3}$
1940	$1.4_0\times10^{-2}$	$1.3_5\times10^{-2}$	$1.4_8\times10^{-2}$

3) I. Langmuir, S. MacLane and K. Blodgett, *Phys. Rev.*, **35**, 478 (1930).
4) The roughness factor of 1.225 was used according to Tonks. L. Tonks, *Phys. Rev.*, **38**, 1030 (1931).

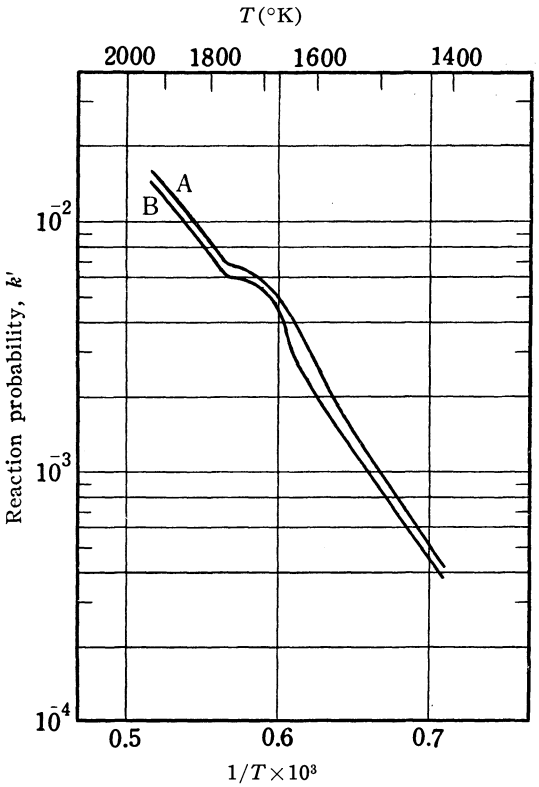


Fig. 6. Effect of filament temperature on the reaction probability k' at 30×10^{-5} and 60×10^{-5} mmHg of water vapor. A—30×10^{-5} mmHg, B—60×10^{-5} mmHg.

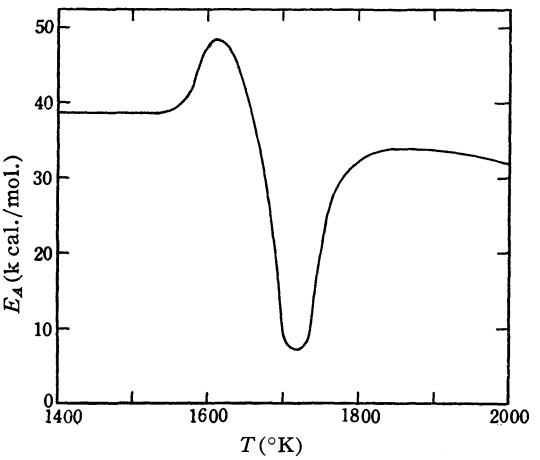


Fig. 7. Apparent heat of activation at 60×10^{-5} mmHg of water vapor.

caused by cooling of the filament by water vapor or by decrease of the reaction probability itself, the lowering of the temperature was not observed by either the optical pyrometer or the resistance of filament.

At filament-temperatures and pressures of water vapor plotted in Fig. 5, the reaction rates were independent of hydrogen pressures. Effect of hydrogen pressure on the reaction rate will be described in the following paper.

From the plot of $\log k'$ vs. $\log P$ the order n of reaction with respect to water vapor can be determined. As described in the previous paper, the rate of reaction D is given by

$$D=k'SBP \tag{5}$$

The reaction rate depends only upon the pressure of water vapor, when the filament temperature is fixed, as

$$D=KP^n \tag{9}$$

where K and n are constants. Eliminating D from Eqs. 5 and 9, k' is given by

$$k'=K/SB\times P^{n-1} \tag{10}$$

or

$$\log k'=\log(K/SB)+(n-1)\log P \tag{11}$$

The value of $n-1$ is thus given as the slope of the curve of $\log k'$ plotted against $\log P$ as in Fig. 5. The order of reaction thus obtained are tabulated in Table III. The reaction is nearly the first order.

TABLE III. ORDER OF REACTION

Temp. of filament (°K)	1505	1610	1710	1850	1940
Order of reaction, n	0.8_0	0.6_0	0.8_6	0.8_0	0.8_0

Summary

1) The end effect of filament upon the reaction probability was eliminated by means of the two-filament method. Its principle and procedure were described.

2) Reaction probabilities were determined at temperatures from 1430 to 1940°K and pressures of water vapor from 12×10^{-5} to 125×10^{-5} mmHg.

3) The reaction probability increased remarkably with the increase of temperature, but the rate of increase became smaller in the vicinity of 1700°K.

4) The order of reaction with respect to water vapor was found to lie between 0.6_0 and 0.8_6.

The author wishes to express sincere thanks to Professor N. Sasaki of Kyoto University and Professor K. Kodera of Kyoto Technical University for their kind discussion and encouragement.

Department of Chemistry
Faculty of Industrial Art
Kyoto Technical University
Sakyo-ku, Kyoto

The Kinetic Study of Surface-chemical Reactions at Extremely Low Pressures. III. The Thermal Reaction between Water Vapor and a Tungsten Filament. Part III

By Takuya HAMAMURA

(Received March 17, 1959)

In continuation of the previous papers[1,2] in which the kinetics of the reaction of water vapor with tungsten was studied, this paper is concerned with the study of the effect of hydrogen pressure on the reaction rate, which seems to give some information about the adsorbed layer on the filaments surface.

Experimental

Apparatus. — The apparatus was essentially the same as that used in the previous experiments, except for an equipment for the control of hydrogen pressure. The pressure of hydrogen in the reaction vessel was changed by an adjustable needle valve placed in the path between trap 6 and diffusion pump 7 in Fig. 1*. If the flow of hydrogen in the path obeys Knudsen's law of molecular flow and the back diffusion through the pump is negligibly small, the quantity D in moles of hydrogen which flow into the balloons per second is given by the following equation similar to Eq. 1'

$$D=A'\bar{B}'P' \tag{12}$$

where A' is the over-all conductance of the path from the reaction vessel to the pump, $\bar{B}'$ is a constant determined experimentally, and P' is the partial pressure of hydrogen in the vessel. Therefore, when A' was changed by varying the conductance of the needle valve, P' was changed correspondingly. The above procedure, however, did not change the pressure of water vapor in the vessel, since the conductance A of the path from the vessel to trap 6 was not changed even if A' was changed. The value of $A'\bar{B}'$ could be determined experimentally by measuring D and P' while hydrogen was flowing through the path. Thus after knowing $A'\bar{B}'$, P' could be calculated from the measured value of D.

The needle valve is shown schematically in Fig. 8. When the mercury was lowered, hydrogen flowed mainly through the wide tube, and when the mercury was raised to cut the wide tube off, it flowed through the capillary with a smaller conductance, then by moving a glass needle containing an iron rod by a solenoid into the capillary, the conductance could be decreased further. The over-all conductance of the path from the reaction vessel to the diffusion pump was 4.90×10^{-3} cm^2 when the mercury was lowered, 1.21×10^{-3} cm^2 when the mercury was raised and the needle was drawn out of the capillary, and 3.15×10^{-4} cm^2 when the whole length of the needle was in the capillary.

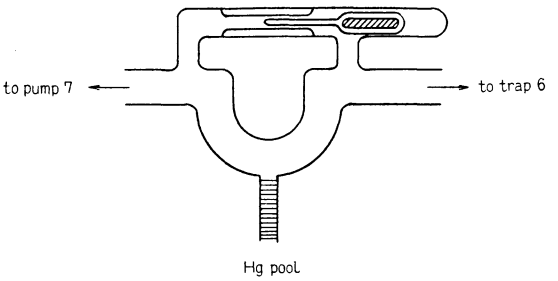


Fig. 8. The needle valve.

A tungsten filament 0.114 mm. in diameter and 81 mm. long was used. This was taken from the same spool as that used in the previous experiments and pretreated in a similar manner. A Pirani gauge of the same type as that attached to the glass balloons was attached to the reaction vessel.

Procedure.—The procedures of evacuating the apparatus, degassing the filament and introducing water vapor into the vessel were described previously. When the flow of water vapor became stationary, the pressure was measured with a quartz fiber manometer, and the filament was then heated to a desired temperature, the conductance of the needle valve being kept at a desired value. The pressure increase of the glass balloons was measured in a similar manner as mentioned previously. The pressure increase gave the reaction rate, and the hydrogen pressure in the vessel was calculated by Eq. 12. Thus, the effect of hydrogen pressure on the reaction rate was determined by the experiments carried out by heating the filament under various conductances of the valve at a fixed temperature and a constant initial pressure of water vapor. The temperature of the reaction vessel remained at room temperature throughout the experiments.

Results

The experiments were carried out at filament temperatures of 1850 and 1940°K

1) N. Sasaki and T. Hamamura, This Bulletin, **29**, 365 (1956).
2) T. Hamamura, ibid., **32**, 845 (1959).
* Eqs. and Figs. are numbered after those of the previous papers.

under 12×10^{-5} and 32×10^{-5} mmHg initial pressures of water vapor and at 1510, 1615, 1850 and 1940°K under 62.5×10^{-5} mmHg.

The reaction rate was independent of the hydrogen pressure below 1850°K at all the initial pressures of water vapor studied. At 1940°K, however, the reaction rate was independent of the hydrogen pressure at 62.5×10^{-5} mmHg of water vapor, but decreased with the increase of hydrogen pressure gradually at 32×10^{-5}

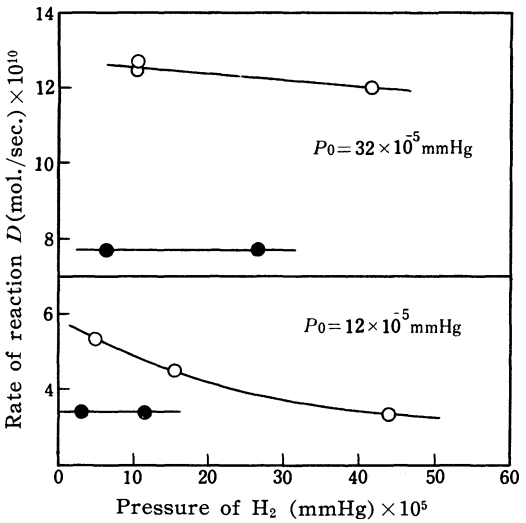


Fig. 9. Effect of hydrogen pressure on the reaction rate. ●-1850°K, ○-1940°K.

mmHg and steeply at 12×10^{-5} mmHg. These are shown in Fig. 9. It was apparent from these results that the reaction rate was independent of the hydrogen pressure at lower filament temperatures or higher pressures of water vapor but decreased with the increase of hydrogen pressure at higher filament temperatures and lower pressures of water vapor. Moreover, the reaction rate decreased more steeply as the temperature increased or the pressure of water vapor decreased.

Discussion

The reaction rate might decrease owing to the retardation of the reaction by hydrogen or might decrease owing to the uptake of hydrogen by the wall, because the rate was calculated from the pressure increase of the glass balloons. The independency of reaction rates upon the hydrogen pressures at lower filament temperatures or higher pressures of water vapor might suggest that neither retardation nor uptake occurred under these conditions. As for the uptake, the following facts are known by the studies[3,4] of Langmuir: when a tungsten filament is heated above 1300°K in hydrogen at low pressure, the hydrogen gradually disappears. This action is caused by the hydrogen dissociated into atoms in contact with the filament, the atom then being driven on to the bulb and there held by adsorption. But the disappearance of hydrogen is suppressed almost completely by a trace of oxygen or water vapor at lower filament temperatures, presumably because of the formation of an adsorbed layer of oxygen acting as a catalytic poison against the dissociation of hydrogen. In the present work, too, the filament surface might be covered with oxygen at lower temperatures or higher pressures of water vapor, and in consequence neither retardation nor uptake occurred. However, the disappearance is known to take place again when the filament temperature rises or the pressure of oxygen or water vapor decreases, probably because of desorption of the adsorbed layer. In the present work, the reaction rate was found to decrease at higher temperatures and lower pressures of water vapor. This seemed to suggest that the decrease was caused by the uptake of hydrogen by the wall, the effect being known as "clean up".

Summary

Hydrogen hardly affected the reaction at lower filament temperatures or higher pressures of water vapor, but it decreased the rate of reaction at higher temperatures and lower pressures, as ascribed to the "clean up" of hydrogen by the filament.

The author wishes to express sincere thanks to Professor N. Sasaki of Kyoto University and Professor K. Kodera of Kyoto Technical University for their kind discussion and encouragement.

Department of Chemistry
Faculty of Industrial Art
Kyoto Technical University
Sakyo-ku, Kyoto

3) I. Langmuir, *J. Am. Chem. Soc.*, 34, 1310 (1912).
4) I. Langmuir, ibid., 38, 2221 (1916).

The Infrared Spectra of Alkane-1-sulfonates

By Kuniaki FUJIMORI

(Received September 13, 1958)

Several investigations have been made on the characteristic infrared absorptions of sulfur-oxygen compounds such as sulfones or sulfone amides, and 1350~1300 cm^{-1} and 1160~1120 cm^{-1} bands were attributed to $-SO_2-$ group[1,2]. On sulfonic acids or their salt, however, there can not be found any systematic studies on their characteristic infrared absorptions. Bellamy[3] proposed 1200~1160 cm^{-1} and 1060~1030 cm^{-1} bands as the characteristic infrared absorptions of $-SO_3-$ group based on his results for aromatic sulfonates. Simon and Kriegsmann[4] investigated Raman and infrared spectra of alkali metal salts of methanesulfonic acid, and discussed these spectra under the assumption that methanesulfonate ion has the symmetry property of C_{3v}. Houlton and Tartar[5] investigated Raman spectra of several *n*-alkane-1-sulfonates in aqueous solution, compared these spectra with those of other sulfur compounds, and proposed some assignments.

Since the assignments so far given seem not to be decisive, the author studied infrared spectra of alkane-1-sulfonates where carbon numbers are 1—8 and 12 in the solid state. Taking into account the theoretical result given in the succeeding paper[6] and the spectra of CXY_3 type molecules, the spectra of methanesulfonate ion were assigned. Furthermore, the characteristic infrared absorptions of sulfonic group and C-S bond in the sulfonic acids were assigned for higher sulfonates.

Results and Discussion

The infrared spectra of sulfonates are shown in Figs. 1—9.

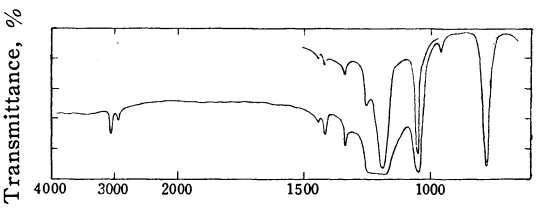


Fig. 1. Methanesulfonate.

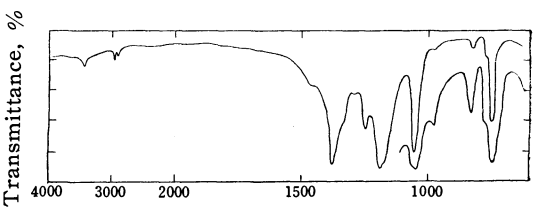


Fig. 2. Ethanesulfonate.

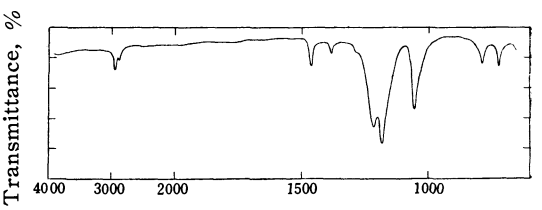


Fig. 3. *n*-Propane-1-sulfonate.

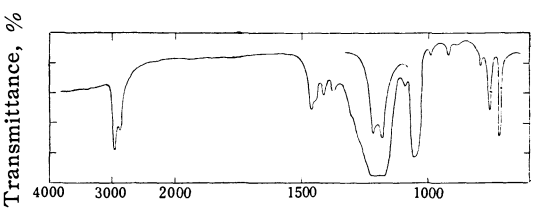


Fig. 4. *n*-Butane-1-sulfonate.

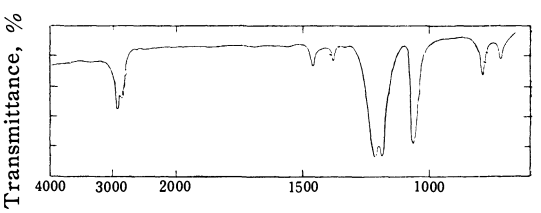


Fig. 5. *n*-Pentane-1-sulfonate.

1) K. C. Schreiber, *Anal, Chem.*, **21**, 1169 (1949).
2) L. J. Bellamy "The Infrared Spectra of Complex Molecules", Methuen & Co., Ltd., London, (1954), p. 297. And also see references cited there.
3) Idem., ibid., p. 301.
4) A. Simon and H. Kriegsmann, *Chem. Ber.*, **89**, 1718 (1956); *Z. physik. Chem.*, **209**, 369 (1955).
5) H. G. Houlton and A. V. Tartar, *J. Am. Chem. Soc.*, **60**, 544 (1938).
6) K. Fujimori, This Bulletin, **32**, 621 (1959).

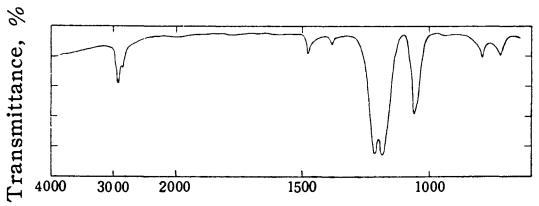


Fig. 6. *n*-Hexane-1-sulfonate.

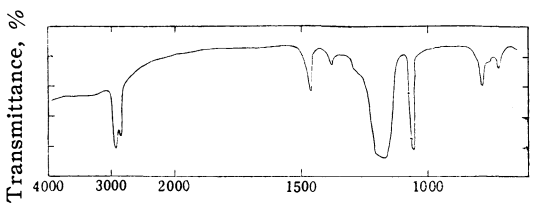


Fig. 7. *n*-Heptane-1-sulfonate.

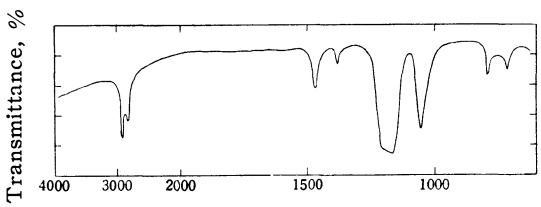


Fig. 8. *n*-Octane-1-sulfonate.

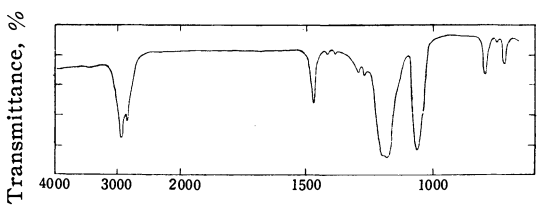


Fig. 9. *n*-Dodecane-1-sulfonate.

For lower homologues the C–H stretching frequencies have wave numbers higher than 2950 cm^{-1}. For higher homologues they decrease and gradually approach to those of hydrocarbons. This result is shown in Table I.

TABLE I. C–H STRETCHING VIBRATIONS (in cm^{-1})

N_C	Wave No.	Wave No.	N_C	Wave No.	Wave No.
1	3024 (w)	2944 (w)	6	2935 (s)	2850 (s)
2	2988 (w)	2944 (w)	7	2926 (s)	2855 (s)
3	2960 (m)	2880 (m)	8	2926 (s)	2855 (s)
4	2944 (s)	2880 (m)	12	2924 (s)	2855 (s)
5	2940 (s)	2870 (s)			

The C–H deformation vibrations are found at 1450~1470 cm^{-1} and at 1380 cm^{-1} and are summarized in Table II.

TABLE II. C–H DEFORMATION VIBRATIONS (in cm^{-1})

N_C	Wave No.	Wave No.	N_C	Wave No.	Wave No.
1	1436 (m)	1418 (m)	6	1462 (m)	1380 (w)
2	1450 (m)	1383 (m)	7	1467 (m)	1380 (w)
3	1461 (m)		8	1468 (m)	1380 (w)
4	1468 (m)	1378 (m)	12	1468 (m)	1380 (w)
5	1464 (m)	1379 (m)			

As to the assignments of S–O stretching and C–S stretching vibrations methanesulfonate ion was dealt with at first. In this case relatively stronger absorptions at 1192, 1060 and 789 cm^{-1} were found. As shown in the preceding paper[6], only three stretching vibrations, ν_1, ν_2 and ν_4, are expected to appear in the rock salt region, where ν_1 is S–CH_3 stretching, ν_2 S–O symmetric stretching, and ν_4 S–O degenerate stretching vibration. From the result of normal coordinate treatment and the comparison of similar molecules given in Table III, the assignments for the spectra of methanesulfonate ion are determined as shown in the table.

TABLE III. COMPARISON OF THE SPECTRA OF $(CH_3)SO_3^-$ AND SIMILAR MOLECULES (in cm^{-1})

Molecules	ν_1	ν_2	ν_4
CH_3D	2205	2982	3030
CH_3F	1050	2863	3009
CCl_3Br	418	710	765
$SO_3(CH_3)^-$	789	1060	1192

The weak absorption at 970 cm^{-1} may be attributed to the rocking vibration of the methyl radical. Simon and Kriegsmann[4] and Siebert[7] reached the same conclusion.

Comparing the absorptions of the higher sulfonates with those of methanesulfonate, the assignments can be made as listed in Tables IV—VI.

About C–S stretching vibration, Simon and Kriegsmann[4] and Siebert[7] reached almost the same conclusion for the cases of

TABLE IV. DOUBLY DEGENERATED AND DOUBLET VIBRATIONS OF S–O STRETCHING VIBRATIONS (in cm^{-1})

N_C	Wave No.	Wave No.	N_C	Wave No.	Wave No.
1		1192	6	1216	1180
2		1180	7		1175
3	1224	1182	8		1175
4	1200	1186	12		1175
5	1210	1184			

All absorptions are strong.

7) H. Siebert, *Z. anorg. u. allgem. Chem.*, **289**, 15 (1957).

TABLE V. SYMMETRIC S-O STRETCHING VIBRATION (in cm^{-1})

N_C	Wave No.	N_C	Wave No.
1	1060	6	1062
2	1056	7	1062
3	1055	8	1062
4	1053	12	1063
5	1060		

All absorptions are strong.

TABLE VI. C-S STRETCHING VIBRATION (in cm^{-1})

N_C	Wave No.	N_C	Wave No.
1	789 (s)	6	787 (m)
2	751 (m)	7	792 (m)
3	783 (m)	8	792 (m)
4	793 (m)	12	798 (m)
5	787 (m)		

TABLE VII. ROCKING VIBRATION OF $-(CH_2)_n-$ GROUP (in cm^{-1})

n	Wave No.	n	Wave No.
2	726 (w)	5	720 (w)
3	759 (m)	6	720 (w)
	723 (m)	7	720 (w)
4	720 (w)	11	721 (w)

methane- and ethane-sulfonates. However, the rocking vibration of $-(CH_2)_n-$ group in the *n*-alkyl radical is expected to be at about 750 cm^{-1} when n is 2 and at 730~720 cm^{-1} when n is greater than 3. Some irregularity found in Table VI may be due to the coupling of C-S stretching vibration with this CH_2 rocking vibration of $-(CH_2)_n-$ group is summarized in Table VII.

The absorptions at 1250 cm^{-1} of methane- and ethane-sulfonates, at 836 cm^{-1} of ethane-sulfonate may be attributed to overtones or combination tones.

Experimental

Samples. — *Methanesulfonate.* — Methanesulfonic acid (pure reagent grade) was distilled in vacuo (b. p. 160°C at 5 mmHg) and the aqueous solution was neutralized with sodium carbonate and evaporated to dryness. Sodium methanesulfonate was recrystallized from 90% ethanol.

Ethanesulfonate.—Ethyl mercaptane (b. p. 37°C) was oxidized with concentrated nitric acid[8] and the reaction mixture was neutralized with sodium carbonate (10% aqueous solution), the sulfonate solution was evaporated to dryness and extracted with hot ethanol to separate inorganic salts. The sulfonate was recrystallized from ethanol.

Other sulfonates.—Sulfonates other than above described were prepared by Strecker reaction[9]. Corresponding chloride was heated from 180 upto 200°C in a stainless steel autoclave for 10~16 hr. with sodium sulfite (anhydride) and water. The reaction mixture was filtered and evaporated to dryness. The residue was washed with petroleum ether (b. p. 30~40°C) and the sulfonate was extracted with hot ethanol and recrystallized from ethanol.

Absorption Measurement. — The infrared spectra were obtained with a Perkin-Elmer Model 21 double beam infrared spectrophotometer using NaCl prism. The KBr disk method was employed to obtain the spectra in solid state.

The author expresses his indebtedness to Dr. A Kotera, Professor of Tokyo University of Education, and Dr. T. Shimanouchi, Assistant Professor of the University of Tokyo, under whose kind direction this work was performed. He also thanks Mr. Y. Ikegami, Fellow of Tohoku University, for his cooperation to obtain infrared spectra and Mr. Y. Akai, Chief of Research Section of Funakawa Refinery, for his encouragement of this research.

Nippon Mining Co., Funakawa Refinery
Oga-shi, Akita

8) D. L. Vivian and E. E. Reid, *J. Am. Chem. Soc.*, **57**, 2559 (1935).
9) R. M. Reed and H. V. Tartar, ibib., **57**, 571 (1935).

LCAO SCF Calculation on Anthracene and Reactivity Indexes in SCF Method

By Kenichi FUKUI, Keiji MOROKUMA and Teijiro YONEZAWA

(Received January 30, 1959)

In order to interpret chemical reactivity of conjugated molecules, there have been proposed several quantum-mechanical methods in LCAO MO treatment, such as the frontier electron method (frontier electron density and superdelocalizability as reactivity indexes[1]), the static method (total π-electron density and self-polarizability for an ionic reaction and free valence for a radical reaction)[2], the localization method (localization energy)[3], and so on.

Within the scope of the simple LCAO MO treatment, where electronic interaction is not explicitly considered, total π-electron density of an alternant hydrocarbon is unity for all the positions[4], and accordingly in terms of the static method the ionic reactivity is to be determined by self-polarizability of each position. But once electronic interaction is taken into account, the uniformity of total π-electron distribution is immediately extinguished, so that its magnitude comes to correspond to the ionic reactivity in a molecule in the static method. For *trans*-butadiene the coefficients of AO's in MO's, calculated in semi-empirical SCF method[5], in non-empirical SCF method[6] and in non-empirical SCF CI method[7], show the larger π-electron density, i. e., the larger electrophilic reactivity, at the position 2, contradictory to the experiments. Further, semi-empirical SCF calculation on naphthalene leads to an erroneous prediction of electrophilic reactivity[8].

For the purpose of obtaining more information on reactivity indexes, in the first two paragraphs of the present paper, we determine the coefficients of AO's in MO's of anthracene by semi-empirical LCAO SCF method and discuss on some physico-chemical properties. In the last paragraph it is examined whether or not each of total π-electron density, free valence and frontier electron density remains a good index of chemical reactivity in SCF treatment.

Method

Roothaan has developed in detail the general formalism of LCAO SCF method for the closed configuration of a molecule[9]. This will not be repeated here for the sake of brevity. Using his theory with only π-electrons considered explicitly, we numerically calculate the coefficients of AO's in SCF MO's of the ground state of anthracene.

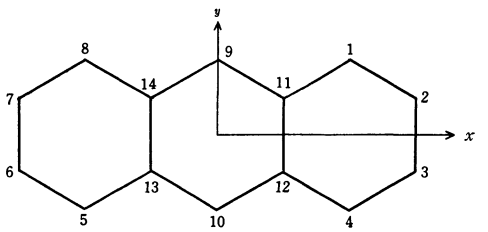


Fig. 1. The numbering of atoms and the coordinate of symmetry operation of anthracene.

The numbering of atoms and the coordinate of symmetry operation are shown in Fig. 1. The bond distances are taken to be 1.370 Å for the bond 1—2, 1.396 Å for 9—11, 1.408 Å for 2—3, 1.423 Å for 1—11 and 1.436 Å for 11—12, and all the bond angles are assumed in a good approximation to be 120° [10].

Necessary numerical evaluation of the reasonance integral, $\beta_{\mu\nu}$, and the coulomb repulsion integral, $\gamma_{\mu\nu}$, are carried out on the semi-empirical formulae proposed by

1) K. Fukui et al., *J. Chem. Phys.*, **20**, 722 (1952); **22**, 1433 (1954); This Bulletin, **27**, 423 (1954).
2) C. A. Coulson and H. C. Longuet-Higgins, *Proc. Roy. Soc. (London)*, **A191**, 39 (1947); **A192**, 16 (1947); F. H. Burkitt et al., *Trans. Faraday Soc.*, **47**, 553 (1951).
3) G. W. Wheland, *J. Am. Chem. Soc.*, **64**, 900 (1940).
4) C. A. Coulson and S. Rushbrooke, *Proc. Cambridge Phil. Soc.*, **36**, 193 (1940).
5) C. M. Moser, *Compt. rend.*, **238**, 1585 (1954).
6) R. G. Parr and R. S. Mulliken, *J. Chem. Phys.* **18**, 1338 (1950).
7) A. Pullman and J. Baudet, *Compt. rend.*, **238**, 241 (1954); A. Pullman *J. chim. phys.*, **51**, 188 (1954).
8) C. M. Moser, ibid., **52**, 24 (1955).
9) C. C. J. Roothaan, *Revs. Mod. Phys.*, **23**, 69 (1951).
10) A. McL. Mathieson et al., *Acta Cryst.*, **3**, 245 (1950); V. C. Sinclair et al., ibid., **3**, 251 (1950). Deviations of all the observed bond angles from 120° are about 1~2°.

TABLE I. SCF MO'S AND THEIR ORBITAL ENERGIES OF ANTHRACENE

Symmetry	Orbital energy[a]	MO	
b_{1u}	$\varepsilon_1 = -5.762$	$\psi_1 = 0.4887\sigma_4 + 0.4448\sigma_5 + 0.3323\sigma_6 + 0.6730\sigma_7$	occupied
b_{2g}	$\varepsilon_2 = -5.190$	$\psi_2 = 0.5818\sigma_8 + 0.6276\sigma_9 + 0.5174\sigma_{10}$	
b_{1u}	$\varepsilon_3 = -3.350$	$\psi_3 = 0.3108\sigma_4 + 0.7098\sigma_5 - 0.3717\sigma_6 - 0.5113\sigma_7$	
b_{3g}	$\varepsilon_4 = -3.196$	$\psi_4 = 0.6278\sigma_{11} + 0.3465\sigma_{12} + 0.4423\sigma_{13} + 0.5386\sigma_{14}$	
a_{1u}	$\varepsilon_5 = -2.433$	$\psi_5 = 0.7932\sigma_1 + 0.4861\sigma_2 + 0.3668\sigma_3$	
b_{2g}	$\varepsilon_6 = -1.9935$	$\psi_6 = 0.0792\sigma_8 + 0.5894\sigma_9 - 0.8039\sigma_{10}$	
b_{3g}	$\varepsilon_7 = -0.2930$	$\psi_7 = 0.5130\sigma_{11} + 0.4221\sigma_{12} - 0.6793\sigma_{13} - 0.3117\sigma_{14}$	
b_{1u}	$\varepsilon_8 = +7.1389$	$\psi_8 = 0.4431\sigma_4 - 0.3746\sigma_5 - 0.7573\sigma_6 + 0.2997\sigma_7$	unoccupied
a_{1u}	$\varepsilon_9 = +7.6451$	$\psi_9 = 0.0811\sigma_1 + 0.5125\sigma_2 - 0.8548\sigma_3$	
b_{2g}	$\varepsilon_{10} = +9.124$	$\psi_{10} = 0.8095\sigma_8 - 0.5087\sigma_9 - 0.2932\sigma_{10}$	
b_{1u}	$\varepsilon_{11} = +9.668$	$\psi_{11} = 0.6843\sigma_4 - 0.3974\sigma_5 + 0.4219\sigma_6 - 0.4425\sigma_7$	
b_{3g}	$\varepsilon_{12} = +9.726$	$\psi_{12} = 0.1781\sigma_{11} - 0.5967\sigma_{12} - 0.5090\sigma_{13} + 0.5943\sigma_{14}$	
a_{1u}	$\varepsilon_{13} = +11.747$	$\psi_{13} = 0.6035\sigma_1 - 0.7079\sigma_2 - 0.3671\sigma_3$	
b_{3g}	$\varepsilon_{14} = +12.069$	$\psi_{14} = 0.5576\sigma_{11} - 0.5880\sigma_{12} + 0.2895\sigma_{13} - 0.5095\sigma_{14}$,	

where[b]

$\sigma_1 = (1/2)(\phi_1 - \phi_4 + \phi_5 - \phi_8)$, $\sigma_2 = (1/2)(\phi_2 - \phi_3 + \phi_6 - \phi_7)$, $\sigma_3 = (1/2)(\phi_{11} - \phi_{12} + \phi_{13} - \phi_{14})$,
$\sigma_4 = (1/2)(\phi_1 + \phi_4 + \phi_5 + \phi_8)$, $\sigma_5 = (1/2)(\phi_2 + \phi_3 + \phi_6 + \phi_7)$, $\sigma_6 = (1/\sqrt{2})(\phi_9 + \phi_{10})$,
$\sigma_7 = (1/2)(\phi_{11} + \phi_{12} + \phi_{13} + \phi_{14})$, $\sigma_8 = (1/2)(\phi_1 + \phi_4 - \phi_5 - \phi_8)$, $\sigma_9 = (1/2)(\phi_2 + \phi_3 - \phi_6 - \phi_7)$,
$\sigma_{10} = (1/2)(\phi_{11} + \phi_{12} - \phi_{13} - \phi_{14})$, $\sigma_{11} = (1/2)(\phi_1 - \phi_4 - \phi_5 + \phi_8)$, $\sigma_{12} = (1/2)(\phi_2 - \phi_3 - \phi_6 + \phi_7)$,
$\sigma_{13} = (1/\sqrt{2})(\phi_9 - \phi_{10})$, $\sigma_{14} = (1/2)(\phi_{11} - \phi_{12} - \phi_{13} + \phi_{14})$

a) W_{2p} as standard. In units of eV. b) ϕ_i is the AO on the i-th atom.

Pariser and Parr[11]. In the expression of the coulomb integral, α_μ,

$$\alpha_\mu = W_{2p} - \sum_{\nu(\neq\mu)} \{\gamma_{\mu\nu} + (\nu : \mu\mu)\} \qquad (1)$$

no particular values of the coulomb penetration integral, $(\nu : \mu\mu)$, have been given by Pariser and Parr, and on the theoretical consideration[12] we have determined its average value as 0.85 eV. when the atoms μ and ν are adjacent, as 0.08 eV. when μ and ν are separated by a single atom, and as zero otherwise. W_{2p} in Eq. 1 is as usual the electronic energy of a carbon atom in its valence state and is regarded as a constant.

Results and Discussion on Anthracene

The obtained SCF MO's, ϕ_i, of the ground state of anthracene and their orbital energies, ε_i, are collected in Table I, together with non-occupied MO's.

Ionization Potential. — Putting $W_{2p} = -11.28$ eV.[11], we obtain 11.57 eV. as the first ionization potential of anthracene, which is, though no experimental results are available, much larger than the estimated value, 7.23 eV., by Matsen[13]. Giving too large calculated value is not particular to the case of anthracene, but the general tendency of SCF calculation[5,6,8]; on this point a discussion shall be made in near future.

Electronic Spectra. — The energies of configurations, the values of interconfigurational matrix elements and wave functions of the excited states are listed in

TABLE II. THE ENERGIES OF CONFIGURATIONS, THE VALUES OF INTERCONFIGURATIONAL MATRIX ELEMENTS AND THE EXCITED STATES WAVE FUNCTIONS[a]

B_{2u}: $[66 \mid 99] = 5.535$, $[69 \mid 96] = 0.551$,
$[77 \mid 88] = 5.419$, $[78 \mid 87] = 0.885$.
$E(V_{78}) - E_0 = 3.782$, $E(V_{69}) - E_0 = 5.206$,
$E(T_{78}) - E_0 = 2.013$, $E(T_{69}) - E_0 = 4.104$.
$[67 \mid 89] = -0.094$, $[69 \mid 87] = 0.369$.
$\langle V_{78} \mid V_{69} \rangle = 0.833$, $\langle T_{78} \mid T_{69} \rangle = 0.094$.
$\Psi(^1B_{2u}^-) = 0.908\ V_{78} - 0.418\ V_{69}$,
$\Psi(^1B_{2u}^+) = 0.418\ V_{78} + 0.908\ V_{69}$,
$\Psi(^3B_{2u}^-) = 0.999\ T_{78} - 0.045\ T_{69}$,
$\Psi(^3B_{2u}^+) = 0.045\ T_{78} + 0.999\ T_{69}$.

B_{3u}: $[66 \mid 88] = 5.145$, $[68 \mid 86] = 0.348$,
$[77 \mid 99] = 5.198$, $[79 \mid 97] = 0.502$.
$E(V_{79}) - E_0 = 3.743$, $E(V_{68}) - E_0 = 4.684$,
$E(T_{79}) - E_0 = 2.740$, $E(T_{68}) - E_0 = 3.987$.
$[76 \mid 89] = -0.094$, $[79 \mid 86] = -0.415$.
$\langle V_{79} \mid V_{68} \rangle = -0.736$, $\langle T_{79} \mid T_{68} \rangle = 0.094$
$\Psi(^1B_{3u}^+) = 0.877\ V_{79} + 0.480\ V_{68}$,
$\Psi(^1B_{3u}^-) = 0.480\ V_{79} - 0.877\ V_{68}$,
$\Psi(^3B_{3u}^-) = 0.997\ T_{79} - 0.075\ T_{68}$,
$\Psi(^3B_{3u}^+) = 0.075\ T_{79} + 0.997\ T_{68}$.

a) In units of eV.

11) P. Pariser and R. G. Parr, *J. Chem. Phys.*, **21**, 465, 767 (1953).
12) R. G. Parr and B. L. Crawford, ibid., **16**, 1049 (1948).
13) F. A. Matsen, ibid., **24**, 602 (1956).

TABLE III. THE EXCITATION ENERGIES AND THE OSCILLATOR STRENGTHS OF ANTHRACENE

Symmetry	Excitation energy (eV.)		Oscillator strength	
	Calcd.	Obsd.	Calcd.	Obsd.
$^1B_{2u}^-$	3.40	3.30[a]	0.15	~0.1[a]
$^1B_{3u}^+$	3.34	3.50[a]	0.20	~0[a]
$^1B_{3u}^-$	5.09	4.80[a]	1.94	2.20[a]
$^1B_{2u}^+$	5.59	5.64[a]	1.01	0.65[a]
$^3B_{2u}^-$	2.01	1.8[b]	0.00	—
$^3B_{3u}^-$	2.73	—	0.00	—
$^3B_{3u}^+$	3.99	—	0.00	—
$^3B_{2u}^+$	4.11	—	0.00	—

a) H. B. Klevens and J. R. Platt, *J. Chem. Phys.*, **17**, 470 (1949).
b) G. N. Lewis and M. Kasha, *J. Am. Chem. Soc.*, **66**, 2100 (1944); S. P. McGlynn, M. R. Padhye and M. Kasha, *J. Chem. Phys.*, **23**, 593 (1955).

Table II, where only four lower excitations are considered. The calculated excitation energies and oscillator strengths are given in Table III, together with the observed values. The agreement with experiments is good, but for the inversion of excitation energies of $^1B_{2u}^-$ band and $^1B_{3u}^+$ band, which will be improved by the inclusion of more possible configurations.

Bond Order and Bond Distance. — Our SCF bond orders and observed bond distances are collected in Table IV, in comparison with the SCF bond orders by Pritchard and Sumner in a rough approximation[14] and with the bond orders in simple LCAO treatment. It is seen in Table IV that SCF bond orders in the present calculation are parallel with the observed bond distances except for the bond 11—12, in accordance with Pritchard and Sumner's result. The discrepancy in the bond 11—12 seems to indicate that the bond order of a bonding is not determined only by its length but by its nature; namely, whether the ending carbons of this bonding are primary, secondary or tertiary.

TABLE IV. THE BOND ORDERS AND OBSERVED BOND DISTANCES OF ANTHRACENE

Bond	Bond order			Obsd. bond distances (Å)[b]
	Present treatment	Pritchard and Sumner[a]	Simple LCAO	
1—2	0.8347	0.8422	0.7374	1.370
9—11	0.6107	0.6318	0.6061	1.396
2—3	0.4542	0.4493	0.5859	1.408
1—11	0.4383	0.4178	0.5354	1.423
11—12	0.5533	0.5484	0.4849	1.436

a) Ref. 14.
b) Ref. 10.

SCF Reactivity Indexes

First of all we define SCF frontier electron density in the same way as in simple LCAO treatment[1], where the frontier orbital denotes the highest occupied one for an electrophilic reaction, the lowest unoccupied one for a nucleophilic reaction, and both for a radical reaction.

The calculated results of total π-electron density, free valence and frontier electron densities of anthracene are given in Table V. Values of these reactivity indexes in SCF method of naphthalene and *trans*-butadiene are collected in Tables VI and VII, respectively.

Total π-electron density of anthracene is the largest at the position 11 and decreases in the order of 2, 1 and 9. The position 11 being out of the question because of its lack of hydrogen to be substituted, an electrophilic substitution should take place at the position 2 and a nucleophilic substitution at the position 9 on the basis of the static method. This prediction contradicts experimental results that the position 9 is the most reactive in an electrophilic substitution. Concerning naphthalene the position 2, where SCF total π-electron density has the largest value as shown in Table VI, does not actually suffer from an electrophilic substitution. Furthermore, as for butadiene Table VII shows that total π-electron densities by semi-empirical SCF method, by non-empirical SCF method and by non-empirical SCF CI method lead to the same erroneous prediction that the position 2 is the most susceptible to an electrophilic reaction. Thus SCF total π-electron density is no longer a good index for chemical reactivity.

On the contrary, it will be valuable to emphasize that SCF frontier electron density correctly predicts the most reactive positions, that is, the position 9 in anthracene, 1 in naphthalene and 1 in

14) H. O. Pritchard and F. H. Sumner, *Proc. Roy. Soc.*, **A226**, 128 (1954); H. O. Pritchard, private communication. Their assumptions are the same as those that are presented by Pople[15], the main points of which are (1) neglect of the coulomb penetration integral, and (2) assumption of equi-bond-length and of regular hexagone of carbon ring, and (3) that the coulomb repulsion integral, $\gamma_{\mu\nu}$, is expressed in the following form.
$\gamma_{\mu\nu}=e^2/R_{\mu\nu}$ ($R_{\mu\nu}$: distance between the atoms μ and ν)
15) J. A. Pople, *Trans. Faraday Soc.*, **49**, 1375 (1953).

TABLE V. VALUES OF SCF REACTIVITY INDEXES OF ANTHRACENE

Position	Total π-electron density	Free valence	Frontier electron density		
			Electrophilic	Nucleophilic	Radical
1	0.983	0.459	0.132	0.098	0.115
2	0.989	0.443	0.089	0.070	0.080
9	0.906	0.511	0.461	0.574	0.517
11	1.075	0.130	0.049	0.045	0.047

TABLE VI. VALUES OF SCF REACTIVITY INDEXES OF NAPHTHALENE[a]

Position	Total π-electron density	Free valence	Frontier electron density		
			Electrophilic	Nucleophilic	Radical
1	0.967	0.453	0.334	0.339	0.343
2	1.003	0.435	0.166	0.162	0.157
9	1.062	0.158	0	0	0

a) Ref. 8.

TABLE VII. VALUES OF SCF REACTIVITY INDEXES OF *trans*-BUTADIENE

Position	Total π-electron density	Free valence	Frontier electron density		
			Electrophilic	Nucleophilic	Radical
A) Semi-empirical SCF method[a]					
1	0.938	0.757	0.575	0.606	0.637
2	1.062	0.545	0.425	0.394	0.363
B) Non-empirical SCF method[b]					
1	0.975	—	0.620	0.633	0.645
2	1.025	—	0.380	0.367	0.355
C) Non-empirical SCF CI method[c]					
1	0.978	—	—	—	—
2	1.022	—	—	—	—

a) Ref. 5. b) Ref. 6. c) Ref. 7.

TABLE VIII. VALUES OF SCF FREE VALENCE OF HYDROCARBONS IN ROUGHER APPROXIMATION[a]

Molecule	Position	Free valence
Naphthalene	1	0.447
	2	0.420
Anthracene	1	0.473
	2	0.441
	9	0.468
Phenanthrene	1	0.431
	2	0.408
	3	0.409
	4	0.428
	9	0.474
Chrysene	1	0.461
	2	0.464
	3	0.439
	4	0.434
	5	0.435
	6	0.436
Pyrene	1	0.432
	2	0.395
	4	0.485

a) Ref. 14.

butadiene for all the three kinds of reactions. It may be, therefore, concluded that frontier electron density remains a good reactivity index even when the electronic interaction is explicitly included.

So far as our approximation is concerned, free valence seems to give correct results in the three hydrocarbons, as shown in Tables V, VI and VII. In comparison with this, we have collected in Table VIII values of free valence of some hydrocarbons, which have been derived from the SCF bond orders obtained by Pritchard and Sumner[14]. It can be seen in Table VIII that this free valence leads to a seriously erroneous conclusion for anthracene and for pyrene: anthracene is, as is well known, the most susceptible to a radical attack at the position 9, and pyrene is so at 1. On inspection of these and other results of SCF calculation[16], it

16) G. Berthier, *J. chim. phys.*, **50**, 344 (1953); I. Tanaka, *J. Chem. Soc. Japan, Pure Chem. Sec.* (*Nippon Kagaku Zasshi*), **75**, 218 (1954); H. O. Pritchard and F. H. Sumner, *Trans. Faraday Soc.*, **51**, 457 (1955); etc.

may be said that the value of bond order, or that of free valence, varies very easily depending on the degree or approximation employed and on the semi-empirical method of evaluating atomic integrals. Such an unstable quantity would probably not deserve a reliable reactivity index.

Department of Fuel Chemistry
Faculty of Engineering
Kyoto University
Sakyo-ku, Kyoto

*Interaction entre les colorants et les surfactifs. II**

Par Tamotsu KONDO, Kenjiro MEGURO et Hidero NITO

(Reçu le 11 février 1959)

Dans le rapport précédent[1], les phénomènes de floculation et de défloculation de la rhodamine et de l'éosine en présence de surfactifs ont été systématiquement étudiés, et les mécanismes de ces phénomènes ont été proposés.

Nous allons essayer, dans le présent travail, d'élucider l'influence de la structure chimique de divers colorants sur les phénomènes de floculation et de défloculation.

Expériences

Matériels. — Les colorants que nous avons utilisés sont classifiés dans le Tableau I.

TABLEAU I. COLORANTS UTILISÉS

Classification	Valence	Nom
Colorants acides	−1	Orange de méthyle
	−1	Orange II
	−1	Na de sulfonate de *p*-hydroxyazobenzène
	−2	Orange G
	−2	Ponceau R
	−2	Tartrazine
Colorants basiques	+1	Jaune d'acridine
	+1	Bleu de méthylène
	+1	Violet de méthyle
	+1	Vert de méthyle
Colorants directs	−2	Benzopurpurine 4B
	−2	Rouge de congo
	−2	Chrysophénine G

Les surfactifs employés sont le bromure de dodécyl-pyridonium et le sodium de dodécyl-sulfate (que nous appellerons B.D.P. et S.D.S.). Leurs préparation et purification ont été déjà décrites dans un autre article[2].

Méthodes expérimentales.—Les méthodes adptées pour observer les phénomènes de floculation et de défloculation des colorants sont les mêmes que nous avons écrites précédemment[1].

Résultats

Floculation et défloculation des colorants par le B.D.P.—L'addition d'un peu de B.D.P. aux solutions de colorants acides a généralement causé la floculation des colorants. Dans le cas de la tartrazine, cependant, on n'a pas observé la floculation, mais on a trouvé seulement l'apparition de la turbidité.

Les floculés colorés ainsi formés étaient solubles dans le chloroforme qui ne dissout pas les colorants acides employés dans ce travail. On a pu extraire un corps coloré dans le chloroforme du mélange de tartrazine et de B.D.P. en solution. On doit alors penser que les floculés et le corps coloré sont des complexes formés entre les colorants et le B.D.P.

On a vu que les floculés ont été remis en solution en présence d'une quantité supérieure de B.D.P. Les concentrations de B.D.P. auxquelles les floculés commencent à défloculer étaient indépendantes de la C.C.M. (concentration critique micellaire) de cet agent cationique.

La valeur de floculation et celle de défloculation du B.D.P. étaient définies comme le minimum des concentrations nécessaires de cet agent pour floculer le colorant, et pour défloculer complètement le floculé[1], respectivement. Celle-là

* Une partie de ce rapport a été présentée à la réunion de chimie colloïdale de la société chimique du Japon qui s'est tenue à Kanazawa, au mois d'octobre 1957.

1) T. Kondo et K. Meguro, Ce Bulletin, **32**, 267 (1959).

2) O. Yoda, K. Meguro, T. Kondo et T. Ino, *J. Chem. Soc. Japan, Pure Chem. Sec.* (*Nippon Kagaku Zasshi*), **75**, 1272 (1954).

était presque indépendante de la structure chimique du colorant et celle-ci ne l'était pas. La différence de ces deux valeurs, que nous appellerons désormais la largeur de la zone de floculation, s'est accrue lorsqu'on a augmenté la concentration de colorant en solution. La Fig. 1 représente la relation entre la largeur de la zone de floculation et la concentration de colorant.

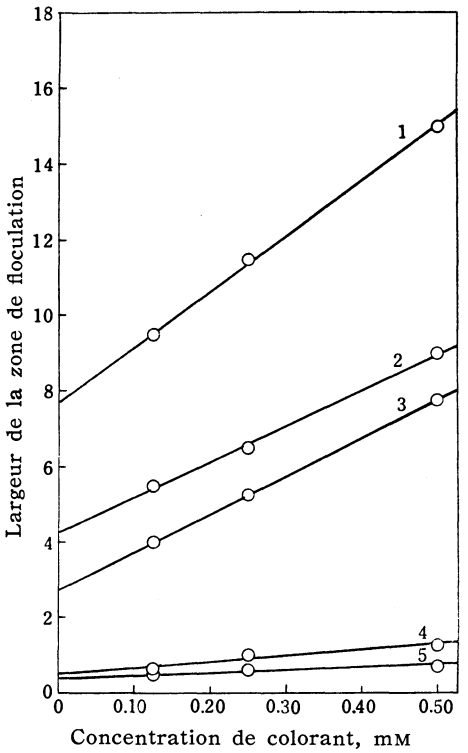


Fig. 1. Relation entre la largeur de la zone de floculation et la concentration de colorant. (1).

TABLEAU II. VALEURS DU N_d DU B.D.P.

Colorant	N_d
Orange de méthyle	14.8
Orange II	9.6
Na de sulfonate de *p*-hydroxyazobenzène	1.6
Orange G	10.2
Ponceau R	0.5

Le talus des lignes droites est caractéristique de chaque colorant et donne le nombre minimum des ions de surfactif qui est nécessaire pour disperser une molécule de complexe. Ce nombre a été nommé le nombre de défloculation, N_d, du surfactif[1]. Les valeurs obtenues sont données dans le Tableau II.

Floculation et défloculation des colorants basiques par le S.D.S.—La floculation du jaune d'acridine et du bleu de méthylène s'est effectuée par le S.D.S., tandis que celle du violet de méthyle et du vert de méthyle n'a jamais lieu par cet agent.

La formation d'un complexe coloré a été vérifiée par l'essai d'extraction dans le chloroforme ou l'acetate d'éthyle pour chaque cas de ces colorants. On a observé la défloculation du floculé en présence d'une quantité supérieure de S.D.S. La Fig. 2 fournit le diagramme qui indique la relation de la largeur de la zone de floculation avec la concentration de colorant.

On obtient la valeur du N_d du S.D.S. qui est de 9.8 et 8.1 pour le jaune d'acridine et le bleu de méthylène, respectivement, en utilisant le talus des lignes droites dans la Fig. 2.

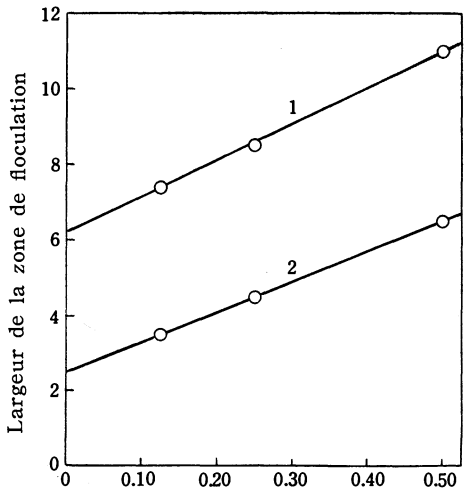


Fig. 2. Relation entre la largeur de la zone de floculation et la concentration de colorant. (2).

Floculation et défloculation des colorants directs.—Tous les colorants directs utilisés ont été floculés par un peu de B.D.P. Les concentrations de B.D.P. qui sont nécessaires pour la floculation des colorants étaient presque égales. Malgré l'addition d'une grande quantité de B.D.P., la défloculation de la benzopurpurine 4B n'a jamais été observée. Dans le cas du rouge de congo, le floculé a dispersé d'abord et ensuite refloculé, lorsque la concentration en agent cationique croît graduellement. On a trouvé pour la chrysophénine G que la zone de floculation et celle de défloculation ont paru deux fois alternativement quand on a graduellement

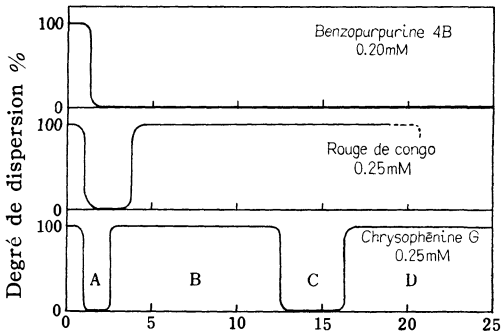


Fig. 3. Schéma de floculation des colorants directs.
A, Première zone de floculation;
B, Première zone de défloculation;
C, Deuxième zone de floculation;
D, Deuxième zone de défloculation.

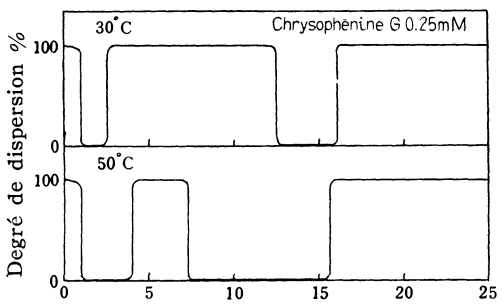


Fig. 4. Influence de la température sur la floculation de la chrysophénine G.

augmenté la de quantité B.D.P. en solution. Lorsqu'on a centrifugé les solutions de la première zone de défloculation, on a constaté qu'il y a eu la précipitation d'un corps coloré. La Fig. 3 donne le schéma de floculation de ces colorants directs.

L'élevation de la température a été accompagnée par la contraction de la première zone de défloculation de la chrysophénine G. Cela est indiqué dans la Fig. 4.

Considérations

Nous avons conclu précédemment[1] que la défloculation d'un complexe est due à la combinaison d'un certain nombre des ions de surfactif avec ce complexe et que le N_d n'y est pas nécessirement égal. A ce point de vue, nous allons examiner les résultats expérimentaux de la défloculation, car la floculation ne dépend pas rigoureusement de la structure chimique des colorants.

L'influence de la structure chimique du colorant sur le N_d.—Comparons d'abord les valeurs du N_d des colorants acides monovalents l'une à l'autre. Ces valeurs sont de 14.8, 9.6 et 1.6 pour l'orange de méthyle, l'orange II et le sodium de sulfonate de *p*-hydroxyazobenzène respectivement. Ces trois colorants ne diffèrent dans leur structure chimique que par le groupe nonionique lié au radical azoïque, comme le montre la Fig. 5.

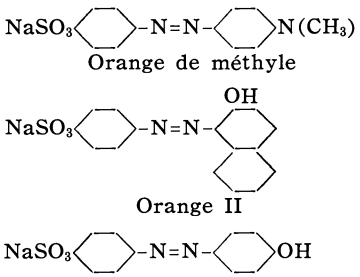


Fig. 5. Structures chimiques des colorants acides.

On doit, par suite, attribuer la différence de la valeur du N_d à celle de la structure du groupe nonionique du colorant.

Les affinités du phénol, du naphthol β et de la diméthylaniline pour l'eau diminuent dans l'ordre suivant:

Phénol > naphthol β > diméthylaniline.

On pourra conclure, en conséquence, que la valeur du N_d dépend profondément de l'affinité du groupe nonionique du colorant pour l'eau. C'est-à-dire, plus grande est l'affinité du groupe nonionique pour l'eau, plus petite est la valeur du N_d. L'ordre des valeurs du N_d pour ces colorants acides est en accord avec celui de leurs solubilités dans l'eau. En ce qui concerne des colorants acides bivalents, on peut aussi constater qu'un petit N_d de colorant amène une grande solubilité dans l'eau. La valeur du N_d du ponceau R, par exemple, est moins grande que celle de l'orange G qui est moins soluble que celui-là.

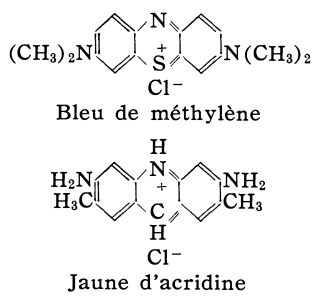
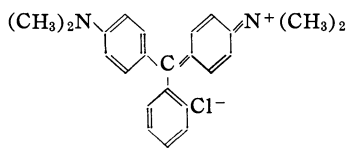


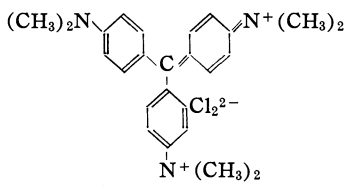
Fig. 6. Structures chimiques des colorants basiques (1).

Le jaune d'acridine et le bleu de méthylène ont les structures chimiques semblables l'une à l'autre comme les montre la Fig. 6. Le fait que les valeurs du N_d pour ces deux colorants sont presque égales sera du à la similarité des structures chimiques de ces colorants.

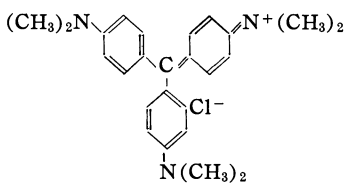
Floculation et défloculation des colorants de triphénylméthane.—On a déjà décrit que le violet de méthyle et le vert de méthyle, colorants de triphénylméthane, ne sont pas floculés par le S.D.S. La comparaison des résultats expérimentaux concernant le vert de malachite, qui est floculé et défloculé par le S.D.S.[3], à ceux du violet de méthyle et du vert de méthyle nous amène à examiner de l'influence de la structure chimique de ces colorants sur leur comportement dans les solutions du S.D.S. La Fig. 7 fournit les structures chimiques de ces trois colorants.



Vert de malachite



Vert de méthyle



Violet de méthyle

Fig. 7. Structures chimiques des colorants basiques (2).

Notons, par exemple, la différence de la structure entre le vert de malachite et le violet de méthyle. Comme le montre cette figure, le vert de malachite et le violet de méthyle ont, respectivement, deux et trois groupes diméthylaminés entre lesquels une charge électrique positive est mise en résonance. Ce fait empêche la localisation d'une charge électrique et amènera, par conséquence, la diminution du pouvoir de la combinaison du colorant avec un ion de sulfate de dodécyl. En outre, plus les structures mises en résonance sont nombreuses, plus le degré de localisation d'une charge sera faible. Alors, le complexe se forme suffisamment en solution pour que l'on puisse observer sa floculation dans le cas du vert de malachite et ne l'est pas dans le cas du violet de méthyle.

Lorsque la quantité de S.D.S. augmente davantage en solution, la combinaison de l'ion de sulfate de dodécyl au complexe a lieu et ce complexe commence à se disperser.

Floculation et défloculation des colorants directs.—Il est bien connu que les molécules de colorant direct se forment l'agrégat dans l'eau, donc l'interaction entre le colorant et le surfactif doit être, dans ce cas, celle entre l'agrégat des molécules de colorant, que nous appellerons le micelle de colorant, et les ions de surfactif.

Cette considération nous amène à conclure que le mécanisme de la floculation du colorant direct sera le même que celui qui a été proposé par les présents auteurs pour la floculation des particules colloïdales par le surfactif[4]. C'est-à-dire, la surface du micelle de colorant perd l'affinité pour l'eau, et il en résulte la floculation.

La tendence vers l'agrégation dépend de la structure chimique du colorant. Pour des colorants directs employés dans ce travail, cette tendence augmente dans l'ordre suivant[5]:

Chrysophénine G < rouge de congo < benzopurpurine 4B.

On pourra expliquer plausiblement les résultats expérimentaux obtenus pour la défloculation, si l'on présume qu'un micelle de colorant est partagé en certains submicelles ou en molécules individuelles par l'addition d'une grande quantité de surfactif et que le micelle de la benzopurpurine est partageable le moins facilement. En d'autres termes, on présume que la défloculation du colorant direct succède au partage du micelle de colorant par le surfactif.

La dispersion du submicelle, correspondant à celle dans la première zone de défloculation, sera due à l'adsorption des ions de surfactif, orientant leur groupe ionique vers l'eau, sur la surface hydrophobique du submicelle floculé.

Lorsque la concentration de surfactif

3) K. Meguro, *J. Chem. Soc. Japan, Pure Chem. Sec.* (*Nippon Kagaku Zasshi*), **77**, 72 (1956).

4) K. Meguro et T. Kondo, *J. Chem. Soc. Japan, Pure Chem. Sec.* (*Nippon Kagaku Zasshi,*), **76**, 642 (1955).

5) T. Vickerstaff, "The Phsical Chemistry of Dyeing", Oxford Univ. Press, London (1954).

croît de plus en plus, le submicelle commence à se diviser. Les charges électriques qui ont été cachées apparaîtront alors et les ions de surfactif se déposeront sur ces charges. La deuxième zone de floculation parait ici.

L'élévation de la température accélère le partage du micelle du colorant[5]. Ce fait causera la contraction de la première zone de défloculation, qui a été observée dans le cas de la chrysophénine G.

Le mécanisme de la défloculation dans la deuxième zone sera le même que celui suggéré pour les colorants acides ou basiques.

Laboratoire de Chimie de Nezu
Université de Musashi
Nérima-ku, Tokyo

Catalytic Hydrogenation of Aromatic Nitriles

By Kazuo HATA and Ken-ichi WATANABE

(Received February 17, 1959)

Catalytic hydrogenation of various aromatic nitriles has been investigated using nickel-copper-kieselguhr catalyst in vapor phase. An earlier study has been made by P. Sabatier[1], but it was only reported that benzonitrile was reduced to toluene and ammonia, while a different result was presented by A. Frébault[2]. Systematic study in this field has never been made and the mechanism of hydrogenation of nitriles has not yet been thoroughly established, although some views have been presented during the past half century[3]. In this paper, results of a systematic study on the catalytic hydrogenation of various aromatic nitriles are presented. The effect of various substituents in aromatic ring is discussed, along with the factor of promotion and retardation in hydrogenation. Further, the mechanism of the hydrogenation of nitriles has been investigated and some views are presented.

1) **Hydrogenation of Aromatic Nitriles in Vapor Phase.**—It was previously reported that nitrile is hyrogenated to methyl compound and ammonia in vapor phase[1] (1), whereas to amines in liquid phase[3] (2).

$$RCN \xrightarrow{H_2} RCH_3 + NH_3 \quad (1)$$

$$RCN \xrightarrow{H_2} RCH_2NH_2,\ (RCH_2)_2NH \quad (2)$$

The original purpose of the present study was to investigate whether or not aromatic nitriles of any kind undergo hydrogenolysis to methyl compounds in vapor phase. Various aromatic nitriles listed in Table I have been hydrogenated. The vapor of nitrile, mixed with an excess of hydrogen, was passed over a catalyst in a reaction tube, which was heated to an appropriate temperature between 200 ~350°C in an electric furnace. The catalyst, which consists of 60% of reduced nickel and 40% of reduced copper, was prepared according to Sabatier's method[1], and supported on purified kieselguhr. Representative experimental results of the hydrogenations are summarized in Table I. As seen in the table, it has been proved that aromatic nitriles are generally hydrogenated to the corresponding methyl compounds according to Formula 1 except for some special cases. However, it is important to note that this cleavage reaction of the nitrile group could not be complete unless sufficient condition for hydrogenation was given[4].

It is now apparent that the reaction temperature at which the hydrogenolysis is effectively carried out is governed by the nature of the compound to be hydrogenated. A well defined range of temperature for the efficient cleavage reaction was found for each compound. It has been found that, in general, a scission of C–C bond between nitrile group and

1) P. Sabatier and J. B. Senderens, *Compt. rend.*, **135**, 226 (1902); **165**, 309 (1917); **140**, 482 (1905).
2) M. A. Frébault, ibid., **140**, 1036 (1905).
3) C. Paal and J. Gerum, *Ber.*, **42**, 1153 (1909); G. Mignonac, *Compt. rend.*, **171**, 114 (1920); J. v. Braun et al., *Ber.*, **56**, 1988 (1923); K. W. Rosenmund et al., ibid., **58**, 51 (1925); K. Kindler, *Ann.*, **485**, 113 (1931); R. Juday and H. Adkins, *J. Am. Chem. Soc.*, **77**, 4559 (1955).
4) M. Obata, K. Watanabe and K. Hata, *J. Chem. Soc. Japan, Pure Chem. Sec.* (*Nippon Kagaku Zasshi*), **78**, 116 (1957).

TABLE I. CATALYTIC HYDROGENATION OF AROMATIC NITRILES IN VAPOR PHASE

Catalyst: ca. 25 g (mixture of NiO and CuO (Ni 60%, Cu 40%) 11 g., purified kieselguhr 14 g., reduced at ca. 300°C before the hydrogenation experiment)
Flow velocity of hydrogen ca. 0.1 l./min.; Flow velocity of sample 0.05～0.1 g./min.

Expt. No.	Nitriles	Temp. (°C)	Time (hr.)	Methyl compounds and yields (%)		Yields of ammonia (%)	Other products (%)	Lit.
1.	Benzonitrile	250	1⅔	Toluene	(87)	100		12
2.	Benzonitrile	358	3½	Toluene	(29)	76	Benzene (39)	12
3.	α-Naphthonitrile	270	3	α-Methylnaphthalene	(74)	97		1—3
4.	β-Naphthonitrile	240	3½	β-Methylnaphthalene	(73)	74		4
5.	*p*-Tolunitrile	205	4	*p*-Xylene	(72)			5
6.	*o*-Tolunitrile	240	3½	*o*-Xylene	(87)	100		6,17
7.	*p*-Nitrobenzonitrile	300	4⅓	*p*-Toluidine	(43)	92	Aminonitrile (32)	7
8.	*m*-Nitrobenzonitrile	250	2⅓	*m*-Toluidine	(56)	73	Aminonitrile (9)	8
9.	*o*-Nitrobenzonitrile	300	1¼	*o*-Toluidine	(17)	79	Aminonitrile (20) Aniline (48)	9
10.	*p*-Aminobenzonitrile	330	3	*p*-Toluidine	(80)	90	Aniline (5)	13
11.	*o*-Aminobenzonitrile	300	3	*o*-Toluidine	(9)	94	Aniline (40)	13
12.	Ethyl *o*-cyano-benzoate	260	2	—		15	Phthalimidine (74)	10
13.	Ethyl *p*-cyano-benzoate	280	2	Ethyl *p*-toluate	(70)	80		16
14.	*p*-Bromobenzonitrile	200～300	1½	—		0	Recovered nitrile	11
15.	*p*-Chlorobenzonitrile	250～350	1½	Toluene (small quantities)		35～60	Recovered nitrile	11
16.	Benzyl cyanide	240	3	Ethylbenzene	(34)	69	Toluene (12) β-Phenylethyl-amine (18)	14
17.	*p*-Hydroxy-benzonitrile	453	2¼	*p*-Cresol	(75)	100	Toluene (10)	15
18.	Salicylonitrile	363	6½	*o*-Cresol	(68)	80	Phenol (11)	18
19.	*p*-Methoxy-benzonitrile	240	1⅓	*p*-Cresyl methyl ether	(70)	100		22
20.	*o*-Methoxy-benzonitrile	300	2¼	*o*-Cresyl methyl ether	(73)	100		19
21.	2,6-Dimethoxy-benzonitrile	300	4	—		86	1,3-Dimethoxy-benzene (55) Recovered nitrile (13)	23
22.	*p*-Cyanobenzalde-hyde	280	2½	*p*-Xylene	(28)	60	Toluene (12)	24
23.	Terephthalo-nitrile	304	2⅓	*p*-Xylene	(46)	81	*p*-Tolunitrile (11)	20
24.	Phthalonitrile	310	1½			78	*o*-Tolunitrile (15) Polymerization	20
25.	Acetylmandelic acid nitrile	250	4½	Ethylbenzene	(70)	74	Acetic acid (68)	21
26.	2,4,6-Trimethyl benzonitrile	240	2½	Isodurene	(ca. 50)	60	Recovered nitrile (34)	25
27.	Cinnamonitrile	260	2½	Propylbenzene	(90)	100		26

1) K. Hata, *Bull. Inst. Phys. Chem. Research (Tokyo)*, **23**, 224 (1944). 2) K. Hata, ibid., **23**, 296 (1944). 3) K. Hata, ibid., **24**, 1 (1945). 4) K. Hata, ibid., **24**, 34 (1945). 5) K. Hasegawa and K. Hata, *J. Chem. Soc. Japan, Pure Chem. Sec. (Nippon Kagaku Zasshi)*, **72**, 54, (1951). 6) Y. Tanaka and K. Hata, ibid., **73**, 85 (1952). 7) K. Watanabe, ibid., **76**, 391 (1955). 8) K. Watanabe, ibid., **76**, 395 (1955). 9) K. Watanabe, ibid., **76**, 398 (1955). 10) K. Watanabe, ibid., **76**, 888 (1955). 11) J. Mukai, K. Watanabe and K. Hata, ibid., **76**, 1354 (1955). 12) M. Tanaka, K. Watanabe and K. Hata, ibid., **76**, 1392 (1955). 13) K. Watanabe, ibid., **77**, 221 (1956). 14) K. Watanabe, ibid., **77**, 977 (1956). 15) M. Tanaka, K. Watanabe and K. Hata, ibid., **77**, 980 (1956). 16) K. Watanabe, ibid., **77**, 1272 (1956). 17) M. Obata, K. Watanabe and K. Hata, ibid., **78**, 116 (1956). 18) M. Tanaka, ibid., **78**, 1385 (1957). 19) F. Iwamoto, K. Watanabe and K. Hata, ibid., **78**, 1390 (1957). 20) M. Tanaka, ibid., **79**, 1302 (1958). 21) M. Tanaka, ibid., **79**, 1318 (1958). 22—26) Unpublished.

aromatic ring occurs as shown in Formula 3, when the hydrogenation is carried out at higher temperature (e. g., Experiment No. 2).

$$RCN \xrightarrow{H_2} RH + CH_3NH_2^* \quad (3)$$

The data given in Table I, are the results of the hydrogenation which give the best yield of the methyl compound among several experiments carried out under various conditions, especially under various reaction temperatures (except for Experiment No. 2). On the other hand, ammonia, which was liberated from the nitrile group during hydrogenation, was introduced to normal sulfuric acid solution and was determined by a titration with baryta water. The yield of ammonia suggests the degree of the cleavage reaction of the nitrile group. When the condition of hydrogenation is changed, somewhat different results can be observed for each compound. It is significant that the cleavage of the nitrile group is largely dependent upon the kinds and the positions of substituents in the aromatic ring.

Besides the normal cleavage reaction of nitriles, various side reactions were observed. For example, reductive cyclization was remarkable in the reaction of ethyl *o*-cyanobenzoate[5]. Sometimes, the side reaction was so complicated that the products could not be identified.

1) Effect of Substituents in Aromatic Ring on the Hydrogenation of Nitriles.— It is very difficult to estimate the effect of substituents on the hydrogenation of the nitrile group, because catalytic reaction is complicated with many factors. Nevertheless, it is conceivable that the relative reactivity of the cleavage reaction may be estimated by comparing the yields of the products, although a vapor phase hydrogenation is carried out ordinarily under such a drastic condition that it may cause undesirable side reactions. In general, it has been proved that a substituent in the aromatic ring exhibits both electronic and steric effects on the hydrogenation of the nitrile group. Any substituent seems to depress the hydrogenation of the nitrile group.

As for the electronic effect, electron-releasing substituents give less effect, while electron-attracting substituents such as nitro, cyano, ethoxycarbonyl and aldehyde groups restrain the hydrogenation of the nitrile group remarkably. However, the effect due to the electronic characteristics of the substituent is not always observed clearly since the catalytic hydrogenation is also governed by many other complicated factors.

In the catalytic reaction, it is the first requisite for the initiation of the reaction that the compound should be adsorbed on the surface of the catalyst. This consideration has led to the inference that the nitrile group will be unfavorably hydrogenated, if another substituent in the same ring undergoes competitive hydrogenation or interferes with the adsorption of the nitrile group on the catalyst by steric effect. As for the steric effect, it is expected that the nearer the substituent to the nitrile group is, the larger is its effect. This effect is observed distinctly about nitro, amino, cyano, hydroxyl and ethoxycarbonyl groups, and may be expressed in terms of "ortho effect" in hydrogenation. When two substituents are introduced in both ortho positions beside the nitrile group, a greater steric effect is observed (Table I, Experiments No. 21 and 26). This "ortho effect" could not be obviously observed in the previous studies of hydrogenation in liquid phase. Further investigation of this effect should be made in connection with a mechanism of the reaction on the surface of catalyst.

A special interfering effect of the nitro and amino groups on the hydrogenation of the nitrile group, has been studied in particular[6]. It was first pointed out in the liquid phase hydrogenation by H. Rupe[7], that the nitro group has an interfering effect on the hydrogenation of the nitrile group, and it was shown extensively that the nearer the nitro group is to the nitrile group, the greater is the effect. Hydrogenation of nitro and aminobenzonitriles in vapor phase also gave less yield of the hydrogenolysis products (Table I, Experiments No. 7—11). In order to solve this problem, some experiments on mixed hydrogenation were made. The vapor of benzonitrile was mixed with that of nitrobenzene, aniline or water, and the mixture was hydrogenated as usual. On the other hand, benzonitrile was hydrogenated on the catalyst which had been previously used for the hydrogenation of nitrobenzene or aniline. The results of the experiments

* Methylamine may be further hydrogenated to methane and ammonia in high reaction temperature.

5) K. Watanabe, *J. Chem. Soc. Japan, Pure Chem. Sec.* (*Nippon Kagaku Zasshi*), **76**, 888 (1955).

6) K. Watanabe, ibid., **77**, 225, 1741 (1956).

7) H. Rupe et al., *Helv. Chim. Acta*, 8, 832, 838 (1925).

TABLE II. MIXED CATALYTIC HYDROGENATION OF AROMATIC NITRILES

Expt. No.	Method	Compounds (g.)	Temp. (°C)	Time (hr.)	Main products and yields (%)	Other products*
1.	A	Benzonitrile (7), Nitrobenzene (7)	250	3½	Toluene (61)	Aniline (74%)
2.	B	Benzonitrile (6)	250	2¼	Toluene (60)	
3.	A	Benzonitrile (8), Water (3)	250	2	Toluene (59)	Amines (+), Recovered nitrile
4.	A	Benzonitrile (6), Aniline (6)	250	3	Toluene (62)	Recovered aniline
5.	C	Benzonitrile (6)	250	2	Toluene (39), Dibenzylamine (18)	Benzylamine (+), Tribenzylamine (+), Recovered nitrile (18%)
6.	A	*p*-Aminobenzonitrile (6.6), Water (3)	330	2	*p*-Toluidine (59)	Recovered nitrile (15%), Aniline (+)

Method A: The mixture of two substances was hydrogenated.
Method B: Catalyst that was used beforehand for the hydrogenation of nitrobenzene (5 g.) was used successively.
Method C: Catalyst that was used beforehand for the hydrogenation of aniline (5 g.) was used successively.
* Products marked with (+) were detected in small quantities.

TABLE III. CATALYTIC HYDROGENATION UNDER INSUFFICIENT CONDITIONS

Expt. No.	Catalyst (g.)	Compounds (g.)	Temp. (°C)	Flow velocity of sample (g./hr.)	Products and yields (%) Methyl compds.	Prim. amine	Sec. amine	Tert. amine	Ammonia	Recovered sample (%)
1.	30	*o*-Tolunitrile (6.7)	240	3	87	—	—	—	100	—
2.	10	〃 (5.9)	260	2	70	1	4	—	91	10
3.	10	〃 (6.0)	〃	6	37	3	8	—	64	37
4.	2	〃 (4.0)	〃	4	16	4	12	—	44	45
5.	0.7	〃 (5.1)	〃	2.5	0	9	11	—	17	61
6.[a]	25	〃 (6.3)	〃	3	62	2	3	—	63	22
7.	10	Benzonitrile (3.0)	260	5	52	2	14	2	68	8
		(12.0)	〃	5	47	7	17	3	70	17
		(5.0)	〃	6	32	6	25	5	64	18
8.	2	〃 (4.0)	〃	4.5	34	7	24	—		18
9.[b]	2	Benzylamine (5.6)	260	6	27	—	27	—		30

a) Flow velocity of hydrogen was diminished to 1.3 l./hr.: in other experiments, excess of hydrogen was used (flow velocity 5~6 l./hr.)
b) Cf. Table V, Experiment No. 6.

are shown in Table II. From these results, it is inferable that the nitro group is first reduced to the amino group and suppresses the hydrogenation of the nitrile group by a competitive reaction. It is further proved that the amino group produced from the nitro group acts poisonously for the catalytic activity (cf. Section 4). However, the hydrogenolysis of *p*-aminobenzonitrile could not be affected by the *p*-substituted amino group. This can be interpreted by the steric ineffectiveness of the *p*-substituted amino group as a poison for the catalyst.

3) **Investigation of Hydrogenation Mechanism of Nitriles.**—The investigation of the behavior of various nitriles in the hydrogenation has led to the study of hydrogenation mechanism of nitriles, which is complicated owing to the presence of secondary products. Generally, it has been known[3] that the main process of the hydrogenation of nitriles may be shown as follows:

$$RCN \rightarrow RCH=NH \rightarrow RCH_2NH_2 \rightarrow RCH_3+NH_3 \quad (4)$$

$$RCH=NH+RCH_2NH_2 \rightarrow RCH=NCH_2R \rightarrow (RCH_2)_2NH \quad (5)$$

$$3\,RCH=NH \rightarrow RCH(N=CHR)_2 \rightarrow RCH=NCH_2R \rightarrow (RCH_2)_2NH \quad (6)$$

It is conceivable that the course of the

TABLE IV. HYDROGENATION OF BENZYLAMINE AND DIBENZYLAMINE

Expt. No.	Compounds (g.)		Temp. (°C)	Time (hr.)	Products and yields[b] (%)		Other products
1.	Benzylamine	(7.3)	250	2	Toluene	(66)	Oil of high boiling point
2.	Benzylamine	(10.0)	360	3	Toluene	(46)	Benzene (9%)
3.[a]	Benzylamine	(7.2)	250	1⅔	Toluene	(81)	
4.	Dibenzylamine	(6.0)	300	2½	Toluene Benzylamine	(34) (+)	Unidentified by-product
5.	Dibenzylamine	(7.3)	350	3½	Toluene Benzylamine	(44) (+)	Unidentified amine
6.	Benzylamine Benzonitrile (Mixture)	(4.0) (4.2)	250	3¼	Toluene (4.3 g.) Benzylamine Dibenzylamine	(68)[c] (+) (+)[d]	Recovered nitrile

a) Before the hydrogenation, 5 mg. of thiophene dissolved in 0.1 g. of benzene was vaporized and passed over the catalyst (cf. Table V, Experiment No. 6).
b) (+) denotes detectable but unestimated.
c) The yield of toluene from benzylamine is also calculated as the yield from benzonitrile.
d) Very small amount: When benzonitrile was hydrogenated with the catalyst treated with benzylamine beforehand, about the same amount of dibenzylamine was obtained (Table V, Experiment No. 10).

TABLE V. EFFECT OF THIOPHENE AND SOME BASES ON THE HYDROGENATION OF NITRILES

Expt. No.	Compounds (g.)		Additional compounds[a] (g.)	Temp. (°C)	Time (hr.)	Products and yields (%) Methyl compds.	Prim. amine	Sec. amine	Recovered sample (%)	Remarks[b]
1.	Benzonitrile	(8)	None	250	1⅔	88	—	—	—	Catalyst 25 g.
2.	〃	(5)	Thiophene (0.003)	250	2	82	+	—	—	Catalyst 10 g.
3.	〃	(5)	〃 (0.2)	250	2	14	—	—	84	Catalyst 10 g.
4.	〃	(7)	〃 (2.0)	250	1½	28	—	—	67	
5.	〃	(7)	〃 (0.005)	350	2	30	+	—	7	Benzene (42%)
6.	Benzylamine	(6)	〃 (0.003)	250	1½	66	—	21	12	Catalyst 10 g.
7.	Benzonitrile	(7.7)	Ammonia	250	2½	69	+	+	—	
8.[c]	〃	(7.1)	〃	250	2	14	14	13	43	
9.	〃	(6)	Aniline (5)	250	2	39	+	18	18	Tribenzylamine
10.	〃	(7.4)	Benzylamine (6.4)	250	3	66	+	+	+	
11.	〃	(10.8)	Dibenzylamine (7.5)	250	2¼	18	14	30	19	
12.	〃	(7)	〃 (2.0)	355	2½	16	11	—	11	Benzene (47%)
13.	〃	(7)	Pyridine (1.0)	250	2⅓	78	+	+	—	

a) The nickel catalyst was previously treated with the vapor of these compounds, and then the nitrile was hydrogenated.
b) 25 g. of catalyst was used except for Experiments No. 2, 3 and 6.
c) The mixture of benzonitrile and ammonia was hydrogenated.

reaction is nearly the same whether in liquid phase or in vapor phase although some differences are found. Some factors in the hydrogenation may forcibly control the process of these reactions. The normal process of the hydrogenation of nitrile in vapor phase follows the course shown in Formula 4, and other side reactions or interruption of the process 4 may be caused by inadequate conditions of the hydrogenation. Such a hydrogenation under insufficient conditions may give ample facilities for the study of hydrogenation mechanism. Therefore, some hydrogenation experiments were tried intentionally under insufficient conditions (quantity of catalyst, feeding velocity of sample and hydrogen, etc.)[4]. It has been shown that the course of the reaction can be controlled in the expected way according to the condition of the hydrogenation. The examples of these experimental results are summarized in Table III.

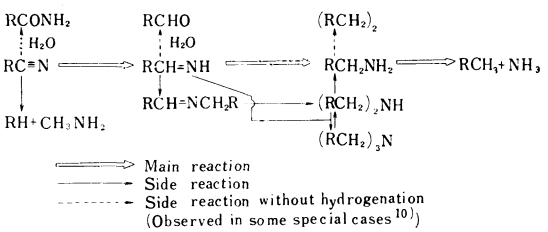
In the hydrogenation of *o*-tolunitrile (Experiments No. 1—5), the yield of the methyl compound through course 4 decreased according to the decreasing quantity of catalyst used, alternatively yielding the increasing quantity of primary and secondary amines. When a small amount of hydrogen was fed during the hydrogenation, a similar result was obtained (Experiment No. 6). In Experiment No. 7, benzonitrile was hydrogenated in three portions successively on the same catalyst, and the products were collected separately for every portion. The components of the reaction products were varied according to the proceeding of the reaction, whereby the changing feature of the reaction was observed.

To ascertain the hydrogenation mechanism, the investigation of the behavior of the intermediate compounds in the process is useful. Thus, the further hydrogenation of amines, which have been found to be intermediate of the process, was carried out[8]. The results of the experiments are summarized in Table IV. When benzylamine was hydrogenated, toluene was obtained and no dibenzylamine was found. But the yield of toluene from benzylamine by the hydrogenation was less than that from benzonitrile, and a small quantity of unidentifiable by-product was obtained from benzylamine. It has been found that benzylamine was smoothly hydrogenated and toluene was obtained in good yield, when a small quantity of thiophene was added to the catalyst (Experiment No. 3). On the other hand, when dibenzylamine was hydrogenated, toluene was obtained in considerable yield, along with a small amount of benzylamine and other unidentified by-product.

It was reported previously by v. Braun[3] that the secondary amine is formed by interaction between a primary amine and an aldimine when aromatic nitrile is hydrogenated in liquid phase (process 5). According to the present investigation in vapor phase, it is evident that dibenzylamine can scarcely be obtained by the hydrogenation of benzylamine, or of the mixture of benzonitrile and benzylamine. It is assumed subsequently that the formation of dibenzylamine in the hydrogenation under insufficient conditions, proceeds through hydrobenzamide and Schiff base as an intermediate according to Formula 6.

It has been found that, when aromatic nitriles are hydrogentated in vapor phase at a higher temperature, the ordinary hydrogenation to methyl compound (reaction 1) is generally accompanied with the hydrogenolysis of C–C bond between the nitrile group and aromatic ring (reaction 3). It has been proved that this cleavage of C–C bond occurs mainly before the hydrogenation of C–N bond does[9]. This cleavage reaction also occurs even at a temperature not so high, when the hydrogenation of the nitrile group happens to be interfered with by the effect of other substituents (Table I, Experiments No. 9 and 11). The cleavage of this type is observed especially in some ortho-substituted benzonitriles (Table I, Experiments No. 21 and 26).

Considering the results of these experiments, the hydrognation mechanism of aromatic nitriles in vapor phase is assumed to be as follows:



8) K. Watanabe, *J. Chem. Soc. Japan, Pure Chem. Sec.* (*Nippon Kagaku Zasshi*), **78**, 1478 (1957).

9) M. Tanaka, K. Watanabe and K. Hata, ibid., **76**, 1392 (1955).

10) K. Watanabe, ibid., **76**, 391, 398 (1955); K. Watanabe, ibid., **77**, 1272 (1956); K. Hasegawa and K.Hata, ibid., **72**, 54 (1951).

TABLE VI. EFFECT OF THIOPHENE ON THE HYDROGENATION OF NITRILE IN LIQUID PHASE

Catalyst: U-Ni-B; Sample: Benzonitrile (7.2 g.); Solvent: 99% Ethanol; Room temperature

Expt. No.	Weight of thiophene (g.)	Hydrogen absorbed (%)	Time (hr.)	Products and yields (%)		
				Prim. amine	Sec. amine	Aldehyde
1.	0	90	1⅔	47	23	11
2.	0.007	93	2⅙	61	13	11
3.	3.5	89	11	56	11	15

4) Factors for Promotion and Retardation in Hydrogenation of Nitriles.—It has been widely known that the result of the hydrogenation reaction varies according to the character of the catalyst, which can be controlled by the addition of appropriate promoter or poisonous matter. The promotion or retardation of the hydrogenation was also observed in aromatic nitriles. The effect of various substances on the character of the nickel catalyst has been investigated[8], and the results of these experiments are summarized in Table V. When benzonitrile was hydrogenated with nickel catalyst which was previously treated with a small amount of thiophene, toluene was obtained in high yield, little by-product being found (Experiment No. 2). On the contrary, when the catalyst was previously treated with ammonia, amine or pyridine, the formation of toluene was suppressed and considerable amounts of by-products were obtained (Experiments No. 7—13). In some experiments, the mixture of benzonitrile and some other basic substances was hydrogenated with the ordinary nickel catalyst, and the results were similar to those in Table V (except the experiment with ammonia, cf. Experiments No. 7 and 8). A similar effect of thiophene has been observed in the liquid phase hydrogenation of benzonitrile (shown in Table VI)[11].

As the result of these experiments, the addition of basic substances (such as amine) has been found to cause retardation of the hydrogenation of nitrile. On the other hand, it has been found that the addition of a small quantity of thiophene causes promotion and increases the yield of the methyl compound, whereas the formation of secondary products is considerably suppressed. Thus, it is evident that the suitable amount of thiophene on the catalyst retards the side reaction of nitriles (e. g., the formation of secondary amine). This effect was especially remarkable in the case of hydrogenation under insufficient conditions. For example, toluene was obtained in high yield from benzonitrile, even when a small quantity of the catalyst was used (Experiment No. 2, compared with Experiment No. 7 in Table III). On the contrary, a large amount of thiophene acts as poison for all the various sorts of the reaction: a large quantity of the nitrile was recovered unchanged (Experiments No. 3 and 4).

Department of Chemistry
Faculty of Science
Tokyo Metropolitan University
Setagaya-ku, Tokyo

11) T. Okazawa, K. Watanabe and K. Hata, unpublished.

On the Dissolution of Na_2O-CaO-SiO_2 Glass in Acid and in Water

By Shoji TSUCHIHASHI and Eiichi SEKIDO

(Received February 26, 1959)

The "chemical durability of glass" is one of the research items of great academic interest, and of leading technical importance as well. Accordingly, there have been many papers published on this subject.

The usual way of representing the results of durability tests is to express them in the equivalent concentration of sodium oxide leached out from the glass surface; sometimes from glass powder to accelerate the attack on glass, or from the glass container itself to make the data more practical. For many purposes this way of presenting data is very useful, because the varying alkalinity of the solution stored in a glass container is often a matter of serious concern.

In multi-component glasses, sodium oxide is not the only substance which passes into solution, even in the initial stage when the silica network remains unchanged. Investigating the change of interference colors produced by the changing thickness of the silica-layer remaining on the surface of some flint glasses immersed in nitric acid solution, the author could confirm the fact that the chemical attack proceeds through the exchange reaction between cations such as Na^+, K^+ and Pb^{2+} in glass on the one hand and H^+, or H_3O^+ in solution on the other[1]. Moreover, the exchange between Na^+, K^+ in glass and H^+ in solution takes place at a rate far greater than that between Pb^{2+} in glass and H^+ in solution, so that the rate of diffusion of Pb^{2+} through glass network determines the rate of reaction.

In studying the mechanism of chemical attack on glass by using soda-lime-silica glass which is simpler in composition and of more practical importance, the optical method fails in its object, because both the rate of reaction and the difference in refractive index between the surface layer and the body are smaller than when we use flint glass.

Hence, in order to draw a clear picture of the complete set of chemical reactions, the components leached out from glass by the conventional powder method were completely analyzed.

1) S. Tsuchihashi, This Bulletin, **24**, 161 (1951).

Experimental Methods

Preparation of the Solution for Analysis. —1) *Sample.*—The glass plates of composition given in Table I were crushed in a percussion mortar, and the powder was sieved to classify it into three meshes, namely, 16~20 (0.833~0.991 mm.), 20~24 (0.701~0.833 mm.), 24~32 (0.495~0.701 mm.), washed thoroughly with methanol to remove all fine particles adhering to the grains, and finally dried at 120°C.

TABLE I. COMPOSITION OF GLASS (weight %)

SiO_2	Na_2O	CaO	MgO	$Fe_2O_3+Al_2O_3$
73.64	13.12	8.44	2.37	2.37

2) *Acid solution.*—As it is necessary to deal exhaustively with an extremely small amount of ions, the water used for the experiments was completely demineralized by treating it successively with ion-exchange resins. This treatment was used also for preparing hydrochloric acid and sulfuric acid solutions, the concentrations of which were 1 N throughout the experiments.

3) *Apparatus.*—The apparatus used for the leaching out experiments is shown in Fig. 1. It is a three-necked flask with a stirrer, both of which are made of Pyrex glass.

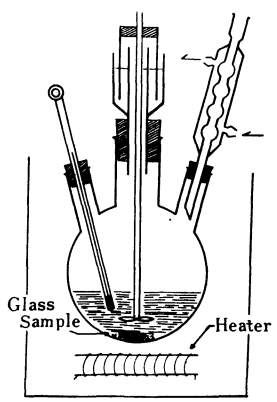


Fig. 1. Apparatus used for the durability test.

4) *Procedure.*—1.00 g. of the glass powder was accurately weighed out and transferred into the flask containing 100 ml. of reagent. Under continuous stirring the temperature was raised as quickly as possible to 100°C, at which it was kept

constant for one or three hours, and then the flask was cooled to room temperature. The solution was separated carefully from the glass powder and subjected to chemical analysis.

A series of blank tests were made in order to determine the amount leached out from the container wall and from the stirrer. The figures obtained, although negligibly small, were subtracted from the results in order to obtain the actual net values.

Chemical Analysis of the Solution.—I. *Silica.*—In order to determine an extremely small amount of silica which had passed from the glass into the liquid, the spectrophotometric method based on the measurement of yellow or blue molybdo-silicic acid was used. There are, however, some points which should be made extremely clear in order to get reliable results. It is known that the color developed changes with the state of existence of silica in solution, namely, whether it is in ionic state, in molecular state or in colloidal state[2-5]. The following conditions should be taken into account.

1) *pH value.*—Quite recently Narita[6] investigated the relation between the quantity of silica in ionic state and the pH of sodium silicate solutions with the result shown in Fig. 2. Since his experiments covered higher percentages of silica than in the present instance, the authors made experiments on the solutions containing smaller amounts of silica, whose compositions are given in Table II.

The silica content was exactly 5 p. p. m. after 6 hr. and 5 p. p. m. after 6 days in pH 12 solution, but was reduced to 0.5 p. p. m. in a 1 N sulfuric acid solution. By adding Ca^{2+} to the solution the

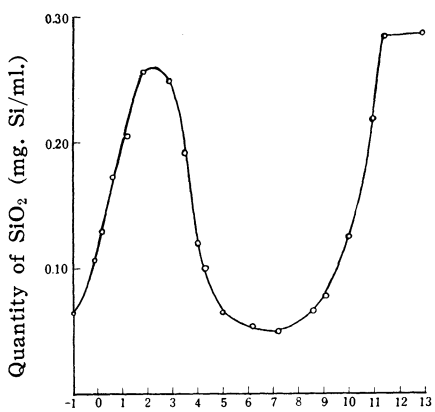


Fig. 2. The relation between the quantity of SiO_2 in ionic state and the pH of solution (after Narita).

TABLE II. DETERMINATION OF SiO_2 INFLUENCED BY OTHER ELEMENTS

Sample solutions	Value of measurements	
	After 6 hr.	After 6 days
5 p.p.m. SiO_2 in 1N H_2SO_4	5 p.p.m.	0.5 p.p.m.
5 p.p.m. SiO_2+5 p.p.m. Ca^{2+}, in 1 N H_2SO_4	5	0
5 p.p.m. SiO_2 in pH 12 solution	5	5
5 p.p.m. SiO_2+5 p.p.m. Ca^{2+}, in pH 12 solution	5	2.9

quantity of ionic silica was reduced; for instance, to 0 in a 1 N sulfuric acid solution, and to 2.9 in an alkaline solution of pH 12. From these observations it may be concluded that the quantity of ionic silica does not depend on the pH of that solution alone. As it has already been shown that the optimum pH value to determine the amount of silica is 1~1.6, we also followed these conditions in performing our experiments.

2) *Quantity of ammonium molybdate.*—The absorption spectra of the solutions, one containing 2 p. p. m. of silica and various amounts of molybdate and the other 20 p. p. m. of silica and various amounts of molybdate, were measured with the result that the addition of 5 ml. of 10% solution of molybdate to 50 ml. solution containing silica gave the greatest sensitivity to the spectra, and that the addition of a larger amount than 5 ml. brought about an undesirable influence[5,7].

3) *Wavelength.*—The published photometric procedures have proved to be of no practical use for measuring the absorption of the yellow molybdo-silicic acid at the optimum wavelength. The recommended wavelengths in millimicrons were: 370[8], 380[7], 390[9], 390 to 400[10], 400[11], 405[12], 416[6,7,13], 420[14], 425[15] and 436[16]. Taking into account these facts, the authors used 410 mμ ("yellow" method) and 810 mμ ("blue" method).

4) *Calibration curve.*—Beer's law was applicable whithin the range from 0 to 60 p. p. m. of silica, and the authors used this calibration curve for the quantitative determination of silica.

We measured the absorbance of the solution as soon as possible after adding the ammonium molybdate to that solution to prevent the influence of Ca^{2+} and other ions. Moreover, in order to examine whether or not any trace of silica might escape as colloid without forming silico-molybdate, alkali was added to the solution to digest the last trace of colloid before it was subjected to analysis.

2) F. Aoki, *J. Chem. Soc. Japan, Pure Chem. Sec.* (*Nippon Kagaku Zasshi*), **72**, 17 (1951).
3) T. Okura, ibid., **72**, 927 (1951).
4) Y. Iwasaki et al., ibid., **75**, 857 (1954).
5) M. A. Desesa and L. B. Roger, *Anal. Chem.*, **26**, 1278 (1954).
6) K. Narita, *J. Chem. Soc. Japan, Pure Chem. Sec.* (*Nippon Kagaku Zasshi*), **76**, 460 (1955).
7) K. Narita, ibid., **77**, 271 (1956).
8) J. Hure and T. Ortis, *Bull. soc. chim. France*, **16**, 834 (1949).
9) R. Guenther and R. H. Gale, *Anal. Chem.*, **22**, 1510 (1950).
10) U. T. Hill, ibid., **21**, 589 (1949).
11) M. Armand and J. Berthaux, *Anal. Chim. Acta*, **5**, 380 (1951).
12) J. R. Boyd, *Anal. Chem.*, **24**, 805 (1952).
13) O. P. Case, *Ind. Eng. Chem., Anal. Ed.*, **16**, 309 (1944).
14) D. Rozental and H. C. Campbell. idid., **17**, 222 (1945).
15) G. N. Cade, ibid., **17**, 372 (1954).
16) H. Pinsl, *Z. Metallkunde*, **27**, 107 (1935).

The results obtained with such treatment and those without it were quite the same, which proves that the present method is satisfactory.

II. *Sodium Oxide.*—Sodium oxide was determined by flame photometry using the spectral line at 589 mμ. As long as the concentration of alkali ions was in the order usually found in the durability tests, all substances except acids[17] were found to be harmless. The disturbance of acids was taken into full account, and the calibration curves were used to prevent the data from being influenced by coexisting anions.

III. *Calcium Oxide.*—Calcium oxide was determined by flame photometry using a calcium oxide band spectrum at 554 mμ. As it was found necessary to make clear the influence of coexisting ions on the result, a series of preliminary experiments were carried out.

1) *Influence of sodium ion.*—A 5 p. p. m. calcium standard solution containing 0 to 100 p. p. m. Na^+ and a 1 p. p. m. solution containing 0 to 20 p. p. m. Na^+ were aspirated to observe the change of the flame intensity, and it was possible to confirm the fact that there was no detectable influence of coexisting Na^+ so far as its concentration did not exceed 15 times the amount of Ca^{2+}.

2) *Influence of iron(III) ion.*—Carrying out the same experiments as the above using a 20 p.p.m. calcium standard solution containing 0 to 50 p.p.m. Fe^{3+}, it was recognized that the limiting concentration of Fe^{3+} was 0.5 times the amount of Ca^{2+}. As the amount of Fe^{3+} in the durability tests never exceeded this limiting value, the influence of coexisting Fe^{3+} may be ignored.

3) *Influence of silica.*—The change of the flame intensity of a 2 p. p. m. calcium standard solution containing silica (up to 5, 10 and 20 p.p. m., respectively) is shown in Figs. 3, 4 and 5. The curves show a general trend indicating that the flame intensity was reduced at first by the addition of silica and brought, by further addition, to a constant value approximately at the point

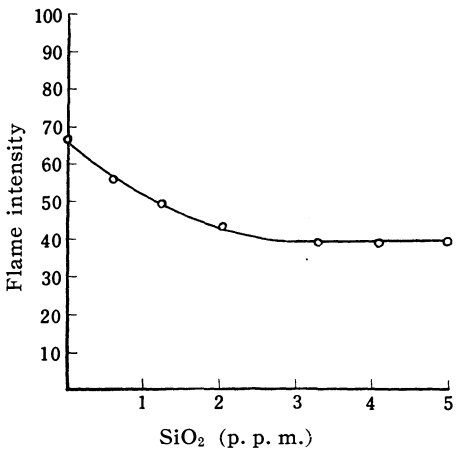


Fig. 3. Flame intensity of Ca^{2+} containing SiO_2
(Ca, 2 p. p. m.; SiO_2, 0～5 p. p. m.)

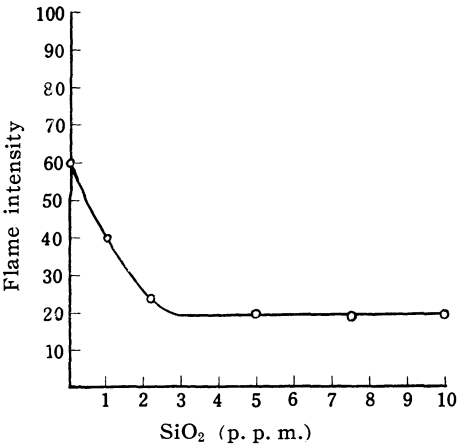


Fig. 4. Flame intensity of Ca^{2+} containing SiO_2
(Ca, 2 p. p. m.; SiO_2, 0～10 p. p. m.)

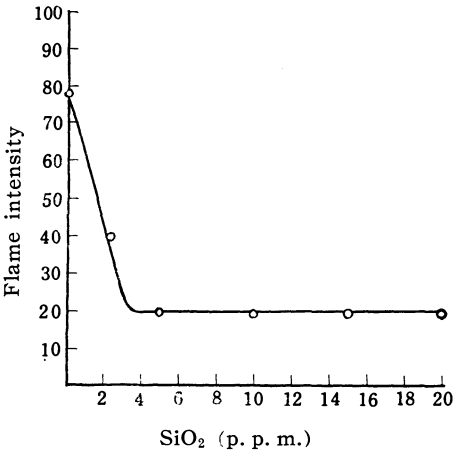


Fig. 5. Flame intensity of Ca^{2+} containing SiO_2
(Ca, 2 p. p. m.; SiO_2, 0～20 p. p. m.)

corresponding to the composition Ca : SiO_2=2 : 3. Thus, for the solution containing silica more than 3/2 of calcium, the calibration curve was drawn by analyzing the solution containing a known quantity of Ca^{2+}.

4) *Influence of acids.*—The disturbance of acids[18] was taken into full account and the calibration curves were made to make the results free from the influence of acids.

Results and Discussion

The data obtained by the durability tests are listed in Table III. The figures indicate that much larger amounts of silica were clearly leached out by water than by acids, and that silica probably placed a check on the rate of dissolution. In

17) P. Portor and C. Wyld, *Anal. Chem.*, **27**, 733 (1955).

18) S. Ikeda, *J. Chem. Soc. Japan, Chem. Sec.* (*Nippon Kagaku Zasshi*), **78**, 1434 (1957).

TABLE III. DURABILITY OF Na_2O-CaO-SiO_2 GLASS

Solution	Time (hr.)	Particle size (mesh)	Amount leached out in mg./100 ml. SiO_2	Na_2O	CaO	Na_2O/SiO_2
H_2O	1	16~20	0.20	0.06	0.01	0.29
		20~24	0.47	0.10	0.04	0.21
		24~32	0.68	0.18	0.04	0.25
	3	16~20	0.40	0.08	0.02	0.20
		20~24	1.05	0.21	0.05	0.20
		24~32	2.10	0.37	0.09	0.18
1N HCl	1	16~20	0.05	0.04	0.01	0.80
		20~24	0.09	0.08	0.04	0.89
		24~32	0.13	0.11	0.08	0.83
	3	16~20	0.06	0.05	0.02	0.80
		20~24	0.12	0.09	0.05	0.80
		24~32	0.20	0.16		0.80
1N H_2SO_4	1	16~20	0.10	0.06	0.07	0.58
		20~24	0.15	0.13	0.05	0.87
		24~32	0.20	0.17	0.07	0.83
	3	16~20	0.12	0.10		0.86
		20~24	0.20	0.15		0.73
		24~32	0.35	0.19		0.55
The ratio in base glass (weight per cent)						0.18

every case, however, larger quantities of silica than those of sodium oxide, and much smaller quantities of calcium oxide than of the other two were found in the solution. As usual, the total amount of dissolved matters inceased in proportion to the length of time, and in inverse proportion to the grain size of the glass powder.

As for the ratio Na_2O/SiO_2, the figures in the sixth and last rows show that the solution had practically the same proportion of sodium oxide to silica as the base glass, and also that the attack of water on glass presumably caused the collapse of the whole structure. The acids did not seem to be so destructive to the network structure, since the ratios were always higher. This indicates that the exchange reaction between H^+ in solution and Na^+, Ca^{2+} in glass is governed by the rate of migration of the ions through the glass network to the surface.

The idea of the collapse of the whole glass structure is strongly supported by the experimental results obtained by Tieze[18] and others[20,21] who confirmed the successive exfoliation of the silica layer during the durability test. This was also proved by the gradual increase of the quantity of dissolved substances.

Action of Water on Glass. — Let us first focus our attention on the network former, silica, which has non-bridging oxygen bonded with Na^+, and try to explain why the ratio of components in the solution was practically the same as that in the base glass when it was attacked by pure water. For this purpose it will be convenient to consider the whole process in two separate stages, i. e., (1) the initial stage and (2) the depth action, although there is no sharp boundary-line between them.

The reactions in the initial stage are illustrated schematically in Fig. 6. At first there will be the migration of Na^+ from the glass into the liquid, which gives rise to the place exchange between H^+ and Na^+. In the meantime Na^+ in the glass

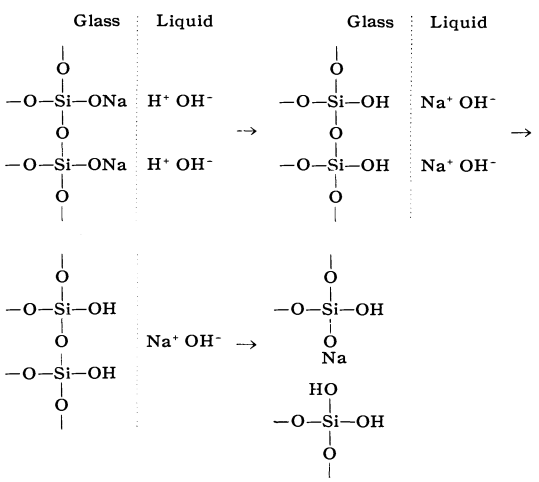


Fig. 6. Schematic representation of the chemical attack of water on glass surface.

19) P. Tieze, *Sprechsaal*, **61**, 809 (1928).
20) Tielsh and Zimmer, ibid., **66**, 285, 303, 319 (1933).
21) I. Sawai, M. Tashiro et al., *J. Ceram. Assoc. Japan (Yogyo Kyokai Shi)*, **52**, 258 (1944).

will diffuse to the surface through the network without producing any appreciable influence upon its structure. The continuous supply of Na^+ from inside, however, will accumulate sodium hydroxide at the surface, which then will begin to attack the bonding oxygen to open the network, so that silica also passes into the solution with gradual increase in its concentration. Hence in the initial stage, more sodium oxide goes into the solution than silica; that is, Na_2O/SiO_2 is higher than that of the base glass. The high value of the ratio Na_2O/SiO_2 in the initial stage is shown in Table III.

In the second stage, the depth action extending inward from the surface should be taken into account. As the reaction proceeds through the mutual diffusion of Na^+ and H^+ (this H^+ can easily migrate through the network and can penetrate deep into the electron cloud of non-bridging oxygen), the structure of sodium silicate changes into that of silicic acid in the layer near the glass surface. Using sodium silicate or dense flint glass, existence of a sharp boundary-line at the surface may easily be observed under a microscope.

Protons penetrate into the electron cloud of oxygen. As a result, the change from ONa to OH brings about the change of electronic configuration around the non-bridging oxygen, which in turn induces the stress in the network. The strain thus developed in the surface layer induces the exfoliation of the skeleton en masse so that all glass components go completely into the solution, with the ratio of components remaining unchanged, whether they are in glass or are dissolved in the solution.

Attack of Acids on Glass.—It requires only a glance at Table III to observe the fact that there is a marked difference between the action of water and of acids. Two remarkable features may be pointed out:

(1) Acids accelerated the leaching of the metallic ions, while they reduced notably the rate of dissolution of silica.

(2) Each component showed different behavior when attacked by different acids.

The question why acids check the dissolution of silica may be answered quite easily, when we take into account the fact that silica network can not be opened until a sodium hydroxide attacks the bridging oxygen, since H^+ in acid solution has no power to open the silica network. In fact, vitreous silica is resistant to the attack of acids, though it is not resistant to that of alkalis.

In the glass containing modifier cations in its network there will be only the place exchange between H^+ and the metallic cation.

It should be noticed that, with a few exceptions, sulfuric acid was stronger than hydrochloric acid in the power of leaching out the cations, while the hydrogen ion concentrations of the solutions are in reverse order, namely,

$$HCl : 0.8 > H_2SO_4 : 0.55$$

This discrepancy may be explained by taking into account the nature of the negative charge distribution in the liquid at the boundary layer surrounding the glass particles. The negative charge of anions reduces the repulsion between the cations which are just going to leave the lattice points and those already existing in the solution. In short, the anion plays an important role in drawing out the cations from the glass network.

Summary

(1) The first step in the attack of water on glass is the exchange reaction between the proton and Na^+ on the glass surface. Sodium hydroxide thus produced in the boundary layer opens the Si-O-Si bond, and consequently silica passes into solution.

(2) When the exchange reaction between Na^+ in glass and H^+ in acid solution takes place, more metallic ions will be drawn out of the network owing to the influence of anions existing in the solution. Consequently more cations pass into the solution, while the silica network will be stabilized by acid so that the silica in the solution will be reduced remarkably.

The authors are indebted to Professor I. Sawai of Kyoto University for his advice and encouragement during the course of this research. Thanks are due also to Mr. S. Nakabayashi and Mr. Y. Nakatani who helped us with the laboratory work.

The cost of this research was defrayed by the Scientific Research Encouragement Grant from the Ministry of Education, to which the writers' thanks are due.

Department of Chemistry
Faculty of Science
Kobe University
Higashinada-ku, Kobe

Complexometric Titration of Rare Earth Elements. Dissolution of the Rare Earth Oxalate with Ethylenediaminetetraacetic Acid and Back Titration with Magnesium Sulfate

By Seizo MISUMI and Tomitsugu TAKETATSU

(Received March 23, 1959)

Complexometric titration of the rare earth ions in solution has been studied widely by many investigators[1-3]. The rare earth oxalate is usually precipitated from a weak acid solution and used for the gravimetric determination of the rare earth elements. Oxalic acid is the most excellent precipitating reagent for the rare earth ion. However, according to the fact that the rare earth oxalate was dissolved in alkaline solution by adding the excess of ethylenediaminetetraacetic acid(EDTA), Marsh[4] studied the fractional precipitation of the rare earth elements, using a different solubility of each rare earth-EDTA-oxalate complex anion in successive decreases of pH of solution. The present authors found that the rare earth ion, in the presence of a large amount of the oxalate ions, could be determined by back titration of the excess of EDTA with standard magnesium sulfate solution using Eriochrome black T as indicator under certain conditions. Thus, the rare earth ion was precipitated as the oxalate, the precipitate was separated and an excess of standard EDTA solution was added to dissolve the precipitate. After the oxalate was completely dissolved, the excess of EDTA in the solution was back titrated with standard magnesium sulfate solution, using Eriochrome black T as indicator. The conditions of dissolution of the rare earth oxalate and of the back titration were studied in detail and the optimum conditions were obtained for the determination of the rare earth elements. This procedure affords good and accurate results for the determination of 1 to 5 mg. of rare earth elements contained in solution under certain conditions. Especially, it is more rapid and rather simpler than the usual gravimetric procedure.

Experimental

Preparation of Standard Solution and Reagents.—*Standard EDTA solution.*—A certain quantity of disodium ethylenediaminetetraacetate dihydrate (analytical grade pure) was dissolved in distilled water and standardized by titration with standard zinc chloride solution, using Eriochrome black T as indicator. Concentration of the standard EDTA solution: 0.01030 mol./l.

Standard magnesium sulfate solution. — The weighed pure magnesium sulfate heptahydrate was dissolved in distilled water and standardized by titration with standard EDTA solution, using Eriochrome black T as indicator. Concentration of the standard magnesium sulfate solution: 0.01131 mol./l.

0.5% *Eriochrome black T (E. B. T.) solution.*— A half gram of E. B. T. and 4.5 g. of hydroxylamine hydrochloride were dissolved in absolute ethanol and the total volume was filled up to 100 ml. with ethanol.

Buffer solution. — Ammonium chloride-ammonium hydroxide buffer was used. Each equivalent quantity of 1 mol. ammonium chloride solution and 1 mol. ammonium hydroxide solution were mixed.

Rare earth chlorides were prepared from the pure rare earth oxides which were all of extra pure grade, specially purified with ion-exchange resins. La_2O_3: more than 99.99%, CeO_2: more than 99.99%, Pr_6O_{11}: more than 99.99%, Nd_2O_3: more than 99.99%, Sm_2O_3: 99.98%.

All other reagents were of analytical reagent grade.

Apparatus.—Two or five ml. microburette (corrected) was used. One drop was equal to 0.005 or 0.006 ml. Micro glass filters (No. 4) and beakers were all boiled in 2% alkaline EDTA solution for about three hours and allowed to stand overnight and washed with distilled water thoroughly before use. The measurements of pH were carried out with the glass electrode pH meter EHM-1 Type of Hitachi & Co.

A sample solution, containing 1 to 5 mg. of the rare earth ion, was taken, the crystalline rare earth oxalate was precipitated, filtered and separated. An excess of the standard EDTA

1) G. Schwarzenbach, "Die Komplexometrische Titration", Ferdinand Enke Verlag, Stuttgart, (1955), p. 61.
2) H. Flaschka, *Mikrochim. Acta*, **1955**, 55.
3) G. Brunisholz and R. Cohen, *Helv. Chim. Acta*, **39**, 324 (1956); ibid., **39**, 2136 (1956).
4) J. K. Marsh, *J. Chem. Soc.*, **1950**, 1819.

solution was added and then the solution was made alkaline with dilute aqueous ammonia. The oxalate was completely dissolved as the rare earth-EDTA-oxalate complex anion[4]. By back titration of the excess of EDTA in the solution with standard magnesium sulfate solution, the rare earth was determined indirectly. The basis of calculation is derived from the fact that the rare earth-EDTA-oxalate complex is known as the 1 : 1 complex[4], which contains one gram atom of rare earth and one molecule of EDTA.

Results and Discussion

Back Titration in the Presence of Oxalate Ion.—Rare earth oxalate was dissolved as the complex anion with an excess of EDTA (HY^{3-}) in the solution and this reaction is supposed to proceed as follows: that is,

$$R_2(C_2O_4)_3+2HY^{3-} \rightarrow 2[RHYC_2O_4]^{2-}+C_2O_4^{2-}$$

in alkaline solution, where R^{3+} indicates the tripositive rare earth ion. When the excess of EDTA in the presence of the rare earth complex ion was back titrated with standard magnesium sulfate solution, using Eriochrome black T as indicator, the interference of the oxalate ion in solution was studied. To the aqueous solution of lanthanum or cerium chloride (content of rare earth ion: 2~4 mg.), about 10 to 70 mg. of oxalic acid was added and the crystalline rare earth oxalate was precipitated. Then an excess of standard EDTA solution was added and the solution was made alkaline with dilute ammonia water solution to dissolve the oxalate completely. After the pH was accurately adjusted to 10.0~10.5 with dilute ammonia water, 5 drops of 0.5% Eriochrome black T solution were added and the excess of EDTA remaining in solution was back titrated with standard magnesium sulfate solution till the blue color of the solution changed into red at the end point. The results are shown in Table I.

It had been supposed that the great excess of the oxalate ions would cause the end point of back titration to be ambiguous. But for 1 to 5 mg. of the rare earth ion, it was found that the addition of 30 mg. of oxalic acid did not interfere with the titration at all. Therefore, provided that the rare earth oxalate can be precipitated, separated and dissolved completely with a known amount of standard EDTA solution, the back titration of the excess of EDTA with standard magnesium sulfate solution is readily carried out in the presence of the oxalate ions and the rare earth-EDTA-oxalate complex ions in solution.

Studies on Various Conditions for the Determination of the Rare Earth Element.—Further, the conditions for this procedure for the determination of the rare earth elements were studied concerning the following matters, i. e.,

a) The process for the precipitation of crystalline rare earth oxalate. The crystalline oxalate was precipitated from a solution of rare earth chloride.

b) The amount of EDTA added for the complete dissolution of the oxalate. The use of 5 ml. of 0.01 M standard EDTA solution was optimum.

c) The amount of the buffer solution added to the solution obtained. The use of 2 ml. of the buffer solution was optimum.

d) The temperature for dissolution of the oxalate with the EDTA solution. 50 to 60°C (5 min.) was the best temperature

TABLE I. EFFECT OF VARIATION IN AMOUNT OF OXALIC ACID ADDED ON THE BACK TITRATION

Lanthanum taken=2.333 mg. pH=10.2~10.5

Oxalic acid added, mg.	La found, mg.	Error, mg.	%	Remarks
10	2.325	−0.008	−0.34	end point sharp
15	2.333	±0.000	±0.00	〃
20	2.333	±0.000	±0.00	〃
30	2.325	−0.008	−0.34	〃
40	2.317	−0.016	−0.69	lacks sharpness
50	2.317	−0.016	−0.69	〃
70	2.270	−0.063	−2.70	obscure

Cerium taken=3.595 mg. pH=10.2

Oxalic acid added, mg.	Ce found, mg.	Error, mg.	%	Remarks
20	3.586	−0.009	−0.25	end point sharp
30	3.576	−0.019	−0.53	〃
40	3.567	−0.028	−0.78	lacks sharpness

for the complete dissolution.

e) Adjustment of the pH for micro titration. The pH 10.2~10.5 was the optimum value which must be accurately kept.

f) On the indication of accurate end point of the back titration with standard magnesium sulfate solution in the presence of oxalate ion, using Eriochrome black T as indicator. The end point was defined to be accurately at the point where the blue color changed completely into the red color.

As the result of these experiments, the optimum conditions are found as follows.

Recommended Procedure.—1) *Precipitation and filtration of the crystalline rare earth oxalate.* — 10 ml. of a weak acid aqueous solution of the tripositive rare earth elements (content of R^{3+} ion: 1~5 mg.) is warmed at 60°C for a few minutes and 20 ml. of the saturated oxalic acid solution is added. The solution is warmed at the same temperature for several hours and then left to stand overnight. Large crystals of the rare earth oxalate are completely precipitated. The precipitate is filtered slowly with the micro glass filter (No. 4) by suction and washed with a saturated oxalic acid solution.

2) *Dissolution of crystalline rare earth oxalate.*—The precipitate is put into a small beaker together with the glass filter, about 25 ml. of distilled water is added and the mixture is warmed at 50~60°C for a few minutes. Then an excess of 0.01 M standard EDTA solution and 2 ml. of 2 N ammonia water are added and the mixed solution is warmed again carefully at 50~60°C for about 5 minutes. The precipitate is thus completely dissolved by this process. After complete dissolution of the precipitate, the solution is cooled rapidly and the glass filter is removed by washing with the distilled water which is added to the original solution.

3) *Back titration with standard magnesium sulfate solution.*—The pH of the solution obtained, must be correctly adjusted to 10.5 with 2 ml. of the buffer solution and dilute ammonia water. Then the total volume of the solution is filled up to about 60 ml. with distilled water. As this indicator, 5 drops of 0.5% E. B. T solution are added and the excess of EDTA in the solution is back titrated with 0.01 M standard magnesium sulfate solution. At the end point, the blue color changes completely into red.

The results obtained by this procedure are given in Table II.

TABLE II. MICROTITRATION OF SOME RARE EARTH ELEMENT

Element	Taken mg.	Found mg.	Error mg.
La	0.935	0.914	−0.021
	2.332	2.332	±0.000
	4.688	4.704	+0.016
Ce	1.798	1.815	+0.017
	3.595	3.605	+0.010
	5.393	5.322	−0.011
Pr	2.582	2.557	−0.025
Nd	1.617	1.627	+0.010
Sm	1.140	1.167	+0.027

It is especially necessary to notice the following matters in this procedure.

a) Determination of the tetrapositive cerium. In the complexometric titration of cerium in alkaline solution, to prevent the oxidation by the tetrapositive ion, it is necessary, in general, to add a reducing agent (e. g., one such as ascorbic acid), but in the presence of the oxalate ion, owing to its reducing property, addition of the reducing agent was not required and the procedure could be applied also to the determination of the tetrapositive cerium ion.

b) Addition of ethanol to the solution for back titration. Wünsch[5] added ethanol for the determination of scandium by complexometric back titration. Generally, in the case of the usual back titration for the determination of rare earth ions, addition of ethanol makes the end point evidently clearer with E. B. T as indicator, but in the presence of the oxalate ion, on the contrary, low value was obtained by adding ethanol.

c) Treatment of the glass vessels with alkaline EDTA solution. As Flaschka and Amin[6] reported, it was seen that the glass vessels were attacked slightly by concentrated EDTA solution and if so, there must be a tendency that a slightly high value for the determination would be obtained. Therefore, the glass vessels which were used in this experiment, were boiled with 2 percent alkaline EDTA solution and left to stand overnight and washed thoroughly with distilled water before use. In this way, such errors, owing to EDTA, were not recognized at

5) L. Wünsch, *Collection Czechoslov. Chem. Communs.*, **20**, 1107 (1955).
6) H. Flashka and A. M. Amin, *Mikrochim. Acta*, **1953**, 410.

all and the value found was accurate and reproducible.

This procedure of complexometric titration to determine the small amount of the rare earth from the oxalate is rapid and precise and more excellent than the usual gravimetric method in its accuracy.

Summary

The processes for dissolution of the oxalate and complexometry to determine the small amounts of rare earth rapidly and accurately, were studied. Crystalline rare earth oxalate was precipitated and filtered. The precipitate was dissolved completely with EDTA in alkaline solution and the excess of EDTA in solution was back titrated with standard magnesium sulfate solution. By this procedure, rare earth in the range of a content about 1 to 5 mg., was determined rapidly with a good accuracy.

The authors desire to thank the Ministry of Education for its financial support of this research.

Department of Chemistry
Faculty of Science
Kyushu University
Hakozaki, Fukuoka

SHORT COMMUNICATIONS

Anion Exchange Studies of Beryllium(II), Cerium(IV), Thorium(IV) and Uranium(VI) Carbonate Complex Ions

By Seizo MISUMI
and Tomitsugu TAKETATSU

(Received December 10, 1958)

Ishimori and Okuno[1] studied anion exchange behavior of uranyl carbonate complex ion in a sodium carbonate solution and Saito and Sekine[2] reported that of thorium carbonate complex ion. No investigation has been reported on the behavior of beryllium and cerium(IV) carbonate complex ions toward anion exchange resins. In this paper, anion exchange behavior of macro amounts of beryllium, cerium, thorium and uranyl carbonate ions formed in ammonium carbonate solution and of tracer amounts of cerium and thorium carbonate complex ions formed in potassium carbonate were studied, using the "Dowex 1, X-8" anion exchanger (50~100 mesh) of carbonate form.

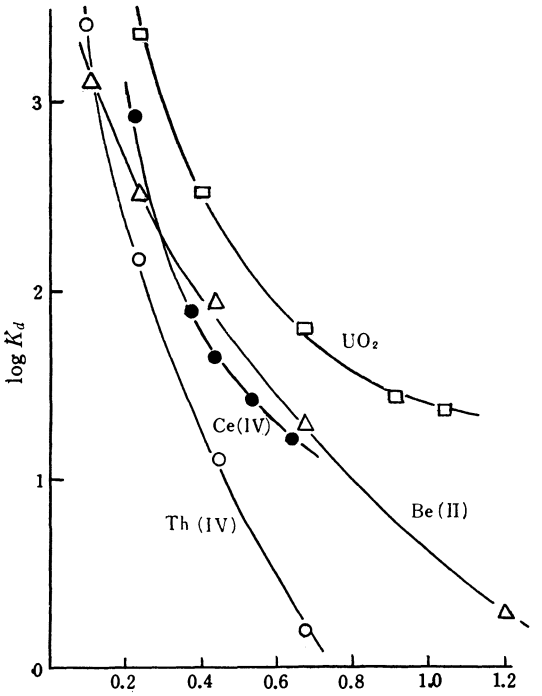
The measurements of distribution coefficients were carried out as follows: one gram of the resin was added to 200 ml. of a series of ammonium carbonate solution of various concentrations containing an equal amount of beryllium carbonate complex ions. The solution was stirred frequently by a magnetic stirrer, allowed to stand for 12 to 20 hr. at about 20°C and the resin was rapidly separated from the solution with a glass filter. The metal ion in the resin was eluted by dilute hydrochloric acid and determined gravimetrically. The distribution coefficient K_d is given by:

$$K_d = [M_r] / [M_s] \quad (\text{ml./g.}) \qquad (1)$$

where M_r is the amount of metal ion in 1 g. of the resin and M_s is that in 1 ml. of the solution. The similar procedure was also applied to the cases of cerium, thorium and uranyl carbonate complex ions. The results are shown in Fig. 1.

It can be seen that beryllium and cerium ions formed the negatively-charged complex ions with ammonium carbonate in the similar manner to thorium and uranyl ions, and that the adsorbabilities of these metal carbonate complex ions decreased as the concentration of ammonium carbonate increased. It is expected from the difference of the values for K_d that

1) T. Ishimori and H. Okuno, This Bulletin, **29**, 78 (1956).
2) N. Saito and T. Sekine, ibid, **30**, 561 (1957).



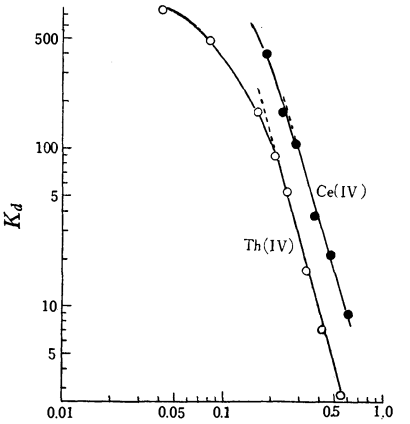
Concentration of ammonium carbonate (M)

Fig. 1. Distribution coefficients of beryllium, cerium, thorium and uranyl ions on anion exchanger in ammonium carbonate solution.
Amounts taken,
Be^{2+}: 11.7 mg (BeO)
Ce^{4+}: 7.3 mg (CeO_2)
Th^{4+}: 26.9 mg (ThO_2)
UO_2^{2+}: 61.0 mg (U_3O_8)

thorium ions can be effectively separated from uranyl ions with the ammonium carbonate solution.

The anion exchanger was saturated with beryllium carbonate complex ions in 0.1 M ammonium carbonate solution, and then washed with dilute ammonium carbonate solution. The results obtained for the exchange capacity by this measurement showed that one mole of beryllium ion corresponds to 1.97 ($\simeq$2.0) equivalents of the resin. This may indicate that the complex anion has a formula such as $[Be(CO_3)_2]^{2-}$ in 0.1 M ammonium carbonate solution.

Distribution coefficients of thorium-234 and cerium-144 in potassium carbonate solutions were determined by a similar procedure. Thorium or cerium in the resin was eluted with hydrochloric acid and the effluent was evaporated on a water bath. The measurements of radioactivities were carried out with a G-M tube. $\log K_d - \log(CO_3^{2-})$ curves plotted in



Concentration of potassium carbonate (M)

Fig. 2. Distribution coefficient of cerium-144 and thorium-234 on anion exchanger in potassium carbonate solution.

Fig. 2 show linearity for both elements from 0.25 to 0.60 M potassium carbonate solution. When only one species of negatively charged complex ion is assumed to be formed between a quadrivalent metal ion (M^{4+}) and carbonate ions, the main reaction would be

$$M^{4+} + xCO_3^{2-} = M(CO_3)_x^{4-2x} \quad (2)$$

$$K_1 = \frac{(M(CO_3)_x^{4-2x})}{(M^{4+})(CO_3^{2-})^x} \quad (2a)$$

Then the following equation is given as to the adsorption of the complex ion on the resin (R_2CO_3).

$$M(CO_3)_x^{4-2x} + (y/2)R_2CO_3 = R_yM(CO_3)_x + (y/2)CO_3^{2-} \quad (3)$$

$$K_2 = \frac{(R_yM(CO_3)_x)(CO_3^{2-})^{y/2}}{(R_2CO_3)^{y/2}(M(CO_3)_x^{4-2x})} \quad (3a)$$

Since the amount of M^{4+} is negligible compared with the amounts of "R_2CO_3", the latter can be regarded as a constant in the above equations. If the concentrations are replaced by thermodynamic activities, Eq. 1 is expressed as follows:

$$K_d = \frac{[M_r]}{[M_s]} = \frac{[R_yM(CO_3)_x]}{[M^{4+}] + [M(CO_3)_x^{4-2x}]} \quad (4)$$

In Eq. 3, y should be equal to $2x-4$ in order to preserve electrical neutrality in the resin. From Eqs. 2a, 3a and 4, the following equation is obtained:

$$\frac{d \log K_d}{d \log(CO_3^{2-})} = 2 - x \quad (5)$$

Since the slopes in Fig. 2 are numerically correspond to $-3.9 \sim -3.8$, the charges of

thorium and cerium(IV) carbonate complex ions could be -8 (their some portions seem to have other values, e.g., -6) in the range between 0.25 and 0.60 M potassium carbonate solutions on the basis of the assumption described above. However, it is probable that these carbonate complex ions include OH^- radicals. Further, it is also supposed that more than one species of negatively charged complex ions may exist and be adsorbed on the resin in other ranges of concentrations of potassium carbonate solutions.

Details of these results will be published elsewhere.

Department of Chemistry
Faculty of Science
Kyushu University
Hakozaki, Fukuoka

The Separation of Thorium(IV) and Cerium(III) Ions by Using Alginate as Cation Exchanger

By Takeo Takahashi and Shingo Miyake

(Received April 3, 1959)

Recently the separation of thorium(IV) and cerium(III) ions by the use of strongly acidic cation exchange resins, such as Dowex 50 or Amberlite IR-120 has been reported by a few workers[1-4].

The present authors will report here a new method for the separation of thorium (IV) and cerium(III) by using alginate as ion exchanger and dilute nitric acid as eluant.

Alginic acid, a natural polyacid, has a property of cation exchanger for several metallic ions in a moderately acid solution of pH 1~3. Metallic ions adsorbed on alginic acid can be eluted easily and separately with dilute acid solutions of varying concentration.

Preparation of Alginate Exchanger and Column.—The alginate exchanger was prepared by swelling the thread* of calcium alginate in a dilute sodium hydroxide solution (less than 0.1 N) for about 30 min. and then by immersing in 0.5 N nitric acid. The product was packed appropriately into a glass tube (1.5 cm. in diameter, 30 cm. in length). The column packed with the adsorption bed of alginate (length, about 20 cm.) was washed successively with 250 ml. each of 0.5 N nitric acid and distilled water. Thus, the alginate was converted completely into acid form.

Procedure.—The mixed solution of thorium(IV) and cerium(III) ions was poured onto the column, the pH being adjusted to 2~2.5 with aqueous ammonia. The bed was then washed with 100 ml. of distilled water, and 200 ml. of 0.075 N nitric acid was passed through the column at a flow rate of about 1 ml./min. By this treatment, all the cerium(III) ions were completely eluted, and then all the thorium-(IV) ions remaining on the column were eluted in the same manner with 100 ml. of 1 N nitric acid.

The amount of throium(IV) and cerium-(III) ions in the effluents was colorimetrically determined with Neo-thoron for thorium(IV) (580 mμ)[5] and with hydrogen peroxide for cerium(III) (320 mμ)[6].

Result.—An example of elution diagrams of the solution containing 35.5 mg. of thorium(IV) and 30 mg. of cerium(III) ions is shown in Fig. 1, and the amounts initially taken are given in Table I in comparison with the amount finally found.

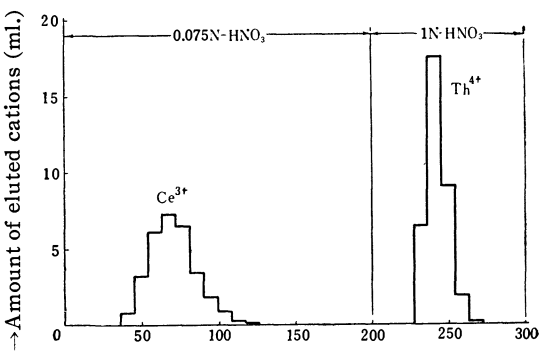


Fig. 1. The elution diagram in the separation of thorium(IV) and cerium(III). The eluants were 0.075 N nitric acid for cerium and 1 N for thorium.

1) L. Gordon et al., *Anal. Chem.*, **28**, 1476 (1956).
2) T. Taketatsu, This Bulletin, **32**, 291 (1959).
3) T. Nishi et al., *III Atomic Energy Symposium (Abstr.), Japan*, 69 (1959). Japan Scientific Council, Tokyo.
4) T. Nozaki, *J. Chem. Soc. Japan, Pure Chem. Sec. (Nippon Kagaku Zasshi)*, **76**, 996 (1955).

* The alginate thread was supplied from Kamogawa Kako Co., Ltd., to whom the authors are indebted to appreciate.

5) Y. Ishibashi and S. Higashi, *Japan Analyst*, **4**, 14 (1955).
6) M. Malinek and L. Klir, *Chem. Abstr.*, **50**, 13659*a* (1956).

TABLE I. ANALYTICAL RESULT
(CALCULATED FROM FIG. 1)

	Taken (mg.)	Found (mg.)	Error (mg.)
Th(IV)	35.5	35.4	0.1
Ce(III)	30·0	30.3	0.3

It would be concluded that the new method with alginate as ion exchanger has an advantage as an industrial and an analytical method for the separation of thorium(IV) and cerium(III).

The authors are grateful for the Grant from the Ministry of Education.

Institute of Industrial Science
The University of Tokyo
Yayoi-cho, Chiba

Decomposition of Solid Ammonium Nitrate by γ-Ray

By Toshiaki SHIRAI
and Masaru NISHIKAWA

(Received May 8, 1959)

When irradiated with ultraviolet light or ionizing radiation, solid metal nitrates are reported to decompose, producing nitrite and oxygen[1]. However, no investigation has been reported on the decomposition of ammonium nitrate. Recently, the authors carried out the irradiation of ammonium nitrate by γ-ray from 1000 Curie ^{60}Co source at the Institute of Physical and Chemical Research. Decomposition products in gaseous phase were analyzed by a mass spectrometer of CEC 21-103A type and the effect of salt addition on the rate of decomposition was studied.

The irradiation of the salt was carried out in vacuo at a dose rate of 4.4×10^5 r/h, at 23°C. The irradiated sample was washed into a clean beaker with CO_2 free water and the resulting solution was titrated for ammonium ion by the method of Marcali and Rieman[2].

On dissolving the irradiated salt in water, copious effervescence occurred, similar phenomenon was reported for some metal nitrates[1b,c,d].

TABLE I. DECOMPOSITION OF AMMONIUM NITRATE BY γ-RAY

Total dose (10^7r)		4.2	7.1	10.5	15.6
W/W_0*		0.99	0.98	0.97	0.97
Total dose (10^7r)		4.1	6.9	11.1	
	Salt** added				
W/W_0*	$LiNO_3$	0.98	0.97	0.98	
	$NaNO_3$	0.98	0.98	0.97	
	KNO_3	0.98	0.97	0.96	

* W: Mass of ammonium nitrate present
W_0: Initial mass of ammonium nitrate
** Concentration, 5 mol. %

In some case, the solution was divided into two parts, one was titrated for the ammonium ion and the other for the nitrate ion with sodium hydroxide after conversion of ammonium nitrate into nitric acid by passing H-form cation exchanger. The amount of NO_3^- was exactly equivalent to that of NH_4^+ plus added metal ion. NO_2^- was not detected, with the method of Griess[3], in contrast to the case of metal nitrates. Table I shows that the decomposition is accelerated by the addition of metal ion. At this stage, however, no definite conclusion may be drawn in this connection, as decomposition was not carried far enough to show the effect clearly.

Following peaks were found in the mass spectrogram of decomposition products in gaseous phase; 14, 16, 17, 18, 28, 29, 30, 32, 44 and by *m/e*. Main peaks were 18, 28, 30 and 44 by *m/e* and they are assigned to be H_2O, N_2, NO, and N_2O, respectively. This feature is qualitatively the same as that obtained for the thermal decomposition of the salt[4]. The effervescence is ascribed to the gas captured in the solid. The quantitative analysis is now being done. This, together with a detailed discussion of the above results, will be reported elsewhere.

The authors wish to thank Dr. N. Matsuura for the valuable discussion and Mr. M. Takizawa in charge of operating the radiation source at the Institute of Physical and Chemical Research.

College of General Education
The University of Tokyo
Komaba, Meguro-ku, Tokyo

1) a. L. Narayanswamy, *Trans. Faraday Soc.*, **31**, 1411 (1935).
b. A. Allen and J. Ghormley, *J. Chem. Phys.*, **15**, 208 (1947).
c. G. Hennig, R. Lees and M. S. Matheson, ibid., **21**, 664 (1953).
d. J. Cunningham and H. G. Heal, *Trans. Faraday Soc.*, **54**, 1355 (1958).
e. C. J. Hochanadel and T. W. Davis, *J. Chem. Phys.*, **27**, 333 (1957).
f. D. Hall and G. N. Walton, *J. Inorg. Nucl. Chem.*, **6**, 288 (1958).
2) K. Marcali and W. Rieman, III, *Ind. Eng. Chem., Anal. Ed.*, **18**, 709 (1946).
3) P. Griess, *Ber.*, **12**, 427 (1879).
4) T. Shirai and M. Nishikawa, *Sci. Pap. Col. Gen. Ed., Univ. of Tokyo*, **9**, 17 (1959).

Cyclooctatetraene Iron Tricarbonyl

By Akira NAKAMURA and Nobue HAGIHARA

(Received May 8, 1959)

Recently Hallam and Pauson[1] investigated butadiene iron tricarbonyl and its derivatives and concluded that the conjugation of the double bonds was essential for the formation of such compounds. However, Pettit[2] reported the preparation of analogous compounds with non-conjugated bicyclo [2.2.1] heptadiene. He considered that a suitable spatial arrangement of the double bonds, not their conjugation was necessary for their effective overlap with the atomic orbitals of the metal which was an essential factor leading to the bond formation.

Since cyclooctatetraene(COT), in its tub form, seems to have such a suitable spatial arrangement of the double bonds, we have tried to prepare cyclooctatetraene iron tricarbonyl, $(C_8H_8)Fe(CO)_3$ (I), and its successful preparation is reported here*.

After irradiation of an equimolar mixture of COT and iron pentacarbonyl with sunlight for 8 hr. and subsequent removal of the unreacted starting materials under reduced pressure, dark red crystals were obtained in 10% yield. These crystals were purified by sublimation under reduced pressure (5 mmHg) at 80°C or by recrystallization from light petroleum.

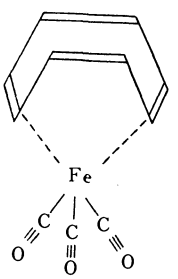
Anal. Found: C, 54.31; H, 3.35; mol. wt. (Rast), 243. Calcd. for $C_{11}H_8FeO_3$: C, 54.14; H, 3.31%; mol. wt., 244.

The combustion analysis apparently conformed to the composition, $(CO)_3Fe.(C_8H_8)$ (I). The purified compound I was beautiful dark red needles, melting at 94°C without decomposition and was stable in air and readily soluble in most organic solvents including pyridine and glacial acetic acid. I dissolved in cold concentrated sulfuric acid and could be recovered unchanged on neutralization, but it decomposed when its solution in concentrated sulfuric acid was heated to 110°C. The solution of I in carbon tetrachloride reacted readily with bromine at room temperature to give ferric bromide and brominated products of COT. I could also be prepared by heating the both components under nitrogen at 120°C for 18 hr.

The infrared spectrum of I (in KBr disk) showed bands at 1961 and 2050 cm^{-1} and at 699, 716 and 720 cm^{-1}. The former group of bands is similar to those of butadiene iron tricarbonyl and the latter group of bands indicates the presence of *cis*-type double bonds.

In the visible region of the spectrum no distinct absorption maxima were observed. In the ultraviolet region it showed a weak absorption maximum at 300 mμ ($\log \varepsilon$: 3.99 in 95% alcohol) similar to that of COT. On treatment with aqueous potassium iodide-iodine solution at 50°C, the solution of I in benzene evolved 3 mol. of carbon monoxide indicating the presence of three $-C\equiv O$ groups in one molecule of I. For further proof of the structure of I, I was decomposed by iodine in toluene. COT was detected in the decomposition products by its reaction with mercuric sulfate to give phenyl acetaldehyde. COT formed was further identified and determined by gas chromatography (the yield of COT was 76%).

From the above results it may be concluded that COT is π-bonded to iron without change in its skeletal structure. It is a well established fact that the molecule of COT is not planar. Therefore, it may be reasonable to assume that COT molecule in I would not be planar, too; and the following structure of I is proposed:



(I)

Fig. 1

When iron pentacarbonyl was used in excess in the photosynthesis of I, yellow crystals were obtained in addtion to I in 3% yield from COT. These crystals were purified by fractional sublimation at 120°C (5 mmHg) followed by recrystallization

1) B. F. Hallam and P. L. Pauson, *J. Chem. Soc.*, **1958**, 642.

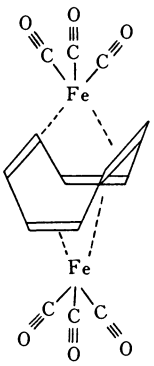
2) R. Pettit, *J. Am. Chem. Soc.*, **81**, 1266 (1959).

* After completion of our work, it has become known to us that T. A. Manuel and F. G. A Stone, (*Proc. Chem. Soc.*, **1959**, 90), also reported the preparation of cyclooctatetraene iron tricarbonyl and the related compounds. They suggested a planar structure to COT which was attached to the iron atom of cyclooctatetraene iron tricarbonyl. In their report, however, no practical description of the preparation of these compounds are given.

from benzene to give orange-yellow needles which decomposed at 185°C.

Anal. Found: C, 43.72; H, 2.35. Calcd. for $C_{14}H_8FeO_6$: C, 43.80; H, 2.11%.

The combustion analysis conformed to the composition, $(CO)_3Fe(C_8H_8)Fe(CO)_3$ (II). This compound II was slightly soluble in light petroleum and methanol, soluble in pyridine, glacial acetic acid and benzene, insoluble in hydrochloric acid and aqueous sodium hydroxide solution. It decomposed in concentrated sulfuric acid at room temperature.



(II)

Fig. 2

The infrared spectrum of II (in KBr disk) showed bands at 1972 and 2035 cm^{-1} for CO stretching region. The characterictic bands indicating the presence of *cis*-type double bonds which were shown in the infrared spectrum of I did not appeared and the whole spectrum was relatively simple compared with that of I, suggesting the higher symmetry of the molecule of II. The ultraviolet absorption spectrum of II had a shoulder at 258 mμ ($\log \varepsilon$: 3.15, in 95% ethanol) and no distinct absorption bands appeared in the visible region. Compared with the absorption band of I the shift of the band toward shorter wavelength and the decrease in intensity are apparent. These spectral changes in the ultraviolet region may be considered to indicate the immobility of the π-electrons of COT in II. From the above results the structure shown in Fig. 2 is proposed.

The Institute of Scientific and Industrial Research
Osaka University
Sakai, Osaka

On the Preparation of Isotopically Pure Light Hydrogen

By Koshiro Miyahara and Takao Kwan

(Received June 8, 1959)

Natural abundance of heavy hydrogen isotope in the water is known to vary depending on the geochemical circumstances in which the water is found[1]. The standardization of the value of D-content in the water or the preparation of isotopically pure light hydrogen was thus needed and became the object of careful investigation particularly by Titani and his co-workers[2,3]. Electrolysis of water is known to produce hydrogen of less D-content. Combustion of the hydrogen followed by re-electrolysis leads to much less concentration in the heavy component. Repeating such procedure, these authors were able to obtain 125 g. light water, the atomic D% of which being $0.0002\pm20\%$, i.e., about one-hundredth of natural abundance.

Current investigation on the chromatography, on the other hand, showed that this technique is powerful for the separation of hydrogen isotopes. Glueckauf and Kitt[4] were able to isolate pure deuterium (99.5%) by a displacement technique using palladium as column packing. The work[5] of this laboratory proved that hydrogen isotopes are separated in the elution chromatogram when synthetic zeolite (Linde molecular sieve) is used as column packing and kept at $-195°C$.

Deuterium was found to adsorb strongly compared with ordinary hydrogen on this packing. As a result, self-displacement of a mixture of hydrogen isotopes through such a cooled column yielded pure hydrogen in the frontal band and then HD and D_2 in the succeeding band[5]. The detection of hydrogen isotopes were made in this case by the thermal conductivity gauge equipped in Shimadzu Gas Chromatograph GC 1A.

---

1) M. Harada and T. Titani, This Bulletin, **10**, 206, 263 (1935); G. R. Clarke, *Nature*, **174**, 469 (1954).
2) T. Titani, S. Horibe and M. Kobayakawa, *Mass Spectroscopy*, **9**, 32 (1957).
3) T. Titani, S. Horibe, T. Komori and M. Kobayakawa, ibid., **9**, 40 (1957).
4) E. Glueckauf and G. P. Kitt, "Vapour Phase Chromatography", Butterworths Scientific Publications, London, (1957), p. 422.
5) S. Ohkoshi, Y. Fujita and T. Kwan, This Bulletin, **31**, 771 (1958).

It is obvious that the latter technique is promising to obtain isotopically pure light hydrogen. An attempt was made therefore to investigate the isolation of light component from ordinary hydrogen by means of such chromatographic technique. A spiral Pyrex column 400 cm. long and 0.5 diameter was filled with molecular sieve 5A and degassed overnight at 300°C by mercury diffusion pump. Two liters hydrogen sample from commercial electrolytic hydrogen* was introduced into the one side of the column immersed in liquid nitrogen. About ten minutes later hydrogen was found to appear on the other side of the column. The initial portion of the hydrogen (100~200 cc. N. T. P.) was then collected in a flask (sample I). The remaining hydrogen, together with those adsorbed on the packing, were collected back to the original flask (sample II). The deuterium content of the two samples were analyzed by Hitachi Mass Spectrometer RMD-3. The result is shown in Table I.

TABLE I

Run	Hydrogen sample	Volume cc. N.T.P.	Atomic D%	Error
1	I	100	0.0000	±0.0005
	II	1900	0.0068	
2	I	200	0.0004	±0.0005
	II	1800	0.0068	

As shown in this table, the sample I was found almost perfectly free from heavy component within the accuracy of the mass spectrometer. Thus, it is quite evident that the chromatographic process is simple and efficient to prepare isotopically pure light hydrogen. At the same time, the process is of practical importance to enrich deuterium or tritium at least in laboratory scale[5].

Research Institute for Catalysis
Hokkaido University, Sapporo

* Supplied by Hokkaido Soda Co., Horobetu.

Photosensitized Oxidation of Isopropylalcohol in the Presence of Zinc Oxide

By Isao Komuro, Yuzaburo Fujita and Takao Kwan

(Received June 8, 1959)

As reported previously[1], two of us (Y.F. and T.K.) found that photodesorption of oxygen takes place on reduced zinc oxide whereas it turns to irreversible sorption on oxidized sample. This opposite fashion of the photoresponse in the adsorption of oxygen stimulated us to investigate how these phenomena should be associated with the photosensitized oxidation reaction[2] known to occur on zinc oxide. Experiments were made, therefore, along with this interest.

The oxidation of isopropylalcohol by oxygen in liquid phase was chosen for the purpose. Commercial zinc oxide powder (guaranteed reagent) supplied by Kanto Kagaku was outgassed at 480°C for one hour in vacuo. On cooling it was poured into isopropylalcohol. This zinc oxide sample is called here as reduced zinc oxide. On the other hand, the commercial zinc oxide was used without any special pretreatment. The sample is supposed to be in oxidized state, since the d.c. electrical resistance measurement has shown that it possesses a resistance value as large as that of oxidized zinc oxide or is much larger than that of reduced zinc oxide.

A 50 ml. dried isopropylalcohol containing 2 g. reduced or oxidized zinc oxide was put into a round Pyrex flask having three openings, two of which being for thermometer and mercury manometer respectively and the remaining being connected to a reflux condenser and then to a gas burette.

Oxygen was introduced from the gas burette into the flask immersed in 65°C thermostat. The oxidation reaction was allowed to proceed with stirring reactant phase operated by magnetic rod placed in the flask. The apparatus was isolated when working. The rate of oxidation was followed by recording the decrease in the gas volume of the burette at a constant

1) Y. Fujita and T. Kwan, This Bulletin, **31**, 380 (1958).
2) For example, see M.C. Markham and K. J. Laidler, *J. Phys. Chem.*, **57**, 363 (1953).

pressure. The partial pressure of oxygen inside the flask was estimated to be 440 mmHg during the reaction.

Irradiation of light was made by Matuda Mercury Lamp SHL 100 UV without filter of any kind but through the window of the thermostat. The reaction product was pipetted and subjected to gas chromatographic and chemical analyses after the measurement of the oxidation rate. The temperature of the oxidation reaction was determined by the thermometer immersed directly in the liquid phase of the reacting system. Illumination caused the temperature of the system to rise less than 2°C.

It was confirmed that without illumination little consumption of oxygen occurs on reduced zinc oxide kept at 65°C. Illumination, however, brought forth distinct consumption of oxygen. On intercepting the light, the consumption occurring steadily was found to cease apparently. Reillumination caused consumption of oxygen again to proceed, so that the photocatalytic oxidation of isopropylalcohol was almost reversible with respect to on or off of the light switch.

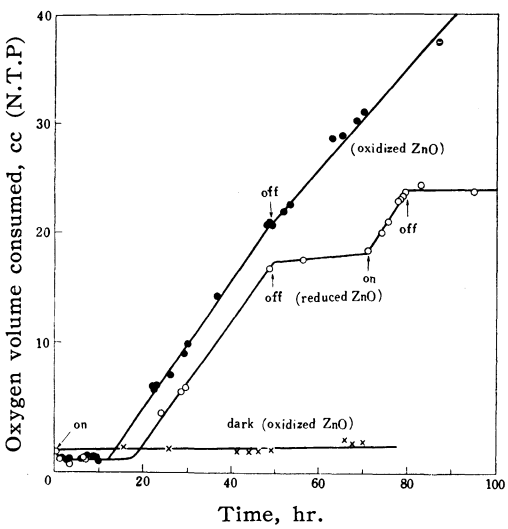


Fig. 1. Oxidation of isopropylalcohol by oxygen on zinc oxide with or without illumination.
T: 65~67°C. P_{O_2}: 440 mmHg.

Now, in the case of oxidized zinc oxide, the photosensitized oxidation reaction took place quite similarly as the case on reduced zinc oxide, while the reaction did not proceed without illumination beyond the period of 70 hr. However, strikingly different behavior was that interception of light still perimits the oxidation reaction to proceed with a speed almost equal to that of illumination. All the rate data for the oxidation of isopropylalcohol are shown in Fig. 1. Gas chromatographic and chemical analyses indicated that the product contains nothing other than acetone and hydrogen peroxide. The oxidation reaction may hence be expressed by

$$CH_3\text{-}\underset{\displaystyle OH}{\underset{|}{CH}}\text{-}CH_3 + O_2 = CH_3\text{-}CO\text{-}CH_3 + H_2O_2$$

As shown previously[1], adsorbed oxygen due to illumination was unable to desorb from the surface of oxidized zinc oxide on intercepting light whereas photodesorption was almost reversible on the surface of reduced zinc oxide. If it is accepted that the photoresponse of this kind should hold even during the oxdation reaction of isopropylalcohol, the different photocatalytic behavior shown above respectively on reduced and oxidized zinc oxide is to be anticipated. Because the catalyzing surface of reduced zinc oxide varies, when oxygen is present, depending on whether the light is switched on or off whereas the surface of oxidized zinc oxide, once experienced illumination, may maintain its state even during the light is intercepted.

On the other hand, almost identical photocatalytic activity shown by the two zinc oxide samples during the initial stage, including the induction period, and later is unexpected and rather embarrassing. Further work is in progress.

Research Institute for Catalysis
Hokkaido University, Sapporo

*Syntheses of Kinetin-analogues. II**

By F. Shigeo Okumura, Yachio Kotani, Tomoyuki Ariga, Mitsuo Masumura and Susumu Kuraishi**

(Received June 8, 1959)

In the previous paper[1] the authors reported the relation between the chemical

* Presented at the 25th Anniversary Meeting of the Botanical Society of Japan, held at Tokyo in October, 1957.

** Biological Institute, College of General Education, The University of Tokyo, Meguro-ku, Tokyo.

1) F. S. Okumura et al., This Bulletin, **30**, 194 (1957).

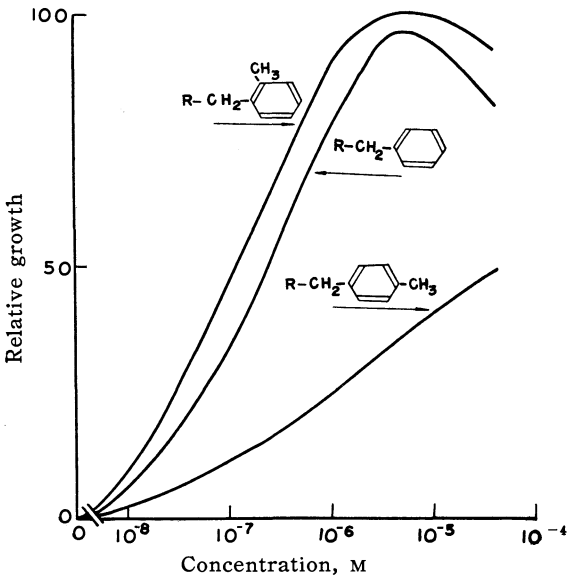


Fig. 1.
R=Aminopurine

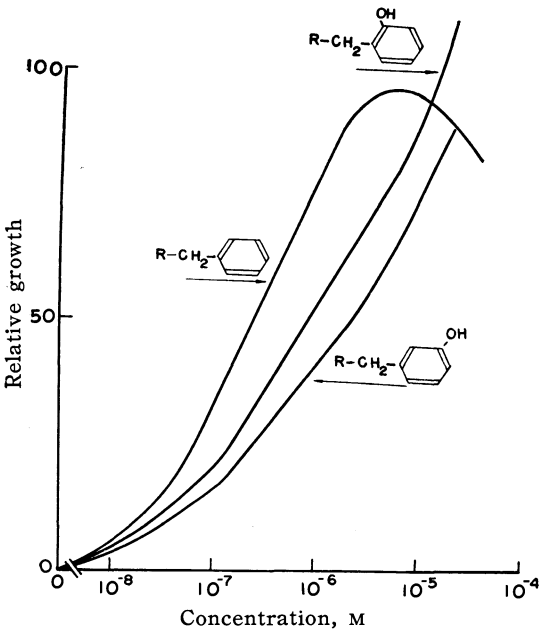


Fig. 2.
R=Aminopurine

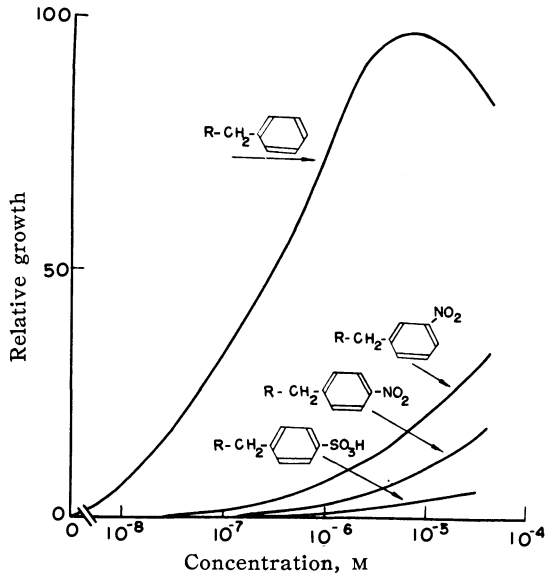


Fig. 3.
R=Aminopurine

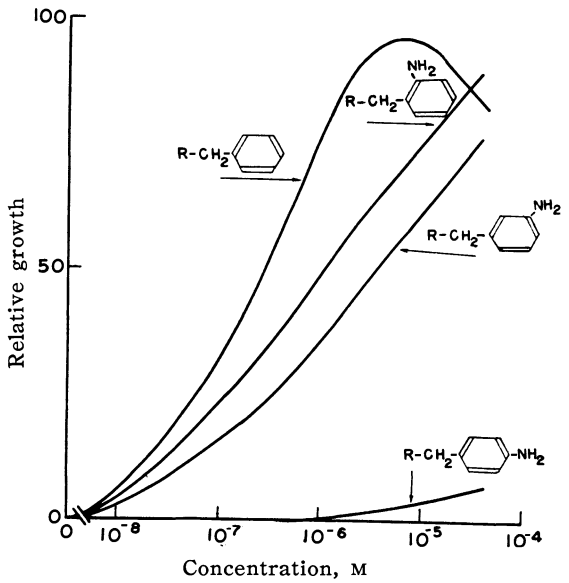


Fig. 4.
R=Aminopurine

structure and the physiological activity of kinetin-analogues by using the leaf test method[2] (*Raphanus sativus L. var. acanthiformis* Makino). It was shown[1] that the kinetin-analogues which have a benzene ring instead of a furan ring have almost the same activity as kinetin on leaf growth.

Seventeen kinetin analogues with various substituents in the benzene ring of 6-(benzylamino)-purine have been synthesized in order to investigate the effect of substituents on leaf growth. Positive and negative substituents, such as methyl, hydroxyl, methoxyl, amino, nitro and sulfonic acid groups were introduced into the ortho, meta or para position of the

2) S. Kuraishi and F. S. Okumura, *Bot. Mag., Tokyo*, **69**, 300 (1956).
3) M. W. Bullock, J. J. Hand and E. L. R. Stockstad, *J. Am. Chem. Soc.*, **78**, 3693 (1956).

TABLE I. SYNTHESES OF SUBSTITUTED 6-(BENZYLAMINO)-PURINES

Substituent	Temp. (°C) and time (hr.) of run	Yield (%)	m.p. (°C)	Analysis N% Found	Calcd.
o-Methyl	130~140[a] 11	67.5	242[b],[e]	29.52	29.27
p-Methyl	130~140[a] 13	65.0	264[c],[e]	29.19	29.27
o-Amino	130~140 5	25.4	279~280[e]	34.81	34.98
m-Amino	120~130 4	49.3	243~244[e]	35.13	34.98
p-Amino	120~130 5	25.2	239~240[e]	35.19	34.98
m-Nitro	130~140 5	34.0	272[e]	31.06	31.15
p-Nitro	90 4	10.3	220~226[d],[e]	29.86	31.15
o-Hydroxy	135 4	23.2	264[h]	29.93	29.04
m-Hydroxy	140~150[a] 18	22.8	284~286[e]	29.20	29.04
m-Methoxy	130~135[a] 13	30.4	248~249[f]	27.46	27.44
o-Chloro	125~130[a] 11	60.8	227~228[e]	27.01	26.97
m-Chloro	130[a] 15	59.0	241~242[e]	26.92	26.97
p-Chloro	120[a] 17	70.5	280~280.5[e]	27.16	26.97
p-Sulfo	160~170 20	12.0	238~242[d],[g]	24.14	22.94

a) in a sealed tube b) 243~244°C[3] c) 263°C[3] d) This compound is still impure.
e) Ethanol f) Methanol g) Water h) Dimethylformamide

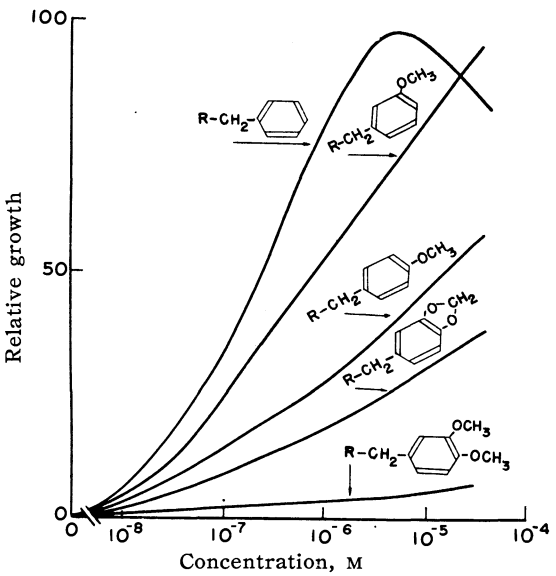


Fig. 5.
R=Aminopurine

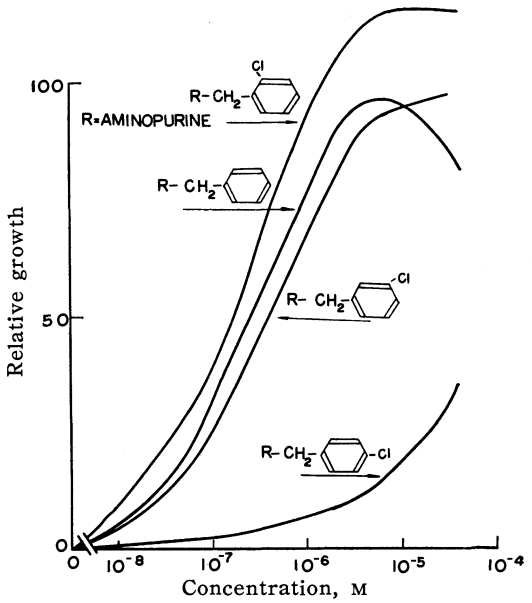


Fig. 6.
R=Aminopurine

benzene ring. In these seventeen analogues, fourteen are new compounds and three have already been reported[1].

The results are shown in Figs. 1, 2, 3, 4, 5 and 6. It is of interest that the ortho substituted isomers are the most active on leaf growth and the activity decreases in the order of the meta and the para isomers. Furthermore, it is noteworthy that the activity of some ortho isomers in higher concentration is stronger than that of 6-(benzylamino)-purine in its optimum concentration, e.g., *o*-methylbenzylaminopurine (Fig. 1), *o*-hydroxybenzylaminopurine (Fig. 2) and *o*-chlorobenzylaminopurine (Fig. 6) and that the kinetin activity is decreased by both meta and para substitution. It is clear from the above facts that the kinetin activity is favored by the ortho-substitution but disfavored by the meta- or para-substitution.

Experimental.—The syntheses of substituted 6-(benzylamino)-purines were achieved by condensing 6-(methylmercapto)purine with various amines. In general, 6-(methylmercapto)-purine was heated with 2 to 3 molecular equivalents of an amine with or without a solvent in a sealed or open tube at the given temperature and for the period given in Table I.

6-(*o*-Chlorobenzylamino) purine.—A mixture of 0.3 g. of 6-(methylmercapto)-purine (3.5 mol.) and 0.87 g. of *o*-chlorobenzylamine (1 mol.) was heated for eleven hours under reflux at 125~130°C. After cooling, the reaction product was precipitated by the addition of acetone, collected, washed with acetone, and then recrystallized from ethanol to give the product, m.p. 227~228°C, in a yield of 60.8%.

Department of Applied Chemistry
Faculty of Engineering
Tokushima University
Tokushima

*Syntheses of Kinetin-analogues. III**

By F. Shigeo Okumura, Noboru Enishi, Hiroyuki Itoh, Mitsuo Masumura and Susumu Kuraishi**

(Received June 8, 1959)

In the first paper of this series[1], the authors showed that 6-(*n*-hexylamino)-purine has almost the same activity on the growth of *Raphanus* leaf as kinetin, and the furan ring of kinetin can be replaced by an alkyl group without causing a remarkable decrease in the kinetin activity. It is very interesting to investigate the relation between the carbon

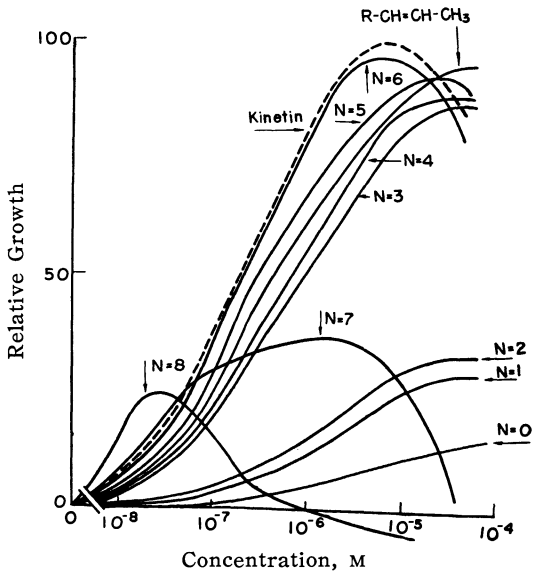


Fig. 1.
R · C_NH_{2N+1}
N=0—8
R=Aminopurine

Table I. Syntheses of 6-(Alkylamino)-purines

Alkyl	Temp. (°C) and time (hr.)	of run	Yield (%)	m.p.	Analysis N% Found	Calcd.
Methyl	130~140	14[a]	74.0	308[b],[j]	46.96	47.00
Ethyl	130~135	17[a]	42.0	234~235[c],[j]	42.76	42.92
n-Propyl	130~140	20[a]	39.5	234[j]	38.59	39.52
Allyl	130~140	10	48.7	221~222[g]	39.60	39.96
n-Butyl	130	20[a]	36.0	228~229[d],[h]	36.58	36.63
n-Amyl	100	15	37.0	164~165[k]	34.21	34.12
n-Hexyl	130~135	9	31.0	177~178[h]	32.81	31.94
n-Heptyl	130~140	14	54.2	175~176[g]	30.00	30.02
n-Octyl	140~145	15[a]	53.0	168~170[j]	28.13	28.34
n-Nonyl	125~135	12	30.1	165~166[h]	26.12	26.79
Geranyl	100~115	8	21.0	146~148[i]	25.90	25.82
n-Dodecyl	150~160	16[a]	50.4	154~156[g]	23.68	23.08
n-Octadecyl	160~165	18[a]	51.0	153~154[g]	18.82	18.12
Dimethyl	130~135	17[a]	45.0	263~264[e],[j]	43.08	42.92
Diethyl	110	8[a]	51.4	217~219[f],[h]	36.70	36.65
Dibutyl	115~125	8[a]	24.8	124~125[h]	28.60	28.32

a) in a sealed tube b) m. p. 312~314°C[2] c) m. p. 238~239°C[2] d) m. p. 233~234°C[2] e) m. p. 251°C[2] f) m.p. 186°C[2] g) Ethanol h) Aq. ethanol i) Aq. methanol j) Water k) Benzene

* Presented at the 25th Anniversary Meeting of the Botanical Society of Japan, held in October, 1957.

** Biological Institute, College of General Education, The University of Tokyo, Meguro-ku, Tokyo.

1) F. S. Okumura et al., This Bulletin, **30**, 194 (1957).
2) G. B. Elison, E. Burgi and G. H. Hitching, *J. Am. Chem. Soc.*, **74**, 411 (1952).

number in the side chain of 6-(alkylamino)-purines and the leaf growth activity.

Sixteen 6-(alkylamino)-purines have been synthesized for this purpose, eleven of which are new compounds, and tested for their physiological activity on the growth of the leaf of *Raphanus sativus L. var. acanthiformis* Makino. The results are shown in Fig. 1.

The activity of the first three members with 0, 1 and 2 carbon atoms in the side chain is very weak, but a sudden increase of activity is observed in 6-(*n*-propylamino)-purine and then the activity gradually increases with the carbon number until the peak of activity is attained in 6-(*n*-hexylamino)-purine, and then the activity decreases rapidly in 6-(*n*-heptylamino)- and 6-(*n*-octylamino)-purines. No activity was observed with higher homologues with 9, 10, 12 and 18 carbon atoms in the side chain.

The activities of 6-(dialkylamino)-purines such as 6-(dimethylamino)-, 6-(diethylamino)- and 6-(dibutylamino)-purines were very weak.

Experimental.—6-(Alkylamino)-purines were prepared by the reaction of 6-(methylmercapto)-purine with aliphatic amines. In general, the 6-(methylmercapto)-purine was heated with an amine in a sealed or open tube without any solvent, but an aqueous solution was used in the case of the volatile amines. After cooling, the reaction product was either precipitated by the addition of acetone, or it was obtained as a residue after evaporation of the excess of the amine under reduced pressure. The product was then recrystallized from an appropriate solvent.

6-(*n*-Hexylamino)-purine. — A mixture of 1.00 g. (1 mol.) of 6-(methylmercapto)-purine and 1.8 g. of *n*-hexylamine (3 mol.) was heated in a sealed tube at 130~135°C for 9 hr. After cooling, the reaction mixture was evaporated to dryness and the residue was recrystallized from 60% ethanol (yield, 0.4 g. or 31.5%).

Department of Applied Chemistry
Faculty of Engineering
Tokushima University
Tokushima

The Rate of the Color Reaction of m-Dinitrobenzene with Sodium Hydroxide in Acetone

By Takehiro Abe

(Received July 6, 1959)

Investigations of kinetics of the color reactions producing Meisenheimer's intermediates[1] have been studied by Caldin, Long and Ainscough[2,3] on the coloration reactions between trinitrobenzenes and ethoxide ion, and also by Nagakura, Oosawa and Tsubomura[4] on the decoloration reaction of the color product between 2, 4-dinitroanisole and hydroxyl.

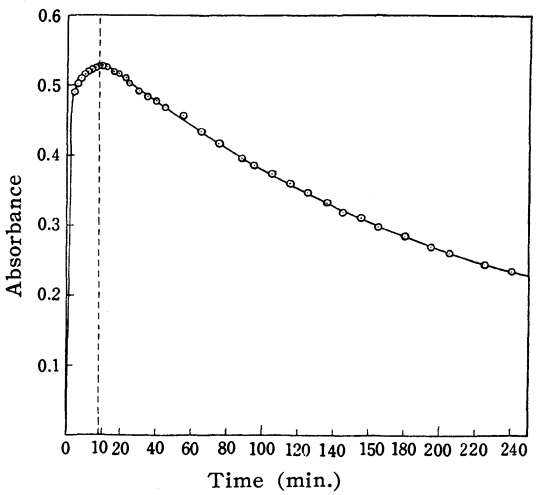
The author has succeeded in pursuing changes in absorbance of a visible absorption of a colored species through both coloration and decoloration reactions in a whole substitution reaction of *m*-dinitrobenzene with sodium hydroxide in acetone.

In the previous paper[5], the author has reported the visible absorption curve (530~600 mμ) of the colored solution produced by adding sodium hydroxide to *m*-dinitrobenzene in acetone. This color becomes more intense for several minutes and then fades slowly. The result in Fig. 1 was obtained by following the absorbance *d* of the 560 mμ absorption of the colored species at 25°C. The coloration and decoloration reactions are formulated provisionally as

$$m\text{-Dinitrobenzene} + \mathrm{NaOH} \xrightarrow{\text{Coloration}} [m\text{-Dinitrobenzene}\cdot\mathrm{OH}]^- \text{ Colored species (transition complex)} \xrightarrow{\text{Decoloration}} \text{A final product}$$

Although both the coloration and the decoloration are actually concurrent, we assume that only coloration reaction proceeds till nine minutes, at which time the maximum absorbance is obtained, and that only the decoloration occurs from that time,

1) J. Meisenheimer, *Ann.*, **323**, 214, 241 (1902).
2) E. F. Caldin and G. Long, *Proc. Roy. Soc.*, **A228**, 263 (1955).
3) J. B. Ainscough and E. F. Caldin, *J. Chem. Soc.*, **1956**, 2528.
4) S. Nagakura, S. Oosawa and H. Tsubomura, Presented at the Symposium on Electron States of Molecules at Kyoto in October, 1958.
5) T. Abe, This Bulletin, **32**, 775 (1959).
6) T. Abe, to be published in ibid., **32**, No. 9 (1959).



Flg. 1. Change in the absorbance of the 560 mμ absorption for the colored solution of *m*-dinitrobenzene (2.33×10^{-5} M) and sodium hydroxide (3.49×10^{-3} N) in acetone, at 25°C (path length of absorption cells, 1 cm.).

since the rate of the coloration reaction is much greater than that of the decoloration, as can be known from Fig. 1. Moreover, on an assumption that *m*-dinitrobenzene completely changes into the colored species just after nine minutes, a value of 2.27×10^{4} can be obtained as a molar extinction coefficient ε of the 560 mμ absorption of the colored species. This value is of the same order, as compared with the molar extinction coefficients of the red complexes of trinitrobenzene and its derivatives with ammonium hydroxide[6]. From this it is, therefore, known that the above assumptions are very good. Under a condition that the concentration of sodium hydroxide is sufficiently larger than that of the colored species produced, the rate constant k_C of the coloration reaction of the second can be derived as follows:

$$k_C=\frac{1}{0.4343(C_{DNB}-C_{OH})(t-t_{0C})}\log\frac{C_{DNB}-d/\varepsilon}{C_{DNB}-d_{0C}/\varepsilon} \quad (1)$$

where C_{DNB} is the initial concentration of *m*-dinitrobenzene, C_{OH}, the initial concentration of sodium hydroxide, d, the absorbance of the colored species after t minutes, and d_{0C}, the value of d after arbitrary t_{0C} minutes. On the other hand, the following empirical formula of the first order satisfactorily represents the observed rate constants, as in the case of the decoloration of 2,4-dinitroanisole[4].

$$k_d=\frac{1}{0.4343(t-t_{0d})}\log\frac{d}{d_{0d}} \quad (2)$$

Here d_{0d} is the value of d after t_{0d}. By taking $t_{0C}=2$ and $t_{0d}=12$ in Eqs. 1 and 2, the values of k_C and k_d at 25°C are calculated respectively, as indicated in Table I.

TABLE I

t(min.)	k_C(mol^{-1}·sec^{-1})	t(min.)	k_d(sec^{-1})$\times10^3$
3	101	25	3.35
4	109	30	3.71
5	99.8	35	3.61
6	104	40	3.37
7	99.7	45	3.47
8	103	55	3.26
	mean 103	65	3.54
t	$k_d\times10^3$	t	$k_d\times10^3$
75	3.64	155	3.64
88	3.71	165	3.68
95	3.64	180	3.64
105	3.68	195	3.64
115	3.64	205	3.61
125	3.61	225	3.57
136	3.64	240	3.54
145	3.75		mean 3.57

The means of k_C and k_d are 103 mol^{-1}·sec^{-1} and 3.57×10^{-3} sec^{-1}, respectively. In the decoloration reaction sodium hydroxide may probably interact with the colored species, because the higher the concentration of alkalies contained, the faster disappear the colors of the complexes of polynitrobenzenes with alkalies[4,6].

It is in progress to investigate the effect of the concentration of sodium hydroxide of the rate of the decoloration reaction, and to obtain energies of activation for the coloration and docoloration.

The author is particularly indebted to Professor Y. Nomura for his suggestion and helpful discussions.

Department of Chemistry
Defense Academy
Yokosuka

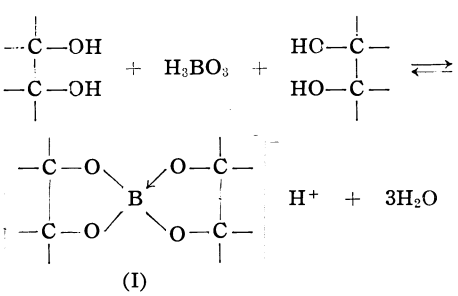
Organic Spot Tests. II. Detection of 1,2-Dihydroxy Compounds (Differentiation of Polyhydroxy Compounds)

By Yujiro NOMURA

(Received July 7, 1959)

The micro detection of acid substances by the color reaction with the mixed solution of sodium sulfanilate, sodium nitrite and α-naphthylamine in aqueous alcohol or dioxan[1] has been developed to a new method of detection of 1,2-dihydroxy compounds.

Boric acid is so weak that the orange to orange red color begins to appear only in 10~15 min. after adding it to the reagent. It has long been known that addition of polyhydroxy compounds, e.g., glycerol, sorbitol and mannitol, to boric acid raises the acidity[2] and thus this weak acid can be titrimetrically determined[3]. This is due to the co-ordinate complex ester (I)[4] of boric acid with 1,2-dihydroxy compounds as follows:



(I)

It has been found that boric acid behaves as a strong acid in the presence of a 1,2-dihydroxy compound also in the above-mentioned reaction to give immediately an intense coloration and that boric acid reciprocally makes it possible to detect 1,2-dihydroxy compounds by the same color reaction. Thus, ethylene glycol, propylene glycol, glycerol and other various polyhydroxy compounds with adjacent hydroxyl groups gave positive reactions with the reagent in the presence of boric acid but trimethylene glycol was indifferent. Catechol also gave a positive reaction, while resorcinol and hydroquinone gave no reaction.

peri-Dihydroxy derivatives of naphthalene behave similarly in this new color reaction. Namely, disodium chromotropate (1,8-dihydroxynaphthalene-3,6-disulfonate) gave the same coloration when the above method was applied.

In the case of a polyhydroxybenzoic acid, its small quantity is evaporated to dryness with one drop of ammonia water in a microcrucible on a water bath and then it may be tested. In this way, 2,3-dihydroxybenzoic acid and gallic acid gave an intense red color, but 2,4-, 2,6- and 3,5-dihydroxybenzoic acids did not.

Accordingly the reaction described above gives a new method of detecting the presence of two hydroxyl groups in 1,2-positions.

General Procedure of the Test.—Several drops of the reagent solution are placed in a depression of a spot plate. A small amount of boric acid is added to it and stirred with a glass rod. One drop of the test solution or a pinch of the solid sample is added to it. An immediate orange red color indicates the presence of a compound with two or more adjacent hydroxyl groups. A blank test without addition of the sample, is recommended if only a small amount of a 1,2-dihydroxy compound is suspected. An acid substance which gives a positive reaction with the reagent solution alone (without the addition of boric acid) must be treated with ammonia water as in the case of the polyhydroxybenzoic acids before the present method is applied.

Department of Chemistry
College of General Education
The University of Tokyo
Meguro-ku, Tokyo

1) Y. Nomura, This Bulletin, 32, 536 (1959).
2) L. Vignon, *Compt. rend.*, **78**, 148 (1874); G. Bouchardat, ibid., **80**, 120 (1875); D. Klein, ibid., **86**, 526 (1878); **99**, 144 (1884).
3) W. Horsch, *Anal. Abstr.*, 2531 (1957).
4) Cf. J. Böeseken, "Advances in Carbohydrate Chemistry", Vol. 4, Academic Press, Inc., New York (1949), p. 193—210.

Measurement of Infrared Dichroism for the Crystal of Lauric Acid in the CsBr Region

By Takehiko SHIMANOUCHI and Michio KAWANO

(Received July 9, 1959)

For the measurement of infrared dichroism the silver chloride transmission polarizer is ordinarily used. However, in the region below 20 μ its performance is not satisfactory owing to its poor transmittance. For the purpose of measuring dichroism for saturated long chain monocarboxylic acids in the range from 600 to 350 cm^{-1} we tested a transmitting polarizer in which six polyethylene films are used instead of silver chloride plates.

The result is very satisfactory and the spectra for lauric acid are shown in Fig. 1. This polarizer is also used in the NaCl region except those about the 2900, 1475, 1375 and 720 cm^{-1} absorptions of polyethylene. In Fig. 2 the dichroism for the oriented crystals of lauric acid in the region from 1300 to 900 cm^{-1} measured by the polyethylene polarizer is given. For the purpose of comparison the same dichroism measured by a Perkin-Elmer AgCl polarizer is shown in Fig. 3. The result indicates that the performance of the present polarizer is as satisfactory as that of the AgCl polarizer.

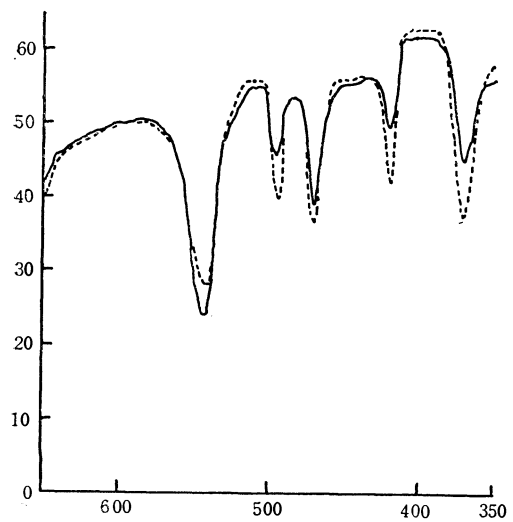


Fig. 1. The infrared dichroism of the oriented crystals of lauric acid (C form) in the CsBr region measured by a polyethylene polarizer.

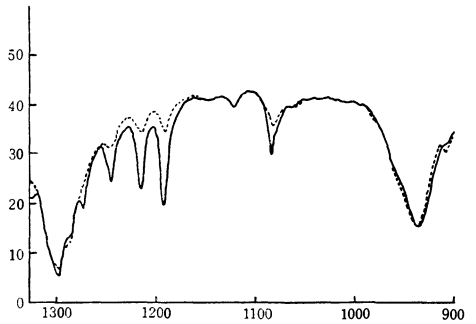


Fig. 2. The infrared dichroism of the oriented crystals of lauric acid (C form) in the NaCl region measured by a polyethylene polarizer.

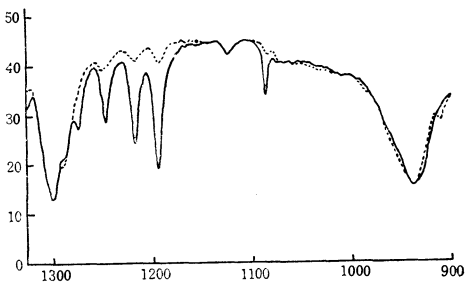


Fig. 3. The infrared dichroism of the oriented crystals of lauric acid (C form) in the NaCl region measured by an AgCl polarizer.

The thickness of the polyethylene film used was 0.02 mm. and an incline of approximately 60 degrees of the films gave the best perfomance. The measurement was made by a Perkin-Elmer Model 21 spectrometer equipped with NaCl or CsBr prism.

In Figs. 1, 2 and 3 the dotted and the full lines give the spectra for the incident light polarized along the *a*- and *b*-axes of the crystal, respectively. It is interesting to note that the four lines in the range from 350 to 500 cm^{-1} given in Fig. 1 have the opposite dichroism to that of the equally spaced progression of bands found in the region from 1180 to 1350 cm^{-1}. The interpretation of the result will be reported afterwards.

Chemical Laboratory, Faculty of Science
The University of Tokyo
Hongo Tokyo (T.S.)

The Railway Technical Research Institute
Minato-ku, Tokyo (M.K.)

Added in Proof:
Recently H. Yoshinaga, S. Fujita, Y. Yamada and A. Mitsuishi have made a polyethylene film polarizer and used this for the region measured by the far-infrared grating spectrometer (Symposium on Molecular Structure and Spectroscopy at Columbus, June, 1959).

Paramagnetic Resonance Absorption in Solutions of the Sodium Adducts of Isoprene

By Keiji Kuwata, Kazuo Morigaki and Kozo Hirota

(Received July 9, 1959)

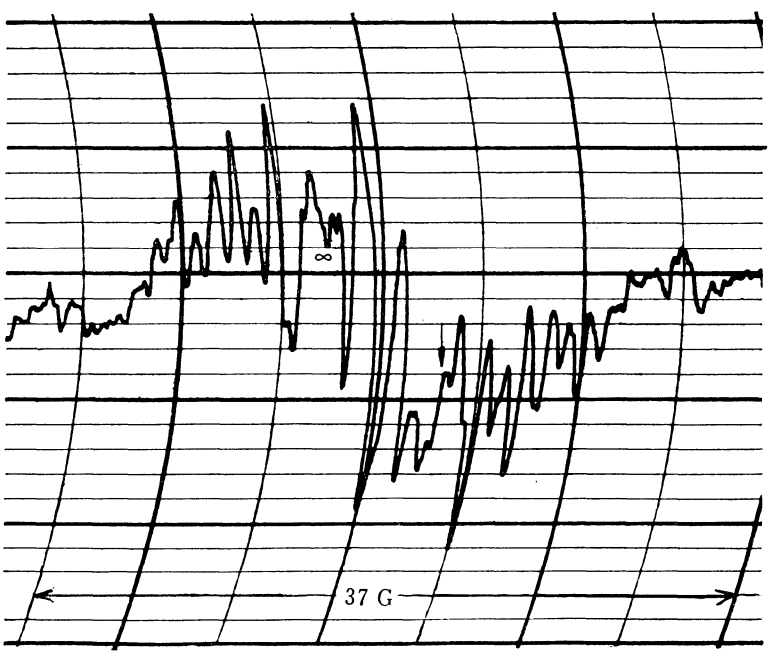
It has been found already by Weissman[1a] and others[2] that paramagnetic resonance absorption spectra are observed in the solutions of the sodium adducts of polynuclear aromatic hydrocarbons, e. g., naphthalene, phenanthrene, naphthacene, etc., and also of benzene derivatives[1b]. Recently, the list of such substances has been enlarged to another kinds of adducts by the present authors, i. e., the adducts of polymerizable vinyl monomers, such as styrene[3], α-methylstyrene[4], 1, 4-diphenylbutadiene[5].

However, since all the above hydrocarbons have one benzene ring at least, it will be interesting to investigate if the adducts of polymerizable vinyl monomers without aromatic rings have the same character. Using the method of preparation as described elsewhere[3], Na-adduct of isoprene was obtained as the solution of tetrahydrofuran. The sample colored brownish yellow, maximum absorption being near 375 mμ. Detailed discussion on the structure of the adduct will be published in a separate paper[6].

Measurement of paramagnetic resonance absorption on the sample gave an affirmative result for the object of the present research. A spectrum of the adduct of isoprene is shown in Fig. 1. Hyperfine structure of the spectra can be explained if a radical anion is assumed to exist, but detailed discussions will appear in future.

The writers express sincere thanks to Professor Junkichi Itoh of Osaka University who gave them much suggestion and convenience in the present research. A part of the expense for the research has been defrayed from a grant given by the Ministry of Education, to which the authors' thanks are due.

Faculty of Science, Osaka University
Nakanoshima, Osaka



Flg. 1. Derivative of paramagnetic resonance absorption of Na-adduct of isoprene. (g=2.0026)

1a) S. I. Weissman et al., *Science*, **117**, 534 (1953); *J. Phys. Chem.*, **57**, 504 (1953), etc. 1b) T. R. Tuttle, Jr. and S. I. Weissman, *J. Am. Chem. Soc.*, **80**, 5342 (1958).
2) A. Carrington, F. Dravnieks and M. C. R. Symons, *J. Chem. Soc.*, **1959**, 947.
3) K. Hirota, K. Kuwata and K. Morigaki, This Bulletin, **31**, 538 (1958); **32**, 99 (1959).
4) K. Morigaki, J. Itoh, K. Kuwata and K. Hirota, "*Sen-i-Kagaku Kenkyusho Hokoku*" (Osaka Univ.), **12**, in press (1959).
5) Unpublished results.
6) K. Kuwata, to be published in This Bulletin.

The Synthesis of dl-4(-3-Furyl)-1-methyl Quinolizidine; Demethyl Analogue of Deoxynupharidine

By Munio KOTAKE, Ichiro KAWASAKI, Tadashi OKAMOTO, Shiro KUSUMOTO and Takeo KANEKO

(Received June 30, 1959)

In 1956, structure (I) was assigned by Kotake, Kusumoto and Ohara[1] to deoxynupharidine; an alkaloid isolated from the roots of *Nuphar japonica* DC. A synthesis of *dl*-4(-3-furyl)-1-methyl quinolizidine is now reported which establishes the synthetic routes to the *dl*-deoxynupharidine*. The stages involved in the synthesis are as follows:

Compound II[2], b. p. 133°C/10^{-2} mmHg; III, (62%) b. p. 130°C/10^{-2} mmHg, I. R. bands at 1645 (amide), 1735 cm^{-1} (ester). *Anal.* Found: C, 64.78; H, 8.89; N, 5.80. Calcd. for $C_{13}H_{21}O_3N$: C, 65.24; H, 8.85; N, 5.85%; IV, (95%) m. p. 102~106°C. *Anal.* Found: C, 53.69; H, 9.13; N, 6.20. Calcd. for $C_{10}H_{19}O_2N$-HCl: C, 54.17; H, 9.09; N, 6.33%; V, (48%) b.p. 154°C/10^{-3} mmHg, I.R. bands at 875, 1505, 3110 (furan), 1573 (conjugated furan), 1625 (amide), 1735 cm^{-1} (ester). *Anal.* Found: C, 65.94; H, 8.24; N, 4.51. Calcd. for $C_{17}H_{25}O_4N$: C, 66.42; H, 8.20; N, 4.56%; VI[3], (56%) b. p. 81~84°C/10^{-3} mmHg, I. R. bands at 875, 1505, 3110 (furan), 1588 (conjugated furan), 1640 cm^{-1} (double bond); VII, (50%) b. p. 87~89°C/10^{-2} mmHg. Perchlorate, m. p. 193~194°C. *Anal.* Found: C, 52.56; H, 6.82; N, 4.34. Calcd. for $C_{14}H_{21}ON \cdot HClO_4$: C, 52.57; H, 6.93; N, 4.38%. Picrate, m. p. 172~174°C. *Anal.* Found: C, 53.30; H, 5.40; N, 12.79. Calcd. for $C_{20}H_{24}O_8N_4$: C, 53.57; H, 5.39; N, 12.50%.

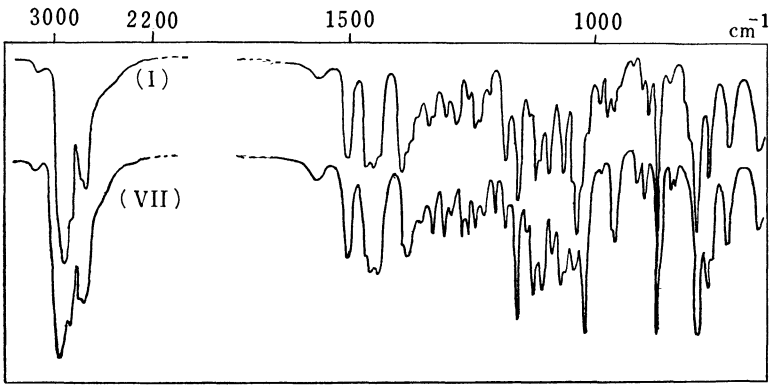


Fig. 1.

The I. R. spectra of compound VII are similar to that of the deoxynupharidine as indicated in Fig. 1.

The authors wish to express their thanks to Professor Takeo Sakan, Professor Takashi Kubota and Professor Yasuhide Yukawa for their encouragement throughout this work.

Department of Chemistry
Faculty of Science
Osaka University
Nakanoshima, Osaka

* The synthesis of *dl*-deoxynupharidine was reported elsewhere.

1) M. Kotake, S. Kusumoto and T. Ohara, *Ann.*, **606**, 148 (1957); This Bulletin, **29**, 157 (1957); *J. Chem. Soc. Japan, Pure Chem. Sec.* (*Nippon Kagaku Zasshi*), **77**, 1302 (1956); **78**, 488 (1957).

2) F. Bohlmann, N. Ottawa and R. Keller, *Ann.*, **587**, 162 (1954); E. E. v. Tamellen and J. S. Baran, *J. Am. Chem. Soc.*, **80**, 4659 (1958).

3) I. Murakoshi, *J. Pham. Soc. Japan* (*Yakugaku Zasshi*), **78**, 594 (1958).

Bond Localization and the Hyperconjugative Effect in the Aromatic Carbonium Ions. II[1]. *Electronic Structures of the Carbonium Ions of Isomeric Xylenes*

By Toshifumi MORITA

(Received October 2, 1958)

Concerning the basic character of unsaturated hydrocarbons, there are several theoretical investigations[2-7] which have their theoretical standpoints on the localization of the C-H_2 bond of their carbonium ions. There are no reasons, however, for fixing the electronic structure of carbonium ions to only the bond localization one; in general, hyperconjugation of H_2 quasi-atom should also be taken into account. In this paper, the need for introduction of hyperconjugation will be revealed for protonated compounds of isomeric xylenes on the basis of the experimental basicity constants[8].

Dependence of Basicity of Isomeric Hydrocarbons on the π-Electron Energies of their Carbonium Ions

Gold and Tye[2], and also Heilbronner and Simonetta[3] have shown that the equilibrium constant K for carbonium ion formation is expressed as

$$-\boldsymbol{R}T \ln K = E_{BH^+} - E_B + \text{constant} \qquad (1)$$

where E_{BH^+} and E_B are π-electron energies of the aromatic carbonium ion, BH^+, and of the parent base, B, respectively. From Eq. 1, the following equation for the ratio of two K's is obtained:

$$K^I/K^{II} = \exp(-A/\boldsymbol{R}T) \qquad (2)$$

where

$$A = (E^I_{BH^+} - E^{II}_{BH^+}) - (E^I_B - E^{II}_B) \qquad (3)$$

Here superscripts I and II refer to either of the two isomeric types of a particular hydrocarbon.

In the case of xylene isomers, $E^I_B - E^{II}_B$ will be estimated from the empirical hyperconjugation energies obtained by Coulson and Crawford[9]. They have indicated that the empirical hyperconjugation energies per methyl group are 1.48, 1.39 and 1.27 kcal./mol. for *m*-, *p*- and *o*-xylenes, respectively. This shows that *m*-xylene is more stable than *p*-xylene by 0.18 kcal./mol., and *o*-xylene is less stable than *p*-xylene by 0.24 kcal./mol.

Now, from the evaluation of π-electron energies of protonated compounds, the basic strengths of *m*- and *o*-xylenes relative to that of *p*-xylene will be estimated by the use of Eqs. 2 and 3.

Consideration of Basicity of Isomeric Xylenes from the Standpoint of Bond Localization Model of their Carbonium Ions

There are several available points of proton attack in each isomer, and the position of highest proton affininity will be determined as that which makes the π-electron energy of the carbonium ion minimum. Now it will be indicated in the following discussion that only by the bond localization hypothesis the basic behaviors of isomeric xylenes can not be understandable. π-Electron energies of carbonium ions necessary for these considerations are calculated for all possible models with respect to the positions of proton attack on the basis of the bond localization hypothesis, using the semi-empirical LCAO MO method and solving numerically the secular equations constructed by the usual variational method. Several assumptions adopted in these calculations are as follows:

(1) the overlaps between the nearest neighboring atomic orbitals are included; (2) the resonance integral including overlap is proportional to the corresponding

1) Part I, T. Morita, This Bulletin, **31**, 322 (1958).
2) V. Gold and F. L. Tye, *J. Chem. Soc.*, **1952**, 2184.
3) E. Heilbronner and M. Simonetta, *Helv. Chim. Acta*, **35**, 1049 (1952).
4) E. L. Mackor, G. Dallinga, J. H. Kruizinga and A. Hofstra, *Rec. trav. chim.*, **75**, 836 (1956).
5) G. Dallinga, A. A. V. Stuart, P. J. Smit and E. L. Mackor, *Z. Elektrochem.*, **61**, 1019 (1957).
6) E. L. Mackor, A. Hofstra and J. H. van der Waals, *Trans. Faraday Soc.*, **54**, 66 (1958).
7) E. L. Mackor, A. Hofstra and J. H. van der Waals, ibid., **54**, 186 (1958).
8) M. Kilpatrick and F. E. Luborsky, *J. Am. Chem. Soc.*, **75**, 577 (1953).
9) C. A. Coulson and V. A. Crawford, *J. Chem. Soc.*, **1953**, 2052.

overlap integral: $\beta_{C\text{-}H_2}=\beta_{C\text{-}H_3}=2.19\beta$ and $\beta_{C(ring)\text{-}C(methyl)}=0.8\beta$, where $\beta_{C\text{-}H_2}$ is the resonance integral between H_2 quasi-atom and the ring carbon atom connecting with it, $\beta_{C\text{-}H_3}$ is that between H_3 quasi-atom and carbon atom in the methyl group, $\beta_{C(ring)\text{-}C(methyl)}$ is that between the ring- and the methyl- carbon atoms, and β is that between the neighboring atoms in the benzene molecule; the other resonance integrals are taken to be β; (3) the Coulomb integral of H_2 or H_3 quasi-atom is taken as $\alpha_{H_2}=\alpha_{H_3}=\alpha-0.3\beta$, and that of the carbon atom next to H_2- or H_3-group is taken as $\alpha_{C(-H_2)}=\alpha_{C(-H_3)}=\alpha-0.1\beta$, where α is the Coulomb integral of a carbon atom of benzene molecule; the other Coulomb integrals are taken to be α.

Computational results are shown in Table I and in Fig. 1. Charge distributions of parent bases calculated by Crawford[10] are 1.0093, 1.0081 and 0.9995 at the positions 2, 4 and 5 in *m*-xylene (1,3-dimethylbenzene) and 1.0044 and 1.0035 at the positions 3 and 4 in *o*-xylene (1,2-dimethylbenzene), respectively. Inspection of these charge distributions predict the order of proton acceptance. Between this order of proton affinity and stabilities of protonated compounds (Table I), a parallel relation exists. This correlation agrees with experimental reactivity of electrophilic substitution except for the position 2 of *m*-xylene, which may be supposed to have low proton affinity because of the steric effect of two neighboring methyl groups, although it is theoretically the most active toward a proton. From their hydrogen isotope exchange reaction studies, Lauer et al.[11] have indicated that relative reactivity of the position 2 to 4 of *m*-xylene is 0.58 : 1.0. We must take such a fact into account. In *m*-xylene, numbers of position of proton attack will be 2.58 and the energy of its probable carbonium ion will be weighted mean of energies of Models I and I′. For *o*-xylene carbonium ion, the stabilities of Models III and III′ are identical, being in agreement with experimental reactivity, halogenation or nitration of *o*-xylene. We assume the energy of protonated *o*-xylene to be the mean of Models III and III′.

TABLE I. π-ELECTRON ENERGIES OF THE CARBONIUM IONS OF XYLENE ISOMERS (BOND LOCALIZATION MODELS)

Carbonium ions	Models	π-Electron energies (units of $-\beta$)
m-Xylene-	I	−11.4819
	I′	−11.5342
	I″	−11.4444
p-Xylene-	II	−11.4905
o-Xylene-	III	−11.4914
	III′	−11.4806

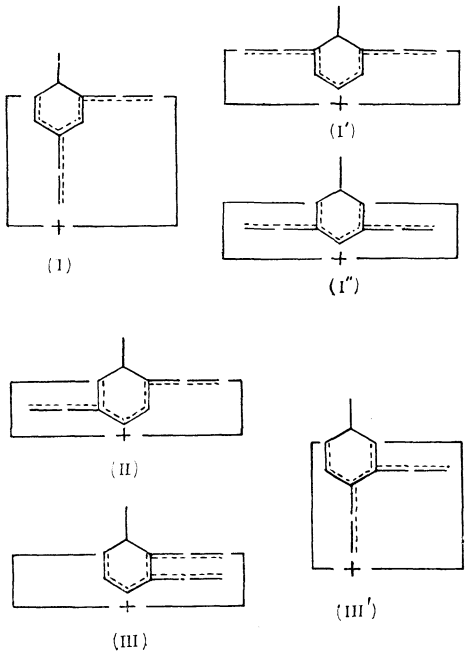


Fig. 1. Models of xylene carbonium ions.
I, I′ and I″: *m*-xylene carbonium ion
II : *p*-xylene carbonium ion
III, III′ : *o*-xylene carbonium ion

The ratio of basicity constants of *m*- and *o*-xylenes to that of *p*-xylene is estimated to be respectively 26 and 1.1 at 20°C from the measurement on the mixtures of these substances with anhydrous hydrogen fluoride[8]. In comparing these values experimentally observed with those theoretically calculated, it must be noticed that the number (Z) of positions of the highest proton affinity of *m*-, *o*- and *p*-xylenes are different from one another. For *m*-xylene, from our treatment mentioned above, $Z=2.58$. For *o*- and *p*-xylenes $Z=4$. Taking these Z values into consideration, the experimentally observed ratio of the reduced basicity constant[6] of *m*-xylene to that of *p*-xylene becomes 40.3 instead of 26, which is in disagreement with the theoretically calculated value, 1.0, using Eqs. 2 and 3. In the case of *o*-xylene, the experimental and theoretical values of K^{III}/K^{II} are 1.1 and 1.0, respectively, so the agreement between these two values

10) V. A. Crawford, ibid., **1953**, 2058.
11) W. M. Lauer, G. W. Matson and G. Stedman, *J. Am. Chem. Soc.*, **80**, 6437 (1958); see also, E. L. Mackor, P. J. Smit and J. H. van der Waals, *Trans. Faraday Soc.*, **53**, 1309 (1957).

is satisfactory[12]. Thus, basic behavior of isomeric xylenes is not understood by the bond localization hypothesis alone. It is natural to take hyperconjugation further into consideration, as is seen in the following section.

π-Electron Structures of Isomeric Xylene Carbonium Ions

In the following, as an example, the relative basicity of *m*-xylene compared to *p*-xylene will be discussed. From Eq. 3, A can be written as follows:

$$A=\{E^{I}_{BH^+}-(E^{I,0}_{BH^+}+0.18)\}-\{E^{II}_{BH^+}-E^{II,0}_{BH^+}\}-\{E^{I}_{B}-E^{II}_{B}\} \quad (4)$$

where, $E^{I}_{BH^+}$ is the π-electron energy for the actual state of the *m*-xylene carbonium ion, $E^{II}_{BH^+}$ is the similar quantity for the *p*-xylene carbonium ion; $E^{I,0}_{BH^+}$ and $E^{II,0}_{BH^+}$ are the π-electron energies for the bond localization models of protonated *m*- and *p*-xylenes, respectively; E^{I}_{B} and E^{II}_{B} are the π-electron energies of *m*- and *p*-xylenes, respectively; the numerical value 0.18 in the right hand side of Eq. 4 is necessary for making $(E^{I,0}_{BH^+}+0.18)=E^{II,0}_{BH^+}$. This value, which is expressed in the unit of kcal./mol. by the use of $\beta=-60$kcal./mol.[12], estimated by comparing the weighted mean of π-electron energies of types I and I′ for protonated *m*-xylene with the energy of type II for protonated *p*-xylene. Taking $E^{I}_{B}-E^{II}_{B}=0.18$ kcal./mol., Eq. 4 becomes as follows:

$$A=-x+c \quad (5)$$

where

$$-x=E^{I}_{BH^+}-E^{I,0}_{BH^+} \quad (6)$$

and

$$-c=E^{II}_{BH^+}-E^{II,0}_{BH^+} \quad (7)$$

The quantities x and c indicate respectively the stabilization energies through hyperconjugation of H_2 quasi-atom in the actual states of *m*- and *p*-xylene carbonium ions compared with their bond localization models. Experiments show $K^{I}/K^{II}=40.3$ [13] at 20°C, consequently from Eqs. 2, 3 and 5, we obtain

$$x=c+8.2 \quad (8)$$

Eq. 8 shows that, if the difference of hyperconjugation energies between protonated *m*- and *p*-xylenes is about eight kcal./mol., the experimentally observed basic behavior of *m*- and *p*-xylenes is understandable. A similar consideration suggests that no change in the hyperconjugation energies exists between *o*- and *p*-xylene carbonium ions. Indeed,

$$x=c+0.09$$

Here it will be noticed that the hyperconjugation energy of protonated *m*-xylene is the weighted mean of hyperconjugation energies by the methylene group for models I and I′, and that of protonated *o*-xylene is the weighted mean for the models III and III′. The value, 8.2 kcal./mol., of change in hyperconjugation energies between protonated *m*- and *p*-xylenes seems too great at first sight. This large difference may not be unreasonable, however, since the substances in question are the so-called "strongly hyperconjugated" systems[14,15].

Discussion

Brown and Brady[16] have shown that change in solvolysis rates between meta- and para-methyl substituted phenyldimethylcarbinyl chloride is explained reasonably, though qualitatively, in terms of valence bond structures. On the stabilities of the protonated isomeric xylenes also, treatment by means of valence bond structures may not be overlooked, and will be tried in the following way.

Model I of protonated *m*-xylene can resonate among three A (AI, AI_1 and AI_2), one B and one C structures (Fig. 2), according to Brown and Brady[16]. However, additional hyperconjugated structures by the two methyl substituents should be taken into account, such as four D, six E, one F, one G and five H structures. The number of resonance structures is altogether twenty-two (Fig. 2). For the models I′, I″, II, III and III′ similar types of resonance structures are considered. Numbers of resonance structures belonging to these types are indicated in Table II. Inspection of Table II suggests that model I is as stable as model I′, model I″ being less stable, and model III will possibly be more stable than model III′. Model I will probably be stable to almost

12) In these calculations, the unit of energy is expressed in kcal./mol. by the use of $\beta=-60$ kcal./mol. See, C. C. J. Roothan and R. S. Mulliken, *J. Chem. Phys.*, **16**, 118 (1948).

13) Here K means the reduced basicity constant.

14) N. Muller and R. S. Mulliken, *J. Am. Chem. Soc.*, **80**, 3489 (1958).

15) N. Muller, L. W. Pickett and R. S. Mulliken, ibid., **76**, 4770 (1954).

16) H. C. Brown and J. D. Brady, ibid., **74**, 3570 (1952).

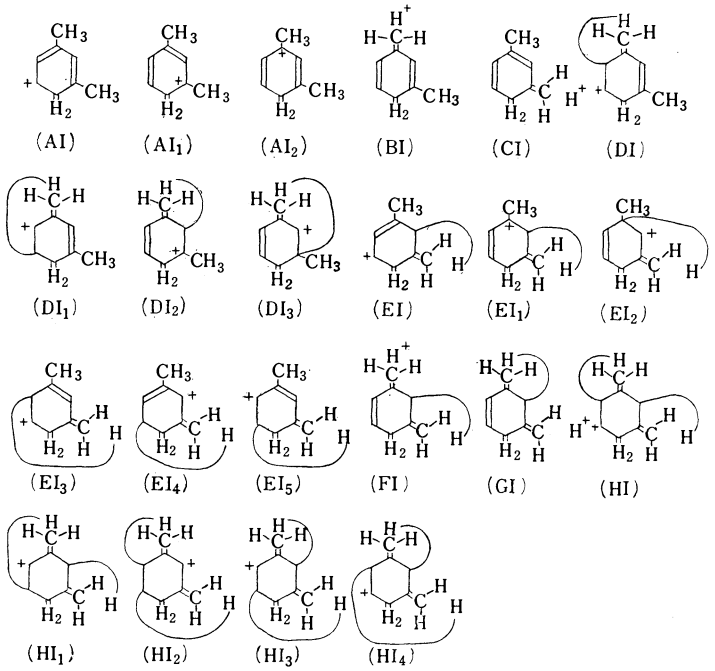


Fig. 2. Valence bond structures of model I of protonated *m*-xylene.

TABLE II. NUMBERS OF THE VALENCE BOND STRUCTURES

Models	A	B	C	D	E	F	G	H	Total
I	3	1	1	4	6	1	1	5	22
I′	3	1	1	5	6	2	2	3	23
I″	3	0	0	0	0	0	0	5	8
II	3	0	1	4	4	1	1	5	19
III	3	0	1	4	7	2	2	3	22
III′	3	1	0	4	4	1	1	2	12

the same extent as model III, which will be more stable than model II. These results are partly in disagreement with experiments. It may be said, however, that the difference of the stability of protonated compounds of xylene isomers will be attributable to that of numbers of hyperconjugation structures by the methyl group, irrespective of hyperconjugation or localization of the methylene.

From their electron spin resonance measurements of isomeric xylene negative ions, Tuttle, Jr. and Weissman[17] have indicated that methyl groups show hyperconjugation in a different manner among these substances and are more hyperconjugated in the *m*-xylene than in the *o*- and *p*-xylene negative ions. As has been hitherto accepted, the hyperconjugation phenomenon seems not so simple but complicated. At all events, it may be likely that the manner in which hyperconjugation occurs depends greatly on the environment of a methyl group.

17) T. R. Tuttle, Jr. and S. I. Weissman, ibid., **80**, 5342 (1958).

Summary

By means of the LCAO MO method, the π-electron energies of xylene carbonium ions are calculated, for all possible models, with respect to the positions of proton attack, on the basis of the bond localization hypothesis. It is indicated that the explanation of the basic behaviors of isomeric xylenes is impossible merely by the bond localization theory of their carbonium ions, and hyperconjugation should be taken into account.

It is indicated that, when the difference of hyperconjugation energies between protonated *m*- and *p*-xylene is about eight kcal./mol., the experimentally observed basic behavior of *m*- and *p*-xylenes is understandable.

The author wishes to thank Professor T. Titani (Tokyo Metropolitan University) for his interest, and Professor A. Kotera (Tokyo University of Education) for his guidance and instructive discussion.

Department of Chemistry
Tokyo Metropolitan University
Setagaya-ku, Tokyo

Studies on Crystal Hydrates. IV. Dehydration and Rehydration, Stable and Metastable Equilibria and Transition between Hydrate Modifications of Potassium Mercury(II) Chloride Monohydrate, $K_2HgCl_4 \cdot H_2O$*

By Hideaki CHIHARA and Syûzô SEKI

(Received February 13, 1959)

Numerous reports may be found in the literature of the subject as to the dehydration and rehydration of crystal hydrates, but there are few investigations based on the exact thermodynamical precautions. Atomistic interpretation of the phenomena related to the behavior of water molecules in the dehydration reaction seems to have insufficient ground to advance. One of the principal reasons for this seems to be that there are complexities which enable us to obtain a material at the well-defined thermodynamical as well as molecular state only with extreme difficulty. Dehydration can frequently produce amorphous or colloidal material which gradually changes to stable crystalline solids[1]. Different methods of preparation sometimes produce materials of different free energy[2].

Many hydrates undergo phase transitions prior to dehydration in the heating experiments[3]. A study of the mechanism of such transitions will assist in understanding the law governing the dehydration reaction.

In the present paper, another example of the difficulty of obtaining the true equilibrium will be presented. It was inferred that $K_2HgCl_4 \cdot H_2O$ might undergo "zeolitic" dehydration, from its crystal structure[4], in which water molecules are packed in channel-like interstices. Although the direct evidence of such type of dehydration was not obtained, a consideration of the entropy of dehydration let us conclude that this is the case. An X-ray diffraction study of the phase transition and the rehydration will be briefly reported.

Experimental

Material. — KCl: Takeda Co., first grade. Purified by recrystallization from water.

$HgCl_2$: Takeda Co., analytical grade. Recrystallized from water. $K_2HgCl_4 \cdot H_2O$: Crystals were prepared according to the phase diagram[5] of the system KCl-$HgCl_2$-H_2O which is reproduced in Fig. 1. Because amorphous samples were often obtained depending on the method of preparation as will be described later, the following procedure was found most satisfactory by analogy of the system $MnCl_2$-NH_4Cl[6]. A saturated solution corresponding to the point a in Fig. 1 (25°C) was

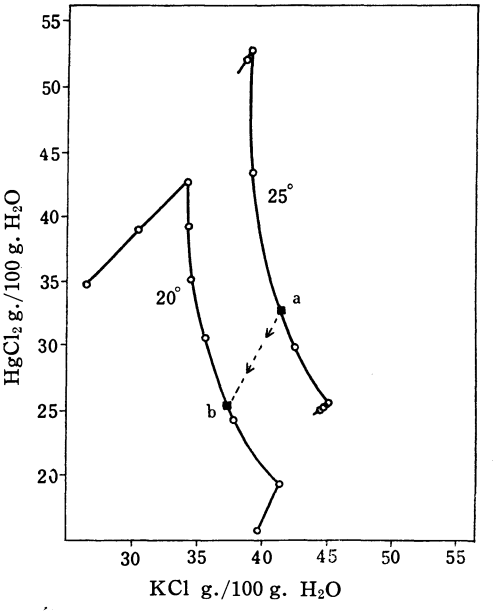


Fig. 1. Solution equilibrium diagram of the system KCl-$HgCl_2$-H_2O. Only a portion corresponding to the solid composition $K_2HgCl_4 \cdot H_2O$ is shown.

slowly cooled down to 20°C. A calculation shows that the solution changes its composition along the line a→b. The precipitate was filtered with a glass filter, pulverized, and then returned to

* The Report III may be found in This Bulletin, **30**, 674 (1957).

1) H. Chihara and S. Seki, This Bulletin, **30**, 674 (1957); G. B. Erost, K. A. Moon and E. H. Tompkins, *Can. J. Chem.*, **29**, 604 (1951); H. W. Quinn, R. W. Missen and G. B. Frost, ibid., **33**, 286 (1955); R. C. W. Wheeler and G. B. Frost, ibid., **33**, 546 (1955).

2) W. F. Giauque, *J. Am. Chem. Soc.*, **71**, 3192 (1949).

3) H. Chihara and S. Seki, This Bulletin, **26**, 88 (1953).

4) C. H. MacGillavry, J. H. de Wilde and J. M. Bijvoet, *Z. Krist.*, **100**, 212 (1938).

5) A. Seidell, "Solubilities of Inorganic and Metal Organic Compounds", 3rd Ed., Vol. 1, D. Van Nostrand Co., New York (1940), p. 624.

6) A. L. Greenberg and G. H. Walden, Jr., *J. Chem. Phys.*, 8, 645 (1940); A. Grenall, ibid., **17**, 1036 (1949).

the mother solution for ten days in a closed vessel, being occasionally shaken. The X-ray photograph of the precipitate finally filtered was entirely consistent with the reported crystal structure[4].

Measurements of the Dehydration Pressures.—The dehydration pressures were measured by a simple mercury-in-glass manometer with the help of a traveling microscope to within ±0.01 mmHg. The water thermostat was kept at constant temperatures to within 0.005°C. In the experiment of the isothermal dehydration, the water vapor was trapped into a small capillary and weighed. The amount dehydrated was corrected for the mercury vapor condensing from the manometer into the trap.

Dehydration Equilibrium

The dehydration pressures of the crystalline $K_2HgCl_4 \cdot H_2O$ were measured between 26 and 40°C and the results are plotted in Fig. 2 by squares. The pressure equation is

$$\log P(\text{mmHg}) = 8.538 - (2161/T) \qquad (1)$$

The heating and cooling data were perfectly coincident within the experimental error and it was ascertained that equilibrium was attained with no hysteresis effect. The heat, the entropy, and the free energy of dehydration are given in Table I.

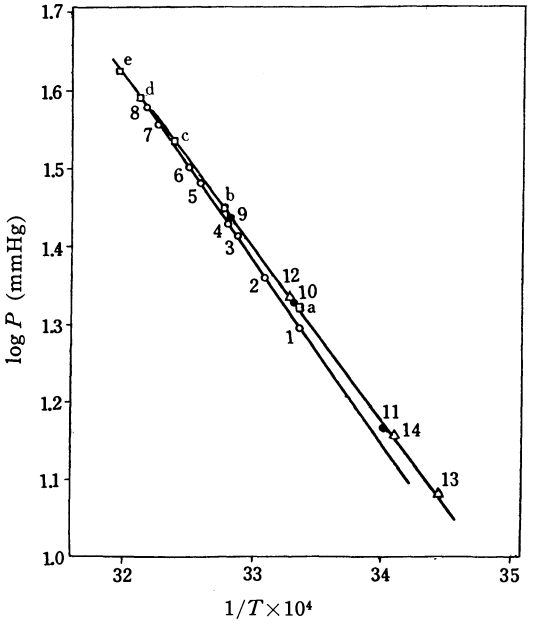


Fig. 2. Dehydration pressures of $K_2HgCl_4 \cdot H_2O$; □, crystalline hydrate (equilibrium data) (a-e); ○, heating direction of partly amorphous hydrate (1-8); ●, cooling direction of partly amorphous hydrate (9-11); △, subsequent heating and cooling measurements with partly amorphous hydrate (12-14).

TABLE I. CHANGES OF THE HEAT CONTENT, THE ENTROPY AND THE FREE ENERGY BY DEHYDRATION OF $K_2HgCl_4 \cdot H_2O$

ΔH kcal./mol.	ΔS cal./mol. deg.	ΔG at 25°C kcal./mol.
9.50	25.9	2.18

Results for Partly Amorphous Samples.—KCl 12.227 g. and $HgCl_2$ 15.459 g. were mixed with water 20 cc. and the solid was dissolved completely at high temperature by preventing evaporation. The solution was then cooled down to and kept at 20°C. It was deeply supercooled and no precipitation occurred before the entire solution reached 20°C. The solid precipitate after a few hours had the composition corresponding to $K_2HgCl_4 \cdot H_2O$ and the solution contained KCl 7.11 g. and $HgCl_2$ 6.13 g. The X-ray powder photograph of the solid thus prepared, however, showed that it was partly amorphous. The Debye rings, though faint, were consistent with the reported crystal structure of the hydrate[4]. The dehydration pressure of the partly amorphous hydrate showed a hysteresis phenomenon according to the pressure equations:

$$\log P(\text{mmHg}) = 9.139 - (2359/T)$$
in heating direction (2)

$$\log P(\text{mmHg}) = 8.595 - (2180/T)$$
in cooling direction (3)

The results are shown by open circles (heating direction) and by solid circles (cooling direction) in Fig. 2. The results of the subsequent heating and cooling experiments are indicated by triangles. It took about 20 days to reach an apparent dehydration equilibrium as compared with a few minutes in the case of the crystalline sample at 24.03°C.

The experiments of isothermal dehydration were made at 34.13°C. The initial formula of the hydrate was $K_2HgCl_4 \cdot 0.997 H_2O$. The constant value of the dehydration pressure was reached only after about 280 days (see Fig. 3). The calculated pressure from Eq. 2 was 31.09 mmHg and the apparent coincidence was good. The second equilibration with the composition $K_2HgCl_4 \cdot 0.965H_2O$ (water 0.032 mol. was taken from the original hydrate) was much slower than the first and then it was felt that further dehydration might accelerate the approach to the equilibrium. The third run, however, was even slower,

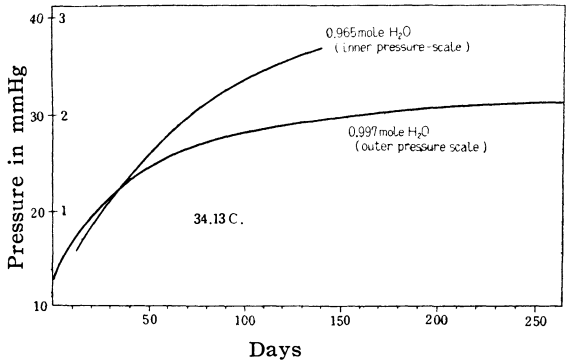


Fig. 3. Approach to the apparent equilibrium of isothermal dehydration of partly amorphous sample.

with 0.809 mol. of water per formula weight. The sample used in this experiment was taken out of the apparatus and examined by the X-rays. It was still partly amorphous but the crystallization seemed to have proceeded during the pressure measurements (longer than two and half years).

The differential thermal analysis of the partly amorphous sample gave only ill-defined peaks in comparison with the result for the crystalline sample which will be discussed below.

These results show that the crystallization of an amorphous solid is a very slow reaction at room temperature and that care must be exercised in the preparation of the solid substances, because an inadequate method of preparation sometimes produces materials of higher free energy than the one for the equilibrium product**.

Entropy of Dehydration

The value of entropy may be assigned to water molecules in the hydrate crystal by subtracting the experimental entropy of dehydration from the standard entropy of water vapor 45.1 cal./deg. mol. This method gives for the present case 19.2 cal./deg. mol. which amounts to roughly twice as large a value as in average hydrate crystals and shows that the dehydration is "zeolitic".

Transition and Dehydration in Air

The results of the differential thermal analysis are given in Fig. 4 which shows two heat-absorption peaks at 114 and 123°C, with a fine structure in the former peak. The shoulder at 107°C always appeared in several runs but one at 117.6°C was not always reproducible.

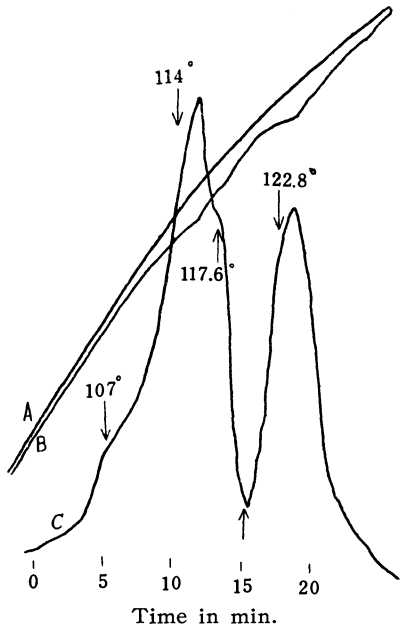


Fig. 4. Differential thermal analysis of crystalline $K_2HgCl_4 \cdot H_2O$; curve A, temperature of the reference NaCl powder; curve B temperature of the sample; curve C the temperature difference.

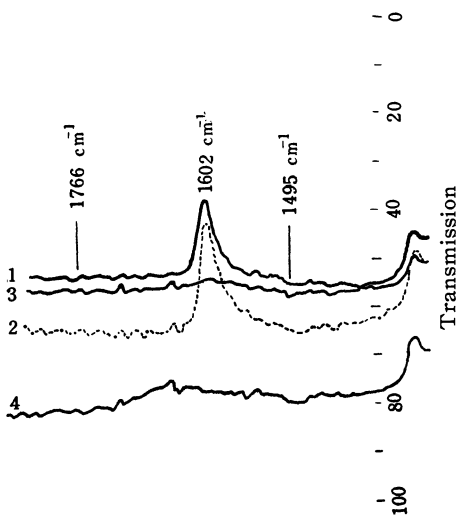


Fig. 5. Infrared spectra. (1) Room-temperature phase, (2) heated to 118°C, (3) heated to 130°C, (4) daifloil background.

There are evidences for the fact that the first peak at 114°C is due to a transition between two hydrate modifications

** A similar case is the dehydration and transition of $NiSO_4$ hexahydrate as reported by Simon and Knauer (*Z. anorg. u. allgem. Chem.*, **242**, 375 (1939)).

7) Full discussion of the entropy of dehydration is given in Part VI (This Bulletin, **32**, 908 (1959)).

and the second peak at 123°C is due to dehydration. There occurred no detectable evaporation and condensation of water in the apparatus of the thermal analysis[3] at the temperature between the two peaks, and also the infrared absorption spectrum*** of the hydrate crystals quenched from 118°C, at which the first heat effect completed its peak, retained the 6-micron absorption band of water (Fig. 5). The hydrate heated beyond the second heat-absorption temperature was not absorbed in this wavelength region; the heat absorption at 123°C is apparently due to dehydration.

An X-ray study was made of the transition of $K_2HgCl_4 \cdot H_2O$ at 114°C. The crystals were heated to 117°C in the apparatus of the differential thermal analysis (the transition was observed) and was rapidly cooled to room temperature and examined by the Norelco X-ray diffractometer. The scanning of the goniometer started about ten minutes after the sample was taken out of the heating vessel, with the scanning rate $2\theta = 0.5°$/min. The scanning was repeated according to the following succession:

12—61°, 35—46, 10—42, 10—35, 34—27 (reversely), 26—34, 10—14, 23—26, 28—31, 45—47, in 2θ values.

It took about 5.5 hr. for this series of scanning. The scanning was then repeated every day for the following six days. The change in the diffraction patterns with time was bewildering during the first few hours. Some of the typical results are reproduced in Fig. 6. The diffraction

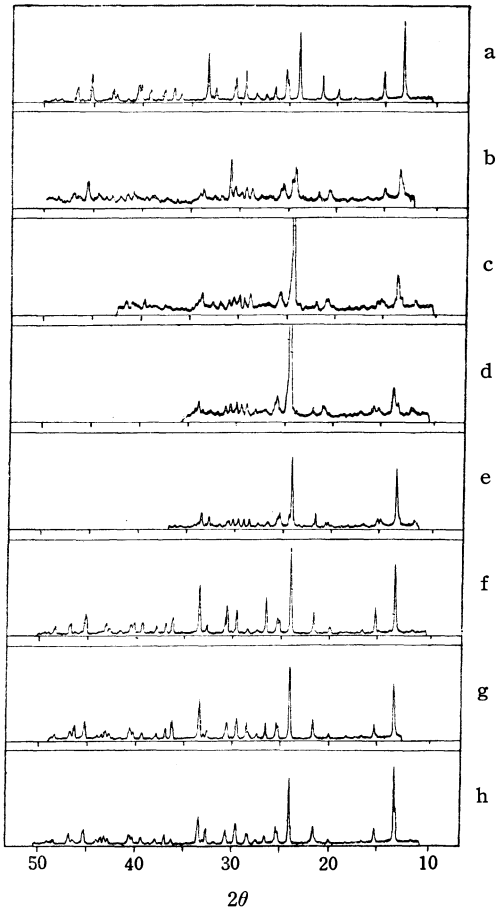


Fig. 6. Change of X-ray diffraction diagrams due to the transition; (a) α-modification of the hydrate, (b) ten minutes after once heating the hydrate to 117°C, (c) 40 min. after b, (d) 60 min. after b, (e) 18 hr. after b, (f) 42 hr. after b, (g) 90 hr. after b, (h) 138 hr. after b.

*** The infrared absorption spectra were recorded with Hilgar Model H800 Spectrophotometer.

TABLE II. POWDER DIFFRACTION LINES IN 2θ VALUES (deg.)

α-Hydrate	β-Hydrate	Anhydrous crystal
13.08 (110)	11.62 (210)	11.25
15.14 (020)	13.16 (021)	11.74
19.9 (002)	13.45 (220)	12.54
21.5 (200)	15.0 (040) (201)	13.14
23.9 (112)	20.7*	13.8
25.1 (022)	21.9 (400)	14.8
25.3 (130)	24.2 (222)	18.2
26.4 (220)	24.5	19.8
27.3 (131)	25.5 (042)	20.2
28.3	25.7 (260)	20.4
29.4 (202)	28.6**	20.6*
30.4 (212)	29.2	21.5
30.6 (040)	29.7* (402)	21.9
32.5 (140)	30.4	23.8
32.9	30.8 (422) (080)	24.1
33.3 (220) (310)	31.8	24.6
36.0 (320)	32.3	25.0
36.1	33.5 (442)	25.4
36.8 (042)	33.6 (620)	27.1
37.7 (240)	34.0	27.4
39.2	36.4 (640)	27.7
40.1 (330)	37.5 (082)	28.3**
40.4 (150) (004) (223)	38.9	28.9
42.6	39.6	29.5
43.0, 43.1 (242)	40.8**	30.0
	41.4	
43.4	42.2	
45.1 (340) (303) (250) (401)	43.0	
	44.4	
46.6 (420)	45.4	
	45.6	

* Diffraction lines due to $HgCl_2$.

** Diffraction lines due to KCl.

patterns of the anhydrous crystal (Fig. 7a) and of the hydrate (Fig. 6a) which is stable at room temperature (α modification) are also given for the sake of reference. The series of patterns shows the change in the crystal structure from the high-temperature modification (β modification) to the low-temperature modification (α modification) slowly occurring at room temperature. Fig. 6b is itself an intermediate or a mixture of the two modifications. Attempts were made to assign the diffraction lines to either α or β modification by comparing the members of the series of the diffraction patterns. The results are summarized in Table II.

Although some of the lines ascribed to the β modification coincide with the lines of the α modification or with the lines of the anhydrous crystal, there exist lines essentially attributable to the β modification. The time change of the intensities also supports this view. The patterns of Fig. 6b and its succeeding changes can not be obtained by a mere superposition of the diffractions from the α-hydrate and those from the β-hydrate. In fact, the intensities of lines belonging to various crystalline forms show intricate changes, for example, (1) 24.1* line first becomes stronger with time, (2) 13.4 and 15.4 are both characteristic to the α-hydrate but their recovery in the intensity is not proportional with each other; the recovery is first more rapid in 15.4 line than 13.4 line, and then the recovery of 13.4 line predominates again, and (3) five lines between 28 and 31 do not change their intensities in a regular, simple way.

It was first supposed that the sample chilled from above the transition temperature might be a mixture of the α and the β modifications, and that the transition might be observed as the decrease in intensity of the characteristic lines of the β form accompanied with the increase in the intensities of lines of the α form by equal fractions. If so, it should be possible to determine the rate of transformation at a supercooled condition which is itself a rare experimental information. Instead, it has become very plausible that the transition is essentially of gradual nature: a structure does not abruptly transform itself into another but there is a continuous series of structures between the β and the α modifications.

This is an analogous situation to the order-disorder transitions in such respect that there are an infinite number of phases between two extreme phases**. But a difference from the order-disorder transition is that nothing like the order parameter may be introduced and that every step of the transition probably corresponds to an ordered state because no regular, proportional change in the diffraction intensities with time was observed in contrast to the case of order-disorder transitions, in which it is possible to calculate the order parameters from the monotonous change of a superstructure-line intensity with temperature[8]. In the case of order-disorder transitions, a unit cell within a crystal has only statistical significance in the sense that a particular unit cell has not necessarily the structure identical with the neighboring unit cell. In the present case of the transition in $K_2HgCl_4 \cdot H_2O$, every unit cell is considered to have the identical structure which gradually changes with time. This type of transition may be termed a slow "Martensite transition" which does not accompany nucleation-and-growth[9].

The determination of the precise structure of the β modification*** seems to be very difficult because the unit cell is relatively large, being

$$a=16.51\text{Å},\ b=23.26\text{Å},\ \text{and}\ c=8.89\text{Å}$$

and containing 16 formula units of $K_2HgCl_4 \cdot H_2O$. This cell is four times as large as the unit cell in the α modification[4] owing to the appearance of the line ($2\theta=11.75°$) which may be indexed as inhibited ($1\,1/2\,0$) on the basis of the structure of the α form.

Rehydration of Anhydrous Crystals

$K_2HgCl_4 \cdot H_2O$ was dehydrated in the apparatus of the differential thermal

* 2θ value (twice the diffraction angle).

** It may not be immediately evident that the transition at 114°C from the α to the β form is of the same nature as that from the β to the α form occuring at room temperature. But there is no reason, at present, to believe otherwise.

8) Y. Saito, *X-sen*, 7, 9 (1952); Z. W. Wilchinsky, *J. Appl. Phys.*, 15, 806 (1944).

9) M. Cohen, "Phase Transformations in Solids", John Wiley & Sons, Inc., New York (1958), p. 588.

*** Kiriyama and Ibamoto[10] reported the structure of the high-temperature form of $K_2HgCl_4 \cdot H_2O$ by use of a high-temperature camera after prolonged heat-treatment at high temperature. Their experimental condition was very different from the present one. There are some discrepancies between their results and the results of the current investigation; for instance, the 11.75 line is missing from their X-ray photographs and therefore the unit cell dimentions are also different from those described here.

10) R. Kiriyama and H. Ibamoto, This Bulletin, 27, 317 (1954).

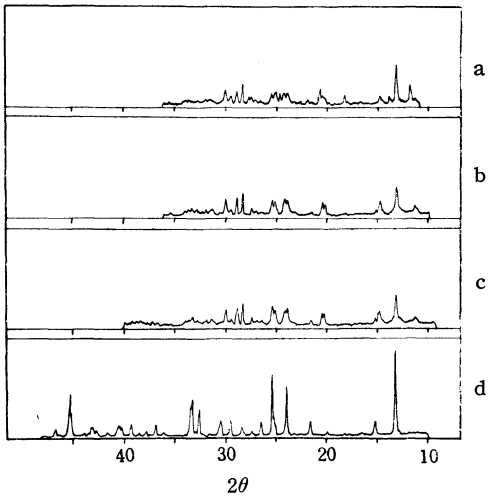


Fig. 7. Change of X-ray diffraction patterns due to rehydration of anhydrous crystal at room temperature; (a) Anhydrous phase, (b) after standing for 60 min. in the open air, (c) after 140 min. (d) after 30 hr. (α-modification of the hydrate).

analysis and it was immediately transferred to the goniometer of the Norelco X-ray diffractometer. It was observed that rehydration occurred in the open air at room temperature, at a measurable rate. This series of diffraction patterns, which is a cinematogram of the rehydration reaction, is reproduced in Fig. 7. It took about 30 hr. at about 30°C for the complete rehydration. This is a comparatively rapid rate of rehydration and therefore it is confirmed that the measurements of the dehydration pressures of the crystalline hydrate correspond to the equilibrium property of the system.

Summary

The dehydration pressures of the crystalline $K_2HgCl_4 \cdot H_2O$ are measured and given by $\log P = 8.538 - (2161/T)$ with P expressed in mmHg. No thermal hysteresis effect was observed. Production and some experiments for partly amorphous hydrate are briefly discussed. A consideration of the entropy of dehydration led to the conclusion that the dehydration is zeolitic. The differential thermal analysis revealed that there is a non-dehydrating transition at 114°C and that the dehydration occurs at 123°C. Infrared spectra of the solids showed that the 6-micron band of water persisted between 114 and 123°C. The X-ray study of the transition at the supercooled condition showed that this is a transition quite different in nature from those of ordinary nucleation-and-growth mechanism. The rehydration of dehydrated crystals was followed by the X-ray diffraction method and found to be relatively rapid at room temperature.

The authors wish to express their sincere thanks to Professor I. Nitta for his interest in the present investigation and to Assistant Professor K. Sakurai and Dr. K. Osaki for their discussions on the X-ray data. The cost of the research was partly defrayed by the financial support of the Ministry of Education to which the authors' appreciation is due.

Department of Chemistry
Faculty of Science
Osaka University
Nakanoshima, Osaka

Studies on Crystal Hydrates. V. Zeolitic Dehydration of DL-Tris-ethylenediamine-cobalt(III) Chloride Hydrate, DL-[Co en$_3$]Cl$_3$·nH$_2$O. Sorption and Desorption of Water Vapor. A Preliminary Study of the Dielectric Properties*

By Hideaki CHIHARA and Kazumi NAKATSU

(Received February 13, 1959)

Crystal hydrates may be classified into two extremes from the standpoint of the dehydration isotherm[1]:

i) crystals which are dehydrated in a stepwise manner (Fig. 1a); $CuSO_4 \cdot 5H_2O$ belongs to this class of hydrates,

ii) crystals which are dehydrated continuously (Fig. 1b); zeolite minerals belong to this class.

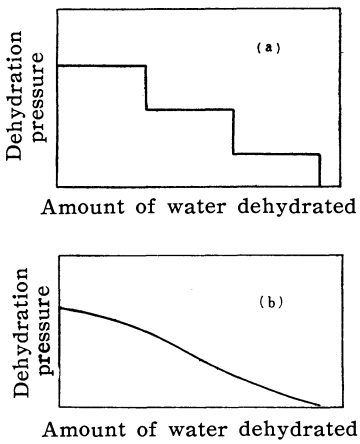


Fig. 1. Two extreme types of dehydration isotherm. (a) the stepwise dehydration, (b) the continuous dehydration.

Zeolites, chabazite, for instance, generally possess two or more kinds of channels of different diameter and each channel crosses with others at cage-like rooms[2]. Analcite has spiral channels which are relatively independent of each other but their diameter is not uniform throughout a channel[3]. We have long been looking for a type of crystal which belongs to the class ii and has only one kind of channel in which positions of water molecules can be located exactly by the method of X-ray analysis. If we can obtain such a crystal, it will provide us with an ideal model substance for examining the role of water in the stabilization of crystal lattice, the capillary condensation theory generally adopted in the adsorption research ane the state of aggregation of water molecules in the channels.

The crystal structure of DL-[Co en$_3$]Cl$_3$·nH$_2$O (n=3) has recently been determined[4] and this was found to be a substance that nearly meets our requirements.

The present paper deals with the experiments aiming at establishing the zeolitic nature of the dehydration of this crystal and with some results obtained in regard to the thermodynamic quantities of dehydration. A preliminary measurement of the dielectric absorption will also be briefly reported.

Experimental

Material.—The preparation of DL-tris-ethylenediamine-cobalt(III) chloride has already been described[4]. Crystals were purified by repeating recrystallization from aqueous solution (Found: C, 20.77; H, 7.01; N, 24.73; Cl, 29.83% on the basis of the anhydrous crystal. From the residue the Co purity was found to be 99.601% by the α-nitroso-β-naphthol method**). The measurements of the dehydration pressure were conducted with powdered crystals unless otherwise stated. Dielectric measurements were made with single crystals grown from the aqueous solutions.

Differential Thermal Analysis.—The differential thermal analysis (Fig. 2) shows that the dehydration takes place over the temperature region between 70 and 170°C. Such gradual

* Report IV may be found in This Bulletin, **32**, 897 (1959).

1) R. Büll, *Angew. Chem.*, **49**, 145 (1936).

2) G. L. Kington and W. Laing, *Trans. Farady Soc.*, **51**, 287 (1955).

3) E. Schiebold, "Kristallstruktur der Silikate" in Ergebnisse der exakten Naturwissenschaften Bd. 12, Verlag von Julius Springer, Berlin (1933).

4) K. Nakatsu, Y. Saito and H. Kuroya, This Bulletin, **29**, 428 (1956).

** The analysis of Co was kindly carried out by Dr. T. Fujino of the Institute of Science and Industry, Osaka University, Sakai, Osaka, to whom the authors are very grateful.

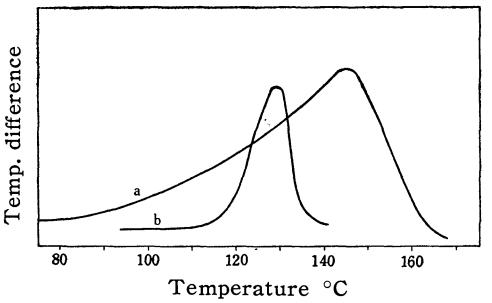


Fig. 2. The differential thermal analysis of (a) DL-$[Co\,en_3]Cl_3$ hydrate and (b) $NiSO_4 \cdot 6H_2O$.

dehydration stands in contrast with the case of nickel sulfate hydrate, for example, and suggests the zeolitic nature of dehydration.

Dehydration Pressures. — The dehydration pressures of the hydrate were measured between 19 and 45°C at various water contents by using the apparatus already described in the preceding paper. The results are summarized in Table I and Fig. 3. The approach to the equilibrium was very rapid, not later than ten minutes after the water bath was thermostated. The pressure values were read by use of a traveling microscope to 0.01 mm. Corrections in the value of the water content for the amount of water present in the vapor phase were not made, since a rough estimate based on the dimensions of the manometer and the sample container showed that it was well within the experimental error. No hysteresis effect was observed: the pressures in the heating and in the cooling directions coincided with each other.

TABLE I. DEHYDRATION PRESSURES. n IS THE NUMBER OF MOLES OF WATER PER FORMULA WEIGHT OF $[Co\,en_3]Cl_3$

n	Pressure equation (in mmHg)
3.35	$\log P = 9.0406 - (2334.0/T)$
3.11	$\log P = 10.003 - (2693.1/T)$
2.96	$\log P = 10.577 - (2910.0/T)$
2.63	$\log P = 10.734 - (3035.9/T)$
2.47	$\log P = 10.699 - (3045.6/T)$
2.02	$\log P = 9.7583 - (2773.2/T)$
1.18	$\log P = 9.7791 - (2782.0/T)$
0.82	$\log P = 9.3500 - (2649.8/T)$
0.39	$\log P = 9.7320 - (2770.1/T)$
0.23	$\log P = 10.119 - (2889.5/T)$
0.02_5	$\log P = 7.5790 - (2206.9/T)$

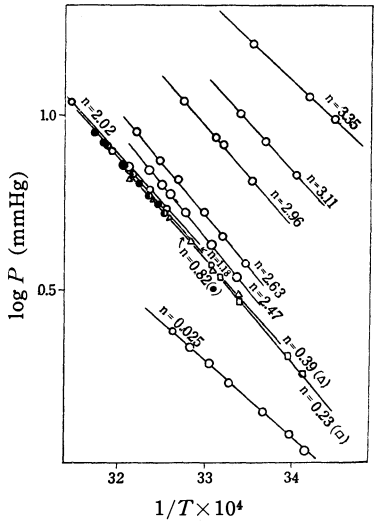


Fig. 3. Dehydration pressure of DL-$[Co\,en_3]Cl_3 \cdot nH_2O$ at different water contents n.

The experiments of dehydration and rehydration (desorption and sorption) of a single crystal was undertaken in order to compare it with the powder data. A single crystal (about 325.6 mg.) placed in a glass vessel (144.9 mg.) was hung under a quartz helical balance, the sensitivity of which was 0.2711 mm./mg. The water vapor pressure in the apparatus was kept constant by use of 72% sulfuric acid solution covering the water vapor pressures up to 13 mmHg. The results are plotted in Fig. 7. No hysteresis was observed between the dehydration and rehydrotion branches.

The differential molar heats and entropies of dehydration were computed from the pressure equations given in Table I. Table II lists these results and Fig. 6 indicates that there is a maximum both in the heat and in the entropy at a certain water content (approximately at $n=2.7$ mol. of water per formula weight of the hydrate).

TABLE II. DIFFERENTIAL MOLAR HEAT AND ENTROPY OF DEHYDRATION AS A FUNCTION OF WATER CONTENT

n	ΔH (kcal./mol.)	ΔS (e.u.)	n	ΔH (kcal./mol.)	ΔS (e.u.)
3.35	10.7	28.2	1.18	12.7	31.6
3.11	12.3	32.6	0.82	12.1	29.6
2.96	13.3	35.2	0.39	12.7	31.2
2.63	13.9	35.9	0.23	13.2	33.1
2.47	13.9	35.8	0.02_5	10.1	21.5
2.02	12.7	31.5			

Description of Crystal Structure

The crystal structure may be briefly outlined here with particular attention to the arrangement of the water molecules. The structure projected on the (0001) plane is represented in Fig. 4. A channel of hexagon cross-section filled with water molecules runs through the origin in the direction of the c-axis. The way in which the water molecules are arranged is schematically shown in Fig. 5 and the crystal data together with the atomic coordinates are reproduced in Table III.

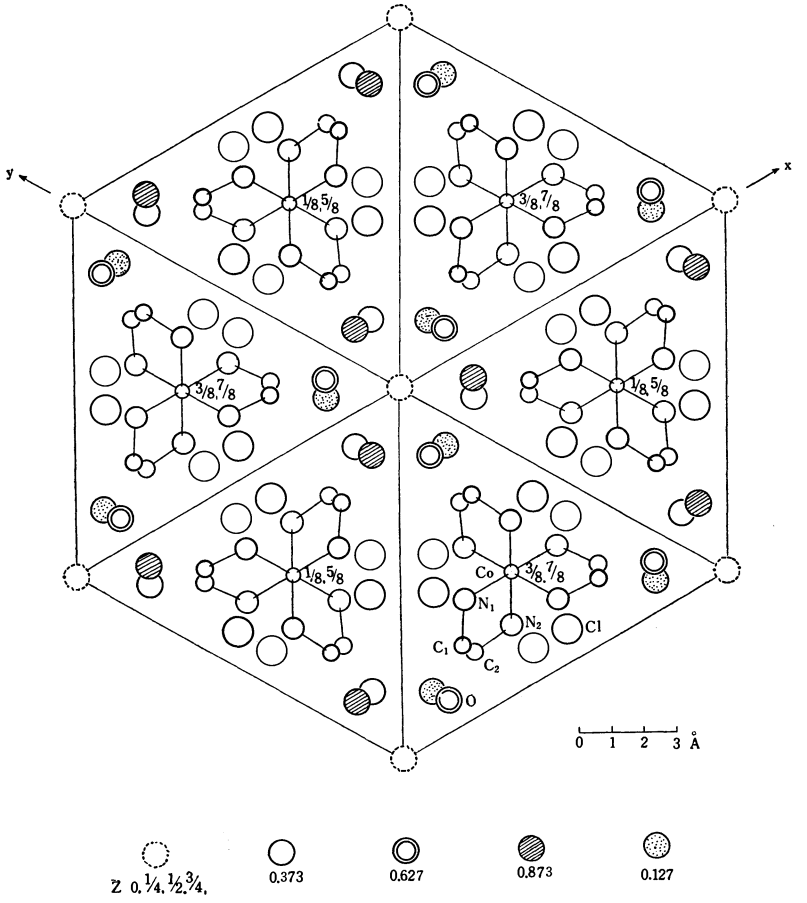


Fig. 4.

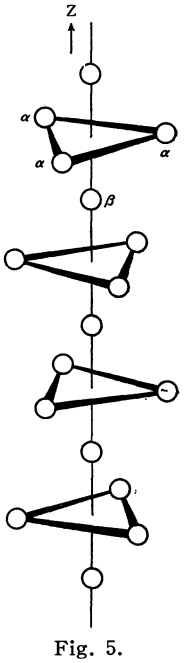


Fig. 5.

TABLE III. CRYSTALLOGRAPHIC DATA

$a=11.50\pm0.02$ Å, $c=15.52\pm0.04$ Å,
Density 1.504 (17°C), $Z=4$,
Space Group $P\bar{3}c1$-D_{3d}^4

Fractional atomic coordinate

Atom	No. of positions & Wyckoff notation	x	y	z
C_0	4d	1/3	2/3	0.125
Cl	12g	0.097	0.493	0.372
O_1	12g	0.087	0.225	0.873
O_2	2a	0	0	1/4
O_3	2b	0	0	0
C_1	12g	0.180	0.397	0.077
C_2	12g	0.215	0.397	0.173
N_1	12g	0.192	0.525	0.050
N_2	12g	0.333	0.535	0.200

TABLE IV. SOME INTERATOMIC DISTANCES

$O_\alpha\cdots Cl$	3.34 Å
$O_\alpha\cdots C_1$	3.36, 3.61 Å
$O_\alpha\cdots C_2$	3.12, 3.55 Å
$O_\alpha\cdots O_\alpha$	3.90, 4.19, 4.54 Å

Water molecules which occupy the 12g positions amount to three moles per formula weight of the hydrate ($n=3$). These positions will be referred to as the α-sites. In view of the long O···O distances listed in Table IV, if water molecules are to occupy only α-sites, and of the improvement of the reliability index by about 2%, it was concluded that water molecules are distributed also on the 2a and 2b special positions (referred to as the β-sites). The fact that the peak at the origin in the electron-density projection on the (0001) plane was not eliminated even at the final stage of the refinement of the structure analysis also led to this conclusion. This addition of water is also consistent with the chemical analysis that the water content of a freshly prepared crystal is $n=3.6$. The $O_\alpha \cdots O_\beta$ distances will then be 2.96 and 3.00 Å corresponding to weak hydrogen bonding.

A single-crystal oscillation photograph was obtained after the crystal was almost dehydrated and its unit cell dimensions were the same as those of the hydrate crystal.

Results and Discussion

The dehydration isotherm derived from the data of Table I by inter- or extrapolating them to 25°C is shown in Fig. 7

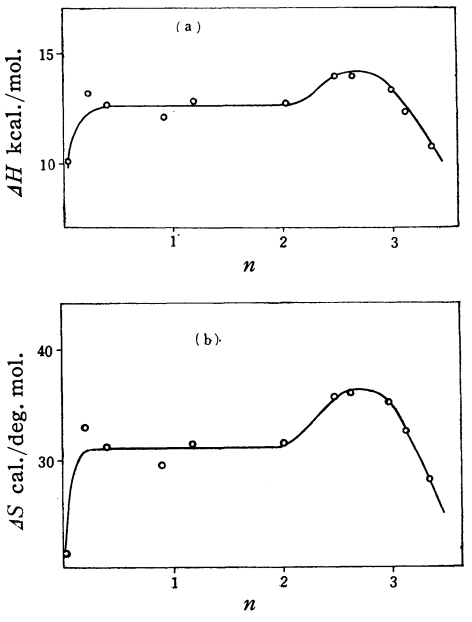


Fig. 6. Differential molar heat (a) and entropy (b) of dehydration as functions of water content n.

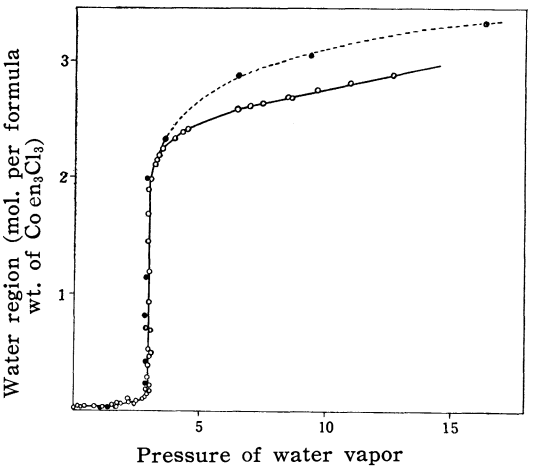


Fig. 7. Dehydration isotherm at 25°C derived from the powder data (solid circle) and determined directly for a single crystal (open circle).

by solid circles. The pressure at 25°C remains almost constant (2.85 mmHg) between the water contents $n=0.2$ and 2.5. Another independent direct measurement of the isotherm at 25°C for a single crystal (denoted by open circles in Fig. 7) gave nearly the same result as that derived from the powder data***. Important conclusions may be drawn from these experimental data.

(a) The fact that the powder and the single-crystal data give the same results clearly shows that the isotherm obtained for the single crystal is not due to adsorption of water vapor on the outer surface of the solid but to the sorption and desorption into and from the interior of the crystal lattice.

(b) That the pressure is constant over a wide range of n reminds us of the character of the destructive dehydration (class i). A close examination, however, shows that the boundary values of n (0.2 and 2.5) do not correspond to any single crystalline phases. In fact there is no set of equivalent positions in the space group $P\bar{3}cl$ that can accommodate the states $n=0.2$ or $n=2.5$. Therefore, it must be emphasized that an appearance of the stepwise dehydration does not always correspond to the destructive dehydration. This conclusion argues against the widely accepted criterion for zeolitic dehydration[1,5-7]. X-ray examination would be necessary for the decision as to whether

*** The small discrepancy at higher pressures is probably due to the larger adsorption of water on the outer surface of powdered crystals.

or not the dehydration is zeolitic.

(c) From the standpoint of the sorption-desorption system, the isotherm of Fig. 7 corresponds to the type V isotherm of the Brunauer-Emmett-Teller classification[8]. It is evident that the horizontal portion of the isotherm corresponds to the capillary condensation into pores of uniform size. Analogous transitions in adsorbed monolayer have been reported and interpreted by many investigators since Harkins and his collaborators observed the first-order phase transition of *n*-heptane on the surface of silver[9], although its reality was open to some discussion[10]. Recent investigations[11] show that such transitions are due to a kind of cooperative phenomena occurring in the assembly of adsorbed vapors. The transitions are sharp on a homogenous surface but they are diffuse on a heterogeneous surface. Capillary condensation phenomena that have been observed at any time are diffuse, because the experiments were carried out on gels which are inevitably inhomogeneous. The transition phenomenon observed in the present study is unique because it occurs in the true equilibrium system (the water regain of the solid did not change during 24 hr. after dosage of vapor; cf. E. V. Ballou, Ref. 10) and also because it is the capillary condensation entirely equivalent, in principle, to the transition on a uniform outer surface of a single crystal.

(d) The maxima in the differential molar heat and entropy in Fig. 6 will be accounted for by the theory of cooperative phenomena. Analogous results were reported by Rhodin[12] for nitrogen adsorbed on single crystals of copper, by Young[13] for argon absorbed on octahedral potassium chloride and by Hayakawa[14]. In all the adsorption systems ever examined, the maximum of the differential heat of adsorption appears when the amount of the gas adsorbed nearly suffices to cover the surface with a monolayer. This is also to be expected theoretically[15]. In the present case the maximum is also near the monolayer coverage of the inner surface of pores ($n=2.7$). The number of pairs of water molecules in a channel interacting with each other increases more rapidly than linearly as the coverage increases, even after the monolayer has been completed. The differential heat thus increases with the coverage on the assumption that the pair interaction energy is constant. On the other hand, the water molecules in the second layer (β-sites) interact with the lattice much more weakly than do the molecules in the first layer (α-sites). Those two counteracting effects give rise to the maximum of the heat of sorption branch.

(e) The differential heat and entropy are very small at very low n values. This is an extraordinary fact as many sorption systems exhibit a great increase in ΔH towards the lower surface coverage. On the surface of a single crystal, the differential heat is constant down to very low pressures[12]. The experimental error involved in the present determination of ΔH does not exceed 0.7 kcal./mol. and, therefore, the small value of ΔH and ΔS may possibly be due to a slight rearrangement of atoms in the completely dehydrated crystal lattice.

The Preliminary Results of Dielectric Measurements.—The dielectric power loss was measured of single crystals ($n=3.6$) between -180°C and room temperature in the frequency range of 300 c/sec. to 10 Mc/sec. The dielectric absorption was found with the electric field in the *c*-axis direction and perpendicular to the *a*-plane of the hexagonal crystal. The activation energies for the relaxation process were 7.7 and 6.3 kcal./mol., respectively. By extrapolation to room temperature, the relaxation times ($\log \tau = (1379/T) - 14.72$ for the *c*-plane) nearly agree with the relaxation time in liquid water and it was inferred that the absorption is due to the hindered rotation of water molecules. In the experiment with the electric field parallel to the *c*-axis, an additional absorption increasing progressively towards lower frequencies was observed. Further precise study of the dielectric properties and the d. c. conduction is going on and will be reported later.

5) W. Eitel, "Physikalische Chemie der Silikate", Johann Ambrosius Barth, Leipzig (1941).
6) O. Glemser, *Z. Elektrochem.* **45**, 820 (1939).
7) G. Tammann, *Z. physik. Chem.* **27**, 323 (1893).
8) S. Brunauer, "Adsorption of Gases and Vapors", Vol. I, Princeton University Press, N. J. (1945), p. 150.
9) G. Jura, E. H. Loser, P. R. Basford and W. D. Harkins, *J. Chem. Phys.* **13**, 535 (1949).
10) R. J. Tykodi, *J. Chem. Phys.*, **22**, 1647 (1954); *J. Phys. Chem.*, **59**, 383 (1955); E. V. Ballou, *J. Am. Chem. Soc.*, **76**, 1199 (1954).
11) B. B. Fisher and W. G. McMillan, *J. Chem. Phys.*, **28**, 549 (1958).
12) T. N. Rhodin, Jr., *J. Am. Chem. Soc.*, **72**, 5691 (1950).
13) D. M. Young, *Trans. Faraday Soc.*, **48**. 548 (1952).
14) J. Hayakawa, This Bulletin, **30**, 124, 236, 243, 332, 337, 343 (1957).
15) W. J. C. Orr, *Trans. Faraday Soc.*, **35**, 1247 (1939).

Summary

The dehydration pressures of DL-$[Co\,en_3]Cl_3 \cdot nH_2O$ ($n \leqq 4$), were measured between 19 and 45°C at various water contents. The dehydration isotherm derived from the data is of type V of the BET classification with a constant pressure (2.85 mmHg at 25°C) region between $n=2.5$ and $n=0.2$, corresponding to the case of capillary condensation into pores of uniform size. The crystal lattice is stable after dehydration, showing the zeolitic nature of dehydration. The usual criterion of stepwise dehydration for the lattice-destructive dehydration does not apply to this type of crystal. The differential molar heat and entropy of dehydration have maximum values around $n=2.7$; this can be accounted for by the theory of co-operative phenomena. At very low water content, there is a possibility of rearrangement of atoms in the crystal as inferred by the entropy consideration. A preliminary study of the dielectric properties showed that the relaxation absorption occurs between −180°C and room temperature in the megacycle region with the activation energy for the relaxation about 7 kcal./mol. The dielectric loss due probably to the d. c. conduction was observed in the *c*-axis direction.

The authors with to thank Professor I. Nitta and Assistant Professor S. Seki of Osaka University and Professor Y. Saito of Osaka City University for their valuable discussions. The present study was partly supported by the financial aid of the Ministry of Education, to which the authors' thanks are also due.

Department of Chemistry
Faculty of Science
Osaka University
Nakanoshima, Osaka (*H. C.*)

Institute of Polytechnics
Osaka City University
Kita-ku, Osaka (*K. N.*)

Studies on Crystal Hydrates. VI[1]*. Thermodynamics of Dehydration of Crystal Hydrates. A New Criterion for the Continuous Zeolitic Dehydration. Capillary Condensation of Water Vapor into Exactly Uniform Pores and an Experimental Test of the Kelvin Equation. Case of* DL*-Tris-ethylenediamine-cobalt(III) Chloride Hydrate*

By Hideaki CHIHARA

(Received February 13, 1959)

A criterion has generally been adopted as to the manner of dehydration of a crystal hydrate, which makes use of the dehydration isotherm[1]. The experimental determination of a complete dehydration isotherm, however, is sometimes quite an elaborate matter owing to difficulty in obtaining the true equilibrium of dehydration[2]. It was found that a new criterion, which is equivalent to the "isotherm criterion", can be obtained by the measurement of dehydration pressures at different temperatures for a fixed content of water in the solid phase; the water content needs not be accurately known. This may be termed "entropy criterion" as it is based on the value of the entropy of dehydration.

Although the entropy criterion is exactly as useful as the isotherm criterion, both were found to fail to apply to a particular case of DL-tris-ethylenediamine-cobalt(III) chloride hydrate, in which only one kind of channel filled with water molecules runs parallel to the direction of the *c*-axis[1]. This cobalt complex presents a remarkable model substance as a crystal

1) Report V: H. Chihara and K. Nakatsu, This Bulletin, **32**, 903 (1959).
2) Report IV: H. Chihara and S. Seki, ibid., **32**, 897 (1959).

hydrate of zeolite type, as a porous adsorbent having exactly uniform capillaries, as a host-lattice of an *Einchluss-verbindung* like a urea adduct, and as an isothermal order-disorder assembly of water molecules.

Thermodynamics of Dehydration

For a dehydration equilibrium

$$A\cdot nH_2O \rightleftarrows A\cdot(n-1)H_2O + H_2O(g)$$

the change in the standard entropy ΔS is given by

$$S_H - S_A = S_W - \Delta S$$

where S_H, S_A and S_W are the standard entropies of the hydrate, the lower hydrate (or the anhydrous crystal) and the water vapor (45.1 cal./deg. mol.), respectively. $S_H - S_A$ can be obtained from the measurements of the heat capacities and ΔS from the tensiometric measurements. Table I lists these values for a few hydrate systems. It is seen in Table I that $S_H - S_A$ is nearly constant being around 10 e. u., which is also nearly equal to the entropy of ice at the standard state. This shows that an additivity rule holds for these crystalline solids. The values of $S_W - \Delta S$, on the other hand, scatter far and wide, being as large as 21.6 e. u. and as small as -2.5 e. u. One of possible reasons for the discrepancies between $S_H - S_A$ and $S_W - \Delta S$ would be that the stable equilibrium may not have been attained in the tensiometric measurements. This may undoubtedly cause a serious discrepancy. However, it is readily shown that a discrepancy can naturally occur even if the equilibrium was obtained in both thermal and tensiometric measurements.

TABLE I. ENTROPY PER MOLE OF WATER IN CRYSTALLINE HYDRATES

Hydrate	$S_H - S_A$[3]	$S_W - \Delta S$
$MgCl_2\cdot 2H_2O$	10.2	10.8[4]
$MgCl_2\cdot 4H_2O$	10.1	10.4[4]
$MgCl_2\cdot 6H_2O$	12.2	13.9[5]
$CaSO_4\cdot \frac{1}{2}H_2O$	11.4	-2.5[6]
$ZnBr_2\cdot 2H_2O$	11.7	21.6[7]
$ZnSO_4\cdot 2H_2O$	10.4	8.5[8]
$ZnSO_4\cdot 7H_2O$	5.6	2.9[8]
$CdBr_2\cdot 4H_2O$	10.7	9.9[9]
$CdSO_4\cdot \frac{8}{3}H_2O$	10.1	12.6[10]
$CuSO_4\cdot H_2O$	8.7	7.9[11]
$CuSO_4\cdot 3H_2O$	9.0	11.6[10]
$CuSO_4\cdot 5H_2O$	9.6	8.0[10]
$NiCl_2\cdot 6H_2O$	8.3	13.2[4]
$BaCl_2\cdot 2H_2O$	8.5	6.8[12]

Let us consider a system consisting of a hydrate phase (denoted by the subscript 1), the anhydrous phase (subscript 2) and the water vapor phase (subscript 3) in equilibrium. The molar Gibbs free energy of the whole system is given by

$$G_m = (1-\theta)\mu_1 + \theta\mu_2 + c\theta\mu_3 \qquad (1)$$

in terms of the chemical potentials μ_i where θ corresponds to the degree of dehydration or the mole fraction of the anhydrous phase in the solid components. One mole of the hydrate is assumed to produce c moles of water vapor. The conditions for the stable equilibrium are

$$\frac{dG_m}{d\theta} = 0 \qquad \frac{d^2G_m}{d\theta^2} > 0 \qquad (2)$$

Case A.—The simplest case in which

$$\left(\frac{\partial\mu_1}{\partial\theta}\right)_{P,T} = \left(\frac{\partial\mu_2}{\partial\theta}\right)_{P,T} = 0 \qquad (3)$$

leads to the ordinary condition of equilibrium

$$\mu_1 = \mu_2 + c\mu_3 \qquad (4)$$

By defining the absolute activity λ_i by

$$\mu_i = kT\log\lambda_i \qquad (5)$$

the equilibrium constant K is then obtained as

$$K \equiv \frac{\lambda_1}{\lambda_2\cdot(\lambda_3^+)^c} = \left(\frac{p}{P^+}\right)^c \qquad (6)$$

where λ^+ and P^+ are the standard-state quantities. The pressure equation will then be

$$\log p - \log P^+ = \frac{1}{c}(\log\lambda_1 - \log\lambda_2 - c\log\lambda_3)$$
$$= -\frac{\Delta h}{kT} + \frac{\Delta s}{k} \qquad (7)$$

where

3) F. D. Rossini et al., "Selected Values of Chemical Thermodynamic Properties", NBS Circular 500, National Bureau of Standards, U. S. Department of Commerce, U. S. Government Printing Office, Washington (1952).
4) I. Sano, *J. Chem. Soc. Japan (Nippon Kwagaku Kwaishi)* **59**, 1145 (1938).
5) J. H. Derby and V. Yngve, *J. Am. Chem. Soc.*, **38**, 1439 (1916).
6) H. Lescoeur, *Ann. chim. Soc.*, **21**, 511 (1890).
7) Y. P. Baxter and R. D. Warren, *J. Am. Chem. Soc.*, **33**, 340 (1911).
8) P. C. F. Frowein, *Z. physik. Chem.*, **1**, 1 (1887).
9) F. Ishikawa and Y. Ueda, *Sci. Rept. Tohoku Univ.*, **22**, 275 (1935).
10) C. D. Carpenter and E. R. Jette, *J. Am. Chem. Soc.*, **45**, 583 (1923).
11) A. Siggel, *Z. Elektrochem.*, **19**, 349 (1913).
12) G. F. Hüttig and Ch. Slonim, *Z. anorg. Chem.*, **181**, 65 (1929).

$$\left.\begin{aligned} \Delta h &= (h_2 + ch_3 - h_1)/c \\ \text{and} \quad \Delta s &= (s_2 + cs_3 - s_1)/c \end{aligned}\right\} \qquad (8)$$

Eq. 7 is the integrated form of the Clapeyron-Clausius equation. The second condition (Eq. 2) gives

$$\frac{\mathrm{d}\log p}{\mathrm{d}\theta} = \frac{\mathrm{d}}{\mathrm{d}\theta}\left\{-\frac{1}{kT}(\mu_1 - \mu_2 - c\mu_3{}^+)\right\} = 0 \qquad (9)$$

showing that the dehydration pressure should be constant over the range of the θ values or, in other words, the dehydration should be stepwise as is the case for $CuSO_4 \cdot 5H_2O$ and its lower hydrates. Eqs. 7 and 8 then indicate that the Clapeyron-type equation gives the integral heat and entropy of dehydration when the condition (3) is satisfied. The heat and entropy thus obtained should be comparable with the third-law values $S_H - S_A$. It is inferred that the condition (3) holds in hydrates for which one sees approximate agreement between $S_H - S_A$ and $S_W - \Delta S$ in Table I.

Case B.—In a general case where the condition (3) is not satisfied,

$$\left(\frac{\partial \mu_1}{\partial \theta}\right)_{P,T} \neq 0 \qquad \left(\frac{\partial \mu_2}{\partial \theta}\right)_{P,T} \neq 0 \qquad (10)$$

the condition for the equilibrium gives

$$-\log \lambda_1 + \log \lambda_2 + c \log \lambda_3 + (1-\theta)\left(\frac{\partial \log \lambda_1}{\partial \theta}\right)_{P,T} + \theta\left(\frac{\partial \log \lambda_2}{\partial \theta}\right)_{P,T} = 0 \qquad (11)$$

which then leads to the pressure equation

$$c \log(p/P^+) = \frac{1}{kT}\{\bar{h}_1 - \bar{h}_2 - ch_3{}^+ - T(\bar{s}_1 - \bar{s}_2 - cs_3{}^+)\} \qquad (12)$$

where $\bar{h}$ and $\bar{s}$ are the differential molar heat and entropy. The shape of the dehydration isotherm must satisfy the second condition for the equilibrium:

$$\frac{\mathrm{d}^2 G_m}{\mathrm{d}\theta^2} = \frac{\mathrm{d}}{\mathrm{d}\theta}\left\{-\mu_1 + \mu_2 + c\mu_3 + (1-\theta)\left(\frac{\partial \mu_1}{\partial \theta}\right)_{P,T} + \theta\left(\frac{\partial \mu_2}{\partial \theta}\right)_{P,T}\right\} > 0 \qquad (13)$$

which then leads to

$$\frac{\mathrm{d}}{\mathrm{d}\theta}(\bar{\mu}_2 + c\mu_3{}^+ - \bar{\mu}_1) = \frac{\mathrm{d}}{\mathrm{d}\theta}(\bar{\mu}_2 - \bar{\mu}_1) > 0 \qquad (14)$$

Differentiating Eq. 12 with respect to θ gives

$$ckT\frac{\mathrm{d}\log(p/P^+)}{\mathrm{d}\theta} = \frac{\mathrm{d}}{\mathrm{d}\theta}(\bar{\mu}_1 - \bar{\mu}_2 - c\mu_3{}^+) = \frac{\mathrm{d}}{\mathrm{d}\theta}(\bar{\mu}_1 - \bar{\mu}_2) \qquad (15)$$

Therefore we have

$$\frac{\mathrm{d}\log p}{\mathrm{d}\theta} < 0 \qquad (16)$$

This shows that the dehydration pressure decreases constantly with increasing θ, or it corresponds to the zeolitic dehydration. The Clapeyron-Clausius equation gives differential molar heat and entropy in this case.

$S_H - S_A$ as obtained from the calorimetric results corresponds to the difference in the integral entropies $s_1 - s_2$ which is related to ΔS by Eq. 8.

Now, it will be evident that the discrepancies between $S_H - S_A$ and $S_W - \Delta S$ may naturally occur if the dehydration proceeds zeolitically as the differential and the integral entropies of dehydration do not usually coincide with each other*, except for accidental coincidence.

In view of the fast that the integral entropy assigned to water molecules within a hyrate lattice is nearly constant being approximately 10 e. u., ΔS values obtained by the tensiometric measurements can be used to determine whether or not the dehydration is zeolitic even if the corresponding calorimetric data are unavailable. In Table I, the discrepancy is appreciable in $CaSO_4 \cdot \frac{1}{2}H_2O$, $ZnBr_2 \cdot 2H_2O$ and $ZnSO_4 \cdot 7H_2O$. The hemihydrate of $CaSO_4$ undergoes zeolitic dehydration as shown by the isotherm reported by Gregg and Willing[13]. The cases of $ZnBr_2$ and $ZnSO_4$ hydrates have not been examined in detail and it is not clear if these are really zeolitic cases.

TABLE II. COMPARISON OF THE ISOTHERM AND ENTROPY CRITERIONS FOR THE TWO TYPES OF DEHYDRATION

	For dehydration by which crystal lattice collapses	For dehydration by which lattice does not collapse
$S_H - S_A$	about 10 e. u.	about 10 e. u.
$S_W - \Delta S$	equal to $S_H - S_A$	not equal to $S_H - S_A$
Clapeyron eq. gives	integral heat and entropy	differential heat and entropy
Pressure vs. deg. of dehydration	constant pressure	monotonous decline

* It is possible to calculate the intergral entropy for zeolitic hrdrates, if complete data of isotherms are available particularly at a very low presure region. See T. L. Hill, P. H. Emmett and L. G. Joyner, *J. Am. Chem. Soc.*, **73**, 5102, 5933 (1951).

13) S. J. Gregg and E. G. G. Willing, *J. Chem. Soc.*, **1951**, 2373, 2916.

Table II summarizes and compares the "isotherm" and "entropy" criterions. The "entropy criterion" is thus entirely equivalent to the "isotherm criterion" which has widely been accepted. The applicability or the inapplicability should be the same for both criterions. The advantage of the "entropy criterion" rests on the fact that the measurements of the dehydration pressure at different water contents are not necessary.

A Notable Case in which the Criterions Fail to Apply

When one correlates a thermodynamic relation to an atomistic interpretation, there is a risk of his over-relying upon empirical rules. Thus the "isotherm criterion" depends on a lot of experimental facts on the isotherm determinations and the structural studies before and after dehydration. This is in a way based on the analogy between zeolitic dehydration and adsorption. The phase rule of course can make judgement if the number of phases is known unambiguously.

The case of DL-$[Co\ en_3]Cl_3 \cdot nH_2O$ ($n \leq 4$), the dehydration of which was reported in the preceding paper[1], provides us with a notable exception to both criterions, which are however mutually consistent. Fig. 1

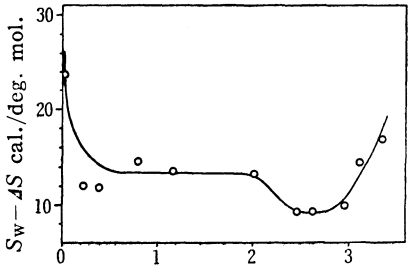


Fig. 1. Change with the water content in the differential molar entropy of water in $[Co\ en_3]Cl_3$ hydrate.

shows the change in $S_W - \Delta S$ as the hydration proceeds. $S_W - \Delta S$ is nearly constant between $n=0.2$ and 3 except for a minimum occurring around $n=2.6$[1]. Below and above this range of values of n, $S_W - \Delta S$ tends to increase, deviating from the additivity value of 10 e. u. The entropy criterion tells that the crystal undergoes zeolitic dehydration when $n \leq 0.2$ and when $n \leq 3$ and the lattice-destructive dehydration when n is between 0.2 and 3. This apparent conclusion is consistent with the isotherm criterion as judged from the isotherm given in Fig. 7 of the preceding paper[1], in which the pressure remains constant between $n=0.2$ and 3. However, as already reported[1], this conclusion is not justified by the crystal structure studies by which we see that the structure is unchanged by dehydration except for the loss of water molecules in the channels. This must evidently correspond to zeolitic dehydration and thus the failure of both criterions is apparent.

The extreme uniformity of the pore structure of this crystal seems to be responsible for the failure. There exists only one kind of pore running parallel in the direction of the *c*-aixs of the crystal. Such uniformity has never been realized in actual hydrate systems or adsorption systems and has been out of reach of empirical rules mentioned in the first paragraph of the present section. This type of isotherm should lead to a sharp distribution function of pore sizes if we treat it by a standard method utilizing the desorption branch of sorption isotherm[14].

The most reliable criterion would be the structure investigation by the X-rays but in most of zeolite minerals and gels there is a broad distribution of pore size, which necessarily gives rise to the isotherm corresponding to the *Case B*; $[Co\ en_3]Cl_3$ hydrate is one of the rarest exceptions. The "entropy criterion" as well as the "isotherm criterion" is, therefore, considered to be still valid in judging which type of dehydration a particular hydrate would undergo.

Comparison of Capillary Radius as Determined by Dehydration Isotherm and by X-ray Study

It will be interesting to see to what extent the well-known Kelvin equation

$$\log(p_r/p) = -2\sigma M/(\rho r \boldsymbol{R} T) \qquad (17)$$

gives reasonable pore radius when it is applied to the system of pores of molecular dimensions. p is the saturation pressure over a plane surface of the adsorbate liquid (water in the present case) whose surface tension is σ, density is ρ, and molecular weight is M. p_r is the saturation pressure over the surface, its radius of curvature being r. This equation has been known to hold for a macroscopic pore or a macroscopic droplet of liquid but we

14) C. Pierce, *J. Phys. Chem.*, **57**, 149 (1953).

seem to have available no direct experimental test of the equation down to pores of a few Ångstroms in radius.

The horizontal portion of the isotherm given in Fig. 7 of the preceding paper[1] gives $r=5.8$Å if $\rho=0.9971$, $\sigma=71.97$ dyn./cm., $p=23.756$ mmHg and $p_r=2.85$ mmHg are inserted in Eq. 17. It would not be necessary to add to r the thickness of a monolayer or of statistical layers as the capillary condensation begins at $n=0.2$, far below the monolayer capacity $n=3$**. On the other hand, the result of the crystal structure analysis[15] gives the distances from the origin (the center of a pore, see Fig. 3 of the preceding paper), in the plane parallel to the base of the hexagonal cell, 2.9 Å to the periphery of the van der Waals radius of the nearest CH_2 group and 3.4Å to the periphery of the nearest chloride ion (the inner wall of the pore is a little pleated).

We are now led to the conclusion that for water vapor as the adsorbate the Kelvin equation gives only the order of magnitude of the pores radius of micropores. We shall undertake experiments with nitrogen as the adsorbate later. For macropores the discrepancy would be much smaller. In view of the fact that the concept of the surface tension would undoubtedly lose its significance in such systems of water molecules, the Kelvin equation has been applied beyond its reasonable limit of application, although the method has been in extensive use for evaluating the pore size distribution in many adsorbents. The use of the Kelvin equation was partly justified for macropores by the experimental results that it gives the pore sizes in good agreement with those obtained by the mercury porosimeter method[16]. The present result gives some clue to the error caused by the use of the Kelvin equation for micropores.

Summary

A simple theory of the thermodynamics of hydrates is developed, which is able to show that the differential molar entropy of dehydration changes with the water content continuously if the hydrate undergoes zeolitic (continuous) dehydration. In this case the integral molar entropy of dehydration does not agree with the differential entropy. The same is true for the heat contents. For stepwise dehydration, on the other hand, both differential and integral entropies coincide in values. A new criterion, termed "entropy criterion", is presented that if the differential entropy of the water of crystallization, obtained by subtracting the entropy of dehydration (determined by the pressure measurements) from the standard entropy of water vapor 45.1 e. u., differs greatly from 10 e. u., the hydrate should undergo zeolitic dehydration and should have water molecules weakly bonded to the crystal lattice, from which water can be removed without causing collapse of the lattice. This new criterion is equivalent to using the current "isotherm criterion".

DL-$[Co\ en_3]Cl_3 \cdot nH_2O$ ($n \leq 4$) presents a notable exception to both criterions in that the crystal undergoes zeolitic dehydration in spite of its entropy of dehydration and its isotherm indicating the stepwise dehydration. The failure of the criterions in this crystal is due to the extreme uniformity of pore structure of the hydrate. The Kelvin equation for calculating the pore radius (giving 5.8Å) from the dehydration isotherm is tested against the pore radius obtained by the X-ray crystal structure analysis (giving 2.9 to 3.4Å). It may be concluded that the Kelvin equation is considered to give only the order of magnitude for micropore size. This cobalt complex hydrate is one of the rarest examples having exactly uniform pores and the criterion for the type of dehydration here presented is still effective in most cases.

The author wishes to express his sincere thanks to Professor I. Nitta and Assistant Professor S. Seki of the Department of Chemistry, Osaka University for illuminating discussions.

Department of Chemistry
Faculty of Science
Osaka University
Nakanoshima, Osaka

** It is rather surprising to note the capillary condensation is completed just befor the monolayer is filled.

15) K. Nakatsu, Y. Saito and H. Kuroya, This Bulletin, **29**, 428 (1956).

16) E. P. Barrett, L. G. Joyner and P. P. Halenda, *J. Am. Chem. Soc.* **73**, 373 (1951).

Quantum-Mechanical Considerations of Chemical Reaction Rates. II. The Transmission through Curved Reaction Path

By Iwao YASUMORI

(Received February 17, 1959)

Previous quantum-mechanical treatments[1-5] of chemical reaction rates deal principally with the behavior of the wave which represents the reacting system, passing from the region of the reactant to that of the resultant on the potential energy surface of reaction. These treatments also may be classed in two ways according to whether their objects are the transmission of the wave through the potential energy barrier[1-4] or through the curve or bend of the reaction path[5], for both the barrier and the bend are the important characteristics of the reaction path on the potential energy surface. Much knowledge of the microscopic feature of reaction rates, was obtained from these studies, but all these results were derived by the use of highly idealized models of potential, for example, one-dimensional square barrier or a path with a perpendicular turn, etc., to avoid mathematical difficulties.

Therefore, it is necessary to examine which of the conclusions correspond to the real behavior of reaction or are due merely to the used model itself.

For the purpose of considering the problem by the use of the more plausible potential models than those used before, Fueki and the present author have recently treated the transmission through the two-dimensional smooth barrier with a parabolic section and have made clear the properties of the quantum-mechanical correction which is necessary for the ordinary estimation of rate by the absolute reaction rate theory[6].

In this paper, another important problem, the transmission through the smoothly curved path with reasonable vibrational potential section is discussed in general and the extent of reflection and transmission is computed for some reaction examples. Then the inspection stated above is made comparing the present results with that of Hulburt and Hirschfelder's work[5] which was previously the first and only detailed one for the effect of the curved path. Also a consideration is made for their predictions of null transmission for the system with particular values of energy and of the availability of this effect for the isotopic separation.

Theoretical

Now we take, as a typical example of reaction, an elementary displacement reaction between atom A and molecule BC, A+BC→AB+C. The general feature of the potential energy surface for linear configuration is as shown in Fig. 1.

In order to discuss the transmission through the bend, we do not take the potential barrier into consideration and use a simplified surface and coordinate system shown in Fig. 2 hereafter.

We assume, as shown in Fig. 2, that the equi-potential lines are parallel with y and y' axes in regions I and II respectvely and that their radii at the bending part are constant. The dotted line shows the reaction path of radius r_e in region II, which traces minima in the direction of x, r or x' in the respective region.

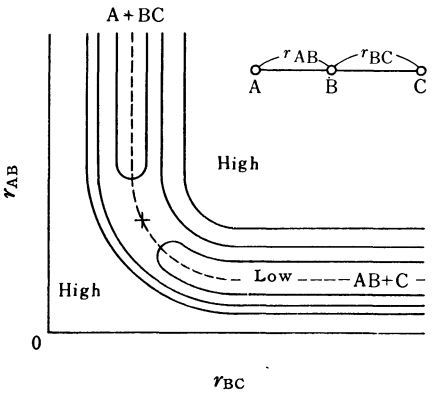


Fig. 1. Potential energy surface of reaction A+BC→AB+C.

1) J. O. Hirschfelder and E. Wigner, *J. Chem. Phys.*, **7**, 616 (1939).
2) E. Wigner, *Z. physik. Chem.*, **B19**, 203 (1932).
3) R. P. Bell, *Proc. Roy. Soc.*, **A139**, 466 (1933).
4) F. A. Matsen, *J. Chem. Phys.*, **22**, 165 (1954).
5) H. M. Hulburt and J. O. Hirschfelder, ibid., **11**, 276 (1943).
6) Paper I of this series: I. Yasumori and K. Fueki, This Bulletin, **29**, 1 (1956).

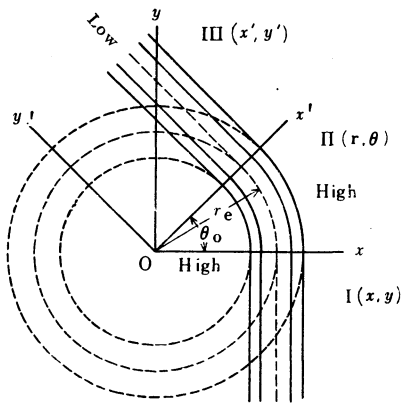


Fig. 2. Coordinate system of curved reaction path.

The wave equation to be satisfied by the system is

$$\nabla^2\Psi+\frac{8\pi^2\mu}{h^2}(E-V)\Psi=0 \tag{1}$$

where μ is the reduced mass of the system. According to the assumed form of potential V, the wave equation is separable with respect to the variables (x,y), (r,θ) and (x',y') in the regions I, II and III, respectively.

Now let us consider an incident wave of unit amplitude in region I, which expresses the state of reactant and comes from $y<0$ to the boundary $y=0$, being partly reflected at the boundary and partly transmitted through the bend.

Now, the wave functions which express the states of the system in each region are given as follows: In region I,

$$\Psi^{\mathrm{I}}=\phi_\kappa{}^{\mathrm{I}}(x)\cdot\exp\left(\frac{2\pi i}{h}p_\kappa\cdot y\right)+\sum_\lambda B_{\kappa\lambda}\phi_\lambda{}^{\mathrm{I}}(x)\cdot\exp\left(-\frac{2\pi i}{h}p_\lambda\cdot y\right) \tag{2}$$

where the first term represents the incident wave and the second the reflected waves. $\phi_\kappa{}^{\mathrm{I}}(x)$ is the eigenfunction of vibrational motion of the system in κ-th state and $\exp[(2\pi i/h)\cdot p_\kappa\cdot y]$ represents the eigenfunction of translational motion with the momentum p_κ. The total energy of the system, E, is equal to the sum of those of each motion, E_{vib} and E_{trans}. $B_{\kappa\lambda}$ is the coefficient of reflected wave referring to the transition between states, κ and λ.

In a similar way, the wave functions in regions II and III are expressed as

$$\Psi^{\mathrm{II}}=\sum_k[C_{\kappa k}\cdot\phi_k{}^{\mathrm{II}}(r)\cdot\exp(im_k\theta)+D_{\kappa k}\cdot\phi_k{}^{\mathrm{II}}(r)\cdot\exp(-im_k\theta)] \tag{3}$$

and

$$\Psi^{\mathrm{III}}=\sum_{\kappa'}F_{\kappa\kappa'}\phi_{\kappa'}{}^{\mathrm{III}}(x')\cdot\exp\left(\frac{2\pi i}{h}p_{\kappa'}\cdot y'\right) \tag{4}$$

where m_k is a constant and we may define a new constant q_k by the equation

$$m_k=\frac{2\pi}{h}\cdot q_k\cdot r_e \tag{5}$$

The coefficients of the transmitted waves, $C_{\kappa k}$ or $D_{\kappa k}$, are defined corresponding to the forward or backward translational motion in k-th state of region II and that of the transmitted wave, $F_{\kappa\kappa'}$ referring to κ'-th state in region III. We assume that all the wave functions for the vibrational motion, $\phi_\kappa{}^{\mathrm{I}}(x)$, $\phi_{\kappa'}{}^{\mathrm{III}}(x')$ and $\phi_k{}^{\mathrm{II}}(r)$ are normalized to unity.

Thus the following equations are readily obtained by the usual procedure of substituting the wave functions into the boundary conditions,

$$\Psi^{\mathrm{I}}=\Psi^{\mathrm{II}}\ \text{and}\ \frac{\partial\Psi^{\mathrm{I}}}{\partial y}=\frac{\partial\Psi^{\mathrm{II}}}{\partial y}=\frac{1}{r}\left(\frac{\partial\Psi^{\mathrm{II}}}{\partial\theta}\right)_{\theta=0} \tag{a), (b)}$$

at $y=0$ and

$$\Psi^{\mathrm{II}}=\Psi^{\mathrm{III}}\ \text{and}\ \frac{\partial\Psi^{\mathrm{III}}}{\partial y'}=\frac{\partial\Psi^{\mathrm{II}}}{\partial y'}=\frac{1}{r}\left(\frac{\partial\Psi^{\mathrm{II}}}{\partial\theta}\right)_{\theta=\theta_0} \tag{c), (d)}$$

at $y'=0$; we have

$$\delta_{\kappa\lambda}+B_{\kappa\lambda}=\sum_k(C_{\kappa k}+D_{\kappa k})u_{k\lambda} \tag{6}$$

$$\delta_{\kappa\lambda}p_\kappa-B_{\kappa\lambda}p_\lambda=\sum_k(C_{\kappa k}-D_{\kappa k})\cdot q_k\cdot v_{k\lambda} \tag{7}$$

$$\sum_k[C_{\kappa k}\cdot\exp(im_k\theta_0)+D_{\kappa k}\times\exp(-im_k\theta_0)]u'_{k\kappa'}=F_{\kappa\kappa'} \tag{8}$$

and

$$\sum[C_{\kappa k}\cdot\exp(im_k\theta_0)-D_{\kappa k}\times\exp(-im_k\theta_0)]\cdot q_k\cdot v'_{k\kappa'}=F_{\kappa\kappa'}\cdot p'_{\kappa'} \tag{9}$$

The expansion coefficients $u_{k\lambda}$'s and $v_{k\lambda}$'s are defined by the equations

$$[\phi_k{}^{\mathrm{II}}(r)]_{\theta=0}=\phi_k{}^{\mathrm{II}}(x)=\sum_\lambda u_{k\lambda}\cdot\phi_\lambda{}^{\mathrm{I}}(x) \tag{10}$$

and

$$\left[\frac{r_e}{r}\cdot\phi_k{}^{\mathrm{II}}(r)\right]_{\theta=0}=\frac{r_e}{x}\cdot\phi_k{}^{\mathrm{II}}(x)=\sum_\lambda v_{\kappa\lambda}\cdot\phi_\lambda{}^{\mathrm{I}}(x) \tag{11}$$

Similarly the coefficients $u'_{k\lambda'}$'s and $v'_{k\lambda'}$'s are also defined by the equations

$$[\phi_k{}^{\mathrm{II}}(r)]_{\theta=\theta_0}=\phi_k{}^{\mathrm{II}}(x')=\sum_{\lambda'}u'_{k\kappa'}\cdot\phi_{\lambda'}{}^{\mathrm{III}}(x') \tag{12}$$

and

$$\left[\frac{r_e}{r}\cdot\phi_k{}^{\mathrm{II}}(r)\right]_{\theta=\theta_0}=\frac{r_e}{x'}\cdot\phi_k{}^{\mathrm{II}}(x')$$

$$=\sum_{\lambda'} v'_{k\lambda'} \cdot \phi_{\lambda'}^{III}(x') \quad (13)$$

Eqs. 6—9 are expressed by the use of the matrix form as

$$1+B=(C+D)u \quad (6')$$

$$p-Bp=(C-D)qv \quad (7')$$

$$(CW+DW^*)u'=F \quad (8')$$

and $$(CW-DW^*)qv'=Fp' \quad (9')$$

where W and its complex conjugate W^* are diagonal matrices whose elements are $\exp(im_k\theta_0)$'s and $\exp(-im_k\theta_0)$'s, respectively. Accordingly the coefficient matrix of the reflected waves, B, and that of the transmitted waves, F, are formally derived as follows: We have

$$B=-(NWM'+MW^*N') \times (MWM'+NW^*N')^{-1} \quad (14)$$

and $$F=1/2\cdot[B(MW+NW^*)+(NW+MW^*)]\cdot u' \quad (15)$$

where

$$M=u^{-1}-pv^{-1}q^{-1} \quad (16)$$

$$N=u^{-1}+pv^{-1}q^{-1} \quad (17)$$

$$M'=u'-qv'p'^{-1} \quad (18)$$

and $$N'=u'+qv'p'^{-1} \quad (19)$$

By the use of the expressions of B and F, the reflection and transmission coefficients $\rho_{\kappa\lambda}$ and $\kappa_{\kappa\kappa'}$ are given by

$$\rho_{\kappa\lambda}=|B_{\kappa\lambda}|^2\cdot p_\lambda/p_\kappa \quad (20)$$

and $$\kappa_{\kappa\kappa'}=|F_{\kappa\kappa'}|^2\cdot p_{\kappa'}/p_\kappa \quad (21)$$

Furthermore, the total reflection and transmission coefficients from a definite initial κ-th state, ρ_κ, and κ_κ, are defined as

$$\rho_\kappa=\sum_\lambda \rho_{\kappa\lambda} \text{ and } \kappa_\kappa=\sum_{\kappa'}\kappa_{\kappa\kappa'} \quad (22), (23)$$

κ_κ may be estimated from the value of ρ_κ by the use of the following equation,

$$\kappa_\kappa=1-\rho_\kappa \quad (24)$$

For the simple case with a single boundary $y=0$, taking

$$D_{\kappa k}=0 \text{ and } F_{\kappa\kappa'}=0$$

the equations to be solved become

$$1+B=Cu \text{ and } p-Bp=Cqv. \quad (25), (26)$$

Then the formal solutions of B and C are

$$B=(S-1)\cdot(S+1)^{-1} \quad (27)$$

and $$C=2S(S+1)^{-1}\cdot u^{-1} \quad (28)$$

where the matrix S has the form of

$$S=pv^{-1}q^{-1}u \quad (29)$$

Therefore, the transmission coefficient, $\kappa_{\kappa k}$ is given by

$$\kappa_{\kappa k}=|C_{\kappa k}|^2\cdot q_k/p_\kappa \quad (30)$$

in this case.

It is very difficult to obtain explicitly the rigorous form of the coefficients $B_{\kappa\lambda}$, $F_{\kappa\kappa'}$ and $C_{\kappa k}$ for general cases. We, therefore, confine ourselves to the simple case where the radius of the path, r_e, is much larger than the classical amplitude of vibration, ρ_{max},

$$r_e \ll \rho_{max}$$

The approximate expressions of the coefficients in this case are given in Appendix I.

Vibrational Wave Function and Computation of the Coefficients

Now we treat the case in which the section of the channel is parabolic and the vibrational motion is simple harmonic. When we put, as the explicit form of vibrational potential,

$$V=2\pi^2\mu\nu_0^2x^2 \quad (31)$$

the normalized vibrational eigenfunction with the quantum number κ in region I is

$$\psi_\kappa^{I}(x)=N_\kappa\cdot\exp\left(-\frac{\alpha}{2}\rho^2\right)H_\kappa(\sqrt{\alpha}\cdot\rho) \quad (32)$$

where

$$\rho=x-r_e \quad \text{and} \quad \alpha=4\pi^2\mu\nu_0/h \quad (33)$$

$N_\kappa=[(\alpha/\pi)^{1/2}/2^\kappa\cdot\kappa!]^{1/2}$ is a normalization factor, $H_\kappa(\sqrt{\alpha}\cdot\rho)$ the κ-th Hermite polynomial and ν_0 the fundamental frequency of vibration. The total energy of the system in region I is

$$E=E_{vib}+E_{trans}=h\nu_0(\kappa+1/2)+(1/2\mu)p_\kappa^2 \quad (34)$$

The eigenfunction of κ'-th state in region III is readily obtained by replacing κ and x in the above expressions with κ' and x' respectively.

The radial function $\psi_k^{II}(r)$ in region II is obtained in the same way as the well-known treatment of the vibrational and rotational motions of diatomic molecule[7], since it is related to the circular potential shown in Fig. 2.

Therefore, under the condition $r_e \gg \rho_{max}$, an approximate form of $\psi_k^{II}(r)$ is given by

$$\psi_k^{II}(r)=\frac{n}{r^{1/2}}\cdot N_k\cdot\exp\left(-\frac{\alpha'}{2}\zeta^2\right)\cdot H_k(\sqrt{\alpha'}\cdot\zeta) \quad (35)$$

where

$$n\simeq[r_e(1+\beta)]^{1/2}\Big/\left[1+\frac{(2k+1)}{2\alpha r_e^2(1+\beta)^2}\right]^{1/2} \quad (36)$$

7) L. Pauling and E. B. Wilson, "Introduction to Quantum Mechanics", McGraw-Hill Book Co., Inc., New York (1935), p. 298.

$$\zeta = \rho - \beta r_e \tag{37}$$

$$\beta = \xi^2/(1+3\xi^2) \tag{38}$$

$$\nu' = \nu_0(1+3\xi^2)^{1/2} \tag{39}$$

$$\xi = q_k/2\pi\mu r_e\nu_0 \tag{40}$$

α' is obtained by replacing ν_0 in α, Eq. 33, with ν' and N_k by replacing κ and α in $N\kappa$ with k and α', respectively.

The total energy in this region is described as

$$E \simeq \boldsymbol{h}\nu'(k+1/2) + (1/2\mu)(1-\beta)q_k^2 \tag{41}$$

The matrix elements of u and v are calculated by Eqs. 32 and 35 as shown in Appendix II.

The above consideration is also applicable, in principle, to the potential with Morse function-type section, but the formulation will be quite tedious.

Few potential energy surfaces with considerable accuracy have been constructed except for the ortho-para hydrogen conversion reaction, $H+H_2 \rightarrow H_2+H$[8,9]. Therefore, we performed the computation of the reflection and transmission coefficients for the potential surfaces which have a similar fearture to that of this reaction except that the barrier is neglected.

The constants used in the computation are

$$\boldsymbol{h}\nu_0 = 12.56 \text{ kcal./mol.}$$

$$\mu = (2/3)\cdot m_H = 1.1156\times10^{-24} \text{ g.}$$

$$\theta_0 = 2\pi/3$$

and $r_e = 1.0$ and 0.5 Å

These values of r_e scarcely satisfy the condition $r_e \gg \rho_{max}$, since the classical amplitudes of vibrational motion for the ground and the first excited levels are 0.09 and 0.15Å, respectively. Calculations were performed for the range of the total energy $E < \boldsymbol{h}\nu_0(2+1/2) = 31.4$ kcal./mol. The obtained values of coefficients are shown in Figs. 3 and 4.

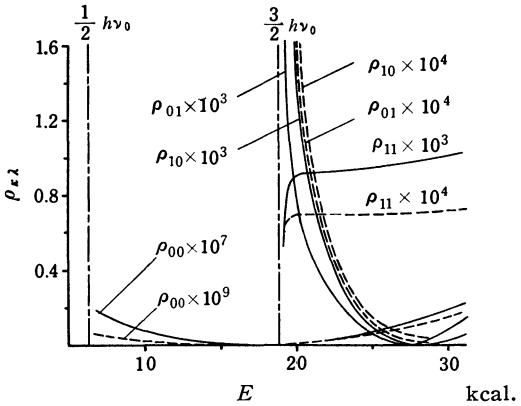


Fig. 3. Reflection coefficients for single boundary.
—— r_e=0.5Å, ---- r_e=1.0Å

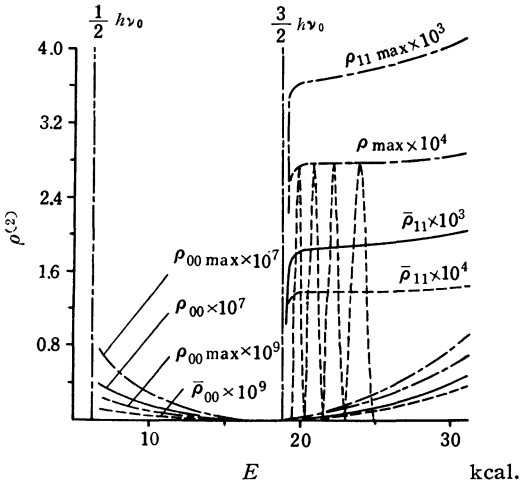


Fig. 4. Reflection coefficients for two boundaries.
—— r_e=0.5Å, ---- r_e=1.0Å, $\theta_0 = 2/3\cdot\pi$

Discussion

The present results agree, in many points, with those of Hulburt and Hirschfelder's in which the potential surface of square-well channel with 90° turn is used, but there are some noticeable differences between them.

That the reflection and transmission coefficients $\rho_{\kappa\lambda}$ and $\kappa_{\kappa\lambda}$ are not zero for $\kappa \neq \lambda$, shows the occurrence of the cross transition between the different vibrational states and also verifies their prediction about this occurrence obtained from the consideration of the classical motion of a particle in smoothly curved channel[10].

Apart from their absolute magnitude, the general properties of the coefficients resemble the results of Hulburt et al. for the case with vibrational transition.

In our case of single boundary with which their results include nothing to be compared, $\rho_{\kappa\kappa}$'s vary slightly with the increase of the translational energy, while $\rho_{\kappa\lambda}$'s, which rise where the translational energy is just equal to $\kappa\boldsymbol{h}\nu_0$ $(\kappa > \lambda)$ or $\lambda\boldsymbol{h}\nu_0$ $(\lambda > \kappa)$, fall rapidly and then increase

8) J. O. Hirschfelder, N. Rosen and H. Eyring, *J. Chem. Phys.*, **4**, 121 (1936).
9) J. O. Hirschfelder, H. Eyring and B. Topley, ibid., **4**, 173 (1936).
10) Ref. 5, p. 280.

gradually as the energy increases. In general, $\rho_{\varepsilon\lambda}$'s are much larger than $\rho_{\varepsilon\varepsilon}$'s in the available range of energy. For the case of two boundaries, the reflection coefficients are oscillating function of energy as shown in Fig. 4. This property is readily seen from the expressions of $B_{\varepsilon\lambda}$'s in Appendix I and those of ρ's, Eq. 20: By the introduction of such approximations as $(v_0^{-1}\cdot u_0)p \simeq q$, etc., the resultant forms are

$$\rho_{\varepsilon\varepsilon} \simeq 4\rho^{(1)}{}_{\varepsilon\varepsilon} \sin^2 m_\varepsilon\theta_0 \quad (42)$$

and $$\rho_{\varepsilon\lambda} \simeq 4\rho^{(1)}{}_{\varepsilon\lambda} \sin^2\{(m_\varepsilon + m_\lambda)/2\cdot\theta_0\} \quad (43)$$

where $\rho^{(1)}$'s represent those of single boundary under the same condition. The angle of bending, θ_0, which is related to the masses of component species, m_A, m_B and m_C, by the equation[11]

$$\sin(\theta_0 - \pi/2) = [m_A m_C/(m_A + m_B)(m_B + m_C)]^{1/2}$$

takes value which is between $\pi/2$ and π. A larger value of θ_0 makes the period of oscillation shorter (Fig. 5).

They also found such an oscillating property of coefficient as stated above and regarded it as an essential one for the transmission of waves through a bend. The present author presumes, however, that the property is partly of artificial nature being due to the form of potential models which have two discontinuous boundaries and is partly of real nature relating to the efficiency of energy transfer between the translational and vibrational motions, by the considerations given below.

The reasons why the form of potential model is responsible are as follows:

(a) Whatever the transmission to be estimated is for a bend or a barrier, all the reflection and transmission coefficients obtained change monotonously with energy in the case of smooth potential without any boundary[3,6], or even in those of single boundary[1], while they always oscillate in the cases of two boundaries[1,5].

(b) From the present result with two boundaries as shown in Fig. 4, it is found that the coefficients which are averaged over each period of oscillation[12] are about twice as large as those of a single boundary under the same condition. This property is based, perhaps, on the fact that the coefficients are the functions of amplitude of the standing waves which exist between boundaries and the amplitude of a wave with a definite phase varies periodically with respect to the momentum q and θ_0 at one of the boundaries. Therefore, when we take the average for each period of oscillation, which corresponds to superposition of all waves with any phase, the results seem to give good approximation for the actual behavior[13]. It goes without saying that such a property as stated above can not be expected in a real case, since the potential energy surface of reaction would be continuous everywhere considering the nature of valence force.

In the next place, their result that the oscillating transmission coefficients get zero values when the energy of translation is just equal to several energy units of quantized motion which is perpendicular to the direction of the above motion, is explained as the complete transfer of translational energy to the vibrational one. This property is also seen from the present result that the value of ρ_{01} rises steeply as the translational energy approaches to $h\nu_0$.

It seems that the speciality of the square-well channel with 90° turn used by them comprises incidentally these effects of real and of virtual: The wave functions which express the translational and vibrational motions are of similar form and their eigenvalues in the bending part are identical to each other.

From these considerations, it will be concluded that the total transmission coefficients κ_ε's decrease stepwise with the increase of energy on account of the entry of reflections in which the higher vibrational states are concerned. This tendency also agrees with that which Hulburt et al. pointed out previously.

Subsequently, the effect of the curvature is examined. A larger curvature (smaller radius) brings about the increase of reflection in both the cases with and without the vibrational transition (Figs. 3 and 4). Because of the smallness of net reflection, however, almost all systems pass through the bend, preserving initial vibration quanta. This persistency of vibrational state was also found for the transmission through the barrier which was treated in

11) S. Glasstone, K. J. Laidler and H. Eyring, "The Theory of Rate Processes", McGraw-Hill Book Co., Inc., New York (1941), p. 102.

12) Since $\frac{1}{\pi}\int_0^\pi \sin^2 x\,dx = 1/2$, the averaged value of $\rho_{\varepsilon\varepsilon}$ in Eq. 43, $\bar{\rho}_{\varepsilon\varepsilon}$, is expressed by $\bar{\rho}_{\varepsilon\varepsilon} \simeq 2\rho_{\varepsilon\varepsilon}{}^{(1)}$, where $\rho_{\varepsilon\varepsilon}{}^{(1)}$ is assumed to be nearly constant in each period. Other coefficients are also treated analogously.

13) A similar situation is held in the case of Ref. 1, p. 621, in which the transmission through an energy barrier was treated.

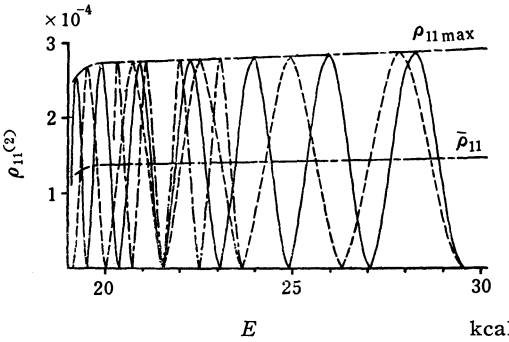


Fig. 5. Variation of $\rho_{11}^{(2)}$ with increase of bending angle θ_0.
r_e=1.0Å,
---- $\theta_0=\pi/2$, —— $\theta_0=2\pi/3$, —·—· $\theta_0=\pi$

Paper I of this series[14]. The case of Hulburt and Hirschfelder's, in which rather large decrease of transmission was estimated, corresponds to that of extremely small radius $r_e=\rho_{\max}$ in our case.

It is expected that the transmission coefficient becomes different for the system including isotopes, since the resultant μ changes its magnitude for the same value of energy. This effect was also pointed out by them and their result of oscillating coefficient with perfect reflection made them expect its availability for the isotopic separation. Since, however, the difference between reflections for isotopic reactions is also very small, the transmission through the bend seems not to be effective for the process.

As a quantum-mechanical correction necessary for the rate-estimation by the usual method, the overall transmission coefficient κ_{bend} is defined by[6]

$$\kappa_{\text{bend}}=\sum_{\varepsilon} e^{-\frac{E_{\text{vib}}}{kT}}\cdot\int_0^{\infty}\kappa_{\varepsilon}\cdot e^{-\frac{p_{\varepsilon}^2}{2\mu kT}}\cdot p_{\varepsilon}\,dp_{\varepsilon}$$
$$\times\left[\sum_{\varepsilon} e^{-\frac{E_{\text{vib}}}{kT}}\cdot\int_0^{\infty} e^{-\frac{p_{\varepsilon}^2}{2\mu kT}}\cdot p_{\varepsilon}\,dp\right]^{-1}$$
$$=1-(\mu kT)^{-1}\cdot(1-e^{-\frac{h\nu_0}{kT}})$$
$$\times\left[\sum_{\varepsilon=0} e^{-\frac{\varepsilon h\nu_0}{kT}}\cdot\int_0^{\infty}\rho_{\varepsilon}e^{-\frac{p_{\varepsilon}^2}{2\mu kT}}\cdot p_{\varepsilon}\,dp_{\varepsilon}\right] \quad (44)$$

Since the individual κ_{ε}'s are nearly equal to unity, the resultant κ_{bend} is also close to unity and gradually decreases as the temperature becomes higher. The values,

14) This effect means that the perturbation at the bend should be very small compared with the total energy of the system. The present condition, $r_e\gg\rho_{\max}$, which is equivalent to that in Ref. 6, p. 2, $a_0\gg aV_r(r)$, satisfies this restriction.

TABLE I. VALUES OF $(1-\kappa_{\text{bend}})$[15]

Temp. °K	300	500	1000	2000
r_e=0.5Å	3.0×10^{-8}	1.3×10^{-6}	3.8×10^{-4}	3.4×10^{-3}
r_e=1.0Å	2.0×10^{-11}	7.3×10^{-7}	2.3×10^{-4}	2.8×10^{-3}

$1-\kappa_{\text{bend}}$, for the hydrogen atom-molecule reaction, for example, are shown in Table I.

Finally, as concerns the reacting system which includes heavier species than hydrogen, it is very difficult to presume the exact behavior of the transmitting waves, because the factors μ, r, ν_0 and θ_0 change markedly for respective cases. In general, increased μ and lowered ν_0 provide an increase of the reflection which is canceled to some extent by an increased r_e. However, the deviation of the total transmission from unity will be very small after all, since the fact that the de Broglie wavelength corresponding to the translational motion becomes shorter than that of hydrogen atom-molecule reaction (1.8Å at 300°K) makes the classical consideration of motion more valid.

The author wishes to thank Professor S. Shida for his kind advice and encouragement. The author is also much indebted to Professor J. Horiuti and Dr. T. Toya of Hokkaido University and Dr. K. Fueki of Osaka University for their valuable discussion and suggestions.

Laboratory of Physical Chemistry
Tokyo Institute of Technology
Meguro-ku, Tokyo

Appendix I. Approximate Formulae of the Coefficients $B_{\varepsilon\lambda}$, $C_{\varepsilon k}$ and $F_{\varepsilon\varepsilon'}$

Under the condition $r_e\gg\rho_{\max}$, it is expected that the vibrational eigenfunction in region II, $\phi_k^{\text{II}}(r)$ becomes close to the function $\phi_{\varepsilon}^{\text{I}}(x)$ with $\varepsilon=k$ in its form at the boundary between regions I and II and that the matrix v is nearly equal to u. Accordingly, when we divide u into the two parts, u_0, the diagonal part of u, and u_1, the offdiagonal part,

$$u=u_0+u_1 \quad (A1)$$

and also
$$v=v_0+v_1 \quad (A2)$$

in a similar manner, it may be assumed that the elements of u_1 (or v_1) are small compared with those of u_0 (or v_0).

(a) The Case of Single Boundary.—We have the matrix S, Eq. 29, of the following approximate form,

$$S=pv_0^{-1}(1-v_1\cdot v_0^{-1})q^{-1}(u_0+u_1) \quad (A3)$$

or neglecting the term including $u_1\cdot v_1$,

15) In the estimation, the values of ρ_{10} and ρ_{01} at $E=3/2\cdot l.\nu_0$ were assumed for convenience to be unity.

$$S=S_0+S_1 \tag{A4}$$

where $S_0=pv_0^{-1}q^{-1}u_0$ (A5)

and $S_1\simeq pv_0^{-1}q^{-1}u_1-pv_0^{-1}v_1v_0^{-1}u_0q^{-1}$ (A6)

Since the matrix B of Eq. 27 is expressed by the use of the above equations, as

$$B=(S_0-1)(S_0+1)^{-1}+2(S_0+1)^{-1}S_1(S_0+1)^{-1} \tag{A7}$$

we can finally get the expressions of the coefficients of reflected waves $B_{\kappa\lambda}$'s and those of transmitted waves $C_{\kappa k}$'s,

$$B_{\kappa\lambda}=\frac{p_\kappa(v_0^{-1}\cdot u_0)_\kappa-q_\kappa}{p_\kappa(v_0^{-1}\cdot u_0)_\kappa+q_\kappa}\delta_{\kappa\lambda}+\frac{2p_\kappa(v_0^{-1})_\kappa[u_{1,\kappa\lambda}q_\lambda-q_\kappa v_{1,\kappa\lambda}(v_0^{-1}\cdot v_0)_\lambda]}{[p_\kappa(v_0^{-1}\cdot u_0)_\kappa+q_\kappa]\cdot[p_\lambda(v_0^{-1}\cdot u_0)_\lambda+q_\lambda]} \tag{A8}$$

and

$$C_{\kappa k}=\frac{2p_\kappa(v_0^{-1}\cdot u_0)_\kappa u^{-1}{}_{\kappa k}}{p_\kappa(v_0^{-1}\cdot u_0)_\kappa+q_\kappa}+\sum_\lambda\frac{2p_\kappa(v_0^{-1})_\kappa[u_{1,\kappa\lambda}q_\lambda-q_\kappa\cdot v_{1,\kappa\lambda}(v_0^{-1}\cdot u_0)_\lambda]u^{-1}{}_{\lambda\kappa}}{[p_\kappa(v_0^{-1}\cdot u_0)_\kappa+q_\kappa]\cdot[p_\lambda(v_0^{-1}\cdot u_0)_\lambda+q_\lambda]} \tag{A9}$$

(b) The Case of Two Boundaries.—By the introduction of the same approximations for u' and v' as those for u and v, the coefficients $B_{\kappa\lambda}$'s are expressed as follows:

$$B_{\kappa\kappa}=L_\kappa[(v_0^{-1}\cdot u_0)_\kappa p_\kappa{}^2-(u_0^{-1}\cdot v_0)_\kappa q_\kappa{}^2]\cdot(Q_\kappa)^{-1} \tag{A10}$$

and

$$\begin{aligned}B_{\kappa\lambda}=&2p_\kappa(Q_\kappa\cdot Q_\lambda)^{-1}\\&\times[(4-G_\kappa\cdot G_\lambda)q_\lambda q_\kappa\{(v_0^{-1})_\kappa v_{1,\kappa\lambda}p_\kappa\\&-(u_0^{-1})_\kappa u_{1,\kappa\lambda}p_\lambda\}\\&-L_\kappa L_\lambda\{(u_0^{-1})_\kappa v_{1,\kappa\lambda}(v_0^{-1}\cdot u_0)_\lambda p_\lambda q_\kappa{}^2\\&-(v_0^{-1})_\kappa\cdot u_{1,\kappa\lambda}(u_0^{-1}\cdot v_0)_\lambda\cdot p_\kappa\cdot q_\lambda{}^2\}\\&+G_\kappa L_\lambda q_\kappa\{(v_0^{-1})_\kappa\cdot v_{1,\kappa\lambda}(v_0^{-1}\cdot u_0)_\lambda p_\kappa p_\lambda\\&-(u_0^{-1})_\kappa\cdot u_{1,\kappa\lambda}(u_0^{-1}\cdot v_0)_\lambda q_\lambda{}^2\}\\&+G_\lambda L_\kappa\{(u_0^{-1})_\kappa\cdot v_{1,\kappa\lambda}q_\kappa{}^2\\&-(v_0^{-1})_\kappa\cdot u_{1,\kappa\lambda}p_\kappa p_\lambda\}]\end{aligned} \tag{A11}$$

where

$$\begin{aligned}Q_\kappa=&L_\kappa\{(v_0^{-1}\cdot u_0)_\kappa\cdot p_\kappa{}^2+(u_0^{-1}\cdot v_0)_\kappa\cdot q_\kappa{}^2\}\\&-2G_\kappa p_\kappa\cdot q_\kappa\end{aligned} \tag{A12}$$

$$G_\kappa=(W+W^*)_\kappa=2\cos m_\kappa\theta_0 \tag{A13}$$

and $$L_\kappa=(W-W^*)_\kappa=2i\sin m_\kappa\theta_0 \tag{A14}$$

The $F_{\kappa\kappa'}$'s is obtained by substituting the above expressions of $B_{\kappa\lambda}$'s into Eq. 15.

Appendix II. Calculations of $u_{k\lambda}$ and $v_{k\lambda}$

The matrix element $u_{k\lambda}$ is defined by

$$\psi_k{}^{\mathrm{II}}(x)\sum_\lambda u_{k\lambda}\cdot\psi_\lambda{}^{\mathrm{I}}(x) \tag{A15}$$

Making use of the property of ψ^{I}, we obtain

$$u_{k\lambda}=\int_{-\infty}^{+\infty}\psi_\lambda{}^{\mathrm{I}*}\cdot\psi_k{}^{\mathrm{II}}\mathrm{d}\rho \tag{A16}$$

where the lower limit of integration with respect to ρ can be practically extended to minus infinity instead of $\rho=-r_e$ because of the rapid diminution of $\psi_\lambda{}^{\mathrm{I}}$ and $\psi_k{}^{\mathrm{II}}$ where ρ is smaller than $-\rho_{\max}$.

From the condition $r_e\gg\rho_{\max}$, $\psi_k{}^{\mathrm{II}}(x)$, Eq. 35, is described approximately by

$$\psi_\kappa{}^{\mathrm{II}}(x)\simeq\frac{n}{r_e{}^{1/2}}\cdot\left(1-\frac{\rho}{2r_e}+\frac{3\rho^2}{8r_e{}^2}\right)\cdot N_k\times\exp\left(-\frac{\alpha'}{2}\zeta^2\right)\cdot H_k(\sqrt{\alpha'}\zeta) \tag{A17}$$

Accordingly, $u_{k\lambda}$ which is given by Eq. A16 consists of the sum of the general term,

$$\text{const.}\times\int_{-\infty}^{+\infty}\rho^n\cdot N_kN_\lambda\cdot\exp\left(-\frac{\alpha'}{2}\zeta^2-\frac{\alpha}{2}\rho^2\right)\times H_k(\sqrt{\alpha'}\cdot\zeta)\cdot H_\lambda(\sqrt{\alpha}\cdot\rho)\,\mathrm{d}\rho$$

which is resolved, furthermore, into the sum of the following integrals with some coefficients[16],

$$I_{\kappa\lambda}=N_kN_\lambda\cdot\int_{-\infty}^{+\infty}\exp\left(-\frac{\alpha'}{2}\zeta^2-\frac{\alpha}{2}\rho^2\right)\times H_k(\sqrt{\alpha'}\cdot\zeta)\cdot H_\lambda(\sqrt{\alpha}\cdot\rho)\cdot\mathrm{d}\rho \tag{A18}$$

Since

$$\alpha'\zeta^2+\alpha\rho^2=(\alpha+\alpha')\left[\rho-\left(\frac{\alpha'}{\alpha+\alpha'}\right)\beta r_e\right]^2=at^2 \tag{A19}$$

where a and t are defined by

$$a=\alpha+\alpha' \quad\text{and}\quad t=\rho-\left(\frac{\alpha'}{\alpha+\alpha'}\right)\beta r_e \tag{A20), (A21}$$

Eq. A18 is also written as

$$I_{k\lambda}=N_kN_\lambda\cdot\exp\left[-\frac{1}{2}\left(\frac{\alpha\alpha'}{\alpha+\alpha'}\right)(\beta r_e)^2\right]\times\int_{-\infty}^{+\infty}\exp\left(-\frac{a}{2}t^2\right)H_kH_\lambda\mathrm{d}\rho \tag{A22}$$

Transforming the variables, $\sqrt{\alpha}\cdot\rho$ in H_λ and $\sqrt{\alpha'}\cdot\zeta$ in H_k, into a new variable,

$$s=\sqrt{a}\cdot t \tag{A23}$$

we can write

$$H_\lambda(\sqrt{\alpha}\cdot\rho)=\sum_l g_{\lambda l}H_l(\sqrt{a}\cdot t) \tag{A24}$$

and $$H_k(\sqrt{\alpha'}\cdot\zeta)=\sum_l h_{kl}H_l(\sqrt{a}\cdot t) \tag{A25}$$

where $g_{\lambda l}$ and h_{kl} are coefficients of expansion.

Substituting Eqs. A24 and A25 into Eq. A22, we can get the final expression of $I_{k\lambda}$,

$$I_{k\lambda}=N_kN_\lambda\cdot\exp\left[-\frac{1}{2}\left(\frac{\alpha\alpha'}{\alpha+\alpha'}\right)(\beta r_e)^2\right]\times\sum_l g_{\lambda l}\cdot h_{kl}(N_l)^{-2} \tag{A26}$$

where N_l is obtained by replacing α and λ in N_λ with a and l respectively. In a similar way, the matrix element $v_{k\lambda}$

$$v_{k\lambda}=\int_{-\infty}^{+\infty}\left(\frac{r_e}{r_e+\rho}\right)\cdot\psi_\lambda{}^{\mathrm{I}*}\cdot\psi_k{}^{\mathrm{II}}\mathrm{d}\rho \tag{A27}$$

is computed, since the function $r_e/(r_e+\rho)\cdot\psi_k{}^{\mathrm{II}}(x)$ has the following approximate form,

16) See, for example, H. Eyring, J. Walter and G. E. Kimball, "Quantum Chemistry", John Wiley & Sons, Inc., New York (1949), p. 60.

$$\left(\frac{r_e}{r_e+\rho}\right)\cdot\psi_k^{\mathrm{II}}(x)\simeq\frac{n}{r_e^{1/2}}\cdot\left(1-\frac{3\rho}{2r_e}+\frac{15\rho^2}{8r_e^2}\right)\cdot N_k \times\exp\left(-\frac{\alpha'}{2}\zeta^2\right)\cdot H_k(\sqrt{\alpha'}\cdot\zeta) \tag{A28}$$

and can also be resolved into the sum of $I_{k\lambda}$ with reasonable coefficient as well as in the case of $u_{k\lambda}$.

The obtained expressions of $u_{k\lambda}$ and $v_{k\lambda}$ for $k,\lambda=0,1$ are shown as follows:

$$u_{00}=A_{00}\cdot\left[\left(1-\frac{1}{2}\varepsilon+\frac{3}{8}\varepsilon^2\right)+\frac{3}{8}\eta\right] \tag{A29}$$

$$u_{10}=2A_{10}\sqrt{\alpha'}r_e\cdot\left[\left(1-\frac{1}{2}\varepsilon+\frac{3}{8}\varepsilon^2\right)(\varepsilon-\beta)+\frac{1}{8}\{9\varepsilon-(4+3\beta)\eta\}\right]$$

$$u_{01}=2A_{01}\sqrt{\bar{\alpha}}\cdot r_e\cdot\left[\left(1-\frac{1}{2}\varepsilon+\frac{3}{8}\varepsilon^2\right)\varepsilon+\frac{1}{8}(9\varepsilon-4)\eta\right]$$

$$u_{11}=4A_{11}\sqrt{\alpha\alpha'}\cdot r_e^2\cdot\left[\left(1-\frac{1}{2}\varepsilon+\frac{3}{8}\varepsilon^2\right)(\varepsilon-\beta)\varepsilon+\frac{3}{8}\eta^2+\left\{\left(1-\frac{1}{2}\varepsilon+\frac{3}{8}\varepsilon^2\right)+\left(\frac{3}{4}\varepsilon-\frac{1}{2}\right)(2\varepsilon-\beta)+\frac{3}{8}(\varepsilon-\beta)\varepsilon\right\}\eta\right]$$

and

$$v_{00}=A_{00}\cdot\left[\left(1-\frac{3}{2}\varepsilon+\frac{15}{8}\varepsilon^2\right)+\frac{15}{8}\eta\right] \tag{A30}$$

$$v_{10}=2A_{10}\sqrt{\alpha'}r_e\cdot\left[\left(1-\frac{3}{2}\varepsilon+\frac{15}{8}\varepsilon^2\right)(\varepsilon-\beta)+\frac{1}{8}\{45\varepsilon-(12+15\beta)\}\eta\right]$$

$$v_{01}=2A_{01}\sqrt{\alpha}\cdot r_e\cdot\left[\left(1-\frac{3}{2}\varepsilon+\frac{15}{8}\varepsilon^2\right)\varepsilon+\frac{1}{8}(45\varepsilon-12)\eta\right]$$

$$v_{11}=4A_{11}\sqrt{\alpha\alpha'}\cdot r_e^2\cdot\left[\left(1-\frac{3}{2}\varepsilon+\frac{15}{8}\varepsilon^2\right)(\varepsilon-\beta)\varepsilon+\frac{15}{8}\eta^2+\left\{\left(1-\frac{3}{2}\varepsilon+\frac{15}{8}\varepsilon^2\right)+\left(\frac{15}{4}\varepsilon-\frac{3}{2}\right)(2\varepsilon-\beta)+\frac{15}{8}(\varepsilon-\beta)\varepsilon\right\}\eta\right]$$

where,

$$A_{k\lambda}=(n_k/r_e^{1/2})\,(N_kN_\lambda/\bar{N}_0^2)\times\exp\left[-\frac{1}{2}\left(\frac{\alpha\alpha'}{\alpha+\alpha'}\right)\cdot(\beta r_e)^2\right] \tag{A31}$$

$$\bar{\alpha}=(\alpha+\alpha')/2 \tag{A32}$$

$$\varepsilon=\{\alpha/(\alpha+\alpha')\}\beta \tag{A33}$$

$$\eta=(2\bar{\alpha}r_e^2)^{-1} \tag{A34}$$

and $\bar{N}_0$ is obtained from the normalization factor N_κ of vibrational eigenfunction by replacing α and κ with $\bar{\alpha}$ and zero.

The expressions of $u'_{k\lambda'}$ and $v'_{k\lambda'}$ are identical with the above, because the form of the potential channel is symmetrical at the two boundaries.

Hydrazinolysis of Nucleic Acids. I. The Formation of Deoxyribopyrimidinic Acid from Herring Sperm Deoxyribonucleic Acid

By Shosuke TAKEMURA

(Received March 23, 1959)

In spite of our recognition of the biological importance of nucleic acid, there are many points on the structure of nucleic acid still left ambiguous, i. e., the nucleotide sequence, the localization in the molecule of certain nucleotides, the structural differences between nucleic acids of different origin, and so on. Some fruitful information on the general structural features of deoxyribonucleic acid has been obtained by Chargaff et al. from chemical degradative studies of a derivative, named apurinic acid, in which deoxyribonucleic acid has been deprived of the purine constituents[1-4]. Many other chemical degradations of deoxyribonucleic acid by which the nucleotide sequence can be studied have been attempted[5-13]. These

1) C. Tamm, M. E. Hodes and E. Chargaff, *J. Biol. Chem.*, **195**, 49 (1952).
2) C. Tamm, H. S. Shapiro, R. Lipshitz and E. Chargaff, ibid., **203**, 673 (1953).
3) C. Tamm and E. Chargaff, ibid., **203**, 689 (1953).
4) M. E. Hodes and E. Chargaff, *Biochim. et Biophys. Acta*, **22**, 348 (1956).
5) A. S. Jones and D. S. Letham, ibid, **14**, 438 (1954).
6) A. S. Jones and D. S. Letham, *J. Chem. Soc.*, **1956**, 2573.
7) A. S. Jones, D. S. Letham. and M. Stacey, ibid., **1956**, 2579.
8) A. S. Jones, D. S. Letham and M. Stacey, ibid., **1956**, 2584.
9) A. S. Jones, M. Stacey and B. E. Watson, ibid., **1957**, 2454.
10) J. A. Lucy and P. W. Kent, *Research*, **6**, 49s (1953).

studies have more or less utilized the particular instability of the purine deoxyribosidic linkages to even a mild acid hydrolysis. Therefore, the information about the nucleotide sequences has been exclusively limited to the pyrimidines in deoxyribonucleic acid. No information was available about the distribution of purines in deoxyribonucleic acid, or of either purines or pyrimidines in ribonucleic acid.

Attention was paid to the reaction of aqueous hydrazine with uracil[14], pyrimidine ribonucleosides[15,16] and ribomononucleotides[16]. Of the latter, uracil and cytosine residues were decomposed to pyrazolone and 3-aminopyrazole, respectively, and simultaneously, ribose 2- and 3-phosphate were obtained from the nucleotide isomers, a and b, respectively. This reaction of hydrazine was successfully applied to both ribo- and deoxyribonucleic acid from which for the first time nondialyzable derivatives almost free from the pyrimidines were obtained and the name ribo- and deoxyribo-apyrimidinic acid were proposed for the products[17,18]. These compounds, especially deoxyribo-apyrimidinic acid, may be useful for structural studies as well as apurinic acid[2,4] and aldehydoapurinic acid di(carboxymethyl)-dithioacetal[7,9].

Anhydrous hydrazine was used for this work, in order to avoid alkaline hydrolysis of the internucleotide linkage which might be caused by the basicity of hydrazine itself even if only a trace of water remained. Since powdered deoxyribonucleic acid of herring sperm took more than 30 min. for its complete dissolution in five parts of anhydrous hydrazine at 60°C, lyophilized preparations were used to prevent a heterogeneous reaction. Experiments using various reaction conditions were carried out and are summarized in Table I. In the course of dissolution in distilled water of the alcohol precipitates after the hydrazinolysis, the viscosity of the solution rapidly decreased. Hydrazine was expected to remain in the precipitates and to cause alkaline hydrolysis. Therefore, in the preparation of DAPYA V, V′ and V″, the alcohol precipitates were dissolved in 0.2 M phosphate buffer of pH 6 and dialyzed. The products thus obtained proved to have longer mean chain lengths and fewer periodate consumptions than others (Table V).

The hydrazinolysis of the deoxyribonucleic acid afforded products the nitrogen content and the N/P ratio of which were lower than those of the parent materials (Table II). Increased removal of the pyrimidines resulted in higher phosphorus contents (Table II). The color intensities by the reaction with diphenylamine were, on the basis of phosphorus content, much more than those given by the parent nucleic acids, although the color intensities were not always parallel to the degree of detachment of the pyrimidines. The estimation of reducing sugar proved that the products had a considerable amount of reducing power, whereas the nucleic acids had only a little. These results, together with the positive qualitative tests for reducing sugar, show that the bulk of the sugar moieties, which in the intact nucleic acid were pyrimidine nucleotides, are in nonglycosidic forms. During the hydrazinolysis and the subsequent treatment, there may be possibilities of side reactions, e. g., formation of hydrazonium salt, hydrazone and sugar alcohol. However, it can be seen from the ratio of N/P that these side reactions occur only slightly if at all.

As shown in Table III the greater part of the pyrimidines was removed from herring sperm deoxyribonucleic acids without impairment of the original interpurine ratios, but small amounts of thymine remained, even in the product obtained through the reaction by which the removal of the pyrimidines was most effective. As for pyrimidine ribomononucleotides, uracil was far more rapidly decomposed by aqueous hydrazine than was cytosine, which was studied by Baron and Brown[16]. Hence it is concluded that thymine is the most resistant to the hydrazinolysis among the main pyrimidine constituents in nucleic acids. The reaction of hydrazine, in the presence of water, gave directly ribose 3-phosphoric acid from pyrimidine ribonucleotides. In the absence of water, however, ureido-deoxyriboside phosphate residues may be formed from the pyrimidine nucleotide residues in the

11) P. W. Kent, J. A. Lucy and P. F. V. Ward, *Biochem. J.*, **61**, 529 (1955).
12) K. Burton and G. B. Peterson, *Biochim et Biophys. Acta*, **26**, 667 (1957).
13) H. S. Shapiro and E. Chargaff, ibid., **23**, 451(1957).
14) H. R. Fosse, J. Hieulle and L. W. Bass, *Compt. rend.*, **178**, 811 (1955).
15) P. A. Levene L. W. Bass, *J. Biol. Chem.*, **71**, 167 (1926).
16) F. Baron and D. M. Brown, *J. Chem. Soc.*, **1955**, 2855.
17) S. Takemura, *J. Biochem.*, **44**, 321 (1957).
18) S. Takemura, *Biochim. et Biophys. Acta*, **29**, 447 (1958).

TABLE I. REACTION OF HERRING SPERM DEOXYRIBONUCLEIC ACID WITH ANHYDROUS HYDRAZINE

Preparation[a]		Amount of DNA	Amount of Anhydrous hydrazine	Reaction temp.	Reaction time	Yield of nondialyzable product	
		mg.	ml.	°C	min.	mg.	%[b]
DAPYA	I	850	3.5	50	30[d]	650	87
DAPYA	II	240	1.0	60	30[d]	170	80
DAPYA	III	120	0.7	60	55	71	72
DAPYA	IV	600	2.8	60	60	389	78
DAPYA	V	248	1.2[c]	37	90	208	95
DAPYA	V′	150	0.7[c]	50	75	113	86
DAPYA	V″	195	1.0[c]	50	150	130	82
APA	II	140	HCl, pH 1.6	37	24 hr.	98	91
APA	IV	250	HCl, pH 1.6	37	26 hr.	183	94
PDRP	ID	150	HCl, pH 1.6	37	26 hr.	39	26
PDRP	IID	70	HCl, pH 1.6	37	26 hr.	17	26
PDRP	IIA	50	0.2	60	60	9.5	17
PDRP	IVD	150	HCl, pH 1.6	37	27 hr.	58	42

a) DAPYA=deoxyribo-apyrimidinic acid; APA=apurinic acid; PDRP=poly-deoxyribose phosphate. DAPYA I and II were obtained from powdered DNA and through acid precipitation; DAPYA III and IV obtained from lyophilized DNA and through acid precipitation; DAPYA V, V′ and V″ obtained from lyophilized DNA and through dissolution in phosphate buffer (See *Experimental*).
b) These are per cent of DNA phosphorus recovered in the product
c) Twice dehydrated hydrazine was used.
d) Reaction times after the complete dissolution of DNA.

TABLE II. COMPOSITION OF THE HYDRAZINOLYSIS PRODUCTS OF HERRING SPERM DEOXYRIBONUCLEIC ACID. PART 1

Preparation[a]		N (%)	P (%)	Atomic N/P	Color reaction with diphenylamine[b]	Reducing deoxyribose residues, mol. per 100 g.-atoms of P[c]
DNA	I	13.4	8.0	3.7	100	5
DNA	II	13.6	8.2	3.7	100	4
DNA	III	13.7	8.2	3.7	100	6
DNA	IV	14.2	8.5	3.7	100	5
DNA	V	13.7	8.2	3.7	100	—
DAPYA	I	12.2	9.1	3.0	135	30
DAPYA	II	12.0	9.6	2.8	156	31
DAPYA	III	12.3	10.0	2.7	133	27
DAPYA	IV	12.2	10.2	2.7	131	36
DAPYA	V	12.3	9.2	3.0	—	—
DAPYA	V′	12.0	9.5	2.8	—	—
DAPYA	V″	11.9	10.1	2.6	—	—
APA	II	6.3	10.6	1.3	116	54
APA	IV	6.5	10.9	1.3	99	51
PDRP	ID	7.4	9.2	1.8	87	51
PDRP	IID	4.7	10.3	1.0	107	63
PDRP	IIA	3.6	9.6	0.85	113	—
PDRP	IVD	3.9	11.0	0.79	110	63

a) See Table I.
b) Compared with each DNA on the basis of P content.
c) Compared with deoxyribose as the standard.

TABLE III. COMPOSITION OF THE HYDRAZINOLYSIS PRODUCTS OF HERRING SPERM DEOXYRIBONUCLEIC ACID. PART 2

Preparation[a]		Mol. of bases/100 g.-atoms of phosphorus[b]						Molar ratios of	
		Adenine	Guanine	Cytosine	Thymine	Total purines	Total pyrimidines	A/G	T/C
DNA	I	29	23	21	27	52	48	1.3	1.3
DNA	II	27	24	22	27	51	49	1.1	1.2
DNA	III	29	23	21	27	52	48	1.3	1.3
DNA	IV	29	23	21	27	52	48	1.3	1.3
DNA	V	28	23	22	27	51	49	1.2	1.2
DAPYA	I	29	23	1.2	19	52	20	1.3	
DAPYA	II	27	24	0.7	8.0	51	8.7	1.1	
DAPYA	III	29	23	0.2	5.4	52	5.6	1.3	
DAPYA	IV	29	23	0.3	4.1	52	4.4	1.3	
DAPYA	V	28	23	1.2	16	51	17	1.2	
DAPYA	V′	28	23	1.0	10	51	11	1.2	
DAPYA	V″	27	24	0.5	5.2	51	5.7	1.1	
APA	II	1.6	2.6	22	27	4.2	49		1.2
APA	IV	0.6	1.0	22	26	1.6	48		1.2
PDRP	IID	2.8	4.3	0.7	6.6	7.1	7.3		
PDRP	IVD	1.8	2.4	0.7	8.3	4.2	9.0		

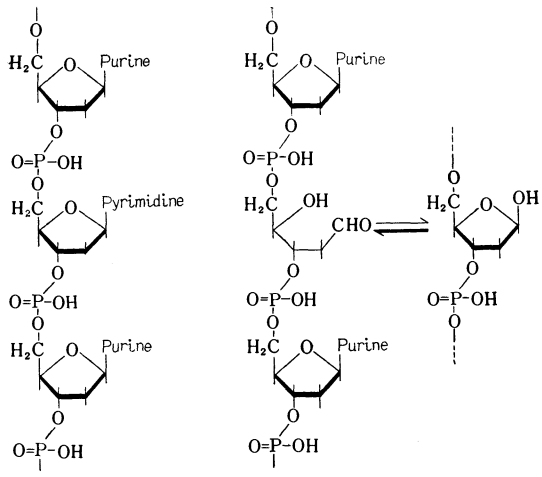
a) See Table I.
b) The values were corrected for a 100% recovery. Actual recoveries of total bases were between 89 and 96%.

TABLE IV. ULTRAVIOLET ABSORPTION SPECTRA OF THF HYDRAZINOLYSIS PRODUCTS OF HERRING SPERM DEOXYRIBONUCLEIC ACID[a]

Preparation[b]		Maximum			Minimum		
		mμ.	E_p*	E_{np}**	mμ.	E_p*	E_{np}**
DNA	I	259	7350		230	3100	
DNA	II	259	7200		230	2950	
DNA	III	258	6850		230	2900	
DNA	IV	258	7700		230	3200	
DAPYA	I	257.5	7200	10000	228	2850	3950
DAPYA	II	256.5	6900	11500	227.5	2800	4650
DAPYA	III	255	6450	11100	227.5	2450	4250
DAPYA	IV	255	6650	11900	227	2600	4650
APA	II	268	4450	8400	238	2700	5100
APA	IV	267.5	4450	8900	237	2650	5300
PDRP	ID	260	5100		232	2500	
PDRP	IID	260	3500		235	2350	
PDRP	IVD	256.5	2400		234	1900	

a) All measurements were carried out in 0.1 M phosphate buffer of pH 7.0.
* The extinction coefficient with respect to one gram-atom of phosphorus per liter.
** The extinction coefficient with respect to one gram-atom of nucleotide phosphorus per liter.
b) See Table I.

deoxyribonucleic acid. The subsequent treatment of the intermediate product may hydrolyze the glycosidic linkage between deoxyribose and urea which seems to be unstable in the presence of water. The deoxyribose phosphate residues thus formed may be present in an equilibrium between the furanose (III) and the free aldehydo-form (II) in the aqueous solution of the deoxyribo-apyrimidinic acid, but are certainly present to a considerable extent in the free aldehydo-form[19-21].



(I) (II) (III)

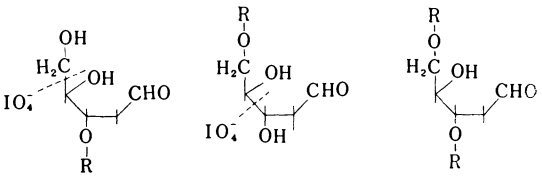
To remove both the purines and the pyrimidines, the apurinic acid from herring sperm deoxyribonucleic acid was treated with anhydrous hydrazine and the deoxyribo-apyrimidinic acid was treated with dilute acid. These products contained bases to the extent of about 10 to 15 mol. % of total phosphorus. The combination of the mild acid hydrolysis with the hydrazinolysis, however, caused greater degradation of the internucleotide linkages than did the hydrazinolysis alone. Moreover, the color intensities with diphenylamine and the estimations of reducing sugar of the products seem to show that a part of the deoxyribose moieties undergo some unknown decompositions.

The mean chain length of apurinic acid (Table V) corresponds to a mean molecular weight of about 5,000. This value is much lower than that obtained by Tamm et al. (15,000; light scattering method)[4] and that by Miura et al. (17,000; surface membrane method)[22]. This discrepancy may be partly due to the quality of the parent deoxyribonucleic acid and also to the presence of many terminal phosphate groups caused by the inclusion in the apurinic acid of a small amount of oligonucleotides. Consequently, it can be assumed that the deoxyriboapyrimidinic acids contain many fragments of much longer chain length than the mean, although fission of the phsophodiester linkages during the hydrazinolysis and the subsequent treatment may have been considerable. Periodate should be consumed only by the nonglycosidic deoxyribose residues which occupy the chain end of nucleotide and do not bear terminal phosphate groups IV and V. If both ends are occupied by nucleotides or bear the terminal phosphate group VI, periodate can not be consumed. Therefore, it is impossible to predict the amount of the periodate consumption of the hydrazinolysis products from their mean chain lengths. The ultraviolet absorption coefficient of the purines are, on the molar basis, greater than that of the pyrimidines. Hence, in addition to the hyperchromic effects of degradation, the removal of the

TABLE V. MEAN CHAIN LENGTH AND PERIODATE CONSUMPTION OF THE HYDRAZINOLYSIS PRODUCTS OF HERRING SPERM DEOXYRIBONUCLEIC ACID

Preparation*		Mean chain length	Periodate consumption, mol. per 1 mol. of P
DAPYA	I	7.3	0.24
DAPYA	III	8.4	0.20
DAPYA	IV	7.0	0.34
DAPYA	V	15	0.17
DAPYA	V'	10	0.17
DAPYA	V''	10	0.19
APA	IV	18	0.14
PDRP	IVD	4.8	0.57

* See Table I.



(IV) (V) (VI)

19) S. M. Cantor and Q. P. Peniston, *J. Am. Chem. Soc.*, **62**, 2113 (1940).
20) Chong-Fu Li, W. G. Overend and M. Stacey, *Nature*, **163**, 538 (1949).
21) W. G. Overend, *J. Chem. Soc.*, **1950**, 2769.
22) K. Miura, K. Imahori and I. Watanabe, *J. Chem. Soc. Japan, Pure Chem. Sec.* (*Nippon Kagaku Zasshi*), **78**, 276 (1957).

pyrimidines results necessarily in the higher absorption coefficient with respect to nucleotide phosphorus (E_{np}) than that of the apurinic acid and the deoxyribonucleic acid (Table IV).

Some fission of the internucleotide linkages occurred during the hydrazinolysis and the subsequent treatment, and small amounts of intact thymine were left in the preparations. However, there will be possibilities to improve the preparative method. Since about 80% of the material was nondialyzable and the interpurine ratios were not distorted during the reaction, the deoxyribo-apyrimidinic acid must be useful for the structural studies of deoxyribonucleic acid. The apyrimidinic acids were used for the study of the specificity of pancreatic deoxyribonuclease which are reported in the subsequent paper.

Experimental

Nitrogen was determined by micro-Kjeldahl method and phosphorus by Allen's method[23]. The color reaction of the hydrazinolysis products with diphenylamine[24] was carried out and compared with each parent deoxyribonucleic acid as the standard. The nonglycosidic deoxysugars which were initially bound to the pyrimidines also participate in the color reaction. Reducing deoxysugar was determined by means of Fujita-Iwatake's method[25]. These results are summarized in Table II. The base composition was determined chromatographically after hydrolyzing samples in a scaled tube with 70% perchloric acid at 100°C for 1 hr.[26] (propan-2-ol—hydrochloric acid[27], Toyo Roshi Co. 51a paper, descending). Each value listed in Table III represents the average of at least three individual determinations. The absorption spectra were determined in 0.1 M phosphate buffer of pH 7.0 (Fig. 1 and Table IV). The mean chain length was determined by the ratio of the total phosphorus to the terminal phosphate which was liberated as inorganic phosphorus by prostatic phosphomonoesterase[28] (Table V). The periodate consumption was carried out at pH 4 with sodium metaperiodate, in the dark at 10°C or below, for 60 min.; excess periodate was reduced with sodium arsenite at pH 8 and the excess arsenite was back titrated with standard iodine solution[29] (Table V).

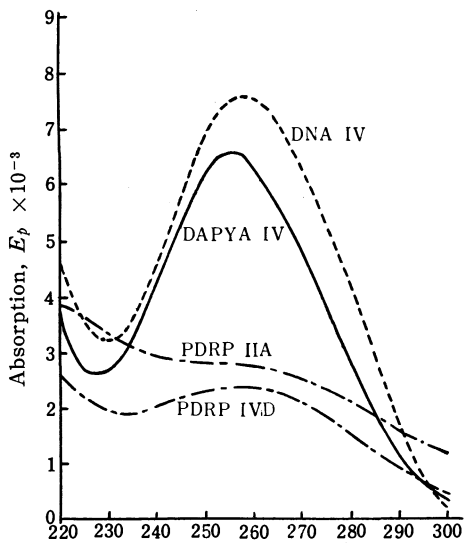


Fig. 1. Ultraviolet absorption curves of the hydrazinolysis products of herring sperm deoxyribonucleic acid in phosphate buffer, pH 7.
E_p=extinction per g.-atom of phosphorus.

Dehydration of Hydrazine.—Eighty per cent hydrazine hydrate was dehydrated with sodium hydroxide pellets at 113°C for 2 hr. and distilled[30]. For more strict dehydration, the distillate was again refluxed with sodium hydroxide pellets at 180°C for 3 hr. and distilled[31].

Deoxyribonucleic Acids.—Five preparations of the sodium deoxyribonucleate of herring sperm, DNA I to V, were used. DNA III was a highly polymerized specimen (MW. ca. 6×10^6)[32]. Before treatment with anhydrous hydrazine, the nucleic acids were dried over concentrated sulfuric acid in vacuo at 60°C for 5 hr. or at 100°C for 3 hr. The compositions of the specimens are summarized in Tables II and III.

Designation of the Reaction Products.—The hydrazinolysis gave products in which the nucleic acid was more or less deprived of the pyrimidines. In order to avoid confusion and to simplify descriprions, the name deoxyribo-apyrimidinic acid (DAPYA) is given to all the hydrazinolysis products and the name polydeoxyribose phosphate (PDRP) to the products obtained either by the hydrazinolysis of the apurinic acid (APA) or by the mild acid hydrolysis, as used for the preparation of apurinic acid, of the hydrazinolysis product. The preparation numbers of the reaction products are the same as those given to the parent deoxyribonucleic acids, i. e., DAPYA II and APA II were obtained from DNA II, PDRP IIA from APA II, and PDRP IID from DAPYA II.

23) F. W. Allen, *Biochem. J.*, **34**, 858 (1940).
24) Z. Dische, *Mikrochem.*, 8, 4 (1930); F. B. Seibert, *J. Biol. Chem.*, **133**, 593 (1940).
25) A. Fujita and D. Iwatake, *Biochem. Z.*, **242**, 43 (1932).
26) A. Marshak and H. J. Vogel, *J. Biol. Chem.* **189**, 597 (1951).
27) G. R. Wyatt, *Biochem. J.*, **48**, 584 (1951).
28) P. R. Whitfeld and R. Markham, *Nature*, **171**, 1151 (1953).
29) J. R. Dyer, "Methods of Biochem. Anal.", Vol. III, Interscience Publishers, Inc., New York, (1955). p. 111.
30) I. M. Kolthoff, *J. Am. Chem. Soc.*, **46**, 2009 (1924).
31) D. H. R. Barton, D. A. J. Ives and B. R. Thomas, *J. Chem. Soc.*, **1955**, 2056.
32) K. Iso and I. Watanabe, *J. Chem. Soc., Japan, Pure Chem. Sec.* (*Nippon Kagaku Zasshi*), **78**, 1268 (1957).

Preparation of the Deoxyribo-apyrimidinic Acids.—The mixture of lyophilized herring sperm deoxyribonucleic acid and anhydrous hydrazine was kept free from moisture under the conditions described in Table I. Within a few minutes, the nucleic acid dissolved in the hydrazine, excepting deoxyribonucleic acid III which took about 10 min. for its complete dissolution. After cooling, absolute alcohol (5 vol.) was added to the highly viscous solution, the fibrous precipitate was made into a powder by scratching, centrifuged, washed with absolute alcohol, with ether, and dried. The dry solid was dissolved with cooling in cold distilled water and the solution dialyzed against running tap water for 20 hr., against frequent changes of distilled water at 4°C for 40 hr. and the inside fluid was freeze-dried. Light yelllow colored products were obtained. The composition of the products thus obtained is listed in Tables II and III.

When the alcohol precipitate was dissolved in 0.2 M phosphate buffer of pH 6 instead of distilled water, the solution was dialyzed against the same buffer at 4°C for 16 hr. against running tap water and finally against distilled water. Faint yellow products were obtained and are described as DAPYA V, V′ and V″ in the tables.

Preparation of Poly-deoxyribose Phosphate.—Apurinic acid was prepared from herring sperm deoxyribonucleic acid in the same way as it was prepared by Tamm et al.[1] Apurinic acid II was dried at 60°C for 5 hr. and then treated with anhydrous hydrazine as above. Deoxyribo-apyrimidinic acids I, II and IV were also treated by the same mild acid hydrolysis as used for the preparation of apurinic acid. The nondialyzable products of yellowish brown color were obtained from each treatment and were incompletely soluble in water, although these gave clear solutions before freeze-drying. The composition of these products is given in Tables II and III.

Qualitative Tests for Nonglycosidic Deoxysugar.—In contrast to the deoxyribonucleic acid, the hydrazinolysis products and the apurinic acid reacted with ammoniacal silver solution yielding brown precipitates, reduced Fehling's solution on warming, reacted with benzidine giving a brown color, reduced mercuric chloride solution yielding a white precipitate, and gave pink color with reduced fuchsin solution, but the reaction of the hydrazinolysis products was much slower than that of the apurinic acid. The hydrazinolysis products spotted on filter paper gave a reddish purple color with the aniline hydrogen phthalate reagent used for the development of chromatogram of reducing sugars[33].

The author thanks Professor F. Egami for his close interest and Professor I. Watanabe, the University of Tokyo, for a supply of herring sperm deoxyribonucleic acids. The expense of this study was defrayed in part by a grant from the Ministry of Education.

Department of Chemistry
Faculty of Science
Nagoya University, Nagoya

33) S. M. Partridge, *Nature*, **164**, 443 (1949).

Hydrazinolysis of Nucleic Acids. II. The Formation of Ribo-apyrimidinic Acid from Yeast Ribonucleic Acid

By Shosuke TAKEMURA and Masazumi MIYAZAKI

(Received March 23, 1959)

In the preceding paper[1], one of the authors has dealt with the formation of a new derivative devoid of pyrimidines, named deoxyribo-apyrimidinic acid, by the hydrazinolysis of herring sperm deoxyribonucleic acid, by the hydrozinolysis of herring sperm deoxyribonucleic acid. In connection with studies on the specificity of pancreatic ribonuclease in which this laboratory is engaged[2-6], it was desired to prepare ribonucleic acid derivatives devoid of the pyrimidines. The hydrazinolysis was first investigated using yeast ribonucleic acid and gave, for the first time, a nondialyzable derivative free from the pyrimidines, for which the name ribo-apyrimidinic acid was proposed[7]. Besides

1) S. Takemura, This Bulletin, **32**, 920 (1959).
2) S. Takemura, *J. Chem. Soc. Japan, Pure Chem. Sec.* (*Nippon Kagaku Zasshi*) **72**, 674 (1951).
3) F. Egami, H. Ishihara and M. Shimomura, *Z. physiol. Chem.*, **295**, 349 (1953).
4) F. Egami, *J. Japan. Biochem. Soc.* (*Sei Kagaku*), **27**, 139 (1955).
5) S. Takemura, *Protein, Nucleic Acid and Enzyme*, **2**, 79 (1957).
6) S. Takemura, "Intern. Kongr. Biochem", Zusammenfassung, IV Kongr., Wien (1958), p. 34.
7) S. Takemura, *J. Biochem.* **44**, 321 (1957).

TABLE I. REACTION OF YEAST RIBONUCLEIC ACID WITH ANHYDROUS HYDRAZINE AND COMPOSITION OF THE NITROGENEOUS CONSTITUENTS OF THE PRODUCTS

Preparation*	Condition of reaction		Yield of nondialyzable product	Mol./10 mol. of adenine[b]			
	t°C	min.	(%)**	Adenine	Guanine	Cytidylic acid	Uridylic acid
RNA, commercial	—	—	—	10.0	12.4	9.4	10.3
RNA, purified	—	—	—	10.0	12.6	11.5	10.2
RAPYA I[a]	0	60	93	10.0 (10.0)	12.4 (12.3)	9.7 (9.5)	7.2 (7.0)
RAPYA II	0	180	—	10.0	12.3	6.2	3.7
RAPYA III	30	120	—	10.0	12.7	1.0	1.8
RAPYA IV[a]	50	60	88	10.0 (10.0)	12.6 (12.3)	0.6 (0.6)	0.7 (0.7)
RAPYA V[a]	70	60	77	10.0 (10.0)	12.5 (12.4)	0.7 (0.7)	0.6 (0.6)
RAPYA VI[a]	50	60	73	10.0	12.3	1.2	2.5
RAPYA VII	80	60	50	10.0	12.9	1.0	1.5
RAPYA VIII	60	60	70	10.0	12.5	1.3	2.8
PAPYA IX	65	90	64	10.0	12.8	0.5	0.5

* RNA=ribonucleic acid; RAPYA=ribo-apyrimidinic acid; RAPYA VI, VII and VIII were obtained from commercial powdered RNA, others from purified and lyophilized RNA.

a) Twice dehydrated hydrazine was used.

** These are per cent of RNA phosphorus recovered in the product.

b) The values in parentheses are the composition of the dialyzable materials.

the problem of the specificity of ribonucleases which are reported in subsequent papers, some information about the general structure of ribonucleic acid may be derived from degradative studies of the derivative.

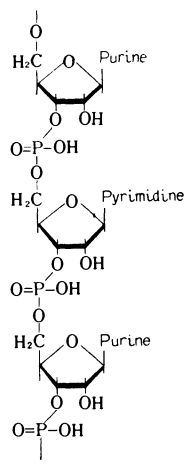
When yeast ribonucleic acid was treated with 80% aqueous hydrazine, a complete hydrolysis of the phosphodiester linkages resulted and only 2′- and 3′-isomers of purine mononucleotides were detected on the paper chromatogram, as the ultraviolet absorbing materials. In the case where anhydrous hydrazine was used, drastic condtions such as reaction at 90°C did not, however, offer any advantages, but indeed resulted in a serious destruction of the phosphodiester linkages and formation of considerable amounts of purine mononucleotide isomers. Experiments using various conditions of time and temperature were carried out and are summarized in Table I. The use of nucleic acid which was not purified and especially not lyophilized resulted in the incomplete removal of the pyrimidines. After treatment with hydrazine and precipitation with alcohol, there were difficulties in obtaining the derivatives without an accompanying serious destruction of the internucleotide linkages. In most cases, the alcohol precipitates were dissolved at 0°C in distilled water and the products precipitated with dilute hydrochloric acid. This procedure was effective for removign hydrazine, which was expected to be included as hydrazonium salt in the alcohol precipitates. However, it was thought that there might be possibilities of the formation of hydrazones or osazones using such acidic conditions. An experiment showed that the use of concentrated phosphate buffer of neutral range converted hydrazonium salts to sodium salts and minimized fissions of the phosphodiester linkages (see Table IV).

The reaction of the lyophilized ribonucleic acid of yeast with anhydrous hydrazine at 50°C for 60 min. was found to be most suitable for the preparation of ribo-apyrimidinic acid. Using these conditions, the product was practically free from pyrimidines and fissions of the phosphodiester linkages were not serious. As attempts to remove the pyrimidines with milder reagents than anhydrous hydrazine, anhydrous methylhydrazine and phenylhydrazine were used. The latter did not react but the former removed considerable amounts of uracil and a little cytosine when the reaction was carried out at 60°C for 90 min. The white product was obtained through acid precipitation and the yield was quantitative. The use of

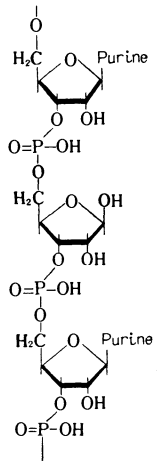
anhydrous methylhydrazine in a more drastic condition is, therefore, of great promise.

The hydrazinolysis products gave slightly higher values for the atomic N/P ratios than those expected from the base composition of the products. The products, excepting that obtained through the dissolution in the buffer, were slightly yellow. A small part of ribose residues may be present as hydrazone or osazone and also as ureido-ribose formed from the pyrimidine riboside moieties by the hydrazinolysis. From the color intensities in the reaction with orcinol and the estimation of reducing sugar, however, it can be seen that these possibilities occure only slightly, if at all. Direct evidence for the presence of free ribose residues in the hydrazinolysis products was obtained by treating one of the products with Takadiastase, which hydrolyses nucleic acids to nucleosides. Much ribose was liberated, as shown by paper chromatography. Qualitative tests for reducing sugar were also strongly positive.

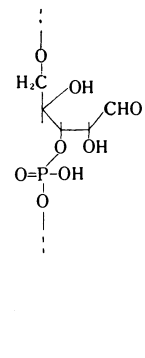
During the hydrazinolysis and the subsequent treatment, the initial interpurine ratios were not distorted. This was most clearly confirmed by analyzing the dialyzable fragments. The base compositions of the dialyzable fragments were the same as those of the corresponding nondialyzable products. The removal of the pyrimidines from yeast ribonucleic acid was easier than that from herring sperm deoxyribonucleic acid. In the initial stage of the reaction, uracil was decomposed faster than was cytosine, but this was reversed later. Yeast ribonucleic acid is presumed to be hydrazinolyzed in a similar way to that shown in the preceding paper on the hydrazinolysis of herring sperm deoxyribonucleic acid[1]. Thus the ribose phosphate residues in the aqueous solution of the ribo-apyrimidinic acid may be present in the furanose form (II) rather than in the free aldehydoform (III)[8].



(I)

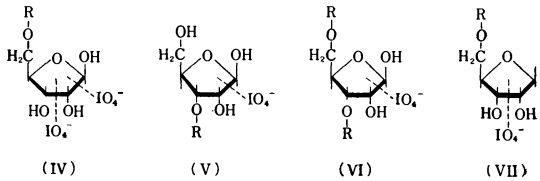


(II)



(III)

In alkaline solutions, the hydrazinolysis products were as unstable as ribonucleic acid. The product which is free from the pyrimidines was unstable, even in solutions of neutral pH or below at 37°C for one day, about 10% of its total phosphorus was rendered soluble in acid—uranyl reagent, but this was greatly reduced at 0°C. In spite of this instability, the product obtained using the most suitable conditions showed a fairly high mean chain length. Periodate should be consumed not only by the nonglycosidic ribose residues within VI or at the end of the chains (IV, V), but also by the purine nucleosides which occupy the chain ends and do not bear a terminal 3′-phosphate group (VII). The periodate consumption



(IV) (V) (VI) (VII)

R=nucleotides or phosphate

of a product obtained through the dissolution in the phosphate buffer was less than that obtained through the acid precipitation. The electrometric titration curve of the product obtained by the reaction at 65°C for 90 min. showed the disappearance of one -NH-CO- dissociation titrating in the range pH 8~12. This can be explained by the removal of uracil. The absence of the amino group of cytosine was, however, not clearly indicated, being obscured by the increased secondary phosphoric acid dissociations which are due to fissions of the phosphodiester linkages.

In the most suitable condition of the hydrazinolysis, about 90% of the material was nondialyzable. Moreover, the interpurine ratio was not distorted during the reaction. Hence, the ribo-apyrimidinic acid must be useful for the structural studies of ribonucleic acid.

8) S. M. Cantor and Q. P. Peniston, *J. Am. Chem. Soc.*, **62**, 2113 (1940).

TABLE II. COMPOSITION OF THE HYDRAZINOLYSIS PRODUCTS OF YEAST RIBONUCLEIC ACID

Preparation*	N (%)	P (%)	Atomic N/P	Color reaction with orcinol[a)]	Reducing ribose residues, mol./100 g.-atoms of P[b)]
RNA, commercial	14.5	8.4	3.8	100	—
RNA, purified	15.0	8.8	3.8	100	3
RAPYA I	14.7	9.3	3.6	127	32
RAPYA IV	13.4	9.9	3.0	164	53
RAPYA V	12.7	9.2	3.0	183	45
RAPYA VIII	12.4	9.1	3.0	163	43
RAPYA IX	13.4	9.9	3.0	153	48

* See Table I.

a) Compared with RNA on the basis of phosphorus content.

b) Compared with ribose as the standard.

Experimental

Nitrogen, phosphorus, reducing sugar (Table II), the ultraviolet absorption spectra (Table III and Fig. 1), the mean chain length and the periodate consumption (Table IV) were determined by methods described in the preceding paper[1]. The nucleotide composition (Table I) was determined chromatographically after hydrolyzing samples in a sealed tube with 1 N hydrochloric acid[9] at 100°C for 1 hr. (propan-2-ol—

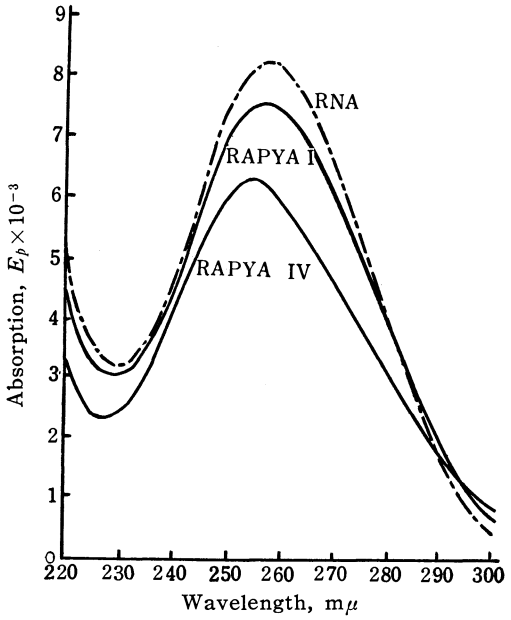


Fig. 1. Ultraviolet absorption curves of the hydrazinolysis products of yeast ribonucleic acid in phosphate buffer, pH 7.
E_p=extinction per g.-atom of phosphorus.

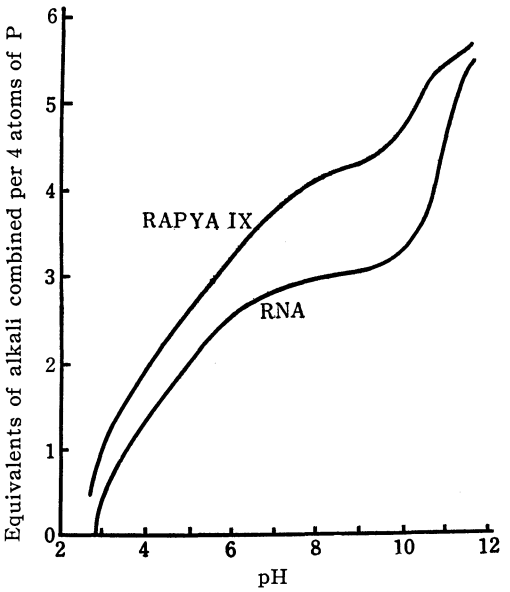


Fig. 2. Electrometric titration curve of the hydrazinolysis product (RAPYA VIII) of yeast ribonucleic acid.

TABLE III. ULTRAVIOLET ABSORPTION SPECTRA OF THE HYDRAZINOLYSIS PRODUCTS OF YEAST RIBONUCLEIC ACID[a)]

Preparation*	Maximum		Minimum	
	mμ	E_p[b)]	mμ	E_p[b)]
RNA, purified	259	8200	230	3200
RAPYA I	259	7600	230	3100
RAPYA IV	255.5	6250	228	2350
RAPYA VIII	255.5	6600	228	2650

a) Measurements were carried out in 0.1 M phosphate buffer of pH 7.

* See Table I.

b) The extinction coefficient with respect to one gram-atom of phosphorus per liter.

9) J. D. Smith and R. Markham, *Biochem. J.*, **46**, 509 (1950).

TABLE IV. MEAN CHAIN LENGTH AND PERIODATE CONSUMPTION OF THE HYDROZINOLYSIS PRODUCTS OF YEAST RIBONUCLEIC ACID

Preparation*	Mean chain length	Periodate consumption, mol. per 1 mol. of P
RNA, purified	21.2	0.05
RAPYA I	19.0	0.46
RAPYA IV	13.5	0.65
RAPYA IV'[a)]	—	1.76
RAPYA IV[a)]''	15.4	0.47
RAPYA V	9.8	0.72

* See Table I.

a) These were obtained by a modified method (see *Experimental*); RAPYA IV'—before treatment with phosphate buffer; RAPYA IV''—after treatment with phosphate buffer.

hydrochloric acid[10], Toyo Roshi Co. No. 51a paper, descending). The color reaction of the hydrazinolysis products with orcinol[11] was compared with the parent ribonucleic acid (Table II). The ribose residues, which in the intact ribonucleic acid were in the pyrimidine nucleotides, also participate in the color reaction. For the electrometric titration of a product (RAPYA IX) a Beckman Type G pH-meter was employed. The measurement was carried out in the absence of carbon dioxide (Fig. 2).

Dehydration of Hydrazines. — Anhydrous hydrazine was prepared as described in the corresponding section of the preceding paper[1]. Fifty per cent aqueous methylhydrazine was dehydrated with sodium hydroxide pellets at 90°C for 12 hr., stood overnight at room temperature and distilled (b. p. 86.6~87.3°C)[12]. Phenylhydrazine was distilled under diminished pressure before use.

Ribonucleic Acid.—A commercial yeast ribonucleic acid, Schwarz Laboratories, Inc., was purified by Sevag's method[13] and freeze-dried. Before treatment with hydrazine, the nucleic acid was dried over concentrated sulfuric acid in vacuo at 60°C for 5 hr. The composition of the nucleic acid is listed in Tables I and II.

Preparation of Ribo-apyrimidinic Acid.— The hydrazinolyses at different conditions gave products in which the ribonucleic acid was more or less deprived of the pyrimidines (Table I). In order to simplify descriptions, the name ribo-apyrimidinic acid (RAPYA) is given to all nondialyzable products obtained by the reaction of the ribonucleic acid with anhydrous hydrazine. A typical preparation was as follows. The mixture of lyophilized and dried yeast ribonucleic acid (1.5 g.) and anhydrous hydrazine (3 ml.) was kept free from moisture at 50°C for 1 hr. Within a few minutes, the nucleic acid dissolved in the hydrazine, making a clear solution, with a slight evolution of heat and foam. After cooling, absolute alcohol (5 vol.) was added to the solution, the white precipitate thus formed washed with absolute alcohol and ether, and dried. The dry solid was then dissolved in cold distilled water at 0°C and the pH adjusted to 1.5 with dilute hydrochloric acid. The slightly yellow precipitate thus formed was washed with absolute alcohol and ether, dried, and then suspended in water and dilute alkali was added carefully until the solid just dissolved. The solution was dialyzed against frequent changes of distilled water at 4°C for 3 days. The nondialyzable fraction was freeze-dried. The light yellow product (RAPYA IV) was obtained in 88% yield with respect to phosphorus recovery. Other reaction products using different conditions were obtained by the same procedure, excepting RAPYA IV' and IV''. For the latter the procedure was modified as mentioned below since yellow materials were obtained at the step where the products were precipitated with acid. This was possibly due to reaction between hydrazine and free ribose residues. After treatment with hydrazine and precipitation with alcohol, the precipitate was dissolved in distilled water at 0°C and the pH was adjusted to 7. This solution was then dialyzed against frequent changes of distilled water and freeze-dried. The white product so obtained still contained hydrazine (RAPYA IV'). This was removed by dissolving the material in ice-cold 0.2 M sodium phosphate buffer (pH 6.2) and dialyzing it against the same buffer at 4°C for 8 hr., then against tap water (24 hr.) and finally against frequent changes of distilled water (48 hr.) and lyophilized (RAPYA IV'').

Reaction of Yeast Ribonucleic Acid with Anhydrous Methylhydrazine. — Lyophilized yeast ribonucleic acid (50 mg.) and anhydrous methylhydrazine (1.5 ml.) were kept free from moisture at 60°C for 90 min., then precipitated with absolute alcohol, dissolved in water, and precipitated with acid. This was again suspended in water and dissolved by the careful addition of dilute alkali and dialyzed. The white product thus obtained, in quantitative yield, contained 10.0 mol. of cytidylic acid and 4.6 mol. of uridylic acid per 10 mol. of adenine. The ratio of guanine to adenine was the same as in the parent nucleic acid.

Reaction of Yeast Ribonucleic Acid with Phenylhydrazine. — Freshly distilled phenylhydrazine (12 g.) and lyophilized yeast ribonucleic acid (0.5 g.) were kept at 150°C for 2 hr. and then treated as mentioned above. The material thus obtained was identical with the parent nucleic acid in the nucleotide composition.

Composition of the Dialyzable Materials. —In the preparation of ribo-apyrimidinc acid I, and also IV and V, the outside fluids of each dialysis were combined, adjusted to pH 7 and freeze-dried. The dialyzable fragments were hydrolyzed with 1 N hydrochloric acid and the products were separated by paper chromatography. The nucleotide compositions are shown

10) G. R. Wyatt, ibid., **48**, 584 (1951).
11) W. Mejbaum, *Z. physiol. Chem.*, **258**, 117 (1939).
12) G. V. Brüning, *Ann.*, **253**, 7 (1889).
13) M. G. Sevag, *Biochem. Z.*, **273**, 419 (1934).

in parentheses in Table I. Practically no differences were shown between the composition of the nondialyzable and the dialyzable materials.

Detection of Ribose and Nucleosides after Enzymic Hydrolysis. — Ribo-apyrimidinic acid IV was dissolved in 0.5 M acetate buffer of pH 5.0 and incubated with dialyzed Takadiastase solution at 37°C for 48 hr. The hydrolyzate was applied on paper and separated with *n*-butanol—ammonia[14]. Ribose was detected by spraying aniline hydrogen phthalate reagent[15]. The ultraviolet photo-print showed only the spots of adenosine and guanosine, whereas yeast ribonucleic acid was completely hydrolyzed to purine and pyrimidine nucleosides by this enzyme.

Qualitative Tests for Nonglycosidic Ribose. —0.2% aqueous solutions of ribo-apyrimidinic acid IV and of yeast ribonucleic acid, and 0.1% ribose solution were used for all tests. Excepting the ribonucleic acid, they reacted with ammoniacal silver solution when heated at 100°C for 15 min., reduced Fehling's solution when heated at 100°C for 5 min., gave a reddish brown color with benzidine in glacial acetic acid at 100°C in a few minutes, and reduced mercuric chloride solution at room temperature. Ribo-apyrimidinic acid IV reacted with phenylhydrazine hydrochloride when heated at 50°C for 15 min. and gave a brownish yellow product. All the hydrazinolysis products spotted on filter paper gave a reddish purple color with aniline hydrogen phthalate reagent used for the development of paper chromatograms of reducing sugars[15].

The authors thank Professor F. Egami for his close interest. The expense of this study was defrayed in part by a grant from the Ministry of Education.

Department of Chemistry
Faculty of Science
Nagoya University
Nagoya

14) R. Markham and J. D. Smith, *Biochem. J.*, **45**, 294 (1949).
15) S. M. Partridge, *Nature*, **164**, 443 (1949).

Amino Acid Synthesis from Nitromalonic Ester. III[1]. *Note on the Synthesis of Glutamic Acid*

By Tôru OKUDA

(Received March 25, 1959)

Several amino acids have been prepared by means of the addition reaction of diethyl nitromalonate with α,β-unsaturated compounds such as acrylonitrile[2] and acrolein[1]. If the similar type of reaction could occur between nitromalonic and acrylic esters, an approach to the synthesis of glutamic acid would be possible. Both the esters have been found to react in the presence of a catalytic amount of triethylamine in alcoholic solution to give 2-carbomethoxyethyl-nitromalonic ester in a good yield. Elimination of one α-ester group of the substituted nitromalonic ester and subsequent hydrogenation[3] gave pyrrolidonecarboxylic ester, which was easily converted into DL-glutamic acid monohydrate. The overall yield was about 50%. Direct reduction of 2-carbomethoxyethyl-nitromalonic ester with Raney nickel in alcoholic solution gave 2-carbomethoxyethyl-malonic ester, indicating the hydrogenolysis occurred during the reaction[4].

Experimental

Diethyl 2-Carbomethoxyethyl-nitromalonate.—Forty-four grams of diethyl nitromalonate and 22 g. of methyl acrylate in 70 ml. of absolute alcohol were heated under reflux in the presence of 3 ml. of triethylamine for 7 hr. and after the concentration of the reaction mixture the residue was dissolved in 400 ml. of ether. The ether solution was extracted with cold aqueous sodium bicarbonate, washed with water and dried. Evaporation of ether gave 55 g. of crude product. When the crude product was distilled in vacuo, there was obtained 49 g. of the pure material boiling at 120~150°C/2 mmHg.

Anal. Found: C, 45.74; H, 6.07; H, 4.83. Calcd. for $C_{11}H_{17}O_8N$: C, 45.36; H, 5.84; N, 4.81%.

1) Paper II of this series; T. Okuda, This Bulletin, **30**, 358 (1957).

2) S. Akabori, Y. Izumi and T. Okuda, *J. Chem. Soc. Japan, Pure Chem. Sec.* (*Nippon Kagaku Zasshi*), **77**,490 (1956).

3) D. I. Weisblat and D. A. Lyttle, U. S. Pat., 2,606,921 (1952).

4) D. I. Weisblat and D. A. Lyttle, *J. Am. Chem. Soc.*, **71**, 3079 (1948).

Ethyl 2-Carbomethoxyethyl-nitroacetate[3,5].—A solution of 51 g. of crude diethyl 2-carbomethoxyethyl-nitromalonate in 450 ml. of dry ether was treated with 4.10 g. of sodium dissolved in 100 ml. of absolute alcohol at 0°C as already reported in the preceding papers[1,2]. The resulting slurry was transferred to a separatory funnel, 150 ml. of ether and 70 ml. of cold 10% hydrochloric acid were added and vigorous shaking was applied. The ether layer was separated and the aqueous layer was extracted with ether. The ether solutions were combined, washed with water and dried. Concentration and vacuum-distillation gave 34 g. of the product of b.p. 115~128°C/2 mmHg.

Anal. Found: C, 43.10; H, 5.95; N, 6.18. Calcd. for $C_8H_{13}O_6N$: C, 43.83; H, 5.98; N, 6.39%.

Ethyl Pyrrolidonecarboxylate.—The pressure-hydrogenation of 34 g. of 2-carbomethoxyethyl-nitroacetate was carried out using 150 ml. of ethanol and 4 g. of Raney nickel. The catalyst was filtered off, and the ethanol was evaporated. Crude ethyl pyrrolidonecarboxylate thus obtained weighed 22 g. This can be purified either by recrystallization from ether-petroleum ether or by distilling at 2 mm., m.p. 48~50°C, b.p. 153°C/2 mmHg.

Anal. Found: C, 53.80; H, 7.14; N, 8.99. Calcd. for $C_7H_{11}O_3N$: C, 53.49; H, 7.05; N, 8.91%.

The ester was converted into DL-glutamic acid monohydrate by acid hydrolysis. The overall yield with respect to diethyl nitromalonate was about 50%.

Anal. Found: C, 36.59; H, 6.62; N, 8.92. Calcd. for $C_5H_{11}O_5N$: C, 36.36; H, 6.71; N, 8.48%.

Diethyl 2-Carbomethoxyethylmalonate.—Twelve grams of diethyl 2-carbomethoxyethyl-nitromalonate was reduced in alcohol with 2 g. of Raney nickel. After the removal of the catalyst and the alcohol the residue was distilled. There was obtained 8 g. of diethyl 2-carbomethoxyethylmalonate boiling at 125~130°C/2 mmHg.

Anal. Found: C, 53.23; H, 7.73. Calcd. for $C_{11}H_{18}O_6$: C, 53.66; H, 7.32%.

Institute for Protein Research
Osaka University
Nishi-ku, Osaka

5) N. Kornblum and J. H. Eeicher, ibid. 78, 1499 (1956).

Studies on the Silk-Palladium Catalyst. I. Preparation and Stability

By Yoshiharu IZUMI

(Received March 27, 1959)

A number of methods have so far been attempted in order to increase the active surface of hydrogenation catalysts of metal or metal oxide nature. Thus, for example, a method has been devised to deposit certain metals or metal oxides onto porous carriers such as carbon or Kieselguhr, to disperse them into colloidal states with the aid of various protective colloids, or to remove a constituent metal from an alloy by chemical treatments as in the case of preparation of Raney nickel. The other methods so far attempted are also based on physical or mechanical dispersion of catalyst metals into colloidal solutions or on the surface of porous substances.

A few years ago, Akabori et al.[1-3] for the first time reported an entirely new type of hydrogenation catalyst and showed that it was capable of catalyzing asymmetric reduction of certain unsaturated compounds. This catalyst was prepared by coordinating palladous chloride with silk fibroin fibers and then hydrogenating the resulting silk-$PdCl_2$ complex. Since palladous can form a chelate compound with silk fibroin, it is not unreasonable to assume that the palladium in the catalyst is firmly fixed to the asymmetric structure of the protein fibers in an almost atomic state. The capacity of asymmetric catalysis may be explained on the basis of the asymmetric structure of the carrier fibroin.

Although this catalyst was originally developed for the purpose of asymmetric synthesis, it also has a number of characteristics suitable for use as a general hydrogenation catalyst. Thus, it is quite easy to mix the catalyst with reacting substances because of its unusual low

1) S. Akabori, Y. Izumi, Y. Fujii and S. Sakurai, *Nature*, 178, 323 (1956).
2) S. Akabori, Y. Izumi, Y. Fujii and S. Sakurai, *J. Chem. Soc. Japan, Pure Chem. Sec.* (*Nippon Kagaku Zasshi*), **77**, 1374 (1956).
3) S. Akabori, Y. Izumi, Y. Fujii and S. Sakurai, ibid., 78, 168 (1957).

density. The catalyst is also unique in that its carrier is a fibrous protein and therefore it can be spun or woven into sheets, cloth or fluffs. In hydrogenation catalysts hitherto devised, the metal is either bound to the carrier by simple mechanical attraction or finely dispersed as colloidal particles. Therefore, it is sometimes not very easy to separate the catalyst from the reaction mixture due to the detachment of the metal from the carrier or to the colloidal nature of the catalyst. With the silk-palladium catalyst, however, the catalyst can be readily separated from the reactants by simple filtration owing to the fact that the metal, though highly dispersed, is tightly held by the micelle structure of silk-fibroin.

The investigations to be reported in this and the following papers were undertaken with an object of obtaining some basic data concerning the applicability of this hydrogenation catalyst for general practical purposes. Also included in this series of papers are observations on the properties of a Nylon-palladium catalyst in which silk fibroin is replaced by the synthetic fiber, 6-Nylon, as the carrier.

Results and Discussion

Activity and Conditions of Preparation of Catalyst.—For the purpose of obtaining the catalyst of a high activity, optimum conditions were sought for the preparation of the catalyst. Table I records the palladium contents of various preparations prepared under different sets of conditions. As can be seen, the highest content was attained when 350 mg. of silk fibroin was boiled for 8 min. with 100 ml. of 0.1 N acetic acid containing 100 mg. of palladous chloride and the resulting chelate was reduced with hydrogen in an autoclave. These conditions were, therefore, used in preparing the catalysts studied in the following sections.

TABLE I. PALLADIUM CONTENTS OF CATALYSTS

Condition for preparation				Pd content in 50 mg. catalyst* (μg.)
Medium (ml.)		$PdCl_2$ (mg.)	Carrier (mg.)	
Water	100	100	Fibroin 350	2590
N/5 HOAc	50	〃	〃	3950
N/10 〃	100	〃	〃	4600
N/10 〃	100	〃	6-Nylon 350	1165
N/15 〃	50	〃	Fibroin 350	3700
N/30 〃	100	〃	〃	4300

* Pd contents were determinated with *p*-nitrosodimethylaniline.

Prolonged boiling for more than 8 min. resulted in an increased palladium content in the catalyst, but this increase was found to be mainly due to an easily detachable form of palladium and did not contribute to the activity. Although the solubility of palladous chloride could be considerably increased by the addition of sodium chloride or sodium acetate to the aqueous solution, these salts were found to inhibit the chelate formation between palladous chloride and fibroin and consequently lead to less active preparations. When silk fibroin was boild with palladous chloride in distilled water, a preparation containing less palladium was obtained as compared with the preparation which was boiled in dilute acetic acid.

The silk-palladium chelate was usually converted into the active catalyst by reducing it with hydrogen in an autoclave. When this activation was carried out by means of formic acid, the resulting catalyst showed appreciably less activity as shown in Table III.

Capacity of Asymmetric Catalysis.—The asymmetric catalyst reported in previous papers was prepared by boiling silk fibroin with palladous chloride in water. This catalyst, as reported previously, was able to catalyze, for example, the asymmetric hydrogenation of 4-benzylidene-2-methyl-oxazol-5-one(4-benzylidenazlacton) to give optically active products. The catalyst prepared in 0.1 N acetic acid instead of in water, and mainly used in this investigation failed to achieve asymmetric catalysis despite its higher palladium content. The reason for such a peculiar behavior of the silk-palladium catalyst is not yet clear. In any event, it seems that the mechanism responsible for the asymmetric catalysis is of a quite delicate nature and can be profoundly affected by slight alterations of the system.

Stability of Catalyst.—Table II is a summary of an investigation in which the activity of the catalyst and its precursor, silk-palladium chelate, was examined both immediately after preparation and after storage for several days in methanol or under dried condition. The activity of the chelate was of course measured after activation. The activity in the table is expressed in terms of "70% reaction time (t)" and reaction velocity (v) observed in the hydrogenation of nitrobenzene to aniline. The results recorded in Table II clearly show that both the catalyst itself and its precursor chelate are quite stable and can be stored for a long period

TABLE II. STABILITY OF CATALYST AND PRECURSOR CHELATE UNDER VARIOUS CONDITIONS

Sample	Storage condition	Storage time	70% Reaction time (min.)	Reaction velocity	Reaction temp. (°C)
Silk-Pd·Cl_2* 350 mg.	In dry state	0	15.5	6.5	16~17
		12 d.	15.0	6.7	〃
Silk-Pd 350 mg.	In methanol	0	18.5	5.4	12~14
		5 d.	20.5	5.0	13~15
		11 d.	18.5	5.4	〃
	In dry state	0	2.1	47.5	40
			9.0	11.1	20~21
		19 h.	9.5	10.5	20
		14 d.	9.0	11.1	20~21
		30 d.	9.5	10.5	18~20

* The activity was measured after conversion to catalyst by hydrogenation.

without loss of activity. Furthermore, no spontaneous combustion took place even when the catalyst was stored in air dried conditions.

TABLE III. ACTIVITY OF CATALYST ACTIVATED WITH FORMIC ACID

Catalyst (mg.)	70% Reaction time (min.)	Reaction velocity	Reaction temp. (°C)
Silk-Pd (350) Activated with HCOOH	15.0	6.7	20

Activation Energy of Hydrogenation Reaction.—The catalytic hydrogenation of nitrobenzene to aniline in the presence of the silk-palladium catalyst was measured at various temperatures. In Fig. 1 is plotted logarithm of reaction velocity (log v) against reciprocal absolute temperature ($^1/_T$). From this graph the activation energy of the catalyzed reaction was computed to be approximately 14.5 kcal./mol.

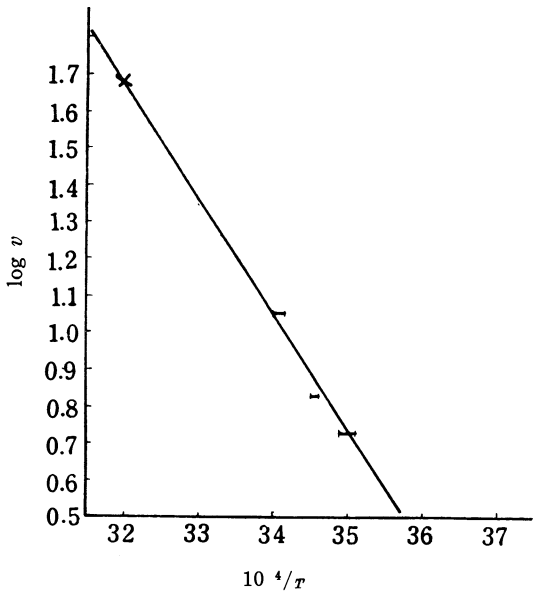


Fig. 1. Dependence of reaction velocity upon temperatures.

Nylon-Palladium Catalyst. — When 6-Nylon (caprolactam polymer) fibers were used as the carrier and treated in the same way as described for silk fibroin fibers, a 6-Nylon-palladium catalyst could be obtained. It was revealed, as shown in Table IV, that the Nylon-palladium catalyst also exhibits a high activity in catalyzing the hydrogenation of nitrobenzene. Nitrobenzene was readily reduced to aniline with hydrogen even at atmospheric pressure in the presence of this catalyst. It was found that the activity was proportional to the palladium content as shown in Table I.

TABLE IV. ACTIVITY OF NYLON-PALLADIUM CATALYST

Catalyst (mg.)	70% Reaction time (min.)	Reaction velocity	Reaction temp. (°C)
Nylon-Pd 350	65	1.5	10
Control (Silk-Pd)		4.9*	10

* Calculated value.

Experimental

I. Preparation of Catalyst. — *1) Palladous Chloridd Solutions.* — *a) Solution in water.*—One hundred milligrams of palladous chloride was added to 100 ml. of cold water and the mixture was stirred for 30 min. in the cold with the aid of a magnetic stirrer.

b) Solution in 0.1 N acetic acid.—One hundred milligrams of palladous chloride were dissolved at 60°C in 10 ml. of 1 N acetic acid and the solution was diluted 10-fold before use.

2) Silk-Palladium Chelate.—Three hundred and fifty milligrams of silk fibroin fibers previously cut into ca. 3 mm. pieces was mixed with 100 ml. of palladous chloride solution (palladous chloride,

100 mg.) and the mixture was boiled for 8 min. The fibers gradually became dense and brownish and finally precipitated as a dark brown mass. After cooling, the precipitated chelate was filtered, washed with water and then methanol, and finally air-dried.

3) Silk-Palladium Catalyst.—The chelate was converted to the active catalyst by the following two methods.

a) The chelate corresponding to 3.5 g. of silk fibroin was suspended in 50 ml. of methanol and reduced with hydrogen (80 kg./cm^2) at 100°C for 1 hr. in a 100 ml. autoclave. (80°C, 2 hr. for the Nylon catalyst).

b) The chelate corresponding to 350 mg. of fibroin was suspended in 30 ml. of 2% formic acid and boiled for 4 min. The chelate became black with vigorous evolution of hydrogen. In both cases, the catalyst, after cooling, was washed with water and methanol and then air-dried.

II. Determination of Palladium.—This was performed by the *p*-nitrosodiethylaniline method of Overholser[4].

III. Reaction Vessel.—A 100 ml. of autoclave was used as the vessel for hydrogenation reactions. The autoclave is illustrated in Fig. 2. The cap A was filled with absorbent cotton in order to prevent the catalyst from invading into the accessory parts of the autoclave. The apparatus was also so designed that the part B could be opened after the reaction. This device rendered it very easy to wash the inside of the tube. Although an aluminum packing was used

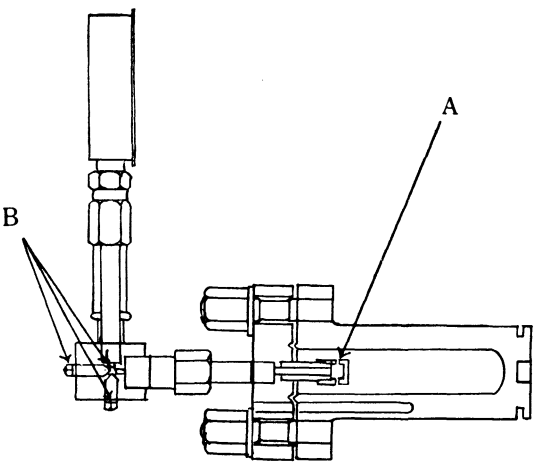


Fig. 2.

at the interface between the lid and the vessel, silver packings were employed in other parts to minimize the unfavorable effects due to metal ions. The autoclave was shaken 100 times per min. with an inclination angle of 15°.

IV. Reaction Velocity Measurement.—*1) Reaction Conditions.*—Four grams of nitrobenzene dissolved in 50 ml. of methanol and the catalyst to be tested were placed in the autoclave and it was filled with hydrogen to 90 kg./cm^2. The initial pressure was read after 15 sec. shaking for equilibriation and the shaking was continued until the theoretical amount of hydrogen was taken up.

2) Calculation of Reaction Velocity.—The reaction velocity (v) was calculated according to the equation,

$$v=\frac{100}{t}$$

where t is the time in minutes required until 70% of the theoretical hydrogen uptake occurred ("70% reaction time").

V. Isolation of Product.—The reaction mixture was filtered and 10 g. of acetic anhydride was added to the filtrate. The mixture was then evaporated to dryness. On cooling the residue after treating with 10 ml. of water, 4.0 g. of crude acetanilide (m. p. 111°C) was obtained. Its melting point was increased to 113°C on recrystallization from water.

VI. Tests of Stability.—*1) Stability Test of Chelate.*—Silk-palladium chelate was dried at 40°C and stored in a stoppered bottle. After 12 days it was activated by hydrogen as described above and its activity for the reduction of nitrobenzene was measured.

2) Stability Tests of Catalyst.—The catalyst preparations prepared by reduction with hydrogen were stored either in methanol or in the dry state (in a stoppered bottle). After suitable periods of storage, their activities were measured as above.

Summary

1. The highest hydrogenation activity was obtained when the silk-palladium catalyst was prepared by boiling the silk fibroin fibers with 0.1% palladous chloride solution in 0.1 N acetic acid for 8 min. and then hydrogenating the resulting chelate.

2. The catalyst prepared as above was, however, devoid of the capacity of asymmetric catalysis, although the same catalyst prepared in distilled water (instead of dilute acetic acid) was able to achieve asymmetric reduction.

3. The catalyst and its precursor chelate could be stored in dry state without any loss of activity.

4. The synthetic fiber, 6-Nylon, could be successfully used as the carrier in place of silk fibroin.

The author wishes to express his sincere thanks to Professor Shiro Akabori for valuable suggestions and encouragement throughout this work. He is also greatly indebted to the Toyo Rayon Co., Ltd. for the supply of 6-Nylon fibers used in this investigation. His thanks are also due to

4) L. G. Overholser and J. H. Yoe, *J. Am. Chem. Soc.*, **63**, 3224 (1941).

Mr. Y. Fujii, for his assistance, and to Dr. R. Sato for his advice on preparing this manuscript.

Division of Organic Chemistry
Institute for Protein Research
Osaka University, Nishi-ku, Osaka

Studies on the Silk-Palladium Catalyst. II. General Properties

By Yoshiharu IZUMI

(Received March 27, 1959)

In the previous paper[1] of this series it was reported that the silk-palladium catalyst possesses a number of excellent characteristics suitable for the purpose of catalytic hydrogenation. In order to obtain further information concerning the fundamental properties of the catalyst and to provide a basis for its practical application, it is intended in the present investigation to study its selectivity, durability and behaviors towards catalytic poisons. The present paper describes the results obtained in these experiments.

Results and Discussion

I. Selectivity of the Catalyst.—The catalytic efficiency of the silk-palladium catalyst was mainly examined in the previous paper[1] on the hydrogenation of nitrobenzene to aniline. In the present study the activity of the catalyst was examined with a variety of unsaturated compounds listed in Table I. The results obtained are also recorded in the same table.

Hydrogenation of C=C Double Bonds.—The C=C double bonds were found to be very easily reduced at low temperatures in the presence of the silk-palladium catalyst. For instance, it was found that mesityl oxide absorbed 70% of the theoretical amount of hydrogen at 30°C for 20 min. if the catalyst (containing ca. 0.08% of palladium metal per substrate) was supplied. This could be compared with the data obtained with 1% (by weight) Raney nickel in the presence of which it took 60 min. at 60°C for mesityl oxide to absorb the same amount of hydrogen. It was further noticed that the catalyst was able to selectively hydrogenate the C=C double bonds in mesityl oxide, crotonaldehyde and acrolein, leaving their carbonyl groups quite unattacked even at higher temperatures.

These results indicate that the silk-palladium catalyst is particularly suitable for the preparation of saturated aliphatic aldehydes and ketones from the corresponding unsaturated compounds. That azlactone and acetaminocinnamic acid are readily hydrogenated by the silk-palladium catalyst was previously reported[2-4]. The catalyst was, however, unable to reduce phenol at all, indicating that the double bonds in benzene rings are inert to the catalytic action.

Hydrogenation of Carbonyl Groups.—As described above, the silk-palladium catalyst was rather inactive in hydrogenating aliphatic carbonyl compounds. This conclusion was further confirmed in an attempt to reduce acetone and methyl ethyl ketone which were not reduced at all. It was, however, found that the hydrogenation of benzaldehyde in the presence of the catalyst readily gave rise to the formation of toluene. It is, therefore, probable that carbonyl groups attached to aromatic rings may be susceptible to the action of the catalyst. The catalyst which was recovered after having been used for the reduction of acetone was found to show no appreciable depression in the activity of hydrogenating nitrobenzene. It therefore seems that the failure in the hydrogenation of acetone (and other aliphatic

1) Y. Izumi, This Bulletin, **32**, 932 (1959).

2) S. Akabori, Y. Izumi, Y. Fujii and S. Sakurai, *Nature*, **178**, 323 (1956).

3) S. Akabori, Y. Izumi, Y. Fujii and S. Sakurai, *J. Chem. Soc. Japan, Pure Chem. Sec.* (*Nippon Kagaku Zasshi*), **77**, 1374 (1956).

4) S. Akabori, Y. Izumi, Y. Fujii and S. Sakurai, ibid., **78**, 168 (1957).

TABLE I. SPECIFICITY OF CATALYST

Substrate (g.)	Product	Yield (%)	Solvent	Catalyst (mg.)	Temp. (°C)	Reaction time (min.) 70%	100%
Mesityl oxide 41	Me-isobutyl ketone	86	—	350	30	21.5	60
Crotonaldehyde 21	Butyraldehyde	70	Ether	100	20	21	102
Acroleine 13	Propionaldehyde	100*	Ether	350	20	4	36
Acrylonitrile 50	Ethyl cyanide	79	—	100	6	47	71
Fumaric acid 12	Succinic acid	88	NaOH	350	53	16	28
Phenol 5	—	—	Methanol	350	170	—	—
Acetone 30	—	—	—	350	120	—	—
Methyl ethyl ketone 30	—	—	—	350	120	—	—
Benzaldehyde 11	Toluene	46	Methanol	350	27	41.3	426
Benzyl cyanide 6	Acetylphenethylamine	79	Ac_2O HOAc	350	75	179	276
Benzaldehyde 10.6	Dibenzylamine	65	Methanol NH_4OH	350	80	145	220
α-Ketoglutaric acid 5	Glutamic acid	50	Methanol NH_4OH	350	60	—	60
Nitrobenzene 4	Aniline	90	Methanol	350	20	9.5	23
MDAN** 12.4	MDAA***	80	Methanol	350	60	38	90
ω-Nitrostyrene 15	Phenylacetoaldoxime	35	Methanol	350	20	9.5	23
Diethyl nitro malonate 6.9	Diethyl aceto-aminomalonate	36	Ac_2O HOAc	350	100	31	90
Azobenzene 5.2	Hydrazobenzene	58	Methanol	100	20	95	185
Azobenzene 10	Aniline	88	Methanol	350	70	20	125
Dimethylglyoxime 3	—	—	Methanol	350	90	—	—
Acetophenonoxime 3	—	—	Methanol	350	70	—	—

* Calculated from dinitrophenylhydrazone.

** $CH_3(CH_3)CH\text{-}CH_2\text{-}CH((CH_3)_2N)\text{-}CH(O\text{-}COC_6H_4NO_2)\text{-}CH_3 \cdot HCl$

*** $CH_3(CH_3)CH\text{-}CH_2\text{-}CH((CH_3)_2N)\text{-}CH(O\text{-}COC_6H_4NH_2)\text{-}CH_3 \cdot HCl$

carbonyl groups) is an intrinsic property of the catalyst and not due to the poisoning by these compounds.

Reduction of Nitrile Groups.—It has already been mentioned that the catalyst was inactive in reducing the nitrile group of acrylonitrile, at least at low temperatures. Using acetic anhydride as a solvent, however, benzyl nitrile was converted to *N*-acetyl-phenethylamine in the presence of hydrogen and the silk-palladium catalyst.

Reductive Amination of α-Ketoglutaric Acid and Benzaldehyde.—The silk-palladium catalyst was able to convert α-ketoglutaric acid to glutamic acid in the presence of ammonia and hydrogen. When benzaldehyde was subjected to reductive amination under similar conditions, the main product obtained was identified as dibenzylamine.

Reduction of Nitro Groups.—In the previous paper[1] the reduction of nitrobenzene to aniline was employed as the test system for comparing the catalytic activity. In the present study, it was further found that 5-methyl-3-dimethyl-aminohexan-2-ol-*p*-nitrobenzoate hydrochloride (MDAN) was also readily hydrogenated by this catalyst to form the corresponding amine hydrochloride (MDAA) in as excellent a yield as in the case of the reduction of nitrobenzene. On the contrary, both ω-nitrostyrene and diethyl nitromalonate were reduced very slowly, yielding phenylacetaldoxime and diethyl acetamidomalonate, respectively; their yields also being low. It may be inferred that the catalyst is able effectively to catalyze the hydrogenation of aromatic nitro groups, but relatively weakly that of aliphatic nitro groups.

Reduction of Azobenzene.—Hydrogenation of azobenzene by means of the silk-palladium catalyst at low temperatures resulted in the formation of hydrazobenzene. At higher temperatures, on the other hand, the hydrogenation proceeded in two steps, as shown in Fig. 1, taking up more than one mole of hydrogen and the main product was aniline.

Reduction of Oximino Groups.—It was already reported[2-4] that the silk-palladium catalyst could catalyze the reduction of

TABLE II. DURABILITY TEST OF CATALYST

Substrate	Catalyst sample (Pd mg.)	Reaction temp. (°C)	Reaction velocity	Temp. at which H_2 uptake starts (°C)
Diethyl maleate 50 g.	Original silk-Pd (9.2)	150	9.5	105
	After 1st recovery	〃	22.0	90
	〃 2nd 〃	〃	18.0	70
	〃 3rd 〃	〃	17.0	50
	〃 4th 〃	〃	25.0	60
〃	Original carbon-Pd (10)	〃	30.0	50
	After 1st recovery	〃	7.4	60
	〃 2nd 〃	〃	9.1	70

benzyldioxime, α-acetoximino-phenylpropionic ethyl ester and glutaric diethyl ester to the corresponding amines. It was, however, found in the present study that both dimethylglyoxime and acetophenone oxime could not be reduced at all.

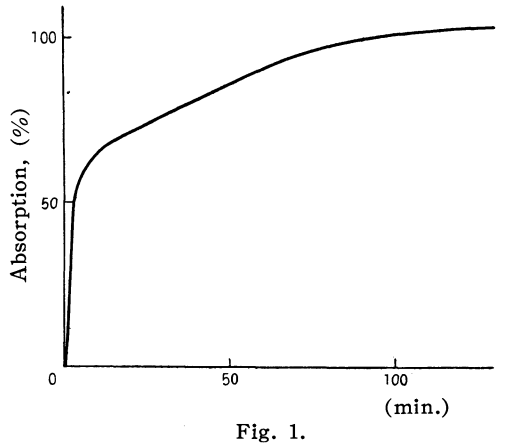


Fig. 1.

II. Durability of Catalyst.—The hydrogenation of diethyl maleate to diethyl succinate was selected as the test system to study the durability of the silk-palladium catalyst. The durability test was conducted in comparison to the carbon-palladium catalyst[5] commonly used as a hydrogenation catalyst.

The results of the test are summarized in Table II. As can be seen from Table II, a very interesting phenomenon was observed concerning the durability of silk-palladium catalyst. When freshly prepared silk-palladium catalyst was used, the temperature at which hydrogen absorption starts was relatively high (105°C) and the reaction proceeded rather slowly. In the hydrogenation using the catalyst recovered from the first run, however, the temperature of initial hydrogen uptake was not only considerably lowered (90°C), but also the reaction itself was accelerated. This elevated activity of pre-used catalyst persisted at least after the fifth run. Such a phenomenon was not observed with the carbon-palladium catalyst which showed the highest activity in the first run and lost it thereafter. It does not seem unreasonable to suppose that such an excellent durability of the silk-palladium catalyst is due to the possibility that the palladium attached to the carrier protein may be sterically rearranged after the first run in favor of the catalytic activity.

In connection with the durability, it might be pointed out that the relatively high ignition point (as compared to the carbon-palladium catalyst) and bulkiness of the fibrous silk-palladium catalyst were very convenient for its handling and recovery.

III. Poisoning of Catalyst.—The silk-palladium catalyst was found to be sensitive to poisonous substances or to various chemical treatments. In Table III are summarized the results of such inhibition studies. In examining the toxic effects, the hydrogenation of either nitrobenzene or diethyl maleate was adopted as the test system and the velocity of hydrogen uptake was calculated and compared as previously described. The carbon-palladium catalyst was also tested as a reference.

Inhibition by Mercaptan.—As can be seen from Table III, the addition of or treatment with ethyl mercaptan markedly decreased the catalytic activity of silk-palladium to hydrogenate both nitrobenzene and diethyl maleate. This poison, which is a well-known inhibitor of palladium catalysts, was also deleterious to the carbon-palladium catalyst. The silk catalyst was, however, much more

5) R. Mozingo, "Organic Syntheses", Vol. 26, John Wiley & Sons., Inc., New York (1947), p. 77, (Procedure D).

TABLE III. EFFECT OF VARIOUS TREATMENTS AND ADDITIONS ON THE ACTIVITY OF SILK AND CARBON-PALLADIUM CATALYSTS

Substrate	Catalyst (Pd mg.)	Addition (mg.)	Reaction temp. (°C)	Reaction velocity
Nitrobenzene 4 g. in 50 ml. MeOH	Silk-Pd (18.4)*	None	50	84
	Carbon-Pd (20)	〃	21	100
	Silk-Pd (18.4)** treated with EtSH	〃	50	22
	Carbon-Pd (20)** treated with EtSH	〃	〃	100
	Silk-Pd (18.4)	EtSH	〃	16.6
	Carbon-Pd (20)	〃	〃	16.6
	Silk-Pd (18.4) acetylated	None	19	1.75
Diethyl maleate 50 ml.	Silk-Pd (18.4)	〃	150	22
	The same after recovery	〃	〃	50
	Silk-Pd (18.4)	EtSH	〃	1.1
	Carbon-Pd (20)	〃	〃	6.25
	Silk-Pd (18.4)	$Fe(NO_3)_3 \cdot 12H_2O$ (40)	〃	1.7
	The same after 1st recovery	〃	〃	22.5
	The same after 2nd recovery	〃	〃	7.4
	The same after 3rd recovery reactivated with EDTA	None	〃	125
	Silk-Pd (18.4)	$Cu(NO_3)_3 \cdot 3H_2O$ (25)	〃	5.3
	The same after 1st recovery	〃	〃	2.7
	The same after 2nd recovery reactivated with EDTA	None	〃	45.0

* Calculated from the activity at 20°C.

** The catalyst was brought in contact with 15 ml. of 0.02% EtSH methanol.

seriously poisoned by the mercaptan than the carbon catalyst. It was, however, noted that no palladium was extracted from the silk catalyst in the presence of ethyl mercaptan, in contrast to the considerable extraction observed in the case of the carbon catalyst. It appears probable that the mercaptan inhibits the catalysts by directly blocking the active palladium.

Inhibition by Metal Ions.—Unlike the carbon palladium and other palladium catalysts, the activity of the silk-palladium catalyst was greatly lowered in the presence of ferric and cupric ions as supplied in the form of nitrates. Cupric ion was somewhat more toxic than ferric ion. It is more likely that these metal ions form chelate linkages with the carrier protein, sometimes three-dimentionally, and thus prevent the reactant from approaching the active palladium atoms which are distributed inside the fibroin micelles.

Reactivation by Ethylenediamine Tetraacetic Acid.—The catalyst poisoned by ferric or cupric ion could be reactivated by treating it with ethylenediamine tetraacetic acid (EDTA). As a matter of especial interest it was revealed that the catalyst thus reactivated exerts very powerful catalytic activity. In fact, EDTA treatments of ferric ion- and cupric ion-poisoned catalysts produced preparations 2.5 and 3 times, respectively, as active as the control catalyst (pre-used once under normal conditions, see above). This peculiar phenomenon suggests that the internal structure of the carrier protein was altered on removal of the metal ions by EDTA to favor the catalytic activity.

Effect of Acetylation.—As previously reported[4], an acetylated silk-palladium catalyst prepared from pre-acetylated silk fibroin and palladous chloride in the usual manner is more active than the unacetylated silk-palladium catalyst in hydrogenating azlactone. Quite unexpectedly, however, it was found in the present investigation that acetylation with acetic anhydride of the pre-formed silk-palladium catalyst greatly depressed the activity. It may be inferred that acetylation of the carrier protein of silk-palladium catalyst blocks the

openings of the fibroin micelles in which the active palladium atoms reside and thus makes it difficult for the substrate to reach the active centers.

In short, there are two types of inhibition; the first, including ethyl mercaptan, inhibits the catalyst by directly combining with palladium atoms and the second, such as ferric ion, cupric ion, and acetylation, by modifying the structure of carrier fibroin. The latter type of inhibition is unique to the silk-palladium catalyst and has special bearings to the structural interpretation of the catalytic activity.

Experimental

I. Preparation of the Catalyst. — The catalyst was prepared by the method of previous papers.

II. Selectivity of the Catalyst.—*1) Reduction of C=C Double Bonds.—a) Reduction of fumaric acid.*—Seventy milliliters of aqueous solution containing 12 g. of fumaric acid adjusted to pH 7.0 with 20% sodium hydroxide and 100 mg. of the catalyst were shaken in 90 kg./cm^2 of hydrogen at 53°C. The reduction was complete after 28 min. The reaction mixture was filtered and the filtrate evaporated to 60 ml. which was then acidified with 20 ml. of concentrated hydrochloric acid. After standing overnight, 9.5 g. succinic acid (m.p. 184°C) was obtained. It was confirmed that the product is devoid of unsaturated bond by infrared spectroscopy.

b) Reduction of mesityl oxide.—Forty-one grams of mesityl oxide was reduced, using 350 mg. of the catalyst with 90 kg./cm^2 hydrogen at 30°C. The reduction was complete after an hour and 1 mol. of hydrogen was absorbed per 1 mol. of mesityl oxide. 36 g. of methyl isobutyl ketone (b. p. 113~115°/760 mm Hg) was obtained from the reaction mixture. Infrared spectroscopy showed a disappearance of unsaturated bond.

c) Preparation of Raney-nickel catalyst.—0.5 g. of Raney-nickel-alloy was added to 6 ml. of 25% sodium hydroxide solution in small portions during 5 min. and then heated for an hour on a water bath. The catalyst sludge was washed three times with each 30 ml. of water and washed with methanol decantation.

d) Reduction of crotonaldehyde. — Twenty-one grams of crotonaldehyde dissolved in 30 ml. of ether was reduced at 20°C with 85 kg./cm^2 hydrogen using 100 mg. of the catalyst. The reduction was continued for 102 min. The reaction mixture was distilled in a 30 cm. dephlegmator. Fifteen grams of butyraldehyde (b. p. 75°C) was obtained and this sample contained no C=C double bonds as examined by infrared spectroscopy.

Analysis of the dinitrophenylhydrazone of this compound showed the following results.

Anal. Found: N, 22.6. Calcd. for $C_{10}H_{12}O_4N_4$: N, 22.2%.

The aldehyde group of crotonaldehyde was never reduced even at higher temperature (130°C).

e) Reduction of acrolein.—When 13 g. acrolein in 20 ml. ether was reduced at 20°C with 85 kg./cm^2 hydrogen using 350 mg. of the catalyst, hydrogen was readily absorbed and the absorption ceased in 36 min.

On adding 2, 4-dinitrophenylhydrazone to 1/100 portion of the reaction mixture, there was obtained 550 mg. propionaldehyde-2, 4-dinitrophenylhydrazone with m.p. 126°C, indicating a yield of 100% in the reduction.

Anal. Found: N, 23.7. Calcd. for $C_9H_{10}O_4N_4$: N, 23.5%.

By distillation of the residue through 15 cm. Widmer column 2 g. of the distillate of b.p. 49°C was obtained. It was proved infrared spectroscopically that this material has no C=C double bond.

This catalyst did not catalyze the reduction of the aldehyde group of this product even when the reduction was carried out at 120°C.

f) Reduction of acrylonitrile. — Fifty grams of acrylonitrile was reduced at 6°C, 100 atm. with 100 mg. of this catalyst and spontaneously the reaction temperature rose to 24°C. The reaction was concluded for 71 min. By fractional distillation, 41 g. of ethyl cyanide (b. p. 96~98°C) was obtained. The product was identified by infrared spectroscopically and gas-chromatographically.

g) Reduction of phenol.—Phenol was not hydrogenated in methanol at 170°C with 80 atm./cm^2 hydrogen by 350 mg. of this catalyst.

2) Reduction of Carbonyl Compounds.—a) Reduction of acetone and methyl ethyl ketone.—Thirty grams of acetone (or methyl ethyl ketone) was not reduced with 90 kg./cm^2 hydrogen at 120°C in the presence of 350 mg. of the catalyst. (Activity of recovered catalyst was tested by the method of previous report[1]. It was clear that the activity of this catalyst was maintained through this condition).

b) Reduction of benzaldehyde.—Eleven grams of benzaldehyde dissolved in 40 ml. of methanol was reduced with 90 kg./cm^2 hydrogen at 27°C using 350 mg. of catalyst. The reduction was continued for 426 min. absorbing of hydrogen per mol. of the aldehyde. 4.3 g. of toluene was obtained from the reaction product, and identified by infrared spectrum.

3) Reduction of Cyanides.—Reduction of benzyl cyanide.—Using 350 mg. of the catalyst 6.0 g. of benzylcyanide was reduced with 100 kg./cm^2 hydrogen at 75°C in a mixture of 15 g. acetic anhydride and 30 g. of acetic acid. The reduction was completed in 276 min. Six grams of acetylphenethylamine (b. p. 145°C/5 mm Hg) was obtained by fractional distillation reaction mixture under reduced pressure.

Anal. Found: N, 8.35. Calcd. for $C_{10}H_{13}ON$: N, 8.58%.

4) Reductive Aminations of Carbonyl Compounds.—a) Reductive amination of benzaldehyde.—Using 350 mg. of the catalyst 10.6 g. of benzaldehyde was reduced in the presence of 6.7 ml. of aqueous ammonia and 25 ml. of methanol with 94 kg./cm^2 hydrogen at 80°C. The reduction was completed in 220 min. By fractional distillation, 6.4 g. of

dibenzylamine (b.p. 156°C/11mmHg) was obtained. The results of analysis were as follows:

Dibenzylamine. *Anal.* Found: N, 6.74. Calcd. for $C_{14}H_{15}N$: N, 7.07%.

Dibenzylamine hydrochloride. *Anal.* Found: N, 5.76. Calcd. for $C_{14}H_{16}NCl$: N, 6.00%.

b) Reductive amination of α-ketoglutaric acid.—Five grams of α-ketoglutaric acid, 14 ml. of 28% ammonia and 36 ml. of methanol were placed in the autoclave. Hydrogenation was carried out at 60°C, 90 kg./cm² for 1 hr. After the reaction mixture was filtered, the filtrate was evaporated in vacuo, dissolved in 5 ml. of water and adjusted to pH 3.2 with hydrochloric acid, then 2.5 g. of glutamic acid was obtained. This product was identified paper-chromatographically and was optically inactive.

5) Reductions of Nitro Compounds.—a) Reduction of nitrobenzene.—This was hydrogenated in the same way as previously reported[1].

b) Reduction of 5-methyl-3-dimethylaminohexyl-(2) p-nitrobenzoate hydrochloride (MDAN).—12.4 g. of MDAN in 40 ml. methanol was reduced at 60°C, 80 atm. for 90 min. with the 350 mg. catalyst. The reaction mixture was concentrated to a volume of 20 ml. and kept at 0°C overnight. There was obtained 8 g. of 5-methyl-3-dimethylaminohexyl-(2) *p*-aminobenzoate hydrochloride (MDAA) with m.p. of 217°C. The mixed melting point with an authentic sample showed no depression.

c) Reduction of ω-nitrostyrene.—When 15 g. of ω-nitrostyrene was hydrogenated at 20°C, 97 atm. in the presence of 350 mg. of the catalyst, the absorption of hydrogen came to an end in 23 min. Filtration, concentration and vacuum-distillation gave 6 g. of the product boiling at 96~108°C/2 mmHg, which crystallized on standing. 4.8 g. of the crystal (m.p. 102°C) obtained. The material was identified as phenylaldoxime.

Anal. Found: N, 10.0. Calcd. for C_8H_9ON: N, 10.4%.

d) Reduction of diethylnitromalonate.—Using 350 mg. of the catalyst 6.9 g. of diethylnitromalonate was reduced in a mixture of 16 ml. of acetic anhydride and 27 ml. of acetic acid with 100 kg./cm² hydrogen at 100°C for 90 min. Two grams of diethyl acetoaminomalonate (m.p. 89°C) was obtained from the reaction mixture after evaporation, addition of 5 ml. of ethyl acetate and overnight standing.

Anal. Found: C, 50.11; H, 7.13; N, 6.52. Calcd. for $C_9H_{15}O_5N$: C, 49.76; H, 6.96; N, 6.45%.

6) Reduction of Azobenzene.—a) Reduction to hydrazobenzene.—5.2 g. of azobenzene was reduced in 50 ml. of ethanol with 94 kg./cm² hydrogen at 20°C. The reduction was concluded for 185 min. absorbing 1 mol. of H_2 per mol. of azobenzene. The reaction mixture was evaporated and the residue was dissolved in 10 ml. of hot methanol. After cooling, 3.0 g. of hydrazobenzene (m.p. 288°C) was obtained as orange crystals. The crystals identified with infrared spectroscopy.

b) Reduction to aniline.—Ten grams of azobenzene was reduced with the 350 mg. catalyst under the same conditions as above except that the reaction temperature was elevated to 70°C. The reduction was concluded for 125 min. Thirteen grams of acetanilide (m.p. 112°C) was obtained from the reaction mixture by the following method. The filtered reaction mixture was evaporated in the presence of 10 g. of acetic anhydride and the residue dissolved in 10 ml. of water and cooled.

III. Durability of Catalyst.—*1) Preparation of the Carbon-Palladium Catalyst.*—The catalyst was prepared by the method of R. Mozingo[5] and stored in wetness.

2) General Procedures.—Hydrogenation experiments were carried out using an autoclave as already reported[1] and the reaction velocity of the hydrogenation of diethyl maleate was calculated according to the equation:

Reaction velocity = 100/reaction time (in min.)

where the reaction time is the time required from 30 to 70% of the hydrogen uptake proceeds.

IV. Poisoning of Catalyst.—*1) General Procedures.*—Hydrogenation velocity of diethyl maleate was measured by the III—*2* method and the reaction velocity of the hydrogenation of nitrobenzene was calculated by the method of the previous paper[1].

2) Inhibition of Mercaptan.—a) Preparation of inhibited catalyst.—Two hundred and fifty milligrams of the silk-palladium or carbon-palladium containing 20 mg. of palladium (In the following experiments, this amount of catalyst was used as a unit.) was mixed with 50 ml. of 0.02% ethyl mercaptan methanol solution, stirred for 15 min. at 20°C, filtered and washed with water and methanol.

b) Poisoning test by substrate containing mercaptan.—b-1) Reduction of nitrobenzene.—The reaction velocity was measured in relation to the reduction system containing 1 mg. of ethylmercaptan, 4 g. of nitrobenzene, 50 ml. of methanol and 1 unit of each catalyst.

b-2) Reduction of dietyl maleate (DEM).—The reaction velocity was measured in relation to 50 g. of DEM containing 4 mg. of ethyl mercaptan.

3) Inhibition by Metal Ions (Metal Ion Effect to the Reduction System of DEM).—Forty milligrams of $Fe(NO_3)_3 \cdot 12H_2O$ or 25 mg. of $Cu(NO_3)_2 \cdot 3H_2O$ was added to the reaction system containing 50 g. of DEM and 1 unit of each catalyst, and the reaction velocity was measured.

4) Reactivation by Ethylenediamine Tetraacetic Acid (EDTA).—Recovered catalysts of experiment (IV-*3*) were boiled with 0.5% EDTA for 5 min., filtered and washed with water and methanol. (Filtered solution was apparently colored with Cu^{2+} or Fe^{3+} EDTA complex.) Using this catalyst, 50 g. of DEM was reduced with hydrogen at 150°C.

5) Effect of Acetylation.—Acetylation of silk-palladium.—Three hundred and fifty milligrams of silk-palladium catalyst was boiled with 50 ml. of an acetic acid anhydride for 2 hr. filtered and washed with water and methanol.

Summary

1. The silk-palladium catalyst was found to catalyze the hydrogenation of

aliphatic C=C double bonds, aldehyde, nitriles and nitro groups directly attached to aromatic rings, azobenzene, and some oximino groups, but relatively weakly that of aliphatic nitro groups. The catalyst was completely inactive to aromatic C=C double bonds, aliphatic carbonyl (with the exception of α-ketoglutarate which was reduced to glutamate in the presence of ammonia), nitriles, and several oximes.

2. The catalyst, when used once, considerably increased its catalytic activity and this elevated activity persisted after several repeated uses.

3. Ethyl mercaptan was poisonous to the catalyst probably due to its combination with the active palladium atoms. Ferric and cupric ions inhibited the catalyst by forming chelate linkages with the carrier protein. The inhibition by these metal ions could be restored by ethylenediamine tetraacetic acid. Acetylation of the catalyst with acetic anhydride markedly reduced the activity, although the treatment of silk fibroin with acetic anhydride prior to the preparation of the catalyst gave a strongly active catalyst.

The author wishes to express his hearty gratitude to Professor Shiro Akabori for encouragement and valuable discussion. He is also indebted to Mr. Yasuo Fujii for cooperation in some phases of this work, to Dr. S. Sakurai and to the Ajinomoto Co., Inc. for the gift of diethyl maleate, and to Dr. R. Sato for his advice on preparing this manuscript.

Division of Organic Chemistry
Institute for Protein Research
Osaka University, Nishi-ku, Osaka

Studies on the Silk-Palladium Catalyst. III. Physicochemical Characterization

By Yoshiharu IZUMI

(Received March 27, 1959)

In the preceding papers of this series[1,2], it was reported that silk and 6-Nylon-palladium catalysts are in a number of respects superior as hydrogenation catalysts to carbon-palladium and other palladium catalysts hitherto described. It was also suggested that these catalysts resemble enzymes in that their activity is considerably affected by metal ions and other agents and some of them are endowed with an ability to catalyze asymmetric hydrogenation reactions[3-5].

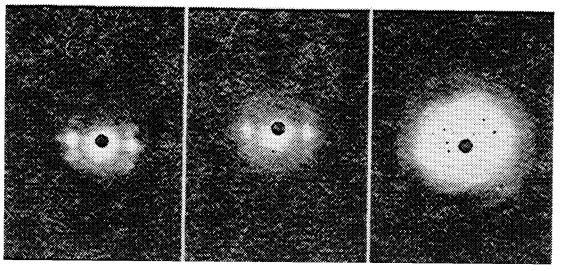
It, therefore, seemed of special interest to study their structure and the process of their activation from physicochemical points of view. It was also hoped that such studies would shed some light on the mechanism by which some of these catalysts achieve the asymmetric reactions.

The present paper describes X-ray diffraction, infrared spectrophotometric experiments on silk fibroin,its palladous chloride chelate compound, and silk-palladium catalyst (samples of silk series) and on the corresponding samples of 6-Nylon* (samples of Nylon series). The behaviors of these samples towards *p*-nitrosodiethylaniline (PNDA), a specific reagent for palladium[6], were also included in this paper.

Results and Discussion

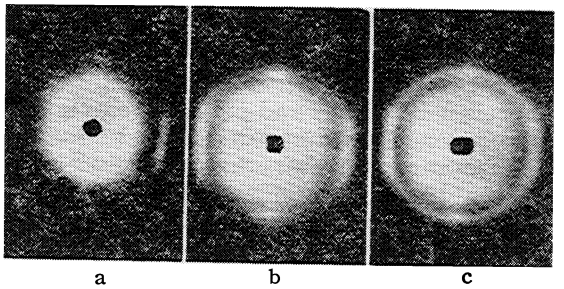
X-Ray Diffraction Studies. — X-ray diffraction pictures of fibrous preparations of the silk series and the Nylon series are shown in Figs. 1 and 2, respectively. X-ray diffraction measurements were also made on powdered samples of the silk series using a Norelco X-ray instrument and the charts obtained are reproduced in Fig. 3.

1) Y. Izumi, This Bulletin, **32**, 932 (1959).
2) Y. Izumi, ibid., **32**, 936 (1959).
3) S. Akabori, S. Sakurai, Y. Izumi and Y. Fujii, *Nature*, **178**, 323 (1956).
4) S. Akabori, Y. Izumi, Y. Fujii and S. Sakurai, *J. Chem. Soc. Japan, Pure Chem. Sec.* (*Nippon Kagaku Zasshi*), **77**, 1374 (1956).
5) S. Akabori, Y. Izumi and Y. Fujii, ibid., **78**, 886 (1957).
* Polycaprolactum.
6) L. G. Overholser and J. H. Yoe, *J. Am. Chem. Soc.*, **63**, 3224 (1941).



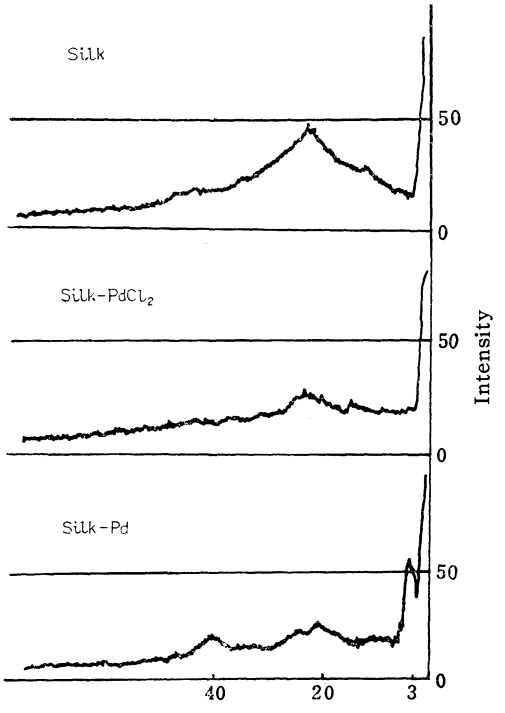
a b c

Fig. 1. X-ray diffraction pictures of silk series.



a b c

Fig. 2. X-ray diffraction pictures of Nylon series.



Diffraction angle (2θ)

Fig. 3. X-ray diffraction patterns of powdered silk series.

As has been known for some time, Figs. 1a and 2a clearly indicate that both silk fibroin and 6-Nylon fibers contain crystalline parts in their structures. The X-ray fiber diagrams of palladous chloride chelates of silk fibroin and 6-Nylon are essentially the same with those of silk fibroin and 6-Nylon, respectively, suggesting that the chelate formation with palladous chloride does not significantly alter the arrangement of these fibers. Conversion of these chelate compounds to catalytic active forms by hydrogenation, however, seems to cause some changes as can be judged from the distinct patterns due to palladium atoms seen in the diagrams of the catalysts.

The Norelco patterns of powdered samples of the silk series are in good agreement with the fiber diagrams of the corresponding preparations. It is noted that the pattern for the powdered silk-palladium catalyst shows in the low-angle region (ca. 3.5°), a peak of which may be due to a ca. 25 Å regular arrangement of the structure.

In summary, it may be concluded that a part of the palladium atoms in the silk-palladium catalysts are assembled in fine crystalline particles and the other part of the palladium probably becomes regularly arranged in the micelle structures of the fibers. However, the possibility that certain regular structures have emerged in the silk protein itself can not be excluded.

Infrared Absorption Measurements. — For the infrared absorption studies powdered samples of the silk series and thin sheet forms of the Nylon series were employed. The spectra of these samples are shown in Fig. 4. As a reference substance carbobenzoxy triglycylleucine and its palladous chloride complex were chosen, the spectra of which are shown in Fig. 4.

Generally speaking, the infrared absorption spectra of the samples of the silk series did not show any remarkable differences, probably due to the high polymeric nature of silk fibroin. Especially, the spectra of the Nylon samples were quite similar to each other, because of the fact that the measurements were made on thin sheet samples, and they contained only a small amount of palladium. However, it can be pointed out, on close examination of the spectra, that the powdered silk-palladium catalyst is similar to the silk fibroin powder rather than to the chelate preparation. A comparison of the infrared absorption spectra of carbobenzoxy triglycylleucine (Cbz. Trigly-Leu) and its palladous chloride complex on one hand and silk fibroin and its palladous chelate on the other hand reveals that an absorption at 3000 cm^{-1} region, which is due

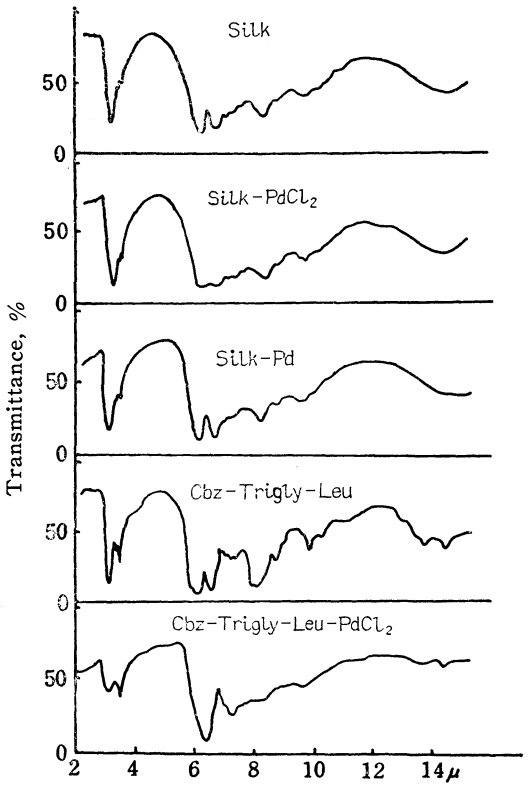


Fig. 4. IR-spectra of silk, silk-$PdCl_2$, silk-Pd, Cbz-Trigly-Leu and Cbz-Grigly-Leu-$PdCl_2$.

to NH groups (probably also OH groups) decreases on the formation of chelates. This suggests that the NH groups (probably also OH groups) of both silk fibroin and the carbobenzoxy tetrapeptide are involved in the chelation with palladous chloride. It may also be noticed that in the spectra of chelate compounds, absorptions at 1640 and 1530 cm^{-1} are diminished and that at 1590 cm^{-1} is increased as compared with the spectra of unchelated forms. The absorptions at 1640 and 1530 cm^{-1} are usually interpreted as caused by CO in COOH and CONH groups, and the absorption at 1590 cm^{-1} as caused by COO^- groups, and Gierer[7] has reported that the complex formation of an amide results in a shift of the absorptions due to CONH to longer wave-lengths. It is therefore probable that the observed changes in the region of 1530 to 1640 cm^{-1} are due to a complicated effect of chelate bond formation between palladous chloride and COOH and/or CONH groups.

It may be concluded that palladous chloride forms chelate linkages with NH_2 (-OH), CONH and COOH groups of fibroin and the dipeptide. These linkages appear to be broken on hydrogenation of the chelate. In the activated chelate, therefore, the palladium seems to be in an almost atomic state.

Behaviors towards *p*-Nitrosodiethylaniline (pNDA). — When silk fibroin and Nylon-$PdCl_2$ chelate compounds were treated with pNDA, a specific reagent for palladium, parts of palladous chloride were released. However, the rest of palladous chloride remained in fibers, although the fibers were strongly colored like pNDA-$PdCl_2$ complex. Furthermore, Fujii[8] observed that silk fibroin-$PdCl_2$ chelate treated with pNDA is more active than silk fibroin-$PdCl_2$ itself and pNDA in catalyzing the decarboxylation of oxalacetic acid. These facts suggest that a considerable part of the palladium is firmly kept in the fiber structure and that on treatment with pNDA the reagent becomes combined with silk fibroin through the mediation of palladium atom or pNDA-$PdCl_2$ complex becomes wrapped into the fiber micelles.

In summary, it can be inferred that palladous chloride is first dispersed in the fiber structures because of the chelate formation. On reduction, palladous chloride in the chelate is converted into an atomic state leaving the carrier protein.

Experimental

I. Preparation of Powdered Silk Fibroin Preparations. — One gram of silk fibroin was dissolved in a modified Schweizer reagent made from 1.6 g. of ethylenediamine and 1.2 g. of $Cu(OH)_2$, and the solution was neutralized with acetic acid and dialyzed. Five milliliters of 1% ethylene diamine tetraacetate solution and 0.1 g. of celite were added to the dialyzed solution and the mixture was filtered under suction. To the filtrate were gradually added 3 volumes of acetone and the precipitate formed was collected by centrifugation. The precipitate was dried at 50°C after washing 4 times with acetone and then once with ethyl ether. The dried silk fibroin was ground in a mortar and passed through a 200 mesh sieve. 0.5 g. of finely powdered silk fibroin was obtained.

This powdered fibroin was converted to palladous chloride chelate and catalyst forms according to the standard methods described in Part I. The chelate was brown in color, and the catalyst resembled active carbon in its appearance.

II. Preparation of 6-Nylon Catalyst Samples for X-ray Measurements. — In order to prevent the tangling of the chelate fibers during the reduction, they were fixed to a holder of the X-ray apparatus. After measurement of the

7) A. Gierer, *Z. Naturforsch*, 8b, 654 (1953).

8) Y. Fujii, *J. Biochem.*, in preparation.

X-ray diffraction, the holder with the chelate fibers in it was wrapped in gauze and then reduced in the autoclave.

III. 6-Nylon-$PdCl_2$ Complex.—The complex was prepared analogously to the silk fibroin-$PdCl_2$ complex.

IV. Triglycyl-carbobenzoxyleucine-$PdCl_2$ Complex. — Forty-four milligrams of triglycyl-carbobenzoxyleucine was boiled for 4 min. with 140 ml. 0.1 N acetic acid containing 140 mg. palladous chloride and the resulting peptide-$PdCl_2$ complex was isolated centrifugally and washed completely with water and then with methanol and dried.

V. X-ray Diffraction Measurements. — X-ray fiber photographs were taken with K_α line of copper filtered through a nickel filter. For powdered samples a Norelco X-ray instrument was used.

VI. Infrared Absorption Measurements. —A Perkin-Elmer apparatus was used. The measurements were made by the KBr tablet method.

Summary

1. From the infrared absorption measurements of silk fibroin, silk fibroin-$PdCl_2$ complex, and silk-palladium catalyst, it was concluded that the NH, OH, COOH and CONH groups of the fibroin participate in the chelate formation with palladous chloride. On reduction of the chelate with hydrogen, the chelate bonds are broken and the fibroin restores its original form.

2. X-ray diffraction pictures of the above-mentioned samples and of the corresponding preparations of the 6-Nylon series suggest that a part of the palladium atoms in the silk-palladium catalyst is assembled in fine crystaline particles and the other part of the palladium probably becomes regularly arranged in the micelle structures of the fibers. However, the possibility that certain regular structures have emerged in the carrier protein itself can not be excluded.

3. Part of the palladium in silk fibroin-$PdCl_2$ complex can be readily released with *p*-nitrosodimethylaniline, while the rest appears to be strongly kept in the fiber structure.

The author wishes to express his sincere thanks to Professor Shiro Akabori for encouragement and valuable advice. He is also indebted to Mr. Yasuo Fujii for skilful collaboration, to Dr. K. Ogawa for measurement of X-ray pictures, to Dr. H. Tadokoro and Mr. T. Inui for infrared measurements, to Mr. F. Sakiyama for the gift of tetrapeptide, to the Toyo Rayon Co. for the gift of 6-Nylon fibers, and to Dr. R. Sato for his advice on preparing this manuscript.

Division of Organic Chemistry
Institute for Protein Research
Osaka University
Nishi-ku, Osaka

*The Reaction of the Aquopentamminechromium(III) Complex Ion in Aqueous Solution. I. Substitution Reaction of a Coordinated Water with a Chloride Ion**

By Shinpei HASHIMOTO

(Received January 6, 1959)

Garrick[1] and Adell[2] have investigated a substitution reaction of aquopentamminecobalt(III) ion in which a coordinated water molecule of the complex ion is replaced by a chloride ion[3]. They have reported that the reaction is of first order with respect to the complex ion and the chloride ion respectively, and that the reaction rate decreases markedly as ionic strength increases.

A similar substitution reaction occurs in the case of aquopentamminechromium (III) ion as well. On addition of hydrochloric acid to the aqueous solution of an aquopentamminechromium (III) complex salt, red crystals precipitate slowly. The

* Presented at the Symposium on Coordination Compounds, held at Nagoya, November, 1957.

1) F. J. Garrick, *Trans. Faraday Soc.*, **33**, 486 (1937).

2) B. Adell, *Z. anorg. u. allgem. Chem.*, **246**, 303 (1941).

3) In Ref. 6b, the reaction of this type was called "anation reaction". This word will be used in this paper for convenience.

absorption spectrum of a solution of the crystallines is identical with that of chloropentamminechromium(III) complex ion. The fact shows that the following substitution reaction occurs in the solution containing aquopentamminechromium(III) complex ion and chloride ion.

$$[Cr(NH_3)_5OH_2]^{3+} + Cl^- \rightarrow [Cr(NH_3)_5Cl]^{2+} + H_2O \quad (1)$$

Since aquopentamminechromium (III) complex ion is very similar to that of cobalt(III) in steric configuration, ionic size and charge, but different only in electronic configuration of the central metal ion, it is interesting to investigate whether this difference in electronic configuration may appear in the reactions of these two metal-ammine-complexes.

This paper presents a study of the substitution reaction in which a coordinated water molecule of aquopentamminechromium(III) complex ion is replaced by a chloride ion in aqueous solution. Furthermore, the influence of ionic strength on the aquation of chloropentamminechromium(III) complex ion is also reported.

Experimental

Materials. — Aquopentamminechromium (III) perchlorate was prepared by the method of Linhard et al.[4] and was purified by recrystallization from perchloric acid solution twice and then from warm water once.

Chloropentamminechromium(III) chloride was prepared according to the direction of Biltz[5]. The chloride was converted by treatment with perchloric acid into perchlorate, and the latter was purified twice by reprecipitation from cold perchloric acid solution.

Sodium chloride of reagent grade was used without further purification. Sodium perchlorate was prepared by neutralizing sodium hydroxide with perchloric acid both of which were of reagent grade. Absorbancies for solutions of sodium chloride and sodium perchlorate were both so small that they could be neglected practically. Their magnitudes for the solutions of unit molarity at 44000 cm^{-1}, where all rate measurements were carried out, were 0.015 and 0.020, respectively against water.

Measurements.—Experimental solutions were prepared as follows. The solution of aquo-complex salt (10^{-3}~10^{-2} M) which was acidified with perchloric acid was placed in a stoppered and brown-colored flask. The solution of sodium chloride (10^{-2}~1 M) whose ionic strength was adjusted with sodium perchlorate was prepared. These two solutions were kept at a constant temperature in a thermostat, and were mixed together quickly; then at intervals of a few minutes, the amount of chloropentamminechromium(III) ion formed was determined spectrophotometrically.

The measurement of absorbancy was made with a Beckman Model DU photoelectric spectrophotometer using stoppered 10 mm. quartz cells. The temperature of the cell compartment was kept constant within ±0.1°C by circulating thermostated water.

The aqueous solution of aquopentamminechromium(III) perchlorate which was acidified with perchloric acid did not change so fast as its neutral solution. When the pH of the solution was lower than approximately 4, no changes in absorbancy nor pH were observed during the course of measurements.

The aquation rate of chloropentamminechromium(III) ion was followed also spectrophotometrically. After dissolving chloropentamminechromium(III) perchlorate in a solution containing appropriate amounts of perchloric acid and sodium perchlorate at an experimental temperature, the change in absorbancy at 44000 cm^{-1} was followed with a thermostated spectrophotometer.

Results

Apparent Molar Extinction Coefficients of Complex Cations. — In order to determine the rate of the formation of chloropentamminechromium(III) complex ion by the measurements of a change in ultraviolet absorption, the correct molar extinction coefficients of complex ions under the reacting condition must be known. Table I shows the temperature dependence of molar extinction coefficients of chloro and aquopentamminechromium (III) ions at 44000 cm^{-1} in aqueous solution containing no chloride ion. These molar extinction coefficients were more or less greater when chloride ion was added.

Fig. 1 shows the variations of molar extinction coefficients of chloro and aquopentamminechromium(III) ions with respect to chloride ion concentration. This increase in extinction coefficients caused with chloride ion may be attributed

TABLE I. MOLAR EXTINCTION COEFFICIENTS OF COMPLEX IONS $\tilde{\nu}$ = 44000 cm^{-1}

Temp., °C	$[Cr(NH_3)_5OH_2]^{3+}$	$[Cr(NH_3)_5Cl]^{2+}$
26		1213
30	21.3	
35	22.2	1236
40	23.3	
45	25.1	1281
50	27.6	
53		1314

4) M. Linhard and W. Berthold, *Z. anorg. u. allgem. Chem.*, **276**, 173 (1955).

5) H. Biltz and W. Biltz, "Laboratory Methods of Inorganic Chemistry", translated by W. T. Hall et al., 2nd Ed., John Wiley & Sons, Inc, New York (1928), p. 185.

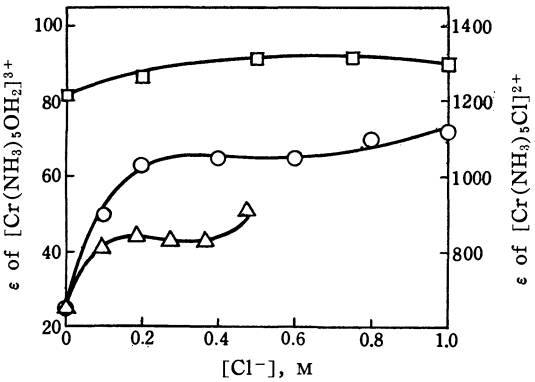


Fig. 1. The change in molar extinction coefficients of complex ions at 44000 cm^{-1} with the chloride ion concentration:
□, $[Cr(NH_3)_5Cl]^{2+}$ (20~23°C);
○, $[Cr(NH_3)_5OH_2]^{3+}$ (45°C);
△, $[Cr(NH_3)_5OH_2]^{3+}$ (45°C, at constant ionic strength).

to the formation of outer sphere association complexes[6] between complex cations and chloride ion. Furthermore, since the formation of the association complex generally depends on the ionic strength of solution[7], the apparent extinction coefficient of a complex ion varies on addition of sodium perchlorate[8] to the solution containing chloride and complex ions. Extinction coefficients of complex ions under various conditions were obtained by extrapolating the absorbancies with regard to the time zero. On the estimation of the molar extinction coefficient of chloropentamminechromium(III) ion under reacting conditions, the small effect of ionic strength mentioned above was neglected. The magnitudes were determined from the data of Table I and Fig. 1, assuming that the temperature dependence of extinction coefficient of outer sphere association complex was similar to that of free complex ion.

The solution of chloropentamminechromium(III) ion obeys the Beer's law strictly where no chloride ion exists, and also satisfies it fairly well even in chloride solution.

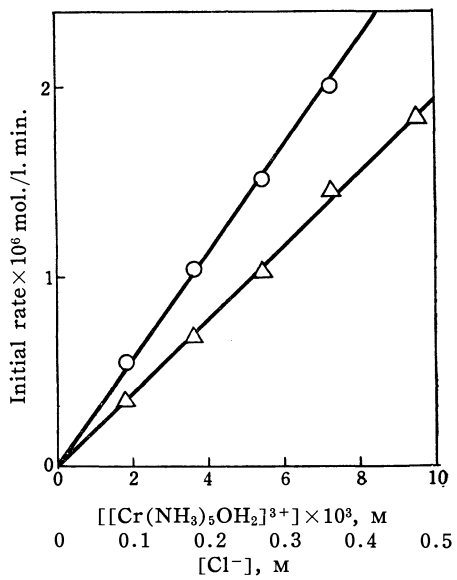


Fig. 2. The first order tests with each of two reactants at 45°C:
○, $[Cr(NH_3)_5OH_2]^{3+}$; △, Cl^-.

The Rate of Formation of Chloropentamminechromium(III) Ion. — It is shown in Fig. 2 that the initial rates of the formation of chloropentamminechromium(III) ion in the solution of the constant ionic strength are proportional to the concentrations of aquo-complex cation and chloride ion, respectively. Accordingly the rate constants of the anation reaction 1 were calculated by the usual method based on Eq. 2, being regarded as a second order reaction. To obtain more correct values of the anation rate, a reverse reaction, that is, an aquation of chloropentammine-complex ion, was taken into account according to the method of Garrick[1].

$$\frac{d[[Cr(NH_3)_5Cl]^{2+}]}{dt} = \vec{k}_2[[Cr(NH_3)_5OH_2]^{3+}][Cl^-] \quad (2)$$

As is shown in Table II, the reaction

TABLE II. TEST FOR THE EFFECT OF HYDROGENE ION ON THE RATE OF ANATION REACTION OF $[Cr(NH_3)_5OH_2]^{3+}$ WITH Cl^- AT 45°C

$[HClO_4]$, mol./l.	Ionic strength, ω	$\vec{k}_2\times10^3$, l./mol. min.
0	0.510	1.55
0.49*	0.500	1.48
0.095	0.625	1.27
0.009	0.630	1.26
0.001	0.631	1.31

* HCl was used.

6) a. M. Linhard, *Z. Elektrochem.*, **50**, 224 (1944).
b. Many other works are summarized and surveyed in the following book: F. Basolo and R. G. Pearson, "Mechanisms of Inorganic Reactions", John Wiley & Sons, Inc., New York (1958), p. 376.
7) a. F. A. Posey and H. Taube, *J. Am. Chem. Soc.*, **78**, 15 (1956).
b. T. Kubota, *J. Chem. Soc. Japan, Pure Chem. Sec. (Nippon Kagaku Zasshi)*, **75**, 552 (1954).
8) Perchlorate ion itself is considered to have hardly any ability of association.

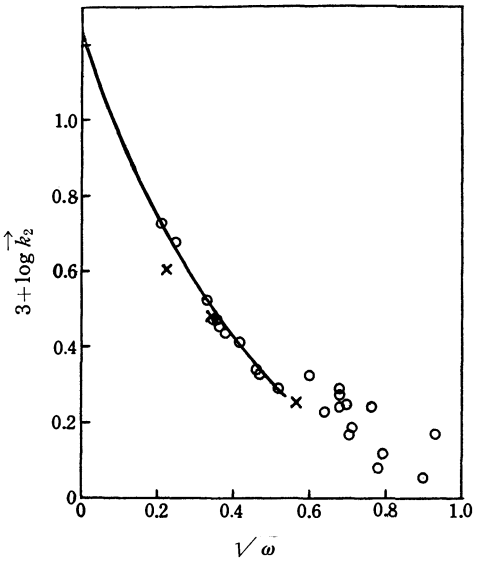


Fig. 3. Influence of ionic strength on the rate of anation:
○, $[Cr(NH_3)_5OH_2]^{3+}$—Cl^- at 45°C;
×, $[Co(NH_3)_5OH_2]^{3+}$—Cl^- [1] at 25°C,
rate scale is for $4+\log \vec{k}_2$. The curve represents Eq. 3.

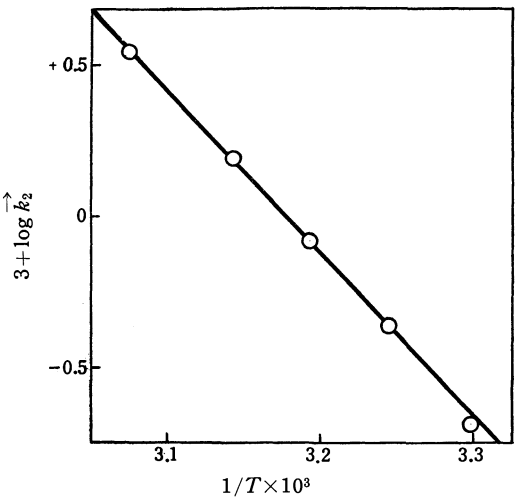


Fig. 4. Arrhenius plot of the anation reaction of $[Cr(NH_3)_5OH_2]^{3+}$ with Cl^- ($\omega=0.52\pm0.01$).

rates are independent of hydrogen ion concentrations so far as the solutions are acidic.

The reaction rate decreases remarkably with increasing ionic strength of solution. The influence is particularly significant in the lower ionic strength region. In Fig. 3, logarithms of rate constants measured at 45°C are plotted against the square root of the ionic strengths in molarity scale, which are calculated from the initial composition of solutions. Observed rates fluctuate markedly in a higher ionic strength region, whereas below a $\sqrt{\omega}$ of about 0.4, experimental results show a good regularity that can be reproduced by Eq. 3. The rate constant at infinite

$$\log \vec{k}_2 = -1.77 - \frac{3.09\sqrt{\omega}}{1+1.36\sqrt{\omega}} \qquad (3)$$

dilution at 45°C was evaluated to be 1.7×10^{-2} l. mol^{-1} min^{-1}.

The results obtained at 30, 35, 40, 45 and 52°C ($\omega=0.52\pm0.01$) give a good Arrhenius plot (see Fig. 4), leading to the value of 24.6 kcal. mol^{-1} for the experimental activation energy, and 1.2×10^{14} l. mol^{-1} min^{-1} for the frequency factor.

Aquation of Chloropentamminechromium (III) Ion.—In order to obtain more correct rate constants of anation reaction 1 it is necessary to take the rate of the aquation[9] into account. Accordingly we were obliged to determine the rate of aquation of chloropentamminechromium(III) ion under various conditions. The results obtained are summarized in Table III.

The influence of ionic strength on the aquation is quite different from that on the anation reaction. In lower ionic strength region, the reaction rate rather increases with increasing ionic strength; then the rate decreases gradually and the gradient of the relation is steepest about $\omega=0.4$, and after that the decrease in rate becomes gradual again. It was observed that the aquation rate was independent of perchloric acid concentration from

TABLE III. RATE CONSTANTS OF AQUATION REACTION OF $[Cr(NH_3)_5Cl]^{2+}$

Temp., °C	$[HClO_4]$, mol./l.	Ionic strength, ω	$\overleftarrow{k}_A\times10^3$, min^{-1}
25			0.58*
26.2	0.00086	0.002	0.589
26.2	0.086	0.087	0.598
35	0.00086	0.002	1.91
35	0.0086	0.009	1.94
35			1.9*
45	0.00086	0.002	5.41
45	0.00082	0.089	5.45
45	0.001	0.263	5.32
45	0.001	0.502	4.67
45	0.00086	0.912	4.31
53.2	0.001	0.002	14.3

* Taken from Ref. 9.

9) Freundlich et al. had studied this aquation, but their data were not sufficient to use for this purpose; H. Freundlich and H. Pape, *Z. physik. Chem.*, **86**, 458 (1914).

10^{-4} M to 10^{-1} M. The experimental activation energy and the frequency factor calculated from the temperature dependence of aquation rate were 22.8 kcal. mol^{-1} and 2.6×10^{13} min^{-1}, respectively. When the transmission coefficient is assumed to be unity, the activation entropy is calculated as -7 e. u.

Discussion

It is shown in Fig. 1 that the absorbancy of aquopentamminechromium(III) ion changes markedly with the concentration of chloride ion. The formation of outer sphere association complex, $[Cr(NH_3)_5\cdot OH_2]^{3+}\cdot Cl^-$, ought to be thought for the reason of this absorbancy change, as was indicated by Linhard[6] in the case of hexamminechromium(III) ion and chloride ion.

The anation reaction 1 is experimentally shown to be of second order and the rate constant varies with the ionic strength of solution as is reproduced by the Brönsted-Bjerrum-Christiansen type Eq. 3[6b], which is the kinetic equivalent of the Debye-Hückel equation. The slope of the line in Fig. 3 is -3.09 at infinite dilution. This value is in good agreement with what is expected from a term $2Az_+z_-$[10] in the Debye-Hückel equation. But it can not be concluded that the anation is a bimolecular reaction. Because these results may also be explained by the following unimolecular path through the outer sphere association complex.

$$[Cr(NH_3)_5OH_2]^{3+}+Cl^- \rightarrow [Cr(NH_3)_5OH_2]^{3+}\cdot Cl^- \quad \text{(fast)}$$

$$[Cr(NH_3)_5OH_2]^{3+}\cdot Cl^- \rightarrow [Cr(NH_3)_5Cl]^{2+}+H_2O \quad \text{(slow)}$$

The formation constant of the outer sphere association complex is about 10^2 under these experimental conditions[11], therefore, a considerable amount of association complex exists in solution. If the reaction proceeds through such an outer sphere association complex, the rate-determining step is not the process of bimolecular association, but the following unimolecular process in which central chromium(III) ion releases a coordinated water molecule.

It is noteworthy that the reaction rate varies regularly according to the Debye-Hückel equation in spite of the considerable formation of the association complex. Moreover, its formation is also found to vary roughly according to the Debye-Hückel equation[11]. These facts indicate that the path through a simple five coordinated intermediate is less probable. In other words, the outer sphere association complex releases its coordinated water molecule more easily than the free complex ion. In the water exchange of hexaquochromium(III) complex ion, Plane et al.[12] have found that various anions speed up the reaction. The fact is also explicable by assuming a higher lability of outer sphere association complex. On the other hand, the results of anation reaction for cobalt(III) complex ion obtained by Garrick[1] seem rather extraordinary from the viewpoint of a gradual slope as is shown in Fig. 3, which is about -1. This gradualness may be explained by assuming an inert association complex and the contribution of another path which has a simple five coordinated intermediate[13] in this case.

The effect of ionic environment on the aquation of chloropentamminechromium (III) ion is quite different from that on the anation reaction. The Brönsted-Bjerrum equation predicts a linear dependence of $\log \overleftarrow{k}_A$ ($\overleftarrow{k}_A$ is the rate constant of aquation) upon ionic strength ω[14] when the Hückel's empirical term is taken into account in the expression of activity coefficients. Though only sodium perchlorate and perchloric acid were used to adjust ionic strength, the dependence was not linear even in the lower ionic strength region. It seems that perchlorate ion may also have some specific effects on the aquation.

Summary

The substitution reaction of aquopentamminechromium(III) ion in which a coordinated water molecule is replaced by a chloride ion was investigated spec-

10) A denotes $0.4343\ e^3(2\pi N)^{1/2}/(10\varepsilon kT)^{3/2}$, and approximately equals 0.53 for aqueous solution at 45°C, z_+ and z_- are the ionic charges of reactants.

11) Result presented by the present author at the Symposium on Coordination Compounds, held in Tokyo, November, 1958. The details will appear elsewhere.

12) R. A. Plane and H. Taube, *J. Phys. Chem.*, **56**, 33 (1952); J. P. Hunt and R. A. Plane, *J. Am. Chem. Soc.*, **76**, 5960 (1954).

13) F. Basolo, *Chem. Revs.*, **52**, 459 (1953).

14) S. Glasstone, K. J. Laidler and H. Eyring, "The Theory of Rate Processes", McGraw-Hill Book Co., New York (1941), p. 441.

trophotometrically. The reaction proceeds according to the second order rate law, $d[[Cr(NH_3)_5Cl]^{2+}]/dt = \vec{k}_2[[Cr(NH_3)_5OH_2]^{3+}].[Cl^-]$, and the rate constant varies regularly with the ionic strength of solution according to the Debye-Hückel type equation. The formation of outer sphere association complex in the solution was detected from the change in ultraviolet absorption. From these results the rate-determining process of this reaction was inferred to be a unimolecular process through the outer sphere association complex. The experimental activation energy and the frequency factor of this reaction were determined to be 24.6 kcal. mol^{-1} and 1.2×10^{14} l. mol^{-1} min^{-1} ($\omega\sim0.52$), respectively.

The aquation of chloropentamminechromium(III) ion was also studied in the solutions of various ionic strengths and the reaction rate was found to vary to some extent with ionic environment.

The author wishes to thank Professor Y. Inamura for his guidance and encouragement throughout this work. Thanks are also due to Professor I. Tanaka for his kind and helpful advice and to Mr. H. Kobayashi and Mr. Y. Mori for many valuable discussions.

Laboratory of Inorganic Chemistry
Tokyo Institute of Technology
Meguro-ku, Tokyo

Intramolecular Interaction between Hydroxyl Group and π-Electrons. IV[1]. *Rotational Isomers of Alcohols and Shift of ν_{O-H} Absorptions in Phenyl Substituted Alcohols*

By Michinori ŌKI and Hiizu IWAMURA

(Received February 16, 1959)

The authors have found[2] an unsymmetric ν_{O-H} absorption band for 10-undecen-1-ol in the course of the investigation of the intramolecular interaction between the hydroxyl group and π-electrons of an isolated double bond. But the origin of the second minor band, obtained by dividing the band on the assumption that the unsymmetric band is an overlap of two symmetric bands which can be expressed by the Lorentz function, has been unknown. The present author expected that saturated aliphatic alcohols, such as ethanol, may also possess two ν_{O-H} absorptions as 10-undecen-1-ol does in spite of the improbable internal interaction. This has been found to be true.

Experimental

Measurement and Calculation.—They were carried out similarly as described previously[2].

Materials. — The materials, all being known compounds, were purified as stated in the literature. Their physical constants agreed with those reported.

Results aud Discussion

The apparent curves for methanol, ethanol, isopropyl alcohol and *tert*-butyl alcohol are given in Fig. 1. The ν_{O-H} absorption is one of the best explored and

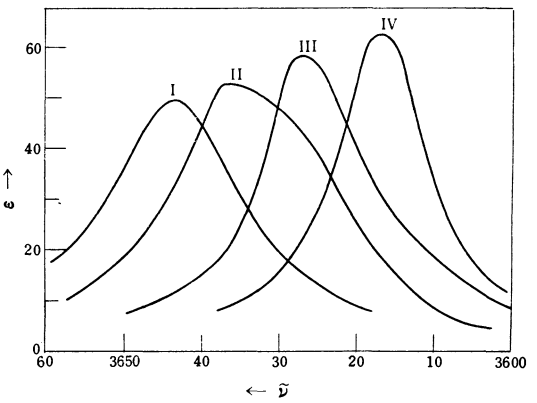


Fig. 1. ν_{O-H} Absorptions of methanol(I), ethanol(II), isopropyl alcohol(III) and *tert*-butyl alcohol(IV).

1) Part III of this series: M. Ōki and H. Iwamura, This Bulletin, **32**, 306 (1959).
2) M. Ōki and H. Iwamura, ibid., **32**, 567 (1959).

it is accepted that the wave number where the absorption maximum appears shifts to the lower side as the alcohol varies from primary to secondary and then to tertiary. The results obtained agree with the above rule, except that ethanol and isopropyl alcohol possess unsymmetric bands which were found with high resolvability of the grating spectrophotometer. The unsymmetric band is divided into two symmetric bands, on the assumption that the unsymmetric curve is an overlap of the two symmetric ones which obey the Lorentz function. The results are given in Table I with those of other aliphatic alcohols.

TABLE I. ν_{O-H} ABSORPTION OF ALIPHATIC ALCOHOLS

R	Band	ν_{max} (cm^{-1})	$\Delta\nu^a_{1/2}$ (cm^{-1})	$A\times10^{-3}$ ($mol^{-1}\cdot l.\cdot cm^{-1}$)	A_I/A_{II}
Primary alcohols (RCH_2OH)					
H		3643.8	22.2	3.99	—
CH_3	I	3637.3	18.2	2.80	1.8
	II	3627	19	1.6	
C_2H_5	I	3639.7	19.5	3.36	2.6
	II	3626	18	1.3	
$C_2H_5CH_2$	I	3639.3	17.6	2.81	2.2
	II	3627	20	1.3	
$(CH_3)_2CH$	I	3641.5	17.9	3.61	2.0
	II	3628	22	1.8	
$(CH_3)_3C$	I	3642.0	20.7	4.83	6.0
	II	3632	18	0.8	
Secondary alcohols (RCH_3CHOH)					
CH_3	I	3627.1	13.8	2.42	1.7
	II	3617	26	1.4	
C_2H_5	I	3628.8	20.0	3.35	3.3
	II	3615	27	1.0	
$(CH_3)_2CH$	I	3631.6	21.0	3.55	2.2
	II	3618	33	1.6	
$(CH_3)_3C$	I	3635.6	17.4	3.42	2.5
	II	3621	23	1.4	
Tertiary alcohols [$R(CH_3)_2COH$]					
CH_3		3616.9	15.2	3.46	—
C_2H_5		3617.3	20.0	3.46	—

The origin of the second minor peak can not be the formation of the dimer, because Liddel and Becker[3] reported that they observed no dimer band at the concentration of 0.001~0.003 mol./l. at which the present measurement was carried out. Neither can be the origin the hydrogen bonding between the solute and the chlorine atom of carbon tetrachloride, since methanol, tertiary alcohols and phenols always show symmetric bands. Therefore it should be sought elsewhere.

Richards[4], Barrow[5] and Flett[6] tried to explain the shift of the ν_{O-H} absorption maxima, as the alcohol varies from primary to secondary and then to tertiary, on the basis of the mesomeric or inductive effect of the substituent. That is to say, the contribution of the resonance structure $H^-CH_2=O^+-H$ or $H^+CH_2=O^--H$ will increase as the result of stabilization due to the presence of the alkyl groups on the carbon atom to which the hydroxyl group is attached, and the resulting weaker force constants cause the ν_{O-H} absorption to appear at a lower wave number. However, this explanation is not convincing, since it does not explain the presence of the two bands for O-H stretching.

Badger and Bauer[7] found two ν_{O-H} absorptions for the primary alcohols and tried without success to assign them to the rotational isomers, because they failed to observe a doublet for the secondary alcohols. However, the idea of the rotational isomerism is attractive to the present authors, since this is a promising explanation for the existence of the two ν_{O-H} absorptions. Though the energy barrier for the rotational isomers around the O-C axis of the alcohols is estimated to be even lower than that of the rotation around the C-C axis of ethane derivatives, a 0.8 or 0.9 kcal./mol. energy barrier would suffice for the presence of the isomers at room temperature. Barrow[8] estimated the energy barrier 0.8 kcal./mol. for ethanol and Weltner and Pitzer[9] estimated 0.9 kcal./mol. for methanol around the O-C axis by comparison of the values obtained by computation and by observation of heat capacities and entropies. The energy barrier is also estimated by the microwave method as 1 kcal./mol.[10]

Now, let us consider the rotational isomers of aliphatic alcohols in respect of the O-C axis. In Fig. 2, the isomers are projected through the O-C axis and the oxygen atom is on the upper side. The circle indicates a carbon atom to which the hydroxyl group is attached.

In type I, the hydrogen atom of the hydroxyl group is situated between the two hydrogen atoms which are attached

3) U. Liddel and E. D. Becker, *Spectrochim. Acta*, **10**, 70 (1957).

4) R. E. Richards, *Trans. Faraday Soc.*, **44**, 40 (1948).
5) G. M. Barrow, *J. Phys. Chem.*, **59**, 1129 (1955).
6) M. St. C. Flett, *Spectrochim. Acta*, **10**, 21 (1957).
7) R. M. Badger and S. H. Bauer, *J. Chem. Phys.*, **4**, 711 (1936).
8) G. N. Barrow, ibid., **20**, 1739 (1952).
9) W. Weltner and K. S. Pitzer, *J. Am. Chem. Soc.*, **73**, 2606 (1951).
10) E. V. Ivash and D. M. Dennison, *J. Chem. Phys.*, **21**, 1804 (1953).

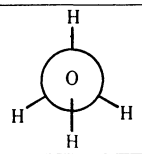
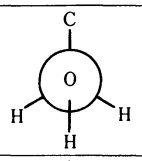
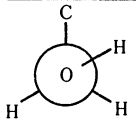
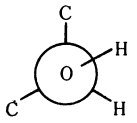
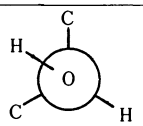
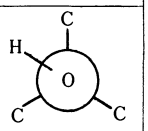
Type	Methanol	Ethanol	Isopropyl alcohol	*tert*-Butyl alcohol
I			—	—
II	—			—
III	—	—		

Fig. 2.

to the next carbon atom; in type II, between carbon and hydrogen atoms; and in type III, between two carbon atoms. Then, it is quite understandable that methanol and *tert*-butyl alcohol have single symmetric bands because they have only one rotational isomer and that also ethanol, higher primary alcohols and secondary alcohols have two bands which form an apparently unsymmetric band because they have two rotational isomers.

It is also expected from the above models that the force field will be almost the same in type I, irrespective of the other part of the molecules, and the same situation is also expected for type II or III. Therefore, the type of the rotational isomers of the alcohols determines the wave number where the ν_{O-H} band appears. This turned out to be really the case. The ν_{O-H} absorption of type I appears at about 3640 cm^{-1}, that of type II at about 3626 cm^{-1} and that of type III at about 3617 cm^{-1} irrespective of the nature of the alcohols. The main peak for the primary alcohols comes from type I and that for the secondary alcohols comes from type II.

The reason for such assignment is as follows. When Table I is examined, it is obvious that primary alcohols possess the property of methanol to some extent, because they show one of the ν_{O-H} bands at about 3640 cm^{-1}. Thus the absorption at ca. 3640 cm^{-1} is assigned to type I. Comparison of the absorptions of secondary alcohols with those of tertiary alcohols in a similar way indicates that the band at about 3617 cm^{-1} must be assigned to type III. The remaining band at about 3626 cm^{-1} is assigned to type II.

The probability of type I for primary alcohols is considered one third and that of type II two thirds. Although such expectation does not agree with the results obtained with the primary alcohols, it does agree with those for the secondary alcohols. One of the possibilities which may explain this phenomenon is repulsion between the hydrogen atom of the hydroxyl group and the alkyl group attached to the alpha carbon. In order to clarify this point, a bulky substituent, such as isopropyl or *tert*-butyl group, is introduced to the primary or secondary alcohols. As to the integrated intensities, the steric effect of the substituent is clearly observed in the primary alcohols but not in the secondary alcohols; since the integrated intensity the ν_{O-H} band, affected by the steric environment, is the minor one in the former, while, in the latter both types are affected as far as the present compounds are concerned. The error included in dividing the unsymmetric band may not allow the drawing of a clear-cut conclusion, but it is still clear that the most stable point for the hydrogen atom of the hydroxyl group is pushed toward the hydrogen rather than the bulky group because of the steric effect and consequently the wave number at which ν_{O-H} absorption appears is heightened. Thus the main peak for *tert*-butylmethylcarbinol

appears very close to the main peak of the primary alcohols (type I). The same phenomenon is also observed in the primary alcohols, but in this case the more outstanding feature is the increase of the ratio of the integrated intensity of type I to that of type II. In other words, in neopentyl alcohol, A_I/A_{II} increased to 6.0 from about 2.0 for the other primary alcohols and the increase in the integrated intensity of type I must be attributed to the greater number of the molecules due to the steric requirement.

Thus, it is now evident that the second minor peaks of ν_{O-H} absorption found in 4-penten-1-ol, 5-hexen-1-ol and 10-undecen-1-ol[2] do not represent the intramolecular interaction between the hydroxyl group and the π-electrons of the double bond, but are attributable to the existence of the two rotational isomers which can be represented by types I and II.

It is expected from the above results that the idea of rotational isomerism will be applicable to the phenyl substituted alcohols and therefore the authors have extended their work to benzyl alcohol and its derivatives. The results are shown in Table II.

TABLE II. ν_{O-H} ABSORPTION OF PHENYLCARBINOLS

Compounds	Band	ν_{max} (cm^{-1})	$\Delta\nu^a_{1/2}$ (cm^{-1})	$A\times10^{-3}$ ($mol^{-1}\cdot l.\cdot cm^{-2}$)
$C_6H_5CH_2OH$	I	3636.3	24.0	2.52
	II	3617.1	17.0	4.26
$C_6H_5CH(CH_3)OH$	I	3627.0	21.0	1.15
	II	3616.0	16.3	4.32
$C_6H_5C(CH_3)_2OH$	I	3620.6	15.4	1.61
	II	3607.1	15.0	3.43
$C_6H_5C(C_2H_5)_2OH$	I	3618.2	17.8	3.49
	II	3608.2	19.0	1.38
$(C_6H_5)_2CHOH$	I	3619.0	15.6	4.92
	II	3609.8	21.4	2.40
$(C_6H_5)_2C(CH_3)OH$	I	3613.0	14.8	4.26
	II	3608.0	20.0	1.85
$(C_6H_5)_2C[CH(CH_3)_2]OH$	I	3617.3	13.2	4.39
	II	3609.7	13.0	0.89
$(C_6H_5)_3COH$		3610.7	15.6	5.95

Ethylmethylphenylcarbinol and ethyldiphenylcarbinol are not included in Table II, because they show a nearly symmetric band which may be an overlap of two similar symmetric bands and can not be divided by the present technique.

It has long been in question why benzyl alcohol and allyl alcohol show an absorption band at about 3620 cm^{-1} in spite of the fact that they are primary alcohols, the only observation of the two bands for benzyl alcohol having been made by Fox and Martin[11]. Quite recently Schleyer, Trifan and Bacskai[12] also reported the existence of the two bands for the O–H stretching absorption of allyl and benzyl alcohols, their results being in good agreement with the present ones. Although the present authors as well as Schleyer et al. attributed the band at 3619 cm^{-1} to the intramolecular interaction between the hydroxyl group and π-electrons, it now seems probably correct to introduce the concept of rotational isomers involving the interaction mentioned above for the explanation of the phenomenon, because type IV shows the absorption band at 3636 cm^{-1} where the normal primary alcohols do, type V at 3618 cm^{-1} and type VI at 3610 cm^{-1}.

The fairly large shifts (7~8 cm^{-1}) between types II and V and between types III and IV are most conveniently explained by introducing the concept of neutralization or the intramolecular interaction between the hydroxyl group and the π-electrons. That is, when a π-electron exists at the β-carbon atom of the alcohol, the interaction takes place and the extension of the O–H bond length occures. Thus the force constant is weakened and the weaker force constant gives rise to the shift of the absorption maximum toward the lower wave number.

Then the rotational isomers represented in Fig. 3 must be somewhat different from those in Fig. 2. In benzyl alcohol it is understood that the hydrogen atom of the hydroxyl group is not in the midst of the two atoms attached to the α-carbon, different from the cases of aliphatic alcohols, but is located closely to the carbon atom which possesses a π-electron. But the O–H bond can not be *cis* in respect of the C_{Ph}–C_α bond; since, if it were, there should not be any difference between types V and VI or between benzhydrol and triphenylcarbinol. The intramolecular interaction in allyl alcohol may be of this type, because its interacted form shows an absorption band at 3619.4 cm^{-1}.

It is also noticed that the band intensity of type V is greater than that of type IV in benzyl alcohol in contrast with the reverse in the primary aliphatic alcohols. This fact can be attributed to greater stabilization of type V in benzyl alcohol

11) J. J. Fox and A. E. Martin, *Trans. Faraday Soc.*, **36**, 897 (1940).
12) P. von R. Schleyer, D. S. Trifan and R. Bacskai, *J. Am. Chem. Soc.*, **80**, 6691 (1958).

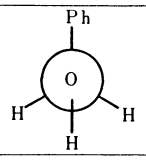
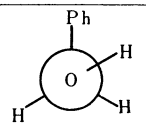
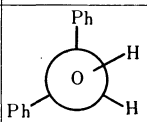
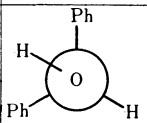
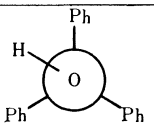
Type	Benzyl alcohol	Benzhyolrol	Triphenylcarbinol
IV		—	—
V			—
VI	—		

Fig. 3.

than of type IV in aliphatic alcohols because of the intermolecular interaction.

The only unknown ν_{O-H} absorption for the rotational isomers in the alcohols now is the one which should be assigned to the type in which the hydrogen atom of the hydroxyl group is situated between the aromatic carbon and the aliphatic carbon (type VII). The example is provided by alkyldiphenylcarbinols. The absorption at 3617 cm^{-1} is assigned to this, since the other absorption at 3609 cm^{-1} has been assigned to type VI.

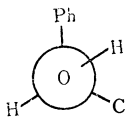


Fig. 4.

Theoretically, it is expected that alkylphenylcarbinols exhibit three ν_{O-H} absorptions, because they have the possibility of taking three types represented by II, V and VII. However, the ν_{O-H} absorptions of the types V and VII are so closely located that it is impossible to resolve them and consequently only two bands are observed for type II and for a mixture of types V and VII with methylphenylcarbinol.

There are some exceptions which are represented by dialkylphenylcarbinols. In these cases, the absorptions occur at 3620 cm^{-1} and at 3607 cm^{-1}, the latter being in the same position as type VI. However, the steric interference between the two alkyl groups and the ortho hydrogen atoms of the benzene nucleus causes the different situation from the others and the case is more complicated. The authors tentatively attribute this abnormality to the internal rotation around the C_{Ph}–C_{α} axis which is forced by the environment. Although the shift in wave number may be too great to assign the bands in an analogous way, it may still be valid that type VII of dialkylphenylcarbinol shows an absorption band at a lower wave number than type III because of the lowered force constant. Thus, the band at 3608 cm^{-1} is tentatively assigned to type VII and that at 3620 cm^{-1} to type III.

Summary

The authors observed symmetric ν_{O-H} absorptions for methanol and tertiary alcohols and unsymmetric bands for primary and secondary alcohols. The unsymmetric band was divided into two bands, assuming that the band is an overlap of the two symmetric bands. The idea of the rotational isomerism was successfully introduced for assigning the band and the following points were concluded.

1) Types I and IV show absorption bands at 3644~3636 cm^{-1}, type II at 3626~3629 cm^{-1}, type III at 3615~3618 cm^{-1}, type V at 3616~3619 cm^{-1}, type VI at 3608~3611 cm^{-1}, and type VII at 3613~3617 cm^{-1}.

2) The exception is dialkylphenylcarbinols which show the ν_{O-H} absorptions at about 3620 cm^{-1} and 3608 cm^{-1}, the former being assigned to type III and the latter to type VII. This ruling-out may be

attributed to the steric effect and the rotation around the C_{Ph}–C_{α} axis.

The steric effect on the integrated intensities and on the wave number where ν_{O-H} absorption falls is also discussed. The differences between types II and IV and between types III and VI were attributed to the existence of the intramolecular interaction between the hydroxyl group and π-electrons of the benzene nucleus. The same reason may cause allyl alcohol to show its main ν_{O-H} absorption at about 3620 cm^{-1}.

The authors are indebted to Professor Y. Urushibara and Professor T. Shimanouchi for their valuable suggestions and discussions. The authors also wish to express their hearty thanks to the Ministry of Education for the Grant in Aid for Fundamental Scientific Research.

Department of Chemistry
Faculty of Science
The University of Tokyo
Hongo, Tokyo

Intramolecular Interaction between Hydroxyl Group and π-Eelctrons. V[1]. *Electronic Effect in Arylcarbinols and a Preliminary Note on the Interaction in Benzylaniline Derivatives*

By Michinori Ōki and Hiizu Iwamura

(Received March 17, 1959)

It has long been in question why absorption due to the O–H stretching vibration of benzyl alcohol or allyl alcohol appears at about 3620 cm^{-1}. However, from the standpoint of the rotational isomerism, the interaction between the hydroxyl group and the π-electrons will be a valuable explanation for the phenomenon, as suggested in the previous paper[1]. If the interaction is the real cause of the shift of the ν_{O-H} absorption, it is expected that the electron density of the carbon atom (C_1) to which the hydroxymethyl group is attached or the next (C_2) to it should have profound effect on the ν_{O-H} absorptions of arylcarbinols. Hence, fourteen meta- and para-substituted benzyl alcohols were prepared and their ν_{O-H} absorptions were determined with a grating spectrophotometer. Ortho-substituted benzyl alcohols are excluded because formation of the internal hydrogen bonding can not be avoided when an atom with a lone pair of electrons is involved.

Experimental

Measurement and Calculation.—They were carried out similarly as reported previously[2].

Materials.—The materials used for the measurement are known compounds, unless otherwise stated. Their physical constants agreed with those in the literature.

m-Cyanobenzyl alcohol.—It was prepared according to the procedure reported by Langguth[3]. Although he reported the compound as an oil, it boiled at 127~127.5°C/3 mm. and solidified to form colorless needles on standing. The melting point is 28~29°C.

m-Phenylbenzyl alcohol. — It was prepared by the lithium aluminum hydride reduction of *m*-phenylbenzoic acid. Although this compound has been reported[4] as syrup, it formed colorless needles, m. p. 55~55.5°C, on recrystallization from carbon tetrachloride—petroleum ether.

Anal. Found: C, 84.70; H, 6.59. Calcd. for $C_{13}H_{12}O$: C, 84.75; H, 6.57%.

m-Benzyloxybenzaldehyde.—To a sodium ethoxide solution prepared from 5.5 g. (0.24 atom) of sodium and 150 ml. of alcohol was added 24.4 g. (0.2 mol.) of *m*-hydroxybenzaldehyde followed by 27.8 g. (0.22 mol.) of benzyl chloride. The mixture was heated under reflux for five hours, cooled and filtered to remove insoluble materials. Evaporation of the solvent gave crystals which were recrystallized to colorless small plates, m. p. 52~53°C, from petroleum ether. Yield, 32.5 g. (82%).

Anal. Found: C, 79.29; H, 5.81. Calcd. for $C_{14}H_{12}O_2$: C, 79.22; H, 5.70%.

m-Benzyloxybenzyl alcohol. — To a slurry prepared from 1.5 g. (0.04 mol.) of lithium aluminum

1) Part IV: M. Ōki and H. Iwamura, This Bulletin, **32**, 950 (1959).
2) M. Ōki and H. Iwamura, ibid., **32**, 567 (1959).
3) St. Langguth, *Ber.*, **38**, 2062 (1905).
4) M. P. Adam, *Ann. Chim. Phys.*, **15**, 245 (1888).

hydride and 50 ml. of ether was gradually added 19.6 g. (0.1 mol.) of *m*-benzyloxybenzaldehyde in 50 ml. of ether and the mixture was stirred at room temperature for two hours. The excessive lithium aluminum hydride was decomposed by adding ethyl acetate in ether and finally the mixture was treated with dilute sulfuric acid. The aqueous layer was extracted with ether and the ethereal extract was washed with aqueous sodium hydroxide and dried over potassium carbonate. Fractional distillation furnished a colorless oil boiling at 160°C/3 mm. which solidified. Recrystallization from benzene-petroleum ether (3 : 7) gave the substance in colorless needles, m. p. 44.5~45°C. Yield, 16.0 g. (81%).

Anal. Found: C, 78.54; H, 6.70. Calcd. for $C_{14}H_{14}O_2$: C, 78.48; H, 6.59%.

N-(p-Methoxybenzyl)-p-anisidine. — A mixture of 3.0 g. of *N*-(*p*-methoxybenzylidene)-*p*-anisidine, 1 g. of Raney nickel T-4 catalyst[5] and 100 ml. of alcohol was stirred in an autoclave at 80~100°C with 100 kg./cm² initial pressure. The heating was discontinued after two hours and, after cooling, the catalyst was removed by filtration. Evaporation of the solvent afforded a crystalline residue which was recrystallized from petroleum ether. Colorless plates, m. p. 94.5~95.5°C, were obtained in 1.5 g. (50%) yield. The rather low yield must be attributed to the hydrogenolysis of the *p*-methoxybenzyl group, since the oder of *p*-cresol methyl ether was distinct in the hydrogenation product.

Anal. Found: C, 74.22; H, 7.23. Calcd. for $C_{15}H_{17}NO_2$: C, 74.05; H, 7.04%.

N-p-Methoxybenzylaniline.—It was prepared in an analogous way. Though the melting point of this material was reported as 64.5°C[6], it melted at 46~47°C (colorless plates from petroleum ether). Since the micro-analyses agreed with the calculated values, it seems that this is one of the polymorphs.

Anal. Found: C, 78.99; H, 7.18. Calcd. for $C_{14}H_{15}NO$: C, 78.84; H, 7.09%.

Results and Discussion

The apparent ν_{O-H} absorption curves of *p*-nitrobenzyl alcohol, *m*-cyanobenzyl alcohol, benzyl alcohol and *p*-benzyloxybenzyl alcohol are shown in Fig. 1. The selection was made because the para-nitro group is the most electron-attracting and the para-benzyloxyl group is the most electron-releasing group in respect of Hammett's σ values[7] among the compounds used in the present work and benzyl alcohol is an intermediate. *m*-Cyanobenzyl alcohol is also included because it gives two apparent maxima.

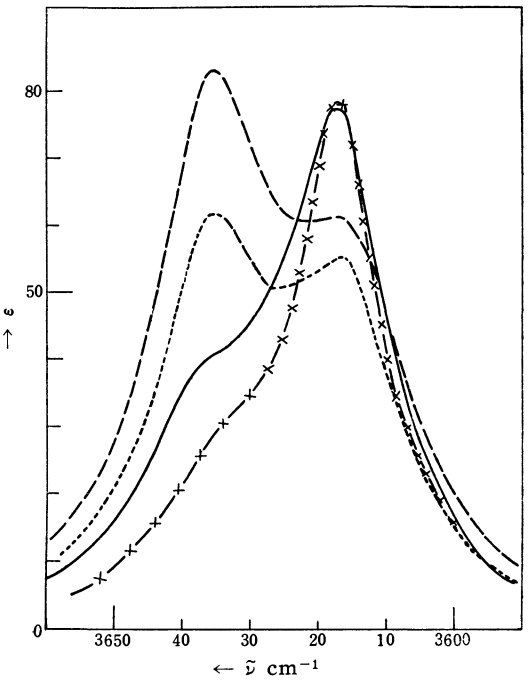


Fig. 1. ν_{O-H} absorption of *p*-nitrobenzyl alcohol (— — —), *m*-cyanobenzyl alcohol (--------), benzyl alcohol (- -) and *p*-benzyloxybenzyl alcohol (—×—).

Introduction of an electron-releasing group such as a benzyloxyl group in the para position in respect of the hydroxymethyl group enhances the intensity of the band at 3617 cm^{-1} and an electron-attracting group such as nitro group in the para position enhances the band at 3636 cm^{-1}. Thus the main peak for the ν_{O-H} absorption of *p*-nitrobenzyl alcohol lies at ca. 3636 cm^{-1}. Splitting of the two bands into the two apparent maxima in *m*-cyanobenzyl alcohol will be a firm proof for the presence of the two ν_{O-H} absorption bands in benzyl alcohol derivatives. The results suggest that the number of molecules which possess internal interaction is greater in the benzyl alcohol with an electron-releasing group and this kind of electronic effect must be caused by the presence of the interaction between the hydroxyl group and the π-electrons, since such enhancement in the band intensities is naturally expected from the assignment suggested in the previous paper[1].

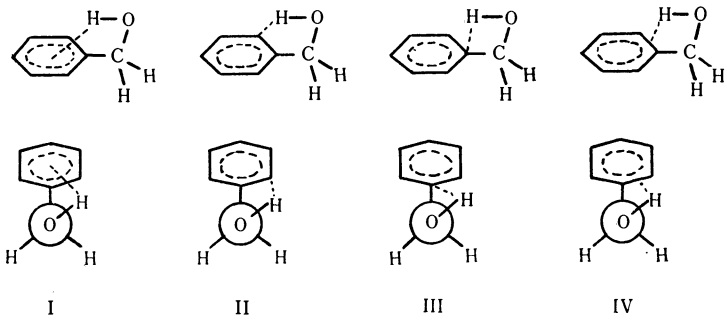
Now, when the internal interaction is taken into account, there are four possibilities in structure as shown in Fig. 2. The figures are presented both as sketches

5) S. Nishimura. This Bulletin, **32**, 61 (1959). The authors are indebted to Dr. Nishimura for preparation of this catalyst.

6) O. F. Steinhart, *Ann.*, **241**, 332 (1887).

7) L. P. Hammentt, "Physical Organic Chemistry", McGraw-Hill Book Co., New York (1940), p. 184. Also see: H. H. Jaffé, *Chem. Revs.*, **53**, 191 (1953).

8) D. S. Trifan, J. L. Weinmann and L. P. Kuhn, *J. Am. Chem. Soc.*, **79**, 6566 (1957).



I II III IV

Fig. 2.

and as projections through the O–C axis. The first (I) is the interaction between the hydroxyl group and the aromatic nucleus as a whole and this type of interaction was empirically quoted by Trifan and his co-workers[8] for α-hydroxyethylferrocene. In the second case (II), the direction of the hydrogen atom of the hydroxyl group points to the carbon atom (C_2) or the π-electron on C_2. This type of interaction has not been suggested, but the suggestion by Lüttke and Mecke[9] for 2-hydroxybiphenyl may fall into this category. In the third (III), the hydrogen atom of the hydroxyl group points to C_1 of the benzene nucleus or the π-electron on C_1. This type of interaction was implied by Goldman and Crisler[10] for phenethyl alcohol derivatives. The fourth case (IV) is the interaction in which the hydrogen atom turns toward the midst of C_1 and C_2, and the overlapping π-electrons on C_1 and C_2, take part in the interaction. The last case was suggested by Baker and Shulgin[11] for *o*-allylphenol and *o*-propenylphenol. Structures I and IV are considered as sorts of π-complexes and structures II and III σ-complexes.

Since the above assignments of the structures are all empirical, it is necessary to assign the structure on the basis of the experimental results. Now it can be hoped that the nature of the interaction may be clarified by changing the substituent on the benzene nucleus, because it is known, as mentioned above, that the interaction is markedly affected by the introduction of certain kinds of substituents. The same substituent was introduced into meta and para positions in respect of the hydroxymethyl group, because electron density on C_2 caused by a substituent in the para position should be roughly reproduced[12] on C_2 by introducing the same substituent into the meta position to the hydroxymethyl group.

If the π-complex (I or IV) is the real case, there should not be much difference between the two arylcarbinols which possess the same substituent, since the electron density of the aromatic ring as a whole must be the same and that in the middle of the two carbon atoms (C_1 and C_2) is considered to be nearly the same, although the effect of the substituent may be seen because of the different electron densities. If II is the case and an electron-releasing group is introduced, the meta-substituted benzyl alcohol would have a stronger absorption band at 3617 cm^{-1} than the para-substituted isomer, because the electron density on C_2 is higher in the meta-substituted compound than in the para-substituted one. And if III is the case, the situation must be opposite to that stated in case II and a compound with an electron-releasing group in the para-position to the hydroxymethyl group must have stronger absorption at 3617 cm^{-1} than the meta-substituted one.

The actual absorption curves are divided into two, assuming that the curves are the overlap of two symmetric bands which are expressed by the Lorentz function and the half widths and the integrated intensities are shown together with absorption maxima in Table I.

As is seen from Table I, an electron-releasing group in the para-position to the

9) W. Lüttke and R. Mecke, *Z. Elektrochem.*, **53**, 241 (1949); *Z. physik. Chem.*, **196**, 56 (1950).
10) I. M. Goldman and R. O. Crisler, *J. Org. Chem.*, **23**, 751 (1958).
11) A. W. Baker and A. T. Shulgin, *J. Am. Chem. Soc.*, **80**, 5358 (1958).

12) In addition to the effect given by σ_p, we must consider σ_o because the ortho positions to the hydroxymethyl group correspond to ortho and para positions to a new substituent for meta-substituted benzyl alcohol. Therefore, the electron density on C_1 or C_2 is different, even if the effect of the hydroxymethyl group is neglected.

TABLE I. ν_{O-H} ABSORPTION OF ARYLCARBINOLS (x-$RC_6H_4CH_2OH$)

R	x	OH	ν_{max} (cm^{-1})	$\Delta\nu_{max}$ (cm^{-1})	$\Delta\nu^a_{1/2}$ (cm^{-1})	$A\times10^{-3}$ ($mol^{-1}\cdot l.\cdot cm^{-2}$)	A_i/A_f
NO_2	*m*	i *	3616.3	18.9	20.4	3.70	0.84
		f **	3635.2		18.8	4.41	
	p	i	3616.0	19.5	23.6	3.98	0.77
		f	3635.5		20.0	5.15	
CN	*m*	i	3616.2	19.2	19.0	2.98	0.75
		f	3635.4		20.8	3.98	
	p	i	3616.4	19.0	19.8	3.49	0.71
		f	3635.4		20.8	4.93	
Cl	*m*	i	3617.0	19.4	18.6	3.74	1.30
		f	3636.4		21.4	2.88	
	p	i	3617.1	18.2	17.6	3.56	1.38
		f	3635.3		21.2	2.58	
C_6H_5	*m*	i	3616.6	19.6	16.6	4.17	1.92
		f	3636.2		21.6	2.18	
	p	i	3617.0	19.4	15.4	3.92	1.88
		f	3636.4		20.4	2.08	
H***		i	3617.1	19.2	17.0	4.26	1.69
		f	3636.3		24.0	2.59	
CH_3	*m*	i	3616.7	20.1	16.6	4.18	1.85
		f	3636.8		22.6	2.26	
	p	i	3617.4	18.4	15.6	3.67	2.02
		f	3635.8		24.2	1.82	
CH_3O	*m*	i	3616.9	19.3	16.6	4.04	1.69
		f	3636.2		25.6	2.40	
	p	i	3617.1	18.9	16.4	4.33	2.48
		f	3636.0		27.8	1.75	
$C_6H_5CH_2O$	*m*	i	3616.1	20.4	16.6	4.32	2.11
		f	3636.5		20.0	2.05	
	p	i	3617.0	18.2	15.0	3.89	2.70
		f	3635.2		20.0	1.44	

* i: denotes interacted form of the hydroxyl group.
** f: denotes free form of the hydroxyl group.
*** Taken from reference 1.

hydroxymethyl group enhances the intensity of the band at 3617 cm^{-1} more than one in the meta position and the tendency is opposite when an electron-attracting group is introduced. This fact excludes the possibility of structure I, II or IV. Hence it is concluded that the interaction between the hydroxyl group and the π-electrons of the aromatic nucleus in benzyl alcohol is of the type expressed by structure III.

The consistency of the wave number (3615.9~3617.4 cm^{-1} and 3635.2~3636.8 cm^{-1}) at which two absorption maxima exist is another proof that the origin of the bands is the rotational isomers, because in phenethyl alcohol derivatives the shift of the wave number, where an absorption of the interacted form appears, is observed[13].

The sum of the integrated intensities of the two bands is not always constant and there is a tendency that a more electron-attracting group gives rise to greater integrated intensity, as has been observed in substituted phenols[14]. However, when $\log \frac{A_i/A_f}{(A_i/A_f)_0}$, where A_i is the integrated intensity of the absorption band due to the interacted form, A_f that of free form and $(A_i/A_f)_0$ is the ratio given by benzyl alcohol, is taken into consideration, this value would represent the equilibrium constant and is in linear relation with

13) See the following paper.
14) P. J. Stone and H. W. Thompson, *Spectrochim. Acta*, **10**, 17 (1957).

TABLE II. ν_{N-H} ABSORPTION OF *N*-ARYLMETHYLARYLAMINES (p-$XC_6H_4CH_2NHC_6H_4$-Y-p)

X	Y	N-H	ν_{max} (cm^{-1})	$\Delta\nu^a_{1/2}$ (cm^{-1})	$A\times10^{-3}$ ($mol^{-1}\cdot l.\cdot cm^{-2}$)	$\Delta\nu_{max}$ (cm^{-1})
H	H	I	3417.4	28.0	2.24	32.8
		II	3450.2	25.6	2.11	
CH_3O	H	I	3418.0	26.8	2.63	32.1
		II	3450.1	23.7	1.73	
H	CH_3O	I	3405.6	35.8	1.93	37.1
		II	3442.7	30.2	1.74	
CH_3O	CH_3O	I	3406.6	35.3	2.03	36.2
		II	3442.8	29.6	1.30	

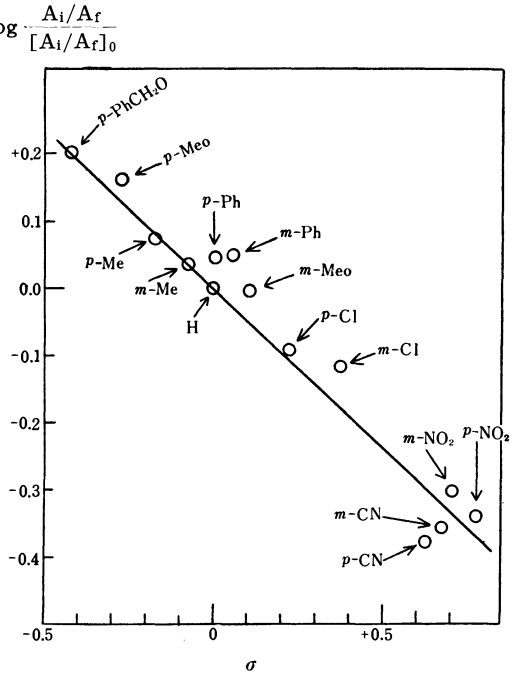


Fig. 3.

Hammett's σ values (Fig. 3). This linear relationship result is again a strong support to the idea of the existence of structure III. Although σ value for the *m*-benzyloxyl group has been unknown, it is now estimated from Fig. 2, by pointing 2.11 on the straight line and projecting to the σ axis, as -0.204.

A similar situation is expected for benzylaniline derivatives, which showed two distinct maxima for N-H stretching 30~40 cm^{-1} apart. The data are given in Table II.

It is understood from Table II, 1) that higher electron density on the benzene nucleus enhances the N-H stretching band at lower wave number, 2) that ν_{N-H} absorption shifts to lower wave number as Colichman & Liu[15] and also Krueger & Thompson[16] have pointed out for the arylamines, and 3) that $\Delta\nu_{max}$ is greater when the basicity of the arylamine increases. The full discussion will be presented in the near future.

Summary

Absorption due to the O-H stretching vibration in the fundamental region was measured with fourteen benzyl alcohol derivatives to see the electronic effect of the substituent on the interaction between the hydroxyl group and the π-electrons and the following conclusions are deduced.

1) The nature of the interaction or the structure of the molecule which gives rise to the ν_{O-H} absorption at 3617 cm^{-1} is discussed and the interaction between the hydroxyl group and the π-electron on the carbon atom to which hydroxymethyl group is attached (structure III) is favored.

2) The consistency of the wave numbers at which two ν_{O-H} absorptions appear, gives further support to the idea that these absorptions originate in the existence of the two rotational isomers.

3) $\mathrm{Log}\dfrac{A_i/A_f}{(A_i/A_f)_0}$ is in linear relation with Hammett's σ values and the σ value of the *m*-benzyloxyl group is estimated as -0.204.

A similar phenomenon is also observed in the substituted benzylanilines.

The authors are indebted to Professor Y. Urushibara and Professor T. Shimanouchi for their valuable advice and encouragement throughout this work, and their thanks are also due to the Ministry of Education for a Grant in Aid for the Fundamental Scientific Research.

Department of Chemistry
Faculty of Science
The University of Tokyo
Hongo, Tokyo

15) E. L. Colichman and S. K. Liu, *J. Am. Chem. Soc.*, **76**, 913 (1954).

16) P. J. Krueger and H. W. Thompson, *Proc. Roy. Soc.*, **A243**, 143 (1957).

Resonance Effect in Hammett Relationship. I. The Substituent Effect in the Acid Catalyzed Decompositions of ω-Diazoacetophenones in Acetic Acid

By Yuho TSUNO, Toshikazu IBATA and Yasuhide YUKAWA

(Received January 28, 1959)

As reported in a previous paper, the Curtius rearrangement of substituted benzazides in toluene did not give a linear Hammett relationship[1], whereas, the decomposition catalyzed by sulfuric acid[2] showed an approximately linear one, which had the negative ρ value. In such an electrophilic reaction, as has been pointed out frequently[3-7], electron releasing para substituents would favor the rate to a greater extent than would be expected from the normal Hammett constants. The same may be anticipated in this reaction. *p*-Hydroxyl and *p*-methoxyl groups indicated the tendency of some higher acceleration, but the scatters of the other groups, especially *p*-nitro group, made it impossible to ascertain this trend. The detailed re-examination as never improved the result. The acid catalyzed solvolytic decomposition of ω-diazoacetophenones is an electrophilic reaction of similar type. Hence, one might anticipate that para substituted derivatives probably show a similar behavior to what is seen in other electrophilic reactions. Furthermore, the rate changes of this reaction might suggest the contribution of substituents at least in such a reaction of which the substituent effects are transmitted through a carbonyl group to an electron deficient reaction center. Lane and coworkers[8], in their study of the substituent effect of this reaction, reported that the rate fitted the Hammett equation, whereas the effect of strongly electron releasing groups has not been reported. Therefore, kinetic study of decomposition of various substituted ω-diazoacetophenones was carried out in acetic acid, and the results are discussed on the basis of the Hammett relationship.

1) Y. Yukawa and Y. Tsuno, *J. Am. Chem. Soc.*, **79**, 5530 (1957).
2) Y. Yukawa and Y. Tsuno, ibid., **81**, 2007 (1959).
3) C. G. Swain and W. P. Langsdorf, Jr., ibid., **73**, 2813 (1951).
4) J. K. Kochi and G. S. Hammond, ibid., **75**, 3445 (1953).
5) (a) N. C. Deno and A. Schriesheim, ibid., **77**, 3051 (1955); (b) N. C. Deno and W. L. Evans, ibid., **79**, 5804 (1957).
6) H. C. Brown and Y. Okamoto, ibid., **79**, 1913 (1957); Y. Okamoto and H. C. Brown, *J. Org. Chem.*, **22**, 485 (1957).
7) J. Miller, *Australian J. Chem.*, **9**, 61 (1956).
8) J. F. Lane and R. L. Feller, *J. Am. Chem. Soc.*, **73**, 4230 (1951).

Experimental

Materials. — Substituted and unsubstituted diazoacetophenones used in this investigation were prepared by the usual procedure[8,9]; all benzoyl chlorides reacted satisfactorily with an excess of diazomethane in ethereal solution with cooling. After this solution was allowed to stand overnight at room temperature, the solvent was removed in vacuo and the residue was collected. Several recrystallizations from ligroin or benzene solution gave pale yellow crystals. The melting points of the diazoketones thus obtained are listed in Table I, together with the boiling points of the starting benzoyl chlorides.

Solvent. — Acetic acid was purified by the same method as that described in a previous paper[2]; b. p. 117.5~118.0°C.

Kinetic Experiments.—The rates of decompositions were determined in 75 ml. of anhydrous acetic acid at 40.00±0.01°C, by collecting the evolved nitrogen by an azotometer. The procedure and the apparatus were the same as those described in several recent papers[1,2,8]. The solution was not stirred but powdered glass was added to the solution in order to prevent the supersaturation of nitrogen gas evolved. In each run, the initial concentration of diazoketone was about 1/200 mol. Volume readings were taken covering the extent of 75% completion of reaction. The infinity reading was determined at the time after a period of 9—10 times as much as the half life of the reaction. The measurements were repeated at least three times for respective diazoketones in order to minimize the experimental error. The total volume of nitrogen collected was close to the theoretical amount. The change in the initial concentration did not show any effect on the rate.

Reaction Product. — The reaction solution was allowed to remain at 40.00°C in a bath until no further evolution of nitrogen occurred, and then the solvent was removed in vacuo. The

9) W. E. Bachmann and W. S. Struve, "Organic Reactions", Vol. 1, John Wiley & Sons, Inc., New York (1942), p. 38.

TABLE I. ω-DIAZOACETOPHENONES, BENZOYL CHLORIDES AND THE DECOMPOSITION PRODUCTS

Subst.	Melting point and boiling point[a] (°C)		
	XC_6H_4COCl	$XC_6H_4COCHN_2$	$XC_6H_4COCH_2Ac$
H	(192~192.7)	47.2~ 48.0[b]	48
p-CH_3O	(152~155/20 mm.)	87.5~ 88.5[c]	57.5~ 58.5
p-C_2H_5O	(161/27 mm.)	80.0~ 80.5[d]	86.0~ 86.8
p-*t*-C_4H_9	(149.9~150.5/14 mm.)	83.5~ 84.0[e]	60.5~ 61.3
p-CH_3	(122/33 mm.)	52.0~ 52.8[b]	84.0~ 85.0
p-C_6H_5	112.5~113.0	119.0~119.5[f]	112.0~112.8
p-Cl	(120~121/28 mm.)	114.0~115.0[b]	68.5~ 69.0
p-Br	(139.0~139.5/33 mm.)	126.0~126.5[b]	85.8~ 86.5
p-NO_2	72.7~73.3	118.0~119.0[b]	122 ~123.5
m-CH_3	(116~117/30 mm.)	64.2~ 64.8[g]	liquid
m-Br	(138.5~139.5/38 mm.)	73.5~ 75.0[h]	liquid
m-NO_2	(169.0/20 mm.)	139.5~140.0[i] (decomp.)	48.5~49.0

a) All melting points are corrected. Boiling points which are given in brackets are uncorrected.
b) J. F. Lane et al., Ref. 8.
c) M. S. Newman and P. Beal, III, *J. Am. Chem. Soc.*, **71**, 1506 (1949).
d) *Anal.* Found: C, 63.56; H, 5.35; N, 14.84%.
Calcd. for $C_{10}H_{10}O_2N_2$: C, 63.16; H, 5.31; N, 14.74%.
e) *Anal.* Found: C, 71.33; H, 6.53; N, 14.17%.
Calcd. for $C_{12}H_{14}ON_2$: C, 71.26; H, 6.98; N, 13.85%.
f) C. E. Blades and A. L. Wilds, *J. Org. Chem.*, **21**, 1013 (1956).
g) *Anal.* Found: C, 67.11; H, 5.21; N, 16.21%.
Calcd. for $C_9H_8ON_2$: C, 67.48; H, 5.03; N, 17.49%.
h) *Anal.* Found: C, 43.01; H, 2.34; N, 12.32%.
Calcd. for $C_8H_5ON_2Br$: C, 42.66; H, 2.22; N, 12.44%.
i) *Anal.* Found: C, 51.02; H, 2.84; N, 20.60%.
Calcd. for $C_8H_5O_3N_3$: C, 50.26; H, 2.62; N, 21.99%.

residues were recrystallized several times from ligroin or ethanol solutions. The corresponding phenacyl acetates having sharp melting points were obtained in quantitative yield (Table I). In the case of *m*-CH_3 and *m*-Br derivatives, the residues were not solidified.

Results and Discussion

The evolution of nitrogen followed strictly the first order equation

$$0.4343 \times kt = \log V_\infty - \log(V_\infty - V)$$

where V_∞ is the volume reading at the infinite time and V the readings at time t. Typical runs of the evolution of nitrogen are given graphically in Fig. 1. The rate constants obtained at 40.00°C are listed in Table II. The average deviations less than 0.7% are obtained in respective runs and the reproducibility of the results is estimated to be about 1%. Some of the rate constants obtained in the present study are slightly lower than those obtained by Lane et al.[8] This appears to be attributable to the difference of acetic acid used as solvent or that of the methods evaluating rate constants.

The mechanism of this reaction proposed is possibly represented as follows:

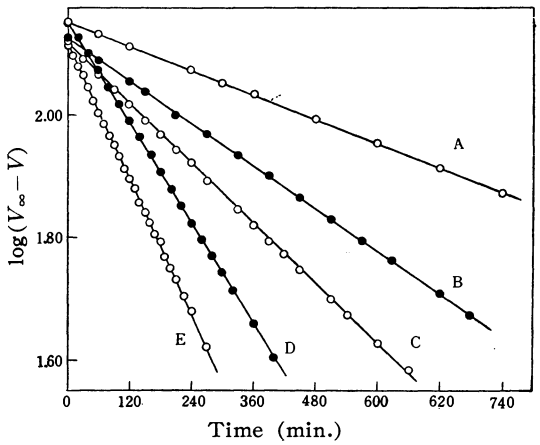


Fig. 1. Typical first order plots for the decomposition of substituted ω-diazoacetophenones in acetic acid at 40.00°C.
A, *m*-NO_2; B, *m*-Br; C, *p*-Cl; D, *m*-CH_3; E, *p*-CH_3.

TABLE II. THE RATE CONSTANTS OF THE DECOMPOSITION OF SUBSTITUTED ω-DIAZOACETOPHENONES IN ACETIC ACID AT 40.00°C

Subst.	$10^3 \times k_1$[a)]	Subst.	$10^3 \times k_1$[a)]
p-CH_3O	7.76±0.06	*p*-Br	1.91 ±0.02
p-C_2H_5O	7.37±0.07	None	2.74 ±0.02[c)]
p-CH_3	4.33±0.04[b)]	*m*-CH_3	3.14 ±0.04
p-*t*-C_4H_9	4.12±0.04	*m*-Br	1.32 ±0.02
p-C_6H_5	3.37±0.02	*m*-NO_2	0.744±0.007
p-Cl	1.98±0.01	*p*-NO_2	0.600±0.006

a) Rate in reciprocal minute.
b) Reported 4.88×10^{-3} at 40.05°C by Lane et al., Ref. 8.
c) Reported 2.94×10^{-3}, Ref. 8.

$$C_6H_5COCHN_2 \xrightarrow{H^+} C_6H_5COCH_2N_2^+$$

$$C_6H_5COCH_2N_2^+ + CH_3CO_2^- \rightarrow C_6H_5COCH_2{-}OCOCH_3 + N_2$$

the first step is the protonation (presumably reversible process) of diazoketone and the second is the rate determining decomposition of the protonated ketodiazonium ion to the acetate. With regard to the second step, two types of mechanism are possible; one is the unimolecular loss of nitrogen followed by the reaction with solvent of the carbonium ion so produced, another is the bimolecular reaction with solvent or acetate ion. Lane et al. suggested the latter one[8].

It will be of interest to discuss the substituent effects on the basis of the Hammett equation[10]. As is shown clearly in Fig. 2, the plot of log *k* against the corresponding Hammett σ-constants fails to give a linear relationship but concaves upward, in contrast to the result by Lane et al.[8] Only with respect to meta substituents and the *p*-nitro group, the linear correlation is obtained. The slope of this correlation line, the ρ_m value, is evaluated using the method of least squares[11] to be −0.830, the probable error of the fit 0.010 in log *k* and the correlation coefficient 0.999. On the other hand, the plots of log *k* vs. σ for para groups lie substantially above the meta line. The deviations appear to be entirely significant in view of the experimental uncertainty.

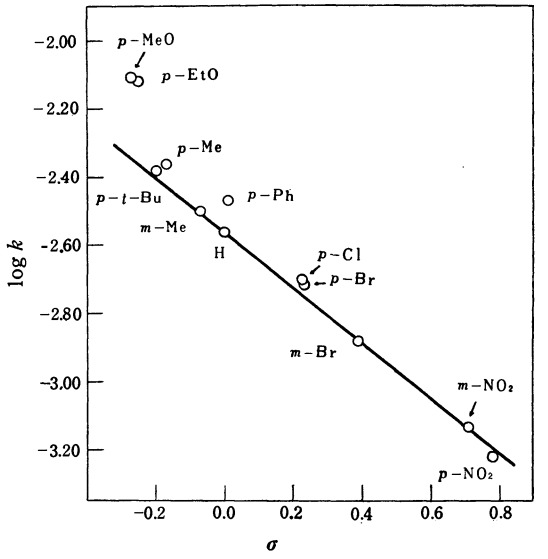


Fig. 2. The Hammett equation applied to the decomposition of ω-diazoacetophenones in acetic acid at 40.00°C.

The above results are not unusual but may be reasonable at least in qualitative consideration. Although the Hammett equation correlates the rates or equilibria of an enormous number of reactions[10,11], some limitations have been noted. One of the limitations is the electrophilic reactions providing the deviations of the plots for electron releasing para substituents such as methoxy, methyl, phenyl and halo groups. In general, these groups show greater electron-release than described by the normal σ-constants in an electrophilic reaction[3-7]. The upward curvature of the plots for these groups is reasonably attributed to differing capacities of the substituents for resonance stabilization of a positively charged transition state. The same considerations as noted above might be employed in the case of the present reaction. If the upward deviations are referred to the resonance capacities, the transition state of this reaction must have a positively charged reaction center, and the charge must be, if possible, delocalized through resonance interaction. This appears to suggest that the driving force of the present reaction may be the elimination of the nitrogen molecule, followed by the attack of acetate ion upon the carbonium ion so produced.

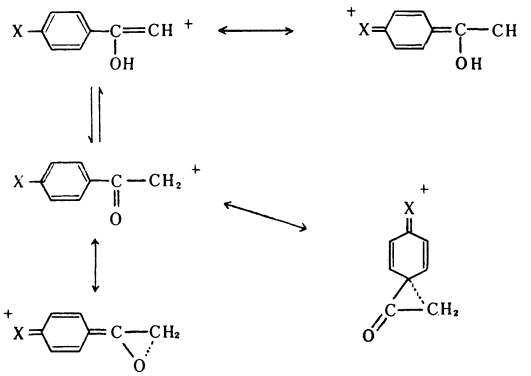
$$C_6H_5{-}CO{-}CH_2N_2^+ \rightarrow C_6H_5CO{-}CH_2^+ + N_2$$

$$\xrightarrow{OAc^-} C_6H_5COCH_2OAc$$

Although this is somewhat inconsistent with Lane's conclusion, this consideration might be reasonable because the decomposition of the diazonium ion into nitrogen and carbonium ion undoubtedly does not

10) L. P. Hammett, *J. Am. Chem. Soc.*, **59**, 96 (1937); "Physical Organic Chemistry", McGraw-Hill Book Co., Inc., New York (1940), p. 194.
11) H. H. Jaffé, *Chem. Revs.*, **53**, 191 (1953).

have high energy requirements[12]. At least the pull factor of the leaving nitrogen may predominate over the push of the attacking species, because of the high stability of the nitrogen molecule. The positive charge so produced at the reaction center would be delocalized through the resonance with powerfully electron releasing aryl groups;



These are consistent with the present data qualitatively. Then, it will be of further interest to treat the deviations in quantitative manner.

The Quantitative Treatment. — The recent advance in this field has prompted us to some attempts to correlate electrophilic reactions with an alternative set of substituent constants. These new substituent constants are denoted by σ^+[13]. Although a number of tentative sets of σ^+ have been proposed by various authors, it is Brown and Okamoto's set[6] that is apparently the most decisive one of general applicability. In Fig. 3 is demonstrated the correlation of present data with Brown and Okamoto's set of σ^+. Least squares treatment[11] indicates that the ρ^+ value, the slope of the regression line, is equal to -0.736 ± 0.0246, the correlation coefficient being 0.994. Brown and Okamoto's set of σ^+ correlates the present data more appropriately than does the normal Hammett constant, whereas it is worthy of remark that all the points for para substituents fall below the ρ_m line to a considerable extent. The ρ^+ value is clearly lower than ρ_m value. This would indicate that the σ^+ values employed for para substituents somewhat overcorrect the present situation. Furthermore, it might possibly be attributed to less availability of the *transition state resonance* of the present reaction than that described on the basis of σ^+. However, this is not surprising, because the contribution of resonance would not always be constant but would vary from reaction to reaction. Such failure of the linear relationship using the set of σ^+ is frequently observed. Some of the examples are provided by the solvolysis of neophyl brosylates[14] in which the resonance effect is less effective than described by Brown and Okamoto's σ^+ values, and the brominolysis of benzeneboronic acids[15] in which the contribution of *transition state resonance* appears greater

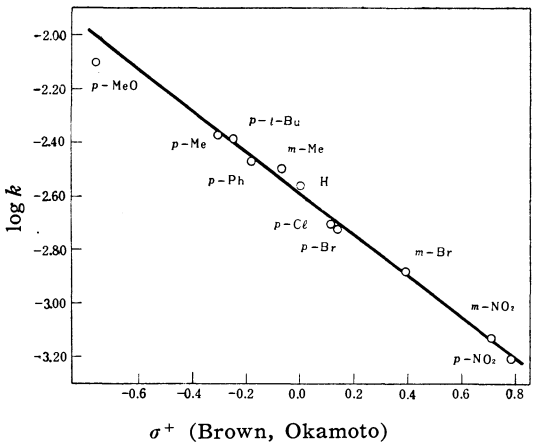


Fig. 3. Plot of decomposition rates of ω-diazoacetophenones against Brown and Okamoto's σ^+.

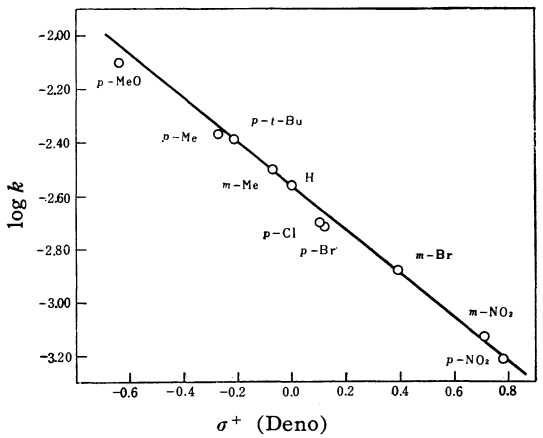


Fig. 4. Correlation of rates of the decomposition of ω-diazoacetophenones with Deno's σ^+.

12) A. Streitwieser, Jr. and W. D. Schaeffer, *J. Am. Chem. Soc.*, **79**, 2888 (1957); A. Streitwieser, Jr., *J. Org. Chem.*, **22**, 861 (1957).

13) See *reference* (*22*) in Y. Okamoto and H. C. Browm, *J. Org. Chem.*, **22**, 485 (1957).

14) R. Heck and S. Winstein, *J. Am. Chem. Soc.*, **79**, 3432 (1957).

15) H. G. Kuivila and A. R. Hendrickson, ibid., **74**, 5069 (1952); H. G. Kuivila and L. E. Benjamin, ibid., **77**, 4834 (1955).

than the estimated. Hence, it is the exsistence of a unique set of σ^+ that would be rather surprising in itself.

On the other hand, through Deno's set of σ^+ [5] the present data can be correlated more successfully than through Brown and Okamoto's, as shown in Fig. 4. The ρ^+ value of this correlation is equal to -0.789 ± 0.024, the correlation coefficient being 0.996. It is evident that the points for para substituents come closer to fitting on the ρ_m line, while the ρ^+ value is not strictly equal to the ρ_m value. The set defined by Pearson from the Beckmann rearrangement[16] also gives a rather more satisfactory result for the present reaction than does Brown and Okamoto's set, although this has not been reported to show any applicability. These facts appear to indicate that the respective sets of σ^+ may be applicable only to respective limited regions of electrophilic reaction series. Then, it would be by no means meaningless to set up tentative σ^+ values from the present reaction. This is encouraged by the success of linear free energy relationship between present data

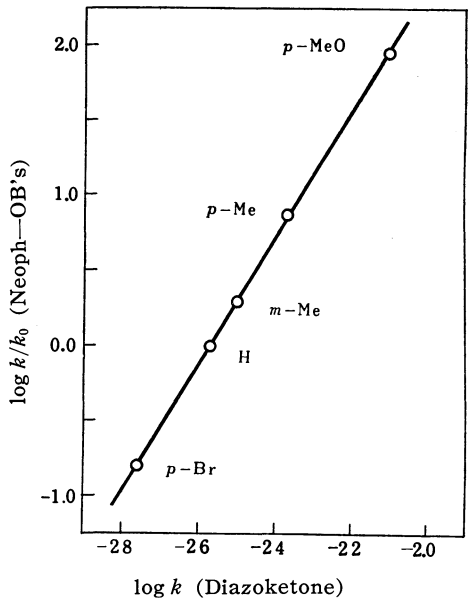


Fig. 5. Correlation of rates of acetolysis of neophyl brosylates and decomposition of ω-diazoacetophenones.

TABLE III. SUBSTITUENT CONSTANTS USED FOR CORRELATING RATES OF DECOMPOSITION OF THE ω-DIAZOACETOPHENONES

Substituent	Hammett[a]	Brown[b]	Deno[c]	σ^+[d]
p-CH_3O	−0.268	−0.764	−0.64	−0.537
p-C_2H_5O	−0.250			−0.512
p-*t*-C_4H_9	−0.197	−0.250	−0.21[f]	−0.209
p-CH_3	−0.170	−0.306	−0.27	−0.234
p-C_6H_5	+0.009	−0.179		−0.103
None	0.000	0.000	0.00	0.000
p-Cl	+0.227	+0.112	+0.11[g]	+0.175
p-Br	+0.232	+0.148		+0.202

a) Taken from the compilation by Jaffé (Ref. 11).
b) Brown and Okamoto's set of σ^+ (Ref. 6).
c) Deno's set of σ^+ (Ref. 5a).
d) The σ^+ values obtained from the present data. These were calculated from the Hammett equation using $\rho = \rho_m = -0.830$ and $\log k_0 = -2.558$.
e) H. C. Brown and Y. Okamoto, *J. Am. Chem. Soc.*, **80**, 4979 (1958).
f) The value derived from the dissociation of benzhydrols (Ref. 5b).
g) The value taken from Ref. 5b. In the original paper (Ref. 5a) +0.08 was given, while the quoted value, +0.11, appears to be more suitable.

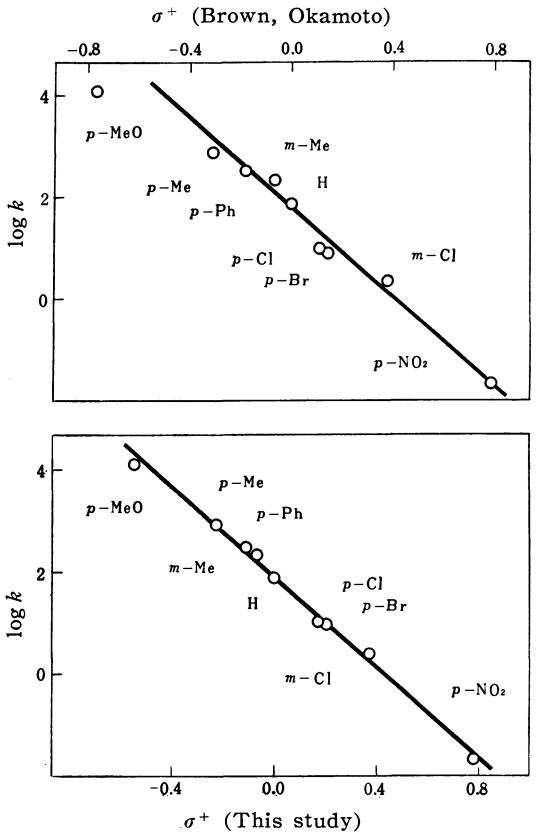


Fig. 6. Correlations of the Beckmann rearrangement of acetophenonoxime picrylethers with Brown and Okamoto's and our σ^+ values.

16) D. E. Pearson, J. F. Baxter and J. C. Martin, *J. Org. Chem.*, **17**, 1511 (1952); D. E. Pearson and J. D. Burton, ibid., **19**, 957 (1954).

and the solvolysis rates of neophyl brosylates[14], as shown in Fig. 5. The new set of σ^+ is given in Table III, along with the values of other sets of substituent constants. The present set does not appear to be applicable to a great many reactions. In some cases, however, it does describe a better correlation than does Brown and Okamoto's. Fig. 6 exhibits the correlations of the Beckmann rearrangement of acetophenone oxime picryl ethers[17] with the present set and with Brown and Okamoto's σ^+. Some other reactions which are satisfactorily correlated by the present set are as follows: the acetolysis of neophyl brosylates[14], the Beckmann rearrangement of acetophenonoximes[16], Diels-Alder reaction of 1-phenyl-1, 3-butadienes with maleic anhydride[18] and acid catalyzed rearrangement of phenylpropenylcarbinols[19].

A particular interest is seen in Table III. For each substituent, σ^+ values become more negative in the following order; the present set $<$Deno's $<$Brown and Okamoto's. The correction relative to the normal substituent constant is great in magnitude in Brown and Okamoto's, small in Deno's and smaller in the present set of σ^+. This parallels presumably the degree of resonance stabilization of electron deficient transition states in respective reference reactions, if the other factors remain constant throughout respective substituted derivatives. Thus, the resonance contribution of substituents would be more important in Brown and Okamoto's reference reaction than in Deno's and of even greater importance than in the present reaction. This is consistent with the facts that in Deno's reference reaction, the dissociation of triphenylcarbinols, the charge delocalization is shared separately by three aryl groups and in the present reaction the resonance contribution of a substituent group is reduced through the carbonyl group.

All one can say is that the σ^+ is not essentially constant but variable with respect to the change in reaction. *Rho—Sigma*$^+$ equation should be applied to the limited reaction series in which the availability of *transition state resonance* is equivalent to that in respective reference reactions. Now, it is highly desirable to correlate these sets of σ^+ with a simple relationship, which will be described in Part II.

The authors are indebted to Mr. T. Shishido for performing microanalysis.

Institute of Scientific and Industrial Research
Osaka University
Sakai, Osaka

17) R. Huisgen, J. Witte, H. Walz and W. Jira, *Ann.*, **604**, 191 (1957).
18) E. J. Dewitt, C. T. Lester and G. A. Ropp, *J. Am. Chem. Soc.*, **78**, 2101 (1956).
19) E. A. Braude and E. S. Stern, *J. Chem. Soc.*, **1947**, 1096.

Resonance Effect in Hammett Relationship. II. Sigma Constants in Electrophilic Reactions and their Intercorrelation

By Yasuhide YUKAWA and Yuho TSUNO

(Received January 28, 1959)

Recently, Brown and Okamoto have demonstrated a practical success in correlating various electrophilic reactions by a single set of σ^+ [1,2], obtained from the substituent effects in solvolysis of phenyldimethylcarbinyl chlorides. Their treatment should involve the assumption that the substituent effects in electrophilic reactions remain constant relative to marked variation in the ρ value. This is inconsistent with our view[3] that the reasonance interactions by a para substituent would depend greatly on the nature of the reactions, so that the effects

1) H. C. Brown and Y. Okamoto, *J. Am. Chem. Soc.*, **79**, 1913 (1957); Y. Okamoto and H. C. Brown, *J. Org. Chem.*, **22**, 485 (1957).

2) H. C. Brown and Y. Okamoto, *J. Am. Chem. Soc.*, **80**, 4979 (1958).

3) Y. Tsuno, T. Ibata and Y. Yukawa, This Bulletin, **32**, 960 (1959).

in electrophilic reactions could not possibly be correlated with a unique set of σ^+. The present view may be reasonable and perhaps the general one[4,5]. Brown and Okamoto's view could be confirmed by the identity of σ^+ values independently derived from other reactions. However, the various sets of σ^+ are varied significantly with respect to changes in the reference reaction[3,6-11]. The reported fact that the σ^+ constant derived from the decomposition of ω-diazoacetophenones differed from the corresponding Brown and Okamoto's[3] constant may afford evidence in favor of the present view.

The variations of σ^+ value for a given para substituent are generally referred to different availabilities of the resonance in various reference reactions, if other factors are maintained constant. On the other hand, failure of the linear $\rho\sigma^+$ relationship could be attributable also to the change in mechanism in a reaction series[12]. Brown has quoted[1], as an example, the solvolysis of benzyl tosylates[5,7], in which the change from S_N1 to S_N2 mechanisms occurred through changes of substituent. In the decomposition of diazoacetophenones, it may be possible to consider that the dissociation of nitrogen molecule competes with the attack of acetate ion in the driving force of the reaction[3]. If this was true, both mechanisms should indicate different responses to the ionizing power of the medium possibly because the stabilization of the carbonium ion produced will be important only in the former mechanism. Therefore, the substituent effects may be sensitive to the changes of solvent. Accordingly, kinetic study of the decomposition of diazoacetophenones was carried out in 75% aqueous acetic acid solution at 25.20°C, in order to confirm the reliability of our σ^+ values.

To the completion of this study, the foregoing view has been concreted and our attention has been directed to correlate empirically these independent sets of σ^+ according to a simple but reasonable relationship. In this paper, the results of the kinetics and of an approach to the correlation of σ^+ are presented.

Experimental

All diazoacetophenones were prepared by the procedure described in the preceding paper[3]. The stock solvent was made up by mixing 75 parts by volume of acetic acid with 25 parts by volume of distilled water. Acetic acid was purified by the usual method[13] and carefully fractionated, b. p. 117.5~118.0°C.

Rate Measurements. — The rates of the decomposition were determined by following the rate of evolution of nitrogen. The apparatus and the procedures were similar to those described in previous papers[3,14]. The temperature of the reaction bath was controlled to 25.20°C within an accuracy of ±0.01°C. Measurements were carried out in 75 ml. of aqueous acetic acid. The quantitative amount of nitrogen was obtained by the decomposition of respective derivatives of diazoacetophenone in aqueous acetic acid at 25.20°C. The rate of evolution of nitrogen followed strictly the first order kinetic law. Individual runs showed average deviations of far less than 1%, and duplicate runs gave rate constants agreeing within 2% or better. *p*-Phenyl-, *p*-bromo- and *m*- and *p*-nitro derivatives are soluble with greater difficulty in this solvent at this reaction temperature than in anhydrous acetic acid. Nitro derivatives were warmed with vigorous shaking at about 40°C to complete dissolution, prior to measurement. But this could not be applied to other derivatives, because of their high reactivities. *p*-Phenyl derivative is far less soluble in this solvent and deviation from the first order kinetic law was observed. The calculated rate constant increased gradually as the reaction proceeded and reached a constant value at 60% completion of the reaction. The rate constants obtained are summarized in Table I.

TABLE I. RATES OF THE DECOMPOSITION OF ω-DIAZOACETOPHENONES IN 75% AQUEOUS ACETIC ACID AT 25.20°C

Subst.	$k_1\times10^3$ a)	Subst.	$k_1\times10^3$ a)
p-CH_3O	28.3 ±0.2	H	5.86 ±0.04
p-C_2H_5O	26.9 ±0.3	*p*-Cl	3.71 ±0.03
p-CH_3	12.07±0.08	*p*-Br	2.94 ±0.07
p-*t*-C_4H_9	10.6 ±0.1	*m*-NO_2	0.816±0.005
m-CH_3	7.43±0.06	*p*-NO_2	0.638±0.004
p-C_6H_5	6.97±0.15		

a) The average rate constant in reciprocal min. and the average deviation.

4) P. B. D. de la Mare, *J. Chem. Soc.*, **1954**, 4450.
5) F. T. Fang, J. K. Kochi and G. S. Hammond, *J. Am. Chem. Soc.*, **80**, 563 (1958); G. S. Hammond, C. E. Reeder, F. T. Fang and J. K. Kochi, ibid., **80**, 568 (1958); G. S. Hammond and C. E. Reeder, ibid., **80**, 573 (1958).
6) D. E. Pearson, J. F. Baxter and J. C. Martin, *J. Org. Chem.*, **17**, 1511 (1952); D. E. Pearson and J. D. Burton, ibid., **19**, 957 (1954).
7) J. K. Kochi and G. S. Hammond, *J. Am. Chem. Soc.*, **75**, 3445 (1953).
8) N. C. Deno and A. Schriesheim, ibid., **77**, 3051 (1955).
9) N. C. Deno and W. L. Evans, ibid., **79**, 5804 (1957).
10) J. Miller, *Australian J. Chem.*, **9**, 61 (1956).
11) J. Packer, J. Vaughan and A. F. Wilson, *J. Org. Chem.*, **23**, 1215 (1958).
12) C. G. Swain and W. P. Langsdorf, *J. Am. Chem. Soc.*, **73**, 2813 (1951).
13) A. Weissberger, "Technique of Organic Chemistry", Vol. VII; "Organic Solvents", 2nd Ed., Interscience Publishers, Inc., New York (1955).
14) Y. Yukawa and Y. Tsuno, *J. Am. Chem. Soc.*, **79**, 5530 (1957); J. F. Lane and R. L. Feller, ibid., **73**, 4230 (1951).

Results

As listed in Table I, rates of the decomposition of diazoacetophenones are significantly increased in aqueous acetic acid relative to those in anhydrous acetic acid. Parallel to this, the sensitivity of the reaction to substituent effects appears to be considerably increased. Whereas the failure of the linear Hammett relationship is also observed in the aqueous medium just as in the case of an anhydrous medium[3]. Electron releasing para substituents supply higher acceleration than would be anticipated by the normal Hammett relationship (Fig. 1). Such a result has been discussed by us[3] and a number of other authors[1,2,4-12] and needs no further elucidation.

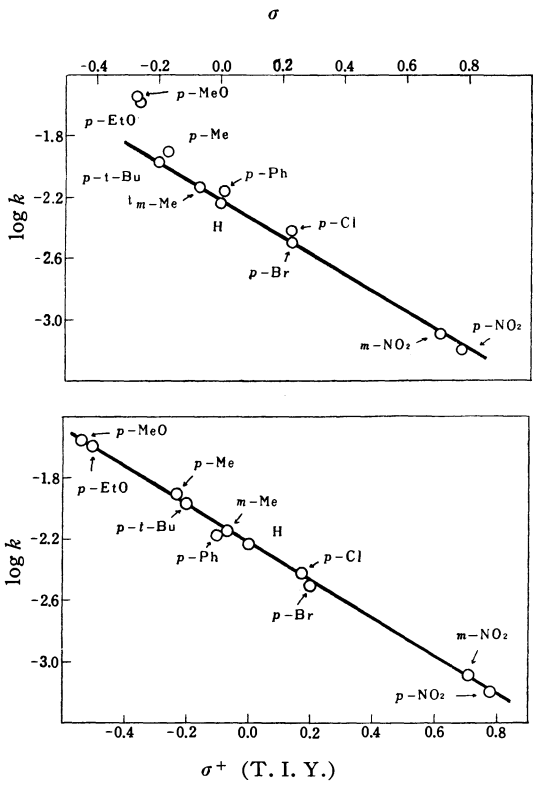


Fig. 1. Plot of the present data against the ordinary σ and our σ^+ constants.

In both reactions, the substituent effects would presumably be invariant, if the transition state remains approximately constant through changes of solvent. An evidence for the identity of substituent effects would generally be provided by a linear relationship between the corresponding $\log k/k_0$ of the two reactions. In fact, all the experimental points of $\log k/k_0$ in aqueous acetic acid fall just on the line expected from the $\log k/k_0$ in anhydrous medium. The correlation is given by an equation

$$\log (k/k_0)_{aq} = 1.510 \log (k/k_0)_{anhyd}$$

This indicates that the changes of medium reflect only ρ value and the substituent effect is not varied in either medium. The above correlation can of course be rewritten in terms of our σ^+ values[3] (Fig. 1). Statistical treatment[15] gives a correlation 1,

$$\log (k/k_0) = (-1.253 \pm 0.020)\sigma^+ \qquad (1)$$

The standard deviation of experimental $\log k$ from the best line is 0.027 and the correlation coefficient is 0.999. The ρ^+ value is closely equal to the ρ_{meta} value, 1.237 ± 0.018, which was obtained from points for m-CH_3, m-nitro, p-nitro and unsubstituted derivatives. On the basis of this ρ^+ value (1), a new set of σ^+ values can be derived from the rates in aqueous acetic acid. They are given in Table II. The present values agree with the previous one. p-Phenyl and p-bromo groups differ considerably in magnitude from the foregoing ones[3]. These are of no doubt attributable to the lower solubilities in aqueous acetic acid (see, *Experimental*). The discrepancies of others are substantially contained within experimental uncertainty. As a result, it may be conclusively suggested that the σ^+ derived from the previous result describes the best situation of the substituent effect in this reaction. Then, it appears to be evidently confirmed that the changes in mechanism as suggested by Brown and Okamoto might not occur through substituent changes in this reaction, and also that the rise in reactivities

TABLE II. σ^+ CONSTANTS

Subst.	σ^+_{aq} [a]	σ^+_{anhyd} [b]	$\sigma^+_{B.O.}$ [c]
p-CH_3O	−0.537	−0.537	−0.764
p-C_2H_5O	−0.519	−0.512	
p-CH_3	−0.241	−0.234	−0.306
p-t-C_4H_9	−0.196	−0.209	−0.250
p-C_6H_5	(−0.051)	−0.103	−0.179 [d]
p-Cl	+0.168	+0.175	+0.112
p-Br	(+0.249)	+0.202	+0.148

a) The present study.
b) The set derived from the decomposition in anhydrous acetic acid (Ref. 3).
c) Brown and Okamoto's set of σ^+, taken from Ref. 1.
d) The value quoted from Ref. 2.

15) H. H. Jaffé, *Chem. Revs.*, **53**, 191 (1953).

of electron releasing para substituents could be attributable entirely to the increase of the resonance contribution.

These facts appear evidently to support the present view in preference to Brown and Okamoto's[1,2].

The linear free energy relationship would essentially hold in more or less limited reaction series in which the substituent effects are close to each other[3]. With the above considerations in mind, a given electrophilic reaction should be correlated with one of these sets of σ^+ most suitable to the resonance effects of substituents in it. However, it appears to be inconvenient practically. Therefore, it is necessary and desirable to correlate these independent sets of σ^+ with a relationship of practical use.

Discussion

The substituent effect can generally be treated as the sum of independent contributions of inductive and resonance components[16]. The former contribution refers to the electron distribution through the *sigma* bonds of a benzene nucleus and the latter to the electron delocalization through the resonance interaction of a substituent with the benzene *pi* electron system. An ordinary Hammett σ constant could be represented according to Eq. 2,

$$\sigma = \sigma_I + \sigma_R \qquad (2)$$

where σ_I is an inductive effect and σ_R is a so-called *resonance polar effect*[16]; σ_R represents the substituent contribution through resonance with the benzene *pi* bonds to the electron density on the nuclear carbon atom at which the functional group is attached.

The substituent effect should be essentially independent of the reaction, whereas it is not always invariant, causing failure of the Hammett linear free energy relationship. The variation of substituent effect would be attributed only to the changes in contribution of the resonance component. The inductive component, the electron distribution through *sigma* bond, should essentially remain constant. The *resonance polar effect* may also be independent of the nature of reactions. However, the resonance component will no longer remain constant in the case of electrophilic reactions. The large electron demand produced at the reaction center of transition state must be delocalized[1-9]. This could be dissipated by the aid of the resonance interactions with electron releasing para substiuents through benzene *pi* orbitals. Then, the resonance effect becomes far greater than the ordinary *resonance polar effect*, σ_R, and σ^+ values result from this reason.

Brown and Okamoto's set of σ^+ may be represented[1]

$$\sigma^+ = \sigma_I + \sigma_R^+ \qquad (3)$$

where σ_R^+ is a resonance effect in the Brown and Okamoto's reference reaction[1,2]. Other authors' sets of σ^+ are also treated in the same manner, although the σ_R^+ are by no means invariant of reactions. In general, the quantity σ_R^+ should be a variable and a function of the resonating capacity of substituent with the electron deficient reaction center through the benzene *pi* electron system. Since σ_I may undoubtedly remain constant through the changes of reaction type[16], the attention could be centered on the changes of σ_R^+. Inductive effect can be eliminated, combining Eqs. 2 and 3

$$\sigma^+ - \sigma = \sigma_R^+ - \sigma_R \equiv G(R) \qquad (4)$$

Here, the quantity $\sigma^+ - \sigma$ should be a function of the resonance effect only, and this quantity just describes the magnitude of respective deviations of para substituents from the meta correlation line. Consequently, it may be anticipated that the analysis of the function $G(R)$ could provide a key to correlate the various sets of σ^+. The formulation of $G(R)$ will be realized practically by tracing changes of the quantity $\sigma^+ - \sigma$.

In actual practice, Brown and Okamoto's and Miller's quantities are plotted linearly against the corresponding quantities of the decomposition of diazoacetophenones, as illustrated in Figs. 2 and 3. These correlations are given by the following equations:

$$(\sigma^+ - \sigma)_{\text{Brown, Okamoto}} = 1.847(\sigma^+ - \sigma)$$

and

$$(\sigma^+ - \sigma)_{\text{Miller}} = 3.185(\sigma^+ - \sigma)$$

The standard deviations of the fits are ± 0.015 and ± 0.007, respectively. Then, the substituent effects in the decomposition of diazoacetophenones can be reproduced

16) R. W. Taft, Jr., in Newman's "Steric Effect in Organic Chemistry", Chapt. 13, John Wiley & Sons, Inc., New York (1956). R. W. Taft, Jr., *J. Am. Chem. Soc.*, **74**, 2729 (1952); ibid., **74**, 3120 (1952); ibid., **75**, 4231 (1953); ibid., **79**, 1045 (1957); R. W. Taft, Jr. and I. C. Lewis, ibid., **80**, 2436 (1958). Y. Yukawa and Y. Tsuno, "Yuki Hannokiko no Shimpo (Recent Advances in the Mechanism of Organic Reactions)", Vol. I, Maki Publishers, Inc., Tokyo (1958), p. 1.

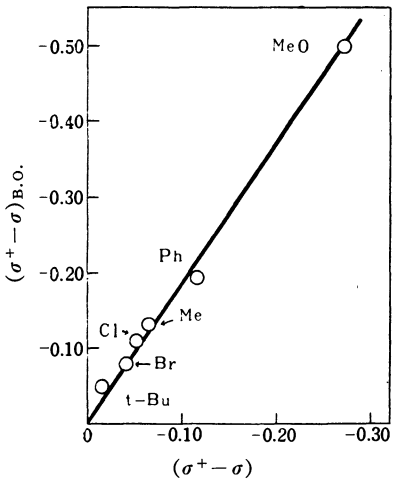


Fig. 2. Plot of Brown and Okamoto's quantity, $\sigma^+-\sigma$, against our quantity.

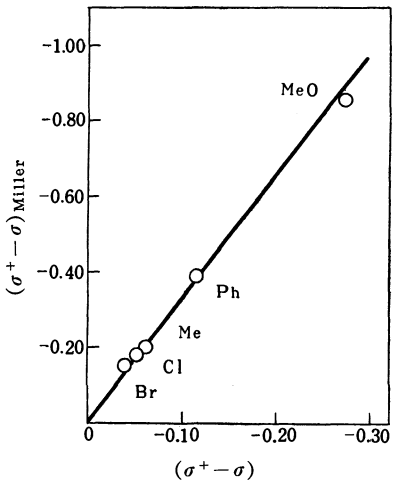


Fig. 3. The correlation between Miller's and our quantities, $\sigma^+-\sigma$.

precisely from various sets of σ^+. This may afford an indirect bit of evidence of our previous discussion of this reaction[3].

Furthermore, strictly linear correlations are observed in respective pairs of other sets of σ^+, as shown clearly in Figs. 4 and 5. These are represented as follows:

$$(\sigma^+-\sigma)_{Brown,\ Okamoto}=0.576(\sigma^+-\sigma)_{Miller}$$

$$(\sigma^+-\sigma)_{Brown,\ Okamoto}=1.347(\sigma^+-\sigma)_{Deno}$$

and

$$(\sigma^+-\sigma)_{Deno}=0.456(\sigma^+-\sigma)_{Miller}$$

The standard deviations are 0.015, 0.002 and 0.025, respectively. Then, these correlations can be held covering a wide range of substituent changes, especially, the last one covers the range from *p*-alkyl to *p*-dimethylamino groups. The same is

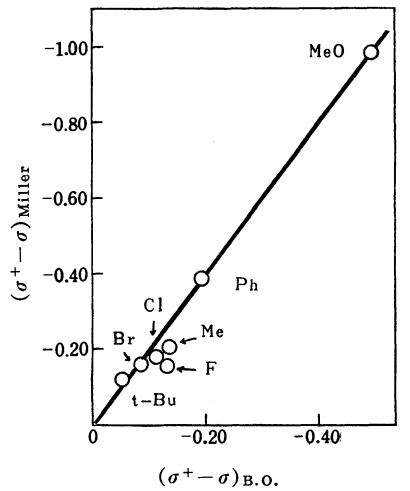


Fig. 4. Correlation of Miller's quantity, $\sigma^+-\sigma$, with Brown and Okamoto's one.

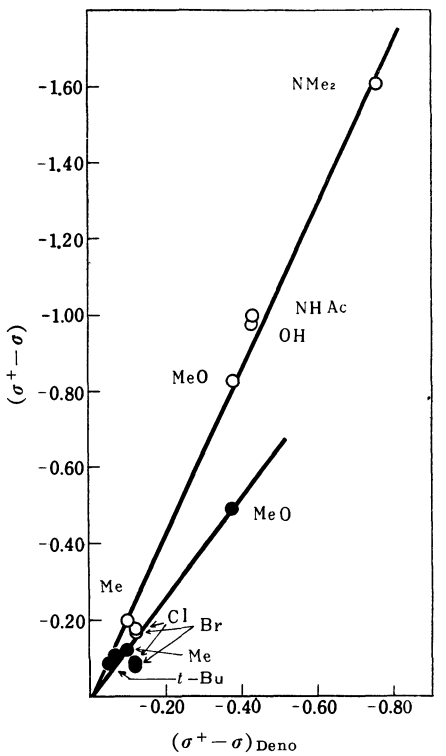


Fig. 5. Correlations of Miller's and Brown and Okamoto's quantities, $\sigma^+-\sigma$, with Deno's one: Open circles, Miller's and closed, Brown and Okamoto's.

true in the case of other sets, such as Packer's[11] and Pearson's[6].

As a conclusion, the function $G(R)$ can be regarded, to a first approximation, as a linear function of the quantity, $\sigma^+-\sigma$. Consequently, the general relationship 5 may be established empirically

TABLE III. CALCULATED VALUE OF BROWN AND OKAMOTO'S σ^+

p-Subst.	Calculated σ^+ value					Exptl.[f] value	Average value	$\sigma^+-\sigma$[h]
	A[a] 1.847[g]	B[b] 0.576[g]	C[c] 1.347[g]	D[d] 0.820[g]	E[e] 0.838[g]	(1.000)		
NMe_2		−1.53	−1.62				−1.60	−1.00
NH_2			−1.40				−1.40	−0.74
NHAc		−0.61	−0.59				−0.60	−0.58
OH		−0.92	−0.91				−0.92	−0.56
CH_3O	−0.765	−0.754	−0.766		−0.729	−0.764	−0.756±0.014[l]	−0.496
C_2H_5O	−0.744						−0.744	−0.494
C_6H_5O		−0.528			−0.559		−0.543	−0.51
CH_3	−0.301[i]	−0.288	−0.305	−0.299	−0.306	−0.306	−0.301±0.006[l]	−0.131
C_2H_5				−0.293	(−0.315)[k]	−0.291	−0.292	−0.141
i-C_3H_7				−0.282		−0.276	−0.279	−0.125
t-C_4H_9	(−0.217)[j]	−0.267	−0.251			−0.250	−0.256±0.010[l]	−0.053
C_6H_5	−0.200	−0.219		−0.177	(−0.240)[k]	−0.179	−0.194±0.020[l]	−0.200
F						−0.071	−0.071	−0.130
Cl	+0.118[i]	+0.122			+0.130	+0.112	+0.121±0.007[l]	−0.106
Br	+0.162	+0.138			+0.154	+0.148	+0.151±0.010[l]	−0.081
I						+0.132	+0.132	−0.144

a) The value calculated on the basis of our σ^+ value (Ref. 3).
b) Calculated from Miller's set of σ^+ (Ref. 10).
c) The value obtained from Deno's set of σ^+ (Refs. 7 and 8).
d) The value on the basis of σ^+ given by Packer et al. (Ref. 11) from the ethanolysis rates of benzhydryl chlorides (E. D. Hughes, C. K. Ingold and N. A. Taher, *J. Chem. Soc.*, **1940**, 949).
e) Calculated from Norris and coworkers' data on the solvolysis of benzhydryl chlorides in absolute ethanol (J. F. Norris and C. Benta, *J. Am. Chem. Soc.*, **50**, 1804 (1928); J. F. Norris and J. T. Blake, ibid., **50**, 1808 (1928): see, the forthcoming paper, (Y. Yukawa and Y. Tsuno, This Bulletin, **32**, 971 (1959).).
f) Brown and Okamoto's σ^+ value (Ref. 1).
g) The r value in the relationship 5; the proportionality constant of the quantity, $\sigma^+-\sigma$, to the corresponding one of Brown and Okamoto.
h) This value should essentially be equal to the difference of Brown and Okamoto's σ^+ from the ordinary Hammett σ constant. This could be regarded as a measure of the resonating power of respective substituents. This has been utilized successfully in regard to the resonance substituent constant, $\Delta\sigma_R^+$, and will be reported in a subsequent paper.
i) The value based on σ^+ obtained in the present study.
j) This group showed deviation from the correlation 5 setting r=1.847, and was omitted from the calculation. Such a deviation was observed in the Pearson's correlation of σ^+ (Ref. 6).
k) This group deviates seriously and was not included in the calculation.
l) Standard deviation.

$$(\sigma^+_A-\sigma)=r(\sigma^+_B-\sigma) \qquad (5)$$

where r is a parameter which remains constant in a reaction series but is a variable of reactions. This parameter may arise without doubt from differing contributions of the resonance effect in reference reactions.

The reliability of the approximation can be substantiated by the close agreement of calculated values on the basis of this relationship with an experimental one. This is clearly exhibited in the comparison of calculated with the experimental values of Brown and Okamoto's σ^+, as shown in Table III. Computed values for respective substituents are in accord with the experimental one, without serious exceptions. The averaged standard deviations of calculated values are estimated to be ±0.009. This is excellent as compared with the agreement of the comparision given by Deno[9], and by Brown and Okamoto[2]. Then, the results in Table III will possibly extend the utility of Brown and Okamoto's set to the substituents having no experimental σ^+ value in their scale.

Through these results, the particular

features of interest have arisen. As mentioned in the above discussion, the quantities $\sigma^+-\sigma$ may be regarded as a function of the resonance capacity of substituents. Therefore, the relationship 5 is in itself a linear resonance energy relationship. The σ^+ values, in turn, could be represented by the following relationship, using a proper set of the quantities $\sigma^+-\sigma$ in a single scale

$$\sigma^+=\sigma+r(\bar{\sigma}^+-\sigma)=\sigma+r\Delta\sigma_R^+$$

where $\bar{\sigma}^+$ is a correct set of σ^+ and $\Delta\sigma_R^+$ represents the standard set of the quantities $\sigma^+-\sigma$. Consequently, electrophilic reactions in general will possibly be correlated by a modified Hammett equation,

$$\log(k/k_0)=\rho(\sigma+r\Delta\sigma_R^+)$$

This has been realized by using the numerical values of $\Delta\sigma_R^+$ in Brown and Okamoto's scale. The utility of this relationship will be described in Part III.

The authors gratefully acknowledge the help of Mr. T. Ibata in the preparation of samples.

Institute of Scientific and Industrial Research
Osaka University
Sakai, Osaka

Resonance Effect in Hammett Relationship. III. The Modified Hammett Relationship for Electrophilic Reactions

By Yasuhide YUKAWA and Yuho TSUNO

(Received January 28, 1959)

As shown in Part II[1] of this series, the substituent constants in Brown and Okamoto's scale were derived for a number of electron releasing para substituents by correlating various sets of σ^+ [2-8]. These values will possibly extend the utility of the Brown and Okamoto's equation[2,10] over a wider range of substituent changes[1,5,10,11]. However, it is clear that the unique set of σ^+ does not always describe the best situation of substituent contributions in various reactions, even though Brown and Okamoto's σ^+ may have an apparent generality. It would be attributed to the changes in availability of the *transition state resonance* in various reactions. The resonance contribution of respective para substituents as well as the magnitude of σ^+ would not be maintained constant but varied from reaction to reaction[1]. Then, the Brown and Okamoto's and also other authors' sets of σ^+ [3-9] should be utilized respectively in the limited extent of reaction series[1,3].

Our success in correlating various sets of σ^+ by Eq. 1[1] appears to imply some suggestions in regard to the Hammett type treatment[12] of electrophilic reactions.

$$(\sigma^+{}_A - \sigma) = r(\sigma^+{}_B - \sigma) \qquad (1)$$

Here r is a proportionality constant, and $\sigma^+{}_A$ represents one of various sets of σ^+ and $\sigma^+{}_B$ another set of σ^+. In a given para substituent, the increments of various σ^+ values relative to the usual σ constant[12]

1) Y. Yukawa and Y. Tsuno, This Bulletin, **32**, 965 (1959).
2) H. C. Brown and Y. Okamoto, *J. Am. Chem. Soc.*, **79**, 1913 (1957); Y. Okamoto and H. C. Brown, *J. Org. Chem.*, **22**, 485 (1957).
3) Y. Tsuno, T. Ibata and Y. Yukawa, This Bulletin, **32**, 960 (1959).
4) N. C. Deno and A. Schriesheim, *J. Am. Chem. Soc.*, **77**, 3051 (1955).
5) N. C. Deno and W. L. Evans, ibid., **79**, 5804 (1957).
6) D. E. Pearson, J. F. Baxter and J. C. Martin, *J. Org. Chem.*, **17**, 1511 (1952); D. E. Pearson and J. D. Burton, ibid., **19**, 957 (1954).
7) J. Miller, *Australian J. Chem.*, **9**, 61 (1956).
8) J. K. Kochi and G. S. Hammond, *J. Am. Chem. Soc.*, **75**, 3445 (1953); G. S. Hammond et al., ibid., **80**, 653, 568, 573 (1958).
9) J. Packer, J. Vaughan and A. F. Wilson, *J. Org. Chem.*, **23**, 1215 (1958).
10) H. C. Brown and Y. Okamoto, *J. Am. Chem. Soc.*, **80**, 4979 (1958).
11) Brown has derived recently the averaged σ^+ values for *p*-NHe_2, *p*-NH_2 and *p*-OH, etc., from σ^+ values of other electrophilic reactions, while the agreement is by no means within satisfactory precision (Ref. 10). Deno's expansion of σ^+ in Brown and Okamoto's scale appears also to be unsuccessful (Ref. 5).
12) L. P. Hammett, *J. Am. Chem. Soc.*, **59**, 96 (1937); "Physical Organic Chemistry", McGraw-Hill Book Co., New York (1940), p. 194; H. H. Jaffé, *Chem. Revs.*, **53**, 191 (1953).

are possibly considered to be a function of its resonance ability. Then, the equation may be a linear resonance energy relationship. Therefore, it appears logical to extend this relationship to general electrophilic reactions combining with Hammett equation[12]. If the above relationship would hold in a variety of electrophilic reactions, the Hammett relationship for electrophilic reactions may be represented empirically according to Eq. 2,

$$\log k/k_0 = \rho(\sigma + r\Delta\sigma_R^+) \qquad (2)$$

where r is a reaction constant describing the degree of the transition state resonance or measuring the magnitude of positive charge to be necessarily stabilized at the transition state, and $\Delta\sigma_R^+$ which corresponds to a proper set of $\sigma^+ - \sigma$ is a substituent constant suggesting the resonating capacity of substituent. From the foregoing point of view, we are free to take one of various sets of the quantities $\sigma^+ - \sigma$ as a proper set of the $\Delta\sigma_R^+$.

The *resonance substituent constant*, $\Delta\sigma_R^+$, is now defined conveniently using the set of quantities $\sigma^+ - \sigma$ in Brown and Okamoto's scale[13]; i.e., the r is taken as unity in Brown and Okamoto's reference reaction, the solvolysis of aryldimethylcarbinyl chlorides in 90% aqueous acetone at 25°C,

$$\Delta\sigma_R^+ \equiv \sigma^+_{\text{Brown and Okamoto}} - \sigma \qquad (3)$$

Eq. 2 is undoubtedly to be satisfied by the reactions to which the Brown and Okamoto's equation was applicable, because the latter equation corresponds to the present Eq. 2 when r is equal to unity. The same is also certain in the electrophilic reactions which are correlated linearly with other sets of σ^+. The second term of Eq. 2 would vanish in the correlation of meta substituents, evidently because the Hammett relationship would hold in general electrophilic reactions as far as the mata substituents are concerned. Accordingly, ρ in Eq. 2 can be replaced by the ρ_{meta} value and the equation may be usually solved on the basis of ρ_{meta} value[14].

An empirical relationship should be required to examine critically the general applicability. Fortunately, in an enormous number of electrophilic reactions, satisfactory results have been realized in terms of this relationship. In the present paper, then, the results of application and generality of this relationship are described.

Correlation of Reactivities

In view of the origin of this relationship, it is a matter of course that the relationship should describe satisfactorily the substituent effect in the respective reference reactions, from which various sets of σ^+ were derived. These are clear in Figs. 1 and 2. The rates of decomposition of ω-diazoacetophenones both in acetic acid at 40.00°C[3] and in 75% aqueous acetic acid at 25.20°C[1] are reproduced strictly in terms of Eq. 2, setting r to be 0.556 and nearly the same value 0.60, respectively.

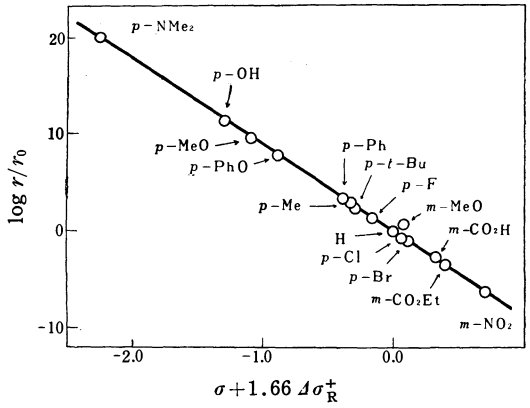


Fig. 1. Relative reactivities in halogenation of monosubstituted benzenes at 25°C (*3*).

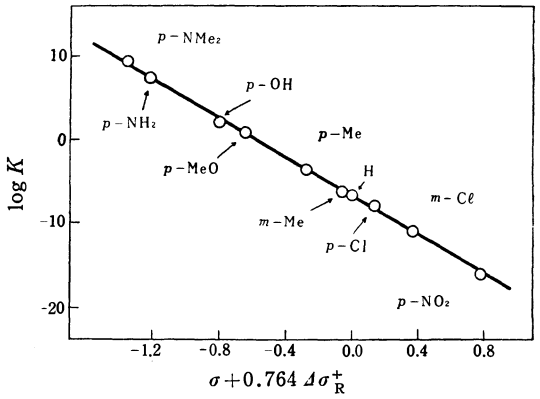


Fig. 2. Dissociation of triphenylcarbinols in sulfuric acid at 25°C (*22*).

13) A tentative set of $\Delta\sigma_R^+$ has been derived on the basis of Deno's reference reaction and applied preliminarily for several electrophilic reactions. [Y. Yukawa and Y. Tsuno, "Yūki Hannōkikō no Shimpo—Recent Advances in the Mechanism of Organic Reactions", (in Japanese) Vol. I, (1958), p. 1.]. However, the present definition of $\Delta\sigma_R^+$ in Brown and Okamoto's scale appears to be more available, in view of its frequent employment encountered in recent literatures.

14) Although various values of σ_{meta}^+ have been given by Brown and others (Refs. 2 and 10), the differences between σ^+_{meta} and σ_{meta} are of magnitude comparable to experimental error. Even if they were significant, the situation of the relationship is unaltered but ρ value must be calculated by solving the regression Eq. 4.

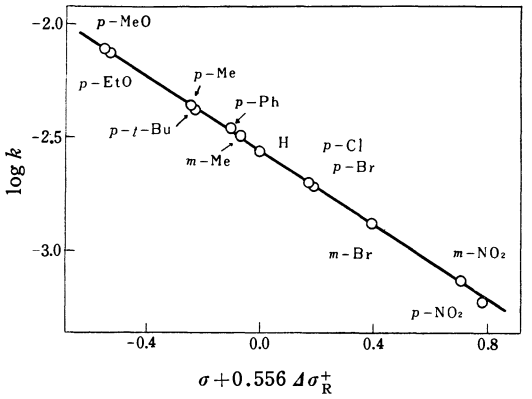


Fig. 3. Decomposition of ω-diazoacetophenones in acetic acid at 40.00°C (*25*).

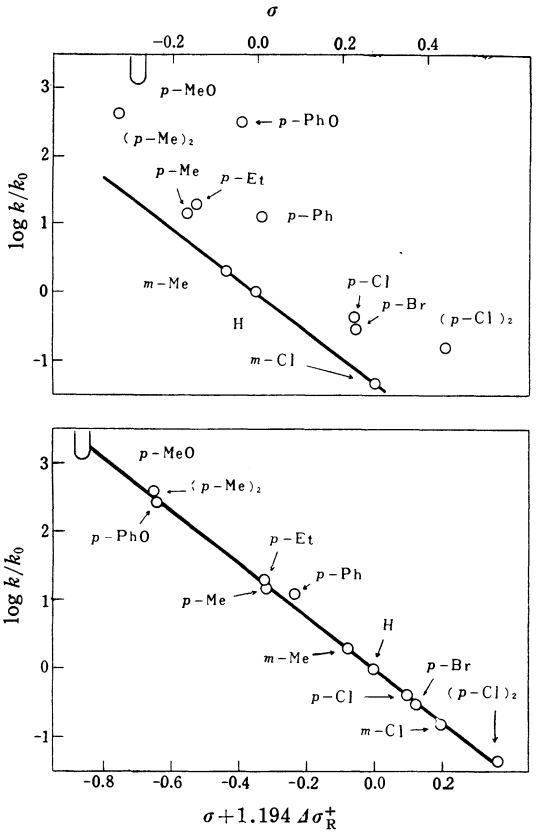


Fig. 4. Ethanolysis of benzhydryl chlorides at 25°C (*10*).

The Pearson's rate data of the Beckmann rearrangement[6] are also correlated in terms of $r=0.434$. The numerical values of $\Delta\sigma_R^+$ used are the one given in Table III of the foregoing paper.

A typical example of electrophilic reactions is the solvolysis of arylalkyl halides. Norris and coworkers[15] reported the ethanolysis rates of benzhydryl chlorides. The Hammett plots of para electron releasing substituents deviate markedly in the upper side of the meta correlation line. With regard to meta substituents, a linear Hammett relationship is obtained, and the slope, ρ_{meta}, is -3.72.

$$\log(k/k_0)_m = -3.72\,\sigma_{meta}$$

Using this ρ value, r is calculated to be 1.194. Then, the rates of the ethanolysis can be expressed by an equation

$$\log k/k_0 = -3.72(\sigma + 1.194\,\Delta\sigma_R^+)$$

In Fig. 4 is demonstrated the fine correlation of $\log k/k_0$ vs. $\sigma+1.194\,\Delta\sigma_R^+$. In the same manner, the rates of ionization of triarylcarbinyl chlorides to form the ion pairs

$$(C_6H_5)_3C\text{-}Cl \rightarrow (C_6H_5)_3C^+//Cl^-$$

in liquid sulfur dioxide[16] are correlated linearly. As is clear in Fig. 5, the correla-

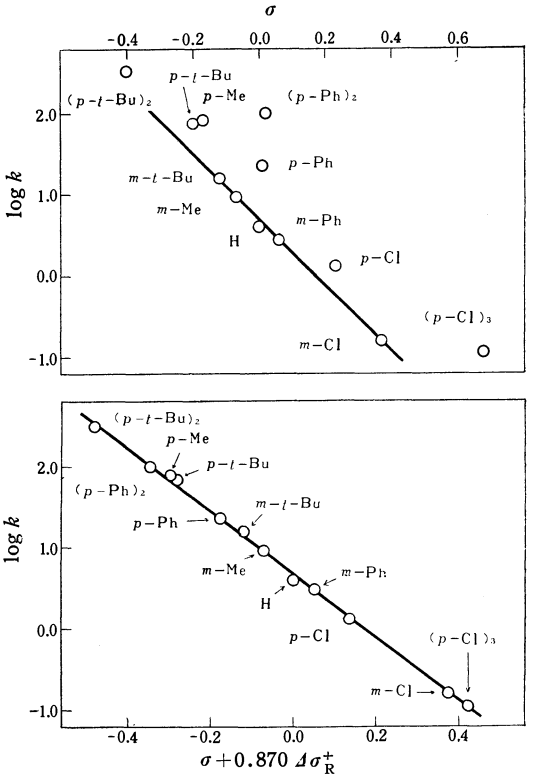


Fig. 5. Dissociations of triphenylcarbinyl chlorides in liquid sulfur dioxide at 0°C (*20*).

15) J. F. Norris and C. Benta, *J. Am. Chem. Soc.*, **50**, 1804 (1928); J. F. Norris and J. T. Blake, ibid., **50**, 1808 (1928).

16) N. N. Lichtin and M. J. Vignale, ibid., **79**, 579 (1957); N. N. Lichtin and P. D. Bartlett, ibid., **73**, 5530 (1951); N. N. Lichtin and H. Glazer, ibid., **73**, 5537 (1951); N. N. Lichtin and H. P. Leftin, *J. Phys. Chem.*, **60**, 164 (1956).

tion is fully satisfactory; $\rho=-4.046$ and $r=0.870$.

At the theoretical ground, the standard of correlation should be based on the meta correlation line, while there are relatively few adequate data which involve the rates of many meta derivatives. For the data involving a few rates of meta derivatives, the correlation is realized by solving the Eq. 4 for a and b on the basis of the method of least squares[17],

$$\log k = a\sigma + b\Delta\sigma_R^+ + \log k_0 \qquad (4)$$

where a and b correspond to ρ and $r\rho$, respectively. In this manner, the solvolysis rates of benzhydryl chlorides in methanol and in isopropanol[18] provide excellent correlations giving $r=1.234$ and 1.350, respectively. Similarly, the dissociation of identically substituted benzhydrols in sulfuric acid at 25°C[5] is correlated linearly in terms of $\rho=-9.112$ and $r=1.175$.

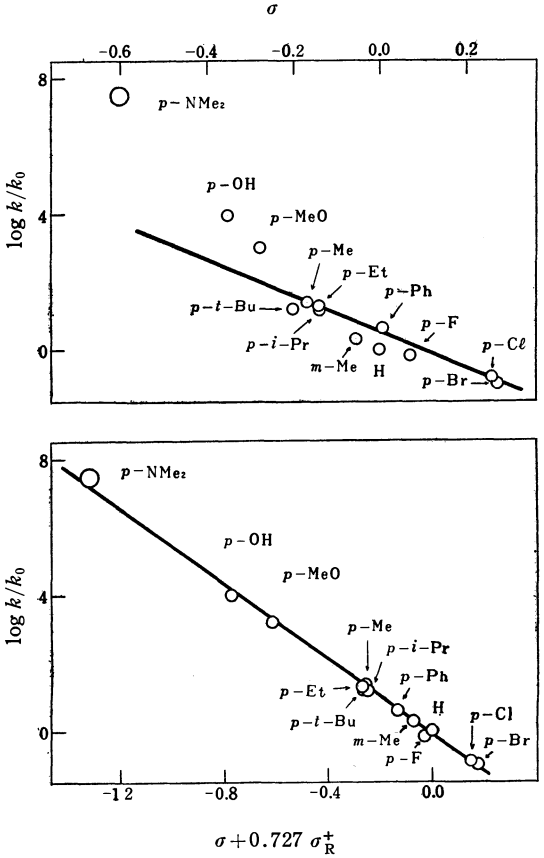


Fig. 6. Protodesilylation of phenyltrimethylsilanes (*23*).

The present treatment is successful not only in the solvolysis but in other types of electrophilic reactions, such as aromatic electrophilic substitutions. Recent data of the nitration[19] and the halogenation[6,20] of substituted benzenes, and protonolysis

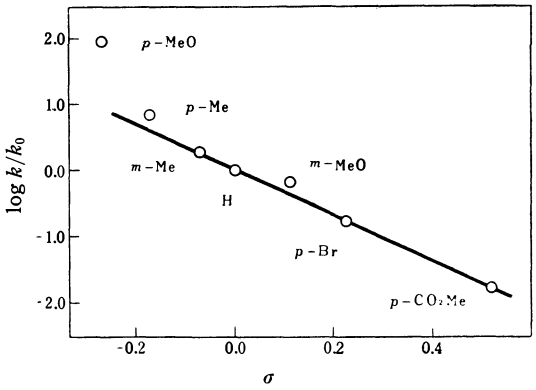


Fig. 7—a. Acetolysis of neophyl brosylates at 70°C (*27*).

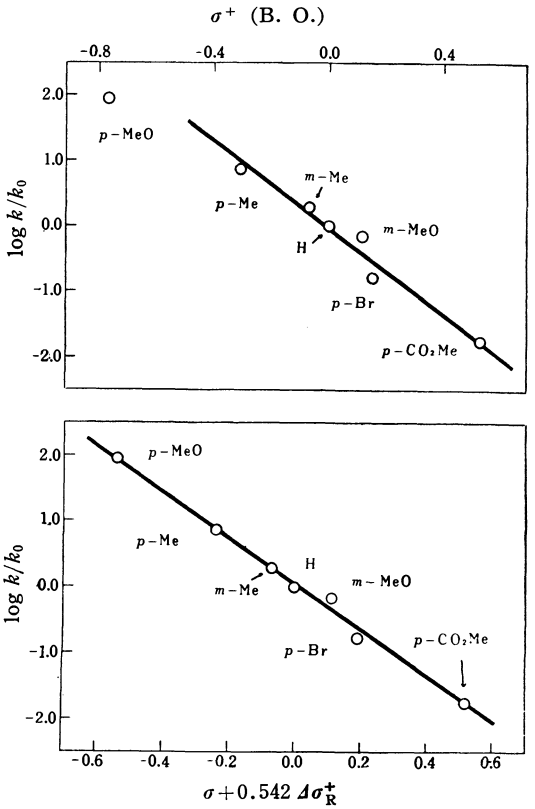


Fig. 7—b. Acetolysis of neophyl brosylates at 70°C (*27*).

17) C. A. Bennett and N. L. Franklin, "Statistical Analysis in Chemistry and the Chemical Industry", John Wiley & Sons, Inc., New York (1954), p. 245.
18) S. Altscher, R. Baltzly and S. W. Blackman, *J. Am. Chem. Soc.*, **74**, 3649 (1952).
19) J. D. Roberts et al., ibid., **76**, 4525 (1954).
20) a) P. B. D. de la Mare, *J. Chem. Soc.*, **1954**, 4450; b) P. B. D. de la Mare and J. T. Harvey, ibid., **1956**, 36; ibid., **1957**, 131; P. B. D. de la Mare and M. Hassan, ibid., **1957**, 3004.

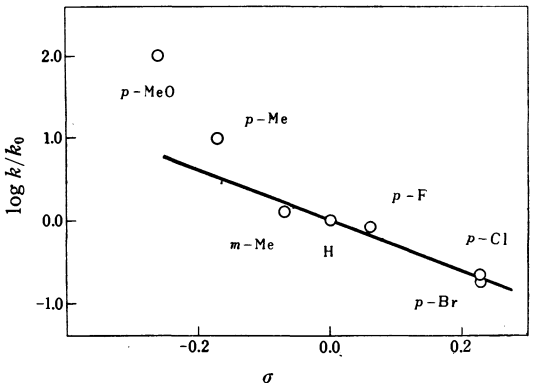


Fig. 8—a. Rearrangement of phenylpropenylcarbinols (*32*).

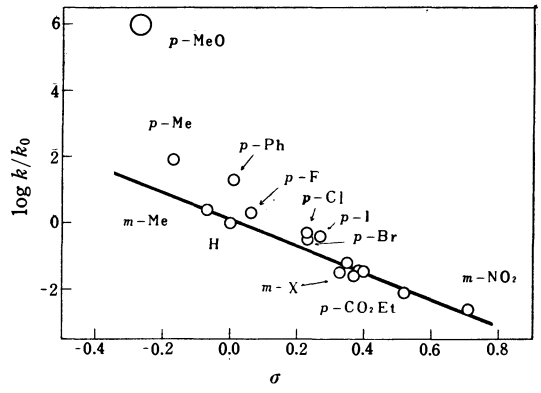


Fig. 9—a. Brominolysis of benzeneboronic acids (*2*).

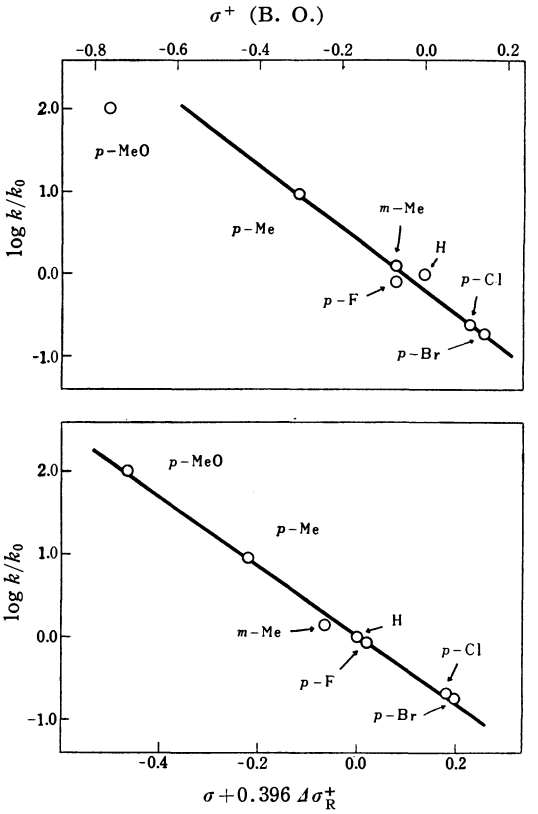


Fig. 8—b. Rearrangement of phenylpropenylcarbinols (*32*).

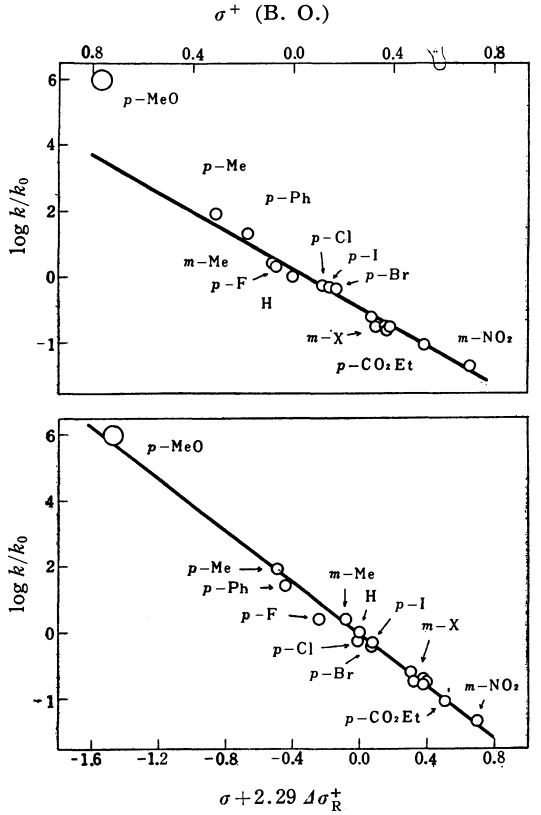


Fig. 9—b. Brominolysis of benzeneboronic acids (*2*).

of phenyltrimethylsilanes[21] (Fig. 6) are described satisfactorily. In the reactions quoted above, the Brown and Okamoto's relationship also results apparently but not strictly linear figures. This may be in accord with the fact that the r factors of these are considerably close to unity (see, Table I).

Recently, Winstein and coworkers[22] reported that the rates of acetolysis of neophyl brosylates failed to give a good result by the Hammett treatment, and also that the correlation was slightly improved by the Brown and Okamoto's. According to the latter treatment, para electron releasing groups fall below the meta line, contrary to the results of the

21) C. Eaborn, ibid., **1956**, 4858.

22) R. Heck and S. Winstein, *J. Am. Chem. Soc.*, **79**, 3432 (1957).

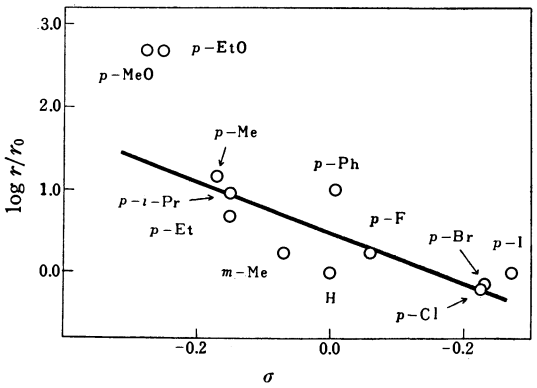


Fig. 10—a, Migratory aptitudes in the pinacol rearrangement (*4*).

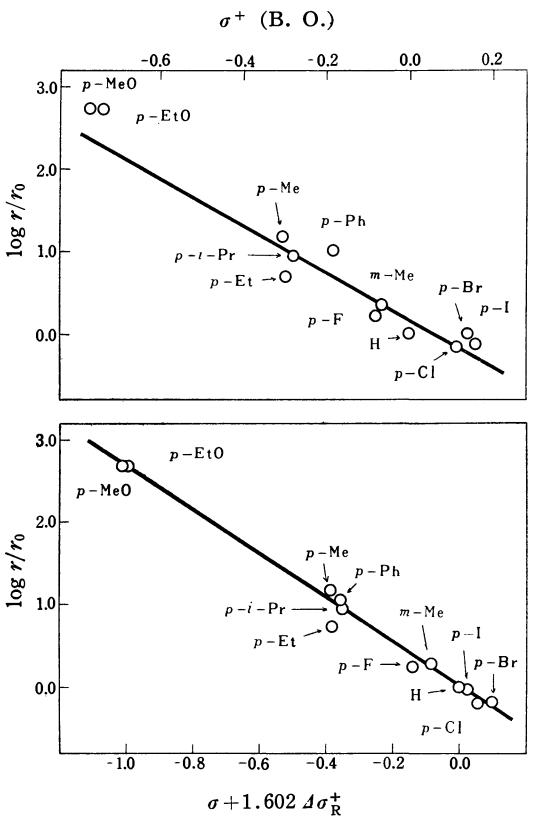


Fig. 10—b. Migratory aptitudes in the pinacol rearrangement (*4*).

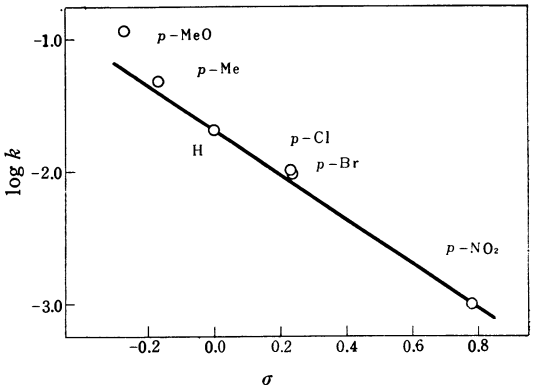


Fig. 11—a. Epoxidation of *cis*-dimethylstilbenes at 30°C (*33*).

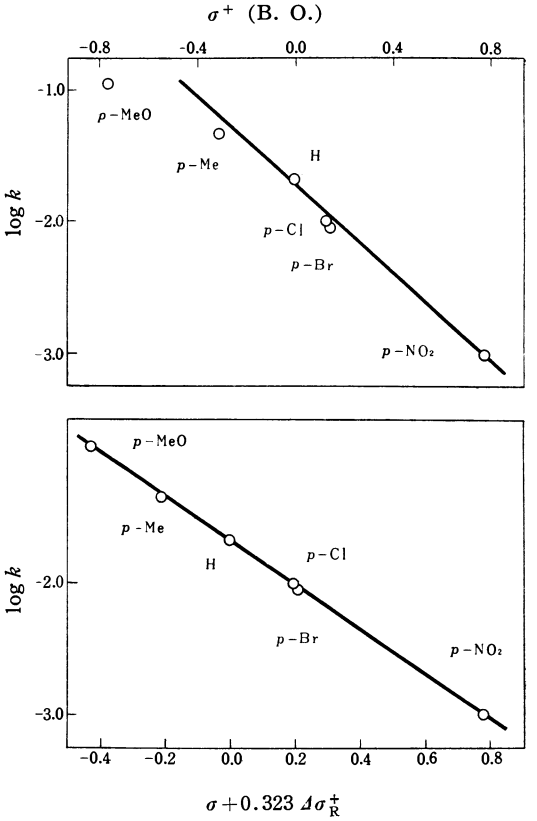


Fig. 11—b. Epoxidation of *cis*-dimethylstilbenes at 30°C (*33*).

Hammett one. However, the present treatment produces a successful figure (Fig. 7) of this reaction, in terms of $r=0.542$. The Beckmann rearrangement of acetophenonoxime picrylethers[23] is correlated with Eq. 2, giving r to be 0.469, although the plot against Brown and Okamoto's σ^+ concaves downward. The rates of the rearrangement of phenylpropenylcarbinols[24] are of the same kind ($r=0.396$), as seen in Fig. 8. The resonance contribution of substituents in these reactions is estimated to be only a half of that in Brown and Okamoto's reference reaction. Therefore, it is natural that Brown and Okamoto's treatment overestimates the

23) R. Huisgen, J. Witte, H. Walz and W. Jira, *Ann.*, **604**, 191 (1957).

24) E. A. Braude and E. S. Stern, *J. Chem. Soc.*, **1947**, 1096.

TABLE I. RESULTS OF APPLICATION OF THE PRESENT RELATIONSHIP

No.	Reaction	ρ	r	s[a]	n[b]	Reference
1	Solvolysis of phenyldimethylcarbinyl chlorides in 90% aqueous acetone at 25°C	−4.518	1.000	0.093	21	2, *d*, *e*
2	Brominolysis of the benzeneboronic acids in 20% acetic acid and 0.40 M sodium bromide at 25°C	−3.84	2.29	0.313	16	25, *c*, *f*
3	Halogenation of substituted benzenes at 25°C	−8.82	1.660	0.414	15	7, *c*
4	Migratory aptitudes in the pinacol rearrangement of symmetrically substituted tetraarylpinacols	−2.523	1.602	0.120	12	26, *d*, *g*
5	Dissociation of monosubstituted benzhydrols in sulfuric acid at 25°C	−5.236	1.492	0.023	7	4, 5, *d*
6	Epoxidation of stilbenes with phthaloyl peroxide in tetrachloromethane at 80°C	−1.630	1.388	0.034	7	27, *c*, *h*
7	Solvolysis of benzhydryl chlorides in isopropyl alcohol at 25°C	−4.004	1.350	0.070	6	18, *d*
8	Solvolysis of benzhydryl chlorides in methanol at 25°C	−4.022	1.234	0.110	6	18, *d*
9	Solvolysis of benzhydryl chlorides in ethanol at 25°C	−4.140	1.198	0.095	10	9, 30, *c*, *j*
10	Solvolysis of benzhydryl chlorides in ethanol at 25°C	−3.721	1.194	0.087	12	15, *c*, *i*
11	Dissociation of identically disubstituted benzhydrols in sulfuric acid at 25°C	−9.112	1.175	0.335	8	4, 5, *d*, *k*
12	Rearrangement of α-phenylethyl chlorocarbonates in dioxane at 70°C	−3.060	1.166	0.048	5	31, *d*
13	Bromination of benzenes by hypobromous acid and perchloric acid in 50% aqueous dioxane at 25°C	−5.276	1.145	0.080	7	20b, *d*, *l*
14	Rearrangement of α-phenylethyl chlorocarbonates in toluene at 80°C	−2.808	1.138	0.117	5	31, *d*
15	Chlorination of benzalacetophenones	−3.413	1.128	0.033	4	32, *c*
16	Solvolysis of monohalobenzhydryl chlorides in 70% aqueous acetone at 25°C	−4.118	1.007	0.023	5	33, *d*
17	Migratory aptitudes in the Schmidt rearrangement of diphenylethylenes	−2.77	0.90	0.10	6	34, *c*
18	Reactivities of substituted benzenes toward nitration in nitromethane or acetic acid at 25°C	−6.377	0.897	0.327	12	19, *c*, *m*
19	Solvolysis of triphenylcarbinyl chlorides in 40% ethanol/60% ethyl ether at 0°C	−2.52	0.88	0.132	8	35, *c*, *n*
20	Dissociation of triphenylcarbinyl chlorides in liquid sulfur dioxide at 0°C	−4.046	0.870	0.101	12	15, *c*, *o*
21	Basicities of monosubstituted azobenzenes	−2.293	0.853	0.100	11	36, *c*
22	Equilibrium constants for carbonium ions from triphenylcarbinols in sulfuric acid at 25°C	−11.73	0.764	0.335	10	4, 5, *d*
23	Phenyltrimethylsilanes with perchloric acid in 72% aqueous methanol at 50°C	−5.597	0.727	0.125	13	21, *d*, *p*
24	Epoxidation of *trans*-stilbenes by perbenzoic acid at 30°C	−1.055	0.713	0.029	9	28, *c*
25	Acid catalyzed decomposition of ω-diazoacetophenones in acetic acid at 40°C	−0.823	0.556	0.008	12	1, 3, *d*, *q*
26	Acid catalyzed decomposition of ω-diazoacetophenones in 75% aqueous acetic acid at 25.20°C	−1.222	0.603	0.025	10	1, *d*, *r*
27	Acetolysis of neophyl brosylates at 70°C	−3.384	0.542	0.077	7	22, *c*
28	Diels-Alder reactions of phenylbutadienes with maleic anhydride in dioxane at 45°C	−0.711	0.475	0.038	5	37, *c*
29	The Beckmann rearrangement of acetophenone oxime picrylethers in dichlorbutane at 70°C	−4.243	0.464	0.233	12	1, 23, *d*
30	The Beckmann rearrangement of acetophenone oximes in 94.5% sulfuric acid at 50.9°C	−1.983	0.434	0.044	9	6, *c*
31	Decomposition of diphenylmethylcarbinyl azides in acetic acid/sulfuric acid at 25°C	−2.092	0.436	0.072	7	38, *d*
32	Rearrangement of phenylpropenylcarbinols in 60% aqueous dioxane at 30°C	−4.056	0.396	0.080	7	24, *d*
33	Epoxidation of *cis*-dimethylstilbenes in benzene at 30°C	−1.692	0.323	0.020	6	29, *c*

34	Epoxidation of *trans*-dimethylstilbenes in benzene at 30°C	−1.554	0.249	0.035	6	29, *c*
35	Diphenyldiazomethanes with benzoic acid in toluene at 25°C	−1.570	0.190	0.036	12	39, *c*

a) The standard deviation of experimental points from the regression line.
b) The number of points involved in the calculation.
c) The correlation obtained on the basis of ρ_{meta} value which were derived from the rates for meta substituted and nonconjugating para substituted derivatives.
d) The correlation obtained in aid of Eq. 4.
e) The correlation obtained by setting a priori $r=1.000$.
f) The correlation of $r=2.05$ and $\rho=-4.31$ was resulted on the basis of Eq. 4.
g) *m*-Methoxy group was omitted from the correlation.
h) The point of *p*-carbethoxy group deviates considerably from meta line and was not included in the calculation of ρ_{meta} value.
i) The point for *p*-*t*-butyl group deviates seriously and was omitted from the calculation of *r* value.
j) *p*-Phenyl group supplies a greater driving force than that expected from this correlation.
k) *p*-Dimethylamino and *p*-phenyl groups were not included in the calculation.
l) *m*-*t*-Butyl group was not included in the calculation and experimental value of −0.078 was resulted for σ_{meta} of this group.
m) Points for meta derivatives deviate from the ρ_{meta} line.
n) *p*-Fluoro group deviates significantly.
o) σ value of +0.06 was employed for *m*-phenyl group. Trisubstituted derivatives were omitted from the calculation, since the cross conjugation effect appeared to be possibly involved.
p) Excepting *p*-dimethylamino and *p*-hydroxy groups, was obtained the partial correlation; $r=0.622$, $\rho=-5.535$ and $s=\pm0.026$. $\Delta\sigma_R^+$ values for these groups were calculated on the basis of this correlation; −1.20 for *p*-dimethylamino and −0.60 for *p*-hydroxy groups.
q) On the basis of ρ_{meta} value of −0.830, *r* value of 0.539 was obtained.
r) *p*-Phenyl group was not included in the calculation.

situation in these reactions. The same is true in the case of the decomposition of diazoacetophenones, as mentioned in the foregoing papers[1,3].

Conversely, the plots against Brown and Okamoto's σ^+ remain to be concaved upward in the brominolysis rates of benzeneboronic acids[25] and the migratory aptitudes of tetraphenyl pinacols[26], to the contrary, the present treatment exhibits fine correlations, whose *r* values are 2.29 and 1.60, respectively. These are the reverse of that mentioned above.

The curved correlation with Brown and Okamoto's σ^+ is fairly often observed in other reaction series, in accordance with the view that the availability of resonance contribution of para substituents is varied to a considerable extent by the changes of reaction series. Recently, Greene pointed out[27] that the rates of epoxidation of *trans*-stilbenes with phthaloyl peroxide satisfied the Brown and Okamoto's relationship. According to the present treatment, this reaction provides a fine figure of $r=1.388$. Similarly, the oxidation with perbenzoic acid is successful in terms of $r=0.713$[28]. Furthermore, the perbenzoic acid oxidation of *cis*- and *trans*-dimethylstilbenes[29] exhibits excellent correlations giving *r* of only 0.2∼0.3, in contrast with the failure of the Brown and Okamoto's. Fig. 11 demonstrates the correlation of

25) H. G. Kuivila and A. R. Hendrikson, *J. Am. Chem. Soc.*, **74**, 5068 (1952); H. G. Kuivila and C. E. Benjamin, ibid., **77**, 4834 (1955).
26) W. E. Bachmann and F. H. Mosher, ibid., **54**, 1124 (1932); W. E. Bachmann and J. W. Ferguson, ibid., **56**, 2081 (1934).
27) F. D. Greene and W. W. Rees, ibid., **80**, 3432 (1958).
28) B. M. Lynch and K. H. Pausacker, *J. Chem. Soc.*, **1955**, 1525.
29) O. Simamura, Private communication. The authors are indebted to Professor O. Simamura who kindly made his data available to us prior to publication.
30) E. D. Hughes, C. K. Ingold and N. A. Taher, *J. Chem. Soc.*, **1940**, 949.
31) K. B. Wiberg and T. M. Skryne, *J. Am. Chem. Soc.*, **77**, 2774 (1955).
32) H. P. Rothbaum, I. Ting and P. W. Robertson, *J. Chem. Soc.*, **1948**, 980.
33) C. K. Ingold, "Structure and Mechanism in Organic Chemistry", Cornell University Press, Ithaca, N. Y. (1953), p. 332.
34) S. N. Ege and K. W. Sherk, *J. Am. Chem. Soc.*, **75**, 354 (1953).
35) A. C. Nixon and G. E. K. Branch, ibid., **58**, 492 (1936).
36) H. H. Jaffé and R. W. Gardner, ibid., **80**, 319 (1958).
37) E. J. DeWitt, C. T. Lester and G. A. Ropp, ibid., **78**, 2101 (1956).
38) C. H. Gudmunsen and W. E. McEwen, ibid., **79**, 329 (1957).
39) C. K. Hancook, R. F. Gilby, Jr. and J. S. Westmoreland, ibid., **79**, 1917 (1957).

oxidation of the *cis*-dimethylstilbenes in benzene at 30°C, with Brown's and the present equations.

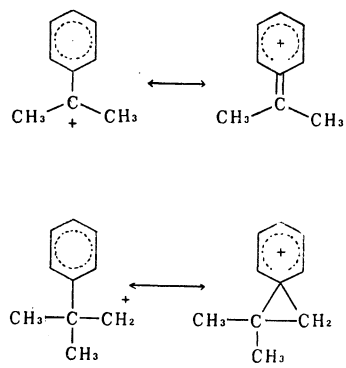
Discussion

As measured by the standard deviations, the fit is as excellent as that seen in the representative Hammett correlation[12]. It is also clear that the present relationship describes rather precisely or is applicable to a greater extent of electrophilic reactions than the Brown and Okamoto's.

According to the results, r varies over a wide range from 0.2 to 2.3 with respect to the change in reaction, and ρ also from -12 to -0.6. Furthermore, it is significant that the magnitudes of $\Delta\sigma_R^+$ are maintained precisely constant with large variation of ρ and r values. The r and ρ values obtained through Eq. 4 are usually equal within experimental uncertainty to those obtained on the basis of meta correlation line.

In comparison with Brown and Okamoto's results[2,10], the following facts may be pointed out. Brown and Okamoto's ρ^+ values appear to be somewhat more negative than ρ of the present paper, in the reactions giving r values greater than unity. Conversely, they are less negative than the present one when $r<1$. Considering that the present ρ values are identified with the corresponding ρ_{meta} values, it is clear that Brown and Okamoto's equation over- or under-corrects the validity of resonance contribution in these reactions. Only in the reactions having r within 0.7~1.3, the Brown and Okamoto's equation would be apparently successful. This indicates the limitation of the application of Brown and Okamoto's relationship[40]. The application for the reactions far out of the limitation would involve the possibility to lead to some erroneous conclusion. However, a relatively large number of reaction series in the literature appears to be involved in the region of r within 0.7~1.3. Then, the Brown and Okamoto's relationship would be applicable to a considerable extent of reaction series at the practical ground[2,10].

The modified Hammett relationship proposed in this paper involves an additional parameter and variable. The former is defined as a resonance parameter for a given substituent, but the latter is merely a proportionality constant in view of the origin of this equation. Accordingly, it is of interest and necessary to know the character of the latter quantity. Although both ρ and r are varied significantly with respect to the change in reaction series, the variation of r value does not appear to be dependent upon the change in ρ value. In the Beckmann rearrangement of acetophenonoximes in sulfuric acid (*30*)[6] and that of oxime picrylethers in dichlorobutane (*29*)[23], ρ differs greatly but r exhibits an identical value. The identical r value may give a good account of the close similarity of both transition states regardless of the different leaving groups and reaction conditions, while, little is described on the transition state model by the different ρ values. In the solvolysis of aryldimethylcarbinyl chlorides[2] and neophyl brosylates[22], the change in r is significant relative to the change in ρ. This may interpret plausibly the different modes of the resonance stabilizations of both transition states.



Therefore, it might be acceptable to say that the r would be a parameter characteristic of the structure of the possible transition state model as well as a parameter measuring the availability of the transition state resonance. As seen in Table I, approximately constant r of 1.2 is given for the reaction series to produce benzhydryl carbonium ions, and r of about 0.8 for those to produce trityl carbonium ions. The relatively small fluctuation would be presumably within experimental uncertainty. Unfortunately, few data are available in the literature to examine this concept more precisely.

40) The reactions quoted by Brown and Okamoto contains the reactions giving r less than 0.6 or more than 1.5. The standard deviations of these are slightly large, but the significant trend of curvature would not always parallel the standard deviation. It is evidently suggested by the difference between ρ^+ resulted and ρ_{meta} values.

The remaining subject of interest will be the theoretical consideration of the present relationship 2, and then the resonance substituent constant, $\Delta\sigma_R^+$.

The substituent effect would be considered to consist of inductive and resonance components[41,42], and the σ constant defined by Hammett is usually expressed by Eq. 5 [2,41,42],

$$\sigma = \sigma_I + \sigma_R \quad (5)$$

where σ_I is the inductive effect and σ_R is the resonance polar effect[42] of the substituent. Recently, Taft has evaluated the σ_I values by modifying his σ^* values for aliphatic series[42,43] on the basis of the Roberts' σ' scale[44], and the σ_R values by subtracting the σ_I values from the corresponding Hammett σ constants. It is well known that the substituent constant would not always be independent of the reaction nature. This would be referred to differing contributions of the resonance component of substituent effect[41], independently of the inductive component.

Furthermore, Taft has suggested that the linear free energy relationship would hold as far as the inductive component of reactivity is concerned[45].

Consequently, the Hammett equation may be expressed by Eq. 6,

$$\log k/k_0 = \rho_I\sigma_I + \boldsymbol{R} \quad (6)$$

In theory, the linear free energy relationship should suffice for the respective one of several components of substituent contribution[46]. If the residual $\boldsymbol{R}$, $\log k/k_0 - \rho_I\sigma_I$, consists of only the resonance contribution, the linear resonance energy relationship may be predictable in regard to the quantity, $\log k/k_0 - \rho_I\sigma_I$.

$$\log k/k_0 - \rho_I\sigma_I = \boldsymbol{R} = \rho_R\bar{\sigma}_R \quad (7)$$

where ρ_R is a reaction constant and $\bar{\sigma}_R$ is a proper parameter representing the resonating capacity of the substituent. Eq. 7 can be rewritten as Eq. 8,

$$\log k/k_0 = \rho(\sigma_I + q\bar{\sigma}_R) \quad (8)$$

where $\rho = \rho_I$ and $q = \rho_R/\rho_I$.

Here, $\bar{\sigma}_R$ should be essentially identical with σ_R in Eq. 5 since the $\bar{\sigma}_R$ corresponds to σ_R in the representative Hammett correlations. This relationship may be reasonably adopted also to electrophilic reactions.

On the other hand, the present equation can be formulated as Eq. 9,

$$\log k/k_0 = \rho(\sigma_I + \sigma_R + r\Delta\sigma_R^+) \quad (9)$$

Combining Eqs. 8 and 9, Eq. 10 is derived.

$$q\bar{\sigma}_R = \sigma_R + r\Delta\sigma_R^+ \quad (10)$$

Then, the linear relationship 11 must be derived, considering $\bar{\sigma}_R$ is identical with σ_R in Eq. 5,

$$\Delta\sigma_R^+ = q'\sigma_R \quad (11)$$

where q' is equal to $(q-1)/r$

The exact value of σ_R is difficult to evaluate, but it is logical to replace conveniently the theoretical values by the corresponding Taft's one. In practice, using the Taft's values instead of the σ_R, an apparently linear plot of $\Delta\sigma_R^+$ is provided, as shown in Fig. 12; given q' is equal to 0.962, the standard deviation of the fit being 0.121. If the Taft's σ_R value could describe suitably the σ_R component, it might be possible to realize generally the linear resonance energy relationship

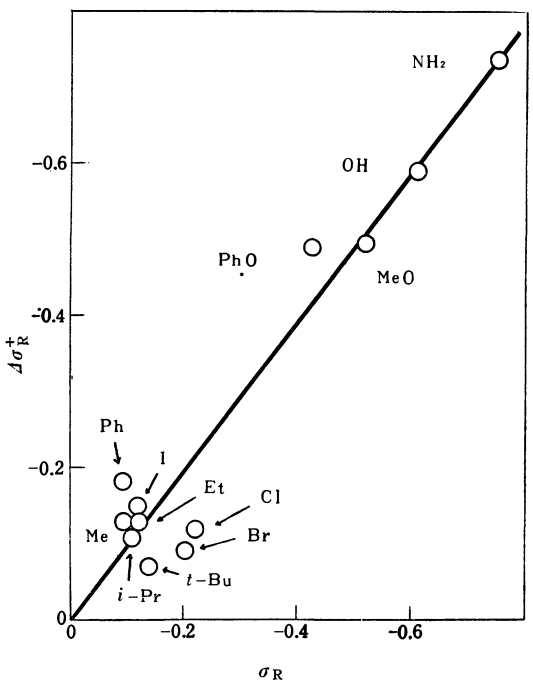


Fig. 12. Correlation of $\Delta\sigma_R^+$ with Taft's σ_R values.

41) The contributions of other specific effects such as solvation and bond energy effects are also involved but they are usually small relative to the above components.

42) R. W. Taft, Jr., in Newman's "Steric Effect in Organic Chemistry", Chapt. 13, John Wiley & Sons, Inc., New York (1956).

43) R. W. Taft, Jr., *J. Am. Chem. Soc.*, **74**, 2729 (1952); ibid., **74**, 3120 (1952); ibid., **74**, 4231 (1953).

44) J. D. Roberts and W. T. Moreland, Jr., ibid., **75**, 2167 (1953).

45) R. W. Taft, Jr., ibid., **80**, 2436 (1958).

46) Y. Yukawa and Y. Tsuno, see the *refrence* under Ref. 13; G. E. K. Branch and M. Calvin, "Theory of Organic Chemistry", Prentice-Hall, Inc., New York (1941), p. 192.

7, therefore, the general Hammett relationship 8. Then, it might be also possible to derive the unique set of σ_R and σ_I on the basis of the present results. However, Taft's σ_R value is by no means excluded from discussion, even though it may be acceptable from a theoretical standpoint. It is a question, at first, whether the Roberts' σ' scale may correspond strictly to that of the inductive effect in benzene system or not. The uncertainty of σ^* increasingly remains in his σ_I value, and must be accumulated in his σ_R value. Furthermore, the actual correlation of electrophilic reactions with his parameters is of considerably poorer precision[47]. On the other hand, $\Delta\sigma_R^+$ stands on a reasonable assumption that the increment of σ^+ relative to σ constant is attributed only to the resonance contribution. The uncertainty derived into this parameter may be entirely referred to only the experimental error of Brown and Okamoto's σ^+.

From these viewpoints, the general Hammett relationship with the parameters derived from $\Delta\sigma_R^+$, if possible, appears to be far more reliable than that with Taft's σ_I and σ_R values. However, it is the generality of Eq. 2, then the $\Delta\sigma_R^+$, that must be settled first. Unfortunately, further examination of the generality is limited by the lack of adequate data in literatures. The adequate literature data which contain rates of many meta derivatives constitute only one third of the data quoted in Table I. Without these reactions, the correlation obtained on the basis of Eq. 4 can not be referred to any standard of correlation such as meta line, although these are believed to be the best descriptions of their respective situations. Moreover, the utilities of $\Delta\sigma_R^+$ values for substituents more negative than *p*-methoxyl group have been scarcely examined at all. Then, the adequate data are highly desirable.

However, the excellent fit of the present relationship for 35 reaction series may be taken to be sufficient support for regarding this as a general relationship. Further investigations now in progress will be reported in forthcoming papers.

Institute of Scientific and Industrial Research
Osaka University
Sakai, Osaka

47) This conclusion is independent of Taft's results (Ref. 45). According to his result in the latest paper on the correlation of Brown and Okamoto's reference reaction, remarkable deviations are observed for *p*-CH_3O and *p*-F derivatives. Full discussion will be made in a proceeding paper, although his treatment disagrees with our concept.

Investigation on Mixed Complexes. II[1]. *Cyano Complexes of Copper and Nickel*

By Sigeo KIDA

(Received October 13, 1958)

A number of studies[2] have been made on the successive formation constants ($k_1, k_2, k_3,\ldots\ldots$) in a solution of metallic complexes, and it was found[3] that in any complex the ratio of the formation constants ($k_1 : k_2 : k_3\ldots\ldots$) is not far different from the statistically expected one, except in some special cases. Furthermore, recent studies of Watters et al.[4], Marcus[5], Yamatera[6] and the present author[1] have shown that the mixed complexes are formed generally in the statistical way.

These facts seem to imply that in a metallic complex the strength of a co-ordination bond is not seriously influenced

1) Part I of this series: S. Kida, This Bulletin, **29**, 809 (1956).

2) For instance, J. Bjerrum, "Metal Ammine Formation in Aqueous Solution", P. Haase and Son, Copenhagen (1941).

3) J. Bjerrum, *Chem. Revs.*, **46**, 381 (1950).

4) J. I. Watters, A. Aaron, and J. Mason, *J. Am. Chem. Soc.*, **75**, 5212 (1953); R. DeWitt and J. Watters, ibid., **76**, 3810 (1954).

5) Y. Marcus, *Acta Chem. Scand.*, **11**, 339, 599, 610, 811 (1957).

6) H. Yamatera and K. Ohashi, Presented at the Symposium on the Co-ordination Compounds, Nagoya, Japan (1957).

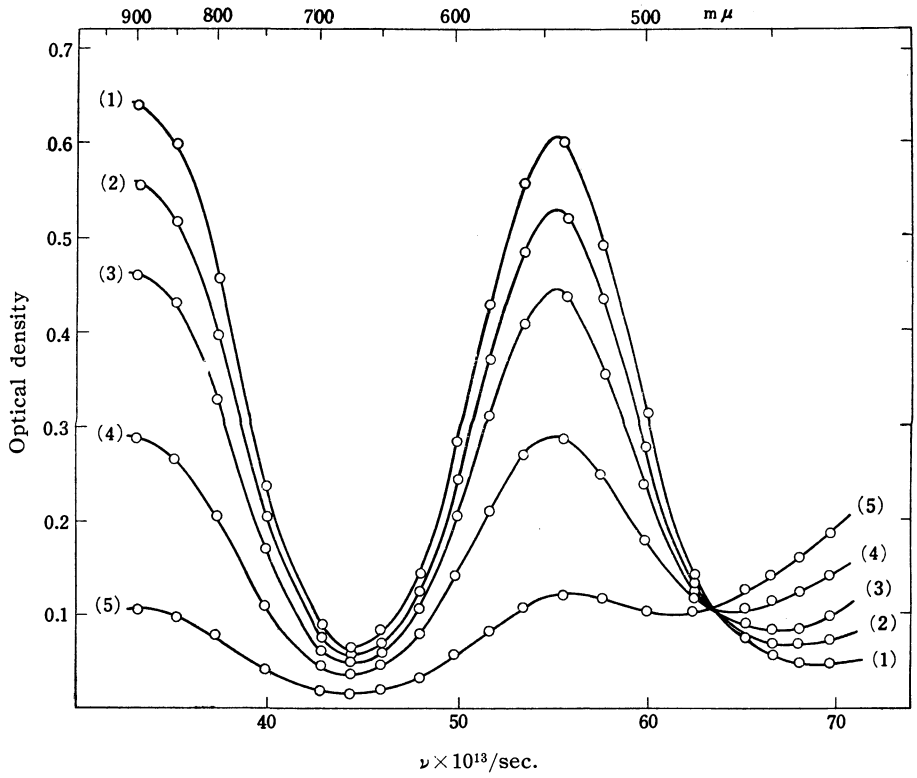


Fig. 1.

by the neighboring ligand; e. g., the strength of the Cu–N bonds are nearly constant in the two complexes, $[Cu\,en_2]^{2+}$ and $[Cu\,en\,C_2O_4]$.

However, it also should be noted that there are many cases in which the formations of the mixed complexes seem not to obey the above-mentioned statistical rule. For instance, the mixed cyano complexes known hitherto are few[7], and difficult to be prepared; this fact would be regarded as suggesting that at least in some cases mixed cyano complexes are not able to be formed or, if it is possibe, they have a strong tendency to be transformed into a complex having only the cyanide ions as ligands. Unfortunately, there is no satisfactory explanation for this phenomenon, since no systematic investigation has ever been made on the conditions leading to the formation of mixed cyano complexes.

This paper will give a report of the investigation which was made for the purpose of getting a clue to this problem.

Results and Discussion

$[Ni\,en_2]^{2+}+CN^-$.—It is well known that the tris-ethylenediamine nickel(II) ion has octahedral configuration, while the tetracyano nickelate(II) ion the planar one. However, it is quite uncertain whether mixed complexes, $[Ni\,en_2(CN)_2]$ and $[Ni\,en(CN)_2]$, which should be closely related to the above-mentioned, can be formed, or not. At first, an attempt, therefore, has been undertaken to clarify this question*.

A sodium cyanide solution was added to a solution of tris-ethylenediamine nickel(II) perchlorate in the ratio as indicated

TABLE I. THE COMPOSITION OF SOLUTIONS

Solution number	(1) cc.	(2) cc.	(3) cc.	(4) cc.	(5) cc.	(6) cc.
0.2 F $[Ni\,en_3](ClO_4)_2$ and 0.1 M en	10	10	10	10	10	10
1.096 F NaCN	0	1	2	4	6	8
Water	10	9	8	6	4	2

7) J. C. Bailar, "The Chemistry of the Coordination Compounds", p. 87; "General Survey", Reinhold Publ. Co., New York (1956).

* Ammine-cyano-nickel(II) compounds, such as $Ni(CN)_2NH_3$, $Ni(CN)_2NH_3H_2O$ and $Ni(CN)_2NH_3C_6H_6$, have been known. [E. E. Aynsley and W. A. Campbell, *J. Chem. Soc.*, **1958**, 1723; K. A. Hofmann and F. Hochtler, *Ber.*, **36**, 1149 (1903)]. However, they are not touched on in this article, since they have complicated structures quite different from that of the mixed complexes in which we are interested here (J. H. Rayner and H. M. Powell, *J. Chem. Soc.*, **1952**, 319).

TABLE II

	(1)	(2)	(3)	(4)	(5)	(6)
([Ni]−1/4[CN])/[Ni]	1.00	0.863	0.726	0.452	0.178	0
D/D_1 for 900 mμ	1.00	0.867	0·719	0.450	0.163	0
for 580 mμ	1.00	0.859	0.714	0.459	0.162	0
for 560 mμ	1.00	0.862	0.718	0.453	0.160	0
1/4[CN]/[Ni]			0.274	0.548	0.822	1.00
D/D_6 for 310 mμ			0.275	0.550	0.841	1.00
for 330 mμ			0.280	0.556	0.816	1.00

Numbers in the first row denote solution numbers in Table I.

in Table I, and extinction measurements were carried out on each of the mixed solutions thus prepared. The results obtained are shown in Fig. 1.

The extinction curves in Fig. 1 tell us that only the tetracyano nickelate(II) and tris-ethylenediamine nickel(II) ions are present, no mixed cyano-amine complex being formed; if any of the mixed complexes were formed, the absorption curve would be more or less subject to deformation, or some new absorption maximum would appear correspondingly.

If we assume all of the added cyanide ion is consumed to form the tetracyano nickelate ion, the calculated values of ([Ni]−1/4[CN])/[Ni] and 1/4[CN]/[Ni] must accord with the experimentally obtainable values, D/D_1 and D/D_6, respectively, where [Ni] and [CN] denote the total concentration of all nickel species and the total concentration of cyanide ion in the solution and D_n is the optical density of the solution, n, shown in Table I and Fig. 1**. Actually, the satisfactory agreement between them can be found as is seen from Table II.

$[Cu\ en_2]^{2+}+CN^-$. — The experiment has been carried out to verify whether the mixed complex such as $[Cu\,en(CN)_2]$ can be formed, or not, when a sodium cyanide solution is added to a solution of bis-ethylenediamine copper(II) perchlorate. Extinction mesurements were made on each of the mixed solutions shown in Table III. The results are shown in Fig. 2.

TABLE III. THE COMPOSITION OF SOLUTIONS

Solution number	(7) cc.	(8) cc.	(9) cc.	(10) cc.	(11) cc.	(12) cc.
0.02 F $[Cu\,en_2](ClO_4)_2$ and 0.01 F NaOH	10	10	10	10	10	10
0.1096 F NaCN	0	1	2	4	6	8
Water	10	9	8	6	4	2

The extinction curves in Fig. 2 indicate that none of the mixed complexes such as $[Cu\,en(CN)_2]$ is existent in the solutions, because the absorption band (due to $[Cu\,en_2]^{2+}$) does not shift at all, being fixed at 500mμ, and yet none of the new absorption bands appears in the shorter wavelength region.

If we assume that four cyanide ions are consumed to convert a copper amine complex into a cyano complex, the calculated value, ([Cu]−1/4[CN])/[Cu], must accord with the experimentally obtainable value, D/D_7, as in the case of nickel. Actually the accordance can be found in Table IV, though it is not so satisfactory as in the case of nickel. Since cyanide complexes of divalent copper can not exist, the following reaction would have possibly occurred:

$$[Cu(en)_2]^{2+}+4CN^- \rightarrow [Cu(CN)_3]^{2-}{}^{***}+1/2(CN)_2+2\,en$$

Stability constants of copper(I) cyanide complexes were determined by Penneman and Jones[8].

$$k_1k_2=[Cu(CN)_2^-]/[Cu^+]\,[CN^-]^2=1\times10^{24}$$

$$k_3=[Cu(CN)_3^{2-}]/[Cu(CN)_2^-]\,[CN^-]=3.8\times10^4$$

$$k_4=[Cu(CN)_4^{3-}]/[Cu(CN)_3^{2-}]\,[CN^-]=50$$

From these data, it seems quite natural that tricyano copper(I) complex is mainly formed.

It must be noted that the possibility of

** If the reaction, $[Ni\,en_3]^{2+}+4\,CN^-\rightarrow[Ni(CN)_4]^{2-}+3\,en$, takes place quantitatively, optical densities of the mixed solutions can be given as follows:

$$D=\varepsilon_1([Ni]-1/4\,[CN])+\varepsilon_2(1/4[CN]),$$

while, for the solutions (1) and (6), $D_1=\varepsilon_1[Ni]$, and $D_6=\varepsilon_2[Ni]$, where ε_1 and ε_2 are extinction coefficients of $[Ni\,en_3]^{2+}$ and $[Ni\,(CN)_4]^{2-}$, respectively. However, the ratios D/D_1 and D/D_6 may be reduced for some wavelength region: for the region of 900~560 mμ, $D/D_1=[(Ni]-1/4[CN])/[Ni]$ with $\varepsilon_2=0$, and for the region of 400~220 mμ, $D/D_6=1/4[CN]/[Ni]$ since ε_1 is quite small as compared with ε_2.

*** For this complex the 4-coordinated configuration such as $[Cu(CN)_3OH_2]^{2-}$ or $[Cu(CN)_3\,en]^{2-}$, may be also considered. However, this is represented tentatively as $[Cu(CN)_3]^{2-}$, and the discussion of this complex will be done in the next section.

8) R. A. Penneman and L. H. Jones, *J. Chem. Phys.*, **24**, 293 (1956).

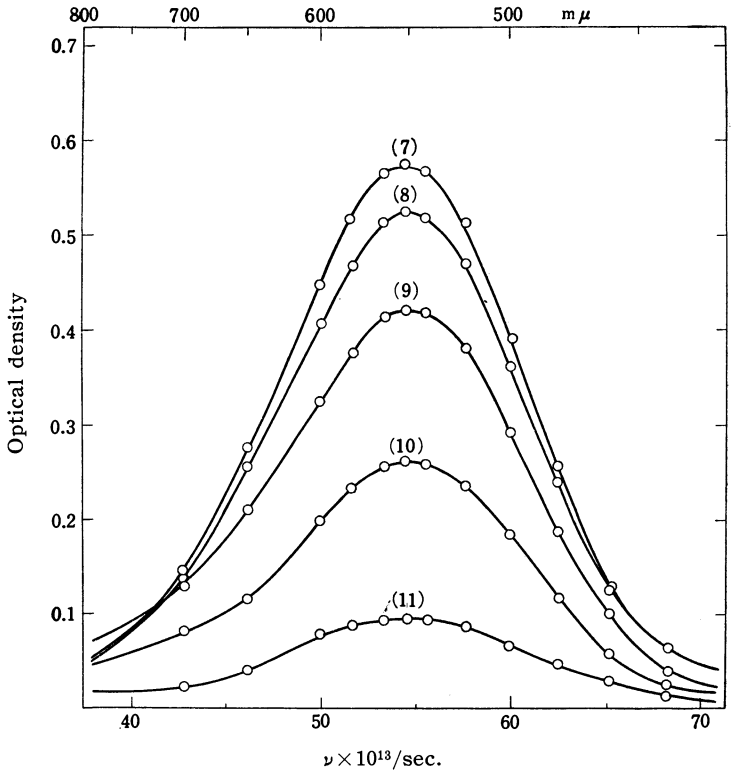


Fig. 2.

TABLE IV

	(7)	(8)	(9)	(10)	(11)	(12)
([Cu]−1/4[CN])/[Cu]	1.00	0.863	0.726	0.452	0.178	0
D/D_7 for 600 mμ	1.00	0.916	0.728	0.450	0.176	0
for 550 mμ	1.00	0.918	0.734	0.458	0.166	0
for 520 mμ	1.00	0.913	0.738	0.456	0.165	0

Numbers in the first row denote solution numbers in Fig. 2.
[Cu] is the total concentration of all copper species in solution.

the existence of a complex of coordination number 5 such as $[Cu\,en_2\,CN]^+$ can not be denied; the formation of this complex might be the cause of the unsatisfactory accordance of the calculated value with the experimental one unlike the case of nickel.

$[Cu(CN)_3]^{2-}$ + en.—Absorption spectra of the tricyano copper(I) complex were measured both with and without excess of ethylenediamine, and it was found that both absorption curves completely coincide within the limit of the experimental error. This fact suggests that the tricyano copper(I) complex does not take an ethylenediamine molecule in the solution to form the mixed complex such as $[Cu(CN)_3\,en]^{2-}$, and that the coordination number of the tricyano copper(I) complex may be 3 (perhaps sp^2 hybridization); if the coordintaion number were 4, the tricyanocopper(I) complex would have the configuration such as $[Cu(CN)_3\,OH_2]^{2-}$, and it would become the mixed complex, $[Cu(CN)_3\,en]^{2-}$, when the ethylenediamine is added to the solution.

$[Cu(CN)_2]^-$ + en.—When ethylenediamine is added to a solution of the dicyano copper(I) complex, the solution becomes turbid and light blue, and then slowly changes into a transparent purple blue solution. The absorption spectrum of this solution completely coincides with that of the bis-ethylenediamine copper(II) complex in the visible region.

From the above results, we can easily understand the fact that neither dicyano nor tetracyano copper(I) complex is formed, but tricyano copper(I) complex, when the cyanide solution is added to the

bis-ethylenediamine copper(II) complex solution.

Experimental

Extinction measurements were made by means of the Beckman D. U. spectrophotometer using 1 cm. quartz cells at room temperature.

In the case of $[Cu\,en_2]^{2+}+CN^-$, each of the solutions prepared as shown in Table III was heated just to boiling, and then cooled to the room temperature before extinction measurements were made; without this treatment, extinction data obtained are not reproducible.

$[Ni\,en_3](ClO_4)_2$ and $[Cu\,en_2](ClO_4)_2$. — The metal quantity of the former was analyzed with dimethylglyoxime, and that of the latter was determined by iodometry.

$[Cu(CN)_2]^-$ and $[Cu(CN)_3]^{2-}$ (in solution). —The copper(I) cyanide was dissolved in the potassium cyanide solution at the ratio of 1 : 1 and 1 : 2 to form these complexes, respectively.

Summary

1. Mixed amino-cyano nickel(II) complexes, such as $[Ni\,en_2(CN)_2]$, $[Ni\,en\cdot(CN_4)_4]^{2-}$ and $[Ni\,en(CN)_2]$ in the solution containing the divalent nickel ion, ethylenediamine and cyanide ion, are not formed.

2. In the solution containing the divalent or the monovalent copper ion, ethylenediamine and the cyanide ion, no mixed amine-cyano copper(I) and copper(II) complexes are formed, except the copper(II) complex of coordination number 5.

3. Among cyano copper(I) complexes, tricyano copper(I) ion is the most stable, and its coordination number may be 3.

The author wishes to express his sincere thanks to Professor R. Tsuchida of Osaka University for his kind advice and encouragement during this work. The author's appreciation is also expressed to Dr. H. Yoneda for his helpful discussion.

Department of Chemistry
Wakayama University
Masago-cho, Wakayama

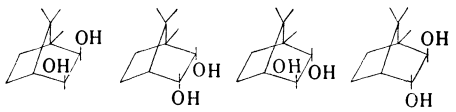
*Stereoisomers of 2,3-Camphane Diols**

By Tsuneichi TAKESHITA and Masayoshi KITAJIMA

(Received November 21, 1958)

There should exist four possible diastereoisomeric camphane-2,3-diols, which in spite of having been prepared by several authors[1], were mostly obtained as mixtures of isomers, with its single epimer believed to have been isolated in fairly pure state by Rupe and Thommen[2]. Therefore, conformation of each epimer has not been established at all. Only Kwart and Gatos[3,4] recently assigned the structure to the one isomer of the Rupe and Thommen diol with positive evidence of infrared spectra and complex formation. It became then the purpose in these studies to isolate all theoretically possible diols and assign conformation; and, if possible, to correlate the isomeric composition of the diols prepared by various methods with the mode of reaction. Several facts which have been clarified are presented in this report. As the authors have hitherto studied *endo-* and *exo-* isomers of borneols and their epimerization[5,6], the hydrogenation of camphorquinone was similarly followed.

Synthesis of Four Stereoisomers.—Four epimers, namely *exo-exo-* (I), *endo-endo-* (II), *endo-exo-* (III), and *exo-endo-* (IV) may possibly result by reduction of camphorquinone. Effective isolation of pure



I II III IV

Fig. 1. Stereoisomers of 2,3-camphane diols.

* Partly presented at the Symposium on Terpenes, Kinki Univ., Nov. 30, 1957.

1) O. Mannase, *Ber.*, **30**, 659 (1897); ibid., **35**, 3811 (1902).

2) H. Rupe and W. Thommen, *Hev. Chim. Acta*, **30**, 933 (1947).

3) H. Kwart and G. C. Gatos, *J. Am. Chem. Soc.*, **80**, 881 (1958). The present author is indebted to Dr. H. Kwart for his kind advice and suggestion, and to Dr. S. J. Angyal for his unpublished reslut.

4) S. J. Angyal recently isolated four diols in fairly pure state. (A. C. S. Meeting, Sept., 1957, New York).

5) T. Takeshita and M. Kitajima, *J. Chem. Soc. Japan, Pure Chem. Sec.* (*Nippon Kagaku Zasshi*), **78**, 994 (1957).

6) T. Takeshita and M. Kitajima, ibid., **79**, 1468 (1958).

TABLE I. INFRARED SPECTA OF *cis*-DIOLS

	Free	Int.	Intra	Int.	Inter	Int.	$\Delta\nu$	OH-O[3]	Ratio (%)	Assignment
I	3630	0.151	3540	0.270	3380	0.440	90	1.5 Å	291.4	*exo-exo-*
II	3630	0.127	3535	0.300	3385	0.529	95	1.5 Å	416.5	*endo-endo-*

Concn. 20.0 mg./ml. CS_2; Cell length 0.5 mm. Free Int., Intra Int. and Inter Int. are peak intensity at free, intra-molecular and inter-molecular O-H stretching.
Ratio Inter, Int./Free, Int.

isomers can be achieved by selecting the procedure yielding the least number of components, and this would be possible by avoiding the method of reduction which may cause isomerization of the hydroxyl group which was entered. As proved in the epimerization of borneol by the authors, such reducing agents as copper chromite, sodium or aluminum isopropylate are effective catalysts of epimerization[6]. Therefore, these were not used for the present purpose. Reduction with lithium aluminum hydride and Raney nickel were the methods mostly utilized for this purpose.

When camphorquinone absorbs 1 molar hydrogen, it leads to hydroxy-ketone and giving a diol on further reduction. As an analogous mode of reduction of camphor, Raney nickel or lithium aluminum hydride should give *exo-* and *endo-* isomer with a preponderance of the former. Hydroxy-ketone obtained by these methods can now be assumed to be isomeric with "α-hydroxycamphor" (V) and "β-hydroxycamphor" (VI) by zinc- acetic acid reduction. $LiAlH_4$ reduction of camphorquinone is expected to yield one *cis-* and two *trans-* isomers. On the other hand, however, further reduction of V or VI, separated from each other, should lead to one *cis-*, one *trans-*, respectively. A *cis*-diol can thus be easily purified in $LiAlH_4$ reduction, but it must be somewhat hard in the case of *trans*-diol to purify one from another.

cis-Diol I.—Camphorquinone in ether was reduced with lithium aluminum hydride after Trevoy and Brown's method[7] at dry-ice temperature. Crude *cis*-diol was converted to acetonide, rectified over a sodium ribbon till no more O-H absorption is detected in the 3500 cm^{-1} region of infrared spectra**. After regeneration of the diol, it was recrystallized from ligroin and repeatedly sublimed in vacuo.

cis-Diol II.—"β-Hydroxycamphor" VI purified through its dimolecular methyl ether[8] was hydrogenated over Raney nickel at room temperature, a *cis*-diol was separated from one *trans*-isomer and purified similarly as in the case of I.

trans-Diol III.—The *trans*-diol separated from II in the foregoing reduction product was repeatedly treated with acetone to remove any trace of remaining *cis*-diol.

trans-Diol IV.—The *trans*-diol isolated from Raney nickelhydrogenated diols of "α-hydroxycamphor" V was further purified like III.

Assignment of Conformation.—Tentative assignment of *cis*-I, II and *trans*-III, IV were separately performed by comparison with I.R. spectra at O-H region.

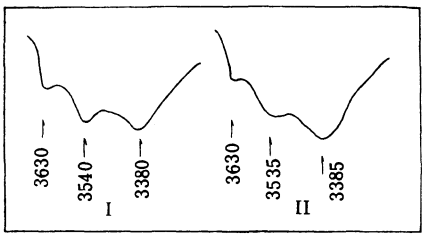


Fig. 2. O-H stretching region (*cis*-diols) CS_2 soln.

The bands at 3540 are intra-molecular O-H; and difference from free O-H, $\Delta\nu=90$, in case of I and 195 in case of II, corresponds to 1.5Å for O-H distance. Concerning the inter-molecular band, intensity of associated O-H/free O-H is a measure of the ease with which solute associates. Thus, as proved in case of borneol[5], the degree of association is far less in *exo-* than that in *endo-*, owing to *gem-* dimethyl hindrance. Of the two *cis*-diols investigated, I can not associate so much as II since the ratio obtained is 291.0 and 416.0%, respectively. Therefore, so far as two *cis*-epimers are concerned, I can be assigned as *exo-*, and II, in turn, as *endo-*. These assigned stuctures of I and II are satisfied with some difference of chemical property,

TABLE II. SAPONIFICATION OF *cis*-DIOL DIACETATES

Isomer	0.1 N KOH, hr.	% Sap'd	25±1°C
I	3	62.9	
II	3	69.1	

7) L. W. Trevoy and W. G. Brown, *J. Am. Chem. Soc.*, 71, 1675 (1949).
** No isomerization of acetonide occurs by distillation over sodium (by I. R.).
8) J. Bredt, *J. prakt. Chem.*, 121, 153 (1929).

TABLE III. INFRARED SPECTRA OF *trans*-DIOLS

	Free	Int.	Inter	Int.	Ratio	Concn.	Assignment
III	3625	0.232	3450	0.064	27.6%	100.0 mg./10 ml.	*endo-exo-*
IV	3620	0.234	3440	0.057	24.4	〃	*exo-endo-*
III	3620	0.280	3440	0.099	35.4	120.0	*endo-exo-*
IV	3620	0.282	3440	0.085	30.1	〃	*exo-endo-*

Cell length 0.5 mm.

that is, the difference of saponification velocity of corresponding diacetate, as shown in Table II.

The slower saponification rate of I coincides well with the assignment by I. R. And as will be reported in a later paper[9], epimerization of I resulted in a great preponderance of II over I. This corresponds with the known stability of *endo*-isomer in case of borneol.

trans-Diols, III and IV, were similarly compared on the infrared spectra. Although associated OH can best be compared in CCl_4 or CS_2 because a solvent molecule such as $CHCl_3$ is known to prevent intermolecular association of solute***, spectra were taken in $CHCl_3$ solution on account of sparing solubility of *trans*-diol in CS_2****. Therefore, the difference of ratio of polymeric OH/free OH between III and IV was not one-sided as in the case of *cis*-diols. Table III shows comparison of spectra.

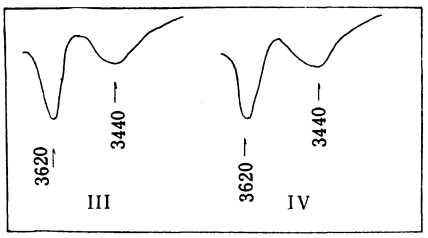


Fig. 3. O-H stretching region (*trans*-diols) $CHCl_3$ soln.

Steric hindrance of *gem*-dimethyl is usually more profound at C_2 than at C_3 because of proximity of adjacent quaternary methyl. That the steric effect of *gem*-dimethyl observed for C_3–OH is not significant has been reported on epi-borneol by Lipp et al.[10] Therefore, an isomer with more bonded OH is suggested to be 2-*endo*-3-*exo*-. This tentative assignment is also supported by the fact that the di-acetate of III is saponified faster than that of IV, as shown in Table IV.

TABLE IV. SAPONIFICATION OF *trans*-DIOL DIACETATES (25±1°C)

Isomer	0.1 N KOH hr.	% Sap'd
III	2	73.1
IV	2	61.3

The properties of four diasteroisomeric diols isolated are summarized in Table V.

TABLE V. PROPERTIES OF DIOLS

Isomer	m. p.(°C)	$[\alpha]_D$	O-H dist.	Conformation
I	262~263	−19.3	1.5 Å	2-*exo*-3-*exo*-
II	224~225	+30.8	1.5	2-*endo*-3-*endo*-
III	253~254	+15.0	(3.3)	2-*endo*-3-*exo*-
IV	251~252	+ 7.7	(3.3)	2-*exo*-3-*endo*-

Isomeric Composion of Diols by Various Methods of Syntheses.—Diols prepared by direct reduction of camphorquinone and by further reduction of hydroxyketone obtained by zinc-acetic acid reduction of camphorquinone were studied then by infrared spectra. The result of one-step hydrogenation is given in Table VI.

Catalytic hydrogenation affords mainly *cis*-I with some II, *trans*-diols increase with rise of reaction temperature. Therefore, reduction at room temperature easily gives *cis*-diols (I+II) in over 90% yield, though *cis*-I is not easy to purify.

$LiAlH_4$ reduction was much influenced by temperature on the reaction product, *cis*-diol obtained at −70°C being exclusively *exo*-, while that of 0°C was contaminated with *endo*-. Thus, the reduction at dry ice temperature is the procedure employed in this paper for the preparation of uncontaminated *cis-exo*-diol. The Meerwein-Pondorff-Verley type reduction of camphorquinone yielded a characteristic product that consisted of *cis*-diols solely, with very few *trans* isomers. And moreover, II increased considerably, compared with other procedures.

Diols Prepared by Hydrogenation of Hydroxy-camphor. — Camphorquinone

9) T. Takeshita, Presented at the Symposium on Terpenes, held at Hiroshima University, Oct. 10, 1958.

*** The association of ROH in $CHCl_3$ is known to be less than in CS_2. The effect of $CHCl_3$ must be the hydrogen bonding power of CH besides the polarity or molecular size of solvent. (Cf. L. J. Bellamy, "The Infra-Red Spectra of Complex Molecules", Methuen and Co, London (1958), p. 100.

**** Limited solubilty of III in $CHCl_3$, less than 130.0 mg./10 ml., makes possible only narrow concentration range for the present purpose, though IV is more soluble.

10) P. Lipp et al., *Ber.*, **68**, 249 (1935).

TABLE VI. REDUCTION PRODUCT OF CAMPHORQUINONE

Expt.	Reducing agent	I	II	III	IV	Remarks	
1	Raney Ni	88	5	1	6	14~20°C	8 hr.
2	〃	75	7	1	17	90~100	9
3	Copper chromite	54	6	9	31	120~150	3
4	Al-(O-*i*Pr)$_3$	60	39	—	1	88	10
5	$LiAlH_4$	89	4	4	3	0	20
6	〃	94	—	3	3	−70	20

TABLE VII. REDUCTION PRODUCT OF HYDROXYCAMPHOR

Expt.	Starting epimer	Reducing agent	I	II	III	IV	Remarks	
7	β-	Raney nickel	—	48	52	—	20~27°C	10 hr.
8	β-	〃	—	41	59	—	29~34	8
9	α-	〃	14	41	—	45	17~18	12
10	α-	〃	12	34	—	54	32~40	6
11	β-	$LiAlH_4$	—	85	15	—	0	20
12	α-	〃	19	69	—	12	0	20
13	β-	Na-EtOH	—	19	16	65	80~90	5
14	α-	〃	—	22	12	66	80~90	5

yields hydroxy-ketone on zinc-acetic acid reduction, which has been reported to consist of α-hydroxycamphor and β-hydroxycamphor[11]. The configuration of this hydroxycamphor is not clear, but must be *endo*-configuration since β-isomer which was regenerated from sparingly soluble dimolecular methyl ether afforded *cis-endo*-diol. The result of reduction of this hydroxyketone also supports this idea as indicated in Table V.

A point to be noticed is that *cis*-diol obtained from β-hydroxycamphor catalytically or with $LiAlH_4$ was *cis-endo*, while that from α-isomer afforded *endo*- mixed with about one third the amount of *exo*-isomer. This shows the homogenity of β-isomer, *endo*- whereas α-isomer was a mixture of *endo*- and *exo*-, in ratio of 3 to 1. The catalytic hydrogenation of hydroxycamphor presents an interesting problem, since predominant *exo*-addition observed in case of camphor[4] was cut to about half to give *trans*-diol. This indicates steric hindrance in opposing direction by *gem*-dimethyl group to that of *endo*-hydroxyl group. Thus, $LiAlH_4$ reduction gives only 15% of *exo*-reduced product because lithium aluminum salt formed with *endo*-hydroxyl group becomes overwhelmingly bulkier than the *gem*-dimethyl, *exo*-directing radical. Sodium with alcohol gave mostly *trans*-diol as the usual mode of *trans*-addition. Similarity of the reduction product is considered to be isomerization of β-hydroxycamphor to α-isomer as seen in Experiments 13 and 14.

11) β-Hydroxycamphor, so designated, is actually α-hydroxy-epicamphor.

Experimental[12]

I. *exo-exo*-2, 3-Camphane-diol.—A solution of camphorquinone (10 g.) in ether was added dropwise at −60°C to −70°C to an ether solution of $LiAlH_4$ (c=1.6 mol./l.) immersed in a methanol-dry ice bath and kept for 20 hr.[6] After decomposition of excess of reagent with water, the whole was washed with dilute sulfuric acid, saturated sodium chloride solution, dried with anhydrous sodium sulfate and the solvent was evaporated to give the *cis*-diol (9.5 g.). Seven grams of crude product was treated with acetone by the procedure of Rupe et al.[2] to give acetonide (8.4 g.), and vacuum distillation afforded some *trans*-isomer (0.43 g.). Acetonide was purified by rectifying over sodium till it showed no more hydroxyl absorption in 3500 region of its infrared spectra, 4 g. of pure acetonide was saponified to regenerate *cis*-diol (2.7 g.), recrystallized from ligroine, and sublimed in vacuo, m. p. 262~263°C, $[\alpha]_D$−19.3 (c=0.50000 g./5 ml.).

II. *endo*-*endo*-2, 3-Camphane-diol. —" β-Hydroxy-camphor " (27.7 g., m. p. 204~205°C), purified through dimolecular methyl ether (m. p. 147~148°C)[8,13] was hydrogenated in alcohol over Raney nickel at 14~20°C to yield *cis*-diol (28.0 g.) mixed with *trans*-isomer. To isolate *cis*-diol, 20 g. of diol was treated as I with acetone. The solid product (21.0 g.), wet with *cis-endo*-acetonide was extracted with boiling hexane to free it from *trans*-diol. Evaporation of hexane afforded acetonide contaminated with some *trans*-isomer; this was further treated over sodium as I, saponified, recrystallized, and vacuum sublimed.

12) All melting points are uncorrected. All rotations were measured in 1 dm. tube as an alcoholic solution. Infrared spectra were taken with a Perkin Elmer Model 21 Infrared Spectrophotometer equipped with sodium chloride prism.

13) J. L. Simonsen mis-stated the m. p. of the compoud as 37~38°C in " Therpenes ", Vol. II, Cambridge University Press, Cambrige (1949), p. 428.

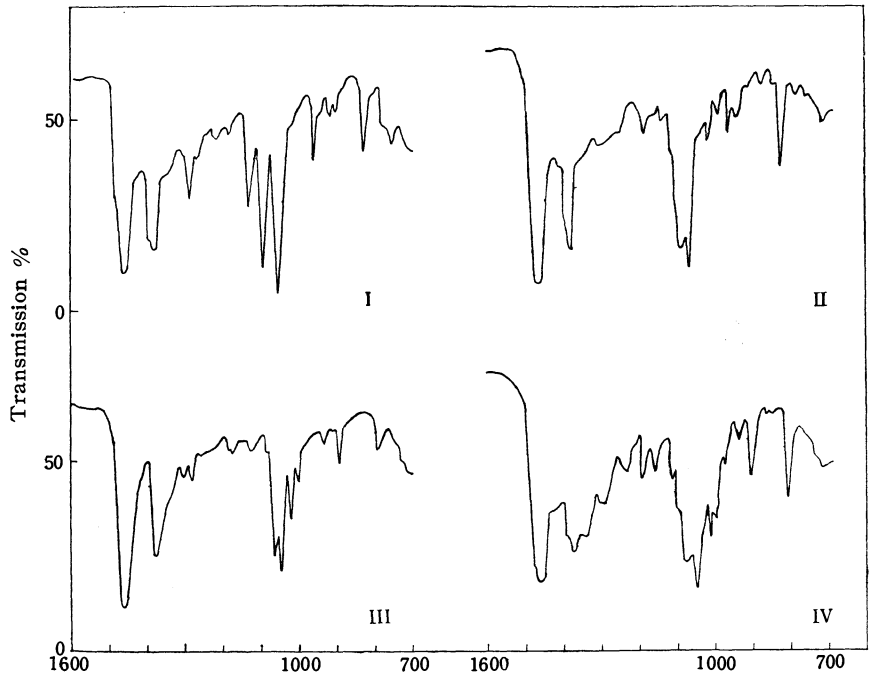


Fig. 4. I. R. of diols (as Nujol mulls)

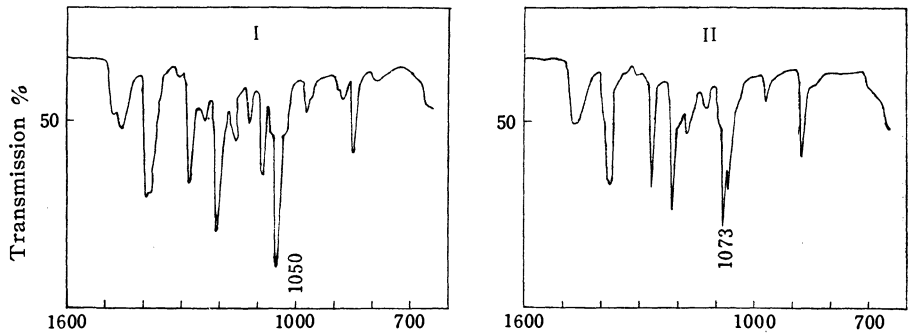


Fig. 5. I. R. of *cis*-acetonide (1600～1650 cm^{-1}) cap.

Yield, 3.6 g., m. p. 224～225°C, $[\alpha]_D$ +30.8 (c= 0.50000 g./5 ml.).

III. *endo*-*exo*-2,3-Camphane-diol. — The *trans*-diol separated (9.2 g.) in isolation of II was further treated with acetone to remove any trace of *cis*-diol present and recrystallized several times from ligroine and sublimed in vacuo. Yield, 7.5 g., m. p. 253～254°C, $[\alpha]_D$+15.0 (c=0.50000 g. /5 ml.).

IV. *exo-endo*-2,3-Camphane-diol.—Similarly as in the case of III, *trans*-isomer separated from hydrogenation of 8.5 g. of "α-hydroxycamphor" was further treated with acetone, to remove *cis*-isomer, recrystallized sublimed in vacuo, m. p. 251～252°C, $[\alpha]_D$ +7.7 (c=0.50000 g./5 ml.).

Infrared Measurement — All the spectra were taken by Perkin Elmer Model 21 with NaCl Optics. The infrared determination of the isomeric composition of diols which resulted as reduction product was developed as follows.

As stereoisomeric cyclic alcohol usually has a characteristic band around the 1000～1100 region like those of *endo*- and *exo*- borneols[5], the spectra of four isomers are distinguishable (Fig. 4) in this region. These are, however, only effective for qualitative analysis because of the overlapping of bands not at the peaks but at the side of absorption maxima. As shown in the preceding discussion, in dilute solution, *cis*-diols absorb both at 3620 and 3520, while *trans*-isomer does so at only 3620 owing to absence of intra-molecular band of 3520. Thus, *cis-trans* composition can be determined by O—H stretching bands. Individual epimers are then determined by C—O stretching region.

1) Intensity of 3620 and 3520 bands measured.

Diols		3620	Average	3520	Average
cis-	I	0.223	0.217	0.166	0.166
	II	0.211		0.165	
trans-	III	0.351	0.354	0.048	0.046
	IV	0.356		0.044	

Concn. 60.0 mg./10 ml. $CHCl_3$
Cell length 1.2 mm. Room temp. 25±2°C

At the concentration indicated, there was not much variation in optical density between isomers within the same geometrical group (*cis-* or *trans-*), and this presents a rapid method of determination of *cis-* and *trans*-isomers. Trial analysis of some synthetic mixtures of known concentration was found to be accomplished with 2% error, this accuracy being sufficient for the present study.

	cis		*trans*		*cis*		*trans*	
Synthetic	II	66.5	IV	33.5	II	33.2	III	66.8
Found		67.2		32.8		34.9		65.1
Synthetic	I	83.2	IV	16.8	III	83.2	III	16.8
Found		85.0		15.0		85.8		14.2

On finding *cis-trans* ratio, determination of each isomer is performed by C—O stretching region.

2) Intensity of C—O stretching region.

Diols	1089	1074	1060
I	0.312	0.095	—
II	0.203	0.282	0.368
III	0.068	0.271	0.168
IV	0.067	0.098	0.401

Concn. 60.0 mg./10 ml. $CHCl_3$
Cell length 0.5 mm.

Fortunately, the 1089 intensity of III and IV does not differ much. *Trans*-contribution at this wave number can be treated as equal in evaluation of *trans* isomers of diols. Compositions III and IV are finally determined after *cis*-diols were removed with acetone as acetonide. Trial analysis was performed with 2% error as follows:

Synthetic	II	66.5	IV	33.5	II	33.2	III	66.8
Found		65.0		35.0		31.0		69.0
Synthetic	I	83.2	IV	16.8	IV	66.5	III	33.5
Found		84.9		15.1		68.3		31.7
Synthetic	III	35.0	IV	65.0				
Found		36.6		64.3				

Thus the ratio of epimers was found to be analyzed on a 2-component system using C—O stretching region with 2% error. However, overall error of analysis amounts to less than 4%, with assay of *cis-trans* ratio combined in analysis of diols. As to *cis*-isomers I and II, characteristic *cis*-acetonide was compared with them. (Fig. 5)

Saponification of Diol Diacetate.—Acetylation of diol was as follows: Each of the diols (3 mmol., 510 mg.) was gently boiled with acetic anhydride (Purity 94.2%, 2.1 g.) and anhydrous sodium acetate (0.4 g.) for 1 hr., settled overnight, the excess of reagent decomposed with 10 ml. of hot water during 2 hr., extracted with ether. After being washed with aqueous solution of sodium chloride, and then sodium bicarbonate, the solution was dried over anhydrous sodium sulfate. Removal of solvent in vacuo, finally by warming at 110°C/7 mmHg afforded slightly colored diacetate oil, in yield ranging from 600 to 700 mg. Purity found. (Theor. Value, Ester Value 441.0 as $(CH_3COO)_2 \cdot C_{10}H_{16}$) Diacetate of I E. V. 427.3, II E. V. 434.5, III E. V. 435.1, IV E. V. 428.1

The diacetate thus prepared was saponified by the usual procedure: Weighed sample, equivalent to 10 ml. of 0.1 N alcoholic KOH, in bottle was immersed in a water bath kept at 25±1°C. To this was added 10 ml. of 0.1 N alcoholic KOH at 25±1°C and maintained at this temperature. Back titration with 0.1 N H_2SO_4 against phenolphthalein gave the amount saponified. (Cf. Table II and IV).

Preparation of Diols by Various Methods.

Expt.	Camphorquinone (g.)	Catalyst		Solvent (ml.)		Temp. (°C)	Time (hr.)	Yield (g.)	m. p. (°C)	$[\alpha]_D$
1	25	Raney Ni	6 g.	EtOH	30	14～20	8	25	253～255	−13.9
2	33.2	〃	6 g.	〃	30	90～100	9	33.3	250～252	− 9.6
3	8.3	Copper chromite	3 g.	Benzene	10	120～150	3	7.8	245～249	− 4.6
4	8.3	Aluminum isopropylate	20 g.	IsoprOH	200	85～88		4.7	241～242	+ 1.9
5	6.6	$LiAlH_4$	0.04mol.	Ether	30	0	20	6.2	256～257	−16.5
6	10.0	〃	0.06mol.	〃	200	−70	〃	9.5	255～257	−15.7
7	β- 27.7	Raney Ni	6 g.	EtOH	20	20～27	10	25.3	232～234	+20.0
8	β- 7	〃	3 g.	〃	15	29～34	8	6.2	232～235	+22.6
9	α- 8.5	〃	3 g.	〃	15	17～18	12	8.2	235～238	+11.2
10	α- 7	〃	3 g.	〃	15	32～40	6	6.8	238～241	+ 8.3
11	α- 4.2	$LiAlH_4$	0.013mol.	Ether	20	0	20	4.0	226～228	+28.7
12	β- 4.2	〃	〃	〃	〃	〃	〃	3.6	229～231	+15.6
13	β- 6.7	Na	9.2 g.	EtOH	150	80～90	5	4.8	229～231	—
14	α- 4.0	〃	6 g.	〃	90	〃	〃	3.2	233～234	+11.9

Expts. 1—3) *Reduction of camphorquinone.*—Camphorquinone was hydrogenated in 100 ml. stainless steel autoclave equipped with magnetic stirring-valve. Initial press., 70～120 kg./cm².

Expt. 4) The Meerwein-Pondorff-Verley reduction of camphorquinone was carried out by the usual method, maintaining the inner temperature below 89°C.

Expts. 5 and 6) Lithium aluminum reduction followed after the procedure of Trevoy and Brown[6]. $LiAlH_4$, ether solution (1.6 M).

Expts. 7—10) *Reduction of hydroxycamphor.*—The hydroxycamphor used in the experiment was synthesized after Bredt's method[8]. Catalytic hydrogenation of α- and β-hydroxycamphor were carried out, using Raney nickel.

Expts. 11 and 12) Lithium aluminum hydride reduction is analogous to that of the foregoing.

Expts. 13 and 14) Reduction of hydroxycamphor with sodium in alcohol was by the usual procedure.

Central Research Institute
Japan Monopoly Corporation
Yutaka-machi, Shinagawa-ku
Tokyo

Decomposition Temperature of Urea Adducts

By Naoki YATA

(Received December 16, 1958)

Decomposition temperatures for urea adducts of *n*-hexadecane, *n*-nonadecane, and *n*-paraffins from C_{19}–C_{20} fraction of mineral oil were determined. The results were compared with the data by Redlich et al.[1] and decomposition temperature of *n*-hexadecane by the author was found to be lower than that of Redlich's.

Addition of benzene to the system (adducts and water) results in the lowering of decomposition temperature. This effect becomes remarkable with a decreasing amount of water.

Experimental

Reagents.—Urea (m. p. 132.6°C) was recrystallized from aqueous solution saturated at 30°C. Methanol (b. p. 64~65°C), benzene (b. p. 80~80.5°C) and petroleum ether (b. p. 40~60°C) were redistilled from the commercial product.

n-Hexadecane (commercial) was treated with activated alumina followed by sulfuric acid and sulfur trioxide treatment, m. p. 16.2°C, $n_D^{20}=1.4251$.

n-Nonadecane and *n*-heneicosane were separated from lubricating oil fraction of Yabase crude (b.p. 104~226°C at 3 mmHg) by urea adduction and chemical treatment as mentioned above. Physical constants of these hydrocarbons were compared with the literature values[2,3] and shown in Table I.

Preparation of Adducts.—Adducts from mineral oil (Yabase lubricating oil fraction as described above) were prepared by adding 120 g of urea and 1 cc. of methanol to 150 g. of oil. After the mixed solution being stirred for 50 min., the adduct produced was filtered off and washed with 1500 cc. of benzene. Yield, 150 g. of adducts. Adducts of *n*-paraffins were made from the petroleum ether solution of them. This solution was treated with 3 times of urea to *n*-paraffins, and 0.3 times of methanol, and was stirred for 50 min. The adducts produced were filtered by suction and washed with 30 times the quantity of benzene.

All of these adducts were dried in vacuo until solvent odor was diminished. Analytical data are shown in Table II. Mole ratios in this table were determined by Schiessler's method[4]. Dissociation temperatures were measured by the method of Knight et al.[5]; according to the present author's experiment, dissociation temperatures of *n*-paraffins are quite similar to that of methyl ester which has been measured by Knight et al.

TABLE I. PHYSICAL CONSTANTS OF *n*-NONADECANE AND *n*-HENEICOSANE

Hydrocarbons	Refractive index (n_D^{60})		Melting point (°C)	
	Found	Lit.	Found	Lit.
n-Nonadecane	1.4268	1.4255	31.0	32.0
n-Heneicosane	1.4300	1.4290	40.5	40.5

Procedure.—A small test tube of 2.5 cm. diameter was connected in a large test tube of 4.5 cm. diameter with a rubber stopper. Two

1) O. Redlich, et al., *J. Am. Chem. Soc.*, **72**, 4153 (1950).
2) C. Kroeger and F. Hallfeld, *Erdöl u. Kohle*, **7**, 811 (1954).
3) M. F. Sawer et al., *J. Inst. Petrol.*, **27**, 1 (1941).
4) R. W. Schiessler and D. J. Flitter., *J. Am. Chem. Soc.*, **74**, 1720 (1952).
5) H. B. Knight et al., *Anal. Chem.*, **24**, 1331 (1951).

TABLE II. COMPOSITIONS AND DISSOCIATION TEMPERATURES OF ADDUCTS

Hydrocarbons in adducts	Urea/*n*-paraffin Wt. ratio	Urea/*n*-paraffin Mol. ratio	Dissociation temp. (°C)
Lub. oil paraffin	3.5	—	125
n-Hexadecane	3.1	11.7(12)[6]	112
n-Nonadecane	3.2	14.1(13.9)	129
n-Heneicosane	3.1	14.6(14.6)	129

grams of adduct samples and water were put into the small test tube with a thermometer and a stirrer made of iron wire.

The large test tube was placed in a 500 cc. beaker where warm water was filled in, and heated. Constant hand stirring was continued with temperature rise of about 5°C/min. until a paraffin portion was separated on the upper layer, and this point was considered as the decomposition temperature.

Results and Discussion

Decomposition Temperature.—Table III shows the decomposition temperature, the average value taken from the two measurements. Decomposition curve was made according to the method of Redlich et al., as shown in Fig. 1. These curves were extrapolated and the intersection with the saturation curve (dotted line) of urea in water were considered as the decomposition point.

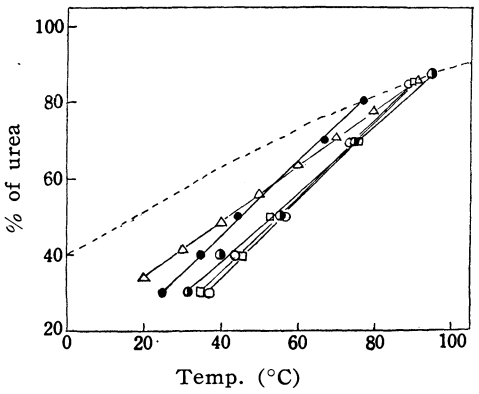


Fig. 1. Decomposition curve of urea adducts.
Dotted line: Urea saturation curve
◑: Mineral oil paraffin adducts
●: *n*-Hexadecane adducts
○: *n*-Nonadecane adducts
□: *n*-Heneicosane adducts
△: *n*-Hexadecane adducts by Redlich

As is shown in Table III, the decomposition point of *n*-hexadecane adduct is 78°C and is lowerthan Redlich's value, 90°C. Schlenk[7] showed that 97.5% of 1 mol. *n*-hexadecane adduct (12 mol. of urea and 1 mol. of *n*-hexadecane) was decomposed in 72 mol. of water at 31°C.

TABLE III. DECOMPOSITION TEMPERATURE OF UREA ADDUCTS

Hydrocarbons in adducts	Decomp. point (°C)	Urea[8] concn. (%)	Decomp. temp. (°C)
Lubricating oil paraffin	95	30	32.0
		40	39.5
		50	55.2
		70	75.0
n-Hexadecane	78	30	24.8
		40	35.0
		50	45.7
		70	67.0
n-Nonadecane	90	30	36.0
		40	43.5
		50	55.2
		70	74.5
n-Heneicosane	90	30	34.5
		40	44.0
		50	53.5
		70	75.0

This result means that 0.975 mol. of *n*-hexadecane adduct is decomposed 72 mol. of water at 31°C and 35.2% aqueous solution of urea is separated. According to the author's result, at the decomposition point of 31°C about 36% aqueous solution of urea is separated, and by Redlich et al. it corresponds to 41%. This deviation of the present result from the data of Redlich et al. was thought to be due to the difference of the determination method.

As *n*-nonadecane and *n*-heneicosane were separated from the same lubricating oil fraction, the decomposition points of these are nearly the same. *n*-Nonadecane sample used in this study is not so pure as is clearly seen from the comparison with the physical properties which have been cited in literature (cf. Table I), but in any case difference of the decomposition point between the carbon number ranges of 1 and 2 seemed to be comparatively small.

Effect of Benzene Addition.—The decomposition of adduct occurs when a sufficient amount of benzene or other hydrocarbon solvents were used at high temperatures. As might be expected, addition of benzene to the system which is composed of adduct and water, lowers the decomposition temperature. Fig. 2 shows the decomposition temperature of adducts containing

6) The values in the brackets were calculated by Redlich's equation[1], $m=0.653n+1.51$, where m is the mole ratio of urea to *n*-paraffin and n is the carbon number.

7) W. Schlenk. Jr., *Ann.*, 565, 204 (1949).

8) Urea concentration means per cent of urea (in adducts) in the urea-water mixture.

43～233% (for urea in adducts) of water and 0～200% (for adducts) of benzene.

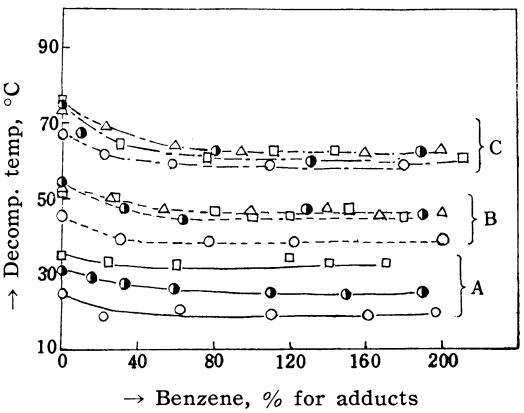


Fig. 2. Effect of benzene addition.
A: 233% water for urea in adducts,
B: 100%, C: 43%
◑: Mineral oil paraffin adducts
○: *n*-Hexadecane adducts
△: *n*-Nonadecane adducts
□: *n*-Heneicosane adducts

When the amount of benzene is increased, the decomposition temperature lowers; but the more the amount of water, the smaller the effect of benzene. The effect of benzene addition of 40～200% for adducts shows almost constant change of decomposition temperature: i. e., on addition of 233% water, temperature change is about 3～5°C, 100% water, 5～8°C, and 43% water, 10～12°C. This unchangeability of the decomposition temperature by the benzene addition may be caused by the limitation of decomposition by benzene itself. Hence, it can be seen that water has greater decomposition velocity than benzene has, and temperature dependence of the benzene decomposition is greater than that of water (Table IV).

Table IV shows the decomposition temperature of *n*-hexadecane adduct by benzene, and complete decomposition is obtained only when the boiling benzene (80°C) is used as 200% for adducts and five hours heating[9].

TABLE IV. DECOMPOSITION OF *n*-HEXADECANE ADDUCT BY BENZENE

Temp. (°C)	Heating time (hr.)	Benzene (% for adduct)	*n*-Hexadecane decomposed (%)
30	4	150	5
50	3	150	19
70	3	150	84
70	6	150	90
80	4	150	93
80	5	150	97.2
30	5	200	7
70	3	200	96
70	5	200	98.7
80	4	200	95
80	5	200	100

Decomposition temperatures of adducts of lower carbon paraffins are lower than those of higher ones, as might be expected from Fig. 2, yet this effect is less striking than water decomposition (Fig. 1).

Thanks are due to Mr. Katsuhiko Ide of this laboratory for many helpful experiments in the course of this work.

Nippon Mining Co.
Funakawa Oil Refinery
Oga-shi, Akita

9) This decomposition is carried out without stirring.

Studies on the Vibrated Dropping Mercury Electrode. I. The Theory of the Limiting Current and its Application to the Electrocapillarity

By Hideo IMAI, Senkichi INOUYE and Shōkichi CHAKI

(Received January 8, 1959)

When the dropping mercury electrode is vibrated by the application of an a. c. electric field, the limiting current of a depolarizer is augmented, the convection current being super-induced on the diffusion-controlled one. We called this new technique for improving the sensitivity of polarographic determinations the "VDME" method, and it was briefly reported in the previous communication[1]. Since the increment of the limiting current beyond the diffusion-controlled one depends upon the electric charge of the mercury-solution interface, this technique has a potentiality for the investigation of the electrocapillarity, especially for the determination of the zero-charge potential, i. e., the Lippmann-potential.

In this report, the theory of the limiting current and an accurate method for determining the Lippmann-potential are presented.

The Theory of the Limiting Current

The a. c. electric field exerts a moment of force as great as $q \cdot E \sin(\omega t) \cdot r \cdot \cos\theta$* on the center of the DME, and causes the forced vibration of the DME about the orifice of the capillary electrode (cf. Fig. 1). Counteracting this vibration, there exists the resistance due to the viscosity of the solution and the restoration of the displacement owing to gravity. Supposing that the former obeys Stokes's law, the moment of force is evaluated as great as $6\pi\eta r \cdot r \cdot r\, \mathrm{d}\theta/\mathrm{d}t$. The latter moment of force is equal to $Mg \cdot r \cdot \sin\theta$. Hence, one obtains the following equation of the vibration.

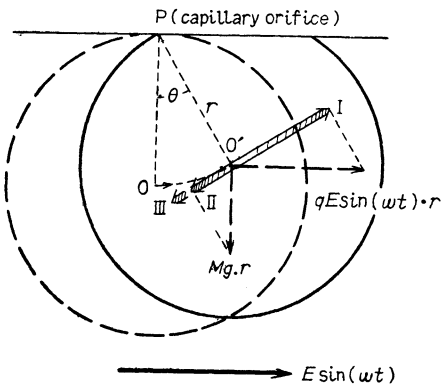


Fig. 1. The schematic representation of the forced vibration of the VDME: The moment of inertia, i, is equal to $q \cdot E \sin(\omega t) \cdot r \cos\theta$, ii is equal to $Mgr \cdot \sin\theta$ and iii is equal to $6\pi\eta r \cdot r \cdot r\, \mathrm{d}\theta/\mathrm{d}t$.

$$I\, \mathrm{d}^2\theta/\mathrm{d}t^2 = q \cdot E \sin(\omega t) \cdot r \cdot \cos\theta - Mg \cdot r \cdot \sin\theta - 6\pi\eta r \cdot r \cdot r\, \mathrm{d}\theta/\mathrm{d}t \quad (1)$$

where the moment of inertia, I, is nearly equal to $2\pi r^2/5$. In Eq. 1, $\cos\theta$ and $\sin\theta$ can be exchanged for one and θ, respectively, provided the amplitude of the vibration is small. It is noteworthy that Eq. 1 holds only in approximation; the reason is that the sphere of the DME may be deformed by the vibration.

The solution of Eq. 1 is given in the following, the term of damped vibration being neglected.

$$\theta = \alpha\{(\beta - \omega^2)\sin\omega t - \gamma\omega\cos\omega t\} / \{(\beta - \omega^2)^2 + \gamma^2\omega^2\} \quad (2)$$

where $\alpha = qEr/I$, $\beta = Mgr/I$

and $\gamma = 6\pi\eta r^3/I$ (3)

Hence, the center of the DME moves at the velocity of

$$r\, \mathrm{d}\theta/\mathrm{d}t = \alpha r\{(\beta - \omega^2)\omega\cos\omega t + \gamma\omega^2\sin\omega t\} / \{(\beta - \omega^2)^2 + \gamma^2\omega^2\} \quad (4)$$

The mean velocity acquired during the motion from the site right under the capillary orifice to the site of the maximum

1) H. Imai, S. Inouye and S. Chaki, This Bulletin, 31, 767 (1958).

* The symbols used in this paper are listed below.
q=the surface charge of the DME.
E=the intensity of the a. c. electric field.
ω=the circular frequency of the a. c. electric field.
M=the mass of the DME.
g=the acceleration of gravity.
r=the radius of the DME.
η=the viscosity coefficient of the solution.
I=the moment of inertia of the DME.

amplitude can be evaluated by Eq. 5, i. e.,

$$(r\,\mathrm{d}\theta/\mathrm{d}t)_{\mathrm{mean}}=T/4\cdot\int_0^{\tau/4}(r\,\mathrm{d}\theta/\mathrm{d}t)\,\mathrm{d}t$$
$$=2\omega\alpha r(\beta-\omega^2+\gamma\omega)/\{(\beta-\omega^2)^2+\gamma^2\omega^2\} \quad (5)$$

where T is the period of the vibration.

Assuming that the concentration of the depolarizer at the vicinity of the electrode surface does not vary owing to the successive vibration, the treatment of Okinaka-Kolthoff's theory[2] developed for the limiting current of the rotated dropping mercury electrode can be applied to this case.

Thus, the following equation is given for the mean limiting current of the VDME;

$$\bar{i}_l=\bar{i}_d+knCD^{1/2}(m\tau)^{1/2}(r\mathrm{d}\theta/\mathrm{d}t)^{1/2}{}_{\mathrm{mean}} \quad (6)$$

where $\bar{i}_d$ is the mean diffusion-controlled current in μA, n is the number of electrons transferred per an ion, C is the bulk concentration of the depolarizer in mF, D is the diffusion constant in cm^2/sec., τ is the life-time of the DME in sec. and k is a numerical constant. In Eq. 6, it is assumed that the streaming velocity of the solution on and near the electrode surface is proportional to the velocity of the vibration. It is noteworthy that the actual surface velocity, and accordingly, the constant, k, are unknown.

Combining Eqs. 3, 5 and 6, one can obtain an expression for the relation between the limiting current and the surface charge of the DME;

$$\bar{i}_l=\bar{i}_d+k'(qE)^{1/2} \quad (7)$$

where k' is a proportionality factor.

The surface charge, q, of the DME in Eq. 7 can be evaluated by the following equation. Assuming Helmholtz's electrical double layer, we get

$$q=\varepsilon\varphi/4\pi\delta \quad (8)$$

where ε is the dielectric constant, φ is the potential of the DME and δ is the thickness of the electrical double layer.

Eqs. 7 and 8 lead to the following expression:

$$\bar{i}_l-\bar{i}_d=k''E^{1/2}(\varphi_{\mathrm{DME}}-\varphi_{\mathrm{max}})^{1/2} \quad (9)$$

where k'' is a proportionality factor, φ_{DME} is the potential of the DME and φ_{max} is the potential of the electrocapillary maximum.

From Eq. 9 it can be forecast that $(\bar{i}_l-\bar{i}_d)$ becomes practically zero at the potential of the electrocapillary maximum, and that the current-voltage curve of the VDME consists of two parabolas which intersect at the potential of the electrocapillary maximum. This curvilinear relation of the current and the potential can be transferred to the linear relation by plotting the square of the $(\bar{i}_l-\bar{i}_d)$ versus the potential of the DME.

The accurate determination of the Lippmann-potential will be carried out by evaluating the intersecting point of two straight lines of the $(\bar{i}_l-\bar{i}_d)^2$ versus φ_{DME} plot in the positive polarization and in the negative polarization, respectively.

Experimental

The current-voltage curve was recorded by a Shimadzu Model RP-2 polarograph. The DME used was of an appreciably long life-time and of the slow rate of mercury flow (τ=ca. 10 sec., $m\leq$1 mg./sec.). It is because the mercury flow on the surface of the DME owing to the rapid growth of the mercury droplet presumably affects the ζ-potential of the mercury-solution interface.

The a. c. source was supplied from a C-R oscillater, and was amplified by a power tube (6L6G) and the cathode-follower out-put was applied to the platinum plate electrodes (Fig. 2).

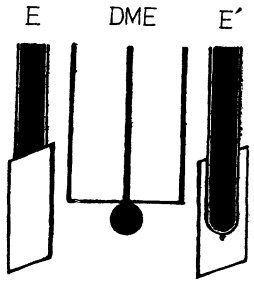


Fig. 2. VDME: E and E' are the platinum plate electrodes to which the a. c. voltage is applied.

Since the impedance of the solution was small, the cathode resistor as small as 30 ohms was used in order to avoid the voltage drop of the out-put. The a. c. voltage was measured by a vacuum tube voltmeter.

All the reagents were of analytical grade. The test solution contained 10^{-3} F Hg^{2+} as the depolarizer. The concentration of the supporting electrolyte ranged from 10^{-3} to 1 F. In the case of the low saline concentration, the depolarizer concentration as small as 10^{-4} F was preferable in order to avoid the migration current. Under these conditions the mercuric ion develops a well-defined wave by a conventional polarograph, and the diffusion-controlled current gives a plateau ranging from -0.1 to -1.7 volts vs. S. C. E. The trace of dissolved oxygen was carefully removed by adding a small quantity of the sodium sulfite solution after the sufficient

2) Y. Okinaka and I. M. Kolthoff, *J. Am. Chem. Soc.*, **79**, 3326 (1957).

bubbling of purified nitrogen. The presence of trace oxygen in the test solution causes the fatal deformation of the current-voltage curve, especially near the potential of the electrocapillary maximum in question.

Results and Discussion

The current-voltage curve of 0.77×10^{-3} F Hg^{2+} in 0.1 F KCl is illustrated in Fig. 3. In Fig. 3 the diffusion-controlled current gives a plateau covering the whole voltage span recorded.

In the region of the positive polarization, the vibration of the DME is gradually retarded as the applied potential is shifted toward more negative potentials, corresponding to the decrease of the surface charge of the DME, and this effect results in the decrease of the limiting current. At the zero-charge potential, that is, the potential of the electrocapillary maximum, the vibration entirely ceases, and accordingly the limiting current will be solely controlled by the diffusion of the depolarizer. Under the appreciably low intensity of the a. c. electric field, the limiting current coincides with the diffusion-controlled one at the potential of the electrocapillary maximum, while it is not so under the sufficiently intense electric field as is illustrated in Fig. 3. This reason is attributable to the fact that the rapid variation of the current at the potential close to the electrocapillary maximum can not be followed by the recorder owing to its damping. In the region of the negative polarization, the limiting current reincreases as the applied potential is shifted toward more negative potentials, corresponding to the increment of the surface charge of the DME. Thus, the limiting current gives a minimum at the potential of the electrocapillary maximum.

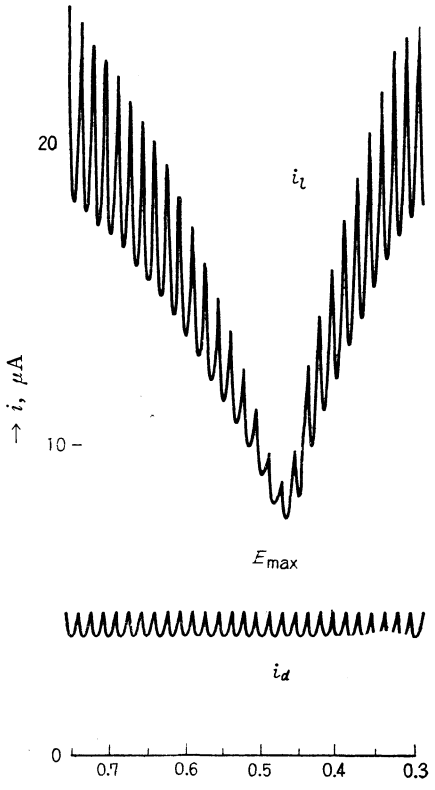


Fig. 3. The VDME current-voltage curve of 0.77×10^{-3} F Hg^{2+} in 0.1 F KCl. The a. c. frequency=25 c. p. s. The intensity of the electric field=0.55 volts/cm. τ= 9.9_4 sec. (open circuit). $m=0.85_5$ mg./sec. Temperature=25°C. (The intensity of the a. c. electric field can be lowered when the trace of surface active materials is removed by adding active charcoal).

The square of $(\bar{i}_l-\bar{i}_d)$ is plotted versus the potential of the DME in Fig. 4. In Fig. 4, the parabolic curvilinear relation of the current-voltage curve in Fig. 3 is transferred to the linear relation as is predicted in Eq. 9. The mean value** of the potential at the intersecting point of

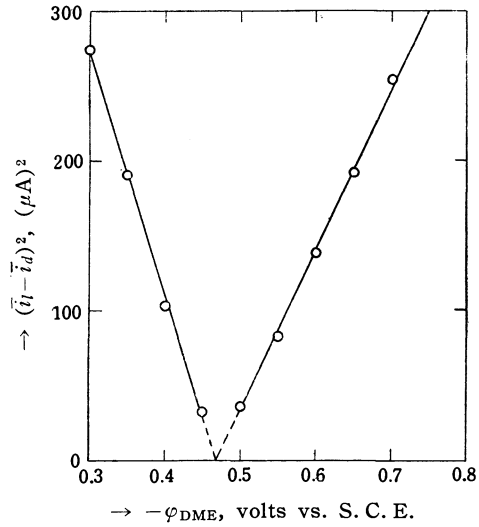


Fig. 4. Variation of the square of $(\bar{i}_l-\bar{i}_d)$ with the potential of the DME. The current was evaluated at the middle point of the saw-tooth oscillation in Fig. 3.

** This value was evaluated as the mean of the data obtained when the applied voltage sweeps toward more negative potentials and when the applied voltage sweeps toward less negative potentials.

two straight lines is -0.467 ± 0.001 volts vs. S. C. E. (in 0.1 F KCl solution). This value shows a very good agreement with the datum obtained by Grahame[3].

This method of determining the Lippmann-potential seems to be better than any other method[4] from the standpoints of the ease and rapidness of the recording, and of its good reproducibility and accuracy.

The authors wish to express their hearty gratitutde to Professor Mutsuaki Shinagawa for his advice and encouragement.

Laboratory of Chemistry, Minami College
Hiroshima University, Hiroshima

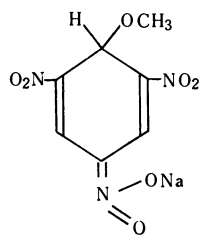
3) D. C. Grahame, *Chem. Revs.*, **41**, 441 (1947).
4) D. C. Grahame, R. P. Larson and M. A. Poth, *J. Am. Chem. Soc.*, **71**, 2978 (1949); T. I. Popova and T. A. Kryukova, *J. physik. Chem.*, **25**, 283 (1951); J. A. V. Butler, "*Electrocapillarity*", Methuen & Co., Ltd., London (1940), p. 56.

Visible and Ultraviolet Absorption Spectra of Red Complexes of 1,3,5-Trinitrobenzene and its Derivatives with Ammonium Hydroxide

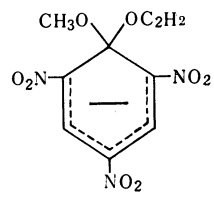
By Takehiro ABE

(Received February 10, 1959)

Trinitrobenzene and its derivatives give red colors with ammonia and with aqueous alkalies. In 1902, Meisenheimer[1] already suggested the following formulae I and II like intermediates in aromatic substitutions, for structures of red products of 1, 3, 5-trinitrobenzene and trinitroanisole with sodium methoxide or sodium ethoxide, respectively.



I



II

By means of the infrared or visible absorption spectra for the red complex of trinitroanisole Meisenheimer's structure II has recently been supported by Hammick and Foster[2,3], by Caldin et al.[4,5], and by Nagakura and Tsubomura[6]. In the previous papers[7,8] the present author also reported the visible absorption spectra of the red colors produced by trinitrobenzene, trinitrotoluene, and tetryl in dilute aqueous solutions of sodium hydroxide. These red colors were reversibly decolorized by addition of weak acids. All the above spectra have been measured directly for the red solutions prepared by adding alkaline solutions into solutions of the nitro compounds, and consequently have been subjected to be influenced by alkalies in the solutions, giving no precise molar absorbancies. In the present study, an attempt has, therefore, been made to determine molar extinction coefficients for the spectra of the red complexes of 1, 3, 5-trinitrobenzene, 2, 4, 6-trinitrotoluene, tetryl, and picryl chloride with ammonium hydroxide without the effect of alkali.

Experimental

Solvents.—All commercial guaranteed solvents were fractionally distilled after usual treatments.

Preparation of the Red Complexes of the Nitro Compounds with Ammonium Hydroxide.—A red-colored solution was prepared by

1) J. Meisenheimer, *Ann.*, **323**, 205, 214, 241 (1902).
2) D. L. Hammick and R. Foster, *J. Chem. Soc.*, **1954**, 2153.
3) R. Foster, *Nature*, **175**, 746 (1955).
4) E. F. Caldin and G. Long, *Proc. Roy. Soc.*, **A228**, 263 (1955).
5) J. B. Ainscough and E. F. Caldin, *J. Chem. Soc.*, **1956**, 2528, 2540, 2546.
6) S. Nagakura and H. Tsubomura, Personal Communication; at the Symposium on Electonic States in Tokyo on May 17, 1958.
7) T. Abe, This Bulletin, **31**, 904 (1958).
8) T. Abe, ibid., **32**, 339 (1959).

adding a little of guaranteed ammonia water (28%) into a solution made by dissolving each of the nitro compounds into acetone. This red solution was evaporated slowly at room temperature by a vacuum pump to remove acetone, ammonia and water, and a dark red residue was obtained. However, the red substance obtained

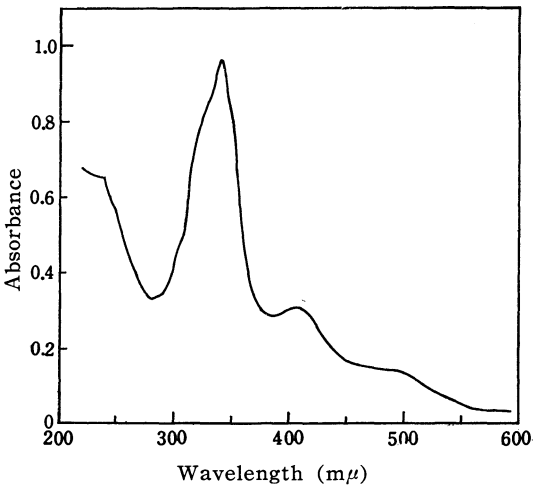


Fig. 1. An absorption spectrum of the red complex of trinitrotoluene with ammonium hydroxide, obtained by evaporation on a water bath, in water.

by evaporation not at room temperature but on a water bath gives an absorption curve illustrated in Fig. 1, which is very different from that indicated in Fig. 2, possibly owing to the further reaction. After being washed with a small quantity of acetone to remove the nitro compound contained, the red substance was dried again at room temperature by a vacuum pump. The powdered dark red product obtained is considered to be the colored complex of the nitro compound with ammonium hydroxide, which is more soluble in water than in acetone, while the nitro compound readily dissolves in acetone but not easily in water. By the above procedure, the red complex of picryl chloride could be obtained easily, although the red color produced by picryl chloride with sodium hydroxide in water disappeared in a few minutes[8].

Spectra.—The spectra of the solutions were measured with a Hitachi quartz spectrophotometer, Model EPU-2 at room temperature. The path length of absorption cells was 1 cm.

Trinitrobenzene forms with sodium methoxide a red product of the empirical composition, trinitrobenzene · CH_3ONa · $1/2H_2O$[9] and with sodium hydroxide a red one having the empirical composition, trinitrobenzene · NaOH[10], respectively. In the present work, the red complexes of the nitro compounds with ammonium hydroxide are assumed to have compositions of nitro compound·NH_4OH in calculating molar extinction coefficients for their spectra. This point is returned to below.

9) L. de Bruyn and van Leent, *Rec. trav. chim.*, **14**, 150 (1895).
10) Giua, *Gazz. chim. ital.*, **45**, II, 351 (1915).

Results and Discussion

The Spectra of the Red Complexes of the Nitro Compounds with Ammonium Hydroxide in Water (Fig. 2).—An absorption spectrum for the red complex of trinitrotoluene is similar to that for the

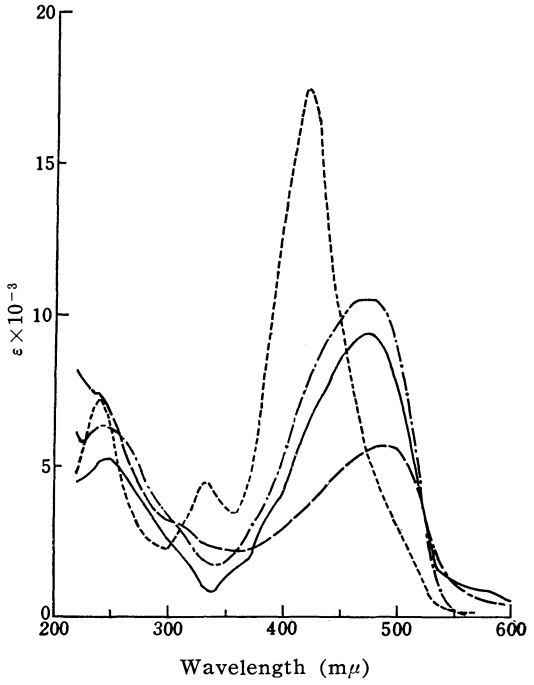


Fig. 2. Absorption spectra of the red complexes of trinitrobenzene (——), trinitrotoluene (—·—), tetryl (— —), and picryl chloride (----) with ammonium hydroxide, all in water.

complex of trinitrobenzene, showing an intense absorption maximum band at about 475 mμ, although a whole molar absorbancy for the former is slightly greater than that for the latter. This similarity implies that both the red complexes are structurally analogous. The red complex of tetryl also shows an analogous absorption curve with those of trinitrobenzene and trinitrotoluene, giving a weaker absorption maximum at about 490 mμ as compared with those for the latter. Only the red complex of picryl chloride shows an intense absorption maximum band at about 420 mμ as compared with those for the other complexes, and a weak band clearly at about 330 mμ. The 330 mμ band seems possibly to be attributed to the complex, although it has not been decided whether the band is due

to the complex itself or to picric acid formed by the further reaction[8], because the band lies at the wavelength close to that of the maximum for the picrate ion. All these red complexes give distinct bands at about 240 mμ.

The Spectra of the Red Complexes in Ethanol (Fig. 3).—These red comlexes in ethanol roughly show the similar spectra

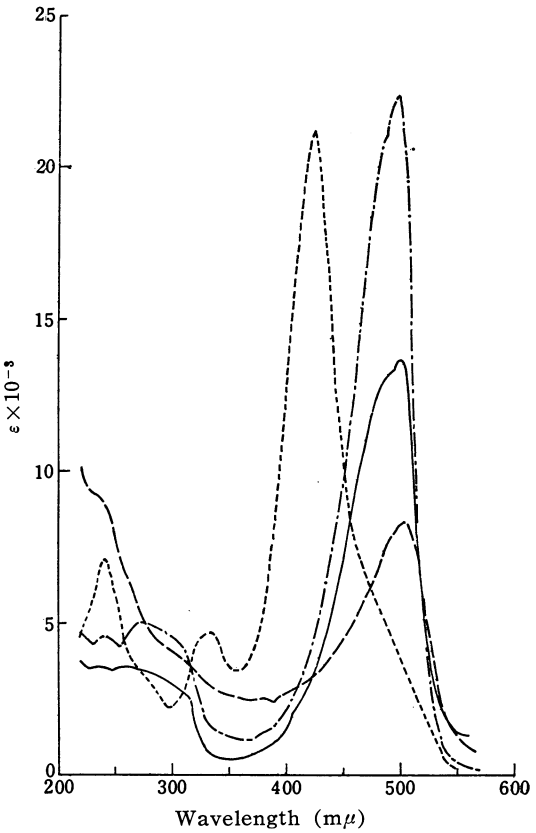
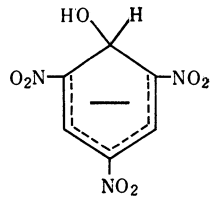


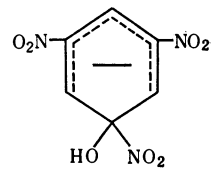
Fig. 3. Absorption spectra of the red complexes of trinitrobenzene (——), trinitrotoluene (—·—), tetryl (—··—), and picryl chloride (----) with ammonium hydroxide, all in ethanol.

as in water. Both in ethanol and in water, the intense visible absorption bands for these complexes shift to the red in the order of picryl chloride, trinitrotoluene, trinitrobenzene, and tetryl with their molar absorbancies decreasing in the same order, except the molar absorbancy for picryl chloride in ethanol. The molar absorbancies for the 240 mμ bands increase in the order of trinitrobenzene, trinitrotoluene, picryl chloride, and tetryl. All the visible bands shift to the red and have greater molar absorbancies in ethanol as compared with those in water. Each of the wide visible bands for the red complexes of trinitrobenzene, trinitrotoluene, and tetryl in water is expected to consist of more than two absorption bands, because a shoulder is observed for the corresponding one in ethanol.

The red complexes between these nitro compounds and ammonium hydroxide may be regarded as the same complexes as those of the nitro compounds with sodium hydroxide or sodium methoxide. Accordingly, the red complexes with ammonium hydroxide can be presumed to have compositions of nitro compound · NH_4OH by analogy with the empirical compositions of trinitrobenzene · CH_3ONa[9], trinitrobenzene · NaOH[10], and trinitroanisole · CH_3ONa[11], as mentioned above. On standing in the cold with dilute aqueous solution of sodium hydroxide, 1,3,5-trinitrobenzene yields 3,5-dinitrophenol[12] through a red intermediate. Considering only this reaction, the red intermediate seems to be more like the following structure IV than like the structure III presented by Meisenheimer, as mentioned in the previous paper[8].

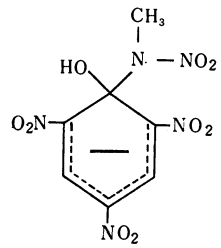


III



IV

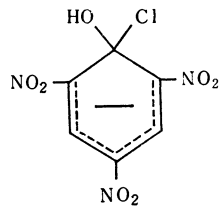
The red color of the complex is certainly owing to transitions of its π-electrons. On the other hand, the complex of tetryl with sodium hydroxide finally produces a product indicating an absorption curve analogous to that for picric acid[8]. The red complex of tetryl with hydroxide anion is, therefore, expected to have Meisenheimer's structure V.



V

11) Jackson, *Am. Chem. J.*, **20**, 448 (1898); **23**, 294 (1901).
12) L. de Bruyn and van Leent, *Rec. trav. chim.*, **13**, 151 (1894).

However, Figs. 2 and 3 indicate that the spectra for the red complex of trinitrobenzene resemble those for the red complex of tetryl, as in the case of the red complexes with sodium hydroxide[8]. This similarity between their spectra can be explained by assuming the structure III for the red complex of trinitrobenzene, since the structure IV is hardly expected to be able to give the similar spectra as those for structure V owing to difference between their π-electron systems. In dilute aqueous solution of sodium hydroxide, picryl chloride finally gives an absorption curve analogous to that of picric acid after the red coloration[8], as in the case of tetryl. The red complex of picryl chloride with ammonium hydroxide is, therefore, expected to have the structure VI such as that for tetryl.



VI

Figs. 2 and 3, though not decisive, appear to be in favor of Meisenheimer's structures such as III, V and VI for all the above red complexes with ammonium hydroxide. Their structures are, however, to be determined hereafter by means of X-rays and infrared spectroscopy.

The difference between the spectra for the red complexes of tetryl and picryl chloride, which both seem to have the same π-electron structures indicated in V and VI, can be interpreted in terms of hyperconjugation of -Cl and $-N(CH_3)NO_2$ to their π-electron systems.

Effect of Sodium Hydroxide on the Spectrum of the Red Complex of 2, 4, 6-Trinitrotoluene with Ammonium Hydroxide in Water (Fig. 4).—As the concentration of sodium hydroxide increases, the molar absorbancy for the spectrum of the red complex of trinitrotoluene with ammonium hydroxide decreases in water, and the decolorization of the red color becomes faster. On the other hand, all these red complexes of the nitro compounds are very stable both in water and in ethanol in absence of alkali. The negative ion OH^- is, therefore, considered

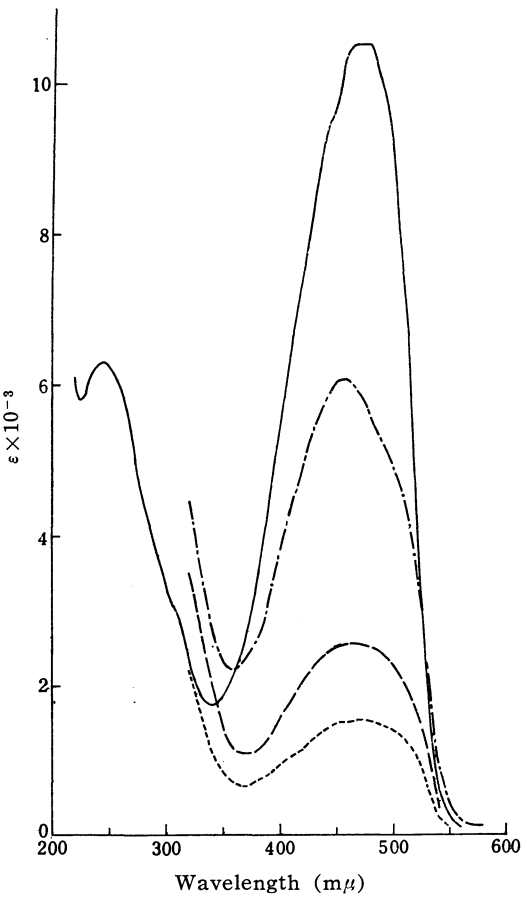


Fig. 4. Absorption spectra of the red complex of trinitroluene with ammonium hydroxide (4.96×10^{-5} M) in water (——) and in aqueous sodium hydroxide solution (0.103 N: —·—, 0.516 N: ——, 1.03 N: ----).

to play an important role for the further decolorization reaction of the red complex. At a low concentration of sodium hydroxide, 0.103 N, the red complex of trinitrotoluene shows an absorption curve similar to that for trinitrotoluene in an aqueous solution of sodium hydroxide[7,8]. This leads to the suggestion that the absorption curves for the red complexes of the nitro compounds, reported in the previous papers[7,8], are somewhat affected by sodium hydroxide.

Summary

The red complexes of trinitrobenzene, trinitrotoluene, tetryl and picryl chloride with ammonium hydroxide, regarded as intermediates in aromatic substitutions, were obtained. Each of these red complexes roughly shows a similar spectrum

both in water and in ethanol. All their visible bands, however, shift to the red and have greater molar absorbancies in ethanol as compared with those in water. The red complex of trinitrobenzene shows an absorption curve analogous to that for the complex of tetryl, although they yield different products after further reactions. As the concentration of sodium hydroxide increases, the molar absorbancy for the spectrum of the red complex of trinitrotoluene decreases in water, probably owing to the action of OH^-.

The author is particularly indebted to Professor Y. Nomura for his suggestion and encouragement throughout this work. Thanks are also due to Dr. S. Maeda for the use of the spectrophotometer.

Department of Chemistry
Defense Academy
Yokosuka

SHORT COMMUNICATIONS

Infrared Spectroscopic Study on Hydrogen Bond Formation between Acetylene and Donor Solvents

By Shunsuke MURAHASHI*, Bunkichi RYUTANI and Koichi HATADA*

(Received June 5, 1959)

It was previously reported by Copley[1], Huemer[2], and Mckinnis[3] that a donor solvent showed a high solvent power for acetylene. They suggested that this could be attributed to hydrogen bond formation between a hydrogen atom of methine group and a donor group of solvent. Any direct experimental evidence, however, has not been given.

In the course of our studies on the solubility of high pressure acetylene in various solvents at low temperature, some evidences which show the hydrogen bond formation have been accumulated by the measurements of the solubility in mixed solvents and of infrared spectra of acetylene. This communication deals with some results obtained from spectroscopic measurements[4].

The spectra were measured by means of a Perkin-Elmer model 21 double beam spectrophotometer equipped with a rock salt prism. The wave numbers of the absorption bands were corrected by the spectral data of a thin film of polystyrene measured right after each run. The error range of the observed wave numbers was about $\pm 5\,cm^{-1}$ at $3000\,cm^{-1}$ and about $\pm 1\,cm^{-1}$ at $700\,cm^{-1}$. Two cells of 0.1 mm. thickness filled with solution and with pure solvent respectively, were used in order to avoid interference of strong bands of the solvent. All the measurements were carried out at 20~25°C.

The spectral data of the acetylene dissolved in various solvents are given in Table I. As shown in Table I, the C–H stretching bands of acetylene in these solutions shift toward lower frequencies and the C–H deformation bands toward higher frequencies than those of gaseous acetylene. The largest shifts of the C–H stretching and deformation frequencies were found for ethyleneglycol dimethyl ether solution. On the other hand, the solution in *n*-octane, which shows the lowest solubility of acetylene, gives negligibly small shifts of the C–H stretching and deformation bands. The last column of Table I shows that the solubility of acetylene in donor solvents can be related to the magnitudes of the shifts of the C–H stretching and deformation frequencies. Therefore, it appears that a close relationship exists between the solubility of acetylene and the donating power of solvent molecules.

Further evidences of these arguments were also obtained by the absorption

* Present address: Department of Chemistry, Faculty of Science, Osaka University, Nakanoshima, Osaka.

1) M. J. Copley et al., *J. Am. Chem. Soc.*, **61**, 1599 (1939).

2) H. Huemer, Library of Congress, Washington 25, D. C., Microfilm file PB. 73508, (1942) p. 7274.

3) A. C. Mckinnis, *Ind. Eng. Chem.*, **47**, 850 (1955).

4) The results of the study of solubility will be reported in *J. Chem. Soc. Japan, Pure Chem. Sec.* (*Nippon Kagaku Zasshi*).

TABLE I. INFRARED ABSORPTION SPECTRA OF ACETYLENE IN VARIOUS SOLUTIONS*

Solvents	C-H stretching vibration		C-H deformation vibration		Solubility of acetylene at 0°C, 6.8 atm. C_2H_2 press., molefractions
	ν cm^{-1}	$\Delta\nu$** cm^{-1}	ν cm^{-1}	$\Delta\nu$** cm^{-1}	
n-Octane	3278	− 5	731	0	0.100
Benzene	3257	−26	742	11	—
n-Hexyl ether	3229	−54	—	—	0.303
Ethyleneglycol dimethyl ether	3205	−78	766	35	0.541

* Saturated solutions were prepared by bubbling dry acetylene through the solvents at 20°C under atmospheric pressure.

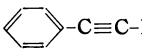
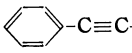
** $\Delta\nu=\nu-\nu_0$

ν_0: the value for gaseous acetylene

ν_0(for C-H stretching) = 3282.5 cm^{-1} [5]

ν_0(for C-H deformation) = 730.74 cm^{-1}

TABLE II. INFRARED ABSORPTION SPECTRA OF MONOSUBSTITUTED ACETYLENES AND THEIR SOLUTIONS IN ETHYLENEGLYCOL DIMETHYL ETHER

Monosubstituted acetylenes	ν_{C-H} or ν_{C-D} cm^{-1}			$\Delta\nu$* cm^{-1}
	Liq. substances	CCl_4 solutions (5 vol. %)	$CH_3OCH_2CH_2OCH_3$ solutions (5 vol. %)	
 -C≡C-H	3281	3313	3241	− 72
 -C≡C-D	2564	2583	2545	− 38
H-C≡C-$CO_2C_2H_5$	3238	3300	3196	−104
H-C≡C-C≡N	3238	3304	3151	−153

* $\Delta\nu=\nu_{C-H(or\ C-D)}$ (in $CH_3OCH_2CH_2OCH_3$ solution) $-\nu_{C-H(or\ C-D)}$ (in CCl_4 solution)

measurement of four monosubstituted acetylene derivatives as shown in Table II. The spectra of these compounds are somewhat complicated on account of an interaction between methine group and substituted group in the molecule. It is, however, of interest to see great differences between the frequencies of their C-H stretching bands in ethyleneglycol dimethyl ether solution and those in carbon tetrachloride solution. In these cases it is seen that the magnitude of the shift of the C-H stretching band depends upon the electronegativity of the substituted groups. All of the above results show that a hydrogen bond is formed between the solute and the donor solvent molecules.

Furthermore some additional evidences of the presence of these intermolecular interaction were also obtained. As shown in Table II, the absorption bands of pure liquid propiolic and cyanoacetylene considerably shift to lower frequencies than those in dilute carbon tetrachloride solution. These shifts may be attributed to the formation of intermolecular hydrogen bond.

Similar shifts were also observed for phenyl acetylene and its deuterated one. The shifts are, however, not so large as those of the above mentioned substances. Therefore, these small shifts may be caused by the "hydrogen-bond-like interaction" between π bonds of benzene nucleus and methine hydrogen[6].

The C-H deformation band was not observed in the rock salt region for the acetylene derivatives except for the case of cyanoacetylene where the frequency of the C-H deformation band was 671 cm^{-1} for the carbon tetrachloride solution and 736 cm^{-1} for the ethyleneglycol dimethyl ether solution. These results of the deformation band may also support the presence of hydrogen bond between the solute and the solvent.

The authors are grateful to Dr. H. Tadokoro in their laboratory for his helpful discussions and to the Research Laboratory

5) E. E. Bell and H. H. Nielsen, *J. Chem. Phys.*, 18, 1382 (1950).

6) A. W. Baker and A. T. Shulgin, *J. Am. Chem. Soc.*, 80, 5358 (1958); P. B. Schleyer et al., ibid., 80, 6691 (1958).

of Dainippon Celluloid Co., Ltd., for the use of the spectrometer.

Institute of Scientific and Industrial Research
Osaka University
Sakai, Osaka

Polarographic Half-Wave Reduction Potentials of Vinyl Compounds and their Molecular Orbital Computation

By Takayuki Fueno, Kameo Asada, Keiji Morokuma and Junji Furukawa

(Received June 25, 1959)

The polarographic half-wave reduction potentials of several vinyl compounds have been determined under essentially identical condition*, and it has been found that these potentials are linearly related to the heights of the lowest vacant π-electronic energy levels of these compounds calculated by the LCAO MO method.

The reduction potentials were determined in a 3 : 1 dioxane-water mixture containing 0.05 M tetra-*n*-butylammonium iodide as a supporting electrolyte. All the compounds were purified by appropriate methods before use. A measured amount of vinyl compound was dissolved into the electrolyte solution so that its concentration was in the region ranging from 10^{-3} to 5×10^{-3} M.

The electrolysis-cell was immersed in a thermostat maintained at 25.0±0.1°C, and any oxygen dissolved in the solution was removed by passing through it a slow stream of oxygen-free and solvent-saturated nitrogen. The dropping-mercury electrode was polarized against a saturated calomel electrode (S. C. E.) connected to the mercury cathode through a pin-hole in the wall of the cell, and the current-voltage curve was recorded. Maxima of the current-voltage curves were suppressed by 10^{-5} M methylene blue incorporated in the sample solution. The half-wave potentials, $E_{1/2}$, were read against S. C. E. and were all corrected for *iR* drop. When tetra-*n*-butylammonium hydroxide was used as the supporting electrolyte, the potentials did not appreciably deviate from those determined in the iodide solution. All the obtained data on $E_{1/2}$ are listed in Table I.

In calculating the energies of the lowest vacant π-levels, the simple LCAO MO method (neglecting overlap integrals) was employed. For each vinyl compound x_{lv}, defined as $\varepsilon_{lv}=\alpha+x_{lv}\beta$, was obtained from the required secular equation. Here α and β are the Coulomb integral of a carbon atom and the resonance integral of a carbon-carbon π-bond, respectively, and ε_{lv} is the energy of the lowest vacant π-level. To empirical integral parameters associated with heteroatoms, were assigned the same values that had previously been used to calculate the localization energies of vinyl compounds[1,2]: $\alpha_O=\alpha+2\beta$ (for carbonyl oxygens), $\alpha_O=\alpha+\beta$ (for ethereal oxygens), $\alpha_N=\alpha+\beta$, $\alpha_{Cl}=\alpha+1.8\beta$, $\alpha_C=\alpha-0.2\beta$ (for carbons bearing a methyl group), $\beta_{CO}=\sqrt{2}\beta$ and $\varepsilon=0.1$**. The

Table I. The interrelation among $E_{l/2}$, x_{lv} and L_{β^-} for vinyl compounds

Vinyl compound	$-E_{l/2}$ a) With Bu_4NI	$-E_{l/2}$ a) With Bu_4NOH	$-x_{lv}$	L_{β^-} b)
Acrylonitrile	2.01	1.95	0.314	1.240
Acrolein	1.53	—	0.315	1.214
Methyl vinyl ketone	1.67	1.63	0.386	1.299
Methyl acrylate	1.95	1.94	0.500	1.428
Methyl methacrylate	2.01	2.00	0.511	1.511
Styrene	2.35	2.35	0.662	1.704
α-Methylstyrene	2.39	2.39	0.692	1.843
β-Methylstyrene	2.54c)	—	0.735	—
Phenyl vinyl ether	3.0	3.0	0.960	2.196
Ethylene	NW	NW	1.000	2.000
Vinyl acetate	NW	NW	1.065	2.130
Vinyl chloride	NW	NW	1.087	2.173
Propylene	NW	NW	1.105	2.210
n-Butyl vinyl ether	NW	NW	1.194	2.387
i-Butyl vinyl ether	NW	NW	1.194	2.387
Isobutylene	NW	NW	1.220	2.440

a) Given in volt vs. S. O. E. The mark NW means "no reduction wave".

b) Given in units of $-\beta$. The values are taken from Ref. 2.

c) H. A. Laitinen and S. Wawzonek, *J. Am. Chem. Soc.*, 64, 1765 (1942).

* Some experimental data determined under different conditions are available, which can not be directly compared.

1) T. Fueno, T. Tsuruta and J. Furukawa, *J. Chem. Soc. Japan, Pure Chem. Sec.* (*Nippon Kagaku Zasshi*), 78, 1075 (1957).

2) T. Fueno, T. Tsuruta and J. Furukawa, ibid., 78, 1080 (1957).

** A carbon atom bearing one or more heteroatoms was assumed to have the Coulomb integral of $\alpha+\varepsilon\beta\Sigma k_X$. Here $\alpha+k_X\beta$ is the Coulomb integral of the heteroatom X.

resonance integrals for π-bonds other than carbonyl bonds were all assumed equal to β. The calculated values of x_{lv} are also listed in Table I. Since both α and β are negative quantities, the lowest vacant level ought to be more stable as x_{lv} takes a smaller negative value.

Inspection of the data given in Table I shows that, the smaller the value of x_{lv} for a vinyl compound, the more easily it can be reduced. Phenyl vinyl ether was found to have the highest reduction potential (ca. -3.0 V.) of all the compounds which could be reduced under the present experimental condition. At about -3.0 V. the residual current began to increase markedly owing to reduction of the supporting electrolyte. Vinyl acetate, vinyl chloride, *n*-butyl vinyl ether, *i*-butyl vinyl ether, ethylene, propylene and isobutylene gave no reduction waves in the range of the applied potential less negative than -3.0 V. vs. S. C. E. The situation may reasonably be explained by their relatively large values of $-x_{lv}$.

The half-wave potentials, $E_{1/2}$, determined with the ammonium iodide as the supporting electrolyte were found to be linearly correlated to x_{lv}'s by

$$E_{1/2} = 2.33\, x_{lv} - 0.80$$

the correlation coefficient being 0.995. The linear equation gives $\beta = -2.33$ eV., if it is assumed that, as in the case of unsaturated hydrocarbons[3,4], the electron transfer step from the electrode to vinyl compounds would be potential-determining. This value of β is in reasonable agreement with -2.23 eV.[4] for unsaturated hydrocarbons.

It seems interesting to note that the value of $-x_{lv}$ increases with increasing magnitude of the anionic β-carbon localization energy, L_{β^-} [2], of vinyl compounds, as seen in Table I. Thus, the polarographic reducibility of vinyl compounds may roughly parallel to their anionic polymerizability. This is to be expected, because vinyl compounds probably possess parallel susceptibilities toward an electron as well as basic substances. The detailed discussion on the present results will be published elsewhere.

Department of Industrial Chemistry
Faculty of Engineering
Kyoto University
Sakyo-ku, Kyoto

3) H. A. Laitinen and S. Wawzonek, *J. Am. Chem. Soc.*, **64**, 1765 (1942).
4) G. J. Hoijtink and J. van Schooten, *Rec. trav. chim.*, 72, 903 (1953).

*The Abnormal Relation between the Viscosities and the Temperatures of Sodium Carbonate Solution**

By Kazuo FUJITA

(Received June 29, 1959)

It has been reported that the ultrasonic velocity and electric conductivity of the dilute solution of sodium sulfate present the abnormalities at the temperatures near the transition points of the saturated solution coexisting with the solid states[1,2].

But the reason why these abnormalities are caused is not fully explained in these reports. Therefore, this communication is to report that the abnormal relation between the viscosities and the temperatures was discovered in sodium carbonate solution.

The author believes that this result is a clue to the behavior of the aqueous solution, containing the inorganic compounds which have the transition-points in the saturated solutions.

In the viscosity measurements was used Ubbelohde suspended level viscometer,

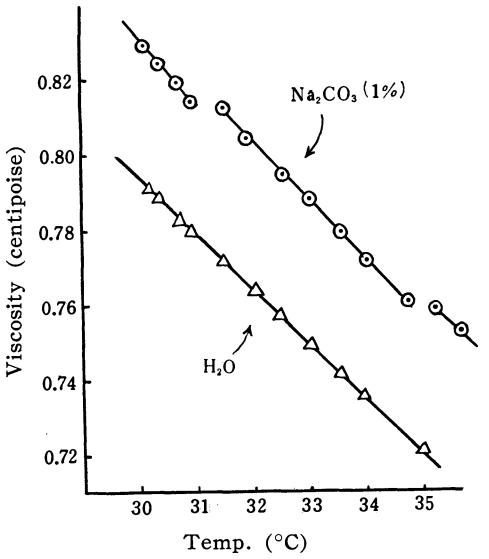


Fig. 1. Plot of viscosity against temperature for 1% Na_2CO_3 aqueous solution and distilled water.

* Presented at 12th Annual Meeting of the Chemical Society of Japan, Kyoto, April 2, 1959.

1) T. Sasaki and T. Yasunaga, *Chem. and Chem. Ind. (Kagaku to Kogyo)*, **7**, 146 (1954).

2) K. Hirano, *J. Chem. Soc. Japan, Pure Chem. Sec. (Nippon Kagaku Zasshi)*, **79**, 648 (1958).

the length and diameter of whose capillary are 20 cm. and 0.33 mm., respectively, and this viscometer being used, the flow time of distilled water 7 cc. was 2280 seconds at 25°C, and in this determination a kinetic energy correction was negligible. The temperature measurements were made with accuracy of ±0.01°C. At intervals of 0.5°C from 25 to 40°C, the flow time of 1% sodium carbonate solution and distilled water were measured using a stop watch. The results were shown in Fig. 1. From these results, it is seen that the changes of viscosity with temperatures were not smooth at about 31 and 35°C.

TABLE I. ENTHALPIES OF ACTIVATION FOR VISCOUS FLOW OF Na_2CO_3

Temp. range (°C)	Enthalpy of activation for viscous flow (kcal./mol.)
Below 30.93	5.11
31.43~34.90	3.11
35.29 and over	2.63

These two points of temperature correspond to the two transition points of the saturated sodium carbonate coexisting with the solid.

Eyring and coworkers[3] have applied the theory of absolute reaction rates to viscous flow and obtained following relation

$$\eta = hN/V \cdot \exp \Delta F^*/RT$$

where ΔF^* is the free energy of activation for viscous flow, V is the molar volume and the other constants have the usual significance. By using this relation the enthalpies of activation for viscous flow were calculated. The values of the enthalpies at below 30.9°C, 31.4~34.9°C and above 35.3°C are different from each other, and the data are shown in Table I.

The viscosity measurements are being made on solutions of sodium carbonate with various concentrations and dilute solutions of other compounds (e.g., Na_2HPO_4).

Department of Chemistry
Wakayama Medical College
Misono-cho, Wakayama

3) S. Glasstone, K. J. Laidler and H. Eyring, "The Theory of Rate Processes", McGraw-Hill Book Co., Inc., New York (1941).

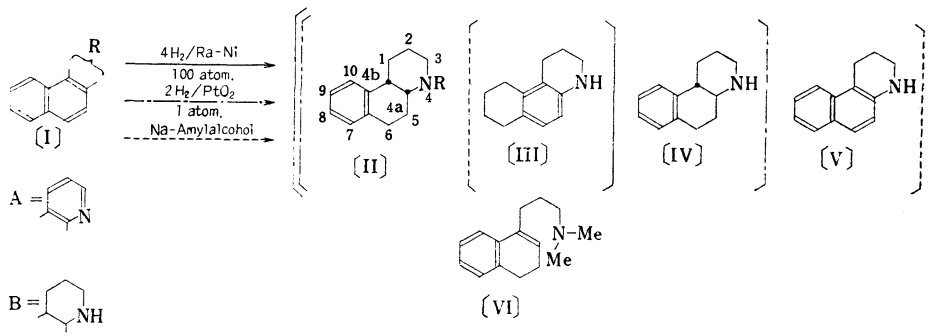
The Syntheses and Exhaustive Methylation of cis- and trans-1, 2, 3, 4, 5, 6, 4a, 4b-Octahydrobenzo [f] quinoline[1]

By Tadashi MASAMUNE
and Masato KOSHI*

(Received July 10, 1959)

A recent paper[2] has described the preparation and also Hofmann's exhaustive methylation of 4-methyl-1, 2, 3, 4, 5, 6, 4a, 4b-octahydrobenzo [f] quinoline (II) R=Me. The stereochemistry of the ring fusion is tentatively assigned as *cis*.

The present paper undertakes to report the syntheses and exhaustive methylation of *cis*- and *trans*-1, 2, 3, 4, 5, 6, 4a, 4b-octahydrobenzo [f] quinoline (II) R=H and (IV). These bases are interesting as 5, 6-benzo-derivatives of decahydroquinoline.



* Present address: Central Research Laboratory of Tōyōkōatsu Industries, Inc., Totsuka-ku, Yokohama.

1) Part X of "The Condensed Polynuclear Perhydrocompounds Containing Nitrogen"; Part IX, T. Masamune, This Bulletin, **30**, 491 (1957).

2) N. A. Nelson, J. E. Ladbury and R. S. Hsi, *J. Am. Chem. Soc.*, **80**, 6633 (1958).

Hydrogenation of benzo[f]quinoline[3] (I) R=A using a catalyst of Raney nickel (150°C) under 100 atm. initial pressure resulted in conversion into the mixture of octahydrobenzo[f]quinoline, consuming four molecular equivalents of hydrogen. From the ethereal solution of oily mixture, *cis*-octahydrobenzo[f]quinoline (II) R=H was isolated as carbonate. *cis*-1,2,3,4,5,6,4a,4b-Octahydrobenzo[f]quinoline[4], which was analyzed as the hydrochloride (Found: C, 64.46; H, 8.09. Calcd. for $C_{13}H_{17}N \cdot HCl \cdot H_2O$; C, 64.65; H, 8.28%.), can be regenerated from the carbonate by adding aqueous caustic alkali. Overall yield, 4.8%. The evaporation of the solvent from mother ethereal solution gave 1,2,3,4,7,8,9,10-octahydrobenzo[f]quinoline (III) in yield of 88%, but no *trans* isomeride could be isolated. On the other hand, hydrogenation of 1,2,3,4-tetrahydrobenzo[f]quinoline[5] (I) R=B in glacial acetic acid with platinum oxide as a catalyst at ordinary pressure, gave the mixture of *cis* and *trans* isomers of octahydrobenzo[f]quinoline in poor yield (*cis* and *trans* 2.4% each). The main product was 1,2,3,4,7,8,9,10-octahydrobenzo[f]quinoline. Yield, 86%. The separation of *cis* and *trans* isomerides was carried out most conveniently by means of the difference between the speed of carbonate formation of the *cis*- and *trans*-bases; thus, on exposing the mixture of *cis* and *trans* isomerides to air for a few hours the *cis* isomeride forms the carbonate preferentially.

Furthermore, the reduction of benzo[f]-quinoline to octahydro-derivatives by sodium and amylalcohol, which has been first described by Bamberger and Müller[3] was reexamined. In this case, *trans*-1,2,-3,4,5,6,4a,4b-octahydrobenzo[f]quinoline (IV) (2.9%) (Found: C, 83.25; H, 9.12; Calcd. for $C_{13}H_{17}N$: C, 83.43; H, 9.08%.), 1,2,3,4,7,8,9,10-octahydrobenzo[f]quinoline (III) (29%) and 1,2,3,4-tetrahydrobenzo-[f]quinoline (V) (39%) were obtained respectively from the reaction mixture.

Though no rigid proof can be given for the configuration of the above isomers,

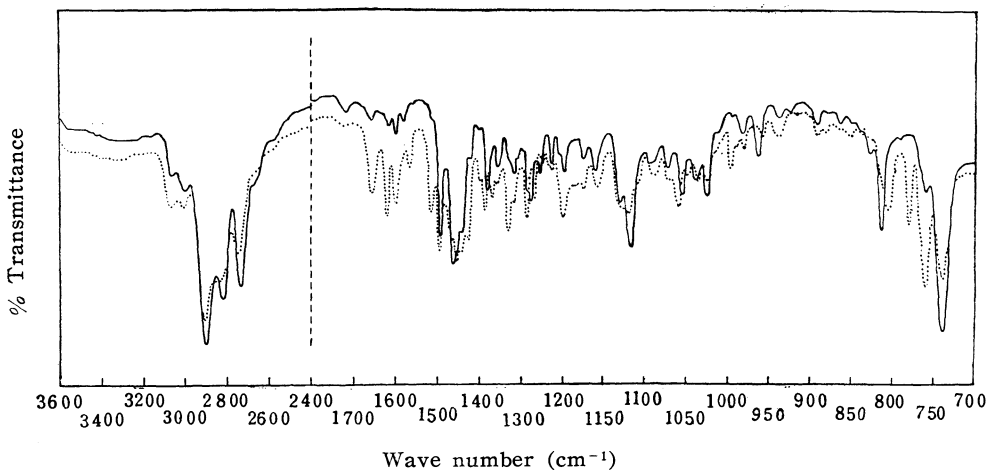


Fig. 1. The infrared spectra of *cis*- and *trans*-4-methyl-1,2,3,4,5,6,4a,4b,-octahydrobenzo[f]-quinolines.
cis: ------ *trans*: ——

TABLE I. PHYSICAL CONSTANTS OE THE *trans* AND *cis* ISOMERS AND THEIR DERIVATIVES

	cis, (°C)	*trans*, (°C)
1,2,3,4,5,6,4a,4b-Octahydrobenzo[f]quinoline	b. p. 160~165/5 mm.	m. p. 88~ 90[b]
Benzoate	m. p. 96~ 97	m. p. 100~102
Picrate	m. p. 197~198.5	m. p. 189~190
Hydrochloride	m. p. 258~259	m. p. 251~253[c]
N-Methylate picrate	m. p. 165~167	m. p. 210~212
Methiodide	m. p. 295[a]	m. p. 238~240

a) N. A. Nelson et al.[2] record m. p. 295°C (decomp.).
b) E. Bamberger et al.[3] record m. p. 91°C.
c) E. Bamberger et al.[3] record m. p. 252°C.

3) E. Bamberger and R. Müller, *Ber.*, **24**, 2648 (1891).
4) Analysis of free base was difficult, owing to rapid absorption of atmospheric carbon dioxide.
5) E. Bamberger and R. Müller, *Ber.*, **24**, 2641 (1891).

in view of the reduction conditions and other considerations[2] there is little doubt that the higher melting product resulting from the reduction with sodium-alcohol system is the *trans* isomeride. The infrared spectra of *cis*- and *trans*-*N*-methyl-octahydrobenzo[f]quinoline are shown in the figure. Physical constants of the *cis* and *trans* isomers and their derivatives are given in Table I.

Exhaustive methylation of *cis*-octahydrobenzo[f]quinoline has been recently carried out by Nelson et al.[2] who found that distillation of *cis*-octahydro-4-methylbenzo[f]quinoline methohydroxide produced 1-(3-dimethylaminopropyl)-3,4-dihydronaphthalene (VI). In the present investigation the Hofmann degradation of *cis*- and *trans*-octahydro-4-methylbenzo[f]-quinoline methohydroxides gave the same oily product in yields of 43% and 32%, respectively, boiling at 150~155°C/4 mm. (picrate m.p. 87~88°C), which was identified as 1-(3-dimethylaminopropyl)-3,4-dihydronaphthalene (VI), and no other compound could be isolated.

Examination of a model of the feasible structures for *cis*- and *trans*-*N*-methyl-octahydrobenzo[f]quinoline shows that in *cis* configuration the necessary conformational requirement for easy Hofmann fission is satisfied by elimination of any one of the equatorial 2-hydrogen, 4b-hydrogen and 5-hydrogen and in *trans* configuration by elimination of the equatorial 2-hydrogen.

Thus, in the exhaustive methylation of both *cis*- and *trans*-octahydrobenzo[f]-quinolines the preferential elimination of a β-proton on C 4b shows vividly that the influence of the electronic character of aromatic substituent at position C 4b is superior to the necessary co-planar *trans*-arrangement for easy Hofmann fission. Several examples[6] of this type of elimination have already been reported. Detailed results of the matters discussed in the present paper will be reported elsewhere.

Department of Chemistry
Faculty of Science
Hokkaido University
Sapporo

6) T. Masamune, This Bulletin, **30**, 491 (1957) and references given there; H. Booth, F. E. King and J. Parrick, *J. Chem. Soc.*, **1958**, 2302.

Thermal Homopolymerization of Lysine and Copolymerization with Neutral and Acidic Amino Acids[1]

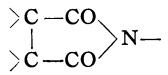
By Kaoru HARADA

(Received July 15, 1959)

Glutamic acid and aspartic acid characteristically yield copolymers[2,3] with unsubstituted amino acids which fail to form polymers when heated individually. By using an excess of acidic amino acids, it is furthermore possible to copolymerize eighteen common amino acids into a *proteinoid*[4].

The special effects of basic amino acids, particularly lysine, are also interesting. Free DL-lysine was converted to its liquid lactam at 150~170°C with vigorous evolution of water vapor and it homopolymerized at 180~230°C.

The free lysine also copolymerized easily with glycine, alanine and other neutral amino acids, glutamic acid, aspartic acid, caprolactam, succinic acid, terephthalic acid and other carboxylic acids. After acidic hydrolysis, component amino acids were identified by paper chromatography. Infrared absorption spectra of lysine homopolymer, lysine-neutral amino acid copolymers and lysine-glutamic acid copolymer indicated that these are typical polypeptides. The salient maxima at 3080, 3280, 1630 and 1540 cm^{-1}; however, lysine-aspartic acid copolymer shows additional bands at 1720 and 1780 cm^{-1} which indicate the 5 membered cyclic imide structure[5],



Some of the yield and amino acid composition of typical polymers are as follows:

DL-Lysine homopolymer*

Temp., °C	Yield after dialysis, g.
180	0.07
190	0.15
200	0.17
210	0.18

1) Contribution No. 116 of the Oceanographic Institute, aided by Grant C-3971 of the National Institutes of Health, U. S. Public Health Service.

2) K. Harada and S. W. Fox, *J. Am. Chem. Soc.*, **80**, 2694 (1958).

3) S. W. Fox, K. Harada and A. Vegotsky, *Experientia*, **15**, 81 (1959).

4) S. W. Fox and K. Harada, *Science*, **128**, 1214 (1958).

5) A. Vegotsky, K. Harada and S. W. Fox, *J. Am. Chem. Soc.*, **80**, 3361 (1958).

DL-Lysine-glycine copolymer**

Reaction conditions		Yield after dialysis	Amino acid composition***	
°C	hr.	g.	Gly %	Lys %
180	2	0.65	77	23
190	1	0.68	62	38
200	1/2	0.64	60	40

DL-Lysine-DL-aspartic acid copolymer****

Temp.	Yield after dialysis	Amino acid composition***	
°C	g.	Asp %	Lys %
170	0.09	33	67
180	0.19	31	69
190	0.99	25	75
200	1.13	24	76
210	1.23	22	78

* DL-Lysine (0.01 mol.) was heated for 2 hr.

** DL-Lysine (0.01 mol.) and glycine (0.01 mol.) were heated.

*** Amino acid compositions were determined by DNP method using column chromatography.

**** DL-Lysine (0.01 mol.) and DL-aspartic acid (0.01 mol.) were heated for 2 hr.

Lysine monohydrochloride did not homopolymerize but did copolymerized with glutamic acid, and with other amino acids in the presence of orthophosphoric acid. Lysine homopolymer was water-soluble (it contained some gel-like material), but it was nondiffusible through cellophane tubing. Lysine-glutamic acid and lysine-glycine copolymers were gel-like materials and lysine-aspartic acid copolymer was sponge-like. The amphoteric polymers of lysine-glutamic acid and also lysine-aspartic acid swelled in alkali and acid, and did not dissolve in either alkali or acid. It is likely that these polymers have a high degree of branching and have a quasi three-dimensional structure. α,ω-Linkage studies of lysine and acidic amino acid residues are now in progress. The lactam formation of lysine is very interesting as is copolymerization of glutamic acid with other amino acids[2]. The lactams serve as reactive intermediates, solvents for the reactions and also basic or acidic catalysts for peptide bond formation. At this time, the studies have revealed a new property of lysine and presented an easy way to prepare lysine-containing polymers.

The Chemistry Department and
Oceanographic Institute of the
Florida State University
Tallahassee, Florida, U.S.A.

Studies on the Mannich Reaction. I. On the Formation of Piperidine Derivatives (1)

By Norito UCHINO

(Received January 30, 1959)

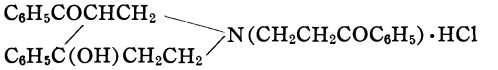
The Mannich reaction of acetophenone with ammonium chloride and formaldehyde[1-3] gives hydrochlorides of mono-(β-benzoylethyl)-amine (I), bis-(β-benzoylethyl)-amine (II), tris-(β-benzoylethyl)-amine (III) and a small quantity of 4-hydroxy-4-phenyl-5-benzoyl-1-(β-benzoylethyl)-piperidine (IV). The last compound is an isomer of the normal product III·HCl. The melting points of the hydrochlorides are 125, 175, 145 and 199~200°C, respectively.

$$C_6H_5COCH_3 + HCHO + NH_4Cl \longrightarrow$$

$C_6H_5COCH_2CH_2NH_2 \cdot HCl$ (I·HCl)

$(C_6H_5COCH_2CH_2)_2NH \cdot HCl$ (II·HCl)

$(C_6H_5COCH_2CH_2)_3N \cdot HCl$ (III·HCl)



(IV·HCl)

In general, this cyclic by-product, having a piperidine ring, is obtained by treating compound III·HCl with alkali[2]. It is not considered that compound III·HCl may be converted into the piperidine derivative IV·HCl in the acidic medium which is the usual condition of the Mannich reaction. Therefore, we can regard compounds I·HCl, II·HCl and III·HCl as the normal products in the Mannich reaction, but it is considered plausible that the piperidine derivative IV·HCl may be produced in some different reactions.

Compound II·HCl or III·HCl undergoes decomposition readily when it is heated in the presence of water to give phenyl vinyl ketone[2]. Therefore, at least a small portion of the products in this Mannich reaction will decompose to give phenyl vinyl ketone, because the reaction is carried out in an aqueous medium at 100°C.

$$(C_6H_5COCH_2CH_2)_3N \cdot HCl \xrightarrow{\text{in water}} (III \cdot HCl)$$

$$(C_6H_5COCH_2CH_2)_2NH \cdot HCl + C_6H_5COCH : CH_2$$
$$(II \cdot HCl)$$

It is well known that phenyl vinyl ketone has a great reactivity to amines[4]. So, it is probable that the phenyl vinyl ketone produced may take part in this Mannich reaction.

The reaction of phenyl vinyl ketone with compound II·HCl was carried out, on trial, under the same conditions as those in the Mannich reaction to give a good yield of compound III·HCl and a small quantity of piperidine derivative IV·HCl. During the reaction, however, the temperature was kept at 40~45°C to avoid the polymerization of the phenyl vinyl ketone. This result shows that the above reaction gives the same products as those in the usual Mannich reaction. The same result was obtained, when aqueous alcohol was used instead of water as the medium. Phenyl vinyl ketone also reacted with compound I·HCl to give compound III·HCl and a small quantity of an unknown substance. In this case, piperidine derivative IV·HCl failed to be isolated.

In view of these facts, phenyl vinyl ketone may be thought to have some concern with the main reaction. But phenyl vinyl ketone failed to react with ammonium chloride under the same conditions. At a higher temperature, only the phenyl vinyl ketone polymerized. On the other hand, acetophenone and formaldehyde reacted with compound I·HCl, II·HCl or ammonium chloride to give compound III·HCl and a small quantity of compound IV·HCl.

These facts show that the Mannich reaction of acetophenone, formaldehyde and ammonium chloride proceeds step by step to give compounds III·HCl and IV·HCl, and that phenyl vinyl ketone has no concern with the main reaction. But it is thought the phenyl vinyl ketone may have some concern with the side reaction,

1) C. M. van Marle and B. Tollens, *Ber.*, **36**, 1351 (1903); H. Schäfer and B. Tollens, ibid., **39**, 2181 (1906).

2) C. Mannich and S. M. Abdullah, ibid., **68**, 113 (1935).

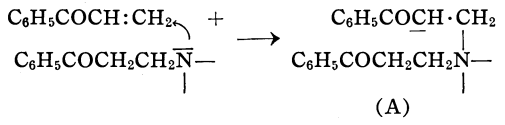
3) Cf. F. F. Blicke, "Organic Reactions", Vol. 1, John Wiley & Sons, Inc., New York (1942), p. 303; E. R. Alexander and E. J. Underhill, *J. Am. Chem. Soc.*, **71**, 4014 (1949); S. V. Liebermann and E. C. Wagner, *J. Org. Chem.*, **14**, 1001 (1949); K. Bodendorf and G. Koralewski, *Arch. Pharm.*, **271**, 101 (1933).

4) E. P. Kohler, *Am. Chem. J.*, **42**, 375 (1909).

and that the benzoylethyl group of compound I·HCl or II·HCl plays an important role in the reaction with phenyl vinyl ketone.

In the reaction between phenyl vinyl ketone and compound II·HCl, IV·HCl was also obtained as in the Mannich reaction. But it was not probable that this IV·HCl was produced by intramolecular aldol-condensation of compound III·HCl, because compound III·HCl did not undergo isomerization, and gave no piperidine derivative IV·HCl, even when it was heated to 45°C in water. Compound III·HCl was recovered quantitatively after the treatment.

Since compound III·HCl or IV·HCl is stable and does not isomerize, it must be considered that neither of them is the secondary product but the primary one. Thus the mechanism of the reaction may be assumed as follows. The primary step of the reaction is the combination of the β-carbon atom of phenyl vinyl ketone with the nitrogen atom of compound II·HCl.



(A)

The intermediate A catches a proton to give compound III·HCl. When the intermediate A undergoes aldol-condensation intramolecularly, it gives compound IV·HCl. More detailed mechanism will be discussed in later papers.

Experimental

Reaction of Phenyl Vinyl Ketone with Bis-(β-benzoylethyl)-amine Hydrochloride (II·HCl).—A mixture of 1.5 g. of compound II·HCl, 1.5 g. of phenyl vinyl ketone and 15 ml. of water was heated with vigorous stirring at 40~45°C for 1.5 hr. A greater part of compound II·HCl dissolved better in the phenyl vinyl ketone than in water, and a crystalline matter was produced as the reaction proceeded. After being cooled for one hour, the crystals were filtered off, washed with water, and dried; yield, 2.0 g.

The crystals were treated with 8 ml. of alcohol with gentle warming, and the soluble matter was extracted. The insoluble residue (about 0.2 g.) was recrystallized from alcohol, giving compound IV·HCl; m. p. and mixed m. p., 199~201°C[5]).

Anal. Found: C, 71.44; H, 6.54; N, 3.07. Calcd. for $C_{27}H_{28}O_3NCl$: C, 72.06; H, 6.27; N, 3.11%.

The alcohol extract was evaporated under reduced pressure, and 1.0 g. of compound III·HCl was obtained; m. p. and mixed m. p., 143~144°C (after drying in vacuo at 78°C).

Anal. Found: C, 72.29; H, 6.20; N, 3.39. Calcd. for $C_{27}H_{28}O_3NCl$: C, 72.06; H, 6.27; N, 3.11%.

The same result was obtained when aqueous alcohol was used in place of water as the medium.

Reaction of Phenyl Vinyl Ketone with Mono-(β-benzoylethyl)-amine Hydrochloride (I·HCl).—A mixture of 2.1 g. of compound I·HCl, 1.5 g. of phenyl vinyl ketone, 5 ml. of water and 5 ml. of alcohol was heated with stirring at 40~45°C for two hours. The mixture was allowed to stand overnight. The crystals produced were filtered off, washed successively with benzene and alcohol-ether mixture, and dried at room temperature; yield, 1.5 g. The crystals were recrystallized from alcohol, giving compound III·HCl; m. p. and mixed m. p., 142~144°C (after drying in vacuo at 78°C).

Anal. Found: C, 71.84; H, 6.55; N, 3.10. Calcd. for $C_{27}H_{28}O_3NCl$: C, 72.06; H, 6.27; N, 3.11%.

The filtrate from compound III·HCl was slightly evaporated to give 0.2 g. of crystals. The crystals were recrystallized from acetone; m. p. 162~164°C. The crystals melted at 174~176°C after repeated recrystallizations. The melting point nearly coincided with that of compound II·HCl (175°C), but the melting point on admixture with an authentic sample depressed exceedingly showing the crystals not to be compound II·HCl. This is further supported by the great solubility of the crystals in alcohol, for the solubility of compound II·HCl is not so great. But it was impossible to make clear whether the crystals were an unknown compound or a mixture of some known compounds, because the yield was too small for the crystals to be identified.

The filtrate from the unknown substance was evaporated under reduced pressure until dry, and 0.5 g. of a residue was obtained. The residue was recrystallized from a mixture of alcohol and acetone; m. p., 121~122°C. The crystals were very soluble in water, and were considered as the starting material I·HCl (m. p., 122~123°C). The melting point on admixture with compound I·HCl did not depress.

Reaction of Bis-(β-benzoylethyl)-amine Hydrochloride (II·HCl) with Acetophenone and Formaldehyde.—A mixture of 3.0 g. of compound II·HCl, 1.2 g. of acetophenone and 1.4 g. of 30% formalin was heated on a steam bath with stirring for 1.5 hr. On cooling, 2.8 g. of crystals were produced. The crystals were filtered off, washed with a mixture of alcohol and ether, and recrystallized from a mixture of alcohol and ether, giving compound III·HCl; m.p. and mixed m. p., 145°C (after drying in vacuo at 78°C).

Anal. Found: C, 71.81; H, 6.18; N, 3.47. Calcd. for $C_{27}H_{28}O_3NCl$: C, 72.06; H, 6.27; N, 3.11%.

The residual mother liquor and washings were concentrated to a syrup under reduced pressure and allowed to stand for about two days to give 0.2 g. of crystals. The crystals were recrystallized from alcohol, giving compound IV·HCl;

5) The melting point of β-benzoylethylamine hydrochloride varies with heating speed because of its instability towards heat.

m. p. and mixed m. p. 199～200°C.

Anal. Found: C, 72.01; H, 6.44; N, 3.03. Calcd. for $C_{27}H_{28}O_3NCl$: C, 72.06; H, 6.27; N, 3.11%.

Reaction of Mono-(β-benzoylethyl)-amine Hydrochloride (I·HCl) with Acetophenone and Formaldehyde.—A mixture of 1.5 g. of compound I·HCl, 2.0 g. of acetophenone and 1.6 g. of 30% formalin was heated on a steam bath with stirring for 1.5 hr. After being cooled for a while, 1.2 g. of crystals were obtained. The crystals were recrystallized from alcohol, giving compound III·HCl; m. p. and mixed m. p., 145°C (after drying in vacuo at 78°C).

Anal. Found: C, 71.41; H, 6.33; N, 3.33. Calcd for $C_{27}H_{28}O_3NCl$: C, 72,06; H, 6.27; N, 3.11%.

The residual mother liquor was allowed to stand for a few days to give 0.1 g. of crystals. The crystals were recrystallized from alcohol, giving compound IV·HCl; m. p. and mixed m. p., 200～201°C.

Anal. Found: C, 70.71; H, 6.32; N, 2.81. Calcd. for $C_{27}H_{28}O_3NCl$: C, 72.06; H, 6.27; N, 3.11%.

Reaction of Phenyl Vinyl Ketone with Ammonium Chloride. — To 10 ml. of water were added 0.25 g. of ammonium chloride and 2.0 g. of phenyl vinyl ketone. The mixture was heated with stirring at 40～45°C for three hours, and was allowed to stand overnight at room temperature to give a resinous matter which was the polymerization product of the phenyl vinyl ketone. The aqueous layer was evaporated until dry under reduced pressure. The residue was confirmed as ammonium chloride by analysis.

Aqueous alcohol (5 : 5 v/v) was used in place of water as the solvent to give the same result. In the case of the higher temperature, the polymerization of phenyl vinyl ketone only was facilitated.

Isomerization of Tris-(β-benzoylethyl)-amine Hydrochloride (III·HCl). — To 7 ml. of water was added 0.5 g. of compound III·HCl, and the mixture was heated with stirring at 45°C for 1.5 hr. On cooling, a crystalline matter was filtered off; yield, 0.5 g. It was recrystallized from alcohol and dried at 78°C in vacuo, giving the starting material III·HCl; m. p., 142～143°C, mixed m. p. on admixture with an authentic sample (143～144°C), 143～144°C.

Summary

1) In the reaction of acetophenone with formaldehyde and ammonium chloride, tris-(β-benzoylethyl)-amine hydrochloride (III·HCl) and 4-hydroxy-4-phenyl-5-benzoyl-1-(β-benzoylethyl)-piperidine hydrochloride (IV·HCl) were produced via bis-(β-benzoylethyl)-amine hydrochloride (II·HCl) after mono-(β-benzoylethyl)-amine hydrochloride (I·HCl).

2) Phenyl vinyl ketone readily reacted with compound I·HCl or II·HCl to give compounds III·HCl and IV·HCl.

The author is particularly indebted to the late Professor Ryuzaburo Nozu and to Professor Ryozo Goto for their discussions and encouragement during this investigation, and also to Professor Seishi Machida for his encouragement.

Chemical Laboratory of Textile Fibres
Kyoto University of Industrial Arts
and Textile Fibres
Kita-ku, Kyoto

Studies on the Mannich Reaction. II. On the Formation of Piperidine Derivatives (2)

By Norito UCHINO

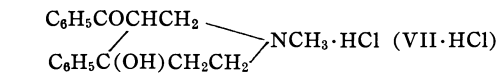
(Received February 19, 1959)

The Mannich reaction of acetophenone with methylamine hydrochloride and formaldehyde gives hydrochlorides of mono-(β-benzoylethyl)-methylamine (V) and bis-(β-benzoylethyl)-methylamine (VI)[1]. The melting points of the hydrochlorides are 139~141°C and 166~169°C, respectively. 4-Hydroxy-4-phenyl-5-benzoyl-1-methyl-piperidine (VII, m. p., 138~140°C) can be obtained by treating compound VI·HCl with alkali, for its isolation is difficult.

$$C_6H_5COCH_3+HCHO+CH_3NH_2\cdot HCl \rightarrow$$

$C_6H_5COCH_2CH_2NH(CH_3)\cdot HCl$ (V·HCl)

$(C_6H_5COCH_2CH_2)_2NCH_3\cdot HCl$ (VI·HCl)



(VII·HCl)

It has been shown that the reaction of phenyl vinyl ketone with compound V·HCl in aqueous alcohol gives a good yield of VI·HCl together with a small quantity of VII·HCl. When water only was used as the medium, the piperidine base failed to be isolated.

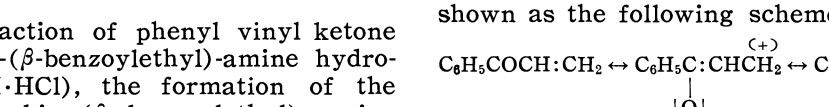
In the reaction of phenyl vinyl ketone with mono-(β-benzoylethyl)-amine hydrochloride (I·HCl), the formation of the isomer of bis-(β-benzoylethyl)-amine hydrochloride (II·HCl) was not certain[2]. But in this case, piperidine derivative VII·HCl could be obtained.

It is necessary to investigate whether or not both of the compounds VI·HCl and VII·HCl were formed at the same time, or whether one of them was formed first and then partly converted into the other. Of course, compound VI·HCl does not isomerize to give compound VII·HCl. Also compound VII·HCl was not converted into compound VI·HCl, under the same conditions as those in the reaction of phenyl vinyl ketone with compound V·HCl.

As the piperidine ring is stable under the above conditions, it is considered that both of the compounds VI·HCl and VII·HCl are primary products of the reaction. The initial step of the reaction may be the combination of the β-carbon atom of phenyl vinyl ketone with the nitrogen atom of compound V·HCl as it has been assumed in the preceding work[2].

If the β-carbon atom of phenyl vinyl ketone can react with the nitrogen atom of β-benzoylethylamine hydrochloride, it seems possible that ammonium chloride or methylamine hydrochloride can also react with phenyl vinyl ketone. Since this is not true, the benzoylethyl group of the amine is likely to play an important role in the reaction.

When a free base of ammonia or methylamine replaced the hydrochloride, it readily reacted with phenyl vinyl ketone to give 4-hydroxy-4-phenyl-5-benzoyl-1-(β-benzoylethyl)-piperidine (IV) or base VII, respectively. The mechanism of this reaction can be considered as follows. The resonance of phenyl vinyl ketone is shown as the following scheme:



This positive carbon atom of phenyl vinyl ketone will combine with ammonia or methylamine by attacking the lone pair of electrons of the nitrogen atom, and give tris-(β-benzoylethyl)-amine (III) or base VI, respectively. As a free base III or VI is very unstable, it isomerizes to give piperidine base IV or VII, respectively[1,3].

From the above, it is concluded that phenyl vinyl ketone can react with a nitrogen atom which has a lone pair of electrons. Here, it is also considered that compound I·HCl, II·HCl or V·HCl may react with phenyl vinyl ketone as the free base which is formed by hydrolysis. To show this, it is necessary for β-benzoylethylamines to be weaker bases than

1) C. Mannich and C. Heilner, *Ber.*, **55**, 356 (1922); F. F. Blicke and J. H. Burckhalter, *J. Am. Chem. Soc.*, **64**, 451 (1942); J. T. Plati and W. Wenner, *J. Org. Chem.*, **14**, 543 (1949); cf. C. Mannich and G. Ball, *Arch. Pharm.*, **264**, 65 (1926).

2) N. Uchino, This Bulletin, **32**, 1009 (1959).

3) C. Mannich and S. M. Abdullah, *Ber.*, **68**, 113 (1935).

ammonia or methylamine, and to give sufficient free bases by hydrolysis of the salts. As the free base of β-benzoylethylamines are very unstable, the basicity of them can not be measured directly. Therefore, the dissociation constant was calculated from the hydrogen ion concentration of the aqueous solution of the salt. The hydrogen ion concentration was measured with 0.05 or 0.1 N solution at 20°C.

Table I. Degree of hydrolysis of β-benzoylethylamine hydrochloride

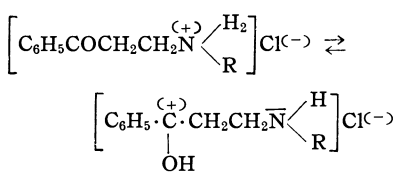
Salt	pH	Dissociation constant of base	Degree of hydrolysis (%)
I·HCl	4.8(0.05 N)	2×10^{-6}	3×10^{-2}
II·HCl	5.0(0.05 N)	5×10^{-6}	2×10^{-2}
V·HCl	5.1(0.1 N)	1×10^{-5}	8×10^{-3}
NH_4Cl		1.79×10^{-5}	
$CH_3NH_2\cdot HCl$		4.38×10^{-4}	

The result of the measurement shows that β-benzoylethylamines are weaker bases than ammonia or methylamine, but their differences are not so great as to elucidate the mechanism of the reaction.

β-Chloropropiophenone was able to react with ammonia to give base IV. As it is well known that phenyl vinyl ketone on being added to hydrogen chloride gives β-chloropropiophenone[4], it may be considered that β-chloropropiophenone is an intermediate product of the reaction. But this consideration is not correct, because it is difficult for ammonium chloride to hydrolyze to give enough hydrochloric acid. In fact, ammonium chloride did not react with phenyl vinyl ketone.

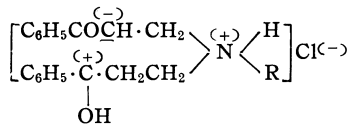
Already it was concluded that (i) the benzoylethyl group plays an important role in the reaction of phenyl vinyl ketone with compound I·HCl, II·HCl or V·HCl, and that (ii) phenyl vinyl ketone can react readily with a nitrogen atom which contains a lone pair of electrons.

Now, we will assume the following prototropy for β-benzoylethylamine hydrochloride.



R=H, CH_3, $C_6H_5COCH_2CH_2$

Here, it is reasonably considered that the β-carbon atom of phenyl vinyl ketone can combine with the lone pair of electrons appearing as in the above equation and gives an intermediate B. The hydrogen



(B)

atom of the hydroxyl group moves to the carbanion as a proton to give the normal product. When the intermediate B undergoes aldol-condensation, it gives the piperidine derivative.

In general, it can be considered that the phenyl vinyl ketone formed by decomposition of the products in the Mannich reaction is concerned with the formation of the piperidine bases which are found in that reaction.

Experimental

Reaction of Mono-(β-benzoylethyl)-methylamine Hydrochloride (V·HCl) with Phenyl Vinyl Ketone.—To a mixture of 5 ml. of water and 3 ml. of alcohol were added 0.5 g. of phenyl vinyl ketone and 0.5 g. of compound V·HCl. The mixture was next heated with stirring at 45~50°C for 2.5 hr. Then the mixture was evaporated until dry under reduced pressure, and washed with benzene to remove the polymerized phenyl vinyl ketone. The residue obtained (0.9 g.) was extracted with a small volume of water, and the insoluble matter (0.8 g.) was recrystallized from alcohol giving compound VI·HCl; m.p. and mixed m. p., 165~167°C.

Anal. Found: C, 68.70; H, 6.83; N, 4.16. Calcd. for $C_{19}H_{22}O_2NCl$: C, 68.76; H, 6.68; N, 4.22%.

The extract was evaporated under reduced pressure. The extraction and evaporation were repeated once more, and the solid matter obtained was recrystallized twice from alcohol giving 0.05 g. of compound VII · HCl; m. p. and mixed m. p., 196~198°C.

Anal. Found: C, 68.71; H, 6.79; N, 4.11. Calcd. for $C_{19}H_{22}O_2NCl$: C, 68.76; H, 6.68; N, 4.22%.

Isomerization of 4-Hydroxy-4-phenyl-5-benzoyl-1-methyl-piperidine Hydrochloride (VII · HCl).—In 5 ml. of water was dissolved 0.2 g. of compound VII·HCl, and the solution was heated to 40~45°C for 1.5 hr. If compound VI·HCl is formed by isomerization, some crystalline matter is expected to appear because of its small solubility. But no crystalline matter appeared. The same result was obtained not only when the temperature of the reaction was kept at 55~60°C, but also when three drops of concentrated hydrochloric acid or a small quantity of alkali was added to the solution, respectively. Removal of the solvent

4) E. P. Kohler, *Am. Chem. J.*, **42**, 289 (1909).

under reduced pressure gave the starting material VII·HCl; m. p. and mixed m. p., 196~198°C.

Reaction of Phenyl Vinyl Ketone with Methylamine Hydrochloride.—Two grams of methylamine hydrochloride were dissolved in 3 ml. of water, and about 1 g. of phenyl vinyl ketone was added to the solution. The solution was heated with stirring at 50~55°C for five hours. Almost all the phenyl vinyl ketone polymerized. The aqueous solution was evaporated until dry under reduced pressure. The residue was confirmed to be only methylamine hydrochloride, and no β-benzoylethylamine hydrochloride was detected.

Reaction of Phenyl Vinyl Ketone with Ammonia.—A mixture of 1 g. of phenyl vinyl ketone, 0.5 ml. of aqueous ammonia (28%) and 10 ml. of water was heated with shaking at 40°C for two minutes. The greater part of the phenyl vinyl ketone polymerized to become viscous, and the liquid phase became turbid. After standing overnight at room temperature, the crystals produced were picked up with a pincette, and were washed with alcohol. As it was difficult to separate the crystals from the resinous matter, the yield was only 0.1 g. The crystals were recrystallized from alcohol, giving base IV; m. p. and mixed m. p., 147~148°C.

Anal. Found: C, 77.90; H, 6.52; N, 3.73. Calcd. for $C_{27}H_{27}O_3N$: C, 78.42; H, 6.58; N, 3.38%.

Reaction of Phenyl Vinyl Ketone with Methylamine.—A gas of excessive methylamine was passed into a solution of 4.5 g. of phenyl vinyl ketone in ether with ice cooling. Then the solution was evaporated to a syrup, which solidified after a while; yield, 4.7 g. The product was recrystallized from methanol giving 2.0 g. of base VII; m. p. and mixed. m. p., 139~140°C.

Anal. Found: C, 77.20; H, 7.25; N, 4.73. Calcd. for $C_{19}H_{21}O_2N$: C, 77.25; H, 7.16; N, 4.74%.

Reaction of β-Chloropropiophenone with Ammonia.—To a solution of 5 ml. of water and 5 ml. of alcohol were added 1 g. of β-chloropropiophenone and 1 ml. of aqueous ammonia (25%), and the mixture was heated with stirring at 40~45°C for an hour. One gram of a crystalline substance was formed. On cooling, the crystals were filtered off and recrystallized from alcohol giving base IV; m. p. and mixed m. p., 148~149°C.

Anal. Found: C, 78.48; H, 6.62; N, 3.63. Calcd. for $C_{27}H_{27}O_3N$: C, 78.42; H, 6.58; N, 3.38%.

β-Chloropropiophenone could react with ammonia, but not with ammonium chloride.

Summary

1) The mechanism of the reaction of phenyl vinyl ketone with β-benzoylethylamine hydrochloride was discussed.

It was concluded that the β-carbon atom of phenyl vinyl ketone combined with β-benzoylethylamine hydrochloride on attacking the lone pair of electrons which appeared in consequence of prototropy, and gave the same products as those in the Mannich reaction.

2) In the Mannich reaction, piperidine bases are found to be produced.

It was concluded that the phenyl vinyl ketone, which was produced by decomposition of the products in the Mannich reaction, was concerned with the formation of these piperidine bases.

The author is particularly indebted to the late Professor Ryuzaburo Nozu and to Professor Ryozo Goto for their discussions and encouragement during this investigation, and also to Professor Seishi Machida for his encouragement.

Chemical Laboratory of Textile Fibres
Kyoto University of Industrial Arts
and Textile Fibres
Kita-ku, Kyoto

Localization Energy with Electronic Interaction

By Kenichi FUKUI, Keiji MOROKUMA and Teijiro YONEZAWA

(Received January 30, 1959)

The localization method by Wheland[1], in which localization energy is employed as the reactivity index, has achieved successes in interpreting chemical reactivity of conjugated molecules[2]. On the other hand, total π-electron density[3], self-polarizability[4], free valence[5], frontier electron density[6] and superdelocalizability[7] are introduced as good reactivity indexes in the approximation of the simple LCAO treatment. Regarding alternant hydrocarbons (AH's) some mathematical relations have been found between localization energy and other reactivity indexes[8].

In the previous paper[9], utilizing LCAO SCF wave function, namely, the wave function where electronic interaction is explicitly included, we have found that the total π-electron density can not predict the correct reactivity of molecules, while the frontier electron density remains a good index for both ionic and radical reactions in LCAO SCF MO treatment just as well as in usual simple LCAO MO treatment. In the present paper we have defined and calculated the localization energy under an explicit consideration of electronic interaction, and comparison of the results obtained by the present method with those in simple LCAO treatment has been made.

Theoretical

Model of Localized System.—According to Wheland's definition the localized system in the transition state has the configuration in which the attacked carbon atom is sp^3-hybridized, so that the resonance integrals between the attacked atom and the neighboring ones are taken to be zero. More precisely the integral does not completely vanish; however, in order to be faithful to the concept of the term "localization", we assume that the resonance integrals between the attacked atom and the others are always zero. This assumption may be reasonable for our approximate calculation.

Here one more problem arises: Simple treatment naturally allows us to deal with the two parts, the localized electrons and the residue, independently from each other; but when we want to take the electronic interaction into account, the interaction between the two parts, and that between those two and the attacking reagent must be considered, as well as the mutual interaction of electrons inside the residue*. Concerning this point, two approximations would be employed. As the first approximation (Approx. 1) we simply assume the two parts to be independent, that is, the only electronic interaction to be taken into account is that which acts inside the residue*. In the second approximation (Approx. 2) the interaction between the two parts shall be treated as a perturbation. The effects of attacking reagent, which do not seem essential to the localization method, are thoroughly neglected for simplicity in both approximations.

Formulation. — The wave function χ_0 of the "isolated" system consisting of $2n$ carbon atoms and $2n$ π-electrons is given as follows:

$$\chi_0 = \frac{1}{\sqrt{(2n)!}} \begin{vmatrix} (\phi_1\alpha)^1 (\phi_1\beta)^1 (\phi_2\alpha)^1 & \cdots\cdots & (\phi_n\beta)^1 \\ (\phi_1\alpha)^2 (\phi_1\beta)^2 (\phi_2\alpha)^2 & \cdots\cdots & (\phi_n\beta)^2 \\ \cdots\cdots & \cdots\cdots & \cdots\cdots \\ \cdots\cdots & \cdots\cdots & \cdots\cdots \\ (\phi_1\alpha)^{2n} (\phi_1\beta)^{2n} (\phi_2\alpha)^{2n} & \cdots\cdots & (\phi_n\beta)^{2n} \end{vmatrix}$$

$$\equiv (1/\sqrt{(2n)!}) [(\phi_1\alpha)^1 (\phi_1\beta)^2 (\phi_2\alpha)^3 \cdots\cdots (\phi_n\beta)^{2n}] \quad (1)$$

1) G. W. Wheland, *J. Am. Chem. Soc.*, **64**, 900 (1940).
2) M. J. S. Dewar, *J. Chem. Soc.*, **1952**, 691; H. C. Longuet-Higgins, *J. Chem. Phys.*, **18**, 283 (1950); T. Yonezawa et al., *Chem. High Polymers* (*Kobunshi Kagaku*), **14**, 533 (1957).
3) G. W. Wheland and L. Pauling, *J. Chem. Phys.*, **1**, 606 (1933); etc.
4) C. A. Coulson and H. C. Longuet-Higgins, *Proc. Roy. Soc.* (*London*), **A191**, 39 (1947); **A192**, 16 (1947).
5) F. H. Burkitt et al., *Trans. Faraday Soc.*, **47**, 553 (1951).
6) K. Fukui, T. Yonezawa and H. Shingu, *J. Chem. Phys.*, **20**, 722 (1952); etc.
7) K. Fukui, T. Yonezawa and C. Nagata, This Bulletin, **27**, 423 (1954).
8) K. Fukui, T. Yonezawa and C. Nagata, *J. Chem. Phys.*, **26**, 831 (1957); H. Baba, This Bulletin, **30**, 147, 154, (1957).
9) K. Fukui, K. Morokuma and T. Yonezawa, This Bulletin, **32**, 853 (1959).

* In electrophilic reaction, the interaction between the two localized electrons is also to be included.

where φ_i is the i-th MO, α and β are the spin functions, and the superscripts denote the numbering of electrons. Each MO should be chosen to minimize the electron energy of the system; but so far as the evaluation of localization energy with electronic interaction is concerned, it seems sufficient to use Hückel MO

$$\psi_i=\sum_\mu c_{i\mu}\phi_\mu \qquad (i=1,2,\cdots\cdots,2n) \tag{2}$$

where ϕ_μ denotes the AO on the μ-th carbon atom.

Introducing a SCF-like procedure proposed by Pople[10], we obtain the following expression of the total electronic energy of the system**.

$$\varepsilon_0=2nU+(\gamma_{\mu\mu}/4)\sum_\mu (P_{\mu\mu})^2+2\beta\sum_{\mu<\nu}^{*} P_{\mu\nu} +\sum_{\mu<\nu}\{(P_{\mu\mu}-1)(P_{\nu\nu}-1)-(1/2)(P_{\mu\nu})^2\}\gamma_{\mu\nu} \tag{3}$$

where U is a core matrix element and is put a constant, β is the resonance integral between the nearest neighbors, and $\gamma_{\mu\nu}$ is the coulomb repulsion integral

$$\gamma_{\mu\nu}=\int \phi_\mu^*(1)\phi_\nu^*(2)\frac{e^2}{r_{12}}\phi_\mu(1)\phi_\nu(2)\mathrm{d}v_1\mathrm{d}v_2 \tag{4}$$

and

$$P_{\mu\nu}=2\sum_{i=1}^{n} c_{i\mu}c_{i\nu} \tag{5}$$

Summation Σ and Σ^* should cover all the atoms and the nearest neighboring atoms, respectively. In deriving Eq. 3 the same assumptions as proposed by Pople[10], for instance, of equi-bond-length, of neglecting the coulomb penetration integrals and so on, are employed.

From the assumption made in the preceding section the wave function χ_E of the "localized" system (transition complex) for electrophilic reaction, in which two electrons are localized on the carbon λ, may be written as follows:

$$\chi_E=(1/\sqrt{(2n-2)!})[(\psi'_1\alpha)^1(\psi'_1\beta)^2\cdots\cdots \times(\varphi'_{n-1}\alpha)^{2n-3}(\psi'_{n-1}\beta)^{2n-2}] \times(1/\sqrt{2!})[(\phi_\lambda\alpha)^{2n-1}(\phi_\lambda\beta)^{2n}] \tag{6}$$

where ψ'_i is the i-th Hückel MO for the residue consisting of $(2n-1)$ carbons.

$$\psi'_i=\sum_\mu c'_{i\mu}\phi_\mu \quad (i=1,2,\cdots\cdots,2n-1) \tag{7}$$

Here we refer the superscript "′" to the residue of the molecule. The two parts being treated separately (Approx. 1), the energy of the system, ε_{E0}, is given as follows[11]:

$$\varepsilon_{E0}=2U+\gamma_{\mu\mu}+(2n-2)U+(\gamma_{\mu\mu}/4)\sum_\mu (P^+_{\mu\mu})^2 +2\beta\sum_{\mu<\nu}^{*} P^+_{\mu\nu}+\sum_{\mu<\nu}\{(P^+_{\mu\mu}-1)(P^+_{\nu\nu}-1) -(1/2)(P^+_{\mu\nu})^2\}\gamma_{\mu\nu} \tag{8}$$

where

$$P^+_{\mu\nu}=2\sum_{i=1}^{n-1} c'_{i\mu}c'_{i\nu} \tag{9}$$

The first two terms correspond to the energy of the localized electrons and the others to that of the residue. When the interaction between the parts is taken into account in higher approximation (Approx. 2), the interaction energy ε_{E1}:

$$\varepsilon_{E1}=\sum_\mu (P^+_{\mu\mu}-1)\gamma_{\mu\lambda} \tag{10}$$

is to be added to the energy ε_{E0}.

Also for nucleophilic reaction, through the similar consideration as for electrophilic one, we easily obtain the following formulae.

$$\chi_N=(1/\sqrt{(2n)!})[(\psi'_1\alpha)^1(\psi'_1\beta)^2\cdots\cdots \times(\psi'_n\alpha)^{2n-1}(\psi'_n\beta)^{2n}] \tag{11}$$

$$\varepsilon_{N0}=2nU+(\gamma_{\mu\mu}/4)\sum_\mu (P^-_{\mu\mu})^2 +2\beta\sum_{\mu<\nu}^{*} P^-_{\mu\nu}+\sum_{\mu<\nu}\{(P^-_{\mu\mu}-1) \times(P^-_{\nu\nu}-1)-(1/2)(P^-_{\mu\nu})^2\}\gamma_{\mu\nu} \tag{12}$$

$$\varepsilon_{N1}=\sum_\mu (1-P^-_{\mu\mu})\gamma_{\mu\lambda} \tag{13}$$

$$P^-_{\mu\nu}=2\sum_{i=1}^{n} c'_{i\mu}c'_{i\nu} \tag{14}$$

For radical reaction,

$$\chi_R=(1/\sqrt{(2n-1)!})[(\psi'_1\alpha)^1(\psi'_1\beta)^2\cdots\cdots \times(\psi'_{n-1}\alpha)^{2n-3}(\psi'_{n-1}\beta)^{2n-2} \times(\psi'_n\alpha)^{2n-1}]\cdot(\phi_\lambda\alpha)^{2n} \tag{15}$$

$$\varepsilon_{R0}=U+(2n-1)U+\gamma_{\mu\mu}\sum_\mu P^\alpha{}_{\mu\mu}P^\beta{}_{\mu\mu} +2\beta\sum_{\mu<\nu}^{*} P^0{}_{\mu\nu}+\sum_{\mu<\nu}\{(P^0{}_{\mu\mu}-1)(P^0{}_{\nu\nu}-1) -[(P^\alpha{}_{\mu\nu})^2+(P^\beta{}_{\mu\nu})^2]\}\gamma_{\mu\nu} \tag{16}$$

$$\varepsilon_{R1}=0 \tag{17}$$

$$\left.\begin{aligned} P^\alpha{}_{\mu\nu}&=\sum_{i=1}^{n} c'_{i\mu}c'_{i\nu}=(1/2)P^-{}_{\mu\nu}\\ P^\beta{}_{\mu\nu}&=\sum_{i=1}^{n-1} c'_{i\mu}c'_{i\nu}=(1/2)P^+{}_{\mu\nu}\\ P^0{}_{\mu\nu}&=P^\alpha{}_{\mu\nu}+P^\beta{}_{\mu\nu}\end{aligned}\right\} \tag{18}$$

10) J. A. Pople, *Trans. Faraday Soc.*, **49**, 1375 (1953).

** Core-core repulsion energies are included in all the expressions of energies in this paper.

11) A. Brickstock and J. A. Pople, *Trans. Faraday Soc.*, **50**, 901 (1954).

TABLE I. LOCALIZATION ENERGIES OF ALTERNANT HYDROCARBONS

Compound	Position	Ionic ($L_N=L_E$)[a] Approx. 1	Ionic ($L_N=L_E$)[a] Approx. 2	Radical (L_R)[a] Approxs. 1 & 2	Simple[b] ($L_N=L_E=L_R$)
Ethylene	—	13.695	6.395	3.165	2.000
Butadiene (*trans*)	1	11.854	6.324	2.590	1.694
	2	14.467	7.167	3.937	2.472
Benzene	—	13.834	7.334	4.995	2.536
Naphthalene	1	12.918	7.134	4.411	2.299
	2	13.470	7.473	4.888	2.480
Anthracene	1	12.575	7.160	4.255	2.240
	2	13.233	7.676	4.755	2.423
	9	11.806	6.882	3.636	2.013
Phenanthrene	1	12.821	7.212	4.604	2.317
	9	12.872	7.147	4.361	2.297
Biphenyl	2	13.157	7.191	4.905	2.400
	4	13.196	7.483	4.944	2.447

a) In units of eV.
b) In units of $(-\beta)$.

TABLE II. LOCALIZATION ENERGIES OF NON-ALTERNANT HYDROCARBONS

Compound	Position	Electrophilic (L_E) Approx. 1[a]	Electrophilic (L_E) Approx. 2[a]	Electrophilic (L_E) Simple[b]	Nucleophilic (L_N) Approx. 1[a]	Nucleophilic (L_N) Approx. 2[a]	Nucleophilic (L_N) Simple[b]	Radical (L_R) Approxs. 1 & 2[a]	Radical (L_R) Simple[b]
Azulene	1	11.392	6.543	1.352	13.265	7.572	2.090	4.177	1.721
	2	12.521	8.100	1.728	12.734	6.694	1.728	4.500	1.728
	4	13.760	8.148	1.808	10.559	5.280	1.231	3.987	1.520
	5	12.654	6.655	1.659	12.595	8.274	1.655	4.485	1.655
	6	13.755	7.349	1.959	11.177	8.959	1.280	4.368	1.620
Fulvalene	1	12.908	5.969	1.987	9.408	5.145	1.365	3.021	1.676
	2	13.702	6.680	2.236	10.507	7.131	1.452	3.783	1.848

a) In units of eV.
b) In units of $(-\beta)$.

The first term in Eq. 16 refers to the localized electron and the others to the residue.

As regards the AH, whose MO has special simplifying properties, Eqs. 8, 10, 12, 13 and 16 can be reduced to simpler ones, that is,

$$\varepsilon_{N0}=\varepsilon_{E0}=2nU+(\gamma_{\mu\mu}/4)\,[(n-1)+\sum_{\mu\nu}^{st}\{1+(c'_{n\mu})^2\}^2]+2\beta\sum_{\mu<\nu}^{*}P^0{}_{\mu\nu}-\{-\sum_{\mu<\nu}^{st,\,st}(c'_{n\mu}c'_{n\nu})^2+\sum_{\mu,\nu}^{st,unst}(P^0{}_{\mu\nu})^2\}(\gamma_{\mu\nu}/2) \tag{19}$$

$$\varepsilon_{N1}=\varepsilon_{E1}=-\sum_{\mu}^{st}(c'_{n\mu})^2\gamma_{\mu\lambda} \tag{20}$$

$$\varepsilon_{R0}=2nU+(\gamma_{\mu\mu}/4)\{(2n-1)-\sum_{\mu}^{st}(c'_{n\mu})^4\}+2\beta\sum_{\mu<\nu}^{*}P^0{}_{\mu\nu}-\{\sum_{\mu<\nu}^{st,\,st}(c'_{n\mu}c'_{n\nu})^2+\sum_{\mu,\nu}^{st,\,unst}(P^0{}_{\mu\nu})^2\}(\gamma_{\mu\nu}/2) \tag{21}$$

Summation $\sum^{st}$ and $\sum^{unst}$ should cover all the starred and the unstarred atoms, respectively.

The localization energies, L, of the λ-th carbon atom are, therefore, obtained from the following equations.

$$\left.\begin{array}{ll}\text{Electrophilic Reaction} & \\ \quad\text{(Approx. 1)} & L_E=\varepsilon_{E0}-\varepsilon_0 \\ \quad\text{(Approx. 2)} & L_E=\varepsilon_{E0}+\varepsilon_{E1}-\varepsilon_0 \\ \text{Nucleophilic Reaction} & \\ \quad\text{(Approx. 1)} & L_N=\varepsilon_{N0}-\varepsilon_0 \\ \quad\text{(Approx. 2)} & L_N=\varepsilon_{N0}+\varepsilon_{N1}-\varepsilon_0 \\ \text{Radical Reaction} & \\ \quad\text{(Approxs. 1 \& 2)} & L_R=\varepsilon_{R0}+\varepsilon_0\end{array}\right\} \tag{22}$$

Evaluation of Atomic Integrals. — For numerical evaluation of β and $\gamma_{\mu\nu}$ are utilized the semi-empirical formulae introduced by Pariser and Parr[12]. For simplicity, as partly stated above, all the

12) R. Pariser and R. G. Parr, *J. Chem. Phys.*, **21**, 767 (1953).

C–C bond distances are assumed the same, 1.39Å, and all the carbon rings (five- and seven-membered rings for azulene and fulvalene, six-membered rings for the other molecules now considered) are supposed to be regular, and polyenyl bond angles to be 120°.

Results and Discussion

The calculated results of localization energy, which is defined in the preceding section, of seven AH's and two non-AH's are listed in Tables I and II***, together with those obtained by simple LCAO treatment.

As is seen from Eq. 20, the interaction energy between the localized electrons and the residue in nucleophilic and in electrophilic reactions is necessarily negative for the AH, namely, there rises some stabilization of the system from the interaction, this seeming true also for the non-AH (cf. Eqs. 10 and 13); and accordingly the values of the localization energies, L_E and L_N, in Approx. 1 are larger than in Approx. 2. For all that we can see in Tables I and II that in both approximations we obtain nearly the same intramolecular orientation, which will be discussed in the later paragraph in detail. In radical reaction, on the other hand, the interaction energy formally vanishes (cf. Eq. 17), and therefore both approximations give the same value of localization energy.

It will be seen in Tables I and II that the magnitude of L_R is generally much smaller than those of L_N and L_E in both approximations, whereas in the simple LCAO treatment the magnitude of L_R lies between those of L_N and L_E. This by no means admits that the activation energy of radical reaction is smaller than those of the others, because effects of reagents and changes in the σ-system are conventionally set aside from this argument. Especially for the AH Eqs. 19 and 20 show the relation $L_E = L_N$ within each approximation in accordance with the result obtained by the simple treatment.

It may be valuable to notice that both approximations indicate the same intramolecular orientation as the simple treatment for all the reactions of the molecules now concerned, except for the ionic reactions of phenanthrene in Approx. 1. Accordingly, its agreement with experimental results is mostly good, but the facts that azulene reacts at the position 1 in radical reaction[13] (L_R is the smallest at 4) and that the position 4 of biphenyl is more reactive than the position 2 both in radical and electrophilic reactions[14] (L_R and L_E indicate 2-orientation) can not be explained on the basis of the localization energy, whether the electronic interaction is taken into account or not. In fulvalene the position 1 is shown to be the most susceptible to attack by localization energies and the position 2 is so by frontier electron density[15], superdelocalizability[16] and total π-electron density[17],

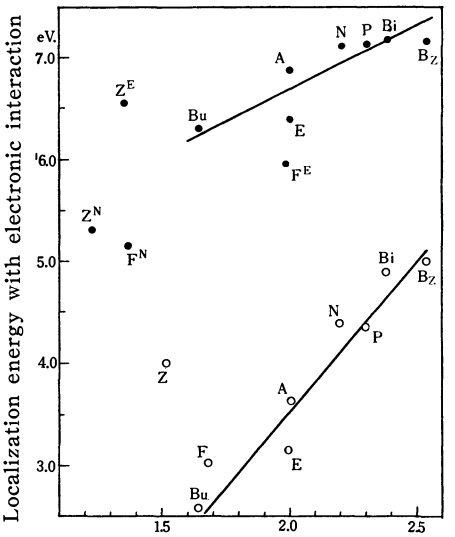


Fig. 1. Relationship between localization energies in simple treatment and with electronic interaction.
○: Radical reaction, ●: Ionic reaction (Approx. 2); E: ethylene, Bu: butadiene, Bz: benzene, N: naphthalene, A: anthracene, P: phenanthrene, F: fulvalene (F^N: nucleophilic, F^E: electrophilic), Z: azulene (Z^N: nucleophilic, Z^E: electrophilic). Only the position of the smallest localization energy of each molecule is plotted. The straight lines are only for AH's.

*** For the position 2 of butadiene, the wave functions of the localized system are expressed in the product of wave functions of three parts, as follows:

$$\chi_E = (1/\sqrt{2})[(\varphi_1'\alpha)^1(\varphi_1'\beta)^2] \times (1/\sqrt{2})[(\phi_2\alpha)^3(\phi_2\beta)^4]$$
$$\chi_R = (1/\sqrt{2})[(\varphi_1'\alpha)^1(\varphi_1'\beta)^2]\cdot(\phi_2\alpha)^3\cdot(\phi_1\alpha)^4$$
$$\chi_N = (1/\sqrt{2})[(\varphi_1'\alpha)^1(\varphi_1'\beta)^2] \times (1/\sqrt{2})[(\phi_1\alpha)^3(\phi_1\beta)^4]$$

In Approx. 1 three parts are treated independently, whereas their mutual interactions are taken into account in Approx. 2.

13) H. Arnold and K. Pahls, *Chem. Ber.*, **89**, 121 (1956).
14) G. Schults, H. Schmidt and H. Strasser, *Ann.*, **207**, *352 (1881); etc.*
15) To be published.
16) To be published.
17) R. D. Brown, *Trans. Faraday Soc.*, **45**, 296 (1949).

further experiments being awaited at this point.

It seems also interesting that, except for the mutual coincidence of the most reactive position, the order of reactivity of each position in azulene does not coincide with one another in the three treatments; in electrophilic reaction, for instance, the reactivity of each position decreases in the order $1>5>2>4>6$ in the simple treatment, $1>2>5>6>4$ in Approx. 1, and $1>5>6>2>4$ in Approx. 2.

As it is seen in Fig. 1, agreement of the intermolecular order of reactivity predicted by the simple treatment with that obtained with electronic interaction is not so good in Approx. 2; and in Approx. 1 the agreement is a little worse. Non-AH's, azulene and fulvalene, largely deviate from the linear relationship of Fig. 1, but unfortunately there are no available data to check which result is correct.

From the above discussion it might be concluded that the localization energy, in which the electronic interaction is taken into account, can be a pretty good index of chemical reactivity.

Department of Fuel Chemistry
Faculty of Engineering
Kyoto University
Sakyo-ku, Kyoto

Added in Proof:

It is easily proved that the following wave functions χ'_E and χ'_R, instead of Eqs. 6 and 15, directly lead to the same energy expressions that were derived in Approx. 2, ε'_E and ε'_R respectively.

$$\chi'_E=(1/\sqrt{(2n)!})[(\psi'_1\alpha)^1(\psi'_1\beta)^2\cdots(\psi'_{n-1}\alpha)^{2n-3}\times(\psi'_{n-1}\beta)^{2n-2}(\phi_\lambda\alpha)^{2n-1}(\phi_\lambda\beta)^{2n}]$$

$$\varepsilon'_E=\varepsilon_{E0}+\varepsilon_{E1}$$

$$\chi'_R=(1/\sqrt{(2n)!})[(\psi'_1\alpha)^1(\psi'_1\beta)^2\cdots(\psi'_{n-1}\alpha)^{2n-3}\times(\psi'_{n-1}\beta)^{2n-2}(1/\sqrt{2})\times\{(\psi'_n\alpha)^{2n-1}(\phi_\lambda\beta)^{2n}-(\psi'_n\beta)^{2n-1}(\phi_\lambda\alpha)^{2n}\}]$$

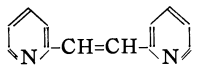
$$\varepsilon_R'=\varepsilon_{R0}$$

Geometrical Isomers of 1,2-Bis-(2-pyridyl)-ethylene

By Takumi KATSUMOTO

(Received February 5, 1959)

1,2-Bis-(2-pyridyl)-ethylene (I) is expected to exhibit geometrical isomerism and to exist in a *cis*- and a *trans*-form. Hitherto, however, only one species has been known. It was first synthesized by Lénárt[1] and melted at 118~119°C. But it has been unknown to which form it belongs. The present author has prepared the other form and concluded from physical properties that the former is the *trans*-isomer and the latter is the *cis*-isomer.



(I)

Experimental

Synthesis of 1,2-Bis-(2-pyridyl)-ethylene. — It was prepared from 2-pyridylformaldehyde, α-picoline and anhydrous zinc chloride. 2-Pyridylformaldehyde, obtained from the Wako Co., was distilled under reduced pressure and the fraction boiling at 76~77°C/17 mmHg was used. α-Picoline, obtained from the Eastman Kodak, was fractionated in an efficient column (b. p., 129.3°C).

A mixture of 2-pyridylformaldehyde (2 g.), α-picoline (3 g.) and anhydrous zinc chloride (2 g.) was heated in a sealed tube at 200°C for 24 hr. After being cooled, the dark brown viscid product was dissolved in aqueous hydrochloric acid. The acid solution was then basified with sodium hydroxide and steam-distilled to remove the unchanged α-picoline. The black oil, which separated on the surface of the solution, was extracted with chloroform and the chloroform extract was dried over anhydrous sodium sulfate and evaporated. The resinous residue was distilled under reduced pressure in a Claisen flask fitted with a wide saber-shaped side tube. A deeply yellow oil distilled out over the interval 150~220°C /15 mmHg and condensed in the side tube. The distillate was extracted with boiling ether, and evaporation of the extract gave 1,2-bis-(2-pyridyl)-ethylene as a brown sticky oil.

Separation of Two Isomers.—The isomers were

1) C. H. Lénárt, *Ann.*, 410, 95 (1915).

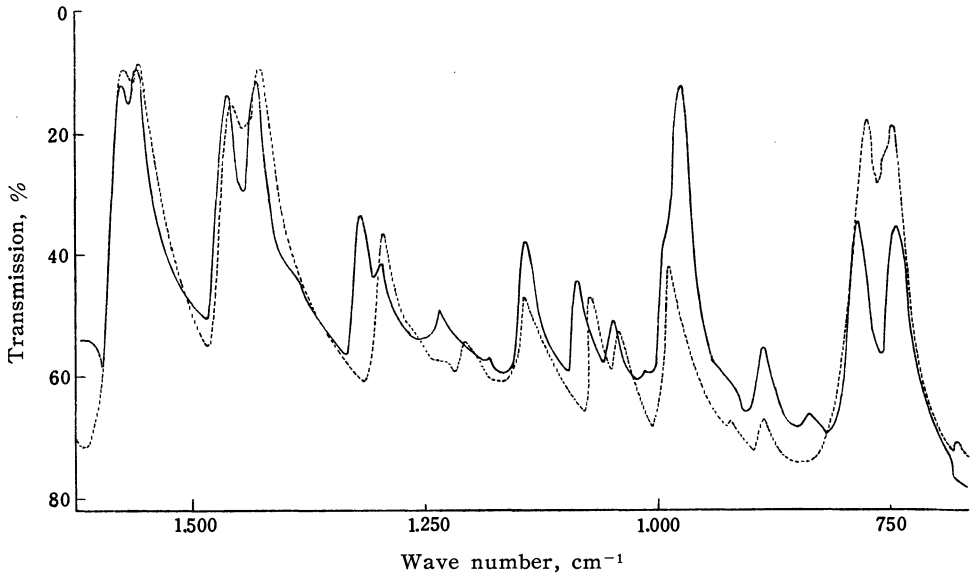


Fig. 1. Infrared spectra of 1,2-bis-(2-pyridyl)-ethylene.
—— compound II (*trans*), ------ compound III (*cis*)

separated by the elution chromatography. The oil was dissolved in chloroform, dried with calcium chloride, and chromatographed on a column (2×13 cm.) of alumina and the column was eluted with the same solvent to give pale brown crystals melting at 70~105°C. Two additional chromatographs on alumina column (2×41 cm.; chloroform) separated them into two parts. One (II), eluted first, forms colorless prisms, m.p. 120~121°C, and corresponds to the compound described by Lénárt. The other (III), contained in the next elute, forms colorless needles and melts sharply at 48.0~48.5°C.

Measurements of Physical Properties. — The boiling points at 15 mmHg pressure were measured by Garcia's method[2]. The pressure was kept constant with a mercury pressure controller fitted with a large buffer bottle (sensitivity, ±0.5 mmHg).

The ultraviolet absorption spectra in cyclohexane were measured with a Shimadzu spectrophotometer. The wavelength of the photometer was calibrated with the absorption band at 301 mμ of an aqueous potassium nitrate solution[3-5]. The infrared spectra in potassium bromide disks were obtained with a Hilger double beam spectrophotometer.

Results and Discussion

The results of the elementary analyses of the two species, II and III, are just the same and consistent with the formula, $C_{12}H_{10}N_2$ (Table I), thus showing that they are isomers.

TABLE I. COMPARISON OF THE TWO ISOMERS OF 1,2-BIS-(2-PYRIDYL)-ETHYLENE

	Compound II	Compound III
Elementary analysis		
Found	C: 78.97% H: 5.738 N: 15.42	C: 78.79% H: 5.729 N: 15.49
Calcd. for $C_{12}H_{10}N_2$	C: 79.09% H: 5.53 N: 15.38	
m. p.	120.0~121.0°C	48.0~ 48.5°C
b. p.	197.0°C	148.5°C
Configuration	*trans*	*cis*

The infrared spectra of the two isomers, II and III, are given in Fig. 1. All bands of II correspond to those of III, except two strong bands located at 968 and 1318 cm^{-1} as shown in Table II. The band at 986 cm^{-1} of III is not clearly noticed in the spectrum of II, but it seems to be hidden by the very strong band at 968 cm^{-1}, because a shoulder is found in this region. Lunde and Zechmeister[6] also found the absorption band at 980 cm^{-1} as a shoulder on the adjacent and intense band at 960 cm^{-1} in the spectra of many *trans*-diphenylpolyenes including *trans*-stilbene.

A number of the common absorption

2) C. R. Garcia, *Ind. Eng. Chem., Anal. Ed.*, **15**, 648 (1943).
3) D. T. Ewing et al., ibid., **12**, 639 (1940).
4) J. M. Vandenbelt et al., ibid., **17**, 235 (1945).
5) H. Ley and F. Volbert, *Z. phisik. Chem.*, **130**, 308 (1927).
6) K. Lunde and L. Zechmeister, *Acta Chem. Scand.*, 8, 1421 (1954).

TABLE II. INFRARED ABSORPTION BANDS OF 1,2-BIS-(2-PYRIDYL)-ETHYLENE

Compound II $\tilde{\nu}_{max}$ (cm^{-1})	Compound III $\tilde{\nu}_{max}$ (cm^{-1})	Assignment**
738 (vs)*	746 (vvs)*	Py-1
780 (vs)	778 (vvs)	Py-1
883 (m)	885 (w)	
968 (vvs)		E
(986 s)	986 (s)	Py-2
1045 (w)	1045 (w)	Py-2
1083 (m)	1073 (m)	Py-2
1138 (s)	1149 (m)	Py-2
1295 (w)	1299 (s)	
1318 (s)		
1428 (vvs)	1430 (vvs)	Py-2
1460 (vvs)	1460 (vs)	Py-3
1559 (vvs)	1561 (vvs)	Py-3
1574 (m)	1578 (s)	Py-3

* The letters shown in the brackets mean the relative intensities. v=very, s=strong, m=medium and w=weak.

** Py-1,2,3 mean the CH out-of-plane deformation, the CH in-plane deformation, and the ring stretching vibration of 2-substituted pyridine ring, respectively. E means the CH out-of-plane deformation of -CH=CH- (*trans*).

bands show that these two compounds have very similar structures. These bands are assigned to the vibrations arising from the 2-substituted pyridine ring as follows:

The infrared spectra of substituted pyridines are closely similar to those of substituted benzenes, although the effect of the electronegative nitrogen appears regularly. All substituted pyridines exhibit strong and characteristic absorptions in the regions 700~850 cm^{-1} due to the out-of-plane bending vibrations of the ring CH. Shindo[7] suggested that 2-substituted pyridines show intense absorptions in the regions 740~780 cm^{-1}, while 3-derivatives do in the regions 770~820 cm^{-1} (m-s) and 690~730 cm^{-1} (vs), and 4-derivatives in the region 790~850 cm^{-1} (s). The 738 cm^{-1} band of II and the 746 cm^{-1} of III suggest that these compounds are 2-derivatives.

Bellamy[8] suggested that a series of weak absorptions in the regions 990~1200 cm^{-1} shown by substituted benzenes are peculiar to the types of substitution. Randall et al.[9] also found that the absorption near 1020 cm^{-1} in monosubstituted benzenes are independent of the nature of the substituent and assigned it to the in-plane bending vibration of CH. Shindo[7] suggested that a series of weak but sharp absorptions in this region are also found in the case of monosubstituted pyridines and the positions are almost constant regardless of the nature of the substituent and that three absorption bands in the regions 988~998 cm^{-1}, 1041~1050 cm^{-1} and 1140~1151 cm^{-1} are characteristic of 2-substituted pyridines. He also attributed them to the in-plane bending mode of the ring involving a considerable ring vibration. Of the four common bands in the spectra of the present compounds, three bands at 986, 1045 and 1138 cm^{-1} of II and those at 986, 1045 and 1149 cm^{-1} of III are respectively in good agreement with the above bands which are characteristic of 2-substituted pyridines. Now, according to Rasmussen[10] the absorption band due to the bending frequencies of CH or the in-plane vibration of hydrogen in the aromatic ring appears in the vicinity of 1429 cm^{-1}. This band corresponds to the fourth, very strong band at 1428 cm^{-1} (II) and at 1430 cm^{-1} (III).

Aromatics have three highly characteristic absorption bands in the regions 1500~1600 cm^{-1} and these bands are assigned to the C=C stretching vibration of the three double bonds round the ring. Of these bands, Randall et al.[11] regarded a band in the regions 1575~1587 cm^{-1} as a positive indication of conjugation of a double bond with the aromatic ring. Brownlie[12] suggested that heterocyclic aromatics such as pyridine also give a similar pair of bands in the region from the C=C and the C=N links, although in this case the third skeletal vibration is usually at appreciably lower frequencies. According to Shindo[7], 2-substituted pyridines have three bands in the regions 1450~1600 cm^{-1} similar to those of substituted benzenes due to their ring double bond stretching vibrations. Compounds II and III show strong bands in this region. The bands at 1460(vvs), 1559(vvs) and 1574(m) cm^{-1} of compound II and 1460(vs), 1561 (vvs) and 1578 (s) cm^{-1} of compound III seem to arise from the 2-substituted pyridine rings, and especially the band at 1574 and 1578 cm^{-1} may be due to the pyridine ring conjugated with C=C double bond. Thus, it seems to be sure that both compounds II and III are 1,2-bis-(2-pyridyl)-ethylene.

7) H. Shindo, *Pharm. Bull. (Japan)*, **5**, 472 (1957).
8) L. J. Bellamy, "The Infrared Spectra of Complex Molecules", Methuen & Co., London(1954), p. 69.
9) R. R. Randall et al., *Trans. Faraday Soc.*, **52**, 9 (1956).
10) R. S. Rasmussen, *Forthscr. Chem. org. Naturstoffe*, **5**, 131 (1948).
11) Randall et al., "The Infrared Determination of Organic Structures", von Nostrand, New York (1949).
12) Brownlie, *J. Chem. Soc.*, **1950**, 3062.

Generally, *trans*-disubstituted ethylenes show intense absorptions near 965 cm^{-1}. Rasmussen and Brattain[13] showed that these absorption bands appear only with *trans* double bond. These absorptions are attributed to the out-of-plane bending vibrations of =CH of the *trans*-disubstituted ethylenes and the absence of these bands can be regarded as conclusive evidence of the absence of *trans* double bond. The strong band at 968 cm^{-1} of II and the lack of this band in the spectrum of III lead to the conclusion that II is the *trans*-form and III is the *cis*-form.

The other sharp band at 1318 cm^{-1} in the spectrum of II is also lacking in the curve of III. According to Lunde et al.[6] *trans*-stilbene gives two weak absorptions at 1312 and 1342 cm^{-1} and these bands are lacking in *cis*-stilbene. Probably, these phenomena have some stereochemical significance which, however, can not be interpreted at the present time.

The melting point of III is lower by about seventy degrees than that of II, as shown in Table I. As the *cis*-isomer always melts at a very much lower temperature than the *trans*-isomer does[14], II and III seem to be a *trans*- and a *cis*-isomer, respectively. Their boiling points at 15 mmHg pressure are also shown in Table I. But it is impossible to distinguish between geometrical isomers from their boiling points, because no general rule as in the case of the melting points holds here.

The ultraviolet spectra of compounds II and III also support the above results as follows: The ultraviolet spectra of geometrical isomers such as those of stilbene[15,16], cinamic acid[16], phenylbutadiene[17] and azobenzene[18] have been investigated. They are composed of the E- (ethylenic) and the K- (conjugated) bands. The absorption intensities of the E-bands of the geometrical isomers are almost equal, while the K-band of the *cis*-form is about half as intense as that of the *trans*-form and lies at somewhat shorter wavelengths. It is well interpreted from the spatial arrangement of groups in these molecules. One of the isomers which approaches more closely to coplanarity exhibits a higher degree of resonance and shows more intense absorption at somewhat longer wavelengths[19]. The ultraviolet absorption curves of II and III are given in Fig. 2. Both have three strong to medium absorption bands in the region of the K-band (Table III). Compound II shows more intense absorption than the compound III and the absorption is located at the longer wavelengths. These curves are typical of geometrical isomers and compound II is a *trans*-isomer and compound III is a *cis*-isomer.

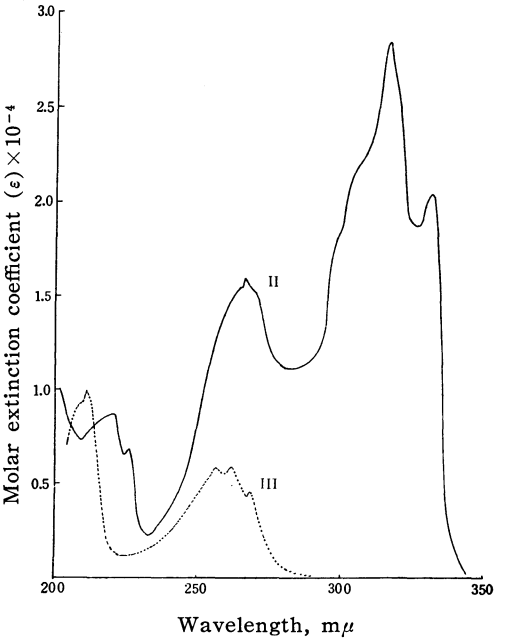


Fig. 2. Ultraviolet spectra of 1,2-bis-(2-pyridyl)-ethylene (II, *trans*; III, *cis*).

TABLE III. ULTRAVIOLET ABSORPTION BANDS OF 1,2-BIS-(2-PYRIDYL)-ETHYLENE

Compound II		Compound III	
$\lambda_{m\mu}$	ε	$\lambda_{m\mu}$	ε
220	8,770	211	9,920
226	6,830		
267	15,750	257	5,790
316	28,470	262	5,910
331	20,510	268	4,420
trans		*cis*	

λ, wavelength; ε, molar extinction coefficient.

The conclusion is that the 1,2-bis-(2-pyridyl)-ethylene described by Lénárt is a *trans*-isomer and the one separated by

13) R. S. Rasmussen and R. R. Brattain, *J. Chem. Phys.*, **15**, 131, 135 (1947).
14) M. Murakami, "Stereo-organic Chemistry (*Kozo-Yuki Kagaku*)", Asakura Publishers, Tokyo (1956), p. 181.
15) U. V. Solmssen, *J. Am. Chem. Soc.*, **65**, 2370 (1943).
16) A. E. Gillam et al., "An Introduction to Electronic Absorption Spectroscopy in Organic Chemistry", Edward Arnold Publishers, London(1957), p. 269.
17) O. Grummitt et al., *J. Am. Chem. Soc.*, **73**, 3479 (1951).
18) R. N. Jones et al., *J. Chem. Soc.*, **1939**, 1315.
19) R. S. Mullikan, *J. Chem. Phys.*, **7**, 364 (1939).

the present author is a *cis*-isomer. The *cis*-isomer(III) is very hygroscopic while the other is not. It may be presumed that the *cis*-structure is very unstable and that it becomes stable by coupling with a water molecule.

The author wishes to thank Professor Sakujiro Kimura of Kyoto University for encouragement, to thank Professor Matsu'ura and his associates of Hiroshima University for recording infrared spectra, and also to thank Mr. Yamaguchi of this Laboratory for helpful assistance.

Chemical Laboratory
Kwansei Gakuin University
Nishinomiya

Synthesis of Aspartic and Glutamic Hydrazides and their Chromatographic and Ionophoretic Separation. C-Terminal Groups of Whale Insulin[1]

By Kozo NARITA and Yumiko OHTA

(Received February 11, 1959)

In the hydrazinolysis of peptides and proteins[2], non-C-terminal acidic amino acids or their amides residues in the polypeptide chain will be converted into α-mono- (derived from aspartyl and glutamyl residues) or di-hydrazides (derived from asparaginyl and glutaminyl residues). C-Terminal aspartic and glutamic acids or their amides will be found as free amino acids or as β- or γ-monohydrazides in the hydrazinolysates of proteins, respectively[3].

By quantitative determination of these hydrazides in the hydrazinolysates of proteins, the number of aspartyl, glutamyl, asparaginyl and glutaminyl residues in the original proteins could be estimated[3]. For that purpose, it is desirable to prepare standard substances for the identification and recovery determination by chromatography or ionophoresis.

Glutamic α- and γ-monohydrazides have previously been prepared[4,5], but the other hydrazides of the acidic amino acids have not heretofore been prepared, as far as we are aware. In the present paper, the synthesis of DL-aspartic α-hydrazide from phthaloyl-DL-aspartic α-methylester, of the isomeric β-hydrazide from L-asparagine, and of the dihydrazides of aspartic and glutamic acids from their diesters will be described. The present contribution also includes separation of these hydrazides by chromatography or ionophoresis, and its application to the hydrazinolysates of beef and whale insulins. The separation methods, however, were not satisfactory, since it was observed that appreciable amounts of some hydrazides were decomposed during the operation.

Experimental

Synthesis of DL-Aspartic α-Hydrazide.—A suspension of 14 g. of phthaloyl-DL-aspartic anhydride[6] in 120 ml. of absolute methanol was refluxed for 30 min. and a small amount of insoluble material was filtered off while it was warm. After being kept overnight, phthaloyl-DL-aspartic α-methyl ester crystallized as prisms. It was recrystallized from methanol; yield, 7.9 g., 43.8%, m.p. 181°C (reported[7] m.p. 182°C). The crude β-methyl ester obtained upon evaporation of the filtrate was recrystallized from water; yield, 3.9 g., 24.8%, m.p. 151~152°C (reported[7] m.p. 147~148°C).

A mixture of 4 g. of the α-ester, 50 ml. of methanol and 2.5 g. of 80% hydrazine hydrate was refluxed for 30 min. The precipitate of phthaloylhydrazine which resulted was filtered off and was washed with hot water. The combined solution of the filtrate and the washings

1) Some parts of this paper were presented at the 9th Annual Meeting of the Chemical Society of Japan, held at Kyoto in April, 1956.

2) S. Akabori, K. Ohno and K. Narita, This Bulletin, **25**, 214 (1952).

3) K. Ohno, *J. Biochem.*, **41**, 345 (1954).

4) S. Akabori and K. Narita, *J. Chem. Soc. Japan, Pure Chem. Sec.* (*Nippon Kagaku Zasshi*), **74**, 829 (1953).

5) K. Narita, ibid., **74**, 832 (1953).

6) F. E. King and D.A.A. Kidd, *J. Chem. Soc.*, **1951**, 2976.

7) F. E. King, J. W. Clark-Lewis and G. R. Smith, ibid., **1954**, 1046.

were adjusted to pH 3.5 with 1 N sulfuric acid. Enough amounts of Amberlite XE-58 (weak anion exchanger, free form) were added to the filtrate to remove sulfate ion, and the resin was filtered off after standing for 30 min. and was washed with water. The combined solution was concentrated in vacuo and two volumes of ethanol were added. An oily material solidified after being kept in a refrigerator and it was recrystallized from dilute ethanol; yield, 2.1 g., m.p. 143°C (with decomp.). It was found by paper chromatography and paper ionophoresis that this material was contaminated with a small amount of free aspartic acid. The aqueous solution of the crude material was again treated with Amberlite XE-58 in a similar manner as mentioned above. On evaporation of the filtrate to a small volume in vacuo, DL-aspartic α-hydrazide crystallized as needles. After addition of ethanol to the filtrate, a second crop of the hydrazide was obtained. The two crops combined were recrystallized from water-ethanol; yield, 1.1 g., 44%, m.p. 180°C (with decomp.).

Anal. Found: N, 27.7. Calcd. for $C_4H_9O_3N_3$: N, 28.6%.

Synthesis of L-Aspartic β-Hydrazide.—A mixture of 3 g. of L-asparagine, 2 ml. of ethanol and 2 g. of 80% hydrazine hydrate was refluxed for 30 min. and held overnight at room temperature. Ethanol was added to the syrup which was obtained on evaporation of the reaction mixture in vacuo and the β-hydrazide crystallized upon scratching of the wall of the vessel under ice cooling. The product was recrystallized from water-ethanol; yield, 2.8 g., 74.5%, m. p. 186°C. When the material was dried over phosphorous pentoxide at 100°C in vacuo, analysis indicated loss of 1.5 mol. water of hydration.

Anal. Found: N, 27.9. Calcd. for $C_4H_9O_3N_3$: N, 28.6%.

Synthesis of L-Aspartic and L-Glutamic Dihydrazides.—L-Aspartic and L-glutamic acids were converted into diethyl ester hydrochlorides, respectively, the free ester was extracted with ether as usual, and the solvent was removed after drying over sodium sulfate. Two and a half moles of hydrazine hydrate were added to the ethanolic solution of the ester, the mixture was held overnight at room temperature and the dihydrazide crystallized in needles. Recrystallization from aqueous ethanol gave about 60% yield in both cases. L-Aspartic α,β-dihydrazide, m.p. 164~165°C (with decomp.).

Anal. Found: N, 42.0. Calcd. for $C_4H_{11}O_2N_5$: N, 43.5%.

L-Glutamic α,γ-dihydrazide, m. p. 134~135°C (with decomp.).

Anal. Found: N, 39.2. Calcd. for $C_5H_{13}O_2N_5$: N, 40.0%.

Paper Chromatography.—Chromatography was performed by an ascending method using lutidine-water mixture (5 : 3, vol.) and Toyo No. 3 filter paper. In the case of multiple development the same solvent was repeatedly used. For the detection of both amino acid and hydrazide, 0.2% ninhydrin *n*-butanol solution (saturated with water) was used and for hydrazide only the ammoniacal silver nitrate solution was sprayed[8].

Paper Ionophoresis.—Toyo No. 3 filter paper (18×40 cm.) was generally used. For the separation of amino acids and hydrazides into three groups, namely, acidic, neutral and basic, neutral buffer of pH 6.4 was prepared in a similar manner as suggested by Lockhart and Abraham[9], except lutidine was used in place of collidine. For the mutual separation of neutral substances, 0.5 M acetic acid (pH 2.64) was used. Potential of 500 V. (12.5 V./cm.) was applied in each case. The current was 6 milliamp. in the case of neutral buffer and 2 milliamp. in dilute acetic acid. The ionophoretic rates of the hydrazides varied from experiment to experiment but the order of the rates did not change. Consequently, in the case of the measurements of relative rates of various hydrazides and the corresponding amides, those on the same paper sheet were compared.

Ion Exchange Chromatography.—Elution chromatography on a Dowex 50−X8 (200~400 mesh) column was tested to separate and estimate amino acid monohydrazides according to the procedure of Moore and Stein[10]. C-Terminal amino acids with the exception of terminal basic amino acids must be present as neutral or acidic substances in the hydrazinolysate of proteins. Since basic materials were adsorbed on the top of the resin column which equilibrated with 0.1 or 0.2 M citrate buffer of pH 3.4, neutral substances were eluted with citrate buffers of several pH's from a short column (0.9×15 cm. or 0.9×30 cm.). In the present experiments, the behaviors of alanine, aspartic β- and glutamic α-hydrazides were mainly studied with regard to the study on insulin.

Hydrazinolysis of Insulin and Treatment of the Product.—Beef and whale insulins studied were kindly supplied by Dr. J. Lens, Organon, Oss, and Shimizu Pharmaceutical Co., respectively. Anhydrous hydrazine was prepared in a similar manner as suggested by Ohno[3]. About 30 mg. of insulin was dissolved in 0.5 ml. of anhydrous hydrazine and heated at 100°C for 8 hr. The hydrazinolysate was taken into dryness over calcium chloride in vacuo at room temperature. In paper ionophoresis, the dried residue was dissolved in a minimum volume of water, an aliquot was applied to Toyo No. 50 paper, thick paper (18×40 cm.), along the starting line, and a potential gradient of 500 V. was applied at pH 6.4 in lutidine-acetic acid buffer. After ionophoresis and air drying, strips from both sides of the paper sheet were cut off and treated with the silver nitrate reagent to detect hydrazides. Using these as a guide, the remainder of the sheet containing neutral substances was cut and they were eluted with water by the technique of Sanger and Tuppy[11]. The wetting top of the cut

8) A mixture of one part of 0.1 N $AgNO_3$ and one part of 0.5 N NH_4OH solution.

9) I. M. Lockhart and E. P. Abraham, *Biochem. J.*, **58**, 633 (1954).

10) S. Moore and W. H. Stein, *J. Biol. Chem.*, **192**, 663 (1951).

11) F. Sanger and H. Tuppy, *Biochem. J.*, **49**, 463 (1951).

paper strip was applied to another paper sheet (Toyo No. 3) and subjected to ionophoresis at pH 2.64 or one- or two-dimensional chromatography.

For the characterization of C-terminal amino acid with the exception of the basic one, asparagine and glutamine, the following technique is also applicable. After ionophoresis of the hydrazinolysate at pH 6.4, the area of hydrazides which traveled to cathode was cut off and the remaining area which contained C-terminal amino acid and monohydrazides of acidic amino acids was then developed with phenol and lutidine two-dimensionally. In this case, it is preferable to develop them first with phenol and then lutidine. During the first development, most of the monohydrazides were destroyed and several very faint unidentified spots could be observed near the phenol front. This procedure might be useful to characterize the C-terminal group of polypeptide of a small molecule, and was successfully used for several cytochromes[12] and for insulin shown in Fig. 1.

In the quantitative determination of the C-terminal groups of insulin, the dried hydrazinolysate was dissolved in 0.5 ml. of 0.05~0.1 N hydrochloric acid 0.5 ml. of 0.2 M citrate buffer (pH 3.5) was added and any insoluble material was centrifuged off, if necessary. A half milliliter of the supernatant was applied to the Dowex 50 column (0.9×15 cm.) equilibrated with 0.2 M citrate of pH 4.23 and elution was started.

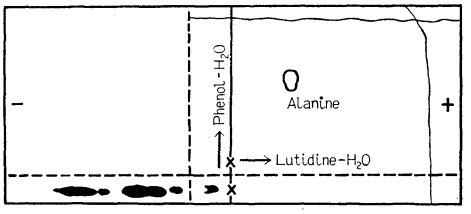


Fig. 1. Ionophoresis at pH 6.40 and subsequent chromatography of the hydrazinolysate of whale insulin. Mark X and broken line indicate original spot and line to be cut before chromatography, respectively. Black and white spots indicate ammoniacal silver nitrate and ninhydrin positive, respectively.

Results and Discussion

Paper Chromatography. — Multiple development technique was used in lutidine-water, since the difference between *Rf* values of the hydrazides was slight in a single development. However, no remarkable effect in resolution of the spots resulted by repeating the development with the same solvent more than twice. *Rf* values of the hydrzaides of acidic amino acids were recorded in Table I.

TABLE I. *Rf* VALUES OF ASPARTIC AND GLUTAMIC HYDRAZIDES*

Number of development	1	2	3
Aspartic α-hydrazide	0.23	0.41	0.48
Aspartic β-hydrazide	0.15	0.33	0.39
Aspartic α,β-dihydrazide	—	0.36	—
Glutamic α-hydrazide	0.24	0.43	0.50
Glutamic γ-hydrazide	0.18	0.37	0.45
Glutamic α,γ-dihydrazide	—	0.44	—

* Lutidine-water (5 : 3, vol.) and the ammoniacal silver nitrate solution were used as the solvent and the reagent, respectively.

Paper Ionophoresis.—Acidic, neutral and basic substances were separated during ionophoresis at pH 6.4, but the acidic amino acid monohydrazides and neutral amino acids could not be separated from each other in this medium. Mutual separation of neutral amino acids has usually been performed in either an acidic or alkaline medium based on the difference of the dissociation constants of their carboxyl or amino group. In the present experiments, acidic pH was used, since amino acid hydrazide seemed to be labile in alkaline medium. The ionophoretic rates of aspartic and glutamic hydrazides to cathode on a paper at pH 2.64 were in the following order:

Glutamic α,γ-dihydrazide>
Aspartic α,β-dihydrazide>
Glutamic α-hydrazide>
Aspartic α-hydrazide>
Glutamic γ-hydrazide>
Aspartic β-hydrazide

The pK'_{COOH} values of aspartic and glutamic monohydrazides are unknown but those of the corresponding amides have been reported[13]. Therefore, the distance that the monohydrazides traveled to cathode during ionophoresis on the

TABLE II. DISTANCES TRAVELED TO CATHODE DURING IONOPHORESIS OF ASPARTIC AND GLUTAMIC HYDRAZIDES AND THE CORRESPONDING AMIDES AT pH 2.64*

	Hydrazid	Amide	
	Distance	Distance	pK'_{COOH}[13]
Aspartic β-	6.1 cm.	4.4 cm.	2.02
Glutamic γ-	6.7	4.8	2.17
Aspartic α-	7.5	—	2.97
Glutamic α-	8.8	8.3	3.81

* Toyo No. 3 filter paper (18×40 cm.), 0.5 M acetic acid, 500 V., 2 milliamp. and 120 min. were used.

12) K. Titani and H. Ishikura, *J. Biochem.*, **44**, 499 (1957).

13) D. M. Greenberg, "Amino Acids and Proteins", Charles C. Thomas Publishers, Springfield (1951), p. 430.

same paper sheet in acidic medium were compared with those of the corresponding amides, to find relationship between the dissociation constant and behavior on the paper (Table II).

The parallel relationship between the ionophoretic rate and the dissociation constant of the amides was observed. Comparing the rates of the amides with those of the corresponding hydrazides, it is apparent that the dissociation constant of the latter is slightly higher than that of the former, and that the difference between the dissociation constant of the hydrazide of α-position and that of ω-position is smaller than that of the corresponding amides. In the ionophoresis performed under the conditions used, the hydrazides in the following pairs were barely separated from one another: Aspartic α-hydrazide and glutamic γ-hydrazide, and glutamic γ-hydrazide and aspartic β-hydrazide. Futhermore, it was observed that the dihydrazides were partially decomposed into both the isomers of the monohydrazides liberating hydrazine in acidic medium.

Ion Exchange Chromatography.—In the ion exchange chromatography, no hydrazides eluted with 0.1 M citrate of pH 3.45 from the 30 cm. column, although aspartic and glutamic acids and alanine eluted each forming a single sharp peak, respectively. When the pH of the buffer was changed to 4.34, leucine, aspartic β- and glutamic γ-hydrazides successively came out from the column. The recoveries of the hydrazides in effluent were only a small percentage using the ninhydrin color yields of the Table III, in which the ratio of ninhydrin color value per mol. hydrazide to that of leucine is listed[10].

TABLE III. NINHYDRIN COLOR YIELDS OF ACIDIC AMINO ACID HYDRAZIDES

Hydrazide	Color yield
Leucine	1.00
Aspartic α-hydrazide	0.93
Aspartic β-hydrazide	1.05
Aspartic α, β-dihydrazide	0.79
Glutamic α-hydrazide	0.85
Glutamic γ-hydrazide	0.69
Glutamic α, γ-dihydrazide	0.48

It was observed that the recoveries of the hydrazides became lower the more acidic the resin surface and the longer the time of contact with the resin. In order to elute hydrazides more rapidly, the length of the column was halved and the ionic strength of the buffer was doubled. Concerning insulin, alanine, aspartic β- and gultamic α-hydrazides could be separated from one another, but aspartic β- and glutamic γ-hydrazides and leucine overlapped in such a column system. Recoveries of the hydrazides were still low under such conditions and further unknown degradation products of the hydrazides eluted gradually and the base line between the peaks of aspartic β- and glutamic α-hydrazides was relatively high. In the quantitative estimation, the base line behind the peak of glutamic α-hydrazide was used.

C-Terminal Groups of Whale and Beef Insulins.—Characterizations of C-terminal amino acids and free carboxyl groups of whale insulin were carried out by means of hydrazinolysis-ionophoresis method described in the experimental section. Alanine, aspartic β- and glutamic α-hydrazides could be identified. These results indicate that the C-terminal groups of the hormone must be alanine and asparagine and that all of the non-C-terminal carboxyl groups belong to glutamic acid residues.

Quantitative estimation of these groups was done by chromatography on a Dowex 50 column. For this purpose it is necessary to determine to what extent known amounts of amino acids could be recovered after treatment with hydrazine and chromatography. A mixture of alanine, asparagine and isoglutamine was heated with anhydrous hydrazine for 8 hr. at 100°C and the reaction mixture was treated according to the procedures described in the experimental section. The recoveries for those are recorded in Table IV. A typical elution curve of the hydrazinolysate of whale insulin is shown in Fig. 2

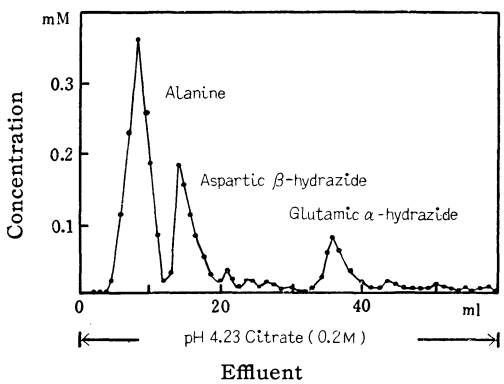


Fig. 2. Elution curve of the hydrazinolysate of whale insulin from Dowex 50 column (0.9×15 cm.).

TABLE IV. RECOVERIES OF AMINO ACIDS AFTER HYDRAZINOLYSIS AND CHROMATOGRAPHY

Material	Product after hydrazinolysis	Recovery after hydrazinolysis and chromatography	Recovery after chromatography	Recovery calculated for hydrazinolysis
Alanine	Alanine	0.48	1.0	0.48
Asparagine	Aspartic β-hydrazide	0.25	0.39	0.64
Isoglutamine	Glutamic α-hydrazide	0.088	0.31	0.29

TABLE V. C-TERMINAL GROUPS AND GLUTAMYL RESIDUES IN WHALE AND BEEF INSULINS*

Insulin		Observed value: Average	Observed value: Range	Corrected value
Whale**	Alanine	0.54	0.41~0.65	1.1
	Aspartic β-hydrazide	0.26	0.22~0.29	1.0
	Glutamic α-hydrazide	0.25	0.20~0.29	2.8
Beef***	Alanine	0.46		1.0
	Aspartic β-hydrazide	0.28		1.1
	Glutamic α-hydrazide	0.14		1.6

* Figures are expressed as mol. per mol. insulin of which molecular weight is assumed to be 6,000.

** Average value for four experiments.

*** Value for single experiment.

and the analytical data of whale and beef insulins are summarized in Table V.

It appears probable that the C-terminal groups of both the insulins (assumed molecular weight, 6,000) are each one mole alanine and asparagine which are consistent with the results of Sanger et al.[14], Harris et at.[15,16] and Chibnall et al.[17] but differ from our previous results[2], in which we reported an additional C-terminal glycine but missed asparagine which escaped from the detection in the earlier method. The main reason which caused such a difference may be attributed to the drastic conditions used in the previous experiments and non-C-terminal glycine might be erroneously identified.

To confirm the singleness of the peak of alanine in Fig. 2, an aliquot of the hydrazinolysate of whale insulin was chromatographed on a Dowex 50 column (0.9×15 cm.) which equilibrated with 0.1 M citrate of pH 3.46. As is shown in Fig. 3, a small peak appeared before alanine and it corresponded to aspartic acid which might be derived from the hydrazide during chromatography. The amount of alanine found in this system was 0.8 mol. per mol. insulin.

In connection with the number of free

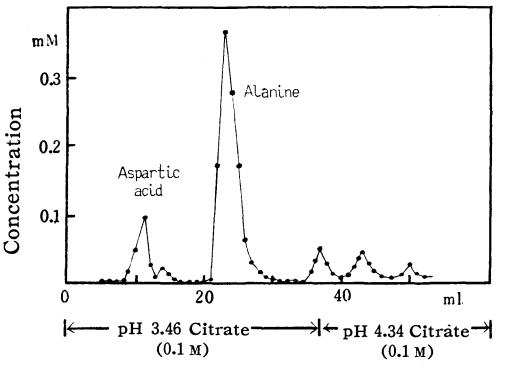
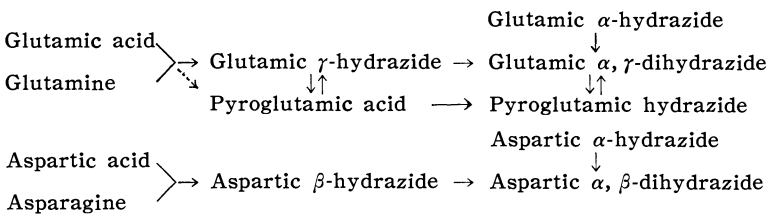


Fig. 3. Chromatogram of the hydrazinolsate of whale insulin on Dowex 50 column (0.9×15 cm.). Concentration and pH of the buffer differ with those in Fig. 2.

carboxyl groups, the present results appear to be of little value, since significant differences were obsereved between the values derived by reduction method and by hydrazinolysis have been obtained with lysozyne[3,18] and the protein of tobacco mosaic virus[19]. As is well known, recoveries of some amino acids, especially aspartic and glutamic acids, after hydrazine treatment are pretty low[20,21]. It was found that one of the main decomposition products was the corresponding hydrazide,

14) F. Sanger, E. O. P. Thompson and R. Kitai, *Biochem. J.*, **59**, 509 (1955).
15) J. I. Harris and C. H. Li, *J. Am. Chem. Soc.*, **74**, 2944 (1952).
16) J. I. Harris, F. Sanger and M. A. Naughton, *Arch. Biochem. Biophys.*, **65**, 427 (1956).
17) A. C. Chibnall and M. W. Rees, *Biochem. J.*, **68**, 105 (1958).
18) A. C. Chibnall, C. H. Haselbach, J. L. Mangan and M. W. Rees, ibid., **68**, 122 (1958).
19) L. K. Ramachandran and K. Narita, *Biochim. et Biophys. Acta*, **30**, 616 (1958).
20) R. H. Locker, ibid., **14**, 533 (1954).
21) C.-I. Niu and H. Fraenkel-Conrat, *J. Am. Chem. Soc.*, **77**, 5882 (1955).

which was identified by paper chromatography. The situation of aspartic and glutamic acids is quite complicated. When glutamic acid alone, for example, was heated with hydrazine and the reaction products were analyzed by chromatography, glutamic acid, glutamic γ-hydrazide, glutamic α, γ-dihydrazide, pyroglutamic acid, pyroglutamic hydrazide and an unknown product were identified. The reaction products of glutamine, glutamic α- and glutamic γ-hydrazides, aspartic acid, asparagine, aspartic α- and aspartic β-hydrazides with hydrazine were analyzed, respectively. Summarizing these results which were obtained, the following reaction scheme could be deduced.



Since free acidic amino acid has never been detected in the reaction mixture of hydrazine with the amide of acidic amino acid, C-terminal asparagine and glutamine can be estimated by hydrazinolysis method by the use of appropriated recovery factors. However, it appears difficult to determine the numbers of non-C-terminal acidic amino acids or their amides residues by hydrazinolysis, owing to the fact that both of them produce the same product, dihydrazide.

In the quantitative determination of C-terminal asparagine or glutamine, elution chromatography described in the present paper seems not to be suitable, since hydrazide derived from the terminal group is decomposed in significant quantity during operation. The dinitrophenyl derivatives of aspartic β- and glutamic γ-hydrazides from the hydrazinolysate of protein by the method III of Akabori et al.[22] or slightly modified method[19], can be separated from one another on two-dimensional paper chromatogram[23,24] developed with Levy's solvent system[25] and this method appears to be more suitable than the present one.

Summary

Aspartic α- and β-monohydrazides and aspartic α, β- and glutamic α, γ-dihydrazides were prepared and their qualitative separation has been performed by means of paper ionophoresis and chromatography. During ionophoresis in acidic medium, the dihydrazide partially decomposed into the isomers of monohydrazides liberating hydrazine. The hydrazinolysis products of whale and beef insulins were analyzed by the aid of elution chromatography on a Dowex 50 column and it was observed that the C-terminal positions were occupied by each one mole of alanine and asparagine in both cases. Furthermore, the present experiments suggested that all of the non-terminal carboxyl groups of the hormone belonged to only glutamic acid residues. Complicated reaction of the acidic amino acids or their amides with hydrazine was discussed.

The present authors are grateful to Professor S. Akabori for his interest and encouragement in these studies, to Shimizu Pharmaceutical Co. and Dr. J. Lens for generous supply of whale and beef insulins, respectively.

Institute for Protein Research
Osaka University
Nakanoshima, Osaka (K.N.)

Department of Chemistry
Ochanomizu Women's University
Bunkyo-ku, Tokyo (Y.O.)

Reprint request should be quoted to K. Narita.

22) S. Akabori, K. Ohno, T. Ikenaka, Y. Okada, H. Hanafusa, I. Haruna, A. Tsugita, K. Sugae and T. Matsushima, This Bulletin, **29**, 507 (1956).
23) K. Narita, unpublished experiments.
24) Y. Kawanishi, K. Iwai and T. Ando, Symposium on Protein Structure, held at Osaka in November, 1958.
25) A. L. Levy, "Methods of Biochemical Analysis", Vol. II, Interscience Publishers, New York (1955), p. 397.

*Thermodynamic Studies on Cobalt Complexes. IV. On the Thermal Dissociation and the Solubility of Aquopentamminecobalt(III) Chloride**

By Motoshichi MORI, Ryokichi TSUCHIYA and Yasuhiro OKANO

(Received February 14, 1959)

In the preceding papers the authors determined the standard free energy of formation of hexamminecobalt(III) chloride in the solid state by measuring its solubility in water[1] and employing the known value of the standard free energy of formation of hexamminecobalt(III) ion. The standard free energy of formation of chloropentamminecobalt(III) chloride in the solid state was also determined by measuring the dissociation pressure of hexamminecobalt(III) chloride[2]. In the present report which is a part of the thermodynamic studies on coordination compounds, the standard free energy of formation of aquopentamminecobalt(III) chloride was determined by measuring its dissociation pressure, and its activity coefficient in the saturated aqueous solution by measuring its solubility. On the basis of these experimental results discussions were conducted on the thermodynamic stability of hexamminecobalt(III), aquopentamminecobalt(III) and chloropentamminecobalt(III) chlorides in the solid state and in the aqueous solution.

Experimental

Aquopentamminecobalt(III) chloride was prepared by the method of Jörgensen[3]. The measurement of its dissociation pressure and rate of thermal dissociation was carried out with the same apparatus described in the preceding paper[2].

The solubility of this complex was determined by analyzing the cobalt content of its saturated aqueous solution by iodometry.

Results and Discussion

Dissociation Pressure of Aquopentamminecobalt(III) Chloride.—As we confirmed by the spectrophotometric measurements the fact that the products of thermal dissociation of aquopentamminecobalt(III) chloride were chloropentamminecobalt(III) chloride and water vapour, the dissociation pressure observed is the vapour tension of water formed by the following reaction;

$$[Co(NH_3)_5OH_2]Cl_3(s) = [Co(NH_3)_5Cl]Cl_2(s) + H_2O(g)$$

The results of measurement of the dissociation pressure are given in Table I. The logarithms of the dissociation

TABLE I. DISSOCIATION PRESSURE OF AQUOPENTAMMINECOBALT(III) CHLORIDE

Temp. °C	$1/T\times10^3$	Dissociation pressure mmHg	$\log p_{mm}$
21	3.400	1.65	0.2175
25	3.356	2.15	0.3324
28	3.310	2.50	0.3979
31	3.288	3.04	0.4829
32	3.278	3.09	0.4900
34	3.256	3.44	0.5366
35	3.246	3.59	0.5551
38	3.214	4.20	0.6233
40	3.195	4.74	0.6758
43	3.164	5.44	0.7356
45	3.144	5.99	0.7774
48	3.114	6.93	0.8407

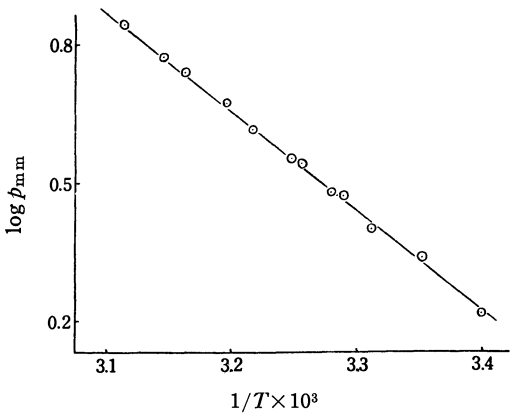


Fig. 1. Relationship between the dissociation pressure of aquopentamminecobalt(III) chloride and the temperature.

* Read at the Symposium on Coordination Compounds of the Chemical Society of Japan held in Nov., 1958.

1) M. Mori, R. Tsuchiya and Y. Okano, This Bulletin, **32**, 462 (1959).

2) M. Mori and R. Tsuchiya, ibid., **32**, 467 (1959).

3) S. M. Jörgensen, *Z. anorg. u. allgem. Chem.*, **17**, 461 (1898).

pressure p_{mm} are plotted against the reciprocal of the absolute temperature in Fig. 1, and an almost straight line is obtained. The equation of the straight line calculated by the method of least squares is

$$\log p_{mm} = 7.5888 - 2166.0/T$$

This equation gives the heat of dissociation ΔH as 9908 cal., and the free energy change of dissociation ΔG° as

$$\Delta G^\circ = -RT \ln p_{atm} = 9908 - 21.54T \quad (1)$$

The value of the free energy change of dissociation at 25°C is $\Delta G^\circ_{298} = 3488$ cal. and that of the entropy change is $\Delta S^\circ_{298} = 21.54$ e. u.

In the preceding paper[2] the standard free energy of formation of chloropentamminecobalt(III) chloride was determined by measuring the dissociation pressure of hexamminecobalt(III) chloride as

$$\Delta G^\circ = -254008 + 365.99T \quad (2)$$

By using the standard free energy of formation of $H_2O(g)$ at 25°C, $\Delta G^\circ_{298} = -54636$ cal.[4] and its heat of formation, $\Delta H_{298} = -57798$ cal.[4], the standard free energy of formation of H_2O as a function of temperature is given by

$$\Delta G^\circ = -57798 + 10.607T \quad (3)$$

Combining Eq. 3 with Eqs. 2 and 1, we get the following equation for the standard free energy of formation of aquopentamminecobalt(III) chloride in the solid state,

$$\Delta G^\circ = -321714 + 398.13T \quad (4)$$

The value of ΔG° at 25°C is $\Delta G^\circ_{298} = -203.024$ kcal.

The Rate of Thermal Dissociation of Aquopentamminecobalt(III) Chloride.—The results of the measurement of the rate of thermal dissociation of aquopentamminecobalt(III) chloride are shown in Table II and Fig. 2.

The velocity constant k at the time when the dissociation begins, is assumed to be given by the tangent of the curve at the origin in Fig. 2. When $\log k$ is plotted against the reciprocal of the absolute temperature, $1/T$, an approximately straight line is obtained as shown

TABLE II. RATE OF DISSOCIATION OF AQUOPENTAMMINECOBALT(III) CHLORIDE

Temp., °C	33	38	43
Time, min.	Dissociation pressure, mmHg		
1	—	—	0.60
2	—	0.55	0.90
3	0.55	0.75	1.10
5	0.70	1.00	1.25
7	—	—	1.40
10	0.90	1.25	1.60
15	1.00	1.35	1.85
20	1.10	1.45	2.10
25	—	1.55	2.35
30	1.15	1.60	2.55
35	—	—	2.70
40	1.20	1.70	2.90
50	—	1.80	3.15
1 hr.	1.25	1.90	3.59
1.5	1.35	2.10	4.33
2	1.45	2.40	—
2.5	1.55	2.70	—
3	1.65	3.05	—
4	1.85	3.45	—
$1/T\times10^3$	3.267	3.214	3.164
k	0.206	0.352	0.628
$\log k$	$\bar{1}.3139$	$\bar{1}.5465$	$\bar{1}.7980$

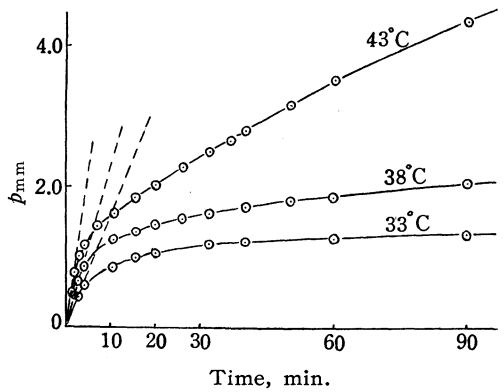


Fig. 2. Rate of dissociation of aquopentamminecobalt(III) chloride.

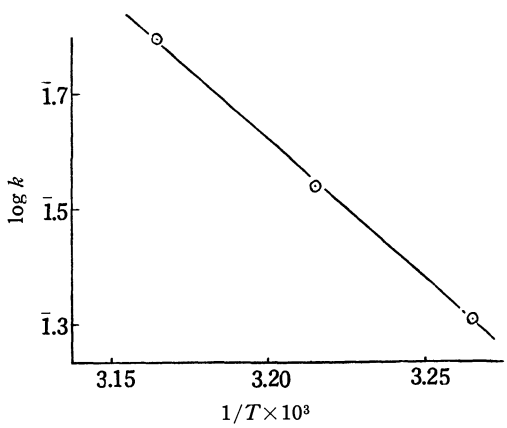


Fig. 3. Relationship between the rate constant and the reciprocal of the absolute temperature.

4) F. D. Rossini et al., "Selected Values of Chemical Thermodynamic Properties", United States Government Printing Office, Washington (1952), p. 9.

in Fig. 3, which gives 21.47 kcal. as the activation energy of the dissociation of aquopentamminecobalt(III) chloride.

Solubility and Activity Coefficient of Aquopentamminecobalt(III) Chloride. — Since the activity coefficient of aquopentamminecobalt(III) chloride has never been found in any literature, the value in the saturated aqueous solution was calculated from the solubility data determined in the present study.

First, by using the standard free energy of formation of aquopentamminecobalt(III) ion in unit activity at 25°C, $\Delta G^\circ_{298} = -104.5$ kcal.[5] and its heat of formation, $\Delta H_{298} = -192.9$ kcal.[6], the standard free energy of formation is obtained as a function of temperature:

$$\Delta G^\circ = -192900 + 296.55T \quad (5)$$

Combining Eq. 5 with Eq. 6 for the standard free energy of formation of chloride ion,

$$\Delta G^\circ = -40023 + 29.1T^{2)} \quad (6)$$

and that of aquopentamminecobalt(III) chloride in the solid state, Eq. 4 obtained above, the free energy change of the solution of aquopentamminecobalt(III) chloride is given by

$$\Delta G^\circ = 8745 - 14.28T \quad (7)$$

The value, 8745 cal. is obtained as the heat of the solution of this complex and $\Delta S^\circ_{298} = 14.28$ e. u. is obtained as the entropy change at 25°C.

On the other hand, the equilibrium constant, K, of the solution of aquopentamminecobalt(III) chloride represented by

$$[Co(NH_3)_5OH_2]Cl_3(s) \rightleftarrows [Co(NH_3)_5OH_2]^{3+}(aq.) + 3Cl^-(aq.)$$

is given by

$$K = \exp(-\Delta G^\circ/RT) \quad (8)$$

If the molality of the solute is expressed by m, the mean activity coefficient, $\gamma_\pm$, in a 1—3 valency type salt[1] is given by

$$\gamma_\pm = \sqrt[4]{K/27}/m \quad (9)$$

Further, if the solubility of aquopentamminecobalt(III) chloride determined by iodometry is expressed by C (mol./l.) and specific gravity of the saturated aqueous solution measured by the hydrometer, d, the molality m is given by

$$m = 1000C/(1000d - MC) \quad (10)$$

where M is the molecular weight of this complex. Thus, the mean activity coefficient $\gamma_\pm$ can be calculated by combining Eqs. 7—10.

The values of the solubility of aquopentamminecobalt(III) chloride and the values of the mean activity coefficient are listed in Table III.

The activity coefficient of aquopentamminecobalt(III) chloride in such concentrated aqueous solutions has never been reported in the past.

Relationship between the Solubility and the Free Energy Change of Solution of Hexamminecobalt(III) and Aquopentamminecobalt(III) Complexes.—From Eqs. 8 and 9, the following equation is derived:

$$\Delta G^\circ = -2.303RT\ (\log 27 + 4\log m + 4\log \gamma_\pm) \quad (11)$$

In the range where $\log \gamma_\pm$ is a linear function of $\log m$ at 25°C, Eq. 11 can be rearranged as

$$\Delta G^\circ_{298} = \alpha + \beta \log m \quad (12)$$

where α and β are constants. Furthermore, if m is approximately proportional to the molar concentration C, Eq. 12 becomes

$$\Delta G^\circ_{298} = \alpha' + \beta' \log C \quad (13)$$

where α' an β' are constants.

When the data of the free energy change, ΔG°_{298}, of the solution of hexamminecobalt(III) chloride, bromide, nitrate and perchlorate reported in the preceding paper[1] as well as that of aquopentamminecobalt(III) chloride listed in Table III are plotted

TABLE III. SOLUBILITY OF AQUOPENTAMMINECOBALT(III) CHLORIDE AND THE RESULTS OF CALCULATION

Temp. °C	Solubility C	Molality m	Free energy change of solution, ΔG°	Equilibrium constant of solution, K	$\gamma_\pm$
15	0.7317	0.8262	4631	3.061×10^4	0.07023
20	0.7661	0.8639	4559	3.976×10^4	0.07171
25	0.8051	0.9106	4488	5.111×10^4	0.07244
30	0.8388	0.9516	4417	6.518×10^4	0.07366

5) A. B. Lamb and A. T. Larson, *J. Am. Chem. Soc.*, **42**, 2038 (1920).

6) F. D. Rossini et al., "Selected Values of Chemical Thermodynamic Properties", United States Government Printing Office, Washington (1952), p. 255.

TABLE IV. THERMODYNAMIC FUNCTIONS IN THE THERMAL DISSOCIATION AND SOLUTION OF HEXAMMINECOBALT(III) AND AQUOPENTAMMINECOBALT(III) CHLORIDES

Reaction	ΔG°_{298}	ΔH_{298}	ΔS°_{298}
$[Co(NH_3)_5NH_3]Cl_3(s) \rightarrow [Co(NH_3)_5Cl]Cl_2(s)+NH_3(g,\ 1\ atm.)$	5672	9612	13.22
$[Co(NH_3)_5OH_2]Cl_3(s) \rightarrow [Co(NH_3)_5Cl]Cl_2(s)+H_2O(g,\ 1\ atm.)$	3488	9908	21.54
$[Co(NH_3)_5NH_3]Cl_3(s) \rightarrow [Co(NH_3)_5NH_3]^{3+}(aq.\ a=1)+3Cl^-(aq.\ a=1)$	6003	8567	8.61
$[Co(NH_3)_5OH_2]Cl_3(s) \rightarrow [Co(NH_3)_5OH_2]^{3+}(aq.\ a=1)+3Cl^-(aq.\ a=1)$	4488	8745	14.28

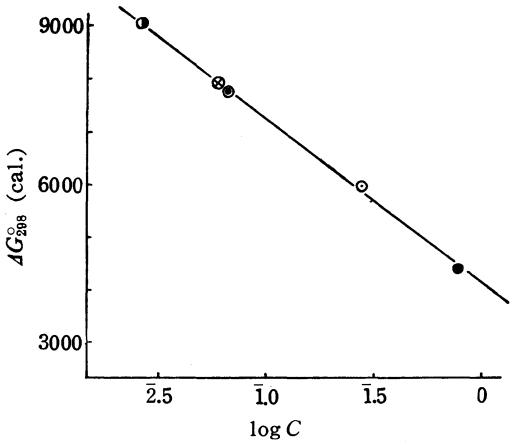


Fig. 4. Relationship between the free energy change of solution and the solubility.
⊙, $[Co(NH_3)_6]Cl_3$
◉, $[Co(NH_3)_6]Br_3$
⊗, $[Co(NH_3)_6](NO_3)_3$
◑, $[Co(NH_3)_6](ClO_4)_3$
●, $[Co(NH_3)_5OH_2]Cl_3$

against the logarithm of their molar concentration C, they all fall on a straight line as shown in Fig. 4. This means that Eq. 13 is applicable to 1—3 valency type complexes described above. Therefore, the free energy change of a solution of a complex of 1—3 valency type can be calculated by using Fig. 4, provided its solubility C is known.

Thermodynamic Stability of Hexamminecobalt(III), Aquopentamminecobalt(III) and Chloropentamminecobalt(III) Chlorides.—The thermodynamic functions in the thermal dissociation and solution of hexamminecobalt(III) and aquopentamminecobalt(III) chlorides at 25°C are summarized in Table IV.

Although the heat of dissociation of hexamminecobalt(III) chloride is close to that of aquopentamminecobalt(III) chloride as shown in Table IV, the entropy change of dissociation of the former is remarkably smaller than that of the latter. Therefore, it is inferred that the difference between the free energy changes of dissociation of the two complexes is due to the difference between the entropy changes. The heat of solution of hexamminecobalt(II) chloride is again close to that of aquopentamminecobalt(III) chloride, and the difference between the free energy changes of solution of these two complexes must be due to the difference between their entropy changes. In other words, it is concluded that the entropy effect plays an important role in those reactions listed in Table IV.

From the solubility data[7] and the activity coefficient[8] of chloropentamminecobalt(III) chloride, its free energy change of solution is calculated as $\Delta G^\circ_{298}=6865$ cal. By using this value and the free energy changes of thermal dissociation and solution of hexamminecobalt(III) and aquopentamminecobalt(III) chlorides, the standard free energy levels of hexamminecobalt(III), aquopentamminecobalt(III) and chloropentamminecobalt(III) chlorides in the solid state and in the aqueous solution in unit activity are computed and shown in Fig. 5. This figure clearly shows the degree of thermodynamic stability of these complexes. The order of the thermodynamic stability is found to coincide with the spectrochemical series[9,10].

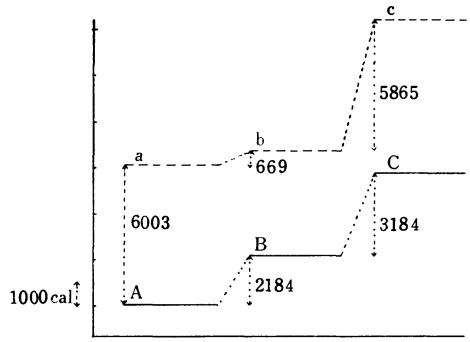


Fig. 5. Standard free energy levels.
A, $[Co(NH_3)_6]Cl_3(s)$
B, $[Co(NH_3)_5OH_2]Cl_3(s)$
C, $[Co(NH_3)Cl]Cl_2(s)$
a, $[Co(NH_3)_6]^{3+}(aq.)+3Cl^-(aq.)$
b, $[Co(NH_3)_5OH_2]^{3+}(aq.)+3Cl^-(aq.)$
c, $[Co(NH_3)_5Cl]^{3+}(aq.)+2Cl^-(aq.)$

7) J. N. Brönsted and A. Petersen, *J. Am. Chem. Soc.*, **43**, 2265 (1921).
8) B. Adell, *Z. anorg. u. allgem. Chem.*, **246**, 303 (1941).
9) R. Tsuchida, This Bulletin, **13**, 388, 436 (1938).
10) Y. Shimura and R. Tsuchida, ibid., **29**, 311 (1956).

Summary

1. The standard free energy of formation of aquopentamminecobalt(III) chloride in the solid state was calculated by measuring its dissociation pressure.

2. From this value and the standard free energy of formation of aquopentamminecobalt(III) ion, the free energy change of the solution of aquopentamminecobalt(III) chloride was calculated. From this value and the solubility data the activity coefficient of aquopentamminecobalt(III) chloride in the saturated aqueous solution was calculated.

The free energy changes of the solutions of hexamminecobalt(III) chloride, bromide, nitrate and perchlorate as well as of aquopentamminecobalt(III) chloride were found to be a linear function of the logarithms of their solubilities.

3. The thermodynamic stability of hexamminecobalt(III), aquopentamminecobalt(III) and chloropentamminecobalt(III) chlorides in the solid state and in the aqueous solution was discussed.

Department of Chemistry
Faculty of Science
Kanazawa University
Kanazawa

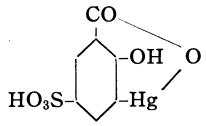
Rheological Properties of Gels. Viscoelasticity of Mercury Sulfosalicylate Solution

By Takaaki DANNO

(Received February 18, 1959)

The study on the visco-elastic properties of agar-agar gel was reported previously[1]. The agar gel shows interesting flow properties superposed on the elastic ones, especially in its softening and melting region. These are interesting from the view point of the relation between the rheological properties and the change of internal structure in the course of the melting of gel. More detailed experiments, however, could not be carried out by reason of the structural limit of our instruments.

On the other hand, mercury sulfosalicylate solution has interesting elasto-viscous properties, as shown by T. Nakagawa[2] who attributed the "Spinnbarkeit" of the solution to its elastic property. The solution is very elastic and also has viscous flow properties. It has been assumed[3] that the structural formula of mercury sulfosalicylate is



It is interesting to seek the origin of strong elasticity of the solution of such a simple substance.

The author measured the visco-elastic parameters of them and studied their dependence on frequency, amplitude, concentration, temperature change, and other factors, by using the coaxial dynamical rheometer.

Experimental

As the experimental procedure for studying the visco-elastic properties of mercury sulfosalicylate solution, the author adopted the method of coaxial type rheometer, which was designed by T. Nakagawa[4].

In this dynamic method for measuring visco-elastic constants, a sinusoidal oscillation is applied at the top of a torsion wire, from which the inner cylinder is suspended, and whose torsion constant is k dyn./cm. Then, the displacement of the top of the torsion wire is given by

$$\Theta = \Theta_0 \sin \omega t \tag{1}$$

and the equation of motion of the inner cylinder is

$$I\ddot{\theta}+R\dot{\theta}+E\theta = k(\Theta-\theta) \tag{2}$$

1) T. Danno, *Bull. Tokyo Gakugei Univ.*, **6**, 103 (1955).
2) T. Nakagawa, This Bulletin, **25**, 93 (1952).
3) Wo. Ostwald and M. Mertens, *Kolloid-Beih.*, **23**, 242 (1926).
4) T. Nakagawa and M. Seno, This Bulletin, **29**, 471 (1956).

where I is the moment of inertia of the inner cylinder, and R and E are the viscous and elastic resistance respectively of the solution between the two cylinders. The stationary solution of this equation is

$$\left.\begin{aligned}\theta &= \frac{k\Theta_0}{\sqrt{\{(E+k)-I\omega^2\}^2+R^2\omega^2}}\sin(\omega t-\phi)\\ &\equiv A\sin(\omega t-\phi)\\ \tan\phi &= \frac{R\omega}{(E+k)-I\omega^2}\end{aligned}\right\} \quad (3)$$

where A is the amplitude of motion of the inner cylinder induced by the sinusoidal torque of the suspension wire, and ϕ is the angle of phase difference between the motion at the top of the suspension wire and the forced oscillation of the inner cylinder. The amplitude ratio m is given by

$$m \equiv \frac{A}{\Theta_0} = \frac{k}{\sqrt{(E+k-I\omega^2)^2+R^2\omega^2}} \quad (4)$$

from Eq. 3, R and E are calculated as

$$\left.\begin{aligned}R &= \frac{kT\sin\phi}{2\pi m}\\ E &= k\left(\frac{\cos\phi}{m}-1\right)+\frac{4\pi^2 I}{T^2}\end{aligned}\right\} \quad (5)$$

where T is the period of oscillation ($\omega=2\pi\nu=2\pi/T$).

When two simple harmonic motions, i.e., the motion at the top of the suspension wire and the forced oscillation of the inner cylinder, whose directions of oscillation are at right angles to each other, are composed, the resulting Lissajous' figure is an ellipse as long as they are of the equal period. Let the area of an ellipse be S_e and that of the rectangle tangent to the ellipse be S_r. Then the next relation is known to hold.

$$\sin\phi = \frac{4}{\pi}\cdot\frac{S_e}{S_r} \quad (6)$$

The scheme of obtaining m and ϕ is realized by a mechanical and optical system. The dynamic viscosity η and the dynamic rigidity G are calculated from the observed R and E by the conventional formulae

$$\left.\begin{aligned}\eta &= \frac{R}{4\pi h}\left(\frac{1}{r_1^2}-\frac{1}{r_2^2}\right)\\ G &= \frac{E}{4\pi h}\left(\frac{1}{r_1^2}-\frac{1}{r_2^2}\right)\end{aligned}\right\} \quad (7)$$

where h, r_1 and r_2 are the length of the immersed portion of the internal cylinder, the radii of the internal and external cylinder, respectively.

Strictly speaking, the inertia effect of the sample which was discussed by S. Oka[5] can not be neglected. But in our present experiments, in which very low frequencies (long period of oscillation) were applied, the rigorous treatment taking into account the inertia of the sample is not necessary.

5) S. Oka et al., *Bull. Kobayashi Inst. Phys. Res.*, 3, 9, 17 (1953).

The experimental condition was as follows: Three hardened steel wires, whose diameter ranged from 0.29 mm. to 0.90 mm. in accordance with the concentration of the sample solution, were used. Coaxial glass vessels of the outer diameter 9.386 cm., and inner one 5.905 cm., were used.

Mercury sulfosalicylate was prepared as follows[6]: An equivalent mass of yellowish mercuric oxide was mixed into the solution of commercial sulfosalicylic acid. When this mixture is heated in a water bath, flesh-colored mercury sulfosalicylate is obtained. The sample thus prepared, mixed with water, is boiled in a flask with reflux condenser for about an hour. After having been dissolved completely in water, it is poured into the space between the two cylinders, cooled and settled for two days in room temperature for conditioning.

The concentration of the solution was determined by evaporation, and was represented in weight per cent. The temperature of the sample to be tested was controlled at 20~65°C, by a water bath thermostat.

Results

Aging of the Solution.—As is usual in all colloidal solutions[7], the marked effect of aging in the physico-chemical properties is observed in our case. The solution of mercury sulfosalicylate, when it is newly prepared, appears as a transparent solution, but gradually loses its transparency and becomes a visco-elastic fluid. Fig. 1 shows the increase of the viscosity and modulus of the rigidity as a function of time.

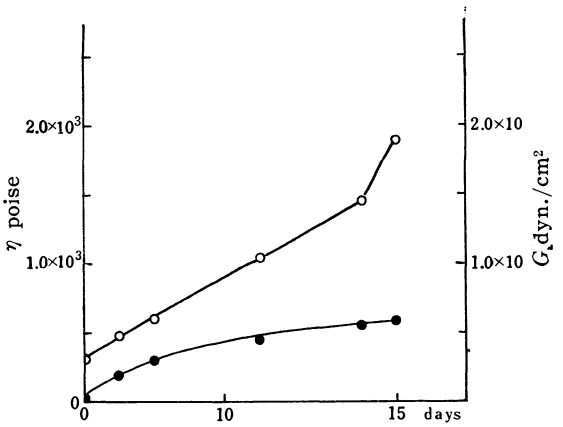


Fig. 1. Viscosity and rigidity of 3.16% mercury sulfosalicylate aq. solution vs. aging time. ○ indicates viscosity and ● rigidity.

6) For instance, J. Samejima, "Koshitsugaku (Colloid Science)", Shokabo, Tokyo (1949), p. 537.

7) For instance, C. Dittmar et al., *J. Poly. Sci.*, 18, 275 (1955).

In our case of mercury sulfosalicylate solution, the viscosity increases rapidly in a few days, while the rigidity increases slowly. In the course of 10 or 15 days, rigidity seems to reach a saturation value, but viscosity continues to increase to a very large value.

Dependence on Frequency. — As is usually observed in the ordinary polymeric solutions, the dynamic viscosity and elasticity of the present system change with frequency.

Fig. 2 shows the viscosity and rigidity of 2.2% mercury sulfosalicylate solution, plotted against the period of oscillation (reciprocal frequency) from 8 sec. to 1286 sec. (about 22 min.). From this figure we see that, in a range of a short period, the viscosity decreases rapidly as the period of oscillation becomes shorter. But, when the period of oscillation is very long, it reaches a constant value.

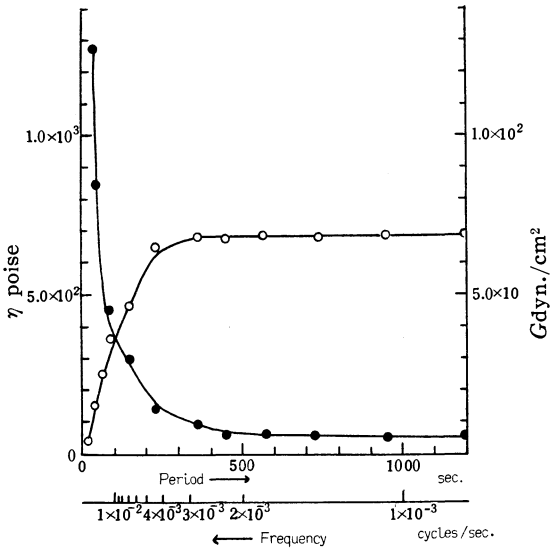


Fig. 2. Frequency dependence of viscosity η and rigidity G of 2.2% mercury sulfosalicylate aq. solution at 24°C. ○ indicates viscosity and ● rigidity.

On the other hand, the rigidity falls steeply in a range of short period. As the viscosity reaches to a certain constant value in a range of a long period, the rigidity also becomes constant. In other words, in a high frequency range, viscosity increases rapidly and rigidity decreases also steeply as the frequency becomes lower. And then, when the frequency is below 2.5×10^{-3} cycl./sec., viz., the period of oscillation is above 400 sec., both viscosity and rigidity are almost constant.

Dependence on Amplitude. — The amplitude effect is shown in Fig. 3, in which $\theta_{\max r=r_1}$ is the amplitude of the shear strain at the wall of the internal cylinder, as given by the following equation,

$$\theta_{\max r=r_1}=\left[\frac{2Ar_1^2r_2^2}{(r_2^2-r_1^2)r^2}\right]_{r=r_1}=\frac{2Ar_2^2}{r_2^2-r_1^2}$$

where A is the amplitude of the oscillation of the internal cylinder and r_1 or r_2 is the radius of the internal and external cylinder, respectively. In the present case, $\theta_{\max r=r}=3.316\ A$ ($r_1=2.953$ cm., $r_2=4.693$ cm.). The concentration of the sample is 1.58 wt. %, and the frequency of oscillation is kept constant. (In the present case, it is 1.29×10^{-1} cycl./sec.).

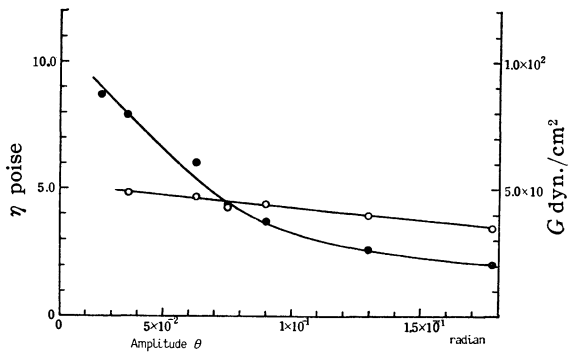


Fig. 3. Amplitude dependence of viscosity η and rigidity G of 1.58% mercury sulfosalicylate aq. solution. ○ indicates viscosity and ● rigidity.

It seems that the viscosity increases as amplitude decreases. But its gradient is fairly slight. As to the rigidity, on the other hand, the situation is somewhat different. It is large in the region of small amplitude, but decreases rapidly as the amplitude increases, and finally tends to a constant value. This is a noticeable experimental result. An explanation of this effect may be given by assuming a sort of structural breakdown by shear strain. An elastic structure breaks into a viscous flow process by a large deformation.

Effect of Concentration of Solution.—So long as we are concerned with dilute solutions, the rigidity seems to be proportional to the third power of concentration as is shown in Fig. 4. This result is in accord with that of agar-agar sol formerly reported[8].

8) T. Danno, *J. Chem. Soc. Japan, Pure Chem. Sec.* (*Nippon Kagaku Zasshi*), **72**, 1061 (1951).

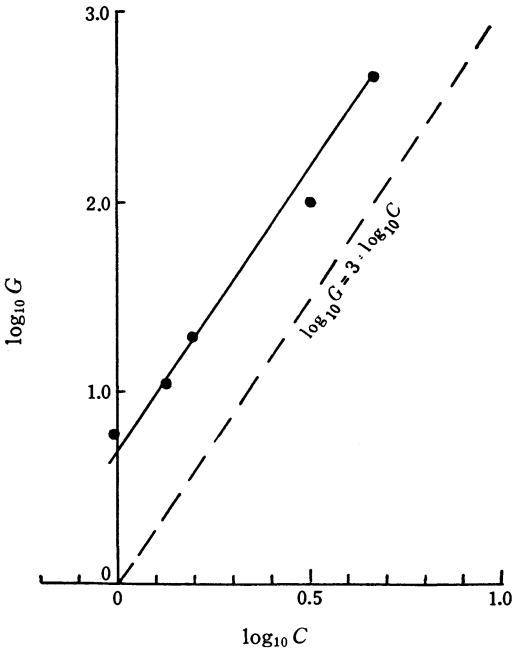


Fig. 4. Effect of concentration of mercury sulfosalicylate aq. solution.

Dependence on Temperature.—Both viscosity and rigidity decrease with the increase of temperature. Fig. 5 shows the results, where viscosity is plotted against the reciprocal of absolute temperature. The author has used the Andrade formula[9]

$$\eta = Ae^{\Delta E/RT}$$

to express the temperature sensitivity of viscosity η; A and ΔE were determined by the method of least square with regard to various periods of oscillation. Results are given in Table I. The apparent heat

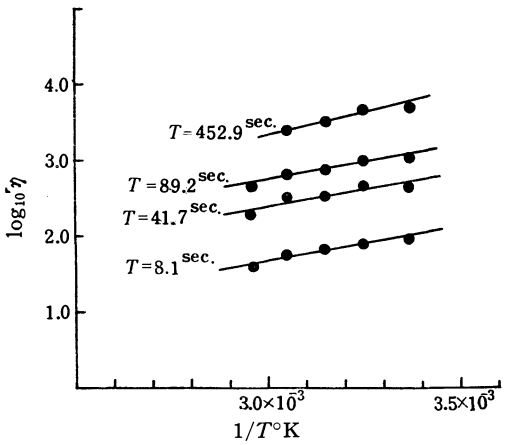


Fig. 5. Temperature dependence of viscosity.

9) E. N. da C. Andrade, *Phil. Mag.*, **17**, 497, 698 (1934).

TABLE I. CONSTANTS OF THE ANDRADE FORMULA

Period, sec.	$-\log A$	E, kcal.
8.1	−0.649	4.11
41.7	−0.210	3.96
89.2	−0.0147	4.10
452.9	−0.147	4.79

(For 4.53 wt. % solution).

of activation in relation to the viscous flow process is about 4 kcal./mol. This value makes one assume the existence of the cross-linking due to the weak secondary bonding like a hydrogen bond.

Discussion

From the results of frequency dependence, it is assumed that this solution has two mechanisms of relaxation. A mechanism which relaxes easily finishes its relaxation during the small period. When the period increases to a certain value, both viscosity and rigidity do not change with frequency due to the nearly complete relaxation of the first mechanism (Fig. 2). We have already seen that viscosity increases, while rigidity does not suffer a remarkable change in the course of aging (Fig. 1). An elastic scaffolding structure is formed in the first stage of gelation, and afterwards the gradual growth of suspending particles in a cavity follows. This is shown in the electron-micrograph

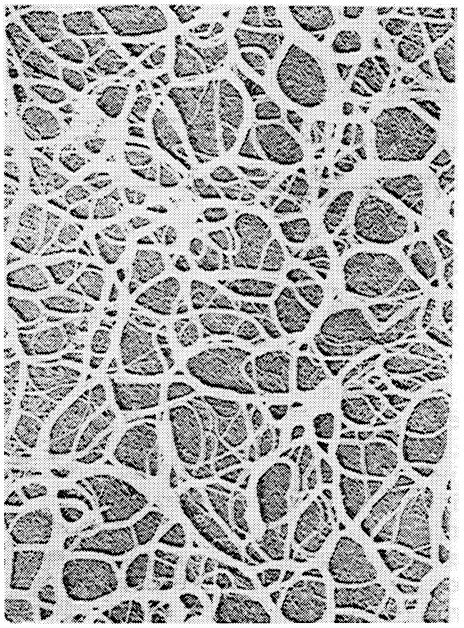


Photo. 1. Electron-micrograph of the aq. solution of mercury sulfosalicylate (×10,000).

(see Photo. 1). This means that the solution of mercury sulfosalicylate has a network structure of two phases.

As to the nature of cross-linking between these submicroscopic network structures, weak secondary bonding, for example, by hydrogenbond, is assumed, because the apparent activation energy of viscosity is calculated to be about 4 kcal./mol.

The author wishes to express his gratitude to Professor H. Akamatsu and Dr. T. Nakagawa both of the University of Tokyo for their leadership and encourgement throughout this investigation. It is also a pleasure to acknowledge the help of the members of Electron-microscope Laboratory of the University of Tokyo.

Department of Chemistry
Tokyo Gakugei University
Setagaya-ku, Tokyo

*Structural Heterogeneity in Viscose Fibers**

By Akiyoshi NAKAI

(Received February 23, 1959)

Though various theories as to the cause and nature of the skin-core effect in viscose fibers have been advanced, none seems to be entirely satisfactory to accout for all the facts so far observed. On the other hand, some observations have been presented which show that the actual structures are far more complicated than the skin-and-core model[1-5], but the results obtained are not yet conclusive.

Dyeing properties of the fiber sections have been studied by various workers, who have dealt almost exclusively with the differential staining of the skin and core. This phenomenon is, as Hermans[6] pointed out, due to a more rapid diffusion of the dye into the core than into the skin.

Generally, dyeing property has two major factors. These are dye diffusion velocity and dye equilibrium absorption. If the picture is oversimplified it would seem that the dye equilibrium absorption is connected with the total spatial per cent of amorphous areas but the dye diffusion velocity is connected with the size and distribution of amorphous areas or the average orientation of the chains in these areas. Then the structural factor which causes the differences in velocity of dye diffusion should not always be identified with that which causes the differences in equilibrium absorption of dye. This suggestion is proved in various experiments.

In addition to the dyeing property of fiber section based on diffusion velocity, therefore, the situation at sorption equilibrium should also be studied. As for this subject, an interesting contribution has been published by Hermans[6], but it seems that there is possibility of further study.

The present investigation is concerned with (1) the observation on the dyeing property of fiber sections and (2) a study of the radial structural gradient by a peeling-off method.

Dyeing Experiment of Fiber Sections

As is well known in ordinary dyeing, the amount of dye absorbed is not sensitively reflected to the depth of color shade beyond the range of fairly low degrees of absorption. In order to distinguish clearly a difference in depth of stained shade on the cross sections prolonged-dyed, dyeing should then be carried out with a diluted dye solution.

Cross sections mounted in the usual way on slides, were dyed for long periods at room temperature with Oxamine Blue 4R which was purified by chromatographing on silica gel.

* Presented before the Meeting of the Fiber Society of Japan, held at Osaka, May 16, 1957.

1) M. Horio et al., *Textile. Research J.*, **17**, 264 (1947).
2) R. L. Royer and C. Maresh, ibid., **17**, 477 (1947).
3) G. G. Taylor and J. C. Brown, *J. Soc. Dyers & Col.*, **69**, 396 (1953).
4) G. D. Joshi and J. M. Preston, *Textile Research J.*, **24**, 971 (1954).
5) K. Kato, *Science [Japan] (Kagaku)*, **25**, 41 (1955).
6) P. H. Hermans, *Textile Research J.*, 18, 9 (1948).

Müller-bath-type Fiber.—The fiber used here was an ordinary rayon (No. 1) spun in a bath containing sulfuric acid 110 g./l., sodium sulfate 350 g./l., and zinc sulfate 15 g./l.

After half an hour of dyeing in a solution of 0.3% Oxamine Blue 4R to which 1% of sodium sulfate had been added, the cross section exhibited the differential staining of skin-and-core with a selectively stained core, as is well known already. This is shown in Fig. 1.

As the dyeing time increased, the intensity of the color increased over all the parts, especially at both the outer circumference of the skin and the boundary between skin and core. After prolonged dyeing—for example, after dyeing for 6 hr. the section showed a finer staining differentiation than the skin-and-core, as shown in Fig. 2. In the section, a narrow zone of the core next to the skin exhibited a darker shade than the central part and was separated from the latter by a rather sharp boundary, and then showed up as a dark band. Moreover, the outer circumference of the skin was seen to stain deeply, but this zone was so thin that it was difficult to distinguish its existence.

Even after further dyeing the above fine differentiation remained, although it was very difficult to distinguish the differences in depth of color shade because of the intensive staining over the whole section.

When such intensively dyed sections were washed with water, the stain was seen to bleed easily off the outermost thin zone and the core but to remain in the main part of the skin. After short washing, the clearness of the boundaries among the various zones became pronounced and the multilayer-like differential staining came again into view. Fig. 3 is a micrograph of such partially washed-out sections mounted in water. As to the phenomenon that by short washing a narrow zone of the core next to the skin became pronounced, drawing a dividing line from the central part, a similar fact was observed already by Hermans, who did not interpret this narrow zone as the differentiated layer different from the central part, but then explained that during washing the former discolored much later than the latter. On the basis of the above observations on both dyeing and washing, however, it seems rather reasonable to assume that the narrow zone has a much greater dye equilibrium absorption than the central part and that there is, moreover, no remarkable difference in velocity of dye diffusion between the two. In the swollen sections in Fig. 3, a very thin deeply-stained outermost zone seems to be seen, but not yet clearly.

When washing had been carried further, the dye disappeared completely from both the outermost thin zone and the core, and remained only in the main part of the skin. Fig. 4 is a micrograph of such a washed-out section after immersion in water, photographed with a contrasting light filter. There is no doubt that a very thin outermost layer exists actually at the outside of the skin, free from the refraction and diffraction effects associated with the cellulose/water interface, as shown previously by Preston and Joshi[7]. This thin outermost layer has a high velocity of dye diffusion and a great dye equilibrium absorption (proved in the next section) and then exhibits a similar property towards dyes as a narrow zone of the core next to the skin.

The above-mentioned phenomena were also observed in other Müller-bath-type fibers (see Fig. 5) and with other dyestuffs such as Sky Blue FF.

In Müller-bath-type fibers there are apparently four distinct layers which differ in dyeing property. The skin itself is composed of two layers which differ in dye equilibrium absorption, and so does the core. These are summarized in Table I.

TABLE I. DYEING PROPERTIES OF FOUR LAYERS IN MÜLLER-BATH-TYPE FIBER (in cross section)

Layer		Velocity of dye diffusion	Equilibrium dye absorption
Skin	1st layer	rapid	high
	2nd layer*	slow	low
Core	3rd layer	rapid	high
	4th layer	rapid	low

* The main part of the skin.

Skinless-type Fiber.—For a sample "Shintoramomen" (No. H-T) was used, which was a high tenacity rayon staple spun from low-alkali viscose in zinc-free and low-acid bath. Fiber of this type is marked by an all-skin structure, as shown in Fig. 6.

Fig. 7 shows a similar section washed-out after prolonged dyeing. In the section, the stain is seen to bleed completely off the outermost thin layer but to remain

7) J. M. Preston and G. D. Joshi, *Kolloid-Z.*, **122**, 6 (1951).

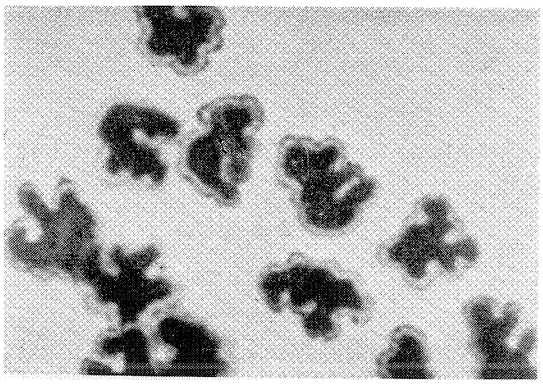


Fig. 1. Cross sections of an ordinary rayon (No. 1), dyed for 30 min. with Oxamine Blue 4R, mounted in canada balsam (×720).

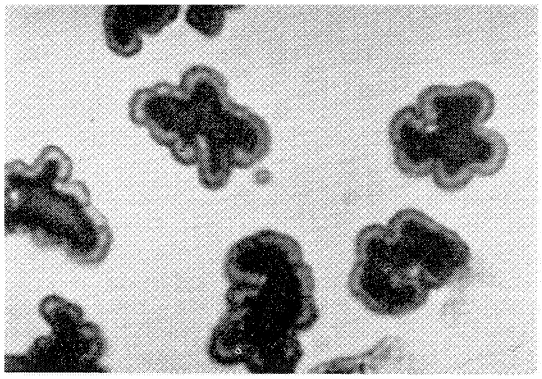


Fig. 2. Same as Fig. 1, except that the dyeing time was prolonged to 6 hr. (×900).

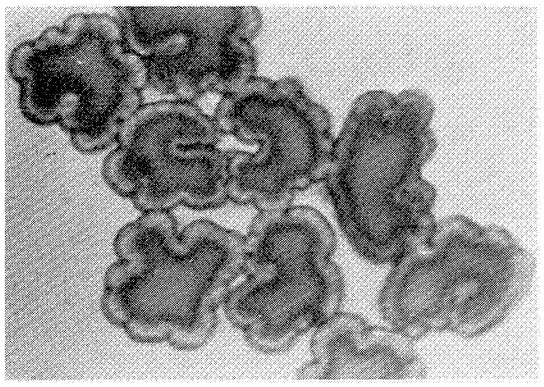


Fig. 3. Partially washed-out sections of an ordinary rayon (No. 1) pre-dyed intensively, mounted in water (×900).

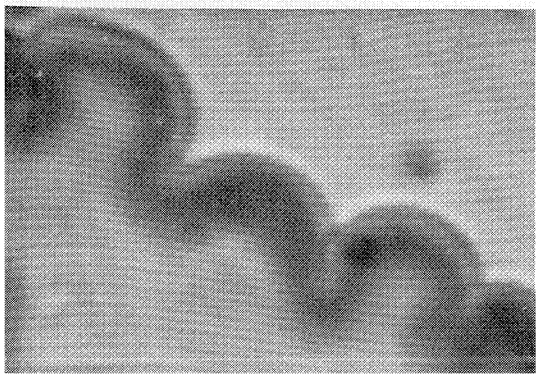


Fig. 4. Same as Fig. 3, except that washing was carried out further, whereas the dye was fixed only in the main part of the skin; mounted in water and examined by a oil-immersion objective (×2000).

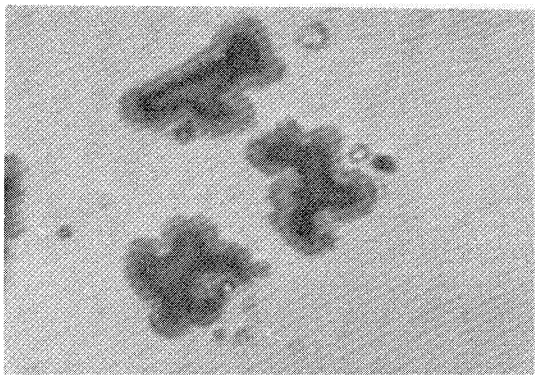


Fig. 5. Cross sections, of a tire-cord yarn, prepared as in Fig. 3 (×900).

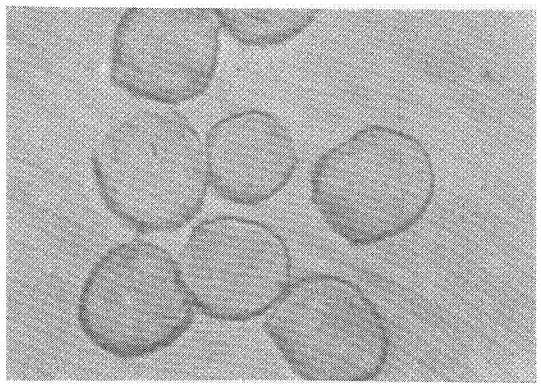


Fig 6. Cross sections of "Shintoramomen" (No. H-T), prepared as in Fig. 1 and mounted in canada balsam (×900).

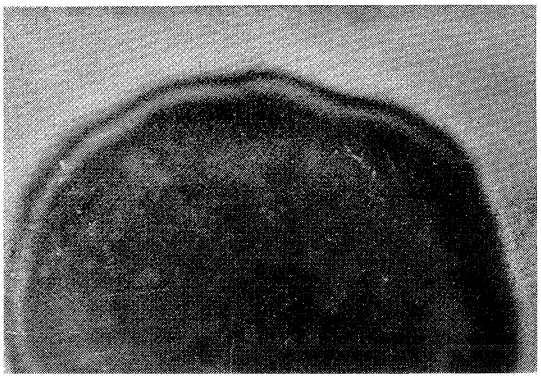


Fig. 7. Same fibre as in Fig. 6; section prepared as in Fig. 4 and mounted in water (×2000).

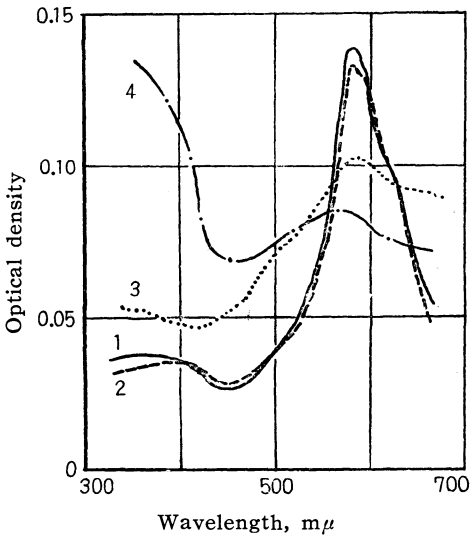


Fig. 8. Spectral sorption curves of dye solutions extracted from (1) the original fiber dyed with Japanol Brilliant Blue 6BKK, (2) the pre-dyed fiber peeled-off to *Pr* 0.23 (before nitration the pre-dyed fiber was vacuum-dried), (3) the pre-dyed fiber peeled-off to *Pr* 0.20 (before nitration the pre-dyed fiber was not vacuum-dried), and (4) the dyestuff decomposed by nitric acid.

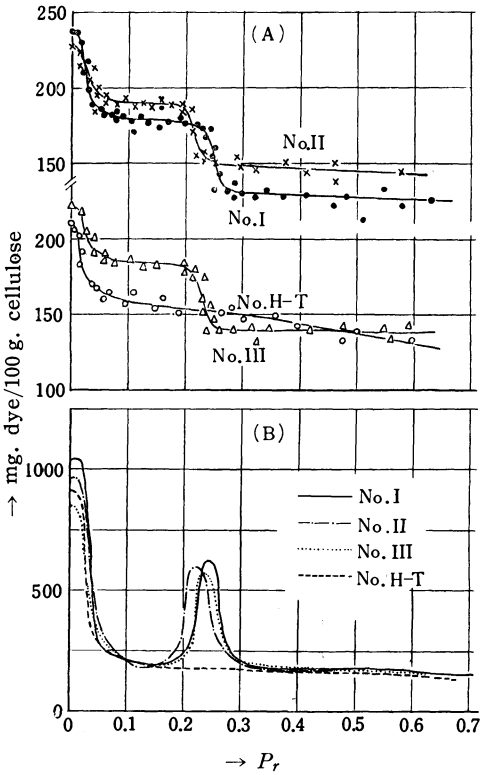


Fig. 9. (A) Amount of dye absorbed as a function of *Pr*. (B) Radial distribution curves in dye equilibrium absorption.

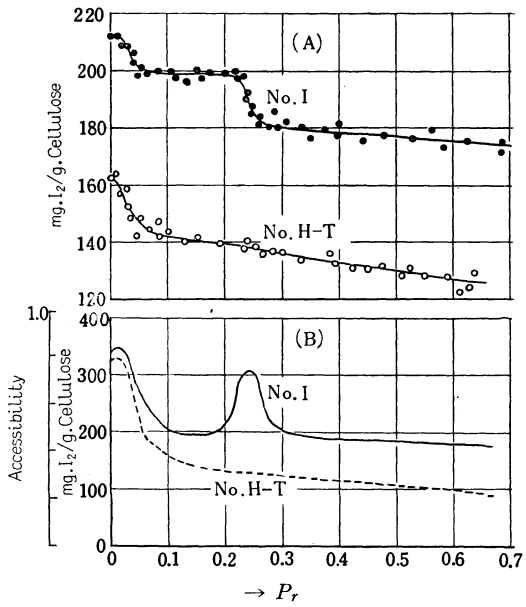


Fig. 10. (A) Amount of iodine absorbed as a function of P_r. (B) Radial distribution curves in iodine absorption and accessibility.

in the inner part, and then two distinct layers are clearly distinguishable. These two layers seem to correspond to the outermost and the second layer in the Müller-bath-type fiber, respectively.

Experiment with Peeling-Off Method

In view of the preceding observations it would seem that the actual structural heterogeneity is far more complicated than that assumed on the basis of the old skin-and-core model. In an investigation with peeling-off technique, therefore, it is necessary to peel the successive layers off as close as possible from the fiber surface toward the center and then to seek the nature of the radial structural gradient existing in fiber to the minutest details.

As a peeling-off technique the heterogeneous nitration presented by Okajima et al.[8] was applied. In a study of this kind, the point is in whether peeling-off is carried on successfully or not. Thereupon, numerous control experiments were carried out carefully.

Experimental Procedure.—A sample of fibers was thoroughly unraveled and vacuum-dried just before use (weight is W). Heterogeneous nitration was carried out at 18°C, and moisture was prevented from entering the reaction vessel. The nitration mixture was made from dry reagents and its composition was as follows:

Nitric acid (1.53) 3 g.
Acetic anhydride 3 g. } per 0.5 g. sample.
Carbon tetrachloride 90 g.

After nitrating the samples to the desired degree, they were washed enough with dry carbon tetrachloride, vacuum-dried and then treated with acetone for removing the nitrate layer.

After applying fresh acetone, they were washed with NH_4SH alcoholic solution recommended by Okajima for the removal of the residual nitrate groups from the fiber surface. Finally they were washed with water, vacuum-dried and weighed (W').

The degree of peeling-off (Pr) was given on the base of the original radius of the filament and obtained by $Pr=1-(W'/W)^{1/2}$.

In order to direct operations properly, microscopical examination of cross sections of the nitrated fibers was carried out using the staining technique. When nitration was carried on much longer, it was seen that the nitrated layer began to show more and more radial flaws, and that nitration proceeded in an irregular fashion. In order to avoid a drawback of this kind, the reaction time was limited to half an hour. If a greater degree of peeling-off was desired, the sample was peeled-off with acetone and then exposed a second time to the nitrating mixture.

Because of the necessity of studying a radial distribution of dye in the dyed fiber—this is the main object in the present investigation — the application of the above peeling-off method to the dyed sample was examined. Fig. 8 shows spectral sorption curves of the dye solutions extracted from the original and peeled-off predyed samples. This figure indicates that, if nitration proceeds under absolutely dry conditions, the dye which remains in the unreacted part has not been decomposed and the acid has not diffused into the inner part beyond the nitrated layer. It was found eventually that the dyed sample was peeled-off satisfactorily as well as the undyed sample. In this case, however, water should not be used for washing, because the dye absorbed in the unreacted part was dissolved away with water.

Samples.—The fibers selected for investigation were "Shintoramomen" (No. H-T) and three ordinary rayons (No. I—III). No. I—III were all spun in the same Müller bath; 1.5, 3.0 and 7.0, deniers, respectively.

Radial Distribution in Dye Equilibrium Absorption.—A sample was dyed to equilibrium at 25°C in a solution of 0.001% Japanol Brilliant Blue 6BKX to which 0.2% of sodium sulfate had been added, and washed briefly with water to remove the mechanically absorbed dye from the fiber surface, vacuum-dried and then peeled-off. In Fig. 9-A is given the amount of dye absorbed as a function of the degree of peeling-off. The radial distribution curves derived therefrom are shown in Fig. 9-B. These are in good agreement with the differential staining based on the differences in equilibrium absorption, irrespective of the differences in dyestuff and even in procedure of dyeing (Ref. Figs. 2, 3 and 7). The fact that a very thin outermost layer has a greater dye equilibrium absorption is experimentally proved here.

Radial Distribution in Crystallinity.—Using the Hessler and Power's method[9], the radial distribution in accessibility was first studied. In Fig. 10-A are given the amount of iodine absorbed on the fibers peeled-off to various degrees. The radial distribution curves derived therefrom are shown in Fig. 10-B, in which a ratio of the absorption value to 412** gives a value for the accessible fraction. Four layers in Müller-bath-type fiber and two in Shintoramomen are clearly distinguished also here.

The accessibility thus obtained is, however, due to the inner surface areas for absorption and seems to be an unsatisfactory measure for crystallinity. In order to seek conclusive evidence on the nature of the fine structure in each layer, the lateral-order (L.O.) distribution of each separated layer was further determined according to the hydrocellulose solubility method presented by Maeda[10]. For example, the L.O. of the outermost layer of No. 1 (P_γ: 0∼about 0.05) was determined by calculation from the L.O. of the original fiber and the observed L.O. of the fiber peeled-off to 0.05 (the outermost layer just about

8) S. Okajima et al., This Bulletin, **26**, 322 (1953).

9) V. J. Hessler and R. E. Power, *Textile Research J.*, **24**, 822 (1954).

** The milligram of iodine absorbed per gram of methocel, as the sample of the completely amorphous cellulose.

10) K. Maeda, *J. Soc. Text. Cellulose Ind. Japan* (*Sen'i-Gakukai-shi*), **12**, 10 (1956).

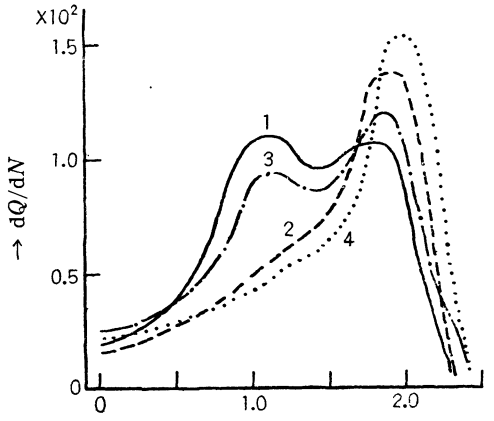


Fig. 11. L.O. distribution curves of each layers in No. 1.
(1) The outermost layer (P_r: 0～ca. 0.05). (2) The second layer (P_r: ca. 0.05～ca. 0.20). (3) The third layer (P_r: ca. 0.20～ca. 0.28). (4) The fourth layer (P_r: ca. 0.28～).

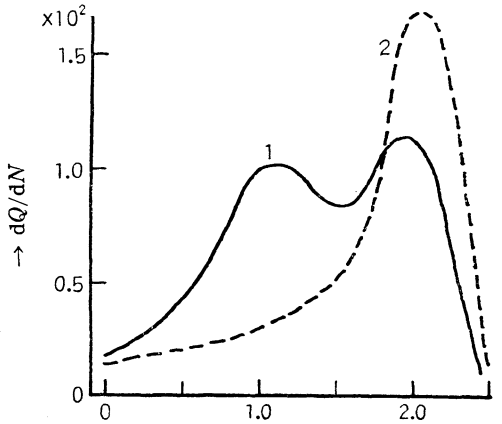


Fig. 12. L.O. distribution curves of each layers in No. H-T.
(1) The outermost layer (P_r: 0～ca. 0.05). (2) The second layer (P_r: ca. 0.05～).

removed). The results are shown in Figs. 11 and 12.

As is seen in the figures, there is an intrinsic difference in L.O. distribution between a layer with greater dye equilibrium absorption and that with less dye equilibrium absorption. The former has two peaks in its distribution curve and, consequently, lower crystallinity. The latter, on the other hand, gives only one peak in the region of considerably high order and, consequently, higher crystallinity. These are in agreement with the information obtained from the radial distribution in iodine absorption described before.

Discussion

As is seen from the above observations, there are two types of differentiated layers.

One is a layer rich in disordered material which shows a lower crystallinity and a greater dye equilibrium absorption. Cellulose gel of this type, which will be termed here "α-type", is formed by a momentary gelatinizing action, such as that of zinc ions[11].

The other is a highly crystallized layer with relatively limited amorphous regions and shows less dye equilibrium absorption. Cellulose gel of this type, which will be termed "β-type", is formed by a relatively slow gelatinizing action, such as those of sodium or hydrogen ions[11].

Consequently, it seems reasonable to assume that viscose fibers consist of the alternative succession of the α-type and β-type layers. In the Müller-bath-type fiber there are four successive layers, i.e., the α_1-, β_1-, α_2- and β_2-layer; the α_1- and β_1-layer altogether correspond to the skin, and the α_2- and β_2-layer to the core. This seems to be in agreement with the result of Joshi and Preston[4], who observed four zones which differ in transverse orientation.

As to the layer succession, there are some interesting facts as follows: (1) Fiber spun in a zinc-free bath has only one combination of the α-type and β-type layer, but fiber spun in a zinc-containing bath has double combinations. (2) The periods of the layer succession are identical in all fibers spun in the same composition of bath, irrespective of the differences of their deniers. These facts seem to lead to the suggestion that the bath composition is of essential importance for the occurrence of the Liesegang-like periodic coagulation which influences the rate of primary gelatination and, consequently, the degree of crystallization.

Moreover, all types of fiber have the outermost thin α-type layer, which will be designated "the cuticle layer"***, irrespective of the existence of zinc salt in their spinning bath. The formation of this layer seems to connect with some inevitable effect occurring when viscose contacts with bath liquid, — maybe, a momentary dehydration carried out in the

11) A. Nakai, ibid., **14**, 905 (1958); **15**, 9, 90, 166, 170 (1959).
*** The cuticle layer was shown also by Heyn, *Textile Research J.*, **27**. 449 (1957). Heyn's paper had not been published when the present investigation was presented at Spring Meeting of the Fiber Society of Japan, held on May 16, 1957.

order of the relaxation time of the macromolecules in viscose, on the surface of the extruded viscose[11].

The most noticeable conclusion to be drawn from the present study is that the main part of the skin has a good crystallinity as well as the central part. This is opposed to the opinions given in the majority of previous works, which maintain that the degree of crystallinity is less in the skin than in the core[12-14]. On the other hand, a few contributions have been reported which show that there is no remarkable difference in crystallinity between the two[15,16]. Since the actual differentiations are far more complicated as proved here, it is doubtful whether the actual nature of the structural heterogeneity can be sought by the methods used in previous works, for example, by a comparative study of the crystallinity of thick- and thin-skin fibers, or by that of the physical properties of fibers peeled-off to various degrees which kept a relatively long interval between the various ones.

The structural difference based on crystallinity is the major factor which causes the differences in dye equilibrium absorption, but not the major factor which causes the differences in velocity of dye diffusion. This is demonstrated by the following facts: (1) There is a remarkable difference in velocity of dye diffusion between the β_1- and β_2-layer, irrespective of the small difference in their crystallinities. (2) There is no difference in velocity of dye diffusion between the α_2- and β_2-layer, irrespective of the great difference in their crystallinities. Consequently, the skin-core effect is not, as Morehead and others believed, due to the differences in degree of crystallinity between the two.

As already shown by various works, the skin part has a higher degree of axial orientation than the core. Accordingly, the main part of the skin (the author's β_1-layer) seems to have a denser structure with good orientation and good crystallinity. The difficulty of the dye permeating into the main part of the skin, and, more generally, the skin effect seems probably to be due to the interdependence of its higher orientation and higher crystallinity.

The course of fiber formation from viscose seems not to be so simple as to be suggested by previous theories. The present investigation seems to demonstrate that some as yet unknown peculiarity in the process of diffusion of the bath components into the viscose is mainly responsible for skin formation.

The author wishes to express his grateful acknowledgment to Professor I. Tachi of Kyoto University for his kind encouragement. He is also indebted to Messrs. S. Hiraoka and S. Omoto for their valuable assistance.

Some of the work reported here was carried out at the Research Institute of the Mitsubishi Rayon Company.

Department of Agricultural Chemistry
Faculty of Agriculture
Kyoto University
Sakyo-ku, Kyoto

12) F. F. Morehead and W. A. Sisson, *Textile Research J.*, **15**, 443 (1945).
13) N. H. Chamberlain and M. P. Khera, *J. Textile Inst.*, **43**, T123 (1952).
14) T. Yurugi, *J. Chem. Soc. Japan, Ind. Chem. Sec.* (*Kogyo Kagaku Zasshi*), **58**, 27 (1955).
15) P. H. Hermans, *Textile Research J.*, **20**, 553 (1950).
16) I. Sakurada and Y. Nukushina, Meeting of the Research Institute of Artificial Fibers, Japan (Oct. 1956).

Infrared Spectrum of α-Aminoisobutyric Acid and the Assignment of the Vibrational Frequencies

By Masamichi TSUBOI and Tadao TAKENISHI

(Received March 3, 1959)

As has been shown in our previous papers[1,2], the infrared absorption measurement is an effective means for detecting differences in the molecular configurations of amino acids in different environments. In order to investigate further in detail such differences in the molecular configurations, it is necessary to know the vibrational mode for each of the bands given by these amino acids. For glycine[3] and DL-alanine[4], complete assignments of the vibrational modes have been made to the bands observed in the NaCl (and also KBr for glycine) region. This paper refers to another simple amino acid, α-aminoisobutyric acid. The vibrational frequencies observed in the solid state infrared spectra of this compound and its deuterated (ND_3^+) one, and also of its hydrochloride will be shown, and then, to all of these observed frequencies, approximate vibrational modes will be assigned on the basis of the results of analyses of normal vibrations made by previous authors for simpler molecules.

It may be worthwhile to point out here that, in these molecules (probably because of their branched-chain structures), the couplings between the skeletal stretching vibrations and the CH_3 or NH_3^+ rocking vibrations are not so strong as in alanine. Therefore, detailed discussions may be made on the couplings between the CH_3 rocking vibrations and the NH_3^+ rocking vibrations.

Experimental

The sample of α-aminoisobutyric acid was purified with active charcoal and repeated recrystallization from water. The deuterated product (ND_3^+) was obtained by dissolving the acid in D_2O and then by evaporating the solvent in vacuum. During the procedure, the D_2O and the acid were kept away from the atmospheric moisture by use of a dry box. By repeating the procedure twice an almost completely deuterated product, practically free from the NDH_2^+ and ND_2H^+ groups, was obtained. α-Aminoisobutyric acid hydrochloride was obtained by dissolving the free acid in concentrated aqueous solution of hydrochloric acid (1.1 equivalents) and was purified by recrystallization from aqueous alcohol.

The infrared absorption measurements were made with Nujol mulls, hexachlorobutadiene mulls, and KBr disks. The instruments used were a Perkin-Elmer 21 spectrometer equipped with an NaCl prism and a Hilger H800 spectrometer equipped with an NaCl prism or with a KBr prism.

Results

Infrared absorption curves obtained for α-aminoisobutyric acid and its deuterated product are shown in Fig. 1, and that for the hydrochloride in Fig. 2. The observed frequencies of the bands are listed in Table I, and are graphically shown in Fig. 3, with their intensities. As to assignments given in the table and Fig. 3, discussions will be given below.

Assignments of the Vibrational Frequencies of Trimethylacetic Acid

Before discussing the vibration frequencies of α-aminoisobutyric acid, considerations will be made on the frequencies of trimethylacetic acid, $(CH_3)_3CCOOH$, which is iso-electronic with α-aminoisobutyric acid cation, $\begin{matrix} NH_3^+ \\ CH_3 \\ CH_3 \end{matrix}\!\!>\!C\text{–}COOH$, the NH_3^+ group of the latter being substituted by the CH_3 group in the former. The frequencies (in the region of 650~1800 cm^{-1}) of $(CH_3)_3CCOOH$, as read from Sadtler Standard Spectrum No. 6355*, are listed in Table II.

For comparison, the frequencies of *tert*-butyl chloride, as observed by Sheppard[5]

1) M. Tsuboi, T. Takenishi and Y. Iitaka, This Bulletin, **32**, 305 (1959).
2) M. Tsuboi and T. Takenishi, ibid., **32**, 726 (1959).
3) M. Tsuboi, T. Onishi, I. Nakagawa, T. Shimanouchi and S. Mizushima, *Spectrochim. Acta*, **12**, 253 (1958).
4) K. Fukushima, T. Onishi, T, Shimanouchi and S. Mizushima, ibid., **13**, 236 (1959).
5) N. Sheppard, *Trans. Faraday Soc.*, **46**, 527 (1950).
* See also reference 7.

are also given in the parallel column. The assignment of the frequencies of *tert*-butyl chloride was made by Nakagawa[6] with the result as given in Table II and Fig. 3.

The vibrational frequencies of trimethylacetic acid can be assigned readily by comparing the frequencies with those of *tert*-butyl chloride and by taking the characteristic frequencies of the carboxyl group[7] into consideration (see Table II and Fig. 3).

The frequencies, 1695, 1408, 1192 and 935 cm^{-1}, (shown in Fig. 3 by thick vertical lines) are assigned to four vibrations of the carboxyl group; i. e., 1695 cm^{-1} to the C=O stretching vibration, 1408 and 1192 cm^{-1} to two vibrations including the C–O stretching and the OH in-plane deformation, and 940 cm^{-1} to the OH out-of-plane deformation vibration. The frequency 865 cm^{-1} is assigned to the C–C (carboxyl) stretching mode, as 895 cm^{-1} in acetic acid dimer[8] or 846 cm^{-1} in acetic acid monomer[8]. All the other frequencies of trimethylacetic acid are correlated (see Fig. 3) with the frequencies of *tert*-butyl chloride, although provisos should be added as follows: The CH_3 degenerate deformation frequency 1460 cm^{-1} in the latter splits into two, 1479 and 1456 cm^{-1}, in trimethylacetic acid. The CH_3 symmetric deformation frequency 1370 cm^{-1} in *tert*-butyl chloride is lowered to 1359 cm^{-1} in trimethylacetic acid; $C\begin{smallmatrix}\diagup C\\ \text{—}C\\ \diagdown C\end{smallmatrix}$ asymmetric stretching frequency 1240 cm^{-1} is raised to 1295 cm^{-1}, and the symmetric stretching frequency 812 cm^{-1} lowered to 766 cm^{-1}. This lowering and raising is explained as the result of interactions of the vibrations of the $(CH_3)_3$–C group with the vibrations of the carboxyl group, interactions between the 1359 and 1408 cm^{-1} vibrations, between 1295 and 1192 cm^{-1} vibrations, and between 766 and 865 cm^{-1} vibrations. The band due to the CH_3 rocking vibration observed at 910 cm^{-1} in *tert*-butyl chloride is probably obscured in trimethylacetic acid by the strong band at 935 cm^{-1}.

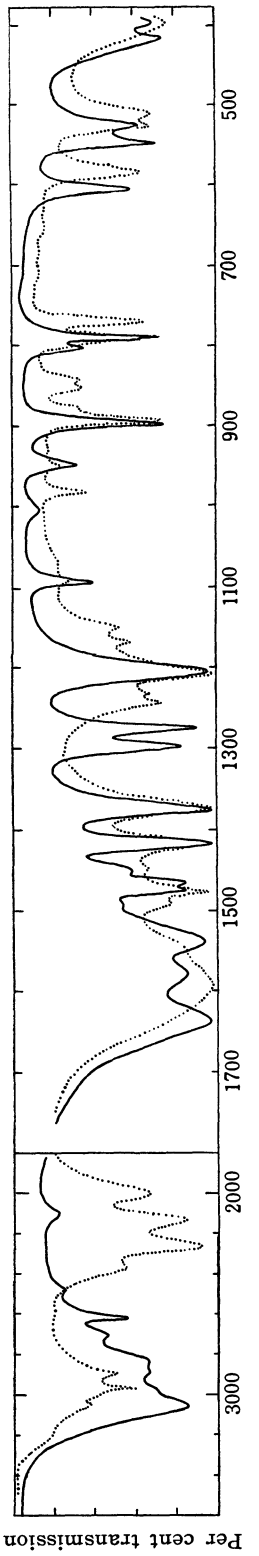


Fig. 1. Infrared absorption spectra of α-aminoisobutyric acid (——) and α-aminoisobutyric acid—ND_3 (·····).

6) I. Nakagawa, *J. Chem. Soc. Japan, Pure Chem. Sec.* (*Nippon Kagaku Zasshi*), **77**, 602 (1956). Nakagawa based his assignment (somewhat different from Sheppard's assignment) on his series of theoretical investigations of the normal vibrations of the molecules with the CH_3 groups and on the comparisons of the frequencies with those of other related molecules such as $CH(CH_3)_3$, etc.

7) D. Hadzi and N. Sheppard, *Proc. Roy. Soc.* (*London*), **A216**, 247 (1953).

8) J. K. Wilmshurst, *J. Chem. Phys.*, **25**, 1171 (1956).

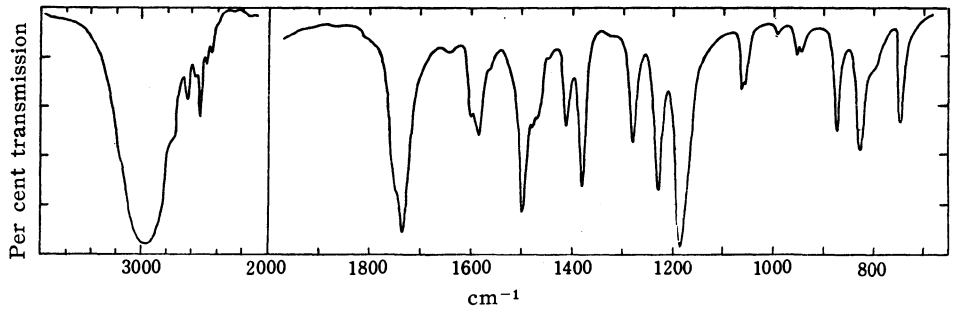


Fig. 2. Infrared absorption spectrum of α-aminoisobutyric acid hydrochloride.

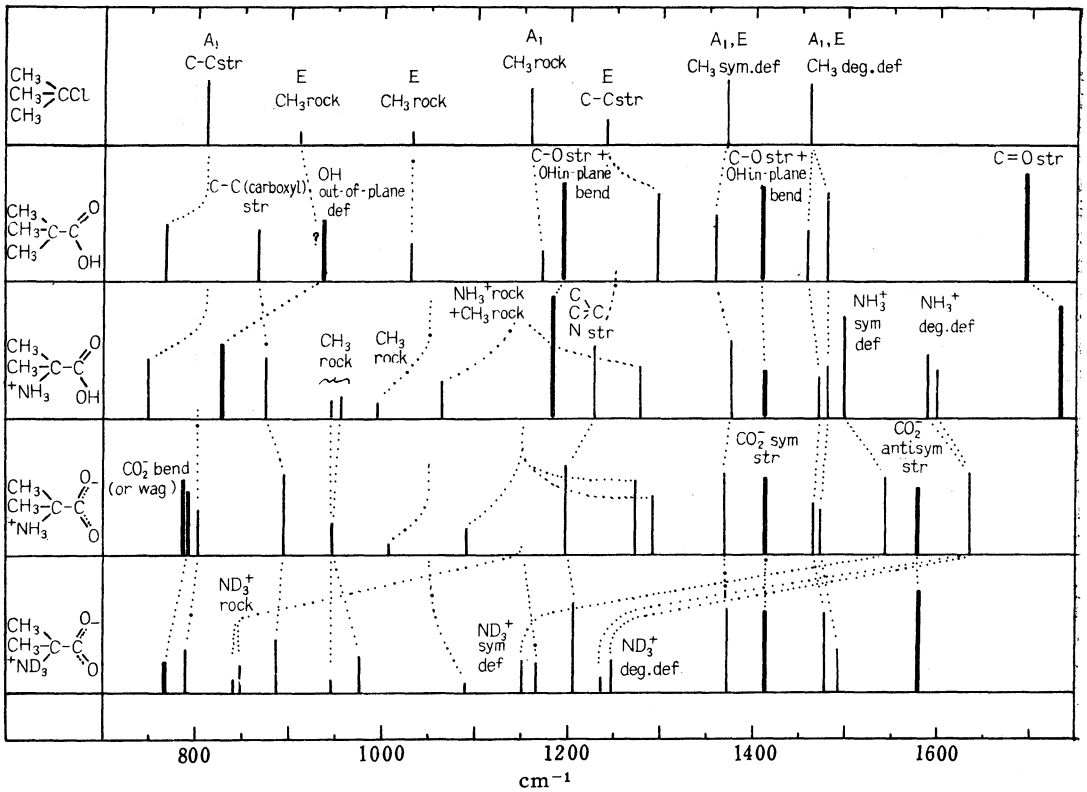


Fig. 3. Positions and intensities of the absorption bands of α-aminoisobutyric acid and related compounds.

Assignments of the Vibrational Frequencies of α-Aminoisobutyric Acid, its Deuterated (ND_3^+) Product, and its Hydrochloride

In the three crystals in question, α-aminoisobutyric acid, its deuterated product, and its hydrochloride, the molecules take the structures expressed by the formulae: $NH_3^+C(CH_3)_2COO^-$, $ND_3^+C(CH_3)_2COO^-$ and $NH_3^+C(CH_3)_2COOH$, respectively. These may be referred to in the following discussions as the zwitterion, the deuterated zwitterion, and the cation, respectively. In all of these three ions there seems to be no strong coupling between the four types of vibrations: the vibrations of the carboxyl group, the skeletal stretching vibrations, the hydrogen deformation vibrations (NH_3^+ and CH_3^+ deformation vibrations), and the hydrogen rocking vibrations. Discussions will, therefore, be presented below of these four types of vibrations in separate paragraphs.

A) Vibrations of the Carboxyl Group (shown in Fig. 3 by thick vertical lines).—In the cation, the carboxyl group takes the form,

TABLE I. OBSERVED FREQUENCIES (cm^{-1}) OF α-AMINOISOBUTYRIC ACID, ITS DEUTERATED PRODUCT (ND_3^+), AND ITS HYDROCHLORIDE, WITH THEIR ASSIGNMENTS
(s: strong, m: medium, w: weak)

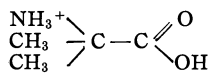
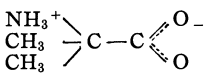
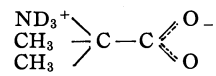
						Assignment
~3000						OH str.
2630 2570 2535 2490 2440		3035 2875 2820 2690 2610 2480 2100				NH_3^+ and CH_3 str.
				2962		CH_3 deg. str.
				2889		CH_3 sym. str.
				2367 2262 2112 2043 1990		ND_3^+ str.
1732	s					C=O str.
1599 1587	s s	1635	s	1237 1247	w w	NH_3^+ or ND_3^+ deg. def.
		1578	s	1580	s	CO_2^- antisym. str.
1495	s	1544	m	1151	m	NH_3^+ or ND_3^+ sym. def.
1480 1470	m m	1473 1465	m m	1492 1478	m s	CH_3 deg. def.
		1413	s	1415	s	CO_2^- sym. str.
1411	m					C-O str.+OH in-plane def.
1376	s	1370	s	1373	s	CH_3 deg. def.
1277	m	1293 1273	s s	849 842	m w	NH_3^+ or ND_3^+ rock.
1229	s	1199	s	1206	s	 asym. str.
1183	s					C-O str.+OH in-plane def.
1064 994	m w	1091 1008	w w	1167 1090	m w	CH_3 rock.
955 945	w w	946	w	976 947	m w	CH_3 rock.
875	m	895	s	888	s	C-C (carbonyl) str.
828	s					OH out-of-plane def.
748	m	803	m	790	m	 sym. str.
↑		792 787	m s	768	m	CO_2^- bend. (or wag.)
		602	m	587	m	CO_2^- wag. (or bend.)
not observed		547 531	m m	529 519	m m	CO_2^- rock.
↓		430 407	m m	404	m	skeletal def.

TABLE II. ASSIGNMENTS OF THE FREQUENCIES (cm^{-1}) OF *tert*-BUTYL CHLORIDE AND TRIMETHYLACETIC ACID
(s: strong, m: medium, w: weak, b: broad)

$(CH_3)_3C-Cl$		$(CH_3)_3C-C(=O)OH$		Assignment
		1695	sb	C=O stretching
1460	s	1479	s	CH_3 deg. def.
		1456	m	
		1408	m	C-O str.+OH in-plane def.
1370	s	1359	m	CH_3 sym. def.
1240	m	1295	sb	C-C str. (E)
		1192	sb	C-O str.+OH in-plane def.
1159	s	1170	w	CH_3 rock. (A_1)
1031	w	1029	m	CH_3 rock. (E)
		935	sb	OH out-of-plane def.
910	w	masked ?		CH_3 rock.
		865	s	C-C (carboxyl) str.
812	m	766	s	C-C str. (A_1)

$C(=O)OH$ The bands due to the vibrations of this group are picked out on account of their frequencies, intensities, or breadth. These are at 1732 (C=O stretching), 1411 (C-O stretching+OH in-plane deformation), 1183 (C-O stretching + OH in-plane deformation), and 828 cm^{-1} (OH out-of-plane deformation).

The frequency of the last vibration is much lower than that (930 cm^{-1}) of carboxylic acids without the NH_3^+ group. This is also the case for glycine hydrochloride and DL-alanine hydrochloride. This fact may be understood, if we assume that the carboxyl groups in amino acid hydrochlorides are in different hydrogen bondings from those of the carboxylic acids containing no NH_3^+ groups; in the latter the ring dimer is mostly formed through the two OH·····O=C bondings, while in the former the NH_3^+ group, a strong proton donor, interrupts the hydrogen bondings in the ring dimer.

In the zwitterion and the deuterated zwitterion, the carboxyl group takes the form, $C(=O)O$ The antisymmetric and symmetric stretching vibrations of this group are observed around the usual positions, 1600 and 1400 cm^{-1},— 1578 and 1413 cm^{-1} in the undeuterated zwitterion, and 1580 and 1415 cm^{-1} in the deuterated zwitterion.

The COO^- rocking vibration has the frequency 504 cm^{-1} in glycine[3], and 540 cm^{-1} in DL-alanine[9]. Therefore, the band at 540 cm^{-1} (doublet with the peaks at 547 and 531 cm^{-1}) in the zwitterion of α-aminoisobutyric acid is assigned to the COO^- rocking vibration. In the deuterated zwitterion, the band at 520 cm^{-1} is picked up as the corresponding one.

The COO^- bending and wagging vibrations have the frequencies 607 and 694 cm^{-1} respectively in glycine[3]. According to the result of the calculation of the normal vibrations in alanine by Fukushima[10], the COO^- bending frequency must be much higher than 607 cm^{-1}, and the band at 746 cm^{-1} was assigned to this vibration. The COO^- wagging vibration in this molecule was assigned to the band at 642 cm^{-1}. α-Aminoisobutyric acid gives two strong bands at 602 cm^{-1} and 790 cm^{-1} (doublet with the peaks at 792 and 787 cm^{-1}) in the region 600~800 cm^{-1}. By analogy with the case of DL-alanine, the band at 602 cm^{-1} is tentatively assigned to the COO^- wagging vibration and that at 790 cm^{-1} to the COO^- bending vibration.

A difficulty of this assignment is due to the fact that, very close to by the band at 790 cm^{-1}, there is another band observed at 805 cm^{-1}, which is later shown to be assigned to the $C-C(-N^+)C$ symmetrical stretching vibration. The two vibrations, COO^- bending and $C-C(-N^+)C$ symmetrical stretching, with dipole oscillations in almost the same direction, would couple strongly, so that the two bands due to these two

9) M. Tsuboi, to be published.

10) K. Fukushima, *J. Chem. Soc. Japan, Pure Chem. Sec.* (*Nippon Kagaku Zasshi*), **79**, 370 (1958).

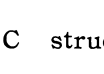
vibrations appear much more apart from each other. From this point of view, the band at 790 cm^{-1} is notlikely due to the COO^- bending vibration. Therefore another choice to assign the 790 cm^{-1} to the COO^- wagging and the 602 cm^{-1} to the COO^- bending is not entirely eliminated.

B) Skeletal Stretching Vibrations. — The skeletal stretching frequencies of the  structure are expected to be close to those of the  structure (see above), the symmetrical one being expected to be around 800 cm^{-1} and the asymmetrical one around 1200 cm^{-1}.

Actually, however, a band in the cation that may be assigned to the  symmetrical stretching vibration is observed at 748 cm^{-1}, a little lower than 800 cm^{-1}. This is attributed to a lowering of the frequency of the vibration in question due to its coupling with the C–C (carboxyl) stretching vibration. The band that may be assigned to the C–C (carboxyl) stretching vibration is observed at 875 cm^{-1}, a little higher than usual (835 cm^{-1} in trichloroacetic acid dimer[7]) just as is expected from the above-mentioned coupling of the two vibrations.

In the zwitterion, the C–C (carboxyl) stretching frequency is 895 cm^{-1}, a little higher than in the cation; and the  symmetrical stretching frequency is 803 cm^{-1}, a usual value.

The band of the cation at 1229 cm^{-1} and that of the zwitterion at 1199 cm^{-1} are assigned to one of the  asymmetrical stretching vibrations**.

In the deuterated zwitterion, the three skeletal stretching frequencies, namely, the symmetrical and asymmetrical stretching frequencies of the  structure and the C–C (carboxyl) stretching frequency, are found to be 790, 1206 and 888 cm^{-1}, respectively.

C) NH_3^+, ND_3^+ and CH_3^+ Deformation Vibrations.—As to the assignments of these vibrations, the results of studies on the vibrations of the glycine molecule[3] as well as of some simple molecules with the CH_3 group[11] are to be referred to. In the cation, the NH_3^+ degenerate deformation vibration is assigned to the doublet with the peaks at 1599 and 1587 cm^{-1}, and the NH_3^+ symmetric deformation vibration to the strong band at 1495 cm^{-1}. In the undeuterated zwitterion, the bands corresponding to the above two are at 1635 and at 1544 cm^{-1} respectively, 30~50 cm^{-1} higher than in the cation. This difference in the positions of bands may be explained by considering that the intermolecular (interionic) hydrogen bonding is stronger for the zwitterion than for the cation.

In the deuterated zwitterion, the doublet with peaks at 1237 and 1247 cm^{-1} and the band at 1151 cm^{-1} are interpreted as corresponding to the above two bands. Then, the factors of the shiftings of these bands are respectively 1.32 and 1.34, in agreement with the expected values, 1.37 and 1.31, respectively.

CH_3 degenerate deformation is assigned to a doublet around 1470 cm^{-1} and CH_3 symmetric deformation to a band near 1370 cm^{-1} in any of the cations, the undeuterated zwitterion, and the deuterated zwitterion.

D) NH_3^+, ND_3^+ and CH_3 Rocking Vibrations.—In any of the above three ions now under discussion, six rocking vibrations are expected, two from the NH_3^+ (or ND_3^+) group and four from the two CH_3 groups. In glycine, both of the two NH_3^+ rocking vibrations are observed in the vicinity of 1150 cm^{-1} [3]; and in isopropyl chloride, the four CH_3 rocking vibrations are observed at 1160, 1062, 949 and 932 cm^{-1} [10]. The location of the bands corresponding to the six rocking vibrations may be made around these frequencies.

Actually, in the cation, there are two weak bands observed, at 955 and 945 cm^{-1}, and these may correspond to the above two frequencies at 949 and 932 cm^{-1} of isopropyl chloride. Instead of bands around 1160 and 1062 cm^{-1}, however, three bands are observed at 1277, 1064 and 994 cm^{-1}. This fact may be explained as a result of interactions of the CH_3 rocking and the NH_3^+ rocking vibrations; thus, the two CH_3 rocking frequencies, originally at 1160 and 1062 cm^{-1} are lowered respectively to 1064 and 994 cm^{-1} and the two

** Only one band could be observed though two are theoretically expected.

11) I. Nakagawa and S. Mizushima, This Bulletin, 28, 589 (1955).

NH_3^+ rocking frequencies, originally around 1150 cm^{-1} are both raised to 1277 cm^{-1}.

In the undeuterated zwitterion, a band with a medium intensity is observed at 946 cm^{-1}. This band is considered to be an unresolved doublet and to correspond to the two CH_3 rocking vibrations observed at 949 and 932 cm^{-1} in isopropyl chloride and at 955 and 945 cm^{-1} in the α-amino-isobutyric acid hydrochloride. Besides this, four bands are observed at 1008, 1091, 1273 and 1293 cm^{-1}. These four bands are again explained as resulting from interactions of two of the four CH_3 rocking vibrations with the two NH_3^+ rocking vibrations, all of which are considered to be originally in the vicinities of 1160 and 1062 cm^{-1} (see Fig. 3).

This explanation is supported by what was observed of the rocking vibrations in the deuterated zwitterion. In the deuterated zwitterion, in which the NH_3^+ group is substituted by the ND_3^+ group, the above-mentioned interactions between the CH_3 and NH_3^+ rocking vibrations should be absent, and hence, the almost pure CH_3 rocking vibrations are expected to occur in the vicinities of 1160 and 1062 cm^{-1}. Actually, two bands are observed at 1167 and 1090 cm^{-1} in the deuterated zwitterion. It is also expected from the above explanation, that the two ND_3^+ rocking vibrations occur around $1160/1.32=880$ cm^{-1}. Actually, two bands are observed at 849 and 842 cm^{-1}. The observed frequencies of the bands are sufficiently close to the expected ones to support the above explanation.

Going into detail, however, the observed frequencies of the two CH_3 rocking vibrations are somewhat higher, and those of the two ND_3^+ rocking vibrations are somewhat lower, than the corresponding expected frequencies. This fact suggests that there are interactions of another type between the CH_3 and ND_3^+ rocking vibrations.

Corresponding to the other two CH_3 rocking vibrations in the deuterated zwitterion, expected around the 940 cm^{-1}, two bands are actually observed at 976 and 947 cm^{-1}. That the band at 976 cm^{-1} is situated at a little higher position than the expected position, 940 cm^{-1}, may again be attributed to the interactions of the CH_3 and ND_3^+ rocking vibrations***.

We wish to express our sincere thanks to Professor San-ichiro Mizushima, Dr. Takehiko Shimanouchi and Dr. Haruomi Oeda for their kind encouragement and valuable suggestions and to Miss Chie Yamazaki for helpful assistance.

Department of Chemistry
Faculty of Science
The University of Tokyo
Hongo, Tokyo (M. T.)

Central Research Laboratory
Ajinomoto Co., Inc.
Kawasaki, Kanagawa (T. T.)

12) N. Sheppard, *Trans. Faraday Soc.*, **46**, 533 (1950); G. Radinger and H. Wittek, *Z. physik. Chem.*, **B45**, 329 (1940); I. Nakagawa, *J. Chem. Soc. Japan, Pure Chem. Sec.* (*Nippon Kagaku Zasshi*), **77**, 602 (1956).

*** Under the assumption that all the rocking vibrations are independent of vibrations of other kinds in the zwitterion and in the deuterated zwitterion, the assignment, above made, of the six rocking frequencies is almost consistent with the product rule. Thus, the observed ratio, $1293\times1274\times1091\times1008\times946\times946/849\times842\times1167\times1090\times976\times947=1.93$, is close to the calculated ratio, 1.81. However, it is to be noted that the observed and calculated ratios are not in complete agreement. This is probably to be explained by considering that the assumption is not entirely valid, in other words, that some other vibrations, e. g., CH_3, NH_3^+, or ND_3^+ degenerate deformation vibrations and C-N stretching vibrations are coupling a little with the rocking vibrations.

Infrared Spectra of Salicylaldehyde, Methylsalicylate and their Sodium Compounds

By Haruka YAMADA

(Received April 2, 1959)

Concerning the infrared spectra of conjugated chelate compounds, it is well known that the absorption bands associated with the OH stretching and the C=O stretching vibrations show some peculiarities that are not observed in the spectra of the usual hydrogen-bonded molecules.

The formation of the intramolecular hydrogen bond in conjugated chelate compounds may be mainly due to electrostatic and charge transfer forces. Though some interpretations of the spectra, common to various conjugated chelate compounds, have been given by considering resonance structures, a question as to what structure contributes predominantly to the resonance has not yet been solved completely. The important contribution of ionic structure to the resonance was pointed out by some investigators[1], based on the infrared studies of the C=O bands, while the ionic structure was disregarded by a few others[2] from the measurements of the OH bands. The OH band seems to be inappropriate for accurate measurement because of its broad band width. The intensity measurement of the C=O band has not yet been made. In these circumstances, more experimental knowledge is required to make an analysis of this problem. Salicylaldehyde and methylsalicylate are suitable for the intensity measurements of the C=O bands and for the present analysis.

The sodium compounds of salicylaldehyde and methylsalicylate are very interesting, because they are expected to have an intermediate character between salts and metal chelate compounds and further will be closely related to the hydrogen-bonded compounds. The measurements for these compounds, therefore, will not only make their structures clear but also give a valuable item of knowledge in regard to the hydrogen-bonded chelation.

Experimental

Measurements were made by a Perkin-Elmer Model 112 Infrared Spectrophotometer equipped with CaF_2 and NaCl prisms. For dilute solutions, fixed cells of 0.01, 0.05 and 1 cm. thicknesses were used, and the thicknesses of the thin cells were determined by the interference method. The slit widths for intensity measurements were kept constant and ranged from 0.07 to 0.15 mm. The integrated absorption intensity of a band, A ($mol^{-1}\cdot l.\cdot cm^{-2}$) was calculated by the following formula;

$$A=(K/Cl)\cdot\Delta\nu_{1/2}\cdot\ln(I_0/I)_{max}$$

where C, l, $\Delta\nu_{1/2}$ and $\ln(I_0/I)_{max}$ have their usual meanings and K is obtained from Ramsay's table[3], by use of the spectral slit width calculated by Kudo's equation[4].

The samples used were purified by distillation. The boiling points were as follows; 68.8~69.0°C/10 mmHg for salicylaldehyde, 73.0~73.5°C/5 mmHg for methylsalicylate and 51.0~51.2°C/9 mmHg for benzaldehyde. *o*-Methoxybenzaldehyde was prepared from salicylaldehyde and dimethylsulfate[5]. The boiling point was 37.3~38.0°C.

The sodium compounds of salicylaldehyde and methylsalicylate were prepared by mixing an excess of salicylaldehyde and methylsalicylate with ethylalcoholate[6]. The sodium compound of methylsalicylate was also prepared by throwing metallic sodium into methylsalicylate. Upon heating, the sodium compound of salicylaldehyde chared at ca. 250°C instead of melting and the sodium compound of methylsalicylate at ca. 180°C. From the titration with hydrochloric acid, it was determined that each compound contained two molecules of salicylaldehyde or methylsalicylate for a sodium ion.

Results and Discussion

The results for the C=O bands of salicylaldehyde and methylsalicylate in

1a) R. S. Rasmussen, D. D. Tunnicliff and R. R. Brattain, *J. Am. Chem. Soc.*, **71**, 1068 (1949).
1b) D. Hadzi and N. Sheppard, *Trans. Faraday Soc.*, **50**, 911 (1954).
2a) M. Tsuboi, This Bulletin, **25**, 385 (1952).
2b) M-L Josein, N. Fuson, J-M Lebas and T. M. Gregory, *J. Chem. Phys.*, **21**, 331 (1953).
2c) H. Tsubomura, ibid., **24**, 927 (1956).
3) D. A. Ramsay, *J. Am. Chem. Soc.*, **74**, 72 (1952).
4) K. Kudo, *J. Spectroscop. Soc. Japan* (*Bunkô Kenkyû*), **9**, 36 (1954).
5) A. Kalschalowsky and St. v. Kostanecki, *Ber.*, **37**, 2347 (1904).
6) N. V. Sidgwick and F. M. Bewer, *J. Chem. Soc.*, **127**, 2379 (1925).

TABLE I. THE C=O BANDS OF SALICYLALDEHYDE AND METHYLSALICYLATE IN CARBON TETRACHLORIDE

		ν_{max} cm^{-1}	Concn. mol.·l^{-1}	$\ln(I_0/I)_{max}$	$\Delta\nu_{1/2}$ cm^{-1}	$A\times10^{-4}$ mol^{-1}·l.·cm^{-2}
Salicylaldehyde	I	1668	0.0942	2.487	7.00	2.60
	II	1668	0.0449	1.276	6.75	2.66
	III	1668	0.0634	1.814	6.80	2.70
	average	1668				2.65
Methylsalicylate		1683	0.0879	1.663	13.6	3.56

TABLE II. THE FREE C=O BANDS AND THE INTERMOLECULAR HYDROGEN-BONDED C=O BANDS OF BENZALDEHYDE AND *o*-METHOXYBENZALDEHYDE IN CARBON TETRACHLORIDE

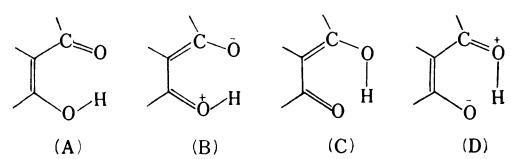
	ν_{max} cm^{-1}	$\Delta\nu_{1/2}$ cm^{-1}	$A\times10^{-4}$ mol^{-1}·l.·cm^{-2}
Benzaldehyde	1708	8.40	2.36
Benzaldehyde+*n*-butanol	1707	15.4	2.96
o-Methoxybenzaldehyde	1694	8.2	2.60*
o-Methoxybenzaldehyde+*n*-butanol	1693	13.2	3.25*

* The intensities are summed up for two ν_{max} assigned to its two isomers, though the intensity of one of them, at 1667 cm^{-1}, is very weak.

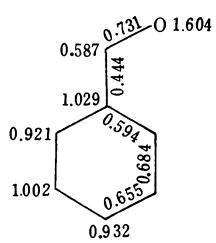
carbon tetrachloride solution are tabulated in Table I. In order to know whether or not the intensity of the band alters with chelating, the spectrum of salicylaldehyde should be compared with that of *o*-methoxybenzaldehyde, as the effect of the conjugation with the benzene ring and that of the ortho-substituted oxygen atom on their C=O groups are the same for both compounds. The results of the measurements for *o*-methoxybenzaldehyde[7] are shown in Table II. Because the intensity of the C=O band for salicylaldehyde is nearly equal to that for *o*-methoxybenzaldehyde, it comes out that the chelation effect does not alter the intensity. As the intensity of the C=O band for methylsalicylate shows the normal value of esters[8], it appears that the chelation effect has a large shift for the C=O stretching frequency towards lower frequency region but hardly affects the intensity. The lack of intensity change may indicate that the change in the bond moment is inappreciable.

In Table II are given the results for the conjugated C=O groups forming the intermolecular hydrogen bond with *n*-butanol. Here, the volume percentages of *n*-butanol in carbon tetrachloride range from 30 to 50%. Almost all the C=O groups of the compound in these solutions form the intermolecular hydrogen bond, since the frequency at the maximum absorption and the intensity of the band do not change with the concentration of *n*-butanol. By the formation of the intermolecular hydrogen bond the intensity noticeably increases, while the change in the frequency is very slight. These phenomena are different from those observed in the chelate compounds and can be explained by Tsubomura's theory[2c].

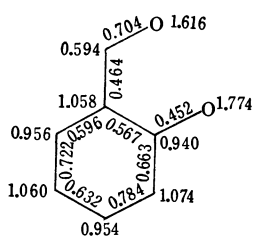
For the conjugated chelate compounds the four possible resonance structures shown below should be taken into account.



7) The ortho-substitution effect can be estimated by the comparison between benzaldehyde and *o*-methoxybenzaldehyde. The decrease of the frequcency and the increase of the intensity for the C=O band were observed by introducing the methoxy group. These changes are due to the migration of the lone pair electrons belonging to the oxygen atom and seem to be explained by the results expected from the molecular diagrams shown below. The molecular diagrams are calculated by a simple LCAO-MO method by use of Orgel's parameters.



Benzaldehyde



o-Methoxybenzaldehyde

8) G. M. Barrow, *J. Chem. Phys.*, 21, 2008 (1953).

TABLE III. SOLVENT EFFECT ON THE C=O BANDS OF SALICYLALDEHYDE AND METHYLSALICYLATE

	Solv.	ν_{max} cm^{-1}	$\Delta\nu_{1/2}$ cm^{-1}	$A\times10^{-4}$ $mol^{-1}\cdot l.\cdot cm^{-2}$
Salicylaldehyde	chloroform	1666	9.3	2.60
	n-butanol	1667	8.8	2.52
	acetonitrile	1666	8.6	2.61
Methylsalicylate	chloroform	1678	19.8	4.16

TABLE IV. THE C=O BAND OF ENOL-FORM OF ACETYLACETONE IN CHLOROFORM

ν_{max} cm^{-1}	Concn. $mol.\cdot l^{-1}$	Enol* content %	$\Delta\nu_{1/2}$ cm^{-1}	$A\times10^{-4}$ $mol^{-1}\cdot l.\cdot cm^{-2}$
1615	0.103	78	62.8	9.15

* K. Kuratani, *Rept. Inst. Sci. and Technol., Univ. Tokyo*, **6**, 217 (1952).

By the formation of the chelate ring the C and D structures newly contribute to the resonance. The important contribution of the B structure was at first pointed out by Rasmussen et al.[1a] and afterwards by Hadzi et al.[1b] again, while the importance of the C structure was reported by Tsuboi[2a], Josein et al.[2b] and Tsubomura[2c]. As it may be true that for a molecule having the carbonyl group the change in ionic character of C=O bond on chelate bonding contributes to the intensity increase of the C=O band, there seem to be two possibilities to account for the present results. First, if the C structure makes a significant contribution to the structure of the chelating compounds, the bond order of the C=O group will decrease and the appreciable change in the bond moment of the group will not occur, in accord with the results. Secondly, if both the structures of B and D equally contribute to the resonance, an increase in the contribution of the B structure will give rise to a decrease of the bond order and hence to the decrease of the C=O frequency, and the equal contribution of both the structures will not significantly alter the bond moment of the C=O group, because the directions of the polarities of both the resonance structures are opposite, and will result in the unaltered intensity of the C=O band. The second interpretation, however, seems to be less reasonable than the first, because in the second the D structure, in spite of its high energy, must contribute to the resonance to the same extent as the increase of the B structure.

In a molecule having a polar resonance structure the per cent contribution of each structure may vary with the change of solvent. As for such a molecule, a slight change in the per cent contribution gives rise to appreciable changes in the dipole moment and in the intensity of the infrared absorption band. The intensity of the C=O band for salicylaldehyde is the same in carbon tetrachloride, in chloroform and even in acetonitrile. This fact indicates the important contribution of non-ionic structures in this molecule. The chelation in methylsalicylate is not so strong as in salicylaldehyde because of the ester resonance[9]. The contribution of the C structure to methylsalicylate, therefore, will be less important than the contribution to salicylaldehyde. In the case of methylsalicylate, the influence of polar solvent on the intensity of the C=O band was found.

As for β-diketones, conjugated chelate compounds take the enol forms. As the C=O bands of these compounds overlap with their C=C bands, the intensities of the bands appear to be very large. Rasmussen et al. described the fact that a very broad band, estimated to be more than a hundred times as strong as the normal carbonyl band, was observed in the range 1639~1538 cm^{-1}.

As is shown in Table IV, the integrated intensity of the broad band including the C=O and C=C bands measured for the enol form of acetylacetone is only about twice as strong as that of the usual conjugated aliphatic C=O band; e.g., the value for isophorone in chloroform is 4.6×10^4 $mol^{-1}\cdot l.\cdot cm^{-2}$. The interpretation for β-diketones will be essentially the same as that for salicylaldehyde. Since the normal value of the intensity of the C=O band for this molecule is expected, this fact indicates

9) A. E. Martell and M. Calvin, "Chemistry of the Metal Chelate Compounds", Prentice-Hall, Inc., New York (1952), p. 164.

that the intensity of the C=C band increases by the chelation effect.

Concerning the band shapes for the chelate compounds, there can be found a relation between the C=O and the OH band. A compound having a sharp C=O band shows a broad OH band, and conversely a compound having a broad C=O band a sharp OH band. Strong chelation is accompanied by a sharp C=O and a broad OH band. Acetic acid is regarded as a sort of chelate compound. The C=O band measured in carbon tetrachloride solution is shown in Table VI. The association of acetic acid to the dimer is so strong that it dissociates with difficulty to the monomer even in 0.05 mol.·l^{-1} concentration. It is interesting to notice that the intensity of the C=O band seems to be normal, though this band is assigned to the antisymmetric stretching vibration caused by the coupling of the two C=O groups.

TABLE V. THE C=O BAND OF ACETIC ACID DIMER IN CARBON TETRACHLORIDE

ν_{max} cm^{-1}	Concn. mol.·l^{-1}	$\Delta\nu_{1/2}$ cm^{-1}	$A\times10^{-4}$ $mol^{-1}\cdot l.\cdot cm^{-2}$
1713.5	0.0481	10.4	3.92

TABLE VI. THE BAND SHAPES OF C=O AND OH STRETCHING VIBRATIONS

	C=O band	OH band
Salicylaldehyde	sharp	broad
Methylsalicylate	broad	sharp
Acetic acid dimer	sharp	broad

TABLE VII. THE WAVE NUMBERS FOR SALICYLALDEHYDE, METHYLSALICYLATE (IN LIQUID) AND THEIR SODIUM COMPOUNDS (IN NUJOL)

Salicylaldehyde	Sodium compound of salicylaldehyde	Methylsalicylate	Sodium compound of methylsalicylate
		701 w	701 w
715 m	731 m		712 m
766 s	766 s	759 s	758 m
	777 m		771 m
		800 m	801 w
		813 sh	806 w
		848 m	850 w
883 s	893 s	866 m	860 sh
		963 m	964 m
1023 m	1036 m	1032 m	1032 m
		1090 m	1085 m
1113 m	1119 s	1136 m	1148 sh
1149 m	1148 s	1158 m	1157 m
1182 s	1180 s	1195 m	1190 m
1201 sh			
1227 s	1246 s	1212 s	1213 s
1276 s	1279 m	1253 m	1257 m
		1301 s	1306 sh
1319 m	1315 m	1325 s	1316 s
		1439 s	1439 s
1577 w		1587 m	1540 m
1619 m	1600 m	1615 m	1607 w
1663 s	1680 s	1679 s	1682 s
3100 w	3344 m	3141 m	3206 m
			3351 m

The wave numbers of the infrared bands for the sodium compounds of salicylaldehyde and methylsalicylate observed in the solid state are tabulated in Table VII, together with the wave numbers for salicylaldehyde and methylsalicylate in the liquid state.

From the infrared measurements and the titration of sodium ion, it can be seen that a sodium ion links to two salicylaldehyde molecules, one of them being a molecular rest ion of salicylaldehyde and the other a salicylaldehyde molecule. The structures of these compounds will be illustrated in Fig. 1.

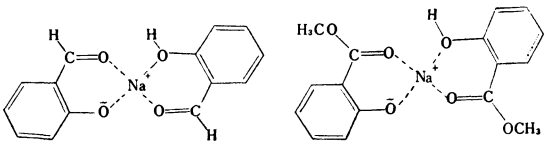


Fig. 1. The sodium compounds of salicylaldehyde and methylsalicylate.

The OH stretching vibrations of the sodium compounds show higher frequencies than those of salicylaldehyde and methylsalicylate. The broad band at 3100 cm^{-1} for salicylaldehyde changes into the sharp band at 3344 cm^{-1} for the sodium compound. The band at 3141 cm^{-1} for methylsalicylate separates into the two bands having their maxima at 3351 cm^{-1} and 3206 cm^{-1} for the sodium compound. The shifts of the OH stretching vibrations caused by changing salicylaldehyde and methylsalicylate into their sodium compounds indicate that the strong intramolecular hydrogen bond in the former varies into the intermolecular hydrogen bond in the latter. The two OH bands for the sodium compound of methylsalicylate may show the existence of the two different types of intermolecular hydrogen bond.

Concerning the sodium compounds, only one band can be assigned to the C=O stretching vibration for each compound. With the vibrations of metal chelate compounds, the couplings between ligand molecules are usually neglected. This approximation may be applied to these

sodium compounds because of the weakness of the metal-oxygen coordinate bonds. The same C=O stretching frequencies for salicylaldehyde and its molecular rest, coordinating to a sodium ion, suggest that the two carbonyl bonds are in the same electronic state. It is deduced that the lone pair electrons on the ionized oxygen in the molecular rest delocalize too little to influence the carbonyl group through the benzene ring. The fact that the carbonyl frequency of the C=O band for sodium compound of salicylaldehyde is higher than that for salicylaldehyde, may be explained by the small value of the electron affinity of sodium ion. As for the electron transfer of the oxygen atom in the carbonyl group, the larger the electron affinity of electron acceptors, the easier the electron transfer. The lone pair electrons on the oxygen atom, therefore, are less drawn by sodium ion than by proton and the frequency of the C=O band is higher for the sodium compound than for salicylaldehyde. The frequency of the C=O band for the sodium compound of methylsalicylate is slightly higher than that for methylsalicylate[10]. Since the coordinate bond between the sodium ion and the carbonyl group is very weak, the carbonyl group of the sodium compound of salicylaldehyde as well as that of *o*-methoxybenzaldehyde will be rather akin to that of virtual non-chelate salicylaldehyde. The difference in the C=O frequency between salicylaldehyde and its sodium compund is 17 cm^{-1}, while that between methylsalicylate and its sodium compound is only 3 cm^{-1}. This fact indicates the strong chelation in salicylaldehyde. This agrees with the results obtained by the solvent effect and the band shapes. The configuration of the sodium compound is probably of a tetrahedral type, since the available orbitals of sodium ion to form the coordinate bond are sp^3 hybrid. However, it has recently been reported[11] that the sodium compound of salicylaldehyde does not form any chelate ring because of the observed high frequency of the C=O band. Based on the present studies this opinion can be left out of consideration.

As regards chelate compounds, the bands assigned to the phenolic C–O stretching vibrations are of considerable interest, because no definite assignment for these bands has yet been made. By comparing the absorption spectrum of salicylaldehyde or methylsalicylate with that of its sodium compound respectively, the phenolic C–O bands are reasonably assigned. The results obtained are listed in Table VIII. The relations between wave numbers of C=O stretching and those of phenolic C–O stretching vibrations are given in Fig. 2.

TABLE VIII. THE WAVE NUMBERS OF C=O AND PHENOLIC C–O STRETCHING VIBRATIONS

	Salicylaldehyde		Methylsalicylate	
	C=O	C–O	C=O	C–O
Na^+	1680	1246	1682	1213
H	1663	1276	1679	1212
Ti^{4+}	1637	1313	1651	1246
Cu^{2+}	1612	1340		

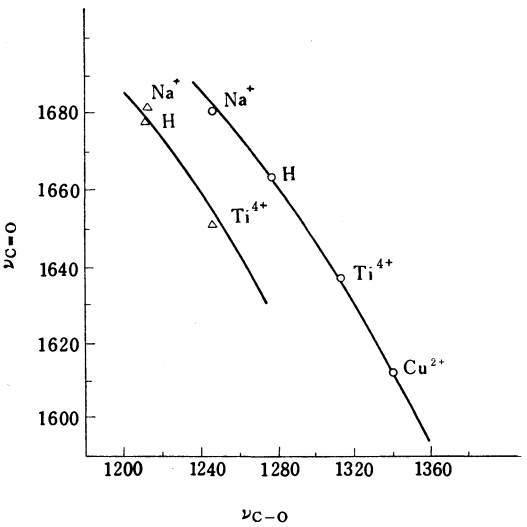


Fig. 2. The relations between the wave numbers of C=O stretching and those of phenolic C–O stretching vibrations. ○ Salicylaldehyde and its metal complexes. △ Methylsalicylate and its metal complexes.

In Table VIII and Fig. 2, copper complex and titanium complexes[12] are shown together. The larger the wave number of C=O stretching vibration, the smaller the wave number of C–O stretching vibration. The reason for this may be as follows. In these chelate compounds, as the double bond character of the C=O bond decreases by the electron migration from the carbon to the oxygen, the electron migration from the oxygen to the benzene ring and the

10) It is supposed that the C=O frequency of the sodium compound of methylsalicylate is hardly affected by the change in the nature of the C–O bond neighboring the C=O bond.

11) P. Chiorboli and P. Mirone, *Ann. chim.*, 48, 363 (1958).

12) A. Yamamoto, to be published.

double bond character of the C–O bond increase. These relations are nearly linear and the curve for salicylaldehyde and its complexes and that for methylsalicylate and its complexes are parallel. From Fig. 2, it follows that the electron affinities of these electron acceptors are probably in the order of $Cu^{2+} > Ti^{4+} > H > Na^{+}$.

The author wishes to express her sincere thanks to Professor K. Kozima for his kind guidance and discussion throughout the course of this study and also to Mr. W. Suetaka for his helpful advice.

Research Laboratory of Spectroscopy
Tokyo Institute of Technology
Meguro-ku, Tokyo

Vinyl-polymerization with Alkylboron Derivatives

By Nobuyuki ASHIKARI

(Received October 22, 1958)

The outline of alkylboron derivatives as the catalysts for the polymerization of vinyl compounds was previously reported[1]. In the present paper, the preparation of these catalysts, the polymerization rates, the relation between the conversion and the molecular weight, and the influence of oxygen on the polymerization rate are described in detail. The catalysts studied were dialkylboron chloride (R_2BCl), dialkylboronous ester (R_2BOR'), dialkylborinic acid (R_2BOH), and dialkylboron oxide [$(R_2B)_2O$]. Furukawa[2] reported that dialkylboron oxide was a good catalyst. The present investigation shows that the organoboron compounds employed in this experiment are effective for comparatively polar monomers.

Experimental and Results

Analytical Methods for Organoboron Compounds.—The synthesized catalysts were analyzed by the following methods. In the case of R_2BCl, hydrogen chloride produced by the decomposition of the sample with water was titrated with sodium hydroxide solution under phenolphthalein indicator. In other cases, quantitative analysis of boron was carried out by the modification of Synder's method[3].

A weighed sample (about 0.2 g.) was taken in a 100 cc. Erlenmeyer flask in which air was previously replaced with nitrogen. After 0.1 N sodium hydroxide solution, the amount of which was nearly equivalent to the theoretical value, was poured into the flask; 30% hydrogen peroxide solution was added slowly to it. The flask was shaken for twenty minutes. Then, the content was transferred into a platinum vessel to be heated gently. After the water was mostly vaporized, the vessel was cooled to room temperature, and the content was poured into a 300 cc. beaker with about 70 cc. of distilled water. To the aqueous solution about 5 cc. of glycerin was added and the titration was carried out with 0.1 N sodium hydroxide solution using phenolphthalein indicator. If the excess of alkaline solution is added at the beginning, the solution containing the sample has to be acidified by the addition of the known volume of hydrochloric acid (0.1 N) before the titration with sodium hydroxide solution is carried out.

The Monomers and the Treatments of the Polymers.—The monomers such as styrene (St), methyl methacrylate (MMA), and vinyl acetate (VA) were purified as mentioned below.

St: The "commercial" was washed with 5% alkaline solution, followed by water, dried over calcium chloride, and distilled.

VA: The "commercial" was steam distilled, dried over sodium sulfate, and distilled.

MMA: It was dried with sodium sulfate and distilled.

The distillation of styrene and methyl methacrylate was carried out under reduced pressure. The polymers except for polyvinyl acetate were treated with methanol, filtered, and dried. In the case of polyvinyl acetate, it was separated from its monomer by steam distillation.

Preparation of the Alkylboron Derivatives.—*Alkylboron chloride.*—The alkylboron chlorides were prepared according to Booth's method[4], i. e., by passing dry hydrogen chloride into trialkylboron. The reaction proceeds as follows:

$$R_3B + HCl = R_2BCl + RH$$

Using this method, diisopropylboron chloride,

1) N. Ashikari, *J. Polymer Sci.*, **28**, 641 (1958).
2) J. Furukawa, T. Tsuruta et al., *J. Chem. Soc. Japan, Ind. Chem. Sec.* (*Kogyo Kagaku Zasshi*), **61**, 733 (1958).
3) H. R. Synder, J. A. Kuck and J. R. Johnson, *J. Am. Chem. Soc.*, **60**, 110 (1938).

diisobutylboron chloride and di-*n*-butylboron chloride were prepared.

To a 100 cc. round bottomed flask, were set an inlet of hydrogen chloride, and a condenser to the top of which a calcium tube was connected. Into this flask 36 g. of triisobutylboron was poured, and hydrogen chloride was introduced. The reaction was continued for 15 hr. at 140°C. Then, the content was distilled under reduced pressure, and the fraction of b. p. $_{31}62\sim65$°C was collected. Thus, 28 g. of diisobutylboron chloride was obtained (87% yield).

Analysis.—A weighing bottle containing 0.3116 g. of the sample was put in a 300 cc. flask containing 100 cc. of distilled water. The weighing bottle was tied with wire to the rubber stopper of the flask as shown in Fig. 1. After the rubber

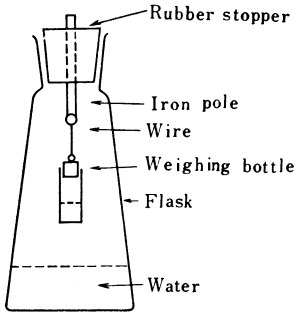


Fig. 1. The vessel for the decomposition of R_2BCl.

stopper was closed, the flask was shaken vigorously to open the stopper of the weighing bottle. The rubber stopper was taken off, and the titration was carried out. The amount of the spent sodium hydroxide solution (0.1 N) was 21.6 cc.

Anal. Found: Cl, 22.42. Calcd. for $(C_4H_9)_2BCl$: Cl, 22.12%.

Similarly, other dialkylboron chlorides were analyzed. The conditions of the preparation and the yields are shown in Table I.

TABLE I. ALKYLBORON CHLORIDE

R in R_2BCl	Temp. °C[a)]	Time hr.	b. p. °C	Yield %
iso-C_3H_7	120	15	125	88
n-C_4H_9	140	15	67/18 mmHg[b)]	82

a) Reaction temperature
b) Booth's value is 173°C[4].

Generally, dialkylboron chloride is rather more unstable to oxygen than the corresponding trialkylboron. For example, diisopropylboron chloride is inflammable in contact with air, but triisopropylboron is not so.

Dialkylboronous ester.—This is easily prepared by the reaction between dialkylboron chloride and alcohol[5]. The reaction formula is as follows:

$$R_2BCl + R'OH = R_2BOR' + HCl$$

Using this method various dialkylboronous esters were prepared. When alcohol was dropped slowly into dialkylboron chloride under nitrogen stream, the reaction took place at once.

The product consisted of two layers. The upper layer was colorless and the lower one, the amount of which was small, was slightly colored. The upper layer was separated from the lower one and distilled. Few studies on the esters of such type as $(iso\text{-}C_3H_7)_2BOR$ have been performed. The yields and the boiling points of these derivatives are shown in Table II.

TABLE II. THE YIELD AND THE BOILING POINT OF $(iso\text{-}C_3H_7)BOR$

R in $(iso\text{-}C_3H_7)_2BOR$	ROH(g.) added	Yield %	b. p. °C
CH_3	3	91.1	117
C_2H_5	4	80.0	132
iso-C_3H_7	5	80.7	51(32 mmHg)
iso-C_4H_9	6	70.1	70(32 mmHg)
tert-C_4H_9	6	35.5	92(30 mmHg)

In Table II, the weigt of the diisopropylboron chloride used was 10 g. in each experiment. Moreover, diisobutylboron isobutyl ester was prepared. This boiled at 97°C/27 mmHg. The yield was 92%.

Analysis of $(iso\text{-}C_3H_7)_2BO(iso\text{-}C_3H_7)$
Sample: 0.1935 g., alkali added: 12.7 cc.
Found B, 7.25%, Calcd. B, 7.05%

Dialkylborinic acid and dialkylboron oxide.—Dialkylborinic acid was prepared according to Eq. 1, but was not always isolated purely because of decomposition by distillation.

$$R_2BCl + H_2O = R_2BOH + HCl \quad (1)$$

Dialkylboron oxide was prepared purely by distillation of the product from dialkylboron chloride and equivalent water. To 28.5 g. of di-*n*-butylboron chloride was added 3.2 g. of pure water under nitrogen stream, and the product was distilled. Thus, 18.5 g. of the product which boiled at 90~92°C/1 mmHg (reported value[6], 136°C/12 mmHg) was obtained (78.3% yield, calculated from di-*n*-butylboron chloride).

Analysis of $[(n\text{-}C_4H_9)_2B]_2O$
Sample: 0.1419 g., alkali added: 10.8 cc.
Found B, 8.41%, Calcd. B, 8.27%

The Rate of the Polymerization of Styrene with these Derivatives.—By observing the polymerization rates, the activities of these catalysts were compared. The catalysts employed in this experiment were isopropylboron derivatives. In

TABLE III. THE SORT AND WEIGHT OF THE CATALYST IN THE POLYMERIZATION OF STYRENE

Catalyst type	Weight, g.	Wt. of St, g.
R_2BOR	0.3681	130
R_2BCl	0.3562	148
$(R_2B)_2O$	0.4022	106

Where, R is iso-C_3H_7.

4) R. B. Booth and C. A. Craus, ibid., **74**, 1415 (1952).
5) M. F. Lappert, *Chem. Revs.*, **56**, 1015 (1956).
6) J. R. Johnson, H. R. Synder and M. G. Van Campen, Jr., *J. Am. Chem. Soc.*, **60**, 115 (1938).

TABLE IV. THE CONDITION OF THE POLYMERIZATION FOR INVESTIGATING THE RELATION BETWEEN THE CONVERSION AND THE INTRINSIC VISCOSITY

Monomer	Temp., °C	Vessel	Cat.[a]/monomer wt. %	O_2 mol. ($\times 10^5$)
MMA	50	flask	0.296	N_2 stream
St	50	flask	0.379	N_2 stream
VA	50	ampoule	0.414	5.0

a) The catalyst is diisopropylboron oxide.

every case, the value of catalyst/monomer was 0.188 in mol. %. The weights of the catalysts and the monomer were shown in Table III.

Each reaction was carried out at 50°C under nitrogen stream in a four necked flask to which a stirrer, an inlet of nitrogen, and a thermometer were connected.

At a certain interval of reaction, 10 g. portions of the sample were taken out and poured into methanol. Then, the polymer was filtered, dried, and weighed. These results were represented in Fig. 2.

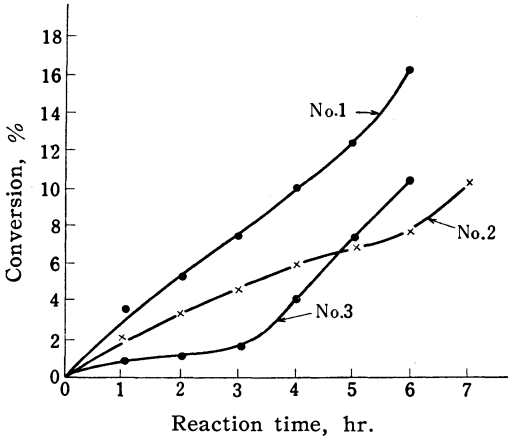


Fig. 2. Polymerization rates of styrene with three types of alkylboron.
No. 1, $(R_2B)_2O$: No. 2, R_2BOR: No. 3, R_2BCl, where, R is iso-C_3H_7.

Usually, in the polymerization with these catalysts, the polymerization rate increased rapidly after a certain reaction time (as shown in Fig. 2).

Relation between the Conversion and the Molecular Weight.—In usual "radical polymerization", the molecular weight is expected to have no relation with the conversion. However, in high conversion, many examples[7] have shown the fact that the former depends on the latter. The same phenomenon was observed, even in low conversion, in the case of the polymerization with alkylboron catalyst. Methyl methacrylate, styrene and vinyl acetate were polymerized in the following conditions (Table IV).

When the reaction was carried out in an ampoule, the apparatus shown in Fig. 4 was used. When a flask was used as a reaction vessel, the reaction was carried out under nitrogen stream, and the sample was taken out after a certain interval of reaction. The relation between the conversion and the intrinsic viscosity was represented in Fig. 3.

In this case, the viscosity of each polymer was measured in the following condition (Table V).

TABLE V. THE CONDITION OF MEASUREMENT OF THE VISCOSITY

Polymer	Solvent	Temp., °C
PMMA	toluene	30
PSt	toluene	30
PVA	benzene	30

Where, "P" means a polymer.

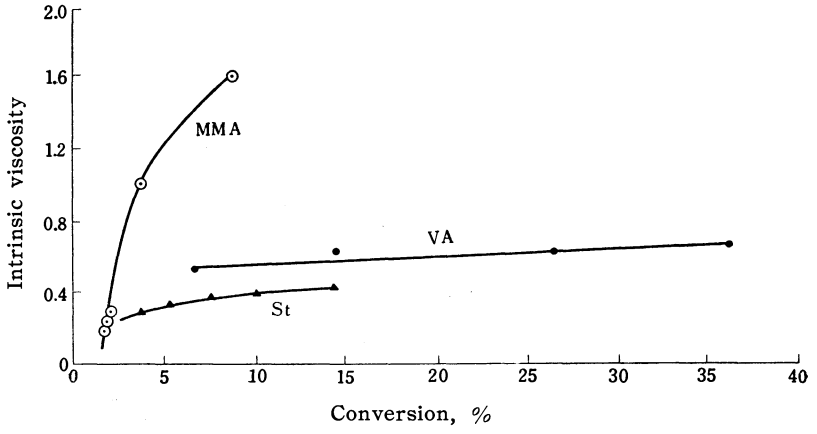


Fig. 3. Relation between the conversion and the intrinsic viscosity.

7) M. Ōiwa, *Chemistry and Chem. Ind.* (*Kagaku to Kogyo*), 11, 792 (1958).

TABLE VI. POLYMERIZATION CONDITIONS FOR INVESTIGATING THE INFLUENCE OF OXYGEN

Monomer	Time, hr.	Temp., °C	Catalyst	Catalyst/monomer, wt. %	Cat., wt.
St	5	40	$R_2BO\cdot iso\text{-}C_3H_7$	0.42	0.0754
MMA	1	40	$R_2BO\cdot iso\text{-}C_3H_7$	0.40	0.0754
VA	0.5	41	$R_2BO\cdot iso\text{-}C_4H_9$	0.41	0.0766

Where, R is iso-C_3H_7.

TABLE VII. MEASUREMENT OF THE VISCOSITIES AND THE EQUATIONS FOR CALCULATING THE MOLECULAR WEIGHT

Polymer	Solvent	Temp., °C	Eq. ($[\eta]=$)	Reference
PSt	toluene	30	$0.55\times10^{-4}M^{0.81}$	8
PMMA	toluene	25	$0.71\times10^{-4}M^{0.73}$	9
PVA	benzene	30	$5.63\times10^{-4}M^{0.62}$	10

Influence of Oxygen on the Polymerization Rate.—To observe the influence of oxygen on the polymerization rate some monomers were polymerized in the following apparatus (Fig. 4).

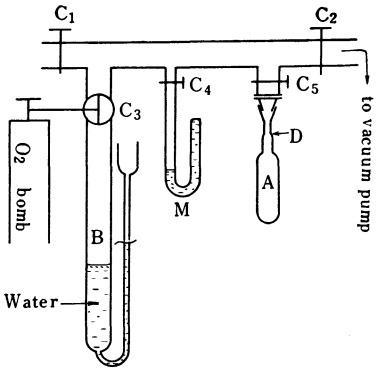


Fig. 4. Apparatus for investigating the influence of oxygen.
M: Manometer
B: Gas burette
A: Polymerization tube

The Explanation of the Apparatus and the Procedure.—The volume of the space enclosed by stopcocks C_1-C_5 is 136 cc., and that of A, polymerization tube, is 70 cc. The volume from C_5 to D is 5 cc.

To tube A in which nitrogen had replaced air, 20 cc. of monomer was introduced and the tube was cooled in dry-ice methanol. After the catalyst, the amount of which was shown in Table VI, was added under a nitrogen stream, the tube was connected to the apparatus. The gas involved in tube A and other spaces enclosed by stopcocks C_1-C_4 was removed by a vacuum pump. After a certain amount of oxygen contained in burette B was introduced to the tube, it was sealed. The sealed tube was transferred into a constant temperature bath. The reaction temperature, the reaction time, etc., were shown in Table VI.

Thus, from the yield obtained after the same reaction time, the influence of oxygen on the polymerization rate was compared. The relation between the amount of oxygen and the conversion was represented in Fig. 5.

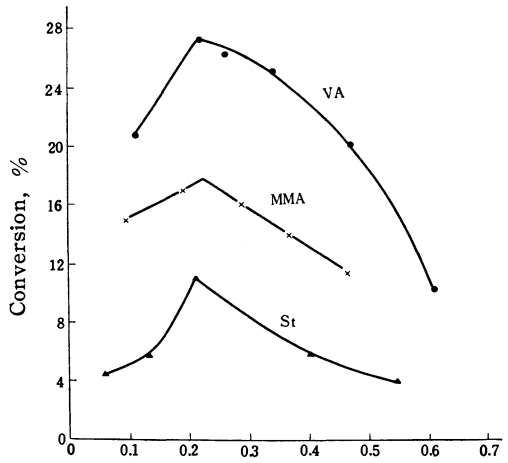


Fig. 5. Diagram of conversion—O_2/catalyst. The influence of oxygen on the polymerization rate.

The viscosity of each sample shown in Fig. 5 was measured to obtain the relation between the molecular weight and the value of O_2/catalyst in mole ratio. These results are represented in Fig. 6. The conditions of measurement of the viscosity and the equations for calculation of the molecular weight are shown in Table VII.

From Fig. 5, it is clear that the polymerization rate is the largest when the value of O_2/catalyst in mole ratio is 0.22. In regard to the molecular weight, the molecular weight at the maximum point of the polymerization rate is minimum except in the case of polyvinyl acetate. The reason why the curve of the molecular weight of PVA against the mole ratio of O_2/catalyst differed from those of polymethyl methacrylate and polystyrene is not clear.

8) T. Alfrey and Batovics, *J. Am. Chem. Soc.*, **65**, 2319 (1943).
9) S. Chinai, J. Matlack and A. Resnick, *J. Polymer Sci.*, **17**, 391 (1955).
10) A. Nakajima, *Chemistry of High Polymers* (*Kobunshi Kagaku*), **11**, 142 (1954).

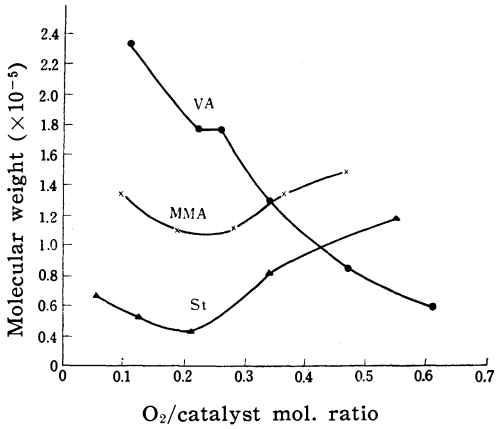


Fig. 6. Relation between the molecular weight and O_2/catalyst mol.-ratio.

Summary

Such alkylboron derivatives as dialkylboron chloride, dialkylborinic acid, dialkylboronous ester, and dialkylboron oxide as the catalysts for the polymerization of vinyl compounds were studied. Although dialkylborinic acid was a good catalyst, it was pretty difficult to isolate it purely, therefore, only a brief description was made in this paper. Of course, some dialkylborinic acids can be isolated purely under suitable conditions. In regard to this, further investigation will be performed.

The polymerization rates of styrene with these catalysts, the relation between the conversion and the intrinsic viscosity, and the influence of oxygen on the polymerization rate were studied. The polymerization rate of some monomers with dialkylboronous ester is maximum when O_2/catalyst in mole ratio is 0.22.

The author wishes to express his sincere thanks to Mr. T. Iwachido in this laboratory who measured the viscosities.

The Electrical Communication Laboratory
Nippon Telegraph and Telephone
Public Corporation
Musashino-shi, Tokyo

Polymerization of Olefins with Trialkylboron Catalyst. III. Copolymerization of Butadiene, Isobutylene and 1-Phenylbutadiene

By Nobuyuki ASHIKARI

(Received April 15, 1959)

As is well known, the monomers having comparatively large polarity easily polymerize with alkylboron catalyst, but those having small polarity do not. The polymerizations of the monomers which polymerize alone, and the copolymerizations of those monomers have already been reported[1,2]. In this paper, the copolymerizations of some monomers which exhibit no tendency to polymerize alone, such as butadiene, isobutylene, and 1-phenylbutadiene were studied. In every pair of the monomers treated in this paper, the copolymerization rates were very small. Particularly, the reaction rate of 1-phenylbutadiene with another monomer was so small that the relative reactivity could not be obtained. The relative reactivities of such pairs as isobutylene-acrylonitrile, butadiene-styrene and butadiene-acrylonitrile were obtained.

1) N. Ashikari, This Bulletin, **31**, 229 (1958).
2) N. Ashikari, *J. Polymer Sci.*, **31**, 249 (1958).

Experimental and Results

1. Monomers.—*1) Isobutylene and butadiene.*—Isobutylene[3] was prepared by dehydration of *tert*-butanol with anhydrous oxalic acid at about 90°C, dried over calcium chloride, and redistilled. Butadiene was prepared according to Blatt's method[4], i.e., thermal decomposition of cyclohexene, dried over calcium chloride, and redistilled.

2) Acrylonitrile, styrene and methyl methacrylate.—The commercial substances were dried and distilled just before use.

3) 1-Phenylbutadiene.—This was synthesized

3) N. Daidan et al., *J. Electrochem. Soc. Japan (Denki Kagaku)*, **13**, 27 (1945).
4) A. H. Blatt et al., "Organic Syntheses", Col. Vol. II, John Wiley & Sons, Inc., New York (1943) p. 655.

from cinnamic aldehyde by the following method[5,6]:

$$\underset{(A)}{RCHO} \xrightarrow{CH_3MgJ} \underset{(B)}{RCH(OMgJ)CH_3} \xrightarrow{NH_4Cl\text{-}H_2O} \underset{(C)}{RCH(OH)CH_3}$$

$$\xrightarrow{HCl} \underset{(D)}{RCHClCH_3} \xrightarrow{-HCl} \underset{(E)}{RCH=CH_2}$$

Where, R is $C_6H_5CH=CH-$.

D was prepared by treating C with dry hydrogen chloride at 0°C, and E was prepared by heating D in pyridin solvent for about one hour. After the reaction was over, unchanged pyridin was distilled off, and the product was washed thoroughly with water to remove the complex of pyridin-hydrogen chloride. Then, the product was dried over calcium chloride and distilled. The yield of pure 1-phenylbutadiene boiling at 56~57°C/3 mmHg was 17~20% of the theoretical amount for cinnamic aldehyde.

II. Procedure of the Copolymerization and the Treatment of the Polymer. — In a polymerization tube, a certain amount of high-boiling monomer such as styrene or acrylonitrile was placed, and the tube was cooled in dry ice-methanol. After the content was thoroughly cooled, the tube was placed on a balance, and a certain amount of second monomer, liquefied by cooling, such as isobutylene or butadiene was poured into the tube. Then, the catalyst, triisobutylboron was added to the tube under nitrogen stream, and the tube was sealed.

The reaction was stopped by cooling the tube in dry ice-methanol. After the tube was opened, the polymer was precipitated by adding the content of the tube into methanol, filtered, dried under reduced pressure at 50°C, and weighed. If the copolymerization was carried out in emulsion system, the polymer was taken out by treating the content with hot water (about 90°C) containing 5% sodium chloride. Thus, the polymer isolated was washed thoroughly with hot water, followed with methanol, dried and weighed.

III. Copolymerization Rates of Butadiene-acrylonitrile in the Bulk and Emulsion Systems. —The copolymerization rate of butadiene-acrylonitrile in emulsion system was compared with that in bulk system.

Generally, the polymerization rate in emulsion system is larger than that in bulk system. In this experiment, the same results were obtained. Moreover, in emulsion system, fairly strong copolymer was obtained.

The total weight of the two monomers in each pair was 11.3 g., and the volume of the catalyst was 0.1 cc. in each experiment. In emulsion system, 12 cc. of distilled water containing 5% emulsifier was used. Each reaction was carried out in a sealed tube at 40°C for five hours. The relation between the conversion and the mole fraction of butadiene in the monomer mixture is shown in Fig. 1.

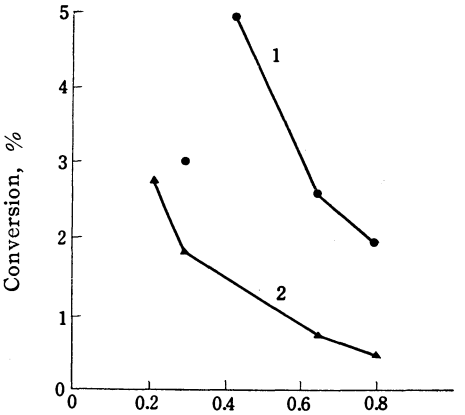


Fig. 1. Copolymerization rates of butadiene-styrene in bulk and emulsion system.
(1) emulsion system
(2) bulk system

IV. Monomer Reactivity Ratios.—The relative reactivities (r_1, r_2) of such pairs as isobutylene-acrylonitrile, butadiene-styrene, and butadiene-acrylonitrile were evaluated graphically using the following equation[7]:

$$r_2 = \frac{\log([M_2]_0/[M_2]) - \frac{1}{p}\log\frac{1-p[M_1]/[M_2]}{1-p[M_1]_0/[M_2]_0}}{\log([M_1]_0/[M_1]) + \log\frac{1-p[M_1]/[M_2]}{1-p[M_1]_0/[M_{02}]}}$$

where $p=(1-r_1)/(1-r_2)$, $[M]_0$ and $[M]$ represent the monomer concentration in the intitial and final states of polymerization, respectively,

TABLE I. ISOBUTYLENE-ACRYLONITRILE

No.	$[M_1]_0$	$[M_2]_0$	Conversion	N%	$[M_1]$	$[M_2]$
1	0.179	0.02	3.44	13.8	0.1757	0.0163
2	0.166	0.04	3.72	14.6	0.1626	0.0356
3	0.179	0.06	3.96	15.2	0.1750	0.0543
4	0.125	0.08	4.77	17.6	0.1218	0.0733
5	0.100	0.10	5.53	18.0	0.0966	0.0923
6	0.116	0.12	5.54	18.7	0.1123	0.1105
7	0.061	0.14	9.02	21.1	0.0575	0.1253
8	0.054	0.18	8.26	21.9	0.0509	0.1638

5) E. C. Coyner and G. A. Ropp, *J. Am. Chem. Soc.*, **69**, 2231 (1947).
6) A. Klages, *Ber.*, **35**, 2650 (1902).
7) F. R. Mayo and C. Walling, *Chem. Revs.*, **46**, 207 (1950).

TABLE II. BUTADIENE-ACRYLONITRILE

No.	$[M_1]_0$	$[M_2]_0$	Conversion	N%	$[M_1]$	$[M_2]$
1	0.0500	0.4490	4.45	15.46	0.04094	0.43599
2	0.1000	0.4000	3.81	13.57	0.09088	0.39019
3	0.0759	0.1755	3.82	12.73	0.07101	0.17084
4	0.1000	0.1509	0.64	11.98	0.09914	0.15017
5	0.2000	0.2000	2.26	11.18	0.19484	0.19614
6	0.2000	0.0509	1.78	8.06	0.19691	0.04951

TABLE III. BUTADIENE-STYRENE

No.	$[M_1]_0$	$[M_2]_0$	Conversion	C%	$[M_1]$	$[M_2]$
1	0.0315	0.200	4.28	90.96	0.02447	0.19439
2	0.0472	0.175	2.99	91.14	0.04512	0.17107
3	0.0631	0.150	2.32	90.78	0.05925	0.14770
4	0.1000	0.100	1.45	89.04	0.09607	0.09983
5	0.0944	0.100	2.01	89.68	0.08996	0.09931
6	0.2202	0.150	1.34	89.20	0.21399	0.14968

and subscripts 1 and 2 mean that the corresponding quantities are concerned with components 1 and 2, respectively.

The values of $[M_1]$, $[M_2]$, conversion, etc., are shown in Tables I—III.

The relative reactivities (r_1, r_2) are shown in Table IV. Table V shows the values in the case of radical type determined by other investigators[8].

TABLE IV. RELATIVE REACTIVITIES

	iB-AN	Bd-AN	Bd-St
r_1	0.02±0.02	0.40±0.02	1.30±0.1
r_2	1.8 ±0.2	0.04±0.01	0.01±0.01
T	50	50	43

iB: isobutylene, AN: acrylonitrile,
Bd: butadiene, T: reaction temp. (°C)

TABLE V. THE VALUES OF (r_1, r_2) REPORTED ON EARLIER PAPER

	Bd-AN	Bd-St
r_1	0.35±0.01	1.48±0.08
r_2	0.05±0.01	0.23±0.07
T	50	50

V. Infrared Spectra and Turbidity Measurement of 1-Phenylbutadiene—Methyl Methacrylate Copolymer.—It had not been clear whether 1-phenylbutadiene enters into a copolymerization reaction or not. In this respect, the copolymerization of this monomer with methyl methacrylate was carried out to make this point clear. As previously mentioned, 1-phenylbutadiene does not polymerize alone with organo boron catalyst, but does thermally. Therefore, even if the two components are present in the product, it does not always mean a copolymer. For the purpose of looking over the product, infrared spectra and turbidity measurement of the product were employed.

V-1) Copolymerization of 1-phenylbutadiene with methyl methacrylate.—The monomer mixture (feed 1 : 1) consisted of 1-phenylbutadiene and methyl methacrylate (0.0237 mol.) was polymerized with 0.1 cc. of triisobutylboron catalyst in a sealed tube at 50°C for 15 hr. The product precipitated with methanol was redissolved in benzene and precipitated with methanol two times. Thus, 0.0702 g. of the polymer was obtained (conversion: 1.3%).

V-2) Infrared spectra.—The infrared spectrum of the sample obtained above was observed in

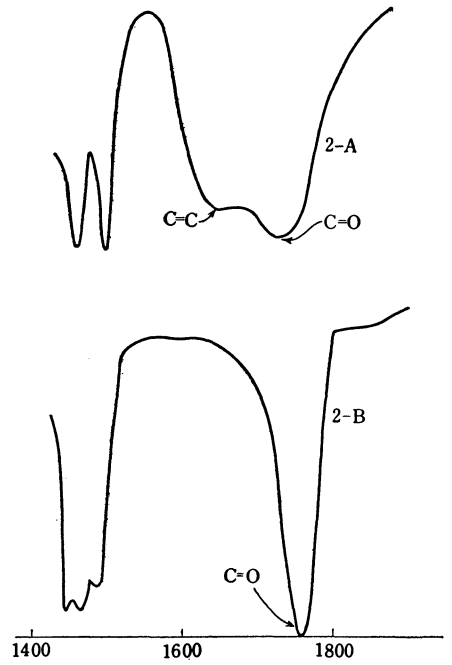


Fig. 2. Infrared spectra of phenylbutadiene-methyl methacrylate copolymer and polymethyl methacrylate.
A, 1-Phenylbutadiene—methyl methacrylate copolymer
B, Polymethyl methacrylate

8) T. Alfrey, J. J. Bohrer and H. Mark, "High Polymers", Vol. VIII, "Copolymerization" Interscience Publishers, Inc., New York (1952), p. 32, 44.

order to confirm the presence of the two components. Fig. 2-A is the spectrum of the sample, and Fig. 2-B is that of polymethyl methacrylate prepared with alkylboron catalyst.

Comparing A with B, it is clear that the product obtained in paragraph V-1 is not identical with polymethyl methacrylate. In Fig. 2-A, the absorption band at about 1650 cm^{-1} owes to C=C, and the band at about 1740 cm^{-1} owes to C=O of methyl methacrylate. Of course, the absorption band of C=C indicates the existence of poly-(1-phenylbutadiene) shown below.

poly(1-phenylbutadiene): $[-CH(C_6H_5)-CH=CH-CH_2-]_n$

V-3) Measurement of turbidity. — The sample obtained in paragraph V-1 was dissolved in 200 cc. of acetone and the turbidity was measured utilizing a nephelo-titrator. The same measurements were carried out with thermally polymerized 1-phenylbutadiene and polymethyl methacrylate prepared with alkylboron catalyst.

In every case, the condition of the measurement was as follows: solvent, acetone; nonsolvent, distilled water; concentration, 0.0070%; temperature, 25°C. These results are represented in Fig. 3.

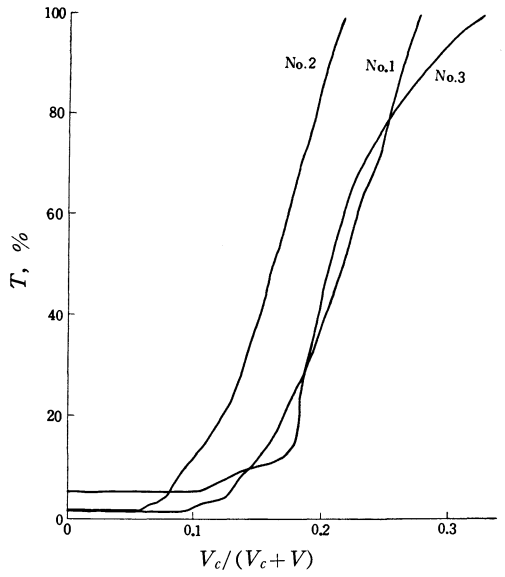


Fig. 3. Diagram of $T-V_c/(V_c+V)$.
T: turbidity, V_c: volume of water,
V: volume of acetone.
No. 1, Copolymer
No. 2, Phenylbutadiene
No. 3, Methyl methacrylate

Comparing No. 1 with No. 2 and 3 in Fig. 3, it may be considered that 1-phenylbutadiene copolymerizes with methyl methacrylate.

Discussion

Diagram of $T-V_c/(V_c+V)$.—If the product (1-phenylbutadiene-methyl methacrylate) is a mixture of the two components, the influence of 1-phenylbutadiene must be more striking around the bottom of No. 1 in Fig. 3. Moreover, the product is a low polymer, so that when it contains the greater part of polymethyl methacrylate, the bottom of No. 1 must be situated on the right side of No. 3. From the viewpoint mentioned above, the product obtained in paragraph V-1 may be considered as a copolymer.

The Relative Reactivities.—The following methods have been employed for obtaining the composition in a copolymer which consists of C and H atoms:

a) from analytical value of C atoms,
b) from refractive index,
c) from ultraviolet absorption.

Any method will contain more or less errors. In this respect, a) is, particularly, apt to contain an error.

Therefore, some questions will be present in the relative reactivity in the copolymerization of butadiene-styrene, reported in this paper. In this respect, the other methods will be employed to the butadiene-styrene copolymer.

As is well known, the mechanism of the polymerization with alkylboron catalyst is a radical type. The propriety of the mechanism is proved in this paper also, comparing the values of the relative reactivities obtained in this experiment with those in the copolymerization with peroxide catalyst.

Summary

The relative reactivities in the copolymerization of some monomers which do not polymerize alone with alkylboron catalyst, with those which polymerize alone, were obtained. The copolymerization rate of 1-phenylbutadiene with another monomer was so small that the relative reactivity could not be obtained. But, from the studies on the reaction product of 1-phenylbutadiene and methyl methacrylate, it was considered that the former copolymerized with the latter.

The author wishes to express his sincere thanks to Messrs. K. Abe and K. Yanagisawa in this laboratory for their kindness observing the infrared spectra.

The Electrical Communication Laboratory
Nippon Telegraph and Telephone
Public Corporation
Musashino-shi, Tokyo

Analytical Chemistry by Means of Organic Compounds. XXV[1]. *1-Hydroxyacridine as a New Reagent (Neo-oxine) (1)*

By Masayoshi ISHIBASHI, Yuroku YAMAMOTO and Hirohiko YAMADA

(Received February 13, 1959)

It is expected that 1-hydroxyacridine will be useful in analytical chemistry, because it has the same functional group as 8-hydroxyquinoline (oxine) which is one of the most valuable organic reagents in various fields such gravimetry, volumetry, or colorimetry. Irving et al.[2] have investigated the behavior of this compound to some metallic ions such as aluminum, chromium, iron(III), gallium, copper and zinc, concerning the study for the effects of steric hindrance of some oxine derivatives. It was found by them that 1-hydroxyacridine and 2-methyl-oxine did not form precipitate with aluminum, while forming precipitate with other metals, and the reason of the failure of these reagents to react with aluminum was attributed to steric hindrance of the groups in the 2-position of oxine. In the presence of aluminum, 2-methyl-oxine was used by Merrit[3] as a precipitant for zinc, or by Motojima[4] as not only a precipitant but also a coloring reagent for beryllium and titanium.

There is, however, no reference for use of 1-hydroxyacridine in analytical chemistry. It is presumed that this compound is more favorable in gravimetry or colorimetry with solvent extraction because of larger molecular weight than that of oxine or its derivatives. Moreover, this compound has the feature of not reacting to aluminum ion and this selective behavior will be advantageously used in determining some metals in the presence of aluminum without preliminary separation.

It is the purpose of this study to investigate the reaction between 1-hyroxyacridine and numerous cations which are used to be reactive with oxine, and to apply the results for gravimetry or colorimetry with solvent extraction.

The present paper is concerned with the results obtained by spectrophotometric method with solvent extraction. Absorption spectra were taken for the reagent in acidic, neutral and alkaline medium. Both acidic and basic ionization constants were then obtained, according to Stenstrom's method[5]. The basis for solvent extraction with chloroform were investigated for the chelate compounds of the reagent with some metals such as copper, cobalt, nickel and zinc. Reactions with other metals and another aspects of the study, such as formula, solubility and thermal stability of the chelate are under investigation and the results will be reported in the near future.

We propose to name this reagent as "neo-oxine".

Experimental and Results

Apparatus.—Spectrophotometric measurements were made with a Beckman quartz spectrophotometer, Model DU, with 1 cm. silica transmission cells having a tight stopper. A Beckman pH meter with glass electrode, Model H-2, was used for all pH measurements.

Materials.—*1-Hydroxyacridine.*—This compound was synthesized by the method described by Irving and his coworkers[2]. The crude product was recrystallized several times from 75% alcohol and dried in vacuo. The melting point of the dried sample was 115~116°C, identical with that in the literature.

Anal. Found: H, 4.82; C, 79.74; N, 7.17; O, 8.36. Calcd. for $C_{13}H_9ON$, H, 4.64; C, 79.99; N, 7.18; O, 8.22%.

The pure substance obtained is brownish yellow needles and slightly soluble in water but easily soluble in organic solvent such as alcohol, or chloroform. The solution of 1-hydroxyacridine was prepared to concentration of 10^{-3} M with 95% alcohol.

Chloroform.—It was purified by distillation.

Buffer solution.—Borate, phosphate and acetate buffers were prepared using each pure acid. To 1/25 M of each acid solution proper amounts of dilute sodium hydroxide solution were added to obtain the desired pH.

1) Paper XXIV of this series: M. Ishibashi and Y. Yamamoto, *Bulletin of the Institute for Chemical Research, Kyoto University*, **31**, 280 (1953).

2) H. Irving, E. J. Butler and M. F. Ring, *J. Chem. Soc.*, **1949**, 1489.

3) L. L. Meritt, *Record. Chem. Progr. (Kresge-Hooker Sci. Lib.)* **10**, 59 (1949).

4) K. Motojima, This Bulletin **29**, 29, 71, 458 (1956).

5) W. Stenstrom and N. Goldsmith, *J. Phys. Chem.*, **30**, 1683 (1926).

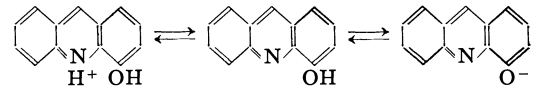
Metal solution.—All of the stock solutions of metals were prepared to concentration of 10^{-3} M. Cupric sulfate which was recrystallized from water and dried in room temperature, was dissolved and then diluted to the desired concentration. Cobaltous sulfate (Merk) was dissolved in water to approximately 10^{-1} M and after the concentration of the metal was checked by electrolysis, the solution was diluted to the desired concentration. Nickel solution was obtained by dissolving pure nickel ammonium sulfate. In the case of zinc the pure metal was dissolved in small amounts of nitric acid and after sulfuric acid was added, the solution was evaporated almost to dryness, and then diluted with water.

All other reagents as ethylenediamine tetraacetic acid, tartaric acid, cuproine (biquinolyl), dimethylglyoxime, etc., were analytical grade ones.

In the preliminary experiments, it was observed that ions such as copper, zinc, nickel, cobalt, iron, etc., were precipitated in slightly acidic (pH 5.1) or in a weak basic (pH 9.5) medium by 1-hydroxyacridine, forming red or reddish orange chelate compounds. It was also confirmed that the compound did not form a precipitate with aluminum in any medium. The filtrate which is obtained by filtrating the precipitate formed in slight excess of reagent, did not react to oxine, and it is presumed that the solubility of the metal chelate of 1-hydroxyacridine may be smaller than that of oxine chelate.

Absorption Spectrum of 1-Hydroxyacridine.—All of the solutions for absorbance measurements were prepared by diluting the required quantity of the stock solution using a buffer solution. The absorbance was measured in the range of 210~450 mμ against the respective buffer solution. Spectra obtained in acidic, neutral and alkaline mediums are shown in Fig. 1.

It is observed that many absorption bands exist in the ultraviolet region, and that the bands in neutral solution shift to longer wavelength with both the decreasing and increasing of pH. The change in absorption spectra with pH may be attributed to structural changes which are due to dissociation of 1-hydroxyacridine as follows, being similar to that of oxine.



Ionization Constant.—To evaluate basic and acidic ionization constants of the reagent, absorbance was then measured for twenty-six solutions having various pH's. In almost all cases, the pH was adjusted using respective buffer solution, but dilute sodium hydroxide or hydrochloric acid solution was used when stronger alkaline or acidic medium was necessary. The absorbance values at four different wavelengths were plotted against pH, as shown in Fig. 2. The phenolic or basic ionization constant was obtained as

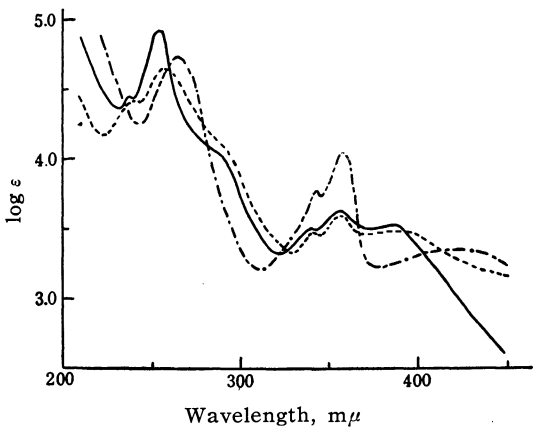


Fig. 1. Absorption spectrum of 1-hydroxyacridine.
—·— pH 4.6, —— pH 7.2, ------ pH 9.5

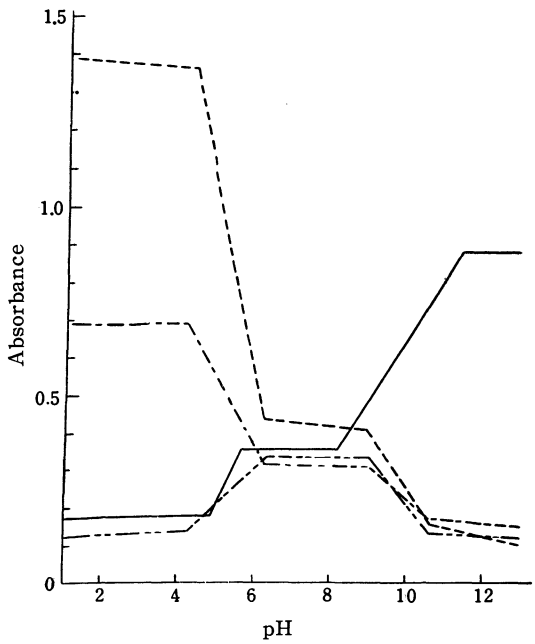


Fig. 2. pK_a and pK_b of 1-hydroxyacridine.
—— at 300 mμ, —·— 343 mμ, ------ 359 mμ, ———— 380 mμ

TABLE I. IONIZATION CONSTANT OF 1-HYDROXYACRIDINE

Wavelength (mμ)	pK_a	pK_b
300	9.85	5.27
343	9.83	5.30
359	9.83	5.31
380	9.86	5.34
Mean	9.84	5.31

pK by a graphical determination of the pH at which the absorbance was half-way between its values in neutral and alkaline or acidic solution. According to Stenstrom and Goldsmith[5], the midpoint pH=pK_a or pK_b. The values obtained are listed in Table I. The pK_a and pK_b of oxine has been reported as 9.70 and 9.08 respectively by Phillips[6]. The pK_a of 1-hydroxyacridine is thus slightly greater than that of oxine, while pK_b is considerably smaller.

Absorption Spectra of 1-Hydroxyacridine and its Chelate in Chloroform. — Procedure of extraction is conducted as follows.

Each 2 ml. of reagent and metal solution (both 10^{-3} M) was pipetted into a separatory funnel having the mark of 20 ml., in which had been contained approximately 15 ml. of the buffer solution having the desired pH and was then diluted to the mark with water. Red or reddish orange precipitate was immediately formed by mixing. After standing for 20 min. or more to digest the precipitate, 10.0 ml. of freshly distilled chloroform was added, and the vessel was vigorously shaken for 2 min. or more. The extraction seemed to be complete, when the lower chloroform layer colored, but the aqueous layer became completely colorless. The organic extract was then transferred into a little Erlenmayer flask containing about 1 g. of anhydrous sodium sulfate. Absorbance was measured for the dried chloroform solution over a range of 300~600 mμ using chloroform as a reference solvent. The pH was measured for the aqueous phase which remained after extraction. Spectra are shown in Fig. 3, and the wavelength of maximum absorption is also listed in Table II. Quite similar experiments were made for the reagent solution, and the results are also shown in Fig. 3 and Table II. In the following experiments, all the extraction procedures are followed as above, unless otherwise indicated. It is seen that a specific absorption band for each chelate appears in the visible region at which the reagent does not show appreciable absorbance.

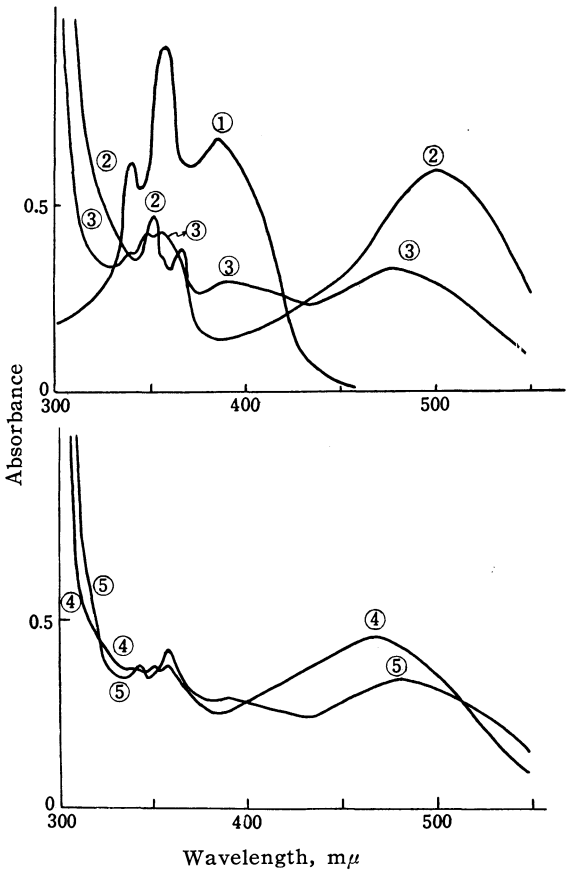


Fig. 3. Absorption spectra in chloroform.
① 1-Hydroxyacridine (extracted from pH 4.6)
② Copper chelate (〃 8.7)
③ Zinc chelate (〃 11.7)
④ Nickel chelate (〃 9.1)
⑤ Cobalt chelate (〃 11.7)

TABLE II. WAVELENGTH OF MAXIMUM IN CHLOROFORM (mμ)

1-Hydroxyacridine	341	358		386	
Copper chelate	353	358		368	502
Cobalt chelate	341	358		388	480
Nickel chelate	340	350		357	468
Zinc chelate	341	350	358	389	478

Effect of pH on Extraction.—To obtain optimum range of pH for the extraction of each element and reagent, the absorbance was measured for the organic extract from aqueous solution, the pH values of which had been adjusted to various values with respective buffer. The pH measurements were made for the aqueous phase after extraction and the absorbance was measured at wavelength of the respective peak of the metal chelate.

The results are shown in Fig. 4. The pH range of optimum extraction for the four metals is somewhat narrow, as compared with the metal chelate of oxine reported by several workers[9], contrary to the expectation. In order to obtain higher selectivity in a solvent extraction using chelate reagents, various masking reagents are extensively used. The effects of some complexing agents as cyanide, ethylenediaminetetraacetic acid and tartaric acid

6) J. P. Phillips and L. L. Meritt, *J. Am. Chem. Soc.*, **70**, 410 (1948).

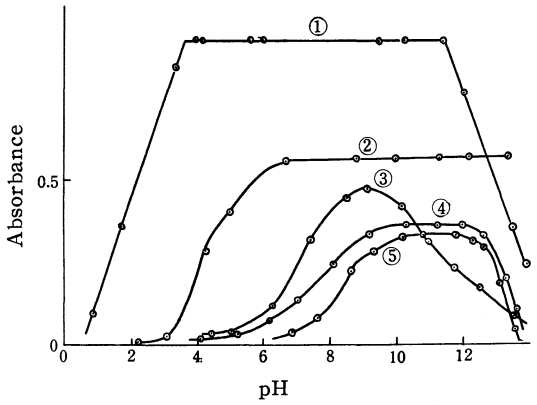


Fig. 4. Effect of pH on extraction.
① 1-Hydroxyacridine
② Copper chelate
③ Nickel chelate
④ Cobalt chelate
⑤ Zinc chelate

were thus investigated. It was found that these complexing agents inhibit the reaction of all metals with 1-hydroxyacridine. When a complexing agent is present in the concentration of 10^{-1} M, the precipitate does not form and the organic extract also does not show appreciable absorbance in the visible region.

Stability of the Metal Chelates.—The effects of time of standing were investigated for the organic extracts of the metal chelates. Standing the dried extract in the transmission cell with a stopper, the absorbance was measured at several intervals. Results are shown in Table III. The result is that the absorbance decreases slightly during the initial several minutes and then remains almost constant during 60~180 min. But when the solution was kept for 1 day, the absorbance had considerably decreased.

TABLE III. EFFECT OF STANDING TO ABSORBANCE

Time min.	Copper 502 mμ	Nickel 468 mμ	Cobalt 480 mμ	Zinc 478 mμ
0	0.554	0.448	0.330	0.305
1	.554	.447	.329	.303
2	.553	.445	.328	.303
3	.553	.443	.327	.303
5	.553	.442	.327	.302
10	.551	.439	.325	.302
20	.551	.438	.324	.300
30	.550	.437	.322	.299
60	.546	.433	.319	.299
90	.545	.433	.319	.299
120	.545	.433	.319	.299
180	.545	.433	.319	.299
1 day	.280	.231	.140	.102

Per Cent Extracted.—The per cent extracted at optimum pH in Fig. 4 was determined for the four elements. For zinc and cobalt, radioactive isotope was used as tracer, and for the other two, the amount of metal ion in aqueous or organic layer was determined by spectrophotometric method using sensitive organic reagents. The procedures are as follows and the results are listed in Table IV.

TABLE IV. PER CENT EXTRACTED

Element	%	pH
Copper	99.71	8.7
Cobalt	99.19	11.7
Nickel	99.10	9.1
Zinc	99.93	11.7

Copper.—Ten milliliters of cupric solution (10^{-3} M) and 5 ml. of the reagent solution (10^{-2} M) were pipetted into a 100 ml. volumetric flask. The solution was then diluted to the mark with the buffer solution. After standing, the red precipitate was extracted with 50 ml. of freshly distilled chloroform. The remaining aqueous solution was then evaporated to about 5 ml. on a sand bath. After cooling, the pH was readjusted to 5.5 with hydrochloric acid and about 1 g. of hydroxylamine hydrochloride was added in order to reduce cupric ion to cuprous. The cuprous ion was then extracted with 10.0 ml. of amyl alcohol containg 0.01% of cuproine[7]. The absorbance was measured at 540 mμ for the reddish violet organic extract. For the standard cupric solution (10^{-5} M), the same extraction procedure with amyl alcohol containing cuproine was done after reduction, and the absorbance was obtained similarly. The per cent of extraction was calculated from the two absorbance values.

Nickel.—The extraction was done under the same condition, except pH, as described above. The organic extract was destroyed by adding proper amount of concentrated perchloric acid and heating to fumes. After destroying organic matter completely, the solution was evaporated to dryness. The residue was dissolved and diluted with water and the amount of nickel ion was determined by dimethylglyoxime following the method described by Sandell[8].

7) J. Hoste and J. Gillis, *Anal. Chim. Acta*, **9**, 263 (1953).
8) E. B. Sandell, "Colorimetric Determination of Traces of Metals", Interscience Publishers, New York (1950), p. 470.

Cobalt.—Two milliliters cobalt (10^{-3} M), 1.0 ml. of the reagent (10^{-2} M) and 1.0 ml. of Co^{60} (carrier free) solution were taken and, after adjusting the pH and diluting to 20 ml., cobalt chelate was extracted as above. A 2.0 ml. of aqueous layer was then pipetted out into a small stainless dish. The solution was evaporated completely to dryness and the counts were determined using Geiger Counter. The per cent extraction was obtained by comparing the counts with that of the standard which was determined similary before extraction.

Zinc.—Zn^{65} was used as tracer. The method of determination for the per cent extracted was quite similar to that for cobalt.

It was found that per cent extracted is more than 99% in all cases under the optimum pH.

Summary

The absorption spectra of 1-hydroxyacridine were obtained both in aqueous and chloroform solution, and the pK_a and the pK_b were determined. The pK_a is slightly greater than that of oxine, and it is suggested that the stability of metal chelate with 1-hydroxyacridine will have values of the same or larger order as that of oxine chelate, because there is a direct relation between the basicity of a chelating agent, as measured pK_a values, and the stability of the chelates it forms, as cited in the literature of Morrison and Friser[9].

The various aspects of solvent extraction using chloroform were then investigated. The optimum pH range on extraction for each element was determined and it was found that the range is narrow as compared with that of the oxine chelate. The per cent extracted was determined and it was found that copper, nickel, cobalt and zinc were almost completely extracted under the conditions investigated.

The authors thank the Ministry of Eduction for the financial support granted for this research.

Department of Chemisty
Faculty of Science
Kyoto University
Sakyo-ku, Kyoto

9) G. H. Morrison and H. Freiser, "Solvent Extraction in Analytical Chemistry", John Wiley & Sons, Inc., New York (1957), p. 26.

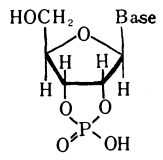
Enzymic Preparation of Guanosine-2′, 3′-cyclic Phosphate, Inosine-2′, 3′-cyclic Phosphate and Xanthosine-2′, 3′-cyclic Phosphate

By Kimiko SATO-ASANO, Yoshiko FUJII and Fujio EGAMI

(Received February 14, 1959)

Our previous studies have shown that ribonuclease T_1(RNase T_1) in Takadiastase hydrolyzes the secondary phosphate ester bonds of guanosine-3′ phosphate in ribonucleic acid (RNA)[1-3]. During the digestion, guanosine-2′, 3′-cyclic phosphate (G-cyclic-p) is accumulated in the reaction mixture as an intermediary product.

It has been also found that RNase T_1 hydrolyzes *deamino*-ribonucleic acid (*deamino*-RNA) splitting preferentially the secondary phosphate ester bonds of inosine-3′ phosphate with an intermediary formation of inosine-2′, 3′-cyclic phosphate (I-cyclic-p). With higher amounts of RNase T_1, the secondary phosphate ester bonds of xanthosine-3′ phosphate is also hydrolyzed with an intermediary formation of xanthosine-2′, 3′-cyclic phosphate (X-cyclic-p)[4].



Nucleoside-2′, 3′-cyclic phosphate

1) K. Sato and F. Egami, *J. Biochem.*, **44**, 753 (1957).
2) K. Sato and F. Egami, *Compt. rend. soc. biol.*, **151**, 1792 (1957).
3) K. Sato-Asano, *J. Biochem.*, **46**, 31, (1959).
4) K. Asano and Y. Fujii, *Symposium on Enzyme Chemistry (Japan)*, **10**, 123 (1958).

It has so far been difficult to synthesize G-cyclic-p by a chemical method with good yield and in high purity[5]. Markham et al. prepared G-cyclic-p and adenosine-2', 3'-cyclic phosphate (A-cyclic-p) by mild alkaline hydrolysis of "RNase I core"[6]; however, the yield was far from satisfactory. On the other hand, I-cyclic-p and X-cylic-p have been neither separated from the natural source nor synthesized.

We succeeded in preparing these purine nucleoside cyclic phosphates with good yield by the enzymic reactions. So the method of preparation of these nucleoside-2', 3'-cyclic phosphates and the properties of new compounds will be reported.

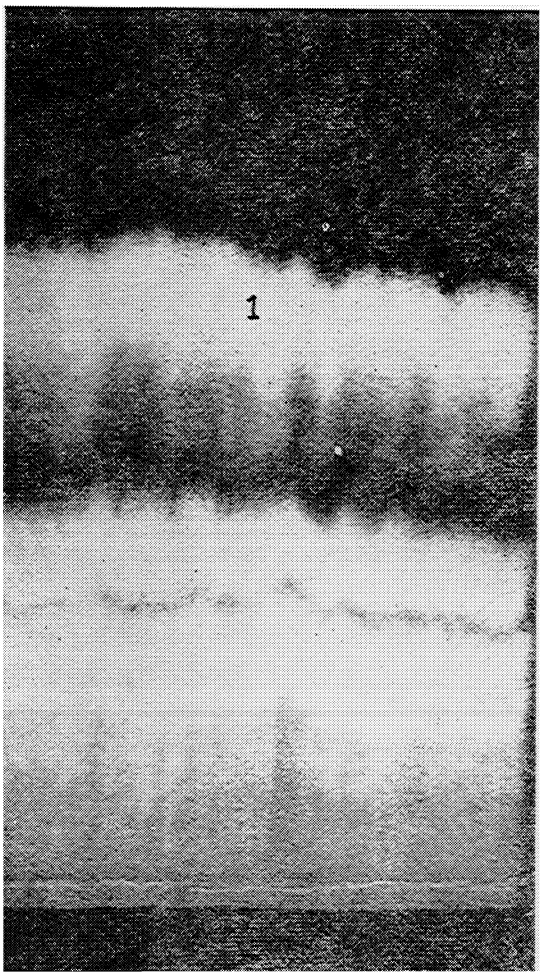


Fig. 1. Paper chromatogram of the dialyzate of the digestion mixture of yeast RNA by RNase T_1. Reaction mixture contains 100 mg. of yeast RNA and 10 μg. of RNase T_1 at pH 7.5. The band 1 is that of G-cyclic-p. Solvent I was used.

Experimental

RNA.—A commercial yeast RNA (Schwarz Laboratories) was deproteinized with chloroform gel formation, dialyzed in a cellophane tubing against distilled water and precipitated with alcohol.

Deamino-RNA.—Yeast RNA was deaminated by the method of Takemura[7]. Details of the preparation and properties of deamino-RNA will be reported elsewhere.

RNase T_1.—The purest sample extracted and prepared from Takadiastase according to the method of Sato and Egami[1] was used.

Paper Chromatography.—*Solvent I*: isopropanol: water (7 : 3) with concentrated aqueous ammonia in the bottom of the vessel (0.5 ml. for each liter of gas phase)[8], descending for 18 to 19 hr.

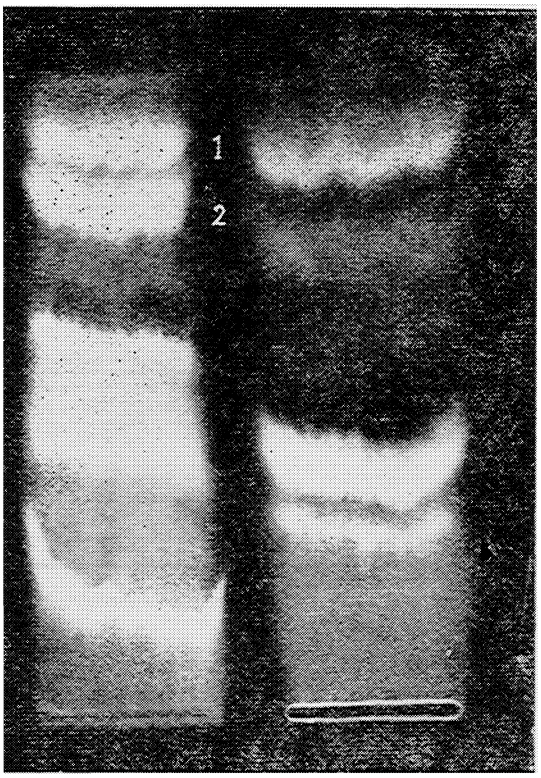


Fig. 2. Paper chromatograms of the dialyzate of the digestion mixture of *deamino*-RNA by RNase T_1. Solvent I was used. The bands are: 1, I-cyclic-p; 2, X-cyclic-p.
a) 20 mg. *deamino*-RNA, 2 μg. RNase T_1/ml.
b) 200 μg. RNase T_1 was added to the nondialyzable fraction in a).

5) D. M. Brown, D. I. Magrath and A. R. Todd, *J. Chem. Soc.*, **1952**, 2708.
6) R. Markham and J. D. Smith, *Biochem. J.*, **52**, 552 (1952); L. A. Heppel and P. R. Whitfeld, ibid., **60**, 1 (1955).
7) S. Takemura, *J. Chem. Soc. Japan, Pure Chem. Sec.* (*Nippon Kagaku Zasshi*), **72**, 674 (1951).
8) R. Markham and J. D. Smith, *Biochem. J.*, **52**, 558 (1952).

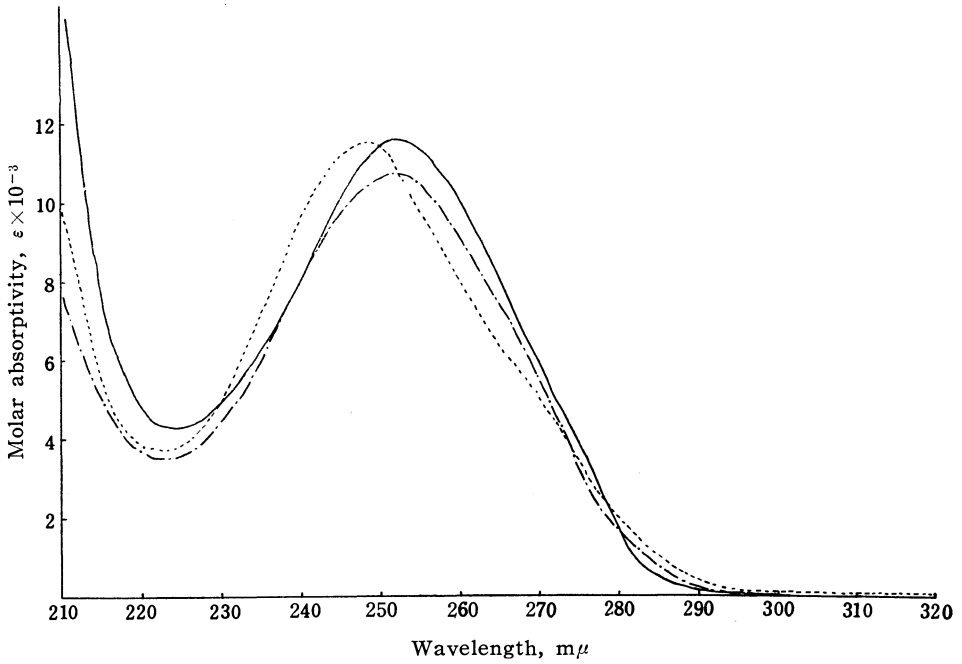


Fig. 3. Absorption spectra of I-cyclic-p.
——, pH 11.2; ------, pH 6.0; ——·——, 2 N HCl.
Beckman spectrophotometer type DK2 was used.

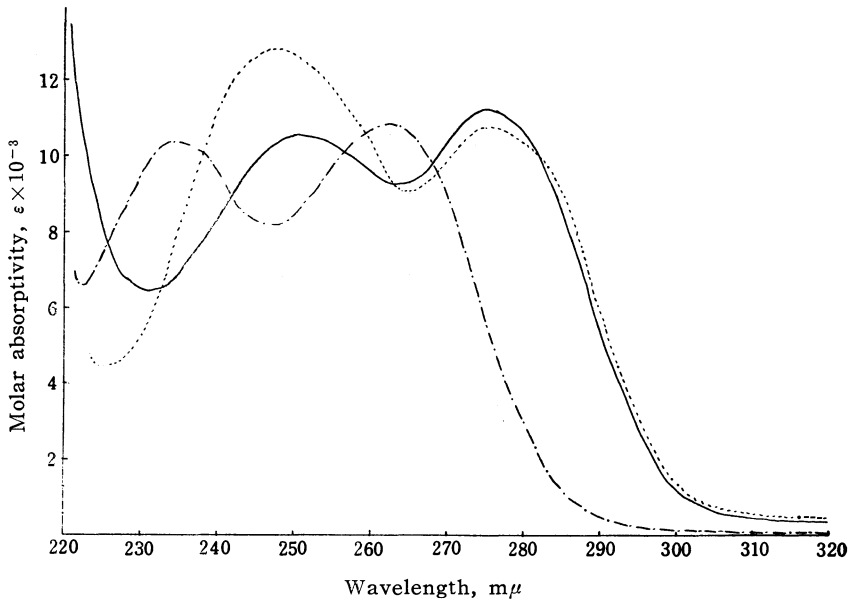


Fig. 4. Absorption spectra of X-cyclic-p.
——, 1 N NaOH; ------, pH 8.1; ——·——, pH 3.0.
Beckman spectrophotometer type DK2 was used.

Solvent II: saturated ammonium sulfate : water: isopropanol (79 : 19 : 2)[9], ascending for 9 hr. Tôyôroshi No. 51 paper was used throughout the studies and the bands on the chromatogram were located by the usual photographic methods.

Organic Phosphorus.—It was measured by the method of Allen[10].

Preparation of G-cyclic-p.—Yeast RNA (100 mg.) was dissolved in 5 ml. of distilled water and pH was adjusted to 7.5. To the solution 10 μg. of RNase T_1 was added. The reaction mixture was incubated at 37°C for 2 hr., then dialyzed against distilled water in a cold room under stirring overnight. The dialyzate was concentrated and subjected to paper chromatography (15~20 cm./100 mg. RNA) using solvent I. As is shown in Fig. 1 the wide intensive band 1 was found, this was identified with that of G-cyclic-p[3]. The band was eluted and lyophilyzed. G-cyclic-p was obtained in an almost pure state by chromatography. After the preparation was rechromatographed with the same solvent, it was proved by another paper chromatography test, paper electrophoresis and its U. V. absorption spectrum that it became completely free from other nucleotides except for a trace amount of guanylic acid (Gp).

Preparation of I-cyclic-p. — One hundred milligrams of *deamino*-RNA was dissolved in 5 ml. of distilled water at pH 7.5 and 10 μg. of RNase T_1 was added, then the reaction mixture was incubated for 5 hr. at 37°C. The reaction mixture was dialyzed against 50 ml. of distilled water in a cold room under stirring, then the dialyzate was concentrated and subjected to paper chromatography (solvent I, descending for 18 hr.). After drying, the paper was rechromatographed with the same solvent for 19 hr. (Fig. 2a). The broad band 1 moving rapidly was identified with that of I-cyclic-p[11]. Band 2 which is that of X-cyclic-p[11] also appeared sightly. Band 1 was eluted with distilled water, the eluate was concentrated and subjected to paper chromatography using solvent I. There was nothing except for a large amount of I-cyclic-p and a trace of inosinic acid (Ip). It was also proved by another paper chromatography test using solvent II that the band was pure I-cyclic-p. The purest preparation was used for the following experiments.

Preparation of X-cyclic-p.—After the pH of the reaction mixture, which remained in the cellophane tubing in the experimental for I-cyclic-p, was adjusted to 7.5, 1.0 ml. of RNase T_1 (1.3 mg./ml.) was added and the reaction mixture was incubated for 5 hr. at 37°C. Then it was dialyzed against 60 ml. of distilled water in a cold room under stirring, then the dialyzate was concentrated and subjected to paper chromatography (solvent I, descending for 18 hr.). After drying, the paper was rechromatographed with the same solvent for 19 hr. (Fig. 2b). The broad band 2 was identified with that of X-cyclic-p[11]. To purify the sample completely, band 2 was eluted with distilled water, the eluate was concentrated and subjected to rechromatography with the same solvent. There was nothing but large amounts of X-cyclic-p and a trace of xanthylic acid (Xp). Moreover, this band 2 was proved to be pure X-cyclic-p by another paper chromatography test with solvent II. This sample was used in the following studies.

9) R. Markham and J. D. Smith, ibid., **49**, 401 (1951).
10) R. J. Allen, ibid., **34**, 858 (1940).
11) K. Sato-Asano and Y. Fujii, *J. Biochem.*, in press.

Results and Discussion

Yields.—The yields were calculated from the optical density. Five milligrams G-cyclic-p from 100 mg. of yeast RNA ; 2 mg. of I-cyclic-p from 100 mg. of *deamino*-yeast RNA ; 2.5 mg. of X-cyclic-p from 100 mg. of *deamino*-yeast RNA.

Absorption Spectra of I-cyclic-p and X-cyclic-p.—Using the purest preparation, their ultraviolet absorption spectra were measured at various pH ranges, and their molar extinction coefficients were determined by measuring phosphate (Figs. 3 and 4).

Rf values were calculated in two solvent systems.

TABLE 1. *Rf* VALUES OF PREPARED CYCLIC NUCLEOTIDES AND OF MONONUCLEOTIDES

	Solvent I	Solvent II
G-cyclic-p	0.28	0.29
I-cyclic-p	0.43	0.33
X-cyclic-p	0.35	0.19
A-cyclic-p	0.48	0.13
C-cyclic-p, U-cyclic-p	0.50	0.54
Gp	0.13	0.45 (3') 0.54 (2')
Ip	0.16	0.52
Xp	0.15	0.33
Ap	0.21	0.23 (3') 0.33 (2')
CP, Up	0.21	0.73

These cyclic nucleotides, especially G-cyclic-p, were rather labile in diluted solution and were hydrolyzed to nucleotides. So all procedures had to be carried out as rapidly as possible.

If two or more cyclic nucleotides were produced from RNA at the same time, the separation might be very difficult. So the stepwise enzymic preparation seems to be a better method. After the preparation of G-cyclic-p from the dialyzate of the digestion mixture of yeast RNA by RNase T_1, the nondialyzable fraction which remained in the cellophane tubing was treated in 0.1 N hydrochloric acid to split the residual cyclic phosphate[2], neutralized and dialyzed completely. What may be

called "RNase T_1 core" thus obtained was useful for the preparation of pyrimidine nucleosidecyclic phosphates by RNase I.

Pyrimidine nucleosidecyclic phosphates were prepared from the dialyzate of yeast RNA digests by RNase I and the residues were further completely digested and dialyzed, and thus the well known "RNase I core" was obtained. It was also a good source for the preparation of G-cyclic-p by RNase T_1.

It was rather difficult to separate a large amount of I-cyclic-p and X-cyclic-p. To solve this difficulty RNase T_1 digestion was divided into two steps: at the first step with a small quantity of RNase T_1, the greater part of I-cyclic-p was separated and at the second step by addition of more RNase T_1, the remaining I-cyclic-p and X-cyclic-p were obtained separately.

Summary

By RNase T_1 digestion, guanosine-2′,3′-cyclic phosphate was obtained with good yield from yeast RNA, and two new compounds, inosine-2′,3′-cyclic phosphate and xanthosine-2′,3′-cyclic phosphate were obtained from *deamino*-yeast RNA. The properties of the new compounds were studied.

We acknowledge the gift of "Taka-diastase Sankyo" by the Sankyo Pharmaceutical Co., Ltd. The expense of this study was defrayed in part by a grant from the Ministry of Education.

Department of Chemistry
Faculty of Science
Nagoya University
Chikusa-ku, Nagoya

Recombination of Hydrogen, Nitrogen and Oxygen Atoms on Copper and Silver Single Crystal Surfaces

By Kazuo NAKADA

(Received March 4, 1959)

Hoping to get information about the bond strength of the chemisorption of hydrogen, the author et al.[1] carried out the recombination of hydrogen atoms on various metal surfaces including single crystal surfaces of copper. In the present work, experiments have been extended to cases of nitrogen and oxygen atoms on single crystal surfaces of copper and silver, considering the fact that comparatively simple electronic band structures of copper and silver will render the theoretical treatment of results possible in future. With regard to oxygen atoms, experiments were conducted only on single crystal surfaces of silver, because the probable formation of relatively thick oxide layers on copper surfaces might complicate the subject for consideration.

Since relatively much information about physical and physico-chemical properties of single crystal surfaces of metals with definite crystal indices are available, execution of any surface reaction on these surfaces seems to be advantageous in considering the mechanism of surface reaction through the comparison of catalytic activity with physical properties. With regard to the research along this line, the works of Gwathmey et al.[2], Sosnovsky[3] and Crocker et al.[4] are noteworthy.

However, few works have yet been undertaken except for the work of Gwathmey et al. in which detailed structures of surfaces during the course of and after the completion of the reaction are fully followed. In the work of Sosnovsky, where the decomposition of formic acid on single crystal surfaces of silver was dealt with, the natural free

1) K. Nakada, T. Sugiura and S. Shida, *J. Chem. Soc. Japan, Pure Chem. Sec.* (*Nippon Kagaku Zasshi*), **76**, 64 (1955); S. Sato, K. Nakada and S. Shida, ibid., **76**, 1308 (1955); K. Nakada, S. Sato and S. Shida, *Proceedings of the Japan Academy*, **31**, 449 (1955); K. Nakada, This Bulletin, **32**, 809 (1959).

2) R. E. Canningham and A. T. Gwathmey, *J. Am. Chem. Soc.*, **76**, 391 (1954).

3) H. M. C. Sosnovsky, *J. Chem. Phys.*, **23**, 1486 (1955).

4) A. J. Crocker and A. T. B. Robertson, *Trans. Faraday Soc.*, **54**, 931 (1958).

surface frozen from the melt was used as a reaction surface. The work of Crocker et al. in which the decomposition of formic acid on single crystal surfaces of copper was dealt with and that of Nakada et al. in which the recombination of hydrogen atoms on the same was dealt with were only concerned with the electropolished surfaces. Although the flatness of these surfaces on the atomic scale was ensured by Rhodin[5] through the adsorption experiment by the use of microbalance technique, there seems still to be doubtful whether or not the electro-polishment would really give such an extreme flatness.

Accordingly, it is highly desirable to know detailed structures of surfaces on which the experiments were made. In the present work, the author devotes himself to the detection of the effect of various kinds of surface pre-treatments on catalytic activity. It seems probable that surfaces subject to such a treatment as chemical etching, which possibly roughen them, will comply with the purpose of this work better than the flattened surfaces, because for such a roughened electron diffraction technique may give the most detailed information on its surface structure. Conversely, it may be expected that from the change in activity resulting from various surface treatments, unknown surface structures lying beyond the limit of the power of the present scientific method, like electron microscopy or electron diffraction technique, would be made clear.

Experimental

An effusion method used in the preceding report* for determining the recombination activity of different transition metals was also adopted this time.

Apparatus. — The apparatus (not shown) described in the above was used without modification, but the sample metal slice was hung only with a Pt/Pt-Rh thermocouple (0.1 mm. in diameter) without any other lead.

Sample Gases.—The hydrogen, oxygen and nitrogen used were all commercial cylinder gases. Hydrogen or oxygen was allowed to bubble through a saturated sodium hydroxide solution and further to diffuse over the platinized asbestos (ca. 400°C) to remove oxygen and hydrogen included in hydrogen and oxygen as an impurity, respectively, but for nitrogen this procedure was not done. They were sent to the discharge tube through a capillary from a reservoir in which the gases were allowed to stay over the saturated sodium hydroxide solution to keep the humidity constant.

Sample Metal Slices.—Single crystals of copper and silver were produced by means of a slow cooling method from electrolytic copper and standard silver for analysis respectively. The single crystals thus obtained were of a cylindrical form (12 mm. in diameter and about 6 cm. long). Single crystal slices (generally in an elliptical form, about 2 to 3 mm. thick) were cut from a cylindrical single crystal in order that their macroscopic-cut planes might coincide with the three principal planes (100), (110) and (111), but in the case of silver only the (110) and (100) slices were prepared.

Pre-treatment of Surfaces.—Two surfaces of a sample slice were generally subjected to two different kinds of pre-treatments, e.g., one pre-treatment was electro-polishment and another, chemical etching with nitric acid or the like. The main conditions of pre-treatment adopted in this work were as follows:

1) Chemical etching was carried out a) in the nitric acid solution (1 : 1 by volume) for 3 min. and b) in the saturated ammonium persulfate solution for 15 min.

2) Electro-polishment of copper was done in the bath of phosphoric acid (90%) at the current densities of 6 to 8 amp./dm^2 for 10 min. and that of silver in the mixed solution of potassium cyanide (10%) and potassium ferrocyanide (10%) at the current densities of 1 to 3 amp./dm^2 for 3 min.

3) For the electric plating, solutions of potassium cuprous cyanide, potassium silver cyanide and ammonium aurocyanide were used as baths of copper-, silver- and gold-plating, respectively.

Procedure.—All free atoms were produced in a discharge tube by use of alternating currents. A sputtering of the electrode material (aluminum) occurred more markedly in the case of nitrogen than in oxygen. Since such a sputtering was localized within the neighborhood of electrodes even in the case of nitrogen, they did not become a serious obstacle to the present experiments.

In the reaction chamber, which was strongly pumped off, the sample metal slice was hung only by a Pt/Pt-Rh thermocouple (0.1 mm.) serving as the temperature measurements at the front of a small hole provided at the end of a side tube of the discharge tube. The temperature of a sample can be followed by measuring the electro-motive force by use of a K-type potentiometer. The electro-motive force was read at intervals of 5 min. The slice was allowed to turn over every twenty or thirty minutes. Before and after this procedure, the temperature was usually shifted from one value to another. From such a shift of the temperature the difference in activities of two surfaces of the same sample subjected to different treatments could readily be detected.

Results

In Fig. 1 is given a plot of temperature, expressed in terms of electro-motive force

5) T. N. Rhodin, *J. Am. Chem. Soc.*, **72**, 5691 (1954).

* This Bulletin, loc. cit. in Ref. 1.

TABLE I. INEQUALITY RELATIONS OF CATALYTIC ACTIVITY

No.	Species of slice	Method of pre-treatment: One side	Method of pre-treatment: The other side	Inequality relation	Kinds of atoms
1	Cu(100)	El. pol. :H_3PO_4	Mech. pol. 06 emery paper	Mech. pol.>El. pol.	N
2	Cu(100)	ditto	Chem. etch. : HNO_3	El. pol.>Chem. etch.	N
3	Cu(100)	Chem. etch.:HNO_3	Chem. etch. : $(NH_4)_2S_2O_8$	$HNO_3<(NH_4)_2S_2O_8$	N, H
4	Cu(110)	El. pol. : H_3PO_4	Mech. pol. 06 emery paper	Mech. pol.>El. pol.	N
5	Cu(110)	ditto	Chem. etch. : HNO_3	El. pol.>Chem. etch.	N
6	Cu(110)	Chem. etch.:HNO_3	Chem. etch. : $(NH_4)_2S_2O_8$	$HNO_3>(NH_4)_2S_2O_8$	N, H
7	Cu(110)/ poly.	Chem. etch. : HNO_3, single	Chem. etch. : HNO_3, poly.	poly.>single	N
8	Cu(110)/ poly.	Chem. etch. : $(NH_4)_2S_2O_8$, single	Chem. etch. : $(NH_4)_2S_2O_8$, poly.	poly.>single	N
9	Cu(111)	El. pol. : H_3PO_4	Chem. etch. : HNO_3	El. pol.>Chem. etch.	N, H
10	Cu(111)	Chem. etch., HNO_3	Chem. etch. : $(NH_4)_2S_2O_8$	$HNO_3<(NH_4)_2S_2O_8$	H
11	Cu(111)	El. pol. : $CuSO_4$	El. pol. : H_3PO_4	$CuSO_4\simeq H_3PO_4$	H
12	Ag(100)	El. pol. : $KCN+K_4FeCN_6$	Chem. etch. : HNO_3	El. pol.>Chem. etch.	H
13	Ag(100)	ditto	Chem. etch. : $(NH_4)_2S_2O_8$	El. pol.≃Chem. etch.	H
14	Ag(100)	ditto	Cu, Ag and Au-plating	(100)>Cu, Ag and Au	H, N
15	Ag(110)	ditto	ditto	(110)>Cu, Ag and Au	H, N
16	Ag(110)	Chem. etch.:HNO_3	Cu-plating	(110)>Cu	H, N
17	Ag(100)	El. pol. : $KCN+K_4FeCN_6$	Cu, Au-plating	Cu, Au>(100)	O
18	Ag(110)	ditto	ditto	(110)>Cu, Au	O

In this table the following abbreviations were adopted. For example, chemical etching in a nitric acid solution was abbreviated as Chem. etch. :HNO_3, electrolytic polishing as El. pol. :H_3PO_4 and electrical plating of silver as Ag-plating.

(μV), against the time (min.) for the case of Ag(110) slice, one side of which is the one electrically plated with silver, while the other side is electrolytically polished. Arrows in Fig. 1 show times when the sample slice was let turn over. From this plot the electrolytically polished Ag(110) surface is found to be more active than the electrically plated silver surface.

Inequality relations thus determined are shown en bloc in Table I. The first column shows species of macroscopic-cut planes of sample slices. In the second and the third columns are shown methods of pre-treatments applied to each side of the surfaces. In the fourth column are given the inequality relations about recombination activities of two surfaces. The last column shows kinds of atoms used.

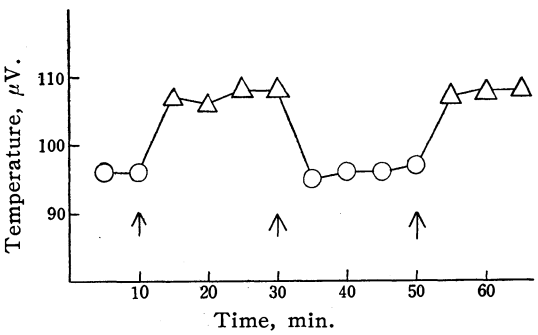


Fig. 1. The shift of the sample slice temperatures on the alternative exposure of two side planes to the reacting gas. This is an example about silver slice corresponding to Table I, No. 15.
○: Silver plating
△: Electrolytic polishing

Some Remarks on the Surface Structures

Since the main purpose of the present work is to make clear the effect of different surface structures on catalytic activity, several bits of information available to date concerning the surface structures of single crystals of some metals will be reviewed below in a little detail.

Among the works along this line the work of Yamaguchi[6] on single crystals of nickel is noteworthy. He made clear their detailed structures when they were etched by a mixed solution of ethyl alcohol and liquid bromine (1 : 1 by volume) by the cooperative uses of electron microscope and electron diffraction technique. In a similar way, structures of the single crystal of copper etched with ammonium

6) S. Yamaguchi, *J. Appl. Phys.*, **22**, 983 (1951).

persulfate was made clear by Ueda et al.[7] According to their result, the surface of a single crystal of copper etched by the saturated solution of ammonium persulfate exposes composite small facets, but all the faces of such facets have (110) family index irrespective of their directions.

Chalmers et al.[8] examined the surface thermally etched in the presence of oxygen or nitrogen. According to their results, the surface heated to 500°C in oxygen was found to show a zonal orientation which should be ascribed to the exposition of (111) face, while surfaces heated in nitrogen show a flat surface having all desired orientations. Pashley[9] examined the single crystal surfaces of silver parallel to the (100), (111), (110) and (311) plane when they were subjected to the electrolytic etching, electrolytic polishing and chemical etching by nitric acid (35%). In this work the electrolytic polishing was found to give very smooth surfaces, while the electrolytic etching or the chemical etching to give well-developed facets which were always of the (100), (110), (210) and (310) types and did not include (111) facets.

Less detailed and less reliable information can be drawn from the optical back reflection image obtained when a very intense light beam is spotted on the single crystal surfaces etched by chemical agents. This optical back reflection method was used in determining the crystal axes of single crystals in this work. Several pieces of information obtained by the use of this method can be found in old works of physicists who were engaged in the study of the anisotropy of work functions of metal single crystals. Farnsworth[10] found that the electrolytic etching of a single crystal of copper at low current densities developed a (111) face and the same treatment at high current densities a (100) face. In the work of Rose[11] the electrolytic etching of the (111) surface in a copper sulfate solution was stated to expose a (111) face and the chemical etching of the (100) surface in a nitric acid solution (65%) to produce a smooth (100) surface with very few undesired faces.

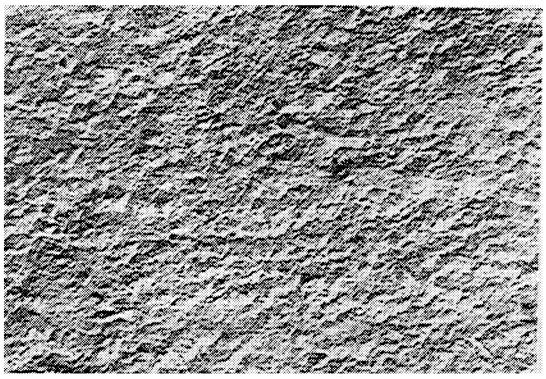
7) R. Ueda et al., presented at the Meeting of the Physical Society of Japan, Osaka, November 2, 1953 (unpublished).
8) B. Chalmers, R. King and R. Shuttleworth, *Proc. Roy. Soc.*, **A192**, 465 (1948).
9) D. W. Pashley, *Proc. Phys. Soc.*, **A64**, 1113 (1951).
10) H. E. Farnsworth, *Phys. Revs.*, **40**, 684 (1932).
11) B. A. Rose, ibid., **44**, 585 (1933).

Discussion

In Fig. 2 is given only a part of the electron micrographs of single crystal surfaces of copper and silver with different crystal indices. From Figs. 2b, c and d, it was clearly recognized that slices with different crystal indices were subjected to corrosion in a considerably different



a) The copper(110) surface electrolytically polished in a phosphoric acid solution (×2000).



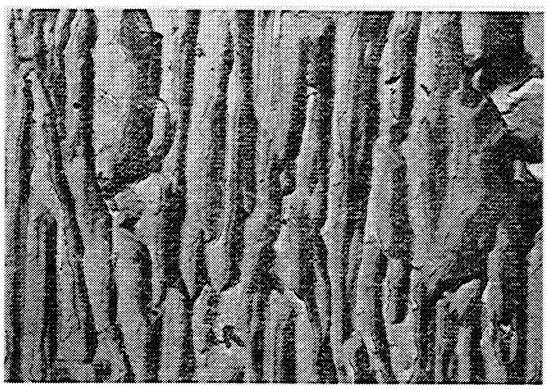
b) The copper(100) surface chemically etched in a nitric acid solution (×3500).



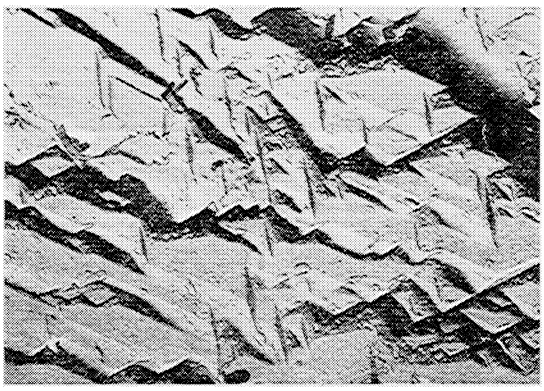
c) The copper(110) surface chemically etched in a nitric acid solution (×3500).



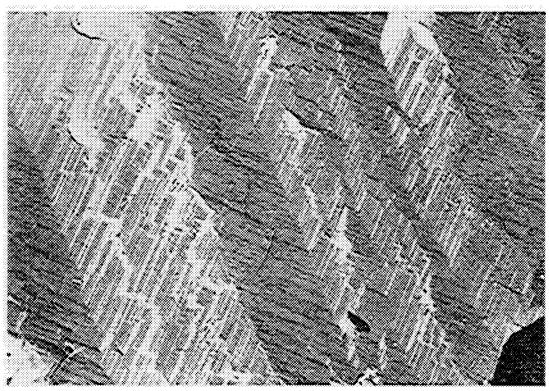
d) The copper(111) surface chemically etched in a nitric acid solution (×3500).



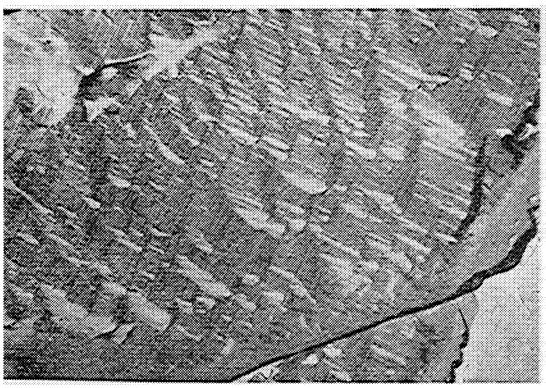
g) The silver(100) surface chemically etched in a nitric acid solution (×3500).



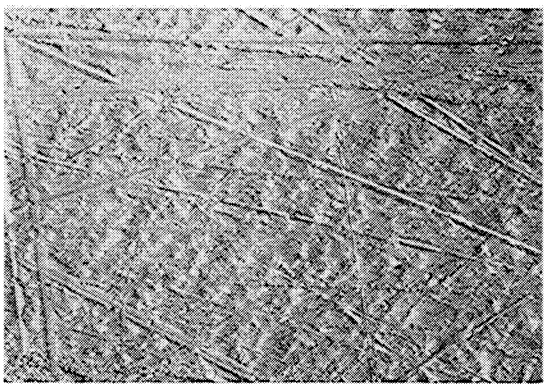
e) The silver(100) surface electrolytically polished in a mixing solution of potassium cyanide and potassium ferrocyanide (×3500).



h) The silver(110) surface chemically etched in a nitric acid solution (×3500).



f) The silver(110) surface electrolytically polished in the same bath as in e) (×3500).



i) The electro-polished silver(110) surface aged under contact with oxygen atoms (×3500).

Fig. 2. Electron micrographs of copper and silver single crystal surfaces subjected to various kinds of pre-treatment.

manner on the attack of the same etching agent. As known from Figs. 2e and f, it seems rather reasonable that the electrolytical polishing of silver surfaces in the bath used in the present work is considered as the electrolytical etching in an electron-microscopic scale. In spite of the significance of determining crystallographic planes of the small facets exposed to the reacting gas, further approach to the true surface structures could not be attained without getting an opportunity to use the electron diffraction method.

No results were obtained in which inequality relations of relative activities for hydrogen atoms and nitrogen atoms disagreed with each other. This suggests that the recombination of hydrogen atoms and nitrogen atoms may proceed probably through the similar mechanism.

In the case of both Cu(100) and Cu(110) slices, the mechanically polished surfaces were more active than electrolytically polished surfaces (Table I, No. 1 and 4). It is supposed that this difference in activity might have originated in strains of Beilby layers formed on the surface. Experiments of No. 7 and 8 were made about the special sample of the Cu(110) slice, the back side of which was changed to a polycrystal state by rapid cooling of only one side after re-heating, while another side remained to be the original single crystal state. From the comparison of activities of these two surfaces for the recombination of nitrogen atoms, both of which are subjected to the attack of the same reagent (nitric acid or ammonium persulfate), were obtained results showing that the polycrystal surface was always more active than the single crystal surface. It seems, however, to be premature to accept the existence of the effect of the crystal boundaries on the catalytic activity.

Bearing in mind the statement of Rose, an experiment of No. 11 was done to know whether the Cu(111) surface electrolytically polished in a copper sulfate solution may be more flat (accordingly less active) than the electrolytically polished surface in phosphoric acid, but any difference in these two treatments could not be detected.

In the previous work of the present author et al. about the recombination of hydrogen atoms on single crystal surfaces of copper which was electrolytically polished, it was made clear that the (110) face is the most active, the (100) face less active than this, and the (111) face the least active. In view of Ueda's work cited above, in which single crystal surfaces of copper etched by ammonium persulfate were shown to be composed of only the (110) family facets, it may be expected that surfaces etched by ammonium persulfate will be more active than those etched by nitric acid which was known to develop the (100) face. Present results show that with the Cu(100) slice this is certainly the case (No. 3), whereas with the Cu(110) slice the reverse order of activity has been obtained (No. 6). These results show that copper surfaces subjected to the chemical etching by nitric acid or ammonium persulfate seem to have more complex structures than expected from the information given above.

Throughout every three slices (100), (110) and (111), electrolytically polished surfaces were found always to be more active than chemically etched surfaces (No. 2, 5 and 9). This suggests that there may exist some other faces with relatively high activity than these principal faces. It is instructive that chemically etched surfaces having a rather complex micro-topography are less active than flat surfaces electrolytically polished. This implies that the recombination does not proceed on the corners or edges of small crystal facets, but rather mainly on plane faces. This has probably originated in such a special circumstance as that reactants are only composed of free atoms which need not be activated further.

Next, let us examine the results on single crystal surfaces of silver. As for the Ag(100) slice, surfaces chemically etched by nitric acid are also less active than those electrolytically polished in accord with the experiment of No. 2 (No. 12), whereas between surfaces chemically etched by ammonium persulfate and those electrolytically polished, no difference in activity was observed (No. 13). Combining the result of the experiment No. 12 with that of No. 13, the surface etched by ammonium persulfate is known to be more active than the one etched by nitric acid in accord with experiment No. 3 about copper. Consequently, it may be said that these chemical agents will have, to some extent, a similar corrosive action against both copper and silver.

For both the recombination of hydrogen atoms and that of nitrogen atoms, Ag(100) and Ag(110) surfaces electrolytically

polished were together more active than the electrically plated surfaces of copper, silver and gold (No. 14 and 15). This shows firstly that activities of these three kinds of metals do not show any wide diversity and secondly that the character of surfaces plays a significant role when the activities of these metals were compared. From the combination of No. 14 and 15, no conclusion could be drawn as to which of the Ag(110) slice and the Ag(100) slice would be more active. With reference to the earlier results of the present author et al. about the recombination of hydrogen atoms on single crystal surfaces of copper, the author has been inclined to ascribe the higher activity to the (110) face.

For the recombination of oxygen atoms on single crystal surfaces of silver subjected to the electro-polishment, inequality relations

$$\text{Ag(110)} > \text{Cu or Au plated surface} > \text{Ag(100)}$$

were obtained (No. 17 and 18). The relation Ag(110)>Ag(100) is in good accordance with the case of the recombination of hydrogen atoms on single crystal surfaces of copper so far as the order is concerned. This accordance seems, however, to be fortuitous in view of the considerably larger nuclear distance of an oxygen molecule, 1.20 Å, than that of a hydrogen molecule, 0.75 Å, even though the larger lattice constant of silver, 4.08Å, compared to that of copper, 3.61 Å, would work favorably for this reaction.

With the recombination of oxygen atoms it was noticed that a kind of polishing action becomes appreciable in repeated runs. Comparing the micro-photograph of Fig. 2a with Fig. 2i, it is immediately perceived that such an aged surface under the contact with oxygen atoms resembles the electrolytically polished surface of copper in its micro-topographic appearance, except that the former possesses somewhat worse flatness than the latter. Experiments No. 17 and 18 are obtained with respect to such aged surfaces, while experiments No. 12 to No. 15 with respect to surfaces polished afresh.

Though it appears probable that this kind of polishing will come from any particular property of oxide layers, such changes of surface structures were not studied further, because this problem is not concerned with the main theme of the present work.

Summary

Recombination of hydrogen atoms, nitrogen atoms and oxygen atoms was carried out on single crystal surfaces of copper and silver subjected to various surface pre-treatments.

With both the recombination of hydrogen atoms and that of nitrogen atoms, copper surfaces electrolytically polished have always higher activity than those chemically polished. The Cu(100) surface chemically etched by ammonium persulfate was more active than that etched by nitric acid for both hydrogen atoms and nitrogen atoms, whereas with the Cu(110) the opposite order of activity was obtained. For both silver and copper, no evidence was found to show the different order of activity between the recombination of hydrogen atoms and that of nitrogen atoms. Concerning the recombination of oxygen atoms on single crystal surfaces of silver, the (110) face was found to be more active than the (100) face in accord with the result of our earlier work about the recombination of hydrogen atoms on single crystal surfaces of copper.

The author wishes to express his gratitude to Professor S. Shida for his help and encouragement during the course of this study.

Laboratory of Physical Chemistry
Tokyo Institute of Technology
Meguro-ku, Tokyo

Polymerization of Methyl Methacrylate Initiated by the System of p-Toluenesulfinic Acid, Dimethylaniline and Oxygen

By Ryoichi UEHARA

(Received December 17, 1958)

Polymerization of vinyl monomers initiated by some sulfinic acids was first reported by Hagger[1]. The present author[2] has reported a self-curing method of methyl methacrylate by the combined action of *p*-toluenesulfinic acid and dimethylaniline in the presence of air. Hagger considered that sulfinic acids by themselves could initiate the polymerization of vinyl monomers and reported an equation representing a relation between the initial rate of polymerization of methyl methacrylate and the concentration of *p*-toluenesulfinic acid.

Recently, Bredereck and others[3] found that absolutely pure *p*-toluenesulfinic acid could not initiate the polymerization of methyl methacrylate, and that for the initiation of the polymerization, the coexistence of oxygen and an "oxygen-acceptor" such as amines or chloide ions was necessary. The polymerization-initiating action of sulfinic acid found by Hagger was explained by Bredereck to be due to the combined action of the sulfinic acid, oxygen in air, and chloride ions containd in the sulfinic acid as an impurity. Moreover, Bredereck[4] has postulated a mechanism for the initiation of the polymerization of methyl methacrylate with an initiating system consisting of oxygen, *p*-toluenesulfinic acid, and an "oxygen-acceptor"; i.e., a peroxide was formed from oxygen and the sulfinic acid, and then a radical was produced from the peroxide and the "oxygen-acceptor" to initiate the polymerization. But no experimental evidence was given by him for this mechanism.

The present author has studied the polymerization of methyl methacrylate initiated by the system of *p*-toluenesulfinic acid, oxygen in air and dimethylaniline from the standpoint of chemical kinetics. In the present paper, correlations of the initial rate of polymerization of methyl methacrylate with the concentration of the components of the inititating system are given, and the initial step of the polymerization is discussed.

The polymerization was carried out in open test tubes under atmospheric pressure of air for the study of the dependence of the initial rate (R) of polymerization upon concentrations of *p*-toluenesulfinic acid (TSA), dimethylaniline (DMA), and methyl methacrylate (MMA). When the effect of the initial pressure of oxygen was tested, the polymerization was carried out in sealed test tubes under various initial pressures of air.

When the concentration of *p*-toluenesulfinic acid was held constant and that of dimethylaniline was varied under atmospheric pressure of air, the initial rate of the bulk polymerization of methyl methacrlate

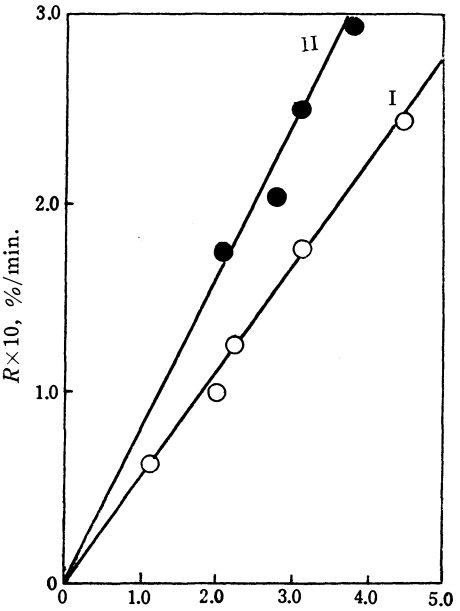


Fig. 1. Correlations of R with [TSA]$^{1/2}$ and [DMA]$^{1/2}$ at 30°C in air.
Line I. [TSA]$=5.1\times10^{-2}$ mol./l.
Line II. [DMA]$=10.0\times10^{-2}$ mol./l.

1) O. Hagger, *Helv. Chim. Acta.*, **31**, 1629 (1948).
2) R. Uehara, *Dental Practice* (*Rinsho Shika*), **196**, 24 (1952).
3) H. Bredereck et al., *Ber.*, **89**, 731 (1956).
4) H. Bredereck et. al., *Angew. Chem.*, **68**, 306 (1956).

was linearly proportional to the square root of the concentration of dimethylaniline. This correlation is shown by line I in Fig. 1, in which 5.01×10^{-2} mol./l. of *p*-toluenesulfinic acid was used at 30°C.

When the concentration of dimethylaniline was kept constant and that of *p*-toluenesulfinic acid was varied, the initial rate of polymerization was linearly dependent upon the square root of the concentration of *p*-toluenesulfinic acid. This relationship is shown by line II in Fig. 1, in which 10×10^{-2} mol./l. of dimethylaniline was used at 30°C. Straight lines I and II in Fig. 1 are brought to a focus at the origin. This fact indicates that neither *p*-toluenesulfinic acid nor dimethylaniline alone can initiate the polymerization in combination with oxygen in air.

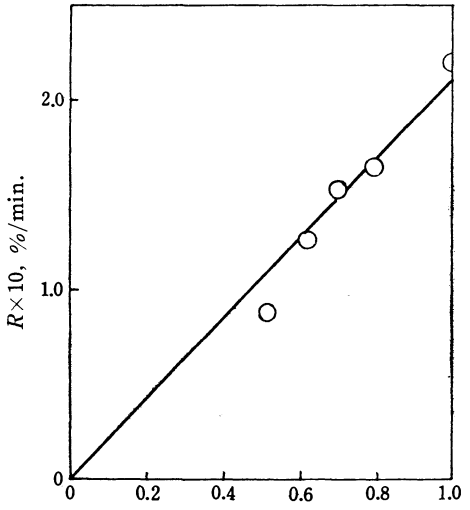


Fig. 2. Correlation of R with the initial pressure of air at 30°C
[TSA] = [DMA] = 8.8×10^{-2} mol./l.

In Fig. 2 the correlation of the initial rate of polymerization with the initial pressure of air in the sealed test tubes is shown. The initial rate of polymerization is linearly proportional to the square root of the initial pressure of air. In this case 8.8×10^{-2} mol./l. of both *p*-toluenesulfinic acid and dimethylaniline were used. The straight line in Fig. 2 gose through the origin. This fact indicates that the polymerization can not be initiated without air. The pressure of air is proportional to that of oxygen, so Fig. 2 shows that the initial rate of polymerization is linearly dependent upon the square root of the initial pressure of oxygen.

In the case of the solution-polymerization in benzene, the initial rate of polymerization was linearly dependent upon the concentration of methyl methacrylate. This correlation is shown in Fig. 3, in which 5.10×10^{-2} mol./l. of both *p*-toluenesulfinic acid and dimethylaniline were used at 40°C, under air of atmospheric pressure.

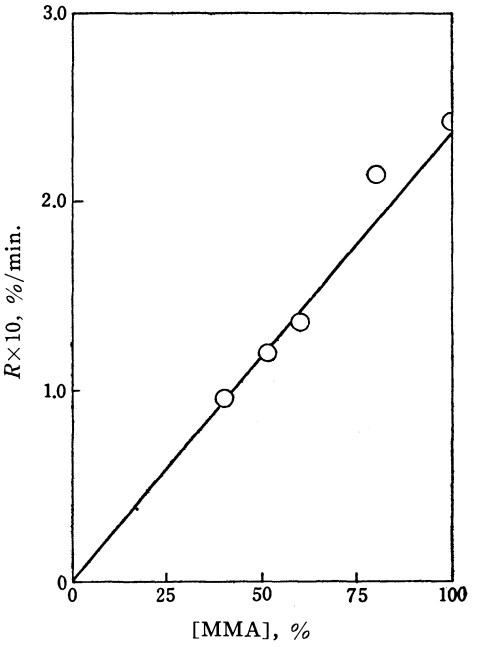


Fig. 3. Relationship between R and [MMA] in case of solution-polymerization in benzene at 40°C.
[TSA] = [DMA] = 5.10×10^{-2} mol./l.

Correlations shown in Figs. 1—3 can be represented by the following equation:

$$R=k[O_2]^{1/2}[TSA]^{1/2}[DMA]^{1/2}[MMA] \quad (1)$$

where k is a constant.

Eq. 1 suggests that oxygen, *p*-toluenesulfinic acid and dimethylaniline, all three, take part in the formation of a radical to initiate the polymerization, but methyl methacrylate is not concerned in the radical formation at the initiation reaction. Moreover, Eq. 1 suggests that there may be several reactions forming the radical from the initiating system. As mentioned above, Bredereck[4] has postulated the formation of a peroxide from oxygen and *p*-toluenesulfinic acid as the first step of the initiation. In another paper, however, Bredereck[3] has reported very briefly without any details of experiments that salts of *p*-toluenesulfinic acid and some aromatic amines initiated the polymerization of methyl methacrylate under air. In addition, it has been reported by

Bredereck[5] and Brauer[6] that salts of the sulfinic acid and amines were efficient accelerators for the polymerization of methyl methacrylate initiated with benzoyl peroxide. Formation of a salt from an amine and *p*-toluenesulfinic acid takes place very smoothly in organic solvent[6]. So, in the case of the combination of *p*-toluenesulfinic acid and dimethylaniline, formation of a salt from the sulfinic acid and the amine is more probable than the formation of a peroxide from the sulfinic acid and oxygen in air. The initiating system, *p*-toluenesulfinic acid-oxygen-chloride ions, must be considered separately from the initiating system under discussion.

To get support for this idea from another point of view, the present author has examined the effects of anhydride, and methyl and ethyl esters of *p*-toluenesulfinic acid for the initiation of the polymerization. The per cent conversions of bulk polymerization by means of equimolar mixtures of these compounds and dimethylaniline are shown in Table I.

TABLE I. THE PER CENT CONVERSIONS OF THE BULK POLYMERIZATION OF METHYL METHACRYLTE UNDER ATMOSPHERIC PRESSURE OF AIR

Initiator*	Conversions, %			
	at 30°C		at 70°C	
	3 hr.	6 hr.	1 hr.	3 hr.
p-Toluenesulfinic acid	22.1	98.7	43.8	96.2
Anhydride	0	0	trace	3.8
Methyl ester	0	0	trace	8.4
Ethyl estr	0	0	trace	4.3

* 5.0×10^{-2} mol./l. of each was used together with equimolar amount of dimethylaniline

Polymerizations were carried out at 30 and 70°C under atomospheric pressure of air. At 30°C, *p*-toluenesulfinic acid was the only material which was responsible for the initiating action. At 70°C, the effect of *p*-toluenesulfinic acid was much greater than those of its derivatives. Namely, the polymerization-initiating action of the sulfinic acid was lost by changing it to its anhydride or esters. Therefore, it appears to be conclusive that the formation of a salt from the sulfinic acid and dimethylaniline is the first step of the polymerization.

By considering the formation of the salt, the following reactions of polymerization are derived:

$$\mathrm{TSA}+\mathrm{DMA}\overset{K}{\rightleftarrows}\mathrm{S}$$

$$\mathrm{S}+\mathrm{O_2}\overset{k_1}{\rightarrow}\mathrm{R}\cdot$$

$$\mathrm{MMA}+\mathrm{R}\cdot\overset{k_2}{\rightarrow}\mathrm{P_1}\cdot$$

$$\mathrm{P}_m\cdot+\mathrm{MMA}\overset{k_3}{\rightarrow}\mathrm{P}_{m+1}\cdot$$

$$\mathrm{P}_m\cdot+\mathrm{P}_n\cdot\overset{k_4}{\rightarrow}\mathrm{P}_{m+n}\ \text{or}\ \mathrm{P}_m+\mathrm{P}_n$$

where S is the salt, R· the radical formed from the salt and oxygen, $P_1\cdot$, $P_m\cdot$, $P_n\cdot$, $P_{m+1}\cdot$ are polymer radicals, P_m, P_n, P_{m+n} polymer molecules, K is the euqilibrium constant, and k_1, k_2, k_3, k_4 are respectively rate constants for each of the reactions.

From these reactions the follwing equation can be deduced by the usual method of chemical kinetics for radical polmerization:

$$R=k_3(Kk_1/k_4)^{1/2}[\mathrm{O_2}]^{1/2}[\mathrm{TSA}]^{1/2}[\mathrm{DMA}]^{1/2}[\mathrm{MMA}] \qquad (2)$$

Eq. 2 completely coincides with Eq. 1.

Experimetal

Materials.—Purification of methyl methacrylate, dimethylaniline and benzene have been reported in a previous paper by the present author[7]. *p*-Toluenesulfinic acid was prepared from *p*-toluenediazonium sulfate by using sulfur dioxide and copper[8]. The crude product was washed with distilled water until ions of heavy metals, chloride and sulfate were not detected in the washing then recrystallized from benzene and methanol, and dried under reduced pressure, m.p. 81°C. The crystallization and the drying of the sulfinic acid were carried out as rapidly as possible, and the purified sulfinic acid was used immediately after drying to avoid deterioration. Anhydride of the sulfinic acid was obtained by treating the acid with acetic anhydride in the presence of a small amount of sulfuric acid, m.p. 75.0°C[9]. Methyl and ethyl esters of the sulfinic acid were prepared from sodium *p*-toluenesulfinate and metyl or ethyl chlorocarbonate, respectively[10]. The esters were used without any purification because of their instability.

Polymerization.—Polymerization under atmospheric pressure of air was carried out in test tubes, each of which was open to the atmosphere

5) H. Bredereck et. al., *Makromol. Chem.*, **12**, 100 (1954).
6) G. M. Brauer and F. R. Burns, *J. Polymer Sci.*, **19**, 311 (1956).
7) R. Uehara, This Bulletin, **31**, 685 (1958).
8) L. Gattermann, *Ber.*, **32**, 1136 (1899).
9) E. Knoevenagel, ibid., **41**, 3326 (1908).
10) R. Otto et. al., ibid., **18**, 2506 (1885).

through a capillary at the top. The test tubes were 15 mm. in diameter and 20 cm. in height, and the capillary was 1 mm. in inner diameter and 4 cm. in length, and fitted to the test tube with a ground glass joint. When the effect of the initial pressure of the air was examined, sealed test tubes, each of which was 20 cc. in capacity, were used in place of the above mentioned open tubes. *p*-Toluenesulfinic acid and dimethylaniline were dissolved separately in methyl methacrylate. Both solutions were chilled in a dry ice-methanol bath for 30 min. Measured amounts of each chilled solution were placed in a test tube and mixed. The polymerization was effected by shaking the tubes in a thermostat. The yield of the polymer was measured at intervals of 10 min. Details of the procedures of polymerization and the determination of the initial rate of polymerization have been reported previously[7].

Summary

Initiation of the polymerization of methyl methacrylate with the initiating system, *p*-toluenesulfinc acid-oxygen-dimethylaniline, has been investigated from the standpoint of chemical kinetics. The initial rate of polymerization of methyl methacrylate was linearly proportional to the square roots of the concentrations of each component of the initiating system, and methyl methacrylate. The polymerization initiating action of the initiating system is lost by changing the sulfinic acid to its anhydride or esters. The formation of a salt from the sulfinic acid and dimethylaniline was suggested as the first step of the initiation of the polymerization.

The present author wishes to express his hearty thanks to Professor Osamu Simamura of the University of Tokyo for his interest in this work.

Tama Kagaku Kogyo Co.
2-28 Minamirokugo
Ota-ku, Tokyo

Polymerization of Methyl Methacrylate Initiated by a Combined Action of p-Tolyl Methyl Sulfone, Dimethylaniline and Oxygen in Air

By Ryoichi UEHARA

(Received December 25, 1958)

p-Tolyl methyl sulfone first reported by Knoevenagel[1] is a compound prepared from sodium *p*-toluenesulfinate and methyl iodide, and an isomer of methyl *p*-toluenesulfinate. The effect of *p*-toluenesulfinic acid for the polymerization of methyl methacrylate has been noted by several authors[2] and that of *p*-tolyl hydroxymethyl sulfone has been reported by Bredereck[3], but about the effect of *p*-tolyl methyl sulfone nothing has been reported up to the present.

It has been found by the present author that the polymerization of methyl methacrylate was initiated by a combined action of *p*-tolyl methyl sulfone, dimethylaniline and oxygen in air. The fact that the system of *p*-toluenesulfinic acid, dimethylaniline and oxygen lost the ability to initiate the polymerization by changing the sulfinic acid to its esters has been reported in a previous paper by the present author[4]. So, it appears of interest that the isomer of the methyl ester initiates the polymerization in combination with dimethylaniline and oxygen. In the present paper, some experimental results concerning the relation between the per cent conversion of the polymerization and the concentrations of the initiating reagents, and effects of various amines on the initiating ability of the system are given. In Fig. 1, per cent conversions versus time of the bulk polymerization of methyl methacrylate in air at 70°C are shown. The concentrations of *p*-tolyl methyl sulfone (TMS) and dimethylaniline (DMA) were respectively 3.01×10^{-2} and 2.98×10^{-2} mol./l. In the case when *p*-tolyl methyl sulfone alone was used

1) E. Knoevenagel, *Ber.*, **21**, 1349 (1888).
2) For example, H. Bredreck et. al., ibid., **89**, 731 (1956).
3) H. Bredereck et. al., *Makromol. Chem.*, **12**, 100 (1954).
4) R. Uehara, This Bulletin, **32**, 1079 (1959).

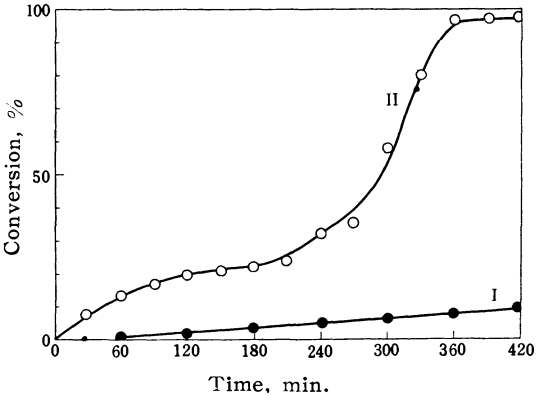


Fig. 1. Conversion versus time relationships of the bulk polymerization at 70°C in air.
([TMS]$=3.01\times10^{-2}$, [DMA]$=2.98\times10^{-2}$ mol./l., I. TMS alone, II. TMS and DMA).

under air, an induction period appeared and then the polymerization took place at a very small rate. When dimethylaniline was used alone, trace of polymethyl methacrylate was formed after 3 hr. By means of *p*-tolyl methyl sulfone and dimethylaniline, the polymerization proceeded at a fairly rapid rate under air. In that case, the time-conversion curve shows an *S*-form which appears usually in the bulk polymerization of methyl methacrylate. The polymerization was completely inhibited by the addition of 0.10×10^{-2} mol./l. of hydroquinone. Under nitrogen the polymerization did not take place.

When equimolar mixture of *p*-tolyl methyl sulfone and dimethylaniline were used in air, per cent conversion after 1 hr. at 60°C were linearly proportional to the initial concentration of *p*-tolyl methyl sulfone or dimethylaniline. At 70°C, the linear dependence of the per cent conversion upon the concentration of *p*-tolyl methyl sulfone can be seen in case the initial concentration of *p*-tolyl methyl sulfone is less than 3.0×10^{-2} mol./l. Those correlations are shown in Fig. 2.

In Table I, per cent conversions after 1 hr. (at 70°C) in the bulk polymerization of methyl methacrylate initiated by equimolar mixtures of *p*-tolyl methyl sulfone and various amines are shown. The mixtures containing heterocyclic, aliphatic, primary and secondary amines were not responsible for the initiation of the polymerization. Only aromatic tertiary amines were effective as the component

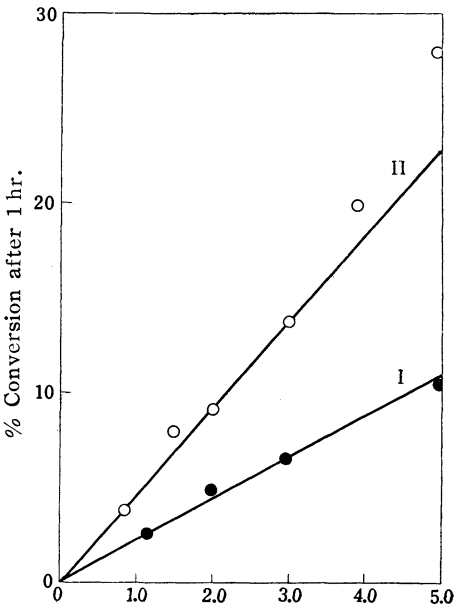


Fig. 2. Correlations of % conversion after 1 hr. with concentration of the initiating reagent.
(I, at 60°C, II, at 70°C)

TABLE I. THE PER CENT CONVERSIONS AFTER 1 HR. AT 70°C IN AIR

Amine*	% Conversion
Dimethylaniline	14.5
N,N-Dimethyl-*p*-anisidine	31.3
N,N-Dimethyl-*p*-toluidine	26.9
N,N-Dimethyl-*p*-chloroaniline	6.03
N,N-Dimethyl-*p*-bromoaniline	5.86
N,N-Dimethyl-*p*-nitrosoaniline	0
N,N-Dimethyl-*p*-nitroaniline	0
N,N-Dimethyl-*p*-phenylazoaniline	0
Aniline	0
N-Methylaniline	0
Diphenylamine	Trace
Quinoline	0
Pyridine	0
Triethylamine	0

* 3.0×10^{-2} mol./l. of each amine and *p*-tolyl methyl sulfone were used.

of the polymerization-initiating system. *p*-Substitution in dimethylaniline influenced significantly its efficiency as a component of the initiating system. Electron-donating groups such as methyl and methoxy increased the yield of the polymer, while electron-withdrawing groups such as chlorine and bromine reduced the yield. When a strongly electron-withdrawing group such as nitro, nitroso, or phenylazo

was present in the para position of dimethylaniline, no polymerization occurred even after 3 hr. The nature of the effects of dimethylaniline will be discussed in future.

Copolymerization of styrene and methyl methacrylate with this initiating system has been examined. To an equimolar mixture of styrene and methyl methacrylate 3.0×10^{-2} mol./l. of each of *p*-tolyl methyl sulfone and dimethylaniline were added, and the polymerization was carried out in air at 70°C for 2 hr. A portion (5.7% by weight) of the copolymer was obtained. *Analysis* found: C, 76.09 and H, 8.13%, calculated for the copolymer in the molar ratio of 1:1, $(C_{13}H_{16}O_2)_n$: C, 76.47 and H, 7.84%, respectively. It was evident that a copolymer containing styrene and methyl methacrylate in a molar ratio of approximately 1:1 was obtained.

Experimental results mentioned above suggest that the polymerization is initiated by a combined action of *p*-tolyl methyl sulfone, dimethylaniline, and oxygen. The facts that the polymerization is inhibited with hydroquinone, and a copolymer in a molar ratio of 1:1 is formed from styrene and methyl methacrylate indicate that the polymerization proceeds through a free radical mechanism[5]. So, it is probable that radicals to initiate the polymerization are produced from *p*-tolyl methyl sulfone, dimethylaniline and oxygen, though the details of the reaction forming the radical are not made clear at present.

Experimental

p-Tolyl methyl sulfone was prepared from sodium *p*-toluenesulfinate and methyl iodide in aqueous methanol[1]. The crude product was carefully washed with 10% aqueous solution of sodium carbonate and distilled water, then recrystallized from ethanol, m. p. 87°C. Purification of methyl methacrylate, dimethylaniline, and hydroquinone were given in a previous paper[6]. Styrene was washed with 10% aqueous solution of sodium hydroxide and pure water, dried over anhydrous sodium sulfate and carefully distilled under a reduced pressure in nitrogen through a fractionating column, b. p. 46°C/20 mmHg. Amines were distilled under reduced pressure of 3 mmHg, or recrystallized from ethanol.

Polymerization was carried out in open test tubes as mentioned in the preceding paper[4]. The procedures of the polymerization and the determination of per cent conversions have been reported in a previous paper[6].

Summary

The polymerization of methyl methacrylate is initiated by a combined action of *p*-tolyl methyl sulfone, dimethylaniline, and oxygen. The efficiency of the initiating system is increased by using dimethylanilines substituted with electron-donating groups in the para position. The fact that the 1:1 copolymer of styrene and methyl methacrylate is formed by means of this initiating system suggests the formation of radicals to initiate the polymerization from the initiating system.

The present author wishes to express his thanks to Professor Osamu Simamura of the University of Tokyo for his interest and also Mr. Tsurahide Cho, the President of Tama Kagaku Kogyo Co., for permission to publish this work.

Tama Kagaku Kogyo Co.
2-28 Minamirokugo,
Ota-ku, Tokyo

5) C. Walling, E. R. Briggs, W. Cummings and F. R. Mayo, *J. Am. Chem. Soc.*, **72**, 48 (1950).

6) R. Uehara, This Bulletin, **31**, 685 (1958).

Polymerization of Methyl Methacrylate Initiated by a Combined Action of Di-p-tolylsulfonylhydroxylamine and Oxygen in Air

By Ryoichi UEHARA

(Received January 13, 1959)

Di-*p*-tolylsulfonylhydroxylamine was first prepared by Koenigs[1] through the reaction of nitrous acid on *p*-toluenesulfinic acid:

$$2CH_3C_6H_4SO_2H + HNO_2 = H_2O + (CH_3C_6H_4SO_2)_2NOH$$

It has been found by the present author that di-*p*-tolylsulfonylhydroxylamine initiates the polymerization of methyl methacrylate by a combined action with oxygen in air, and this effect is accelerated by the addition of dimethylaniline[2]. Although some compounds related to di-*p*-tolylsulfonylhydroxylamine such as *p*-toluenesulfinic acid[3] and di-*p*-tolylsulfonylmethylamine[4] are noted as components of the initiating system for the polymerization of methyl methacrylate, nothing has been reported up to the present about the effect of di-*p*-tolylsulfonylhydroxylamine for the polymerization.

In the present paper, experimental results concerning the polymerization of methyl methacrylate intiated by the combined action of di-*p*-tolylsulfonylhydroxylamine and oxygen in air, with or without dimethylaniline, are given.

Fig. 1 shows the per cent conversion versus time of the bulk polymerization of methyl methacrylate in air. The polymerization proceeded at a moderate rate by means of 1.86×10^{-2} mol./l. of di-*p*-tolylsulfonylhydroxylamine (DTSH) alone. By the addition of 2.0×10^{-2} mol./l. of dimethylaniline (DMA) the polymerization proceeded fairly rapidly. 3.1×10^{-2} mol./l. of hydroquinone (HQ) retarded the polymerization initiated with 1.86×10^{-2} mol./l. of di-*p*-tolylsulfonylhydroxylamine, i.e., the rate of polymerization was not affected until the conversion reached approximately 5%, but after that the reaction hardly proceeded at all. In the atmosphere of nitrogen, the polymerization occured with difficulty by means of di-*p*-tolylsulfonylhydroxylamine and dimethylaniline. So, it is evident that oxygen is necessary for the initiation of the polymerization.

Copolymerization of methyl methacrylate

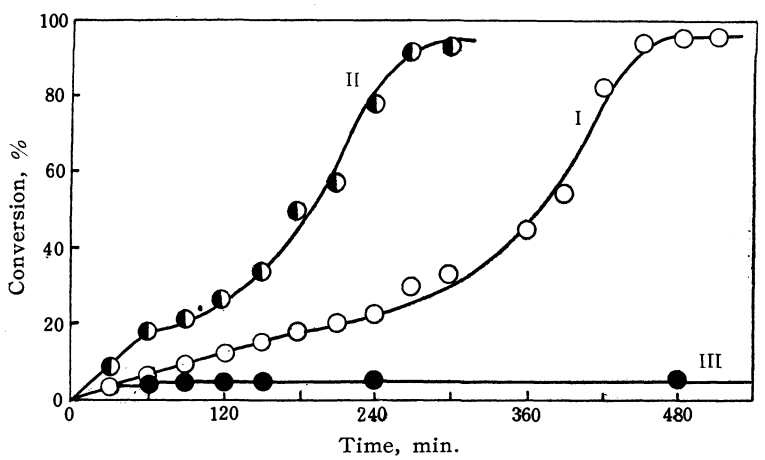


Fig. 1. Per cent conversion versus time of bulk polymerization of methyl methacrylate at 70°C in air. I. DTSH 1.86×10^{-2} mol./l., II. DTSH 1.86×10^{-2} and DMA 2.0×10^{-2} mol./l., III. DTSH 1.86×10^{-2} and HQ 3.1×10^{-2} mol./l.

1) P. Koenigs, *Ber.*, 11, 616 (1878).
2) R. Uehara, *J. Japan. Chem.* (*Kagaku-no-Ryoiki*), 7, 291 (1953).
3) For example, H. Bredereck et al., *Ber.*, 89, 731 (1956).
4) H. Bredereck et. al., *Makromol. Chem.*, 12, 100 (1954).

and styrene was examined by the initiating system of di-*p*-tolylsulfonylhydroxylamine, oxygen and dimethylaniline. An equimolar mixture of methyl methacrylate and styrene containing 1.7×10^{-2} mol./l. each of di-*p*-tolylsulfonylhydroxylamine and dimethylaniline was heated at 70°C in air. After 2 hr., 9.1% by weight of the copolymer was obtained. Analysis of the copolymer shows that a copolymer in the molar ratio of 1 : 1 has been formed; i. e., found: C, 76.31 and H, 8.03%, calculated for the copolymer in the molar ratio of 1 : 1, $(C_{13}H_{16}O_2)_n$: C, 76.47 and H, 7.84%, respectively. This fact indicates that the polymerization proceeds through a free radical mechanism[5].

Average degrees of polymerization of polymethyl methacrylate formed by means of the initiating system are shown in Table I. In a course of the bulk polymerization by means of 1.86×10^{-2} mol./l. of di-*p*-tolylsulfonylhydroxylamine, the average degrees were approximately constant until the conversion reached 20% (after about 240 min.), while, after that period, they increased gradually corresponding to the extent of the polymerization. Fig. 2 shows the correlation of the average degree of polymerization of

TABLE I. AVERAGE DEGREE OF POLYMERIZATION, $\overline{P}$, OF POLYMETHYL METHACRYLATE FORMED BY MEANS OF DTSH AT 70°C IN AIR

DTSH (mol./l.×10²)	Time (min.)	Conversion (%)	$\overline{P}$
1.86	30	3.1	2280
〃	60	6.1	2540
〃	90	9.8	2570
〃	120	13.0	2580
〃	240	23.1	2880
〃	300	33.5	3820
〃	360	45.1	3910
〃	420	79.6	3940
〃	480	95.8	3990
〃*	60	16.2	1310
〃*	120	26.8	1560
〃*	180	49.5	1830
3.13	30	4.5	1760
4.50	〃	4.8	1490
5.12	〃	5.0	1310
6.30	〃	6.0	1280
7.19	〃	6.3	1110
8.20	〃	6.5	1080
9.00	〃	6.6	940

* With an equimolar amount of dimethylaniline.

5) C. Walling, F. R. Briggs, W. Cummings and F. R. Mayo, *J. Am. Chem. Soc.*, 72, 48 (1950).

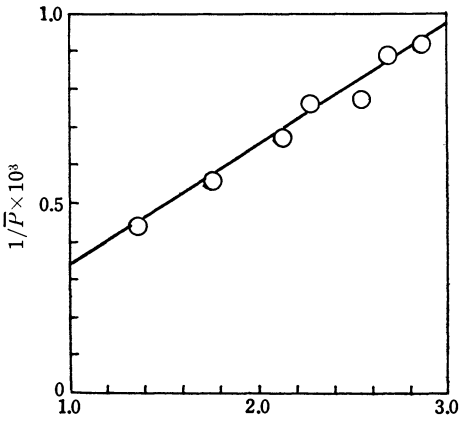
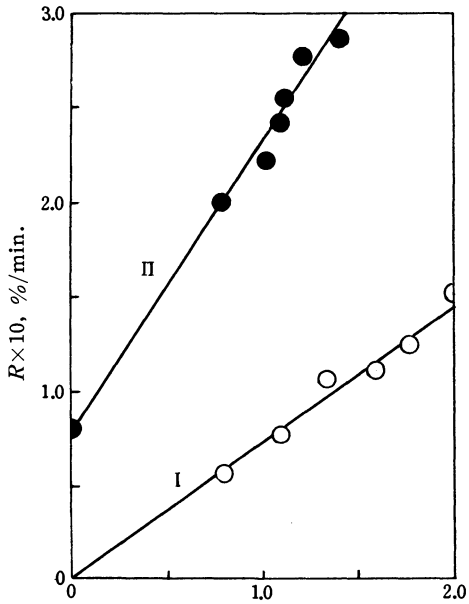


Fig. 2. Correlation of the average degree of polymerization of polymethyl methacrylate with the initial concentration of DTSH at 70°C in air.

polymethyl methacrylate formed during the course of the first 30 min. of the polymerization with the initial concentration of di-*p*-tolylsulfonylhydroxylamine. It is seen that the reciprocal of the average degree of polymerization is linearly dependent upon the square root of the intial concentration of di-*p*-tolylsulfonylhydroxylamine. This fact also indicates the radical character of the polymerization.

The relation between the initial rate of polymerization and concentrations of di-*p*-tolylsulfonylhydroxylamine and dimethylaniline has been investigated. The correlation of the initial rate of polymerization in air with the concentration of di-*p*-tolylsulfonylhydroxylamine is shown in Fig. 3 by line I. The initial rate of polymerization is linearly proportional to the square root of the initial concentration of di-*p*-tolylsulfonylhydroxylamine. When the concentration of di-*p*-tolylsulfonylhydroxylamine was kept constant and various amounts of dimethylaniline were added, the initial rate of polymerization was linearly dependent upon the square root of the initial concentration of dimethylaniline. Line II in Fig. 3 shows this relation in a case when 1.2×10^{-2} mol./l. of di-*p*-tolylsulfonylhydroxylamine was used. It is evident that the so-called square root dependence which is typically seen in the radical polymerization of vinyl monomers holds between the initial rate of polymerization and the initial concentration of both di-*p*-tolylsulfonylhydroxylamine and dimethylaniline. This fact can be regarded as supporting the



[DTSH]$^{1/2}\times 10$ for I
[DMA]$^{1/2}\times 10$ (with 1.20×10^{-2} of DTSH) for II
mol./l.

Fig. 3. Correlations of the initial rate of polymerization with concentrations of DTSH and DMA at 70°C in air.

radical character of the polymerization reaction.

The accelerating effect of dimethylanilne is significantly influenced by groups substituted in its para position. The per cent conversions of the polymerization after 1 hr. at 70°C accelerated by using various amines are compared in Table II. Electron-donating groups such as methyl and methoxy promote, and electron-withdrawing groups such as chloro and bromo reduce the efficiency of the initiating system. By strongly electron-withdrawing groups such as nitro and nitroso, the polymerization-initiating action of the initiating system is completely lost.

TABLE II. EFFECTS OF *p*-SUBSTITUTED DIMETHYLANILINE ON THE EFFICIENCY OF THE INITIATING SYSTEM

Substituted group	% Conversion after 1 hr.
CH_3O	30.4
CH_3	23.5
H	16.0
Cl	8.1
Br	7.3
NO	0
NO_2	0

Di-*p*-tolylsulfonylhydroxylamine (1.86×10^{-2} mol./l.) and the amine (2.0×10^{-2} mol./l.) were used at 70°C in air.

From the above mentioned experimental results, it is evident that the polymerization of methyl methacrylate initiated by a combined action of di-*p*-tolylsulfonylhydroxylamine and oxygen, with or without dimethylaniline as an accelerator, proceeds through a free radical mechanism. Therefore, it is very probable that a radical to initiate the polymerization is produced from the initiating system, though the nature of the initiating reactions will be the subject of further investigations.

Experimental

Purification of methyl methacrylate, dimethylaniline, and hydroquinone have been reported in a previous paper by the present author[6]. Di-*p*-tolylsulfonylhydroxylamine was prepared from sodium *p*-toluenesulfinate, sodium nitrite, and hydrochloric acid at 0°C[1]. The crude product was washed with distilled water until no ions of chloride and heavy metals were detected in the washing to eliminate water soluble impurities, and recrystallized from benzene and methanol, m. p. 127°C, with decomposition.

Polymerizations were carried out in open test tubes which have been mentioned in a previous paper by the author[7]. Di-*p*-tolylsulfonylhydroxylamine and dimethylaniline were dissolved in methyl methacrylate cooled in an ice-salt bath. The solution (2 cc.) was placed in each of the tubes and heated in a thermostat bath with shaking. The procedures of the polymerization and determination of the initial rate of polymerization have been given previously[6]. The initial rate was expressed in unit of per cent per minute. The average degree of polymethyl methacrylate was estimated from its intrinsic viscosity in chloroform by using the equation of Sakurada[8].

Summary

The polymerization of methyl methacrylate is initiated by a combined action of di-*p*-tolylsulfonylhydroxylamine and oxygen. The polymerization is accelerated with dimethylaniline and retarded with hydroquinone. The initial rate of polymerization is linearly dependent upon the square roots of concentrations of di-*p*-tolylsulfonylhydroxylamine and dimethylaniline in air. The reciprocal of the average degree of polymerization of the

6) R. Uehara, This Bulletin, **31**, 685 (1958).
7) R. Uehara, This Bulletin **32**, 1079 (1959).
8) I. Sakurada, *Chem. High Polymers* (*Kobunshi Kagaku*), **2**, 253 (1945).

polymethyl methacrylate formed by means of the present initiating system is proportional to the square root of the initial concentration of di-*p*-tolylsulfonylhydroxylamine. A copolymer (1 : 1) is obtained from an equimolar mixture of styrene and methyl methacrylate. These facts suggest that the polymerization is initiated by a radical produced from the initiating system.

The present author thanks Professor Osamu Simamura of the University of Tokyo for his continued interest and Mr. Tsurahide Cho, the President of Tama Kagaku Kogyo Co., for permission to publish this work.

Tama Kagaku Kogyo Co.
2-28 Minamirokugo
Ota-ku, Tokyo

On the Phase Transition of Hexamethyldisilane

By Hiroshi SUGA* and Syûzô SEKI

(Received March 7, 1959)

So-called plastic crystal was first defined by Timmermans[1] in 1938 as a class of crystals which have the entropy of fusion less than about 5 e.u., being miscible together regardless of the difference in the molecular shape, and show much larger plastic flow than the ordinary crystals. This kind of crystal usually undergoes phase transition with much larger entropy change than that at the melting point and the phase just below the melting point possesses a peculiar nature such as that mentioned above. Since then, a number of crystals were found to belong to this category. In general, most of these crystals were composed of more or less globular molecules and these molecules having methyl or methylene groups at the molecular peripheries are the typical case; i.e., $C(CH_3)_4$[2], $C(SCH_3)_4$[3], cyclohexane[4], $Be_4O(CH_3COO)_6$[6], camphor[6], etc. These kinds of molecules in the lattice are considered to be held together mainly by the weak van der Waals force in respect of the rather small heat of sublimation, and the molecules are characterized by the violent thermal motions such as statistical randomness of molecular orientation or, moreover, by such a factor as self-diffusion which was revealed by recent investigations with nuclear magnetic resonance absorption[7] or in other ways.

In the previous paper[8], the present authors and others have reported the results of preliminary investigations of the phase transition of hexamethyldisilane by thermal and X-ray methods and found that this material really belongs to the category of the plastic crystal. We have also published already the result of the investigation by use of the nuclear magnetic resonance method on the present crystal[9]. So, in the present paper we should like to confine ourselves to reporting mainly the results obtained by the thermal method.

Experimental

Material.—The hexamethyldisilane used in this investigation was prepared by the courtesy of Dr. Nozakura from hexachlorodisilane and the methyl Grignard reagent[10] and purified by

* Present address: Department of Physics, Osaka University, Nakanoshima, Osaka.

1) J. Timmermans, *J. chim. phys.*, **35**, 331 (1938).

2) J. G. Aston and G. H. Messerly, *J. Am. Chem. Soc.*, **58**, 2354 (1936); J. G. Powles and H. S. Gutowsky, *J. Chem. Phys.*, **21**, 1695 (1953).

3) H. J. Backer and W. G. Perdok, *Rec. trav. chim.*, **61**, 533 (1943); W. G. Perdok and P. Terpstra, ibid., **62**, 687 (1943); **65**, 493 (1946).

4) J. G. Aston, G. J. Szasz and H. L. Fink, *J. Am. Chem. Soc.*, **65**, 1135 (1943); E. R. Andrew and R. G. Eades, *Proc. Roy. Soc.* (*London*), **A216**, 398 (1953).

5) T. Watanabé, Y. Saito, *Nature*, **163**, 225 (1949); T. Watanabé, Y. Saito and H. Koyama, ibid., **164**, 1056 (1949); M. Momotani, S. Seki, H. Chihara and H. Suga, This Bulletin, **28**, 325 (1955).

6) A. H. White and S. O. Morgan, *J. Am. Chem. Soc.*, **57**, 2078 (1935); K. Schäfer and O. Frey, *Z. Elektrochem.*, **56**, 882 (1953).

7) E. R. Andrews, "Nuclear Magnetic Resonance", Cambridge Univ. Press, Cambridge (1955).

8) H. Suga, S. Seki, Y. Chatani and I. Taguchi, *Ann. Report Inst. Fiber Res.* (Osaka Univ.), 8, 51 (1954), (in Japanese); Y. Chatani, H. Suga and I. Taguchi, Annual Meeting of the Chemical Society of Japan, held at Tokyo, April, 1955.

9) T. Yukitoshi, H. Suga, S. Seki and J. Itoh, *J. Phys. Soc. Japan*, **12**, 506 (1957).

10) W. C. Schumb and C. M. Saffer, Jr., *J. Am. Chem. Soc.*, **61**, 363 (1939).

fractional distillation under ordinary pressure, b.p. 112.8~113.0°C. After repeated fractional crystallizations, the sample obtained was finally purified by vacuum distillation, m. p. 14.2~14.4°C. It has been found in the course of purification that this crystal showed remarkably the so-called "vapor snake" phenomenon[11] which seemed to be characteristic of the crystal having low heat of fusion and high triple-point pressure.

Procedure and Apparatus.—For the reaffirmation of the occurrence of the phase transition, the method of the differential thermal analysis (DTA) was employed by using alumina powder as a reference substance. The sample was distilled into a DTA test tube and then sealed off in vacuo. After cooling down to the liquid nitrogen temperature, the sample was heated at a nearly constant rate 0.75°C/min. The apparatus was similar to that[12] used hitherto in our laboratory except for the automatic controller device for the constant heating rate with the reference substance and also the automatic recording of the temperature difference between the sample and the reference substance. The details of the automatic controller and recorder will be reported elsewhere in the near future. In order to determine the accurate temperatures and enthalpy changes associated with the polymorphic transition and fusion, respectively, the heat capacity was determined over the temperature range from −80 to +40°C with the conduction calorimeter which was the same one[13] used in our laboratory with a slight modification. The sample-containing cell was made anew of eighteen-carat gold plate with a wall thickness of 0.03 cm. and was approximately 2.5 cm. in height and 1.5 cm. in diameter. Eight radial fines of thin platinum sheet were silver-soldered inside the calorimeter to aid in establishing good heat distribution. In order to ensure thermal equilibrium, the heating rate employed was 0.25~0.30°C/min. except for around the transition and fusion points where a much slower heating rate was necessary. The vapor pressure measurements were carried out below and above the melting point of this crystal by using a simple glass-made mercury manometer with a sufficiently degassed sample.

Results and Discussion

Fig. 1. gives the result of the differential thermal analysis. The heat effect accompanied by the phase transition (at about −52°C) was three times as large as that corresponding to the fusion and consistent with the previous preliminary result[8]. The high temperature phase looks uniformly transparent, to a glassy mass, and always accompanies the vapor snake phenomenon as far as the air is absent. The microscopic observation indicates that this phase is optically isotropic. On cooling this phase, it is observed to be converted into a polycrystalline, opaque mass at the transition point where the appearance of the birefringence was observed under the microscopic observation.

The heat capacity data are tabulated in Table I and their variation with temperature is plotted in Fig. 2. Table II gives enthalpy and entropy changes accompanying the transition and fusion processes, respectively. In order to determine the true melting point of hexamethyldisilane and also to test the amout of impurity

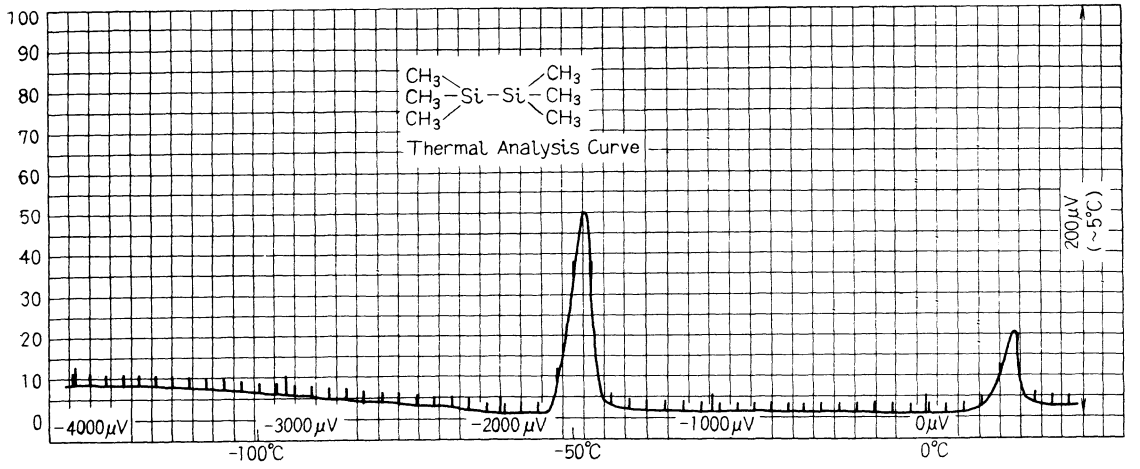


Fig. 1. Automatic recording curve of the differential thermal analysis for hexamethyldisilane.

11) S. Seki, *Science [Japan]* (*Kagaku*), **18**, 277 (1948); M. K. Phibbs and H. I. Schiff, *J. Chem. Phys.*, **17**, 843 (1949); F. C. Frank, ibid., **18**, 231 (1950); S. Seki, ibid., **18**, 397 (1950); R. Verschingel and H. I. Schiff, ibid., **22**, 723 (1954).

12) H. Chihara and S. Seki, This Bulletin, **26**, 88 (1953).

13) I. Nitta, S. Seki and M. Momotani, *Proc. Japan Acad.*, **26**·9, 25 (1950); S. Seki, M. Momotani, K. Nakatsu and T. Ōshima, This Bulletin, **28**, 411 (1955).

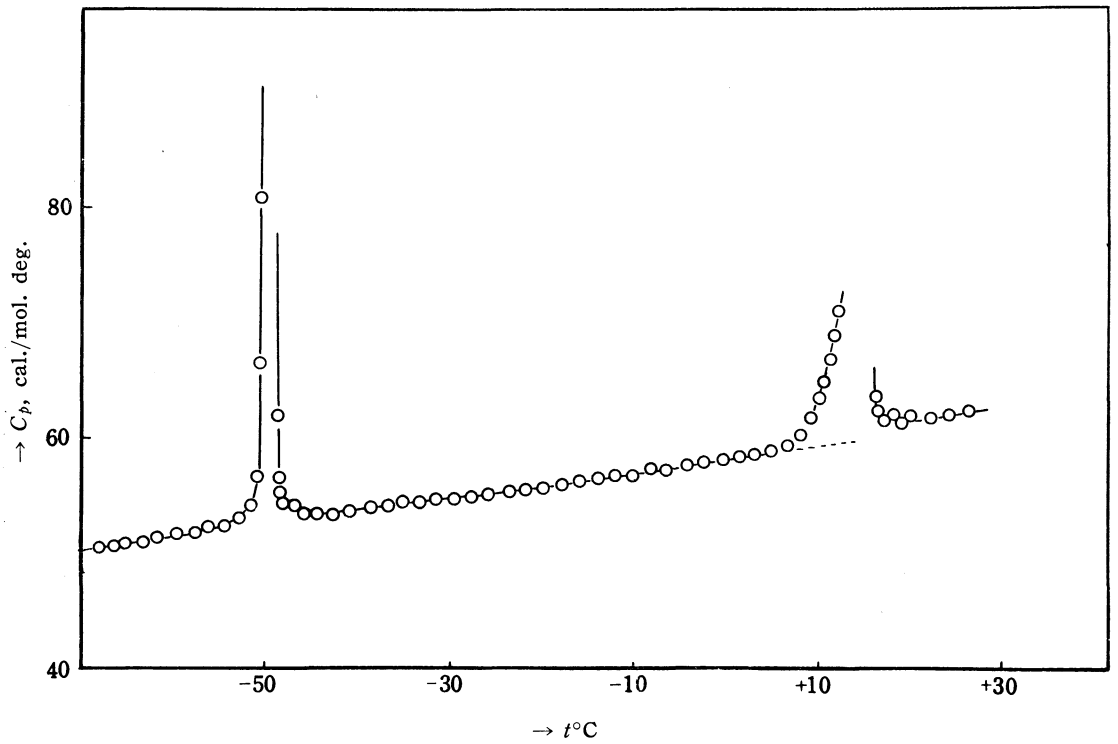


Fig. 2. Heat capacity of hexamethyldisilane as a function of temperature.

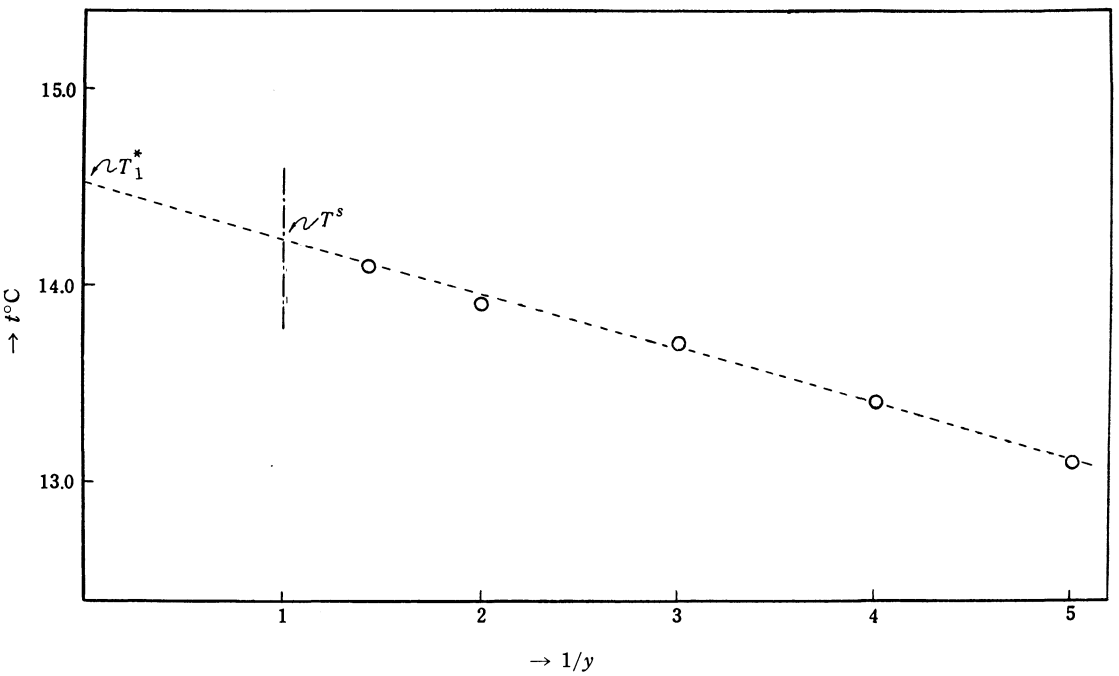


Fig. 3. Plot of the temperature of the liquid-solid equilibrium for hexamethyldisilane as a function of the reciprocal of the fraction of sample melted. T^s is the m.p. of the actual sample, and T_1^* is the m.p. of an absolutely pure sample.

TABLE I. C_p OF HEXAMETHYLDISILANE AS A FUNCTION OF TEMPERATURE

t°C	C_p (cal./mol. deg.)	t°C	C_p (cal./mol. deg.)
−66.96	50.76	−21.36	55.10
−63.42	50.46	−18.13	55.08
−61.21	51.40	−12.76	55.45
−57.18	52.21	−10.07	55.58
−55.30	52.27	− 7.59	55.69
−54.39	52.66	− 4.41	56.26
−53.49	53.33	− 1.21	56.64
−52.87	53.77	2.91	58.12
−52.58	62.16	5.28	61.45
— transition —		8.42	66.68
−49.37	74.67	11.39	96.30
−48.13	53.88	12.55	141.32
−47.39	52.96	— fusion —	
−44.70	53.49	16.71	60.19
−41.11	53.61	17.70	61.41
−38.20	53.79	19.22	60.84
−34.39	53.74	21.78	61.44
−30.09	54.27	22.52	61.16
−26.23	54.64		

TABLE II. TEMPERATURES, ENTHALPIES AND ENTROPIES OF TRANSITION AND FUSION OF HEXAMETHYLDISILANE

	T°K	ΔH (cal./mol.)	ΔS(e. u.)
Transition	221.8	2330	10.5
Fusion	287.7_2	721	2.51

involved in the used sample, the well-known thermodynamic equation[14]

$$T = T_1^* - (\boldsymbol{R}T_1^{*2}/\Delta H_f)(N/y)$$

was used. Here, T and T_1^* are the apparent and true melting points of the material, respectively; $\boldsymbol{R}$, gas constant; ΔH_f, the enthalpy of fusion; N, the number of moles of impurity; and y, the number of moles of material melted. Fig. 3 represents a plot of equilibrium temperatures against the various amounts melted. As is shown, the observed T versus $1/y$ relationship gives a straight line whose slope makes it possible to determine the value of N, by using the measured value of ΔH_f. As the result, we have determined the true melting point of hexamethyldisilane to be 14.5_6°C and the purity of the sample was 99.87% pure (the m. p. reported in the literature is 14.0~14.4°C[15]).

Table III gives the vapor pressure data of the liquid and solid states. The observed values in the liquid range are in good agreement with those of Brockway and Davidson[15]. By applying the method of least squares, good linear relations are obtained between $\log P$ and $1/T$ in both phases. The table also includes the changes of free energy, enthalpy and entropy accompanying the vaporization and sublimation processes, respectively. As the difference between the heat of vaporization and of sublimation, one can obtain the heat of fusion 697±41 cal./mol. which agrees within their experimental errors with the calorimetric value mentioned above.

We summarize in Table IV the entropies

TABLE III. VAPOR PRESSURE DATA OF HEXAMETHYLDISILANE IN THE SOLID AND LIQUID STATES

Solid state		Liquid state	
T°K	P, mmHg	T°K	P, mmHg
274.52	7.648	287.62	16.546
275.27	7.917	289.45	18.286
279.14	10.179	291.87	20.850
280.51	11.075	294.34	23.758
282.04	12.190	296.78	26.884
283.61	13.405	299.32	30.664
284.34	14.867	301.54	34.124
286.56	15.831	303.01	36.830
		304.19	38.940
		307.09	44.853
		310.39	52.037

$\log P = -2105.37/T + 8.550$ (in the solid state)

$\log P = -1953.12/T + 8.011$ (in the liquid state)

	ΔH(cal./mol.)	ΔS (e. u.)	$\Delta G^0_{298.16}$
Sublimation	9640±25	25.96±0.17	1900±76
Vaporization	8943±16	23.49±0.05	1940±32
Fusion	697±41 (obsd. 721)		

TABLE IV. ENTROPIES OF TRANSITION AND FUSION OF HEXAMETHYLDISILANE AND ALSO OF RELATED COMPOUNDS AVAILABLE FOR COMPARISON

	$Si_2(CH_3)_6$[a]	Si_2F_6[b]	$C_2(CH_3)_6$[c]	C_2F_6[d]	C_2Cl_6[e]
ΔS_{tr}	10.5	—	3.13	8.59	1.93 5.70
ΔS_f	2.51	13.8	4.82	3.71	5.50
ΔS_{total}	13.0	13.8	8.0	12.3	13.1

a) Present study.

b) The values were quoted from F. D. Rossini et al., "Selected values of Chemical Thermodynamic Properties", U.S. Government Printing Office, Washington (1952).

c) D. W. Scott and H. M. Huffman, *J. Am. Chem. Soc.*, 74, 883 (1952). Recent dilatometric observation revealed another instance of polymorphism near the m. p. [W. F. Seyer, R. B. Sennet and F. C. Williams, *J. Am. Chem. Soc.*, 71, 3447 (1949)].

d) S. Seki and M. Momotani, This Bulletin, 23, 30 (1950).

14) For example, S. Seki, *Japan Analyst (Bunseki Kagaku)*, 6, 737 (1957).

15) L. O. Brockway and N. R. Davidson, *J. Am. Chem. Soc.*, 63, 3287 (1941).

of the transition and of the fusion of the present substance together with those of the related compounds. As is evident for all compounds except for C_2Me_6, the sum of both entropies of the transition and fusion is nearly equal to 13.0 e. u., the value predicted from the Walden rule[16], which holds for the entropy of fusion of usual organic compounds. Accordingly, the transition phenomenon of these compounds may be reckoned as the beginning of the melting process. In other words, the total amount of entropy change which ordinarily should be gained at the melting point is divided between the transition and the melting processes. In the case of hexamethyldisilane, the observed entropy of fusion is very close to the value 2.0 e. u. calculated theoretically for a communal entropy of fusion[17], which comes from the communal sharing of free volume in the liquid state. Considering the reverse (freezing) process, it may be reasonable to infer that the liquid of hexamethyldisilane freezes only with respect to the translational motion** of the molecule at the freezing point and does not do so with respect to the rotational or orientational motion until the transition point is reached. And, even at the transition point, it seems that the stopping of the rotational motion of the methyl group about the Si–C axis does not take place yet. This is because the sum of the entropies of fusion and of transition for hexamethyldisilane is almost equal to that for hexachlorodisilane which is isoelectronic with the former and possesses no corresponding rotational group. This thermodynamical conclusion coincides with the result obtained from the nuclear magnetic resonance experiment[9] which revealed that the rotational motion of the methyl group about the Si–C axis was already excited even at temperatures far below the transition point.

In the X-ray investigation[8] of hexamethyldisilane, it was found that the high temperature phase belongs to body-centered cubic lattice with the cell constant of 8.47Å (at 0°C) containing two molecular units and that the molecular axis (Si–Si axis) is orientated randomly among the four body-diagonals. The observed reflection lines were also interpreted semi-quantitatively by assuming a D'_{3h} model (internal free rotation about the Si–Si axis), or alternatively assuming either a D_{3d} or a D_{3h} model combined with overall rotation of the molecule about the molecular axis, by using the value 18 for the temperature factor in all cases. On the other hand, the crystal structure of the low temperature phase was not yet determined, owing to the difficulty of preparing a single crystal available for the X-ray analysis (it may be hexagonal or orthorhombic crystal system[8]). The anomalously large value of the temperature factor in the high temperature phase is qualitatively in accordance with the large value of the entropy of transition. In passing it may be added here that the studies of Raman and infrared spectra[18] of hexamethyldisilane revealed that the molecule in the liquid state has a D_{3h} or a D'_{3h} equilibrium configuration, excluding a D_{3d}-type.

Now, we shall infer from the entropy consideration what sorts of molecular motions will be excited on passing through the transition point from the ordered low-temperature phase to the plastic crystal phase. Referring to the results of X-ray and spectroscopic investigations mentioned above, the following model may be assumed reasonably. In the high temperature phase, the molecular orientation (motion 1) is randomly distributed among the four body-diagonals and the two kinds of internal rotation (motion 2, about Si–Si axis ; motion 3, about Si–C axis) combined with the overall molecular rotation about the molecular axis (motion 4) are fully excited, whereas the motions are highly hindered except for motion 3 in the low temperature phase though not so below the transition point[9]. Then each contribution from the enhancement of such a kind of motion to the entropy of transition can be estimated in terms of statistical mechanics. The contribution from the increase of the orientational freedom (motion 1) is $R \ln 4$ which amounts to 2.54 e. u. The contribution from motion 2 is calculable by use of Pitzer's table[19], assuming the symmetry number 3 and the potential barrier hindering the internal rotation in the low temperature phase 5.7 kcal./mol.[9] In this case, the moment of inertia is computed

** It may be noted that even in the plastic crystal phase a kind of self-diffusion process seems to occur (see Ref. 9).

16) P. Walden, *Z. Elektrochem.*, **14**, 763 (1908).

17) H. Eyring and J. Hirschfelder, *J. Phys. Chem.*, **41**, 249 (1937).

18) C. C. Cerato, J. L. Lauer and H. C. Beachell, *J. Chem. Phys.*, **22**, 1 (1954). H. Murata and S. Kumada, ibid., **21**, 945 (1953); H. Murata and K. Shimizu, ibid., **25**, 1968 (1955).

19) K. S. Pitzer, *J. Chem. Phys.*, **5**, 469 (1937); K. S. Pitzer and W. D. Gwinn, ibid., **10**, 428 (1942).

using tetrahedral angle for ∠Si–Si–C and the interatomic distance of Si–C, 1.88 Å[20], and also assuming that the three rotating hydrogen atoms in methyl group lie at the position of the carbon atom. This contribution amounts approximately to 2.58 e. u. The sum of both entropies, 5.1 e. u., is only half of the observed entropy of transition, 10.5 e. u., so the remaining contribution from motion 4 seems to amount to nearly equal magnitude. Although the precise estimation of the latter is difficult at the present stage owing to the lack of knowledge about the crystal structure of the low temperature phase and also about the heights of the potential barrier hindering this motion in both phases, we assume tentatively that the rotation is fully excited in the high temperature phase whereas the motion is entirely fixed in the low temperature phase. Then the contribution can be calculated with the following equation

$$\Delta S = \boldsymbol{R}\left[\ln\frac{1}{\pi\sigma}\left(\frac{8\pi^3 I_m \boldsymbol{k} T}{\boldsymbol{h}^2}\right)^{1/2} + \frac{1}{2}\right]$$

where I_m is the moment of inertia about the molecular axis, and σ the symmetry number. The calculated value becomes 5.50 e. u. with the values of $T=222$°K and $\sigma=3$. Thus, the calculated total amount of these three entropies, 10.6 e. u., comes out to be nearly equal to the observed one, 10.5 e.u. Here it may be noticed that we have not completely ignored the overall rotational motions about the other two principal axes, since these motions were partly involved already in motion 1. Probably this fortuitous agreement arises from the situation that the over-estimated entropy value of motion 4 might be canceled by the under-estimaton of motion 1.

In conclusion, we may say that although our discussion on the mechanism of the phase transition in hexamethyldisilane from the point of view of entropy is of semi-quantitative nature, its main feature was explained by combining our thermodynamical study with those of the X-ray crystal analysis and the nuclear magnetic resonance.

20) M. L. Huggins, *J. Am. Chem. Soc.*, **75**, 4123 (1953).

Summary

Measurements of the heat capacity (200~300°K) and the vapor pressure (274~310°K) were carried out covering the transition and melting points of hexamethyldisilane. The following results were obtained; T_{tr} 221.8°K, ΔH(transition) 2330 cal./mol., ΔS(transition) 10.5 e. u.; T_f 287.7$_2$°K, ΔH(fusion) 721 cal./mol., ΔS (fusion) 2.51 e. u.; vapor pressure equations,

$$\log P(\text{mmHg}) = -2105.4/T + 8.5503 \quad (274.5\sim286.6\text{°K})$$

$$\log P(\text{mmHg}) = -1953.1/T + 8.0105 \quad (287.6\sim310.4\text{°K});$$

ΔH_{sub} 9640±25 cal./mol., ΔS_{sub} 26.0±0.17 e.u., $\Delta G°_{298.16}$(sub.) 1900±76 cal./mol.; ΔH_{vap} 8943±16 cal./mol., ΔS_{vap} 23.5±0.05 e. u., $\Delta G°_{298.16}$(vap.) 1940±31 cal./mol.

These data showed that the present crystal belongs to the class of plastic crystal. We have discussed the qualitative nature of the phase transition in the present crystal from the point of view of entropy, referring to the X-ray and the nuclear magnetic resonance studies. The remarkable "vapor snake" phenomenon was also observed on this material.

In conclusion, the authors wish to express their sincere thanks to Professor I. Nitta for his valuable advice and continued interest in the present study. The cost of this research has been defrayed from the Scientific Research Encouragement Grant from the Ministry of Education to which the authors' thanks are due.

Department of Chemistry
Faculty of Science
Osaka University
Nakanoshima, Osaka

*Stereoregular Polymers. I. Polymerization of Styrene by Triethylaluminum-Titanium Tetrachloride Catalysts**

By Shunsuke MURAHASHI, Shun'ichi NOZAKURA, Masao SUMI and Kōichi HATADA

(Received November 17, 1958)

Much information is now accumulating in regard to the isotactic polymerization of α-olefins. In particular, the reports of Natta and his collaborators[1] are very instructive about the mechanisms of stereospecific polymerization of propylene. These experiments, however, are mainly based on the heterogeneous catalysts composed of triethylaluminum ($AlEt_3$) and titanium trichloride ($TiCl_3$) (Natta's type). Catalysts derived from $AlEt_3$ and $TiCl_4$ (Ziegler's Type) have not been examined in detail mainly because of their poor reproducibility. Recently, Yamazaki has reported some aspects of polymerization of styrene with this type of catalysts[2].

The authors carried out the polymerization of styrene with the heterogeneous catalysts prepared from $AlEt_3$ and $TiCl_4$, and found that the stereospecificity of the catalysts varied very much with the method of preparation of catalytic mixtures.

The object of the present work is to investigate the relationship between property and stereospecificity of the catalysts.

Results and Discussion

Effect of Preparative Conditions of Triethylaluminum-Titanium Tetrachloride Catalysts upon the Stereospecificities of the Catalysts.— Even in the catalysts of the same ratio of $AlEt_3$ to $TiCl_4$ the stereospecificities of the catalytic mixtures varied intensively according to the method of mixing the two components. Some of the experimental data are listed in Table I.

When $AlEt_3$ and the monomer were charged before the introduction of $TiCl_4$, the stereospecificity was very low, and this is probably due to the cationic polymerization with $TiCl_4$. There was only a small difference between two kinds of catalysts that were prepared under the reverse orders of addition of $AlEt_3$ and $TiCl_4$. A very pronounced effect was observed when the catalysts were prepared with or without stirring. In some cases ultrasonic wave was applied in order to effect an efficient agitation. The catalyst that was prepared without stirring had an appearance of solid mass and was colored orange-brown. Such a catalyst yielded a high stereospecificity. When, on the other hand, the catalyst was prepared under mixing, it was a fine black powder and showed a poor stereospecificity. An explanation for this difference will be given later.

Influence of the Ratio of Triethylaluminum to Titanium Tetrachloride. — Preparation of catalysts and polymerization were carried out under stirring by magnetic stirrer. Yields of the atactic and the isotactic polystyrene polymerized on varying the ratios of $AlEt_3$ to $TiCl_4$ are shown in Fig. 1.

The yield of atactic polystyrene decreased rapidly up to the molar ratio (r) of unity and remained almost constant at

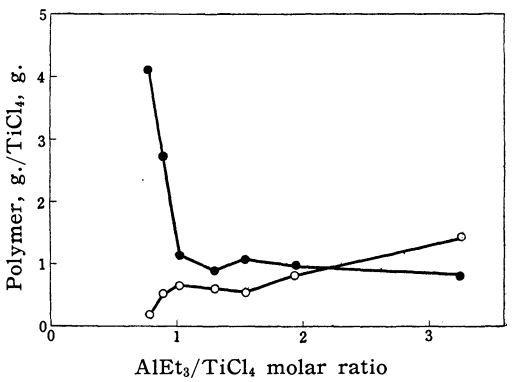


Fig. 1. Polymerization of styrene with Ziegler catalysts.
○ Isotactic polystyrene
● Atactic polystyrene

* Part of this work was presented at the 10th Meeting of the Chemical Society of Japan, Tokyo, April 6, 1957.

1) G. Natta, I. Pasquon and E. Giachetti, *Angew. Chem.*, **69**, 213 (1957); *Makromol. Chem.*, **24**, 258 (1957).

2) N. Yamazaki, *Chem. of High Polymers* (*Kōbunshi Kagaku*), **15**, 49 (1958).

TABLE I. POLYMERIZATION OF STYRENE WITH $AlEt_3$-$TiCl_4$ CATALYSTS PREPARED UNDER VARIOUS CONDITIONS

$TiCl_4$ 0.20 g., *n*-Heptane 15 ml.
$AlEt_3$ 0.36 g., Styrene 5.00 ml.

No.	Preparation of catalysts		Temp., °C	Time, hr.	Conversion, %	Insoluble part in M.E.K., %[c]
	The order of addition	Agitation				
1	Monomer-$AlEt_3$-$TiCl_4$	Stirring[a]	70	4	27.4	23
2	$AlEt_3$-$TiCl_4$-Monomer	Without stirring	70	3	28.0	84
3	〃	Without stirring	15	3	5.2	66
4	〃	Stirring	70	4	15.8	60
5	〃	Stirring and ultrasonic wave[b]	70	4	18.4	39
6	$TiCl_4$-$AlEt_3$-Monomer	Without stirring	70	4	19.5	81
7	〃	Stirring	70	4	7.9	64
8	〃	Stirring and ultrasonic wave[b]	70	4	13.3	4.4

a) Stirring was carried out by a magnetic stirrer.
b) After mixing by a magnetic stirrer, ultrasonic wave (450 KC, ca. 2W./cm^2) was applied for about ten minutes.
c) The percentage fraction of extraction residue with hot methylethylketone in total polymer.

increasing ratios. On the other hand, the yield of isotactic polymer showed a small but gradual increase over the whole range examined.

The high content of atactic polymer that was formed in a condition $r<1$ may reasonably be ascribed to the existence of remaining $TiCl_4$. Furthermore, the appearance of a break on the atactic curve in Fig. 1 seems to indicate the disappearance of $TiCl_4$ and the appearance of another kind of catalyst which also promotes the atactic polymerization of styrene with minor activity, and this kind of catalyst may probably be soluble complex compounds containing titanium and aluminum.

Valency States of Titanium in Catalytic Mixtures.—The reaction between $AlEt_3$ and $TiCl_4$ may be considered to be analogous to that of Grignard's reagent on alkyl orthotitanate[3]. Therefore, the reaction scheme may be written in the following manner:

Alkylation (fast)

$$Et_3Al+TiCl_4\rightarrow EtTiCl_3+Et_2AlCl \quad (1)$$

$$Et_3Al+EtTiCl_3\rightarrow Et_2TiCl_2+Et_2AlCl \quad (2)$$

Decomposition (slow)

$$EtTiCl_3\rightarrow Et\cdot+TiCl_3 \quad (3)$$

$$Et_2TiCl_2\rightarrow 2Et\cdot+TiCl_2 \quad (4)$$

The alkylation reaction may be fast and the decomposition which yields titanium of lower valencies may be comparatively slow.

3) D. F. Herman, W. K. Nelson, *J. Am. Chem. Soc.*, 75, 3877,3882 (1952).

In order to elucidate the results obtained above, the distribution of the valency states of titanium in catalysts was examined. When $AlEt_3$ and $TiCl_4$ was mixed to produce a heterogeneous catalyst, a gas evolved. According to the gas chromatographic analysis, the gas consisted of a large portion of ethane and small portions of butane and hydrogen. Ethane might be derived from the disproportionation reaction of ethyl radical which occurred in reactions 3 and 4. Ethylene, which is another procuct of disproportionation, was not found. It probably had polymerized in this condition.

On the other hand, the gas, which evolved when the solid catalyst was decomposed by dilute sulfuric acid, was found to be composed mainly of ethane and hydrogen, a small amount of butane, and a trace of ethylene. Ethane might be derived from the hydrolysis of ethyl-metal bond in the catalyst mixture. Hydrogen can be assumed to evolve according to the following reaction[3]:

$$Ti^{2+}+H_2O\rightarrow Ti^{3+}+\frac{1}{2}H_2+OH^- \quad (5)$$

Therefore, the amount of hydrogen was measured volumetrically by absoption with colloidal palladium and one mole of hydrogen was assumed to be equivalent to two moles of divalent titanium. The total trivalent titanium in the hydrolyzate was then determined by redox titration with ceric sulfate. The results are given in Table II. As expected, the catalyst which was prepared in a condition $r=1$

TABLE II. VALENCY STATES OF TITANIUM IN SOLID CATALYSTS

The catalysts were prepared at 70°C in 15 ml. of *n*-heptane from 0.37 g. of $AlEt_3$ and the appropriate amount of $TiCl_4$.

$AlEt_3/TiCl_4$ molar ratio	Preparation of catalyst	Gas evolved		Ti(IV) %	Ti(III) %	Ti(II) %
		When catalyst was prepared, ml.	When catalyst was decomposed, ml.[c]			
1.09	Stirring[a]	41	65	2	98	0
2.44	Stirring[a]	30	116	0	35	65
2.74	Stirring[a]	30	113	0	23	77
2.51	Without stirring[b]	13	133	4	80	16

a) $TiCl_4$ and $AlEt_3$ were added in this order under stirring by a magnetic stirrer.
b) Catalyst components were added in the order of $AlEt_3$ and $TiCl_4$ without stirring.
c) Decomposition was carried out about half an hour after preparation of the catalyst, when evolution of gas had almost entirely ended.

TABLE III. POLYMERIZATION AFTER WASHING THE SOLID CATALYSTS

Styrene (5.00 ml.) was polymerized for 3.0 hr. at 70°C without stirring.

No.	Preparation of catalyst[a]			$AlEt_3$ added after washing, g.	Conversion, %	Insoluble part in M.E.K. %
	$TiCl_4$, g.	$AlEt_3$, g.	Temp., °C			
1	0.44	0.33	70	0.33	28.7	91
2[b]	0.45	0.33	b. p. of *n*-heptane	0.34	33.3	90
3	0.45	0.13	b. p. of xylene[c]	0.33	27.3	92
4	0.40	0.33	b. p. of *n*-heptane	0	79.4	Trace
5	0.23	0.33	b. p. of *n*-heptane	0	45.5	17
6[d]	0.44	0.32 0.32	b. p. of *n*-heptane	Without washing	32.7	86
7[e]	0.44	0.67	70	0.32	2.4	65

a) Generally heterogeneous catalysts were prepared in 15 ml. of *n*-heptane under stirring by a magnetic stirrer. $TiCl_4$ and $AlEt_3$ were added in this order.
b) Polymerization time was 3.2 hr.
c) Xylene wae used as solvent for preparing the catalyst. The catalyst was washed with *n*-heptane as usual, and then the polymerization was carried out in *n*-heptane.
d) $AlEt_3$ (0.32 g.) was added dropwise into the solution of $TiCl_4$ at the boiling temperature of *n*-heptane and the mixture was refluxed for ten minutes and kept for one hour at room temperature, and then the remaining half (0.32 g.) of $AlEt_3$ and monomer was added at 70°C.
e) The order of adding two components was reversed. Into 0.67 g. of $AlEt_3$ was added $TiCl_4$ rapidly under stirring at 70°C and the black, fine precipitate was washed with *n*-heptane and the polymerization was carried out as usual with the secondary addition of $AlEt_3$ and monomer.

contained a small amount of tetravalent titanium, which is responsible for a relatively large amount of atactic polymer. The catalyst, in which *r* is more than unity, was found to be mainly composed of divalent and trivalent titanium. The reduction of titanium over trivalent state does not seem to have a marked effect upon stereospecificity. In fact, the catalyst that was prepared without agitation, although it included a certain amount of tetravalent titanium and a large amount of trivalent titanium, showed a good stereospecificity and a good catalytic activity.

Influence of Washing the Solid Catalyst.—In order to remove the soluble catalysts which were considered to be responsible for the atactic polymerization, catalyst mixtures were washed with *n*-heptane by decantation and then polymerizations were carried out with or without addition

of further $AlEt_3$. Experimental data are summarized in Table III.

Without the secondary addition of $AlEt_3$ after washing only amorphous polystyrene was obtained, while with its addition the catalyst acquired a very high stereospecificity and also good catalytic activity. However, when $TiCl_4$ was reduced gradually by an equivalent amount of $AlEt_3$ and then an additional equivalent amount of $AlEt_3$ and styrene was added, a good result was obtained (Table III, No. 6).

The catalyst which was prepared by adding $TiCl_4$ to 2.5 times on molar base of $AlEt_3$ under stirring showed a very poor catalytic activity even after washing (Table III, No. 7).

The results seem to suggest the importance of the physical nature of solid catalyst. This subject will be discussed in detail in the later part of this paper.

Recently similar experiments were described in a patent publication where the catalyst was filtered through a glass filter and the effect of filtration was explained there to be due to the removal of the finely dispersed parts of the catalyst[4].

X-ray Study of Solid Catalysts.—The solid catalysts, which were prepared in similar manners to those of Tables I and II, were washed with *n*-heptane and sealed in a small ampoule with a thin wall (Fig. 2), and then exposed to X-ray. It was found in general that the more stereospecific and active catalyst showed the sharper diffraction pattern. X-ray photographs of the catalysts prepared under various conditions are shown in Fig. 3. In the case of the catalyst that was prepared by dropping $TiCl_4$ quickly into the solution

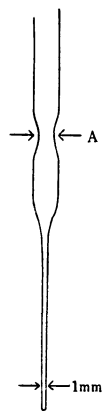


Fig. 2. A capillary ampoule for the X-ray study.

4) S. G. Montecatini and K. Ziegler, Irish Pat., 66,855 (1955).

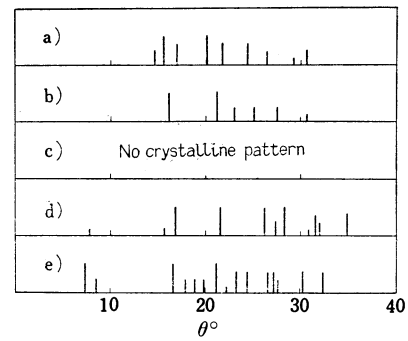


Fig. 3. X-ray powder patterns of catalytic masses (CuKα radiation).
a) $TiCl_4$ (1 mol. equivalent) was added into $AlEt_3$ (2.3 mol. equivalents) at 70°C without agitation.
b) $AlEt_3$ (1 mol. equivalents) was added to $TiCl_4$ 1 mol. equivalent) at 70°C under agitation.
c) $AlEt_3$ (2.3 mol. equivalents) was added quickly into $TiCl_4$ (1 mol. equivalent) at 70°C under agitation.
d) $TiCl_3$, the product of Stauffer Chem. Co.
e) $TiCl_2$[6].

of 2.5 mol. equivalents of $AlEt_3$ at 70°C under agitation, there was found no crystalline reflection but a diffuse halo. Such a catalyst had a poor stereospecificity and catalytic activity.

On the contrary, when either (a) 1 mol. equivalent of $TiCl_4$ was added into 2.4 mol. equivalents of $AlEt_3$ without agitation or (b) 1 mol. equivalent of $AlEt_3$ into the solution of 1 mol. equivalent of $TiCl_4$ under agitation, the solid mass showed moderately crystalline reflections. These reflections are rather diffuse as compared with that of commercial $TiCl_3$, indicating an imperfect growth of the crystals. The reflections coincide with neither that of $TiCl_3$[5] nor that of $TiCl_2$[6]. This fact might suggest the existence of some crystalline complex compound containing Al and Ti or another modification of $TiCl_3$ and $TiCl_2$[7].

The solid mass prepared by method a showed a good stereospecificity and catalytic activity. But in the case of the catalyst b, also good results were obtained

5) W. Klemm and E. Krose, *Z. anorg. u. allgem. Chem.*, **253**, 218 (1947).
6) M. Farber, A. J. Darnell and F. Brown, *J. Chem. Phys.*, **23**, 1556 (1955).
7) F. Böck and L. Moser, *Monatsch.*, **34**, 1825 (1913). The existence of two modifications of $TiCl_3$ was first suggested by Böck and Moser in the study of the heat of solution. Two kinds of $TiCl_3$ were described by them to be violet colored and brown. The violet is the one that is obtaind by reduction of $TiCl_4$ at high temperture and is now available commercially.

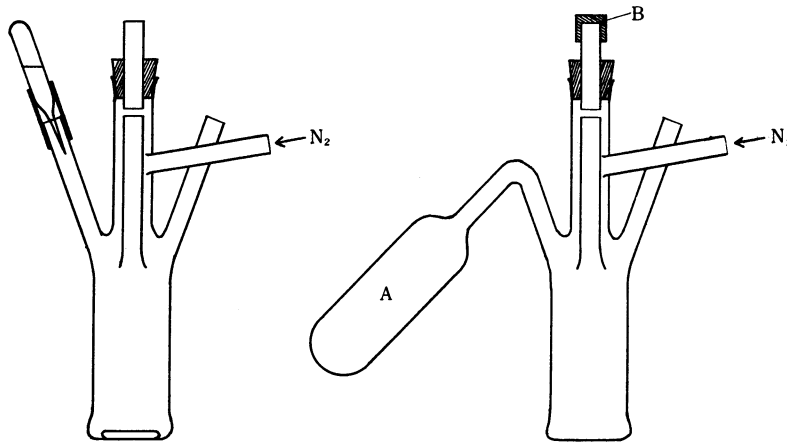


Fig. 4. Vessels for the polymerization.

by washing with *n*-heptane. (Table III, No. 1—3). Although both the catalysts (a and b) gave the crystalline patterns, they showed some differences in details of X-ray diagram. Further study of this point would be necessary, but was not pursued.

Conclusion

Titanium tetrachloride, ethylaluminum chlorides, soluble aluminum-titanium complex compounds, and amorphous insoluble solid are conceivable for the formation of atactic polymer. Titanium tetrachloride is the one that remained unreacted when the molar ratio of $AlEt_3$ to $TiCl_4$ did not exceed unity. The others are considered to be formed by the reaction between $AlEt_3$ and $TiCl_4$. Although the first three can be removed by washing with *n*-heptane, the last one can not.

The content of the crystalline component in solid mass depends upon the condition of reaction between $AlEt_3$ and $TiCl_4$. If the alkylation of $TiCl_4$ proceeded beyond the stage of $EtTiCl_3$ (or Et_2TiCl_2), the sufficient growth of the crystallites of the compound containing $TiCl_3$ (or $TiCl_2$) could not be expected. Moreover, it is a factor to be considered that some amorphous titanium compound would be produced if the alkylation of the unstable compound containing titanium chlorides occurred preferentially before the sufficient growth of crystallites was permitted.

In order to prepare a crystalline catalytic mass, therefore, it is preferable to use $AlEt_3$ in an amount not more than an equivalent of $TiCl_4$. As shown in the experiments, it may be a convenient method for obtaining a crystalline catalytic mass to combine the solutions of two reactants without agitation.

It is noteworthy that the crystalline component of the effective solid catalyst is neither $TiCl_3$ nor $TiCl_2$, and is probably some complex compound containing Al and Ti or the other modification of $TiCl_3$ (or $TiCl_2$). The fact seems to be one of the important differences between catalysts of Ziegler's type (i. e., $AlEt_3$ and $TiCl_4$) and Natta's type (i. e., $AlEt_3$ and $TiCl_3$).

Experimental

Meterials. — Commercial styrene was washed with 10% solution of sodium hydroxide and water, dried over calcium chloride, and distilled in a nitrogen stream before use[8].

n-Heptane was shaken with fuming sulfuric acid, washed with water and dilute alkali, dried over calcium chloride, distilled and stored over sodium chips.

$AlEt_3$ was the product of Mitsui Chem. Ind. Co. and was used as 30% solution in *n*-heptane. Concentration was checked by the amount of ethane evolved when the solution was hydrolyzed.

$TiCl_4$ was the product of Osaka Titanium Co. and used as 21% solution in *n*-heptane. The concentration was checked by determining titanium by redox titration with ceric solution after reduction with zinc amalgam.

Polymerization.—The polymerization vessel is shown in Fig. 4a. *n*-Heptane was placed in the vessel of about 100 ml. capacity and the ampoules of monomer, $TiCl_4$, $AlEt_3$, and a thermometer if necessary were mounted on it through rubber tubings. The air in the apparatus was replaced by dry nitrogen by repeated evacuation and introduction of nitrogen. Then the lower half

8) E. R. Blout and H. Mark, "Monomers", Interscience Publishers, Inc., New York (1949).

of the apparatus was immersed in the thermostat and the contents of the ampoules were dropped in by breaking the top of the ampoule which was previously scratched at the capillar part in order to ease the breaking.

Polymerization was stopped by the introduction of 2 ml. of methanol and 0.3 ml. of concentrated hydrochloric acid and then all the contents were poured onto a large amount of methanol. After standing overnight, the polymer was collected and washed with methanol, and dried.

If the washing of the solid catalyst with *n*-heptane was needed the vessel shown in Fig. 4b was used. The supernatant liquid was decanted into the side flask (A) and 15 ml. of *n*-heptane was injected through a silicone rubber cap (B). The decantation and the injection were repeated three times. The ampoule of $AlEt_3$ now emptied was exchanged with another one in the stream of nitrogen and charged, and then the monomer was dropped in.

Extraction of the Atactic Polymer from the Crude Polymer.—About 0.4 g. of polymer was refluxed with 40 ml. of methylethylketone for several hours. After standing overnight at room temperature, the remaining isotactic polymer was collected, washed with methylethylketone, dried in vacuo at 100°C.

Valency States of Titanium in Catalytic Mixtures.—A gas buret was connected to the reaction vessel of Fig. 4a and an ampoule containing 8 ml. of 10% sulfuric acid was mounted in place of styrene. After the mixing of the catalyst components, 30 to 40 min. was required for almost complete evolution of gas. The reaction vessel was cooled to 0°C and the gas in the vessel was replaced by nitrogen by repeated evacuation and filling. Then the catalyst mixture was hydrolyzed by dropping the aqueous sulfuric acid and the amount of the gas evolved was measured by the gas buret.

An aliquot of the mixed gas was analyzed for hydrogen using colloidal palladium as absorbent.

The hydrolyzed aqueous layer was separated from the organic layer in an atmosphere of carbon dioxide and analyzed for Ti(III) by titration with ceric standard solution using diphenylamine as an indicator. The amount of Ti(III) thus measured was taken as the sum of Ti(II) and Ti(III) in the catalyst mixture. Some of the results are given in Table III.

X-ray Study of Solid Catalyst—The solid catalytic mass was washed with *n*-heptane by decantation, and the slurry of catalyst was brought into a small thin-walled ampoule made of Terex glass (Fig. 2). All the operations were carried out in a nitrogen atmosphere. The ampoule was sealed at A. The solid powder was packed down to the bottom by a centrifuge and exposed to X-ray.

Summary

Styrene was polymerized by the heterogeneous catalysts of Ziegler's type which were prepared under various conditions. The important factors which have pronounced effects on the stereospecificity and the catalytic activity of the mixture are concluded to be the existence of the remaining titanium tetrachloride, ethylaluminum chlorides and some soluble aluminum-titanium complex compounds, and the crystalline nature of the solid catalytic mass. The first three are considered to be responsible for the atactic polymerization of styrene and can be removed by washing with *n*-heptane. The crystallinity of the solid catalyst seems to be necessary for its high stereospecificity and catalytic activity.

The solid catalyst was examined by X-ray. It was found that the crystalline component of the catalyst did not correspond to $TiCl_3$ or $TiCl_2$, and thus it was suggested that some crystalline complex compounds containing Al and Ti or some other modifications of $TiCl_3$ (or $TiCl_2$) would be responsible for the effective catalytic component of Ziegler catalyst. The authors also suggested that the fact might be one of the important differences between the heterogeneous catalysts of Ziegler's type and Natta's type.

The authors wish to thank Mitsui Chem. Ind. Co. for the generous supply of triethylaluminum and Osaka Titanium Co. for titanium tetrachloride. We are also very grateful to Mr. Y. Chatani of Nitta Laboratory who helped us in the experiment of X-ray.

Department of Chemistry
Faculty of Science
Osaka University
Nakanoshima, Osaka

Derivatives of 1,8(9)-p-Menthadien-10-yl-carbinol

By Kyoichi SUGA and Shoji WATANABE

(Received February 10, 1959)

In the previous paper[1], the preparation of a limonenylcarbinol and the determination of its structure as 1,8(9)-*p*-menthadien-10-yl-carbinol (I) were reported. The present paper describes various derivatives of the limonenylcarbinol.

When a mixture of I and paraformaldehyde was heated at 130~150°C for several hours, a pale yellow viscous oil was obtained. Analysis ($C_{12}H_{20}O_2$) and the molecular weight (192) indicated that the product was an adduct of one mole of formaldehyde to I. The presence of a primary hydroxyl group was proved by a qualitative analysis and an infrared absorption spectrum (9.6 μ). Quantitative acetylation with pyridine and acetic anhydride[2] showed that it was a monohydric alcohol. The infrared absorption spectrum showed characteristic absorption bands of the acetal type at 8.05, 8.6 and 9.0 μ (Fig. 1). From the above results, it was concluded that the structure of the substance is formaldehyde mono-1,8(9)-*p*-menthadien-10-yl-carbinyl acetal (II).

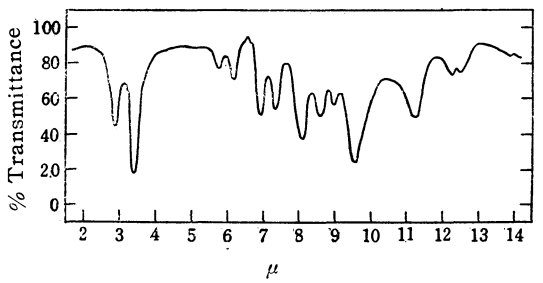


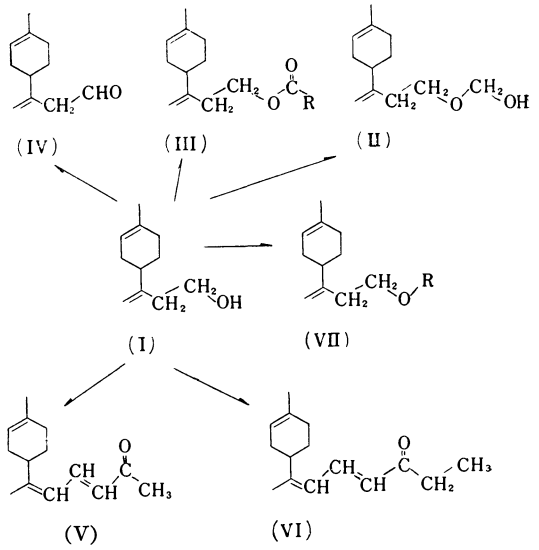
Fig. 1. Infrared absorption spectrum of II.

Various esters (III) were prepared from I. The monoesters of maleic acid, phthalic acid and succinic acid were prepared. The sodium salt of the acid maleate shows remarkable surface activity, and the foaming force is equal to that of the cetylsulfate (Table I). By the action of palmitoyl chloride, capryloyl chloride, isovaleryl chloride, phenylacetyl chloride and cinnamoyl chloride, I gave the esters of the corresponding acids (Table II). The caprylate and the phenylacetate are fragrant.

TABLE I. THE FOAMING FORCE OF SODIUM LIMONENYLCARBINYL MALEATE

%	Numbers of foams after (min.) 2	5	Quantities of foams after (min.) 2	5
Na limonenylcarbinyl maleate				
0.50	25.5	13.8	216	184
0.25	19.8	12.3	195	173
0.10	14.0	10.0	114	90
Na laurylsulfate (SO_3: 27.2%)				
0.24	7.4	2.2	857	852
0.15	8.4	2.7	758	753
Na cetylsulfate (SO_3: 22.1%)				
0.30	24.8	16.2	265	256
0.15	19.8	13.4	180	173

By the action of chromic anhydride in glacial acetic acid, a limonenylformaldehyde, 3-(4-methyl-3-cyclohexen-1-yl)-3-buten-1-al (IV) was obtained. Its odor is more fragrant than that of I. It gives positive reactions with Schiff's reagent and Tollen's reagent. The composition was confirmed from those of the 2,4-dinitrophenylhydrazone and semicarbazone.



1) K. Suga, J. Ishii and S. Watanabe, This Bulletin, 32, 711 (1959).

2) N. Sugiyama, "Micro Identification of Organic Compounds (Yukikagobutsu no Biryo Kakuninho)", Baifukan Co, Ltd., Tokyo (1957), p. 60.

TABLE II. MONO-BASIC ACID ESTERS OF THE LIMONENYLCARBINOL

	Refining procedure	Physical constants	Molecular weight Found	Calcd.
Palmitate	Chromatography	n_D^{19} 1.4794	378	404
Caprylate	Chromatography	n_D^{18} 1.4797 $[\alpha]_D^{15}$ +11.7	301	320
Isovalerate	Chromatography	n_D^{19} 1.4884	244	250
Phenylacetate	Vacuum distillation	n_D^{17} 1.5270 b. p. 150C°/4 mmHg $[\alpha]_D^{15}$ +26.0	279	284
Cinnamate	Chromatography	n_D^{11} 1.4822 $[\alpha]_D^{15}$ +15.1	290	296

TABLE III. LIMONENYLCARBINYL ETHERS

	Boiling point °C/mmHg	Refractive index	Specific gravity	Molecular refraction Found	Calcd.	Yield %
Methyl	85~86/12	n_D^{25} 1.4870	$d_4^{24.5}$ 0.9317	55.39	52.61	80
Ethyl	96~97/4~5	n_D^{23} 1.4921	d_4^{23} 0.9353	59.98	59.64	90
Allyl	115~118/17	n_D^{23} 1.4927	$d_4^{24.5}$ 0.9293	64.26	63.79	80
Benzyl	175~179/10	n_D^{23} 1.5300	d_4^{23} 0.9885	80.17	79.13	90

Action of a large excess of acetone and aluminum isopropoxide on I gave a limonenylmethyleneacetone, as a viscous oil with burning odor. The structure of 6-(4-methyl-3-cyclohexen-1-yl)-3,5-heptadien-2-one(V) was demonstrated as follows: The substance gave a 2,4-dinitrophenylhydrazone and a positive iodoform reaction, which showed that it was a methyl ketone. The major absorption peaks at 295 and 223 mμ in the ultraviolet spectrum (Fig. 2) suggested the presence of a conjugated dienone grouping.

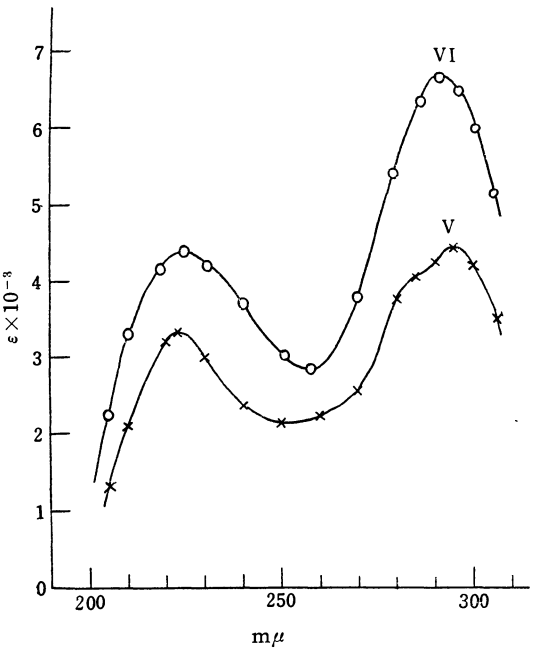


Fig. 2. Ultraviolet absorption spectra of V and VI.

Similarly, 7-(4-methyl-3-cyclohexen-1-yl)-4,6-octadien-3-one(VI) was prepared from I and methyl ethyl ketone. It is more viscous than V and also possesses a burning odor. The composition was confirmed by an elementary analysis of its 2,4-dinitrophenylhydrazone. It showed absorption peaks at 291 and 225 mμ (Fig. 2) corresponding to the conjugated dienone structure(VI). The iodoform reaction was negative.

Some ethers of I were also prepared. I was converted into the sodium compound by the action of sodamide in benzene. The ethyl limonenylcarbinyl ether VII ($R=C_2H_5$) was obtained in a yield of 90% from ethyl bromide and the sodium compound. Its ethoxyl radical was detected by Zeisel's method[3]. Similarly, methyl, ethyl, benzyl and allyl ethers were prepared (Table III).

Experimental

1,8(9)-*p*-Menthadien-10-yl-carbinol(I). — Prepared from *d*-limonene and paraformaldehyde as reported previously[1]: b. p. 102~106°C/4 mm.; d_4^{17} 0.9603; n_D^{17} 1.5020; $[\alpha]_D^{10}$+37.2; phenylurethan, m. p. 56~57°C.

Formaldehyde Mono-1,8(9)-*p*-menthadien-10-yl-carbinyl Acetal.—In a glass tube, 4 g. of I and 0.8 g. of paraformaldehyde were sealed and heated

3) R. L. Shriner, R. C. Fuson and D. Y. Curtin, "The Systematic Identification of Organic Compounds", 4th Ed., John Wiley & Sons, Inc., New York; Maruzen Co., Ltd., Tokyo (1956), p. 116.

at 150~170°C for 6 hr. By fractional distillation, 1.5 g. of II was given: b. p. 155~162°C/5 mm.; $n_D^{20.5}$ 1.5066; $d_4^{20.5}$ 1.0306; molecular refraction 56.64 (calcd. for $C_{11}H_{17}OCH_2OH$: F_2, 57.65); hydroxyl group, 6.03% (calcd. for monohydric alcohol, 8.68%); molecular weight, 192 (calcd. for $C_{12}H_{20}O_2$: 196.2).

Anal. Found: C, 72.17; H, 9.41. Calcd. for $C_{12}H_{20}O_2$: C, 73.40; H, 10.27%.

The Limonenylcarbinyl Monoesters of Dibasic Acids.—*1,8(9)-p-Menthadien-10-yl-carbinyl hydrogen maleate.*—A mixture of 2 g. maleic anhydride and 2 g. of I was heated at 100°C for 3 hr. The reaction mixture was thoroughly washed with water of 60°C, dried in vacuo, and 3 g. of a pale yellow monoester was obtained, n_D^{12} 1.4921. Molecular weight, 264.25[4] (calcd. for $C_{15}H_{20}O_4$: 264.2). The silver salt was prepared by adding silver nitrate solution to the sodium salt of the acid maleate.

Anal. Found: Ag, 29.75; Calcd. for $C_{15}H_{19}O_4Ag$: Ag, 29.08%.

The foaming force of the sodium salt solution was measured by Nakajima's method[5] (Table I).

Acid phthalate and acid succinate of I.—They were prepared similarly.

The Limonenylcarbinyl Esters of Monobasic Acids. — *1, 8(9)-p-Menthadien-10-yl-carbinyl palmitate.*—To a mixture of 1.5 g. of I and 20 cc. of anhydrous ether, a dry ethereal solution of 3.0 g. of palmitoyl chloride was added with stirring. The reaction mixture was left overnight at room temperature. The crude palmitate was extracted with ether and the extract was washed three times with 30% aqueous methanolic solution containing 5% potassium hydroxide, and several times with water, and dried over anhydrous sodium sulfate. The crude palmitate, obtained by evaporation of the solvent, was chromatographed on active alumina and the pale yellow part in the middle of the chromatogram was eluted with methanol. By removing the methanol, 2.0 g. of the palmitate was obtained.

Caprylate, phenylacetate and cinnamate.—They were prepared similarly (Table II).

3-(4-Methyl-3-cyclohexen-1-yl)-3-buten-1-al (IV).—To a mixture of 4 g. of chromic anhydride, 5 cc. of water and 100 cc. of glacial acetic acid, a mixture of 9 g. of I, 30 cc. of acetone and 20 cc. of glacial acetic acid was added in 25 min. at 50~55°C with vigorous agitation, and the mixture was stirred for 4.5 hr. Then this was poured into a large amount of water and extracted with ether. The extracts were washed with water and dried over anhydrous sodium sulfate. By fractional distillation, 3.5 g. of IV was obtained: b. p. 88°C/4 mm.; n_D^8 1.5045. It gave a positive reaction with Schiff's reagent and reduced an ammoniacal silver nitrate solution.

2, 4-Dinitrophenylhydrazone.—It was prepared as usual and recrystallized twice from a mixture of pyridine and methanol. Fine red crystals, m. p. higher than 220°C.

Anal. Found: N, 16.14. Calcd. for $C_{17}H_{20}O_4N_4$: N, 16.27%.

Semicarbazone.—A mixture of IV, semicarbazide hydrochloride, sodium acetate and methanol was allowed to stand for about a month, and the crystals produced were collected and recrystallized twice from methanol. Colorless needles, m. p. 192°C.

Anal. Found: N, 18.35. Calcd. for $C_{12}H_{19}ON_3$: N, 18.98%.

6-(4-Methyl-3-cyclohexen-1-yl)-3, 5-heptadien-2-one (V).—A mixture of 5 g. of I, 18.5 g. of aluminum isopropoxide, 150 g. of refined acetone and 150 g. of anhydrous benzene was refluxed for 40 hr. Then 300 g. of benzene was added to the reaction mixture, and the benzene solution was separated, washed with 30% sulfuric acid three times and with water several times, and dried over anhydrous sodium sulfate. After benzene was evaporated, 1.0 g. of V was obtained by fractional distillation: b. p. 125~133°C/3 mm.; n_D^{10} 1.5271; λ_{max} 295 mμ, ε 4480; λ_{max} 223 mμ, ε 3340. The substance gave a positive iodoform reaction.

2, 4-Dinitrophenylhydrazone.—This was prepared as usual and recrystallized from ethylacetate. Red needles, m. p. 179~180°C.

Anal. Found: N, 14.50. Calcd. for $C_{20}H_{24}O_4N_4$: N, 14.50%.

7-(4-Methyl-3-cyclohexen-1-yl)-4, 6-octadien-3-one (VI).—A mixture of 7 g. of I, 24 g. of aluminum isopropoxide, 200 g. of refined methyl ethyl ketone and 200 g. of dry benzene was refluxed for 60 hr. It was poured into 30% sulfuric acid and extracted with ether. The extracts were washed with water and dried over anhydrous sodium sulfate. By fractional distillation, 2.0g. of VI was obtained: b. p. 125~132°C/2 mm.; n_D^{23} 1.4806; λ_{max} 291 mμ, ε 6650; λ_{max} 225 mμ, ε 4340. It did not give a positive iodoform reaction.

2, 4-Dinitrophenylhydrazone.—This was prepared as usual and recrystallized twice from a mixture of ethyl acetate and ethanol. Red needles, m. p. 203°C.

Anal. Found: N, 14.11. Calcd. for $C_{21}H_{26}N_4O_4$; N, 13.99%.

The Ethers of the Limonenylcarbinol (VII).—*Ethyl 1, 8(9)-p-menthadien-10-yl-carbinyl ether* (R=C_2H_5).—To a benzene solution (100 cc.) of 4.3 g. of sodamide, 12.4 g. of I was added gradually at 60~65°C with vigorous agitation. When ammonia gas was no more generated, 13.3 g. of ethyl bromide was added in drops and the mixture was stirred for three hours. After leaving it overnight, the benzene solution was washed with water, and dried over anhydrous sodium sulfate. By fractional distillation 13.1 g. of VII was given.

Anal. Found: C, 80.04; H, 11.61. Calcd. for $C_{13}H_{22}O$: C, 80.34; H, 11.41%.

The ethoxyl radical was detected by Zeisel's method.

Methyl, benzyl and allyl ethers.—These were prepared similarly.

Absorption Spectra. — Infrared absorption spectra were measured by using a Perkin-Elmer spectrophotometer and ultraviolet absorption

4) It was measured by using 0.3971 N sodium hydroxide solution.

5) H. Nakajima, *J. Chem. Soc. Japan, Ind. Chem. Sec.* (*Kogyo Kagaku Zasshi*), **56**, 611 (1953).

spectra by a "Shimadzu" photometric spectrophotometer Type QB-50 using isopropyl alcohol as a solvent.

The authors are indebted to Mr. Michiaki Miura for technical assistance.

Department of Applied Chemistry
Faculty of Technology
Chiba University
Matsudo-shi, Chiba

Modified Bond Eigenfunction Method of Constructing Potential Energy Surface of Reaction. I. Theory and General Remarks

By Iwao YASUMORI

(Received February 28, 1959)

In order to evaluate the chemical reaction rates theoretically, it is necessary to know the detailed feature of the interaction potential between the reacting species, i. e., the potential energy surfaces of the reaction. These surfaces are formed, in principle, from the eigenvalues of the wave equation for all electrons in the system at all orientations of atomic nuclei. Because of mathematical difficulties, however, which are the same as those in the calculation of "molecular energy", it is extremely difficult to construct the surface with the required accuracy, e. g., 0.1 kcal.

This situation of the problem has been a main cause of the fact that there is no available method for this purpose except Eyring's semi-empirical one[1] which is based on London's formula. Also it has been frequently pointed out by several investigators[2] that this approximate procedure contains many inadequacies, for instance, neglect of non-orthogonality between the orbitals of different atoms, introduction of *s*-electron approximation disregarding the direction of valence and the arbitrary choice of coulombic fraction ρ, etc. Nevertheless, this method has the distinctive character of giving an interpolation formula utilizing the experimental bond energies of component species.

Based on the idea of making use of the observed data for the component species, Moffitt[3] recently developed the "atoms-in-molecules" method in the field of "molecular theory" and succeeded in improving the calculated energy values for oxygen, ethylene, allyl radical, etc. If we regard the reacting system as a "complex molecule" and take molecular species as components, instead of atoms in Moffitt's method, it is possible to develop the corresponding "molecules-in-molecules" or "modified bond eigenfunction" method of constructing potential energy surfaces[4].

According to this idea, the author presents an improved method which stands on a firm basis and has wider applicability. The outline of the method and remarks on its application are given in this paper. The practical application and the inspection of the availability of the method will be made in relation to the hydrogen atom-molecule reaction in the following paper[5].

Theory

Elementary chemical reaction

$$A_1+B_1 \rightarrow A_2+A_2$$

is here considered, where A_1, B_1, A_2 and B_2 denote component molecular species. The potential energy surfaces of this reaction are constructed by the eigenvalues E of the wave equation for all n electrons,

$$\boldsymbol{H}\Psi(1,2,\cdots,n)=E(R_1,R_2,\cdots,R_N)\Psi(1,2\cdots,n) \quad (1)$$

1) S. Glasstone, K. J. Laidler and H. Eyring, "The Theory of Rate Processes", McGraw-Hill Book Co., Inc., New York (1941), p. 91.

2) H. M. James and A. S. Coolidge, *J. Chem. Phys.*, **1**, 825 (1933).

3) W. Moffitt, *Proc. Roy. Soc.*, **A210**, 224, 245 (1951); ibid., **A218**, 464, 486 (1953).

4) Also this idea has been independently found by Dr. P. Lykos, Argonne National Laboratory, U. S. A., private communication.

5) This series of papers contains the detailed account of the communication which was presented in *J. Chem. Phys.*, **23**, 1566 (1955).

at every set of fixed orientation of all N nuclei, $R_1, R_2, \cdots R_N$ in the system. Total Hamiltonian $\boldsymbol{H}$ has the usual form as

$$\boldsymbol{H}=-\sum_i \frac{1}{2}\Delta_i+\sum_{i>j}\frac{1}{r_{ij}}+\sum_{p>q}\frac{Z_pZ_q}{R_{pq}}-\sum_p\sum_i\frac{Z_p}{r_{pi}} \tag{2}$$

where p, q, and i, j, denote atomic nuclei and electrons, respectively; Z, nuclear charge, R and r, mutual distances between nuclei and electrons, respectively.

It is almost impossible to solve this equation in general; we must, therefore, be contented with merely some approximate solution. Now, when the distances between each species in the system become infinitely large, the wave function will have the following asymptotic form for any set of reactant or of any product, i. e., A_m+B_m, A_n+B_n, $\cdots$,

$$\Psi=\boldsymbol{A}\phi_{A_m^\mu}\cdot\phi_{B_m^\nu} \tag{3}$$

or

$$\Psi=\boldsymbol{A}\phi_{A_n^{\mu'}}\cdot\phi_{B_n^{\nu'}} \tag{3'}$$

$\phi_{A_m^\mu}$ and $\phi_{B_m^\nu}$ are the exact eigenfunctions of species A_m and B_m in the states μ and ν, respectively, and satisfy the equations

$$\boldsymbol{H}_{A_m}\phi_{A_m^\mu}=E_{A_m^\mu}\phi_{A_m^\mu} \tag{4}$$

and

$$\boldsymbol{H}_{B_m}\phi_{B_m^\nu}=E_{B_m^\nu}\phi_{B_m^\nu} \tag{4'}$$

where $\boldsymbol{H}_{A_m}$ and $\boldsymbol{H}_{B_m}$ are partial Hamiltonians for A_m and B_m, respectively, having the form of

$$\boldsymbol{H}_{A_m}=-\frac{1}{2}\sum_i\Delta_i+\sum_{i>j}\frac{1}{r_{ij}}+\sum_{p>q}\frac{Z_pZ_q}{R_{pq}}-\sum_p\sum_i\frac{Z_p}{r_{pi}} \tag{5}$$

and

$$\boldsymbol{H}_{B_m}=-\frac{1}{2}\sum_k\Delta_k+\sum_{k>l}\frac{1}{r_{kl}}+\sum_{r>s}\frac{Z_rZ_s}{R_{rs}}-\sum_s\sum_k\frac{Z_s}{r_{sk}} \tag{5'}$$

The nuclei p, q, and electrons i, j, belong to A_m and the nuclei r, s, and electrons k, l, to B_m. Also the eigenvalues $E_{A_m^\mu}$ and $E_{B_m^\nu}$ are those for the states of species, respectively. $\boldsymbol{A}$ in Eq. 3 is an antisymmetrizer[3] which makes the product functions $\phi_{A_m^\mu}\cdot\phi_{B_m^\nu}$ totally antisymmetrical for the exchange between any pair of electrons in the system, and has the form

$$\boldsymbol{A}=\{n!/n_A!\cdot n_B!\}^{1/2}\sum_t P_tv_t \tag{6}$$

where n_A, n_B and n are the numbers of electrons in A_m, B_m and their total respectively, P_t is any operator for inter-species exchange of electrons and $v_t=\pm1$ according to whether P_t gives an even or odd permutation.

Corresponding to all sets of species in their respective electronic states, $A_m^\mu+B_m^\nu$ $(m, \mu, \nu=1, 2, \cdots)$, we take the "composite functions" defined by

$$\phi_{m\mu\nu}=\boldsymbol{A}\phi_{A_m^\mu}\cdot\phi_{B_m^\nu} \tag{7}$$

and we assume that the total wave function is constructed approximately from these sets of composite functions,

$$\Psi=\sum_{m,\mu,\nu}C_{m\mu\nu}\cdot\phi_{m\mu\nu} \tag{8}$$

The eigenvalues $E(R_1, R_2, \cdots, R_N)$ for each orientation of nuclei are given by

$$E=\int\bar{\Psi}\boldsymbol{H}\Psi\,\mathrm{d}\tau\Big/\int\bar{\Psi}\Psi\,\mathrm{d}\tau \tag{9}$$

When the usual variation method is adopted, the above relations are converted into the secular determinant,

$$\mathrm{Det.}\,|H_{m\mu\nu,n\mu'\nu'}-ES_{m\mu\nu,n\mu'\nu'}|=0 \tag{10}$$

where

$$H_{m\mu\nu,n\mu'\nu'}=\int\bar{\phi}_{m\mu\nu}\boldsymbol{H}\phi_{n\mu'\nu'}\,\mathrm{d}\tau \tag{11}$$

and

$$S_{m\mu\nu,n\mu'\nu'}=\int\bar{\phi}_{m\mu\nu}\phi_{n\mu'\nu'}\,\mathrm{d}\tau \tag{12}$$

Moreover, when we take an assumption of neglecting the contribution of spin angular momentum to the energy, the whole electronic state is classified with their total spin S and its component S_z values and the determinant is factorized into several smaller ones in which all the elements of H and S are those for the same electronic states $\kappa(S, S_z)$'s,

$$\mathrm{Det.}\,|H^\kappa_{m\mu\nu,n\mu'\nu'}-E^\kappa S^\kappa_{m\mu\nu,n\mu'\nu'}|=0 \qquad \kappa=1, 2, \cdots \tag{13}$$

Next, let us divide the total Hamiltonian into the partial Hamiltonians $\boldsymbol{H}_{A_n}+\boldsymbol{H}_{B_n}$ for the composite species A_n+B_n and the remaining interaction term $\boldsymbol{I}_n$, that is,

$$\boldsymbol{H}=\boldsymbol{H}_{A_n}+\boldsymbol{H}_{B_n}+\boldsymbol{I}_n \tag{14}$$

where

$$\boldsymbol{I}_n=\sum_i\sum_k\frac{1}{r_{ik}}+\sum_p\sum_s\frac{Z_pZ_s}{R_{ps}}-\sum_p\sum_k\frac{Z_p}{r_{pk}}-\sum_s\sum_i\frac{Z_s}{r_{si}} \tag{15}$$

the nuclei p's and electrons i's belong to A_n and the nuclei s's and electrons k's to B_n. $\boldsymbol{H}_{A_n}$ and $\boldsymbol{H}_{B_n}$ have forms similar to $\boldsymbol{H}_{A_m}$ and $\boldsymbol{H}_{B_m}$, Eqs. 5 and 5'. Accordingly, $H^\kappa_{m\mu\nu,n\mu'\nu'}$ is rewritten as

$$H^{\kappa}_{m\mu\nu,\, n\mu'\nu'} = (E_{A^{\mu'}_n} + E_{B^{\nu'}_n})\, S^{\kappa}_{m\mu\nu,\, n\mu'\nu'} + I^{\kappa}_{m\mu\nu,\, n\mu'\nu'} \quad (16)$$

where

$$I^{\kappa}_{m\mu\nu,\, n\mu'\nu'} = \int \bar{\psi}_{m\mu\nu} \boldsymbol{I}_n \psi_{n\mu'\nu'} \mathrm{d}\tau \quad (17)$$

The number of bonds which take part in the reaction is usually one or two in each species and if we take an energy scale in which the bond energy of the composite state $A^{\mu'}_n + B^{\nu'}_n$, $\varepsilon_{n\mu'\nu'}$ is measured from the state where all these "reacting bonds" break down and the species A_n and B_n are separated into several fragments (radicals), then the eigenvalues for the composite state is described as a sum of "fragment-state energy" $E_{n\mu'\nu'}$ and "bond energy" $\varepsilon_{n\mu'\nu'}$

$$E_{A^{\mu'}_n} + E_{B^{\nu'}_n} = E_{n\mu'\nu'} + \varepsilon_{n\mu'\nu'} \quad (18)$$

Further, we take conveniently one of these "fragment-states" as a standard state and define its energy, E^{κ}_0. For this standard, the energies of the whole system E and of any composite state which belongs to the same $\kappa(S, S_z)$, $E_{A^{\mu'}_n} + E_{B^{\nu'}_n}$, are rewritten as follows:

$$E^{\kappa} = E^{\kappa}_0 + \varepsilon^{\kappa} \quad (19)$$

and

$$E_{A^{\mu'}_n} + E_{B^{\nu'}_n} = E^{\kappa}_0 + \varepsilon^{\kappa}_{n\mu'\nu'} = E^{\kappa}_0 + (\varepsilon_{A^{\mu'}_n} + \varepsilon_{B^{\nu'}_n}) \quad (20)$$

ε^{κ}, $\varepsilon^{\kappa}_{n\mu'\nu'}$, $\varepsilon_{A^{\mu'}_n}$ and $\varepsilon_{B^{\nu'}_n}$ in Eqs. 19 and 20 are respective "bond energies" of the system, of the composite state and of the species A_n and B_n newly measured from the level E_0. Substituting Eqs. 16, 19 and 20 into 10,

$$\mathrm{Det.}\,|I^{\kappa}_{m\mu\nu,\, n\mu'\nu'} + (\varepsilon^{\kappa}_{n\mu'\nu'} - \varepsilon^{\kappa}) S_{m\mu\nu,\, n\mu'\nu'}| = 0 \quad (21)$$

is obtained finally. Since $\varepsilon_{A^{\mu'}_n}$ and $\varepsilon_{B^{\nu'}_n}$ in Eq. 20 are bond energies[6] for molecules, we can frequently utilize their observed values[7]. The remaining unknown quantities, $S_{m\mu\nu,\, n\mu'\nu'}$ and $I_{m\mu\nu,\, n\mu'\nu'}$ can be evaluated, in principle, if we know the exact forms of the composite functions. Unfortunately, this is not the case except for a few states of hydrogen molecule and also the direct use of the function in exact form for the present purpose is unsuitable because of complicated calculations. Therefore, we may use their values calculated by the use of approximate composite functions with a simple analytic form[8].

Some Limitations for the Composite Functions

According to the above considerations the reactions proceed "adiabatically" on each surface. It is expected that this adiabatic condition brings some limitations on the character of states (wave functions) of species to be combined. Furthermore, when the reacting system has some symmetrical configurations during the reaction, the limitations become finer. This correlation between limited states of species was recently studied by Shuler and Laidler for the polyatomic system by the use of spin and orbital correlation rules[9,10].

Their conclusion shows that three or four atomic systems lie frequently on a

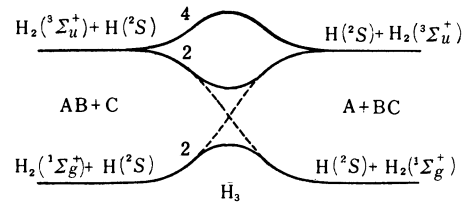


Fig. 1a. Lower potential energy surfaces of H-H-H system.

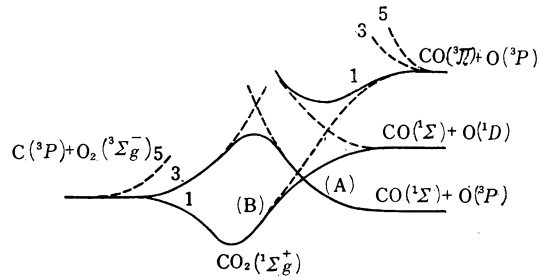


Fig. 1b. Lower potential energy surfaces of C-O-O system.

6) Here, the definition of "bond energy" is used also for the energy of the repulsive state of a molecule.

7) For example, when A_n is a diatomic molecule, some of its bond energies are given as functions of nuclear distance based on the spectroscopic data. (Morse function etc.)

8) The matrix, $\boldsymbol{H} = \boldsymbol{I} + \boldsymbol{ES}$, is not always Hermitian in this case. In order to avoid this theoretial defect, adoption of approximation for the elements such as

$$\bar{H}_{m\mu\nu,\, n\mu'\nu'} = \bar{H}_{n\mu'\nu',\, m\mu\nu} = \frac{1}{2}[H_{m\mu\nu,\, n\mu'\nu'} + H_{n\mu'\nu',\, m\mu\nu}]$$

may be required. Similar cosideration also has been given by Moffitt. See Ref. 3.

9) K. E. Shuler, *J. Chem. Phys.*, **21**, 624 (1953).

10) K. J. Laidler, ibid., **22**, 1740 (1954).

straight line or a plane where the orbital correlation may have an important part, while the general polyatomic system scarcely has these constraints at all as long as special symmetry does not exist. These results and the correlation tables given by Shuler[9] are available for the present consideration. Typical examples of correlation for the lower energy surfaces are shown in Fig. 1. In the figure, the numbers on the curves representing adiabatic surfaces are for spin multiplicity, $2S+1$, and the states of reactants and resultants are shown in both ends of each curve. Relative orientation and shapes of the curves are arbitrary.

Some explanations are added to the system H_3 (Fig. 1a). The lowest surface of this reaction is clearly one of doublet. When all the nuclei are orientated on a line, the system has a symmetry of $C_{\infty v}$ and so the lowest state will be classified to $^2\Sigma^+$. Then the states of composite species which satisfy this designation are confined

$$H_2(^{1,3}\Sigma^+)+H(^2S_g),\quad H_2(^{1,3}\Sigma^+)+H(^2P_u)$$
$$H_2(^{1,3}\Pi)+H(^2P_u),\ \text{etc.}$$

However, it is known that elements, $S_{m\mu\nu,\,n\mu'\nu'}$ and $I_{m\mu\nu,\,n\mu'\nu'}$ which relate to states of higher energy hardly contribute to the lowest state, so we can conveniently neglect these composite states of high energy and can reduce the order of the determinant. Further, when this system has higher symmetries such as equidistance-on-a-line ($D_{\infty h}$) or equilateral triangle (D_{3h}), new relations appear among the coefficients of composite functions $C_{m\mu\nu}$'s, so as to reduce the order of determinant[11].

As for the C-O-O system, the reaction, $CO_2(^1\Sigma^+)\rightarrow CO(^1\Sigma)+O(^3P)$ is a forbidden process in the present treatment. The intersection of the surfaces A and B in Fig. 1b will give, however, the zeroth approximation for the surface of this reaction.

Approximate Estimation of $S_{m\mu\nu,\,n\mu'\nu'}$ and $I_{m\mu\nu,\,n\mu'\nu'}$ for the Three-atom System

Discussion is focused here on the reaction, as an example,

$$AB+C\rightarrow A+BC \quad \text{or} \quad AC+B$$

which is composed of three atoms having one valence electron. One of composite functions which express its lowest state with $S=1/2$ and $S_z=1/2$ is

$$\psi_1=\boldsymbol{A}\psi_{AB}(1,2)\cdot\psi_C(3)$$
$$=\sum_n P_c^n\varphi_{AB}(1,2)\cdot\varphi_C(3)$$
$$\times\frac{1}{\sqrt{2}}\{\alpha(1)\beta(2)-\alpha(2)\beta(1)\}\cdot\alpha(3) \quad (22)$$

where P_c means cyclic exchange of electrons 1, 2 and 3 in this order; φ's are the orbital parts and the bond orbital, $\varphi_{AB}(1,2)$, is symmetrical for the exchange of electrons 1 and 2. Analogous forms are taken for the functions ψ_2 and ψ_3 of other composite states, BC+A and CA+B, respectively.

Now, we neglect the contributions from all higher composite states and assume φ_{AB}, $\varphi_{BC},\cdots$, and φ_A, $\varphi_B,\cdots$, to be the ones of their lowest states, and then the order of determinant can be reduced to three. We take, furthermore, the simplest form of these functions by the use of atomic orbital approximation,

$$\varphi_{AB}(1,2)=a(1)b(2)+a(2)b(1) \quad (23)$$

and

$$\varphi_C(3)=c(3) \quad (24)$$

and so on. In these functions, $a(1)$, $b(2)$ and $c(3)$ express the valence orbitals of atom A, B and C, respectively. By the use of these expressions, the formulae of S_{mn} and I_{mn} (m, $n=1$, 2, 3) are described as shown in the Appendix.

Since the numerical values of molecular integrals including atomic orbitals with the principal quantum number $n=1,2,3$ are available at present[12], it is possible to evaluate the formulae directly except for several multiple-center integrals. Also these integrals are estimated exactly for some simple systems and also are approximately given by, e.g., Rudenberg-Mulliken's procedure[13].

Here, it is interesting to examine the simplification neglecting all these multiple-center integrals in the formulae. In this case, I_{mn} can be described as the function of coulombic energies Q_{AB}, $Q_{BC},\cdots$, and exchange energies J_{AB}, $J_{BC},\cdots$, of respective bonds, AB, $BC,\cdots$, for example,

$$I_{11}=2Q_{CA}+Q_{BC}-J_{CA}-J_{BC}$$

where

$$Q_{CA}=\bar{R}_{CA}^{-1}+(c^2|a^2)-(c^2|A)-(a^2|C)^{14}$$

11) See, for example, H. Eyring, J. Walter and G. E. Kimball, "Quantum Chemistry", John Wiley & Sons, Inc., New York (1949), Chap. X, p. 172; Chap. XIII, p. 252.

12) M. Kotani, A. Amemiya, E. Ishiguro and T. Kimura, "Table of Molecular Integrals", Maruzen Co., Ltd., Tokyo (1955).

13) K. Rudenberg, *J. Chem. Phys.*, **19**, 1433 (1951); R. S. Mulliken and R. G. Parr, ibid., **18**, 1338 (1950).

and

$$J_{CA}=(ac)^2\bar{R}_{CA}^{-1}+(ac|ac)-(ac)(ac|A+C),$$

etc.

Moreover, when the non-orthogonality between orbitals of different atoms is disregarded in S_{mn}'s, the expressions for I_{mn}'s and S_{mn}'s exactly correspond to those obtained by the well-known method of bond eigenfunction[15].

Eyring's semi-empirical method is derived readily by the use of these expressions and by taking the values of Q_{AB}, $J_{AB},\cdots$, from the assumption,

$$\varepsilon_{AB}=Q_{AB}+J_{AB},\quad \varepsilon_{BC}=Q_{BC}+J_{BC},\cdots, \tag{25}$$

and

$$\rho_{AB}=Q_{AB}/\varepsilon_{AB},\quad \rho_{BC}=Q_{BC}/\varepsilon_{BC},\cdots, \tag{26}$$

where ε_{AB}, $\varepsilon_{BC},\cdots$ and ρ_{AB}, $\rho_{BC},\cdots$ are bond energies and coulombic fractions of bonds AB, $BC,\cdots$. Therefore, this procedure may be regarded as one of the methods for estimating the elements I_{mn}'s conveniently by the use of ε_{AB}'s and ρ_{AB}'s.

Another basis of the present method will be examined below with respect to this reaction example. It is known theoretically that the wave functions which express the doublet states with $S_z=1/2$ are written as follows, by the use of orbital approximation;

$$\Phi_1=\sum_n P_c^n\{\psi(1,2,3)+\psi(2,1,3)\}\times\frac{1}{\sqrt{2}}\{\alpha(1)\beta(2)-\alpha(2)\beta(1)\}\alpha(3) \tag{27}$$

and

$$\Phi_2=\sum_n P_c^n\{(\psi1,2,3)-\psi(2,1,3)\}\times\frac{1}{\sqrt{6}}[\{\alpha(1)\beta(2)+\alpha(2)\beta(1)\}\alpha(3)-2\alpha(1)\alpha(2)\beta(3)] \tag{28}$$

where $\psi(1,2,3)$ is the orbital function[16]. When we take the simplest form of ψ's, $\psi(1,2,3)=a(1)b(2)c(3)$, etc., Φ_1 is identified with the composite function $\boldsymbol{A}\psi_{AB}\cdot\psi_C$ and Φ_2 is also rewritten as

$$\Phi_2=\sum_n P_c^n\{a(1)b(2)-a(2)b(1)\}c(3)\times\frac{1}{\sqrt{6}}[\{\alpha(1)\beta(2)+\alpha(2)\beta(1)\}\alpha(3)-2\alpha(1)\alpha(2)\beta(3)] \tag{29}$$

or

$$=\sum_n P_c^n[\{b(1)c(2)+b(2)c(1)\}a(3)+\{c(1)a(2)+c(2)a(1)\}b(3)]\times\frac{1}{\sqrt{6}}\{\alpha(1)\beta(2)-\alpha(2)\beta(1)\}\alpha(3) \tag{29'}$$

These expressions correspond apparently to the state composed of AB in a triplet state and C in a doublet state or the combination of composite states, BC in a singlet state and A in a doublet state, and CA and B in the analogous states.

Since the eigenvalues of these doublet states of the whole system are determined from the wave function,

$$\Psi=c_1\Phi_1+c_2\Phi_2 \tag{30}$$

the utilization of Φ_1 and Φ_2 as the basic functions is equivalent to the adoption of the set of composite functions, $\boldsymbol{A}\psi_{AB}\cdot\psi_C$, $\boldsymbol{A}\psi_{BC}\cdot\psi_A$ and $\boldsymbol{A}\psi_{CA}\cdot\psi_B$.

The conclusion from the above consideration and also the method of bond-eigenfunction shows that one of these three functions is linearly dependent on the others. But, in the present method, such a relation does not always hold, for the present choice of a functional set is effectively to make use of the observed values of bond energies, ε_{AB}, ε_{BC} and ε_{CA}.

Remarks on the Application to the General System

In several reactions, bonds have frequently a directional character such as p-, d- orbitals or their hybridization. Also other important cases are the reactions in multielectronic systems with inner-shell and incompleted shell electrons. Any polyatomic system is comprised in the combination of these cases. Some remarks will be made on the application to these systems.

System with Directed Valence Bond. — A typical example is the hydrogen-halogen reaction

$$X(^2P)+H_2(^1\Sigma^+)\rightarrow HX(^1\Sigma^+)+H(^2S)$$

For simplicity, the halogen atom is assumed to have only a p-valence electron. This system has been studied only by Magee with crude approximation[17].

Denoting two independent p-orbitals of halogen, which lie on the plane involving three atoms, by p_x and p_y, we can readily see that these p-orbitals and s-orbitals of two hydrogen atoms form a basis for an

14) For these notations, see the definitions given in Appendix.
15) Ref. 11, Chap. XIII, p. 232.
16) Ref. 12, p. 15.
17) J. L. Magee, *J. Chem. Phys.*, 8, 677 (1940).

irreducible representation of the group of surface symmetry C_s. Accordingly, the p-bonding orbital on the plane is expressed by linear combination of p_x and p_y,

$$p_\sigma = \lambda p_x + \mu p_y \tag{31}$$

Since the total wave function is described as

$$\Psi = C_1 A\psi_{XH_A}\cdot\psi_{H_B} + C_2 A\psi_{XH_B}\cdot\psi_{H_A} + C_3 A\psi_{H_2}\cdot\psi_X \tag{32}$$

respective bond functions are given by

$$\psi_{XH_A} = \lambda_1\psi(p_x - h_A) + \mu_1\psi(p_y - h_A)$$

$$\psi_{XH_B} = \lambda_2\psi(p_x - h_B) + \mu_2\psi(p_y - h_B)$$

and $\psi_X = \lambda_3\psi(p_x) + \mu_3\psi(p_y)$

where h's are the valence orbitals of the hydrogen atom.

Even if all states of higher energy are neglected, the determinant is still so great. But when the ratios λ_i/μ_i's are fixed so as to minimize the energy of each composite state, the order of determinant can be reduced to three and the bond energy of HX is utilized effectively, for the p_σ orbital lies along the line joining H and X in this case[18].

System with Inner-shell Electrons. — The simplest example is the reaction including alkali metal,

$$LiH(^1\Sigma^+) + H(^2S) \rightarrow Li(^2S) + H_2(^1\Sigma^+)$$

of which one of the composite functions is

$$\phi_1 = A\phi_{LiH}(1,2,3,4)\cdot\phi_H(5)$$

The orbital part of molecular function, ϕ_{LiH} may be factorized by the use of the inner shell orbital ϕ_i[19] and the bond orbital ϕ_{LiH} which are symmetrical for exchange of electrons, respectively. Expressing these orbitals by the introduction of atomic orbital approximation, it is found that I_{mn}'s consist of two parts, (1) integrals with exchange of electrons between inner-shell and bond orbitals of other species and (2) integrals in which inner-shell electrons remain un-exchanged.

Now, we take a simplification neglecting the former because of the small overlapping between inner-shell and valence orbital of different species. The electrons in closed shell distribute almost spherically round the Li nucleus and then contribute to energy only by coulombic repulsion. Since this effect is estimated effectively by adjusting the nuclear charge of Li atom, the system is regarded as the one consisting of three valence electrons only.

The effect of an incomplete shell, lone pair and even that of radicals which are not concerned directly with the reaction, are similar in principle to the above case. However, an important difference between them is that the charge distributions in these cases are not spherically symmetrical for the nuclei noticed. Therefore, it may be necessary to take such an approximation as the replacement of these distributions to several point charges distributed around the nucleus.

Finally, a remark is briefly made on the system having multiple bond. When the bond breaks completely or is newly formed as a result of reaction, all electrons relating to the bond must be taken into the treatment. On the other hand, when the bond is partially subjected to reaction, electrons in the remaining part of the bond behave in the same manner as those of the incompleted shell stated above and then are treated in a similar way too. The above consideration has been taken for the displacement reaction $A+BC \rightarrow AB+C$. Conclusions obtained here, however, are readily extended to other types of reaction, for instance, double decomposition, $AB+CD \rightarrow AC+BD$.

If the ground states of molecules are all singlet in this case, the lowest surface will also belong to singlet and composite functions, which can be constructed in a way quite analogous to that shown in the previous sections.

The author wishes to thank Professor S. Shida of Tokyo Institute of Technology and Professor K. Hirota of Osaka University for their valuable suggestions and kind encouragement. Also the author is indebted to Mr. Y. Mori for many helpful discussions.

Laboratory of Physical Chemistry
Tokyo Institute of Technology
Meguro-ku, Tokyo

Appendix

Formulae of S_{mn} and I_{mn} for the System of Three Atoms with One Valence Electron. — In a way similar to ϕ_1 of Eq. 22, ϕ_2 and ϕ_3 for the other composite states are described as follows:

18) When the direction of the valence orbital is fixed during the reaction for some reason, for example, the hindrance of atoms or radicals attached to the noticed atom, and it does not accord with the joining line, some correction may be required for full insertion of observed bond energies.

19) This orbital almost coincides with inner shell orbital of Li atom.

$$\psi_2=\boldsymbol{A}\psi_{BC}(1,2)\cdot\psi_A(3)$$

and $$\psi_3=\boldsymbol{A}\psi_{CA}(1,2)\cdot\psi_B(3)$$

Total Hamiltonian operator and wave function are

$$\boldsymbol{H}=-\frac{1}{2}\sum_{i=1}^{3}\Delta_i+\sum_{i>j}\frac{1}{r_{ij}}+\sum_{p>q}\frac{Z_pZ_q}{R_{pq}}-\sum_p\sum_i\frac{Z_p}{r_{pi}} \tag{A.1}$$

and

$$\Psi=C_1\psi_1+C_2\psi_2+C_3\psi_3 \tag{A.2}$$

Accordingly, the determinant to be solved is

$$\text{Det.}\,|I_{mn}+(\varepsilon_{mn}-\varepsilon)S_{mn}|=0 \quad m,n=1,2,3 \tag{A.3}$$

I_{mn}'s are further resolved into several terms for convenience,

$$I_{mn}=K_{mn}-J_{mn}+R_{mn}\cdot S_{mn} \tag{A.4}$$

The formulae of ε_{mn}, S_{mn}, R_{mn}, K_{mn} and J_{mn} are shown below. The notation of integrals used in the expressions is as follows:

$$(ab)=\int a(1)b(1)\,d\tau_1$$

$$(a^2|b^2)=\int a^2(1)\frac{1}{r_{12}}b^2(2)\,d\tau_1d\tau_2$$

$$(ab|ab)=\int a(1)b(1)\frac{1}{r_{12}}a(2)b(2)\,d\tau_1d\tau_2$$

$$(a^2|B)=\int a^2(1)\cdot\frac{Z_B}{r_{B1}}\,d\tau_1 \qquad \text{etc.}$$

Also, in the expressions below, ε_{m1} $(A\rightleftarrows C)$ means the exchange of letters "A" and "C" in that of ε_{m1} and so on.

(1) ε_{mn}; $\varepsilon_{m1}=\varepsilon_{AB}$

$\varepsilon_{m2}=\varepsilon_{m1}(A\rightleftarrows C)$ $\quad m=1,2,3$

$\varepsilon_{m3}=\varepsilon_{m1}(B\rightleftarrows C)$

(2) R_{mn}; $R_{m1}=\bar{R}_{BC}^{-1}+\bar{R}_{AC}^{-1}$ $\quad \bar{R}_{BC}^{-1}=Z_BZ_C\cdot R_{BC}^{-1}$ etc.,

$R_{m2}=R_{m1}(A\rightleftarrows C)$ $\quad m=1,2,3$

$R_{m3}=R_{m1}(B\rightleftarrows C)$

(3) S_{mn}; $S_{11}=2+2(ab)^2-(bc)^2-(ac)^2-2(ab)(bc)(ca)$

$S_{22}=S_{11}(a\rightleftarrows c)$

$S_{33}=S_{11}(b\rightleftarrows c)$

$S_{12}=S_{21}=-1+2(ac)^2-(ab)^2-(bc)^2$
$+(ab)(bc)(ca)$

$S_{13}=S_{31}=S_{12}(a\rightleftarrows b)$

$S_{23}=S_{32}=S_{12}(b\rightleftarrows c)$

(4) K_{mn}; $K_{11}=2(a^2|c^2)+2(b^2|c^2)$
$+4(ab)(ab|c^2)-(ac|ac)$
$-(bc|bc)-(bc)\cdot\{(a^2|bc)+(ab|ac)\}$
$-(ac)\{(b^2|ac)+(ab|bc)\}$
$-2(ab)(ac|bc)$

$K_{22}=K_{11}(a\rightleftarrows c)$

$K_{33}=K_{11}(b\rightleftarrows c)$

$K_{12}=2[(ac|ac)+(ac)(b^2|ac)]$
$+(bc)(ab|ac)+(ab)(bc|ac)$
$-[(a^2|c^2)+(b^2|a^2)+(ab|ab)$
$+(ab)(c^2|ab)+(ac)(bc|ab)$
$+(bc)\{2(bc|a^2)+(ab|ac)\}]$

$K_{32}=K_{12}(b\rightleftarrows c)$

$K_{21}=K_{12}(a\rightleftarrows c)$

$K_{31}=K_{21}(a\rightleftarrows b)$

$K_{13}=K_{12}(a\rightleftarrows b)$

$K_{23}=K_{13}(a\rightleftarrows c)$

(5) J_{mn}; $J_{11}=\{2-(bc)^2\}\cdot(a^2|C)+\{2-(ac)^2\}\cdot(b^2|C)$
$+\{4(ab)-2(ac)(bc)\}\cdot(ab|C)$
$+\{2+2(ab)^2\}\cdot(c^2|A+B)$
$-\{(bc)+(ab)(ac)\}\cdot(bc|A+B+C)$
$-\{(ac)+(ab)(bc)\}\cdot(ac|A+B+C)$

$J_{22}=J_{11}(a\rightleftarrows c,\ A\rightleftarrows C)$

$J_{33}=J_{11}(b\rightleftarrows c,\ B\rightleftarrows C)$

$J_{12}=\{2(ac)+2(ab)(bc)\}(ac|B+C)$
$-\{(ab)+(ac)(bc)\}(ab|B+C)$
$-\{1+(bc)^2\}(a^2|B+C)$
$-\{1+(ab)^2\}(c^2|A)$
$-\{1-2(ac)^2\}(b^2|A)$
$+\{2(ac)-(ab)(bc)\}(ac|A)$
$+\{(ac)(ab)-2(bc)\}(bc|A)$
$+\{2(bc)(ac)-(ab)\}(ab|A)$

$J_{32}=J_{12}(b\rightleftarrows c,\ B\rightleftarrows C)$

$J_{21}=J_{12}(a\rightleftarrows c,\ A\rightleftarrows C)$

$J_{31}=J_{21}(a\rightleftarrows b,\ A\rightleftarrows B)$

$J_{13}=J_{12}(a\rightleftarrows b,\ A\rightleftarrows B)$

$J_{23}=J_{13}(a\rightleftarrows c,\ A\rightleftarrows C)$

Modified Bond Eigenfunction Method of Constructing Potential Energy Surface of Reaction. II. Application to the Hydrogen Atom-Molecule Reaction

By Iwao YASUMORI

(Received March 3, 1959)

A new method of constructing the potential energy surface of a chemical reaction was presented in the previous paper and some remarks on the procedure of application were also given. In order to examine its availability, the method is effectively applied to the hydrogen atom-molecule reaction, since much theoretical and experimental knowledge has been accumulated on its component species, H_2 and H.

As is well known, the potential energy surfaces of this reaction have been evaluated by Hirschfelder et al.[1] in a purely theoretical manner and by Eyring et al.[2] semi-empirically. Also, recently several investigators[3] have given some considerations about this system from the standpoint of molecular orbital method.

In this paper, besides the examination of the applicability of the method, surface properties obtained here are discussed comparing them with those obtained in the previous works. Calculation of reaction rate based on the surface is carried out also.

Composite Wave Functions

We denote three hydrogen atoms in the systems, A, B and C, and, for simplicity, confine ourselves to the lowest surface of linear configuration. Therefore, it is assumed that the reaction proceeds by the equation

$$H_AH_B+H_C \rightarrow H_A+H_BH_C$$

on a straight line.

According to the considerations given in Paper 1, the total wave function which expresses the state with the total spin $S=1/2$ and its component $S_z=1/2$ is described as follows:

$$\begin{aligned}\Psi=\sum_{m=1}^{3} C_m\psi_m &= C_1\boldsymbol{A}\varphi_{AB}(1,2)\varphi_C(3)\\ &\times\frac{1}{\sqrt{2}}\{\alpha(1)\beta(2)-\alpha(2)\beta(1)\}\alpha(3)\\ &+C_2\boldsymbol{A}\varphi_{BC}(1,2)\varphi_A(3)\\ &\times\frac{1}{\sqrt{2}}\{\alpha(1)\beta(2)-\alpha(2)\beta(1)\}\alpha(3)\\ &+C_3\boldsymbol{A}\varphi_{CA}(1,2)\varphi_B(3)\\ &\times\frac{1}{\sqrt{2}}\{\alpha(1)\beta(2)-\alpha(2)\beta(1)\}\alpha(3)\end{aligned} \tag{1}$$

where each term represents the composite functions for bond structures $AB+C$, $BC+A$ and $CA+B$, respectively. In the equation, $\varphi_{AB}(1,2),\cdots$ are ${}^1\Sigma^+_g$ orbital functions of H_2 and $\varphi_c(3),\cdots$ are atomic $1s$ orbital functions of hydrogen. Spin functions $\frac{1}{\sqrt{2}}\{\alpha(1)\beta(2)-\alpha(2)\beta(1)\}$ and $\alpha(3)$ correspond to singlet state of molecule and doublet state of atom, respectively. There are many higher energy states which correlate to the lowest surface such as $H_2({}^{1,3}\Sigma^+)+H({}^2S_g,{}^2P_u)$, $H_2({}^1{}^3\Pi)+H({}^2P_u)$, etc. But all these composite states were excluded in the present calculation[4], since, apart from the simplification of procedure, their contributions to the energy of the lowest state are rather small and also some of them are hardly available because of the lack of experimental data.

By the operation of antisymmetrizer,

$$\boldsymbol{A}=\frac{1}{\sqrt{3}}\Sigma_t P_t v_t \tag{2}$$

each composite function is expressed as

$$\begin{aligned}\psi_1=&\frac{1}{\sqrt{6}}\varphi_{AB}(1,2)\cdot\varphi_C(3)\{\alpha(1)\beta(2)-\alpha(2)\beta(1)\}\alpha(3)\\ &+\frac{1}{\sqrt{6}}\varphi_{AB}(2,3)\cdot\varphi_C(1)\{\alpha(2)\beta(3)-\alpha(3)\beta(2)\}\alpha(1)\\ &+\frac{1}{\sqrt{6}}\varphi_{AB}(3,1)\cdot\varphi_C(2)\{\alpha(3)\beta(1)-\alpha(1)\beta(3)\}\alpha(2)\end{aligned} \tag{3}$$

and so on. The determinant, from which energy values for all configurations of atoms are deduced, is described as

$$\text{Det.}\,|I_{mn}+(\varepsilon_{mn}-\varepsilon)S_{mn}|=0 \qquad m,n=1,2,3 \tag{4}$$

1) J. O. Hirschfelder, N. Rosen and H. Eyring, *J. Chem. Phys.*, **4**, 121 (1936).

2) J. O. Hirschfelder, H. Eyring and B. Topley, ibid., **4**, 170 (1936).

3) J. M. Walsh and F. A. Matsen, ibid., **19**, 526 (1951); V. Griffing and J. T. Vanderslice, ibid., **23**, 1035 (1955); G. E. Kimball and J. G. Trulio, ibid., **28**, 493 (1958).

4) However, the composite states $H_2({}^3\Sigma^+_u)+H({}^2S_g,1s)$, are automatically included in the wave function. See Paper I.

where $$S_{mn}=\int \bar{\psi}_m \psi_n d\tau \quad (5)$$

$$I_{mn}=\int \bar{\psi}_m \boldsymbol{I}_n \psi_n d\tau \quad (6)$$

When we take the lowest state of free atoms 3H as a standard of energy of system, bond energies of species are given by

$$\varepsilon_{m1}=\varepsilon_{H_2}(AB),\quad \varepsilon_{m2}=\varepsilon_{H_2}(BC),\quad \varepsilon_{m3}=\varepsilon_{H_2}(CA)$$
$$m=1,2,3$$

and interaction operators $\boldsymbol{I}_n$'s are also defined as

$$\boldsymbol{I}_1=\boldsymbol{H}-\boldsymbol{H}_{AB}-\boldsymbol{H}_C \quad (7)$$
$$\boldsymbol{I}_2=\boldsymbol{H}-\boldsymbol{H}_{BC}-\boldsymbol{H}_A \text{ and } \boldsymbol{I}_3=\boldsymbol{H}-\boldsymbol{H}_{CA}-\boldsymbol{H}_B$$

where $\boldsymbol{H}$ is the total Hamiltonian of three electrons in the system and $\boldsymbol{H}_{AB}$ and $\boldsymbol{H}_C$ are the partial ones for molecule AB and atom C, respectively, and so on.

Molecular functions taken into the calculation are as follows:

(a) Heitler-London type function,

$$\varphi_{AB}(1,2)=a(1)b(2)+a(2)b(1)$$

where $a(1)$ and $b(2)$ are 1s orbital functions of hydrogen,

$$a(1)=(1/\pi)^{1/2}\exp(-r_{A1})$$

and $$b(2)=(1/\pi)^{1/2}\exp(-r_{B2}),\text{ etc.}$$

(b) Wang type function obtained by introduction of effective nuclear charge z into the atomic orbitals of the function a,

$$a(1)=(z^3/\pi)^{1/2}\exp(-zr_{A1})\quad \text{etc.}$$

(c) Weinbaum type function composed of the above functions, that is, the covalent term, and the ionic term,

$$\varphi^{ion}{}_{AB}(1,2)=a(1)a(2)+b(1)b(2)$$

Since these functions are described by the use of atomic orbital approximation, formulae of elements I_{mn} and S_{mn} given in the Appendix of Paper I are available for the present calculation. In addition to this, it is to be noted that when we estimate the values of ε_{H_2} also by the use of these approximate functions, the results are reduced to those of Hirschfelder et al.[1] The present method differs from theirs in the point that the interaction energies are evaluated by making use of approximate functions, while the observed values, that is, those deduced from the exact functions, are utilized for the bond energies of H_2.

Details of Calculation and Results

Detailed procedure of energy calculations which were performed by the use of approximate functions are shown below for the respective cases.

(a) Calculation of Symmetrical Linear Configuration with Heitler-London Type Function of H_2.—Making use of the formulae in the Appendix of Paper I, we can express the elements S_{mn} and I_{mn} as the sum of several molecular integrals, i. e., two-center and three-center ones. The values of two-center integrals were obtained from the tables by Kotani et al.[5] and by Hirschfelder and Linnett[6] (being abbreviated to L.-H. hereafter). For the three-center integrals, values of one electron integrals such as

$$(bc\mid A)=\int b(1)c(1)\frac{1}{r_{A1}}d\tau_1$$

were taken from the table by Hirschfelder and Weygandt[7] and values of two electron ones, for example,

$$(bc\mid a^2)=\int b(1)c(1)\frac{1}{r_{12}}a^2(2)\,d\tau_1 d\tau_2$$

were calculated in a similar way as those of Hirchfelder's[1].

Also some of their values were taken from the table in the paper of Baker et al.[8] Therefore, such an approximate calculation as Rudenberg-Mulliken's procedure[9],

$$(bc\mid a^2)\cong\frac{1}{2}(bc)\cdot[(b^2\mid a^2)+(c^2\mid a^2)]\quad \text{etc.},$$

was not required in this case.

(b) Calculation with Heitler-London-plus-Ionic Type Function.—Strictly speaking, the coefficient of ionic term added to covalent function must be taken so as to minimize the energy value, since the ionic term is another function contributing $^1\Sigma^+$ state of molecule. However, the coefficient was fixed to the value, $C_{ion}=0.1607$ take from L.-H.'s work, in order only to examine the effect of electronic distribution in hydrogen molecular function. In this case, the ionic integrals of two-center type, for example,

$$(ac\mid a^2)=\int a(1)c(1)\frac{1}{r_{12}}a^2(2)\,d\tau_1 d\tau_2\quad \text{etc.},$$

newly appear. The values were obtained also from the table by Kotani et al.

(c) Calculation with Wang Type Function.—At the values of effective nuclear charge in atomic orbital function, the following values were used for the calculation; (i) the values from original Wang function, $z=1.166$[10] and (ii) the values from L.-H.'s work shown in Table I.

When we adopt these functions for the strict procedure of calculation, the molecular integrals which appear, are of unsymmetrical type including the atomic orbital functions with effective nuclear charge, z and $z=1$. The values of these

5) M. Kotani, A. Amemiya, E. Ishiguro and T. Kimura, "The Table of Molecular Integrals", Maruzen Co., Ltd., Tokyo (1955); M. Kotani, A. Amemiya and T. Simose, *Proc. Phys.-Math. Soc. Japan*, **20**, Extra 1 (1938); **22**, Extra 1 (1940).

6) J. O. Hirschfelder and J. W. Linnett, *J. Chem. Phys.*, **18**, 130 (1950).

7) J. O. Hirschfelder and C. N. Weygandt, ibid., **6**, 806 (1938).

8) R. S. Baker, H. Eyring, C. J. Thorne and D. A. Baker, ibid., **22**, 699 (1954).

9) K. Rudenberg, ibid., **19**, 1433 (1951): R. G. Parr and R. S. Mulliken, ibid., **18**, 1338 (1950).

10) S. C. Wang, *Phys. Rev.*, **31**, 579 (1928).

TABLE I. VARIATION OF z WITH INTERNUCLEAR SEPARATION IN THE WANG TYPE FUNCTION OF H_2

zR(a. u.)*	1.0	1.5	1.75	2.0	2.5	3.0
z	1.3911	1.2145	1.1388	1.0823	1.0151	1.0000

* 1 a. u.=0.5292 Å.

unsymmetrical integrals were estimated accurately by James[11] for 1s and 2s orbitals of lithium atom and approximately be Mulligan[12] for carbon dioxide calculation. Here, for simplicity, the effective nuclear charges in all orbitals were assumed to be equally z, so as to utilize the results of calculations a) and b). The effect of this approximation will be discussed later.

(d) Calculation with Wang-plus-Ionic Type Function.—Used values of effective nuclear charge and coefficients of ionic term are as follows: (i) the values used in original Weinbaum's function[13], $z=1.193$ and $C_{ion}=0.256$ and (ii) the values obtained from L.-H's treatment of H_2 which are shown in Table II.

TABLE II. VARIATION OF z AND C_{ion} IN THE WANG-PLUS-IONIC TYPE FUNCTION OF H_2

zR(a. u.)	1.0	1.5	1.75	2.0	2.5	3.0
z	1.3976	1.2411	1.1746	1.1195	1.0472	1.0000
C_{ion}	−0.01603	0.1361	0.1664	0.1780	0.1681	0.1200

Further calculations were performed for the following cases.

(e) Effect of Varying Nuclear Charge z.—For the linear configuration of equi-distance, calculation was carried out varying z in Wang type function as $z=1.0$, 1.166, 1.3, 1.4 and 1.5, respectively.

(f) Comparison of Energy Values on Various Stages of Approximation.—The effects of various approximations such as (i) use of three-center integral values calculated by Rudenberg-Mulliken type approximation, (ii) neglect of these integrals and (iii) ii plus neglect of non-orthogonality of orbitals in S_{mn}'s, were examined utilizing Heitler-London type function for the same configuration as described in e).

(g) Variaton of Energy by Bending.—Increase of energy owing to bend of R_{BC} to R_{AB} was calculated for several equi-distant configurations by the use of Heitler-London and Wang type functions.

(h) Energy Values of Some Unsymmetrical Configuration. — Three-center integrals which appear in this case have need of complicated calculations. However, it is possible that, by an analogy of Mulligan approximation for the unsymmetrical integrals with different z's, these integrals are expressed approximately in terms of symmetrical configurations.

For example, denoting $R_{AB}=R_1$ and $R_{BC}=R_2$, we have

$$(ab \mid bc)_{R_1,R_2}=(ab)_{R_1}\cdot(bc)_{R_2}\times\frac{1}{2}\left[\left(\frac{(ab\mid bc)}{(ab)(bc)}\right)_{R_1}+\left(\frac{(ab\mid bc)}{(ab)(bc)}\right)_{R_2}\right]$$

Otherwise, these integrals may be resolved into the sum of several two-center integrals by the use of Rudenberg-Mulliken type approximation. Calculation was carried out for the configurations of

$R_{AB}=1.5$ a. u., $R_{BC}=2.0$ a. u.
$R_{AB}=1.75$ a. u., $R_{BC}=2.0$ a. u.
$zR_{AB}=2.00$ a. u., $zR_{BC}=2.50$ a. u.
and $zR_{AB}=2.25$ a. u., $zR_{BC}=2.50$ a. u.

by the use of Heitler-London and Wang ($z=1.4$) type functions and of approximate values of integrals.

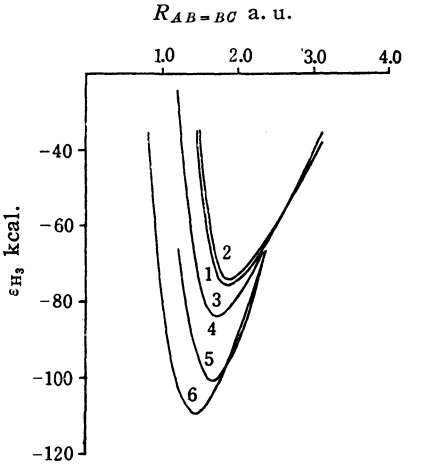


Fig. 1. Energies of symmetrical linea H_3.
1. Heitler-London function
2. H.-L.-plus-Ion function
3. Wang function (L.-H.)
4. Wang-plus-Ion function (L.-H.)
5. Wang function ($z=1.4$)
6. Observed H_2

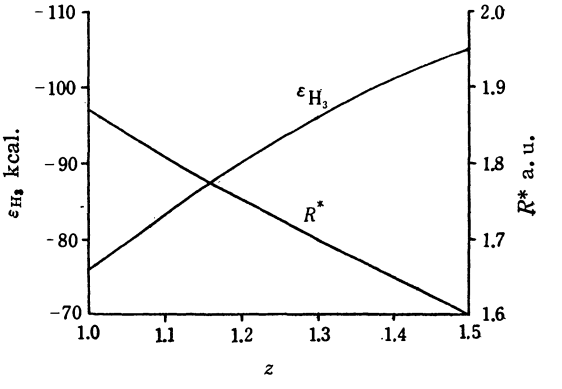


Fig. 2. Variation of energy and nuclear separation of H_3 with increase of z.

11) H. M. James, *J. Chem. Phys.*, **2**, 794 (1934).
12) J. F. Mulligan, ibid., **19**, 347 (1951).
13) S. Weinbaum, ibid., **1**, 593 (1933).

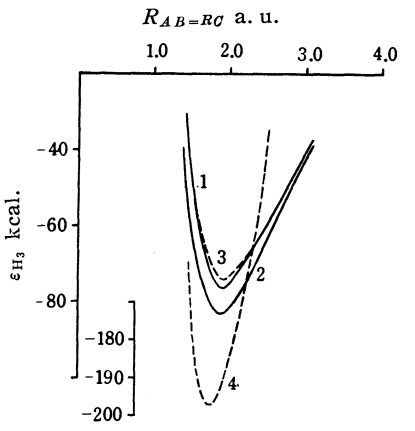


Fig. 3. Energies of H_3 by the use of various approximations.
1. Heitler-London function
2. Three-center integrals by R.-M. approximation
3. Neglect of three-center integrals
4. Neglect of three-center integrals and of non-orthogonality of atomic orbitals

TABLE III. VARIATION OF ENERGY BY BENDING*

(i) $R_{AB}=R_{BC}=2.00$ a. u. (Heitler-London type function)

ϕ (rad.)**	0.000	0.314	0.711
E (kcal.)	−81.8	−81.1	−77.4

(ii) $zR_{AB}=zR_{BC}=2.25$ a. u. (Wang type function $z=1.4$)

ϕ (rad.)	0.000	0.952
E (kcal.)	−100.1	−92.6

(iii) $zR_{AB}=zR_{BC}=2.50$ a. u. (Wang type function $z=1.4$)

ϕ (rad.)	0.000	0.902
E (kcal.)	−101.6	−95.7

* Values of three-center integrals with R.-M. approximation were used.
** ϕ is the angle between lines A-B and B-C.

TABLE IV. ENERGIES OF H_3 FOR UNSYMMETRICAL LINEAR CONFIGURATIONS*

	(z=1)		(z=1.4)	
zR_{AB} (a. u.)	1.50	1.75	2.00	2.25
zR_{BC} (a. u.)	2.00	2.00	2.50	2.50
E (kcal.)	−81.1	−83.7	−99.6	−103.4

* Values of three-center integrals with R.-M. approximation were used.

Results obtaind from calculations a)—h) are shown in Figs. 1—3 and Tables III and IV. An example of potential enegy surface constructed from these data is also shown in Fig. 4.

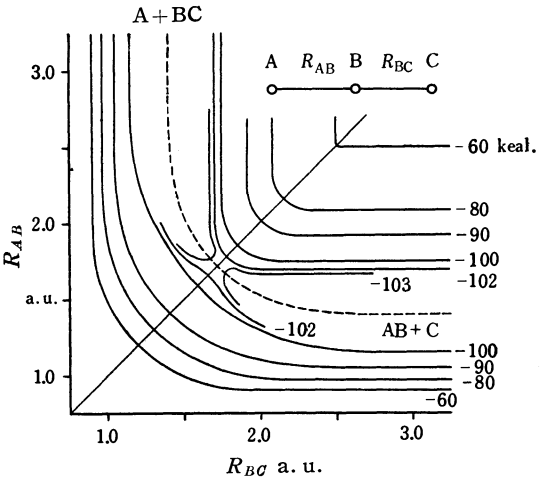


Fig. 4. Potential energy surface of reaction $H_2+H\rightarrow H+H_2$ (Wang type function $z=1.4$).

Discussion

Activation energies obtained by the present method (Table V) are not always satisfactory compared with the observed value[14] or the previous ones by Hirschfelder et al.[1], except the result with Wang

TABLE V. VALUES OF ENERGY OF H_3, E_{H_3}, NUCLEAR SEPARATION, R^*, AT ACTIVATED STATE AND OF ACTIVATION ENERGY, E_a, OBTAINED BY VARIOUS TREATMENTS

Used molecular function	(kcal.) E_{H_3}	E_{H_2}	E_a	(a. u.) R^*
Heitler-London	−76.0	−109.5	33.5	1.87
(R.-M. approx.)	−83.0	−109.5	26.5	1.87
(H.-E.-R.)*	−53.11	− 72.18	19.07	2.00
H.-L.-plus-Ion.	−75.0	−109.5	34.5	1.88
(H.-E.-R.)	−60.39	− 74.02	13.63	2.00
Wang.	−88.0	−109.5	21.5	1.77
(L.-H.)**	−84.0	−109.5	25.5	1.72
(H.-E.-R.)	−56.16	− 86.94	30.78	1.89
Wang-plus-Ion	−88.0	−109.5	21.5	1.73
(L.-H.)	−84.0	−109.5	25.5	1.72
(H.-E.-R)	−67.09	− 92.24	25.15	1.84
Wang. (z=1.4)	−101.0	−109.5	8.5	1.65
(R.-M. approx.)	−102.4	−109.5	7.1	1.72
Griffing et al.[3]***	−63.0	− 71.76	8.76	1.82
Kimball et al.[3]***	−72.4	—	—	1.93
Observed value[14]	—	−109.5	4∼8	—

* Values calculated by Hirschfelder, Eyring and Rosen.
** Values calculated by the use of Hirschfelder-Linnett's coefficients.
*** Values calculated by the LCAO-MO method with configuration interaction.

14) K. H. Gelb and P. Harteck, *Z. physik. Chem.* (*Bodenstein Festband*), 849(1931); A. Farkas and L. Farkas, *Proc. Roy. Soc.*, **A152**, 124 (1935).

type function in which $z=1.4$. However, marked improvements from their work are found in the absolute energy values of H_3 complex state, that is, the lowering 15~30 kcal. Besides, it is apparent that the activation energies estimated by them are of relative character; the use of improved function of H_2 brings, on the contrary, large increase for the values.

Interesting results are seen for the influence of an added ionic term. The introduction of this term lowers energies of H_3 complex slightly in the case of Hirschfelder et al., while it has almost no effect in the present treatment. These results are owing partly to the small contribution of ionic state to the lowest one and partly to the use of fixed coefficient of that term.

Also the results are explained phenomenally as that addition of this state brought an increase of interaction energy allowing superposition of electrons on the same atom. Considerations shall be done again later relating to the distribution of electrons in the system.

Next, the effect of nuclear charge z is examined. The lowering of energy and the contraction of the dimension of activated complex with increase of z are shown in Fig. 2. When z is increased to 1.4 or larger, the activation energy calculated attains the observed one. This effect may be explained qualitatively as that the use of atomic orbital shrunk by larger z diminishes the interaction between species and then energy of complex and nuclear distance decrease to those of the initial molecule.

If the energies of molecular species are estimated by the use of the same approximate function, this decrease of interaction energy will be compensated by the increase of molecular energy, and then an optimum value of z will be obtained. Accordingly, the variational principle does not always hold in the present method which makes use of the experimental value of molecular energy. However, this "half-theoretical" character of the present method gives an advantage of taking the nuclear charge z as an arbitrary parameter. According to this idea, it becomes possible to choose the z value from such a different point of view as will be discussed below.

When the atom C is separated infinitely from the molecule AB, the energy of the lowest state is apparently equal to that of molecule AB and that of the next higher state belonging to another doublet is expressed, by the use of Wang type function, as follows:

$$E_1=\frac{1}{R_{AB}}+\frac{Q-J}{1-S^2} \tag{8}$$

where

$$S=(ab) \tag{9}$$

$$Q=(a^2 \mid b^2)-(a^2 \mid B)-(b^2 \mid A) \tag{10}$$

and

$$J=(ab \mid ab)-(ab)(ab \mid A+B) \tag{11}$$

This equation corresponds clearly to the theoretical expression of the repulsive ${}^3\Sigma_u^+$ state of H_2.

Since the energy of this state was evaluated accurately by James, Coolidge and Present[15] by the aid of the variation method, we can choose the parameter z so as to coincide the energy by Eq. 8 with the calculated value by them.

The result is satisfactory as shown in Fig. 5; when the nuclear distances R_{AB} and R_{BC} come near the configuration of activated state, z value approaches 1.4. This

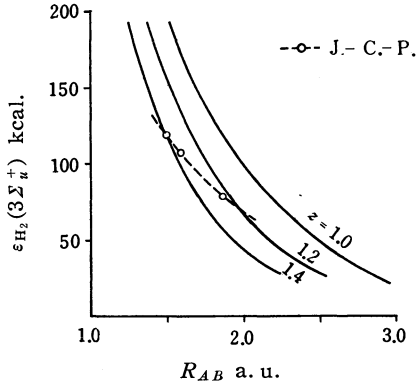


Fig. 5. Energy of triplet state of H_2.

fact suggests that the use of a composite function which gives better value for the energy of the state correlating strongly to the noticed one, improves the result markedly. Another qualitative reason of taking a larger value of z is in its effect upon the electronic distribution in the molecule. The present results will be improved if we make use of exact molecular function, e. g., James-Coolidge type one[16]. The distinction of J.-C. function from usual orbital ones is in its electronic distribution in which the overlapping of electrons is diminished by the introduction of inter-electronic coordinate r_{12}. This effect is

15) H. M. James, A. S. Coolidge and R. D. Present, *J. Chem. Phys.*, 4, 187 (1936).
16) H. M. James and A. S. Coolidge, ibid., 1, 825 (1933).

attained to some extent by the use of orbital functions with increasing z value. Also the addition of an ionic term, on the contrary, estranges the distribution from J.-C.'s. It is expected, therefore, that the utilization of larger z takes in partly the energy of electronic correlation in molecules, and then in the reacting system. It goes without saying that this correlation is partly included by the use of experimental data for the component species.

Potential Energy Basin

Here, the existence of so-called "potential energy basin" is briefly discussed.

By applying straightforwardly Eyring's semi-empirical method to the H_3 system of linear configuration, the obtained surface has two distinct basins[17], i.e., (a) a markedly deep one occurring where the distances between neighboring atoms, R_{AB} and R_{BC} are smaller than 1.0 a.u. and (b) a shallow one near the activated state.

Neither the results of the present calculation nor that of Hirschfelder et al.[1] show such basins as those above. The fact that these basins are apparent ones, being induced from the assumption of constant coulombic fraction, is explained as follows; for the shrunken configuration where both R_{AB} and R_{BC} are nearly equal to those giving zero bond energies, ε_{AB}, $\varepsilon_{BC}\simeq 0$, the coulombic and exchange parts of these bonds, Q_i and J_i $(i=AB, CB)$ are in the relation as

$$Q_i \simeq -J_i \gg 0 \tag{12}$$

while their values by Eyring's procedure are

$$(1-\rho)Q_1=\rho\cdot J_i\simeq 0 \tag{12'}$$

Therefore, the energy value which is obtained from London's formula,

$$E=Q_{AB}+Q_{BC}+Q_{CA}-[J_{AB}^2+J_{BC}^2+J_{CA}^2 - J_{AB}J_{BC}-J_{BC}J_{CA}-J_{CA}J_{AB}]^{1/2} \tag{13}$$

and these Q's and J's, is underestimated extremely as

$$E'=\varepsilon_{AC}=Q_{AC}+J_{AC} \tag{14'}$$

instead of exact value,

$$E=\varepsilon_{AC}+3Q_{AB}\gg E' \tag{14}$$

This situation is apparently the cause of basin a).

Next, the origin of basin b) is examined. For the equi-distant configuration "P" as shown in Fig. 7, the energy change ΔE,

17) S. Sato, This Bulletin, 28, 450 (1955).

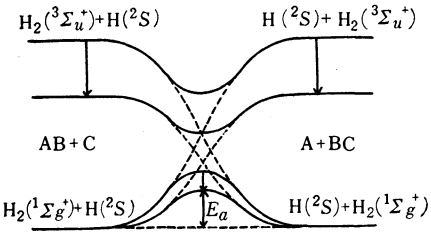


Fig. 6. Variation of activation energy with lowering of upper surface.

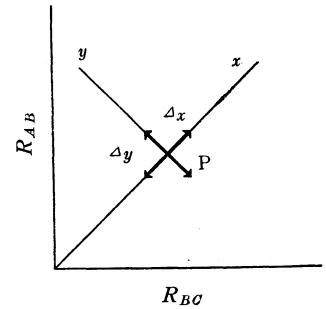


Fig. 7. Displacements around P.

induced from the small displacements around P is expressed as

$$\begin{aligned}\Delta E_x &\simeq \sqrt{2}\left[\left(\frac{\partial Q_{AB}}{\partial R_{AB}}\right)+\frac{1}{2}\left(\frac{\partial J_{AB}}{\partial R_{AB}}\right)\right.\\ &\quad\left.+\left(\frac{\partial Q_{AC}}{\partial R_{AC}}\right)-\left(\frac{\partial J_{AC}}{\partial R_{AC}}\right)\right]\cdot(\Delta x)\\ &\quad+\left[\frac{1}{2}\left(\frac{\partial^2 Q_{AB}}{\partial R_{AB}^2}\right)+\frac{1}{4}\left(\frac{\partial^2 J_{AB}}{\partial R_{AB}^2}\right)\right.\\ &\quad\left.+\left(\frac{\partial^2 Q_{AC}}{\partial R_{AC}^2}\right)-\left(\frac{\partial^2 J_{AC}}{\partial R_{AC}^2}\right)\right]\cdot(\Delta x)^2\\ &=A_1(\Delta x)+A_2(\Delta x)^2\end{aligned}$$

along the x axis and

$$\begin{aligned}\Delta E_y &\simeq \left[\frac{1}{2}\left(\frac{\partial^2 Q_{AB}}{\partial R_{AB}^2}\right)+\frac{1}{4}\left(\frac{\partial^2 J_{AB}}{\partial R_{AB}^2}\right)\right.\\ &\quad\left.-\frac{3}{4}\cdot\frac{1}{|J_{AB}-J_{AC}|}\cdot\left(\frac{\partial J_{AB}}{\partial R_{AB}}\right)^2\right]\cdot(\Delta y)^2\\ &=B_2(\Delta y)^2\end{aligned}$$

along the y axis. According to Eyring's assumption of constant ρ, the minimum point appears at the position where the coefficient of (Δx), A_1, is equal to zero and the nuclear separation $R_{AB}^*(=R_{BC}^*)$ is slightly larger than the equilibrium distance r_e of H_2 (1.40 a.u.), for example, $R_{AB}^*=1.6$ and 1.9 a.u. for $\rho=0.2$ and 0.1, respectively. In the case of large coulombic fraction, therefore, this point is apparently in a basin, for $A_2>0$ and B_2, the coefficient of $(\Delta y)^2$, estimated approximately by the

use of equation

$$B_2 \simeq \frac{1}{4}\left(\frac{\partial^2 J_{AB}}{\partial R_{AB}^2}\right) - \frac{3}{4}\cdot\frac{1}{|J_{AB}-J_{AC}|}\cdot\left(\frac{\partial J_{AB}}{\partial R_{AB}}\right)^2$$

$$J_{AB} = (1-\rho)\cdot\varepsilon_{H_2}(R_{AB})$$

and of Morse function of H_2, is positive where

$$R_{AB}^{*} < 1.74 \text{ a. u.}$$

Alternatively, when we give up this assumption of constant ρ, the nuclear distances at the minimum point are somewhat extended. The value of B_2 estimated by making use of the following expression of J_{AB},

$$J_{AB} = D'\left[e^{-2a(r-r_e')} - 2e^{-a(r-r_e')}\right]$$ [18]

where $D' = 0.9\, D_{H_2} = 98.51$ kcal./mol.

$r_e' = 0.9\, r_e = 1.261$ a. u.

and $a = 1.0298$,

is negative where

$$R_{AB}^{*} > 1.60 \text{ a. u.}$$

This result shows that the surface near the activated state is a saddle-like one or, at least, has not such a depression as was expected by Eyring et al.

Computation of Reaction Rate

Now, we shall evaluate the rate of the reaction on the knowledge of the surface derived here. Such a detailed calculation has been done only by Eyring et al.[19] According to the activated complex theory, the rate v and rate constant k of the elementary reaction $H_2(AB) + H(C) \rightarrow H(A) + H_2(BC)$ are expressed by

$$v = kC_{H_2}\cdot C_H \qquad (20)$$

and

$$k = \kappa\frac{I_{H_3}\sigma_{H_2}}{I_{H_2}\sigma_{H_3}}\cdot\frac{h^2}{(4\pi m_H/3)^{3/2}\cdot(kT)^{1/2}} \times\frac{1}{4}\cdot\frac{\sinh\left(\frac{1}{2}h\nu_{H_2}/kT\right)e^{-E_c/kT}}{\sinh\left(\frac{1}{2}h\nu_s/kT\right)\cdot\sinh^2\left(\frac{1}{2}h\nu_\phi/kT\right)} \qquad (21)$$

The notations in these equations are as follows:

C; concentration of species.
κ; the transmission coefficient.
I; a moment of inertia.
σ; symmetry number.
m_H; mass of hydrogen atom.
ν_{H_2}; vibrational frequency of H_2.
ν_s and ν_ϕ; stretching and bending vibrational frequencies of activated complex respectively.
E_c; classical energy of activation.

The quantities belonging to molecule or complex are distinguished by the addition of subscripts, e. g., "H_2" or "H_3". Since the complex in the present result is a symmetrical linear one, $\sigma_{H_2} = \sigma_{H_3} = 2$ holds. Constants deduced from the surface constructed by the use of Wang type function ($z = 1.4$) are shown in Table VI with Eyring's ones.

TABLE VI. CONSTANTS FOR THE HYDROGEN ATOM-MOLECULE REACTION

	Present result*	Eyring et al.**
R_{AB}^{*} (Å)	0.88 (0.91)	1.354
R_{BC}^{*} (Å)	0.88	0.753
I_{H_3} (10^{-40} gcm^2)	2.62	3.79
I_{H_2} (〃)	0.458	0.458
$1/2\cdot h\nu_s$ (kcal.)	4.78	5.18
$1/2\cdot h\nu_\phi$ (kcal.)	1.35	0.95
$1/2\cdot h\nu_{H_2}$ (kcal.)	6.27	6.21
E_c (kcal.)	8.5 (7.1)	7.63

* Values obtained by the use of Wang type function with $z = 1.4$. In parentheses, those with R.-M. approximation are shown.
** Values obtained from Ref. 19. Coulombic fraction $\rho = 0.20$.

TABLE VII. RATE CONSTANTS OF HYDROGEN ATOM-MOLECULE REACTION, k (cc. mol^{-1} sec^{-1})

Temperature °K	300	600	1000
Observed values	9.0×10^7	—	2.2×10^{12}
Present results a.	3.6×10^6	1.0×10^{10}	0.4×10^{12}
〃 b.*	3.9×10^7	3.5×10^{10}	0.7×10^{12}
Eyring et al.	7.3×10^7	7.3×10^{10}	1.5×10^{12}

* Values obtained by the use of constants in parentheses, Table VI.

The evaluated rate values are given in Table VII, with the observed ones by Geib and Harteck and Farkas et al.[14] and also with the calculated ones by Eyring et al. Although detailed comparison is rather difficult because of few experimental data, the agreement with the evaluated ones is reasonably good. The reason why Eyring's values are slightly large compared with the present ones is in the use of larger moment-of-inertia value of the complex deduced from its unsymmetrical form. Accordingly, when we give up the assumption of constant ρ, the moment-of-inertia and therefore rate

18) The corresponding coulombic fractions obtained from this function are 0.13, 0.18 and 0.20 at $R_{AB} = 1.5$, 2.0 and 2.5 a. u., respectively.
19) H. Eyring et al., "The Theory of Rate Processes", McGraw-Hill Book Co. Inc., New York, (1941), p. 203.

also are reduced to those near the present ones.

Besides, it is necessary to use corrected values of transmission coefficient for this reaction consisting of light atoms in low temperatures.

Since it is known that the bending of the reaction path scarcely affects the extent of transmission at all, the evaluation of κ is confined to that through potential energy barrier[20]. Now taking Wigner's correction, $\kappa=1-\frac{1}{24}\left(\frac{h\nu_t}{kT}\right)^2$, where ν_t is the imaginary vibrational frequency of complex along the reaction path, we obtain κ's values to be 6.3, 2.3 and 1.5 at 300, 600 and 1000°K respectively from the value $ih\nu_t=6.8$ kcal. The rate values are then corrected to

$$2.5\times10^8,\ 8.1\times10^{10} \text{ and } 1.1\times10^{12}$$

at respective temperatures. Since Wigner's correction may give upper limit of κ, it is sure that the rate in lower temperatures were well improved.

Conculusion

The method of modified bond eigenfunction was applied to construct the potential energy surface of the hydrogen atom-molecule reaction. Also it was shown that the reaction rates estimated on this surface were in agreement with the observed ones.

In the calculation of surface, we took effective nuclear charge z in orbital function as an arbitrary parameter and showed the propriety of employing a larger z value than unity. Accordingly, it is to be noted that the functions of component species near the configuration of activated state are different from those of "free species" and that, by the use of these deformations, some parts of electronic correlation energy are taken into calculation.

Recently, Arai et al.[21] have developed, in the field of "molecular theory", the method of "deformed-atoms-in-molecules" which differs from the original Moffitt's method by taking deformed atomic orbitals in the molecule. Then, it may be said that the method by the present author corresponds to a further extension of theirs for the reacting system.

Although, the electronic correlation is considered partly in the above-mentioned manner, its full inclusion by the device of more valid approximation for wave function will be the important problem to be studied hereafter.

The author wishes to thank Professor S. Shida of Tokyo Institute of Technology and Professor K. Hirota of Osaka University for their valuable suggestions and kind encouragement. Also the auther is indebted to Mr. Y. Mori for helpful discussion.

Laboratory of Physical Chemistry
Tokyo Institute of Technology
Meguro-ku, Tokyo

20) I. Yasumori and K. Fueki, This Bulletin, **29**, 1 (1956). For the effect of curved reaction path, I. Yasumori, ibid.. **32**, 913 (1959).

21) T. Arai, *J. Chem. Phys.*, **26**, 435, 451 (1957); T. Arai and M. Sakamoto, ibid., **28**, 32 (1958).

The Mannich Base of Troponoid and its Application. II. On 5-Bromomethyltropolone Derivative

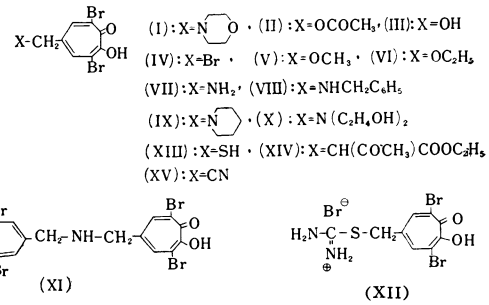
By Shuichi SETO and Kyozo OGURA

(Received March 26, 1959)

In the preceding paper[1], the authors reported on the derivation of 5-hydroxymethyl- and 5-formyltropolones from 3,7-dibromo-5-morpholinomethyltropolone, and on their reactions. In the present series of experiments, the 5-hydroxymethyl derivative was further led to 5-bromomethyl derivative and examination of this reaction showed some interesting results which are described herein.

Warming of 3,7-dibromo-5-hydroxymethyltropolone(III), obtained from 3,7-dibromo-5-morpholinomethyltropolone (I), in hydrobromic acid affords 3,7-dibromo-5-bromomethyltropolone(IV) as colorless needless, m. p. 140°C, in a good yield. IV is very reactive and reacts with various anionoid reagents to undergo substitution of bromine in the bromomethyl group as *p*-bromomethylphenol does[2].

Under some conditions, for example, treatment with sodium hydroxide solution, it forms a bis(tropolonyl)methane derivative. When IV is heated in methanol or ethanol, 5-methoxymethyl-(V) or 5-ethoxymethyltropolone derivative(VI) is obtained. These substances are the same as the compounds obtained on refluxing 5-acetoxymethyltropolone derivative(II) in methanol or ethanol. Reaction of IV with sodium acetate afforded II. Reaction with amines occurs easily at room temperature to afford the corresponding aminoalkyltropolone derivatives. Treatment with liquid ammonia, benzylamine, morpholine, piperidine and diethanolamine, respectively, affords 5-aminomethyl-(VII), 5-benzylaminomethyl-(VIII), 5-morpholinomethyl-(I), 5-piperidinomethyl-(IX), and 5-bis (β-hydroxyethyl) aminomethyltropolone (X) derivatives. I and IX are also obtained by the Mannich reaction of 3,7-dibromotropolone, and VII is also obtained in some cases by treatment of II with liquid ammonia. Reaction of IV with concentrated ammonium hydroxide gives bis (3,7-dibromotropolon-5-ylmethyl) amine (XI). All these aminoalkyltropolone derivatives form a water-soluble green iron complex with ferric chloride. IV undergoes reaction with thiourea in *tert*-butanol at room temperature to form *S*-(3,7-dibromotropolon-5-ylmethyl) isothiuronium bromide(XII) whose treatment with alkali affords 3,7-dibromo-5-mercaptomethyltropolone (XIII). IV forms a bis(tropolonyl)-methane derivative in strong alkali and its reaction with carbanions is not possible by the conventional method. Application of a large excess of the reagent to a dilute solution of IV gives the desired compound. For example, dropwise addition of a dilute solution of IV in ethyl acetoacetate with stirring, into a solution of a large excess of potassium compound of ethyl acetoacetate affords the anticipated 5-(β-acetyl-β-ethoxycarbonyl)tropolone derivative(XIV). Application of a large excess of potassium cyanide to a solution of IV in dioxane and water gives 5-cyanomethyltropolone derivative(XV).



Experimental[3]

3,7-Dibromo-5-bromomethyltropolone (IV). — A mixture of 2 g. of 3,7-dibromo-5-hydroxymethyltropolone(III) and 40 ml. of hydrobromic acid (sp. g., 1.38) was warmed for 15 min. and the colorless needle crystals that separated out were recrystallized from a benzene-cyclohexane mixture: m. p. 139~140°C. Yield, 2 g.

Anal. Found: C, 25.91; H, 1.89. Calcd. for $C_8H_5O_2Br_3$: C, 25.73; H, 1.34%. U. V. λ_{max}^{MeOH} mμ (log ε): 265(4.53), 350(4.21), 428(421).

1) S. Seto and K. Ogura, This Bulletin, **32**, 493 (1959).
2) K. Auwers, *Ber.*, **34**, 4264 (1901).
3) All melting points are not corrected.

3, 7-Dibromo-5-methoxymethyltropolone (V). — A solution of 10 mg. of IV in 1 ml. of methanol was heated on a water bath for about 10 minutes and the removal of methanol left colorless needles, m. p. 135°C, which showed no depression on admixture with the substance[1] obtained by refluxing II in methanol.

Anal. Found: C, 33.98; H, 2.73. Calcd. for $C_9H_8O_3Br_2$: C, 33.33; H, 2.47%. U. V. λ_{max}^{MeOH} mμ (log ε): 267(4.63), 346(4.29), 428(4.30).

3, 7-Dibromo-5-ethoxymethyltropolone (VI). — In exactly the same manner as in the cases of V and IV was heated in ethanol and colorless needles, m. p. 100°C, were obtained. These showed no depression on admixture with the substance[1] obtained by the refluxing of II in ethanol.

Anal. Found: C, 35.62; H, 2.91. Calcd. for $C_{10}H_{10}O_3Br_2$: 35.54; H, 2.96%.

3, 7-Dibromo-5-aminomethyltropolone (VII).—(a) A solution of 100 mg. of IV dissolved in ca. 5 ml. of liquid ammonia was allowed to stand at room temperature for 4 days. The yellowish brown residue which was obtained by removal of liquid ammonia was extracted with 1.5 N hydrochloric acid. The extract was neutralized to pH 2.5 and the precipitate thereby formed was collected. Washing of this precipitate with water and methanol afforded yellow powder, m. p. 225°C (decomp.).

b) A solution of 100 mg. of II dissolved in ca. 100 ml. of liquid ammonia was allowed to stand for a week. VII was obtained by treating the residue in the same manner as in the case of a).

Anal. Found: C, 29.62; H, 3.27; N, 4.04. Calcd. for $C_8H_7O_2NBr_2 \cdot H_2O$: C, 29.35; H, 2.75; N, 4.28%. U. V. λ_{max}^{MeOH} mμ (log ε): 268(4.44), 345 (3.95), 430(3.98).

3,7-Dibromo-5-benzylaminomethyltropolone(VIII). —About 30 mg. of IV was dissolved in one drop of benzylamine and the solution was warmed at 50°C for a few minutes. By this process yellow crystals separated out. About 1 ml. of acetic acid-water was added to this mixture, the crystals were collected by filtration, and recrystallized from ethanol; m. p. 180°C. Yield, ca. 30 mg.

Anal. Found: C, 43.94; H, 3.57; N, 3.10. Calcd. for $C_{15}H_{13}O_2NBr_2 \cdot 2H_2O$: C, 43.17; H, 3.59; N, 3.35%. U. V. λ_{max}^{MeOH} mμ (log ε): 267(4.32), 347 (3.95), 430(3.87).

3, 7-Dibromo-5-piperidinomethyltropolone (IX).— a) The addition of 0.5 ml. of piperidine to 50 mg. of IV resulted in excessive generation of heat and a solution was effected. Addition of water to this solution produced a yellow precipitate. This mixture was adjusted to pH 5 with hydrochloric acid, the precipitate was collected, and washed with water and ethanol. m. p. 189~190°C (decomp.). Yield, ca. 20 mg.

b) A mixture of 400 mg. of 3,7-dibromotropolone(I) in 0.6 ml. of acetic acid and 0.4 ml. of piperidine was heated at 100°C and when in solution, 0.2 ml. of formaldehyde solution (37%) was added dropwise, with stirring. After about 10 min. of stirring and heating, the yellow precipitate that formed was collected and washed with water and ethanol, m. p. 190°C (decomp.). Yield, 490 mg. This substance showed no depression of melting point on admixture with the substance obtained by method a).

Anal. Found: C, 41.69; H, 3.95; N, 3.74. Calcd. for $C_{13}H_{15}O_2NBr_2$: C, 41.38; H, 3.98; N, 3.72%. U. V. λ_{max}^{MeOH} mμ (log ε): 268(4.02), 350 (3.71), 425(3.71).

3, 7-Dibromo-5-bis(β-hydroxyethyl)aminomethyltropolone (X). — A solution of 30 mg. of IV dissolved in 3 drops of diethanolamine was neutralized with 2 N hydrochloric acid and the yellow precipitate that formed was collected, washed with water and methanol; m. p. 160°C.

Anal. Found: C, 35.60; H, 3.89; N, 3.69. Calcd. for $C_{12}H_{15}O_4NBr_2$: C, 36.27; H, 3.78; N, 3.52%. U. V. λ_{max}^{MeOH} mμ (log ε): 267(4.21), 350 (3.90), 430(3.87).

Bis(3, 7-dibromotropolon-5-ylmethyl)amine (XI). —A mixture of ca. 30 mg. of IV in 0.5 ml. of concentrated ammonium hydroxide was stirred for a few minutes at room temperature. By this process yellow crystals precipitated out. This mixture was neutralized with 2 N hydrochloric acid, the yellow powder so formed was collected, and washed with water and methanol; m. p. 196°C.

Anal. Found: C, 31.31; H, 1.98; N, 2.59. Calcd. for $C_{16}H_{11}O_4NBr_4$: C, 31.94; H, 1.83; N, 2.31%. U. V. λ_{max}^{MeOH} mμ (log ε): 268(4.40), 345 (4.06), 425(4.00).

S-(3,7-Dibromotropolon-5-ylmethyl)isothiuronium Bromide (XII).—A solution of 40 mg. of IV and 20 mg. of thiourea dissolved in 3 ml. of *tert*-butanol was stirred at room temperature for a few minutes and the colorless crystals that separated out were collected, and washed with ethanol; m. p. 223~224°C (decomp.). Yield, 50 mg.

Anal. Found: C, 24.59; H, 2.42; N, 6.51. Calcd. for $C_9H_9O_2N_2SBr_3$: C, 24.05; H, 2.00; N, 6.24%. U. V. λ_{max}^{MeOH} mμ (log ε): 268(4.59), 335 (3.88), 387(3.71), 420(3.58).

3, 7-Dibromo-5-mercaptomethyltropolone (XIII). —A mixture of 50 mg. of XII in 0.5 mol. of 45% sodium hydroxide solution was heated for a few minutes on a water bath and neutralized by pouring this mixture into 6 N hydrochloric acid containing cracked ice. The precipitate that formed was collected and recrystallized from ethanol to give pale yellow needles, m. p. 128°C. Yield, 20 mg.

Anal. Found: C, 30.10; H, 1.84. Calcd. for $C_8H_6O_2Br_2S$: C, 29.45; H, 1.82%. U. V. λ_{max}^{MeOH} mμ (log ε): 267(4.46), 350(4.01), 430(3.86).

3, 7-Dibromo-5-(β-acetyl-β-ethoxycarbonylethyl)-tropolone (XIV). — A solution of 500 mg. of IV dissolved in 50 ml. of ethyl acetoacetate was added dropwise into a solution of 1 g. of potassium dissolved in 50 ml. of ethyl acetoacetate, with stirring at room temperature. The solution was further stirred for 2 hr. at room temperature,

neutralized with 6 N sulfuric acid to pH 5, and the ethyl acetoacetate layer was separated. The acetate layer was washed with water and evaporated under reduced pressure to remove the acetate. The dark red, oily residue crystallized on addition of ether, the crystals were collected, washed with ether, and recrystallized from a mixture of benzene and petroleum ether; m. p. 114~115°C. Yield, 350 mg.

Anal. Found: C, 39.83; H, 3.74. Calcd. for $C_{14}H_{14}O_5Br_2$: C, 39.81; H, 3.32%. U. V. λ_{max}^{MeOH} mμ (log ε): 268(4.55), 345(4.07), 430(3.96).

3, 7-Dibromo-5-cyanomethyltropolone (XV). — A solution of 150 mg. of IV dissolved in 3 ml. of dioxane was added dropwise, with stirring, into a solution of 150 mg. of potassium cyanide dissolved in 6 ml. of dioxane and 1 ml. of water at room temperature, the drops causing a transitory red color to appear. After completion of addition, the mixture was stirred for 1 hr., the solvent was removed under reduced pressure at room temperature, and the residue was acidified with hydrochloric acid. The brown precipitate that formed was collected and recrystallized from benzene; m. p. 148~151°C. Yield, 100 mg. During recrystallization, bis(3,7-dibromotropolon-5-yl)-methane formed as a benzene-insoluble by-product.

Anal. Found: C, 34.04; H, 1.80; N, 3.82. Calcd. for $C_9H_5O_2NBr_2$: C, 33.86; H, 1.57; N, 4.39%. U. V. λ_{max}^{MeOH} mμ (log ε): 267(4.50), 345(4.04), 430(3.98).

Summary

Reaction of 3,7-dibromo-5-hydroxymethyltropolone with hydrobromic acid affords 3, 7-dibromo-5-bromomethyltropolone, which has a high reactivity and reacts with various anionoid reagents to undergo substitution of bromine in the bromomethyl group. In this manner it is possible to extend the substituent by forming C–O, C–N, C–S and C–C bonding at the tip of the methyl group in position 5 of the tropolone ring.

A part of the expense for the present research was defrayed by Sankyo Co., Ltd. The microanalyses were carried out by Messrs. S. Oyama and S. Azumi and Miss A. Iwanaga. The authors wish to express their sincere gratitude to the above-mentioned people.

The Chemical Research Institute of Non-Aqueous Solutions
Tohoku University
Katahira-cho, Sendai

Synthesis of Polyanhydride. I. Mixed Anhydride of Aromatic and Aliphatic Dibasic Acids*

By Naoya YODA and Akihisa MIYAKE

(Received February 4, 1959)

The polyanhydride of aromatic dibasic acid was first prepared by Bucher and Slade[1], who reported that the crystalline polymer of the melting point above 300°C was obtained by heating isophthalic acid or terephthalic acid with acetic anhydride. Aliphatic polyanhydride was synthesized in 1932 by Hill and Carothers[2] who have investigated the preparation of polyanhydride from sebacic acid. Although possessing fiber-forming properties, it was reported that the aliphatic polyanhydride melted at too low a point to be of practical interest and the polymer gradually disintegrated in the presence of moisture due to hydrolytic degradation. On account of these unfavorable properties, the study of polyanhydride has not been taken into consideration since then. In 1957, however, Conix[3] reported that aromatic polyanhydride prepared from di-(*p*-carboxyphenoxy)-α,ω-alkane has shown excellent film and fiber-forming properties. This might be ascribed to the hydrophobic nature of polymer molecules, caused by the accumulation of phenylene nuclei along the polymer chain to form a regular molecular structure very closely packed as observed in polyethylene terephthalate.

The present investigation has been undertaken in order to study the synthesis

* Presented before the 4th Autumnal Meeting of the Chemical Society of Japan, held in Tokyo, November 23, 1958.

1) J. E. Bucher and W. C. Slade, *J. Am. Chem. Soc.*, **32**, 1319 (1909).

2) J. W. Hill and W. H. Carothers, ibid., **54**, 1569 (1932).

3) A. Conix, *Makromol. Chem.*, **24**, (1) 76 (1957); *J. Polymer Sci.*, **29**, 343 (1958).

of mixed polyanhydrides of aromatic and aliphatic dibasic acids. As described herein, the mixed polyanhydrides of random structure were obtained when the calculated amount of aromatic and aliphatic dibasic acids had been mixed and treated with acetic anhydride which caused them to polymerize by heating in vacus. When suitable amounts of aromatic and aliphatic dibasic acids were used, it was possible to obtain mixed polyanhydrides of practical interest having their melting points in the range of 200 to 250°C. Using terephthalic acid as aromatic dibasic acid and adipic acid or sebacic acid as aliphatic dibasic acid, the mixed dibasic acids can be transformed into mixed anhydride with acetic anhydride. These mixed anhydrides polymerize by splitting off acetic anhydride. The diagram of composition versus melting point was obtained. From this the composition of mixed polyanhydride having its melting point in the range of 200°C to 250°C has been obtained for terephthalic acid-adipic acid, and terephthalic acid-sebacic acid copolymers.

Furthermore, the preparation of aromatic and aliphatic mixed polyanhydrides of regular structure have been investigated by the polycondensation reaction of diacid halide with dibasic acid in organic solvent pairs such as pyridine-benzene and pyridine-ether. The mixed polyanhydrides of regular structure having their melting points at 225°C (adipic acid) and 215°C (sebacic acid) have been synthesized, and the influence of chemical structure on the physical properties of these polymers was discussed[4].

Experimental and Results

Materials.—Commercially available sebacic acid and adipic acid were recrystallized from ethanol. The melting point was 133°C and 151~153°C, respectively. The purified terephthalic acid was obtained by converting it into dimethyl ester, followed by vacuum distillation and alkaline hydrolysis. Thus, carefully purified aliphatic and aromatic dibasic acids were used as a starting material for each polymerization.

Mixed Polyanhydride of Random Structure.—The mixed polyanhydride of terephthalic acid and adipic acid was obtained by polycondensation reaction using the excess of acetic anhydride. The detailed procedure is described as follows.

A 13.3 g. (0.08 mol.) portion of terephthalic acid and 17.5 g. (0.12 mol.) of adipic acid were mixed together and 415 ml. of acetic anhydride (b. p. 130°C) were added to the mixture. The combined solution was refluxed on an oil bath at 150~160°C for 8 hr. After the dibasic acids were completely dissolved into acetic anhydride, reflux was continued for an additional one hour and the excess of acetic anhydride was distilled off under water jet pump pressure to form mixed anhydride of low melting crystalline solid. The prepolymer thus formed was heated under dry nitrogen atmosphere in vacuo at 240°C for 1.5 hr. The resulting polyanhydride has its melting point at 235°C and possesses fiber-forming property. The intrinsic viscosity of polymer measured in 1,4-dioxane at 30°C was 0.130. However, it becomes brittle shortly after spinning due to its hydrolytic degradation by absorbing moisture. When purified terephthalic acid and adipic acid were used, it was possible to avoid coloration by impurities on heating.

The relationship between the melting point and the composition of terephalic acid and adipic acid was measured and its mole fraction was plotted against the melting point of copolymer as shown in Fig. 1. It gives the minimum melting point at 47~48°C where the composition of copolymer

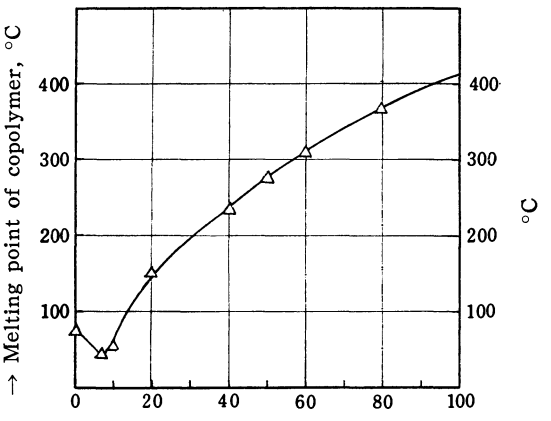


Fig. 1. Relation between composition and melting point of adipic acid-terephthalic acid anhydride copolymer.

is 93 mol. % of adipic acid. Polyanhydride of terephthalic acid itself has its melting point above 410°C. Two acids, e. g., terephthalic acid and aliphatic acid, furnish a series of copolymers in which the melting point and degree of crystallinity increase as the proportion of terephthalic acid is increased over 10 mol. %.

The experimental results are summarized in Table 1. The infrared spectrum of the polymerization product has absorption bands of anhydride carbonyl group at 5.56 and 5.78 μ as illustrated in Fig. 2[5].

The polycondensation proceeds smoothly upon heating in vacuo to obtain a linear polymer and

4) N. Yoda, *Makromol. Chem.* **32**, (1) 1 (1959).

5) L. J. Bellamy, "The Infrared Spectra of Complex Molecules", 2nd. Ed., Methuen & Co., London (1958), p. 127—129.

TABLE I. COMPOSITION AND MELTING POINT OF TEREPHTHALIC ACID-ADIPIC ACID ANHYDRIDE COPOLYMERS

Expt. No.	Terephthalic acid mol. %	Adipic acid mol. %	m. p., °C	Properties	$[\eta]^{30°C}_{1,4\text{-Dioxane}}$
1	0	100	75～ 77	Crystallizes readily	—
2	7	93	47～ 48	Crystallizes readily	—
3	10	90	53～ 55	Crystallizes readily	—
4	20	80	150～155	Crystallizes, fiber-forming	0.116
5	40	60	235	Crystallizes, fiber-forming	0.130
6	50	50	275	Crystalline solid	—
7	60	40	310	Crystalline solid	—
8	80	20	365	Crystalline solid	—

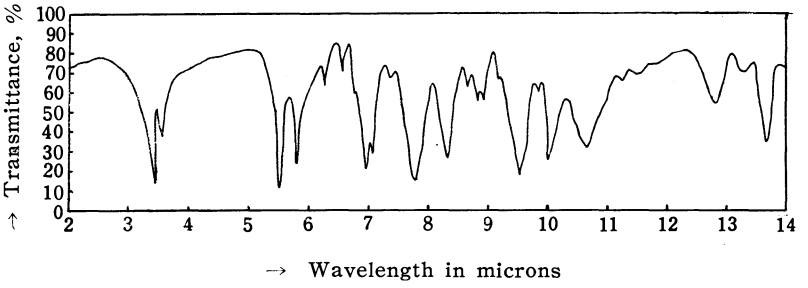


Fig. 2. The infrared spectrum of polyanhydride of adipic acid-terephthalic acid system (KBr).

the infrared data support the fact that the chains link with each other by anhydride groups and are terminated by acetyl groups derived from the reagent used in bringing about the anhydride formation.

The polymerization is started even by simple heating at 220～250°C at atmospheric pressure. A much faster reaction, leading to the formation of polyanhydride of higher molecular weights is observed, however, on heating the mixed anhydrides in vacuo under dry nitrogen atmosphere at elevated temperatures in order to facilitate the removal of acetic anhydride.

In the same manner, the mixed polyanhydride of terephthalic acid and sebacic acid was prepared by polycondensation of purified sebacic acid and terephthalic acid. The detailed procedure is illustrated below.

A 17 g. portion (0.10 mol.) of terephthalic acid and 40 g. (0.20 mol.) of sebacic acid were pulverized and 1000 ml. of acetic anhydride was added to the mixture. The solution was refluxed at 150～160°C for 8 hr. After distilling off the excess of acetic anhydride, a mixed anhydride of low melting crystalline solid was obtained. The prepolymer was heated under dry nitrogen atmosphere in vacuo at 230°C for 1.5 hr. to form polyanhydride having its melting poing at 220°C. This possesses a fiber-forming property and it is somewhat elastic. It becomes brittle shortly after spinning due to its hydrolytic degradation by absorbing moisture. The intrinsic viscosity of polymer measured in *p*-dioxane at 30°C immediately after spinning was 0.162.

The relationship between the melting point versus the composition of terephthalic acid and

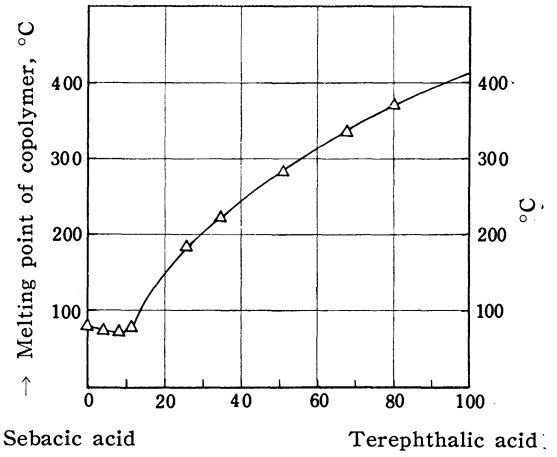


Fig. 3. Relation between composition and melting point of sebacic acid-terephthalic acid anhydride copolymer.

sebacic acid was obtained and its mole fraction was plotted against the melting point of copolymer as shown in Fig. 3. It was found that the minimum melting point was at 75°C where the composition of copolymer was 95.6 mol. % of sebacic acid and 4.4 mol. % of terephthalic acid. The experimental results are summarized in Table II. The infrared spectrum of copolymer has carbonyl absorption bands at 5.56 and 5.78 μ as shown in Fig. 4[5].

Infrared spectra indicate that polyanhydride before hydrolysis has two carbonyl absorption

TABLE II. COMPOSITION AND MELTING POINT OF TEREPHTHALIC ACID-SEBACIC ACID ANHYDRIDE COPOLYMERS

Expt. No.	Terephthalic acid mol. %	Sebacic acid mol. %	m. p., °C	Properties	$[\eta]_{1,4\text{-Dioxane}}^{30°C}$
1	0	100	79~80	Crystallizes readily	—
2	4.4	95.6	78	Crystallizes readily	—
3	8.5	91.5	75	Crystallizes readily	—
4	11.0	89.0	80	Crystallizes readily	—
5	25.9	74.1	185	Crystallizes, fiber-forming	0.081
6	34.4	65.6	220	Crystallizes, fiber-forming	0.162
7	51.1	48.9	280	Crystalline solid	—
8	67.7	32.3	335	Crystalline solid	—
9	80.7	19.3	370	Crystalline solid	—

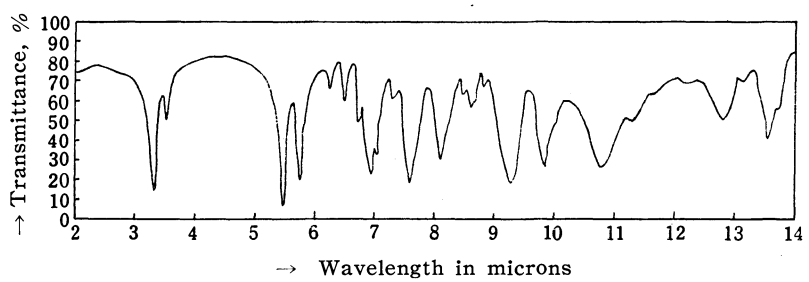


Fig. 4. The infrared spectrum of polyanhydride of sebacic acid-terephthalic acid system (KBr)

bands of the anhydride group at 5.56 and 5.78 μ. In addition to the carbonyl absorptions, the anhydride group also shows a strong band due to the C-O-C stretching vibration at 9.56 μ. When the polymer is exposed to moisture, the carbonyl absorption band at 5.86 to 5.95 μ appears. This indicates the existence of aliphatic and aromatic carboxylic acid carbonyl groups. The absorption bands at 3.71 and 3.95 μ are also observed. These can be taken as a strong evidence for the presence of dimeric carboxylic acid by taking account of bands existing in the carbonyl region.

When polyanhydrides of random structure are exposed to alkaline solution, it leads to the complete hydrolysis of anhydride to form aromatic and aliphatic dicarboxylic acids. An infrared spectrum shows neither anhydride carbonyl bands at 5.56 and 5.78 μ nor an ether band at 9.56 μ. On the contrary, the typical carboxylic acid bands appear at 3.71 and 3.95 μ of dimeric carboxylic acid bands and the strong carbonyl band at 5.86 μ[5].

The mixed anhydride of three components of dibasic acid such as the terephthalic acid, the adipic acid and the sebacic acid system was prepared by polycondensation reaction using the excess of acetic anhydride. The polymerization procedure is described as follows.

A 8.3 g. portion (0.05 mol.) of terephthalic acid, 7.3 g. of adipic acid (0.05 mol.) and 10.1 g. (0.05 mol.) of sebacic acid were thoroughly mixed in a mortar and refluxed with 550 ml. of acetic anhydride at 150~160°C for 8 hr. After all the acids were completely dissolved into acetic anhydride, the excess of acetic anhydride was distilled off under reduced pressure to form a mixed anhydride which was a low-melting crystalline solid. Then the prepolymer was heated under dry nitrogen atmosphere in vacuo at 250°C for 1.5 hr. to form a polyanhydride having a melting point at 245°C, which possesses a fiber-forming property.

Polymerization with acetyl chloride was also studied for dibasic acid anhydride of terephthalic acid and adipic acid or sebacic acid. In this case, the fiber-forming copolymer having a melting point at 210~230°C was also obtained with the mole fraction of 40 mol. % of terephthalic acid and 60 mol. % of adipic acid or sebacic acid.

Mixed Polyanhydride of Regular Structure.— Attempting to prepare the polyanhydride in which aromatic dibasic acid and aliphatic dibasic acid link with each other in a regularly bonded form, the polycondensation reaction of dibasic acid and dibasic acid chloride by dehydrochorination was studied in organic solvent pairs such as pyridine-ether, pyridine-benzene and dimethyl formamide-dimethyl aniline. Furthermore, the reaction of dibasic acid chloride with dimethyl ester of dibasic acid was investigated. In this case, terephthalic acid was again used for aromatic dibasic acid, and adipic acid or sebacic acid was chosen for aliphatic dibasic acid.

Preparation of Dibasic Acid Chloride.— Terephthalic acid chloride was prepared by the action of phosphorus pentachloride on terephthalic acid. After extraction with ether, it was dried over anhydrous sodium sulfate and the ether was evaporated off. The recrystallizations from ligroin after decolorization with activated charcoal

gave colorless needles, m.p. 83.0°C (yield, 67%).

Adipic acid chloride was also obtained by refluxing adipic acid with the excess of thionyl chloride on a water bath for 4 hr. After evaporating off the excess of thionyl chloride, it gave adipic acid chloride which boiled at 112~115°C/10 mmHg (yield, 60%). Sebacic acid chloride was prepared in the same manner mentioned above with thionyl chloride to obtain a product boiling at 161°C/14 mmHg (yield, 45%). In order to avoid hydrolysis, the solvents used for the polymerization were carefully purified each time before use. Pyridine (C. P. grade) was refluxed with barium oxide and distilled, and the fraction at 115.5°C was taken. Benzene and ether were dried over metallic sodium and distilled immediately before use.

Polymerization in Pyridine-Ether Medium —A 4.5 g. portion (0.03 mol.) of terephthalic acid was dissolved into 120 ml. of pyridine and 5 g. (0.03 mol.) of adipic acid chloride dissolved into 100 ml. of ether were added dropwise into the reaction system with ice cooling under dry nitrogen atmosphere.

When acid chloride is added into pyridine, the pyridine complex is formed[6]. The reaction temperature was gradually raised to 25~30°C and stirring was continued for 4 hr. at this temperature. The resulting polymer was filtered, washed and dried to obtain polyanhydride having a melting point at 250°C. The existence of the anhydride group was confirmed by the infrared spectrum which showed acid anhydride absorption bands in a carbonyl region[5].

Polyanhydride of sebacic acid-terephthalic acid obtained under the same reaction condition has its melting point at 240°C, and the infrared spectrum has acid anhydride absorption bands in a carbonyl region[5].

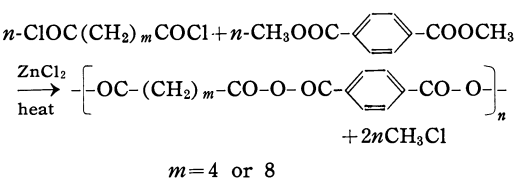
On the contrary, polyanhydride of terephthalic acid chloride and aliphatic acid forms a white crystalline solid, melting at 300°C with decomposition. The infrared spectrum shows acid anhydride and carboxylic acid absorption bands in a carbonyl region.

Polymerization in Pyridine-Benzene Medium.— When a pyridine-benzene solvent pair is used for the dehydrochlorination of terephthalic acid and aliphatic dibasic acid chloride, it was observed that the reaction proceeded more smoothly than in a pyridine-ether medium to form a white crystalline solid having its melting point at 225°C. The infrared spectrum shows carbonyl absorption band at 5.50 and 5.70 μ.

The reaction of sebacic acid chloride and terephthalic acid was also studied under the same reaction conditions, and white crystalline polymer melting at 215°C was obtained. The percent conversion of polyanhydrides in pyridine-benzene was found to be higher than that of polyanhydrides in pyridine-ether. The infrared spectrum indicates the existence of the acid anhydride group in a carbonyl region.

Polymerization of Dibasic Acid Chloride with Dibasic Acid Methyl Ester in the Presence of Zinc Chloride Catalyst.—As one of the processes to prepare polyanhydrides of regular structure, the polymerization reaction of dibasic acid chloride with dibasic acid methyl ester in the presence of zinc chloride was studied. The polyanhydrides of regular structure having their melting points at 203°C (adipic acid-terephthalic acid) and at 195°C (sebacic acid-terephthalic acid) were obtained.

Kyrides and Dvornikoff[7] reported the reaction of dialkyl phthalate and phthalyl chloride to give anhydride and the alkyl chloride. The improved method of the reaction of diacid chloride and diacid ester was employed in the presence of zinc chloride as a catalyst. The following reaction takes place for the polymerization in this case.



$m=4$ or 8

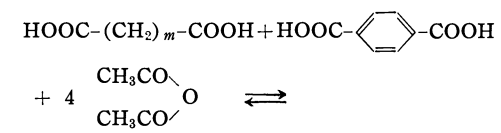
Although it is relatively stable against hydrolytic degradation, coloration of the polymer was observed when it was heated above 200°C.

In the same manner, polyanhydride obtained from sebacic acid chloride melts at 195°C and coloration occurs when it is heated above 200°C. It was found that the polymer thus obtained was relatively stable towards hydrolysis and it has a melting point with thermal decomposition. The polycondensation in dimethyl formamide medium was also studied and the polymers thus obtained failed to show good hydrolytic and thermal stability. It was found from the experimental results obtained above that the dehydrochlorination reaction of acid chloride and dibasic acid in pyridine-benzene medium gave the most satisfactory results.

Infrared Absorption Measurements. — The spectra were recorded with a Perkin-Elmer Model 21 spectrophotometer using an NaCl prism. Potassium bromide disks were used. The die and handpress were those supplied by the Shimadzu Co., Ltd.

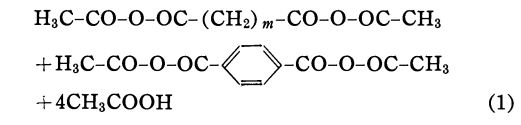
Discussion

The polycondensation reaction of aromatic and aliphatic dibasic acids with acetic anhydride proceeds through the following equations; firstly, the dibasic acids are converted into mixed anhydrides with acetic anhydride as shown in Eq. 1.



6) E. C. Harning, "Organic Syntheses", Col. Vol. III, John Wiley & Sons, Inc., New York (1955), p. 28.

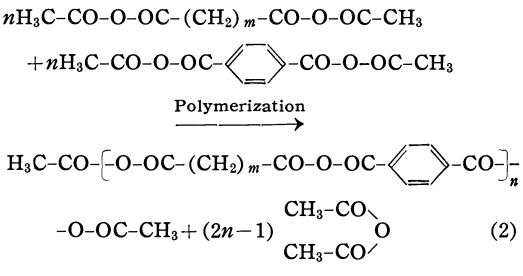
7) L. P. Kyrides and M. N. Dvornikoff, *J. Am. Chem. Soc.*, **55**, 4630 (1933).



(1)

$m=4$ or 8

Secondly, these mixed anhydrides thus formed, which bear terminal acetyl end-groups and are low-melting crystalline solids, polymerize upon heating by splitting off acetic anhydride to form polyanhydride with high molecular weights as indicated in the following Eq. 2.

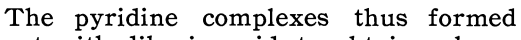


(2)

$m=4$ or 8

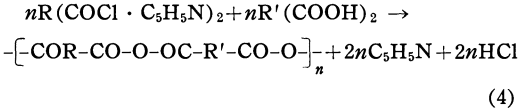
As to the mixed polyanhydride of random structure from aliphatic and aromatic dibasic acids, it was observed that the melting point and the degree of crystallinity increase with an increase in the proportion of aromatic dibasic acid. Presumably this can be explained by the fact that the introduction of aromatic nuclei into the polymer chain results in the formation of the polymer having rigid molecular structure due to the accumulation of phenylene nuclei along the polymer chain.

In the polymerization of polyanhydride of regular structure in pyridine-ether and pyridine-benzene media, the pyridine complexes of diacid chloride are first formed as shown in the following scheme:

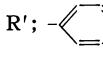


(3)

The pyridine complexes thus formed react with dibasic acid to obtain polyanhydride of regular structure as follows:



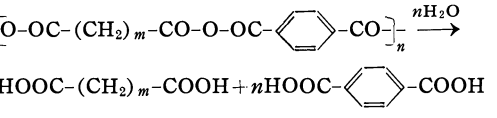
(4)

A. R; $-(CH_2)_4-$, $-(CH_2)_8-$, R'; 

B. R;  , R'; $-(CH_2)_4-$, $-(CH_2)_8-$

There are possibilities that anhydride interchange reaction takes place during the dehydrochlorination process at an elevated temperature to be transformed into the polyanhydride of random structure. This can be avoided, however, when the polymerization is performed at room temperature or at slightly elevated temperature under atmospheric pressure.

It is reasonably presumed that acid anhydride groups in a less closely packed polymer chain (e. g., polyanhydride of random structure) are easily hydrolyzed in the presence of moisture[8], and the polyanhydride chain is disintegrated into low molecular weight dicarboxylic acid, as shown below:



(5)

The authors have further given their attention to the application of interfacial polycondensation[9] for the polymerization of polyanhydride, which involves a similar concept already mentioned in the case of polymerization in solvent pairs, using diacid chloride for one component in such organic solvent as chloroform or benzene, and sodium or potassium salt of dibasic acid or dimethyl ester of dibasic acid for another in aqueous alcohol phase at room temperature under nitrogen atmosphere[10]. Much room is left for the detailed study of polyanhydride synthesis in this field, and further investigation is necessary before it can be applied for general purposes.

Summary

Copolymerization reactions of mixed anhydrides of aliphatic and aromatic dibasic acids have been investigated. It has been shown that a polyanhydride of regular structure was obtained from diacid chlorides and dibasic acids in organic medium, and that polyanhydrides of random structure were obtained from the mixed aromatic and aliphatic dibasic acids. A polyanhydride having its melting point at 225°C was prepared for terephthalic acid and adipic acid copolymer of regularly linked structure and that having its melting point at 215°C for terephthalic acid and sebacic acid copolymer. It was found that the stability of copolymer towards hydrolytic and thermal degradations was greater for those with regularly

8) C. K. Ingold, "Structure and Mechanism In Organic Chemistry" Cornell Univ. Press, Ithaca, New York (1953), p. 754.

9) E. L. Wittbecker and P. W. Morgan, Abstracts of the 134th Am. Chem. Soc. Meeting, Chicago, Illinois, (September, 1958), p. 8T—12T.

10) N. Yoda, unpublished work.

linked structure than for a polyanhydride of random structure. The mixed polyanhydrides of random structure were prepared and the diagram of composition versus melting point was obtained. The mole fractions of the two acid components were found to be 35~40 mol. % of terephthalic acid and 60~65 mol. % of aliphatic dibasic acid for copolymers melting at 220 to 240°C. It has further been shown that aliphatic and aromatic dibasic acids furnish a series of copolymers in which the solubility decreases and the melting point and the degree of crystallinity increase as the proportion of aromatic dibasic acid is increased.

The authors wish to express their gratitude to Dr. K. Hoshino, the Director of the Research Department, and Dr. M. Watanabe for their interest in this research and the permission for its publication. Sincere thanks are also due to Professor Y. Ishii of Nagoya University for helpful discussion. The authors are indebted to Messrs. S. Tanaka and Y. Bamba for their cooperation in carrying out the experiments.

Central Research Laboratories
Research Department
Toyo Rayon Co., Ltd.
Otsu, Shiga

The Isolation of Technetium by Coprecipitation or Anion Exchange

By Fujio ICHIKAWA

(Received January 17, 1959)

1. Coprecipitation of Technetium with Molybdate. — Technetium-99 having a long half-life is usually separated from fission products of uranium-235 after a long irradiation and cooling time. But technetium-99m is easily prepared as a decay product of molybdenum-99 from neutron irradiated molybdenum. Articles[1-3] on the coprecipitation of technetium mainly refer to that with sulfide, perrhenate and perchlorate. In this paper, the coprecipitation behavior in connection with the separation of technetium from molybdenum is reported.

Experimental. — Technetium-99m is not a β emitter but a γ emitter, whereas molybdenum-99 is a β and γ emitter. Accordingly the γ-ray spectrum peak of technetium-99m (0.140 MeV.) is measured with 256 channel pulse height analyzer, whereas molybdenum-99 is simply determined by measurement of β-ray activity with G-M counter.

Fifty milligrams of ammonium molybdate is irradiated in a J. R. R.-1 Reactor for 2 hr. at a flux of 10^{11} neutrons/cm^2/sec. Since the half-life of molybdenum-99 is 67 hr. and that of technetium-99m is 6.04 hr., radioactive equilibrium is reached after 23.08 hr. The irradiated sample is dissolved in 10 ml. of water after a day.

Two milliliters each of various precipitants is added to 1 ml. portion of this sample solution. A 5% solution of lead nitrate, calcium chloride, barium chloride, silver nitrate or uranyl nitrate is used as the precipitant. When calcium chloride is used, 1 ml. of 3 M aqueous ammonia is required for the complete precipitation of calcium molybdate. The precipitate formed is separated

TABLE I-1. COPRECIPITATION RATIO OF TECHNETIUM-99 m WITH SOME MOLYBDATES

Form of precipitate	Precipitation ratio of Mo-99 %	Precipitation ratio of Tc-99m %
$PbMoO_4$	99.2	99.6
	96.0	99.6
	86.4	87.5
$CaMoO_4$	94.4	23.1
	93.3	12.3
	96.5	20.1
	97.7	33.7
$BaMoO_4$	96.3	10.9
	94.7	41.4
	75.1	39.6
Ag_2MoO_4	85.5	51.6
	95.9	67.8
	96.7	41.8
UO_2MoO_4	85.0	35.2

1) J. B. Gerlit; "International Conference on the Peaceful Uses of Atomic Energy", Vol. 7, United Nations Publication, New York (1955), p. 145.
2) G. W. Parker, J. Reed and J. W. Ruch, AECD-2043.
3) N. Matsuura, M. Kojima and A. Iguchi, *Japan Analyst* (*Bunseki Kagaku*), **7**, 792 (1958).

from the supernatant solution by the aid of a centrifuge, a filter tube or an usual filtering funnel. The β and γ-ray activities of precipitates and supernatant solutions are measured by comparing them with the activities of the sample solution to which no precipitant was added. The separation ratio is calculated from those data and is shown in Table I-1.

Results. — A 99.6% portion of technetium-99m is coprecipitated with lead molybdate. About 70% of technetium-99m remains in the solution after calcium molybdate is precipitated, but a few per cent of molybdenum also remains by single precipitation. Seventy per cent of technetium-99m is not precipitated with barium molybdate or uranyl molybdate. J. A. Swartout[4] used silver molybdate in order to isolate technetium from molybdenum, but in the present study 50~60% of technetium is coprecipitated with silver molybdate.

The results mentioned above, are applied in two ways. One is an easy preparation of technetium-99m solution from irradiated calcium molybdate, and the other is an isolation of technetium-99m and molybdenum-99 from fission products by coprecipitation with lead molybdate.

(1) Fifty milligrams of calcium molybdate irradiated in J. R. R.-1 Reactor for 2 hr. is washed on a Toyo 5B filter paper with 10 ml. of water or 1% ammonium hydroxide and the β and γ activities of washings are measured. The results are shown in Table I-2.

The absorption curve of β-ray shows that calcium-45 coexists in the washings. This solution is passed through a cation-exchange column and almost all of the β contaminations are removed by this treatment.

TABLE I-2. SEPARATION OF TECHNETIUM-99m FROM IRRADIATED $CaMoO_4$

Washing	γ Activity of Tc-99m cpm/ml.	β Activity of impurities cpm/ml.	β Activity after resin treatment cpm/ml.
H_2O	129000	6240	691
1% NH_4OH	74565	12250	—

(2) Twenty milligrams of uranyl nitrate is irradiated in J. R. R.-1 for 2 hr. Neptunium-239 is separated by nitrate form anion exchanger[5]. Then the solution containing uranium and fission products is neutralized with ammonium hydroxide and ammonium biuranate formed is removed by filtering. A few milligrams of ammonium molybdate and lead nitrate are added to this solution. Lead moybdate is separated and washed with water. This precipitate shows a γ-ray spectrum of technetium-99m free from other fission products. (Fig. 1-1)

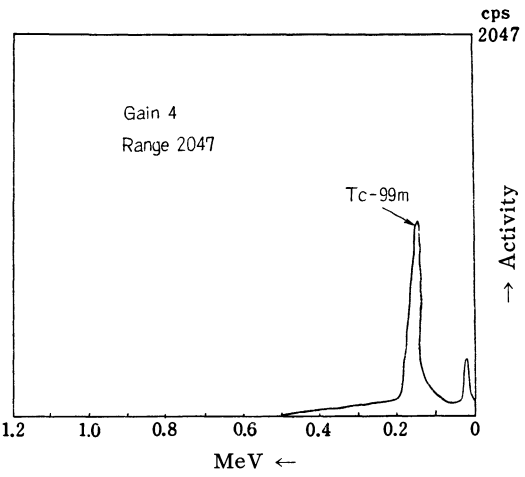


Fig. 1. γ-Ray spectrum of $PbMoO_4$ precipitation.

2. Isolation of Technetium from Fission Products by Anion Exchanger. — Several methods[1,2,6,7] were reported on the separation of technetium-99m from irradiated uranium. These were mainly based on the coprecipitation with sulfide or the solvent extraction. Hall and Johns[8] reported an anion-exchange separation of molybdenum and technetium. According to their results, molybdenum is eluted from a perchlorate form anion exchanger with 10% sodium hydroxide solution, and the technetium is then washed out with 2.0 M ammonium thiocyanate solution. This is a good separation method but thiocyanate solution is unfavorable for further treatment. In another report[9], the dependence of distribution coefficient of technetium on the nitric acid and hydrochloric acid concentrations was measured, and it is known that technetium forms a chloride complex anion within the 0.1~12 N hydrochloric acid concentration range and that it is strongly absorbed at lower nitric acid concentrations, but eluted easily with nitric acid of higher acidity. In the

4) J. A. Swartout, Nat. Nucl. Energy Series, "The Fission Products", Book 2, McGraw-Hill Book Co., Inc., London (1951), Paper 97.
5) F. Ichikawa, This Bulletin, **31**, 778 (1958).
6) D. C. Lincoln and W. H. Sullivan, Nat. Nucl. Energy Series, "The Fission Products", Book 2, McGraw-Hill Book Co., Inc., London (1951), Paper 99.
7) R. P. Schuman, ibid., Paper 100.
8) N. F. Hall and D. H. Johns, *J. Am. Chem. Soc.*, **75**, 5787 (1953).
9) E. H. Huffman, R. L. Oswalt and L. A. Williams, *J. Inorg. Nucl. Chem.*, **3**, 49 (1956).

present paper, the separation of technetium from irradiated uranium by anion exchangers is studied, following the papers mentioned above.

Experimental.—Fifty milligrams of ammonium molybdate is irradiated as mentioned in section 1. The sample is dissolved into 1 or 2 ml. of water and poured on the top of hydroxide form anion exchanger Dowex 1 column (100~200 mesh, 1 cm.×5 cm.). The column is washed with 100 ml. of 10% sodium hydroxide and then technetium is eluted with nitric, hydrochloric or sulfuric acid of various concentrations. Results are shown in Fig. 2-1. From these data, it is shown that technetium is not eluted with 10% sodium hydroxide or 0.7 N nitric acid, but easily eluted with 7 N nitric acid. Then these behaviors are applied to the following experiment.

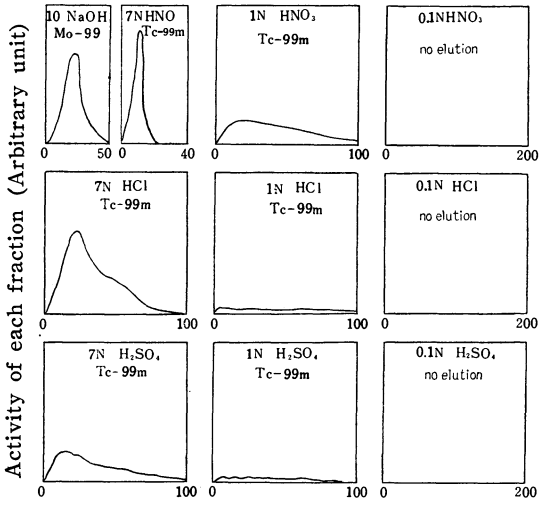


Fig. 2-1. Elution curves of Tc-99m with HNO_3, HCl and H_2SO_4 after elution of Mo-99.

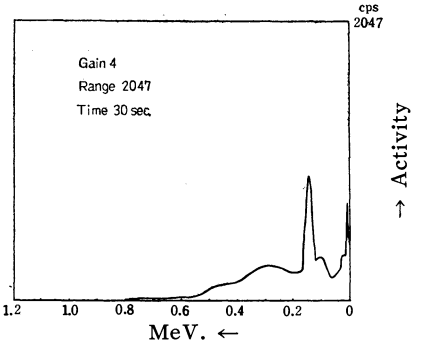


Fig. 2-2. γ-Ray spectrum of total fission products after removal of Np-239.

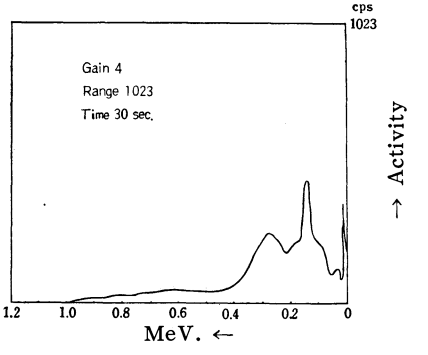


Fig. 2-3. γ-Ray spectrum of 10% NaOH fraction.

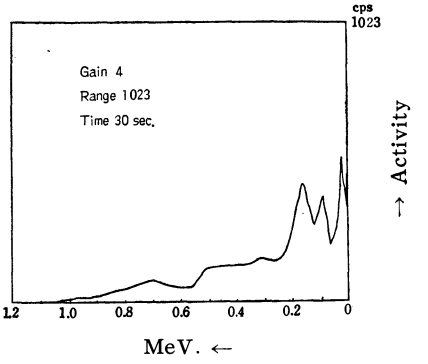


Fig. 2-4. γ-Ray spectrum of 0.7 N HNO_3

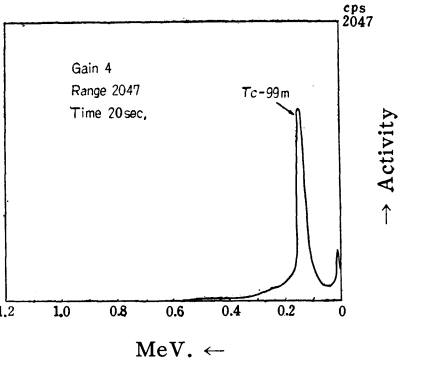


Fig. 2-5. γ-Ray spectrum of 7.5 N HNO_3 fraction.

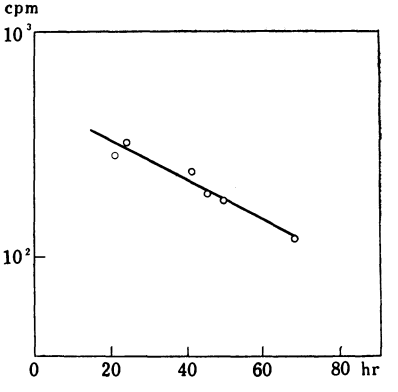


Fig. 2-6. β-Ray decay curve of 7.5 N HNO_3 fraction.

TABLE II. RECOVERY OF TECHNETIUM-99m FROM FISSION PRODUCTS

Exp. No.	Fraction	Total volume of fraction	Sample volume for γ spectrometry	Range of γ spectrometer	Time for measurement	Peak height of Tc-99m	Recovery ratio of Tc-99m
		ml.	ml.	cps	sec.		%
1*	Σ F. p.	50	2	1000	—	27.8	100
	7 N HNO_3	20	2	300	—	62.5	27
				Counts per channel			
2	Σ F. P.	50	2	2047	30	32.3	100
	10% NaOH	70	5	1023	30	26.1	**
	0.7 N HNO_3	50	5	1023	30	0	0
	7 N HNO_3	20	5	2047	20	59.8	46.3

* Data of Expt. No. 1 are measured by single channel pulse height analyzer.

** Tc-99m found in NaOH fraction may be a decay product of Mo-99.

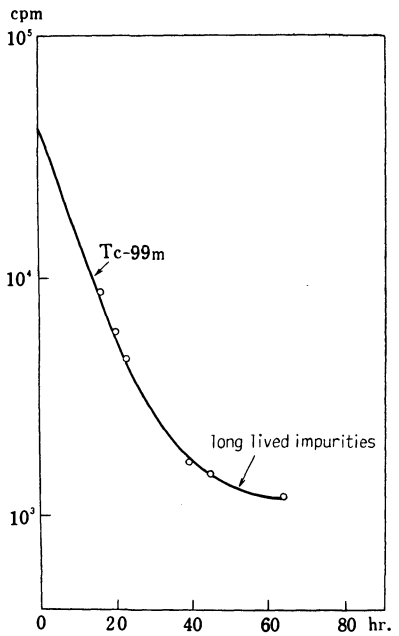


Fig. 2-7. γ-Ray decay curve of 7.5 N HNO_3 fraction.

Twenty milligrams of irradiated uranyl nitrate is used as a starting material. Neptunium-239 is removed by a nitrate form anion exchanger[5]. Thus, about 50 ml. of 7.5 N nitric acid solution of fission products is obtained. This solution is dried up and redissolved in 1 ml. of water and poured onto the hydroxide form anion exchanger. The column is washed with 150 ml. of 10% sodium hydroxide, with 200 ml. of 0.7 N nitric acid and finally with 20 ml. of 7.5 N nitric acid. γ-ray spectra of each fraction are measured by a 256 channel pulse height analyzer. They are shown in Figs. 2-2~5. As Fig. 2-5 shows, the pure spectrum of technetium-99m is found in 7.5 N nitric acid fraction. Decay of β and γ activities are shown in Figs. 2-6 and -7. After 3 days technetium 99m is disintegrated away almost completely, leaving impurities of long half-life.

Results.—Technetium is not eluted with 10% sodium hydroxide and eluted with 3~7 N nitric acid. But with other kinds of acid or dilute nitric acid, the elution of technetium is very slow or unpredictable. This is probably due to the complex formation. Some species of fission products may behave as an anion, and some others may form insoluble hydroxides in these chemical circumstances. These will be caught on a hydroxide form anion exchanger. Species which may form insoluble hydroxide will be eluted with 0.7 N nitric acid. Molybdenum-99 is washed out with sodium hydroxide and other anionic species will be removed with sodium hydroxide and 0.7 N nitric acid.

Recovery of technetium is calculated and shown in Table II. About 40~45% of technetium-99m is recovered in 7.5 N nitric acid solution. Purity in γ-ray activity is about 95% at the separation time.

Thanks are due to Dr. T. Ishimori for his advice and also to Miss S. Uruno, for her able assistance.

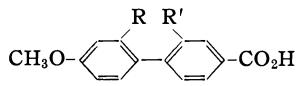
Chemistry Division
Japan Atomic Energy
Research Institute
Tokai, Ibaraki

Estrogenic Biphenyls. V[1]. *Steric Effect in 2,2'-Dialkyl-4-methoxybiphenyl-4'-carboxylic Acids*

By Takeo SATO

(Received February 17, 1959)

Enhancement in the estrogenic activity of the 2- or 2'-alkyl homologs of 4-methoxybiphenyl-4'-carboxylic acid (I) in comparison with the parent compound I was attributed to the increase in the interplanar angle of the two benzene nuclei to attain a favorable conformation[2] for the development of the activity[3].



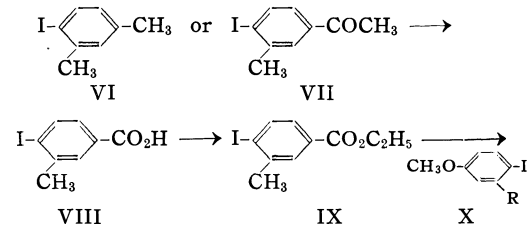
I: R=R'=H
II: R=CH_3, R'=H
III: R=H, R'=CH_3
IV: R=R'=CH_3
V: R=C_2H_5, R'=CH_3

The present author and Ōki also pointed out in the part III[4] of this series that the increase in the chain-length of the alkyl group at position 2 has little effect, as was deduced from the ultraviolet absorption spectra, and, consequently, essentially the same estrogenic potency was found in those compounds.

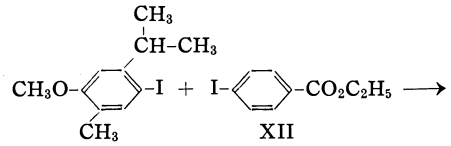
Since the minimum active dose in mice of the most potent compound of this series was found to be 100 γ, compared with 2.5 γ of stilbestrol dimethyl ether, it is considered that the methylene group at position 2 affords a steric effect which is not optimum for the development of the estrogenic potency as far as the biphenyl derivatives are concerned. Then the author sought higher estrogenic activity in more sterically hindered biphenyl derivatives.

4-Methoxy-2'-methylbiphenyl-4'-carboxylic acid (III) should have a similar conformation with 4-methoxy-2-methylbiphenyl-4'-carboxylic acid (II)[4], as was proved in 2,3'-diethyl-4-methoxybiphenyl-4'-carboxylic acid and 2',5'-diethyl-4-methoxybiphenyl-4'-carboxylic acid[5], because the steric interference by the methyl group must be equivalent at positions 2 and 2'. It is expected that the introduction of another alkyl group into position 2 of the compound III will give more steric interference and will result in a greater rotation of the benzene rings toward each other to relieve the steric hindrance. Thus the thicker models will be given.

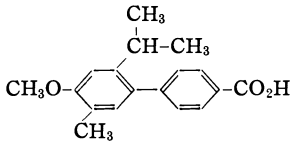
The method of preparation is illustrated in the following chart. Although 4-iodo-3-methylbenzoic acid (VIII) was obtained by Klingel[6] through a sequence of reactions starting from *o*-toluidine, the present author largely modified the method as is described in *Experimental Part*. The compound VIII is also obtainable through nitric acid oxidation[7] of 4-iodo-*m*-xylene (VI). The Ullmann reaction between appropriate 4-iodoanisoles (X) and ethyl 4-iodo-3-methylbenzoate (IX) followed by alkaline hydrolysis gave the desired biphenyls.



As a reference compound 2-isopropyl-4-methoxy-5-methylbiphenyl-4'-carboxylic acid (XIII) was prepared from ethyl 4-iodobenzoate (XII) and 4-iodo-3-isopropyl-6-methylanisole (XI). The compound XIII is expected to involve greater rotation of the benzene nuclei toward each other than the corresponding straight-side-chain compounds because of the greater steric interference of the isopropyl group.



1) Part IV: T. Sato and M. Ōki, This Bulletin, **30**, 958 (1957).
2) M. Ōki and Y. Urushibara, ibid., **25**, 109 (1952): See also J. Grundy, *Chem. Revs.*, **57**, 281 (1957).
3) M. Ōki and T. Sato, This Bulletin, **30**, 508 (1957).
4) T. Sato and M. Ōki, ibid., **30**, 859 (1957).
5) M. Ōki and T. Sato, ibid., **30**, 702 (1957).
6) J. Klingel, *Ber.*, **18**, 2687 (1885).
7) A. Grahl, ibid., **28**, 84 (1895).



XIII

The ultraviolet absorption maxima with the estrogenic activities in mice of the compounds I, II, III, IV, V and XIII are given in Table I.

TABLE I. ULTRAVIOLET ABSORPTION MAXIMA AND ESTROGENIC ACTIVITIES OF 4-METHOXY-BIPHENYL-4'-CARBOXYLIC ACID DERIVATIVES

Compound	K-Band maxima λ, mμ	log ε	Active dose in mice, γ (%)
I	289	4.36	1000 (50)
II	280	4.17	200 (100)
III	271	4.21	
IV			100 (80)
V			100 (60)
XIII	273	4.06	

The ultraviolet absorption maximum of the compound III is located at 271 mμ and the curve is similar with that of compound II. The hypsochromic shift in the type of the compound III compared with the compound II is always observed and may be attributed to the hyperconjugation of the methyl group[8]. The compound XIII, even though the bulkiness of the isopropyl group is expected to exert a greater steric interference and to cause a greater deterioration in conjugation, still possesses a strong K-band of the biphenyl system. The hypsochromic shift of the absorption maximum of the compound XIII, which can be compared with the compound II in term of hyperconjugation, can be attributed to the deterioration in conjugation, since the methyl group at position 5 is known to have little effect on the ultraviolet absorption[9]. On the other hand, the compounds IV and V show weak absorption at about 280 mμ, possess instead the strong absorption at about 230 mμ, indicating the two moieties of the biphenyl system absorb the light almost independently. Thus the two benzene nuclei in the compounds IV and V are considered nearly perpendicular to each other.

The estrogenic activity in ovariectomized mice was determined by the vaginal smear test. It is striking to find out that the estrogenic potency is not greatly altered by the introduction of the alkyl groups into position 2 and/or posititon 2', but it is evident that the estrogenic action is enhanced by the introduction of the alkyl groups.

Experimental[10]

4-Amino-3-methylacetophenone. — To a well stirred mixture of 115 g. (0.77 mol.) of *o*-acetotoluidide, 70 g. (0.89 mol.) of acetyl chloride and 700 ml. of carbon disulfide, was added 350 g. (2.62 mol.) of anhydrous aluminum chloride in small portions in the course of one hour, during which time the whole was gently refluxed on a bath. The refluxing was continued for one hour and the viscous oil at the bottom, after cooling, was decomposed with an excess of concentrated hydrochloric acid. The acidic mixture was hydrolyzed by refluxing for two hours without isolation of the acetamido compound. The solution was made alkaline with sodium hydroxide and the organic material was extracted with ether. The ethereal solution was washed as usual and evaporated to give 44 g. (38% of the theoretical) of 4-amino-3-methylacetophenone, colorless needles, which melted at 110°C on recrystallization from benzene-petroleum ether. The reported melting point is 102°C[5].

Anal. Found: N, 9.52. Calcd. for $C_9H_{11}NO$: N, 9.39%.

4-Iodo-3-methylacetophenone (VII).—To a diazonium solution obtained from 16 g. (0.11 mol.) of 4-amino-3-methylacetophenone, 30 ml. of concentrated sulfuric acid, 100 ml. of water and 7 g. (0.10 mol.) of sodium nitrite in minimum quantity of water, was added a solution of 17 g. (0.1 mol.) of potassium iodide in 20 ml. of water in the course of 10 min. Stirring was continued for thirty minutes below 10°C and then at 50°C for one hour. The mixture was extracted with ether and the ethereal extract was successively washed with aqueous sodium hydroxide, aqueous sodium thiosulfate and water. The iodo-acetophenone boiled at 146~148°C/8 mm. and solidified on standing. Pale yellow crystals, m.p. 42~43°C. Yield, 15.5 g. or 60% of the theoretical. It was prepared by Klingel[6] in the same way and the reported melting point was 39°C.

4-Iodo-3-methylbenzoic acid (VIII).—A solution of 45 g. (0.17 mol.) of iodoketone VII in 170 ml. of dioxane was dropped slowly into a sodium hypobromite solution, made from 56 g. (1.4 mol.) of sodium hydroxide, 82 g. (0.51 mol.) of bromine and 450 ml. of water, at the temperature below 10°C. After the excess of sodium hypobromite was decomposed with sodium bisulfite and bromoform was removed by steam distillation, the solution was acidified to give a crystalline substance, which was recrystallized from ethanol-water. Colorless needles, m.p. 198~199°C. Yield, 39 g. (88% of the theoretical). According to

8) Private communication from Dr. M. Ōki, the University of Tokyo.
9) T. Sato and M. Fujii, unpublished work.
10) All melting and boiling points are uncorrected. The microanalyses were carried out by Mr. Mizushima to whom the author's thanks are due.

Klingel[6] the same acid, m. p. 203~204°C, was obtained by chromic acid oxidation of the iodoketone VII.

Anal. Found: C, 36.72; H, 2.72. Calcd. for $C_8H_7O_2I$: C, 36.66; H, 2.69%.

Ethyl 4-iodo-3-methylbenzoate (IX).—The iodobenzoate was obtained as a colorless oil boiling at 145~147°C/8 mm. by usual esterification of the acid VIII.

Anal. Found: C, 41.21; H, 3.79. Calcd. for $C_{10}H_{11}O_2I$: C, 41.41; H, 3.82%.

4-Methoxy-2'-methylbiphenyl-4'-carboxylic acid (III).—As a general procedure of the Ullmann reaction, the preparation of 4-methoxy-2'-methylbiphenyl-4'-carboxylic acid (III) is described. To a well-stirred mixture of 3 g. (0.010 mol.) of ethyl 3-methyl-4-iodobenzoate (IX) and 10 g. (0.043 mol.) of 4-iodoanisole (X, R=H), 10 g. (0.16 atom) of copper bronze, activated by Kleiderer and Adams' method[11], was added in 20 min. at 220~230°C. The reaction mixture was then heated to 270~280°C for 25 min. and extracted with acetone after cooling. The extract was hydrolyzed by refluxing with a mixture consisting of 50 ml. of 10% sodium hydroxide solution and 100 ml. of ethanol for about two hours. The solvent was evaporated and the residue was diluted with water. Insoluble dimethoxybiphenyl was removed by filtration. On acidification, the filtrate afforded an acid mixture, which was purified by chromatography on alumina. Repeated recrystallizations from ethanol gave 500 mg. of colorless needles, m. p. 183~184°C.

Anal. Found: C, 73.92; H, 5.59. Calcd. for $C_{15}H_{14}O_3$: C, 74.36; H, 5.83%.

2, 2'-Dimethyl-4-methoxybiphenyl-4'-carboxylic acid (IV).—The dimethylbiphenyl was prepared from compound IX and 4-iodo-3-methylanisole (X, R=CH_3)[4]. It was necessary to remove unchanged starting materials in vacuo before hydrolysis for the easier purification of the product. The acid was obtained as colorless prisms on recrystallization from ethanol-water, m. p. 142~144°C.

Anal. Found: C, 74.99; H, 6.39. Calcd. for $C_{16}H_{16}O_3$: C, 74.98; H, 6.29%.

2-Ethyl-4-methoxy-2'-methylbiphenyl-4'-carboxylic acid (V).—It was prepared from IX and 3-ethyl-4-iodoanisole (X, R=C_2H_5)[3]. Removal of the unchanged materials in vacuo was required and the distillate up to 180°C/5 mm. was discarded. Colorless needles, m. p. 139~140°C were obtained on recrystallization from benzene-petroleum ether.

Anal. Found: C, 75.55; H, 6.75. Calcd. for $C_{17}H_{18}O_3$: C, 75.53; H, 6.71%.

2-Isopropyl-5-methyl-4-iodoanisole (XI). — To a solution of 80 g. (0.49 mol.) of carvacrol methyl ether in 100 ml. of ethanol were alternatively added 130 g. (0.51 mol.) of iodine and 130 g. (0.60 mol.) of yellow mercuric oxide in small portions in the course of 30 min., while the mixture was well stirred and cooled in ice-water below 20°C. Stirring was continued for an additional 30 min. The mixture was heated on a water bath for 10 min. and filtered with suction. After the filtrate was diluted with water, the heavy oil was extracted with ether. The ethereal solution was washed with aqueous potassium iodide and dried over calcium chloride. The product boiling at 130~150°C/6~7 mm. was collected and then refractionated. The pure compound was obtained as brown oil, b. p. 135~137°C/6 mm.

Anal. Found: C, 46.16; H, 5.21. Calcd. for $C_{11}H_{15}OI$: C, 45.53; H, 5.21%.

2-Isopropyl-4-methoxy-5-methylbiphenyl-4'-carboxylic acid (XIII). — It was prepared from the compound XI and ethyl 4-iodobenzoate (XII). After hydrolysis the acidic portion was extracted with ethanol and the extract was recrystallized from ethanol to give colorless plates, m. p. 227.5~229°C.

Anal. Found: C, 76.06; H, 6.98. Calcd. for $C_{18}H_{20}O_3$: C, 76.03; H, 7.09%.

Ultraviolet absorption spectra. — They were measured with a Hitachi photoelectric spectrophotometer Model EPU-2, the compounds being in dissolved 95% ethanol.

The author wishes to express his hearty thanks to Professor Y. Urushibara, the University of Tokyo, Professor K. Hata, Tokyo Metropolitan University, and Dr. M. Ōki for their kind guidance and encouragement throughout this study and to the members of the Research Department, Teikoku Hormone Manufacturing Co., Ltd., Kawasaki, for bioassays. The author is also indebted to the Ministry of Education for the Grant in Aid for Fundamental Scientific Research.

Department of Chemistry
Faculty of Science
Tokyo Metropolitan University
Setagaya-ku, Tokyo

11) E. C. Kleiderer and R. Adams, *J. Am. Chem. Soc.*, **55**, 4219 (1933).

The Aconite Alkaloids. XXXII[1]. *On Lucidusculine. Part II*[2]

By Takashi AMIYA

(Received March 2, 1959)

In the previous report[2] the extended formula of lucidusculine (I) has been proposed as follows:

$$C_{18}H_{23}\begin{cases}(OH)_2\\ OCOCH_3\\ >N-C_2H_5\\ >C=CH_2\end{cases}$$

Some new derivatives of lucidusculine are described in the present paper.

Catalytic hydrogenation[3] of I with platinum oxide in glacial acetic acid yielded dihydrolucidusculine(II), $C_{24}H_{37}O_4N$, m. p. 192~198°C, $[\alpha]_D^{18}$ −58.6°. On acetylation with acetic anhydride in pyridine, II gave dihydrolucidusculine diacetate(III), $C_{28}H_{41}O_6N$, m. p. 140~144°C, $[\alpha]_D^{18}$ −55.5°.

The infrared absorption spectrum of compound I gave two peaks at 6.06 and 11.26 μ and that of lucidusculine diacetate (IV)[4,5], $C_{28}H_{39}O_6N$, gave peaks at 6.08 and 11.32 μ due to presence of a terminal methylene group. Compounds II and III, on the other hand, showed no peak near the above-mentioned wavelengths. Therefore, it seems very probable that the hydrogenation of compound I proceeds as:

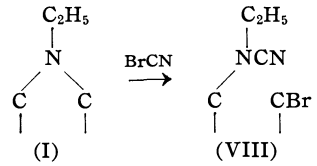
$$>C=CH_2 \xrightarrow{2H} >\overset{*}{C}H-CH_3$$

On account of a newly formed asymmetric carbon atom (asterisked) the formation of an epimer of compound II might be suspected[6].

Luciculine(V), $C_{22}H_{33}O_3N\cdot H_2O$, obtained from compound I upon hydrolysis with alcoholic potassium hydroxide[5], also showed two peaks in the infrared spectrum at 6.09 and 11.27 μ characteristic of a terminal methylene group.

Hofmann degradation of luciculine methiodide(VI) yielded a basic substance, named isomesoluciculine[7](VII), $C_{21}H_{31}O_3N\cdot H_2O$, m. p. 123~127°C (decomp.), $[\alpha]_D^{19}$ −17.0°. Compound VII showed peaks in the infrared spectrum at 6.08 and 11.28 μ characteristic of a terminal methylene group.

On treatment of compound I with cyanogen bromide, two reaction products were obtained. One of them was easily isolated because of its high solubility in water; it was named bromolucidusculine cyanamide (VIII), $C_{24}H_{35}O_4N(CN)Br\cdot 2H_2O$, m. p. 157~162°C (decomp.), $[\alpha]_D^{17}$ −76.0°, in which cleavage of the N-containing ring was noticed. It showed a peak in the infrared spectrum at 4.74 μ due to presence of a cyano group. The other was easily soluble in acetone but found to crystallize with difficulty. This cyanogen bromide degradation may proceed as follows:



(I) (VIII)

The ultraviolet absorption spectra of all these compounds showed only end absorptions and are reminiscent of those of aconite alkaloids, i. e., atisine, dihydroatisine, aconine, delphonine[8] and lycoctonine[9].

Experimental

Lucidusculine (I).—The ultraviolet absorption spectrum of this compound in methanol showed end absorption and no maximum. The infrared absorption spectrum in Nujol showed the presence of hydroxyl groups (2.95 μ), an acetoxyl group (5.82 and 8.10 μ) and a terminal methylene group (6.06 and 11.26 μ).

Dihydrolucidusculine (II).—Lucidusculine (1 g.)

1) This constitutes a part of a series entitled "The Aconite Alkaloids" by H. Suginome. Part XXXI: T. Shima and T. Amiya, This Bulletin, **31**, 657 (1958).

2) Part I: H. Suginome, T. Amiya and T. Shima, ibid., **32**, 824 (1959).

3) Cf. H. Suginome and F. Shimanouchi, *Ann.*, **545**, 220 (1940), Foot Note 4).

4) H. Suginome, S. Kakimoto and J. Sonoda, *J. Fac. Sci., Hokkaido Univ., Ser. III. Chem.*, **4**, 25 (1950).

5) R. Majima and S. Morio, *Ber.*, **65**, 599 (1932).

6) This point will be mentioned later.

7) By the same treatment, H. Suginome and S. Umezawa obtained mesoluciculine, $C_{21}H_{31}O_3N\cdot H_2O$, m.p. 199~200°C with sintering point 114°C, $[\alpha]_D^{15}$−12.8°, H. Suginome and S. Umezawa, *J. Fac. Sci., Hokkaido Univ., Ser. III. Chem.*, **4**, 44 (1950). The relation between mesoluciculine and isomesoluciculine seems to be that of polymorphism.

8) L. C. Craig, L. Michaelis, S. Granick and W. A. Jacobs, *J. Biol. Chem.*, **154**, 293 (1944).

9) O. E. Edwards and Léo Marion, *Canad. J. Chem.*, **30**, 627 (1952).

was dissolved in 16 cc. of glacial acetic acid and hydrogenated with 0.5 g. of platinum oxide for six hours. After removal of platinum, the solution was evaporated to dryness. On treatment of the residue with water and then with aqueous ammonia, a precipitate was obtained. On recrystallization from ethyl acetate, crystals were yielded, which melted at 192~198°C. $[\alpha]_D^{18}$ −58.6° (methanol). Yield, 0.5 g. The ultraviolet absorption spectrum of this compound in methanol showed end absorption and no maximum. The infrared absorption spectrum in Nujol showed the presence of hydroxyl groups (2.96 μ) and an acetoxyl group (5.80 and 8.12 μ).

Anal. Found: C, 70.61; H, 9.15. Calcd. for $C_{24}H_{37}O_4N$: C, 71.43; H, 9.24%.

Dihydroluciduscuiline Diacetate (III). — A mixture of dihydroluciduscuiline (0.6 g.), acetic anhydride (1 cc.) and pyridine (4 cc.) was allowed to stand in a sealed tube at room temperature for two days. After removal of the solvents, the residue was dissolved in water and then precipitated with aqueous ammonia. The precipitate was recrystallized from ethanol. Crystals melted at 140~144°C. $[\alpha]_D^{18}$ −55.5° (methanol). Yield was quantitative. The ultraviolet absorption spectrum of this compound in methanol showed end absorption and no maximum. The infrared absorption spectrum in Nujol had no peak attributable to a hydroxyl group but showed the presence of acetoxyl groups (5.82 and 7.95 μ).

Anal. Found: C, 68.45; H, 8.84. Calcd. for $C_{28}H_{41}O_6N$: C, 68.96; H, 8.48%.

Luciduscuiline Diacetate (IV). — A mixture of luciduscuiline (0.6 g.), acetic anhydride (1 cc.) and pyridine (4 cc.) was allowed to stand in a sealed tube at room temperature for two days. After removal of the solvents, the residue was dissolved in water and then precipitated with aqueous ammonia. The precipitate was recrystallized from ethanol. Crystals melted at 159~167°C alone and on admixture with luciduscuiline diacetate prepared according to the direction of Majima and Morio[4,5]. Yield was quantitative. The ultraviolet absorption spectrum of this compound in methanol showed end absorption and no maximum. The infrared absorption spectrum in Nujol showed the presence of acetoxyl groups (5.82 and 8.01 μ) and a terminal methylene group (6.08 and 11.32 μ).

Luciculine (V). — The ultraviolet absorption spectrum of this compound in methanol showed end absorption and no maximum. The infrared absorption spectrum in Nujol showed the presence of hydroxyl groups (2.98 μ) and a terminal methylene group (6.09 and 11.27 μ).

Luciculine Methiodide (VI). — The ultraviolet absorption spectrum of this compound in methanol showed end absorption and no maximum. The infrared absorption spectrum in Nujol had a peak at 2.98 μ attributable to hydroxyl groups and peaks at 6.11 and 11.22 μ attributable to a terminal methylene group.

Isomesoluciculine (VII). — The base was prepared from luciculine methiodide (0.5 g.) by Hofmann degradation. Recrystallization from acetone gave crystals, which melted at 123~127°C (decomp.). $[\alpha]_D^{19}$ −17.0° (methanol). The ultraviolet absorption spectrum of this compound in methanol showed end absorption and no maximum. The infrared spectrum in Nujol showed the presence of hydroxyl groups (2.98 μ) and a terminal methylene group (6.08 and 11.28 μ).

Anal. Found: C, 68.79; H, 9.31; (N)CH_3, 4.52; H_2O, 5.04. Calcd. for $C_{21}H_{31}O_3N \cdot H_2O$: C, 69.39; H, 9.15; (N)$CH_3$, 4.13; H_2O, 4.95%.

Bromoluciduscuiline Cyanamide (VIII). — To cyanogen bromide (0.25 g.) dissolved in 7.5 cc. of benzene, luciduscuiline (0.45 g.) dissolved in benzene (16 cc.) was added. The reaction mixture, which became turbid after 10 min., was allowed to stand at room temperature for 24 hr. and then was filtered. The crystalline precipitate collected by filtration was hygroscopic and then treated with water. The residue, obtained from the water-soluble portion, was crystallized from acetone and melted at 157~162°C (decomp.). $[\alpha]_D^{17}$ −76.0° (methanol). The ultraviolet absorption spectrum of this compound in methanol showed end absorption and no maximum. The infrared absorption spectrum in Nujol showed the presence of hydroxyl groups (2.94 and 3.10 μ), a cyano group (4.74 μ), an acetoxyl group (5.88 and 7.97 μ) and a terminal methylene group (6.06 and 11.23 μ).

Anal. Found: C, 55.92; H, 7.89; N, 4.52; Br, 13.66; (N)C_2H_5, 4.94; H_2O, 5.5. Calcd. for $C_{24}H_{35}O_4N(CN)Br \cdot 2H_2O$; C, 55.23; H, 7.23; N, 5.13; Br, 14.70; (N)C_2H_5, 5.34; H_2O, 6.62%.

The water-insoluble portion did not crystallize from acetone. These portions were nearly equal in amounts.

The author wishes to express his sincere thanks to Professor Harusada Suginome, President of Hokkaido University, for his kind guidance throughout this work and to Mr. Mineo Yakushiji for the determination of *N*-alkyl groups.

Department of Chemistry
Faculty of Science
Hokkaido University
Sapporo

Intramolecular Interaction between Hydroxyl Group and π-Electrons. VI[1]*. Electronic Effect on the Interaction in ω-Arylalkanols*

By Michinori Ōki and Hiizu Iwamura

(Received March 17, 1959)

In connection with the intramolecular interaction between hydroxyl group and π-electrons, the authors have measured the ν_{O-H} absorption of various substituted benzyl alcohols and concluded that the hydrogen atom of the hydroxyl group interacts with the π-electron on the carbon atom to which the hydroxymethyl group is attached. On the other hand, Goldman and Crisler[2] examined three phenethyl alcohol derivatives on the O–H stretching absorption and concluded that the hydrogen atom of the hydroxyl group interacts with the π-electron on the carbon atom to which the 2-hydroxyethyl group is attached. Meanwhile, the present authors predicted[3], by comparison of the two band intensities of the interacting forms in allyl alcohol and 3-buten-1-ol, that the interaction occurring in them might be different in nature, since allyl alcohol gives a larger band intensity of the interacting form than 3-buten-1-ol in spite of the fact that $\Delta\nu_{max}$ is smaller in allyl alcohol than in 3-buten-1-ol. Moreover, it is reasonable to consider that allyl alcohol with benzyl alcohol and 3-buten-1-ol with phenethyl alcohol possess the same type of interaction. Therefore, it may be thought that there is a contradiction between the conclusion by Goldman and Crisler and that by the present authors. Since it is dangerous to draw a conclusion from a small number of examples, the ν_{O-H} absorptions of various ω-arylalkanols have been re-examined.

Experimental

Measurement.—It was performed similarly as described previously[3]. When a small peak was present (3-arylpropanols) or the presence of a peak was suspected (4-arylbutanol), the measurement was carried out with a quartz cell of 5 cm. length without alteration of concentration.

Calculation of Integrated Intensities.—It was carried out similarly as reported previously[3], when only two bands were present. However, the presence of three bands, two of which were derived from the presence of the rotational isomers and the third by the internal interaction, required modification to some extent. The two stronger bands were first obtained in the usual manner and the summation of the bands was subtracted from the apparent curve. This procedure usually gave rise to an unsymmetric band. The process was repeated through the trial-and-error method until the third band became symmetric.

Materials. — The compounds used for the measurement are known compounds, unless otherwise stated, and their physical constants well agree with those in the literature.

Preparation of ω-Arylalkanols by Lithium Aluminum Hydride Reduction of Esters.—To a slurry prepared from 2.5 g. (0.07 mol.) of lithium aluminum hydride and 100 ml. of ether, was added 0.1 mol. (0.05 mol. for amino-esters) of the corresponding ester[4]. After stirring for two hours at the room temperature, the excessive lithium aluminum hydride was decomposed by adding ethyl acetate in ether and then dilute sulfuric acid (aqueous sodium hydroxide in the case of aminoalcohols) was added. The aqueous layer was extracted with ether and ethereal extract was washed with aqueous sodium hydroxide. After drying over potassium carbonate followed by evaporation, the residue was either fractionally distilled or recrystallized from an appropriate solvent. Compounds with low melting points were once distilled and then recrystallized. The results are summarized in Table I.

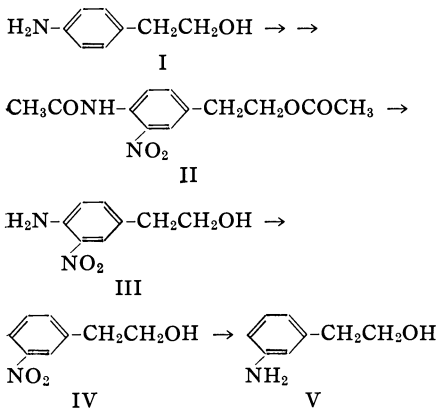
Preparation of 2-(*m*-Aminophenyl)-ethanol.—2-(*m*-Aminophenyl)-ethanol (V) was prepared as illustrated in the following chart.

1) Part V of this series: This Bulletin, **32**, 955 (1959).
2) I. M. Goldman and R. O. Crisler, *J. Org. Chem.*, **23**, 751 (1958).
3) M. Ōki and H. Iwamura, This Bulletin, **32**, 567 (1959).
4) Amino-esters were conveniently prepared by hydrogenation of the corresponding nitro-esters or alkyl nitrocinnamates in the presence of U-Ni-A catalyst [Y. Urushibara, S. Nishimura and H. Uehara, This Bulletin, **28**, 466 (1955)]. Substituted cinnamic acids were also reduced with the same catalyst in excellent yields, when their sodium salts in water were used. The authors are grateful to Dr. S. Nishimura for hydrogenation.
5) See; N. Carmack and M. A. Spielman, "*Organic Reactions*", John Wiley & Sons, Inc., New York, Vol. III, (1946), p. 83; E. Schwenk and E. Bloch, *J. Am. Chem. Soc.*, **64**, 3051 (1942).
6) C. J. Collins, ibid., **73**, 1038 (1951).
7) D. Sontag, *Compt. rend.*, **197**, 159 (1933).

TABLE I. ω-ARYLALKANOLS [x-$RC_6H_4(CH_2)_nOH$]

R	x	n	b. p. (°C) (3 mmHg)	m. p. (°C)	Crystal form	n_D	*Anal.* Calcd.	Found
Cl[a]	*m*	2	100.5	—	—	1.5475 (23°C)	C: 61.35 H: 5.73	61.59 6.00
CH_3[b]	*p*	3	97～98	23～25	plates	—	C: 79.95 H: 9.39	79.68 9.28
H_2N[c]	*p*	3	145～150	54～55	needles	—	C: 71.49 H: 8.67	71.26 8.70
Cl[d]	*p*	3	111～112	—	—	1.5428 (15.5°C)	C: 63.35 H: 6.49	63.87 6.59
H_2N[e]	*p*	4	—	71～72	needles	—	C: 72.69 H: 9.15	72.50 9.24

a) The starting material, methyl *m*-chlorophenylacetate, was conveniently prepared through the modified Wilgerodt reaction[5] using morpholine and *m*-chloroacetophenone followed by hydrolysis and then esterification. The over-all yield of the ester was 70%.
b) The melting point has not been reported[6].
c) Recrystallized from benzene containing a small amount of alcohol.
d) Refractive index was reported as 1.5424 (21°C) for substance obtained by the chlorination of 3-phenylpropanol[7].
e) This compound is rather unstable and discolors quickly in the air. Benzene was used as the recrystallization solvent.



2-(p-Acetamido-m-nitrophenyl)-ethyl acetate (*II*). To 102 g. (1 mol.) of acetic anhydride, 118 g. (0.86 mol.) of 2-(*p*-aminophenyl)-ethanol[8] was added and the mixture was heated on a water bath for thirty minutes. After cooling, 79 g. (1 mol.) of acetyl chloride was slowly added, and the mixture was heated under reflux on a water bath for one hour. Hydrogen chloride and the excessive reagents were removed in vacuo and the residue was dissolved in 400 ml. of acetic anhydride. The solution was cooled in an ice-salt bath and 106.5 ml. (1.7 mol.) of nitric acid (d=1.42) was carefully added at 10～20°C with good stirring. The mixture was stirred for further fifteen minutes at that temperature and then poured into 3 l. of ice-water. The crystals were collected and the major portion was submitted to the subsequent hydrolysis. The analytical sample was obtained by recrystallization from benzene-petroleum ether. It was obtained as yellow needles, m. p. 77°C.

Anal. Found: C, 53.95; H, 5.48. Calcd. for $C_{12}H_{14}N_2O_5$: C, 54.15; H, 5.25%.

2-(p-Amino-m-nitrophenyl)-ethanol (*III*). — The crude compound II was heated with 500 ml. of 6 N hydrochloric acid under reflux for three hours. The cooled reaction mixture was basified with aqueous sodium hydroxide and organic material was extracted with ether. The ethereal extract was dried over potassium carbonate and evaporated. The residue solidified on standing and was recrystallized from benzene. Orange flat needles, m. p. 85～87°C. Over-all yield, 88 g. (56%).

Anal. Found: C, 52.86; H, 5.63. Calcd. for $C_8H_{10}N_2O_3$: C, 52.74; H, 5.53%.

2-(m-Nitrophenyl)-ethanol (*IV*).—To a solution of 54.6 g. (0.2 mol.) of compound III in 80 ml. of concentrated hydrochloric acid and 20 ml. of water, was added 20.7 g. (0.3 mol.) of sodium nitrite in a minimal quantity of water at −5～−3°C. The mixture was stirred at 0°C for ten minutes and then 325 g. (1.5 mol.) of 30% hypophosphorus acid precooled to 0°C was added, the temperature being maintained at 0～3°C. The mixture was stirred for another hour and then allowed to stand in an ice-bath containing ca. 5 kg. of ice which melted in about twelve hours. After twenty-four hours, the mixture was extracted with ether and the ethereal extract was washed with aqueous sodium hydroxide. Drying with potassium carbonate followed by fractional distillation afforded 25.0 g. (50%) of an orange-yellow oil, b. p. 141～146°C/4 mm., which set to needles. The analytical sample was obtained through recrystallization from benzene-petroleum ether. It was obtained as faintly yellow needles, m. p. 50～51°C.

Anal. Found: C, 57.58; H, 5.55. Calcd. for $C_8H_9NO_3$: C, 57.38; H, 5.43%.

2-(m-Aminophenyl)-ethanol (*V*)[9].—To a solution

8) H. M. Woodburn and C. F. Stuntz, *J. Am. Chem. Soc.*, **72**, 1362 (1950).

9) This compound has been prepared by lithium aluminum hydride reduction of *m*-aminophenylacetic acid [J. B. Dickey and E. B. Towne, Brit. Pat., 722,367; *Chem. Abstr.*, **49**, 9935 (1955)]. They reported only the boiling point as 135～138°C/2 mm. but no melting point.

TABLE II. ν_{O-H} ABSORPTIONS OF 2-ARYLETHANOLS (x-$RC_6H_4CH_2CH_2OH$)

R	x	OH	ν_{max} (cm^{-1})	$\Delta\nu^a_{1/2}$ (cm^{-1})	$A\times10^{-3}$ ($mol^{-1}\cdot l.\cdot cm^{-2}$)	$\Delta\nu_{III-I}$ (cm^{-1})	$A_I/(A_{II}+A_{III})$
		I	3598.0	25.6	3.62		
	m	II	3625	18	0.60	37.5	1.50
H_2N		III	3635.5	17.6	1.82		
		I	3597.8	24.4	3.14		
	p	II	3623	18	0.53	37.2	1.14
		III	3635.0	19.8	2.23		
		I	3602.3	24.8	3.34		
	m	II	3624	18	0.66	33.5	1.19
CH_3O		III	3635.8	17.9	2.14		
		I	3602.5	26.4	2.96		
	p	II	3623	18	0.69	33.3	1.03
		III	3635.8	18.0	2.19		
		I	3603.1	27.3	3.28		
	m	II	3625	20	0.82	32.7	1.06
CH_3		III	3635.8	18.1	2.27		
		I	3602.1	22.4	2.72		
	p	II	3623	20	0.74	33.2	0.93
		III	3635.5	17.0	2.19		
		I	3606.4	24.4	2.62		
H		II	3626	17	0.68	29.6	0.86
		III	3636.0	18.4	2.36		
		I	3611.0	23.0	2.25		
	m	II	3625	16	0.71	24.2	0.645
Cl		III	3635.2	15.8	2.78		
		I	3610.2	24.4	2.23		
	p	II	3625	17	0.88	25.3	0.64
		III	3635.5	15.2	2.61		
		I	3615.0	21.6	1.20		
	m	II	3625	17	1.52	2.00	0.207
O_2N		III	3635.0	15.4	4.29		
		I	3614.0	22.4	1.37		
	p	II	3626	18	1.42	21.0	0.253
		III	3635.0	14.6	3.99		

of 90 g. (0.36 mol.) of 90% stannous chloride in 80 ml. of concentrated hydrochloric acid, was added 20 g. (0.12 mol.) of compound IV and the mixture was stirred, when the spontaneous reaction set in. After the reaction subsided, the mixture was heated on a water bath for thirty minutes, cooled and decomposed with an excess of aqueous sodium hydroxide. When the mixture was chilled, the aminoalcohol solidified and was collected by filtration. It was recrystallized from benzene, m. p. 68~69°C. It sometimes forms needles and sometimes plates. Yield, 13 g. (80%).

Anal. Found: C, 70.00; H, 7.98. Calcd. for $C_8H_{11}NO$: C, 70.04; H, 8.08%.

Results and Discussion

2-Arylethanols. — The apparent O–H stretching absorption curves are divided into three, assuming that they are the overlap of the three symmetric bands which are expressed by Lorentz function. The apparent curves refuse to be divided into two to fit in, as was pointed out in the earlier paper[3]. The results are shown in Table II.

The actual features of division are shown in Fig. 1 and Fig. 2, 2-(*p*-aminophenyl)-ethanol and 2-(*p*-nitrophenyl)-ethanol being taken as the examples because of the extremity of Hammett's σ-values of the substituents.

Two (bands II and III) of the three ν_{O-H} absorption bands are derived from the rotational isomers of primary alcohols and their positions (3635 cm^{-1} and 3625 cm^{-1}) are in good agreement with the previous assignment[10]. The third band (band I) must be attributed to the presence of the intramolecular interation between the hydroxyl group and the π-electrons as

10) M. Ōki and H. Iwamura, This Bulletin, **32**, 950 (1959).

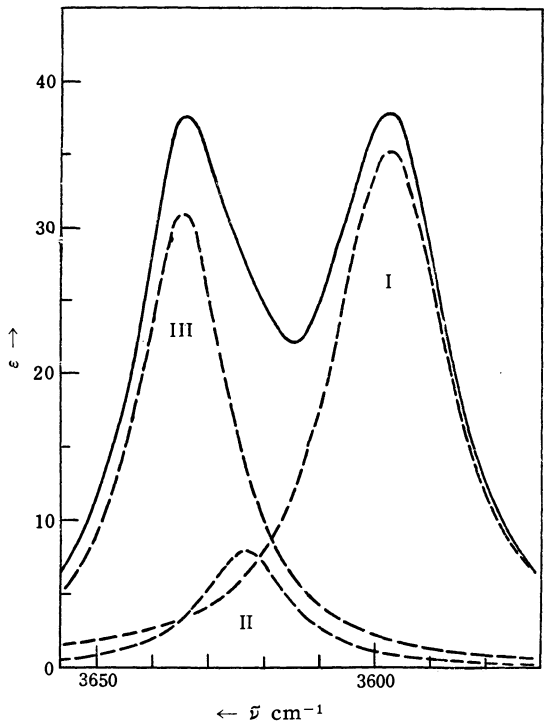


Fig. 1. ν_{O-H} absorption of 2-(*p*-aminophenyl)-ethanol.

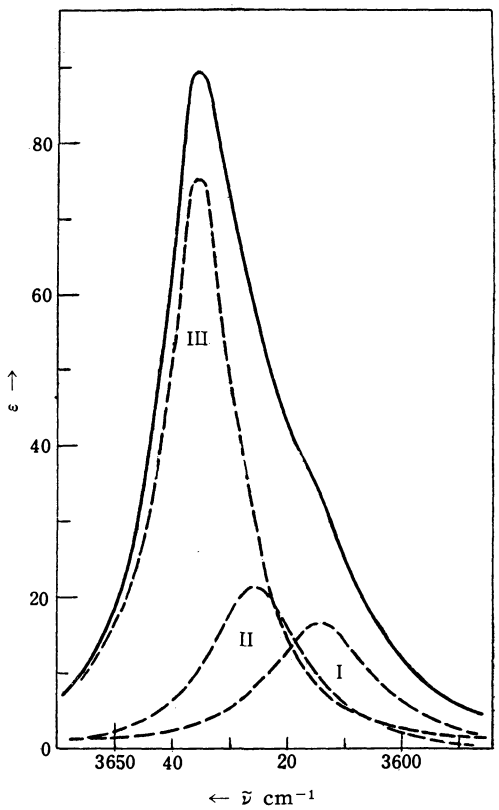


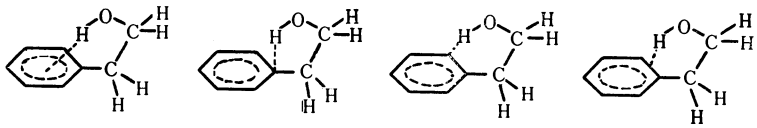
Fig. 2. ν_{O-H} absorption of 2-(*p*-nitrophenyl)-ethanol.

Trifan and his coworkers[11,12], Anet and Bavin[13] and Goldman and Crisler[2] have assigned. Since the error involved in dividing the original band into three is rather great, especially for band II, it is not allowable to use the integrated intensity of band II for discussion, although molecular scale models tell that band II is derived from the only rotational form that makes the interaction possible. Hence, the difference of the wave numbers is shown by $\nu_{III}-\nu_I$ rather than by $\nu_{II}-\nu_I$ and the ratio of the integrated intensities is also exemplified by $A_I/(A_{II}+A_{III})$ rather than by A_I/A_{II}.

As clearly understood from Table II, the electronic effect from the substituent is observed. The wave number of the ν_{O-H} absorption maximum (band I) of the interacting form shifts to a lower wave number as the substituent becomes more electron-releasing, and the electron-attracting substituent causes the wave number of band I to shift and approach to the absorption of normal primary alcohols, this phenomenon having not been observed in benzyl alcohol derivatives. The integrated intensity of band I also increases as the electron-releasing group is introduced.

As to the molecular structure of the internally interacting form, the authors pointed out four possibilities as shown in Fig. 3[1]. Structure VI indicates the interaction between the hydroxyl group and the benzene nucleus as a whole, the case having been suggested by Trifan and his coworkers[11]. Structure VII, representing the interaction which includes C_1 of the benzene nucleus, was deduced by Goldman and Crisler[2] by comparison of three ν_{O-H} curves of 2-phenylethanol, 2-(*p*-methoxyphenyl)-ethanol and 2-(*p*-nitrophenyl)-ethanol. Structure VIII with the participation of C_2 of the benzene nucleus was suggested by Lüttke and Mecke[14], and structure IX, in which C_1 and C_2 take part, by Baker and Shulgin[15].

11) D. S. Trifan, J. L. Weinmann and L. P. Kuhn, *J. Am. Chem. Soc.*, **76**, 6566 (1957).
12) P. von Schleyer, D. S. Trifan and R. Bacskai, ibid., **80**, 6691 (1958).
13) F. A. L. Anet and P. M. G. Bavin, *Can. J. Chem.*, **34**, 1756 (1956).
14) W. Lüttke and R. Mecke, *Z. Elektrochem.*, **53**, 241 (1949): *Z. physik. Chem.*, **196**, 56 (1950).
15) A. W. Baker and A. T. Shulgin, *J. Am. Chem. Soc.*, **80**, 5358 (1958).



VI VII VIII IX

Fig. 3.

Structure VII is first excluded on the basis of the experimental results given in Table II, because compounds with the same substituent in the meta and in the para positions to the 2-hydroxyethyl group give similar curves. Structure VII expects a favored interaction in the 2-phenylethanol with a strongly electron-donating group in the para position over the compound possessing the same substituent in the meta.

Structure VI is rather improbable because it has no orbital which would couple with that of the hydrogen atom. If such interaction took place, further lengthening of the O–H bond should be expected, which would give rise to further lowering of the wave number of band I because of a weaker force constant. Structure VI is made improbable also by the theoretical treatment of the complex of benzene with hydrogen ion or silver ion as discussed below. The structure should not be hexagonally symmetrical, nor should the positive ion be on the plane of the benzene nucleus[16].

Thus, there are two possibilities left for the structure. It seems that structure VIII is more convincing when Hammett's σ values[17] of the ortho position in respect of 2-hydroxyethyl group is taken for the ordinate and $\log\frac{A_I/(A_{II}+A_{III})}{[A_I/(A_{II}+A_{III})]_0}$, where $[A_I/(A_{II}+A_{III})]_0$ is the ratio obtained with 2-phenylethanol, for the abscissa (Fig. 4), because they are nearly in linear relation. However, the defect of this structure can be pointed out immediately because of the far deviation of 2-(*p*-methoxyphenyl)-ethanol from a straight line, or, in other words, because 2-(*p*-methoxyphenyl)-ethanol and 2-(*m*-methoxyphenyl)-ethanol show almost the same internal interaction in spite of the great distance between σ constants ($\sigma_m=+0.115$, $\sigma_p=-0.268$). Even the correction which will be discussed in the following paragraph modifies only σ_m but does not affect σ_p. The deviation of 2-(nitrophenyl)-ethanols can be attributed to the error in dividing the apparent curves into three, since the bands I of these compounds are the smallest comprising no maxima nor distinct shoulders.

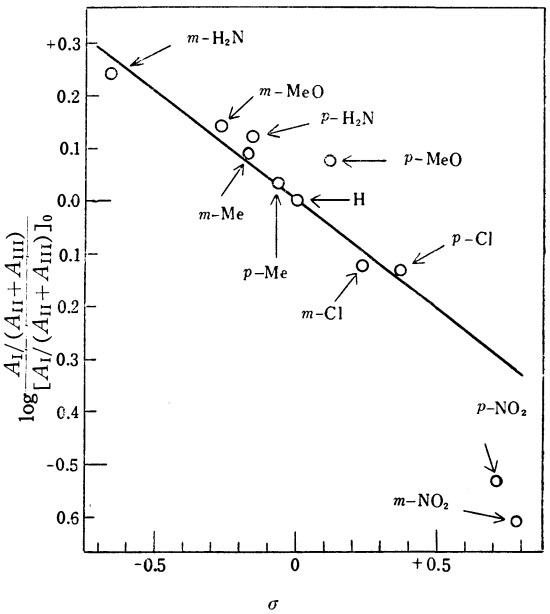


Fig. 4. Relation between $\log\frac{A_I/(A_{II}+A_{III})}{[A_I/(A_{II}+A_{III})]_0}$ in 2-arylethanol and σ constants for structure VIII.

The relation between the σ constants and $\log\frac{A_I/(A_{II}+A_{III})}{[A_I/(A_{II}+A_{III})]_0}$ for structure IX is shown in Fig. 5. The σ constants for the para-substituted compounds should be the mean values of those for meta and for para and those for the meta-substituted compounds should be expressed by $\left(\frac{\sigma_o+\sigma_p}{2}+\sigma_m\right)\Big/2$. Unfortunately, however, few σ values for ortho-substitution have been known, the only example having been provided by Shulgin and Baker[18]

16) R. S. Mulliken, *J. Chem. Phys.*, **19**, 514 (1951); *J. Am. Chem. Soc.*, **74**, 811 (1952).

17) L. P. Hammett, "Physical Organic Chemistry", McGraw-Hill Book Co., New York (1940), p. 184. Also see: H. H. Jaffé, *Chem. Revs.*, **53**, 191 (1953).

18) A. T. Shulgin and A. W. Baker, *Nature*, **182**, 1299 (1958).

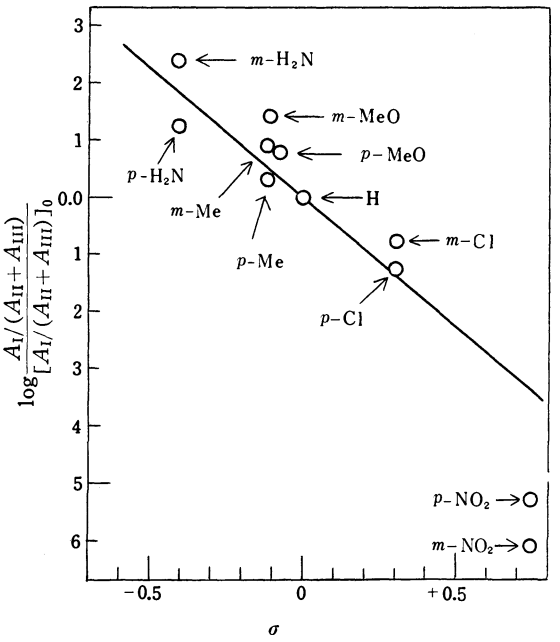


Fig. 5. Relation between $\log\frac{A_I/(A_{II}+A_{III})}{[A_I/(A_{II}+A_{III})]_0}$ in 2-arylethanol and σ constants for structure IX.

who found the same values for ortho-chloro and para-chloro within the experimental error and a slightly more negative value for ortho-methoxyl than for para-methoxyl. Electron densities computed by the molecular orbital method have been reported in some instances and slight differences between ortho- and para-position have been reported, although they do not cover all the substituents used in the present work. Hence, $(\sigma_m+\sigma_p)/2$ is used as an approximation for the substituents in the meta-position except the methoxyl group for which respective values for ortho and for para are available.

There are deviations from a straight line, even though the results are better than those considered from structure VIII. In other words, the meta-substituted 2-phenylethanol is always favored in the internal interaction over the para-substituted, or the former always gives a greater integrated intensity of band I, when an electron-releasing group is introduced. The deviations may be caused by neglecting the electron density of the ortho-position and/or by the contribution of structure VIII to some extent, which favors 2-phenylethanols with an electron-donating group in the meta-position for the interaction. The deviation may be also caused by using $A_{II}+A_{III}$ instead of A_{II} as the integrated intensity of the free form, since the scale model indicates that the free form capable of producing such an interaction is only one, of which integrated intensity is given by A_{II}.

If the intramolecular interaction between the hydroxyl group and the π-electrons is considered as a complex formation between a cation and an aromatic nucleus, structure IX can be supported. Namely, Rundle and Goring[19] observed on the basis of diffraction data that the silver ion in the complex with benzene is bonded equally with the two carbon atoms of the benzene nucleus and is located above the surface. Judged from the present results shown in Table II, the wave number of the ν_{O-H} absorption of the interacting form can be said just the same for a given substituent irrespective of its position. This fact strongly supports structure IX as the internally interacting form of 2-phenylethanol.

Strictly speaking, however, structure VIII can not be totally rejected, because it is one of the possibilities that favor the meta-substituted compounds in the internal interaction more than the para-substituted. Doering et al.[20] studied the structure of the heptamethylbenzenonium compound and postulated the 1,1,2,3,4,5,6-heptamethylbenzenonium ion with C_1 of the tetrahedral structure, without totally rejecting another with the methyl ion located between the two carbon atoms of the benzene nucleus and out of the plane. On the contrary, the present conclusion is that structure IX is the main contribution[21].

3-Arylpropanols.—As the representatives of 3-arylpropanols the ν_{O-H} absorption curves of 3-(*p*-aminophenyl)-propanol and 3-(*p*-chlorophenyl)-propanol and the corresponding divided values are shown in Figs. 6 and 7, respectively. The results are summarized in Table III.

It may be suspected that the lowest

19) R. E. Rundle and J. H. Goring, *J. Am. Chem. Soc.*, **72**, 5337 (1950).

20) W. von Doering, M. Saunders, H. G. Boyton, H. W. Earhart, E. F. Wadley, W. R. Edwards and G. Laber, *Tetrahedron*, **4**, 178 (1958).

21) It may be pointed out that another possibility exists in which either structure VII or VIII contributes. Namely, the direction of the hydroxyl group points to either C_1 or C_2 depending on the favorable electron density on the carbon atom. This is improbable, however, since interacting forms of both meta- and para-substituted compounds absorb at nearly the same wave number, while, in O-H···O hydrogen bonding, ν_{O-H} absorption generally appears at lower wave numer in the formation of a six-membered ring than of a five-membered ring.

TABLE III. ν_{O-H} ABSORPTIONS OF 3-ARYLPROPANOLS (x-$RC_6H_4CH_2CH_2CH_2OH$)

R	x	OH	ν_{max} (cm^{-1})	$\Delta\nu^a_{1/2}$ (cm^{-1})	$A\times10^{-3}$ ($mol^{-1}\cdot l.\cdot cm^{-2}$)	$\Delta\nu_{III-I}$ (cm^{-})	$\Delta\nu_{III-II}$ (cm^{-1})
		I	3587.0	33.0	1.11		
	m	II	3627.2	24.0	2.15	52.9	12.7
H_2N		III	3639.9	17.6	3.33		
		I	3590.0	29.0	0.98		
	p	II	3625.8	20.0	1.92	49.9	14.1
		III	3639.9	16.7	3.32		
		I	3593.0	35.0	0.50		
	m	II	3625.2	24.0	2.28	47.2	15.0
CH_3O		III	3640.2	16.6	3.62		
		I	3595.0	27.0	0.39		
	p	II	3626.8	21.2	2.05	45.0	13.4
		III	3640.2	14.6	2.92		
		I	3593.2	30.6	0.43		
	m	II	3627.0	23.0	1.97	46.8	13.0
CH_3		III	3640.0	15.8	2.99		
		I	3598.0	31.4	0.51		
	p	II	3628.5	22.6	2.23	42.6	12.1
		III	3640.6	15.6	3.01		
H		II	3623.0	21.6	1.93		16.7
		III	3639.9	16.0	3.57		
Cl	*p*	II	3627.8	24.8	2.53		12.6
		III	3640.4	16.6	3.40		

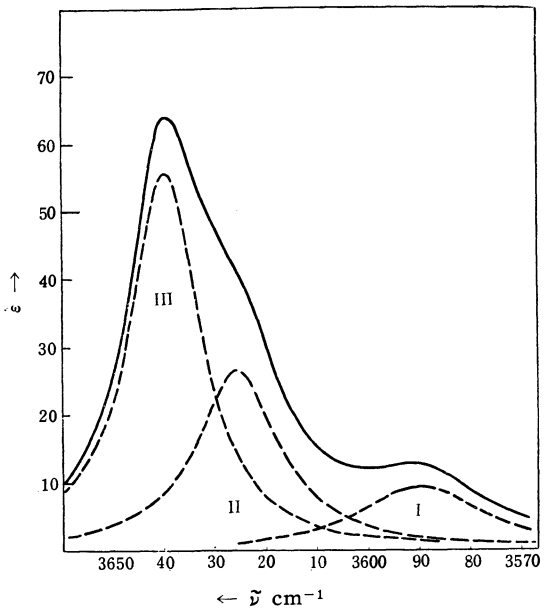


Fig. 6. ν_{O-H} absorption of 3-(*p*-aminophenyl)-propanol.

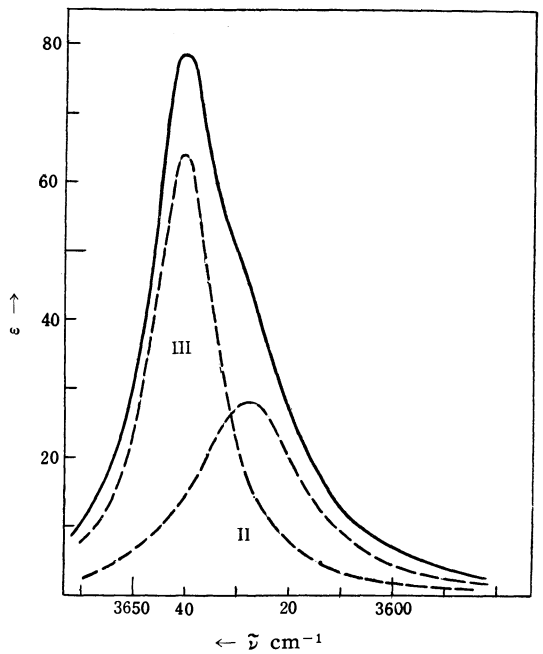


Fig. 7. ν_{O-H} absorption of 3-(*p*-chlorophenyl)-propanol.

ν_{O-H} absorption (band I) of 3-(aminophenyl)-propanols might be the ν_{N-H} absorption, but actually ν_{N-H} absorptions are found at 3479 cm^{-1} and 3393 cm^{-1} for 3-(*m*-aminophenyl)-propanol. The shift in the wave numbers of the ν_{O-H} absorption of the interacting form is consistent with the results obtained with 2-arylethanols. Namely, the methoxyl and the methyl groups give bands I at nearly the same wave number and the amino group further lowers the wave number. The difference between the meta- and the para-substituted compounds can not be taken as an

TABLE IV. ν_{O-H} ABSORPTIONS OF 4-ARYLBUTANOLS (p-$RC_6H_4CH_2CH_2CH_2CH_2OH$)

R	OH	ν_{max} (cm^{-1})	$\Delta\nu^a_{1/2}$ (cm^{-1})	$A\times10^{-3}$ ($mol^{-1}\cdot l.\cdot cm^{-2}$)	$\Delta\nu_{max}$ (cm^{-1})
H_2N	II	3626.1	19.8	2.21	13.0
	III	3639.1	17.4	3.26	
H	II	3626.6	23.2	2.36	13.3
	III	3639.9	17.6	3.43	

important indication, because bands I constitute the smallest peaks and errors involved in dividing the apparent absorption do not allow to discuss such a small difference.

It is apparent that the interaction is less favored in 3-arylpropanols than in 2-arylethanols, because even 3-(aminophenyl)-propanols give the smaller integrated intensities of band I. 3-Phenylpropanol itself does not show any absorption corresponding to band I of the other compounds with an electron-releasing group. However, the close examination of band II reveals that band II of 3-phenylpropanol is located at a rather low wave number, $\Delta\nu_{III-II}$ being as large as 16.7 cm^{-1}, in comparison with 12~15 cm^{-1} of others. It may be attributed to the fact that the peak corresponding to band I of 3-phenylpropanol is too small to be separated from others by the present technique. The above assumption seems verifiable because 3-(p-chlorophenyl)-propanol gives bands II and III in the normal positions for primary alcohols, $\Delta\nu_{III-II}$ being 12.6 cm^{-1}. In this case, the electron-attracting power of the chlorine atom seems to prohibit the interaction from taking place.

It is rather strange that 3-arylpropanols possess smaller numbers of internally interacting molecules even though the interacting form seems to be more stabilized than that in 2-arylethanol, because the wave numbers of bands I of 3-arylpropanols are lower than those of 2-arylethanols[22]. It must be attributed either to the unfavorable change in entropy and energy or to the difference in nature, as the authors pointed out for allyl alcohol and 3-buten-1-ol[3]. In this case, however, the present authors will choose the former for the following reasons. Firstly, the electronic effect in 3-arylpropanols shows the same trend as that in 2-arylethanol, and, secondly, the interacting form in 3-arylpropanol requires the all-*gauche* form including two carbon and one oxygen atoms, while that in 2-arylethanol requires the *gauche* form including one each of carbon and oxygen atoms. Hence, even though the interacting form of 3-arylpropanols will be more stabilized, if once formed, the unfavorable change in entropy and energy will limit the number of the molecules.

As to the nature of the interaction, 3-arylpropanols do not provide further information. The authors again come to a difficulty because of the weakness of bands I, but would like to assign tentatively the same structure as 2-arylethanols, because the meta- and the para-substituted compounds give nearly the same ν_{O-H} absorptions.

4-Arylbutanols.—The results of 4-arylbutanols are shown in Table IV.

From Table IV, it is obvious that 4-phenylbutanol does not possess any intramolecular interaction between the hydroxyl group and the π-electrons, since its ν_{O-H} absorption is normal for primary alcohols. Even 4-(p-aminophenyl)-butanol shows the normal absorption for primary alcohols in spite of the favorable electron density on the aromatic nucleus due to the presence of the strongly electron-releasing amino group. And again, this fact must be attributed to the unfavorable change in both entropy and energy.

Thus, it can be concluded that the internal interaction between the hydroxyl group and the π-electrons of the benzene nucleus occurs, when the hydroxyl group is an alcoholic O-H and the carbon chain is not fixed, up to 3-phenylpropanol in the series of ω-arylalkanols.

Summary

The electronic effect on the intramolecular interaction between the hydroxyl group and the π-electrons of the benzene nucleus was studied with various ω-arylalkanols. In 2-arylethanols, introduction of an electron-releasing group into the benzene nucleus gives rise to the shift of the ν_{O-H} absorption maxima to a lower wave number and to greater integrated

22) For example, see R. M. Badger and S. H Bauer, *J. Chem. Phys.*, 5, 839 (1937).

intensities of the band due to the interacting form, and introduction of an electron-attracting group to a higher wave number and smaller integrated intensities. However, the wave number of the band due to the interacting form is not affected by the position of the substituent, as far as the substituent is the same. Thus, the structure represented by IX is favored. On the other hand, a compound with an electron-releasing group in the meta position always shows greater integrated intensities of the band due to the interacting form than the para-substituted isomer and this fact saves structure VIII from entire rejection. Hence, the authors tentatively assign structure IX as the most favorable with participation of structure VIII to some extent.

In 3-arylpropanols the interaction is observed only in the compounds with an electron-releasing group and 3-(*p*-chlorophenyl)-propanol shows the normal ν_{O-H} absorption for primary alcohols. The phenomenon that 3-arylpropanols show smaller interaction in spite of the appearance of the band due to the interacting form at a lower wave number is attributed to the unfavorable change in both energy and entropy.

In 4-arylbutanol no interaction is observed, even though a strongly electron-donating group is introduced.

Thus, as the authors predicted, it has been proved that the intramolecular interaction occurring in 2-phenylethanol is different in nature from that in benzyl alcohol.

The authors wish to express their hearty thanks to Professor Y. Urushibara and Professor T. Shimanouchi for their valuable suggestions and discussions. The authors are also indebted to the Ministry of Education for a Grant in Aid for Fundamental Scientific Research.

Department of Chemistry
Faculty of Science
The University of Tokyo
Hongo, Tokyo

Self-diffusion of Iodide Ion and Strontium Ion in Strontium Iodide Solutions

By Ryohei MATUURA and Yasushi KOGA

(Received April 3, 1959)

Self-diffusion coefficients of iodide ion in hydrogen iodide, sodium iodide, potassium iodide and rubidium iodide solutions were measured by Mills and Kennedy[1]. They showed that in every iodide solution studied the product of self-diffusion coefficient of iodide ion and relative viscosity of the solution, i.e., $D\eta/\eta_0$, was linear against the square root of the concentration, $\sqrt{c}$, up to considerably high concentrations. In the case of self-diffusion of sodium, potassium, chloride and sulfate ions, however, no such linear relations were found. Matuura and Shimozawa[2] showed that the self-diffusion of calcium and strontium ions in chloride solutions was very complicated with respect to the concentration of the solution and found that the $D\eta/\eta_0$ vs. $\sqrt{c}$ curves had two minima and one maximum. The important difference of iodide ion from the other ions cited above in connection with the kinetic behaviors in aqueous solutions may be in its large size and poor hydration. A simple picture of the self-diffusion process for such "unhydrated" ions was suggested by Mills and Kennedy, which, in the case of monovalent counter ions, seems to explain the iodide ion self-diffusion satisfactorily. It is very interesting to investigate whether or not the same picture could be extended to the iodide of the divalent counter ions. The present work has been performed with the solution of strontium iodide in order to check this point and to obtain further knowledge

1) R. Mills and J. W. Kennedy, *J. Am. Chem. Soc.*, **75**, 5696 (1953).
2) R. Matuura and R. Shimozawa, *Mem. Faculty of Science, Kyushu University, Ser. C*, **2**, 53 (1955).

of the behavior of ions in electrolyte solutions.

Experimental

Apparatus. — The diffusion apparatus was essentially the same as that proposed by Anderson and Saddington[3] and modified by Wang[4]. The schematic diagram of the apparatus is shown in Fig. 1. A three-necked flask of one liter capacity

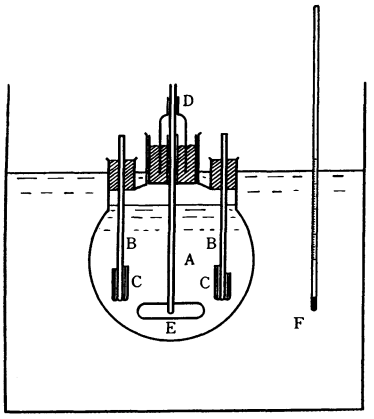


Fig. 1. Diffusion apparatus.

(A) was fitted with capillary holders (B) and a mercury seal stirrer (D). A plastic paddle (E) was turned slowly by an electric motor. The flask and contents were immersed in a thermostat (F) of 25±0.01°C. The capillary diffusion cells (C) were prepared as follows. The different diameter capillaries of Pyrex glass were used and the inside diameter was calibrated by filling with pure mercury. They were 0.0612 and 0.0780 cm. The capillaries were cut to different lengths and the top end of each capillary was ground flat with fine carborundum. The other end was sealed with glass to make a flat bottom. The length of each capillary was measured precisely with a micrometer caliper. These lengths varied from 2.97 to 5.19 cm.

Procedure.—Capillaries were filled with a radiotracer solution of known concentration by using a fine pipette drawn from a glass tubing. They were then held vertically in a flask containing one liter of inactive strontium iodide solution of the same concentration as the capillary solution. The air above the solution in the flask had been replaced by nitrogen gas so that the strontium iodide solution might not be decomposed by oxygen in air. Also, in order to avoid the effect of light, the outer surface of the flask had been coated with black paint. Each capillary was immersed in the flask solution up to just below the upper end of the capillary and left standing for about 30 min. in order to secure thermal equilibrium between the solution inside and outside of the capillary. Then the capillaries were dipped completely into the flask solution and the diffusion was allowed to start. The nitrogen gas in the flask was renewed after setting the capillary cells in it. During the diffusion period the flask solution was stirred by turning a paddle (see Fig. 1) at a constant rate 90 r. p. m. This turning rate was chosen in order to minimize the Δl correction according to Mills and Kennedy[1]. After each diffusion period (3 to 7 days) the capilliaries were taken out of the flask and the radioactivity of the solution in each capillary was measured by a counter. The radioactivity of the original solution was also measured at the same time and two values of radioactivity, that is, before and after diffusion corrected for natural decay, was compared on the same volume unit.

The viscosity of the solution was measured with an Ostwald viscometer at 25°C.

Materials. — The tracers used in the present experiment were ^{131}I and ^{89}Sr. ^{131}I (half-life 8.0 days) was obtained in the form of chloride in weak basic sodium bisulfite solution. The bisulfite was removed by titration with hydrogen iodide to a pH of about 5. A drop of this solution was added to a quantity of strontium iodide solution. The concentration of iodide in this solution was measured volumetrically. Since the concentration of cations other than strontium in this solution was negligibly small, this was used as a tracer solution for iodide ion diffusion in strontium iodide solutions. The radioactivity of ^{131}I in the solution was measured by a proportional gas counter.

^{89}Sr (half-life 54 days) was obtained as a carrier-free chloride. This contained less than 10% ^{90}Sr (half-life 25 years) which decays into ^{90}Y (half-life 65 hr.). A drop of the original solution was dried up and dissolved in the strontium iodide solution of known concentration to make a capillary solution. After diffusion the solution was drawn out of a capillary by means of a fine pipette. The capillary was washed several times with a large excess of distilled water. The sample solution, together with all washings, was evaporated to dryness and its radioactivity (c_{av}) was measured by a G. M. counter. The radioactivity (c_0) of the original solution was also measured at the same time. It was found that the ratio c_{av}/c_0 depended upon the duration after the diffusion had been stopped, because of the destruction of equilibrium between ^{90}Sr and ^{90}Y caused by the difference in the diffusion rate of the two species. So the measurement of c_{av} and c_0 was made week by week until the constant value of c_{av}/c_0 was obtained. It took two to four weeks to attain the complete equilibrium between ^{90}Sr and ^{90}Y. From this constant value of c_{av}/c_0 the diffusion coefficient of strontium ion in strontium iodide solutions was calculated.

It was found that strontium iodide decomposes gradually in air and by light, resulting in the liberation of iodine which makes the solution colored. So it was necessary to use a fresh sample for each experiment. The strontium

3) J. S. Anderson and K. Saddington, *J. Chem. Soc.*, **1949**, S 381.
4) J. H. Wang, *J. Am. Chem. Soc.*, **73**, 4181 (1951).

iodide solution was prepared from strontium carbonate and hydrogen iodide just before each run of diffusion and viscosity measurement. Rigorous precautions were made for the solution not to change by air and light during the experiment, as already mentioned. The solution was slightly acidic. Its concentration was determined gravimetrically as strontium sulfate and also volumetrically as silver iodide. Both methods agreed well.

Calculations

Under the present experimental conditions the Fick's diffusion equation is solved as follows[5].

$$\frac{c_{av}}{c_0}=\frac{8}{\pi^2}\sum_{n=0}^{\infty}\frac{1}{(2n+1)^2}\exp\left[-(2n+1)^2\pi^2Dt/4l^2\right] \tag{1}$$

where, c_{av} is the average concentration of the tracer ion in the capillary solution after diffusion, c_0 is its initial concentration, l is the length of the capillary, t is the diffusion time and D is the self-diffusion coefficient. For the value of Dt/l^2 greater than 0.2 the series in the Eq. 1 converges so rapidly that all terms following the first can be neglected with an error smaller than 0.2%. This condition was always kept in the present experiment. Thus the equation

$$2.303\log\frac{\pi^2}{8}\cdot\frac{c_{av}}{c_0}=-\frac{\pi^2Dt}{4l^2} \tag{2}$$

was always used for the calculation of the self-diffusion coefficient of iodide ion and strontium ion in the strontium iodide solutions.

TABLE I. SELF-DIFFUSION COEFFICIENT OF IODIDE ION IN STRONTIUM IODIDE SOLUTIONS AT 25°C

c (mol. SrI_2/l.)	$D_{I^-}\times10^5$ (cm²/sec.)
0.00042	1.995±0.03
0.0024	1.991±0.02
0.0042	1.928±0.02
0.0111	1.869±0.03
0.0128	1.881±0.02
0.0138	1.880±0.03
0.056	1.841±0.03
0.187	1.791±0.02
0.223	1.76 ±0.03
0.375	1.694±0.02
0.438	1.663±0.01
0.713	1.613±0.04

Results

Self-diffusion coefficients of iodide ion and strontium ion in strontium iodide solution of various concentrations are shown in Tables I and II, respectively.

TABLE II. SELF-DIFFUSION COEFFICIENT OF STRONTIUM ION IN STRONTIUM IODIDE SOLUTIONS AT 25°C

c (mol. SrI_2/l.)	$D_{Sr^{2+}}\times10^5$ (cm²/sec.)
0.0038	0.788±0.002
0.0116	0.744±0.003
0.0125	0.762±0.012
0.0242	0.748±0.013
0.096	0.743±0.010
0.0985	0.734±0.003
0.2197	0.719±0.02
0.500	0.704±0.018
0.7245	0.681±0.008
0.985	0.630±0.017

Values of relative viscosity of strontium iodide solutions at 25°C are shown in Table III.

TABLE III. RELATIVE VISCOSITY OF STRONTIUM IODIDE SOLUTIONS AT 25°C

c (mol. SrI_2/l.)	η/η_0
0.001	0.995
0.01	0.993
0.1	1.012
0.2	1.033
0.4	1.059
0.6	1.096
0.8	1.139
1.0	1.186
1.2	1.248
1.4	1.322
1.6	1.391
1.8	1.469
2.0	1.588
2.2	1.741
2.4	1.884

Discussion

In the dilute solution the self-diffusion of an ion is mainly controlled by the relaxation of ionic atmosphere around the ion. On the basis of Onsager's limiting law for the diffusion coefficient[6], Gosting and Harned[7] derived an equation for the variation of self-diffusion coefficient of the ion with its concentration, which in the case of self-diffusion of the ion (chemical

5) A. C. Wahl and N. A. Bonner, "Radioactivity Applied to Chemistry", John Wiley & Sons, Inc., New York (1951), p. 77.

6) L. Onsager, *Ann. N. Y. Acad. Sci.*, **46**, 241 (1945).

7) L. J. Gosting and H. S. Harned, *J. Am. Chem. Soc.*, **73**, 159 (1951).

species 1) in its binary electrolyte (chemical species 1 and 2) solutions, may be put into the following form.

$$D_1=\frac{\boldsymbol{R}T\lambda^0{}_1}{|Z_1|\boldsymbol{F}^2}-2.694\times10^{16}\frac{\lambda^0{}_1|Z_1|\boldsymbol{F}}{3\boldsymbol{N}\varepsilon}\sqrt{\frac{4\pi}{\varepsilon\boldsymbol{R}T}}\times\left(1-\sqrt{d(\omega_1)}\right)\sqrt{\sum_i c_i Z_i{}^2} \quad (3)$$

where, D_1 is the self-diffusion coefficient of the ion (in cm²/sec.), Z_1 and $\lambda^0{}_1$ are its number of the charge and limiting equivalent conductance (in coulomb/sec.×cm²/V.), respectively, c_i is the concentration of the i-th ion (in mol./l.), ε is dielectric constant of the solvent, and $\boldsymbol{R}$, $\boldsymbol{F}$, $\boldsymbol{N}$ and T are gas constant (in joule/deg. mol.), Faraday constant (in coulomb), Avogadro number and absolute temperature, respectively. $d(\omega_1)$ in Eq. 3 is given by

$$d(\omega_1)=\left(\frac{|Z_1|}{|Z_1|+|Z_2|}\right)\left(\frac{1}{2}+\frac{|Z_2|\lambda^0{}_2}{|Z_2|\lambda^0{}_1+|Z_1|\lambda^0{}_2}\right) \quad (4)$$

For the self-diffusion of iodide ion and strontium ion in strontium iodide solutions we use[8]

$$\lambda_{I^-}=76.8$$
$$\lambda_{Sr^{2+}}=59.46$$

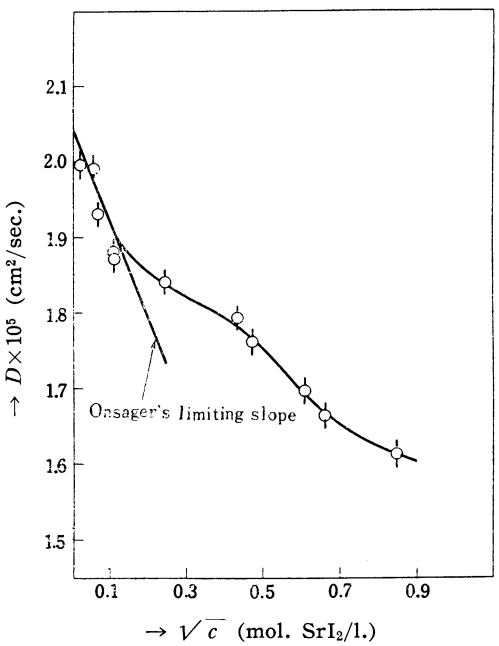


Fig. 2. Self-diffusion coefficient of I^- in SrI_2 solutions against square root of the concentration at 25°C.

8) D. A. McInnes, "The Principles of Electrochemistry", Reinhold Publishers Corp., New York (1950), p. 342.

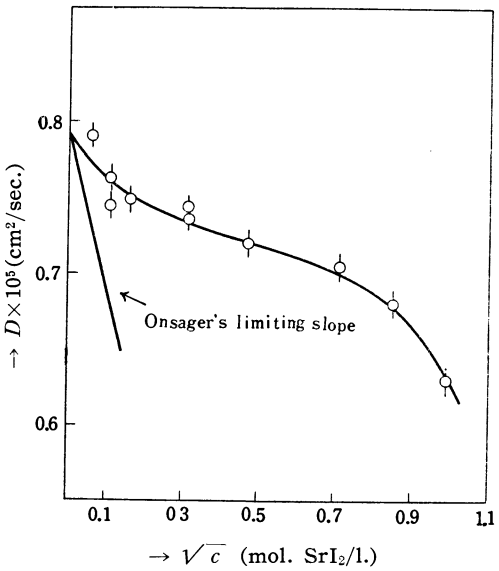


Fig. 3. Self-diffusion coefficient of Sr^{2+} in SrI_2 solutions against square root of the concentration at 25°C.

and we obtain the following equations by inserting the numerical values in Eq. 3:

$$D_{I^-}\times10^5=2.045-1.12\sqrt{c} \quad (5)$$

$$D_{Sr^{2+}}\times10^5=0.792-1.04\sqrt{c} \quad (6)$$

where, c is expressed in mol. SrI_2/l. These are limiting laws for the self-diffusion in the present case. In Figs. 2 and 3 are shown measured D_{I^-} and $D_{Sr^{2+}}$ against $\sqrt{c}$, respectively. It is seen that the experimental data fit the limiting law fairly well.

At higher concentrations the situation is much more complicated. Of various factors which control the ionic self-diffusion three may be considered most important, i.e., the viscosity of the solution, the hydration of the diffusing ion (i.e., the interaction between ion and solvent) and the state of ionic atmosphere (i.e., the interaction between ions). The correction for viscosity of the solution is usually made simply by multiplying D with η/η_0. In Fig. 4 $D\eta/\eta_0$ for iodide ion is plotted against $\sqrt{c}$. The curve for iodide ion is approximated by two straight lines. The straight line of lower concentrations can be extrapolated exactly to the Nernst limiting value, D_0, while that of higher concentrations gives a lower value by extrapolation to the zero concentration. Mills and Kennedy[1] showed that the $D\eta/\eta_0$ vs. $\sqrt{c}$ relation for iodide ion in the solution of iodide of monovalent

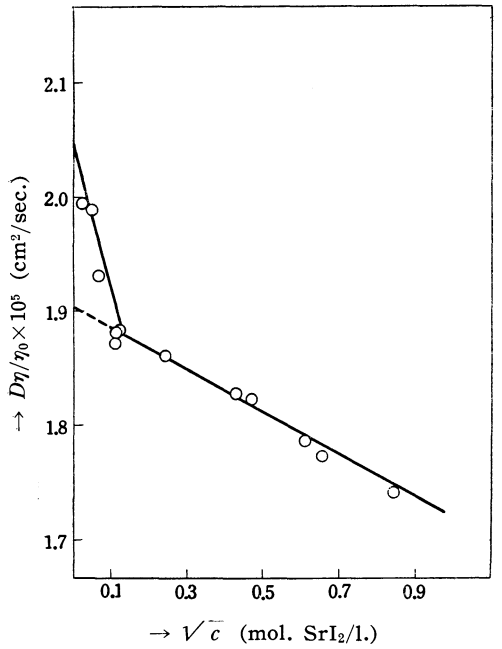


Fig. 4. $D\eta/\eta_0$ vs. $\sqrt{c}$ relation for I^- in SrI_2 solutions at 25°C.

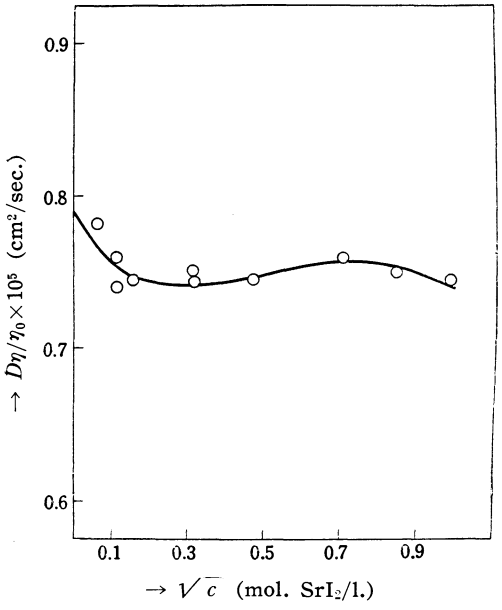


Fig. 5. $D\eta/\eta_0$ vs. $\sqrt{c}$ relation for Sr^{2+} in SrI_2 solutions at 25°C.

metal or hydrogen is linear all through from low to considerably high concentrations and extrapolated to the Nernst limiting value. It is not perfectly evident why the self-diffusion of iodide ion in strontium iodide is markedly different from that in the iodides which Mills and Kennedy studied, but one might ascribe it to the difference in the state of ionic atmosphere around the diffusing iodide ion.

The $D\eta/\eta_0$ vs. $\sqrt{c}$ relation for strontium ion in the solution of strontium iodide is shown in Fig. 5. This curve is much more complicated than and quite different in nature from the curve for iodide ion. It is well known that strontium ion is strongly hydrated, while iodide ion is "unhydrated". Matuura and Shimozawa[2] applied an empirical equation to the self-diffusion of strongly hydrated ions, which is

$$D\eta/\eta_0 = D_0 - k_1\sqrt{c} + k_2 c \log c + k_3 c \qquad (7)$$

where, k_1, k_2 and k_3 are constants. Of these k_1 is a limiting slope $D\eta/\eta_0$ vs. $\sqrt{c}$ relation and can be calculated from Fig. 5. Eq. 7 may be checked by plotting

$$F(D) \equiv \frac{D\eta/\eta_0 - D_0 + k_1\sqrt{c}}{c} \qquad (8)$$

against $\log c$. In Fig. 6 this plot is shown. It is seen that Eq. 7 is a fair expression for the self-diffusion of strontium ion in strontium iodide solutions.

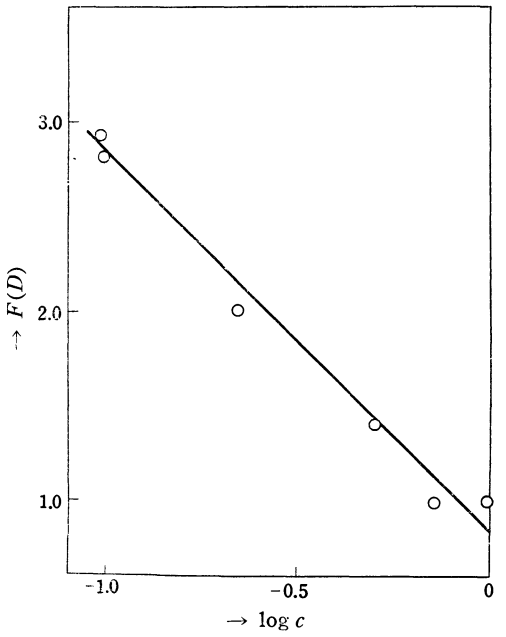


Fig. 6. $F(D)$ vs. $\log c$ relation for Sr^{2+} in SrI_2 solutions.

From the straight line in Fig. 6 the values of k_2 and k_3 are calculated as shown in Table IV. In the same table the data are given for the self-diffusion of strontium ion in strontium chloride

solutions and of sodium ion in sodium iodide and sodium chloride solutions[2].

TABLE IV. VALUES OF k_2 AND k_3 FOR STRONTIUM AND SODIUM ION

System	k_2	k_3
Sr^{2+} in SrI_2	−1.98	0.84
Sr^{2+} in $SrCl_2$	−1.54	0.93
Na^+ in NaI	−0.67	0.24
Na^+ in NaCl	−0.51	0.35

It is clear from Table IV that the absolute values of both k_2 and k_3 are larger for strontium ion than for sodium ion. Since Eq. 7 is an empirical one, the physical meaning of k_2 and k_3 is not definitely given, but one may conclude that k_2 and k_3 are mainly concerned with the charge (and of course also with the hydration) and size of the diffusing ion.

Summary

The self-diffusion coefficient of iodide ion and strontium ion in aqueous strontium iodide solutions has been measured by a capillary method. It has been found that the Onsager's limiting equation can be applied to the self-diffusion of both ions. The $D\eta/\eta_0$ vs. $\sqrt{c}$ relation for iodide ion has been represented by two straight lines, while that for strontium ion has been shown by a much more complicated curve. The latter has been represented successfully by an empirical equation for strongly hydrated ions presented by Matuura and Shimozawa.

A part of this work was performed at the Department of Chemistry, Washington University, St. Louis, Mo., U. S. A. The authors wish to express their thanks to Professor Joseph W. Kennedy of Washington University for his kind advice and encouragement.

Department of Chemistry
Faculty of Science
Kyushu University
Hakozaki, Fukuoka

SHORT COMMUNICATIONS

*Infrared Spectra of Polyvinyl Chloride**

By Akihiro KAWASAKI, Shigeo SHIOTANI, Junji FURUKAWA and Teiji TSURUTA

(Received June 10, 1959)

There exist many reports on infrared spectra of polyvinyl chloride, but are found only a few studies[1-5] which deal with crystalline and amorphous bands in the infrared spectra of this polymer.

With respect to some samples of polyvinyl chloride, we have examined correlation between the specific gravity and the optical density in the absorption bands ranging from 4,000 to 700 cm^{-1}.

Polyvinyl chloride was prepared at room temperature with a binary mixture of triethylaluminum and di-*tert*-butyl peroxide as catalyst. The viscosity average molecular weight of the polymer was 32,000. The samples were in the form of thin solid films, which were prepared from tetrahydrofuran solution of the polymer. By heat treatment in the Wood alloy, the specific gravity, d_4^{30}, of the sample was controlled from 1.3887 to 1.4022.

The examination of the infrared spectra of the polymer having various specific gravity has made clear that the ratios of any two of the optical densities at 2920, 1375 and 1092 cm^{-1} remain almost unchanged irrespective of the change in the specific gravity of the samples. Since it was considered, from this result, that each of the bands mentioned above varied in the same way with the specific gravity, the band at 2920 cm^{-1} was taken as standard and the ratio of optical densities at every absorption band to 2920 cm^{-1} band was calculated.

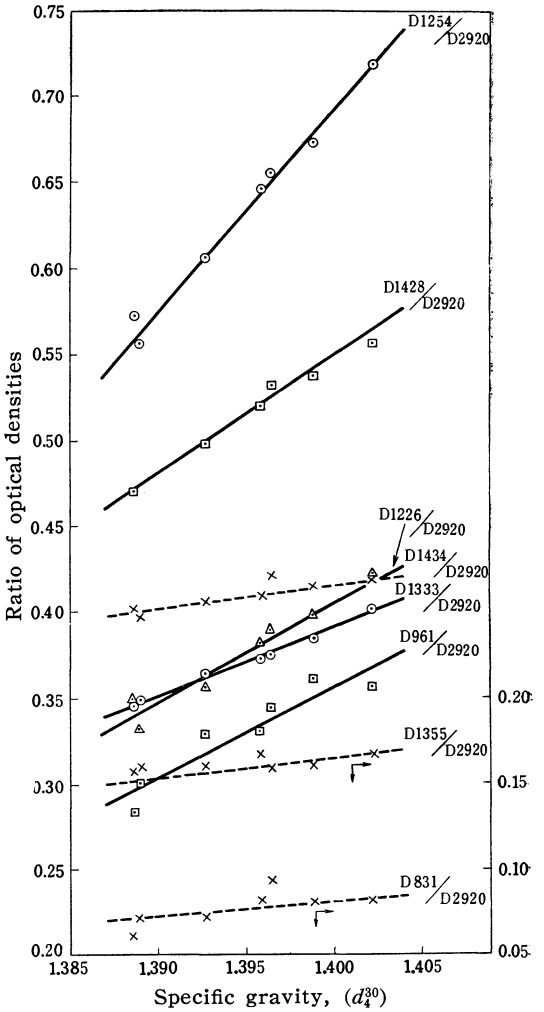


Fig. 1. Relation between optical density and specific gravity.

The liner relationship in Fig. 1 between the specific gravity and the optical density at bands 1428, 1333, 1254, 1226 (distinct parallel band) and 961 cm^{-1}, and the differential absorption band between two polymers having different specific gravity in Fig. 2 lead to the conclusion that these five absorption bands correlate with the specific gravity or crystallinity of the sample. A similar relation was observed

* Presented before the Symposium on Raman and Infraed Spectra at Kyoto, October 16, 1958.

1) S. Krimm and C. Y. Lang, *J. Polymer Sci.*, **22**, 95 (1956).
2) R. J. Grisenthwaite and R. F. Hunter, *Chem. & Ind.*, **1958**, 719.
3) S. Mizushima, T. Shimanouchi and S. Tsuchiya, Abstract of the Paper read in the 11th Annual Meeting of the Chemical Society of Japan, Tokyo (1958), p. 147.
4) S. Mizushima, T. Shimanouchi and S. Tsuchiya, Abstract of the Paper read in the Sympsoium on High Polymer, Osaka (1958), p. 127.
5) H. Watanabe and T. Hotta, Abstract of the paper read in the Symposium on High Polymer, Nagoya (1957), p. 54.

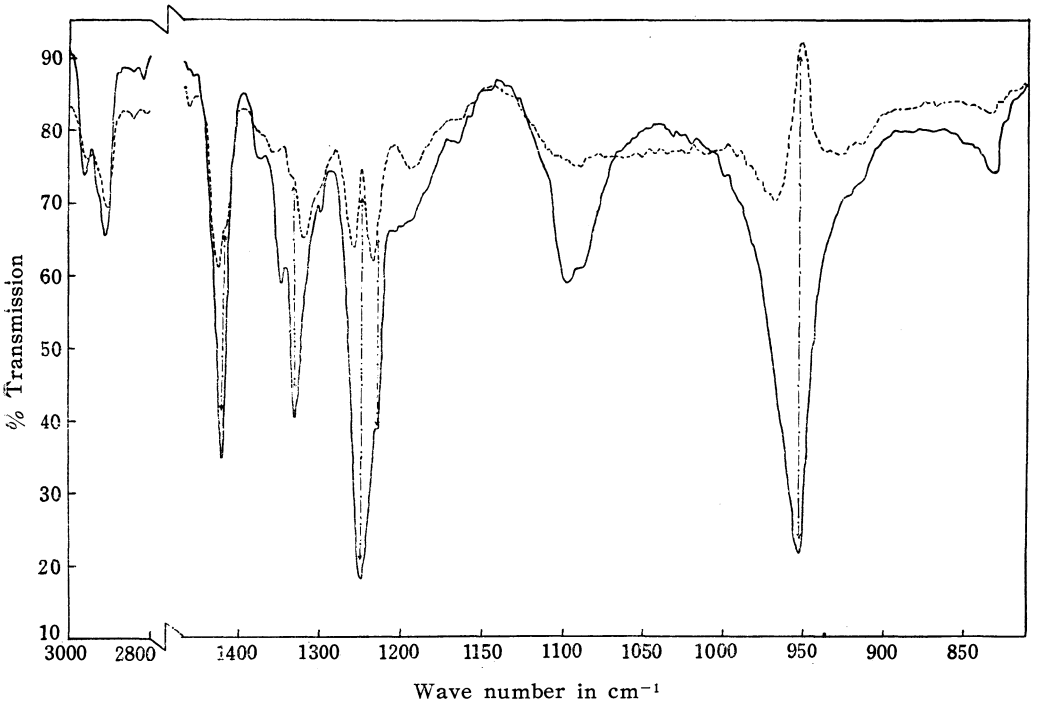


Fig. 2. Differential infrared spectra (——: reference, lower density polymer, ----: reference, higher density polymer.)

also in the absorption bands at 1434, 1355 and 831 cm^{-1} but its dependency upon the specific gravity was much smaller than the above case.

The analysis of these results is under study in our laboratory. Full dentails will be reported in this bulletin.

The authors wish to express their gratitude to Dr. H. Tadokoro, Faculty of Science, Osaka University, and to Dr. Z. Kumazawa, Faculty of Agriculture, Kyoto University, for advice and kindness in infrared analysis.

Department of Industrial Chemistry
Faculty of Engineering
Kyoto University
Sakyo-ku, Kyoto

Infrared Spectra of Crystalline and Amorphous Polystyrene

By Masatami TAKEDA, Kazuyoshi IIMURA
Akira YAMADA and Yoshio IMAMURA

(Received June 30, 1959)

It has been reported[1] that crystalline polystyrene (CPS) prepared by Ziegler type catalyst shows a quite different infrared spectrum from that of amorphous polystyrene (APS) prepared by radical catalyst. It has been also suggested[2] that some bands in the spectrum of CPS could be associated with the three fold herical structure[3] of isotactic polystyrene.

We have studied the infrared spectrum of CPS-I* in the solid state, in the solution of carbon disulfide***, and in the molten state, and have compared them with the corresponding spectra of APS**. Another

1) G. Natta, *Makromol. Chem.*, **16**, 213 (1955).
2) H. Tadokoro et al., This Bulletin, **32**, 313 (1959).
3) C. W. Bunn and E. R. Howelles, *J. Polymer Sci.*, **18**, 307 (1955).

* Prepared by Ziegler catalyst and separated from insoluble parts with cold methyl ethyl ketone after treating with *n*-heptane.

** Commercial polystyrene, "Styron-666".

*** The solution was prepared by extraction of CPS-I at the boiling point of carbon disulfide.

crystalline polystyrene, CPS-II****, prepared by Alfin catalyst has been studied in the solid state.

The spectra of these samples in various states are shown in Fig. 1. The most remarkable differences between CPS-I and APS in solid are found in the bands at 1085, 1054 and 567 cm^{-1}. These absorption bands of CPS-I in solution are very similar to those of solid CPS-I, but some of the other bands observed in the solid state disappear.

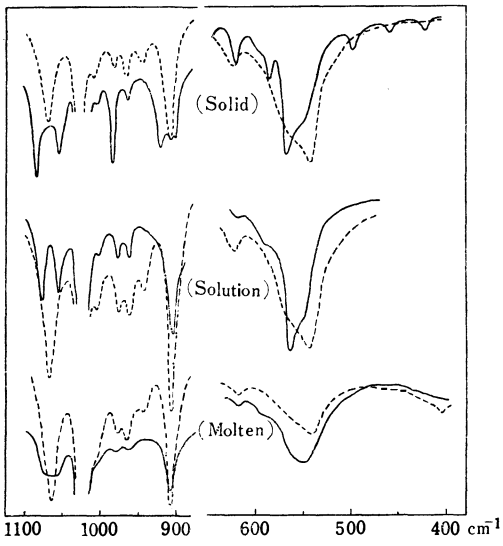


Fig. 1. Infrared spectra of CPS-I and APS in various states.
—— CPS-I ---- APS

In the molten state, the spectrum of CPS-I is almost similar to the spectrum of APS, except for the following points: the doublet at 1085 and 1054 cm^{-1} of solid CPS-I changes into a single and broad band with the maximum at 1070 cm^{-1} with melting, whereas molten APS shows a rather sharp absorption at 1070 cm^{-1}.

The asymmetric band with the maximum at 567 cm^{-1} of solid CPS-I becomes a symmetric and broad band with the maximum at 552 cm^{-1}, while the absorption maximum of molten APS at 543 cm^{-1} remains unchanged.

The observed absorption frequencies are shown in Table I. Complete assignment of the bands at 1085, 1054 and 567 cm^{-1} in both polystyrenes in various states are not yet obtained.

However, the differences between the spectra of CPS-I in various states can be used to classify the observed bands in three groups.

TABLE I. FREQUENCIES IN VARIOUS STATES OF CPS AND APS

CPS-I			APS		Classification of the band
solid	soln.	molten	solid, soln., molten		
1364	1364	1370 w	1370		B
1314	1314	1314 w	1312		B
1297	1297	1295 w	1295		B
1185	1190	1185 w	1182		B
1085	1080				C
		1063 b	1070	s	C
1054	1057				C
984	978 w	978 w	980		A
965	963	963	965		
			945		
923					A
910	908	905	905		
901					A
620 s	620 b	620 b	620	b	A
587					A
567	560				C
		552 b			C
			543		C
499					A
465					A
426					A

s: sharp
b: broad
w: weak in solution and in molten state

(A) Under the first group come the bands at 984, 923, 901, 620, 587, 499, 465 and 426 cm^{-1}. They disappear instantly or are very much weakened when CPS-I dissolves in solution or melts. These bands, which are not observed in the spectrum of APS, may be assigned to the vibrational bands caused by the perturbation by rather long range intra- and intermolecular interactions in the CPS-I crystal. The band at 984 cm^{-1} is considered as a typical crystalline band by Tadokoro et al[4].

(B) Under the second group come the bands at 1365, 1314, 1297 and 1185 cm^{-1}. They are stronger in crystallized CPS-I than in quenched one, and persist in the spectrum of the solution. These bands have been assigned[2] to the CH or CH_2 deformation vibrations, which are closely associated with the intramolecular interaction in the herical chain having a three-fold screw axis.

(C) The doublet at 1085~1054 cm^{-1} and

**** Separated from insoluble parts in cold methyl ethyl ketone after treating with *n*-heptane.

4) H. Tadokoro et al., Symposium of High Polymer, Osaka, Oct., 1958.

the asymmetric bands at 567 cm^{-1} in solid CPS-I and at 543 cm^{-1} in APS could form the third group, because they appear differently in the spectra of molten CPS-I and APS.

The band at 567 cm^{-1} is tentatively assigned by the following reason: The Raman band at 558 cm^{-1} of APS has been assigned to the ν_{6A} mode, an in-plane vibration of benzene nuclei of A_1 mode, by Liang and Krimm[5], which derives from a Raman active and infrared inactive mode of benzene. If all the phenyl radicals in the herical conformation of a polystyrene molecule vibrate in the same phase in the ν_{6A} mode, the dipole moment of the molecule changes along the screw axis of the conformation. It is possible in this case that the ν_{6A} mode is infrared active and shows parallel dichroism which is actually found in our experimental data shown in Fig. 2. Thus we may expect that the band at 567 cm^{-1} is an *X*-sensitive vibration of monosubstituted benzene[6], and sensitive to the short range interaction between the phenyl group and the herical C–C main chain which has alternate *trans* and *gauche* conformations[7].

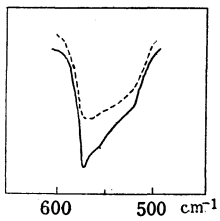


Fig. 2. Dichroism of the 567 cm^{-1} band in solid CPS-I.
—— Electric vector parallel to elongation
---- Electric vector perpendicular to elongation

The band at 543 cm^{-1} of APS is assigned to an *X*-sensitive vibration which is affected by another short range interaction between the phenyl group and the C–C main chain of APS which may have mainly *trans-trans* conformation sequence in their syndiotactic parts.

The doublet at 1085~1054 cm^{-1} of CPS-I and singlet at 1070 cm^{-1} of APS are probably assigned also to the same type of vibration.

On the basis of the above empirical classification of characteristic bands of CPS-I and APS, as a possible interpretation of the origin of these absorption bands, the following tentative conclusions are drawn.

Based on the behavior of C class band, the conformation of CPS-I along the C–C main of a few monomer units seems to differ from that of APS in their molten states. This may lead us to expect that the change of the bands at 1085, 1054 and 567 cm^{-1} must be connected with the content of the isotactic configuration of CPS-I. If this is assumed, it should be suggested that the isotactic contents in the chain configuration of CPS-II is smaller than that of CPS-I, since the C band of CPS-II in the solid state is quite similar to that of molten CPS-I as is shown in Fig. 3.

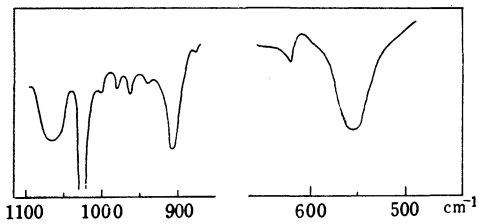


Fig. 3. Infrared spectrum of solid CPS-II.

In solution, it is interesting to note that the herical conformation of isotactic polystyrene is partly reserved, because the persistence of the bands at 567, 1085, 1054 and also 1364, 1314, 1297, 1185 cm^{-1} of crystallized CPS are well recognized.

The authors are grateful to Professor T. Shimanouchi of the University of Tokyo for his discussion and kind cooperation in the measurement of dichroism.

Tokyo College of Science
Kagurazaka, Shinjuku-ku
Tokyo

5) C. Y. Liang and S. Krimm, *J. Polymer Sci.*, **27**, 241 (1958).
6) D. H. Whiffen, *J. Chem. Soc.*, **1956**, 1350.
7) W. R. Krigbaum, D. K. Carpenter and S. Newman, *J. Phys. Chem.*, **62**, 1586 (1958).

On Miyaconitine and Miyaconitinone

Shichiro KAKIMOTO, Nobukatsu KATSUI and Yoshiyuki ICHINOSE

(Received August 7, 1959)

In an earlier paper[1], the extended formulae of miyaconitine(I) $C_{23}H_{29}O_6N$ and miyaconitinone(II) $C_{23}H_{27}O_6N$ were given respectively as follows:

(I) $C_{19}H_{20}(OAc)(OH)(=O)_3(N\text{-}Et)$

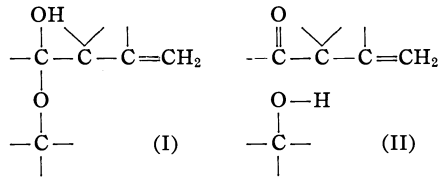
(II) $C_{19}H_{19}(OAc)(=O)_4(N\text{-}Et)$

The present communication presents further consideration of the empirical and extended formulae of I and II:

(I) $C_{24}H_{31}O_6N$: $C_{20}H_{22}(OAc)(OH)(-O-)\cdot(=O)_2(N\text{-}Et)$. λ_{max}^{EtOH} 295 mμ (log ε 1.6), ν_{max}^{KBr} 3470(OH), 1726, 1678(CO), 3090, 1648, 877 cm^{-1} ($\rangle C=CH_2$)

(II) $C_{24}H_{31}O_6N$: $C_{20}H_{22}(OAc)(OH)(=O)_3\cdot(N\text{-}Et)$. pK_a' 6.5 λ_{max}^{EtOH} 290 mμ(log ε 2.6), ν_{max}^{KBr} 3410(OH) 1728, 1715, 1676(CO), 3090, 1648, 883 cm^{-1} ($\rangle C=CH_2$)

The presence of the terminal methylene group was confirmed not only by the observation of infrared spectra, but also by ozonolysis and novel Lemieux oxidation[2] to give formaldehyde. Compound I showed extreme susceptibility to aldehyde reagents (viz., Fehling, Tollens and TTC, etc.), but II did not. The oxidation of I with bismuth oxide in refluxing acetic acid yielded II. The infrared spectrum of II showed a band at 3410 cm^{-1} probably due to a tertiary hydroxyl group. These observations are explained by the consideration that the conversion of I to II is not a simple oxidation of a secondary hydroxyl group to a carbonyl group but is an oxidation of a hemiketal moeity existing in I. Ultraviolet absorption of II and its alkamine, miyaconinone(III), $C_{22}H_{25}O_5N$ showed abnormal intensity due to a β,γ-unsaturated carbonyl group[3]: λ_{max}^{EtOH} 294 mμ (log ε 2.6), ν_{max}^{Nujol} 3460, 3310 (OH) 1724, 1673 (CO) 1649, 888 cm^{-1} ($\rangle C=CH_2$). Therefore, the partial structures of I and II may be represented by the following schemata.



Alkaline hydrolysis of II gave ψ-miyaconinone*(IV), m. p. 254~256°C, $[\alpha]_D^{20}$ −1.0°, pK_a 4.2, λ_{max}^{EtOH} 284 mμ(log ε 1.2). ν_{max}^{Nujol} 3600, 3510 (OH) 1783, 1727(CO) 1648, 889 cm^{-1} ($\rangle C=CH_2$) (*Anal.* Found: C, 68.58, H, 7.48. Calcd. for $C_{22}H_{25}O_5N$: C, 68.19; H, 7.54%). This compound was obtained also by alkaline treatment of III. In the ultraviolet absorption of IV, the maximum displayed no longer the abnormal intensity as shown in those of II and III. On the other hand, the infrared spectrum of IV showed three peaks due to hydroxyl group although that of III had two peaks. Then it is considered that the reaction of II to IV involves the base-catalyzed conversion of the carbonyl group to a hydroxyl group. A plausible explanation of this reaction is that the carbonyl group showing abnormal intensity in II or III has undergone an internal aldol condensation. It has been previously reported that an α-diketone group adjacent to the nitrogen atom is present[4]. Accordingly, the condensation must have occurred in the methylene group adjacent to the α-diketone. The lower basicity of IV also supports these considerations.

In the titrations of periodate and lead tetraacetate, III and IV took up rapidly one mole more than II in one hour. It is suggested then that III and IV have a vicinal glycol system.

The composition of the fundamental base, $C_{20}H_{31}N$, and the exsistence of terminal methylene group suggest that I and II may be belonged to atisine or garryine type alkaloids.

Furthermore, it has been already reported that songorine[3b,5], one of aconite alkaloids, has the same β,γ-unsaturated ketonic system with II. And so it is considered tentatively that I and II have

1) H. Suginome, S. Furusawa, Y. Chiba and S. Kakimoto, *J. Fac. Sci. Hokkaido Univ. Ser. III Chem.*, **4**, 1 (1950).

2) R. Pappo, D. S. Allen, R. V. Lemieux and W. S. Johnson, *J. Org. Chem.*, **21**, 478 (1956).

3a) R. C. Cookson and N. S. Wariyar, *J. Chem. Soc.*, **1956**, 2302.

3b) K. Wiesner, Z. Valenta, J. F. King, R. K. Maudgal, L. G. Humber and S. Itô, *Chem. & Ind.*, **1957**, 173.

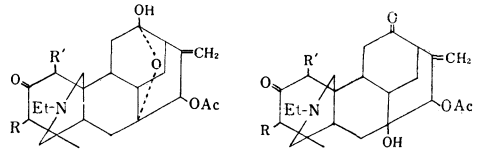
* In a previous paper[1], it has been reported that the hydrolysis of II gave miyaconine which was obtained also from I by the same hydrolysis. But the infrared spectrum of the former was different from that of the latter.

4) S. Kakimoto, This Bulletin, **32**, 349 (1959).

5) K. Wiesner, S. Itô and Z. Valenta, *Experientia*, **14**, 167 (1958).

closely related ring structures with these alkaloids.

Above all, it has been reported that selenium dehydrogenation of II gives phenanthrene and anthracene[6]. If anthracene ring occurred without rearrangement in the course of dehydrogenation, this fact, above consideration and the partial structures may lead possible structures for I and II as follows:



(I) R=O R'=H₂ (II)

As for the α-diketone system, R=O is more probable than R'=O**. The infrared absorption of I or II is similar*** to that of kobusine diacetate which has an allylic acetate function[7]. It is suggested that the acetyl group in I and II covers an allylic hydroxyl group which is observed generally in alkaloids of the atisine group. Some experimental studies in order to confirm the above considerations are in progress.

The authors wish to express their deep thanks to Professor Harusada Suginome, President of Hokkaido University, for his exceedingly kind direction throughout this work.

Department of Chemistry
Faculty of Science
Hokkaido University, Sapporo

6) H. Suginome and S. Kakimoto, This Bulletin, **32**, 352 (1959).

** In the molecular model of II, the active methylene group concerning the aldol condensation is more plausible R' than R.

*** In the comparison of infrared spectra of kobusine and kobusine diacetate, and II and III, similar shifts of the peaks were observed in the region of 870~930 cm^{-1}. These data will be reported in a later paper.

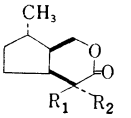
7) T. Okamoto, *Chem. Pharm. Bull. Japan*, **7**, 44 (1959).

The Structure of Matatabilactone

By Takeo Sakan, Akira Fujino, Fujio Murai, Akio Suzui and Yasuo Butsugan

(Received August 18, 1959)

In the preceding communication[1], the authors presented the structural formula of dihydronepetalactone for matatabilactone which was isolated as one of the physiologically active components for the Felidae animals from the leaves of *Actinidia polygama* Miq. (Matatabi). This estimation was principally based on the fact that two known epimeric nepetalinic acids were obtained by the oxidation of the corresponding hydroxy acid with potassium permanganate. It was pointed out that the alternative formula, i. e., that of isoiridomyrmecin(Ia)[2] or iridomyrmecin (Ib)[2] was unlikely to be the case because of the quite clear differences among the $\nu_{C=O}$ values in the infrared spectra of these substances. The examination thereafter has, however, led to some new informations in regard to the structural problem.



Ia $R_1=CH_3$, $R_2=H$

Ib $R_1=H$, $R_2=CH_3$

A hydroxy acid, $C_{10}H_{18}O_3$(II) of m. p. 109~110°C (*Anal.* Found: C, 63.86; H, 9.72. Calcd: C, 64.49; H, 9.74%) was isolated when I (*Anal.* Found: C, 71.54; H, 9.88. Calcd. for $C_{10}H_{16}O_2$: C, 71.39; H, 9.59%) was, after alkali hydrolysis, treated carefully with acetic acid. By vacuum sublimation II was converted into a lactone, m. p. 60°C, $[\alpha]_D^{21}-67.6°$ (c 0.10, carbon tetrachloride)(III), from which the hydrazide(IV) of II, m. p. 119~120°C (*Anal.* Found: N, 14.11. Calcd. for $C_{10}H_{20}O_2N_2$: N, 13.99%) was derived. The physical properties of II—IV are respectively very similar to those of the compounds of Ia series. The mixed fusion tests and the

1) T. Sakan, A. Fujino, F. Murai. Y. Butsugan and A. Suzui., This Bulletin, **32**, 315 (1959).
2) G. W. K. Cavill and H. D. Locksley, *Australian J. Chem.*, **10**, 352 (1957).

comparisons of the infrared spectra of the samples of III and IV proved their identities with those that have been found by the Australian chemists. The authors are deeply indebted to Dr. G. W. K. Cavill for his kind offers.

It was difficult to seperate II completely from I, and accordingly, the residual part is as yet non-crystalline. Although attempts to obtain the other component in a pure state have been up to now without success, it is likely that matatabilactone is a mixture of Ia and Ib.

Institute of Polytechnics
Osaka City University
Kita-ku, Osaka

Calcd. for $C_{10}H_{13}O_2N$: C, 67.02; H, 7.31; N, 7.82%) was obtained. Chlorination of IV with phosphorus oxychloride and successive catalytic hydrogenation of the dechloro-compound (oil) afforded DL-actinidine(V), b.p. 100~103°C/12 mmHg (picrate: m. p. 142~143°C). V was then resolved into an optically active form through the mono-salt of dibenzoyltartaric acid. The less soluble salt in absolute ethanol yielded, on regeneration of the base, a laevorotatory oil(VI), $[\alpha]_D^{21}$ −8.01° (c 2.17, chloroform), the infrared spectrum of which was in all respects identical with that of natural actinidine. Identity between the picrates of VI, m.p. 146~147°C, and of I, was also established through the mixed melting point determination and the comparison of the infrared spectra.

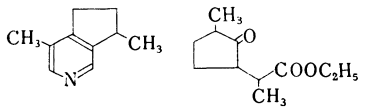
Institute of Polytechnics
Osaka City University
Kita-ku, Osaka

The Synthesis of Actinidine

By Takeo SAKAN, Akira FUJINO, Fujio MURAI, Akio SUZUI and Yasuo BUTSUGAN

(Received August 18, 1959)

Actinidine(I)[1], a basic effective component for the Felidae animals in *Actinidia polygama* Miq. (Matatabi), was synthesized from ethyl α-(3-methyl-2-oxo-cyclopentyl)-propionate(II)[2] as follows.



(I) (II)

The cyanohydrin of II was dehydrated to a cyanoester(III), b. p. 106~120°C/2 mmHg by the action of thionyl chloride in the presence of pyridine. The position of the double bond in III is not conclusive, and both possible isomers seem to have been actually produced. Attempts to separate them with alkali or ethoxide solution resulted in failure. On acid or alkali hydrolysis of III, the dihydroxy-pyridine derivative(IV), m. p. 167~168°C (*Anal.* Found: C, 66.71; H, 7.32; N, 7.77.

1) T. Sakan, A. Fujino, F. Murai, Y. Butsugan and A. Suzui, This Bulletin, **32**, 315 (1959).
2) R. L. Jones and R. P. Linstead, *J. Chem. Soc.*, **1936**, 616.

Dialkylthioboronates

By Nobuyuki ASHIKARI

(Received September 7, 1959)

Many organo boron compounds are known to be effective catalysts for vinyl-polymerization[1-3]. Accordingly, several dialkylthioboronates have been prepared for testing the catalytic activity. It was found that though the activites of the compounds as polymerization catalysts were low, they reacted in a characteristic manner with ammonia. These compounds are new substances, and the synthetic method and some properties of them are described in this paper.

The only known dialkylthioboronate is dimethylthioboronate[4], $(CH_3)_2BSCH_3$, which was prepared by the interaction of methylmercaptan and tetramethyl diborane.

$$2CH_3SH + B_2H_2(CH_3)_4 = 2(CH_3)_2BSCH_3 + 2H_2$$

In the present studies, the dialkylthioboronates have been prepared by reaction between dialkylboron chloride and the sodium salt of mercaptan. While alcohols react readily with dialkylboron chloride to produce dialkylboronous esters[5], mercaptans do not react at least at room temperature. Dialkylthioboronate reacts readily with ammonia to produce a white solid at about $-60°C$, which appears to be an unstable 1 : 1 addition product. This product easily decomposes to dialkylamino borine, R_2BNH_2, on distillation. The reaction is considered to be as follows:

$$R_2BSR' \xrightarrow{\text{liq. } NH_3} R_2BSR' : NH_3$$
$$\xrightarrow{\text{distill.}} R_2BNH_2 + R'SH$$

The details of this aspect will be reported in the near future.

Experimental and Results. — In a 300 cc. three necked round-bottomed flask, fitted with a mechanical stirrer with a mercury seal, a reflux condenser, and a dropping funnel, were placed about 100 cc. of anhydrous ether and the various amonts of sodium shown in Table I. To the mixture,

TABLE I. YIELDS OF R_2BSR'

R in R_2BCl	Wt., g.	R in $R'SH$[a]	Na, g.	Product, g.	Yield, %[b]
iso-C_3H_7	33	C_2H_5	10	18	30.0
n-C_4H_9	45	C_2H_5	10	30	40.0
n-C_4H_9	30	*iso*-C_3H	7	16	36.6
n-C_4H_9	31	*n*-C_4H_9	6	34	38.0

a) The amount of R'SH is 25 g. in each experiment.
b) The yield was calculated from R'SH employed.

25 g. of mercaptan was dropped slowly, with stirring. After completion of addition, the system was heated for about three hours, and the mixture was cooled to room temerature. The unchanged sodium was removed, and about 100 cc. of ethereal solution containing a certain amount of dialkylboron chloride (shown in Table I) was added slowly from the dropping funnel. The reaction proceeds as follows:

$$R_2BCl + R'SNa = R_2BSR' + NaCl$$

After the dropping had been completed, the mixture was heated for about four hours. The solvent was distilled off, and further distillation was carried out under reduced pressure. The products were redistilled for measurements of physical constants. The results are shown in Table II.

1) G. S. Kolesnikov and L. S. Fedorova, *Izv. AN. USSR*, No. 2, 236 (1957).
2) J. Furukawa et al., *J. Chem. Soc. Japan, Ind. Chem. Sec.* (*Kogyo Kagaku Zasshi*), **61**, 728 (1958).
3) N. Ashikari, *J. Polymer Sci.*, **28**, 641 (1958).
4) A. B. Burg and R. I. Wagner, *J. Am. Chem. Soc.*, **76**, 3307 (1954).

TABLE II. PHYSICAL CONSTANTS OF R_2BSR'

R_2BSR'	b.p.,°C	d_4^{20}	Calcd. B%	Found B%[c]
(*iso*-C_3H_7)$_2$BSC_2H_5	80/20 mm.	0.8490	6.96	7.04
(*n*-C_4H_9)$_2$BSC_2H_5	142/60 mm.	0.8400	5.91	6.11
(*n*-C_4H_9)$_2$BS(*iso*-C_3H_7)	74/4 mm.	0.8525	5.50	5.58
(*n*-C_4H_9)$_2$BS(*n*-C_4H_9)	78/3 mm.	0.8318	5.14	5.42

c) Quantitative analysis of boron was carried out by Synder's method[5].

Dialkylthioboronate is a colorless liquid having an unpleasant odor and is oxidized slowly in air. It seems, however, to be stable in cold water.

The Electrical Communication Laboratory
Nippon Telegraph and Telephone
Public Corporation
Musashino-shi, Tokyo

5) H. R. Synder, J. A. Kuck and J. R. Johnson, ibid., **60**, 110 (1938).

Calculated Thermodynamic Properties of Trimethylchlorosilane

By Kazuhiro Shimizu and Hiromu Murata

(Received September 10, 1959)

The vibrational assignment of trimethylchlorosilane has been revised, based on a normal coordinate treatment as a fourteen body problem[1]. The probable values of the wave numbers of the normal vibrations were used to calculate the values of the heat content, free energy, entropy and heat capacity for the ideal gaseous state at 1 atmospheric pressure (rigid rotator, harmonic oscillator approximation). The bond distances and the interbond angles in the previous Table I[1] and the Hirschfelder formula[2] were used to calculate the product of the principal moments of inertia, $I_aI_bI_b=3.85961\ 10^{-113}$ g^3 cm^6. The molecular weight used was 108.652 and the symmetry number was 3. The three torsional vibrational frequencies of the methyl groups belong to the species a_2 and e. No information about their frequencies has been given. Therefore, the total contributions of the translational, rotational and vibrational frequencies are listed in Table I, except those of the three unknown methyl torsional modes. When the contributions of the three ones are evaluated, they have to be added.

TABLE I. HEAT CAPACITY, FREE ENERGY AND HEAT CONTENT OF TRIMETHYLCHLOROSILANE FOR THE IDEAL CASEOUS STATE AT 1 ATMOSPHERIC PRESSURE (cal. deg^{-1} mol^{-1}), EXCEPT THE CONTRIBUTIONS OF THE THREE METHYL TORSIONAL FREQUENCIES

T°K	$(H^0-E_0^0)/T$	$-(F^0-E_0^0)T$	S^0	C_p^0
100	9.39	49.03	58.43	12.67
200	12.59	56.54	69.13	18.79
273.15	14.87	60.72	75.59	23.47
300	15.72	62.24	77.96	25.23
400	18.89	67.19	86.08	31.43
500	21.95	71.74	93.69	36.75
600	24.80	75.99	100.79	41.20
700	27.41	80.02	107.43	44.96
800	29.82	83.76	113.57	48.21
900	32.02	87.47	119.50	51.04
1000	34.05	91.01	125.05	53.51

The authors wish to thank Professor H. Shingu of Kyoto University for making valuable discussions.

Osaka Municipal Technical Research Institute
Kita-ku, Osaka

1) K. Shimizu and H. Murata, to be published in *J. Mol. Spectroscopy*.

2) J. O. Hirschfelder, *J. Chem. Phys.*, 8, 431 (1940).

Polarographic Studies on the Rare Earths. II. Europium

By Seizo MISUMI and Yasushi IDE

(Received March 22, 1959)

Europium has the stable dipositive oxidation state similar to samarium and ytterbium among the rare earth elements. It is also clearly recognized that this intermediate dipositive oxidation state exists during the reduction process of the tripositive europium ions on dropping mercury electrode and this fact has already been studied by some investigators. Laitinen and Taebel[1], and also Noddack and Brukl[2] obtained only a single wave having the half-wave potential of −0.77 V. vs. S. C. E. in acidic solution and −0.67 V. vs. S. C. E. in neutral solution. On the other hand, Holleck[3] obtained double wave for europium. Namely, the half-wave potential of the first wave was −0.78 V. vs. S. C. E. and that of the second wave, −2.14 V. vs. S. C. E. with lithium chloride as the supporting electrolyte, and −0.82 V. and −2.14 V. vs. S. C. E. respectively when with tetramethylammonium iodide. Many other polarographic studies on the europium complexes with various complex-forming agents were reported by Holleck[4], Onstott[5] and Vlček[6].

In this paper, the authors have reported the behaviors of europium ion in the process of reduction on the dropping mercury electrode. The reduction waves were studied in detail under various conditions, especially in order to know the electrode reactions.

Experimental

All current-voltage curves were recorded by the Yanagimoto photographic polarograph PEL-Model 3 Type. All potentials were corrected and referred to saturated calomel electrode (S. C. E). The capillary used had the flowing weight of mercury, $m=0.789$ mg./sec. at the height of 58.5 cm. (corr.) Hg and the drop time, $t=5.20$ and 3.10 sec./drop at the applied potentials of −0.8 V. and −2.0 V. vs. S. C. E. respectively (the factor $m^{2/3}\,t^{1/6}$ was from 1.021 to 1.135 $mg^{2/3}\,sec^{-1/2}$ in the same potential range). pH value of the solution was measured with the Hitachi glass electrode pH meter EHM-1 Type for micro amount. All experiments were carried out in a thermostat of 25.0±0.1°C.

Europium solution was prepared by dissolving pure europium oxide (Eu_2O_3: more than 99.9%), purified with ion exchange resin. The concentration of the stock solution was 0.01 M/l. Lithium chloride and lithium perchlorate used as supporting electrolytes were guaranteed grade pure Shikajirushi. The concentrations of these stock solutions were 1 mol./l. The gelatin solution used as maximum suppressor, was prepared freshly in every experiment.

To the sample solution of europium, certain quantities of the supporting electrolyte and of gelatin were added to be the final concentrations, 0.1 M/l. and 0.01%, respectively. And then a micro amount of 0.01 N sulfuric acid was added to prevent the hydrolysis of the aquo europium ion and to adjust pH at the same time. The total volume of the solution was made up to 5 ml. with distilled water. The concentration of europium ion was in the range from 0.5 to 1.6 mM/l. and pH of the solution was varied from 2.75 to 3.90. Dissolved oxygen was removed by passing purified nitrogen gas through the solution for at least 20 min. Then polarograms were recorded.

Results and Discussion

1) The Reduction Wave of Aquo Tripositive Europium Ion. — Typical reduction waves of aquo tripositive europium ion are shown in Fig. 1. At pH less than 3.9, three stepped waves were obtained and the first and the third waves are due to the

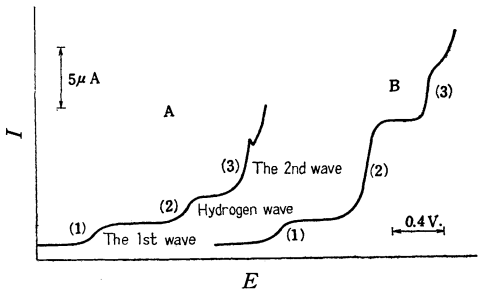


Fig. 1. The reduction waves of europium. Eu^{3+} ion: 1.104 mM in 0.1 M LiCl and 0.01% gelatin medium. pH: A=3.50, B=3.05.

1) H. A. Laitinen and W. A. Taebel, *Ind. Eng. Chem., Anal. Ed.*, **13**, 825 (1941).
2) W. Noddack and A. Brukl, *Angew. Chem.*, **50**, 362 (1937).
3) L. Holleck, *Z. Naturforsch.*, **2b**, 81 (1947).
4) L. Holleck and D. Eckardt, *Z. Elektrochem.*, **59**, 202 (1955).
5) E. I. Onstott, *J. Am. Chem. Soc.*, **74**, 3773 (1952).
6) A. A. Vlček, *Collection Czechoslov. Chem. Communs.*, **20**, 1507 (1955).

TABLE I. DEPENDENCE OF LIMITING CURRENTS OF THE FIRST AND THE SECOND WAVES ON THE HEIGHTS OF THE MERCURY COLUMN

h cm.	h_{corr} cm.		i_l, μA		$i_l/\sqrt{h_{corr}}$	
	$h_{1.corr}$	$h_{2.corr}$	i_{l_1}	i_{l_2}	$i_{l_1}/\sqrt{h_{1.corr}}$	$i_{l_2}/\sqrt{h_{2.corr}}$
40	38.4	38.1	1.60	3.29	0.258	0.535
50	48.4	48.1	1.79	3.62	0.257	0.522
90	58.5	58.1	1.94	3.97	0.254	0.521

(Eu^{3+} ion: 1.023 mM in 0.1 M LiCl and 0.01% gelatin medium, pH: 3.10)

reduction of aquo europium ion and the second wave is the hydrogen wave. In this paper hereafter, the first step is called "the first wave" and the third step "the second wave" of europium.

Owing to the variation in pH and the concentration of europium, the differences between the forms of the reduction waves were indicated. From the polarograms obtained, the following results were derived as the common characteristics, i. e., 1) at pH more than 3.2, independent of concentration, the second wave had a small maximum, but as the pH decreased, this maximum usually disappeared; 2) at pH less than 2.7, a well defined second wave could not be obtained. It is supposed that the large diffusion current of the hydrogen wave probably disturbed the second wave. The effect of various supporting electrolytes on the forms of the reduction waves were rather small and negligible, giving polarograms of similar types.

2) Dependence of Limiting Current of the First and the Second Waves on the Pressure of Dropping Mercury and Influence of Temperature on the Diffusion Current. — The relation between limiting currents and various heights of the mercury column is shown in Table I. The results obviously indicate the fact that the limiting current is proportional to the square root of the height of the mercury column, corrected for the back pressure. Accordingly, the limiting current is diffusion controlled.

The temperature coefficient of the half-wave potential of the first wave at 20~30°C, was 0.4 mV./deg. and that of the limiting current 1.9%/deg., which would be expected in the case of diffusion controlled process for the reduction of tripositive ion.

3) Reversibility. — The reduction waves were analyzed by logarithmic plot. The results are shown in Table II. As the reciprocal slope of the first wave was nearly constant, the average value 0.087 V., in the range of pH 3.50 to 2.75, the first reduction wave was irreversible and due to one electron transfer. The value of $\alpha_1 n_1$, was about 0.68 on the average. The transfer coefficient α was equal to 0.68 if the number of electrons associated with the electrode reaction was assumed to be one (α is a transfer coefficient in the equation of potential on irreversible wave, $E=E_{1/2}-\boldsymbol{RT}/\alpha n\boldsymbol{F}\cdot\ln(i/i_d-i)$. The plots of E against $\log(i/i_d-i)$ indicated an almost straight line. The reciprocal slope of the second wave decreased gradually with decrease of pH and approached a constant value, about 0.030 and the value of $\alpha_2 n_2$ increased reversely up to about 2.0. The plots of E against $\log(i/i_d-i)$ for the second wave indicated the slightly curved line near a pH about 3.50, but with decrease of pH it approached a straight line. Therefore, it is considered that the electrode reaction of the second wave was irreversible or quasi-reversible and according to the decrease of pH, it approached the reversible wave and the reaction was accompanied with two electron transfer. Many investigators have reported the reduction process of aquo tripositive europium ion as reversible except Vlček[6] who suggested that it was irreversible. The results in this experiment were also in good agreement with those of Vlček's report on the confirmation of irreversibility in the reduction process of the aquo europium ion.

TABLE II. THE RECIPROCAL SLOPE OF E VS. $\log(i/i_d-i)$ AND THE VALUE OF αn

pH	Reciprocal slope, V.		$\alpha_1 n_1$	$\alpha_2 n_2$
	1st wave	2nd wave		
3.50	0.087	0.045	0.63	1.3
3.15	0.085	0.045	0.78	1.7
3.05	0.086	0.034	0.69	1.7
2.95	0.087	0.030	0.68	2.0
2.75	0.090	0.030	0.66	2.0
(Eu^{3+} ion: 1.104 mM in 0.1 M LiCl and 0.01% gelatin medium)				
2.90	0.090	0.048	0.65	1.2
2.80	0.082	0.036	0.71	1.6
(Eu^{3+} ion: 1.000 mM in 0.1 M $LiClO_4$ and 0.01% gelatin medium)				

The oxidation wave of aquo dipositive europium ions (Eu^{2+} aq.), which were obtained by the reduction of aquo tripositive europium ions (Eu^{3+} aq.) with John's reductor, was studied. The half-wave potential of the oxidation wave of aquo dipositive europium ions was −0.292 V. vs. S. C. E. at pH 2.55 and this value did not coincide with the half-wave potential of the reduction wave of aquo tripositive europium ions under the same conditions. Thus, from this fact, the electrode reaction of the first wave was shown evidently to be irreversible (the potential difference of anodic and cathodic waves was about 0.440 V.).

4) The Effects of Variation in pH Value on the Reduction Waves.—The results of variation in pH value are shown in Table III, by which the effects on half-wave potentials and diffusion currents were studied. Both the half-wave potential of the first wave $(E_1)_{1/2}$ and the second wave $(E_2)_{1/2}$ shifted all to the more negative side as pH values were decreased. The extent of the shift for the first wave was somewhat greater especially in the range of pH 3.50 to 3.15 than at pH less than 3.15. This fact is probably due to the existence of various hydroxo europium complex ions, produced by hydrolysis of aquo europium complex ions in each step of variation in pH of solution, owing to the basicity of europium. The diffusion currents were independent of pH, almost constant at the same concentration in the range of pH, given in Table III.

5) The Effects of Variation in Concentration on the Reduction Wave. — In the various concentrations of europium ion, i. e., 0.552, 1.104 and 1.656 mM/l. at the constant pH (adjusted to ca. 2.95), the reduction waves were recorded. These effects of variations in concentrations of europium ions on half-wave potentials and diffusion currents were studied. Results are shown in Table IV.

The half-wave potentials of the first and the second wave, $(E_1)_{1/2}$ and $(E_2)_{1/2}$, were constant, independent of concentrations. The diffusion current of the first wave i_d, increased proportionally to concentration and thus the ratio i_{d_1}/c (c : concentration of europium ion) indicated constant value too, i. e., there exists a linear relationship between diffusion current and concentration, which can be used for determination of europium. Especially, since in the potential range where the first wave of tripositive europium ion appears, the reduction waves of all other rare earth ions are absent, it is possible to determine polarographically the contents of europium in a mixture of several kinds of rare earth elements. The diffusion current constant of the first wave, I_{d_1}, was also constant. The diffusion current of the second wave, i_{d_2}, however, increased anomalously with the increase of the concentration and the value of the ratio i_{d_2}/c and the diffusion current constant of the second wave, I_{d_2}, decreased gradually

TABLE III. THE EFFECTS OF VARIATION IN pH ON HALF-WAVE POTENTIAL, DIFFUSION CURRENT AND DIFFUSION CURRENT CONSTANT

pH	Half-wave potential V. vs. S. C. E.		Diffusion current μA		Diffusion current constant	
	$(E_1)_{1/2}$	$(E_2)_{1/2}$	i_{d_1}	i_{d_2}	I_{d_1}	I_{d_2}
3.50	−0.731	−1.948	1.94	3.97	1.55	3.43
3.15	−0.760	−1.958	1.98	3.89	1.58	3.40
3.05	−0.762	−1.967	1.95	3.92	1.56	3.42
2.95	−0.767	−1.971	1.94	3.95	1.55	3.44
2.75	−0.771	−1.975	2.00	3.99	1.60	3.45

(Eu^{3+} ion: 1.104 mM in 0.1 M LiCl and 0.01% gelatin medium)

TABLE IV. THE EFFECTS OF VARIATION IN CONCENTRATION OF EUROPIUM ION ON HALF-WAVE POTENTIALS AND DIFFUSION CURRENTS

Concn. of Eu^{3+} ion mM	Half-wave potential V. vs. S. C. E.		Diffusion current μA		i_d/c		Diffusion current constant	
	$(E_1)_{1/2}$	$(E_2)_{1/2}$	i_{d_1}	i_{d_2}	i_{d_1}/c	i_{d_2}/c	I_{d_1}	I_{d_2}
0.552	−0.761	−1.972	0.99	2.33	1.79	4.22	1.59	4.10
1.104	−0.767	−1.971	1.94	3.99	1.76	3.58	1.55	3.44
1.659	−0.764	−1.976	2.94	5.07	1.78	3.42	1.58	3.55

(pH: 2.95, 0.1 M LiCl, 0.01% gelatin)

with rise of concentration. These anomalies may be attributed to precipitation or adsorption of the basic substances of europium on the electrode surfaces.

6) The Effects by the Kinds of Anions Contained in the Supporting Electrolytes.—The reduction process of aquo europium ion on dropping mercury electrode, often depends on its ionic states. These ionic states show considerably different dependence upon the kinds of electrolytes dissolved in the solution. Therefore, the kinds of supporting electrolytes added, are frequently able to cause remarkably different results to the reduction wave. Particularly, by the anion species of supporting electrolytes and further by the differences of their concentrations, the reversibility of the electrode reaction and the rate-determining step are influenced. From this standpoint, under the same conditions, by varying the anion species of the supporting electrolytes, the effects on the reduction waves were studied. The results are shown in Table V.

At the same concentration, somewhat large effects by the species of anions in the supporting electrolytes on the reduction wave could be seen as shown in Table V. Although pH was not kept strictly the same, the trend of the effects on the reduction wave could be seen. The half-wave potential of the second wave shifted to the more negative side in the order of $I^- < Cl^- < ClO_4^-$. Since the ionic strength was kept always constant, the half-wave potential should have the same value under the same conditions, but owing to the kinds of the anion species the different values were indicated. It is considered that the aquo europium ion forms the halogeno aquo complex ion with halogen ion, which takes part in the electrode reaction. However, as the perchlorate ion is the anion which does not form complex generally with the metal ions, it is also considered that the aquo europium ion exists in the same ionic state (single ion) in the solution with lithium perchlorate as the supporting electrolyte. If the halogeno aquo europium complex ion exists in the solution with the halides as the supporting electrolytes, it is known that this complex ion becomes more reducible than the aquo europium ion (single ion) and as the results of the electrode reaction approaches the reversible one from the irreversible. These facts were recognized from the reciprocal slope and the half-wave potential in this experiment. That is to say, in the presence of the halogen ions, the half-wave potential of the second wave shifted to the positive side and the reversibility increased at the same time. The value of the diffusion current constant of the first wave, I_{d_1}, was nearly constant in the case of the halide ions, but in the case of the perchlorate ions, the diffusion current constant of the second wave, I_{d_2}, was greater, which means the irreversible reaction. Thus, the aquo complex ion (single ion) is more difficult to be reduced than the halogeno aquo complex ion. This fact

TABLE V. EFFECTS OF THE VARIOUS ANION SPECIES OF THE SUPPORTING ELECTROLYTES ON THE REDUCTION WAVES

Supporting electrolytes 0.1 M	Concn. of Eu^{3+} ion mM	pH	Half-wave potential V. vs. S. C. E.		Diffusion current constant		Reciprocal slope, V.	
			$(E_1)_{1/2}$	$(E_2)_{1/2}$	I_{d_1}	I_{d_2}	1st wave	2nd wave
LiI	1.000	3.15	−0.635	−1.965	1.56	3.44	0.089	0.034
LiCl	1.023	3.10	−0.766	−1.967	1.55	3.47	0.082	0.030
$LiClO_4$	1.000	2.90	−0.733	−2.048	1.58	4.18	0.090	0.048

(Concn. of gelatin: 0.01%)

TABLE VI. EFFECTS OF THE CONCENTRATION OF THE SUPPORTING ELECTROLYTES ON THE REDUCTION WAVE

Concn. of LiCl M	Half-wave potential V. vs. S. C. E.		Diffusion current constant, μA		Reciprocal slope, V.	
	$(E_1)_{1/2}$	$(E_2)_{1/2}$	I_{d_1}	I_{d_2}	1st wave	2nd wave
0.1	−0.766	−1.967	1.55	3.47	0.092	0.035
0.2	−0.768	−1.960	1.48	3.42	0.088	0.037
0.5	−0.767	−1.953	1.57	3.51	0.096	0.034
0.7	−0.750	−1.954	1.52	3.30	0.103	0.037

(Concn. of the gelatin: 0.01%, concn. of Eu^{3+} ion: 1.000 mM, pH: 3.10)

was in good agreement with the values of the reciprocal slopes for the second waves.

The results concerning the variation in the concentration of lithium chloride as supporting electrolyte are given in Table VI, in which effects of the chloride ion on the reduction wave are shown.

The half-wave potential of polarography is generally represented by the term containing activity coefficients and diffusion coefficients. If either the activity coefficient or the diffusion coefficient is varied, the half-wave potential will probably indicate a different value. With increasing ocncentratoins of total electrolytes the activity coefficient tends to decrease and as the result, the half-wave potential is likely to shift to the more negative potential. Moreover the stability of halogeno aquo europium complex ion is thermodynamically greater than the aquo europium ion and the negative shift will probably take place.

But, on the contrary, as shown in the results of Table VI, there can be seen a tendency for the half-wave potential to shift apparently to the more positive side according to the increase of the concentration of lithium chloride as the supporting electrolyte. At the concentration of 0.5 to 0.7 mmol., the extent of the shift was considerably great. With the increase of chloride ions, the increased chloro aquo complex ions caused the overpotentials to decrease and this large decrease in this overpotential, i. e., the easiness of reduction, outweighed the shift in the equilibrium relation. Thus the half-wave potential seems to shift apparently to the more positive side. In spite of these facts, the value of the reciprocal slope increased with the increase of the concentration of lithium chloride, that is, the irreversibility in the electrode reaction increased too.

7) The Effects of Concentration of Gelatin as Maximum Suppressor, on the Reduction Wave. — By the variation in concentration of gelatin from 0 to 0.05%, the effects on the reduction waves were studied. With the increase of the concentration of gelatin, the half-wave potentials of both the first and the second waves shifted to the more negative side respectively and the values of the reciprocal slopes increased. At pH less than 3.2, without gelatin, a large maximum appeared in the second wave, but with the increase of concentration of gelatin added as maximum suppressor, the maximum decreased gradually and, when 0.01% concentration of gelatin was added, it disappeared completely. At pH more than 3.2, even at concentration of gelatin 0.01%, the maximum could be seen slightly.

8) The Electrode Reduction and the Relation between Reduction Process and Electronic Structure of Aquo Europium Ion.—The reduction of aquo europium ion on dropping mercury electrode, proceeds irreversibly or quasi reversible as described in section 3. In the equation of the current-voltage curve for the irreversible reaction, $E=E_{1/2}-0.0591/\alpha n\cdot\log(i/i_d-i)$ $(0<\alpha<1)$, it was derived that n_1 was equal to 1 and n_2 to 2, by using the results given in Table II. Consequently, the electrode reaction for the first wave was one electron change and that for the second wave two electrons. As the limiting current was diffusion controlled, with Ilkovic's equation, the following relation could be held theoretically between diffusion currents of the first wave and of the second wave, i. e., $i_{d_1} : i_{d_2}=1 : 2$. Therefore, the ratio of the diffusion current constants for the first and the second wave, $I_{d_1} : I_{d_2}=1 : 2$ is obtained.

The experimental average values of diffusion current constants were as follows, namely, $(I_{d_1})_{av}=1.57$ and $(I_{d_2})_{av}=3.46$. Hence, the ratio $(I_{d_1})_{av} : (I_{d_2})_{av}=1 : 2.2$ was obtained, which was in fairly good agreement with the value of the theoretical ratio. Thus, it is considered that the electrode reaction in the reduction of aquo tripositive europium ion proceeds as follows:

The first wave,

$$Eu^{3+}\,aq.+\,e^-\rightarrow Eu^{2+}aq.$$

The second wave,

$$Eu^{2+}\,aq.+\,2e^-\rightarrow Eu^0$$

For the rate determining steps of the irreversible electrode reaction, the following main factors are supposedly considered.

a) The overpotential required for dehydration of the coordinated water molecules.

b) The stepwise dissociation of the aquo complex ion.

c) The overpotential required for the changes of the inner electronic configuration (in some $(n-2)f$ orbitals).

d) The stability in the oxidation state of the aquo complex ion.

e) The others.

The results of the irreversible reduction process of the aquo europium complex ion at the dropping mercury electrode, was

TABLE VII. POLAROGRAPHIC REDUCTION (ELECTRON TRANSFER AND ELECTRONIC CONFIGURATION)

Electrode reaction	Electronic configuration (Oxidized form) 1st wave	(Reduced form) 2nd wave	
Eu^{3+} aq. → Eu^{2+} aq. Irreversible	$f^6s^2p^6d^0d^0d^0[d^2sp^3]+e^-$		
		→ $f^6s^2p^6d^1d^0d^0[d^2sp^3]$	(2 step electron transfer)
		→ $f^7s^2p^6d^0d^0d^0[d^2sp^3]+2e^-$	
Eu^{2+} aq. → Eu^0 Irreversible			→ $f^7s^2p^6d^1d^1d^0[d^2sp^3]$
			→ $f^7s^2p^6s^2$—ligand

(Eu: $4f^75s^25p^66s^2$)

in good agreement with the conclusions of Vlček's rule[7], concerning the mechanism of the electron transfer by polarographic reduction. The dipositive stable oxidation state of europium is already known in solution. As Vlček pointed out, the true two step reduction wave as *f*-transition element was seen for the aquo europium complex ion. Generally, the rate of the electrode reaction is determined always by the slowest of the processes and the change by the electron transfer in reduction processes may always have a tendency to produce the most stable electronic configuration. The aquo europium complex ion is assumed to have simply the coordination number 6 and to be $Eu(H_2O)_6^{3+}$ complex ions. The probable relation between electron transfer and electronic configuration is shown in Table VII.

Summary

The double reduction waves of pure aquo tripositive europium ion, under various conditions, at dropping mercury electrode were studied. The effects of the variations in pH, the concentration of europium ion, the anion species of supporting electrolytes, and the concentration of gelatin as maximum suppressor, etc. were examined. The electrode reaction of the first wave was irreversible and one electron reduction, and that of the second wave was the irreversible or quasi reversible two electrons reduction. The half-wave potentials of the first wave and the second wave at pH 2.95 were as follows.

$(E_1)_{1/2}$: −0.767 V. vs. S. C. E.

$(E_2)_{1/2}$: −1.971 V. vs. S. C. E.

where concentration of Eu^{3+} ion: 1.104 mM in 0.1 M LiCl and 0.01% gelatin medium.

The authors wish to thank the Ministry of Education for the financial support given to this research.

Department of Chemistry
Faculty of Science
Kyushu University
Hakozaki, Fukuoka

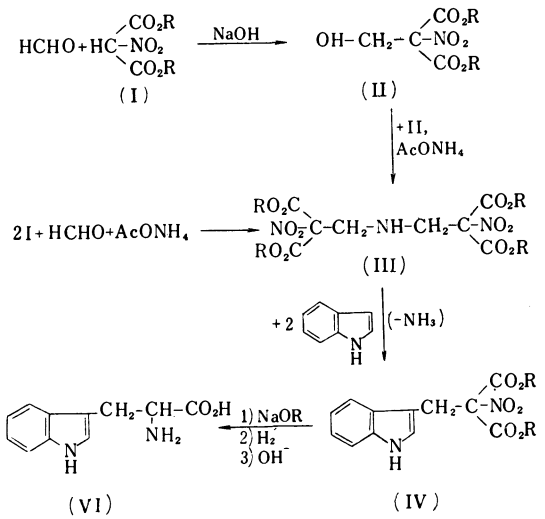
7) A. A. Vlček, *Collection Czechoslov. Chem. Communs.*, **20**, 894 (1955).

Aminosäure-Synthese aus Nitromalonester. IV[1]. *Eine neue Synthese von Tryptophan mit Hilfe der Alkylierung des Indols mit 1, 1, 5, 5-Tetracarbalkoxy-1, 5-dinitro-3-azapentan**

Von Tôru OKUDA

(Eingegangen am 25. März 1959)

Seitdem Hopkins und Cole[2] zum erstenmal im Jahre 1901 Tryptophan aus dem Caseinhydrolysat isolierten, sind bisher zahlreiche Untersuchungen über die synthetische Darstellung dieser Aminosäure gemacht worden, von denen nur die praktischen im folgenden angeführt seien: (1) Umsetzung von Gramin mit Acylaminomalonestern[3-5], Nitroessigester[6] bzw. Nitromalonester[7]; (2) Umsetzung von Indol mit Dialkylaminomethyl-acylaminomalonestern[8]; (3) Fischer-Indol-Ringschluß des aus Acetamino-malonester, Acrolein und Phenylhydrazin dargestellten Phenylhydrazons[9]; (4) reduzierende Aminierung von α-Keto-β-(3-indolyl)propionsäure[10]; (5) Decarboxylierung von 2-Carboxytryptophan, welches von γ-Butyrolacton[11], Acetessigester[12] bzw. α-Ketoglutarsäure[13] abgeleitet wird; (6) Addition von Indol zu α-Acetaminoacrylsäure[14]. Es bleibt trotzdem noch die einfachere Synthese dieser Aminosäure in besserer Ausbeute wünschenswert.



* Auszugsweise vorgetragen an der XI. Versammlung der Japanischen Chemischen Gesellschaft, Tokio, 4. April 1958.

1) III. Mitteil.: T. Okuda, Dieses Bulletin, **32**, 931 (1959).

2) F. G. Hopkins und S. W. Cole, *Proc. Roy. Soc. (London)*, **68**, 21 (1901); *J. Physiol.*, **27**, 418 (1902).

Wie das oben angegebene Reaktionsschema zeigt, stellt die vorliegende Arbeit eine neue Synthese des Tryptophans dar, in der, Nitromalonester als Ausgangsstoff dient. In früheren Mitteilungen haben wir über Synthesen von Ornithin[15], Prolin[16], Glutaminsäure-γ-semialdehydacetal[16] und Glutaminsäure[1] aus dem gleichen Ester (I) berichtet.

Wie schon zitiert, haben Weisblat und Lyttle ein Verfahren zur Darstellung des Tryptophans mittels Nitromalonesters entdeckt[7], indem sie zunächst I in siedendem Toluol mit Gramin zur Reaktion brachten und anschließend das Kondensationsprodukt reduzierten und verseiften.

Unsere Synthese geht auch von dem gleichen Nitromalonester (I) aus, aber, wie aus dem Reaktionsschema ersichtlich ist, unterscheidet sich dieser von dem von ihnen entdeckten Verfahren darin, daß bei uns eine bisher unbekannte, neuartige Alkylierungsreaktion mittels 1,1,5,5-Tetracarbalkoxy-1, 5-dinitro-3-azapentans (III), einer Art bis-substituierten Amins, welches durch eine Mannich-Reaktion von Nitromalonester (I), Formaldehyd und Ammoniak gewonnen wird, angewandt ist.

Mannich-Reaktion von Nitromalonester mit Formaldehyd und Ammoniak. — Durch Einwirkung von wässriger Formaldehyd-

3) E. E. Howe, A. T. Zambito, H. R. Snyder und M. Tishler, *J. Am. Chem. Soc.*, **67**, 38 (1945).

4) H. Hellmann, *Z. physiol. Chem.*, **284**, 163 (1949).

5) N. F. Albertson, S. Archer und C. M. Suter, *J. Am. Chem. Soc.*, **67**, 36 (1945).

6) D. A. Lyttle und D. I. Weisblat, ebenda, **69**, 2118 (1947).

7) D. I. Weisblat und D. A. Lyttle, ebenda, **71**, 3079 (1948).

8) A. Butenandt und H. Hellmann, *Z. physiol. Chem.*, **284**, 168 (1949).

9) O. A. Moe und D. T. Warner, *J. Am. Chem. Soc.*, **70**, 2763 (1948).

10) S. Sakurai, *J. Biochem. (Tokio)*, **44**, 47 (1957).

11) H. Plieninger, *Chem. Ber.*, **83**, 268 (1950).

12) B. Hegedüs, *Helv. Chim. Acta*, **29**, 1499 (1946).

13) S. Sakurai und Y. Komachiya, nicht veröffentlicht.

14) H. R. Snyder und J. A. MacDonald, *J. Am. Chem. Soc.*, **77**, 1257 (1955).

15) S. Akabori, Y. Izumi und T. Okuda, *J. Chem. Soc. Japan, Pure Chem. Sec. (Nippon Kagaku Zasshi)*, **77**, 490 (1955).

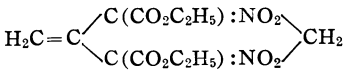
16) T. Okuda, Dieses Bulletin, **30**, 358 (1957).

Lösung auf Nitromalonester (I) in Gegenwart einer katalytischen Menge Natronlauge als Kondensationsmittel konnten wir Hydroxymethyl-nitromalonsäure-dimethylester (IIa) als weiße Kristalle vom Schmp. 90~91°C und den Äthylester (IIb) als farblose Flüssigkeit vom Sdp 1 mm. 120~125°C in guten Ausbeuten erhalten. Versuche, α-Carbalkoxy-α-nitro-β-(3-indolyl)-propionsäureester (III) direkt durch Umsetzung von Indol mit Hydroxymethyl-nitromalonester (II) oder mit dessen acetyliertem Derivate darzustellen, waren alle ohne Erfolg, was uns einen andern Weg einschlagen ließ.

Kürzlich haben Feuer und Mitarb.[17] sowie Fränkel und Mitarb.[18] gefunden, daß 2, 2-Dinitroalkanole, die aus *gem*-Dinitroparaffinen und Formaldehyd gewonnen wurden, unter Bildung von Bis-(2, 2-dinitroalkyl)-aminen mit Ammoniak in wässriger Essigsäure-Lösung kondensieren.

Auch für die Mannich-Reaktion von Hydroxymethyl-nitromalonester (II) mit Ammoniak galten die Bedingungen, unter denen Bis-(2, 2-dinitroalkyl)-amine dargestellt wurden. Wenn man also II mit 2 Mol. Ammoniumacetat in Wasser auf etwa 60°C behandelte, so erhielt man leicht das Kondensationsprodukt. Anderseits gelang es uns, auch durch Versetzung von Nitromalonester (I) mit Ammoniumacetat und Formaldehyd das gleiche Mannich-Kondensationsprodukt direkt zu gewinnen.

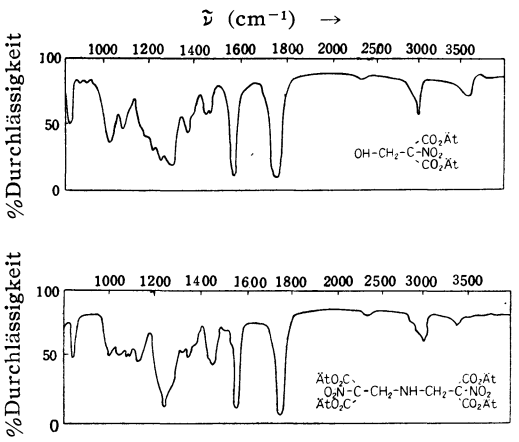
Im Jahre 1903 erhielten Ulpiani und Mitarb.[19] durch Umsetzung von Ammoniumsalz des *aci*-Nitromalonsäure-diäthylesters mit einem großen Überschuß von Formaldehyd ein kristallinisches Produkt vom Schmp. 46°C, das vermutlich mit dem von uns dargestellten als identisch anzusehen ist. Sie gaben aber aus falschen experimentellen Daten die Formel VII an. Bald darauf wurde diese



VII

auf Grund der ebullioskopischen und kryoskopischen Molekulargewichtsbestimmung derart korrigiert, daß dieser Verbindung statt der Formel VII wohl eher die Formel IIIb zukommen sollte[20].

Zur endgültigen Entscheidung der



Abbild 1. IR-Spektren von Hydroxymethyl-nitromalonsäure-diäthylester (IIb) und 1,1, 5,5-Tetracarbäthoxy-1,5-dinitro-3-azapentan (IIIb). (in Flüssigkeit)

Konstitution des Kondensationsprodukts, dessen Formel trotz der Battagliaschen Berichtigung im Beilsteins Handbuch mit dem Wort "vielleicht" aufgeschrieben ist[21], wiederholten wir die Elementaranalyse und die Molekulargewichtsbestimmung nach der Rast-Methode und konnten dabei bestätigen, daß die von Battaglia angegebene Formel III als ein bis-substituierten Amin richtig ist. Die Struktur von III ergibt sich auch aus folgenden Befunden: das Infrarot-Spektrum (Abbild. 1) zeigt lediglich eine NH-Bande (3300 cm^{-1}), aber keine NH_2-Doppelbande (3300~3500 cm^{-1}).

Alkylierung des Kohlenstoffatoms in β-Stellung von Indol mit 1, 1, 5, 5-Tetracarbalkoxy-1, 5-dinitro-3-azapentan. — An der Molekularstruktur von 1, 1, 5, 5-Tetracarbalkoxy-1, 5-dinitro-3-azapentan (III) ist anzunehmen, daß durch die Einflüsse der Carbalkoxyl- und Nitro-Gruppen, welche elektronenanziehend wirken können, an beiden Enden des Moleküls die Bindungen zwischen dem mittelständigen Stickstoffatom und den benachbarten Kohlenstoffatomen aufgelockert genug seien, um sich unter gewissen Bedingungen abzuspalten. Es wäre daher denkbar, das Ziel der Substitution eines Wasserstoffatoms von nucleophilen oder potentiell nucleophilen Verbindungen durch Dicarbalkoxy-nitroäthyl-Gruppe $\left(\begin{matrix}RO_2C\\O_2N\end{matrix}\!\!>\!C\!-\!CH_2\!-\right)$ mittels dieses bis-substituierten Amins anzustreben.

Es ist wohl bekannt, daß im allgemeinen

17) H. Feuer, G. B. Bachman und W. May, *J. Am. Chem. Soc.*, **76**, 5124 (1954).
18) M. B. Fränkel und K. Klager, ebenda, **79**, 2953 (1957).
19) C. Ulpiani und E. Pannain, *Gazz. chim. ital.*, **33I**, 379 (1903).
20) A. Battaglia, ebenda, **38I**, 356 (1908).
21) "Beilsteins Handbuch der Organischen Chemie", 2. Band, Julius Springer, Berlin (1920), S. 597.

die *C*-Alkylierungsreaktion von *H*-aciden Verbindungen mittels tertiärer Mannich-Basen oder quartärer Ammoniumsalze in Anwesenheit von Natriumhydroxyd als Kondensationsmittel mit Erfolg durchgeführt werden kann[22].

Aber bisher ist unseres Wissens keine Literaturangabe über die *C*-Alkylierungsreaktion mittels sekundärer Aminen bekanntgeworden.

Bei den Vorversuchen beobachteten wir, daß beim Erhitzen von Indol und 1, 1, 5, 5-Tatracarbalkoxy-1, 5-dinitro-3-azapentan (III) in Xylol unter Stickstoff-Strom auf 130~140°C die Entwicklung des Ammoniaks eintrat. Diese und andere Versuche, die hintenan beschrieben sind, deuten auf die Umsetzung von 2 Mol. Indol mit 1 Mol. Azapentan (III) unter Abspaltung von 1 Mol. Ammoniak hin (s. das Reaktionsschema).

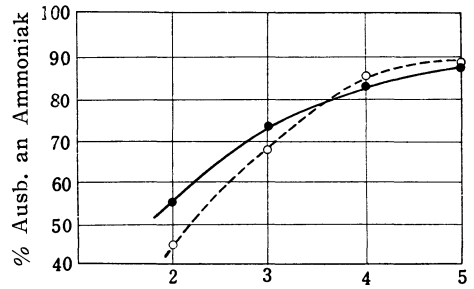
Beim Arbeiten mit äquivalenten Mengen von beiden Reagenzien war jedoch die Entwicklungsmenge des Ammoniaks ziemlich gering (etwa 50% d. Theorie), was uns zur Bestimmung optimaler Bedingungen auf dieser Reaktionsetappe veranließ. In Tabelle I sind einige typische Versuchsergebnisse mit verschiedenen Molenverhältnissen von Indol zu Azapentan (III) in An- oder Abwensenheit von Kondensationsmitteln zusammengestellt.

TABELLE I. VERGLEICH DER AMMONIAKENTWICKLUNGSMENGE BEI DER ALKYLIERUNG VON INDOL MIT AZAPENTAN UNTER VERSCHIEDENEN BEDINGUNGEN

Mol.-Verhältnis von Indol zu III	Lösungsmittel	Katalysator	Reaktionsdauer Std	Ausb. %
2	Xylol	kein	4	45
2	Xylol	K_2CO_3	2	6
2	kein	kein	5	52
5	Xylol	kein	8	89
4	Xylol	kein	6	84

Die Kurven auf Abbild. 2 zeigen Einflüsse von Molenverhältnissen auf die Ammoniakentwicklung ohne Zusatz von einem Katalysator.

Wie aus Tabelle I und Abbild. 2 ersichtlich ist, sind die befriedigenden Ausbeuten (über 80% d. Theorie) durch Verwendung von über 4 Mol. Indol zu 1 Mol. Azapentan (III) erreicht worden**. Hierbei ist auch berichtenswert, daß die Anwesenheit einer



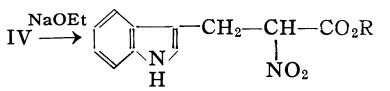
Abbild. 2. Einfluß des Molenverhältnisses von Indol zu Azapentan auf die Ammoniakentwicklung.
—●— IIIa, ---○--- IIIb

katalytischen Menge Alkali die Entwicklung von Ammoniakgas erheblich verhinderte, während die Abwesenheit des Lösungsmittels wenigstens auf die Gasentwicklung keinen wesentlichen Einfluß ausübte.

Das Kondensationsprodukt (IV) war zwar nicht zur Kristallisation zu bringen, sondern immer als zähflüssiges Öl zu erhalten, dessen Konstitution jedoch durch die weiteren Umsetzungen gesichert wurde.

Eine von den günstigen Voraussetzungen für Gelingen dieser Alkylierungsreaktion scheint die bereits erwähnte Auflockerung der *N-C*-Bindungen im alkylierenden Amin (III) zu sein. Zugleich dürfte dabei eine sterische Assistenz[23] eine Rolle spielen, die dem großen Umfang der Amino-Gruppe zuzuschreiben ist. Auch die Flüchtigkeit des dabei abgespalteten Ammoniaks begünstigt vermutlich den Verlauf der Reaktion; denn das Kondensationsprodukt (IV) ist gegen Alkali sehr empfindlich.

Auch in Gegenwart von Indol wurde die Eliminierung einer Carbalkoxy-Gruppe von IV mit Natriumalkoholat ebenso[7] bequem



V

durchgeführt. Bei Zugabe von Eiswasser in das Reaktionsgemisch ging das entstandene Natriumsalz des *α-aci*-Nitro-*β*-(3-indolyl)propionsäureester (V) in wässrige

22) Vgl. J. H. Brewster und E. L. Eliel, "Organic Reactions", Vol. VII, John Wiley & Sons, Inc., New York (1953), S. 99.

** Unter ähnlichen Bedingungen wurden Phenol und Azapentan zur Reaktion gebracht, wobei heftige Ammoiakgasentwicklung beobachtet wurde. Die Chromatographie einer Probe des Hydrolysats ergab, daß es Tyrosin und wahrscheinlich 2-Oxyphenylalanin enthält. Die Reaktion wurde präparativ nicht weiter untersucht, zeigt aber an, daß sich auch Phenol in *o*- und *p*-Stellung alkylieren läßt.

23) G. L. Shoemaker und R. W. Keown, *J. Am. Chem. Soc.*, **76**, 6374 (1954).

Schicht über, während das an der Alkylierungsreaktion nicht beteiligte Indol in ätherischer Schicht zurückblieb, womit das Ziel der Trennung von V aus Indol einfach erreicht werden konnte. Der beim Ansäuern der Natriumsalz-Lösung gewonnene, freie Nitroester (V) wurde unter Druck hydriert. Die Gesamtausbeute an Tryptophan, bezogen auf Nitromalonester (I), war 50～60%.

Beschreibung der Versuche

Hydroxymethyl-nitromalonsäure-dimethylester (IIa).—Ein Gemisch von 8.5 g (0.105 Mol, 3.15 g Formaldehyd) 37 proz. Formalin und 17.7 g (0.1 Mol) Nitromalonsäure-dimethylester in 20 ccm Methanol wurde in Gegenwart von 0.5 ccm 1 N NaOH unter gelindem Rühren 2 Stdn auf 40°C erwärmt. Dabei entstand anfangs eine klare gelbliche Lösung, aus der sich im Verlauf der Reaktion weiße Kristalle des Kondensationsproduktes abschied. Nach Erkalten wurde die Reaktionsmischung mit 200 ccm eisgekühltem Wasser verdünnt und über Nacht im Eisschrank stehengelassen. Man saugte die Kristalle ab, wusch mit wenig kaltem Wasser und trocknete. Die Ausbeute an Hydroxymethyl-nitromalonsäure-dimethylester (IIa) vom Schmp. 83～84°C betrug 20.5 g (nahezu quantitativ). Der durch Umkristallisation aus Methanol-Wasser analysenrein erhaltene Ester schmolz bei 92～93°C.

$C_6H_9O_7N_2$(207.1) Ber. C 34.37 H 4.38 N 6.76
Gef. C 34.59 H 4.21 N 6.37

Hydroxymethyl-nitromalonsäure-diäthylester (IIb).—Ein Gemisch von 82.0 g (0.4 Mol) Nitromalonsäure-diäthylester, 34 g (12.6 g Formaldehyd, 0.42 Mol) 37% Formalin in 60 ccm Methanol wurde in Gegenwart von 3 ccm 1 N Natronlauge unter Schüttelung 3 Stdn auf 35～45°C erwärmt. Nach Erkalten und Neutralisierung des als Kondensationsmittel verwendeten Natriumhydroxyds mit Salzsäure wurde die gelblich klare Lösung in 500 ccm Eiswasser gegossen, wobei sich ein Öl ausschied. Die obere wässrige Schicht wurde dreimal mit je 200 ccm Benzol extrahiert. Die Auszüge und das ausgeschiedene Öl wurden vereinigt, die benzolische Lösung wurde mit Wasser gewaschen und auf Natriumsulfat getrocknet. Nach dem Abdampfen des Benzols destillierte man *i. Vak.* den Rückstand. 83 g Hydroxymethyl-nitromalonsäure-diäthylester(IIb) wurden als farblose Flüssigkeit vom Sdp $_{1\,mm}$. 120～125°C erhalten. Ausbeute 94%.

$C_8H_{13}O_7N$(235.2) Ber. C 40.85 H 5.57 N 5.96
Gef. C 40.77 H 5.57 N 5.93

Banden im IR-Spektrum bei: 3554 cm^{-1} (—OH); 1755 cm^{-1} (>C=O); 1572 cm^{-1} ($—NO^2$) (s. Abbild. 1).

Acetoxymethyl-nitromalonsäure-diäthylester.—11 g (0.047 Mol) Hydroxymethyl-nitromalonsäure-diäthylester (IIb) wurden in Gegenwart einer katalytischen Menge *p*-Toluolsulfonsäure mit 20 ccm Acetanhydrid 30 Min zum Sieden erhitzt. Nach dem Einengen des Reaktionsgemisches erhielt man durch Vakuumdestillation die acetylierte Verbindung als farblose Flüssigkeit. Sdp $_{1\,mm}$. 123～127°C. Ausbeute 12 g.

$C_{10}H_{15}O_8N$(277.2) Ber. C 43.32 H 5.45 N 5.05
Gef. C 43.32 H 5.74 N 4.84

1, 1, 5, 5-Tetracarbomethoxy-1, 5-dinitro-3-azapentan (IIIa).—25.4 g (0.2 Mol) Nitromalonsäure-dimethylester (Ia) wurden in einer Lösung von 23.1 g (0.3 Mol) Ammoniumacetat in 120 ccm Wasser auf 40°C gelöst, dann zu dieser Lösung wurden 17 g (6.2 g Formaldehyd, 0.21 Mol) 37% Formalin schnell hinzugefügt. Bald darauf begann sie sich unter Wärmeentwicklung zu trüben. Nach 20 minutigem Erwärmen bei 40°C ließ man das Gemisch im Eisschrank 2–3 Tage stehen, wobei die anfangs ölige Substanz kristallinisch erstarrte. Man saugte die Kristalle ab, wusch mit eiskaltem Wasser und trocknete. Für die Weiterverarbeitung wurde das so erhaltene Präparat ohne besondere Reinigung verwendet. Ausbeute 35～38 g (88～96% d. Theorie) Das aus Äther-Petroläther umkristallisierte 1, 1, 5, 5-Tetracarbomethoxy-1, 5-dinitro-3-azapentan (IIIa) zeigte den Schmp. 69～71°C.

$C_{12}H_{17}O_{12}N_3$ (395.3)
Ber. C 36.46 H 4.34 N 10.63
Gef. C 36.29 H 4.29 N 10.39

Molekulargewicht (nach Rast): 416.

1, 1, 5, 5-Tetracarbäthoxy-1, 5-dinitro-3-azapentan (IIIb). — *a) Aus Hydroxymethyl-nitromalonsäure-diäthylester (IIb).* — Aus 23.5 g (0.1 Mol) Hydroxymethyl-nitromalonsäure-diäthylester (IIb) und 15.2 g (0.2 Mol) Ammoniumacetat in 30 ccm Wasser. Ausbeute 21 g (93% d. Theorie). Schmp. 40～42°C.

$C_{16}H_{25}O_{12}N_3$ (451.4)
Ber. C 42.57 H 5.58 N 9.31
Gef. C 42.57 H 5.50 N 9.30

Molekulargewicht (nach Rast): 427; 470.

b) Aus Nitromalonsäure-diäthylester (Ib). —20.5 g (0.1 Mol) Nitromalonsäure-diäthylester(Ib) wurden in eine Lösung von 13.8 g (0.2 Mol) Ammoniumacetat in 130 ccm warmen Wasser unter Schüttelung gelöst

und mit 10 g (3.7 g Formaldehyd, 0.12 Mol) 37% Formalin versetzt. Dabei schied sich ein schweres Öl unter Wärmeentwicklung ab. Man schüttelte die Reaktionsmischung 30 Min auf 60°C und ließ sie über Nacht im Eisschrank stehen. Gelegentliche Schüttelung oder Reibung mit dem Glasstab förderte die Kristallisation. Die cremefarbigen Kristalle wurden kalt abgesaugt, mit eiskaltem 50 proz. Alkohol nachgewaschen und getrocknet. 21.0~22.5 g (94~100% d. Theorie). Schmp. 30~35°C. Nach Umkristallisierung aus Alkohol- oder Essigsäure-Wasser erhielt man weiße, grobe Kristalle vom Schmp. 42~43°C.

$C_{16}H_{25}O_{12}N_3$(451.4)

Ber. C 42.57 H 5.58 N 9.31
Gef. C 42.76 H 5.63 N 9.32

Banden im IR-Spektrum bei: 3384 cm^{-1} (>NH); 1755 cm^{-1} (>C=O) 1570 cm^{-1} ($-NO_2$).

Beim Mischschmelzen von den aus Ib und den aus IIb dargestellten Kristallen wurde keine Schmelzpunkterniedrigung beobachtet.

Bestimmung optimaler Bedingung für Alkylierung des Indols mit Azapentan (III).—Da sich bei dieser Alkylierungsreaktion Ammoniakgas entwickelte, wurde seine Menge durch Rücktitrierung mit Natronlauge bestimmt, nachdem es sich in Schwefelsäure absorbieren ließ. Der unten geschilderte Versuch stellt ein typisches Beispiel für solche Bedingungsbestimmung dar.

Zu 4 ccm trocknem Xylol, welches sich im langen 20 ccm-Kolben mit einem Stickstoff-Einleitungsröhrchen und einem Kühler befindet, wurden 395 mg (0.001 Mol) 1, 1, 5, 5-Tetracarbomethoxy-1, 5-dinitro-3-azapentans (IIIa) und 468 mg (0.004 Mol) Indol gegeben. Der Kolben wurde im Ölbade von 140°C gehalten; während des Erhitzens wurde durch das in die Lösung eintauchendes Glasröhrchen ein lebhafter Strom des mit Calciumchlorid getrockneten Stockstoffs geleitet, welcher zusammen mit dem abgespalteten Ammoniakgas zu verd. Schwefelsäure mit bekannter Normalität geführt wurde. Nach 6 stdg. Kochen wurde die Reaktion abgebrochen. Aliquote der Schwefelsäure-Lösung wurden aufgenommen und mit N/50 NaOH rücktitriert. Molzahl des abgespalteten Ammoniaks während der Reaktion war 0.000840. Also 84% der Theorie. Über andere Versuchsergebnisse siehe Tabelle I und Abbild. 2.

α-Nitro-α-carbomethoxy-β-(3-indolyl)propionsäure-methylester (IVa). — 3.95 g (0.01 Mol) 1, 1, 5, 5-Tetracarbomethoxy-1, 5-dinitro-3-azapentan (IIIa) und 5.85 g (0.015 Mol) Indol wurden in 20 ccm trocknem Xylol gelöst und unter kräftigem Rühren 8 Stdn lang auf 130°C erhitzt. Während des Erhitzens wurde ein lebhafter Strom des Stickstoffs geleitet. Schon bei einer Temperatur von 110°C begann eine Entwicklung des Ammoniaks und war auf dem Siedepunkt von Xylol sehr lebhaft. Nach beendeter Reaktion verdampfte man Xylol unter vermindertem Druck und unterwarf dann den Rückstand einer kontinuierlichen Extraktion mit Petroläther. Nach 36 stdg. Extraktion wurde das hinterbliebene rote Öl in 80 ccm Äther aufgenommen und die ätherische Lösung wurde zweimal mit je 10 ccm 10 proz. Salzsäure, zweimal mit 15 ccm Wasser, dann zweimal mit je 10 ccm 5 proz. Na_2CO_3 und schließlich dreimal mit je 15 ccm Wasser ausgeschüttelt und über Natriumsulfat getrocknet. Das nach dem Abdampfen des Äthers erhaltene Öl wurde auf 100°C unter 1 mmHg gehalten. α-Nitro-α-carbomethoxy-β-(3-indolyl)propionsäure-methylester (IVa) war ein viskoses rotes Öl, das weder kristallisierbar noch unzersetzt destillierbar war. Ausb. 4.2 g.

$C_{14}H_{14}O_6N_2$(306.3) Ber. N 9.15 Gef. N 9.64.

α-Nitro-α-carbäthoxy-β-(3-indolyl)propionsäure-äthylester (IVb).—Nach der oben bei der Darstellung von IVa beschriebenen Methode. Zähflüssiges, rotes Öl.

α-Nitro-β-(3-indolyl)propionsäure-methylester (Va). — Der Ester (Va) kann nach dem bekannten Verfahren[7] aus IVa gewonnen werden. Wir konnten auch aus IIIa den Ester(Va) direkt darstellen, ohne daß man IVa isolierte. Denn bei unsrer Synthese wurde ein Überschuß Indol verwendet und dessen Entfernung nahm zur Gewinnung von IVa, wie bereits erwähnt, viel Zeit in Anspruch.

Eine Lösung von 11 g (0.0279 Mol) rohem 1, 1, 5, 5-Tetracarbomethoxy-1, 5-dinitro-3-azapentan (IIIa) und 13 g (0.111 Mol) Indol in 50 ccm trocknem Xylol wurden in einen 200 ccm-Vierhalskolben gesetzt, welcher mit Rührer, Einleitungsrohr und Rückflußkühler versehen war. Die Lösung wurde unter kräftigem Rühren und lebhaftem Strom des Stickstoffs 5 Stdn lang auf 130~140°C erhitzt. Nach Erkalten fügte man zum Reaktionsgemisch 50 ccm Äther hinzu, schüttelte die Lösung mit 5 proz. HCl, H_2O, 5 proz. Na_2CO_3 und H_2O aus und trocknete diese über Natriumsulfat. Die getrocknete Lösung wurde unter Feuchtigkeitsausschluß und Rühren mit einer Lösung von 1.3 g Natrium in 40 ccm absol. Alkohol im Verlauf von 40

min. tropfenweise versetzt. Nach 5 stdg. Weiterrühren ließ man die Reaktionsmischung im Eisschrank stehen, sodann ließ man 100 ccm eiskaltes Wasser unter kräftigem Rühren hinzufließen, wodurch das Natriumsalz von *α-aci*-Nitro-*β*-(3-indolyl)propionsäure-methylester in die wässrige Phase überging, während das an der Reaktion nicht beteiligte Indol im organischen Lösungsmittel blieb. Man trennte die beiden Schichten voneinander, extrahierte die organische Schicht dreimal mit je 30 ccm eiskaltem Wasser, und vereinigte die Auszüge mit der wässrigen Schicht. Die wässrige Lösung wurde dann mit wenig Chloroform ausgezogen, mit 100 ccm Äther überschichtet und mit 10 ccm 10 proz. HCl unter kräftiger Schüttelung angesäuert, wobei der freie Ester (Va) in Äther überging. Nach dreimaliger Extraktion der wässrigen Lösung mit 30 ccm Äther wurde die vereinigte ätherische Lösung zweimal mit je 30 ccm Wasser gewaschen und auf Natriumsulfat getrocknet. Nach der Abdestillation des Äthers erhielt man 11.2 g *α*-Nitro-*β*-(3-indolyl)-propionsäuremethylester(Va) als ein zähflüssiges rotes Öl. Ein Teil des rohen Produktes wurde *i. Vak.* destilliert und das Destillat erstarrte kristallinisch beim Stehenlassen. $Sdp_{0.04\ mm}$. 160～165°C. Schmp. 44～46°C.

Das Kaliumsalz zersetzte sich unter Aufschäumung bei 218～219°C.

$C_{12}H_{11}O_4N_2K$(286.3)

Ber. C 50.34 H 3.87 N 9.78
Gef. C 49.27 H 4.11 N 9.69

Banden im IR-Spektrum bei: 3400 cm^{-1} (>NH); 3043 cm^{-1} (=CH—); 1756 cm^{-1} (Ester C=O); 1550 cm^{-1} (—NO_2).

α-Nitro-β-(3-indolyl)propionsäure-äthylester (Vb). — Nach der beim entsprechenden Methylester (Vb) angegebenen oder der früher durch Weisblat[7] angegebenen Vorschrift wurde Vb dargestellt, das aber bei uns keinesfalls zur Kristallisation gebracht werden konnte.

Tryptophan (VI) und Tryptophan-äthylester.— 11.2 g (0.0452 Mol) *α*-Nitro-*β*-(3-indolyl)-propionsäure-methylester (Va) in 50 ccm Methanol wurden in Gegenwart von 2 g Nickel-Aluminium-Legierungen dargestellten Raney-Nickel-Katalysatoren in einem Stahlhochdruckautoklav unter mechanischer Schüttelung bei 80～90°C und 100 Atm Wasserstoffdruck hydriert. Innerhalb von 2 Stdn nahm die Lösung die berechnete Menge Wasserstoff auf. Nach Einengen der vom Katalysator abfiltrierten Lösung blieb ein rotes Öl, welches mit 30 ccm 10 proz. Natronlauge auf dem Wasserbade 2 Stdn auf 80～90°C erwärmt wurde. Danach gab man der Lösung 20 ccm Alkohol, entfärbte mit Kohle und stellte sie heiß mit Essigsäure auf pH 5.9 ein. Nach 3 tägigem Stehenlassen im Eisschrank wurden weiße Blättchen von DL-Tryptophan (VI) abgesaugt. Die Ausbeute betrug. 7.1 g (77% d. Theorie). Es zersetzte sich bei 263～265°C.

$C_{11}H_{12}O_2N_2$(204.2)

Ber. C 64.69 H 5.92 N 13.72
Gef. C 64.55 H 6.20 N 13.84

Beim Arbeiten mit *α*-Nitro-*β*-(3-indolyl)-propionsäure-äthylester (Vb) erhielt man Tryptophan in fast gleicher Ausbeute.

$C_{11}H_{12}O_2N_2$(204.2)

Ber. C 64.69 H 5.92 N 13.72
Gef. C 64.59 H 6.27 N 13.72

Aus rohem Reduktionsprodukt wurde Tryptophan-äthylester-hydrochlorid isoliert. Schmp. 233°C (Zers.) (aus Alkohol-Äther).

$C_{13}H_{17}O_2N_2Cl$(268.7)

Ber. C 58.10 H 6.38 N 10.43
Gef. C 57.76 H 6.14 N 10.42

Zusammenfassung

1. Es wird eine neue Synthese des Tryptophans aus Nitromalonester in einer Gesamtausbeute von rund 50-Prozent beschrieben.

2. Die Schlüsselreaktion, die auf diese Synthese angewandt ist, ist eine neue Alkylierung des Indols mit 1, 1, 5, 5-Tetracarbäthoxy-1, 5-dinitro-3-azapentan, einem bis-substituierten Amin, welches leicht erhältlich ist durch Mannich-Reaktion von Nitromalonester, Ammoniak und Formaldehyd. Die optimale Bedingung für die Alkylierungsreaktion wurde auch untersucht.

Meinem verehrten Lehrer, Herrn Prof. Dr. S. Akabori bin ich für die Förderung dieser Arbeit zu großem Dank verpflichtet. Ebenso danke ich Herren Dr. S. Sakurai und Dr. Y. Izumi für freundliche Unterstüzung.

Institut für Eiweißforschung
der Universität Osaka
Tosabori, Nishi-ku, Osaka

*Total Synthesis of Isorenieratene**, **

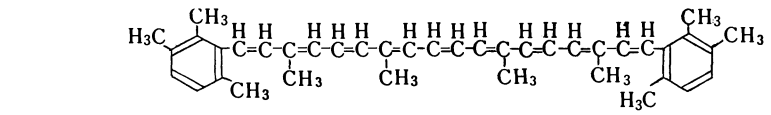
By Masaru YAMAGUCHI

(Received April 3, 1959)

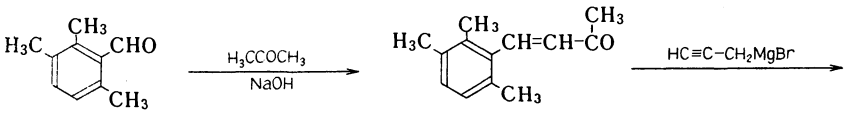
It has been shown by degradative oxidation that isorenieratene, one of the C_{40}-carotenoid hydrocarbons discovered in a sea-sponge, *Reniera japonica*[1], has a remarkable constitution I[2], in which substituted benzene rings are present as terminal groups in place of ionone rings. As the natural carotenoids have so far been aliphatic or alicyclic compounds, the above finding is very significant, and, therefore, it is of importance to make a further confirmation of this exceptional structure of isorenieratene by a synthetic study.

Recently, several routes involving many interesting intermediates have been developed for the total syntheses of carotenoids[3], some of these routes giving considerably good yields. For the present study, however, a method established by Karrer et al.[4] has been applied for the reason of the simplicity of the method, though the overall yields attained by them are not so satisfactory.

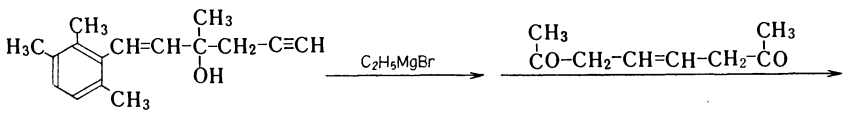
The starting material, 2,3,6-trimethylbenzaldehyde (II), was condensed with acetone to give 2,3,6-trimethylbenzalacetone (III), which corresponds to β-ionone, a starting material in the β-carotene syntheses. The ketone (III) was converted into an acetylenic alcohol (IV), which by condensation with 4-octene-2,7-dione gave a C_{40}-diynetetraol (V). Partial hydrogenation of V followed by dehydration gave



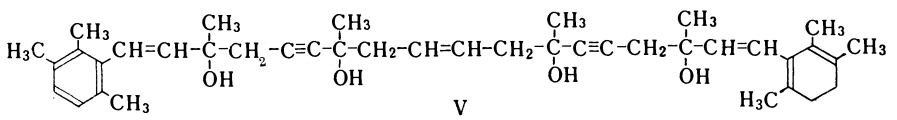
I



II III



IV



V



* "Pigments of Marine Animals", VIII. VII of this series: T. Mukai, *Memoirs of the Faculty of Science, Kyushu University, Series C., Chemistry*, **3**, No. 2, 29 (1958).

** Read before the 12th Annual Meeting of the Chemical Society of Japan, Kyoto, April, 1959.

1) T. Tsumaki, M. Yamaguchi and T. Tsumaki, *J. Chem. Soc. Japan, Pure Chem. Sec.* (*Nippon Kagaku Zasshi*), **75**, 297 (1954).

2) M. Yamaguchi, This Bulletin, **31**, 51 (1958).

3) For example: H. H. Inhoffen and H. Siemer, *Fortschr. Chem. org. Naturstoffe*, **9**, 1 (1952); O. Isler et al., *Helv. Chim. Acta*, **39**, 249,274,449,454,463,2041(1956); **40**, 456,1242,1256(1957); B. C. L. Weedon et al., *J. Chem. Soc.*, **1953**, 3286,3294,3299.

4) P. Karrer and C. H. Eugster, *Helv. Chim. Acta*, **33**, 1172 (1950); C. H. Eugster, C. Garbers and P. Karrer, ibid., **35**, 1179 (1952).

isorenieratene (I) in a small yield.

Isorenieratene thus obtained forms purplish-red fine needles, m. p. 199~200°C, and is indistinguishable in the appearance from the specimen isolated from the sea-sponge. Furthermore, a mixed melting point, a mixed chromatography, and UV- and IR-spectra established perfect identity. (IR-spectra : Fig. 1).

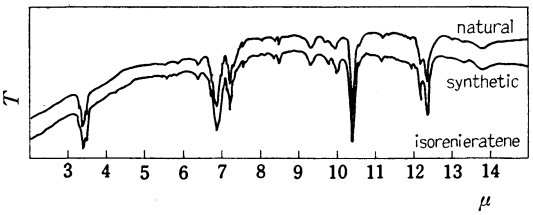


Fig. 1. Infrared spectra of isorenieratene (nujol mull).

Experimental

Solutions were evaporated under diminished pressure unless otherwise mentioned. Anhydrous sodium sulfate was employed for drying solutions.

4-(2, 3, 6-Trimethylphenyl)-3-buten-2-one (III).—A 10% aqueous sodium hydroxide solution (3.1 cc.) was added dropwise during five minutes to a stirred mixture of 2, 3, 6-trimethylbenzaldehyde (14 g.), acetone (16 g.) and water (10 cc.) at room temperature. After stirring for eight hours, the upper layer was separated, combined with the extract (benzene, 20 cc.) of the lower aqueous layer, washed successively with water, 3% hydrochloric acid and water, dried and evaporated. Distillation of the residue gave at first trimethylbenzaldehyde (2.5 g.) and then 4-(2, 3, 6-trimethylphenyl)-3-buten-2-one (11 g.) as an almost colorless oil, b.p. 127~132°C/6 mmHg.

Anal. Found: C, 82.98; H, 8.67. Calcd. for $C_{13}H_{16}O$: C, 82.93; H, 8.57%.

The semicarbazone, colorless needles, m.p. 223~225°C.

Anal. Found: C, 68.37; H, 7.83. Calcd. for $C_{14}H_{19}ON_3$: C, 68.54; H, 7.81%.

The 2, 4-dinitrophenylhydrazone, red plates, m.p. 178~180°C.

Anal. Found: C, 61.79; H, 5.37. Calcd. for $C_{19}H_{20}O_4N_4$: C, 61.95; H, 5.47%.

The residue of the distillation solidified on cooling, which on recrystallization from benzene-ethanol gave 1, 5-bis(2, 3, 6-trimethylphenyl)-1, 4-pentadien-3-one (1.9 g.) in pale yellow plates, m.p. 153~154°C.

Anal. Found: C, 86.67; H, 8.15. Calcd. for $C_{23}H_{26}O$: C, 86.74; H, 8.23%.

The 2, 4-dinitrophenylhydrazone, red needles from acetic acid, m.p. 166~168°C.

Anal. Found: C, 70.11; H, 5.95. Cacld. for $C_{29}H_{30}O_4N_4$: 69.86; H, 6.07%.

1-(2, 3, 6-Trimethylphenyl)-3-methyl-1-hexen-5-yn-3-ol (IV).—A Grignard solution was prepared by dropwise addition (1.5 hr.) of propargyl bromide (5.9 g.) in dry ether (20 cc.) to magnesium (1.5 g.) covered with dry ether (60 cc.) under vigorous stirring. Magnesium was previously activated with a 1% aqueous solution of mercuric chloride. The excess of magnesium was removed by filtration and the solution was added during a half hour to a well stirred solution of the above C_{13}-ketone (III) (9 g.) in dry ether (20 cc.). The mixture was refluxed under stirring for additional one hour, and then decomposed with ice and 5% aqueous sulfuric acid. The ethereal layer was washed with water, dried and evaporated. The oily residue was dissolved in absolute ethanol (80 cc.), a solution of Girard reagent P (6 g.) in acetic acid (6.3 g.) was added, and the mixture was refluxed for an hour. The cooled solution was poured into ice water (300 cc.) containing sodium hydrogen carbonate (7.95 g.) and extracted with ether (3×50 cc.). The ethereal solution was washed, dried and evaporated. Distillation of the residue gave 1-(2, 3, 6-trimethylphenyl)-3-methyl-1-hexen-5-yn-3-ol (4.3 g.) as a faint colored viscus oil, b.p. 110~115°C/0.04 mmHg.

Anal. Found: C, 83.92; H, 9.05. Calcd. for $C_{16}H_{20}O$: C, 84.16; H, 8.83%.

C_{40}-diyntetraol (V).—A solution (ca. 30 cc.) of ethylmagnesium bromide prepared from ethyl bromide (3.9 g.) was filtered, and added dropwise during one and a half hour to a well stirred mixture of above acetylenic alcohol (4.1 g.), cuprous chloride (50 mg.) and dry ether (16 cc.). The mixture was refluxed for an additional one hour. A solution of 4-octene-2, 7-dione[5] (840 mg.) in dry ether (18 cc.) was then added dropwise during thirty minutes under efficient stirring. After refluxing for one hour, the mixture was allowed to stand overnight, and decomposed with 1 N sulfuric acid under ice-cooling. Ether (30 cc.) was added, and the ethereal layer was washed with dilute sulfuric acid, an aqueous solution of sodium hydrogen carbonate and water, dried and evaporated. The yellow brown oily residue was adsorbed on alumina (95 g., standardized according to Brockmann), from a benzene solution (15 cc.). The column was washed successively with benzene (115 cc., the elute gave an oily residue, 1.7 g.), with ether (100 cc., it gave 1.4 g. of residue), and with ether-methanol (10:1, 180 cc.). The last fraction contained C_{40}-tetraol, which is obtained by evaporation of the solvent as a yellowish colored glasslike mass (1.8 g.).

Anal. Found: C, 79.39; H, 8.82. Calcd. for $C_{40}H_{52}O_4$: C, 80.50; H, 8.78%.

It showed somewhat low C-value, and was employed for the next step without further purification.

Isorenieratene (I).—A solution of tetraol (300 mg.) in ethyl acetate (10 cc.) was agitated with active charcoal (100 mg.) for 10 min., filtered, and shaken with palladium barium sulfate catalyst (1%, 20 mg.) in an atmosphere of hydrogen. Occasional additions of the catalyst (ca. 5 mg.) were necessary until 2 mol. (23.6 cc., 13°C/760 mmHg) of hydrogen was adsorbed (2.5

5) P. Karrer and C. H. Eugster, ibid. ,32, 1934 (1949).

hr.). The catalyst was removed and the solution was evaporated to give a glassy residue. A boiling solution of toluene-*p*-sulfonic acid (40 mg., dehydrated by melting in vacuo) in toluene (5 cc.) was added at a time to a boiling solution of the above residue in toluene (10 cc.) and the mixture was boiled for ca. eighty seconds, the water which formed being removed by azeotropic distillation. The greenish brown solution was cooled and poured into a mixture of a saturated aqueous solution of sodium hydrogen carbonate and petroleum ether (50 cc.). On shaking, the color changed into deep red. The petroleum ether solution was then washed once with water and thrice with 90% methanol, dried and evaporated. The reddish brown residue was dissolved in petroleum ether and chromatographed on alumina (2×20 cm.). The chromatogram was developed with petroleum ether, giving (i) a diffuse faint yellow band (least strongly adsorbed); (ii) an orange zone which is somewhat heterogeneous due to the presence of *cis*-isomer; (iii) a small orange brown zone; (iv) a small brown zone. The orange zone (ii) was eluted with benzene-methanol (10:1). The residue of the elute was treated with a mixture of petroleum ether and ethanol (1 : 1, 3 cc.), and left to stand overnight in an ice chamber to giv a red precipitate (4.5 mg.). From the mother liquor was obtained an additional quantity of the pigment (1 mg.) after isomerization with iodine. In this way, 900 mg. in total of the tetraol was worked up giving 14 mg. of the pigment. Several recrystallizations from benzene-methanol gave the analytically pure pigment (9 mg.), in purplish red fine needles, m.p. 199～200°C. The mixed melting point with isorenieratene (m.p. 199～200°C) which was isolated from the sea-sponge, *Reniera japonica*, was 199～200°C. A mixed chromatography of the synthetic and the natural pigments showed no separation. They gave the same UV-curves with maxima at 492 ($\varepsilon=12.3\times10^4$) and 463 m$\mu$ ($\varepsilon=10.4\times10^4$) (in benzene, spectrophotoelectric method). IR-curves: Fig. 1.

Anal. Found: C, 90.58; H, 9.24. Calcd. for $C_{40}H_{48}$: C, 90.85; H, 9.15%.

The author wishes to express his thanks to Professor Tokuichi Tsumaki for his exceedingly kind direction throughout this work. The author also thanks Mr. Ryoichi Shimada for UV-spectra measurement and Mr.Michio Shido for microanalysis. The cost of this work has been partially covered by the Scientific Research Grant of the Ministry of Education.

Department of Chemistry
Faculty of Science
Kyushu University
Hakozaki, Fukuoka

*Magnetochemical Investigation on Thermal Decomposition of Silver Oxide**

By Shōtaro TOBISAWA

(Received April 20, 1959)

The thermal decomposition of silver oxide in oxygen under atmospheric pressure, was investigated by Lewis[1], and was found to follow the equation $dx/dt = kx(1-x)$, where x is the fraction of silver produced. His result was confirmed by Hood and Murphy[2]. On the other hand, it was found by Garner and Reeves[3] that the decomposition in vacuo did not hold Lewis' equation but gave the equation $\sqrt[3]{p} = kt - C$ for the initial part of the decomposition, where p is the pressure of oxygen evolved with the progress of decomposition. The rates of thermal decompositions of the type A (solid)→B (solid) + C (gas) have been interpreted in terms of the formation and growth of nuclei by many investigators[4]. It may, therefore, be considered that the formation and growth of nuclei depend on the origins of silver oxide and also on the experimental conditions under which the decompositions are carried out.

All the previous work on the kinetics of the decomposition of silver oxide had been carried out by measuring the pressures of the oxygen gas evolved. Although this pressure-method is the most common for kinetic measurements of solid decomposition, it is undesirable for an accurate

* Presented before the 11th Annual Meeting of the Chemical Society of Japan, Tokyo, April, 1958.

1) G. N. Lewis, *Z. physik. Chem.*, **52**, 310 (1905); *J. Am. Chem. Soc.*, **28**, 139 (1906).

2) G. C. Hood and G. W. Murphy, *J. Chem. Educ.*, **26**, 169 (1949).

3) W. E. Garner and L. W. Reeves, *Trans. Faraday Soc.*, **50**, 254 (1954).

4) W. E. Garner, "Chemistry of the Solid State", Butterworths Scientific Publications, London (1955), p. 213.

measurement of the reaction rate on account of the existence of a considerable space from a reaction chamber to a piece of equipment for pressure measurement. The present author has constructed a recording magnetic balance of Hirone's type[5] with many improvements. This balance has been used continuously with very high sensitivity for many hours and as a thermal balance without magnetic field. By using it as the magnetic balance, the kinetics of the decomposition of silver oxide can be investigated by the measurement of change in magnetic susceptibility, due to the oxygen gas evolved. By using it as the thermal balance, the kinetics can be studied by the measurement of the loss in weight with the progress of decomposition. In the case of magnetic balance, silver oxide was charged into a small bulb and was sealed after being evacuated. The pressure of oxygen in contact with the undecomposed silver oxide became higher as the reaction proceeded. However, in the case of thermal balance, the sample was packed in an open bulb and the decomposition was carried out under costant reduced pressure.

The purpose of the present work is to show the results of kinetic measurements obtained under the above two experimental conditions, together with the measurements of the magnetic susceptibility of silver oxide and of metallic silver produced by the complete decomposition of silver oxide.

Experimental

Materials.—In the present work, four samples were used. Samples A and B were guaranteed reagents of the Kanto Chemical Co. Ltd., and of Kahlbaum, respectively. Silver carbonate contained in the above samples could easily be converted into silver oxide by heating under vacuum according to the equation, $Ag_2CO_3 = Ag_2O + CO_2$. Samples C and D were obtained by heating the samples A and B at 250°C for an hour under the vacuum of 10^{-5} mmHg, respectively. This treatment was carried out before each measurement.

Apparatus.—The magnetic balance was operated by the Faraday method, because this method is convenient to measure the change in magnetic susceptibility of the reaction system at high temperatures. As indicated in Fig. la, a small bulb of fused quartz was suspended in the position giving the maximum value of $H \cdot \partial H/\partial x$, which was determined from Fig. 2. Here H is the field strength and $\partial H/\partial x$ is its gradient along the vertical line passing through the center of the gap between the pole pieces. The bulb 4 mm. high could be held within the error of about one per cent of the maximum value of $H \cdot \partial H/\partial x$.

The recorder used here could plot three values, the magnetic forces acting on a bulb containing a sample, the temperatures of a sample, and the currents supplied to an electromagnet, on a chart at regular intervals of 15 sec., respectively. The

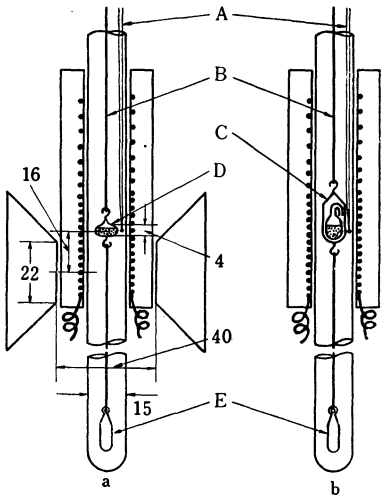


Fig. 1. Positions of sample bulbs in the magnetic balance a and the thermal balance b, showing in mm. unit.
A: $P_t - P_t \cdot Rh$ (13%) thermocouple (0.3 mm. in diameter)
B: Fused quartz rod (1.2 mm. in diameter)
C: Fused quartz basket
D: Fused quartz bulb (ca. 0.10 cc. in volume)
E: Weight of copper

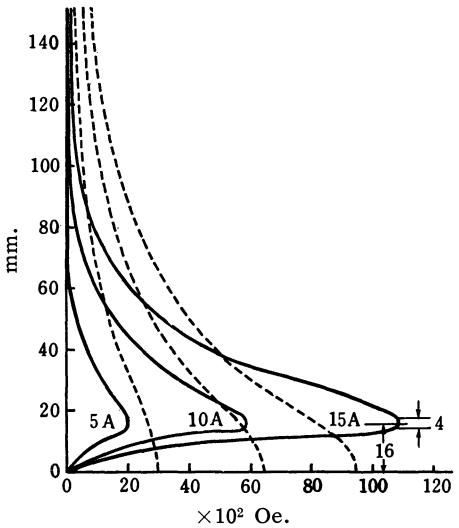


Fig. 2. Diagram of H (---) and $H \cdot \partial H/\partial x$ (—). The origin is the middle point between two centers of pole pieces.

5) T. Hirone, S. Maeda and N. Tuya, *Rev. Sci. Instr.*, **25**, 516 (1954); *Sci. Rep. Res. Inst. Tohoku Univ.*, **A6**, 67 (1954).

magnetic force could be indicated by the current which was proportional to the force, and was calibrated by the magnetic susceptibility of the empty bulb of fused quartz in each measurement. The susceptibility of the fused quartz was -0.46×10^{-6} units per gram[6], and it scarcely depended on temperature at all. The full scale of the recording chart was 10 milliamp. The apparatus was modulated to make it possible to indicate changes of 0.1 milliamp. corresponding to -0.58×10^{-6} e. m. u. in magnetic susceptibility, on a recording chart. The temperature scale of the recorder was calibrated by using the freezing points of four Kahlbaum reagents: tin, zinc, antimonium and silver. Each measurement was carried out in the constant magnetic field of 8250 Oersteds.

When the balance was used as a thermal balance, the recorder could give the losses in weight and the corresponding temperatures of the sample. One millimeter on the recording chart corresponded to 0.015 mg. A sample was packed in the bulb shown in Fig. 1b and was thermally decomposed under the constant pressure of 50 mmHg.

Results

Decomposition Temperature.—The decomposition temperature of silver oxide was determined by the above two methods by raising the temperature at constant rate, 200°C per hour. The results obtained by means of the thermal balance, are shown in Figs. 3 (for the samples A and B) and 4 (for the samples C and D). The first losses in weight for the samples A and B occur at 148°C and the second ones at 372°C. The first losses in weight for the samples C and D are negligibly small and the second ones occur at 354°C.

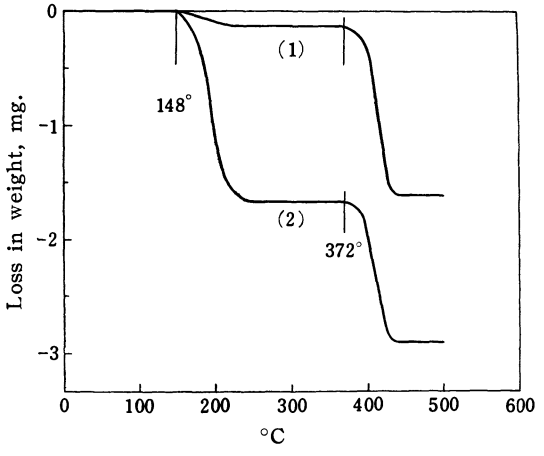


Fig. 3. Loss in weight-temperature curves. (1) Sample A (wt. 20.0 mg.); (2) Sample B (wt. 20.0 mg.).

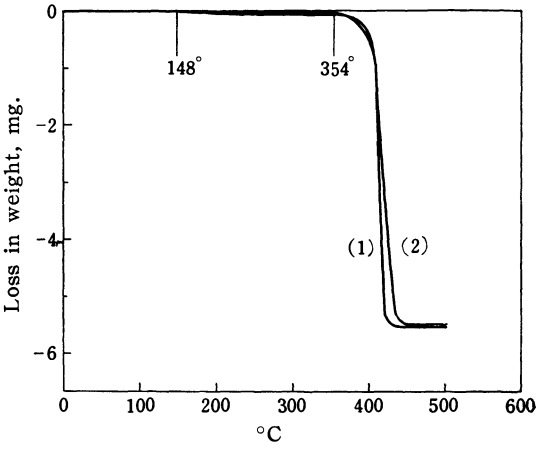


Fig. 4. Loss in weight-temperature curves. (1) Sample C (wt. 80.0 mg.); (2) Sample D (wt. 80.0 mg.).

The curves of magnetic susceptibility against temperature for the reaction system are given in Fig. 5. The sample used in each measurement was about 50 mg. and was sealed in a bulb after being evacuated for several hours under a vacuum of 10^{-5} mmHg. The curves for the samples A and B deflect obviously toward the paramagnetic sides owing to the paramagnetism of oxygen gas evolved at the decomposition at 372°C. The curve of the sample C shown in a broken line in Fig. 5, indicates that the silver oxide decomposes at 354°C. All the samples treated with heating under evacuation, decomposed at the same temperature. It is apparent from the magnetic measurements that the first losses at 148°C are not due to oxygen gas.

Moisture had no responsibility for the loss in weight at 148°C, because each sample was freed from moisture by evacuation. A preliminary qualitative analysis of carbon dioxide with barium hydroxide solution, showed that the silver oxide was partly converted into silver carbonate. The first loss in weight at 148°C in Fig. 3 is, therefore, due to the thermal decomposition of silver carbonate contained in the sample. The negligibly small amount of loss in weight in Fig. 4 can be ascribed to the decomposition of silver carbonate which had been formed by combining the silver oxide with carbon dioxide in air, within two hours or so before the beginning of the measurement. From the above experimental results, it

6) S. S. Bhatnagar and K. N. Mathur, "Physical Principles and Applications of Magnetochemistry", Macmillan & Co., Ltd., London (1935), p. 354.

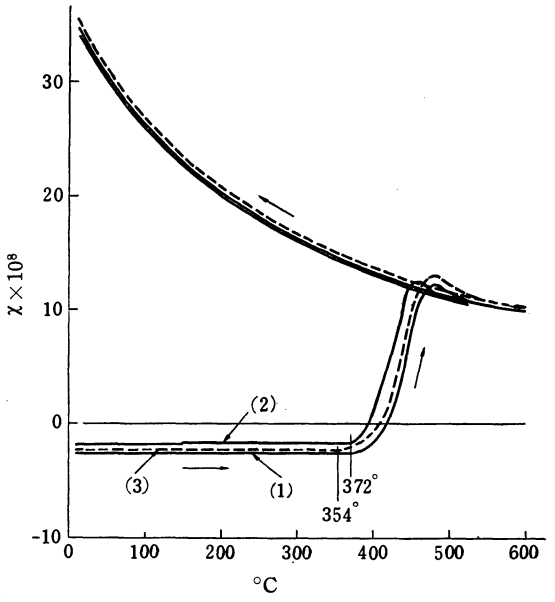


Fig. 5. Magnetic susceptibility-temperature curves.
(1) Sample A (wt. 50.0 mg.); (2) Sample B (wt. 50.0 mg.); (3) Sample C (wt. 49.3 mg.).

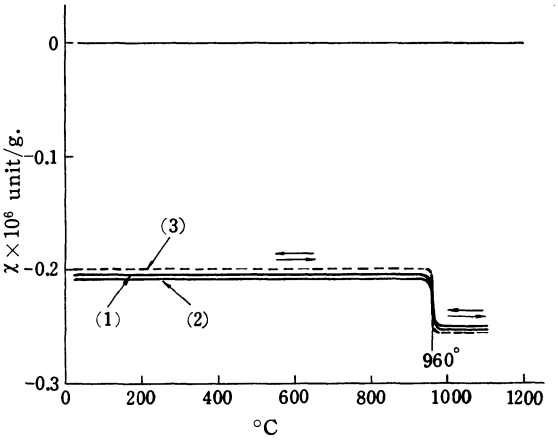


Fig. 6. Magnetic susceptibility-temperature curves.
(1) Metallic silver obtained from sample A;
(2) Metallic silver obtained from sample B;
(3) Kahlbaum silver metal.

is found that the decomposition temperature of silver oxide is apparently affected by silver carbonate contained in the oxide.

Magnetic Susceptibilities of Metallic Silver and Silver Oxide.—In order to know whether paramagnetic or ferromagnetic impurity was present in the samples A and B, the magnetic susceptibilities of metallic silver obtained by the complete decomposition, were measured. In addition, the susceptibility of Kahlbaum silver was measured. The curves obtained are shown in Fig. 6. The magnetic susceptibilities of metallic silver produced by the decomposition of the samples A and B were -0.21×10^{-6} units per gram and that of Kahlbaum silver was -0.20×10^{-6} units per gram at room temperature. The curves in Fig. 6 show that the magnetic susceptibility of metallic silver is independent of temperature below 1100°C, except for a slight increase at the melting point. These facts indicate that no magnetic impurities are involved in either sample, and that the metallic silver is normally diamagnetic and takes no supercooling. The curve obtained by Honda[7] shows that the magnetic susceptibility of metallic silver increases with increasing temperature. On the other hand, Selwood[8] mentioned that the magnetic susceptibility of metallic silver was almost independent of temperature.

The magnetic susceptibility of silver oxide from which carbon dioxide was removed, was -0.48×10^{-6} units per gram at room temperature. It was less than the value of -0.58×10^{-6} units per gram[9], reported previously.

Kinetic Measurements.—(1) Photo. 1 is an example of the chart obtained by means of the thermal balance, showing the losses in weight and the corresponding temperatures. In each measurement a required constant temperature could be obtained within a few minutes. Curves of the loss in weight (x) against time (t) at 380, 390, 400 and 410°C for 80 mg. of the sample D are shown in Fig. 7. It was ascertained that the rate of decomposition held neither

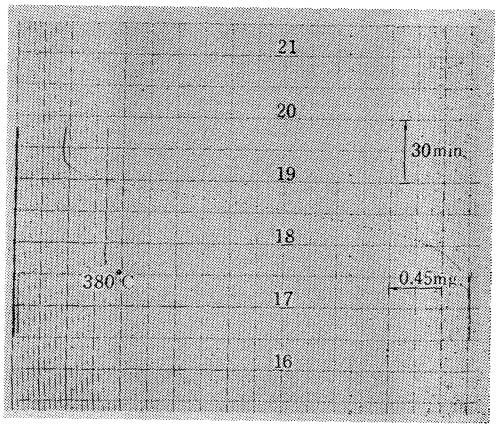


Photo. 1. An example of chart obtained by means of the thermal balance.

7) K. Honda, *Ann. Physik*, **32**, 1027 (1910).
8) P. W. Selwood, "Magnetochemistry", 2nd Ed., Interscience Publishers, New York (1956), p. 362.
9) See reference 8, p. 214.

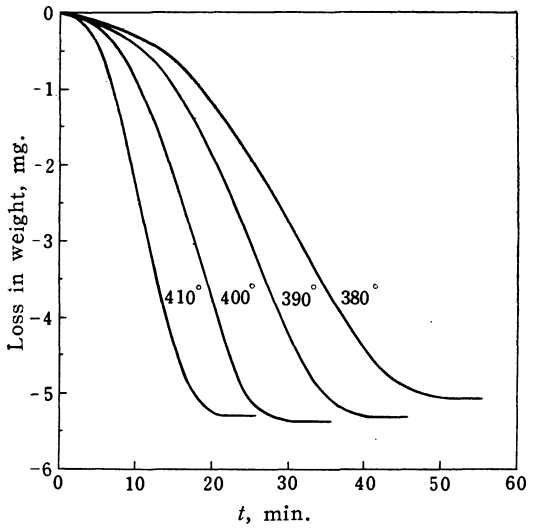


Fig. 7. Loss in weight-time curves for sample D.

Lewis' equation nor that of Prout-Tompkins[10]. The validity of the equation, $\sqrt[3]{x}=kt-C$, presented by Garner et al. for the initial part of the decomposition, was examined by plotting $\sqrt[3]{x}$ against t in Fig. 8. The values of k were obtained from the figure. The activation energy of 29.4 kcal. per mole was estimated from the slope of line which was obtained by plotting $\log k$ against $1/T$. The activation energies reported for this decomposition are as follows: 31.8[1] 35~36[11], 10.5[12] and 45.6~46.2 kcal. per mole[2].

(2) Examining in detail the plots in Fig. 8, it is seen that these plots show the curves with several inflection points. The plots of dx/dt against t are shown in Fig. 9. The time was calculated by setting zero time at the point where the half of

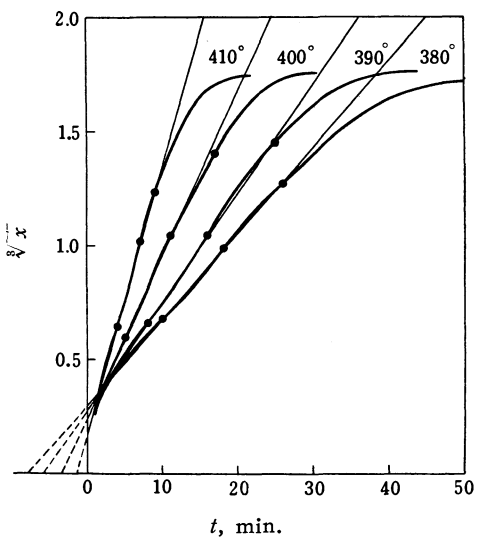


Fig. 8. Curves obtained according to Garner's equation.
●: Inflection point.

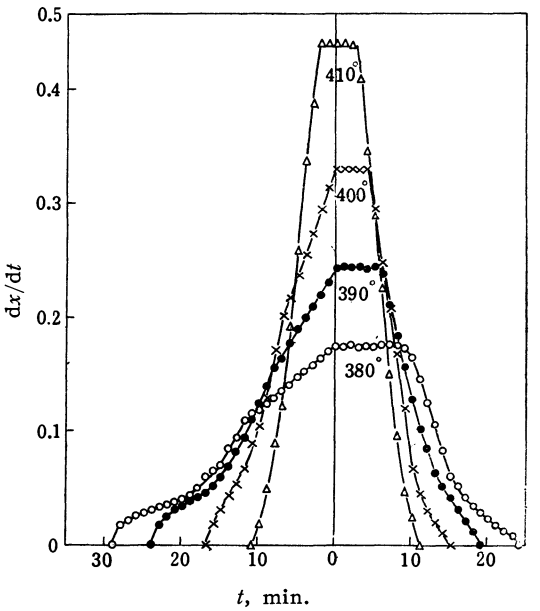


Fig. 9. Plots of dx/dt against time for sample D.

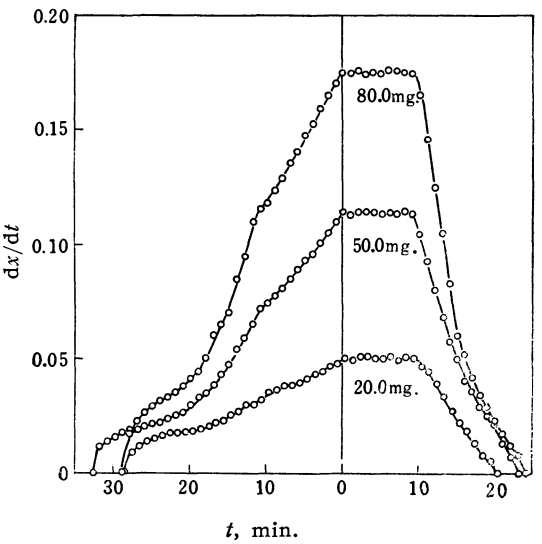


Fig. 10. Plots of dx/dt against time for sample D at 380°C.

10) E. G. Prout and F. C. Tompkins, *Trans. Faraday Soc.*, **40**, 488 (1944).
11) A. F. Benton and L. C. Drake, *J. Am. Chem. Soc.*, **28**, 139 (1906).
12) M. M. Pavlyuchenko and E. Gurevich, *Zhur. Obshchei Khim.*, **21**, 467 (1951); *Chem. Abstr.*, **45**, 5006 (1951).

TABLE I. VALUES FOR α AND β

Stage	380°C		390°C		400°C		410°C	
	α	β	α	β	α	β	α	β
1	1.72×10^{-2}	0.39	1.74×10^{-2}	0.52	1.75×10^{-2}	0.83	1.79×10^{-2}	1.44
2	0.09×10^{-2}	1.65	0.16×10^{-2}	1.65	0.42×10^{-2}	1.65	1.32×10^{-2}	1.65
3	0.81×10^{-2}	0.91	0.79×10^{-2}	1.09	2.29×10^{-2}	0.95	3.76×10^{-2}	1.13
4	1.77×10^{-1}	0	2.45×10^{-1}	0	3.30×10^{-1}	0	4.42×10^{-1}	0
5	1.44×10^{12}	− 7.50	3.69×10^{11}	− 7.50	1.61×10^{7}	− 5.00	6.63×10^{4}	− 3.64
6	1.35×10^{23}	−14.14	2.95×10^{28}	−18.14	1.15×10^{20}	−14.14	1.95×10^{16}	−12.00

silver oxide was decomposed. All the curves in Fig. 9 indicate that the rate of decomposition varies discontinuously, and that the period constant rate is recognized in the curve. The plots of dx/dt against t obtained for 20, 50 and 80 mg. of the sample D at the same temperature, 380°C, are given in Fig. 10. The figure shows that the period of constant rate is not affected by the difference in weight of sample. By plotting $\log dx/dt$ against $\log t$ in Fig. 11, the breaking points become very distinctive. The curve for the whole course of the decomposition can be divided into several linear parts. Each linear part can be represented by the equation $\log dx/dt = \log\alpha + \beta\log t$ or $dx/dt = \alpha t^{\beta}$. The estimated values for α and β from Fig. 11 are listed in Table I. The value of α depends on temperature except in the case of the first stage, and β also varies with temperature except in the cases of the certain stages.

As indicated in Fig. 12, the curves of

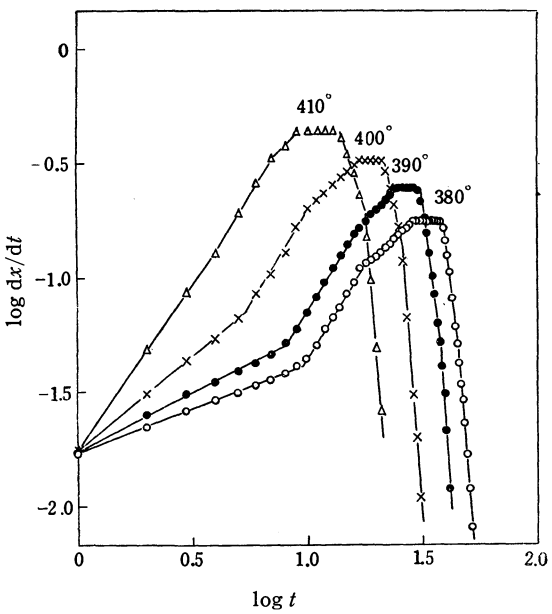


Fig. 11. Plots of $\log dx/dt$ against $\log t$ for sample D.

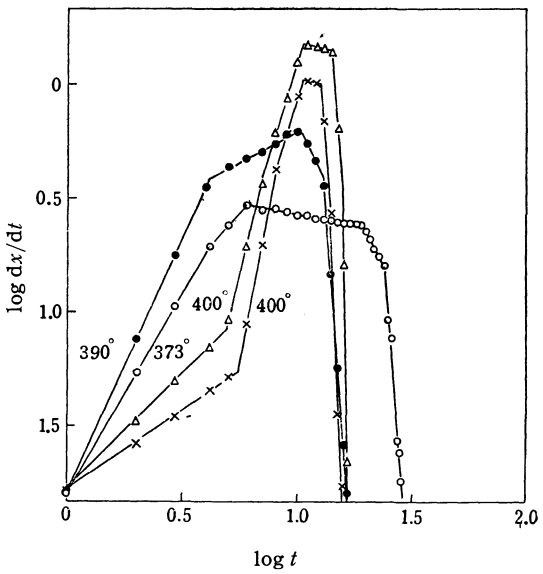


Fig. 12. Plots of $\log dx/dt$ against $\log t$ for sample C (wt. 80.0 mg.).
—△—: wt. 150.0 mg.

$\log dx/dt$ against $\log t$ for the sample C can also be divided into several linear parts for the whole course of the decomposition, as found in the case of sample D.

(3) In the magnetic measurements, the balance was modulated to make it possible to indicate only the change of paramagnetic nature with very high sensitivity. Thus, the small values of diamagnetic susceptibilities of silver oxide and of metallic silver produced by decomposition could be neglected. To determine the weight of oxygen gas evolved in the bulb, the value of paramagnetic susceptibility obtained under a constant temperature was compared with the theoretical value calculated from Van Vleck's equation[13]. In each experiment, the estimated weight of oxygen gas evolved in the bulb at the end of the experiment, was in good agreement with the difference between an initial

13) J. H. Van Vleck, "The Theory of Electric and Magnetic Susceptibilities", Oxford University Press, London (1932), p. 266.

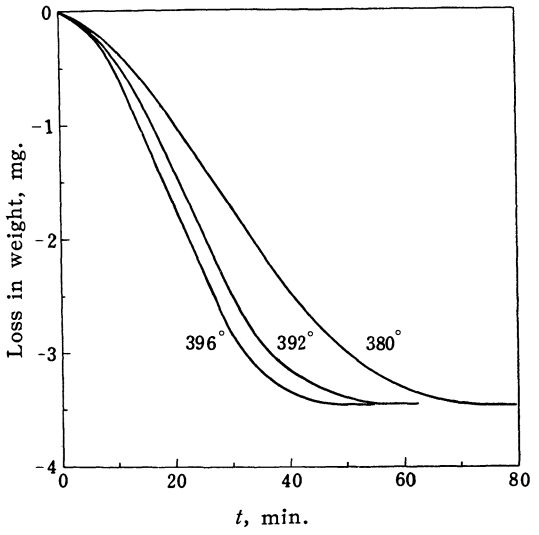


Fig. 13. Loss in weight-time curves for sample D.

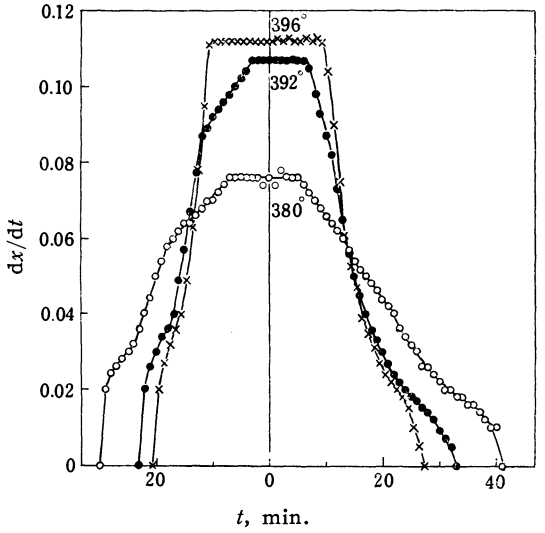


Fig. 14. Plots of dx/dt against time for sample D.

weight of bulb containing a sample and the one containing the residue obtained by removing the oxygen gas evolved in the bulb. In every measurement, the sample used was about 50 mg., and the temperature of the sample was controlled similarly as in the case of the thermal balance. The curves of x against t for the sample D at 380, 392 and 396°C, and the curves of dx/dt against t are shown in Figs. 13 and 14, respectively. The rate of decomposition is represented by the curves with the period of constant rate, as found in the case of the thermal balance. From the plots of $\log dx/dt$ against $\log t$ in Fig. 15, it is apparent that the curves can be divided into the several linear parts. The equation $dx/dt=\alpha' t^{\beta'}$ can, therefore, be applied to the result obtained under the condition in which the sample is decomposed in contact with the evolved gas. The estimated values for α' and β' are given in Table II. The value of α' depends on temperature except for the first stage, β' also varies with temperature except for certain stages. These features are similar to those found in the

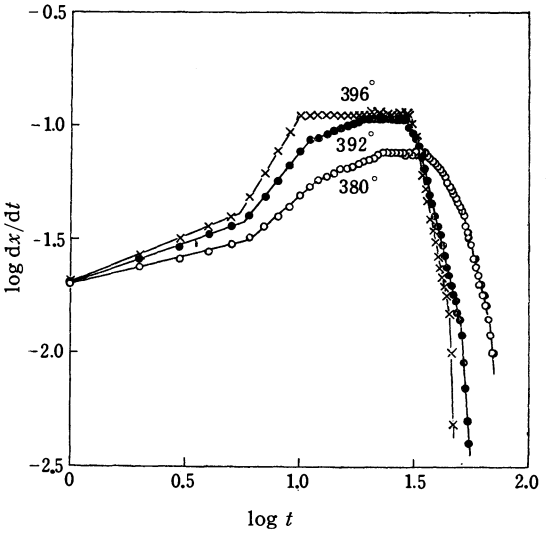


Fig. 15. Plots of $\log dx/dt$ against $\log t$ for sample D.

TABLE II. VALUES FOR α' AND β'

Stage	380°C		392°C		396°C	
	α'	β'	α'	β'	α'	β'
1	2.00×10^{-2}	0.26	2.03×10^{-2}	0.35	2.04×10^{-2}	0.42
2	0.65×10^{-2}	0.88	0.42×10^{-2}	1.26	0.29×10^{-2}	1.61
3	2.04×10^{-2}	0.42	3.80×10^{-2}	0.34	0.29×10^{-2}	1.61
4	0.76×10^{-1}	0	1.07×10^{-1}	0	1.12×10^{-1}	0
5	4.10	−1.12	7.95×10	−1.95	3.93×10^{7}	−5.09
6	9.04×10	−1.95	3.76×10^{6}	−4.35	3.93×10^{7}	−5.09
7	4.34×10^{6}	−4.10	3.76×10^{6}	−4.35	3.93×10^{7}	−5.09
8	5.01×10^{18}	−10.70	1.10×10^{22}	−13.40	3.38×10^{39}	−24.40

experimental results obtained by the thermal balance.

It was noteworthy that several breaking points appear on the curve in each constant temperature, in spite of the entirely different origins and experimental conditions. This fact shows that fresh potential sites at which nuclei can be formed, are created at intervals as the reaction proceeds. It may be considered that the formation of fresh potential sites is due to a strain which is induced by the reaction product at a surrounding undecomposed portion when the reaction product grows to a certain magnitude.

Summary

(1) It was found, by means of the thermal and magnetic balance, that the decomposition temperatures of silver oxide and of silver oxide containing silver carbonate are 354 and 372°C, respectively.

(2) The magnetic susceptibilities of metallic silver obtained by the decomposition and of silver oxide are -0.21×10^{-6} and -0.48×10^{-6} units per gram at room temperature, respectively. Metallic silver is normally diamagnetic from room temperature to 1100°C.

(3) Under the present experimental conditions, the rate of decomposition is represented by the equation $dx/dt=a_i t^{b_i}$ for the whole course of the decomposition, where i is the subscript for each stage, and generally both a_i and b_i depend on the temperature. It is considered that nuclei are created at intervals as the reaction proceeds.

The author wishes to express his sincere gratitude to Professor Y. Nomura for his suggestions regarding this work and for his helpful advice during the course of the construction of the apparatus.

Department of Chemistry
Defense Academy
Yokosuka

The Kinetic Study of Surface-chemical Reactions at Extremely Low Pressures. IV. The Thermal Reaction between Water Vapor and a Tungsten Filament. Part IV

By Takuya HAMAMURA

(Received April 21, 1959)

Tungsten compound formed by the reaction of water vapor with tungsten at high temperatures has been studied by some investigators. Smithells[1] has studied the reaction by using a gas-filled electric bulb and reported that tungsten was removed from the hotter part of the filament as WO_2 and deposited as W on the colder part. Alterthum[2] assumed the formation of WO_2 in their estimation of equilibrium constants of the system W-H_2O at high temperatures, and Dushman[3] showed thermodynamically that water vapor could oxidize W to WO_2 or W_2O_5. In the previous experiments[4-6] concerning the heating of a tungsten filament in water vapor at low pressures, however, it was found that a blue deposit was formed on the wall of the reaction vessel as the reaction proceeded.

Since WO_2 is brown, this deposit seemed to correspond to another compound. This difference may come from the fact that other authors' results are those at the equilibrium state and not applicable to the present case. It is the aim of the present work to identify the blue deposit and to explain the process of its formation.

1) C. J. Smithells, "Tungsten", Chapman & Hall, Ltd., London (1952), p. 141.
2) H. Alterthum and F. Koref, *Z. Elektrochem.*, **31**, 508 (1925).
3) S. Dushman, "Vacuum Technique", John Wiley & Sons, Inc., New York (1949), p. 822.
4) N. Sasaki and T. Hamamura, This Bulletin, **29**, 365 (1956).
5) T. Hamamura, ibid., **32**, 845 (1959).
6) T. Hamamura, ibid., **32**, 848 (1959).

Experimental

The tungsten compound formed by the reaction vaporizes from the filament at high temperatures to produce the deposit on the wall of the vessel. The composition of deposit was determined by means of an electron diffraction method and an indirect method mentioned below.

Electron Diffraction Method. — A film of formval attached on a sheet mesh was placed in the reaction vessel to deposit the product on it; and after the reaction ended, it was taken out of the vessel and a diffraction pattern was taken with a micro-diffraction apparatus.

Indirect Method. — Composition of the deposit was determined from the weight loss of the filament and the amount of hydrogen produced. Since no layer of the product was formed on the filament above 1200°K and the evaporation of tungsten was negligible below 2400°K, the weight loss of filament gave the weight of tungsten converted to the product. On the other hand, if one molecule of hydrogen was assumed to be formed from one molecule of water vapor, the quantity in moles of hydrogen was equal to twice that of oxygen combined with tungsten. Therefore, the mean apparent composition was determined from the weight loss of filament and the amount of hydrogen produced.

Apparatus. — The experimental apparatus was the same as that described in the previous papers, except that the filaments were made removable from the lead wires for weighing, i. e., they were clamped at both ends by nickel strips welded to the leads. The filaments used were taken from the same spool as that used in the previous experiments and pretreated in a similar manner. Six filaments, 0.114 mm. in diameter and 75 mm. long each, were mounted perpendicular to the axis of the reaction vessel at a distance of 5 cm. from each other. One of them was used for a standard to compensate all the weight changes that were not caused by the reaction itself; for example, the change caused by the oxidation and adsorption during the weighing process and the evaporation during the degassing process and so on. The filament was degassed in a similar manner as the others, but not heated in water vapor. The other five filaments were used for the determination of the composition. A glass balloon of 10.278 l. was used to introduce hydrogen into it and the pressure was measured with a McLeod manometer.

Procedure.—Prior to the mounting, each filament was weighed with a micro-balance and mounted in the vessel in a manner such as that mentioned above. The procedures of evacuating the apparatus, degassing the filaments and introducing water vapor into the vessel were similar to those of the previous experiments, except that the filaments were degassed at 2200°K for 6 hr. When the flow of water vapor became stationary, one of the filaments was heated at a definite temperature and the hydrogen liberated was carried by the diffusion pump into the balloon. After a certain interval of time, the filament was cooled and the pressure of the balloon was measured to obtain the amount of hydrogen. Thus, five filaments were heated one by one under different filament temperatures and pressures of water vapor. After five filaments had been heated, all the filaments were heated again in high vacuum at 2000°K for twenty minutes. Then the filaments were taken out of the vessel, removed from the leads and weighed again with a micro-balance. The net weight loss was obtained as a difference of weight loss of the respective filament and the weight change of the standard filament.

The experiments were made at temperatures from 1480 to 1950°K and initial pressures of water vapor from 63×10^{-5} to 200×10^{-5} mmHg. The hydrogen pressure in the vessel was controlled whenever it was necessary. The temperature of the vessel remained at room temperature throughout the experiments.

The hydrogen in the balloon was compressed by a diffusion pump into a sampling bulb of one liter up to about 0.1 mmHg and analyzed with a Consolidated Electrodynamics Corporation mass-spectrometer model 21-401.

Results and Discussion

Electron Diffraction Method. — All the diffraction patterns obtained consisted of diffused lines, presumably because the deposits were too fine crystalline or amorphous. Therefore, this method was not used for identification of the products.

Indirect Method. — Results obtained are given in Table IV*, representing the composition in form of WO_x. It is evident from this table that the compositions are about $WO_{2.80}$ independent of filament temperatures, pressures of water vapor and hydrogen pressures. The colors of all the deposits were blue by transmitted light.

From the color and composition the deposits seem to be composed of some of the following oxides[7,8] or hydroxides[9-11] of tungsten, e. g., β-($WO_{2.9}$) and γ-($WO_{2.72}$) for oxide and $H_{0.1}WO_3$, $H_{0.33}WO_3$ and $H_{0.5}\cdot WO_3$ for hydroxide. These are blue or violet, respectively, and have compositions close to those of the blue deposits, (hydroxide has the apparent composition of $WO_{2.95}$, $WO_{2.83}$ and $WO_{2.75}$ respectively, if determined by means of the indirect

* Tables, figures and equations in the present paper are numbered after those of the previous papers.

7) O. Glemser and H. Sauer, *Z. anorg. u. allgem. Chem.*, **252**, 144 (1943).

8) A. J. Hegedüs, T. Millner, J. Neugebauer and U. Sasvari, ibid., **281**, 64 (1955).

9) O. Glemser and C. Neuman, ibid., **265**, 288 (1951).

10) O. Glemser, U. Hauschild and G. Lutz, ibid., **269**, 93 (1952).

11) F. Ebert and H. Flasch, ibid., **226**, 65 (1935).

TABLE IV

Temp. of filament K°	Initial press. of H_2O mmHg$\times 10^5$	Press. of H_2 in vessel mmHg$\times 10^5$	Net weight loss of filament mol.$\times 10^6$	Amount of H_2 produced mol.$\times 10^5$	Composition	Gas. product mass No. %
1480	176	2	3.96	1.11	$WO_{2.81}$	
1580	63	2	4.04	1.12	$WO_{2.78}$	
1580	179	5	4.22	1.19	$WO_{2.82}$	
1700	63	6	4.59	1.28	$WO_{2.79}$	
1700	200	16	4.86	1.35	$WO_{2.77}$	28 0.4% 32 —
1730	103	8	3.89	1.09	$WO_{2.80}$	
1730	103	9	5.17	1.46	$WO_{2.83}$	
1730	103	127	5.56	1.55	$WO_{2.79}$	
1800	103	11	5.07	1.43	$WO_{2.82}$	
1900	103	16.5	7.00	1.97	$WO_{2.82}$	
1950	103	24	3.88	1.09	$WO_{2.81}$	
1950	103	24	7.94	2.20	$WO_{2.78}$	

method). It is known that these oxides are formed by reduction of WO_3 with hydrogen and the hydroxides by reduction of WO_3 with atomic hydrogen.

The following two processes may be considered for the production of the blue deposit:

1) the product vaporizes from the filament as a blue compound to make a blue deposit on the wall.

2) the product vaporizes from the filament as trioxide and its colorless deposit is secondarily reduced on the wall to form a blue deposit.

The process, by which the deposit was, produced was studied by vaporizing γ-oxide from the filament in high vacuum. When a tungsten filament was heated at 700°C in about 0.01 mmHg pressure of oxygen, a dark violet layer of γ-oxide[12] was formed on the filament. After forming a certain thickness of the layer, excess oxygen was evacuated and the filament was heated above 1500°K. Then the oxide layer vaporized from the filament and made a deposit on the wall of the vessel. The experiments were carried out at various thicknesses of deposit up to about 1000 Å and vaporizing temperatures up to about 2200°K. It was found that the deposits produced were always colorless regardless of the thickness of the deposit and the vaporizing temperature and the blue deposit was not formed at all. The thickness was estimated from the amount of oxygen combined with the filament to make γ-oxide. It was found experimentally that deposit of about 100 Å thick was detectable as a blue film when it was formed by the reaction of water vapor with tungsten. Blackburn[13] has found that WO_2 decomposed completely to W and WO_3 above 1300°K and made WO_3 deposit on the wall. γ-Oxide and probably β-oxide, too, would behave similarly. Hydroxides are not likely to vaporize from the filament as they are. $H_{0.5}WO_3$ is known[9] to decompose into $WO_{2.9}$, hydrogen and water vapor above 60°C. Other hydroxides seem to behave in a similar manner, although their thermal stability is not known. As a result, it is probable that the blue deposit was formed not primarily by the deposition of blue compounds, but secondarily by the reduction of a colorless deposit of WO_3 with hydrogen on the wall.

As for the reduction, the following facts are known in the present stage of research. It is evident that the reduction was not carried out with hydrogen in gas phase, because the composition of the deposit and the reaction rate[6] were independent of the hydrogen pressure in the vessel. Accordingly, the reduction should be carried out with hydrogen liberated by the reaction of water vapor with tungsten. The hydrogen would contain the molecules excited in the electronic or the vibrational energy and even the atoms, if generated. These will be discussed in a subsequent paper.

The independence of the composition $WO_{2.80}$ of deposit upon the filament temperatures and others mentioned above may be due to the fact that the reduction rate becomes smaller at the lower oxidation state. The reduction rate was studied by means of a static method by heating

12) H. Hashimoto, K. Tanaka and E. Yoda, *J. Electron-Microscopy*, **6**, 8 (1958).

13) P. E. Blackburn, M. Hoch and H. L. Johnston, *J. Phys. Chem.*, **62**, 769 (1958).

a tungsten filament in hydrogen within a reaction vessel whose wall had been covered with WO_3 deposit formed by heating the filament in a definite amount of oxygen. The hydrogen pressure was measured as a function of the heating time of the filament and the extent of reduction was determined from the pressure decrease of hydrogen. Two examples are shown in Fig. 10, where the filament

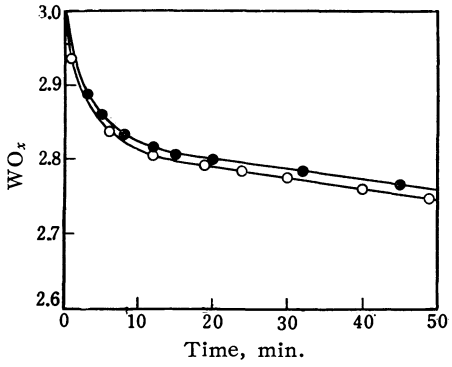


Fig. 10. Reduction of WO_3 with atomic hydrogen.
● 100 Å, 100×10^{-4} mmHg
○ 50 Å, 50×10^{-4} mmHg

temperature was 1740°K and the thickness of WO_3 was about 50 and 100 Å, respectively, and the initial pressure of hydrogen was 50×10^{-4} and 100×10^{-4} mmHg each. It is evident from the figure that the reduction proceeds swiftly down to about $WO_{2.80}$ but the rate slows down appreciably at the lower oxidation state. It is obvious in these experiments that the reduction is carried out mainly with atomic hydrogen formed from the molecules by the dissociation in contact with the filament, and not with hydrogen molecules which rebound from the filament, because the mean temperature of rebounding molecules is about 280°C (for the filament temperature of 1740°K) which is too low to reduce WO_3, since the accomodation coefficient of hydrogen on tungsten surface is 0.19[14].

Result of analysis of hydrogen is shown in Table IV. Only a small amount of gas of mass number 28, presumably carbon monoxide formed from carbon in the filament and water vapor, is contained. The fact that oxygen was not detected in hydrogen suggests that WO_3 was formed by a direct reaction of water vapor with tungsten and not by the reactions through the thermal decomposition of water vapor

$$2H_2O \rightarrow 2H_2 + O_2$$
$$W + 3/2O_2 \rightarrow WO_3$$

If oxygen was liberated, a part of it would leave the vessel without reacting with the filament and be introduced into the balloon, and a part would react with the filament to form WO_3 deposit. The ratio of the former oxygen to the latter can be evaluated by the kinetic theory of gases as follows; the quantity in moles of oxygen which leaves the vessel per second is given similar to Eq. 12 by

$$A'\bar{B}''P'' \qquad (13)$$

where $A'\bar{B}''$ is a constant determined experimentally and P'' the partial pressure of oxygen in the vessel. While the quantity which reacts with the filament per second is given similar to Eq. 2 by

$$k''SB''P'' \qquad (14)$$

where k'' is the reaction probability of oxygen with tungsten. From these formulae, the ratio is calculated as a function of filament temperature as shown in Table V, where values of k'' are determined experimentally by using a filament taken from the same spool. It is evident that if WO_3 was formed by a reaction of gaseous oxygen with tungsten at 1700°K, oxygen had to be detected by the mass spectrometer which was able to detect 0.1% oxygen in hydrogen.

TABLE V

Temp. of filament °K,	1600	1700	1800	1900
Ratio	1.7	1.1	0.64	0.51

Summary

1) Reaction product vaporizes from the filament as tungsten trioxide and its colorless deposit is reduced with hydrogen liberated by the reaction. Consequently, the blue deposit having the mean apparent composition of $WO_{2.80}$ can be obtained.

2) The WO_3 deposit is reduced readily with atomic hydrogen down to $WO_{2.80}$, but the reduction rate becomes appreciably slower at the lower oxidation state.

3) Oxygen is not contained in hydrogen. This suggests that WO_3 is not formed by a reaction of tungsten with gaseous oxygen liberated by thermal decomposition of water vapor, but is formed directly by a reaction of tungsten with water vapor.

The author wishes to express sincere thanks to Professor N. Sasaki of Kyoto

14) I. Langmuir, *J. Am. Chem. Soc.*, **38**, 1145 (1916).

University and Professor K. Kodera of Kyoto Technical University for their kind discussions and encouragement, to Messrs. R. Ueda and T. Makita of Kyoto University for electron diffraction and mass spectrometer, respectively, and to Mr. T. Naiki of Kyoto Technical University for electron diffraction.

Department of Chemistry
Faculty of Industrial Art
Kyoto Technical University
Sakyo-ku, Kyoto

Crystallinity Studies of Polychlorotrifluoroethylene by the Infrared Method. II. Kinetics of the Crystallization

By Hiroshi MATSUO

(Received April 30, 1959)

The isothermal rate of spherulitic growth of polychlorotrifluoroethylene (PCTFE) was studied by Price[1] by direct microscopic observation. He observed, however, that there was an ordering process, detectable by X-rays, which developed much more rapidly than did the spherulites. Allen[2] also suggested that there would be no necessary simple connection between the rate of growth of a spherulite and the rate of change of density. On the other hand, Morgan[3] and Flory[4] demonstrated that spherulitic growth was a true measure of the crystallization rate in the cases of polyethylene terephthalate and polydecamethylene sebacate, respectively.

In the preceding paper[5] it was shown that the infrared method was available for reliable estimates of crystallinity in PCTFE, completely independent of other methods. Furthermore, this method is responsive to crystallinity changes taking place rapidly. The investigation reported in the present paper was undertaken with the objective of measuring the isothermal rate of crystallization and to understand the crystallization kinetics of PCTFE by employing this technique. These results were discussed, comparing them with those obtained by other methods.

Experimental

The crystalline band at 440 cm^{-1} of the infrared spectrum was used to follow the production of crystalline material as the crystallization proceeded.

To determine the isothermal rate of crystallization, a procedure was used similar to that used by Reding and Brown[6] to measure the rate of crystallization of polyethylene. Two ovens, one directly over the other, were mounted on a Perkin-Elmer Model 112 infrared spectrometer with potassium bromide optics. The ovens were separately controlled; the upper oven was heated to 230°C of melting temperature and the lower one was heated to any desired growth temperature between 190 and 170°C by circulating a rapid stream of air through an insulated duct from the heaters. A calibrated thermocouple inserted in the lower oven very close to the sample led to a recorder-controller. The controller served to keep the growth temperature within the accuracy of ±0.5°C.

A thin film (0.03~0.06 mm. thick) of commercial PCTFE (NST 270) was clamped in a thin metal holder and placed in the upper oven. After five minutes at 230°C the sample holder was dropped into the lower oven so that it was in the path of the infrared radiation. The melt sample was estimated to reach the desired growth temperature in less than ten seconds. Since the spectrometer was responsive to changes taking place in three seconds or more, this technique proved adequate to follow the crystallization at high rates.

Results

The crystallized fraction of the sample was calculated from the experimental curves. Measurements of the rate of crystallization were carried out at temperatures between 174 and 190°C. Fig. 1 is

1) F. P. Price, *J. Am. Chem. Soc.*, **74**, 311 (1952).
2) P. W. Allen, *Trans. Faraday Soc.*, **48**, 1178 (1952).
3) L. B. Morgan, *Phil. Trans. (London)*, **A247**, 23 (1954).
4) P. J. Flory and A. D. McIntyre, *J. Polymer Sci.*, **18**, 592 (1955).
5) H. Matsuo. ibid., **25**, 234 (1957); This Bulletin, **30**, 593 (1957).
6) F. P. Reding and A. Brown, *J. Appl. Phys.*, **25**, 848 (1954).

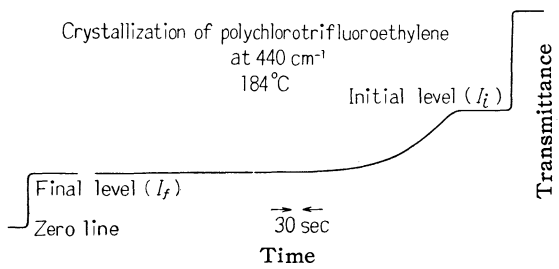


Fig. 1. Typical experimental record.

a typical experimental record obtained in this manner at 184°C. The optical density at time t is defined as

$$D_t \log = (I_i/I_t)$$

Similarly, obtical densities at final and initial states of the crystallization process are obtained by

$$D_f = \log(I_i/I_f), \quad \text{and} \quad D_i = 0$$

The continuously determined data for one curve at each growth temperature were plotted to form Fig. 2. The sigmoid-shaped curves seem to indicate that the crystallization process consists of an induction period, an intermediate period of accelerating rate of crystallization, and a final period to approach an equilibrium state. The degree of crystallinity of the sample, which completed the crystallization process, was measured by the infrared method[5] at room temperature. It is shown in Fig. 3.

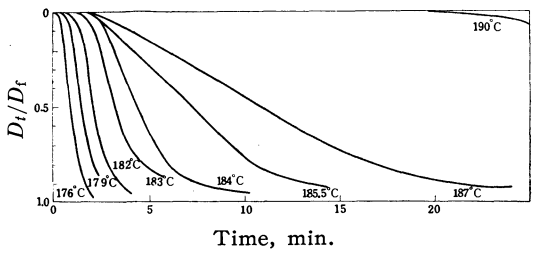


Fig. 2. Ratio of optical density at time t to that at completion of the process, plotted against t at various growth temperatures.

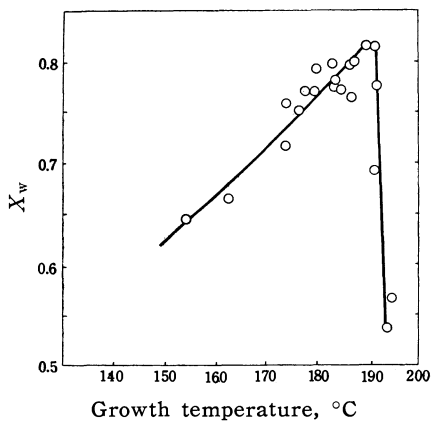


Fig. 3. Degree of crystallinity at completion of crystallization vs. growth temperature.

Discussion

In general, it is found[7] that

$$\ln(V_f - V_t)/(V_f - V_i) = (-1/X_w)kt^n \quad (1)$$

where V_t, V_f and V_i denote the specific volumes at time t, final and initial states of the crystallization process, respectively. X_w is the degree of crystallinity at the completion of the process, and k is the crystallization rate constant. Since the proportionality between the optical density of 440 cm^{-1} and the specific volume for the crystallization process of the polymer is known[5], Eq. 1 becomes

$$\ln(D_f - D_t)/D_f = (-1/X_w)kt^n \quad (2)$$

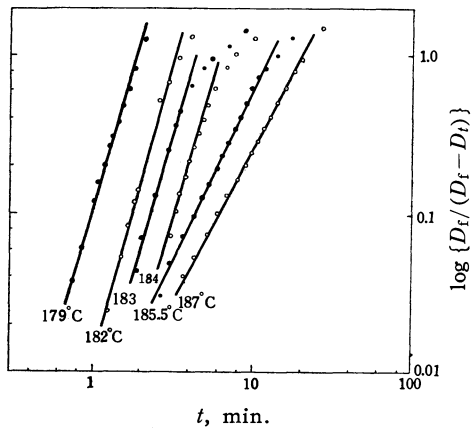


Fig. 4. Plot of log log $[D_f/D_f - D_t)$ vs. log t.

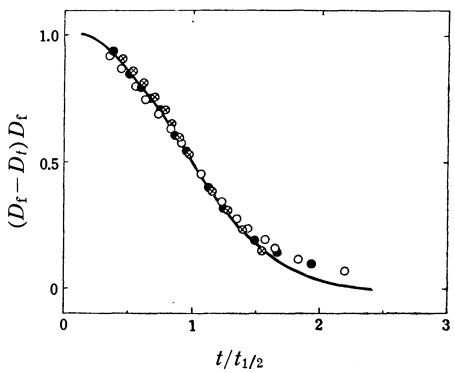


Fig. 5a. Superposition of isotherms at 188°C (⊗); 187°C (○); 185.5°C (●) to Eq. 2 for $n=2.2$.

7) L. Mandelkern, ibid., **26**, 443 (1955); *Chem. Revs.*, **56**, 903 (1956).

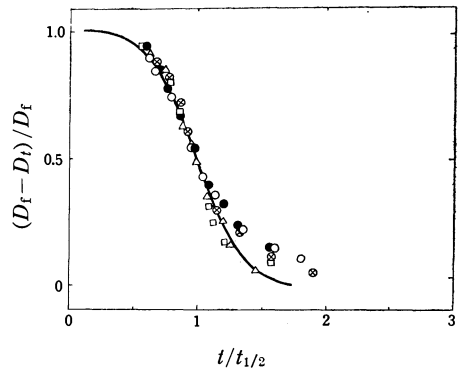


Fig. 5b. Superposition of isotherms at 184°C (●); 183°C (○); 182°C (⊗); 179°C (△); 178°C (□) to Eq. 2 for $n=3.4$.

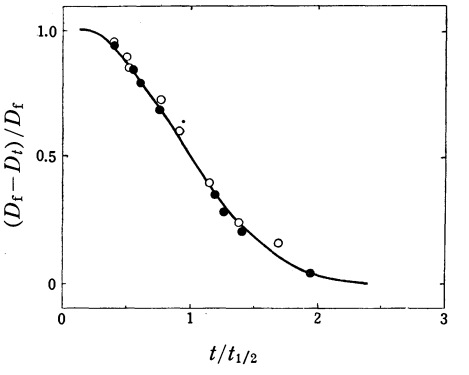


Fig. 5c. Superposition of isotherms at 176°C (●); 174°C (○) to Eq. 2 for $n=2.2$.

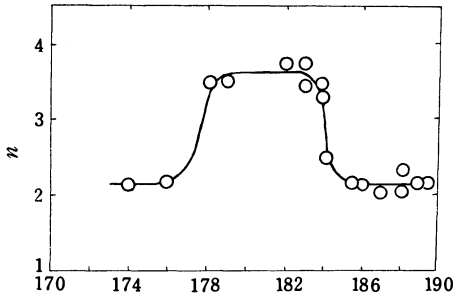


Fig. 6. Values of n at various growth temperatures.

By plotting ln $\ln(D_f-D_t)/D_f$ against ln t, the value of n can be obtained from the slope of the resultant straight line in Fig. 4. In Fig. 5 typical isotherms are plotted according to Eq. 2, where the half time $t_{1/2}$ indicates that the time at $D_t=1/2\,D_f$. The solid lines represent the theoretical isotherms. Good agreement can be obtained for the early stages of the process, but as the crystallization proceeds, the calculated amount of crystallinity is systematically greater than the observed.

The experimental values of n at various growth temperatures are plotted in Fig. 6. The value of n in Avrami's analysis[8] is dependent upon the type of crystallites in nucleation and growth as Table I shows.

TABLE I

Type of growth	Type of nucleation	n
spherical	homogeneous	4
disk	homogeneous	3
spherical	heterogeneous	3
disk	heterogeneous	2

It is, therefore, conceivable that at the growth temperature between 190 and 185°C the nucleation process will be promoted by any heterogeneities which are present in the melt. A fixed number of stable nuclei are present and subsequent transformation is a consequence only of the disk-type lineal growth of these centers. At the growth temperature between 184 and 178°C the nucleation process will be mainly governed by homogeneous nucleation. Price[1] observed by the microscopic method that at temperatures between 190 and 175°C the spherulites are heterogeneously nucleated, and at 170°C and below they are both heterogeneously and homogeneously nucleated. The difference in the results obtained by Price and the present method will be mainly due to the differences in molecular weight, thickness, form of the sample, and in the melting temperature and time, just as has been pointed out in the case of polyethylene terephthalate[3]. In this experiment samples could not be preserved physically as films at higher melting temperatures for a long time prior to the initiation of the crystallization process. Therefore, it will be difficult to say whether the variation of the exponent n with growth temperature is an inherent property of the polymer or not. Very recently, Hoffman[9] indicated that crystallization of the polymer is a results of one-dimensional growth of primary nuclei that are born at later and later dates, and that no obvious relation exists between the growth of primary nuclei and that of spherulites. Furthermore, he pointed out that the polymer has to be heated to the vicinity of 305°C prior to crystallization so as to destroy virtually all of the embryos in the crevices of the heterogeneities.

8) M. Avrami, *J. Chem. Phys.*, **7**, 1103 (1939); **8**, 212 (1940); **9**, 177 (1941).

Next, the temperature coefficient of the crystallization rate was examined. In the vicinity of $T_m(\Delta T=25-30°C)$ the growth rate of crystallites shows a great negative temperature coefficient, in contradiction to the concept of growth controlled by diffusion. The fact leads to the concept of growth governed by secondary nucleation at the spherulite surface[4]. Accurate measurement of the rate of crystallization in the lower growth temperature range was prevented by the rapid onset of crystallization as the material was cooled from the melt through the temperature region of the maximum rate of crystallization, however short the time spent there. It will be, however, expected by Fig. 7 that the maximum rate of crystallization of the polymer locates at a lower temperature near 170°C[9].

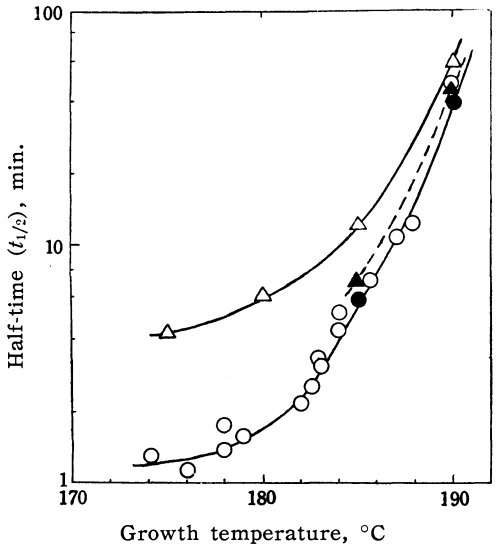


Fig. 7. Half-time vs. growth temperature.
(○) obtained by the infrared method (NST 270);
(●) obtained by the density method (NST 270);
(▲ and △) obtained by the microscopic method (NST 240 and 300).

Considering the formation of disk nuclei of fixed thickness which possess only lateral surface energy, the free energy, ΔF_d, can be expressed as

$$\Delta F = 2\pi rl\sigma - \pi r^2 l\Delta f_0 \qquad (3)$$

where σ is the interfacial free energy per unit area for the cylindrical surface, and Δf_0 is the bulk free energy of fusion per unit volume. Maximizing Eq. 3 with respect to r and equating Δf_0 to $(\Delta T/T_m)\Delta h_u$, where Δh_u is the heat of fusion per unit volume of repeating unit, there is obtained

$$\Delta F^* = (\pi l\sigma^2/\Delta h_u)(T_m/\Delta T) \qquad (4)$$

The rate of nucleation in condensed systems may be expressed by

$$A = A_0 \exp(-E/kT - \Delta F^*/kT) \qquad (5)$$

Furthermore, assuming the growth to be mainly diffusion controlled, then

$$G = G_0 \exp(-E/kT) \qquad (6)$$

Therefore, the rate constant may be expressed[10]

$$k = k_0 \exp\{-3E/kT - (\pi l\sigma^2/H_u)T_m/\Delta T \cdot kT\} \qquad (7)$$

Over the small temperature range of the present experiments the pre-exponential factor may be considered to remain constant, then

$$\log k = A - B(T_m/\Delta T \cdot T) \qquad (8)$$

The plot of $\log k$ against $T_m/T \cdot T$ is shown in Fig. 8. Here the melting point of the polymer is taken as 215°C and the values of k in the microscopic method[1] are calculated by

$$k = \frac{4}{3}NS^3$$

where N is the number density and S is the growth rate of spherulites. In this

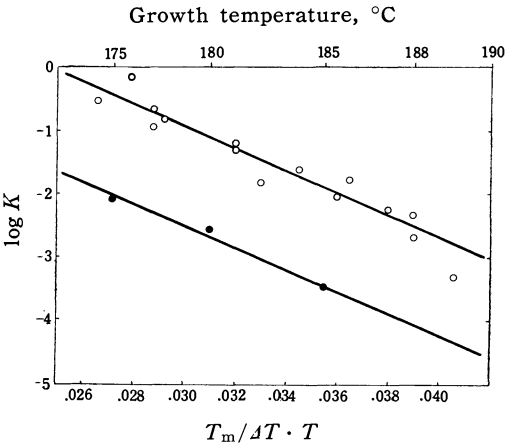


Fig. 8. Plot of $\log k$ vs. $T_m/\Delta T \cdot T$.
(○) obtained by the infrared method;
(●) obtained by the microscopic method.

9) J. D. Hoffman of the National Bureau of Standards, private communications.

10) M. Takayanagi and T. Yamashita, *J. Polymer Sci.*, 22, 552 (1956).

figure the results obtained by both the microscopic and the infrared methods can be approximated by straight lines which indicate the same negative temperature coefficient.

Finally, the effect of melting temperature on the rate of crystallization of the polymer was examined by the present method. After samples had been maintained at different melting temperatures (273~210°C) for five minutes, the half-times of crystallization at 188, 187 and 183°C were measured. They are shown in Fig. 9. The increase in the rate of

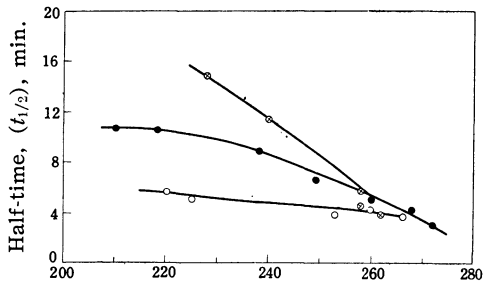


Fig. 9. Half-times as a function of melting temperature for crystallizations at 188°C (⊗), 187°C (●), and 183°C (○).

crystallization with an increase of the melting temperature was indicated contrary to the cases of Nylon 66[2] and polyethylene terephthalate[3]. The fact had been explained by Price[1] as due to degradation of the polymer at a higher melting temperature. Recently, thin films of the polymer of NST 300 and 290 were supplied. The average molecular weight of the polymers were estimated to be approximately 81,000 and 78,000, respectively. Using these samples the half-time of crystallization at 183°C and the degree of crystallinity at the completion of the crystallization process were measured. The half-times were 4.6 and 7.4 min., respectively; the degree of crystallinity at the completion of the crystallization process were 74 and 64%, respectively. It will be expected that both the rate of crystallization and the degree of crystallinity at the completion of the crystallization process increase as the molecular weight of the polymer decreases.

Summary

The isothermal rate of crystallization in polychlorotrifluoroethylene was measured at temperatures ranging from 172 to 190°C below the melting point by following the change of observed absorbance of crystalline band at 440 cm^{-1}. The isothermal rate of crystallization and apparent induction time are dependent on temperature. The data on the kinetics of the crystallization are compared with the result of Avrami's analysis. At temperatures between 190 and 185°C the nucleation process will be promoted by heterogeneities which exist in the melt. Between 184 and 178°C it will be mainly governed by homogeneous nucleation.

Electrical Communication Laboratory
Nippon Telegraph and Telephone
Public Corporation
Musashino-shi, Tokyo

Ultraviolet Absorption Spectra of Substituted Phenylureas

By Yojiro TSUZUKI, Shinichi MOTOKI and Kazuko MIGITA

(Received April 30, 1959)

Dulcin(*p*-ethoxypenylurea) has been a well known substance as one of the strongest sweetening agents, whereas the ortho isomer is tasteless and the *m*-ethoxyphenylurea rather bitter.

In an earlier work on the sweetness of organic compounds one of the authors has pointed out that the sweetness of aromatic compounds is closely related to the resonance structures, and has shown that the greater the sweetness of the compound, the greater is the resonance energy[1]; thus, the resonance energy in dulcin isomers decreases in the order of $p>o>m$.

Since the ethoxy group, being associated with the carbamide group, would contribute to the resonance stabilization of the molecule in different ways to cause electronic effects according to the relative position of the two groups, the mode of the resonance in these compounds could be analyzed, provided the electronic nature of the carbamide group is elucidated. The purpose of this paper is to obtain whatever information is possible on these problems.

As is well known the ultraviolet absorption spectrum of benzene exhibits the characteristic peaks at 203.5 mμ (K-band, $\varepsilon=7400$) and 240~260 mμ (B-band, $\varepsilon=250$). When a substituent is introduced into the nucleus, both of the absorption bands are displaced towards the region of longer wavelengths owing to the resonance attributed to the conjugation of the substituent with the nucleus. In disubstituted benzenes the following semiquantitative relations have been established by Doub and Vandenbelt[2,3] between the absorption displacement and the electronic properties of the two groups, thus:

1. In the absorption spectrum of the disubstituted benzenes, one substituent of which is electron-attracting and the other electron-releasing.

a) The absorption shift of the 203.5 mμ band of benzene is, in the case of *p*-compounds ($\Delta\lambda$), considerably greater than the sum of those of the corresponding monosubstituted compounds ($\Delta\lambda_1+\Delta\lambda_2$), namely,

$$\Delta\lambda \gg \Delta\lambda_1+\Delta\lambda_2$$

Example:

	p-$H_2N\cdot C_6H_4\cdot NO_2$		$C_6H_5NO_2$		$C_6H_5NH_2$
λ_{max} (mμ)	381		268.5		230
$\Delta\lambda$ (mμ)	177.5	$\gg$	65	+	26.5
	$\Delta\lambda$		$\Delta\lambda_1$		$\Delta\lambda_2$

b) As to the orientation effect, the following order of red-shift is observed:

$$\lambda_{max}\ p>o>m$$

Example:

$H_2N\cdot C_6H_4\cdot NO_2$	p	o	m
K-band	381	282.5	280
B-band	—*	412	358

2. In the spectra of disubstituted benzenes the groups of which are both electron-attracting or both electron-releasing.

a) In the case of *p*-compounds:

$$\Delta\lambda<\Delta\lambda_1+\Delta\lambda_2$$

Example:

p-$NO_2\cdot C_6H_4\cdot CO_2H$	$C_6H_5NO_2$		$C_6H_5\cdot CO_2H$
$\Delta\lambda$ (mμ) 55	<	65	+ 26.5

b) In the case of nuclear isomers:

$$\lambda_{max}\ p>m>o$$

Example:

$H_2N\cdot C_6H_4\cdot NH_2$	p		m		o
K-band	245	>	240	>	233
B-band	320	>	289	$\geqq$	289

3. In the spectra of disubstituted benzenes, one substituent of which is a halogen atom or a methyl radical.

a) In the case of *p*-compounds:

$$\Delta\lambda \geqq \Delta\lambda_1+\Delta\lambda_2$$

This relation always holds, regardless of whether the electronic property of the other substituent be electron-attracting or electron-releasing.

b) In the case of three isomers:

$$\lambda_{max}\ p>m>o$$

1) Y. Tsuzuki, S. Kato and H. Okazaki, *Science [Japan] (Kagaku)*, **24**, 523 (1954).
2) L. Doub and J. M. Vandenbelt, *J. Am. Chem. Soc.*, **69**, 2714 (1947).
3) L. Doub and J. M. Vandenbelt, ibid., **71**, 2414 (1949).

* The absorption corresponding to the B-band often disappeared with *p*-compounds.

Few exceptions have been, however, found in this case.

On the basis of these empirical rules, one might determine, by means of spectroscopy, the stabilization due to resonance in disubstituted benzenes and the electronic effect of the substituent.

In the present investigation several substituted phenylureas containing various substituents of typical electronic nature such as NO_2, EtO, CH_3, Br were prepared and the spectra of these compounds were measured for the purpose of determining the electronic effect of the carbamide group and comparing with each other the magnitudes of the resonance of the nuclear isomers of dulcin.

Results and Discussion

The experimental results are shown in Table I.

TABLE I. ULTRAVIOLET ABSORPTION SPECTRA OF SUBSTITUTED PHENYLUREAS ($R \cdot C_6H_4 \cdot NHCONH_2$)

Substituent R	K-band		B-band	
	λ_{max}	ε_{max}	λ_{max}	ε_{max}
o-NO_2	275	4350	365	3260
m-NO_2	270	5130	338	1660
p-NO_2	322	13200	—	—
o-EtO	241	15400	281	3830
m-EtO	240.5	13500	280	2550
p-EtO	242	18200	290	1980
o-CH_3	236	10400	270	660
m-CH_3	240	17600	277	770
p-CH_3	240	18400	281	1090
p-Br	247	25300	276	1370

Table II is given to see how the above stated relations are applicable to the present results. It is seen from this table that the absorption maxima of the three isomers $EtO \cdot C_6H_4 \cdot NHCONH_2$ appear in the order of $p>o>m$ for both K- and B-bands. The results may be interpreted as indicating the resonance energy decreasing in the order $p>o>m$, which shows that the carbamide group is electron-attracting. The conclusion is well in accordance with the tentative theory of the relation between the sweetness and the resonance. On the other hand, the slight resemblance of the spectra of nitrophenylureas to those of nitroaniline rather leads us to a somewhat opposite conclusion that the carbamide group is slightly electron-releasing.

TABLE II. ANALYSIS OF ABSORPTION DATA

a) *p*-Substituted phenylureas

p-$R \cdot C_6H_4 \cdot NHCONH_2$

Substituent R	Relation				
	$\Delta\lambda$	>	$\Delta\lambda_1$**	+	$\Delta\lambda_2$
NO_2	118.5	>	33.5	+	65
	$\Delta\lambda$	<	$\Delta\lambda_1$	+	$\Delta\lambda_2$
EtO	38.5	<	33.5	+	16
	$\Delta\lambda$	=	$\Delta\lambda_1$	+	$\Delta\lambda_2$
CH_3	36.5	=	33.5	+	3
	$\Delta\lambda$	>	$\Delta\lambda_1$	+	$\Delta\lambda_2$
Br	43.5	>	33.5	+	6.5

b) Nuclear isomers of substituted phenylureas

Substituent R	Relation	
	K-band	B-band
NO_2	$p>o>m$	$o>m$
EtO	$p>o>m$	$p>o>m$
CH_3	$p=m>o$	$p>m>o$

It follows therefore that this group is to be regarded as electronically amphoteric, behaving in an electron-attracting or releasing manner, depending on the other group.

Since such a peculiar organic group has never been known in the chemical literature, further investigation is now being made to ascertain the new interpretation of these structural problems, the results of which will be published in the near future.

Experimental

Preparation of Samples. — Commercial dulcin was used after purification by repeated recrystallization from water.

o-Nitrophenylurea was synthesized according to the direction of Arndt[4] with slight modification.

$$o\text{-}NO_2C_6H_4NH_2HCl \xrightarrow[NaOH]{Pb(SCN)_2} (o\text{-}NO_2C_6H_4NHCSNH_2)$$

$$\xrightarrow[-H_2S]{} o\text{-}NO_2C_6H_4NHCN \xrightarrow[HCl]{H_2O} o\text{-}NO_2C_6H_4NHCONH_2$$

The other substituted phenylureas were prepared from potassium cyanate and the corresponding nuclear substituted anilines by the methods given in "Organic Syntheses"[5].

o-Nitrophenylurea, m. p. 183~184°C, the *m*-isomer, m. p. 189°C, the para, m. p. 235°C.

o-Ethoxyphenylurea, m. p. 134°C, the *m*-isomer, m. p. 112°C, the para, m. p. 175°C.

o-Methylphenylurea, m. p. 195°C, the *m*-compound, m. p. 145°C, the para, m. p. 183°C.

p-Bromophenylurea m. p. 220°C.

** Phenylurea has two absorption peaks at 237 mμ (ε=17700) and 266~275 mμ (ε=1100) corresponding to K-band and B-band, respectively. W. A. Schroeder et al., *Anal. Chem.*, **23**, 1740 (1951).

4) F. Arndt, *Ber.*, **46**, 3528 (1913).

5) F. Kurzer, "Organic Syntheses", Vol. 31, John Wiley & Sons, Inc., New York (1951), p. 8.

Absorption Spectra.—The absorption spectra were measured in the region of 200~350 mμ by means of a Beckman Model DU Quartz spectrophotometer with the above samples dissolved in absolute ethanol to the concentration of ca. 1/10,000 mol./l.

Summary

Ultraviolet absorption spectra of several nuclear substituted phenylureas have been measured with the attempt to study the electronic effect of the carbamide group, and the resonance stabilization in three dulcin isomers.

Department of Chemistry
Tokyo College of Science
Kagurazaka, Shinjuku-ku
Tokyo

Analysis of Non-Newtonian Flow by Falling-Sphere Method

By Sadao HIROTA and Masao TAKADA

(Received May 12, 1959)

Thixotropic solution must be handled without any strong agitation in order to obtain so-called "virgin-state viscosity". Neither the capillary nor the rotating cylinder viscometer is suitable for this purpose, while the falling-sphere method is applicable, because (a) the agitation of the sample in this measunement is far less compared with that in other methods, and (b) the sphere always falls contacting with a new, so-called "virgin-state" solution.

In order to devise the falling-sphere method for this purpose it is necessary to obtain general flow curves by this method because the fluidity of these solutions normally shows shear dependence as well as time dependence.

Shear stress S_R at the equator of a sphere was given[1] by

$$S_R = R\Delta\rho g/3 \tag{1}$$

where R is the radius of the sphere and $\Delta\rho$ is the density difference between sphere and fluid. Eq. 1 was later proved to be applicable also to non-Newtonian flow. And a necessary shear stress could be obtained by selecting a sphere of suitable radius.

For Newtonian flow, the shear rate at the equator of the sphere $(du/dr)_R$ followed immediately from Stokes' equation.

$$(du/dr)_R = 3U_0/2R \tag{2}$$

Sheppard[2], however, pointed out that Eq. 2 fails to express the true shear rate in a non-Newtonian nitrocellulose solution. Phipps[3] claimed the necessity of non-Newtonian correction for Eq. 2. Many attempts[4-9] have been made to utilize the falling-sphere method for non-Newtonian systems without success establishing the corrected equation for Eq. 2 so far. The aim of this paper is to find it and to examine its applicability.

In the previous study[10] we obtained empirically

$$(du/dr)_R = (3U_0/2R) \times [1 + 2.4(d\log U_0/d\log R - 2)] \tag{3}$$

adopting the capillary viscometer method as the standard for which a standardized treatment of data had been proposed by Krieger and Maron[11]. In the present study, a similar result has been obtained theoretically.

Theoretical

In Newtonian Flow. — Consider a steady flow around a sphere of radius R falling

1) H. Lamb, "Hydrodynamics", 3rd Ed., Cambridge Univ. Press, London (1906), p. 553.
2) S. E. Sheppard, *J. Ind. Eng. Chem.*, **9**, 523 (1917).
3) H. E. Phipps, *Colloid Symposium Monograph*, **5**, 259, (1928).
4) A. G. Pasynskii and A. I. Ravinovich, *Zhur. Fiz. Khim.*, **5**, 521 (1934); *Chem. Abstr.*, **29**, 7753 (1935).
5) A. De Waele, *J. Rheology*, **2**, 141 (1936).
6) A. K. Skrjabin, *Lief.*, **17**, 7 (1936); cited from Kulakoff's paper.
7) N. N. Kulakoff, *Kolloid-Z.*, **80**, 204 (1937).
8) J. C. Williams and E. I. Fulmer, *J. Appl. Phys.*, **9**, 760 (1938).
9) J. Schurz, *Naturwissenschaften*, **42**, 339 (1955).
10) M. Takada and S. Hirota, *J. Chem. Soc. Japan, Pure Chem. Sec.* (*Nippon Kagaku Zasshi*), **80**, 956 (1956).
11) I. M. Krieger and S. H. Maron, *J. Appl. Phys.*, **25**, 72 (1954).

slowly at the velocity U_0 in a Newtonian fluid. The rate of flow U at the distance r from the center is given[12] by

$$U = -R^3 \Delta\rho g(3+R^2/r^2)\phi/18r \quad (4)$$

Where ϕ = fluidity = 1/viscosity

Differentiating Eq. 4 by r, we obtain the shear rate.

$$du/dr = R^3 \Delta\rho g(1+R^2/r^2)\phi/6r^2 \quad (5)$$

Shear stress S is then

$$S = (du/dr)/\phi = R^3 \Delta\rho g(1+R^2/r^2)/6r^2 \quad (6)$$

At $r=R$, Eq. 6 becomes Eq. 1. Eq. 1 has also been obtained directly from the calculation based on the balance between shear force and gravity without being confined to the Newtonian flow[9]. And Eq. 1 is also applicable to the non-Newtonian flow.

In Non-Newtonian Flow. — Non-Newtonian fluidity $P(S)$ is a function of S. Since the latter is a function of R and r, $P(S)$ may be regarded as a function of R and r.

$$(du/dr)/S \equiv P(S) = F(R, r) \quad (7)$$

If we assume that only the shear rate is responsible for the non-Newtonian anomaly, and that Eq. 6 is still applicable* to the non-Newtonian flow, we may introduce Eq. 6 into Eq. 7.

$$du/dr = R^3 \Delta\rho g(1+R^2/r^2)\cdot F(R, r)/6r^2 \quad (8)$$

Though the form of $F(R, r)$ or du/dr is unknown, the following functional equation holds.

$$U_0 = \int_R^\infty (du/dr)dr = \int_R^\infty R^3 \Delta\rho g(1+R^2/r^2) \times F(R, r)/6r^2 \cdot dr \quad (9)$$

Since non-Newtonian fluidity increases with increasing S in many cases, it increases with increasing R and decreases with increasing r. Therefore, if we assume

$$P(S) \equiv F(R, r) = f(R)\cdot g(r) \quad (10)$$

$f(R)$ is an increasing function of R and $g(r)$ is a decreasing function of r.

Defining apparent fluidity, F_a, analogous to Stokes' equation, as

$$F_a = 9U_0/2R^2 \Delta\rho g \quad (11)$$

and substituting Eqs. 10 and 11 into Eq. 9, we obtain

$$4F_a/3R^3 \cdot f(R) = (1/R^2)\cdot \int_R^\infty g(r)/r^4 \cdot dr + \int_R^\infty g(r)/r^4 \cdot dr \quad (12)$$

which may be differentiated by R to become

$$2F_a/3R \cdot f(R) \cdot [(d\log F_a/d\log R) - (d\log f(R)/d\log R) - 3] = -g(R)/R - \int_R^\infty g(r)/r^2 \cdot dr \quad (13)$$

At $r=R$, since $F(R, R) \propto F_a$**

$$d\log F(R, R)/d\log R = d\log F_a/d\log R = H \quad (14)$$

From Eq. 10

$$\log F(R, R) = \log f(R) + \log g(R) \quad (15)$$

$$H = (d\log f(R)/d\log R) + G \quad (16)$$

where

$$G = d\log g(R)/d\log R \quad (17)$$

Introducing Eq. 16 into Eq. 13 and differentiating it again by R

$$F(R, R) = 2F_a[(G-1)(G-3) + dG/d\log R]/3(2-G) \quad (18)$$

From Eq. 10

$$(\partial \log P(S)/\partial \log r)_R = (d\log P(S)/d\log S)\cdot(\partial \log S/\partial \log r)_R = d\log g(r)/d\log r \quad (19)$$

where, from Eq. 6

$$\partial \log S/\partial \log r = [2r^2/(r^2+R^2)] - 4 = -3 \quad (\text{at } r=R) \quad (20)$$

and from Eq. 1, $d\log S_R = d\log R$, then

$$d\log P(S)/d\log S = d\log F(R, R)/d\log R = H \quad (21)$$

$$d\log g(r)/d\log r = d\log g(R)/d\log R = G \quad (22)$$

Substituting Eqs. 20—22 into Eq. 19,

$$\left.\begin{aligned} G &= -3H \\ dG &= -3dH \end{aligned}\right\} \quad (23)$$

Thus, Eq. 18 becomes

$$F(R, R) = F_a(1+4H+3H^2-dH/d\log R) \times [1-(3H/2)+(3H/2)^2\cdots\cdots] \quad (24)$$

There is an empirical fact that, for many non-Newtonian fluids, the slope of a plot of $\log F_a$ vs. $\log R$ is constant over a wide range of shear stress and is usually small as compared with unity. For example, $H=0.143$ in 1% NaCMC aq. (MW.$=8\times10^4$, Deg.Eth.$=0.654$) as in Fig. 1.

12) Derived from, for example, B. Fujimoto, "Ōyō Ryutairikigaku (Applied Fluid Dynamics)", Maruzen Co., Ltd., Tokyo (1941), p. 340.

* Discussion on the applicability will be given in another paper.

** This proportionality follows from Krieger-Maron's relation, $P(S)=F_a[1+\Delta(S)]$, where $\Delta(S)$ has been known to be constant over a wide range of S[11].

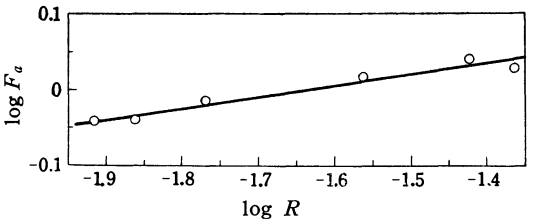


Fig. 1. Plot of $\log F_a$ vs. $\log R$ for 1% NaCMC. aq. (MW.$=8\times10^4$, Deg. Eth.$=$ 0.654) by falling sphere method at 25°C.

Thus,

$$\left.\begin{aligned} &\mathrm{d}\log F_a/\mathrm{d}\log R = H = \text{const.} < 1 \\ &\mathrm{d}H/\mathrm{d}\log R = 0,\ H^3 \fallingdotseq 0,\ H^4 \fallingdotseq 0, \cdots \end{aligned}\right\} \quad (25)$$

Substituting Eq. 25 into Eq. 24, we have

$$F(R,R) \fallingdotseq F_a[1+2.5(\mathrm{d}\log F_a/\mathrm{d}\log S_R) - (3/4)(\mathrm{d}\log F_a/\mathrm{d}\log S_R)^2] \quad (26)$$

or

$$(\mathrm{d}u/\mathrm{d}r)_R \fallingdotseq (3U_0/2R) \times [1+2.5(\mathrm{d}\log U_0/\mathrm{d}\log R-2) - (3/4)(\mathrm{d}\log U_0/\mathrm{d}\log R-2)^2] \quad (27)$$

which agrees very well with the empirical equation (Eq. 3).

Now, using Eqs. 1 and 27, we can obtain the exact flow curve, and hence the true viscosity by the falling-sphere method.

Experimental

For the measurement a glass tube about 20 cm. long and of 2.0 cm. in inside diameter was used, fixed in a thermostat regulated to 25±0.1°C. Glass spheres were made in the manner reported previously[10]. The fall of the sphere (density 2.50) was measured by a stop-watch over a definite distance in the sample. From these data, S_R and $(\mathrm{d}u/\mathrm{d}r)_R$ were calculated by means of Eqs. 1 and 27. Table I gives some examples of data and calculations. Values of $\mathrm{d}\log F_a/\mathrm{d}\log R$ in Table I were obtained from the slope in Fig. 1. The resulting flow curve is shown in Fig. 2.

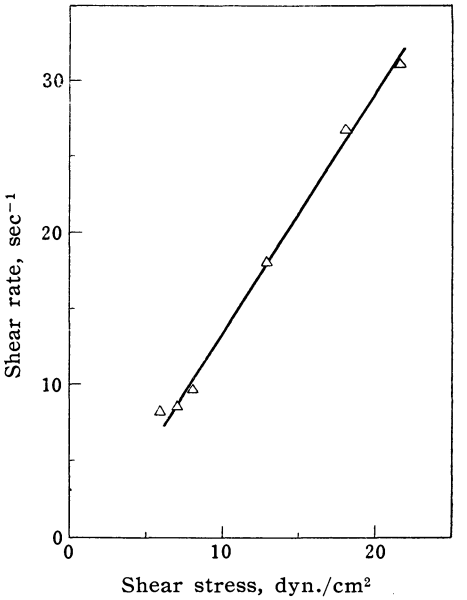


Fig. 2. Flow curve for 1% NaCMC. aq. (MW. 8×10^4, Deg. Eth. 0.654) by falling sphere method at 25°C.

Table I. Falling-sphere method. Data and sample calculations for 1% NaCMC. aq. (MW.$=8\times10^4$, Deg. E.$=0.654$) at 25°C

$R\times10^2$	cm.	4.35	3.78	2.74	1.70	1.37	1.21
S_R	dyn./cm^2	21.35	18.5	13.4	8.36	6.72	5.95
Eq. 1							
U_0	cm./sec.	0.666	0.515	0.250	0.0913	0.0558	0.0435
F_a	l./pois.	1.071	1.10	1.04	0.963	0.908	0.904
$\log F_a$		0.030	0.041	0.017	−0.016	−0.042	−0.044
$\log R$		−1.363	−1.423	−1.563	−1.769	−1.863	−1.917
$\mathrm{d}\log F_a/\mathrm{d}\log R$		0.143	0.143	0.143	0.143	0.143	0.143
$(\mathrm{d}u/\mathrm{d}r)_R$	1/sec.	31.2	27.8	18.6	10.9	8.26	7.30
Eq. 27							

Table II. Samples used for the experiment (Fig. 3)

No.	Solution	Mol. wt.	Deg. eth.	Concn., %
I	Methylcellulose aq.		0.654	1.0
II	NaCMC. aq.	8×10^4	0.654	1.0
III	NaCMC. aq.	8×10^4	0.301	1.0
IV	NaCMC. aq.	$(10\sim12)\times10^4$	0.649	1.0
V	NaCMC. aq.	8×10^4	0.654	1.2
VI	Nitrocellulose in butylacetate			12.0

Results

From Fig. 3 it is seen that the flow curves from the proposed falling-sphere method coincide very well with those from Krieger and Maron's capillary method. The difference between the empirical equation (Eq. 3) and the theoretical one (Eq. 27) is also negligibly small. These results seem to indicate the validity of our formula.

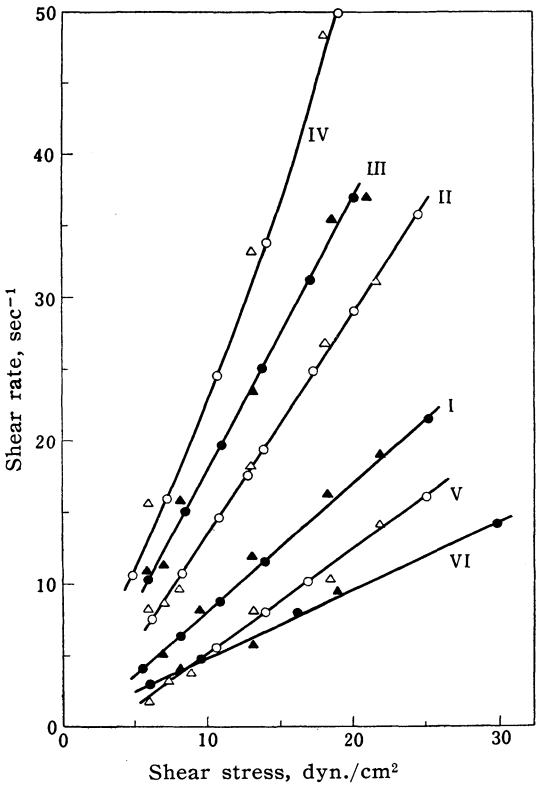


Fig. 3. Flow curves for samples in Table II at 25°C.
Falling sphere method·····▲△
Capillary method ·····●○

Summary

A procedure to obtain a general flow curve by falling-sphere method is presented. The shear stress S_R and shear rate $(du/dr)_R$ at the equator of the sphere are given as

$$S_R = R\Delta\rho g/3$$

$$(du/dr)_R = (3U_0/2R) \times [1+2.5(d\log U_0/d\log R-2) - (3/4)(d\log U_0/d\log R-2)^2]$$

where $\Delta\rho$ is the density difference between sphere and fluid, R the radius and U_0 the falling velocity of the sphere.

The authors wish to express their hearty thanks to Dr. Tsurutaro Nakagawa and Dr. Hirotaro Kambe of the University of Tokyo for their valuable suggestion and discussion and also to Dr. Junzo Shinoda and Dr. Kazuo Miyatake of Daiichi Pharmaceutical Company, Limited for their kind encouragement and permission to publish this paper.

Yanagishima Plant
Daiichi Pharmaceutical Co., Ltd.
Sumida-ku, Tokyo

The Preparation and Properties of N-Salicylideneglycinato-aquo-copper(II), Sodium N-Salicylideneglycylglycinato-cuprate(II) and Related Compounds

By Akitsugu NAKAHARA

(Received May 13, 1959)

It was demonstrated by Eichhorn and Marchand[1] that the coordination of copper(II) ion with the Schiff base produced from salicylaldehyde and glycine results in a stabilization of the >C=N-double bond under conditions that would promote its rupture in the absence of the metal. However, the formation of the copper(II) chelate of salicylideneglycine was observed only in a solution on the basis of a spectroscopic investigation; and the composition of the complex was deduced from an extension of the method of continuous variation to a three component system, copper : salicylaldehyde : glycine. In the present work the same compound, *N*-salicylideneglycinato-aquo-copper(II), **A**, was isolated in the crystalline state and investigated as to its properties. Sodium *N*-salicylideneglycylglycinato-cuprate(II), **B**, was also prepared and investigated as to its structure.

Experimental

Preparation of Copper(II) Chelates.—*N-Salicylideneglycinato-aquo-copper(II).*— To a solution of 6 g. of glycine in 100 ml. water was added 10 g. of salicylaldehyde. The resulting mixture was stirred and heated at about 60°C.

Upon the addition of 16 g. of crystalline cupric acetate, a dark-green solution was formed. A yellowish-green crystalline solid of *N*-salicylideneglycinato-aquo-copper(II) was then gradually deposited within half an hour. The reaction mixture was allowed to cool and filtered by suction. The additional crude product was also obtained by evaporating the filtrate. The yield, in total, was almost quantitative. Recrystallization from a large amount of water gave acicular crystals which decomposed at 240°C.

Anal. Found: C, 32.46; H, 5.39; N, 4.21; H_2O, 26.9. Calcd. for tetrahydrate of **A**: C, 32.60; H, 5.14; N, 4.23; H_2O, 27.2%.

In the above procedure cupric sulfate in place of acetate was observed to give the same result. Furthermore, the same compound was prepared also by reactions between: (1) bis-glycinato-copper(II) and bis-salicylaldehyde-copper(II) in 1:1 molar ratio; (2) bis-glycinato-copper(II) and salicylaldehyde in 1:2 molar ratio; (3) glycine and bis-salicylaldehyde-copper(II) in 2:1 molar ratio.

However, the yield of reaction 2) or 3) was only half of that of 1), since the copper was not sufficient to give the same amount of the product.

The compound is soluble in water, methanol and ethanol, though the solubility is comparatively small, especially in the latter two solvents.

Sodium N-salicylideneglycylglycinato-cuprate(II).— To a solution of 5.3 g. of glycylglycine and 3.2 g. of sodium hydroxide in 100 ml. water was added 8 g. of crystalline cupric acetate. After heating the resulting mixture on a water bath, a deep-blue solution characteristic of copper(II) chelates of peptides was gradually formed. Upon the addition of 5 g. of salicylaldehyde the color of the solution changed to violet. The solution was stirred and heated for thirty more minutes, and was then filtered. The filtrate was concentrated to a small volume and allowed to stand, whereupon beautiful violet needles were obtained. These were recrystallized from their concentrated aqueous solution by adding alcohol or acetone.

Anal. Found: C, 30.69; H, 5.02; N, 6.32; H_2O, 25.8. Calcd. for hexahydrate of **B**: C, 30.81; H, 4.91; N, 6.54; H_2O, 25.2%.

A complete dehydration of the compound was performed by heating the crystals in vacuo at 56°C.

Anal. Found: C, 41.00; H, 3.04; N, 8.89. Calcd. for **B**: C, 41.2; H, 2.81; N, 8.75%.

As described above, an aqueous solution of the compound is violet, but reversibly changes to green in an acid solution.

Potassium salt of the same copper(II) chelate was also obtained in the same way by employing potassium hydroxide instead of sodium hydroxide.

In order to identify the potassium salt, a precipitation of potassium hexanitro-cobaltate(III) was ascertained.

Copper(II) chelate of N-salicylideneglycineethylester.—This compound, **F**, was prepared according to the direction of Pfeiffer et al.[2] by treating the copper(II) complex of salicylaldehyde with hydrochloride of glycineethylester in the presence of sodium acetate in alcohol. It was also confirmed that a reaction in an aqueous suspension between bis-salicylaldehyde-copper(II) and hydrochloride

1) G. L. Eichhorn and N. D. Marchand, *J. Am. Chem. Soc.*, **78**, 2688 (1956).

2) P. Pfeiffer, W. Offermann and H. Werner, *J. prakt. Chem.*, **159**, 313 (1942).

of glycineethylester in the presence of sodium hydroxide is more convenient than the previously reported one[2]. After recrystallization from pyridine or ethanol olive-green crystals were obtained, which decomposed at 200°C, showing a good agreement with the previous datum[2].

Glycylglycinato-aquo-copper(II)[3]. — Freshly precipitated cupric hydroxide was treated in an aqueous suspension with a slight excess of glycylglycine. The resulting deep-blue solution was filtered and concentrated to a small volume, and was then filtered again. The filtrate was allowed to stand for several days over sodium hydroxide, whereupon deep-blue prisms were obtained. These were recrystallized from their concentrated aqueous solution by adding alcohol.

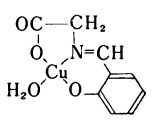
Anal. Found: C, 20.99; H, 4.53; N, 12.09; H_2O, 14.73. Calcd. for monohydrate of **C**: C, 20.85; H, 4.35; N, 12.18; H_2O, 15.65%.

Measurements. — The visible and ultraviolet absorption spectra were determined with a Beckman DU Spectrophotometer at room temperature. The concentration of the solutions varied from 10^{-2} to 10^{-5} F/l.

The infrared spectra were obtained by a Hilger H 800 Infrared Spectrophotometer using a sodium chloride prism. The potassium bromide disk method was employed.

Discussion

The result of analyses and other small tests described in the preceding section afford good reasons to assign structures **A** and **B** for the copper(II) chelate of *N*-salicylideneglycine and that of *N*-salicylideneglycylglycine, respectively. Structure **A** is exactly the same as that postulated by Eichhorn and Marchand[1] on the basis of a spectroscopic investigation. Though they reported also on the formation of 1 : 2 : 2 copper : salicylaldehyde : glycine complex at pH 5, no such compound was isolated in the present investigation even under conditions that would favor its formation. For example, in the case of the reaction between bis-glycinato-copper(II) and salicylaldehyde or between glycine and bis-salicylaldehyde-copper(II) a 1 : 2 : 2 ratio of copper, salicylaldehyde and glycine was employed in a neutral solution, but the reaction product was only the 1 : 1 : 1 complex, **A**. The disagreement might be understood by taking the low solubility of **A** into consideration, since there might be an equilibrium between 1 : 1 : 1- and 1 : 2 : 2-complex in the system.



A

Inspection of the chemical quations of the reactions used in this work reveals that the formation of **A** is accompanied by a liberation of acid:

$$CuSO_4 + C_6H_4\langle^{OH}_{CHO} + NH_2CH_2COOH \rightarrow \mathbf{A} + H_2SO_4$$

$$Cu(CH_3COO)_2 + C_6H_4\langle^{OH}_{CHO} + NH_2CH_2COOH \rightarrow \mathbf{A} + 2CH_3COOH$$

In fact, it was ascertained that the solution was considerably strong acid when the reaction was over. Thus, the present work supports the previous conclusion[1] that the cordination of copper(II) with salicylideneglycine stabilizes >C=N- double bond to such an extent that the Schiff base complex is capable of existence even in acid media, where the uncomplexed Schiff base is dissociated.

It may further be speculated that the tremendous effect of this kind, of metal, may play an important role also in the case of the non-enzymatic transamination reaction of pyridoxal[4-6].

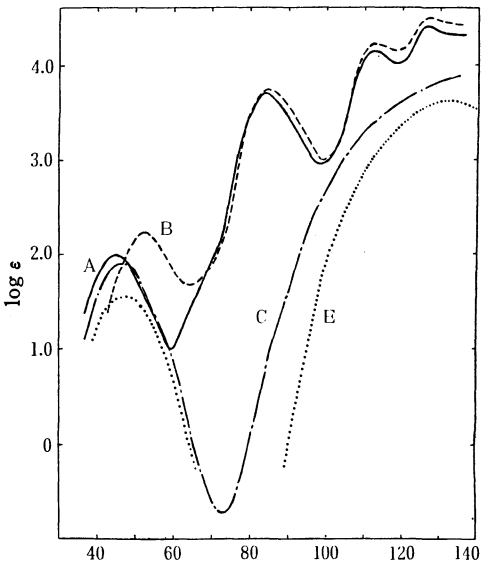


Fig. 1. Visible and ultraviolet absorption spectra of: **A**, *N*-salicylideneglycinato-aquo-copper(II); **B**, sodium *N*-salicylideneglycylglycinato-cuprate (II); **C**, glycylglycinato-aquo-copper(II); **E**, bis-glycinato-copper(II), in aqueous solutions.

3) A. R. Manyak, C. B. Murphy and A. E. Martell, *Arch. Biochem. Biophys.*, **59**, 373 (1955).
4) F. Schlenk and A. Fischer, *Arch. Biochem.*, **12**, 69 (1947).
5) D. E. Metzler, M. Ikawa and E. E. Snell, *J. Am. Chem. Soc.*, **76**, 648 (1954).
6) J. B. Longenecker and E. E. Snell, *Proc. Natl. Acad. Sci.*, **42**, 221 (1956).

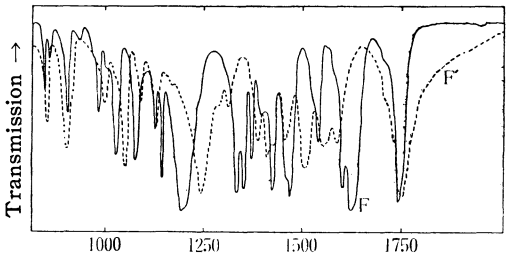


Fig. 2. Infrared absorption spectra of: **F**, copper(II) chelate of *N*-salicylideneglycineethylester; **F'**, hydrochloride of glycineethylester.

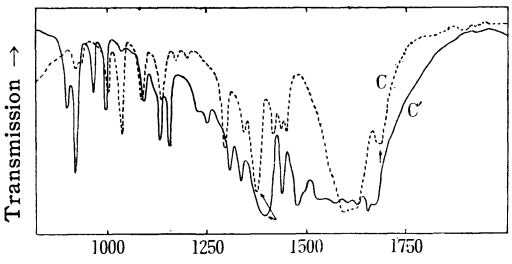


Fig. 3. Infrared absorption spectra of: **C**, glycylglycinato-aquo-copper; **C'**, glycylglycine.

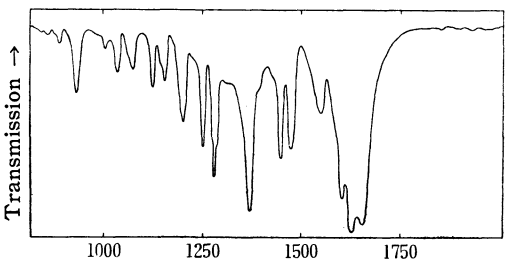


Fig. 4. Infrared absorption spectrum of *N*-salicylideneglycinato-aquo-copper(II), **A**.

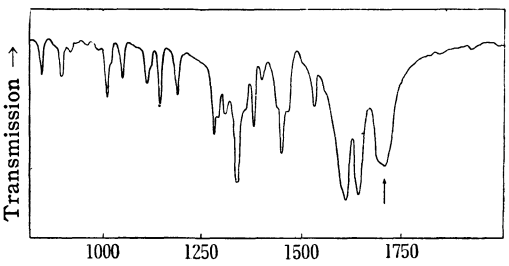
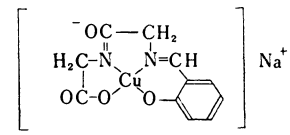


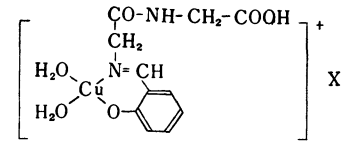
Fig. 5. Infrared absorption spectrum of sodium *N*-salicylideneglycylglycinatocuprate(II), **B**.

Contrary to the case of *N*-salicylideneglycine which is coordinated to copper(II) ion as a terdentate chelate ligand even at a low pH value, *N*-salicylideneglycylglycine behaves as a quadridentate ligand in neutral or basic media and perhaps as a bidentate in acid media.

Formula **B** corresponds to the structure of the copper(II) chelate in neutral or basic media, while **D** would correspond to that in acid media.



B



D

Though there is no decisive reason for the latter the fact that it is green in acid media seems to favor the formula, **D**, in which the peptide nitrogen and carboxylate oxygen are detached from the copper.

As to the process of the formation of **A** the first step may be the coordination of copper(II) with glycinate ion, since a deep-blue solution characteristic of copper(II) chelates of amino acids was first observed before any other marked change occurred, regardless of the methods of preparation employed in this investigation. A chelate ligand in coordination very often increases its reactivity on account of the effect of the metal[7]. Therefore, it may be considered that the glycinate ligand in coordination gains greater activity and becomes easier to form the Schiff base with salicylaldehyde. In contrast with this type of reactions, Sato et al.[8] already reported that bis-glycinato-copper(II) reacts with acetaldehyde in a basic solution to give threonine in a very good yield. The difference between the above two reactions may be attributed to the effect of the -OH group in the molecule of salicylaldehyde.

Visible and Ultraviolet Absorption Spectra.—

7) A. E. Martell and M. Calvin, "Chemistry of the Metal Chelate Compounds", New York Prentice-Hall, Inc., New York (1952) p. 336.

8) M. Sato, K. Okawa and S. Akabori, This Bulletin, **30**, 937 (1957).

TABLE I. ABSORPTION MAXIMA OF COPPER(II) COMPLEXES IN THE VISIBLE REGION

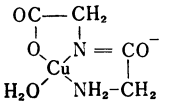
Compounds	Solvent	ν_{max} 10^{13} sec^{-1}	log ε_{max}	Type of complexes with respect to the kind of donor atoms
$CuSO_4 \cdot 5H_2O$*	water	36.5	1.09	40
$(NH_4)_4[CuO_6Mo_6O_{18}H_6] \cdot 5H_2O$*,a)	〃	37.1	1.06	
$[Cusalgly(H_2O)] \cdot 4H_2O$, **A**	〃	45.3	1.98	1 N 30
$CuSO_4 \cdot en \cdot 3H_2O$*	1/4 F en·2HClO$_4$ solution	45.3	1.51	
$[Cugly_2] \cdot H_2O$, **E**	water	48.0	1.54	
$[Cuala_2] \cdot H_2O$	〃	48.8	1.54	
$[Cu(C_5H_{10}O_2N)_2] \cdot 2H_2O$*b)	1/100 F ligand solution	49.5	2.04	2 N 20
$[Cuglygly(H_2O)] \cdot H_2O$, **C**	water	46.5	1.89	
$Na[Cusalglygly] \cdot 6H_2O$, **B**	〃	52.2	2.20	
$[Cu(NH_3)_4]SO_4 \cdot H_2O$*	$(NH_4)_2SO_4 + NH_3$ solution	49.2	1.76	4 N
$[Cuen_2]SO_4 \cdot 2H_2O$*	water	54.0	1.85	

* Reported by H. Ito[9].

a) Ammonium hexa-molybdato-cuprate(II).

b) Di-α-methylamino-isobutyrato-copper(II).

Absorption curves of **A** and **B**, and of the copper(II) chelate of glycine, **E**, and glycylglycine, **C**, are shown in Fig. 1. The curves of **C** and **E** consist of two each

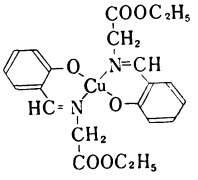


C

of typical absorption bands, whereas both **A** and **B** contain some additional absorption bands in the ultraviolet region. These additional bands apparently belong to the specific absorption bands, being due to the salicylaldimino group of the ligand in coordination. On the other hand, the small absorption bands on each curve in the visible region are the characteristic band of copper(II) complexes. Their numerical data together with those of some other copper(II) complexes are tabulated in Table I. Inspection of Table I reveals that the absorption maximum of **B** is hypsochromically shifted to a considerable degree compared with those of the same type of complexes with respect to the kind of donor atoms. In fact, the color of **B** rather resembles that of bis-ethylenediamine-copper(II) complex, in which all the four donor atoms are nitrogens. From this point of view, it may be supposed[9] that *N*-salicylideneglycylglycinato-cuprate-(II), **B**, belongs to a typical dsp^2-type complex.

Infrared Absorption Spectra. — Infrared absorption curves of **A**, **B**, **C**, and of the copper(II) chelate of *N*-salicylideneglycine-ester, **F**, are shown in Figs. 2—5.

From a comparison of the spectrum of **A** with that of **F**, in which two carboxylate groups of the ligand are protected from coordination by being bound to ethyl groups, it may be concluded that the carboxylate group of **A** is apparently coordinates to copper(II). This is owing to the fact that there is no very strong absorption band in the region of 1700~1740 cm^{-1} on the curve of **A**, contrary to the case of **F**.



E

The carbonyl peak of the carboxylate groups is usually shifted toward lower frequencies upon coordination[10,11]. In the present case, however, the carbonyl peak which is expected to shift toward lower frequencies can not be assigned, since there are some very strong absorptions of salicylaldimino group of the ligand in the expected region.

In the case of the curve, **C**, the carbonyl peak of the coordinated carboxyl group

9) H. Ito, *J. Chem. Soc. Japan, Pure Chem. Sec.* (*Nippon Kagaku Zasshi*), **78**, 1395 (1956).

10) D. H. Busch and J. C. Bailar, Jr., *J. Am. Chem. Soc.*, **75**, 4574 (1953).

11) S. Kirschner, ibid., **78**, 2372 (1956).

is observed at about 1600 cm^{-1}. Not only the anti-symmetric C–O stretching band, but also the shifting of the symmetric stretching band from 1400 to 1370 cm^{-1} affords an additional evidence for the structure with a coordinated carboxyl group[12].

Of interest is a weak absorption at 1680 cm^{-1}, which is supposed to be concerned with the carbonyl group of the peptide link. The concerned band in the free peptide molecule normally appears at about 1655 cm^{-1} [13].

However, the coordination of copper(II) with the nitrogen atom of peptide may shift the band to some extent. Richard and Thompson[14] have pointed out, for example, that electrophilic substituents on the nitrogen atom can give rise to an increase in the frequency up to 1680 cm^{-1}.

The same kind of shifting of the peptide carbonyl band is more effectively presented in **B**. In this case, however, the absorption band is much stronger than that of **C**; and the degree of shifting is even greater. This fact may indicate that the linkage between copper(II) and peptide nitrogen is stronger in **B** than in **C**, and is consistent with the conclusion that **B** might be a typical dsp^2-type complex.

12) K. Nakamoto, J. Fujita, S. Tanaka and M. Kobayashi, ibid., **79**, 4904 (1957).
13) L. J. Bellamy, "The Infra-red Spectra of Complex Molecules", John Wiley & Sons, Inc., New York (1954), p. 192.
14) R. E. Richards and H. W. Thompson, *J. Chem. Soc.*, **1947**, 1248.

Summary

The two new compounds, *N*-salicylideneglycinato-aquo-copper(II) and sodium *N*-salicylideneglycylglycinato-cuprate(II) were prepared and investigated as to their structure.

Their infrared, visible and ultraviolet absorption spectra together with those of some related compounds were measured and discussed.

The author wishes to express his sincere thanks to Professor R. Tsuchida for his encouragement throughout the course of this work, and to Dr. S. Yamada and Mr. Y. Yamamoto for their valuable discussion.

Inorganic Chemistry Laboratory
South College, Osaka University
Abeno-ku, Osaka

Polymerization of Methyl Methacrylate Initiated by Phenylazo p-Tolyl Sulfone

By Ryoichi UEHARA

(Received May 15, 1959)

Phenylazo *p*-tolyl sulfone was first prepared by Koenigs[1] through the reaction of benzenediazonium chloride with sodium *p*-toluenesulfinate:

$$C_6H_5N_2Cl + CH_3C_6H_4SO_2Na = C_6H_5N_2SO_2C_6H_4CH_3 + NaCl$$

Copolymerization of butadiene and styrene (GR-S rubber) by the use of various arylazo aryl sulfones as initiators have been carried out by Brown[2]. It has been reported by Theobold[3] that solution-polymerization of acrylonitrile in ethanol takes place very smoothly at 40°C by means of phenylazo *p*-tolyl sulfone and a very small amount of cupric chloride. The present author has examined the effect of phenylazo *p*-tolyl sulfone upon the polymerization of methyl methacrylate. Phenylazo *p*-tolyl sulfone was an efficient initiator of the polymerization, but it was not suitable for use in manufacture of polymethyl methacrylate, because the polymer formed was dark orange in color. On the other hand, it appears of interest that dimethylaniline acted as an accelerator for this polymerization. In the present paper, results of experiments about the

1) P. Koenigs, *Ber.*, **10**., 1531 (1877).
2) R. S. Brown, U. S. Pat., 2,527,393 (1950); *Chem. Abstr.*, **45**, 383 (1951).
3) C. W. Theobold, U. S. Pat., 2,584,306 (1952); *Chem. Abstr.*, **46**, 3798 (1952).

relation between the initial rate of polymerization and the concentrations of phenylazo *p*-tolyl sulfone, dimethylaniline and methyl methacrylate are given, and the nature of the initiating reaction is discussed from the standpoint of the reaction kinetics.

The dependence of the initial rate of polymerization (R) upon the concentration of phenylazo *p*-tolyl sulfone ([AZS]) in the solution-polymerization in benzene (concentration of methyl methacrylate, 30%) were studied at 41, 51 and 60°C. As are shown in Fig. 1, the square root dependence of the rate upon the concentration was observed at each temperature. When the logarithms of the initial rates

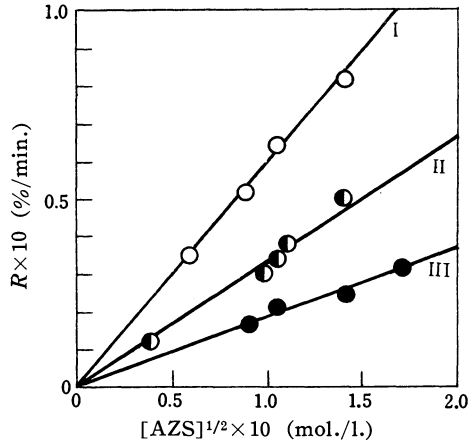


Fig. 1. Dependences of R upon $[AZS]^{1/2}$ at 60 (I), 51 (II) and 41°C (III) ([MMA]=30% in benzene).

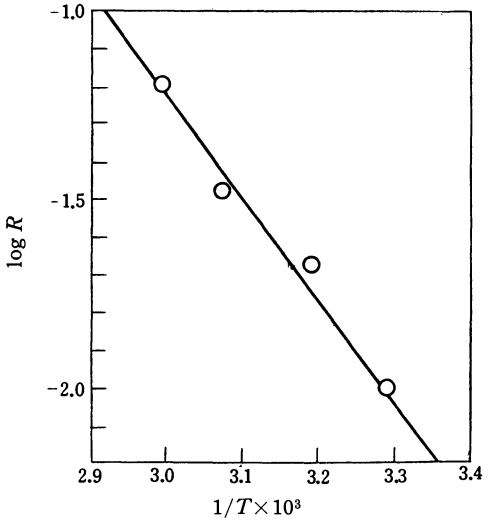


Fig. 2. Relationship between $\log R$ and $1/T$ ([AZS]=1.1×10^{-2} mol./l. and [MMA]=30% in benzene).

(phenylazo *p*-tolyl sulfone 1.1×10^{-2} mol./l.) were plotted against the reciprocals of the temperatures, a straight line was obtained (Fig. 2). The overall activation energy of the polymerization calculated from the slope of the straight line in Fig. 2 was found to be 12.2 kcal./mol.

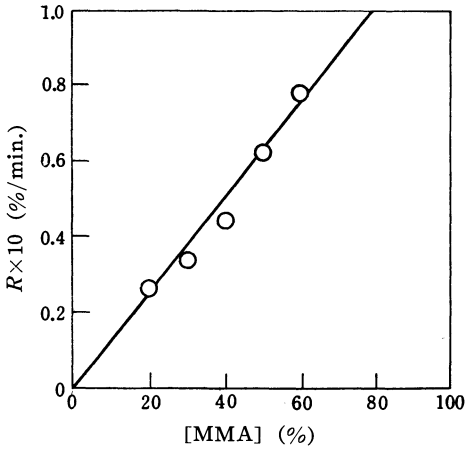


Fig. 3. Correlation of R with [MMA] at 51°C ([AZS]=1.1×10^{-2} mol./l.).

Fig. 3 shows a relationship between the initial rate and the concentration of methyl methacrylate ([MMA]) in benzene (at 51°C and phenlazo *p*-tolyl sulfone 1.1×10^{-2} mol./l.). The rate was linearly proportional to the concentration of methyl methacrylate.

Relationships shown in Figs. 1 and 3 are represented by Eq. 1:

$$R=k_0[AZS]^{1/2}[MMA] \quad (1)$$

where k_0 is a constant. This equation is quite similar to that which is usually known to hold in the polymerization of vinyl monomers initiated by benzoyl peroxide or α,α'-azo-bis-isobutyronitrile[4]. Eq. 1, therefore, suggests a unimolecular first order decomposition of phenylazo *p*-tolyl sulfone as the initiating reaction of the polymerization.

The polymerization of methyl methacrylate initiated by phenylazo *p*-tolyl sulfone is accelerated by addition of dimethylaniline. When the concentration of phenylazo *p*-tolyl sulfone was kept constant and various amounts of dimethylaniline were added, the initial rate of polymerization was linearly dependent upon the square root of the concentration of dimethylaniline ([DMA]). Fig. 4 shows

4) P. J. Flory, "Principles of Polymer Chemistry", Cornell University Press, Ithaca, N. Y. (1953), p. 116.

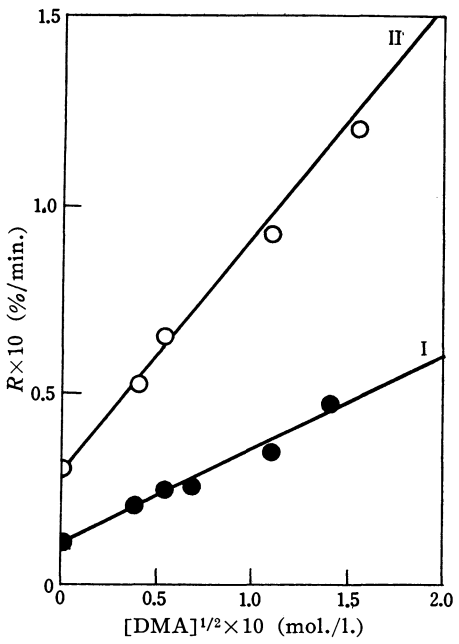


Fig. 4. Correlations of R with $[DMA]^{1/2}$ at 51°C ($[MMA]=30\%$, $[AZS]=0.15\times10^{-2}$ for line I and 0.96×10^{-2} mol./l. for line II).

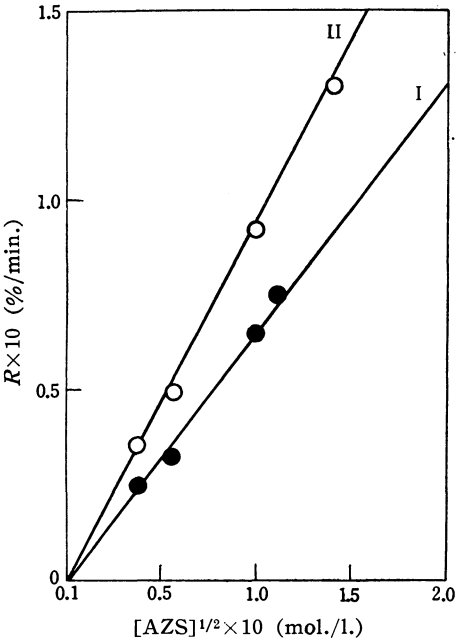


Fig. 5. Correlations of R with $[AZS]^{1/2}$ at 51°C ($[MMA]=30\%$, $[DMA]=0.29\times10^{-2}$ for line I and 1.2×10^{-2} mol./l. for line II).

examples of this relationship (concentration of methyl methacrylate 30%; concentration of phenylazo *p*-tolyl sulfone 0.15×10^{-2} and 0.95×10^{-2} mol./l. at 51°C). In the case when the concentration of dimethylaniline was held constant and that of phenylazo *p*-tolyl sulfone was varied, the initial rate of polymerization was proportional to the square root of the concentration of phenylazo *p*-tolyl sulfone. Examples of this correlation are shown in Fig. 5 (methyl methacrylate 30%, and dimethyl- aniline 0.29×10^{-2} and 1.2×10^{-2} mol./l. at 51°C). It is evident from Figs. 1 and 4 that the polymerization takes place at measurable rates at 51°C by means of phenylazo *p*-tolyl sulfone alone. Therefore, in the case where the concentration of methyl methacrylate is kept constant, the correlations shown in Figs. 4 and 5 can be represented by the following equation:

$$R=k[AZS]^{1/2}+k'[AZS]^{1/2}[DMA]^{1/2} \quad (2)$$

where k and k' are constants.

Eq. 2 suggests that the polymerization of methyl methacrylate by means of phenylazo *p*-tolyl sulfone and dimethylaniline is initiated by two reactions, i. e., a unimolecular first order decomposition of phenylazo *p*-tolyl sulfone and a bimolecular reaction between phenylazo *p*-tolyl sulfone and dimethylaniline, k and k' being the rate constants respectively. From Eq. 2, the following equation is derived:

$$R=k[AZS]^{1/2}(1+k'/k[DMA]^{1/2}) \quad (3)$$

k'/k, the ratio of the rate constants of the two initiating reactions of the polymerization, can be calculated from the slops of the straight lines in Fig. 4. It was found to be 2.00 from line I and 2.18 from line II (at 51°C and methyl methacrylate 30% in benzene).

Imoto and others[5] have reported a rate-concentration equation similar to Eq. 2 or 3 for the polymerization of methyl methacrylate initiated with benzoyl peroxide and dimethylaniline, and suggested a similar mechanism to that mentioned above.

Experimental

Materials.—Purification of methyl methacrylate, dimethylaniline and benzene have been mentioned in a previous paper by the present author[6]. Phenylazo *p*-tolyl sulfone was obtained by addition of sodium *p*-toluenesulfinate (21 g.) into an aqueous solution of benzenediazonium chloride which was prepared from aniline (10 g.), 30%

5) M. Imoto et al., *J. Chem. Soc. Japan, Ind. Chem. Sec.* (*Kogyo Kagaku Zasshi*), **58**, 451 (1955).
6) R. Uehara, This Bulletin, **31**, 685 (1958).

aqueous HCl (40 cc.) and $NaNO_2$ (8 g.). The crude product was recrystallized three times from pure methanol, giving pure phenylazo *p*-tolyl sulfone (17.5 g.), m. p. 87.5°C with decomposition (83.5°C by Brown[2]). This compound was not quite stable at room temperature under sunlight. In a colorless, transparent glass vessel, it changed into a resinous meterial during several weeks in summer.

Polymerization. — Polymerization was carried out in sealed test tubes which were 15 mm. in diameter and 10 cm. in height and made of brown-colored glass so as to reduce the effects of sunlight upon the polymerization. Phenylazo *p*-tolyl sulfone was dissolved in benzene. Methyl methacrylate was cooled in an ice-salt bath. Measured amounts of the benzene-solution and methyl methacrylate were placed in a test tube and mixed. The test tube was immersed in a dry ice-methanol bath and flushed with nitrogen and sealed. The extent of the polymerization was estimated from the weight of polymethyl methacrylate, and the rate of polymerization was expressed in unit of per cent per minute. Details of the procedures of the polymerization and the determination of the initial rate of polymerization have been reported previously[6].

Summary

The effects of phenylazo *p*-tolyl sulfone upon the polymerization of methyl methacrylate were examined. In the solution-polymerization in benzene, the initial rate of polymerization was linearly dependent respectively upon the square root of the concentration of phenylazo *p*-tolyl sulfone and upon the concentration of methyl methacrylate. A unimolecular first order decomposition of phenylazo *p*-tolyl sulfone is suggeted as the initiating reaction of the polymerization. Dimethylaniline acted as an accelerator for this polymerization. In this case, the initial rate of polymerization was linearly proportional to the square root of each of the concentrations of phenylazo *p*-tolyl sulfone and dimethylaniline. A bimolecular reaction between phenylazo *p*-tolyl sulfone and dimethylaniline has been proposed for the acceleration of the polymerization.

The author wishes to express his hearty thanks to Professor Osamu Simamura of the University of Tokyo for his interests in this work and Mr. Tsurahide Cho, the President of Tama Kagaku Kogyo Co. for permission to publish this work.

Tama Kagaku Kogyo Co.
2-28 *Minamirokugo*
Ota-ku, Tokyo

*Synthesis of 3, 6-Dimethyl-2, 3-dihydro-1H-cyclopent[a]anthracene. A Possible Dehydrogenation Product of Anthranoid Rearrangement Product of Steroids**

By Masao NAKAZAKI and Sachihiko ISOE

(Received February 11, 1959)

A number of works have been accumulated on the dienone-phenol rearrangement of the steroid A ring, and there can be found scrupulous studies on the structures of the products of this rearrangement[1], the relation between the products and the reaction conditions[2], and the effects of the structures on the rearrangement course[3]. Stimulated by these studies on steroids, various model compounds were synthesized and the same pattern of reaction was demonstrated[4].

* A preliminary note appeared in *Chem. & Ind.*, **1958**, 43.

1) H. Minlon, *Naturwissenschaften*, **36**, 765 (1938); R. B. Woodward, H. H. Inhoffen, H. O. Larson and K. H. Menzel, *Chem. Ber.*, **86**, 594 (1955); and Inhoffen's preceeding papers, **1940—1953**.

2) A. S. Dreiding and Ann Voltman, *J. Am. Chem. Soc.*, **68**, 1715 (1946); A. S. Dreiding, W. J. Pummer and A. J. Tomosewski, ibid., **75**, 3159 (1953).

3) A. L. Wilds and C. Djerassi., ibid., **68**, 1715 (1946); and numerous studies by Djerassi, ibid., **70**, 1911, 3962 (1948); **72**, 4540 (1950); **73**, 990, 1523 (1951); **76**, 1741 (1954); and *J. Org. Chem.*, **15**, 896 (1950).

4) R. B. Woodward and T. Singh, *J. Am. Chem. Soc.*, **72**, 494 (1950); R. T. Arnold, ibid., **71**, 1781 (1949); **69**, 2322 (1947); **72**, 3153 (1950); F. M. Marbell and E. Magoon, ibid., **77**, 2542 (1955); **76**, 5118 (1954).

But, as to the dienone-phenol rearrangement of the steroid B ring[5], thorough study is still lacking and the structures of the rearrangement products have remained obscure. Tsuda's group[6] was the first to carry out the structural study of a dienone-phenol rearrangement product of the steroid B ring. Namely, 7-keto-5,8(9)-cholestadien-3β-yl acetate (I)[6,7], prepared by chromic acid oxidation of 5,8(9)-cholestadien-3β-yl acetate in acetic acid, was treated with concentrated sulfuric acid in acetic anhydride to give phenol acetate(IIa). After hydrolysis of IIa with ethanolic potassium hydroxide to a phenol IIb, m. p. 261~265°C, they submitted this phenol to selenium dehydrogenation to obtain, among other products, a hydrocarbon (oil) $C_{19}H_{18}$ in the form of picrate, m. p. 133.5~134°C. The ultraviolet absorption which showed an anthracene type pattern, was attributed by them to the structure IV, and consequently structure IIb was assumed for the phenol, m. p. 261~265°C.

This type of rearrangement is not the only one which can convert the perhydrophenanthrene skeleton of steroids into the perhydroanthracene skeleton, but a smooth "anthrasteroid" rearrangement studied by Mosettig and coworkers[8] can be counted as another type of conversion leading to the anthracene skeleton. Tsuda and coworker[9] also carried out a modification of "anthrasteroid" rearrangement of $\Delta^{5,8}$-cholestadien-3β-ol to the product III, in the presence of mercuric acetate and toluenesulfonic acid in ethanol under the influence of strong irradiation[10]. Dehydrogenation of product III with selenium afforded the same hydrocarbon $C_{19}H_{18}$, which they obtained from II previously. Since 3,6-dimethyl-2,3-dihydro-1-*H*-cyclopent[*a*]anthracene (IV) is a dehydrogenation product to be expected from the "anthranoid rearrangement" product and corresponds to Diels' hydrocarbon usually obtained by the dehydrogenation of steroids, the synthesis of this compound IV is considered to be important[11]. In this paper we report the synthesis of compound IV.

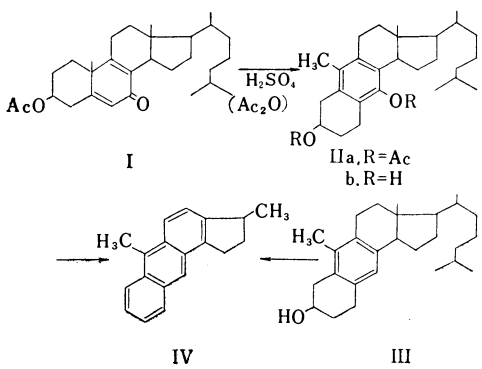


Fig. 1

Whereas the synthetic routes to the phenanthrene type dehydrogenation products of steroids have been well explored[12], there have been few to prepare the anthracene type like IV. Compound VII appears to be the most promising starting material which could be transformed into IX by Johnson's modification of Stobbe condensation[13](Fig. 2). 1-Methyl-2-naphthoic acid (VIa), prepared either

5) D. H. R. Barton and B. R. Thomas, *J. Chem. Soc.*, **1953**, 1842, converted 7-ketolanosta-5,8-dien-3β-yl acetate into "isomeric phenol" by bolling with acetic acid and zinc dust. P. Bladon, *J. Chem. Soc.*, **1955**, 2176, obtained a phenol from 3β-acetoxylumista-5,8 (9), 20-trien-7-one (λ_{max} 246 mμ, ε 11,800) by the action of acetic acid and zinc dust, and discussed the structure. They also pointed out another possible route of dienone-phenol rearrangement by methyl migration.

6) K. Tsuda, K. Arima and R. Hayatsu, *J. Am. Chem. Soc.*, **76**. 2933 (1954). Compound I shows ultraviolet absorption at λ_{max} 238 mμ (log ε 4.475), $[\alpha]_D^{22}$ −67.3°. m. p. 151~152°C. Semicarbazone: m. p. 210~212°C (decomp.). The same compound prepared by Inhoffen by another route has m. p. 169~170°C $[\alpha]_D^{20}$ −9°, λ_{max} 248 mμ, ε 12,800 (methanol). H. H. Inhoffen and W. Menzel, *Chem. Ber.*, **87**, 146 (1954).

7) Other steroids possessing 5,8(9)-dien-7-one structure show maxima of ultraviolet absorption as follows: 3β-hydroxy-5,8(9), 20-ergostatrien-7-one, λ_{max} 247 mμ (ε 21,000) (D. C. Burke, J. H. Turnbull and W. Wilson, *J. Chem. Soc.*, **1953**, 3237); 3β-acetoxy-5,8(9). 20-ergostatrien-7-one, λ_{max} 245 mμ (ε 11,800) (J. Elks, R. M. Evans, A. G. Long and G. H. Thomas, ibid., **1954**, 451); λ_{max} 246 mμ (ε 12,800) (J. Elks, R. M. Evans, J. F. Oughton and G. H. Thomas, ibid., **1954**, 463).

8) E. Mosettig and I. Scheer, *J. Org. Chem.*, **17**, 764 (1952); W. R. Nes and E. Mosettig, *J. Am. Chem. Soc.*, **75**, 2787 (1953); **76**, 3182, 3186 (1954); W. R. Nes, ibid., **78**, 193 (1956); I. Scheer, W. R. Nes and P. B. Smeltzer, ibid., **77**, 3300 (1955); W. R. Nes, R. B. Kostic and E. Mosettig, ibid., **78**, 36 (1956). We would like to propose the general term "anthranoid rearrangement" for all rearrangements of steroids to the compounds possessing an anthracene skeleton, and to restrict the term "anthrasteroid rearrangement" to the type of Mosettig's reaction.

9) K. Tsuda and R. Hayatsu, *J. Am. Chem. Soc.*, **77**, 3089 (1955).

10) Being a photochemical reaction accompanied by simultaneous dehydrogenation, the mechanism appears complicated. But the product is in sharp contrast to the product of Mosettig's rearrangement in maintaining the 3-hydroxyl group unattacked.

11) After we completed the synthesis of IV, A. W. Burgstahler, *J. Am. Chem. Soc.*, **79**, 6047 (1957), published a paper in which he described an elegant proof of the structure of anthracholestatetraene proposed by Mosettig et al.

12) L. F. Fieser and M. Fieser, "Natural Products Related to Phenanthrene", 3rd Ed., Reinhold Pub. Corp., New York (1949), p. 148—154.

13) W. S. Johnson and G. H. Daub, "Organic Reactions", Vol. **6**, John Wiley & Sons, Inc., New York (1951), p. 1.

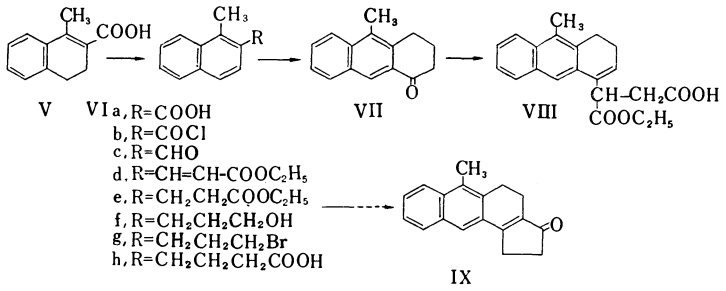


Fig. 2.

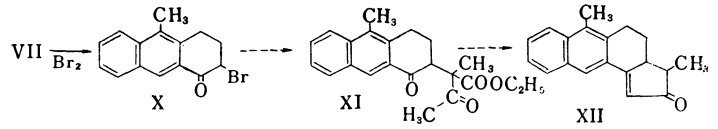


Fig. 3.

by dehydrogenation[14] of V by means of bromine or by the Grignard synthesis from α-(chloromethyl)naphthalene, was converted into the aldehyde VIc via the aicd chloride VIb by means of the Rosenmund reduction with Pd-$BaSO_4$. By the Claisen condensation with ethyl acetate, VIc gave the unsaturated ester VId, which in turn was catalytically hydrogenated to VIe. The alcohol VIf, obtained by lithium aluminum hydride reduction of VIe, was treated with phosphorus tribromide to afford the bromide VIg, which gave the acid VIh by the usual nitrile synthesis and hydrolysis.

The Stobbe condensation of the ketone VII, easily accessible from the acid VIh by Wilds' method[15], led to the formation of VIII, but the ring closure to IX by Johnson's method[16] using zinc chloride was unsuccessful, probably owing to the vulnerability of the α-position of the naphthalene nucleus to the cationoid attack which would direct the ring closure in an undesired direction. Although the plan to build up the D ring by Johnson's method failed, various synthetic routes which can be carried out in a basic medium so as to avoid the complicated side reaction encountered above, were tried with the ketone VII to secure the D ring.

Condensation of the bromoketone X, provided by the bromination of the ketone VII in ether, with potassium ethyl methylacetoacetate[17] in *tert*-butanol failed to give XI, which was expected to afford XII by ring closure.

Another route tried was an indirect one (Fig. 4). The alcohol XVII which would be prepared following the scheme whereby Johnson achieved his brilliant equilenine synthesis[18], might give IV on dehydrogenation accompanied by the simultaneous migration of the angular methyl group to the position originally occupied by the hydroxyl group.

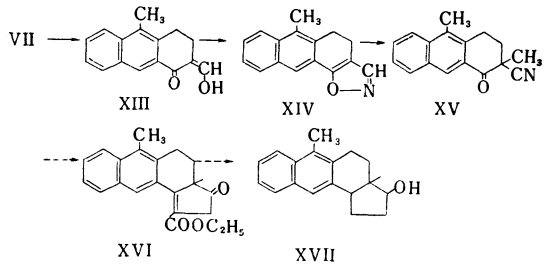
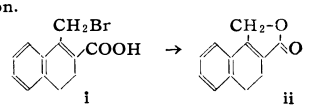


Fig. 4.

The process leading to XV was carried out smoothly, but again the Stobbe condensation of the α-cyanomethylketone to afford XVI was fruitless, probably owing to the ready opening of the ketone XV with the base. The sequence of the steps which finally led to IV is shown in Fig. 5.

14) When dehydrogenation was carried out in acetic acid, the bromination product i was the main product, which could be converted into the lactone ii by hydrolysis with methanolic potassium hydroxide followed by acidification.



15) A. L. Wilds, *J. Am. Chem. Soc.*, **64**, 1424 (1942).
16) W. S. Johnson and J. W. Peterson, ibid., **67**, 1367 (1945).
17) Wilds succeeded in the same type of condensation using ethyl acetoacetate, *J. Am. Chem. Soc.*, **64**, 1421 (1949).
18) W. S. Johnson et al., ibid., **69**, 2942 (1947).

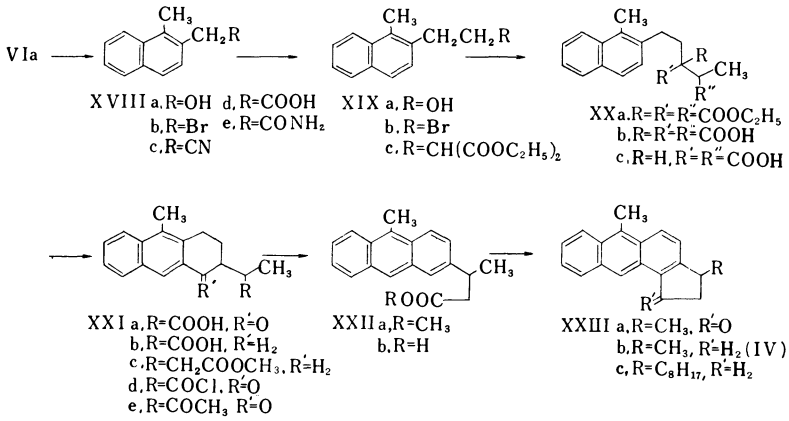


Fig. 5.

1-Methyl-2-naphthoic acid (VIa) was reduced with lithium aluminum hydride to give the alcohol XVIIIa, and its side chain was extended to the homologous alcohol XIXa by the usual sequence of reactions (bromide XVIIIb→cyanide XVIIIc →acid XVIIId→alcohol XIXa). The alcohol XIXa was treated with phosphorus tribromide in benzene to yield the bromide XIXb, which gave the condensation product XIXc with ethyl sodiomalonate.

Condensation of XIXc with ethyl α-bromopropionate in the presence of potassium *tert*-butoxide led to the triester XXa. The tricarboxylic acid XXb obtained by the hydrolysis of XXa with methanolic potassium hydroxide was decomposed to the dicarboxylic acid XXc, which was cyclized to the ketocarboxylic acid XXIa by PCl_5-$SnCl_4$ method of Wilds[15,19], whereas the ring closure using polyphosphoric acid[20] resulted only in the recovery of the starting material.

After the carbonyl group of XXIa was removed by the Clemensen-Martin reduction, the resulting acid XXIb[21] was transformed into the methyl ester of the homologous acid XXIc by the Arndt-Eistert method. Heating with 30% Pd-C at 290~300°C, followed by hydrolysis, converted the ester XXIc into the anthracene derivative XXIIb, m. p. 160~160.5°C, which showed an ultraviolet absorption spectrum characteristic of an anthracene type (see *Experimental*).

The appearance of new bands in the infrared absorption spectrum (11.90 and 12.30 μ) which can be attributed to the 1,2,4-trisubstituted benzene structure[22], together with the characteristic absorption in ultraviolet region, leaves no doubt about the anthracene structure of the compound. The ring closure[23] of the acid XXIIb by PCl_5-$SnCl_4$ method accomplished the ketone XXIIIa, which exhibited infrared absorption band at 5.93 μ (indanone)[24] and 12.2 μ (two adjacent hydrogens on aromatic hydrocarbon). The ultraviolet absorption spectrum which is very close to α-acetylanthracene (see Table I) also confirms the structure of the ketone.

The final stage to IV was the Clemensen-Martin reduction of the ketone XXIIIa. The oily product was purified by chromatography on alumina column to provide colorless crystals, m. p. 78~79.5°C after recrystallization from methanol. The picrate melted at 128~128.5°C (the picrate of Tsuda's hydrocarbon, m. p. 133~134°C), and the 2,4,6-trinitrobenzolate at 142~142.5°C. The ultraviolet absorption spectrum of the hydrocarbon XXIIIb (IV) could in almost every detail be overlapped on the spectrum of Mosettig's hydrocarbon XXIIIc (dehydroanthracholesterol), whereas Tsuda's hydrocarbon showed an anomalous absorption in the long wavelength, presumably owing to impurity[25].

19) To get the methyl ketone XXIe, which would give a five membered D ring was tried in vain. Cf. A. L. Wilds et al., *J. Am. Chem. Soc.*, **69**, 3079 (1947); **66**, 1688 (1944).

20) D. D. Gardner and W. J. Horton, ibid., **74**, 4976 (1953).

21) Two racemates of compound XXIb can be expected, but no attempt was made to separate them.

22) H. Dannenberg, U. Shiedt and W. Sheidle, *Z. Naturforsh.* **B8**, 269 (1953).

23) The reactivity to cationoid attack is much greater at α-position on anthracene than at β-position. Cf. L. F. Fieser and H. Heymann, *J. Am. Chem. Soc.*, **63**, 2333 (1941) and W. S. Johnson, "Organic Reactions", Vol. 2, John Wiley & Sons, Inc., New York (1946). p. 114.

24) H. Dannenberg and D. D. Dannenberg, *Ann.*, **585**, 1 (1954), reported the absorption at 5.92 μ in the similar system.

25) The selenium dehydrognation of IIb may lead, although it is highly unlikely, to another structure than IV, but in the case of dehydrogenation of III to IV, there is no reason to expect serious change of the skeleton.

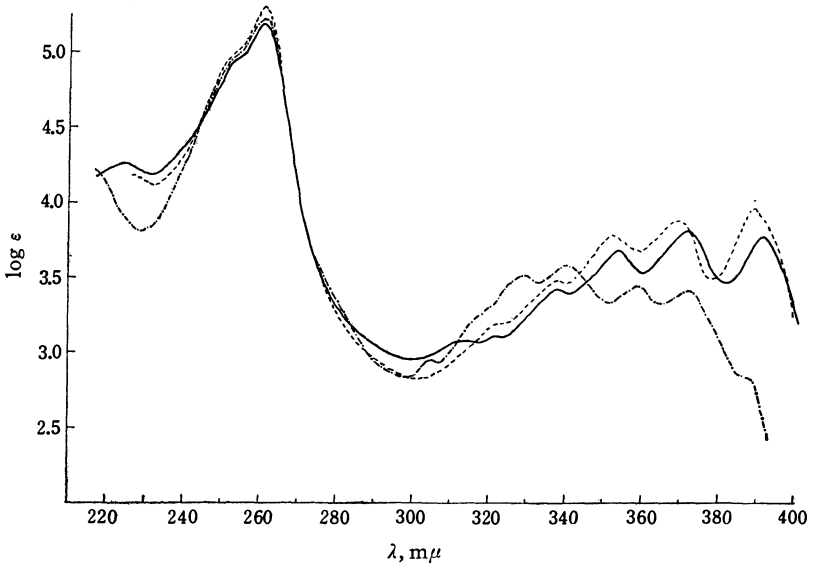
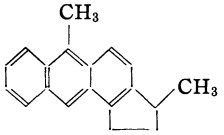
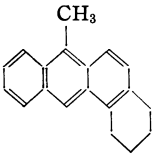


Fig. 6.



——— Synthetic
—·—·— Tsuda et al.



------ Fieser et al.

TABLE I.

XXIIIa[1]		α-Acetyl anthracene[2]		IV (synthetic)[3]		IV (Tsuda)[4]		XXIIIc (Mosettig)[5]		1,2,3,4-Tetrahydro-10-methylbeazanthrene[6]	
λ_{max}	log ε	λ_{max}	log ε	λ_{max}	ε	λ_{max}	ε	λ_{max}	ε	λ_{max}	log ε
245	4.72	241	4.76	226	18,040			227	16,550		
263	4.73	254	4.84	238	21,530			234	17,550		
332	3.22	330	3.24	255	93,750						
346	3.49	346	3.53	261	145,200	262	123,600	262	165,000	261	5.3
363	3.66	366	3.71	308	1,270	303	790				
395	3.77	385	3.73	323	1,317	328	3,170				
				338	2,650	341	4,150	338	2,750	336	3.5
				354	4,765	358	4,000	354	5,000	351	3.8
				372	6,690	372	2,980	372	7,420	368	3.9
				393	6,260	388	710	391	7,520	388	4.0

1) In ethanol.
2) In ethanol: R. N. Jones, *J. Am. Chem. Soc.*, **67**, 2127 (1945). β-Acetylanthracene: see R. N. Jones, *Chem. Revs.*, **41**, 353 (1947).
3) In ethanol.
4) In solvent unspecified: K. Tsuda, K. Arima and R. Hayatsu, *J. Am. Chem. Soc.*, **76**, 2933 (1954); K. Tsuda and R. Hayatsu, ibid., **77**, 3089 (1955).
5) In isooctane: W. R. Nes, R. B. Kostic and E. Mosettig, ibid., **78**, 436 (1956).
6) In ethanol: L. F. Fieser and E. B. Hershberg, ibid., **60**, 940, (1938).

Experimental**

Ethyl α-Aceto-γ-phenylbutyrate.—To a stirred and cooled solution of sodium ethoxide prepared from 450 cc. of absolute ethanol and 23 g. of sodium, 143 g. of ethyl acetoacetate was added in an atmosphere of nitrogen, and the reaction mixture was warmed to 60~70°C. After the addition of 197 g. of phenethyl bromide (b. p. 96~98°C/11 mmHg) over a period of 2 hr., the mixture was heated at 70~75°C for 5 hr., 80~85°C

** All ultraviolet spectra were measured with a Beckmann spectrophotometer DK 2, and infrared spectra with a Perkin Elmer Model 12 C. The anlyses were performed in the Microanalytical Laboratory of the Institute of Polytechnics, Osaka City University, Osaka.

for an additional 5 hr., and refluxed for 6 hr. on a water bath. After the solvent was removed, the residue was poured into water, made sligitly acidic with hydrochloric acid, and extracted with ether. The organic layer was washed with water and dried over anhydrous sodium sulfate, and the ether was removed.

The ester distilled at 124~127°C/1 mmHg, and weighed 163 g. (Yield, 69.5%).

1-Methyl-3, 4-dihydro-2-naphthoic Acid.—Ninety grams of ethyl α-aceto-γ-phenylbutyrate was added dropwise to 375 cc. of concentrated sulfuric acid chilled at −4°C with stirring more than 40 min., and the mixture was kept at this temperature for 2 hr. After the reaction mixture was poured on crushed ice, the crystals were collected and washed thoroughly with water. After being dried, they weighed 64.5 g. (yield, 84.2%), and were used in dehydrogenation without further purification. A small portion was recrystallized from petroleum ether, m. p. 127~130°C. (literature[26]: m. p. 129~130°C).

1-Methyl-2-naphthoic Acid (VIa).—*Dehydrogenation of V.*—To a solution of 58 g. of V in 300 cc. of carbon tetrachloride, 54 g. of bromine was added at 65~70°C over a period of 2 hr. with stirring. After additional heating (70~75°C) for 2 hr. with stirring, the mixture was cooled to deposite crystals.

The crude crystalline product (55.6 g.) was dissolved in a solution of 40 g. of sodium hydroxide in 750 cc. of water and the solution was heated on a water bath for 2 hr., and treated with Norit. The alkaline solution was freed from Norit, and made acidic with 1 N hydrochloric acid to afford 34.5 g. of crude VIa (yield, 44.1%), which was recrystallized, m. p. 177.5~178°C (literature[26]: 177~178°C).

Grignard synthesis from α-(chloromethyl)naphthalene.—To a suspension of 35 g. of magnesium in 360 cc. of absolute ether, was added 85 g. of α-(chloromethyl) naphthalene in 200 cc. of ether with stirring for more than 5 hr., and the mixture was refluxed for 1 hr.

The Grignard solution was filtered through glass wool to remove excessive magnesium, and added to a chilled solution of 215 g. of ethyl chlorocarbonate in 160 cc. of ether taking more than 40 min. After being kept at room temperature for 30 min., the mixture was decomposed with dilute sulfuric acid and ice, and the organic layer was washed in turn with water and dilute sodium carbonate solution. Romoval of the solvent gave a liquid, which boiled at 140~143°C/2~3 mmHg and weighed 46.6 g. Hydrolysis of the ester with 20 g. of potassium hydroxide, 25 cc. of water and 50 cc. of methanol gave 28.6 g. of VIa, m. p. 160~170°C. Recrystallization from benzene raised the m. p. to 175~176°C.

1-Bromomethyl-3, 4-dihydro-2-naphthoic Acid (i).—To a solution of 15 g. of V (m. p. 127~130°C) in 60 cc. of glacial acetic acid, a mixture of 13.8 g. of bromine and 20 cc. of acetic acid was added with stirring for more than 1.5 hr. The color of bromine disappeared rather rapidly. The solution was warmed at 55°C for 30 min., and a small amount of sodium sulfite was added to discharge the bromine color.

Crystals, precipitated by the addition of water, were collected and washed with water to give 20 g. of the bromide i, which was recrystallized from benzene to give prismatic crystals, m. p. 177°C (decomp.).

Anal. Found: C, 54.44; H, 4.23; Br, 29.96. Calcd. for $C_{12}H_{11}O_2Br$: C, 53.50; H, 4.15; Br, 29.93%.

The Lactone (ii).—Five grams of i was dissolved in a solution of 5 g. of potassium hydroxide in 1 cc. of water and 30 cc. of methanol, and the solution was refluxed on a water bath for 40 min. After the addition of 30 cc. of water, the alkaline solution was made acidic to precipitate an oil, which was decanted from superfluous liquid. The viscous oil could be crystallized by trituration with a cold dilute sodium hydroxide solution.

Recrystallization from petroleum ether gave the lactone ii melting at 112~113°C.

Anal. Found C, 77.48; H, 5.68. Calcd. for $C_{12}H_{10}O_2$: C, 77.42; H, 5.38%.

1-Methyl-2-naphthoyl Chloride (VIb).—A mixture of 35.0 g. of VIa and 44.5 g. of thionyl chloride was refluxed on a water bath for 2 hr. The excess of thionyl chloride was removed to give an oil, which distilled at 136~138°C/2 mmHg, m. p. 79~80.5°C and weighed 36.5 g. The anilide was recrystallized from ethanol m. p. 212~214°C.

Anal. Found: C, 82.75; H, 6.04; N, 5.55. Calcd. for $C_{18}H_{15}ON$: C, 82.73; H, 5.79; N, 5.36%.

1-Methyl-2-naphthaldehyde (VIc).—A stream of hydrogen was introduced into a stirred mixture of 36.5 g. of VIb and 3.4 g. of 5% Pd/$BaSO_4$[27] in 330 cc. of xylene at 110°C. When the evolution of hydrogen chloride ceased (in about 2 hr.), the reaction mixture was cooled and freed from the catalyst. Removal of the solvent in vacuo followed by distillation gave 15.4 g. of an oil (yield, 50.6%), which solidified gradually on standing. The semicarbazone was recrystallized from dilute acetic acid, m. p. 227~231°C (decomp.).

Anal. Found: C, 69.16; H, 5.61. Calcd. for $C_{13}H_{13}ON_3$: C, 68.70; H, 5.77%.

Ethyl β-(1-Methyl-2-naphthyl)acrylate (VId).—A mixture of 42 cc. of ethyl acetate and 0.3 cc. of absolute ethanol was added all at once to the cooled powdered sodium[28] provided by vigorous stirring of 2.7 g. of molten sodium under refluxing xylene followed by decantation from the xylene. After stirring for 10 min. at −5°C, a solution of 15.2 g. of the aldehyde VIc in 30 cc. of ethyl acetate was added over a period of 1.5 hr. and the mixture was stirred for 1.5 hr. at −6°C. The dark red reaction mixture was decomposed by adding 9 cc. of acetic acid and then 200 g. of ice, and the aqueous layer was extracted with ethyl acetate twice. The combined extract was washed

26) K. V. Auwers and K. Möller, *J. prakt. Chem.*, **109**, 124 (1925).

27) R. Mozingo "Organic Syntheses", Vol. 26, John Wiley & Sons, Inc., New York (1946), p. 77.

28) C. S. Marvel and W. B. King, ibid., Col. Vol. 1, (1948), p. 252.

with water, 5% sodium bicarbonate solution and water. After drying, the solvent was removed to afford a pale yellow liquid, which was distilled to give 10.1 g. of a colorless liquid, b. p. 167~173°C/2 mmHg, (yield, 47%), which solidified on standing and recrystallized from petroleum ether, m. p. 62~63°C.

Anal. Found: C, 80.25; H, 6.97. Calcd. for $C_{16}H_{16}O_2$: C, 79.97; H, 6.71%.

Ethyl β-(1-Methyl-2-naphthyl)propionate (VIe).—Catalytic hydrogenation of 15.3 g. of the unsaturated ester VId with 0.4 g. of 10% Pd/C in 180 cc. of ethanol gave an oil which boiled at 161~162°C/2 mmHg and weighed 11.4 g. (yield, 75%).

Anal. Found: C, 79.59; H, 7.71. Calcd. for $C_{15}H_{18}O_2$: C, 79.31; H, 7.49%.

3-(1-Methyl-2-naphthyl)-1-propanol (VIf).—To a slurry of 0.95 g. of lithium aluminum hydride in 40 cc. of ether, a solution of 5.4 g. of the ester VIe in 20 cc. of ether was added with stirring. After refluxing for 1 hr., the excess of the reducing reagent was decomposed by adding 4 cc. of ethyl acetate and then 25 cc. of water and 15 cc. of concentrated hydrochloric acid. The organic layer was washed with water, 5% sodium bicarbonate solution and water again. After drying over anhydrous magnesium sulfate, the solvent was removed to give an oil, which was purified by distillation in vacuo, b. p. 173~174°C/3 mmHg. 4.1 g. (yield, 91.9%). The phenylurethane was recrystallized from benzene-petroleum ether, m. p. 113~114°C.

Anal. Found; C, 78.96; H, 7.03. Calcd. for $C_{21}H_{21}O_2N$: C, 78.97; H, 6.63%.

1-Bromo-3-(1-methyl-2-naphthyl)-propane (VIg).—A solution of 5.0 g. of the alcohol VIf in 19 cc. of benzene was added dropwise to a stirred mixture of 5.0 g. of phosphorus tribromide and 125 cc. of benzene. After heating at 70~75°C for 4 hr., the mixture was poured into ice water and saturated with sodium chloride. The benzene layer was separated, and the aqueous layer was extracted with ether. The combined benzene solution and ether were washed with water and dried over anhydrous magnesium sulfate. The residue freed from the solvent was distilled at 135~136°C/0.002 mmHg, to give the bromide VIg weighing 5.2 g. (yield, 80.4%).

3-(1-Methyl-2-naphthyl)-1-propanecarboxylic Acid (VIh).—A mixture of 5.2 g. of the bromide VIg, 89 cc. of ethanol, 5.0 g. of potassium cyanide and 20 cc. of water was refluxed for 26 hr. After removal of the ethanol, the mixture was poured onto ice, acidified with 20 cc. of concentrated hydrochloric aicd, and extracted with ether.

After removal of the ether the residual oil was hydrolyzed by boiling with 59 cc. of acetic acid and 33 cc. of concentrated hydrochloric acid for 7 hr., while 1.2 cc. of concentrated hydrochloric acid was added every hour. The crystals deposited on cooling melted at 123~125°C and weighed 4.3 g. (yield, 94.6%). Recrystallization from benzene-petroleum ether raised the melting point to 126~127°C.

Anal. Found: C, 79.62; H, 7.05. Calcd. for $C_{15}H_{16}O_2$: C, 78.92; H, 7.06%.

1-Oxo-10-methyl-1, 2, 3, 4-tetrahydroanthracene (VII).—To a solution of 5.1 g. of the carboxylic acid VIh in 44 cc. of dry benzene, 9.2 g. of phosphorus pentachloride was added. After stirring at room temperature for 1 hr., the mixture was heated for 10 min. at 45~50°C, and then a solution of 28.6 g. of stannic chloride in 22 cc. of benzene was added to the chilled solution. The orange-red solution was stirred for 50 min. with cooling in an ice bath, and was decomposed with 200 cc. of water. Addition of 22 cc. of concentrated hydrochloric acid was followed by extraction with ether, and the organic layer was washed with water, 1 N sodium hydroxide solution and water. After drying over anhydrous magnesium sulfate, the solvent was removed to give a solid weighing 4.3 g. (yield, 91.7 g.), which was recrystallized from methanol, m. p. 99.5~100.5°C, 4.0 g. An infrared absorption spectrum indicated a peak at 5.97 μ.

Anal. Found: C, 85.95; H, 7.62. Calcd. for $C_{15}H_{14}O$: C, 85.68; H, 6.71%.

The Stobbe Condensation of VII.—In a stream of nitrogen, 1.2 g. of potassium was dissolved in 22 cc. of *tert*-butanol. To the solution was added a mixture of 5.4 g. of the ketone VII, 7.2 g. of diethyl succinate and 7.5 g. of *tert*-butanol and the mixture was heated at 110°C for 50 min. To the cooled solution, 8.5 cc. of concentrated hydrochloric acid and 50 cc. of water was added, the separated brown oil was extracted with ether. After being washed with water, the ether layer was extracted with three portions of 160 cc. of 1 N ammonia water to separate the half ester VIII. The turbid solution was cleared with Norit, and was acidified with 4 N hydrochloric acid to precipitate an oil, which was extracted with ether. The ether extract was washed with water and dried over anhydrous magnesium sulfate. To the brown residue (5.3 g.) was added 50 cc. of acetic acid and then a solution of 25 cc. of acetic acid and 1.5 g. of zinc chloride. The solution was heated on a free flame for 5 hr. The reaction mixture turned blue-black in color, and was filled with a voluminous amorphous solid, from which no traceable material was isolated.

1-Oxo-2-bromo-10-methyl-1, 2, 3, 4-tetrahydroanthracene (X).—To a chilled suspension of 2.6 g. of the ketone VII in 20 cc. of ether, a solution of 2.0 g. of bromine in 10 cc. of ether was added over a period of 10 min. with stirring. After stirring at room temperature for 2 hr., precipitated crystals were collected and recrystallized from methanol-acetone (3 : 1), m. p. 136~137°C. Yield, 2.7 g.

Anal. Found: C, 62.46; H, 4.71. Calcd. for $C_{15}H_{13}OBr$: C, 62.28; H, 4.50%.

The Condensation of the Bromoketone X with Ethyl Methylacetoacetate.—To a cold solution of potassium *tert*-butoxide prepared from 0.33 g. of potassium and 11 cc. of *tert*-butanol, 1.35 g. of ethyl methylacetoacetate was added and the mixture was stirred for 5 hr. at room temperature in an atmosphere of nitrogen. After a solution

of 2.4 g. of the bromoketone X in 28 cc. of dry benzene was added taking more than 10 min., the reaction mixture was stirred at room temperature for 5 min., and refluxed for 1.5 hr. The solution was acidified with 10 cc. of 1 N hydrochloric acid and ice, and the organic layer was in turn washed with water and 2% sodium hydroxide solution. Removal of the solvent gave a brown oil (3.4 g.) from which no traceable material was isolated by chromatographic adsorption on alumina.

1-Oxo-2-oxymethylene-10-methyl-1,2,3,4-tetrahydroanthracene (XIII).—To pulverized sodium methoxide prepared from 0.82 g. of sodium and 20 cc. of methanol, a solution of 2.64 g. of ethyl formate in 30 cc. of benzene was added with stirring and cooling in a gentle stream of nitrogen. A mixture of 3.7 g. of the ketone VII and 40 cc. of benzene was added dropwise with stirring for more than 17 min. The color of the solution changed from yellow-green to green-yellow. After heating at 8~20°C for 6 hr., ice water was added to precipitate the sodium salt of the oxymethylene ketone XIII, which was separated and washed with water. A reddish brown oil, separated on addition of hydrochloric acid to the aqueous solution of the sodium salt, was extracted with ether and the extract was washed with water and dried. Removal of the solvent gave 3.9 g. of a viscous oil, which showed a violet color reaction with ferric chloride and was used directly to prepare the isoxazole XIV.

The Isoxazole XIV.—To a solution of 3.90 g. of the crude oxymethylene ketone XIII in 144 cc. of acetic acid, was added 1.67 g. hydroxylamine hydrochloride and the mixture was heated at 75~80°C for 7 hr. After the solvent (about 120 cc.) was removed by evaporation in vacuo, 100 cc. of water was added to the mixture to precipitate an oil, which solidified upon standing. The crude isoxazole (3.65 g.) was recrystallized from diluted methanol to give needles melting at 111~112°C.

Anal. Found: C, 81.61; H, 5.67; N, 6.46. Calcd. for $C_{16}H_{13}ON$: C, 81.68; H, 5.57; N, 5.94%.

The Cyanoketone XV.—To a solution of potassium *tert*-butoxide provided from 1.68 g. of potassium and 47 cc. of *tert*-butanol, was added 3.15 g. of the isoxazole XIV, and the mixture was heated for 10 min. at 70°C. To the orange-red solution, 13.5 cc. of methyl iodide was added taking more than 7 min. at 70~73°C. After heating at 75°C for 25 min. the solvent was removed and water was added to precipitate crystals. They were collected and washed with water, m. p. 141~142°C. Yield, 3.25 g. The melting point was raised by recrystallization from ethanol to 142~143°C.

Anal. Found: C, 82.21; H, 6.16; N, 5.93. Calcd. for $C_{17}H_{15}ON$: C, 81.90; H, 6.06; N, 5.62%.

The Stobbe Condensation of the Cyanoketone XV.—To a solution of potassium *tert*-butoxide prepared from 0.75 g. of potassium and 30.5 cc. of *tert*-butanol, was added 6.8 cc. of diethyl succinate taking more than 5 min. with stirring and cooling, and then 2.15 g. of the cyanoketone XV. The mixture was stirred for 2 hr. at room temperature, heated at 50°C for 1 hr., and then stirred for 5 hr. at room temperature. After being kept overnight, 20 cc. of 2 N hydrochloric acid solution was added with cooling, when carbon dioxide was evolved. After removal of the solvent in vacuo at 40°C, the aqueous layer was extracted with ether, from which the acidic material was transferred into 5% potassium hydroxide solution. Upon evaporation of the ether, the organic layer gave a small amount of a solid melting at 220~221°C after recrystallization from benzene.

Anal. Found: C, 81.22; H, 6.90%.

This was not investigated further because of the small amount available. The alkaline solution which contained the acidic material was acidified with hydrochloric acid to afford a very viscous oil, which was not studied further.

1-Methyl-2-hydroxymethyl-naphthalene (XVIIIa).—To a slurry of 5.75 g. of lithium aluminum hydride in 120 cc. of ether, a solution of 16 g. of 1-methyl-2-naphthoic acid in 340 cc. of ether was added taking more than 30 min., and the mixture was refluxed for 1 hr. on a water bath. After the excess of the reducing reagent was destroyed with ethyl acetate, the white voluminous precipitate was dissolved in dilute hydrochloric acid, and extracted with ether. The ether extract was washed with water, sodium bicarbonate solution and water. Removal of the solvent gave 14.0 g. of crystals melting at 124~126°C, which were recrystallized from benzene, m. p. 126~126.5°C.

Anal. Found: C, 83.88; H, 7.26. Calcd. for $C_{12}H_{12}O$: C, 83,69; H, 7.02%.

1-Methyl-2-bromomethyl-naphthalene (XVIIIb).—To a solution of 25.3 g. of the alcohol XVIIIa in 90 cc. of acetic acid, 63 g. of acetic acid saturated with hydrobromic acid was added for more than 15 min. After the solution was heated at 50~52°C for 20 min., the precipitate was collected (35.1 g.). Recrystallization from acetic acid afforded crystals melting at 68~69°C, 41.3 g. (yield, 90.6%).

For analysis this was further recrystallized from ligroin to give crystals melting at 69~70°C.

Anal. Found: C, 61.37; H, 4.97. Calcd. for $C_{12}H_{11}Br$: C, 61.28; H, 4.68%.

1-Methyl-2-cyanomethyl-naphthalene (XVIIIc).—A mixture of 10 g. of the bromide XVIIIb, 100cc. of ethanol, 5.0 g. of potassium cyanide and 20 cc. of water was refluxed for 5.5 hr. After the ethanol was removed, 300 cc. of water was added to the solution to precipitate a solid which showed m. p. at 75.5~76.5°C after recrystallization from ligroin, and weighed 7.2 g. (yield, 93.5%).

Anal. Found: C, 85.97; H, 6.24; N, 7.98. Calcd. for $C_{13}H_{11}N$: C, 86.16; H, 6.12; N, 7.73%.

(1-Methyl-2-naphthyl)-acetic Acid (XVIIId) and its Amide (XVIIIe).—A mixture of 6.8 g. of the cyanide XVIIIc, 10 cc. of acetic acid, 10 cc. of concentrated hydrochloric acid and 10 cc. of water was refluxed for 30 min. After cooling, crystals (m. p. 146~158°C) were collected and washed with 5% sodium hydroxide solution to remove the acid XVIIId. The amide could be further hydrolyzed with concentrated hydrochloric acid and acetic acid to give the acid

XVIIId.

Anal. Found: C, 78.36; H, 6.60; N, 7.05. Calcd. for $C_{13}H_{13}ON$: C, 78.36; H, 6.58; N, 7.03%.

The alkaline extract was acidified to precipitate the acid XVIIId which was recrystallized from benzene to afford prisms, m. p. 165~166°C, weighed 5.7 g.

Anal. Found: C, 78.00; H, 6.03. Calcd. for $C_{13}H_{12}O_2$: C, 77.98; H, 6.04%.

When an attempt was made to hydrolyze the crude cyanide XVIIIc directly, the overall yield of the acid was 83%.

2-(1-Methyl-2-naphthyl)-ethanol (XIXa).—To a slurry of 5.03 g. of lithium aluminum hydride in 120 cc. of ether, was added a solution of 14 g. of the acid XVIIId in 300 cc. of ether with stirring for more than 30 min., and the mixture was refluxed for 3 hr. The excess of the reducing reagent was destroyed with 20 cc. of ethyl acetate, and the mixture was decomposed with dilute hydrochloric acid.

The organic layer was separated and the aqueous layer was extracted with ether. After drying, removal of the ether gave an oil, which was distilled to give a liquid boiling at 140~143°C/1 mmHg and weighing 11.7 g. (yield, 90.0%). For analysis a small sample was recrystallized from ligroin, m. p. 54~55°C.

Anal. Found: C, 83.95; H, 7.63. Calcd. for $C_{13}H_{14}O$: C, 83.83; H, 7.58%.

1-Bromo-2-(1-methyl-2-naphthyl)-ethane (XIXb).—To a solution of 17.5 g. of the alcohol XIXa in 60 cc. of benzene, 19 g. of phosphorus tribromide in 24 cc. of benzene was added taking more than 25 min., and the mixture was stirred for 3 hr. at 60~70°C. The reaction mixture was poured onto crushed ice, and the bromide was taken into ether. After the ether layer was washed with saturated sodium chloride solution and water, it was dried over anhydrous sodium sulfate. Removal of the solvent gave a liquid, which was distilled to afford the bromide XIXb, boiling at 124~126°C/0.006 mmHg and weighing 14.4 g. (yield, 61.5%).

Anal. Found: C, 63.10; H, 5.50. Calcd. for $C_{13}H_{13}Br$: C, 62.60; H, 5.23%.

Diethyl 1-(1-Methyl-2-naphthyl)-3, 3-propanedicarboxylate (XIXc).—Under 40 cc. of xylene, 2.52 g. of sodium was pulverized, and the xylene was decanted off and replaced by 18 cc. of benzene. To this mixture, 16.2 cc. of absolute ethanol was added for more than 5 min., and heated for 5 min. After 25.2 cc. of diethyl malonate was added over a period of 10 min., the solution was heated for 10 min. on a water bath, and a solution of 14.3 g. of the bromide XIXb in 118 cc. of benzene was added taking more than 20 min. Then the mixture was heated at 60~63°C for 8 hr. at 70°C for 2 hr., and refluxed for an additional 4 hr. The solution was poured onto ice, acidified with diluted hydrochloric acid, and extracted with ether. The ether extract was washed with water and dried. The residue, obtained by evaporation of the solvent, was distilled to give an oil, b. p. 160~165°C/0.005 mmHg. Yield, 18.1 g. (96.3%).

Anal. Found: C, 72.00; H, 7.41. Calcd. for $C_{20}H_{24}O$: C, 73.14; H, 7.37%.

Triethyl 5-(1-Methyl-2-naphthyl)-2, 3, 3-pentanetricarboxylate (XXa).—To a solution of potassium *tert*-butoxide in *tert*-butanol, provided from 1.1 g. of potassium and 26 cc. of *tert*-butanol in an atmospher of nitrogen, 8.0 g. of the diethyl ester XIXc was added, the mixture was stirred for 3 min. at room temperature, and 5.4 g. of ethyl α-bromopropionate was added for more than 10 min. The solution was stirred for an additional 30 min. After the *tert*-butanol was removed, the residue was poured into ice water and extracted with ether. After washing with water and drying, the solvent was removed to leave an oil, which was distilled at 195~200°C/0.006~0.008 mmHg. Yield, 9.5 g. (91.5%).

Anal. Found: C, 70.08; H, 7.59. Calcd. for $C_{25}H_{32}O_6$: C, 70.07; H, 7.53%.

5-(1-Methyl-2-naphthyl)-2, 3-pentanedicarboxylic Acid (XXc).—A solution of 11.7 g. of the ester XXa in 40 cc. of methanol was added to a solution of 26.5 g. of potassium hydroxide in 93 cc. of methanol and the mixture was refluxed for 1hr., to precipitate the potassium salt. Water (34 cc.) was added and the mixture was refluxed for 2 hr. After the addition of 30 cc. of water, the methanol was removed and 50 cc. of water was added to the solution. Unsaponified material was removed with ether, and the aqueous layer was acidified with 6 N hydrochloric acid. The tricarboxylic acid was extracted with ether. The ether was removed to give a semisolid which was decarboxylated by heating at 180~185°C. The acid was taken into 10% sodium hydorxide solution, precipitated with 6 N hydrochloric acid, and then extracted with ether. Removal of the ether gave 8.5 g. of tan-yellow semisolid, which was cyclized to XXa without further purification.

α-2-(10-Methyl-1-oxo-1, 2, 3, 4-tetrahydroanthryl)-propionic Acid (XXIa).—To a solution of 3.8 g. of the dicarboxylic acid XXc in 30 cc. of benzene, 9.7 g. of phosphorus pentachloride was added with stirring, and the mixture was heated at 20°C for 1 hr., and at 45°C for 5 min. To the cold stirred solution, a solution of 37.0 g. of stannic chloride in 15 cc. of benzene was added taking more than 5 min., and the mixture was stirred for 1 hr. at room temperature. The mixture was poured onto a mixture of 200 g. of ice and 30 cc. of concentrated hydrochloric acid, and extracted with ether. The ether extract was washed with water and shaken with 10% sodium hydroxide solution to extract the acid XXIa. The ketoacid (1.15 g., m.p. 179.5~181.5°C) was obtained by acidification followed by extraction with ether, and recrystallized from benzene to give needles melting at 181~182°C.

Anal. Found: C, 76.58; H, 6.59. Calcd. for $C_{18}H_{18}O_3$: C, 76.57; H, 6.45%.

The infrared spectrum indicated peaks at 6.00 and 5.90 μ.

α-2-(10-Methyl-1, 2, 3, 4-tetrahydroanthryl)-propionic Acid (XXIb).—A mixture of 1.0 g. of the ketoacid XXIa, 5 g. of zinc amalgam, 6 cc. of acetic acid and 6 cc. of concentrated hydrochloric acid was covered with a layer of 4 cc. of toluene

and the whole was refluxed for 24 hr., while 1 cc. of concentrated hydrochloric acid was added to the solution every four hours (5 cc. in total). The solution, freed from excessive zinc, was diluted with water and extrated with ether. After the ether layer was washed with water and dried over anhydrous sodium sulfate, the solvent was removed to give crystals melting at 133~154°C and weighing 0.48 g. From mother liquor the second crop (0.28 g.) was obtained, m. p. 133~138°C. The combined material was recrystallized from dilute methanol to give a mixture of stereoisomers of the acid XXIb. The infrared spectrum showed peaks at 5.85 μ and lacked the carbonyl band at 6.00 μ of the ketocarboxylic acid XXIa.

Anal. Found: C, 80.87; H, 7.66. Calcd. for $C_{18}H_{20}O_2$: C, 80.56; H, 7.51%.

Methyl β-2-(10-Methyl-1, 2, 3, 4-tetrahydroanthryl)-butyrate (XXIc).—To a solution of 1.58 g. of the carboxylic acid XXIb in 19 cc. of benzene, 5 cc. of thionyl chloride was added and the mixture was heated on a water bath for 1 hr. After removal of the thionyl chloride and benzene in vacuo, 10 cc. of benzene was added and the solvent was evaporated so as to remove the excess of the thionyl chloride completely, and the residue was dissolved in 20 cc. of cold benzene. This solution of the acid chloride was added to a dried etheral solution of diazomethane provided from 6.3 g. of nitrosomethylurea. The reaction mixture was allowed to stand in an ice bath for 50 min., and at room temperature for 3 hr., while vigorous effervescence was observed. After the solvent was evaporated below 25°C, the residue was dissolved in 20 cc. of methanol and the solution was added to a slurry of 0.4 g. of silver oxide in 40 cc. of methanol and the mixture was refluxed for 2 hr.[29] The solution was filtered, and 0.2 g of silver oxide was added. After refluxing for 30 min., again 0.2 g. of silver oxide was added and the mixture was refluxed for an additional 30 min. After filtering off the silver and silver oxide, the solvent was removed to give a viscous liquid weighing 1.38 g., which was directly dehydrogenated to the ester XXIIa.

β-(10-Methyl-2-anthryl)-butyric Acid (XXIIb).—A mixture of 1.35 g. of the methyl ester XXIc and 0.2 g. of 30% Pd/C[30] was heated in an atmosphere of nitrogen at 250~280°C for 12 min. at 290~300°C for 1 hr. and at 310°C for 30 min. The reaction mixture was taken into boiling benzene, and freed from the catalyst. Removal of the solvent afforded a viscous orange oil possessing violet-green fluorescence. Beside the carbonyl band at 5.75 μ, the infrared spectrum showed peaks at 12.3 and 11.9 μ which are characteristic of the 1, 2, 4-trisubstituted benzene nucleus. The methyl ester was directly hydrolyzed. The mixture of 1.11 g. of the ester, 3 cc. of 40% potassium hydroxide solution, 5 cc. of water and 5 cc. of methanol was refluxed for 2 hr. in an atmosphere of nitrogen. After cooling, water was added and the solution was washed with ether to remove unsaponified material. The aqueous layer was acidified with hydrochloric acid, and extracted with ether. The ether extract was washed with water and dried. Removal of the solvent left an oil, which could be brought to crystallization by trituration with a small amount of benzene. The crystals collected weighed 0.60 g. and melted at 148~153°C. These were recrystallized from benzene to yield 0.5 g. of the acid XXIIb, m. p. 154~157°C. From mother liquor, the second crop (0.28 g., m. p. 157~158°C) was obtained by sublimation at 0.5 mmHg. The combined crystals were recrystallized from benzene, m. p. 160~160.5°C. The infrared spectrum showed peaks at 5.90 μ (carboxyl group) and 12.3 μ (1, 2, 4-trisubstituted benzen nucleus). The ultraviolet spectrum in ethanol indicated the following maxima: λ_{max} mμ (log ε): 258 (5.20), 332 (3.41), 347 (3.66), 365 (3.80), 385 (3.75).

Anal. Found: C, 82.07; H, 6.74. Calcd. for $C_{19}H_{18}O_2$: C, 81.98; H, 6.52%.

1-Oxo-3,6-dimethyl-2, 3-dihydro-1*H*-cyclopent[*a*]-anthracene (XXIIIa).—To a solution of 0.68 g. of the carboxylic acid XXIIb in 20 cc. of benzene, 0.9 g. of phosphorus pentachloride was added and the mixture was stirred for 30 min. at 0°C and 1 hr. at room temperature. To the well chilled and stirred solution, a solution of 0.6 g. of stannic chloride in 2 cc. of benzene was added and the mixture was stirred for 30 min. at 0°C and 1 hr. at room temperature. The reaction mixture was decomposed with a cold solution of 7 cc. of concentrated hydrochloric acid in 30 cc. of water, and extracted with ether. The ether extract was washed with 6 N hydrochloric acid, water, 5% sodium carbonate solution, and water. After drying, the solvent was removed to yield a residue which gave 0.41 g. of crystals, m. p. 135~141.5°C, upon trituration with methanol. For analysis they were recrystallized from methanol to afford needles, m. p. 142~143.5°C. The infrared spectrum indicated peaks at 5.93 μ, and the ultravioled spectrum is shown in Table I.

Anal. Found: C, 87.47; H, 6.23. Calcd. for $C_{19}H_{16}O$: C, 87.66; H, 6.17%.

3, 6-Dimethyl-2, 3-dihydro-1*H*-cyclopent[*a*]-anthracene (IV).—A mixture of 0.32 g. of the ketone XXIIIa, 5 g. of zinc amalgam, 5 cc. of concentrated hydrochloric acid, 5 cc. of acetic acid and 5 cc. of toluene was refluxed for 22 hr., while 7.5 cc. in total of concentrated hydrochloric acid was added from time to time. After the solution was cooled, the toluene layer was separated and the aqueous layer was extracted with ether. The combined toluene solution and ether were washed with water and dried over anhydrous sodium sulfate. Removal of the solvent yielded 0.265 g. of an orange oil with blue green fluorescence, which was dissolved in 40 cc. of benzene and chromatographed on 15 g. of alumina. Elution with 40 cc. of benzene gave 216 mg. of a pale yellow liquid. This was dissolved in 15 cc. of petroleum ether, and chromatographed again on

29) W. E. Bachmann and W. S. Struve, "Organic Reactions", Vol. 3, John Wiley & Sons, Inc., New York (1943), p. 38.

30) N. D. Zelinsky and M. B. Turowa Pollak, *Ber.*, **58**, 1298 (1925); H. St. Pfau and Pl. A. Plattner, *Helv. Chim. Acta.*, **23**, 78, (1940).

10 g. of alumina. Elution with 60 cc. of petroleum ether gave first 64 mg. of an almost colorless liquid, which was followed by 134 mg. of a pale yellow liquid eluted with 20 cc. of petroleum ether-benzene (1 : 1) and 30 cc. of benzene. The yellow oil solidified on standing to give crystals, m. p. 64~68°C, which were recrystallized twice from methanol, m. p. 78~79.5°C. The ultraviolet spectrum is given in Fig. 6 and Table I. The molecular weight determination by Rast's method gave the value 236 ($C_{19}H_{18}$: 246.33).

Anal. Found: C, 92.06; H, 7.86. Calcd. for $C_{19}H_{18}$: C, 92.63; H, 7.37%.

The picrate was recrystallized from ethanol to give reddish brown needles, m. p. 128~128.5°C.

Anal. Found: C, 63.25; H, 4.66; N, 9.13. Calcd. for $C_{25}H_{21}O_7N_3$: C, 63.15; H, 4.45; N, 8.84%.

The 2, 4, 6-trinitrobenzolate was recrystallized from ethanol to afford scarlet needles, m. p. 142~142.5°C.

Anal. Found: C, 65.48; H, 4.65; N, 9.12. Calcd. for $C_{25}H_{21}O_6N_3$; C, 65.35; H, 4.61; N, 9.15%.

The authors are indebted to Dr. Takeo Sakan and Dr. Masazumi Nakagawa for many helpful suggestions. The authors wish also to thank Mr. Eiichi Togashi, Shiono Koryo Kaisha, for a generous gift of phenethyl alcohol.

Department of Chemistry
Institute of Polytechnics
Osaka City University
Kita-ku, Osaka

Spectrophotometric Study of the Iodine-Complexes of cis- and trans-Stilbene

By Shigeru YAMASHITA

(Received March 25, 1959)

Results of the experiments[1], carried out recently in this laboratory, on the iodine-catalyzed *cis-trans* isomerization of stilbene in *n*-hexane led to the suggestion that the molecular complex formed between iodine and stilbene may play an important role in the photochemical as well as in the thermal isomerization at low temperatures around room temperature. It seemed then desirable to investigate the equilibria in the formation of iodine-complexes of both *cis-* and *trans*-stilbene quantitatively, since only limited information was available about these equilibria and related thermodynamic quantities. The present paper reports a spectrophotometric study of these complexes. The equilibrium constants, the heats and the entropy changes for the formation of iodine-complexes of *cis*-stilbene in *n*-hexane and of *trans*-stilbene in *n*-hexane and in carbon tetrachloride have been determined.

Experimental

Materials.—*Iodine.*—The commercial reagent of special grade was used without any further purification.

cis-Stilbene.—The preparation described in "Organic Syntheses"[2] was followed. After several repetitions of vacuum distillation, the product (b. p. 114~119°C/3.5~4.0 mmHg) was stored in the dark under reduced pressure. The absorption curve was in good agreement with that previously reported[3].

trans-Stilbene.—The commercial reagent (m. p. 119~120°C) was used without any further purification. The absorption curve was again in good agreement with that previously reported[3].

n-Hexane.—The commercial reagent of chemically pure grade was treated with fuming sulfuric acid, concentrated sulfuric acid and an aqueous solution of potassium permanganate, successively. After drying over anhydrous calcium chloride, the product was fractionally distilled.

Carbon tetrachloride.—The commercial reagent was successively treated with potassium hydroxide and anhydrous calcium chloride and then fractionally distilled.

Methods.—The absorption spectra were measured with an EPB-U type Hitachi-spectrophotometer. A quartz cell with a glass stopper (10.0 mm. light path) was used for the measurement in all wavelength regions.

The temperature of the absorption cell was kept constant in a water-circulating thermostat equipped with windows, as described by Bell[4].

1) To be published in a later paper.

2) R. E. Buckles and N. G. Wheeler, "Organic Syntheses", Vol. 33, John Wiley & Sons, New York (1953), p.88.

3) G. P. Mueller and D. Pickens, *J. Am. Chem. Soc.*, **72**, 3626 (1950); M. Orchin et al., *J. Chem. Educ.*, **34**, 493 (1957).

4) P. H. Bell, *Science*, **105**, 15 (1947).

All the operations were carried out in a dark place in order to avoid the occurrence of iodine-catalyzed *cis-trans* photoisomerization of stilbene.

Results and Discussion

Visible Absorption Bands of Iodine-Stilbene Complexes.—Iodine has an absorption maximum at 520 mμ in *n*-hexane, its absorbance over the range from 430 to 270 mμ being very weak. *cis*-Stilbene shows no absorbance in the range longer than 350 mμ in the same solvent. As *cis*-stilbene is added in increasing amounts to a dilute solution of iodine in *n*-hexane, the absorption peak at 520 mμ characteristic of the free iodine diminishes and is replaced by a new peak at 420 mμ as shown in Fig. 1. This new peak at 420 mμ may, therefore, be interpreted as a blue shift of iodine such as is frequently observed for iodine-complexes[5]. The charge-transfer band of the complex which may also be expected to appear in a still shorter wavelength region has not been studied in this work on account of difficulties due to the overlapping intense absorption of *cis*-stilbene.

Preliminary experiments in which the ratio of concentration of iodine to that of *cis*-stilbene was varied, keeping the sum of these constant, showed that the optical density at the absorption maximum was greatest in the equimolar mixture,

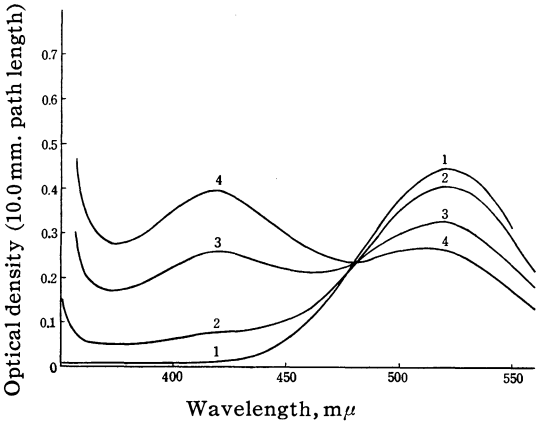


Fig. 1. Variation of the absorption band of iodine with increasing concentration of *cis*-stilbene: solvent, *n*-hexane; temperature, 24°C; concentration of I_2, 5.0×10^{-4} M; concentrations of *cis*-stilbene, 0, 2.0×10^{-2}, 1.0×10^{-1}, and 1.9×10^{-1} M for curves 1—4, respectively.

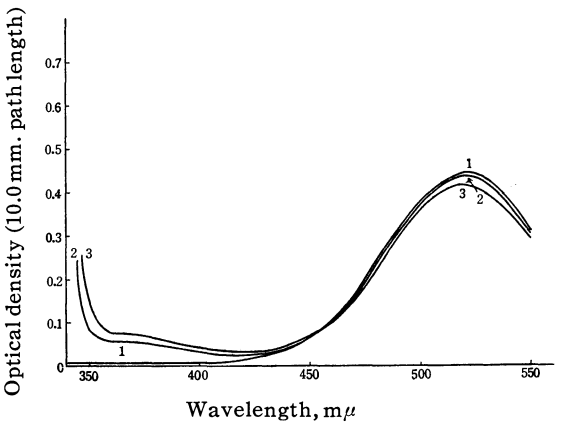


Fig. 2. Variation of the absorption band of iodine with increasing concentration of *trans*-stilbene: solvent, *n*-hexane; temperature, 24°C; concentration of I_2, 50×10^{-4} M; concentrations of *trans*-stilbene, 0, 5.0×10^{-2}, 9.5×10^{-2} M for curves 1—3, respectively.

indicating that the composition of the complex formed is 1 : 1. Isosbestic points such as those seen in Fig. 1 and less clearly in Fig. 2 have frequently been observed for 1 : 1 complexes.

Results obtained with *trans*-stilbene in the same solvent were, on the whole, similar to those with *cis*-stilbene. Here, however, the equilibrium constant for the complex formation has a lower value than for *cis*-stilbene as shown below. Consequently, the new maximum at 365 mμ which may again be taken as a blue shift of iodine is, as seen in Fig. 2, less sharp than that for *cis*-stilbene.

Andrews and Keefer[6a] reported an absorption maximum at 373 mμ, and a molar extinction coefficient of 7140 at this wavelength for the iodine-complex of *trans*-stilbene in carbon tetrachloride. In order to compare them with these results[6], measurements in carbon tetrachloride have been traced for the iodine-complex of *trans*-stilbene. The results obtained, together with those in *n*-hexane, are given in Table I where molar extinction coefficients determined as described below are included. As for the *trans*-stilbene complex in carbon tetrachloride, the values of λ_{max} obtained by the present author and by Andrews and Keefer agree with each other, but those of ε_{max} differ considerably from each other. Though the reason for the discrepancy in ε_{max} is not

5) H. A. Benesi and J. H. Hildebrand, *J. Am. Chem. Soc.*, **71**, 2703 (1949); C. Reid and R. S. Mulliken, ibid., **76**, 3869 (1954); S. Nagakura, ibid., **80**, 520 (1958); P. A. D. de Maine, *J. Chem. Phys.*, **26**, 1192 (1957).

6) (a) L. J. Andrews and R. M. Keefer, *J. Am. Chem. Soc.*, **74**, 4500 (1952); see also (b) R. Bhattacharya and S. Basu, *Trans. Faraday Soc.*, **54**, 1286 (1958).

clear yet*, Table I shows that all the values of ε_{max} found in this work for the iodine-stilbene complexes are nearly equal to each other and are of the same order of magnitude as those for free iodine. This is consistent with the interpretation that the observed absorption maxima are caused by the blue shifts of iodine since ε_{max} of the blue shift does not differ much from that of free iodine for many iodine-complexes, while far greater values, around 10000, have been reported for charge-transfer bands[5,7].

Equilibrium Constants.—Equilibrium constants for the iodine-stilbene complexes were determined, as usual, by a series of experiments in which the concentration of the donor component was varied, keeping that of iodine constant. As the latter concentration was relatively low in this work, the following equation[8,9] was applied to the optical densities obtained at respective absorption maxima.

$$1/(\varepsilon_A-\varepsilon_F) = 1/(\varepsilon_C-\varepsilon_F)(1/K_C)(1/C_D) + 1/(\varepsilon_C-\varepsilon_F) \quad (1)$$

n this equation ε_F and ε_C are, respectively, the molar extinction coefficients for free iodine and the complex in the mixture, and $\varepsilon_A = d/[(I_2)l]$, where d is the measured optical density of the solution containing the complex, (I_2) is the total concentration of iodine (free and complexed) and l is the path length of the absorption cell (1 cm.); C_D is actually the concentration of donor left free in the mixture but can be equated to its total concentration when an amount much greater than that of iodine is employed, as was the case in the present work; K_C is the equilibrium constant for the formation of the 1:1 complex.

Figs. 3 and 4 show that the linear relation required by Eq. 1 between $1/(\varepsilon_A-\varepsilon_F)$ and $1/C_D$ holds for *cis*- as well as for *trans*-stilbene in *n*-hexane, indicating that the compositions of these complexes are equally 1:1, as already inferred for

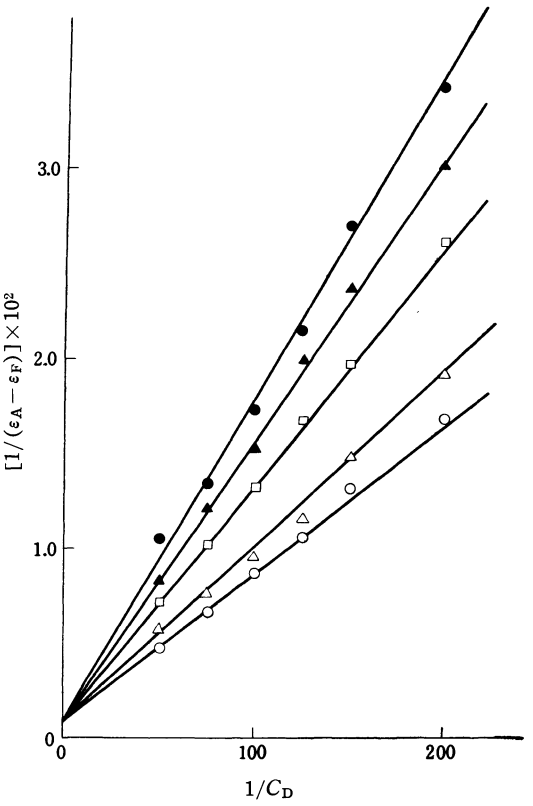


Fig. 3. $1/(\varepsilon_A-\varepsilon_F)$—$1/C_D$ diagram for the *cis*-stilbene—iodine system in *n*-hexane.
—●— 30°C, —▲— 25°C, —□— 20°C,
—△— 15°C, —○— 10°C.

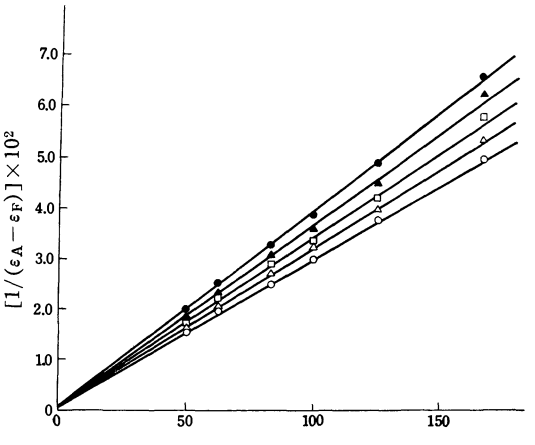


Fig. 4. $1/(\varepsilon_A-\varepsilon_F)$—$1/C_D$ diagram for the *trans*-stilbene-iodine system in *n*-hexane.
—●— 30°C, —▲— 25°C, —□— 20°C,
—△— 15°C, —○— 10°C.

cis-stilbene. Silmilar results were obtained with *trans*-stilbene in carbon tetrachloride. Values of ε_C calculated from intercepts of these straight lines have already been

* Andrews and Keefer determined ε_{max} from the intercept of a Benesi-Hildebrand plot at 25°C using the optical densities corrected for free iodine. Their extrapola tion at a single temperature is liable to produce a considerable error; however, it is not clear whether this is the sole reason for the large discrepancy in question. In the present work, as seen in Figs. 3 and 4, extrapolations at five different tempertures gave a constant intercept, making the value of ε_{max} thus determined much more reliable.

7) L. E. Orgel, *Quart. Revs.*, 8, 422 (1954).

8) L. J. Andrews and R. M. Keefer, *J. Am. Chem. Soc.*, 77, 4202 (1955).

9) J. A. A. Ketelaar et al., *Rec. trav. chim.*, 71, 1104 (1952).

TABLE I. ABSORPTION MAXIMA AND MOLAR EXTINCTION COEFFICIENTS FOR IODINE AND IODINE-STILBENE COMPLEXES

Absorbing species	Solvent	λ_{max} mμ	ε_{max}
I_2	*n*-Hexane	520	8.40×10^2
I_2	Carbon tetrachloride	520	1.20×10^3
I_2—*cis*-Stilbene	*n*-Hexane	420	1.32×10^3
I_2—*trans*-Stilbene	*n*-Hexane	365	1.38×10^3
I_2—*trans*-Stilbene	Carbon tetrachloride	374	1.48×10^3

TABLE II. EQUILIBRIUM CONSTANTS FOR IODINE-STILBENE COMPLEXES

Complex	Solvent	K_C				
		10°C	15°C	20°C	25°C	30°C
I_2—*cis*-Stilbene	*n*-Hexane	9.74	8.35	6.13	5.10	4.42
I_2—*trans*-Stilbene	*n*-Hexane	2.42	2.22	2.10	1.97	1.82
I_2—*trans*-Stilbene	Carbon tetrachloride	—	1.68	1.53	1.45	1.36

TABLE III. THERMODYNAMIC CONSTANTS FOR COMPLEX FORMATION AT 25°C

Complex	Solvent	$-\Delta H$ kcal./mol.	$-\Delta F$ kcal./mol.	$-\Delta S$ e. u./mol.
I_2—*cis*-Stilbene	*n*-Hexane	7.54	0.965	22.1
I_2—*trans*-Stilbene	*n*-Hexane	2.54	0.402	7.18
I_2—*trans*-Stilbene	Carbon tetrachloride	2.40	0.220	7.32

given in Table I as ε_{max}'s and those of K_C obtained from the slopes are listed in Table II.

Heats and Entropy Changes.—Fig. 5 shows plots of $\log K_C$ against the reciprocal temperature for the three systems investigated. The heats of the complex formation obtained from these plots are given in Table III, together with free energy and entropy changes calculated at 25°C. As seen in the table, the change of solvent from *n*-hexane to carbon tetrachloride produces only slight changes, as would usually be expected, while there exist significant differences between the values for *cis*- and *trans*-stilbene. Apparently, *cis*-stilbene forms a more stable and rigid complex with iodine than *trans*-stilbene. A plausible explanation for such a difference may be given as follows. Since the molecule of stilbene is planar in the *trans*-form and also nearly planar in the *cis*-form[10], iodine will attach to either form of stilbene on either side of its molecular plane to form a molecular complex.

trans-Stilbene has, however, two phenyl groups projected almost in the opposite direction, while *cis*-stilbene has a bent and therefore much more compact structure. Hence the complex of *cis*-stilbene may have a more rigid structure than that of *trans*-stilbene, and, at the same time, the former complex may be more stable owing primarily to a greater van der Waals attraction.

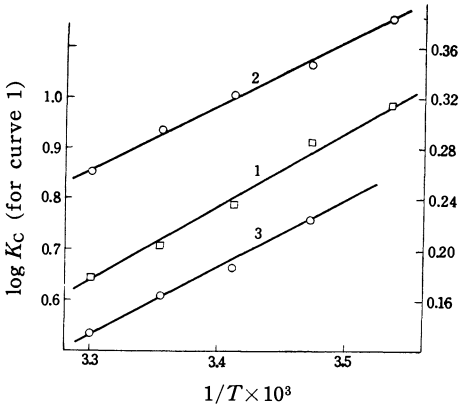


Fig. 5. Plots of $\log K_C$ vs. $1/T$:
1, I_2+*cis*-stilbene in *n*-hexane;
2, I_2+*trans*-stilbene in *n*-hexane;
3, I_2+*trans*-stilbene in carbon tetrachloride.

The author is particularly indebted to Professor O. Toyama of the College of Engineering and to Dr. T. Hayakawa for their discussions and encouragement during this investigation. The author wishes also to thank Mr. Y. Hayashibara for his assistance. A part of the expense of this study has been defrayed by the Scientific Research Grant from the Ministry of Education.

Department of Chemistry
College of General Education
The University of Osaka Prefecture
Mozu-higashino-cho, Sakai

10) G. N. Lewis, T. T. Magel and D. Lipkin, *J. Am. Chem. Soc.*, **62**, 2973 (1940).

The Crystal Structure of Bis(glutaronitrilo)copper(I) Nitrate

By Yukio KINOSHITA, Ikuo MATSUBARA and Yoshihiko SAITO*

(Received April 2, 1959)

In a previous paper[1] the authors have reported the crystal structure of bis-(succinonitrilo)copper(I) nitrate. As a continuation of our crystallographic study of a series of complexes prepared from nitriles of aliphatic dibasic acids and univalent copper, the present paper reports the determination of the crystal structure of bis(glutaronitrilo)copper(I) nitrate, $[Cu(NC\text{-}CH_2\text{-}CH_2\text{-}CH_2\text{-}CN)_2]NO_3$. This work was undertaken to elucidate the mechanism of cuprous ion dyeing of polyacrylonitrile fibers[2], and the structure of bis(glutaronitrilo)copper(I) nitrate may be particularly interesting in this complex series, because, as Rath et al.[3] have suggested, it is considered to be most suitable as the model substance of the polyacrylonitrile fibers dyed with cuprous ion technique.

Experimental

Bis(glutaronitrilo)copper(I) nitrate was prepared according to the directions of Rath et al.[3] similar to those described in the previous paper[1].

Anal. Found: C, 38.15; H, 4.08; N, 22.12; Cu, 20.27. Calcd. for $C_{10}H_{12}N_5O_3Cu$: C, 38.28; H, 3.86; N, 22.32; Cu, 20.25%.

Minute prismatic crystals were chosen for X-ray study in order to minimize the effects of absorption.

Rotation and Weissenberg photographs, taken with Cu $K\alpha$ radiation ($\lambda=1.542$ Å), showed the crystals to be tetragonal with $a=8.25\pm0.01$ Å, and $c=9.71\pm0.01$ Å.

The observed extinction, $(h\,h\,l)$ with $l=2n+1$ and $(h\,0\,0)$ with $h=2n+1$, is characteristic of the space group $P\bar{4}2_1c$–D_{2d}^4.

The observed density of the crystals, measured by flotation, is 1.587 g./cc., while the density calculated on the basis of two formula units in each unit cell is 1.577 g./cc.

Complete intensity data for the $(h\,k\,0)$ and $(0\,k\,l)$ zones were obtained from Weissenberg photographs in conjunction with the multiple film technique. The $(h\,k\,0)$ data comprise 41 different reflections out of a total of 48 that are accessible, and the $(0\,k\,l)$ data represent 95 forms out of all 106 forms available.

All intensities were estimated visually. After being corrected for the Lorentz and polarization factors, the intensities were reduced to relative F_o values which were later converted into absolute values by comparison with calculated ones.

Determination of Atomic Positions

In the space group $P\bar{4}2_1c$ there are two independent sets of twofold positions: 000; $\frac{1}{2}\frac{1}{2}\frac{1}{2}$ and $00\frac{1}{2}$; $\frac{1}{2}\frac{1}{2}0$. Since there are two formula units of $[Cu(NC\text{-}CH_2\text{-}CH_2\text{-}CH_2\text{-}CN)_2]NO_3$ in each unit cell, the copper atoms and the nitrogen atoms of nitrate ions must occupy these positions; the copper atom may be placed arbitrarily at the origin and the nitrogen atoms at $00\frac{1}{2}$. The point symmetry of these twofold positions is $\bar{4}$. This is in accordance with the expected tetrahedral coordination of a univalent copper atom. The nitrate ions thus centered at $00\frac{1}{2}$ are also required to have the same symmetry. However, trigonal nitrate ions could have the apparent symmetry $\bar{4}$ only if disorder exists in the crystal. The central carbon atom of each glutaronitrile molecule must occupy one of the two sets of fourfold positions and all other atoms probably lie on general positions. Consequently a glutaronitrile molecule must have a twofold axis of symmetry. Patterson projections upon (001) and (100) were calculated. These served to confirm the arrangement of heavy atoms. Both Patterson projections could be readily solved on the basis of the knowledge of interatomic distances and bond angles obtained for crystals of bis(succinonitrilo)copper(I) nitrate[1], and the orientation of the glutaronitrile molecule in the crystal could be successfully deduced. In this way, all the coordinates of atoms except those of oxygen atoms were approximately fixed. It is almost evident that the phase angles of the structure factors for a complete set can be determined on the

* Institute of Polytechnics, Osaka City University, Kita-ku. Osaka.

1) Y. Kinoshita, I. Matsubara and Y. Saito, This Bulletin, **32**, 741 (1959).

2) R. H. Blaker, S. M. Katz, J. F. Laucius, W. R. Remington and H. E. Schroeder, *Discussions Faraday Soc.*, No. **16**, 210 (1954).

3) H. Rath, H. Rehm, H. Rummler and E. Specht, *Melliand Textilber.*, **38**, 431, 538 (1957).

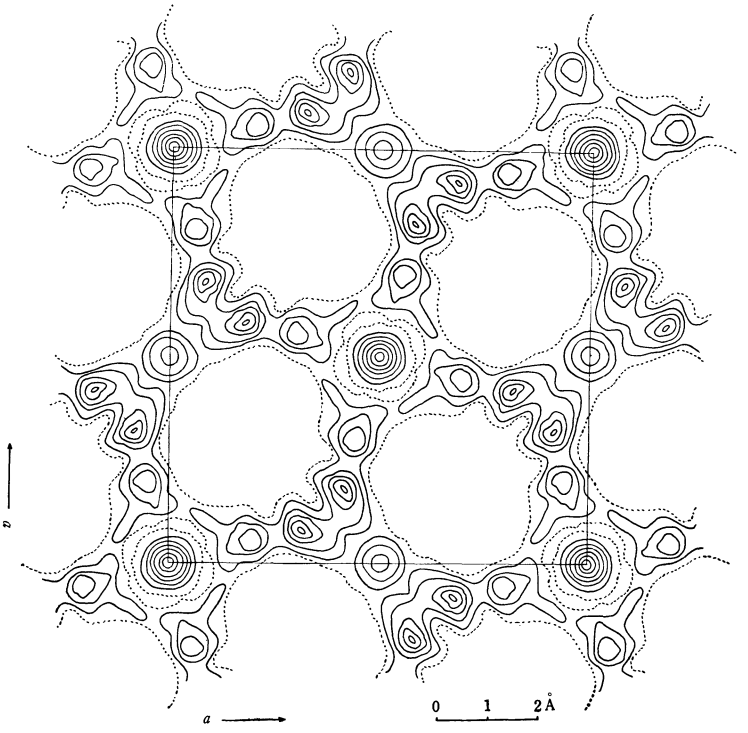


Fig. 1. Final Fourier projection of electron density upon (001). Contours are drawn at intervals of 8e Å^{-2} for copper and those for other atoms are at intervals of 2e Å^{-2}, the lowest being 2e Å^{-2}.

basis of these parameters. Fourier projections of electron density, $\rho(xy)$ and $\rho(yz)$ were then evaluated, the phase angles of which were calculated from the above mentioned parameter values. The projections so obtained showed the heavy copper atoms as well as ligand molecules clearly resolved, together with rather faint outlines of oxygen atoms in the nitrate ions. From the distribution of peaks around the nitrogen atoms, statistical orientations of nitrate ions were deduced. Calculation of structure amplitudes including the contribution of oxygen atoms improved the agreement

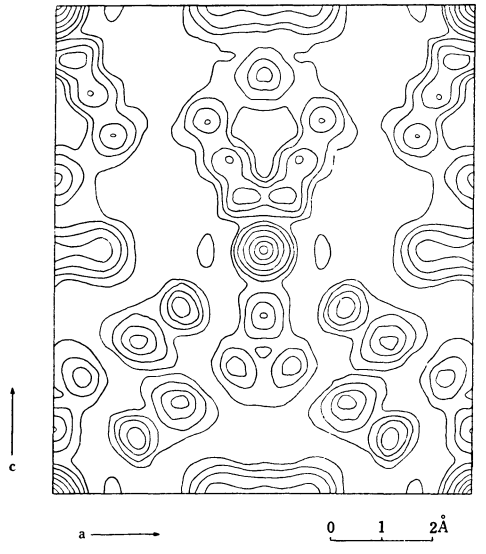


Fig. 2. Final Fourier projection of electron density upon (100). Contours are drawn at intervals of 6e Å^{-2} for copper and those for other atoms are at intervals of 2e Å^{-2}, the lowest being 2e Å^{-2}.

TABLE I. FINAL ATOMIC COORDINATES

Atom	Number of positions and Wyckoff notation	x/a	y/b	z/c
Cu	2 *a*	0.000	0.000	0.000
N_1	8 *e*	0.192	0.053	0.113
C_1	8 *e*	0.297	0.088	0.183
C_2	8 *e*	0.447	0.138	0.267
C_3	4 *d*	0.500	0.000	0.362
N_2*	2 *b*	0.000	0.000	0.500
O**	8 *e*	0.150	0.000	0.500
	8 *e*	0.130	0.075	0.500
	8 *e*	0.075	0.130	0.500

* Nitrogen atom of nitrate ion.

** Six oxygen atoms are statistically distributed on these three sets of eightfold positions with weights 1/4.

TABLE II. COMPARISON OF OBSERVED AND CALCULATED STRUCTURE FACTORS

Index	$\|F_o\|/4$	$F_c/4$	Index	$\|F_o\|/4$	$\|F_c\|/4$	$\alpha°$	Index	$\|F_o\|/4$	$\|F_c\|/4$	$\alpha°$
200	22.4	+24.3	011	8.1	9.1	0	006	11.6	11.9	0
400	8.0	+ 9.9	021	5.9	6.4	90	016	< 0.3	0.2	270
600	6.8	+ 7.9	031	9.7	10.5	0	026	7.8	8.3	0
800	2.6	+ 2.6	041	4.1	5.0	270	036	2.0	1.5	270
1000	3.1	+ 2.7	051	8.3	7.6	0	046	4.9	5.8	0
			061	1.2	1.4	270	056	2.3	2.5	90
110	10.6	+12.9	071	2.1	1.9	0	066	4.0	4.0	0
210	12.0	+10.4	081	1.8	1.8	90	076	< 0.3	0.1	270
310	8.2	+ 8.7	091	1.4	1.3	0	086	3.2	3.3	0
410	6.2	+ 6.3	0101	0.8	0.7	270	096	1.1	1.3	90
510	6.9	+ 7.5								
610	1.4	+ 2.1	002	11.8	11.1	0	017	3.8	2.5	0
710	4.7	+ 4.4	012	0.6	1.1	90	027	< 0.3	0.2	90
810	0.6	− 0.1	022	13.4	14.6	0	037	3.2	3.4	0
910	2.5	+ 2.1	032	1.1	0.8	90	047	0.5	0.3	270
1010	< 0.3	− 0.3	042	9.6	10.2	0	057	4.2	4.1	0
			052	3.6	3.8	270	067	0.6	0.6	270
220	7.1	− 7.1	062	6.6	7.1	0	077	3.1	2.2	0
320	< 0.2	− 0.2	072	2.1	2.6	270	087	0.3	0.5	270
420	10.6	+ 9.7	082	4.3	4.5	0				
520	1.2	+ 0.6	092	0.4	0.8	270	008	9.6	10.7	0
620	11.6	+11.4	0102	1.4	2.2	0	018	< 0.3	0.5	90
720	< 0.4	− 0.7					028	6.9	7.5	0
820	5.3	+ 5.6	013	3.6	3.4	180	038	2.0	2.0	270
920	1.7	+ 0.9	023	7.4	7.1	90	048	4.3	4.1	0
1020	3.3	+ 2.9	033	6.7	6.6	0	058	1.1	0.2	270
			043	3.3	3.2	90	068	4.1	4.1	0
330	4.9	+ 4.6	053	8.2	8.4	0	078	0.3	0.4	270
430	1.9	− 1.4	063	2.2	1.9	270	088	1.6	2.1	0
530	6.2	+ 6.1	073	3.9	4.1	0				
630	0.7	− 0.6	083	1.4	1.3	270	019	3.7	3.0	0
730	2.6	+ 2.9	093	2.3	2.6	0	029	0.9	1.3	270
830	< 0.3	+ 0.5	0103	0.6	0.9	270	039	3.4	3.4	0
930	2.6	+ 2.1					049	0.6	0.1	90
1030	0.8	+ 0.8	004	13.7	14.0	0	059	3.6	4.0	0
			014	0.3	0.2	90	069	< 0.2	0.7	90
440	8.3	+ 7.6	024	11.0	11.9	0	079	< 0.2	0.1	180
540	0.7	+ 0.8	034	2.4	3.5	90				
640	6.7	+ 7.1	044	2.0	2.9	0	0010	5.0	5.6	0
740	2.6	− 2.0	054	1.1	0.5	90	0110	1.5	1.9	270
840	4.6	+ 4.7	064	3.0	4.4	0	0210	2.2	2.8	0
940	< 0.3	− 0.1	074	1.7	1.8	90	0310	1.5	1.0	90
			084	4.4	4.4	0	0410	2.1	2.0	0
550	6.3	+ 6.6	094	0.3	0.6	270	0510	0.6	0.6	270
650	2.4	− 2.4	0104	< 0.2	0.6	0	0610	1.1	1.5	0
750	1.8	+ 2.2								
850	< 0.3	− 0.0	015	1.8	1.2	0	0111	1.5	1.2	0
950	0.9	+ 0.9	025	4.1	4.6	270	0211	1.6	1.2	90
			035	9.5	10.0	0	0311	2.1	2.1	0
660	2.9	+ 3.6	045	< 0.3	0.9	270	0411	< 0.2	0.3	90
760	0.6	+ 0.9	055	1.8	2.1	0	0511	< 0.1	0.6	0
860	2.6	+ 2.5	065	2.5	1.9	90				
			075	2.7	2.8	0	0012	1.7	2.6	0
770	2.8	+ 2.0	085	0.4	0.2	90	0112	1.9	1.9	90
870	< 0.2	+ 0.4	095	1.7	1.8	0	0212	2.0	1.9	0
							0312	< 0.1	0.4	90

between calculated and observed intensities. The best agreement is found if the nitrate ions lie perpendicularly to the *c*-axis, taking four different azimuthal orientations in such a way that the direction of one N–O bond coincides with one of the *a*-axis. Thus the apparent symmetry of the nitrate ions becomes $\bar{4}$, in accordance with the requirement of the space group. Although structure factors were also calculated under the assumption of free rotation of nitrate ions, the result gave a slightly greater *R*-value.

By the usual method of successive approximation the final projections were obtained. The final Fourier projections upon (001) and (100) are shown in Figs. 1 and 2, respectively. The final atomic coordinates are listed in Table I. Observed and calculated structure factors as well as phase angles are listed in Table II. The agreement on the whole is quite good and values of $R=\sum||F_o|-|F_c||/\sum|F_o|$ are 0.106 and 0.117 for $(h\,k\,0)$ and $(0\,k\,l)$, respectively. In the calculation of the structure factors, the atomic scattering curves calculated by Berghuis et al.[4] were employed. A temperature correction, $\exp -B(\sin\theta/\lambda)^2$, was applied with $B=3.0$ Å^2.

Interatomic distances and bond angles calculated on the basis of the atomic parameters listed in Table I are given in Table III.

TABLE III. INTERATOMIC DISTANCES AND BOND ANGLES

$Cu-N_1$	1.98 Å	$\angle CuN_1C_1$	176°
C_1-N_1	1.14	$\angle N_1C_1C_2$	176
C_1-C_2	1.54	$\angle C_1C_2C_3$	110
C_2-C_3	1.53	$\angle C_2C_3C_{2'}$	106
N_2-O	1.24		

Calculation of the structure factors as well as that of the electron density was carried out with a Remington Rand UNIVAC 120 electronic computer quite effectively.

Description of the Structure

The projections of the structure of bis-(glutaronitrilo)copper(I) nitrate upon (001) and (100) are shown in Figs. 3 and 4, respectively. It consists of infinite two-dimensional networks of the complex ion $[Cu(NC-CH_2-CH_2-CH_2-CN)_2]_n^{n+}$ and nitrate ions. A copper atom is tetrahedrally surrounded by four nitrogen atoms at a distance of 1.98 Å. Each glutaronitrile molecule is coordinated to two different copper atoms with nitrogen atoms at both ends. As a consequence, all the copper atoms in a plane perpendicular to the *c*-axis are linked together with ligand molecules, forming a two-dimensional network of complex ions. A glutaronitrile molecule possesses a twofold axis of symmetry and takes a *gauche-gauche* configuration with respect to the C_2–C_3 and C_3–$C_{2'}$ bonds. The angles of internal rotation were found to be 115° with the *trans* position taken as the origin. The carbon-carbon distances and bond angles agree well with those usually found in other organic crystals. The carbon-nitrogen bond distance is 1.14 Å and the Cu–N–C–C group is close to linear, which is similar to the case of bis(succinonitrilo)copper(I) nitrate. These facts indicate that the bond character of the carbon-nitrogen bond may be expressed as C≡N. Because of the rigidity of the triple bond and the tetrahedral coordination of copper atoms, the network of the complex ion is puckered. Nevertheless, the mode of packing of each layer is considered to be satisfactory with reasonable van der Waals distances between successive sheets. At the center of each mesh of the network of the complex ion a nitrate ion is located perpendicularly to the *c*-axis. The trigonal nitrate ion seems to have statistical azimuthal orientations and its apparent symmetry becomes $\bar{4}$. Just above and below the nitrate ion lie two copper atoms of adjacent layers at a distance of 4.86 Å, which should be compared with the corresponding distance of 4.77 Å found for the crystals of bis(succinonitrilo)copper(I) nitrate. That is to say, there is a cavity in the packed layers of the two-dimensional complex ions and a nitrate ion is at the center of the cavity. The interatomic distances between oxygen atoms of nitrate ions and the carbon atoms of the nearest methylene groups in the complex ion are longer than 3.14 Å. This is to be compared with the distance of 3.12 Å found between the carbon atom of a methylene group and the oxygen atom of a water molecule in the crystals of $[Co\,en_3]Cl_3\cdot 3H_2O$[5].

Further discussions of the structure will be made after the crystal structure of bis(adiponitrilo)copper(I) nitrate[6] has been determined.

4) J. Berghuis et al., *Acta Cryst.*, 8, 478 (1955).

5) K. Nakatsu, Y. Saito and H. Kuroya, This Bulletin, **29**, 428 (1956).

6) Y. Kinoshita, I. Matsubara, T. Higuchi and Y. Saito, ibid., **32**, 1221 (1959).

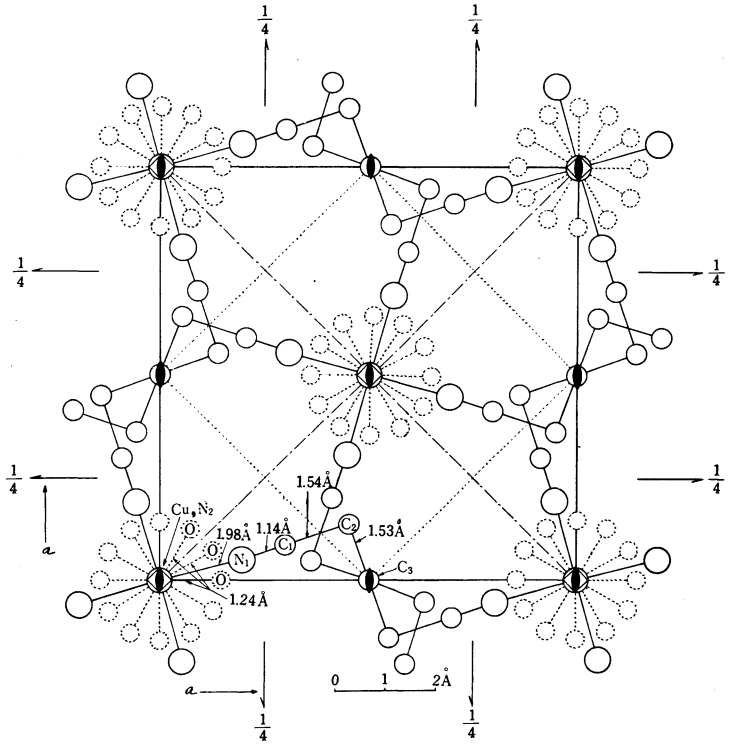


Fig. 3. Projection of the structure upon (001).

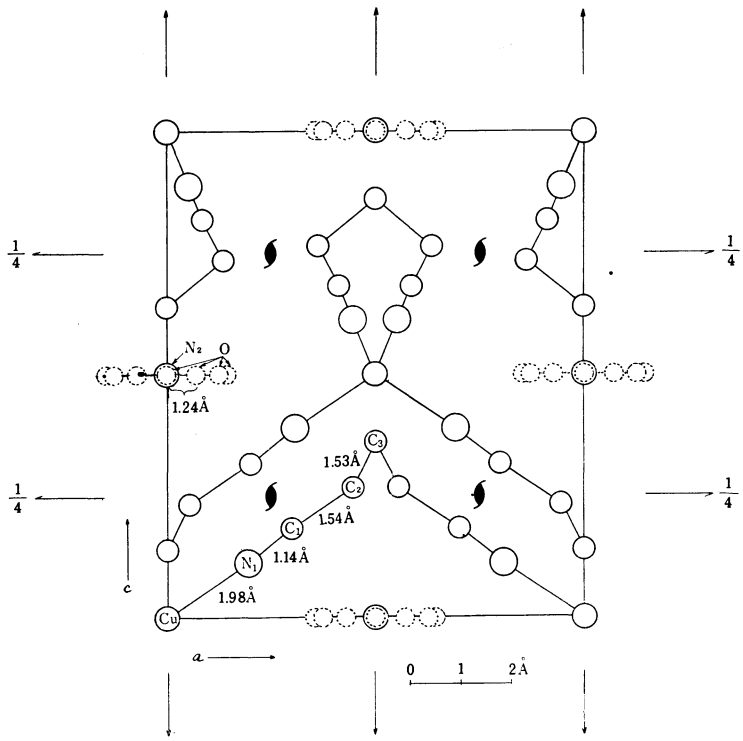


Fig. 4. Projection of the structure upon (100).

Summary

The crystal structure of bis(glutaronitrilo)copper(I) nitrate has been determined by the two-dimensional Fourier method. It is tetragonal $P\bar{4}2_1c$ with two formula units in a cell of dimensions: $a=8.25\pm0.01$ Å and $c=9.71\pm0.01$ Å.

The crystal consists of infinite two-dimensional networks of complex ion $[Cu(NC-CH_2-CH_2-CH_2-CN)_2]_n^{n+}$ and nitrate ions. A copper atom is tetrahedrally surrounded by four nitrogen atoms at a distance of 1.98 Å. Each glutaronitrile molecule is coordinated to two different copper atoms with nitrogen atoms at both ends and takes a *gauche-gauche* configuration with respect to the two C–C bonds. The nitrate ions lie perpendicularly to the *c*-axis. The trigonal nitrate ions seem to have statistical azimuthal orientations in the crystal and the apparent symmetry of the nitrate ion is $\bar{4}$.

All the atoms in the group Cu–N–C–C lie approximately on a straight line. This fact and the observed carbon-nitrogen distance of 1.14 Å suggest that the bond character in the carbon-nitrogen group may essentially be expressed as C≡N.

The authors wish to express their hearty thanks to Dr. K. Hoshino and Dr. K. Kato of the Central Research Laboratories of Toyo Rayon Co., Ltd. for their kind encouragement in the course of this study. They also wish to thank Mr. K. Yoshida of Toyo Rayon Co., Ltd. for carrying out the mechanical computations.

Central Research Laboratories
Toyo Rayon Co., Ltd.
Otsu, Shiga

The Crystal Structure of Bis(adiponitrilo)copper(I) Nitrate

By Yukio KINOSHITA, Ikuo MATSUBARA, Taiichi HIGUCHI* and Yoshihiko SAITO*

(Received April 27, 1959)

We have previously reported on the crystal structures of some complexes prepared from nitriles of aliphatic dibasic acids and univalent copper[1,2], which may be of interest in relation to the mechanism of cuprous ion dyeing of polyacrylonitrile fibers. In the course of our study on crystal structures of this series of complexes, the crystal structure of bis(adiponitrilo)copper(I) nitrate, $[Cu(NC-CH_2-CH_2-CH_2-CH_2-CN)_2]NO_3$, has been determined by means of two-dimensional Fourier methods.

The crystal structure will be discussed together with those of homologues reported in the previous papers, and some remarks will be made on the mechanism of dyeing polyacrylonitrile fibers.

* Institute of Polytechnics, Osaka City University, Kita-ku, Osaka.

1) Y. Kinoshita, I. Matsubara and Y. Saito, This Bulletin, **32**, 741 (1959).

2) Y. Kinoshita, I. Matsubara and Y. Saito, ibid., **32**, 1216 (1959).

3) H. Rath, H. Rehm, H. Rummler and E. Specht, *Melliand Textilber.*, **38**, 431, 538 (1957).

Experimental

Bis(adiponitrilo)copper(I) nitrate was prepared according to the method of Rath et al.[3] by dissolving silver nitrate into adiponitrile at 60°C and adding an excess of copper powder. After some black spongy silver was deposited, the mixture was filtered. On cooling, the clear filtrate deposited yellowish crystals.

Anal. Found: C, 42.05; H, 4.70; N, 20.54; Cu, 18.52. Calcd. for $C_{12}H_{16}N_5O_3Cu$: C, 42.16; H, 4.72; N, 20.49; Cu, 18.59%.

The crystals are orthorhombic and the unit cell dimensions, as determined from rotation and Weissenberg photographs taken with Cu $K\alpha$ radiation ($\lambda=1.542$ Å), are $a=9.41\pm0.02$ Å, $b=13.73\pm0.02$ Å and $c=5.85\pm0.01$ Å. Systematic extinctions occur only for $(h\,k\,0)$ with $h+k$ odd, $(0\,k\,l)$ with $k+l$ odd and $(h\,0\,l)$ for $h+l$ odd. The space group is therefore $Pnnn-D_{2h}^2$.

Assuming two formula units in the unit cell, the calculated density is 1.502 g./cc., in good agreement with the measured density 1.516 g./cc.

The intensities of the spectra recorded on multiple-film zero-layer Weissenberg photographs were estimated visually and corrected for Lorentz and polarization factors. In view of the small size of the crystals no corrections were made

for the absorption effect. The resulting F^2's were correlated so that all observed data were on the same relative intensity scale. They were later converted into an absolute scale by comparison with calculated values.

Determination of Atomic Positions

Since the general point position in the space group *Pnnn* is eightfold, and since there are only two formula units of $[Cu(NC-CH_2-CH_2-CH_2-CH_2-CN)_2]NO_3$ in the unit cell, it follows that the copper atom must occupy one of the four sets of special positions; 0, 0, 0; 1/2, 1/2, 1/2, etc. All these positions are the intersecting points of three twofold axes which are parallel to the three principal axes respectively. Should the copper atoms occupy a set of these positions, the $(h\,k\,l)$ intensities should conform approximately to the extinction condition of body centered lattice. Equi-inclination Weissenberg photographs revealed that this condition was actually fulfilled. The positions of the copper atoms are, therefore, arbitrarily chosen as 0, 0, 0; 1/2, 1/2, 1/2.

Similarly the nitrogen atoms of nitrate ions must lie on a set of these special positions. The point symmetry of these twofold positions is 222. This is not in accordance with the trigonal symmetry of the nitrate ion. The nitrate ion could have apparent symmetry 222 only if disorder exists in the crystal.

The Patterson projections onto (001), (010) and (100) are very similar to the corresponding Fourier projections, since copper atoms at the origin and the center of the unit cell make all signs of zero-layer reflections positive and moreover the plane group symmetry of the Patterson projections are similar to that of Fourier projections. Therefore, preliminary Fourier projections were computed with all signs positive. Because the *c*-axis is as short as 5.85 Å, the extended chain form of methylene groups in the adiponitrile molecule, which apparently connects the copper atom at the origin with that at the center of the unit cell, is clearly shown on $P(uv)$ and $\rho(xy)$. Further, it has been found from $(0\,k\,l)$ data that the atoms in adiponitrile molecules are concentrated in (031) planes, because the orders of reflection from (031) are exceptionally intense and the intensity decreases through four orders according to a normal decline. Consideration of the above facts with the aid of the Patterson projection upon (100) has led to the conclusion that an adiponitrile molecule is coordinated with the nitrogen atoms of both ends to two copper atoms at 0, 0, 0 and at 1/2, 1/2, 3/2, taking a planar zigzag configuration. Thus the approximate coordinates of all the atoms in the ligand molecule could be fixed. However, from the Patterson projections and the preliminary Fourier maps of electron density only, locations of the atoms in the nitrate ions could not be fixed unequivocally. As a consequence, the approximate parameters of these atoms were determined by trial calculations of structure amplitudes. The best agreement between observed and calculated structure amplitudes was obtained when the nitrate ion was placed perpendicularly to the *a*-axis, taking four different azimuthal orientations as shown in Table I. Thus, the apparent symmetry of the nitrate ion becomes 222 in accordance with the requirement of the space group. Determination of the more precise atomic parameters was achieved by successive

TABLE I. FINAL ATOMIC COORDINATES

Atom	Number of positions and Wyckoff notation		x/a	y/b	z/c
Cu	2 *a*		0.000	0.000	0.000
N_1	8 *m*		0.129	0.076	0.200
C_1	8 *m*		0.194	0.110	0.341
C_2	8 *m*		0.292	0.164	0.509
C_3	8 *m*		0.201	0.223	0.667
N_2	2 *b*		0.000	0.500	0.500
O_1	4 *j*	(1/4)*	0.000	0.410	0.500
O_2	4 *l*	(1/4)*	0.000	0.500	0.288
O_3	8 *m*	(1/4)*	0.000	0.455	0.317
O_4	8 *m*	(1/4)*	0.000	0.422	0.394

* Oxygen atoms are statistically distributed with weights shown in parentheses.

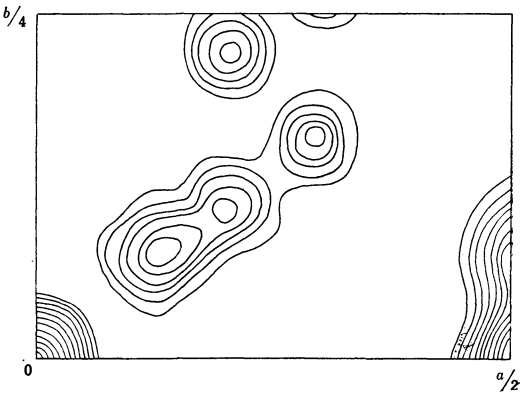


Fig. 1. Final Fourier projection of electron density upon (001). Contours are drawn at intervals of 4e $Å^{-2}$ for copper and those for other atoms are at intervals of 1e $Å^{-2}$, the lowest being 2e $Å^{-2}$.

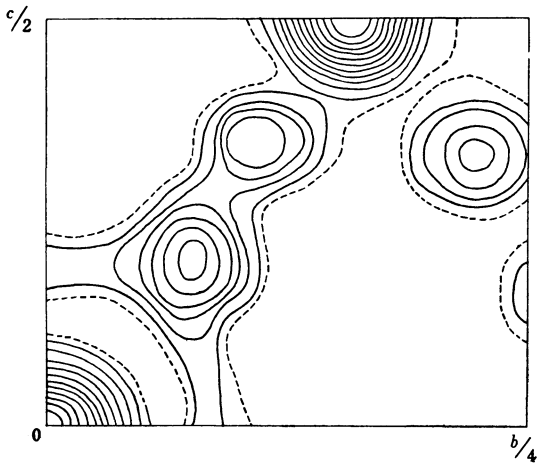


Fig. 2. Final Fourier projection of electron density upon (100). Contours are drawn at intervals of 5e Å^{-2} for copper and those for other atoms are at intervals of 1e Å^{-2}, the lowest being 2e Å^{-2} (broken).

Fourier syntheses. The final Fourier projections upon (001) and (100) are shown in Figs. 1 and 2, respectively.

The atomic parameters of the asymmetric unit are recorded in Table I and the calculated interatomic distances and bond angles are shown in Table II. The comparison of observed and calculated structure amplitudes is given in Table III, the reliability factors $R=\sum||F_o|-|F_c||/\sum|F_o|$ being 0.107, 0.116 and 0.112 for ($h\,k\,0$), ($h\,0\,l$) and ($0\,k\,l$), respectively, with a weighted mean value of 0.110.

TABLE II. INTERATOMIC DISTANCES AND BOND ANGLES

$Cu-N_1$	1.98 Å	$\angle CuN_1C_1$	169°
C_1-N_1	1.13	$\angle N_1C_1C_2$	172
C_1-C_2	1.54	$\angle C_1C_2C_3$	108
C_2-C_3	1.50	$\angle C_2C_3C_{3'}$	108
$C_3-C_{3'}$	1.53		
N_2-O	1.24		

A mean isotropic temperature factor with $B=3.0$ Å^2 was found to be satisfactory for the three principal zones. Calculation of electron density as well as that of structure factors were carried out on a Remington Rand UNIVAC 120 electronic computer quite effectively.

Description of the Structure

The projections of the structure of bis(adiponitrilo)copper(I) nitrate upon (001) and (100) are shown in Figs. 3 and 4, respectively.

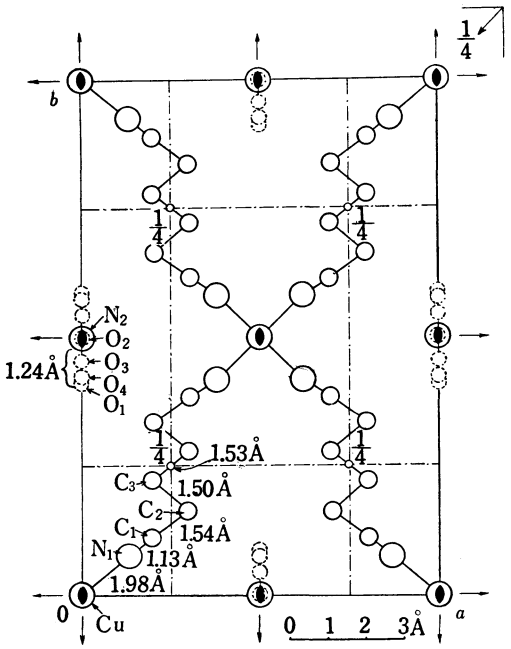


Fig. 3. Projection of the structure upon (001).

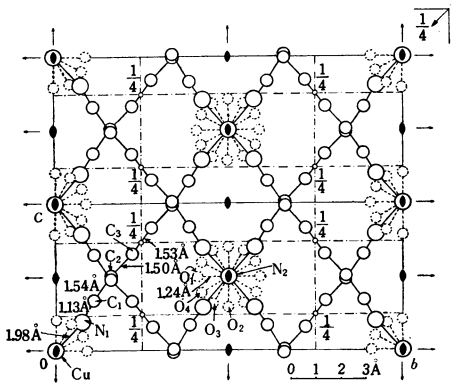


Fig. 4. Projection of the structure upon (100).

It is evident from the figures that the structure consists of infinite three-dimensional networks of the complex ion $[Cu(NC-CH_2-CH_2-CH_2-CH_2-CN)_2]_n^{n+}$ and nitrate ions. A copper atom is surrounded tetrahedrally by four nitrogen atoms at a distance of 1.98 Å, which is in good agreement with the corresponding values observed for the related compounds reported previously[1,2]. Each adiponitrile molecule is coordinated to two different copper atoms, resulting in a complicated three-dimensional network of the complex ion. A copper atom at the origin is linked to four copper atoms belonging to different unit cells at 1/2, 1/2, 3/2; −1/2, −1/2, 3/2; 1/2,

TABLE III. COMPARISON OF OBSERVED AND CALCULATED STRUCTURE FACTORS

Index	F_o	F_c	Index	F_o	F_c	Index	F_o	F_c
200	6	7	280	22	23	705	12	9
400	72	70	480	40	35	802	14	12
600	70	64	680	22	16	804	18	16
800	26	28	880	7	3	901	14	12
1000	32	33	1080	10	11	903	17	14
1200	< 2	−1	190	41	33	905	< 2	8
020	64	69	390	< 5	−1	1002	11	12
040	22	24	590	43	47	1004	7	6
060	5	4	790	9	−6	1101	< 3	0
080	26	23	990	10	12	1103	< 2	12
0100	31	28	2100	29	25	011	54	60
0120	30	28	4100	23	20	031	102	117
0140	19	20	6100	16	14	051	28	26
0160	4	4	8100	11	9	071	18	29
002	24	23	1110	20	16	091	25	24
004	34	32	3110	14	16	0111	30	27
006	34	35	5110	< 5	1	0131	12	16
110	34	39	7110	14	17	0151	16	21
310	34	−35	9110	< 3	4	0171	< 4	4
510	< 4	3	2120	22	20	022	28	31
710	18	16	4120	13	13	042	30	31
910	13	7	6120	13	13	062	71	74
1110	< 4	2	8120	10	14	082	32	33
220	113	124	1130	14	14	0102	13	15
420	40	37	3130	9	8	0122	21	24
620	37	37	5130	< 5	0	0142	8	7
820	34	40	7130	11	12	0162	< 5	7
1020	7	9	2140	16	17	013	28	23
1220	10	15	4140	7	7	033	32	30
130	29	25	6140	7	9	053	34	32
330	19	21	1150	10	10	073	19	23
530	18	17	3150	6	6	093	51	55
730	14	13	5150	< 4	4	0113	10	8
930	12	13	2160	13	16	0133	< 7	4
1130	< 4	0	4160	< 3	5	0153	4	7
240	78	72	101	26	21	024	38	30
440	55	47	103	40	41	044	24	23
640	30	26	105	26	19	064	37	37
840	20	21	107	5	4	084	12	11
1040	8	9	202	49	44	0104	8	8
150	19	18	204	39	41	0124	17	20
350	66	61	206	< 4	0	0144	8	9
550	28	27	301	10	12	015	28	25
750	15	16	303	6	8	035	38	34
950	11	9	305	6	−2	055	12	9
1150	< 3	10	307	11	6	075	10	8
260	38	35	402	56	60	095	10	11
460	50	50	404	24	21	0115	11	13
660	15	13	406	18	15	0135	< 3	7
860	10	9	501	11	9	026	8	8
1060	10	9	503	66	64	046	8	9
170	13	14	505	7	6	066	9	9
370	68	64	602	23	20	086	11	10
570	16	19	604	18	14	0106	7	8
770	22	20	606	13	13	017	< 5	0
970	< 5	2	701	14	13	037	13	13
1170	< 2	10	703	17	12	057	10	9

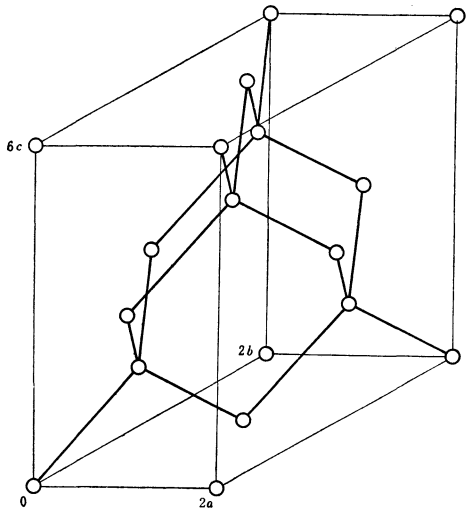


Fig. 5. Schematic diagram of a single 4-connected network in the crystal of bis(adiponitrilo)copper(I) nitrate.

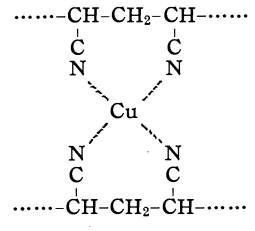
$-1/2, -3/2; -1/2, 1/2, -3/2$. In this way the copper atoms and the ligand molecules form a three-dimensional 4-connected network[4], in which all the copper atoms are arranged on a distorted diamond lattice and are linked by the ligand molecules with each other. Fig. 5 schematically illustrates the constitution of the network. The figure shows a single 4-connected network. For simplicity, adiponitrile molecules are drawn as straight lines connecting two copper atoms. The structure of bis(adiponitrilo)copper(I) nitrate consists of a superposition of six sets of this 4-connected network displaced through c with respect to each other.

Each adiponitrile molecule has a center of symmetry between the two central carbon atoms. All the carbon atoms of the adiponitrile molecule are less than 0.06 Å from the plane (031) and constitute a planar zigzag chain configuration, while the nitrogen atoms of nitrile groups are 0.10 Å distant from that plane. All the carbon-carbon bond lengths and bond angles in the methylene groups are close to normal values. The carbon-nitrogen bond distance is 1.13 Å and the Cu-N-C-C group is close to linear as in the cases of the related compounds reported previously[1,2]. These facts indicate that the bond character of the carbon-nitrogen bond may be expressed as C≡N.

The nitrate ions lie perpendicularly to the a-axis. The trigonal nitrate ion seems to have statistical azimuthal orientations in the crystal and its apparent symmetry becomes 222. The interatomic distances between the oxygen atoms of the nitrate ions and the carbon atoms of the nearest methylene groups in the complex ion are longer than 3.19 Å. This is to be compared with the corresponding value of 3.14 Å found in the crystals of bis(glutaronitrilo)-copper(I) nitrate[2].

Remarks on the Mechanism of Cuprous Ion Dyeing of Polyacrylonitrile Fibers

As pointed out in the previous paper[1], cuprous ion is readily absorbed by polyacrylonitrile fibers which then acquire an almost unlimited affinity for anionic dyes, which ordinarily can not be applied to this class of fibers. Blaker et al.[5] and Rath et al.[3] have suggested that the high affinity of cuprous ion for polyacrylonitrile is due to the inherent capability of nitrile groups in the fibers to absorb cuprous ion through formation of complexes, which may act as positive sites for fixation of dye anions. It has been established by the present investigations that, in the complexes prepared from univalent copper and nitriles of aliphatic dibasic acids, four nitrogen atoms of nitrile groups enter into combination with a cuprous ion, forming a stable tetrahedral complex. This fact strongly indicates that there may exist a strong interaction of the same kind between cuprous ions and nitrile groups of polyacrylonitrile molecules in the dyeing of fibers with cuprous ion technique. However, by analogy with the structures of these complexes it is very unlikely that stable chelate rings of the type,



are formed between cuprous ions and polyacrylonitrile molecules. In fact, it can easily be understood that such a chelate ring with reasonable bond distances and bond angles can never be obtained, owing to the rigidity of the Cu-N-C-C

4) For the definition of the term, see A. F. Wells, *Acta Cryst.*, **7**, 545 (1954).

5) R. H. Blaker, S. M. Katz, J. F. Laucius, W. R. Remington and H. E. Schroeder, *Discussions Faraday Soc.*, No. **16**, 210 (1954).

group. Therefore, Blaker and Rath's suggestion is only valid in the sense that the nitrile groups of polyacrylonitrile molecules are involved in the formation of complexes similar to those of simple nitriles as described in this and the preceding papers.

In the structures of these complexes, nitrate ions are located in cavities which are formed in the polymeric chain or network of complex ions owing to the rigidity of the Cu–NC–CH_2– group and the tetrahedral nature of the Cu–N bonds. This fact may suggest that in the polyacrylonitrile-Cu(I) complex the dye anions are trapped in cavities analogous to those mentioned above and are fixed by electrostatic interactions with the positive cuprous ions.

Summary

The crystal structure of bis(adiponitrilo)-copper(I) nitrate has been determined by the two-dimensional Fourier method. It is orthorhombic *Pnnn* with two formula units in a cell of dimensions: $a=9.41\pm0.02$ Å, $b=13.73\pm0.02$ Å and $c=5.85\pm0.01$ Å.

The crystal consists of infinite three-dimensional networks of complex ion $[Cu(NC-CH_2-CH_2-CH_2-CH_2-CN)_2]_n^{n+}$ and nitrate ions. A copper atom is tetrahedrally surrounded by four nitrogen atoms at a distance of 1.98 Å. Each adiponitrile molecule is coordinated to two different copper atoms with nitrogen atoms of both ends, forming a planar zigzag configuration of methylene groups. Thus the copper atoms and the ligand molecules form a complicated three-dimensional 4-connected network. The nitrate ions lie perpendicularly to the *a*-axis. The trigonal nitrate ion seems to have statistical azimuthal orientations in the crystal and its apparent symmetry becomes 222.

All the atoms in the group Cu–N–C–C lie approximately on a straight line. This fact and the observed carbon-nitrogen distance of 1.13 Å suggest that the bond character in the carbon-nitrogen group may essentially be expressed as C≡N.

On the basis of the structures of this and the other related complexes, some remarks have been made on the mechanism of cuprous ion dyeing of polyacrylonitrile fibers.

The authors wish to express their hearty thanks to Dr. K. Hoshino and Dr. K. Kato of the Central Research Laboratories of Toyo Rayon Co., Ltd. for their kind encouragement in the course of this study. They also wish to thank Mr. K. Yoshida of Toyo Rayon Co., Ltd. for carrying out the mechanical computations.

Central Research Laboratories
Toyo Rayon Co., Ltd.
Otsu, Shiga

π-Electronic Structures of o-Quinones

By Akira KUBOYAMA

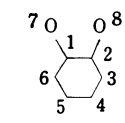
(Received April 17, 1959)

Previously[1], we studied the π-electronic structures of *p*-quinones (*p*-benzoquinone, α-naphthoquinone and anthraquinone) by the aid of the simple LCAO MO method and succeeded in explaining the following problems concerning the near UV absorption bands of the *p*-quinones: 1) a similarity among the $\pi-\pi$ transition bands of these *p*-quinones, 2) a relative magnitude of the $n-\pi$ transition energy of *p*-benzoquinone, α-naphthoquinone, and anthraquinone, 3) the effect of the electron-donating group on the $\pi-\pi$ transition bands of α-naphthoquinone and anthraquinone. In the present paper, similar theoretical studies have been extended to absorption spectra of *o*-quinones such as *o*-benzoquinone, β-naphthoquinone, and phenanthrenequinone. The calculations on β-naphthoquinone and phenanthrenequinone by the MO method have never been carried out. The obtained results are now reported.

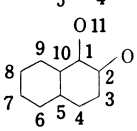
1) A. Kuboyama, This Bulletin, 31, 752 (1958).

Method of Calculation

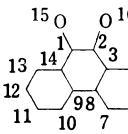
The method employed in the present calculation is exactly the same as that used in the case of *p*-quinones. The coulomb (α_i) and exchange (β_{ij}) integrals were determined on the basis of the same principles as described in the previous paper. They are as follows:



$\alpha_7=\alpha+1.3\beta$, $\alpha_1=\alpha+0.2\beta$
$\alpha_3=\alpha_4=\alpha$
$\beta_{17}=\beta_{34}=\beta$, $\beta_{12}=0.8\beta$
$\beta_{23}=\beta_{45}=0.9\beta$



$\alpha_{11}=\alpha_{12}=\alpha+1.3\beta$
$\alpha_1=\alpha_2=\alpha+0.2\beta$
$\alpha_3=\alpha_4=\cdots\cdots=\alpha_9=\alpha_{10}=\alpha$
$\beta_{1-11}=\beta_{2-12}=\beta_{34}=\beta_{56}=\beta_{67}$
$=\cdots\cdots=\beta_{9-10}=\beta_{5-10}=\beta$
$\beta_{12}=0.8\beta$,
$\beta_{23}=\beta_{45}=\beta_{1-10}=0.9\beta$



$\alpha_{15}=\alpha+1.3\beta$, $\alpha_1=\alpha+0.2\beta$
$\alpha_3=\alpha_4=\alpha_5=\alpha_6=\alpha_7=\alpha_8=\alpha$
$\beta_{1-15}=\beta_{34}=\beta_{45}=\beta_{56}=\beta_{67}$
$=\beta_{78}=\beta_{38}=\beta$
$\beta_{12}=0.8\beta$, $\beta_{23}=\beta_{89}=0.9\beta$

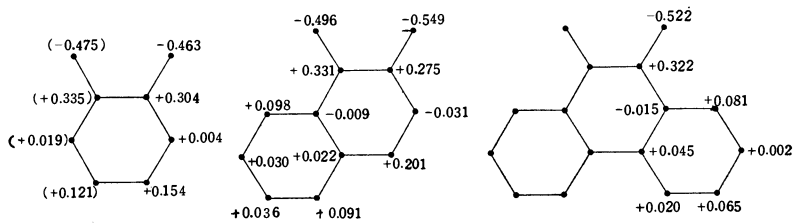
Among these values, those concerning the quinone nuclei were set equal to the values evaluated for *o*-benzoquinone by the self-consistent method[2].

Results

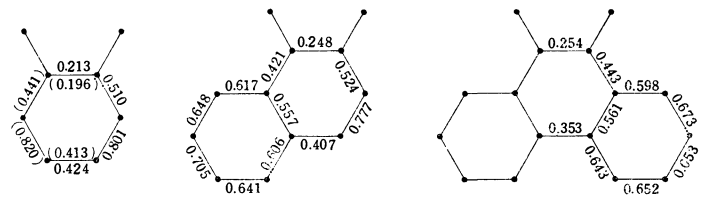
The obtained molecular diagrams are given below.

In the above diagram, the unpaired electron densities are the ones in the lowest unfilled orbitals[3]. In the molecular diagram for *o*-benzoquinone the values in brackets are the ones previously calculated by the self-consistent method. The agreement between these two molecular diagrams for *o*-benzoquinone is substantially good. Further, the energy levels of *o*-benzoquinone calculated by the two methods mentioned above are in good agreement with each other. The energy levels evaluated with these quinones are given in Fig. 1. Furthermore, the dependence* of the energy levels upon the coulomb integral of the oxygen atom was

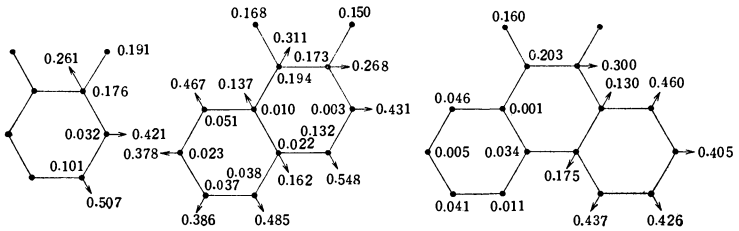
Charge densities



Bond orders



Free valences and unpaired electron densities



2) S. Nagakura and A. Kuboyama, *J. Chem. Soc. Japan, Pure Chem. Sec.* (*Nippon Kagaku Zasshi*), **74**, 499 (1953); S. Nagakura and A. Kuboyama, *J. Am. Chem. Soc.*, **76**, 1003 (1954).

3) H. M. McConnell, *J. Chem. Phys.*, **24**, 632 (1956).

* The similar figure for *p*-benzoquinone was given by L. E. Orgel, *Trans. Faraday Soc.*, **52**, 1172 (1956).

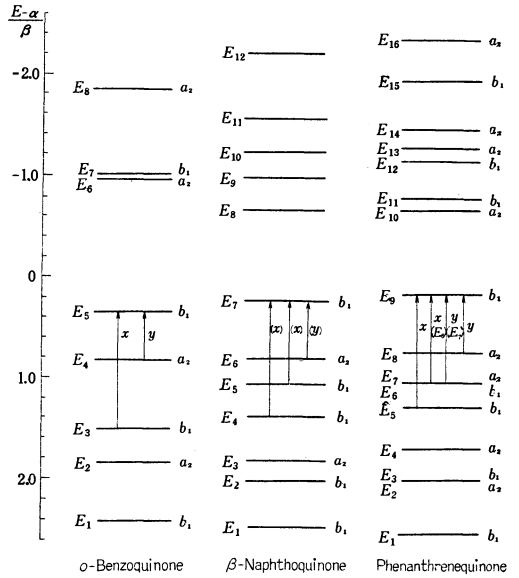


Fig. 1.

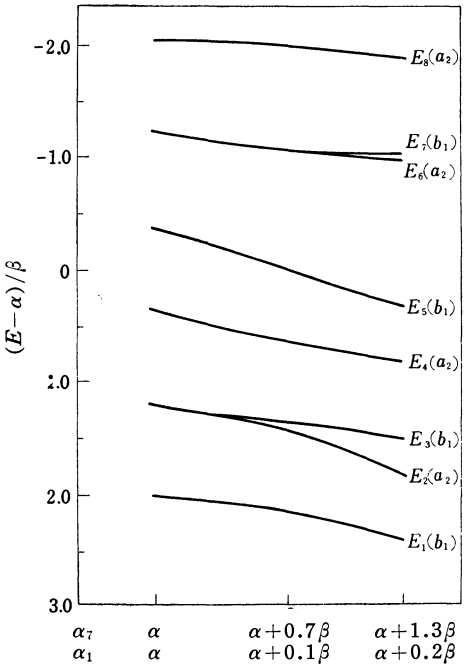


Fig. 2.

studied with *o*-benzoquinone. The result is shown in Fig. 2. The energy levels are classified according to the symmetry properties of the corresponding orbitals in the symmetry groups of these *o*-quinones (C_{2v}), taking the molecular symmetry axis as the x-axis and the molecular plane as the xy plane. For β-naphthoquinone which has no molecular symmetry axis, the symmetry properties of the orbitals are considered in relation to the quinone nucleus. The letters x and y attached to the arrow showing the transition between the energy levels denote the directions of the polarization in the allowed transitions. In phenanthrenequinone, the E_2 and E_6 orbital energies are a little lower than the E_3 and E_7 orbital energies, respectively.

Discussion

Molecular Diagrams. — The molecular diagrams of the three *o*-quinones are also similar in many points as well as those of the *p*-quinones. As for charge distributions, the negative charges of oxygen atoms slightly increase in the order of *o*-benzoquinone < β-naphthoquinone < phenanthrenequinone. In β-naphthoquinone, the carbonyl group (C_1–O_{11}) is relatively electronically more negative than the one (C_2–O_{12}). Positions 3 and 4 of β-naphthoquinone are relatively electronically more negative and positive, respectively, than the corresponding positions of *o*-benzoquinone. The result that position 3 of β-naphthoquinone is electronically somewhat negative explains the remarkable fact[4] that at this position the nitro group substitution reaction occurs. The calculated dipole moments of *o*-benzoquinone, β-naphthoquinone, and phenanthrenequinone are ca. 8.1, 11.0, and 9.9 D, relatively. If the contribution of the inductive effect between two large dipoles belonging to adjacent carbonyl bonds (ca. 1.5 D)** is in every case subtracted from these values, the final values are 6.6, 9.5 and 8.4 D, respectively, which are considerably greater than the experimental values (5.1[2], 5.6[2] and 5.6 D[5], respectively). These differences between the calculated and the experimental values are commonly observed in the simple MO calculations. As for bond orders, in β-naphthoquinone the value for the C_2–C_3 bond is greater than the one for the C_{10}–C_1 bond and the value for the C_3–C_4 bond is nearly equal to the corresponding one of *o*-benzoquinone. The diagrams also show that the six-membered carbon rings attached to the quinone nuclei of β-naphthoquinone and

4) L. F. Fieser and M. Fieser, "Organic Chemistry", 2nd Ed. (1950), translated into Japanese, Maruzen Co., Ltd., Tokyo (1957), p. 748.

** The contribution of the inductive effect was calculated by the same method as that described in the following reference: H. M. Smallwood and K. F. Herzfeld, *J. Am. Chem. Soc.*, **52**, 1919 (1930).

5) C. C. Caldwell and R. J. W. LeFèvre, *J. Chem. Soc.*, **1939**, 1614.

phenanthrenequinone are correctly approximated by the benzene nucleus. Free valence values for position 4 of *o*-benzoquinone and β-naphthoquinone are great, particularly in the case of the latter. The unpaired electron densities in the lowest unfilled orbitals are thought to be roughly equal to the unpaired electron densities in the corresponding semiquinone ions[3]. In the three *o*-quinones, the parts greater than seventy per cent of the total unpaired electron densities exist at the carbonyl groups. Previously, McConnell[3] reported that between the splitting constant, α_i, in the hfs in the electron paramagnetic resonance absorption of semiquinone ions and the unpaired electron density, ρ_i (i denotes the position of a carbon atom to which a proton bonds), the following relationship can be formulated.

$$\alpha_i = 34\,\rho_i \qquad (1)$$

Recently M. Adams[6] reported the measured values of the splitting constants of various semiquinone ions. In *o*-benzoquinone, the values calculated following formula 1 (3.44 and 1.07 gauss) are in good agreement with the measured values (3.65 and 0.95 gauss). In β-naphthoquinone, the unpaired electron density of position 4 is considerably great and the value calculated by formula 1 is 4.48 gauss. As in β-naphthoquinone the measured values are 1.3 and 0.24 gauss, a doublet with a large splitting constant is probably overlooked. In accordance with the experimental result that in phenanthrenequinone 5 quintets resulting from the two sets of four equivalent protons were found, the calculated results show that the unpaired electron densities at positions 4, 6, 11, 13 and positions 5, 7, 10, 12 are mutually nearly equal in each group, respectively.

The Energy Levels. — From the energy levels given above, the following two points are noticeable, as in the *p*-quinones. First, the differences between the high filled and the lowest vacant orbitals are similar in these *o*-quinones. In the region 300 ~ 400 mμ, *o*-benzoquinone has one $\pi-\pi$ transition band, and β-naphthoquinone and phenanthrenequinone have two $\pi-\pi$ transition bands and all these bands are relatively weak***. Further, these three *o*-quinones have one $\pi-\pi$ transition band near 250 mμ***. Those of β-naphthoquinone and phenanthrenequinone are strong, and the one of *o*-benzoquinone is relatively weak. In the above energy levels all the transitions are allowed. Now, it is thought that the longest wavelength $\pi-\pi$ bands are assigned as $E_4 \rightarrow E_5$ (*o*-benzoquinone), $E_6 \rightarrow E_7$ (β-naphthoquinone) and $E_8 \rightarrow E_9$ (phenanthrenequinone), and the second long wavelength $\pi-\pi$ transition bands as $E_5 \rightarrow E_7$ (β-naphthoquinone) and $E_6, E_7 \rightarrow E_9$ (phenanthrenequinone), and the bands near 250 mμ as $E_3 \rightarrow E_5$ (*o*-benzoquinone), $E_4 \rightarrow E_7$ (β-naphthoquinone), and $E_5 \rightarrow E_9$ (phenanthrenequinone), respectively. Though there remains a π unfavorable point that the band near 250 mμ of *o*-benzoquinone alone is relatively weak, the above assignments are thought to be reasonable, considering the similarity of the energy levels among the three *o*-quinones. Second, the energy levels are as a whole a little elevated as the size of the *o*-quinone molecule becomes larger. Now, the lone-pair orbital energies of the oxygen atoms in the three *o*-quinones are thought to be nearly equal. Thus, as was previously reported[1], this result explains the fact that the $n-\pi$ transition energy becomes greater as the size of the *o*-quinone molecule becomes larger. The average value of the highest filled and the lowest vacant orbital energies of each *o*-quinone as a measure of the elevation of the energy levels is $\alpha+0.628\beta$, $\alpha+0.514\beta$ and $\alpha+0.469\beta$ for *o*-benzoquinone, β-naphthoquinone and phenanthrenequinone, respectively.

The Effect of the Electron-Donating Substituent on the $\pi-\pi$ Transition Bands. — As was previously reported[7,1], the greater the C_{mi}^2 value is, and the smaller the C_{ni}^2 value, the greater the extent of the red-shift of the band corresponding to the transition ($m \rightarrow n$) is, and the C_{mi}^2 value has a much greater effect than the C_{ni}^2 value, where C_{mi} and C_{ni} are the coefficients of the i-th atomic orbital in the LCAO MO, m and n, respectively. Now, let us examine this rule for *o*-benzoquinone and β-naphthoquinone. In Figs. 3[8] and 4[9], the absorption spectra of some methyl group substituted *o*-benzoquinones and methoxyl group substituted β-naphthoquinones are given, respectively. All the π-orbitals of the three *o*-quinones are intrinsically non-degenerate and we can reasonably assume that the quasi-π-orbital energy of the methyl group and the lone-pair orbital

6) M. Adams, *J. Chem. Phys.*, 28, 774 (1958).

*** In view of the intensity and the solvent effect[2], these bands are thought to be due to $\pi-\pi$ transition.

7) A. Kuboyama, *J. Chem. Soc. Japan, Pure Chem. Sec.* (*Nippon Kagaku Zasshi*), 77, 1062 (1956).

8) H. J. Teuber and G. Steiger, *Ber.*, 88, 802 (1955).

9) H. J. Teuber and N. Götz, ibid., 87, 1236 (1954).

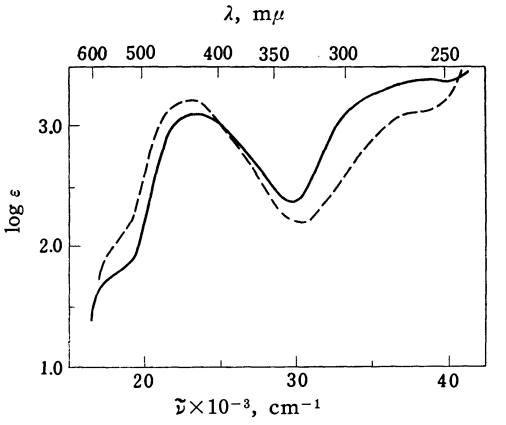


Fig. 3[8]. —— 3,4,5-Trimethyl-*o*-benzoquinone
---- 3,4,6-Trimethyl-*o*-benzoquinone
Solvent, chloroform.

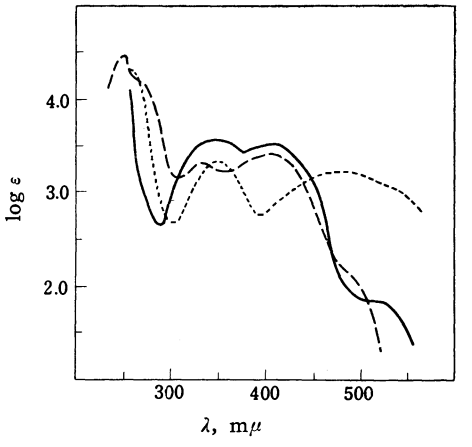


Fig. 4[9]. —— β-Naphthoquinone
----- 3-Methoxy- 〃
---- 4-Methoxy- 〃
Solvent, chloroform.

TABLE I. THE SQUARE VALUES OF THE COEFFICIENTS IN *o*-BENZOQUINONE
(The numbers in the first row denote the positions of the substitutions)

	3	4
$E_3(b_1)$	0.103	0.290
$E_4(a_2)$	0.296	0.101
$E_5(b_1)$	0.032	0.101

TABLE II. THE SQUARE VALUES OF THE COEFFICIENTS IN β-NAPHTHOQUINONE

	3	4
$E_4(b_1)$	0.113	0.231
$E_5(b_1)$	0.001	0.002
$E_6(a_2)$	0.290	0.074
$E_7(b_1)$	0.003	0.132

energy of the oxygen atom in the methoxyl group as a substituent are lower than the E_3 (*o*-benzoquinone) and the E_4 (β-naphthoquinone) orbital energies, respectively. Thus, the above method can be applied to these cases. In Fig. 3, the longer and the shorter wavelength $\pi-\pi$ transition bands of *o*-benzoquinone largely shift toward longer wavelengths for 3- and 4-substitutions, respectively. The data in Table I clearly fit these facts. In Fig. 4, the band near 400 mμ and the band near 250 mμ of β-naphthoquinone largely shift toward longer wavelengths for 3- and 4-substitutions, respectively. The data in Table II clearly explain these facts. In addition, the absorption spectra of some hydroxyl group substituted at the benzene nucleus attached to the quinone nucleus of β-naphthoquinones are also generally explained by the calculated results. Thus, in general, the effect of the electron-donating substituent on the $\pi-\pi$ transition bands in the near UV region of *o*-benzoquinone and β-naphthoquinone can be clearly explained by the above method as well as in the case of the *p*-quinones.

The good agreements between the results calculated by the simple MO method and the experimental results, concerning the near UV absorption spectra in the *o*- and the *p*-quinones, are thought to be due to the quinoid field****, characteristic of quinone compounds, which differs from the round fields, characteristic of the aromatics, presented by J. R. Platt[10].

Summary

Electronic structures of *o*-benzoquinone, β-naphthoquinone and phenanthrenequinone were studied with the simple MO method, using the same integral values as those adopted in the self-consistent MO calculation for *o*-benzoquinone. As for charge distributions, the negative charges of oxygen atoms slightly increase in the order of *o*-benzoquinone, β-naphthoquinone, and phenanthrenequinone. The calculated dipole moments (6.6, 9.5 and 8.4 D for *o*-benzoquinone, β-naphthoquinone and phenanthrenequinone, respectively) seem a little greater than the experimental values. As for bond orders, reasonable results were obtained. The calculated results predict the existence of a doublet with a large splitting constant (ca. 4.5 gauss) in the hfs of the electron paramagnetic resonance absorption of β-naphtho-semiquinone ion. Three problems

**** The similar discussion was given in J. W. Sidman's work: *J. Am. Chem. Soc.*, 78, 4567 (1956).

10) J. R. Platt, *J. Chem. Phys.*, 18, 1168 (1950).

concerning the near UV absorption bands [1) the similarity among the $\pi-\pi$ transition bands of the three *o*-quinones, 2) the relative magnitude of the $n-\pi$ transition energy of *o*-benzoquinone, β-naphthoquinone, and phenanthrenequinone, 3) the effect of the electron-donating group on the $\pi-\pi$ transition bands of *o*-benzoquinone and β-naphthoquinone] can be clearly explained by the calculated results, as in the cases of the *p*-quinones.

The author wishes to express his sincere thanks to Professor S. Nagakura of the Institute for Solid State Physics, the University of Tokyo, for his kind guidance. The author's thanks are also due to Mr. H. Kônosu for his kind cooperation in this research.

Government Chemical Industrial Research Institute, Tokyo
Shibuya-ku, Tokyo

*Behavior of Surface Active Molecules at an Interface. II. Statistical Thermodynamics of Monolayers of Rod-Like Molecules**

By Masayuki NAKAGAKI

(Received May 20, 1959)

A monolayer is often considered to be a two-dimensional system. However, this standpoint is not acceptable in detailed discussions, because a monolayer has a certain thickness and has a thermodynamic freedom in the direction perpendicular to the monolayer as well as in the two directions along the interface. An effort to consider the monolayer as a three-dimensional existence has been made in the preceding paper of this series[1] by considering the possibility that the end groups of the molecules in a monolayer are not necessarily on one plane, in order to explain the shape of the pressure-area curves of condensed monolayers.

Another example that definitely requires the three-dimensional consideration comes out from rather expanded monolayers in which molecules are supposed to be inclined to the normal of the interface so that the collision diameter of the molecules in the monolayer depends on the degree of the inclination of the molecules. This will be discussed in the present paper.

As for the equation of the state of the monolayer insoluble in the substrate, it has already been pointed out by Akamatsu and the present author[2] that the two dimensional analogue of the van der Waals equation can be used. Then, the equation applicable, at least empirically, is:

$$(F+a/A^2)(A-A_0)=kT \qquad (1)$$

where F is the surface pressure, A is the area per one molecule, k is the Boltzmann constant, T is the absolute temperature and a and A_0 are constants. A_0 corresponding to the constant b in the van der Waals equation is given by

$$A_0=(\pi/2)d^2 \qquad (2)$$

if the molecules are spherical and the diameter is d. However, fatty acid molecules and substances of much interest in surface chemistry is not spherical but is rod-like. If all the rod-like molecules are vertical to the interface and thickness of each molecule is d in diameter, it is then obvious that Eq. 2 can be used. Generally the rod-like molecules are, however, inclined to the interface or lying flat on the interface, so that Eq. 2 can not be used. For the molecules inclined to the interface, theoretical equations to be used instead of Eq. 2 will be derived, and the equations will be applied to experimental data already known in literature.

Theoretical Calculation of the Constant A_0

Principle of the Calculation. — For three-dimensional solutions, Zimm[3] calculated the van der Waals constant b for rod-like

* Presented before the 11th Symposium on Colloid Chemistry, the Chemical Soeiety of Japan, Sendai, Sept. 5, 1958.

1) M. Nakagaki, This Bulletin, **29**, 64 (1956).

2) H. Akamatsu and M. Nakagaki, ibid., **23**, 232 (1950).

3) B. Zimm, *J. Chem. Phys.*, **14**, 164 (1946).

molecules by using the method of McMillan and Mayer[4]. This method is to obtain the second virial coefficient from the value of the phase integral over the entire range of the overlapping of two molecules. By analogy with the three-dimensional osmotic pressure equation in the above mentioned papers, the second virial coefficient A_2 in the expression of the surface pressure F as a power series of surface concentration c:

$$F=\boldsymbol{R}T\{(1/M)c+A_2c^2+\cdots\cdots\} \quad (3)$$

is given by the equation,

$$A_2=-(\boldsymbol{N}_0/2SM^2)\int g_2\{2\}\,\mathrm{d}\,\{2\} \quad (4)$$

where $\boldsymbol{N}_0$ is the Avogadro number, M is the molecular weight of the surface active substance, S is the area of the interface. The integral will be explained later on. Since the surface concentration c is related to the area per one molecule A by the equation:

$$c = M/\boldsymbol{N}_0A \quad (5)$$

Eq. 3 is rewritten as

$$FA/\boldsymbol{k}T=1+(A_2M^2/\boldsymbol{N}_0)(1/A)+\cdots\cdots \quad (6)$$

On the other hand, Eq. 1 expanded in a power series of $(1/A)$ is

$$FA/\boldsymbol{k}T=1+(A_0-a/\boldsymbol{k}T)(1/A)+\cdots\cdots \quad (7)$$

where the term A_0 comes from the repulsion due to the overlapping of two molecules and the term $(a/\boldsymbol{k}T)$ comes from the intermolecular attraction.

On comparing Eqs. 6 and 7, two methods will be suggested for further calculations. The one, which is theoretically accurate but difficult to put in practice, is to calculate the integral in Eq. 4 by taking both the overlapping and the attraction into account, and to assign the value of $(A_2M^2/\boldsymbol{N}_0)$ thus obtained to $(A_0-a/\boldsymbol{k}T)$. The other method, which is theoretically rather arbitrary but easy to put in practice, is to calculate the integral in Eq. 4 by taking only the overlapping into account and neglecting the intermolecular attraction, and to assign the value of $(A_2M^2/\boldsymbol{N}_0)$ thus obtained to A_0. The latter method is adopted in the present paper because the term A_0 is of main interest and because the calculation of the integral is very complicated if the first method is used. Therefore,

$$A_0=-(1/2S)\int g_2\{2\}\,\mathrm{d}\,\{2\} \quad (8)$$

4) McMillan and Mayer, *J. Chem. Phys.*, **13**, 376 (1954).

The g-function of two molecules g_2 is calculated from distribution functions F_n by the equation

$$g_2(1,2)=F_2(1,2)-F_1(1)F_1(2) \quad (9)$$

where the suffix of both g- and F-functions designates the number of molecules in the system considered, and $\{n\}$ means the assembly of all the coordinates of n molecules, while (i) means the coordinates of the i-th molecule. The distribution function $F_2(1,2)$ must be zero in the region where the two molecules overlap. On the other hand, in the region where the molecules do not overlap, the function must be a constant, since the intermolecular attraction is to be neglected in the present method of the calculation. The value of the constant is determined by a normalization equation,

$$(1/S^n)\int F_n\{n\}\,\mathrm{d}\,\{n\}=1 \quad (10)$$

This equation can be rewritten as

$$F_n\{n\}=S^n/\int \mathrm{d}\,\{n\} \quad (11)$$

if $F_n\{n\}$ is a constant.

The Case in which All Molecules are Vertical to the Interface ($\theta=0°$).—Since all the rod-like molecules are assumed to be vertical to the interface, the overlapping of two circles of diameter d in one plane is to be considered. Therefore, the result must be identical with the case of spherical molecules given by Eq. 2. The calculation will be described in some detail for this simplest case in order to explain the process followed repeatedly in the later part of this paper.

As shown in Fig. 1a, the location of the axis of rod 1 is given by the coordinates X and Y, and that of rod 2 relative to rod 1 is given by the coordinates r and φ. Then,

$$\mathrm{d}\{2\} = \mathrm{d}X\mathrm{d}Y r\mathrm{d}r\mathrm{d}\varphi \quad (12)$$

By using Eq. 11,

$$F_2(1,2)=\begin{cases}1 & \text{when rods 1 and 2 do not overlap}\\ 0 & \text{when rods 1 and 2 overlap}\end{cases} \quad (13)$$

$$F_1(1)=F_1(2)=1$$

Now, rods 1 and 2 overlap when $0<r<d$, so that by Eq. 9,

$$\begin{aligned} &g_2(1,2)=-1 \quad \text{when } 0<r<d\\ &g_2(1,2)=0 \quad \text{in all other ranges of coordinates}\end{aligned} \quad (14)$$

Therefore,

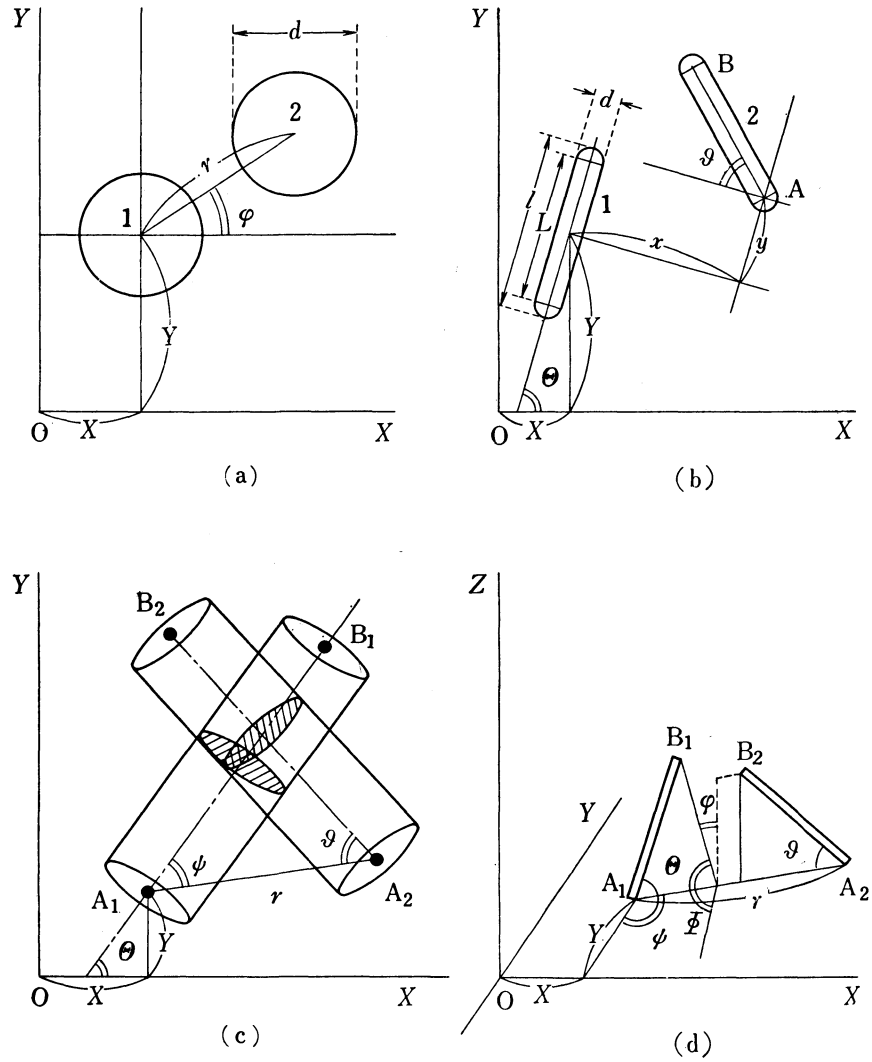


Fig. 1. Coordinate systems used in the cases of (a) $\theta=0°$; (b) $\theta=90°$; (c) $\theta=\theta_0$; and (d) θ is indefinite.

$$\int g_2\{2\}\,\mathrm{d}\{2\} = -\int_S \mathrm{d}X\mathrm{d}Y\int_0^{2\pi}\mathrm{d}\varphi\int_0^d r\,\mathrm{d}r$$
$$= -\pi S d^2 \qquad (15)$$

By combining this with Eq. 8, an equation exactly identical with Eq. 2 is obtained.

The Case in which All Molecules are Lying Flat upon the Interface ($\theta=90°$).—In order to avoid the complication arising from the overlapping of the edges of the rods, and to make the results of the present calculation comparable to the preceding results, the molecules are assumed to have round edges. To describe this shape of the molecule, it is assumed that a rod is composed of a circular cylinder of length L and diameter d and two hemispheres of diameter d at both ends of the circular cylinder, the center of the hemispheres being A and B, as shown in Fig. 1b.

When all rods are lying flat on the interface, the position and the orientation of a rod are designated by using three coordinates. For the three coordinates of rod 1, Cartesian coordinates X and Y of the center of gravity and the angle Θ between the X-axis and the axis of the rod may be used. For rod 2, the Cartesian coordinates x and y of the center of a hemisphere A (the origin of which is the center of gravity of rod 1 and the direction of the coordinate axes is perpendicular and

parallel to the direction of the axis of rod 1), and the angle ϑ between the axis of rod 2 and the coordinate axis $(-x)$ may be used as shown in Fig. 1b.

Then, $d\{2\}$ is $dXdYd\Theta dxdyd\vartheta$, $F_2\{2\}$ is $(1/4\pi^2)$ when two rods do not overlap with each other and is zero when they overlap, and $F_1\{1\}$ is $(1/2\pi)$. Therefore, the value of $g_2(1,2)$ is equal to $(-1/4\pi^2)$ when the rods overlap and is equal to zero when they do not. Therefore, the value of the integral calculated over the entire range of the coordinates corresponding to the overlapping of the rods is

$$\int g_2\{2\}d\{2\} = -(2S/\pi)(L^2+2\pi dL+\pi^2d^2/2) \tag{16}$$

This agrees with Eq. 15 if $L=0$. If the total length of the rod (that is $L+d$) is designated by l, and the value of A_0 is calculated from Eq. 8 by the aid of Eq. 16, then,

$$A_0=(1/\pi)l^2+2(1-1/\pi)dl+(\pi/2-2+1/\pi)d^2 \tag{17}$$

This agrees with Eq. 2 if $d=l$. Now, if the rods are very thin, $(d \ll l)$,

$$A_0 = (1/\pi)l^2 \tag{18}$$

The Case in which All Molecules are Inclined by the Same Angle($\theta=\theta_0$). — When all rods are inclined to the normal of the surface by the same angle θ_0, the position and the orientation of a rod may be specified by three coordinates. Fig. 1c shows the projection of rod 1 (A_1B_1) and of rod 2 (A_2B_2) onto the plane XY parallel to the interface. The three coordinates of rod 1 may be X and Y to give the location of the lower end A_1 of the axis and angle Θ to give the direction of the rod. The three coordinates of rod 2 may be r and ψ to give the location of A_2 and ϑ to give the direction. Then, $d\{2\}$ is $dXdYd\Theta rdrd\psi d\vartheta$, and $g_2\{2\}$ is $(-1/4\pi^2)$ when two rods overlap and is zero when they do not.

The calculation of the range of overlapping is rather complicated in this case and needs some approximation. If the rods are sufficiently thin, rods 1 and 2 overlap with each other when $\vartheta=\psi$, and the height of the intersection h from the surface is $r/2\cos\psi\tan\theta_0$. Now, considering the rods of some thickness, the cross section of the rods will be an ellipse when the cross section is parallel to the interface. The range of the angle ϑ to give the overlapping of the ellipses at the hight of h will give the condition of the overlapping of the rods. It is not easy, however, to estimate this range of ϑ, because the mutual orientation of the ellipses depends on the value of r and ψ. To avoid this mathematical complication, the ellipses will be replaced in this approximate calculation with circles of the same area. Then, the diameter of the equivalent circles d_0 will be $(d/\sqrt{\cos\theta_0})$ where d is the diameter of the rods. If the rods are sufficiently thin and long, that is, $2\sin\theta_0 > d_0/l$, the rods overlap approximately when

$$\psi-(2d_0/r)\cos\psi<\vartheta<\psi+(2d_0/r)\cos\psi \tag{19}$$

The final results thus obtained and applicable when $d/2l<\theta_0<\pi/2-d/l$ are

$$A_0=(\pi-4/\pi)d^2/2\cos\theta_0 + (\sin\theta_0/\sqrt{\cos\theta_0})dl \tag{20}$$

If $d \ll l$,

$$A_0=(\sin\theta_0/\sqrt{\cos\theta_0})dl \tag{21}$$

The Case in which Molecules can be Inclined at Any Angle with Equal Probability ($0<\theta<\pi/2$). — In this case, the position and the orientation of two rods 1 and 2 are defined by eight coordinates, X, Y, r, ψ, Θ, ϑ, Φ and φ. As is shown in a perspective, Fig. 1d, X and Y give the position of A_1. r gives the distance between A_1 and A_2. ψ gives the direction of A_1A_2. Θ gives the angle $B_1A_1A_2$. ϑ gives the angle $B_2A_2A_1$. Φ gives the angle between the plane $B_1A_1A_2$ and the plane XY. φ gives the angle between the plane $B_1A_1A_2$ and $B_2A_2A_1$. Here A_1 and A_2 are the lower end of rods 1 and 2, respectively, and B_1 and B_2 are the upper ends of rods 1 and 2. If the rods are sufficiently thin and $d \ll l$, the two rods overlap in the following three cases:

(1) $0<\Theta<\pi/2$, $0<\vartheta<\pi/2$,
$0<r<l(\cos\Theta+\cos\vartheta)$ and
$-(d/r)(1/\tan\Theta+1/\tan\vartheta)$
$<\varphi<(d/r)(1/\tan\Theta+1/\tan\vartheta)$;

(2) $\pi/2<\Theta<\pi$, $0<\vartheta<\pi-\Theta$,
$0<r<l(\cos\vartheta+\sin\vartheta/\tan\Theta)$ and
$-(d/r)(1/\tan\Theta+1/\tan\vartheta)$
$<\varphi<(d/r)(1/\tan\Theta+1/\tan\vartheta)$;

(3) $\pi/2<\vartheta<\pi$, $0<\Theta<\pi-\vartheta$,
$0<r<l(\cos\Theta+\sin\Theta/\tan\vartheta)$ and
$-(d/r)(1/\tan\Theta+1/\tan\vartheta)$
$<\varphi<(d/r)(1/\tan\Theta+1/\tan\vartheta)$.

Then, by using the value of a definite integral, $\int_0^1(\tan^{-1}x/x)dx=0.9160$, the following equation can be obtained under the

assumption that $d \ll l$.

$$A_0 = 1.7014\, dl \qquad (22)$$

Eq. 22 corresponds to Eq. 21 with $\theta_0 = 71.8°$. This value of θ_0 is considered to be the statistically averaged value of θ for freely orienting molecules.

Applications for Gaseous Films of Fatty Acids

The theoretical equations derived above are to be applied to gaseous films and not to condensed films because multiple collisions, important in condensed films, are not taken into account in the derivations of these theoretical equations.

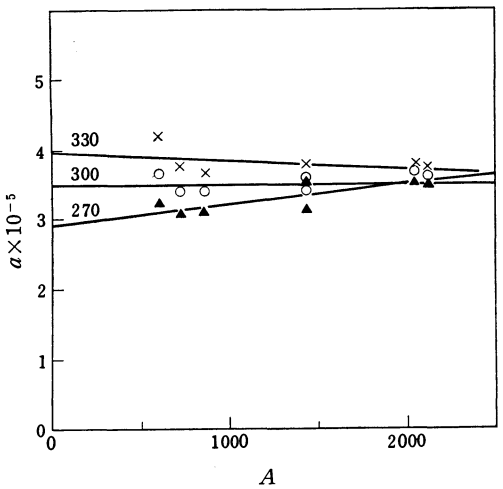


Fig. 2. The dependence of a on A for tridecylic acid, the parameter being A_0.

Therefore, the equations are applied to gaseous films of fatty acid using the experimental data given by Adam and Jessop[5]. In order to obtain the values of the constants a and A_0 of the van der Waals type equation, Eq. 1 was rewritten in the following form:

$$a = [kT/(A - A_0) - F]\, A^2 \qquad (23)$$

and the value of a for systematically varied values of A_0 are calculated by using experimental values of A and F given by Adam and Jessop. The value of a thus calculated for tridecylic acid are shown in Fig. 2. It is seen that the value of a is independent of A if the value of A_0 is assumed to be 300 Å^2. The values of a and A_0 thus obtained for tridecylic acid and myristic acid are shown in Table I.

TABLE I. CONSTANTS OF GASEOUS FILMS

	A_0	$a\times10^{-5}$	M	a/M^2	
Myristic acid	320	4.02	228	7.74	7.71
Tridecylic acid	300	3.52	214	7.68	

The data used for these calculations are shown in Fig. 3 with ○ for myristic acid and with △ for tridecylic acid. Curves in the figure shows the values calculated by Eq. 1, using the values of constants given in Table I. These curves explain well the experimental plots. Horizontal lines in the figure show where a two-dimensional phase change occurs. It is obvious that Eq. 1 does not hold over the pressure of the phase change.

As for the constant a, it is often said

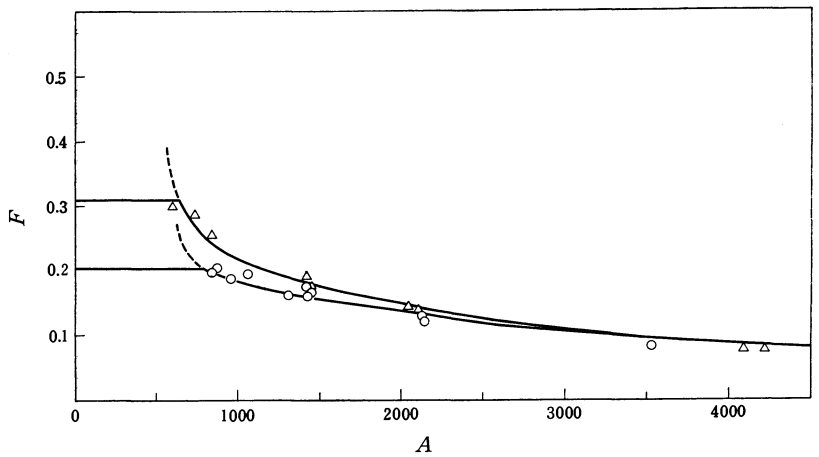


Fig. 3. Gaseous films of myristic acid and tridecylic acid.
○: Myristic acid △: Tridecylic acid

5) N. K. Adam and G. Jessop, *Proc. Roy. Soc.* (*London*), **A110**, 423 (1926).

that its value is proportional to the square of the molecular weight. This is valid in this case since the value of a/M^2 in Table I gives the relation,

$$a = 7.71 \times M^2 \qquad (24)$$

In order to compare the values of A_0 given in Table I with the theoretical equations derived above, the molecules are assumed to be rods of 5.0 Å in diameter and of $(6.0+1.3m)$ Å in length, where m is the number of carbon atoms in the hydrocarbon chain of the molecule. The values thus assumed are cited in Table II.

TABLE II. THE CONSTANT A_0 FOR GASEOUS FILMS

	d Å	l Å	A_0 $\theta=0°$ Å^2	A_0 $\theta=71.8°$ Å^2	A_0 $\theta=90°$ Å^2
Myristic acid	5.0	22.9	39.3	270	320
Tridecylic acid	5.0	21.6	39.3	258	294
Lauric acid	5.0	20.3	39.3	247	267

These values seem reasonable on the basis of various surface chemical studies and are compatible with the values already used by the present author[6]. Using these values of d and l, values of A_0 are calculated for vertical orientation, $\theta=0°$, by Eq. 2; for free orientation by Eq. 20 with $\theta_0=71.8°$; and for horizontal orientation, $\theta=90°$, by Eq. 17. The values thus calculated are shown in Table II. Comparing these with those in Table I, it may be concluded that the molecules of myristic acid and tridecylic acid are lying flat upon the interface.

In the case of lauric acid, the F–A curve obtained experimentally by Adam and Jessop is different from those of myristic and tridecylic acid, because lauric acid does not show any definite phase transition at the range of some hundred Å^2, as shown with ○ in Fig. 4. If it is assumed that the molecules of lauric acid are rods of $d=5.0$ Å and $l=20.3$ Å, and lying flat on the interface, A_0 should be 267 Å^2 as shown in Table II. On the other hand, a should be 3.08×10^5 for lauric acid according to Eq. 24. By using these values with Eq. 1, the solid curve in Fig. 4 is obtained. The curve can explain the experimental data to some extent in the region of larger A values, but the experimental data for smaller A values neither coincide with the van der Waals equation shown by the solid curve nor show any phase transition. The data will be explained by the assumption that the molecules at first lying flat on the interface gradually stand up according to the compression of the monolayer.

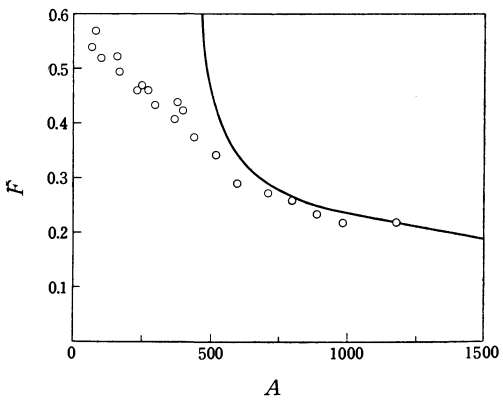


Fig. 4. Gaseous film of lauric acid.

Assuming that the molecules of lauric acid are rods of the above described dimensions, the value of A_0 is calculated as a function of the angle θ, that is the angle between the normal of the interface and the axis of the molecule. The curve in Fig. 5 is thus obtained by using Eqs. 2, 17 and 20. The point f in the figure shows the value of A_0 for the case in which the molecules can take any value of θ with equal likelihood.

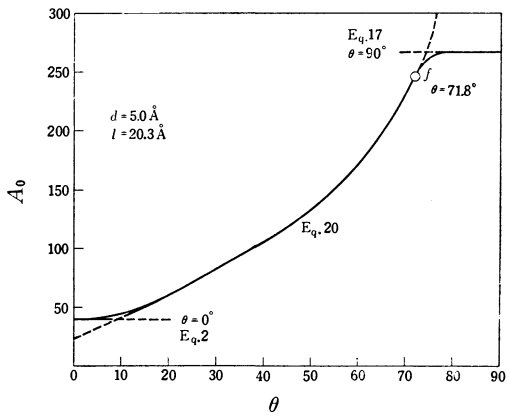


Fig. 5. The relationship between A_0 and θ for lauric acid.

By using, on the other hand, Eq. 1 together with the value of $a=3.08\times10^5$, the value of A_0 can be calculated as a function of the area A from the experimental data shown in Fig. 4. From this value of A_0, the value of θ can be obtained on the basis of Fig. 5. The relation between θ and A thus obtained are shown in Fig. 6. The horizontal line in the

6) M. Nakagaki, *J. Chem. Soc. Japan, Pure Chem. Sec.* (*Nippon Kagaku Zasshi*), **72**, 113 (1951).

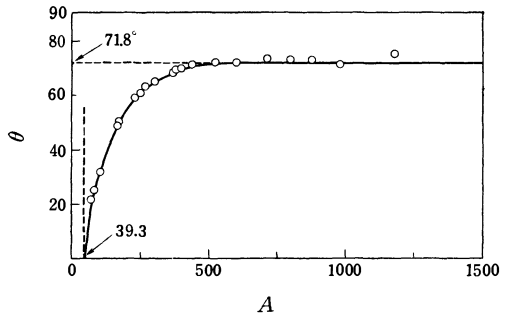


Fig. 6. The orientation of lauric acid molecules as a function of A.

figure shows the case of free orientation, in which the statistically averaged value of θ is 71.8°, and the vertical line shows the case in which all molecules are vertical to the interface. Molecules of lauric acid are in free orientation when the area A is very large, but the molecules interfere with each other and θ becomes smaller when A is les than about 500 Å^2. At last, all the molecules are vertical when A is 39.3 Å^2.

Summary

On the basis of the two-dimensional analogy of the method of McMillan and Mayer, the van der Waals constant A_0 for monolayers of rigid rod-like molecules is calculated theoretically for the cases in which all molecules are (1) vertical to the interface; (2) lying flat upon the interface; (3) inclined by a constant angle θ_0; and (4) orienting freely.

The theoretical equations thus obtained are used to discuss the orientation of molecules in gaseous films of myristic acid, tridecylic acid and lauric acid. As the results, it is concluded that the molecules of myristic acid and tridecylic acid are lying flat upon the interface in the gaseous film until the phase transition to a condensed film occurs. On the other hand, molecules of lauric acid are freely orienting when the area per one molecule is large, and the orientation becomes the more vertical, the more the monolayer is compresssed. The molecular orientations during this compression process were described quantitatively.

Faculty of the Science of Living
Osaka City University
Nishi-ku, Osaka

Dielectric Constants of Binary Mixtures; 1,2-Dichloroethane and Nonpolar Solvents

By Ryoichi FUJISHIRO and Ko KIMURA

(Received May 25, 1959)

The molecular structure of 1,2-dichloroethane has been studied in detail by many authors[1]. This molecule has steric isomers arising from the internal rotation and the equilibrium between these isomers in solutions is determined by the intramolecular interaction in the dichloroethane molecule and by the intermolecular interaction with solvent molecules. For example, the greater part of the dichloroethane molecules exists as the *gauche* form in the liquid state, whereas the dilution by adding nonpolar solvents causes decrease of the fraction of the *gauche* form. This is particular interest and worth being examined from various standpoints, that is, the dielectric and the thermodynamic behaviors of mixtures.

The thermodynamic behavior of such mixtures has already been discussed from the measurements of heats of mixing[2], and the excessive enthalpy was explained to some extent by considering the equilibrium between the steric isomers. The dielectric behavior of mixtures of dichloroethane with nonpolar solvents, however, has not been studied in detail except in the low concentration range of dichloroethane.

In this report the dielectric properties of mixtures of dichloroethane with nonpolar solvents such as carbon tetrachloride,

1) S. Mizushima, "Structure of Molecules and Internal Rotation", Academic Press, New York (1954).

2) K. Amaya and R. Fujishiro, This Bulletin, **31**, 90 (1958).

cyclohexane, benzene and carbon disulfide, will be examined experimentally over all the concentrations and discussed on the basis of the Onsager theory and the theory extended by Fujishiro[3] and Scholte[4].

Outlines of the Theory

According to Onsager, we select the spheroidal cavity of the molecular dimension and put a point dipole in the center of this cavity. The surroundings of the spheroidal cavity are replaced by the continuum of the macroscopic dielectric constant. When the long and the short axes of the spheroid are $2a$ and $2b$, respectively, and the dipole is located along the long axis, the local field $\vec{f}$[5] is given by

$$\vec{f}=\vec{G}+\vec{R}=\varepsilon/[\varepsilon+(1-\varepsilon)A]\vec{E}+g\vec{m} \qquad (1)$$

where $\vec{G}$, $\vec{R}$ and $\vec{E}$ express the cavity, the reaction and the external fields, respectively, and $\vec{m}$ is the electric dipole moment in dielectrics in the presence of an external field. A is the constant determined by the geometric shape of the cavity and has the following expression[6],

$$A=\frac{ab^2}{2}\int_0^\infty \frac{\mathrm{d}\xi}{(\xi+a^2)^{3/2}(\xi+b^2)}$$

g is called the factor of the reaction field and is given by

$$g=\frac{3}{ab^2}\cdot\frac{A(1-A)\cdot(\varepsilon-1)}{\varepsilon+(1-\varepsilon)A}$$

When we assume the optical polarizability of dichloroethane to be isotropic, $\vec{m}$ is generally related to both $\vec{\mu}$ and $\vec{f}$ by the formula,

$$\vec{m}=\vec{\mu}_v+\alpha\vec{f} \qquad (2)$$

μ_v and α being the electric dipole moment and the optical palarizability of the *gauche* form of dichloroethane, respectively. From Eqs. 1 and 2, we obtain

$$\vec{f}=\frac{g}{1-\alpha g}\vec{\mu}_v+\frac{\varepsilon}{\varepsilon+(1-\varepsilon)A}\cdot\frac{\vec{E}}{1-\alpha g} \qquad (3)$$

Then the average dipole moment $\bar{m}$ is written as follows:

$$\begin{aligned}\bar{m}&=<\vec{m}\cdot\vec{e}>\\&=\int_\Omega(\vec{m}\cdot\vec{e})e^{-U/kT}\mathrm{d}\Omega\Big/\int_\Omega e^{-U/kT}\cdot\mathrm{d}\Omega\\&=\frac{\varepsilon}{\varepsilon+(1-\varepsilon)A}\left\{\frac{\alpha}{1-\alpha g}+\frac{1}{(1-\alpha g)^2}\cdot\frac{\mu_v^2}{3kT}\right\}E\end{aligned} \qquad (4)$$

The symbols $\vec{e}$ and U are a unit vector in the direction of the external field and the potential energy of the system in the presence of the external field, respectively. Then the dielectric constant of a mixture containing N_1 molecules of 1-compound, N_2 molecules of 2-compound and so on per cc., is given by the following formula,

$$\varepsilon-1=4\pi\textstyle\sum_z\cdot N_z\bar{m}_z/E \qquad (5)$$

If we take the mixture containing N_g molecules of the *gauche* form of dichloroethane, N_t molecules of the *trans* form ($N_d=N_g+N_t$) and N_s molecules of a non-polar solvent per cc., we obtain from Eqs. 4 and 5

$$\begin{aligned}\varepsilon-1=4\pi\Bigg[&N_g\cdot\frac{\varepsilon}{\varepsilon+(1-\varepsilon)A}\left\{\frac{1}{(1-\alpha g)^2}\cdot\frac{\mu_v^2}{3kT}\right\}\\&+N_d\cdot\frac{\varepsilon}{\varepsilon+(1-\varepsilon)A}\cdot\frac{\alpha}{1-\alpha g}\\&+N_s\frac{\varepsilon}{2\varepsilon+n_s^2}a_s^3(n_s^2-1)\Bigg]\end{aligned} \qquad (6)$$

In the derivation of this equation, we used the following assumption and relation:

(i) A or α for the *trans* form is equal to that for the *gauche* from, though this assumption is not strictly correct.

(ii) Assuming that a solvent molecule is spherical, A for the solvent molecule may be substituted by the value 1/3 for the spherical cavity, and the polarizability of the solvent molecule is replaced by the Lorentz-Lorenz relation,

$$\frac{n_s^2-1}{n_s^2+2}=\frac{\alpha}{a^3}$$

n and a being the refractive index and the radius of the spherical solvent molecule, respectively. Strictly speaking, as there is the contribution of atomic polarization to α, it is expressed by the Clausius-Mossotti relation instead by that of Lorentz-Lorenz. However, the atomic polarization is generally equal to only a few per cent of the electronic polarization. Hence we have conventionally used the latter relation.

Now, as the dielectric constant of the

3) R. Fujishiro, *J. Chem. Soc. Japan, Pure Chem. Sec.* (*Nippon Kagaku Zasshi*), **65**, 352 (1949).
4) T. G. Scholte, *Physica*, **15**, 437 (1949).
5) H. Fröhlich, "Theory of Dielectrics", Oxford University Press, London (1949).
6) C. G. Bötter, "Theory of Electric Polarisation", Elsevier Publishing Co., Houston (1952).

mixture itself is concerned not only with N_d, but also with N_g in the mixture as already shown in Eq. 6, we need to know the ratio N_g/N_d in the equilibrium state of the mixture. Factors determining the equilibrium are the intramolecular energy difference ΔE between the *gauche* and the *trans* forms of dichloroethane, the free energy ΔG for the electrostatic stabilization of the polar *gauche* form in the dielectrics, and the intermolecular dispersion energy between dichloroethane and solvent molecules. As is well known, ΔG is given by

$$\Delta G=\frac{1}{2}\cdot\frac{g}{1-\alpha g}\mu_v^2 \tag{7}$$

So far as the dispersion energy is concerned, it is natural to consider that the interaction of the *gauche* form of dichloroethane with a solvent molecule is approximately equal to that of the *trans* form. Thus, one interaction parameter w instead of two may be introduced as follows:

$$w=w_{ds}-\frac{1}{2}(w_{dd}+w_{ss})$$

where w_{ij} is the ordinary dispersion energy between i and j molecules and d or s expresses dichloroethane or a solvent. Then the configurational partition function[7] may be written as

$$Z=2^{N_g}\phi_d^{N_d}\phi_s^{N_s}\frac{(N_d+N_s)!}{N_t!\,N_g!\,N_s!}\exp\left(\frac{-Xw}{kT}\right)\times\exp\left\{\frac{-N_g(\Delta E-\Delta G)}{kT}\right\} \tag{8}$$

where ϕ_d and ϕ_s represent the internal partition functions of dichloroethane and a solvent molecule respectively, and X is the number of dichloroethane solvent pairs. As the chemical potential of the *gauche* form of dichloroethane is equal to that of the *trans* form in the equilibrium state, we write

$$\frac{\partial \ln Z}{\partial N_g}=\frac{\partial \ln Z}{\partial N_t} \tag{9}$$

Hence the ratio of N_g/N_t is easily derived by using Eqs. 8 and 9 as follows:

$$N_g/N_t=2\exp\left\{\left(-\Delta E+\Delta G+N_g\cdot\frac{\partial \Delta G}{\partial N_g}\right)\Big/kT\right\} \tag{10}$$

The value ε and at the same time the ratio N_g/N_t are determined at any composition and temperature by the method of "trials and errors" from Eqs. 6, 7 and 10.

7) The detailed description was given in a previous paper. See reference 2.

Experimental

In order to compare the theoretical results with the experimental ones, we measured the dielectric constants of the mixture of dichloroethane and nonpolar solvents such as carbon tetrachloride, cyclohexane, benzene and carbon disulfide. The apparatus[8] for the measurement of the dielectric constant was already described and the capacity of a dielectric cell used in this experiment was about 5 pf. All materials were purified according to the standard method[9].

Comparison of the Theoretical Results with the Observed Values

Fig. 1 shows the theoretical curves of the dielectric constants plotted against the mole fraction of dichloroethane for the dichloroethane-carbon tetrachloride mixture at 25 and 60°C. In this calculation the following values are used;

$\mu=2.55$ D, $\alpha=0.838\times10^{-23}$ cc.
E[10]$=1.27$ kcal./mol.

	n_s^2	v_d (molecular volume of dichloroethane)	v_s (molecular volume of carbon tetrachloride)
25°C	2.124	1.325×10^{-22}	1.612×10^{-22}
60°C	2.072	1.375×10^{-22} cc.	1.676×10^{-22} cc.

All the calculations were carried out on the assumption that there is no volume change on mixing, i.e., $N_dv_d+N_sv_s=1$. This

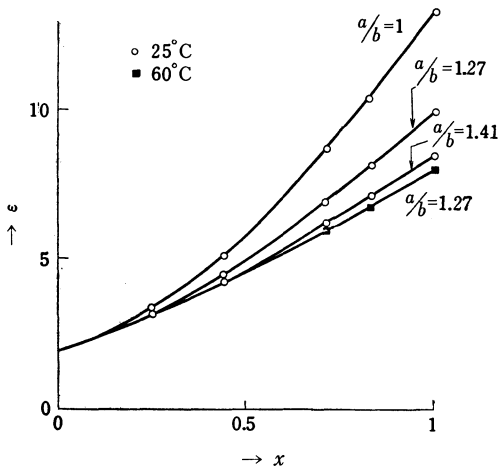


Fig. 1. The calculated dielectric constants of the mixture; dichloroethane-carbon tetrachloride.

8) I. Nakagawa, *J. Chem. Soc. Japan, Pure Chem. Sec.* (*Nippon Kagaku Zasshi*), **79**, 1353 (1958); K. Kimura and R. Fujishiro, This Bulletin, **32**, 433 (1959).
9) A. Weissberger et al., "Organic Solvents", Interscience Publishers, Inc., New York (1955).
10) A. Wada, *J. Chem. Phys.*, **22**, 198 (1954).

assumption was confirmed to be reasonable by the measurements of densities of the mixture.

The ratio a/b of the *gauche* form of dichloroethane is to be estimated by the use of the atomic distances and van der Waals radii of component atoms of the dichloroethane molecule. But the dichloroethane molecule is not strictly spheroidal. Only the long axis along which the dipole

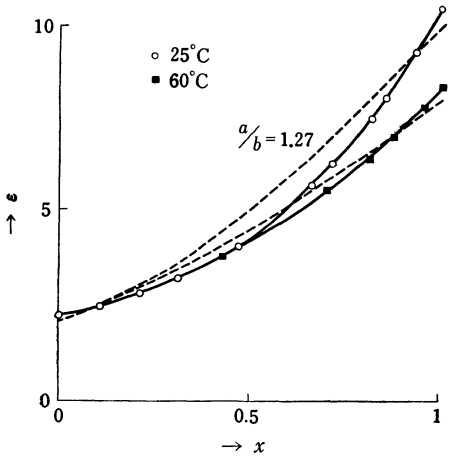


Fig. 2. Comparison of the calculated dielectric constants of the mixture, dichloroethane - carbon tetrachloride, with the observed dielectric constants. ------ Calculated, —— Observed

is located is determined uniquely, whereas the selection of the short axis is arbitrary. The ratio a/b, therefore, can take any value from 1.27 in the case of the maximum short axis to 1.57 of minimum short axis. Values of a/b used in the actual calculation are 1.27 and 1.41, the latter of which is the geometric mean of 1.27 and 1.57. For the sake of comparison the theoretical results in the case of $a/b=1$ are also shown in Fig. 1. From this figure, we may infer that the modification of the shape of the cavity leads to considerable variation of the calculated values of the dielectric constants. This means that the reaction field is overestimated in the Onsager model, i. e., $a/b=1$ and underestimated in the case of $a/b=1.41$. Fig. 2 shows the experimental results corresponding to those of Fig. 1. As seen from these figures, the most satisfactory agreement with experiments is obtained when we adopt as a/b a value 1.27 which corresponds to the allowed maximum of the short axis. This result is of particular interest from the viewpoint of the selection of the short axis. Moreover, the experimental curves representing the dielectric constants of the mixture against the mole fraction x of dichloroethane are more concave than the theoretical curves. The curvatures of the experimental curves themselves are different for different solvents as is seen later, and for different temperatures.

When we compare the theoretical values with the observed ones at 25 and 60°C, we find a better agreement with the experimental results at 60°C than at 25°C as is

TABLE I. THE OBSERVED DIELECTRIC CONSTANTS OF THE MIXTURE; DICHLOROETHANE-CARBON TETRACHLORIDE AT 25° AND 60°C

25°C x	ε	60°C x	ε
0	2.227	0	2.165
0.098	2.501	0.248	2.879
0.207	2.889	0.450	3.774
0.333	3.478	0.679	5.282
0.475	4.347	0.766	5.998
0.667	5.875	0.851	6.823
0.722	6.428	0.940	7.776
0.841	7.778	1	8.492
0.928	8.948		
1	10.022		

shown in Fig. 2 and Table I. This result is the same as that deduced from the equation for the dielectric constants of polar liquids proposed by Yasumi-Komooka[11]. Their conclusion was that a better agreement with the experimental data is obtained near the boiling point than near the melting point.

On the other hand, when we examine the calculated ratio N_g/N_d, we find that it decreases more gradually in the spheroidal model than in the spherical, as is shown in Fig. 3. The calculated ratio N_g/N_d in $x=1$ at 25°C is about 0.75 which

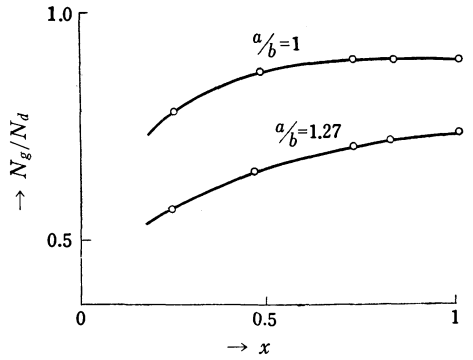


Fig. 3. The calculated ratio N_g/N_d in the mixture, dichloroethane-carbon tetrachloride at 25°C.

11) M. Yasumi and H. Komooka, This Bulletin, **29**, 407 (1956).

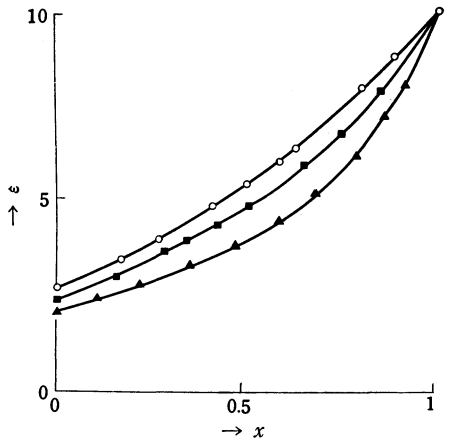


Fig. 4. The experimental results of mixtures, dichloroethane-cyclohexane —○—, dichloroethane-benzene —■— and dichloroethane-carbon disulfide —▲—.

TABLE II. THE OBSERVED DIELECTRIC CONSTANTS OF THE MIXTURES AT 25°C

Dichloroethane-cyclohexane		Dichloroethane-benzene		Dichloroethane-carbon disulfide	
x	ε	x	ε	x	ε
0	2.018	0	2.273	0	2.601
0.101	2.246	0.117	2.803	0.152	3.298
0.232	2.655	0.226	3.345	0.241	3.774
0.350	3.163	0.326	3.897	0.407	4.865
0.475	3.863	0.419	4.468	0.607	6.413
0.548	4.379	0.510	5.084	0.629	6.594
0.649	5.239	0.613	5.863	0.779	7.892
0.743	6.213	0.721	6.801	0.876	8.839
0.826	7.249	0.815	7.779	1	10.073
0.888	8.163	1	10.070		
1	10.073				

is somewhat larger than the value 2/3 measured by the spectroscopic method, but the apparent dipole moment calculated from N_g/N_d when $x \to 0$ agrees fairly well with that estimated experimentally by the use of Debye's equation for dilute solutions.

Finally, the experimental results on mixtures of dichloroethane with other nonpolar solvents at 25°C are summarized in Fig. 4 and Table II. By comparing the experimental curves representing the dielectric constants of mixtures against x with one another, it will be found that the curvatures of the curves are different for different mixtures, and diminish in the following order; cyclohexane and carbon tetrachloride > benzene > carbon disulfide. The excess enthalpy[2] of each mixture decreases in the same order, that is, cyclohexane > carbon tetrachloride > benzene, although the heats of mixing for the carbon disulfide solution have not been measured as yet. Now, the actual calculation of the dielectric constants was carried out only for the mixture dichloroethane-carbon tetrachloride. However, the concentration dependence of the dielectric constants in other mixtures may be inferred to some extent from the calculated results for the mixture dichloroethane-carbon tetrachloride. The case in which the best agreement of the theoretical results with experiments is obtained is the carbon disulfide solution, and next to it, the satisfactory agreement of the theoretical values with the experimental ones is found in the case of benzene solution. The reason why the better agreement even in this simple model is obtained in the case of the carbon disulfide and the benzene solutions is not clear, but some specific interaction may be responsible for this coincidence, considering that the thermodynamic and the spectroscopic[12] measurements suggest the anomalous behavior in the benzene solution. This interesting point may be elucidated partly by examining in detail the temperature dependence of the dielectric constants of the mixtures.

Summary

The dielectric constant for the mixture dichloroethane-carbon tetrachloride was calculated by making use of a model proposed by Onsager, Fujishiro and Scholte. The calculated values agree rather well with the experimental. The higher the temperature is, the better is the agreement. The dielectric constants of other mixtures such as dichloroethane-cyclohexane, dichloroethane-benzene and dichloroethane-carbon disulfide were also measured only at 25°C and compared with one another. The coincidence of the theoretical values with the experimental was obtained in the following order; carbon disulfide, benzene, carbon tetrachloride and cyclohexane.

The cost of this research has been partly defrayed by a grant from the Ministry of Education.

Department of Chemistry
Faculty of Science
Osaka City University
Kita-ku, Osaka

12) A. Wada and Y. Morino, *J. Chem. Phys.*, **22**, 1276 (1954).

Estimation of the Energy of Hydrogen Bonds Formed in Crystals. I. Sublimation Pressures of Some Organic Molecular Crystals and the Additivity of Lattice Energy

By Ariyuki AIHARA

(Received May 25, 1959)

A considerable number of investigations have been done on the problem of hydrogen bonds from both experimental and theoretical points of view, especially since the introduction of the infrared technique in this field of study. Thus, it may safely be said that there is little left to be studied on these topics, so far as they are concerned with hydrogen bondings in solutions of, e. g., phenols, amides and amines in appropriate solvents. One of the questions, however, which is not completely solved as yet, is how to estimate the strength of hydrogen bonds when they are formed in the crystalline state. In this connection, the author has been engaged in the measurement of sublimation pressures of a number of amides and amines with the hope of getting knowledge concerning the relation between the energy of hydrogen bonds in crystals and the heat of sublimation[1].

The principle of estimating the energy of hydrogen bonds in crystals, which has hitherto been adopted by several investigators[1-3], is first to measure the heat of sublimation of a substance in question and then to subtract from it the amount of contribution to the lattice energy due to dispersive and dipolar interaction between molecules in the lattice. Here, the interaction energy due to dispersive force can be calculated theoretically by the Slater-Kirkwood formula[4] if the crystal structure is fully analyzed by X-ray diffraction or by any other methods, while the dipolar interaction can be estimated by the usual procedure or by assuming point charge models.

In case the crystal structure is too complicated to permit theoretical calculation of lattice energy or if it is not analyzed yet, a conventional method has been used in which one assumes the heat of sublimation of a substance, isoelectronic with that in question, as equivalent to the portion of lattice energy due to dispersive and dipolar interaction between molecules in the crystal of a substance forming a hydrogen bond, thereby estimating the energy of the hydrogen bond according to the method already mentioned. A trouble is that an appropriate isoelectronic molecule is not always available to follow the above procedure.

To overcome this difficulty the author has tried first to establish the approximate method of estimating the lattice energy of molecular crystals empirically, assuming its additivity, and then to make use of this method to estimate the energy of hydrogen bonds in crystals of phenols, amides and amines. In this paper, the additivity rule for lattice energy of organic molecular crystals will be examined together with experimental results of sublimation pressure measurement for a number of molecular crystals.

Experimental

Sublimation pressures were measured with a viscosity gauge of the type first designed by Haber[5], Langmuir[6] and later modified by Sasaki[7]. It consists of a Λ shaped fine quartz fiber mounted on a piece of a quartz rod and set in a measuring cell. The diameter of the fiber is 0.1 mm. and the length of the isosceles side of the triangle formed is nearly 10 cm. To facilitate the setting of vibration of the fiber from outside of the cell by a small magnet, a piece of iron wire is attached to the top of the fiber. Samples are fractionally sublimed or distilled under high vacuum and are introduced directly into the cell without allowing them to

1) A. Aihara, *J. Chem. Soc. Japan, Pure Chem. Sec. (Nippon Kagaku Zasshi)*, **73**, 855 (1952); ibid., **74**, 437, 631, 634 (1953); ibid., **76**, 492, 495, 497 (1955).
2) L. Pauling, "The Nature of the Chemical Bnod", Cornell Univ. Press, Ithaca, N. Y. (1945), p. 304—306.
3) S. Seki et al., This Bulletin, **29**, 127 (1956); ibid., **32**, 137 (1959).
4) J. C. Slater and J. G. Kirkwood, *Phys. Rev.*, **37**, 682 (1931).
5) F. Haber and F. Kerschbaum, *Z. Elektrochem.*, **20**, 296 (1914).
6) I. Langmuir, *J. Am. Chem. Soc.*, **35**, 107 (1913).
7) N. Sasaki, "Handbook Experimental Chemistry (Kagaku Jikken Gaku)", Vol. I—3, Kawade Shobo Co., Ltd., Tokyo (1950), p. 321.

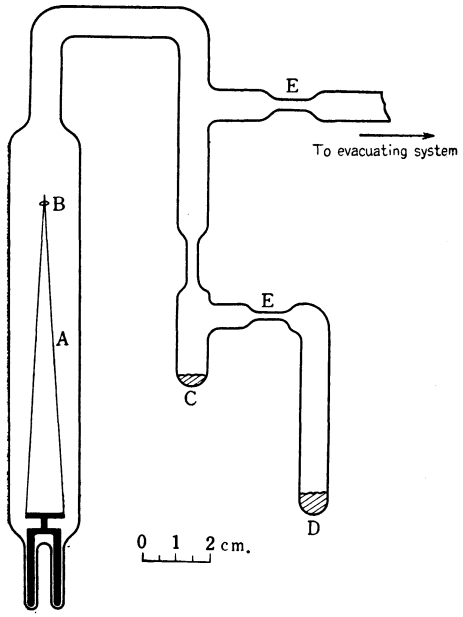


Fig. 1. Viscosity gauge.
A, quartz fiber; B, iron ring
C, sample (purified); D, sample (crude);
E, to be sealed off after evacuation.

make contact with air. The device is shown in Fig. 1[1].

Like most of other vapor pressure measuring gauges, the viscosity gauge must be calibrated with an absolute manometer, such as the McLeod or Knudsen gauge. Here, the calibration was made by subjecting the gauge to saturated vapor of carefully purified benzophenone at several temperatures at which the vapor pressure of benzophenone was already known[8]. According to Haber and Kerschbaum[5], the relation between the pressure in the gauge, P, and the damping time rebuired for the amplitude of the vibration of the fiber to decrease to its half value, t, can be expressed as follows; $P\sqrt{M}=b/t-a$. Here a and b are constants of the gauge and M is the molecular weight of the vapor in it. Thus by observing the damping time, t, at several temperatures and putting the corresponding values of vapor pressures into the above equation, the values of a and b can be determined by the method of least squares. An example of the above procedure is shown in Table I. The values of vapor pressure in the last column of the table were calculated by an equation obtained by Nitta and Seki[8]: $\log P = 12.434-4654.3/T$. The constants, a and b, thus obtained are the average values at 30°C, and correction must be made as they vary with $\sqrt{T}$ when measurements are made at different temperatures.

Most of the materials used are commercial products of high grade and are purified several times by fractional sublimation or distillation under high vacuum. Their melting points are shown in the following tables together with sublimation pressure obtained.

8) I. Nitta and S. Seki, *J. Chem. Soc. Japan, Pure Chem. Sec. (Nippon Kagaku Zasshi)*, **71**, 378 (1950).

Table I. Relation between the damping time and the vapor pressure of benzophenone at several temperatures

T°C	t sec.	P(mmHg)$\times 10^4$
20.3	351	3.78
23.0	261	5.26
25.4	197	7.03
28.1	144	9.91
30.5	110	12.8
33.2	81.7	17.7
36.0	59.1	25.2
38.8	44.1	32.9

$a=5.66\times10^{-4}$, $b=2.00$

Results

The observed sublimation pressures of biphenyl, diphenylmethane, dibenzyl, triphenylmethane, benzil, benzoylacetone, naphthalene, 2,3-dimethylnaphthalene, 2,6-dimethylnaphthalene, 2-acetylnaphthalene,

Table II. Sublimation pressure of biphenyl

T°K	P(mmHg)$\times 10^3$	T°K	P(mmHg)$\times 10^3$
279.3	0.972	290.6	3.51
281.7	1.28	292.7	4.61
282.8	1.49	295.9	6.16
285.8	2.11	297.5	7.04
288.1	2.59	299.1	8.43
289.7	3.23		

$\log P(\text{mmHg}) = 11.168-3959.4/T$: m. p. 69.5°C

Table III. Sublimation pressure of diphenylmethane

T°K	P(mmHg)$\times 10^3$	T°K	P(mmHg)$\times 10^3$
277.9	1.26	288.4	4.52
279.3	1.48	290.8	5.70
280.9	1.79	292.3	6.44
282.6	2.22	294.4	7.75
284.1	2.71	296.0	9.16
286.4	3.57	297.9	10.26

$\log P(\text{mmHg}) = 12.594-4307.8/T$: m. p. 26.8°C

Table IV. Sublimation pressure of dibenzyl

T°K	P(mmHg)$\times 10^4$	T°K	P(mmHg)$\times 10^4$
286.6	7.77	295.0	23.6
288.6	10.1	298.5	31.8
290.7	12.7	299.6	36.3
293.1	16.8	301.4	44.0
294.3	19.8	307.4	83.7

$\log P(\text{mmHg}) = 12.194-4386.0/T$: m. p. 53.2°C

acenaphthene, and *p*-acetylanisole are shown in Tables II—XIII, respectively. Vapor pressure equations for these substances, obtained by the method of least squares, are also shown together with their melting points.

TABLE V. SUBLIMATION PRESSURE OF TRIPHENYLMETHANE

T°K	P(mmHg)$\times 10^4$	T°K	P(mmHg)$\times 10^4$
325.6	4.04	336.2	13.2
327.3	4.93	336.6	13.7
329.0	5.75	340.0	19.4
330.0	6.61	344.3	30.2
333.0	8.99	349.3	48.7

$\log P(\text{mmHg}) = 12.661 - 5227.9/T$: m. p. 94.0°C

TABLE VI. SUBLIMATION PRESSURE OF BENZIL

T°K	P(mmHg)$\times 10^4$	T°K	P(mmHg)$\times 10^4$
318.7	3.83	328.1	10.9
321.1	5.07	329.7	12.8
322.4	5.89	333.1	18.2
324.1	6.92	336.1	25.7
325.2	7.83	340.1	41.1

$\log P(\text{mmHg}) = 12.708 - 5140.8/T$: m. p. 95.5°C

TABLE VII. SUBLIMATION PRESSURE OF BENZOYLACETONE

T°K	P(mmHg)$\times 10^4$	T°K	P(mmHg)$\times 10^4$
278.6	4.12	288.8	14.9
280.4	5.28	290.5	18.6
282.8	7.06	294.4	28.4
284.6	8.88	296.6	36.2
286.7	11.3	299.5	51.0

$\log P(\text{mmHg}) = 12.317 - 4374.6/T$: m. p. 58.3°C

TABLE VIII. SUBLIMATION PRESSURE OF NAPHTHALENE

T°K	P(mmHg)$\times 10^3$	T°K	P(mmHg)$\times 10^3$
275.9	6.63	281.1	11.6
277.8	8.32	283.2	14.1
279.5	9.47		

$\log P(\text{mmHg}) = 10.376 - 3462.6/T$: m. p. 81.7°C

TABLE IX. SUBLIMATION PRESSURE OF 2,3-DIMETHYLNAPHTHALENE

T°K	P(mmHg)$\times 10^4$	T°K	P(mmHg)$\times 10^4$
278.5	3.32	287.4	9.91
280.4	4.27	290.0	13.5
282.6	5.59	291.6	15.9
283.0	5.80	293.8	20.5
283.7	6.31	295.4	24.3
284.9	7.44	297.3	29.7
285.6	7.89	301.3	45.9
286.3	8.55		

$\log P(\text{mmHg}) = 11.510 - 4172.6/T$: m. p. 105.3°C

TABLE X. SUBLIMATION PRESSURE OF 2,6-DIMETHYLNAPHTHALENE

T°K	P(mmHg)$\times 10^4$	T°K	P(mmHg)$\times 10^4$
279.0	2.72	289.3	10.2
280.5	3.32	290.5	11.7
282.1	4.13	293.7	16.9
283.8	5.17	296.7	24.2
285.6	6.55	299.7	33.8
286.8	7.44	303.8	52.2

$\log P(\text{mmHg}) = 12.165 - 4386.4/T$: m. p. 106.2°C

TABLE XI. SUBLIMATION PRESSURE OF 2-ACETYLNAPHTHALENE

T°K	P(mmHg)$\times 10^4$	T°K	P(mmHg)$\times 10^4$
295.1	3.95	305.5	13.3
297.2	5.16	309.5	21.3
299.3	6.59	315.8	41.4
302.5	9.49		

$\log P(\text{mmHg}) = 12.153 - 4589.9/T$: m. p. 55.8°C

TABLE XII. SUBLIMATION PRESSURE OF ACENAPHTHENE

T°K	P(mmHg)$\times 10^3$	T°K	P(mmHg)$\times 10^3$
291.1	1.03	298.3	2.40
292.2	1.20	301.0	3.22
292.9	1.29	304.4	4.64
293.8	1.44	307.3	6.20
295.8	1.79	310.6	8.54
297.3	2.09		

$\log P(\text{mmHg}) = 11.758 - 4290.5/T$: m. p. 95.0°C

TABLE XIII. SUBLIMATION PRESSURE OF *p*-ACETYLANISOLE

T°K	P(mmHg)$\times 10^4$	T°K	P(mmHg)$\times 10^4$
275.8	4.53	287.4	18.1
277.7	5.72	289.1	21.9
280.3	7.78	293.1	33.9
282.0	9.76	296.4	48.3
284.4	12.8	298.8	61.6
285.1	13.8	300.4	72.4

$\log P(\text{mmHg}) = 11.367 - 4056.1/T$: m. p. 38.4°C

Some of the results of the measurements of sublimation pressure of biphenyl, published previously by several investigators[9-11], are compared in Fig. 2 with the author's. As can be seen in the figure, the author's result is in good agreement with that of Seki and Suzuki, while the others show considerable deviations from the author's, Bradley's data being too high and Bright's too low. The fact that the results obtained by different methods, i. e., a method using viscosity gauge by the

9) N. F. H. Bright, *J. Chem. Soc.*, **1951**, 624.
10) S. Seki and K. Suzuki, This Bulletin, **26**, 209 (1953).
11) R. S. Bradley, *J. Chem. Soc.*, **1953**, 1690.

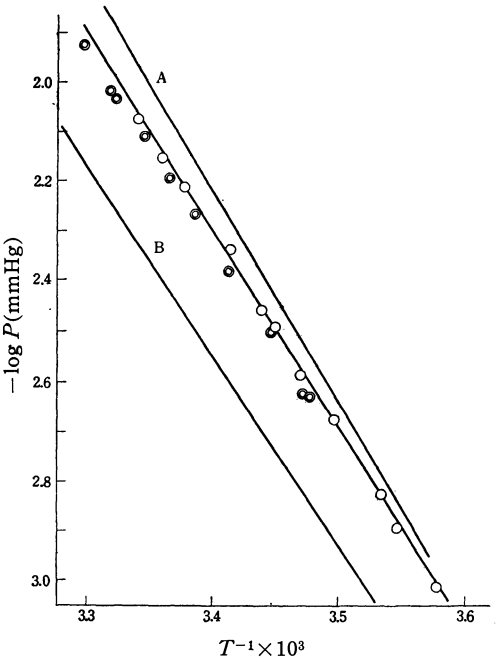


Fig. 2. Sublimation pressure of biphenyl.
○, Aihara; ◎, Seki & Suzuki;
A, Bradley; B, Bright.

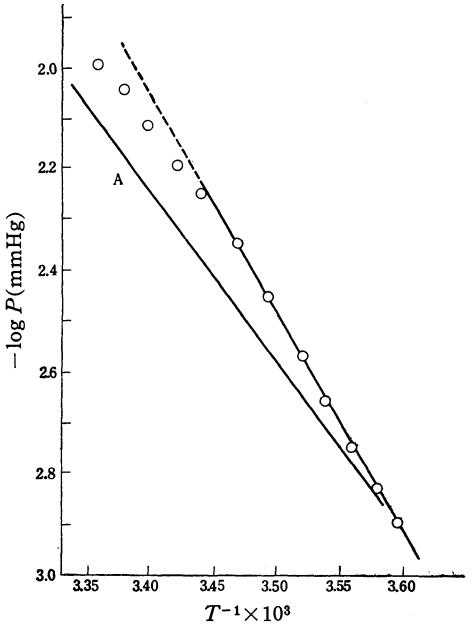


Fig. 3. Sublimation pressure of diphenylmethane.
○, Aihara; A, Bright.

author and an effusion method by Seki and Suzuki, give a good agreement, clearly shows the reliability of these data.

The sublimation pressure of diphenylmethane measured by Bright[9] is again lower than the author's result, the linear relation between $\log P$ and T^{-1} showing a smaller inclination compared with the author's. (Fig. 3). Plotting the experimental values of $\log P$ against T^{-1}, it is noticed in the author's measurement that there occurs a change in the linear relation between $\log P$ and T^{-1} at about 15°C and upward. Roughly speaking, the relation between $\log P$ and T^{-1} after this change goes almost parallel with that of Bright's. Also a simple dilatometric measurement revealed the occurrence of a change in the expansion coefficient of diphenylmethane at about 15°C. (Fig. 4). Although the nature of this transitional change is not clear as yet, it is likely that Bright missed it, putting too much weight on observed values of sublimation pressure above 15°C. The vapor pressure equation shown in Table III is, thus, valid for the temperature range below 15°C.

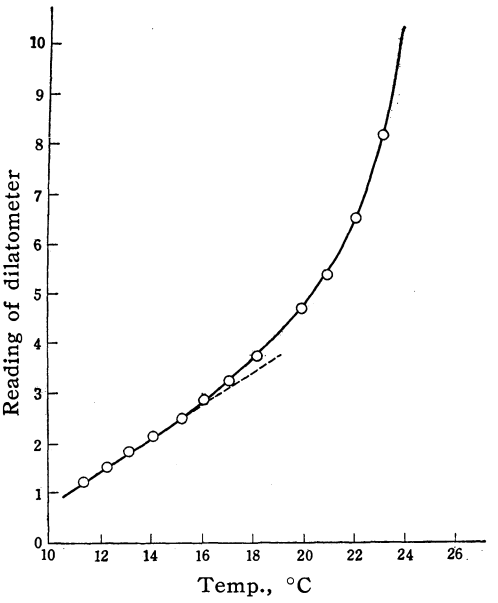
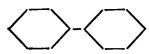
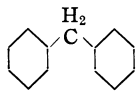
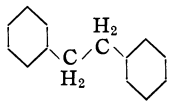
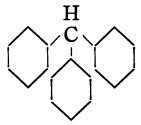
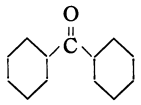
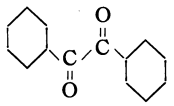
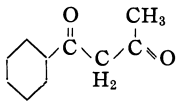
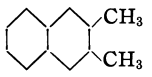
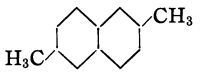
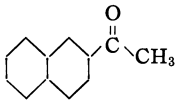
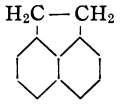
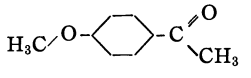


Fig. 4. Dilatometry of diphenylmethane. Reading of dilatometer is in an arbitrary scale.

Bright's[9] result on the sublimation pressure of dibenzyl deviates similarly from the author's as was seen in the two cases mentioned above: the vapor pressure equation and the heat of sublimation obtained by Bright are, $\log P=9.86-3783/T$, $\Delta H=17.3$ kcal./mol., while the author's are $\log P=12.194-4386.0/T$ and $\Delta H=20.07$ kcal./mol.

Of the other substances dealt with in this paper, mention should be made of the

TABLE XIV. VALUES OF THERMODYNAMIC FUNCTIONS

Compounds	ΔH_{obs} kcal./mol.	ΔH_{calc} kcal./mol.	$\Delta G^{298.2°K}$ kcal./mol.	ΔS cal./deg. mol.
	18.12±0.14	18.0	6.81±0.28	37.9±0.5
	19.71±0.15	20.0	6.45±0.31	44.5±0.5
	20.07±0.11	22.0	7.36±0.22	42.6±0.4
	23.92±0.14	29.0	10.58±0.26	44.8±0.4
	21.30 [8]	21.5	8.26 [8]	43.7 [8]
	23.52±0.27	25.0	10.11±0.55	45.0±0.9
	20.02±0.10	20.0	7.14±0.21	43.2±0.4
	15.84±0.54	15.5	5.61±1.12	34.3±1.9
	19.09±0.07	19.5	7.31±0.14	39.5±0.2
	20.07±0.09	19.5	7.40±0.18	42.5±0.3
	21.00±0.10	21.0	8.35±0.20	42.4±0.3
	19.63±0.10	19.5	7.52±0.21	40.6±0.4
	18.56±0.05	18.5	6.98±0.11	38.8±0.2

result of sublimation pressure of naphthalene. There are plenty of data on the sublimation pressure of naphthalene published already in literatures[11-13], but strangely none of them coincide with one another. The author's value of sublimation pressure lies between those of Bradley[11]* and Andrews[13], while $\Delta H=15.84$ kcal./mol. by the author agrees well with Zilberman-Granovskaya's[12] value, $\Delta H=15.7$ kcal./mol., and Wolf's[14] value, $\Delta H=15.9$ kcal./mol. The differences between the various results must be due to different degrees of purity of the samples with which the determinations were made, and also due to the inaccuracy of the methods of determination.

The values of some thermodynamic functions of the substances derived from vapor pressure equations are shown in Table XIV.

Additivity of Lattice Energy

Inspection of the relation between the heats of sublimation and the molecular structures of the compounds listed in Table XIV suggests that an additivity rule may be applied to the lattice energies of these crystals, at least as a first approximation. Now let it be assumed that each constituent group of a molecule, such as methyl, carbonyl, phenyl, etc., makes a contribution to the lattice energy independently. Then, if we allot an appropriate energy to each group, it should be possible to get a "calculated lattice energy" of a compound in question. The third column of Table XIV shows the values of lattice energies thus calculated for compounds dealt with in this paper, with the following values of allotted lattice energies for constituent groups. (Table XV). Notwithstanding the approximate nature of the method of calculation, the agreement between observed and calculated values of lattice energies, i. e., ΔH_{obs} and ΔH_{calc}, is quite satisfactory, as can be seen in Table XIV. Disagreement noticed in a few cases, such as dibenzyl, triphenylmethane and benzil, can be ascribed to the bulky structure of the molecules which prevents the close approach of constituent groups to each other, thus decreasing the amount of contribution to the lattice energy to some extent.

Table XV. Allotment of lattice energies to groups

Groups	Energy kcal./mol.	Groups	Energy kcal./mol.
CH, CH_2, CH_3	2.0	O-CH_3	4.0
NH, NH_2	2.0	C_6H_5	9.0
OH	2.0	$C_{10}H_7$	15.5
C=O	3.5	*t*-Butyl	5.5

In Table XV, the value for phenyl group, 9.0 kcal./mol., was determined by dividing the heat of sublimation of biphenyl, 18.1 kcal./mol., by two: this value is very close to the heat of sublimation of benzene obtaind by Trieschmann, 9.2 kcal./mol.[15] The value for naphthyl group, 15.5 kcal./mol. is close to the average of the heat of sublimation of naphthalene determined by the author, Wolf[14], and Zilberman-Granovskaya[12]. As to the increment of lattice energy due to a methyl (or methylene) group, several investigators have published the following values: 2.3 kcal./mol. by Müller[16], 1.5 kcal./mol. by Inokuchi[17], 1.7~2.2 kcal. mol. by Moelwyn-Hughes[18], 1.1~1.7 kcal./mol. by Davies[19]. The author's value, 2.0 kcal./mol., is the average of the above values and those obtained by analyzing the data in Table XIV. The same value is assigned to amino and hydroxyl groups as that of a methyl group, because these molecules are all isoelectronic. The validity of assigning the same value to these groups will be confirmed in succeeding papers where the lattice energies of phenols, amides and amines will be discussed. Also Bondi and Simkin[20] have discussed this problem. The value for a carbonyl group, 3.5 kcal./mol., was obtained by analyzing the heats of sublimation of benzophenone, benzoylacetone, 2-acetylnaphthalene and some other compounds having a carbonyl group. The value for a *tert*-butyl group was derived from the heat of sublimation of 1, 4-di*tert*-butylbenzene[21]. 4.0 kcal./mol. for

12) Zilberman-Granovskaya, *J. Phys. Chem.* (*U.S.S.R.*), **14**, 759 (1940):
log $P=10.41-3429/T$, $\Delta H=15.7$ kcal./mol.

13) M. R. Andrews, *J. Phys. Chem.*, **30**, 1497 (1926):
log $P=12.275-4000/T$, $\Delta H=18.28$ kcal./mol.

* Bradley's data:
log $P=11.597-3783/T$, $\Delta H=17.3$ kcal./mol.

14) K. L. Wolf and H. Weghofer, *Z. physik. Chem.*, **B39**, 194 (1938).

15) H. G. Trieschmann, Dissertation, Kiel (1935).

16) A. Müller, *Proc. Roy. Soc.* (*London*), **A154**, 124 (1936).

17) H. Inokuchi, *J. Chem. Soc. Japan, Pure Chem. Sec.* (*Nippon Kagaku Zasshi*), **72**, 552 (1951).

18) E. A. Moelwyn-Hughes, "Physical Chemistry", Pergamon Press, London (1957), p. 682.

19) M. Davies, private communication.

20) A. Bondi and D. J. Simkin, *J. Chem. Phys.*, **25**, 1073 (1956).

21) E. R. Hopke and G. W. Sears, *J. Chem. Phys.*, **19**, 1345 (1951).

a methoxyl group was determined by subtracting the allotted lattice energies for methyl and carbonyl groups from the heat of sublimation of *p*-acetylanisole.

It must be admitted that the treatment of lattice energies of organic molecular crystals discussed above is quite rough and could not be applied to more complicated cases without further refinement. Still, an orthodox way of calculating lattice energies, such as by Slater-Kirkwood formula[4] or by other ways, does not necessarily give a satisfactory agreement between calculated and observed lattice energies, as has been pointed out by Seki and his collaborators[22]. Therefore, it would be helpful, at the present stage, to have an approximate way of estimating lattice energies of molecular crystals empirically, as is proposed in this paper. This procedure will be used later to get the energy of hydrogen bond in crystals of phenols, amides and amines.

22) S. Takagi, R. Shintani, H. Chihara and S. Seki, This Bulletin, **32**, 137 (1959).

Summary

Sublimation pressures of a number of organic molecular crystals were measured by a viscosity gauge. The heats of sublimation of these compounds were examined in relation to their molecular structures, and it was concluded that an additivity rule could be applied to the lattice energies of these crystals as a first approximation.

The author wishes to thank Professor M. Davies, the University of Wales, for informing the author about some of his results prior to publication. The cost of the work was partly defrayed by the financial support of the Ministry of Education to which the author's thanks are due.

Department of Chemistry
Faculty of Liberal Arts & Science
Shinshu University
Agata-machi, Matsumoto

Stress Relaxation of Thermo-Reversible Gels. Polyvinyl Alcohol—Congo Red—Water System

By Kiyoshi ARAKAWA

(Received June 1, 1959)

In the previous paper the author reported the result of the stress relaxation experiment made on the gel of the polyvinyl alcohol-glycerin-water system[1]. As another example of thermo-reversible gels of polymeric nature, the gel of the polyvinyl alcohol-congo red-water system is known, and several studies on the properties of the gel have been reported[2].

As a part of the series of rheological studies of thermo-reversible gels[1,3] a stress relaxation experiment has been attempted on the gel, and the result is reported in the present paper.

1) K. Arakawa, This Bulletin, **31**, 842 (1958).
2) C. Dittmar and W. J. Priest, *J. Polymer Sci.*, **18**, 275 (1955); N. Hirai, *J. Chem. Soc. Japan, Pure Chem. Sec.* (*Nippon Kagaku Zasshi*), **75**, 693 (1954); T. Danno, The 10th Annual Meeting of the Chemical Society of Japan, Tokyo, April, 1957.
3) K. Arakawa, *J. Chem. Soc. Japan, Pure Chem. Soc.* (*Nippon Kagaku Zasshi*), **80**, 133 (1959).

Experimental

Apparatus. — The apparatus to measure the relaxing stress produced in the specimen under a given strain is the same one as that used previously[1,3]. The chainomatic balance part of the apparatus is shown in Fig. 1. A specimen is compressed between a plate attached to a bar and a bottom plate connected to a screw gauge by the rotation of the gauge, which is graduated to 0.01 mm. The stress in the specimen is calculated from the vertical length of the suspended chain which is balancing automatically with the stress. The specimen is dipped in liquid paraffin, as was done in the preceding studies[1,3].

Sample. — A commercial sample of polyvinyl alcohol was purified by precipitation from aqueous solution. The amount of residual acetate groups in the sample was 1.5% by mole. The intrinsic viscosity $[\eta]_{30}$ was 0.96 100 cc./g., which was determined by a capillary viscometer. The viscosity-average molecular weight M_V was calculated to be 8.5×10^4 according to the formula by

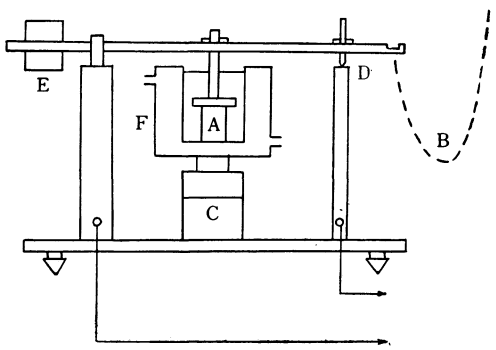


Fig. 1. Chainomatic balance relaxometer
A: specimen
B: chain
C: screw gauge
D: point contact
E: balancing weight
F: double jacket

A. Nakajima et al.[4] Congo red used was Merck's analytical grade chemical.

The preparation of specimens was as follows. A definite quantity of dried polyvinyl alcohol was mixed with dried congo red powder, the amount of which was adjusted to be accurately 1/10 of polyvinyl alcohol by weight (this weight ratio of congo red and polyvinyl alcohol was taken to be the same for all specimens used in the present study), and a calculated quantity of water was added to the mixture in a conical beaker. After being covered with liquid paraffin, the mixture was dissolved slowly by heating in a water bath. After complete dissolution the solution was poured into cylindrical moulds kept at about 85°C in a thermostat and was cooled down slowly to 50°C (the rate of temperature decrease: 5°C per hour), and then was aged at room temperature. After several days the specimens (diameter, 2 cm.; height, about 3 cm.) were taken out from the moulds, and were aged moreover at room temperature in liquid paraffin for about a month. The composition of the prepared specimens is described in Table I.

TABLE I. THE COMPOSITION OF GELS

Sample	Polyvinyl alcohol wt. %	Congo red wt. %
A	17.5	1.75
B	15.0	1.50

Samples A and B have typical rubber-like elasticity at ordinary temperature and make the sol-gel transition reversibly at about 80°C.

Results and Discussion

Stress Relaxation Data.—The data of stress relaxation of samples A and B are plotted in the form $(298/T)E_r$ vs. $\log t$, where $E_r=f/\gamma$ is relaxation Young's modulus; t time, and f stress, in Figs. 2a and 2b. The strain γ applied in the present experiment was 15% for all specimens. This value was in the range where the linear relation between stress and strain was almost maintained. These data are reduced to 25°C by multiplying E_r by a factor $298/T$.

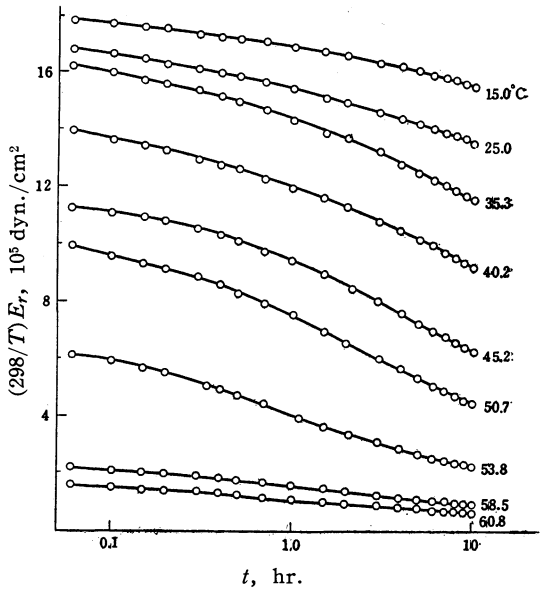


Fig. 2a. Reduced relaxation Young's modulus of 17.5% gel.

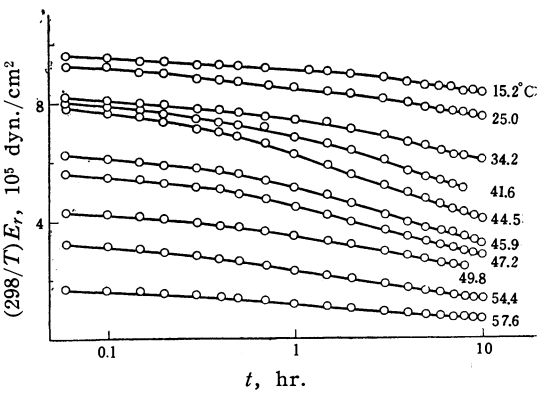


Fig. 2b. Reduced relaxation Young's modulus of 15% gel.

The master relaxation curve[5] at 25°C for each sample is obtained by means of arbitrary shift factors a_T. The curves,

4) A. Nakajima and K. Furutate, *Chem. High Polymers (Kobunshi Kagaku)*, **6**, 460 (1949).

5) J. D. Ferry, *J. Am. Chem. Soc.*, **72**, 3746 (1950); F. Schwarzl and A. J. Staverman, *J. Appl. Phys.*, **23**, 838 (1952); C. A. Dahlquist and M. R. Hatfield, *J. Colloid Sci.*, **7**, 253 (1952).

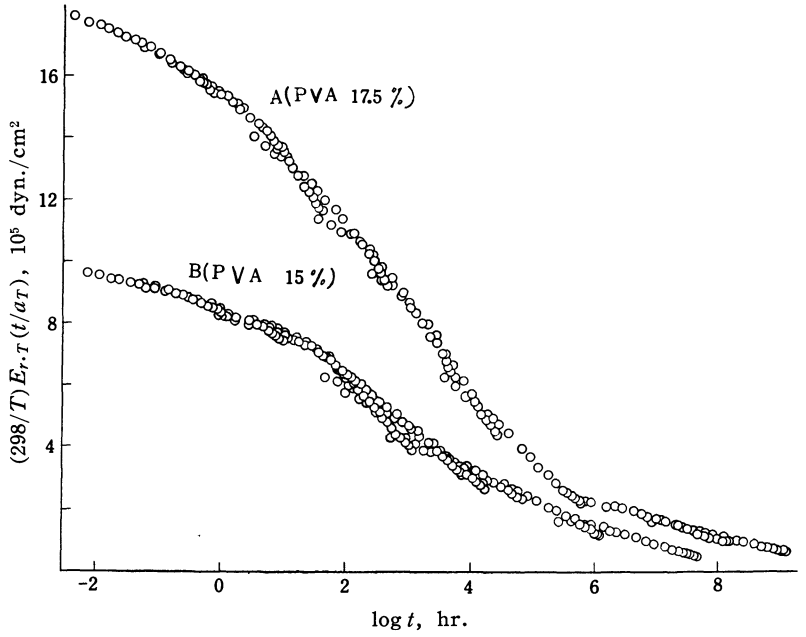


Fig. 3. Master relaxation curves at 25°C.

thus obtained, are plotted in Fig. 3. The superposition of each relaxation curve is seen to be fairly good.

Shift factors $\log a_T$ are plotted against $1/T$ in Fig. 4. It seems the $\log a_T$ vs. $1/T$ curve is approximately linear in the low temperature region, and that the deviation from linearity occurs at about 43°C. The apparent activation energy H_a which is calculated from the $\log a_T$ vs. $1/T$ curve is a constant value, 42 kcal., below 43°C. This value of H_a is smaller than that of the gel of polyvinyl alcohol, glycerin, and water system. The value of H_a increases with temperature above 43°C. This tendency differs from that observed in the polyvinyl alcohol-glycerin-water gel, but is similar to that observed in the hydrogel of agar-agar in which the deviation from linearity appears at about the same temperature, but the value of H_a below the temperature is much smaller*,[3].

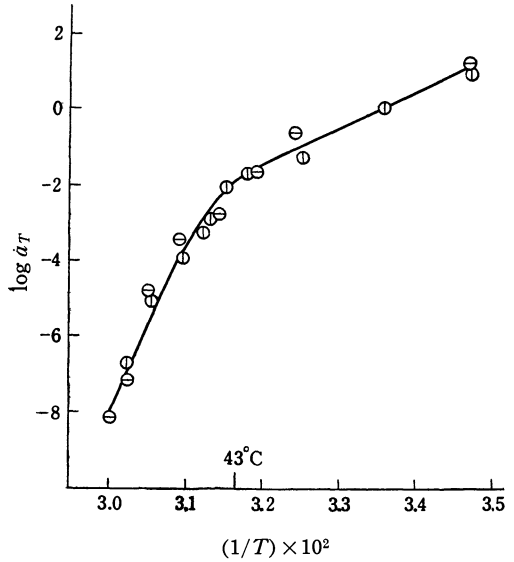


Fig. 4. Log a_T vs. $1/T$ relation.
⊖ Sample A
⊕ Sample B

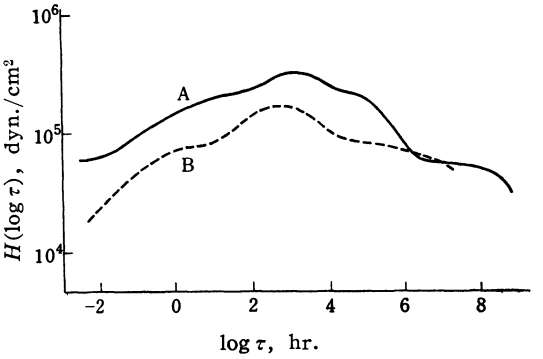


Fig. 5. Relaxation spectra

* In the hydrogels of agar-agar the superposition of each relaxation curve is not so good, except in the case of 2.6% gel, above ca. 40°C. The mechanical behavior of 2.6% gel was as described in the text. In the gels of the other concentration a similar tendency was seen, though exact master curves were not obtained.

As seen in the fact described above, the $\log a_T$ vs. T relation does not obey the equation of WLF form[6].

Distribution Functions of Relaxation Times.— The relaxation spectra $H(\log \tau)$ are shown in Fig. 5, which were calculated from the master relaxation curves shown in Fig. 3 by the second order approximation[7].

$$H\left(\log\frac{\tau}{2}\right)=2.303\left[E_r\left\{-\frac{\mathrm{d}\log E_r}{\mathrm{d}\log t}+\frac{1}{2.303}\frac{\mathrm{d}^2(\log E_r)}{\mathrm{d}(\log t)^2}+\left(\frac{\mathrm{d}\log E_r}{\mathrm{d}\log t}\right)^2\right\}\right]_{t=\tau}$$

Each curve in Fig. 5 is seen to exhibit the character of the box type region of the whole spectrum, which corresponds to the rubbery and fluid state of materials.

Each spectrum is similar in shape except at the long time end, and the spectrum for 15% gel is seen to conform to that for 17.5% gel when slid upwards and to the right.

From the above facts it seems to be possible that two curves shown in Fig. 3 are composed to a single curve approximately, but this reduction on concentration has turned out to need the multiplication factor $(C_0/C)^n$, where the value of n is 3.5~4 and C_0 is a reference concentration. This value of n is too large, being compared with the value, 2, reported previously by DeWitt et al.[8] on the solution of polyisobutylene. More data are required.

6) M. L. Williams, R. F. Landel and J. D. Ferry, *J. Am. Chem. Soc.*, **77**, 3701 (1955).
7) R. D. Andrews, *Ind. Eng. Chem.*, **44**, 707 (1952); F. Schwarzl and A. J. Staverman, *Physica*, **18**, 791 (1952).
8) T. W. DeWitt, H. Markovitz, F. J. Padden and L. J. Zapas, *J. Colloid Sci.*, **10**, 174 (1955).

Summary

Stress relaxation curves were obtained for the gels of the polyvinyl alcohol-congo red-water system in the temperature range, 15~60°C, by means of a chainomatic relaxometer. The molecular weight of polyvinyl alcohol was 8.5×10^4, and gels of 15.0 and 17.5% were used, where the concentration of congo red was adjusted to be 1/10 of that of polyvinyl alcohol. Master relaxation curves were obtained for each concentration over the range, 10^{-2}~10^9 hr, and relaxation spectra were calculated by the second order approximation. The following results were obtained.

1) The $\log a_T$ vs. T relation gives a single curve for two concentrations, and does not obey the equation of WLF form. Also it has characteristics similar to that of agar-agar gels.

2) The apparent activation energy is kept constant to be 42 kcal. below about 43°C, and above this temperature it sharply increases with temperature.

3) The reduction on concentration to a single composite relaxation curve seems to be possible in rough approximation.

The author is indebted to Mr. Morio Kamisho and Mr. Yoshio Daicho for their cooperation in carrying out the experiment.

Department of Chemical Industry
Faculty of Engineering
Shizuoka University
Oiwake, Hamamatsu

Infrared Studies of Polyvinyl Alcohol by Deuteration of its OH Groups

By Hiroyuki TADOKORO

(Received May 29, 1959)

In the previous paper[1] we have studied the density, the sorption of water vapor, and the infrared absorption spectrum of polyvinyl alcohol (PVA) films subjected to heat-treatments at different temperatures from the point of view of crystallinity, and have concluded as follows: (1) the degree of crystallinity determined by these methods is parallel unless the thermal decomposition is considerable, and (2) the 1141 cm^{-1} (8.76 μ)* band is a so-called "crystallization-sensitive" band[2-4]. Succeeding the previous work, we have carried out further studies on PVA by means of infrared spectrum, X-ray diffraction and density measurements in the hope of making some contribution to the studies of the crystallinity and fine texture[3] of high polymers.

The purpose of the present paper is to report some new information obtained by the results of deuteration of the OH groups of PVA.

We have made the infrared spectroscopic measurements of the deuterated PVA for the following purposes. The first is for the elucidation of the nature of the crystallization-sensitive band at 1141 cm^{-1}. As to the crystallization-sensitive band, a considerable number of reports have been published during these several years on polyethylene and many other polymers. Although some reasonable interpretations on the absorption mechanism of the crystallization-sensitive bands have been proposed in the cases of polyethylene, there is no conclusive one for the 1141 cm^{-1} band of PVA. The second purpose is for the assignments of the absorption bands in the region of 1500~800 cm^{-1}. There are already many publications on this problem[5-8], but it is not yet settled at all. The third is to test whether we can determine the crystallinity (or accessibilty) of PVA by means of the deuterium exchange method or not. In the case of cellulose, for instance, it is well known that the velocity of deuterium exchange reaction of the hydroxyl group in the amorphous region is much faster than it is in the crystalline region[9-11]. The fourth is to examine the fine structure of the OH stretching bands of the spectrum arising from the crystalline region, if the amorphous region is to be exclusively deuterated. Marrinan and Mann[11] have investigated the fine structure of the OH bands of various kinds of cellulose by the use of this method.

As to the infrared absorption spectrum of deuterated PVA, Ukita, Nishino and Kominami[12] and also Krimm, Liang and Sutherland[8] have reported quite independently. Ukita and his coworkers have recognized no appreciable change of the spectrum, except the new appearance of the broad band at 4.01 μ due to the OD stretching vibration, because of the low degree of deuteration in their case. Krimm and his coworkers have measured the spectrum of PVA-*d* (degree of deuteration: about 90%) in the region of 3600~400 cm^{-1}, and have obtained experimental results similar to ours. As the assignments of the absorption bands of polymers are generally very complicated problems, we have carried out other experiments such

1) H. Tadokoro, S. Seki and I. Nitta, This Bulletin, **28**, 559 (1955).

* Although the value 1146 cm^{-1} (8.74μ) was used in the previous paper[1], 1141 cm^{-1} seems to be more precise according to the subsequent more accurate measurements.

2) J. B. Nichols, *J. Appl. Phys.*, **25**, 840 (1954).

3) I. Nitta and H. Tadokoro, *High Polymer* (*Kobunshi*), **5**, 296, 345 (1956). (A review of the crystallinity of high polymers).

4) H. Tadokoro, *J. Chem. Soc. Japan, Ind. Chem. Soc.* (*Kogyo Kagaku Zasshi*), **59**, 731 (1956). (A review of the application of the infrared spectroscopy for the study of the structure of high polymers).

5) H. W. Thompson and P. Torkington, *Trans. Faraday Soc.*, **41**, 246 (1945).

6) E. R. Blout and R. Karplus, *J. Am. Chem. Soc.*, **70**, 862 (1948).

7) A. Elliott, E. J. Ambrose and R. B. Temple, *J. Chem. Phys.*, **16**, 877 (1948).

8) S. Krimm, C. Y. Liang and G. B. B. M. Sutherland, *J. Polymer Sci.*, **22**, 227 (1956).

9) V. J. Frilette, J. Hanle and H. Mark, *J. Am. Chem. Soc.*, **70**, 1107 (1948).

10) K. E. Almin, *Svensk Paperstidn.* **55**, 767 (1952).

11) H. J. Marrinan and J. Mann, *J. Appl. Chem.*, **4**, 204 (1954); *Trans. Faraday Soc.*, **52**, 481, 487, 492 (1956); *J. Polymer Sci.*, **21**, 301 (1956).

12) J. Ukita, Y. Nishino and T. Kominami, *J. Chem. Soc. Japan, Ind. Chem. Sec.* (*Kogyo Kagaku Zasshi*), **58**, 158 (1955).

TABLE I. SAMPLES

Samples	Conditions of heat-treatment	Density at 25°C (g./cc.)	Crystallinity (density method)
I	No heat-treatment	1.291_0	0.29
III	160°C, 15 min.	1.300_7	0.42

as infrared spectroscopic measurements of oriented PVA-*d* and of doubly oriented PVA[13,14], density measurements[15], etc., to get some useful data for this purpose.

Experimental

a) Polyvinyl Alcohol Samples.—Film specimens were prepared from the same starting material (PVA of average degree of polymerization: 1650) by the same method as that described already in the previous papers[1,16]. (See Table I). In the present work the films were cast on a polystyrene plate instead of a glass plate, because the most suitable thickness of the film for infrared measurements is about 7~10 μ, and it is difficult to strip off such a thin film from a glass plate.

The oriented film was prepared by stretching it by hand in one direction over a small flame until it could be stretched no more. Examination of the film between crossed polaroid sheets confirmed the orientation in the direction of stretching.

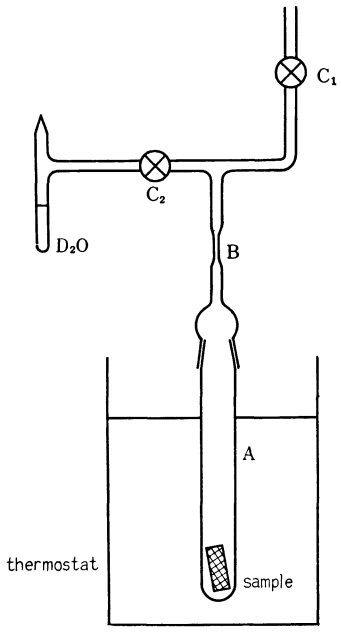


Fig. 1. Apparatus for deuteration.

b) Deuteration, Formalization and Infrared Measurements.—The deuteration of PVA was carried out by using 99.7% heavy water** in a vessel shown in Fig. 1. A PVA film (ca. 20 mm. ×30 mm.) put between the parts of folded stainless steel wire gauze (350 mesh), was inserted in a glass tube A, and was dried at 60°C for about 48 hr. under high vacuum (10^{-4} mmHg or below) by using a liquid air trap (stopcock C_1 being open, and C_2 being closed). After the drying was over, C_1 was closed, the temperature was lowered to room temperature, and then by opening C_2, the sample was equilibrated to the saturated vapor pressure of heavy water. After "being allowed to stand" for about 24 hr., the sample was dried again, and such procedures were repeated several times. At last the glass tube was sealed off at B. The measurements were carried out by putting the films between rock salt plates, with or without polychlorotrifluorocarbon oil (Difloil #3, kindly supplied by Osaka Kinzoku Kôgyô Co., Ltd.).

The oriented and deuterated PVA film for the measurement of dichroism could be prepared by successive procedures in a series of stretching, heat-treatment and deuteration.

Samples I and III were also subjected to formalization and then to deuteration. The formalization was carried out in an aqueous solution of sulfuric acid (200 g./l.), sodium sulfate (250 g./l.) and formaldehyde (40 g./l.) at about 50°C for 15 min. and 2 hr. for each sample. During the formalization treatment the film was held between the parts of a folded wire gauze of bronze (300 mesh) to be free from deformation.

Infrared absorption spectra were taken by using a Hilger H800 Recording Infrared Spectrophotometer with sodium chloride prism, and a Perkin-Elmer Model 21 Double Beam Recording Infrared Spectrophotometer with sodium chloride prism and silver chloride polarizer.

Results and Discussion

a) Deuteration.—The obtained spectra of PVA and of deuterated PVA are shown in Fig. 2a and Table II. The possible errors of the wave number are $\pm 10\,cm^{-1}$ and $\pm 5\,cm^{-1}$ in the regions of $4000 \sim 2000\,cm^{-1}$ and $2000 \sim 700\,cm^{-1}$, respectively. Thus, our spectral data shown in Fig. 2 and Table II are in substantial agreement with those obtained by Krimm et al.[8]

It is well known that OH or NH groups are easily converted into OD or ND by exchange reaction with heavy water, but CH groups are not converted easily unless

13) H. Tadokoro, S. Seki and I. Nitta, *J. Polymer Sci.*, **22**, 563 (1956).
14) H. Tadokoro, S. Seki, I. Nitta and R. Yamadera, ibid., **28**, 244 (1958).
15) H. Tadokoro, K. Kôzai, S. Seki and I. Nitta, ibid., **26**, 379 (1957).
** The product of Norsk Hydro-Electrisk Kvoelstofaktieselskab.
16) H. Tadokoro, S. Seki and I. Nitta, This Bulletin, **27**, 451 (1954).
17) Y. Nishino, J. Ukita and T. Kominami, *J. Chem. Soc. Japan, Ind. Chem. Sec.* (*Kogyo Kagaku Zasshi*), **58**, 159 (1955).
18) E. Nagai and S. Kuribayashi, *Chem. High Polymers* (*Kobunshi Kagaku*), **12**, 322, 368 (1955).
19) L. Glatt, D. S. Webber, C. Seaman and J. W. Ellis, *J. Chem., Phys.*, **18**, 413 (1950).

TABLE II. INFRARED SPECTRA AND VIBRATIONAL ASSIGNMENTS OF PVA AND PVA-*d*

PVA			PVA-*d*			Assignments[e]	
Frequency in cm^{-1}	Dichroism	Intensity	Frequency in cm^{-1}	Dichroism	Intensity	Previous work	This work
3340[a]		vs				ν(OH)	ν(OH)
2945	⊥	s	2945	⊥	s	ν_a(CH_2) (T, E, B, K)[d]	ν_a(CH_2)
2910	⊥	s	2910	⊥	s	ν_s(CH_2)	ν_s(CH_2)
2840	⊥	sh	2840	⊥	sh	ν(CH) (K)	
			2470[a]		vs	ν(OD)	ν(OD)
1440[b]	∥	s	1428	⊥	m	δ(CH_2) (T, B); δ(OH) or superposition of δ(OH) and δ(CH_2) (E); δ(CH+OH), 1428 cm^{-1} is δ(CH_2) (K)	superposition of δ(CH_2) and a coupling band (coupling of δ(OH) and 1383 cm^{-1} band of PVA-*d*). 1428 cm^{-1} band of PVA-*d* is δ(CH_2)
1420[b]	⊥	s					
			1383	∥	s		w(CH) or w(CH_2)
1376	⊥	w	1376	⊥?	m	δ(CH_3-C) (B); w(CH_2) (K)	δ(CH)?
			1360	⊥	sh		
1326[c] 1315	⊥	m				hydrogen deformation (E); δ(CH+OH) (K)	coupling of δ(OH) and 1383 cm^{-1} band of PVA-*d*
			1256	⊥?	sh		
1232	∥	w	1230	∥	m	acetyl group (T, E) not to be acetyl group (B) w(CH) (K)	w(CH_2) or w(CH)
1141	⊥	m	1148	⊥	s	associated with hydrogen-bond (Ni, Na) ν(C-O-C) (K) associated with oxygen-atom (E)	crystallization-sensitive band (see subsequent paper)
			1122	⊥	s		
1093	⊥	s				associated with oxygen-atom (T) ν(C-O) (B, E, K)	ν(C-O)
1083	∥	m	1083	∥	m		
			1049	⊥	s		ν(C-O)
			977	⊥	m		δ(O-D)
			930	⊥	sh		
913	⊥	w				r(CH_2) (K)	skeletal or CH_2
890	⊥	vw					
849	⊥	m				ν(C-C) (K)	
			842	⊥	m		skeletal or CH_2
835	⊥	sh	825	⊥	sh		r(CH_2)
640[f]	∥	sh				w(OH) (K)	
610	⊥	m					
480	⊥	w				δ(C-O) (K)	
410	?	w				w(C-O) (K)	
360	⊥	w					

a) The ν(OH) band at about 3340 cm^{-1} shows no appreciable dichroism at the band maximum, but perpendicular and parallel nature at the higher frequency and lower frequency side, respectively, agreeing with the descriptions of Glatt et al.[19] and Krimm et al.[8] The ν(OD) band at about 2470 cm^{-1} was also found to show the same behavior.

b) The band at about 1430 cm^{-1} splits to 1440 and 1420 cm^{-1} in the polarized spectra because of the difference of their dichroism.

c) The band at about 1325 cm^{-1} has its absorption maximum at 1326 and 1315 cm^{-1} in the case of perpendicular and parallel radiation, respectively.

d) T: Thompson and Torkington[5], E: Elliott, Ambrose and Temple[7], B: Blout and Karplus[6], K: Krimm, Liang and Sutherland[8], Ni: Nishino, Ukita and Kominami[17], Na: Nagai and Kuribayashi[18].

e) ν: stretching, ν_a: antisymmetric stretching, ν_s: symmetric stretching, δ: bending, w: wagging, r: rocking.

f) The data in the region lower than 640 cm^{-1} was reproduced from the paper by Krimm et al.[8]

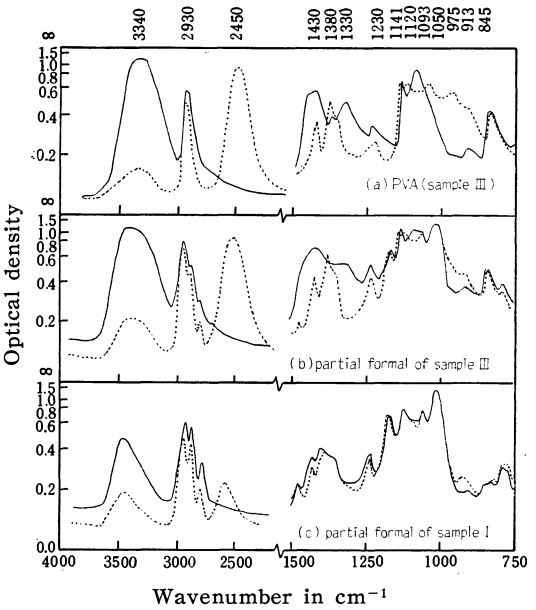


Fig. 2. Infrared spectra of (a) PVA, (b) partial formal of sample III and (c) that of sample I and their deuterated samples (broken line).

under some special conditions[20]. Thus, when PVA is brought into contact with heavy water, the following reaction will take place and the change of the structure will be detected in the infrared spectrum of the sample.

$$-(-CH_2-\underset{\displaystyle OH}{\underset{|}{CH}}-)_{\bar{p}} \xrightarrow{D_2O} -(-CH_2-\underset{\displaystyle OD}{\underset{|}{CH}}-)_{\bar{p}}$$

As a result of the deuteration, the intensity of the ν(O–H) band at 3340 cm^{-1} decreases and at the same time a new intense band appears at 2450 cm^{-1}. This latter band evidently corresponds to the ν(O–D) band. While the ν(C–H) band at 2940 cm^{-1} is not affected appreciably by deuteration, this band could be used as the standard for the intensity measurements. The diminution of the optical density of the ν(O–H) band referred to this C–H band, may be used as a measure of degree of deuteration. The extent of deuteration of the sample shown in Fig. 2a is found to be about 90% by this method of estimation.

Now, the deuterations for samples I and III of Table I were studied under various conditions. When the procedures of drying and of exposure to heavy water vapor were repeated alternately several times, both the samples were deuterated up to about 90% regardless of the degree of crystallinity. On the contrary, the extent of deuteration of nylon 6 which had undergone the same procedure as the PVA sample, was much lower than that of PVA. Moreover, the lower the degree of crystallinity of the sample of nylon 6 is, the higher is the extent of deuteration as is shown in Fig. 3. The same results have been reported on the celluloses as mentioned above[9-11].

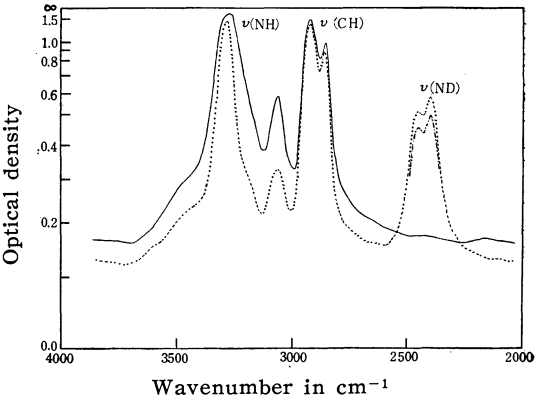


Fig. 3. Infrared spectra of nylon 6 (——) and deuterated nylon 6 (------): ———— sample subjected to heat-treatment.

In relation to these evidences, it will be quite interesting to examine whether the crystalline region of PVA, which is considered to be inaccessible to formalization[21,22], could be deuterated or not. The solid lines of Figs. 2b and 2c show the infrared spectra of samples I and III subjected to formalization. For sample I, the remarkable decrease of the intensity of the OH stretching band at 3340 cm^{-1} and its shift to the shorter wavelength side on formalization may indicate the high degree of formalization. However, for sample III the intensity of the OH stretching band decreases only to a slight extent. This result reconfirmed the fact that the crystalline region is not formalized appreciably as was reported previously by some authors[21,22]. The spectra of these partial formals after deuteration were also shown in the same figure with broken lines. This result indicates that the residual OH groups of the formal of sample III were

20) For example, M. Koizumi, Organic Deuterocompounds, "Advances in Organic Chemistry (Yûkikagaku no Shimpo)" Vol. II. Edited by M. Kotake and S. Akabori, Kyôritsu Shuppan Co. Ltd., Tokyo (1939), p. 27.

21) K. Hirabayashi and N. Fujimoto, *Chem. High Polymers (Kobunshi Kagaku)*, **7**, 159 (1950).

22) Y. Yoshioka and M. Nagano, ibid., **9**, 36 (1952).

deuterated up to about 84%. Thus, the crystalline region of sample III, which was not accessible to formalization, was found to be highly deuterated. These facts seem to show that the difference between the velocity of deuterium exchange in the crystalline region and that in the amorphous region, is considerable in the cases of nylon 6 and cellulose, while this difference is negligibly small in PVA. In this respect, the mechanism of the deuteration reaction of the crystalline region of PVA seems to be a very interesting problem.

b) Interpretation of the Spectra. — The infrared dichroism of the deuterated PVA is shown in Fig. 4, together with that of ordinary PVA for the purpose of comparison. This sample could be prepared by the successive procedures of stretching, heat-treatment and finally deuteration. This method of preparation is based upon the aforementioned remarkable fact that the crystalline region of PVA film even after subjected to heat-treatment can be easily deuterated by exposing it to D_2O vapor.

Although we can not make conclusive assignments of the absorption bands in the region of 1500~700 cm^{-1} at present, we may give here our tentative assignments on the main bands in this region. The band at about 1430 cm^{-1} was assigned by Thompson and Torkington[5] and also by Blout and Karplus[6] to a deformation mode of CH_2 group. On the other hand, Elliott, Ambrose and Temple[7] considered this band to be the δ(O–H), or to be the superposition of the δ(O–H) and the $\delta(CH_2)$ modes. However, this band should be a superposition of the CH_2 bending and some other band connected with hydroxyl group, or probably the O–H deformation, since the intensity of this band decreases sensitively on deuteration and there remains a sharp band which is certainly attributed to the CH_2 bending mode, because of its perpendicular nature. The perpendicular band at 1325 cm^{-1} should also be related to the hydroxyl group because of the intensity decrease on deuteration, whereas Elliott and his coworkers[7] merely referred this band to a hydrogen deformation mode. Just at the middle of the above-mentioned two bands, i.e., at 1380 cm^{-1}, a new intense and sharp band appears on deuteration. We have already suggested[23] that this fact is well interpreted by assuming that these two bands (1430 and 1325 cm^{-1}) are associated with the coupling of the δ(OH) and some other mode such as the CH deformation, and the coupling is removed on deuteration. Krimm and his coworkers[8] independently made a more or less similar interpretation on the results of deuterated PVA (no orientation), and concluded that these two bands come from the interaction between the δ(OH) and δ(CH) modes. However, we have found from the dichroic data with the oriented PVA-*d* that the new band at 1383 cm^{-1} has the nature of distinguished parallel dichroism, and there appear also two perpendicular bands at 1376 and 1361 cm^{-1}, superposed with the 1383 cm^{-1} band. Thus Krimm and his coworkers' assignment of the 1383 cm^{-1} band to δ(CH) can not explain the parallel dichroism of this band. The problem of the assignments of the bands in this region is very complex, but our suggestion in the previous paper[21] does not contradict the present experimental results***.

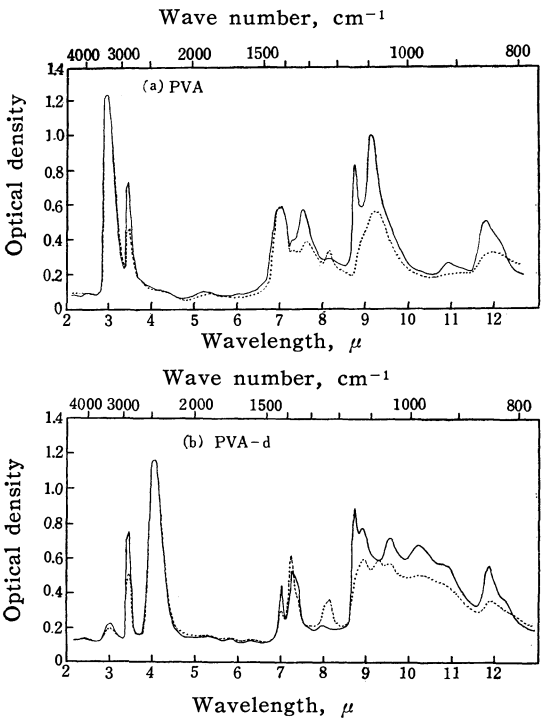


Fig. 4. Infrared dichroism of (a) PVA and (b) PVA-*d* (degree of deuteration ca. 92%): —— electric vector perpendicular to elongation: ------ electric vector parallel to elongation.

23) H. Tadokoro, S. Seki and I. Nitta, *J. Chem. Phys.*, **23**, 1351 (1955).

*** Possibile assignments will be that the 1383 cm^{-1} band is the w(CH) or the $w(CH_2)$[24], and 1376 cm^{-1} band the δ(CH).

24) I. Nakagawa, *J. Chem. Soc. Japan, Pure Chem. Sec.* (*Nippon Kagaku Zasshi*), **76**, 540 (1955).

The parallel band at 1230 cm^{-1} was reported to be associated with the residual acetyl group by Thompson et al.[5] and Elliott et al.[7] But later this assignment was shown to be inadequate by Blout and Karplus[6] from the experimental fact that this band is not removed by acid hydrolysis, although the 1256 cm^{-1} band in unpurified samples is removed simultaneously with the 1710 cm^{-1} band. From the facts that this band is not affected by deuteration and that it becomes intense on formalization with preserving the parallel dichroic nature, this band may be supposed to be $w(CH_2)$, although Krimm and his coworkers' assignment[8] to w(CH) is also undeniable.

The 1148 cm^{-1} band of PVA-*d* is supposed to correspond to the 1141 cm^{-1} band of PVA, because of the distinct perpendicular dichroism. As to the assignment of this band, various interpretations have been proposed, and this seems to be one of the most interesting problems in the infrared studies of this substance. Detailed discussions of this band will be reported in subsequent paper.

The 1093 cm^{-1} band may be mainly associated to the ν(C–O) mode from its location, perpendicular dichroism and the reasonable wave number shift by deuteration, in accordance with the interpretations of Blout et al.[6], Elliott et al.[7], and Krimm et al.[8] The parallel band at 1083 cm^{-1}, superposing the 1093 cm^{-1} band, seems not to be affected by deuteration. On deuteration the 1093 cm^{-1} band disappears and three perpendicular bands appear at 1122, 1049 and 977 cm^{-1}. Of these three bands, the 1049 cm^{-1} band may be assigned to the ν(C–O), and 977 cm^{-1} band to the δ(O–D) tentatively from the consideration of the wave number ratios of the shifts on deuteration.

The perpendicular bands at 913 and 845 cm^{-1} are considered not to be directly associated with the OH group, because of the negligibly small effect of deuteration.

Finally, we wish to refer to the results of our infrared microspectroscopic measurement on the highly doubly oriented PVA sample[14]. In this experiment the measurements were made so that the direction of the polarized infrared beam was parallel to the direction of rolling (the same as that of the carbon zigzag chain). The spectra obtained in this experiment were partly reproduced in Fig. 5. The solid line represents the spectrum with the electric vector parallel to the rolled plane (i. e., the plane of the carbon zigzag chain), and the broken line that with the electric vector perpendicular to the rolled plane. It was found that the 913 and 845 cm^{-1} bands have weak pleochroism, and the latter is a superposition of two bands. The direction of the transition moment of the $r(CH_2)$ mode is perpendicular to the plane of the carbon zigzag chain. The 835 cm^{-1} band, the transition moment of which is in this direction as is evident from the curves in Fig. 5, may be considered as assigned to this mode. The assignment of the 913 cm^{-1} band to $r(CH_2)$ by Krimm et al.[8] is not consistent with our experimental result that the transition moment of this band is parallel to the plane of the carbon zigzag chain.

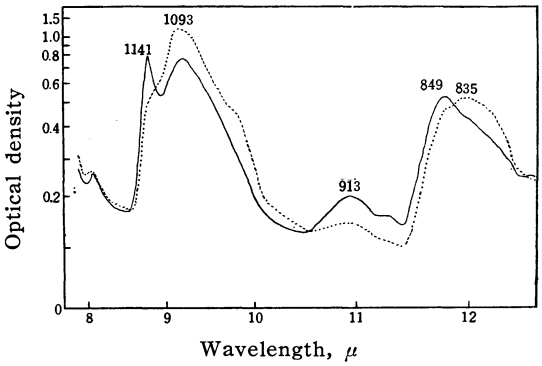


Fig. 5. Infrared spectra of highly doubly oriented PVA specimen[14]. The direction of the infrared beam is parallel to that of rolling.
—— electric vector ∥ rolled plane.
------ electric vector ⊥ rolled plane.

The author wishes to express his gratitude to Professor I. Nitta and Assistant Professor S. Seki, under whose guidance this research was carried out. He also expresses his sincere thanks to Professor T. Shimanouchi of the University of Tokyo for helpful advice and criticism, to Dr. T. Kanzawa and Mr. H. Kamio of Takeda Pharmaceutical Industries Co., Ltd. for preparing part of the charts of the infrared absorption spectra, and to Kurashiki Rayon Co., Ltd. for kindly giving him the PVA samples.

Department of Polymer Science
Faculty of Science
Osaka University
Nakanoshima, Osaka

Heats of Combustion and Formation of Lower Members of Methyl- and Ethyl-methoxypolysiloxanes

By Toshio TANAKA

(Received May 29, 1959)

The heats of combustion of lower members of polydimethylsiloxanes were measured by Thompson[1], and with the aid of the results, average values of bond energy terms for Si–O and Si–C bonds were found to be 117 and 64 kcal./mol., respectively. Of these energy values, the former seems to be too great and the latter somewhat too small, in comparison with those calculated from heats of formation of silica and carborundum. In fact, the Si–O bond energy term has been calculated to be 102 kcal./mol. as the reasonable value, from the heats of formation of methoxy-polysilanes and -polysiloxanes in the preceding paper[2].

In the present work, the heats of combustion of lower members of methyl- and ethyl-methoxypolysiloxanes represented by L_n and L'_2 have been measured, and thermal data derived therefrom have been discussed.

$$L_n:\ CH_3O\left[\begin{array}{l}CH_3\\ |\\ Si\cdot O\\ |\\ OCH_3\end{array}\right]_n\cdot CH_3,\quad n=1\sim3$$

$$L'_2:\ CH_3O\left[\begin{array}{l}C_2H_5\\ |\\ Si\cdot O\\ |\\ OCH_3\end{array}\right]_2\cdot CH_3$$

Experimental

Materials. — The preparation and the physical constants of the members of L_n [3] and L'_2 [4] used in the present work were already reported.

Calorimetry. — The apparatus and procedure used in the combustion experiment have been similar to that described elsewhere[2,5]. The calibration experiment of the calorimeter was carried out at 20°C using benzoic acid (39f) supplied from National Bureau of Standards, Washington, and its energy equivalent value was determined to be 2459 cal./deg. (relative mean deviation ±0.1%).

A thin walled glass ampoule[5] has been used for the purpose of making possible complete combustion of each member of L_n. The completeness of combustion has been ascertained by the method as described in the previous paper[5]. A few other techniques which cause organosilicon compounds to burn completely was reported[1,6]. It seems, however, that satisfactory combustion is not always attained even when these techniques are employed. In the experiment of L'_2, the techniques which are troublesome about the procedure have not been applied; a sample of about 0.4 g. has been weighed in a gelatine capsule, with a known heat of combustion, and the capsule has been vertically supported on a platinum combustion vessel by a platinum ignition wire, a piece of cotton being tied to it, which passes through two small holes at the top of capsule. The evaporation of L'_2 through the very small holes on the capsule has been neglected in quantity, because of its high boiling point (97°C/20 mmHg). This neglect has no influence on the experimental results of L'_2. After burning the sample by electrical ignition, carbon monoxide has not been identified by Winkler's reagent[7] in gaseous phase of bomb contents, and a bulky product, consisting of silica and an incomplete combustion product in a part, has been yielded on the combustion vessel. The incomplete combustion product contains amorphous carbon and, sometimes, a trace of carborundum, and these have been determined in quantity by the procedure described elsewhere[8]. Thermal corrections for carbon and carborundum have been calculated using the values of 7.84 cal./mg. (=32.8 joules/mg.)[9] and 6.86 cal./mg. for their heats of combustion, respectively. The latter value has been calculated from the figures of −26.7 kcal./mol. for the heat of formation of carborundum[10], and is that at standard constant volume process. The completeness of combustion in L'_2 has been found to be 98.5~99.7% by the analysis of incomplete combustion product.

Results and Discussion

Four to six combustion experiments have been made with each liquid sample, and the results are shown in Table I.

1) R. Thompson, *J. Chem. Soc.*, **1953**, 1908.
2) T. Tanaka and T. Watase, This Bulletin, **28**, 258 (1955).
3) T. Tanaka, A. Tasaka, R. Ōkawara and T. Watase, *Technol. Repts. Osaka Univ.*, **7**, 193 (1957).
4) R. Ōkawara, This Bulletin, **28**, 360 (1955).
5) T. Tanaka, U. Takahashi, R. Ōkawara and T. Watase, ibid., **28**, 15 (1955).
6) S. Tannenbaum, S. Kaye and G. F. Lewenz, *J. Am. Chem. Soc.*, **75**, 3753 (1953).
7) L. W. Winkler, *Z. anal. Chem.*, **102**, 99 (1935).
8) T. Tanaka, *Technol. Repts. Osaka Univ.*, **8**, 437 (1958).
9) F. D. Rossini, "Experimental Thermochemistry", Interscience Publishers, Inc., New York (1956), p. 46.
10) F. D. Rossini et al., "Selected Values of Chemical Thermodynamic Properties", Natl. Bur. Standards, Washington (1952).

TABLE I. HEAT OF COMBUSTION AT CONSTANT VOLUME, cal./g.

Compound							Mean
L_1	5632	5629	5617	5609	—	—	5622
L_2	5213	5228	5221	5212	5219	—	5219
L_3	5083	5055	5074	5072	—	—	5071
L'_2	5875	5865	5903	5856	5891	5868	5876

The relative mean deviation in each run is somewhat high compared with modern precision measurements, but of sufficient precision for bond energy term purpose in view of the other uncertainties involved.

Table II is the summary of important thermal data of four organosilicon compounds, calculated from the results of combustion experiments. Notations in Table II are as follows: $-\Delta U_R$, the heats of combustion at standard constant volume process where the reactants are one atmospheric pressure; $-\Delta H_c$, the heats of combustion in isobaric process at one atmospheric pressure; $-\Delta H_f$, the heats of formation of liquid compounds under consideration from standard elements (gaseous H_2 and O_2, graphitic carbon and metallic silicon); $-\Sigma E$, the heats of formation of the gaseous compounds from monoatomic gases. These energy values, except that in the last column of Table II, have been calculated by the same method as that used in the preceding paper[2], and in the calculation of $-\Sigma E$, heats of vaporization have been estimated to be 7.9, 9.1, 10.3 and 9.5 kcal./mol. for L_1, L_2, L_3 and L'_2, respectively, from Trouton's rule.

Bond Energy Term. — According to the additive law of bond energy, the value ΣE obtained experimentally in such a way may also be expressed by the formula

$$\Sigma E = pE_{Si-O} + qE_{Si-C} + rE_{C-O} + sE_{C-H} + tE_{C-C} \quad (1)$$

where E represents the energy value of bond corresponding to each suffix, and the factors p, q, r, s and t the number of bonds in the molecule under consideration. The energy terms of C–O, C–H and C–C bonds are well known, and if it is assumed that each value is not varied with the change of molecule, the bond energy values of bonds concerning the silicon atom may be estimated by formula 1. The value of $-E\left[\begin{smallmatrix} & C & \\ & | & \\ O-Si-O & & \end{smallmatrix}\right]$ presented in the last column of Table II has been estimated in this manner, using 98.8, 83.2 and 83.2 kcal./mol. for C–H, C–C and C–O bond energy terms, respectively. The former two values have been calculated by the method of least squares from heats of formation of lower members (from ethane to hexane) in normal paraffin[11], other than methane, and the latter from the heat of formation of dimethylether[10] using the C–H bond energy obtained there. Two kinds of Si–O bond are contained in the molecules of L_n and L'_2; that of Si–O–CH_3 linkage and of Si–O–Si linkage. However, no energy difference between the two kinds of Si–O bond were observed in the preceding work on methoxy-polysiloxanes[2], and so these bonds will not be distinguished in the following discussion.

The $-E\left[\begin{smallmatrix} & C & \\ & | & \\ O-Si-O & & \end{smallmatrix}\right]$ in L_2 and L'_2 is in good agreement. However, this value increases with the polymer size of L_n, and further its energy difference between L_2 and L_3 is not so large as that between L_1 and L_2. This tendency has also been found in our recent investigation on heats of formation of methoxy end-blocked dimethylpolysiloxanes[12], and suggests that the $-E\left[\begin{smallmatrix} & C & \\ & | & \\ O-Si-O & & \end{smallmatrix}\right]$ may be close to a constant value as the polymer size increases*.

TABLE II. HEATS OF COMBUSTION AND FORMATION, AND BOND ENERGY, kcal./mol.

Compound	Mol. wt.	$-\Delta U_R$	$-\Delta H_c$	$-\Delta H_f$	$-\Sigma E$	$-E\left[\begin{smallmatrix} & C & \\ & | & \\ O-Si-O & & \end{smallmatrix}\right]$
L_1	136.23	766	767	227	1799	364
L_2	226.38	1181	1183	412	2847	368
L_3	316.54	1605	1608	589	3887	370
L'_2	254.43	1495	1498	422	3408	368

11) F. D. Rossini et al., "Selected Values of Physical and Thermodynamic Properties of Hydrocarbons and Related Compounds", Carnegie Institute of Technology, Pittsburgh, Pennsylvania (1953).

12) T. Tanaka, to be published in *J. Inorg. Nuclear Chem.*

* Such a tendency for bond energy will always be found in lower members of a homologous series; for example, in calculation of C-C bond energy from heats of formation of normal paraffin, assuming that C-H bond energy is constant in the members.

The heats of combustion of various alkylsilanes were already measured by Tannenbaum[6], and Si-C bond energy estimated therefrom[13]. There was found an interesting tendency; namely, that the Si-C bond energy decreased as the size of the alkyl group joined to the silicon atom increased. It will here be assumed for the convenience of discussion that Si-O bond energy in $Si(OCH_3)_4$ (103 kcal./mol.**), which is 1 kcal. lower than that in amorphous silica, is the normal value for its bond energy. Similarly, if Si-C bond energy calculated from the heat of formation of $Si(CH_3)_4$ [6] is assumed to be its normal value, it may be estimated to be 71 kcal./mol. using the heats of atomization and the C-H bond energy adopted in the present work. This value for Si-C bond energy is 1 kcal. lower than that*** in carborundum, and seems to be reasonable for its normal bond energy. If such assumptions are accepted for the normal bond energies of Si-O and Si-C bonds, the calculated value for $-E\left[\begin{array}{c} C \\ | \\ O\text{-}Si\text{-}O \\ | \\ O \end{array}\right]$ results in 380 kcal./mol. under the additive law of bond energy, and is considerably higher than the observed value in L_3, not to speak of L_1, L_2 and L'_2. Such a deviation from the additive law of bond energy may be attributed to all of the bonds in the molecule under consideration. However, silicon atom has small electronegativity (1.8)[14] and its covalent radius is considerably larger than that of the carbon atom. Also it is well known that the silicon atom is, frequently, able to form a partially double bonding character with other atoms having lone-pair electron or electron donating power, by accepting the electron in its vacant *d*-orbital[15]. Considering these characteristics, the bonding orbital of the silicon atom seems to be liable to undergo any sort of distortion by the effect of neighboring groups.

The observed atomic distance of Si-O bond[16] is abnormally shorter than that (1.91 Å) expected from covalent radii, and this shortening has been considered to be due to the contribution of d_π-p_π bond character[17]. The π-bond character of each Si-O bond in structural unit, $\begin{array}{c} C \\ | \\ O\text{-}Si\text{-}O \\ | \\ O \end{array}$, of the molecules considered in this paper will be undoubtedly less than that in $\begin{array}{c} O \\ | \\ O\text{-}Si\text{-}O, \\ | \\ O \end{array}$ being the structural unit of methoxypolysiloxanes, considering the numbers of resonance structures between Si-O bonds in both the structural units. As the result, the energy value of Si-O bond in L_n and L'_2 will be supposed to be lower than that in methoxy-polysiloxanes. In this manner, the considerable lowering of bond energy should be expected in the case of methoxy end-blocked dimethylpolysiloxanes, $CH_3O[Si(CH_3)_2 \cdot O]_n \cdot CH_3$, the structural unit being $\begin{array}{c} C \\ | \\ O\text{-}Si\text{-}O \\ | \\ C \end{array}$, and this expectation has been ascertained in the recent investigation on their lower members. This supposition on Si-O bond energy will correspond to the shortening of the silicon-halogen bond distance with the decrease of the number of halogen atoms attached to silicon[18].

Summary

1. The heats of combustion of lower members of methyl- and ethyl-methoxypolysiloxanes have been measured at 20°C and constant volume, and the corresponding heats of combustion and formation in isobaric process have been calculated.

2. The bond energy term in structural unit of $\begin{array}{c} C \\ | \\ O\text{-}Si\text{-}O \\ | \\ O \end{array}$ has been calculated from the heat of formation, and it has been found that its value increases with the polymer sizes of the members. Finally, the $-E\left[\begin{array}{c} C \\ | \\ O\text{-}Si\text{-}O \\ | \\ O \end{array}\right]$ has been compared with

13) S. Tannenbaum, *J. Am. Chem. Soc.*, **76**, 1027 (1954).

** The Si-O bond energy has been calculated to be 103, 102 and 103 kcal./mol. from heats of formation of $Si(OCH_3)_4$, $Si_2O(OCH_3)_6$ and $Si_3O_2(OCH_3)_8$, respectively, using 98.8 and 83.2 kcal./mol., instead of 98.9 and 84.1 kcal./mol. adopted in the preceding paper[2], for C-H and C-O bond energies.

*** Calculated to be 72 kcal./mol. from heat of formation of carborundum[10].

14) O. Pritchard and H. A. Skinner, *Chem. Revs.*, **55**, 745 (1955).

15) For example, E. L. Reilly, C. Curran and P. A. McCusker, *J. Am. Chem. Soc.*, **76**, 3311 (1954).

16) 1.64±0.03 Å in $\left(\begin{array}{c} (CH_3)_2 \\ O\langle \begin{array}{c} Si\text{—}O \\ Si\text{—}O \end{array} \rangle \\ (CH_3)_2 \end{array}\right)_2$ Si, W. L. Roth and D. Harker, *Acta Cryst.*, **1**, 34 (1948); 1.66±0.04 Å in $[(CH_3)_2SiO]_3$, E. H. Aggarwal and S. H. Bauer, *J. Chem. Phys.*, 18, 42 (1950); 1.64±0.03 Å in $Si(OCH_3)_4$, 1.63±0.05 Å in $((CH_3)_3Si)_2O$, see Ref. 18.

17) L. Pauling, *J. Phys. Chem.*, **56**, 361 (1952).

18) M. Yokoi, This Bulletin, **30**, 106 (1957).

that expected from the additive law of bond energy, and the lowering of bond energy in these molecules has been discussed in view of the resonance effect.

The author wishes to express his sincere thanks to Professor T. Watase for his gracious encouragement, Dr. R. Ōkawara for providing him with a part of the sample used in the present work, and Messrs. A. Tasaka and T. Ōtsuka for their aid during this experiment.

Department of Applied Chemistry
Faculty of Engineering
Osaka University
Miyakojima-ku, Osaka

Studies on the State of Formic Acid Adsorbed on Silica and Alumina by a Combined Method of Nuclear Magnetic Resonance and Infrared Absorption

By Kozo HIROTA, Kenji FUEKI, Kotaro SHINDO and Yasuo NAKAI

(Received June 6, 1959)

As reported already[1], formic acid is chemisorbed as the formate ion on several metallic powders (Ag, Cu, Ni, Rh, Pd, Pt and Zn), while the acid chemisorbed on silica does not dissociate[2]. However, it was found in the present study that the conclusion obtained in the case of silica can not be applied to alumina, especially in the case of low coverage of adsorption. Such a conclusion may be worthy to be reported, considering the fact[3] that the catalytic role of alumina is similar to that of silica rather than that of metals, e. g., these oxides have dehydrating activity in addition to dehydrogenating activity, contrary to the case of metals which have only dehydrogenating activity.

Experimental

Formic Acid.—The reagent of C. P. grade made by Edogawa Kagaku Kogyo Co. was repeatedly dehydrated by crystallization and then vacuum-distilled in the presence of anhydrous copper sulfate.

Silica—Silica gel for chromatographic use made by Mallinkrodt Chemical Works was dehydrated at 300°C for 150 hr. It was confirmed by X-ray analysis that the amorphous structure of silica was not changed by dehydration. The specific surface area of the silica was found to be 520 m^2/g. by the BET method (adsorbate: nitrogen).

Alumina.—Alumina gel, precipitated by the reaction between aluminum nitrate and ammonia in aqueous solution, was dehydrated at 300°C for 50 hr. The specific surface area was found to be 310 m^2/g.

Measurement.—Formic acid was adsorbed on each adsorbent which was enclosed in a glass sample tube in vacuo. In the case of nuclear magnetic resonance measurement, a capillary tube filled with water as a standard substance was put in the center of the sample tube. The proton resonance spectra were obtained with a high resolution spectrometer (Varian V-4300B)* at a fixed frequency of 40 Mc/sec. The tube was always rotating around its axis during the measurement. The infrared spectra were obtained using the paste method[4], in which the sample was quickly mulled with Nujol, and a part of the sample was held between the plates of sodium chloride and then offered for measurement (apparatus: Hilger H800). During this procedure a small amount of formic acid may be lost in the atmosphere, but it was checked that this amount was small enough not to alter the conclusion. Taking such a situation into account, the coverage was conventionally designated by θ' instead of the true coverage θ in the case of samples used in infrared absorption measurement. Measurements were made at room temperature.

Results and Discussion

Proton Magnetic Resonance Absorption.—The proton resonace spectrum of formic acid

1) K. Hirota, K. Kuwata and Y. Nakai, This Bulletin, **31**, 861 (1958); K. Hirota, K. Kuwata and S. Asai, *J. Chem. Soc. Japan, Pure Chem. Sec.* (*Nippon Kagaku Zasshi*), **80**, 701 (1959).

2) K. Hirota, K. Fueki, K. Shindo and Y. Nakai, This Bulletin, **31**, 783 (1958).

3) G. M. Schwab and E. Schwab-Agallidis, *J. Am. Chem. Soc.*, **71**, 1806 (1949).

* In the preliminary report, the apparatus was referred to as Varian V-4310C, because some part of the apparatus is so named.

4) G. C. Pimentel, C. V. Gerland and G. Jura, *J. Am. Chem. Soc.*, **75**, 803 (1953).

adsorbed on silica is quite different from that in the liquid state, especially when the amount of adsorption is small, (e. g., $\theta=0.5$); only one signal**, corresponding to the hydrogen atom bonded to the carbon atom, appears as a broad one and, moreover, its position shifts by 33 cps to a higher magnetic field. However, as the coverage is increased up to 2.7, the signal becomes narrower in width and that of the hydrogen atom bonded to the oxygen atom also appears as a very broad one. Thus it may be concluded that the motion of hydrogen in the carboxyl group is fixed in the state of monomolecular adsorption, and such a restriction of the motion is relaxed gradually according as the adsorption layer is the upper. Furthermore, it is pointed out that the observed shifts may be mainly of apparent nature, and therefore, the effect of the magnetic susceptibility of bulk substance was taken into consideration. The chemical shifts, corrected for this effect[5], are shown in the last column of Table I. Though it seems that there is a relation between the amount of adsorbed formic acid and the chemical shift, it is too small for the meaning to be discussed in detail.

TABLE I. CHEMICAL SHIFT OF FORMIC ACID ADSORBED ON SILICA***
(Unit: cps)

δ_{ads}: Shift from reference (water)
δ_{meas}: Shift from liquid formic acid
δ_{cor}: Value to be corrected for bulk magnetic susceptibility
$\delta=\delta_{meas}-\delta_{cor}$: Chemical shift

θ	δ_{ads}	δ_{meas}	δ_{cor}	δ
0.5	97	33	26	7
1.1	100	30	25	5
1.7	103	27	23	4
2.7	109	21	19	2

On the other hand, we could not detect any appreciable signal for the formic acid adsorbed on alumina in the monomolecular state. This is probably due partly to the small amount of adsorption and partly to stronger interaction with alumina than with silica.

Furthermore, the difference in the adsorbed state between silica and alumina could be made clear by the infrared absorption measurement as shown below.

Infrared Absorption.—*Silica.*—In the case of silica two adsorption bands are observed at 3450 (broad) and 1620 cm^{-1}. Both bands may be ascribed to associated water on the surface[6]. However, the stretching band due to the isolated hydroxyl group on the silica surface[7] does not appear at 3749 cm^{-1}, probably being masked by the broad band at 3450 cm^{-1} [8].

Now, when formic acid is adsorbed on silica, new absorption bands appear at 1714 and 960 cm^{-1} in addition to the band near 3520 cm^{-1} (Fig. 1, Table II). The absorption band at 1714 cm^{-1} can be ascribed to

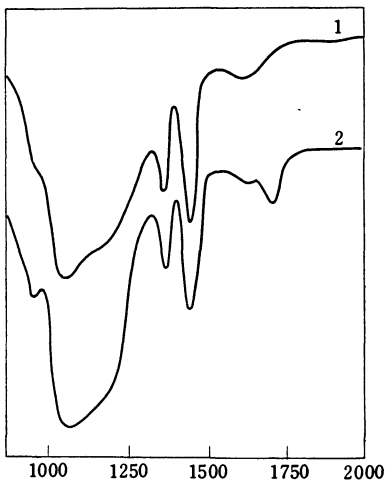


Fig. 1. Infrared spectrum of formic acid adsorbed on silica.
1: silica, 2: $\theta'=0.7$

the C=O stretching vibration, while the band at 960 cm^{-1} to the OH out-of-plane deformation vibration. Thus, it may be said that formic acid is adsorbed on silica in a non-dissociated state. The C=O stretching band shifts to lower frequency as compared to that of the monomer and also of the dimer. This band is rather similar in frequency to that of formic acid in the crystalline state. The same situation holds for the OH deformation band[9]. Considering these facts, it seems that the adsorbed formic acid forms hydrogen bonding not only to the silica surface, but also to each other, forming thus a two-dimensional net structure. Such a model

** The assignment of the signal was made by the use of deuteroformic acid HCOOD.

5) J. R. Zimmerman and M. R. Foster, *J. Phys. Chem.*, **61**, 282 (1957).

*** The resonance of proton bonded to the carbon atom is shown.

6) A. Chevet, *J. Phys. Radium*, **14**, 493 (1953).

7a) R. S. McDonald, *J. Am. Chem. Soc.*, **79**, 850 (1957); *J. Phys. Chem.*, **62**, 1168 (1958).

b) A. N. Terenin, N. G. Yaroslavskii, A. V. Karyakin and A. I. Sidorova, *Microchim. Acta*, 467 (1955).

8) K. Naito, presented at the Symposium on Infrared and Raman Spectra, Kyoto, October, 1958.

9) R. C. Millikan and K. S. Pitzer, *J. Chem. Phys.*, **27**, 1305 (1957); *J. Am. Chem. Soc.*, **20**, 3515 (1958).

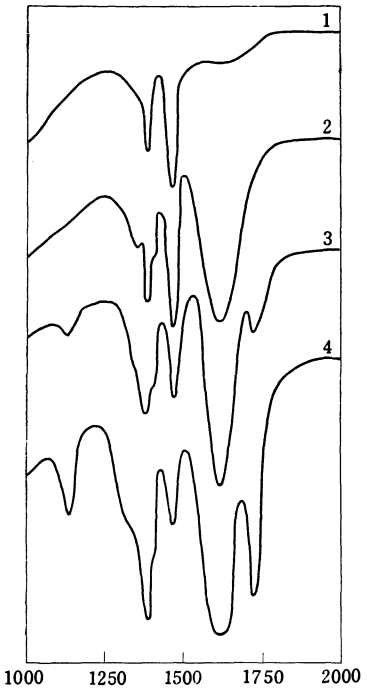


Fig. 2. Infrared spectrum of formic acid adsorbed on alumina.
1: alumina, 2: $\theta'=0.7$, 3: $\theta'=1.3$, 4: $\theta'=2.4$.

was already proposed in the case of the adsorption of water and ethanol on silica from the results of the dielectric measurement of these systems[10,11].

Alumina. — In the infrared spectrum of alumina, not only the absorption bands (3450 and 1620 cm^{-1}) of associated water on the surface, but also that (3760 cm^{-1}) of the isolated hydroxyl group are observed. When formic acid is adsorbed in a monomolecular layer, new absorption bands appear at 1344 and 1402 cm^{-1} besides 1620 cm^{-1} (strong), while the intensity of the band at 3450 cm^{-1} does not vary (Fig. 2, Table II). As the bands at 1344, 1402 and 1620 cm^{-1} can be assigned to the fundamental modes of vibration, ν_2, ν_5 and ν_4, of the formate ion[12], respectively, the state of formic acid adsorbed on alumina is similar to that on metals. However, when the amount of adsorbed formic acid is increased and a monomolecular layer is completed, new absorption bands appear at 1733 and 1124 cm^{-1}, and the band near 3520 cm^{-1} increases in intensity. These results show that non-dissociated formic acid can exist in the upper layer of adsorption on alumina.

TABLE II. SUMMARIZED RESULTS OF INFRARED ABSORPTION****

Adsorbent	θ' 0.3	0.7	1.3	2.4
Silica	1714	1714	1714	—
	960	960	960	—
Alumina			1733 (1705)	1733 (1705)
	1620 (1602)	1620 (1602)	1620 (1602)	1620 (1602)
	1402 (1377)	1402 (1377)	1402 (1377)	1402 (1377)
	1344 (1329)	1344 (1329)	1344 (1329)	1344 (1329)
			1124 (1100)	1124 (1100)

In short, it has been found that the adsorbed formic acid in a monomolecular layer exists as a dissociated or non-dissociated state, according as the adsorbent is alumina or silica. Such difference of state may be noteworthy, in the light of the fact that the catalytic activity of both oxides is similar, i. e., formic acid is dehydrated rather than dehydrogenated, in contrast with the overwhelmingly dehydrogenating activity of metallic powders. It seems, therefore, that there is no direct relation between the adsorbed state and the activated state of decomposition. Concerning this result further research is in progress.

Summary

The state of formic acid adsorbed on silica and alumina has been studied by a combined method of nuclear magnetic resonance and infrared absorption. The adsorbed formic acid in a monomolecular layer has been found not to be dissociated in the case of silica, but to be dissociated in the case of alumina.

A part of the expense for the present investigation has been defrayed from a grant given by the Ministry of Education, to which the authors' thanks are due.

Department of Chemistry
Faculty of Science
Osaka University
Nakanoshima, Osaka

10) M. Shimizu, *J. Chem. Soc. Japan, Pure Chem. Sec.* (*Nippon Kagaku Zasshi*), **78**, 21 (1957).
11) S. Kurosaki, T. Tsuchiya and R. Kawai, ibid., **78**, 1806 (1957).
12) Landolt-Börnstein, "Zahlenwerte und Funktionen", 1, 2. Teil, Springer, Berlin (1951), p. 237.

**** In this table, only the bands in low frequency region were shown. Values in parenthese were obtained by the measurement in which Nujol was not used.

Study on the Reductive Spinel—A New Spinel Formula AlN-Al_2O_3 instead of the Previous One Al_3O_4

By Goro YAMAGUCHI and Hiroaki YANAGIDA

(Received March 4, 1959)

It was proposed in the previous papers[1-3] that a lower valent aluminum ion Al^+ or Al^{2+} may exist in a spinel form Al_2O-$5Al_2O_3$ or Al_3O_4. L. M. Foster, however, suggested[4] that the spinel-like material contains nitride as its component and, therefore, the reducing ability is probably due to the nitride component.

In order to determine whether the reducing ability is due to the lower valent aluminum ion or to the nitride component, the chemical behaviors, the conditions of the formation, the magnetic susceptibility, the cell constant, and the density of the reductive spinel have been investigated.

Experimental

Synthesis of the Reductive Spinel.—Alumina and the reducing agent, aluminum or graphite, were mixed together and heated in the Tammann furnace (Fig. 1).

The X-ray diffraction patterns of the products were investigated at first, and the formation of the reductive spinel was confirmed with a number of methods as shown in Table I. The purity was confirmed also with the slow scanning X-ray diffraction recording.

Chemical Behaviors (Analysis of Nitrogen).—

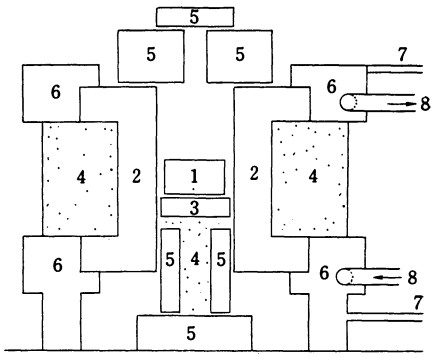


Fig. 1. Tammann furnace for the reductive spinel synthesis.
(1) sample, (2) graphite cylinder, resistance heater, (3) sintered alumina sample holder, (4) graphite powder, (5) refractory, (6) iron frame heater holder, (7) lead wire, (8) water, coolant.

The decomposition of the reductive spinel was tried by using the following reagents: (1) alkali or acid at room temperature; (2) PbO 90: B_2O_3 glass as a flux at 800°C in vacuo (Fig. 2); (3) air above 1000°C. The spinel employed in these experiments was confirmed not to show any X-ray diffraction pattern originating in crystalline aluminum nitride. The evolved gases in the

TABLE I. CONFIRMATION OF THE FORMATION OF THE REDUCTIVE SPINEL AND CHARACTERISTICS WHICH DISTINGUISH IT FROM OTHER SPINEL MgO-Al_2O_3 AND γ-Al_2O_3

	Methods	Reductive spinel	$MgO \cdot Al_2O_3$	γ-Al_2O_3
1)	X-ray diffraction recording (geigerflex, filtered Cu$K\alpha$ radiation) Scanning speed 4°2 θ per minute	Diffraction pattern of spinel structure Sharp peak	Diffraction pattern of spinel structure Sharp peak	Diffraction pattern of spinel structure Broad
2)	X-ray diffraction recording Scanning speed 1/4°2 θ per minute	Unit cell dimension about 7.94 Å	Unit cell dimension about 8.06 Å	Unit cell dimension about 7.89 Å
3)	Observation of Becke's line; comparison with the refractive index 1.74 of CH_2I_2	>1.74	<1.74	<1.74
4)	Observation of weight increase above 1000°C through heating in air	Increase	—	—

1) G. Yamaguchi, *J. Electrochem. Soc. Japan* (*Denki-Kagaku*), **14**, 106 (1946).
2) G. Yamaguchi, *J. Ceram. Assoc. Japan* (*Yogyo Kyokai Shi*), **61**, 549 (1953); *Ceram. Abstr.*, **33**, 87*e* (1954); *Chem. Abstr.*, **48**, 3652*b* (1954).
3) G. Yamaguchi, This Bulletin, **23**, 89 (1950).
4) Private communication from Dr. L. M. Foster (ALCOA).

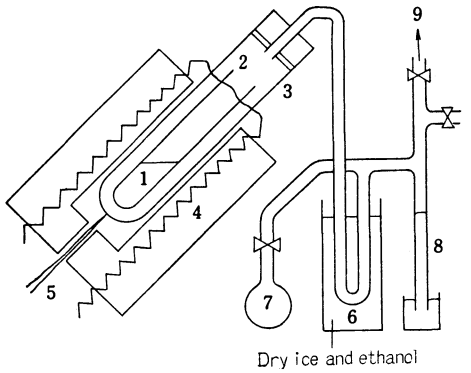


Fig. 2. Apparatus for nitrogen analysis.
(1) sample and flux, (2) silica tube, (3) transparent silica tube, (4) heater, (5) thermo-couple, (6) condenser, (7) gas sample flask, (8) pressure gauge, (9) vacuum pump.

decomposition process were analyzed by a mass-spectrometer.

Other Properties of the Spinel.—The magnetic susceptibility was measured by the Gouy method. The applied magnetic field was 8500 or 13000 gauss.

The mean dielelectric constant of the system of the spinel and air was measured. The frequency applied was 1 MC. The size of the spinel was 60~80 in Tyler mesh. Its packing ratios were from 0.48 to 0.53.

Results

Formation of the Reductive Spinel.—The reductive spinel can be formed through reduction of alumina in a reductive atmosphere above 1650°C, but in vacuo, alumina evaporates. The best procedure in the present study is as follows: (1) mixing 0.2 g. of graphite with 5 g. of γ-alumina thoroughly; (2) heating it at 1700°C for 2 hr. in the Tammann furnace through which only a little air can pass; (3) quenching it. When the reduction of alumina is insufficient α-alumina remains, whereas crystalline aluminum nitride is isolated when the reduction has proceeded too far.

Chemical Behaviors. — The decomposition of the reductive spinel by acid or alkali can not be noticed at room temperature. Products of the reaction between the reductive spinel and the glass as a flux were lead metal and nitrogen gas. The volume of the emitted nitrogen gas corresponds to 85% of the calculated value from the formula of $AlN-Al_2O_3$. The volume of nitrogen gas was fluctuated because of the difficulties of complete fusing. The emitted gas moved the flux to a lower temperature part. The sample increased in weight by 6.90% when it was kept in air above 1000°C, and turned into α-alumina.

Other Properties.—The observed magnetic susceptibility was $\chi = -0.34\times10^{-6}$/g. The dielectric constant was calculated to be 23.8. The refractive index 1.80 was also calculated from data[3]. Then, the ionic refraction of nitrogen N^{3-} in the reductive spinel should be 4.30. This calculation was made by the Lorentz-Lorenz equation. The unit cell dimension is 7.940 Å (in spinel structure *Fd3m*), and the density is 3.78 g./cc.

Discussion

The synthetic experiments show that the presence of nitrogen is inevitable in the conditions of the formation of the reductive spinel, and alumina turns into aluminum suboxide and evaporates in vacuo[5]. Emission of nitrogen gas and the weight increase of the reductive spinel through oxidation lead us to conclude that the reducing ability is due to the nitride component. The weight increase by 6.90% corresponds approximately to that of $AlN-Al_2O_3$ by 6.95%. The magnetic susceptibility shows an absence of lower valent aluminum ion Al^{2+}. The ionic refraction of nitrogen ion 4.30 in the spinel structure is only 1.14 times larger than that of oxygen ion 3.77[3]. This shows that the ionic radii of nitrogen ion is not much greater than that of oxygen ion. The density 3.78 g./cc. and the cell dimension 7.940Å are coincident with a spinel formula $AlN-Al_2O_3$.

Summary

A compound between aluminum oxide and aluminum nitride can be produced in a reductive atmosphere above 1650°C.

A new spinel formula $AlN-Al_2O_3$ should be adopted instead of the previous one $Al_2O-5Al_2O_3$ or Al_3O_4.

The physical constants of $AlN-Al_2O_3$ are as follows: crystal structure *Fd3m*, $Z=8$, $a=7.940$ Å; density 3.78 g./cc.; dielectric constant 23.8; refractive index 1.80; magnetic susceptibility -0.34×10^{-6}/g.

Department of Applied Chemistry
Faculty of Engineering
The University of Tokyo
Hongo, Tokyo

5) R. Kiyoura and T. Sata, *J. Ceram. Assoc. Japan (Yogyo Kyokai Shi)*, **66**, 44 (1958).

*The Molecular Structure of the Monomer and the Dimer of Acrylic Acid**

By Takeshi UKAJI

(Received June 2, 1959)

Acrylic acid is known as an important source of some highly polymeric products, however its molecular structure has been left unsolved.

Recent electron diffraction study[1] of the monomer of formic and acetic acids has indicated that the two distances between the carbon atom and oxygen atoms in carboxyl group are not the same. This result essentially agreed with the structure of the monomer of formic acid of the electron diffraction sector-photometer method proposed by Karle and Karle[2]. Furthermore, various data[3] on the conjugated system show that the C–C single bond distance between two double bonds is shorter than its normal distance of 1.54 Å.

The present investigation was undertaken for the purpose of clarifying the stereochemical structure of acrylic acid, and also to elucidate the question as to what changes may occur on association of the monomer of the acid.

Experimental

Acrylic acid was prepared by hydrolysis of commercial grade methyl acrylate. On careful distillation of the acid, a fraction boiling at 50~51°C/20 mmHg was collected.

Electron diffraction photographs were taken according to the usual manner using a camera reported in the previous paper[4] (camera distance, ca. 9 cm., electron wavelength, 0.056~0.063 Å, determined by gold foil). The diffraction pattern were visually measured to the extent of ca. 70 of q-values.

Interpretation of Diffraction Patterns and Results

The well known formula for the calculation of the theoretical intensity curves are as follows:

$$I_{(q)}=\sum_i\sum_j \frac{Z_iZ_j}{r_{ij}} \exp(-a_{ij}q^2) \sin\frac{\pi}{10}qr_{ij}$$

$$q=(40/\lambda)\sin(\theta/2), \quad a_{ij}=(\pi^2/200) \ <\Delta r_{ij}^2>$$

where r_{ij} is the distance between the i-th and j-th atom, λ the electron wavelength, θ the scattering angle, Z_i the atomic number of i-th atom, and $<\Delta r_{ij}>$ the mean square amplitude of r_{ij}. The exponential term is omitted as a first approximation, i.e., $\exp(-a_{ij}q^2)=0$.

Monomer of Acrylic Acid. — To obtain the monomer of the acid, a fine nozzle through which its vapor flowed out was heated at 170~200°C by a spiral nichrome wire. No available data concerning the thermal equilibrium between the dimer and monomer of the vapor of this acid have appeared in literature. Also the temperature of the nozzle was controlled to obtain diffraction patterns different from those of the dimer. Some photographs were taken and these were then carefully compared with that of the dimer of the acid. In the regions of 20~30 of q-values, a remarkable change was observed in these patterns. Eight satisfactory photographs were obtained.

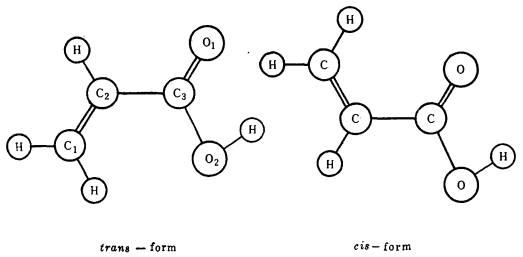


Fig. 1. Schematic model showing the *trans*- and *cis*-forms of acrylic acid.

It is assumed that all the atoms in this molecule are coplanar, and that the C–H distance and ∠CCH are 1.08 Å and 120°, respectively. The hydrogen atom in OH group was neglected, because its contribution to the total theoretical intensity curve was small. The parameters C_1=C_2, C_2–C_3, C_3=O_1 and C_3–O_2 used in the calculation of theoretical intensity curves, were varied from 1.32 to 1.45 Å, from 1.40 to 1.54 Å, from 1.18 to 1.24 Å and from 1.32 to 1.50 Å in steps of 0.02 or 0.03 Å, respectively, while the angles of $C_1C_2C_3$, $C_2C_3O_1$ and $O_1C_3O_2$ were varied from 110 to 130°, from 110 to 130° and from 110 to 135° in steps of 2 or 3°, respectively. In Fig. 2, the solid lines are the theoretical intensity curves of *trans*-form, and the chain lines are of *cis*-form.

*Presented partly at the Symposium on Structural Chemistry, Fukuoka, Nov. 22, 1957.

1) J. Karle and L. O. Brockway, *J. Am. Chem. Soc.*, **66**, 574 (1944).
2) I. Karle and J. Karle, *J. Chem. Phys.*, **22**, 43 (1954).
3) P. W. Allen and L. E. Sutton, *Acta Cryst.*, **3**, 46 (1950).
4) T. Yuzawa and M. Yamaha, This Bulletin, **26**, 414 (1953).

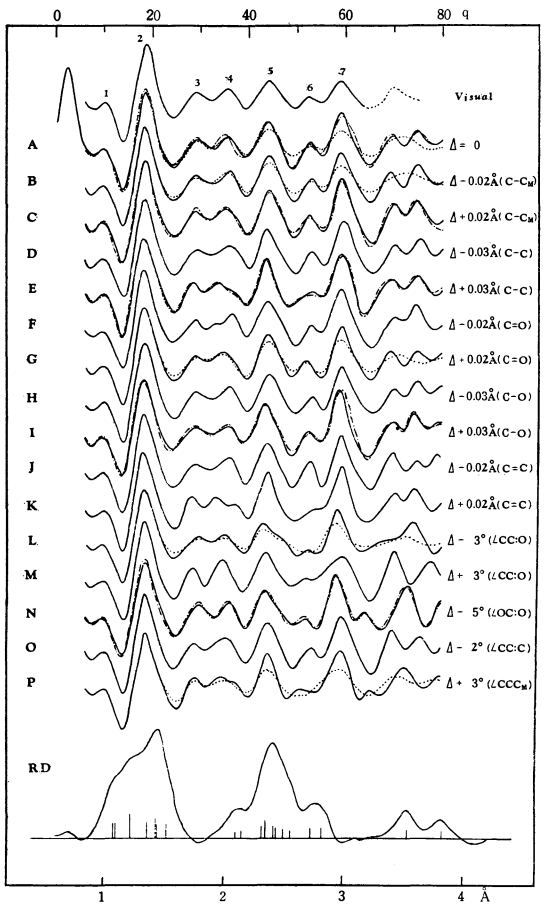


Fig. 2. Visual, theoretical intensity curves and radial distribution curve for acrylic acid. The notations on the right hand side of this figure show that the models deviate from the most probable model, for example, $\Delta=0$ is the most probable model which has the parameter as follows: C-H, 1.08; C=C, 1.36; C-C, 1.44; C=O, 1.22; C-O, 1.43 Å; $\angle$C : CH=$\angle$C : CC=$\angle$CC : O, 120° and $\angle$OC : O, 125°.

The effect of thermal vibration on the theoretical curves was examined, the vibration factors a's listed in Table I being used, and the curves including these effects were shown in the dotted lines in the same figure.

A careful comparison was made between the visual and theoretical intensity curves. Curve A is in the best agreement with the visual one. The curves of several other models resemble the visual one, but they differ from it in some features. The 4th, 5th and 6th maxima of curve B shift outward, while in curve C the 3rd and 4th maxima shift inward. Curves D and E are taken for the purpose of ascertaining the limit of acceptability for C=O distance, both curves being in good agreement with the visual one in all respects, except for the small displacement of the positions of the 3rd, 4th and 6th maxima. Likewise curves F and G are used to show the limit for C-O distance. These curves are also rejected because of the disagreement with the visual curve in the range $q>45$. In curve H, the 4th and 6th maxima shift outward, while in curve I the 3rd and 5th maxima shift outward, while in curve I the 3rd and 5th maxima shift inward. Curves J and K are taken as typical ones for models which have values accepted as borderline: the features of these curves in the range $q>50$ disagree with the visual curve. In curve L, the 4th minimum and the 7th maxima both shift inward, while the 4th and 5th maximum shift outward. Curves M and N are shown as the acceptable limit for the angle $C_1C_2C_3$. In curve M, the 6th and 7th maxima shift outward greatly, on the other hand, in curve N the positions of the 5th maximum and minimum shift inward.

As shown in Fig. 2, the theoretical curves of the *trans*- and *cis*-forms remain almost unchanged in all features. Therefore, we could not distinguish the difference between the *trans*- and *cis*-configurations of this molecule.

From the above considerations, model A is regarded as the most acceptable one, while the others are all accepted as borderline fits. Seven models are selected from them, and their q_C/q_O values are summarized in Table II.

TABLE I. APPROXIMATE VIBRATION FACTORS a_{ij} USED IN CALCULATION FOR THE MONOMER AND DIMER OF ACRYLIC ACID

a_{ij}	Atom pairs	
	Monomer	Dimer
0	C_1=C_2, C_2-C_3, C_3=O_1, C_3-O_2	C_1=C_2, C_2-C_3, C_3=O_1, C_3-O_2
0.00010	$O_1'\cdots C_2$, $O_2'\cdots C_2$	$O_1'\cdots C_2$, $O_2'\cdots C_2$
0.00015	C-H, $O_1'\cdots O_2$, $C_1'\cdots C_3$	C-H, $O_1'\cdots O_2$, $C_1'\cdots C_3$
0.00020	$C'\cdots$H, $O_2''\cdots C_1$	$C'\cdots$H, $O_2''\cdots C_1$
0.00035	$O_1''\cdots C_1$	$O_1''\cdots C_1$
0.00040		OH$\cdots$O'
0.00060		$O_1\cdots O_1'$, $O_2\cdots O_2'$, $O_1\cdots C_3'$, $O_2\cdots C_3'$, $C_3\cdots C_3'$
0.00080		$O_1\cdots C_2'$, $O_2\cdots C_2'$, $C_3\cdots C_2'$, $C_2\cdots C_2'$, $O_1\cdots C_1'$, $O_2\cdots C_1'$
0.00100		$C_3\cdots C_1'$, $C_2\cdots C_1'$, $C_1\cdots C_1'$

TABLE II. q_C/q_O VALUES FOR ACRYLIC ACID

Feature Max.	Feature Min.	q_O	q_C/q_O Model A	C	D	F	G	I	M	Wt.
1		10.37	0.984	0.964	0.945	0.984	0.964	0.984	0.984	1
	1	14.25	0.983	0.983	0.983	0.969	0.982	0.976	0.982	1
2		19.06	0.995	0.971	0.984	0.979	0.997	0.976	0.984	2
	2	24.34	0.998	1.017	1.018	0.998	0.998	0.994	1.007	2
3		29.53	0.999	0.958	0.992	0.999	0.974	0.974	0.999	4
	3	32.48	0.998	0.939	0.970	0.964	0.959	0.985	0.978	2
4		35.57	1.001	0.984	1.012	1.006	0.990	0.984	0.998	4
	4	40.57	0.993	0.998	0.986	0.990	0.974	0.992	0.986	2
5		45.35	1.000	0.979	0.995	1.006	1.003	0.985	0.999	4
	5	49.08	1.006	0.993	1.007	1.011	1.009	1.007	1.006	1
6		52.38	1.004	1.008	1.012	0.998	1.009	1.016	1.016	2
	6	56.15	0.996	1.002	0.996	0.988	0.997	1.011	1.000	1
7		60.04	1.003	1.004	0.999	0.983	1.020	1.002	1.016	1
Wt. mean			0.998	0.981	0.995	0.994	0.989	0.988	0.996	
Wt. mean dev.			0.004	0.023	0.014	0.010	0.015	0.016	0.008	

The radial distribution curve for this molecule (RD curve in Fig. 2) was calculated using the following equation:

$$rD_{(r)}=\sum_{q=1}^{q_{max}} I_{(q)O} \exp(-bq^2) \sin\frac{\pi}{10}qr$$

where $I_{(q)O}$ is the intensity read from the visual curve. The value of b was determined by setting the $\exp(-bq^2) = 0.1$ at $q=70$. The curve shows that the first peak corresponds to the C–H, C_1=C_2, C_2–C_3, C_3=O_1 and C_3–O_2 distances, the second to the C′···H, C_1′···C_3, O_1′···O_2, O_1′···C_2 and O_2′···C_2 distances, the third to the O_2″···C_1 and fourth to the O_1″···C_1 distance, respectively. Owing to the complex nature of the peaks, no attempt was made to resolve them. It is found, however, that the positions determined from the most probable model agree fairly well with the peaks observed in this radial distribution curve.

The following values are obtained for the structure of the monomer of acrylic acid: C_1=C_2=1.36±0.02 Å; C_2–C_3=1.44±0.03 Å; C_3=O_1=1.22±0.02 Å; C_3–O_2=1.43±0.03 Å; ∠$C_1C_2C_3$=120±2°; ∠$C_2C_3O_1$=120±3°; ∠$O_1C_3O_2$=125±5°.

Dimer of Acrylic Acid. — It was assumed that the association of acrylic acid was the hydrogen bond coupling of two single molecules of the same type as in the case of formic and acetic acids, that the two planar acrylic acid molecules were coplanar, and also that the C_2, C_3, C_2′ and C_3′ atoms were laid on the same axis (as shown in Fig. 3). Many parameters were involved, so that the complete analysis on the molecular structure of the dimer of this acid would be very laborious. Therefore, some of the parameters of the most probable model obtained from

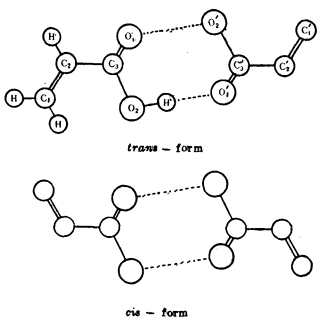


Fig. 3. Schematic model showing the skeletons and the numbering of atoms of the dimer of acrylic acid.

the above-mentioned analysis of monomer of this acid were assumed to be as follows: C–H, C_1=C_2, ∠C_2C_1H and ∠$C_1C_2C_3$ are assumed to be 1.08, 1.36 Å, 120 and 120°, respectively. Then the other parameters determining the structure C_2–C_3, C_3=O_1 and C_3–O_2 distances were varied from 1.40 to 1.50 Å, from 1.18 to 1.24 Å and from 1.30 to 1.43 Å in steps of 0.02 or 0.03 Å and O–H···O separation was varied from 2.65 to 2.80 Å with the same increment, while the angles of ∠$C_2C_3O_1$ and ∠$O_1C_3O_2$ were varied from 110 to 130° and from 120 to 135° in steps of 2 or 3°, respectively.

Some of the intensity curves are shown in Fig. 4. In this figure, the solid lines are the theoretical intensity curves of the *trans*-form, and the chain lines are of the *cis*-form. The effect of thermal vibration factors listed in Table I being used, the curves including these effects are shown in a dotted line in the same figure.

Curve E is in the best agreement with the visual one. In curve A, the 3rd and 4th maxima shift inward, while in curve B these maxima shift outward. A comparison of curves C and D, which possess 0.02 Å longer and shorter parameters, respectively, for C_3=O_1 distance, show that there are remarkable changes of the features

TABLE III. q_C/q_O VALUES FOR THE DIMER OF ACRYLIC ACID

Feature		q_O	q_C/q_O Model				Wt.
Max.	Min.		E	B	G	K	
1		12.28	1.005	0.915	0.968	0.982	1
	1	14.30	1.008	1.015	1.028	0.969	1
2		18.45	1.001	0.995	1.011	0.995	2
4		35.53	0.998	0.991	0.986	0.949	3
	4	40.24	1.005	0.989	1.025	1.016	2
5		45.18	1.000	1.022	1.014	0.999	3
	5	49.32	0.997	1.015	0.983	0.997	1
6		51.86	1.005	1.022	1.016	0.995	2
	6	55.45	0.989	0.996	0.997	0.983	1
7		60.48	1.009	1.011	1.011	1.007	1
Wt. mean			1.001	1.002	1.005	0.988	
Wt. mean dev.			0.005	0.017	0.016	0.017	

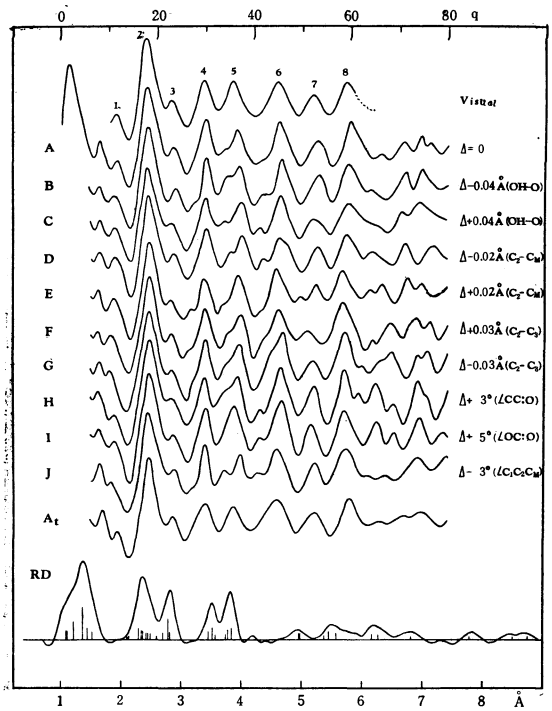


Fig. 4. Visual, theoretical intensity curves and radial distribution curve for the dimer of acrylic acid.
The notations on the right hand side of this figure show that the models deviate from the most probable model, for example, $\Delta=0$ is the most probable model which has the parameter as follows; C-H, 1.08; C=C, 1.36; C-C, 1.44; C=O, 1.22; C-O, 1.36 Å; ∠C:CH=∠C:CC=∠CC:O, 120°; ∠OC:O, 1.25° and OH···O distance, 2.76 Å.

in the region of 20 to 30 q-values. Curve F differs from E, the former possessing a parameter of an OH···O distance which is 0.04 Å longer than in the latter; and curve G differs from E, the former possessing the same distance by 0.04 Å shorter. These curves disagree with the visual one in the positions of the 3rd and 4th maxima. In curves H and I, remarkable differences from the visual one are found in features between 20 and 30 of q-values and in positions of 3rd and 4th maxima. Curves J and K were examined for the purpose of ascertaining the limit of acceptability for C_2–C_3 distance, both curves being in good agreement with the visual one in all respects, except the 3rd and 6th maxima.

The radial distribution curve for the dimer of acrylic acid is shown in Fig. 2 (RD curve). The positions determined from the most acceptable model (shown in vertical lines in this curve) fairly well agree with the peaks observed in this radial distribution curve. A relatively small peaks is found at 2.76 Å corresponding to the separation across the bridge O–H···O.

The structure determined for the dimer of acrylic acid, which is in agreement with the quantitative results (q_C/q_O values in Table III), is as follows: C_1=C_2=1.36 Å (assumed); C_2–C_3=1.44±0.03 Å; C_3=O_1=1.22±0.02 Å; C_3–O_2=1.36±0.03 Å; ∠$C_1C_2C_3$=120° (assumed); ∠$C_2C_3O_1$=120±3°; ∠$O_1C_3O_2$=125±5°; O–H···O=2.76±0.04 Å.

Discussion

The C=O and C–O distances in acrylic acid are the same as those observed in several interesting structural studies of the carboxyl group on formic and acetic acids. Therefore, no differences between a saturated and an unsaturated substituent attached to the carboxyl group could be found in this work.

Moreover, the C=C, C–C and C=O distances and the valence angles in this

molecule generally agree with the corresponding bond lengths and valence angles of acrolein[5] and acrylyl chloride[6] which are obtained by electron diffraction studies. Bond shortening and bond elongation of C–C and C=C bonds in conjugated molecules were plausibly explained by the delocalization of π-electron. As a matter of fact, it may be considered that the order of conjugation in this molecule is the same as that calculated on acrolein by C. A. Coulson[7].

In the dimer, the C–O bond becomes 0.07 Å shorter than that in the monomer, while the C=O bond remains unchanged. Within the limits of accuracy of this work, the circumstances are the same as in the case of association of formic and acetic acids. Several investigations show that the heat of dimerization of some carboxylic acids is of the order of 13~18 kcal./mol. The C–O bond shortening may be attributed for considerable part to the formation of a ring by two carboxyl groups across the hydrogen bridges.

The author wishes to express his sincere gratitude to Professor A. Kotera and Mr. M. Igarashi of Tokyo University of Education for their kind guidance and encouragement throughout this work, and for the free use of the apparatus located at their university. Thanks are also due to Professor J. Kurahashi and Dr. T. Takeshima of this university for their helpful advice.

Department of Chemistry
Faculty of Science
Ibaraki University, Mito

5) H. Mackle and L. E. Sutton, *Trans. Faraday Soc.*, **47**, 691 (1951).
6) T. Ukaji, This Bulletin, **30**, 737 (1957).
7) C. A. Coulson, *Trans. Faraday Soc.*, **42**, 106 (1946).
8) O. Z. Foz and J. Marcills, *Chem. Abstr.*, **44**, 8716*b* (1950); J. J. Fox and A. E. Martin, *Trans. Faraday Soc.*, **36**, 397 (1940); F. H. MacDougall, *J. Am. Chem. Soc.*, **63**, 3420 (1941).

*The Molecular Structure of the Monomer and the Dimer of Methacrylic Acid**

By Takeshi UKAJI

(Received June 2, 1959)

It has been commonly recognized that the derivatives of acrylic acid which have a methyl group on the α-carbon atom are reactive than the one having no substituent. Theoretical and structural explanation of this chemical fact seems not yet to have been given. The present work is directed to clarifying the stereochemical structure of methacrylic acid, and also to elucidate the question concerning the changes which may occur on the introduction of the methyl group into the α-position of the acid and on the association of the monomeric acid.

Experimental

Methacrylic acid was prepared by hydrolysis of commercial grade methacrylate. On careful distillation of the acid, a fraction boiling at 75~76°C/20 mmHg was collected. It was stocked over hydroquinone.

The electron diffraction photographs were taken according to the usual manner using a camera reported in the previous paper[1] (camera distance, ca. 9 cm.; electron wavelength, 0.053~0.061 Å, determined by calibration with gold foil). The experimental technique concerning the photographs of the monomer of this acid was essentially the same in the case of the monomer of acrylic acid. The diffraction pattern was visually measured to an extent of ca. 70 of q-values.

Interpretations of Diffraction Patterns and Results

For the calculation of theoretical intensity curves, the authorized formula[3b] was used. The thermal vibration factor is omitted as a first approximation.

Monomer of Methacrylic Acid.—To examine if the temperature of the present experiment is sufficient for the thermal dissociation of the acid, some photographs were taken and these were carefully compared with that of the dimer of this acid. A remarkable change was observed.

* Presented partly at the Symposium on Structural Chemistry, Fukuoka, Nov. 22, 1957.

1) T. Yuzawa and N. Yamaha, This Bulletin, **26**, 414 (1953).

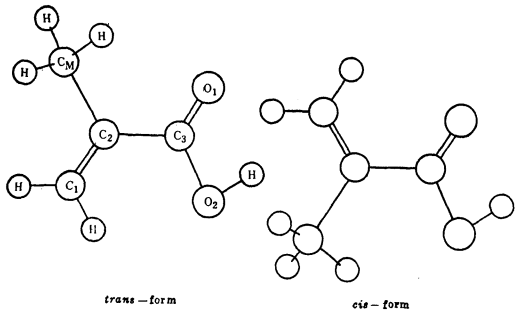


Fig. 1. Schematic model showing the *trans*- and *cis*-forms of methacrylic acid.

in the feature at about 23 of q-values in these patterns. Six satisfactory photographs were obtained.

On the basis of foregoing information[2,3], it is assumed that all the carbon and oxygen atoms in this molecule are coplanar, and that the C-H bond distance in the methyl group is 1.10 Å, in which each hydrogen atom forms tetrahedral configuration, and the C-H distance and ∠CCH in methylene group are 1.08 Å and 120°, respectively. The hydrogen atom in the hydroxyl group was neglected for the same reason as that described in the previous paper[3b]. The parameters C_1=C_2, C_2-C_3, C_3=O_1, C_3-C_2 and C_2-C_M (in methyl group), used in the calculation of theoretical intensity curves, were varied from 1.32 to 1.45 Å, from 1.40 to 1.54 Å, from 1.18 to 1.24 Å, from 1.32 to 1.50 Å and from 1.40 to 1.54 Å in steps of 0.02 or 0.03 Å, while the angles of $C_1C_2C_3$, $C_3C_2C_M$, $C_2C_3O_1$ and $O_1C_3O_2$ were varied from 110 to 130°, from 110 to 130°, and from 110 to 135° in steps of 2 or 3°, respectively.

In Fig. 2, the solid lines are descriptive of the theoretical intensity curves of the *trans*-form, and the chain lines those of the *cis*-form. The effect of thermal vibration (the factors are listed in Table I) was then examined and the curves including these effects were shown in the dotted lines in the same figure.

A careful comparison was made between the visual and theoretical intensity curves. Curve A is in the best agreement with the visual one. The curves of several other models quoted in this figure also resemble the observed intensity curve, but they differ from it in the features of some maxima and minima. Curves B and C agree with the visual one in all features, except for the position of the 4th maximum. While in curves D and E, the positions of the 3rd minimum and the 4th maximum and minimum, and the feature of the 6th peak differs from the visual curve. Curves F, G, H and I are taken for the purpose of ascertaining the limit of acceptability for C_3=O_1 and C_3-O_2 distances; these curves are in good agreement with the observed one in all features, except for the positions of the 4th and

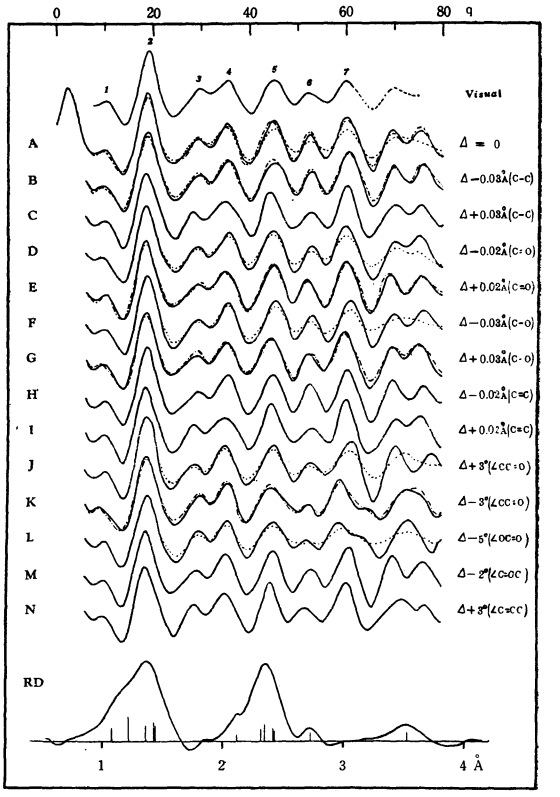


Fig. 2. Visual, theoretical intensity curves and radial distribution curve for methacrylic acid. The notations on the right hand side of this figure show that the models deviate from the most probable model, for example, Δ=0 is the most probable model which has the following parameters; C-H=1.08, C_M-H (in methyl group)=1.10, C=C=1.36, C-C=1.44, C=C=1.22, C-O=1.43 Å, $\angle CC_MH$=109.5°, $\angle$C:CH=$\angle$C:CC=$\angle$CCC=$\angle$CC:O=120° and $\angle$OC:O=125°.

6th maxima. In curves J and K, the positions of the 4th maximum and the intensity relations of the 6th peak are different from those of the visual one. Curves L and M are used to examine the limit of angle $C_2C_3O_1$. These curves are rejected because of the disagreement with the visual one in the range of q>45. Curves from N to P show the acceptable limit of the angles of $O_1C_3O_2$, $C_1C_2C_3$ and $C_2C_3C_M$, respectively. These curves have small differences in the positions and features of the 3rd minimum, the 4th and the 6th maximum.

The theoretical intensity curves of the *trans*- and the *cis*-forms remain almost unchanged throughout all the features. Therefore, we could not distinguish between the *trans*- and *cis*-configuration of this molecule.

From the above considerations, model A is regarded as the most acceptable one, while others are all accepted as on the borderline.

2) T. Ukaji, This Bulletin, **32**, 1266 (1959).
3) (a) H. Mackle and L. E. Sutton, *Trans. Faraday Soc.*, **47**, 691 (1951). (b) T. Ukaji, This Bulletin, **30**, 737 (1957).

TABLE I. APPROXIMATE VIBRATION FACTORS USED IN CALCULATION FOR THE MONOMER AND DIMER OF METHACRYLIC ACID

Values of factor	Atom pairs	
	Monomer	Dimer
0	C_1=C_2, C_2–C_3, C_3–C_M, C_3=O_1, C_3–O_2	C_1=C_2, C_2–C_3, C_2–C_M, C_3=O_1, C_3–O_2
0.00010	$O'_1\cdots C_2$, $O'_2\cdots C_2$, $C'_1\cdots C_M$, $C'_3\cdots C_M$, $C'_1\cdots C_3$	$O'_1\cdots C_2$, $O'_2\cdots C_2$, $C'_1\cdots C_M$, $C'_3\cdots C_M$, $C'_1\cdots C_3$
0.00015	C–H, C_M–H (in methyl group), $O'_1\cdots O_2$	C–H, C_M–H (in methyl group), $O'_1\cdots O_2$
0.00020	$C'_2\cdots$H, $C'_2\cdots$H (in methyl group)	$C_2\cdots$H, $C'_2\cdots$H (in methyl group)
0.00035	$O_2''\cdots C_1$, $O_1''\cdots C_M$	$O_2''\cdots C_1$, $O_1''\cdots C_M$
0.00040	$O_1''\cdots C_1$	$O_1''\cdots C_1$, OH$\cdots$O'
0.00060	$O_2''\cdots C_M$	$O_2\cdots C'_M$, $O_1\cdots O_1'$, $O_2\cdots O'_2$, $O_1\cdots C'_3$, $O_2\cdots C'_3$, $C_3\cdots C_3'$
0.00080		$O_1\cdots C'_2$, $O_2\cdots C'_2$, $C_3\cdots C'_3$, $O_1\cdots C'_1$, $O_2\cdots C'_1$, $C_3\cdots C'_M$, $O_1\cdots C'_M$, $O_2\cdots C_M$
0.00100		$C_3\cdots C'_1$, $C_2\cdots C'_1$ $C_1\cdots C'_1$, $C_1\cdots C'_M$, $C_2\cdots C'_M$
0.00120		$C_M\cdots C'_M$

TABLE II. q_C/q_O VALUES FOR METHACRYLIC ACID

Feature		q_O	q_C/q_O Model							Wt.
Max.	Min.		A	B	E	G	H	M	N	
1		10.44	0.982	0.986	0.982	0.977	0.987	0.982	0.977	1
	1	14.06	0.996	0.982	0.982	0.996	0.996	0.996	0.982	1
2		18.66	0.997	0.994	0.993	0.993	0.997	0.993	0.989	2
	2	24.27	1.001	1.009	1.009	1.009	1.009	1.001	1.003	2
3		29.02	1.004	1.004	0.982	0.999	1.004	1.009	1.020	4
	3	32.41	1.009	1.003	0.941	0.964	1.003	0.957	0.957	2
4		35.74	0.996	1.007	0.951	0.972	1.002	0.968	1.021	4
	4	39.21	1.002	1.005	1.000	1.005	1.014	0.992	1.002	2
5		44.00	1.000	1.007	0.995	1.005	1.006	0.994	0.989	3
	5	49.30	0.998	0.999	0.999	0.992	1.004	0.999	1.008	2
6		52.25	1.005	1.014	1.014	0.995	1.019	0.993	0.991	1
	6	55.02	0.999	1.009	1.004	0.999	1.007	0.967	0.985	1
7		58.96	1.001	1.001	1.005	1.006	0.997	1.009	0.986	1
Wt. mean			1.001	1.003	0.984	0.992	1.003	0.989	0.998	
Wt. mean dev.			0.004	0.007	0.020	0.012	0.006	0.014	0.016	

Seven models are selected from them, and their q_C/q_O values are summarized in Table II. The structural information deduced from the values of averages and the average deviations of q_C/q_O ratios is consistent with the above correlation analyses.

The RD curve in Fig. 2 is the radial distribution curve for this molecule. In this curve, the first peak corresponds to the C–H, C_M–H (in methyl group), C_1=C_2, C_2–C_3, C_2–C_M, C_3=O_1 and C_3–O_2 distances, the second, third and fourth to the C'$\cdots$H, $C'_2\cdots$H, $O'_1\cdots C_2$, $O'_2\cdots C_2$, $C'_1\cdots C_M$, $C'_3\cdots C_M$, $C'_1\cdots C_3$, $O''_2\cdots C_1$ and $O''_1\cdots C_M$, the fifth to the $O''_1\cdots C_1$ and the sixth to the $O''_2\cdots C_M$ distances, respectively. The interatomic distances determined from the most probable model (shown in vertical lines in this RD curve) are in good agreement with the peaks observed in this radial distribution curve.

The following values are obtained for the structure of the monomer of methacrylic acid: C_1=1.36±0.02 Å; C_2–C_3=1.44±0.03 Å; C_2–C_M=1.52±0.02 Å; C_3=O_1=1.22±0.02 Å; C_3–O_2=1.43±0.03 Å; $\angle C_1C_2C_3$=120±2°; $\angle C_3C_2C_M$=120±3°; $\angle C_2C_3O_1$=120±3°; $\angle O_1C_3O_2$=125±5°.

Dimer of Methacrylic Acid.—The circumstances of the association of methacrylic acid is assumed to be the same as in the case of the dimer of acrylic acid. The complete analysis on the molecular structure of the dimer of this acid may be very laborious because of the inclusion of so many parameters. Therefore, some parameters of the most probable model of the

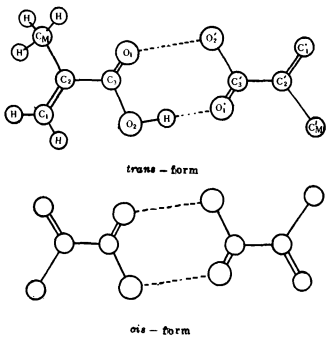


Fig. 3. Schematic model showing the skeletons and the numbering of atoms of the dimer of methacrylic acid.

monomer of this acid obtained from the above analysis were assumed to be as follows: C-H (in methyl group), C_M-H (in methyl group), C_1=C_2, C_3=O_1, $\angle C_2C_1H$, $\angle C_2C_MH$, $\angle C_1C_2C_3$, $\angle C_2C_3O_1$ and $\angle O_1C_3O_2$ were taken to be 1.08 Å, 1.10 Å, 1.36 Å, 1.22 Å, 120°, 109.5°, 120°, 120° and 125°, respectively. In the thirty models examined in this analysis, the parameters C_2-C_3, C_2-C_M and $C_1C_2C_M$ were varied from 1.40 to 1.50 Å, from 1.45 to 1.54 Å and from 110 to 130°, respectively.

Some of the theoretical intensity curves are shown in Fig. 4. These curves are representative of the theoretical intensity curves of the *trans*-form, and those of the *cis*-form are omitted in this figure for the reason that few differences are found between them. Curve A is in the best agreement with the visual one, and has parameters described in the notations of Fig. 4. In curves B and C, the 5th and 6th maxima have some different features from the visual curve; the position of the 7th maximum shifts outward in the former curve and the same maximum

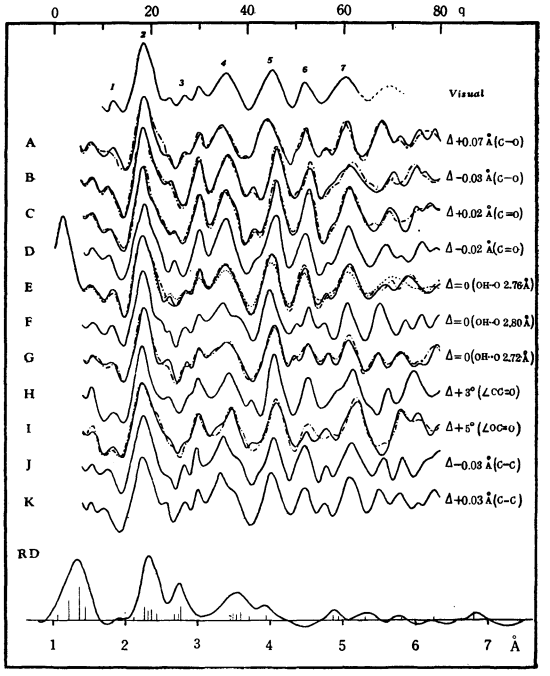


Fig. 4. Visual, theoretical intensity curves and radial distribution curve for the dimer of methacrylic acid. The notations on the right hand side of this figure show that the models deviate from the most probable model, for example, $\Delta=0$ is the most probable model which has the following parameters; C-H=1.08, C_M-H (in methyl group)=1.10, C=C=1.36, C-C=1.44, C=O=1.22, C-O=1.36 Å, $\angle$C : CH=$\angle$C : CC=$\angle CCC_M$=$\angle$CC : O=120°, $\angle CC_MH$=109.5°, $\angle$OC:O=125° and OH···O=2.75Å.

TABLE III. q_C/q_O VALUES FOR THE DIMER OF METHACRYLIC ACID

Feature		q_O	q_C/q_O Model				Wt.
Max.	Min.		A	C	E	G	J	
1		11.35	1.007	0.978	0.965	0.951	0.933	1
	1	14.21	1.002	0.993	0.999	0.968	0.968	1
2		17.86	1.003	0.994	1.011	1.025	1.008	1
	2	21.65	1.000	0.998	0.995	1.016	1.025	1
3		23.02	1.000	0.991	0.984	0.995	1.021	2
	3	26.41	0.983	0.985	0.962	1.003	0.996	2
4		29.63	1.006	1.012	0.996	1.012	1.006	4
	4	32.57	0.998	0.998	0.996	0.998	0.981	3
5		35.65	1.005	1.036	1.023	1.035	1.014	2
	5	40.23	0.998	0.989	0.997	0.994	0.982	1
6		44.77	1.002	1.014	0.994	1.026	0.999	2
	6	49.15	1.005	1.001	0.983	1.001	1.000	1
7		52.28	1.010	0.997	1.002	0.999	1.006	1
	7	55.51	1.006	0.999	0.999	0.991	0.993	1
8		59.05	1.005	1.004	0.986	0.999	1.001	1
Wt. mean			1.001	1.002	0.993	1.004	0.994	
Wt. mean dev.			0.005	0.011	0.012	0.015	0.014	

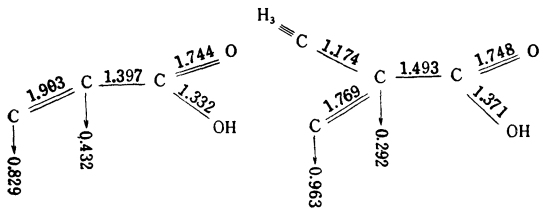
shifts inward in the latter. Curves D and F are taken for the purpose of ascertaining the limit of acceptability for C_2–C_M distance, both curves being in good agreement with the visual one in all the positions of maxima and minima; however, small peaks and shoulders appear among them. In curve F, the 3rd minimum and 7th and 8th maxima shift inward and the 5th maximum outward, while in curve G, the 5th and 6th maxima shift outward. In curves H and I, the 4th and 5th minima and 6th maximum have different positions, but in curve J small peaks appear between the 4th and 5th and 6th maxima. Curve A shows the effect of thermal vibration on curve A, using the vibration factors listed in Table I.

The radial distribution curve for the dimer of methacrylic acid is shown in Fig. 4 (RD curve). The curve shows that the positions and their relative height of peaks determined from the most probable model (as shown in vertical lines) agree fairly well in general with the peaks observed in this radial distribution curve.

The structure of the dimer of methacrylic acid, which is in agreement with the quantitative results in Table III, is determined as follows: C_2–C_M=1.52±0.02 Å, $\angle C_1C_2C_M$=120±3° and O_1–H···O_2 separation 2.75±0.04 Å; and all other parameters are the same as in the dimer of acrylic acid.

Discussion

The C_1=C_2, C_2–C_3, C_3=O_1 and C_3–O_2 distances and the valence angles of $C_1C_2C_3$, $C_2C_3O_1$ and $O_1C_3O_2$ in this molecule are essentially the same as the corresponding bond lengths and valence angles of acrylic acid which is obtained in a previous paper[2]. The C_2–C_M distance in this molecule is shorter than the normal C–C single bond distance 1.54 Å. This bond shortening is explained by the term hyperconjugation. The result of the theoretical calculation by Coulson and Crawford[4] shows that the bond compression energy of C–C single bond, from 1.54 to 1.52 Å, is 0.13 kcal./mol. In our preliminary calculation by a simple MO method** (neglecting overlap integral) acrylic and methacrylic acid, the values of bond order and free valence are shown schematically as follows:



When the values obtained here of the bond order and the bond lengths were treated following the method of Mulliken and others[5], the results compared favorably with the criterion regarding the bond order and the bond lengths which included the idea of hyperconjugation of them (the values concerned with C=C and C–C of acrylic acid, C=C, C–C and C–C_M (in methyl group) of methacrylic acid). In the above figure, the comparison of free valence shows that methacrylic acid has a tendency to possess somewhat greater sensibility than acrylic acid in radical reaction.

In the dimer of this acid, the circumstances are the same as in the case of the association of acrylic acid.

The author wishes to express his sincere gratitude to Professor A. Kotera, Mr. M. Igarashi and Mr. M. I'Haya of Tokyo University of Education for their kind guidance and encouragement throughout this work, and for the free use of the

4) C. A. Coulson and V. A. Crawford, *J. Chem. Soc.*, **1953**, 2052.

** The well-known LCAO molecular orbital treatment is conducted as follows: the effect of the σ electron, assumed to be constant, is neglected, and the π-electrons are considered, as an approximation, to occupy the molecular orbital formulated below.

$$\Psi_i=\sum_{r=1}^{n} c_{ir}\phi_r$$

Then, we have the equatin:

$$(\alpha_r-E)C_r+\sum_{s\neq r}(\gamma_{rs}-S_{rs}E)C_s=0 \qquad (r=1,2,\cdots\cdots,n)$$

in which α is the coulomb integral, E's the energies of LCAO MO's, γ_{rs} the exchange integral and S_{rs} the overlap integral. The details of the calculations of the lower energy levels of these molecules and the empirical parameters adopted are essentially the same as in the case of the calculation of hyperconjugation by I'Haya except for the parameters assigned of oxygen atoms which are: α_O(carbonyl oxygen)=α_C+2.0 and α_O(carboxyl oxygen)=α_C+1.5. Here α_C is the coulomb integral of the carbon atom. According to Coluson's*** definition, the charge density (q_r) of π-electron on the atom r and the bond order (p_{rs}) of the bond between atoms r and s are given by the following equations:

$$q_r=2\sum_i C_{ir}^2$$

$$q_{rs}=2\sum_i C_{ir}\cdot C_{is}$$

where the summations are taken overall occupied MO's.

The calculation of the free valence F_r at atom r in a molecule followed the definition formulated by Coulson****

$$F_r=N_{max}-N_r$$

The values of N_{max} is $3+\sqrt{3}$ and the N_r is

$$N_r=3+\sum_i p_{rs}$$

in which p_{rs} is the π-bond order of the r-s bond, where s is adjacent to r atom.

*** C. A. Coulson, *Proc. Roy. Soc.* (*London*), **A169**, 413 (1939).

**** C. A. Coulson, *Discussions Faraday Soc.*, **2**, 9 (1947).

5) R. S. Mulliken et al. *J. Am. Chem. Soc.*, **63**, 41 (1941).

apparatus located at their university. Thanks are also due to Dr. T. Takeshima of this university for his helpful advice.

Department of Chemistry
Faculty of Science
Ibaraki University, Mito

*The Molecular Structure of Methyl Acrylate and Methyl Methacrylate**

By Takeshi UKAJI

(Received June 2, 1959)

Investigations of methyl formate and methyl acetate by electron diffraction have been reported[1], but no information seems to have been proposed regarding the stereochemical structure of methyl acrylate and methyl methacrylate which are important materials for high polymeric products.

In the present work, structural studies on methyl acrylate and methyl methacrylate by the electron diffraction method are undertaken to determine the most probable location of the methyl group of ester in these two compounds and to inspect the effect of hyperconjugation on the C-C single bond between the methyl group and the α-carbon atom in methyl methacrylate.

Experimental

Samples were purified by careful distillation. Methyl acrylate, b. p. 84.5~85.5°C. Methyl methacrylate, b. p. 100~101°C. These were stocked over hydroquinone.

The electron diffraction photographs were taken in the usual manner using a camera similar to the one reported in the previous paper[2] (camera distance, ca. 9 cm., electron wavelength, 0.059~0.063 Å, determined by calibration with gold foil). Fifteen satisfactory photographs were obtained in the case of methyl acrylate and eight in the case of methyl methacrylate. The diffraction patterns were visually measured to an extent of about $q=80$ in both cases.

Interpretation of Diffraction Patterns and Results

For the calculation of theoretical intensity curves, the authorized formula[3] was used. The exponential term of the formula is omitted as a first approximation.

Methyl Acrylate.—In the models of this molecule only four parameters are changed. In these the C_3-O_2 distance in carboxyl bond is varied from 1.32 to 1.45 Å in steps of 0.02 or 0.04 Å, and the O_2-C_4 distance in methoxyl bond from 1.40 to 1.50 Å with the same increments. The angle of $C_3O_2C_4$ of methoxyl group varied from 105 to 130° in steps of 5° and the angle between $C_3O_2C_4$ plane and the plane composed of the other atoms in the molecule is varied from 0 to 60°. The other parameters of this molecule were assumed to be those of the most probable model of acrylic

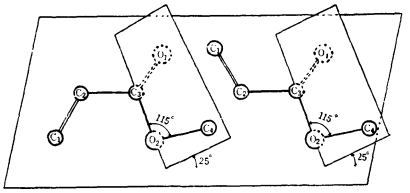


Fig. 1. Schematic models showing the skeletons and the numbering of atoms of methyl acrylate. The left model is *trans*-form and the right *cis*-form.

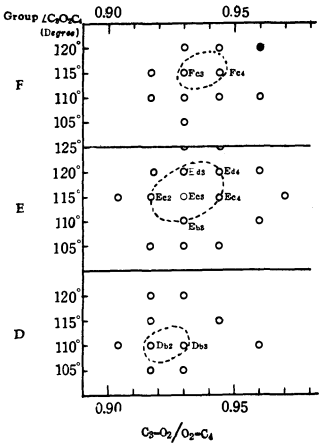


Fig. 2. Parameter chart for methyl acrylate.

* Partly presented at the 9th Annual Meeting of the Chemical Society of Japan, Kyoto, April, 1956.

1) A survey of the results of electron diffraction through 1949 is found in the tabulation by P. W. Allen and L. E. Sutton, *Acta Cryst.*, **3**, 46 (1950).

2) T. Yuzawa and M. Yamaha, This Bulletin, **26**, 414 (1953).

3) P. A. Shffer, V. Schomaker and L. Pauling, *J. Chem. Phys.*, **14**, 659 (1946).

4) T. Ukaji, This Bulletin, **32**, 1266 (1959).

acid[4]. Careful comparison was made between the visual intensity curve and the theoretical ones.

Fig. 2 shows the parameter chart for this molecule. The groupings of the models in the following discussions are made according to the qualitative similarity of the theoretical intensity curves. Groups D, E and F correspond to the models of which methyl groups are inclined by 20, 25 and 30°, respectively, to the molecular plane, and others are all rejected because of the disagreement with the visual curve.

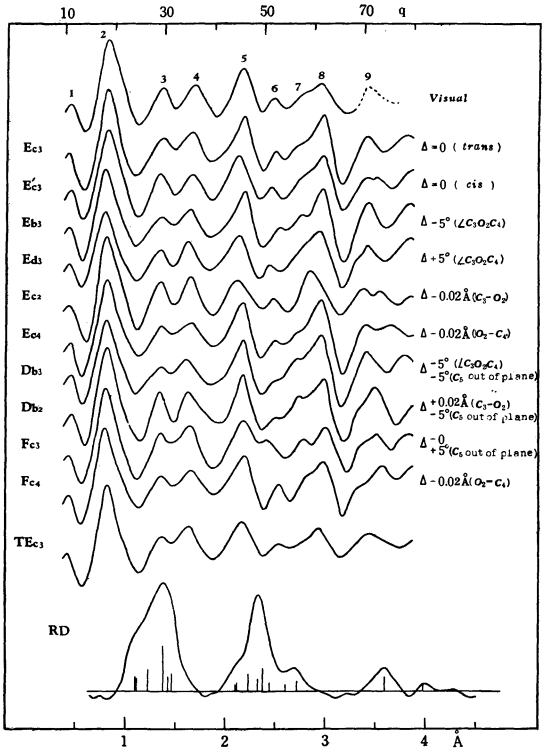


Fig. 3. Visual, theoretical intensity curves and radial distribution curve for methyl acrylate. The notations on the right hand side of this figure show that the models deviate from the most probable model, for example, $\Delta=0$ is the most probable model which has the following parameters; C_1–H $=1.08$, C_5–H (in methyl geoup) $=1.10$, C_1=C_2 $=1.36$, C_2–$C_3=1.44$, C_3=$O_1=1.22$, C_3–$O_2=1.36$, O_2–$C_4=1.46$ Å, $\angle C_2C_1H=\angle C_1C_2C_3=\angle C_2C_3O_1$ $=120°$, $\angle O_2C_4H$ (in methyl ester group) $=$ $109.5°$, $\angle O_1C_3O_2=125°$, $\angle C_3O_2C_4=115°$ and C_4 atom is 25° out of plane configuration.

Of curves of the *trans*-form of the models E_{c2}, E_{b3}, E_{c3}, E_{d3} and E_{c4}, curve E_{c3} is in excellent agreement with the visual curve in all respects (Fig. 2). Curve E'_{c3} is taken as the typical one of which the model has a *cis*-configuration as regards C_1=C_2 and C_3=O_1. No remarkable discrepancies in the positions of maxima, minima and their intensity relations of the theoretical intensity curves are found throughout this work between the *trans*- and *cis*-configurations. Therefore, that of the *cis*'s of all the other models are omitted in Fig. 3. Curves E_{c3}, E_{b3}, E_{d3} and E_{c4} are given in order to show the limits of acceptability for the positions and relative intensities of the 5th, 6th and 8th maxima, and of the acceptable range of shapes of the 7th shelf. All curves with 4th maximum and minimum shifting inward and with the resolution of the 7th shelf greater than that in curve E_{b3} were rejected. Curve E_{d3} was the lower limit of acceptability for the 4th, 5th and 6th maxima shifting inward and for the prominence of the 7th shelf.

Curves D_{b2} and D_{b3} are given as acceptable curves of the D group. The height of the 5th maximum is slightly increased in both curves, and that of the 3rd maximum in the D_{b2} curve decreased, but that in D_{b3} increased. These discrepancies are not regarded as sufficient to justify the rejection of these models, and both models are considered to be acceptable borderline ones.

Of models in the F group, curves F_{c3} and F_{c4} are taken as representative ones. The features of the 6th maximum and the 7th shelf are both accepted as the limit of permission.

The effect of the thermal vibration on the theoretical curve was then examined. The vibration factor is listed in Table I. Curve TE_{c3} is a representative one showing this effect on the theoretical curve calculated from model E_{c3}. This curve has the same feature in all respects as the visual one has.

From the above considerations, model E_{c3} may be regarded as the most acceptable one, while the others are all accepted as borderline cases. The q_C/q_O values of these eight models are summarized in Table II. The weighing for each feature is indicative of its reliability in comparison with theoretical curves. Low weighing is given to the inner features, because these have generally been found to give less satisfactory agreement than do those at somewhat greater q values. Features for which reproducible measurements could not be obtained are also given lower weights. To the features farther out are assigned relatively low weights.

TABLE I. APPROXIMATE VIBRATION FACTORS USED IN THE CALCULATION FOR METHYL ACRYLATE

Factors	Atom pairs
0.00008	for C_3=O_1 and C_1=C_2
0.00012	for C_3–O_2, C_4–O_2 and C_2–C_3
0.00015	for $O_1'\cdots O_2$, $C_2'\cdots O_1$, $C_2'\cdots O_2$ and $C_1'\cdots C_3$
0.00030	for C–H, $O_1'\cdots C_4$ and $C_1'\cdots O_2$
0.00040	for $C'\cdots$H, $O_2'\cdots$H, $C_2''\cdots C_4$ and $C_1''\cdots O_1$
0.00045	for $C_1'''\cdots C_4$

TABLE II. q_C/q_O VALUES FOR METHYL ACRYLATE

Feature Max.	Min.	q_O	q_C Model E_{c4}	E'_{c3}	E_{b3}	E_{d3}	E_{c2}	E_{c4}	D_{b3}	F_{c3}	Wt.
1		11.70	0.992	1.000	0.983	0.983	0.992	0.992	0.992	0.983	1
	1	14.25	0.986	0.986	0.976	0.975	1.013	0.990	0.983	0.997	1
2		18.70	1.003	1.000	0.974	0.979	1.000	1.005	0.974	1.000	2
	2	24.81	0.992	1.017	1.008	1.008	1.019	1.015	1.003	1.003	1
3		29.56	1.001	0.990	1.014	0.998	0.998	1.008	1.011	0.988	2
	3	32.55	0.999	1.004	0.984	0.984	0.992	0.999	0.968	0.992	1
4		36.00	1.000	0.992	0.979	0.976	0.987	1.000	0.967	0.981	2
	4	40.50	0.993	0.978	0.976	0.981	0.993	1.002	0.956	0.993	1
5		45.67	1.001	0.986	1.012	0.990	0.990	1.007	1.007	1.009	2
	5	49.44	1.011	0.995	1.011	0.995	1.011	1.011	1.005	1.001	1
6		52.20	1.001	0.990	1.019	0.983	1.002	1.006	—	0.978	1
	6	54.73	0.987	0.989	1.003	0.982	1.015	0.996	—	0.996	1
7		(57.50)	1.000	1.008	0.992	—	—	1.000	0.988	1.008	0
8		61.84	1.002	0.996	0.999	0.990	0.963	1.001	0.996	1.011	1
	8	66.15	0.997	0.998	1.002	0.998	1.005	1.001	0.998	1.008	1
Wt. mean			0.998	0.994	0.994	0.986	0.997	1.003	0.987	0.996	
Av. dev.			0.006	0.011	0.017	0.016	0.013	0.018	0.022	0.011	

TABLE III. APPROXIMATE VIBRATION FACTORS USED IN THE CALCULATION FOR METHYL METHACRYLATE

Factors	Atom pairs
0.00008	for C_1=O_1 and C_1=C_2
0.00012	for C_3–O_2, C_4–O_2, C_2–C_3 and C_2–C_5
0.00015	for $C_1'\cdots O_2$, $O_1'\cdots C_2$, $O_2'\cdots C_2$ and $C_3'\cdots C_4$
0.00018	for $C_1'\cdots C_3$, $C_3'\cdots C_5$ and $C_1'\cdots C_5$
0.00030	for C–H, $O_1'\cdots C_4$, $O_1''\cdots C_5$ and $O_2''\cdots C_1$
0.00040	for $C_2'\cdots H$, $O_2'\cdots H$, $O_1''\cdots C_1$, $O_2''\cdots C_5$ and $C_1'''\cdots C_4$
0.00050	for $C_4'''\cdots C_5$

TABLE IV. q_C/q_O VALUES FOR METHYL METHACRYLATE

Feature Max.	Min.	q_O	q_C/q_O Model I	II	III	IV	V	Wt.
1		10.43	1.030	1.004	1.015	0.992	1.045	1
	1	14.26	1.013	0.982	0.978	0.972	0.982	1
2		18.08	0.999	1.013	0.999	1.001	1.006	2
	2	24.72	0.983	0.996	0.992	1.021	0.992	1
3		29.23	0.975	1.004	0.989	1.016	0.987	2
	3	32.18	0.988	1.011	0.979	0.995	0.979	1
4		35.80	0.987	1.002	0.978	0.957	0.971	2
	4	39.52	0.992	0.995	0.998	0.942	0.975	2
5		41.75	1.029	1.007	—	0.958	—	1
	5	43.08	1.010	1.015	—	0.963	—	1
6		45.05	1.021	1.021	1.011	1.003	0.999	2
	6	49.00	1.031	1.004	1.005	1.010	1.020	1
7		57.03	0.995	0.999	1.007	0.988	0.993	2
	7	59.59	1.002	0.993	1.006	0.987	0.974	1
8		61.41	1.023	1.003	1.014	0.989	0.998	1
	8	66.52	1.015	0.992	0.995	1.015	0.993	1
9		71.10	1.009	0.997	1.005	1.019	0.985	1
	9	75.03	0.999	0.984	0.999	1.010	0.973	1
Wt. mean			1.003	1.002	0.997	0.989	0.991	
Av. dev.			0.014	0.010	0.014	0.026	0.018	

The radial distribution function for this molecule is calculated by the use of the following equation, (RD curve in Fig. 3):

$$rD_{(r)}=\sum_{q=1}^{q_{max}} I_{(q)_O}\exp(-bq^2)\sin\frac{\pi}{10}qr$$

where $I_{(q)_O}$ is the intensity read from the visual curve. The value b is determined by setting $\exp(-bq^2)=0.1$ at $q=80$. The curve shows that the first peak corresponds to the C–H, C_3–O_1, C_2–C_3, C_3–O_2 (in carboxyl) and O_2–C_4 (in methoxyl) distance, the second and the third to the nonbonding atom pairs, i. e., $C'\cdots H$, $O'_2\cdots H$, $O_1'\cdots O_2$, $O_1'\cdots C_2$, $O_2'\cdots C_2$, $C_1'\cdots C_3$, $C_1'\cdots O_2$ and $C_2''\cdots C_4$, the fourth to the $C_1''\cdots O_1$, and the fifth to the $C_1'''\cdots C_4$, respectively. Owing to the complex nature of the peaks, no attempt was made to resolve the distances. It may be noted, however, that the position determined from the most acceptable model agrees fairly well with the peaks observed in this radial distribution curve.

The results obtained from the examination of theoretical intensity curves and the visual ones are as follows.

Assumption: C–H=1.08 Å, C–H (in methyl group)=1.10 Å, C_1=C_2=1.36 Å, C_2–C_3=1.44 Å, C_3=O_1=1.22 Å, $\angle CCH=\angle C_1C_2C_3=\angle C_2C_3O_1=120°$, $\angle O_1C_3O_2=125°$ and $\angle O_2C_4H=109.5°$ (in methyl group).

Results: C_3–O_2 (in carboxyl)=1.36±0.02 Å, O_2–C_4 (in methoxyl)=1.46±0.02 Å, $\angle C_3O_2C_4=115\pm5°$ and out-of-plane angle of methyl group is 25±5°.

Methyl Methacrylate.—On account of the many parameters involved, a complete analysis on the molecular structure of methyl methacrylate may be very laborious. The present analysis was based upon the following assumption: C–H (in methylene group)=1.08 Å, C–H (in methyl group)=1.10 Å, the hydrogen atoms in two methyl groups have tetrahedral configuration, C_1=C_2=1.36 Å, C_2–C_3=1.44 Å, C_3=O_1=1.22 Å, C_3–O_2 (in carboxyl)=1.36 Å, O_2–C_4 (in methoxyl)=1.46 Å, $\angle C_2C_1H=\angle C_1C_2C_3=\angle C_2C_3O_1=120°$, $\angle O_1C_3O_2=125°$, $\angle C_3O_2C_4=115°$ and the C_4 atom is inclined by 25° to the molecular plane. Therefore, in the models examined in this work, only two parameters are changed; the C_2–C_5 distance between C_5 atom of methyl group and α-carbon atom is varied from 1.45 to 1.54 Å in steps of 0.02 or 0.03 Å and the angle of $C_5C_2C_3$ from 110 to 130° in steps of 2 or 3°.

The theoretical intensity curves which are calculated through the above mentioned equation are carefully compared with the visual one. In Fig. 5, visual and theoretical intensity curves and also the radial distribution curve are shown. Curve B is the most acceptable one, and curves A and from C to E can be considered to show the limit of acceptability for the resolution and

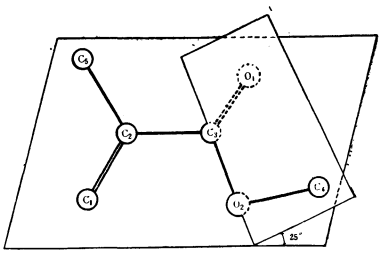


Fig. 4. Schematic model showing the skeleton and the numbering of atoms of methyl methacrylate. This model shows the *trans*-form.

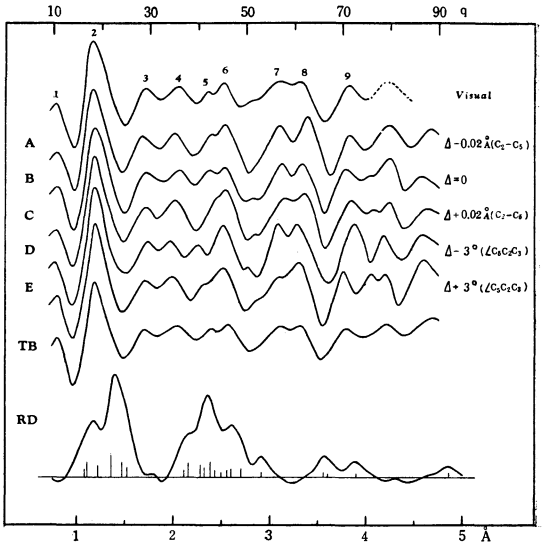


Fig. 5. Visual, theoretical intensity curves and radial distribution curve for methyl methacrylate. The notations on the right hand side of this figure show that the models deviate from the most probable one, for example, $\Delta=0$ is the most probable model which has the following parameters; C_1–H=1.08, C_4–H=C_5–H=1.10, C_1=C_2=1.36, C_2–C_3=1.44, C_3=O_1=1.22, C_3–O_2=1.36, O_2–C_4=1.46 Å, $\angle C_2C_1H=\angle C_1C_2C_3=\angle C_2C_3O_1=120°$, $\angle C_2C_5H=\angle O_2C_4H=109.5°$, $\angle O_1C_3O_2=125°$, $\angle C_3O_2C_4=115°$ and C_4 atom is 25° out of plane configuration.

for the relative intensities of the 7th and 8th maxima and the feature of the 5th shelf. Curve TB shows the effect of thermal vibration. The thermal vibration factors examined in this case are listed in Table III. The q_C/q_O values of these models are summarized in Table IV. The weighing of these features followed the same consideration as in the case of methyl acrylate.

The radial distribution curve (RD curve in Fig. 5) is drawn according to the above equation. The value of b is determined by setting $\exp(-bq^2)=0.1$ at $q=90$. The curve shows that the positions determined from the most acceptable model agree

well with the peaks observed in this radial distribution curve.

The results obtained from the above analyses in this molecule are as follows.

Assumption: All parameters of the most probable model of methyl acrylate were assumed, and the C_5 atom in the methyl group was coplanar, H atoms in this group were of tetrahedral configuration and C_5–H bond lengths were 1.10 Å.

Results: C_2–C_5 = 1.52±0.02 Å and $\angle C_5C_2C_3$ = 129±3°

Discussion of the Results

The results obtained from electron diffraction investigation of acrylic acid generally agree with the corresponding bond lengths and valence angles of acrolein and acetic acid which were obtained by electron diffraction study by Sutton et al.[5] and by Brockway et al.[6] On the basis of the above reason, it was assumed that the skeletons of methyl acrylate and methyl methacrylate were of the same dimension as in the case of acrylic acid.

Unfortunately, no data have appeared which make possible the valid comparison of the C=C, C–C and C=O distances in these esters with those in other compounds. However, the configuration of the methyl group in methyl acrylate agrees with that of methyl acetate. The values for the $C_3O_2C_4$ angle (115±5°) and for the out-of-plane configuration (25±5°) obtained in this work do not differ significantly from the values reported for methyl acetate.

Regarding methyl methacrylate, the value of C_2–C_5 distance obtained here is comparable with the recent value obtained by Keidel and Bauer[7] in the case of toluene, and with the results of I'Haya's theoretical calculation on hyperconjugation[8] of the methyl group in ethylacetylene.

The author wishes to express his sincere thanks to Professor A. Kotera and Mr. M. Igarashi of Tokyo University of Education for their kind guidance and encouragement throughout this work. Thanks are also due to Dr. T. Takeshima of this university for his helpful advice.

Department of Chemistry
Faculty of Science
Ibaraki University, Mito

5) H. Mackel and L. E. Sutton, *Trans. Faraday Soc.*, **47**, 691 (1951).
6) J. Karle and L. O. Brockway, *J. Am. Chem. Soc.*, **66**, 574 (1944).
7) F. A. Keidel and S. H. Bauer, *J. Chem. Phys.*, **25**, 1218 (1956).
8) Y. I'Haya, This Bulletin, **28**, 369 (1955).

SHORT COMMUNICATIONS

The Glass Transition Temperatures of Various Kinds of Polyethylenes

By Kōji TANAKA

(Received August 18, 1959)

It is well known that various physical properties of polyethylene are considerably affected by the chain branching. According to C. A. Sperati et al.[1], for instance, short chain branching controls crystallinity, and long chain branching the viscoelastic properties of the molten polymer and the ultimate strength of the solid.

The author performed an experiment in order to know whether chain branching affects the glass transition temperature or not.

Samples used in this investigation are Marlex 50, Ziegler type polyethylene, and eight kinds of high-pressure polyethylene which are different in their molecular weights, melt index and numbers of short and long chain branchings. These high-pressure samples were provided by courtesy of E. I. du Pont de Nemours and Company. Marlex 50 and Ziegler were commercial polymers. In Table I are shown molecular parameters for these high-pressure polyethylenes. For Marlex 50 and Ziegler these data were not available hitherto, but since the number of short chain branchings was found for

1) C. A. Sperati, W. A. Franta and H. W. Starkweather, Jr., *J. Am. Chem. Soc.*, **75**, 6127 (1953).

the two materials in the paper by R. C. Rempel et al.[2], those were adopted for reference. These are 0.15 and 0.25 for Marlex 50 and Ziegler, respectively. Prior to a series of measurements these ten samples were sufficiently crystallized by thermal treatment.

TABLE I. MOLECULAR PARAMETERS[a] FOR HIGH-PRESSURE POLYETHYLENES

Sample	Melt index	$Mn \times 10^{-3}$	Nc[b]	Nw[c]
A	0.2	34	1.6	20
B	2.1	32	1.6	18
C	2.1	21	2.2	27
D	2.1	18	3.0	34
E	3.8	20	1.6	13
F	2.0	50	2.0	18
G	1.8	27	0.6	10
H	1.6	12	3.2	29

a) These data were determined at E. I. du Pont de Nemours and Company according to the method described in *J. Am. Chem. Soc.*, **75**, 6110 (1953).

b) Short chain branching index in CH_3 groups per 100 CH_2 groups.

c) Long chain weight average number of branch points per molecule[3].

Measurements were carried out by volume dilatometry[4]. As confining liquid mercury and absolute alcohol were used for the run above −40°C and for that from −70°C to room temperature, respectively. A Dewar vessel containing toluene was used as a bath. Cooling and heating of the bath were conducted at the rate of 0.3°C per min. by throwing dry ice and inserting nichrom wire into the bath.

Glass transition temperature, T_g, was determined from intersection of two straight lines on the volume-temperature curve and from discontinuity of the curve obtained by plotting the volume-temperature derivatives as a function of temperature.

Glass transition temperatures obtained from this experiment were plotted as a function of the short chain branching index (Fig. 1). From the figure it seems that the glass transition temperature of these samples lowers proportionally with the increase of the short chain branchings, though Marlex and Ziegler appear to deviate somewhat from this tendency. Then the relation between the glass

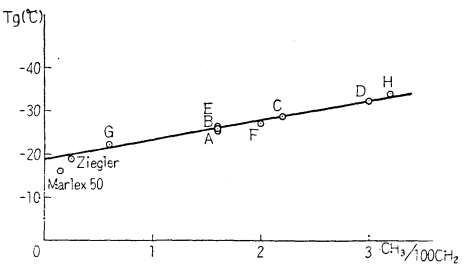


Fig. 1. Glass transition temperatures of various polyethylene samples different in their short chain branching index.

transition temperature and the short chain branching index of these high-pressure polyethylenes was led to the following equation:

$$T_g = -4.6\ \mathrm{Nc} - 18.7$$

On the other hand, long chain branching does not appear to affect the glass transition temperature so much as short chain branching does.

The author thanks Professor M. Takeda for many helpful suggestions and discussion.

Department of Chemistry
Tokyo College of Science
Shinjuku-ku, Tokyo

2) R. C. Rempel, H. E. Weaver, R. H. Sands and R. L. Miller, *J. Appl. Phys.*, **28**, 1082 (1957).
3) B. H. Zimm and W. H. Stockmayer, *J. Chem. Phys.*, **17**, 1301 (1949).
4) N. Bekkedahl, *J. Research Natl. Bur. Standards*, **42**, 145 (1949).

Studies on Organic Catalytic Reactions. I

By Ken-ichi WATANABE

(Received October 3, 1959)

It is interesting to study the application of metallic catalysts to new organic reactions beyond the customary catalytic reactions. Various reactions of organic compounds may be accelerated with the aid of catalysts and subsequently some new catalytic reactions are expected to be found. In this paper, general aspects of hydrolysis of aromatic nitriles and esters with nickel catalysts—mainly the Urushibara nickel catalyst[1]— are reported, and reactions of aromatic halogen compounds with the catalyst are also described.

When aromatic nitriles were refluxed with water in the presence of the catalyst, they were found to be hydrolyzed to the

1) Y. Urushibara and S. Nishimura, This Bulletin, 27, 480 (1954).

TABLE I. HYDROLYSIS OF BENZONITRILE WITH URUSHIBARA NICKEL CATALYST

Benzonitrile g.	U-Ni-B g.	Solvent cc.	Time hr.	Products, g. Amide	Amine	acid	Remarks
5	4	Water 80	11	4.2 (73%)	0.4	+	
5	4	Ethanol 60	9	0.6 (11%)	4.0	+	
10	8	Ethanol 100	8	3.6 (19%)	3.6	+	Recovered 0.1 g.
10	8	Dioxane 100	12	4.0 (34%)	1.5	−	Recovered 0.4 g. White crystals m.p. 220°C

corresponding acid amides in fairly good yields even though the reaction medium was neutral to litmus. The hydrolysis was generally stopped at the amide stage and very small amounts of acids were obtained. Further hydrolysis of amides to acids could not be observed even when the amides were treated again with a newly prepared catalyst. Small quantities of nitriles were hydrogenated to amines by hydrogen absorbed on the nickel catalyst. Some factors, effective for the reaction, were examined in regard to the kind of catalyst, promoter or poison, solvent and duration of refluxing. In most of the reactions, the Urushibara nickel was used as the catalyst, and representative results of the experiments with benzonitrile are shown in Table I. Stabilized nickel catalysts (K. S. Y. Catalysts)[2] were also used in some experiments, and similar results could be observed.

Among the varieties of the Urushibara catalyst, U-Ni-B was the most advantageous for the hydrolysis; U-Ni-A[3], BA[4], AA[5] and U-Cu-B were not so admirable because some undesirable side reactions were induced. When precipitated nickel prepared from nickel chloride and zinc dust was used in place of the Urushibara catalyst, the product was found to be a complex of a primary amine and zinc, which can be decomposed to the amine by treating with alkali. Zinc powder by itself did not show any catalytic activity for hydrolysis.

As for the reaction solvents, water, ethanol, dioxane and *n*-butanol were used, and water was proved to be the most excellent of all as shown in Table I. A small quantity of thiophene or pyridine was added to the U-Ni-B catalyst in order to examine specific behavior as a promoter for the catalyst. However, they were of no use but rather gave an unfavorable effect.

The hydrolysis of the nitrile group was also observed in *p*-tolunitrile, *o*-nitrobenzonitrile and benzyl cyanide, yielding the appreciable amounts of the corresponding amides. On the contrary, hydrolysis of ethyl benzoate hardly proceeded with the same method, and benzoic acid could scarcely be obtained.

On the other hand, some aromatic halogen compounds were treated with the nickel catalyst in the same procedure mentioned above. Chlorobenzene, bromobenzene and iodobenzene were mainly dehalogenated to bezene along with a small quantity of biphenyl, although the reaction velocity of chlorobenzene was very slow compared with those of the others. When a small quantity of thiophene was added to the catalyst in the reaction of bromobenzene, alternative obscure reaction occurred yielding an unidentifiable oily product of a high boiling point. Reactions of nitro or amino derivatives of halogenobenzenes were more complicated. Among the reactions of this series, remarkable result was obtained with benzyl chloride. When benzyl chloride was refluxed with U-Ni-B in ethanol, a Wurtz type reaction was observed and bibenzyl was obtained in a good yield (above 70%). However, when the mixture was refluxed for a long time, the production of bibenzyl was accompanied with the formation of a highly boiling oil.

As the results of the studies on these catalytic reactions, it was found that amides are obtained from nitriles without acidic or alkaline hydrolysis, and that bibenzyl is obtained from benzyl chloride without sodium metal. These reactions are simple in procedure, and the yields of products are fairly good when the reactions are carried out under suitable conditions. The details of these experiments and discussion will be published in a following paper.

2) T. Yamanaka et al., *J. Sci. Res. Inst.*, **51**, 168 (1957); **52**, 143, 224 (1958).
3) Y. Urushibara, S. Nishimura and H. Uehara, This Bulletin, **28**, 446 (1955).
4) K. Hata, S. Taira and I. Motoyama, ibid., **31**, 776 (1958).
5) K. Hata, K. Watanabe and H. Watanabe, ibid., **32**, 6 (1959).

The author wishes to express his hearty thanks to Professor Kazuo Hata for his kind advice.

Department of Chemistry
Faculty of Science
Tokyo Metropolitan University
Setagaya-ku, Tokyo

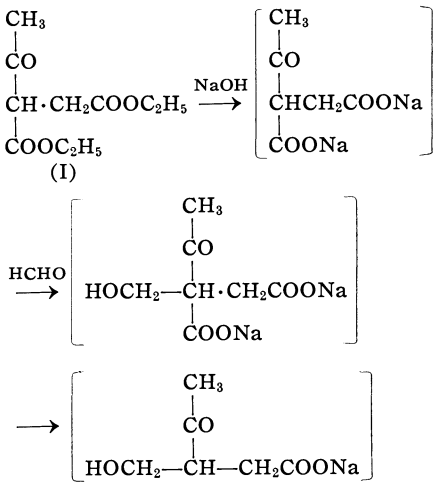
The New Synthetic Method of β-Acetyl-butyrolactone

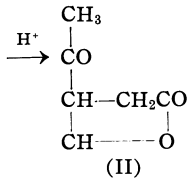
By Yoshihiko NISHIZAWA

(Received October 3, 1959)

B. R. Baker[1] has prepared β-acetyl-butyrolactone (II) from itaconic acid half ester or dimethyl methoxy-succinate. This method, however, gave a very poor yield and β-acetyl-butyrolactone (II) was only isolated as 2,4-dinitrophenylhydrazone derivative.

The present author found that β-acetyl-butyrolactone (II) is synthesized in a smooth way from diethyl acetyl-succinate[2] (I) according to the following equation[3].





(II)

One hundred and eight grams (0.5 mol.) of diethyl acetyl-succinate (I) (b. p. 140~ ~142°C/14 mmHg, n_D^{16} 1.4380) were added to 480 ml. of 10% sodium hydroxide aqueous solution at 0°C and left for twenty four hours at room temperature (ca. 15~20°C). After the oil was dissolved completely, the aqueous solution was neutralized with 30% sulfuric acid to pH 8~8.2 and then 20 g. of sodium bicarbonate and 54 ml. of 37% formaline were added. After the mixture was allowed to stand overnight at room temperature, acidified with 30% sulfuric acid and extracted continuously with ether. The ether layer was dried with anhydrous sodium sulfate and then ether was evaporated. The residual oil was distillated under the diminish pressure; yield, 28.0 g. (43.8%), b. p. 140~143°C/6 mmHg, n_D^{31} 1.4600.

Anal. Found: C, 55.98; H, 6.41. Calcd. for $C_6H_8O_3$: C, 56.24; H, 6.29%.

2,4-Dinitrophenylhydrazone; m. p. 191~ 192°C (recrystallized from acetic acid).

Anal. Found: C, 46.61; H, 3.70; N, 18.20. Calcd. for $C_{12}H_{12}O_6N_4$: C, 46.76; H, 3.92; N, 18.18%.

The 2,4-dinitrophenylhydrazone was soluble in sodium bicarbonate aqueous solution and the mixed melting point with the authentic 2,4-dinitrophenylhydrazone[1] was not depressed.

The author is much indebted to Mr. S. Kitamura for his earnest assistance and wishes to express his thanks to his coworkers for the microanalysis.

Sumitomo Chemical Co., Ltd.
Osaka Works
Konohana-ku, Osaka

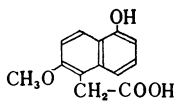
1) B. R. Baker, *J. Org. Chem.*, **17**, 116 (1952).
2) C. Rach, *Ann.*, **234**, 35 (1886).
3) Y. Nishizawa, Japan. Pat., No. 254,740.

*Abnormal Reduction of 2-Methoxy-5-hydroxy-1-naphthylacetic Acid**

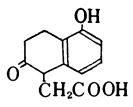
By Takeshi MATSUMOTO and Akira SUZUKI

(Received February 20, 1959)

In the previous paper[1] the synthesis of 2-methoxy-5-hydroxy-1-naphthylacetic acid (I) was described. The present work was undertaken in an attempt to prepare 1,2,-3,4-tetrahydro-2-oxo-5-hydroxy-1-naphthylacetic acid (II), a potential intermediate for building up the diterpenoid alkaloid framework, by reduction I.



(I)



(II)

It is well known that the reduction of a variety of 2-methoxynaphthalene derivatives by alkali metal in alcohol[2] or in alcohol-liquid ammonia[3] yields the corresponding 2-oxotetralins. At first sight, therefore, it seemed easy to prepare tetrahydro-2-oxo-5-hydroxy-1-naphthylacetic acid (II). However, attempted reduction along this line led to unusual results. Depending upon the procedure employed, tetrahydro-5-hydroxy-1-naphthylacetic acid (III) or a mixture of compound III and tetrahydro-2-oxo-4,5-dihydroxy-1-naphthylacetic acid (IV) has been obtained.

At first, the reduction was effected by employing a large excess of sodium (ca. 0.03 mol. per 0.001 mol. of I) in butanol. Product A, which was obtained in good yield, unexpectedly did not react with dinitrophenylhydrazine. The elemental composition corresponded to $C_{12}H_{14}O_3$ rather than to that of the expected product II, $C_{12}H_{12}O_4$. The tests for a methoxyl group (Zeisel) and for a secondary alcohol group (Nessler) were both negative. The infrared spectrum in nujol mull possessed a single sharp band at 1700 cm^{-1} (carboxyl group) and a broad absorption band at 3200~3400 cm^{-1}. Of three oxygen atoms, two have thus been shown to be present in a carboxyl group, and one probably as a hydroxyl group. The presence of a hydroxyl group was confirmed by the formation of monoacetate, $C_{14}H_{16}O_4$. The ultraviolet spectrum (Fig 2. curve b) of product A could be superimposed upon that of 1,2,3,4-tetrahydro-5-naphthol (curve c). These results clearly indicate that product A should be expressed by formula III. So far as the authors are aware, the ready conversion of methoxynaphthalenes to desoxygenated tetralins has not hitherto been reported[4]. The formation of the abnormal reduction product must be attributed, at least in part, to the presence

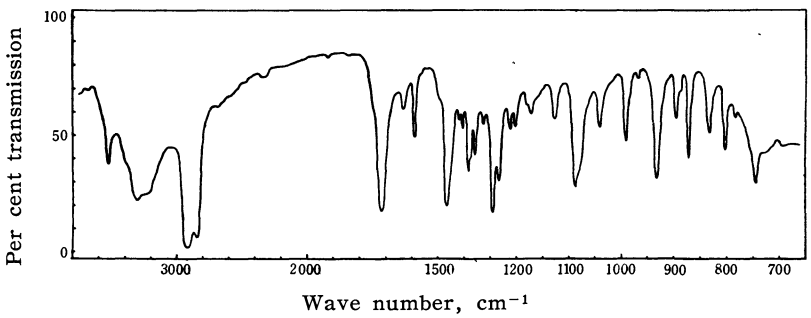


Fig. 1. Infrared spectrum of 1,2,3,4-tetrahydro-2-oxo-4,5-dihydroxy-1-naphthylacetic acid (IV).

* Approaches to the Synthesis of Diterpenoid Alkaloid Models. II.

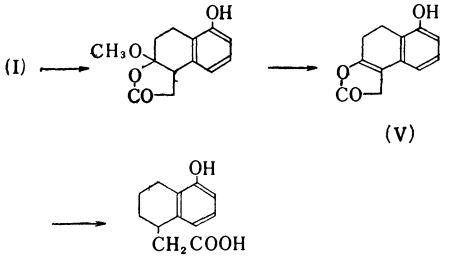
1) T. Matsumoto and A. Suzuki, This Bulletin, in preparation.

2) For example, U. W. Cornforth and R. Robinson, *J. Chem. Soc.*, **1949**, 1861.

3) A. J. Birch and H. Smith, *Quart. Revs.*, **12**, 17 (1958).

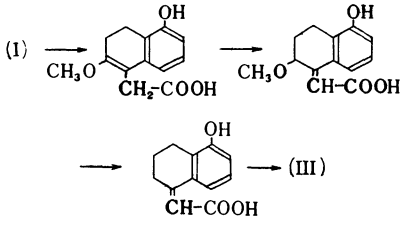
4) A. L. Wilds et al., *J. Am. Chem. Soc.*, **95**, 5360 (1953), have obtained Δ^{9-10}-octahydronaphthalene as a by-product (10~16%) from 5,6,7,8-tetrahydro-1-methoxynaphthalene by reduction with lithium in alcohol-liquid ammonia.

of a carboxyl group, since 1-methyl-2-methoxy-5-hydroxynaphthalene is reported to give smoothly tetrahydro-1-methyl-2-oxo-5-hydroxynaphthalene[5]. On the other hand, Jacobs and Scott[6] have observed that $\beta\gamma$-unsaturated-γ-lactones are susceptible to catalytic hydrogenolysis to form saturated acids, whereas $\alpha\beta$-isomers give saturated lactones on catalytic hydrogenation. The authors are not aware of any example of reductive cleavage of $\beta\gamma$-unsaturated-γ-lactone by means of sodium and alcohol. Nevertheless, it seemed likely at that time that the abnormal reduction proceeds under the participation of the carboxyl group through a $\beta\gamma$-unsaturated-γ-lactone such as V as shown below:



(III)

According to this assumption, treatment of methyl ester of I, rather than I itself, under the same conditions was expected to afford methyl ester of the desired tetralone (II). However, reduction of the methyl ester of I with subsequent hydrolysis gave again the tetralin derivative III as a main product. The above assumption therefore became improbable; the tetralin derivative III might be formed through a process which involves reductive elimination of the allylic methoxyl group as outlined below, but further evidence is required to elucidate the pathway.



The authors next examined the reduction employing sodium and boiling ethanol as well as sodium and ethanol-liquid ammonia (Birch's conditions). In both

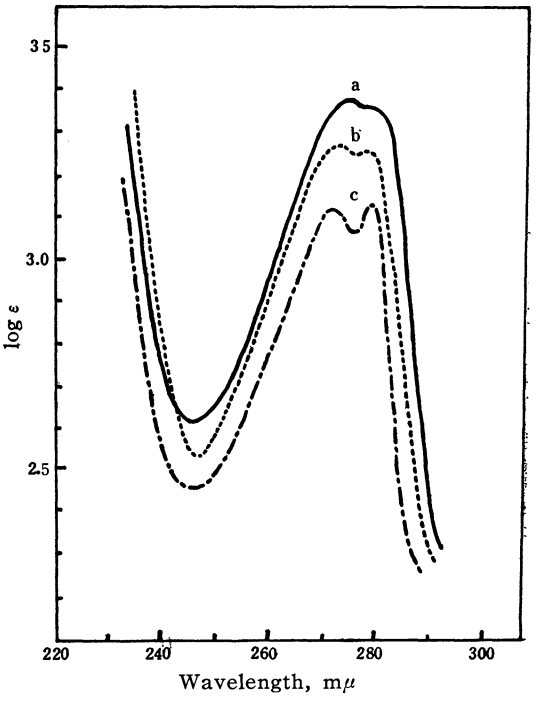


Fig. 2. Ultraviolet spectra.
a (——): 1,2,3,4-Tetrahydro-2-oxo-4,5-dihydroxy-1-naphthylacetic acid (IV) in methanol.
b (------): 1,2,3,4-Tetrahydro-5-hydroxy-1-naphthylacetic acid (III) in methanol.
c (-----): 1,2,3,4-Tetrahydro-5-naphthol in cyclohexane.

cases most of the starting material was recovered, in the former case, probably because of the low reaction temperature and in the latter case, probably owing to the extreme low solubility[7] of the naphthylacetic acid in liquid ammonia. Attempts to reduce I by means of lithium in ethanol-liquid ammonia-dimethoxyethane (Wild's procedure) led to the formation of tetrahydro-5-hydroxy-1-naphthylacetic acid (III) in good yield, even when only 4.7 g. atoms per mol. of lithium was used[8].

Since all efforts to prepare III were thus unsuccessful, attention was turned again to the first method. The reduction was carried out at this time employing a smaller amount than before (8 atoms per mol.) of sodium. From the resulting reaction mixture, an appreciable amount of a carbonyl compound B, m. p. 121.5~123°C was isolated through its triethylamine salt, together with tetrahydro-5-hydroxy-1-naphthylacetic acid (III) and the

5) Ref. 2.
6) W. A. Jacobs and A. B. Scott, *J. Biol. Chem.*, 87, 601 (1930).
7) For similar examples, see Ref. 3.
8) In this case a portion of the starting material was recovered; see *Experimental Section* below.

unchanged starting material I. Elemental analysis of the carbonyl compound B indicated the formula $C_{12}H_{14}O_6$. The infrared spectrum (Fig. 1) of this compound exhibited absorption bands at 3550 and 1635 cm^{-1} (solvated water), which disappear in a sample dried at 80°C in high vacuum, a broad band extending from 3400 to 3200 cm^{-1} (associated OH) and a single broad band at the carbonyl region (probably superimposed carboxyl and carbonyl bands). The ultraviolet spectrum (Fig. 2, curve a) of the hydrated substance showed almost the same shape as those of 1,2,3,4-tetrahydro-5-naphthol (curve c) and 1,2,3,4-tetrahydro-5-hydroxy-1-naphthylacetic acid (III) (curve b).

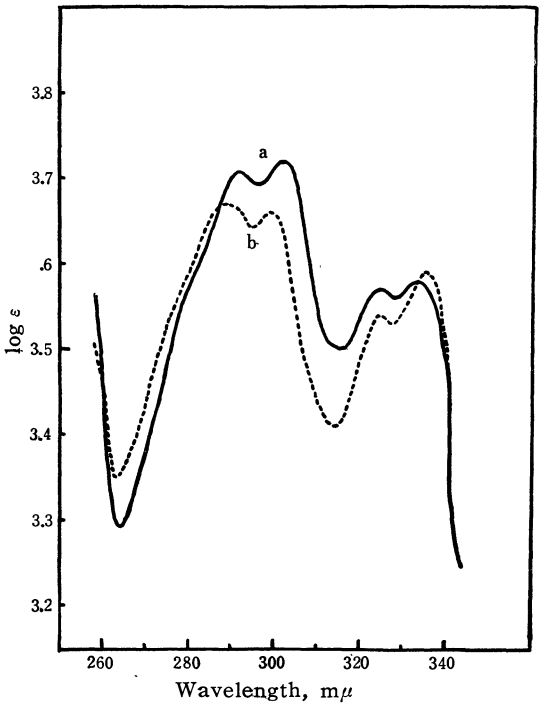


Fig. 3. Ultraviolet spectra in methanol.
a (——): 2-Methoxy-5-hydroxyl-1-naphthylacetic acid (I).
b (------): Methyl 2,5-dihydroxy-1-naphthylacetate (VI).

At this stage the authors supposed that they had the desired product II ($C_{12}H_{12}O_4$) with two moles of water of crystallization at hand, although analytical values for carbon and hydrogen agreed better with $C_{12}H_{14}O_6$. Drying at 80°C in high vacuum was accompanied by decomposition of product B and an analytically pure anhydrous sample could not be obtained. To confirm the above hypothesis, preparation of the methyl ester was then attempted. Contrary to the expectation, treatment with methanolic hydrogen chloride led to two naphthalene derivatives. Presence of the 1-naphthol chromophore in both the products was clearly demonstrated by their ultraviolet spectra. One of the products, $C_{14}H_{14}O_4$, m. p. 155.5~156.5°C, ν_{max}^{nujol} 3420(OH) and 1735 cm^{-1} (ester) exhibited positive Zeisel test and was readily identified with methyl 2-methoxy-5-hydroxy-1-naphthylacetate (VII)[1], which was obtained separately by esterification of I. The other product, $C_{13}H_{12}O_4$, m. p. 183~184°C, ν_{max}^{nujol} 3480 (OH) and 1740 cm^{-1} (ester) was formulated as methyl 2,5-dihydroxy-1-naphthylacetate (VI) on the basis of analytical and spectral data (ultraviolet spectrum; Fig. 3, curve b). Formation of these naphthalene derivatives suggests strongly that product B, $C_{12}H_{14}O_6$, is actually a monohydrate of tetrahydro-2-oxo-5-hydroxy-1-naphthylacetic acid with an additional hydroxyl group on the aliphatic portion. Presence of two hydroxyl groups was proved by the formation of a diacetate, $C_{16}H_{14}O_6$. The infrared spectrum (Fig. 4) of the diacetate showed complete absence of a hydroxyl function and presence of the following groups: $\beta\gamma$-unsaturated-γ-lactone (1795 cm^{-1}), phenyl acetate (1765 cm^{-1}) and saturated ester (1745 cm^{-1}). Therefore, a structural formula like VIII is concluded for this

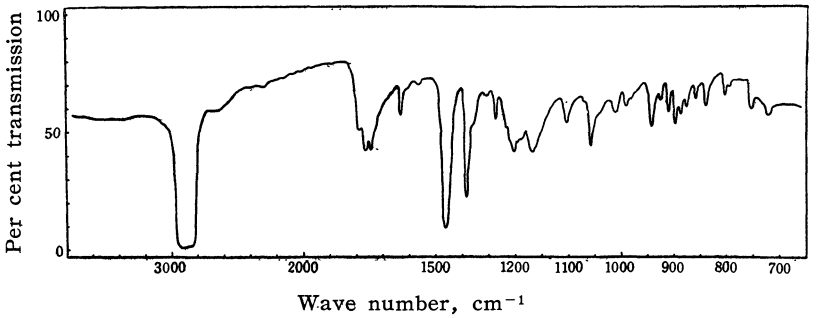
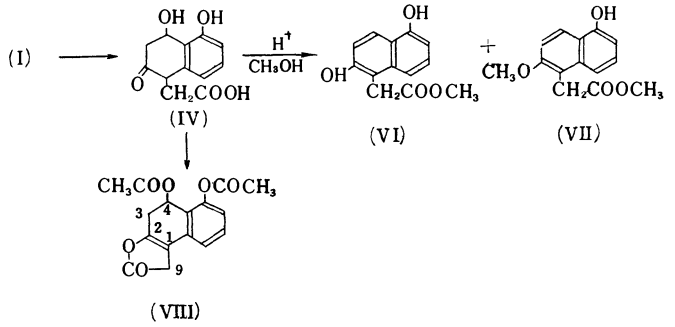


Fig. 4. Infrared spectrum of VIII.



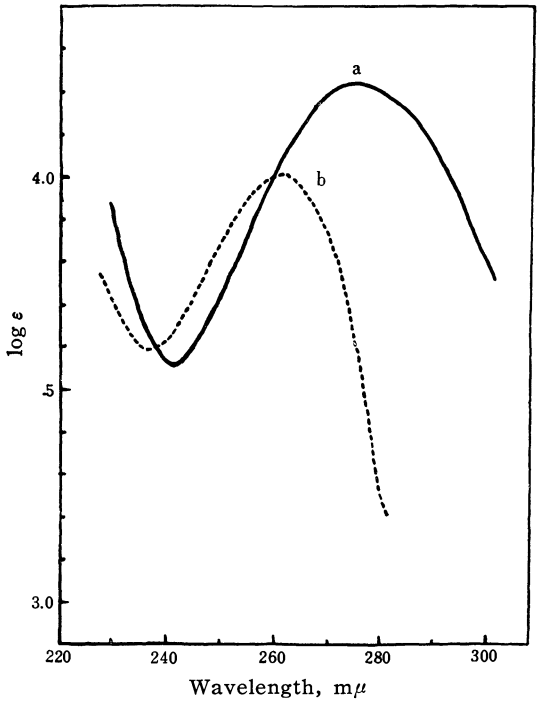
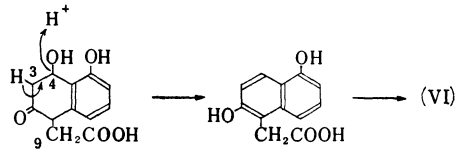


Fig. 5. Ultraviolet spectra.
a (——): VIII in methanol.
b (------): 1,2-Dihydronaphthalene in *n*-hexane.

compound*. The ultraviolet spectrum[9] (Fig. 5, curve a) seems also to agree with this formula. There is a bathochromic shift and an increase in absorption intensity as compared with the spectrum (curve b) of the parent hydrocarbon, 1,2-dihydronaphthalene; these changes can be reasonably ascribed to the presence of an enolic and of a phenolic acyloxy group on the conjugated system.

From formula VIII thus assigned to the diacetate, it follows that two hydroxyl groups (except one hydroxyl group of water of crystallization) are present in product B, and moreover, the hydroxyl group does not occupy the 1-position.

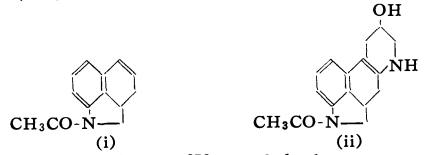
Concerning the position of the aliphatic hydroxyl group in compound B, there remain possibilities of its presence at C_3, C_4 and C_9 positions, of which the C_4 position is the most likely one, since the formation of the naphthalene derivatives[10] is readily explained by a β-elimination reaction:



However, the possibilities of C_3 and C_9 positions can not be conclusively excluded at this stage, since substituents at these positions, being placed respectively at $\alpha\beta$-position to the phenyl and carbonyl groups, are expected to be also susceptible to undergoing an elimination reaction. In the case of C_9 position, subsequent rearrangement of the resultant unsaturated compound would lead to the naphthalene derivatives. The presence of the hydroxyl group at the C_4 position, however, has been demonstrated by the following evidence: product B does not reduce triphenyltetrazolium chloride and hence does not contain an α-ketol system, and moreover, the fact that p*K*a value (6.20) of the product is very close to that (6.12)

* At this stage the position of the alicyclic acetoxyl group is uncertain.

9) Compound i has been reported to possess bands at 241, (ε 22500), 254 (ε 23000), 307 (ε 1600) and 316 (ε 1300) mμ; absorption bands at 252 (ε 2060) and 328 (ε 1500) mμ are recorded for compound ii. E. C. Kornfeld, E. J. Kornfeld, G. B. Kline, M. T. Mann, D. E. Morrison, R. G. Jones and R. B. Woodward, *J. Am. Chem. Soc.*, 78, 3087 (1956).



Low ε max value at 252 mμ of the latter compound is quite unusual.

10) 2-Naphthols are readily methylated by methanol in the presence of acidic catalysts; W. A. Davis, *J. Chem. Soc.*, 77, 33 (1900).

of the tetrahydro-5-hydroxy-1-naphthylacetic acid (III), clearly indicates that the hydroxyl group is not located at the α-position (C_9) relative to carboxylic function. Although the structure of product B has thus been shown to be IV, the mechanism of conversion I→IV is quite obscure. No example of this kind of reaction seems ever to have been recorded. Although it is out of the scope of the authors' immediate purpose to study in detail the reaction process, it may be noted that the effective reagent which causes the conversion seems not to be sodium butoxide, but to be sodium itself; IV could not be obtained by a mere boiling of I in butanolic sodium butoxide solution.

Experimental[11]

Reduction of 2-Methoxy-5-hydroxy-1-naphthylacetic Acid (I) with Sodium and *n*-Butanol.—A solution of I (230 mg.; 0.001 mol.) in butanol (7 cc.) was boiled under reflux in an oil-bath at 120～130°C with stirring, sodium (730 mg.; 0.032 g. atom) was added in small pieces during 15 min. A further quantity of butanol (3 cc.) was then added to dissolve precipitated sodium butoxide. When the sodium had completely dissolved, the mixture was poured into an equal volume of water. The alkaline aqueous layer was separated, extracted twice with ether, acidified with concentrated hydrochloric acid and allowed to stand overnight. The crude reduction product, which separated out, was collected by filtration. When the filtrate was extracted three times with ether and the ether was evaporated, an additional amount of the above product was obtained. Total yield, 130 mg. (63%). After recrystallization from water, product A (tetrahydro-5-hydroxy-1-naphthylacetic acid) had m. p. 144～145°C and exhibited ν_{max}^{nujol} 3200～3400 (OH) and 1700 cm^{-1} (CO_2H). Ultraviolet absorption bands at 272 (log ε 3.27) and 278 mμ (log ε 3.26).

Anal. Found: C, 69.79; H, 6.98. Calcd. for $C_{12}H_{14}O_3$: C, 69.88; H, 6.84%.

1, 2, 3, 4-Tetrahydro-5-acetoxy-1-naphthylacetic Acid.—The above acid (III) (100 mg.) was dissolved in absolute pyridine (1.5 ml.). Pure acetic anhydride (0.5 ml.) was added with shaking and the reaction mixture was set aside overnight. The most of pyridine and excess of acetic anhydride was then evaporated. To the residue was added 2 N hydrochloric acid and the mixture was extracted three times with ethyl acetate. The extract was washed twice with water, dried and evaporated. The solid residue on being crystallized from ligroin afforded 100 mg. (83.5%) of the acetoxy acid. Recrystallization from ligroin gave an analytical sample as colorless needles, m. p. 125～126.5°C, ν_{max}^{nujol} 1750 (phenylacetate) and 1700 cm^{-1} (CO_2H).

Anal. Found: C, 67.74; H, 6.60. Calcd. for $C_{14}H_{16}O_4$: C, 67.73; H, 6.50%.

1, 2, 3, 4-Tetrahydro-2-oxo-4, 5-dihydroxy-1-naphthylacetic Acid (IV).—To a boiling solution of I (1.84 g.; 0.008 mol.) in 40 cc. of butanol, sodium (1.47 g.; 0.064 g. atom) was added rapidly in small pieces during 10 min. with stirring. After the sodium had completely dissolved, the mixture was treated with 40 cc. of water, and the two layers were separated. After the aqueous layer had been washed twice with ether, 8 cc. of concentrated hydrochloric acid was added under ice cooling and the solution was warmed in a water bath at 70～80°C for 30 min. When the mixture had cooled, an oily substance was separated out; the aqueous layer was then extracted three times with ethyl acetate. The oil and the ethyl acetate extract were combined and the whole was washed twice with water, dried with sodium sulfate, and evaporated to dryness. The oily residue (1.82 g.) was then dissolved in 50 cc. of ethyl acetate; to this solution an excess of triethylamine was added in small portions and the solution was allowed to stand for 5 days. At the end of this period, a considerable amount of triethylamine salt and viscous gum precipitated on the bottom of the flask. The solvent was removed by decantation and the viscous gum was removed by washing the residue quickly with a small amount of cold absolute ethanol. The crystalline triethylamine salt thus obtained melted at 152°C with decomposition.

The salt was then dissolved in 5 cc. of water; the solution was acidified with 6 N hydrochloric acid and extracted with ethyl acetate; the extract was washed with water, dried and evaporated. On being triturated with ether, the residue crystallized to furnish crude tetrahydro-2-oxo-4, 5-dihydroxy-1-naphthylacetic acid (IV), which was recrystallized from water as colorless solvated prisms (0.3 g.; 15%), m. p. 121.5～123°C. Ultraviolet absorption band at 274 mμ (log ε 3.38).

Anal. Found: C, 56.92; H, 5.75. Calcd. for $C_{12}H_{12}O_5 \cdot H_2O$: C, 56.69; H, 5.55%.

The viscous part, which was separated from the triethylamine salt of IV, on being acidified with hydrochloric acid afforded a mixture of the starting material and III, which was separated by virtue of higher solubility of the latter compound in water.

Reduction of I by Nelson-Wild's Method.—Sample of compound I (920 mg.; 0.004 mol.) was placed in a three-necked flask equipped with stirrer, dropping funnel and drying tube (soda-lime). To the vessel was added enough anhydrous dimethoxyethane (20 ml.) to dissolve I. The flask was cooled to −40～−50°C. Liquid ammonia (45 ml.) was added to the solution and then lithium (0.5 g.; 0.072 g. atom) in small pieces during 2 min. After stirring for 10 min. absolute

11) All melting points are uncorrected. Infrared spectra were taken on a Koken model DS-301 infrared spectrophotometer with sodium chloride optics. Ultraviolet spectra were measured by means of a Beckman model DK-2 spectrophotometer. The authors are indebted to Mr. O. Yonemitsu of the Pharmaceutical Institute of Hokkaido University for infrared spectra data and to Miss Noriko Fujino for microanalyses.

ethanol was added dropwise for a period of 15 min. When the blue color of the solution had disappeared, ammonia was expelled, the residue was then treated with cold water and acidified with 6 N hydrochloric acid. The acidic aqueous solution was extracted three times with ethyl acetate. After the combined extracts had been washed with saturated sodium chloride solution and dried over sodium sulfate, the solvent was evaporated and the residue was crystallized from water. A yield of 500 mg. (61%) of 1, 2, 3, 4-tetrahydro-5-hydroxy-1-naphthylacetic acid (III) was obtained. Recrystallization from water gave a pure material of m. p. 144~145°C as colorless needles. No depression at the melting point was observed on admixture with the product obtained by the use of sodium and butanol.

When reduction had been effected employing 0.92 g. (0.004 mol.) of compound I, 20 cc. of dimethoxyethane, 50 cc. of ammonia, 0.13 g. (0.0188 mol.) of lithium and 1.2 cc. of ethanol, there were obtained 310 mg. of III and 560 mg. of I. Presence of a small amount of carbonyl compound in the crude reaction product was indicated by the dinitrophenylhydrazine test, but the compound could not be isolated.

Aromatization of Product B.—Sample of product B (210 mg.) was suspended in 5% methanolic hydrogen chloride (10 cc.). The reaction mixture was refluxed on a steam bath for a period of 2 hr. After it had cooled, the solution was evaporated to dryness in vacuo. To the viscous residue were added water and ethyl acetate; the aqueous layer was separated and was re-extracted with ethyl acetate. The combined extracts were washed successively with water, 5% sodium bicarbonate and saturated sodium chloride solution, and dried over anhydrous sodium sulfate. After removal of the solvent, 192 mg. of a solid product was obtained. Crystallization of the product from benzene gave 50 mg. of methyl 2,5-dihydroxy-1-naphthylacetate (VI) with a melting point 180~183°C, which raised to 183~184°C (decomp.) on recrystallization from benzene. Ultraviolet absorption bands at 288 (log ε 3.67), 299 (log ε 3.66), 324 (log ε 3.54) and 335 mμ (log ε 3.59). Infrared spectrum (nujol): 3480 (OH) and 1740 cm^{-1} (ester group).

Anal. Found: C, 67.46; H, 5.51. Calcd. for $C_{13}H_{12}O_4$: C, 67.23; H, 5.21%.

From the above benzene filtrate, after removal of the solvent and crystallization from aqueous methanol, 100 mg. of methyl 2-methoxy-5-hydroxy-1-naphthyl acetate (VII), m. p. 146~149°C, was obtained. An analytical sample, obtained by recrystallization from a small amount of benzene, had m. p. 155.5~156.5°C.

Infrared spectrum[12]: 3400 (OH) and 1720 cm^{-1} (ester group).

Anal. Found: C, 68.15; H, 5.95. Calcd. for $C_{14}H_{14}O_4$: C, 68.28; H, 5.73%.

Acetylation of the Tetralon Derivative (IV).—The keto acid (IV) (47 mg.) was added to a solution of acetic anhydride (0.5 cc.) in anhydrous pyridine (1.5 cc.) and the mixture was allowed to stand overnight. After concentration of the reaction mixture to a small volume, water and 2 N hydrochloric acid were added. The mixture was then shaken three times with ethyl acetate. The organic layers were combined, washed twice with water and dried over sodium sulfate. Removal of the solvent in vacuo left 33 mg. of an oily residue from which on trituration with petroleum ether, 24 mg. of crystalline material was obtained. For analysis the product was recrystallized from benzene, m. p. 176~176.5°C.

Ultraviolet absorption band at 276 mμ (log ε 4.22).

Anal. Found: C, 63.86; H, 4.67. Calcd. for $C_{16}H_{14}O_6$: C, 63.57; H, 4.67%.

Dissociation constants of III and IV were measured at 25°C in 50% ethanol using HRL model M-3 pH meter.

Summary

1,2,3,4-Tetrahydro-5-hydroxy-1-naphthylacetic acid has been obtained from 2-methoxy-5-hydroxy-1-naphthylacetic acid by reduction either with sodium and *n*-butanol, or with lithium and liquid ammonia-ethanol. In the former case, under moderate conditions, 1,2,3,4-tetrahydro-2-oxo-4,5-dihydroxy-1-naphthylacetic acid has been isolated as a by-product.

Department of Chemistry
Faculty of Science
Hokkaido University
Sapporo

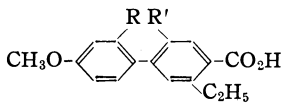
12) In the 1650~1500 cm^{-1} region, the dihydroxynaphthylacetate (VI) absorbs at 1630, 1608, 1590, 1524 cm^{-1}. See Ref. 1.

Estrogenic Biphenyls. VI[1]. *2- and 6'-Alkyl Derivatives of 3'-Ethyl-4-methoxy-biphenyl-4'-carboxylic Acid*

By Takeo SATO and Michinori ŌKI*

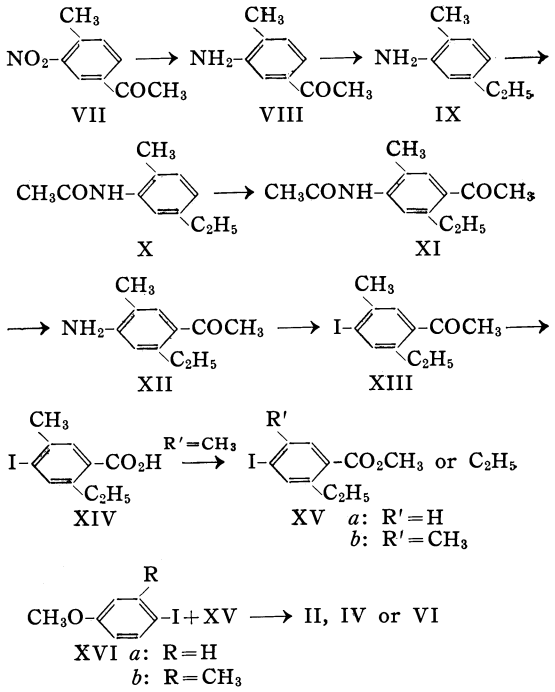
(Received March 16, 1959)

It was reported[2] that 3'-ethyl-4-methoxybiphenyl-4'-carboxylic acid (I) was fully estrogenic at the dose of 250 γ when injected subcutaneously to ovariectomized mice. Introduction of an additional ethyl group into position 2 or 6' of compound I increased the activity to a minimum active dose of 100 γ, thus 2,3'-diethyl-4-methoxybiphenyl-4'-carboxylic acid (III)[3] and 2',5'- (for 3',6')-diethyl-4-methoxybiphenyl-4'-carboxylic acid (V)[4] being the most active members of this series hitherto known. Enhancement of the estrogenic activity in compounds III and V in comparison with compound I was taken as an indication of a favorable molecular conformation in III and V as had already been observed in dialkylstilbestrol dimethyl ethers and related compounds[5]. The ethyl group introduced into position 2 or 6' was found to force the two benzene rings to a non-planar arrangement from the ultraviolet absorption spectra.



	R	R'		R	R'
I	H	H	IV	H	CH_3
II	CH_3	H	V	H	C_2H_5
III	C_2H_5	H	VI	CH_3	CH_3

The present communication deals with further studies on the effect of the 2- and 6'-alkyl substituents on the conformation and on the estrogenic activity of compound I and with the discussion on the relation between the physiological activity and the molecular structure in this series. 3'-Ethyl-4-methoxy-2-methylbiphenyl-4'-carboxylic acid (II) was prepared from 4-iodo-3-methylanisole (XVIb)[6] and ethyl 2-ethyl-4-iodobenzoate (XVa)[3] through the Ullmann reaction. The 6'-methyl isomer, namely, 5'-ethyl-4-methoxy-2'-methylbiphenyl-4'-carboxylic acid (IV), and the 2,6'-dimethyl derivative, namely, 5'-ethyl-4-methoxy-2,2'-dimethylbiphenyl-4'-carboxylic acid (VI), were prepared from methyl 2-ethyl-4-iodo-5-methylbenzoate (XVb) and the corresponding iodoanisoles (XVIa or b). The preparation of the ester XVb is shown in the accompanying diagram.



Modified Wolff-Kishner reduction[7] of 3-amino-4-methylacetophenone (VIII)[8] afforded 5-ethyl-2-methylaniline (IX) in an excellent yield which was acetylated in the usual manner to give 5-ethyl-2-methylacetanilide (X). The acetanilide was treated with acetyl chloride and aluminum chloride in carbon disulfide and resulting 4-acetamido-2-ethyl-5-methylacetophenone (XI) was refluxed with dilute hydrochloric acid to give 4-amino-2-ethyl-

* Present address: Department of Chemistry, Faculty of Science, The University of Tokyo, Hongo, Tokyo.

1) Part V: T. Sato, This Bulletin, **32**, 1130 (1959).
2) T. Sato and M. Ōki, ibid., **30**, 958 (1957).
3) M. Ōki and T. Sato, ibid., **30**, 508 (1957).
4) M. Ōki and T. Sato, ibid., **30**, 702 (1957).
5) M. Ōki and Y. Urushibara, ibid., **25**, 109 (1952).
6) T. Sato and M. Ōki, ibid., **30**, 859 (1957).
7) Huang-Minlon, *J. Am. Chem. Soc.*, **68**, 2487 (1946); **70**, 2802 (1948); **71**, 3301 (1949).
8) I. J. Rinkes, *Rec. trav. chim.*, **64**, 205 (1945).

5-methylacetophenone (XII). Diazotization of the aminoketone XII followed by treatment of the diazonium salt with potassium iodide yielded 2-ethyl-4-iodo-5-methylacetophenone (XIII), which was oxidized with sodium hypobromite to 2-ethyl-4-iodo-5-methylbenzoic acid (XIV). Esterification of compound XIV gave the desired ester XVb.

The ultraviolet absorption data of compounds II, IV and VI are recorded in Table I together with those of compounds I[6], III[4] and V[4]. Compounds II and IV showed the K-band at 272 and 270 mμ, respectively, approximately in the regular intensities characteristic of this system. Hypsochromic shift of some 15 mμ caused by the introduction of the methyl substituent into an ortho position to the pivot bond is the result of an increase in the interplanar angle of the two benzene nuclei to relieve the steric hindrance. The shift is, however, smaller by 2 mμ than in the corresponding compounds with the ethyl group (III and V), and it agrees with the data of the present authors[6] and others[9]. It is noteworthy that the 6′-alkyl derivative of compound I gives an absorption maximum at a shorter wavelength than the 2-alkyl derivative whether the alkyl is methyl or ethyl. The result is in good agreement with the idea of hyperconjugation of the alkyl group with the carboxyl group through the benzene nucleus, with which the 2-alkyl derivative is favored[10]. In the 2,6′-dimethyl derivative (VI), no K-band maximum was found in the region examined but a shoulder at ca. 270 mμ was noticed. This is undoubtedly caused by further deterioration in conjugation of the biphenyl skeleton.

TABLE I. ULTRAVIOLET ABSORPTION MAXIMA[a] AND ESTROGENIC ACTIVITIES OF 2- AND 6′-ALKYL DERIVATIVES OF 3′-ETHYL-4-METHOXYBIPHENYL-4′-CARBOXYLIC ACID

Compound	λ, mμ	log ε	Active dose in mice, γ
I	286	4.36	250
II	272	4.13	100
III	270	4.09	100
IV	270	4.17	100[c]
V	268	4.14	100
VI	~270[b]	3.92	500

a) In 95% ethanol. b) ~: Indicates a shoulder. c) Active in 80% animals.

9) E. A. Braude, F. Sondheimer and W. F. Forbes, *Nature*, **173**, 117 (1954).
10) M. Ōki and H. Iwamura, unpublished work; also see Ref. 1.

The physiological data in Table I were obtained by the usual vaginal smear test with ovariectomized mice. The activities of the compounds with a methyl group were nearly the same as those with an ethyl group at the same position. The estrogenic potency is surely raised by the introduction of an alkyl group into position 2 or 6′, but again no difference due to the change in the alkyl group was observed. Although the minimum active dose of compound VI to produce estrus in 100% animals was found to be 500 γ, it is not certain whether the excessive thickness of the molecule as indicated by the greater deterioration in conjugation really weakened the estrogenic activity of this compound, because it was active in 80% animals at 100 γ.

Experimental[11]

5-Ethyl-2-methylacetanilide (X).—A mixture of 149 g. (1 mol.) of 3-amino-4-methylacetophenone (VIII), obtained from 3-nitro-4-methylacetophenone (VII) according to Rinkes[8], 69 g. (1.1 mol.) of 80% hydrazine hydrate, 280 g. of potassium hydroxide and 1 kg. of diethylene glycol, was heated under reflux for two hours. Then the low boiling fraction was distilled off until the pot temperature reached 180°C. After the remaining mixture was refluxed for further three hours, the whole was steam-distilled and the distillate was combined with the low boiling fraction collected previously. The combined distillate was extracted with ether and the extract was dried over potassium carbonate. 5-Ethyl-2-methylaniline (IX) was obtained as a colorless liquid boiling at 78~79°C/3 mm. in 90% yield. The acetanilide X was obtained by acetylation with acetic anhydride, m. p. 136~137°C. The reported melting point is 138°C[8].

4-Acetamido-2-ethyl-5-methylacetophenone (XI).—To a well stirred suspension of 165 g. (0.93 mol.) of compound X in 78 g. (1 mol.) of acetyl chloride and 750 ml. of carbon disulfide, was added 415 g. (3.1 mol.) of anhydrous aluminum chloride in small portions in the course of one hour, while the mixture was gently refluxed. It was refluxed for another hour and then allowed to stand for two hours. The upper layer was decanted off and the viscous oil was decomposed with ice water and hydrochloric acid. The crystals were collected and recrystallized from aqueous ethanol to give 170 g. (79% yield) of colorless needles, m. p. 139~140°C.

Anal. Found: N, 6.56. Calcd. for $C_{13}H_{17}NO_2$: N, 6.39%.

4-Amino-2-ethyl-5-methylacetophenone (XII).—The acetamido compound XI was hydrolyzed with 1:1 aqueous hydrochloric acid. Colorless needles, m. p. 105~106°C, were obtained on recrystallization from benzene-petroleum ether.

11) All melting and boiling points are uncorrected.

Anal. Found: N, 8.22. Calcd. for $C_{11}H_{15}NO$: N, 7.91%.

2-Ethyl-4-iodo-5-methylacetophenone (XIII).—To a diazonium salt solution obtained from 32 g. (0.18 mol.) of compound XII, 39 ml. of concentrated sulfuric acid, 54 ml. of water and 13 g. (0.19 mol.) of sodium nitrite in a minimum quantity of water, was added a solution of 31 g. (0.19 mol.) of potassium iodide in a small amount of water. Stirring was continued for 30 min. at a low temperature and then at 50~60°C for two hours. The mixture was extracted with ether and the extract was washed with aqueous sodium hydroxide, aqueous sodium thiosulfate and water. The iodoacetophenone was obtained in a 50% yield as a brown oil boiling at 127~128°C/2.5 mm. On standing it solidified and colorless needles melting at 51~52°C were obtained on recrystallization from petroleum ether.

Anal. Found: I, 43.88. Calcd. for $C_{11}H_{13}IO$: I, 44.08%.

2,4-Dinitrophenylhydrazone.—It was obtained as orange needles, m. p. 165~166°C, on recrystallization from ethyl acetate.

Anal. Found: N, 11.54. Calcd. for $C_{18}H_{19}IN_4O_4$: N, 11.62%.

2-Ethyl-4-iodo-5-methylbenzoic Acid (XIV).—To a well stirred sodium hypobromite solution prepared from 28 g. (0.18 mol.) of bromine, 20 g. (0.50 mol.) of sodium hydroxide and 120 ml. of water, was added a solution of 17 g. (0.057 mol.) of compound XIII in 60 ml. of dioxan in one hour. The temperature was kept below 10°C during the addition and then at 50~60°C for one hour. After excessive hypobromite was decomposed with sodium sulfite, the whole was steam-distilled. The remaining solution was acidified with hydrochloric acid and the product was recrystallized from aqueous ethanol. Colorless needles, m. p. 157~158°C, were obtained in 90% yield.

Anal. Found: I, 44.41. Calcd. for $C_{10}H_{11}IO_2$: I, 43.77%.

Methyl 2-Ethyl-4-iodo-5-methylbenzoate (XVb).—The acid XIV was esterified in the usual manner. The ester, b. p. 125°C/2.5 mm., was obtained in a 78% yield.

Anal. Found: I, 42.08. Calcd. for $C_{11}H_{13}IO_2$: I, 41.76%.

3'-Ethyl-4-methoxy-2-methylbiphenyl-4'-carboxylic Acid (II).—With vigorous stirring 15 g. (0.24 atom) of copper bronze activated by Kleiderer and Adams' method[12] was added in small portions to a mixture of 9 g. (0.036 mol.) of 4-iodo-2-methylanisole (XVIb) and 5 g. (0.016 mol.) of ethyl 2-ethyl-4-iodobenzoate[3] over a period of 30 min., while the temperature was maintained at 215~220°C. The mixture was then heated to 280~285°C and was stirred for 30 min. at that temperature. After cooling, the whole was extracted with boiling acetone and the extract was refluxed with 40 ml. of 10% aqueous sodium hydroxide and 70 ml. of ethanol for two hours. A part of ethanol was removed by distillation and the residue was diluted with water to make up 500 ml. and an insoluble oil was removed by extraction with ether. The aqueous layer was acidified with hydrochloric acid and the acid mixture thus collected was extracted with hot benzene. On concentration of the solution it afforded a crude product, which on repeated recrystallization from aqueous ethanol gave 500 mg. of colorless needles melting at 150.5~151°C.

Anal. Found: C, 75.32; H, 6.80. Calcd. for $C_{17}H_{18}O_3$: C, 75.53; H, 6.71%.

5'-Ethyl-4-methoxy-2'-methylbiphenyl-4'-carboxylic Acid (IV).—The Ullmann reaction was carried out in the same way as described above with 15 g. (0.064 mol.) of 4-iodoanisole (XVIa), 9 g. (0.030 mol.) of methyl 2-ethyl-4-iodo-5-methylbenzoate (XVb) and 20 g. (0.32 atom) of activated copper bronze. The temperature for the addition of copper bronze was 230~240°C and then raised to 280~290°C. The acidic portion was digested with ether and the ethereal solution was passed through an alumina column. The elute was evaporated and repeated recrystallization of the residue from ethanol gave colorless needles melting at 188~189°C. It weighed 900 mg.

Anal. Found: C, 75.35; H, 6.51. Calcd. for $C_{17}H_{18}O_3$: C, 75.53; H, 6.71%.

5'-Ethyl-4-methoxy-2,2'-dimethylbiphenyl-4'-carboxylic Acid (VI).—The reaction was carried out in the same way as described for the preparation of II, with 18 g. (0.073 mol.) of compound XVIb, 10 g. (0.033 mol.) of compound XVb and 30 g. (0.47 atom) of activated copper bronze. The reaction temperatures were the same as in the preparation of IV. The acetone extract was distilled under reduced pressure to remove any unchanged materials, and the distillate up to 190°C/5 mm. was discarded. Colorless plates, melting at 127~128°C after recrystallization from ethanol-water, were obtained by handling the residue of vacuum distillation as described before. It weighed 600 mg.

Anal. Found: C, 76.27; H, 7.39. Calcd. for $C_{18}H_{20}O_3$; C, 76.03; H, 7.09%.

Ultraviolet Absorption Spectra.—The ultraviolet absorption spectra were measured with a Hitachi photo-electric spectrophotometer Model EPU-2. The samples were dissolved in 95% ethanol.

The authors wish to express their hearty thanks to Professor Y. Urushibara, the University of Tokyo, and Professor K. Hata, Tokyo Metropolitan University, for encouragement throughout this work, and to the Research Department of Teikoku Hormone Manufacturing Co., Kawasaki, for bioassays. The authors' thanks are also due to the Ministry of Education for the Grant in Aid for Fundamental Research.

Department of Chemistry
Faculty of Science
Tokyo Metropolitan University
Setagaya-ku, Tokyo

12) E. C. Kleiderer and R. Adams, *J. Am. Chem. Soc.*, **55**, 4219 (1933).

Estrogenic Biphenyls. VII. Preparation and Estrogenic Action of Methoxyl Derivatives of 4-Methoxybiphenyl-4'-carboxylic Acid

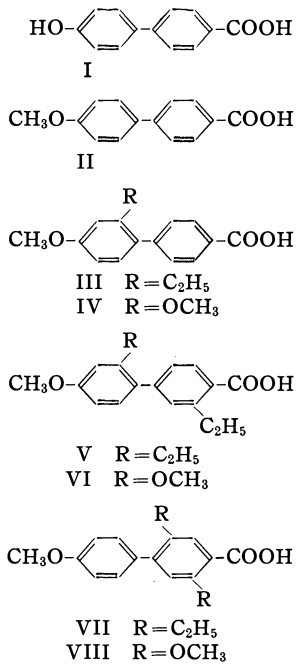
By Takeo SATO

(Received April 20, 1959)

In the study on the relation between the estrogenic activity and the molecular structure it has been found that in 4-hydroxybiphenyl-4'-carboxylic acid (I) and its methyl ether (II) the introduction of alkyl groups into suitable positions of the biphenyl skeleton increases the activity[1-6]. That the introduction of alkyl groups into position 2 or 2' of 4-methoxybiphenyl-4'-carboxylic acid (II) largely modifies the otherwise planar conformation of the biphenyl skeleton is apparent from the ultraviolet absorption spectra. The enhancement of the activity caused by the alkyl groups is explained on the basis of the steric effect of the alkyl groups, which makes the molecular structure or the conformation more suitable for the development of the physiological activity.

The minimum active doses of typical compounds of this series were found to be as follows: The parent compound II[3] was active only in 50% of ovariectomized mice at the dose of 1 mg., while full estrus was produced in 100% animals by a dose of 500 γ of compound III[3] and by 100 γ of either compound V[1] or compound VII[2]. The substances with a methyl or a propyl group in place of the ethyl group in compound III showed an activity similar to that of compound III in contrast to the case of the stilbene series[7]. This may be understood, when the similar ultraviolet absorption spectra of these homologous compounds are interpreted as the indication of their similar basic biphenyl skeletons which are not altered by the chain length of the straight-chain alkyl groups at position 2[2,3,8].

It was not explained, however, that the estrogenic activity of 2,2'-disubstituted



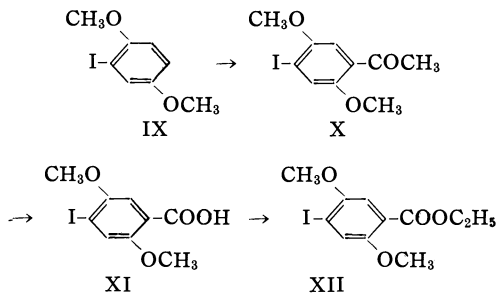
derivatives[5,6], whose ultraviolet spectra differed markedly from those of the monoalkyl derivatives in missing the characteristic K-band in the region examined, was nearly the same as that of the monoalkyl derivatives. The fact was striking because the physiological activity such as estrogenic activity is considered to be very sensitive even to a slight deformation of the structure.

In this connection it is interesting to prepare the alkoxyl analogues in which the alkoxyl group will take the same arrangement as alkyl groups but will produce less steric hindrance. The present communication describes the preparation of three such methoxyl analogues, IV, VI and VIII. The effect of the replacement of the alkyl group by the methoxyl group on the estrogenic activity may be compared with the case of the methoxyl analogues of hexestrol. Takahashi reported that 1, 2-dimethoxy-1,2-bis-(*p*-hydroxyphenyl)-ethane was fully active at 0.5 γ while the ethoxyl analogue was so at

1) M. Ōki and T. Sato, This Bulletin, **30**, 508 (1957).
2) M. Ōki and T. Sato, ibid., **30**, 702 (1957).
3) T. Sato and M. Ōki, ibid., **30**, 859 (1957).
4) T. Sato and M. Ōki, ibid., **30**, 958 (1957).
5) T. Sato, ibid., **32**, 1130 (1959).
6) T. Sato and M. Ōki, ibid., **32**, 1289 (1959).
7) M. Ōki, *J. Chem. Soc. Japan, Pure Chem. Sec.* (*Nippon Kagaku Zasshi*), **73**, 252 (1952); M. Ōki and Y. Urushibara, This Bulletin, **25**, 109 (1952).
8) E. A. Braude, F. Sondheimer and W. F. Forbes, *Nature*, **173**, 117 (1954).

10 γ[9]. The compound in which only one of the ethyl groups of hexestrol was replaced by a methoxyl group was less active than the dimethoxyl compound[10].

2,4-Dimethoxybiphenyl-4'-carboxylic acid (IV) was prepared by the Ullmann reaction of 2,4-dimethoxyiodobenzene and ethyl 4-iodobenzoate. The 2-methoxyl analogue (VI) of 2,3'-diethyl-4-methoxybiphenyl-4'-carboxylic acid (V), one of the most active members of the alkyl series, was prepared from 2,4-dimethoxyiodobenzene and ethyl 2-ethyl-4-iodobenzoate[1] through the same method. 2',4,5'-Trimethoxybiphenyl-4'-carboxylic acid (VIII), the totally methoxylated analogue of the diethyl compound VII, was obtained from 4-iodoanisole and ethyl 4-iodo-2,5-dimethoxybenzoate (XII), which was prepared by the following reaction sequence:



2,5-Dimethoxyiodobenzene (IX), prepared either from hydroquinone dimethyl ether by direct iodination or from 2,5-dimethoxyaniline by diazo reaction, was treated with acetyl chloride and aluminum chloride in carbon disulfide. 4-Iodo-2,5-dimethoxyacetophenone (X), thus produced, was oxidized with sodium hypobromite to give the corresponding benzoic acid XI, which was esterified to XII in the usual manner. Attempted Friedel-Crafts reaction of 2,5-dimethoxyacetanilide in carbon disulfide with the aim of obtaining 4-acetamido-2,5-dimethoxyacetophenone, which might be another intermediate for the preparation of XII, failed and the starting material was recovered.

The estrogenic activities were determined by the vaginal smear test with ovariectomized mice, substances in oil solution being injected subcutaneously. Compound IV was found active at 400 γ, while the corresponding ethyl compound (III) at 500 γ, as stated above. Compound VI was active only to 20% of the test animals at 100 γ, while the corresponding diethyl compound (V) was fully estrogenic at this level. The same situation is also observed in 2',5'-disubstituted compounds. Namely, while the 2',5'-diethyl compound (VII) was active equally to compound V, the 2',5'-dimethoxyl analogue (VIII) was active to 40% of the animals even at 200 γ. Although these 2-methoxyl compounds may be represented by thinner structural models than the corresponding alkyl compounds, the weaker activities of the former may be attributed to the thinner structures only with a reserve, since the direct physiological effect of the methoxyl group itself is obscure.

Experimental*

2,4-Dimethoxybiphenyl-4'-carboxylic Acid (IV).—With good stirring, 15 g. (0.057 mol.) of 2,4-dimethoxyiodobenzene, prepared by iodination of resorcinol dimethyl ether with iodine and yellow mercuric oxide according to Kauffmann and Kieser[11], and 5 g. (0.018 mol.) of ethyl 4-iodobenzoate were heated to 230°C and 15 g. (0.24 atom) of activated copper bronze[12] was added in small portions over a period of twenty minutes, while the temperature was maintained at 230~250°C. When the addition was over, the reaction mixture was heated to 280~290°C and kept at that temperature for thirty minutes. The acetone extract was subjected to vacuum distillation and the distillate up to 120°C/5 mm. was discarded. The residue was hydrolyzed with aqueous-alcoholic alkali and tetramethoxybiphenyl was removed by filtration. Acidification of the aqueous solution gave a crude product, which was extracted with hot acetic acid, and the substance obtained from the extract was recrystallized from ethanol to yield 1 g. of colorless plates melting at 199~200°C.

Anal. Found: C, 69.39; H, 5.99. Calcd. for $C_{15}H_{14}O_4$: C, 69.75; H, 5.46%.

3'-Ethyl-2,4-dimethoxybiphenyl-4'-carboxylic Acid (VI).—In the same way as described for the preparation of compound IV, 11 g. (0.042 mol.) of 2,4-dimethoxyiodobenzene and 5.5 g. (0.018 mol.) of ethyl 2-ethyl-4-iodobenzoate[1] were condensed with 15 g. (0.24 atom) of activated copper bronze. The acetone extract was concentrated until the temperature of the distilling vapor reached 152°C at 5 mm. The crude acid, obtained by hydrolysis of the product, was extracted with hot benzene. Repeated recrystallization from ethanol gave 200 mg. of colorless needles melting at 187~187.5°C.

Anal. Found: C, 71.24; H, 6.10. Calcd. for $C_{17}H_{18}O_4$: C, 71.31; H, 6.34%.

9) T. Takahashi, *J. Chem. Soc. Japan, Pure Chem. Sec.* (*Nippon Kagaku Zasshi*), **73**, 765 (1952); Y. Urushibara and T. Takahashi, This Bulletin, **23**, 53 (1950).
10) T. Takahashi, *J. Chem. Soc. Japan, Pure Chem. Sec.* (*Nippon Kagaku Zasshi*), **73**, 629 (1952).

* All boiling and melting points are uncorrected. The author is indebted to Mr. T. Mizushima for carrying out the microanalyses.
11) H. Kauffmann and F. Kieser, *Ber.*, **45**, 2333 (1912).
12) E. C. Kleiderer and R. Adams, *J. Am. Chem. Soc.*, **55**, 4219 (1933).

2,5-Dimethoxyiodobenzene. — Hydroquinone dimethyl ether was iodinated with iodine and mercuric oxide[13]. It was also prepared[14] from 2,5-dimethoxyaniline by diazotization followed by decomposition in the presence of potassium iodide.

4-Iodo-2, 5-dimethoxyacetophenone (X).—To a well stirred mixture of 100 ml. of carbon disulfide and about one fifth of 33 g. (0.25 mol.) of powdered aluminum chloride was added dropwise a solution consisting of 16 g. (0.20 mol.) of acetyl chloride and 50 g. (0.19 mol.) of 2, 5-dimethoxyiodobenzene in the course of thirty minutes, while the rest of the aluminum chloride was added occasionally through another opening of the flask. The reaction mixture was gently refluxed for one hour and then poured into ice water containing hydrochloric acid. The carbon disulfide layer was concentrated and the residue was extracted with ether. The ethereal solution was successively washed with water, aqueous alkali, sodium thiosulfate and again water. Evaporation of the solution afforded 15 g. (26% of the theoretical) of light brown needles melting at 98～99°C on recrystallization from ethanol.

Anal. Found: C, 39.28; H, 3.60. Calcd. for $C_{10}H_{11}O_3I$: C, 39.23; H, 3.62%.

The 2, 4-Dinitrophenylhydrazone was obtained as deep-orange plates, m. p. 210～212°C, on recrystallization from ethyl acetate.

Anal. Found: N, 11.72. Calcd. for $C_{16}H_{15}O_6N_4I$: N, 11.53%.

4-Iodo-2, 5-dimethoxybenzoic Acid (XI).—To a sodium hypobromite solution, prepared by dropping 21 g. (0.13 mol.) of bromine into 15 g. (0.38 mol.) of sodium hydroxide in 130 ml. of water below 0°C, was added 14 g. (0.046 mol.) of compound X dissolved in 50 ml. of dioxan over a period of one hour, the temperature being kept below 20°C. After the excessive hypobromite was decomposed with sodium bisulfite, the whole was steam-distilled and the remainder was acidified with hydrochloric acid. Colorless needles melting at 175～177°C were obtained on recrystallization of the product from ethanol. Yield, 10 g. or 71% of the theoretical.

Anal. Found: C, 35.25; H, 3.00. Calcd. for $C_9H_9O_4I$: C, 35.09; H, 2.94%.

Ethyl 4-Iodo-2, 5-dimethoxybenzoate (XII).—A solution of 5 g. (0.016 mol.) of compound XI in 50 ml. of ethanol, saturated with dry hydrogen chloride, was heated under reflux for five hours. After the solvent was removed the residue was diluted with water and extracted with ether. The ethereal solution was successively washed with water, sodium bicarbonate solution, sodium thiosulfate solution and again water. Colorless plates melting at 65～66°C were obtained on recrystallization from petroleum ether. Yield, 5 g. or 93% of the theoretical.

Anal. Found: C, 39.30; H, 3.95. Calcd. for $C_{11}H_{13}O_4I$: C, 39.30; H, 3.90%.

2', 4, 5'-Trimethoxybiphenyl-4'-carboxylic Acid (VIII).—The Ullmann reaction was carried out in the same way as described for the preparation of compound IV, using 8 g. (0.034 mol.) of 4-iodoanisole, 5 g. (0.015 mol.) of compound XII and 15 g. (0.24 atom) of activated copper bronze. The acidic part was extracted with hot benzene and the extract was concentrated to yield 200 mg. of colorless plates melting at 142～143°C.

Anal. Found: C, 66.84; H, 5.48. Calcd. for $C_{16}H_{16}O_5$: C, 66.66; H, 5.59%.

The author wishes to express his hearty thanks to Professor K. Hata, Tokyo Metropolitan University, and Professors Y. Urushibara and M. Ōki, the University of Tokyo, for their kind guidance and encouragement and to the Research Department of Teikoku Hormone Manufacturing Co., Ltd., Kawasaki, for bioassays. The author's thanks are also due to the Ministry of Education for the Grant in Aid for Fundamental Scientific Research.

Department of Chemistry
Faculty of Science
Tokyo Metropolitan University
Setagaya-ku, Tokyo

13) H. Kauffmann and I. Fritz, *Ber.*, **41**, 4413 (1908).
14) F. Ullmann et al., *Ann.*, **332**, 38 (1904).

Synthesis and Physical Properties of Normal Higher Alcohols. I. Synthesis of Normal Higher Primary Alcohols of Odd Carbon Numbers from Undecanol to Pentacosanol

By Akira WATANABE*

(Received March 17, 1959)

As part of a broad program of investigating the synthesis and physical properties of long chain compounds, the present author has taken up normal primary alcohols. Since Müller[1] reported an X-ray investigation of a series of normal paraffins, a phenomenon of phase transitions in the solid state of long chain compounds has drawn much attention of chemists and physicists.

Although several communications dealing with the transition phenomenon of long chain compounds have appeared in the literature, higher alcohols have not been studied as fully as paraffins and consequently the results are rather fragmentary and somewhat ambiguous. Moreover, only few reports are found on the alcohols with odd carbon numbers and more than eighteen carbon atoms[2]. A reason for this may have been the difficulty of obtaining a series of higher alcohols in high purity. Therefore, it is desirable to investigate in more detail and more systematically the synthesis and the physical properties of the series of alcohols. From this point of view, the author has undertaken to synthesize alcohols having more than ten carbon atoms and in this paper the preparation of higher alcohols of odd carbon numbers from undecanol $C_{11}H_{23}OH$ to pentacosanol $C_{25}H_{51}OH$ is reported.

Until recently, all the alcohols up to hexatriacontanol $C_{36}H_{73}OH$ have been synthesized by other workers for the purpose of making comparison with naturally occurring products. In the present investigation, the three synthetic routes were chosen depending upon the availability of starting materials and close attention was paid to obtain the products having sufficient purity for physical studies.

(A) $RCO_2H \rightarrow RCO_2Ag \xrightarrow[(\text{in } CCl_4)]{Br_2} RBr \xrightarrow{CH_3CO_2Ag} CH_3CO_2R \xrightarrow{H_2O} ROH$

(B) $RCO_2H \xrightarrow{SOCl_2} RCOCl \xrightarrow{CH_2N_2} RCOCHN_2 \xrightarrow[(\text{in } CH_3OH)]{Ag_2O} RCH_2CO_2CH_3 \xrightarrow{LiAlH_4} RCH_2CH_2OH$

(C) $C_2H_5O_2C(CH_2)_5Br \xrightarrow{\text{Ethyl malonate}}$

(I)

$C_2H_5O_2C(CH_2)_5CH(CO_2C_2H_5)_2 \xrightarrow[Na]{C_6H_5CH_2OH}$

(II)

$C_6H_5CH_2O_2C(CH_2)_5CNa(CO_2CH_2C_6H_5)_2 \xrightarrow{RCOCl}$

(III)

$C_6H_5CH_2O_2C(CH_2)_5C(CO_2CH_2C_6H_5)_2COR \xrightarrow[2.-CO_2]{1.\ H_2}$

(IV)

$RCO(CH_2)_6CO_2H \xrightarrow{\text{Huang-Minlon reduction}}$

(V)

$R(CH_2)_7CO_2H \rightarrow R(CH_2)_7CO_2C_2H_5$

(VI) (VII)

$\xrightarrow{LiAlH_4} R(CH_2)_8OH$

(VIII)

Undecanol $C_{11}H_{23}OH$, tridecanol $C_{13}H_{27}OH$, pentadecanol $C_{15}H_{31}OH$, heptadecanol $C_{17}H_{35}OH$ and heneicosanol $C_{21}H_{43}OH$ were prepared by method A. The process of degradative bromination of silver salts of fatty acids is the well known Hunsdiecker reaction[3]. The alkyl bromides obtained by this method were heated with silver acetate at 150°C without a solvent to yield the acetyl compounds which were converted into the desired alcohols by hydrolysis with alcoholic potassium hydroxide. Overall yields were about 40%.

Nonadecanol $C_{19}H_{39}OH$ was prepared by the Arndt-Eistert reaction (method B) from stearic acid. Stearoyl chloride, obtained from stearic acid and thionyl chloride, and diazomethane in ether gave

* Some parts of this work were perfomed of Department of Chemisty, Faculty of Science, Kyoto University Sakyo-ku, Kyoto.

1) A. Müller, *Proc. Roy. Soc.*, A138, 514 (1932).

2) Review of the literature is presented in a paper by Kakiuchi et al., *J. Phys. Soc. Japan*, 75, 291 (1950).

3) H. Hunsdiecker and Cl. Hunsdiecker, *Ber.*, 75, 291 (1942).

TABLE I. ALCOHOLS

Alcohols	Formula	Analyses, %. Calcd. C	Calcd. H	Found C	Found H	m. p.*, °C		t. p.**, °C
Undecyl	$C_{11}H_{24}O$	76.67	14.04	76.55	13.19	14.0	14.3[a]	—
Tridecyl	$C_{13}H_{28}O$	77.93	14.09	77.80	13.93	30.5	30.5[b]	27.7
Pentadecyl	$C_{15}H_{32}O$	78.87	14.12	79.11	14.17	45.0	45.0[c]	38.0
Heptadecyl	$C_{17}H_{36}O$	79.61	14.15	79.47	14.23	54.0	54.0[d]	46.0
Nonadecyl	$C_{19}H_{40}O$	80.20	14.17	80.38	14.12	62.5	63.0[e]	51.0
Heneicosyl	$C_{21}H_{44}O$	80.69	14.19	80.53	14.10	69.0	69.0[e]	55.0
Tricosyl	$C_{23}H_{48}O$	81.10	14.20	81.30	14.14	72.5	73.1[f]	63.0
Pentacosyl	$C_{25}H_{52}O$	81.44	14.21	81.45	14.16	77.5	77.3[f]	68.0

* Melting points are uncorrected.

** When a sample is cooled below its freezing point, transition appears with change of the transparent waxy material into an opaque crystalline state.

a) R. Robinson, *J. Chem. Soc.*, **125**, 229 (1924).
b) J. Blau, *Monatshe. Chem.*, **26**, 106 (1905).
c) E. Jeffreys, *Am. Chem. J.*, **22**, 28 (1899).
d) P. A. Leven et al., *J. Boil. Chem.*, **20**, 531 (1915).
e) P. A. Leven et al., ibid., **59**, 915 (1924).
f) S. Shiina, *J. Soc. Chem. Ind., Japan* (*Kōgyō Kwagaku Zassi*), **39**, 345 (1936).

TABLE II. FATTY ACIDS

Acids	m. p., °C	Acid value Expt.	Acid value Calcd.	Iodine value	Methyl esters m. p., °C	Methyl esters b. p., °C
Lauric	43.0	279.0	280.2	0	—	110/4 mm.
Myristic	53.5	244.2	245.8	0	18.0	140/4 mm.
Palmitic	62.3	218.6	219.0	0.02	29.0	160/5 mm.
Stearic	69.6	196.5	197.4	0	38.5	178/4 mm.
Behenic	79.5	164.0	164.9	0.1	48.0*	185/1.8 mm.

* Ethyl ester.

diazononadecanone which had been synthesized by Grundmann previously[4]. The conversion of the diazoketone into methyl nonadecanoate with silver oxide in methanol was carried out easily. The ester was reduced with lithium aluminum hydride to nonadecanol in almost quantitative yield.

Method C which was used for the synthesis of tricosanol $C_{23}H_{47}OH$ and pentacosanol $C_{25}H_{51}OH$ is analogous to that of Bowman's ketone synthesis[5]. Ethyl *n*-hexane-1,1,6-tricarboxylate (II) which served as the starting material was prepared from ethyl malonate and ethyl bromocaproate which was obtained from cyclohexanone by the method of Brown[6]. Benzyl *n*-hexane-1,1,6-tricarboxylate derived from the ethyl ester by transesterification with benzyl alcohol was condensed with palmitoyl chloride or stearoyl chloride, to give, after hydrogenation and decarboxylation, 8-ketotricosanoic acid or 8-ketopentacosanoic acid. Reduction to the corresponding fatty acid by Huang-Minlon's method[7] was efficient. Ethyl tricosanoate and ethyl pentacosanoate were readily reduced to the desired alcohols with lithium aluminum hydride.

The physical constants and analytical data of the alcohols are given in Table I together with those reported by other workers who had previously synthesized them by different methods. The transition points of C_{19}, C_{21}, C_{23}, C_{25} alcohols were unknown.

Since it is known that sometimes minor impurities, especially homologues, have a marked influence on the transition behavior of long chain compounds, it was felt necessary to obtain the starting fatty acids in high purity. Commercial fatty acids such as lauric, myristic, palmitic, stearic,

4) C. Grundmann, *Ann.*, **524**, 37 (1936).
5) R. E. Bowman, *J. Chem. Soc.*, **1950**, 174.
6) G. B. Brown and C. W. H. Partridge, *J. Am. Chem. Soc.*, **66**, 839 (1944).
7) Huang-Minlon, ibid., 68, 2487 (1946).

and behenic acids were obtained in a pure state by fractionation of the methyl ester through four feet Fenske column followed by saponification and recrystallization. Physical constants and analytical data of these fatty acids are given in Table II.

Experimental

Undecanol, Tridecanol, Pentadecanol, Heptadecanol and Heneicosanol.—These alcohols were prepared from the corresponding fatty acids by method A involving Hunsdiecker's reaction[3]. A typical example is given for the preparation of heneicosanol.

Silver behenate: $C_{21}H_{43}CO_2Ag$—A solution of 20 g. of potassium behenate in 200 ml. of ethanol was stirred on a steam bath while a solution of 13 g. of silver nitrate in 50% aqueous ethanol was added dropwise. The resulting bulky white precipitate was collected on a filter, thoroughly washed four times by suspension in 500 ml. of hot water, air-dried, and brought to complete dryness at 150°C under reduced pressure (2 mm.). The yield was almost quantitative.

Heneicosyl bromide: $C_{21}H_{43}Br$—The reaction was carried out under strict exclusion of moisture. To a suspension of 12 g. of silver behenate in 80 ml. of carbon tetrachloride was added a solution of 10 g. of bromine in 50 ml. of carbon tetrachloride which had previously been dried over phosphorus pentoxide. Reaction began immediately, with the evolution of carbon dioxide. When the reaction almost ceased, the reaction mixture was heated at the boiling point for a short period to complete the reaction. Silver bromide formed was filtered off and the solution was washed successively with water, sodium thiosulfate solution, 5% sodium hydroxide solution, and water, and dried over sodium sulfate. Evaporation of the solution gave 8.5 g. of an oily product, which solidified on standing at room temperature. Recrystallization from ethanol yielded the pure bromide which melted at 44.5~45°C and weighed 5.3 g. (53%).

Anal. Found: C, 67.5; H, 11.49. Calcd. for $C_{21}H_{43}Br$: C, 67.2; H, 11.47%.

The melting point is higher than that of docosyl bromide $C_{22}H_{45}Br$ (44°C)[8]. This is consistent with the fact that the melting points of normal alkyl bromides of odd carbon numbers are slightly higher than those of next higher homologue.

Heneicosanol: $C_{21}H_{43}CH$ — An intimate mixture of 5 g. of heneicosyl bromide and 2.3 g. of silver acetate was kept at 150°C for 3 hr. The reaction mixture was extracted three times with hot benzene. The benzene solution free from silver bromide was washed with water and dried over sodium sulfate. Evaporation of the solution gave 4.2 g. of a residue which was saponified without purification. The crude ester was refluxed for 3 hr. with 10 ml. of 30% alcoholic potassium hydroxide. The resulting alcohol was recrystallized twice from ethanol and twice from benzene to give heneicosanol in platelets, m. p. 68.5~69°C. Overall yield was 40% (3 g.).

Nonadecanol. — The intermediate diazoketone was prepared by the method of Grundmann[4]. The melting point of this compound was 69~70°C (reported 69°C).

Methyl nonadecanoate: $C_{18}H_{37}CO_2CH_3$—A slurry of freshly prepared silver oxide in methanol was added portionwise to a stirred solution of 18 g. of 1-diazo-2-nonadecanone in 160 ml. of methanol which was heated beforehand at 65°C. The addition required about 4 hr. and the temperature of the reaction mixture was kept at 60~65°C during the course of the reaction. At the end of this period a 2 ml. portion was taken from the solution and added to concentrated hydrochloric acid. An evolution of nitrogen was not observed, and then the solution was cooled and filtered. Partial removal of the methanol and subsequent cooling gave a white solid which was recrystallized from methanol, m. p. 42~43°C. The yield was 17 g. (95%). It was identified by the mixed melting point with an authentic sample.

Reduction of methyl nonadecanoate.—To a stirred suspension of 0.2 g. of lithium aluminum hydride in 25 ml. of dry ether was added a solution of 3 g. of methyl nonadecanoate in 15 ml. of ether dropwise at such a rate that a gentle reflux of the solvent was maintained. After the addition was complete, the solution was refluxed for 15 min. The excess of lithium aluminum hydride was decomposed by cautious addition of water and the reaction mixture was acidified with dilute sulfuric acid. The ether layer was removed, and washed with water to neutral reaction. The solid residue, obtained by removal of the solvent from the dried solution, was recrystallized four times from benzene to give nonadecanol in platelets, m. p. 62~62.5°C. Yield was 90% (2.3 g.).

Tricosanol. — The preparation of intermediate ethyl ε-bromocaproate (I) was modelled after that of Brown and Partridge[6]. From 50 g. of purified cyclohexanone 52 g. of the bromoester was obtained, b. p. 118°C/14 mm. or 98°C/4.5 mm., n_D^{32} 1.4561 (reported: b. p. 120~125°C/14 mm., n_D^{21} 1.4566).

Ethyl n-hexane 1,1,6-tricarboxylate (II).—The bromoester (33 g.) was refluxed with a solution of 48 g. of sodiomalonic ester in 150 ml. of absolute ethanol for 8 hr. After removal of the solvent the cooled mixture was treated with dilute solfuric acid and the triethylester was isolated in a usual manner as a colorless liquid, b. p. 150~151°C/1 mm. Yield, 28 g. (63%). n_D^{28}, 1.4360.

Anal. Found: C, 59.91; H, 9.01; Calcd. for $C_{15}H_{26}O_6$: C, 59.58; H, 8.67%.

8-Ketotricosanoic acid (V): $CH_3(CH_2)_{14}CO(CH_2)_6CO_2H$—In a 200 ml. three-necked flask equipped with a mechanical stirrer, a dropping funnel and a reflux condenser fitted with a calcium chloride tube, were placed 0.75 g. of finely powdered sodium sand and 70 ml. of dry benzene. To the mixture was added from the dropping funnel 11.3 g. of ethyl *n*-hexane-1,1,6-tricarboxylate.

8) V. Braun et at., *Ann.*, **472**, 132 (1929).

The mixture was refluxed with stirring until the sodium sand disappeared. It required about 8 hr. After 7.5 g. of benzyl alcohol (purified by oximation followed by distillation: b. p. 79~80°C/7 mm., odorless) was added, the reflux condenser was replaced by a Fenske column and the mixture was heated to distill off ethanol as the benzene-ethanol azeotrope. Then the Fenske column was again replaced by the reflux condenser. Palmitoyl chloride (9 g.) b. p. 148°C/1.5 mm. was added with stirring, and the resulting solution was refluxed for 1 hr. The neutral solution obtained was distilled under reduced pressure to give a yellow oil which could not be crystallized and was subjected to hydrogenation without purification. A solution of 25 g. of tribenzyl compound IV in 50 ml. of ethyl acetate was shaken with Pd-C (0.5 g.) and Pd-$SrCO_3$ (0.5 g.) in a hydrogen atmosphere of slightly positive pressure. After 10 hr. the absorption of hydrogen ceased, but during this period the fresh catalyst was added from time to time because of its poisoning, the total amount of catalyst being 4 g. The solution freed from the catalyst was refluxed for 30 min. to decarboxylate the product. After the solvent was partially removed, white small crystals separated out from the cooled solution. Repeated recrystallization from acetone gave white crystals having the constant melting point of 93.5~94°C. Yield was 23% (2.8 g.).

Anal. Found: C, 75.16; H, 12.00. Calcd. for $C_{23}H_{44}O_3$: C, 74.94; H, 12.03%.

Tricosanoic acid (VI): $C_{22}H_{45}CO_2H$—To a solution of 2.5 g. of potassium hydroxide in 30 ml. of diethylene glycol was added 2.5 g. of the ketonic acid and 2.5 ml. of hydrazine hydrate. The mixture was heated to 165°C in an oil bath. After 1 hr. of heating the water formed distilled off through a take-off condenser. The contents of the flask were held at 200°C for 6 hr., and cooled. The fatty acid was isolated by pouring the reaction mixture into an equal volume of water followed by acidification with dilute sulfuric acid. Recrystallization from benzene gave 2.2 g. of platelets, m. p. 78.5°C (reported: 79~79.3°C[9]). The ethyl ester of the acid was obtained by the usual method and purified by vacuum distillation followed by recrystallization from benzene, m. p. 51~52°C (reported: 51.2~51.4°C[9]), b. p. 207°C/1.5 mm.

Tricosanol: $C_{23}H_{47}OH$ — From 2 g. of ethyl tricosanoate, 0.15 g. of lithium aluminum hydride in absolute ether was obtained 1.3 g. of the pure alcohol which melted at 72.5°C.

Pentacosanol.—It was prepared analogously to tricosanol stearic acid, being used in place of palmitic acid. The experimental results are given briefly.

Condensation product of benzyl n-hexane-1,1,6-tricarboxylate with stearoyl chloride. — From 17 g. of the tribenzyl compound and 11 g. of stearoyl chloride (b. p. 169°C/1.5 mm.) were obtained 24 g. of a crude product in a state of viscous brown liquid.

8-Ketopentacosanoic acid: $CH_3(CH_2)_{16}CO(CH_2)_6CO_2H$—From 24 g. of the above benzyl compound, 2.5 g. of the ketonic acid was obtained. The product was recrystallized from acetone and then from benzene to a constant melting point of 97°C.

Anal. Found: C, 75.91; H, 12.05. Calcd. for $C_{25}H_{48}O_3$: C, 75.70; H, 12.20%.

Pentacosanoic acid: $C_{24}H_{49}CO_2H$ — The Huang-Minlon reduction of 2.5 g. of the ketonic acid gave 2.2 g. of pentacosanoic acid, m. p. 83.1°C (reported: 83.2~83.4°C[9]). Ethyl pentacosanoate, m. p. 57~58°C (reported: 57.1~57.4°C[9]), b. p. 215°C/0.7 mm.

Pentacosanol: $C_{25}H_{51}OH$ — By use of lithium aluminum hydride (0.15 g.), 1.7 g. of the pure product was obtanied from 2.1 g. the ethyl pentacosanoate. m.p. 77.5°C (from ligroin).

The author expresses his sincere thanks to Professor Ryozo Goto for his kind guidance througout this study. Thanks are also due to the Ministry of Education for a Grant-in-Aid for Scientific Research.

Department of Applied Chemistry
Himeji Technical College
Idei, Himeji

9) S. Shiina, *J. Soc. Chem. Ind., Japan* (*Kôgyô Kwagaku Zassi*), **39**, 345 (1936).

Competitive Hydrogenation of Acetylenic Compounds

By Tosao FUKUDA

(Received March 18, 1959)

1, 4-Butynediol can be partially hydrogenated on the Pd-$CaCO_3$ catalyst, with quinoline as a poison, and also on the Pd-$BaCO_3$ catalyst poisoned by lead acetate and quinoline, but not on the ordinary palladium catalyst[1,2]. The effect of lead acetate on the Pd-$CaCO_3$ catalyst was different from that of quinoline. It was explained that lead acetate is adsorbed more strongly than 1, 4-butynediol or 1, 4-butenediol, while quinoline is adsorbed in competition with 1, 4-butynediol and 1, 4-butenediol[3].

It seems to be an interesting problem to study in more detail how the properties of the Pd-$CaCO_3$ catalyst are affected by such an additive as quinoline. Thus, the properties of the catalyst for the hydrogenation of phenylacetylene and propargyl alcohol were studied.

Experimental

Procedure. — The hydrogenation experiments were carried out with Pd-$CaCO_3$ catalyst[4] (Pd-content, 5% by wt.), at 25°C and at the atmospheric pressure in methyl alcohol. Phenylacetylene was prepared according to J. C. Hessler[5], and propargyl alcohol was a commercial product[6]. These were purified by distillation. The hydrogenation products were analyzed by gas chromatography.

The gas chromatography experiments were carried out at 100°C by a glass gas chromatography apparatus[7]. Polyethyleneglycol-400 column (P.E.G.-column) and polyethyleneglycol-400-dinonyl phthalate column (P.E.G.-D.N.P-column) were used. With P.E.G.- and P.E.G.-D.N.P.-columns, phenylacetylene, styrene, ethylbenzene, propargyl alcohol, allyl alcohol, and propyl alcohol eluted as shown in Fig. 1.

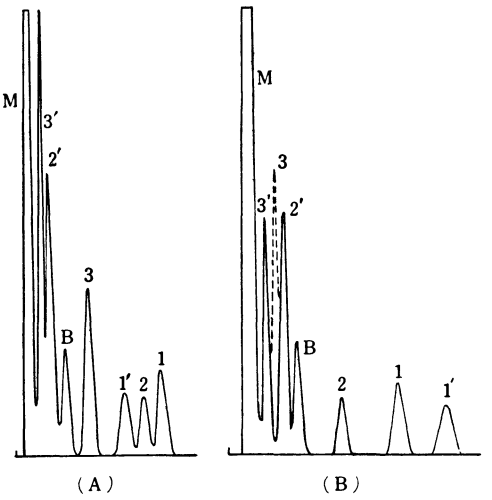


Fig. 1. Chromatogram on P.E.G-D.N.P-column and P.E.G.-column, at 100°C.
(A) P.E.G-D.N.P-column : [P.E.G-400-(20%)-celite : D.N.P (20%)-celite =9 : 12 (by wt.)]
length : 2 m., diameter : 4 mm.
(B) P.E.G-column : [P.E.G-400-(20%)-celite] length : 1 m., diameter : 4 mm.
carrier gas : H_2 (50 cc/min.)
1 : Phenylacetylene
2 : Styrene
3 : Ethylbenzene
1' : Propargyl alcohol
2' : Allyl alcohol
3' : Propyl alcohol
B : *n*-Butyl alcohol
M : Methyl alcohol

Results

The hydrogenation of phenylacetylene and propargyl alcohol on the Pd-$CaCO_3$ catalyst took place as shown in Fig. 2. It was shown that phenylacetylene and propargyl alcohol could not be partially hydrogenated in the presence of quinoline.

When 20 millimol. of phenylacetylene or propargyl alcohol in a concentration of 2 millimol./ml. was used, the reaction products were shown in Fig. 3. In these experiments, a mixture of methyl alcohol

1) T. Fukuda and T. Kusama, This Bulletin, **31**, 339 (1958).
2) T. Fukuda, ibid., **31**, 343 (1958).
3) T. Fukuda, ibid., **32**, 420 (1959).
4) H. Lindler, *Helv. Chim. Acta*, **30**, 1911 (1947).
5) J. C. Hessler, "Organic Syntheses", Col. Vol. 1, John Wiley & Sons, Inc., New York, p. 428.
6) A commercial extra pure grade (Tokyo Kasei Co., Tokyo).
7) T. Fukuda, *Japan Analyst* (*Bunseki Kagaku*), 8, 627 (1959).

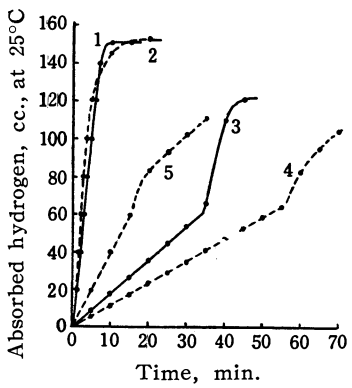


Fig. 2. The absorption of hydrogen in the hydrogenation of phenylacetylene and propargyl alcohol.
$Pd\text{-}CaO_3$ catalyst 100 mg.
1: Phenylacetylene (ca. 3.6 millimol.) ···methyl alcohol solution (20 cc.)
2: Phenylacetylene (ca. 3.6 millimol.) ···methyl alcohol-quinoline solution (20 cc.)
3: Propargyl alcohol (ca. 2.8 millimol.) ···aqueous solution (20 cc.)
4: Propargyl alcohol (ca. 2.8 millimol.) ···water-quinoline solution (20 cc.)
5: Propargyl alcohol (ca. 2.8 millimol.) ···quinoline solution (20 cc.)

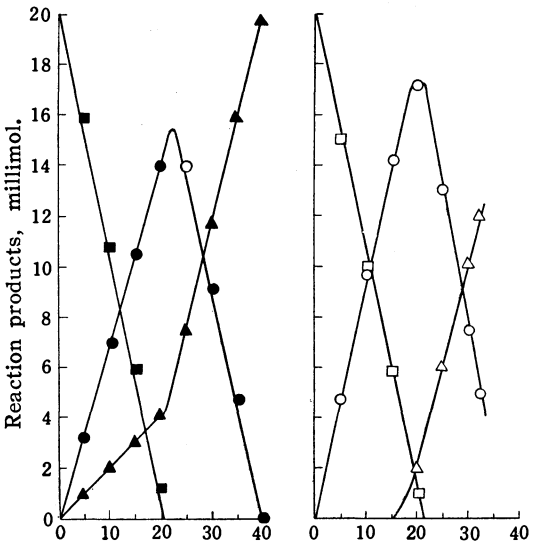


Fig. 3. The reaction products in the hydrogenation of phenylacetylene and propargyl alcohol.
$Pd\text{-}CaO_3$ catalyst 1.00 g.
■ Phenylacetylene □ Propargyl alcohol
● Styrene ○ Allyl alcohol
▲ Ethylbenzene △ Propyl alcohol

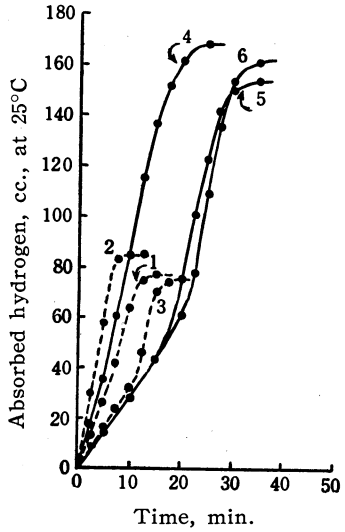


Fig. 4. The absorption rate of hydrogen in the competitive hydrogenation of acetylenic compounds.
$Pd\text{-}CaO_3$ catalyst 100 mg.
Methyl alcohol solution (20 cc.)
1: 1,4-Butynediol (2 millimol.)
2: Phenylacetylene (2 millimol.)
3: Propargyl alcohol (2 millimol.)
4: Phenylacetylene (2 millimol.) +1,4-butynediol (2 millimol.)
5: Propargyl alcohol (2 millimol.) +1,4-butynediol (2 millimol.)
6: Phenylacetylene (2 millimol.) +propargyl alcohol (2 millimol.)

and *n*-butyl alcohol (an internal standard for the gas chromatographic analysis) was used as a solvent. The hydrogenation of phenylacetylene took place with simultaneous hydrogenation of about 20 mol. % of styrene. On the other hand, in the hydrogenation of propargyl alcohol, allyl alcohol was scarcely hydrogenated.

The competitive hydrogenation took place as shown in Fig. 4. When the concentration of the each acetylenic compound was 2 millimol./ml., the reaction products came out as shown in Figs. 5—7, with the absorbed amount of hydrogen. In these experiments, a mixture of methyl alcohol and *n*-butyl alcohol was used as a solvent. The peak of 1,4-butynediol, 1,4-butenediol, and 1,4-butanediol did not appear under the experimental conditions of the gas chromatography. However, the contents of these substances in the product could be roughly estimated from the absorbed amount of hydrogen as shown by the dotted lines, assuming that 1,4-butynediol and 1,4-butenediol were hydrogenated selectively.

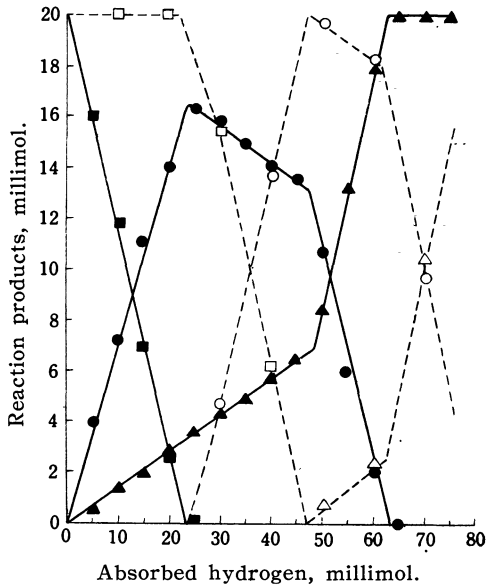


Fig. 5: The reaction products in the competitive hydrogenation of phenylacetylene and 1,4-butynediol.
$Pd\text{-}CaCO_3$ catalyst 1.00 g.
Phenylacetylene (20 millimol.)
1,4-Butynediol (20 millimol.)
■ Phenylacetylene □ 1,4-Butynediol
● Styrene ○ 1,4-Butenediol
▲ Ethylbenzene △ 1,4-Butanediol

It was shown that, in the competitive hydrogenation of 1,4-butynediol and phenylacetylene, the latter was hydrogenated first and the former was then hydrogenated, and both steps were accompanied by the hydrogenaion of a small amount of styrene.

The hydrogenation of 1,4-butenediol took place after that of styrene was completed. In the competitive hydrogenation of 1,4-butynediol and propargyl alcohol, the latter was hydrogenated first, and the hydrogenation of 1,4-butynediol with a small amount of allyl alcohol followed. The remaining allyl alcohol was hydrogenated with 1,4-butenediol. In the competitive hydrogenation of phenylacetylene and propargyl alcohol, the latter was hydrogenated with about 35 mol. % of the former. The remaining phenylacetylene was hydrogenated with a small amount of styrene and allyl alcohol. Styrene was hydrogenated with allyl alcohol.

Even when 0.2 millimol./ml. of phenylacetylene (or propargyl alcohol) and 1.8 millimol./ml. of 1,4-butynediol were used, the competitive hydrogenation took place similarly as explained above.

It was observed that an appreciable amount of allyl alcohol was consumed by

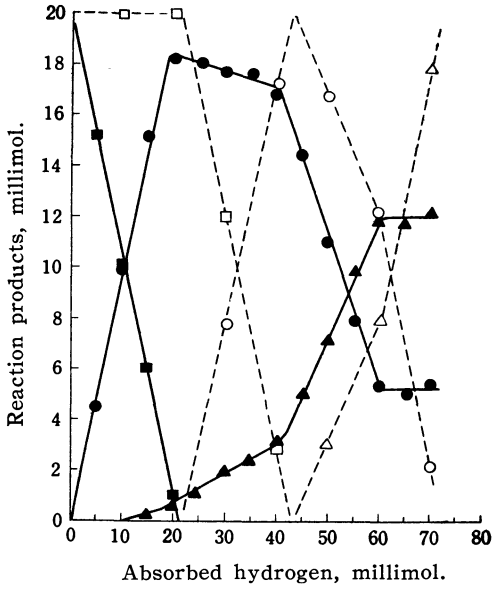


Fig. 6. The reaction products in the competitive hydrogenation propargyl alcohol and 1,4-butynediol.
$Pd\text{-}CaCO_3$ catalyst 1.00 g.
Propargyl alcohol (20 millimol.)
1,4-Butynediol (20 millimol.)
■ Propargyl alcohol □ 1,4-Butynediol
● Allyl alcohol ○ 1,4-Butenediol
▲ Propyl alcohol △ 1,4-Butanediol

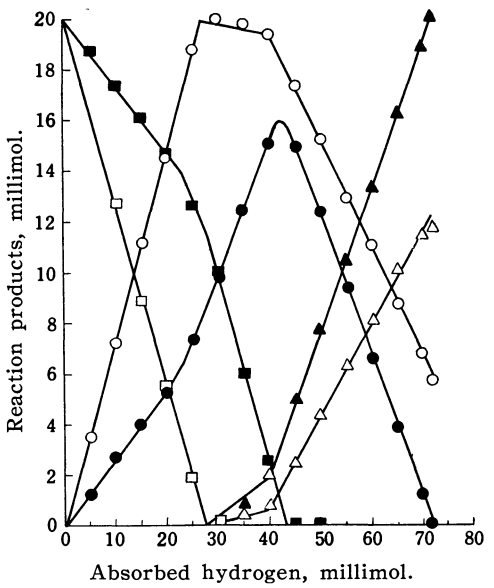


Fig. 7. The reaction products in the competitive hydrogenation of phenylacetylene and propargyl alcohol.
$Pd\text{-}CaCO_3$ catalyst 1.00 g.
Phenylacetylene (20 millimol.)
Propargyl alcohol (20 millimol.)
■ Phenylacetylene □ Propargyl alcohol
● Styrene ○ Allyl alcohol
▲ Ethylbenzene △ Propyl alcohol

the side reaction, and its hydrogenation was interrupted with the occurrence of the side reaction. The product from the side reaction was mainly propionaldehyde. However, it was found that propionaldehyde could not retard the hydrogenation of allyl alcohol, a mixture of methyl alcohol and propionaldehyde being used as a solvent.

Consideration

It is interesting to note that, when phenylacetylene has been absorbed on the catalyst surface, styrene is hydrogenated more easily than 1,4-butynediol, but, when the hydrogenation of phenylacetylene has been completed, 1,4-butynediol is hydrogenated more easily than styrene. Allyl alcohol is hydrogenated more easily than 1,4-butenediol. However, 1,4-butenediol is hydrogenated, even when the hydrogenation of allyl alcohol has been interrupted.

These results show that the catalyst properties are affeced by the adsorption of 1,4-butynediol, phenylacetylene, propargyl alcohol and so on. It is generally admitted that the catalyst properties are changed by the adsorbed substance[8]. When phenylacetylene or propargyl alcohol is adsorbed on the catalyst surface, the catalyst properties may be different from those when 1,4-butynediol is adsorbed. Accordingly, the partial hydrogenation of 1,4-butynediol might have been achieved on the Pd-$CaCO_3$ catalyst, with quinoline as a beneficial poison, but not phenylacetylene and propargyl alcohol.

It was shown that the gas chromatography is very useful to study the reactions.

The author is grateful to Professor T. Kusama, Yokohama National University, for his unfailing kindness in encouraging this work. The author is also indebted to Professor K. Tamaru, Yokohama National University, for his valuable advice, and Mr. Y. Suzuki, for his assistance.

Department of Chemistry
Faculty of Engineering
Yokohama National University
Minami-ku, Yokohama

8) R. Suhrman and K. Schultz, *Z. physik. Chem.*, 1, 69 (1954); W. H. Sachtler, *J. Chem. Phys.*, 35, 751 (1956); L. E. Moore and P. W. Selwood, *J. Am. Chem. Soc.*, 78, 697 (1956).

Dehydration of Bile Acids and their Derivatives. VII. Isomerization of Methyl 3α-Hydroxy-Δ^7-cholenate to Methyl 3α-Hydroxy-Δ^{14}-cholenate

By Ryuzaburo OSAWA and Kazumi YAMASAKI

(Received April 3, 1959)

Yamasaki[1] reported previously that the action of concentrated hydrochloric acid on chenodeoxycholic acid gave three isomeric 3α-hydroxycholenic acids, but the localization of their double bonds has not yet been settled. In order to obtain any further information about these acids, the authors have attempted to isomerize 3α-hydroxy-Δ^7-cholenic acid derived from chenodeoxycholic acid and to compare the product obtained with the isomers reported by Yamasaki[1]. Methyl 3α-ethoxycarbonyloxy-7α-hydroxycholanate (Ib) was prepared from methyl chenodeoxycholate (Ia) according to Fieser et al.[2] and dehydrated with phosphorus oxychloride in pyridine[3] to give methyl 3α-ethoxycarbonyloxy-Δ^7-cholenate[4] in a fairly good yield, m. p. 136°C, $\alpha_D^{24} = +81.20°$ (Chf.) [Herz[5]: m. p. 126°C, $\alpha_D^{21} + 80 \pm 2°$ (Di)].

Methyl 3α-hydroxy-Δ^7-cholenate (IIc)

1) K. Yamasaki and K. Takahashi, *Z. physiol. Chem.*, **256**, 21 (1938); K. Yamasaki, *J. Chem. Soc. Japan, Pure Chm. Sec.* (*Nippon Kagaku Zasshi*), **72**, 680 (1951).

2) L. F. Fieser, J. E. Herz, M. W. Klohs, M. A. Romero and T. Utne, *J. Am. Chem. Soc.*, **74**, 3309 (1952).

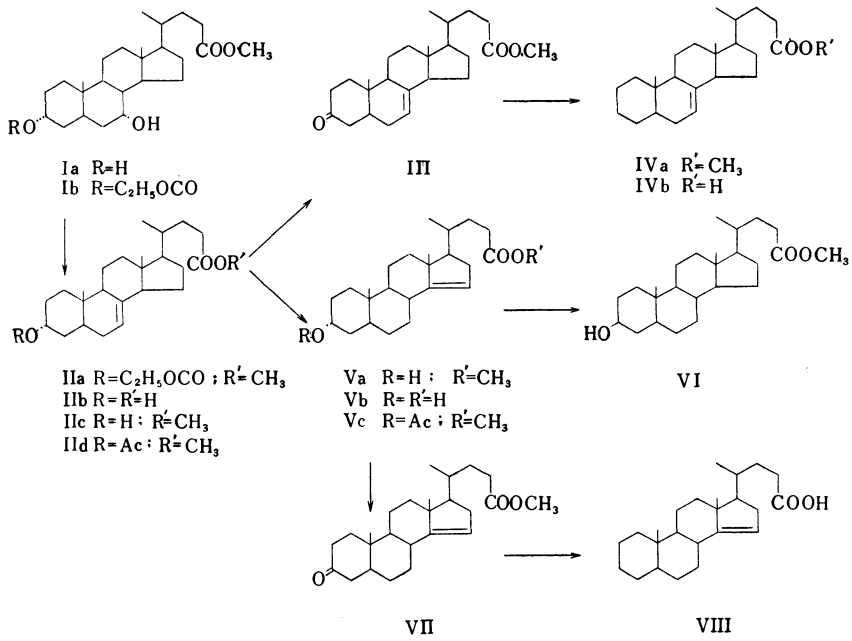
3) E. Berner, A. Lardon and T. Reichstein, *Helv. Chim. Acta*, **30**, 1542 (1947).

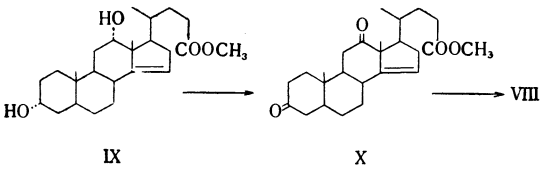
4) Although the proposed position (Δ^7) of the double bond of this acid has not yet been studied, the position is highly probable, because the C_7 OH-group of chenodeoxycholic acid is apt to be dehydrated (*trans*-dehydration) exactly like cholic acid[3], and any possible shift of the double bond then formed can be excluded under the condition here described.

5) J. E. Herz, A thesis submitted to the Department of Chemistry, Harvard University (1951).

TABLE I. 3α-HYDROXYCHOLENIC ACIDS DERIVED FROM CHENODEOXYCHOLIC ACID

3α-Hydroxy-cholenic acid	m. p. °C	$[\alpha]_D$	Methyl ester, m. p., °C	Methyl ester acetate, m. p. °C
β-Apochenodeoxycholic acid[1]	195～196	+83.67° (alc.)	—	83～84
γ-Apochenodeoxycholic acid[1]	182～183	+101.73° (MeOH)	—	77～78
Chenocholenic acid[1]	211～213	+30.0° (MeOH)	—	—
3α-Hydroxy-Δ^7-cholenic acid	189～190	+62.0° (Di.)	108～109	127
3α-Hydroxy-Δ^{14}-cholenic acid	160	+62.8° (Chf.)	140～141	110





was subjected to isomerization by the action of dry hydrogen chloride gas[6], and a crystalline mixture was obtained. A fraction melting higher than the starting material was purified to afford crystals of m. p. 140～141°C, $\alpha_D^{20}=+55.8°$ (Chf.). The isomerized ester showed a distinct depression of the melting point on admixture with the starting substance and gave a negative selenium dioxide test, while the latter did a positive test, contrary to Fieser's report[7].

The corresponding free acid dissolved in ethanol showed an absorption maximum at 211 mμ with an extinction coefficient of ε_{max}^{EtOH} 2390, while $\Delta^{8(14)}$-cholenic acid as a reference substance, obtained from apocholic acid[8], showed an extinction coefficient of $\varepsilon_{max}^{EtOH}=6170$. According to Bladon et al.[9], this finding suggests that the new 3α-hydroxycholenate possesses either a tri- or a disubstituted ethylenic grouping. As was expected, the ester absorbed one mole of hydrogen on catalytic hydrogenation to give methyl lithocholate (VI) (m.p. 130°C). These results provide a strong evidence for the Δ^{14}-structure (V) of the new acid.

In order to ascertain the structure, the 3-hydroxy-ester (Va) was transformed into a cholenic acid by the Huang-Minlon reduction[10] of the corresponding 3-keto-ester (VII). The cholenic acid obtained was identified with Δ^{14}-cholenic acid (VIII) which was derived from 3α,12α-dihydroxy-Δ^{14}-cholenic acid[11] (IX) through its dehydro-acid (X).

6) K. Yamasaki, *Z. physiol. Chem.*, **233**, 10 (1935).
7) L. F. Fieser, *J. Am. Chem. Soc.*, **75**, 4395 (1953).
8) To be published.
9) P. Bladon, H. B. Henbest and G. W. Wood, *J. Chem. Soc.*, **1952**, 2737.
10) Huang-Minlon, *J. Am. Chem. Soc.*, **71**, 3301 (1949).
11) Cf. L. F. Fieser and M. Fieser, "Natural Products Related to Phenanthrene", 3rd Ed., Reinhold Publishing Corp., New York (1949), p. 118.

Thus it is concluded that the isomerized product from methyl 3α-hydroxy-Δ^7-cholenate (IIc) is methyl 3α-hydroxy-Δ^{14}-cholenate (Va), but, as shown in Table I, the 3α-hydroxy-Δ^{14}-cholenic acid (Vb) was found to be different from any of the three 3α-hydroxycholenic acids obtained by Yamasaki[1]. The expected presence of the isomeric 3α-hydroxy-$\Delta^{8(14)}$-cholenate together with the Δ^{14}-ester in the isomerization product is now under investigation.

Experimental

Preparation of 3α-Hydroxy-Δ^7-cholenic Acid and Derivatives. — *Methyl 3α-ethoxycarbonyloxy-7α-hydroxycholanate (Ib).* — Two grams of methyl chenodeoxycholate (Ia) (the free acid, m.p. 140°C, was prepared according to Fieser and Rajagopalan[12] from cholic acid and the non-crystalline methyl ester was prepared with diazomethane as ususl) dissolved in 20 ml. of dioxane containing 3.2 ml. of pyridine was treated with 4 ml. of ethyl chloroformate with cooling in ice water. After standing at room temperature for 2 hr., the mixture was diluted with water, and extracted twice with ether. The combined extract was washed with dilute hydrochloric acid and with water, dried over sodium sulfate, and evaporated to dryness in vacuo. The residue was treated with a small quantity of methanol, warmed and allowed to stand at room temperature to crystallization. Recrystallization from methanol gave the ethoxycarbonyl derivative (Ib) in colorless blades, m. p. 136°C, $\alpha_D^{20}=+30.55°$ (Chf.).

Methyl 3α-ethoxycarbonyloxy-Δ^7-cholenate (IIa).— The above ester (Ib) (1.8 g.) was dissolved in 20 ml. of pyridine, 6 ml. of phosphorous oxychloride was added, and the mixture was kept at room temperature overnight. The reaction mixture was poured cautiously into 300 ml. of ice water, and extracted 3 times with ether. The combined ethereal extract was washed with water, dilute hydrochloric acid, aqueous sodium hydroxide solution and again water, successively, and dried over sodium sulfate. Removal of the solvent gave a crystalline residue, to which was added a small quantity of methanol, and the solution was warmed and allowed to stand at room temperature to give a crystalline product, m.p. 120~121°C. Yield, 1.65 g. Recrystallization from acetone gave the product in blades, m. p. 132~133°C, $\alpha_D^{24}=+81.2°$ (Chf.).

Anal. Found: C, 73.00; H, 9.63. Calcd. for $C_{28}H_{44}O_5$ (460.32): C, 73.01; H, 9.89%.

3α-Hydroxy-Δ^7-cholenic acid (IIb). — The above ester (IIa) (1.5 g.) was dissolved in 20 ml. of methanol containing 10 ml. of 10% aqueous potassium hydroxide and the solution was refluxed for 1.5 hr. The hydrolyzate was diluted with water and acidified with dilute hydrochloric acid. The precipitates were collected, washed with water and dried to give the free acid, m. p. 183~184°C. Yield, 1.17 g. Recrystallization from ethyl acetate and methanol gave the substance in needles, m. p. 189~190°C, $\alpha_D^{21}=+62.0°$ (Di). The selenium dioxide test was positive.

Anal. Found: C, 76.64; H, 10.05. Calcd. for $C_{24}H_{38}O_3$ (374.54): C, 76.94; H, 10.23%.

Methyl 3α-hydroxy-Δ^7-cholenate (IIc).—The above acid (IIb) (m. p. 190~191°C, 0.5 g.) was refluxed with 10 ml. of methanol containing two drops of concentrated hydrochloric acid for 1/2 hr., and the solution was concentrated by passing a stream of air to crystallization. After completion of crystallization, the crystals were collected and washed with a small volume of methanol, m. p. 104~105°C. Yield, 0.49 g.

Recrystallized twice from aqueous methanol, the substance was obtained in glistening leaflets, m. p. 108~109°C, $\alpha_D^{24}=+61.8\pm1.4°$ (Chf.).

Methyl 3α-acetoxy-Δ^7-cholenate (IId).—The above ester (IIc) (200 mg.) in 4 ml. of pyridine was treated with 2 ml. of acetic anhydride. After standing for 24 hr., water and concentrated hydrochloric acid (3.5 ml.) were added and the mixture was warmed for 20 min. on a steam bath. The solid was collected, and weighed 200 mg. Recrystallized once from methanol, the substance was obtained in glistening plates, m. p. 126~127°C, $\alpha_D^{23}=+86.0°$ (Chf.), λ_{max} 211 mμ, ε_{max}^{EtOH} 2075.

Anal. Found: C, 74.80; H, 9.64. Calcd. for $C_{27}H_{42}O_4$ (430.61): C, 75.30; H, 9.85%.

Methyl 3-keto-Δ^7-cholenate (III). — Methyl 3α-hydroxy-Δ^7-cholenate (IIc) (800 mg.) was oxidized in acetone with the chromic acid-H_2SO_4 mixture according to Baldon et al.[13] When the reaction was completed, the solution was diluted with water. After completion of crystallization in an ice box, the crystals were collected, m. p. 123~124°C. Yield, 770 mg. Recrystallized once, the substance was obtained in a pure state, m. p. 125°C, $\alpha_D^{23}=+53.3$ (Chf.).

Anal. Found: C, 77.22; H, 9.77. Calcd. for $C_{25}H_{38}O_3$ (386.55): C, 77.67; H, 9.91%.

Methyl Δ^7-cholenate (IVa). — Methyl 3-keto-Δ^7-cholenate (III) (0.51 g.) was heated with a mixture of triethylene glycol (30 ml.), hydrazine hydrate (1.5 ml.) and potassium hydroxide (1 g.) by the modified Wolff-Kishner method (Huang-Minlon[10] reduction).

The reaction mixture was diluted with water and acidified with dilute hydrochloric acid. The solid was collected, washed with water, and dried. The crude acid in methanol was treated with an ether solution of diazomethane and concentrated. The first crop (0.37 g.) showed m. p. 95.5~97°C, and the second (0.05 g.), m. p. 85~86°C.

Recrystallization of the combined crops from methanol-acetone gave thin rectangular plates of m. p. 98~99°C, undepressed by the sample obtained by the phosphorous oxychloride dehydration of methyl 7-hydroxycholanate (Herz[5]); $\alpha_D^{23}=+53\pm3°$ (Chf.) [$\alpha_D^{21}=+56\pm2°$ (Di.) (Herz[5])].

Anal. Found: C, 80.25; H, 10.58. Calcd. for $C_{25}H_{40}O_2$ (372.57): C, 80.62; H, 10.82%.

12) L. F. Fieser and S. Rajagopalan, *J. Am. Chem. Soc.*, **72**, 5530 (1950).

13) P. Bladon, J. M. Fabian, H. B. Henbest, H. P. Koch and G. W. Wood, *J. Chem. Soc.*, **1951**, 2402.

Δ^7-Cholenic acid (IVb).—The above ester (IVa) (100 mg.) was refluxed for 1 hr. with 7 ml. of methanol and 3 ml. of 10% aqueous potassium hydroxide, and the reaction mixture was diluted with water and acidified with dilute hydrochloric acid. The crystalline solid was collected. Recrystallized twice from methanol, Δ^7-cholenic acid was obtained in a pure state, m. p. 150~151°C, undepressed on admixture with the specimen (m. p. 151°C) prepared by Herz[5].

Anal. Found: C, 80.78; H, 10.47. Calcd. for $C_{24}H_{38}O_2$ (558.54): C, 80.80; H, 10.68%.

Isomerization of Methyl 3-Hydroxy-Δ^7-cholenate.—*Methyl 3α-hydroxy-Δ^{14}-cholenate (Va).*—A stream of dry hydrogen chloride gas was passed into a solution of methyl hydroxy-Δ^7-cholenate (IIc) (1.0 g.) in anhydrous chloroform (20 ml.) for 2 hr. at 0°C. The solution was diluted with chloroform with cooling in ice water, washed with water, soda solution and again with water, successively, and dried over sodium sulfate. Removal of the solvent gave a crystalline residue. This was dissolved in 1 ml. of benzene, passed throngh a Brockmann-alumina column and eluted with petroleum ether, benzene, ether and methanol, successively. The first portions of the elute contained the original substance, and a substance of higher melting point was obtained from the fractions eluted with ether. Rechromatography of the fractions of the higher melting point gave an ester of m. p. 139°C, and recrystallization from ethanol-water afforded crystals of m. p. 140~141°C, $\alpha_D^{20}=+55.8°$ (Chf.), which showed a depression in the melting point on admixture with the starting substance and was negative in the selenium dioxide test.

Anal. Found: C, 77.40; H, 10.13. Calcd. for $C_{25}H_{40}O_3$ (388.32): C, 77.69; H, 9.91%.

Methyl 3α-acetoxy-Δ^{14}-cholenate (Vc).—Methyl 3α-hydroxy-Δ^{14}-cholenate (Va) (m. p. 141°C, 100 mg.) in 2 ml. of pyridine was treated with 1 ml. of acetic anhydride. After standing for 24 hr., water and concentrated hydrochloric acid (3.5 ml.) were added to the reaction mixture, and the whole was warmed for 20 min. on a steam bath. The solid was collected. Yield, 100 mg. Recrystallized once from methanol, the product was obtained in glistening leaflets of m. p. 110°C, $\alpha_D^{20}=+86.7°$ (Chf.).

Anal. Found: C, 75.30; H, 9.85. Calcd. for $C_{27}H_{42}O_4$ (430.61): C, 75.30; H, 9.85%.

3α-Hydroxy-Δ^{14}-cholenic acid (Vb).—Methyl 3α-hydroxy-Δ^{14}-cholenate (Va) (100 mg.) was dissolved in 7 ml. of methanol containing 3 ml. of 10% aqueous potassium hydroxide and the mixture was refluxed for 1 hr. The solution was acidified with dilute hydrochloric acid. The crystalline solid was collected. Recrystallized twice from methanol containing ethyl acetate, the substance was obtained in a pure state, m. p. 161°C, $\alpha_D^{24}=+62.8°$ (Chf.), λ_{max} 211 mμ, ε_{max}^{EtOH} 2390.

Anal. Found: C, 76.27; H, 10.37. Calcd. for $C_{24}H_{38}O_3$ (374.54): C, 76.94; H, 10.23%.

Methyl lithocholate (VI).—Methyl 3α-hydroxy-Δ^{14}-cholenate (Va) (m. p. 141°C, 50 mg.) in 10 ml. of glacial acetic acid was shaken for 3 hr. with 10 mg. of PtO_2 (Adams) and hydrogen, 3.1 ml. of hydrogen being absorbed (the calculated amount: 3.07 ml.). Concentration of the solution, addition of a small amount of methanol and heating gave needles. Recrystallization from methanol afforded a sample of m. p. 130°C, $\alpha_D^{20}=+24.2°$ (Chf.). This showed no depression in the melting point on admixture with authentic methyl lithocholate (m. p. 129~130°C).

Anal. Found: C, 77.48; H, 10.17. Calcd. for $C_{25}H_{42}O_2$ (375.58): C, 76.78; H, 10.83%.

Methyl 3-keto-Δ^{14}-cholenate (VII).—Methyl 3α-hydroxy-Δ^{14}-cholenate (Va) (m. p. 141°C, 200 mg.) in 20 ml. of acetone was oxidized with the chromic acid-H_2SO_4 mixture according to Bladon et al.[13] After completion of oxidation, the excess of the oxidant was destroyed by addition of a small quantity of methanol. The solution was diluted with water and extracted with ether. The ether extract was washed with water, soda solution and again with water, successively, dried over sodium sulfate and evaporated. The residue was triturated with a small quantity of methanol, and kept at room temperature. The yield of colorless needles, m. p. 78~79°C, was 155 mg. Recrystallized twice from aqueous methanol, the substance was obtained in a pure state, m. p. 89~90°C, $\alpha_D^{24}=+38.8°$ (Chf.).

Anal. Found: C, 77.40; H, 10.13. Calcd. for $C_{25}H_{38}O_3$ (386.55); C, 77.69, H. 9.09%.

Δ^{14}-Cholenic acid (VIII).—Reduction of methyl 3-keto-Δ^{14}-cholenate (VII) (100 mg.) was conducted according to the modified Huang-Minlon procedure[10] with a mixture of triethylene glycol (10 ml.), hydrazine (1 ml.) and potassium hydroxide (1 g.). The reaction mixture was diluted with water and acidified with dilute hydrochloric acid. The solid was collected, washed with water, dried over sodium sulfate, and evaporated. Recrystallization from ethyl acetate and then from aqueous methanol afforded colorless needles of m. p. 143~144°C, $\alpha_D^{22}=+61.8°$ (Chf.), ε_{max}^{EtOH} 3404.

Anal. Found: C, 80.44, H, 10.71. Calcd. for $C_{24}H_{38}O_2$ (358.54): C, 80.39; H, 10.68%.

Derivation of Δ^{14}-cholenic Acid from 3,12-Dihydroxy-Δ^{14}-cholenic Acid.—*Methyl 3,12-diketo-Δ^{14}-cholenate (X).*—Methyl 3,12-dihydroxy-Δ^{14}-cholenate (IX) (200 mg.) was oxidized with the chromic acid-H_2SO_4 mixture according to Bladon et al.[13] Recrystallization from methanol gave fine needles of m. p. 134°C, $\alpha_D^{22}=+60.3$ (Chf.). Yield, 0.175 g.

Anal. Found: C, 75.18; H, 9.15. Calcd. for $C_{25}H_{36}O_4$ (400.56): C, 74.96; H, 9.06%.

Δ^{14}-Cholenic acid (VIII).—The above diketoester (X) (200 mg.) was reduced by the Huang-Minlon procedure[10] (25 ml. of triethylene glycol, 2 ml. of hydrazine hydrate, 2 g. of potassium hydroxide). Recrystallization from acetone and then from acetic acid gave crystals of m.p. 142~143°C, $\alpha_D^{20}=+62.1°$ (Chf.). This acid showed no depression of the melting point on admixture with the specimen obtained above from 3α-hydroxy-Δ^{14}-cholenic acid.

Anal. Found: C, 79.59; H, 10.75. Calcd. for $C_{24}H_{38}O_2$ (358.54): C, 80.39; H, 10.68%.

The preparation of methyl Δ^7-cholenate from methyl 3α-hydroxy-Δ^7-cholenate was carried out, when Yamasaki was working in L. F. Fieser's Laboratory, Harvard University. The elementary analyses were carried out by Mr. Okada of the Analysis Room of Shionogi Laboratory, to whom the authors' gratitude is due.

The authors are greatly indebted to Professor Itô of the Pharmaceutical Institute, the University of Tokyo, for his valuable suggestion and encouragement.

Department of Biochemistry
Tottori University
School of Medicine
Yonago (K. Y.)

Laboratory of the Nippon
Eiyô Kagaku Co.
Katsushika-ku, Tokyo (R. O.)

The Silver Catalyzed Oxidation of Arsenious Acid by Persulfate

By Yugul Kishore GUPTA and Deen Dayal MISRA

(Received April 13, 1959)

The uncatalyzed oxidation of arsenious acid by persulfate has been studied by Gupta & Ghosh[1] and Gupta[2] has found the specific influence of several ions in this oxidation. The oxidation is similar to other uncatalyzed oxidations such as those of thiosulfate[3] and oxalate[4,5] ions. Catalysis by silver ion has been reported by Gupta and Ghosh, but no systematic study was made by them. Silver catalyzed oxidations by persulfate are reported to be of three types. Hence a detailed study of this silver catalyzed reaction was made to evaluate a possible mechanism and to compare the results with those of other silver catalyzed oxidations.

Experimental

Persulfate oxidations are very susceptible to impurities of the solutions and the nature of the glass vessel, and hence all the vessels and apparatus used in this investigation, were of Jena glass. The medium of reaction was redistilled water.

All the chemicals used were of B.D.H.A.R. or E. Merck G.R. quality. A stock solution of 0.20 N arsenious acid was prepared. For this, a requisite amount of arsenious oxide, sufficient to give a little more than 0.20 N acid, was dissolved by boiling in redistilled water. After allowing it to cool, it was filtered and standardized against permanganate solution. Persulfate solution was always freshly prepared and its concentration checked by Eckardt's method[6]. All other solutions were prepared in the usual way.

The reaction was studied at 24°C in a thermostat and silver nitrate was added at the end. A preliminary study indicated that there was practically no reaction between persulfate and arsenious acid at 24°C for about 30~40 min., the time for which they were kept together in the reaction vessel. The reaction speed becomes measurable only at higher temperatures. Gupta and Ghosh studied the uncatalyzed reaction at 45°C.

Five milliliters of the reaction mixture were pipetted out at suitable intervals of time, in a beaker containing 3 ml. of pure and concentrated hydrochloric acid and 10~15 ml. of distilled water. One drop of 0.0025 M KIO_3 added and the contents were titrated against 0.01 N $KMnO_4$ from a microburette. Persulfate did not interfere with this titration. The reaction was completely checked by inhibiting chloride ions[2].

Results and Discussion

The oxidation is of the first order in persulfate and the constants have been calculated from the relation,

$$k = (2.303/t) \times (1/C_{Ag^+}) \times \log [a/(a-x)]$$

where 'a' and '$a-x$' are the concentrations of the persulfate initially and after time 't', respectively, and C_{Ag^+} is the concentration of the silver ions. The reaction is in fact bimolecular, but has a first order rate constant because the concentration of the catalyst Ag^+ does not change during the course of the reaction. Hence k, though a first order constant, has the units of l. equi^{-1} min^{-1}.

1) Y. K. Gupta and S. Ghosh, *J. Inorg. & Nuclear Chem.*, **11**, 62 (1959).
2) Y. K. Gupta, *J. Ind. Chem. Soc.*, **36**, No. 9 (1959).
3) C. V. King and O. F. Steinbach, *J. Am. Chem. Soc.*, **52**, 4779 (1930).
4) C. V. King, ibid., **50**, 2089 (1928).
5) T. L. Allen, ibid., **73**, 3589 (1951).
6) Le Blank Eckardt, *Chem. News*, **81**, 38 (1900).

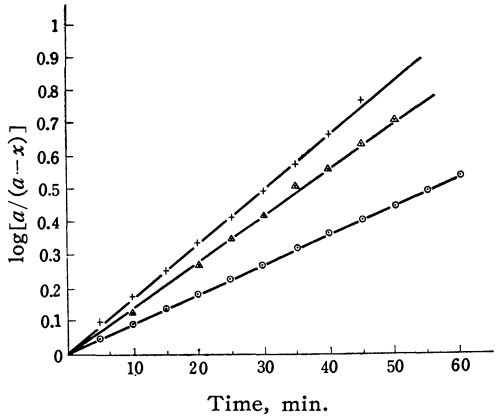


Fig. 1. Silver catalyzed oxidation of H_3AsO_3 by $K_2S_2O_8$.
⊙ Sample 1; k=23.96
△ Sample 2; k=31.49
× Sample 3; k=36.77

Gupta and Ghosh[1] obtained different results with different samples of arsenious acid solution. It was, therefore, imperative to study also the catalyzed reaction with different samples of acid solution. Three experiments out of 20 are shown in Fig. 1 where the average k varied within appreciable limits.

However, the results are quite reproducible with the same sample of arsenious acid solution and hence in order to compare the results amongst themselves, it was necessary to use the same stock solution of arsenious acid as was done by Gupta and Ghosh. Efforts were made to eradicate the cause of this trouble, but without any success. The present paper reports the results of experiments using sample 1 of Fig. 1. The reaction is specifically influenced by the ions and hence no electrolyte was added to keep the ionic strength constant. Nor was there any need for it, because in any particular experiment no change in k was observed as the reaction progressed.

Table I shows the results using different concentrations of the reactants.

It may be seen that the reaction is independent of the concentration of arsenious acid — a fact found in other persulfate oxidations where it is independent of the concentration of the reductant. The rate of reaction increases with the increase in the concentration of the persulfate, but the constants decrease, probably due to the inhibition by potassium ions. The inhibiting character of the potassium ions have been reported in the oxidation of formate[7], oxalic acid[8] and oxalate[9], and the decomposition of persulfate[10]. Alkali metal ions, in general, inhibit many persulfate oxidations.

TABLE I

$K_2S_2O_8$, N	H_3AsO_3, N	k
0.005	0.0102	25.80
0.01	0.0102	23.96
0.02	0.0102	19.80
0.04	0.0102	13.82
0.01	0.0051	24.01
0.01	0.0102	23.96
0.01	0.0204	24.59

Specific Effect of the Ions.—Table II gives the average values of k for the kinetics of this reaction in the presence of several electrolytes.

TABLE II

$K_2S_2O_8$=0.01 N; H_3AsO_3=0.0102 N; $AgNO_3$=0.001 M

Electrolyte	Concn., M	k
—	—	23.96
K_2SO_4	0.25	7.49
K_2SO_4	0.125	8.49
$(NH_4)_2SO_4$	0.25	11.22
$(NH_4)_2SO_4$	0.125	11.71
$MgSO_4$	0.25	7.93
$MgSO_4$	0.125	9.88
KNO_3	0.50	10.72
KNO_3	0.25	11.44
$NaNO_3$	0.25	16.50
$NaNO_3$	0.125	18.96
NH_4NO_3	0.50	13.80
NH_4NO_3	0.25	18.21

There is no regular variation in k with the change in the ionic strength of the reaction mixture and hence no conclusion regarding the salt effect could be obtained. A comparison of the results shows that the inhibiting action is in the order $K^+ > Na^+ > NH_4^+$——a conclusion similar to that of uncatalyzed oxidation[2]. When the results for nitrates and sulfates are compared, it may be seen that either sulfate ion inhibits or the nitrate ion accelerates. However, the possibilty of both is also considered. In any reaction a sulfate ion is gradually produced, but no increase or decrease in the constants was observed as the reaction progressed. Hence the sulfate ion seems to have no effect or little effect in this reaction and the reaction rate is higher in presence of nitrates than

7) S. P. Srivastava and S. Ghosh, *Z. physik. Chem.*, **202**, 198 (1953).
8) S. P. Srivastava and S. Ghosh, ibid., **205**, 332 (1956).
9) Y. K. Gupta and S. Ghosh, *J. Inorg. & Nuclear Chem.*, accepted (1959).
10) A. Kailan and L. Olbrich, *Monatshe. Chem.*, **47**, 449 (1927).

of sulfates, due to the acceleration by nitrate ions.

Reaction in Presence of CH_3COONa, CH_3COONH_4 and CH_3COOH.—Five concentrations of CH_3COONa were investigated and it was found that there exists an optimum concentration of sodium acetate for which the reaction is fastest. Fig. 2 shows the average constants for different concentrations of sodium acetate.

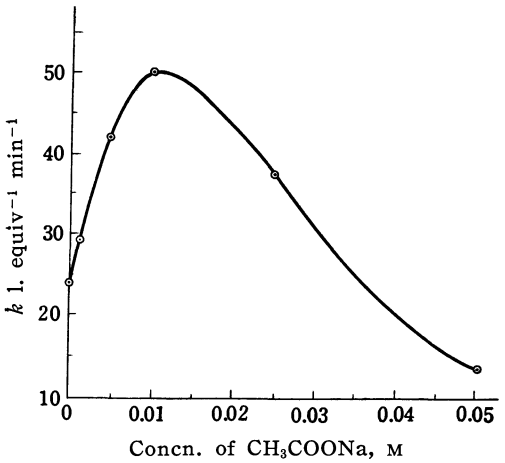


Fig. 2. Effect of CH_3COONa in the silver catalyzed oxidation of H_3AsO_3 by $K_2S_2O_8$.

The sodium ion has been found to inhibit and hence the acetate ion must catalyze the reaction. It appears that at lower concentrations of CH_3COONa, the catalyzing influence of acetate ions predominates over the inhibiting action of sodium ions; whereas the reverse is true at higher concentrations of sodium acetate. The accelerating action of acetate ions may further be seen in Table III where the results with acetic acid and ammonium acetate are shown.

TABLE III

$K_2S_2O_8$=0.01 N; H_3AsO_3=0.0102 N; $AgNO_3$=0.001 M

Electrolyte	Concn., M	k
CH_3COOH	0.40	40.27
CH_3COOH	0.10	39.70
CH_3COONH_4	0.50	4.94
CH_3COONH_4	0.25	6.16

Higher concentrations of sodium acetate could not be employed because a precipitate of possibly sodium arsenite formed. This, however, disappeared as the reaction progressed. Results with ammonium acetate are quite as expected.

Reaction in Presence of Sulfuric Acid.—Seven

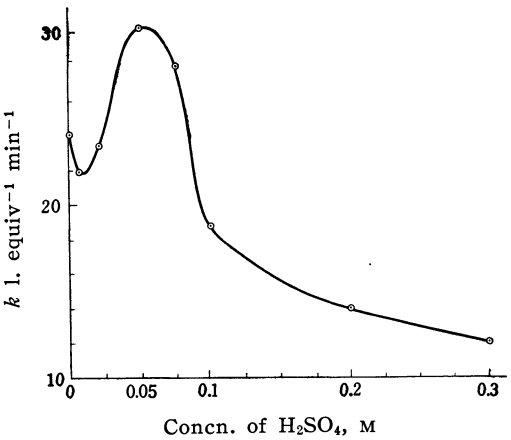


Fig. 3. Effect of H_2SO_4 in the silver catalyzed oxidation of H_3AsO_3 by $K_2S_2O_8$.

concentrations of sulfuric acid were employed and the results are graphically shown in Fig. 3.

There is a concentration of sulfuric acid for which the reaction is fastest. The rate decreases below or above that concentration. The rate constant is 30.26 l. $equi^{-1}$ min^{-1} at this concentration. It may appear from Fig. 3 that hydrogen ions inhibit and sulfate ions slightly accelerate, although the latter have been found to be without any effect. The actual mechanism is not clear. In fact, it is difficult to explain the behavior of sulfuric acid in persulfate oxidations. In the silver catalyzed oxidations of oxalic acid[11] and hydrogen peroxide[12], sulfuric acid retards the rate, whereas it accelerates the rate in the uncatalyzed oxidation of oxalic acid[8] and silver catalyzed oxidation of potassium oxalate[9].

Action of Nitrate, Aluminum and Manganous Ions.—When nitric acid is used, the reaction is very slow in the initial stages, but the rate increases quickly with time. The average constants as shown in Table IV, are found to increase till the end of the reaction.

It seems that there is some impurity in nitric acid which helds up the reaction in the beginning. Further on comparing these results with those in the presence of sulfuric acid, it is evident that the rate is higher in the presence of nitric acid. Hence nitrate ions accelerate the rate.

The results with aluminum nitrate and

11) Y. K. Gupta and S. Ghosh, *Proc. Nat. Acad. Sci., India*, **27A Part V**, 258 (1958).
12) S. P. Srivastava and S. Ghosh, ibid., **23A Part VI**, 44 (1954).

TABLE IV

$K_2S_2O=0.01$ N; $H_3AsO_3=0.0102$ N; $AgNO_3=0.001$ M

Time min.	0.016 M HNO_3		0.16 M HNO_3	
	$KMnO_4$ ml.	k	$KMnO_4$ ml.	k
0	5.10	—	5.10	—
5	4.96	1.61	—	—
10	4.28	15.57	—	—
15	3.66	20.80	—	—
20	3.16	22.95	4.92	0.86
25	2.68	24.91	4.52	4.04
30	2.24	26.76	4.04	7.10
35	1.90	27.64	3.62	9.51
40	1.58	28.82	3.20	11.16
45	1.38	28.60	—	—
50	1.18	28.88	2.56	13.38
55	0.98	29.63	2.28	14.28
60	—	—	2.00	15.33

TABLE V

$K_2S_2O_8=0.01$ N; $H_3AsO_3=0.0102$ N; $AgNO_3=0.001$ M

Electrolyte	Concn., M	k
$Al(NO_3)_3$	0.0625	80.60
$Al(NO_3)_3$	0.01	80.01
$Al_2(SO_4)_3$	0.0625	28.66
$Al_2(SO_4)_3$	0.01	25.93
$MnSO_4$	0.002	7.32
$MnSO_4$	0.001	11.45

aluminum sulfate are shown in Table V. The reaction is very fast in the presence of aluminum nitrate. The rate only slightly increases in the presence of aluminum sulfate.

From this it appears that nitrate ions greatly catalyze the reaction and sulfate does so only slightly, whereas aluminum is without any effect. It may, however, be mentioned that the rate constants gradually decreased in the case of aluminum nitrate and increased in the case of aluminum sulfate till the end of the reaction, and that the above table gives only the average constants. The increase or decrease was 15 to 20%.

Manganous sulfate was used because it has been found to act as a catalyst or an anticatalyst in many of the persulfate oxidations. The authors believe that Mn(II) has a specific inhibiting effect.

Energy and Entropy of Activation.—The energy of activation has been calculated from the results of experiments at three different temperatures. Table VI gives the constants at these temperatures.

The average energy of activation was 18941 cal. The frequency factor[13] and the entropy[14] calculated from this, are 1.55×10^6 l. equiv^{-1} sec^{-1} and -31.06 E.U., respectively. These values correspond to the overall reaction and they may be quite different for the rate determining step. Also these values may vary from sample to sample of arsenious acid, but their nature and order of magnitude do help us to arrive at a possible mechanism.

TABLE VI

$K_2S_2O_8=0.01$ N; $H_3AsO_3=0.0102$ N; $AgNO_3=0.001$ M

Temp. °C	k
24	23.96
29	30.54
39	50.00

The rate is the first order in persulfate and independent of the concentration of arsenious acid. No conclusion regarding the salt effect could be obtained. The authors propose the following mechanism for the silver catalyzed oxidation of arsenious acid by persulfate.

$$S_2O_8^{2-} \rightleftarrows 2SO_4^- \quad \text{rapid (1)}$$

$$2SO_4^- + Ag^+ \rightarrow 2SO_4^{2-} + Ag^{3+} \quad \text{slow (2)}$$

$$Ag^{3+} + 2H_2O \rightarrow Ag^+ + 2H^+ + 2OH \quad \text{fast (3)}$$

$$H_3AsO_3 + 2OH \rightarrow H_3AsO_3 + H_2O \quad \text{fast (4)}$$

The existence of free radicals[15] SO_4^- and OH, and higher valent silver, Ag^{3+} is now beyond doubt. Gupta and Ghosh[16] have discussed the possibilty of higher valent silver in a paper on the silver catalyzed oxidation of Mn(II) by persulfate. The rate determining step 2 is preceded by an equilibrium which has a very small equilibrium constant K, of the order of 10^{-8} or even less. Step 2 is really bimolecular or rather termolecular, but has a first order dependence on the concentration of the persulfate as shown below.

$$-dc/dt = k_2[Ag^+][SO_4^-]^2$$

but $K[S_2O_8^{2-}] = [SO_4^-]^2$ from reaction 1.

Hence $-dc/dt = k_2K[S_2O_8^{2-}][Ag^+]$

$= k_r[S_2O_8^{2-}]$ where $k_r = k_2K[Ag^+]$

The silver ion concentration remains constant and hence the slow step is the first order in persulfate. Experimentally determined k is equal to $k_r/[Ag^+]$. Hence

13) Calculated from the relation $k=A\times e^{-E/RT}$ where A is the frequency factor.

14) Calculated from the relation $k=(KT/h)\cdot e^{\Delta S/R}\cdot e^{-\Delta H/RT}$ where ΔS the entropy change and ΔH is not much different than E.

15) N. Uri, *Chem. Revs.*, **50**, 375 (1952).

16) Y. K. Gupta and S. Ghosh, *J. Inorg. & Nuclear Chem.*, **9**, 178 (1959).

$k=k_2K$ or $k_2=k/K=23.96/10^{-8}$ or 23.96×10^8 l. equiv^{-1} min^{-1}. Based on this value of k_2, the entropy change for the slow step is +5.47 E.U. Absolute entropy values have no meaning. Reactions are faster or slower according as their entropy changes are positive or negative as compared to standard values. A standard value for comparision for bimolecular reactions is about −12 E.U. (calculated for the frequency factor, 10^{11}). There is an entropy increase[17] if the reactants are oppositely charged ions and hence the slow step 2 is supported by a positive entropy change. The generally accepted mechanism is, $S_2O_8^{2-}+Ag^+=2SO_4^{2-}+Ag^{3+}$. If this were the rate determining step, entropy change for the overall reaction should directly support this. The overall entropy change is negative and hence the authors disapprove the slow step between $S_2O_8^{2-}$ and Ag^+. With a prior equilibrium, the entropy change for the slow step 2 is positive and hence step 2 must be preferably between oppositely charged ions, i. e. the reaction is between positively charged silver ion and a negative ion from persulfate, but not persulfate itself.

Gupta and Ghosh[1] have proposed two mechanisms for the uncatalyzed oxidation of arsenious acid by persulfate.

$$S_2O_8^{2-} \rightleftarrows SO_4+SO_4^{2-} \quad \text{slow}$$

or

$$S_2O_8^{2-}+2H_2O \rightleftarrows 2HSO_4^-+2OH \quad \text{slow}$$

Since the silver catalyzed oxidation of arsenious acid is very similar to the uncatalyzed oxidation, particularly in so far as the specific effect of the ions is concerned, it is reasonable to conclude that reaction mechanisms must also be similar. Hence it is believed that OH is preferably the radical responsible for oxidation in the uncatalyzed reaction.

This silver catalyzed oxidation is comparable to the fast oxidation of oxalate[9], and is much faster than the other type of catalyzed reactions wherein the specific rate constant lies between 0.2 and 0.3 at 25°C. Such oxidations are those of Cr(III)[18], VO(II)[19], Mn(II)[20], Ce(II)[21] and many other ions.

17) A. A. Frost and R. G. Pearson, "Kinetics and Mechanism", John Wiley & Sons, Inc., New York (1953), p. 132.

Summary

The kinetics of silver catalyzed oxidation of arsenious acid has been followed by estimating the acid with the permanganate. The results are reproducible only with the same stock solution of arsenious acid. This oxidation is much faster than other silver catalyzed oxidations, such as those of Cr^{3+}, VO^{2+}, Mn^{2+}, Ce^{2+}, etc. The oxidation is of the first order in persulfate and independent of the concentration of the acid. The entropy of activation has been calculated and a mechanism has been suggested. No conclusion regarding the salt effect could be obtained due to the specific effect of the ions. K^+, Na^+, NH_4^+ and Mg^{2+} inhibit in the order given. Nitrate ion accelerates the rate and sulfate ion seems to have no effect.

Department of Chemistry
D.A.V. College
Kanpur, India

18) D. M. Yost, *J. Am. Chem. Soc.*, **48**, 152 (1926).
19) D. M. Yost and W. Claussen, ibid., **53**, 3349 (1931).
20) A. O. Dekker, H. A. Levy and D. M. Yost, ibid., **59**, 2129 (1937).
21) W. H. Cone., ibid., **67**, 78 (1945).

Zur Darstellung von Polymethoxy-o-phthalaldehydsäuren

Von Eturô MAEKAWA und Seiko NAN'YA

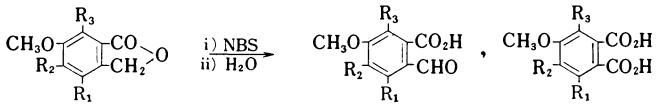
(Eingegangen am 18. Mai 1959)

Polymethoxyphthalaldehydsäuren sind von Bedeutung, weil sie durch Grignardreaktion mit Methylmagnesiumjodid 3-Methylphthalide geben, die als Ausgangsprodukte zur Darstellung von Seeigelfarbstoffen interessant sind[1]. Edwards, Perkin und Stoyle[2] oxydierten Mekonin mit Braunstein in verdünnter Schwefelsäure zur Opiansäure. Es ist aber schwierig, die Oxydation genau zu kontrollieren. Stevens und Robertson[3] versuchten, 5.6-Methylendioxyphthalid mit Bleidioxyd oder Chromsäure zu 4.5-Methylendioxyphthalaldehydsäure zu oxydieren, konnten jedoch keine günstigen Ergebnisse bekommen. Da der Phthalidring im alkalischen Medium geöffnet wird, kann man die Oxydation besser alkalisch durchführen. Obgleich in den stark alkalischen Lösungen die durch Oxydation zuerst entstandene Phthalaldehydsäure sogar die Neigung zeigt[4], durch Cannizarosche Reaktion zu Phthalsäure und Phthalalkoholsäure, nämlich dem Ausgangsprodukt, zu disproportionieren, scheinen die Phthalide in schwach alkalischen Medien leicht zu Phthalaldehydsäuren oxydiert zu werden. Blair, Brown und Newbold[5] erhielten z. B. aus Mekonin bzw. 5.6.7-Trimethoxyphthalid (XIII) und Dimethylamin in Alkohol bei Raumtemperatur 2-Hydroxymethyl-5.6-dimethoxy- bzw. 2-Hydroxymethyl-4.5.6-trimethoxybenzoesäuredimethylamid, das durch Chromsäureoxydation in Eisessig in der Kälte und durch anschließende Verseifung mit verdünnter Salzsäure Opiansäure bzw. 4.5.6-Trimethoxyphthalaldehydsäure (XIV) in etwa 40%-iger Ausbeute ergab. Andererseits wird aus 3-Bromphthalid durch Hydrolyse mit Wasser *o*-Phthalaldehydsäure leicht hergestellt[6], welcher man aus Phthalid durch direktes Bromieren bei erhöhter Temperatur[6] oder durch Versetzen mit *N*-Bromsuccinimid (abgekürzt NBS) nach Hirshberg, Lavie und Bergmann[7] in guten Ausbeuten erhalten kann. Zur Darstellung der Polymethoxyphthalaldehydsäuren scheint sich das direkte bromieren schlechter zu eignen als das Verfahren mit NBS, weil die Gefahr darin besteht, daß der, während der Reaktion der Phthalide mit Brom entwickelte Bromwasserstoff bei der Reaktionstemperatur, nämlich bei 130~150°C, die Methoxygruppe abspaltet. Brown und Newbold[8] erhielten durch die Methode mit NBS *m*-Opiansäure und 4.5-Methylendioxyphthalaldehydsäure aus den entsprechenden Phthaliden in guten Ausbeuten, erwähnten jedoch, daß diese Reaktion auf die Phthalide, die, wie Mekonin, am Benzolkern leicht substituierbare Stelle besitzen, im allgemeinen nicht anwendbar ist[5]. Nach der in der Literatur beschriebenen Vorschrift[7,8] mit etwa doppelter molekularer Menge an NBS konnte in der früheren Arbeit[1] aus 4.5.6-Trimethoxyphthalid (I) keine erwartete Aldehydsäure (II) erhalten werden, wobei die Reaktion aber nicht weiter probiert wurde. Unter Verwendung von äquimolekularer Menge an NBS wird jedoch 3.4.5.6-Tetramethoxyphthalaldehydsäure (V) aus 4.5.6.7-Tetramethoxyphthalid (IV) in 85%-iger Ausbeute hergestellt[1]. Um optimale Bedingungen zur Darstellung der Polymethoxyphthalaldehydsäuren aus den entsprechenden Phthaliden zu finden, wird deren Reaktion mit NBS weiter untersucht.

IV ergibt durch Behandeln mit doppelter molekularer Menge an NBS und durch anschließende Hydrolyse des Produktes mit Wasser in nah-quantitativer Ausbeute 3.4.5.6-Tetramethoxyphthalsäure(VI), deren Konstitution durch Elementaranalyse sowie durch die Bildung des Anhydrids beim Erhitzen und durch IR-Absorptionsspektrum* festgestellt wurde.

1) F. Weygand, H. Weber und E. Maekawa, *Chem. Ber.*, **90**, 1879, (1957).
2) G. A. Edwards, W. H. Perkin und F. W. Stoyle, *J. Chem. Soc.*, **127**, 195 (1925).
3) T. S. Stevens und M. C. Robertson, ebenda, **1927**, 2790.
4) G. H. Beckett und C. R. A. Wright, ebenda, **29**, 281 (1876).
5) J. Blair, J. J. Brown und G. T. Newbold, ebenda, **1955**, 708.
6) R. L. Shrine und E. J. Wolf, „Organic Syntheses", Col. Vol. 3, John Wiley & Sons, Inc., New York (1955), S. 737.
7) Y. Hirshberg, D. Lavie und E. D. Bergmann, *J. Chem. Soc.*, **1951**, 1030.
8) I. J. Brown und G. T. Newbold, ebenda, **1952**, 4397.

* Für die Aufnahme der IR-Spektren danken wir Herrn Prof. Dr. Y. Ishii (Organ.-Chem. Inst. der Techn. Fak. der Univ. Nagoya) bestens.



I: $R_1=R_2=OCH_3$, $R_3=H$ II: $R_1=R_2=OCH_3$, $R_3=H$ III: $R_1=R_2=OCH_3$, $R_3=H$
IV: $R_1=R_2=R_3=OCH_3$ V: $R_1=R_2=R_3=OCH_3$ VI: $R_1=R_2=R_3=OCH_3$
VII: $R_1=R_2=H$, $R_3=OCH_3$ VIII: $R_1=R_2=H$, $R_3=OCH_3$ IX: $R_1=R_2=H$, $R_3=OCH_3$
X: $R_1=R_3=H$, $R_2=OCH_3$ XI: $R_1=R_3=H$, $R_2=OCH_3$ XII: $R_1=R_3=H$, $R_2=OCH_3$
XIII: $R_1=H$, $R_2=R_3=OCH_3$ XIV: $R_1=H$, $R_2=R_3=OCH_3$
XV: $R_1=R_2=OCH_3$, $R_3=CH_3$ XVI: $R_1=R_2=OCH_3$, $R_3=CH_3$

Aus I konnte durch Behandeln mit äquimolekularer Menge an NBS und durch anschließende Hydrolyse 3.4.5-Trimethoxyphthalaldehydsäure (II) in einer Ausbeute von 77% hergestellt werden. Unter Verwendung von doppelter molekularer Menge an NBS bildete sich nach der Hydrolyse als Hauptprodukt 3. 4. 5-Trimethoxyphthalsäure (III) und daneben auch eine kleine Menge II. Die auf diese Weise hergestellte Aldehydsäure II fällt aus Wasser zum größten Teil als Nadeln aus, die bei 129°C schmelzen, und aus Äthanol oder Chloroform zum größten Teil als Nadeln, die bei 135°C schmelzen. Beide Kristalle unterscheiden sich durch ihr Aussehen sowie durch die Geschwindigkeit der Auflösung in verschiedenen Lösungsmitteln, wobei der höherschmelzende Kristall sich im allgemeinen langsamer löst, ergeben jedoch identisches 2. 4-Dinitrophenylhydrazon. Phthalaldehydsäuren können bekanntlich nicht nur als Aldehydsäuren sondern unter Umständen auch als 3-Oxyphthalide reagieren. Opiansäure reagiert z. B. sowohl mit den Aldehydreagenzien als auch mit Alkoholen unter Bildung von 3-Alkoxymekoninen[9,10], die in die normalen Ester der Opiansäure übergehen können. Buu-Hoï stellte fest[11], daß *o*-Phthalaldehydsäure und ihre kernsubstituierten Derivate nach UV-Spektren in Wasser fast ausschließlich als echte Aldehydsäure, in Chloroform zum größten Teil als 3-Oxyphthalid und in Alkoholen als ein Gleichgewichtsgemisch aus beiden Isomeren existieren. Die IR-Spektren der beiden Kristallarten von II in KBr (Abb. 1 u. 2) unterscheiden sich durch Absorptionen bei 1700~1800 cm^{-1}, sind beide jedoch sehr ähnlich dem der *o*-Phthalaldehydsäure in KBr[12], während das IR-Spektrum der Chloroformlösung von II (Abb. 3) eine dem Phthalidring typische Bande bei 1768 cm^{-1} zeight und keine Bande, die der echten Phthalaldehydsäure zuzuordnen ist. Daher wird angenommen, daß der Unterschied zwischen beiden Kristallarten von der Säure II, die im kristallinischen Zustand als echte Phthalaldehydsäure existiert, auf den der Kristallstruktur zurückzuführen ist, obgleich, wie unten erwähnt, der niedrigerschmelzende Kristall nicht fähig ist, durch Grignardreaktion mit Methylmagnesiumjodid 3-Methyl-4. 5. 6-trimethoxyphthalid zu ergeben.

Die oben beschriebenen Polymethoxyphthalsäuren, nämlich III und VI, reagieren mit 2. 4-Dinitrophenylhydrazin viel schneller als Phthalsäure selbst unter Bildung der 2. 4-Dinitrophenylhydrazone ihrer Anhydride.

Gegen die Meinung von Blair u. a.[5] ergibt Mekonin (VII) Opiansäure in relativ guter Ausbeute unter Verwendung von äquimolekularer Menge an NBS und 3. 4-Dimethoxyphthalsäure (IX) mit doppelter Menge an NBS. Zur Darstellung von *m*-Opiansäure (XI) aus X ist auch unsere Vorschrift mit äquimolekularer Menge an NBS besser geeignet als die von Brown u. a.[8] mit überschüssigem NBS, nach welcher sich beim Nachprüfen in unserem Laboratorium *m*-Hemipinsäure in erheblicher Menge ergab. Auch der aus *m*-Mekonin nach McRae u. a.[13] hergestellte 5. 6. 7-Trimethoxyphthalid (XIII) gibt 4. 5. 6-Trimethoxyphthalaldehydsäure (XIV) bzw. 3. 4. 5-Trimethoxyphthalsäure (III) je nach der Menge an verwendetem NBS. 4. 5. 6-Trimethoxy-7-chlormethylphthalid, der aus Gallussäuretrimethyläther nach King und King[14] hergestellt wurde, ergibt durch Reduktion mit Zinkstaub und Essigsäure 4. 5. 6-Trimethoxy-7-methylphthalid (XV), der durch Versetzen mit äquimolekularer Menge an NBS 3. 4. 5-Trimethoxy-6-methylphthalaldehydsäure (XVI) ergab. XVI kristallisierte wieder in zwei verschiedenen

9) A. Kirpal, *Ber. dtsch. chem. Ges.*, **60**, 382 (1927).
10) W. M. Radionowa und A. M. Fedorowa, ebenda, **59**, 2949 (1926).
11) Buu-Hoï und Lin-Chen Kin, *Compt. rend.*, **209**, 221 u. 346 (1939), **212**, 242 u. 268 (1941).
12) *DMS-Kartei*, S-Karte Nr. 3423.
13) J. A. McRae, R. B. VanOrder, F. H. Grifith und Th. E. Habgood, *Canadian J. Chem.*, **29**, 482 (1951).
14) F. E. King und T. J. King, *J. Chem. Soc.*, **1942**, 726.

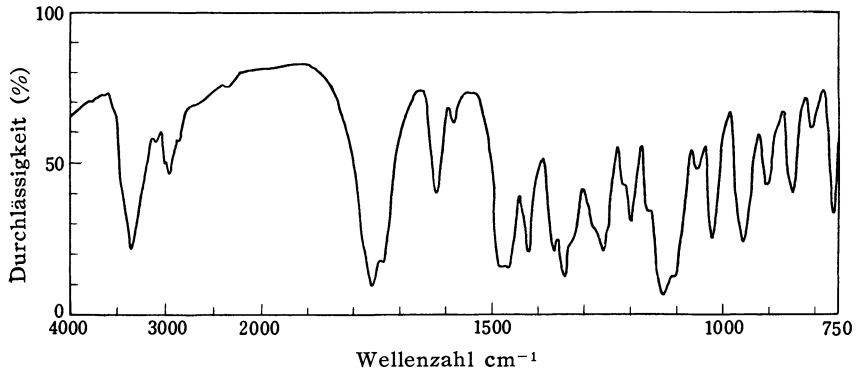


Abb. 1. IR-Absorption der 3.4.5-Trimethoxy-*o*-phthalaldehydsäure (Fp. 129°C).

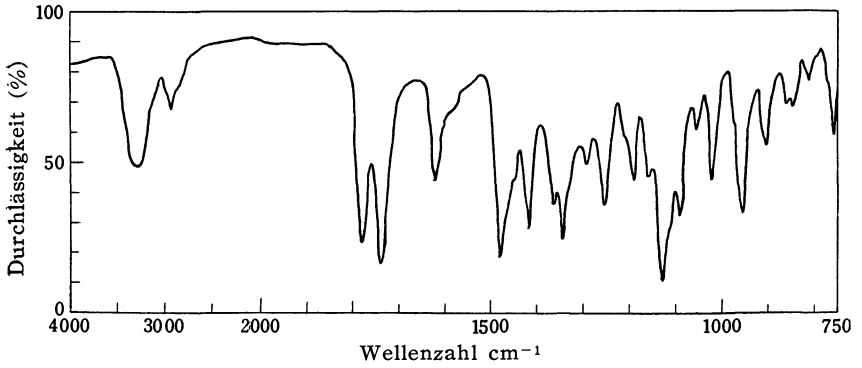


Abb. 2. IR-Absorption der 3.4.5-Trimethoxy-*o*-phthalaldehydsäure (Fp. 135°C).

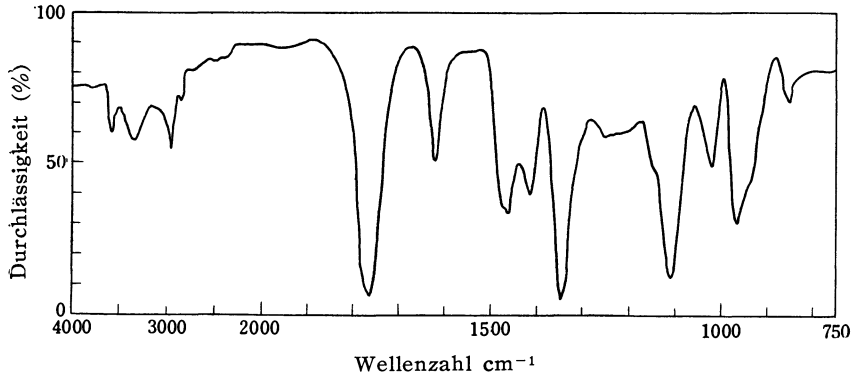


Abb. 3. IR-Absorption der 3.4.5-Trimethoxy-*o*-phthalaldehydsäure (in Chlf.).

Kristallarten von den Schmelzpunkten 114 und 124°C, deren Unterschied nach den IR-Spektren auf dem der Kristallstruktur beruhen muß. Ein Molekül der Verbindung XVI besitzt insgesammt 5 aktive Wasserstoffatome, und seine Reaktionen mit überschüssigem NBS sind sehr komplex; sie werden weiter untersucht.

Die Ergebnisse der NBS-Oxydation der Polymethoxyphthalide sind zusammenfassend in der Tabelle I angegeben.

Aus Phthalaldehydsäure wurden 3-Alkylphthalide durch Grignardreaktion mit Alkylmagnesiumjodiden in guter Ausbeute hergestellt[15,16] und andere kernsubstituierte 3-Alkylphthalide können auch auf diese Weise aus den entsprechenden substituierten Phthalaldehydsäuren gewonnen werden[1,16]. Bei den polymethoxylierten

15) H. Simonis, E. Marben und E. Mermod, *Ber. dtsch. chem. Ges.*, 38, 3981 (1905).
16) E. Mermod und H. Simonis, ebenda, 41, 982 (1908).

TABELLE I. NBS-OXYDATION DER POLYMETHOXYPHTHALIDE

Phthalid	Produkte	
	Phthalid : NBS=1 : 1 (°C)	Phthalid : NBS=1 : 2 (°C)
I	II, Fp. 129 u. 135 (77%)[a]	III, Fp. 174,5[b] (51%) u. daneben II (16%)
IV	V, Fp. 98,5 (85%)[c]	VI, Fp. 192,3 (87%)
VII[d]	VIII, Fp. 147,5[e] (81%)	IX, Fp. 187[f] (56%) u. daneben VIII (32%)
X[d]	XI, Fp. 184[g] (48%)	XII, Fp. 204[h] (28%) u. daneben XI (55%)
XIII	XVI, Fp. 136[i] (53%)	III, Fp. 174 (43%)
XV	XVI, Fp. 114 u. 124 (50%)	

a) In Klammern Ausbeute; b) G. Bargellini u. a., *Atti Acad. Lincei*, **21 II**, 146 (1912), Fp. 174°C; c) Daten aus Lit. 1 zitiert; d) Lösungsmittel Benzol u. CCl_4 (1 : 2 in Volumen); e) Lit. 2, Fp. 150°C; f) Lit. 2, Fp. 187°C; g) Lit. 8, Fp. 187~188°C; h) R. G. Fargher u. a., *J. Chem. Soc.*, **119**, 1724 (1921), Fp. 202°C; i) Lit. 8, Fp. 136°C, Mischprobe mit der höher schmelzenden II zeigte eine Depression von ca. 10°C.

Derivaten, besonders bie Opiansäure, nimmt die Ausbeute ab, offenbar weil die Löslichkeit von Polymethoxyphthalaldehydsäuren in Äther viel geringer ist. Es gelang uns also 3-Methyl-4.5.6-trimethoxyphthalid aus der ätherischen Suspension der höherschmelzenden Aldehydsäure II herzustellen. Die niedrigerschmelzende II war unter allen Bedingungen—soweit versucht—nicht fähig, mit Methylmagnesiumjodid zu reagieren. Der Unterschied der Reaktivität beider Kristallarten, der auch auf dem der Kristallstruktur beruhen mag, ist jedoch noch nicht völlig aufgeklärt.

Organische Bromide können auch aus den entsprechenden um ein Kohlenstoffatom höheren Carbonsäuresilbersalzen durch Behandeln mit Brom hergestellt werden[17,18]. Um andere Möglichkeiten zur Darstellung der 3-Bromphthalide und dadurch die der Darstellung der Phthalaldehydsäuren zu finden, wurde nun die Reaktion des Silbersalzes der aus 3-Trichlormethyl-4.5.6-trimethoxyphthalid hergestellten 4.5.6-Trimethoxyphthalid-3-carbonsäure (XVII)[19] mit Brom probiert. Obgleich XVII in einer äquimolekularen Kalilauge beim Versetzen mit Silbernitrat kein Silbersalz ausfallen läßt, ergibt sie jedoch in einer wässerigen Lösung, die die zweifach-molekulare Menge Kaliumhydroxyd enthält, beim Zusatz des Silbernitrats Disilbersalz der 2-(Hydroxy-carboxy-methyl)-3.4.5-trimethoxybenzoesäure. Da Silbersalze aromatischer Carbonsäuren nach unseren Versuchen im allgemeinen langsamer als Salze aliphatischer Säuren mit Brom unter Decarboxylieren reagieren und da Salze der α-Hydroxycarbonsäuren Aldehyde geben[20], wird das Disilbersalz mit einer äquimolekularen Menge Brom in Tetrachlorkohlenstoff behandelt, wobei 4.5.6-Trimethoxy-7-bromphthalid-3-carbonsäure (XVIII) statt der erwarteten Aldehydsäure II erhalten wird. XVIII enthält ein Molekül Kristallwasser und gibt das Wasser beim Schmelzen ab. Eine andere Konstitutionsmöglichkeit, nämlich 2-(Hydroxy-carboxy-methyl)-3.4.5-trimethoxy-6-brombenzoesäure, wird aber nach dem IR-Absorptionsspektrum, wegen des undeutlichen Schmelzpunktes sowie auf Grund der Tatsache, daß die wasserfreie Säure XVIII viel höher schmilzt als die wasserhaltige, verneint. Die kristallwasserfreie Säure XVIII geht beim Erhitzen in 4.5.6-Trimethoxy-7-bromphthalid über. Die Totalausbeute beträgt auf XVII bezogen ca. 50%. Derselbe Bromphthalid wird auch aus 4.5.6-Trimethoxy-7-aminophthalid, der aus XVII über 4.5.6-Trimethoxyphthalid und 4.5.6-Trimethoxy-7-nitrophthalid hergestellt wurde[1], nach Sandmeyer hergestellt, wobei die Ausbeute auf XVII bezogen höchstens 5% beträgt.

17) A. Lüttringhaus und D. Schade, ebenda, **74B**, 1565 (1941).
18) H. Hunsdiecker und Cl. Hunsdiecker, ebenda, **75B**, 291 (1942).
19) R. L. Alimchandani, *J. Chem. Soc.*, **125**, 540 (1924).
20) J. Kleinberg, *Chem. Revs.*, **40**, 381 (1947).

Beschreibung der Versuche

1. 4.5.6-Trimethoxyphthalid (I)[14].—Ein Gemisch aus 10 g Gallussäuretrimethyläther, 33 ccm 30%-igem Formalin und 9 ccm konz. Salzsäure wurde 20 Min. am Rückfluß erhitzt, 5 g (47%) farblose Nadeln, Fp. 136°C** (aus Äthanol) (Lit.[14] 135~136°C).

2. 4.5.6.7-Tetramethoxyphthalid (IV)[1]. — Eine Lösung von 10 g 3.4.5.6-Tetramethoxyphthalalkohol in 60 ccm Eisessig wurde mit einer Lösung von 8 g Natriumbichromat in 60 ccm Eisessig bei 60°C tropfenweise oxydiert, 3,5 g

** Schmelzpunkte wurden mikroskopisch bestimmt, aber nicht korrigiert.

(36%) leicht gelbe Nadeln, Fp. 52°C (aus Äther) (Lit.[1] 52°C).

3. Mekonin (VII)[2].—Ein Gemisch aus 8 g 2.3-Dimethoxybenzoesäure, 35 ccm konz. Salzsäure und 30 ccm 30%-igem Formalin wurde 15 Min. am Rückfluß erhitzt, 2 g (24%) farblose Nadeln, Fp. 101～103°C (aus Wasser) (Lit.[2] 102°C).

4. *m*-Mekonin (X)[13]. — 50 g Veratrumsäure wurden in 250 ccm Eisessig mit 80 ccm 40%-igem Formalin und 200 g konz. Salzsäure 10 Std. auf 90～95°C und noch 3 Std. auf 100°C erhitzt. 25 g (47%) farblose Nadeln, Fp. 155°C (aus Wasser) (Lit.[13] 155°C).

5. 5.6.7-Trimethoxyphthalid (XIII)[13]. — 20 g X wurden durch Versetzen mit 10 ccm konz. Schwefelsäure und 140 ccm konz. Salpetersäure zu 8 g 7-Nitro-*m*-mekonin nitriert, dessen Reduktion in Essigester mit Raney-Nickel 6,5 g 5.6-Dimethoxy-7-aminophthalid [Fp. 181～182°C (aus Äthanol)] ergibt. 5,9 g des Hydrochlorids dieses Amins geben durch Diazotieren mit Natriumnitrit und durch anschließendes Versetzen mit Kaliumjodid 3,5 g 5.6-Dimethoxy-7-jodphthalid [Fp. 169°C (aus Essigsäure)], dessen 3,2 g bei 12-stündigem Kochen in einer methanolischen Lösung von 0,8 g Kalium in Gegenwart von wenig Kupferbronze (Merck) in 2,0 g XIII übergehen, Fp. 136～136,5°C (aus Wasser) (Lit.[13] 136,6～137°C). Mischprobe mit I zeigte eine Depression von ca. 10°C.

6. 4.5.6-Trimethoxy-7-chlormethylphthalid[14].—Ein Gemisch aus 10 g Gallussäuretrimethyläther, 33 ccm 30%-igem Formalin und 40 ccm konz. Salzsäure 20 Min. am Rückfluß erhitzt, 6,5 g (51%) farblose Nadeln, Fp. 85°C (aus Äthanol) (Lit.[14] 85°C).

7. 4.5.6-Trimethoxy-7-methylphthalid (XV).—5 g der vorstehenden Chlormethylverbindung wurden in 70 ccm Eisessig mit 13,5 g Zinkstaub 30 Min. am Rückfluß gekocht, das Filtrat nach dem Erkalten im Vakuum eingeengt und dann mit Wasser versetzt. Der ausgeschiedene Niederschlag wurde aus verdünnter Essigsäure umkristallisiert, 4,4～4,5 g (ca. 90%) farblose Nadeln, Fp. 80～82°C.

*Anal.**** Gef.: C 58,07; H 5,88. Ber. für $C_{12}H_{14}O_5 \cdot 1/2CH_3CO_2H$ (268,2): C 58,20; H 6,01.

8. 3.4.5-Trimethoxyphthalaldehydsäure (II). — 4 g I wurden in 350 ccm Tetrachlorkohlenstoff mit 3,2 g NBS in Gegenwart von einer Messerspitze Dibenzoylperoxyd (abgekürzt BPO) unter Bestrahlung mit einer 500W-Wolframlampe 1 Std. am Rückfluß gekocht. Das gebildete Succinimid wurde abgesaugt und das Filtrat eingeengt. Der Rückstand wurde mit ca. 150 ccm Wasser unter mechanischem Rühren 2 Std. auf dem siedenden Wasserbad erwärmt, das Reaktionsgemisch abfiltriert und die Lösung langsam abdunsten gelassen. Dabei fielen gelbe Nadeln aus, Ausbeute 3,4 g (77%), Fp. 128,5～129°C (aus Wasser) und Fp. 134～135°C (aus Äthanol oder Chloroform).

Anal. Gef.: C 55,13; H 5,11. Ber. für $C_{11}H_{12}O_6$ (240,2): C 55,00; H 5,04.

2.4-Dinitrophenylhydrazon.—Orange Nadeln, Fp. 235～236°C (aus 95%-igem Äthanol).

Anal. Gef.: C 48,73; H 4,13; N 13,28. Ber. für $C_{17}H_{16}N_4O_9$ (420,4): C 48,58; H 3,84; N 13,33.

9. 3.4.5-Trimethoxyphthalsäure (III).—11,2 g I wurden in 1000 ccm Tetrachlorkohlenstoff mit 18 g NBS und wenig BPO 1 Std. unter Bestrahlung am Rückfluß gekocht, das gebildete Succinimid abgesaugt und das Filtrat eingeengt. Der Rückstand wurde mit 150 ccm Wasser 2 Std. auf dem siedenden Wasserbad erwärmt und das Gemisch noch heiß abfiltriert. Es fielen zuerst 1,3 g (16%) II beim Abkühlen der Lösung und dann 6,6 g (51%) III beim Einengen der Mutterlauge in Prismen aus, Fp. 173,5～174,5°C (aus Wasser) (Lit.[10] 174°C), IR-Absorption in KBr: 1680～1720 cm^{-1} (breite Bande).

Anhydrid.—Nadeln, Fp. 143～144°C (aus Benzol) (Lit.[10] 143°C), IR-Absorptionen in KBr: 1724 u. 1831 cm^{-1}.

2.4-Dinitrophenylhydrazon des Anhydrids.—Gelbe Nadeln, Fp. 254,5～256°C (aus Äthanol).

Anal. Gef.: C 49,00; H 3,73; N 13,79. Ber. für $C_{17}H_{14}N_4O_9$ (418,3): C 48,81; H 3,37; N 13,39.

10. 3.4.5.6-Tetramethoxyphthalsäure (VI).—1,5 g IV wurden in 30 ccm Tetrachlorkohlenstoff mit 2,1 g NBS und wenig BPO unter Bestrahlung 1 Std. am Rückfluß gekocht und das Gemisch wie vorstehend aufgearbeitet, wobei 1,3 g (86%) VI in farblosen Nadeln erhalten wurden. Fp. 191,7～192,3°C (aus Wasser), IR-Absorption in KBr: 1690～1710 cm^{-1} (breite Bande).

Anal. Gef.: C 50,43; H 5,00. Ber. für $C_{12}H_{14}O_8$ (286,2): C 50,35; H 4,93.

Anhydrid bildete sich beim Schmelzen von VI quantitativ, Fp. 137,5～138°C (aus Benzol).

Anal. Gef.: C 53,50; H 4,75. Ber. für $C_{12}H_{12}O_7$ (268,2): C 53,73; H, 4,51.

2.4-Dinitrophenylhydrazon des Anhydrids.—Gelbe Nadeln, Fp. 220,5～221°C (aus Äthanol).

Anal. Gef.: C 48,58; H 3,86; N 12,41. Ber. für $C_{18}H_{16}N_4O_{10}$ (448,4): C 48,22; H 3,60; N 12,50.

11. 3.4.5-Trimethoxy-6-methylphthalaldehydsäure (XVI).—Eine Lösung von 2 g XV in 150 ccm Tetrachlorkohlenstoff wurde mit 2 g NBS und wenig BPO unter Bestrahlung 2 Std. am Rückfluß erhitzt und das Gemisch wie vorstehend aufgearbeitet, 0,98 g (50%) farblose Nadeln, Fp. 114°C (aus Wasser), IR-Absorptionen in KBr: 1690 u. 1703 cm^{-1}, und Fp. 122°C (aus Chloroform), IR-Absorptionen in KBr: 1689 u. 1703 cm^{-1}.

Anal. Gef.: C 56,44; H 4,88. Ber. für $C_{12}H_{14}O_6$ (254,2): C 56,69; H 4,55.

2.4-Dinitrophenylhydrazon. — Rote Nadeln, Fp. 214°C (aus 95%-igem Äthanol und Essigester).

Anal. Gef.: C 50,02; H 3,86; N 12,84. Ber. für $C_{18}H_{18}N_4O_9$ (434,4): C 49,72; H 4,12; N 12,89.

12. 3-Methyl-4.5.6-trimethoxyphthalid.—Einem Grignardreagens aus 0,50 g Magnesiumspänen und 3,0 g Methyljodid wurde eine Suspension von 1,5 g II vom Fp. 135°C in 500 ccm absolutem Äther unter Eiskühlung zugetropft. Es wurde 1 Std. unter Eiskühlung und noch 1 Std. am Rückfluß umgerührt. Das Reaktionsgemisch wurde auf Eis gegossen und mit 2 N Schwefelsäure angesäuert. Die wässerige Schicht wurde mehrmals mit Äther ausgezogen, die ätherische Lösung mit verdünnter Natriumhydrogencarbonatlösung

*** Für Mikroanalysen der Verbindungen sind wir der Zentralen Mikroanalysenstelle der Univ. Kyôto sehr dankbar.

gewaschen, mit Natriumsulfat getrocknet und eingeengt. Es blieb ein gelbes Fett zurück, das aus Wasser kristallisiert wurde, 0,75 g (49%) farblose Nadeln, Fp. 52°C, IR-Absorption in KBr: 1765 cm^{-1}.

Anal. Gef.: C 60,56; H 5,98. Ber. für $C_{12}H_{14}O_5$ (238,2): C 60,50; H 5,92.

13. 2.4-Dinitrophenylhydrazon des Phthalsäureanhydrids. — Gelbe Nadeln, Fp. 280~282°C (aus 95%-igem Äthanol und Essigester).

Anal. Gef.: C 51,09; H 2,62; N 17,65. Ber. für $C_{14}H_8N_4O_6$ (328,2): C 51,23; H 2,46; N 17,07.

14. 4.5.6-Trimethoxyphthalid-3-carbonsäure (XVIII)[20]. — 5 g 3-Trichlormethyl-4.5.6-trimethoxyphthalid wurden in einer Natronlauge aus 5 g Natriumhydroxyd und 20 ccm Wasser 45 Min. erhitzt und das abgekühlte Gemisch mit Salzsäure angesäuert, 3,5 g (90%) farblose Nadeln, Fp. 147~148°C (aus Wasser) (Lit.[20] 147~148°C).

15. Disilbersalz der 2-(Hydroxy-carboxy-methyl)-3.4.5-trimethoxybenzoesäure. — Eine Lösung von 2,68 g XVII in einer Kalilauge aus 1,12 g Kaliumhydroxyd und 100 ccm Wasser wurde mit 3,4 g Silbernitrat in 100 ccm Wasser versetzt. Der Niederschlag wurde mit Methanol gewaschen und im Vakuumexsikkator getrocknet, 3,04 g (76%).

Anal. Gef.: Ag 42,75. Ber. für $C_{12}H_{12}Ag_2O_8$ (499,8): Ag 43,18.

16. 4.5.6-Trimethoxy-7-bromphthalid-3-carbonsäure (XVIII).—Eine Suspension von 3,0g vorstehenden Silbersalzes in 100 ccm Tetrachlorkohlenstoff wurde bei ihrem Siedepunkt mit 1,2 g Brom in 20 ccm Tetrachlorkohlenstoff tropfenweise versetzt, das Gemisch mit 150 ccm 0,1 N Brom-Wasserstoffsäure 10 Min. umgerührt und das Silberbromid abfiltriert (2,70 g). Beim Einengen des Filtrats fielen farblose Nadeln aus, 3,50 g (90%), Fp. 75~90°C (aus Wasser). IR-Absorptionen in KBr: 1721 cm^{-1} (COOH) u. 1761 cm^{-1} (Phthalid).

Anal. Gef.: C 39,81; H 3,84; Br 22,04. Ber. für $C_{12}H_{11}BrO_7 \cdot H_2O$ (365,1): C 39,49; H 3,59; Br 21,89.

Beim Schmelzen bildete sich die wasserfreie XVIII, Fp. 137~138°C.

Anal. Gef.: C 41,40; H 3,32; Br 23,27. Ber. für $C_{12}H_{11}BrO_7$ (347,1): C 41,55; H 3,19; Br 23,02.

17. 4.5.6-Trimethoxy-7-bromphthalid (XIX).— 2,92 g der wasserfreien XVIII wurden auf 185°C erhitzt, 1,91 g (76%) (nach einer Umkristallisation aus Methanol), Fp. 103~104°C.

18. XIX aus 4.5.6-Trimethoxy-7-aminophthalid. —Eine Lösung von 4 g 4.5.6-Trimethoxy-7-aminophthalid[1] in 3 ccm konz. Schwefelsäure und 20 ccm Wasser wurde mit 2 g festem Natriumnitrit diazotiert, die überschüssige salpetrige Säure mit Harnstoff zersetzt, das Gemisch mit 2,4 g Kupfer(I)-bromid mit überschüssiger Bromwasserstoffsäure versetzt und dann erhitzt. Das dabei getrennte Öl wurde nach dem Erkalten aus Methanol kristallisiert, 1,5 g (29%), farblose Nadeln, Fp. 103~104°C. Mischschmelzpunkt mit dem obenstehenden Präparat 103~104°C.

Zusammenfassung

Polymethoxyphthalaldehydsäuren wurden aus den entsprechenden Phthaliden durch Bromieren mit äquimolekularer Menge an NBS und durch anschließende Hydrolyse der Produkte in guten Ausbeuten hergestellt, während die Verwendung von überschüssigem Reagens Phthalsäuren ergab. 3.4.5-Trimethoxyphthalaldehydsäure existiert in Chloroformlösung als 3-Hydroxy-4.5.6-trimethoxyphthalid und fällt aus den Lösungen als echte Phthalaldehydsäure in zwei verschiedenen Kristallarten aus, von denen nur die höher schmelzende durch Grignardreaktion mit Methylmagnesiumjodid 3-Methyl-4.5.6-trimethoxyphthalid ergeben konnte. Das aus 4.5.6-Trimethoxyphthalid-3-carbonsäure hergestellte Disilbersalz ergab durch Versetzen mit Brom statt der erwarteten Phthalaldehydsäure das 7-Bromderivat.

Herrn Prof. Dr. F. Weygand, München sagen wir an diesser Stelle unseren aufrichtigsten Dank für seine Anleitung und Anregung zu vorstehender Arbeit. Dem Unterrichtsministerium Japan sind wir für seine Unterstützung dieser Arbeit durch eine Beihilfe für individuelle Forschung 1958 zum Dank verpflichtet.

Technisch-Chemisches Institut der Technischen Hochschule Nagoya Shôwa-ku, Nagoya

Studies on the Cobalt(III) Complexes of Monothiophosphate Ion

By Jinsai HIDAKA, Junnosuke FUJITA, Yoichi SHIMURA and Ryutaro TSUCHIDA

(Received June 11, 1959)

Recently, Yasuda and Lambert[1] reported that the monothiophosphate ion shows an interesting color reaction with the cobalt-(II) ion in aqueous solution. Except for this report there has been no description heretofore about the coordinative nature of the monothiophosphate ion. In the present paper, the syntheses of di-monothiophosphato - bis - ethylenediamine and monothiophosphato - bis - ethylenediamine cobalt(III) complexes will be reported. Furthermore, their visible and ultraviolet and also the infrared absorption spectra will be discussed mainly in comparison with those of the known thiosulfato complexes of cobalt(III).

Experimental

Preparation.—*1) Dark green complex*: $Na_3[Co\,en_2(SPO_3)_2]\cdot 8H_2O$. — This complex was prepared as follows: 3.2 g. anhydrous sodium monothiophosphate[1,2], was completely dissolved in 80 ml. of water, and the solution was added to the aqueous solution (20 ml.) of 2.5 g. *trans*-$[Co\,en_2Cl_2]Cl$. The color of the mixture changed from dark red to dark greenish red. To complete the reaction the mixture was preserved for one hour. The resulting solution was filtered quickly, and ethanol was added carefully to the clear filtrate on cooling. Dark greenish crystalline powder was obtained. The crude product was recrystallized from a small quantity of cold water by the addition of ethanol. The fine crystals obtained were dried in a desiccator over sulfuric acid.

Anal. Found: Co, 9.58; P, 9.72; N, 8.97; C, 7.67; H, 5.05; H_2O, 23.66. Calcd. for $Na_3[Co\,en_2(SPO_3)_2]\cdot 8H_2O = C_4H_{16}O_6S_2N_4P_2Na_3Co\cdot 8H_2O$: Co, 9.59; P, 10.10; N, 9.12; C, 7.82; H, 5.25; H_2O, 23.46%.

2) Dark red complex: $[Co\,en_2(SPO_3)]\cdot 2H_2O$.— To the aqueous solution (30 ml.) of 5 g. *trans*-$[Co\,en_2Cl_2]Cl$, was added on cooling an aqueous solution (70 ml.) of 3.2 g. of anhydrous sodium monothiophosphate. The resulting solution was dark red. A large amount of ethanol was added carefully to the solution. The desired complex was obtained as dark reddish crystalline powder.

Anal. Found: Co, 17.8; P, 9.35; N, 16.93; C, 14.37; H, 6.51; H_2O, 11.82. Calcd. for $[Co\,en_2(SPO_3)]\cdot 2H_2O = C_4H_{16}O_3SN_4PCo\cdot 2H_2O$: Co, 18.07; P, 9.5; N, 17.18; C, 14.73; H, 6.19; H_2O, 11.05%.

Measurements. — The visible and ultraviolet absorption measurements were made by a Beckman DU spectrophotometer in cold aqueous solutions to prevent the aquation of the complexes. The concentration of the solutions varied from $1/2\times10^{-2}$ to $1/8\times10^{-3}$ F. The infrared spectra were obtained by a Parkin-Elmer Model 21 (double beam) and a Hilger H-800 infrared spectrophotometer using sodium chloride prisms. The potassium bromide disk method and nujol mull technique were employed.

Materials.—Thiosulfato-pentammine cobalt(III) chloride, $[Co(NH_3)_5(SSO_3)]Cl$[3], and sodium dithiosulfato - bis - ethylenediamine cobaltate(III), $Na[Co\,en_2(SSO_3)_2]$[4], were obtained as dark red and green crystals, respectively, in the usual way as done by Rây and his coworker. The visible and ultraviolet absorption curves of these compounds are shown in Figs. 1 and 2. These absorption curves were in good agreement with those obtained by Kiss et al.[5,6].

Results and Discussion

Dark green complex: $Na_3[Co\,en_2(SPO_3)_2]\cdot 8H_2O$.—The visible and ultraviolet absorption curve of this compound is shown in Fig. 1, in which the spectrum of the corresponding thiosulfato-complex, $Na[Co\,en_2(SSO_3)_2]$, is also plotted for comparison. These two absorption curves are similar to each other on the whole. The frequencies of the absorption maxima for each complex are listed in Table I.

The first absorption bands of these complexes are shifted towards longer wavelengths than those of complexes of $[Co^{III}N_4O_2]$ type[7,8] and distinctly split into two components. Moreover, the type of these splittings differ from those of $[Co^{III}N_4O_2]$ and $[Co^{III}N_5O]$ type complexes.

1) S. K. Yasuda and J. L. Lambert, *J. Chem. Educ.*, **31**, 572 (1954).
2) J. W. Mellor, "A Comprehensive Treatise on Inorganic and Theoretical Chemistry", Vol. 8, Longmans, Green & Co., New York (1931), p. 1068—1069.
3) P. R. Rây, *J. Indian Chem. Soc.*, **4**, 71 (1927).
4) P. R. Rây and S. N. Maulik, ibid., **10**, 655 (1933).
5) A. Kiss and D. Czeglédy, *Z. anorg. u. allgem. Chem.*, **235**, 407 (1938).
6) A. Kiss, G. Auer and E. Major, ibid., **264**, 28 (1941).
7) M. Linhard and M. Weigel, ibid., **264**, 321 (1951).
8) Y. Shimura and R. Tsuchida, This Bulletin, **29**, 311 (1956).

TABLE I. THE FIRST, SECOND AND THE CHARGE-TRANSFER BANDS OF MONOTHIOPHOSPHATO AND THIOSULFATO Co(III) COMPLEXES
(in frequency unit 10^{13}/sec.)

Complex salt	First band ν_{max} (log ε)	Second band ν_{max} (log ε)	Charge-transfer band ν_{max} (log ε)
$[Co(NH_3)_5(SSO_3)]Cl$	58.8 (1.82)	ca. 82 (2.3)	103.4 (4.9) 126 (3.6)
$Na[Co\,en_2(SSO_3)_2]$	54.9 (1.93)		89.6 (4.28)
$Na_3[Co\,en_2(SPO_3)_2]$	53.9 (2.10)		87.0 (4.36) 108 (3.83)
$[Co\,en_2(SPO_3)]$	56.0 (2.31)	ca. 82 (2.6)	107.3 (4.16)

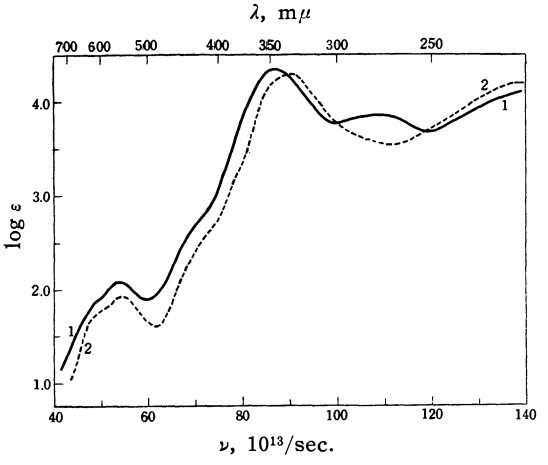


Fig. 1. Absorption spectra of:
1, $Na_3[Co\,en_2(SPO_3)_2]\cdot 8H_2O$;
2, $Na[Co\,en_2(SSO_3)_2]$.

These facts indicate that the cobalt(III) ion in these complex ions coordinates monothiophosphate or thiosulfate ions by their sulfur atoms. This conclusion is also supported by the fact that these complexes show intense absorption bands in the near ultraviolet, which are probably originated from charge transfer between the central cobalt(III) ion and the coordinated monothiophosphate or thiosulfate ion. As to the charge transfer band of di-thiosulfato-bis-ethylenediamine cobalt(III) ion, it is located at a longer wavelength than that of thiosulfato-pentammine cobalt(III) ion. Judging from the position of the thiosulfate ion in the spectrochemical series, it is evident that $[Co\,en_2(SSO_3)_2]^-$ has *trans* structure with regard to two thiosulfate ions in coordination[8]. It may be concluded, therefore, that the structure of $[Co\,en_2(SPO_3)_2]^{3-}$ is also *trans*, since its absorption curve is quite similar to the corresponding thiosulfato-complex.

Structure of the Dark Red Complex.—From the result of the chemical analysis, there was two possibilities of the structure of the "dark red complex". The one is $[Co\,en_2(OH_2)(SPO_3)]\cdot H_2O$ in which the monothiophosphate ion is coordinated as a monodentate ligand, and the other, $[Co\,en_2(SPO_3)]\cdot 2H_2O$ in which the monothiophosphate ion is coordinated as a chelate ligand.

Being heated for dehydration, sodium di-monothiophosphato-bis-ethylenediamine cobaltate(III) is rather unstable and changes into black sulfide of cobalt at about 110°C with evolution of hydrogen sulfide. On the contrary, the dark red complex is more stable against heating. Even after the two molecules of water were expelled at 110°C, the dark red color of the complex was well preserved and no indication of the decomposition of the complex was observed. These facts suggest that the structure of the dark red complex is $[Co\,en_2(SPO_3)]\cdot 2H_2O$ and not $[Co\,en_2(OH_2)(SPO_3)]\cdot H_2O$.

The visible and ultraviolet absorption curve of the dark red complex is shown in Fig. 2, in which the spectrum of thiosulfato-pentammine cobalt(III) ion is also plotted for comparison.

The trend that the two absorption curves resemble each other on the whole, is similar to the case of Fig. 1. There are, however, a few important differences between the two curves in Fig. 2. In the

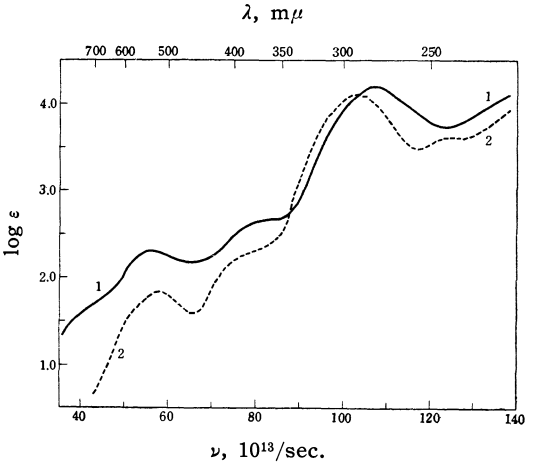


Fig. 2. Absorption spectra of:
1, $[Co\,en_2(SPO_3)]\cdot 2H_2O$;
2, $[Co(NH_3)_5(SSO_3)]Cl$.

first place, the charge transfer band of the dark red complex ($\nu=107.3\times10^{13}$/sec.) is in a shorter wavelength than that of the thiosulfato-pentammine complex. The second difference is seen in the first and the second absorption bands. In this region, the absorption of the dark red complex is stronger in intensity than that of the thiosulfato-pentammine complex. These phenomena may be considered as a proof for the structural difference between the two complexes, especially the difference in the type of coordination of the sulfur-containing ligands.

Infrared Absorption Spectra. — Fig. 3 indicates the infrared spectra of the thiosulfato cobalt(III) complexes and of sodium thiosulfate pentahydrate in 1250~850 cm^{-1} region. Except for the absorption bands which are due to the vibration of ethylenediamine, two absorption bands appear in this region, which are assigned as the S–O vibration[9].

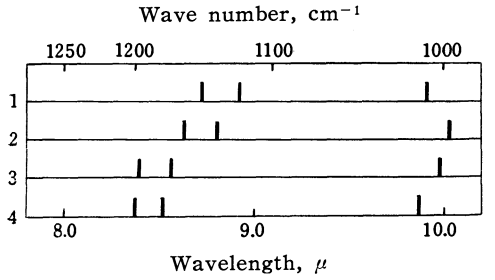


Fig. 3. Infrared absorption bands of:
1, $Na_2S_2O_3\cdot5H_2O$ (KBr disk);
2, $[Co(NH_3)_5(SSO_3)]Cl$ (nujol mull);
3, $Na[Co\,en_2(SSO_3)_2]$ (nujol mull);
4, $K_4[Co(CN)_5(SSO_3)]$ (KBr disk).

The free thiosulfate ion has the symmetry of C_{3v}, and the symmetry is not altered by coordination, because the central cobalt(III) ion is attached to the sulfur atom of the monodentate thiosulfate ion in these complexes. As is seen in Fig. 3, although the band at 1000 cm^{-1} is hardly shifted by coordination, the bands at 1120 cm^{-1} are shifted to higher frequencies by coordination. A similar trend is seen in the cobalt(III) complex which contains monothiophosphate ions as monodentate ligand (Fig. 4).

These facts will be explained from the assumption that the free ligand (SPO_3^{3-}) and the coordinated ligand have the same symmetry C_{3v}. The two sharp bands of the free ligand are due to the PO_3 group

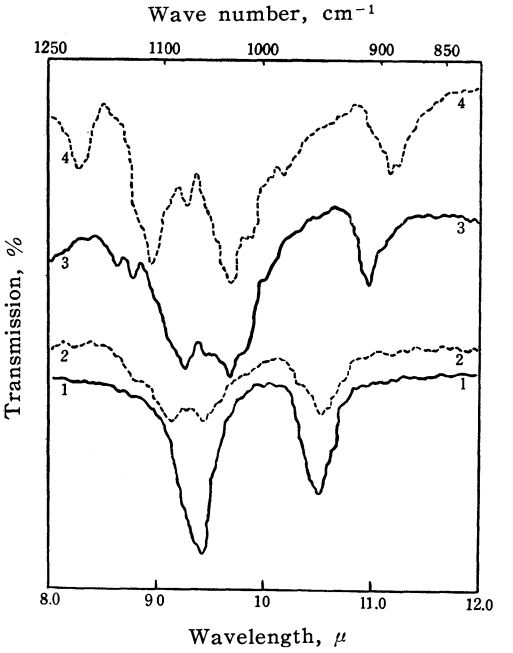


Fig. 4. Infrared absorption spectra of:
1, Na_3SPO_3 (KBr disk);
2, $Na_3[Co\,en_2(SPO_3)_2]\cdot8H_2O$ (KBr disk);
3, $[Co\,en_2(SPO_3)]\cdot2H_2O$ (nujol mull);
4, $[Co\,en_2(SPO_3)]$ (nujol mull).

and the vibrations are assumed to be symmetric PO_3 stretching vibration (950 cm^{-1}) and degenerate PO_3 asymmetric vibration (1064 cm^{-1}), respectively[10]. In the di-monothiophosphato-bis-ethylenediammine cobalt(III) ion, the band at 950 cm^{-1} is hardly shifted, but the band at 1064 cm^{-1} is shifted to a higher frequency and splits into two peaks. This trend is in good accordance with that of the thiosulfato complexes mentioned above. These relationships led us to the conclusion that the cobalt(III) ion in this complex coordinates the monothiophosphate ion by the sulfur atom, in good agreement with the conclusion from the visible and ultraviolet spectra. On the contrary, in the spectra of the dark red complex, the symmetric PO_3 stretching vibration of the monothiophosphate ion is shifted to a lower frequency by coordination. If it is assumed that the dark red complex has the structure containing the monodentate monothiophosphate ligand, namely, $[Co\,en_2(OH_2)(SPO_3)]\cdot H_2O$, the symmetry of the coordinated SPO_3^{3-} ions is C_{3v}, but if the chelate structure in $[Co\,en_2(SPO_3)]\cdot2H_2O$, is assumed, the symmetry of the ligand is lowered to C_s. It is presumed, therefore,

9) K. Nakamoto, J. Fujita, S. Tanaka and M. Kobayashi, *J. Am. Chem. Soc.*, **79**, 4909 (1957).

10) M. Tsuboi, ibid., **79**, 1351 (1957).

that the shift of the band at 950 cm^{-1} is caused by the chelate coordination. Furthermore, in the spectra of the dehydrated complex (Fig. 4), no new band by degradation symmetry appears, though the bands are more or less shifted. These shifts probably result from the vanishing of the hydrogen-bond between the water molecules and the SPO_3^{3-} group. Similar shifts were reported for some inorganic phosphorus compounds[11].

Summary

Two new complexes, sodium di-monothiophosphato-bis-ethylenediamine cobaltate(III) octa-hydrate and monothiophosphato-bis-ethylenediamine-cobalt(III) dihydrate, have been synthesized by the reaction of *trans*-dichloro-bis-ethylenediamine cobalt(III) chloride with anhydrous sodium monothiophosphate in cold aqueous solution. The infrared and the visible and ultraviolet absorption spectra of these compounds and of the corresponding thiosulfato-Co(III) complexes have been measured and discussed in relation to the structures of the complexes.

This study was supported by a grant from the Ministry of Education.

Department of Chemistry
Faculty of Science
Osaka University
Nakanoshima, Osaka

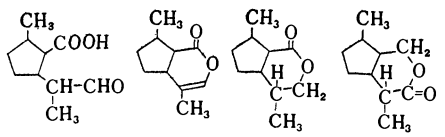
11) D. E. C. Corbridge and E. J. Lowe., *J. Chem. Soc.*, **1957**, 493.

The Synthesis of Cyclopentane Derivatives. I

By Tsuguo TANAKA

(Received April 11, 1959)

Recently, several methylcyclopentane derivative from natural sources have been reported. Among them, nepetalic acid (I) and nepetalactone (II) from the oil of cat-nip (Nepeta cataria)[1], matatabilactone (III) from the oil of the wormseed of matatabi (Actinidia poligama Miq.,)[2] and iridolactone (IV) from ant (Iridomyrmex species)[3] are particularly interesting because of their close relationship concerning both physiological activities and chemical structures.

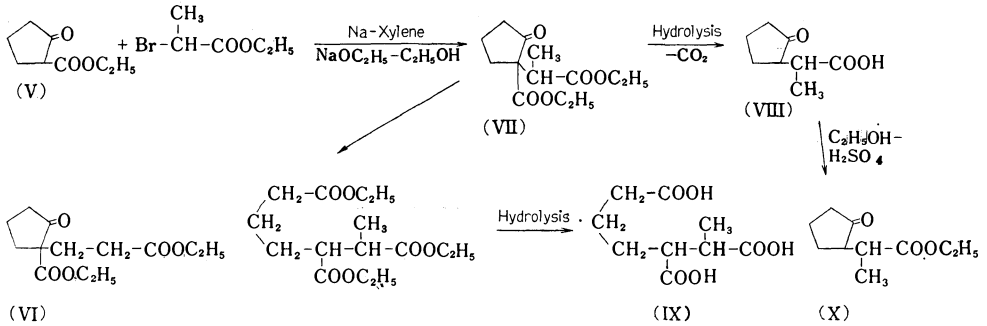


(I) (II) (III) (IV)

The determination of conformations of these compounds[4] in relation to their physical and chemical properties seems worthy of further considerations. Now, synthesis of several cyclopentane derivatives was attempted with a view to obtain some informations about conformational problems and to find out a new synthetic route.

In the present experiment, *cis*- and *trans*-lactones of 2-α-carboxyethylcyclopentanol were prepared as the first step in a series of this investigation attempted, which lead to the compounds having no methyl substituent in the ring, and thus alleviating stereochemical difficulties. The condensation of carbethoxycyclopentanone (V) with ethyl α-bromopropionate, reported by Šorm et al.[5] and Sen et al.[6], respectively, was re-examined and some new results were obtained. The condensation was conducted by use of either sodium metal in toluene[5,7] or sodium ethoxide in absolute alcohol[8]. 2-Carbethoxy-2-α-carbethoxyethyl cyclopentanone (VII) was obtained

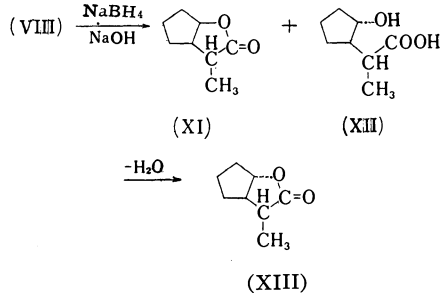
1) S. M. McElvain, R. D. Bright and P. R. Johnson, *J. Am. Chem. Soc.*, **63**, 1558 (1941); E. J. Eisenbraun and S. M. McElvain, ibid., **77**, 1599 (1955).
2) T. Sakan, A. Fujino, F. Murai, Y. Butsugan and A. Suzui, This Bulletin, **32**, 315 (1959).
3) G. W. K. Cavill, D. L. Ford and H. D. Locksley, *Chem. & Ind.*, **75**, 465 (1956).
4) R. B. Bates, E. J. Eisenbraun and S. M. McElvain, *J. Am. Chem. Soc.*, **80**, 3420 (1958); ibid., **80**, 3413 (1958).
5) F. Šorm, Z. Šormová and L. Šedivý, *Collection Czechoslov. Chem. Communs.*, **12**, 554 (1947); *Chem. Abstr*, **42**, 7742*c* (1948).
6) K. Sen and P. Bagchi, *Science and Culture (India)*, **20**, 254 (1954); *Chem. Abstr.*, **49**, 14652*e* (1955).
7) W. Herz. *J. Am. Chem. Soc.*, **78**, 1485 (1956).
8) (a) E. D. Bergmann and R. Ikan, ibid., **80**, 3135 (1958). (b) A. Kötz, *Ann.*, **350**, 235 (1906).



in 70 and 60% yield, respectively. Here, in the latter case, an acid, m.p. 147°C, was newly detected as the by-product of the cleavage of the ring in VII[9,8b] followed by hydrolysis of the ester group. The acid was identified as hexane-tricarboxylic acid-1,4,5 (IX) obtained by Sen et al.[10] from 2-methyl-2,3-dicarbethoxy-cyclohexanone; the formation substantiates structure VII for the condensation product.

2-Carbethoxy-2-β-carbethoxyethyl-cyclopentanone (VI) which might be the product of dehydrobromination and Michael addition[11] of ethyl α-bromopropionate to carbethoxycyclopentanone (V) could not be detected. The ketoester (VII) was converted into 2-α-carboxyethyl-cyclopentanone (VIII), m.p. 66°C, which on esterification yielded ethyl ester (X), as indicated in the formulation.

On the other hand, VIII was treated with sodium borohydride, when a selective reduction of the keto group[12] was realized;



from the reduction product a lactone of possibly *cis*-2-α-carboxyethyl-cyclopentanol (*cis*-lactone) (XI) and a hardly lactonized one, possibly *trans*-hydroxyacid (XII) were obtained. Structure XII was ascertained by analysis and also by the comparison of the absorption spectrum of the reduction product with that of keto-acid (VIII). 288 mμ band in the ultraviolet spectrum and 5.80 μ peak in the infrared spectrum of the keto-acid were not observed in the spectrum of the reduction product as illustrated in Figs. 1 and 2, respectively.

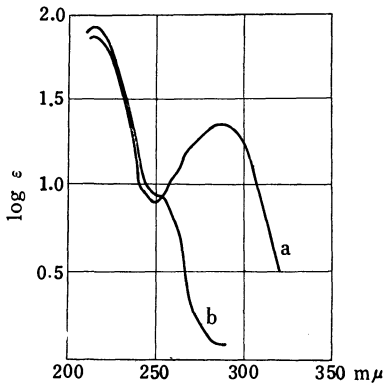


Fig. 1. Ultraviolet spectra of 2-α-carboxyethyl-cyclopentanone (a) and *trans*-2-α-carboxyethyl-cyclopentanol (b) in alcoholic solutions.

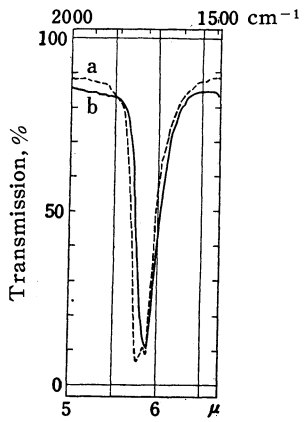


Fig. 2. Infrared spectra of 2-α-carboxyethyl-cyclopentanone (a) and *trans*-2-α-carboxyethyl-cyclopentanol (b).

9) A. H. Cook and R. P. Linstead, *J. Chem. Soc.*, **1934**, 964.
10) K. Sen and P. Bagchi, *Science and Culture (India)*., **19**, 312 (1953); *Chem. Abstr.*, **49**, 2338*f* (1955).
11) P. B. Talukdar and P. Bagchi, *J. Org. Chem.*, **20**, 25 (1955).
12) E. B. Reid and J. R. Siegel, *J. Chem. Soc.*, **1954**, 520; R. P. Zelinski, B. W. Turnquest and E. C. Martin, *J. Am. Chem. Soc.*, **73**, 5521 (1951).

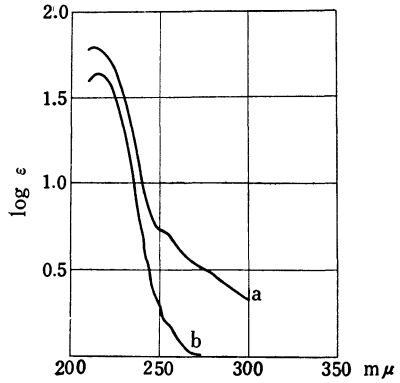


Fig. 3. Ultraviolet spectra of *trans*-lactone (a) and *cis*-lactone (b) in alcoholic solutions.

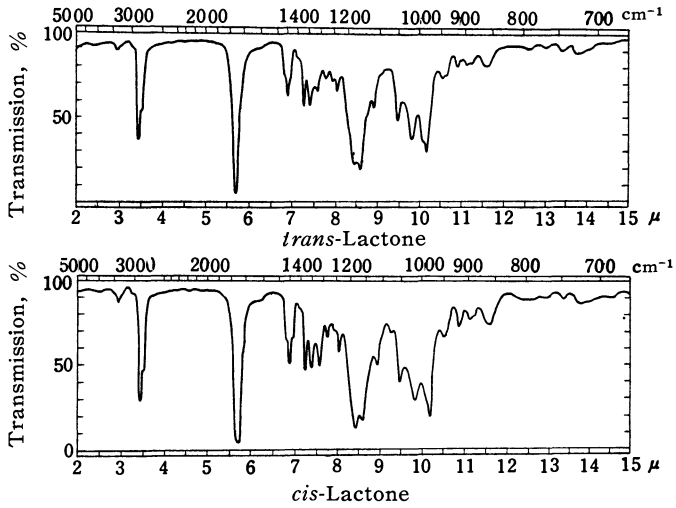


Fig. 4. Infrared spectra of *trans*-lactone and *cis*-lactone.

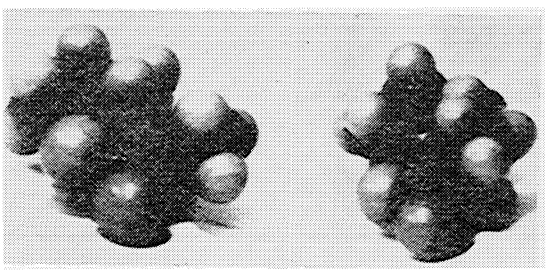
The reduction of 2-carboxymethyl-cyclopentanone with sodium amalgam in sodium hydroxide solution was reported by Linstead et al.[13] to yield *cis*-lactone in 28% yield. The lactonization of XII gave a sweet smelling *trans*-lactone (XIII) (heated under diminished pressure); a trace of concentrated sulfuric acid facilitated the reaction. In this way the reduction of keto-acid (VIII) yielded 37% of *cis*-lactone and 38% of *trans*-lactone (consult Table I).

TABLE I. PHYSICAL CONSTANTS OF *cis*- AND *trans*-LACTONES

	Density $d_4^{13.5}$	Refractive index $n_D^{13.5}$	b. p., °C
cis-Lactone	1.08462	1.4712	73~74/2 mm.
trans-Lactone	1.09688	1.4725	67/2 mm.

Some differences between these lactones were also revealed in the ultraviolet (Fig. 3) and infrared (Fig. 4) spectra of them. In the ultraviolet spectra, the extinction coefficient of *trans*-lactone is a little higher than that of *cis*-lactone particularly at longer wavelengths.

In the infrared spectra, comparison of relative intensity of absorption peaks 8.44 μ (a) and 8.60 μ (b) (C–O stretching) gives a convenient method of characterizing these lactones. In the spectra of *cis*- and *trans*- lactones, a>b and b>a are recognized, respectively. And the singlet absorption peaks 10.50 μ, 11.13 μ in the spectrum of *cis*-lactone, appear as doublet peaks 10.50, 10.64 μ; 11.13, 11.25 μ respectively in that of *trans*-lactone. By the examination of the molecular models in Fig. 5, it is ascertained that *cis*-lactone is a staggered molecule having *cis*-orientation at C_1 and C_2, while *trans*-lactone is a planar molecule having a *gauche*-orientation at C_1 and C_2.



trans-Lactone *cis*-Lactone

Fig. 5. The molecular models of *trans*-lactone and *cis*-lactone.

Experimental[14]

2-Carbethoxy-2-α-carbethoxyethyl-cyclopentanone.—(a) The Condensation of 73 g. of ethyl α-bromopropionate with 62 g. of 2-carbethoxy-cyclopentanone by use of 9.2 g. of sodium in 500 ml. of toluene was completed by refluxing the mixture for ten hours. The reaction product, being treated in the usual way, yielded 61 g. of fraction b. p. 128~129°C/2.5 mm., 7 g. of fraction b. p. 123~128°C/2.5 mm. The latter was also used for further work. Yield, 70%. λ_{max} 249 mμ log ε 3.09; ν_{max} 5.74 μ, 5.82 μ (C=O).

Anal. Found: C, 60.30; H, 7.85. Calcd. for $C_{12}H_{20}O_5$: C, 59.00; H, 8.25%.

2-α-Carboxyethyl-cyclopentanone. — Forty-five grams of 2-carbethoxy-2-α-carbethoxyethyl-cyclo-

13) R. R. Linstead and E. M. Mead, *J. Chem. Soc.*, **1934**, 935.

14) Infrared spectra were measured with Perkin Elmer Model 21 spectrophotometer and ultraviolet spectra in alcoholic solutions with Beckman E. P. U. spectrophotometer.

TABLE II. PHYSICAL CONSTANTS OF 2-α-CARBOXYETHYL-CYCLOPENTANONE AND ITS DERIVATIVES

	b. p., °C	m. p., °C	Melting point of semi-carbazone °C	Melting point of 2,4-dinitro-phenylhydrazone °C	Boiling point of ethylester °C
Šorm et al.	154/15 mm.	—	188	—	81～83/0.5 mm.
Sen et al.	150/3 mm.	—	—	220	—
Experiment	118～119/0.4 mm.	66	189	220	93.5～94/3 mm.

pentanone was gently refluxed with 100 ml. of concentrated hydrochloric acid for sixteen hours at 135～145°C in an oil bath. The reaction mixture was cooled and extracted with ether. Benzene was added to the ether solution and the solvents were evaporated and the residue was vacuum-distilled. A portion (18.4 g.) of the acid b. p. 118～119°C/0.4 mm. was obtained. Yield, 64%. On standing in the ice box, it gradually crystallized; m. p. 45°C. Recrystallized from benzene-petroleum ether as feathery needles; m. p. 66°C, λ_{max} 214 mμ log ε 1.86, 288 mμ log ε 1.34; ν_{max} 5.80 μ, 5.90 μ (C=O).

Anal. Found: C, 60.72; H, 7.84. Calcd. for $C_8H_{12}O_3$: C, 61.52; H, 7.75%.

An additional amount (ca. 1 g.) was obtained by evaporating the hydrochloric acid solution in vacuum and extracting the residual tar with ether. Physical constants by three different authors are listed in Table II.

(b) To a solution of 7.6 g. of sodium in 120 ml. of absolute alcohol was added 54 g. of carbethoxy-cyclopentanone in twenty minutes at 20°C with efficient stirring. Sixty-four grams of ethyl α-bromopropionate was added to the mixture and refluxed for four hours. A clear red solution resulted. Fifty milliliters of alcohol was distilled off from it and the residue was diluted with 250 ml. of ice water and extracted with ether. The ether solution, after washing with water, dried with sodium sulfate and the ether was evaporated and the residue vacuum-distilled. Fifty and a half grams of fraction boiling 126.5～130°C/2.5 mm. was obtained. Yield, 60%.

2-α-Carboxyethyl-cyclopentanone and Hexane-tricarboxylic Acid-1, 4, 5.—Hydrolysis was effected in the same way as in a) by using 47.5 g. of ketodiester b. p. 126.5～130°C/2.5 mm. and 105 ml. of concentrated hydrochloric acid. On evaporation of ether and redissolving the residue in a small amount of dry ether, 850 mg. of colorless crystals which were difficult to solve in ether, separated, which on crystallization from ethyl acetate-petroleum ether melted at 147°C. Analysis and titration conformed to hexane-tricarboxylic acid-1, 4, 5.

Anal. Found: C, 49.40; H, 6.71. Calcd. for $C_9H_{14}O_6$: C, 49.54; H, 6.47%. Titration. 9.00 mg. required 12.4 ml. of 0.010 N sodium hydroxide. Calcd. for $C_6H_{11}(COOH)_3$: 12.4 ml. From the ether solution after distillation in vacuum was obtained 14 g. of 2-α-carboxyethyl-cyclopentanone b. p. 119～120°C/0.4 mm. Yield, 46%.

2-α-Carbethoxyethyl-cyclopentanone. — Seven grams of 2-α-carboxyethyl-cyclopentanone was dissolved in 20 ml. of absolute alcohol containing 0.7 ml. of concentrated sulfuric acid and refluxed for six hours in a water bath. Twelve milliliters of ethanol was distilled off from the reaction mixture and the residue was poured into 120 ml. of ice water.

The product was extracted with ether and the ether solution was washed with 5% aqueous sodium carbonate solution and with water successively, and dried with sodium sulfate. Evaporation of ether and vacuum-distillation of the residue produced 5.8 g. of 2-α-carbethoxyethyl-cyclopentanone b. p. 93.5～94°C/3 mm. Yield, 70%. λ_{max} 214 mμ log ε 2.02, 288 mμ log ε 1.36; ν_{max} 5.80 μ (C=O).

Anal. Found: C, 64.91; H, 9.21. Calcd. for $C_{10}H_{16}O_3$: C, 65.19; H, 8.75%.

***cis*-Lactone, *trans*-2-α-Carboxyethyl-cyclopentanol and *trans*-Lactone.**—The aqueous sodium hydroxide solution (4.2 g. of sodium hydroxide in 94 ml. of water) of 14.4 g. of 2-α-carboxyethyl-cyclopentanone was gradually (in one hour) added to a solution of 2.3 g. of sodium borohydride in 35 ml. water. The mixture was well shaken after each addition and left to stand for two days at room temperature after the addition was over. It was cooled in an ice bath, and 50 ml. of concentrated hydrochloric acid was added to it with stirring. After the addition was over, it was warmed on a water bath for fifteen minutes, cooled in an ice bath and extracted three times with benzene followed by four times with ether. The combined benzene solution after washing three times with water was dried with sodium sulfate. Benzene was evaporated under reduced pressure and the residue vacuum-distilled. Four and four-fifth grams of *cis*-lactone (3.8 g. of fraction b. p. 73～74°C/2 mm., 1 g. of fraction b. p. 71～72.5°C/2 mm.) was obtained. The latter fraction was also used for further work. Yield, 37%. λ_{max} 215 mμ log ε 1.65; ν_{max} 5.70 μ (C=O) 8.44 μ, 8.60 μ (C-O).

Anal. Found: C, 67.96; H, 8.89. Calcd, for $C_8H_{12}O_2$: C, 68.54; H, 8.63%.

To the combined ether solution was added 100 ml. of benzene. Ether and moisture were azeotropically distilled. And the residue was vacuum-distilled. *trans*-2-α-Carboxyethyl-cyclopentanol b. p. 125～126°C/0.4 mm., m. p. 58°C, was obtained. λ_{max} 215 mμ log ε 1.93; ν_{max} 5.90 μ (C=O).

Anal. Found: C, 61.37; H, 9.21. Calcd. for $C_8H_{14}O_3$: C, 60.74; H, 8.92%.

***trans*-Lactone Prepared from *trans*-2-α-Carboxyethyl-cyclopentanol.** — In the usual pro-

cedure the residue of the ether extract was directly lactonized by heating it at 180~195°C under 30 mm. pressure from thirty minutes to three hours. *trans*-Lactone mixed with water slowly distilled out. But when one drop of concentrated sulfuric acid was added to the hydroxyacid, lactonization was completed in a few minutes. The product was dissolved in benzene, dried with sodium sulfate. Benzene was evaporated and the residue vacuum-distilled. Four and nine-tenths grams of *trans*-lactone b. p. 67°C/2 mm. was obtained. Yield, 38%. λ_{max} 213.5 mμ log ε 1.81; ν_{max} 5.70 μ (C=O) 8.44 μ, 8.60 μ (C-O).

Anal. Found: C, 68.52; H, 8.80. Calcd. for $C_8H_{12}O_2$: C, 68.54; H, 8.63%.

The author is grateful to Mr. H. Kotsuma* for infrared spectra and Mr. M. Shito and Miss S. Indo for the microanalysis.

Faculty of Liberal Arts
Saga University
Honjo, Saga

* Present address: Shin-Nihon-Chisso Fertilizers Co., Minamata, Kumamoto.

Characteristics of Alginic Acid as a Cation Exchanger and its Application to the Separation of Thorium(IV) and Cerium(III) Ions

By Takeo TAKAHASHI and Shingo MIYAKE

(Received June 6, 1959)

Alginic acid belongs to one of the polyacids with carboxylic groups as the dissociation group. It is generally soluble in water, either neutral or basic, but can maintain a solid state in an acidic salt solution, showing an excellent cation exchange property[1] and although its analytical and industrial applications have also been investigated[2], the characteristics as cation exchanger or situation in cation exchangers have not yet been explained clearly. It is the principle object of the present research to discuss the cation exchange property of alginic acid from the viewpoint of acidity. Alginic acid indicates somewhat stronger acidity in the aqueous solution than acetic acid[3] and polyacrylic acid which is also one of the polycarboxylic acids. From the viewpoint of the acidity, it is expected that the characteristics of alginic acid as cation exchanger would be placed between a strongly acidic and a weakly acidic exchanger. Thus it may be used advantageously for the ion-exchange separation of some multivalent cations, which are separated with difficulty with conventional exchangers, either strongly or weakly acidic. For example, the separation of thorium(IV) and cerium(III) with alginic acid as exchanger was briefly described in the previous communication[4]. The present paper discusses the characteristics of alginic acid as cation exchanger and the same subject was described in a previous paper in some detail.

Experimental

Alginic acid employed for the measurement of the ion exchange equilibrium was prepared by the following procedure. A commercial sodium alginate was dissolved in water to make about 0.5% solution. The insoluble residue was congelated by warming the solution to 50~60°C on a water bath, and removed by filtering through a filter bed composed of Toyo filter paper No. 2 and No. 5c. Alginic acid, coagulated by the addition of hydrochloric acid to the filtrate, was, after a few hours, collected on a piece of silk gauze of about 60 mesh, and washed with about 50% methanol until the absence of chlorine ions in the washing was confirmed. After the methanol was pressed out, the swelled alginic acid was stored in a closed container with water in the bottom.

Amberlite IR-120, a strongly acidic exchanger and IRC-50, a weakly acidic one were similarly stored in a wet state. Table I shows the properties of these exchangers available for the experiment.

1) J. L. Monger and A. Wassermann, *Nature*, **159**, 746 (1947).
2) H. Specker and H. Hartkamp, *Z. anal. Chem.*, **140**, 167 (1953); **141**, 33 (1954).
3) S. Miyake, *J. Chem. Soc. Japan, Ind. Chem. Sec.* (*Kogyo Kagaku Zasshi*), **61**, 1278 (1958).
4) T. Takahashi and S. Miyake, This Bulletin, **32**, 878 (1959).

TABLE I. THE PROPERTIES OF THE EXCHANGERS

Exchanger	Humidity %	0.1 N NaOH (ml.) for neutralization of 1 g. of exchanger
IR-120	43.1	23.56
H alg.	66.6	18.96
IRC-50	48.5	53.70

The alginic acid used in the column (1.5 cm. in diameter and 20 cm. in length) for the separation of thorium (IV) and cerium (III) ions was prepared from calcium alginate thread* by the procedure described in the previous paper[4].

Other reagents were all of the special grade (G. R.) available commercially.

Spectrophotometric methods were used for the analysis of thorium(IV) and cerium(III) ions, using Neo-thorone for thorium(IV) (580 mμ) and hydrogen peroxide for cerium(III) (320 mμ).

Results and Discussion

Characteristics of Alginic Acid as an Exchanger.—*Apparent dissociation constant.*—IR-120 (0.22 g.), IRC-50 (0.10 g.) and alginic acid (0.28 g.) weighed exactly within a deviation of 1 mg. were immersed in 10 ml. of the mixed solution containing $(10-x)$ ml. of 1 N potassium chloride and x ml. of potassium chloride and potassium hydroxide mixture (1 N KCl–0.1 N KOH), respectively. After the ion exchange equilibrium was achieved by allowing the mixed solution to stand for 24 hr. (for 3 days in the case of IRC-50) with occasional agitation, the pH of each supernatant solution was measured by means of Toa Denpa Model HM-3 glass electrode pH meter. Fig. 1 shows the relationship between the pH of the supernatant solution in its equilibrium state and the volume of 0.1 N potassium hydroxide added.

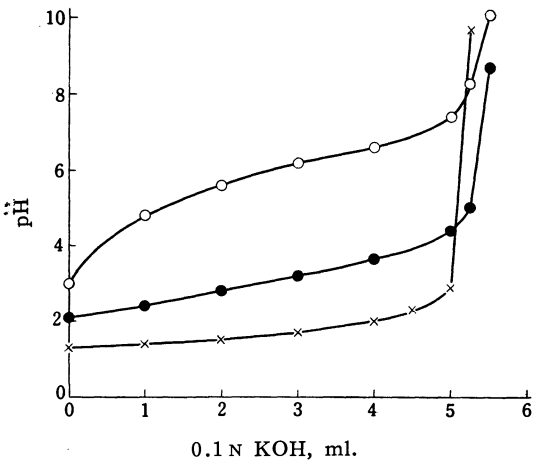


Fig. 1. Titration curves of exchangers.
○: IRC-50, ●: H alg., ×: IR-120

Such curves as those shown in Fig. 1 correspond to the titration curves of the exchangers as polyacids, and have been used for a mean in the characterization of the dissociation group of ion exchangers. For the purpose of expressing the apparent dissociation constant, pK, in the case of a weak polyacid, it is useful to take the value of pH at which half of the polyacid is exactly neutralized.

From Fig. 1, the values of pK for the exchangers are found to be 1.6 for IR-120, 3.1 for alginic acid and 6.0 for IRC-50. Now, attention must be paid to the fact that the values of pH cited above are of the external solution with which the exchangers are in equilibrium, and the true pH[5] in the internal body of the exchangers may show lower values. However, it is concluded that alginic acid is situated between the strongly acidic and the weakly acidic exchangers from the viewpoint of acidity. In fact, it is well known that alginic acid is one of the strongest acids among all the weak polyacids with the carboxylic group. The most valuable characteristic of alginic acid is that it has an intermediate acidity as cation exchanger.

On the other hand, in a cation exchange reaction under a given condition, the difference between the selectivity of different cations is independent in principle of the kind of functional group of exchangers, with the exception of some special exchangers, but the effect of the kind of functional group upon the property of the exchanger is due to the difference of their acidities. When the exchangers have the same functional group and different acidities, a difference in property as ion exchanger should be found. Accordingly, it is expected that alginic acid would have an intermediate property for cations, and that it may be available for the separation of several cations, which are separated with difficulty by means of conventional exchangers.

Distribution constant of thorium(IV) and cerium(III) ions.—Each exchanger, weighed in the same manner as that described above, is immersed in 20 ml. of 3.8×10^{-3} M thorium nitrate solution or 7.1×10^{-3} M cerous nitrate solution, with nitric acid of various concentrations. After equilibrium is reached through the same procedure as

* The alginate thread was supplied from Kamogawa Kato Co., Ltd., to whom the authors are indebted and to whom they express their thanks.

5) M. Honda, *J. Am. Chem. Soc.*, **73**, 2943 (1951).

that described above, thorium(IV) or cerium(III) ions in an aliquot of the supernatant solution were determined.

The distribution constant, K_d, for thorium(IV) and cerium(III) ions in regard to each exchanger was calculated from the following equation.

$$K_d = \frac{\text{Concn. of cation in the exchanger (dry base) (mg./g.)}}{\text{Concn. of cation in the supernatant soln. (mg./ml.)}}$$

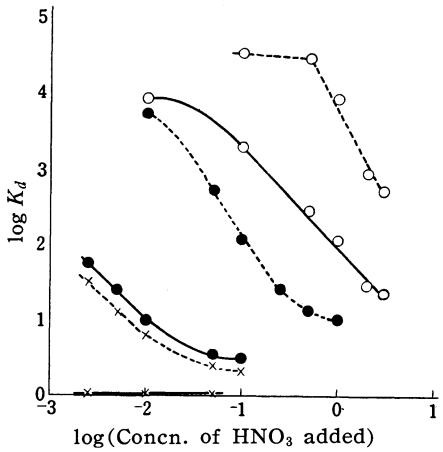


Fig. 2. Effect of concentration of nitric acid upon K_d of thorium(IV) and cerium(III).
------: Th, ——: Ce
○: IR-120, ●: H alg., ×: IRC-50

Fig. 2 shows the relationship between log K_d and logarithm of concentration of nitric acid in the solution. Now, for the concentrations of nitric acid, the stoichiometrical concentrations in the initial periods of the reaction were used instead of pH at the equilibrium, because of the difficulty of the measurement of pH in a concentrated nitric acid.

It is clear that IRC-50 adsorbs these cations little or not at all from an acid solution which keeps them without hydrolysis, and that these cations are adsorbed by IR-120 too tightly to be eluted fractionally with a dilute solution of conventional mineral acid. The values of K_d for thorium(IV) and cerium(III) ions in regard to alginic acid is placed between those in regard to IR-120 and IRC-50.

For the separation of thorium(IV) and cerium(III) ions by cation exchanger, it has been, heretofore, usual to use strongly acidic exchangers such as Amberlite IR-120 or Dowex-50 and to use complex reagents such as EDTA[6,7], citrate[8] and oxalate[9] for the fractional elution. This is because of the difficulty with which these cations are eluted from strongly acidic exchangers with a dilute acid solution. On the other hand, it is not always easy to convert the complex ions into simple metallic ions. However, it seems likely that thorium(IV) and cerium(III) ions can be easily eluted fractionally with a conventional mineral acid as shown in Fig. 2, provided that alginic acid is used as exchanger. It has never been suggested that an intermediately acidic exchanger such as alginic acid be used for the separation of thorium(IV) and cerium(III) ions.

Separation of Thorium(IV) and Cerium(III) Ions by the Use of Alginic Acid Column.—*Synthetic solution.*—The synthetic solutions containing thorium(IV) and cerium(III) ions in various concentrations were made pH 2 to 2.5 with aqueous ammonia and poured over the top of the column. Thorium(IV) and cerium(III) ions are adsorbed on alginic acid. After the column is washed with 100 ml. of water, cerium(III) ion is eluted with nitric acid of a concentration below 0.1 N at a flow rate of about 1 ml./min., and then the thorium(IV) ion is eluted with 1 N nitric acid. An example of the elution diagram has been shown in the previous paper[4]. Some analytical results are given in Table II.

TABLE II. SEPARATION OF THORIUM(IV) AND CERIUM(III) IONS FROM THEIR SYNTHETIC SOLUTION

Taken mg.		Found mg.		Concn. and vol. of eluted soln. for Ce		for Th	
Th	Ce	Th	Ce	N	ml.	N	ml.
35.5	30.0	35.5	30.1	0.05	250	1	100
35.5	30.0	35.4	30.3	0.075	200	〃	〃
70.0	30.0	69.9	30.0	〃	〃	〃	150
35.5	45.0	35.5	44.8	0.1	〃	〃	100
70.0	45.0	70.1	44.9	〃	〃	〃	150
70.0	60.0	70.0	47.4	〃	300	〃	〃
105.5	45.0	105.7	45.0	〃	200	〃	〃

It is shown that the present method can be feasible for the quantitative separation of thorium(IV) and cerium(III) ions and that the column employed in this experiment has a dimension suitable for the adsorption of the cerium(III) ion below 45 mg.

6) L. Gordon et al., *Anal. Chem.*, **28**, 1476 (1956).
7) T. Taketatsu, This Bulletin, **32**, 291 (1959).
8) T. Nishi et al., *III Atomic Energy Symposium, Japan*, 69 (1959).
9) T. Nozaki, *J. Chem. Soc. Japan, Pure Chem. Sec.* (*Nippon Kagaku Zasshi*), **76**, 996 (1955).

Application to monazite. — The monazite employed in this experiment was mined in 1940 at Ishikawa-yama, Fukushima-ken. Monazite ore was digested with concentrated sulfuric acid in the usual way. Mixed oxalates of thorium(IV) and rare earth metals were separated from other metallic ions through reprecipitation with oxalic acid. The oxalate mixture was converted into hydroxide by immersing into a warm sodium hydroxide solution and then dissolved in nitric acid. After the ceric ion contained in the mixed solution was reduced with a small amount of sodium nitrite to the cerous ion, and after the pH was adjusted with nitric acid to about 1, an aliquot of the solution was poured over the top of the column, which then was washed with 250 ml. of 0.1 N nitric acid at a flow rate of about 1 ml./min. Thus, the thorium(IV) ion is adsorbed entirely on alginic acid in the column, while all rare earth metal ions pass through the column. The results are shown in Table III.

TABLE III. SEPARATION OF THORIUM(IV) AND RARE EARTH IONS FROM MONAZITE

Mixed oxide	ThO_2 found in the column	Oxides of R.E. found in the effluent	Other oxides eluted with 1 N H_2SO_4
mg.	mg.	mg.	mg.
298	42.5	237.1	18.3
〃	42.8	237.3	17.8
〃	43.1	236.8	19.1

The "other oxides" shown in the last column of Table III are the oxides not eluted with 1 N nitric acid but eluted with 1 N sulfric acid. They seem to be composed of the oxides of titanium, zirconium and hafnium. In this experiment, the mixed oxide, the oxides of rare earth elements and "other oxides" were precipitated with aqueous ammonia from respective solutions and determined gravimetrically.

Summary

The apparent dissociation constant of alginic acid was measured by means of the neutralization with 0.1 N potassium hydroxide in 1 N potassium chloride solution and found to have a value of 3.1. This value is between that of IR-120 and of IRC-50, which is obtained by the same manner of measurement. The values of K_d for thorium(IV) and cerium(III) ions in regard to these three exchangers were measured, showing that the value in regard to alginic acid is also situated between the other two.

The application of alginic acid to the fractional separation of thorium(IV) and cerium(III) ions gave a satisfactory result.

The authors are grateful for the Grant from the Ministry of Education.

Institute of Industrial Science
The University of Tokyo
Yayoi-cho, Chiba

*Studies on 3-(Anthraquinon-1-yl)oxazolidin-2-ones. II. 3-(Bromoanthraquinon-1-yl)oxazolidin-2-ones and their Related Compounds**

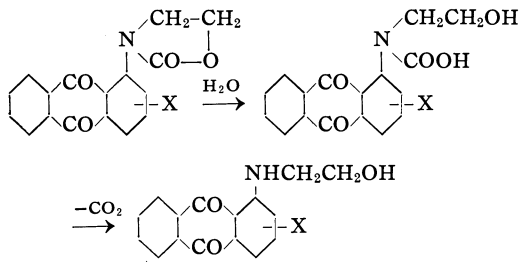
By Kō Naiki

(Recieved June 10, 1959)

It was shown in a previous paper[1] that an introduction of a methyl group into an anthraquinone nucleus of 3-(anthraquinon-1-yl)oxazolidin-2-one decreases the reactivity with an aqueous solution of potassium hydroxide. In other words, the existence of a steric hindrance of the 2-methyl group plays an important part in the hydrolysis process (Scheme I), inhibiting the conversion of the anthraquinon-1-yl-oxazolidin-2-ones into the 1-*N*-2-hydroxyethylamino-anthraquinones to a certain extent.

* Presented at the 12th Annual Meeting of the Chemical Society of Japan, Kyoto, April, 1959.

1) K. Naiki, This Bulletin, **32**, 361 (1959).



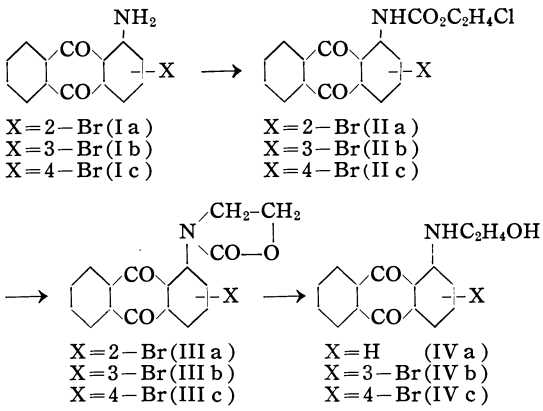
Scheme I

Furthermore, it was shown that in the case of the spectra of 2-chloroethyl methylanthraquinon-1-ylcarbamates the steric inhibition of the $\pi-p$ conjugation, i. e. interaction between an anthraquinone ring and an unshared electron pair of the nitrogen atom, plays an important role. Thus the introduction of the 2-methyl group into the anthraquinone ring results in the lowering of the intensity of the band near 400 mμ ascribed to the Aq-N̈ chromophore, where Aq represents the anthraquinone ring, and results in the displacement by 43 mμ towards shorter wavelength as compared with 2-chloroethyl 4-methylanthraquinon-1-ylcarbamate. In 3-(methylanthraquinon-1-yl) oxazolidin-2-ones, the steric inhibition of the $\pi-p$ conjugation due to a bulky *N*-substituent, oxazolidin-2-onyl, results in the lowering of the intensity of the band near 400 mμ to a greater extent, and the introduction of the 2-methyl group into the anthraquinone ring weakens the band associated with Aq-N̈ chromophore.

In the present study, 3-(bromoanthraquinon-1-yl)oxazolidin-2-ones, 2-chloroethyl bromoanthraquinon-1-ylcarbamates and 1-*N*-2-hydroxyethylamino-bromoanthraquinones were synthesized and the effect of the bromine atom according to its position on absorption spectra of 2-chloroethyl bromoanthraquinon-1-ylcarbamates and 3-(bromoanthraquinon-1-yl) oxazolidin-2-ones was discussed in terms of the steric hindrance. None of them has yet been prepared. Furthermore, the effect of the bromine atom according to its position on the reactivity of bromoanthraquinon-1-yloxazolidin-2-ones with potassium hydroxide was investigated.

Preparation and Results

The syntheses of the compounds were carried out according to the following processes (Scheme II).



Scheme II

2-Chloroethyl 2-bromoanthraquinon-1-ylcarbamate(IIa), 3-bromoanthraquinon-1-ylcarbamate(IIb) and 4-bromoanthraquinon-1-ylcarbamate(IIc) were obtained from the corresponding 1-amino-bromoanthraquinones (Ia, Ib and Ic, respectively) by the action of 2-chloroethyl chloroformate in the presence of sodium carbonate in boiling xylene.

3-(2-Bromoanthraquinon-1-yl)oxazolidin-2-one(IIIa) was prepared from 2-chloroethyl 2-bromoanthraquinon-1-ylcarbamate by the action of a 20% aqueous solution of potassium hydroxide at 98~99°C for 1 hr. The mixture of 1-*N*-2-hydroxyethylaminoanthraquinone(IVa) and 3-(2-bromoanthraquinon-1-yl)oxazolidin-2-one(IIIa) was obtained from 2-chloroethyl 2-bromoanthraquinon-1-ylcarbamate by the action of a 20% aqueous solution of potassium hydroxide at 105~107°C for 1 hr. Each of the constituents was separated by a column chromatography from benzene on alumina.

The mixture of 1-*N*-2-hydroxyethylamino-3-bromoanthraquinone(IVb), 3-(3-bromoanthraquinon-1-yl)oxazolidin-2-one(IIIb) and 2-chloroethyl 3-bromoanthraquinon-1-ylcarbamate was obtained from 2-chloroethyl 3-bromoanthraquinon-1-ylcarbamate by the action of a 20% aqueous solution of potassium hydroxide at 98~99°C for 1 hr. and each of the constituents was separated by a column chromatography from benzene on alumina. In the same way, 1-*N*-2-hydroxyethylamino-4-bromoanthraquinone(IVc) and 3-(4-bromoanthraquinon-1-yl)oxazolidin-2-one(IIIc) were obtained from 2-chloroethyl 4-bromoanthraquinon-1-ylcarbamate.

The proportion of constituents of the reaction mixture from the corresponding 2-chloroethyl bromoanthraquinon-1-ylcarbamates by the action of a 20% aqueous

TABLE I. THE PROPORTIONS OF THE CONSTITUENTS OF THE REACTION PRODUCTS OBTAINED FROM 2-CHLOROETHYL BROMOANTHRAQUINON-1-YLCARBAMATES AND A 20% AQUEOUS SOLUTION OF POTASSIUM HYDROXIDE

Position of Br	II %	III %	IV %
2	0	100	0
3	29	7	64
4	44	26	30

solution of potassium hydroxide at 98~99°C for 1 hr. was determined.

The results are shown in Table I. The reaction mixture obtained from the chloroethyl bromoanthraquinon-1-ylcarbamate and potassium hydroxide can be separated into the constituents by a column chromatography from benzene on alumina, but it is observed that the 2-chloroethyl bromoanthraquinon-1-ylcarbamate is gradually converted into the corresponding bromoanthraquinon-1-yloxazolidin-2-one on alumina. For this reason, the determination of the proportion of constituents was carried out by a spectrophotometry. Since the absorption bands of the constituents are separated from each other, the determination was carried out exactly. The absorption spectra of 2-chloroethyl bromoanthraquinon-1-ylcarbamates, 3-(bromoanthraquinon-1-yl)oxazolidin-2-ones and 1-*N*-2-hydroxyethylamino-bromoanthraquinones are shown in Figs. 1—3, respectively.

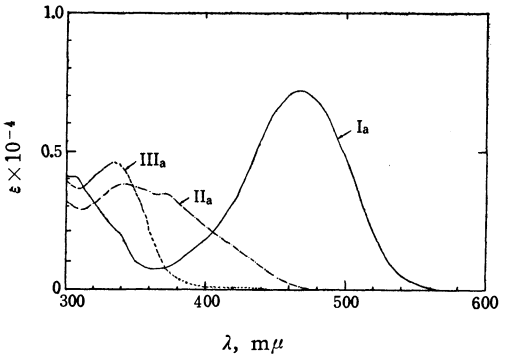


Fig. 1. Absorption spectra of 1-amino-2-bromoanthraquinones.
Ia: 1-Amino-2-bromoanthraquinone (in ethanol)
IIa: 2-Chloroethyl 2-bromoanthraquinon-1-ylcarbamate (in toluene)
IIIa: 3-(2-Bromoanthraquinon-1-yl)-oxazolidin-2-one (in toluene)

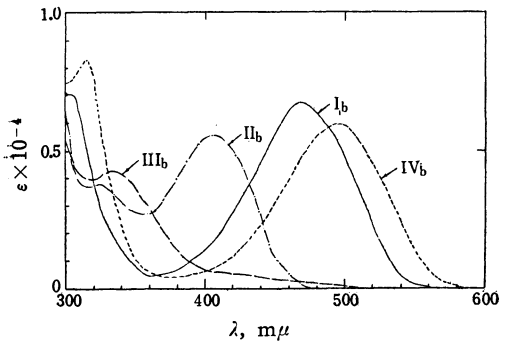


Fig. 2. Absorption spectra of 1-amino-3-bromoanthraquinones.
Ib: 1-Amino-3-bromoanthraquinone (in ethanol)
IIb: 2-Chloroethyl 3-bromoanthraquinon-1-ylcarbamate (in toluene)
IIIb: 3-(3-Bromoanthraquinon-1-yl)-oxazolidin-2-one (in toluene)
IVb: 1-*N*-2-Hydroxyethylamino-3-bromoanthraquinone (in toluene)

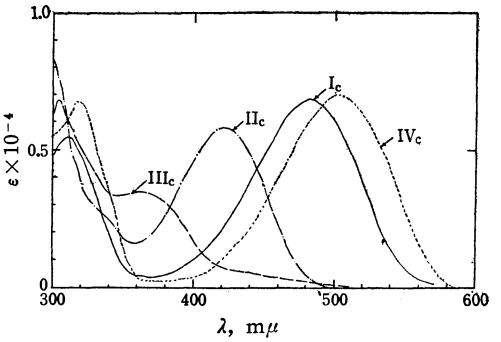


Fig. 3. Absorption spectra of 1-amino-4-bromoanthraquinones.
Ic: 1-Amino-4-bromoanthraquinone (in ethanol)
IIc: 2-Chloroethyl 4-bromoanthraquinon-1-ylcarbamate (in toluene)
IIIc: 3-(4-Bromoanthraquinon-1-yl)-oxazolidin-2-one (in toluene)
IVc: 1-*N*-2-Hydroxyethylamino-4-bromoanthraquinone (in toluene)

TABLE II. ABSORPTION MAXIMA AND EXTINCTION COEFFICIENTS OF 1-AMINO-BROMOANTHRAQUINONES

Compound	λ_{max}, mμ		$\varepsilon_{max}\times10^{-4}$	
I a *	308	469	0.436	0.760
I b *	~305	471	(0.732)	0.689
I c *	312	483	0.570	0.701
II a **	342	370	0.386	0.346
II b **	325	406	0.375	0.555
II c **	~335	423	(0.269)	0.580
III a **	334	~395	0.472	(0.031)***
III b **	335	~410	0.417	(0.062)***
III c **	342	~420	0.347	(0.064)***
IV b **	313	496	0.821	0.593
IV c **	318	503	0.683	0.697

Bracketed values are absorption bands of low intensity.
* Solvent: ethanol; concn. 1×10^{-4} mol./l.
** Solvent: toluene; concn. 1×10^{-4} mol./l.
*** Solvent: toluene; concn. 1×10^{-3} mol./l.

Absorption maxima and extinction coefficients are given in Table II.

Discussion

Effect of the Bromine Atom according to its Position on Absorption Spectra.—In the case of the spectra of 2-chloroethyl anthraquinon-1-ylcarbamates, the introduction of the 2-bromine atom into an anthraquinone ring results in the lowering of an intensity of the band near 400 mμ ascribed to Aq-N̈ chromophore and the displacement by 53 mμ towards a shorter wavelength as compared with 2-chloroethyl 4-bromoanthraquinon-1-ylcarbamate. This fact may be explicable in terms of the steric hindrance of the $\pi-p$ conjugation, between the anthraquinone ring and an unshared electron pair of the nitrogen atom, due to a repulsion between the carbonyl group and the 2-bromine atom which arises from the overlapping of the van der Waals radii. It is pointed out that $\varepsilon_2/\varepsilon_4$ is considerably smaller for 2-chloroethyl bromoanthraquinon-1-ylcarbamates than for 2-chloroethyl methylanthraquinon-1-ylcarbamates. Projection diagrams (Fig. 4) of uniplanar

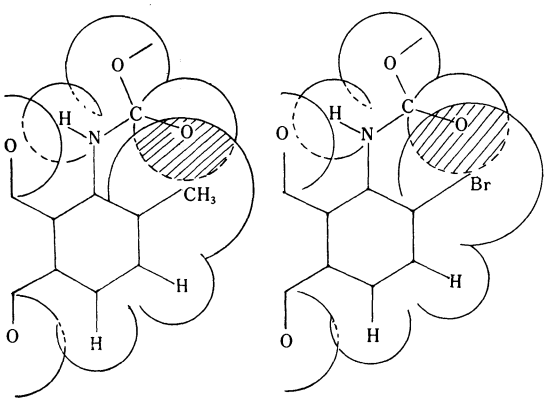


Fig. 4. Projection diagrams of 2-chloroethyl 2-bromo- and 2-methyl-anthraquinon-1-yl-carbamates.

structures, employing van der Waals radii, indicate only a slightly larger overlapping for 2-chloroethyl 2-bromoanthraquinon-1-ylcarbamate than for 2-chloroethyl 2-methylanthraquinon-1-ylcarbamate. Hence additional effects, i. e. the coulombic interaction of the carbonyl group with the 2-bromine atom and the hydrogen bonding between the carbonyl group and the 2-methyl group, must be considered in an explanation of the spectral diffrence between 2-chloroethyl 2-bromoanthraquinon-1-ylcarbamate and 2-methylanthraquinon-1-ylcarbamate (Table III).

Table III. Absorption maxima and extinction coefficients of the primary bands of 2-chloroethyl anthraquinon-1-ylcarbamates

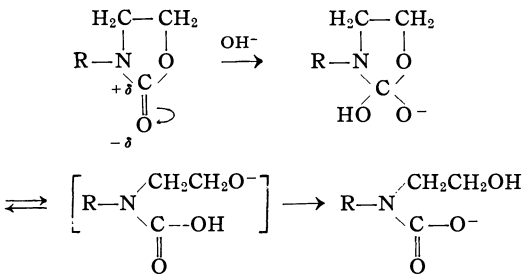
Substituent of anthraquinone nucleus	λ_{max} mμ	$\varepsilon\times10^{-4}$	$\varepsilon_2/\varepsilon_4$
2-Methyl	378	0.520(ε_2)	0.84
4-Methyl	421	0.618(ε_4)	
2-Bromo	370	0.346(ε_2)	0.60
4-Bromo	423	0.580(ε_4)	

In the spectra of 3-(anthraquinon-1-yl)-oxazolidin-2-ones, it is expected that an absence of intermolecular hydrogen bonding possibility results in the lowering of the intensity of the band near 400 mμ as compared with the compounds which have intermolecular hydrogen bonding possibility, 2-chloroethyl anthraquinon-1-ylcarbamates. It is further expected that the introduction of a bulky group, such as oxazolin-2-onyl, into the 1-position of the anthraquinone ring increases the extent of steric inhibition of the $\pi-p$ conjugation, between the anthraquinone ring and the unshared electron pair of the nitrogen atom, and results in the lowering of the intensity of the band near 400 mμ ascribed to Aq-N̈ chromophore. If the 2-bromine atom is introduced into the anthraquinone ring, the steric hindrance inhibits the $\pi-p$ conjugation between the ring and the unshared electron pair of the nitrogen atom to a greater extent. This is illustrated in Table II.

The Effect of the 2-Bromine Atom on the Reactivity of 3-(Bromoanthraquinon-1-yl)-oxazolidin-2-ones with the Hydroxide Ion.—On account of an aqueous dispersion of solid material, various difficulties may be introduced in the discussion when the reactivities are compared with each other. Nevertheless, it may be probable that some close relation exists between the reactivity and factors such as electronic and steric effects of groups in the anthraquinone nucleus. Table I shows clearly that the 2-bromine atom decreases the reactivity of the 3-(bromoanthraquinon-1-yl)-oxazolidin-2-ones with potassium hydroxide to a considerable extent. In other words, it shows the existence of a steric hindrance of the 2-bromine atom in the hydrolysis, this effect inhibiting the conversion of 3-(2-bromoanthraquinon-1-yl)oxazolidin-2-one into 1-*N*-2-hydroxyethylamino-2-bromoanthraquinone.

In the basic hydrolysis of 3-substituted oxazolidin-2-ones, there is a carbonyl carbon atom at which attack would be

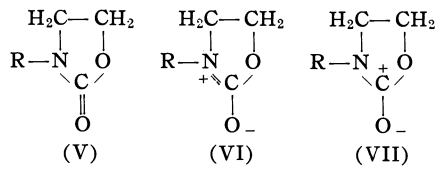
expected to occur. A mechanism of the hydrolysis reaction may be illustrated as follows (Scheme III).



Scheme III

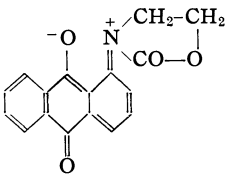
The addition complex has a more or less tetrahedral configuration at the site of substitution. Its formation controls the rate of the reaction. It may be probable, therefore, that the steric hindrance to the formation of the addition complex, due to overlapping of the van der Waals radii and the coulombic interaction of the 2-bromine atom with the hydroxide ion, inhibits the conversion of 3-(2-bromoanthraquinon-1-yl)-oxazolidin-2-one into 1-*N*-2-hydroxyethyl-amino-2-bromoanthraquinone. Further effects must, however, be considered in an explanation of the experimental results.

3-Substituted oxazolidin-2-ones may be described as a resonance hybrid of structures V—VII.



(V) (VI) (VII)

If the -N̈-C=O system is planar, there will be a flow of a charge away from the nitrogen atom into the carbonyl oxygen atom; in other words, structure VI is much more important than structure VII, in which the positive charge is on the carbonyl carbon atom. In 3-anthraquinon-1-yloxazolidin-2-ones, an additional structure VIII contributes to the resonance hybrid. This means that if the Aq-N̈ system is planar, there will be a flow of a charge away from the nitrogen atom into the anthraquinone ring, this resulting in a decrease of the contribution of structure VI to the resonance hybrid. The steric hindrance of the 2-bromine atom to the planar configuration of the Aq-N̈ system decreases the contribution of structure VIII, increasing the contribution of structure VI to the resonance hybrid.



(VIII)

On the other hand, a nucleophilic attack occurs readily at the position at which an open sextet of electrons can be provided readily. It is therefore reasonable to suppose that the contribution of structure VI is unfavorable for the formation of an addition complex in the reaction of 3-(anthraquinon-1-yl)oxazolidin-2-ones with the hydroxide ion. The steric hindrance of the 2-bromine atom to the planar configuration of the Aq-N̈ system inhibits the conversion of 3-(2-bromoantraquinon-1-yl)-oxazolidin-2-one into 1-*N*-2-hydroxyethyl-amino-2-bromoanthraquinone.

It is also expected that the introduction of electron attracting groups into the anthraquinone ring results in the decrease of contribution of strueture VI to the resonance hybrid and the formation of the addition complex will be facilitated, increasing the rate of conversion of 3-(anthraquinon-1-yl)oxazolidin-2-ones into 1-*N*-2-hydroxyethylaminoanthraquinones. This is illustrated by the comparison of reactivities of 3-(bromoanthraquinon-1-yl)-oxazolidin-2-ones with those of 3-(methyl-anthraquinon-1-yl)oxazolidin-2-ones (Table IV).

TABLE IV. CONVERSION OF 3-(ANTHRAQUINON-1-YL)OXAZOLIDIN-2-ONES INTO 1-*N*-2-HYDROXY-ETHYLAMINOANTHRAQUINONES*

Compound	Conversion, %
3-(2-Methylanthraquinon-1-yl)oxazolidin-2-one	17
3-(2-Bromoanthraquinon-1-yl)oxazolidin-2-one	0
3-(3-Methylanthraquinon-1-yl)oxazolidin-2-one	73
3-(3-Bromoanthraquinon-1-yl)oxazolidin-2-one	90
3-(4-Methylanthraquinon-1-yl)oxazolidin-2-one	41
3-(4-Bromoanthraquinon-1-yl)oxazolidin-2-one	54

* KOH, 20%; Temp., 98~99°C; Reaction time, 1 hr.

Experimental

1-Amino-2-bromoanthraquinone (Ia).—Red plates (glacial acetic acid), m. p. 179~180°C.

Anal. Found: N, 4.62. Calcd. for $C_{14}H_8O_2NBr$: N, 4.64%.

1-Amino-3-bromoanthraquinone (Ib)[2]. — Red prisms (glacial acetic acid), m. p. 242~243°C.

Anal. Found: N, 4.70. Calcd. for $C_{14}H_8O_2NBr$: N, 4.64%.

2) F. Ullmann and O. Fisher, *Ber.*, **49**, 2154 (1956).

1-Amino-4-bromoanthraquinone (Ic)[3].—The compound was separated by a column chromatography from benzene on alumina and recrystallized from ligroin, giving red needles, m. p. 179~180°C.

Anal. Found: N, 4.69. Calcd. for $C_{14}H_8O_2NBr$: N, 4.64%.

2-Chloroethyl 2-Bromoanthraquinon-1-ylcarbamate (IIa)[4].—Yellow needles (ethyl alcohol), m. p. 188~189°C.

Anal. Found: N, 3.48. Calcd. for $C_{17}H_{11}O_4NBrCl$: N, 3.42%.

2-Chloroethyl 3-Bromoanthraquinon-1-ylcarbamate (IIb).—A mixture of 2.00 g. of 1-amino-3-bromoanthraquinone (m. p. 240~241°C), 1.20 g. of 2-chloroethyl chloroformate (b. p. 150~151°C), 0.90 g. of sodium carbonate and 30 ml. of xylene was refluxed with stirring for 8 hr. The insoluble material was removed by hot filtration and the filtrate was evaporated to a volume of about 15 ml. for crystallization. Yield, 2.65 g. (99% of the theory) of yellow needles, m. p. 215~216°C. It was recrystallized from ethanol, giving yellow needles, m. p. 220~221°C.

Anal. Found: N, 3.53. Calcd. for $C_{17}H_{11}O_4NBrCl$: N, 3.42%.

2-Chloroethyl 4-Bromoanthraquinon-1-ylcarbamate (IIc).—A mixture of 2.00 g. of 1-amino-4-bromoanthraquinone (m. p. 175~176°C) 1.20 g. of 2-chloroethyl chloroformate (b. p. 150~151°C), 0.90 g. of sodium carbonate and 20 ml. of xylene was refluxed with stirring for 2 hr. The insoluble material was removed by hot filtration and the filtrate was evaporated to a volume of about 10 ml. for crystallization. Yield, 2.55 g. (94% of the theory) of yellow needles, m. p. 201~202°C. It was recrystallized from ethanol, giving yellow needles, m. p. 203~204°C.

Anal. Found: N, 3.67. Calcd. for $C_{17}H_{11}O_4NBrCl$: N, 3.42%.

3-(2-Bromoanthraquinon-1-yl)oxazolidin-2-one (IIIa)[4].—Pale brown plates (toluene), m. p. 284°C (decomp.).

Anal. Found: N, 4.09. Calcd. for $C_{17}H_{10}O_4NBr$: N, 4.11%.

3-(3-Bromoanthraquinon-1-yl)oxazolidin-2-one (IIIb) and 1-*N*-2-Hydroxyethylamino-3-bromoanthraquinone (IVb).—A mixture of 1.00 g. of finely powdered 2-chloroethyl 3-bromoanthraquinon-1-ylcarbamate and 30 g. of a 20% aqueous solution of potassium hydroxide was heated with vigorous stirring in a boiling water bath for 1 hr. After being diluted with water, the precipitate was collected, washed with water, and dried. Yield, 0.92 g. of reddish brown powder. The product, consisting of 1-*N*-2-hydroxyethylamino-3-bromoanthraquinone, 3-(3-bromoanthraquinon-1-yl)oxazolidin-2-one and 2-chloroethyl 3-bromoanthraquinon-1-ylcarbamate, was dissolved in benzene and chromatographed on alumina. 1-*N*-2-Hydroxyethylamino-3-bromoanthraquinone is most strongly adsorbed and 3-(3-bromoanthraquinon-1-yl)oxazolidin-2-one is more strongly adsorbed than 2-chloroethyl 3-bromoanthraquinon-1-ylcarbamate, which is gradually converted into 3-(3-bromoanthraquinon-1-yl)oxazolidin-2-one on alumina in the column. The red band, containing 1-*N*-2-hydroxylamino-3-bromoanthraquinone, was eluted by the use of ethanol. Yield, 0.15 g. of red needles, m. p. 213~214°C. It was recrystallized from toluene, giving red needles, m. p. 213~214°C.

Anal. Found: N, 4.08. Calcd. for $C_{16}H_{12}O_3NBr$: N, 4.11%.

The pale brown band, containing 3-(3-bromoanthraquinon-1-yl)oxazolidin-2-one, was eluted by the use of ethanol. Yield, 0.07 g. of pale brown crystalline powder, m. p. 215~229°C. It was recrystallized from ethanol, giving pale brown needles, m. p. 243~244°C.

Anal. Found: N, 3.73. Calcd. for $C_{17}H_{10}O_4NBr$: N, 3.76%.

The yellow elute, containing 2-chloroethyl 3-bromoanthraquinon-1-ylcarbamate, was evaporated for crystallization. Yield, 0.70 g. of yellow needles, m. p. 212~215°C.

3-(4-Bromoanthraquinon-1-yl)oxazolidin-2-one (IIIc) and 1-*N*-2-Hydroxyethylamino-4-bromoanthraquinone (IVc).—A mixture of 1.00 g. of finely powdered 2-chloroethyl 4-bromoanthraquinon-1-ylcarbamate (m. p. 201~202°C) and 30 g. of a 20% aqueous solution of potassium hydroxide was heated with vigorous stirring in a boiling water bath for 1 hr. After being diluted with water, the precipitate was collected, washed with water and dried. Yield, 0.88 g. of reddish brown powder. The product was treated as in the foregoing experiment. The red band, containing 1-*N*-2-hydroxyethylamino-4-bromoanthraquinone, was eluted by the use of ethanol. Yield, 0.45 g. of red needles, m. p. 176~177°C. It was recrystallized from ethanol, giving red needles, m. p. 181~182°C.

Anal. Found: N, 4.09. Calcd. for $C_{16}H_{12}O_3NBr$: N, 4.11%.

The pale brown band, containing 3-(4-bromoanthraquinon-1-yl)oxazolidin-2-one, was eluted by the use of ethanol. Yield, 0.20 g. of pale brown needles, m. p. 197~202°C. It was recrystallized from ethanol, giving pale brown needles, m. p. 208~209°C.

Anal. Found: N, 3.98. Calcd. for $C_{17}H_{10}O_4NBr$: N, 3.76%.

The yellow elute, containing 2-chloroethyl 4-bromoanthraquinon-1-yl-carbamate, was evaporated for crystallization. Yield, 0.10 g. of yellow needles, m. p. 184~190°C.

1-*N*-2-Hydroxyethylaminoanthraquinone (IVa).—A mixture of 0.50 g. of 2-chloroethyl 2-bromoanthraquinon-1-ylcarbamate (m. p. 191~192°C) and 15 g. of a 20% aqueous solution of potassium hydroxide was refluxed with vigorous stirring for 1 hr. After being diluted with water, the precipitate was collected, washed with water and dried. Yield, 0.40 g. of brownish red powder. It was treated as in the foregoing experiment. The red band, containing 1-*N*-2-hydroxyethylaminoanthraquinone, was eluted by the use of ethanol. Yield, 0.05 g. of red needles, m. p. 169~171°C. A mixed m. p. with authentic 1-*N*-2-hydroxyethylaminoanthraquinone[5] (m.p. 172°C) was 170~171°C.

3) Ger. Pat., 266,563 (1913).

4) K. Naiki, *J. Soc. Org. Syn. Chem., Japan* (*Yūki Gōsei Kagaku Kyōkaishi*), **14**, 84 (1954).

5) K. Naiki, ibid., **12**, 401 (1954).

The pale brown band, containing 3-(2-bromoanthraquinon-1-yl)oxazolidin-2-one, was eluted by the use of ethanol. Yield, 0.30 g. of pale brown plates, m. p. 265°C (decomp.).

Determination of the Proportion of the Constituents of the Reaction Product Obtained from 2-Chloroethyl Bromoanthraquinon-1-ylcarbamate and a 20% Aqueous Solution of Potassium Hydroxide.—A mixture of 0.20 g. of finely powdered 2-chloroethyl bromoanthraquinon-1-ylcarbamate and 6.0 g. of a 20% aqueous solution of potassium hydroxide was heated with vigorous stirring in a boiling water bath for 1 hr. After being diluted with water, the precipitate was colleted, washed with water and dried. Yield, 0.18 g. of brownish red powder from 2-chloroethyl 2-bromoanthraquinon-1-ylcarbamate; 0.18 g. of brownish red powder from 2-chloroethyl 3-bromoanthraquinon-1-ylcarbamate; 0.18 g. of brownish red powder from 2-chloroethyl 4-bromoanthraquinon-1-ylcarbamate. The proportion of the constituents of the products obtained above was determined by a Shimadzu QB-50 electrophotometer. Optical densities (D) of the toluene solution of the products are shown in Tables V—VII. It was found by simple calculation that the reaction product obtained from 2-chloroethyl 2-bromoanthraquinon-1-ylcarbamate contains 174 mg. of 3-(2-bromoanthraquinon-1-yl)oxazolidin-2-one; the product obtained from 2-chloroethyl 3-bromoanthraquinon-1-ylcarbamate contains 10 mg. of 3-(3-bromoanthraquinon-1-yl)oxazolidin-2-one, 106 mg. of 1-*N*-2-hydroxyethylamino-3-bromoanthraquinone and 57 mg. of 2-chloroethyl 3-bromoanthraquinon-1-ylcarbamate; the product obtained from 2-chloroethyl 4-bromoanthraquinon-1-ylcarbamate contains 46 mg. of 3-(4-bromoanthraquinon-1-yl)oxazolidin-2-one, 49 mg. of 1-*N*-2-hydroxyethylamino-4-bromoanthraquinone and 86 mg. of 2-chloroethyl 4-bromoanthraquinon-1-ylcarbamate.

TABLE V. OPTICAL DENSITIES OF THE PRODUCT OBTAINED FROM 2-CHLOROETHYL 2-BROMOANTHRAQUINON-1-YLCARBAMATE*

λ mμ	D	$\varepsilon \times 10^{-4}$	
		IIa	IIIa
330	0.480	0.370	0.466
370	0.125	0.346	0.124

* Solvent: toluene; concn. 38 mg./l.

TABLE VI. OPTICAL DENSITIES OE THE PRODUCT OBTAINED FROM 2-CHLOROETHYL 3-BROMOANTHRAQUINON-1-YLCARBAMATE*

λ mμ	D	$\varepsilon \times 10^{-4}$		
		IIb	IIIb	IVb
330	0.528	0.372	0.417	0.432
410	0.281	0.556	0.064	0.076
500	0.446	0.020	0.007	0.590

* Solvent: toluene; concn. 43 mg./l.

TABLE VII. OPTICAL DENSITIES OF THE PRODUCT OBTAINED FROM 2-CHLOROETHYL 4-BROMOANTHRAQUINON-1-YLCARBAMATE*

λ mμ	D	$\varepsilon \times 10^{-4}$		
		IIc	IIIc	IVc
340	0.336	0.240	0.347	0.353
420	0.324	0.560	0.054	0.098
500	0.255	0.051	0.007	0.696

* Solvent: toluene; concn. 42 mg./l.

The author is indebted to Mr. Yoshié Tanizaki for his helpful advice, to Mr. Toshirō Iijima for his helpful discussions and also Professor S. Tsuruoka for his encouragement throughout the present study.

The Laboratory of Dyestuff Chemistry
Tokyo Institute of Technology
Meguro-ku, Tokyo

Crystallization-sensitive Band of Polyvinyl Alcohol

By Hiroyuki TADOKORO

(Received June 11, 1959)

So-called "crystallization-sensitive bands" in the infrared absorption spectra have recently been found with various kinds of high polymers, such as polyethylene[1-5], polyethylene terephthalate[6-8], polychlorotrifluoroethylene[9], rubber hydrochloride[10], neoprene[11], polyamides[12-14], polyethylene glycol[15], polyvinylidene chloride[16], gutta percha[17], etc. Bands of this kind have at present interested many investigators as one of the powerful measures of the degree of crystallinity, or as a useful clue for the elucidation of the fine structure of the crystalline high polymers[12].

As to the 1141 cm^{-1} band in the infrared spectrum of polyvinyl alcohol (PVA), Elliott, Ambrose and Temple[18] reported that this band shows strong dichroism, and Nagai and his coworkers[19] found that this band becomes more and more intense as heat-treatment proceeds, up to the temperature at which the sample becomes colored. In a previous paper[20] they have concluded that degrees of crystallinity determined by density, sorption of water vapor and infrared absorption methods are approximately in linear relationship unless the thermal decomposition is considerable, and that the 1141 cm^{-1} band is recognized as a so-called crystallization-sensitive band. The nature of this band has been discussed by several authors as will be described below, but is still in a stage of speculation. Accordingly it is highly desirable that further new experimental facts should be accumulated. In the present paper the author will report the experimental results obtained on the proposed crystallization-sensitive band of PVA.

Experimental

a) Samples.—Film specimens were prepared by the same procedures as those described in the previous paper[21].

b) Measurements of the Pleochroism.—A doubly oriented specimen was prepared as follows. A uniaxially oriented PVA film* was rolled with a hot roller at about 90°C (to about four times its length compared with the original one) by holding it between two sheets of nylon 610**. In this procedure the direction of rolling was the same as that of stretching. The double orientation of the sample prepared in this way was ascertained by taking an X-ray Sauter photograph.

Fig. 1 shows schematically the relation between the cross-section perpendicular to the direction of rolling (the direction of the molecular chain axis) of the doubly oriented PVA film and the incident polarized infrared radiation***. As is shown in this figure, both the electric vector and the direction of propagation of the polarized infrared beam are perpendicular to the direction of rolling which is normal to the plane of the figure. The infrared spectra were observed at various angles of the incident beam, namely, 0, 45, 60, 70 and 75°. These infrared measurements were carried out by using a Perkin-Elmer Model 21 Infrared Spectrophotometer with AgCl polarizer.

1) R. B. Richards, *J. Appl. Chem.*, **1**, 370 (1951).
2) R. S. Stein and G. B. B. M. Sutherland, *J. Chem. Phys.*, **22**, 1993 (1954); R. S. Stein, ibid., **23**, 734 (1955).
3) A. Keller and I. Sandeman, *J. Polymer Sci.*, **15**, 133 (1955).
4) S. Krimm, C. Y. Liang and G. B. B. M. Sutherland, *J. Chem. Phys.*, **25**, 549 (1956).
5) M. C. Tobin, ibid., **23**, 891 (1955).
6) W. H. Cobbs, Jr. and R. L. Burton, *J. Polymer Sci.*, **10**, 275 (1953).
7) R. G. J. Miller and H. A. Willis, ibid., **19**, 485 (1956).
8) A. B. Thompson and D. W. Wood, *Nature*, **176**, 78 (1955).
9) H. Matsuo, *J. Polymer Sci.*, **21**, 331 (1956); This Bulletin, **30**, 593 (1957).
10) P. B. Checkland and W. H. T. Davison, *Trans. Faraday Soc.*, **52**, 151 (1956).
11) W. E. Mochel and M. B. Hall, *J. Am. Chem. Soc.*, **71**, 4082 (1949); J. T. Maynard and W. E. Mochel, *J. Polymer Sci.*, **13**, 235 (1954).
12) J. B. Nichols, *J. Appl. Phys.*, **25**, 840 (1954).
13) I. Sandeman and A. Keller, *J. Polymer Sci.*, **19**, 401 (1956).
14) H. W. Starkweather, Jr. and R. E. Moynihan, ibid., **22**, 363 (1956).
15) W. H. Davison, *J. Chem. Soc.*, **1955**, 3270.
16) R. L. Burton, W. H. Cobbs, Jr. and V. C. Haskell, *J. Polymer Sci.*, **7**, 569 (1951).
17) G. B. B. M. Sutherland and A. V. Jones, *Discussions Faraday Soc.*, **9**, 281 (1950).
18) A. Elliott, E. J. Ambrose and R. B. Temple. *J. Chem. Phys.*, **16**, 877 (1948).
19) E. Nagai, S. Mima, S. Kuribayashi and N. Sagane, *Chem. High Polymers (Kobunshi Kagaku)*, **12**, 199 (1955).
20) H. Tadokoro, S. Seki and I. Nitta, This Bulletin, **28**, 559 (1955).
21) H. Tadokoro, ibid., **32**, 1252 (1959).

* See Ref. 21.

** Kindly supplied by Dr. H. Yumoto of Tôyô Rayon Co., Ltd.

*** It may be noticed that the angle β of the crystal lattice given in the text of Bunn's paper[22] is different from that of the figure. Fig. 1 in the present paper was reproduced according to the text of Bunn's paper.

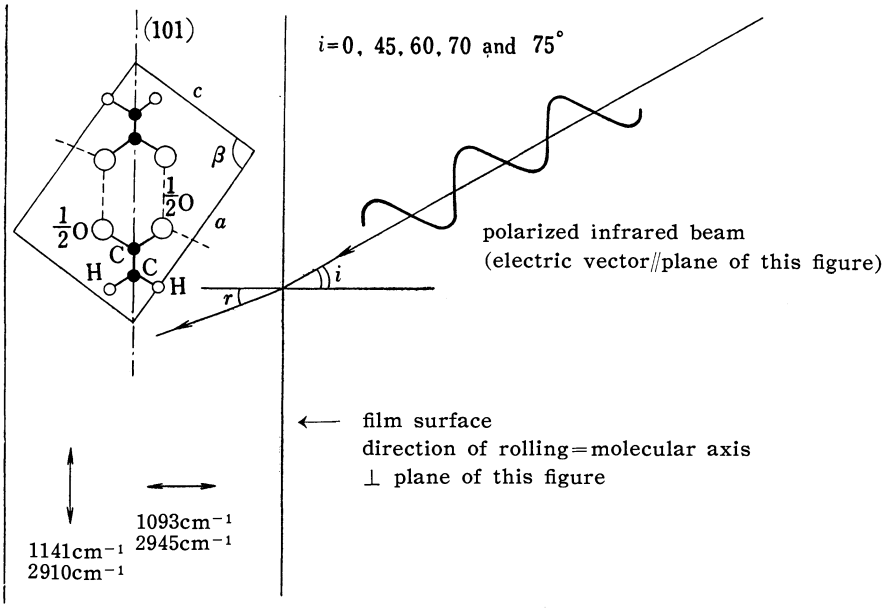


Fig. 1. The relation between the cross-section of the doubly oriented PVA film and the incident polarized infrared beam.

c) Formalization and Swelling in Water.—The PVA samples used for the experiments of formalization and swelling in water, were the same as samples I and III described in the previous papers[20,21]. The details of the experimental condition of the formalization was also given in the previous paper[22]. Those samples were also subjected to swelling in water at room temperature for 2 days. The degrees of swelling for samples I and III in this experimental condition are about 4.7 and 0.7, respectively. The infrared absorption spectra and X-ray diffraction photographs were taken by using a Hilger H800 Infrared Spectrophotometer and an ordinary Laue camera, respectively, before and after the treatment of formalization and swelling in water. During the X-ray measurements the swollen samples were held between aluminum foils in order to prevent the vaporization of water from the samples.

Results and Discussion

a) Pleochroism of the 1141 cm^{-1} Band.—When a polymer is stretched, the crystallites (or molecular chains) are so oriented that the molecular chain axes will be arranged parallel to the stretched direction, but the orientation of the molecular plane in the cross-section perpendicular to the direction of stretching remains completely random. Such a kind of orientation is called a "uniaxial orientation" and the usual fibers have more or less this kind of orientation. When the uniaxially oriented film is rolled in an adequate condition, a certain plane parallel to the molecular axis (in the case of PVA, the plane of carbon zigzag chain) is oriented further parallel to the rolled plane. Such a mode of orientation is called "double orientation". This possibility of double orientation was found for the first time by Bunn et al. on polyethylene[23] and nylon 66[24] by the use of X-ray diffraction, and afterwards this procedure was applied to the infrared studies of nylon 66, PVA and polyethylene by Ambrose and his coworkers[25] in the 3 μ region, and of polyethylene terephthalate by Miller and Willis in the 5~15 μ region[26].

The infrared studies of the doubly oriented PVA sample were carried out in the 3 μ region by Glatt et al.[27] and Elliott et al.[25] By the use of the pleochroism of the CH_2 stretching modes, they found that the plane of the carbon zigzag chain is parallel to the rolled plane of the film.

If the transition moment of an absorption band is perpendicular to the direction of rolling and exists in the rolled plane of

22) C. W. Bunn, *Nature*, **161**, 929 (1948).

23) C. W. Bunn, *Trans. Faraday Soc.*, **35**, 482 (1939).
24) C. W. Bunn and E. V. Garner, *Proc. Roy. Soc.*, **A181**, 45 (1947).
25) A. Elliott, E. J. Ambrose and R. B. Temple, *Nature*, **163**, 567 (1949); E. J. Ambrose, A. Elliott and R. B. Temple, *Proc. Roy. Soc.*, **A199**, 183 (1949).
26) R. G. J. Miller and H. A. Willis, *Trans. Faraday Soc.*, **49**, 433 (1953).
27) S. Krimm, C. Y. Liang and G. B. B. M. Sutherland, *J. Polymer Sci.*, **22**, 227 (1956).

the doubly oriented film, the intensity of the band must be strongest when the angle of incidence, $i=0°$, and must be weaker as i increases (see Fig. 1). On the contrary, in the case when the direction of the transition moment is normal to the rolled plane, the intensity of the band should behave in the reverse manner. Utilizing this fact, it is possible to know the appoximate direction of the transition moment from the results of the absorption measurements on the doubly oriented sample.

The spectra taken with the doubly oriented specimen at different inclinations to the incident polarized beam is partly reproduced in Fig. 2. The relation between the optical density of the bands and the angle of incidence i is also given in Fig. 3.

From these measurements, it was possible to draw the following experimental conclusions: (1) the directions of the transition moments of the CH_2 symmetric stretching band at 2910 cm^{-1} and of the band at 1141 cm^{-1} are preferentially parallel to the surface of the rolled film, and (2) that of the CH_2 antisymmetric stretching band at 2945 cm^{-1} and of the band at 1093 cm^{-1} are more or less normal to the film surface, while (3) those of the other bands do not show any remarkable polarization**** (see Fig. 3).

Prior to the discussion on the nature of 1141 cm^{-1} band, it should be liked to make

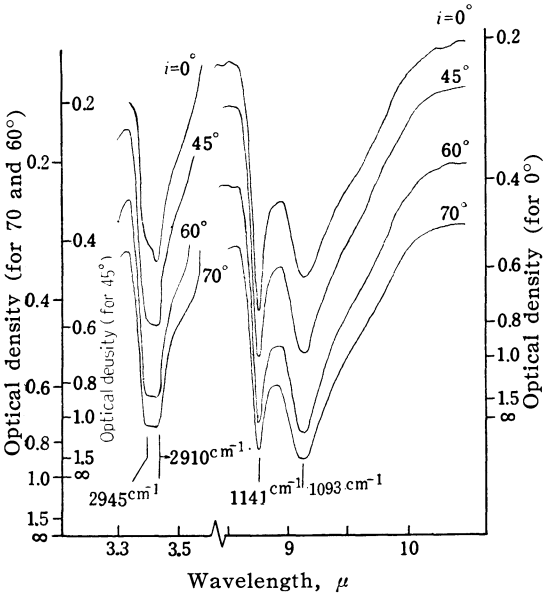


Fig. 2. Infrared spectra of doubly oriented PVA film taken at different inclinations (i means the angle of incidence).

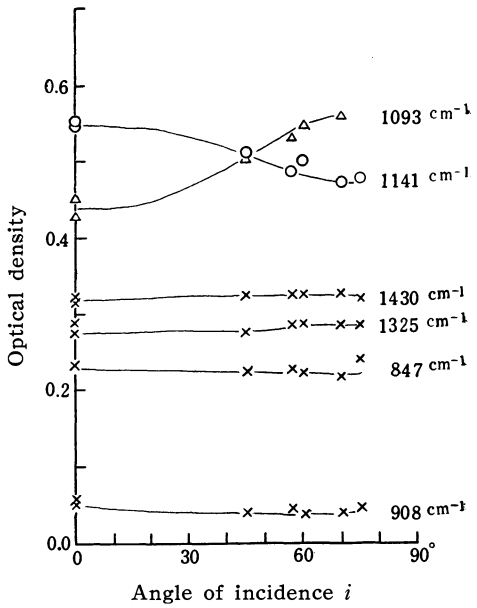
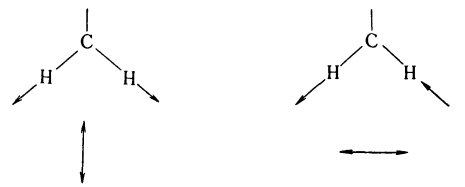


Fig. 3. Relation between the optical density of the bands and the angle of incidence i (doubly oriented PVA film).



CH_2 symmetric stretching 2910 cm^{-1}

CH_2 antisymmetric stretching 2945 cm^{-1}

Fig. 4. Two vibration types of CH_2 stretching of PVA.

a short comment on the modes of vibrations of CH_2 group. As shown in Fig. 4, there are two kinds of C-H stretching vibrations of the CH_2 group of PVA[25]. The transition moment of the symmetric stretching mode at 2910 cm^{-1} should be parallel to the bisector of the angle H-C-H, and that of the antisymmetric mode at 2945 cm^{-1} perpendicular to it. The results on the CH_2 stretching modes inform us of the fact that the plane of the zigzag chain of carbon atoms is parallel to the surface of the film, in agreement with the observation of Ambrose and his coworkers[25].

Krimm, Liang and Sutherland[27] assigned this 1141 cm^{-1} band to the stretching of

**** Of the other bands, 913, 849 and 835 cm^{-1} bands were found to have weak pleochroism by the infrared microspectroscopic measurements on a highly and doubly oriented PVA sample[28].

28) H. Tadokoro, S. Seki, I. Nitta and R. Yamadera, *J, Polymer Sci.*, 28, 244 (1958).

ether linkage produced by heat-treatment and they stated that the authors' conclusion[20] that this 1141 cm^{-1} band is the crystallization-sensitive band, is open to question. However, the experimental fact presented here together with the following sections b), c) and d) are believed to support the authors' conclusion.

b) Density Consideration. — Of the four samples (Table I) studied in the previous paper[20], sample IV subjected to heat-treatment in air at highest temperature (at 193°C for 2.5 min.) showed a deviation from the linear relationship between the optical density of the 1141 cm^{-1} band and the density of the samples, and this was interpreted as the result of a chemical change on the basis of the ultraviolet absorption spectrum. This deviation was pointed out by Krimm et al.[27] as one of the evidences for their objection to the authors' view[20]. Here, the author wishes to refer to the results of the authors' density measurements by the density gradient tube method on PVA films[29]. The samples for the measurements were treated in silicone oil for various durations at various temperatures as shown in the explanation of Fig. 5. The density of the samples was determined at 25°C by using the mixture of xylene and carbon tetrachloride as flotation medium. The ultraviolet absorption spectra of these samples were also measured with a Beckman Model DU Quartz Spectrophotometer in order to examine whether or not some chemical change occurs. Fig. 5 shows the correlation between the optical density of the 1141 cm^{-1} band and the density of the samples. As the thicknesses of the films were not the same in each case, the relative intensity of the 1141 cm^{-1} band of the samples was obtained by adjusting the intensities of the other bands to fit one another as closely as possible. This procedure was based upon the fact that the intensity of the 1141 cm^{-1} band is very sensitive to heat-treatment, whereas those of others are not. In Fig. 5 the samples denoted by △ show two strong absorption bands (280 and 330 mμ) in the ultraviolet region similarly to that for sample IV in the previous paper[20]. Twelve samples denoted by ○ clearly satisfy the linear relationship, while the samples denoted by △ deviate downwards from this. This fact indicates that this deviation is to be attributed to the thermal decomposition, and so it is less significant in the discussion of the crystallinity of PVA. Thus the observed linear relationship between the intensity of the 1141 cm^{-1} band and the density of the samples is in good agreement with the previous conclusion that the 1141 cm^{-1} band is a crystallization-sensitive band.

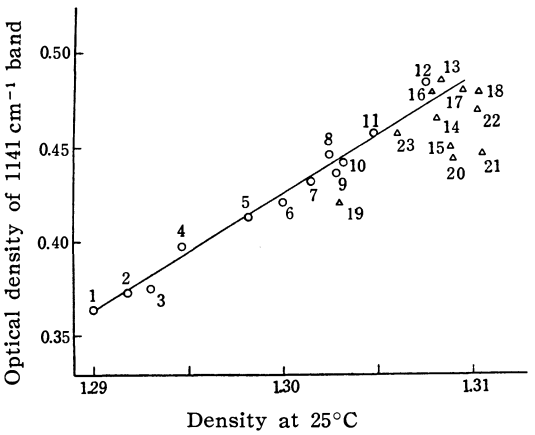


Fig. 5. Optical density of 1141 cm^{-1} band plotted against density for PVA samples subjected to heat-treatments at various conditions in silicone oil[29].

1.	no treatment		13.	180°C	60 min.
2.	100°C	5 min.	14.	190	2
3.	100	100	15.	190	5
4.	140	2	16.	190	21
5.	140	10	17.	220	1
6.	160	5	18.	220	2
7.	160	10	19.	220	15
8.	160	20	20.	240	10 sec.
9.	160	40	21.	240	40
10.	160	85	22.	240	90
11.	180	5	23.	240	120
12.	180	30			

c) Formalization and Swelling in Water. — Fig. 6 shows infrared spectra of dry and swollen PVA samples I and III, and their partial formals. The curves below the swollen samples are for those of the drying process, and were measured successively about 7 min. after the measurement on the swollen sample was done, and so on. In the case of sample I, the 1141 cm^{-1} band was observed to disappear on formalization. On the other hand, for sample III the 1141 cm^{-1} band is not affected remarkably. The 1141 cm^{-1} band of the partial formal of sample III is identified with that of sample III by its similar behavior to deuteration, namely, this band shifts slightly to a shorter wavelength side on deuteration in both cases of PVA and the partial formal of

29) H. Tadokoro, K. Kôzai, S. Seki and I. Nitta, ibid., **26**, 379 (1957).

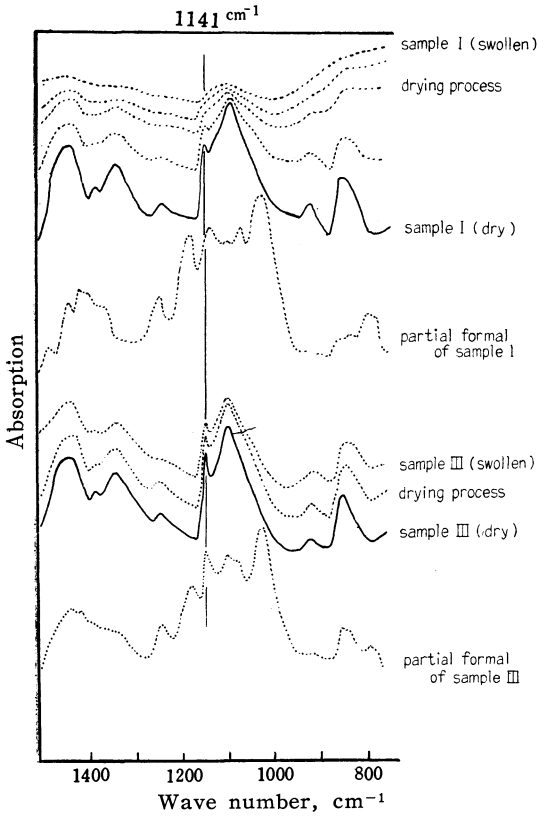


Fig. 6. Infrared spectra of dry and swollen PVA samples I and III and of their partial formals. The curves below the swollen one were measured successively ca. 7 min. after the measurement of the swollen sample was done, and so on.

sample III[30]. The 1141 cm^{-1} band is hardly found in the spectra of the swollen sample I, but appears progressively as the samples are being dried. On the other hand, in the case of sample III this band seems not to be influenced strongly by swelling.

Fig. 7 shows the X-ray photographs of the samples in Fig. 6. In Fig. 7, a) is for dried sample I, b) swollen sample I, c) partial formal of sample I, d) dried sample III, e) swollen sample III, and f) partial formal of sample III. The spots in the photographs a), b) and e) arise from the aluminum foil used for sealing the samples in order to prevent vaporization of water from the samples. The spots in c) and f) are due to the residual sodium sulfate being used for formalization. The haloes in b) and e) are due to liquid water. The diffraction rings due to PVA disappear in photograph b) of the swollen sample I, but the rings seem not to be affected remarkably in the case e) of sample III. In photograph c) of the partial formal of sample I, the intense diffraction rings of PVA give place to a new halo of smaller diffraction angle. This change corresponds to the increase of the apparent lattice distance from 4.51 to 4.72 Å.

The authors' previous observations by use of the infrared absorption and X-ray photographs indicate evidently that the 1141 cm^{-1} band behaves in parallel with the diffraction rings due to the crystalline region of PVA on formalization and swelling in water; namely, both the band and the rings disappear in the case of sample I, but are not affected remarkably in the case of sample III. This fact may also be considered to support the conclusion that this band is a crystallization-sensitive band.

d) On the Assignment of the 1141 cm^{-1} Band.—As to the assigment of the 1141 cm^{-1} band, various interpretations have already been proposed. Elliott and his coworkers[18] explained that this band is connected with the presence of the oxygen atom because of the lack of this band in the case of polyvinyl chloride. Nishino and his coworkers[31] as well as Nagai and his coworkers[32] considered this band to be associated with the formation of hydrogen bond. Krimm and his coworkers[27] suggested that this band may be the stretching of C–O–C linkage produced as the result of the heat-treatment of the sample.

It is considered to be necessary that the assignment of this band should satisfy the following experimental facts:

(1) The strongly perpendicular dichroism of this band (Fig. 4 of Ref. 21).

(2) The fact that the transition moment of the band is nearly parallel to the plane of the zigzag chain (Fig. 2).

(3) The parallel relationship between the intensity of the band and the density of the sample (Fig. 5).

(4) The location of the band in the observed spectrum.

(5) The only slight shift of this band on deuteration (about 7 cm^{-1} or 0.994 in wave number ratio, to higher frequency).

(6) The crystal structure of this substance[22], etc.

As the shift of this band on deuteration is so small, this band seems to be not

30) See Fig. 2 of Ref. 21.

31) Y. Nishino, J. Ukita and T. Kominami, *J. Chem. Soc. Japan, Ind. Chem. Sec.* (*Kogyo Kagaku Zasshi*), **58**, 159 (1955).

32) E. Nagai and S. Kuribayashi, *Chem. High Polymers* (*Kobunshi Kagaku*), **12**, 322, 368 (1955).

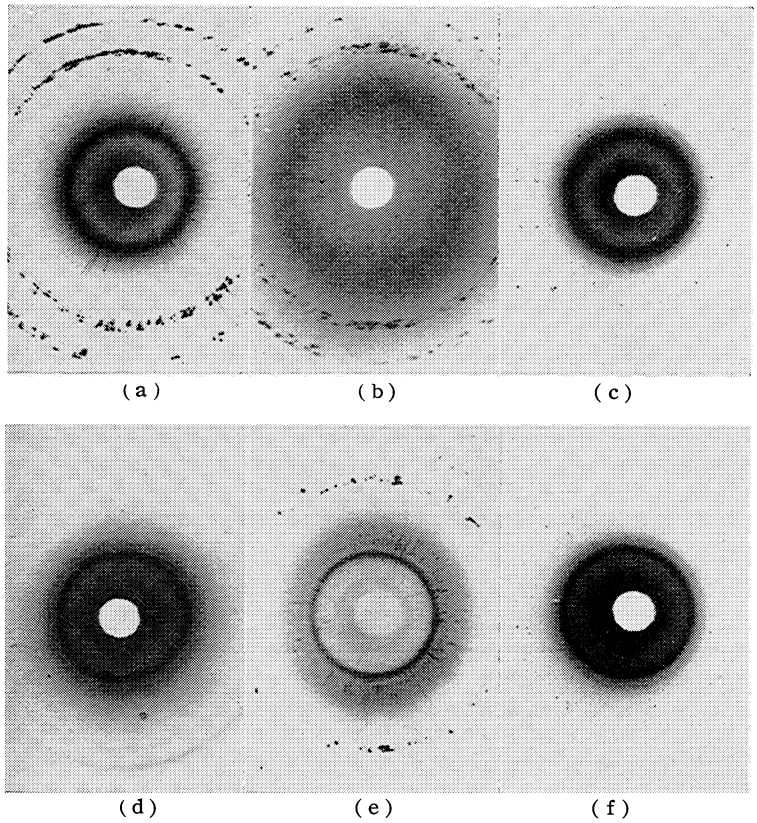


Fig. 7. X-ray photographs corresponding to the samples in Fig. 6: (a) sample I (dry); (b) sample I (swollen); (c) partial formal of sample I; (d) sample III (dry); (e) sample III (swollen); (f) partial formal of sample III.

directly associated with the motion of the hydrogen atom of hydroxyl group such as O–H deformation. The assignment of this band to the stretching of C–O–C linkage does not seem to be able to explain the experimental facts mentioned above [sections a), b) and c)] and the fact that this band exists distinctly even in the spectrum of the sample with no heat-treatment (such a sample is hardly considered to contain ether linkage). In this respect, Haas[33] has recently concluded that (1) the suggestion by Krimm et al.[27] relating this band to C–O–C vibration must be rejected, and (2) a hypothesis which relates the band with some vibrational modes associated only with crystallization is favored.

At the present stage it is still difficult to make the final assignment of this band from the present experimental data, but this band is undoubtedly due to the crystalline arrangements of the molecules and is thought to be intimately related to the regular repetition of the *trans*-configuration of the zigzag chains. For further elucidation of the nature of this band the total syntheses of $-(-CD_2-\underset{\underset{OH}{|}}{CD}-)_p-$ are now being carried out. (D)

The author wishes to express his gratitude to Professor I. Nitta and Assistant Professor S. Seki, under whose guidance this research was carried out. He also expresses his sincere thanks to Professor T. Shimanouchi of the University of Tokyo for helpful advice and criticism, to Dr. T. Kanzawa and Mr. H. Kamio of Takeda Pharmaceutical Industries, Ltd. for preparing part of the charts of the infrared absorption spectra, and to Kurashiki Rayon Co., Ltd. for kindly giving him the PVA samples.

Department of Polymer Science
Faculty of Science
Osaka University
Nakanoshima, Osaka

33) H. C. Haas, *J. Polymer Sci.*, **26**, 391 (1957).

Relations between Electronic Absorption Spectra and Spatial Configurations of Conjugated Systems. I. Biphenyl

By Hiroshi SUZUKI

(Received June 12, 1959)

A twist of a "single" bond in a conjugated system caused by steric effects affects the electronic absorption spectrum of the molecule. Since the interaction of the π-orbitals across the bond and hence the conjugation of the system are maximal when the system is planar, as is well known, any deviation from the planarity of the molecular configuration reduces the degree of conjugation to the corresponding extent, and consequently alters the spectral feature.

The relation between the spatial configuration and the electronic absorption spectrum of a conjugated system may conveniently be divided into the following three kinds; (A) that between the spatial configuration and the shape of the absorption curve (mainly an appearance of fine structure), (B) that between the spatial configuration and the intensity of the conjugation band, and (C) that between the spatial configuration and the position of the conjugation band.

Concerning the relation of A, Merkel and Wiegand[1] proposed the hypothesis that the appearance of fine structure depended on the planarity of the molecular configuration. Thus, the spectra of fluorene and of carbazole, for example, which are thought to be planar, and also that of biphenyl in the crystalline state exhibit fine structures. On the basis of this hypothesis, Merkel and Wiegand suggested that the lack of structure in the spectrum of biphenyl in solution might indicate the non-planarity of the molecule in solution. However, this hypothesis has been denied by Kortüm and Dreesen[2]. According to their opinion, the appearance of fine structure does not depend on planarity of the molecular configuration, but depends rather on its rigidity. However, whether there is an unconditional relation between the molecular configuration and the appearance of fine structure or not has not yet been clarified, since this problem is considerably complicated, and since an appearance of fine structure depends on techniques of measurement, on solvents, etc.

A change in spatial configuration about a "single" bond in a conjugated system has conventionally been thought to affect the position and the intensity of the conjugation band in any of the following three ways, depending on the degree of deviation from the coplanarity[3]: (1) No change in the position of the absorption maximum but a decrease in the intensity. This effect is caused by relatively small twists. (2) A shift of the absorption maximum to shorter wavelengths in addition to a decrease in the intensity. This effect is caused by larger twists than the first effect. (3) When the twist is large enough to eliminate almost completely the $\pi-\pi$ interaction across the twisted bond, the spectrum is similar to the sum of the spectra of the component parts of the molecule on either side of the bond.

On the basis of such a classification, Braude and his coworker[4] assumed the following relation between the angle of twist θ and the molar extinction coefficient ε of the absorption maximum of the conjugation band for the cases of type 1, namely the cases in which the steric effect changes the absorption intensity alone;

$$\varepsilon/\varepsilon_0 = \cos^2\theta$$

where ε_0 is the molar extinction coefficient of the corresponding absorption maximum of the planar reference compound. Braude and his coworkers applied this postulated relation to some sterically hindered derivatives of benzaldehyde[4], of acetophenone[4], of styrene[5], and of biphenyl[6],

1) (a) Chr. Wiegand and E. Merkel, *Ann.*, **557**, 242 (1947). (b) E. Merkel and Chr. Wiegand, *Naturwiss.*, **34**, 122 (1947). (c) E. Merkel and Chr. Wiegand, *Z. Naturforsch.*, **3b**, 93 (1948).

2) G. Kortüm and G. Dreesen, *Chem. Ber.*, **84**, 182 (1951).

3) See, for example: M. S. Newman, "Steric Effects in Organic Chemistry", John Wiley & Sons, Inc., New York (1956), p. 484.

4) E. A. Braude and F. Sondheimer, *J. Chem. Soc.*, **1955**, 3754.

5) E. A. Braude and F. Sondheimer, ibid., **1955**, 3773.

6) E. A. Braude and W. F. Forbes, ibid., **1955**, 3776.

and stated that the satisfactory value of the angle of twist θ was obtained for each of the compounds. However, it can not be recognized that only a change of the intensity of the conjugation band occurs without any significant displacement of the position in each of the systems of compounds cited by Braude and others, in spite of their assumption. And further, it seems that the derivation of their equation and its basic theory are open to considerable criticism.

However, independently from Braude and others' works, a relation bearing a close similarity to the one mentioned above has been proposed. Thus, Klevens and Platt[7] have stated that the oscillator strength of the conjugation band is linearly related to the van der Waals radius of the interfering group and to the $\cos^2$ of the calculated angle of the C–N bond twist in some ortho-substituted dimethylanilines. In addition, Beale and Roe[8] have found that the changes in oscillator strength of the conjugation band for substitution with methyl groups in stilbene are additive, and that the ortho-substitution reduces the oscillator strength.

Regarding the relation of C, that is, the relation between the spatial configuration of a molecule and the position of the conjugation band, the following examples may be cited: *trans*-Stilbene has the conjugation band at about 294 mμ, which is progressively shifted toward shorter wavelengths with the concurrent decreases in the intensity as one, and then two methyl groups are introduced into the α- and α'-positions of the molecule[9,10]. Biphenyl has the conjugation band at about 247 mμ, which is markedly shifted toward shorter wavelengths in the spectrum of o,o'-dimethylbiphenyl[11]. Further, bimesityl does not exhibit the characteristic conjugation band, but absorbs as two molecules of mesitylene[11,12]. These hypsochromic wavelength displacements are explained in terms of the steric interference of the substituents which prevents the molecule from assuming a coplanar configuration.

Although these phenomena had been known for a considerably long time as the references cited show, no theoretical explanation had been established satisfactorily, and consequently, the quantitative relation between the dimensions of the spatial configuration of the molecule, especially the angle of twist, and the position of the conjugation band had not been clarified[13]. Thus, the prevailing explanations were rather unsatisfactory or unreasonable ones such as, for example, the following: The appearance of the conjugation band is related to the conjugation, and therefore requires the coplanarity of the molecular configuration. On the basis of such an assumption, the hypsochromic shifts observed in, for example, the spectra of α- and α,α'-substituted stilbenes as well as in that of *cis*-stilbene as compared with that of *trans*-stilbene needed to be explained by a rather implausible hypothesis based on a concept of "partial chromophore"[14]. The alternative prevailing explanation was as follows: The extent of the contribution of the dipolar structure in the electronic excited state is larger than in the ground state. Since the dipolar structure requires a coplanarity of the molecular configuration, steric hindrance to such a configuration will raise the potential energy of the excited state more than that of the ground state, and hence, the transition energy will be increased[15].

Previously, the present author calculated the quantitative relations between the degree of deviation from coplanarity of the molecular configuration and the position of the conjugation band as well as the extent of conjugation for stilbenes[16] and also for biphenyls[17,18], by the method based on the simple LCAO molecular orbital method. By the results of the calculations he clarified the fact that the perfect coplanarity is not prerequisite to the occurrence of conjugation and to the appearance of the characteristic conjugation band, and that the conjugation band is gradually shifted toward shorter wavelengths as the degree of deviation from the coplanarity increases. Further he showed that the values of the angle of

7) H. B. Klevens and J. R. Platt, *J. Am. Chem. Soc.*, **71**, 1714 (1949).
8) R. N. Beale and E. M. F. Roe, ibid., **74**, 2302 (1952).
9) (a) H. Ley and F. Rinke, *Ber.*, **56**, 771 (1923). (b) B. Arends, ibid., **64**, 1936 (1931).
10) R. N. Jones, *J. Am. Chem. Soc.*, **65**, 1818 (1943).
11) M. T. O'Shaughnessy and W. H. Rodebush. ibid., **62**, 2906 (1940).
12) L. W. Pickett, G. F. Walter and H. France, ibid., **58**, 2296 (1936).
13) See, for example: (a) R. N. Beale and E. M. F. Roe, *J. Chem. Soc.*, **1953**, 2755. (b) W. Klyne, "Progress in Stereochemistry", Vol. 1, Butterworths Scientific Publications, London (1954), p. 142.
14) See, for example: E. A. Braude, *J. Chem. Soc.*, **1949**, 1902. See also Ref. 10.
15) For examples: W. R. Remington, *J. Am. Chem. Soc.*, **67**, 1838 (1945). And also: Refs. 6, and 13b, p. 131.
16) H. Suzuki. This Bulletin, **25**, 145 (1952).
17) H. Suzuki, ibid., **27**, 597 (1954).
18) H. Suzuki, ibid., **29**, 945 (1956).

twist as well as the effective resonance energy can be satisfactorily computed from the observed position of the conjugation band.

Although these previous treatments seem fairly satisfactory in principle, it was found afterwards that they included an inadequate assumption. Thus, the choice of the absorption maximum corresponding to the planar molecule of biphenyl in the previous paper[17] was found to be probably inadequate. In addition, it seems that there are some aspects which were not given adequate consideration in the previous papers. Thus, first, the spectrum of *trans*-stilbene in solution was assumed to be that of the planar molecule of the compound without sufficient consideration. Strictly speaking, there is no evidence to indicate that *trans*-stilbene in the solution state has the planar configuration. Secondly, the electronic bathochromic effects of substituents such as methyl groups were ignored, and this ignoring seems to be an over-simplification. These electronic effects of substituents should not be ignored particularly when the substituents are on the benzene nuclei. Lastly, the position of absorption maximum varies more or less with the solvent, so the solvent effect should also be taken into account.

In this series of papers, the erroneous assumption mentioned above being corrected, and the aspects which were not given sufficient consideration being re-examined, a method similar to the previous one is applied to the greater range of conjugated compounds, and the relation between the spatial configuration of the molecule and the electronic absorption spectrum, especially the position of the conjugation band, is discussed more comprehensively and more fully. The relation of the intensity of the band and that of the appearance of fine structure to the spatial configuration of the molecule will also be referred to at suitable places in this series.

The present series is concerned mainly with the spatial configurations and the electronic states of the molecules in solution. This subject is certain to be very important in studying the relations between molecular structures and reactivities of organic compounds. In this connection, it seems that there is no precise and direct means to determine the spatial configurations of molecules in solution, such as the X-ray analysis for the crystalline states or the electron diffraction analysis for the vapor states. Therefore, information from the analysis of the electonic absorption spectra is conceivably important and useful in this respect. From this point of view, in this series the spatial configurations of the compounds inferred from the electronic absorption spectra are correlated as much as possible with the other properties, especially the reactivities of the compounds.

In this part of series, the ultraviolet absorption spectra of biphenyl in the various states, i.e. the crystalline, the solution, and the vapor state, and their relations to the spatial configurations of the molecule are discussed in detail as the basis of the present treatment.

Calculation

Although the procedures of calculation were already outlined in the previous papers[16,17], those for biphenyl are shown below in somewhat more refined form.

(1) Correlation of a Parameter for the Resonance Integral for the Pivot Bond with the Bond Length and the Interplanar Angle. — The π—π resonance integral for the 1-1′ bond, namely the co-annular or pivot bond, is denoted by $\mu\beta$, in which β is the π—π resonance integral for the C-C bond in the benzene ring and μ is a parameter by which allowance is made for changes of the resonance integral with the bond length and the angle of twist, i.e. the angle between the planes of the two benzene rings, which is subsequently referred to also as the interplanar angle. (The symbol α in the previous papers was replaced by μ.)

The π—π resonance integral for C-C bond can be taken to be approximately proportional to the π—π overlap integral[19], and, as easily verified, the π—π overlap integral $S(R, \theta)$ in the case where the bond length is R and the angle of twist is θ is equal to the overlap integral $S(R, 0°)$ in the case where the bond length is R and the angle of twist is 0°, multiplied by $\cos\theta$. Accordingly, the parameter μ can approximately be expressed by the following equation;

$$\mu = S(R, 0°)\cos\theta / S(1.39, 0°) \qquad (1)$$

where $S(1.39, 0°)$ represents the π—π overlap integral for the C-C bond in the benzene ring, the length of which is 1.39 Å.

The relation between the bond length R and the corresponding overlap integral $S(R, 0°)$ can be obtained from Mulliken's Tables[20]. According to results of calculation based on the tables, the values of $S(R, 0°)$ and hence of $S(R, 0°)/S(1.39, 0°)$ vary linearly with R, at least in the range of R

19) (a) R. S. Mulliken, C. A. Rieke and W. G. Brown, *J. Am. Chem. Soc.*, **63**, 41 (1941). (b) J. van Dranen and J. A. A. Ketelaar, *J. Chem. Phys.*, **17**, 1338 (1949).
20) R. S. Mulliken, C. A. Rieke, D. Orloff and H. Orloff, ibid., **17**, 1248 (1949).

between 1.44 and 1.54 Å, and the relations can approximately be expressed as follows:

$$S(R,0°)=0.1920+(1.54-R)\times 0.36 \quad (2)$$

$$S(R,0°)/S(1.39,0°)=0.77108+(1.54-R)\times 1.4458 \quad (3)$$

where the value of $S(1.39,0°)$ is 0.249.

According to the result of X-ray crystal analysis by Dhar[21], R is 1.48 Å and θ is 0° in biphenyl in the crystalline state. Consequently, the corresponding value of μ is evaluated at 0.858.

Any deviation from the coplanar configuration must inevitably reduce the π—π interaction across the co-annular bond to the corresponding extent, and consequently must be accompanied by change in the bond length. Thus, the value of R will vary from 1.48 Å in the planar biphenyl molecule to 1.54 Å, i. e. the length of the normal C-C single bond, as θ varies from 0° to 90°. Therefore, the following relation may tentatively be assumed between R and θ:

$$\{S(R,0°)-S(1.54,0°)\}/\{S(1.48,0°)-S(1.54,0°)\}=S(R,\theta)/S(R,0°)=\cos\theta \quad (4)$$

Hence, evidently from Eq. 2,

$$R=1.54-(1.54-1.48)\times\cos\theta \quad (5)$$

Then, from Eqs. 1 and 4 one obtains;

$$\mu=\cos\theta\times S(1.54,0°)/S(1.39,0°)+\cos^2\theta\times\{S(1.48,0°)/S(1.39,0°)-S(1.54,0°)/S(1.39,0°)\} \quad (6)$$

And further, from Eqs. 3 and 6

$$\mu=\cos\theta\times 0.77108+\cos^2\theta\times(1.54-1.48)\times 1.4458 \quad (7)$$

It is evident that the value of μ becomes gradually smaller as the value of θ becomes larger and that μ becomes 0 when θ is 90°.

(2) Solution of the Secular Equation for the Determination of the Molecular Orbitals. — By solving the secular equation for the determination of the molecular orbitals as linear combinations of $2p\pi$ atomic orbitals, one can obtain the values of energies of the molecular orbital corresponding to the value of the parameter μ. Consequently, the values of the extra-resonance energy (subsequently referred to as *R.E.*), of the coefficients of the $2p\pi$ atomic orbitals in the molecular orbital functions, and of the quantities such as the π-bond orders corresponding to the molecular configuration prescribed by the value of μ can also be obtained by the usual procedures[22].

The biphenyl molecule can be considered as belonging to the symmetry group D_2. Then, the highest occupied π-orbital (π_1) in the biphenyl molecule belongs to the representation B_3, and coincides with the φ_1 orbital in benzene when μ is 0. On the other hand, the lowest vacant π-orbital (π_1*) belongs to A_1, and coincides with the φ_2 orbital in benzene when μ is 0. (The notation for orbitals in benzene is according to Sklar[23].) Transitions from orbitals belonging to B_2 to those belonging to A_1 are allowed by absorption of light polarized along the direction of the long-axis of the molecule. Accordingly, the energy difference (referred to as ΔE_A) between the lowest vacant orbital π_1* and the highest occupied orbital π_1 is considered to be the transition energy corresponding to the conjugation band (the A-band) in the spectrum of biphenyl.

In addition to the eight orbitals belonging to B_1 and B_3, energies of which vary with μ, there are two sets of doubly degenerate orbitals belonging to A_1 and B_2, energies of which do not vary with μ. These orbitals may be considered as ones localized in the benzene rings. Thus, the two of these orbitals whose energy is $+\beta$ (φ) correspond to the φ_{-1} orbital in benzene, and another two whose energy is $-\beta$ (φ*) correspond to the φ_{-2} orbital in benzene. In other words, it can be considered that one orbital of each of the two sets of doubly degenerate orbitals in each benzene ring interacts with the neighboring π-orbitals to give whole-molecular orbitals when two benzene rings are linked with each other, whereas the other orbital of each set remains isolated. The intense bands observed at about 200 mμ in the spectra of biphenyl and its related compounds are presumably due to transitions between the orbitals localized in the benzene rings.

The results of calculations are shown in Table I. In this table, $\Delta E_A(-\beta)$ and $R.E.(-\beta)$ are values obtained by ignoring the π—π overlap integral, and $\Delta E_A(-\gamma)$ and $R.E.(-\gamma)$ are values obtained by taking the overlap integral into account, assuming the value of the overlap integral for the C-C bond in benzene as 0.25. The symbol $p_{1-1'}$ represents the π-bond order of the 1-1' bond.

It is evident that the values of ΔE_A increase as the value of μ decreases, and agree with the values for benzene when μ is 0. This means that the conjugation band is gradually shifted toward shorter wavelengths as the value of μ decreases, and therefore as the value of θ increases, and that the band will coincide with that of benzene when μ is 0 and therefore θ is 90°.

It appears that there is no simple quantitative relation between μ and ΔE_A, or between ΔE_A and *R.E.* On the other hand, examination of the data in Table I reveals that *R.E.* $(-\beta)$ is almost completely proportional to μ^2 and can approximately be expressed as $0.385\times\mu^2$, a fact which coincides with the qualitative generalization by Dewar[24]. In addition, $p_{1-1'}$ is roughly proportional to μ and can roughly be expressed as

21) (a) J. Dhar, *Indian J. Phys.*, **7**, 43 (1932); *Chem. Abstr.*, **26**, 4517 (1932). (b) J. Dhar, *Proc. Natl. Inst. Sci. India*, **15**, 11 (1949); *Chem. Abstr.*, **43**, 4655 (1949).

22) See, for example: H. Eyring, J. Walter and G. E. Kimball, "Quantum Chemistry", John Wiley & Sons, Inc., New York (1944), p. 254 ff. See also: C. A. Coulson, "Valence", Clarendon Press, Oxford (1952), p. 250 ff.

23) A. L. Sklar, *J. Chem. Phys.*, **7**, 984 (1939).

24) M. J. S. Dewar, *J. Am. Chem. Soc.*, **74**, 3345 (1952). (*Theorem 14*).

TABLE I

μ	1.1	1.0	0.9	0.8	0.7	0.6
$\Delta E_A(-\beta)$	1.3610	1.4092	1.4596	1.5120	1.5666	1.6232
$\Delta E_A(-\gamma)$	1.4016	1.4544	1.5099	1.5680	1.6290	1.6929
$R.E.(-\beta)$	0.4606	0.3832	0.3128	0.2484	0.1914	0.1414
$R.E.(-\gamma)$	0.1416	0.1184	0.0972	0.0774	0.0600	0.0446
$p_{1-1'}$		0.370	0.334	0.298	0.264	0.228
μ	0.5	0.4	0.3	0.2	0.1	0
$\Delta E_A(-\beta)$	1.6820	1.7424	1.8048	1.8686	1.9338	2
$\Delta E_A(-\gamma)$	1.7598	1.8292	1.9016	1.9764	2.0538	2.1333
$R.E.(-\beta)$	0.0988	0.0632	0.0358	0.0160	0.0040	0
$R.E.(-\gamma)$	0.0312	0.0200	0.0114	0.0052	0.0014	0
$p_{1-1'}$	0.193	0.156	0.118	0.079	0.040	0

$0.375\times\mu$. The value of $p_{1-1'}$ is 0.319 when μ is 0.858.

(3) Correlation of the Calculated Transition Energy with the Observed Position of the Conjugation Band. — The present calculations are concerned with the vertical excitations according to the Franck-Condon principle, namely, to electron jumps without change in the configuration of the molecular skeleton.

In general, the most probable spatial configuration of a conjugated compound and its stability are believed to be determined mainly by the combined effect of the resonance stabilization and the steric repulsion. The steric repulsion will raise the potential energy of the molecule in the ground state. Accordingly, in the problem which is concerned with, for example, the difference of stability between the geometrical isomers, the steric repulsion energy must be taken into account in principle.

On the other hand, since the spatial configuration of the molecule is assumed not to change between in the ground state and in the electronic excited state, the magnitudes of the steric repulsion energies involved in both the states may be the same at least approximately, and therefore, it seems that the electronic transition energy must not contain any significant contribution of the steric repulsion energy itself, and must be determined as a function of the spatial configuration of the molecule alone. That is, the values of ΔE_A shown in Table I may be correlated directly with the observed wave numbers of the absorption maxima of the conjugation bands. (In this connection, the interpretations by Braude and others on the relation between the steric effect and the position of the conjugation band are highly questionable. This will be referred to in detail in later parts of this series.)

The correlation of the calculated transition energy ΔE_A with the observed position ν_A (in wave number) of the conjugation band is accomplished as follows. When there are two compounds whose spatial configurations are already known and whose corresponding electronic absorption spectra are already observed, the linear relation of ΔE_A to ν_A is assumed between the two points prescribed by the two reference compounds.

As one of the two reference compounds, the planar compound is chosen in most cases. This is subsequently referred to as the longer-wavelength-side reference compound. The corresponding ΔE_A and ν_A are denoted by ΔE_L and ν_L, respectively. On the other hand, as the shorter-wavelength-side reference compound the one which corresponds to the value 0 of the parameter μ or the analogous one is chosen in most cases. The corresponding ΔE_A and ν_A are denoted by ΔE_S and ν_S, respectively. Then, the value of ΔE_A for a given compound of the type under consideration is obtained from the observed value of ν_A by the following equation:

$$\Delta E_A = \Delta E_S - (\Delta E_S - \Delta E_L)(\nu_S - \nu_A)/(\nu_S - \nu_L) \quad (8)$$

Consequently, the corresponding value of μ and then the values of θ, R, $R.E.$, etc. can be calculated in turn.

In the case of biphenyl, biphenyl in the crystalline state is chosen as the longer-wavelength-side reference compound. In this molecule, θ is 0°, and R is 1.48 Å as mentioned already, and consequently, the corresponding values of μ and of ΔE_A (i.e. ΔE_L) are computed to be 0.858 and $1.482(-\beta)$, respectively. On the other hand, as the shorter-wavelength-side reference compound, benzene is chosen, which corresponds to the case where the values of μ and of ΔE_A (i.e. ΔE_S) are 0 and $2(-\beta)$, respectively. However, it requires sufficient consideration to determine what values of ν are to be taken as ν_L and ν_S, corresponding to ΔE_L and ΔE_S, respectively. Therefore, these choices of the references are discussed in detail in the next sections.

The Shorter-wavelength-side Reference

When the value of the parameter μ is 0, the energy levels in biphenyl coincide with those in benzene, and the value of ΔE_A (i.e. ΔE_S) is $2(-\beta)$. According to Platt[25], the "center of gravity of singlets", 48000 cm^{-1} in the absorption spectrum of benzene, that is, the weighted mean of the energies of the three singlet-singlet transitions at 48000 cm^{-1} (208.3 mμ, B_{1u}), at 38200 cm^{-1} (261.8 mμ, B_{2u}), and at 53000 cm^{-1} (188.7 mμ, E_{1u}) measured in solution[26], corresponds to the energy

25) J. R. Platt, *J. Chem. Phys.*, 18, 1168 (1950).
26) H. B. Klevens and J. R. Platt, ibid., 17, 470 (1949).

difference of $2(-\beta)$ calculated by the molecular orbital method of the same order of approximation as the present treatment. Therefore, the value of 48000 cm^{-1} was taken as ν_S in the previous papers.

The same assumption is used also in the present treatment, since this assumption seems to be supported by the following facts. First, Dewar[27] has used the value of 208 mμ for the wavelength of the band of benzene in his application of the NBMO method to spectra of catacondensed aromatic compounds. Secondly, Dale[28] has used a value of about 205 mμ for benzene in his attempt to correlate the wavelength positions of the main bands of linear polyphenyls with the numbers of linked chain benzene nuclei. Furthermore, according to Wenzel[29], the intense conjugation band at about 250 mμ in the spectrum of biphenyl corresponds to the band at about 210 mμ of benzene. All these values for benzene are closely similar to the "center of gravity of singlets" mentioned above.

The Longer-wavelength-side Reference

Spectra of Biphenyl in the Crystalline State.— The value of ΔE_A (i.e. ΔE_L), $1.482(-\beta)$, calculated by using the values of the dimensions of the spatial configuration of biphenyl in the crystalline state is to correspond to the wave number of the absorption maximum of the conjugation band of the "isolated" planar molecule of biphenyl. The spectrum of biphenyl in solution has the conjugation band at about 247 mμ, but this band should not be taken as the band corresponding to ΔE_L, because there is no evidence to indicate that the molecule of biphenyl in solution would have the same spatial configuration as in the crystalline state. In the earlier paper[17], the wave number 36306 cm^{-1} of the first absorption maximum in the spectrum of biphenyl in the crystalline state measured by Deb[30] was taken as ν_L, i.e. the wave number corresponding to ΔE_L. According to Deb, the characteristic (conjugation) band in the spectrum of biphenyl in the liquid state is split up into two broad bands at 36306 cm^{-1} (2754 Å) and at 37386 cm^{-1} (2675 Å) in the spectrum of the solid at 30°C, and the band at 36306 cm^{-1} was presumed to be the intrinsic band. This assignment of the band is evidently inadequate, in view of the studies by Wenzel[29] and by Dale[28].

Wenzel[29] has proposed the hypothesis that the intense transition at about 250 mμ in biphenyl in solution is interpreted as a superposition of a strong and a weak transition corresponding to the 210 mμ and the 260 mμ transition in benzene, respectively. According to her, the weak transition is hidden by the strong one in the spectrum of biphenyl in solution. From comparison of spectra of some 3- and 3,3'-substituted biphenyl derivatives with pairs of spectra of benzene and the correspondingly substituted benzene derivatives and with pairs of spectra of naphthalene and its correspondingly substituted derivatives, she has inferred that the "hidden transition" of biphenyl may be located at about 275 mμ or at about 271 mμ, and that the intensity of this transition may be of the same order as the weak transitions in benzene and naphthalene.

The existence of the hidden transition in biphenyl has experimentally been corroborated by Dale[28]. He has measured the spectrum of biphenyl in the crystalline state by the pressed KCl-disk technique, and found that the spectrum is very similar to the solution spectrum. Thus, the spectrum of the solid showed an intense, structureless band with a maximum at 253 mμ, which is to be compared with the band at about 246 mμ in the solution spectrum. On the other hand, the spectra measured on thin films of solidified melt, on those by evaporation of a thin layer of solution, and on those of sublimed crystals of biphenyl revealed a band showing fine structure with a maximum at about 275 mμ. The molar extinction coefficient of the absorption maximum has been very roughly estimated to be about 1000~2000. In addition, whereas the spectra of *p*-terphenyl and of *p,p'*-quaterphenyl either in solution or in the crystalline states measured by the pressed KCl-disk technique showed the intense bands without structure at considerably longer wavelengths than that of biphenyl, the spectra of solidified melts or sublimed crystals of these compounds showed bands with structure at about 275 mμ, similarly to the corresponding one of biphenyl. These weak bands at about 275 mμ are probably due to the transversely polarized transitions normally hidden by the stronger conjugation bands. This revelation of the hidden transitions in biphenyl and *p*-polyphenyls has been interpreted as follows. Since the incident light is almost parallel to the long molecular axes in the thin films of crystals prepared by solidification of melts, by evaporation of solutions, or by sublimation, owing to the orientation of molecules in these samples, the conjugation bands due to transitions polarized along the long molecular axes are so reduced that the weak hidden transitions are revealed.

In view of the evidences mentioned above, the band at about 275 mμ in the spectrum of the solid biphenyl measured by Deb[30] is probably the "hidden transition". In this connection, Merkel and Wiegand[1] reported that the spectrum of biphenyl in the crystalline state exhibited a band showing fine structure in sharp contrast with that in the solution, and assumed this fact as one of the bases for their hypothesis concerning the relation between the appearance of fine structure and the coplanarity of the molecular configuration. Probably they compared impertinently the "hidden transition" revealed in the solid spectrum with the conjugation band in the solution spectrum.

Besides the bands at about 275 mμ and at 267 mμ mentioned above, Deb[30] found a very feeble band at about 290 mμ with structure in spectra

27) M. J. S. Dewar, *J. Chem. Soc.*, **1952**, 3532.
28) J. Dale, *Acta Chem. Scand.*, **11**, 650 (1957).
29) A. Wenzel, *J. Chem. Phys.*, **21**, 403 (1953).
30) A. R. Deb, *Indian. J. Phys.*, **27**, 305 (1953).

of biphenyl measured on the liquid films and on the solid films of larger thickness. This feeble band was resolved as sharp absorption peaks when the temperature of the solid film was reduced to −180°C. Deb has assumed that this feeble band at about 290 mμ belongs to a system different from the one to which the bands at 275 mμ and at 267 mμ belong, and that this feeble system is due to the transition in one of the two benzene rings in biphenyl when the second one is in the excited state. Perhaps the same feeble band at about 290 mμ was recently found by Coffman and McClure[31] and by Broude and his collaborators[32] in the spectrum of a single crystal of biphenyl at 20°K with polarized light, and also by Kanda[33] in the spectrum of the solution at low temperature. In addition, biphenyl appears to have a very feeble band at longer wavelengths than 300 mμ. Although the assignments of these feeble bands have not yet been established with certainty, it may be safe to say that these bands are to be excluded from the present consideration.

Although it may be somewhat open to criticism that the state of biphenyl in the pressed KCl-disk is the same as that in the crystal, it is assumed to be so. Then, from the above considerations, the intense band detected by the pressed KCl-disk technique may be taken as the conjugation band of the planar molecule of biphenyl in the crystalline state. Consequently, one would assume that the wave number 39526 cm^{-1} (253 mμ) of the position of the maximum might be ν_L, corresponding to the calculated transition energy $1.482(-\beta)$, ΔE_L, for the planar molecule of biphenyl. However, there is the possibility that interactions between the molecules in the crystal may affect the energy levels in the molecule and consequently the absorption spectrum of the compound. Accordingly, although such intermolecular interactions are supposed to be weak in nonpolar aromatic crystals[34], it is necessary to make allowances for this effect in the choice of the references for the correlation between ν_A and ΔE_A.

Normal Red-shift.—According to the results of measurements by Dale[28], the absorption maximum in the spectrum measured by the pressed KCl-disk technique is always at longer wavelengths than the corresponding one in the spectrum of the solution. The magnitude of the wavelength displacement of a band of a rigid molecule due to the change of the state from the solution in hexane to the solid state, which was referred to as the "normal red-shift", was found to vary regularly with the wavelength of the corresponding band, by measuring the spectra of naphthalene and of anthracene in both the states. Thus, the normal red-shift increases regularly from about 2 mμ at 220 mμ to 8 mμ at 300 mμ, and to 19 mμ at 400 mμ, with increasing wavelength of the position of the band. This normal red-shift is supposed to be due to the effect of interactions between the molecules in the crystals. From the analogy of the solvent effect[35] and of the Davydov effect[36-41] in a single crystal, it would be expected that the magnitude of the normal red-shift might be related to the intensity of the band. But, in fact, it is not so. The band cited by Dale includes the bands of considerably different intensity from each other, and no regularity between the magnitude of the normal red-shift and the intensity of the band can be found. Thus, the logarithms of the molar extinction coefficients of the bands of naphthalene at about 275 mμ and at about 221 mμ are 3.82 and 5.02, respectively[42], and the oscillator strengths of these bands are 0.11 and 1.7, respectively[41]. The logarithms of the molar extinction coefficients of the bands of anthracene at about 376 mμ and at about 252 mμ are 3.88 and 5.25, respectively[42], and the oscillator strengths of these bands are 0.1 and 2.3, respectively[37]. And further, according to Craig and others, the band of naphthalene[41] at about 275 mμ and that of anthracene[37-39] at about 380 mμ are assigned as "short-axis transitions", and that of naphthalene at about 220 mμ and that of anthracene at about 250 mμ are assigned as "long-axis transitions". From these considerations, the regular relation between the magnitude of the normal red-shift and the wavelength of the position of the absorption band seems to hold regardless of kinds of compounds, of characters of bands, and of intensities of bands. Accordingly, by application of this relation, the magnitude of the normal red-shift corresponding to the wavelength 253 mμ of the maximum of the conjugation band in the spectrum of biphenyl in the crystalline state (measured by the pressed KCl-disk technique) may be estimated to be about 3.5 mμ. (The oscillator strength of the conjugation band of biphenyl is 0.411 in solution, according to Almasy and Laemmel[43].)

On the other hand, according to the results of the measurements by the present author, which will be reported in detail in Part V of this series, the intense bands at 294.1 mμ and at 306.9 mμ in the spectrum of *trans*-stilbene in *n*-heptane are shifted toward longer wavelengths by about 4.5 mμ and by about 5.5 mμ, respectively, in the spectrum measured by the pressed KCl-disk

31) R. Coffman and D. S. McClure, *Can. J. Chem.*, **36**, 48 (1958); D. S. McClure, ibid., **36**, 59 (1958).
32) V. L. Broude, E. A. Izrailevich, A. L. Liberman, M. I. Onoprienko, O. S. Pakhomova, A. F. Prikhot'ko and A. I. Shatenshtein, *Optika i Spektroskopiya*, **5**, 113 (1958).
33) Yoshiya Kanda (Kyushu Univ.), a personal communication.
34) R. S. Mulliken, *J. Phys. Chem.*, **56**, 801 (1952).
35) N. S. Bayliss, *J. Chem. Phys.*, **18**, 292 (1950).
36) (a) A. S. Davydov, *Zhur. Eksptl. Teoret. Fiz.* (*J. Exptl. Theoret. Phys.*), **18**, 210 (1948). (Translated by M. Kasha.) (b) V. L. Broude, V. S. Medvedev and A. F. Prikhot'ko, ibid., **21**, 665 (1951). (c) A. S. Davydov, ibid., **21**, 673 (1951).
37) D. P. Craig and P. C. Hobbins, *J. Chem. Soc.*, **1955**, 539.
38) D. P. Craig, ibid., **1955**, 2302.
39) D. P. Craig and P. C. Hobbins, ibid., **1955**, 2309.
40) D. P. Craig and J. R. Walsh, *J. Chem. Phys.*, **25**, 588 (1956).
41) D. P. Craig and J. R Walsh, *J. Chem. Soc.*, **1958**, 1613.
42) E. Clar, *Spectrochim. Acta*, **4**, 116 (1950).
43) F. Almasy and H. Laemmel, *Helv. Chim. Acta*, **33**, 2092 (1950).

TABLE II. ULTRAVIOLET ABSORPTION SPECTRA OF BIPHENYL IN VARIOUS SOLVENTS

Solvent	A-band		B-band		C-band	
	λ_{max}	ε	λ_{max}	ε	λ_{max}	ε
n-Heptane	247.0	16450	(205.0)	41400	200.5	45100
Methanol	247.2	17300	—		—	
95% Ethanol	247.7	18050	(204.5)	42000	201.5	43000
Chloroform	249.5	16700	—		—	
Carbon tetrachloride	256.5	16450	—		—	

Wavelengths (mμ) in parentheses denote inflections.

technique. (The oscillator strength of the conjugation band in the spectrum of *trans*-stilbene in solution is 0.745, according to Beale and Roe[8].) These values, probably corresponding to the normal red-shifts of the conjugation band of *trans*-stilbene, are considerably smaller than those (about 8 and 9 mμ) anticipated from the relation mentioned above between the shift and the position of the band.

The crystals of naphthalene[41], anthracene[37], biphenyl[44], and *trans*-stilbene[44,45] all belong to the monoclinic space group C_{2h}^5, and bear a certain similarity to each other. However, whereas in each of these compounds except for the last the number of molecules in a unit cell is 2, in the crystal of *trans*-stilbene the number of molecules in a unit cell is 4. On the other hand, the molecular structure of biphenyl may be said to have greater similarity to that of *trans*-stilbene than to those of naphthalene and anthracene. From such considerations, it seems that there may be a possibility that the magnitude of the normal red-shift of the conjugation band of biphenyl is smaller than the value estimated above and is probably about 2 mμ, on the analogy of the case of *trans*-stilbene.

Since the estimation of the magnitude of the normal red-shift of the conjugation band of the "planar" molecule of biphenyl, at any rate, includes inevitable uncertainty, the alternative values of 3.5 and 2 mμ are assumed in the present calculation. After being corrected for the normal red-shift by these values, the position of the absorption maximum of the conjugation band of the "isolated" planar biphenyl molecule is assumed to be 249.5 mμ (a) or alternatively 251 mμ (b), and the corresponding wave numbers, (a) 40080 cm^{-1} and (b) 39841 cm^{-1}, are assumed to be ν_L.

The difference between the above assumed position of the conjugation band of the "isolated" planar biphenyl molecule, 249.5 or 251 mμ, and the corresponding one of biphenyl in solution, 247 mμ (in *n*-heptane, the present work) or 246 mμ (in hexane[28]), is assumed to be due to the difference in the most probable spatial configuration of the molecule between in the solution state and in the crystalline state.

44) J. Hengstenberg and H. Mark, *Z. Kristallogr. Kristallgeometr., Kristallphysik, Kristallchem.*, **70**, 283 (1929); *Chem. Zentr.*, **C1**, 3668 (1930).

45) (a) J. M. Robertson, M. Prasad and I. Woodward, *Proc. Roy. Soc.* (London), **A154**, 187 (1936). (b) J. M. Robertson and I. Woodward, ibid., **A162**, 568 (1937).

Spectra of Biphenyl in Solution

The ultraviolet absorption spectra of biphenyl in various solvents measured by the present author on a Cary recording spectrophotometer Model 14 M-50 are shown in Table II and Fig. 1. In Fig. 1, the spectra of biphenyl in the crystalline state and in the vapor state found in the literature are also shown for comparison.

The band represented as A-band in Table II is the conjugation band (the so-called K-band). The C-band is the one presumably due to transitions between the orbitals localized on each of the benzene rings, as already mentioned. The B-band (inflection) is probably the vestigial band due to transitions from the highest

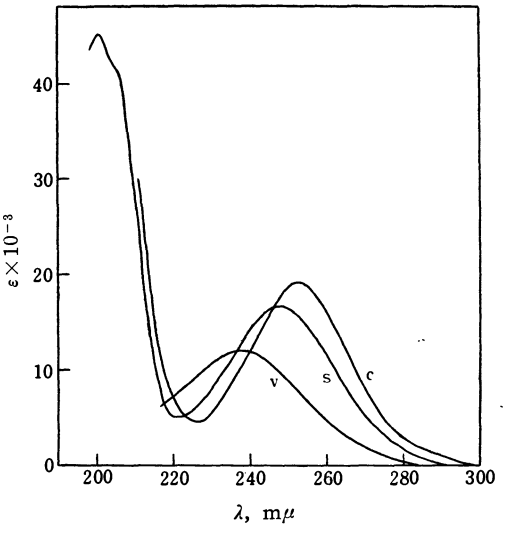


Fig. 1. Ultraviolet absorption spectra of biphenyl in various states.
c. The crystal spectrum measured by Dale[28] by the pressed KCl-disk technique. (The extinction scale is arbitrary for the reliable absolute extinction value could not be obtained.)
s. The solution spectrum (solvent: *n*-heptane).
v. The vapor spectrum measured by Almasy and Laemmel[43] at 170°C.

occupied orbital $\pi_1(B_2)$ to the orbitals φ^* belonging to A_1 or B_2 whose energy is $-\beta$, or from the orbitals φ belonging to A_1 or B_2 whose energy is $+\beta$ to the lowest vacant orbital $\pi_1^*(B_1)$.

It is seen that the spectrum is affected more or less by the solvents. Thus, the conjugation band at 247 mμ in the spectrum of the solution in *n*-heptane is shifted more or less toward longer wavelengths in the spectra in other solvents. The magnitude of the bathochromic shift by the solvent effect is small in methanol and in ethanol, is considerably larger in chloroform, and is extraordinarily large in carbon tetrachloride. In view of these solvent effects, data of spectra in the same solvent should in principle be compared at least in each of the systems of compounds in the treatment. In this part, the data of the spectra in non-polar hydrocarbon solvents being taken as the basis for comparison, and being corrected for the wavelength displacements of the band resulting from changes in phase (i. e. the normal red-shift mentioned above for the crystalline state and the solvent effect for the vapor state which will be mentioned later), the data of the spectra of biphenyl in the various states are compared.

Since the difference of the solvent effect between that of *n*-heptane and of *n*-hexane is supposed to be very small, the difference between the result of the measurement by the present author using *n*-heptane as solvent and that by Dale[28] using *n*-hexane as solvent may be ascribed to experimental errors. At any rate, the position of the maximum of the conjugation band in the spectra of biphenyl in the non-polar hydrocarbon solvents is located at slightly shorter wavelengths than that assumed above for the "isolated" planar molecule of biphenyl. This fact may be supposed to indicate that the most probable conformation of the molecule of biphenyl in solution is slightly non-planar, agreeing with the inference by Dale[46] from comparison of the results of measurements of the infrared absorption spectra of biphenyl in the solutions and in the pressed KBr-disk.

Spectra of Biphenyl in Vapor State

The spectra of biphenyl in the vapor state were studied thoroughly by Almasy and Laemmel[43]. They measured the spectra of biphenyl vapor at the various temperatures from 170 to 520°C and investigated also effects of various foreign gases.

It is noteworthy that the spectrum of pure biphenyl vapor is not largely affected by temperature at least in the range mentioned above, and that whereas the intensity ε of the absorption maximum of the conjugation band decreases gradually from 12050 at 170°C to 9400 at 520°C when the temperature is raised, the oscillator strength of the band is maintained almost constant regardless of the temperature. (The oscillator strength at 170°C is 0.316. The average of the values at 170, 260, 360 and 520°C is 0.311±0.0035.)

The position of the absorption maximum is gradually shifted toward longer wavelengths from 42000 cm^{-1} at 170°C to 41750 cm^{-1} at 520°C, as the temperature is raised. From these results, the position of the maximum at 20°C was inferred by extrapolation as 42100 cm^{-1} (ε, 19000).

Whereas these spectra of the vapor, showing no fine structure, resemble in shape the spectra of the solutions and that of the crystal by the pressed KCl-disk technique, the absorption maximum is considerably shifted toward shorter wavelengths in the vapor spectra than in the solution spectra, and further than the assumed position of the maximum for the "isolated" planar molecule. This fact is supposed to indicate that the degree of deviation from the planarity of the molecular configuration is larger in the vapor state than in the solution state.

Correction for Solvent Effect.—In order to compare the position of the absorption maximum in the vapour spectrum with that in the solution spectrum and with that for the "isolated" planar molecule, the solvent effect must be taken into account.

According to Bayliss[35], the magnitude of the displacement $\Delta\nu$ (in cm^{-1}) of the absorption maximum of a nonpolar molecule to lower frequencies by a nonpolar solvent is related to the refractivity of the solvent, and is expressed as the following equation:

$$\Delta\nu = \frac{3e^2}{8\pi^2c^2m}\cdot\frac{f}{\nu a^3}\cdot\frac{n^2-1}{2n^2+1}$$

$$= 10.71\times10^9\frac{f}{\nu a^3}\cdot\frac{n^2-1}{2n^2+1}$$

where n is the refractive index of the solvent at the frequency concerned, f is

46) J. Dale, *Acta Chem. Scand.*, 11, 640 (1957).

TABLE III. RESULTS OF CALCULATIONS FOR BIPHENYL IN VARIOUS STATES

State	λ_{max}, mμ	ν_{max}, cm^{-1}	ΔE_A, $-\beta$	μ	$\theta°$	R, Å	$R.E.$, $-\beta$
Crystal	a) 249.5*	40080	1.482	0.858	0	1.48	0.286
	b) 251*	39841	〃	〃	〃	〃	〃
Solution	247.0	40486	a) 1.509	0.807	19	1.484	0.253
	(*n*-heptane)		b) 1.523	0.780	23	1.485	0.237
	246	40650	a) 1.519	0.787	22	1.485	0.241
	(*n*-hexane)		b) 1.533	0.762	26	1.486	0.227
Vapor	238.8**	41866	a) 1.599	0.643	40	1.494	0.163
	(170°C)		b) 1.611	0.621	42	1.495	0.152
	238.3**	41966	a) 1.605	0.631	41	1.495	0.157
	(20°C)		b) 1.617	0.611	43	1.496	0.147

* Values corrected for the normal red-shift.
** Values corrected for the solvent effect.

the oscillator strength of the band, ν is the wave number of the position of the absorption maximum, and a is the radius of the (spherical) solute molecule. This relation was experimentally verified by Coggeshal and Pozefsky[47] in their study on the spectra of naphthacene and some other cata-condensed aromatic hydrocarbons. By application of this equation, the magnitude of the shift toward lower frequencies of the maximum of the conjugation band of biphenyl resulting from change in the state from the vapor to the solution in *n*-hexane is computed to be about 134 cm^{-1}, the following values being used; f=0.316 (the value at 170°C); ν=42000 cm^{-1} (the absorption maximum at 170°C); n=1.438 (the refractive index of *n*-hexane[48] at 42000 cm^{-1}); a=5 Å (as the radius a of the molecule, the round value of the half length of the long molecular axis of biphenyl along which the transition is polarized was provisionally taken by consulting the study by Lippert[49] on *p,p'*-disubstituted stilbenes, although this evaluation is inevitably still somewhat arbitrary).

This calculated value of $\Delta\nu$ may approximately apply to the inferred position of the maximum at 20°C and also to the case where the solvent is *n*-heptane instead of *n*-hexane. Accordingly, being corrected for this solvent effect, the wave number of the position of the maximum of the conjugation band of biphenyl in the vapor state, which is to be compared with the corresponding ones in the spectra of the solutions of biphenyl in *n*-hexane and in *n*-heptane, is evaluated to be 41866 cm^{-1} (at 170°C) or 41966 cm^{-1} (at 20°C).

47) N. D. Coggeshall and A. Pozefsky, *J. Chem. Phys.*, **19**, 980 (1951).
43) J. L. Lauer, ibid., **16**, 612 (1948).
49) E. Lippert, *Z. Naturforsch.*, **10a**, 541 (1955).
50) O. Bastiansen, *Acta Chem. Scand.*, **4**, 926 (1950).

Application of Calculation

On the basis of the above considerations, from the observed positions of the absorption maxima in the solution spectra and the positions in the vapor spectra corrected for the solvent effect, the respectively corresponding values of ΔE_A can be evaluated according to the assumption that ΔE_A varies linearly with μ_A from ΔE_L [1.482$(-\beta)$] for ν_L (40080 or 39841 cm^{-1}) to ΔE_S [2$(-\beta)$] for ν_S (48000 cm^{-1}). Consequently, the corresponding values of μ, θ, R and $R.E.$ can be evaluated in turn. The results are summarized in Table III.

It is shown that the values calculated for the interplanar angles in the most probable conformations of biphenyl in the solution state and in the vapor state are about 20° and about 40~43°, respectively. These values coincide fairly well with those estimated by other workers on different grounds. Thus, Bastiansen[50] deduced the value of 45±10° for the angle in the vapor state from the result of his study by the electron diffraction sector method. This value agrees almost completely with the present one. On the other hand, Samoilov and Dyatkina[51] inferred the value to be about 30° from calculations of resonance energy and steric repulsion energy between the nearest hydrogen atoms by the molecular orbital method. Recently, Adrian[52] concluded, from calculations somewhat similar to those by Samoilov and Dyatkina, that the angle is probably between 20° and 30°. In addition, calculations by Coulson and Longuet-Higgins[53] are said to indicate that

51) S. Samoilov and M. Dyatkina, *Zhur. Fiz. Khim.*, **22**, 1294 (1948); *Chem. Abstr.*, **43**, 2606 (1949).
52) F. J. Adrian, *J. Chem., Phys.*, **28**, 608 (1958).
53) C. A. Coulson, presented at a Conference on Quantum-Mechanical Methods in Valence Theory, Washington, 1951. (According to Refs. 6 and 52.)

the decrease in repulsion energy between the ortho-hydrogen atoms and the decrease in resonance energy resulting from non-planarity are practically balanced for interplanar angles of up to about 20°. All these values are compatible with the values calculated here for the solution state.

Summary

1) The ultraviolet absorption spectra of biphenyl in the crystalline state, in the solution state, and in the vapor state have been discussed in detail.

2) The relation between the position of conjugation band in the spectra of biphenyl and the spatial configuration of the molecule has been clarified by calculations based on the simple LCAO molecular orbital method.

3) By using the results of the calculations, it has been inferred from the analysis of the absorption spectra that the angles between the planes of the two benzene rings in the most probable conformations of biphenyl in the solution state and in the vapor state are about 20° and about 40~43°, respectively. These values coincide fairly well with the values estimated by other workers on different grounds.

The author thanks Professor Kengo Shiomi for his encouragement and for reading the manuscript, Professor Osamu Simamura for his encouragement, and Dr. Yoshiya Kanda of Kyushu University for helpful advice and especially for drawing his attention to Dale's papers which furnished one of the important bases for the present work.

Department of Chemistry
College of General Education
The University of Tokyo
Meguro-ku, Tokyo

Relations between Electronic Absorption Spectra and Spatial Configurations of Conjugated Systems. II. o-Alkyl- and o, o'-Dialkylbiphenyls

By Hiroshi SUZUKI

(Received June 22, 1959)

In the preceding part[1] of this series the relation between the ultraviolet absorption spectra and the most probable spatial configurations of biphenyl in the various states has been discussed in detail on the basis of the calculation carried out by the simple LCAO molecular orbital method. In the present part, the same method is applied to some ortho-alkyl substituted biphenyl derivatives, and the relation between the spectra and the most probable spatial configurations of these compounds is discussed.

It is well known that atrop-isomerism occurs when two or more, especially when all, of the four ortho hydrogen atoms in biphenyl are replaced by larger atoms or groups. This phenomenon is explained as being due to steric hindrance caused by the substituents which prevents rotation about the central 1—1′ bond, namely the co-annular bond, in the biphenyl derivatives. Therefore, the most probable configurations of these compounds must be non-coplanar.

This inference is supported by information from the electronic absorption spectroscopy. Thus, for example, the spectrum of bimesityl does not exhibit the conjugation band characteristic of biphenyl-type compounds, but is closely similar to the sum of the spectra of two mesitylene molecules[2]. This fact is considered to indicate that the twist of the co-annular bond is large enough to eliminate almost completely the $\pi-\pi$ interaction across the

1) H. Suzuki, This Bulletin, **32**, 1340 (1959).

2) (a) L. W. Pickett, G. F. Walter and H. France, *J. Am. Chem. Soc.*, **58**, 2296 (1936). (b) M. T. O'Shaughnessy and W. H. Rodebush, ibid., **62**, 2906 (1940). (c) E. Marcus, W. M. Lauer and R. T. Arnold, ibid., **80**, 3742 (1958).

bond in this compound. That is, it is inferred that the two benzene rings in this compound are almost perpendicularly oriented, as suggested by Guy by means of calculations of the energy associated with the tortion about the central linkage in 2, 2', 6, 6'-tetramethylbiphenyl[3].

In either *o*- or *o*, *o*'-substituted biphenyls, the substituents do not confer, unless they are exceptionally large, measurable optical stability on the rotational enantiomorphs at room temperature[4], but contrariwise, they affect markedly the spectral feature. Thus, for example, the conjugation band of *o*-methylbiphenyl is at a considerably shorter wavelength and of considerably lower intensity than that of biphenyl. This hypsochromic shift is believed to indicate that the interplanar angle θ, i. e. the angle of twist of the co-annular bond, in the most probable spatial configuration of *o*-methylbiphenyl is considerably larger than the corresponding one of biphenyl itself. Further, the spectrum of *o*, *o*'-dimethylbiphenyl exhibits no distinct maximum of the conjugation band, but exhibits only an inflection at a further shorter wavelength than the position of the conjugation band of *o*-methylbiphenyl (Fig. 1.).

It is to be noted here that the effect of the substituents upon the spectra of these biphenyl derivatives must include not only the hypsochromic effect due to steric interference of the substituents, but also the electronic (probably bathochromic) effect of the substituents. As is seen in Fig. 1, the absorption maximum of the conjugation band of *p*, *p*'-dimethylbiphenyl

TABLE I. ULTRAVIOLET ABSORPTION SPECTRA OF BIPHENYL AND ALKYLBIPHENYLS

Compound	Solvent	Conjugation band		Ref.
		λ_{max}	ε	
Biphenyl	E	247.7	18050	1)
	Hp	247.0	16450	1)
p-Methyl-	E	253	13300	5)
o-Methyl-	E	235	10500	6)
	E	ca. 237	9960	a
	E	ca. 235		8)
	Cy	ca. 235		8)
	Hp	235	10000	7)
o-Ethyl-	E	233	10500	6)
o-*n*-Propyl-	E	233	10000	6)
o-Isopropyl-	E	233	11000	6)
o-*n*-Butyl-	E	233	10500	6)
p, *p*'-Dimethyl-	E	255.6	20500	a
	E	ca. 260	20000	9)
	Hp	255.2	21200	a
	Hx	256	21400	10)
o, *o*'-Dimethyl-	E	(ca. 227)	6800	11)
	E	(228～229)	(6000～6500)	a
p, *p*'-Diethyl-	E	256.5	22500	12)
p, *p*'-Diisopropyl-	E	256.5	23500	12)
o, *o*'-Diethyl-	E	(ca. 277)	6000	12)
o, *o*'-Diisopropyl-	E	(ca. 277)	5500	12)
o, *o*'-Di-*tirt*-butyl-	E	No conjugation band		12)
Bimesityl		No conjugation band		2)

Solvent: E, ethanol; Hp, *n*-heptane; Cy, cyclohexane; Hx, *n*-hexane.
Wavelengths (mμ) in parentheses denote inflections.
Ref. a refers to the present work.

3) J. Guy, *J. chim. phys.*, **46**, 469 (1949).
4) R. Adams and H. C. Yuan, *Chem. Revs.*, **12**, 261 (1933).
5) The Chemical Society of Japan, "Jikken Kagaku Koza" Vol. 1, Maruzen Co., Ltd., Tokyo (1957), p. 191 (K. Hirayama).
6) E. A. Braude and W. F. Forbes, *J. Chem. Soc.*, **1955**, 3776.
7) H. Suzuki, This Bulletin, **27**, 597 (1954).
8) R. A. Friedel, M. Orchin and L. Reggel, *J. Am. Chem. Soc.*, **70**, 199 (1948).
9) B. Williamson and W. H. Rodebush, ibid., **63**, 3018 (1941).
10) R. A. Friedel and M. Orchin. "Ultraviolet Absorption of Aromatic Compounds", John Wiley & Sons, Inc., New York (1951).
11) G. H. Beaven, D. M. Hall, M. S. Lesslie, E. E. Turner and G. R. Bird, *J. Chem. Soc.*, **1954**, 131.
12) P. M. Everitt, D. M. Hall and E. E. Turner, ibid., **1956**, 2286.

from which the steric interference of the substituents is absent is at a considerably longer wavelengths as compared with the corresponding one of biphenyl. This bathochromic displacement of the band is probably due to the hyperconjugation effect of methyl groups. The similar bathochromic effect due to hyperconjugation must operate also in the spectra of ortho-substituted biphenyl derivatives such as *o*-methyl- and *o*, *o'*-dimethylbiphenyl. Accordingly, in order to clarify the relation between the spectra and the spatial configurations of *o*-alkyl- and *o*, *o*-dialkylbiphenyls, it is necessary to make allowance for the electronic bathochromic effect of the substituents.

Spectra of Alkylbiphenyls

The data of the ultraviolet absorption spectra of some alkylbiphenyls are summarized in Table I, in which that of biphenyl is included for comparison. Of the spectra measured by the present author, those of biphenyl and of *p*, *p'*-dimethylbiphenyl were measured with a Cary recording spectrophotometer Model 14 and those of *o*-methyl- and of *o*, *o'*-dimethylbiphenyl with a Beckman quartz spectrophotometer Model DU. These spectra are shown also in Fig. 1[13].

***o*-Alkylbiphenyls.**—The absorption maximum of the conjugation band of *p*-methylbiphenyl is at 253 mμ. The bathochromic effect due to the hyperconjugation effect of a *p*-methyl group and that of an *o*-methyl group are considered to be approximately of the same magnitude, as supported by the comparison of the results of calculations of the energy levels in *p*-terphenyl and in *o*-terphenyl, which will be reported in Part IV of this series.

Accordingly, if the steric effect of the ortho methyl substituent were absent, *o*-methylbiphenyl would exhibit the conjugation band at approximately the same position as that of the *p*-isomer. Hence *p*-methylbiphenyl may reasonably be taken as the longer-wavelength-side reference compound in this case.

It was reported in the preceding part that the value of the parameter μ in the $\pi-\pi$ resonance integral $\mu\beta$ for the 1–1′ bond in biphenyl in solution is 0.780 and that the corresponding calculated transition energy ΔE_A is 1.523 $(-\beta)$ (cf. Table III in Ref. 1). From the above consideration, these values are assumed here to correspond approximately to the position of the maximum of the conjugation band of *p*-methylbiphenyl. That is, the values of ΔE_L and of ν_L in the present treatment of *o*-methylbiphenyl are assumed to be 1.523 $(-\beta)$ and 39526 cm^{-1} (253 mμ), respectively.

On the other hand, as the value of ν_S corresponding to ΔE_S $[2(-\beta)]$ when μ is 0, analogously to the choice of the "center of gravity of singlets" 48000 cm^{-1} of benzene[14] in the case of biphenyl itself[1], the corresponding value of toluene may be taken here.

In Table II, a collection of the relevant data of the spectra of benzene and of several alkylbenzenes is assembled. In this table also the data of *m*-xylene and of mesitylene which are not needed in the present part are conveniently included for the sake of reference in the later parts (probably VIII and XI) of this series.

It is seen in Table II that each of the bands of toluene is at a longer wavelength by about 5 mμ than the corresponding band of benzene. Therefore, as the value of toluene corresponding to the center of gravity of singlets 48000 cm^{-1} (208.3 mμ) of benzene, the value of 46882 cm^{-1} (213.3 mμ) may be taken. Accordingly, the value of ν_S is assumed here to be 46882 cm^{-1}.

In this manner, the allowance for the electronic bathochromic effect of the substituent is made by the choice of the

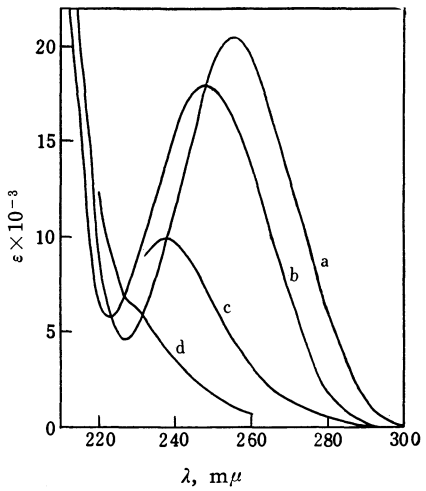


Fig. 1. The ultraviolet absorption spectra of biphenyl and of methylbipenyls in ethanol.
a: *p*, *p'*-Dimethylbiphenyl. b: Biphenyl. c: *o*-Methylbiphenyl. *d*: *o*, *o'*-Dimethylbiphenyl.

13) The author is indebted to Dr. Makoto Takahashi for a generous supply of the sample of *p*, *p'*-dimethylbiphenyl. Preparations of *o*-methyl- and of *o*,*o'*-dimethylbipheyl wer reported in Ref. 7.

14) J. R. Platt, *J. Chem. Phys.*, 18, 1168 (1950).

TABLE II-1. ULTRAVIOLET ABSORPTION SPECTRA OF BENZENE AND ALKYLBENZENES (in *n*-heptane)[15]

Compound	Allowed transition			Forbidden transition		
	λ_{max}, mμ	ε	f	λ_{max}, mμ	ε	f
Benzene	183.5	46000	0.69	195.0	6900	0.10
Toluene	188.5	55000	0.97	200.0	8100	0.12
Ethylbenzene	189.0	57000	1.00	200.0	7400	0.11
m-Xylene	193.0	76000	1.28	203.0	10500	0.18

TABLE II-2. ULTRAVIOLET ABSORPTION SPECTRA OF BENZENE AND ALKYLBENZENES

Compound	Approx. center of band[16] (in *n*-hexane)		O-O band[17] (vapor)	O-O band[18]
	λ, mμ	ε	λ_{max}, mμ	λ_{max}, mμ
Benzene	255	230	262.54	262.46
Toluene	261	300	266.78	266.75
Ethylbenzene	261	220		266.43
n-Propylbenzene	261	245		266.52
Isopropylbenzene				265.87
n-Butylbenzene	260	235		266.63
m-Xylene	266	400		
Mesitylene	266	305	274.06	

references for correlation between the observed position of the conjugation band and the calculated transition energy. Thus, quite analogously to the treatment in the preceding part, the value of the transition energy ΔE_A corresponding to the wave number of the absorption maximum of the conjugation band of *o*-methylbiphenyl can be computed (cf. Eq. 8 in Ref. 1). In this case, it is assumed that ΔE_A varies linearly with ν_A in the range of ΔE_L [1.523 $(-\beta)$] to ΔE_S [2$(-\beta)$]. By the way, ΔE_L and ΔE_S correspond to ν_L (39526 cm^{-1}) and ν_S (46882 cm^{-1}), respectively. Then, one can obtain the corresponding values of μ, θ, R, etc. in turn according to the relation between ΔE_A and μ (cf. Table I in Ref. 1), and to the relation between μ and θ as well as R (the length of the 1–1′ bond) (cf. Eqs. 1—7 in Ref. 1), which were postulated in the preceding part.

The absorption maxima of ethyl-, *n*-propyl- and *n*-butylbenzene are located at about the same wavelength, 260~261 mμ, as that of toluene. On the other hand, *o*-ethyl- *o*-*n*-propyl-, *o*-isopropyl-, and *o*-*n*-butylbiphenyl all exhibit the maxima of the conjugation bands at about the same wavelength, 233 mμ. Hence it is obvious that these *o*-alkylbiphenyls can be approximately treated also by application of the relation between ΔE_A and ν_A assumed above for the case of the *o*-methyl analogue.

o, o′ - Dialkylbiphenyls. — The absorption spectra of *o*, *o*′-dimethyl-, *o*, *o*′-diethyl-, and *o*, *o*′ - diisopropylbiphenyl are markedly different from those of the corresponding *o*-monoalkylbiphenyls. Each of the spectra of these *o*, *o*′-dialkylbiphenyls shows no distinct absorption maximum of the conjugation band, but merely an inflection at about 227 mμ, which is regarded as the vestigial or submerged conjugation band. According to Everitt and his coworkers[12], the spectra of these *o*, *o*′-dialkylbiphenyls exhibit feeble bands at about 263.5 mμ and at about 270~271 mμ (the molar extinction coefficients are lower than 1000) in addition to the vestigial conjugation band mentioned above. These feeble bands are believed to correspond to the "hidden transition" in biphenyl[19], and this revelation is probably due to the marked hypsochromic shift and the reduction in the intensity of the conjugation band caused by larger deviation from coplanarity of the configuration in these sterically hindered biphenyl derivatives, as compared with biphenyl itself.

In order to infer the most probable spatial configurations of these *o*, *o*′-dialkylbiphenyls by application of the present

15) J. R. Platt and H. B. Klevens, *Chem. Revs*, **41**, 301 (1947).
16) A. E. Gillam and E. S. Stern, "An Introduction to Electronic Absorption Spectroscopy", 2nd Ed., Edward Arnold Publishers, Ltd., London (1957), p. 134.
17) K. F. Herzfeld, *Chem. Revs.*, **41**, 233 (1947).
18) W. West, "Chemical Applications of Spectroscopy" (Technique of Organic Chemistry IX), Interscience Publishers., Inc., New York (1956), p. 677 (F. A. Matsen).
19) A. Wenzel, *J. Chem. Phys.*, **21**, 403 (1953). See also Ref. 1.

TABLE III. RESULTS OF CALCULATION

Biphenyl derivative	λ_{max}, mμ	ν_A, cm^{-1}	ΔE_A, $-\beta$	μ	θ	R, Å
o-Methyl-	235	42553	1.719	0.438	58°	1.508
o-Ethyl-, *o*-*n*-propyl, *o*-isopropyl-, *o*-*n*-butyl-	233	42918	1.743	0.399	60.7	1.5105
o,*o*'-Dimethyl-	(227)	44053	1.826	0.267	70	1.5193
o,*o*'-Diethyl-, *o*,*o*'-diisopropyl-	(227)	44053	1.829	0.262	70.3	1.5195

method, allowance for the electronic bathochromic effects of the substituents is made analogously to the case of *o*-monoalkylbiphenyls by choice of the references for correlation between the calculated transition energy and the observed position of the conjugation band. Thus, as ν_L corresponding to ΔE_L 1.523 $(-\beta)$, the wave number 39124 cm^{-1} (255.6 mμ) of the maximum of the conjugation band of *p*,*p*'-dimethylbiphenyl is taken in the case of *o*,*o*'-dimethylbiphenyl, and the wave number 38986 cm^{-1} (256.5 mμ) of the maxima of the conjugation bands of *p*,*p*'-diethyl- and *p*, *p*'-diisopropylbiphenyl is taken in the case of the corresponding *o*,*o*'-isomers. On the other hand, as ν_S corresponding to ΔE_S $2(-\beta)$, the value of monoalkylbenzene 46882 cm^{-1} (213.3 mμ) corresponding to the center of gravity of singlets of benzene is taken, quite similarly to the case of *o*-monoalkylbiphenyls.

Results of Calculations and Discussion

The results of the calculations are shown in Table III. The calculated value of the angle of twist in *o*-methylbiphenyl is in considerably good agreement with the value 62° deduced from the scale model in which the length of the 1–1' bond is 1.51 Å, the lengths of C_6H_5–H bond and of the C_6H_5–CH_3 bond are 1.08 and 1.54 Å, respectively, the radii of hydrogen atom and of methyl group are 0.9 and 2.0 Å, respectively, and an ortho hydrogen atom just touches the ortho methyl group.

It is noteworthy that the values of the angle of twist in *o*-ethyl-, *o*-*n*-propyl-, *o*-isopropyl-, and *o*-*n*-butylbiphenyl are equal to each other, and that they are merely slightly larger than that in the methyl analogue. This fact may be considered to indicate that all but the methylene group attached directly to the phenyl ring can adopt conformations such that they cause little or no additional interference, as suggested already by Braude and Forbes[6].

The calculated value of the interplanar angle in *o*,*o*'-dimethylbiphenyl is eventually closely similar to the value estimated in the earlier paper[7], 70.5°. Therefore, the discussion in the earlier paper may apply also to the present result. Thus, this value 70° of the interplanar angle in *o*,*o*'-dimethylbiphenyl coincides almost exactly with the corresponding value, 70.6°, found for 2,2'-dimethylbenzidine dihydrochloride by the X-ray crystal analysis[20], and it is inferred that the preferred configuration of the former is similar to the configuration of the latter which has been found to have the two ortho methyl groups in the *cis*-disposition. This inference of the *cis*-configuration of *o*,*o*'-dimethylbiphenyl seems to be supported also by the fact that the interplanar angle in gaseous 2,2'-dichlorobiphenyl found by the electron diffraction method[21] and that in crystalline 2,2'-dichlorobenzidine found by the X-ray crystal analysis[22] are 74° and 72°, respectively, and that both these compounds have been found to have *cis*-configurations.

If the molecule of *o*,*o*'-dimethylbiphenyl assumed the *trans*-configuration in which the ortho hydrogen atoms just contact with the ortho methyl groups, the configuration of the biphenyl skeleton would be similar to that in *o*-methylbiphenyl, and consequently *o*,*o*-'dimethylbiphenyl would show a closely similar spectrum to that of *o*-methylbiphenyl. In fact it is not so. Thus, as already mentioned, the hypsochromic shift of the conjugation band is observed to be markedly larger in the spectrum of *o*,*o*'-dimethylbiphenyl than in that of *o*-methylbiphenyl.

This fact has been interpreted by Braude and Forbes[6] as follows: "The hypsochromic shift from 2500 to 2350 Å due to one *o*-methyl substituent actually corresponds to an increase in transition energy of 7 kcal./mol., which is the amount by which the energy level of the electronic excited

20) (a) F. Fowwether and A. Hargreaves, *Acta Cryst.*, **3**, 81 (1950); *Chem. Abstr.*, **44**, 7118 (1950). (b) A. Hargreaves and W. H. Taylor, *J. Sci. Instruments*, **18**, 138 (1941); *Chem. Abstr.*, **35**, 7261 (1941).
21) O. Bastiansen, *Acta Chem. Scand.*, **4**, 926 (1950).
22) D. L. Smare, *Acta Cryst.*, **1**, 150 (1948); *Chem. Abstr.*, **42**, 8045 (1948).

state has been raised relative to that of the ground state and it is obviously reasonable that the effect of two such substituents should be about twice as great". It seems that they have attributed the hypsochromic shift, viz. an increase in transition energy, to an increase in the difference between the steric repulsion energy in the electronic excited state and that in the ground state.

However, as mentioned already in the preceding part[1] of this series, since the transition is considered to be an electron jump without change in nuclear configuration according to the Franck-Condon principle, the steric repulsion energy in the electronic excited state and that in the ground state must be at least approximately of the same magnitude. Therefore, whereas the steric repulsion energy is a contributing factor to the stability of the molecule and hence to determination of the most probable spatial configuration of the molecule, the electronic transition energy must not depend directly on the steric repulsion energy in the ground state, but on the spatial configuration itself. And further, of course, there should be no direct relation between the electronic transition energy and the height of the energy barrier to rotation about the co-annular bond which depends mainly on the difference between the steric repulsion energy in the coplanar configuration and that in the most probable configuration.

From such considerations, the difference between the spectrum of *o*-methylbiphenyl and that of *o*, *o'*-dimethylbiphenyl should be ascribed to the difference of the most probable spatial configurations of the biphenyl skeleton in these compounds. It is obvious that the interpretation by Braude and his coworker is quite unreasonable.

o, *o'*-Diethyl- and *o*, *o'*-diisopropylbiphenyl are inferred to have configurations similar to that of *o*, *o'*-dimethylbiphenyl, although the estimation of the interplanar angle in these compounds is inevitably somewhat uncertain since the conjugation bands of these compounds are vestigial, the positions of the maxima of which can not accurately be determined.

o, *o'*-Di-*tert*-butylbiphenyl exhibits no trace of a discrete conjugation band. This fact may be considered to indicate that the interplanar angle in this compound is so large owing to the bulkiness of the substituents that the $\pi-\pi$ interaction across the co-annular bond is almost completely eliminated.

23) W. Theilacker and W. Ozegowski, *Ber.*, **73**, 33 (1940).

Relation of Spatial Configurations with Other Properties

The difference of the spatial configurations of the compounds must undoubtedly affect also certain physical and chemical properties of the compounds besides the electronic absorption spectra. Accordingly, the spatial configurations of the biphenyls inferred above on the basis of the absorption spectra may be correlated with various other properties of the compounds. A few examples are given below.

Theilacker and Ozegowsky[23] found that 2, 2'-dimethyl-4, 4'-biphenylene-bis-diphenylmethyl has properties closely similar to those of the 2, 2', 6,6'-tetrachloro analogue which is known to be a true biradical[24]. In addition, Müller and Hertel[25] concluded from the result of measurement of the magnetic susceptibility that this 2, 2'-dimethyl compound is paramagnetic and hence a true biradical in contrast to its parent compound, Chichibabin's hydrocarbon, which had been found to be completely diamagnetic and not a biradical[26]. Although the latter compound was found afterwards by application of the paramagnetic resonance absorption method to contain about 4% of the biradical form in solution in benzene[27], it may be safe to state that in the equilibrium between the diphenoquinone form and the biradical form the latter form is more favorable in the 2, 2'-dimethyl compound than in the parent compound, and that this fact is to be related to the reduced $\pi-\pi$ interaction across the co-annular bond in the former compound as compared with the latter compound.

According to Sherwood and Calvin[28], in *p*-amino-*p'*-nitrobiphenyl the *p'*-nitro group exerts a marked effect upon the basicity of the *p*-amino group and this effect is diminished by ortho substitution by two methyl groups. This effect of ortho methyl groups has been ascribed to the blocking of nitro-amino resonance by the forced non-coplanarity of the configuration of the biphenyl skeleton.

Castro, Andrews and Keefer[29] recently measured the equilibrium constants and the heats of formation of 1 : 1 complexes of a series of methylbiphenyls with 1, 3, 5-trinitrobenzene. According to their results, whereas the complexes increase in stability as the number of *p*-methyl substituents on the biphenyl nucleus is increased, the complex stability decreases in the order

24) E. Müller, ibid., **72**, 2063 (1939).
25) E. Müller and E. Hertel, *Ann.*, **555**, 157 (1944).
26) E. Müller and I. Müller-Rodloff, ibid., **517**, 134 (1935).
27) C. A. Hutchison, Jr., A. Kowalsky, R. C. Pastor and G. W. Wheland, *J. Chem. Phys.*, **20**, 1485 (1952).
28) D. W. Sherwood and M. Calvin, *J. Am. Chem. Soc.*, **64**, 1350 (1942).
29) C. E. Castro, L. J. Andrews and R. M. Keefer, ibid., **80**, 2322 (1958).

biphenyl> *o*-methylbiphenyl > *o*, *o*'-dimethylbiphenyl>bimesityl, as the number of *o*-methyl substituents is increased. This fact is indicative of the dependence of the complex stability on the factors which prevent coplanarity of the two benzene rings in the biphenyl derivatives, and supports the present conclusion that the degree of deviation from planarity of the configuration of biphenyl skeleton increases as the number of *o*-methyl substituents is increased.

Furthermore, Brownstein[30] measured the nuclear magnetic resonance absorption spectra of some 2-halo- and 4-halobiphenyls and attributed shifts in proton resonance absorption toward a higher field observed for some of the protons in 2-halobiphenyls to steric effects of the halogen upon the ortho protons of the unsubstituted benzene ring. In addition, he explained the melting points of these compounds by the twisting of the benzene rings as the size of the 2-substituent is increased. Thus, whereas a heightening of melting point is observed with increasing molecular weight for the 4-halobiphenyl as would be expected, the melting point of the 2-halobiphenyl is lowered as the molecular weight increases. This was believed to be caused by the decreasing symmetry of the molecule as the benzene rings are twisted further out of plane by the steric effect of the *o*-substituent.

Although the melting point is a very complex property, it may be sure that the spatial configuration of the molecule is an important factor to govern the melting point. A somewhat similar phenomenon to the one mentioned above is observed in the series of methylbiphenyls. Thus, whereas the melting points of biphenyl and of *p*-methylbiphenyl are 69 and 49~50°C (47~48°C), respectively, *o*-methylbiphenyl is liquid at room temperature. In addition, whereas the melting point of *p*, *p*'-dimethylbiphenyl is 125°C (121°C), that of the *o*, *o*'-isomer is 18°C. (Data of the melting points are according to Dictionary edited by Heilbron[31]). The fact that the melting point of the *o*-isomer is invariably markedly lower than that of the corresponding *p*-isomer may be at least partly due to the non-planarity of the configuration of the *o*-isomer.

30) S. Brownstein, ibid., **80**, 2057 (1958).

31) I. Heilbron, "Dictionary of Organic Compounds", Oxford University Presss, Inc., New York (1953).

Summary

The method described in the preceding part of this series has been applied with allowance for the electronic bathochromic effect of the substituents to *o*-alkyl- and *o*, *o*'-dialkylbiphenyls, and the relation between the ultraviolet absorption spectra and the most probable spatial configurations of these compounds has been clarified, resulting in the conclusion that the interplanar angle in *o*-methylbiphenyl as well as its analogues is about 60° and that *o*, *o*'-dimethylbiphenyl as well as its analogues has the *cis*-configuration in which the interplanar angle is about 70°.

On the basis of the result, the interpretation by Braude and Forbes of the spectra of *o*-methyl- and *o*, *o*'-dimethylbiphenyl has been criticized.

In addition, the inferred spatial configurations of these biphenyl derivatives have been correlated with some physical and chemical properties of these and some related compounds.

The author thanks Professor Kengo Shiomi for reading the manuscript and for valuable advice.

Department of Chemistry
College of General Education
The University of Tokyo
Meguro-ku, Tokyo

Relations between Electronic Absorption Spectra and Spatial Configurations of Conjugated Systems. III. o,o'-Bridged Biphenyls

By Hiroshi SUZUKI

(Received June 22, 1959)

The method developed in the earlier parts[1,2] of this series is applied to some *o,o'*-bridged biphenyls, and the relation between the ultraviolet absorption spectra and the spatial configurations of these compounds is discussed.

A collection of the data of the spectra of some *o,o'*-bridged biphenyls is assembled in Table I.

o,o'-One-atom-bridged and Two-atom-bridged Biphenyls

The spectra of fluorene and of 9,10-dihydrophenanthrene exhibit besides the intense bands at about 260 mμ lower bands at about 300 mμ. The former bands are probably the conjugation bands characteristic of the biphenyl-type compounds. The

TALBE I. ULTRAVIOLET ABSORPTION SPECTRA OF *o,o'*-BRIDGED BIPHENYLS

Entry No.	Compound	Solvent	Conjugation band		Ref.
			λ_{max}, mμ	ε	
1	Fluorene	Hp	261.5*	18900	a
		E	ca. 260*	19000	3)
2	9,10-Dihydrophenanthrene	Hx	263.5	18000	4)
		E	264	17000	4)
3	4,5-Methylene-9,10-dihydrophenanthrene	E	ca. 272	ca. 18500	5)
o,o'-Three-atom-bridged biphenyls					
4	2,7-Dihydro-3,4-5,6-dibenzoxepin	Hx	250	16500	4)
5	3,4-5,6-Dibenzocyclohepta-3,5-diene-1-carboxylic acid	E	249	15300	6)
6	6,6-Dicarbethoxydibenzo-[a,c][1,3]-cycloheptadiene	E	249	16980	7)
7	Methyl 3,4-5,6-dibenzocyclohepta-3,5-diene-1-carboxylate	E	248.5	15500	6)
8	1-Hydroxymethyl-3,4-5,6-dibenzocyclohepta-3,5-diene	E	248.5	15400	6)
9	2,7-Dihydro-3,4-5,6-dibenzazepinium-1-*spiro*-1'''-piperidinium bromide	W	248	15000	4)
o,o'-Four-atom-bridged biphenyls					
10	Ethyl 4,5-6,7-dibenzocycloocta-4,6-diene-1,1,2,2-tetracarboxylate	E	239.5	13100	6)
11	Methyl 4,5-6,7-dibenzocycloocta-4,6-diene-1,2-dicarboxylate	E	236.5	12700	6)

Solvent: E, ethanol; Hp, *n*-heptane; Hx, *n*-hexane; W, water.
* The most intense maximum of fine structure.
Ref. a refers to the present work (cf. Table II and Fig. 1).

1) H. Suzuki, This Bulletin, **32**, 1340 (1959).
2) H. Suzuki, ibid., **32**, 1350 (1959).
3) W. V. Mayneord and E. M. F. Roe, *Proc. Roy. Soc.* (*London*), **A158**, 634 (1937).
4) G. H. Beaven, D. M. Hall, M. S. Lesslie and E. E. Turner, *J. Chem. Soc.*, **1952**, 854.
5) R. N. Jones, *J. Am. Chem. Soc.*, **63**, 1658 (1941).
6) G. H. Beaven, G. R. Bird, D. M. Hall, E. A. Johnson, J. E. Ladburg, M. S. Lesslie and E. E. Turner, *J. Chem. Soc.*, **1955**, 2708.
7) D. C. Iffland and H. Siegel, *J. Am. Chem. Soc.*, **80**, 1947 (1958).

latter, which are absent from biphenyl, are difficult to interpret. Braude[8,9] seems to have attempted to explain these feeble bands by means of an assumption of C–C hyperconjugative interaction of the two benzene rings through the methylene bridge. Perhaps these bands may be considered to correspond to the "hidden transition" in biphenyl[10].

The spectrum of fluorene and that of 9,10-dihydrophenanthrene resemble each other considerably on the whole[11]. However, while the latter shows no fine structure, the former shows a remarkably well-resolved fine structure (Table II and Fig. 1). This may be related to the fact that fluorene has probably a strained or forced coplanar or near-coplanar configuration.

TABLE II. THE ULTRAVIOLET ABSORPTION SPECTRUM OF FLUORENE IN *n*-HEPTANE MEASURED ON A CARY RECORDING SPECTROPHOTOMETER MODEL 14 M-50 (cf. Fig. 1)

		Conjugation band			
λ_{max}, mμ	ε	λ_{max}, mμ	ε	λ_{max}, mμ	ε
300.3	10070	(277.4)	8350	226.5	5680
293.6	5020	272.2	13050	220.4	16250
288.9	6190	264.2	18720	208.5	42500
		261.5	18900	204.3	44500
		(255.5)	16630		

Wavelengths in parentheses denote inflections.

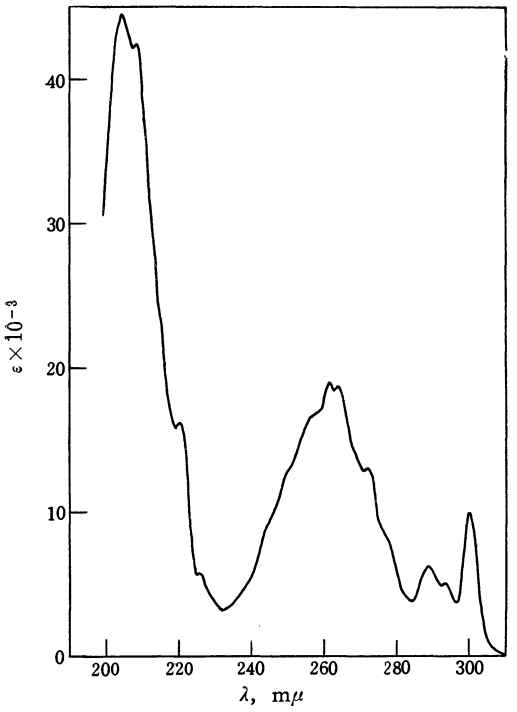


Fig. 1. The ultraviolet absorption spectrum of fluorene in *n*-heptane (cf. Table II).

The conjugation band of fluorene is at considerably longer wavelengths than that of biphenyl. This bathochromic shift of the band may be partly due to the forced coplanarity or near-coplanarity of the molecular configuration of fluorene, and partly to the hyperconjugation of the methylene group. When the relation postulated for biphenyl[1] between the calculated electronic transition energy ΔE_A and the observed position ν_A (in wave number) of the maximum of the conjugation band is provisionally applied without allowance for the bathochromic (hyperconjugation) effect of the substituent to fluorene, the value of the parameter μ in the π—π resonance integral $\mu\beta$ for the co-annular bond in fluorene is estimated to be about 1.060 from the position 261.5 mμ (in *n*-heptane) of the most intense maximum of the conjugation band. This value is to be compared with the corresponding value 0.780 or 0.762 for biphenyl in solution, although this value for fluorene should be considered as a measure of the degree of "conjugation" in fluorene including hyperconjugation of the methylene group as well as intrinsic conjugation which depends on the spatial configuration of the biphenyl skeleton. The fact that the degree of conjugation in fluorene is considerably larger than in biphenyl may explain at least partly the extraordinarily larger reactivity of fluorene as compared with biphenyl in some kinds of reactions. A few examples are given below.

The reactivity of fluorene to nitration is much higher than that of biphenyl. Thus, while the "partial rate factor" (the rate constant of separate nuclear position of the compound relative to one nuclear position of benzene being taken as unity) at *p*-position and that at *o*-position in biphenyl are 38 and 41, respectively[12], or 11.0 and 18.5, respectively[13], the values at the corresponding positions (i. e. the 2- or 7- and the 4- or 5-positions) in fluorene are 2040 and 944, respectively[14].

8) E. A. Braude, *J. Chem. Soc.*, **1949**, 1902.
9) E. A. Braude and F. C. Nachod, "Determination of Organic Structures by Physical Methods", Academic Press, Inc., New York (1955), p. 154 ff. (E. A. Braude).
10) A. Wenzel, *J. Chem. Phys.*, **21**. 403 (1953). See also Ref. 1.
11) R. N. Jones, *J. Am. Chem. Soc.* **67**, 2127 (1945).
12) O. Simamura and Y. Mizuno, This Bulletin, **30**, 196 (1957).
13) P. B. D. de la Mare and M. Hassan, *J. Chem. Soc.*, **1957**, 3004.
14) M. J. S. Dewar and D. S. Urch, ibid., **1958**, 3079.

Berliner and Shieh[15] have correlated the rate constants of solvolysis of α-arylethyl chlorides with the atom localization energies calculated by Dewar and others for the aryl radicals, and found that the reactivity of 2-fluorenyl compound is extraordinarily higher than expectation.

In addition, Sandin and coworkers[16] have compared the carcinogenic activities of 2-acetylaminofluorene, 4-acetylaminobiphenyl, and their related compounds, and found the fact that 2-acetylaminofluorene has a much higher activity as compared with 4-acetylaminobiphenyl and especially its *o*-methyl substituted derivatives. They have ascribed this fact to the greater planarity of the configuration of the biphenyl skeleton in 2-acetylaminofluorene than in the other compounds.

The interplanar angle in 9,10-dihydrophenanthrene has been estimated by Beaven and coworkers[4] to be about 20° by means of a model in which the saturated carbon atoms maintain their tetrahedral valency angle. Accordingly the bathochromic displacement of the conjugation band of this compound relative to that of biphenyl may be due mainly to the normal electronic substituent effect (probably hyperconjugation effect) of the alkyl group.

The maximum of the conjugation band of 4,5-methylene-9,10-dihydrophenanthrene is at even longer wavelengths than those of fluorene and 9,10-dihydrophenanthrene. In this compound the conflicting steric requirements of the two bridges would appear to be most favorably compromised in an approximately planar configuration. Accordingly the bathochromic shift of the conjugation band of this compound relative to those of fluorene and of 9,10-dihydrophenanthrene may be ascribed partly to the planarity or nearer-planarity of the configuration, and partly to the electronic substituent effect of the additional dimethylene or methylene bridge.

o, *o'*-Three-atom-bridged and Four-atom-bridged Biphenyls

Each of the spectra of the compounds in which the *o*,*o'*-positions of biphenyl are bridged by a 7-membered ring (which are subsequently referred to as the *o*,*o'*-three-atom-bridged biphenyls) (entries 4—9, Table I) shows the conjugation band at considerably shorter wavelengths than those of fluorene and of 9,10-dihydrophenanthrene. The corresponding band of each of the compounds in which the *o*,*o'*-positions of biphenyl are bridged by an 8-membered ring (the *o*,*o'*-four-atom-bridged biphenyls, entries 10 and 11) is further shifted toward shorter wavelengths.

These *o*,*o'*-three-atom-bridged and four-atom-bridged biphenyls are considered to have non-planar configurations. Accordingly, the hypsochromic displacements of the conjugation band observed in these compounds with respect to fluorene or 9,10-dihydrophenanthrene are probably ascribed to the non-planarity of the configurations, and therefore, their configurations may be inferred from their spectra by application of the method described in the earlier parts of this series.

In application of the method to these compounds, 9,10-dihydrophenanthrene is taken as the longer-wavelength-side reference compound. The justification for taking this compound rather than fluorene as the reference compound is that this makes a pertinent allowance for the bathochromic effect of two methylene groups attached at the *o*- and the *o'*-positions of biphenyl, and further justification is found in the fact that the molecule of fluorene is presumed to contain a considerably large strain.

The previously assumed relation between the length of the co-annular bond R and the interplanar angle θ (Eqs. 4 and 5 in Part I of this series) may not be pertinent to this case. However, a slight change in the value of R does not substantially affect the calculated value of the interplanar angle θ, as suggested by the results of calculations in the case of terphenyls which will be described in the next part of this series. Hence the relation is applied to the present case for simplification. Then, adopting the value (about 20°) estimated by Beaven and coworkers from the scale model for the interplanar angle in 9,10-dihydrophenanthrene, the corresponding value of R is computed to be 1.4837 Å, and the parameter μ in the $\pi-\pi$ resonance integral $\mu\beta$ for the co-annular bond is evaluated to be 0.801. Consequently, the value of the calculated transition energy $1.5115(-\beta)$, viz. ΔE_L, when μ is 0.801 is assumed to correspond to the wave number 37879 cm^{-1} (264 mμ),

15) E. Berliner and N. Shieh, *J. Am. Chem. Soc.*, **79**, 3849 (1957).
16) R. B. Sandin, R. Melley, A. S. Hay, R. N. Jones, E. C. Miller and J. A. Miller, ibid., **74**, 5073 (1952).

viz. ν_L, of the position of the maximum of the conjugation band in the spectrum of 9,10-dihydrophenanthrene in ethanol. (In the present treatment the data of the spectra of the solutions in ethanol are compared in principle.)

As the shorter-wavelength-side reference, quite similarly to the previous treatment of *o*-alkyl- and *o,o'*-dialkylbiphenyls[2], the value of toluene, 46882 cm^{-1} (213.3 mμ), corresponding to the "center of gravity of singlets" of benzene is taken, because the effect of a methylene group upon the positions of the bands of benzene is considered to be approximately of the same magnitude as that of a methyl group (cf. Table II in Part II of this series). That is, the value of 46882 cm^{-1} (viz. ν_S) is assumed to correspond to the value of the calculated transition energy $2(-\beta)$ (viz. ΔE_S) when μ is 0.

On the basis of the above assumptions, the value of ΔE_A, μ, θ, R, etc. for each of the *o,o'*-three-atom-bridged and the *o,o'*-four-atom-bridged biphenyls can be computed by the usual procedure from the position of the conjugation band in its spectrum. The results of calculations are summarized in Table III.

TABLE III. RESULTS OF CALCULATION

Compound	λ_{max} mμ	ν_A cm^{-1}	$\Delta E_A/-\beta$	μ	θ	R Å
o,o'-Three-atom-bridged biphenyls						
4	250	40000	1.627	0.594	44.5°	1.497
5, 6	249	40161	1.635	0.579	46.0	1.498
7, 8	248.5	40241	1.640	0.572	46.7	1.499
9	248	40323	1.644	0.565	47.3	1.499
(Average)	249	40161	1.635	0.579	46.0	1.498
o,o'-Four-atom-bridged biphenyls						
10	239.5	41754	1.722	0.434	58.0	1.508
11	236.5	42283	1.751	0.387	61.5	1.511
(Average)	238	42017	1.736	0.411	59.8	1.510

Compounds are represented by the entry numbers in Table I.

Beaven and coworkers have estimated the interplanar angle in *o,o'*-three-atom-bridged biphenyls as about 50°[4], and that in *o,o'*-four-atom-bridged biphenyls as about 60~65°[6] from models. The values have been computed here to be 44.5~47.3° average, 46°) and 58.0~61.5° (average, 59.8°), respectively, which agree fairly well with the values estimated from models.

From the close similarity between the spectrum of 2,7-dihydro-3,4-5,6-dibenzoxepin (entry 4,Table I)and that of biphenyl Beaven and others[4] have presumed that "in the oxepin the phenyl groups are no less conjugated and hence no less coplanar than in biphenyl", and concluded that "the biphenyl-type spectrum does not provide sure evidence for a coplanar configuration" "since the oxepin can not be coplanar". In addition, the present author considered in the previous paper[17] that the estimation of the value of the interplanar angle in biphenyl as about 50° was supported by this spectral similarity. A common flaw in these considerations is that the bathochromic effect of the substituents was not sufficiently taken into account.

On the other hand, Braude and Forbes[18] have estimated the interplanar angles in ortho-bridged biphenyls and their related compounds by applying the equation $\cos\theta = \varepsilon/\varepsilon_0$, assuming that ε_0 is equal to the molar extinction coefficient of the conjugation band of fluorene, and obtained the following values; 21° for 2,7-dihydro-3,4-5,6-dibenzoxepin (entry 4, Table I), 41° for its *o,o'*-dimethyl derivative, 47° for its *o,o'*-dimethoxy-derivative, and 27° for 2,7-dihydro-3,4-5,6-dibenzazepinium-1-*spiro*-1'''-piperidinium bromide (entry 9).

Their equation mentioned above has been assumed to be true on the basis of the hypothesis of transitions from the non-planar ground state to the uniplanar or near-planar excited state, and the starting point of their theory is the assumption that the absorption intensity is determined by the transition probability which is in turn governed mainly by the probability in which the molecule in the ground state assumes the uniplanar or near-planar configuration[19]. However, this probability must be governed by the shape of the potential energy curve for the tortional vibration, and hence mainly by the energy difference between the uniplanar or near-planar configuration and the most probable configuration. In spite of the hypothesis by Braude and others, it seems to be very questionable whether or not there is any direct relation between this probability, namely, the height of the energy barrier to the rotation about the pivot bond and the interplanar angle in the most probable configuration.

Furthermore, according to its basic theory, the equation mentioned above

17) H. Suzuki, This Bulletin, **27**, 597 (1954).
18) E. A. Braude and W. F. Forbes, *J. Chem. Soc.*, **1955**, 3776.
19) E. A. Braude and F. Sondheimer, ibid., **1955**, 3754.

should be applied only to the case in which the so-called steric effect of type 1 is exerted, that is, to the case in which a reduction in the intensity of the conjugation band occurs alone without any significant hypsochromic shift. Nevertheless, it is evident that in the spectra of the compounds cited by Braude and Forbes remarkable hypsochromic shifts are involved. The application of the equation to these compounds is, therefore, inconsistent with its basic theory itself.

The introduction of two *o*-methyl groups or of two *o*-methoxyl groups into dihydrodibenzoxepin (entry 4, Table I) causes a remarkable decrease in the intensity of the "biphenyl-type" conjugation band. Considering this effect as being mainly due to the steric effect, Braude and Forbes[18] have stated that the assumption by Beaven and others of an angle of 50° between the benzene rings in the parent oxepin is questionable. Thus, adopting the assumption of Beaven and others, since the benzene rings in this compound are already at an angle of about 50°, the introduction of the *o*-substituents should have no steric consequences. On the other hand, Beaven and others[4] have attempted to explain this effect of the substituents by electronic interaction between the substituents and the separate benzene rings to which they are attached.

However, in the preceding part of this series, the interplanar angle in *o,o'*-dimethylbiphenyl was estimated to be about 70°, and this compound was inferred to have the *cis*-configuration. This value of the interplanar angle is considerably larger than that for dihydrodibenzoxepin, 50°, estimated by Beaven et al., or 44.5°, by the present author. Therefore, even when the value, 50° or 44.5°, is adopted as the interplanar angle in dihydrodibenzoxepin, the introduction of the substituents into the ortho positions can evidently increase the interplanar angle, and hence a decrease in the intensity and the hypsochromic shift caused by the introduction of two *o*-methyl groups can be explained sufficiently, contrary to the opinion of Braude and others. A decrease in the intensity of the band caused by the introduction of two *o*-methoxyl groups may be similarly explained by steric effect, but the fact that the band of *o,o'*-dimethoxy-derivative is at, though slightly, longer wavelengths than that of the parent compound may be attributed to the electronic effect of the substituents.

Finally, in connection with the spatial configuration of the *o,o'*-bridged biphenyls, it is noteworthy that recently Iffland and Siegel[7] succeeded first in preparing an optically active biphenyl derivative whose optical activity is due to non-planarity of the biphenyl skeleton as a consequence of the requirement of a three-carbon-atom-bridge across the *o,o'*-positions. According to them, this compound, *d*-6,6-dicarbethoxy-dibenzo-[a, c] [1, 3]-cycloheptadiene (entry 6, Table I), is optically stable in the crystalline state, and loses half of its activity ($[\alpha]_D^{32.5}$ +2.25° in cyclohexane) in 80 min. in cyclohexane solution.

Summary

The ultraviolet absorption spectra of some *o,o'*-bridged biphenyls and their relations to the spatial configurations have been discussed. The method developed in the earlier parts of this series has been applied to these compounds, especially *o,o'*-three-atom-bridged (*o,o'*-7-membered-ring-bridged) and *o,o'*-four-atom-bridged (*o,o'*-8-membered-ring-bridged) biphenyls, and the interplanar angles have been calculated to be about 44.5~47.3° (average, 46°) for the former compounds and about 58.0~61.5° (average, 59.8°) for the latter.

The author thanks Professor Kengo Shiomi for reading the manuscript and for valuable advice.

Department of Chemistry
College of General Education
The University of Tokyo
Meguro-ku, Tokyo

The Relation between the Deformation of Substrate of PVA Sheet by Stretching and the Stretch Ratio R_s

By Yoshié TANIZAKI, Teruaki KOBAYASHI and Noboru ANDO

(Received June 24, 1959)

In the hope of analyzing relative directions of transition moments of dyes by their dichroism in stretched polyvinyl alcohol (PVA) sheets, the following equation has been derived previously in reference to the relation between the observed optical density ratio R_d and the stretch ratio R_s[1],

$$R_d=\frac{2+2(2r^2-1)\,T(R_s)}{(2r^2+1)-(2r^2-1)\,T(R_s)} \qquad (1)$$

where

$$\left.\begin{aligned} T(R_s)&=\frac{R_s^2}{R_s^2-1}\\ &\times\left\{1-\frac{N(R_s)}{\sqrt{R_s^2-1}}\ln(R_s+\sqrt{R_s^2+1})\right\}\\ N(R_s)&=2\\ &\times\left\{\frac{1}{\sqrt{R_s^2-1}}\ln(R_s+\sqrt{R_s^2-1})+R_s\right\}^{-1}\\ R_s&>1 \end{aligned}\right\} \qquad (2)$$

and the angle between the orientation axis of a molecule and the direction of its transition moment is given by $\cot^{-1}r$. When Eq. 1 was derived, it was assumed that an imaginary sphere in substrate of PVA sheet changes into a spheroid, keeping its volume constant, with the stretching of the PVA sheet. The relation between R_d and R_s expressed by Eq. 1, which was derived on the basis of such an assumption, coincided well with the experimental results of the dyes which the authors used. However, it has become necessary to ascertain whether the assumption is practically correct or not. This inspection was carried out by a very simple check measurement. Therefore, the method and the results obtained will be reported.

The object of this paper is to confirm the following subjects: 1) whether the width and the thickness of a PVA sheet decrease in the same ratio, when the sheet is stretched; 2) whether the relation between two quantities used when R_s was defined—namely the lengths of both long and short axes of an ellipse deformed from a circle drawn on the sheet by stretching it—coincides with the theoretical relation derived by assuming an ellipsoid of constant volume as just mentioned; 3) and whether if the two facts are just as expected, the relation between R_d and R_s of poly-iodine ions in PVA sheet[2], which seem to have both their transition moment and orientation axis in the same direction, must have the same behavior both experimentally and theoretically.

The Change in Width and Thickness of PVA Sheet When It Is Stretched.—The width and the thickness of PVA sheet were measured with a caliper and a micrometer. Let w_0 be the initial length of PVA sheet perpendicular to the stretching direction (the width), t_0 be the initial thickness, and w and t be their respective values corresponding to any R_s. Values of $(w/w_0)/(t/t_0)$ are plotted in Fig. 1, in which the white circles mean values when the ratio of the initial lengths of sheet parallel and perpendicular to the stretching direction is about 1 : 1, and the black circles those corresponding to the ratio of about 1 : 3. The figure shows clearly that the width and the thickness decrease in the same ratio at least in the former case (which has the same condition as the others which the authors have reported).

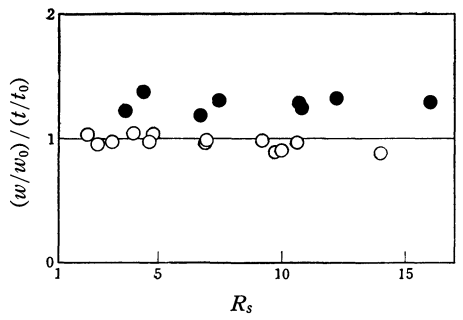


Fig. 1

1) Y. Tanizaki, This Bulletin, **32**, 75 (1959).

2) Y. Tanizaki, T. Kobayashi and N. Ando, *J. Chem. Soc. Japan, Pure Chem. Sec.* (*Nippon Kagaku Zasshi*), **80**, 445 (1959).

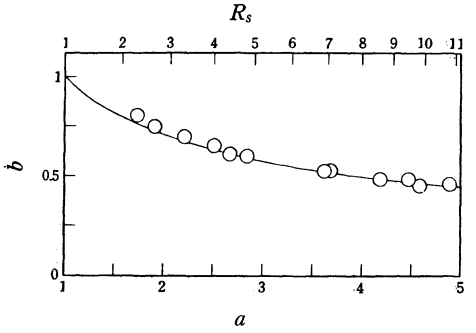


Fig. 2

The Relation between Lengths of Long and Short Axes. — Let a be the length of the long axis and b that of the short one of an ellipsoid, and then its volume is proportional to ab^2 and R_s is defined by a/b, with $a=b$ before stretching. Now, taking up a case in which the width decreases in proportion to the thickness as shown in Fig. 1, the authors searched for the following relation, to see whether the values of R_s actually used were correct. If an assumed sphere in a PVA sheet changes into ellipsoids, keeping its volume constant, when it is stretched, then the theoretical relation of $b-a$ or $b-R_s$ will be expressed by the curve shown in Fig. 2. Observed values corresponding to the curve are also shown in the figure, and they fit it satisfactorily.

The Relation between R_d and R_s of Poly-iodine Ions in PVA Sheet. — The absorption at about 600 mμ of iodine in PVA is due to linear poly-iodine ions constituted by many iodine atoms[3]. Therefore, in such a polyatomic molecule, its orientation axis coincides with the direction of its transition moment, and then the value of r mentioned above becomes infinity and Eq. 1 has the simple form of

$$R_d = [2T(R_s)] / [1 - T(R_s)] \qquad (3)$$

In Fig. 3 a curve drawn by Eq. 3 is shown, and corresponding observed values are also shown by white circles. This experiment was performed as follows.

Iodine was adsorbed by PVA sheets in solutions containing boric acid ~5 g.%, potassium iodide 1~2 g.%, ammonium iodide 1~2 g.% and iodine 0.2~0.5 g.%. The sheets, which were swollen beforehand in water, were dehydrated in alcohol to be put back in a hard state, in order to

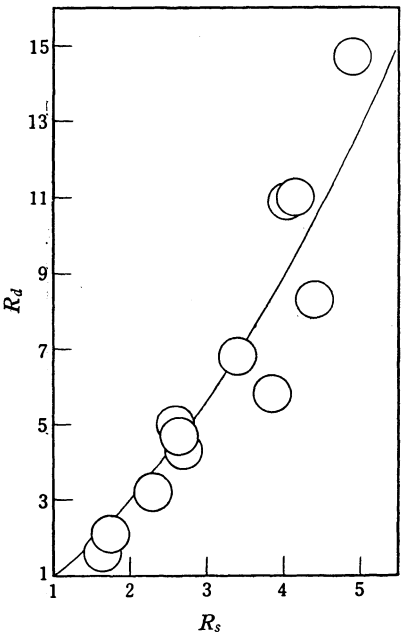


Fig. 3

prevent adsorbed iodine from fleeing from the sheets. However, even by this method, iodine could not be adsorbed in a satisfactorily uniform manner. The PVA sheets which adsorbed iodine were stretched after they were dried well at room temperature. The absorption spectra by polarized light of any stretched iodine-PVA sheet did not always show the same values at corresponding angles, when the sample sheet was rotated (0° to 360°); that is, $D_{\parallel}$ (or $D_{\perp}$) of a sample was measured at two angles, but the two observed values did not always coincide with each other. Therefore, it is their average values that are shown in Fig. 3.

The agreement between the curve drawn by Eq. 3 and the observed values is a direct verification of the propriety of distribution function which was used when Eq. 1 was derived. Therefore, if only samples which are sufficiently long as compared with their width are used, when PVA sheets are stretched, it may be considered that the deformation of their substrate occurs with a constant volume (at least when $R_s<15$). This shows that the fundamental assumption employed for the derivation of the equation was proper.

Laboratory of Physical Chemistry
Tokyo Institute of Technology
Meguro-ku, Tokyo

3) See Ref. 2 and those cited in it.

Effect of Dry Grinding on Gibbsite

By Goro YAMAGUCHI and Kenichi SAKAMOTO

(Received May 26, 1959)

The crystal structure of gibbsite, one of the aluminum-trihydroxides, is a double-layered structure, and the binding force between layers is a rather weak hydrogen bond. So, when gibbsite is ground, it is supposed that the dimension of crystal particles is reduced and the stacking disorder of layers may occur. The authors examined the structural change of ground gibbsite, and confirmed the fact that very fine gibbsite (diameter of the particles is less than 1 micron) decomposes to χ-alumina directly, and in this process boehmite is not produced. The authors also studied the thermal decomposition of ground gibbsite and checked the difference of thermal properties between unground and ground gibbsite.

Experimental

Material. — Gibbsite employed in this study is a commercial product. It consists of aggregates of small crystals of a few microns and the dimension of the aggregates is 20~30 microns. Impurities are shown in Table I.

TABLE I. IMPURITIES IN GIBBSITE

Na_2O	0.35 %
Fe_2O_3	0.009
SiO_2	0.008

Procedure. — This gibbsite was ground in a ball mill and sampled. The samples were examined by X-ray methods, including X-ray small-angle diffraction procedure, and also by differential thermal analysis (DTA). Also their ignition loss was determined.

Results

Gibbsite was ground for 100 hr., and sampled at a definite time during grinding. The ignition loss was nearly constant through this process (Table II). The result of X-ray analysis was shown in Fig. 1. It is seen from this result that

TABLE II. IGNITION LOSS OF GROUND GIBBSITE

Time of grinding	Igniton loss
0 hr.	34.4 %
1	34.4
3	34.7
6	33.9
10	34.1
20	33.7
40	34.2
100	35.0

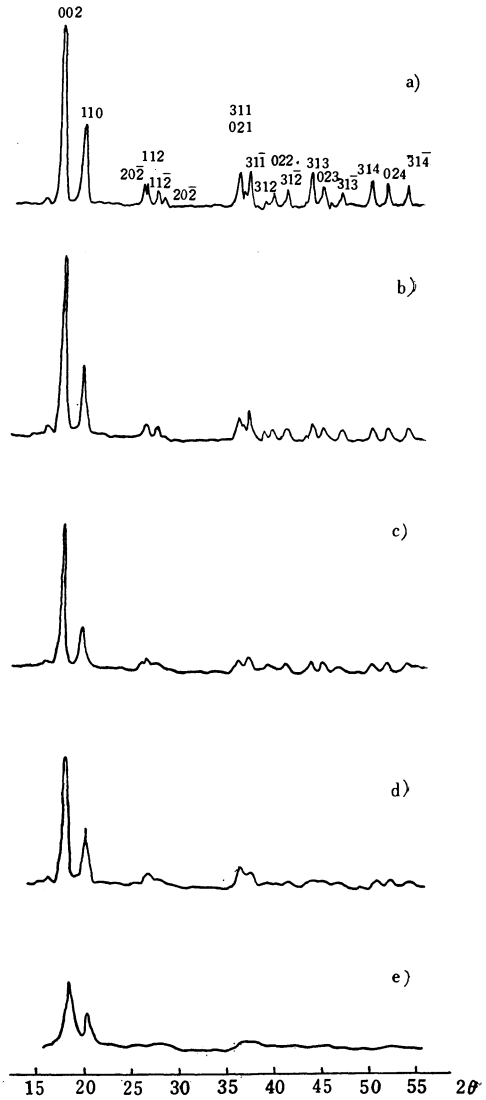


Fig. 1. X-ray diffraction diagrams of gibbsite.
a) Original gibbsite
b) Ground for 6 hr.
c) Ground for 10 hr.
d) Ground for 20 hr.
e) Ground for 100 hr.

the intensities of diffracted lines decreased gradually, and only two lines (002) and (110) were observed after 40 hr. On the contrary, the result of the small-angle scattering suffered little change (Fig. 2). From this, the authors can calculate the diameter of gibbsite by using Warren's formula[1]. Diameters of unground gibbsite and of that ground for 100 hr. are about 3500 and 2000 Å respectively. The diameter of gibbsite, ground less than 100 hr., lies between 3500 and 2000 Å. Microscopic observation reveals that an aggregate was released into some single particles, and a single particle was broken to a few fragments which have the size of about a micron. From above facts, it may be said that a particle of gibbsite which seems to be a single crystal is not continuous in the sense of X-ray crystallography. This continuous domain which is sensible for small-angle diffraction remained almost unchanged during grinding. The result of DTA was shown in Fig. 3. When the grinding time is within a few hours, ground gibbsite decomposes similarly as unground gibbsite does, that is, it reveals three endothermic peaks. But after a longer period of grinding, the DTA-curve of gibbsite changes gradually from the normal curve. The first peak becomes smaller and

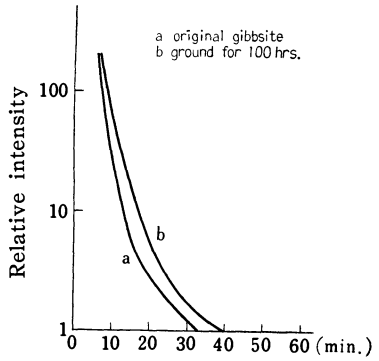


Fig. 2. X-ray small angle diffraction of gibbisite.

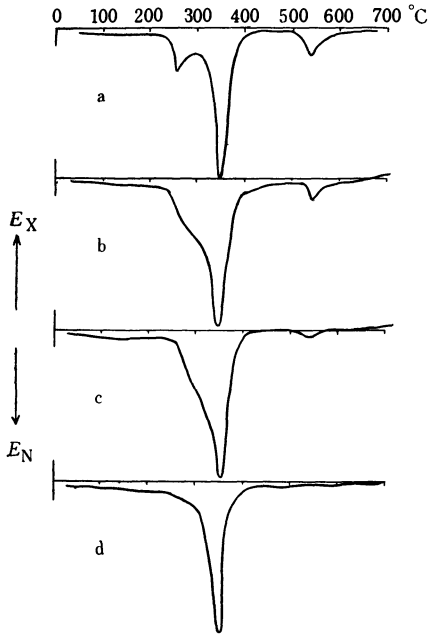


Fig. 3. DTA-curves of ground gibbsite.
a) Original gibbsite
b) Ground 6 hr.
c) Ground 20 hr.
d) Ground 40 hr.

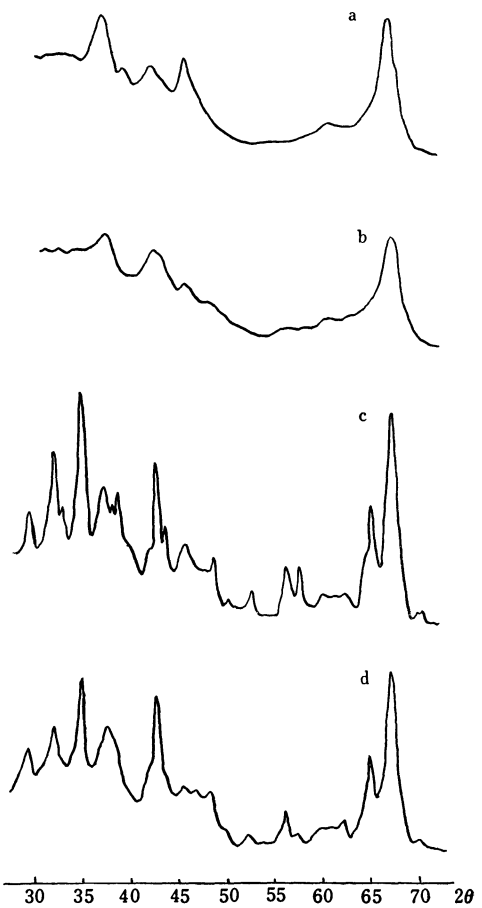


Fig. 4. X-ray diffraction diagrams of calcined gibbsite.
a) Calcined at 800°C after 3 hour-grinding [($\chi+\gamma$) alumina]
b) Calcined at 800°C after 20 hour-grinding (χ-alumina)
c) Calcined at 1000°C after 3 hour-grinding [($\kappa+\theta$) alumina]
d) Calcined at 1000°C after 20 hour-grinding (κ-alumina)

1) B. E. Warren, *J. Appl. Phys.*, **13**, 364 (1942).

only a knob is seen at this point. Parallel with this, the third peak becomes smaller. After the grinding of 40 hr., only the main peak is observed. This leads us to the conclusion that ground gibbsite decomposes directly into alumina; diffracted lines of alumina at 700~900°C were different from each other according to their grinding times. The diffraction of 1.99 Å became weaker and the diffraction of 2.12 Å became relatively intense (Fig. 4).

Consideration

There are many minerals, such as clay minerals, which have layered structures. In these substances the binding force within the layer is covalent and very rigid, but the interlayer force is rather weak. Lately it has been reported that there are many disordered clay minerals and theoretical calculation has been made by many authors[2].

Gibbsite, which has a composition of aluminum-trihydroxide and does not contain silicon oxide, may be said to be one of the most simple layered minerals. Therefore, it is possible to anticipate the fact that the various types of stacking along *c*-axis will occur in aluminum-trihydroxide. Thus it can also be anticipated that gibbsite, one of aluminum-trihydroxide-polytypes, is naturally supposed to be easily disordered by grinding. In this study, the authors can indicate that the properties of ground gibbsite are as follows: 1) gibbsite retains its composition during grinding; 2) the X-ray small-angle diffraction behavior suffers little change by grinding and appears within a very narrow range; 3) the intensities of diffracted lines become weak gradually with grinding; 4) (002) reflection does not diminish at first but becomes weak after a grinding of about 10 hr.; 5) (110) reflection still exists with (002) reflection after the disappearence of other lines.

From the facts mentioned above, it is clear that the disintegration of crystal occurred by grinding and the intensity of diffracted lines became weak. It may be said that only a slipping of layers took place so long as (002) reflection did not change, and after that the order along *c*-axis began to be lost with the diminution of (002) intensity. But the fact that (110) reflection remained as well as (002) after the other reflections had vanished indicates the direction of the slipping of the layers. The crystal structure of gibbsite is shown in Fig. 5 and Table III[3]. As explained already the packing of (OH) is an unusual packing of 1—2 2—1, so the direction of the slipping of layers would be [110]. In fact, it is proved that $F(110)$ is unchanged so long as the slipping of layers proceeds in the direction [110].

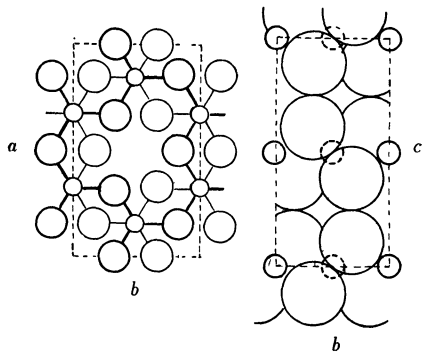


Fig. 5. Crystal structure of gibbsite.

TABLE III. CRYSTAL STRUCTURE OF GIBBSITE

Crystal class	Monoclinic
Space group	$P\,2_1/n$ (C_{2h}^5)
Unit cell	$a=8.6236$ Å, $b=5.0602$ Å
	$c=9.699$ Å, $\beta=85°26'$
Z	8 $Al(OH)_3$
Atomic coordinates	$4(e)$; $\pm(X,Y,Z;\ 1/2-X,$ $Y+1/2,\ 1/2-Z)$

As seen from Fig. 5, there are two layers with a distance of $c/2$ in a unit cell and the structure within the layer is unchanged. Thus F is separated to parts F_1 and F_2, each of which is an F-factor of its own layer. Also it is assumed that a lower layer keeps its position and an upper layer slips by $\Delta r(\Delta X+\Delta Y)$. So the displacement of any atom of an upper layer is equal to Δr. Thus

$$\begin{aligned} F(110)_{\text{slipped}} &= F_1(110)+F_2(110) \\ &= \Sigma\, 2f\cdot\cos 2\pi(X+Y) \\ &\quad +\Sigma\, 2f\cdot\cos 2\pi[(1/2-X-\Delta X) \\ &\quad +(1/2+Y+\Delta Y)] \\ &= \Sigma\, 2f\cdot\cos 2\pi(X+Y) \\ &\quad +\Sigma\, 2f\cdot\cos 2\pi[(Y-X) \\ &\quad +(\Delta Y-\Delta X)] \end{aligned}$$

2) G. W. Brindley, "X-ray Identification and Crystal Structures of Clay Minerals", Mineralogical Society, London (1951); S. B. Hendricks and E. Teller, *J. Chem. Phys.*, **10**, 147 (1942); W. H. Zachariasen, *Phys. Rev.*, **71**, 715 (1947); C. R. Houska and B. F. Warren, *J. Appl. Phys.*, **25**, 1503 (1954).

3) H. D. Megaw, *Z. Krist.*, **A87**, 185 (1934).

$$= \Sigma 2f \cdot \cos 2\pi (X+Y) + \Sigma 2f \cdot \cos 2\pi (Y-X) \quad (\Delta X = \Delta Y) = F(110)_{\text{original}}$$

In a disordered structure, the magnitude of the slipping is not constant but it is natural that (OH) of disordered gibbsite has nearly hexagonal close stacking in short range.

Many reports about the thermal decomposition of gibbsite have been published[4]. Brown and coworkers proposed the dual decomposition hypothesis of gibbsite as follows[5].

$$\begin{array}{l} \text{Gibbsite} \rightarrow \chi \rightarrow \kappa \rightarrow \alpha \\ \quad\downarrow \qquad\qquad\qquad\uparrow \\ \text{Boehmite} \rightarrow \gamma \rightarrow \delta \rightarrow \theta \end{array}$$

Also Tertian and coworker showed that very fine gibbsite decomposed directly to χ-alumina without being contaminated with boehmite[6].

$$\text{Gibbsite} \rightarrow \chi \rightarrow \kappa \rightarrow \alpha$$

When the authors were writing this report, Dr. Tertian sent us kindly very fine gibbsite which had the diameter of about 0.5 micron. So the thermal transformation of this gibbsite was checked and, consequently, it could be recognize that Tertian's result was correct. (Fig. 6)

In reference to the above facts, it is expected that after long grinding, it is possible to get fine gibbsite which does not decompose into boehmite but is transformed directly into χ-alumina. The result of DTA shows that the first peak and the third peak which indicate respectively formation and decomposition of boehmite become smaller with the duration of grinding. Parallel to this, the dimension of ground crystal decreased to a micron. After 40 hr. grinding, gibbsite decomposed to alumina which did not contain boehmite. This alumina exhibited the characteristic diffraction of 2.12 Å for χ-alumina and was transformed to κ-alumina. So it may be concluded that the ground gibbsite has the same properties as the fine gibbsite. But there are some questions in this explanation. This ground gibbsite shows only two diffraction lines and is no longer true gibbsite. But it may be supposed that this

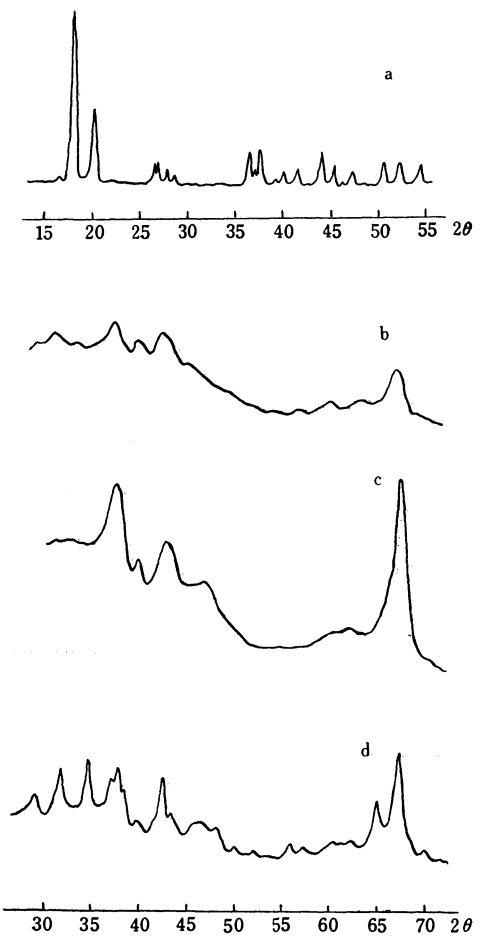


Fig. 6. X-ray diffraction diagrams of fine gibbsite.
a) Original gibbsite
b) Calcined at 350°C
c) Calcined at 800°C (χ-alumina)
d) Calcined at 1000°C (κ-alumina)

gibbsite retains the essential property and structure after being ground, so the thermal property of this gibbsite would have the true character of gibbsite.

The difference of thermal property between large and small particles of gibbsite is explained as follows. When large particles of gibbsite is heated to about 200°C, the hydrothermal reaction begins to form interior crystals and dissolution of gibbsite and crystallization of boehmite occur[7]. But in the case of fine particles, the small crystal can not keep the vapor pressure in it, and the vapor evaporates, so the formation of boehmite ceases. Then the gibbsite decomposes to χ-alumina. That is, the formation

4) A. S. Russell et al., "Alumina Properties, Technical Paper No. 10", Aluminum Company of America, Pittsburgh, Penn. (1956).
5) J. F. Brown et al., *J. Chem. Soc.*, **1953**, 84.
6) R. Tertian and D. Papee, *Compt rend.*, **241**, 1575 (1955).
7) G. Yamaguchi and K. Sakamoto, This Bulletin, **32**, 696 (1959).

of boehmite is not the result of direct decomposition but the result of hydrothermic reaction as in an autoclave, while the small particles of gibbsite can not keep the vapor pressure in it. Thus the hydrothermic reaction does not occur and boehmite is not produced from this gibbsite.

Summary

The effect of dry grinding on gibbsite was examined by X-ray diffraction, X-ray small angle diffraction and differential thermal analysis. It has been found that there are two sorts of structural change in the process of dry grinding. One, which occurs early in this process, is the slip of layers. In this stage (002) reflection retains its intensity. The other, which takes place after grinding of about 10 hr., is the three-dimensional disintegration of the crystal structure and the intensities of all diffractions become weak. Since only two reflections (002) and (110) are observed after 40 hr., it can be known that the direction of the slipping of layers is [110].

DTA-curve of gibbsite exhibits three endothermic peaks in the beginning of grinding but comes to exhibit only one peak which indicates the decomposition of gibbsite to alumina. This means that ground gibbsite decomposes directly to χ-alumina as fine gibbsite and boehmite is not produced in this process.

The authors wish to express hearty thanks to Dr. R. Tertian of Pechiney for his favor.

Department of Applied Chemistry
Faculty of Engineering
The University of Tokyo
Hongo, Tokyo

Sur la dissolution des minerais sulfurés en divers milieux. I. Dissolution d'un minerai sulfuré de fer en milieu acide

Par Masami ICHIKUNI et Hiroshi KAMIYA

(Reçu le 29 mai 1959)

La désagrégation des minerais sulfurés a été étudiée au point de vue de prospection géochimique par Ohashi[1], qui s'est préoccupé à la dissolution du fer, cuivre, zinc et plomb dans les conditions des eaux naturelles. Garrels en a développé une discussion se basant sur les notions thermodynamiques d'équilibre des reactions[2]. La connaissance du comportement du soufre n'est pas pourtant satisfaisante pour l'explication complète de la désagrégation. D'ailleurs l'influence des facteurs de milieu sur ce phénomène reste encore peu claire. L'examen détaillé du phénomène, par voie de cinétique de la réaction, serait d'une importance particulière dans la géochimie.

On pourrait désigner le pH, le potentiel d'oxydo-réduction, la température, la concentration en ion sulfate et d'autres comme facteurs de milieu participant à la désagrégation. Dans ce rapport on présentera une étude fondamentale sur l'influence du pH et de l'air, celui-ci se rapportant avec le pH au potentiel d'oxydoréduction.

1) S. Ohashi, *J. Chem. Soc. Japan, Pure Chem. Sec.* (*Nippon Kagaku Zasshi*), **74**, 845, 901 (1953).
2) R. M. Garrels, *Geochim. et Cosmochim. Acta*, **5**, 153 (1954).

Expérience

Généralité. — On pulvérise du minerai sulfuré de fer frais, en traite en milieu acide ou neutre en conduisant de l'air dans la suspension du minerai et poursuit la concentration de composants dissous en fonction du temps.

Echantillon.—Un minerai siliceux (nom populaire donné à un minerai sulfuré consistant en

TABLEAU I. RÉSULTAT D'ANALYSE DU MINERAI

Composant	Teneur, %
SiO_2	71,0
Fe	13,3
S combiné	15,0
S libre	0,15
Cu	0,048
Total	99,5

sulfure de fer et en acide silicique qui se produit autour d'un filon de minerai sulfuré chalcophile) produit à la mine de Kosaka, département d'Akita. On l'a pulvérisé de manière à ce que la poudre passe par un tamis avec un nombre de maille à 100. Le tableau I en montre le résultat d'analyse et révèle que le minerai consiste presque entièrement en pyrite et en acide silicique.

La présence du soufre libre dans le minerai pulvérisé suggère la décomposition du minerai provoquée par l'oxydation lors de la pulvérisation. Il y a donc une possibilité d'altération partielle du minerai sulfuré en d'autres composés que le sulfure, tels que l'oxyde, le sulfate.

Traitement. — On prend 200 ml. d'acide chlorhydrique à une concentration connue ou d'eau bidistillée dans un ballon à fond plat à 300 ml. et le met sur un bain-marie. On en attache à l'entrée un tuyau de verre qui a 4 mm. de diamètre et qui sert à introduire de l'air dans la liqueur et un condensateur à reflux dont la sortie est reliée à une trompe, réglée de manière à ce que l'air barbote dans la liqueur à un débit constant. La température de la liqueur est réglée à 80°C. On y ajoute 5 g. de minerai pulvérisé et effectue le prélèvement d'une petite quantité de liqueur, à peu près 10 ml., à 10 min., une, deux, trois et quatre heures à partir du moment de l'addition du minerai. Le dosage du cuivre, fer et sulfate s'effectue sur la liqueur filtrée.

Conditions du traitement.—Les facteurs à examiner sont le débit de l'air et le pH. Etant donné que la désagrégation des minerais sulfurés donne de l'acide sulfurique, les essais de la dissolution en milieu acide sulfurique se conformeraient aux conditions dans la nature. Mais le dosage du sulfate formé par le traitement rencontrera une difficulté, l'augmentation de la concentration en sulfate devant être très légère. Par suite de cette considération, on s'est permis d'employer l'acide chlorhydrique. On maintient la température constamment à 80°C sur toute la série des expériences, afin de supprimer l'effet de la température lors de la comparaison des résultats.

TABLEAU II. CONDITIONS DU TRAITEMENT ET CONCENTRATION DE COMPOSANT DISSOUSS

Conditions		Durée du traitement	Concn. des composants dissous				
Concn. en HCl N	Débit de l'air l./min.	hr.	Cu^{2+}	Fe^{2+}	Fe^{3+}	SO_4^{2-}	acidité
					mé/l.		
		1/6	0,039	1,69	0,06	1,50	
		1	0,070	1,85	0,01	1,50	
0,1	0	2	0,090	1,86	0,04	1,56	
		3	0,099	1,87	0,03	1,56	
		4	0,114	1,93	0,09	1,63	
		1/6	0,031	1,43	0,10	1,25	
		1	0,041	1,72	0,00	1,37	
0,1	0,5	2	0,062	1,74	0,06	1,50	
		3	0,091	1,75	0,05	1,50	
		4	0,108	1,87	0,00	1,54	
		1/6	0,031	1,61	0,03	1,25	
		1	0,049	1,95	0,03	1,58	
0,1	1,5	2	0,077	2,10	0,04	—	
		3	0,083	2,25	0,14	2,08	
		4	0,100	2,48	0,02	2,13	
		1/6	0,013	1,58	0,00	1,21	
		1	0,024	1,93	0,00	1,46	
0,01	1,5	2	0,049	2,12	0,00	1,73	
		3	0,062	2,35	0,00	1,88	
		4	0,079	2,56	0,04	2,19	
		1/6	0,007	1,36	0,01	1,35	
		1	0,012	1,68	0,01	1,46	
0,001	1,5	2	0,020	1,82	0,00	1,83	
		3	0,028	2,12	0,02	2,08	
		4	0,032	2,39	0,00	2,50	0,11
		1/6	0,002	1,15	0,03	1,46	0,31
		1	0,002	1,31	0,00	1,67	0,36
Eau bidistillée	1,5	2	0,003	1,36	0,00	1,81	0,45
		3	0,008	1,43	0,00	2,19	0,76
		4	0,012	1,49	0,02	2,71	1,22

Les essais du débit de l'air s'effectuent en milieu acide chlorhydrique 0,1 N. Le débit de l'air est varié d'une façon suivante: 1) sans introduction de l'air, 2) 0,5 l./min., et 3) 1,5 l./min. Le premier essai ne signifie pas l'exclusion entière de l'air, mais la diminution la plus possible de contact avec l'air. On a recours en même temps à un agitateur mécanique dans le but de maintenir l'efficacité constante de l'agitation.

Les essais du pH s'effectuent sous un débit de l'air de 1,5 l./min., en milieu acide chlorhydrique: 1) 0,1 N, 2) 0,01 N, 3) 0,001 N, et 4) dans l'eau bidistillée.

Analyse. — Une quantité limitée de liqueur prélevée ayant empêché d'effectuer une analyse complète, on se borne à faire le dosage du cuivre, fer divalent, fer total et sulfate. Le cuivre et le fer sont dosés par la colorimétrie, avec la dithizone et l'*o*-phénanthroline, respectivement. Le sulfate, par la turbidimétrie après la formation du sulfate de baryum.

On ne décèle pas dans la liqueur d'autres composants de soufre que le sulfate.

Résultats et discussion

Le tableau II montre le résultat obtenu. Lors du traitement avec de l'eau bidistillée ou de l'acide très dilué, on a remarqué la formation de l'acide sulfurique dont la quantité est estimée par la soustraction du fer du sulfate, les deux étant exprimés en mé/l. Par des essais effectués à part, on a constaté que la somme du fer et de l'acidité s'accorde bien avec la quantité de sulfate dans la limite d'erreur du dosage.

D'autre part, la teneur en fer trivalent est donnée par la différence entre le fer total et le fer divalent.

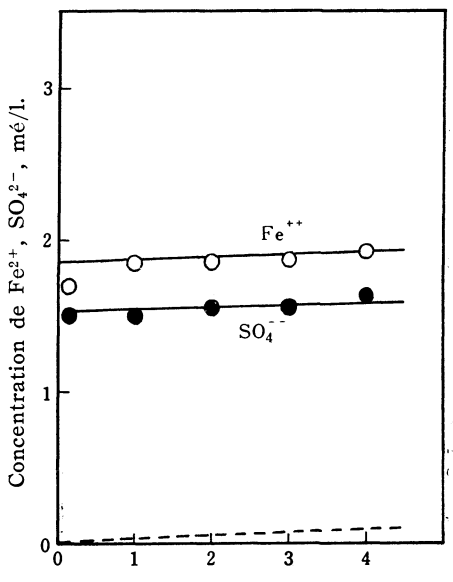
Interprétation des données. — Le minerai utilisé pour ces essais a subi une décomposition partielle par la pulvérisation, ce qui cause quelques irrégularités de dissolution au début du traitement. On développera la discussion en tenant compte de la quantité de composants dissous provenant de la partie préalablement décomposée du minerai.

Les figures sont dessinées avec les données du tableau II. La figure 1 représente la dissolution du fer et du sulfate, et la figure 2, celle du cuivre.

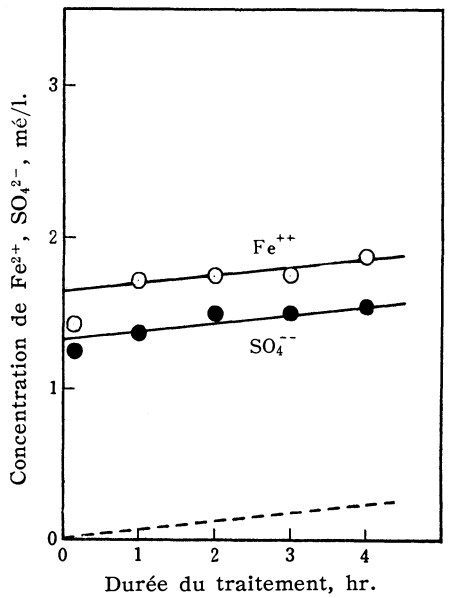
Dans les figures, le trait plein représente la concentration de composants telle qu'on l'a trouvée, et le trait discontinu, tracé de l'origine parallèlement à celui-là, en montre la concentration correspondant à la dissolution par le traitement. La pente du trait discontinu permet de comparer la vitesse de dissolution d'un composant avec celle d'autres.

Influence du débit de l'air. — Ces essais, effectués en milieu acide chlorhydrique 0,1 N, montrent que la dissolution du cuivre en subit peu d'influence, tandis que celle du fer et du soufre est favorisée par l'augmentation du débit de l'air.

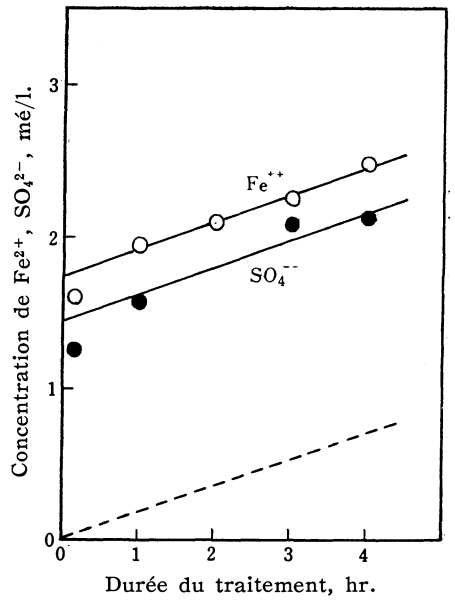
Influence du pH.—La vitesse de dissolution du fer est la même dans l'acide chlorhydrique 0,1 N que dans l'acide 0,01 N. Il en est de même du cuivre et du soufre. L'élévation du pH empêche la dissolution du cuivre et du fer, et accélère celle du soufre.



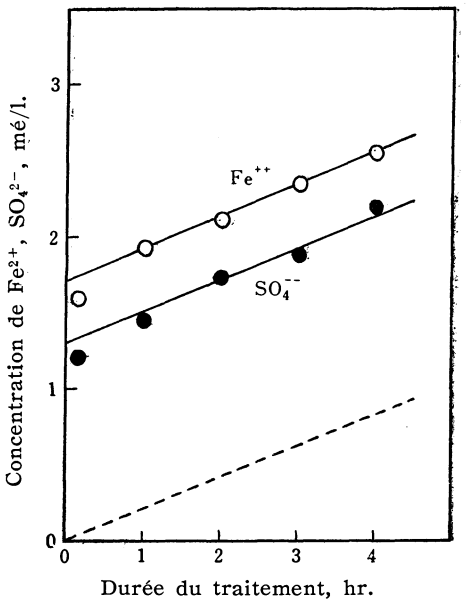
(a) HCl 0,1 N; Air 0 l./min.



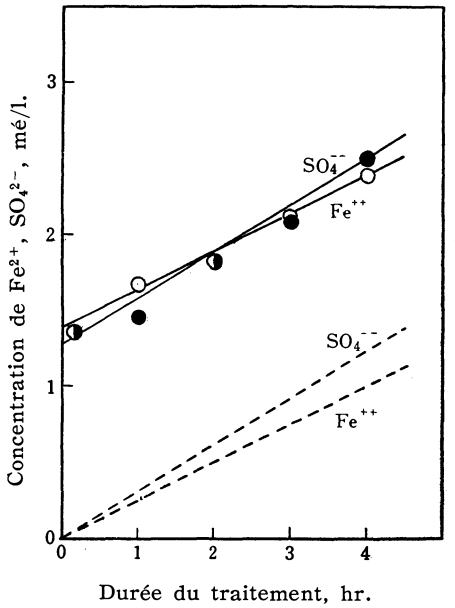
(b) HCl 0,1 N; Air 0,5 l./min.



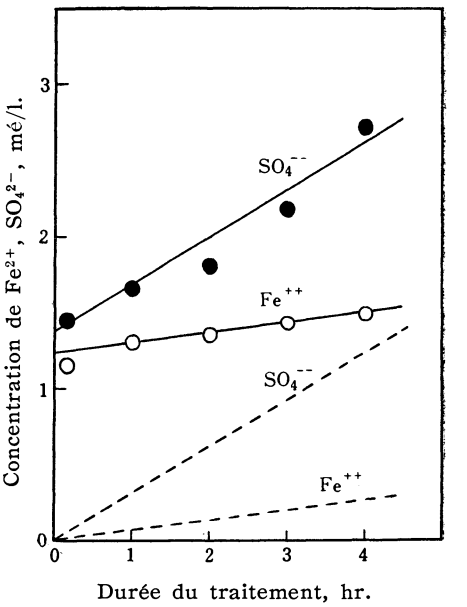
(c) HCl 0,1 N; Air 1,5 l./min.



(d) HCl 0,01 N; Air 1,5 l./min.



(e) HCl 0,001 N; Air 1,5 l./min.



(f) Eau bidistillée; Air 1,5 l./min.

Fig. 1. Dissolution du fer et du sulfate.
Trait plein: concentration totale.
Trait discontinu: concentration correspondant à la dissolution par le traitement.

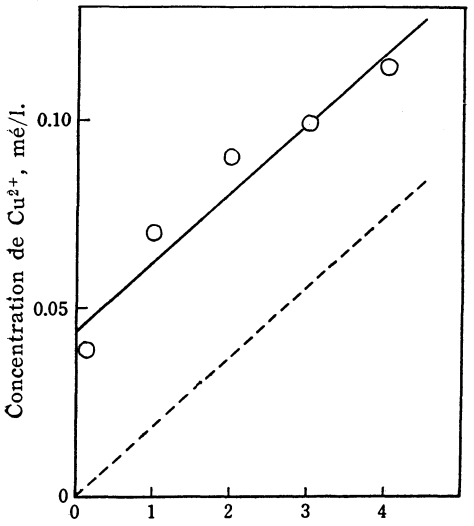
Aucune variation de pH n'a été trouvée pour les expériences effectuées en milieu acide 0,1 N et 0,01 N. Cependant on a remarqué l'abaissement du pH au cours du traitement dans l'acide 0,001 N et l'eau bidistillée. Dans le premier cas, le pH de la liqueur était de 3,0 avant l'addition du minerai, et de 2,8 après quatre heures du traitement. On discutera plus loin le dernier cas, dissolution du minerai par l'eau.

Composition de composants dissous. — La quantité de cuivre dissous étant très petite par rapport à celle de fer et de sulfate,

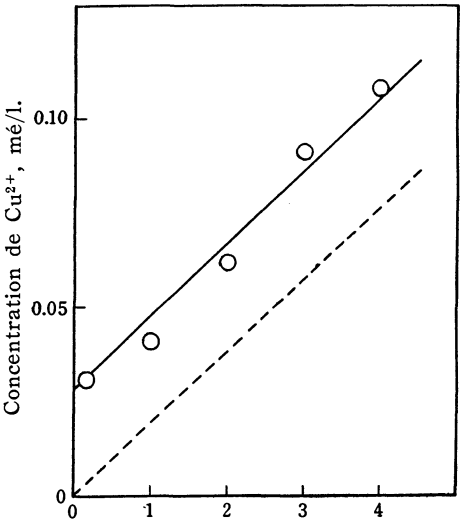
on étudie ici simplement la relation entre le fer et le sulfate. La concentration de fer trivalent ne dépassant pas quelques pourcents de celle de fer divalent, on ne prend pas non plus celui-là en considération. Comme l'indique la figure 1, le rapport de la quantité de fer divalent sur celle de sulfate est l'unité, tous deux étant produits par le traitement et exprimés en unité de mé. On voit bien que l'oxydation du minerai sulfuré par l'air donne le sulfate de fer(II). La présence du fer trivalent serait attribuable à l'oxydation du fer divalent sous forme duquel le fer contenu dans le minerai se dissout dans l'eau.

Si la réaction a lieu dans un milieu à pH relativement grand, le sulfate se dissout plus que le fer. Cela s'explique par la formation de l'acide sulfurique. Ce phénomène devient plus remarquable lors du traitement avec de l'eau bidistillée.

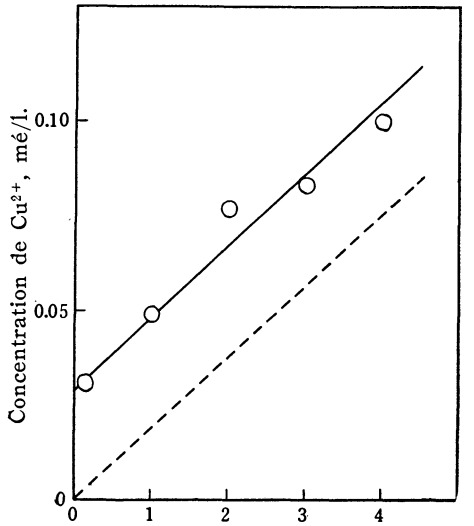
Dissolution du minerai par l'eau.—Le résultat de cet essai, considéré comme reproduction de la désagrégation du minerai sulfuré par les eaux naturelles de caractère normal, serait indispensable pour la connaissance des réactions qui ont lieu dans la nature. La dissolution du fer devient



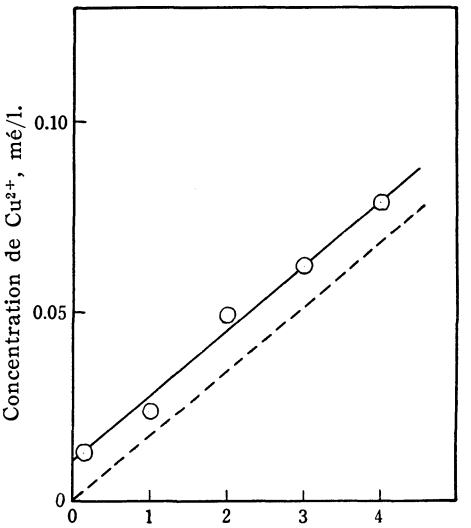
(a) HCl 0,1 N; Air 0 l./min.



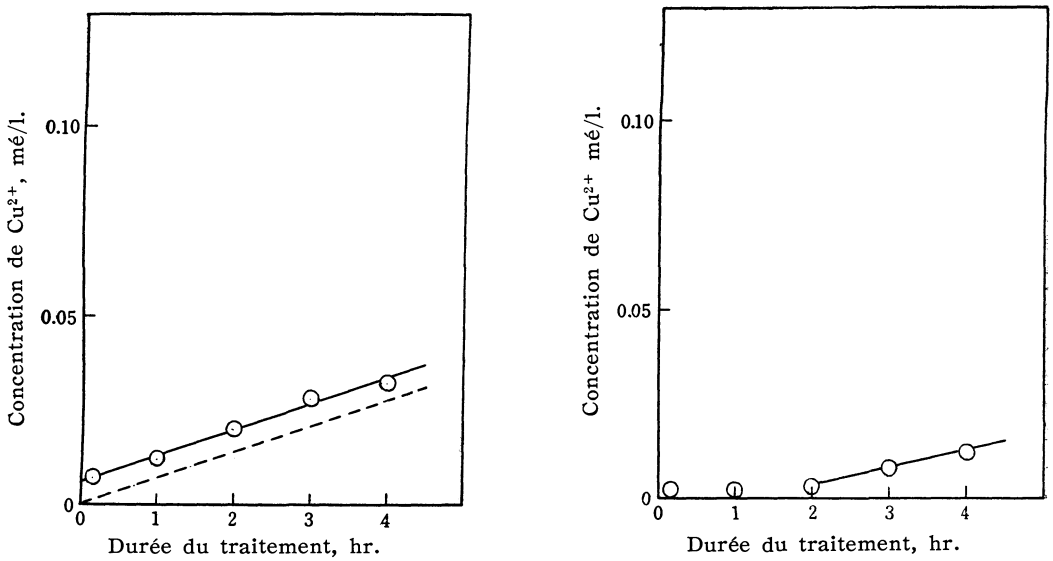
(b) HCl 0,1 N; Air 0,5 l./min.



(c) HCl 0,1 N; Air 1,5 l./min.



(d) HCl 0,01 N; Air 1,5 l./min.



(e) HCl 0,001 N; Air 1,5 l./min. (f) Eau bidistillée; Air 1,5 l./min.

Fig. 2. Dissolution du cuivre
Trait plein: concentration totale.
Trait discontinu: concentration correspondant à la dissolution par le traitement.

extrêmement petite, et on ne décèle presque pas de cuivre. Celle du sulfate, au contraire, s'accélère dans ce milieu.

Pourtant on n'arrive pas à différer si une faible concentration en fer est causée par la précipitation du fer hydrolysé ou par la prédominance de la réaction de formation de l'acide sulfurique.

La liqueur devient acide avec la durée du traitement, et au bout de quatre heures, le pH en est inférieur à 3. La dissolution du cuivre augmente avec l'abaissement du pH. Cette tendance est prévue par des essais décrits ci-dessus.

Comportements des composants.—*Cuivre.*—Le facteur règnant sur la dissolution du cuivre contenu dans le minerai sulfuré est vraisemblablement le pH du milieu. Dans un milieu à pH inférieur à 2, la vitesse de dissolution reste constante, indépendamment du pH. Elle est peu influencée par le débit de l'air introduit dans la liqueur.

Fer. — Le débit de l'air exerce une influence considérable sur la dissolution de ce métal. Le résultat des essais fait présumer que la pyrite est relativement stable, même en milieu acide, s'il s'agit des conditions non-oxydantes.

Soufre. — Cet élément se dissout sous forme de sulfate, en milieu acide ou neutre, et en présence de l'air. Sous ces conditions oxydantes, le sulfate est toujours le plus stable parmi les espèces de composés de soufre[3]. La vitesse de dissolution en est d'autant plus grande que le pH est grand, mais le mécanisme de la formation de l'acide sulfurique restera comme un problème à résoudre. Le comportement du soufre résiduel après la dissolution du sulfate de fer, $FeSO_4$, à partir de la pyrite, FeS_2, exigera une étude plus approfondie.

Les auteurs expriment leurs remerciements profonds à Monsieur le professeur K. Noguchi qui leur a permis l'exécution de cette étude et qui leur a accordé toutes les aides possibles, et à Monsieur le professeur T. Hanya qui a bien voulu leur donner des conseils utiles.

Laboratoire de Chimie, Faculté des Sciences
Université Métropolitaine de Tokyo
Setagaya-ku, Tokyo

3) R. M. Garrels et C. R. Naeser, ibid., 15, 113 (1958).

The Infrared Spectrum of Dimethyl Sulfone

By Kuniaki FUJIMORI

(Received June 5, 1959)

In the preceding paper[1] normal vibrations and force constants of the methanesulfonate ion were determined empirically. In this paper the infrared spectrum of dimethyl sulfone was measured, the normal vibrations of this molecule were calculated using force constants of the methanesulfonate ion, and they were compared with the experimental values.

Calculation of Normal Vibrations

The calculation was done by means of Wilson's method[2] and treated as a five-body problem assuming the methyl radical to be one particle. As the intramolecular potential, Urey-Bradley field[3] was assumed as done in the case of the methanesulfonate ion[1]. By assuming all the valence angles of sulfur to be tetrahedral, the following elements of G and F materices were obtained[4].

Elements of G matrix for A_1 type vibrations

$$g_{11}=\frac{2}{3}\mu_S+\mu_{Me}$$

$$g_{12}=-\frac{2}{3}\mu_S$$

$$g_{13}=\frac{2}{\sqrt{3}}(\sigma'-1)\mu_S$$

$$g_{14}=-\frac{\sqrt{8}}{3}(\sigma'+1)\mu_S$$

$$g_{22}=\frac{2}{3}\mu_S+\mu_O$$

$$g_{23}=-\frac{2}{\sqrt{3}}(\sigma'-1)\mu_S$$

$$g_{24}=\frac{\sqrt{8}}{3}(\sigma'+1)\mu_S$$

$$g_{33}=\frac{3}{2}(\sigma'^2\mu_{Me}+\mu_O)+2(\sigma'-1)^2\mu_S$$

$$g_{34}=-\frac{1}{\sqrt{6}}\{3(\sigma'^2\mu_{Me}-\mu_O)+4\sigma'(\sigma'-1)\mu_S\}$$

$$g_{44}=\sigma'^2\mu_{Me}+\mu_O+\frac{4}{3}(\sigma'+1)^2\mu_S$$

Elements of F matrix for A_1 type vibrations

$$f_{11}=K_{SMe}+2(s^2_{Me}F_{Me}+t^2_{MeO}F'_{MeO}+s^2_{MeO}F_{MeO})$$

$$f_{12}=-2(t_{MeO}t_{OMe}F'_{MeO}+s_{MeO}s_{OMe}F_{MeO})$$

$$f_{13}=\sqrt{\frac{2}{3}}\{(t_{MeO}s_{OMe}F'_{MeO}+t_{OMe}s_{MeO}F_{MeO})+\sigma t_{Me}s_{Me}(F'_{Me}+F_{Me})\}$$

$$f_{14}=\sigma t_{Me}s_{Me}(F'_{Me}+F_{Me})$$

$$f_{22}=K_{SO}+2(t^2_{OMe}F'_{MeO}+s^2_{OMe}F_{MeO}+s^2_OF_O)$$

$$f_{23}=\sqrt{\frac{2}{3}}(t_{OMe}s_{MeO}F'_{MeO}+t_{MeO}s_{OMe}F_{MeO})-t_Os_O(F'_O+F_O)\}$$

$$f_{24}=-t_Os_O(F'_O+F_O)$$

$$f_{33}=\frac{1}{3}\{\sigma^2(H_{Me}-s^2_{Me}F'_{Me}+t^2_{Me}F_{Me})+(H_O-s^2_OF'_O+t^2_OF_O)\}$$

$$f_{34}=\frac{1}{\sqrt{6}}\{-\sigma^2(H_{Me}-s^2_{Me}F'_{Me}+t^2_{Me}F_{Me})+(H_O-s^2_OF'_O+t^2_OF_O)\}$$

$$f_{44}=\frac{1}{2}\{\sigma^2(H_{Me}-s^2_{Me}F'_{Me}+t^2_{Me}F_{Me})+(H_O-s^2_OF'_O+t^2_OF_O)\}+\frac{3}{\sqrt{8}}\kappa/r^2_{SO}$$

Elements of G and F matrices for A_2 type vibration

$$g=\frac{3}{2}\sigma'^2\mu_{Me}+\frac{3}{2}\mu_O+\frac{1}{3}(5\sigma'^2+2\sigma'+5)\mu_S$$

$$f=\sigma(H_{MeO}-s_{MeO}s_{OMe}F'_{MeO}+t_{MeO}t_{OMe}F_{MeO})-\frac{1}{\sqrt{8}}\kappa/r^2_{SO}$$

Elements of G matrix for B_1 type vibrations

$$g_{11}=\frac{4}{3}\mu_S+\mu_{Me}$$

$$g_{12}=-\frac{2}{3}(\sigma'+3)\mu_S$$

$$g_{22}=\frac{1}{2}\sigma'^2\mu_{Me}+\frac{3}{2}\mu_O+\frac{1}{3}(\sigma'+3)^2\mu_S$$

1) K. Fujimori, This Bulletin, **32**, 621 (1959).
2) E. B. Wilson, *J. Chem. Phys.*, **7**, 1047 (1939); **9**, 76 (1941).
3) H. C. Urey and C. A. Bradley, *Phys. Rev.*, **38**, 1946 (1931).
4) T. Shimanouchi, *Bulletin Inst. Phys. Chem. Research, Tokyo (Riken Iho)*, **21**, 825 (1941).

Elements of F matrix for B_1 type vibrations

$$f_{11}=K_{SMe}+2(t^2_{Me}F'_{Me}+t^2_{MeO}F'_{MeO}+s^2_{MeO}F_{MeO})$$

$$f_{12}=\sqrt{2}\,(t_{MeO}s_{OMe}F'_{MeO}+t_{OMe}s_{MeO}F_{MeO})$$

$$f_{22}=\sigma(H_{MeO}-s_{OMe}s_{MeO}F'_{MeO}+t_{MeO}t_{OMe}F_{MeO})+\frac{3}{\sqrt{8}}\kappa/r^2_{SO}$$

Elements of G matrix for B_2 type vibrations

$$g_{11}=\frac{4}{3}\mu_S+\mu_O$$

$$g_{12}=-\frac{2}{3}(3\sigma'+1)\mu_S$$

$$g_{22}=\frac{3}{2}\sigma'^2\mu_{Me}+\frac{1}{2}\mu_O+\frac{1}{3}(3\sigma'+1)^2\mu_S$$

Elements of F matrix for B_2 type vibrations

$$f_{11}=K_{SO}+2(t^2_{OMe}F'_{MeO}+s^2_{OMe}F_{MeO}+t^2_{O}F'_{O})$$

$$f_{12}=\sqrt{2}\,\sigma(t_{OMe}s_{MeO}F'_{MeO}+t_{MeO}s_{OMe}F_{MeO})$$

$$f_{22}=\sigma(H_{MeO}-s_{OMe}s_{MeO}F'_{MeO}+t_{MeO}t_{OMe}F_{MeO})+\frac{3}{\sqrt{8}}\kappa/r^2_{SO}$$

where, K is the stretching force constant, H is the bending force constant and F and F' are repulsive force constants. And μ is the reciprocal of the atomic weight of sulfur, oxygen or the methyl radical.

The following notations are also used:

$$s_{ij}=(r_i-r_j\cos\alpha_{ij})/q_{ij},$$

$$s_{ji}=(r_i-r_j\cos\alpha_i)/q_{ij},\quad t_{ij}=r_j\sin\alpha_{ij}/q_{ij},$$

$$t_{ji}=r_i\sin\alpha_{ij}/q_{ij},\quad \sigma=r_{SMe}/r_{SO},\quad \sigma'=1/\sigma,$$

κ (intramolecular tension)

$$=-(K'_i r_{ij}^2+H'_{ij}r_{ij}q_{ij}\sqrt{t_{ij}t_{ji}}),$$

where r denotes S–O or S–Me bond length, q_{ij} denotes distance between non-bonded atoms, α_{ij} denotes valence angle and $r^2_{ij}=r_ir_j$.

For the S–O and S–Me bond length, the following values were assumed. S–O= 1.43 Å, S–Me=1.80 Å[5].

Force constants were transferred from methanesulfonate ion[1], diethyl sulfide[6], tetramethyl silane[7] and sulfur dioxide[8]. Their values are given in Table I.

TABLE I. FORCE CONSTANTS

F.C.	10^5 dyn./cm.	Ref.	F. C.	10^5 dyn./cm.	Ref.
K_{SMe}	3.05	1)	F'_{Me}	−0.020	7)
K_{SO}	9.86	8)	F_O	0.64	1)
H_{Me}	0.157	6)	F'_O	−0.064	1)
H_O	0.552	1)	F_{MeO}	0.35	1)
H_{MeO}	0.250	1)	F'_{MeO}	−0.035	1)
F_{Me}	0.200	7)	κ	0.328*	1)

* Unit is 10^{-11} dyn./cm.

Results and Discussion

The calculated normal vibrations are given in Table II. The infrared spectrum of dimethyl sulfone in a solid state is shown in Fig. 1. The absorption frequencies are compared with the observed values and their assignments are made as shown in Table III.

TABLE II. CALCULATED NORMAL VIBRATIONS (in cm^{-1})

Type	Wave number	Assignment
A_1	741	S-Me stretching
	314	$S(Me)_2$ bending
	1252	S-O stretching
	521	SO_2 bending
A_2	408	twisting
B_1	795	S-Me stretching
	472	$S(Me)_2$ rocking SO_2 wagging
B_2	1345	S-O stretching
	428	$S(Me)_2$ wagging SO_2 rocking

TABLE III. ABSORPTIONS AND ASSIGNMENTS (in cm^{-1})

Wave number	Assignment	Calcd.
3024 (m), 2962 (w)	C-H stretching	
1430 (m), 1412 (m)	CH_3 degenerated bending	
1337 (s)	CH_3 symmetric bending	
1315 (s), 1290 (s)	S-O stretching	1345
1130 (s)	S-O stretching	1252
938 (s)	Me rocking	
761 (s)	S-Me stretching	795
695 (m)	S-Me stretching	741

C-H stretching frequencies have higher wave numbers than those of hydrocarbons because of strong electronegativity of $-SO_2-$ group. This phenomenon was also found in the case of lower sulfonates[9]. Methyl rocking vibration at 938 cm^{-1} has lower wave number than that of methanesulfonate ion. The reason may be attributed to the coupling with S–O stretching vibration.

5) Chem. Soc. Japan, "Kagaku Binran" (Handbook of Chemistry), New Edition, Maruzen Co., Ltd., Tokyo (1958), p. 1027.
6) M. Hayashi, *J. Chem. Soc. Japan, Pure Chem. Sec.* (*Nippon Kagaku Zasshi*), **77**, 1692 (1956).
7) T. Shimanouchi, ibid., **74**, 226 (1953).
8) A. Simon and H. Kriegsmann, *Z. physik. Chem.*, **209**, 369 (1956).
9) K. Fujimori. This Bulletin, **32**, 850 (1959).

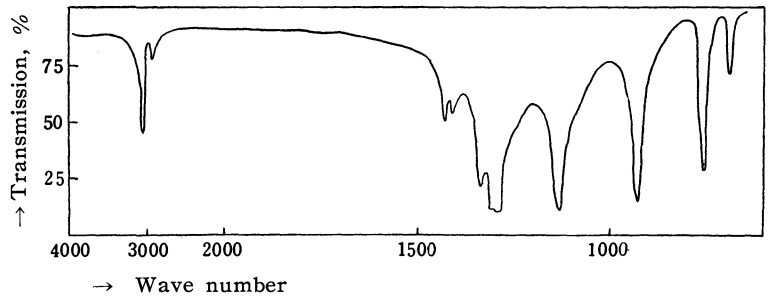


Fig. 1. Infrared spectrum of dimethyl sulfone.

The deviation between the observed and calculated frequencies may be attributed to the high value of S–O stretching force constant and the low value of O–O repulsive force constants.

Experimental

The infrared spectrum was obtained by a Perkin-Elmer Model 21 double-beam infrared spectrophotometer using NaCl prism. The KBr disk method was employed to obtain the spectrum in solid state.

Dimethyl sulfone was prepared by oxidation of dimethyl sulfoxide with hydrogen peroxide in acetic acid solution[10]. After the reaction mixture was treated with acetaldehyde and the solvent was removed, dimethyl sulfone was recrystallized from ethanol. The melting point of this compound is 108.5°C and the referenced value is 109°C[11].

The author wishes to express his indebtedness to Dr. A. Kotera, Professor of Tokyo University of Education, and Dr. T. Shimanouchi, Professor of the University of Tokyo, under whose kind direction this work was performed. The author also wishes to thank Mr. Y. Ikegami, Fellow of Tohoku University, for his co-operation in obtaining infrared spectrum, and to Mr. Y. Akai, Chief of Research Section of Funakawa Refinery, for his encouragement of this research.

Nippon Mining Co., Funakawa Refinery
Oga-shi, Akita

10) L. Fied and J. W. McFarland, *J. Am.. Chem. Soc.*, 75, 5582 (1953).

11) "Beilsteins Handbuch der Organischen Chemie", E. II 1, Julius Springer, Berlin (1941), p. 277.

The Kinetics of Substitution Reactions Involving Metal Complexes. II. Effect of Acetate Ions on the Reaction between Copper(II) and Lead-Ethylenediaminetetraacetate Complexes

By Nobuyuki TANAKA and Kiyoko KATO*

(Received July 3, 1959)

In the previous paper[1], the substitution reaction of copper(II) ions and lead-ethylenediaminetetraacetate(EDTA) complexes was reported. The rate of the reaction was followed by measuring the change of the polarographic diffusion current of copper(II) ions with time in acetate buffer solutions. The reaction was found to proceed, under the experimental conditions, simultaneously through three different reaction paths, and the rate constants of the elementary reactions of those reaction paths were determined.

Although the reaction rate was measured in acetate buffer solutions, the effect of acetate ion concentration was not taken into consideration, all measurements being

* Present address: The Women's Department, Tokyo College of Pharmacy, 31, Uenosakuragi-cho, Taito-ku, Tokyo.

1) N. Tanaka, K. Kato and R. Tamamushi, This Bulletin, 31, 283 (1958).

carried out at 0.1 M of acetate in concentration. Ackermann and Schwarzenbach[2] found that the overall reaction rate of the substitution reaction of copper(II) ions and cadmium-EDTA complexes increased with the decreasing concentration of acetate ions, but they gave no quantitative explanation of this phenomenon. The increase of the reaction rate with the decrease of the acetate ion concentration was also found by the present authors in the case of the substitution reaction of copper(II) ions and lead-EDTA complexes.

In this paper, the effect of acetate ions on the rate of the substitution reaction of copper(II) ions and lead-EDTA complexes is investigated. The experimental results reported in the previous paper[1] are treated on the basis of the formation of acetato complexes of metal ions in acetate media and on the assumption that the substitution reaction proceeds through the hydrated metal ions which are in equilibrium with the acetato complexes. The rate constants of the elementary reactions reported previously are recalculated with the equations newly derived.

Derivation of the Rate Equation

Let us consider the acetate buffer solution which contains copper(II) ions and lead-EDTA complexes. In the solution containing acetate ions less than 0.2 M in concentration, copper(II) and lead(II) form mono- and diacetato complexes[3]. Therefore, the overall substitution reaction is represented by the equations

$$Cu^{2+}+2\ OAc^- \rightleftarrows CuOAc^+ + OAc^- \rightleftarrows Cu(OAc)_2 \quad (1)$$

$$Cu^{2+}+PbY^{2-} \rightleftarrows CuY^{2-}+Pb^{2+} \quad (2)$$

$$Pb^{2+}+2\ OAc^- \rightleftarrows PbOAc^+ + OAc^- \rightleftarrows Pb(OAc)_2 \quad (3)$$

where Y^{4-} means a completely dissociated EDTA anion. Under the condition that lead ions and lead-EDTA complexes are present in a large excess over copper(II) ions, the substitution reaction 2 can be simplified to

$$Cu^{2+} \underset{k^-}{\overset{k^+}{\rightleftarrows}} CuY^{2-}$$

In the polarographic measurement in acetate media, it is impossible to determine separately either the concentration of hydrated copper(II) ions or that of acetato-copper(II) complexes. On the contrary, the diffusion current of copper(II) obtained in acetate media corresponds to the sum of the diffusion current of the hydrated copper(II) ions and that of the acetato-copper(II) complexes. In other words, the concentration that can be determined polarographically is $[Cu^{2+}]_{app}$ given by the equation[4]

$$[Cu^{2+}]_{app} = [Cu^{2+}] + [CuOAc^+] + [Cu(OAc)_2] \quad (5)$$

The rate equation for reaction 4, therefore, is expressed as

$$-\frac{d[Cu^{2+}]_{app}}{dt} = k^+[Cu^{2+}]_{app} - k^-[CuY^{2-}] \quad (6)$$

Integrating Eq. 6,

$$\ln\{[Cu^{2+}]_{app} - [Cu^{2+}]_{e,app}\} = -(k^+ + k^-)t + \ln\{[Cu^{2+}]_{0,app} - [Cu^{2+}]_{e,app}\}$$

is obtained. At the equilibrium of the reaction, the relation

$$\frac{k^+}{k^-} = \frac{[CuY^{2-}]_e}{[Cu^{2+}]_{e,app}} \doteqdot K^{Cu}_{Pb,app}\frac{[PbY^{2-}]_0}{[Pb^{2+}]_{0,app}}$$

may be satisfied, where $K^{Cu}_{Pb,app}$ represents the apparent equilibrium constant expressed as

$$K^{Cu}_{Pb,app} = \frac{[Pb^{2+}]_{e,app}[CuY^{2-}]_e}{[Cu^{2+}]_{e,app}[PbY^{2-}]_e}$$

Subscripts e and 0 mean equilibrium and zero time, respectively. The value of $K^{Cu}_{Pb,app}$ must be determined polarographically as the same concentration of acetate as the reaction rate is observed.

In the previous study[1], it was found that the substitution reaction between copper(II) and lead-EDTA complexes proceeds through the simultaneous reaction paths

$$\text{(i)}\quad Cu^{2+}+PbY^{2-} \underset{k_1^-}{\overset{k_1^+}{\rightleftarrows}} CuY^{2-}+Pb^{2+} \quad (7)$$

$$\text{(ii)}\quad PbY^{2-}+H^+ \rightleftarrows PbHY^- \quad (8a)$$

$$Cu^{2+}+PbHY^- \underset{k_{II}^-}{\overset{k_{II}^+}{\rightleftarrows}} CuHY^- + Pb^{2+} \quad (8b)$$

$$CuHY^- \rightleftarrows CuY^{2-}+H^+ \quad (8c)$$

$$\text{(iii)}\quad PbY^{2-}+H^+ \rightleftarrows Pb^{2+}+HY^{3-} \quad (9a)$$

$$Cu^{2+}+HY^{3-} \underset{k_{III}^-}{\overset{k_{III}^+}{\rightleftarrows}} CuY^{2-}+H^+ \quad (9b)$$

and the rate equation

2) H. Ackermann and G. Schwarzenbach, *Helv. Chim. Acta*, **35**, 485 (1952).

3) N. Tanaka and K. Kato, unpublished work.

4) Cf., N. Tanaka and K. Kato, This Bulletin, **32**, 516 (1959).

$$-\frac{d[Cu^{2+}]}{dt}=\left\{k_1^{+}+k_2^{+}[H^+]+k_3^{+}\frac{[H^+]}{[Pb^{2+}]}\right\}\times[Cu^{2+}][PbY^{2-}]-\left\{k_1^{-}+k_2^{-}[H^+]+k_3^{-}\frac{[H^+]}{[Pb^{2+}]}\right\}[Pb^{2+}][CuY^{2-}] \quad (10)$$

was derived, where

$$\left.\begin{aligned} k_2^{+}&=k_{II}^{+}K_{PbHY}^{H}, & k_2^{-}&=k_{II}^{-}K_{CuHY}^{H}\\ k_3^{+}&=k_{III}^{+}/(K_{PbY}K_{HY}), & k_3^{-}&=k_{III}^{-}\end{aligned}\right\} \quad (11)$$

As has been mentioned above, the concentration which was actually measured polarographically was not the concentration of hydrated copper(II) ions in Eq. 10, but the sum of the concentrations of hydrated ions and acetato complexes. If it is assumed that the substitution reaction proceeds through only the hydrated ions which are in equilibrium with the acetato complexes, the apparent rate of the reaction ($=-d[Cu^{2+}]_{app}/dt$) which is determined polarographically is expressed as

$$-\frac{d[Cu^{2+}]_{app}}{dt}=\left\{k_1^{+}+k_2^{+}[H^+]+k_3^{+}\frac{[H^+]}{[Pb^{2+}]}\right\}\times[Cu^{2+}][PbY^{2-}]-\left\{k_1^{-}+k_2^{-}[H^+]+k_3^{-}\frac{[H^+]}{[Pb^{2+}]}\right\}[Pb^{2+}][CuY^{2-}] \quad (12)$$

From Eq. 5, the concentration of the hydrated copper(II) ions is given as

$$[Cu^{2+}]=\frac{[Cu^{2+}]_{app}}{1+\sum_{n=1}^{2}K_{Cu(OAc)_n}[OAc^-]^n} \quad (13)$$

where $K_{Cu(OAc)_n}$ represents the overall formation constant of acetatocopper(II) complexes expressed with

$$K_{Cu(OAc)_n}=\frac{[Cu(OAc)_n^{(2-n)+}]}{[Cu^{2+}][OAc^-]^n}$$

Similarly the concentration of the hydrated lead(II) ions is given as

$$[Pb^{2+}]=\frac{[Pb^{2+}]_{app}}{1+\sum_{n=1}^{2}K_{Pb(OAc)_n}[OAc^-]^n}$$

where $K_{Pb(OAc)_n}$ means the overall formation constant of acetatolead(II) complexes.

Introducing Eqs. 13 and 14 into Eq. 12, Eq. 15 is obtained. Eq. 15 is now considered to be a general formula which expresses the rate of the substitution reaction between copper(II) and lead-EDTA complexes in acetate media.

Determination of the Rate Constants

From Eqs. 6 and 15, the relations given by Eqs. 16 and 17 are obtained, where the initial concentrations, $[Pb^{2+}]_0$ and $[PbY^{2-}]_0$, are substituted for $[Pb^{2+}]$ and $[PbY^{2-}]$, respectively. Since both $[Pb^{2+}]$ and $[PbY^{2-}]$ are present in the reaction mixture in a large excess over the concentration of copper(II), the changes of their concentrations during the reaction can be neglected.

$$-\frac{d[Cu^{2+}]_{app}}{dt}=\left\{\frac{k_1^{+}+k_2^{+}[H^+]+k_3^{+}[H^+]\dfrac{1+\sum_{n=1}^{2}K_{Pb(OAc)_n}[OAc^-]^n}{[Pb^{2+}]_{app}}}{1+\sum_{n=1}^{2}K_{Cu(OAc)_n}[OAc^-]^n}\right\}[Cu^{2+}]_{app}[PbY^{2-}]-\left\{\frac{k_1^{-}+k_2^{-}[H^+]+k_3^{-}[H^+]\dfrac{1+\sum_{n=1}^{2}K_{Pb(OAc)_n}[OAc^-]^n}{[Pb^{2+}]_{app}}}{1+\sum_{n=1}^{2}K_{Pb(OAc)_n}[OAc^-]^n}\right\}[Pb^{2+}]_{app}[CuY^{2-}] \quad (15)$$

$$\frac{k^{+}}{[PbY^{2-}]_0}\equiv\frac{k_1^{+}+k_2^{+}[H^+]+k_3^{+}[H^+]\dfrac{1+\sum_{n=1}^{2}K_{Pb(OAc)_n}[OAc^-]^n}{[Pb^{2+}]_{0,app}}}{1+\sum_{n=1}^{2}K_{Cu(OAc)_n}[OAc^-]^n} \quad (16)$$

$$\frac{k^{-}}{[Pb^{2+}]_{0,app}}\equiv\frac{k_1^{-}+k_2^{-}[H^+]+k_3^{-}[H^+]\dfrac{1+\sum_{n=1}^{2}K_{Pb(OAc)_n}[OAc^-]^n}{[Pb^{2+}]_{0,app}}}{1+\sum_{n=1}^{2}K_{Pb(OAc)_n}[OAc^-]^n} \quad (17)$$

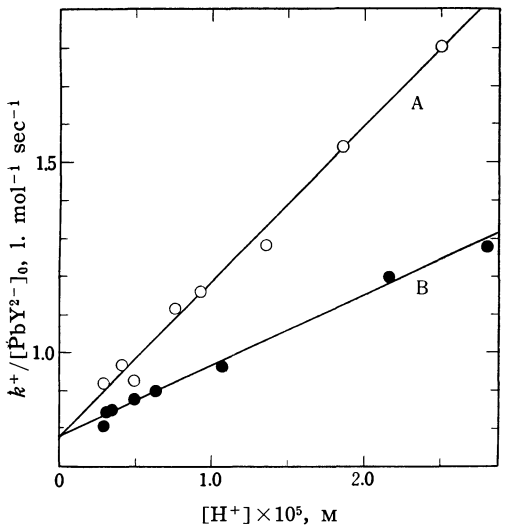


Fig. 1. $k^+/[PbY^{2-}]_0$ as a function of the hydrogen ion concentration in acetate buffer—potassium nitrate solutions of ionic strength 0.2 at 25°C. Initial concentrations are: $[Cu^{2+}]_{0,app}=1.86\times10^{-4}$ M; $[PbY^{2-}]_0=4.05\times10^{-3}$ M; $[Pb^{2+}]_{0,app}=3.95\times10^{-3}$ M (curve A) and 9.97×10^{-3} M (curve B). Concentratrations of free acetate are: 0.095 M(A) and 0.088 M (B).

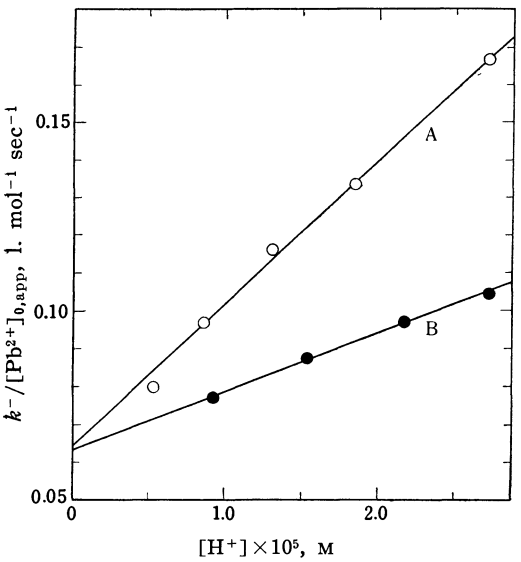


Fig. 2. $k^-/[Pb^{2+}]_{0,app}$ as a function of the hydrogen ion concentration in acetate buffer—potassium nitrate solutions of ionic strength 0.2 at 25°C. Initial concentrations are: $[CuY^{2-}]_0=4.65\times10^{-4}$ M; $[PbY^{2-}]_0=4.05\times10^{-3}$ M; $[Pb^{2+}]_{0,app}=3.95\times10^{-3}$ M (curve A) and 9.97×10^{-3} M (curve B). Concentrations of free acetate are: 0.095 M (A) and 0.088 M (B).

The experimental results which were reported in the previous paper[1] were utilized for the calculation of the rate constants in Eq. 15. The relations of $k^+/[PbY^{2-}]_0$ vs. $[H^+]$ and $k^-/[Pb^{2+}]_{0,app}$ vs. $[H^+]$ are plotted in Figs. 1 and 2. The values of the rate constants calculated are given in Table I. The formation constants of acetatocopper(II) and acetatolead(II) complexes which were used in the calculation are those which were determined polarographically at ionic strength 0.2 at 15, 25 and 35°C[3]. They are given in Table II. The concentration of uncomplexed acetate in the solution was calculated by successive approximation.

The rate constants of both elementary reactions 8b and 9b can be calculated from the relations given in Eqs. 11, using the values of K^{H}_{PbHY}, K_{PbY} and K_{HY} which are given in Table III. The values of K_{PbY} at 15, 25 and 35°C were obtained by dividing the values of K_{CuY} by those of K^{Cu}_{Pb}. The

Table I. Rate constants in Eq. 15 obtained experimentally at ionic strength 0.2 at various temperatures

Temp., °C	Rate constant, l. mol^{-1} sec^{-1}					
	k_1^+	k_2^+	k_3^+	k_1^-	k_2^-	k_3^-
15	1.7	6×10^3	18			
25	5.1	3×10^4	58	1.0	3×10^3	14
35	17	1.5×10^5	160			

Table II. Formation constants of acetato complexes of copper(II) and lead(II) at ionic strength 0.2 at various temperatures

Temp., °C	K_{CuOAc}	$K_{Cu(OAc)_2}$	K_{PbOAc}	$K_{Pb(OAc)_2}$
15	41	190	130	750
25	52	93	130	390
35	69	82	120	380

Table III. Equilibrium constants at ionic strength 0.2 at various temperatures

Temp., °C	log K_{PbY}	pK_{HY}	log K^{H}_{PbHY}
15	18.17	10.20	—
20	—	—	2.7
25	17.76	10.04	—
35	17.36	9.91	—

Table IV. Rate constants for reactions 7, 8b and 9b at ionic strength 0.2 at various temperatures

Temp., °C	Rate constant, l. mol^{-1} sec^{-1}		
	k_1^+	k_{II}^+	k_{III}^+
15	1.7	10	1.7×10^9
25	5.1	60	3.0×10^9
35	17	300	4.5×10^9

TABLE V. RATE CONSTANTS, HEAT OF ACTIVATION AND ENTROPY OF ACTIVATION FOR REACTIONS 7, 8b AND 9b

Reaction	Rate constant, expressed in l. mol^{-1} sec^{-1}	$\Delta H^{\ddagger}$, kcal. mol^{-1}	$\Delta S^{\ddagger}$, e. u.
$Cu^{2+}+PbY^{2-} \rightarrow CuY^{2-}+Pb^{2+}$	$k_1^+=2.7\times10^{15}\ \exp(-20{,}000/\boldsymbol{RT})$	19	10
$Cu^{2+}+PbHY^{-} \rightarrow CuHY^{-}+Pb^{2+}$	$k_{II}^+=2.5\times10^{22}\ \exp(-28{,}000/\boldsymbol{RT})$	27	42
$Cu^{2+}+HY^{3-} \rightarrow CuY^{2-}+H^+$	$k_{III}^+=3.2\times10^{15}\ \exp(-\ 8{,}200/\boldsymbol{RT})$	7.6	10

formation constants of CuY^{2-}, K_{CuY}, at 15, 25 and 35°C at ionic strength 0.2 were calculated, from the value obtained by Schwarzenbach et al.[5] at 20°C at ionic strength 0.1, with the aid of the Debye-Hückel equation and the heat of formation of CuY^{2-}, −8.2 kcal./mol., reported by Charles[6]. The equilibrium constants of reaction 2 at zero acetate concentration, K_{Pb}^{Cu}, used in this calculation are those determined by the present authors[3]. The rate constants of three elementary reactions 7, 8b and 9b thus calculated are summarized in Table IV.

Discussion

Linear relations were found between the logarithm of rate constant and the reciprocal of absolute temperature for three elementary reactions 7, 8b and 9b.

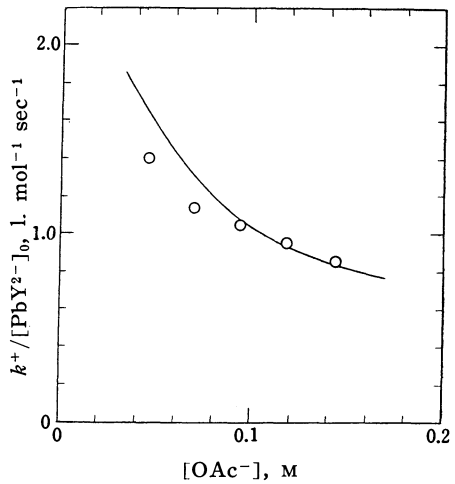


Fig. 3. $k^+/[PbY^{2-}]_0$ as a function of the acetate concentration in acetate buffer—potassium nitrate solutions of pH 5.14 and ionic strength 0.2 at 25°C. Initial concentrations are: $[Cu^{2+}]_{0,app}=1.96\times10^{-4}$ M; $[PbY^{2-}]_0=4.90\times10^{-3}$ M; $[Pb^{2+}]_{0,app}=4.90\times10^{-3}$ M. — indicates the theoretical curve and ○, the experimental value.

5) G. Schwarzenbach, R. Gut and G. Anderegg, *Helv. Chim. Acta*, **37**, 937 (1954).
6) R. G. Charles, *J. Am. Chem. Soc.*, **76**, 5854 (1954).

This made it possible to express the rate constants in the form of the Arrhenius equation and to calculate the heat of activation and the entropy of activation. The results are given in Table V.

From Eq. 15, it is predicted that the reaction rate decreases with the increase of acetate concentration. Using Eq. 16, the values of $k^+/[PbY^{2-}]_0$ were calculated at various acetate concentrations with the rate constants given in Table I and the formation constants of the acetato complexes. They are plotted against acetate concentration as shown in Fig. 3. The reaction rates were experimentally measured at various acetate concentrations, keeping the other conditions constant, with the same procedure as given in the previous paper[1]. Those values are also shown in Fig. 3, which are in fair agreement with the calculated ones. The deviation of the expermental values from the calculated ones is apparent at lower acetate concentration. This has not been clearly understood, but is considered to be due to a contribution of the reactions in which acetatocopper(II) complexes participate.

Summary

The effect of acetate ions on the rate of the substitution reaction of copper(II) and lead-EDTA complexes is explained quantitatively on the basis of the formation of acetato complexes of copper(II) and lead(II) in acetate media and on the assumption that the substitution reaction proceeds only through the hydrated metal ions. The rate constants, the heats of activation and the entropies of activation for three elementary reactions are recalculated with the experimental results obtained previously.

The authors thank the Ministry of Education for the financial support granted for this research.

Department of Chemistry
Faculty of Science
Tohoku University
Katahira-cho, Sendai

SHORT COMMUNICATIONS

Infrared Spectra of Glycols Coordinated to Metal Ions

By Akihisa MIYAKE

(Received October 12, 1959)

Ethylene glycol has received attention in discussion of the infrared spectrum of polyethylene glycol[1]. Certain problems with regard to the rotational isomerism of this molecule still remain to be solved. It has been known that ethylene glycol forms coordination compound with cobalt or nickel ion[2]. In an attempt to provide some new information on the vibrational assignments for this molecule, the infrared spectra of these coordination complexes were investigated.

Cobalt(II) chloride or nickel(II) chloride was dehydrated by heating at about 150°C. The coordination complexes were prepared by adding ethylene glycol to these dehydrated salts. There is a marked spectral difference between the free molecule and the molecule coordinated about a metal ion (Fig. 1). The coordinated ligand shows two kinds of spectra according to the water content of the dehydrated salts, both for cobalt and nickel. When the water contents of the salts exceed a value of about 15%, the complexes obtained from them (complex I) exhibit the spectrum shown in Fig. 1B. When the water contents are lower than this value, the complexes obtained (complex II) exhibit the spectrum shown in Fig. 1C. On the other hand, there is no difference between the cobalt and nickel complexes.

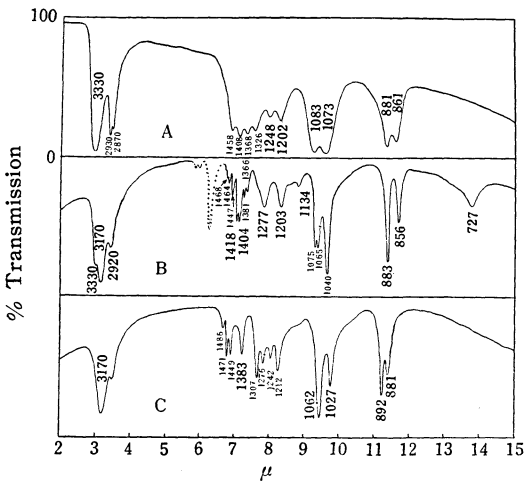


Fig. 1. Infrared spectra of ethylene glycol: (A) Liquid, (B) (C) metal complex (Nujol and polytrifluoroethylene mull, ---- water).

Two bands at 881 and 861 cm^{-1} in liquid ethylene glycol are undoubtedly assigned to the CH_2 rocking vibrations, because no other fundamental vibrations are expected in this region. The appearance of two CH_2 rocking bands indicates that ethylene glycol is present in the *gauche* form, because two CH_2 rocking bands (A and B types) are expected for the *gauche* form but only one (A_u type) for the *trans* form. The other CH_2 rocking vibration (B_g type) of the *trans* form is forbidden to appear in an infrared spectrum. An alternative interpretation is possible, however, assuming that two vibrations coalesce into a single band. In this way Kuroda and Kubo[1] have assigned the band at 881 cm^{-1} to the *gauche* form and the band at 861 cm^{-1} to the *trans* form, considering that the two *gauche* vibrations overlap. Experimental results obtained in the present work provide data as to which one of these contradictory interpretations is more reasonable.

The number of absorption bands observed in the spectra of the complexes is a little larger than that observed for the liquid state. This indicates that the number of molecular forms present in the complex is at least not smaller than that present in the liquid. Thus, if the *trans* and *gauche* forms coexist in the liquid, they must also coexist in the complexes. Then the bands at 887 cm^{-1} (complex I) and 892 cm^{-1} (complex II) must be assigned to the *gauche* form, and the bands at

1) Y. Kuroda and M. Kubo, *J. Polymer Sci.*, **26**, 323 (1957).
2) A. Grün and E. Boedecker, *Ber.*, **43**, 1051 (1910).

856 cm^{-1} (complex I) and 881 cm^{-1} (complex II) to the *trans* form. Relative intensities of these two bands attributed to different molecular forms do not change appreciably through the three states, liquid, complex I and complex II. Therefore, the assignment based on the coexistence of both *trans* and *gauche* forms leads to a very improbable conclusion that the equilibrium ratio of the two kinds of molecular form and hence the energy difference between them do not change through the three different states.

All the bands change their positions more or less on going from liquid to complex I and from complex I to complex II, indicating that some small differences in the molecular form are present among the three states. If the band at 881 cm^{-1} in liquid ethylene glycol is composed of two *gauche* vibrations, it is reasonably expected that these two separate from each other in the complexes because the CH_2 rocking frequencies are particularly sensitive to conformation[3]. Although the bands of the complexes at 887 and 892 cm^{-1} are much sharper than the band of the liquid at 881 cm^{-1}, there is no indication of such a separation. It is too accidental that the two *gauche* frequencies coincide through the three states.

From these considerations it is more reasonable to assign both the CH_2 rocking bands to the *gauche* form than to assign one of them to the *gauche* and the other to the *trans* form. The presence of only the *gauche* form is sufficient to account for the number of observed bands in the region 1500~800 cm^{-1}, ten for the liquid, fifteen for complex I, and thirteen for complex II. The number of fundamental frequencies expected to appear in this range are thirteen for the *gauche* form and six for the *trans* form.

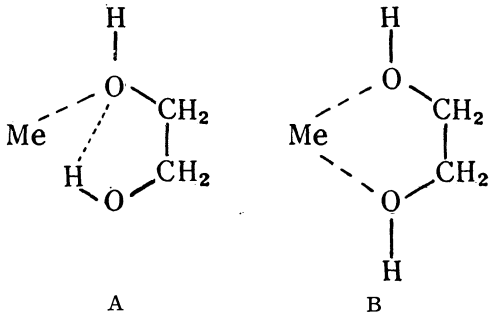


Fig. 2. Two types of coordination.

3) I. Nakagawa and S. Mizushima, This Bulletin, 28, 589 (1955).

The ligand in complex I can be considered to coordinate in a manner shown in Fig. 2A. This is based on the existence of two OH bands (3330 and 3170 cm^{-1}) indicating the presence of two kinds of OH groups. [The OH frequencies of the coexisting water are higher (ca. 3400 cm^{-1}) even if they appear.] The ligand in complex II shows a single OH band and probably coordinates in a manner shown in Fig. 2B. Spectral features of the liquid ethylene glycol, especially the positions of the CH_2 rocking frequencies, are more close to those of complex I than to those of complex II. Thus one of the OH groups of ethylene glycol molecule seems to form an intramolecular hydrogen bond in the liquid state.

Besides ethylene glycol, diethylene glycol and triethylene glycol were also investigated. Again, there are significant changes of the spectra on passing from

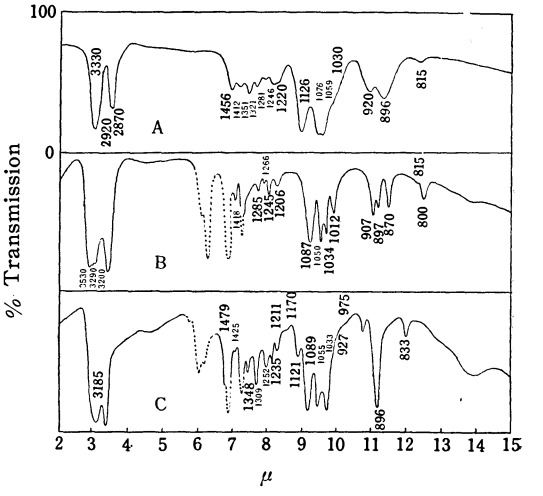


Fig. 3. Infrared spectra of diethylene glycol: (A) Liquid, (B) cobalt complex, (C) nickel complex (Nujol mull, ---- water and Nujol).

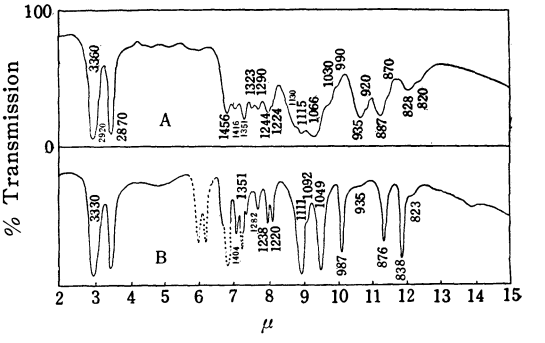


Fig. 4. Infrared spectra of triethylene glycol: (A) Liquid, (B) metal complex (Nujol mull, ---- water and Nujol).

liquid to complex compound. In the case of triethylene glycol, there is no difference between the spectra of nickel and cobalt complexes. On the other hand, in the case of diethylene glycol, the spectrum of the nickel complex differs profoundly from that of the cobalt complex (Fig. 3).

Central Research Laboratories
Toyo Rayon Co.
Otsu, Shiga

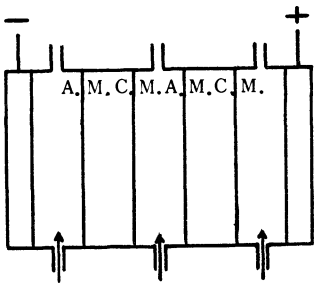


Fig. 1. Five compartment cell for electrodialysis.
C. M., cation exchange membrane
A. M., anion exchange membrane

Permeability of Amino Acid across Ion Exchange Membranes

By Takeo YAMABE, Manabu SENŌ and Nobuharu TAKAI

(Received October 17, 1959)

The bulk of experimental work[1] has published on the separation of amino acids by ion exchange resins and a few studies[2], which dealt with electro-chemical desalting of amino acid solution using ion exchange membranes, have recently been presented. These electrodialyses of amino acids using ion exchange membranes were carried out in the range of pH higher than the isoelectric point of the amino acids and deep concerns were not paid for hydrogen ion concentration of sample solution by these authors. Since the charge carried by an ion of amino acid in its aqueous solution is greatly affected by pH of the medium, it is natural to expect that pH of sample solution is one of the greatest factors in the electrodialysis operation of amino acid.

In the present study, permeability of amino acid across ion exchange membranes was examined in the whole range of pH and some interesting results were found.

The apparatus consisted mainly of five-compartment cell which is shown shematically in Fig. 1. Into the center compartment, 0.05 N aqueous solution of glutamic acid containing sodium chloride (0.1 N), whose pH was adjusted with hydrochloric acid or sodium hydroxide beforehand, was fed at the flow-rate of 500 ml./hr. The two adjacent compartments, which are filled with 0.1 N sodium chloride, are separated from the center compartment by cation and anion exchange membranes, respectively. Amino acid transferred across each of these ion exchange membranes was measured.

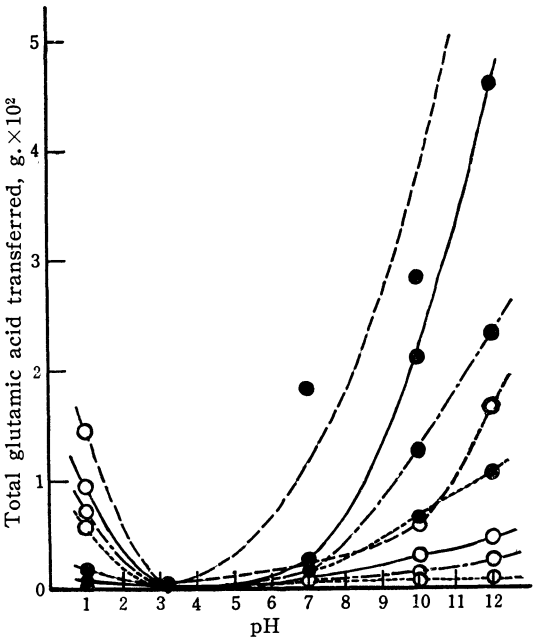


Fig. 2. Relation between pH and permeation of glutamic acid across ion exchange membranes.
○ permeation across cation exchange membrane
● permeation across anion exchange membrane
---------- 0.2×10^{-2} amp./cm²
—·—·— 0.5 〃
———— 1.0 〃
———— 2.0 〃

1) C. Calmon and T. R. E. Kressman, "Ion Exchangers in Organic and Biochemistry", Interscience Publishers, Inc., New York (1957).
2) J. D. Blainey and H. J. Yardley, *Nature*, **177**, 83 (1956); A. T. Di Benedetto and E. N. Lightfoot, *Ind. Eng. Chem.*, **50**, 691 (1958); A. M. Peers, *J. Appl. Chem.*, 8, 59 (1958).

All the electrodialysis experiments were carried out for one hour at four fixed current densities. Ion exchange membranes used are heterogeneous and strongly dissociated ones are prepared in the authors' laboratory.

The results were given in Fig. 2. As seen in this figure, the permeability of amino acid depends greatly on the pH of medium and it is the lowest at the isoelectric point, pI 3.2, of glutamic acid. In the range of pH higher than pI, the larger parts of glutamic acid migrate through the anion exchange membrane to the anode-side and the permeation across the cation exchange membrane is predominant in the lower pH range. This behavior becomes more remarkable with the rise of current density. This result is reasonable in view of amphoteric nature of amino acid.

It must be pointed out that some parts of amino acid migrate in the direction unexpected and some amounts of amino acid permeate across the anion and the cation exchange membranes at the isoelectric point. It appears that both positively and negatively charged molecules of amino acid may exist in the moderate pH range, since it is clear that such a permeation of amino acid does not always take place only by the simple diffusion process through membranes as revealed by the experimental data when no electric current runs*. Further investigation must be done on this behavior.

The similar results were also obtained concerning the electro-chemical permeation of glycine and lysine. The full data will be presented in the near future.

From these results, the optimum pH in the separation of amino acids and the demineralization of amino acid solution by ion exchange membranes may be predicted. These experiments are now under study.

Institute of Industrial Science
The University of Tokyo
Yayoi-cho, Chiba

* When no electric current is passed, the total amounts of glutamic acid transferred across ion exchange membranes are as follows:

pH	Total amounts of glutamic acid transferred across A. M.	C. M.
1.0	0	15.1×10^{-4} g.
3.2	0	0
12.0	95×10^{-4} g.	0

Absorption Spectra of 1,4-Diaminoanthraquinone in Mixed Solvents of Carbon Tetrachloride and Ethyl Alcohol

By Yoshio SUDA

(Received October 21, 1959)

It was previously discussed by Arban[1,2] that the absorption spectra of methylene blue in mixed solvents of water and organic solvents showed characteristic shifts which might be attributed to the change in aggregation states of the dye ion in the mixed solvents.

In this paper, characteristic changes in spectra of 1,4-diaminoanthraquinone (DAA) in mixed solvents are reported. The spectra were measured by means of a Hitachi recording spectrophotometer model EPR and all the measurements were carried out with the 1.0×10^{-4} mol./l. solution of DAA. As shown in Fig. 1, the spectrum of DAA in carbon tetrachloride has one absorption peak I at

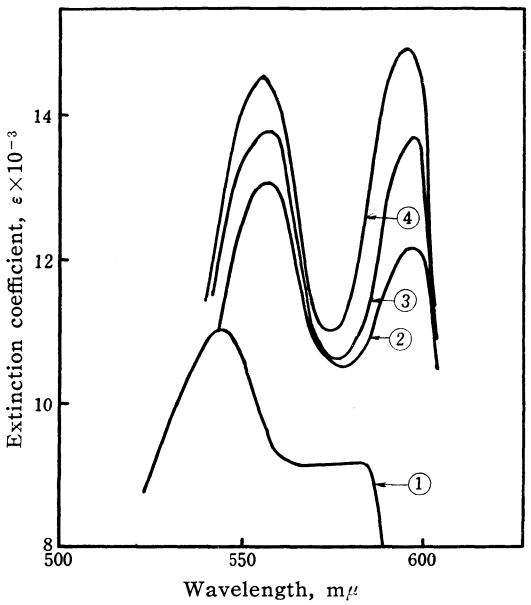


Fig. 1. Absorption spectra of 1,4-diaminoanthraquinone in mixed solvents; in CCl_4 ①, in CCl_4 80%: C_2H_5OH 20% ②, in CCl_4 40%: C_2H_5OH 60% ③, and in C_2H_5OH ④.

1) Kh. L. Arban, *Izves. Acad. Nauk USSR, Series Phys.*, **22**, 443 (1956).
2) Kh. L. Arban and N. V. Ivanova, *Doklady Acad. Nauk USSR*, **114**, 1043 (1957).

544 mμ and one horizontal shoulder at 565~584 mμ. On addition of ethanol to the solution, the latter changes to the second peak II, and simultaneously a shift of the peak location occurs. With the increasing ethanol concentration, the extinction coefficient at peak II increases rapidly as compared with that at peak I, and consequently, the ratio of both coefficients $r=\varepsilon_{II}/\varepsilon_{I}$ increases. The spectral data of DAA in various organic solvents are given in Table I. Solvents which belong to the first group are non-polar and the spectra in these solvents show one maximum and one shoulder, and a small value of r. In contrast to this, the spectra in solvents of the second group which are polar and have hydrogen-bonding ability, show the two absorption peaks and a large value of r.

TABLE I. ABSORPTION SPECTRA DAA IN VARIOUS SOLVENTS

Solvents	Refractive Index	Absorption peak I mμ	r
The first group			
n-Hexane	1.38	534	0.83
Cyclohexane	1.43	539	0.82
Carbon tetrachloride	1.46	544	0.83
Benzene	1.50	545	0.85
The second group			
Methanol	1.33	551	0.98
Ethanol	1.36	554	1.03
Acetic acid	1.37	552	1.03
Glycerine	1.47	557	1.05
Pyridine	1.51	558	0.94

An addition of ethanol to pure solvent exerts another effect on the spectrum. When the concentration of ethanol is increased, the location of the peak shifts to longer wavelengths at first and via the point of the maximum shift return back to shorter wavelengths. Similar shifts are also observed with methanol and others. As examples, absorption curves in mixed solvents of carbon tetrachloride with methanol and ethanol are shown in Fig. 2.

This characteristic change can not be explained by the simple solvent-effect (Kundt's law) alone, because the law says only that the larger the refractive index of solvent is, the larger the degree of shift to longer wavelengths becomes. DAA satisfies Beer's law both in ethanol and in carbon tetrachloride, and disperses as the monomer or a uniformly aggregated

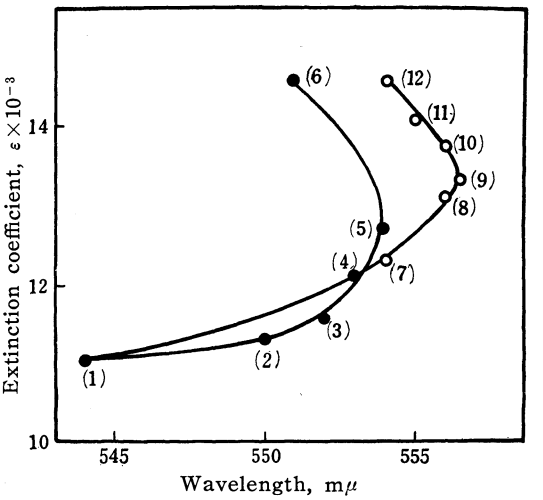


Fig. 2. Effects of solvent composition on wavelength and extinction coefficient at peak I.
—●— CH_3OH-HCl_4 mixtures
(1) 0 : 100, (2) 4 : 96, (3) 8 : 92
(4) 20 : 80, (5) 40 : 60 (6) 100 : 0
—○— C_2H_5OH-CCl_4 mixtures
(1) 0 : 100, (7) 6 : 94, (8) 20 : 80
(9) 40 : 60, (10) 60 : 40, (11) 80 : 20
(12) 100 : 0

particle. Arban's suggestion for methylene blue does not explain the case of DAA, if it can be assumed that dispersed particles are monomers in both solutions.

Spectral differences such as a number of peaks, the ratio of extinction coefficients and characteristic changes of locations of peaks indicate that mutual interaction between DAA and carbon tetrachloride (the first group) differs from that between DAA and ethanol (the second group). The essential difference in the interaction has been studied by the present author from the view points of solubility. The detailed discussion on the results will be reproted elsewhere.

The author wishes to express his sincere thanks to Mr. H. Uedaira for helpful discussion and for a gift of copies of Arban's papers.

The Textile Research Institute of Japanese Government Kanagawa-ku, Yokohama

Detection of Atomic Oxygen in the Decomposition Products of Nitrous Oxide by the Platinum Catalyst at Low Pressures

By Kazuo MITANI and Yoshio HARANŌ

(Received November 4, 1959)

Nitrous oxide is decomposed by platinum catalyst into oxygen and nitrogen. It is generally accepted that the first step of this reaction is $N_2O \rightarrow N_2+O$; and that the nitrogen is given off from the surface, while the oxygen atom remains adsorbed. The authors have investigated to find whether this oxygen atom is given off in the atomic state into the gas phase at low pressures.

The main part of the apparatus is shown in Fig. 1.

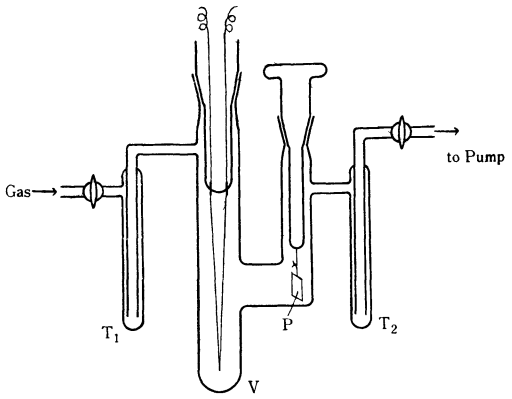


Fig. 1.

In the reaction vessel V, a platinum ribbon ($0.024\times0.28\times363$ mm.) is stretched, which can be heated by electric current. Atomic oxygen is detected by the change of color of molybdenum trioxide from pale yellow to deep blue according to the following equation[1]:

$$3\,MoO_3+O=Mo_3O_8+O_2$$

Molybdenum trioxide is deposited on a glass plate P, which is hung in the side tube of the reaction vessel. All the apparatus can be evacuated by a diffusion pump through a trap cooled by dry ice.

After decomposing nitrous oxide, it was found that atomic oxygen is given off from the platinum surface heated in vacuo for a long time[2]. Therefore, the following preliminary treatment of the platinum ribbon is necessary before every experiment. The platinum ribbon is heated in hydrogen first, and then in vacuo, to a high temperature. Subsequently oxygen is admitted, and the ribbon is heated again. Finally the ribbon is heated once more in vacuo to 1400°C for an hour. After this treatment, the platinum ribbon does not give off atomic oxygen. Now, nitrous oxide is conducted from the reservoir to the pump through the reaction vessel, the pressure in the reaction vessel being kept at $1\times10^{-3}\sim5\times10^{-4}$ mmHg. When the platinum ribbon is heated to 1400°C, molybdenum trioxide changes its color distinctly from plale yellow to deep blue within 30 min. From this experiment it is certain that atomic oxygen is given off when nitrous oxide is decomposed by the platinum catalyst at low pressures. When the pressure of nitrous oxide is higher (0.1~0.03 mmHg), no atomic oxygen is detected in a similar experiment. In the latter experiment, oxygen atoms given off from the platinum surface may recombine to form molecular oxygen before reaching the detector of atomic oxygen. But it is also probable that nitrous oxide molecules collide from the gas phase to the adsorbed oxygen atoms very frequently when the pressure of nitrous oxide is higher, and that consequently adsorbed oxygen atoms are given off as molecular oxygen according to the following reaction:

$$O_{ads}+N_2O \rightarrow N_2+O_2$$

In order to decide which mechanism is true, further investigations are necessary.

Institute of Chemistry
Kyoto Prefectural University of Medicine
Taishōgun, Kita-ku, Kyoto

1) W. H. Rodebush and W. A. Nichols, *J. Am. Chem. Soc.*, **52**, 3864 (1930).

2) A detailed report will be published in the near future.

Electrometric Estimation of Bismuth

By V. D. Anand, B. N. Prasad and Aqil Ahmed Amani

(Received June 8, 1959)

Thiourea and its derivatives, which are good sulfur coordinators[1], have been used for the detection and determination of a number of ions. Bismuth ion forms a yellow compound on the addition of thiourea[2]. Recently an electrometric study of the bismuth complexes with thiourea and substituted thioureas employing the bimetallic electrode system has been communicated by the anthors' laboratories[3]. During the course of this work it was observed that the method can be easily adopted for the quantitative determination of bismuth. The present communication reports in detail the application of the bimetallic electrode system to the estimation of bismuth with thiourea, substituted thioureas and urea.

B.D.H. reagent grade bismuth trichloride was recrystallized twice from acetone and its solutions of varying concentrations in anhydrous methanol, ethanol and acetone were prepared. The strength of these solutions was determined by the oxychloride method[4]. Thiourea solutions were standardized by the Volhard procedure[5] as modified by Cuthil and Atkins[6].

The bimetallic electrode system was used, employing the Pt : W bimetallic couple, first proposed by Furman and Wilson[7]. The Bi : W electrode system was also used. An aliquot of the bismuth chloride solution was taken in a pyrex cell fitted with the platinum and tungsten (or the bismuth and tungsten) electrodes. The electrical circuit was similar to that used by Gay[8], and consisted of a 1.5 V. cell with its negative pole connected to the tungsten electrode, a 1 kΩ fixed resistance, a 200 Ω variable rheostat and a suitably shunted galvanometer, all connected in series. Galvanometer deflections were noted after successive additions, from the burette, of small amounts of standard thiourea solution and thorough stirring.

The addition of the titrant near the end point was dropwise. Maxima in the galvanometric deflection mark the equivalence points, corresponding to the formation of different complexes.

A representative curve from an actual determination of bismuth against thiourea in acetone medium, using the Pt : W bimetallic electrode system, is shown in Fig. 1. The curve shows two peaks corresponding to the two complexes of bismuth with thiourea reported in the earlier communication[3].

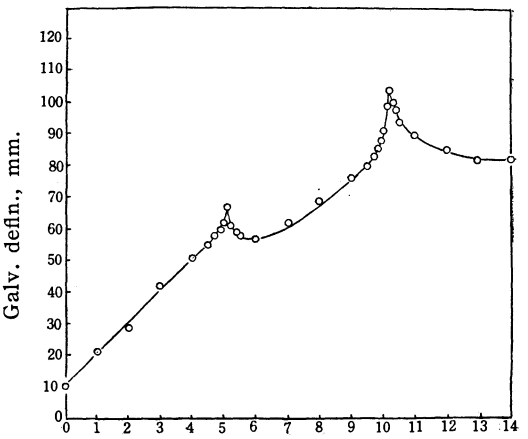


Fig. 1. Titration of bismuth against thiourea in acetone medium, using Pt: W bimetallic electrode system.

Table I shows the results of determination of bismuth against thiourea, phenyl thiourea, *p*-toluyl thiourea and urea in different non-aquous media using the Pt: W bimetallic system.

The estimation of bismuth against the same ligands was also done with the Bi: W bimetallic electrode couple. The results are recorded in Table II. The titrations with urea had to be restricted to methanol and ethanol medium only because of the low solubility of urea in acetone.

The two peaks in the titration curve correspond to the two end points in these titrations. This agrees with the formation of the two complexes viz., $2BiCl_3 \cdot 3X$ and

1) J. H. Yoe and L. G. Overholser, *Ind. Eng. Chem., Anal. Ed.*, **14**, 435 (1942).
2) C. Mahr, *Z. anal. Chem.*, **94**, 161 (1933); **97**, 96 (1934).
3) V. D. Anand and B. N. Prasad, communicated to *Z. anorg. u. allgem. Chem.* (accepted for publication).
4) "Scotts Standard Methods of Chemical Analysis", 5th Ed., D. Van Nostrand Co., Inc., New York (1944), p. 153.
5) J. Volhard, *Ber.*, **7**, 100 (1847).
6) R. Cuthil and C. Atkins, *J. Soc. Chem. Ind.*, **56**, 5T (1937).
7) N. H. Furman and E. B. Wilson, *J. Am. Chem. Soc.*, **50**, 277 (1928).
8) J. R. Gay, *Ind. Eng. Chem., Anal. Ed.*, **11**, 383 (1939); cf. A. Findlay, "Practical Physical Chemistry", Longman Green and Co., Inc., London (1949), p. 240.

TABLE I. ELECTROMETRIC DETERMINATION OF BISMUTH
(Pt : W Bimetallic electrode system)

Solvent medium	Weight of the bismuth complex: $2BiCl_3 \cdot 3X$* Calculated g.	Found g.	Error mg.	$BiCl_3 \cdot 3X$* Calculated g.	Found g.	Error mg.
			Thiourea			
Acetone	0.1428	0.1430	+0.2	0.1809	0.1811	+0.2
	0.0142	0.0142	—	0.0180	0.0181	+0.1
	0.0072	0.0072	—	0.0091	0.0090	−0.1
Methanol	0.0812	0.0815	+0.3	0.1028	0.1026	−0.2
	0.0162	0.0164	+0.2	0.0205	0.0204	−0.1
	0.0041	0.0040	−0.1	0.0052	0.0052	—
Ethanol	0.1290	0.1293	+0.3	0.1631	0.1635	+0.4
	0.0257	0.0258	+0.1	0.0325	0.0327	+0.2
	0.0129	0.0129	—	0.0163	0.0162	−0.1
			Phenyl thiourea			
Acetone	0.0180	0.0184	+0.4	0.0255	0.0252	−0.3
	0.0091	0.0092	+0.1	0.0129	0.0128	−0.1
	0.0044	0.0046	+0.2	0.0063	0.0064	+0.1
Methanol	0.0689	0.0685	−0.4	0.0979	0.0972	−0.7
	0.0346	0.0344	−0.2	0.0491	0.0488	−0.3
	0.0138	0.0137	−0.1	0.0196	0.0194	−0.2
Ethanol	0.0359	0.0357	−0.2	0.0510	0.0514	+0.4
	0.0180	0.0180	—	0.0255	0.0256	+0.1
	0.0073	0.0073	—	0.0103	0.0102	−0.1
			p-Toluyl thiourea			
Acetone	0.0426	0.0423	−0.3	0.0614	0.0609	−0.5
	0.0212	0.0212	—	0.0305	0.0302	−0.3
	0.0084	0.0083	−0.1	0.0121	0.0121	—
Methanol	0.0513	0.0508	−0.5	0.0739	0.0745	+0.6
	0.0258	0.0255	−0.3	0.0371	0.0372	+0.1
	0.0103	0.0102	−0.1	0.0149	0.0149	—
Ethanol	0.0253	0.0250	−0.3	0.0365	0.0363	−0.2
	0.0128	0.0128	—	0.0184	0.0185	+0.1
	0.0052	0.0052	—	0.0074	0.0074	—
			Urea			
Methanol	0.0764	0.0768	+0.4	0.0934	0.0939	+0.5
	0.0382	0.0383	+0.1	0.0467	0.0465	−0.2
	0.0192	0.0192	—	0.0234	0.0233	−0.1
Ethanol	0.1125	0.1133	+0.8	0.1375	0.1364	+1.1
	0.0225	0.0227	+0.2	0.0275	0.0272	−0.3
	0.0112	0.0111	−0.1	0.0137	0.0137	—

* X denotes the complexing ligand.

$BiCl \cdot 3X$ (Where X stands for the complexing group). The two end points afford a convenint internal check on the accuracy of the procedure. The titration may, however, be stopped at either stage, since both equivalence points give accurate values within the limits of experimental error and results are easily reproducible.

It is evident from an examination of Tables I and II that the error is generally small and far less than is usually met with in the ordinary estimations. This is indicative of the fact that the electrometric determination is a simple, convenient and rapid procedure, easily applicable to the quantitative determination of bismuth.

TABLE II. ELECTROMETRIC DETERMINATION OF BISMUTH
(Bi : W Bimetallic electrode system)

Solvent medium	Weight of the bismuth complex: $2BiCl_3 \cdot 3X$* Calculated g.	$2BiCl_3 \cdot 3X$* Found g.	$2BiCl_3 \cdot 3X$* Error mg.	$BiCl_3 \cdot 3X$* Calculated g.	$BiCl_3 \cdot 3X$* Found g.	$BiCl_3 \cdot 3X$* Error mg.
			Thiourea			
Acetone	0.1428	0.1437	+0.9	0.1809	0.1823	+1.4
	0.0142	0.0143	+0.1	0.0180	0.0182	+0.2
	0.0072	0.0072	—	0.0091	0.0090	−0.1
Methanol	0.0812	0.0806	−0.6	0.1028	0.1020	−0.8
	0.0162	0.0163	+0.1	0.0205	0.0208	+0.3
	0.0041	0.0041	—	0.0052	0.0052	—
Ethanol	0.1290	0.1298	+0.8	0.1631	0.1640	+0.9
	0.0257	0.0259	+0.2	0.0325	0.0328	+0.3
	0.0129	0.0128	−0.1	0.0163	0.0164	+0.1
			Phenyl thiourea			
Acetone	0.0180	0.0182	+0.2	0.0255	0.0258	+0.3
	0.0091	0.0091	—	0.0129	0.0131	+0.2
	0.0044	0.0045	+0.1	0.0063	0.0063	—
Methanol	0.0689	0.0684	−0.5	0.0979	0.0983	+0.4
	0.0346	0.0344	−0.2	0.0491	0.0493	+0.2
	0.0138	0.0138	—	0.0196	0.0195	−0.1
Ethanol	0.0359	0.0362	+0.3	0.0510	0.0506	−0.4
	0.0180	0.0180	—	0.0255	0.0254	−0.1
	0.0073	0.0072	−0.1	0.0103	0.0103	—
			p-Toluyl thiourea			
Acetone	0.0426	0.0429	+0.3	0.0614	0.0618	+0.4
	0.0212	0.0214	+0.2	0.0305	0.0303	−0.2
	0.0084	0.0084	—	0.0121	0.0122	+0.1
Methanol	0.0513	0.0508	−0.5	0.0739	0.0733	−0.6
	0.0258	0.0256	−0.2	0.0371	0.0368	−0.3
	0.0103	0.0104	+0.1	0.0149	0.0149	—
Ethanol	0.0253	0.0255	+0.2	0.0365	0.0361	−0.4
	0.0128	0.0126	−0.2	0.0184	0.0182	−0.2
	0.0052	0.0052	—	0.0074	0.0073	−0.1
			Urea			
Methanol	0.0764	0.0769	+0.5	0.0934	0.0944	+1.0
	0.0382	0.0384	+0.2	0.0467	0.0470	+0.3
	0.0192	0.0193	+0.1	0.0234	0.0236	+0.2
Ethanol	0.1125	0.1136	+1.1	0.1375	0.1361	−1.4
	0.0226	0.0228	+0.2	0.0275	0.0272	−0.3
	0.0112	0.0113	+0.1	0.0137	0.0136	−0.1

* X denotes the complexing ligand.

Sincere thanks of the authors are due to Professor S. S. Joshi, D. Sc. (London), Head of Chemistry Department for facilities and keen interest and the Ministry of Scientific Research and Cultural Affairs for the award of a scholarship to one of them (V. D. A.).

Chemical Laboratories
Banaras Hindu University
Banaras-5, India